Studies on Disease Prevention and Control, Decontamination and Sterilization, Microbial Adaptive Responses and Survival, Alternative Therapies, and Sustainability

Submitted by

Neil J. Rowan (M.Sc. Ph.D.)

September 2024

A Thesis Submitted in Fulfilment of the Requirements for the Higher Degree of Doctor of Science (D.Sc) in the Faculty of Science

Declaration

This thesis is the result of the author's original research. It has been composed by the author and has not been previously submitted for examination which has led to the award of a degree.

Signed:  Date: 27th September, 2024

Abstract

This thesis describes my independent research studies starting in 1996 on five related areas that have advanced disease prevention and control including sustainable technologies to meet significant societal challenges. There are ever increasing demands for specialist foods and sophisticated devices to meet complexities of modern society including serving vulnerable groups. Whilst there is an expanding volume of published literature on developing food production, and to a much lesser degree medical devices, there is a need to understand why traditional and emerging decontamination and sterilization modalities work and what conditions or circumstances operating at the interface between microbial destruction and maintaining a desired product functionality could support microbial survivors and potentially foodborne or iatrogenic-mediated infection. There is also a dearth in knowledge surrounding the real-time detection of viable fastidious pathogenic microorganisms (such as complex parasites or drug-resistant fungi) post selection of appropriate technologies to safely treat foods and to decontaminate complex reusable medical devices. There is also a dearth of published information on appropriate cellular and molecular indicators to inform critical mechanistic information underpinning testing, verification and validation of new decontamination technologies. Elucidating holistically, the key parameters governing reliable and effective decontamination, provides evidence-based data to inform next-generation products from design thinking to automation in order to meet emerging societal needs.

The **first section** provides critical new insights and knowledge on conditions promoting the potential survival of microbial pathogens in sensitive foods such as reconstituted foods destined for vulnerable populations. It describes preparation and storage-abuse conditions promoting adaptive microbial survival and toxin production leading. It describes occurrence of such abuse conditions in hospital-prepared feeds in a HIV ward along with implemented of my recommended solutions that informed new guidelines of practice and helped to mitigate against future food-borne illnesses. This section characterizes processing conditions promoting the occurrence of atypical pathogens in sensitive foods, such as thermal-stresses leading to atypical cellular appearance and virulence factor expression *Listeria monocytogenes* that also enabled survival in human polymorphonuclear leukocytes.

The **second section** elucidates the first reporting on reliable and repeatable operational conditions underpinning non-thermal processing technologies (pulsed UV light, pulsed-plasma gas-discharge, pulsed electric fields), which also encompasses key mechanistic knowledge on critical cellular and molecular determinants governing irreversible microbial cell death. Commensurate studies report on development of alternative biomarkers to monitor and evaluate real-time disinfection performance including first report of a combined cell culture-qPCR assay for complex entero-parasites. New methodologies for toxicological end-point determinations in processing technologies are described.

First reporting on microbial kinetic inactivation and modelling for non-thermal technologies. Studies also elucidate appropriate treatment dose for effective killing of biological indicators including development of vaporized hydrogen peroxide as a new thermal sterilization modality for medtech.

The third section elucidates and develops non-thermal decontamination and sterilization technologies at commercial scale for established and new applications including for medical devices, food/feed, and for pollination industry (such as for decontaminating heat-sensitive pollen of complex pathogens fed to bees). Depending on the application, these studies include technologies encompassing x-ray, electron-beam, gamma-irradiation, pulsed UV and the co-development of real-8578/-+parametric release for treated products. Understanding the holistic interplay of all applied and inimical stresses governing effective microbial lethality *defines* critical knowledge including desirable end-to-end sterility assurance conditions ranging from elucidation to verification and validation of technological applications that meets safety. This section describes first classification system for effective cleaning of complex features in reusable medical devices and revisits efficacy of Spaulding's classification for device sterilisation and patient safety using this combinational new cleaning method. A holistic subject-matter knowledge of decontamination helps society meet unforeseen threats such as my elucidation and the first published recommendation of appropriate sterilization technologies and conditions for the safe reuse of PPE arising from critical supplying chain shortages during COVID-19 pandemic along with for sustainable waste management. Studies advance shellfish depuration and decontamination for recalcitrant fastidious norovirus pathogens attached to bivalve tissue.

The **fourth** section elucidates and develops novel alternative therapies and approaches for combatting antimicrobial-drug resistant (AMR) pathogens including bacteria and fungi, such as for lung delivery and for animal feed applications. Studies also address diagnostics for AMR pathogens that are at crisis point for society linked to decontamination. Studies also address elucidation of alternative antimicrobial and biofilm-disrupting bioactives used synergistically and in combination, yet tolerant of and suitable for medical device production-processes for smart coating applications.

The **last section** describes development of sustainable innovation including use of appropriate disinfection technologies. This includes first studies on development of an integrated multi-trophic aquaculture system in the peatlands aligned with zero-waste, zero pollution and climate action principles. It addresses digital transformation including new 'in-field' real-time monitoring and combined use of bioinformatics and next-generation sequencing to advance sustainable food innovation. It develops and applies new models including life cycle assessment and ecological tools.

Acknowledgements

Life is a journey that we are told is taking one step after another, that is lonely road. When we have someone to walk with us and support us along the way, that is living. I dedicate this thesis to my parents Ruth and Breffni, to my wife Michelle, to my daughter Chloe and to my sons Kevin and Liam for their endless love, support and encouragement! This thesis has been a psychological journey that captured precious time that was not shared enough with them. I apologise to them for when I have been distant and not focusing on their needs. I discussed this higher DSc submission with my father Breffni sadly before he passed way in 2014; it's a real relief (catharsis) that have I eventually managed to address it.

I was the first of many generations to have attended University. I feel this background has positively influenced my steadfast commitment to pursuit of research excellence and has helped with my engagement with students who attend university from all walks of life. I am grateful to the University of Galway for awarding me a professional soccer scholarship during my undergraduate years as a microbiology student. I am grateful to the late Professor John E Smith offering me an AFRC educational scholarship to pursue postgraduate studies at Strathclyde University. Thank you to Prof John G. Anderson and Prof Scott MacGregor for their friendship and encouragement at Strathclyde University as I forged an independent research pathway. I was pleased that my grading of 5* during the UK Research Assessment Exercise of 2023 reflected my commitment to this pursuit of academic excellence and to growing research and innovation at the University of Strathclyde.

To my friends at Dublin Institute of Technology, thank you for keeping me sane given that I commuted ca. 6 hours every day for 3 years to lecture there; thus, affording our children the opportunity of attend school locally in Athlone. Thank you to the School of Medicine at the University of Galway for appointing me as an Adjunct Professor. Also, to the University of KwaZulu Natal, and the University of Malaysia for Honorary Professorship appointments in Biotechnology. To the University of Stanford for recognising my contributions to these fields of study as reflected in my appearance on 2023 list of top 2% scientists globally. To the Technological University of Shannon (TUS), for bestowing the inaugural 'Outstanding Contribution to Research' award earlier this year. I have spent the past 20 years working at TUS here in Ireland (formerly Athlone Institute of Technology (AIT)) that was predominantly teaching-led. I thank TUS for my appointment as the first Director of the Bioscience Research Institute since 2012 and for its trust in me to inform process changes to grow research scale and capacity that contributed to it becoming a new university in October 2020.

Table of Content **Page**

Rowan, N.J., Kirf, D. and Tomkins, P. (2009). Studies on the susceptibility of different culture morphotypes of *Listeria monocytogenes* to uptake and survival in human polymorphonuclear leukocytes. *FEMS Immunology and Medical Microbiology*, **57** (2), 183-192. 86

Rowan, N.J. (1999). Evidence that inimical food-preservation barriers alter microbial resistance, cell morphology and virulence. *Trends in Food Science and Technology*, **10** (8), 261-270. 96

Geraghty, L., Booth, M., Rowan, N.J. and Fogarty, A. (2013). Investigations on the efficacy of routinely used phenotypic methods compared to genotypic approaches for the identification of staphylococcal species isolated from companion animals in Irish veterinary hospitals. Ir Vet J 66, 7 (2013). https://doi.org/10.1186/2046-0481-66-7 106

Rowan, N. (2004). Viable but non-culturable forms of food and waterborne bacteria: quo vadis? *Trends in Food Science and Technology*, **15** (9), 462-467. 115

Section 2: Adaptive Microbial Stress Responses and Inactivation Performance under Non-thermal Processing and Decontamination 121

Rowan, N.J., MacGregor, S.J., Anderson, J.G., Fouracre, R.A., McIIvaney, L. and Farish, O. (1999). Pulsed light inaction of food related microorganisms. *Applied and Environmental Microbiology*, **65** (3), https://doi.org/10.1128/AEM.65.3.1312-1315.1999 123

Garvey, M., Fernandes, J.P.A. and Rowan, N.J. (2015). Pulsed light for the inactivation of fungal biofilms of clinically-relevant pathogenic *Candida* species. *Yeast*, **32**, 533-542. 127

Farrell, H.P., Garvey, M., Cormican, M., Laffey, J.G., Rowan, N.J. (2010). Investigation of critical inter-related factors affecting the efficacy of pulsed light for inactivating clinically relevant bacterial pathogens. *Journal of Applied Microbiology*, **108** (5), 1494-1508. 135

Farrell, H., Hayes, J., Laffey, J and Rowan, N. J. (2011). Studies on the relationship between pulsed UV light irradiation and the simultaneous occurrence of molecular and cellular damage in clinically-relevant *Candida albicans*. *Journal of Microbiological Methods*, **84** (2), 317-326. 150

Garvey, M., Farrell, H., Cormican, M. and Rowan, N.J. (2010). Investigations of the relationship between use of in vitro cell culture-quantitative PCR and a mouse-based bioassay for evaluating critical factors affecting the disinfection performance of pulsed UV light for treating *Cryptosporidium parvum* oocysts in saline. *Journal of Microbiological Methods*, **80** (3), 267-273. 160

Garvey, M., Stocca, A and Rowan, N.J. (2014). Development of a combined *in vitro* cell culture – Quantitative PCR assay for evaluating the disinfection performance of pulsed light for treating the waterborne enteroparasite *Giardia lamblia*. *Experimental Parasitology*, **144**, 6-13. 167

Garvey, M., Clifford, E., O'Reilly, E., Rowan, N.J. (2013). Efficacy of Using Harmless *Bacillus* Endospores to Estimate the Inactivation *of Cryptosporidium parvum* Oocysts in Water. *The Journal of Parasitology*, **99** (3), 448-452. 176

Garvey, M., Rabbitt, D., Stocca, A. and Rowan, N.J. (2014). Pulsed ultraviolet light inactivation of *Pseudomonas aeruginosa* and *Staphylococcus aureus* biofilms. *Water and the Environmental Journal*, **29** (1), 36-42.

Hayes, J.C., Laffey, J.G., McNeil, B. and Rowan, N.J. (2012). Relationship between growth of food-spoilage yeast in high-sugar environments and sensitivity to high-intensity pulsed UV light irradiation. *International Journal of Food Science and Technology*, **47** (9) 1925-1934.

Garvey, M., Stocca, A. and Rowan, N.J. (2016). Use of a real-time PCR assay to assess the effect of pulsed light inactivation on bacterial cell membranes and associated cell viability. *Water Environment Research*, **88** (2) 168-174.

Rowan, N.J., Valdramidis, V.P. and Gomez-Lopez, V.M (2015). A review of quantitative methods to describe efficacy of pulsed light generated inactivation data that embraces the occurrence of viable but non culturable state microorganisms. *Trends in Food Science and Technology*, **44** (1), 79-92.

Fitzhenry, K., Clifford, E., Rowan, N.J. and Val de Rio, A. (2021). Bacterial inactivation, photoreactivation and dark repair post flow-through pulsed UV disinfection. *Journal of Water Processing Engineering*, **41**, https://doi.org/10.1016/j.jwpe.2021.102070

Garvey, M., Coughlan, G., Murphy, N. and Rowan, N.J. (2016). The pulsed light inactivation of veterinary relevant microbial biofilms and the use of a RTPCR assay to detect parasite species within biofilm structures. *Open Veterinary Journal*, **6** (1), https://doi.org/10.4314/ovj.v6i1.3

Garvey, M., Hayes, J., Clifford, E., Kirf, D. and Rowan, N.J. (2013). Efficacy of measuring cellular ATP levels to determine the inactivation of pulsed UV treated *Cryptosporidium parvum* oocysts suspended in water. *Water Supply*, **13** (2), 202-213.

Rowan, N.J. (2019). Pulsed light as an emerging technology to cause disruption for food and adjacent industries – Quo vadis? Trends in Food Science and Technology, 88, 316-332.

Rowan, N.J., MacGregor, S.J., Anderson, J.G., Fouracre, R.A. and Farish, O. (2000). Pulsed electric field inactivation of diarrhoeagenic *Bacillus cereus* through irreversible electroporation. *Letters in Applied Microbiology*, **31** (2), 110-114.

Yaqub, S., Anderson, J.G., MacGregor, S.J. and Rowan, N.J. (2004). Use of a fluorescent viability stain to assess lethal and sublethal injury in food-borne bacteria exposed to high-intensity pulsed electric fields. *Letters in Applied Microbiology*, **39** (30, 246-251.

Beveridge, J.R., Wall, K., MacGregor, S.J., Anderson, J.G. and Rowan, N.J. (2003). Pulsed electric field inactivation of spoilage microorganisms in alcoholic beverages and the influence of pulse profile. Digest of Technical Papers. PPC-2003. 14th IEEE International Pulsed Power Conference (IEEE Cat. No.03CH37472), Dallas, TX, USA, 2003, pp. 1132-1135 Vol.2, doi: 10.1109/PPC.2003.1278011.

Rowan, N.J. MacGregor, S.J., Anderson, J.G., Cameron, D. and Farish, O. (2001). Inactivation of *Mycobacterium paratuberculosis* by Pulsed Electric Fields. *Applied and Environmental Microbiology*, **67** (6), https://doi.org/10.1128/AEM.67.6.2833-2836.2001

Rowan, N.J., Espie, S., Harrower, J., Anderson, J.G., Marsili, L., MacGregor, S.J. (2007). Pulsed-Plasma Gas-Discharge Inactivation of Microbial Pathogens in Chilled Poultry Wash Water. *Journal of Food Protection*, **70** (12), 2805-2810.

Hayes, J., Kirf, D., Garvey, M. and Rowan, N. (2013). Disinfection and toxicological assessments of pulsed UV and pulsed-plasma gas-discharge treated-water containing the waterborne protozoan enteroparasite *Cryptosporidium parvum. Journal of Microbiological Methods*, **94** (3), 325-337.

Rowan, N.J., Espie, S., Harrower, J., Farrell, H., Marsili, L., Anderson, J.G. and MacGregor, S. J. (2008). Evidence of lethal and sublethal injury in food-borne bacterial pathogens exposed to high-intensity pulsed-plasma gas discharges. *Letters in Applied Microbiology*, **46** (1), 80-86.

McEvoy, B. and Rowan, N.J. (2019). Terminal sterilization of medical devices using vaporized hydrogen peroxide: a review of current methods and emerging opportunities. *Journal of Applied Microbiology*, **127** (5), 1403-1420.

Rowan, N.J., Kremer, T., McDonnell, G. (2023). A review of Spaulding's classification system for effective cleaning, disinfection and sterilization of reusable medical devices: Viewed through a modern-day lens that will inform and enable future sustainability. *Science of the Total Environment*, **878**, https://doi.org/10.1016/j.scitotenv.2023.162976

Chen, Y., Neff, M., McEvoy, B., Cao, Z., Pessoli, R., Murphy, A., Gately, N., Hopkins Jnr, M., Rowan, N.J. and Devine, M. (2019). 3D printed polymers are less stable than injection moulded counterparts when exposed to terminal sterilization processes using novel vaporized hydrogen peroxide and electron beam processes. *Polymer*, **183**, https://doi.org/10.1016/j.polymer.2019.121870

Garvey, M. and Rowan, N.J. (2023). Pathogenic Drug Resistant Fungi: A Review of Mitigation Strategies. *International Journal of Molecular Sciences*, **24** (2), https://doi.org/10.3390/ijms24021584

Garvey, M., Meade, E. and Rowan, N.J. (2022). Effectiveness of front line and emerging fungal disease prevention and control interventions and opportunities to address appropriate eco-sustainable solutions. *Science of the Total Environment*, **851** (2), https://doi.org/10.1016/j.scitotenv.2022.158284

Rowan, N.J., and Laffey, J.G. (2020). Challenges and solutions for addressing critical shortage of supply chain for personal and protective equipment (PPE) arising from Coronavirus disease (COVID19) pandemic – Case study from the Republic of Ireland. Science of the Total Environment. 725, https://doi.org/10.1016/j.scitotenv.2020.138532

Rowan, N., J. and Laffey, J.G. (2020). Unlocking the surge in demand for personal and protective equipment (PPE) and improvised face coverings arising from coronavirus disease (COVID-19) pandemic – Implications for efficacy, re-use and sustainable waste management. *Science of the Total Environment*, **752**, https://doi.org/10.1016/j.scitotenv.2020.142259

Rowan, N.J. and Moral, R.A. (2016). Disposable face masks and reusable face coverings as non-pharmaceutical interventions (NPIs) to prevent transmission of SARS-CoV-2 variants that cause coronavirus disease (COVID-19): Role of new sustainable NPI design innovations and predictive mathematical modelling. *Science of the Total Environment*, **772**, https://doi.org/10.1016/j.scitotenv.2021.145530

Section 3: Scaling Disinfection and Sterilisation Technologies

Eakins, J., Lynch, M., Carolan, J.C. and Rowan, N.J. (2023). Studies on the novel effects of electron beam treated pollen on colony reproductive output in commercially-reared bumblebees (*Bombus terrestris*) for mass pollination applications. *Science of the Total Environment*, **899**, https://doi.org/10.1016/j.scitotenv.2023.165614

Naughton, J., Tiedeken, E.J., Garvey, M., Stout, J.C. and Rowan, N.J. (2017). Pulsed light inactivation of the bumble bee trypanosome parasite *Crithidia bombi*. *Pathology and Parasitology*, 144-154.

Goblirsch, M., Eakins, J. and Rowan, N.J. (2021). Disease-mitigating innovations for the pollination service industry: Challenges and opportunities. *Current Opinion in Environmental Science and Health*, **22**, https://doi.org/10.1016/j.coesh.2021.100265

McEvoy, B., Maksimovic, A. and Rowan, N.J. (2022). *Geobacillus stearothermophilus* and *Bacillus atrophaeus* spores exhibit linear inactivation kinetic performance when treated with an industrial scale vaporized hydrogen peroxide (VH2O2) sterilization process. *Journal of Applied Microbiology*, **134** (1), https://doi.org/10.1093/jambio/lxac028

McEvoy, B., Maksimovic, A., Howell, D., Reppert, P., Ryan, D., Rowan, N.J. and Herve, M. (2023). Studies on the comparative effectiveness of X-rays, gamma rays and electron beams to inactivate microorganisms at different dose rates in industrial sterilization of medical devices. *Radiation Physics and Chemistry*, **208**, https://doi.org/10.1016/j.radphyschem.2023.110915

McEvoy, B., Lynch, M. and Rowan, N.J. (2021). Opportunities for the application of real-time bacterial cell analysis using flow cytometry for the advancement of sterilization microbiology. *Journal of Applied Microbiology*, **130** (6), 1794-1812.

McFadden, E., Costa Ramos, A., Bradley, D., Vrain, O., McEvoy, B. and Rowan, N.J. (2016). Comparative studies on the novel sterilisation of Irish retailed infant milk formula using electron beam and pulsed light treatments. *International Journal of Science, Environment and Technology*, **5** (6), 4375-4377.

Kremer, T., Rowan, N.J. and McDonnell, G. (2024). A proposed cleaning classification system for reusable medical devices to complement the Spaulding classification. *Journal of Hospital Infection*, **145**, 88-98.

Kremer, T.A., Felgar, J., Rowan, N.J. and McDonnell, G. (2023). Validation of the Device Feature Approach for Reusable Medical Device Cleaning Evaluations. *Biomedical Instrumentation and Technology*, https://doi.org/10.2345/0899-8205-57.4.143

Rowan, N.J., Johnstone, C.M., McLean, R.C., Anderson, J.G. and Clarke, J.A.(1999). Prediction of Toxigenic Fungal Growth in Buildings by Using a Novel Modelling System. *Applied and Environmental Microbiology*, **65** (11), https://doi.org/10.1128/AEM.65.11.4814-4821.1999

Rowan, N.J (2024). Digital technologies to unlock safe and sustainable opportunities for medical device and healthcare sectors with a focus on the combined use of digital twin and extended reality applications: A review. *Science of the Total Environment*, **926**, https://doi.org/10.1016/j.scitotenv.2024.171672

Franssen, F., Gerard, C., Cozma-Petrut, A., Vieira-Pinto, M., Rezek Jambrak, A, Rowan, N.J., Paulsen, P., Rozcki, M., Tysnes, K., Rodrigues-Lasaro, D and Roberston, L. (2019). Inactivation of parasite transmission stages: Efficacy of treatments on food of animal origin. *Trends in Food Science and Technology***, 83,** 114-128.

Gerard, C., Franssen, F., La Barbona, S., Monteiro, S., Cozma-Petrut, A., Uttaker, K.S., Rezek Jambrak, A., Rowan, R., Rodriguez-Lasaro, D., Tysnes, K and Robertson, L..J. (2019). Inactivation of parasite transmission stages: Efficacy of treatments on foods of non-animal origin. *Trends in Food Science and Technology*, **91**, 12-23.

Kremer, T., Murray, N., Buckley, J. and Rowan, N.J. (2023). Use of real-time immersive digital training and educational technologies to improve patient safety during the processing of reusable medical devices: Quo Vadis? *Science of the Total Environment*, **900**, https://doi.org/10.1016/j.scitotenv.2023.165673

Byrne, T., Murray, N., McDonnell-Naughton, M. and Rowan, N.J. (2023). Perceived factors informing the pre-acceptability of digital health innovation by aging respiratory patients: a case study from the Republic of Ireland. *Frontiers in Public Health*, **11**, https://doi.org/10.3389/fpubh.2023.1203937

Section 4: Complementary and Alternative Therapies and Approaches

Masterson, C.H., Murphy, E.J., Gonzalez, H., Major, I., McCarthy, S.D., O'Toole, D., Laffey, J.393G. and Rowan, N.J (2020). Purified β-glucans from the Shiitake mushroom ameliorates a405ntibiotic-resistant *Klebsiella pneumoniae*-induced pulmonary sepsis. *Letters in Applie424d Microbiology* **71** (4), 405-412.

Murphy, E.J., Masterons, C., Rezoagli, E., O'Toole, D., Major, I., Stack, D., Lynch, M., Laffey, J.G. and Rowan, N.J (2020). β-Glucan extracts from the same edible shiitake mushroom *Lentinus edodes* produce differential in-vitro immunomodulatory and pulmonary cytoprotective effects — Implications for coronavirus disease (COVID-19) immunotherapies. *Science of the Total Environment*, **732**, https://doi.org/10.1016/j.scitotenv.2020.139330

Murphy, E.J., Rezoagli, E, Pogue, R., Simonassi-Paiva, B., Aldin, I., Fehrenbach, G.W., O'Niell, E., Major, I., Laffey, J.G. and Rowan, N. (2022). Immunomodulatory activity of β-glucan polysaccharides isolated from different species of mushroom – A potential treatment for inflammatory lung conditions. *Science of the Total Environment*, **809**, https://doi.org/10.1016/j.scitotenv.2021.152177

Murphy, E.J., Rezoagli, E., Major, I., Rowan, N.J., Laffey, J.G (2020). β-Glucan Metabolic and Immunomodulatory Properties and Potential for Clinical Application. *Journal of Fungi*, **6** (4), https://doi.org/10.3390/jof6040356

Galanakis, C.M., Aldawoud, T.M., Rizou, M., Rowan, N.J. and Ibrahim, S.A. (2020). Food Ingredients and Active Compounds against the Coronavirus Disease (COVID-19) Pandemic: A Comprehensive Review. *Foods*, **9 (**11), https://doi.org/10.3390/foods9111701

Wan Mohtar, W.A.A.Q.I, IIham, Z., Jamaludin, A.A and Rowan, N.J (2021). Use of Zebrafish Embryo Assay to Evaluate Toxicity and Safety of Bioreactor-Grown Exopolysaccharides and Endopolysaccharides from European *Ganoderma applanatum*

Mycelium for Future Aquaculture Applications. *International Journal of Molecular Sciences*, **22** (4), https://doi.org/10.3390/ijms22041675

Wan Mohtar, W.A.A.Q.I., Fafek, N.A., Thiran, J.P., Rahman, J.F.P., Yerima, G., Subramaniam, K. and Rowan, N.J. (2021). Investigations on the use of exopolysaccharide derived from mycelial extract of Ganoderma lucidum as functional feed ingredient for aquaculture-farmed red hybrid Tilapia (Oreochromis sp.). *Future Foods*, **3**, https://doi.org/10.1016/j.fufo.2021.100018

Usuldin, S.R.A., Wan-Mohtar, W.A.A.Q.I., IIham, Z., Abdullah, N.R. and Rowan, N. (2021). *In vivo* toxicity of bioreactor-grown biomass and exopolysaccharides from Malaysian tiger milk mushroom mycelium for potential future health applications. *Nature Scientific Reports*, **11**, https://doi.org/10.1038/s41598-021-02486-7

Masterson, K., Meade, E., Garvey, M., Lynch, M, Major, I and Rowan, N.J (2021). Development of a low-temperature extrusion process for production of GRAS bioactive-polymer loaded compounds for targeting antimicrobial-resistant (AMR) bacteria. *Science of the Total Environment*, **80**0, https://doi.org/10.1016/j.scitotenv.2021.149545

Masterson, K., Major, I., Lynch, M. and Rowan, N.J. (2023). Synergy Assessment of Four Antimicrobial Bioactive Compounds for the Combinational Treatment of Bacterial Pathogens. *Biomedicine*s, **1**1 (8), https://doi.org/10.3390/biomedicines11082216

Rowan, N.J., Meade, E., Garvey, M. (2021). Efficacy of frontline chemical biocides and disinfection approaches for inactivating SARS-CoV-2 variants of concern that cause coronavirus disease with the emergence of opportunities for green eco-solutions. *Current Opinion in Environmental Science and Health*, **23,** https://doi.org/10.1016/j.coesh.2021.100290

Meade, E., Hehir, S., Rowan, N.J. and Garvey, M. (2022). Mycotherapy: Potential of Fungal Bioactives for the Treatment of Mental Health Disorders and Morbidities of Chronic Pain. *Journal of Fungi*, **8** (3), https://doi.org/10.3390/jof8030290

Section 5: Elucidating and Developing New Sustainable Technologies and Frameworks

Naughton, S., Kavanagh, S., Lynch, M. and Rowan, N.J. (2020). Synchronizing use of sophisticated wet-laboratory and in-field handheld technologies for real-time monitoring of key microalgae, bacteria and physicochemical parameters influencing efficacy of water quality in a freshwater aquaculture recirculation system: A case study from the Republic of Ireland. *Aquaculture*, **526**, https://doi.org/10.1016/j.aquaculture.2020.735377

Tahar, A., Kennedy, A.M., Fitzgerald, R.D., Clifford, E. and Rowan, N.J. (2018) Longitudinal evaluation of the impact of traditional rainbow trout farming on receiving water quality in Ireland. *PeerJ 6 Aquatic Biology*, **e5281**, https://doi.org/10.7717/peerj.5281

Tahar, A., Kennedy, A., Fitzgerald, R., Clifford, E. and Rowan, N.J. (2018). Full water quality monitoring of a traditional flow-through rainbow trout farm. *Fishes* **3** (3),https://doi.org/10.3390/fishes3030028

Rowan, N.J., Fort, A., O'Neill, E.A., Clifford, E., Jansen, M., Helfert, M., Toner, D., Maguire, J. and Tiwari, B. (2024). Development of a novel recirculatory multitrophic peatland system for the production of high-value bio-based products at scale embracing zero waste and pollution principles to unlock sustainable development goals. *Case Studies*

in Chemical and Environmental Engineering, **9**, https://doi.org/10.1016/j.cscee.2024.100763

O'Neill, E.A. and Rowan, N.J. (2022). Microalgae as a natural ecological bioindicator for the simple real-time monitoring of aquaculture wastewater quality including provision for assessing impact of extremes in climate variance – A comparative case study from the Republic of Ireland. *Science of the Total Environment*, **802**, https://doi.org/10.1016/j.scitotenv.2021.149800

O'Neill, E.A., Morse, A.P. and Rowan, N.J. (2022). Effects of climate and environmental variance on the performance of a novel peatland-based integrated multi-trophic aquaculture (IMTA) system: Implications and opportunities for advancing research and disruptive innovation post COVID-19 era. *Science of the Total Environment*, **819**, https://doi.org/10.1016/j.scitotenv.2022.153073

O'Neill, E.A., Rowan, N.J. and Fogarty, A.M. (2019). Novel use of the alga *Pseudokirchneriella subcapitata*, as an early-warning indicator to identify climate change ambiguity in aquatic environments using freshwater finfish as a case study. *Science of the Total Environment*, 692, 209-218.

O'Neill, E.A., Fehrenbach, G., Murphy, E., Alencar, S.A., Pogue, R. and Rowan, N.J. (2022). Use of next generation sequencing and bioinformatics for profiling freshwater eukaryotic microalgae in a novel peatland integrated multi-trophic aquaculture (IMTA) system: Case study from the Republic of Ireland. Science of the Total Environment, 851 (2), https://doi.org/10.1016/j.scitotenv.2022.158392

O'Neill, E.A. and Rowan, N.J. (2023). Potential disruptive effects of zoosporic parasites on peatland-based organic freshwater aquaculture: Case study from the Republic of Ireland. Science of the Total Environment, 868, https://doi.org/10.1016/j.scitotenv.2023.161495

Rowan, N.J., Murray, N., Qiao, Y., O'Neill, E., Clifford, E., Barcelo, D. and Power, D.M. (2022). Digital transformation of peatland eco-innovations ('Paludiculture'): Enabling a paradigm shift towards the real-time sustainable production of 'green-friendly' products and services. *Science of the Total Environment*, **838** (3), https://doi.org/10.1016/j.scitotenv.2022.156328

Galanakis, C.M., Rizou, M., Aldawoud, T.M.S., Ucak. I. and Rowan, N.J. (2021). Innovations and technology disruptions in the food sector within the COVID-19 pandemic and post-lockdown era. Trends in Food Science and Technology, 110, 193-200

Fehrenbach, G.W., Murphy, E., Pogue, R., Carter, F., Clifford, E., Major, I. and Rowan, N. (2023). Pulsed ultraviolet disinfection of artificially contaminated seawater seeded with high levels of pathogen disease indicators as an alternative for the shellfish industry depuration systems. *Environmental Science and Pollution Research*, **30,** 70771-70782.

Fehrenbach, G.W., Pogue, R., Carter, F., Clifford, E. and Rowan, N.J. (2022). Implications for the seafood industry, consumers and the environment arising from contamination of shellfish with pharmaceuticals, plastics and potentially toxic elements: A case study from Irish waters with a global orientation. *Science of the Total Environment*, **844**, https://doi.org/10.1016/j.scitotenv.2022.157067

Finnegan, W., Clifford, E., Goggins, J., O'Leary N., Dobson, A., Rowan, N., Xiao, L., Miao, S., Fitzhenry, K., Leonard, P., Tarpey, E., Gil-Pulido, B., Gao, F. and Zhan, X.

(2018). Dairywater – striving for sustainability within the diary processing industry in the Republic of Ireland. *Journal of Diary Research*, **85** (3), 366-374.

Tiedeken, E.J., Tahar, A., McHugh, B. and Rowan, N.J. (2017). Monitoring, sources, receptors, and control measures for three European Union watch list substances of emerging concern in receiving waters – A 20 year systematic review. *Science of the Total Environment*, **574**, 1140-1163.

Tahar, A., Tiedeken, E.J., Clifford, E., Cummins, E. and Rowan N.J. (2017). Development of a semi-quantitative risk assessment model for evaluating environmental threat posed by the three first EU watch-list pharmaceuticals to urban wastewater treatment plants: An Irish case study. *Science of The Total Environment***, 603-604**-, 627-638.

Tahar, A., Tiedeken, E.J. and Rowan, N.J. (2018). Occurrence and geodatabase mapping of three contaminants of emerging concern in receiving water and at effluent from waste water treatment plants – A first overview of the situation in the Republic of Ireland. *Science of the Total Environment*, **616-617**-, 187-197.

Rowan, N.J. (2023). Current decontamination challenges and potentially complementary solutions to safeguard the vulnerable seafood industry from recalcitrant human norovirus in live shellfish: Quo Vadis? *Science of the Total Environment*, **874**, https://doi.org/10.1016/j.scitotenv.2023.162380

Ruiz-Salmon, I., Laso, J., Margallo, M., Villanaueva-Rey, P., Rodriguez, E., Quinteiro, P., Claudia Dias, A., Almeida, C., Clifford, E., Reguiero, L., Mendez, D., Anglada, C., Noirot, C., Rowan, N.J., Vazquez-Rowe, I. and Aldaco, R. (2021). Life cycle assessment of fish and seafood processed products – A review of methodologies and new challenges. *Science of the Total Environment*, **761**, https://doi.org/10.1016/j.scitotenv.2020.144094

Almeida, C., Laso, J., Baptista de Sousa, Cooney, R., Quinterio, P., Rowan, N.J., Dias, A.C., Clifford E., Reboredo, R.G., Margallo, M., Nunes, M.L. and Marques, A. (2023). Seafood consumers engagement in reducing environmental impacts from packaging. *Science of the Total Environment*, **863**, https://doi.org/10.1016/j.scitotenv.2022.160846

Rowan, N.,J. and Casey, O. (2021). 'Empower Eco' multi-actor HUB: A triple helix 'academia-industry-authority' approach to creating and sharing potentially disruptive tools for addressing novel and emerging new Green Deal opportunities under a United Nations Sustainable Development Goals framework. *Current Opinion in Environmental Science and Health*, **21**, https://doi.org/10.1016/j.coesh.2021.100254

Cooney, R., Baptista de Sousa, D., Fernandez Rios, Mellett, S., Rowan, N., Morse, A.P., Hayes, M., Laso, J., Regueiro, L., Wan, A., Clifford, E. (2023). A circular economy framework for seafood waste valorisation to meet challenges and opportunities for intensive production and sustainability. *Journal of Cleaner Production*, **392**, https://doi.org/10.1016/j.jclepro.2023.136283

Rowan, N.J. and Galanakis, C.M. (2020). Unlocking challenges and opportunities presented by COVID-19 pandemic for cross-cutting disruption in agri-food and green deal innovations: Quo Vadis? *Science of the Total Environment*. **748**, https://doi.org/10.1016/j.scitotenv.2020.141362

Rowan, N.J. (2023). Challenges and future opportunities to unlock the critical supply chain of personal and protective equipment (PPE) encompassing decontamination and reuse under emergency use authorization (EUA) conditions during the COVID-19

Section One: Food Safety Microbiology

My independent studies started with studies that profiled and detected a range of *Bacillus* species contaminating sensitive foods such as in hospital-feeds used by HIV patients. These investigations are described in the first section 'Food Safety Microbiology'. *Bacillus* are aerobic endospore forming bacteria that survive extreme processing conditions. My studies revealed that *B. cereus* and other atypical members of this *Bacillus* genus were capable of producing enterotoxins under various conditions of storage including refrigeration. Lack for appropriate healthcare processes and presence of utilizable carbohydrate source can lead to food-borne intoxication such as in a HIV-ward.

Appropriate practical solutions comprise an understanding and mitigating the occurrence of key factors governing *Bacillus* germination and toxin production in these foods for the hospital. My related research also revealed that atypical *Bacillu*s species can cause veterinary infections, which highlights emergence of atypical pathogenic species. *Bacillus cereus* were isolated that could grow and produce diarrhogeanic enterotoxins in reconstituted infant milk formulae under refrigeration storage. Thermal-stress studies associated with milk-based products, including artificially-spiked reconstituted infant milk formulae, can affect the physiology of the bacterial pathogen where studies revealed that sub-lethally stressed *Listeria monocytogenes* cells can alter their characteristic morphological appearance from short rods to very long chains influencing routine detection. These culture variants of *L. monocytogenes* can grow under refrigerated storage. Studies using molecular probes elucidated key housekeeping and virulence determinants governing this morphological and physiological transformation in *L. monocytogenes* associated with applied stresses. Immunological studies demonstrated that atypical rough cultures of *L. monocytogenes* can be taken up and survive in human polymorphonuclear leukocytes. Studies conducted under osmotic food-stress revealed variance in microbial survivors and the emergence of a sub-population of viable but non-culturable (VBNC) microorganisms. The existence and potential implications for food industry and consumers of this VBNC is addressed. This earlier research was conduction in food safety laboratories at Strathclyde University where Prof John G. Anderson provided collaborative valuable insights particularly on accessing and using automated bacterial plate readers.

Journal of Food Protection, Vol. 60, No. 9, 1997, Pages 1089–1094

Bacteriological Quality of Infant Milk Formulae Examined under a Variety of Preparation and Storage Conditions

N. J. ROWAN,* J. G. ANDERSON, and A. ANDERTON

Department of Bioscience & Biotechnology, University of Strathclyde, Royal College Building, 204 George Street, Glasgow G1 1XW, Scotland

(MS# 96-271: Received 27 September 1996/Accepted 20 January 1997)

ABSTRACT

One hundred infant milk formulae (IMFs), representative of the 10 leading brands available in the UK, were subjected to a variety of preparation and storage conditions. Each IMF was the subject of triplicate trials in which duplicate samples were analyzed. All IMFs analyzed immediately after reconstitution were of satisfactory bacteriological quality, exhibiting a total aerobic count of $<10^4$ CFU g^{-1} (mean 2.3×10^2 CFU g^{-1}) and a *Bacillus cereus* count of $<10^3$ CFU g^{-1} of powder (mean 1.3×10^2 CFU g^{-1} for formulae containing this bacterium). Seventeen percent of all dried IMF examined contained *B. cereus;* subsequent reconstitution and storage over a 24-h period at ≥30°C resulted in this organism being detected in a further 46% (63 of 100), so that the majority of these foods exceeded the International Dietetics Association of the European Community (IDAEC) proposed reconstitution safety limit of 10^3 CFU g^{-1}. Variations in preparation conditions did not significantly influence the numbers of *Bacillus* CFU present ($P < 0.05$). The bacteriological quality of an IMF depended on the type and number of organisms initially present and on product temperature and duration of product storage. Microbial numbers in IMFs were influenced by storage temperatures of ≥20°C for 14 h, while incubation at ≤10°C for 24 h had no effect ($P < 0.05$). Although the microflora of dried IMFs predominantly consisted of *B. licheniformis* (46%) and *B. subtilis* (30%), subsequent reconstitution and incubation resulted in the shift to *B. cereus* I (31%) and II (38%) as dominant organisms. The latter often grew to the exclusion of the former two *Bacillus* spp. Diarrheagenic enterotoxin was detected in 4% of IMFs analyzed after 14 h of storage at ≥25°C.

Key words: Infant milk formulae, bacteriological quality, *Bacillus* spp., diarrheagenic enterotoxin, preparation and storage effects

Despite the strong supporting evidence for breast milk as the choice food for the nutritional and immunological development of infants, not all mothers are eager or medically capable of breast-feeding *(19).* For babies who do not receive breast milk, a powdered or ready-to-feed infant milk formula (IMF) substitute is required *(18).*

Reconstituted baby foods are however considered to be a food class of high risk due to the susceptibility of infants to enteric bacterial pathogens, their severe response to toxins, and increased mortality *(12).* Despite the elevated temperatures employed in the manufacture of IMF, there have been a number of food-related illnesses where infant milk powder has been implicated as the vehicle of infection *(7, 16).* The numbers of *Salmonella* cells in IMFs implicated in previous food-borne infections were very low; e.g., in the 1985 UK outbreak only three *S. ealing* cells kg^{-1} were present *(20).* The vulnerability of infants to low numbers of pathogenic organisms may be due to the host's underdeveloped immune system *(2).*

Generally, dried milk-based infant foods are known to be contaminated with aerobic sporeformers of the genus *Bacillus* via raw milk that frequently contains these bacteria in low numbers. Of particular concern is the occurrence of enterotoxigenic *B. cereus* in these products *(3).* These authors reported that 54% of 261 samples of infant food distributed in 17 countries were contaminated with *B. cereus,* reaching levels of 0.3 to 600 viable cells per g. When samples contaminated with approximately 100 cells per ml were reconstituted and incubated at 27°C, levels of 10^5 organisms per ml were reached in 7 to 9 h. While the infectious dose of *B. cereus* is in the range of 10^5 to 10^7 cells, diarrheal enterotoxin is produced before cells reach the level of 10^7 cells per ml *(11).* Outbreaks associated with infants, aged, and/or infirm persons have been attributed previously to the consumption of foods containing low numbers of *B. cereus* in the range of 10^3 to 10^5 cells per g *(8).* Granum et al. *(10)* suggested that the food industry should be concerned about levels as low as 10^3 to 10^4 cells per ml or g of food, as it is likely that food intoxication is caused by ingestion of *B. cereus* cells or spores rather than of preformed enterotoxin. Aas et al. *(1)* revealed that ingestion of cells and/or spores ($>10^4$ ml^{-1}) was the main source of *B. cereus* food poisoning in Norway.

In the past, it has been the practice of many clinical laboratories to simply discard isolates of *Bacillus* spp. (often described as "inconsequential aerobic spore-forming bacteria") other than *B. anthracis* or *B. cereus,* as contaminants of the skin, hair, etc., which were in fact of unappreciated relevance to the infections from which they were isolated *(15).* However, several reports have recently implicated other members of the genus *Bacillus* (i.e., *B. subtilis, B. licheniformis, B. pumilus, B. brevis, B. thuringiensis,* and *B.*

* Author for correspondence. Tel: 0044 141 552 4400 X2531; Fax: 0044 141 553 1161; E-mail: n.j.rowan@pop-hub.strath.ac.uk

sphaericus) as etiological agents in proven food-borne illness outbreaks *(9, 13)*.

The principle objectives of this research were to determine the type and number of *Bacillus* spp. present in infant milk formulae available in the UK, to examine the effects of various methods of preparation, cooling, and storage on the microflora of these products, and to examine these infant formulations for the presence of diarrheal enterotoxin.

MATERIALS AND METHODS

Preparation of samples

Each month for 12 months, 8 to 10 infant milk formulae (IMF) products representative of the main brands available in the UK were purchased and analyzed. Care was taken to ensure that contamination of the infant powder did not occur by wearing vinyl gloves and swabbing the outer package with 70% alcohol. The package integrity of each sample container was checked prior to analysis. Infant powder (25 g) was aseptically added into duplicate 500-ml Duran bottles containing 225 ml of sterile distilled water and 6 to 8 glass beads to aid mixing. The IMF was reconstituted at a water temperature of either 56°C and/or 90°C (±0.2°C) by shaking 25 times through an excursion of 30 cm. These temperatures were achieved by equilibrating the Duran bottles containing the sterile water in preheated waterbaths (Techne Tempette Junior TE-8J) prior to reconstitution.

Cooling and storage of the reconstituted infant milk formulae

The cooling procedures used were table-top cooling (where the foods were left to cool at room temperature), water cooling (where the bottles of foods were held under cold running water), and immediate refrigeration (where the foods were placed directly into a refrigerator). Following a 30-min cooling period, the reconstituted formulae were incubated at either 4, 10, 20, 25, 30, and/or 35°C for periods up to and including 24 h, in order to simulate the "temperature abuse" which may be encountered in hospital wards *(2; 4)* and in the home.

Bacteriological analysis

The bacteria present were enumerated and identified at 0, 8, 14, and 24 h sample time intervals by spread and spiral plating (Spiral plater model B, Spiral Systems Inc.) duplicate samples onto tryptone soya agar supplemented with 0.6% yeast extract (TSYEA), nutrient agar no 2 supplemented with 0.5 mg liter^{-1} $MnSO_4 \cdot H_2O$ (NAMS), blood agar no. 2 supplemented with 7% defribrinated horse blood (BA) and *Bacillus cereus* selective agar (BCSA) (Oxoid products). Undiluted samples were also analyzed in TSEYA using the pour plate technique. The plates were incubated aerobically at 25 and 30°C for 48 or 72 h. This procedure was repeated in duplicate for 3 separate samples analyzed from each infant formulation.

Cultures obtained on the above media were examined for the following morphological and/or biochemical properties: Gram and catalase reactions, cell width and length determined via an image analyzer (Solitaire 512, Seescan Plc.) (TSYEA), lecithovitellin and lecthinase production (BCSA), hemolytic reaction and gross colony morphology (BA), and spore stain to determine shape, position and swelling of sporangium (NAMS). Other morphological and physiological tests performed included examination for motility, hydrolysis of starch, casein and/or gelatin, growth in the presence of 7.5% NaCl or 0.001% lysozyme, formation of acetoin from glucose, and growth under anaerobic conditions. The identity of each *Bacillus* isolate was confirmed using the API 50 CHB and API 20 E galleries (bioMérieux Ltd.).

Detection of diarrheagenic enterotoxin

The bacterial isolate was inoculated into brain heart infusion broth supplemented with 0.25% filter-sterilized glucose and incubated at 30°C for 18 h on a rotary shaker (250 rpm). After growth, duplicate 1-ml samples were centrifuged (Microcentaur MSE) at 11,500 × *g* for 10 min at 4°C. The filtrate was retained for subsequent assay of enterotoxin via the *Bacillus cereus* enterotoxin reverse passive latex agglutination test system (BCET-RPLA, Oxoid). The infant foods were assessed for the presence of enterotoxin by using the BCET-RPLA system after initially obtaining a fat-free fraction via the Filtron® Stirred Cell Ultrafiltration System fitted with a membrane having a 300-kDa molecular weight cutoff point (Filtron® Technology Corporation).

Statistical analysis

The Fisher's exact test was used to compare the bacteriological quality of the 10 leading brands of infant powder. The effects of IMF preparation temperature, cooling method, and storage temperature on microbial numbers (where total aerobic counts for 100 IMFs were pooled and compared as a unit under these conditions) were examined using three-way ANOVA analysis (Minitab version 11, Minitab Ltd). All significant differences were reported at the 95% level of confidence ($P < 0.05$).

RESULTS

Bacteriological quality of reconstituted infant milk formulations before incubation

All 100 IMFs examined immediately after reconstitution were of satisfactory bacteriological quality, having total aerobic counts less than the International Dietetics Association of the European Community (IDAEC) proposed safety limit of 10^4 CFU g^{-1} (Table 1) and a *B. cereus* count less than 10^3 CFU g^{-1} of power (Table 2) *(3)*. In the subsequent text these recommended values are referred to as the "reconstitution safety limit." The IMFs examined, which were representative of the 10 leading brands currently available in the UK, were of similar bacteriological quality ($P < 0.05$).

The temperature of the water used for formula reconstitution (Tables 1, 2 and 3) and/or the cooling method (Table 3) did not affect the type or number of organisms in IMFs examined collectively under brand type (Tables 1 and 2) or when examined as a unit of 100 infant milk products (Table 3) ($P < 0.05$). Large variations in microbial numbers shown in tables 1 and 3 were due to the wide range of total aerobic counts obtained for IMFs examined under brand type or as a unit of IMF (data not shown); e.g., microbial numbers in brand A products ranged from the detection limit of $\geq 1.0 \times 10^1$ to 6.1×10^3 CFU g^{-1} (Table 1). The temperature of the water used for IMF preparation and/or the cooling method did not result in products of different bacteriological quality from that of the dry samples ($P < 0.05$) when analyzed individually (data not shown).

The largest concentration of organisms present in any IMF product was 6.1×10^3 CFU g^{-1} (consisting solely of *B. licheniformis*), while the mean total aerobic count for all

TABLE 1. *Variation in total aerobic counts exhibited by 100 IMFs examined immediately after reconstitution at a water temperature of either 56 or 90°C*

IMF brand	No. samples (*n*)	No. IMF with total aerobic count (log CFU g^{-1}) after reconstitution in the range: <1.0[a] 56°C	<1.0[a] 90°C	≤2.0 56°C	≤2.0 90°C	≤3.0 56°C	≤3.0 90°C	≤4.0 56°C	≤4.0 90°C	Total aerobic count (log CFU g^{-1})[b] Mean 56°C	Mean 90°C	SD 56°C	SD 90°C
A	13	3	3	5	3	4	6	1	1	2.8	2.9	2.4	2.4
B	12	2	2	4	1	5	8	1	1	2.9	2.9	2.7	2.8
C	12	0	0	3	6	8	5	1	1	2.5	2.4	2.7	2.7
D	11	1	1	4	4	3	5	3	1	2.8	2.6	2.5	2.3
E	14	1	1	6	8	7	5	0	0	2.3	2.2	1.9	1.9
F	11	0	0	6	7	5	4	0	0	2.0	2.0	1.9	1.9
G	11	2	2	6	7	3	2	0	0	2.1	2.2	1.6	1.7
H	11	0	0	2	3	6	7	3	1	2.7	2.3	2.8	2.4
I	3	0	0	2	1	1	2	0	0	1.9	1.9	1.8	1.8
J	2	0	0	1	0	1	2	0	0	1.7	1.8	1.9	1.9
All	100	9	9	39	40	43	46	9	5	2.4	2.3	2.2	2.2

[a] IMF with total aerobic counts below the detection limit of 1 log CFU g^{-1}.

[b] Mean and standard deviation refer to the variation in total aerobic counts (log CFU g^{-1}) among IMF in each brand prepared at either 56 or 90°C. IMF with counts lower than the detection limit were not included in the calculation of the mean and standard deviation. No significant difference in microbial numbers was observed between brands ($P < 0.05$).

infant foods analyzed was 2.3×10^2 CFU g^{-1} (Table 1). Although *B. cereus* was present in 17% of the IMFs examined, of which 6 foods (35.3%) contained the enterotoxigenic form of this organism, diarrheal enterotoxin was not detected in these infant powders. The largest number of *B. cereus* recovered from any formulation was 4.8×10^2 CFU g^{-1}, while the mean *B. cereus* count for IMFs shown to contain this organism was 1.3×10^2 CFU g^{-1} (Table 2).

The microbial flora of the IMF consisted mainly of aerobic sporeformers of the genus *Bacillus,* with the most prominent species isolated belonged to members of the subgroup *B. subtilis,* such as *B. subtilis* (30%), *B. licheniformis* (46%), and *B. pumilus* (9%) (Table 4).

Bacteriological quality of reconstituted infant formulae after periods of storage abuse

As no differences were observed in the bacteriological qualities of individually examined IMFs ($P < 0.05$) or among these products when they were compared under brand type (Tables 1 and 2), microbial numbers in each reconstituted IMF were pooled and examined collectively as a unit of 100 foods under various preparation and storage

TABLE 2. *Variation in* Bacillus cereus *counts among IMFs examined immediately after reconstitution at a water temperature of 56 or 90°C*

IMF brand	No. samples (*n*)	No. IMF with *B. cereus* recovered in the range: (log CFU g^{-1}) <1.0[a] 56°C	<1.0[a] 90°C	≤2.0 56°C	≤2.0 90°C	≥2.01 to <3.0 56°C	≥2.01 to <3.0 90°C	*Bacillus cereus* (log CFU g^{-1})[b] Mean 56°C	Mean 90°C	SD 56°C	SD 90°C
A	13	9	9	4	4	0	0	1.9	1.9	0.07	0.08
B	12	12	12	0	0	0	0	LDL[c]	LDL	LDL	LDL
C	12	7	7	4	4	1	1	1.9	2.0	0.39	0.27
D	11	10	10	1	1	0	0	1.9	1.9	0	0
E	14	13	13	0	0	1	1	2.4	2.4	0	0
F	11	10	10	1	1	0	0	2.2	2.1	0	0
G	11	11	11	0	0	0	0	LDL	LDL	LDL	LDL
H	11	8	8	3	3	0	0	1.9	1.9	0.08	0.03
I	3	2	2	0	0	1	1	2.6	2.6	0	0
J	2	1	1	1	1	0	0	2.0	2.0	0	0
All	100	83	83	14	14	3	3	2.1	2.1	0.07	0.05

[a] IMF with *B. cereus* counts below detection limit of 1 log CFU g^{-1}.

[b] Mean and standard deviation refer to the variation in *B. cereus* counts (log CFU g^{-1}) among IMF in each brand prepared at either 56 or 90°C. IMF with counts less than detection limit were not included in calculations of mean and standard deviation.

[c] LDL: IMF with *B. cereus* counts less than the detection limit. No significant difference in microbial numbers was observed between brands ($P < 0.05$).

TABLE 3. *Total aerobic counts for 100 IMFs examined under a variety of preparation, cooling, and storage conditions*

Storage temperature (°C)	Preparation temperature (°C)	Mean (SD) total aerobic counts: log CFU g^{-1} for 100 reconstituted IMF stored 24 h											
		Tap cooled				Table top cooled				Refrigerated			
		0 h	8 h	14 h	24 h	0 h	8 h	14 h	24 h	0 h	8 h	14 h	24 h
35	56	2.4 (2.1)	3.4AB[a] (2.4)	4.2AB (2.5)	8.0AB (3.1)	2.4 (2.3)	3.5AB (2.5)	4.4AB (2.6)	8.3AB (2.9)	2.4 (2.1)	3.4AB (2.4)	4.5AB (2.5)	8.2AB (3.1)
	90	2.4 (2.2)	3.4AB (2.5)	4.3AB (2.5)	8.1AB (3.1)	2.4 (2.2)	3.4AB (2.4)	4.3AB (2.4)	8.0AB (3.0)	2.3 (2.2)	3.4AB (2.5)	4.4AB (2.6)	8.0AB (2.8)
30	56	2.5 (2.2)	3.1AB (2.3)	3.7AB (2.5)	6.9AB (2.8)	2.4 (2.1)	3.2AB (2.4)	3.7AB (2.5)	6.9AB (3.0)	2.4 (2.3)	2.9AB (2.4)	3.7AB (2.7)	7.2AB (2.9)
	90	2.4 (2.2)	3.2AB (2.4)	3.8AB (2.4)	7.0AB (2.9)	2.3 (2.2)	2.9AB (2.5)	3.7AB (2.5)	7.0AB (2.8)	2.4 (2.1)	2.9AB (2.5)	3.9AB (2.7)	7.2AB (3.0)
25	56	2.4 (2.3)	2.8AB (2.3)	3.1AB (2.4)	6.3AB (2.7)	2.4 (2.0)	2.7AB (2.4)	3.1AB (2.4)	5.8AB (2.7)	2.4 (2.2)	2.8AB (2.5)	2.9AB (2.5)	5.9AB (2.8)
	90	2.3 (2.2)	2.8AB (2.4)	3.2AB (2.5)	6.1 (2.7)	2.3 (2.2)	2.9AB (2.5)	3.3AB (2.5)	5.8AB (2.4)	2.4 (2.0)	2.8AB (2.3)	3.0AB (2.6)	5.7AB (2.8)
20	56	2.4 (2.1)	2.6 (2.2)	2.8AB (2.4)	3.2AB (2.5)	2.5 (2.2)	2.6 (2.4)	2.8AB (2.5)	3.1AB (2.6)	2.3 (2.2)	2.5 (2.3)	2.8AB (2.5)	3.2AB (2.7)
	90	2.4 (2.2)	2.6 (2.4)	2.9AB (2.4)	3.3AB (2.6)	2.3 (2.0)	2.5 (2.2)	2.9AB (2.3)	3.0AB (2.5)	2.4 (2.1)	2.5 (2.3)	2.8AB (2.5)	3.3AB (2.6)
≤10	56	2.3 (2.3)	2.4 (2.0)	2.4 (2.2)	2.4 (2.1)	2.3 (2.2)	2.4 (2.2)	2.3 (2.2)	2.4 (2.1)	2.4 (2.2)	2.4 (2.3)	2.4 (2.2)	2.4 (2.2)
	90	2.4 (2.1)	2.4 (2.1)	2.3 (2.2)	2.4 (2.3)	2.4 (2.2)	2.5 (2.2)	2.4 (2.1)	2.3 (2.3)	2.3 (2.3)	2.4 (2.2)	2.3 (2.1)	2.4 (2.2)

[a] A: IMF differing at $P < 0.05$ level compared to these 100 infant foods treated under the same preparation, cooling conditions for shorter storage times and B: for shorter time periods at lower storage temperatures.

TABLE 4. *Number of IMF from which different* Bacillus *spp. were isolated over a 24 hour incubation period at temperatures ≥20°C*

Bacillus spp. isolated	No. IMF in which species was isolated after incubation period of:			
	0 h	8 h	14 h	24 h
B. cereus I	10	30 (3)[b]	31 (3)	31 (3)
B. cereus II	7	34 (5)	37 (6)	38 (6)
B. licheniformis	46	46	47	31
B. subtilis	30	36	36	32
B. pumilus	9	13	13	11
B. megaterium	3	12 (2)	13 (3)	13 (3)
B. sphaericus	8	20	21 (5)	21 (6)
B. amyloliquefaciens	1	2	2	2
B. lentus	ND[a]	3	3	3
B. coagulans	6	8	8	8
B. circulans II	4	6	6	6
B. brevis	1	3	3	3
B. laterosporus	ND	ND	1	1
B. polymyxa	3	4	4	4
B. firmus	4	4	4	4
B. mycoides	5	12 (2)	13 (2)	13 (2)
Non-*Bacillus* spp. (cocci)	3	6	6	6
Bacillus spp. not detected	9	2	1	0

[a] ND: the named *Bacillus* spp. was not detected at this sample period.

[b] Numbers in parentheses: number of IMF prepared at 90°C supporting growth of *Bacillus* spp. not isolated from the same feeds prepared at 56°C.

conditions. The type and/or number of organisms in IMF examined under conditions of storage abuse were not altered by either the temperature of water used for formulae preparation and/or subsequent cooling conditions (Table 3). Some individually examined IMFs differed however, in microbial numbers when reconstituted at 90°C (±0.2°C) and incubated at ≥20°C for ≥14 h ($P < 0.05$): 11 and 7 formulations exhibited either lower or higher total aerobic counts compared to the same products prepared at 56°C respectively (data not shown). Incubation of IMFs at temperatures ≥20°C for ≥14 h resulted in an increase in the number of organisms present in each formulation (Table 3).

Improper storage of reconstituted IMF at ≥20°C for 24 h (or ≥25°C for ≥14 h) resulted in the microbiological quality of a number of formulations exceeding potentially hazardous levels (Fig. 1 and 2), with all 63 foods containing *B. cereus* (6 foods contained both *B. cereus* I and II) being above the reconstitution safety limit of 10^3 cells per g after 24 h at 30°C (Fig. 2). Products held at these higher storage temperatures were found to contain greater microbial numbers sooner; e.g., 20% of foods exceeded the satisfactory reconstitution limit of 10^3 *B. cereus* cells per g after only 8 h at 35°C (Fig. 2). While incubation of IMFs at ≤10°C for 24 h did not alter the bacteriological quality of these formulations ($P < 0.05$), an increase in the number and/or type of organisms present correlated with longer exposures at higher temperatures (Table 3). The bacteriological quality of each IMF depended on the number of organisms initially

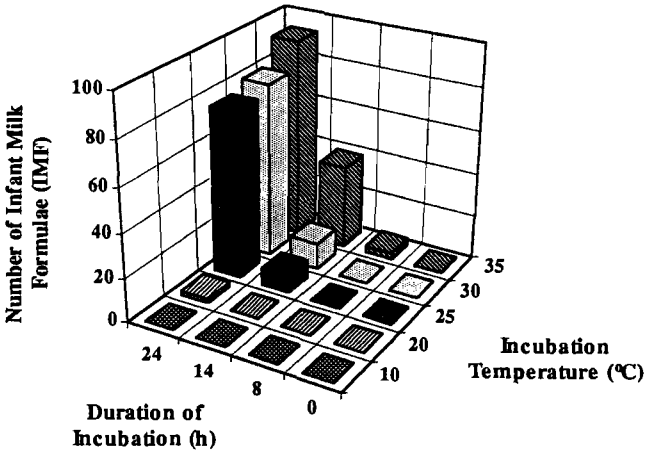

FIGURE 1. *The effects of temperature and duration of incubation on the number of infant milk formulae having a total aerobic count which exceeds the reconstitution safety limit of 10^4 CFU g^{-1}.*

present and on the product temperature and duration of product storage (Table 3).

While incubation of formulations at 20°C for 8 h did not affect microbial numbers ($P < 0.05$) (Table 3), storage at ≥20°C for ≥8 h resulted in an increase in the number of foods containing different types of *Bacillus* spp.; e.g., of *B. lentus* and *B. laterosporus,* which had not been recovered from earlier samples, emerged (Table 4). Some IMFs prepared at 90°C contained organisms that were not isolated from the same IMF products prepared at 56°C, such as *B. cereus, B. mycoides, B. sphaericus,* and *B. megaterium* (Table 4). *Bacillus licheniformis* and *B. subtilis* were initially predominant in IMF examined immediately after reconstitution. Additional storage of IMF resulted in the emergence of *B. cereus* I and II as dominant organisms, often growing to the exclusion of the former *Bacillus* spp. (Table 4).

Of the 38 IMFs supporting the growth of *B. cereus* II, diarrheal enterotoxin was detected in 4 IMFs after 14 h at ≥25°C. Additional storage at higher temperatures for longer

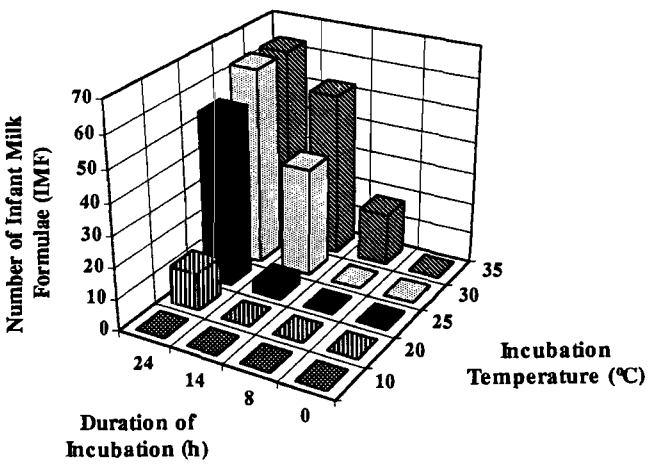

FIGURE 2. *The effects of temperature and duration of incubation on the number of infant milk formulae containing* B. cereus *at a level exceeding the reconstitution safety limit of 10^3 CFU g^{-1}.*

periods did not alter the number of products which contained toxin. However, subsequent enterotoxin studies involving the cultivation of all *B. cereus* II isolates in BHI broth supplemented with 0.25% glucose at 25°C for 14 h or more resulted in a further six isolates exhibiting diarrheal toxin production. Infant formulations produced by the 10 leading brands did not significantly differ in bacteriological quality when examined under varying conditions of preparation and storage ($P < 0.05$).

DISCUSSION

The bacteriological quality of infant milk formulae currently available in the UK is superior to that of infant formulations sold in Scotland in 1987, where a preliminary survey by the Scottish Food Co-ordinating Committee reported that the numbers of organisms present in these dried products ranged from 0 to 4.5×10^6 CFU ml^{-1} *(21).* In a later study carried out by Anderton *(2),* the author reported that milk-based powders used in the preparation of nasogastric feeds in Scottish hospitals contained 50 to 300 *Bacillus* spp. cells per g. These findings are consistent with the quality of dried infant formulae examined in other countries, where the mean total aerobic counts obtained from 26 Italian and 78 Japanese infant formulae did not exceed the recommended 10^4 CFU g^{-1} *(5, 23).*

Becker et al. *(3)* reported that of 261 samples of infant food distributed in 17 countries, 54% were contaminated with levels of *B. cereus* in the range of 0.3 to 600 CFU g^{-1}. While only 17% of UK dried IMF products contained *B. cereus,* a similar concentration of the organism was recovered, i.e., ≥10 to 480 CFU g^{-1}.

The microbial flora of the infant formulations are consistent with the type of organisms isolated by previous researchers; Lovell *(17)* and Kwee et al. *(14)* established that the bacterial flora of powdered milks consisted primarily of aerobic sporeformers, thermoduric cocci, and/or members of the genus *Corynebacterium.* Veda et al. *(23)* also showed that the most frequently isolated organisms from dried baby formulae in Japan were *B. licheniformis* and *B. subtilis,* while other *Bacillus* spp. recovered included *B. cereus, B. pumilus, B. megaterium, B. circulans,* and *B. coagulans.*

By far the greatest factors influencing the bacteriological quality of each infant feed were the number of organisms initially present and the temperature and duration of incubation. Formulae containing approximately 10^2 *B. cereus* spores per g may become unfit for consumption when subjected to storage at or above 25°C for 14 h, reaching levels of 1.3×10^3 CFU g^{-1}. Becker et al. *(3)* revealed that reconstituted infant formulae containing the same initial concentration of viable cells may reach levels as high as 10^5 *B. cereus* cells per g in 7 to 9 h when incubated at 27°C.

While the variation in IMF preparation and cooling method did not influence the number of *Bacillus* spp. present, incubation of IMF which had been initially reconstituted at 90°C often resulted in the emergence of aerobic sporeformers that were not recovered in the same samples prepared at the lower water temperature of 56°C. It is

possible that these *Bacillus* spp. emerged from slow-germinating endospores that require higher preparation temperatures in order to bring about germination. Stadhouders et al. *(22)* showed that heating milk at temperatures from 65 to 95°C for various holding times heat activated slow-germinating endospores of *B. cereus*, which for the main part did not germinate within 24 h in HTST (high-temperature short-time treated) milk stored under similar conditions.

Incubation at ≥25°C of reconstituted IMF which initially contained members of the *B. subtilis* subgroup often resulted in emergence of *B. cereus* as the dominant organism, which frequently grew to the exclusion of the former *Bacillus* spp. Wong et al. *(24)* reported that when *B. cereus* organisms started to multiply in milk products, the growth of other bacteria was inhibited. They attributed this inhibitory effect to the bacteriostatic activity of the organic acids produced by *B. cereus*.

Diarrheal enterotoxin was detected in 4 infant formulations after a 14 h incubation period at or above 25°C. All these foods had been supplemented with maltodextrin by the food companies. While maltodextrin is a harmless by-product of starch hydrolysis, Garcia-Arribas and Kramer *(6)* detected that besides glucose, starch is a good carbon source for both *B. cereus* growth and subsequent diarrheal toxin production. By supplementing IMF with maltodextrin in order to enhance the nutritional value of this product, the food industry may have inadvertently provided a suitable environment where improperly stored IMF containing enterotoxigenic *B. cereus* may produce toxin.

Of the aerobic sporeformers isolated from the dried IMF samples during this study, *B. subtilis, B. licheniformis, B. pumilus, B. cereus* I and II, *B. mycoides, B. brevis, B. megaterium, B. circulans* II, and *B. coagulans* have been occasionally implicated in either food-borne-related illness and/or opportunist infections *(13, 15)*.

In conclusion, dried infant milk formulae commercially available to Scottish retailers is of satisfactory microbiological quality and should not present any health problems to consumers if properly reconstituted (at water temperatures ≥56°C) under hygienic conditions. As the bacterial flora of inadequately stored IMF may proliferate to unacceptable levels, with possible production of diarrheal enterotoxin, these foods should be consumed within 4 h of preparation and not retained as leftovers for future use, storage of feeds during this period should occur in a properly maintained refrigerator (i.e., at ≤8°C), leftover feeds should never be re-used or topped up with fresh formulae, and feeding bottles (and teat) should be thoroughly cleaned and sterilized before re-use.

ACKNOWLEDGMENTS

The authors would like to thank Scottish Home and Health Department for funding this project (K/MRS/50/C2005), Dr. Irene Watson-Craik (Department of Bioscience and Biotechnology, University of Strathclyde) for the use of her image analysis equipment and Prof. George Gettinby (Department of Statistics and Modelling Science, University of Strathclyde) for his assistance with the statistical analysis.

REFERENCES

1. Aas, N., B. Gondrosen, and G. Langeland. 1992. Norwegian Food Control Authority's report on food associated diseases in 1990. SNT-Report 3. Oslo.
2. Anderton, A. 1993. Bacterial contamination of enteral foods and feeding systems. Clin. Nutr. 12:97–113.
3. Becker, H., G. Schaller, W. von Wiese, and G. Terplan. 1994. *Bacillus cereus* in infant foods and dried milk products. Int. J. Food Microbiol. 23:1–15.
4. Burnett, I. A., B. L. Wardley, and J. T. Magee. 1989. The milk kitchen, Sheffield Children's Hospital, before and after a review. J. Hosp. Infect. 13:179–185.
5. Fininoli, C., and G. Rondini. 1989. Evaluation of infant formula contamination in Italy. Food Chem. 32:1–8.
6. Garcia-Arribas, M. L., and J. M. Kramer. 1991. The effect of glucose, starch and pH on the growth, enterotoxin and haemolysin production by strains of *Bacillus cereus* associated with food poisoning and non-gastrointestinal infections. Int. J. Food Microbiol. 11:21–31.
7. Gericke, B., and V. Thurn. 1994. Identification of infant food as a vehicle in a nosocomial outbreak of *Citrobacter freundii:* epidemiological subtyping by allozyme whole cell protein and antibiotic resistance. J. Appl. Bacteriol. 76:553–558.
8. Giannella, R. A., and L. Brasile. 1979. A hospital food-borne outbreak of diarrhea caused by *Bacillus cereus:* clinical, epidemiologic, and microbiologic studies. J. Infect. Dis. 139:366–370.
9. Granum, P. E. 1994. *Bacillus cereus* and its toxins. J. Appl. Bacteriol. 76:615–665.
10. Granum, P. E., S. Brynestad, and J. M. Kramer. 1993. Analysis of enterotoxin production by *Bacillus cereus* from dairy products, food poisoning incidents and non-gastrointestinal infections. Int. J. Food Microbiol. 17:269–279.
11. Granum, P. E., S. Brynestad, K., O'Sullivan, and H. Nissen. 1993. The enterotoxin from *Bacillus cereus:* production and biochemical characterisation. Neth. Milk Dairy J. 47:63–70.
12. International Commission on Microbiological Specifications for Foods. 1986. Microorganisms in Foods, Vol. 1. Their significance and methods of enumeration. University of Toronto Press, Toronto.
13. Jackson, S. G., R. B. Goodbrand, R. Ahmed, and S. Rasatiya. 1995. *Bacillus cereus* and *Bacillus thuringiensis* isolated in gastro-enteritis outbreak investigation. Lett. Appl. Microbiol. 21:603–605.
14. Kwee, W. S., T. W. Dommett, J. E. Giles, R. Roberts, and R. A. D. Smith. 1986. Microbiological parameters during powdered milk manufacture—variation between processes and stages. Aust. J. Dairy Technol. 53: 3–8.
15. Logan, N. A. 1988. *Bacillus* species of medical and veterinary importance. J. Med. Microbiol. 25:157–165.
16. Louie, K. K. 1993. *Salmonella* serotype *tennessee* in powdered milk products and infant formula—Canada and the United States. JAMA 270(4):432.
17. Lovell, H. R. 1981. The microbiology of milk. *In* R. K. Robinson (ed.), Dairy microbiology, vol. 1. Applied Science Publishers, London.
18. Retallack, S. J., K. Simmer, M. Makrides, and R. A. Gibson. 1994. Infant weaning practices in Adelaide: the results of a shopping complex survey. Aust. Paediatr. J. 30:28–32.
19. Rowan, N. J. 1996. Studies on the growth, survival, interaction, and detection of potentially pathogenic *Listeria* and *Bacillus* spp. in infant milk formulae. Ph.D. Thesis. University of Strathclyde, Glasgow, Scotland.
20. Rowe, B. 1987. *Salmonella ealing* infections associated with consumption of infant dried milk. Lancet ii:900–903.
21. Scottish Food Co-ordinating Committee. 1990. Report of a working party on food surveillance. A survey of the bacteriological and chemical qualities of dried milk and related products in Scotland in 1987.
22. Stadhouders, J., G. Hup, and C. P. M. Langeveld. 1980. Some observations on the germination, heat resistance and outgrowth of fast germinating and slow germinating spores of *Bacillus cereus* in pasteurised milk. Neth. Milk Dairy J. 34:215–228.
23. Veda, S., S. Asakusa, and Y. Kuwabara. 1980. *Bacillus* in commercial baby foods. J. Jpn. Soc. Food Technol. 27:30–37.
24. Wong, H. C., Y.-L. Chen, and C. L. F. Chen. 1988. Growth, germination and toxigenic activity of *Bacillus cereus* in milk products. J. Food Prot. 51:707–710.

Journal of Hospital Infection (1997) **36**, 259–267

The bacteriological quality of hospital-prepared infant feeds

N. J. Rowan, J. G. Anderson and A. Anderton

Department of Bioscience and Biotechnology, University of Strathclyde, Royal College Building, 204 George Street, Glasgow, Scotland, UK

Received 11 September 1996; revised manuscript accepted 20 November 1996

Summary: Twenty-four pasteurized infant feeds, prepared in a Glasgow hospital, were examined microbiologically. All produced a satisfactory total aerobic mesophilic count of $\leq 1{\cdot}0 \times 10^4$ cfu/g (mean $6{\cdot}3 \times 10^1$ cfu/g) within 1 h of preparation. *Bacillus cereus* was detected in two infant feeds immediately after preparation and one of these had a *B. cereus* count of $1{\cdot}4 \times 10^3$ cfu/g exceeding the recommended safety limit of $\leq 1{\cdot}0 \times 10^3$ cfu/g. Subsequent storage over a 14 h period at 25°C or greater resulted in the appearance of *B. cereus* in a further eight feeds, the majority of which exceeded the safety limit of 10^3 cfu/g. The microbiological quality of each infant feed depended on the type and number of organisms initially present, and on the temperature and duration of storage. Incubation of feeds at ≤10°C for 14 h did not alter the microbiological quality ($P=0{\cdot}05$). While *Bacillus licheniformis* and *Bacillus subtilis* were the predominant organisms isolated within 8 h of incubation (45·8 and 20·8% of feeds, respectively), additional storage resulted in the emergence of *B. cereus* I (25%) and II (20·8%) as dominant *Bacillus* spp. The addition of glucose polymers and other supplements to infant formulae did not affect the type and number of organisms present ($P=0{\cdot}05$). Diarrhoeal enterotoxin was detected in three of the five formulations which supported the growth of *B. cereus* II via the *B. cereus* enterotoxin reverse phase latex agglutination test BCET-RPLA system. Although the infant feeds were of similar microbiological quality ($P=0{\cdot}05$), the majority of *Bacillus* spp. isolated have been previously implicated in either foodborne illnesses and/or opportunist infections.

Keywords: Infant feeds; microbiological quality; *Bacillus* spp.; enterotoxin; hospital study.

Introduction

Reconstituted baby foods are considered to be a high-risk food because of the susceptibility of the consumer population to enteric microbial pathogens, but there is no requirement that these foods should be sterile and many milk-based products are only subjected to pasteurization before spray-drying.[1]

Correspondence to: Dr. Neil Rowan, Department of Bioscience and Biotechnology, University of Strathclyde, Royal College Building, 204 George Street, Glasgow, Scotland, UK.

0195–6701/97/040259+09 $12.00/0

Despite the elevated temperatures employed in the manufacture of infant milk formulae and a commitment to product quality and safety, there have been a number of food related poisonings where infant milk powder has been implicated as the vehicle of infection.[2,3] The number of *Salmonella* present in the infant milk formulae implicated in some food poisonings were very low, e.g., in the 1988 Canadian outbreak, nine *Salmonella newport* cells/100 g formula, while in a UK outbreak only three *Salmonella ealing* cells/kg were present.[4] The vulnerability of infants to low numbers of pathogenic organisms may be due to an immature immune system.[5]

Dried-milk products are known to be frequently contaminated with *Bacillus* spp. Becker *et al.*[6] reported that when 261 samples of infant food distributed in 17 countries were examined for *B. cereus*, 54% of them were contaminated with *B. cereus* reaching levels of 0·3–600 viable cells/g. When samples contaminated with approximately 100 *B. cereus* cells/mL were reconstituted and incubated at 27°C, levels of 10^5 organisms/mL were reached in 7–9 h. While the infectious dose of *B. cereus* is in the range 10^5–10^8 cells,[7] diarrhoeal enterotoxin is produced before cells reach a level of 10^7 cells/mL. Granum *et al.*[8] suggested that the food industry should be concerned about levels as low as 10^3–10^4 cells/g food. This concern has been substantiated by Aas *et al.*[9] where the authors revealed that ingestion of cells or spores at $\geq 10^4$/mL was the main source of *B. cereus* food poisoning in Norway.

In the past, it has been the practice of many clinical laboratories to simply disregard isolates of *Bacillus* spp.—often described as 'inconsequential aerobic spore-forming bacteria'. Strains other than *B. anthracis* or *B. cereus* were considered to be contaminants of the skin, hair etc., but were later found to be clinically relevant.[10] Several reports have recently implicated other members of the genus *Bacillus* (i.e., *Bacillus subtilis, Bacillus licheniformis, Bacillus pumilus, Bacillus brevis, Bacillus thuringiensis* and *Bacillus sphaericus*) as the aetiological agent in proven foodborne illness outbreaks.[11,12]

Concern about Gram-negative bacteria introduced during reconstitution of feeds means that many hospitals now pasteurize infant feeds after reconstitution.[13] Counts of aerobic spore-forming bacilli are little affected by pasteurization, however, and the authors reported counts of 10^2/mL post-heat treatment. This situation may be of particular concern because pasteurized infant feeds and/or enteral feeds are routinely used in hospitals for the tube feeding of babies who are unable to suck because they are premature or ill. The feed may be held at ward temperature (25–30°C) for many hours, allowing the proliferation of micro-organisms.[14] The principal objective of this research, therefore, was to determine the type and number of organisms present in infant feeds prepared at a special feeding unit in a Glasgow hospital, and to examine the effects of temperature and duration of storage on the microflora of these products. Finally, infant formulations were assessed for the presence of diarrhoeal enterotoxin.

Materials and methods

Preparation and transportation of samples
Each month for four months, triplicate batches of six infant formulae (with or without thickeners, hydrolysed protein, glucose polymers and fat calorie supplements and/or soya supplements) were collected for microbiological analysis. They were prepared at a water temperature of 56°C and pasteurized at 63°C for 30 min in the Special Feeding Unit. Infant feed (25 mL) was transferred to separate sterile universal containers and labelled with the date, time of preparation and description of formulation. These infant formulations were representative of the main types of feed supplied to the hospital wards. The samples were transported to the laboratory in a cooler bag containing ice packs and a maximum/minimum thermometer (i.e., temperature maintained at 2 ± 3°C), and analysed within 1 h of collection. The package integrity of each sample container was checked before analysis.

Storage of the reconstituted infant feeds
The reconstituted formulae were incubated at either 4, 10, 25 and/or 30°C for up to 14 h in order to simulate the 'temperature abuse' conditions that may be encountered in hospital wards and incubators for premature infants.

Microbiological analysis
The bacteria present were isolated and enumerated at 0, 8 and 14 h sample time intervals by spread and spiral plating (Spiral plater model B, Spiral Systems Inc.) duplicate samples onto tryptone soya agar supplemented with 0·6% yeast extract (TSYEA), nutrient agar No. 2 supplemented with 0·5 mg/L $MnSO_4.H_2O$ (NAMS), blood agar No. 2, supplemented with 7% defribrinated horse blood (BA) and *B. cereus* selective agar (BCSA) (Oxoid products). The plates were incubated aerobically at 25 and 30°C for 48/72 h. This procedure was repeated in duplicate for three separate samples analysed from the same infant formulation. Colonies obtained on the above culture media were examined for the following properties: Gram and catalase reactions, cell width and length (μm) determined via image analyser (Solitaire 512, Seescan Plc.) (TSYEA), lecithovitellin/lecthinase production (BCSA), haemolytic reaction and gross colonial morphology (mm) (BA) and spore stain to determine shape and whether or not the sporangium was distended (NAMS). Other tests performed included motility, hydrolysis of starch, casein and/or gelatine, growth in the presence of 7·5% NaCl or 0·001% lysozyme, formation of acetoin from glucose and growth under anaerobic conditions. The identity of each *Bacillus* isolate was confirmed using the API 50 CHB and API 20 E galleries (bioMérieux Ltd.).

Detection of diarrhoeal enterotoxin
The bacterial isolate was inoculated into brain–heart infusion broth supplemented with 0·25% filter-sterilized glucose and incubated at 30°C for

18 h under orbital conditions (250 rpm). After growth, duplicate 1 mL aliquots were centrifuged (Microcentaur MSE) at 11 500 ***g*** for 10 min at 4°C. The filtrate was retained for enterotoxin assay via the *B. cereus* enterotoxin reverse phase latex agglutination test system (BCET-RPLA, Oxoid). Infant feeds were assessed for the presence of enterotoxin using the BCET-RPLA system after initially obtaining a fat-free fraction via the 'Filtron' stirred cell ultrafiltration system fitted with a membrane with a 300 kDa molecular weight cutoff point ('Filtron' Technology Corporation).

Statistical analysis

Each infant feed was the subject of triplicate trials where duplicate samples were analysed. The type and number of *Bacillus* spp. present in each infant milk formula product were compared using the Mann–Whitney U-test and the Wilcoxon ranked sign test at the $P=0{\cdot}05$ level.

Results

Microbial quality of pasteurized infant feeds before incubation

Of the 24 infant feeds analysed within 1 h of preparation, 23 (96%) were of satisfactory microbiological quality having a total aerobic mesophilic count of $\leq 1{\cdot}0 \times 10^4$ cfu (colony-forming units)/g and a *B. cereus* count of $\leq 1{\cdot}0 \times 10^3$ cfu/g powder (Table I).[1] The total aerobic mesophilic count (cfu/g) is the sum of the predominant organisms detected in each infant feed. One infant formulation was deemed unsafe for infant consumption because it had a *B. cereus* count of $1{\cdot}4 \times 10^3$ cfu/g powder. The microbiological quality amongst these infant feeds varied over the range $0–1{\cdot}4 \times 10^3$ cfu/g, with a mean total aerobic mesophilic count of $6{\cdot}3 \times 10^1$ cfu/g. A description of the infant formulations presented in Table I is given in Table II. Diarrhoeal enterotoxin was not detected in any of the feeds analysed. The microbial flora of the infant formulations mainly consisted of aerobic spore formers from the genus *Bacillus*. The most prominent species were *B. licheniformis* and *B. subtilis*; these were isolated from 45·8 and 20·8% of feeds analysed, respectively (Table I).

Microbial quality of infant feeds after periods of storage abuse

Improper storage of these infant feeds at temperatures ± 25°C over a 14 h period resulted in an increased number of formulations becoming unsafe for consumption, with 60% (at 25°C) and 90% (at 30°C) of feeds containing *B. cereus* exceeding the recommended $1{\cdot}0 \times 10^3$ cfu/g level after 14 h (Table III). Feeds containing levels as low as 100 *B. cereus* cells/g after the initial preparation may become unacceptable for consumption after 8 h incubation at 25°C (Table I). While incubation of feeds for 14 h at ≤ 10°C did not significantly alter the bacterial quality of these feeds ($P=0{\cdot}05$), an increase in either the type and/or number of organisms was shown to be commensurate with exposure to higher temperatures and longer storage periods (Table I).

Table I. *The effects of temperature (°C) and duration (h) of incubation on the type and number (log_{10} cfu/g) of organisms present in 24 infant feeds*

Infant feed*	Predominant organisms	Aerobic count of named organisms (log_{10} cfu g^{-1})						
		≤10°C			25°C		30°C	
		0 h	8 h	14 h	8 h	14 h	8 h	14 h
B	*B. licheniformis*	2·301	2·602	2·066	2·602	2·845	2·447	3·447
	B. sphaericus	—	—	—	2·000	2·447	2·125	3·125
A + N + P	*B. licheniformis*	2·602	2·556	2·544	2·602	3·398	2·740	3·662
	B. sphaericus	—	—	—	2·335	2·653	2·452	3·041
D + ½N + P†	*B. cereus* II	—	—	—	—	2·066	2·000	3·491
	B. pumilus	—	—	—	—	2·698	—	2·633
E	*B. cereus* I	—	—	—	—	2·000	—	2·263
	B. mycoides	—	—	—	—	2·125	—	2·681
C + O	*B. licheniformis*	2·176	—	2·263	2·335	2·778	2·653	3·380
	B. subtilis	—	2·221	2·368	2·066	2·602	2·716	3·380
F	*B. licheniformis*	2·823	2·875	2·845	2·912	3·505	3·000	3·959
	B. cereus I	—	—	—	1·920	3·114	2·000	3·491
	B. megaterium	—	—	—	2·176	2·602	2·066	3·322
C + N	*B. subtilis*	—	—	—	2·125	2·790	2·602	3·342
D + P	*B. licheniformis*	2·221	2·000	2·325	2·176	2·698	2·447	3·204
	B. sphaericus	—	—	—	—	2·125	—	2·452
H + O	*B. licheniformis*	3·716	3·746	3·690	3·813	4·716	4·230	4·934
Q	*B. subtilis*	2·452	2·397	2·452	2·000	2·602	2·724	3·278
	B. mycoides	2·000	2.176	—	2·447	2·845	3·204	4·041
D + P†	*B. sphaericus*	—	—	—	—	2·000	—	2·225
	B. mycoides	—	—	—	—	2·447	—	2·066
	B. cereus II	—	—	—	2·066	2·698	2·176	3·322
J	*B. sphaericus*	—	—	—	2·176	2·263	2·000	3·230
	B. megaterium	—	—	—	—	2·066	—	2·221
K	*B. licheniformis*	—	—	—	—	2·125	—	2·335
D	*B. licheniformis*	2·000	2·335	2·176	2·125	2·402	2·623	3·204
A	*B. cereus* II	—	—	—	2·125	3·000	2·176	3·518
	B. megaterium	—	—	—	2·066	2·698	2·447	3·342
B	*B. subtilis*	2·125	2·066	2·125	2·335	2·740	2·778	3·452
	B. pumilus	2·000	2·066	2·066	2·518	2·903	2·602	3·278
I	*B. cereus* I	—	—	—	2·447	3·146	2·176	3·579
	B. polymyxa	2·301	2·176	2·301	2·452	2·643	3·000	3·556
G	*B. licheniformis*	2·477	2·221	2·221	2·301	2·778	2·732	3·332
	B. sphaericus	—	—	—	2·125	2·633	2·698	3·225
	B. circulans II	—	—	—	—	2·519	—	2·000
F	*B. licheniformis*	2·491	2·602	2·447	2·698	3·322	2·716	3·518
	B. cereus I	—	—	—	2·066	3·204	2·125	3·623
C + P	*B. cereus* I	—	—	—	2·335	2·973	2·452	3·544
	B. cereus II	2·000	2·125	—	3·146	3·579	3·716	4·643
	Cocci	3·176	3·146	3·041	3·230	3·708	2·519	3·880
A + O	*B. licheniformis*	—	—	—	—	2·452	—	2·397
	B. megaterium	—	—	—	2·000	2·447	2·301	2·900
	B. brevis	—	—	—	—	2·125	—	2·477
B + ½M + P†	*B. licheniformis*	2·125	2·518	2·066	2·602	2·857	2·633	3·176
	B. subtilis	2·301	2·301	2·125	2·176	2·447	2·613	3·342
	B. cereus II	—	—	—	—	2·778	2·452	3·397
B	*B. licheniformis*	2·447	2·518	2·301	2·698	2·977	2·778	3·397
C + ½M	*B. cereus* I	3.146	3·079	3·146	3·149	5·041	3·643	5·792
	Mean Count ($N = 24$)	1·801	1·742	1·670	2·260	3·251	2·679	3·758

*The letters represent either the infant formula or supplement analysed and are described fully in Table II. The fraction ½ refers to the supplement being employed at half its usual concentration.
†Detection of diarrhoeal enterotoxin in feeds supporting the growth of *B. cereus* II.

Table II. *Description of infant formulae and/or supplements analysed during this study*

Product	Code	Description
SMA White Cap	A	Normal brand of infant milk formula
SMA Gold Cap	B	Normal brand of infant milk formula
Nutrilon Plus	C	Normal brand of infant milk formula
Premcare	D	Infant formula for premature babies
Generaid Plus	E	Enteral feed for liver disease
Monogen	F	Nutritionally complete feed: high in medium chain triglycerides
Wysoy	G	Soya formula
Nutramigen	H	Hydrolysed protein formula
Pregestimil	I	Hydrolysed protein formula
Nutrison Energy Plus	J	High energy, high protein enteral feed
Elemental 028	K	Elemental formula
Paediatric Nutrison	L	Paediatric enteral feed
Nestargel	M	Feed thickener
Carobel	N	Feed thickener
Maxijul	O	Glucose polymer
Duocal	P	Glucose polymer and fat calorie supplement
Farleys Oster Milk 2	Q	Normal brand of infant milk formula

Table III. *Number of infant feeds (*N*=24) exceeding the recommended total aerobic mesophilic count ($\geq 10^4$ cfu/g) and/or* Bacillus cereus *count ($\geq 10^3$ cfu/g) over a 14 h period at a variety of incubation temperatures*

Microbiological quality	Incubation temperature								
	≤10°C			25°C			30°C		
	0 h	8 h	14 h	0 h	8 h	14 h	0 h	8 h	14 h
Total aerobic mesophilic count ($\geq 10^4$ cfu/g)*	0	0	0	0	0	3	0	2	5
Bacillus cereus count ($\geq 10^3$ cfu/g)†	1	1	1	1	2	6	1	2	9

*Number of infant feeds ($N=24$) which exceeded the ICMSF recommended total aerobic mesophilic count of 10^4 cfu/g^{-1}.
†Number of infant feeds where *B. cereus* was isolated (i.e. $N=10$) which exceeded the ICMSF recommended *B. cereus* count of 10^3 cfu/g^{-1}.

Incubation of the feeds at ≥25°C for ≥8 h resulted in an increase in the number of feeds containing *Bacillus* spp., with the emergence of *Bacillus megaterium*, *Bacillus circulans* II, *B. brevis* and *B. sphaericus* which had not been previously recovered from earlier samples ($P=0{\cdot}05$). Furthermore, *B. cereus* I and II were isolated from a greater number of feeds and emerged as dominant organisms (Figure 1). The addition of glucose polymers and fat calorie supplements, thickeners, hydrolysed protein and/or soya to infant formulae did not affect the type or number of organisms present ($P=0{\cdot}05$).

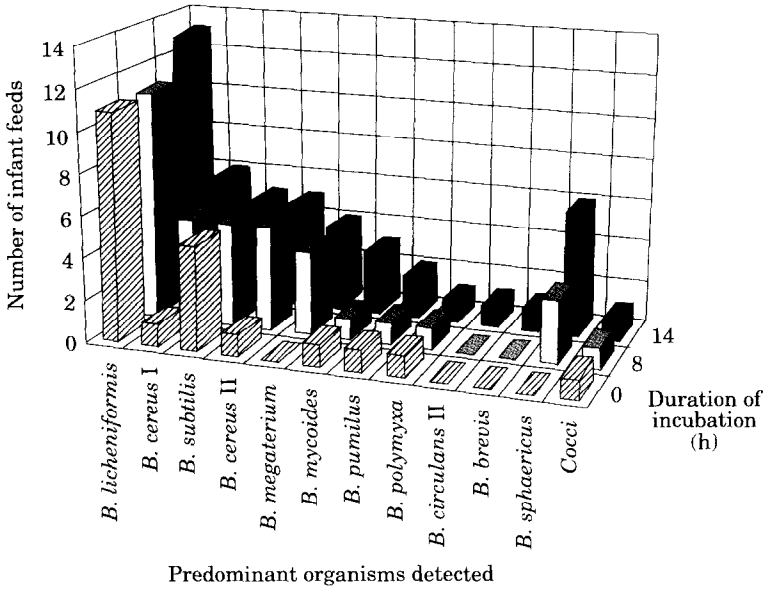

Figure 1. Predominant organisms present in 24 infant formulations incubated over a 14 h period at $\geq 25°C$.

Diarrhoeal exterotoxin was detected after 14 h at $\leq 25°C$ in three of the five feeds which supported the growth of *B. cereus* II (symbolized by † in Table I). Additional incubation for up to 24 h at 30°C did not lead to an increase in the number of feeds containing enterotoxin. However, cultivation of five *B. cereus* II isolates in BHI broth supplemented with 0·25% glucose under orbital conditions (250 rpm) at 30°C resulted in four isolates demonstrating enterotoxin production.

Discussion

The microbiological quality of infant feeds analysed within 1 h of preparation from a Glasgow hospital was superior to that of infant milk formulae commercially available in Scotland in 1987, when a preliminary survey by the Scotish Food Co-ordinating Committee reported that the bacterial quality of dried milk ranged from $0–4·5 \times 10^6$ cfu/mL.[15] In a later study carried out by Anderton,[14] the author reported that milk-based powders used in the preparation of nasogastric feeds contained 50–300 cfu *Bacillus* spp./g. These findings are consistent with the quality of dried infant formulae examined in other developed countries, where the mean total aerobic counts obtained from 26 Italian and 78 Japanese infant formulae did not exceed the recommended 10^4 cfu/g powder.[5,16]

Becker *et al.*[6] reported that of 261 samples of infant food (distributed in

17 countries), 54% were contaminated with levels of *B. cereus* between the range of $0{\cdot}3–6{\cdot}0 \times 10^2$ cfu/g. In the present study only two infant feeds (8·3%) sampled within 1 h of reconstitution contained this organism. The microbial flora of the infant formulations are consistent with bacterial species isolated by previous researchers, for example Lovell[17] and Kwee *et al.*[18] established that the bacterial flora of powdered milk consists of aerobic spore formers, thermoduric cocci and/or *Corynebacteria*. Veda *et al.*[16] also showed that the most frequently-isolated organisms from baby formulae were *B. licheniformis* and *B. subtilis*, followed by *B. cereus*, *B. pumilus*, *B. megaterium*, *B. circulans* and *B. coagulans*.

By far the greatest factors influencing the bacteriological quality of each infant feed were the type and number of organisms initially present and the temperature and duration of incubation ($P=0{\cdot}05$). Pasteurized feeds containing approximately 10^2 *B. cereus* cells/g may become unfit for infant consumption when subjected to storage at or above 25°C for 8 h after reaching levels of $1{\cdot}4 \times 10^3$ cfu/g. Becker *et al.*[6] revealed that reconstituted infant formulae containing the same initial concentration of *B. cereus* may reach levels as high as 10^5 organisms/g in 7–9 h at 27°C.

Diarrhoeal enterotoxin was detected in infant formulations that had been supplemented with glucose polymers after a 14 h incubation period at or above 25°C. One pasteurized feed containing enterotoxigenic *B. cereus* II cells, which was not supplemented with glucose, did not support enterotoxin production. By culturing *B. cereus* II in BHI broth supplemented with 0·1% (w/v) glucose, Granum *et al.*[8] showed that this carbon source was important for enterotoxin production.

Of the aerobic spore-formers isolated from these infant feeds during this study, *B. subtilis*, *B. licheniformis*, *B. pumilus*, *B. cereus* I and II, *B. mycoides*, *B. brevis*, *B. megaterium* and *B. circulans* II, have been previously implicated in either food-related illness and/or opportunist infections.[10,12]

In conclusion, while the bacteriological quality of 96% of infant feeds prepared at the Special Feeding Unit was satisfactory, pasteurization did not successfully reduce *B. cereus* numbers in one feed to a level safe for infant consumption. Bacteria in inadequately stored feeds may proliferate to unacceptable levels and there may thus be significant production of diarrhoeal enterotoxin. The following recommendations should be adhered to: infant formulations should be consumed shortly after preparation (within 4 h), storage of feeds during this period should occur in a properly-maintained refrigerator, left over feeds should never be re-used or topped up with fresh formula and feeding bottles (and teat) should be thoroughly cleaned and sterilized before re-use.

In order to provide a safe food supply for the developing infant, parents, healthcare workers, nursing and medical staff should be informed of the microbiological hazards associated with keeping reconstituted infant formulae at ambient temperatures for prolonged storage periods.

The authors would like to thank Dr Irene Watson-Craik for the use of her image analysis equipment and to the staff of a Glasgow hospital for their participation in this study.

References

1. International Commission on Microbiological Specifications for Foods 1. Their significance and methods of enumeration. Toronto 1986: University of Toronto Press.
2. Gericke B, Thurn V. Identification of infant food as a vehicle in a nosocomial outbreak of *Citrobacter freundii*: epidemiological subtyping by allozyme whole cell protein and antibiotic resistance. *J Appl Bacteriol* 1994; **76**: 553–558.
3. Louie KK. *Salmonella* serotype *tennessee* in powdered milk products and infant formula—Canada and the United States, *JAMA* 1993; **270**: 432.
4. Rowan NJ. Studies on the growth, survival, interaction, and detection of potentially pathogenic *Listeria* and *Bacillus* spp. in infant milk formulae. PhD Thesis 1996. University of Strathclyde, Glasgow, Scotland.
5. Finoli C, Rondini G. Evaluation of infant formula contamination in Italy. *Food Chem* 1989; **32**: 1–8.
6. Becker H, Schaller G, von Wiese W, Terplan G. *Bacillus cereus* in infant foods and dried milk products. *Int J Food Microbiol* 1994; **23**: 1–15.
7. Granum PE, Brynestad S, O'Sullivan K, Nissen H. The enterotoxin from B. cereus: production and biochemical characterization. *Neth Milk Dairy J* 1993; **47**: 63–70.
8. Granum PE, Brynestad S, Kramer JM. Analysis of enterotoxin production by *Bacillus cereus* from dairy products, food poisoning incidents and non-gastrointestinal infections. *Int J Food Microbiol* 1993; **17**: 269–279.
9. Aas N, Gondrosen B, Langeland G. *Norwegian Food Control Authority's Report on Food Associated Diseases in 1990*. SNT-Report 3 1992; Oslo.
10. Logan NA. *Bacillus* species of medical and veterinary importance. *J Med Microbiol* 1988; **25**: 157–165.
11. Granum PE. *Bacillus cereus* and its toxins. *J Appl Bacteriol* 1994; **76**: 615–665.
12. Jackson SG, Goodbrand RB, Ahmed R, Rasatiya S. *Bacillus cereus* and *Bacillus thuringiensis* isolated in gastro-enteritis outbreak investigation. *Lett Appl Microbiol* 1995; **21**: 603–605.
13. Burnett IA, Wardley BL, Magee JT. The milk kitchen, Sheffield Children's Hospital, before and after—a review. *J Hosp Infect* 1989; **13**: 179–185.
14. Anderton A. Bacterial contamination of enteral feeds and feeding systems. *Clin Nutr* 1993; **12**: 97–113.
15. Scottish Food Co-ordinating Committee. Report of a working party on food surveillance. *A Survey of the Microbiological and Chemical Qualities of Dried Milk and Related Products in Scotland in 1987*. Scottish Food Co-ordinating Committee, 1990.
16. Veda S, Asakusa S, Kuwabara Y. *Bacillus* in commercial baby foods. *J Jap Soc Fd Technol* 1980; **27**: 30–37.
17. Lovell HR. In: Robinson RK, Ed. The microbiology of milk. *Dairy Microbiology*. Volume 1. London: Applied Science Publishers 1981.
18. Kwee WS, Dommett TW, Giles JE, Roberts R, Smith RAD. Microbiological parameters during powdered milk manufacture-variation between processes and stages. *Aust J Dairy Technol* 1986; March: 3–8.

Journal of Hospital Infection (1998) **38**, 139–146

Growth and enterotoxin production by diarrhoeagenic *Bacillus cereus* in dietary supplements prepared for hospitalized HIV patients

N. J. Rowan and J. G. Anderson

Department of Bioscience and Biotechnology, University of Strathclyde, Glasgow, Scotland

Received 21 May 1994; revised manuscript accepted 3 September 1997

Summary: This study was initiated because of an increase in diarrhoeal episodes in a ward caring for patients infected with the human immunodeficiency virus (HIV). An examination of hospital-prepared dietary supplements (build-up food) found *Bacillus cereus* to be a potential problem. Due in part to inadequate refrigeration conditions (13 ± 4°C), the microbial flora in commercially pasteurized semi-skimmed milk (PSSM) reached potentially hazardous levels ($>10^6$ cfu/mL). While refrigerated PSSM did not support enterotoxin production, reconstitution of build-up powder in PSSM followed by storage in the HIV ward (4 h at 28 ± 3°C) resulted in growth of *B. cereus* ($>10^7$ cfu/mL) and synthesis of diarrhoeal enterotoxin. While insufficient epidemiological data was available to establish conclusively a causal relationship between patients' symptoms and source, the study highlights a potential *B. cereus* problem with hospital-prepared dietary supplements and recommendations are proposed to prevent this re-occurrence.

Keywords: Diarrhoeagenic enterotoxin; *Bacillus cereus*; hospital-prepared dietary supplements; HIV patients.

Introduction

Immunocompromised individuals, e.g., human immunodeficiency virus (HIV) or acquired immunodeficiency syndrome (AIDS) patients,[1,2] and those with underlying conditions such as cancer,[3] trauma,[4] central venous catheters,[5] rheumatoid arthritis,[4] are particularly susceptible to food-borne bacterial enteropathogens and nosocomial/opportunistic infections.[1] For these vulnerable groups, the number of enteropathogenic organisms required to cause illness may be significantly lower than for those with a healthy immune system.[1,2] Thus, the bacteriological quality of hospital-prepared foods is of paramount importance.

Correspondence to: Dr N. J. Rowan, Department of Bioscience and Biotechnology, University of Strathclyde, Royal College Building, 204 George St., Glasgow, Scotland, UK.

0195–6701/98/020139 + 08 $12.00/0

To guard against possible deleterious effects of food-borne, Gram-negative enteric bacteria, milk-based products such as infant milk formulations[6] and enteral feeds[7] are routinely pasteurized in hospitals, or commercially pasteurized milk-based foods are used (e.g., for immunocompromised and other patients requiring a complemented diet of high-energy build-up food.[8] However counts of aerobic spore-forming bacilli and of other thermoduric bacteria in these pasteurized foods are little affected by pasteurization).[9,10] In general, resident lactic acid bacteria (LAB) protect unprocessed milk against the growth of many bacterial pathogens by producing antimicrobial metabolic products such as organic acids, hydrogen peroxide, lactoperoxidase, CO_2, ethanol, diacetyl, antibiotics and bacteriocins.[11,12] As LAB are heat labile and do not survive pasteurization, [10] improper storage of food after pasteurization may allow growth of certain enteropathogens and synthesis of toxins.[13]

Of particular concern is the occurrence of *Bacillus cereus* and other opportunist pathogenic *Bacillus* spp.[7,14] Rowan *et al.*[6] reported that hospital-prepared pasteurized infant milk formulae were contaminated with low numbers of these ubiquitous aerobic spore-forming bacteria. While the infectious dose of *B. cereus* is considered to be 10^5–10^7 cells/mL;[15,16] Granum[17] suggested counts as low as 10^3–10^4/mL could cause concern as food intoxication may be caused by ingestion of bacteria which could subsequently form enterotoxin in the small intestine. There is insufficient evidence, however, to show that *B. cereus* food intoxication results from consumption of pre-formed toxin,[18] or production of toxin by ingested bacteria.[16] Here, we present evidence that inadequately refrigerated and stored hospital-prepared build-up food can be a source of hazardous levels of enterotoxigenic *B. cereus*.

Materials and methods

Preparation and transportation of samples

During two visits to a HIV ward in a Glasgow hospital, triplicate samples of the complemented dietary food supplement 'build-up' (a high calory powder, reconstituted in commercially pasteurized semi-skimmed milk, (PSSM), administered orally to patients) were prepared by the hospital staff for bacteriological and toxicological analysis. A sachet of lemon and lime flavoured build-up powder (BUP_1) was blended with 300 mL of $PSSM_1$ (BUP + PSSM). Separate 25 mL samples of $PSSM_1$ and $BUP_1 + PSSM_1$ were transferred to 30 mL sterile containers. This procedure was repeated on the second visit using a different carton of PSSM($PSSM_2$) and a different batch of BUP(BUP_2). The blender and polystyrene cup were swabbed on each occasion and the swabs were transferred to Amies' transport medium (Oxoid). Duplicate sachets of BUP (with batch numbers corresponding to samples prepared by hospital staff) were retained for

analysis. Products had not passed their expiry date before sampling. A maximum/minimum thermometer was placed in the refrigerator (i.e., where PSSM was stored before use). Samples were transported to the laboratory in a cooler bag containing ice packs and a maximum/minimum thermometer (i.e., temperature maintained at $1 \pm 3°C$).

Microbiological analysis

Samples were examined within 1 h of collection and after 4 h at 30°C (i.e., simulation of consumption period where food may rest at a ward temperature of $28 \pm 3°C$). Enumeration of micro-organisms was carried out using both the spread plate method and the spiral plating technique (Spiral plater model B, Spiral Systems Inc.). The media used were tryptone soya agar (supplemented with 0·6% yeast extract), blood agar base (supplemented with 0·7% defibrinated horse blood), nutrient agar (supplemented with 0·5 mg $MnSO_4H_2O$ to aid sporulation) and *B. cereus* selective agar (Oxoid CM617). Plates were examined at 24 h and after two and three days incubation at 30°C. *B. cereus* isolates were identified by the morphological and biochemical properties as described by Rowan and Anderson.[13] Other *Bacillus* spp. were identified by morphological, physiological and biochemical tests.[8] The identity of *Bacillus* isolates was confirmed using the API 50 CHB and API 20 E galleries (Biomérieux Ltd., France). *Micrococcus* spp. were identified by morphological and biochemical properties.[14]

Detection of diarrhoeagenic enterotoxin

Foods contaminated with *B. cereus* were assessed for diarrhoeal enterotoxin by the *B. cereus* enterotoxin—reverse passive latex agglutination assay kit (BCET-RPLA TD950; Oxoid)—which has a sensitivity of 4 ng enterotoxin per mL^5 using a non-turbid, fat free extract obtained with an Omega 300 kDa molecular weight cut-off polyethersulphone membrane (Filtron Technology Corporation). *B. cereus* NCTC 11145 and *Bacillus licheniformis* NCTC 10341 were used as positive and negative controls.

Statistical analysis

Fisher's exact test was used to compare the total microbial numbers and the levels of *B. cereus* (cfu/mL or /g) in samples obtained from the above mentioned materials. All significant differences were reported at the 95% level of confidence ($P<0·05$).

Results

Enterotoxigenic Bacillus cereus *in dietary supplements prepared for hospitalized HIV patients*

Results of the microbiological examination are listed in Table I. Although various bacteria were detected in the BUP samples, numbers were low.

Table I. *Bacteriological quality of inadequately refrigerated and stored hospital-prepared build-up food*

Products analysed	Predominant organisms	Microbial numbers present (log_{10} cfu/mL or /g)	
		Initial analysis	Analysis after 4 h storage at 30°C
$PSSM_1$	*Micrococcus* spp.	6·26	7·56
	Bacillus subtilis	5·74	5·72
BUP_1	*Bacillus licheniformis*	2·42	2·40
	Bacillus subtilis	1·30	1·30
	Bacillus cereus (emetic type)	1·11	1·10
$BUP_1 + PSSM_1$	*Micrococcus* spp.	6·38	7·54
	Bacillus subtilis	5·75	6·54
$PSSM_2$	*Bacillus cereus* (diarrhoeal type)*	5·86	7·55
	Bacillus licheniformis	4·63	ND‡
BUP_2	*Bacillus licheniformis*	1·95	1·90
	Bacillus circulans	1·49	1·47
	Bacillus cereus (diarrhoeal type)	1·30	1·30
	Bacillus sphaericus	1·34	1·34
$BUP_2 + PSSM_2$	*Bacillus cereus* (diarrhoeal type)*	5·86	7·63†
	Bacillus lichenformis	4·62	ND‡

* Diarrhoeagenic strain of *B. cereus*—as detected with the BCET-RPLA assay kit.
† Diarrhoeal enterotoxin detected in food sample.
‡ Organism not detected on BCSA plates at 10^{-4} dilution.
$PSSM_1$, $PSSM_2$ Pasteurized semi-skimmed milk, 1 and 2.
BUP_1, BUP_2 Build-up powder, 1 and 2.

Potentially hazardous levels of various bacteria were however recovered from both PSSM samples; counts were above the recommended safety limit of 2 ± 10^5 cfu/mL.[10] Because of this, the prepared build-up food (BUP+PSSM) also contained unacceptably high levels of bacteria.

The bacterial flora of most samples was dominated by members of the genus *Bacillus*, as is frequently the case with pasteurized[9] and/or powdered food products.[19] *B. cereus* (diarrhoeagenic strain) was recovered from samples of BUP_2 and $PSSM_2$ with the latter at high levels, and consequently the prepared food ($BUP_2 + PSSM_2$) was also highly contaminated. Diarrhoeal enterotoxin was not detected in either $PSSM_2$ or $BUP_2 + PSSM_2$ on initial examination, but was present in the latter after storage for 4 h at 30°C at a level of 16 ng/mL (Table I).

The thermoduric Gram-positive cocci recovered from both PSSM and BUP+PSSM belonged to the genus *Micrococcus* (Table I). As members of this genus are generally of little medical significance, the organism was not identified further.[14] Microbial counts obtained from the blender and

Table II. *Recommendations proposed to improve the bacteriological quality of hospital-prepared build-up foods*

Number	Recommendations
1	The hospital refrigerator should be maintained at or below 4°C.
2	The refrigerator should be serviced and monitored (i.e., maximum/minimum thermometer) at regular intervals.
3	Items should not be tightly packed in the refrigerator, as this will prevent the circulation of cold air throughout compartments.
4	Opening and closing the refrigerator door should be kept to a minimum.
5	All refrigerated foods should be used before their expiry date.
6	The time between food preparation and consumption should be kept to a minimum.*
7	Close attention should be paid to personal hygiene and all preparative equipment should be thoroughly cleaned before use.

* If hospital staff are confident that they can satisfy recommendations 1–5 and 7, then on the basis of our findings we recommend that these supplementary foods may remain for up to 4 h at ward temperature. However, if the hospital cannot satisfy these points, we recommend a reduced storage period, i.e., keeping foods for up to 1 h at ambient ward temperature.

polystyrene cup were below the lower detection limit of 10 cfu. The type and number of organisms isolated from BUP did not influence the bacterial quality of the reconstituted build-up food ($P<0{\cdot}05$). The PSSM contaminated with high levels of bacteria (Table I), had been stored under inadequate conditions. The refrigerator was operating at approximately 9°C above the specified temperature of 4°C (i.e. 13 ± 4°C). On the basis of the above findings, a list of recommendations was proposed to reduce bacterial counts in dietary supplemented foods to an acceptable level (Table II).

Bacteriological quality of properly refrigerated and stored hospital-prepared build-up foods

The study was repeated one month after the hospital had acted on the recommendations proposed in Table II. Microbial numbers in BUP_3+PSSM_3 and BUP_4+PSSM_4 were reduced to $<10^3$ cfu/mL, well within the acceptable limit for bacteriological quality.[10] Although a diarrhoeagenic strain of *B. cereus* was isolated from BUP_3, no enterotoxin was detected in BUP_3+PSSM_3 after 4 h storage at 30°C (Table III). Although epidemiological data was not released by the hospital, the incidence of diarrhoeal episodes among HIV patients was reported to be reduced.

Discussion

Unacceptably high levels of enterotoxigenic *B. cereus* ($>10^5$ cfu/mL) were detected in hospital-prepared foods (BUP+PSSM). The high microbial numbers were attributed in part to the storage of PSSM in an inadequately

Table III. *Bacteriological quality of properly refrigerated and stored hospital-prepared build-up food*

Products analysed	Predominant organisms	Microbial numbers present (log_{10} cfu/mL or /g)	
		Initial analysis	Analysis after 4 h storage at 30°C
Pasteurized semi-skimmed milk ($PSSM_3$)	*Bacillus subtilis*	2·28	2·84
	Bacillus sphaericus	1·50	1·88
	Bacillus cereus (diarrhoeal type)*	1·18	1·39
Build-up powder (BUP_3)	*Bacillus licheniformis*	1·74	1·69
	Bacillus megaterium	1·47	1·47
BUP_3+PSSM_3	*Bacillus subtilis*	2·30	2·86
	Bacillus licheniformis	1·69	2·10
	Bacillus sphaericus	1·50	1·90
	Bacillus megaterium	1·43	1·90
	Bacillus cereus (diarrhoeal type)*	1·12	1·36
$PSSM_4$	*Micrococcus* spp.	2·87	3·74
	Bacillus cereus var mycoides	1·30	1·54
BUP_4	*Bacillus licheniformis*	1·55	1·94
BUP_4+PSSM_4	*Micrococcus* spp.	2·86	3·76
	Bacillus cereus var mycoides	1·30	1·54
	Bacillus licheniformis	1·60	1·86

* Diarrhoeagenic strain of *B. cereus*—as detected with the BCET-RPLA assay kit.
$PSSM_3$, $PSSM_4$ Pasteurised semi-skimmed with 3 and 4
BUP_3, BUP_4 Build up powder, 3 and 4.

maintained refrigerator. Particular attention has been drawn to the importance of both the design and effective operation of refrigerators for the prevention of food-poisoning in the domestic environment.[20] Similar considerations must apply with even greater force in hospitals.

Storage of *B. cereus* contaminated BUP+PSSM for 4 h at 30°C (i.e., simulating the consumption period where the food may rest in the ward) resulted in growth of this enterotoxigenic strain and synthesis of diarrhoeal toxin. Although PSSM did not support toxin production (due in part to milk being a poor medium as it has a low free amino acid content and lacks glucose),[8,24] addition of BUP (which contains glucose) to PSSM allowed contaminating *B. cereus* cells to produce diarrhoeal enterotoxin. Rowan and Anderson[13] recently demonstrated that improperly stored reconstituted infant milk formulae supplemented with >0·1% glucose or maltodextrin also supported both growth of *B. cereus* and synthesis of diarrhoeal enterotoxin.

Implementation of the recommendations significantly improved the bacteriological and toxicological quality of hospital-prepared build-up foods ($P<0·05$). Thus, despite the absence of epidemiological data, diarrhoeal episodes among HIV patients may have been caused by the consumption

of hospital-prepared build-up food contaminated with enterotoxigenic *B. cereus* cells and/or enterotoxin; and illness induced by the effects of pre-formed toxin[18] or by growth of *B. cereus* in the ileum with subsequent synthesis of enterotoxin.[16]

Despite the fact that *Bacillus* spp. (apart from *Bacillus anthracis*) isolated occasionally from human pathological samples (e.g., blood, cerebrospinal fluid, wounds and stools),[21] are often described as 'inconsequential aerobic spore-forming contaminants' and to be of little clinical significance;[1,3] those recovered from hospital-prepared dietary supplements during this study (i.e., *B. cereus*, *B. licheniformis*, *Bacillus subtilis*, *Bacillus sphaericus* and *Bacillus circulans*) have been implicated in food-borne illnesses[8] and/or opportunist infections.[3,5,22–24]

As the number of people infected with HIV and AIDS,[25] is expected to reach 40 million by the year 2000,[26] far more immunocompromised individuals will be admitted to hospital. Indeed HIV and AIDS patients already account for more than 50% of adult medical admissions in many African national and provincial hospitals.[27,28] In view of the immunological status of these and other vulnerable groups, the storage and preparation of their food is of paramount importance.

We thank the Scottish Office Home and Health Department for funding this work (K/MRS/50/C2205). We also thank Dr Irene Watson-Craik for the use of her image analysis equipment and to the staff of a Glasgow hospital for their participation in this study.

References

1. Drobniewski FA. *Bacillus cereus* and related species. *Clin Microbiol Rev* 1993; **6**: 324–338.
2. Mueller GP, Williams SA. Surgical infections in AIDS patients. *Am J Surg* 1995; **169**: 34–38.
3. Banerjee C, Bustamante CI, Wharton R, Talley E, Wade C. *Bacillus* infections in patients with cancer. *Arch Intern Med* 1988; **148**: 1769–1774.
4. Cotton DJ, Gill VJ, Marshall DJ, Gress J, Thaler M, Pizzo P. Clinical features and therapeutic interventions in 17 cases of Bacillus bacteremia in an immunosuppressed patient population. *J Clin Microbiol* 1987; **25**: 672–674.
5. Blue SR, Singh VR, Saubolle MA. *Bacillus licheniformis* bacteremia, five cases associated with indwelling central venous catheters. *Clin Infect Dis* 1995; **20**: 629–633.
6. Rowan NJ, Anderson JG, Anderton A. The bacteriological quality of hospital-prepared infant feeds. *J Hosp Infect* 1997; **35**: 259–267.
7. Burnett IA, Wardley BL, Magee J. The milk kitchen, Sheffield Children's Hospital, before and after a review. *J Hosp Infect* 1989; **13**: 179–185.
8. Rowan NJ. Studies on the growth, survival, interaction and detection of potentially pathogenic *Listeria* and *Bacillus* species in infant milk formulae. Ph.D. thesis 1996, University of Strathclyde, Glasgow, Scotland.
9. Craven HM, Macauley BJ. Microorganisms in pasteurized milk after refrigeration storage—Identification of types. *Austral J Dairy Technol* 1992; **47**: 38–45.
10. Nelson FE. In: Robinson RK, Ed. *Dairy Microbiology Vol. 1. The Microbiology of Milk*. London and New York: Elsevier Applied Science Publishers, 1985; 165–208.
11. Daeschel MA. Antimicrobial substances from lactic acid bacteria for use as food preservatives. *Food Technol* 1989; **43**: 164–167.
12. Jack RW, Tagg JR, Ray B. Bacteriocins of Gram positive bacteria. *Microbiol Rev* 1995; **59**: 171–200.

13. Rowan NJ, Anderson JG. Maltodextrin stimulates growth of *Bacillus cereus* and synthesis of diarrhoeal enterotoxin in infant milk formulae. *Appl Environ Microbiol* 1997; **63**: 1182–1184.
14. Gilmour A, Rowe MT. In: Robinson RK, Ed. *Dairy Microbiology Vol. 1. The Microbiology of Milk*. London and New York: Elsevier Applied Science Publishers, 1985; 35–76.
15. Granum PE, Brynestad S, Kramer JM. Analysis of enterotoxin production caused by *Bacillus cereus* from dairy products, food poisoning incidents and non-gastrointestinal infections. *Int J Food Microbiol* 1993; **17**: 269–279.
16. Granum PE, Brynestad S, O'Sullivan K, Nissen H. Enterotoxin from *Bacillus cereus*: production and biochemical characterisation. *Neth Milk Dairy J* 1993; **47**: 63–70.
17. Granum PE. *Bacillus cereus* and its toxins. *J Appl Bacteriol* 1994; **76**: 61–66.
18. Baker JM, Griffiths WM. Evidence for increased thermostability of *Bacillus cereus* enterotoxin in milk. *J Food Protect* 1995; **58**: 443–445.
19. Buchanan RL, Schultz FJ. Evaluation of the Oxoid BCET-PRLA kit for the detection of *Bacillus cereus* diarrhoeal enterotoxin as compared to cell culture cytotoxicity. *J Food Protect* 1992; **55**: 440–443.
20. Becker H, Schaller G, von Wiese W, Terplan G. *Bacillus cereus* in infant foods and dried milk products. *Int J Food Microbiol* 1994; **23**: 1–15.
21. Richmond Report. *The Microbiological Safety of Food, Part II*. Report of the Committee on the Microbiological Safety of Food. Her Majesty's Stationery Office, London, 1991.
22. Young RF, Yoshimori RH, Murray DL, Chou PJ. Postoperative neurosurgical infections due to *Bacillus* species. *Surg Neurol* 1982; **18**: 271–273.
23. Goudswaard WB, Dammer MH, Hol C. *Bacillus circulans* infection of a proximal interphalangeal joint after a clenched-fist injury caused by human teeth. *Eur J Clin Microbiol Infect Dis* 1995; **14**: 1015–1016.
24. Marley EF, Saini NK, Venkatraman C, Orenstein JM. Fatal *Bacillus cereus* meningoencephalitis in an adult with acute myelogenous leukemia. *South Med J* 1995; **88**: 969–972.
25. Sliman R, Rehm S, Shlaes DM. Serious infections caused by *Bacillus* species. *Med* 1987; **66**: 218–223.
26. Quinn TC. Global burden of the HIV pandemic. *Lancet* 1996; **348**: 99–106.
27. Mertens TE, Lowbeer D. HIV and AIDS—Where is the epidemic going? *Bull W.H.O.* 1996; **74**: 121–129.
28. Mhalu FS, Lyamuya E. Human immunodeficiency virus infection and AIDS in East Africa—Challenges and possibilities for prevention and control. *East Afr Med J* 1996; **73**: 13–19.

APPLIED AND ENVIRONMENTAL MICROBIOLOGY, Mar. 1997, p. 1182–1184 Vol. 63, No. 3
0099-2240/97/$04.00+0

Maltodextrin Stimulates Growth of *Bacillus cereus* and Synthesis of Diarrheal Enterotoxin in Infant Milk Formulae

N. J. ROWAN* AND J. G. ANDERSON

Department of Bioscience and Biotechnology, University of Strathclyde, Glasgow, Scotland

Received 10 October 1996/Accepted 5 December 1996

One hundred reconstituted milk-based infant formulae (IMF) representative of 10 leading brands available in many European Economic Community countries were examined for *Bacillus cereus* and for the presence of diarrheal enterotoxin. Sixty-three reconstituted IMF supported growth of the organism after 14 h at 25°C, and in 4 of these, which contained maltodextrin, enterotoxin was detected. Reconstituted IMF (and basal synthetic media) supplemented with ≥0.1% maltodextrin supported both growth of *B. cereus* and diarrheal toxin production when incubated for 14 h or more at 25°C.

Reconstituted infant foods are considered to be a food class of high risk due to the susceptibility of infants to enteric bacterial pathogens, their severe response to enterotoxins, and their increased mortality (14). There is, however, no requirement that these foods should be sterile, and many powdered milk products are subjected only to pasteurization prior to spray drying (11). Of particular concern is the occurrence of enterotoxigenic *Bacillus cereus* in these products; Becker et al. (2) reported that 54% of 261 samples of infant food examined (distributed in 17 countries) were contaminated with this organism, reaching levels of 0.3 to 600 cells g^{-1}.

While the infectious dose of *B. cereus* is considered to be in the range of 10^5 to 10^7 cells ml^{-1} (8), outbreaks of food-borne illness associated with infants and other vulnerable groups have been attributed previously to the consumption of foods containing low numbers of this bacterium, in the range of 10^3 to 10^5 cells g^{-1} (6). Fortunately, despite the inherent ability of *B. cereus* spores to survive harsh environmental conditions (12) and the increasing number of food-related illnesses associated with the consumption of either proteinaceous (13) or farinaceous (9) foods containing this organism, the incidence of *B. cereus* food poisoning attributable to milk and milk products remains remarkably low (2). The low incidence of *B. cereus* food intoxication from these products may be due in part to milk being a poor medium for toxin production, as it has a very low free-amino-acid content and lacks glucose (2, 12). Christiansson et al. (4) reported however, that milk inoculated with *B. cereus* strains showed cytotoxicity in culture supernatant after periods of storage at different temperatures.

There is insufficient evidence to establish conclusively whether *B. cereus* diarrheal-type food intoxication results from consumption of preformed toxin (1, 12) or from production of enterotoxin by ingested cells or spores in the ileum (7). However, all of the studies on the stability of the diarrheal enterotoxin that are cited in the literature have been performed in nonfood systems, and recent evidence suggests that this stability may be significantly greater when the toxin is preformed in foods such as milk (1).

Many leading baby food companies now incorporate ingredients of a high calorific value, such as maltodextrin (a derivative of starch hydrolysis), in infant formula products which are intended for premature and weaning babies (1, 14). Here, we present evidence that maltodextrin stimulates growth of *B. cereus* in reconstituted infant milk-based formulae (IMF) (and in basal synthetic media) and synthesis of enterotoxin.

A correlation was made between maltodextrin content (kindly supplied by Cerestar Gruppo Ferruzzi) and synthesis of diarrheal enterotoxin by using three diarrheagenic *B. cereus* II strains, namely, *B. cereus* SU11 and SU58, isolated from analyzed IMF, and *B. cereus* NCTC 11145, obtained from the National Collection of Type Cultures. *Bacillus licheniformis* NCTC 10341 was used as a negative control for enterotoxin production. Cultures were grown at 30°C and maintained on nutrient agar (Oxoid Products); they were subcultured every 2 weeks. Fisher's exact test was used to compare levels of diarrheal enterotoxin (in nanograms per milliliter) produced in test media by *B. cereus*. All significant differences were reported at the 95% level of confidence ($P < 0.05$).

An examination of 100 IMF for *B. cereus* diarrheal enterotoxin. One hundred IMF (i.e., products in which the only protein source was cow's milk), representative of 10 leading brands available in many European Economic Community countries, were analyzed for the presence of *B. cereus* and for diarrheal enterotoxin production. Triplicate 25-g IMF samples were reconstituted in 225 ml of sterile water at 56°C (±0.2°C) by shaking 25 times through an excursion of 30 cm and were then incubated at 25 and 30°C for periods up to and including 24 h. Samples were spread and spiral plated (Spiral plater model B, Spiral Systems Inc.) onto tryptone soy agar (supplemented with 0.6% yeast extract), blood agar (supplemented with 0.7% defibrinated horse blood), nutrient agar (supplemented with 0.5 mg of $MnSO_4H_2O$ $liter^{-1}$ to aid sporulation), and *B. cereus* selective agar (Oxoid Products) and were incubated for up to 72 h at 30°C. *B. cereus* isolates were identified by establishing the following morphological and biochemical properties: positive Gram and catalase reactions; cell width (>1 μm) and length (>3 μm) (Solitaire 512 Image Analyzer; Seescan Plc); motility and lecithovitellin/lecithinase production; β-hemolytic reaction and gross colony morphological appearance (millimeters); an ellipsoidal endospore, centrally or subterminally positioned with nondistention of the sporangium; hydrolysis of starch, casein, and gelatin; and growth in the presence of 7.5% NaCl or 0.001% lysozyme. The identity of each isolate was confirmed by using the API 50 CHB and API 20 E galleries (Biomérieux Ltd.).

Infant foods contaminated with *B. cereus* were assessed for the presence of diarrheal enterotoxin with the *B. cereus* enter-

* Corresponding author. Mailing address: Department of Bioscience and Biotechnology, University of Strathclyde, Royal College Building, 204 George St., Glasgow, Scotland. Phone: 0044 41 552 4400, ext. 2085. Fax: 0044 41 553 1161. E-mail: n.j.rowan@pop-hub.strath.ac.uk.

TABLE 1. Influence of duration of storage at ≥25°C on number of reconstituted IMF contaminated with *B. cereus* strains, with or without diarrheal enterotoxin

Duration of storage (h)	No. of IMF contaminated with:[a]			
	B. cereus I	*B. cereus* II	Diarrheagenic *B. cereus* II	Diarrheagenic *B. cereus* II and diarrheal toxin
0	10	7	6	0
8	30	34	10	0
14	31	37	10	4
24	31	38	10	4

[a] One hundred IMF were examined for *B. cereus* and for the presence of diarrheal enterotoxin.

otoxin-reverse passive latex agglutination assay kit (BCET-RPLA TD950; Oxoid) after a nonturbid, fat-free extract was initially obtained via the Filtron stirred cell ultrafiltration system fitted with an Omega 300-kDa cutoff polyethersulfone membrane (Filtron Technology Corporation). *B. cereus* isolates producing enterotoxin after overnight cultivation in brain heart infusion (BHI) broth supplemented with 0.1% glucose (BHIG) at 30°C were designated as potentially enterotoxigenic.

B. cereus was detected in 17 IMF examined immediately after reconstitution at levels up to 4.8×10^2 CFU g^{-1} (mean, 1.3×10^2 CFU g^{-1}); only 6 (35.3%) of these contained the enterotoxigenic form of this organism (Table 1). Diarrheal enterotoxin, however, was not detected in any dried IMF product. In agreement with other studies (2, 12), these experiments demonstrated that the dried IMF available in many European Economic Community countries is of acceptable bacteriological quality, having *B. cereus* counts lower than the safety limit of 10^3 CFU g^{-1} proposed by the Association of Dietetic Food Industries of the European Community (data not shown) (2). Subsequent reconstitution and storage resulted in 63 infant foods containing this organism, where 6 products contained both *B. cereus* I and II (Table 1). Of the 38 IMF supporting growth of *B. cereus* II (of which 10 isolates were shown to be enterotoxigenic after cultivation in BHIG), diarrheal enterotoxin was detected in only 4 formulations after 14 h at ≥25°C (Table 1). The level of enterotoxin in cultured IMF varied over the range of 16 to ≥124 ng ml^{-1}, where the reported sensitivity of the BCET-RPLA test in detecting this enterotoxin is 2 ng ml^{-1} (3). All four infant formulations supporting enterotoxin production contained maltodextrin (three also had lactose), while the six toxin-free baby foods containing enterotoxigenic *B. cereus* II had lactose as their sole carbohydrate source. These studies showed that improperly stored IMF containing maltodextrin may pose a threat to consumer safety, as they may be contaminated with diarrheagenic *B. cereus* capable of both growth and enterotoxin production in these products.

Effect of maltodextrin on growth of *B. cereus* and synthesis of diarrheal enterotoxin. To confirm the possible link between maltodextrin and stimulation of diarrheal enterotoxin production, additional studies, using three enterotoxigenic *B. cereus* II isolates (i.e., *B. cereus* SU11, SU58, and NCTC 11145) and a nonenterotoxigenic *B. licheniformis*, NCTC 10341, were carried out. After an initial 24-h cultivation period at 125 rpm in BHI broth at 30°C, each test organism was washed three times in phosphate-buffered saline (0.01 M sodium phosphate [pH 7.2]–0.15 M NaCl) and centrifuged at $11,500 \times g$ for 10 min at 4°C (Microcentaur MSE). Decimal serial dilution of the suspended cells was carried out in phosphate-buffered saline, and a 1-ml sample of the 10^{-4} dilution was inoculated into either basal synthetic media or tyndallized IMF test media to give an initial cell count of 10 to 100 cells ml^{-1}.

Inoculated basal synthetic media (pH 7.2) and tyndallized IMF test media, supplemented with 0.01, 0.1, 1.0, or 3.52% filter-sterilized maltodextrin, glucose, or lactose, were incubated for 14 and 24 h at 25°C. Confirmation that each test sugar had passed through the 0.45-μm-pore-size membrane filter (Millipore) was achieved by carrying out separate sugar assays with a 10% stock solution of each sugar before and after filtration. Following cultivation at 25°C, filtrates obtained from the test cultures (via the Filtron stirred cell ultrafiltration system) were examined for the number of cells present (CFU per milliliter) and for the presence of enterotoxin as described earlier. Reconstituted IMF used in these enterotoxin studies were tyndallized to sterility prior to supplementation with the above-mentioned sugars.

Basal synthetic media (Table 2) and reconstituted IMF (Table 3) supplemented with ≥0.1% maltodextrin both supported growth of *B. cereus* SU11, SU58, and NCTC 11145 and stimulated diarrheal enterotoxin production (Tables 2 and 3). Higher levels of enterotoxin (in nanograms per milliliter) were produced in basal synthetic media containing 1% maltodextrin or glucose (Table 2) and in reconstituted IMF containing 1.6% maltodextrin (Table 3) than in media containing either higher or lower concentrations of these sugars. While lactose supported growth of each test culture, no enterotoxin was produced in these cultured media (Tables 2 and 3). IMF used in these toxin studies either contained or were supplemented with infant formula-grade maltodextrin at levels normally found in certain brands of these products (Table 3). It was not unexpected that maltodextrin (a derivative of starch hydrolysis) had the potential to stimulate diarrheal enterotoxin production, as

TABLE 2. Diarrheal enterotoxin production by *B. cereus* strains at 30°C in basal synthetic media containing different carbohydrate sources

Test organism	ng of enterotoxin ml^{-1}[a] (no. of cells[b]) in basal media containing:									
	Maltodextrin				Glucose				Lactose	
	3.52%	1.0%	0.1%	0.01%	3.52%	1.0%	0.1%	0.01%	3.52%	≤1.0%
B. cereus SU11	2 (7.01)	32 (7.23)	—[c] (6.81)	— (6.75)	2 (7.24)	32 (7.08)	— (6.89)	— (6.79)	— (7.06)	— (6.98)
B. cereus SU58	4 (6.91)	32 (7.20)	2 (6.86)	— (6.78)	4 (7.26)	32 (7.29)	2 (6.97)	— (6.87)	— (6.98)	— (6.92)
B. cereus NCTC 11145	4 (7.04)	32 (7.18)	4 (7.01)	— (6.92)	8 (7.36)	32 (7.18)	4 (7.08)	— (6.98)	— (7.01)	— (6.98)
B. licheniformis NCTC 10341	— (6.80)	— (6.78)	— (6.61)	— (6.38)	— (6.85)	— (6.78)	— (6.66)	— (6.49)	— (6.68)	— (6.61)

[a] Detected by the BCET-RPLA system.
[b] Measured as $\log_{10}$ CFU per milliliter.
[c] —, no toxin detected.

TABLE 3. Diarrheal enterotoxin production by *B. cereus* strains in a variety of commercially available IMF containing or supplemented with maltodextrin

IMF (% maltodextrin)	ng of enterotoxin ml^{-1}[a] produced (no. of cells[b]) in test media			
	B. cereus SU11	*B. cereus* SU58	*B. cereus* NCTC 11145	*B. licheniformis* NCTC 10341
A (3.78)	16 (7.37)	32 (7.29)	64 (7.36)	—[c] (6.90)
B (1.6)	32 (7.32)	64 (7.27)	≥128 (7.37)	— (6.90)
C (3.52)	32 (7.39)	64 (7.28)	64 (7.34)	— (6.88)
D (0)	— (7.29)	— (7.27)	— (7.30)	— (6.86)
D+[d] (3.52)	32 (7.30)	64 (7.30)	64 (7.32)	— (6.86)
E (0)	— (7.22)	— (7.25)	— (7.31)	— (6.90)
E+ (1.6)	32 (7.28)	64 (7.26)	≥128 (7.32)	— (6.91)

[a] Detected by BCET-RPLA assay in fat-free IMF extract.
[b] Measured as $\log_{10}$ CFU per milliliter.
[c] —, no toxin detected.
[d] +, composition of original infant formulations altered by the addition of maltodextrin.

starch has been shown previously to be a suitable carbohydrate source for both growth of *B. cereus* and subsequent diarrheal toxin production (5).

Despite worldwide occurrence of diarrheagenic *B. cereus* in milk, there are remarkably few reports of food intoxication in which this organism was implicated as the etiological agent (2, 12). While the mechanism of *B. cereus* diarrheal-type food poisoning remains unclear, one factor contributing to this low incidence is the unsuitability of milk as a medium for enterotoxin production, as it lacks glucose and free amino acids (12). This study has shown that *B. cereus* occasionally contaminated dried IMF at acceptably low levels and should not present a health problem to the consumer population if IMF is reconstituted under hygienic conditions and consumed within 4 h of preparation. However, improperly stored formulations containing maltodextrin may pose a threat to consumer safety, as they may be contaminated with diarrheagenic *B. cereus* capable of both growth and diarrheal toxin production in these products. By supplementing IMF with maltodextrin in order to enhance the nutritive value of this product (2), food companies may have unwittingly produced a suitable environment in which improperly stored infant foods containing diarrheagenic *B. cereus* may produce enterotoxin.

We thank the Scottish Home and Health Department for funding this research (K/MRS/50/C2005).

We also thank Irene Watson-Craik (Department of Bioscience and Biotechnology, University of Strathclyde) for the use of her image analysis equipment and George Gettinby (Department of Statistics and Modelling Science, University of Strathclyde) for his assistance with the statistical analysis.

REFERENCES

1. **Baker, J. M., and W. M. Griffiths.** 1995. Evidence for increased thermostability of *Bacillus cereus* enterotoxin in milk. J. Food Prot. **58:**443–445.
2. **Becker, H., G. Schaller, W. von Wiese, and G. Terplan.** 1994. *Bacillus cereus* in infant foods and dried milk products. Int. J. Food Microbiol. **23:**1–15.
3. **Beecher, D. J., and A. C. L. Wong.** 1994. Identification and analysis of the antigens detected by two commercial *Bacillus cereus* enterotoxin immunoassay kits. Appl. Environ. Microbiol. **60:**4614–4616.
4. **Christiansson, A., A. S. Naidu, I. Nilsson, T. Wadstrom, and H.-E. Pettersson.** 1989. Toxin production by *Bacillus cereus* dairy isolates in milk at low temperatures. Appl. Environ. Microbiol. **55:**2595–2600.
5. **Garcia-Arribas, M. L., and J. M. Kramer.** 1990. The effect of glucose, starch and pH on the growth, enterotoxin and haemolysin production by strains of *Bacillus cereus* associated with food poisoning and non-gastrointestinal infections. Int. J. Food Microbiol. **11:**21–31.
6. **Giannella, R. A., and L. Brasile.** 1979. A hospital food-borne outbreak of diarrhea caused by *Bacillus cereus*: clinical, epidemiologic and microbiologic studies. J. Infect. Dis. **139:**366–370.
7. **Granum, P. E., S. Brynestad, and J. M. Kramer.** 1993. Analysis of enterotoxin production by *Bacillus cereus* from dairy products, food poisoning incidents and non-gastrointestinal infections. Int. J. Food Microbiol. **17:**269–279.
8. **Granum, P. E., S. Brynestad, K. O'Sullivan, and H. Nissen.** 1993. The enterotoxin from *B. cereus*: production and biochemical characterization. Neth. Milk Dairy J. **47:**63–70.
9. **Granum, P. E.** 1994. *Bacillus cereus* and its toxins. J. Appl. Bacteriol. **76:** 615–665.
10. **Hostacka, A., A. Kosiarova, V. Majtan, and S. Kohutova.** 1992. Toxic properties of *Bacillus cereus* strains isolated from different foodstuffs. Zentralbl. Bakteriol. **276:**303–312.
11. **International Commission on Microbiological Specifications for Foods.** 1986. International Commission on Microbiological Specifications for Foods, vol. 1. Their significance and methods of enumeration. University of Toronto Press, Toronto, Ontario, Canada.
12. **International Dairy Federation.** 1992. *Bacillus cereus* in milk and milk products, p. 1–48. Bulletin No. 275. International Dairy Federation, Brussels, Belgium.
13. **Jackson, S. G., R. B. Goodbrand, R. Ahmed, and S. Rasatiya.** 1995. *Bacillus cereus* and *Bacillus thuringiensis* isolated in gastro-enteritis outbreak investigation. Lett. Appl. Microbiol. **21:**603–605.
14. **Rowan, N. J.** 1996. Studies on the growth, survival, interaction, and detection of potentially pathogenic *Listeria* and *Bacillus* spp. in infant milk formulae. Ph.D. thesis. University of Strathclyde, Glasgow, Scotland.

Diarrhoeal enterotoxin production by psychrotrophic *Bacillus cereus* present in reconstituted milk-based infant formulae (MIF)

N.J. Rowan and J.G. Anderson

Department of Bioscience and Biotechnology, University of Strathclyde, Glasgow, UK

1625/97: received 18 September 1997 and accepted 23 September 1997

N.J. ROWAN AND J.G. ANDERSON. 1998. One hundred reconstituted milk-based infant formulae (MIF) representative of 10 leading brands available in many European Economic Community countries were examined for psychrotrophic *Bacillus cereus* and for the presence of diarrhoeal enterotoxin. Of the 38 *B. cereus* isolates recovered from MIF, one, four and 16 strains grew at 4, 6 and 8 °C after 15 d. One (2·6%), two (5·3%) and six (15·8%) of the isolates were identified as potential psychrotrophic food poisoning strains as they were both enterotoxigenic and exhibited good growth at 4, 6 and 8 °C, respectively. Enterotoxin was not detected in MIF in which less than 5·36 $\log_{10}$ cfu of *B. cereus* ml^{-1} had grown. While psychrotrophic enterotoxigenic *B. cereus* strains occur occasionally in MIF, brief storage of reconstituted MIF at the recommended refrigeration temperature of 4 °C will allow this product to remain safe for consumption.

INTRODUCTION

Bacillus cereus, a ubiquitously distributed aerobic spore-former, tolerates adverse environmental conditions better than most other bacterial pathogens (Rowan 1996). Becker *et al*. (1994) reported that 54% of 261 samples of infant food distributed in 17 countries was contaminated with *B. cereus*, reaching levels of 0·3–600 viable cells g^{-1}. Also, Rowan *et al*. (1997) demonstrated that hospital prepared infant food may be contaminated with enterotoxigenic *B. cereus* at levels above the Association of Dietetic Food Industries of the European Communities (IDAEC) proposed safety limit of 10^3 cfu ml^{-1}. To guard against possible deleterious effects of food-borne Gram-negative enteric bacteria, hospitals are routinely pasteurizing many milk-based products (Anderton 1993). Several researchers have shown, however, that counts of aerobic spore-forming bacteria in these pasteurized foods are little affected by this thermal process (Rowan 1996).

Observations that psychrotrophic *B. cereus* strains have been implicated in outbreaks of food-related illness (Turner *et al*. 1996) and are capable of producing toxins (Christiansson *et al*. 1989; Griffiths 1990; van Netten *et al*. 1990; Granum *et al*. 1993a), have raised concern about their growth and enterotoxin production abilities in refrigerated foods (International Dairy Federation 1992). There is insufficient evidence to establish conclusively whether *B. cereus* diarrhoeal-type food intoxication results from consumption of preformed toxin (Baker and Griffiths 1995) or from production of enterotoxin by ingested cells or spores in the ileum (Granum *et al*. 1993b). However, all of the studies on the stability of the diarrhoeal enterotoxins that are cited in the literature have been performed in non-food systems, and recent evidence suggests that this stability may be significantly greater when the toxin is preformed in foods such as milk (Baker and Griffiths 1995). The existence is reported here of psychrotrophic strains of *B. cereus* capable of growth and enterotoxin production in reconstituted milk-based infant formulae.

Correspondence to : Dr N. J. Rowan, Department of Bioscience and Biotechnology, University of Strathclyde, Royal College Building, 204 George Street, Glasgow G1 1XW, UK.

MATERIALS AND METHODS

Strains

Bacillus cereus NCTC 11145 and *B. licheniformis* NCTC 10341, obtained from the National Collection of Typed Cultures, were used as positive and negative control strains for diarrhoeal enterotoxin production respectively. Cultures were grown at 30 °C and maintained on Nutrient Agar; they were subcultured every 2 weeks.

Preparation of infant powder samples

One hundred milk-based infant formulae products (MIF), representative of 10 leading brands available in many European Economic Community countries, were purchased and examined for the presence of *B. cereus* and for diarrhoeal enterotoxin. Triplicate 25 g MIF samples were reconstituted in 225 ml of sterile water at 56 °C (±0·2 °C) by shaking 25 times through an excursion of 30 cm and were then incubated at 30 °C for periods up to and including 24 h.

Bacteriological analysis

Milk-based infant formulae samples were spread and spiral plated (Spiral plater model B, Sprial Systems Inc., Don Whitley Scientific, Ltd, Shipley, UK) onto Tryptone Soya Agar (supplemented with 0·6% yeast extract), Blood Agar Base (supplemented with 0·7% defibrinated horse blood), Nutrient Agar (supplemented with 0·5 mg of $MnSO_4H_2O$ l^{-1} to aid sporulation) (NAMS), and *B. cereus* Selective Agar (Oxoid, Basingstoke, UK) and incubated for 72 h at 30 °C. *Bacillus cereus* isolates were identified and confirmed by establishing certain key morphological and biochemical characteristics as described in Rowan *et al.* (1997).

Detection of diarrhoeagenic *B. cereus* strains

After overnight cultivation of *B. cereus* isolates in Brain Heart Infusion broth supplemented with 0·25% filter-sterilized glucose (BHIG) at 30 °C for 18 h on a rotary shaker (250 rev min^{-1}), duplicate 1 ml samples were examined in diarrhoeagenic properties via the *B. cereus* enterotoxin—reverse passive latex agglutination assay kit (BCET-RPLA TD950; Oxoid) as described in Rowan and Anderson (1997). *Bacillus cereus* isolates producing enterotoxin after cultivation in BHIG were designated as potentially enterotoxigenic.

Growth of *B. cereus* isolates in MIF at psychrotrophic temperatures

Milk-based infant formulae used to study growth profiles as affected by temperature of incubation were pre-tempered for at least 24 h at the temperature used in the challenge. Triplicate pre-cleaned and sterilized infant feeding bottles containing 250 ml of tyndallized Farleys second milk (a milk-based infant formula containing maltodextrin shown previously to support diarrhoeal enterotoxin production (Rowan and Anderson 1997)), were seeded with approximately 10^2 *B. cereus* spores ml^{-1} and were then incubated at 4, 6, 8 and 30 °C (a control temperature for toxin production) for periods up to and including 15 d.

The study was done in triplicate and the incubation temperatures varied less than 0·5 °C throughout the study. Diarrhoeagenic *B. cereus* NCTC 11145 and atoxigenic *B. licheniformis* NCTC 10341 were used as positive and negative controls, respectively. The starting inoculum (reflecting *B. cereus* counts obtained occasionally from dried MIF products (Rowan 1996)) was achieved by inoculating MIF with a spectrophotometrically (A_{600}) adjusted (Shimadzu uv-120-02; Shimadzu Corporation, Kyoto, Japan) spore suspension prepared in phosphate buffered saline (PBS, 0·01 mol l^{-1} sodium phosphate pH 7·2, 0·15 mol l^{-1} NaCl), where the test strains and isolates had been harvested from a 72 h culture grown at 30 °C on NAMS. Before MIF inoculation, the PBS cell/spore suspension was tempered in a waterbath (Techne Tempette Junior TE-8J; Techne Inc., Princetown, USA) at 70 °C for 10 min (simulating the water temperature used occasionally to reconstitute infant powder in the home (Rowan 1996)) to eliminate vegetative cells. Microbial numbers in the feeding bottles were confirmed by plating (1 : 10) dilutions on NAMS plates that were then incubated at 30 °C for 48 h.

Detection of diarrhoeal enterotoxin in MIF samples

Milk-based infant formulae seeded with *B. cereus* were assessed for the presence of diarrhoeal enterotoxin, with the BCET-RPLA assay kit, after a non-turbid, fat-free extract was initially obtained via the Filtron stirred cell ultrafiltration system fitted with an Omega 300 kDa cut-off polyethersulfone membrane (Filtron Technology Corporation; Flowgen, Lichfield, UK).

Statistical analysis

Fisher's exact test was used to compare levels of diarrhoeal enterotoxin (ng ml^{-1}) and/or microbial numbers (cfu ml^{-1}) in MIF. All significant differences were reported at the 95% levels of confidence ($P < 0·05$).

RESULTS AND DISCUSSION

Thirty-eight diarrhoeal-type *B. cereus* isolates were recovered from the 100 MIF products analysed, of which only 10 (26·3%) isolates were designated as potentially enterotoxigenic, producing varying levels of enterotoxin in BHIG after 18 h at 30 °C (results not shown). van Netten *et al.* (1990) reported that 8% of 483 pasteurized milk samples were positive for *B. cereus*, with approximately half of the isolates capable of growth at 7 °C.

This study showed that of the 38 *B. cereus* isolates seeded in MIF at low temperatures, one (2·6%), two (5·3%) and six (15·8%) isolates were identified as potential psychrotrophic food poisoning strains as they were both diarrhoeagenic and exhibited good growth at 4, 6 and 8 °C, respectively (Table 1). Enterotoxin was detected sooner in MIF incubated at higher

Table 1 *Bacillus cereus* isolates supporting diarrhoeal enterotoxin production and/or growth in reconstituted milk-based infant formulae (MIF) after 15 days at ⩽8 °C and 2 days at 30 °C

		ng of enterotoxin ml^{-1}* (no. of cells†) in MIF			
		Incubation temperature (°C)			
Strains	Source of strains	4	6	8	30
SU02/95	SMA white cap	—‡	— (5·75)	— (7·98)	— (8·17)
SU03/95	Nutrilon plus	— (4·76)	13 (6·52)	43 (7·37)	171 (7·48)
SU11/95	Nutrilon premium	—	—	32 (8·08)	213 (8·00)
SU27/95	Nutrilon premium	—	—	— (7·46)	— (7·78)
SU30/95	Milupa milumil	—	—	96 (7·80)	226 (8·04)
SU36/95	Milupa milumil	—	—	—	128 (7·96)
SU38/95	SMA gold cap	—	—	— (7·64)	— (7·58)
SU46/95	Nutrilon plus	—	—	—	213 (8·08)
SU48/95	Milupa aptamil	—	—	— (6·45)	— (7·76)
SU53/95	Nutrilon plus	—	—	—	64 (7·37)
SU58/95	Farleys first milk	—	—	— (5·88)	— (7·48)
SU62/95	Nutrilon premium	—	—	107 (7·28)	192 (7·56)
SU70/95	Milupa aptamil	—	—	— (7·77)	— (7·80)
SU99/95	Farleys second milk	—	3 (6·25)	96 (7·91)	64 (7·84)
SU108/96	Nutrilon plus	—	—	— (6·04)	— (8·08)
SU109/96	SMA white cap	—	—	—	132 (7·67)
SU114/96	SMA white cap	—	— (6·37)	— (7·57)	— (8·08)
SU123/96	Nutrilon premium	—	—	— (7·42)	— (7·45)
SU125/96	Farleys first milk	—	—	16 (6·78)	128 (7·85)
SU126/96	SMA gold cap	—	—	— (8·17)	— (8·08)
11145	NCTC	—	—	—	64 (7·37)
Bacillus licheniformis (10341)	NCTC	—	—	—	—

* Detected by the BCET-RPLA system, where values are averages of three replicate trials.
† Measured as $\log_{10}$ cfu ml^{-1}, where counts are averages of three replicate trials.
‡ No significant growth ($P < 0{\cdot}05$) or enterotoxin detected.

temperatures, where tests became positive after 23 d at 4 °C, 15 d at 6 °C and 10 d at 8 °C (Table 2). However, enterotoxin was not detected until *B. cereus* populations reached 5·36 $\log_{10}$ cfu ml^{-1}. This appears to be in agreement with the infective dose proposed by Kramer and Gilbert (1989), where the authors stated that at least 10^5 cfu ml^{-1} (g^{-1}) were necessary to cause illness. In an outbreak of *B. cereus* gastroenteritis linked to the consumption of stew, the estimated infective dose was 10^4–10^5 cfu g^{-1} (Beuchat *et al.* 1997).

While typical environmental isolates of *B. cereus* do not normally grow at temperatures below 10 °C (Granum *et al.* 1993a), other research groups have recently reported the existence of psychrotrophic strains capable of diarrhoeal enterotoxin production in microbiological media (Christiansson *et al.* 1989; Griffiths 1990), dairy products (Christiansson *et al.* 1989; Griffiths 1990; van Netten *et al.* 1990; Granum *et al.* 1993a), and convenience meals (Griffiths 1990; Beuchat *et al.* 1997) at or near refrigeration temperatures. These strains are causing increasing concern in the food industry as they have been implicated in a number of food poisoning incidents (van Netten *et al.* 1990). Granum *et al.* (1993a) demonstrated that 6% of 85 strains of psychrotrophic *B. cereus* (isolated from Norwegian dairy products) were enterotoxigenic, while Christiansson *et al.* (1989) showed that 75% of 136 *B. cereus* isolates produced an extracellular verocytotoxin when grown in milk or whipped cream at 8 °C.

In conclusion, as infant foods are considered to be a food class of high risk due to the susceptibility of infants to enteric bacterial pathogens, their response to enterotoxins and increased mortality (International Dairy Federation 1992),

Table 2 Titres of diarrhoeal enterotoxin produced in reconstituted MIF inoculated with spores of *Bacillus cereus* and incubated for up to 15 days at 4, 6 and 8 °C

Strains	Incubation temperature (°C)	ng of enterotoxin ml^{-1}* (no. of cells†) in MIF at incubation time (days)			
		3	6	10	15
SU03/95	4	—	—(2·65)	—(3·52)	—(4·76)§
	6	—	—(3·36)	—(4·93)	13 (6·52)
	8	—(2·86)	—(4·22)	5 (5·91)	43 (7·37)
SU11/95	4	—	—	—	—
	6	—	—	—	—
	8	—(2·94)	—(4·42)	3 (6·26)	32 (8·08)
SU30/95	4	—	—	—	—
	6	—	—	—	—
	8	—(2·60)	—(3·90)	—(5·65)	96 (7·80)
SU62/95	4	—	—	—	—
	6	—	—	—	—
	8	—	—(3·45)	—(5·45)	107 (7·28)
SU99/95	4	—	—	—	—
	6	—	—(3·08)	—(4·60)	3 (6·25)
	8	—(3·00)	—(4·50)	13 (6·35)	96 (7·91)
SU125/96	4	—	—	—	—
	6	—	—	—	—
	8	—	—(3·18)	—(5·17)	16 (6·78)
NCTC 11145	4	—	—	—	—
	6	—	—	—	—
	8	—	—	—	—

* Detected by the BCET-RPLA system, where values are averages of three replicate trials.
† Measured as $\log_{10}$ cfu ml^{-1}, where counts are averages of three replicate trials.
‡ No significant difference ($P < 0{\cdot}05$) or enterotoxin produced.
§ 16 ng of enterotoxin ml^{-1} detected after 23 days at 4 °C.

improper cold storage of infant formulations may pose a threat to consumer safety as the products may be contaminated with psychrotrophic *B. cereus* capable of both growth and enterotoxin production in these products.

ACKNOWLEDGEMENTS

The authors thank the Scottish Office, Home and Health Department (K/MRS/50/C2205) for funding this research.

REFERENCES

Anderton, A. (1993) Bacterial contamination of enteral feeds and feeding systems. *Clinical Nutrition* **12**, 97–113.

Baker, J.M. and Griffiths, M.W. (1995) Evidence for increased thermostability of *Bacillus cereus* enterotoxin in milk. *Journal of Food Protection* **58**, 443–445.

Becker, H., Schaller, G., von Wiese, W. and Terplan, G. (1994) *Bacillus cereus* in infant foods and dried milk products. *International Journal of Food Microbiology* **23**, 1–15.

Beuchat, L.R., Clavero, M.R.S. and Jaquette, C.B. (1997) Effects of nisin and temperature on survival, growth and enterotoxin production characteristics of psychrotrophic *Bacillus cereus* in beef gravy. *Applied and Environmental Microbiology* **63**, 1953–1958.

Christiansson, A., Naidu, A.S., Nilsson, I., Waldstrom, T. and Petterson, H.-E. (1989) Toxin production by *Bacillus cereus* dairy isolates in milk at low temperatures. *Applied and Environmental Microbiology* **55**, 2595–2600.

Granum, P.E., Brynestad, S. and Kramer, J.M. (1993a) Analysis of enterotoxin production by *Bacillus cereus* from dairy isolates, food poisoning incidents and non-gastrointestinal infections. *International Journal of Food Microbiology* **17**, 269–279.

Granum, P.E., Brynestad, S., O'Sullivan, K. and Nissen, H. (1993b) Enterotoxin from *Bacillus cereus*: production and biochemical characterisation. *Netherlands Milk Dairy Journal* **47**, 63–70.

Griffiths, M.N. (1990) Toxin production by *Bacillus* spp. present in milk. *Journal of Food Protection* **53**, 790–792.

International Dairy Federation (1992) *Bacillus cereus* in milk and milk products. In *Bulletin No. 275. International Dairy Federation* pp. 1–48. Brussels, Belgium.

Kramer, J.M. and Gilbert, R.J. (1989) *Bacillus cereus* and other *Bacillus* species. In *Foodborne Bacterial Pathogens* ed. Doyle, M.P. pp. 22–70. New York : Marcel Dekker.

Rowan, N.J. (1996) Studies on the growth, survival, interaction and detection of potentially pathogenic *Listeria* and *Bacillus* species in infant milk formulae. Ph.D. thesis, University of Strathclyde, Glasgow, UK.

Rowan, N.J. and Anderson, J.G. (1997) Maltodextrin stimulates growth of *Bacillus cereus* and synthesis of diarrhoeal enterotoxin in infant milk formula. *Applied and Environmental Microbiology* **63**, 1182–1184.

Rowan, N.J., Anderson, J.G. and Anderton, A. (1997) The bacteriological quality of hospital-prepared infant feeds. *Journal of Hospital Infection* **35**, 259–267.

Turner, B.E., Foegeding, P.M., Larick, D.K. and Murphy, A.H. (1996) Control of *Bacillus cereus* spores and spoilage microflora in sous vide chicken breast. *Journal of Food Science* **61**, 217–219, 234.

van Netten, P., van de Moosdijk, A., van Hoensel, P., Mossel, D.A.A. and Perales, I. (1990) Psychrotrophic strains of *Bacillus cereus* producing enterotoxin. *Journal of Applied Bacteriology* **69**, 73–79.

Journal of Food Protection, Vol. 61, No. 2, 1998, Pages 196–200

Effectiveness of Cleaning and Disinfection Procedures on the Removal of Enterotoxigenic *Bacillus cereus* From Infant Feeding Bottles

NEIL J. ROWAN* AND JOHN G. ANDERSON

Department of Bioscience and Biotechnology, University of Strathclyde, Royal College Building, 204 George Street, Glasgow, Scotland

MS 97-53: Received 21 March 1997/Accepted 2 May 1997

ABSTRACT

Reconstituted infant milk formulas are considered a food class of high risk because of the susceptibility of the infant population to enteric bacterial pathogens, severe response to enterotoxins, and increased mortality. Twenty infant feeding bottles, contaminated with different levels of enterotoxigenic *Bacillus cereus,* were subjected in triplicate to a variety of commonly used cleaning and disinfecting procedures. Although thorough cleaning reduced microbial numbers, it did not remove all *B. cereus* present. Three commercially available disinfection procedures (i.e., one chemical and two thermal) successfully eliminated this organism when the level of contamination was $<10^5$ organisms ml^{-1}. However, the chemical disinfection method failed to eliminate enterotoxigenic *B. cereus* totally at potentially hazardous contamination levels (i.e., $\geq 10^5$ organisms ml^{-1}) that may be encountered under storage abuse conditions in the home.

Infant populations are highly vulnerable to foods contaminated at low levels with enteric bacterial pathogens and their toxins, in part because of their immature immune system *(13).* Infant foods have been implicated occasionally as the etiological agents in a number of food-related illnesses *(8, 15).* Numbers of *Salmonella* spp. in infant milk formulas (IMF) implicated in previous foodborne outbreaks were very low, e.g., in the 1985 UK outbreak only three *Salmonella ealing* cells kg^{-1} were present *(23).*

Bacillus cereus, an occasional contaminant of dried infant milks, tolerates adverse environmental conditions better than most other bacterial enteropathogens *(14).* Becker et al. *(3)* reported that 54% of 261 samples of infant food distributed in 17 countries were contaminated with diarrheagenic *B. cereus,* reaching levels of 0.3–600 viable cells g^{-1}. When samples contaminated with approximately 100 cells ml^{-1} were reconstituted and incubated at 27°C, levels of 10^5 ml^{-1} were reached in 7–9 h. Rowan et al. *(22)* demonstrated that hospital-prepared infant food may be contaminated with diarrheagenic *B. cereus* at levels above the Association of Dietetic Food Industries of the European Communities (IDAEC) proposed safety limit of 10^3 colony-forming units (CFU)g^{-1}. In general, growth of enteric microbial pathogens in unprocessed milk is inhibited by the antagonistic action of resident lactic acid bacteria (LAB) *(5, 18).* Because LAB do not survive the spray-drying process, however *(16, 17),* contaminating deleterious organisms may proliferate in reconstituted baby foods under improper storage conditions *(21–23).*

Although the infectious dose of *B. cereus* is considered to be 10^5–10^7 cells ml^{-1} *(10),* outbreaks of foodborne illness associated with infants have been attributed to consumption of foods containing 10^3–10^5 cells g^{-1} *(9).* Granum et al. *(11)* suggested that the food industry should be concerned with levels as low as 10^3–10^4 ml^{-1} of food because food intoxication may be caused by ingestion of *B. cereus* cells or spores that may subsequently form enterotoxins in the ileum. In Norway, *B. cereus* was the most common cause of foodborne outbreaks in 1990 *(1).*

Donovan *(6)* showed that the main source of *B. cereus* contamination of raw milk obtained from creameries was derived chiefly from emptied cans that were allowed to stand for long periods before washing. The author suggested that vegetative cells of *B. cereus* readily formed spores in thin films of diluted milk in the rinsed cans. Hypochlorite disinfectants (e.g., Milton solution) are inactivated by food debris, organic matter, and catonic detergents *(2);* Hobbs and Roberts *(12)* showed that traces of milk remaining in baby bottles after careless washing totally inactivated 200 ppm available chlorine (i.e., the maximum amount recommended for disinfection). Other researchers showed wide variations in *B. cereus* spore thermal resistance, e.g., $D_{100°C}$ values ranged from 0.3 to 11.2 min in milk *(14),* which may play an important role in determining the efficacy of many commercially available thermal baby bottle disinfection procedures.

The principle objectives of this research were to determine the efficacy of commonly used cleaning and disinfection procedures on the removal of enterotoxigenic *Bacillus cereus* from infant feeding bottles subjected to periods of storage abuse which may occur in the home.

MATERIALS AND METHODS

Bacterial culture. The efficacy of infant feeding bottle cleaning and disinfection procedures was evaluated by use of *B.*

* Author for correspondence. Tel: 0044 141 552 4400, ext. 2531; Fax: 0044 141 553 1161; E-mail: n.j.rowan@pop-hub.strath.ac.uk.

cereus NCTC 11145, a diarrheagenic strain obtained from the National Collection of Typed Cultures. The diarrheagenic capability of this strain was previously demonstrated in reconstituted IMF *(20),* in which enterotoxin produced was detected with the *B. cereus* enterotoxin–reverse passive latex agglutination (BCET-RPLA) assay kit (Oxoid). Cultures were grown at 30°C and maintained on nutrient agar no. 2 (Oxoid Product); they were subcultured every 2 wk.

Infant feeding bottle cleaning procedures. Twenty precleaned and sterilized infant feeding bottles containing 250 ml of milk-based infant formula (in which 25 g of infant milk powder was reconstituted in 225 ml of sterile water at 56 ± 0.2°C, shaken 25 times through an excursion of 30 cm, and then tyndallized to sterility) were seeded with approximately 10^2 *B. cereus* spores ml^{-1} and then stored at 25°C for periods of up to 18 h (simulating storage abuse conditions that may occur in the home). Tyndallization consists of heating IMF on three successive days at 100°C for 30 min and leaving it at storage temperatures during the intervening times, during which spores can germinate so that resulting vegetative cells will be killed by the following period of heating at 100°C *(19).* The study was performed in triplicate. The starting inoculum was achieved by inoculating IMF with a spectrophotometrically (A_{600}) adjusted (Shimadzu uv-120-02) spore suspension prepared in phosphate-buffered saline (PBS; 0.01M; sodium phosphate, pH 7.2; 0.15M NaCl), in which *B. cereus* had been harvested from a 72-h culture grown at 30°C on nutrient agar no. 2 supplemented with 0.5 mg of $MnSo_4H_2O$ l^{-1} to aid sporulation (NMSA). Before IMF inoculation, the PBS cell/spore suspension was heat-treated in a water bath (Techne Tempette Junior TE-8J) at 65°C for 30 min to eliminate vegetative cells. Microbial numbers in the feeding bottles were confirmed by plating (1:10) dilutions onto NMSA plates that were then incubated at 30°C for 48 h.

Simulating the range of "after-use" situations that may be encountered in the home, the seeded baby bottles were subjected to the following range of commonly used handling procedures: (i) emptied of milk, (ii) emptied of milk and rinsed three times in warm water containing household detergent, and (iii) emptied of milk, washed, and brushed thoroughly in warm water containing household detergent (care was taken to ensure that all visible milk deposits were removed). In the subsequent text, baby bottlestreated with these procedures are referred to as uncleaned, partially cleaned, and thoroughly cleaned, respectively.

The extent to which *B. cereus* remained in these treated bottles was determined by filling each bottle with 250 ml of tyndallized IMF; the bottles were then shaken 25 times through an excursion of 30 cm before enumeration (to avoid ambiguity, IMF used as a bottle wash is referred to as IMF*). Microbial numbers were determined immediately after cleaning by spread and spiral plating (Spiral Plater Model B, Spiral Systems Inc.) duplicate samples of IMF* bottle wash onto *B. cereus* selective agar (BCSA). Plates were incubated aerobically at 25°C for 48–72 h. The identity of three representative cultures obtained on BCSA was confirmed by establishing the following morphological and biochemical properties: positive gram and catalase reactions, cell width (>1 μm) and length (>3 μm), motility and lecithovitellin/lecithinase production, β-haemolytic reaction and gross colony morphological appearance (millimeters), and an ellipsoidal endospore, centrally or subterminally positioned with nondistention of sporangium and characteristic API 50 CHB and API 20 E biochemical reaction profiles (Biomérieux Ltd.).

Infant feeding bottle disinfection methods. The following commercially available disinfection methods were tested: (i) feedtime steam sterilization (Boots), a thermal method in which feeding bottles were automatically steamed at 100°C for 15 min, (ii) microwave feedtime bottle steam sterilization (Boots), a thermal method in which bottles were placed in a sterilizing unit and steamed at 100°C in a microwave oven (Toshiba ER-686.E/EW) for 9 min, and (iii) complete baby feedtime sterilization (Boots), a chemical method in which bottles were immersed in 125 ppm sodium hypochlorite for 90 min. These methods are referred to as steam, microwave, and chemical, respectively, in Tables 1, 2, and 3.

These disinfection methods were carried out following details outlined in the manufacture's instructions. To examine the efficacy of each disinfection method, uncleaned, partially cleaned, and thoroughly cleaned feeding bottles containing different levels of *B. cereus* (described in the previous section) were subjected to each disinfection procedure. After disinfection, the bottles were filled with 250 ml of IMF* and incubated for periods of up to 18 h at 25°C. Microbial numbers in IMF* bottle wash were determined immediately after disinfection and after 14 and 18 h of incubation at 25°C.

TABLE 1. *Efficacy of different disinfection methods at eliminating enterotoxigenic* B. cereus *from untreated, partially cleaned, and thoroughly cleaned infant bottles in which the initial level of contamination was approximately 10^2 spores ml^{-1}*

	Disinfection method[a]								
	Steam			Microwave			Chemical		
Extent of cleaning	0 h	14 h	18 h[b]	0 h	14 h	18 h	0 h	14 h	18 h
Emptied	<1.0	<1.0	2.36[c]	<1.0	<1.0	1.85	<1.0	1.63	3.52
	—[d]	—	(1.28)	—	—	(0.87)	—	(0.73)	(1.49)
Emptied and rinsed	<1.0	<1.0	<1.0	<1.0	<1.0	<1.0	<1.0	<1.0	<1.0
	—	—	—	—	—	—	—	—	—
Emptied, washed, and brushed	<1.0	<1.0	<1.0	<1.0	<1.0	<1.0	<1.0	<1.0	<1.0
	—	—	—	—	—	—	—	—	—

[a] Microbial numbers in disinfected baby bottles were measured as $\log_{10}$ CFU ml^{-1}.

[b] Disinfected infant bottles, subjected previously to various cleaning regimes, were filled with 250 ml of IMF* and incubated for periods of up to 18 h at 25°C before enumeration.

[c] Mean *B. cereus* count for 20 feeding bottles analysed; the standard deviation is shown below the mean in parentheses. <1.0 refers to baby bottles having a *B. cereus* count below the lower detection limit of 1.0 $\log_{10}$ CFU ml^{-1}.

[d] —, Standard deviation of 0, in which all 20 bottles had *B. cereus* counts below the lower detection limit.

TABLE 2. *Efficacy of different disinfection methods at eliminating enterotoxigenic* B. cereus *from untreated, partially cleaned, and thoroughly cleaned infant feeding bottles that had been stored for 14 h at 25°C before disinfection*

	Disinfection method[a]								
	Steam			Microwave			Chemical		
Extent of cleaning	0 h	14 h	18 h[b]	0 h	14 h	18 h	0 h	14 h	18 h
Emptied	<1.0	2.64[c]	5.72	<1.0	2.40	5.58	2.49	4.79	6.52
	—[d]	(1.52)	(1.73)	—	(1.13)	(1.42)	(1.23)	(1.47)	(1.79)
Emptied and rinsed	<1.0	<1.0	3.74	<1.0	<1.0	3.57	<1.0	2.32	5.71
	—	—	(1.30)	—	—	(1.51)	—	(1.37)	(1.52)
Emptied, washed, and brushed	<1.0	<1.0	2.04	<1.0	<1.0	1.70	<1.0	1.13	3.64
	—	—	(0.83)	—	—	(1.23)	—	(0.47)	(1.32)

[a] Microbial numbers in disinfected baby bottles were measured as $\log_{10}$ CFU ml^{-1}.
[b] Disinfected infant bottles, subjected previously to various cleaning regimens, were filled with 250 ml of IMF* and incubated for periods of up to 18 h at 25°C before enumeration.
[c] Mean *B. cereus* count for 20 feeding bottles analysed; the standard deviation is shown below the mean in parentheses. <1.0 refers to baby bottles having a *B. cereus* count below the lower detection limit of 1.0 $\log_{10}$ CFU ml^{-1}.
[d] —, Standard deviation of 0, in which all 20 bottles had *B. cereus* counts below the lower detection limit.

TABLE 3. *Efficacy of different disinfection methods at eliminating enterotoxigenic* B. cereus *from untreated, partially cleaned, and thoroughly cleaned infant feeding bottles that had been stored for 18 h at 25°C before disinfection*

	Disinfection method[a]								
	Steam			Microwave			Chemical		
Extent of cleaning	0 h	14 h	18 h[b]	0 h	14 h	18 h	0 h	14 h	18 h
Emptied	<1.0	4.82	7.32[c]	<1.0	4.67	6.92	4.32	5.82	7.65
	—[d]	(1.15)	(1.92)	—	(1.47)	(1.79)	(1.30)	(1.82)	(1.63)
Emptied and rinsed	<1.0	2.60	5.20	<1.0	2.70	4.96	<1.0	4.93	6.79
	—	(1.57)	(1.57)	—	(0.95)	(1.82)	—	(1.51)	(1.79)
Emptied, washed, and brushed	<1.0	<1.0	4.18	<1.0	<1.0	3.92	<1.0	3.70	5.88
	—	—	(1.42)	—	—	(1.17)	—	(1.42)	(1.37)

[a] Microbial numbers in disinfected baby bottles were measured as $\log_{10}$ CFU ml^{-1}.
[b] Disinfected infant bottles, subjected previously to various cleaning regimens, were filled with 250 ml of IMF* and incubated for periods of up to 18 h at 25°C before enumeration.
[c] Mean *B. cereus* count for 20 feeding bottles analysed; the standard deviation is shown below the mean in parentheses. <1.0 refers to baby bottles having a *B. cereus* count below the lower detection limit of 1.0 $\log_{10}$ CFU ml^{-1}.
[d] —, Standard deviation of 0, in which all 20 bottles had *B. cereus* counts below the lower detection limit.

Statistical analysis. Fisher's exact test was used to compare microbial numbers in infant feeding bottles subjected to various cleaning and/or disinfecting procedures (Minitab Statistical Software Version 11; Minitab Plc.). All significant differences were reported at the 95% level of confidence ($P < 0.05$).

RESULTS AND DISCUSSION

Efficacy of commonly used infant feeding bottle cleaning procedures. The study showed that the greater the level of infant bottle cleaning, the larger the reduction in microbial numbers (Figure 1); the effectiveness of each cleaning stage at removing diarrheagenic *B. cereus* differed at the $P < 0.05$ level. Thorough cleaning of bottles contaminated with 10–100 spores ml^{-1}, a level of contamination occurring occasionally in IMF *(21)*, did not remove all of the spores present. Potentially hazardous levels of *B. cereus* remained in more heavily contaminated bottles (i.e., those in which the level of IMF contamination was approximately 10^5 organisms ml^{-1} after 14 h of storage) subjected to rigorous washing and brushing (Figure 1). Because thorough cleaning did not totally remove *B. cereus* from feeding

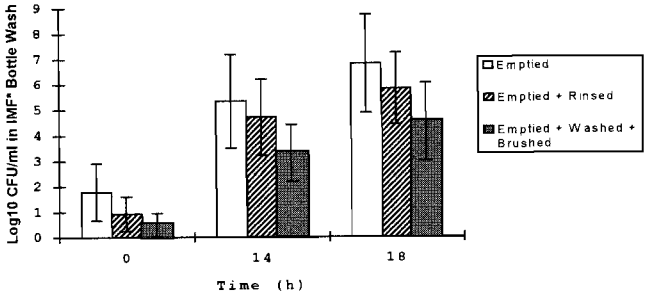

Figure 1. *Effect of extent of cleaning on the removal of enterotoxigenic* B. cereus *from infant feeding bottles stored for periods of up to 18 h at 25°C before treatment.* □, *Emptied;* ▨, *emptied and rinsed;* ■, *emptied, washed, and brushed.*

bottles (i.e., removal of visible milk deposits did not provide microbial free bottles), baby bottle cleaning must be supplemented with an appropriate disinfection method to provide safe food for infant consumption.

Efficacy of commercially available infant feeding bottle disinfection procedures. All disinfection methods successfully reduced diarrheagenic *B. cereus* to a nondetectable level (i.e., <10 CFU ml^{-1}) when the initial level of contamination was $\leq 10^5$ CFU ml^{-1} (Tables 1 and 2). In IMF* bottle wash, *B. cereus* emerged earlier (i.e., after 14 h of incubation at 25°C) in uncleaned baby bottles that had been subjected to the chemical disinfection method (Table 1). Application of both thermal disinfection methods did not totally eliminate *B. cereus;* reemergence was detected in IMF* after 18 h of incubation (Table 1). The level of contamination (i.e., period during which bottles were held under storage abuse) and the degree of bottle cleaning before disinfection affected the length of time that bottles remained with *B. cereus* at undetectable levels ($P < 0.05$); *B. cereus* emerged earlier in uncleaned bottles that had been stored for longer periods before disinfection (Tables 2 and 3).

The chemical method failed to disinfect uncleaned feeding bottles contaminated with approximately 10^5 organisms ml^{-1} (Tables 2 and 3). Subsequent storage of thermally disinfected bottles resulted in the detection of this organism at potentially hazardous levels in IMF* after 14 h of incubation at 25°C. Both steam disinfection procedures were equally efficient at removing *B. cereus* from baby bottles contaminated with $\geq 10^5$ CFU ml^{-1} ($P < 0.05$), and both methods were significantly better than the chemical method ($P < 0.05$) (Tables 2 and 3). Ayliffe et al. *(2)* reported the isolation of *Klebsiella aerogenes* and *Pseudomonas* spp. from baby bottles even after they had been thoroughly cleaned and disinfected in a sodium hypochlorite solution. The authors showed that this chemical disinfection process may occasionally be hazardous even when cleaning appeared to be efficient. Hypochlorite solution must be changed daily because the activity of this disinfection procedure diminishes with time *(2),* a requirement that may be prone to neglect.

This study has reaffirmed that infant bottle cleaning practices must be supplemented with a disinfection method to provide bottles free of potentially hazardous organisms. Although both heat and chemical disinfection procedures successfully removed *B. cereus* spores from contaminated baby bottles (at levels occurring occasionally in freshly prepared infant feeds), the latter method was inefficient at disinfecting uncleaned and partially cleaned bottles contaminated with the large numbers of this organism that occur during storage abuse. Failure to eliminate *B. cereus* will result in an increased inoculum and enhanced contamination of subsequently prepared infant feeds. Although *B. cereus* was the focus of this study, other *Bacillus* spp. (i.e., *B. licheniformis, B. subtilis, B. pumilus, B. brevis, B. thuringiensis,* and *B. sphaericus*) occurring occasionally in dried IMF products *(21)* have been implicated as the etiological agents in proven foodborne illness outbreaks *(16)* and opportunistic infections *(4, 7);* the majority of these organisms show greater heat resistance than *B. cereus (19).* Recent evidence has shown that IMF supplemented with maltodextrin stimulated growth of *B. cereus* and synthesis of diarrheal enterotoxins under improper storage conditions *(20);* therefore, extra care should be taken to ensure that baby bottles are thoroughly cleaned and disinfected before use.

ACKNOWLEDGMENTS

The authors thank the Scottish Home and Health Department for funding this research (K/MRS/50/C2005). They also thank George Gettinby (Department of Statistics and Modelling Science, University of Strathclyde) for his assistance with the statistical analysis.

REFERENCES

1. Aas, N., B. Gondrosen, and G. Langeland. 1992. Norwegian Food Control Authority's report on food associated diseases in 1990. SNT-Report 3, Oslo.
2. Ayliffe, G. A. J., B. J. Collins, and F. Pettit. 1970. Contamination of infant feeds in a Milton milk kitchen. Lancet i:559–560.
3. Becker, H., G. Schaller, W. von Wiese, and G. Terplan. 1994. *Bacillus cereus* in infant foods and dried milk products. Int. J. Food Microbiol. 23:1–15.
4. Blue, S. R., V. R. Singh and M. A. Saubolle. 1995. *Bacillus licheniformis* bacteremia, five cases associated with indwelling central venous catheters. Clin. Infect. Dis. 20:629–338.
5. Daeschel, M. A. 1989. Antimicrobial substances from lactic acid bacteria for use as food preservatives. Food Technol. 43:164–167.
6. Donovan, K. O. 1959. The occurrence of *Bacillus cereus* in milk and on dairy equipment. J. Appl. Bacteriol. 23:131–137.
7. Drobniewski, F. A. 1993. *Bacillus cereus* and related species. Clin. Microbiol. Rev. 6:324–338.
8. Gericke, B., and V. Thurn. 1994. Identification of infant food as a vehicle in a nosocomial outbreak of *Citrobacter freundii:* epidemiological subtyping by allozyme whole cell protein and antibiotic resistance. J. Appl. Bacteriol. 76:553–558.
9. Giannella, R. A., and L. Brasile. 1979. A hospital food-borne outbreak of diarrhea caused by *B. cereus:* clinical, epidemiologic, and microbiologic studies. J. Infect. Dis. 139:366–370.
10. Granum, P. E., S. Brynestad, and J. M. Kramer. 1993. Analysis of enterotoxin production by *Bacillus cereus* from dairy products, food poisoning incidents and non-gastrointestinal infections. Int. J. Food Microbiol. 17:269–279.
11. Granum, P. E., S. Brynestad, K. O'Sullivan, and H. Nissen. 1993. The enterotoxin from *B. cereus:* production and biochemical characterization. Neth. Milk Dairy J. 47:63–70.
12. Hobbs, B. C., and D. Roberts. 1987. *In* B. C. Hobbs and D. Roberts (eds), Food poisoning and food hygiene. Edward Arnold Publishers Ltd., London.
13. International Commission on Microbiological Specifications for Foods. 1986. *In* International Commission on Microbiological Specifications for Foods, vol 1. Their significance and methods of enumeration. University of Toronto Press, Toronto, Ontario, Canada.
14. International Dairy Federation. 1992. *Bacillus cereus* in milk and milk products, p. 1–48. *In* Bulletin no. 275. International Dairy Federation, 41, Square Vergote, Brussels, Belgium.
15. Louie, K. K. 1993. *Salmonella* serotype *tennessee* in powdered milk products and infant formula—Canada and the United States. JAMA 270:432.
16. Lovell, H. R. 1985. The microbiology of dried milk powders, p. 209–232. *In* R. K. Robinson (ed.), Dairy microbiology, vol. 1. The microbiology of milk. Elsevier, London.
17. Mettler, A. E. 1989. Pathogens in milk powders—have we learned the lesson? J. Soc. Dairy Technol. 42:48–54.
18. Nelson, F. E. 1985. The microbiology of market milk, p165–208. *In* R. K. Robinson (ed.), Dairy microbiology, vol. 1. The microbiology of milk. Elsevier, London.

19. Rowan, N. J. 1996. Studies on the growth, survival, interaction, and detection of potentially pathogenic *Listeria* and *Bacillus* spp. in infant milk formulae. Ph.D. thesis. University of Strathclyde, Glasgow, Scotland.
20. Rowan, N. J. and J. G. Anderson. 1997. Maltodextrin stimulates growth of *Bacillus cereus* and synthesis of diarrheal enterotoxin in infant milk formulae. Appl. Environ. Microbiol. 63:1182–1184.
21. Rowan, N. J., J. G. Anderson, and A. Anderton. 1997. Bacteriological quality of infant milk formulae examined under a variety of preparation and storage conditions. J. Food Prot. 60:1089–1094.
22. Rowan, N. J., J. G. Anderson, and A. Anderton. 1997. The bacteriological quality of hospital-prepared infant feeds. J. Hosp. Infect. 35:259–267.
23. Rowe, B. 1987. *Salmonella ealing* infections associated with consumption of infant dried milk. Lancet ii:900–903.

APPLIED AND ENVIRONMENTAL MICROBIOLOGY, Apr. 2003, p. 2372–2376 Vol. 69, No. 4
0099-2240/03/$08.00+0 DOI: 10.1128/AEM.69.4.2372–2376.2003

Production of Diarrheal Enterotoxins and Other Potential Virulence Factors by Veterinary Isolates of *Bacillus* Species Associated with Nongastrointestinal Infections

Neil J. Rowan,[1]* George Caldow,[2] Curtis G. Gemmell,[3] and Iain S. Hunter[1]

Department of Bioscience, University of Strathclyde,[1] and Department of Bacteriology and Immunology, University of Glasgow Medical School, Glasgow Royal Infirmary,[3] Glasgow, and Veterinary Science Division, Scottish Agricultural College, St. Boswells,[2] Scotland

Received 11 September 2002/Accepted 16 January 2003

With the exceptions of *Bacillus cereus* and *Bacillus anthracis*, *Bacillus* species are generally perceived to be inconsequential. However, the relevance of other *Bacillus* species as food poisoning organisms and etiological agents in nongastrointestinal infections is being increasingly recognized. Eleven *Bacillus* species isolated from veterinary samples associated with severe nongastrointestinal infections were assessed for the presence and expression of diarrheagenic enterotoxins and other potential virulence factors. PCR studies revealed the presence of DNA sequences encoding hemolysin BL (HBL) enterotoxin complex and *B. cereus* enterotoxin T (BceT) in five *B. cereus* strains and in *Bacillus coagulans* NB11. Enterotoxin HBL was also harbored by *Bacillus polymyxa* NB6. After 18 h of growth in brain heart infusion broth, all seven *Bacillus* isolates carrying genes encoding enterotoxin HBL produced this toxin. Cell-free supernatant fluids from all 11 *Bacillus* isolates demonstrated cytotoxicity toward human HEp-2 cells; only one *Bacillus licheniformis* strain adhered to this test cell line, and none of the *Bacillus* isolates were invasive. This study constitutes the first demonstration that *Bacillus* spp. associated with serious nongastrointestinal infections in animals may harbor and express diarrheagenic enterotoxins traditionally linked to toxigenic *B. cereus*.

Members of the *Bacillus* genus are ubiquitous soil microorganisms that frequently contaminate foods (21, 22, 26). With the exceptions of *Bacillus anthracis* and *Bacillus cereus*, *Bacillus* species are generally perceived to be inconsequential and of little clinical significance (8). A number of food poisoning incidents can be attributed to *B. cereus*, and this bacterium is known to cause a variety of nongastrointestinal diseases as well as two different types of food poisoning (for reviews, see references 12, 19, 21, and 22), which are characterized by either diarrhea or emesis. The diarrheal type is attributed to heat-labile enterotoxins, namely, the hemolysin BL (HBL) and non-hemolytic enterotoxin protein complexes, and to a *B. cereus*-related enterotoxic protein T (BceT). In *B. cereus* strain F837/76, the three HBL components are encoded by an operon containing *hblC*, *hblD*, and *hblA*, in that order, which respectively encode two lytic components designated L_2 and L_1 and a binding component designated B (30). We recently reported on the abilities of different clinical and food isolates of *B. cereus* and other *Bacillus* spp. to express diarrheal enterotoxins HBL and BceT after growth in reconstituted infant milk formulae (26). Previous research has also shown that 14 different *Bacillus* species isolated from raw milk and from the farm environment may have the potential to produce diarrheal enterotoxins (4). The emetic type is caused by a heat-stable dodecadepsideptide, cereulide (21).

The relevance of other *Bacillus* species as food poisoning organisms and as etiological agents in nongastrointestinal infections, including local, deep-tissue, and systemic infections, is being increasingly recognized (8). Nongastrointestinal infections have been seen primarily in individuals who are intravenous drug abusers or immunocompromised as a consequence of infection with human immunodeficiency virus, chemotherapy, or malignancy (4, 28). *B. cereus* strains isolated from nongastrointestinal infections have shown the ability to synthesize many virulence factors, including necrotizing exotoxin-like hemolysins, phospholipases, collagenases, and proteases (8).

Due to their endospore-forming abilities, these bacteria tolerate adverse conditions better than most bacterial enteropathogens do and may proliferate in a wide range of environments, including processed and untreated foods (22, 26). Raw milk is frequently contaminated by *Bacillus* endospores that originate from bedding, fodder, dung, soil, improperly cleaned milking utensils, and the surrounding environment (35). Contamination of raw milk may also occur through infection of a cow's udder, and serious herd outbreaks of bovine mastitis have been previously attributed to members of this genus (17, 35). *Bacillus* spp. have also been implicated as causative agents of mastitis and abortions in other animals, including cows (17), pigs (18), horses (23), water buffalo (10), and dromedary camels (37).

We report the detection of diarrheagenic enterotoxins HBL and BceT (traditionally harbored by toxigenic *B. cereus*) in a number of veterinary isolates of *Bacillus* spp. that were associated with serious nongastrointestinal infections in animals. We also report on the ability of these *Bacillus* isolates to be cytotoxic towards human HEp-2 cells and to express HBL enterotoxins. All experiments were performed in triplicate, with averages and standard errors of results shown. Differences in bacterial adherence, invasion, and cytotoxicity were exam-

* Corresponding author. Mailing address: Department of Bioscience, University of Strathclyde, Royal College, 204 George St., Glasgow G1 1XW, Scotland. Phone: 44 (0)141 548 2531. Fax: 44 (0)141 553 4124. E-mail: n.j.rowan@strath.ac.uk.

TABLE 1. Bacterial strains used

Bacterial species	Isolate	Provider	Reference no.	Isolate source	Gross lesion(s)	Associated disease
B. cereus	NB3	SAC	C20593	Bovine milk	None recorded	Bovine mastitis
	NB23	SAC	PC181	FSC, placenta, foetal lung, and liver	None recorded	Bovine abortion
	NB27	SAC	C175	Bovine milk	None found	Bovine mastitis
	NB35	SAC	S20247	Ovine FSC	None found	Ovine abortion
	NB40	SAC	S20254	Ovine FSC	None recorded	Ovine abortion
	NB50	SAC	AYRS31375	Lamb brain	—[b]	
	NB51	SAC	AURM31973	Caprine milk	None recorded	Caprine mastitis
	SU52	NCTC	11145	Human stool	—	Diarrheal food poisoning[a]
B. licheniformis	NB42	SAC	S20282	Ovine FSC	None found	Ovine abortion
	NB14	SAC	C205	Bovine placenta, FSC, fotal lung and liver	None recorded	Bovine abortion
B. polymyxa	NB6	SAC	C83	Bovine fotal lung	None recorded	Bovine abortion
B. coagulans	NB11	SAC	C70	Bovine FSC, fotal lung and liver	None recorded	Bovine abortion
L. monocytogenes	SU1	NCTC	11994	Cerebrospinal fluid	—	Adult meningitis[a]
E. coli	HB101	ATCC	33694	Laboratory K-strain	—	None

[a] Associated with disease in humans only.
[b] —, not known.

ined in HEp-2 cells at 95 or 99.9% confidence intervals by using analysis of variance (one-way or balanced models) with Minitab (State College, Pa.) software (release 11).

Isolation and identification of *Bacillus* species associated with serious nongastrointestinal infections in animals. The *Bacillus* strains used in this study (Table 1) were obtained from the diagnostic laboratories of the Scottish Agricultural College (SAC), Veterinary Science Division, Scotland; the American Type Culture Collection (ATCC), Manassas, Va.; and the National Collection of Type Cultures (NCTC), Public Health Laboratory Service, Colindale, United Kingdom. Eleven members of the genus *Bacillus* comprising seven *B. cereus* strains, two *Bacillus licheniformis* strains, one *Bacillus polymyxa* strain, and one *Bacillus coagulans* strain were isolated from veterinary samples associated with serious nongastrointestinal infections (Table 1); of these veterinary samples, 25-g amounts from the placenta, fetal stomach contents (FSC), and fetal brain, lung, and liver were aseptically transferred to Todd-Hewitt broth (Oxoid, Basingstoke, United Kingdom) for 24 h at 37°C. These particular organs and materials are routinely examined in cases of animal abortions. Samples were transferred directly and after the aforementioned overnight enrichment onto 7% (vol/vol) horse erythrocyte-blood agar plates (Oxoid) and were incubated for 48 h at 37°C in a 5% CO_2 atmosphere (CO_2 incubator; LEEC Ltd., Nottingham, England). The diseases associated with the veterinary *Bacillus* isolates ranged from severe infections, such as induction of fetal abortions in sheep and cattle (e.g., from isolates *B. cereus* NB35, *B. licheniformis* NB42, *B. polymyxa* NB6, and *B. coagulans* NB11), to the less serious mastitis (e.g., from *B. cereus* NB3) (Table 1).

The identity of each *Bacillus* isolate was confirmed by performing a sequence of characteristic morphological and physiological tests described previously (29) and by using miniaturized biochemical API 50 CHB and API 20E galleries (bioMérieux, Marcy l'Etoile, France). All *Bacillus* isolates exhibited characteristic morphological, physiological, and biochemical properties to the species level. The bacteria were stored at −70°C (Microbank System; Pro-Lab Diagnostics, Richmond Hill, Ontario, Canada) to prevent loss of virulence characteristics.

Ability of *Bacillus* veterinary strains to adhere to, invade, and produce a cytotoxic effect on epithelial cells. The ability of *Bacillus* test strains to adhere to and invade HEp-2 cells was determined after 18 h of growth in brain heart infusion (BHI) broth by previously described procedures (25), with minor modifications. HEp-2 monolayers were grown for 24 h in a 5% CO_2 atmosphere (CO_2 incubator; LEEC Ltd.) at 37°C in Dulbecco's modified Eagle medium (DMEM) supplemented with 10% fetal calf serum (FCS) (Gibco Life Sciences, Paisley, Scotland) in 24-well tissue culture plates (Scientific Lab Supplies, Nottingham, England) seeded with approximately 10^5 cells per well. Prior to assay, the monolayers were washed three times with DMEM and the monolayers were inoculated with 1 ml of bacterial culture containing $\sim 10^7$ CFU ml^{-1} (in DMEM with 10% FCS) in triplicate followed by a 2-h incubation at 37°C in a 5% CO_2 atmosphere. After incubation, the monolayers were washed three times with DMEM to remove any nonadherent cells and then 1 ml of DMEM containing 10% FCS was added to each well of one of the test plates, which were incubated for 2 h. For the invasion assays, 1 ml of DMEM containing 10% FCS and 100 μg of gentamicin ml^{-1} (Gibco) was added to each well of the other 24-well plate, which was similarly incubated for 2 h. The monolayers were then washed three times with DMEM, and the tissue culture cells were lysed with 1 ml of 1% (vol/vol) Triton X-100 in distilled water (Sigma, Dorset, England) for 5 min at 37°C. Samples (0.1 ml) of lysate from each tissue culture plate were serially diluted in 0.9 ml of sterile distilled water, with subsequent enumeration by plating 20 μl of appropriate 10-fold dilutions on BHI agar plates. *Listeria monocytogenes* NCTC 11994 and *Escherichia coli* ATCC 33694 were used as positive and negative control strains, respectively, in tests of adherence to and invasion of HEp-2 cells.

Results showed that 10 (91%) of 11 *Bacillus* spp. isolated from the veterinary environment were unable to adhere to or invade HEp-2 cells. Only *B. licheniformis* NB14 adhered to

TABLE 2. Potential virulence factor expression by *Bacillus* spp. isolated from veterinary and clinical samples

Bacterial species	Isolate	Toxin concn detected (ng/ml)[a]	% Cytotoxic activity[b]			Detection of the indicated diarrheagenic genes by PCR[d]				% of bacteria showing[c]:	
			Normal	HT	TT	*hblA*	*hblC*	*hblD*	*bceT*	Adherence	Invasion
B. cereus	NB3	—	85 ± 4	15	10 ± 1	−	−	−	−	−	−
	NB23	≥128	77 ± 6	20 ± 6	26 ± 6	+	+	+	+	−	−
	NB27	—	82 ± 5	—	—	−	−	−	+	−	−
	NB35	64	88 ± 3	16 ± 1	24 ± 6	+	+	+	+	−	−
	NB40	≥128	78 ± 3	18 ± 2	10	+	+	+	+	−	−
	NB50	≥128	89 ± 1	22 ± 3	—	+	+	+	+	−	−
	NB51	64	93	13 ± 1	11 ± 2	+	+	+	+	−	−
	SU52	≥128	85 ± 2	12 ± 1	28 ± 6	+	+	+	+	0.03 ± 0.005	−
B. licheniformis	NB42	—	39 ± 5	9 ± 2	—	−	−	−	−	−	−
	NB14	—	66 ± 3	12 ± 2	22 ± 6	−	−	−	−	2.8 ± 0.22	−
B. polymyxa	NB6	16	88 ± 4	13 ± 1	18 ± 1	+	+	+	−	−	−
B. coagulans	NB11	64	89 ± 6	10 ± 3	5 ± 1	+	+	+	+	−	−
L. monocytogenes	SU1	—	82 ± 5	14 ± 3	24 ± 5	−	−	−	−	3.88 ± 0.37	1.15 ± 0.23
E. coli	HB101	—	—	—	—	−	−	−	−	−	−

[a] Detection of diarrheal enterotoxin in test media by the RPLA test. —, no diarrheal enterotoxin detected.
[b] Supernatant fluids were untreated (Normal), heated (HT), or trypsin treated (TT) prior to assessment of toxicity to HEp-2 cells. Values shown are means ± standard errors for results from triplicate trials where samples were examined three times. —, no effect.
[c] Values are reported as means ± standard errors. −, no adherence or invasion.
[d] +, gene was detected; −, gene was not detected.

HEp-2 cells (Table 2). These findings contrasted markedly with those of previous infectivity studies, where 43 (91%) of the 47 strains isolated from clinical or food samples adhered to HEp-2 or Caco-2 cells and 23 (49%) demonstrated various levels of invasion (26). Other researchers have also reported that *Bacillus* spp. may occasionally cause mastitis or abortions in animals (10, 16, 33, 37). Recent evidence suggests that many members of the *Bacillus* genus may also be the causes of serious systemic diseases, such as septicemia, endocarditis, peritonitis, ophthalmitis, liver failure, and meningitis in humans (8, 20, 31).

Assessment of cytotoxicity was based on a method described previously (6) for measuring total cellular metabolic activity by using the tetrazolium salt 3-(4,5,-dimethylthiazole-2-yl)-2,5-diphenyl tetrazolium bromide (MTT; Sigma), with some minor modifications. HEp-2 monolayers were grown overnight at 37°C in a 5% CO_2 atmosphere in DMEM supplemented with 10% FCS in 96-well microplates seeded with approximately 5×10^4 cells per well. Bacterial cultures were grown for 18 h as described above, and 0.1-ml samples were filter sterilized (0.2-μm-pore-size membranes; Sarstedt, Nümbrecht, Germany) and added in triplicate to the test plates immediately, after heating of the supernatant at 95°C for 10 min, or after enzymatic treatment with 0.1% trypsin. Positive and negative assay controls were 1% Triton X-100 (Sigma) and phosphate-buffered saline, respectively. Tissue culture monolayers containing the bacterial culture supernatants were incubated overnight at 37°C in a 5% CO_2 atmosphere, followed by the addition of phosphate-buffered saline containing 0.5% MTT (Sigma) to each well for 4 h at 37°C. The suspensions in the wells were then removed, and the formazan product was solubilized by the addition of 100 μl of 0.04 M HCl in dimethyl sulfoxide (Sigma, Poole, United Kingdom). The contents of the plates were measured spectrophotometrically at 540 nm in a microplate reader (Labsystems EMS reader). The toxic effect of the cell-free bacterial culture supernatant on the HEp-2 cell line was calculated from the following equation: [(1 − optical density of test sample)/(optical density of negative control)] × 100. Cytotoxic effects produced in HEp-2 cells were also confirmed by light microscopy.

While results showed that there were species-to-species variations in the levels of cytotoxicity produced, the culture supernatant fluids from all 11 *Bacillus* isolates were cytotoxic for this epithelial cell line (Table 2). Six *Bacillus* isolates exhibited levels of toxicity (85.5% ± 5% [mean ± standard deviation]) that were similar to or greater than those produced by clinical isolates of *B. cereus* SU52 and *L. monocytogenes* SU1, which are associated with gastrointestinal and nongastrointestinal infections in humans, respectively (Table 2). A marked variation in the range of toxicity levels exhibited by *Bacillus* isolates associated with more serious veterinary infections, such as ovine and bovine abortions, was apparent (Table 2). Separate heat and trypsin treatments of culture supernatant fluids either reduced or eliminated toxicity in HEp-2 cells, which suggests that the cytotoxic activity was attributed to the proteinaceous fractions of the culture supernatants (Table 2). Cell-free culture supernatants from all 11 *Bacillus* species examined for cytotoxicity in this study showed toxicity in HEp-2 cells. The variation in toxicity levels observed was similar ($P < 0.05$) to that reported previously for cell-free supernatant fluids from 38 strains representing 14 different *Bacillus* species from clinical and food samples (26).

Others have also shown that MTT can be used to assess the cytotoxic effect of culture supernatant fluids of *Bacillus* species isolated from raw milk (4, 9). Only live eukaryotic cells are recognized by this assay because the tetrazolium ring of MTT is cleaved in the mitochondria of metabolically active cells. By using this assay, Beattie and Williams (4) showed that some isolates of *Bacillus circulans*, *Bacillus laterosporus*, *Bacillus lentus*, *B. licheniformis*, *Bacillus mycoides*, *Bacillus subtilis*, *B. cereus*, and *Bacillus thuringiensis* were toxigenic to Chinese hamster ovary cells. Tetrazolium salts have also been used to

assess the cytotoxicities of other pathogens, such as *Mannheimia haemolytica* biotype A serotype 1 leukotoxin (7) and the cytotoxin of *Campylobacter jejuni* (6), and they were recently used to investigate *B. cereus* toxicity (36). Finlay et al. (9) advocated the use of MTT, as the currently used HEp-2 cell vacuolation assay for *Bacillus* emetic toxin is laborious, subjective, and unreliable.

Detection of diarrheagenic enterotoxins by PCR and measurement of other potential virulence factors. *B. cereus* NCTC 11145 was used as a positive control strain in assays for the presence of HBL and BceT enterotoxins, as shown previously (26). *L. monocytogenes* NCTC 11994 and *E. coli* ATCC 33694 were used as negative control strains in assays for the presence of genes encoding HBL and BceT enterotoxins. Chromosomal DNA was isolated from the test *Bacillus* spp. by use of a previously described procedure (26). The DNA sequences encompassing the diarrheagenic genes *bceT* (1), *hblC* and *hblA* (30), and *hblD* (13) were used to design primers that would amplify segments of the genes, if present, in a selection of the above-mentioned test *Bacillus* strains. Amplification was carried out in a DNA thermal cycler for 36 cycles of 30s at 94°C; 1 min at 54°C, 58°C, 62°C, and 63°C for *hblD*, *bceT*, *hblC*, and *hblA* genes, respectively; and 1 min at 72°C. PCR products of 439, 428, 399, and 873 bp were detected when the following pairs of oligonucleotide primers were used, respectively: HBLD-N (5′-AATCAAGAGCTGTCACGAAT-3′) and HBLD-C (5′-CACCA ATTGACCATGCTAAT-3′), BCET-N (5′-TTACATTACCAGGACGTGCTT-3′) and BCET-C (5′-T GTTTGTGATTGTAATTCAGG-3′), HBLC-N (5′-AATAG GTACAGATGGAACAGG-3′) and HBLC-C (5′-GGCTTTC ATCAGGTCATACTC-3′), and HBLA-N (5′-GCTAATG TAGTTTCACCTAGCAAC-3′) and HBLA-C (5′-AATCAT GCCACTGCGTG GACATATAA-3′). Findings from PCR primer studies revealed that seven veterinary *Bacillus* isolates contained *hblA*, *hblC*, and *hblD* genes that encode the tripartite HBL enterotoxin complex traditionally harbored by toxigenic *B. cereus* (Table 2). With the exception of *B. polymyxa* NB6, all *Bacillus* isolates encoding the HBL enterotoxin were also shown to have the *bceT* gene that encodes the BceT enterotoxin (Table 2). None of the other *Bacillus* species contained diarrheagenic enterotoxin genes (Table 2).

Analysis of cell-free culture supernatants from all seven veterinary *Bacillus* isolates displaying positive signals for all three HBL toxin genes tested positive by the *B. cereus* enterotoxin (diarrheal type) reversed passive latex agglutination (RPLA) assay that is specific for the L_2 component of the HBL complex (Table 2). The presence of diarrheal HBL enterotoxin was measured by using the RPLA kit according to the manufacturer's instructions (Oxoid). This finding suggests that after 18 h of growth in BHI broth, these other *Bacillus* isolates produced protein toxins that were very similar to those of *B. cereus* and that these species may have presented a potential hazard if they had entered the food chain. The level of enterotoxin HBL produced by these particular *Bacillus* spp. ranged from 16 to $\geq$128 ng ml^{-1}; the reported sensitivity of the RPLA test is 2 ng ml^{-1} (5). There was good agreement between carriage of *hblA*, *hblC*, and *hblD* genes and detection of secreted HBL enterotoxin in culture supernatants (Table 2).

These results contrasted markedly with findings from a previous study, in which only 4 (22%) of 18 *Bacillus* isolates from the clinical and food environments harboring all three *hbl* genes produced HBL enterotoxin in cultured BHI broth (26). However, a further eight isolates belonging to *B. cereus*, *B. licheniformis*, *B. circulans*, and *Bacillus megaterium* were found to produce HBL enterotoxin after growth in reconstituted baby food, which suggests that many *Bacillus* isolates that have the necessary diarrheagenic genes require a specific environmental signal(s) for transcriptional activation. Environmental signals have been shown previously to modulate virulence factor expression in *B. cereus* and in other bacterial enteropathogens (24, 27). Schoeni and Wong (32) have previously reported that HBL enterotoxin was secreted by more than 200 tested *B. cereus*, *B. thuringiensis*, and *B. mycoides* strains. Beattie and Williams (4) showed that the supernatant fluids from isolates of *B. thuringiensis*, *B. circulans*, *B. licheniformis*, *B. lentus*, *B. laterosporus*, and *B. mycoides* reacted positively with both the *Bacillus* diarrheal enterotoxin visual immunoassay (BDE; Tecra) or RPLA immunoassays. *B. subtilis*, *B. licheniformis*, *Bacillus pumilus*, and *B. thuringiensis* have been previously implicated in outbreaks of foodborne disease (15, 31).

It has been shown that some *B. cereus* strains may contain multiple copies of the *hbl* genes that arose from duplication of a single gene (32). *hbl* has been mapped to a portion of the *B. cereus* chromosome that exhibits greater variability than do other regions and this variable region is sometimes located on large extrachromosomal DNA fragments that appear to be stable but might also prove to be large mobile plasmids (32). Interestingly, evidence of chromosomal gene mobilization and transfer of plasmids coding for δ-endotoxin among strains of the well-characterized insect pathogen *B. thuringiensis* and *B. cereus* have been provided previously (2, 11). Many survival trait genes, such as those for virulence factors and antibiotic resistance, are located on plasmids (16). *B. anthracis*, belonging to the *B. cereus* group and thus a close relative of *B. cereus* and *B. thuringiensis* (and the causative agent of anthrax) (3), has its crucial virulence factors located on two plasmids, and when one or both are lost the *B. anthracis* becomes avirulent (34). The aforementioned finding, combined with the high degree of phylogenetic relatedness among members of this genus (14), possibly explains why many different *Bacillus* species isolated from the veterinary, clinical, and food environments carry similar enterotoxins traditionally harbored by toxigenic *B. cereus*.

All *Bacillus* veterinary isolates were also tested for lecithinase (phosphatidylinositol-specific phospholipase C) activity after overnight growth on nutrient agar supplemented with 8% egg yolk (Oxoid) and by overlaying 1% L-*d*-phosphatidylinositol substrate (Sigma) in 0.7% agarose on overnight cultures of the bacteria on L agar plates. Lecithinase-positive strains produced a halo of precipitation (the insoluble diacylglycerol) around the bacterial colonies. Production of catalase was assayed by using an ID Color Catalase testing kit (bioMérieux). The ability to induce hemolysis in a 7% concentration of horse erythrocytes (blood agar) was examined. Results showed that only *B. cereus* strains produced lecithinase, whereas beta-hemolysis and catalase activities were exhibited by all *Bacillus* isolates.

In summary, this study constitutes the first demonstration that isolates of many *Bacillus* spp., from samples associated with serious nongastrointestinal infections in animals, may carry diarrheagenic enterotoxin genes traditionally harbored

by toxigenic *B. cereus*. We also have shown that these veterinary *Bacillus* isolates are cytotoxic towards HEp-2 cells and have expressed HBL enterotoxins. While the roles of diarrheagenic enterotoxins and other potential virulence factors in the aforementioned animal infections have yet to be elucidated, this study has demonstrated that a variety of *Bacillus* spp. isolated from the veterinary environment may contain pathogenicity traits that may enhance their fitness for survival and to elicit disease.

We are grateful to V. Gill and D. Currie for their excellent technical assistance and the scientific staff of the Veterinary Science Division of the Scottish Agricultural College who made the isolations in the course of the routine diagnostic work.

REFERENCES

1. **Agata, N., M. Ohta, Y. Arakawa, and M. Mori.** 1995. The *bceT* gene of *Bacillus cereus* encodes an enterotoxic protein. Microbiology **141:**983–988.
2. **Aronson, A. I., and W. Beckman.** 1987. Transfer of chromosomal genes and plasmids in *Bacillus thuringiensis.* Appl. Environ. Microbiol. **53:**1525–1530.
3. **Ash, C., J. A. E. Farrow, M. Dorsch, E. Stackebrandt, and M. D. Collins.** 1991. Comparative analysis of *Bacillus anthracis*, *Bacillus cereus*, and related species on the basis of reverse transcriptase sequencing of 16S rRNA. Int. J. Syst. Bacteriol. **41:**343–346.
4. **Beattie, S. H., and A. G. Williams.** 1999. Detection of toxigenic strains of *Bacillus cereus* and other *Bacillus* spp. with an improved cytotoxicity assay. Lett. Appl. Microbiol. **28:**221–225.
5. **Becker, H., G. Schaller, W. von Wiese, and G. Terplan.** 1994. *Bacillus cereus* in infant foods and dried milk products. Int. J. Food Microbiol. **23:**1–15.
6. **Coote, J. G., and T. Arian.** 1996. A rapid, colorimetric assay for cytotoxin activity in *Campylobacter jejuni*. FEMS Immunol. Med. Microbiol. **13:**65–70.
7. **Craig, F. F., R. Dalgleish, and A. D. Sutherland.** 1990. A colorimetric, microplate assay for the leucotoxin of *Pasteurella haemolytica*. Vet. Microbiol. **22:**309–340.
8. **Drobniewski, F. A.** 1993. *Bacillus cereus* and related species. Clin. Microbiol. Rev. **6:**324–338.
9. **Finlay, W. J. J., N. A. Logan, and A. D. Sutherland.** 1999. Semiautomated metabolic staining assay for *Bacillus cereus* emetic toxin. Appl. Environ. Microbiol. **65:**1811–1812.
10. **Galiero, G., and E. De Carlo.** 1998. Abortion in water buffalo (*Bubalus bubalis*) associated with *Bacillus licheniformis*. Vet. Rec. **143:**640–641.
11. **Gonzalez, J. M., B. J. Brown, and B. C. Carlton.** 1982. Transfer of *Bacillus thuringiensis* plasmids coding for δ-enterotoxin among strains of *B. thuringiensis* and *B. cereus*. Proc. Natl. Acad. Sci. USA **79:**6951–6955.
12. **Granum, P. E., and T. Lund.** 1997. *Bacillus cereus* and its food poisoning toxins. FEMS Microbiol. Lett. **157:**223–228.
13. **Hansen, B. M., and N. B. Hendriksen.** 2001. Detection of enterotoxic *Bacillus cereus* and *Bacillus thuringiensis* strains by PCR analysis. Appl. Environ. Microbiol. **67:**185–189.
14. **Helgason, E., O. A. Økstad, D. A. Caugant, H. A. Johansen, A. Fouet, M. Mock, I. Hegna, and A.-B. Kolstø.** 2000. *Bacillus anthracis*, *Bacillus cereus*, and *Bacillus thuringiensis*–one species on the basis of genetic evidence. Appl. Environ. Microbiol. **66:**2627–2630.
15. **Jackson, S. G., R. B. Goodbrand, R. Ahemd, and S. Kasatiya.** 1995. *Bacillus cereus* and *Bacillus thuringiensis* isolated in a gastroenteritis outbreak investigation. Lett. Appl. Microbiol. **21:**103–105.
16. **Kado, C. I.** 1998. Origin and evolution of plasmids. Antonie Leeuwenhoek **73:**117–126.
17. **Kirkbride, C. A.** Bacterial agents detected in a 10-year study of bovine abortions and stillbirths. J. Vet. Diagn. Investig. **5:**64–68.
18. **Kirkbride, C. A., and J. Collins.** 1996. Porcine abortion caused by *Bacillus* spp. 1986. J. Am. Vet. Med. Assoc. **188:**1060–1061.
19. **Kotiranta, A., K. Lounatmaa, and M. Haapasalo.** 2000. Epidemiology and pathogenesis of *Bacillus cereus* infections. Microbes Infect. **2:**189–198.
20. **Mahler, H., A. Pasi, J. M. Kramer, P. Schulte, A. C. Scoging, W. Baer, and S. Kraehenbuehl.** 1997. Fulminant liver failure in association with the emetic toxin of *Bacillus cereus*. N. Engl. J. Med. **336:**1142–1148.
21. **McKillip, J. L.** 2000. Prevalence and expression of enterotoxins in *Bacillus cereus* and other *Bacillus* spp., a literature review. Antonie Leeuwenhoek **77:**393–399.
22. **Phelps, R. J., and J. L. McKillip.** 2002. Enterotoxin production in natural isolates of *Bacillaceae* outside the *Bacillus cereus* group. Appl. Environ. Microbiol. **68:**3147–3151.
23. **Ranganatha, H. G., and S. Saki.** 1981. *Bacillus cereus* as a cause of abortion in a mare. Curr. Sci. **50:**458.
24. **Rowan, N. J.** 1999. Evidence that inimical food preservation barriers alter microbial resistance, virulence and cell morphology. Trends Food Sci. Technol. **10:**261–272.
25. **Rowan, N. J., A. A. G. Candlish, A. Bubert, J. G. Anderson, K. Kramer, and J. McLauchlin.** 2000. Virulent rough filaments of *Listeria monocytogenes* from clinical and food samples secreting wild-type levels of cell-free p60 protein. J. Clin. Microbiol. **38:**2643–2648.
26. **Rowan, N. J., K. Deans, J. G. Anderson, C. G. Gemmell, I. S. Hunter, and T. Chaithong.** 2001. Putative virulence factor expression by clinical and food isolates of *Bacillus* spp. after growth in reconstituted infant milk formulae. Appl. Environ. Microbiol. **67:**3873–3881.
27. **Rowan, N. J., and J. G. Anderson.** 1997. Maltodextrin stimulates growth of *Bacillus cereus* and synthesis of diarrheal enterotoxin in infant milk formulae. Appl. Environ. Microbiol. **63:**1182–1184.
28. **Rowan, N. J., and J. G. Anderson.** 1998. Growth and enterotoxin production by diarrhoeagenic *Bacillus cereus* in dietary supplements prepared for hospitalised HIV patients. J. Hosp. Infect. **38:**139–146.
29. **Rowan, N. J., J. G. Anderson, and A. Anderton.** 1997. Bacteriological quality of infant milk formulae examined under a variety of preparation and storage conditions. J. Food Prot. **60:**1089–1094.
30. **Ryan, P. A., J. D. Macmillan, and B. A. Zilinkas.** 1997. Molecular cloning and characterization of the genes encoding the L_1 and L_2 components of hemolysin BL from *Bacillus cereus*. J. Bacteriol. **179:**2551–2556.
31. **Salkinoja-Salonen, M. S., R. Vuorio, M. A. Andersson, P. Kämpfer, M. C. Andersson, T. Honkanen-Buzalski, and A. C. Scoging.** 1999. Toxigenic strains of *Bacillus licheniformis* related to food poisoning. Appl. Environ. Microbiol. **65:**4637–4645.
32. **Schoeni, J. L., and A. C. Wong.** 1999. Heterogeneity observed in the components of hemolysin BL, an enterotoxin produced by *Bacillus cereus*. Int. J. Food Microbiol. **53:**159–167.
33. **Schuh, J., and D. Weinstock.** 1985. Bovine abortion caused by *Bacillus cereus*. J. Am. Vet. Med. Assoc. **187:**1047–1048.
34. **Turnbull, P. C., R. A. Hutson, M. J. Ward, M. N. Jones, C. P. Quinn, N. J. Finnie, C. J. Duggleby, J. M. Kramer, and J. Melling.** 1992. *Bacillus anthracis* but not always anthrax. J. Appl. Bacteriol. **72:**21–28.
35. **Van Heddeghem, A., and G. Vlaemynck.** 1992. Sources of contamination of milk with *Bacillus cereus* on the farm and in the factory. Bull. Int. Dairy Fed. **275:**19–22.
36. **von Dietrich, R., K. Mauersberger, and E. Martlbauer.** 1997. Zur anwendbarkeit des MTT zytotoxizitatstests zum nachwies von *B. cereus* enterotoxin. Arch. Lebensmittelhyg. **48:**73–96.
37. **Wernery, U., and M. Ali.** 1996. *Bacillus cereus* abortion in a nine-year-old dromedary camel–a case report. J. Camel Pract. Res. **3:**153.

APPLIED AND ENVIRONMENTAL MICROBIOLOGY, June 1998, p. 2065–2071 Vol. 64, No. 6
0099-2240/98/$04.00+0

Effects of Above-Optimum Growth Temperature and Cell Morphology on Thermotolerance of *Listeria monocytogenes* Cells Suspended in Bovine Milk

NEIL J. ROWAN* AND JOHN G. ANDERSON

Department of Bioscience and Biotechnology, University of Strathclyde, Glasgow, Scotland

Received 21 November 1997/Accepted 20 March 1998

The thermotolerances of two different cell forms of *Listeria monocytogenes* (serotype 4b) grown at 37 and 42.8°C in commercially pasteurized and laboratory-tyndallized whole milk (WM) were investigated. Test strains, after growth at 37 or 42.8°C, were suspended in WM at concentrations of approximately 1.5×10^8 to 3.0×10^8 cells/ml and were then heated at 56, 60, and 63°C for various exposure times. Survival was determined by enumeration on tryptone-soya-yeast extract agar and *Listeria* selective agar, and D values (decimal reduction times) and Z values (numbers of degrees Celsius required to cause a 10-fold change in the D value) were calculated. Higher average recovery and higher D values (i.e., seen as a 2.5- to 3-fold increase in thermotolerance) were obtained when cells were grown at 42.8°C prior to heat treatment. A relationship was observed between thermotolerance and cell morphology of *L. monocytogenes*. Atypical *Listeria* cell types (consisting predominantly of long cell chains measuring up to 60 μm in length) associated with rough (R) culture variants were shown to be 1.2-fold more thermotolerant than the typical dispersed cell form associated with normal smooth (S) cultures ($P \leq 0.001$). The thermal death-time (TDT) curves of R-cell forms contained a tail section in addition to the shoulder section characteristic of TDT curves of normal single to paired cells (i.e., S form). The factors shown to influence the thermoresistance of suspended *Listeria* cells ($P \leq 0.001$) were as follows: growth and heating temperatures, type of plating medium, recovery method, and cell morphology. Regression analysis of nonlinear data can underestimate survival of *L. monocytogenes*; the end point recovery method was shown to be a better method for determining thermotolerance because it takes both shoulders and tails into consideration. Despite their enhanced heat resistance, atypical R-cell forms of *L. monocytogenes* were unable to survive the low-temperature, long-time pasteurization process when freely suspended and heated in WM.

Listeria monocytogenes is a facultative anaerobic bacterium that is distributed ubiquitously in the environment (19) and has a higher thermotolerance than many other nonsporeforming food-borne pathogens (14, 21). Because this potentially lethal pathogen is found occasionally in raw milk (2, 10, 11, 14, 36) and in other nonprocessed foods (2, 19, 25, 26) and can grow in foods under refrigerated storage (22), considerable emphasis has been placed on its complete destruction during pasteurization and during other minimal thermal food processes (3, 4, 6–8, 12–14, 31, 32).

Many factors are known to influence microbial thermotolerance in foods such as the composition of the food and the physiological condition of vegetative cells and spores (15, 24, 52). Bacterial thermotolerance can also increase after exposure to a variety of environmental stress conditions including heating at sublethal temperatures, presence of deleterious chemicals in the growth medium (e.g., hydrogen peroxide, dyes, and antibiotics, etc.), viral infections, and osmotic and acidic shocks (18, 19, 29).

Any temperature above the optimum growth temperature will exert a stress effect (24); while the optimum temperature for growth of *L. monocytogenes* lies between 30 and 37°C, it can grow between 1 and 45°C (19, 48). For most microbial species growth at or short-term exposure to temperatures above optimum induces higher thermotolerances (1, 37–40). It is believed that these temperatures trigger physiological responses that lead to the synthesis of special proteins known as heat shock proteins (HSPs) (31, 33). In *Escherichia coli* K-12, when cells were shifted to 42°C from an incubation temperature of 30°C, the rate of HSP formation increased 5 to 20-fold (cited in reference 48). Gram-positive and -negative bacteria appear to behave similarly: *Streptococcus faecalis* grown at 45°C were more heat resistant than when grown at 27°C (53), while the $D_{55°C}$ value for *Salmonella senftenberg* 775W increased as growth temperature was raised from 15 to 44°C (43).

Many authors have reported an increase in the thermotolerance of *L. monocytogenes* as a result of heat shock prior to heating (20, 28, 31, 34, 35, 44). Results from Linton et al. (35) and Pagán et al. (44) are particularly interesting as they suggest that the magnitude of the effect of heat shock treatments is highly dependent on the temperature and duration of the treatment, with higher heating temperatures and longer treatments favoring an increase in heat resistance. Whereas the former researchers observed that *L. monocytogenes* attained its greatest thermotolerance after 20 min of heat shocking at 48°C, Pagán et al. (44) reported a sevenfold increase in thermotolerance achieved by extending the duration of heat shock to 180 min at 45°C. While most thermotolerance studies have utilized *L. monocytogenes* cells at or below 37°C (3, 4, 6–8, 10, 12, 13, 23, 51), the body temperature of a cow suffering from listeriosis can reach as high as 42.8°C (10, 14). Doyle et al. (14) reported the low-level survival of *L. monocytogenes* in high-temperature short-time (HTST)-pasteurized milk from a cow that had been artificially infected with the organism. Also, Knabel et al. (31) showed that growth of *Listeria* at temperatures above 37°C for 18 h (39 to 43°C) resulted in cells that were sixfold more thermotolerant than cells grown at 37°C.

* Corresponding author. Mailing address: Department of Bioscience and Biotechnology, University of Strathclyde, Royal College Bldg., 204 George St., Glasgow G1 1XW, Scotland. Phone: 44 141 548 2531. Fax: 44 141 553 1161. E-mail: n.j.rowan@strath.ac.uk.

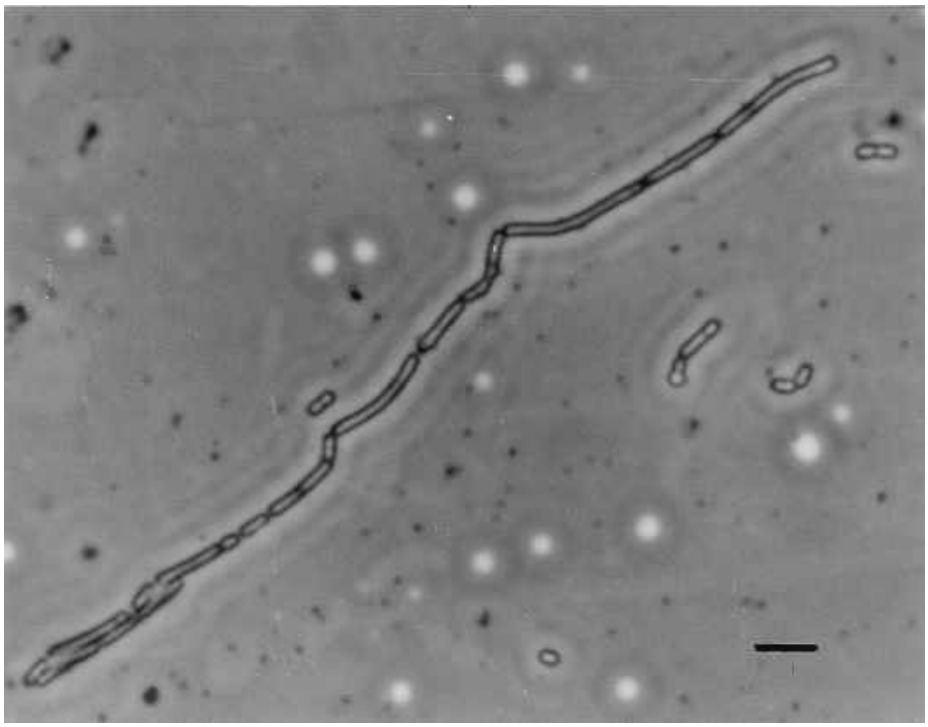

FIG. 1. Cell chain development in *L. monocytogenes* NCTC 11994 (R_1). A phase contrast micrograph (Nikon Optiphot-2 light microscope) is shown. Bar = 5μm.

Interestingly, both research groups used serotype 4b strains, a serotype implicated in a number of fatal food-borne outbreaks (19, 21, 25, 26) and shown recently by Sörqvist to be the second-most heat resistant of seven serotypes examined (49). While production of HSPs are typically a response to temperature upshifts, extended growth at above-optimum temperatures has been shown to result in the expression of HSPs (45).

Microbial cell morphology has been linked with increased thermotolerance (41, 46). The acquisition of thermotolerance in heat-shocked *Aquaspirillum arcticum* was shown to be directly related to the formation of long cells (40). Jørgensen et al. (29) showed that *L. monocytogenes* cells grown in medium containing 1.5 mol of NaCl $liter^{-1}$ prior to heating were 22-fold more heat tolerant than similarly treated cells grown with 0.09 mol of NaCl $liter^{-1}$. Cells grown in medium containing 1.5 mol of NaCl $liter^{-1}$ became 50 times longer, but no link to thermotolerance could be made. The change from short rods to long cell chains also occurs under nonstress conditions; Kuhn and Goebel (32) showed that spontaneous mutants of *L. monocytogenes* that form long cell chains occur at a relatively high frequency (about 1 in 10,000 colonies). These long cell chain forms exhibited thermal death-time (TDT) curves that were characterized by both shoulder and tail sections. Other researchers have reported similar TDT curves in *L. monocytogenes* as a result of heat shocking (20, 31, 34, 35); none, however, have mentioned whether the cell morphology of this organism had altered as a result of heating.

The present study was undertaken to investigate the effect of growth at the above-optimum temperature of 42.8°C (i.e., similar to the body temperature of a cow infected with *L. monocytogenes*) on the heat resistance of different cell forms of *L. monocytogenes* (serotype 4b). Thermotolerance was calculated by determining both D values (decimal reduction times) and Z values (numbers of degrees Celsius required to cause a 10-fold change in the D value) and by using the end point recovery method.

MATERIALS AND METHODS

Bacterial culture and media. Two different morphological culture forms of *L. monocytogenes* were used, the normal smooth or S type, consisting of short single and/or paired rods (0.4 to 0.5 μm in diameter and 0.5 to 2 μm in length), and the atypical rough or R type, predominantly consisting of long cell chains of up to 60 μm in length (Fig. 1). The two S-type strains used were NCTC 9863 and 11994 (both of these serotype 4b strains were originally isolated from patients with meningitis and are referred to as S_1 and S_2, respectively, throughout the text) and were obtained from the National Collection of Type Cultures, Public Health Laboratories, Colindale, London, United Kingdom. The two R-form culture variants, R_1 and R_2, were derived previously from the S_1 and S_2 strains, respectively (46), via heating studies as follows: the parent S_1 and S_2 cultures were grown in tyndallized whole milk (WM) at 42.8°C for 24 h without shaking prior to being heated at 60°C for 7 min and at 63°C for 3 min. The R_1 and R_2 culture variants were obtained on tryptone-soya agar plates supplemented with 0.6% yeast extract (TSYEA). The cultures were plated immediately after the 7- and 3-min intervals described above and were incubated for 48 h at 37°C. The purity of the strains was confirmed by Gram, catalase, and oxidase reactions; tumbling motility at 25°C; CAMP test reaction; and biochemical profiling with the API *Listeria* gallery (Biomérieux Ltd.). Stock cultures were grown on TSYEA at 37°C for 18 to 20 h and were maintained at 4°C with monthly transfer.

Fifty milliliters of tryptone-soya broth supplemented with 0.6% yeast extract (TSYEB) contained in a 250-ml flask was inoculated with the test strain and incubated at 30°C with shaking at 150 rpm on a rotary incubator (model RFI-125; INFORS AG, Botlmingen, Switzerland). Growth was monitored by measuring the optical density at 625 nm (OD_{625}) of the culture with a spectrophotometer (model UV-120-02; Shimadzu Corp., Kyoto, Japan). Cells from the late-exponential phase (an absorbance of 0.2 at OD_{625}, yielding approximately 10^9 *Listeria* cells/ml) were harvested by centrifugation at 3,000 × *g* in a refrigerated (4°C) centrifuge, washed twice, and resuspended in 5 ml of precooled phosphate-buffered water (0.01 M, pH 7 at 4°C). Two duplicate 250-ml flasks each containing 50 ml of commercially pasteurized WM were tyndallized to sterility and inoculated to give initial cell densities of approximately 10^3 cells/ml. Cultures were grown without shaking for 24 h at 37 or 42.8°C to the respective maximum stationary stage.

Thermal resistance studies and enumeration. Heat treatments were performed using screw-cap 28-ml dilution bottles containing 10 ml of WM. The bottles were equilibrated at 56, 60, or 63°C utilizing a circulating constant tem-

TABLE 1. Heat resistance of S- and R-culture forms of *L. monocytogenes* grown in WM at 37 or 42.8°C prior to heating at 56, 60, and 63°C as determined by the interval sample plating method

Heating Temp (°C)	Growth Temp (°C)	D or Z value (min) for culture forms plated on indicated media[a]							
		S_1		R_1		S_2		R_2	
		TSYEA	LSA	TSYEA	LSA	TSYEA	LSA	TSYEA	LSA
56	42.8	24.5 (0.7)^{Aa}	16.5 (0.3)^{Ad}	29.1 (0.3)^{Ab}	18.1 (0.1)^{Ac}	26.5 (0.8)^{Aa}	17.8 (0.3)^{Ac}	31.5 (0.8)^{Ab}	19.5 (0.2)^{Ac}
	37	9.6 (0.2)^{Ba}	6.4 (0.2)^{Bc}	10.5 (0.1)^{Bb}	6.5 (0.2)^{Bc}	10.1 (0.2)^{Ba}	6.4 (0.2)^{Bc}	11.4 (0.2)^{Bb}	6.6 (0.1)^{Bc}
60	42.8	3.7 (0.2)^{Aa}	1.8 (0.2)^{Ad}	4.4 (0.2)^{Ab}	2.1 (0.1)^{Ac}	3.9 (0.1)^{Aa}	2.0 (0.1)^{Ac}	4.8^{Ab}	2.3 (0.2)^{Ac}
	37	1.5^{Ba}	0.7 (0.1)^{Bc}	1.7 (0.1)^{Bb}	0.8 (0.1)^{Bc}	1.5 (0.2)^{Ba}	0.8 (0.1)^{Bc}	1.8 (0.1)^{Bb}	0.9 (0.1)^{Bc}
63	42.8	1.1 (0.1)^{Aa}	0.4 (0.1)^{Ac}	1.4 (0.1)^{Ab}	0.6^{Ac}	1.2^{Aa}	0.5 (0.1)^{Ac}	1.4 (0.1)^{Ab}	0.6 (0.1)^{Ac}
	37	0.4 (0.1)^{Ba}	0.1 (0.1)^{Bb}	0.4^{Ba}	0.2^{Bb}	0.4 (0.1)^{Ba}	0.2 (0.1)^{Bb}	0.5 (0.1)^{Ba}	0.2^{Bb}
Z-values	42.8	**5.1 (0.1)**^{Aa}	**4.4 (0.1)**^{Ab}	**5.2**^{Aa}	**4.6 (0.1)**^{Ab}	**5.1**^{Aa}	**4.4**^{Ab}	**5.2**^{Aa}	**4.6 (0.1)**^{Ab}
	37	**5.0 (0.1)**^{Aa}	**4.3**^{Ab}	**5.0 (0.1)**^{Ba}	**4.4 (0.1)**^{Bb}	**5.0**^{Aa}	**4.3 (0.1)**^{Ab}	**5.1**^{Aa}	**4.4 (0.1)**^{Bb}

[a] Values are means of three replicates. Numbers in parentheses are standard deviations. Values in the same column within each heating temperature with different superscript uppercase letters are significantly different ($P \leq 0.05$). Values in the same row with different superscript lowercase letters are significantly different ($P \leq 0.05$). Numbers in boldface are Z values, which were determined by simple linear regression.

perature water bath (model HE30; Grant Instruments Ltd., Cambridge, United Kingdom) equipped with a thermoregulator capable of maintaining temperature to within ± 0.05°C (model TE-8A; Techne Ltd., Cambridge, United Kingdom); the level of the water in the water bath was maintained ca. 5 cm above the submerged bottles. A mercury thermometer was inserted into an uninoculated bottle and was checked periodically during the experimental runs to ascertain that the heating temperatures were maintained. One milliliter of the overnight-grown cells was then added to give 1.5×10^8 to 3×10^8 CFU/ml of WM. At predetermined heating intervals (over 2 h at 56°C, 1 h at 60°C, and 30 min at 63°C), a 1-ml sample was removed from each of the bottles and added to 9 ml of WM. The bottles containing heat-treated samples were transferred quickly into a beaker containing tap water at 22°C and held for 1 min (which ensured near-instantaneous cooling of the samples) and then placed into a beaker containing an ice-water mixture. Preliminary experiments showed no growth during this period of time (data not shown) (46). Heat treatments at each temperature were repeated at least twice.

Recovery of surviving cell populations was determined at each heating interval in the heat-treated suspensions, and dilutions thereof, by spread, pour, and spiral plating samples (model B; Spiral Systems Inc., Shipley, United Kingdom) onto TSYEA and *Listeria* selective agar (LSA) (Oxford formulation; Oxoid). Successive dilutions were performed with 9 ml of WM, and all counts were done with triplicate plates. WM was used as the diluent to provide greater protection against the deleterious effects of heat treatment when *L. monocytogenes* cells were grown, heat treated, and enriched in the same nutrient medium compared with that provided by changing the nutritional composition of the heating menstruum and/or the diluent (data not shown) (46). Plates were incubated aerobically at 37°C for 48 h, and colonies were counted. The cell morphologies of three randomly selected colonies were examined per plate. All bottles containing treated cultures from each sample heating interval were then incubated and/or resuscitated without shaking at 30°C for 2 days, and total aerobic counts were carried out by using both plating media as described above. This latter recovery method is referred to herein as the end point recovery method, where the end point is defined as the last sample interval resulting in growth of heat-injured cells (i.e., the last sample interval just before reaching the interval yielding total inactivation of suspended cells) at each treatment temperature. Near the end point, samples were removed at 2-, 1-, and 1-min intervals at 56, 60, and 63°C, respectively.

Statistical methods. All experiments in this study were performed in triplicate, and results are reported as averages. Estimates of thermal resistance at each heating temperature were expressed as D values calculated as the absolute value of the inverse slope of the least square regression line fitted to $\log_{10}$ reduction in viable cell numbers versus heating time. A linear regression was computed from $\log_{10}$ D value versus heating temperature, and the Z value was computed as the absolute value of the inverse of the slope. Temperatures used to determine Z values were 56, 60, and 63°C, and thermotolerance was computed by using both selective and nonselective media. Effects of growth and heat treatment temperatures, plating media, type of recovery method, and cell morphology on thermal resistance were calculated at the 95 and 99.9% confidence intervals by analysis of variance (balanced model) with Minitab software Release 11 (Minitab Inc., State College, Pa.).

RESULTS AND DISCUSSION

Effects of growth temperature and other factors on the thermotolerance of *L. monocytogenes*. Growth and heating temperatures and types of plating media and recovery methods had significant effects ($P < 0.001$) on the survival of heated *L. monocytogenes* (Tables 1 and 2). Growth of *Listeria* cells in bovine WM at the above-optimum temperature of 42.8°C resulted in a 2.5- to 3-fold increase in thermotolerance ($P \leq 0.001$) compared to that for growth at 37°C (Table 1). This enhanced thermotolerance was seen at each heating temperature (Table 1). Table 2 lists the factors that significantly influenced the heat resistance of *Listeria* cells shown in Table 1. While treatment temperature was shown to have the most significant effect on thermotolerance (i.e., the higher heating temperatures resulting in greater reductions in cell numbers), other factors which provided greater levels of cell protection were growth at 42.8°C prior to heat treatment and recovery of thermally injured cells on the nonselective TSYEA medium (Tables 1 and 2). Greater recovery of heat-injured *Listeria* cells was obtained after a 2-day enrichment period in WM (Table

TABLE 2. Factors shown to influence the thermotolerance of *L. monocytogenes* suspended in bovine WM as determined by analysis of variance (balance design)

Source of variance[a]	Statistical result[b]				
	DF	SS	MS	*F*	*P*
TT	2	4,406.1	2,203.1	8,428.3	≤0.001
GT	1	768.4	768.4	2,939.7	≤0.001
PM	1	211.2	211.2	808.1	≤0.001
CM	1	14.9	14.9	56.9	≤0.001
TT · CT	2	944.1	472.1	1,806.0	≤0.001
TT · PM	2	191.5	95.7	366.3	≤0.001
TT · CM	2	15.2	7.6	29.1	≤0.001
CT · PM	1	41.9	41.9	160.2	≤0.001
CT · CM	1	7.5	7.5	28.6	≤0.001
PM · CM	1	4.3	4.3	16.6	≤0.001
TT · CT · PM	2	35.5	17.7	67.9	≤0.001
TT · CT · CM	2	7.0	3.5	13.3	≤0.001
TT · PM · CM	2	4.5	2.3	8.7	≤0.001
CT · PM · CM	1	1.6	1.6	5.9	≤0.017
TT · CT · PM · CM	2	1.2	0.6	2.2	≤0.115
Error	72	18.8	0.3		
Total	95	6,673.6			

[a] TT, treatment temperature; GT, growth temperature; PM, plating medium; CM, cell morphology (differences between atypical R- and typical S-cell forms.
[b] DF, degrees of freedom; SS, sum of squares; MS, mean squares; *F*, *f* statistic. *F* value compares the spread of results in data sets to determine if they could reasonably be considered to come from the same parent distribution.

TABLE 3. Effects of growth temperature on the thermotolerances of S- and R-cell forms of *L. monocytogenes* using the end point recovery method[a]

Growth temp (°C)	Plating medium	$D_{63°C}$ for indicated cell form with[a]:							
		Immediate plating of heated samples				Plating after 2-day enrichment period at 30°C			
		S_1	S_2	R_1	R_2	S_1	S_2	R_1	R_2
42.8	TSYEA	7.3 (0.5)^{Aa}	7.6 (0.6)^{Aa}	9.6 (0.6)^{Ab}	10.3 (1.2)^{Ab}	21.6 (1.5)^{Ac}	21.3 (1.2)^{Ac}	24.3 (2.1)^{Ac}	24.6 (2.6)^{Ac}
37	TSYEA	3.0^{Ba}	3.0 (1.0)^{Ba}	4.0^{Ba}	4.3 (0.6)^{Ba}	7.6 (0.6)^{Bb}	7.6 (1.5)^{Bb}	10.3 (1.5)^{Bc}	10.3 (0.6)^{Bc}
42.8	LSA	3.0^{Aa}	4.3 (0.6)^{Aa}	5.0 (1.0)^{Aa}	5.0 (1.0)^{Aa}	17.6 (0.6)^{Ab}	18.0 (1.5)^{Ab}	21.6 (1.5)^{Ac}	22.3 (1.7)^{Ac}
37	LSA	0.7 (0.7)^{Ba}	1.0^{Ba}	2.0 (1.0)^{Ba}	1.6 (1.2)^{Ba}	4.0^{Bb}	5.6 (0.6)^{Bb}	6.0 (1.0)^{Bb}	7.3 (1.5)^{Bb}

[a] Values are means (± standard deviations). Values in the same column within each heating temperature with different superscript uppercase letters are significantly different ($P \leq 0.05$). Values in the same row with different superscript lowercase letters are significantly different ($P \leq 0.05$).

3). Results from total viable counts (data not shown) showed that growth occurred in the enriched bottles at each sample interval up to and including the end point.

The results of the present study are in agreement with the findings of other researchers (14, 31), who showed that growth of *L. monocytogenes* cells at an above-optimum temperature (i.e., 39 to 43°C) resulted in an increase in thermotolerance. Growth of *L. monocytogenes* F5069 under anaerobic conditions at 43°C prior to heat treatment and enumeration of survivors resulted in $D_{62.8°C}$ values that were at least sixfold greater than those previously obtained by using cells grown at 37°C and with aerobic plating (31). Whereas Knabel et al. (31) reported that under their test conditions, high levels of *L. monocytogenes* survived the minimum low-temperature, long-time (LTLT) pasteurization process, we showed that *L. monocytogenes* cells grown at 42.8°C were less heat tolerant, surviving approximately 27 min of heating at 63°C when enumerated after a 2-day enrichment period. Knabel and coworkers attributed the greater recovery of severely heat-injured *L. monocytogenes* cells to the absence of O_2 in the enrichment medium (i.e., the O_2 sensitivity of heat-injured *Listeria* cells has been attributed in part to the inactivation of catalase and superoxide dismutase). Dallmier and Martin (9) reported that catalase and sodium dismutase were rapidly inactivated when *Listeria* cells were heated at temperatures of 55 to 60°C. Inactivation of these two enzymes was thought to result in the accumulation of toxic levels of O_2 products, such as O_2^- and H_2O_2.

The production and action of a specific set of HSPs, synthesized during the growth of *L. monocytogenes* cells at 42.8°C, may also account for the acquired thermotolerance in the present study (27, 31, 45). While the precise role of HSPs in acquired heat resistance remains controversial, HSPs might help cells cope with stress-induced damage by promoting the degradation of abnormal proteins (e.g., lon and Clp proteases) and/or the reactivation of stress-damaged proteins by functioning as molecular chaperones, preventing the aggregation and promoting the proper refolding of denatured proteins (45). Rapid degradation of damaged proteins reduces the possibility of deleterious interactions between polypeptides and functional proteins, prevents accumulation of insoluble aggregates, and releases the amino acids contained in nonfunctional polypeptides for synthesis of new proteins (45). As is the case for all organisms studied so far, *L. monocytogenes* responds to sudden increases in temperature by synthesizing a particular set of HSPS (28). Some stress-induced proteins are also produced in organisms in order to sustain long-term survival at above-optimum temperatures (45). For instance, in *Saccharomyces cerevisiae*, some HSPs are required for growth at temperatures near the upper end of the normal growth range (e.g., HSP70), others are required for long-term survival at moderately high temperatures (e.g., ubiquitin), and still others are required for tolerance to extreme temperatures (e.g., HSP104) (45). In some cases, expression of genes encoding for the production of proteins associated with one stimulus (e.g., heat shock) can be induced during other stresses; for example, various HSPs in *E. coli* cells are also synthesized when the cells are exposed to hydrogen peroxide, ethanol, UV, puromycin, and nutrient or amino acid deprivation (27). Therefore, the large increase in heat resistance observed when *L. monocytogenes* cells were grown at 42.8°C, compared with that of cells grown at 37°C, may have been due to the accumulation of large amounts of postexponential HSPs that were induced by elevated growth temperature, nutrient deprivation, and/or other stresses (27, 45). Jenkins et al. (27) concluded that the increased heat resistance of stationary-phase *E. coli* cells could have been a result of synthesis of postexponential HSPs that were induced during glucose starvation. The induction of HSPs, therefore, may prepare cells for growth at elevated sublethal temperatures while playing only a minor role in acquired thermotolerance at lethal temperatures.

Under the present test conditions, heat-injured *Listeria* cells suspended in the heating menstruum were subjected to minimal mixing before enumeration and then enriched for 2-days without shaking. Due to the differences in cell recovery between immediate aerobic plating and 2-day enrichment methods (Table 3), it is probable that the enhanced thermotolerance seen with the latter method was due in part to the provision of a reduced O_2 environment in the enrichment bottles. Nonetheless, R-form cells cultivated at 42.8°C prior to heating at 63°C were recovered from the 27-min sample interval, i.e., an additional heat tolerance of 16 min compared with that of the immediate plating method resulted (Table 3). As heat-injured cells grew in WM over the 2-day enrichment period, it was not possible to convert end point survivor data to D values (Table 3). The enhanced recovery of cells grown at 42.8°C seen after enrichment in WM at 30°C is important in terms of milk safety, because HTST pasteurization (which is used commercially) has been shown to result in approximately 10-fold fewer log reductions of *L. monocytogenes* than the LTLT pasteurization process used in this study (6). Therefore, under similar growth and recovery conditions (enrichment in WM at 30°C), HTST pasteurization might yield survivors that can grow in milk.

The significance of *L. monocytogenes* in relation to food safety is mainly due to its ability to grow in foods under refrigerated storage (2, 10, 11, 14, 28). Many authors have reported that in non-heat-shocked cells of different bacterial species, higher growth temperatures lead to higher thermotolerance (31, 37–39). There is little knowledge, however, about the influence of growth at above-optimal temperatures in relation to the acquisition and maintenance of thermotolerance in foods during refrigeration. Whereas the thermotolerance de-

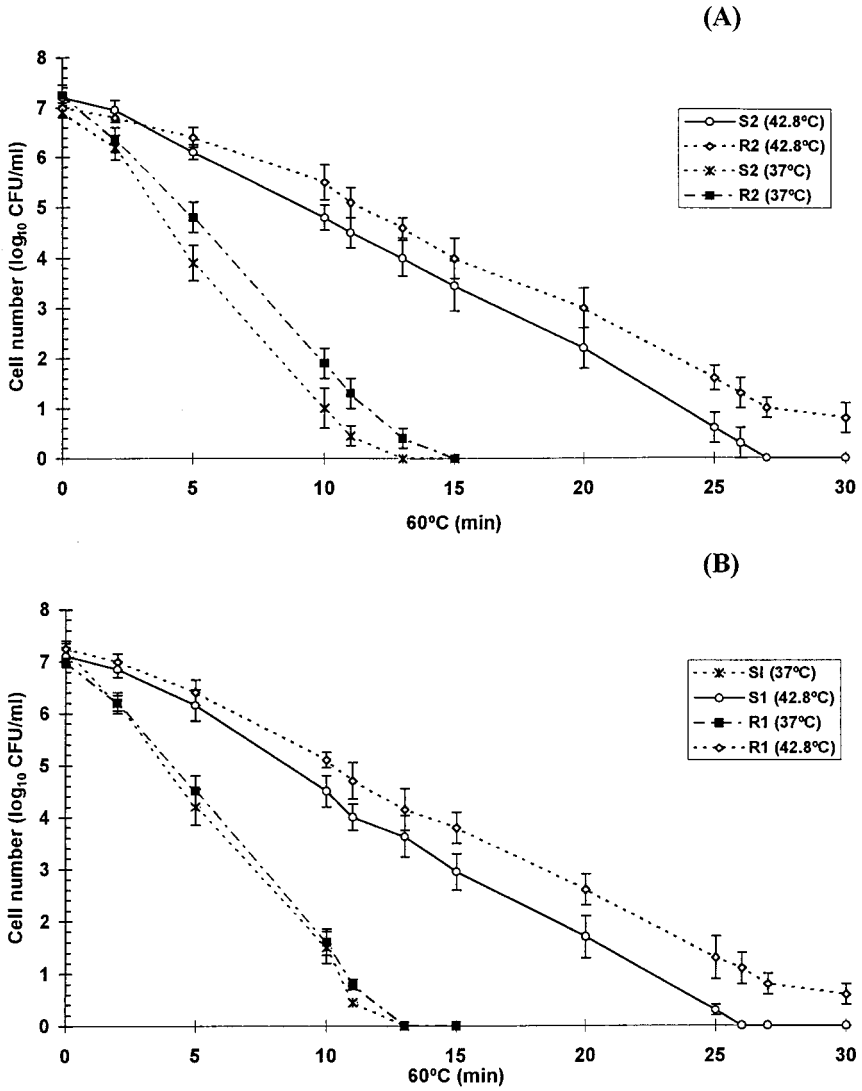

FIG. 2. Thermal resistance of S- and R-cell forms of *L. monocytogenes* NCTC 11994 (A) and NCTC 9863 (B) grown at 37 and 42.8°C prior to heating at 60°C.

veloped by *Salmonella typhimurium* after heat shocking was lost during storage in just 1 h (37), Farber and Brown (17) reported that *L. monocytogenes* still maintained, after a 24-h period at 6°C, the heat resistance developed after a 2-h heat shock at 48°C. Smith and Marmer (47) showed that *L. monocytogenes* grown at 10°C did not attain the heat resistance of non-heat-shocked cells grown at 37°C. Pagán and coworkers (44), however, showed that storage of heat-shocked *L. monocytogenes* (42.5°C for 180 min) for 24 h at 4°C before heating did not affect the D values seen for heat-shocked cells. These authors also reported that for non-heat-shocked *Listeria* cells stored for 7 and 14 days at 4°C, the proportion of cells responding to heat shock not only depended on the duration of heat shock but also on the duration of previous storage. The longer the duration of heat shock and the shorter the duration of storage, the greater the proportion of cells responding to heat shock. For instance, after a 14-day storage at 4°C, Pagán et al. (44) reported that only 10% of the cells given the longest heat shock of 120 min responded, while only 1.5% of those given the mildest heat shock of 15 min did so.

Factors affecting the thermotolerance of *L. monocytogenes* R- and S-cell forms. The thermotolerance of the R- and S-cell forms varied as a result of the various growth, heating, and recovery conditions used in the present study. Atypical R-type culture forms (predominantly consisting of long cell chains) exhibited higher D and Z values (Table 1) than those of typical S forms (consisting of single and paired cells). R-cell forms were 1.2-fold more heat tolerant as measured by D value ratios at each heating temperature (Table 1). R cultures obtained from the two *L. monocytogenes* strains (NCTC 11994 and 9863) did not differ in thermotolerance nor did the parent S forms ($P \leq 0.001$). Both cell forms of *L. monocytogenes* grown at 37 and 42.8°C showed nonlinear TDT curves (Fig. 2). Whereas the R-form TDT curves contained both a shoulder and tail section, S-form survivor curves exhibited a shoulder section only (Fig. 2).

Atypical R-form cells consistently survived longer at 62.8°C than S-form cells as shown by both recovery methods (Table 3). Both cell forms were recovered after a longer duration of heating when enumerated on TSYEA immediately after heat-

ing and after a 2-day enrichment period (Table 3). Other researchers also reported inferior recovery of heat-injured *L. monocytogenes* as a result of enumeration on selective plating media (31, 34, 35, 47, 48). Despite their enhanced thermotolerance, atypical cell forms of *L. monocytogenes* were unable to survive the LTLT pasteurization process (Table 3). Jørgensen et al. (29) also reported the existence of long cell chains in *L. monocytogenes* which exhibited TDT curves that contained both a shoulder and tail section post heating. These atypical *Listeria* cells, however, were obtained by severe osmotic shock due to growth in medium containing 1.5 mol of NaCl/liter, and these cells became up to 50 times longer than cells grown in medium containing 0.09 mol of NaCl/liter. Cells which had adapted to a high salinity before heat treatment showed a 10-fold increase in thermotolerance in minced beef compared to a 22-fold increase in tryptic phosphate broth. However, no link between the acquisition of thermotolerance and cell morphology was made. While TDT curves obtained during the present study, as a result of growth at an above-optimum temperature, were similar to the type of survivor curves obtained by Jørgensen et al. (29), atypical *Listeria* cells were shown to be 1.2-fold more heat tolerant than single-celled cultures at each heating temperature (Table 1). McCallum and Inniss (41) reported a direct link between thermotolerance and cell morphology, where the acquisition of thermotolerance in *A. arcticum* was related to the formation of filamentous cells.

It is particularly interesting that the majority of researchers reporting greater thermotolerance in *L. monocytogenes*, as a result of growth at above-optimal temperatures and/or heat shock, showed nonlinear TDT curves that contained both a shoulder and tail section (16, 20, 37, 44) or just an initial shoulder section (30, 35, 50). In addition, the majority of researchers reporting survivor curves in *L. monocytogenes* used the same serotype, 4b (16, 20, 29, 31, 35, 37, 50); this serotype has been isolated from patients with meningitis and from foods implicated in a number of food-related illnesses (19, 21, 25, 26).

Irrespective of the shape of the thermal death kinetic data, calculations on the level of thermotolerance in *Listeria* cells have been based on logarithmic death kinetics (i.e., D values that were calculated as the absolute value of the inverse slope of the least square regression line fitted to log reduction in viable cell numbers versus heating time) (16, 20, 31, 35, 37, 50). Very often no allowance has been made in these calculations for the shoulder and/or tail section in survivor curves. King et al. (30) showed that the function $(\log N_0 - \log N)^a = kt + c$ could be successfully used to linearize the survivor curves obtained from *B. fulva*, a mold that produced heat-resistant ascospores. N_0 and N are the initial and surviving number of organisms, respectively, at time t, the death rate constant is given by k, and c is a constant for a set of data. The a value is derived from the least squares slope of a plot of $\log(\log N_0 - \log N)$ versus log time.

King and coworkers showed that the function does not change significantly as the severity of the lethal treatment is increased. When comparing the survival of microbial species under different thermal processes in foods, a large number of log units of kill should be used so the final calculations will incorporate the shoulder and the rapid death phase of the curve. For instance, a 1 log unit destruction of *L. monocytogenes* NCTC 11994 (i.e., S_1 in Fig. 2) takes 6.1 min at 60°C, but the second log unit takes 3.4 min, the third takes 3.3 min, the fourth takes 3.1 min, and the fifth takes 2.6 min. Because of the shoulder of the curve, a third of the total time for a 5 log unit reduction is required for the first log unit of destruction. While the $D_{60°C}$ for S_1 was 3.7 min, the analogous value for a 1-log unit destruction (using the linearizing function) increased to 3.9 min. Application of this function also showed that the thermotolerance of other bacterial pathogens was underestimated. The time taken for a 6-log unit reduction in *Salmonella seftenberg* 750W was observed to be 119 min but was calculated to be 132 min using the function (43). However, use of this formula did not apply to TDT curves containing both shoulder and tail sections (data not shown) (46). Shoulders of TDT curves have been postulated to be due to spore activation, repair of heat injury, cell disaggregation, or even methodological problems (24, 42). Moats et al. (42) reported extensive tailing in the survivor curves for *E. coli*, *S. faecalis*, *Salmonella senftenberg* 775W, and *S. antum* and attributed these deviations from the exponential death rates to differences in heat resistances in a single bacterial culture and/or clumping (i.e., where clumps of two or more cells produce a colony as long as one cell in the clump is viable). Therefore, while measurement of thermotolerance by the TDT curve method (i.e., D value determination) provides detailed data on thermal death rate kinetics that cannot be obtained by the end point recovery method (24, 44, 52), regression analysis of nonlinear data can underestimate survival of *L. monocytogenes* (Table 3). The end point recovery method appears to be a better method for determining microbial thermotolerance because it takes both shoulders and tails into consideration.

Little knowledge is available on the putative virulence capability of R-transformed *L. monocytogenes*. Kuhn and Goebel (32) reported that long cell chains of this organism result from an impairment in the synthesis of a major extracellular protein, p60 (considered an important housekeeping protein for virulent strains of *L. monocytogenes*). It was suggested that p60 protein may be a murein hydrolase and that its synthesis is not under the control of the transcriptional activator, PrfA (which regulates the synthesis of many virulence factors in the gene cluster). The p60 mutants form long cell chains (also designated R forms), with unseparated septae between the individual bacterial cells, which disaggregate to normal-sized single bacteria upon treatment with partially purified p60. R-mutant forms were reported to be avirulent as they were unable to invade phagocytic 3T6 mouse fibroblast cells (5, 32). These researchers showed, however, that these R-mutant forms were still capable of adhering to and invading epithelial human colon carcinoma cells (CaCo-2), albeit at a reduced level of invasiveness (5). As spontaneously occurring mutants of *L. monocytogenes* with R-form cell characteristics were isolated previously at a relatively high frequency (1 in 10,000 colonies) (32), and were also shown to emerge under conditions of severe osmotic (29) and heat stress (46), the potential pathogenicity of ingested R-form *L. monocytogenes* in vulnerable groups remains unanswered. In the present study, the reversion rate from R form to normal-sized single bacteria was shown to be approximately 3 in 500 colonies (data not shown) (46).

In view of the fact that many foods are subject to mild heat treatments followed by lengthy periods of refrigerated storage, e.g., sous-vide (19), greater research is needed to determine the pathogenicity of long cell chain forms of *L. monocytogenes*, their frequency of occurrence in foods, and the relevance of survivor curves (particularly TDT curves with tail sections) in food systems. The D value concept, which assumes a linear response between the log number of cell survivors and heating time, accurately described only some of the data presented. More importantly, D values calculated from linear sections of the TDT curve, and not from the entire curve, could lead to an underestimation of the time and temperature required to achieve the desired level of cell destruction. Therefore, the end point method may be the best approach for determining mi-

crobial thermotolerance as it takes both shoulders and tails into account.

ACKNOWLEDGMENT

We thank the Ministry of Agriculture, Fisheries and Food (MAFF) for funding this research.

REFERENCES

1. **Argüelles, J. C.** 1997. Thermotolerance and trehalose accumulation induced by heat shock in yeast cells of *Candida albicans*. FEMS Microbiol. Lett. **146:**65–71.
2. **Beckers, H. J., P. S. S. Soentoro, and E. H. M. Delfgou-van Asch.** 1987. The occurrence of *Listeria monocytogenes* in soft cheeses and raw milk and its resistance to heat. Int. J. Food Microbiol. **4:**249–256.
3. **Bradshaw, J. G., J. T. Peeler, J. J. Corwin, J. M. Hunt, and R. M. Twedt.** 1987. Thermal resistance of *Listeria monocytogenes* in dairy products. J. Food Prot. **50:**54–544,556.
4. **Bradshaw, J. G., J. T. Peeler, J. J. Corwin, J. M. Hunt, J. T. Tierney, E. P. Larkin, and R. M. Twedt.** 1985. Thermal resistance of *Listeria monocytogenes* in milk. J. Food Prot. **48:**743–745.
5. **Bubert, A., M. Kuhn, W. Goebel, and S. Kohler.** 1992. Structural and functional properties of the p60 proteins from different *Listeria* species. J. Bacteriol. **174:**8166–8171.
6. **Bunning, V. K., C. W. Donnelly, J. T. Peeler, E. H. Briggs, J. G. Bradshaw, R. G. Crawford, C. M. Beliveau, and J. T. Tierney.** 1988. Thermal inactivation of *Listeria monocytogenes* within bovine milk phagocytes. Appl. Environ. Microbiol. **54:**364–370.
7. **Bunning, V. K., R. G. Crawford, J. G. Bradshaw, J. T. Peeler, J. T. Tierney, and R. M. Twedt.** 1986. Thermal resistance of intracellular *Listeria monocytogenes* cells suspended in raw bovine milk. Appl. Environ. Microbiol. **52:** 1398–1402.
8. **Crawford, R. G., C. M. Beliveau, J. T. Peeler, C. W. Donnelly, and V. K. Bunning.** 1989. Comparative recovery of uninjured and heat-injured *Listeria monocytogenes* cells from bovine milk. Appl. Environ. Microbiol. **55:**1490–1494.
9. **Dallmier, A. W., and S. E. Martin.** 1988. Catalase and superoxide dismutase activities after heat injury of *Listeria monocytogenes*. Appl. Environ. Microbiol. **54:**581–582.
10. **Donker-Voet, J.** 1963. My view of the epidemiology of *Listeria* infections, p. 133–139. *In* M. L. Gray (ed.), Second symposium on listeric infection. Montana State College, Bozeman.
11. **Donnelly, C. W.** 1994. *Listeria monocytogenes*, p. 215–251. *In* Y. H. Hui, J. R. Gorham, K. D. Murrell and D. O. Cliver (ed.). Foodborne disease handbook. Diseases caused by bacteria. Marcel Dekker, Inc., New York, N.Y.
12. **Donnelly, C. W., and E. H. Briggs.** 1986. Psychrotrophic growth and thermal inactivation of *Listeria monocytogenes* as a function of milk composition. J. Food Prot. **49:**994–998, 1002.
13. **Donnelly, C. W., E. H. Briggs, and L. S. Donnelly.** 1987. Comparison of heat resistance of *Listeria monocytogenes* in milk as determined by two methods. J. Food Prot. **50:**14–17, 20.
14. **Doyle, M. P., K. A. Glass, J. T. Berry, G. A. Garcia, D. J. Pollard, and R. D. Schultz.** 1987. Survival of *Listeria monocytogenes* in milk during high-temperature, short-time pasteurization. Appl. Environ. Microbiol. **53:**1433–1438.
15. **Elliker, P. R., and W. C. Frazier.** 1938. Influence of time and temperature of incubation on heat resistance of *Escherichia coli*. J. Bacteriol. **36:**83–98.
16. **Fain, A. R., J. E. Line, A. B. Moran, L. M. Martin, R. V. Lechowich, J. M. Carosella, and W. L. Brown.** 1991. Lethality of heat to *Listeria monocytogenes* Scott A: D-value and Z-value determinations in ground beef and turkey. J. Food Prot. **54:**756–761.
17. **Farber, J. M., and B. E. Brown.** 1990. Effect of prior heat shock on heat resistance of *Listeria monocytogenes* in meat. Appl. Environ. Microbiol. **56:** 1584–1587.
18. **Farber, J. M., and F. Pagotto.** 1992. The effect of acid shock on the resistance of *Listeria monocytogenes*. Lett. Appl. Microbiol. **15:**197–201.
19. **Farber, J. M., and P. I. Peterkin.** 1991. *Listeria monocytogenes*, a food-borne pathogen. Microbiol. Rev. **55:**476–511.
20. **Fedio, W. M., and H. Jackson.** 1989. Effect of tempering on the heat resistance of *Listeria monocytogenes*. Lett. Appl. Microbiol. **9:**157–160.
21. **Flemming, D. W., S. L. Cochi, K. L. MacDonald, J. Brondum, P. S. Hayes, B. D. Plikaytis, M. B. Holmes, A. Audurier, C. V. Broome, and A. L. Reingold.** 1985. Pasteurized milk as a vehicle of infection in an outbreak of listeriosis. N. Engl. J. Med. **312:**404–407.
22. **Gill, C. O., and M. P. Reichel.** 1989. Growth of the acid-tolerant pathogens *Yersinia enterocolitica*, *Aeromonas hydrophilia* and *Listeria monocytogenes* on high-pH beef packaged under vacuum or carbon dioxide. Food Microbiol. **6:**223–230.
23. **Golden, D. A., L. R. Beuchat, and R. E. Brackett.** 1988. Inactivation and injury of *Listeria monocytogenes* as affected by heating and freezing. Food Microbiol. **5:**17–23.
24. **Hansen, N. H., and H. Riemann.** 1963. Factors affecting the heat resistance of nonsporing organisms. J. Appl. Bacteriol. **26:**314–333.
25. **Jacquet, C., B. Catimel, R. Brosch, C. Buchrieser, P. Dehaumont, V. Goulet, A. Lepoutre, P. Veit, and J. Rocourt.** 1995. Investigations related to the epidemic strain involved in the French listeriosis outbreak in 1992. Appl. Environ. Microbiol. **61:**2242–2246.
26. **James, S. M., S. L. Fannin, B. A. Agree, B. Hall, E. Parker, J. Vogt, G. Run, J. Williams, L. Lieb, C. Salminen, T. Prendergast, S. B. Werner, and J. Chin.** 1985. Listeriosis outbreak associated with Mexican-style cheese—California. Morbid. Mortal. Weekly Rep. **34:**357–359.
27. **Jenkins, D. E., J. E. Schultz, and A. Martin.** 1988. Starvation-induced cross protection against heat or H_2O_2 challenge in *Escherichia coli*. J. Bacteriol. **170:**3910–3914.
28. **Jørgensen, F., B. Panaretou, P. J. Stephens, and S. Knøchel.** 1996. Effect of pre- and post-heat shock temperature on the persistence of thermotolerance and heat-shock induced proteins in *Listeria monocytogenes*. J. Appl. Bacteriol. **80:**216–224.
29. **Jørgensen, F., P. J. Stephens, and S. Knøochel.** 1995. The effect of osmotic shock and subsequent adaptation on the thermotolerance and cell morphology of *Listeria monocytogenes*. J. Appl. Bacteriol. **79:**274–281.
30. **King, A. D., H. G. Bayne, and G. Alderton.** 1979. Nonlogarithmic death rate calculations for *Byssochlamys fulva* and other microorganisms. Appl. Environ. Microbiol. **37:**596–600.
31. **Knabel, S. J., H. W. Walker, P. A. Hartman, and A. F. Mendonca.** 1990. Effects of growth temperature and strictly anaerobic recovery on the survival of *Listeria monocytogenes* during pasteurization. Appl. Environ. Microbiol. **56:**370–376.
32. **Kuhn, M., and E. Goebel.** 1989. Identification of an extracellular protein of *Listeria monocytogenes* possibly involved in intracellular uptake by mammalian cells. Infect. Immun. **57:**55–61.
33. **Lindquist, S.** 1986. The heat shock-response. Annu. Rev. Biochem. **55:**1151–1191.
34. **Linton, R. H., J. B. Webster, M. D. Pierson, J. R. Bishop, and C. R. Hackney.** 1992. The effect of sublethal heat shock and growth atmosphere on the heat resistance of *Listeria monocytogenes* Scott A. J. Food Prot. **55:**84–87.
35. **Linton, R. H., M. D. Pierson, and J. R. Bishop.** 1990. Increase in heat resistance of *Listeria monocytogenes* Scott A by sublethal heat shock. J. Food Prot. **53:**924–927.
36. **Lovett, J., D. W. Francis, and J. M. Hunt.** 1987. *Listeria monocytogenes* in raw milk: detection, incidence, and pathogenicity. J. Food Prot. **50:**188–192.
37. **Mackey, B. M., and C. Derrick.** 1990. Heat shock synthesis and thermotolerance in *Salmonella typhimurium*. J. Appl. Bacteriol. **69:**373–383.
38. **Mackey, B. M., and C. M. Derrick.** 1986. Elevation of the heat resistance of *Salmonella typhimurium* by sublethal heat shock. J. Appl. Bacteriol. **61:**389–393.
39. **Mackey, B. M., and C. M. Derrick.** 1987. Changes in the heat resistance of *Salmonella typhimurium* during heating at rising temperatures. Lett. Appl. Microbiol. **4:**13–16.
40. **Mackey, B. M., C. Pritchet, A. Norris, and G. C. Mead.** 1990. Heat resistance of *Listeria*: strain differences and effects of meat type and curing salts. Lett. Appl. Microbiol. **10:**251–255.
41. **McCallum, K. L., and W. E. Inniss.** 1990. Thermotolerance, cell filamentation, and induced protein synthesis in psychrophilic and psychrotrophic bacteria. Arch. Microbiol. **153:**585–590.
42. **Moats, W. A., R. Dabbah, and V. M. Edwards.** 1971. Interpretation of nonlogarithmic curves of heated bacteria. J. Food Sci. **36:**526.
43. **Ng, H., H. G. Bayne, and J. A. Garibaldi.** 1969. Heat resistance of *Salmonella*: the uniqueness of *Salmonella senftenberg* 775W. Appl. Microbiol. **17:**78–82.
44. **Pagán, R., S. Condon, and F. J. Sala.** 1997. Effects of several factors on the heat-shock induced thermotolerance of *Listeria monocytogenes*. Appl. Environ. Microbiol. **63:**3225–3232.
45. **Parsell, D. A., and S. Lindquist.** 1993. The function of heat-shock proteins in stress tolerance: degradation and reactivation of damaged proteins. Annu. Rev. Genet. **27:**437–496.
46. **Rowan, N. J.** 1996. Studies on the growth, survival, interaction and detection of potentially pathogenic *Listeria* and *Bacillus* species in infant milk formulae. Ph.D. thesis. University of Strathclyde, Glasgow, United Kingdom.
47. **Smith, J. L., and B. S. Marmer.** 1991. Temperature shift effects on injury and death in *Listeria monocytogenes* Scott A. J. Food Saf. **11:**73–80.
48. **Smith, J. L., B. S. Marmer, and R. C. Benedict.** 1991. Influence of growth temperature on injury and death of *Listeria monocytogenes* Scott A during a mild heat treatment. J. Food Prot. **54:**166–169.
49. **Sörqvist, S.** 1994. Heat resistance of different serovars of *Listeria monocytogenes*. J. Appl. Bacteriol. **56:**383–368.
50. **Sörqvist, S.** 1993. Heat resistance of *Listeria monocytogenes* by two recovery media used with and without cold pre-incubation. J. Appl. Bacteriol. **74:**428–432.
51. **Stephens, P. J., M. B. Cole, and M. V. Jones.** 1994. Effect of heating rate on the thermal inactivation of *Listeria monocytogenes*. J. Appl. Bacteriol. **77:** 702–708.
52. **Tomlins, R. I., and Z. J. Ordal.** 1976. Thermal injury and inactivation in vegetative bacteria, p. 153–191. *In* F. A. Skinner and W. B. Hugo (ed.), Inhibition and inactivation of vegetative microbes. Academic Press, London, United Kingdom.
53. **White, H. R.** 1953. The heat resistance of *Streptococcus faecalis*. J. Gen. Microbiol. **8:**27–37.

Trinity College Library Dublin

The University of Dublin

Trinity College Inter-Library Loans Copyright Regulations

Copies of articles ordered through Trinity College Inter-Library Loans and utilized by users are subject to copyright regulations. By accepting material, the user commits to observing these regulations, most notably that the copies are for personal use and not to be disclosed to third parties.

In the case of electronically delivered material, the copy may only be printed once and the file must be permanently deleted afterwards.

Trinity College Library Inter-Library Loans

College Street Dublin 2 Ireland
Telephone (+353 1) 896 1654 Fax (+353 1) 896 3524
e-mail loans@tcd.ie

Food Microbiology 30 (2012) 330–339

Contents lists available at SciVerse ScienceDirect

Food Microbiology

journal homepage: www.elsevier.com/locate/fm

Studies on the pathogenesis and survival of different culture forms of *Listeria monocytogenes* to pulsed UV-light irradiation after exposure to mild-food processing stresses

Derek Bradley [a], Brian McNeil [b], John G. Laffey [c], Neil J. Rowan [a,*]

[a] Department of Nursing and Health Science, Athlone Institute of Technology, Dublin Road, Athlone, Co. Westmeath, Ireland
[b] Strathclyde Institute of Biomedical and Pharmaceutical Sciences, Strathclyde University, Glasgow, Scotland, UK
[c] Department of Anaesthesia and Intensive Care Medicine, School of Medicine, National University of Ireland Galway, Ireland

ARTICLE INFO

Article history:
Received 23 August 2011
Received in revised form
27 December 2011
Accepted 28 December 2011
Available online 3 January 2012

Keywords:
Listeria monocytogenes
Morphotypes
Food-related stresses
Invasiveness
Pulsed UV light

ABSTRACT

The effects of mild conventional food-processing conditions on *Listeria monocytogenes* survival to pulsed UV (PUV) irradiation and virulence-associated characteristics were investigated. Specifically, this study describes the inability of 10 strains representative of 3 different culture forms or morphotypes of *L. monocytogenes* to adapt to normally lethal levels of PUV-irradiation after exposure to sub-lethal concentrations of salt (7.5% (w/v) NaCl for 1 h), acid (pH 5.5 for 1 h), heating (48 °C for 1 h) or PUV (UV dose 0.08 μJ/cm^2). Findings showed that the order of increasing sensitivity of *L. monocytogenes* of non-adapted and stressed morphotypes to low pH (pH 3.5 for 5 h, adjusted with lactic), high salt (17.5% w/v NaCl for 5 h), heating (60 °C for 1 h) and PUV-irradiation (100 pulses at 7.2 J and 12.8 J, equivalent to UV doses of 2.7 and 8.4 μJ/cm^2 respectively) was typical wild-type smooth (S/WT), atypical filamentous rough (FR) and atypical multiple-cell-chain (MCR) variants. Exposure of *L. monocytogenes* cells to sub-lethal acid, salt or heating conditions resulted in similar or increased susceptibility to PUV treatments. Only prior exposure to mild heat stressing significantly enhanced invasion of Caco-2 cells, whereas subjection of *L. monocytogenes* cells to combined sub-lethal salt, acid and heating conditions produced the greatest reduction in invasiveness. Implications of these findings are discussed. This constitutes the first study to show that pre-exposure to mild conventional food-processing stresses enhances sensitivity of different culture morphotypes of *L. monocytogenes* to PUV, which is growing in popularity as an alternative or complementary approach for decontamination in the food environment.

1. Introduction

The opportunistic pathogen *Listeria monocytogenes* causes listeriosis, a serious infection with high hosptialization and mortality rates, with consumption of contaminated food principle mode of its transmission to humans (Tompkin, 2002). Increased ready-to-eat (RTE) food consumption makes *L. monocytogenes* a serious threat since the pathogen is able to survive a wide range of environmental stress conditions, such as low temperature, acidic pH, and high osmolarity (Sue et al., 2004). According to the European Centre for Disease Control and Prevention, listeriosis was the fifth most common zoonotic infection in Europe in 2006 (EFSA-EDSC, 2007), while it is estimated to account for approximately 28% of the deaths resulting from food-borne illnesses in the UK (cited in Chorianopoulus et al., 2011). Because *L. monocytogenes* is ubiquitous it may be introduced into food-processing plants through many different routes. *L. monocytogenes* has been shown to colonize processing environments and to contaminate products during processing. Certain strains may become persistent in a plant and cause continuous contamination (Lünden et al., 2008; Van Boeijen et al., 2008; Van Boeijen et al., 2010). Although the origin of persistence can be different, overall persisters can have specific qualities, such as acid and heat tolerance and adherence to surfaces, contributing to the establishment of house strains. A number of studies have shown persistence of *L. monocytogenes* in various food-processing plants (Lünden et al., 2008). Some of these persistent strains dominated and persisted in a plant or production line for years and caused food contamination and human disease.

Adaptation to hostile environmental conditions has been demonstrated to alter cellular physiology of a number of food-borne persister pathogens such that they become resistant to further extreme food-processing stresses (Hill et al., 2002; Chorianopoulus

* Corresponding author.
E-mail address: nrowan@ait.ie (N.J. Rowan).

0740-0020/$ – see front matter © 2011 Elsevier Ltd. All rights reserved.
doi:10.1016/j.fm.2011.12.024

et al., 2011). Our group has demonstrated that exposure of microbial pathogens, including *L. monocytogenes*, to a plethora of sub-lethal stressors may alter their cellular structure and appearance producing atypical rough cultures or morphotypes that often exhibit greater tolerance to extreme stresses compared to parent wild-type cells (Rowan, 1999). Characterization of molecular determinants involved in conversion to the atypical culture variant forms or morphotypes has been previously described by a number of researchers (Kuhn and Goebel, 1989; Monk et al., 2004), with specific involvement of a peptidoglycan hydrolase CwhA (formerly termed invasion-associated protein or p60) in the formation of the rough colony appearance. Regarding *L. monocytogenes*, one of the most important and intensively investigated adaptive responses is to acid stress, the so-called acid tolerance response (ATR) (Gahan et al., 1996; Lou and Yousef, 1997; Chorianopoulus et al., 2011). The ATR normally results from pre-exposure of microbial cells to mild-acid conditions (pH 5.0–6.0) and besides enabling augmented tolerance to extreme acid challenges (Koutsoumanis and Sofos, 2004), it has also been found to offer *L. monocytogenes* cross-protection against heat, ethanol, oxidative and osmotic stresses, as well as against the bacteriocin nisin and other ionophores (Lou and Yousef, 1997; Rowan, 1999; Chorianopoulus et al., 2011). Of note, heterogeneity in a microbial population with an effect on resistance was also recently observed in the use of the high hydrostatic pressure that is an emerging non-thermal food-processing technique (Van Boeijen et al., 2010). The advantages of developing the latter and other non-thermal processing technologies for food applications include the potential retention of fresh-food characteristics and organoleptic qualities such as flavour, aroma and texture. However, as exposure to mild conventional food-processing conditions represent extensions of the natural variation that a microorganism may also encounter during infection, it is not surprising to learn that many bacteria capable of persistence (including *L. monocytogenes*) are capable of mounting adaptive responses to these applied sub-lethal stress conditions (Rowan, 1999; Hill et al., 2002). With current consumer preferences for foods that avoid the extreme use of a single preservation hurdle, there has been an awakening towards studies that focus on stress-adaptation and cross-protection to multiple stresses, particularly in minimally processed foods. The "stress-hardening phenomenon" has significant food-safety implications, especially in situations where the food industry explores levels of lethality that are close to the boundaries of microbial control. The ability of *L. monocytogenes* to alter morphological appearance together with its peculiar ability to adapt to hostile environments (Lou and Yousef, 1997) and to persist on food-contact surfaces (Chorianopoulus et al., 2011) are of particular interest for food processors, since these microbial attributes may pose serious risks to food safety.

Pulsed light (PUV) is a non-thermal approach that has received considerable attention as a strategy for decontaminating food, packaging, water and air (Gómez-López et al., 2007). This approach kills microorganisms by using ultra-short duration pulses of an intense broadband emission spectrum that is rich in UV-C germicidal light (200–280 nm band). PUV is produced using techniques that multiplies power manifold by storing electricity in a capacitor over relatively long times (fractions of a second) and releasing it in a short time (millionths or thousandths of a second) using sophisticated pulse compression techniques (Gómez-López et al., 2007). The emitted flash has a high peak power and usually consists of wavelengths from 200 to 1100 nm broad spectrum light enriched with shorter germicidal wavelengths (Gómez-López et al., 2007). Thus, significant microbial reductions in ultra-short treatment times, the limited energy cost of PUV, the lack of residual compounds, and its great flexibility are some of the major benefits of this technique (Oms-Oliu et al., 2010). Seminal developments pertaining to PUV technologies has been the subject of recent reviews (Gómez-López et al., 2007; Oms-Oliu et al., 2010), with emphasis strongly placed on decontamination efficacy for food and water applications that aptly reflects the focus of research in this field of study to date. Given that *L. monocytogenes* may encounter various hurdles (stresses) in food-processing environments (e.g. acidity, salinity, sanitizers etc.), it is possible that prior exposure to these inimical stresses may alter the resistance of *L. monocytogenes* to normally lethal levels of pulsed UV light. Consequently, the objectives of the present work were to: (i) investigate the relationship (if any) between prior exposure to sub-lethal food-related stresses (acid, salt and heating) and subsequent tolerance to extreme levels of the same for 3 different morphotypes of *L. monocytogenes*, (ii) determine if prior exposure to these conventional food-processing stresses or/and to mild-PUV conditions affects resistance of these *L. monocytogenes* morphotypes to normally lethal levels of high-intensity pulsed UV irradiation, (iii) determine that relationship (if any) between prior exposure of *L. monocytogenes* to sub-lethal salt, acid, heating and PUV conditions (stresses applied singly and combined) on their subsequent adherence and invasiveness to human Caco-2 cells. To the best of our knowledge, no published study to date has investigated the relationship between exposure to mild-food processing stress conditions and adaptive bacterial tolerance to normally lethal levels of pulsed UV light.

2. Materials and methods

2.1. Bacterial strains used and preparation of inocula

The *Listeria* strains used in the study were, if not otherwise indicated, derived or obtained from the Special *Listeria* Culture Collection [SLCC] of H. P. R. Seeliger, Würzburg, Germany, from C. Hill, University College Cork (UCC), Ireland, or from the National Collection of Type Cultures [NCTC], Public Health Laboratory Service [PHLS], Central Public Health Laboratory, Colindale, UK (Table 1). Strains exhibiting typical wild-type coccobacilli appearance were designated S/WT (**s**mooth entire colony morphotype); strains exhibiting atypical long filaments separated by one or two septa were designated FR (**f**ilamentous **r**ough colony morphotype), while strains exhibiting atypical long cell chains with multiple septa were designated MCR (**m**ultiple coccobacilli cells in long **c**hain arrangement producing **r**ough colony morphotype). The clinical rough strains FR2 and FR3 were blood-culture isolates from a 76 and 72 year-old female and male respectively, both individuals had sepsis and pyrexia. Strains of *L. monocytogenes* were grown separately to single colonies on *Listeria* Selective agar (LSA, Oxiod, Basingstoke, UK) agar respectively at 37 °C for 48 h aerobically. All test strains were maintained in Microbank storage vials (Cruinn Diagnostic, Ireland) at −80 °C in bead vials and were resuscitated by adding one bead in 10 ml of Tryptone Soy Broth (TSB, Difco Laboratories, Detroit, Mich.) and incubating at 30 °C for 24 h (preculture).

2.2. ELISA for the detection of CwhA protein

Detection of CwhA protein (formerly p60) in all test *L. monocytogenes* strains occurred using indirect ELISA involved the addition of 100 μl of cell-free supernatant per well of microtitre plates (supernatant from an overnight culture and harvested by centrifugation) and incubation for 2 h at 37 °C. Coated proteins were washed three times with wash buffer (PBS containing 0.1% v/v Tween 20) and the *L. monocytogenes*-specific monoclonal antibody CwhA-mAb K3A7 was added. This mAb was generated against the *L. monocytogenes*-specific epitope, peptide D, of the Cwha protein, which has been described previously (Bubert et al., 1997). Generation

Table 1
Listeria monocytogenes strains used and their characteristic morphological and physiological properties identified in this study.

Strain	Serotype	Reference Strain No.	Origin	Tumbling Motility	Cell Morphology and Physiological Properties			Colony Area (μm^2)[f]	Titre by ELISA (A_{492}) with anti-CwhA MAb[h]
					Cell form	Cell Type Designation	Cell Length (μm)[e]		
S1/WT	4b	NCTC 11994	Adult meningitis	+[g]	Single, paired cells	Wild-type smooth	3.0 ± 1.0 A	$(1.9 \pm 0.6) \times 10^5$ A	0.61 ± 0.05 B
S2/WT	4b	NCTC 9863	Infantile meningitis	+	Single, paired cells	Wild-type smooth	3.7 ± 1.2 A	$(2.3 \pm 0.8) \times 10^5$ A	0.53 ± 0.09 B
S3/WT[a]	1/2c	LO28	Begley et al. (2002)	+	Single, paired cells	Wild-type smooth	3.3 ± 1.0 A	$(2.7 \pm 0.5) \times 10^5$ A	0.57 ± 0.06 B
S4/WT	1/2a	NCTC 10357	Type strain (rabbit)	+	Single, paired cells	Wild-type smooth	3.3 ± 1.2 A	$(1.7 \pm 0.3) \times 10^5$ A	0.55 ± 0.08 B
MCR1[b]	1/2a	SLCC 5764	Kathariou et al. (1987)	+	Long cell chains	MCR variant	72.3 ± 20.9 B	$(1.9 \pm 0.7) \times 10^6$ B	0.26 ± 0.08 A
MCR2	1/2a		Kathariou et al. (1987)	+	Long cell chains	MCR variant	80.1 ± 27.4 B	$(1.6 \pm 0.9) \times 10^6$ B	0.28 ± 0.03 A
MCR3	1/2a	SL 5779	J. Potel (see text below)[d]	+	Long cell chains	MCR variant	81.3 ± 19.0 B	$(2.1 \pm 0.8) \times 10^6$ B	0.23 ± 0.03 A
FR1	4b		Derived from NCTC 4885[c]	−	Long filaments	FR variant	75.3 ± 37.9 B	$(9.3 \pm 0.6) \times 10^6$ C	0.73 ± 0.06 C
FR2	*	L6705	Dried Custard powder	−	Long filaments	FR variant	49.9 ± 34.1 B	$(9.3 \pm 0.6) \times 10^6$ C	0.75 ± 0.06 C
FR3	*	L1342	Blood culture	−	Long filaments	FR variant	73.5 ± 18.3 B	$(9.5 \pm 1.1) \times 10^5$ C	0.65 ± 0.04 B

*Autoagglutinable cultures (and therefore not serotypable), were kindly provided by J. McLauchlin, PHLS, Food Safety Laboratory, Colindale, UK.
[a] Kindly provided by Colin Hill, UCC, Ireland.
[b] Derived from *L. monocytogenes* Mackaness (SLCC 5764).
[c] Kindly provided by J. Potel (via A. Bubert), Institute for Medical Microbiology, Medical Academy, Hannover, Germany.
[d] Derived from *L. monocytogenes* NCTC 4885 after 5 min exposure to high-intensity, pulsed-plasma, gas-discharge (PPGD) stressing conditions (Rowan et al., 2007). Note, NCTC denotes the National Collection for Typed Cultures, Colindale, London, UK, which was original source for strain.
[e] Mean length (μm) from ten measurements (±standard deviation). Single and paired cells were measured and averaged for the smooth-cell forms. Values in the same column followed by the same letter did not differ at the $p \leq 0.05$ level, while values with different letters differed at the $p < 0.05$ level.
[f] Mean of area measurements for ten colonies grown for 48 h on LSA plates.
[g] + indicates a positive motility test for *L monocytogenes.*
[h] OD_{492} values greater than 0.1 were considered a positive result. BHI broth controls gave a value of 0.004 ± 0.01.

of K3A7 was achieved by using standard protocols (Kuhn and Goebel, 1989). The anti-CwhA-mAb was prepared as a tissue-culture supernatant diluted 1/200 (v/v) in wash buffer and incubated for 1 h at room temperature. The microtitre wells were washed three times with wash buffer and sheep anti-mouse horseradish peroxidase conjugate (Sigma) was added at 100 µl well^{-1} at a dilution of 1/1000 in wash buffer and incubated for 1 h at room temperature. Excess conjugate was washed five times with wash buffer and the substrate SIGMA FAST™ OPD tablets (Sigma) were added at 100 µl well^{-1} with 0.5 h incubation at room temperature. The A_{492nm} was measured after the addition of 50 µl well^{-1} 3 M H_2SO_4.

2.3. Cell or filament length and colony appearance determination

Overnight cultures of all *L. monocytogenes* strains described in Table 1 were separately incubated in brain heart infusion broth at 37 °C with aeration. At various time intervals, the lengths of the cells were determined using image analysis (Nikon Optiphot-2 microscope that was connected to a Solitaire 512 Image Analyzer, Seescan Plc.) as per methods described previously (Jones et al., 1994). Ten cells were measured per sample. Overnight cultures were also grown at 37 °C on *Listeria* selective agar (LSA; Oxford formulation; Oxoid) to investigate differences in colony appearance. The area (in square micrometers) of ten colonies per sample were measured with the image analysis system mentioned above.

2.4. Electron microscopy

Strains representative of the 3 different morphotypes of *L. monocytogenes* were examined by transmission electron microscopy as per methods described by Rowan et al. (2001) with modifications. Cells were grown to their stationary phase, washed twice with PBS and resuspended in sterile-distilled water before application to formvar-coated grids. After the grid was dried, one drop of a solution containing 3% v/v tungstophosphoric acid and 0.3% v/v sucrose (pH 6.8–7.4) was added. The solution was removed after 30–60 s, and the grid was dried and examined on a Zeiss 902 transmission electron microscope.

2.5. Assays for induction of prior heating, acid, osmotic stress

The procedures of Lou and Yousef (1997) and Buchanan and Edelson (1996) were followed to prepare cells under conditions of mild acid, salt or heating, with modifications. Briefly, 10 µl of bacterial preculture was inoculated into 100 ml of Tryptone Soy broth containing 1% v/v glucose (TSB + G) or TSB without any glucose (TSB − G), and grown in an orbital shaker at 125 rpm for 24 h at 37 °C where the pH of cultures following incubation in TSB + G and TSB − G were *ca.* 4.7 and *ca.* 6.7, respectively. Cells from final working cultures where harvested by centrifugation (5000 × *g*, 10 min, at room temperature (RT)), washed twice with 0.1 M phosphate buffered saline (PBS) and finally resuspended in PBS where the optical density was adjusted at 540 nm to 2.0 (*ca.* 10^9 CFU ml^{-1}) by spectrophotometric (Model UV-120-02 instrument, Shimadzu Corp., Kyoto, Japan) determination. *L. monocytogenes* strains grown in TSB − G were subjected to short sub-lethal acid and salt stress conditions by initially washing 10 ml of working cultures by centrifugation as described earlier followed by resuspension directly in 10 ml of fresh TSB − G for 1 h by centrifugation where the salt content was adjusted to 7.5% w/v NaCl or the pH was adjusted to 5.5. Following NaCl addition or/and pH adjustment, these 10 ml mildly-stressed working cultures were subsequently resuspended in 10 ml fresh TSB − G containing high salt (17.5% NaCl) or low acid (pH 3.5, adjusted with lactic) for 5 h (extreme acid and salt challenge). Lactic acid was used as acidulant for pH adjustment in the pH adaptation (pH 5.5) and for the challenge medium (pH 3.5). For mild-heat stress studies, 10 ml of non-adapted working TSB − G cultures were heated at 48 °C for 1 h in a circulating constant temperature waterbath (Model HE30, Grant Instruments Ltd, Uk) equipped with a thermoregulator capable of maintaining temperature to within ±0.05 °C (model TE-8A, Techne Ltd, Cambridge, UK), followed by a 2 h incubation at RT with subsequent exposure to 60 °C for 1 h (extreme heat challenge) as per method described previously by Rowan and Anderson (1998). Samples were treated in triplicate and were spread, pour and spiral plated on Tryptone Soy Agar supplemented with 6% yeast extract (TSYEA) followed by incubation for 24 and 48 h at 37 °C before enumeration. Survivors were recorded as $\log_{10}$ colony forming units (CFU) per ml.

2.6. PUV treatment of test cultures

A bench-top pulsed power source (PUV-1, Samtech Ltd., Glasgow) was used to power a low-pressure (60 kPa) xenon-filled flashlamp (Heraeus Noblelight XAP type NL4006 series constructed from a clear UV transparent quartz tube), that produced a high-intensity diverging beam of polychromatic pulsed light, was used in this study as per method described by Farrell et al. (2010) with modifications. The pulsed light has a broadband emission spectrum extending from the UV to the infrared region with a rich UV content and its intensity also depends on the level of the voltage applied. The fabricant stated that the discharge tube represents a line-source of limited length and consequently the light formed an elliptical, equi-intensity profile over the sample plane eliminating shading effects. This resulted in a ~30% variation in luminous intensity between the centre and the edge of the sample. The light source has an automatic frequency-control function that allows it to operate at one pulse per second that was used throughout this study. Light exposure was homogenous as the xenon lamp measuring 9 cm × 0.75 cm was longer than the 8.5 cm diameter polystyrene Petri dishes used in the tests which were placed directly below the lamp. For standard treatments, the light source was mounted at 8 cm above the treatment area that was designed specifically to accommodate a standard Petri dish containing 10 ml of sample and was set as the minimum or lower threshold distance by the fabricant. This was to ensure that full coverage of the Petri dish occurred and to eliminate possible shading effects. The optical density of test samples was then spectrophotometrically adjusted at 540 nm to 2 units (*ca.* 10^9 CFU/ml) as described earlier. Standard PUV treatments involved spread-plating 0.1 ml aliquots of non-adapted and prior-acid, osmotic and heat-stressed working cultures on TSYEA and LSA plates followed by application of a pre-determined number of pulses ranging from 0 (untreated control) to 100 pulses using lamp discharge energies of 7.2 J and 12.8 J at a distance of 8 cm from the light source. Mild-PUV treated cultures were exposed to 3 pulses at 7.2 J (UV dose 0.08 μJ/cm^2) followed by 2 h incubation under conditions of light and dark repair before exposure to more extreme PUV conditions. This low level PUV regime reduced a pre-determined population of *L. monocytogenes* by less than 0.5 log CFU/ml. Measurement of corresponding fluence rate (or 'irradiance') (Joule/cm^2) at each applied pulsed was also determined using chemical actinometry as per Farrell et al. (2011), as the non-continuous emitted spectrum did not facilitate use of a calibrated radiometer. The lethality of the PUV process under varying experimental conditions was determined by treating pre-determined numbers of test cultures that were inoculated on agar surfaces, and by enumerating survivors post treatments (expressed in terms of $\log_{10}$ colony forming units or CFU cm^{-2}). Subtraction of the logarithm of the count after different combinations of pulsing, discharge energies and distances from light source, from the logarithm of the count before processing provided a measure of process lethality. As it is not appropriate to determine log-linear death rate kinetic data from PUV-treated test bacteria as a function of time (as total duration of treatment comprises the pulse-pause sequence as well as the actual duration of pulsing), inactivation plots were measured following a modified first order dependence formulae of Farrell et al. (2010): ($\log_{10}$ (N_p/N_0) = $-kp$, where k = rate constant). N_0 is the initial concentration of bacteria and N_p is the microbial concentration after applying a defined number of pulses (p) at discharge energy (J). This rate constant k defines the sensitivity of a microorganism to a defined PUV treatment and is unique to each microbial species; the higher the k value the more sensitive the test strain to the treatment process. The former approach was also employed to determine k values for all samples subjected to varying combinations of low acid, high salt, heating and PUV conditions so as to facilitate comparisons between samples for bacterial tolerance to each combination of applied stressors. All experiments were carried out in triplicate using same culture to avoid sample variability.

2.7. Tissue-culture invasion assay

Invasion assays using the tumor-derived Caco-2 human colorectal epithelial cell line (Cat no. 8601202, Health Protection Agency, Salisbury, UK; passage number 46) were performed as previously described (Rowan et al., 2000), with slight modifications. Briefly, Caco-2 monolayers were grown overnight in a 5% CO_2 atmosphere at 37 °C in D-MEM supplemented with 10% foetal calf serum (FCS, Gibco BRL) in 24-well culture tissue plates seeded with approximately 3 × 10^5 cells per well. Prior to invasion assays, monolayers were washed three times in D-MEM followed by the addition of 1 ml of D-MEM containing 10% FCS to each well. Bacterial cultures were resuspended in 1 ml of D-MEM to an optical density at 580 nm of 2.0 (model UV-120-02 spectrophotometer, Shimadzu Corp., Kyotoa, Japan). For adherence assays, triplicate monolayers were infected with 0.1 ml of bacteria culture followed by a 2-h incubation at 37 °C in a 5% CO_2 atmosphere. After incubation, nonadherent bacteria were removed by three washes with 3 ml of D-MEM. The tissue-culture cells were lysed with 1 ml of 1% Triton X-100 (v/v distilled water) for 5 min at 37 °C, followed by serial dilution in 0.9 ml of PBS, with subsequent enumeration by plating 0.1 ml of appropriate 10-fold dilutions on BHI agar. For invasion assays, 1-ml of fresh D-MEM containing 10% FCS and 100 μg/ml of gentamicin was added to the infected tissue-culture monolayers followed by a 2-h incubation at 37 °C. The tissue-culture cells were washed three times in 3 ml of D-MEM and were then lysed with 1 ml of 1% Triton X-100 (v/v distilled water) for 5 min at 37 °C. Invasion efficiency is reported as follows: (the number of bacteria recovered from each well following Caco-2 cell lysis divided by the number of bacteria that had been used for inoculation) × 100.

2.8. Statistical analysis

Analysis of variance – balanced model (Minitab software Release 14, Minitab Inc., State College, PA) was used to compare the effects of food-processing related stresses on microbial adaptation and tolerance. Experiments were replicated three times with duplicate treatments in each replication, and results are reported as means ± standard deviations. Significant differences were reported at 95% confidence intervals.

3. Results and discussion

3.1. Studies on morphological and physiological characteristics of different culture morphotypes of L. monocytogenes tested

All strains described in Table 1 were identified as *L monocytogenes* by establishing the characteristic morphological, physiological and biochemical properties associated with this pathogen. All cultures produced catalase, were CAMP test positive with *Staphylococcus aureus* and were identified as *L. monocytogenes* by use of API *Listeria* biochemical profiling. Confirmation of species identification occurred by analysis of culture supernatant for CwhA protein by indirect ELISA with an *L. monocytogenes*-specific anti-CwhA MAb (Table 1). The cell and colony appearances of all rough variants were shown to significantly differ from those of the wild-type *L. monocytogenes* strains, which had a typical smooth wild-type morphology (S/WT). Unlike the latter smooth strains,

whose cells have characteristic cocco-bacillus appearance (*ca.* 0.5 μm in diameter by 2 μm in length), cell types associated with the rough variants were shown to be atypically long. Some rough variants consisted of unseptated or paired filaments that measured up to 113 μm in length (designated FR variants), whereas others formed long chains that were up to 107 μm in length and that consisted of multiple cells of similar size (designated MCR variants) (Table 1). Rough variants isolated from clinical specimen or derived under conditions of stress produced by exposure to pulsed plasma gas discharge showed the FR filamentous phenotype. The mean cell lengths for the various culture variants of *L. monocytogenes* were shown to be 3.3 ± 1.1 (wild-type normal S type), 77.9 ± 22.4 (MCR variant) and 66.2 ± 30.1 (FR variant). MCR and FR variants were found to be incapable of characteristic tumbling motility and formed irregular or rough colonies that no longer produced a blue–green sheen upon oblique illumination. Image analysis data showed that irregular rough colonies consistently had different areas (in square micrometer) and appearances ($p \leq 0.05$) to that of smaller, wild-type S-form colonies after 48 h growth on LSA plates (Table 1). Indirect ELISA studies (Table 1) with an anti-CwhA MAb showed that these MCR variants secrete a considerably reduced amount of a peptidoglycan hydrolase protein. The addition of partially purified CwhA led to a decay of the cell chains to normal size within 3 h of treatment. Unlike MCR variants that secreted diminished levels of cell-free CwhA, indirect ELISA studies showed that FR variants produced wild-type or greater amounts of Cwha indicating the latter FR morphotypes were type II in nature (Table 1). The addition of partially purified CwhA from wild-type *L. monocytogenes* to FR variants did not decay the lengths of the filaments to the normal *Listeria* cell size.

Changes in bacterial colony morphology often accompany microbial adaptation to new environments and ecological niches (Monk et al., 2004). *L. monocytogenes* has also been reported to form atypical elongated (filamentous) cells when exposed to a range of adverse growth conditions, such as high concentrations of NaCl (8–9%) in the presence (Bereski et al., 2002) or absence of acid (Bereski et al., 2002; Isom et al., 1995; Jørgensen et al., 1995), increased CO_2 environments (Lie et al., 2003; Nilsson et al., 2000), high hydrostatic pressure (Ritz et al., 2001), osmotic stress (Jørgensen et al., 1995), alkaline stress (Giotis et al., 2007), above optimum growth temperature, i.e., 42.5 °C (Rowan and Anderson, 1998), and the presence of antimicrobial growth agents such as trimethorpim and co-trimoxazole (Minkowski et al., 2001). In the present study, conversion of S2/WT and S3/WT strains to the filamentous FR morphotype occurred under conditions of acid and heat stressing with wild-type levels of the peptidoglycan hydrolase Cwha detected. A number of earlier studies suggest that in some cases, removal of such deleterious stresses results in a slow return to normal wild-type cell forms within 24 h (Isom et al., 1995), suggesting that filamentation of *L. monocytogenes* may be an adaptive response to adverse growth conditions. Variant rough colony morphotypes were thought to occur spontaneously and irreversibly at low frequency during prolonged culture in the laboratory. Monk et al. (2004) had previously observed that chaining cells exhibited enhanced biofilm-forming capabilities, and therefore further studies investigating the relationship between susceptibility of planktonic versus biofilm morphotypes of *L. monocytogenes* to non-thermal processing technologies is also merited. The colonization of the murine gall bladder by *L. monocytogenes* also resulted in a change in cellular morphology (chaining), subsequently leading to the formation of biofilms within the gall bladder, which resembles a dynamic rather than static environment (Hardy et al., 2006). Apart from obvious physical differences, such as absence of blue–green sheen upon Henri oblique illumination and impaired cell separation that gave chaining cells without coordinated motility, the fermentative and biochemical profiles of rough and smooth colonies were considered identical (Gutekunst et al., 1992; Rowan et al., 2000; Monk et al., 2004). Characterization of molecular determinants involved in conversion to the filamentous FR colony variants has been previously described by a number of researchers (Kuhn and Goebel, 1989; Gutekunst et al., 1992; Monk et al., 2004), with specific involvement of a peptidoglycan hydrolase CwhA (formerly termed invasion-associated protein or p60; Pilgrim et al., 2003) in the formation of the rough colony morphotype. These so-called type 1 rough colony isolates showed reduced CwhA secretion plus decreased attachment and invasion of certain nonphagocytic cell lines (Gutekunst et al., 1992). The isolation of a filamentous rough colony variant (termed type II) showing wild-type levels of CwhA secretion and cellular invasion have also been previously described (Lenz and Portnoy, 2002). While the specific mechanisms governing these morphological changes still remain unclear (Gardan et al., 2003; Monk et al., 2004; Giotis et al., 2007), conversion to the atypical rough culture forms may result in failure to accurately detect and/or enumerate this enteropathogen from adverse conditions such as food preservation or inimical stresses associated with exposure to host immune system. Although FR variants have been isolated previously from clinical specimens and food samples, the multiple long cell chain form (MCR type) secreting reduced levels of CwhA has not.

Different culture variants of microbial pathogens, including *L. monocytogenes*, may arise from exposure to harsh growth conditions and may alter their morphological, physiological and virulence characteristics in order to protect itself from subsequent exposure to lethal levels of same or different stresses (Rowan, 1999; Leistner, 2000; Hardy et al., 2006). However, despite the growing number published work on the impact of food-processing stresses on the adaptive survival of *L. monocytogenes*, very little information currently exists on the susceptibility of non-adapted and mildly-stressed culture morphotypes of this pathogen to novel non-thermal food processing technologies or to conventional preservation techniques.

3.2. Relationship between exposure to prior food-related sub-lethal stressors and tolerance to normally lethal levels of the same stress

Findings showed a clear pattern where 3 culture morphotypes of *L. monocytogenes* tested demonstrated variable tolerance to normally lethal food-related stressors depending on type of prior-sub-lethal stress applied and the type of morphotype challenged. Fig. 1a shows that strains representative of the normal wild-type coccobacilli cells (designated S/WT) were shown to be significantly more tolerant to low acid conditions (pH 3.5 for 5 h) compared to similarly treated filamentous rough (FR) and multiple-cell-chain (MCR) phenotypes. Fig. 1b also shows that prior exposure to sub-lethal acid-stress conditions (pH 5.5 for 1 h) significantly enhanced resistance to normally lethal levels of acid exposure (pH 3.5 for 5 h) for all strains tested. Corresponding *k*-value determinations for the salt-stressed (7.5% w/v NaCl for 1 h) representative strains S1/WT, FR1 and MCR1 that were subsequently exposed to high salt conditions (17.5% w/v NaCl for 5 h) are shown in Fig. 2. For ease of comparisons between multiple strains under various treatment regimes, corresponding *k*-value determinations were then compared for different heat, acid and salt treatments (Table 2). Prior exposure to sub-lethal heating, salt and acid-stress conditions augmented resistance to normally lethal levels of the same stress for all morphotypes tested following the order S/WT, FR and then MCR as least resistant (Table 2). Strains that had been acid-adapted by growth to stationary phase in TSB + G were more tolerant compared to similar strains cultured under similar conditions in

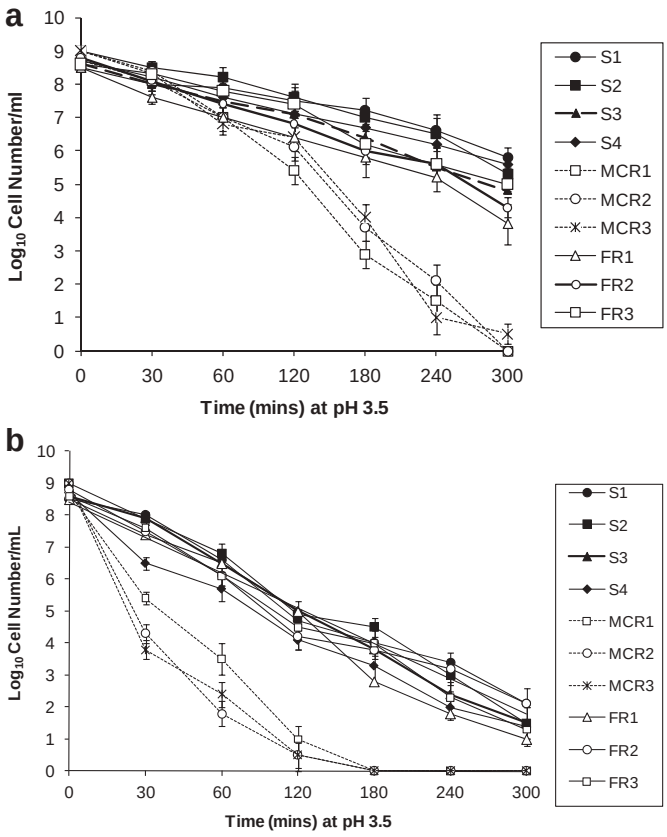

Fig. 1. (a) Influence of exposure of different culture morphotypes of *L. monocytogenes* to pH 5.5 for 1 h (adjusted with lactic acid) followed by subjection to extreme acid (pH 3.5 for 5 h) compared to (b) non-adapted controls.

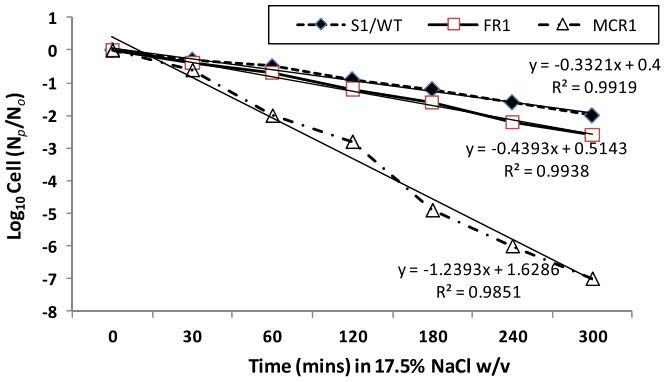

Fig. 2. Determination of inactivation rate constant *k* values for *L. monocytogenes* S1/WT (◆), MCR1 (□) and FR1 (△) strains after exposure to combination of sub-lethal salt (7.5% w/v for 1 h) and high salt (17.5% w/v NaCl for 5 h) conditions.

TSB − G combined with mild-acid stress at pH 5.5 for 1 h (Table 2), and compared to non-adapted cells (mean *k* values: 1.45 ± 0.06, 1.68 ± 0.04 and 1.72 ± 0.05 respectively) (Table 2). Strain *L. monocytogenes* MCR3 exhibited the least resistance to all combinations of sub-lethal and lethal stressors ($p \leq 0.05$) (Table 2).

Acids, salts and heating are commonly used as major barriers to prevent microbial growth in foods (Chorianopoulus et al., 2011), where often these treatments are applied simultaneously as their combinational use may act synergistically (Leistner, 2000). However, this present work is in agreement with the findings of previous researchers who demonstrated that prior exposure to mild-food-related stressors augments resistance of *L. monocytogenes* to the same and cross-protects against different stressors (Lou and Yousef, 1997; Chorianopoulus et al., 2011). Chorianopoulus et al. (2011) also observed that regardless of acidity/salinity conditions during attachment to stainless steel, the adaptive stationary-phase acid-tolerance response (ATR) enhanced the resistance of sessile cells to subsequent lethal challenge (exposure to pH 2 for 6 min; adjusted with either hydrochloric or lactic acid). In the present study, a similar pattern emerged where ATR grown strains of *L. monocytogenes* exhibited greater tolerance to more extreme low acid conditions (pH 3.5 for 5 h; adjusted also with either hydrochloric or lactic acid) compared to non-adapted cells or to cells subjected to mild-acid conditions (pH 5.5 for 1 h). Lactic acid is commonly used for decontamination in the meat environments (Gordon Greer and Dilts, 1995). Adriao et al. (2008) also observed that a 2 h exposure of exponential growing planktonic cells of *L. monocytogenes* to moderate acid (pH 5.5) promoted subsequent survival of these cells once they became attached to stainless steel coupons at low pH (3.5) during a 2 h period, compared to cells that had not previously been exposed to acid. This study also corroborates findings of Koutsoumanis et al. (2003) who found that *L. monocytogenes* cultured in the presence of 1% glucose till stationary phase was more tolerant to low pH 3.5 compared with non-acid adapted cells. However, the latter study only focused on typical wild-type cultures of *L. monocytogenes*. The authors previously demonstrated that FR morphotype strains of *L. monocytogenes* were more tolerant of subsequent extreme heating at 56 °C, 60 °C and 65 °C compared to typical wild-type S-form cells if grown at the elevated temperature of 42 °C. However, this difference in microbial thermotolerance was attributed to the fact that FR strains exhibited a pronounced tailing effect in their death rate kinetic data plots that was not observed in similar strains grown at ≤37 °C prior to heating (such as described in the present study).

Previous studies have also shown that stressed pathogens such as *L. monocytogenes* and *Escherichia coli* O157:H7 are able to adapt to acidic food environments, allowing the cells to stay viable under conditions long enough to cause illness if sufficient present in sufficient numbers (Gabriel and Nakano, 2010). This acid habituation or acid tolerance is a response of bacterial pathogens towards nonlethal acidic pH which helps in genetic and physiologic changes that protect such stress-hardened cells from inactivation (Gabriel and Nakano, 2010). Acid adaptation of *E. coli* O157:H7 and *L. monocytogenes* has also been shown to induce cross-protection against thermal inactivation in fruit juices, milk and chicken broth (Sharma et al., 2005). In addition to degrading of nucleic acids by exposures to heating (Gabriel and Nakano, 2010), other researchers such as Wu (2008) observed that exposure of microbial cells to high temperatures and desiccation damages the cell walls of microorganisms leading to losses in vital cellular materials including ions such as Mg^{2+} and K^{+}, amino acids and peptides, and nucleic acids. Therefore, different food-processing stresses induce different types and amounts of damage to different sites in a microbial cell that also consequently result in variations in cellular repair mechanisms (Wu, 2008).

3.3. Relationship between exposure to prior food-related stresses and adaptive tolerance to pulse UV-light irradiation

Prior exposure to sub-lethal levels of acid (pH 5.5 for 1 h) or salt (7.5% NaCl for 1 h) significantly reduced the ability to all morphotypes of *L. monocytogenes* to cope with extreme pulsed UV-light irradiation at lamp discharge energies of 7.2 J and 12.8 J (Table 3). Acid adaptation by growth of all strains in TSB + G to their respective stationary phase did not significantly influence tolerance

Table 2
Influence of prior sub-lethal exposure to mild acid, salt and heat stressing on subsequent resistance of different morphotypes of *Listeria monocytogenes* to normally lethal levels of the same stress.

Test Strain[a]	Reduction rate (k) values at different combinations of prior sub-lethal and lethal stress conditions[b]						
	pH 4.7[c]	pH 3.5 for 5 h[d]		17.5% (w/v) NaCl for 5 h		60 °C for 1 h	
	[Growth in TSY + G]	Pre-exposure: pH 5.5 for 1 h	Non-acid stress control	Pre-exposure: 7.5% (w/v) NaCl for 1 h	Non-osmotic stress control	Pre-exposure: 48 °C for 1 h	Non-heat stress control
S1/WT	0.43 ± 0.01 C	0.48 ± 0.04 C	1.42 ± 0.07 I	0.33 ± 0.02 A	1.56 ± 0.03 I	0.38 ± 0.02 B	1.22 ± 0.03 H
S2/WT	0.46 ± 0.03 C	0.49 ± 0.01 C	1.47 ± 0.11 I	0.29 ± 0.05 A	1.42 ± 0.06 I	0.38 ± 0.02 B	1.15 ± 0.02 G
S3/WT	0.44 ± 0.03 C	0.51 ± 0.02 C	1.39 ± 0.03 I	0.34 ± 0.01 A	1.44 ± 0.08 I	0.40 ± 0.02 B	1.27 ± 0.06 H
S4/WT	0.40 ± 0.01 C	0.49 ± 0.02 C	1.52 ± 0.04 I	0.38 ± 0.02 B	1.52 ± 0.02 I	0.39 ± 0.01 B	1.31 ± 0.04 H
	0.43 ± 0.02 C	0.49 ± 0.02 C	1.45 ± 0.06 I	0.33 ± 0.04 A	1.49 ± 0.06 I	0.39 ± 0.02 B	1.24 ± 0.06 H
FR1	0.49 ± 0.05 C	0.51 ± 0.03 C	1.66 ± 0.06 J	0.44 ± 0.02 B	1.64 ± 0.05 J	0.51 ± 0.04 C	1.12 ± 0.03 G
FR2	0.56 ± 0.03 C	0.66 ± 0.03 D	1.72 ± 0.07 J	0.61 ± 0.04 D	1.73 ± 0.08 J	0.53 ± 0.04 C	1.38 ± 0.03 I
FR3	0.54 ± 0.03 C	0.64 ± 0.04 D	1.68 ± 0.07 J	0.52 ± 0.04 C	1.63 ± 0.07 J	0.49 ± 0.03 C	1.15 ± 0.05 G
	0.53 ± 0.06 C	0.60 ± 0.08 D	1.68 ± 0.04 J	0.52 ± 0.08 C	1.66 ± 0.06 J	0.51 ± 0.02 C	1.22 ± 0.14 G
MCR1	0.83 ± 0.03 E	0.98 ± 0.03 F	1.71 ± 0.04 J	1.24 ± 0.06 H	1.63 ± 0.11 J	0.89 ± 0.01 F	1.51 ± 0.04 I
MCR2	0.94 ± 0.02 F	1.11 ± 0.02 G	1.67 ± 0.10 J	1.30 ± 0.05 H	1.82 ± 0.07 J	0.82 ± 0.05 E	1.50 ± 0.03 I
MCR3	0.93 ± 0.04 F	1.08 ± 0.04 G	1.77 ± 0.05 J	1.24 ± 0.05 H	1.76 ± 0.10 J	1.01 ± 0.05 F	1.47 ± 0.04 I
	0.90 ± 0.05 F	1.06 ± 0.04 G	1.72 ± 0.05 J	1.26 ± 0.03 H	1.74 ± 0.09 J	0.91 ± 0.09 F	1.49 ± 0.02 I

[a] Full description of different test pleomorphic strains of *L. monocytogenes* provided in Table 1.
[b] Inactivation kinetic k data. Values with different capitalized letter are significantly different at $p \leq 0.05$.
[c] *L. monocytogenes* strains grown in TSB + G to stationary phase (pH 4.7) without subsequent adjustment to pH 3.5. Cells were exposed to pH 4.7 for approximately 14 h.
[d] *L. monocytogenes* strains grown in TSB − G to stationary phase (pH 6.7) before exposure to pH 5.5 (adjusted with lactic acid) for 1 h.

to PUV challenges (data not shown). However, exposure to prior heating (48 °C for 1 h) did not significantly affect PUV tolerance compared to non-adapted cells where similar k-values were observed between these samples (Table 3). A similar pattern of general sensitivity to PUV-irradiation was observed for *L. monocytogenes* tested with the order of decreasing resistance to applied PUV at low discharge energies seen as S/WT, FR and MCR (Table 3). These findings are also in an agreement with recent unpublished work from our laboratory which demonstrated that prior short exposure or growth of *Saccharomyces cerevisiae*, *Candida albicans*, *L. monocytogenes* or *E. coli* under osmotic stress conditions (i.e., using increasing concentrations of dextrose ranging from 10 to 50 g/L) resulted in reduced susceptibility of these tempered strains to pulsed UV-light irradiation compared to non-adapted controls.

There is currently a dearth of information on the influence of prior food-processing conditions (applied sequentially or simultaneously) on the subsequent resistance of such adaptive strains to non-thermal technologies such as pulsed UV. The authors have previously reported on the relationship between pulsed UV-light irradiation and the simultaneous occurrence of molecular and cellular damage in clinical strains of *C. albicans*. PUV-irradiation inactivates *C. albicans* through a complex multi-hit cellular process that included inflicting irreversible damage to DNA and destabilizing the functionality and integrity of plasma cell membrane (Farrell et al., 2011). Takeshita et al. (2003) also noted that the concentration of eluted proteins varied significantly between pulsed UV and low-pressure UV irradiated yeast cell suspensions, with the latter showing minimal protein leakage.

Table 3
Influence of prior exposure to sub-lethal salt, acid and heat stressing on the subsequent resistance of different culture morphotypes of *L. monocytogenes* to pulsed UV-light irradiation at lamp discharge energies of 7.2 J or 12.8 J (equivalent to UV doses of 2.7 and 8.4 μJ/cm^2 resp.).

Test Strain[a]	Reduction rate (k) values at separate PUV treatments post exposure to different sub-lethal stress conditions [b]									
	Non-stressed control		pH 4.7 for *ca.* 14 h[c]		pH 5.5 for 5 h[d]		7.5% (w/v) NaCl for 1 h		48 °C for 1 h	
	7.2 J	12.8 J	7.2 J	12.8 J	7.2 J	12.8 J	7.2 J	12.8 J	7.2 J	12.8 J
S1/WT	0.40 ± 0.02 A	0.94 ± 0.01 E	0.50 ± 0.02 B	1.10 ± 0.02 G	0.53 ± 0.02 B	1.16 ± 0.04 G	0.66 ± 0.02 C	1.11 ± 0.02 G	0.45 ± 0.03 A	0.93 ± 0.02 E
S2/WT	0.39 ± 0.03 A	0.92 ± 0.03 E	0.54 ± 0.04 B	1.11 ± 0.03 G	0.56 ± 0.03 B	1.13 ± 0.04 G	0.56 ± 0.02 B	1.00 ± 0.01 F	0.41 ± 0.04 A	0.90 ± 0.03 E
S3/WT	0.42 ± 0.02 A	0.98 ± 0.01 E	0.46 ± 0.01 A	1.05 ± 0.01 F	0.51 ± 0.02 B	1.08 ± 0.03 G	0.64 ± 0.01 C	1.01 ± 0.01 F	0.45 ± 0.01 A	1.02 ± 0.01 F
S4/WT	0.45 ± 0.04 A	0.90 ± 0.03 E	0.53 ± 0.03 B	1.08 ± 0.04 G	0.57 ± 0.04 B	1.15 ± 0.02 G	0.65 ± 0.01 C	1.13 ± 0.03 G	0.43 ± 0.02 A	0.95 ± 0.01 E
	0.42 ± 0.02 A	0.94 ± 0.03 E	0.51 ± 0.01 B	1.09 ± 0.03 G	0.54 ± 0.03 B	1.13 ± 0.04 G	0.63 ± 0.04 C	1.06 ± 0.06 G	0.44 ± 0.02 A	0.95 ± 0.05 E
FR1	0.46 ± 0.04 A	0.88 ± 0.03 E	0.61 ± 0.03 C	1.01 ± 0.03 F	0.67 ± 0.03 C	1.08 ± 0.04 G	0.71 ± 0.05 C	1.09 ± 0.04 G	0.52 ± 0.02 B	0.89 ± 0.02 E
FR2	0.41 ± 0.04 A	0.93 ± 0.04 E	0.60 ± 0.03 C	1.15 ± 0.03 G	0.69 ± 0.03 C	1.28 ± 0.02 H	0.66 ± 0.04 C	1.15 ± 0.05 G	0.43 ± 0.01 A	0.91 ± 0.03 E
FR3	0.48 ± 0.02 A	0.96 ± 0.04 E	0.66 ± 0.01 C	1.19 ± 0.01 G	0.76 ± 0.01 D	1.29 ± 0.01 H	0.79 ± 0.01 D	1.19 ± 0.06 G	0.53 ± 0.02 B	0.93 ± 0.03 E
	0.45 ± 0.03 A	0.93 ± 0.04 E	0.62 ± 0.04 C	1.12 ± 0.04 G	0.71 ± 0.04 D	1.21 ± 0.11 H	0.72 ± 0.06 C	1.14 ± 0.05 G	0.49 ± 0.06 B	0.90 ± 0.01 E
MCR1	0.83 ± 0.01 D	1.16 ± 0.05 G	0.92 ± 0.02 F	1.09 ± 0.01 G	1.01 ± 0.01 F	1.13 ± 0.04 G	1.09 ± 0.03 G	1.35 ± 0.03 H	0.80 ± 0.03 C	1.13 ± 0.05 G
MCR2	0.77 ± 0.04 D	1.14 ± 0.06 G	1.02 ± 0.04 G	1.28 ± 0.04 H	1.09 ± 0.04 G	1.31 ± 0.01 H	1.18 ± 0.04 G	1.48 ± 0.01 I	0.80 ± 0.04 C	1.09 ± 0.03 G
MCR3	0.79 ± 0.03 D	1.16 ± 0.04 G	0.94 ± 0.02 F	1.10 ± 0.01 G	0.99 ± 0.01 F	1.15 ± 0.06 G	1.13 ± 0.06 G	1.35 ± 0.04 H	0.78 ± 0.01 C	1.15 ± 0.04 G
	0.80 ± 0.03 D	1.13 ± 0.03 G	0.96 ± 0.04 F	1.16 ± 0.05 G	1.04 ± 0.05 F	1.19 ± 0.09 G	1.13 ± 0.05 G	1.39 ± 0.08 H	0.79 ± 0.01 C	1.12 ± 0.03 G

[a] Full description of different test pleomorphic strains of *L. monocytogenes* provided in Table 1.
[b] Inactivation kinetic k data. Values with different capitalized letter are significantly different at $p \leq 0.05$.
[c] *L. monocytogenes* strains grown in TSB + G to stationary phase (pH 4.7) without subsequent adjustment to pH 3.5. Cells were exposed to pH 4.7 for approximately 14 h.
[d] *L. monocytogenes* strains grown in TSB − G to stationary phase (pH 6.7) before exposure to pH 5.5 (adjusted with lactic acid) for 1 h.

Farrell et al. (2011) also advocated use of novel intracellular viability markers (such as onset of late apoptosis or early stage necrosis) as an alternative or complementary approach to use of plate count or redox probes for the real-time detection of microbial lethality post decontamination. These conventional viability enumeration methods that are routinely used to confirm disinfection or preservation efficacy of food processes are limited by the recognised fact that a sub-population of treated microorganisms may be capable of repair after resuscitation (Rowan et al., 2008; Rowan, 2011). Whereas, confirmation of the detection of a late necrotic marker in PUV-treated microorganisms appears to be related to a treatment regime that inflicts irreversible damage and is beyond that identified by use of plate count and vital respiratory or redox staining. Our findings also supports the viewpoint of Guerrero-Beltrán and Barbosa-Cánovas (2004), which highlights the pressing need to optimise all inter-related (synergistic) inimical factors to achieve target inactivation level for specific food applications. Future studies that explore and quantify the relationship between application of minimal conventional combined with emerging (non-thermal) food-processing conditions and onset of irreversible microbial cell damage post treatments will facilitate optimisation of PUV for safe food applications. Identifying the right combination of mild preservation techniques known as "hurdles" is a very powerful tool in preventing microbial growth and in minimising organoleptic changes in foods. The latter is particularly relevant as use of PUV is gaining in popularity as a novel approach for treating liquid foods such as clover honey and infant foods (Choi et al., 2010) and for decontaminating dried foods such as wheat flour and black pepper (Fine and Gervais, 2004). Kelik et al. (2009) also reported on the potential of PUV for decontaminating unpackaged and vacuum-packaged chicken frankfurters.

3.4. Influence of prior sub-lethal stressing on invasion of human Caco-2 cells

Findings showed that prior exposure to mild-heating (48 °C for 1 h), acid (pH 5.5 for 1 h), salt (7.5% w/v NaCl for 1 h) and PUV (UV does 0.08 μJ/cm^2) treatments had variable effects on the ability of different morphotypes of *L. monocytogenes* to invade Caco-2 cells when compared with non-adapted controls grown at 37 °C (Fig. 3). Adherence and invasion data for strains S2/WT, FR2 and MRC3 were selected for illustration in Fig. 3 as they consistently demonstrated greater tolerance to applied stresses including PUV-irradiation compared to other test strains challenged. Prior exposure to mild-acid and salt stressors reduced the ability of all morphotypes to invade Caco-2 cells (Fig. 3), while mild-heating significantly augmented this virulence-associated characteristic in *L. monocytogenes* S/WT and FR strains ($p \leq 0.05$). Acid-adapted stationary-phase *L. monocytogenes* strains showed similar virulence attributes to samples exposed to mild-acid stress and cultured in TSB – G (data not shown). Test strains exposed to mild-PUV irradiation showed similar invasion abilities compared to non-stressed controls ($p \leq 0.05$) (Fig. 3). This corroborates previous studies investigating the influence on environmental signals or stresses such as mild heating on the up-regulation of *PrfA* gene, which is a transcriptional activator governing virulence factor expression in *L. monocytogenes* (Portnoy et al., 1992; Chakroborty et al., 1992). Interestingly, exposure of *L. monocytogenes* to temperatures below human body temperature such as refrigeration (4 °C) also causes down-regulation of *PrfA* and an associated reduction in virulence factor expression. Irrespective to the type of prior stressor applied, MCR strains were shown to be less invasive and also demonstrated reduced ability to adhere to Caco-2 cells (Fig. 3). A clear pattern emerged where the order to decreased ability to invade Caco-2 cells was S/WT, FR and MCR morphotypes. Note worthily, exposure of all morphotypes to a simultaneous combination of acid (pH 5.5 for 1 h, adjusted with lactic acid), salt (7.5% w/v NaCl for 1 h) and mild heating (48 °C for 1 h) produced the greatest reduction in invasion of Caco-2 cells (Fig. 3). This present study also agrees with the previous findings of Faith et al. (2007) who demonstrated that Cwha (or p60) mutant of *L. monocytogenes* was less capable to cause systemic infection in A/J mice following intragrastric inoculation than the parental wild-type strain (SLCC 5764, serotype 1/2a). Similar to MCR strains studied in this work, this latter Cwha mutant also exhibited a diminished ability to invade and multiply within Caco-2 cells (Faith et al., 2007). Collectively, these findings intimate that expression of the *Cwha* gene is required for maximal virulence of *L. monocytogenes* in addition to possibly playing a housekeeping role in adaptive tolerance to environmental stresses.

This study is in agreement with the findings of Lorentzen and co-workers (2011) who recently observed a reduced ability of 7 salt-stressed strains of *L. monocytogenes* grown to either early or late stationary phase at 4 °C to invade Caco-2 cells compared to non-salt stressed control strains. At both growth phases, the strains were exposed to either no salt or to salt stress comparable to that applied in the production of rehydrated salt-cured cod, i.e., 21% (w/v) NaCl followed by dilution to 2% (w/v) NaCl. The authors contend that as the ability to invade Caco-2 cells correlates with bacterial virulence, the results of their study suggests *L. monocytogenes* represent a lower food-safety risk when exposed to salt-curing with extreme NaCl concentrations. This present study also corroborates the landmark work of Garner and co-workers (2006) who demonstrated a decreased invasion of stationary-phase grown *L. monocytogenes* 10403S cells into Caco-2 epithelial cells after a 1 h challenge at 37 °C post bacterial exposure to gastric

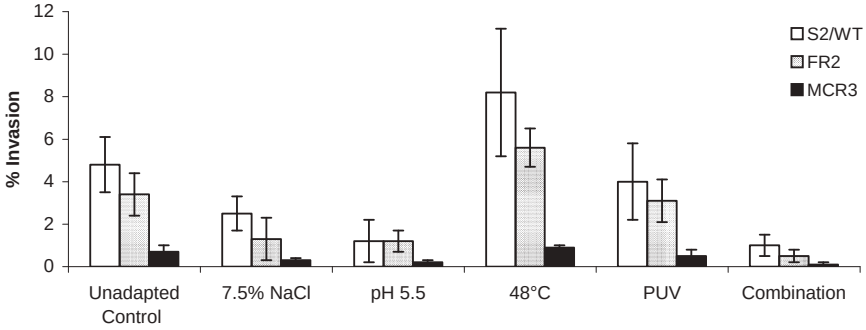

Fig. 3. Influence of prior exposure of *L. monocytogenes* S2/WT, FR2 and MCR2 strains to sub-lethal salt, acid, heating and PUV (singly and combined) stresses on their subsequent invasiveness to Caco-2 cells. Invasion efficiency is reported as follows: (the number of bacteria recovered from each well following Caco-2 cell lysis divided by the number of bacteria that had been used for inoculation) × 100.

fluid (pH 4.5 containing 2.2% (w/v) NaCl or 2.5% (w/v) sodium lactate) compared to unadjusted gastric acid control samples (pH 4.5 without added salt or lactate). Invasion of Caco-2 cells post salt and organic acid challenge in gastric acid (pH 4.5) was shown to less than 5% for both mild stressors after 1 h exposure. However, these authors also observed a marked increase in the invasion of similar *L. monocytogenes* into Caco-2 cells where bacteria were grown in brain heart infusion broth containing 2.2% w/v NaCl (median 28% invasion) or 275 mM sodium lactate (median 37% invasion) at 37 °C and pH 7.4. These researchers also observed a significant reduction in invasion when *L. monocytogenes* cells were grown at 7 °C compared to 37 °C. Loepfe et al. (2010) also observed a significant reduction in the invasiveness of cold-stressed *L. monocytogenes* when investigated using human Caco-2 and murine macrophage *in vitro* cell infection models. Walecka et al. (2011) recently demonstrated that although stationary-phase *L. monocytogenes* exhibit lower invasiveness to human enterocytic HT-29 cells than log-phase cells, the latter have a greater capacity to enhance their pathogenicity in response to salt stress. However, Jaradat and Bhunia (2003) advocated caution in interpreting results from *in vitro* Caco-2 adhesion profiles as this might not be an accurate assessment of a strain's ability to invade human organs or tissues in a mouse model.

Akin to the hostile environment encountered in food, *L. monocytogenes* must survive the human body defences that include gastric acid (ranging from pH 2.5 to 4.5 depending on feeding status), bile salts and organic acids within the gastrointestinal tract in order to elicit an infection (Gahan and Hill, 2005; Gray et al., 2006). Begley et al. (2002) observed that while exponential-phase *L. monocytogenes* LO28 cells were sensitive to unconjugated bile acids, prior adaptation to sub-lethal levels of bile acids or heterologous stresses, such as acid, heat, or salt significantly enhanced bile resistance. Thus, to survive extreme and rapidly changing conditions, bacteria must sense these changes and then respond with appropriate alternations in gene expression and protein activity. Therefore, another important scientific challenge is to identify mechanisms that control the switch(es) that allow free-living bacteria to adjust to and invade a host organism that also embraces prior exposure or adaptation to mild stressors (Olsen et al., 2009; Lorentzen et al., 2011). It was shown previously that bacteria which modify their metabolism in response to stress alter their virulence (Walecka et al., 2011). Thus, Roche et al. (2005) postulate that strains efficiently responding to environmental changes should be more virulent. However, exposure to food-related stress conditions commonly found in ready-to-eat (RTE) products (currently thought to be the most common cause of human listeriosis infections in the United States (cited in Garner et al., 2006)) combined with passage through the human gastrointestinal tract appears to reduce the invasion of *L. monocytogenes* to Caco-2 cells, which brings in the question the reliability and efficacy of interpreting data from this *in vitro* infection model alone for estimating human pathogenesis potential.

In conclusion, typical and atypical culture forms of *L. monocytogenes* appear to respond differently to applied conventional food-related stresses and to pulsed UV-light irradiation. These findings support the development of PUV for the decontamination of foods and should be considered as a complementary treatment technology for future applications in the food industry. While use of linearized inactivation kinetic plots provided succinct comparisons between strains and treatments in this study, there is also merit in considering use of alternative approaches such as the Weibull model that may take greater account of the variation in the shape between inactivation plots (Mafart et al., 2002). Future research should focus on expanding the range of stresses studied such as the impact of refrigeration conditions on subsequent PUV survival and pathogenesis. Research is also needed to simulate conditions encountered in real complex food-processing ecosystems and to develop more appropriate infection models to elucidate the impact of stress-hardening on microbial pathogenesis with a nexus to food safety and risk assessment. Studies on the possible difference in sensitivity between planktonic compared to more recalcitrant biofilm-challenged cultures of *L. monocytogenes* are also merited. Additionally, elucidating knowledge and understanding of molecular events jointly involved in the *L. monocytogenes* stress-adaptive-responses to emerging non-thermal food preservation techniques combined with their attachment to abiotic surfaces will provide further valuable information.

Acknowledgement

The authors kindly acknowledge the financial support of the Technical Research Sector Strand 1 Programme, Ireland, and of the Ministry of Agriculture, Fisheries and Food (MAFF), UK.

References

Adriao, A., Vieira, M., Fernandes, I., Barbosa, M., Sol, M., Tanreiro, R.P., Chambel, L., 2008. Marked intra-strain variation in response of *Listeria monocytogenes* dairy isolates to acid or salt stress and the effect of acid or salt adaptation on adherence to abiotic surfaces. Int. J. Food Microbiol. 123, 142–150.

Begley, M., Gahan, C.G.M., Hill, C., 2002. Bile stress response in *Listeria monocytogenes* LO28: adaptation, cross-protection, and identification of genetic loci involved in bile resistance. Appl. Environ. Microbiol. 68, 6005–6012.

Bereski, F., Gavini, F., Benezech, T., Faille, C., 2002. Growth, morphology and surface properties of *Listeria monocytogenes* Scott A and LO28 under saline and acid environments. J. Appl. Microbiol. 92, 556–565.

Bubert, A., Riebe, J., Schnitzler, N., Schönberg, A., Goebel, W., Schubert, P., 1997. Isolation of catalase negative *Listeria monocytogenes* strains from listeriosis patients and their rapid identification by anti-p60 antibodies and/or PCR. J. Clin. Micrbiol. 35, 179–183.

Buchanan, R.L., Edelson, S.G., 1996. Culturing enterohemorrhagic *Escherichia coli* in the presence and absence of glucose as a single means of evaluating the acid tolerance response of stationary-phase cells. Appl. Environ. Microbiol. 62, 4009–4013.

Chakroborty, T., Leimester-Wächter, M., Donann, E., Hartl, M., Goebel, W., Nichterlein, T., Notermans, S., 1992. Co-ordinate regulation of virulence genes in *L. monocytogenes* requires product of the PrfA gene. J. Bacteriol. 174, 568–574.

Choi, M.S., Cheigh, C.I., Jeong, E.A., Shin, J.K., Chung, M.S., 2010. Nonthermal sterilization of *Listeria monocytogenes* in infant foods by intense pulsed light treatment. J. Food Eng. 97, 504–509.

Chorianopoulus, N., Giouris, E., Grigoraki, I., Skandamis, P., Nychas, G.-J., 2011. Effect of acid tolerance response (ATR) on attachment of *Listeria monocytogenes* Scott A to steel under extended exposure to acid and/or salt stress and resistance of sessile cells to subsequent strong acid challenge. Int. J. Food Microbiol. 145, 400–406.

EFSA-ECDC, 2007. The community summary report on trends and sources of zoonoses, zoonotic agents, antimicrobial resistance and foodborne outbreaks in the European Union in 2006. EFSA J. 130, 2–352.

Faith, G.M., Kathariou, S., Neudeck, B.L., Luchansky, J.B., Czuprynski, C.J., 2007. A p60 mutant of *Listeria monocytogenes* is impaired in its ability to cause infection in intragastrically inoculated mice. Microb. Pathog. 42, 237–241.

Farrell, H.P., Garvey, M., Rowan, N.J., 2010. Critical inter-related factors governing the efficacy of pulsed light for the inactivation of clinically relevant bacteria. J. Appl. Microbiol. 108, 1494–1508.

Farrell, H.P., Hayes, J., Laffey, J.G., Rowan, N.J., 2011. Studies on the relationship between pulsed UV light and the simultaneous occurrence of molecular and cellular damage in clinically-relevant *Candida albicans*. J. Microbiol. Methods 84, 317–326.

Fine, F., Gervais, P., 2004. Efficiency of pulsed UV light for microbial decontamination of food powders. J. Food Protect. 67, 787–792.

Gabriel, A.A., Nakano, H., 2010. Influences of simultaneous physicochemical stress exposures on injury and subsequent responses of *E. coli* O157:H7 to resuscitative and inactivative challenges. Int. J. Food Microbiol. 139, 182–192.

Gahan, C.G., Hill, C., 2005. Gastrointestinal phase of *Listeria monocytogenes* infection. J. Appl. Microbiol. 98, 1345–1353.

Gahan, C.G.B., O'Driscoll, B., Hill, C., 1996. Acid adaptation of *L. monocytogenes* can enhance survival with increased resistance to surface sanitizers and heat. J. Food Protect. 53, 3128–3132.

Gardan, R., Cossart, P., Labadie, J., 2003. Identification of *Listeria monocytogenes* genes involved in salt and alkaline-pH tolerance. Appl. Environ. Microbiol. 69, 3137–3143.

Garner, M.R., James, K.E., Callahan, M.C., Wiedmann, M., Boor, K.J., 2006. Exposure to salt and organic acids increases the ability of *Listeria monocytogenes* to invade Caco-2 cells but decreases its ability to survive gastric stress. Appl. Environ. Microbiol. 72, 5384–5395.

Giotis, E.S., Blair, I.S., McDowell, D.A., 2007. Morphological changes in *Listeria monocytogenes* subjected to sublethal alkaline stress. Int. J. Food Microbiol. 120, 250–258.

Gómez-López, V.M., Ragaert, P., Debevere, J., Devlieghere, F., 2007. Pulsed light for food decontamination: a review. Trends Food Sci. Technol. 18, 464–473.
Gordon Greer, G., Dilts, B.D., 1995. Lactic acid inhibition of the growth of spoilage bacteria and cold tolerant pathogens on pork. Int. J. Food Microbiol. 25, 141–151.
Gray, M.J., Freitag, N.E., Boor, K.J., 2006. How the bacterial pathogen *Listeria monocytogenes* mediates the switch from environmental Dr. Jekyll to pathogenic Mr. Hyde. Infect. Immun. 74, 2505–2512.
Guerrero-Beltrán, J.A., Barbosa-Cánovas, G.V., 2004. Review: advantages and limitations on processing foods by UV light. Food Sci. Technol. Int. 10, 137–147.
Gutekunst, K.A., Pine, L., White, E., Kathariou, S., Carlone, G.M., 1992. A filamentous like mutant of *L. monocytogenes* with reduced expression of a 60-kilodalton extracellular protein invades and grows in 3T6 and Caco-2 cells. Can. J. Microbiol. 38, 843–851.
Hardy, J., Morgolis, J.J., Contag, C.H., 2006. Induced biliary excretion of *Listeria monocytogenes*. Infect. Immun. 74, 1819–1827.
Hill, C., Cotter, P.D., Sleator, R.D., Gahan, C.G.M., 2002. Bacterial stress response in *Listeria monocytogenes*: jumping the hurdles imposed by minimal processing. Int. Dairy J. 12, 273–283.
Isom, L.L., Khambatta, Z.S., Moluf, J.L., Akers, D.F., Martin, S.E., 1995. Filament formation in *Listeria monocytogenes*. J. Food Protect. 58, 1031–1033.
Jaradat, Z.W., Bhunia, A.K., 2003. Adhesion, invasion and translocation characteristics of *Listeria monocytogenes* serotypes in Caco-2 cell and mouse models. Appl. Environ. Microbiol. 69, 3640–3645.
Jones, L.R., Watson-Craik, I.A., Senior, E., 1994. Image analysis of the effects of different materials on surface colonization by anaerobic microbial associates from landfill. Binary 6, 78–80.
Jørgensen, F., Stephens, P.J., Knøchel, S., 1995. The effect of osmotic shock and subsequent adaptation on the thermotolerance and cell morphology of *Listeria monocytogenes*. J. Appl. Microbiol. 79, 274–281.
Kathariou, S., Hacker, J., Hof, H., Then, I., Wagner, W., Kuhn, M., Goebel, W., 1987. Bacterial cytotoxins – extracellular proteins and virulence factors. In: Rott, R., Goebel, W. (Eds.), Molecular Basis of Viral and Microbial Pathogenesis. Springer-Verlag, Berlin, pp. 141–150.
Kelik, N.M., Demirci, A., Puri, V.M., 2009. Inactivation of *Listeria monocytogenes* on unpackaged and vacuum-packaged chicken frankfurters using pulsed UV-light. J. Food Sci. 74, 431–439.
Koutsoumanis, K.P., Sofos, J.N., 2004. Comparative acid stress of *Listeria monocytogenes, Escherichia coli* O157:H7 and *Salmonella typhimurium* after habituation at different pH conditions. Lett. Appl. Microbiol. 38, 321–326.
Koutsoumanis, K.P., Kendal, P.A., Sofos, J.N., 2003. Effect of food processing-related stresses on acid-tolerance of *Listeria monocytogenes*. Appl. Enviorn. Microbiol. 69, 7514–7516.
Kuhn, M., Goebel, W., 1989. Identification of an extracellular protein of *Listeria monocytogenes* possibly involved in intracellular uptake by mammalian cells. Infect. Immun. 57, 55–61.
Leistner, L., 2000. Basic aspects of food preservation by hurdle technology. Int. J. Food Microbiol. 55, 181–186.
Lenz, L.L., Portnoy, D.A., 2002. Identification of a second *Listeria secA* gene associated with protein secretion and the rough phenotype. Mol. Microbiol. 45, 1043–1056.
Lie, J., Kolling, G.L., Matthews, K.R., Chikindas, M.L., 2003. Cold and carbon dioxide used as multi-hurdle preservation do not induce appearance of viable but non-culturable *Listeria monocytogenes*. J. Appl. Microbiol. 94, 48–53.
Loepfe, C., Raimann, E., Stephan, R., Tasara, T., 2010. Reduced host cell invasiveness and oxidative stress tolerance in double and triple csp gene family deletion mutants of *Listeria monocytogenes*. Foodborne Pathog. Dis. 7, 775–783.
Lorentzen, G., Mennen, S., Olsen, R.L., Skjerdal, T., 2011. Invasiveness of *Listeria monocytogenes* strains of Caco-2 cells in response to a period of extreme salt stress reflecting salt-curing and rehydration of cod (*Gadus morhua* L.). Food Control 22, 1040–1045.
Lou, Y., Yousef, A.H., 1997. Adaptation of sub-lethal environmental stresses protects against lethal preservation factors. Appl. Environ. Microbiol. 63, 1252–1255.
Lünden, J.M., Tolvanen, R., Korkeala, H., 2008. Acid and heat tolerance of persistent and nonpersistent food plant strains. Lett. Appl. Microbiol. 46, 276–280.
Mafart, P., Couver, O., Gaillard, S., Leguerinel, I., 2002. On calculating sterility in thermal preservation methods: application of the Weibull frequency distribution model. Inter. J. Food Microbiol. 72, 107–113.
Minkowski, P., Staege, H., Groscurth, P., Schaffner, A., 2001. Effects of trimethoprim and co-trimoxazole on the morphology of *Listeria monocytogenes* in culture medium and after phagocytosis. J. Antimicrobial. Chemother. 48, 185–193.
Monk, I.R., Cook, G.M., Monk, B.C., Bremer, P.J., 2004. Morphotypic conversion in *Listeria monocytogenes* biofilm formation: biological significance of rough colony isolates. Appl. Environ. Microbiol. 70, 6686–6694.
Nilsson, L., Chen, Y.H., Chikindas, M.L., Huss, H.H., Gram, L., Montiville, T.J., 2000. Carbon dioxide and nisin act synergistically on *Listeria monocytogenes*. Appl. Environ. Micobiol. 66, 769–774.
Olsen, I., Vogensen, F.K., Jespersen, I., 2009. Gene transcription and virulence potential of *Listeria monocytogenes* strains after exposure to acidic and NaCl stress. Foodborne Pathog. Dis. 6, 669–680.
Oms-Oliu, G., Martin-Belloso, O., Soliva-Fortuny, R., 2010. Pulsed light treatments for food preservation: a review. Food Bioprocess. Technol. 3, 13–23.
Pilgrim, S., Klob-Maurer, A., Gentschev, I., Goebel, W., Kuhn, M., 2003. Deletion of the gene encoding p60 in *Listeria monocytogenes* leads to abnormal cell division and loss of actin-based motility. Infect. Immun. 71, 3473–3484.
Portnoy, D.A., Chakroborty, T., Goebel, W., Cossart, P., 1992. Molecular determinants of *Listeria monocytogenes* pathogenesis. Infect. Immun. 60, 1263–1267.
Ritz, M., Tholozan, J.L., Federighi, M., Pilet, M.F., 2001. Morphological and physiological characterization of *Listeria monocytogenes* subjected to high hydrostatic pressure. Appl. Environ. Microbiol. 67, 2240–2247.
Roche, S.M., Gracieux, P., Milohanic, E., Albert, I., Virlogeus-Payant, I., Temoin, S., Grepinet, O., Kerouanton, A., Jacquet, C., Cossart, P., Velge, P., 2005. Investigation of specific substitutions in virulence genes characterizing phenotypic groups of low-virulence field strains of *Listeria monocytogenes*. Appl. Environ. Microbiol. 71, 6039–6048.
Rowan, N.J., Anderson, J.G., 1998. Effects of above-optimum growth temperature and cell morphology on thermotolerance of *Listeria monocytogenes* cells suspended in bovine milk. Appl. Environ. Microbiol. 64, 2065–2071.
Rowan, N.J., Anderson, J.G., MacGregor, S.J., 2000. Pulsed electric fields inactivation of diarrhoegenic *Bacillus cereus* in caused by irreversible electroporation. Lett. Appl. Microbiol. 31, 110–114.
Rowan, N.J., MacGregor, S.J., Anderson, J.G., Cameron, D., Farish, O., 2001. Inactivation of *Mycobacterium paratuberculosis* by pulsed electric fields. Appl. Environ. Microbiol. 67, 2833–2838.
Rowan, N.J., Espie, S., Harrower, J., Anderson, J.G., Marsili, L., MacGregor, S.J., 2007. Pulsed plasma gas inactivation of microbial pathogens in chilled poultry wash water. J. Food Protect. 70, 2805–2810.
Rowan, N.J., Espie, S., Harrower, J., Farrell, H., MacGregor, S.J., 2008. Evidence of lethal and sublethal injury in food-borne pathogens exposed to high-intensity pulsed -plasma gas discharges. Lett. Appl. Microbiol. 46, 80–86.
Rowan, N.J., 1999. Evidence that inimical food-preservation barriers alter microbial resistance, cell morphology and virulence. Trends Food Sci. Technol. 10, 261–270.
Rowan, N.J., 2011. Defining established and emerging microbial risks in the aquatic environment: current knowledge, implications and outlooks. Int. J. Microbiol. 65, 1196–1215.
Sharma, M., Adler, B.B., Harrison, M.D., Beuchat, L.R., 2005. Thermal tolerance of acid-adapted and unadapted *Salmonella, Escherichia coli* O157:H7 and *Listeria monocytogenes* in cantaloupe juice and watermelon juice. Lett. Appl. Microbiol. 41, 448–453.
Sue, D., Fink, D., Wiedmann, M., Boor, K.J., 2004. Sigma B-dependent gene induction and expression in *Listeria monocytogenes* during osmotic and acid stress conditions simulating the intestinal environment. Microbiology 150, 3843–3855.
Takeshita, K., Shibato, J., Sameshima, T., Fukunaga, S., Isobe, S., Arihara, K., Itoh, M., 2003. Damage of yeast cells induced by pulsed UV light irradiation. Int. J. Food Microbiol. 85, 151–158.
Tompkin, R.B., 2002. Control of *Listeria monocytogenes* in the food-processing environment. J. Food Protect. 65, 709–725.
Van Boeijen, I.K.H., Moezelaar, R., Abee, T., Zwietering, M.H., 2008. Inactivation kinetics of three *Listeria monocytogenes* strains under high hydrostatic pressure. J. Food Protect. 71, 19–27.
Van Boeijen, I.K.H., Chavaroche, A.A.E., Valderrama, W.B., Moezelaar, R., Zwietering, M.H., Abee, T., 2010. Population diversity of *Listeria monocytogenes* LO28: phenotypic and genotypic characterization of variants resistant to high hydrostatic pressure. Appl. Environ. Microbiol. 76, 2225–2233.
Walecka, E., Molenda, J., Karpiskova, R., Bania, J., 2011. Effect of osmotic stress and culture density on invasiveness of *Listeria monocytogenes* strains. Int. J. Food Microbiol. 144, 440–445.
Wu, V.C.H., 2008. A review of microbial injury and recovery methods in food. Food Microbiol. 25, 725–744.

Letters in Applied Microbiology 2000, **31**, 319–322

Cellular morphology of rough forms of *Listeria monocytogenes* isolated from clinical and food samples

N.J. Rowan, J.G. Anderson and A.A.G. Candlish

Department of Bioscience and Biotechnology, University of Strathclyde, Glasgow, UK

172/2000: received 14 April 2000, revised 23 June 2000 and accepted 27 June 2000

N.J. ROWAN, J.G. ANDERSON AND A.A.G. CANDLISH. 2000. Transmission electron microscopy (TEM) studies revealed that rough cell-forms of *L. monocytogenes* (designated FR variants), isolated from clinical and food samples (and under conditions of sublethal heat stress), consist of either single or paired long-filaments. These FR variants markedly contrast in cell morphology from other previously described avirulent rough-mutants of *L. monocytogenes* that form long chains consisting of multiple cells of similar size (designated MCR variants). The identity of these *Listeria* isolates was determined using a commercially available, anti-*Listeria* polyclonal KPL antibody and by the API *Listeria* biochemical gallery. This study shows that filamentous rough-forms of *L. monocytogenes* may occur in clinical and food samples that are of undetermined pathogenicity.

INTRODUCTION

Listeria monocytogenes is a facultative intracellular bacterial pathogen responsible for serious disease in immunocompromised individuals and pregnant women (McLauchlin 1997). Epidemiological observations and electron microscopic studies of tissues of infected guinea pigs (Racz *et al.* 1972) provided evidence that the gastrointestinal tract is an important route of infection and that the epithelial cells of the intestine may be the primary site of entry for these bacteria.

Spontaneously occurring, rough mutants of *L. monocytogenes* secreting greatly reduced levels of a 60-kDa major extracellular housekeeping-protein (termed p60) and forming long chains of cells were previously described (designated MCR variants in this study) (Kathariou *et al.* 1987; Kuhn and Goebel 1989). This p60 protein is required for normal cell division (Bubert *et al.* 1992), and is transcribed independently of the central virulence regulator PrfA (Chakraborty *et al.* 1992). Although septum formation still occurs, separation of the divided cells does not take place (Wuenscher *et al.* 1993).

MCR variants were shown to have reduced virulence in the mouse model of infection and did not efficiently invade mouse 3T6-fibroblasts (Kuhn and Goebel 1989). Treatment of MCR variants with partially purified cell-free p60 led to disaggregation of cell chains to normal-sized single bacteria with restored invasiveness (Kathariou *et al.* 1987; Kuhn and Goebel 1989). Thus, for these MCR variants, cell-free p60 not only causes decay of cell chains but participates actively in the invasion process. We recently described atypical rough cell forms of *L. monocytogenes* from clinical and food samples that showed wild-type levels of adherence, invasion and cytotoxicity to human epithelial HEp-2 and HeLa cells (Rowan *et al.* 1999). Here, we show that these invasive rough forms of *L. monocytogenes* consist of single or paired long-filaments (designated FR variants).

Correspondence to: N.J. Rowan, Department of Bioscience and Biotechnology, University of Strathclyde, Royal College Bldng, 204 George St, Glasgow G1 1XW, UK (e-mail: n.j.rowan@strath.ac.uk).

MATERIALS AND METHODS

Bacterial strains

The *L. monocytogenes* strains used in the study were, if not otherwise indicated, derived or obtained from the Special *Listeria* Culture Collection [SLCC] of H. P. R. Seeliger, Würzburg, Germany, or from the National Collection of Type Cultures [NCTC], Public Health Laboratory Service [PHLS], Central Public Health Laboratory, Colindale, London, UK. (Table 1). Two auto-agglutinable blood culture and food isolates of *L. monocytogenes* exhibiting a rough phenotype were obtained from Dr Jim McLauchlin, Food Safety Microbiology Laboratory, PHLS, Colindale, London, UK. The clinical strains PHLRIII and PHLRIV were blood-culture isolates from a 76 and 72 years-old female and male, respectively; both individuals had sepsis and pyrexia. The spontaneously rough variants *L. monocytogenes* RI, RII and RIII were kindly supplied by Dr Andreas Bubert, Microbiological Analytics, Merck KGaA, 64271 Darmstadt, Germany. Where the rough variants RI and RII were previously derived from *L. monocytogenes*

Table 1 *L. monocytogenes* strains used

Strain	Serotype	Reference No.	Origin	Cell morphology		ELISA (A_{492})¶ KPL pAb
				Form	Designation	
S1	4b	NCTC 11994	Adult meningitis	Single, paired cells	WT smooth	0·56 ± 0·12
S2	4b	NCTC 9863	Infantile meningitis	Single, paired cells	WT smooth	0·82 ± 0·16
RI‡	1/2a	SLCC 5764	Kathariou *et al.* (1987)	Long cell chains	MCR variant	0·64 ± 0·05
RII§	1/2a		Kathariou *et al.* (1987)	Long cell chains	MCR variant	0·78 ± 0·12
RIII	1/2a	SLCC 5779	J. Potel (see text)	Long cell chains	MCR variant	0·39 ± 0·06
PHLRII		L7071	Dried custard powder	Long cell chains	MCR variant	1·23 ± 0·16
SURI*	4b		Rowan and Anderson (1998)	Long filaments	FR variant	0·62 ± 0·06
SURII†	4b		Rowan and Anderson (1998)	Long filaments	FR variant	0·93 ± 0·15
PHLRI		L6705	Dried custard powder	Long filaments	FR variant	1·05 ± 0·14
PHLRIII		L7346	Blood culture	Long filaments	FR variant	1·23 ± 0·16
PHLRIV		L1342	Blood culture	Long filaments	FR variant	1·16 ± 0·19

*Derived from *L. monocytogenes* NCTC 11994.
†Derived from *L. monocytogenes* NCTC 9863.
‡Derived from *L. monocytogenes* Mackaness (SLCC 5764).
§Derived from *L. monocytogenes* EGD
¶O.D.$_{492}$ values greater than 0·1 were considered a positive result. BHI broth controls gave a value of 0·03 ± 0·01.

Mackaness and EGD, respectively (Kuhn and Goebel 1989). Strain RII (SLCC 5779), was originally obtained from J. Potel (Institute for Medical Microbiology, Medical Academy, Hannover, Germany). *L. monocytogenes* RIII, another rough mutant derived from a smooth strain of serovar 1/2a, was obtained from J. Potel (Institute for Medical Microbiology, Medical Academy, Hannover, Germany). The rough variants SURI and SURII were derived from parent S1 and S2 strains, respectively, under conditions of heat stress (Rowan and Anderson 1998). Stored bacteria were kept at −70 °C in phosphate-buffered saline (PBS) with 20% glycerol (v/v) until used.

Biochemical and physiological methods

Catalase production was determined by applying a drop of 30% H_2O_2 to the colonies and observing the occurrence of O_2 bubbles, as described elsewhere (Bubert *et al.* 1997). The CAMP test was performed using standard procedures by streaking out bacteria perpendicular to *Staphylococcus aureus* on 5% sheep blood agar plates and observing zones of augmented haemolysis, as described elsewhere (Bubert *et al.* 1997). Characteristic blue-green sheen from colonies by obliquely transmitted light and tumbling motility of *Listeria* cells were determined as described elsewhere (Rowan and Anderson 1998). The commercial biochemical API *Listeria* test (bioMerieux, Marcy l'Etoile, France) was used according to the manufactures instructions.

Indirect ELISA

Detection of heat stable antigens in cell-free supernatants was achieved by indirect ELISA using an anti-*Listeria* affinity-purified polyclonal antibody that was obtained from Kirkegaard and Perry Laboratories (KPL, Gaithersburg, Maryland) in a lyophilized form. Preparation of antigen from overnight cultures involved centrifugation followed by the addition of 100 μl of supernatant per well of microtitre plates and incubation for 2 h at 37 °C. Antigen-coated plates were washed three times with wash buffer and the KPL-antibody was added at a dilution of 1/1000 (v/v) in wash buffer and incubated overnight for 1 h at room temperature. Unbound antibody was removed by washing three times with wash buffer, and rabbit antigoat horseradish peroxidase conjugate (Sigma) was added at 100 μl/well with a dilution of 1/1000 (v/v) in wash buffer and incubated for 1 h at room temperature. Excess conjugate was washed five times with wash buffer and the substrate, Sigma FAST^{TM} OPD tablets (Sigma), were added at 100 μl/well with 0·5 h incubation at room temperature. The A_{492nm} was measured after the addition of 50 μl per well 3 mol l^{-1} H_2SO_4.

Transmission electron microscopy (TEM)

Cells were grown to mid-log phase in brain heart infusion broth, washed twice with PBS and resuspended in sterile-distilled water before application to formvar-coated grids.

After the grid was dried, one drop of a solution containing 3% v/v tungstophosphoric acid and 0·3% v/v sucrose (pH 6·8–7·4) was added. The solution was removed after 30–60 s, and the grid was dried and examined on a Zeiss 902 transmission electron microscope.

RESULTS AND DISCUSSION

Due to the severity of listeriosis in predisposed-individuals, the identification of atypical rough cell-forms of *L. monocytogenes* in clinical or food samples (which are of undetermined pathogenicity) is of clinical relevance (McLauchlin 1997; Rowan 1999). All of the bacterial strains described in Table 1 were previously identified as *L. monocytogenes* by establishing characteristic morphological, physiological and biochemical properties associated with this bacterial pathogen and by analysing secretions of p60 in culture supernatants by indirect ELISA using a *L. monocytogenes*-specific antip60 monoclonal antibody (Rowan *et al*. 1999). The use of this *L. monocytogenes* p60-specific mAb for the unequivocal identification of this species has been previously demonstrated (Bubert *et al*. 1997). In this study, we have shown that these rough isolates of *L. monocytogenes* can also be identified by indirect ELISA using the commercially available anti-*Listeria* KPL pAb (Table 1) and with the API *Listeria* biochemical galleries.

Unlike typical wild-type smooth (S) *L. monocytogenes* strains that are characteristically 'coccobacillus' in cell appearance (approximately 2 μm in length), cell types associated with the rough or R variants were previously shown to be atypically long, measuring up to approximately 100 μm in length (Rowan *et al*. 1999). In the present study, we have shown that some R variants consisted of unseptated or paired-filaments (designated FR variants), whereas others formed long chains that consisted of multiple cells of similar size (designated MCR variants) (Table 1). Rough variants isolated from clinical specimens and food samples, or derived under conditions of heat stress predominately showed a FR-filamentous phenotype (Fig. 1a). Whereas spontaneously occurring *L. monocytogenes* RI, RII and RIII, and the food sample isolate PHLRII, exhibited a MCR-cell phenotype (Fig. 1b), which confirmed previous observations (Kuhn and Goebel 1989). MCR and FR variants were previously shown to be incapable of characteristic tumbling motility, and formed irregular or rough colonies that no longer produced a blue-green sheen upon oblique illumination (Rowan *et al*. 1999).

Here, we have shown that FR variants of *L. monocytogenes* differ from the wild-type smooth or S form of *L. monocytogenes* by forming single or paired filaments (Fig. 1a). Unlike MCR variants, the filamentous forms are not impaired in the synthesis of the major extracellular protein p60 (Rowan *et al*. 1999) which is required for a late step in cell division (Kuhn and Goebel 1989). We have previously shown that exposure of wild-type smooth forms of *L. monocytogenes* to environmental stress conditions, such as heat shock and growth at above-optimal temperatures, resulted in the generation of atypical cell forms of *Listeria* with a FR phenotype (Rowan and Anderson 1998; Rowan 1999). It has also been observed that long filamentous forms of *L. monocytogenes* with a rough phenotype similar

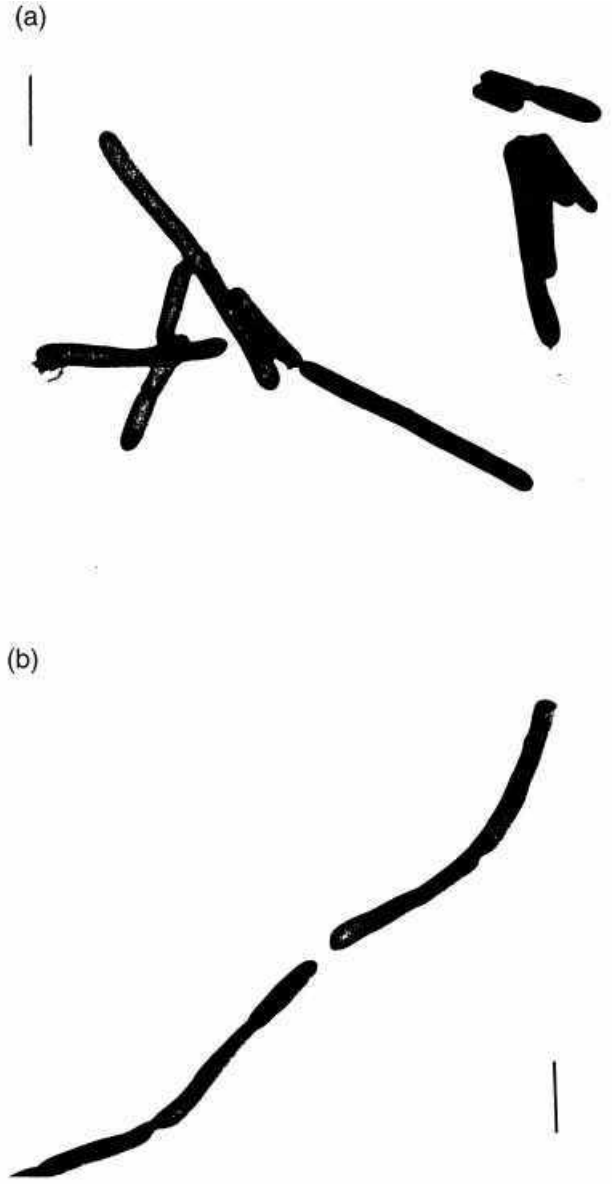

Fig. 1 Transmission electron micrographs of FR variant *L. monocytogenes* PHLRI (a) and MCR variant *L. monocytogenes* RI (b). Bar, 4 μm.

to that of lactobacilli or filamentous forms with a smooth phenotype can appear, in the latter case under the influence of suboptimal antibiotic concentrations (cited in Bubert *et al*. 1997).

In conclusion, rough cell-forms of *L. monocytogenes*, obtained from clinical and food samples and demonstrating wild-type levels of invasiveness in HEp-2 and HeLa epithelial cell lines (Rowan *et al*. 1999), were shown to consist of atypical paired or single filaments by TEM. While these rough forms of *L. monocytogenes* possess some unusual physiological and morphological properties, these variants can be identified by conventional biochemical and serological tests.

ACKNOWLEDGMENTS

We thank the University of Strathclyde for funding this research. We also thank Dr Jim McLauchlin (Food Safety Microbiology Laboratory, Central Public Health Laboratory Service, Colindale, London, UK) and Dr Andreas Bubert (Microbiological Analytics, Merck KGaA, 64271 Darmstadt, Germany) for the kind gift of rough *L. monocytogenes* strains.

REFERENCES

Bubert, A., Kuhn, M., Goebel, W. and Köhler, S. (1992) Structural and functional properties of the p60 proteins from different *Listeria* species. *Journal of Bacteriology* **174**, 8166–8171.

Bubert, A., Riebe, J., Schnitzler, N., Schönberg, A., Goebel, W. and Schubert, P. (1997) Isolation of catalase-negative *Listeria monocytogenes* strains from listeriosis patients and their rapid identification by anti-p60 antibodies and/or PCR. *Journal of Clinical Microbiology* **35**, 179–183.

Chakraborty, T., Leimeister-Wächter, M., Domann, E., Hartl, M., Goebel, W., Nichterlein, T. and Notermans, S. (1992) Coordinate regulation of virulence genes in *Listeria monocytogenes* requires the product of the *prfA* gene. *Journal of Bacteriology* **174**, 568–574.

Kathariou, S., Hacker, J., Hof, H., Then, I., Wagner, W., Kuhn, M. and Goebel, W. (1987) Bacterial cytotoxins – extracellular proteins and virulence factors. In *Molecular Basis of Viral and Microbial Pathogenesis* ed. Rott, R. and Goebel, W. pp. 141–150. Berlin: Springer-Verlag.

Kuhn, M. and Goebel, W. (1989) Identification of an extracellular protein of *Listeria monocytogenes* possibly involved in intracellular uptake by mammalian cells. *Infection and Immunity* **57**, 55–61.

McLauchlin, J. (1997) The pathogenicity of *Listeria monocytogenes*: a public health perspective. *Reviews in Medical Microbiology* **8**, 1–14.

Racz, P., Tenner, K. and Mero, E. (1972) Experimental *Listeria* enteritis. 1. An electron microscopic study of the epithelial phase in experimental *Listeria* infection. *Laboratory Investigations* **26**, 694–700.

Rowan, N.J. (1999) Evidence that inimical food-preservation barriers alter microbial resistance, cell morphology and virulence. *Trends in Food Science and Technology* **10**, 261–270.

Rowan, N.J. and Anderson, J.G. (1998) Effects of above-optimum growth temperature and cell morphology on thermotolerance of *Listeria monocytogenes* cells suspended in bovine milk. *Applied and Environmental Microbiology* **64**, 2065–2071.

Rowan, N.J., Bubert, A. and McLauchlin, J. (1999) Characterisation of virulent atypical cell forms of *Listeria monocytogenes* from the clinical environment secreting wild-type levels of p60. *Federation of Infection Societies, 6th International Conference*, Manchester, 1–3 December, p.45.

Wuenscher, M.D., Köhler, S., Bubert, A., Gerike, U. and Goebel, W. (1993) The *iap* gene of *Listeria monocytogenes* is essential for cell viability, and its gene product, p60, has bacteriolytic activity. *Journal of Bacteriology* **175**, 3491–3501.

JOURNAL OF CLINICAL MICROBIOLOGY, July 2000, p. 2643–2648 Vol. 38, No. 7
0095-1137/00/$04.00+0

Virulent Rough Filaments of *Listeria monocytogenes* from Clinical and Food Samples Secreting Wild-Type Levels of Cell-Free p60 Protein

NEIL J. ROWAN,[1]* ALAN A. G. CANDLISH,[1] ANDREAS BUBERT,[2] JOHN G. ANDERSON,[1] KARL KRAMER,[3] AND JIM MCLAUCHLIN[4]

Department of Bioscience and Biotechnology, University of Strathclyde, Glasgow,[1] and Food Safety Microbiology Laboratory, Public Health Laboratory Service, Colindale, London,[4] United Kingdom, and Microbiological Analytics, Merck KGaA, 64271 Darmstadt,[2] and Department of Botany, Technical University Munich-Weihenstephan, 85350 Freising,[3] Germany

Received 21 December 1999/Returned for modification 21 March 2000/Accepted 17 April 2000

Atypical rough cell filaments of *Listeria monocytogenes* (designated FR variants), isolated from clinical and food samples, form long filaments up to 96 μm in length and demonstrated wild-type levels of adherence, invasion, and cytotoxicity to human epithelial HEp-2, Caco-2, and HeLa cells. Unlike previously described avirulent rough mutants of *L. monocytogenes* that secrete diminished levels of the major extracellular protein p60 and that form long chains that consist of multiple cells of similar size (designated MCR variants), FR variants secreted wild-type or greater levels of p60. This study shows that virulent filamentous forms of *L. monocytogenes* occur in clinical and food environments and have atypical morphological characteristics compared to those of the wild-type form.

Listeria monocytogenes is a facultative intracellular bacterial pathogen that can cause severe food-borne infections such as meningitis, encephalitis, and septicemia in humans (16). The major risk groups are immunocompromised individuals and pregnant women (16). Virulent strains of *L. monocytogenes* are able to survive and multiply within host macrophages and can invade, replicate, and multiply in nonprofessional phagocytes such as mouse 3T6 fibroblasts, hepatocytes, and human colon carcinoma Caco-2 epithelial cells (9, 10, 11). Epidemiological observations and electron microscopic studies of tissues of infected guinea pigs (20) provided evidence that the gastrointestinal tract is an important route of infection and that the epithelial cells of the intestine may be the primary site of entry for these bacteria.

L. monocytogenes requires a 60-kDa major extracellular housekeeping protein (termed p60) for normal cell division (6). This p60 protein is transcribed independently of the central virulence regulator PrfA, and it is also involved in the attachment of *L. monocytogenes* to certain eukaryotic cells and the internalization of *L. monocytogenes* into certain eukaryotic cells (6, 14). Spontaneously occurring, rough mutants of *L. monocytogenes* that secrete greatly reduced levels of p60 and that form long chains of cells (designated MCR variants in this study) were described previously (13, 14, 25). Although septum formation still occurs, separation of the divided cells does not take place (25). MCR variants were shown to have reduced virulence in the mouse model of infection and did not efficiently invade mouse 3T6 fibroblasts (14). Treatment of MCR variants with partially purified cell-free p60 led to disaggregation of cell chains to normal-sized single bacterial cells whose invasiveness was restored (6, 14, 25). Thus, for these MCR variants, cell-free p60 not only causes decay of cell chains but participates actively in the invasion process.

Here, we report on the identification and characterization of atypical rough filaments of *L. monocytogenes* (designated FR variants) from clinical specimens (isolated from patients with sepsis and pyrexia) and food samples that show wild-type levels of adherence, invasion, and cytotoxicity to human epithelial HEp-2, Caco-2, and HeLa cells. In addition, we show that these virulent FR isolates differ from previously reported avirulent MCR strains in that they secrete wild-type or greater levels of cell-free p60.

* Corresponding author. Mailing address: Department of Bioscience and Biotechnology, University of Strathclyde, Royal College Bldg., 204 George St., Glasgow G1 1XW, United Kingdom. Phone: 44 (0) 141 548 2531. Fax: 44 (0) 141 553 4124. E-mail: n.j.rowan@strath.ac.uk.

MATERIALS AND METHODS

Bacterial strains and growth media. The *Listeria* strains used in the study were, if not otherwise indicated, derived or obtained from the Special *Listeria* Culture Collection (SLCC) of H. P. R. Seeliger, Würzburg, Germany, or from the National Collection of Type Cultures (NCTC), Public Health Laboratory Service (PHLS), Central Public Health Laboratory, Colindale, United Kingdom (Table 1). Two autoagglutinable blood culture and food isolates of *L. monocytogenes* that exhibited a rough phenotype were obtained from the Food Safety Microbiology Laboratory, PHLS, Colindale, United Kingdom. Clinical strains PHLRIII and PHLRIV were blood culture isolates from a 76-year-old female and a 72-year-old male, respectively, both of whom had sepsis and pyrexia. Strain RII (SLCC 5779) was originally obtained from J. Potel (Institute for Medical Microbiology, Medical Academy, Hannover, Germany). The rough variants SURI, SURII, and SURIII were derived from parent strains S1, S2, and S3, respectively, via heating studies (23). Isolation of spontaneous rough variant RI and *L. monocytogenes* rough variants RII and RIV, derived from *L. monocytogenes* Mackaness and EGD, respectively, was reported elsewhere (14). *L. monocytogenes* RIII, another rough mutant derived from a smooth strain of serovar 1/2a, was obtained from J. Potel (Institute for Medical Microbiology).

Listeria cells were grown in brain heart infusion (BHI) broth (Oxoid Ltd., Basingstoke, England) at 37°C with agitation. For adhesion and invasion assays, the bacteria were harvested in the logarithmic growth phase and were washed three times by centrifugation (MSE Centaur 1) at 3,000 rpm for 10 min in Dulbecco's minimum essential medium (DMEM; Gibco BRL, Life Technologies Ltd., Paisley, Scotland). The stored bacteria were kept at −70°C in phosphate-buffered saline (PBS) with 20% (vol/vol) glycerol until they were used.

Biochemical and physiological methods. Catalase production was determined by applying a drop of 30% H_2O_2 to the colonies and observing the occurrence of O_2 bubbles, as described elsewhere (4). The CAMP test was performed by standard procedures by streaking out bacteria perpendicular to *Staphylococcus aureus* on 5% sheep blood agar plates and observing zones of augmented hemolysis, as described elsewhere (4). The characteristic blue-green sheen from the colonies as detected with obliquely transmitted light and the tumbling motility of *Listeria* cells were determined as described elsewhere (23). The test strains were examined for arsenic and cadmium sensitivities as described elsewhere (17). The commercial biochemical API *Listeria* test (bioMerieux, Marcy l'Etoile, France) was used according to the manufacturer's instructions.

TABLE 1. *L. monocytogenes* strains used and their characteristic morphological and physiological properties identified in this study

Strain	Serotype	Reference strain no.	Origin	Cell morphology			Colony area (μm^2)[a]		Titer by ELISA (A_{492}) with anti-p60 MAb[b]
				Form	Designation	Length (μm)[c]	TSYEA	LSA	
S1	4b	NCTC 11994	Adult meningitis	Single, paired cells	Wild-type smooth	3.0 ± 1.0 A	$(6.1 \pm 0.6) \times 10^5$ A	$(9.4 \pm 0.6) \times 10^4$ A	0.63 ± 0.06 B
S2	4b	NCTC 9863	Infantile meningitis	Single, paired cells	Wild-type smooth	3.7 ± 1.2 A	$(6.4 \pm 0.4) \times 10^5$ A	$(2.1 \pm 1.1) \times 10^5$ B	0.53 ± 0.09 B
S3	1/2a	NCTC 10357	Type strain (rabbit)	Single, paired cells	Wild-type smooth	3.3 ± 0.9 A	$(5.9 \pm 0.3) \times 10^5$ A	$(1.7 \pm 0.7) \times 10^5$ B	0.55 ± 0.04 B
RI[d]	1/2a	SLCC 5764	Kathariou et al. (13)	Long cell chains	MCR variant	71 ± 18.9 B	$(1.1 \pm 0.8) \times 10^6$ B	$(1.2 \pm 0.7) \times 10^6$ C	0.26 ± 0.08 D
RII[e]	1/2a		Kathariou et al. (13)	Long cell chains	MCR variant	80 ± 28.1 B	$(1.6 \pm 1.3) \times 10^6$ B	$(1.8 \pm 0.8) \times 10^6$ C	0.28 ± 0.02 D
RIII	1/2a	SLCC 5779	J. Potel (see text)	Long cell chains	MCR variant	81.5 ± 19.1 B	$(1.8 \pm 0.9) \times 10^6$ B	$(2.1 \pm 0.8) \times 10^6$ C	0.23 ± 0.03 D
PHLRII		L7071	Dried custard powder	Long cell chains	MCR variant	68.8 ± 22.4 B	$(9.1 \pm 1.1) \times 10^5$ B	$(9.4 \pm 0.7) \times 10^5$ C	0.31 ± 0.05 D
SURI[f]	4b		Rowan and Anderson (23)	Long filaments	FR variant	56.1 ± 31 B	$(9.5 \pm 0.5) \times 10^5$ B	$(9.8 \pm 1.3) \times 10^5$ C	0.60 ± 0.06 B
SURII[g]	4b		Rowan and Anderson (23)	Long filaments	FR variant	59.2 ± 37.9 B	$(9.7 \pm 1.1) \times 10^5$ B	$(1.0 \pm 0.8) \times 10^6$ C	0.49 ± 0.08 C
SURIII[h]	1/2a		This study	Long filaments	FR variant	61.7 ± 42.1 B	$(9.5 \pm 0.5) \times 10^5$ B	$(9.7 \pm 0.6) \times 10^5$ C	0.58 ± 0.05 B
PHLRI		L6705	Dried custard powder	Long filaments	FR variant	49.9 ± 34.1 B	$(9.2 \pm 0.6) \times 10^5$ B	$(9.3 \pm 0.6) \times 10^6$ C	0.75 ± 0.04 A
PHLRIII		L7346	Blood culture	Long filaments	FR variant	58.2 ± 25.3 B	$(8.9 \pm 0.7) \times 10^5$ B	$(9.1 \pm 1.0) \times 10^5$ C	0.71 ± 0.06 B
PHLRIV		L1342	Blood culture	Long filaments	FR variant	73.5 ± 18.3 B	$(9.9 \pm 0.5) \times 10^5$ B	$(1.4 \pm 1.1) \times 10^6$ C	0.65 ± 0.04 B
RIV[d]	1/2a		Kathariou et al. (13)	Cells and long filaments	IR variant	62 ± 28.3 B	$(9.6 \pm 1.0) \times 10^5$ B	$(8.5 \pm 1.6) \times 10^5$ C	0.72 ± 0.06 A

[a] Mean of area measurements for 20 colonies.
[b] ODs at 492 nm of greater than 0.1 were considered a positive result. BHI broth controls gave a value of 0.03 ± 0.01.
[c] Average length from 20 measurements. Single and paired cells were measured and averaged for the smooth-cell forms. Values in the same column followed by the same letter did not differ at the level of $P < 0.05$, while values with different letters differed at the level of $P < 0.05$.
[d] Derived from *L. monocytogenes* Mackaness (SLCC 5764).
[e] Derived from *L. monocytogenes* EGD.
[f] Derived from *L. monocytogenes* NCTC 11994.
[g] Derived from *L. monocytogenes* NCTC 9863.
[h] Derived from *L. monocytogenes* NCTC 10357.

Adhesion and invasion assays. The ability of *Listeria* test strains to adhere to and invade HeLa, HEp-2, and Caco-2 cells was determined by previously described procedures (24), with minor modifications. HeLa, HEp-2, and Caco-2 cell monolayers were grown overnight in a 5% CO_2 atmosphere at 37°C in DMEM supplemented with 10% fetal calf serum (FCS; Gibco BRL) in 24-well tissue culture plates seeded with approximately 3×10^5 cells per well. Prior to adhesion and invasion assays, the monolayers were washed three times in DMEM followed by the addition of 1 ml of DMEM containing 10% FCS to each well. Bacterial cultures were resuspended in 1 ml of DMEM to optical densities (ODs; model UV-120-02 spectrophotometer; Shimadzu Corp., Kyoto, Japan) at 580 nm of 2.0 for wild-type cells, 2.2 for FR-type cells, and 2.3 for MCR-type cells (corresponding to cell populations of $\sim 3.5 \times 10^9$ CFU/ml). For adherence assays, triplicate monolayers were infected with 0.1 ml of bacterial culture, followed by a 2-h incubation at 37°C in a 5% CO_2 atmosphere. After incubation, nonadherent bacteria were removed by three washes with 3 ml of DMEM. The tissue culture cells were lysed with 1 ml of 1% (vol/vol) Triton X-100 (in distilled water) for 5 min at 37°C, followed by serial dilution in 0.9 ml of PBS, with subsequent enumeration by plating 0.1 ml of appropriate 10-fold dilutions on BHI agar. For invasion and intracellular growth assays, 1 ml of fresh DMEM containing 10% FCS and 100 μg of gentamicin per ml was added to the infected tissue culture monolayers, followed by a 2-h incubation at 37°C. The tissue culture cells were washed three times in 3 ml of DMEM and were then lysed with 1 ml of 1% (vol/vol) Triton X-100 (in distilled water) for 5 min at 37°C. The surviving bacteria were quantified by the same method outlined above.

Cytotoxicity assay. Assessment of the cytotoxic effect was made by measuring total cellular metabolic activity with the tetrazolium salt 3-(4,5-dimethylthiazole-2-yl)-2,5-phenyl tetrazolium bromide (MTT; Sigma). The cytotoxicity assay of Coote and Arain (8) was used, with minor modifications. HEp-2 and HeLa cell monolayers were grown overnight at 37°C in a 5% CO_2 atmosphere in DMEM supplemented with 10% FCS in 96-well microplates seeded with $\sim 5 \times 10^4$ cells per well. Bacterial culture supernatants, prepared as described above, were added in triplicate to the test plates immediately or after heating of the supernatants at 95°C for 10 min. Positive and negative assay controls were 1% Triton X-100 (Sigma) and PBS, respectively. Microplates that contained the infected tissue culture monolayers were incubated overnight at 37°C in a 5% CO_2 atmosphere, followed by the addition of PBS containing 0.5% MTT (Sigma) to each well for 4 h at 37°C. The suspension in the wells was then removed and the formazan product was solubilized by the addition of 100 μl of 0.04 N HCl in dimethyl sulfoxide (Sigma). The contents of the wells were measured spectrophotometrically at 620 nm in a microplate reader (Bio-Rad). The toxic effect of the cell-free bacterial culture supernatant on the HEp-2 and HeLa cell lines was calculated from the following equation: (1 − OD of test sample/OD of negative control) × 100.

ELISA for detection of p60 protein. Detection of p60 protein by an indirect enzyme-linked immunosorbent assay (ELISA) involved the addition of 100 μl of cell-free supernatant (supernatant from an overnight culture harvested by centrifugation) to each well of the microtiter plates and incubation for 2 h at 37°C. Coating proteins were washed three times with wash buffer (PBS containing 0.1% [vol/vol] Tween 20), and the *L. monocytogenes*-specific anti-p60 monoclonal antibody (MAb) K3A7 (7) was added. This MAb was generated against the *L. monocytogenes*-specific epitope, peptide D, of the p60 protein, which has been described previously (6, 12). The anti-p60 MAb was prepared as a tissue culture supernatant that was diluted 1/200 (vol/vol) in wash buffer and incubated for 1 h at room temperature. The microtiter wells were washed three times with wash buffer, sheep anti-mouse horseradish peroxidase conjugate (Sigma) was added at 100 μl $well^{-1}$ and a dilution of 1/1,000 in wash buffer, and the plates were incubated for 1 h at room temperature. Excess conjugate was washed five times with wash buffer, as the substrate SIGMA FAST OPD tablets (Sigma) were added at 100 μl/well, and the plates were incubated for 0.5 h at room temperature. The A_{492} was measured after the addition of 50 μl of 3 M H_2SO_4 to each well.

Biological assay for p60. The cell chain disruption activity of p60 was tested with rough *L. monocytogenes* strains (Table 1) as described elsewhere (25), with minor modifications. Strains were grown in BHI broth to the early stationary phase; cell chains were washed with PBS, resuspended to ODs of 2.0, 2.2, and 2.3 at 580 nm (for reasons described earlier) in PBS containing 20% (vol/vol) glycerol, and stored at −20°C until use. The culture supernatant from *L. monocytogenes* S1, which contained extracellular proteins including p60, was concentrated 100-fold with a 10-kDa-molecular-mass-cutoff Omega membrane (Microsep Microconcentrators; Filtron Technology Corp., Northborough, United Kingdom), after which the culture supernatant was filter sterilized (pore size, 0.2 μm; Sartorius). To test for chain disruption activity, 30 μl of concentrated supernatant was diluted serially twofold in PBS containing 2 mM dithiothreitol (Sigma) and was separately incubated with 30 μl of the *Listeria* test strains for 1 to 3 h (samples were assessed at 30-min intervals). At the indicated time points, 10 μl of the mixture was examined by phase-contrast microscopy to evaluate the lengths of the bacteria.

Cell chain length and colony appearance determination. Overnight cultures of all *L. monocytogenes* strains described in Table 1 were separately incubated in BHI broth at 37°C with aeration. At various time intervals, the lengths of the cells were determined by image analysis (with a Nikon Optiphot-2 microscope that was connected to a Solitaire 512 Image Analyzer [Seescan Plc.]). Twenty cells

were measured per sample. Overnight cultures were also grown at 30°C on *Listeria* selective agar (LSA; Oxford formulation; Oxoid) and on Tryptone soya yeast extract agar (TSYEA; Oxoid) to investigate differences in colony appearance. The areas (in square micrometers) of 20 colonies per sample were measured with the image analysis system mentioned above.

Electron microscopy. The cells were grown to the mid-log phase, washed twice with PBS, and resuspended in sterile-distilled water before application to Formvar-coated grids. After the grid was dried, 1 drop of a solution containing 3% (vol/vol) tungstophosphoric acid and 0.3% (vol/vol) sucrose (pH 6.8 to 7.4) was added. The solution was removed after 30 to 60 s, and the grid was dried and examined on a Zeiss 902 transmission electron microscope.

Statistical methods. All experiments in this study were performed in triplicate, and the results are reported as averages. Differences in secreted levels of cell-free p60, cell chain or filament length, colony appearance, and putative virulence properties such as levels of cytotoxicity, adherence, and penetration into human epithelial HeLa, HEp-2, and Caco-2 cells were calculated at the 95 or 99.9% confidence intervals by analysis of variance (one-way or balanced model) with Minitab software, release 11 (Minitab Inc., State College, Pa.).

RESULTS

Identification of rough variants of *L. monocytogenes* from clinical and food samples. All of the bacterial strains described in Table 1 were identified as *L. monocytogenes* by establishing the characteristic morphological, physiological, and biochemical properties associated with this bacterial pathogen. All cultures produced catalase, were CAMP test positive with *S. aureus*, and were identified as *L. monocytogenes* by the API *Listeria* tests. Confirmation of the species identification occurred by analysis of culture supernatant for p60 protein by indirect ELISA with an *L. monocytogenes*-specific anti-p60 MAb (Table 1).

The cell and colony appearances of all rough variants were shown to differ from those of the wild-type *L. monocytogenes* strains, which had the typical smooth morphology. Unlike wild-type smooth strains, whose cells have the characteristic coccobacillus appearance (approximately 0.5 μm in diameter by 2 μm in length), cell types associated with the rough variants were shown to be atypically long. Some rough variants consisted of unseptated or paired filaments that measured up to 96 μm in length (designated FR variants), whereas others formed long chains that were up to 110 μm in length and that consisted of multiple cells of similar size (designated MCR variants) (Table 1). Rough variants isolated from clinical specimens and food samples or derived under conditions of heat stress predominately showed an FR filamentous phenotype (Table 1). MCR and FR variants were found to be incapable of characteristic tumbling motility and formed irregular or rough colonies that no longer produced a blue-green sheen upon oblique illumination. Image analysis data also showed that irregular rough-form colonies consistently had different areas (in square micrometers) and appearances ($P < 0.05$) compared to those of the smaller, wild-type smooth-form colonies after 48 h of growth on both TSYEA and LSA plates (Table 1). The MCR and FR variants of *L. monocytogenes* were not shown to differ in colony size or appearance on either plating medium (Table 1).

It is unlikely that the FR variants PHLRI, PHLRIII, and PHLRIV were epidemiologically linked, as they differed in their sensitivities to arsenic and cadmium on biotyping. The sensitivities to arsenic and cadmium were as follows: PHLRIII and PHLRIV, arsenic sensitive and cadmium resistant; PHLRI, arsenic and cadmium resistant. Serotyping of these particular strains was not possible as they autoagglutinate.

FR variants of *L. monocytogenes* secrete wild-type levels of p60 and vary in the degree of cell septation. Spontaneously occurring MCR variants of *L. monocytogenes* with a rough colony appearance, namely, RI, RII, RIII, and RIV (14), and the food sample isolate PHLRII exhibited similar phenotypes; they tended to form cell chains in which septum formation between individual cells still occurred, but the cells did not separate. However, *L. monocytogenes* RIV differed from the other MCR variants by the random formation of septa along the length of the cell chains, resulting in cells of dissimilar lengths within the long chains. Indirect ELISA studies (Table 1) with an anti-p60 MAb showed that four of these MCR variants secrete a considerably reduced amount of the major extracellular protein p60, whereas the fifth one (variant RIV) synthesized a wild-type level or an even larger amount of this protein, as described previously (15). The addition of partially purified p60 to *L. monocytogenes* RI, RII, RIII, and PHLRII variants led to a decay of the cell chains (mean, 75.3 ± 22.1 μm) to the normal size (mean, 3.5 ± 1.1 μm) within 3 h of treatment. However, treatment of *L. monocytogenes* RIV with partially purified p60 of wild-type *L. monocytogenes* did not lead to a decay of the cell chains, as the cell chain lengths before (62 ± 28.3 μm) and after (66.4 ± 23.7 μm) 3 h of p60 treatment did not differ significantly ($P < 0.05$), which confirmed previous observations (14).

The two blood culture isolates PHLRIII and PHLRIV, the food sample isolate *L. monocytogenes* PHLRI, and the three *L. monocytogenes* variants SURI, SURII, and SURIII that we previously derived from wild-type smooth-form cultures under conditions of sublethal heat stress (Table 1) (23) also exhibited a rough colony appearance. However, these rough strains differed in cell morphology from the aforementioned MCR variants, as these FR variants formed long filaments that either were unseptated or contained a single septum (Table 1). These filaments were often of dissimilar size, as septum formation occurred at different locations. Unlike MCR variants that secrete diminished levels of cell-free p60, indirect ELISA studies showed that these FR variants produced wild-type and larger amounts of p60 (Table 1). The addition of partially purified p60 from wild-type *L. monocytogenes* to all FR variants did not decay the lengths of the filaments to the normal *Listeria* cell size.

FR variants are invasive and show wild-type *L. monocytogenes* levels of cytotoxicity to human epithelial HEp-2 and HeLa cells. All MCR variants tested showed a considerably reduced ability to adhere to and invade HEp-2 and HeLa epithelial cells under conditions that were appropriate for the efficient attachment and uptake of the three wild-type smooth *L. monocytogenes* strains (Fig. 1). In marked contrast, FR variants showed levels of adherence to and invasiveness of HEp-2 and HeLa cells that were similar to those of wild-type smooth-form *L. monocytogenes* strains (Fig. 1). With the exception of *L. monocytogenes* RIV, neither epithelial cell line was more susceptible to adherence or penetration by the *Listeria* test strains (Fig. 1). Addition of partially purified p60 from wild-type *L. monocytogenes* S1 to the MCR variants *L. monocytogenes* RI, RII, RIII, and PHLRII not only caused a decay of cell chains but also resulted in a restoration of *L. monocytogenes* invasiveness to wild-type levels in HEp-2 and HeLa cells (Fig. 2). While treatment of the MCR variant *L. monocytogenes* RIV with p60 did not lead to a disruption of the cell chains, it did restore invasiveness to a significant extent in these human epithelial cell lines (Fig. 2). An interesting aspect of RIV is that it appears to be an intermediary morphological form (or IR variant), as it possesses both normal-sized bacterial cells and long filaments within its cell chain.

It has also been reported that the ability of mutant RIII to adhere to Caco-2 cells is not affected; however, no data regarding the ability of this variant to invade this cell line were presented (5). Thus, the ability of a limited number of test *L. monocytogenes* strains that varied in their cell morphologies

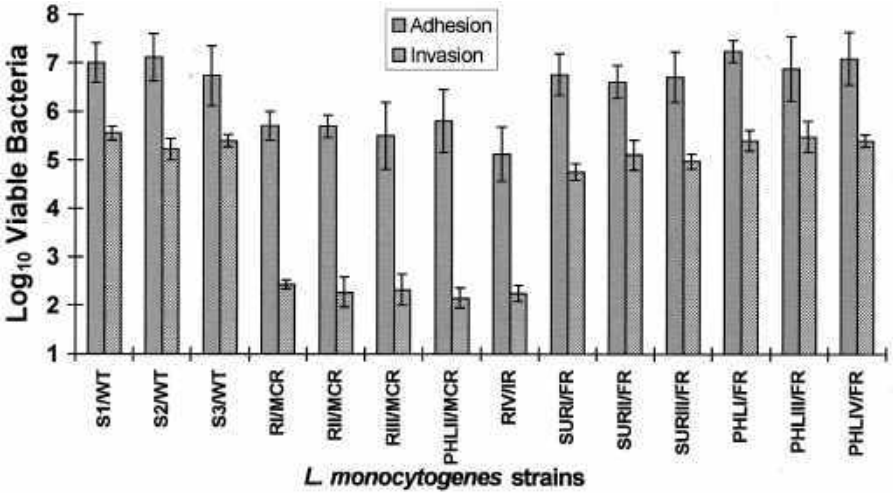

FIG. 1. Adherence of different *L. monocytogenes* strains to HEp-2 cells and invasion of different *L. monocytogenes* strains into HEp-2 cells. Due to similarities in adhesion and invasion data for HEp-2 and HeLa cell lines ($P < 0.05$), only invasion results for HEp-2 cells are illustrated here.

(namely, the wild-type strain S1, the MCR variants RIII and PHLRII, and the FR variant PHLRI) to adhere to and invade Caco-2 cells was investigated. These particular bacteria showed similar levels of adhesion ($P < 0.05$) to this epithelial cell line (approximately 1.4% ± 0.5% adherence for all bacterial cells challenged). However, the MCR variants *L. monocytogenes* RIII and PHLRII showed markedly reduced levels of invasion of Caco-2 cells (approximately 0.0009% ± 0.0003% and 0.0004% ± 0.0002% invasion of the cells that adhered, respectively) compared to the penetrating abilities of the wild-type *L. monocytogenes* S1 (2.3% ± 0.6% invasion) and the FR variant PHLRI (1.9% ± 0.4% invasion). This ability of the MCR variants of *L. monocytogenes* to show wild-type levels of adherence to Caco-2 cells is in marked contrast to the reduced adherence evident for these strains in other epithelial cell lines (i.e., 0.22% ± 0.04% and 0.18% ± 0.05% adherence to HEp-2 and HeLa cells, respectively), as described above (Fig. 1).

Due to earlier described differences in cell morphology and physiology between *L. monocytogenes* MCR and FR variants and smooth-form cells, the ability of these *Listeria* strains to elicit a cytotoxic response in HEp-2 and HeLa cells was investigated. All *L. monocytogenes* test strains showed similar levels of cytotoxicity for both HEp-2 and HeLa cells ($P < 0.05$), where the average toxicities for all 14 *Listeria* test strains were 68.3% ± 6.1% and 69.5% ± 4.7%, respectively. Both HEp-2 and HeLa cell lines were similarly affected by the levels of toxicity produced by the test *L. monocytogenes* strains ($P < 0.05$).

DISCUSSION

Due to the severity of listeriosis in predisposed individuals and the uncertainty as to the infectious dose of this pathogenic bacterium, the identification of atypical, virulent cell forms of *L. monocytogenes* in clinical or food samples is of paramount importance (16, 23). In this study we report on the characterization of atypical filaments of *L. monocytogenes* that were isolated from the blood of patients with pyrexia and sepsis and that showed wild-type levels of adherence, invasion, and cytotoxicity to human epithelial cells. Virulent filamentous cell forms of *L. monocytogenes* were also obtained from food samples and under conditions of sublethal environmental stress (23). These FR variants of *L. monocytogenes* not only had atypical cell and colony morphologies but were also unable to produce tumbling motility and failed to provide a characteristic blue-green sheen upon oblique illumination. While identification of irregular colonies as *L. monocytogenes* by conventional methods would appear to be problematic, once isolated, the identities of these atypical *Listeria* strains can be rapidly determined by conventional biochemical tests or by an indirect ELISA with an *L. monocytogenes*-specific MAb that recognizes a secreted p60 protein. The use of *L. monocytogenes* p60-specific antibodies for the unequivocal identification of this species, including other avirulent rough isolates, has been demonstrated in a series of publications (2, 4, 6). The test *Listeria* strains can also be successfully identified by indirect ELISA with the commercially available, polyclonal KPL antibody (Kirkegaard & Perry Laboratories, Gaithersburg, Md.) (data not shown).

Here, we have characterized rough variants of *L. monocytogenes* which differ from the wild-type smooth form of *L. monocytogenes* either by the formation of long chains that consist of multiple cells (MCR variants) or by the formation of single or paired filaments (FR variants). MCR variants are impaired in the synthesis of the major extracellular protein p60 and, con-

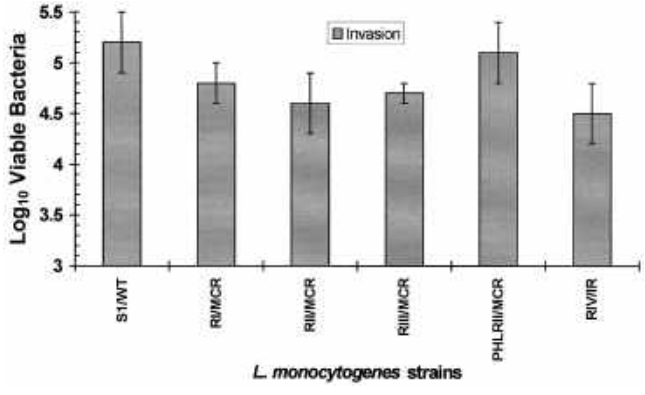

FIG. 2. Reconstitution of invasiveness of *L. monocytogenes* MCR variants by treatment of cells with p60 (concentrated supernatant of *L. monocytogenes* S1). Due to similarities in adhesion and invasion data for HEp-2 and HeLa cell lines ($P < 0.05$), only invasion results for HEp-2 cells are illustrated here.

sequently, tend to form cell chains in which septum formation between the individual cells still occurs but the cells do not separate. Other researchers have shown that p60 possesses a murein hydrolase activity which is required for a late step in cell division (3, 25). Cell-chain-disruption activity can be blocked by inhibition of the single cysteine residue that occurs in all p60 proteins at the same position in the C terminus (25).

All MCR variants that we tested showed a considerably reduced ability to invade the human epithelial HEp-2, Caco-2, and HeLa cell lines under conditions that were appropriate for efficient penetration by wild-type *L. monocytogenes* cells. This finding is in agreement with those of other researchers, who showed that spontaneously occurring MCR variants have a reduced ability to adhere to and invade embryo mouse fibroblast 3T6 cells (14). These data suggest that the reduced invasiveness of this MCR variant for HEp-2 and HeLa cells was due at least in part to the reduced adherence of this long-cell-chain variant. This reduction in adherence appears to be directly related to the reduced amount of cell-free p60 synthesized by these MCR mutants, since the addition of purified or partially purified p60 restored the invasiveness of this variant (14). It could be demonstrated that the addition of p60 to *L. monocytogenes* RIII restored adherence to and invasiveness into 3T6 fibroblasts to levels comparable to those demonstrated by wild-type *L. monocytogenes* (6, 14). Our study also corroborates the work of Kuhn and Goebel (14), who first described wild-type levels of p60 secretion by *L. monocytogenes* RIV and further showed that the addition of wild-type p60 did not disrupt these long cell chains but restored invasiveness into nonprofessional phagocytic 3T6 mouse fibroblast cells.

In contrast to MCR variants, we have described clinical and food isolates of *L. monocytogenes* that showed a long filamentous-like cell morphology and that secreted wild-type levels of cell-free p60. The appearance of FR variants was not altered by the addition of p60, and this atypical cell form demonstrated wild-type levels of invasiveness to HEp-2 and HeLa cells (and to Caco-2 cells for a limited number of FR variants tested). It has been observed that long filamentous forms of *L. monocytogenes* with a rough phenotype similar to that of lactobacilli or filamentous forms with a smooth phenotype can appear, in the latter case under the influence of suboptimal antibiotic concentrations (as cited in reference 4). However, to our knowledge, this is the only description of virulent filamentous forms of *L. monocytogenes* that have naturally occurred in clinical and food environments. It would appear that these autoagglutinable FR variants isolated from clinical (*L. monocytogenes* PHLRIII and PHLRIV) and food (*L. monocytogenes* PHLRI) samples are not epidemiologically linked, as the strains were isolated from different parts of the United Kingdom and have different biotypes, as a result of which they vary in their sensitivities to arsenic and cadmium. The FR phenotype is very stable on agar plates, and we assume that the FR phenotype was also presented by the clinical isolates during infection, since we also observed cell chain formation during multiplication inside host cells in our tissue culture studies (data not shown). Thus, it is not clear at which time point a mutation led to this phenotype. It must be appreciated, however, that while these clinical and food *L. monocytogenes* FR isolates exhibited wild-type *L. monocytogenes* levels of virulence in a variety of human epithelial cell lines, this does not necessarily allow one to infer that these cultures can cause disease in a complete animal.

However, in the laboratory it is possible to transform *L. monocytogenes* from the wild-type smooth form to the rough form. We previously showed that exposure of wild-type smooth forms of *L. monocytogenes* to environmental stress conditions, such as heat shock and growth at above-optimal temperatures, resulted in the generation of atypical cell forms of *Listeria* with an FR phenotype (23). Other researchers have also shown that exposure of *L. monocytogenes* to other environmental stresses results in a marked change in the lengths of treated cells (22). It is likely that the ability of *L. monocytogenes* to react and respond to changes in its surroundings is crucial to its survival (1, 18). It has recently been shown that exposure of bacterial enteropathogens such as *Salmonella enterica* serotype Typhimurium and verocytotoxigenic *Escherichia coli* to sublethal environmental stresses protects these problematic bacteria from lethal levels of the same and different stresses and may also increase their virulence (22). Acid-adapted *L. monocytogenes* cells demonstrated increased tolerance to thermal stress, osmotic stress, crystal violet, and ethanol; and emerging acid-tolerant *L. monocytogenes* cells were often shown to be more virulent when injected interperitoneally into mice (15). Recent evidence shows that there is expressional cross talk between the central virulence regulator PrfA and the stress response mediator ClpC in *L. monocytogenes* (21). The reasons for the difference in cell morphology and virulence of FR variants compared with those of the wild-type smooth form of *L. monocytogenes* and other types of R variants are still not known. However, other studies have shown that double mutations of the molecular chaperones ClpC and ClpE in *Listeria* cells also affect both cell division and virulence (19).

In summary, we have described the occurrence and unequivocal identification of three different rough forms of *L. monocytogenes* from clinical and food samples and from strains derived under conditions of sublethal heat stress. As the occurrence of virulent FR variants in clinical and food environments may be underestimated because of misidentification and underrecognition, we suggest that irregularly shaped bacterial cultures from clinical and food samples that produce a characteristic black precipitate on LSA plates should be further investigated.

ACKNOWLEDGMENTS

We thank the University of Strathclyde for funding this research.

We thank K. Deans for tissue culture assistance and V. Gill and D. McLaughlin for excellent technical support.

REFERENCES

1. **Abee, T., and J. A. Wouters.** 1999. Microbial stress response in minimal processing. Int. J. Food Microbiol. **50:**65–92.
2. **Allerberger, F., M. Dierich, G. Petranyi, M. Lalic, and A. Bubert.** 1997. Nonhemolytic strains of *Listeria monocytogenes* detected in milk products using VIDAS immunoassay kit. Zentbl. Bakteriol. Parasitenkd. Infektkrankh. Hyg. Abt. 1 Orig. **200:**189–195.
3. **Bubert, A., H. Kestler, M. Götz, R. Böckmann, and W. Goebel.** 1997. The *Listeria monocytogenes* iap gene as an indicator gene for the study of PrfA-dependent regulation. Mol. Gen. Genet. **256:**54–62.
4. **Bubert, A., J. Riebe, N. Schnitzler, A. Schönberg, W. Goebel, and P. Schubert.** 1997. Isolation of catalase-negative *Listeria monocytogenes* strains from listeriosis patients and their rapid identification by anti-p60 antibodies and/or PCR. J. Clin. Microbiol. **35:**179–183.
5. **Bubert, A., M. Kuhn, W. Goebel, and S. Köhler.** 1992. Structural and functional properties of the p60 proteins from different *Listeria* species. J. Bacteriol. **174:**8166–8171.
6. **Bubert, A., P. Schubert, S. Köhler, R. Frank, and W. Goebel.** 1994. Synthetic peptides derived from the *Listeria monocytogenes* p60 protein as antigens for the generation of polyclonal antibodies specific for secreted cell-free *L. monocytogenes* p60 proteins. Appl. Environ. Microbiol. **60:**3120–3127.
7. **Chakraborty, T., M. Leimeister-Wächter, E. Domann, M. Hartl, W. Goebel, T. Nichterlein, and S. Notermans.** 1992. Coordinate regulation of virulence genes in *Listeria monocytogenes* requires the product of the *prfA* gene. J. Bacteriol. **174:**568–574.
8. **Coote, J. G., and T. Arain.** 1996. A rapid, colourimetric assay for cytotoxin activity in *Campylobacter jejuni*. FEMS Immunol. Med. Microbiol. **13:**65–70.
9. **Dramsi, S., I. Biswas, E. Maguin, L. Braun, P. Mastroeni, and P. Cossart.** 1995. Entry of *Listeria monocytogenes* into hepatocytes requires expression of

inlB, a surface protein of the internalin multigene family. Mol. Microbiol. **16:** 251–261.
10. **Drevets, D. A., R. T. Sawyer, T. A. Potter, and P. A. Campbell.** 1995. *Listeria monocytogenes* infects human endothelial cells by two distinct mechanisms. Infect. Immun. **63:**4268–4276.
11. **Gaillard, J. L., P. Berche, J. Mounier, S. Richard, and P. Sansonetti.** 1987. In vitro model of penetration and intracellular growth of *Listeria monocytogenes* in the human enterocyte-like cell line Caco-2. Infect. Immun. **55:** 2822–2829.
12. **Harlow, E., and D. Lane.** 1988. Antibodies: a laboratory manual. Cold Spring Harbor Laboratory, Cold Spring Harbor, N.Y.
13. **Kathariou, S., J. Hacker, H. Hof, I. Then, W. Wagner, M. Kuhn, and W. Goebel.** 1987. Bacterial cytotoxins—extracellular proteins and virulence factors, p. 141–150. *In* R. Rott and W. Goebel (ed.), Molecular basis of viral and microbial pathogenesis. Springer-Verlag, Berlin, Germany.
14. **Kuhn, M., and W. Goebel.** 1989. Identification of an extracellular protein of *Listeria monocytogenes* possibly involved in intracellular uptake by mammalian cells. Infect. Immun. **57:**55–61.
15. **Marron, L., N. Emerson, C. G. M. Gahan, and C. Hill.** 1997. A mutant of *Listeria monocytogenes* L028 unable to induce an acid tolerance response displays diminished virulence in a murine model. Appl. Environ. Microbiol. **63:**4945–4947.
16. **McLauchlin, J.** 1997. The pathogenicity of *Listeria monocytogenes*: a public health perspective. Rev. Med. Microbiol. **8:**1–14.
17. **McLauchlin, J., M. D. Hampton, S. Shah, J. Threlfall, A. A. Wieneke, and G. D. W. Curtis.** 1997. The subtyping of *Listeria monocytogenes* on the basis of plasmid profiles and arsenic and cadmium susceptibilities. J. Appl. Microbiol. **83:**381–388.
18. **Mekalanos, J. J.** 1992. Environmental signals controlling expression of virulence determinants in bacteria. J. Bacteriol. **174:**1–7.
19. **Nair, S., C. Frehel, L. Nguyen, V. Escuyer, and P. Berche.** 1999. ClpE, a novel member of the HSP100 family, is involved in cell division and virulence of *Listeria monocytogenes*. Mol. Microbiol. **31:**185–196.
20. **Racz, P., K. Tenner, and E. Mero.** 1972. Experimental *Listeria* enteritis. 1. An electron microscopic study of the epithelial phase in experimental *Listeria* infection. Lab. Investig. **26:**694–700.
21. **Ripio, M.-T., J.-A. Vázquez-Boland, Y. Vega, S. Nair, and P. Berche.** 1998. Evidence for expressional crosstalk between the central virulence regulator PrfA and the stress response mediator ClpC in *Listeria monocytogenes*. FEMS Microbiol. Lett. **158:**45–50.
22. **Rowan, N. J.** 1999. Evidence that inimical food-preservation barriers alter microbial resistance, cell morphology and virulence. Trends Food Sci. Technol. **10:**261–270.
23. **Rowan, N. J., and J. G. Anderson.** 1998. Effects of above-optimum growth temperature and cell morphology on thermotolerance of *Listeria monocytogenes* cells suspended in bovine milk. Appl. Environ. Microbiol. **64:**2065–2071.
24. **Strom, M. S.** 1998. Phenotypic and genetic characterization of a non-hemolytic variant of *Listeria monocytogenes* from cold-smoked salmon. Food Microbiol. **15:**329–337.
25. **Wuenscher, M. D., S. Köhler, A. Bubert, U. Gerike, and W. Goebel.** 1993. The *iap* gene of *Listeria monocytogenes* is essential for cell viability, and its gene product, p60, has bacteriolytic activity. J. Bacteriol. **175:**3491–3501.

FEMS IMMUNOLOGY & MEDICAL MICROBIOLOGY

RESEARCH ARTICLE

Studies on the susceptibility of different culture morphotypes of *Listeria monocytogenes* to uptake and survival in human polymorphonuclear leukocytes

Neil J. Rowan, Dominik Kirf & Paul Tomkins

Department of Nursing and Health Science, Athlone Institute of Technology, Athlone, Ireland

Correspondence: Neil J. Rowan, Department of Nursing and Health Science, Athlone Institute of Technology, Dublin Road, Athlone, Ireland. Tel.: +353 9064 71838; fax: +353 9064 86135; e-mail: nrowan@ait.ie

Received 29 April 2009; revised 24 June 2009; accepted 30 July 2009.
Final version published online 7 September 2009.

DOI:10.1111/j.1574-695X.2009.00597.x

Editor: Patrick Brennan

Keywords
Listeria monocytogenes; atypical cell morphotypes; opsonization; survival; PMNLs.

Abstract

This study demonstrated that atypical virulent filaments of *Listeria monocytogenes* (rough variant type II and designated FR for this study), isolated from clinical specimens or generated during exposure to pulsed-plasma gas discharge in liquids, were shown to be capable of survival when engulfed by human polymorphonuclear leukocytes (PMNLs). Factors shown to significantly influence the maximal respiratory burst response in PMNLs and survival of different internalized cell or filament forms of *L. monocytogenes* were bacterial strain, culture form, degree of opsonization (with and without the use of 10% serum) and composition of the bacterial growth media used before uptake by PMNLs. Opsonized regular-sized *L. monocytogenes* cells grown on blood agar (BA) elicited the greatest respiratory burst response and survived best in PMNLs. The filamentous (FR) and multiple cell chain (MCR) rough variants were significantly less susceptible to uptake and survival in PMNLs. Supplementation of tryptone soya agar with hemin resulted in significantly reduced chemiluminescence responses in phagocytosing PMNLs compared with the maximal levels observed from prior bacterial growth on BA or brain heart infusion agar that also contained a source of iron. The MCR variants secreting decreased levels of a peptidoglycan hydrolase CwhA protein exhibited the lowest percentage survival when internalized in PMNLs compared with wild-type smooth or FR culture variants as determined by the macrophage-killing assay.

Introduction

Listeria monocytogenes is a Gram-positive, rod-shaped, facultative intracellular bacterium that can cause severe food-borne infections in humans and animals (Vázquez-Boland *et al.*, 2001). The major risk groups are immunocompromised individuals and pregnant women. The infective dose of this organism is yet to be determined, and is most probably complicated by a number of factors, including the susceptibility of the host and the virulence of the infecting strain. Virulent strains of *L. monocytogenes* are able to survive and multiply within host macrophages, and can invade, replicate and multiply in nonprofessional phagocytes such as mouse 3T6 fibroblasts, hepatocytes and human colon carcinoma Caco-2 cells (Gaillard *et al.*, 1987; Dramsi *et al.*, 1995; Drevets *et al.*, 1995; Ohya *et al.*, 1998). Its ability to replicate in the cytoplasm of the cells of the host is critical for virulence, as evidenced by the significant attenuation of *L. monocytogenes* when intracellular replication is compromised by mutation (Hardy *et al.*, 2004).

Changes in bacterial colony morphology often accompany microbial adaptation to new environments and ecological niches (Medina *et al.*, 2003; Monk *et al.*, 2004). *Listeria monocytogenes* has also been reported to form atypical elongated (filamentous) cells when exposed to a range of adverse growth conditions, such as high concentrations of NaCl (8–9%) in the presence (Bereski *et al.*, 2002) or absence of acid (Brezin, 1973; Isom *et al.*, 1995; Jørgensen *et al.*, 1995; Bereski *et al.*, 2002), acidic conditions, i.e. pH 5.0 at 37 °C (Isom *et al.*, 1995), increased CO_2 environments (Nilsson *et al.*, 2000; Lie *et al.*, 2003), high hydrostatic pressure (Ritz *et al.*, 2001), osmotic stress (Jørgensen *et al.*,

1995), alkaline stress (Giotis *et al.*, 2007), above optimum growth temperature, i.e. 42.5 °C (Rowan & Anderson, 1998), and the presence of antimicrobial growth agents such as trimethorpim and cotrimoxazole (Minkowski *et al.*, 2001). A number of studies suggest that, in some cases, removal of such deleterious stresses results in a slow return to normal wild-type cell forms within 24 h (Brezin, 1973; Isom *et al.*, 1995), suggesting that filamentation of *L. monocytogenes* may be an adaptive response to adverse growth conditions. Monk *et al.* (2004) had previously observed that chaining cells exhibited enhanced biofilm-forming capabilities. The colonization of the murine gall bladder by *L. monocytogenes* also resulted in a change in cellular morphology (chaining), subsequently leading to the formation of biofilms within the gall bladder, which resembles a dynamic rather than a static environment (Hardy *et al.*, 2006). Variant rough colony morphotypes were thought to occur spontaneously and irreversibly at a low frequency during prolonged culture in the laboratory. Apart from obvious physical differences, such as the absence of a blue-green sheen upon Henri oblique illumination and impaired cell separation that produced chaining cells without coordinated motility, the fermentative and biochemical profiles of rough and smooth colonies were considered identical (Gutekunst *et al.*, 1992; Rowan *et al.*, 2000; Monk *et al.*, 2004).

Characterization of the molecular determinants involved in conversion to the filamentous FR colony variants has been previously described by a number of researchers (Kuhn & Goebel, 1989; Gutekunst *et al.*, 1992; Monk *et al.*, 2004), with the specific involvement of a peptidoglycan hydrolase CwhA (formerly termed invasion-associated protein or p60; Wuenscher *et al.*, 1993) in the formation of the rough colony morphotype. These so-called type 1 rough colony isolates showed reduced CwhA secretion plus decreased attachment and invasion of certain nonphagocytic cell lines (Gutekunst *et al.*, 1992), while a CwhA null mutant was previously used to clarify the role of the CwhA protein during infection (Pilgrim *et al.*, 2003). The isolation of a filamentous rough colony variant (termed type II) showing wild-type levels of CwhA secretion and cellular invasion has also been described previously (Rowan *et al.*, 2000; Lenz & Portnoy, 2002). While the specific mechanisms governing these morphological changes still remain unclear (Gardan *et al.*, 2003; Monk *et al.*, 2004; Giotis *et al.*, 2007), conversion to the atypical rough culture forms may result in a failure to accurately detect and/or enumerate this enteropathogen from adverse conditions such as food preservation or inimical stresses associated with exposure to the host immune system. Although FR variants have been isolated previously from clinical specimens and food samples (Rowan *et al.*, 2000), the multiple long cell chain form (MCR type) secreting reduced levels of CwhA has not. Despite a plethora of published data on the impact of food-processing stresses and associated similarities to deleterious stresses encountered by bacterial pathogens on exposure to host immune cells on the survival and morphological stability of *L. monocytogenes*, very little information currently exists on the susceptibility and/or the survival of different culture morphotypes of this pathogen to a phagocytic attack by human polymorphonuclear leucocytes (PMNLs).

In this report, we examined inter-related factors that affect the susceptibility of different culture morphotypes of *L. monocytogenes* to phagocytosis and survival in human PMNLs.

Materials and methods

Bacterial strains and growth media

The *Listeria* strains used in the study were, if not otherwise indicated, derived or obtained from the National Collection of Type Cultures (NCTC), Public Health Laboratory Service (PHLS), Central Public Health Laboratory, Colindale, UK (Table 1). Autoagglutinable MCR2 and FR2 isolates of *L. monocytogenes* exhibiting rough culture phenotypes were obtained from Dr Jim McLauchlin, Food Safety Microbiology Laboratory, PHLS, Colindale, UK. The FR2 clinical strain of *L. monocytogenes* was obtained from a 72-year-old male with sepsis and pyrexia. The rough filamentous variant FR1 was derived from a wild-type smooth form of *L. monocytogenes* NCTC 4885 after exposure to adverse culture conditions created by high-intensity pulsed-plasma gas discharge treatments according to the method described in Rowan *et al.* (2008).

The *Listeria* cells were grown for 48 h at 37 °C on brain heart infusion agar (BHIA), 7% (v/v) sheep blood agar (BA) and on tryptone soya agar supplemented with 15 μg mL^{-1} hemin (TSHA) and tryptone soya agar without hemin (TSA), before challenging with human PMNLs. Hemin supplements were purchased from Sigma-Aldrich Chemical Co. Ltd, dissolved in hot water, adjusted to pH 7 and filter sterilized before adding to TSA as per the recommendations of Tsai & Hodgson (2003). Stored bacteria were maintained at 4 °C on TSA slopes until use; fresh isolates of each test strain were also recultured every 2 weeks from original vials that were kept at −70 °C in the Microbank™ system.

Biochemical and physiological methods

Catalase production was determined by applying a drop of 3% H_2O_2 to the colonies and observing the occurrence of O_2 bubbles, as described elsewhere (Bubert *et al.*, 1997). The Christie, Atkins, Munch–Petersen (CAMP) test was performed using standard procedures by streaking out

Table 1. *Listeria monocytogenes* strains used and their characteristic morphological and physiological properties identified in this study

Strain	Serotype	Reference strain no.	Origin	Cell morphology and physiological properties					Titer by ELISA ($A_{492\,nm}$) with anti-CwhA mAb‡
				Tumbling motility	Cell form	Cell-type designation	Cell length (μm)*	Colony area (μm^2)†	
S1	4b	NCTC 11994	Adult meningitis	+	Single, paired cells	Wild-type smooth	3.0 ± 1.0 A	(1.9 ± 0.6) × 10^5 A	0.61 ± 0.05 B
S2	4b	NCTC 9863	Infantile meningitis	+	Single, paired cells	Wild-type smooth	3.7 ± 1.2 A	(2.3 ± 0.8) × 10^5 A	0.55 ± 0.08 B
MCR1§	1/2a	SLCC 5764	Kathariou *et al.* (1987)	+	Long cell chains	MCR variant	42.3 ± 20.9 B	(3.9 ± 0.7) × 10^6 B	0.23 ± 0.06 A
MCR2	¶	L7071	Dried custard powder	—	Long cell chains	MCR variant	56.1 ± 32.3 B	(1.7 ± 0.8) × 10^6 B	0.25 ± 0.03 A
FR1	4b		Derived from NCTC 4885‖	—	Long filaments	FR variant	65.2 ± 37.9 B	(9.3 ± 0.6) × 10^6 C	0.73 ± 0.06 C
FR2	¶	L1342	Blood culture	—	Long filaments	FR variant	63.5 ± 38.3 B	(9.5 ± 1.1) × 10^6 C	0.59 ± 0.05 B

*Mean length (μm) from 10 measurements (±SD). Single and paired cells were measured and averaged for the smooth-cell forms. Values in the same column followed by the same letter did not differ at the $P < 0.05$ level, while values with different letters differed at the $P < 0.05$ level.

†Mean of area measurements for 10 colonies grown for 48 h on LSA plates.

‡$OD_{492\,nm}$ values > 0.1 were considered a positive result. BHI broth controls gave a value of 0.004 ± 0.01.

§Derived from *Listeria monocytogenes* Mackaness (SLCC 5764).

¶Autoagglutinable cultures and therefore not serotypable.

‖Derived from *L. monocytogenes* NCTC 4885 after a 5-min exposure to high-intensity, pulsed-plasma, gas discharge decontamination conditions.

+, a positive motility test for *L. monocytogenes*.

bacteria perpendicular to *Staphylococcus aureus* on 7% sheep BA plates containing and observing zones of augmented hemolysis, as described elsewhere (Rowan *et al.*, 2000). A characteristic blue-green sheen from colonies by obliquely transmitted light and tumbling motility of *Listeria* cells was observed as described elsewhere (Rowan *et al.*, 2000). The commercial biochemical API *Listeria* test (BioMerieux, Marcy l'Etoile, France) was used according to the manufacturer's instructions.

Enzyme-linked immunosorbent assay (ELISA) for the detection of CwhA protein

Detection of CwhA protein (formerly p60) in all test *Listeria* strains using indirect ELISA involved the addition of 100 μL of cell-free supernatant per well of microtiter plates (supernatant from an overnight culture and harvested by centrifugation) and incubation for 2 h at 37 °C. Coated proteins were washed three times with wash buffer [phosphate-buffered saline (PBS) containing 0.1% v/v Tween 20] and the *L. monocytogenes*-specific monoclonal antibody CwhA-mAb K3A7 was added. This mAb was generated against the *L. monocytogenes*-specific epitope, peptide D, of the p60 protein, which has been described previously (Bubert *et al.*, 1997). Generation of K3A7 was achieved using standard protocols (Kuhn & Goebel, 1989). The anti CwhA-mAb was prepared as a tissue culture supernatant diluted 1/200 (v/v) in wash buffer and incubated for 1 h at room temperature. The microtiter wells were washed three times with wash buffer, and sheep anti-mouse horseradish peroxidase conjugate (Sigma-Aldrich Chemical Co. Ltd) was added at 100 μL per well at a dilution of 1/1000 in wash buffer and incubated for 1 h at room temperature. Excess conjugate was washed five times with wash buffer and the substrate SIGMA FAST™ OPD tablets (Sigma-Aldrich Chemical Co. Ltd) was added at 100 μL per well with 0.5 h of incubation at room temperature. The $A_{492\,nm}$ was measured after the addition of 50 μL per well 3 M H_2SO_4.

Cell or filament length and colony appearance determination

Overnight cultures of all the *L. monocytogenes* strains described in Table 1 were separately incubated in BHI broth at 37 °C with aeration. At various time intervals, the lengths of the cells were determined using image analysis (Nikon Optiphot-2 microscope that was connected to a Solitaire 512 Image Analyzer, Seescan Plc.). Ten cells were measured per sample. Overnight cultures were also grown at 37 °C on *Listeria*-selective agar (LSA; Oxford formulation; Oxoid) to investigate differences in colony appearance. The area (μm^2) of 10 colonies per sample was measured using the image analysis system mentioned above.

Electron microscopy

Cells were grown to the stationary phase (30 h) on BA plates, washed twice with PBS and resuspended in sterile-distilled water before application to formvar-coated grids. After the grid was dried, one drop of a solution containing 3% v/v tungstophosphoric acid and 0.3% v/v sucrose (pH 6.8–7.4) was added. The solution was removed after 30–60 s, and the grid was dried and examined on a Zeiss 902 transmission electron microscope.

Measurement of bacterial susceptibility to opsonophagocytosis

Preparation of bacteria

Bacteria were separately grown for 16 and 30 h on BA, BHIA and TSYEA at 37 °C. Bacteria were then harvested, washed and standardized spectrophotometrically ($OD_{560\,nm}$) so that suspensions containing 1×10^8 CFU mL^{-1} (PMNL ingestion studies) or 5×10^8 CFU mL^{-1} (measurement of respiratory burst) were available for investigation.

Bacterial opsonization

The standard bacterial suspensions were opsonized in 1 mL of 10% (v/v) normal human pooled serum containing 0.1% gel-HBSS (Hanks basal salt solution with 0.1% gelatin) for 15 min at 37 °C; the opsonized cells were harvested by centrifugation and resuspended in diluent (PBS, pH 7.1) at the original concentration. Unopsonized bacteria (no serum) were used for comparison.

Isolation of neutrophils (PMNLs)

PMNLs were isolated from 20 to 30 mL of fresh blood taken from healthy human donors in heparin vacutainers (and inverted to mix) using density gradient centrifugation through Ficoll-Hypaque (Polymorphprep; Nycomed, Amersham, UK) as per Gemmell & Ford (2002). The neutrophil-rich layer was harvested and washed gently with 0.1% gel-HBSS before standardization to a concentration of *c.* 1×10^7 cells mL^{-1} (as determined using a hematocrit chamber). Purity was $\geq$95% and viability, as measured by exclusion of trypan blue (0.1% solution), was also $\geq$95%.

Phagocytosis and bacterial killing by PMNLs

The ability of PMNLs to phagocytose and kill opsonized cells of *L. monocytogenes* was assessed using the previously published method of Gemmell & Ford (2002). Briefly, 0.1 mL of a suspension of opsonized or nonopsonized bacteria grown separately on BA plates for 16 and 30 h were added to duplicate polypropylene vials, followed by the addition of 0.1 mL of PMNLs. The vials were then incubated for various time intervals up to and including 45 min at 37 °C in an orbital shaking incubator at 250 r.p.m. Experiments were performed using a bacteria/PMNL ratio of 50 : 1. Immediately after removal from the incubator at the indicated times, 2.5 mL of ice-cold 0.1% gel-HBSS was added and the phagocytic cells were washed three times in PBS by differential centrifugation at 1000 ***g*** (4 °C) for 5 min. Washing and shaking with PBS was carried out to remove trapped or loosely adherent bacteria from neutrophils. Slide preparations were then made of a selection of the bacteria/PMNL mixtures, as follows: after the washing stages, the reaction mixture was resuspended in 50 μL of PBS and centrifuged at 21 ***g*** for 5 min on a silane-coated glass slide using a cytocentrifuge (Cytospin 2, Shandon, Southern Products Ltd, Runcorn, UK) in order to visually assess phagocytic cells. After drying for 10 min, the slides were stained with Giemsa stain and examined microscopically at $\times$1000 magnification. The phagocytic index was determined as percent positive macrophages (those containing more than one bacterium) times the mean number of bacteria per positive macrophage as described previously by Alford *et al.* (1991).

The bacterial killing process was measured by constituting mixtures as for the phagocytosis assay above and determining CFUs at specific times. Four sets of vials were made up for each assay, one to be sampled immediately upon the addition of PMNL (zero time) and the other three to be sampled at 15, 30 and 45 min, respectively. Volumes of 0.1 mL of opsonized or nonopsonized bacteria were added to each vial, followed by the addition of 0.1 mL of PMNL. Then, after the desired incubation intervals (0, 15, 30 or 45 min), 0.1 mL of cold sterile water was added to each vial; the vials were mixed thoroughly, and appropriate dilutions were prepared. Samples of these dilutions were pipetted into sterile Petri dishes, and 15 mL of sterile molten BHIA was added, mixed well and allowed to solidify. Survivors (expressed in terms of CFU) were enumerated after an overnight incubation at 37 °C and percent change in CFU at 15, 30 and 45 min, relative to CFU at zero time, was calculated. Experiments were repeated in triplicate on at least 3 separate days with PMNL from different normal donors.

The phagocytic process was measured using the peak chemiluminescence assay of Gemmell & Ford (2002), which follows the respiratory burst in neutrophils exposed to serum-opsonized (and nonopsonized) bacteria that had been grown separately on BA, BHIA or TSHA and TSA plates. Opsonized bacteria (5×10^7 CFU) were added to a reaction mixture consisting of 5×10^5 PMNL and 50 μL of 1×10^{-5} M luminol in the dark. Light release was then measured from the chemiluminescence counter (BioOrbit 1253, BioOrbit, Turku, Finland) over a 45-min period and peak response (mV) was noted.

Statistical methods

All experiments in this study were performed in triplicate, and results are reported as averages with SDs. The influence of strain type, culture form (wild-type smooth vs. cell-chain and filamentous rough forms), opsonization and plating medium on the uptake and survival of *L. monocytogenes* cells in PMNLs was determined at the 95% or greater confidence intervals using ANOVA (one-way or balanced model) with MINITAB software Release 13 (Minitab Inc., State College, PA).

Results

Confirmation of the morphological and physiological characteristics of different culture types isolated previously from clinical and food samples

All the bacterial strains described in Table 1 were identified as *L. monocytogenes* by establishing the characteristic morphological, physiological and biochemical properties associated with this pathogen. All cultures produced catalase, were CAMP test positive with *S. aureus* and were identified as *L. monocytogenes* using API *Listeria* biochemical profiling. Confirmation of species identification was performed by analysis of culture supernatant for CwhA protein by indirect ELISA with an *L. monocytogenes*-specific anti-CwhA mAb (Table 1).

The cell and colony appearances of all rough variants were shown to differ significantly from those of the wild-type *L. monocytogenes* strains, which had a typical smooth morphology. Unlike wild-type smooth strains, whose cells have a characteristic coccobacillus appearance (*c.* 0.5 μm in diameter × 2 μm in length), cell types associated with the rough variants were shown to be atypically long. Some rough variants consisted of unseptated or paired filaments that measured up to 103 μm in length (designated FR variants), whereas others formed long chains that were up to 88 μm in length and consisted of multiple cells of similar size (designated MCR variants) (Table 1). Rough variants isolated from clinical specimens or derived under conditions of stress produced by exposure to pulsed-plasma gas discharge showed the FR filamentous phenotype. The mean cell lengths for the various culture variants of *L. monocytogenes* were shown to be 3.3 ± 1.1 (wild-type normal S type), 49.2 ± 26.6 (MCR variant) and 64.3 ± 38.1 (FR variant). MCR and FR variants were found to be incapable of the characteristic tumbling motility and formed irregular or rough colonies that no longer produced a blue-green sheen upon oblique illumination. Image analysis data showed that irregular rough colonies consistently had areas (μm^2) and appearances ($P < 0.05$) different from that of smaller, wild-type form colonies after 48 h of growth on LSA plates (Table 1). Spontaneously occurring MCR1 variant and food sample isolate MCR2 with a rough colony appearance exhibited similar phenotypes, tending to form long chains in which septum formation between individual cells still occurred, but the cells were not separate.

Indirect ELISA studies (Table 1) with an anti-CwhA mAb showed that these MCR variants secrete a considerably reduced amount of a peptidoglycan hydrolase protein. The addition of partially purified CwhA led to a decay of the cell chains (mean 49.2 ± 26.6 μm) to normal size (mean 3.3 ± 1.0 μm) within 3 h of treatment. The blood culture isolate FR2 and the FR1 variant of *L. monocytogenes* derived from the wild-type S form culture after exposure to pulsed-plasma gas discharge treatment also exhibited a rough filamentous cell appearance. However, unlike MCR variants that secreted diminished levels of cell-free CwhA, indirect ELISA studies showed that FR variants produced wild type or greater amounts of Cwha, indicating that the latter FR morphotypes were type II in nature (Table 1). The addition of partially purified CwhA from wild-type *L. monocytogenes* to FR variants did not decay the lengths of the filaments (mean 64.3 ± 38.1 μm) to the normal *Listeria* cell size.

Effect of opsonization and composition of bacterial growth medium on the susceptibility of different culture forms of *L. monocytogenes* to phagocytosis by human PMNLs

The induction of a respiratory burst by human PMNL following exposure to different culture forms of *L. monocytogenes* was measured as the maximal chemiluminescence (mV) response, usually occurring 15–20 min after addition of the bacterium/luminol reaction mixture in the dark. The level of respiratory burst of PMNL exposed to 10% opsonized bacteria was significantly different ($P = 0.00003$) from similar nonopsonized bacteria (Table 2). Studies revealed that prior growth of all test bacteria on media containing or supplemented with iron augmented respiratory burst activity in PMNLs ($P = 0.0016$), with mean (mV) measurements of 56.2 ± 4.4, 45.6 ± 5.6, 43.0 ± 4.7 and 34.3 ± 3.3 for bacteria grown on BA, BHIA, TSHA and TSA, respectively (Table 2). Albeit in lower measured amounts, a similar pattern of respiratory burst activity was observed for nonopsonized bacteria with mean (mV) measurements of 14.4 ± 3.6, 7.8 ± 2.7, 7.6 ± 1.7 and 5.5 ± 1.3 for BA, BHIA, TSHA and TSA, respectively. Wild-type smooth *Listeria* elicited the greatest respiratory burst in PMNLs ($P = 0.008$) compared with MCR or FR variants. No significant difference was observed between rough MCR and FR culture variants in eliciting maximal chemiluminescence responses ($P = 0.497$). However, wild-type smooth S2 elicited a stronger respiratory burst response compared with S1 ($P = 0.006$), while there was no difference in the chemiluminescence responses between individual strains of either

Table 2. Effect of *Listeria monocytogenes* strain type, culture morphotype, opsonization and composition of agar media on the maximal chemiluminescence response (mV) elicited by phagocytosing PMNLs

	Maximal chemiluminescence (mV)† after ingestion of different morphotypes of *L. monocytogenes* by PMNLs							
	Opsonized cells (10% serum)				Nonopsonized cells (0% serum)			
Strain*	BA	BHIA	TSHA	TSA	BA	BHIA	TSHA	TSA
S1	62.7 ± 4.1 C	54.3 ± 8.3 D	48.1 ± 4.4 D	39.6 ± 3.4 E	12.9 ± 2.3 G	7.6 ± 1.4 H	7.2 ± 1.4 H	4.6 ± 1.2 I
S2	80.8 ± 7.1 A	70.8 ± 3.5 B	64.6 ± 5.3 C	52.3 ± 4.5 D	23.5 ± 8.8 F	9.9 ± 3.8 G	9.1 ± 1.8 G	6.9 ± 1.4 H
MCR1	45.2 ± 3.4 D	37.5 ± 5.0 E	35.1 ± 4.1 F	30.1 ± 2.7 F	13.1 ± 4.7 G	5.8 ± 2.0 H	7.5 ± 2.1 H	4.1 ± 1.1 I
MCR2	47.8 ± 3.9 D	37.0 ± 6.4 E	39.8 ± 5.4 E	30.0 ± 2.9 F	10.8 ± 1.1 G	7.3 ± 6.8 H	6.7 ± 2.0 H	4.1 ± 1.2 I
FR1	50.3 ± 2.9 D	39.3 ± 4.8 E	33.3 ± 4.1 F	26.2 ± 4.1 F	11.4 ± 2.7 G	6.8 ± 1.3 H	6.5 ± 1.3 H	6.2 ± 1.8 H
FR2	50.6 ± 5.5 D	34.9 ± 5.8 E	37.5 ± 5.3 E	28.1 ± 2.2 F	14.9 ± 2.5 G	9.3 ± 1.4 G	8.5 ± 1.4 H	6.7 ± 1.3 H

*Description of the strains provided in Table 1.
†Mean (± SD) of triplicate samples measured from triplicate trials. Values (mV) having different uppercase letters differ at the $P < 0.05$ level.
BA and BHIA contain a source of iron, whereas TSHA is artificially supplemented with hemin.

MCR or FR variants ($P = 0.513$). Visualization of the bacterium/phagocyte mixture using light microscopy revealed greater numbers of intracellular smooth-type bacteria compared with PMNLs containing MCR or FR variants. The mean numbers of bacteria ingested by phagocytosing macrophages after 45-min exposure were shown to be 12 ± 4, 7 ± 4 and 6 ± 3 for the smooth, MCR and FR cell types, respectively (Fig. 1). A quantitative measurement of PMNL-ingested bacteria (phagocytic index) revealed significant differences ($P < 0.05$) between the wild-type smooth form (984 ± 286) compared with similarly exposed rough MCR (441 ± 213) and FR (330 ± 151) variants (Fig. 1).

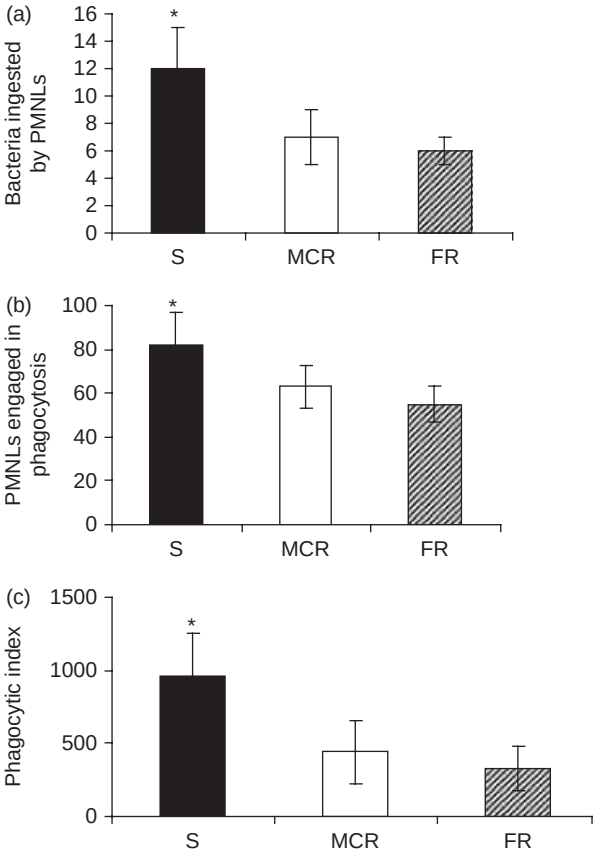

Fig. 1. Influence of bacterial load on the phagocytosis of different morphotypes of *Listeria monocytogenes*: (a) number of bacteria ingested by phagocytosing PMNLs, (b) proportion of PMNLs engaged in phagocytosis, and (c) phagocytic index (mean ± SD of three experiments). *Statistical difference at the $P < 0.05$ level.

Survival of different opsonized culture variants of *L. monocytogenes* in human PMNLs

Survival of different opsonized (10% serum) culture forms of *L. monocytogenes* in PMNLs was examined over a 45-min exposure period (Fig. 2). A clear pattern emerged where the percentage of bacterial survivors post-PMNL ingestion decreased over the 45-min exposure for all *Listeria* culture forms studied. While wild-type smooth and FR variants exhibited a similar percentage survival in PMNLs, strains belonging to MCR variant were significantly less resistant to exposure to deleterious stresses associated with internalization in PMNLs. Greater survival of all culture forms of *L. monocytogenes* occurred in PMNLs where bacteria were either grown before on BA plates (Fig. 3) and/or when older 30-h cultures were used compared with younger 16-h strains (Fig. 4) ($P < 0.05$). Interestingly, less pronounced survival in PMNLs occurred after 45-min exposure, where bacteria had been grown before on TSA supplemented with hemin (Fig. 5) compared with similar samples grown on BA (Fig. 3b) plates. However, although the mean survival percentages were generally higher for the majority of morphotypes studied compared with prior growth of similar samples on TSA alone (Figs 3 and 5), only S2 grown on BA was observed to be significantly different at the $P < 0.05$ level after 45 min of exposure to PMNLs (Fig. 3b). Greater survival ($P < 0.05$) occurred for all S and FR morphotypes studied after shorter

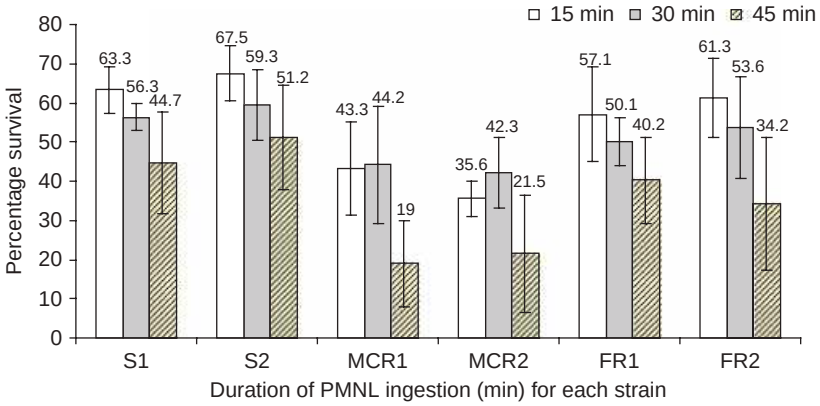

Fig. 2. Percentage survival of different morphotypes of *Listeria monocytogenes* in human PMNLs challenged over a 45-min exposure period (mean ± SD of three experiments).

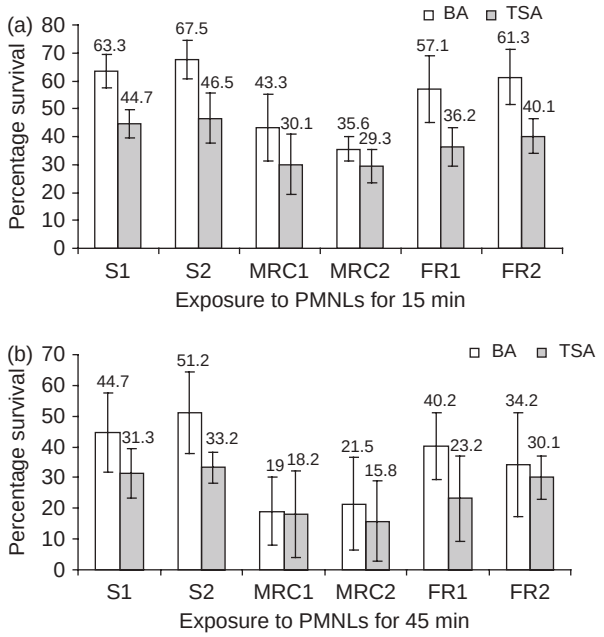

Fig. 3. Effect of growth of bacteria on BA media containing a source of iron on the survival response (percentage) of different morphotypes of *Listeria monocytogenes* in human PMNLs challenged for (a) 15 min and (b) 45 min (mean ± SD of three experiments).

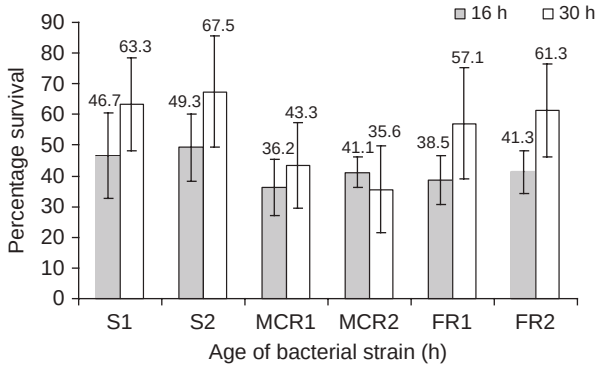

Fig. 4. Effect of bacterial cell age on the survival response (percentage) of different morphotypes of *Listeria monocytogenes* in human PMNLs challenged over a 45-min exposure period (mean ± SD of three experiments).

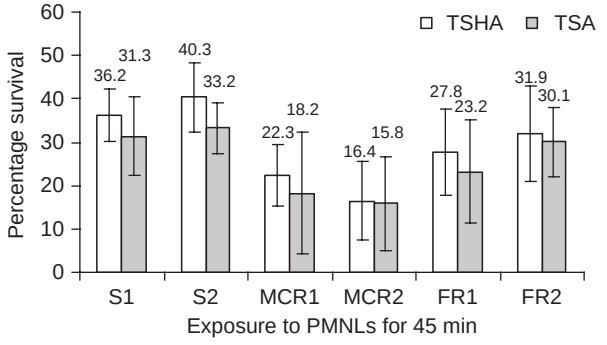

Fig. 5. Effect of supplementation of TSA with hemin on the survival response (percentage) of different morphotypes of *Listeria monocytogenes* in human PMNLs challenged for 45 min (mean ± SD of three experiments).

durations of exposure to PMNLs, where the latter had been grown before on BA plates (Fig. 3a).

Discussion

This study demonstrated that human PMNLs are capable of engulfing and internalizing different cell or filament morphotypes of *L. monocytogenes* that were isolated from clinical specimens and food samples. However, the efficacy of this phagocytosis process was shown to depend on many factors namely bacterial strain, culture form (normal smooth vs. atypical rough variants), degree of opsonization and the composition of bacterial culture media used before uptake by PMNLs. The much smaller normal cell type of *L. monocytogenes* (*c.* 2 μm in length) was shown to be much more susceptible to phagocytic uptake compared with

atypical rough chains of cells or filaments that measured up to *c.* 100 μm in length. Studies reporting previously on the pathogenicity of different culture variants of *L. monocytogenes* are very limited. Wilder & Edberg (1973) appear to be the first researchers to report on the interaction of regular-sized smooth and atypical rough cells of *L. monocytogenes* with normal mouse peritoneal macrophages in culture and revealed that after 24 h the latter rough variants were almost completely killed, whereas the smooth strain tended to show complete survival. The authors did not indicate whether the rough variants constituted a filamentous or the long cell chain of cell arrangement. However, the findings of Wilder & Edberg (1973) appear to markedly contrast similar PMNL studies carried out earlier by Mackaness (1962), where the latter reported that macrophages initially infected with *L. monocytogenes* released their content of pathogens at 20 h. In the present study, the viability of all culture morphotypes of *L. monocytogenes* was reduced within 45 min of engulfment by human PMNLs.

Visual observation of *L. monocytogenes* S2 cells engulfed in PMNLs revealed that some bacteria had converted to longer chains of cells. The numbers of internalized *Listeria* were shown to be < 16 cells or filaments in positive PMNLs. Kingdon & Sword (1970) previously reported that *L. monocytogenes* killed the host macrophage when the intracellular population increased to approximately 16 bacteria per cell. Hardy *et al.* (2004) also observed the conversion to chains of cells from normal-sized *L. monocytogenes* cells during replication in murine gall bladder. Interestingly, chain morphology was not observed during intracellular growth of wild-type bacteria in an ordinary broth culture. The significance of bacterial growth in the gall bladder with respect to the pathogenesis and the spread of listeriosis depends on the ability of the bacterium to leave this organ and be disseminated to other tissues and into the environment. Rowan *et al.* (2000) previously demonstrated that atypical rough filaments of *L. monocytogenes*, isolated from clinical specimens and food samples, demonstrated wild-type levels of adherence, invasion and cytotoxicity to human epithelial HEp-2, Caco-2 and HeLa cells.

Use of 10% serum in the present study augmented phagocytosis of all different culture variants of *L. monocytogenes*, which appears to agree with findings from recent studies of Vahidy & Jehan (2006), who demonstrated the role of immune serum in augmenting the *in vitro* engulfment of typical short cells of *L. monocytogenes* by PMNLs of rabbits. Growth of different variants of *L. monocytogenes* on BA resulted in increased respiratory burst activity and bacterial survival in human PMNLs. This also correlated with visible inspection of bacteria/phagocytes mixtures (phagocytic indices) that revealed greater numbers of internalized *Listeria* cells in PMNLs when these bacteria were grown on BA compared with similar cells grown on TSA plates before PMNL challenge. While BA contains a source of iron, supplementation of TSA with hemin did not produce similar levels of respiratory burst activity in engulfed bacteria, indicating that other constituents in BA (and to a lesser degree in BHIA) contribute to the augmented chemiluminescence responses. The presence of hemin augmented respiratory activity in PMNLs compared with the use of TSA alone for many opsonized morphotypes alone, indicating that prior microbial exposure to iron in bacterial growth media influenced respiratory burst activity in PMNLs. However, supplementation of bacterial growth media with hemin did not significantly enhance survival in this present study. The augmented respiratory burst activity in the presence of iron may be indirectly mediated by the Haber–Weiss–Fenton and related reactions (Yuan *et al.*, 1995). In these reactions, hydroxyl radicals are generated from hydrogen peroxide in the presence of Fe^{2+}, which is oxidized to Fe^{3+}. Generation of more hydroxyl radicals and Fe^{3+} results from the reaction between superoxide and Fe^{2+}. It is likely that, in activated macrophages, the concentration of superoxide ions and hydrogen peroxide increases due to the above-summarized reactions. It is also well documented that the level of iron determines the expression of several virulence factors and that survival of bacteria during infection also depends on the ability to interact with and acquire iron from the host (Braun, 2005). It has been reported previously that during listerial infection, the availability of iron determines the survival and invasiveness of the bacterium (Rea *et al.*, 2004).

It is interesting to note that the filamentous morphotype of *L. monocytogenes* can also arise after exposure to deleterious conditions associated with novel food processing or environmental decontamination (Giotis *et al.*, 2007). In the present study, we describe the occurrence of an FR1 variant that was generated after sublethal exposure to high-intensity pulsed-plasma gas discharge conditions, which is a technique similar in design to that of high-intensity pulsed electric fields with the inclusion of a gas-sparging stage (Rowan et al., 2008). Hahn *et al.* (1999) suggest that the switch to the filamentous state in bacteria may be a survival response defending the latter against flagellate grazing. While human PMNLs were capable of engulfing type II filaments of *L. monocytogenes*, it is not apparent from this present study as to whether or not there was an upper limit or threshold in terms of filament size. Although lower numbers of rough cell chain or filament types were engulfed by macrophages compared with normal short cell types of *L. monocytogenes*, studies were not carried out to elucidate the ability of macrophages to engulf *Listeria* based on the degree of filament or chain length. Different culture variants of microbial pathogens, including *L. monocytogenes*, may arise from exposure to harsh growth conditions that may alter their morphological, physiological and virulence

characteristics. Prior exposure to hostile growth conditions can protect these bacteria from subsequent exposure to lethal levels of the same or different stresses (Aldsworth *et al*., 1999; Rowan, 1999; Hardy *et al*., 2006). During the parasitic lifecycle, *L. monocytogenes* must cope with a series of challenges that arise during different stages of infection. These challenges include low nutrient availability, resistance to various physical stresses (e.g. temperature, acid, bile; Gahan & Hill, 2005) and the host immune system (Pamer, 2004). Stress resistance and dramatic switches in cellular morphology and survival characteristics in *L. monocytogenes* are undoubtedly governed by the expression of specific gene products, which is possibly coordinated and regulated by PrfA and by other presently unknown transcriptional controlling factors (Hardy *et al*., 2006; Riedel *et al*., 2009). Interestingly, the latter authors also observed that differences in culture media formulations used for biofilm production (i.e. use of 10-diluted BHI vs. TSB) had a dramatic effect on the ability of an Δ*agrD*-mutant strain of *L. monocytogenes* to form biofilms. A clear trend also emerged where older cultures of *L. monocytogenes* survived better in human PMNLs compared with similarly prepared and exposed younger variants. Previous researchers have also demonstrated that pathogens in their stationary growth phase survive adverse conditions associated with food processing, in part, due to the fact that their metabolic processes have slowed down and are less susceptible to the lethal action of extrinsic stresses (Rowan, 1999; Giotis *et al*., 2007).

In conclusion, while human PMNLs are capable of engulfing different culture morphotypes of *L. monocytogenes*, typical short and atypical type II filamentous types of this pathogen appear to survive this immune challenge better than multiple cell chain variants that secrete reduced levels of the peptidoglycan hydrolase CwhA protein. All esculin-positive culture isolates growing on LSA plates should be tested further to confirm their identity using an immunological or equivalent molecular-based probe that is species specific for *L. monocytogenes*.

Acknowledgements

We thank Dr Jim McLauchlin, Food Safety Microbiology Laboratory, Public Health Laboratory Service (PHLS), Colindale, UK, for the provision of *L. monocytogenes* MRC2 and FR2. We also thank Dr Andreas Bubert, Microbiological Analytics, Merck KgaA, 64271 Darmstadt, Germany, for the kind gift of the *L. monocytogenes*-specific anti-Cwha (formerly p60) monoclonal antibody. This work was supported, in part, by the Republic of Ireland, Technical Sector Research: Strand 1 program.

References

Aldsworth TG, Sharman RL & Dodd CER (1999) Bacterial suicide through stress. *Cell Mol Life Sci* **56**: 378–383.

Alford CE, King TE & Campbell PA (1991) Role of transferring, transferring receptors, and iron in macrophage listericidal activity. *J Exp Med* **174**: 459–466.

Bereski F, Gavini F, Benezech T & Faille C (2002) Growth, morphology and surface properties of *Listeria monocytogenes* Scott A and LO28 under saline and acid environments. *J Appl Microbiol* **92**: 556–565.

Braun V (2005) Bacterial iron transport related to virulence. *Contrib Microbiol* **12**: 210–213.

Brezin B (1973) The effect of NaCl on the morphology of *Listeria monocytogenes*. *Zbl Bakt Mik Hyg* **225**: 80–84.

Bubert A, Riebe J, Schnitzler N, Schönberg A, Goebel W & Schubert P (1997) Isolation of catalase negative *Listeria monocytogenes* strains from listeriosis patients and their rapid identification by anti-p60 antibodies and/or PCR. *J Clin Microbiol* **35**: 179–183.

Dramsi S, Biswas I, Maguin E, Braun L, Mastroeni P & Cossart P (1995) Entry of *Listeria monocytogenes* into hepatocytes requires expression of *inlB*, a surface protein of the internalin multigene family. *Mol Microbiol* **16**: 251–261.

Drevets DA, Sawyer RT, Potter TA & Campbell PA (1995) *Listeria monocytogenes* infects human endothelial-cells by two distinct mechanisms. *Infect Immun* **63**: 4268–4276.

Gahan CG & Hill C (2005) Gastrointestinal phase of *Listeria monocytogenes* infection. *J Appl Microbiol* **98**: 1345–1353.

Gaillard J, Berche LP, Mounier J, Richard S & Sansonetti P (1987) *In vitro* model of penetration and intracellular growth of *Listeria monocytogenes* in the human enterocyte-like cell line Caco-2. *Infect Immun* **55**: 2822–2829.

Gardan R, Cossart P & Labadie J (2003) Identification of *Listeria monocytogenes* genes involved in salt and alkaline-pH tolerance. *Appl Environ Microb* **69**: 3137–3143.

Gemmell CG & Ford CW (2002) Virulent factor expression by Gram-positive cocci exposed to subinhibitory concentrations of linezolid. *J Antimicrob Chemoth* **50**: 665–672.

Giotis ES, Blair IS & McDowell DA (2007) Morphological changes in *Listeria monocytogenes* subjected to sublethal alkaline stress. *Int J Food Microbiol* **120**: 250–258.

Gutekunst KA, Pine L, White E, Kathariou S & Carlone GM (1992) A filamentous like mutant of *L. monocytogenes* with reduced expression of a 60-kilodalton extracellular protein invades and grows in 3T6 and Caco-2 cells. *Can J Microbiol* **38**: 843–851.

Hahn MW, Moore ERB & Hofle MG (1999) Bacterial filament formation, a defense mechanism against flagellate grazing, is growth rate controlled in bacteria of different phyla. *Appl Environ Microb* **65**: 25–35.

Hardy J, Francis KP, DeBoer M, Chu P, Gibbs K & Contag CH (2004) Extracellular replication of *Listeria monocytogenes* in the murine gallbladder. *Science* **303**: 851–853.

Hardy J, Morgolis JJ & Contag CH (2006) Induced biliary excretion of *Listeria monocytogenes*. *Infect Immun* **74**: 1819–1827.

Isom LL, Khambatta ZS, Moluf JL, Akers DF & Martin SE (1995) Filament formation in *Listeria monocytogenes*. *J Food Protect* **58**: 1031–1033.

Jørgensen F, Stephens PJ & Knøchel S (1995) The effect of osmotic shock and subsequent adaptation on the thermotolerance and cell morphology of *Listeria monocytogenes*. *J Appl Microbiol* **79**: 274–281.

Kathariou S, Hacker J, Hof H, Then I, Wagner W, Kuhn M & Goebel W (1987) Bacterial cytotoxins – extracellular proteins and virulence factors. *Molecular Basis of Viral and Microbial Pathogenesis* (Rott R & Goebel W, eds), pp. 141–150. Springer-Verlag, Berlin.

Kingdon GC & Sword P (1970) Biochemical and immunological effects of *Listeria monocytogenes* haemolysin. *Infect Immun* **1**: 363–372.

Kuhn M & Goebel W (1989) Identification of an extracellular protein of *Listeria monocytogenes* possibly involved in intracellular uptake by mammalian cells. *Infect Immun* **57**: 55–61.

Lenz LL & Portnoy DA (2002) Identification of a second *Listeria secA* gene associated with protein secretion and the rough phenotype. *Mol Microbiol* **45**: 1043–1056.

Lie J, Kolling GL, Matthews KR & Chikindas ML (2003) Cold and carbon dioxide used as multi-hurdle preservation do not induce appearance of viable but non-culturable *Listeria monocytogenes*. *J Appl Microbiol* **94**: 48–53.

Mackaness GB (1962) Cellular resistance to infection. *J Exp Med* **116**: 381–406.

Medina E, Rohde M & Chhatwal GS (2003) Intracellular survival of *Streptococcus pyogenes* in polymorphonuclear cells results in increased bacterial virulence. *Infect Immun* **71**: 5376–5380.

Minkowski P, Staege H, Groscurth P & Schaffner A (2001) Effects of trimethoprim and co-trimoxazole on the morphology of *Listeria monocytogenes* in culture medium and after phagocytosis. *J Antimicrob Chemoth* **48**: 185–193.

Monk IR, Cook GM, Monk BC & Bremer PJ (2004) Morphotypic conversion in *Listeria monocytogenes* biofilm formation: biological significance of rough colony isolates. *Appl Environ Microb* **70**: 6686–6694.

Nilsson L, Chen YH, Chikindas ML, Huss HH, Gram L & Montiville TJ (2000) Carbon dioxide and nisin act synergistically on *Listeria monocytogenes*. *Appl Environ Microb* **66**: 769–774.

Ohya S, Xiong H, Tanabe Y, Arakawa M & Mitsuyama M (1998) Killing mechanism of *Listeria monocytogenes* in activated macrophages as determined by an improved assay system. *J Med Microbiol* **47**: 211–215.

Pamer EG (2004) Immune responses to *Listeria monocytogenes*. *Nat Rev Immun* **4**: 812–823.

Pilgrim S, Klob-Maurer A, Gentschev I, Goebel W & Kuhn M (2003) Deletion of the gene encoding p60 in *Listeria monocytogenes* leads to abnormal cell division and loss of actin-based motility. *Infect Immun* **71**: 3473–3484.

Rea RB, Gahan RC & Hill C (2004) Disruption of putative regulatory loci in *Listeria monocytogenes* demonstrates a significant for Fur and PerR in virulence. *Infect Immun* **72**: 717–727.

Riedel CU, Monk IR, Casey PG, Waidmann MS, Gahan CGM & Hill C (2009) AgrD-dependent quorum sensing affects biofilm formation, invasion, virulence and global gene expression profiles in *Listeria monocytogenes*. *Mol Microbiol* **71**: 1177–1189.

Ritz M, Tholozan JL, Federighi M & Pilet MF (2001) Morphological and physiological characterization of *Listeria monocytogenes* subjected to high hydrostatic pressure. *Appl Environ Microb* **67**: 2240–2247.

Rowan NJ (1999) Evidence that inimical food-preservation barriers alter microbial resistance, cell morphology and virulence. *Trends Food Sci Tech* **10**: 261–270.

Rowan NJ & Anderson JG (1998) Effects of above-optimum growth temperature and cell morphology on thermotolerance of *Listeria monocytogenes* cells suspended in bovine milk. *Appl Environ Microb* **64**: 2065–2071.

Rowan NJ, Candlish AAG, Bubert A, Anderson JG, Kramer K & McLaughlin J (2000) Virulent rough filaments of *Listeria monocytogenes* from clinical and food samples secreting wild-type levels of cell-free p60 protein. *J Clin Microbiol* **38**: 2643–2648.

Rowan NJ, Espie S, Harrower J, Farrell H & MacGregor SJ (2008) Evidence of lethal and sublethal injury in food-borne pathogens exposed to high-intensity pulsed-plasma gas discharges. *Lett Appl Microbiol* **46**: 80–86.

Tsai HN & Hodgson (2003) Development of a synthetic minimal medium for *Listeria monocytogenes*. *Appl Environ Microb* **69**: 6943–6945.

Vahidy R & Jehan F (2006) Enhanced *in vitro* engulfment of *Listeria monocytogenes* by rabbit polymorphonuclear leukocytes in the presence of sera from immune rabbits. *FEMS Immunol Med Mic* **14**: 103–107.

Vázquez-Boland JA, Kuhn M, Berche P, Chakraborty T, Dominguez-Bernal G, Goebel W, González-Zorn B, Wehland J & Kreft J (2001) *Listeria* pathogenesis and molecular virulent determinants. *Clin Microbiol Rev* **14**: 584–640.

Wilder MS & Edberg JC (1973) Interaction of virulent and avirulent *Listeria monocytogenes* with cultured mouse peritoneal macrophages. *Infect Immun* **7**: 409–415.

Wuenscher MD, Kohler S, Bubert A, Gerike U & Goebel W (1993) The *iap* gene of *Listeria monocytogenes* is essential for cell viability, and its gene product, p60, has bacteriolytic activity. *Bacteriology* **175**: 3491–3501.

Yuan XM, Brunk UT & Olsson A (1995) Effects of iron and hemoglobin loaded human monocyte-derived macrophages on oxidation and uptake of LDL. *Arterioscl Throm Vas* **15**: 1345–1351.

ELSEVIER

Trends in Food Science & Technology 10 (1999) 261–270

TRENDS IN FOOD SCIENCE & TECHNOLOGY

Viewpoint

Evidence that inimical food-preservation barriers alter microbial resistance, cell morphology and virulence

Neil J. Rowan

Department of Bioscience and Biotechnology, University of Strathclyde, Royal College Building, 204 George St., Glasgow G1 1XW, UK (tel: +44-(0)-141-548-2531; fax: +44-(0)-141-553-4124; e-mail: nj.rowan@strath.ac.uk)

Food manufacturing, distribution and storage rely on well-placed deleterious stresses or hurdles that either inhibit or inactivate contaminating microorganisms in food systems. Recent molecular and physiological evidence points to the fact that many food-borne pathogenic bacteria are adapting to these sub-lethal inimical stresses, and as a consequence, becoming more resistant to lethal levels of the same (homologous) or cross-protected against other (heterologous) stresses. Many stress-adapted microbial pathogens are also showing an enhanced virulence. As non-stressed exponentially-growing bacteria are often used in food safety studies, it is likely that predictive models using such data may be underestimating the actual survival capabilities of stress-challenged microorganisms. The 'stress-hardening' phenomenon has significant food-safety implications, especially in situations where the food industry explores levels of lethality that are close to the boundaries of microbial control. In this Viewpoint article, I wish to focus on the ability of environmental stress to augment or modulate virulence; the ability of stress-adapted microbial-pathogens to survive homologous or heterologous stresses commonly encountered in foods and in the mammalian host; and also to alter microbial cell morphological and physiological characteristics as a consequence of these inimical stresses.

In developed countries, we enjoy increased health and longevity, and we take, as our right, the 'safety' of the foods and beverages we consume. However, as we enter a new millennium current epidemiological and clinical data poignantly show that we are not winning the battle against food-borne diseases which represent a major cause of suffering, morbidity and mortality in both developed and under-developed countries. This unacceptable and rising trend is very evident, despite having attained better knowledge and understanding of the infection processes of many pathogenic bacteria that contaminate our foods, together with better understanding of methods for controlling these microorganisms in foods and much stricter regulations being applied to food manufacturing, distribution and storage [1–3].

It has been estimated that there are more than 1000 million yearly cases of gastroenteritis amongst children under the age of five and up to 5 million deaths in underdeveloped countries and most are caused by the consumption of contaminated foods [2]. As pointed out by Baird-Parker, the level of food-borne disease in technology-advanced Europe is also unacceptably high. While precise figures are lacking, recent estimates of food-borne illness would indicate that in many European countries there are at least 50,000 cases of acute gastroenteritis per million population per year with a figure of 300,000 recently suggested for The Netherlands [2]. Estimates for the USA are even higher, with one recent estimate suggesting between 6 and 80 million illnesses per year (resulting in up to 9000 deaths), with an associated annual economic burden estimated at 5 billion U.S. Dollars [1]. However, as there is considerable under-reporting of cases of food-borne illness to the authorities, the true extent of food-borne illness in all countries, even in countries that have well-adapted epidemiological surveillance systems may even be greater.

0924-2244/00/$ - see front matter
PII: S0924-2244(99)00060-6

While death rates from food-related illness are considerably lower in developed countries, it has been pointed out that 'up to 5% of episodes of acute gastroenteritis lead to serious, and often chronic, sequelae (including rheumatoid conditions such as Reiter's syndrome and ankylosing spondylitis), nutritional and malabsorption problems, haemolytic-uraemic syndrome (caused by verotoxin-producing strains of *Eschericia coli*), and other illnesses such as aserosclerosis and Guillain-Barré syndrome following infection by *Campylobacter* species' [2]. The reason for the increase in the reported illness is probably the result of a combination of factors, including: better reporting; changes in agricultural practices (e.g, a strong correlation between the increase in human salmonellosis, and campylobacter enteritidis and the increased consumption of poultry); changes in food marketing and eating habits (e.g. preference for foods that are perceived to be more natural, fresher, healthier, and more convenient, and increased consumption of pre-prepared 'convenience' food in the home and greater consumption of food outside the home); international travel and commerce; changing population sensitivities (although it is well-recognized that the young, old, immunodeficient and pregnant women are particularly vulnerable, there are some indications that our quest for pathogen-free food may lead to increased susceptibility to disease as a result of loss of natural immunity caused by failure to prime the immune system with subclinical numbers of pathogens); and the identification of new bacterial pathogens (including stress-adaptive microbial strains).

In a recent Viewpoint article in this journal, Knøchel and Gould [4] commented on the fact that consumers are increasingly demanding more natural, healthy, and convenient foods that are low in salt and low or lacking in preservatives, and that the use of multiple hurdles in foods is influencing the physiology of food spoilage and pathogenic microorganisms. In their article they posed the question 'With such a reduction taking place in the preservation of foods, how are we going to achieve a real reduction in the incidence of food-poisoning from manufactured foods?' Both Archer [5] and I are in agreement with Knøchel and Gould [4] regarding the effects of stresses on the physiology of food-related pathogenic microorganisms. However, as milder preservation processes still rely on well-placed inimical stresses to control the growth of microbial contaminants, it is unlikely that a reduction in preservation will lead to a reduction in the immediate virulence of certain pathogens and to a lowering to the rate of emergence of new and better host-adapted microorganisms. In this Viewpoint article, I intend to address the under-recognized issues of adaptive-stress response and enhanced virulence in *Listeria monocytogenes*, *Escherichia coli* and *Salmonella typhimurium* (and where relevant, other *Salmonella* spp., *Campylobacter jejuni*, *Aeromonas hydrophila*, *Bacillus subtilis*, and *Yersinia enterocolitica*). Evidence will be presented to show that the stress-hardening phenomenon can also result in adaptive-changes to cell morphology and physiology in certain food-borne bacterial pathogens.

Stress-adaptation and cross-protection of lethal preservation factors

As addressed by Leistner [6], food-borne bacterial pathogens are commonly stressed during food processing, distribution and storage. For instance, in cheese manufacture, pathogens existing in the raw milk undergo a series of deleterious stresses, which include heat (e.g. during milk thermal treatment), hydrogen peroxide (e.g. that may be added to the raw milk), acid (e.g. produced by starter cultures during the fermentation), and salt (e.g. added to the curd). For effective food preservation and safety assurance, the food industry relies on combination of intrinsic, extrinsic and implicit inhibitory and lethal factors (hurdles) which when applied simultaneously or sequentially, are intended to curtail or inactivate the development of contaminating pathogenic microoorganisms in food. However, as these conditions represent extensions of the natural variation that a microorganism may encounter, it should not be surprising that many problematic bacteria are capable of mounting an adaptive-response. Compelling evidence has been gathered over the last five years which shows that this is the case, where for many food-borne bacterial pathogens, exposure to sub-lethal environmental stresses hardens these bacteria, and as a consequence, stress-adaptive strains have increased resistance to normally lethal levels of the same (homologous) or different (heterologous) inimical stresses [7–10]. In effect, stress adaptation to the first encountered hurdle, hardens or 'arms' the pathogens and increases the resistance to subsequent stresses, which may counteract the effectiveness of food preservation hurdles and compromise food safety.

Indeed, the ability of food-borne pathogens to react and respond to changes in their surroundings is crucial to their survival. Numerous researchers have previously shown that certain food-borne bacterial pathogens can adapt and survive single preservation hurdles [11–13]. For instance, the survival of *L. monocytogenes* after 15 days in cabbage juice (5% NaCl) and 21 days in orange juice (pH 3.6) [7], or the isolation of verocytotoxigenic *E. coli* serotype O157:H7 from apple-cider which was implicated as the vehicle of infection in a number of food-borne illnesses [14]. Because of the importance of heat processing to the food industry, the focus of much research has been temperature (in particular the heat shock response and its impact on thermotolerance of food pathogens) [5,11,15], and until recently, little attention had been placed on the relevance of other cross-protecting inimical factors to microbial stress-

adaptation and survival. With current consumer preferences for foods that have avoided the extreme use of a single preservation hurdle, there has been an awakening towards studies that focus on stress-adaptation and cross-protection against multiple stresses, particularly in minimally processed foods. Lou and Yousef [8] recently showed that adaptation of *L. monocytogenes* to sub-lethal doses of ethanol, hydrogen peroxide, salt, acid, heat or nutrient deprivation, significantly increased the resistance of this pathogen to lethal levels of the same and cross-protected the organism to different stresses [e.g. acid (pH 3.5), ethanol (15.7% vol/vol), H_2O_2 (0.1% wt/vol), 25% NaCl, heat, and starvation (survival in 0.lM phosphate buffer after 300 h)]. Marron *et al.* [16] reported that *L. monocytogenes* exhibited a significant acid-tolerance response following a 1 h exposure to milk acid (pH 5.5), which was capable of subsequently protecting cells from severe acid stress (pH 3.5) and against lethal levels of other stresses such as heat, ethanol, salt and crystal violet. Acid-adaptation enhanced the survival of *L. monocytogenes* in foods containing lactic acid (yogurt [pH 3.8] and cottage cheese [pH 4.7]), citric acid (orange juice [pH 3.6]), or acetic acid (salad dressing [pH 3.0]) [7]. Indeed, following prolonged exposure of this pathogen to pH 3.5, mutants constitutively demonstrated increased acid tolerance at all stages of the growth cycle [7]. Thus, prior adaptation of *L. monocytogenes* to mildly acidic conditions can greatly enhance the survival of this pathogen in low-pH foods.

Recent evidence also shows that environmental stress-adaptation and cross-protection against other lethal or inimical preservation factors occurs in other food-borne bacterial enteropathogens. For instance, adaptation of *S. typhimurium* cells to sub-lethal acid stress greatly increased their resistance to organic acids (lactic, propionic, acetic), heat inactivation, osmotic stress, an activated lactoperoxidase system, and hydrophobic and surface-active compounds [9]. Acid-adapted *E. coli* were found to be more resistant to weak organic acids (propionic, lactic, acetic, benzoic, sorbic and trans-cinnamic) [12]. Because a number of foods rely on low pH to prevent the growth of pathogens and spoilage organisms, the ability of food-borne pathogens to initiate an acid-tolerance response (ATR) may be an important factor influencing their survival in normally lethal food environments. Other pathogenic bacteria acquiring increased resistance to low pH following exposure to sub-lethal acidic conditions include *Salmonella typhi*, and *Aeromonas hydrophila* [17,18].

The physiological and molecular responses by which certain food-borne bacterial pathogens adapt and acquire resistance to these complex inimical stresses, such as heat, acid, salt, low iron, and starvation, have been recently addressed in a number of seminal review articles [5, 19–21]. Consequently, it is not the intention in this review to delve into these stress-response systems in fine detail. On the contrary, I will describe however, some of the more broader and salient aspects of microbial-stress adaptation that appear to have a bearing on microbial virulence that will be addressed later. The physiological response by bacteria to heterologous inimical stresses that cause protein denaturation or loss of function of some cell structures, is varied and complex. The two main stress-response systems for which we have insights are the physiological responses to osmotic stress and to the heat-shock response [20]. The latter stress-response system involves transiently augmented rates of synthesis of stress or chaperone proteins [such as heat shock proteins (Hsp) in the case of heat shock] that alter the kinetics of protein folding in favour of correctly assembled molecules and protein complexes. Bacterial cells containing these stress proteins appear to have enhanced potential to repair damaged, to resist further homologous or heterologous stresses and to prevent cell death [19]. In enteric bacteria, such as *E. coli* and *S. typhimurium*, the induced synthesis of stress proteins involved in the general stress response, including heat shock proteins (e.g, GroEL and DnaK) and certain outer membrane proteins, is thought to provide a mechanism for maintaining intracellular homeostatsis in normally lethal environments [18,19]. Mekalonos [22] pointed out that the induction of stress proteins or molecular chaperons (e.g. as a consequence of the ATR), also provides cross protection against a wide-variety of other stresses.

Underpinning the tolerance of microorganisms to sub-lethal stresses, such as salt and acid, is the activation of extant enzymes and transport systems which are governed by changes in gene expression. Both specific and general regulons (i.e. a group of coordinately-regulated genes activated in response to an environmental parameter), are involved in reducing susceptibility of an organism to stress. As pointed out by Booth [20] a major advancement in our understanding of stress-response systems has been the recognition that bacterial cells that have stopped growing (stationary-phase cells) are more resistant to stresses. In the enteric bacteria, the stationary-phase gene regulon is controlled by the RpoS protein. It has been observed with *E. coli* O157:H7, that entry into the stationary growth phase or starvation induces the synthesis of protective proteins encoded for by the *rpoS* gene, which confers resistance to a range of chemical and physical challenges. Rowe and Kirk [10] recently showed that cross protection of *E. coli* O157:H7 to lethal levels of acid and salt is mediated, at least in part, by the *rpoS* gene.

An unnerving hypothesis recently tendered by many, is that in a situation where *E. coli* is faced with starvation or survival, it appears to 'direct' the mutation necessary to utilize the substrate that was available, and thus survived the starvation stress [23,24]. Indeed, Archer [5] pointed out that 'the occurrence of acceler-

ated or adaptive genetic change, either in the form of mutation or extinction, in microorganisms faced with stress is now accepted, only the mechanism(s) is debated'. Moxon [24] recently postulated that if the deleterious environment persists, and if gene expression by the classical stress response is not adequate, then either the bacterium adapts genetically or it dies. Proposed theories for adaptive mutations include; increase in transciption activity triggered by stress leads to mutation; recombination between homologous repeats; the existence of error-prone DNA-polymerase; or defects in the mismatch-repair system. Moxon [24] suggests that mutation rates will be higher in 'genes whose products interact with the environment in unpredictable ways'.

While the use of multiple inimical hurdles is sufficient to control the growth and toxin production of certain contaminating bacterial pathogens (such as *Staphyloccus aureus* and *Clostridium botulinum* that need to grow to large cell populations in order to secrete toxins), low level survival of other stress-adapted enteric bacteria (such as *E. coli* serotype O157:H7, *S. typhimurium,* and *L. monocytogenes*), may be sufficient to cause food-borne infections, particularly in sensitive individuals. Therefore, the stress response could be classified as a putative virulence mechanism, as unless pathogenic bacteria can cope with multiple preservation hurdles in food and in other deleterious environments, they will not go on to elicit a food-borne infection.

Microbial stress-adaptation and enhanced virulence

Whilst the induction of a stress-resistant phenotype in sublethally stressed bacterial enteropathogens has profound implications for their survival in foods, there is strong evidence that sublethal environmental stressors can also modulate the synthesis of virulence factors in these microorganisms. Over the past five years, researchers have shown that for many stress-hardened bacterial pathogens, the expression of important virulence determinants is modulated by environmental signals, such as inimical stresses [5,22,25]. For instance, environmental cues that are currently recognized as having a modulating influence on the expression of coordinately regulated virulence determinants in bacteria include CO_2 (*Bacillus anthracis* and *Vibrio Cholera*), temperature (*Bordetealla pertussis*, *Escherichia coli, Salmonella typhimurium, Listeria monocytogenes, Vibrio cholerae, Shigella* and *Yersinia* species), iron (*Corynebacterium diphtheriae*, *E. coli*, *L. monocytogenes, Pseudomonas aeruginosa*, *S. typhimurium* and *Vibrio cholerae*), pH (*Salmonella typhimurium, E. coli*, *L. monocytogenes, H. Vibrio cholerae,* and *Agrobacterium tumefaciens*), starvation (*L. monocytogenes, E. coli* and *S. typhimurium*), carbon source (*L. monocytogenes* and *E. coli*), osmolarity (*Pseudomonas aeruginosa*, *L. monocytogenes*), growth phase (*S. typhimurium* and *Staphylococcus aureus*), Ca^{2+} (*Yersinia* species), oxidative stress (*S. typhimurium),* phenolic compounds, monosaccharides, and phosphate (*Agrobacterium tumefaciens*), SO_4 and nicotinic acid (*Bordella Pertussis*) and amino acids (*Vibrio cholerae*) [13,17,19,22]. The regulatory affect of many of these environmental signals on microbial virulence to the human host has recently received much attention.

The ability of *L. monocytogenes,* and other bacterial pathogens such as *E. coli* O157:H7 and *S. typhimurium* to adapt to low-pH environments is of particular interest because the organism encounters such environments in foods and during passage through the stomach (~pH 3.5) and during its transient residence in the macrophage phagosome (~pH 4.4–5.7) [17,19]. The isolation of acid-tolerant mutants *of L. monocytogenes* and of *S. typhimurium* suggests that these low-pH environments have the potential to select for strains with increased acid resistance. However, acid-tolerant variants of *L. monocytogenes* were recently reported to have increased lethality for mice relative to that of the non-stressed wild type when inoculated by the intraperitoneal route [16]. The increased capacity of the acid-tolerant mutants of *L. monocytogenes* to grow under conditions of low pH may account for their increased virulence in the mouse model.

The induction of virulence determinants in *L. monocytogenes* is also modulated by a variety of other environmental cues. Indeed, with the exception of the *iap* gene, all of the known virulence genes of *L. monocytogenes* are coordinately regulated by the pleiotropic transcriptional activator PrfA [26,27]. It would appear that for PrfA-mediated virulence gene regulation, PrfA switches between transcriptionally inactive and active forms depending upon interaction with a protein factor termed Paf [PrfA activating factor(s)] that is responsible for transducing signals from the environment to the PrfA system [28]. Increased expression of the *prfA* gene occurs in response to osmotic stress and heat shock, and during the stationary phase of growth [29,30]. Other environmental stimuli that were recently shown to influence expression of PrfA include the preservatives nitrite and sorbate, carbon source (e.g. downregulated in the presence of glucose), low levels of iron, charcoal, and starvation [26,31].

There is also evidence for expressional crosstalk between the central virulence regulator PrfA and the stress response mediator ClpC in *L. monocytogenes* where the ClcC ATPase downregulates the synthesis of the PrfA. However, modulated *prfA* expression occurs in the presence of carbohydrates such as cellobiose and arabutin (commonly found in soil), and at temperatures at or below 26°C, indicating that *L. monocytogenes* is capable of sensing environmental stimuli outside the host and reacts by downregulating the expression of virulence genes [32]. Indeed, using molecular techniques such as reverse-transcriptase polymerase chain reaction

(RT-PCR) and green fluorescent protein (GFP)-mediated fluorescence to analyse the regulation of PrfA-dependent virulence genes of *L. monocytogenes,* it was recently shown that this pathogen (like other intracellular bacterial pathogens such as *S. typhimurium* and *Legionella pneumophila*) has the ability to preferentially and coordinately express virulence genes depending on its location within the host cell [26,28]. Alarmingly, and returning to the earlier theme of 'adaptive-mutations', Ripo *et al.* [33] recently showed that several *L. monocytogenes* strains that express elevated levels of virulence factors all carry a point mutation within prfA that converts the gene product to an 'activated' state. Gahan and Hill [34] reported that both *L. monocytogenes* and *S. typhimurium* adapt to intracellular growth environments by the synthesis of specific proteins, many of which are stress-associated proteins In *S. typhimurium*, these proteins represent some of the components of the regulon involved in the adaptation to heat shock, oxidative stress and acid stress.

Expression of the general stress response RpoS sigma factor is necessary for both environmental-stress adaptation and virulence in enteric bacteria such as *E. coli* and *S. typhimurium* [19]. However, the general stress sigma factor σ^B, that is required for acid tolerance in *L. monocytogenes,* has minimal influence on survival of *L. monocytogenes* in the mouse model of infection, however a role in the overall infection process cannot be ruled out [35]. Interestingly, there appears to be a link with normal expression of the verocytotoxin gene in *E. coli* O157:H7 and the ability of this pathogen to tolerate inimical stresses. Daboob [14] recently reported that under certain osmotic stress and heat shock conditions, the attenuated strain of *E. coli* O157:H7 (which does not produce verocytotoxin) is less resistant and adapts poorly to these stresses compared to wild-type *E. coli* O157:H7 strains that syntheses this toxin. This indicates a dual-function of this particular virulence determinant in both environmental stress-adaptation and pathogenicity. Due to the severity of the haemolytic-ureamic illness associated with *E. coli* 0157:H7, this strain has been re-designated a category III pathogen, which limits most researchers to using attenuated strains for food-safety studies. Whilst culture characteristics of the *E. coli* O157:H7 verocytotoxin-negative strains are similar, food safety studies using these attenuated strains as a measurement of the survival capabilities of normal wild-type *E.* coli O157:H7 are likely to be underestimating the true resistance of this important pathogen, and are likely to be flawed.

It has recently been proposed that 'molecular chaperones act as microbial virulence factors' [36]. They point out that while molecular chaperones are normally considered to be intracellular proteins, several bacteria have been shown to express Hsps on their outer surface that also function as adhesins. For instance, the chaperone 60 of *Helicobacter pylori* has been found on the bacterial surface, and this pathogen binds to sulphoglycolipids that are present on the gastric epithelium at acid pH. If this pathogen is heat-shocked at 42°C, then binding at neutral pH is also achieved. Whereas, binding is blocked by inhibitors of protein synthesis or antibodies to chaperonin 60 or Hsp 70, showing that the synthesis of both molecular chaperones is needed for sulphatide binding. *Haemophilis influenza,* and the intracellular bacterium *Mycobacterium avium* utilize surface-associated Hsp70 to bind to eukaryotic cells.

Environmental stress and changes in microbial cell morphology and physiology

Under conditions of sublethal environmental stress, in addition to producing a host of protective factors that arise due to preferential gene expression, adapted-mutations or for reasons presently unknown, stressed-bacteria may also alter their characteristic cell morphology. Clinical microbiologists and food technologists rely on the identification of characteristic morphological and physiological properties (such as cell shape, colony appearance, motility) when routinely identifying pathogenic bacteria from clinical and food samples. In our laboratory, atypical 'Rough' cell forms of *L. monocytogenes* have been isolated from laboratory-based culture media, bovine milk and reconstituted infant milk formulae, under conditions of brief heat shock or growth at above-optimal temperatures [13]. These stable but 'Rough' variants produced cell filaments up to 110 μm in length, and although the identity of these stress-altered microorganisms was confirmed by using *L. monocytogenes*-specific anti-p60 antisera and by commercial biochemical test kits, these bacteria had altered morphological (e.g. having an atypical, irregular colony morphology with an associated loss of characteristic blue–green sheen upon Henry illumination) and physiological (e.g. being unable to tumble in motion) properties [37]. Such stress-induced changes may result in the mis-identification of these variants in clinical and food laboratories. Interestingly, these unusual stress-derived filamentous organisms were shown to be more heat resistant than wild type *L. monocytogenes,* due in part to prominent shoulder and tailing sections in their thermal death kinetic response. The rough-filaments exhibited wild-type levels of adhesion to and invasion of human epithelial CaCo-2, HeLa and HEp-2 cells [37]. There is evidence to suggest that these rough variants do exist outside the laboratory, as atypical cultures of *L. monocytogenes* exhibiting similar filamentous cell-morphology and virulence capabilities were recently isolated from blood cultures and food samples by the Public Health Laboratory, London. As the infective dose of *L. monocytogenes* is possibly very low for sensitive individuals, the finding of atypical and potentially virulent filamentous-forms of this pathogen

in the environment (and under conditions of sublethal stress) has obvious food safety and clinical implications [26].

While there appears to be a propensity towards long cell forms of *L. monocytogenes* in aged-cultures (6–9 days old), spontaneously-occurring mutants of this pathogen producing long cell chains do occur at a relatively high frequency (1 in 10,000 generations) [38], and these mutants (designated SR-mutants) have been very thoroughly characterized by Goebel and his colleagues at the molecular, immunological and virulence levels [26,27,38]. These SR-mutants differ from the above-mentioned stress-derived filamentous cultures, in that they produce long cell chains (comprised of normal sized *Listeria* cells that are separated by a double-septum), they produce diminished levels of p60 and are unable to invade 3T6 fibroblasts, hepatocytes, epithelial and endothelial mammalian cells. For many of these SR-variants, the deficiency in virulence is due predominantly to a diminished secretion of p60 (encoded by the *iap* gene) which is an important virulence determinant for adhesion to and internalization of non-professional phagocytic cells.

The above findings should not be considered in isolation, as stress-induced changes in cell morphologies have been described in *L. monocytogenes* and other microorganisms by other researchers. Jørgensen and co-researchers [39] showed that there was a relationship between the time of exposure to different stressful levels of NaCl (incorporated in laboratory based media and minced beef) and the corresponding changes in thermotolerance and cell morphology of *L. monocytogenes*. Bacterial cells grown in media with 0.09 mol/L NaCl subjected to a short osmotic up-shock in media containing 0.5, 1.0 and 1.5 mol/L showed a 1.3, 2.5 and 8-fold increase in thermotolerance, respectively. The morphology of this pathogen was markedly affected by the osmolarity of the growth medium as cells grown in media containing 1.5 mol/L NaCl became up to 50 times longer than cells grown in media with 0.09 mol/L. It was not mentioned, however, whether these elongated cells were in chains or if they were filaments. In the early 1970's, Brazin [40] also demonstrated that *L. monocytogenes* underwent various morphological changes when grown in foods containing high salt levels (NaCl 8–9%).

Besides enhancing thermotolerance, an elevated osmolarity of the growth medium has also been linked to changes in cell morphology in other bacteria, such as *E. coli* and *Bacillus subtilis* [41–43]. Whilst low-osmolality was recently shown to alter the cell morphology of *Campylobacter jejuni* to an atypical coccoid-form (a possible association with the so-called 'viable non-culturable' state) [44]. Other researchers have also reported on a correlation between the acquisition of thermotolerance in psychrophilic and phychrotrophic microorganisms, and a change in cell morphology (to long filaments). McCallum and Inniss [45] showed that both the psychrophile *Aquaspirillium arcticum* and the psychrotroph *Bacillus psychrophilus* acquired thermotolerance when either heat shocked or treated with 50 μg/ml nalidixic acid (DNA synthesis inhibitor); both treatments resulted in the induction of heat shock or stress proteins and a marked change in cell morphology to a filamentous state. However, with the exception of the earlier-mentioned filamentous *L. monocytogenes,* the virulence potential of these pleomorphic microorganisms was not ascertained.

There is evidence, at the molecular level, to suggest that microbial stress-response and cell-division may be linked. The ClpC and ClpE ATPases (both Hsp 100 proteins) which are necessary for the heat shock response in *L. monocytogenes* are downregulated during infection by virulence transcriptional activator PrfA [46]. This is particularly interesting as a double ClpC-ClpE mutation influences cell division and virulence where these mutants form long cell chains and are avirulent [47]. The transcriptional levels of the *iap* gene are also very low during infection, which is also interesting as this gene is a general house-keeping protein needed for both cell division and infection.

Under-estimation of microbial survival and virulence using standard culture media

An artefact of current microbiological practice is to measure the effects of inimical processes using laboratory rich culture media where the challenged microorganisms are commonly assessed during their exponential growth phase. As pointed out by Archer [5] and Hopkins [48], 'although life on a petri plate with a few simple sugars and a handful of amino acids might not seem like much, to a bacterium it's a night in Trump Tower with a breakfast in bed'. In reality, bacteria experience and must adapt to multifaceted hostile environments, let it be in food (containing a mixture of complex substrates and natural antimicrobial compounds such as lysozyme or hydrogen perioxide, a low water activity perhaps, and acids and other deleterious products that are inherent to the food or produced by other competing microflora), or during passage through the environments of the stomach (such as low pH) and on internalization by host macrophages (where the bacteria must overcome the host's immunological defenses). To properly evaluate the survival capabilities of established or emerging food-borne pathogens in these complex environments, microbiologist and food technologists must holistically consider the effects of these multiple stresses, and endeavour to replicate these deleterious environments in food safety studies.

A well-appreciated phenomenon in microbiology is that bacterial cells in the stationary growth phase are more resistant to preservation hurdles than exponential-

phase ones [10]. In addition, it has been observed that bacteria are better recovered from environmental isolation or from sub-lethal stresses in the laboratory, if they are plated on minimal rather than rich media. The single cellular process that has been suggested to link these two phenomena is 'bacterial cell suicide' [15,20,49]. The idea arose from studies assessing the effects of competing microflora (using 10^8 living cells) on the resistance of *S. typhimurium* to heat and freeze injury. A mixed flora of exponential-phase competitor bacteria (containing equal numbers of *E. coli*, *Citrobacter freundi and Pseudomonas aeruginosa*) increased the heat resistance of 10^5 cful/ml exponential-phase *S. typhimurium* from a D-value of 0.43 min to 2.09 min at 55°C, equivalent to the resistance level of stationary-phase cells. D-value or decimal reduction value, is the time taken to reduce a population of cells by one log order i.e. 90%, under a given process condition [20]. Aldsworth [49] also showed that the presence of viable competitive microflora at cell densities of 10^8 cfu ml^{-1} protected an underlying population of 10^5 cfu of *S. typhimurium* against freeze thaw. The mechanism of enhanced resistance was initially postulated to be via an RpoS-mediated adaptive response. However, while the onset of the RpoS-mediated gene expression was brought forward by the addition of competitive bacteria, the time taken for induction was measured in hours, and since the protective effect was observed to be essentially instantaneous, the 'stationary-phase adaptive response' was excluded as the physiological medium. The only instantaneous physiological effect of the competitive microflora was a reduction in the percent saturation of oxygen from 100% to less than 10%. Thus, for both milk heat treatment (55°C) and freeze injury, this alteration in oxygen tension affords *S. typhimurium* a substantive (i.e. 2 orders of magnitude) augmentation in survival.

Aldsworth *et al.* [49] pointed out that the self-destruction is attributed to an oxidative-burst when rapidly growing bacterial cells are growth-arrested following sub-lethal injury. The greater sensitivity of exponential-phase cells is due to the production of intracellular free radicals rather than the direct physical action of the applied process, where the inimical process disturbs cell growth but does not affect the metabolic rate. What should be a sub-lethal injury becomes lethal, through growth arrest, leading to a decoupling of catabolic and anabolic metabolism (i.e. some stressed bacterial cells are unable to cope metabolically with nutritious growth media and die though oxidative suicide). The supplementation of oxygen scavengers such as sodium pyruvate or glutathione to nutritionally restricted growth media was shown to assist in the recovery of stress-damaged bacteria. Dodd *et al.* [15] also reported that protection against self destruction can be provided by reducing the oxygen tension, or by expression of the genes associated with the stationary phase, which allow cells to adapt to stress responses and which protect the cell against DNA damage, free radical damage and protein denaturation. Oxoid Limited, Basingstoke, UK, and Unilever Research Colworth, UK, have recently developed the S.P.R.I.N.T. *Salmonella* enrichment broth that contains an Oxyrase® enzyme system to overcome the oxidative stress within a medium which is detrimental to the growth of the sub-lethally stressed cells [20]. It has been shown that the addition of Oxyrase® is equivalent to the addition of 10^8 competing bacteria cells per millilitre.

This 'suicide hypothesis' may provide an explanation for the so called 'viable but non-culturable (VNC)' phenomenon (i.e. where stressed bacterial cells are metabolically active but unable to grow in standard culture media), where sub-lethally stressed bacteria exhibit normal respiratory and metabolic functions yet fail to grow on standard culture media [50]. Indeed, a daunting aspect of microbial stress-hardening shrouds the probability that the survival rate of inimically treated bacteria may even be higher than currently reported. Food safety studies predominately use standard culture media that do not cater for the possibility that a small section of the stressed bacterial population may be in the so-called VNC state. Recent advances in fluorescent microscopy should also help to re-address this issue. One particular method measures the single-cell activity of natural bacteria using the intracellular fluorescent probe 5-cyano-2,3-ditolyl tetrazolium chloride (CTC) [44]. This method results in the production of a fluorescent CTC-formazon product of reduction that can be quantified at low concentrations in individual cells and is thought to indicate that cell electron transport system activity or respiration is occurring. This CTC-staining method was recently used to show that VNC forms of *Campylobacter jejuni* do occur as a consequence of osmotic stress [44]. Indeed, the consequence of low level survival of VNC forms of the bacterial enteropathogens *E. coli* O157:H7 and *L. monocytogenes* is significant, as the infective dose of these bacteria may be as low as 50 cells [14,26].

Another problem of notoriety that bedevils the food industry is the inherent variability of bacterial cells, which when translated in terms of food safety often reveals that for many important bacterial pathogens (treated singly or in a mixed culture of competing microbes), death may not be exponential. For instance, food-borne enteric pathogens such as *L. monocytogenes* frequently exhibit an initial exponential kill proceeded by a 'tail section' that indicates an apparently increased resistance in the later stages of exposure to inimical processes. Booth [20] pointed out that these survivors are likely to be physiologically protected from the stress and are not mutants, as re-growth of the surviving cell population from the tail section, and exposure to stress,

repeats almost exactly the pattern of survival seen in the initial study. However, for food safety studies that use the above-mentioned D-values from linearized death rate data, an under-estimation of survival capabilities is highly probable. Interestingly, recent physiological data shows that 'laboratory-trained' strains do not show tailing in survival studies, and Booth [20] postulates that this tailing phenomenon may have been bred out of them by the continuous culture on relatively rich media.

Are we also under-estimating the virulence capabilities of food-borne pathogens when these microorganisms are grown under normal conditions on standard laboratory rich media? Recent studies using *L. monocytogenes* show that while a number of important virulence genes (such as *hly and plcA* which encode listeriolysin and a phospholipase respectively) are induced by growth in laboratory rich media such as brain heart infusion (BHI) broth, other important virulence determinants (such as *mpl*, *actA and plcB* which are required for escape of this pathogen from macrophages and cell-to-cell motility) are not expressed unless BHI is prior-treated with activated charcoal [26,28,33]. Indeed, unless this growth medium had been charcoal-treated, the role of the *bvr* gene and β-glucosidases, such as cellobiose, in the suppression of the pleiotrophic virulence transcriptional activator PrfA would have remained cryptic [32]. Interestingly, charcoal-treatment of BHI is required for the expression of virulence genes in *L. monocytogenes* irrespective as to whether or not the pathogen had been prior heat stressed. Considering the perceived 'better knowledge and understanding' of microbial resistance and pathogenesis in foods, are we still significantly behind in our appreciation of environmental-stress adaptation and associated virulence when it comes to media formulation for parasite-host interactive studies?

Conclusions and outlooks

There is little room for complacency in the food industry, as borne out by a relatively recent catastrophic breakdown in equipment at a Chicago milk-pasteurising plant, which resulted in an estimated 150,000 persons becoming ill from salmonellosis [2]. The implications of the aforementioned, are that the food industry may currently consider certain homologous or heterologous stresses as lethal, when in fact these inimical preservation treatments are actually sub-lethal. Given the current short falls (particularly where predictive models base bacterial survival against diverse inimical processes using rapidly growing and rapidly metabolising exponential-phase cells), the true level of susceptibility of stress-resistant microbial populations has yet to be determined. It is not to suggest that such predictive models are intrinsically unsafe, rather to infer that where these models explore levels of lethality that are close to the boundaries of microbial control, then there is scope for error [8]. For example, where the food industry contemplates modification to existing preservation strategies, or develops new ones (e.g. where there appears to be a trend towards more natural foods that are preserved using a combination of novel electrotechnologies and sub-lethal traditional methods).

In addition, not only are many problematic food-borne bacterial pathogens adapting to these deleterious stresses, it also would appear that certain pathogens are altering their characteristic cell morphology and physiology as a consequence of these inimical processes. While the precise mechanisms for these stress-induced cellular changes are currently unknown, adaptive-mutations brought on by stress cannot be ruled-out. For the immediate future, there is an urgent need for food preservation and safety studies to focus on the multiplicity of sub-lethal stresses that are commonly experienced by food-borne bacterial pathogens during food manufacture, distribution and storage, and to translate this valuable data into current predictive models. It is equally important to be mindful of microbial-stress adaptation and enhanced virulence when investigating parasite-host interactions. Best-published knowledge currently recommends researchers to be aware of 'bacterial cell-suicide' due to oxidative stress and to compensate for this phenomenon in their studies. Finally, it's not all doom and gloom, the idea of applying sub-lethal stresses to boost the survival of beneficial microorganisms in foods, such as *Bifidobacterium*, might have significant merit.

References

1 Slutsker, L., Alterkruse, S.F. and Swerdlow, D.L. (1998) 'Food-borne Diseases: Emerging Pathogens and Trends' in *Emerg. Infect. Dis*. 12, 199–218

2 Baird-Parker, A.C. (1994) 'Foods and Microbiological Risk' in *Microbiol*. 140, 687–695

3 Buchanan, R.L. (1997) 'Identifying and Controlling Emerging Foodborne Pathogens: Research Needs' in *Emerg. Infect. Dis*. 3, 517–521

4 Knøchel, S. and Gould, G. (1995) 'Preservation Microbiology and Safety: Quo Vadis?' in *Trends Food Sci. Technol*. 6, 127–131

5 Archer, D. (1996) 'Preservation Microbiology and Safety: Evidence That Stress Enhances Virulence and Triggers Adaptive Mutations' in *Trends Food Sci. Technol*. 7, 91–95

6 Leistner, L. (1995) 'Principles and Applications of Hurdle Technology' in *New Methods of Food Preservation* (Gould, G.W., ed), pp. 1–21, Blackie Academic & Professional

7 Gahan, C.G., O'Driscoll, B. and Hill, C. (1996) 'Acid Adaptation of *Listeria monocytogenes* Can Enhance Survival in Acid Foods and During Milk Fermentation' in *Appl. Environ. Microbiol*. 62, 3123–3128

8 Lou, Y. and Yousef, A.H. (1997) 'Adaptation of Sublethal Environmental Stresses Protects Against Lethal Preservation Factors' in *Appl. Environ. Microbiol*. 63, 1252–1255

9 Leyer, G.J. and Johnson, E.A. (1993) 'Acid Adaptation Induces Cross-protection Against Environmental Stresses in *Salmonella typhimurium*' in *Appl. Environ. Microbiol*. 59, 1842–1847

10 Rowe, M.T. and Kirk, R. (1999) 'An Investigation into the Phenomenon of Cross-protection in *Escherichia coli* 0157:H7' in *Food Microbiol*. 16, 157–164

11 Farber, J.M. and Pagotto, F. (1992) 'The Effect of Acid Shock on the Heat Resistance of *L. monocytogenes*' in *Lett. Appl. Microbiol* 15, 197–201

12 Goodson, M. and Rowbury, R.J. (1989) 'Resistance of Acid-habituated *Escherichia coli* to Organic Acids and its Medical and Applied Significance' in *Lett. Appl. Microbiol*. 8, 211–214

13 Rowan, N.J. and Anderson, J.G. (1998) 'Effects of Above-optimum Growth Temperature and Cell Morphology on Thermotolerance of *L. monocytogenes* Cells Suspended in Bovine Milk' in *Appl. Environ. Microbiol*. 64, 2065–2071

14 Daboob, A.A. (1999) 'Studies on Factors Affecting the Growth and Thermotolerance of *Escherichia coli* Including the Pathogenic Serotype O157:H7'. Ph.D. thesis, University of Strathcylde, Glasgow, UK

15 Dodd, C.E.R., Sharman, R.L., Bloomfield, S.F., Booth, I.R. and Stewart, G.S.A.B. (1997) 'Inimical Processes: Bacterial Self Destruction and Sub-lethal Injury' in *Trends Food Sci. Technol*. 8, 238–241

16 Marron, L., Emerson, N., Gahan, C.G.M. and Hill, C. (1997) 'A Mutant of *Listeria monocytogenes* L028 Unable to Induce an Acid Tolerance Response Displays Diminished Virulence In a Murine Model' in *Appl. Environ. Microbiol*. 63, 4945–4947

17 Hill, C., O'Driscoll, B. and Booth, I.R. (1995) 'Acid Adaptation and Food Poisoning Microorganisms' in *Int. J. Food Microbiol*. 28, 245–254

18 Karem, K.L., Foster, J.W. and Bej, A.K. (1994) 'Adaptive Acid Tolerance in *Aeromonas hydrophila*' in *Microbiol*. 140, 1731–1737

19 Foster, J.W. and Specter, M.P. (1995) 'How *Salmonella* Survive Against the Odds' in *Annu. Rev. Microbiol*. 49, 145–174

20 Booth, I.R. (1998) 'The Bacteria Strike Back' in *The Biochemist* April, 8–11.

21 Abee, T. and Wouters, J.A. (1999) 'Microbial Stress and Minimal Processing' in *Int. J. Food Microbiol*. 50, 65–92

22 Mekalonos, J.J. (1992) 'Environmental Signals Controlling Expression of Virulence Determinants in Bacteria' in *J. Bacteriol*. 174, 1–7

23 LeClerc, J.E., Li, B., Payne, W.L. and Cebula, T.A. (1996) 'High Mutation Frequencies Among *Escherichia coli* and *Salmonella* Pathogens' in *Science* 274, 1208–1211

24 Moxon, E.R., Rainey, P.B., Nowak, M.A. and Lenski, R.E. (1994) 'Adaptive Evolution of Highly Mutable Loci in Pathogenic Bacteria' in *Curr. Biol*. 4, 24–33

25 Lee, I.S., Lin, J., Hall, H.K., Bearson, B. and Foster, J.W. (1995) 'The Stationary-phase Sigma Factor σ^S (RpoS) is Required for a Sustained Acid Tolerance Response in Virulent *Salmonella typhimurium*' in *Mol. Microbiol*. 17, 155–167

26 Bubert, A., Sokolovic, Z., Chun, S.-K., Papatheodoru, L., Simm, A. and Goebel, W. (1999) 'Differential Expression of *Listeria monocytogenes* Virulence Genes in Mammalian Host Cells' in *Mol. Gen. Genet*. 261, 323–336

27 Chakraborty, T., Leimeister-Wachter, M., Domann, E., Harti, M., Goebel, W., Nichterlein, T. and Notermans, S. (1992) 'Coordinate Regulation of Virulence Genes in *Listeria monocytogenes* Requires the Product of the *prfA* Gene' in *J. Bacteriol*. 174, 568–574

28 Freitag, N.E. and Jacobs, K.E. (1999) 'Examination of *Listeria monocytogenes* Intracellular Gene Expression by Using the Green Fluorescent Protein of *Aequorea victoria*' in *Infect. Immun*. 67, 1844–1852

29 Park, S.F., Stewart, G.S.A.B. and Krol, R.G. (1992) 'The Use of Bacterial Luciferase for Monitoring the Environmental Regulation of Expression of Genes Encoding Virulence Factors in *Listeria monocytogenes*' in *J. Gen. Microbiol*. 138, 2619–2627

30 Sokolovic, Z., Reidel, J., Wuenscher, M. and Goebel, W. (1993) 'Surface-associated, PrfA-regulated Proteins of *Listeria monocytogenes* Synthesized Under Stress Conditions' in *Mol. Microbiol*. 8, 219–227

31 McKeller, R.C. (1993) 'Effect of Preservatives and Growth Factors on Secretion of Listeriolysin O by *Listeria monocytogenes*' in *J. Food Protect*. 56, 380–384

31 Brehm, K., Ripio, M-T., Kreft, J. and Vazquez-Boland, J.-A. (1999) 'The *bvr* Locus of *Listeria monocytogenes* Mediates Virulence Gene Expression by β-Glucosides' in *J. Bacteriol*. 181, 5024–5032

33 Ripio, M-T., Vazquez-Boland, J-A., Vega, Y., Nair, S. and Berche, P. (1998) 'Evidence of Expressional Crosstalk Between the Central Virulence Regulator PrfA and the Stress Response Mediator ClpC in *Listeria monocytogenes*' in *FEMS Microbiol. Lett*. 158, 45–50

34 Gahan, C.G.M. and Hill, C. (1999) 'The Relationship Between Acid Stress Responses and Virulence in *Salmonella typhimurium* and *Listeria monocytogenes*' in *Int. J. Food Microbiol*. 50, 93–100

35 Wiedmann, M., Arvik, T.J., Hurley, R.J. and Boor, K.J. (1998) 'General Stress Transcription Factor σ^B and its Role in Acid Tolerance and Virulence of *Listeria monocytogenes*' in *J. Bacteriol*. 180, 3650–3656

36 Lewthwaite, J., Skinner, A. and Henderson, B. (1998) 'Are Molecular Chaperones Microbial Virulence Factors?' in *Trends in Microbiol*. 6, 426–428

37 Rowan, N.J., McLauchlin, J. and Bubert, A. (1999) 'Virulent Atypical Cell Forms of *Listeria monocytogenes* Secreting Wild-type Levels of p60' Proceedings of the 6th Conference of the Federation of Infection Societies, Manchester, UK, 1–3 December, p. 45

38 Kuhn, M. and Goebel, W. (1989) 'Identification of an Extracellular Protein of *Listeria monocytogenes* Possibly Involved in Intracellular Uptake by Mammalian Cells' in *Infect. Immun*. 57, 55–61

39 Jørgensen, F., Stephens, P.J. and Knøchel, S. (1995) 'The Effect of Osmotic Shock and Subsequent Adaptation on Thermotolerance and Cell Morphology of *Listeria monocytogenes*' in *J. Appl. Bacteriol*. 79, 274–281

40 Brazin, B. (1973) 'The Effect of NaCl on the Morphology of *Listeria monocytogenes*' in *Zbl. Bakteriol. Hyg. I. Abt. Orig. A* 225, 80–84

41 Roth, W.G., Porter, S.E., Leckir, M.P., Porter, B.E. and Dietzler, D.N. (1985) 'Restoration of Cell Volume and the Reversal of Carbohydrate Transport and Growth Inhibition of Osmotically Upshocked *Escherichia coli*' in *Biochem. Biophys. Res. Comm*. 126, 442–449

42 Ruzal, S.M. and Sanchez-Rivas, C (1993) 'Physiological and Genetic Characterisation of the Osmotic Stress Response in *Bacillus subtilis* ' in *Can. J. Microbiol*. 40, 140–144

43 Schleyer, M., Schmid, R. and Bakker, E.P. (1993) 'Transient, Specific and Extremely Rapid Release of Osmolytes from Growing Cells of *Escherichia coli* K-12 Exposed to Hypoosmotic Shock' in *Arch. Microbiol*. 160, 424–431

44 Reezal, A., McNeil, B. and Anderson, J.G. (1998) 'Effect of Low-osmolality Nutrient Media on Growth and Culturability of *Campylobacter* Species' in *Appl. Environ. Microbiol*. 64, 4643–4649

45 McCallum, K.L. and Inniss, W.E. (1990) 'Thermotolerance, Cell Filamentation, and Induced Protein Synthesis in Psychrotrophilic and Psychrotropic Bacteria' in *Arch. Microbiol*. 153, 585–590

46 Rouquette, C., Ripio, M.-T., Pellegrini, E., Bolla, J.-M., Tascon, R.I., Vasquez-Boland, J.-A. and Berche, P. (1996) 'Identification of a ClpC ATPase Required for Stress Response and *in vivo* Survival of *Listeria monocytogenes*' in *Mol. Microbiol*. 21, 977–987

47 Nair, S., Frehel, C., Nguyen, L., Escuyer, V. and Berche, P. (1999) 'ClpE, a Novel Member of the HSP100 Family, is Involved in Cell Division and Virulence of *Listeria monocytogenes*' in *Mol. Microbiol.* 31, 185–196
48 Hopkins, K. (1994) 'Theory of Adaptive Mutations Makes a Comeback in *E. coli*' in *J. NIH Res.* 6, 57–62
49 Aldsworth, T.G., Sharman, R.L., Dodd, C.E.R. and Stewart, G.S.A.B. (1998) 'A Competitive Microflora Increases the Resistance of *Salmonella typhimurium* to Inimical Processes: Evidence for a Suicide Response' in *Appl. Environ. Microbiol.* 64, 1323–1327
50 Bloomfield, S.F., Stewart, G.S.A.B., Dodd, C.E.R., Booth, I.R. and Power, E.G.N. (1998) 'The Viable but Not-culturable Phenomenon Explained' in *Microbiol.* 144, 1–3

IRISH VETERINARY JOURNAL
Iris Tréidliachta Éireann

RESEARCH Open Access

Investigations on the efficacy of routinely used phenotypic methods compared to genotypic approaches for the identification of staphylococcal species isolated from companion animals in Irish veterinary hospitals

Lisa Geraghty[1,2*], Mary Booth[1,2], Neil Rowan[1] and Andrew Fogarty[1,2]

Abstract

Background: Identification of Staphylococci to species level in veterinary microbiology is important to inform therapeutic intervention and management. We report on the efficacy of three routinely used commercial phenotypic methods for staphylococcal species identification, namely API Staph 32 (bioMérieux), RapID (Remel) and Staph-Zym (Rosco Diagnostica) compared to genotyping as a reference method to identify 52 staphylococcal clinical isolates (23 coagulase positive; 29 coagulase negative) from companion animals in Irish veterinary hospitals.

Results: Genotyping of a 412 bp fragment of the staphylococcal *tuf* gene and coagulase testing were carried out on all 52 veterinary samples along with 7 reference strains. In addition, genotyping of the staphylococcal *rpo*B gene, as well as PCR-RFLP of the *pta* gene, were performed to definitively identify members of the *Staphylococcus intermedius* group (SIG). The API Staph 32 correctly identified all *S. aureus* isolates (11/11), 83% (10/12) of the SIG species, and 66% (19/29) of the coagulase negative species. RapID and Staph-Zym correctly identified 61% (14/23) and 0% (0/23) respectively of the coagulase-positives, and 10% (3/29) and 3% (1/29) respectively of the coagulase-negative species.

Conclusions: Commercially available phenotypic species identification tests are inadequate for the correct identification of both coagulase negative and coagulase positive staphylococcal species from companion animals. Genotyping using the *tuf* gene sequence is superior to phenotyping for identification of staphylococcal species of animal origin. However, use of PCR-RFLP of *pta* gene or *rpo*B sequencing is recommended as a confirmatory method for discriminating between SIG isolates.

Keywords: Companion animals, Staphylococci species identification, Genotyping, tuf, *rpo*B

Background

Staphylococcal species are considered to be opportunistic pathogens, colonising the skin and mucous membranes of humans and animals. In animals, both coagulase positive and coagulase negative Staphylococci have been associated with infection, with a variety of sources identified [1,2]. International animal surveillance programmes on emerging trends in antibiotic resistance typically focus on food animals. Consequently, there is a dearth of similar information for pets or companion animals that frequently are administered with antibiotics, particularly in veterinary hospitals. Recent studies have reported a link between the isolation of multi-drug resistant bacteria from pet owners with companion animal carriage [1]. Antibiotic resistance to beta-lactams, including methicillin resistance, has been found in both coagulase negative and coagulase positive Staphylococci carried by healthy and infected cats, dogs and horses [3-5] reported that various coagulase negative species of

* Correspondence: lgeraghty@ait.ie
[1]Biosciences Research Institute, Athlone Institute of Technology, Dublin Rd., Athlone, Co. Westmeath, Ireland
[2]Department of Life and Physical Science, School of Science, Athlone Institute of Technology, Dublin Rd., Athlone, Ireland

Staphylococci from bovine milk differed significantly from each other in antimicrobial resistance profiles (both genotypic and phenotypic) with implications for treatment and management decisions. Accurate speciation of Staphylococci is vital to establish critical links between bacterial species of clinical origin and emerging trends in antibiotic resistance.

Historically, identification of bacterial specimens has been based on conventional microbiological procedures, which include growth on various media, cell morphology, staining reactions and biochemical profiles [6]. Currently in Ireland commercial systems such as API Staph 32 (bioMérieux), Rap-ID (Remel) and Staph-Zym (Rosco Diagnostica) are regularly used to identify species of Staphylococci. There is an absence of published information on the efficacy of using these commercial phenotypic methods for routine Staphylococcal identification particularly from companion animals. Recent reports suggest that phenotypic methods have inherent weaknesses due to the variability in expression of phenotypic characteristics by isolates belonging to the same species and their reliance on subjective interpretation of test results that can also introduce variability [7-11]. Blaiotta and co-workers [8,12] reported a large variation in phenotypic properties of Staphylococci isolated from fermented sausages using laboratory-prepared basal media supplemented separately with fermentable sugars. This group also reported that 25% of these Staphylococci were not identifiable using phenotypic methods. Most phenotypic identification systems have been developed for human healthcare and validated using clinical isolates obtained from human infections [9,11]. When employed on isolates of animal origin, the identification system may be less reliable due to the lack of animal isolates in the reference databases [13,14].

Genotypic methods are reported to have higher discriminatory power, reproducibility and typeability compared to phenotypic methods [10,11,15,16]. Several approaches are available for genotyping bacterial isolates including AFLP (amplified fragment length polymorphism), ribotyping, PCR-RFLP and DNA sequencing. DNA sequence based species identification of Staphylococci is currently the most accurate method with the largest reference database, and is considered to be the gold standard method [10,11]. Traditionally, the most common target for DNA sequencing in bacteria is 16S-rRNA [11,17]. However, this gene is highly conserved among Staphylococci, and often does not provide sufficient discriminatory power to differentiate closely related staphylococcal species [11]. Alternatives to the 16S rRNA gene which have been successfully applied to staphylococcal genotyping include *gap* [17], *cpn* 60 [18], *tuf* [9], *rpo*B [19], *nuc* [20] and *sod*A [21]. Heikens et al., [9] first proposed partial amplification and sequencing of the *tuf* gene as a reliable and reproducible method for the identification of species of Staphylococci. Subsequent studies have confirmed *tuf* gene sequencing as an accurate method for speciating coagulase negative Staphylococci, [22,23]. Blaiotta et al. [24] revealed diversity among coagulase positive *Staphylococcus* species strains based on partial *kat* (catalase) gene sequences and reported a PCR-RFLP assay for identification of coagulase-positive species (*S. aureus, S. delphini, S. hyicus, S. intermedius, S. pseudomedius, S. schleiferi* subsp. *coagulans*). Similarly, Sasaki et al. [25] used a multiplex-PCR method targeting the staphylococcal thermonuclease gene (*nuc*) to successfully differentiate between the same species.

Based upon best-published literature, there is a dearth of critical information on the efficacy of using phenotypic "quick tests" to identify staphylococcal species associated with companion animals. Therefore, this study aimed to compare the efficacy of three routinely-used phenotypic staphylococcal identification test kits with genotypic methods in order to identify the most accurate method of speciating clinical isolates of Staphylococci from a variety of companion animals (dogs, cats, horses) in primary care veterinary hospitals throughout Ireland.

Methods

Bacterial strains

Fifty two staphylococcal clinical isolates of veterinary origin and 7 reference control strains were analysed in this study. Clinical specimens were isolated from infection site swabs taken at primary care veterinary clinics (Table 1). Animal species included feline (n=21), canine (n=18), equine (n=11) and bovine (n=2). Infection types included flesh wounds and superficial abscesses (n=38), deep seated infections (n=9), post-operative infections (n=4), and ocular infections (n=3). Swabs were streaked onto Columbia blood agar and Staphylococci were identified by colony morphology, haemolysis patterns, Gram's stain characteristics, catalase activity, growth on Baird Parker agar, coagulase activity and Voges-Proskauer (VP) testing. Two different coagulase tests were performed: a tube test for free coagulase and a slide test for bound coagulase of clumping factor. Seven control strains and fifty-two clinical isolates were tube coagulase tested according to Murray et al. [6] as follows: a mixture of a 0.1 ml nutrient broth incubated with overnight culture was mixed with 0.5 ml of reconstituted rabbit plasma containing EDTA (Rabbit Coagulase Plasma, Cruinn Diagnostics) in a sterile glass tube and incubated at 37°C in a water bath for 4 hrs. The tubes were observed for clot formation by gently tilting at a 90° angle from the vertical. The tubes were then re-incubated and re-read at 24 hrs. Any degree of clotting was read as a positive result. The slide coagulase test was performed using a Staphylase test kit (Oxoid) according to manufacturer's instructions. A positive result

Table 1 Source of Staphylococci isolated from companion animals in veterinary hospitals

Isolate no.	Staphylococcal species	Companion animal	Infection type	Location of veterinary hospital (Region of Ireland)
1	*S. aureus*	equine	Joint infection	north
2	*S. aureus*	feline	Flesh wound	north
3	*S. aureus*	feline	Face abscess	west
4	*S. aureus*	bovine	Post caesarian	west
5	*S. aureus*	feline	Interdigital infection	west
6	*S. aureus*	feline	Interdigital infection	west
7	*S. aureus*	equine	Abdominal trauma	south
8	*S. aureus*	canine	Post ortho op	east
9	*S. aureus*	feline	Cat fight abscess	west
10	*S. aureus*	feline	Flesh wound	west
11	*S. aureus*	equine	Flesh wound	west
12	*S. pseudintermedius*	canine	Post ortho op	west
13	*S. pseudintermedius*	canine	Granuloma type	north
14	*S. pseudintermedius*	canine	Pyoderma	north
15	*S. pseudintermedius*	canine	Flesh wound	north
16	*S. pseudintermedius*	feline	Deglove wound	west
17	*S. pseudintermedius*	canine	Flesh wound	south
18	*S. pseudintermedius*	canine	Flesh trauma	west
19	*S. pseudintermedius*	equine	Abdominal wound	south
20	*S. pseudintermedius*	equine	Joint infection	north
21	*S. pseudintermedius*	canine	Ear tip infection	west
22	*S. pseudintermedius*	feline	Granuloma type	east
23	*S. pseudintermedius*	canine	Flesh wound	south
24	*S. felis*	canine	Flesh wound	north
25	*S. felis*	feline	Ocular infection	east
26	*S. felis*	canine	Post hysterectomy	west
27	*S. equorum*	canine	Eyelid infection	south
28	*S equorum*	canine	Flesh wound	north
29	*S. equorum*	canine	Face pyoderma	north
30	*S. equorum*	canine	Ear infection	north
31	*S. equorum*	feline	Trauma to face	south
32	*S. equorum*	feline	Cat fight abscess	south
33	*S equorum*	equine	Uterine infection	east
34	*S. equorum*	feline	Flesh wound	south
35	*S. succinus*	equine	Uterine infection	west
36	*S. warneri/pasteuri*	canine	Eyelid infection	south
37	*S. warneri/pasteuri*	bovine	Chronic mastitis	west
38	*S. carnosus/simulans*	feline	Abscess	south
49	*S. carnosus*	feline	Rhinitis	north
40	*S. carnosus*	feline	Pyoderma	north
41	*S. carnosus /simulans*	feline	Puncture wound	west
42	*S. carnosus/simulans*	equine	Chronic flesh wound	west
43	*S. carnosus/simulans*	feline	Abscess	south
44	*S. carnosus*	feline	Ear infection	west
45	*S. carnosus/simulans*	feline	Puncture wound	west

Table 1 Source of Staphylococci isolated from companion animals in veterinary hospitals *(Continued)*

46	*S. carnosus /simulans*	equine	Uterine infection	east
47	*S. xylosus*	feline	Laceration flesh	east
48	*S. xylosus*	canine	Flesh wound	east
49	*S. xylosus*	equine	Uterine infection	west
50	*S. xylosus*	canine	Deglove RTA	south
51	*S. saprophyticus*	feline	Flesh wound	north
52	*S saprophyticus*	feline	Infection in paw	south

was read when clumping occurred within 10 seconds. Reference strain identity and source are shown in Table 2.

Phenotypic identification testing

Phenotypic identification to species level was carried out using three test kits which are commercially available to veterinary laboratories in Ireland, i.e. API Staph 32 (bioMérieux), RapID (Remel) and Staph-Zym (Rosco Diagnostica). Prior to testing, isolates were cultured overnight at 37°C on Columbia blood agar. Tests were carried out according to manufacturers' instructions and results were interpreted using the appropriate laboratory computer software or reference indices recommended by the manufacturer. The results of the phenotypic tests in this study are also described in terms of sensitivity, specificity and predictive value positive (PVP) of the three test kits and were calculated in comparison with *tuf* genotyping [5]. Sensitivity was calculated as the proportion of the true positive isolates that are correctly identified with the phenotypic tests. Specificity was calculated as the proportion of the true negatives that are correctly identified with the phenotypic tests. The predictive value positive (PVP) for each test was calculated as the proportion of isolates identified as a specific species based on phenotypic testing that truly represented that particular species.

Genotypic identification testing

Genomic DNA from overnight liquid cultures in nutrient broth was extracted using a DNeasy kit (QIAGEN) according to manufacturer's instructions. For genotyping, a 412 bp fragment of the *tuf* gene was amplified for all clinical isolates and reference strains according to Heikens et al. [9]. Amplification of a 750 bp *rpoB* gene segment was carried out on all SIG isolates (3 reference strains and 12 clinical isolates) according to Drancourt and Raoult [19], with the following modifications in PCR cycling conditions: 2 minutes at 95°C for 1 cycle, 30 seconds at 94°C, 30 seconds at 47°C, 1 minute at 72°C for 35 cycles, and 5 minutes at 72°C for 1 cycle.

DNA sequencing

A total of 59 *tuf* amplicons (from 7 reference and 52 clinical isolates) and 15 *rpoB* amplicons (3 reference and 12 clinical isolates) were sequenced by Sequiserve, Germany and Functional Biosciences, USA using amplification primers [9,19]. Forward and reverse sequences were analysed using the BLASTn alignment program and the NCBI nucleotide database NCBI [26].

PCR-RFLP to differentiate SIG species

Twelve clinical isolates were identified by both *tuf* and *rpo*B genotyping as members of the *Staphylococcus intermedius* group (SIG). PCR-RFLP involving amplification of the *pta*

Table 2 Identification of staphylococcal reference strains

Species ID	Source*	*tuf*	*rpo*B	*pta*-RFLP	API Staph 32	RapID	Staph-Zym
S. aureus IMD247	Athlone Institute of Technology	*S. aureus*	-	-	*S. aureus*	*S. aureus*	*S. vitulans*
S. hycius 11249	University College Dublin	*S. hycius*	-	-	*S. hycius*	*S. aureus*	*S. hycius*
S. aureus 25923	ATCC	*S. aureus*	-	-	*S. aureus*	*S. aureus*	*No result*
S. aureus 43300	ATCC	*S. aureus*	-	-	*S. aureus*	*S. aureus*	*S. vitulans*
S. intermedius CCUG 6520	University of Copenhagen	*S. intermedius*	*S. intermedius*	*S. intermedius*	*S. intermedius*	*S. intermedius*	*No result*
S. delphini M4	University of Copenhagen	*S. delphini*	*S. delphini*	*S. delphini*	*S. intermedius*	*No result*	*S. vitulans*
S. pseudinter -medius Y19	University of Copenhagen	*S. pseudinter - medius*	*S. pseudinter - medius*	*S. pseudinter - medius*	*S. intermedius*	*S. intermedius*	*S. vitulans*

*American Typed Culture Collection (ATCC).

gene followed by digestion with *Alu*1 was used in this study to distinguish between the three known species in the SIG group according to Bannhoer et al., [27] and Kadlec et al. [28].

Results

Comparative use of phenotypic 'quick tests' and genotypic methods to identify reference strains of staphylococcal species

Seven reference staphylococcal strains were analysed in this study using each of the speciation methods: *tuf* genotyping, API Staph 32, RapID and Staph-Zym. The results are displayed in Table 2. The *tuf* genotyping correctly identified all reference strains. The API Staph 32 test correctly identified *S. aureus*, *S. hycius*, and *S. intermedius* reference strains. However *S. pseudintermedius* and *S. delphini,* were both misidentified indicating that this test does not distinguish SIG species. The RapID test correctly identified all of the *S. aureus* reference strains and *S. intermedius*, but misidentified *S. hycius* and *S. pseudintermedius.* RapID gave no result for *S. delphini*. Staph-Zym identified only one (*S. hycius*) of the 7 control strains, correctly. The three SIG reference strains in the study were also analysed by *rpo*B genotyping and PCR-RFLP of the *pta* gene and were correctly identified by both tests.

Speciation of staphylococcal clinical isolates

Based on using *tuf* genotyping as the reference identification method for this study, the clinical isolate collection (n=52) was found to comprise of a range of staphylococcal species. The results are shown in Table 3. Forty four percent (23/52) were identified as coagulase positive species, of which 47.8% (11/23) were *S. aureus* and 43% (10/23) were *S. pseudintermedius* (Table 3). For two of the coagulase positive isolates, *tuf* did not distinguish between *S. pseudintermedius* and *S. delphini* (Isolate No's. 18 and 23). All twelve SIG clinical isolates were confirmed to be *S. pseudintermedius* according to banding patterns using PCR-RFLP of the *pta* gene and *rpo*B genotyping. Fifty six percent (29/52) of isolates were identified by *tuf* genotyping as coagulase negative Staphylococci (CONS) (Table 3). These included, *S. equorum* (n=8), *S. xylosus* (n=4), *S. carnosus/simulans* (n=6), *S. carnosus* (n=3), *S. felis* (n=3), *S. warneri*/*pasteuri* (n=2), *S. saprophyticus* (n=2) and *S. succinus* (n=1). For six of the CONS isolates, *tuf* genotyping did not distinguish between two closely related coagulase negative species, identifying them as *S. carnosus* or *S. simulans,* a finding which correlates with research carried out by Ghebremedhin et al. [29]. For two additional isolates a result of *S. pasteuri* or *S. warneri* was obtained. The results of *tuf* genotyping were consistent with the coagulase test results in all cases with five exceptions, namely *S. aureus* (Isolate No. 1) and *S. pseudintermedius* (Isolate No's 16, 17, 22 and 23). These strains failed to coagulate plasma in both slide and tube coagulation tests, but were subsequently confirmed as coagulase positive species by PCR-RPLP of the *pta* gene and *rpo*B sequencing.

The results of the phenotypic tests in this study are summarised in Table 4, where the sensitivity, specificity and predictive value positive (PVP) of the three test kits are calculated in comparison with *tuf* species identification. The API Staph 32 test showed greatest sensitivity for *S. aureus* isolates (100%). A majority (10/12) of the *S. pseudintermedius* isolates were positively identified as members of the SIG group (83.3%), however, none were accurately speciated. The remaining *S. pseudintermedius* isolates gave either no result (n=1) or was misidentified (n=1). Specificity was 100% for *S. aureus*, and 95% for the SIG group. For the remaining 29 isolates, which were CONS, 31% (9/29) were correctly identified. Isolates identified by *tuf* genotyping as *S. carnosus/simulans* were correctly identified by API Staph 32 as either *S. carnosus* or *S. simulans* in six out of nine cases (66.6% sensitivity). *S. xylosus* species were correctly identified by API Staph 32 with a sensitivity of 75%. In this test, specificity for these two species was 95.3 and 83.3% respectively. Sensitivity was 0% for *S. equorum*, *S. felis* and *S. succinus* while specificity was 97.7, 98 and 100% respectively. In the case of *S. warneri* and *S. saprophyticus* sensitivity was 50%, with 100% specificity in each case. The API Staph 32 demonstrated the highest PVP with the coagulase positive isolates, with *S. aureus* at 100% and the SIG group at 83.3%. PVP values could not be interpreted for some coagulase negative species, as the test did not identify the species in some cases. *S. xylosus* demonstrated a PVP of 27.2%, due to the high number of false positive results and low specificity (83.3%). Overall, the API Staph 32 had a sensitivity value of 61.5%, a specificity value of 98% and a PVP value of 80% compared to identification of staphylococcal species by *tuf* genotyping.

RapID correctly identified 81.8% (9/11) of the *S. aureus* isolates (sensitivity 81.8%, specificity 100%), but misidentified all of the *S. pseudintermedius* isolates. On consideration of ability to identify the SIG group, the RapID test had a sensitivity of 41.6% and specificity of 95.2%. Only 7% (2/29) of the CONS were correctly identified, 58.6% (17/29) were misidentified, and no result was obtained for 34% (10/29). When attempting to identify *S. xylosus*, RapID demonstrated a sensitivity value of 50%, but with a specificity of 66.6%, resulting in a PVP of just 15.8%. Overall, the RapID Staph had a sensitivity value of 32.7%, a specificity value of 95.4% and a PVP value of 47.2% compared to identification of staphylococcal species by *tuf* genotyping.

Staph-Zym correctly identified none of the coagulase positive isolates in this study, and only one of the CONS isolates (Isolate No. 39; *S. carnosus*). For 11.5% (6/52) of isolates, Staph-Zym yielded more than one species name. For 44.2% (23/52) Staph-Zym yielded "no result".

Table 3 Identification of coagulase positive and negative staphylococcal clinical isolates

No	*tuf*	API Staph 32	RapID	Staph-Zym
1	*S. aureus*	*S. aureus*	*S. aureus*	no result
2	*S. aureus*	*S. aureus*	*S. aureus*	*S. capitus*
3	*S. aureus*	*S. aureus*	*S. capitus*	no result
4	*S. aureus*	*S. aureus*	*S. aureus*	no result
5	*S. aureus*	*S. aureus*	*S. aureus*	no result
6	*S. aureus*	*S. aureus*	*S. aureus*	no result
7	*S. aureus*	*S. aureus*	*S. aureus*	*S. warneri*
8	*S. aureus*	*S. aureus*	*S. aureus*	*S. warneri*
9	*S. aureus*	*S. aureus*	*S. aureus*	*S. vitulans*
10	*S. aureus st398*	*S. aureus*	*S. aureus*	no result
11	*S. aureus st398*	*S. aureus*	*S. gallinarum/xylosus*	*S. warneri*
12	*S. pseudintermedius*	*S. intermedius*	*S. xylosus*	*no result*
13	*S. pseudintermedius*	*S. intermedius*	*S. gallinarum/xylosus*	*no result*
14	*S. pseudintermedius*	*S. intermedius*	*S. xylosus*	*no result*
15	*S. pseudintermedius*	*S. intermedius*	*S. intermedius/xylosus*	*S. capitus*
16	*S. pseudintermedius*	*S. intermedius*	*S. capitus*	*no result*
17	*S. pseudintermedius*	*S. intermedius*	*S. intermedius*	*S. capitus/hycius*
18	*S. pseud/delphini**	*S. intermedius*	*S. gallinarum/xylosus*	*no result*
19	*S. pseudintermedius*	*S. intermedius*	*S. epidermidis*	*S. vitulans*
20	*S. pseudintermedius*	no result	*no result*	*no result*
21	*S. pseudintermedius*	*S. intermedius*	*S. intermedius*	*no result*
22	*S. pseudintermedius*	*S. intermedius*	*S. intermedius*	*no result*
23	*S. pseud/delphini**	*Kocuria rosea*	*S. hominus/ capitus*	*S. lentus/fleurettii*
No	***tuf***	**API 32**	**RapID**	**Staph-Zym**
24	*S. felis*	*S.chromogens*	*S.chromogenes*	*S. vitulans*
25	*S. felis*	*S. carnosus*	*S. intermedius*	*S. capitus*
26	*S. felis*	*s. xylosus*	*S. xylosus*	no result
27	*S. equorum*	*S. xylosus*	*S. xylosus*	no result
28	*S. equorum*	*S. warnerei*	*S. warnerei*	no result
29	*S. equorum*	no result	*S. xylosus*	*S.xylosus/scuiri*
30	*S. equorum*	*S. xylosus*	*S. xylosus*	no result
31	*S. equorum*	no result	no result	no result
32	*S. equorum*	*S. xylosus*	*S. xylosus*	*S. lentus*
33	*S. equorum*	*S. xylosus*	*S. xylosus*	no result
34	*S. equorum*	*S. epidermidis*	*S. epidermidis*	no result
35	*S. succinus*	*S. xylosus*	*S. xylosus*	*no result*
36	*S.warnerei/ pasteureii*	*S. warnerei*	*no result*	*S. vitulans*
37	*S.warnerei/ pasteureii*	*S. carnosus*	no result	*S.lentus/fleurettii*
38	*S. carnosus /simulans*	*S. carnosus*	no result	*S. warnerei*
39	*S. carnosus*	*S. simluans*	*S. simulans*	*S. carnosus*
40	*S. carnosus*	*S. carnosus*	no result	no result
41	*S. carnosus/simulans*	*S. simulans*	no result	*S.capitus/ hyicus*
42	*S. carnosus/simulans*	*S. simulans*	no result	*S. vitulans*
43	*S. carnosus/simulans*	*s. xylosus*	*S. xylosus*	*S. lentus*
44	*S. carnosus*	no result	no result	no result
45	*S. carnosus/simulans*	*S. xylosus*	*S. xylosus*	no result
46	*S. carnosus/simulans*	*S. equorum*	*S. xylosus*	*S.xylosus/conhii*

Table 3 Identification of coagulase positive and negative staphylococcal clinical isolates *(Continued)*

47	*S. xylosus*	*S. xylosus*	*S. xylosus*	*no result*
48	*S. xylosus*	*S. xylosus*	*no result*	*no result*
49	*S. xylosus*	*S. intermedius*	*no result*	*S. vitulans*
50	*S. xylosus*	*S. xylosus*	*S. xylosus*	*S. scuiri*
51	*S. sapraphyticus*	*S.sapraphytics*	*S. xylosus*	*S. lentus*
52	*S. sapraphyticus*	*S. xylosus*	*S. xylosus*	*no result*

*= *S. pseudintermedius* or S. delphini.

Discussion

The results presented herein emphasise the importance of choosing the correct identification test for accurate speciation of staphylococcal species of animal origin. The accurate identification of staphylococcal species impacts directly and positively on treatment outcomes and on the epidemiological analysis of emerging trends in multi-drug resistant staphylococcal infections in veterinary medicine.

This present study revealed that all three phenotypic test systems yielded inaccurate speciation results when compared to *tuf* genotyping (Table 3). When considering phenotypic test kits on their own, one must consider the reliability of reading a result with a high "apparent" accuracy. For example, RapID identified one isolate as *S. xylosus* with a 97% probability value; however this isolate was subsequently identified by *tuf* as *S. pseudintermedius*, which could mislead the diagnostician. One of the arguments for using phenotypic test kits is that they are less costly than genotyping. When comparing the costs of phenotyping one must consider the potential consequences of misidentification including unnecessary morbidity and mortality of infected animals.

Of the phenotypic tests utilized, the API Staph 32 correctly identified 100% of *S. aureus* isolates, 83.3% of SIG isolates and 31% of the CONS; the RapID test correctly identified 81.8% of *S. aureus*, 33% of SIG isolates and 6.8% of the CONS; while the Staph-Zym test correctly identified only 2% of all isolates. Each of these tests is based on the evaluation of expression of genetically encoded characteristics by bacterial isolates. Inaccurate speciation may be due to variable expression of biochemical traits within species, as previously reported by Blaiotta et al. [8]. This is supported in the present study where it was observed that in each of the test systems, some biochemical tests frequently gave a misleading response for a given species tested. In particular, tests for arginine dihydrolase, arginine arlyamidase, β-glucuronidase, fructose and mannitol fermentation, novobiocin resistance and nitrate reduction, were observed in one or more systems to generate a response contrary to the expected result for a given species (data not shown). In addition, species identification kits such as these are manufactured for the human diagnostics market and are interpreted against databases with reference strains of human origin. This suggests that the reproducibility and therefore reliability of these tests is questionable when applied to veterinary isolates. When the identification of *S. aureus* by the three phenotyping test kits is considered, it was observed that while all of the *S. aureus* isolates were identified by API Staph 32, they were not consistently identified by either Rap-ID or Staph-Zym, demonstrating a lack of correlation between tests systems for a

Table 4 Sensitivity, specificity and predictive value positive of API Staph 32, RapID Staph and Staph-Zym tests showing individual results for species isolated in this study and overall values for test kits

Species	API Staph 32			RapID			Staph-Zym		
	Sens[1]	Spec[2]	PVP[3]	Sens	Spec	PVP	Sens	Spec	PVP
Overall	61.5	98	80	32.7	95.4	47.2	1.9	99	20
S. aureus	100	100	100	81.8	100	100	0	100	n/a
SIG	83.3	95	83.3	41.6	95.2	71.4	0	95	n/a
S. felis	0	98	n/a[4]	0	98	n/a	0	98	n/a
S. equorum	0	97.7	n/a	0	100	n/a	0	100	n/a
S. succinus	0	100	n/a	0	100	n/a	0	100	n/a
S. warneri	50	98	50	0	98	n/a	0	98	n/a
S. carnosus	66.6	95.3	75	11.1	100	100	11.1	100	100
S. xylosus	77	83.3	27.2	50	66.6	15.8	0	66.6	n/a
S. saprophyticus	50	100	50	0	100	n/a	0	100	n/a

Values calculated using *tuf* genotyping as a reference method.
[1]Sensitivity [2]specificity [3]predictive value positive [4]not applicable.

commonly isolated species. In addition, of the eight *S. equorum* isolates identified by genotyping, API Staph 32 identified four as *S. xylosus*, one as *S. epidermidis,* one as *S. warneri* and did not identify two, suggesting within species variability for the test system. With respect to the newly recognised *Staphylococcus intermedius* group [30], the failure of the phenotypic test kits to correctly speciate members of this group is of concern due to the relevance of *S. pseudintermedius,* not only as a veterinary pathogen, but as a source of nosocomial infection [31].

DNA sequencing of housekeeping genes is regularly used to definitively type staphylococcal isolates, [9,18-21,32]. In this study, *tuf* and *rpoB* gene segments were amplified by PCR and sequenced according to published methods ([9,19], respectively). Both genes constitute more discriminatory targets than the 16S-rRNA gene to differentiate closely related staphylococcal species. The results of this study demonstrated 100% accuracy for reference strains using *tuf* genotyping. Among the clinical isolates, 23 were identified by *tuf* genotyping as coagulase positive species (Table 3). Interestingly, five of these isolates failed to coagulate in both the tube and slide agglutination tests. These findings are not atypical however. According to Murray et al. [6] up to 30% of *S. aureus* field isolates fail to display coagulase activity. Reduced coagulase activity in *S. aureus* is also reported to be associated with reduced susceptibility to vancomycin [33]. It is worth noting that in the present study, each of the four *S. pseudintermedius* isolates which failed to coagulate also showed reduced susceptibility to vancomycin (data not shown). *tuf* genotyping identified 29 coagulase negative isolates and 5 distinct species (Table 3). The species *S. carnosus* and *S. simulans,* however, could not be definitively differentiated from each other by *tuf* genotyping. Likewise, *S. warneri* and *S. pasteuri* were not differentiated by this method. Previous authors have documented a close phylogenetic link between these pairs of species [29,34,35] and the current findings support this.

All three of the reference SIG species were identified correctly by *tuf* genotyping (*S. intermedius, S. delphini, S. pseudintermedius*). Ten of the clinical isolates were identified as *S. pseudintermedius*, but for two additional isolates, *tuf* could not differentiate between *S. pseudintermedius* and *S. delphini*. In an attempt to clarify the identity of these two isolates, both of canine origin, *rpo*B sequencing and PCR-RFLP of the *pta* gene were performed. Both isolates were confirmed as *S. pseudintermedius* by the two methods. Given the clinical significance of *S. pseudintermedius* in veterinary medicine, and the published evidence that MRSP (methicillin resistant *S. pseudintermedius*) is emerging as a nosocomial infection, the importance of an accurate identification is paramount. Our findings suggest the use of *rpo*B genotyping or PCR-RFLP of the *pta* gene as a confirmatory method for discriminating between SIG isolates until a larger cohort of these species are entered into the *tuf* gene database, thereby enhancing its accuracy.

Conclusion

Of the three biochemical tests used, the API Staph 32 test performed with the highest degree of accuracy for the coagulase positive Staphylococci. When compared to *tuf* genotyping all three of the rapid biochemical tests performed poorly for the speciation of coagulase negative Staphylococci. This study highlights the importance of choosing the correct identification test for accurate speciation of staphylococcal species of companion animal origin, as failure to correctly identify specific pathogens may impact on subsequent antimicrobial interventions.

Competing interests

The authors declare no competing interests.

Authors' contributions

LG collected all experimental the data, participated in the study design, sequence alignment and drafting of the manuscript. MB participated in the study design, sequence alignment and drafting of the manuscript. AF participated in the design of the study and drafting the manuscript. NR participated in the study design and drafting of the manuscript. All authors read and approved the final manuscript.

Acknowledgements

The authors would like to acknowledge the help of Dr. Arshnee Moodley, University of Copenhagen, in the preparation of this paper, and for the donation of some of the reference strains used. We would also like to thank Dr. Damien Brady, Athlone Institute of Technology, and Ms. Yvonne Abbott, University College Dublin, for the donation of reference strains. We would like to thank Dr. Rory Breathnach, University College Dublin, for his contribution to this research work. This work was jointly funded by Irish Strand 1 Technological Sector Research Funding programme and by the President's Seed Funding Initiative at Athlone Institute of Technology, Ireland.

Received: 12 January 2013 Accepted: 2 April 2013
Published: 1 May 2013

References

1. Guardabassi L, Loeber ME, Jacobson A: **Transmission of multiple antimicrobial-resistant *Staphylococcus intermedius* between dogs affected by deep pyoderma and their owners.** *Vet Microbiol* 2004, **98:**23–27.
2. Leonard FC, Abbott Y, Rossney A, Quinn PJ, O'Mahony R, Markey BK: **Methicillin-resistant *Staphylococcus aureus* isolated from a veterinary surgeon and five dogs in one practice.** *Vet Res* 2006, **58:**155–159.
3. Malik S, Peng H, Barton MD: **Partial nucleotide sequencing of the *mec*A genes of *Staphylococcus aureus* isolates from cats and dogs.** *J Clin Microbiol* 2006, **44:**413–416.
4. Weese JS, Dick H, Willey BM, McGeer A, Kreiswirth BN, Innis B, Low DE: **Suspected transmission of methicillin-resistant *Staphylococcus aureus* between domestic pets and humans in veterinary clinics and in the household.** *Vet Microbiol* 2006, **115:**148–155.
5. Sampimon AC, Lam TG, Mevius DJ, Schukken YH, Zadoks RN: **Antimicrobial susceptibility of coagulase negative staphylococci isolated from bovine milk samples.** *Vet Microbiol* 2011, **150:**173–179.
6. Murray PR, Baron EJ, Jorgensen JH, Landry ML, Pfaller MA: **Manual of Clinical Microbiology, 9th Edition.** *American Society Microbiology* 2007:390–411.
7. Coppola R, Mauriello G, Aponte M, Moscheitti G, Villani F: **Microbial succession during ripening of Naples-type salami, a southern Italian fermented product.** *Meat Sci* 2000, **56:**321–329.

8. Blaiotta G, Pennacchia C, Villani F, Ricciardi R, Tofalo R, Parente E: **Diversity and dynamics of communities of coagulase-negative staphylococci in traditional fermented sausages.** *J Appl Microbiol* 2004, **97:**271–284.
9. Heikens E, Fleer A, Paauw A, Florijn A, Fluit AC: **Comparison of genotypic and phenotypic methods for species-level identification of clinical isolates of coagulase-negative staphylococci.** *J Clin Microbiol* 2005, **43:**2286–2290.
10. Capurro A, Artursson K, Waller KP, Bengtsson B, Ericsson-Unnerstad H, Aspán A: **Comparison of a commercialized phenotyping system, antimicrobial susceptibility testing, and *tuf* gene sequence-based genotyping for species-level identification of coagulase-negative staphylococci isolated from cases of bovine mastitis.** *Vet Microbiol* 2009, **134:**327–233.
11. Zadoks RN, Watts JL: **Species identification of coagulase-negative staphylococci: genotyping is superior to phenotyping.** *Vet Microbiol* 2009, **134:**20–28.
12. Blaiotta G, Pennachia C, Ercolin D, Moschetti G, Villani F: **Combining denaturing gradient gel electrophoresis of 16S rDNA V3 region and 16S-23S rDNA spacer region polymorphism analyses for the identification of staphylococci from Italian fermented sausages.** *Sys Appl Microbiol* 2003, **26:**423–433.
13. Burriel AR, Scott M: **A comparison of methods used in species identification of coagulase-negative staphylococci isolated from the milk of sheep.** *Vet J* 1998, **155:**183–188.
14. Jousson O, Di Bello D, Vanni M, Cardini G, Soldani G, Pretti C, Intorre L: **Genotypic versus phenotypic identification of staphylococcal species of canine origin with special reference to *Staphylococcus schleiferi* subsp. coagulans.** *Vet Microbiol* 2007, **123:**238–244.
15. Thorberg BM, Brändström B: **Evaluation of two commercial systems and a new identification scheme based on solid substrates for identifying coagulase-negative staphylococci from bovine mastitis.** *J Vet Med* 2000, **47:**683–691.
16. Taponen S, Pyörälä S: **Coagulase-negative staphylococci as cause of bovine mastitis- not so different from *Staphylococcus aureus*?** *Vet Microbiol* 2009, **134:**29–36.
17. Park JY, Fox LK, Seo KS, McGuire MA, Park YH, Rurangirwa FW, Sischo WM, Bohach GA: **Comparison of genotypic and phenotypic methods for the phenotypic identification of coagulase-negative Staphylococcal isolates from bovine intramammary infections.** *Vet Microbiol* 2010, **147:**142–148.
18. Shah MM, Iihara H, Noda M, Song SX, Nhung PH, Ohkusu K, Kawamura Y, Ezaki T: ***DnaJ*** **gene sequence-based assay for species identification and phylogenetic grouping in the genus *Staphylococcus*.** *Int J Syst Evol Microbiol* 2007, **57:**25–30.
19. Drancourt M, Raoult D: ***Rpo*****B Gene Sequence-Based Identification of *Staphylococcus* Species.** *J Clin Microbiol* 2002, **40:**1333–1338.
20. Becker K, von Eiff C, Keller B, Brück M, Etienne J, Peters G: **Thermonuclease gene as a target for specific identification of *Staphylococcus intermedius* isolates: use of a PCR-DNA enzyme immunoassay.** *Diagn Microbiol Infect Dis* 2005, **51:**237–244.
21. Poyart C, Quesne G, Boumaila C, Trieu-Cuot P: **Rapid and accurate species-level identification of coagulase-negative staphylococci by using the *sod*A gene as a target.** *J Clin Microbiol* 2001, **39:**4296–4301.
22. Bergeron M, Dauwalderm O, Gouym M, Freydiere AM, Bes M, Meugnier H, Benito Y, Etienne J, Lina G, Vandenesch F, Boisset S: **Species identification of staphylococci by amplification and sequencing of the *tuf* gene compared to the *gap* gene and by matrix-assisted laser desorption ionization time-of-flight mass spectrometry.** *Eur J Clin Microbiol Infect Dis* 2010, **30:**343–354.
23. Hwang SM, Kim MS, Park KU, Song J, Kim EC: ***tuf*** **gene sequence analysis has greater discriminatory power than 16S rRNA sequence analysis in identification of clinical isolates of coagulase-negative staphylococci.** *J Clin Microbiol* 2011, **49:**4142–4149.
24. Blaiotta G, Fusco V, Ercolini D, Pepe O, Coppola S: **Diversity of *Staphylcoccus* species strains based on partial *kat* (catalase) gene sequences and design of a PCR-restriction fragment length polymorphism assay for identification and differentiation of coagulase-positive species (*S. aureus, S. delphini, S. hyicus, S. schleiferi subsep. coagulans).*** *J Clin Microbiol* 2010, **48:**192–201.
25. Sasaki T, Tsubakishita S, Tanaka Y, Ohtsuka M, Hirotaki S, Kawakami T, Fukata T, Hiramatsu K: **Multiplex- PCR method for species identification of coagulase positive staphylococci.** *J Clin Microbiol* 2010, **48:**765–769.
26. NCBI; 2012. http://www.ncbi.nlm.nih.gov/Taxonomy/Browser/wwwtax.cgi?id=1279.
27. Bannoehr J, Franco A, Iurescia M, Battisti A, Fitzgerald JR: **Molecular diagnostic identification of *Staphylococcus pseudintermedius*.** *J Clin Microbiol* 2009, **47:**469–471.
28. Kadlec K, Rohde J, Schwar S: **Identification and presence of different staphylococcal species within the *Staphylococcus intermedius* group among various animal hosts.** In *Methicillin-resistant Staphylococci in animals: Veterinary and public health implications.* ASM conference; 2009:42.
29. Ghebremedhin B, Layer F, König W, König B: **Genetic classification and distinguishing of Staphylococcus species based on different partial gap, 16S rRNA, *hsp*60, *rpo*B, *sod*A, and *tuf* gene sequences.** *J Clin Microbiol* 2008, **46:**1019–1025.
30. Devriese LA, Vancanneyt M, Baele M, Vaneechoutte M, De Graef E, Snauwaert C, Cleenwerck I, Dawyndt P, Swings J, Decostere A, Haesebrouck F: ***Staphylococcus pseudintermedius*** **sp. nov., a coagulase-positive species from animals.** *Int J Syst Evol Microbiol* 2005, **55:**1569–1573.
31. Paul NC, Moodley A, Ghibaudo G, Guardabassi L: **Carriage of methicillin-resistant Staphylococcus pseudintermedius in small animal veterinarians: indirect evidence of zoonotic transmission.** *Zoonoses Public Health* 2011, **58:**533–539.
32. Barros EM, Iório NL, Bastos Mdo C, dos Santos KR, Giambiagi-deMarval M: **Species-level identification of clinical staphylococcal isolates based on polymerase chain reaction–restriction fragment length polymorphism analysis of a partial groEL gene sequence.** *Diagn Microbiol Infect Dis* 2007, **59:**251–257.
33. Moreira B, Boyle-Varva S, deLonge BL, Daum RS: **Increased production of penicillin binding protein 2, increased detection of other penicillin-binding proteins, and decreased activity associated with glycopeptide resistance in *Staphylococcus aureus*.** *Antimicrob Agents Chemother* 1997, **41:**1788–1793.
34. Mellman A, Becker K, van Eiff C, Keckevoet U, Schumann P, Harmsen D: **Sequencing and Staphylococci identification.** *Emerg Infect Dis* 2006, **12:**333–336.
35. Shin JH, Kim SH, Jeong HS, Oh SH, Kim HR, Lee JN, Yoon YC, Kim YW, Kim YH: **(Identification of coagulase-negative staphylococci isolated from continuous ambulatory peritoneal dialysis fluid using 16S ribosomal RNA, *tuf*, and *sod*A gene sequencing.** *Perit Dial Int* 2011, **31:**340–346.

doi:10.1186/2046-0481-66-7
Cite this article as: Geraghty *et al.*: Investigations on the efficacy of routinely used phenotypic methods compared to genotypic approaches for the identification of staphylococcal species isolated from companion animals in Irish veterinary hospitals. *Irish Veterinary Journal* 2013 **66**:7.

ELSEVIER

Trends in Food Science & Technology 15 (2004) 462–467

TRENDS IN FOOD SCIENCE & TECHNOLOGY

Viewpoint

Viable but non-culturable forms of food and waterborne bacteria: Quo Vadis?

Neil J. Rowan*

School of Biological Sciences, Dublin Institute of Technology, Kevin Street, Dublin 8, Ireland (tel.: +353-14024747; e-mail: neil.rowan@dit.ie)

There is increasing evidence for a viable but non-culturable (VBNC) state in microbes, particularly in the stressing environment presented by modern foods with their varied pre-treatment and packaging strategies. This is a cause for concern because of evidence that microbial pathogens in such a state may retain their capacity to cause infections after ingestion by the consumer despite their inability to grow under the conditions employed in procedures for determining their presence in foods. Heavily stressed pathogenic species of bacteria in a VBNC or not immediately culturable state are potentially dangerous public health problems, particularly as stressed cells may be more virulent than well-fed bacteria. In this viewpoint article, I wish to focus on possible procedures for detecting such organisms and assessing their physiological state.

Safe food processing, distribution, and storage rely on a high degree of assurance (close to 100%) that a food ready to be consumed is free from pathogenic microorganisms and/or their toxins (Rowan, 1999). Microbial population in foods, food ingredients, and the food contact environment normally constitute many different species that have markedly varied growth requirements and come from different sources. As microorganisms are extremely diverse and highly dynamic, it is not surprising that the many different types of microbial species present in food exist in a number of physiological states that possess different requirements for survival and to sustain growth.

The microbiological safety of food has benefited significantly from advances made in predictive microbiological modelling and by the introduction and implementation of Hazard Analysis and Critical Control Points (HACCP) (Buchanan, 1997). HACCP, when applied appropriately, provides a systematic conceptual framework for identifying hazards and critical control points (i.e. the places during processing of a food where proper control measures need to be implemented in order to prevent any risk to consumers) thereby focusing efforts on the proper functioning of key food production, processing and distribution steps. Such methods of examining microbiological safety, storage stability, and sanitary quality of food depend on testing representative portions (or samples) from identified control points (which may include the final product) for the presence of appropriate pathogens (e.g. *Salmonella*) or the number or level of selected pathogens (e.g. *Staphylococcus aureus*), different microbiological groups (e.g. aerobic plate counts, psychrotrophic counts, thermoduric counts, and yeast and moulds), and indicator bacteria (e.g. coliforms and enterococci) per gram or millilitre of food (Ray, 2001).

Because substantial knowledge is required, current HACCP strategies cannot be expected to control all unknown hazards such as emerging foodborne pathogens or the occurrence of heavily stressed bacteria that are in a viable but non-culturable (VBNC) or not immediately culturable state (Buchanan, 1997; Kell, Kaprelyants, Weichant, Harwood, & Barer, 1998). Emerging and VBNC pathogens are unknown hazards; therefore, to control them, key data must be acquired to convert these pathogens from unknown to known hazards. Accurate enumeration of total microbial load and identification of types present in food and food ingredients are pivotal to hazard identification and characterisation and contributing significantly to assuring food safety (Rowan, 1999). Underestimation in the levels of problematic microbes in food products, and failure to identify the presence of pathogenic organisms in representative food samples are significant threats to public health. In addition, a reliable microbiological examination of foods and food ingredients helps food technologists and microbiologists to assess their safety to consumers, their stability and shelf life under normal storage conditions, and the level of sanitation used during handling. In addition, microbial load and type can

* Corresponding author.

0924-2244/$ - see front matter © 2004 Elsevier Ltd. All rights reserved.
doi:10.1016/j.tifs.2004.02.009

also provide important information about untreated foods and/or treatments, usually some form of heat-processing parameters that would be necessary to meet appropriate microbiological standards, specifications or guidelines for an acceptable food product (Ray, 2001).

Food preservation and microbial stress responses

The art of food preservation is principally, to poise conditions within food close to an organism's tolerance threshold (Booth, 1998). Food manufacture, distribution and storage rely on well-placed deleterious stresses or hurdles which can be applied simultaneously or sequentially and are intended to inhibit or inactivate the development of contaminating organisms in food systems (Leistner, 1995). Indeed, with current consumer preferences for foods that have avoided the extreme use of a single preservation hurdle, there has been an awakening towards studies that have demonstrated microbial stress-adaptation and cross-protection against multiple-stresses, particularly in modified foods (Lou & Yousef, 1997). For instance, recent research has shown that adaptation of *Listeria monocytogenes* to sub-lethal doses of ethanol, hydrogen peroxide, salt, acid, heat or nutrient deprivation, significantly increased the resistance of this pathogen to lethal levels of the same and cross-protected this problematic bacterium to different stresses [e.g. acid (pH 3.5), ethanol (15.7% vol/vol), H_2O_2 (0.1% wt/vol), 25% NaCl, heat, and starvation (survival in 0.1 M phosphate buffer for 300 h)] (Lou & Yousef). Stress adaptation and cross-protection has also been shown in other foodborne bacterial pathogens, particularly in *Escherichia coli* and *Salmonella enterica* serovar Typhimurium (Foster & Spector, 1995).

However, while there is a body of evidence to show that many microbes have the potential to adapt to food processing, adaptation and survival to inherent sub-lethal stresses that are intrinsically associated with food puts considerable pressure on microbial physiology and on critical metabolic processes. Bacteria that have been subjected to environmental stresses often have reduced capacity for gene expression, thus the rate at which new proteins are completed is slower than in a similar cell growing under optimum conditions (Rowan, 1999). Normal practice for enumerating surviving cell population is to grow sub-lethally stressed organisms on artificial culture media (traditional agar plate count method), where microbial counts are typically expressed as colony forming units (CFU) per millilitre or gram of sample. However, use of the traditional plate count method alone may not be suitable for the enumeration of some sub-lethally stressed bacteria that are not capable of growth on nutritionally rich laboratory-based agar.

Bacterial cultures, especially in nature and under conditions of stress (such as freezing, drying and starvation), have been previously reported to display significant heterogeneity in terms of the percentage of viable cells, and with respect to their gross cellular metabolic activities (Kaprelyants & Kell, 1993). In marine microbiology the vast differences between bacterial numbers enumerated by direct microscopic counts and by the agar-plate method have been reported by many workers as far back as the late 1950s (Jannasch & Jones, 1959). Although the differences can be partly attributable to the clumping of cells and non-living particles in seawater samples, it was suggested that the viable plate count method may considerably underestimate the bacterial cells actually living in natural seawaters.

Viable but non-culturable microbial cells

The introduction of the concept of viable but non-culturable (VBNC) cells by Byrd and Colwell in the 1980s has led to important research concerning the possible existence and significance of these kind of cells in foodstuffs (Byrd, Xu, & Colwell, 1991). Xu *et al*. (1982) were the first to bring experimental evidence of the existence of the VBNC state in pathogenic bacteria. They showed that *E. coli* and *Vibrio cholerae* cells that were suspended in artificial seawater quickly lost their ability to grow on the culture media normally used for their detection. According to Oliver (1993), a bacterium in the VBNC state is defined as "a cell which is metabolically active, while being incapable of undergoing the cellular division required for growth in or on a medium normally supporting growth of that cell". Besnard, Federighi, and Cappelier (2000) suggest that the transition to the VBNC state in *L. monocytogenes* represents a survival strategy that bacteria can adopt under adverse conditions (starvation, acid stress, etc.). VBNC bacteria are considered to represent a sub-population of cells which are not able to grow in the usual culture media and which cannot be resuscitated by traditional resuscitation techniques, but yet remain physically active for several functions such as cellular elongation (Roszak & Colwell, 1987), respiratory chain activity (Besnard *et al*., 2000; Rodriguez, Phipps, Ishiguro, & Ridgway, 1992) or incorporation of radio-labelled substrates (Rollins & Colwell, 1986). Alternatively, it has been suggested that the VBNC state may be a survival mechanism adopted by many bacteria when exposed to adverse environmental conditions (Barer & Harwood, 1999).

The number of food and waterborne bacteria in which the VBNC state has been reported has greatly increased, particularly over the last two decades which mirrors technical advances (Table 1). For instance, *Campylobacter jejuni* has been shown to exist in two different cellular morphologies, where the atypical coccus-form (currently associated with the non-growing VBNC state) occurs under adverse growth conditions (Reezal, McNeil, & Anderson, 1998). Jones, Sutcliffe, and Curry (1991) showed that the non-culturable coccal forms of the organism were capable of infecting mice; however, this property differed between strains. Other methods, such as the chick model, were also used to investigate and demonstrate infectivity of the VBNC forms of *C. jejuni* (Cappelier, Megras, Jouve, & Federighi, 1999).

The use of fluorescent redox probes for direct visualization of actively respiring bacteria is gaining in popularity

Table 1. Food and waterborne bacteria that were reported previously to exist in a VBNC state

Bacteria reported to exist in a VBNC state	Reference cited
Escherichia coli	Gunasekera *et al*. (2002), Reissbrodt *et al*. (2002), Wang and Doyle (1998), Xu *et al*. (1982)
Vibrio cholerae	Wolf and Oliver (1992), Xu *et al*. (1982)
Listeria monocytogenes	Besnard *et al*. (2000), Rowan (2001)
Legionella pneumophilia	Hussong *et al*. (1987)
Salmonella enteritidis	Roszak *et al*. (1984)
Salmonella enterica serovar Typhimurium	Reissbrodt *et al*. (2002)
Citrobacter freundii	Reissbrodt *et al*. (2002)
Campylobacter jejuni	Cappelier *et al*. (1999), Jones *et al*. (1991), Reezal *et al*. (1998), Rollins and Colwell (1986)
Pseudomonas putida	Gunasekera *et al*. (2002)
Shigella dysenteriae type 1	Rahman, Shahamat, Chowdhury, and Colwell (1996)
Enterobacter agglomerans	Besnard *et al*. (2000)
Bacillus cereus	Rowan (2001)

The purpose of this table is to intimate commonly occurring food and waterborne bacteria that were reported previously to exist in a VBNC state. As such, it should not be considered nor serve as a definitive list of all bacteria that were reported previously to exist in this viable nonculturable form.

amongst research groups investigating this VBNC phenomenon (Besnard *et al*., 2000). For instance, use has been made of the redox dye 5-cyano-2, 3-ditolyl tetrazolium chloride (CTC) as an artificial electron acceptor that directly competes with molecular oxygen. The reducing power generated by the electron transport system converts CTC into insoluble, fluorescent CTC-formazon crystals (i.e. clearly visible with UV optics and epi-illumination), which accumulate in metabolically active bacteria. A number of research groups have used this metabolic staining technique to illustrate enumeration differences between agar-plate counts and total cell numbers that were still capable of active respiration (Besnard *et al*.). Research in my laboratory has shown previously that sub-populations of *Bacillus cereus* and *L. monocytogenes* that were treated with novel, high-intensity, pulsed electric fields were capable of reducing the CTC stain, yet unable to form colonies on a variety of laboratory-based culture media (Rowan, MacGregor, & Anderson, 2001). That said, a demonstration of active respiration does not necessarily infer that these stressed bacteria are capable of future growth.

However, this redox staining method has recently been used in combination with a novel direct viable count (DVC) procedure to highlight differences in agar-plate counts. The DVC method is based on the incubation of treated microbial samples with an antimicrobial agent such as nalidixic acid or ciprofloxacin, and nutrients (Besnard *et al*., 2000). These antimicrobial agents act as specific inhibitors of DNA synthesis and prevent cell division without affecting other cellular metabolic activities. The resulting cells can continue to metabolise nutrients and become elongated and/or flattened during incubation. Thus, the size of metabolically active cells increases, while inactive cells remain unchanged as measured by epifluorescence microscopy and image analysis. In addition to using cell membrane integrity staining (based on propidium iodide exclusion), Gunasekera, Sørensen, Attfield, Sørensen, and Duncan (2002) recently employed inducible gene expression (i.e. *de novo* expression of a green fluorescent protein (*gfp*) reporter gene) to highlight differences in plate counts for *Pseudomonas putida* and *E. coli* that have been heat-treated in milk. Gene expression using inducible genetic markers may be considered as another complementary approach for assessing microbial viability.

However, many research groups investigating the existence of viable non-culturable states in sub-lethally stressed bacteria have not included an enrichment or resuscitation stage, and have used laboratory-based media that are nutritionally rich. As pointed out by Archer (1996), "although life on a Petri plate with a few simple sugars and a handful of amino acids might not seem like much, to a bacterium it's a night in Trump Tower with a breakfast in bed". In reality, bacteria experience and must adapt to multifaceted hostile environments as seen in foodstuffs. To properly evaluate the survival capabilities (and true numbers of living cells) of established and emerging foodborne pathogens in complex environments, microbiologists and food technologists must holistically consider the effects of multiple stresses, and endeavour to replicate these environments in food safety studies. It has been previously reported that greater recovery of stress-damaged bacteria (e.g. isolated from environmental samples or exposed to sub-lethal stresses in the laboratory) occurs when these organisms are plated on minimal rather than rich media (Rowan, 1999). The single cellular process that may be responsible for this phenomenon is 'bacterial cell suicide' (Aldsworth, Sharman, Dodd, & Stewart, 1998), where self-destruction is attributed to an oxidative-burst when rapidly growing bacterial cells are growth arrested following sub-lethal injury. The greater sensitivity of exponential-phase cells is due to the production of intracellular free radicals rather than the direct physical action of the applied process, where the inimical process disturbs cell growth but does not affect the metabolic process, e.g. what should be a sub-lethal injury becomes lethal, through growth arrest, leading to a decoupling of catabolic and anabolic metabolism (i.e. some stressed bacterial cells are unable to cope metabolically with nutritious growth media and die through oxidative suicide). Supplementation with oxygen scavengers such as sodium pyruvate or glutathione to nutritionally restricted growth media was shown to assist in the recovery of stress-damaged bacteria (Dodd, Sharmon, Bloomfield, Booth, & Stewart, 1997).

Indeed, the recent work of Reissbrodt and co-workers has provided good evidence that supports my viewpoint that

heavily stress-damaged bacterial cells shown to be in a VBNC or not immediately culturable state can be resuscitated by the inclusion of various growth factors in a non-selective recovery medium (Reissbrodt *et al*., 2002). The authors showed that the addition of trihyhdroxanamate siderophore ferrioxamine E, the commercially available antioxidant Oxyrase, and a heat-stable autoinducer of growth secreted by enterobacterial species in response to norepinephrine, resuscitated cells of either *Salmonella enterica* serovar Typhimurium and/or enterohemorrhagic *E. coli* that were stressed by prolonged incubation in water microcosoms or by heat treatment. The enterbacterial autoinducer (AI) also resuscitated stressed populations of *Citrobacter freundii* and *Enterobacter agglomerans*. That said, the study showed marked variations in the ability of the aforementioned growth factors to restore growth of stress-damaged cells on laboratory-based culture media. Whilst the mechanism of action of AI was not established, it could possibly function as a quorum sensor for stressed bacteria or by interaction with components of the bacterial global stress responses such as RpoS (i.e. σ^S subunit of RNA polymerase which is a central stress response regulator for many enterobacterial bacterial pathogens).

In the case of pathogenic species of bacteria, the VBNC state is a potentially dangerous public health problem, particularly as stressed bacteria are apparently more virulent than well-fed bacteria (Sylvester, Taylor, & LaHann, 2001). Whilst the induction of a stress-resistant phenotype in sub-lethally stressed bacterial enteropathogens has profound implications for their survival in foods, there is strong evidence that sub-lethal environmental stressors can also modulate the synthesis of virulence factors in these microorganisms (Rowan, 1999). Therefore, bacteria which adapt to a heavily stressed environment are more likely to survive levels of stress that would previously be considered lethal (Gahan, O'Driscoll, & Hill, 1996) and also acquire a heightened state of virulence (Marron, Emerson, Gahan, & Hill, 1997).

Use of genotypic and phylogenetic studies to unravel the viable nonculturable phenomenon in food and waterborne bacteria

The advent of computer technology in the 1950s along with other dramatic breakthroughs in molecular biology and immunology has significantly advanced the field of bacterial taxonomy. This has enabled a holistic polyphasic system of bacterial classification to be adapted which combines key characteristics identified by practical (e.g. phenotypic, genotypic, chemotaxonomic) and evolutional (e.g. phylogenetic) taxonomic schemes (Vandamme, 2003). Through technological advances made particularly in whole genome DNA–DNA hybridisation and rRNA/DNA homology studies (where the latter approach focuses on important macromolecular chronometers such as rRNA genes), we are now capable of amplifying and sequencing genetic information from bacteria from disparate environments, irrespective as to whether or not they have been cultured previously or not. While the efficacy of this approach depends on having an extensive genebank of reference sequences that can be used to correlate newly sequenced data from nonculturable bacteria, it is critically important to have a broad, yet uniform technical base with expertise to analyse and interpret properly such data. The International Committee on Systematic Bacteriology have recognised a new category for nonculturable bacteria which is named '*Candidatus*' (Murray & Stackebrandt, 1995). This is considered a taxonomic status for uncultured 'candidate' species for which relatedness has been determined (e.g. for which phylogenetic relatedness has been determined by amplification and sequence analysis of prokayotic RNA genes with universal prokaryotic primers) and authenticity has been verified by use of *in situ* probes.

Members of the taxa *Candidatus* failed to grow using traditional culturing approaches, yet their presence was identified using by genotypic and phylogenetic methods (Vandamme, 2003). For instance, it was shown recently that a new non-culturable bacterial species present in human faeces samples correlated well with partial 16S rDNA sequence information obtained by *Campylobacter* genus-specific PCR. It was proposed that this organism be named *Candidatus Campylobacter hominis* as it could not be cultured by the classic methods of culturing enteric campylobacters. As phylogenetic analysis clustered this organism in a group of *Campylobacter* species, some of which prefer anaerobic conditions for optimal growth, application of anaerobic culture conditions in a subsequent study allowed the organism to be cultured and the classical binomial species name *Campylobacter hominis* was adopted (Lawson, On, Logan, & Stanley, 2001). Using this information, the organism was successfully cultured under anaerobic conditions. There are other recent examples where molecular information was used to identify and delineate appropriate conditions, and subsequently isolate in pure culture strains of *Desulfovibrio* and *Arcobacter* which had not been cultured previously in isolation (Teske, Sigalvich, Cohen, & Muyzer, 1996). Thus, among the minority of bacteria that have been discovered, it is estimated that more than 90% are as yet nonculturable. Such nonculturable organisms may be detected only by molecular techniques based on probes such as 16S and 23S rRNAs or on determination of mRNA, either by reverse transcriptase PCR (Sheridan, Masters, Shallcross, & MacKey, 1998) or by fluorescent techniques such as *in situ* hybridisation, microradiography, epifluorescence microscopy, and flow cytometry (Reissbrodt *et al*., 2002).

Conclusions and outlooks

There is compelling evidence that foodstuffs, particularly after processing, could harbour microorganisms which cannot be detected by conventional techniques such as cultivation on standard broth or agar media, although other tests show that these organisms retain various levels of

metabolic activity. There is evidence that they may, in suitable conditions, regain the ability to grow and/or produce toxins and other harmful changes that can be pathological to those consuming the food. This seemingly anomalous situation may result from damage caused by exposure to the nutrient-rich conditions in conventional media. In at least some cases, 'lean' (low nutrient) media supplemented with suitable anti-oxidants may improve recovery of sub-lethally stressed microbes. Methods such as staining with redox compounds can reveal which cells retain some metabolic activity, but the links between this and possible resumption of growth are not yet established. Furthermore, these methods are difficult to apply in routine screening of foods. The need to clarify these matters is becoming more urgent as consumers exercise preference for lightly treated foods. In order to successfully meet such challenges, it is important that we holistically harness the tremendous wealth of information that is steadily becoming available in the fields of microbial genomics and proteomics, and that we continue to make strides to expedite the speed and quality of data interpretation by utilising combatant advances in information and computer technologies. It is equally important that effective strategies for data dissemination be adopted, whereby both research scientists and front-line food technologists benefit mutually from seminal breakthroughs in this area (Roszak, Grimes, & Colwell, 1984).

References

Aldsworth, T. G., Sharman, R. L., Dodd, C. E. R., & Stewart, G. S. A. B. (1998). A competitive microflora increases the resistance of *Salmonella typhimurium* to inimical processes: Evidence for a suicide response. *Applied and Environmental Microbiology, 64*, 1323–1327.

Archer, D. (1996). Preservation microbiology and safety: Evidence that stress enhances virulence and triggers adaptive mutations. *Trends in Food Science and Technology, 7*, 91–95.

Barer, M. R., & Harwood, C. R. (1999). Bacterial viability and culturability. *Advances in Microbial Physiology, 41*, 93–137.

Besnard, V., Federighi, M., & Cappelier, J. M. (2000). Evidence of viable but non-culturable state in *Listeria monocytogenes* by direct viable count and CTC-DAPI double staining. *Food Microbiology, 17*, 697–704.

Booth, I. R. (1998). The bacteria strike back. *The Biochemist, April*, 1–8.

Buchanan, R. L. (1997). Identifying and controlling emerging foodborne pathogens: Research needs. *Emerging Infectious Diseases, 3*, 517–521.

Byrd, J. J., Xu, H. S., & Colwell, R. R. (1991). Viable but non-culturable bacteria in drinking water. *Applied and Environmental Microbiology, 57*, 875–878.

Cappelier, J. M., Megras, C., Jouve, J. L., & Federighi, M. (1999). Recovery of viable but non-culturable *Campylobacter jejuni* in two animal models. *Food Microbiology, 16*, 375–383.

Dodd, C. E. R., Sharmon, R. L., Bloomfield, S. F., Booth, I. R., & Stewart, G. S. A. B. (1997). Inimical processes: Bacterial self destruction and sub-lethal injury. *Trends in Food Science and Technology, 8*, 238–241.

Foster, J. W., & Spector, M. P. (1995). How *Salmonella* survive against the odds. *Annual Review of Microbiology, 140*, 1731–1737.

Gahan, C. G., O'Driscoll, B., & Hill, C. (1996). Acid adaptation of *Listeria monocytogenes* can enhance survival in acid foods and during milk fermentation. *Applied and Environmental Microbiology, 63*, 1252–1255.

Gunasekera, T. S., Sørensen, A., Attfield, P., Sørensen, S. J., & Duncan, A. V. (2002). Inducible gene expression by non-culturable bacteria in milk after pasteurisation. *Applied and Environmental Microbiology, 68*, 1988–1993.

Hussong, D., Colwell, R. R., O'Brien, M., Weiss, R., Person, A. D., Weimer, R. M., & Burge, W. D. (1987). Viable *Legionella pneumophilia* not detectable by culture on agar media. *Biotechnology, 5*, 947–950.

Jannasch, J. W., & Jones, E. W. (1959). Bacterial populations in seawater as determined by different methods of enumeration. *Limnology and Oceanography, 4*, 128–139.

Jones, M., Sutcliffe, E. M., & Curry, M. (1991). Recovery of viable but non-culturable forms of *Campylobacter jejuni*. *Journal of General Microbiology, 137*, 2477–2482.

Kaprelyants, A., & Kell, D. B. (1993). The use of 5-cyano-2,3-ditolyl tetrazolium chloride and flow cytometry for the visualization of respiratory activity in individual cells of *Micrococcus luteus*. *Journal of Microbiological Methods, 17*, 115–122.

Kell, D. B., Kaprelyants, A. S., Weichant, D. H., Harwood, C. R., & Barer, M. R. (1998). Viability and activity in readily culturable bacteria: A review and discussion of the practical issues. *Antonie Leeuwenhoek, 73*, 169–187.

Lawson, A. J., On, S. L. W., Logan, J. M. J., & Stanley, J. (2001). *Campylobacter hominis* sp. nov. from the human gastrointestinal tract. *International Journal of Systematic and Evolutionary Microbiology, 51*, 651–660.

Leistner, L. (1995). Principles and applications of hurdle technology. In G. W. Gould (Ed.), *New methods of food preservation* (pp. 1–21). Glasgow: Blackie Academic and Professional.

Lou, Y., & Yousef, A. H. (1997). Adaptation to sublethal environmental stresses protects against lethal preservation factors. *Applied and Environmental Microbiology, 63*, 1252–1255.

Marron, L., Emerson, N., Gahan, C. G. M., & Hill, C. (1997). A mutant of *Listeria monocytogenes* L028 unable to induce an acid tolerance response displays diminished virulence in a murine model. *Applied and Environmental Microbiology, 63*, 4945–4947.

Murray, R. G. E., & Stackebrandt, E. (1995). Taxonomic note: Implementation of the provisional status *Candidatus* for imcompletely described procaryotes. *International Journal of Bacteriology, 45*, 186–187.

Oliver, J. D. (1993). Formation of viable but nonculturable cells. In S. Kjelleberg (Ed.), *Starvation in bacteria. Journal of Applied Bacteriology* (72).

Rahman, I., Shahamat, M., Chowdhury, M. A. R., & Colwell, R. R. (1996). Potential virulence of viable but nonculturalbe *Shigella dysenteriae* type 1. *Applied and Environmental Microbiology, 62*, 115–120.

Ray, B. (2001). Hazard analysis critical control points. In *Fundamental food microbiology* (pp. 515–518). London: CRC Press.

Reezal, A., McNeil, B., & Anderson, J. G. (1998). Effect of low-osmolality nutrient media on growth and culturability of *Campylobacter* species. *Applied and Environmental Microbiology, 64*, 4643–4649.

Reissbrodt, R., Rienaecker, I., Romonova, M., Freestone, P. P. E., Haigh, R. D., Lyte, M., Tschape, H., & Williams, P. H. (2002). Resuscitation of *Salmonella enterica* serovar Typhimurium and enterohemorrhagic *Escherichia coli* from viable but nonculturable state by heat-stable enterobacterial autoinducer. *Applied and Environmental Microbiology, 68*, 4788–4794.

Rodriguez, G. G., Phipps, D., Ishiguro, K., & Ridgway, H. F. (1992). Use of a fluorescent redox probe for direct visualisation of actively respiring bacteria. *Applied and Environmental Microbiology, 58*, 1801–1808.

Rollins, D. M., & Colwell, R. R. (1986). Viable but non-culturable stage of *Campylobacter jejuni* and its role in survival in the natural aquatic environment. *Applied and Environmental Microbiology, 52*, 531–538.

Roszak, D. B., & Colwell, R. R. (1987). Metabolic activity of bacterial cells enumerated by direct viable count. *Applied and Environmental Microbiology, 53*, 2889–2893.

Roszak, D. B., Grimes, D. J., & Colwell, R. R. (1984). Viable but non-culturable forms of *Salmonella enteritidis* in aquatic systems. *Canadian Journal of Microbiology, 30*, 334–338.

Rowan, N. J. (1999). Evidence that inimical food-preservation barriers alter microbial resistance, cell morphology and virulence. *Trends in Food Science and Technology, 10*, 261–270.

Rowan, N. J., MacGregor, S., & Anderson, J. G. (2001). Rapid fluorescence assessment of actively respiring bacteria after treatment with pulsed electric fields. In *2nd International Symposium on Nonthermal Medical/Biological Treatments Using Electromagnetic Fields and Ionized Gases*. April 12–14, Norfolk, Virginia, USA.

Sheridan, G. E., Masters, C. I., Shallcross, J. A., & MacKey, B. M. (1998). Detection of mRNA by reverse transcriptase-PCR as an indicator of viability in *Escherichia coli* cells. *Applied and Environmental Microbiology, 64*, 1313–1318.

Sylvester, D. M., Taylor, M., & LaHann, T. R. (2001). Viable but nonculturable bacteria: A public heath threat. *Infectious Disease Review, 3*, 70–82.

Teske, A., Sigalvich, P., Cohen, Y., & Muyzer, G. (1996). Molecular identification of bacteria from a coculture by denaturing gradient gel electrophoresis of 16S ribosomal DNA fragments as a tool for isolation in pure cultures. *Applied and Environmental Microbiology, 62*, 4210–4215.

Vandamme, P. A. R. (2003). Taxonomy and classification of bacteria. In P. R. Murray, J. E. Baron, J. H. Johgensen, M. A. Pfaller, & R. H. Yolken (Eds.), *Manual of clinical microbiology,* 8th ed. (pp. 271–285). Washington, DC: ASM Press.

Wang, G., & Doyle, M. P. (1998). Survival of enterohemorrhagic *Escherichia coli* O157:H7 in water. *Journal of Food Protection, 61*, 662–667.

Wolf, P. W., & Oliver, J. D. (1992). Temperature effects on viable but non-culturable forms of *Vibro vulnificus*. *FEMS Microbiology Ecology, 101*, 33–39.

Xu, H. S., Robert, N., Singleton, F. L., Attwel, R. W., Grimes, D. J., & Colwell, R. R. (1982). Survival and viability of non-culturable *Escherichia coli* and *Vibrio cholerae* in the estuarine and marine environment. *Microbial Ecology, 8*, 313–323.

Section Two- Adaptive Microbial Stress Responses and Inactivation Performance under Non-thermal Processing and Decontamination

The **second section** of this thesis describes development of 'nonthermal food and water Technologies – Elucidation and Development'. It was as an evolution of earlier bacterial pathogen detection and survival post traditional food treatments and involved collaborations with Professor Scott MacGregor (High Voltage Engineering, Strathclyde University). Studies describe first reports on important operational factors governing reliable and repeatable destruction of bacterial and fungal pathogens using high intensity pulsed light (PUV), pulsed electric fields (PEF) and pulsed-plasma gas-discharge (PPGD) technologies. A growing number of published papers failed to incorporate appropriate levels of microbial killing (log reductions or biological load) nor described methods in sufficient detail to inform development of international standards for the safe and effective safe deployment of appropriate non-thermal technologies. Studies describe the use of a new biocidal wash from PPGD technology including first reporting on cellular imaging using fluorescent, confocal, transmission and electron microscopy. Studies were reported on the role in microbial inactivation kinetic modelling to elucidate efficacy of technology applications including addressing the occurrence of different survivor curves. At this time I was employed as Senior Lecturer and first Enterprise Manager for the Roberston Laboratories for Electronic Sterilisation Technologies at Strathclyde University. Thereafter, I moved to Dublin Institute of Technology and Athlone Institute of Technology (now Technological University of the Shannon), where the first studies advanced the combinational effects of simultaneous and sequential stresses produced by emerging. Technologies. This study revealed the pulsed-UV light kills pathogenic yeast using a multi-hit lethal cascade process encompassing membrane permeabilization, lipid peroxidation, genomic damage, reactive oxygen species generation, necrosis and apoptosis. It revealed that detection of latter apoptosis phase after increasing UV pulse coincides with occurrence of irreversible lethality in clinical isolates of *Candida albicans*. Detection of biomarker for apoptosis in such treated-pathogens can be potentially used as rapid real-time approach to elucidate rapid irreversible destruction of such contaminating pathogens that supplement alternative plate counts that demands a lengthy resuscitation and enumeration process. Studies describe the development of appropriate surrogate or bioindicators (chemical and biological) for real-time evaluation of non-thermal treatment technology development and performance that hurdles limitations of traditional culture-based approaches. Critical bacterial inactivation, photo inactivation and dark repair are also described for Pulsed UV compared with similarly treated

low pressure UV light sources. Subsequent studies were also conducted using PPGD for complex water borne parasites *Cryptosporidium parvum* and *Giardia lamblia*. These studies revealed efficacy of PUV dose but required the co-development of a combined cell culture-quantitative PCR assay (along with Gold Standard Mice assay) to prove disinfection efficacy for suspended water applications. These parasites don't grow on normal agar plates. Studies revealed that these non-thermal treatment technologies can also kill pathogen harboured in complex biofilms. Studies were also conducted to determine other surrogate bioindicators for complex pathogens post non-thermal treatment technologies including use of ATP and safe *Bacillus* endospores. Studies revealed the importance of design and PPGD configuration, as the earlier prototype model was shown to produce undesired toxicological and eco-toxicological endpoints due to corrosion of unshielded electrodes during pulsing; thus, deemed to be unsafe for follow on industrial treatment applications.

APPLIED AND ENVIRONMENTAL MICROBIOLOGY, Mar. 1999, p. 1312–1315 Vol. 65, No. 3
0099-2240/99/$04.00+0

Pulsed-Light Inactivation of Food-Related Microorganisms

N. J. ROWAN,[1]* S. J. MACGREGOR,[2] J. G. ANDERSON,[1] R. A. FOURACRE,[2] L. MCILVANEY,[2] AND O. FARISH[2]

Department of Bioscience & Biotechnology,[1] and the Department of Electronic & Electrical Engineering,[2] University of Strathclyde, Glasgow, Scotland

Received 17 August 1998/Accepted 25 November 1998

The effects of high-intensity pulsed-light emissions of high or low UV content on the survival of predetermined populations of *Listeria monocytogenes*, *Escherichia coli*, *Salmonella enteritidis*, *Pseudomonas aeruginosa*, *Bacillus cereus*, and *Staphylococcus aureus* were investigated. Bacterial cultures were seeded separately on the surface of tryptone soya-yeast extract agar and were reduced by up to 2 or 6 $\log_{10}$ orders with 200 light pulses (pulse duration, ~100 ns) of low or high UV content, respectively ($P < 0.001$).

Despite significant advances made towards a better understanding of bacterial transmission and pathogenicity in foods, the incidence of reported food-borne illnesses associated with bacterial enteropathogens continues to be a major problem in the United Kingdom (5) and North America (7). It is generally accepted that contamination of both unprocessed and uncooked foods with pathogenic bacteria is a major source of concern, and any method of either reducing or eliminating food contamination will have a significant effect on the incidence of food-borne disease (5). A possible approach to reducing the level of microbial contamination on food surfaces in slaughterhouses, and in other food preparation environments, is UV irradiation (1–3, 5, 8, 9). Stermer et al. (8) indicated that the bacterial load on fresh meat can be effectively reduced by UV irradiation, while Wallner-Pendleton and coworkers (9) showed that this method of disinfection reduced *Salmonella* surface contamination without adversely affecting poultry carcass color or increasing meat rancidity. These studies indicate that if an effective and economic method of UV generation can be developed, then UV irradiation may have a practical application in the disinfection of food and contact surfaces.

While conventional alternating-current systems produce light with a power dissipation in the range of 100 to 1,000 W per device, a pulse power energization technique (PPET) can dissipate many megawatts of electrical power in the light source (4). PPET also tends to produce a greater intensity of the shorter bactericidal wavelengths of light, and, by using this approach, it is possible to design an extremely short energization time of the light source (~100 ns). For modest energy input (e.g., 3 J), this results in high peak power dissipation (~35 MW). Here we present evidence that PPET may lend itself to surface disinfection since it significantly reduces large populations of various food-related microorganisms on laboratory-based media.

The effectiveness of PPET, with two different light sources, in reducing predetermined microbial numbers on agar surfaces was determined by using a variety of proven bacterial pathogens, namely, *Escherichia coli* NCTC 12079 (serotype O157:H7), *Listeria monocytogenes* NCTC 11994 (serotype 4b), diarrheagenic *Bacillus cereus* NCTC 11145, *Salmonella enteritidis* NCTC 4444, *Staphylococcus aureus* NCTC 4135, *Pseudomonas aeruginosa* NCTC 8203, and the yeast *Saccharomyces cerevisiae* NCTC 10716, obtained from the National Collection of Type Cultures, Colindale, London, United Kingdom. Bacterial cultures were grown at 30°C and maintained on tryptone soya agar supplemented with 0.6% yeast extract (TSYEA). The yeast culture was grown at 25°C and maintained on malt extract agar supplemented with 0.3% yeast extract, 1% glucose, and 0.3% mycological peptone (MYGPA). Analysis of variance, balanced model (Minitab software release 11; Minitab Inc., State College, Pa.), was used to compare the effects of pulsed-light irradiation, number of pulses applied, and the type of microorganism treated. The studies were performed in quadruplicate, and all significant differences are reported at 95% ($P < 0.05$) and 99.9% ($P < 0.001$) confidence intervals.

Pulsed-light inactivation of food-related microorganisms. The bacterial test strains were inoculated into 100 ml of tryptone soya broth supplemented with 0.6% yeast extract (TSYEB) and cultivated on a shaker at 125 oscillations per minute to a population density of $\sim 10^9$ cells ml^{-1} (confirmed via plate counts). A 0.1-ml aliquot of a 10^{-5} dilution of this culture (the diluent used was 0.01 M sodium phosphate [pH 7.2]–0.15 M NaCl) was transferred to 100 ml of fresh TSYEB. The bacterial test strains were again grown to a density of $\sim 10^9$ cells ml^{-1}. *S. cerevisiae* was grown to a cell density of $\sim 10^9$ cells ml^{-1} (confirmed via plate counts) in 100 ml of malt extract broth supplemented with 0.3% yeast extract, 1% glucose, and 0.3% mycological peptone (MYGPB) at 25°C. Ten samples, each containing 20 μl of a bacterial or yeast test culture, were surface inoculated on separate TSYEA or MYGPA plates, respectively, by using the Miles and Misra method (6).

The test assembly consisted of a rectangular polyvinyl chloride housing, a pulse generator, and associated switching with controlling circuitry as shown in Fig. 1. The light source was mounted 4.5 cm above two sample holders that were set at a position 45 degrees to the horizontal. This allowed two samples to be irradiated simultaneously, with each sample receiving the same average exposure. Two light sources were employed. The first of these was a Heraeus Noblelight XAP series (type NL4006) constructed from a clear fused-quartz tube (UV transparent) filled with xenon to a pressure of 59 kPa. The second light source was a Heraeus Noblelight XFP series (type NL4320) with a cerium-doped quartz envelope, again filled with xenon to a pressure of 59 kPa. The envelope of this tube (NL4320) restricted the light output in the UV region. Both light sources produced a broad spectrum of white light with peak spectral emissions at wavelengths of ~550 nm, as shown in Fig. 2A for the low-UV-content tube and in Fig. 2B for the

* Corresponding author. Mailing address: Department of Bioscience and Biotechnology, University of Strathclyde, Royal College, 204 George St., Glasgow G1 1XW, Scotland. Phone: 44 141 548 2531. Fax: 44 141 553 1161. E-mail: n.j.rowan@strath.ac.uk.

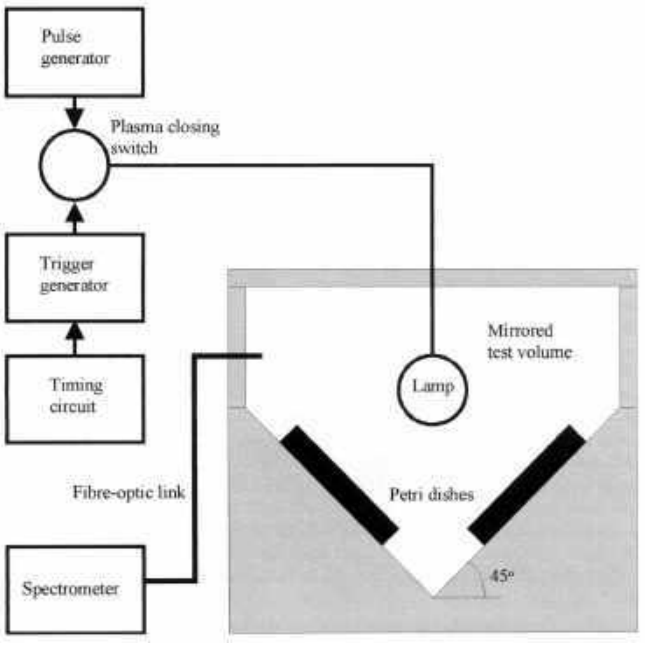

FIG. 1. Schematic layout of experimental facility for microbial inactivation with a pulsed-light source.

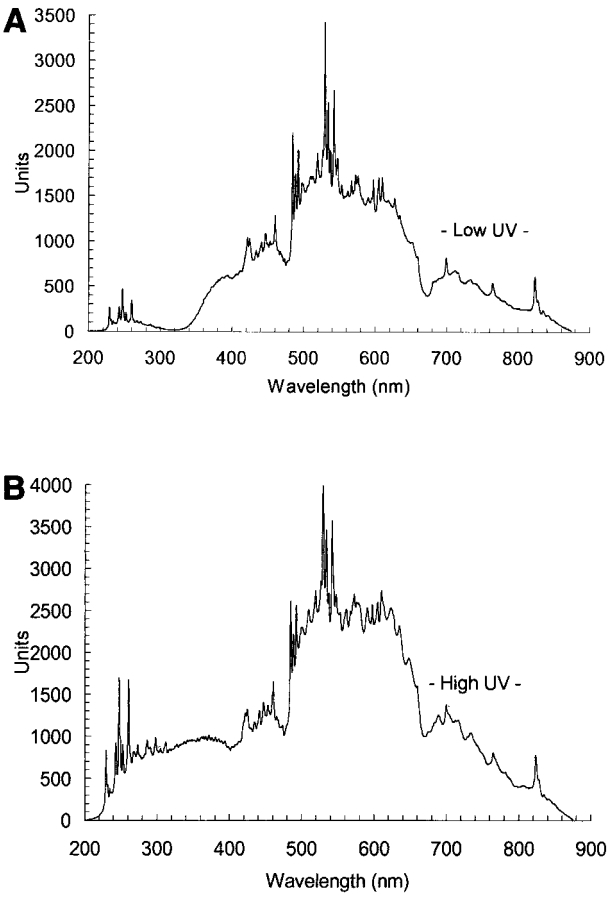

FIG. 2. Emission spectra (range, 200 to 900 nm) from two different light sources; one shows a low UV content (A), and the other shows a higher UV content (B).

high-UV-content tube. The major differences in emission spectra occur between 200 and 450 nm.

A single-stage, inverting, pulse-forming-network Marx generator was used to create a high-peak-power discharge. The generator was charged to a DC voltage of 30 kV for all experiments and was discharged directly into the light source by using a plasma switch triggered via a high-voltage autotransformer. The generator source capacitance was 6.4 nF, and the source impedance, when fired, was 6.25 Ω. A fiber-optic link and timing control circuit were used to activate the pulse generator at a pulse repetition rate of 1 pulse per s. The generator was charged by using a Brandenburg 50-kV, 1-mA DC supply, and, at full voltage, the pulse-forming-network Marx generator contained a stored energy of 3 J. The nominal duration of the output pulse was 85 ns, representing an average peak electrical power, per pulse, of 35 MW. This should be compared with the ~100-W average power rating of the light source when operated continuously. At 1 pulse per s, the average power consumption of the system was 3 W, and consequently no discern-

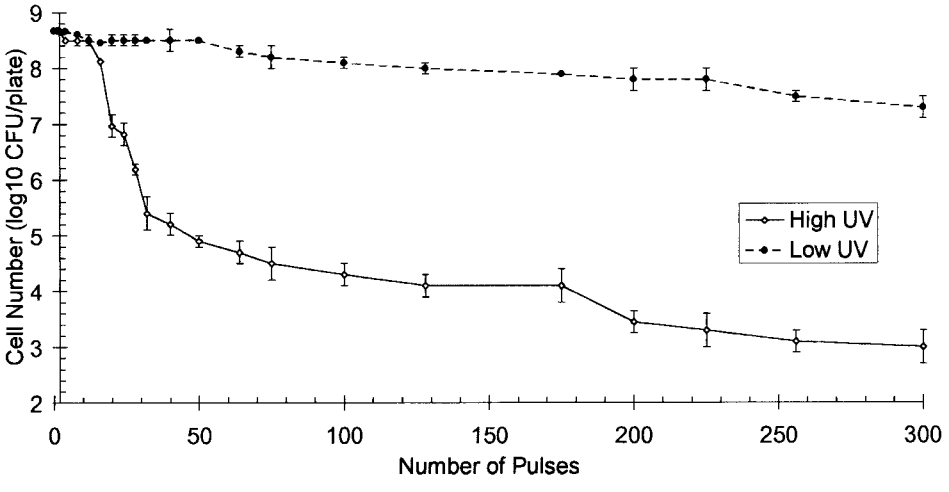

FIG. 3. Pulsed-light inactivation of surface-inoculated *E. coli* using two light sources which contained either a low- or high-UV content.

TABLE 1. Influence of two different pulsed-light sources on the viability of a variety of microbial populations

Treatment		No. of food-related microorganisms present (log_{10} CFU per plate [mean ± SD])[a]						
Light Source	No. of pulses	*B. cereus*	*L. monocytogenes*	*S. aureus*	*E. coli*	*S. enteritidis*	*P. aeruginosa*	*S. cerevisiae*
Untreated control	0	8.3 ± 0.1 B	9.4 ± 0.2 A	9.4 ± 0.1 A	9.6 ± 0.3 A	9.7 ± 0.2 A	8.7 ± 0.1 B	8.4 ± 0.2 B
High UV	100	4.5 ± 0.3 G	5.8 ± 0.4 E	5.2 ± 0.3 F	4.5 ± 0.1 G	5.2 F	4.3 ± 0.2 G	4.7 ± 0.2 G
	200	3.4 ± 0.3 H	5.0 ± 0.2 F	4.3 ± 0.1 G	3.4 ± 0.1 H	4.1 ± 0.2 G	2.9 ± 0.3 I	3.5 ± 0.1 H
Low UV	100	8.0 B	9.3 ± 0.1 A	8.9 ± 0.2 A	9.1 ± 0.1 A	9.1 ± 0.2 A	6.9 ± 0.3 D	8.0 ± 0.3 B
	200	7.9 ± 0.4 B	9.2 ± 0.1 A	8.1 ± 0.4 B	7.8 ± 0.2 C	8.1 ± 0.1 B	6.5 ± 0.1 D	7.7 ± 0.2 C

[a] Measured as log_{10} CFU per plate, where counts are averages of four replicate trials. Values followed by the same letter do not differ at the $P < 0.05$ level, whereas values followed by different letters differ at the $P < 0.05$ level.

ible increase in sample temperature was observed during treatment. The electrical diagnostics consisted of a high-voltage DC probe, used to measure the charging voltage, and a high-speed transient probe to monitor the pulsed voltage applied to the light source. With the line-source geometry employed, the light intensity profile varied by −30% from the center to the edge of the sample. The light emission was monitored with a four-channel Ocean Optics SQ2000 fiber-optic spectrometer. The spectral resolution was 1.25 nm for each channel (50-mm slit width), and the detectors (Sony 1LX511) were enhanced to allow UV detection. Continuous monitoring of the optical emissions verified that the emission spectra were constant throughout the experiment.

Surface-inoculated TSYEA and MYGPA plates containing approximately 10^9 cells ml of test culture^{-1} were positioned in the PPET assembly (Fig. 1). Samples of each test culture were treated with either 100 or 200 pulses of high-intensity light which contained either a low or high level of UV. Following treatment, the plates were wrapped in aluminium foil to prevent photoreactivation and were incubated for 48 h at 30°C. The study was carried out in quadruplicate with duplicate plates for each set of exposures. The surviving populations were enumerated and expressed as log_{10} CFU per plate.

Initial experiments with *E. coli* (Fig. 3) showed that the type of light source used had a significant effect on the level of inactivation ($P < 0.001$). A 5- and 6-log_{10}-order inactivation occurred after treatment with 100 and 200 pulses, respectively, with the higher UV light source, whereas 300 pulses of low-UV light gave a reduction of only 1 log_{10} order. Subsequently, 100 and 200 pulses were selected to test *Salmonella enteritidis*, *Staphylococcus aureus*, *Escherichia coli*, *Pseudomonas aeruginosa*, *Bacillus cereus*, *Listeria monocytogenes*, and the yeast *Saccharomyces cerevisiae*.

The results showed with each test culture that significantly greater levels of microbial inactivation ($P < 0.001$) occurred with light pulses of high-UV content. With 200 pulses of high-UV light, all of the microbial populations treated were reduced by 5 to 6 log_{10} orders, whereas with low-UV light, only a 1- to 2-log_{10}-order reduction in cell numbers occurred. It was found that there were variations in the susceptibility of test cultures (Table 1). The levels of resistance of the following bacteria differed (and are listed in order of decreasing resistance): *L. monocytogenes*, *Staphylococcus aureus*, *Salmonella enteritidis*, *E. coli*, *B. cereus*, *Saccharomyces cerevisiae*, and *P. aeruginosa* (the levels of resistance between *S. aureus* and *S. enteritidis* and those between *B. cereus*, and *S. cerevisiae* did not significantly differ at the $P < 0.05$ level). These findings are in agreement with the work of Jay (2), in which gram-positive bacteria were shown to be more resistant to the effects of UV light than gram-negative bacteria and pseudomonads and flavobacteria were shown to be the most sensitive.

By using this PPET approach for high-intensity light generation, it was possible to produce significant levels of peak power in the light source which are not achievable under conventional continuous excitation (4). This in turn results in a greater relative production of light in the shorter biocidal wavelengths. It has been well documented that UV is effective in killing microorganisms contaminating the surfaces of a variety of materials, including food (2, 3, 8, 9). The lethal action of high-intensity broad-spectrum light is due predominantly to either photothermal and/or photochemical mechanisms (e.g., the formation of lethal thymine dimers on the microbial DNA) (1, 2). Since only a negligible rise in temperature (i.e., less than 1°C) occurred in the treated agar, there were no appreciable photothermal effects. Therefore, it is likely that the lethality of this PPET approach can be attributed to the photochemical action of the shorter UV wavelengths. This is supported by the data in Fig. 2, which compares the spectral emissions produced by both PPET light sources and shows that they differ in the level of the shorter wavelengths in the range of 200 to 450 nm.

Bank and coworkers (1) have shown previously that a 6-log_{10} decrease in viable bacterial numbers, which had been surface inoculated onto trypticase soy agar plates, could be achieved by using a computer-controlled modulated UV-C light source (100 to 280 nm). Their light system used exposures of up to 60 s at 40-W peak power compared to an 85-ns exposure at 35-MW peak power in the present study, demonstrating the antimicrobial effectiveness of the PPET. This approach may be further improved by optimizing the emission spectra to enhance the antimicrobial UV-C content.

In conclusion, this study has shown that a 6-log_{10} reduction in microbial populations was achieved after exposure to 200 pulses of light containing high-intensity UV. The energy delivery system has modest energy requirements, ~3 J, and if this is delivered in a short period of time, with a high repetition rate, then rapid treatment can be achieved.

We thank S. M. Turnbull, Y. Koutsoubis, F. A. Tuema, and D. A. Currie (University of Strathclyde) for their assistance in this study.

REFERENCES

1. **Bank, H. L., J. John, M. K. Schmehl, and R. J. Dratch.** 1990. Bacteriocidal effectiveness of modulated UV light. Appl. Environ. Microbiol. **56:**3888–3889.
2. **Jay, J. M.** 1997. Radiation preservation of foods and nature of microbial radiation resistance, p. 304–323. *In* J. M. Jay (ed.), Modern food microbiology. Chapman and Hall, New York, N.Y.
3. **Kuo, F.-L., J. B. Carey, and S. C. Ricke.** 1997. UV irradiation of shell eggs:

effect of populations of aerobes, moulds and inoculated *Salmonella typhimurium*. J. Food Prot. **60:**639–643.
4. **MacGregor, S. J., S. M. Turnbull, F. A. Tuema, and O. Farish.** 1997. Factors affecting and methods of improving the pulse repetition frequency of pulse-charged and de-charged high pressure gas switches. IEEE Trans Plasma Sci. **25:**110–117.
5. **Pennington, T. H.** 1997. The Pennington Group: report on the circumstances leading to the 1996 outbreak of *E. coli* O157 in Central Scotland, the implications for food safety and the lessons to be learned. Stationery Office Publishers, Edinburgh, United Kingdom.
6. **Roberts, D., W. Hooper, and M. Greenwood.** 1995. Practical food microbiology. Public Health Laboratory Service, London, United Kingdom.
7. **Slutsher, L., S. F. Altekruse, and D. L. Swerdlow.** 1998. Foodborne diseases: emerging pathogens and trends. Emerg. Infect. Dis. **12:**199–216.
8. **Stermer, R. A., M. Lasater-Smith, and C. F. Brasington.** 1987. Ultraviolet radiation—an effective bactericide for fresh meat. J. Food Prot. **50:**108–111.
9. **Wallner-Pendleton, E. A., S. S. Summer, G. W. Froning, and L. E. Stetson.** 1994. The use of ultraviolet radiation to reduce *Salmonella* and psychrotrophic bacterial contamination on poultry carcasses. Poult. Sci. **73:**1327–1333.

Yeast
Yeast 2015; **32**: 533–540
Published online 5 June 2015 in Wiley Online Library
(wileyonlinelibrary.com) **DOI:** 10.1002/yea.3077

Research Article

Pulsed light for the inactivation of fungal biofilms of clinically important pathogenic *Candida* species

Mary Garvey[1]*, Joao Paulo Andrade Fernandes[2,3] and Neil Rowan[2]
[1]*Department of Life Sciences, Institute of Technology Sligo, Ireland*
[2]*Bioscience Research Institute, Athlone Institute of Technology, Ireland*
[3]*CAPES Foundation, Ministry of Education of Brazil, Universidade Federal do Rio de Janeiro, Brazil*

**Correspondence to:*
M. Garvey, Department of Life Sciences, Institute of Technology Sligo, Ash Lane, Sligo, Ireland.
E-mail: garvey.mary@itsligo.ie

Received: 21 October 2014
Accepted: 3 May 2015

Abstract

Microorganisms are naturally found as biofilm communities more than planktonic free-floating cells; however, planktonic culture remains the current model for microbiological studies, such as disinfection techniques. The presence of fungal biofilms in the clinical setting has a negative impact on patient mortality, as *Candida* biofilms have proved to be resistant to biocides in numerous *in vitro* studies; however, there is limited information on the effect of pulsed light on sessile communities. Here we report on the use of pulsed UV light for the effective inactivation of clinically relevant *Candida* species. Fungal biofilms were grown by use of a CDC reactor on clinically relevant surfaces. Following a maximal 72 h formation period, the densely populated biofilms were exposed to pulsed light at varying fluences to determine biofilm sensitivity to pulsed-light inactivation. The results were then compared to planktonic cell inactivation. High levels of inactivation of *C. albicans* and *C. parapsilosis* biofilms were achieved with pulsed light for both 48 and 72 h biofilm structures. The findings suggest that pulsed light has the potential to provide a means of surface decontamination, subsequently reducing the risk of infection to patients. The research described herein deals with an important aspect of disease prevention and public health.

Keywords: **pathogenic; yeast; UV inactivation; sessile communities; surfaces; *Candida***

Introduction

In the last three decades, fungi have appeared as a major cause of human disease, predominantly among immunocompromised individuals, neonates, burns patients and patients with serious underlying illnesses (Trofa *et al.,* 2008). *Candida* species are opportunistic eukaryotic fungal pathogens commonly associated with clinical infections resulting in deep tissue infection, high mortality rates and financial burden.

Biofilms (sessile communities) are a form of microbial growth where cells grow in a self-produced protective environment, which allows the cells to escape the dangers of their surrounding location. Biofilms are usually associated with wet or damp surfaces, such as indwelling medical devices and/or tubing on medical equipment. However, it is now known that microbes can survive for extended periods in a dehydrated state on dry hospital surfaces. Indeed, biofilms have recently been discovered on dry hospital surfaces (Otter *et al.,* 2014). *Candida* biofilms are composed of yeast cells and filaments that are structurally attached to biotic or abiotic surfaces and embedded in an extracellular matrix (Nailis *et al.,* 2010). Research has shown that such biofilm cell communities are more resistant to chemical disinfection techniques than planktonic (free-floating) cells, due to their extracellular matrix, structural complexity, gene upregulation and metabolic heterogeneity (Fanning and Mitchell, 2012). Biofilm formation by pathogenic microorganisms such as *Candida* plays a key role in infections resulting

from intravascular devices in the clinical setting. Indeed, the association between *Candida* species biofilm formation and continued host infection has become more evident. Once a biofilm forms, it can continuously supply cells which detach from the main structure into the bloodstream, acting as a source of infection.

It has been reported by Kumanoto (2002) that conditions with a high flow rate, such as that encountered within the circulatory system, may favour the development of persistent biofilms on devices placed in the bloodstream. Furthermore, *Candida* species biofilms are quite resistant to antifungals such as fluconazole, amphotericin B, nystatin and voriconazole (Kumanoto, 2002). In recent years there has been a marked increase in non-*C. albicans*-related bloodstream infections from *Candida* species, mainly *C. parapsilosis*, *C. krusei* and *C. tropicalis* (Trofa *et al.,* 2008). The resistance of this species to antibiotics and the ability of *Candida* biofilms to tolerate chemical disinfection suggest the need for alternative methods of removing this pathogen from clinical settings.

Prevention of infection is a superior method than infection treatment in terms of cost and patient well-being. An alternative or supplementary means of control is to minimize the extent of exposure of the patient to these fungal pathogens, thereby preventing an infection from occurring. Typical clinical surfaces, such as plastics, have been shown to act as reservoirs for viable pathogenic fungi, such as *Candida albicans* and *C. parapsilosis* (Neely and Orloff, 2001). Proper cleaning regimens that include the use of effective surface decontamination techniques can help prevent patient exposure to pathogenic species.

The use of ultraviolet (UV) light has proved effective for the inactivation of a range of microbial species; however, there is limited information available on its use for the removal of clinically relevant *Candida* species or *Candida* biofilms. UV disinfection occurs following exposure of test species to UV energy at 254 nm, which has a negative effect on genetic material, preventing microbial replication. Standard UV lamps emit UV energy as a continuous wave from either a low-pressure (LP) or a medium-pressure (MP) lamp source at set wavelengths. Ultraviolet C (UVC) has been found to be efficient at sterilizing the inner surface of catheters contaminated with bacterial biofilms and subsequently preventing catheter-related infections (Bak *et al.,* 2009). Studies by this research group have focused on the use of an alternative means of delivering UV energy, referred to as 'pulsed UV' (PUV), which delivers UV light in short-duration pulses of high-intensity light with a broader range of wavelengths in the range 100–1100 nm, enriched with shorter germicidal wavelengths (Farrell *et al.,* 2011). These wavelengths may potentially affect more cellular targets, such as cell membranes and protein structures, than DNA alone, producing irreparable cellular damage. Due to the delivery mechanism of short-duration pulses, PUV also has a better penetration depth than LPUV. Additionally, PUV has proved effective for the inactivation of numerous microbial species, bacterial endospores, biofilms and parasite species in a shorter treatment time than LP- or MP-UV, leading to a reduction in operation costs (Garvey *et al.,* 2014). Considering these important advantages of PUV over LP-UV, the aim of this study was to determine the potential of a PUV light system for the inactivation of clinically important *Candida* species in both planktonic and biofilm form on surfaces commonly found in the health care setting.

Methods

Test strain culture conditions

All *Candida* test strains used in this study were sourced from the American Type Tissue Culture Collection (ATCC), with the exception of a *C. albicans* hospital isolate, which was sourced from a blood culture at the National University of Ireland, Galway Hospital. *Saccharomyces cerevisiae* (ATCC 9763) was also sourced from the ATCC and used for PUV studies as a comparative strain to *Candida*. Strains were cultured and maintained on malt extract agar (Cruinn Diagnostics, Ireland) at 37 °C following removal from storage in microbank vials (Cruinn Diagnostics, Ireland) at −80 °C. *C. parapsilosis* (ATCC 22019) was cultured and maintained on Sabouraud agar (Cruinn Diagnostics, Ireland) at 30 °C and incubated at 5 °C for short-term storage on agar slopes. Strains were identity confirmed by Gram staining and the germ-tube assay, according to Farrell *et al.* (2011), following a maximal 2 week storage period. For treatment studies, single colonies were

Yeast 2015; **32**: 533–540.
DOI: 10.1002/yea

aseptically transferred to 100 ml malt extract broth and incubated at 37 °C under rotary conditions at 125 rpm for *S. cerevisiae*, *C. albicans* (ATCC 10231), *C. albicans* (clinical isolate NUIG 6250), *C. krusei* (ATCC 14243) and *C. tropicalis* (ATCC 13803); *C. parapsilosis* was cultured in 100 ml Sabouraud broth at 30 °C at 125 rpm for 18 h.

CDC reactor biofilm growth

All fungal biofilm growth was achieved by the use of a CDC biofilm reactor (Biosurface Technologies Corp., Bozeman, MT, USA). The CDC reactor is a recognized method for the growth of microbial biofilms under high shear and continuous flow (Coenye and Nelis, 2010) and is the standard method in use by the American Society for Testing and Materials (ASTM 2012).

The CDC reactor is composed of a glass vessel, which holds the reactor medium. Placed into this vessel is a polyethylene top which holds eight removable polypropylene rods, each of which in turn has three inserts for holding the coupons on which the microbial cells attach. Therefore, each biofilm reactor has the capacity for 24 coupons equivalent to 24 separate biofilms, which makes it an ideal apparatus for inactivation studies. In the centre of the reactor a magnetic stirrer is present, which provides a continuous flow of nutrients over the colonized surface of the coupons. Continuous mixing of the culture liquid is achieved by placing the reactor on a magnetic stir plate (RCT Basic Stir Plate IKA®, Staufen, Germany) at 130 rpm. The reactor vessel was filled with 300 ml malt extract broth for *C. albicans* (ATCC), hospital strains and *C. krusei*; 300 ml Sabouraud broth was added for *C. parapsilosis*; 1 ml of an 18 h culture of the test strain, grown in suitable broth, was then added to the reactor vessel and incubated at 37 °C (30 °C for *C. parapsilosis*) under rotary conditions at 130 rpm. The reactor was incubated for 48 and 72 h to allow for biofilm growth to a maximal cell density, according to the method of Nailis *et al.* (2010). Fungal cell counts were performed at inoculation of the reactor broth and at 48 and 72 h of incubation to determine the planktonic cell density of the reactor. The cell density of sessile cells was determined for stainless steel and PVC surfaces by scraping the surface with a sterile cell scraper (Sarstedt, Germany) into 10 ml sterile phosphate-buffered saline (sPBS; Sigma-Aldrich, Ireland), according to the ASTM-recommended procedure for biofilm cell density analysis. Colony forming units (cfu/ml) were determined by spreading 100 µl serially diluted sessile cells on suitable agar, followed by incubation for 24 h at 30 °C or 37 °C.

Pulsed UV studies

Pulsed-light inactivation was conducted on test strains in planktonic form in suspension and on agar surfaces for comparative studies to that of the biofilm communities on PVC and stainless steel surfaces. The PUV system used throughout this study was the PUV-01 (Samtech Ltd, Glasgow, UK), consisting of two main components, a treatment chamber and a driver circuit. The driver unit consists of the trigger and discharge outputs, frequency control, trigger control and the discharge voltage control. The trigger cable connects the trigger output of the driver unit with the trigger electrode of the flashlamp, while the discharge cable connects the discharge output of the driver unit with the lamp anode and cathode. The treatment chamber consists of a polyvinyl chloride housing containing a xenon light source and a circular treatment table. The light source has an automatic frequency control function that allows it to operate at 1 pulse/s (pps), which was used throughout this study. Petri dishes used in the tests were placed directly below the lamp, which ensured that full coverage of the plate surface occurred and eliminated possible shading effects. In this study, standard treatments involved exposing the test samples to lamp discharge energy of 16.2 J at 8 cm distance from the light source.

PUV treatment of planktonic cells

Planktonic cells of all *Candida* test strains and *S. cerevisiae* were treated by PUV for analysis compared to the sessile cells. For PUV studies, a single colony of the test strain was aseptically transferred to 100 ml sterile malt extract broth, followed by incubation at 37 °C for 18 h at 125 rpm. For surface treatment, 100 µl of an appropriate dilution was spread onto malt agar surfaces. Sabouraud broth and agar were used as previously described for the growth of *C. parapsilosis*. Test plates were then exposed to pulses of UV light at 16.2 J at varying fluences at a rate of 1 pulse/s, according to Garvey *et al.* (2014), up to a PUV

Yeast 2015; **32**: 533–540.
DOI: 10.1002/yea

fluence of 8 μJ/cm^2 (treatment time of 80 s) for surfaces and 11 μJ/cm^2 (treatment time of 100 s) for fungal suspensions. PUV studies were also conducted on samples diluted from the 18 h broth in 20 ml final volumes of sterile PBS at 8 cm from the light source, after which 100 μl treated liquid was transferred to suitable agar and incubated at 37 °C for 24 h, or 30 °C for *C. parapsilosis*.

PUV treatment of biofilm structures

PVC and stainless steel coupons were aseptically removed from the reactor, rinsed with sPBS and transferred to a sterile Petri dish. Samples were exposed to pulses of UV light at 16.2 J at 8 cm from the light source at varying UV fluence (μJ/cm^2) up to a PUV fluence of 6.48 μJ/cm^2 (equivalent to a treatment time of 60 s). Once treated, the coupons were immersed in 10 ml sterile PBS and the surface scraped, using a sterile cell scraper, to remove the treated biofilms and to determine fungal cell viability. The liquid was then transferred to a sterile 20 ml container and centrifuged at 800 × *g* for 10 min to pellet the cells. The sample was then resuspended and agitated to ensure biofilm dispersion. Serial dilutions were made from the biofilm suspensions and 100 μl spread on triplicate agar plates to determine the cfu/ml of treated samples. This process was repeated for coupons at varying UV fluences to determine the $\log_{10}$ reduction obtained with increasing UV fluence compared to an untreated control. A cell count was also conducted on the medium present in the reactor vessel, using the spread plate technique.

Statistics

All the experiments were performed three times, with three plate replicates for each experimental data point, providing a mean result for each experimental batch. The log reduction was calculated as $\log_{10}$ of the ratio of the concentration (cfu/ml) of the non-treated (N_0) and UV-treated (N) samples [$\log_{10}$ (N_0/N)]. Linear regression analysis was used to determine the rate of inactivation for each test species under the regime of PUV treatments applied at the 95% significance level. Student's *t*-test and one-way ANOVA model (Minitab software release 16; Mintab Inc., State College, PA, USA) were used to determine the sensitivity of each test strain to PUV light.

Results and discussion

Candida biofilm formation

The CDC reactor proved an effective tool for the formation and growth of fungal biofilms. Sessile colony counts showed that high-density biofilms formed at the 48 and 72 h incubation time points for both surface types in the reactor (Table 1). After 48 h, a 4.7, 4.2 and 4.6 $\log_{10}$ cfu/ml biofilm formed for *C. albicans*, *C. albicans* (clinical isolate) and *C. parapsilosis*, respectively, on PVC surfaces. There was a significant difference ($p < 0.05$) in the sessile population density on stainless steel surfaces, where a 4.2 $\log_{10}$ cfu/ml biofilm formed for each test species. A similar trend was observed following 72 h of incubation with 4.8, 5.2, 5.1 and 4.3, 4.0 and 5.0 $\log_{10}$ cfu/ml biofilm growths for *C. albicans*, *C. albicans* (clinical isolate) and *C. parapsilosis* on PVC and stainless steel coupons, respectively. These data suggest that both surface types can support the formation of densely populated *Candida* biofilm structures; however, PVC appears more favourable for growth, evident from the significantly higher sessile cell count than on stainless steel surfaces.

Table 1. Clinically relevant *Candida* species biofilm cell density after 48 and 72 h of growth in a CDC biofilm reactor (± SD)

	Biofilms cell density ($\log_{10}$ cfu/ml)			
	48 h		72 h	
	PVC	SS	PVC	SS
C. albicans	4.7 (±0.2)^A	4.2 (±0.01)^B	4.8 (±0.1)^A	4.3 (±0.05)^D
C. albicans (clinical)	4.2 (±0.1)^B	4.2 (±0.05)^B	5.2 (±0.03)^F	4.0 (±0.1)^C
C. parapsilosis	4.2 (±0.05)^B	4.2 (±0.1)^B	5.1 (±0.02)^E	5.0 (±0.04)^E

A–E, significant differences in cfu/ml; SS, stainless steel.

Yeast 2015; **32**: 533–540.
DOI: 10.1002/yea

Furthermore, it was found that, with further incubation (>72 h), there was no significant increase in the number of sessile cells present. Biofilm cell counts reached a maximum at 72 h, after which there was no increase in cell number on either surface material, a similar trend to that reported by Nailis *et al.* (2010). Indeed, research by this group concluded that the CDC reactor allows for the formation of more densely populated *Candida* biofilms than alternative methods, such as microtitre plates (Nailis *et al.,* 2010), and attributed this to the availability of nutrients within the reactor. Studies assessing *in vivo* models for catheter-associated *Candida* infections, such as microscopic structure analysis, indicate that *in vitro* techniques such as the CDC reactor show structured biofilm communities similar to those found *in vivo* (Lopez-Ribot, 2005). Furthermore, *in vitro* studies have shown that *Candida* can survive in the low-iron environment found in the tissues surrounding implanted devices, such as catheters, with the additional factor of its filamentous life cycle making it proficient at colonizing inert surfaces such as PVC (Suci and Tyler, 2002). These studies suggest that *in vitro* model systems do mimic *in vivo* events, indicating that the research outputs made are clinically relevant.

Pulsed UV inactivation of planktonic and sessile *Candida* test strains

The *Candida* and *Saccharomyces* test strains under study proved sensitive to PUV inactivation, albeit to varying extents. Figure 1 details the inactivation of test strains on agar surfaces following exposure to PUV irradiation. Interestingly, the *C. albicans* clinical isolate proved significantly ($p < 0.05$) more sensitive to UV disinfection that the reference strain *C. albicans* (ATCC), with 5.6 and 3.25 $\log_{10}$ cfu/ml inactivation obtained with a PUV fluence of 1.08 μJ/cm^2 for each strain, respectively, on agar surfaces. This trend of an increased sensitivity of the clinical isolate continued for all applied treatment fluences up to 5.39 μJ/cm^2 (treatment time of 50 s). A fluence of 5.39 μJ/cm^2 was needed to obtain a 5.8 $\log_{10}$ cfu/ml of *C. albicans* reference strain, with 2.15 μJ/cm^2 giving a similar inactivation rate of the clinical isolate (Figure 1). *C. albicans* (ATCC) and *S. cerevisiae* showed similar levels of inactivation (ca. 3.2 $\log_{10}$) at 1.08 μJ/cm^2 (treatment time of 10 s). This UV fluence resulted in a ca. 5 $\log_{10}$ cfu/ml inactivation of *C. albicans* (clinical), *C. krusei* and *C. parapsilosis* and 4 $\log_{10}$ cfu/ml inactivation of *C. tropicalis*. A fluence of 5.39 μJ/cm^2 resulted in a ca. 5.8 $\log_{10}$ cfu/ml inactivation of *S. cerevisiae*, *C. tropicalis* and *C. albicans* and a ca. 7.5 $\log_{10}$ cfu/ml inactivation of *C. parapsilosis*, *C. krusei* and *C. albicans* (clinical), indicating that levels of sensitivity to treatment varied with the UV fluence on agar surfaces. The order of sensitivity from least to most resistant to PUV at 5.39 μJ/cm^2/pulse on agar surfaces was: *C. parapsilosis*, *C. krusei*, *C. albicans* (clinical), *C. tropicalis*, *S. cerevisiae* and *C. albicans* (ATCC).

A similar trend was observed when treated in suspension, where *C. albicans* (clinical) proved

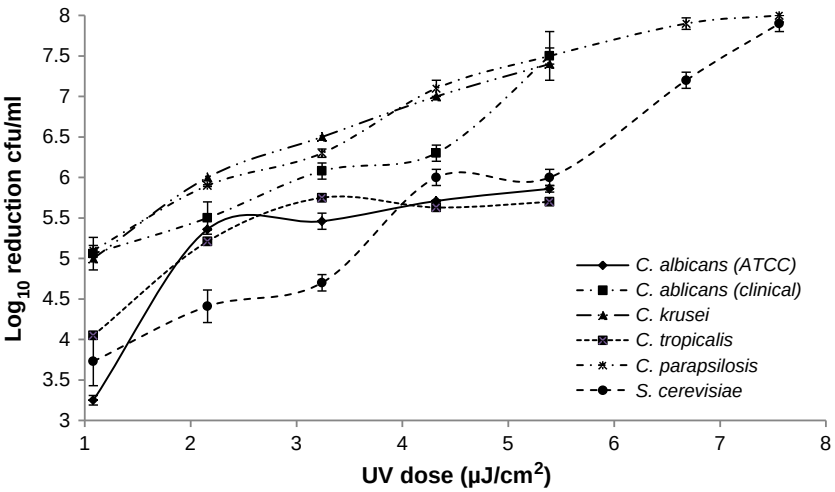

Figure 1. Pulsed light inactivation of *Candida* and *Saccharomyces* test species on agar surfaces (± SD)

Yeast 2015; **32**: 533–540.
DOI: 10.1002/yea

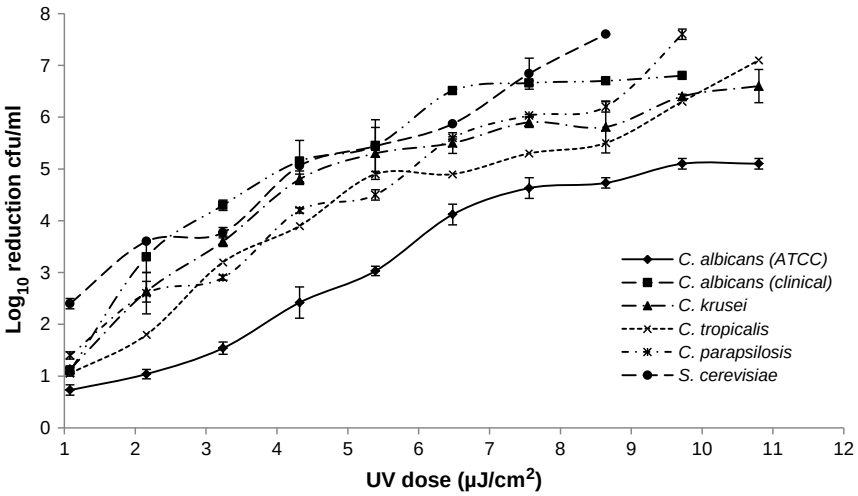

Figure 2. Pulsed light inactivation of 20 ml fungal suspensions of *Candida* and *Saccharomyces* test strains (± SD)

more sensitive to UV exposure than the reference strain (Figure 2) at all treatment fluences. There was no significant difference between the inactivation of *S. cerevisiae* and *C. albicans* (clinical) at treatment fluences of 4.32, 5.39 and 7.56 µJ/cm^2 in suspension, with complete inactivation of both strains achieved with 8.64 µJ/cm^2 (Figure 2). Additionally, *C. krusei* and *C. parapsilosis* showed similar levels of sensitivity to PUV with *C. tropicalis* proving significantly more resistant than both strains in suspension. Significantly more UV fluence was needed to obtain similar levels of inactivation with fungal suspension compared to surface spread for all test strains. The order of sensitivity from least to most resistant to PUV for fungal suspensions at 7.56 µJ/cm^2 was *S. cerevisiae*, *C. albicans* (clinical), *C. parapsilosis*, *C. krusei*, *C. tropicalis* and *C. albicans* (ATCC).

Neely and Orloff (2001) have shown that fungal pathogens have the ability to survive on clinical surfaces. Established biofilms on these surfaces pose a difficult challenge to hospital cleaning and disinfection, due to their resistance to biocides and difficulty in removing them by detergent cleaning (Otter *et al.,* 2014). Fungal infections are increasing at a disturbing rate, affecting a growing population of severely ill patients, which poses important challenges for health care professionals. Studies by Chandra *et al.* (2001) have shown that cellular resistance to biocides increased as the biofilm structure matured, with a 72 h biofilm of *C. albicans* showing a dramatically increased level of resistance than earlier-stage biofilm counterparts (Chandra *et al.,* 2001). A means of inactivating planktonic and sessile cells that renders the surface free of pathogenic species is essential to prevent patient infection or the contamination of medical materials. The PUV system used in this study repeatedly inactivated *Candida* species biofilms on both PVC and stainless steel surfaces. Significant levels of inactivation were obtained for *C. albicans* (ATCC), *C. albicans* (clinical) and *C. parapsilosis* for 48 h (Figure 3) and 72 h (Figure 4) biofilm structures. For both time points, ca. 3.5–4 $\log_{10}$ cfu/ml inactivation of all test strains was achieved with a fluence of 6.68 µJ/cm^2. There was no difference in the inactivation rates of *C. parapsilosis* 48 and 72 h biofilms on PVC surfaces. *C. albicans* biofilms appear more UV sensitive at 48 h, with a significant ($p < 0.05$) increase in inactivation obtained for each PUV fluence. The *C. albicans* clinical isolate showed similar or a slightly decreased level of inactivation at 48 h compared to 72 h biofilm formation; 48 h biofilms on stainless steel surfaces appear more UV-sensitive, with an increase in inactivation achieved for *C. albicans* up to a UV fluence of 4.32 µJ/cm^2 and for all treatment fluences for *C. albicans* (clinical) and *C. parapsilosis*. At 48 h biofilm formation, *C. parapsilosis* appears most resistant to UV pulses, with both *C. albicans* strains showing similar levels of sensitivity on PVC surfaces. A similar trend was observed for biofilms grown for 48 h on stainless steel surfaces. The order of increasing sensitivity to UV fluence was *C. parapsilosis*, *C. albicans* and *C. albicans*

Yeast 2015; **32**: 533–540.
DOI: 10.1002/yea

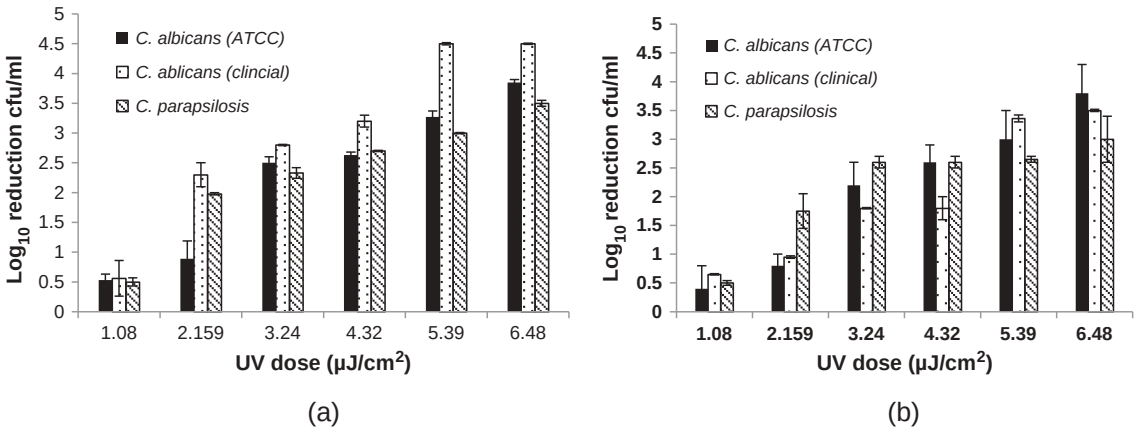

Figure 3. Pulsed-light inactivation of 48 h *Candida* species biofilms grown on (a) PVC and (b) stainless steel surfaces (± SD)

(clinical) on PVC surfaces and *C. albicans* (clinical), *C. parapsilosis* and *C. albicans* on stainless surfaces for 72 h biofilm structures. In general it was found that planktonic cells are more sensitive to PUV than attached cells on either surface material. The order of sensitivity to UV pulses was the same for fungal suspensions and biofilms on stainless steel surfaces, meaning that planktonic cells treated in suspension had the same level of susceptibility to pulsed light as cells in biofilms on stainless steel surfaces. *C. parapsilosis* proved the most sensitive test strain on agar surfaces and PVC-attached biofilms.

Biofilm communities are the natural state of microbial habitat, where they are found attached to biotic or abiotic surfaces, more so than planktonic free-floating cells. Regardless of this, planktonic culture remains the main mechanism for microbiological studies, such as disinfection (Otter *et al.*, 2014). This study assessing the sensitivity of fungal biofilm structures to pulsed-light treatment provides a direct relationship between treatment fluence and loss of viability in sessile cells. Here we have dealt with an important aspect of clinical disinfection and disease prevention. The findings demonstrate the effective use of pulsed UV light for the effective inactivation of clinically relevant *Candida* species on surfaces commonly associated with the health care setting. Although these initial studies are promising, further studies are warranted to assess the disinfection of multi-species biofilm communities. Biofilms often develop as a multi-species structure, with a synergistic relationship providing protection from a range of environmental stresses. Additionally, studies are merited to assess the potential of fungal biofilms to harbour

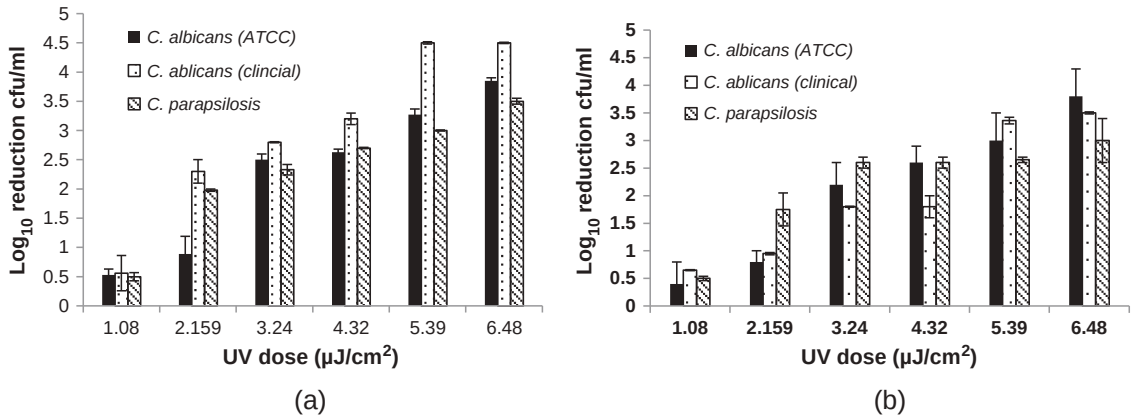

Figure 4. Pulsed-light inactivation of 72 h *Candida* species biofilms cells grown on (a) PVC and (b) stainless steel surfaces (± SD)

Yeast 2015; **32**: 533–540.
DOI: 10.1002/yea

other opportunistic pathogens, such as viruses and parasite species.

Acknowledgements

The authors wish to express their gratitude to Professor Martin Cormican, National University of Ireland, Galway (NUIG Ireland), who kindly donated the clinical isolates for use in this study.

References

American Society for Testing and Materials (ASTM). 2012. Standard No. E2562–12. Standard test method for quantification of *Pseudomonas aeruginosa* biofilm grown with high shear and continuous flow using a CDC biofilm reactor. ASTM: West Conshohocken, PA, USA.

Bak J, Ladefoged SD, Tvede M, *et al*. 2009. Fluence requirements for UVC disinfection of catheter biofilms. *Biofouling* **25**: 289–296.

Chandra J, Kuhn MD, Mukherjee KP, *et al*. 2001. Biofilm formation by the fungal pathogen *Candida albicans*: development, architecture, and drug resistance. *J Bacteriol* **183**: 5385–5394.

Coenye T, Nelis JJ. 2010. *In vitro* and *in vivo* model systems to study microbial biofilm formation. *J Microbiol Methods* **83**: 89–105.

Fanning S, Mitchell AP. 2012. Fungal biofilms. *PLoS Pathog* **8**: e1002585.

Farrell H, Hayes J, Laffey J, Rowan N. 2011. Studies on the relationship between pulsed UV light irradiation and the simultaneous occurrence of molecular and cellular damage in clinically relevant *Candida albicans*. *J Microbiol Methods* **84**: 317–326.

Garvey M, Thokala N, Rowan N. 2014. A comparative study on the pulsed UV and the low pressure UV inactivation of waterborne microorganisms. *J Water Environ Res* **86**: doi:10.2175/WER-D-13-00062.1.

Kumanoto AC. 2002. *Candida* biofilms. *Curr Opin Microbiol* **5**: 608–611.

López-Ribot LJ. 2005. *Candida albicans* Biofilms: more than filamentation. *Curr Biol* **15**: doi:10.1016/j.cub.2005.06.020.

Nailis H, Kucharikova S, Ricicova M, *et al*. 2010. PCR expression profiling of genes encoding potential virulence factors in *Candida albicans* biofilms: identification of model-dependent and -independent gene expression. *BMC Microbiol* **10**: 114.

Neely NA, Orloff MM. 2001. Survival of some medically important fungi on hospital fabrics and plastics. *J Clin Microbiol* **39**: 3360–3361.

Otter AJ, Vickery K, Walker J, *et al*. 2014. Surface-attached cells, biofilms and biocide susceptibility: implications for hospital cleaning and disinfection. *J Hosp Infect* **1**: 1–12.

Suci AP, Tyler JB. 2002. Action of chlorexidine digluconate against yeast and filamentous forms in an early stage *Candida albicans* biofilm. *Antimicrob Agents Chemother* **46**: 3522–3530.

Trofa D, Ga'cser A, Nosanchuk JD. 2008. *Candida parapsilosis*, an emerging fungal pathogen. *Clin Microbiol Rev* **21**: 606–625.

Yeast 2015; **32**: 533–540.
DOI: 10.1002/yea

Journal of Applied Microbiology

Journal of Applied Microbiology ISSN 1364-5072

ORIGINAL ARTICLE

Investigation of critical inter-related factors affecting the efficacy of pulsed light for inactivating clinically relevant bacterial pathogens

H.P. Farrell[1], M. Garvey[1], M. Cormican[2], J.G. Laffey[3] and N.J. Rowan[1]

1 Department of Nursing and Health Science, Athlone Institute of Technology, Athlone, Westmeath, Ireland
2 Department of Bacteriology, School of Medicine, National University of Ireland, Galway, Ireland
3 Department of Anaesthesia, School of Medicine, National University of Ireland, Galway, Ireland

Keywords
bacterial pathogens, clinical environment, decontamination, intense broad-spectrum pulsed light, nonthermal or minimal processing technologies, pigments, ultraviolet.

Correspondence
Hugh P. Farrell, Department of Nursing and Health Science, Athlone Institute of Technology, Dublin Road, Athlone, Co. Westmeath, Ireland. E-mail: nrowan@ait.ie

2009/0389: received 2 March 2009, revised 21 May 2009 and accepted 12 August 2009

doi:10.1111/j.1365-2672.2009.04545.x

Abstract

Aims: To investigate critical electrical and biological factors governing the efficacy of pulsed light (PL) for the *in vitro* inactivation of bacteria isolated from the clinical environment. Development of this alternative PL decontamination approach is timely, as the incidence of health care–related infections remains unacceptably high.

Methods and Results: Predetermined cell numbers of clinically relevant Gram-positive and Gram-negative bacteria were inoculated separately on agar plates and were flashed with ≤60 pulses of broad-spectrum light under varying operating conditions, and their inactivation measured. Significant differences in inactivation largely occurred depending on the level of the applied lamp discharge energy (range 3·2–20 J per pulse), the amount of pulsing applied (range 0–60 pulses) and the distance between light source and treatment surface (range 8–20 cm) used. Greater decontamination levels were achieved using a combination of higher lamp discharge energies, increased number of pulses and shorter distances between treatment surface and the xenon light source. Levels of microbial sensitivity also varied depending on the population type, size and age of cultures treated. Production of pigment pyocynanin and alginate slime in mucoid strains of *Pseudomonas aeruginosa* afforded some protection against lethal action of PL; however, this was evident only by using a combination of reduced amount of pulsing at the lower lamp discharge energies tested. A clear pattern was observed where Gram-positive bacterial pathogens were more resistant to cidal effects of PL compared to Gram negatives. While negligible photoreactivation of PL-treated bacterial strains occurred after full pulsing regimes at the different lamp discharge energies tested, some repair was evident when using a combination of reduced pulsing at the lower lamp discharge energies. Strains harbouring genes for multiple resistances to antibiotics were not significantly more resistant to PL treatments. Slight temperature rises (≤4·2°C) were measured on agar surfaces after extended pulsing at higher lamp discharge energies. Presence of organic matter on treatment surface did not significantly affect PL decontamination efficacy, nor did growth of PL-treated bacteria on selective agar diminish survival compared to similarly treated bacteria inoculated and enumerated on nonselective agar plates.

Conclusions: Critical inter-related factors affecting the effective and repeatable *in vitro* decontamination performance of PL were identified during this study that will aid further development of this athermal process technology for applications in health care and in industry. Very rapid reductions (*c.* 7 $\log_{10}$ CFU cm^{-2}

within ≤10 pulses) occurred using discharge energy of 20 J for all tested clinically relevant bacteria under study when treated at 8 cm distance from xenon light source. While no resistant flora is expected to develop for treatment of microbial pathogens on two-dimensional surfaces, careful consideration of scale up factors such as design and operational usage of this PL technique will be required to assure operator safety.

Significance and Impact of the Study: Findings and conclusions derived from this study will enable further development and optimization of this decontamination technique in health care and in food preparation settings, and will advance the field of nonthermal processing technologies.

Introduction

There is growing international concern regarding the unacceptably high levels of health care–related infections due in part to the continued development of antimicrobial resistance. Prevention of infection is a superior approach compared to the cost and consequences of treatment of infection, with strong emphasis placed on hand hygiene compliance and proper cleaning regimens that include use of effective surface decontamination techniques (Solberg 2000). However, conventional surface decontamination approaches such as chemical biocides have recognized limitations that include unwanted microbial adaptation, subsequent cross-resistance to front line antibiotics, and lingering chemical residues (Lambert *et al.* 2001; Randall *et al.* 2001; Gebel *et al.* 2002). Numerous studies have also highlighted limitations of decontamination techniques such as conventional, continuous-wave (CW) UV mercury lamps of low pressure designed to produce energy at 254 nm (called monochromatic or germicidal light) that include microbial repair and the necessity for lengthy durations of exposure to obtain suitable levels of decontamination (Bintsis *et al.* 2000). More recently, medium-pressure mercury UV lamps have been used because of their much higher germicidal UV power per unit length and because of their ability to emit polychromatic light comprising germicidal wavelengths from 200 to 300 nm (Bolton and Linden 2003).

Pulsed light (PL) is an approach that has received considerable attention as a strategy for decontaminating food, packaging, water and air (Dunn *et al.* 1997; Gómez-López *et al.* 2007). However, PL technology is also a strong candidate for contact surface decontamination in the health care setting. This approach kills micro-organisms by using ultrashort-duration pulses of an intense broadband emission spectrum that is rich in UV-C germicidal light (200–280 nm band). PL is produced using techniques that multiplies power manifold by storing electricity in a capacitor over relatively long times (fractions of a second) and releasing it in a short time (millionths or thousandths of a second) using sophisticated pulse compression techniques (Rowan *et al.* 1999; Gómez-López *et al.* 2007). The emitted flash has a high peak power and usually consists of wavelengths from 200 to 1100 nm broad-spectrum light enriched with shorter germicidal wavelengths (MacGregor *et al.* 1998; Gómez-López *et al.* 2007). This technology has received several names in the scientific literature: pulsed UV (PUV) light (Anderson *et al.* 2000; Sharma and Demirci 2003; Wang *et al.* 2005), high-intensity broad-spectrum PL (Roberts and Hope 2003), PL (Rowan *et al.* 1999), intense PL (Gómez-López *et al.* 2007) and pulsed white light (Marquenie *et al.* 2003). Seminal developments pertaining to these next generation light-flashing technologies has been the subject of recent review (Elmnasser *et al.* 2007; Gómez-López *et al.* 2007), with emphasis strongly placed on decontamination efficacy for food and water applications that aptly reflects the focus of research in this field of study to date. A strong advantage of using pulsed xenon lamps over continuous low-to-medium pressure conventional UV lamps is that the latter has a characteristic high peak power dissipation, which allows for more rapid microbial inactivation. A continuous 10 W lamp needs to be operated for 10 s to achieve the same decontamination efficacy (supplying same energy) as a pulsed lamp of typically 1 MW operated for just 100 μs. Otaki *et al.* (2003) also reported that adaptive microbial survival (tailing phenomenon) occurs when samples are treated in high turbidity solutions using continuous UV sources, whereas tailing did not occur when similar samples were treated with pulsed xenon lamp.

While current findings from the literature suggests that development of a pulse light approach appears promising, most of the studies to date have focused on food or water applications using a limited range of electro-physical or biological parameters, such as use of a single lamp discharge energy (J) or fluence (UV dose cm^{-2}) and/or employing a single distance from light source to target treatment area. These landmark *in vitro* and *in vivo* PL

studies have been recently reviewed for efficacy in terms of inactivating food-related spoilage organisms and potential microbial pathogens (Elmnasser *et al.* 2007; Gómez-López *et al.* 2007), and include studies carried out using lamp discharge energies of 3 J (MacGregor *et al.* 1998; Rowan *et al.* 1999), 7 J cm^{-2} (Marquenie *et al.* 2003 and Gómez-López *et al.* 2005), 0·99 J cm^{-2} (Krishmanmurthy *et al.* 2004, 0·7 J cm^{-2} (Takeshita *et al.* 2003) and 1 J cm^{-2} (Wekhof *et al.* 2001). These studies demonstrated that factors such as number of light pulses applied, lamp discharge intensity, distance from lamp to treatment surfaces, shading, microbial species, age and density affected the efficacy of PL decontamination performances. To the best of our knowledge, no published study to date has investigated the *in vitro* decontamination efficacy of varying critical electro-physical parameters and biological conditions on PL-treated bacteria that were originally isolated from patients in health care environment.

Despite advances highlighted earlier, more extensive basic research is required to understand comprehensively how PL affects clinically relevant bacteria with view to maximizing the potential of this decontamination technique for application in various settings. This study therefore (i) includes a critical evaluation of the effect of varying key electrical parameters such as lamp discharge energy and pulse number on the sensitivity of a wide range of bacteria isolated from patients from clinical environment to PL treatments, (ii) the influence of bacterial population size, age and type on the level of decontamination by PL, (iii) the influence of bacterial production of light absorbing pigments and alginate slime on PL decontamination efficacy, (iv) the influence of antimicrobial drug resistance status on treated bacteria and presence of organic mater on sensitivity to PL treatments, (v) investigate how the relative position of the sample with respect to xenon lamp affects lethality of PL using different discharge energies, (vi) verifying the existence of the photoreactivation phenomenon and possible development of resistance in flashed clinically relevant bacteria, (vii) the heating of supporting agar medium by PL irradiation; emphasizing the implications of these findings for application of PL in health care settings.

Materials and methods

PL equipment

These studies used a bench-top pulsed power source (PUV-1; Samtech Ltd, Glasgow, UK), a low-pressure (60 kPa) xenon-filled flashlamp (Heraeus Noblelight XAP type NL4006 series constructed from a clear UV transparent quartz tube; Heraeus Noblelight Inc., Duluth, GA) that produced a high-intensity diverging beam of polychromatic PL as per the system arrangement described recently by Wang *et al.* (2005). The solid-state pulsed power source utilizes power-compression to transfer stored electrical energy to the xenon flashlamp in a short duration but with peak power. When the pulsed power source operates at 1 kV, as in this study, the energy of 20 J is stored in a 40 μF capacitor, and the energy is dissipated in the flashlamp within 30 μs, thereby producing a peak power of 1 MW. The PL has a broadband emission spectrum extending from the UV to the infrared region with a rich UV content and its intensity also depends on the level of the voltage applied as shown by the UV/visible lamp spectra in Fig. 1 as reported by the fabricant. The fabricant stated that the discharge tube represents a line source of limited length and as a consequence of this, the light formed an elliptical, equi-intensity profile over the sample plane eliminating shading effects. This resulted in a *c.* 30% variation in luminous intensity between the centre and the edge of the sample. The light emission spectrum was monitored using a four channel Ocean Optics SQ2000 fibre optic spectrometer (Ocean Optics, Dunedin, FL) (Fig. 1). The spectral resolution was 1·25 nm on each channel and the optical detector (Sony 1LX511; StellarNet Inc., Tampa, FL) had been enhanced to allow UV detection. The pulsed broadband emission spectra exhibit rich output in the UV-C region from 220 to 280 nm comprising three distinct peaks at 229, 247 and 260 nm. This xenon lamp is therefore capable of providing high-energy UV output using a small number of short-duration pulses. The light source has an automatic frequency-control function that allows it to operate at 1 pulse per second that was used throughout this study. Light exposure was homogenous as the xenon lamp (9·0 cm × 0·75 cm in length and width, respectively) was longer than the 8·5 cm diameter polystyrene Petri dishes used in the tests, which were placed directly below the lamp. For standard treatments (unless

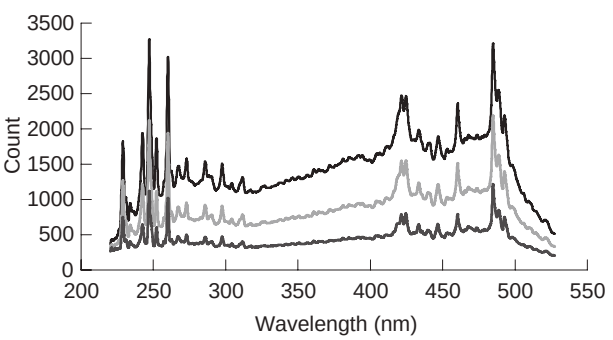

Figure 1 Spectral distribution of used xenon lamp at different applied voltages with equivalent discharge energies. (—) 1000 V or 20 J; (–) 800 V or 12·8 J and (—) 600 V or 7·2 J.
Source and permission: Samtech, Glasgow, UK.

otherwise noted), the light source was mounted at 8 cm above the treatment area that was designed specifically to accommodate a standard Petri dish.

PL inactivation procedures

In this study, standard treatments involved surface spread-inoculating 8·5 cm Petri dishes that were positioned at 8 cm distance from the light source (unless otherwise noted), and separately subjected to lamp discharge energies of 3·2, 5, 7·2, 9, 12·8 and 20 J. The number of pulses of light applied ranged from 0 (control) to 60 pulses. The influence of varying distance from the light source from the inoculated Petri dishes (range 8–20 cm) on inactivation efficacy was also investigated by rotating the treatment shelf in the PL system to the desired distance. The PL system was manually adjusted to deliver 1 pulse per second for all studies. The lethality of the PL process under varying experimental conditions was determined by treating predetermined numbers of test organisms that were inoculated on agar surfaces and by enumerating survivors post treatments (expressed in terms of $\log_{10}$ CFU cm^{-2}). Subtraction of the logarithm of the count after different combinations of pulsing, discharge energies and distances from light source, from the logarithm of the count before processing provided a measure of process lethality. As it is not appropriate to determine log-linear death rate kinetic data from PL-treated test bacteria as a function of time (as total duration of treatment comprises the pulse-pause sequence as well as the actual duration of pulsing), inactivation plots were measured following a modified first-order dependence formulae of Kühn *et al.* (2003): $(\log_{10}\ (N_P/N_0) = -k_p$, where k = rate constant). N_0 is the initial concentration of bacteria and N_p is the microbial concentration after applying a defined number of pulses at discharge energy (J). This rate constant k defines the sensitivity of a micro-organism to a defined PL treatment and is unique to each microbial species; the higher the k value the more sensitive the test strain to the treatment process. The former approach was employed to determine k values for PL-treated test bacteria, as individual fluence values (μW cm^{-2}) were not available for all combinations of lamp discharge energy and distance from light source . All experiments were carried out in triplicate using same culture to avoid sample variability.

Bacterial strains used and preparation

The species of test bacteria used in these experiments, their origin, clinical relevance and corresponding selective culture media are summarized in Table 1. Initially (and unless otherwise stated), emphasis was placed on using an extensive number of *Pseudomonas aeruginosa* test strains for investigating electrical and biological factors affecting PL decontamination efficacy with subsequent comparisons of tolerances to a range of other clinically significant Gram-positive and Gram-negative bacteria isolated from patients in health care environment. Test bacteria also comprised multiple antimicrobial drug–resistant (MDR) strains, methicillin-resistant *Staphylococcus aureus* (MRSA), vancomycin-resistant *Enterococcus* species (VRE) and *Klebsiella pneumoniae* ATCC 700721. Confirmation of MDR strain status was performed in a clinical laboratory using recommended disc diffusion susceptibility testing as per standard procedures (Clinical and Laboratory Standards Institute 2008). *Staphylococcus aureus* D3187 was shown to be resistant to erythromycin, cefoxitin 30, fucidin, ofloxacin and oxacillin/flucloxacillin, while sensitive to chloramphenicol, linezolid and vancomycin. *Enterococcus faecium* J5616 and J5810 were resistant to amoxicillin/ampicillin and vancomycin, while sensitive to gentamicin, linezolid and quinupristin/dalfopristin. E-testing confirmed resistance to vancomycin for both *Ent. faecium* J5616 and J5810, where minimum inhibitory concentration was shown to be >256 μg ml^{-1}. *Klebsiella pneumoniae* ATCC 700721 was resistant to ampicillin, ticarcillin, trimethoprim–sulfamethoxazole and gentamicin, but was susceptible to amikacin, ciprofloxacin and imipenem. The vegetative form of *Bacillus cereus* were prepared as per methods described previously (Rowan *et al.* 1999). All test strains were maintained in Microbank storage vials (Cruinn Diagnostics, Dublin 12, Ireland) at −70°C. The identity of three randomly selected isolates of each bacterial pathogen was confirmed before and after experimental studies as per methods described by Barrow and Feltham (2003). Strains were stored at 4°C on agar slopes of tryptone soya agar supplemented with 0·6% yeast extract (TSYEA) (Oxoid, Basingstoke, UK) and monthly checked for purity and renewed. To prepare the test samples, bacterial test strains were streaked to purity from porous beads taken from Microbank vials, and an isolated colony then transferred to 50 ml tryptone soya broth supplemented with 0·6% yeast extract and cultivated with shaking at 125 oscillations per minute for 24 h at 37°C to reach early stationary phase. The optical density was then adjusted at 540 nm to 2·0 (*c.* 10^9 CFU ml^{-1}) by spectrophotometric (Model UV-120-02 instrument; Shimadzu Corp., Kyoto, Japan) determination using 0·1 mol l^{-1} phosphate buffered saline (PBS) (pH 7·2) (confirmed via aerobic plate count). Using the spread plate technique, 0·5 ml aliquots of the 24-h OD_{540}-adjusted cultures were then inoculated onto triplicate TSYEA agar plates. After drying for 1 h on the laboratory bench to avoid light attenuation because of PBS, plates were flashed and then incubated without further treatment at 37°C for 48 h. Care was taken to ensure that samples were centrally inoculated on each agar plate and were subsequently spread

Table 1 Origin, clinical significance and culture media of used test bacteria

Bacterium	Code	Source*		Clinical relevance†	Selective media (solid)‡
		Origin	Clinical site		
Gram-positive bacteria					
Enterococcus faecium	J952	NUIG	Yes	Bloodstream	ESA
	J5616	NUIG	Yes	VRE	ESA
	J5810	NUIG	Yes	VRE	ESA
Enterococcus faecalis	D46209	NUIG	Yes	Bloodstream	ESA
Enterobacter cloacae	04B3311	DIT	Yes	Bloodstream	VRBGA
Enterobacter sakazakii	8155	NCTC	No	Food poisoning	HESA
Staphylococcus aureus	25923	ATCC	No	None reported	BPA
	5624	NUIG	Yes	Bloodstream	BPA
	J2860	NUIG	Yes	Bloodstream	BPA
	D3187	NUIG	Yes	MRSA	BPA
Staphylococcus epidermidis	10221	NUIG	Yes	Bloodstream	CA
	03B2511	DIT	Yes	Device implant	CA
Bacillus cereus	11143	NCTC	No	Vomit	BCSA
	22728	LMG	No	Food poisoning	BCSA
Listeria monocytogenes	11994	NCTC	No	Meningitis	LSA
	9863	NCTC	No	Meningitis	LSA
Gram-negative bacteria					
Acinetobacter baumanii	D3953	NUIG	Yes	Bloodstream	MLAA
Escherichia coli	25922	ATCC	No	None reported	MacCA
	411	NUIG	Yes	–	MacCA
	02B1173	DIT	Yes	UTI	MacCA
Pseudomonas aeruginosa	5449	NUIG	Yes	–	KAA
	R5137	NUIG	Yes	Sputum	KAA
	R1460	NUIG	Yes	Sputum	KAA
	2605	NUIG	Yes	–	KAA
	2633	NUIG	Yes	Sputum	KAA
	02B7570	DIT	Yes	UTI	KAA
	2502	NUIG	Yes	–	KAA
	02B710	DIT	Yes	Otitis media	KAA
	03B8474	DIT	Yes	–	KAA
	03B6908	DIT	Yes	–	KAA
	03B3922	DIT	Yes	Bloodstream	KAA
	04B2325	DIT	Yes	Sputum	KAA
	03B3694	DIT	Yes	–	KAA
	03B3845	DIT	Yes	Bloodstream	KAA
	27853	ATCC	No	None reported	KAA
Klebsiella pneumoniae	04B4415	DIT	Yes	Liver abscess	SCAI
	700721	ATCC	Yes	Sputum (MDR)	SCAI
Proteus mirabilis	02B1121	DIT	Yes	UTI	TMSA

–, not known.

*Code for cultures used: ATCC, American Type Culture Collection, Rockville, MD, USA; NCTC, National Collection of Type Cultures, Colindale, London, UK; LGM, Laboratorium Microbiologie, Universiteit Gent, Belgium; NUIG, National University of Ireland Galway, Department of Bacteriology, Ireland; DIT, Dublin Institute of Technology, Kevin Street, Dublin, Ireland.

†Clinical codes: VRE, vacomycin-resistant enterococcus; MRSA, methicillin-resistant *Staph. aureus*; UTI, urinary tract infection; MDR, multiple drug resistant.

‡Selective media codes and sources: ESA, enterococcus selective agar (SIFIN, Berlin, Germany); VRBGA, violet red bile glucose agar (Oxoid, Hampshire, UK); BPA, Baird Parker agar (Oxoid); MLAA, modified Leeds *Acinetobacter* agar (Oxoid); MacCA, MacConkey agar (Oxoid); BCSA, *B. cereus* selective agar (Oxoid); LSA, *Listeria selective* agar (Oxoid); SCAI, Simmons citrate agar with 1% (w/v) inositol (Difco); TMSA, Thayer–Martin selective agar (Difco); HESA, hi-crome *Enterobacter sakazaki* agar (Biochemika); CA, Chapman agar (Merck).

up to a distance of *c.* 0·5 cm from the perimeter of the polystyrene Petri dish in or to minimize or eliminate any shading effects. The latter procedure was adopted as it also is recognized that polystyrene absorbs considerably in the UV range. 15 ± 0·1 ml of molten agar was aseptically transferred by pipette to Petri dishes thus maintaining

standardized depth of agar for all studies. After incubation, separate colonies were enumerated and survivors were expressed in terms of $\log_{10}$ CFU cm^{-2}. Samples were also similarly spread inoculated on selective agar media for each respective test bacteria to investigate the influence of antimicrobial agents and/or dye present in selective agars on survival of PL-treated samples (Table 1). The limit of detection was one colony. Typical colonies of each test strain were randomly selected from respective agar plates after 24 and 48 h at 37°C with the highest dilution, and were confirmed by use of appropriate physiological and biochemical tests as described earlier.

Influence of population size and age on decontamination efficacy

To determine the influence of bacterial population size on the decontamination efficacy of PL, several agar media in Petri dishes were inoculated with 0·5 ml aliquots of the tenfold dilution of 24 h OD_{540} adjusted culture on TSYEA plates to give initial cell populations of *c.* 3, 5, 7 and 9 $\log_{10}$ CFU cm^{-2}. Plates were removed from the PL treatment chamber after predetermined number of flashes and survivors were enumerated by means of the above plating method. To determine the influence of population age on sensitivity of test strains to PL treatments, cultures were grown for 16 h (late exponential) and the OD was spectrophotometrically adjusted to *c.* 2·0 at 540 nm giving an initial cell population of *c.* 9 $\log_{10}$ CFU ml^{-1} (confirmed by plate count). Plates were then inoculated, PL treated and survivors enumerated as per method described earlier.

Media heating

Heating of the surface of agar plates inoculated with test bacteria was investigated using thermal imaging (IRI 4010; InfraRed Integrated Systems Ltd, Northampton, UK) as per modified method of Nugent and Higginbotham (2007). Plates were positioned 8 cm from light source and were flashed with 60, 45 and 20 pulses of 3·2, 12·8 and 20 J, respectively. An image was taken of the treated plates immediately post treatment and examined for thermal data using relevant software (IRISYS 4000 Series Imager, ver. 1.0.0.14; Infra Red Integrated Systems Ltd, Northampton, UK). Each data point represents a mean value of 12 randomly selected points over three replicate treatments.

Influence of photoreactivation on decontamination efficacy

This experiment was designed to investigate the effect of sunlight on the reactivation of damaged bacteria under typical real-life conditions as per method described by Gómez-López *et al.* (2005) with modifications. To test the possibility that photoreactivation occurs, agar plates were inoculated with test bacteria and were exposed to PL treatments according to standard method and then subjected to the following. The first three plates were immediately wrapped in aluminium foil post treatment; the other three similarly treated plates were exposed to direct sunlight by placement on laboratory bench illuminated by sunlight for 4 h. The plates were incubated for 48 h at 37°C as described earlier and survivors enumerated (expressed as $\log_{10}$ CFU ml^{-2}). The experiment was conducted in triplicate.

Determination of alginate levels from *Pseudomonas aeruginosa* test strains

The purpose of this experiment is to investigate whether production of mucoid (or slime) by *Ps. aeruginosa*, which is directly attributed to synthesis of exopolysaccharide alginate, confers resistance to PL exposure. Fifteen strains of *Ps. aeruginosa* comprising seven mucoid and eight nonmucoid strains as noted in Table 1 were grown on MacConkey agar supplemented with 5% (v/v) glycerol and *Ps. aeruginosa* chromogenic agar (bioMérieux, La Balme-les-Grottes, France) at 37°C and visually checked thereafter for mucoid colony development after 24 and 48 h incubation as recommended by Laine *et al.* (2009) (Table 2). Isolated colonies of mucoid strains (and nonmucoid control strain ATCC 27853) were then separately grown with shaking at 150 rev min^{-1} for 20 h at 37°C in 50 ml of chemically defined alginate promoting medium of Terry *et al.* (1991) that was adjusted to pH 7 before media sterilization. To confirm alginate production in culture suspensions for PL studies, cells were pelleted after incubation by centrifugation at 10 000 rev min^{-1} for 10 min at 4°C. Thereafter, the culture supernatant was precipitated using an equal volume of 2% (w/v) cetylpyridinium chloride (Sigma) followed by centrifugation at 10 000 rev min^{-1} for 10 min at 4°C (Knutson and Jeans 1968). The alginate pellet was resuspended in 5 ml of 1 mol l^{-1} NaCl and precipitated with 5 ml of 2-propanol and centrifuged at 10 000 rev min^{-1} for 10 min at 4°C. The final alginate pellet was resuspended in 500–4000 μl PBS depending on the quantity of alginate recovered. The amount of alginate was determined using a borate/carbazole method for which sodium alginate (Sigma) was used to create a standard curve. A 30 μl solution of purified alginate was mixed with 1·0 ml borate/sulfuric acid reagent (10 mmol l^{-1} H_2BO_2 in concentrated H_2SO_4) and 30 μl carbazole reagent (Sigma) [0·1% (v/v) in ethanol] was added. The mixture was heated to 55°C for 30 min and

Table 2 Comparison of the relationship between pyocyanin and alginate slime and *in vitro* inactivation of *Pseudomonas aeruginosa* strains treated at 8 cm distance from light source with discharge energy of 7·2 J

Test strain	Pyocynanin (μg 5 ml^{-1})	Alginate slime	Population reduction* Pulse number 5	10	15	20	Inactivation rate† at 7·2 J *k* value	R^2
5449	–	–	3·4 ± 0·1	6·8 ± 0·3	7·2 ± 0·4	7·2 ± 0·1	0·64 ± 0·04D	0·99
R1460	–	–	2·4 ± 0·1	5·5 ± 0·2	5·6 ± 0·4	6·4 ± 0·4	0·54 ± 0·02B	0·97
R5137	–	+	1·4 ± 0·1	4·1 ± 0·2	5·8 ± 0·3	6·7 ± 0·5	0·41 ± 0·03A	0·99
2605	8·3 ± 0·3	+	2·0 ± 0·1	4·2 ± 0·2	5·9 ± 0·3	6·3 ± 0·2	0·37 ± 0·01A	0·99
2633	–	+	1·9 ± 0·1	4·8 ± 0·1	5·4 ± 0·4	6·1 ± 0·3	0·42 ± 0·03A	0·96
02B7570	2·9 ± 1·1	+	1·5 ± 0·1	4·0 ± 0·2	5·9 ± 0·2	6·7 ± 0·5	0·41 ± 0·03A	0·99
02B710	12·2 ± 0·2	+	2·0 ± 0·1	4·4 ± 0·2	5·8 ± 0·3	6·8 ± 0·4	0·39 ± 0·02A	0·99
03B8474	3·7 ± 1·1	–	2·5 ± 0·2	5·5 ± 0·3	5·7 ± 0·4	6·5 ± 0·5	0·54 ± 0·01B	0·98
03B6908	4·6 ± 1·0	–	3·6 ± 0·1	7·0 ± 0·2	7·2 ± 0·2	7·2 ± 0·3	0·67 ± 0·02D	0·99
03B3694	2·4 ± 0·9	–	3·5 ± 0·2	6·9 ± 0·1	7·1 ± 0·3	7·2 ± 0·1	0·64 ± 0·02D	0·96
03B3922	4·3 ± 0·3	–	3·0 ± 0·1	5·6 ± 0·2	6·2 ± 0·2	6·4 ± 0·3	0·58 ± 0·02C	0·98
04B2325	–	+	3·8 ± 0·2	6·0 ± 0·2	6·9 ± 0·4	7·0 ± 0·3	0·56 ± 0·03C	0·98
2508	–	+	3·3 ± 0·2	6·3 ± 0·3	6·5 ± 0·1	7·0 ± 0·4	0·61 ± 0·03C	0·98
27853	6·5 ± 0·5	–	3·4 ± 0·1	6·3 ± 0·2	6·6 ± 0·4	6·9 ± 0·3	0·61 ± 0·02C	0·98
03B3845	2·2 ± 0·3	–	3·3 ± 0·2	6·3 ± 0·1	6·6 ± 0·2	7·0 ± 0·2	0·61 ± 0·02C	0·98

(–), Not detected; (+) detected.

*Population reduction, expressed in $\log_{10}$ CFU cm^{-2}, achieved after pulsing at 7·2 J where initial population was inoculated on agar surfaces at *c.* 9 $\log_{10}$ CFU cm^{-2}.

†Reduction rate constant (*k*) is the mean rate (±SD) of log cell reductions per pulse, which is measure of inactivation of test strain per pulse. The higher the *k* value the more sensitive the strain to pulsed light treatments. R^2 is correlation co-efficient from linear regression data. Values with different capitalized letter in same column are significantly different at $P \leq 0{\cdot}05$ level.

the alginate concentration was determined spectrophotometrically at 500 nm.

Determination of pyocyanin levels from *Pseudomonas aeruginosa* test strains

The relationship between production of the light absorbing pigment pyocyanin by some *Ps. aeruginosa* strains and sensitivity to PL irradiation was examined. The method of Essar *et al.* (1990) was followed with slight modifications. The pyocyanin assay is based on the absorbance of pyocyanin at 520 nm in acidic solution. The strains were grown with shaking (125 rev min^{-1}) at 37°C for 24 h in 50 ml Cetrimide broth medium (Watman, Kent, UK) that is similar in formulation to King's A medium and known to promote pyocyanin production in *Ps. aeruginosa* (Brown and Lowbury 1965). A 5 ml aliquot was transferred to a sterile universal and centrifuged at 4000 rev min^{-1} for 10 min at 4°C. The supernatant was filtered through a 0·2-μm filter (Millipore), and pyocyanin was subsequently extracted from the filtered supernatant with 3 ml of chloroform. The solution was vortexed to mix before centrifugation at 4000 rev min^{-1} for 10 min at 4°C. The upper layer was carefully removed using a micropipette and discarded. The pyocyanin, if present in the bottom layer, was subsequently transferred to a fresh universal and 1 ml of 0·2 mol l^{-1} HCl was added. The solution was vortexed and centrifuged as described earlier. The resulting pink-coloured upper layer was carefully extracted and transferred to a cuvette and the absorbance was determined at A_{520}. Micrograms quantities were calculated by multiplying the absorbance at 520 nm by 17·072 as per method of Kurachi (1958).

Statistical analyses

Analysis of variance, balanced model (Minitab software release 13; Minitab Inc., State College, PA, USA) was used to compare the effects of relationship of independent variables on light treatments.

Results

Sensitivity of test bacteria to PL treatments

The sensitivity of all clinical isolates of *Ps. aeruginosa* to PL treatments was initially investigated at lamp discharge energy of 7·2 J and is summarized in Table 2. Based on PL inactivation rates shown in Table 2, all test *Ps. aeruginosa* strains were reduced by *c.* 7 $\log_{10}$ CFU cm^{-2} within 20 pulses at 7·2 J. There were marked variations in sensitivity to treatments amongst strains of *Ps. aeruginosa*.

Table 3 Comparison of inactivation rate constant *k* values obtained for test bacteria using increasing lamp discharge energies ranging from 3·2 to 20 J at 8 cm distance from light source to sample

Test bacterium	Code	Reduction rate (*k*) at different discharge energies* (J)			
		3·4	7·2	12·8	20
Gram-positive bacteria					
Enterococcus faecium	J952	0·07 ± 0·03A	0·24 ± 0·02C	0·55 ± 0·02H	0·93 ± 0·05J
	J5616†	0·06 ± 0·02A	0·24 ± 0·01C	0·50 ± 0·04H	0·95 ± 0·04J
	J5810†	0·10 ± 0·01A	0·29 ± 0·04D	0·61 ± 0·03G	0·98 ± 0·03J
Enterococcus faecalis	D46209	0·09 ± 0·01A	0·29 ± 0·02D	0·65 ± 0·02G	1·07 ± 0·03K
Enterobacter cloacae	04B3311	0·16 ± 0·03B	0·39 ± 0·03E	0·89 ± 0·04J	1·21 ± 0·02L
Enterobacter sakazakii	8155	0·17 ± 0·04B	0·47 ± 0·02F	1·11 ± 0·03K	1·33 ± 0·03M
Staphylococcus aureus	25923	0·13 ± 0·01B	0·38 ± 0·03E	0·90 ± 0·02J	1·29 ± 0·03M
	5624	0·16 ± 0·02B	0·49 ± 0·01F	1·07 ± 0·04K	1·42 ± 0·04N
	J2860	0·15 ± 0·03B	0·37 ± 0·04E	0·81 ± 0·02I	1·42 ± 0·05N
	D3187†	0·14 ± 0·02B	0·40 ± 0·03E	1·12 ± 0·05K	1·45 ± 0·05N
Staphylococcus epidermidis	10221	0·13 ± 0·01B	0·37 ± 0·03E	0·90 ± 0·03J	1·33 ± 0·02M
	03B2511	0·15 ± 0·02B	0·40 ± 0·02E	0·88 ± 0·05J	1·29 ± 0·03M
Bacillus cereus	11143	0·09 ± 0·01A	0·24 ± 0·02C	0·56 ± 0·02H	1·06 ± 0·03K
	22728	0·14 ± 0·02B	0·25 ± 0·02C	0·57 ± 0·04H	1·08 ± 0·03K
Listeria monocytogenes	11994	0·16 ± 0·03B	0·39 ± 0·02E	0·92 ± 0·03J	1·41 ± 0·02N
	9863	0·18 ± 0·03B	0·40 ± 0·03E	0·90 ± 0·04J	1·33 ± 0·03M
Gram-negative bacteria					
Acinetobacter baumanii	D3953	0·15 ± 0·02B	0·35 ± 0·02E	0·77 ± 0·02I	1·19 ± 0·04L
Escherichia coli	25922	0·19 ± 0·02B	0·52 ± 0·04F	1·41 ± 0·03N	1·61 ± 0·05O
	411	0·17 ± 0·03B	0·44 ± 0·03E	0·93 ± 0·04J	1·35 ± 0·04M
	02B1173	0·24 ± 0·02C	0·51 ± 0·03F	1·31 ± 0·02M	1·65 ± 0·03O
Pseudomonas aeruginosa	02B710	0·14 ± 0·02B	0·39 ± 0·02E	0·86 ± 0·04J	1·36 ± 0·04K
	2633	0·16 ± 0·03B	0·42 ± 0·03E	0·91 ± 0·02J	1·33 ± 0·03K
	2605	0·16 ± 0·01B	0·37 ± 0·01E	1·10 ± 0·03K	1·35 ± 0·03K
	R5137	0·23 ± 0·02C	0·67 ± 0·02G	1·49 ± 0·04N	1·59 ± 0·02O
Klebsiella pneumoniae	04B4415	0·24 ± 0·01C	0·53 ± 0·03F	0·88 ± 0·02J	1·36 ± 0·03M
	700721†	0·23 ± 0·01C	0·50 ± 0·02F	1·29 ± 0·2M	1·42 ± 0·04N
Proteus mirabilis	02B1121	0·25 ± 0·03C	0·67 ± 0·02G	1·31 ± 0·3M	1·61 ± 0·03O

*Inactivation kinetic *k* data. Values with different capitalized letter are significantly different at $P \leq 0{\cdot}05$.
†Designates strains that harbour genes for multiple resistance to antibiotics.

A clear pattern was observed regarding strains expressing mucoid or slime phenotype as these in general were shown to be less sensitive to treatments at 7·2 J. The sensitivity of a select number of mucoid and nonmucoid *Ps. aeruginosa* strains was then compared to other clinically relevant bacteria over an extended range of energy densities (Table 3). A clear significant pattern was observed where more rapid reductions in predetermined populations of all test bacteria occurred with increased levels of pulsing and with use of higher discharge energies. For instance, rapid reductions in all test organisms (*c.* 7 log orders) occurred in ≤10 pulses at 20 J compared to a requirement to use up to 45 pulses to attain same level of inactivation for these test pathogens at the lower 3·2 J. This overall trend of greater susceptibility to PL with use of increasing discharge energies for test bacteria is clearly shown for *Ps. aeruginosa* 2605 in Fig. 2, which illustrates determination of the death rate constant *k* values for

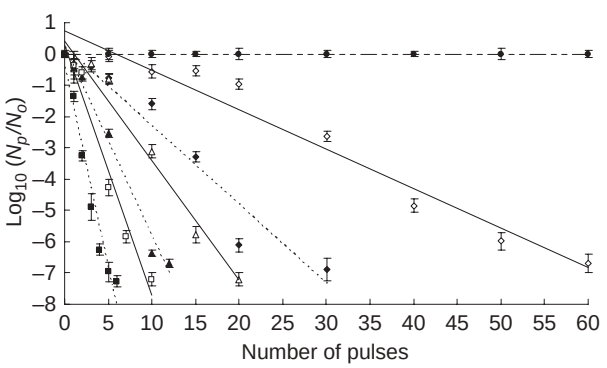

Figure 2 Determination of inactivation rate constant *k* value for *Staphylococcus aureus* D3187 (methicillin-resistant *Staph. aureus*) after pulsing at 8 cm using decreasing lamp discharge energies: (●) untreated control; (■) 20 J; (□) 12·8 J; (▲) 9 J; (△) 7·2 J; (◆) 5 J and (◇) 3·2 J.

linearized inactivation data where the slope (or k value) provides a measure of the log reduction in cell population ($\log_{10}$ CFU cm^{-2}) per pulse. While k value determinations where established for all test strains in a similar manner, it is neither practical nor beneficial to illustrate all linearized data plots for each strain in this study. However, the lower the k value the greater the resistance to the applied PL treatment, and this means of evaluating *in vitro* inactivation performance was used to compare sensitivities of all clinical bacteria under similar studies using increasing discharge energies at 8 cm from light source (Table 3).

Staphylococci and enterococci were significantly less sensitive to lethal action of PUV at all discharge energies tested compared to other Gram-positive and Gram-negative bacteria under study. The level of resistance, expressed in terms of k value determinations, of test bacteria to PL treatments differed significantly ($P < 0{\cdot}05$) and are listed in order of decreasing resistance: *Enterococcus* spp., *Staphylococcus* spp., *B. cereus*, *Enterobacter* spp., *Listeria monocytogenes*, *Acinetobacter baumanii*, *Ps. aeruginosa*, *Escherichia coli*, *Kl. pneumoniae* and *Proteus mirabilis* (Table 3). In particular, there was no significant difference in inactivation levels amongst all *Ps. aeruginosa* test strains at the uppermost test discharge energy of 20 J, irrespective of production of slime or pigments ($P < 0{\cdot}05$). The harbouring of genes encoding multiple resistances to antibiotics in certain test bacteria, such MRSA, VRE and MDR-*Kl. pneumonia*e, did not confer greater resistance to pulse light treatment when compared to similar strains of the same species or different species of test bacteria (Table 3). However, studies were not carried out to determine whether these microbial antibiotic resistance genes were plasmid or chromosomally carried. The influence of the relative position between test sample and light source on decontamination efficacy was also investigated. A clear pattern was observed where Gram-positive and Gram-negative bacteria treated at a shorter distance from treatment surface to the PL light source were more sensitive to this decontamination approach (Fig. 3). An even distribution of microbial killing was produced on the PL-treated plates as observed by the random locations of survivor colonies on agar surfaces, indicating that the central positioning of the agar plates directly under the light source coupled with the spread plate technique carried out in this study helped to minimize any possible shading effects.

Influence of microbial population size and age on decontamination efficacy

Test bacteria may react differently to PL exposure depending on population size and stage in growth cycle.

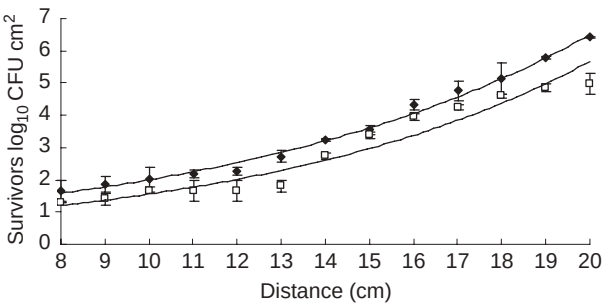

Figure 3 Effect of the distance between the lamp source and the surface of spread-inoculated Petri dishes on the inactivation of *Staphylococcus aureus* D3187 (◆) and *Escherichia coli* 411 (□) at lamp discharge energy of 12·8 J. Bars indicate ±SD. N and N_o: number of test bacteria, respectively, before and after flashing. Solid line is the trend line.

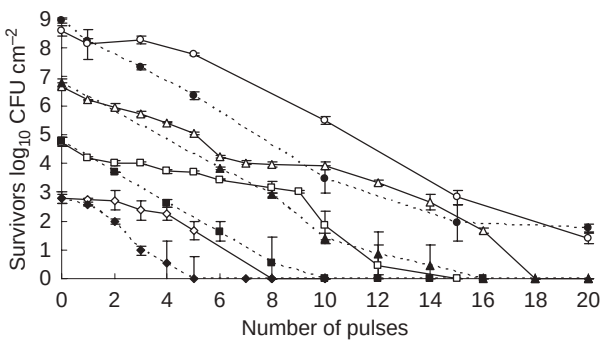

Figure 4 Effect of initial population size (expressed in $\log_{10}$ CFU cm^{-2}) and pulse number on the inactivation of *Staphylococcus aureus* D3127 and *Pseudomonas aeruginosa* 2605 using lamp discharge energy of 7·2 J at 8 cm distance from xenon light source. Bars indicate ±SD. Initial count for *Ps. aeruginosa* 2605, (◇) 3 $\log_{10}$; (□) 5 $\log_{10}$; (△) 7 $\log_{10}$ and (○) 9 $\log_{10}$. Initial count for *Staph. aureus* D3127, (◆) 3 $\log_{10}$; (■) 5 $\log_{10}$; (▲) 7 $\log_{10}$ and (●) 9 $\log_{10}$.

Figure 4 shows changes in level of inactivation as a function of the number of *Staph. aureus* D3127 (MRSA) and *Ps. aeruginosa* cells present on the surface of agar before treatment. A clear pattern emerged where the lower the initial starting cell population treated, the faster the reduction in numbers observed. PL-treated *Staph. aureus* cells produced an initial shoulder effect in sigmoidal-shaped kinetic inactivation plots. With the exception of samples treated at the lamp lowest discharge of 3·2 J, this shoulder effect was absent from similarly treated *Ps. aeruginosa* cells that exhibited linear inactivation data during early to mid ranges of treatment using discharge energies ≥5 J. The presence of this shoulder effect was a pattern that was observed for all tested Gram-positive bacteria, whereas all Gram negatives were devoid of this shoulder phenomenon. It is important to note that death

rate kinetic data was determined from Gram-positive bacteria using log-linear portion of curve avoiding use of the shoulder section. Figure 4 also illustrated a distinct tailing or tolerance effect in the inactivation data for both *Staph. aureus* and *Ps. aeruginosa*, and this is a clear pattern that emerged for all test bacteria where initial cell population inoculated on plates was *c.* 9 $\log_{10}$ CFU cm^{-2}. The effect of microbial population size had a significant effect on the sensitivity of slime and pigment producers of *Ps. aeruginosa* to PL treatments. At starting cell populations of $\leq 10^5$ $\log_{10}$ CFU cm^{-2}, all strains were equally sensitive to PL, but at high starting cell populations, slime and pigment producers were more tolerant to PL (Fig. 4). Figure 5 shows that *Ps. aeruginosa* was more sensitive to lethal action of PL treatments during late exponential (16 h) phase of growth compared to similarly treated samples that had been grown and treated in their stationary (24 h) phase when exposed to combinations of low number of pulses using lower lamp discharge energies. No significant difference in inactivation data was observed between 16 and 24 h cultures exposed to full treatment regimes of flashing at different range of discharge energies used in this study (data not shown).

Influence of selective antimicrobial composition of agar, soiling of agar and photoreactivation on PUV decontamination efficacy

Antimicrobial or selective nature of agar

To test the possibility that the presence of antibiotics and dyes present in selective agar may impact negatively on the survival of subpopulations of PL-treated test bacteria, samples were separately inoculated on both nonselective TSYEA and selective agar (listed in Table 1) and similarly pulsed at 7·2 J at 8 cm from light source and thereafter enumerated after 48 h incubation at 37°C. A clear pattern emerged where presence of selective agents in agar did not significantly affect levels of survivors compared to similarly treated samples grown and enumerated on TSYEA plates. For example, Fig. 6 shows similar inactivation kinetic data for *E. coli* 411 initially inoculated separately on selective MacConkey agar and nonselective TSYEA, flashed at 7·2 J at 8 cm distance from light source, and survivors enumerated after 48 h. Data are not presented for the other clinical bacteria treated and subsequently enumerated on respective selective agar (as per Table 1) and on nonselective agar (TSYEA), as there was no significant difference observed for survivor counts using different plating media ($P > 0{\cdot}05$).

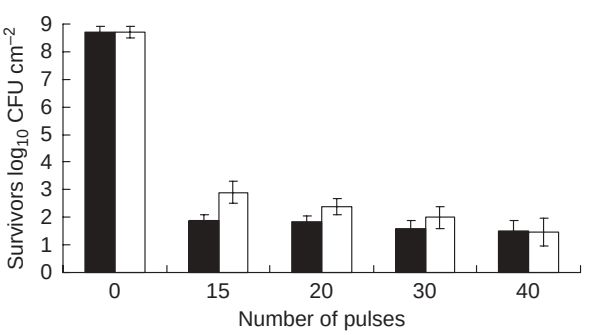

Figure 5 Effect of population age on sensitivity of *Escherichia coli* 411 to lethal action of pulsed light at 7·2 J at 8 cm from light sources. (■) 16 h and (□) 24 h cultures. Bars indicate ±SD.

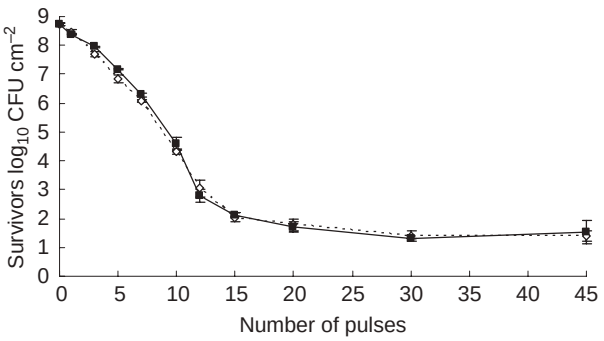

Figure 6 Survivor data (expressed in terms of $\log_{10}$ CFU cm^{-2}) for *Escherichia coli* 411 inoculated separately on selective MacConkey agar and nonselective tryptone soya agar supplemented with 0·6% yeast extract (TSYEA) plates and flashed at 7·2 J at 8 cm from light source. (■) MacConkey count and (□) TSYEA count. Bars indicate ±SD.

Artificial soiling of agar surface

To test the possibility that presence of organic matter artificially seeded on agar surfaces may impact negatively of PL inactivation efficacy, test populations of bacteria were suspended in PBS solutions containing increasing concentrations (0% control, 5%, 10% and 20% v/v) of foetal calf serum (FCS) and were subjected to 50 pulses using the mid range discharge energy of 7·2 J. No significant difference in levels of inactivation was evident based on these agar surface seeding studies ($P = 0{\cdot}445$). However, a significant difference in PL efficacy was observed when similar suspensions of test organisms were treated in corresponding PBS–FCS solutions (separate 10 ml volumes treated in Petri dish) (Fig. 7). PL treatments reduced test populations by 7·2 ± 0·3 $\log_{10}$ CFU cm^{-2} (PBS control; $P = 0{\cdot}545$), 7·0 ± 0·3 $\log_{10}$ CFU cm^{-2} (5% FCS; $P = 0{\cdot}475$), 6·5 ± 0·2 $\log_{10}$ CFU cm^{-2} (10% FCS; $P = 0{\cdot}035$) and 3·6 ± 0·4 $\log_{10}$ CFU cm^{-2} (20% FCS; $P = 0{\cdot}001$). Figure 8 shows that there is a clear linear correlation in increased absorbance with increasing concentrations of FCS at wavelengths of known biocidal efficacy (254, 260, 265 and 270 nm).

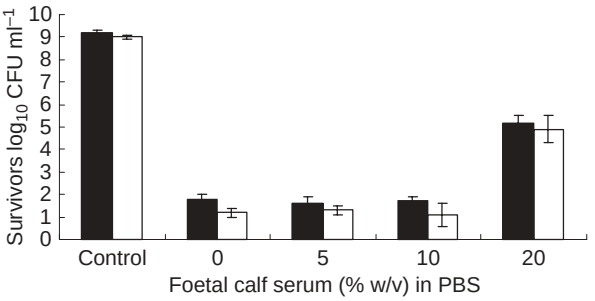

Figure 7 Effect of presence of organic matter on sensitivity of *Pseudomonas aeruginosa* 2605 (■) and *Staphylococcus aureus* D3127 (□) to pulsed light after 40 pulses using 7·2 J at 8 cm distance from light source.

Photoreactivation

To test the possibility that photoreactivation occurs, inoculated plates of *Ps. aeruginosa* were pulsed at 20, 7·2 and 3·2 J and then were exposed for 4 h of sunlight post treatment. Untreated and treated control plates (wrapped in aluminium foil for equivalent 4 h photoreactivation period) were incubated and enumerated post treatment. Some photoreactivation was evident after 15 and 45 pulses at the lower discharge energies of 3·2 and 7·2 J, respectively (Fig. 9). However, a clear pattern was demonstrated where no photoreactivation effect was evident after full flash treatment regimes at all discharge energies tested. No photoreactivation was evident after 5 and 10 pulses at 20 J for *Ps. aeruginosa* (Fig. 6).

Heating of agar surface during PUV treatments

Because of the presence of visible and infrared light (together with UV light) in the pulsed spectrum emitted by the xenon lamp, test samples and surrounding surface media can warm up during flashing. Significant change in surface media temperature can contribute in part to inactivation performance achieved by PUV system. Findings from this study showed that limiting pulse number to 60, 50, 40, 30 and 15 pulses at lamp discharge energies of 3·2, 5, 7·8, 12·2 and 20 J respectively did not significantly alter surface temperature beyond 4·2 ± 0·2°C. A distance of 8 cm between the light source and the treatment agar surface was used for these studies.

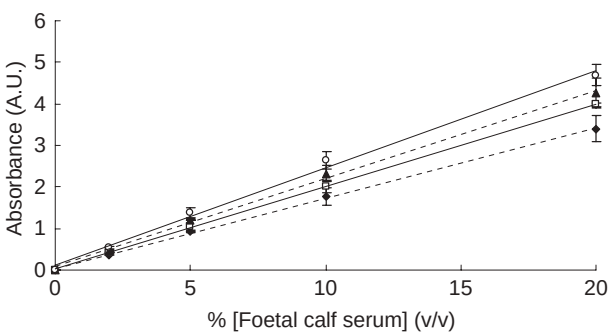

Figure 8 Best fit plots of absorbance *vs* increasing percentage of foetal calf serum (*v*/v). (◆) 254 nm; (□) 260 nm; (▲) 265 nm and (○) 270 nm. Bars indicate ±SD.

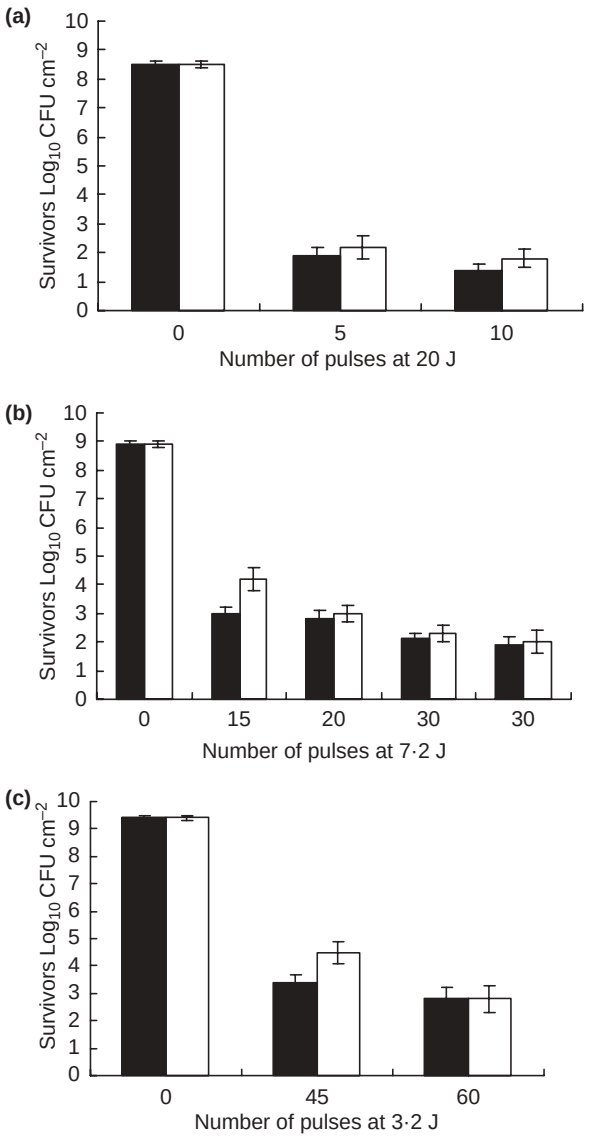

Figure 9 Effect of photoreactivation and repair for *Pseudomonas aeruginosa* 2605 treated at lamp discharge energies of (a) 20 J, (b) 7·2 J and (c) 3·2 J. Bars indicate ±SD. Reductions in populations expressed in $\log_{10}$ CFU cm^{-2} with (□) and without provision for conditions inductive to (■) photoreactivation.

Discussion

Results presented in this study showed that all clinically relevant bacteria tested were reduced by *c.* 7 $\log_{10}$ CFU cm^{-2} on artificially seeded agar surfaces by the lethal action of pulsed UV light. The inactivation rates achieved for all test bacteria was shown to be directly related to intensity of the lamp discharge energy, the number of pulses applied, the distance from the light source, microbial type and microbial population size and age studied. Greater variations in sensitivity of test bacteria to PL treatments was observed using combinations of low discharge energies and reduced pulse number. For instance, ≤40 and 30 pulses were required to reduce predetermined populations by *c.* 7 $\log_{10}$ CFU cm^{-2} using 3·2–5 J, respectively, at 8 cm from light source, compared to use of ≤10 pulses to achieve similar levels of inactivation for samples treated at 20 J. Gram-positive bacteria were shown to be more resistant than Gram negatives, a similar trend was reported by Anderson *et al.* (2000). All Gram positives tested exhibited a characteristic shoulder effect in their sigmoid shaped inactivation kinetic data. However, the latter shoulder feature was absent from similarly PL-treated Gram negatives. Other researchers reported that the shape of inactivation curves for microbial inactivation by CW UV light and by PL was sigmoid in shape, but did not report specific differences in the shape of death rate kinetic data as a function of Gram reaction. Previous researchers have reported that the initial plateau in death rate plots is because of injury phase and once the maximum amount of injury has been surpassed, minimal additional UV exposure would be lethal for micro-organisms with commensurate rapid reductions in survivor numbers (Gómez-López *et al.* 2007). The latter section of the death rate plot has been characterized by a tailing phase for which there are several possible explanations: lack of homogenous population, multi-hit killing phenomena, varying abilities of cells to repair DNA damage, shading effect that may have been produced by the edge of the Petri dishes used in some experiments (Yaun *et al.* 2003). Use of large initial cell populations inoculated on agar plates will provide a shading protection effect because of heterogeneous sample seeding, where cells in the underneath layers are not illuminated because of overcrowding effect. However, in this present study, tailing was not evident for lower cell population sizes, particularly when studying inactivation plots of treated Gram-negative bacteria. Complete inactivation of micro-organisms and absence of tailing have also been reported (Otaki *et al.* 2003; Wang *et al.* 2005); however, Gómez-López *et al.* (2007) noted in their review of these findings that the effect on the detection limit of the enumeration method should have been better assessed. The latter authors also cautioned about the potential for overestimation of the lethality because of the possibility that two or more survivors situated very close to each other on agar surfaces can form just one colony, and therefore be enumerated as one survivor. Bacterial strains harbouring multiple resistance to antimicrobial agents were not more tolerant to PL irradiation compared to similar strains of the same bacteria species or different types of test bacteria. This is a promising finding as these particular MDR pathogens have been reported to exhibit cross-resistance to chemical biocides and to other antibiotics (Lambert *et al.* 2001; Randall *et al.* 2001; Gebel *et al.* 2002).

Pseudomonas aeruginosa is notorious for its resistance to antibiotics primarily due to the permeability barrier afforded by its Gram-negative outer membrane. *Pseudomonas aeruginosa* strains produce two types of soluble pigments, the fluorescent pyoverdin and the blue green pigment pyocyanin (often referred to as 'blue pus') that is a characteristic of suppurative infections caused by this pathogen. Previous researchers have demonstrated that pyocyanin, a water soluble pigment, helps to protect *Ps. aeruginosa* strains from UV-C exposure because of their capacity to absorb wavelengths of light in this germicidal region (Kerr *et al.* 1999). This present study showed that production of pyocyanin by certain *Ps. aeruginosa* test strains provided some protection against germicidal action of PL exposure where low levels of flash discharge energies (3·2–5 J) were used to treat initial cell populations of ≤10^7 CFU cm^{-2}. The ability of pigments and/or slime to afford protection against PL exposure was observed to be a direct function of cell population, lamp discharge energy and number of pulses applied. It is possible that only beyond a significant cell population threshold does *Ps. aeruginosa* produce protective pigmentation, which is tightly regulated via complex quorum sensing and inter-cell signalling. A recent *in vivo* study carried out by Feuilloley *et al.* (2006) reported that a single light pulse of a dose of 1 J cm^{-2} is sufficient to entirely reduce a 6 log CFU ml^{-1} population of *Ps. aeruginosa* suspended in ampoules of solution for injection.

Mucoid strains of *Ps. aeruginosa* produce an exopolysaccharide (alginate) slime that forms the matrix for *Pseudomonas* biofilm, which anchors this bacterium to various contact environments. In medical situations, the exopolysaccharide protects the pathogen from the human host immune defences. A clear pattern emerged where mucoid-producing test strains of *Ps. aeruginosa* at high population densities (*c.* 10^9 CFU cm^{-2}) may exhibit increased tolerance perhaps related to additional shading via formation of complex slime. However, there was no significant evidence of a protective effect from pigments and/or slime in *Ps. aeruginosa* test strains when discharge energies of ≥12·8 J were used at a distance of 8 cm from

inoculated agar surfaces. The contributing role of functional housekeeping enzymes involved in either mopping up toxic free radicals produced during PUV irradiation and/or chaperoning (protecting) critical internal cell constituents cannot be discounted. Anderson *et al.* (2000) demonstrated that the darker pigmented fungal spores of *Aspergillus niger* were more resistant than spores of *Fusarium culmorum* due perhaps to the pigment of the former absorbing more in the UV-C region, thus protecting *Aspergillus* in part from UV damage. However, the authors did not corroborate these assumptions by obtaining absorbance data for pigments extracted from spores. In contrast, Gómez-López *et al.* (2005) did not observe any sensitivity pattern among different groups of bacteria, yeast and moulds to intense pulse light treatments. However, *Ps. aeruginosa* was not included in their study.

The lethal effects of PL can be attributed to its rich broad-spectrum UV-C content, its short duration, high peak power, and its ability to regulate both the pulse duration and frequency output of the flash lamps, which plays a major role in microbial destruction. Despite advances in applied research for this nonthermal processing approach, findings from same of the effects of PUV are frequently explained using current knowledge from studies on the effect of continuous conventional UV irradiation. However, despite PUV containing a UV-C enriched component in its broad spectrum, the mechanistic underpinnings governing microbial inactivation are not equivalent for both approaches (Gómez-López *et al.* 2005). Considerable research has been performed to elucidate the different mechanisms underpinning microbial inactivation by PL, all of them emphasizing pivotal role of UV component of the pulsed spectrum along with intimating other minor photochemical and photothermal effects (Anderson *et al.* 2000; Wekhof *et al.* 2001; Takeshita *et al.* 2003; Wuytack *et al.* 2003; Wang *et al.* 2005). Gómez-López *et al.* (2007) astutely emphasized the duality or co-existence of both mechanisms, and that the relative importance of each one would depend on the fluence and target micro-organism. The germicidal effect of UV light on treated bacteria is mainly because of formation of pyrimidine dimers inhibiting formation of new DNA that ultimately derails the vital process of cell replication (called clonogenic death). Without sufficient repair mechanisms, such damage results in lethal irreversible mutations. Thus, the UV region is crucial to the decontamination efficiency of PL treatments. It has been confirmed that no microbial inactivation occurs if a filter is included to remove the UV wavelength region lower than 320 (Takeshita *et al.* 2003). Wang *et al.* (2005) also corroborated this finding, where they demonstrated that the filtered removal of broadband emission spectrum of light at wavelengths above 300 nm had no significant bearing on microbial inactivation performance of a pulsed xenon flashlamp. Maximum lethality to PL-treated *E. coli* occurred at around 270 nm. The latter corroborated earlier work of Wekhof (2000) who demonstrated that UV-C fluxes alone are sufficient for full inactivation using a flash lamp.

However, it is also important to note that the photothermal effect can occur and that intercellular heating may contribute significantly to overall germicidal efficacy of PL. Although the increase in surface temperature of the inoculated agar did not exceed 4·2 ± 0·2°C after full treatments in this present study, localized overheating of the internal cellular constituents cannot be dismissed. For example, Wekhof (2000) proposed that with a fluence exceeding 0·5 J cm^{-2}, the disinfection is achieved through rupture of the bacteria during their momentous overheating caused by absorption of all UV light from a flash lamp. Wekhof *et al.* (2001) later illustrated electron micrographs of deformed and ruptured PL-treated *A. niger* spores that provided evidence of the escape of overheated contents of these fungal spores. However, Takeshita *et al.* (2003) reported that the process of irreversible electropermeabilization of cell membrane induced by action of PL exposure cannot be ruled out, particularly as the yeast cell structure of CW UV light–treated cells was almost the same as that of nonexposed cells. It is likely that the mechanism of cellular killing is multi-targeted as this is also in line with relative inactivation of clinical bacteria plated on selective and nonselective agars in this study. This also corroborates findings of Wuytack *et al.* (2003) who concluded that pulsed white light inactivation should be regarding as a multi-hit process based on enumeration of treated *Salmonella* cells plated on selective and nonselective agar. This is in marked contrast to recovery and enumeration of microorganisms exposed to deleterious stress commonly associated with conventional decontamination approaches, such heating or use of chemical preservatives in food processing, where sublethal damage of treated cells occurs (Rowan *et al.* 1999; Yaqub *et al.* 2004).

It must also be stated that use of PL enriched in UV has operational limitations because of its potential detrimental effects on skin tissue and components of the eye. While such operational issues can be addressed, other research groups are alternatively exploring the potential of photodynamically inactivating bacterial pathogens using visible light at 400–420 nm (Ashkenazi *et al.* 2003; Ganz *et al.* 2005; Lukšiene 2005). The mechanism of cellular destruction attributed to photosensitization involves using visible light where blue wavelength component photoactivates endogenous porphyrins (photosensitizers) that accumulate within the bacterial cells in oxygen dependent process that ultimately kill the illuminated

cells. This porphyrin excitation leads to energy transfer and ultimately, the production of highly cytotoxic, oxygen-derived free-radical species (Wainwright 1998). While photosensitization is another milder technique that might be useful to decontaminate surfaces and air using light, a comparison of inactivation data reported previously by other researchers as a function of wavelength suggests that visible light inactivation of bacteria (Guffey and Wilborn 2006) is a significantly less efficient process than is ultraviolet light inactivation (Wang *et al.* 2005).

Acknowledgements

The authors thank the Health Research Board (Grant no. RP/2005/187) for the PhD scholarship of H. Farrell. We also greatly appreciate the technical assistance of V. Buckley (NUIG) with work pertaining to antimicrobial susceptibility testing of test strains.

References

Anderson, J.G., Rowan, N.J., MacGregor, S.J., Fouracre, R.A. and Farish, O. (2000) Inactivation of food-borne enteropathogenic bacteria and spoilage fungi using pulsed light. *IEEE Trans Plasma Sci* **28**, 83–88.

Ashkenazi, H., Malik, Z., Harth, Y. and Nitzan, Y. (2003) Eradication of *Propionibacterium* acnes by its endogenic porphyrins after irradiation with high intensity blue light. *FEMS Immunol Med Microbiol* **35**, 17–24.

Barrow, G.I. and Feltham, R.K.A. (2003) *Cowan and Steel's Manual for the Identification of Medical Bacteria*, 3rd edn. Cambridge, UK: Cambridge University Press.

Bintsis, T., Litopoulou-Tzanetaki, E. and Robinson, R.K. (2000) Existing and potential application of ultraviolet light in the food industry – a critical review. *J Sci Food Agric* **90**, 637–645.

Bolton, J.R. and Linden, K.G. (2003) Standardization of methods for fluence (UV dose) determination in bench-scale UV experiments. *J Environ Sci Eng* **129**, 209–215.

Brown, V.L. and Lowbury, E.J.L. (1965) Use of an improved cetrimide agar medium and culture methods for *Pseudomonas aeruginosa*. *J Clin Pathol* **18**, 752–756.

Clinical and Laboratory Standards Institute (2008) *Performance Standards for Antimicrobial Susceptibility Testing M100-S18, M2-A9 and M37-A3*. Wayne, PA: CLSI.

Dunn, J., Bushnell, A., Ott, T. and Clark, W. (1997) Pulsed white light food processing. *Cereal Foods World* **42**, 510–515.

Elmnasser, N., Guillou, S., Leroi, F., Orange, N., Bakhrouf, A. and Federighi, M. (2007) Pulsed-light system as a novel food decontamination technology: a review. *Can J Microbiol* **53**, 813–821.

Essar, D.W., Eberly, L., Hadero, A. and Crawford, I.P. (1990) Identification and characterization of genes for a second anthranilate synthase in *Pseudomonas aeruginosa*: interchangeability of the two anthranilate synthases and evolutionary implications. *J Bacteriol* **172**, 884–900.

Feuilloley, M.G.R., Bourdet, G. and Orange, N. (2006) Effect of white pulsed light on *Pseudomonas aeruginosa* culturability and its endotoxin when present in ampoules for injection. *Eur J Parenteral Pharm Sci* **11**, 37–43.

Ganz, R.A., Viveiros, J., Ahmad, A., Ahmadi, A., Khalil, A., Tolkoff, M.J., Nishioka, S. and Hamblin, M.R. (2005) *Helicobacter pylori* in patients can be killed by visible light. *Lasers Surg Med* **36**, 260–265.

Gebel, J.H., Sonntag, G., Werner, H.P., Vacata, V., Exner, M. and Kistemann, T. (2002) The higher disinfectant resistance of nosocomial isolates of *Klebsiella oxytoca*: how reliable are indicator organisms in disinfectant testing? *J Hosp Infect* **50**, 309–311.

Gómez-López, V.M., Deviehere, F., Bonduelle, V. and Debevere, J. (2005) Factors affecting the inactivation of micro-organisms by intense light pulses. *J Appl Microbiol* **99**, 460–470.

Gómez-López, V.M., Ragaert, P., Debevere, J. and Devlieghere, F. (2007) Pulsed light for food decontamination: a review. *Trends Food Sci Technol* **18**, 464–473.

Guffey, J.S. and Wilborn, J. (2006) Effects of combined 405 nm and 880 nm lighto on *Staphylococcus aureus* and *Pseudomonas aeruginosa* in vitro. *Photomed Laser Surg* **24**, 680–683.

Kerr, J.R., Taylor, G.W., Rutman, A., Hoiby, N., Cole, P.J. and Wilson, R. (1999) *Pseudomonas aeruginosa* pyocyanin and 1-hydroxyphenazine inhibit fungal growth. *J Clin Pathol* **52**, 385–387.

Knutson, C.A. and Jeans, A. (1968) A new modification of the carbazole analysis: application of heteropolysaccharides. *Anal Biochem* **24**, 470–481.

Krishmanmurthy, K., Demirci, A. and Irudayaraj, J. (2004) Inactivation of *Staphylococcus aureus* by pulsed UV-light sterilization. *J Food Prot* **67**, 1027–1030.

Kühn, K.P., Chabreny, I.F., Massholder, K., Stickler, M., Benz, V.W., Sonntag, H.G. and Erdinger, L. (2003) Disinfection of surfaces by photocatalytic oxidation with titanium dioxide and UVA light. *Chemosphere* **53**, 71–77.

Kurachi, M. (1958) Studies on the biosynthesis of pyocyanine. *Bull Inst Chem Res* **36**, 188–196.

Laine, L., Perry, J.D., Lee, M., Oliver, M., James, A.L., Foata, C., Halimi, D., Orenga, S. *et al.* (2009) A novel chromogenic medium for isolation of *Pseudomonas aeruginosa* from the sputa of cystic fibrosis patients. *J Cyst Fibros* **8**, 143–149.

Lambert, R.J., Joynson, J. and Forbes, B. (2001) The relationships and susceptibilities of some industrial, laboratory and clinical isolates of *Pseudomonas aeruginosa* to some antibiotics and biocides. *J Appl Microbiol.* **91**, 972–984.

Lukšiene, Z. (2005) New approach to inactivation of harmful and pathogenic microorganisms by photosensitization. *Food Technol Biotechnol* **43**, 411–418.

MacGregor, S.J., Rowan, N.J., McIlvaney, L., Anderson, J.G., Fouracre, R.A. and Farish, O. (1998) Light inactivation of food-related pathogenic bacteria using a pulsed power source. *Lett Appl Microbiol* **27**, 67–70.

Marquenie, D., Geeraed, A.H., Lammertyn, J., Soontjens, C., Van Impe, J.F., Michiels, C.W. and Nicolaï, B.M. (2003) Combinations of pulsed white light and UV-C or mild heat treatment to inactivate conidia of *Botrytis cinerea* and *Monilia fructigena*. *Int J Food Microbiol* **85**, 185–196.

Nugent, M.J.D. and Higginbotham, C.L. (2007) Preparation of a novel freeze thawed poly(vinyl alcohol) composite hydrogel for drug delivery applications. *Eur J Pharm Biopharm* **67**, 377–386.

Otaki, M., Okuda, A., Tajima, K., Iwasaki, T., Kinoshita, S. and Ohgaki, S. (2003) Inactivation differences of microorganisms by low pressure UV and pulsed xenon lamps. *Water Sci Technol* **47**, 185–190.

Randall, L.P., Cooles, S.W., Sayers, A.R. and Woodward, M.J. (2001) Association between cyclohexane resistance in *Salmonella* of different serovars and increased resistance to multiple antibiotics, disinfectants and dyes. *J Med Microbiol* **50**, 919–924.

Roberts, P. and Hope, A. (2003) Virus inactivation by high intensity broad spectrum pulsed light. *J Virol Methods* **110**, 61–65.

Rowan, N.J., MacGregor, S.J., Anderson, J.G., Fouracre, R.A., McIlvaney, L. and Farish, O. (1999) Pulsed-light inactivation of food-related microorganisms. *Appl Environ Microbiol* **65**, 1312–1315.

Sharma, R.R. and Demirci, A. (2003) Inactivation of *Escherichia coli* O157:H7 on inoculated alfalfa seeds with pulsed ultraviolet light and response surface modelling. *J Food Sci* **68**, 1448–1453.

Solberg, C.O. (2000) Spread of *Staphylococcus aureus* in hospitals: causes and prevention. *Scand J Infect Dis* **32**, 587–595.

Takeshita, K., Shibato, J., Sameshima, T., Fukunaga, S., Isobe, S., Arihara, K. and Itoh, M. (2003) Damage of yeast cells induced by pulsed light irradiation. *Int J Food Microbiol* **85**, 151–158.

Terry, J.M., Piňa, S.E. and Mattingly, S.J. (1991) Environmental conditions which influence mucoid conversion in *Pseudomonas aeruginosa* PAO1. *Infect Immun* **59**, 471–477.

Wainwright, M. (1998) Photodynamic antimicrobial chemotherapy (PACT). *J Antimicrob Chemother* **42**, 13–28.

Wang, T., MacGregor, S.J., Anderson, J.G. and Woolsey, G.A. (2005) Pulsed ultra-violet inactivation spectrum of *Escherichia coli*. *Water Res* **39**, 2921–2925.

Wekhof, A. (2000) Disinfection with flash lamps. *PDA J Pharma Sci Technol* **54**, 264–276.

Wekhof, A., Trompeter, F.J. and Franken, O. (2001). Pulsed UV-disintegration (PUVD): a new sterilization mechanism for packaging and broad medical-hospital applications. In *Proceedings of the First International Conference on Ultraviolet Technologies*, Washington, DC, USA, 14–16 June, pp. 1–15. Ontaria, Canada: International Ultraviolet Association.

Wuytack, E.Y., Phuong, L.D.T., Aertsen, A., Reyns, K.M., Marquenie, D. and De Ketelaere, B. (2003) Comparison of sublethal injury induced in *Salmonella enterica* serovar Typhimurium by heat and by different non-thermal treatments. *J Food Prot* **66**, 31–37.

Yaqub, S., Anderson, J.G., MacGregor, S.J. and Rowan, N.J. (2004) Use of fluorescent metabolic stain to assess lethal and sub-lethal injury in food-borne bacteria exposed to pulsed electric fields. *Lett Appl Microbiol* **39**, 246–251.

Yaun, B.R., Summer, S.S., Eifert, J.D. and Marcy, J.E. (2003) Response of *Salmonella* and *Escherichia coli* O157: H7 to UV energy. *J Food Prot* **66**, 1071–1073.

Journal of Microbiological Methods 84 (2011) 317–326

Contents lists available at ScienceDirect

Journal of Microbiological Methods

journal homepage: www.elsevier.com/locate/jmicmeth

Studies on the relationship between pulsed UV light irradiation and the simultaneous occurrence of molecular and cellular damage in clinically-relevant *Candida albicans*

Hugh Farrell [a], Jennifer Hayes [a], John Laffey [b], Neil Rowan [a,*]

[a] Department of Nursing and Health Science, Athlone Institute of Technology, Ireland
[b] Department of Anaesthesia and Critical Care Medicine, National University of Ireland Galway, Ireland

ARTICLE INFO

Article history:
Received 18 October 2010
Received in revised form 15 December 2010
Accepted 15 December 2010
Available online 23 December 2010

Keywords:
Pulsed UV irradiation
Candida albicans
Molecular and cellular damage
Apoptosis
Novel decontamination process

ABSTRACT

This constitutes the first study to report on the relationship between pulsed UV light (PL) irradiation and the simultaneous occurrence of molecular and cellular damage in clinical strains of *Candida albicans*. Microbial protein leakage and propidium iodide (PI) uptake assays demonstrated significant increases in cell membrane permeability in PL-treated yeast that depended on the amount of UV pulses applied. This finding correlated well with the measurement of increased levels of lipid hydroperoxidation in the cell membrane of PL-treated yeast. PL-treated yeast cells also displayed a specific pattern of intracellular reactive oxygen species (ROS) generation, where ROS were initially localised in the mitochondria after low levels of pulsing (UV dose 0.82 μJ/cm^2) before more wide-spread cytosolic ROS production occurred with enhanced pulsing. Intracellular ROS levels were measured using the specific mitochondrial peroxide stain dihydrorhodamine 123 and the cytosolic oxidation stain dichloroflurescin diacetate. Use of the dihydroethidium stain also revealed increased levels of intracellular superoxide as a consequence of augmented pulsing. The ROS bursts observed during the initial phases of PL treatment was consistent with the occurrence of apoptotic cells as confirmed by detection of specific apoptotic markers, abnormal chromatin condensation and externalisation of cell membrane lipid phosphatidylserine. Increased amount of PL-irradiation (ca. UV does 1.24–1.65 μJ/cm^2) also resulted in the occurrence of late apoptotic and necrotic yeast phenotypes, which coincided with the transition from mitochondrial to cytosolic localisation of ROS and with irreversible cell membrane leakage. Use of the comet assay also revealed significant nuclear damage in similarly treated PL samples. Although some level of cellular repair was observed in all test strains during sub-lethal exposure to PL-treatments (≤20 pulses or UV dose 0.55 μJ/cm^2), this was absent in similar samples exposed to increased amounts of pulsing. This study showed that PL-irradiation inactivates *C. albicans* test strains through a multi-targeted process with no evidence of microbial ability to support cell growth after ≤20 pulses. Implications of our findings in terms of application of PL for contact-surface disinfection are discussed.

1. Introduction

The incidence of nosocomial yeast infections has increased markedly in recent time and has become a major cause of morbidity and mortality in vulnerable groups including neonates, cancer patients and the elderly (Fanello et al., 2001). More than 90% of persons infected with HIV who are not receiving highly active antiretroviral therapy eventually develop oropharyngeal candidiasis (de Repentigny et al., 2004). Prevention of infection is a superior approach compared to the cost and consequences of treatment of infection, with strong emphasis placed on hand hygiene compliance and proper cleaning regimens that include use of effective surface decontamination techniques (Solberg, 2000).

Pulsed UV light (PL) technology has received considerable attention as a promising next-generation approach for decontaminating food, packaging, water and air (Gómez-López et al., 2007; Elmnasser et al., 2007; Garvey et al., 2010). This approach kills microorganisms by using ultrashort duration pulses of an intense broadband emission spectrum that is rich in UV-C germicidal light (200–280 nm band). PL is produced using techniques that multiplies power manifold by storing electricity in a capacitor over relatively long times (fractions of a second) and releasing it in a short time (millionths or thousandths of a second) using sophisticated pulse compression techniques (Rowan et al., 1999; Gómez-López et al., 2007). The emitted flash has a high peak power and usually consists of wavelengths from 200 to 1100 nm broad spectrum light enriched with shorter germicidal wavelengths (Wang et al., 2005; Gómez-López et al., 2007). A strong advantage of using pulsed xenon lamps over continuous low to medium pressure conventional UV lamps is that the former has a characteristic high peak-power dissipation, which allows for more rapid microbial inactivation. A continuous 10 W lamp needs

* Corresponding author. Department of Nursing and Health Science, Athlone Institute of Technology, Dublin Road, Athlone, Co. Westmeath, Ireland. Tel.: +353 906473081; fax: +353 906486135.
E-mail address: nrowan@ait.ie (N. Rowan).

0167-7012/$ – see front matter © 2010 Elsevier B.V. All rights reserved.
doi:10.1016/j.mimet.2010.12.021

to be operated for 10 s to achieve the same decontamination efficacy (supplying same energy) as a pulsed lamp of typically 1 MW operated for just 100 μs. Despite significant interest in the development of PL as an alternative or complementary means of disinfection, most published studies to date have only used conventional aerobic plate counts to report on gross microbial viability post UV irradiation. Moreover, with the exception of a limited study undertaken by Takeshita et al. (2003) no other published research has reported on the inter-related cellular responses involved in microbial response to pulsed light treatments. This dearth in microbial physiology data is critical as it may unlock key information for the subsequent development and optimization of this novel decontamination technology for surface, water and air applications.

This constitutes the first study to report on the relationship between the occurrence and augmentation of nuclear and cellular damage and apoptosis in clinically-relevant *Candida albicans* cells as a consequence of increased amounts of pulsed UV light treatments.

2. Materials and methods

2.1. Preparation and pulsing of C. albicans stains with UV rich light

A bench-top pulsed power source (PUV-1, Samtech Ltd., Glasgow) was used to power a low-pressure (60 kPa) xenon-filled flashlamp (Heraeus Noblelight XAP type NL4006 series constructed from a clear UV transparent quartz tube), that produced a high-intensity diverging beam of polychromatic pulsed light, was used in this study following the method of Farrell et al. (2009) with modifications. The pulsed light has a broadband emission spectrum extending from the UV to the infrared region with a rich UV content and its intensity also depends on the level of the voltage applied. The manufacturer stated that the discharge tube represents a line-source of limited length and consequently the light formed an elliptical, equi-intensity profile over the sample plane eliminating shading effects. This resulted in a ~30% variation in luminous intensity between the centre and the edge of the sample. The light source has an automatic frequency-control function that allows it to operate at one pulse per second that was used throughout this study. Light exposure was homogeneous as the xenon lamp measuring 9 cm × 0.75 cm was longer than the 8.5 cm diameter polystyrene Petri dishes used in the tests, which were placed directly below the lamp. For standard treatments, the light source was mounted at 8 cm above the treatment area that was designed specifically to accommodate a standard Petri dish containing 10 ml of sample and was set as the minimum or lower threshold distance by the fabricant. This was to ensure that full coverage of the Petri dish occurred and to eliminate possible shading effects.

Test microorganisms used in these experiments, their origin and clinical relevance are summarized in Table 1. All test strains were maintained in Microbank storage vials (Cruinn Diagnostic, Ireland) at −70 °C. Identification of three randomly selected isolates of each yeast strain was confirmed before and after experimental studies by use of the germ-tube assay with occasionally use of the VITEK yeast biochemical card and API-32 C systems (bioMérieux, France) as per methods described by Hsu et al. (2003). Strains were stored at 4 °C on agar slopes of Malt Extract agar (MEA; Oxoid, Basingstoke, UK) and checked monthly for purity and renewed. To prepare the test samples, yeast test strains were streaked to purity from porous beads taken from Microbank vials, and an isolated colony was then transferred to 50 ml Malt Extract broth (MEB adjusted to pH 5.6 ± 0.2 °C; Oxoid, Basingstoke, UK) and cultivated with shaking at 125 oscillations per minute for 14 h at 35 °C until each test organism (listed in Table 1) reached late exponential phase as reported previously by Farrell et al. (2009). The optical densities of test samples were then spectrophotometrically adjusted at 640 nm to 0.2 units (ca. 10^8 CFU/ml) [Model UV-120-02 instrument, Shimadzu Corp., Kyoto, Japan] using 0.1 M phosphate buffered saline (PBS) [pH 7.2] (confirmed via aerobic plate count). Standard UV treatments involved re-suspending OD_{640nm}-adjusted yeast samples in sterile 10 ml of 0.1 M PBS, which was aseptically transferred to 8.5 cm Petri dishes and subjected to UV light treatments. The number of pulses of light used ranged from 0 (untreated control) to 150 pulses using a lamp discharge energy of 7.2 J at a distance of 8 cm from the light source that was shown previously to inactivate test yeast populations by ca. 7 log CFU/ml over this treatment regime (Farrell et al., 2009). Measurement of corresponding fluence rate (or 'irradiance) (Joule/cm^2) at each applied pulse was determined using chemical actinometry as described by Rahn et al. (2003), as the non-continuous emitted spectrum did not facilitate use of a calibrated radiometer. Dose is sometimes used as a synonym of fluence. The lethality of this PL process was confirmed by enumerating survivors post-treatments on triplicate Sabouraud dextrose agar (SDA; Oxoid) and MEA plates (both adjusted to pH 5.6 ± 0.2 °C) using the spread plate technique (expressed in terms of $\log_{10}$ colony forming units or CFU ml^{-1}). After 48 h at 35 °C, typically with the highest dilution, identify was confirmed as described above. All experiments were carried out in triplicate using the same culture to avoid sample variability. Heating of the yeast suspensions was measured using a thermocouple and by thermal imaging (IRI 4010, InfraRed Integrated Systems Ltd, Northampton, England) using modifications of Nugent and Higginbotham (2007). There was no discernable increase in saline temperature during UV treatments.

Table 1
Origin and clinical significance of test strains.

Strain	Source[a]	Code	Clinical significance
Candida albicans	NUHG	6250	Human blood isolate
Candida albicans	NUHG	R810	Human sputum isolate
Candida albicans	NUHG	R854	Human sputum isolate
Candida albicans	NUHG	D7100	Human wound isolate
Candida albicans	ATCC	10231	Human bronchomycosis

[a] National University Hospital Galway (NUHG), American Type Culture Collection (ATCC).

2.2. Determining yeast cell membrane integrity post UV treatments using microbial protein leakage and propidium iodide dye uptake assays

Damage or disruption to the cell membrane of test yeast was determined by measuring loss of intracellular proteins released into sample supernatant post-UV-irradiation at each PL-treatment endpoint. Treated and untreated yeast cell suspensions were kept on ice to prevent protease activity, centrifuged at 10,000 rpm for 10 min at 10 °C, and the supernatant was collected thereafter. The concentrations of eluted yeast protein in the supernatants were determined spectrophotometrically using the BSA Protein assay kit (Pierce Chemical) using 150 μl sample aliquots. The absorbances of PL-treated samples, untreated controls and BSA standards (range 0–200 μg BSA/ml) were measured at 560 nm after 2 h incubation at 37 °C on a micro-titre plate reader (Wallac 1420 VICTOR$^{2™}$ Turku, Finland). The standard curve of increasing concentration of BSA standard (μg/ml) against corresponding absorbance (560 nm) (data not shown) was used to determine the protein concentration of all PL-treated samples and untreated controls.

Non-permeable propidium iodide (PI) dye was also used to investigate disruption of cell membranes in similarly treated samples. When used in combination with the membrane-permeable fluorescent 4′,6-diamidino-2-phenylindole (DAPI) stain that binds strongly to DNA, it is possible to determine the proportion of cells with permeabilized cell membranes post UV treatments. 500 μl aliquots of treated cell suspensions (approx 10^7 cell ml^{-1}) were transferred to sterile Eppendorf tubes. Propidium iodide (Sigma) was added to a concentration of 100 μg/ml and the tubes were then incubated in the dark for 30 min at 4 °C. The cell suspension was subsequently counter

stained with 1 μg/ml DAPI. The cell suspension was then washed twice and resuspended in fresh PBS. A 20 μl aliquot of cell suspension from treated and control samples was transferred to a clean microscope slide, then mounted with glycerol gelatin (Sigma) and subsequently examined by fluorescence microscopy (Leitz Diaplan, Germany). All samples were examined in triplicate.

2.3. Measurement of reactive oxygen species (ROS) produced in UV irradiated test yeast

Overproduction of ROS in yeast cells as a consequence of UV irradiation was determined by using a number of oxidative-stress-sensitive probes namely: dihydrorhodamine 123 (DHR 123), 2′,7′-dichlorodihydrofluorescein diacetate (DCFH-DA) and dihydroethidium (DHE) (all probes were purchased from Sigma). Following UV treatments, 500 μl aliquots samples were separately transferred to a sterile Eppendorf tube. Thereafter, DHR-123 was added to a concentration of 5 μg/ml, and the tube was then incubated for 2 h at 30 °C in the dark. The oxidation of nonfluoresecnt DHR 123 to the fluorescent rhodamine 123 is catalysed by the enzyme peroxidase that accumulates in mitochondrial membranes (Nomura et al., 1999; Qin et al., 2008). The oxidation of DHR 123 was measured fluorimetrically using excitation and emission wavelengths of 505 and 535 nm. DCFH-DA was added to similarly treated samples at a final concentration of 10 μM from a 1 mM stock solution in ethanol, and then incubated at 30 °C for 1 h in the dark. The acetyl groups in DCFH-DA are removed by membrane esterases to form 2′,7′-dichlorodihydrofluorescein (DCFH) when this probe is taken up by viable cells. DCFH is not fluorescent but is highly sensitive to ROS (such as RO_2, RO, OH, HOCl, and $ONOO^-$) and is oxidised to the highly fluorescent compound 2′,7′-dichlorofluorescein via reactions described previously by Ischiropoulos et al. (1999). Exposure of samples to light was minimised, and fluorescence was measured spectrofluorometrically (Wallac 1420 VICTOR^{2}™ Turku, Finland). Dihydroethidium (DHE) was added to a concentration of 5 μg/ml, and then incubated for 10 min at room temperature (DHE) is oxidised to the fluorescent ethidium (ET) and is relatively specific for $O_{\bar{2}}$, with minimal oxidation induced by H_2O_2, $ONOO^-$, or HOCl as observed previously by Tarpey and Fridovich (2001). The cell suspension was subsequently counter-stained with 1 μg/ml DAPI. The cell suspension was then washed twice and resuspended in fresh PBS. 20 μl aliquot test samples and untreated controls were transferred to a clean microscope slide, mounted with glycerol gelatin (Sigma) and examined by fluorescence microscopy (Leitz Diaplan, Germany).

2.4. Measurement of lipid hydroperoxides production in UV irradiated yeast

A PeroxiDetect™ kit was used to determine the levels of lipid hydroperoxides in yeast cell lysate, which is based on a modified ferrous oxidation/xylenol orange assay of Jiang et al. (1991). Lipid peroxides oxidize Fe^{2+} to Fe^{3+} ions at acidic pH that form a colour adduct with xylenol orange (XO, 3,3′-bis[N,N–bis (carboxymethyl) aminomethyl]-o-cresolsulfonephthalein, sodium salt), which is observed at 560 nm. The cell lysate was prepared as described by Jiang et al. (1991). Test yeast cell suspensions were UV-treated as outlined above. Samples (5 ml) were harvested and washed twice with distilled water (15,000 rpm for 5 min at 4 °C). Cell pellets were subsequently transferred to 13×100-mm glass culture tubes and resuspended in 300 μl of methanol/0.01% butylated hydrotoluene (BHT). Approximately 1 g of glass beads was added, and the cells were lysed by vortexing (4 cycles of 30 s vortex, 30 s on ice), and the upper methanol layer was transferred to a microcentrifuge tube. The glass beads were then washed once with 1 ml of methanol/0.01% BHT, the methanol layers were pooled, and following centrifugation (100,000 rpm for 10 min at 4 °C) the supernatants were assayed for oxidation products. A *tert*-butyl hydroperoxide (*tert*-BuOOH) standard curve was prepared in 90% methanol [data not shown]. Working reagent was prepared by mixing 100 μL of ferrous ammonium sulphate Reagent (2.5 mM ammonium ferrous (II) sulphate/0.25 M sulphuric acid), and 10 ml of organic peroxide colour reagent (4 mM BHT/125 μM xylenol orange in 90% methanol). Samples of yeast cell lysate (100 μL) were added to 1 ml of working reagent. Samples were incubated at room temperature for 30 min, and the absorbance at 560 nm was measured.

2.5. Measurement of apoptosis in UV irradiated yeast

The following studies were undertaken to investigate the occurrence of cellular apoptosis and necrosis in PL-treated test yeast. Translocation of lipid phosphatidylserine (PS) from the inner leaflet to the extracellular side of the plasma membrane is an early stage event in apoptosis and was detected by using the Annexin V-FITC Apoptosis Detection kit (Sigma) as described by Madeo et al. (1999) with modifications. Annexin V stain has a strong binding affinity for PS. After PL-treatments, cells were harvested and washed with sorbitol buffer (1·2 M sorbitol, 0·5 mM $MgCl_2$, 35 mM K_2HPO_4, pH 6·8). Cell walls were digested with 60 U lyticase ml/L in sorbitol buffer (Sigma) for about 60 min at 28 °C, where digestion with this enzyme was carefully monitored by phase-contrast microscopy in order to prevent damage to the unfixed protoplasts. Cells were then washed twice with binding buffer (10 mM HEPES/NaOH, pH 7·4, 140 mM NaCl, 2·5 mM $CaCl_2$; CLONTECH Laboratories) containing 1·2 M sorbitol. To 38 μl cell suspensions in binding/sorbitol buffer were added 2 μl Annexin V (20 μg/ml) and 2 μl of a prodidium iodide (PI) working solution and incubated for 20 min at room temperature. The cells were then washed three times and resuspended in binding/sorbitol buffer. Finally the 10 μl of cell suspensions were transferred to clean microscope slides and mounted with the glycerol gelatine. Slides were observed using a Hamamatsu Colour chilled 3cco camera, attached to fluorescence microscope (Leitz Diaplan, Germany) at 40× and 100× magnification. For quantitative assessment of Annexin V^- PI staining, at least 200 yeast cells were counted per sample and trials were repeated in duplicate. This combined Annexin V/PI staining approach enables distinction of early apoptotic (designated as Annexin V^+/PI^-), late apoptotic (designated as Annexin V^+/PI^+) and necrotic (designated as Annexin V^-/PI^+) cells. Chromatin morphology was also examined using DAPI stain as apoptotic cells demonstrate abnormal chromatin condensation with fragments forming a semicircle as described previously by Herker et al. (2004). The chromatin of untreated control samples appear as a single round spot in the middle of the cell. The standard protocol for DAPI nuclei staining was used as described by Klassen and Meinhardt (2004). Treated and untreated cells were collected by centrifugation at 10,000 rpm for 10 min, then resuspended in 70% (v/v) ethanol and incubated for 1 h for fixation and permeabilisation. Following washing and rehydration in PBS, cells were resuspended in PBS containing 1 μg ml/L DAPI and visualized under a fluorescence microscope (Leitz Diaplan, Germany).

2.6. Detection of genotoxic damage in PL-irradiated test yeast using the comet assay

A modified alkaline comet assay procedure of Miloshev et al. (2002) was used in the present study for detecting and analyzing the ability of PL irradiation to cause DNA damage that includes strand breaks. *C. albicans* test strains were inoculated into separate 100 mL malt extract broth (Fluka) and incubated in a shaking incubator (New Brunswick Scientific Innova 4000) at 35 °C and 125 oscillations per minute for 18–24 h. The broth was centrifuged at 1400 rpm (Mistral MSE 1000 benchtop centrifuge), the supernatant discarded and the pelleted yeast cells resuspended in sterile PBS to a population density of ~10^7 cells/mL (confirmed via plate counts). 10 mL aliquots were

distributed into sterile Petri dishes and each dish was individually exposed to UV irradiation regimes as outlined earlier. Three 10 mL aliquots were incubated in 0.1 mM, 0.5 mM and 1 mM H_2O_2 respectively. These samples served as positive controls. A solution (referred to hereafter as SCE) containing 1.0 M sorbitol, 0.1 M sodium citrate and 60 mM EDTA was prepared. The irradiated yeast suspensions were collected in centrifuge tubes and centrifuged at 1000 rpm for 10 min. The pellets were washed twice in 10 mL 40 mM EDTA/90 mM 2-mercaptoethanol (known hereafter as 2-ME), discarding the supernatant. 2 mL SCE, 16 μL 2-ME and 0.2 mg lyticase were added to each centrifuge tube to resuspend the washed pellets. The tubes were incubated at 37 °C for 2 h in order to produce spheroplasts. A lysis buffer was prepared, consisting of 50 mM TrisHCl; 25 mM EDTA; 0.5 M NaCl; 3 mM $MgCl_2$; 3 mM 2-mercaptoethanol; 0.1% (v/v) Triton-X-100; and 10% (v/v) SDS. After the 2 h incubation period, the tubes were again centrifuged at 650 rpm for 10 min and the supernatant discarded. Each pellet was resuspended in 700 μL lysis buffer and incubated at 68 °C for 15 min, vortexing intermittently during this time. 200 μL of each sample was mixed with 400 μL 0.7% (w/v) low-melting point (LMP) agarose (previously boiled and then cooled to ~40 °C prior to mixing) and then spread thinly and evenly on to glass slide and immediately covered with a Gelbond®, Electrophoresis Film, (Sigma-Aldrich, Ireland) strip and stored at 4 °C for 10 min until the gel had set. Alkaline electrophoresis was preceded by a 20 min unwinding step in electrophoresis buffer pH13. Electrophoresis was performed in at 25 V and 300 mA for 12 min in a 2 L capacity 35 cm tank connected to Power Pac 300 (Bio-Rad), with gelbond strips placed horizontally side by side avoiding gaps. Yeast cells were neutralized by rinsing 3 times with Tris–Cl buffer pH 7.4 before fixation in 100% methanol for a minimum of 3 h at 4 °C. Prior to analysis, DNA was stained by placing gelbond strips in freshly prepared SYBR® Gold nucleic acid stain (Invitrogen GmbH, Germany) for 40 min at room temperature. Finally, the gels were cover-slipped and viewed at 400× magnification using a fluorescent microscope (Leitz Diaplan) equipped with an excitation filter of 475–490 nm.

2.7. Detection of photo-reactivation in UV-irradiated yeast

This experiment was designed to investigate the degree of photo-reactivation in PL-treated test yeast following the method of Farrell et al. (2010). Briefly, plates were prepared by spread plating 50 μl of cell suspension on relevant solid media in triplicate for each exposure. The plates were exposed to increasing doses UV irradiation as per regimes described earlier. The first three plates were immediately wrapped in aluminium foil post treatment; the remaining three plates were exposed to direct sunlight for 4 h post-treatment. The plates were incubated for 48 h at 37 °C. To determine the number of surviving cells, colonies were counted and expressed as $\log_{10}$ colony forming units (CFU)/cm^2.The experiment was conducted in triplicate and variance determined.

2.8. Statistical analysis

Student's *t*-tests and ANOVA one-way model (MINITAB software release 13; Mintab Inc., State College, PA) were used to compare the effects of the relationship of independent variables on light treatments.

3. Results and discussion

3.1. Determination of cell membrane integrity and functionality post pulsed light treatments

The integrity of yeast cell membrane in response to separate PL was determined using protein leakage and the combined PI/DAPI cell staining assays. Propidium iodide (PI) has been previously used as an indicator of microbial cell membrane functionality (Helmerhorst et al., 1999) as PI is able to enter permeabilised cells. Once in the microbial cytoplasm PI binds to nucleic acids yielding fluorescence in the red wavelength region (Virto et al., 2005). The relationships between cell vitality (determined by PI/DAPI staining), cell viability (determined by total aerobic plate counts) and concentration of eluted fungal proteins from PL-treated *C. albicans* D7100 are shown in Fig. 1. These results demonstrated a UV dose-dependent increase in both protein leakage and membrane permeability, which was also strongly correlated with a commensurate decrease in cell viability over similar PL treatment regimes. 15.3 ± 0.5 μg/ml of fungal protein was lost from the cell after 150 pulses (or UV dose of 4.1 μJ/cm^2), which corresponded to a 7.8 log order reduction in cell viability (Fig. 1). A similar pattern of protein loss with increased PL exposure was exhibited by all *C. albicans* strains tested ($r^2 = 0.89$) (data not shown).

Plasma membrane permeabilisation in response to PL was estimated by fluorescence microscopy based on the influx of PI that is excluded by test yeast cells with intact plasma membranes. The proportions of *C. albicans* test cells exhibiting PI permeability were plotted versus increasing exposure to PL at 7.2 J (Fig. 2). PL-treated cells demonstrated increased PI fluorescence in response to increasing amounts of UV exposure. This UV dose-dependent increase in cell permeability correlated strongly with a commensurate decrease in cell viability in PL treatment (Fig. 2). During the initial 15 pulses of PL-irradiation (UV dose 0.41 μJ/cm^2) less than 1% of treated cell were found to exhibit PI permeability (Fig. 2). However, following 20 pulses (UV dose 0.55 μJ/cm^2) there was an exponential increase in the numbers of PI positive cells with a corresponding decrease in cell viability. After 90 and 150 pulses (equivalent to UV doses of 2.4 and 4.1 μJ/cm^2 respectively), approximately 90% and 99% of treated yeast cells displayed PI fluorescence. The overall trend observed with the PI cellular uptake assay was consistent with that observed with the protein leakage assay for similarly treated samples; suggesting that loss of plasma membrane selective permeability coincides with loss of membrane integrity with increasing exposure to PL-irradiation.

The latter highlights the importance of cell membrane integrity and functionally in maintaining viable clinically-relevant yeast. Previous studies have shown that the ability of yeast to cope with environmental stresses that affect plasma membrane organisation and functionality depends upon maintenance of its physical characteristics such as organization of fatty acyl chains in the phospholipid membrane (van der Rest et al., 1995). A similar phenomenon was observed by Takeshita et al. (2003), who noted that the concentration of eluted proteins varied significantly between pulsed light and low-pressure UV (LP-UV) irradiated yeast cell suspensions, with LP-UV treated samples showing minimal protein leakage. These

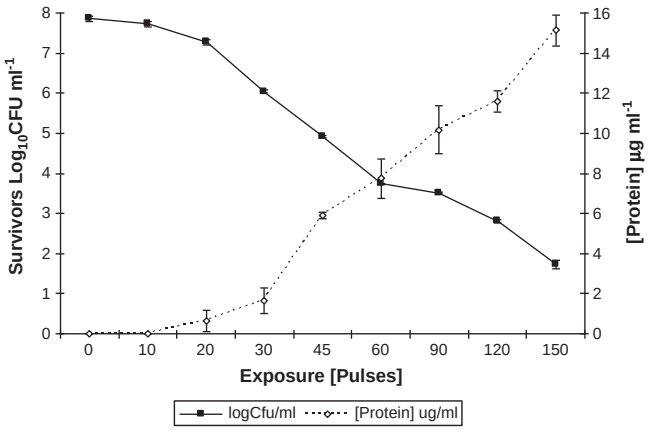

Fig. 1. Reduction in total fungal proteins levels (μg/ml) in *C. albicans* D7100 as a consequence of increased pulsing or amount of pulses applied.

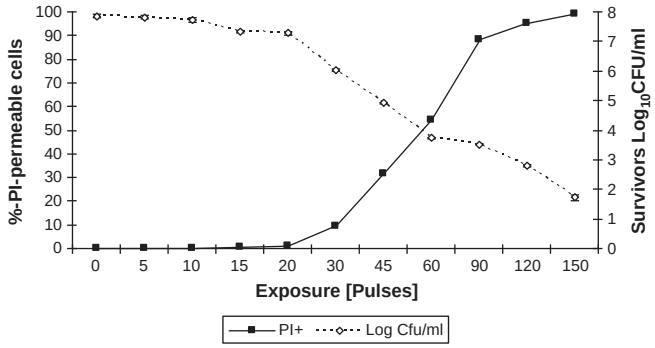

Fig. 2. Relationship between pulsed light inactivation of *C. albicans* D7100 and prodidium iodide (% PI) permeable cells.

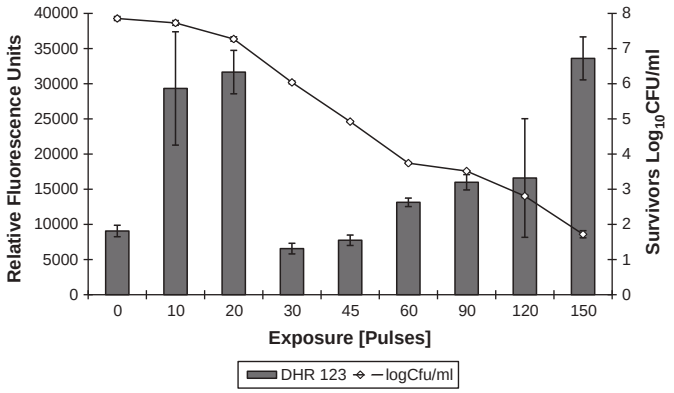

Fig. 3. Relationship between mitochondrial ROS generation and localization profile as measured by specific DHR-123 fluorescence and microbial inactivation (Survivors Log_{10} CFU/ml) in pulsed-light treated *C. albicans* D7100.

authors reported that this observed difference in cell membrane integrity post UV irradiation may be attributed to the contribution of spectral components of pulsed light that is not present in LP-UV lamp spectrum. Other researchers have reported previously that exposing *Saccharomyces cerevisiae* cells to near-UV radiation (300–400 nm) caused damage to the yeast cell membrane functionality due to loss of permeability and to membrane-associated active transport processes (Arami et al., 1993).

3.2. Generation of reactive oxygen species (ROS) in UV irradiated test yeast

Oxidative stress is an unavoidable consequence of life in an oxygen-rich atmosphere. Oxygen radicals and other activated oxygen species are generated as by-products of aerobic metabolism and exposure to various natural and synthetic toxicants. Redox homeostasis in cells is important for the maintenance of proper cellular functions (Adler et al., 1999) including intracellular communication (Karu, 2008) as well as initiation and propagation of apoptosis (Madeo et al., 1999). Elevated levels of intracellular reactive oxygen species (ROS) can be biologically deleterious, potentially damaging a wide range of macromolecules including nucleic acids, proteins and lipids. The production of intracellular ROS was monitored in test yeast during the course of PL-treatments using the specific ROS mitochondrial stain dihydrorhodamine-123 (DHR-123) and cytosolic stain 2′,7′-dichlorodihydrofluorescein diacetate (DCFH-DA). Previous researchers have that DRH is no fluorescent, uncharged, and readily taken up by cells, whereas DHR-123, the product of DHR oxidation, is fluorescent, is positively charged, and binds selectively to the inner mitochondrial membrane of living cells (Royall and Ischiropoulos, 1993; Qin et al., 2008). Qin et al. (2008) reported that the fluorescence of this dye is an indicator of mitochondrial reactive oxygen intermediate production and membrane integrity. Our findings revealed a distinct shift in the localisation of intracellular ROS generation in test yeast over the 150 pulse regime at 7.2 J (Figs. 3, 4 and 5). A low basic level of ROS with distinct mitochondrial localisation was initially observed within the first 20 pulses by visualization of DHR-123 fluorescence, which also included localised ROS clusters about the periphery of the cells (data not shown). A sudden drop in mitochondrial ROS levels was observed after 20 pulses in PL-treated test yeast with a subsequent steady UV dose-dependent increase in ROS levels occurring with increased pulsing. Maximal levels of ROS induced fluorescence were observed following 20 pulses at 7.2 J, with similar levels observed after the terminal 150 pulse end point.

The ROS profile measured using the cytosolic specific 2′,7′-dichlorofluorescein (DCFH-DA) stain revealed a significantly different pattern of activity in similarly treated PL-samples (Fig 4). Previous researchers have reported that DCFH-DA is also readily taken up by cells and, after deacetylation to DCFH, is oxidised to its fluorescent derivative, DCF, and remains in the cytosol (Royall and Ischiropoulos, 1993; Qin et al., 2008). The DCFH-DA method has become a standard technique for measuring ROS formed in cells by ionizing radiation (Hafer et al., 2008). The DCFH-DA plot for PL-treated cell suspensions demonstrated marginally increased levels from 30 pulses (corresponding to DHR-123 pattern) with a substantial dose-dependent increase in ROS load evident at 90, 120 and 150 pulse end-points. The levels of cytosolic ROS observed following 150 pulses in test yeast were approximately 20 times those observed following 30 pulses and 10 times those observed following 90 pulses in similarly treated samples at 7.2 J. DCFH can be oxidised by several reactive species, including RO_2, RO, OH, HOCl, and $ONOO^-$, but only longer-lived radicals contribute to the increase in fluorescence (Ischiropoulos et al., 1999).

The intracellular superoxide levels in PL-treated yeast were measured using the ROS stain dihydroethidium (DHE) (Fig. 5). This superoxide-specific stain had been used successfully by other research groups to investigate ROS activity in microbial cultures (Carter et al., 1994; Henderson and Chappell, 1993). The oxidation of DHE to ethidium (ET) is relatively specific for O_2^-, with minimal oxidation induced by H_2O_2, $ONOO^-$, HOCl (Tarpey and Fridovich, 2001). DHE is dehydrogenated to ethidium, which then intercalates with negatively charged DNA and emits a red fluorescent signal. Our findings showed that PL-treated samples demonstrated a UV dose-dependent increase in intracellular superoxide levels (Fig. 5). Specifically, a UV dose-dependent increase in superoxide levels was observed following 30 pulses, which culminated in ca 98% of PL-treated yeast cells exhibiting intense DHE-mediated fluorescence

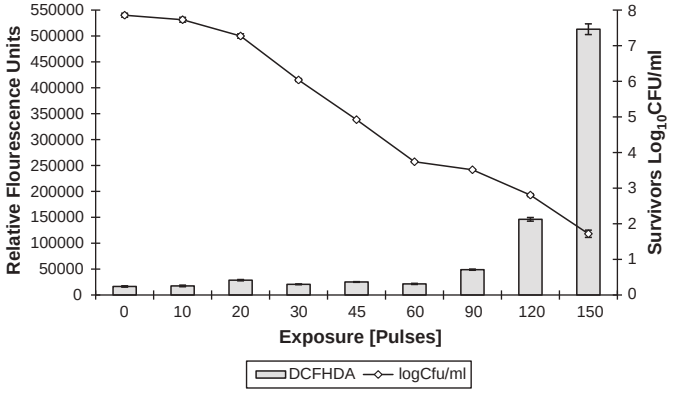

Fig. 4. Relationship between cytosolic ROS generation and localization profile as measured by specific DFCH-FA fluorescence and microbial inactivation (Survivors Log_{10} CFU/ml) in pulsed light treated *C. albicans* D7100.

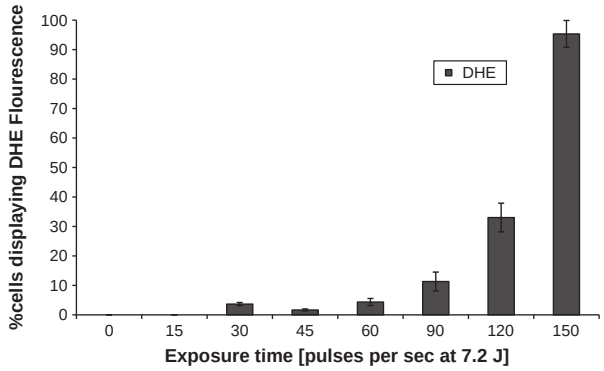

Fig. 5. Percentage of *C. albicans* D7100 exhibiting DHE fluorescence over 150 pulsing regime at lamp discharge energy of 7.2 J.

following 150 pulses (Fig. 5). The presence of high levels of superoxide anion at higher PL exposures is in agreement with the observations of Rowe et al. (2008) who noted that as the redox state of yeast cells continues to move toward an oxidised state as a consequence of high levels of DNA damage caused by increased intracellular levels of O_2^-, such ROS-stressed cell can no longer survive due to extensive nuclear and macromolecular damage. There was a degree of variation observed in ROS levels between the strains, however, the patterns of distribution remained consistent where all strains exhibited enhanced ROS activity when exposed to increased amount of pulsing [data not shown].

Under normal physiological conditions, intracellular ROS generated during respiration are retained by the mitochondria and reduced by protective enzymes such as superoxide dismutase, catalase and glutathione peroxidise (Chang et al., 2004). However, a reduction in protective enzyme activity or an event such as mitochondrial membrane depolarisation can result in the accumulation of ROS in the cytoplasm that imparts an oxidative stress burden on the cell (Gourlay and Ayscough, 2005) The diversity of ROS species that can be generated in cells is matched by a variety and complexity of cellular responses to detoxification, repair of damage, or maintenance of metal ion homeostasis, with at least 450 genes required to maintain cellular resistance to ROS (Perrone et al., 2008). Such intracellular defence mechanisms in yeast involve antioxidant enzymes, such as superoxide dismutases (SODs), catalases and peroxidises (Kwon et al., 1994) are susceptible to damage by ROS. Previous studies have demonstrated that oxidative processes result in the loss of key antioxidant enzymes (Hodgson and Fridovich, 1975; Kono and Fridovich, 1982; Tabatabaie and Floyd, 1994), which may exacerbate oxidative stress-mediated cytotoxicity (Lee et al., 2001). A reduction in superoxide-dismutase activity has been shown to reduce cell viability (Longo et al., 1996; Wawryn et al., 1999). Both superoxide dismutase and catalase are readily deactivated by singlet oxygen and by the radicals (Escobar et al., 1996). Thus, there is a growing consensus that ROS, such as hydroxyl radicals, superoxide anions, and organic hydroperoxides, play a role in cellular damage caused by ionizing radiation such as DNA strand breaks, lipid peroxidation and protein modification (Lee et al., 2001). Lee et al. (2001) showed that cytosolic and mitochondrial SODs play an essential role in the protection of yeast cells against ionizing radiation. This observation is further supported by the significant increases in ROS levels such as superoxide and organic hydroperoxides in PL-treated *C. albicans* strains in this present study.

3.3. Role of PL-mediated lipid peroxidation of cellular membranes on the viability of treated yeast

Lipid hydroperoxides are prominent non-radical intermediates of lipid peroxidation whose identification can often provide valuable mechanistic information such as whether a primary reaction is mediated by singlet oxygen or oxyradicals (Girotti et al., 1985). The endogenous oxidative degradation of membrane lipids by lipid peroxidation result in the formation of a very complex mixture of lipid hydroperoxides, chain-cleavage products, and polymeric material (Girotti, 1998). Once initiated, lipid peroxidation can self-perpetuate as a radical chain reaction, impairing membrane integrity and membrane-associated functions (Alic et al., 2001; Davis, 2000). The presence of lipid peroxides in PL-treated yeast was determined using the peroxiDetect™ Kit (Fig. 6). Examination of the findings for lipid peroxidation production in this study (Fig. 6) revealed a similar pattern of microbial lethality aligned with enhanced protein leakage (Fig. 1) and PI fluorescence (Fig. 2) due to increased pulsing. Test yeast demonstrated a dramatic initial increase in lipid hydroperoxide levels with c.a. 26, 43 and 67 nM peroxide ml/L measured following 45 (UV dose 1.24 μJ/cm^2), 90 (UV dose 2.48 μJ/cm^2) and 150 (UV dose 4.13 μJ/cm^2) pulses at 7.2 J respectively. This also corroborates previous observations from other research groups which reported that peroxidised membranes become rigid and lose their selective permeability and integrity when exposed to lethal extrinsic stresses (Davis, 2000). Lipid hydroperoxides are by-products of the interaction of ROS with lipid components of plasma membrane. Examination of the results outlined in Fig. 6 revealed a UV dose dependent increase in the levels of lipid hydroperoxides in response to increasing exposure to PL irradiation. There was also a strong correlation between increasing levels of lipid hydroperoxides and decreasing cell viability.

The relationship between intracellular ROS generation, lipid peroxidation and cellular responses to sub-lethal and lethal stress exposures is best understood by examination of the model outlined by Girotti (1998). Under normal physiological growth condition, the cell is in homeostasis with a pro-oxidant/antioxidant balance. However, exposure to low levels of an oxidant inducing stress such as PL causes low levels of lipid peroxidation in treated cell membranes of test yeast. There also appears to be a threshold for repair in PL-treated test yeast that was limited to the first 20 pulses (UV dose 0.55 μJ/cm^2). With moderate levels of lipid peroxidation, stress signalling may lead to the death program induction culminating in apoptotic death. Higher levels of PL-mediated lipid peroxidation in test yeast caused structural and metabolic damage leading to cell membrane lysis (Figs. 1 and 2) and necrotic cell death became evident (Fig. 7). The loss of membrane selective permeability is further supported by the presence of extracellular aqueous hydroperoxides and superoxide anions that accumulate after increasing amounts of high pulsed light exposures [data not shown]. Arami et al. (1997) demonstrated that photo-decomposition of ergosterol following exposure to near-UV radiation caused cell death. This may also be in part attributed to alteration to the sterol structure as a result of singlet oxygen-mediated oxidation of ergosterol in the plasma membrane of PL-

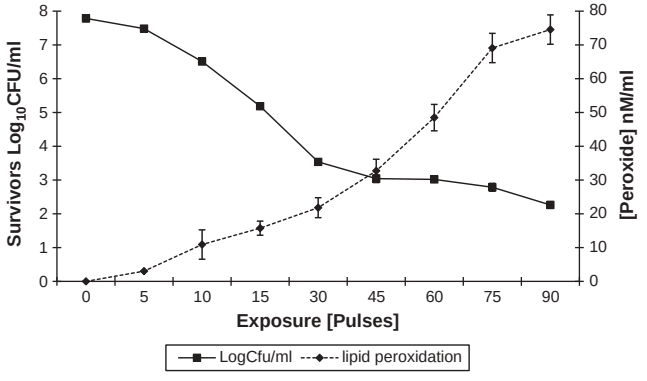

Fig. 6. Relationship between lipid peroxidation (mM/ml) and microbial cell reductions (Survivors Log_{10} CFU/ml) in pulsed UV light treated *C. albicans* D7100.

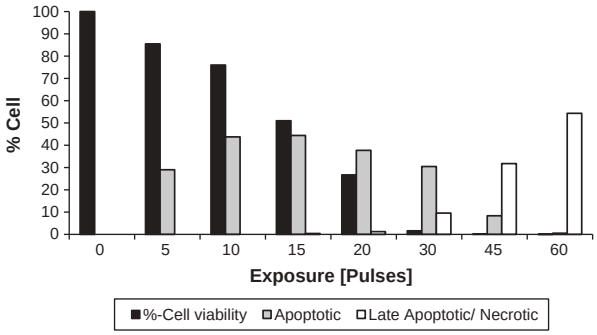

Fig. 7. Percentage occurrence of apoptotic (late and early) and necrotic *C. albicans* D7100 cells at various end-point determinations post pulsed light exposure at 7.2 J.

treated yeast leading to the formation of oxysterols that do not optimally support membrane function and cell growth (Böcking et al., 2000). Such alterations in the structure and functioning of ergosterol in PL-treated yeast may cause destabilisation of membrane with commensurate loss of fluidity leading to cell death. Böcking et al. (2000) also indicated that the fatty acid composition of cellular membrane lipids accounted for different sensitivities to oxidative damage, where the cell membrane also acts as a primary site for oxidative attack. These findings indicate that irreversible disruption of cell membrane functionality contributes to PL mediated inactivation in clinical-relevant *C. albicans*.

3.4. Determination of apoptosis and necrosis in PL-treated C. albicans

Apoptosis is a highly regulated form of programmed cell death in higher eukaryotes. Apoptosis is defined by a set of cytological alterations including externalisation of lipid phosphatidylserine (PS), chromatin condensation, DNA breakage and uncontrolled accumulation of ROS (Madeo et al., 2002). DNA fragmentation and formation of membrane-enclosed cell fragments termed “apoptotic bodies” (Martin et al., 1995) also occurs. Programmed cell death is found in many eukaryotes and is crucial for embryogenesis, tissue homeostasis and disease control in multicellular organisms (Madeo et al., 2002). Recently, it was discovered that simple unicellular organisms like budding *S. cerevisiae*, *Candida* spp., *Aspergillus* and bacteria also have the potential to undergo apoptosis (Phillips and Vousden, 2001; Madeo et al., 2002). Measurement of DAPI-stained yeast cells post PL-treatments in this study (data not shown) revealed fuzzy and prolate spheroid chromatin characteristics typical of apoptotic cell phenotypes. These PL-treated cells showed sickle-shaped DNA (ca. 1–10% of treated cells) and randomly distributed nuclear fragments (ca. 10–40% of treated cells) after 30 pulses (UV dose 0.82 μJ/cm^2). Increased fragmentation was observed with subsequent PL treatments beyond 30 pulses with 80–90% of the cells displaying abnormal chromatin distribution.

The translocation of lipid PS from the inner leaflet to the extracellular side of the plasma membrane is recognised as an early stage event in apoptosis and was detected using Annexin V that has a strong affinity for PS. When combined with PI that stains DNA of injured cells with permeable membranes, this combined Annexin V/PI staining approach facilitates distinction of early apoptotic (designated as Annexin V$^+$/PI$^-$), late apoptotic (designated as Annexin V$^+$/PI$^+$) and necrotic (designated as Annexin V$^-$/PI$^+$) cells. These differences, where apoptotic and necrotic yeast cells emitted green light and red fluorescence respectively, allowed discrimination of apoptotic and late apoptotic/necrotic cells (Fig. 7). Early and late stage apoptosis was confined to the initial 30 to 45 pulses in treated test yeast. Following 5 pulses approximately 30% demonstrated early-stage apoptotic cell characteristics with maximal Annexin V$^+$/PI$^-$ types evident after 15 pulses. The latter measure of cell injury also coincides with the localisation of mitochondrial ROS in similarly treated cells. After augmented PL-treatments the numbers of early-stage apoptotic cells decreased significantly with only 38, 31 and 4% of cells exhibiting this Annexin V$^+$/PI$^-$ characteristic after 20, 30 and 45 pulses respectively (Fig. 7). Following 15 pulses a UV dose-dependent increase in the numbers of PI$^+$ cell types was observed with ca. 10% displaying late apoptotic or Annexin $^+$/PI$^+$ characteristics. After 45 pulses (UV dose 1.24 μ/cm^2) cells were characterised as being late apoptotic or necrotic in appearance. A marked pattern emerged where with increased pulsing a decrease in late-apoptotic type cells occurred that was matched by an increase in necrotic cell (Annexin−/PI$^+$) numbers, with only necrotic cells observed following 150 pulses at 7.2 J. This general pattern was not unexpected as previous researchers have reported that numerous cytotoxic substances that cause necrosis when applied at elevated concentrations also induce apoptosis in similar cells when used at lower concentrations (Liberthal and Levin, 1996). However, to the best of the author's knowledge no other study exploring the occurrence of apoptosis in PL-treated microorganisms has been published.

Akin to mammalian cells, apoptosis in yeast cells can be induced by cell–cell communication, by external stresses such as conventional UV, toxins, starvation, heat or by reactive oxygen species (Madeo et al., 1999; del Carratore et al., 2002). One of the key factors differentiating apoptotic and necrotic cell death is the utilisation of energy by the former phenotype. Apoptosis is an energy dependent process and, therefore, if the energy depletion occurs above a critical threshold then necrosis will ensue (Gabai et al., 2000). Therefore, the mitochondria are not only important for the energetic status of the cell but are also pivotal organelles governing microbial life and death (Eisenberg et al., 2007). Damage to mitochondrial macromolecules may also lead to increased ROS production and further damage to mitochondrial components thereby causing a vicious downward spiral in terms of ROS production and damage accumulation in yeast cells (Madeo et al., 2002). Perrone et al. (2008) proposed that increased ROS production is due to reduced oxygen consumption by respiratory chain, which is associated with increased availability of intracellular oxygen for ROS production. Interestingly, the presence of extensive intracellular levels of ROS early in PL treatments (Figs. 3, 4 and 5) coincided with the appearance of apoptotic cell phenotypes. Another feature of apoptotic cell death process is an increase in the intracellular levels of superoxide anion (Simon et al., 2002), which also occurred in PL-treated cells as measured by mitochondrial ROS specific DHR-123 staining (Fig. 3). However, it is not clear as to what event comes first, the generation or accumulation of intracellular ROS leading to cell death, or the onset of apoptosis leading to cellular damage resulting in augmented ROS production in treated cells.

As with mammalian cell, yeast has an asymmetric distribution of phospholipids within the cytoplasmic membrane. However, on induction of apoptosis 90% of lipid phosphatidylserine (PS) that are initially orientated towards the cytoplasm are translocated to the outer leaflet (Martin et al., 1995). Therefore, lipid PS exposure serves as a sensitive marker for early stage apoptosis, which was detected in PL-treated *C. albicans* test strains using annexin V stain that has a high binding affinity for PS in the presence of Ca^{2+}. Also, other research groups have recently stated that an apoptotic yeast cell, such as *C. albicans* treated with acetic acid (Phillips and Vousden, 2001), will eventually suffer from a collapse of metabolism causing the breakdown of plasma membrane integrity leading to the appearance of a necrotic morphology. Eisenberg et al. (2010) have recently reported that the process of necrosis may still be regulated by defined molecular events, which is distinguishable from unregulated necrosis inflicted by brutal chemical or physical insults such as by PL-irradiation reported in this study. However as the effects are pleiotropic, further studies are needed in order to establish whether PL-induced apoptosis in *C. albicans* is initiated by general damage responses or by the alteration of specific cellular components.

3.5. Use of comet assay to investigate nuclear damage in PL-irradiated test yeast

The comet assay is a widely adopted rapid and sensitive technique for detecting and analyzing the potential of substances to cause DNA damage which includes strand breaks, alkali-labile sites, DNA cross-links, and incomplete excision repair sites in virtually all singles (Tice et al., 2000; Kirf et al., 2010). The basic principle of the comet assay is the migration of different sized DNA molecules in an agarose gel under an electrophoretic current. More specifically, induced DNA strand breakage leads to fragmentation of the supercoiled duplex DNA which can be stretched out by electrophoresis. Under an electric current, due to their reduced molecular size, fragments of damaged DNA move further within the pores of the agarose gel than intact DNA. This process leads to the microscopic appearance of the cell as a comet-like shape as the broken strands of the negatively changed DNA molecule become free to migrate in the electric field toward the anode. The intact DNA of the nucleus form the head of the comet and the small DNA fragments appear as the tail. The presence of strand breaks in PL-treated test yeast was visualized after 15 pulses (UV dose 0.41 μJ/cm^2) by the emergence of comet tails from the nuclei of the cells (Fig. 8). Greater tail moment and tail DNA were observed with enhanced pulses in treated test yeast ($p<0.05$). This constitutes the first occasion where the comet assay was used to confirm that damage to DNA occurs in PL-treated test yeast. Examination of test yeast post PL-treatments revealed that *C. albicans* did retain some capacity for repair that occurred within the first 20 pulses (or UV dose 0.55 μJ/cm^2) (Fig. 9). Previous researchers have reported that germicidal effect of PL-irradiation on pathogenic yeast is related in-part to the formation of pyrmidine dimmers inhibiting formation of new DNA that derails the process of cell replications (referred to as clonogenic death) (Farrell et al., 2009). This trend also coincides with the large variation in colony size and appearance that was observed in PL-treated test yeast

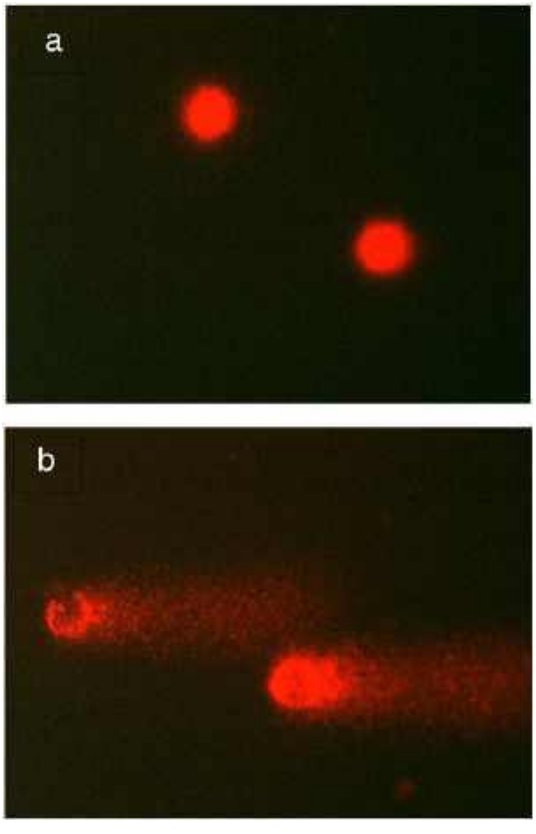

Fig. 8. Fluorescent images of DNA from untreated (a) and pulsed light-treated (b) *C. albicans* D7100 post comet assay.

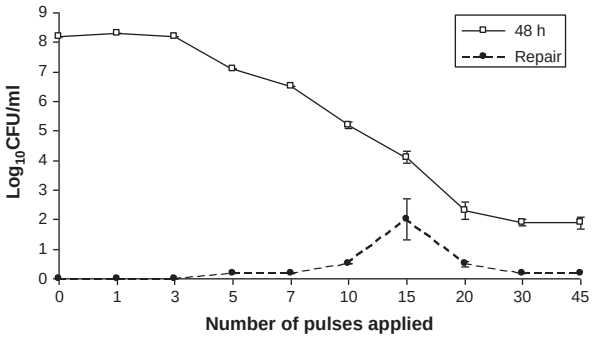

Fig. 9. Examination of the levels of *C. albicans* D7100 repair (expressed in Survivors Log_{10} CFU/ml) after exposure to pulsed light at 7.2 J/pulse.

following 24 and 48 h incubation at 30 °C. This difference in colony size and appearance was absent or less pronounced in similar samples exposed to more lethal levels of PL (60 pulses or UV does 1.65 μJ/cm^2). It is therefore likely that vital pathways mediating repair of damaged DNA in test yeast (such as direct reversal, base excision repair, nucleotide excision repair, mismatch repair, translesion synthesis and recombination direct reversal as reported by Rowe et al., 2008) are either decoupled or unable to function properly in PL-treated cells that also experience simultaneous damage to other vital cellular components. An early response of mitotic cells to low level stress injury is to enter a transient growth-arrested state in which the DNA is largely supercoiled, replication is halted and only a few stress genes are transcribed and translated (Crawford et al., 1996; Davis, 2000). This is not unexpected given the high levels of ROS measured PL treated test yeast in this study. Only when the cell is damaged severely by ROS, resulting in delay in cell division and some apoptosis, are specific antioxidant and repair functions induced strongly (Alic et al., 2001). Therefore, it is probable that a proportion of the PL-treated test yeast entered growth arrest as a protective measure against oxidative stress and were able to repair associated damage. If the oxidative stress is not severe enough to cause apoptosis or necrosis, cells will re-enter the growth cycle after a period of transient growth arrest (Davis, 2000). This would account for the appearance of new colonies following 48 h incubation, which were not observed during enumeration following 24 h incubation. Takeshita et al. (2003) reported that greater level of DNA damage occurs using conventional low-pressure UV light compared with treating similar *S. cerevisiae* samples with pulsed light.

Despite the fact that PL-irradiation has been approved for food surface decontamination by the US Food and Drug Administration (FDA) since 1999, significant variability in the efficacy of PL for treating similar spoilage and pathogenic microorganisms has been reported (Oms-Oliu et al., 2010). While the main mechanism of microbial inactivation is explained through photochemical effect that prevents the treated cell from replicating (Wang et al., 2005), our findings have also demonstrated that photophysical effects also play a significant contributory role in PL-mediated microbial lethality. Krishnamurty et al. (2008) also reported that PL-treated *Staphylococcus aureus* exhibited cell wall damage, cytoplasmic membrane shrinkage, cellular content leakage, and mesosome disintegration based on visualization with transmission electron microscopy and Fourier transform infrared spectroscopy observations.

4. Conclusion

Our findings clearly demonstrated that PL-irradiation inactivates *C. albicans* through a multi-hit cellular process that includes inflicting irreversible damage to DNA and destabilizing the functionality and integrity of plasma cell membranes. These findings have significant implications for PL-technology development, in particular for surface and water decontamination applications. PL has also significant

potential applications for the treatment of packaging material surfaces or food contact materials that require rapid disinfection, particularly as this approach is characterised by the lack of residual compounds that eliminates the need for use of chemical disinfectants and preservatives (Oms-Oliu et al., 2010). Despite growing evidence to support use of PL for the aforementioned applications, there is a pressing need to identify an intracellular marker such as onset of late apoptosis or early stage necrosis in PL-treated microbial pathogens so as to standardize and optimise treatments for different applications. Our findings clearly demonstrate that onset of necrosis in PL-treated *C. albicans* reflects lethality and can be used as an *in-vitro* real-time marker to confirm disinfection efficacy. Our findings have also significant broader implications as it is envisaged that this approach may be adopted, in time, as a complementary or alternative method to that of using conventional plate count and redox probes for the real-time detection of microbial lethality post decontamination. These conventional viability methods used to confirm disinfection efficacy are limited by the recognised fact that a sub-population of treated microorganisms may be capable of repair after resuscitation (Rowan, 2011). Whereas, confirmation of the detection of a late necrotic marker in PL-treated microorganisms appears to be related to a treatment regime that inflicts irreversible damage and is beyond that identified by use of plate count and possibly vital respiratory or redox staining. Our findings also corroborate the viewpoint of Guerrero-Beltrán and Barbosa-Cánovas (2004), which highlights the need to optimise all inter-related factors to achieve target inactivation level for specific food applications.

Additional future studies should focus on investigating and confirming that the relationship between microbial lethality and onset of necrosis in a broad range of PL-treated microbial spoilage and pathogenic microorganisms is an accurate and repeatable measurement of PL-process efficiency. Additional studies also merited including use of more ROS specific probes such as *N*-can-acetyl-3, 7-dihydroxyphenoxazine (Amplex Red) and 2-[6-(4′-hydroxy) phenoxy-3 H-xanthen-3-on-9-yl] benzoic acid (HPF) for the determination of $OH^{\cdot}$ and H_2O_2 levels respectively, which will help unravel roles of specific reactive oxygen species in PL-mediated cell death process. There is also the possibility that visible light component of the PL lamp spectrum contributed to yeast inactivation, which was not specifically investigated in this study. It is known that endogenous protoporphyrin IX is an efficient photosensitiser of photodynamic processes in biological objects exposed to visible light (Shumarina et al., 2003). The phototoxicity of endogenous protoporphyrin IX is due to its ability to generate ROS (predominantly singlet oxygen), which readily react with biologically important macromolecules and thereby cause their photo-oxidation, impairment of their functional activity and eventually cell death.

Acknowledgements

The authors thank the Science Foundation Ireland (Grant No. 07/RFP/ENMF374) and the Irish Health Research Board (Grant No. RP/2005/187) for funding this study. We also thank Dr. Dominik Kirf for his technical assistance with the comet assay. We also greatly appreciate the kind donation of clinical yeast strains from Prof. Martin Cormican at NUI, Galway, Ireland.

References

Adler, V., Yin, Z., Tew, K.D., Ronai, Z., 1999. Role of redox potential and reactive oxygen species in stress signaling. Oncogene 18, 6104–6111.
Alic, N., Higgins, V.J., Dawes, I.W., 2001. Identification of a *Saccharomyces cerevisiae*gene that is required for G_1 arrest in response to the lipid oxidation product linoleic acid hydroperoxide. Mol. Biol. Cell 12, 1801–1810.
Arami, S., Hada, M., Itadani, A., Yamashita, S., Hachiya, K., Kanayama, M., Tada, M., 1993. Damage of the membrane function in the yeast *Saccharomyces cerevisiae* by near-UV irradiation. Scientific Reports of the Faculty Agriculture Okayama University, 82, pp. 1–7.
Arami, S., Ada, M., Tada, M., 1997. Reduction of ATPase activity accompanied by photodecomposition of ergosterol by near-UV irradiation in plasma membranes prepared from Saccharomyces cerevisiae. Microbiology 143, 2465–2471.
Böcking, T., Barrow, K.D., Netting, A.G., Chicott, T.C., Coster, H.G., Hofer, M., 2000. Effects of single oxygen on membrane sterols in the yeast *Saccharomyces cerevisiae*. Eur. J. Biochem. 267, 1607–1618.
Carter, W.O., Narayanan, P.K., Robinson, J.P., 1994. Intracellular hydrogen peroxide and superoxide anion detection in endothelial cells. J. Leukocyte Biol. 55, 253–256.
Chang, T.-S., Cho, C.-S., Park, S., Yu, S., Kang, S.W., Rhee, S.G., 2004. Peroxiredoxin III, a mitochondrion-specific peroxidase, regulates apoptotic signaling by mitochondria. J. Biol. Chem. 279, 41975–41984.
Crawford, D.R., Schools, G.P., Salmon, S.L., Davies, K.J.A., 1996. Hydrogen peroxide induces the expression of *adapt15*, a novel RNA associated with polysomes in hamster HA-1 cells. Arch. Biochem. Biophys. 325, 256–264.
Davis, K.J.A., 2000. Oxidative stress, antioxidant defenses, and damage removal, repair, and replacement systems. IUBMB Life 50, 279–289.
de Repentigny, L., Daniel Lewandowski, D., Jolicoeur, P., 2004. Immunopathogenesis of oropharyngeal candidiasis in human immunodeficiency virus infection. Clin. Microbiol. Rev. 17, 729–759.
del Carratore, R., Della Croce, C., Simili, M., Taccinie, E., Scavuzzo, M., Sbrana, S., 2002. Cell cycle and morphological alterations as indicative of apoptosis promoted by UV irradiation in *S. cerevisiae*. Mutation Res 513, 183–191.
Eisenberg, T., Bultner, S., Kroemer, G., Madeo, F., 2007. The mitochondrial pathways in yeast apoptosis. Apoptosis 12, 1011–1023.
Eisenberg, T., Carmona-Gutierrez, D., Büttner, S., Tavernarakis, N., Madeo, F., 2010. Necrosis in yeast. Apoptosis 15, 257–268.
Elmnasser, N., Guillou, S., Leroi, F., Orange, N., Bakhrouf, A., Federighi, M., 2007. Pulsed-light system as a novel food decontamination technology: a review. Can. J. Microbiol. 53, 813–821.
Escobar, J.A., Rubio, M.A., Lissi, E.A., 1996. SOD and catalase inactivation by singlet oxygen and peroxyl radicals. Free Radical Biol. Med. 20, 285–290.
Fanello, S., Bouchara, J.-P., Jousset, N., Delbos, V., LeFlohic, A.-M., 2001. Nosocomial *Candida albicans* acquisition in a geriatric unit: epidemiology and evidence for person-to-person transmission. J. Hosp. Infect. 47, 46–52.
Farrell, H.P., Garvey, M., Rowan, N.J., 2009. Studies on the inactivation of medically important *Candida* species on agar surfaces using pulsed light. FEMS Yeast Res. 9, 956–966.
Farrell, H.P., Garvey, M., Cormican, M., Laffey, J.G., Rowan, N.J., 2010. Investigation of critical inter-related factors affecting the efficacy of pulsed light for inactivating clinically relevant bacterial pathogens. J. Appl. Microbiol. 108, 1494–1508.
Gabai, U.L., Vaglom, J.A., Volloch, U., Merlin, A.B., Force, T., Koutroumanis, M., Massie, B., Mosser, D.D., Sherman, M.Y., 2000. Hsp72-mediated suppression of c-jun n-terminal kinase is implicated in development of tolerance to caspase independent cell death. Mol. Cell. Biol. 20, 6828–6836.
Garvey, M., Farrell, H.P., Cormican, M., Rowan, N.J., 2010. Investigations of the relationship between use of *in vitro* cell culture-quantitative PCR and a mouse-based bioassay for evaluating critical factors affecting the disinfection performance of pulsed light for treating *Cryptosporidium parvum* oocysts in saline. J. Microbiol. Methods 80, 267–273.
Girotti, A.W., 1998. Lipid hydroperoxide generation, turnover and effector action in biological systems. J. Lipid Res. 39, 1529–1542.
Girotti, A.W., Thomas, J.P., Jordan, J.E., 1985. Inhibitory effect of zinc (II) on free radical lipid peroxidation in the erythrocyte membranes. J. Free Radical Biol. Med. 1, 385–401.
Gómez-López, V.M., Ragaert, P., Debevere, J., Devlieghere, F., 2007. Pulsed light for food decontamination: a review. Trends Food Sci. Technol. 18, 464–473.
Gourlay, C.W., Ayscough, K.R., 2005. The actin cytoskeleton: a key regulator of apoptosis and ageing? Nature Rev. Mol. Cell Biol. 6, 583–589.
Guerrero-Beltrán, J.A., Barbosa-Cánovas, G.V., 2004. Review: advantages and limitations on processing foods by UV light. Food Sci. Technol. Intern. 10, 137–147.
Hafer, K., Konishi, T., Schiestl, R.H., 2008. Radiation-induced long lived extracellular radicals do not contributed to measurement of intracellular reactive oxygen species using dichlorofluorescein method. Radiat. Res. 169, 469–473.
Helmerhorst, E.J., Breeuwer, P., van 't Hof, W., Walgreen-Weterings, E., Oomen, L.C.J.M., Veerman, E.C.I., Nieuw Amerongen, A.V., Abee, T., 1999. The cellular target of histatin 5 on *Candida albicans* is the energized mitochondrion. J. Biol. Chem. 274, 7286–7291.
Henderson, L.M., Chappell, J.B., 1993. Dihydrorhodamine 123: a fluorescent probe for superoxide generation? Eur. J. Biochem. 217, 973–980.
Herker, E., Jungwirth, H., Lehmann, K.A., Maldener, C., Fröhlich, K.U., Wissing, S., Büttner, S., Fehr, M., Sigrist, S., Madeo, F., 2004. Chronological aging leads to apoptosis in yeast. J. Cell Biol. 164, 501–507.
Hodgson, E.K., Fridovich, I., 1975. The interaction of bovine erythrocyte superoxide dismutase with hydrogen peroxide: inactivation of the enzyme. Biochemistry 14, 5294–5299.
Hsu, M.C., Chen, K.W., Lo, H.J., Chen, Y.C., Liao, M.H., Lin, Y.H., Li, S.Y., 2003. Species identification of medically important fungi by use of real-time LightCycler PCR. J. Med. Microbiol. 23, 1071–1076.
Ischiropoulos, H., Gow, A., Thom, S.R., Kooy, N., Royall, J.A., Crow, J.P., 1999. Detection of reactive nitrogen species using 2, 7-dichlorodihydrofluorescein and dihydrorhodamine 123. Methods Enzymol. 301, 367–373.
Jiang, Z., Woollard, A.C.S., Wolff, S.P., 1991. Lipid peroxide measurement by oxidation of Fe^{++} in the presence of xylenol orange: comparison with the thiobarbituric acid assay and an iodometric method. Lipids 26, 853–856.

Karu, T.I., 2008. Mitochondrial signaling in mammalian cells activated by red and near-IR radiation. Photochem. Photobiol. 84, 1091–1099.
Kirf, D., Higginbotham, D.L., Rowan, N.J., Devery, S.M., 2010. Cyto- and genotoxicological assessment and functional characterization of *N*-vinyl-2-pyrrolidone–acrylic acid-based copolymeric hydrogels with potential for future use in wound healing applications. Biomed. Mater. 5.
Klassen, R., Meinhardt, F., 2004. Induction of DNA damage and apoptosis in *Saccharomyces cerevisiae* by a yeast killer toxin. Cell. Microbiol. 7, 393–401.
Kono, Y., Fridovich, I., 1982. Superoxide radical inhibits catalase. J. Biol. Chem. 257, 5751–5754.
Krishnamurty, K., Tewari, J.C., Irudayaray, J., Demirici, A., 2008. Microscopic and spectroscopic evaluation of inactivation of *Staphylococcus aureus* by pulsed UV light and infrared heating. Food Bioproc. Technol. doi:10.1007/s11947-008-0084-8.
Kwon, S.J., Park, J.W., Kim, K., 1994. Inhibition of metal-catalysed oxidation systems by a yeast protector protein in the presence of thiol. Biochem. Mol. Biol. Int. 32, 419–427.
Lee, J.H., Choi, I.Y., Kil, I.S., Kim, S.Y., Yang, E.S., Park, J.W., 2001. Protective role of superoxide dismutases against ionizing radiation in yeast. Biochim. Biophys. Acta 1526, 191–198.
Liberthal, W., Levin, J.S., 1996. Mechanisms of apoptosis and its potential role in renal tubular epithelial cell injury. Am. J. Physiol. 271, 477–488.
Longo, V.D., Gralla, E.B., Valentine, J.S., 1996. Superoxide dismutase activity is essential for stationary phase survival in *Saccharomyces cerevisiae*: mitochondrial production of toxic oxygen species in vivo. J. Biol. Chem. 27, 12275–12280.
Madeo, F., Fröhlich, E., Ligr, M., Grey, M., Sigrist, S.J., Wolf, D.H., Fröhlich, K.U., 1999. Oxygen stress: a regulator of apoptosis in yeast. J. Cell Biol. 145, 757–767 K.U.
Madeo, F., Englhardt, S., Herker, E., Lehmann, X.I., Maldener, C., Proksch, A., Wissing, S., Fröhlich, K.U., 2002. Apoptosis in yeast: a new system with applications in cell biology and medicine. Curr. Gen. 41, 208–216.
Martin, S.J., Reutelingsperger, C.P., McGahon, A.J., Rader, J.A., van Schie, R.C., LaFace, D.M., Green, D.R., 1995. Early redistribution of plasma membrane phosphatidylserine is a general feature of apoptosis regardless of the initiating stimulus: inhibition by overexpression of Bcl-2 and Abl. J. Exper. Med. 182, 1545–1556.
Miloshev, G., Mihaylov, I., Anachkova, B., 2002. Application of the single cell gel electrophoresis on yeast cells. Mutation Res. 513, 69–74.
Nomura, K., Imai, H., Koumura, T., Arai, M., Nakagawa, Y., 1999. Mitochondrial phospholipid hydroperoxide glutathione peroxidase suppresses apoptosis mediated by a mitochondrial death pathway. J. Biol. Chem. 274, 29294–29302.
Nugent, M.J.D., Higginbotham, C.L., 2007. Preparation of a novel freeze thawed poly (vinly alcohol) composite hydrogel for drug delivery applications. Eur. J. Pharma. Biopharm. 67, 377–386.
Oms-Oliu, G., Martin-Belloso, O., Soliva-Fortuny, R., 2010. Pulsed light treatments for food preservation. A review. Food Bioproc. Technol. 3, 13–23.
Perrone, G.G., Tan, S.X., Dawes, I.W., 2008. Reactive oxygen species and yeast apoptosis. Bioch. Biophys. Acta. Mol. Cell. Res. 1783, 1354–1368.
Phillips, A.C., Vousden, K.H., 2001. E2F-1 induced apoptosis. Apoptosis 6, 173–182.
Qin, Y., Lu, M., Gong, X., 2008. Dihydrorhodamine 123 is superior to 2, 7-dichlorodihydorfluorescein diacetate and dihydrorhodamine 6 G in detecting intracellular hydrogen peroxide in tumor cells. Cell Biol. Intern. 32, 224–228.
Rahn, R.O., Stefan, M.I., Bolton, J.R., Goren, E., Shaw, P.S., Lykke, K.R., 2003. Quantum yield of the iodide–iodate chemical actinometer: dependence on wavelength and concentration. Photochem. Photobiol. 78, 146–152.
Rowan, N.J., 2011. Defining established and emerging microbial risks in the aquatic environment: current knowledge, implications and outlooks. Inter. J. Microbiol. doi:10.1155/2011/462832.
Rowan, N.J., MacGregor, S.J., Anderson, J.G., Fouracre, R.A., McIlvaney, L., Farish, O., 1999. Pulsed-light inactivation of food-related micro-organisms. Appl. Environ. Microbiol. 65, 1312–1315.
Rowe, L.A., Degtyareva, N., Doetsch, P.W., 2008. DNA damage-induced reactive oxygen species (ROS) stress response in *Saccharomyces cerevisiae*. J. Free Radical Biol. Med. 45, 1167–1177.
Royall, J.A., Ischiropoulos, H., 1993. Evaluation of 2′, 7′-dichlorofluorescein and dihydrorhodamine 123 as fluorescent probes for intracellular H2O2 in cultured endothelial cells. Arch. Biochem. Biophys. 302, 348.
Shumarina, A.O., Strakhovskaya, M.G., Turovetskii, V.B., Fraikin, G.Y., 2003. Photodynamic damage to yeast subcellular organelles induced by elevated levels of endogenous protoporphyrin IX. Microbiology 72, 434–437.
Simon, H.U., Hay-Yehia, A., Levi-Schaffer, F., 2002. Role of reactive oxygen species in apoptosis induction. Apoptosis 5, 415–418.
Solberg, C.O., 2000. Spread of *Staphylococcus aureus* in hospitals: causes and prevention. Scand. J. Infect. Dis. 32, 587–595.
Tabatabaie, T., Floyd, R.A., 1994. Susceptibility of glutathione peroxidase and glutathione reductase to oxidative damage and the protective effect of spin trapping agents. Arch. Biochem. Biophys. 314, 112–119.
Takeshita, K., Shitato, J., Sameshima, T., Fukunaga, S., Isobe, S., Arihara, K., Itoh, M., 2003. Damage of yeast cells induced by pulsed light irradiation. Intern. J. Food Microbiol. 85, 151–158.
Tarpey, M.M., Fridovich, I., 2001. Methods of detection of vascular reactive species. Nitric oxide, superoxide, hydrogen peroxide, and peroxynitrite. Circ. Res. 89, 224–236.
Tice, R.R., Agurell, E., Anderson, D., Burlinson, B., Hartmann, A., Kobayashi, H., Miyamal, Y., Rojas, E., Ryu, J.-C., Gasaki, Y.F., 2000. Single cell gel/comet assay: guidelines for in vitro and in vivo genetic toxicology testing. Environ. Mol. Mutagenesis 35, 206–221.
van der Rest, M.E., Kamminga, A.H., Nakano, A., Anraku, Y., Poolman, B., Konings, W.N., 1995. The plasma membrane of *Saccharomyces cerevisiae*: structure, function and biogenesis. Microbiol. Rev. 59, 304–322.
Virto, R., Mañas, P., Álvarez, I., Condon, S., Raso, J., 2005. Membrane damage and microbial inactivation by chlorine in the absence and presence of a chlorine-demanding substrate. Appl. Environ. Microbiol. 71, 5022–5028.
Wang, T., MacGregor, S.J., Anderson, J.G., Woolsey, G.A., 2005. Pulsed ultra-violet inactivation spectrum of *Escherichia coli*. Water Res. 39, 2921–2925.
Wawryn, J., Krzepilko, A., Myszka, A., Bilinski, T., 1999. Deficiency in superoxide dismutases shortens life span of yeast cells. Acta Biochim. Pol. 46, 249–353.

Journal of Microbiological Methods 80 (2010) 267–273

Contents lists available at ScienceDirect

Journal of Microbiological Methods

journal homepage: www.elsevier.com/locate/jmicmeth

Investigations of the relationship between use of *in vitro* cell culture-quantitative PCR and a mouse-based bioassay for evaluating critical factors affecting the disinfection performance of pulsed UV light for treating *Cryptosporidium parvum* oocysts in saline

Mary Garvey [a], Hugh Farrell [a], Martin Cormican [b], Neil Rowan [a,*]

[a] Department of Nursing and Health Science, Athlone Institute of Technology, Ireland
[b] Department of Bacteriology, National University of Ireland, Galway, Ireland

ARTICLE INFO

Article history:
Received 1 December 2009
Received in revised form 7 January 2010
Accepted 9 January 2010
Available online 21 January 2010

Keywords:
Cryptosporidium parvum
Pulsed light
In vitro HCT-8 cell culture-*q*PCR assay
Mouse-infectivity bioassay
Humic acid

ABSTRACT

Cryptosporidium parvum is an enteric coccidian parasite that is recognised as a frequent cause of water-borne disease in humans. We report for the first time on use of the *in vitro* HCT-8 cell culture-quantitative PCR (*q*PCR) assay and the *in vivo* SCID-mouse bioassay for evaluating critical factors that reduce or eliminate infectivity of *C. parvum* after irradiating oocysts in saline solution under varying operational conditions with pulsed UV light. Infections post UV treatments were detected by immunofluorescence (IF) microscopy and by quantitative PCR in cell culture, and by IF staining of faeces and by hematoxylin and eosin staining of intestinal villi in mice. There was a good agreement between using cell culture-*q*PCR and the mouse assay for determining reduction or elimination of *C. parvum* infectivity as a consequence of varying UV operating conditions. Reduction in infectivity depended on the intensity of lamp discharge energy applied, amount of pulsing and population size of oocysts ($P \leq 0.05$). Conventional radiometer was unable to measure fluence or UV dose in saline samples due to the ultra-short non-continuous nature of the high-energy light pulses. Incorporation of humic acid at a concentration above that found in surface water (i.e., ≤ 10 ppm) did not significantly affect PUV disinfection capability irrespective of parameters tested ($P \leq 0.05$). These observations show that use of this HCT-8 cell culture assay is equivalent to using the 'gold standard' mouse-based infectivity assay for determining disinfection performances of PUV for treating *C. parvum* in saline solution.

1. Introduction

Cryptosporidium parvum is an enteric coccidian parasite that is recognised as a frequent cause of water-borne disease in humans (Hunter and Syed, 2001). The occurrence of the environmentally resistant thick-walled oocyst stage of this organism has become a worldwide concern due to its resistance to disinfection with chlorine at concentrations typically applied in drinking water treatment plants (2 to 6 mg/L) (Rochelle et al., 2002). Development of alternative methods of *Cryptosporidium* disinfection for water applications (such as ozone and/or UV) has been hindered by the uncertainty surrounding efficacy of using *in vitro* surrogate viability assays due to their overestimation of oocysts survivors post treatments and the lack of critical data on the preferred use of *in vitro* cell culture and/or *in vivo* animal-based infectivity assays to determine inter-related factors governing repeatable disinfection of oocysts suspended in water (Johnson et al., 2005). Although recent studies that utilized at least 20 different cell lines have advocated the preferential use of the human ileocecal adenocarcinoma HCT-8 cell line as an equivalent *in vitro* method to that of using the "gold standard" mouse assay for measuring infectivity of *Cryptosporidium* (Rochelle et al., 2002), there is no evidence to date on the combined use of these approaches for assessing critical operational parameters governing pulsed UV light (PUV) as a means of disinfecting water contaminated with this enteroparasite. Development of PUV has recently received attention as a potentially novel strategy for decontaminating water as it offers many benefits including rapid microbial reductions and efficiency of energy usage due to underpinning high peak-power dissipation during treatments (Elmnasser et al., 2007; Gómez-López et al., 2007).

This constitutes the first study to report on the relationship between use of *in vitro* HCT-8 cell culture and mouse-based infectivity assays to determine critical operational factors affecting the disinfection performance of PUV for treating *C. parvum* oocysts suspended in saline solution.

* Corresponding author. Department of Nursing and Health Science, Athlone Institute of Technology, Dublin Road, Athlone, Co. Westmeath, Ireland. Tel.: +353 906473081; fax: +353 906486135.
E-mail address: nrowan@ait.ie (N. Rowan).

0167-7012/$ – see front matter © 2010 Elsevier B.V. All rights reserved.
doi:10.1016/j.mimet.2010.01.017

2. Materials and methods

2.1. C. parvum oocysts

C. parvum oocysts (Iowa isolate derived from a bovine calf) were purchased from Waterborne Inc USA. Oocysts were stored in sterile PBS (0.01 M phosphate buffer, containing 0.0027 M KCL and 0.137 MNaCl at a pH of 7.4) with 100 U of penicillin/ml, 100 µg of streptomycin/ml and 100 µg of gentamicin/ml and stored at 4 °C until they were used for UV treatment studies. The excystation rate was determined for each batch of oocysts by microscopic observation following sequential incubation at 37 °C in acidified Hanks balanced salt solution for 1 h and in 0.8% trypsin–0.75% sodium taurocholate for 1 h, followed by incubation at room temperature for 30 min as described elsewhere (Rochelle et al., 2002). Identification of *C. parvum* oocysts was confirmed by PCR targeting of a 620 bp polymorphic region of the β-tubulin gene by previously published procedures (Rochelle et al., 1999) [data not shown]. For negative infection studies, oocysts were inactivated by heating at 70 °C for 30 min. All experiments were carried using oocysts with greater than 80% viability, as determined by *in vitro* excystation as per Korich et al. (2000).

2.2. Enumeration of oocysts

Standard counts were determined for all oocyst stocks. Viable oocysts were enumerated by serial dilution in PBS containing the aforementioned antibiotics using both fluorescence microscopy (confocal microscopy, Leica DM 600 CS Germany), and real-time quantitative PCR (*q*PCR) post infection in HCT-8 cell line as per method of Keegan et al. (2003) with modifications (described below). Use of a combined surrogate dye staining method comprising propidium iodide (PI) and a fluorescein-labelled mouse-derived monoclonal antibody A400FLR-1X Crypt-a-Glo™ (having corresponding epitope on oocyst cell wall; Waterborne Inc, New Orleans, USA) was used to confirm the viability of oocysts. Oocyst suspensions at different population sizes were initially centrifuged at 3000 rpm for 15 min at 4 °C, then re-suspended in acidified Hanks Balanced Salt Solution pH 2.7 for 1 h at 37 °C before filtration onto polycarbonate black 0.8 µm-pore-size membrane filters (Fischer Scientific) using a filter system (Millipore) at a vacuum pressure of 200 mbar (1 bar = 10^5 Pa.). 10 µl of propidium iodide (PI) (Sigma), prepared by dissolving 1 mg of PI in 1 ml of 0.1 M sterile PBS, and 1 drop (ca. 45 µl) of A400FLR-1X Crypt-a-Glo™ were then applied to oocysts on the membrane and incubated for 2 h at room temperature in the dark. The membranes were mounted on glass microscope slides with 4 µl mounting medium (glycerol [nonphotoreactive], 2 ml; 100 mg of DABCO {1,4-diazabiccyclo[2,2,2] octane} per ml of double distilled water, 2.4 ml; 0.1 ml Tris buffer, 4.8 ml, formalin 0.5 ml; and 5 MNaCl, 0.5 ml) and sealed with coverslips and clear nail varnish. Non-viable oocysts stained bright red due to uptake of PI when viewed at an excitation wavelength of 460 to 500 nm and an emission spectrum of 510 nm to 560 nm. Whereas all viable and non-viable oocysts stained apple-green when stained with A400 FlR-1X at an excitation wavelength of 460 to 500 nm and an emission wavelength of 510 to 560 nm. Entire membranes were scanned and all oocysts suspensions were counted by fluorescence microscopy. All counts were determined in triplicate.

2.3. Pulsing of Cryptosporidium with UV rich light

A bench-top pulsed power source (PUV-1, Samtech Ltd., Glasgow) was used to power a low-pressure (60 kPa) xenon-filled flashlamp (Heraeus Noblelight XAP type NL4006 series constructed from a clear UV transparent quartz tube), that produced a high-intensity diverging beam of polychromatic pulsed light, was used in this study as per Farrell et al. (2009) with modifications. The pulsed light has a broad-band emission spectrum extending from the UV to the infrared region with a rich UV content and its intensity also depends on the level of the voltage applied. The light source has an automatic frequency-control function that allows it to operate at 1pulse/s that was used throughout this study. Light exposure was homogenous as the xenon lamp measuring 9 cm × 0.75 cm was longer than the 8.5 cm diameter Petri dishes used in the tests which were placed directly below the lamp, which ensured that full coverage of the agar surface occurred and eliminated possible shading effects. For standard treatments (unless otherwise noted), the light source was mounted at 8 cm above the treatment area, which was set as the minimum threshold distance by the fabricant and was shown recently to provide optimal inactivation for a range of other recalcitrant microbial pathogens (Farrell et al., 2009). In this study, standard treatments involved suspending predetermined numbers of *C. parvum* in 10 ml of PBS that were transferred to Petri dishes that was then subjected to lamp discharge energies of 3.2 J, 12.8 J, 16.2 J, and 20 J at 8 cm distance from the light source. Due to the nature of the ultra-short high-energy pulses (i.e., non-continuous approach), the UVX radiometer (UVP Ultra-Violet Products) used for these present studies was not capable of measuring fluence or UV doses for PUV. Therefore, all treatments were characterized in terms of lamp discharge energy (J) for all PUV experiments. However, it was possible to measure fluence or UV dose (mJ/cm^2) for control studies using a continuous LP UV system in water samples, where values were determined after considering important inter-related factors described by Bolton and Linden (2003). The number of pulses of light used ranged from 0 (untreated control) to 350 pulses. The influence of population size of oocysts (range 10^1 to 10^5 oocysts/ml) on the decontamination efficacy of PL was also determined by challenging viable oocysts to both cell culture and mouse-infectivity assays post UV treatments as described below. Heating of the oocyst supensions was measured using a thermocouple and by thermal imaging (IRI 4010, InfraRed Integrated Systems Ltd, Northampton, England) as per modified method of Nugent and Higginbotham (2007). There was no discernable increase in water temperature during each treatment. All studies were run in triplicate.

2.4. In vitro cell culture infectivity assay

Monolayers of the human ileocecal adenocarcinoma cell line HCT-8 (ATCC CCL-244: American Type Culture Collection, Rockville, Md.) were grown with regular subcultering in RPMI 1640 growth media (Sigma) with L glutamine and supplemented antibiotics (penicillin G, 100,000 U/L, streptomycin, 0.5 g/L and amphotericin B, 0.5 g/L), sodium bicarbonate, 2 g/L, and 10% fetal calf serum adjusted to pH 7.4. HCT-8 cells were grown in T75 cm^{-2} cell culture flasks (Sarstedt, Germany) in a humidified incubator at 37 °C in an atmosphere containing 5% (vol/vol) CO_2 for ca. 24 h until 80 to 90% confluent monolayers had formed. Cell monolayers were then detached with 0.25% (vol/vol) trypsin-EDTA and subsequently seeded into each of 8 well chambered slides (Lab Tec II, Nunc) at a concentration ca.1×10^5 cells per well. After UV or heat treatments, the oocysts were stimulated by re-suspension in acidified HBSS (Hank Balanced Salt Solution, pH 2.7) and then in 1.0% (wt/vol) bile salts (Sigma, pH 7) for 1 h at 37 °C. After two washing steps with sterile PBS, oocysts were re-suspended in cell culture media and thereafter 350 µl aliquots were then added to each well. Untreated oocysts were also stimulated to infect the cell monolayer as described above and provided a positive control. Duplicate sample of oocysts was heat treated at 70 °C for 30 min and this preparation was used as a negative control as per Rochelle et al. (2002). Samples were incubated for 48 h at 37 °C in 5% (vol/vol) CO_2 atmosphere, which included the addition of fresh RPMI media after 24 h incubation. Each individual well containing a separate monolayer was fixed by flooding with 100% (vol/vol) methanol (Sigma) which was subsequently left to stand for 10 min at room temperature. After removal of methanol, 75 µl of the fluorescein stain Sporo-Glo™A600FLR-20X (Waterborne Inc, UK) was added to each well for

45 min (at 37 °C), which detects different life cycle stages of *Cryptosporidium in vitro*. The inoculated HCT-8 cell monolayers were then counterstained for 1 min with C101 containing Evans blue dye (Waterborne Inc, USA). All slides were examined under fluorescence microscopy (Leitz Diaplan fluorescence microscope) at an excitation wavelength of 460 to 500 nm and an emission wavelength of 510 to 560 nm for Sporo-Glo™ and an excitation wavelength of 550 nm and emissions wavelength of 610 nm for the counterstain C101. All wells containing separate monolayers was examined and noted as positive or negative for sites of parasitic infection or foci of infection. Images of *C. parvum* life cycle stages were captured using of a camera (Hamamatsu Colour Chilled 3cco Camera) mounted on the aforementioned fluorescence microscope. All studies were performed in triplicate.

2.5. Combined cell culture-quantitative PCR (CC qPCR) assay for enumerating viable C. parvum post treatments

Real-time, Taqman-quantitative PCR (*q*PCR) was performed using primers (TIB MOLBIOL, Berlin, Germany) specific for the 18S region of *Cryptosporidium* following the method of Keegan et al. (2003) with some slight modifications. The sequence of the Taqman probe was based on the conserved eukaryotic probe of Amman et al. (1990) with the following sequence: 5-′-(6-FAM) ACC AGA CTT GCC CTC C (TAMRA). An aliquot (4 µl) of the Lightcycler Taqman® Master kit (Roche Diagnostics, West Sussex, England) comprising Taq DNA polymerase, reaction buffer, $MgCl_2$ and dNTP was used in each reaction. Cycling parameters were initial denaturation for 10 min at 95 °C followed by 50 cycles of denaturation for 10 s at 95 °C, annealing for 40 s at 40 °C, extension for 1 s at 70 °C and cooling for 30 s at 40 °C on a LightCycler® device (Model 1.5, Roche Diagnostics, West Sussex, England). The large number of cycles was used to ensure detection of low levels of infection. On completion of each *q*PCR run amplification curves were analyzed by LightCycler® software (version 3.5, Roche) and a standard curve of oocyst DNA concentration determined. When required, PCR amplicons were visualized by UV illumination following electrophoresis in 1% agarose gels containing ethidium bromide. DNA standards were prepared from fresh oocysts ranging in concentration from 10^1 to 10^7 oocysts/ml by dilution in PBS following standard viable count determinations. Aliquots of oocysts at different densities were then stimulated to infect the HCT-8 cell line that were seeded into 24 well plates (Sarstedt) at a concentration of ca. 1×10^4 cells/ml at 90% confluency. The latter cell line stimulation occurred by re-suspension and separate incubations for 1 h in acidified HBSS and in bile salts as described earlier. 1 ml aliquots of each concentration range of excysted oocysts were re-suspended in RPMI cell culture growth media and added to one well of the 24 well plate. Following a 48 h incubation at 37 °C in a humidified atmosphere of 5% (vol/vol) CO_2, the cell culture media with non-adherent or internalized *C. parvum* was removed by aspiration and discarded. Mammalian cells were then washed with sterile PBS and trypsinized using 200 µl of 0.25% (vol/vol) trypsin/EDTA (Sigma) and left for 15 min at 37 °C until complete detachment of the monolayer had occurred. Cells were then centrifuged at 1000 rpm for 10 min and re-suspended in 200 µl sterile PBS, thereafter the mammalian cells and *C. parvum* sporozoite cell membranes were lysed using PCR template preparation kit (Roche Diagnostics, West Sussex, England) in order to produce DNA (template) and standard curve (Fig. 1). The aforementioned procedure was then repeated to determine infectivity of oocysts subjected to varying UV parameters or heating at 70 °C for 30 min (negative control). Log inactivation of oocysts (L) is defined by $L=\log_{10}[Nd/No]$, where No is the initial concentration of oocysts and Nd is the concentration of viable infectious oocysts post disinfection treatments as detected by combined cell culture-*q*PCR assay as per method of Lee et al. (2008)).

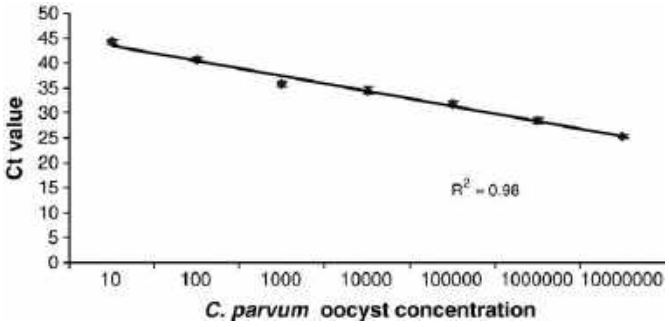

Fig. 1. Standard curve for serially diluted *Cryptosporidium* DNA standards.

2.6. Mice infectivity studies

Twenty day old SCID mice were obtained from Charles River Laboratories, Inc. (England). On arrival the mice were placed in mice cages (2 per cage) in a temperature controlled animal house at Athlone Institute of Technology. Appropriate bedding, food in the form of high protein food pellets and water were supplied. Different population densities of oocysts of *C. parvum* were suspended in warmed (37+/−2 °C) sterile PBS without and with the addition of humic acid (10 mg/l). After exposure to different regimes of PUV or monochromatic light, samples were wrapped in tin foil to prevent photoreactivation and centrifuged at 3000 rpm for 15 min. The supernatant was removed and the pellet re-suspended in 10 ml sterile H_2O, which replaced use of PBS as the latter caused the mice unnecessary discomfort that was possibly related to the salinity of the solution. Following UV and heat (control) treatments, mice were inoculated by delivering a 1 ml aliquot of each dose of oocysts to the back of the throat with a sterile syringe that contained a feeding needle. Each set of UV parameters under study encompassed the use of four mice where two were inoculated with oocysts after exposure to pre-determined UV parameters while the two mice were administered with sterile water (negative control). Positive control studies involved inoculating mice with different concentrations of viable oocysts (as determined by viability staining). Once dosed, the mice were placed in a new animal cage with fresh bedding, food and water. Once satisfied that all mice were suitably comfortable, they were housed in the animal house with daily monitoring. Faeces was collected each day and subjected to the fluorescent stain Auramine O [bis(*p*-dimethylaminophenyl)-methylenimine hydrochloride]with Thiazine red counterstain to determine if infectivity had occurred. Samples of faeces were also stained with the *Cryptosporidium* specific stain ST103R Crypto-a-glo™ (Waterborne Inc) as per the manufacturer's instructions to confirm that infection was present. Slides were examined using confocal microscopy (Leica DM 600 CS) for the presence of *C. parvum* oocysts, which appeared as green fluorescent discs against a red background (excitation filter 490 nm; emission filter 510 nm). Six weeks after inoculation the mice were sacrificed by cervical dislocation and intestinal samples were embedded in wax (Lambwax, pelletized paraffin wax) using a histokinette (Leica, TP 120, Germany) before being cut into thin slices by use of a microtome (Reichert-jung 2035 Biocut, Germany) for subsequent microscope examination. Infections were detected by examining formalin-fixed (Bouins solution, Sigma), slide-mounted (glycerine coated,Sigma, Ireland), hematoxylin-(Mayer, Fluka BioChemika, Sigma, Germany) and eosin (Ehrlich, Fluka BioChemika, Sigma, Germany) stained sections (5 um by 2 to 3 cm) of the terminal ileum that was removed from each mouse at necropsy (Korich et al., 2000). After the latter H and E staining, slides were examined by microscopy (Nikon Eclipse E200 microscope with attached Pixelink micron optical Nikon camera utilising Adobe Photoshop Elements 3.0 software for imaging analysis) to determine if areas of parasitic infection were present. The ileum was chosen as it is the first region of the gut to be colonized by the parasite and harbors

the majority of developmental stages (Rochelle et al., 2002). 10 µl samples of intestinal sample stained with 45 µl of A400FLR-1X Crypt-a-glo™ (Waterborne Inc) for 2 h at 37 °C were also examined by IF microscopy for the presence of *C. parvum* life cycle stages. Evidence of infection was defined as the presence of *C. parvum* parasite developmental stages in the microvilli of any of the prepared histological sections. Use of animals for this particular study was assessed by the ethics reviewing panel at AIT, and externally by the Department of Health and Children (Ireland) after which an animal license [B100/4061 was issued.

2.7. Statistical analysis

Student's *t*- tests and ANOVA one-way model (MINITAB software release 13; Mintab Inc., State College, PA) were used to compare the effects of the relationship of independent variables on light treatments.

3. Results and discussion

3.1. Use of in vitro cell culture-qPCR assay for measuring infectivity of C. parvum post UV treatments

Studies showed that there was a good agreement between use of immunofluorescence (IF) microscopy and *q*PCR for detecting infectious *C. parvum* following 48 h exposure to HCT-8 cell monolayers post PUV treatments (Table 1). Studies also showed more rapid reductions in *C. parvum* numbers occurred using higher levels of lamp discharge energy and with greater pulsing at 8 cm distance from the light source. *q*PCR revealed that approximately 4-$\log_{10}$ reductions in *C. parvum* infectivity occurred using 350, 250, 90 and 60 pulses at lamp discharge energies of 3.2 J, 12.8 J, 16.2 J and 20 J respectively. It was not possible to confirm complete elimination of *C. parvum* infectivity post PUV studies at the lower detection limit of the *q*PCR assay was 10 oocysts as set by standard curve for increasing concentrations of *Cryptosporidium* DNA (Fig. 1).

Table 1
Influence of lamp discharge energy and pulse number on reduction of *C. parvum* infectivity as determined by use of the combined *in vitro* HCT-8 cell culture-quantitative PCR assay. PUV treatments were performed at 8 cm distance from light source.

PUV parameters		HCT-8 cell culture infectivity assay			
Lamp discharge energy (J)	Number of pulses	No. of infected monolayers[a]	IF microscopic detection	Presence of foci of infection	$\log_{10}$ reduction (infectivity)[b]
0	0	4	High	+	0
3.2	≤150	4	High	+	1.9 ± 0.1
	200	3	High	+	2.3 ± 0.2
	250	2	Low	−[c]	2.8 ± 0.3
	300	1	Low	−	3.5 ± 0.3
	350	0	−[c]	−	≥4
12.8	≤100	4	High	+	2.2 ± 0.1
	150	3	Medium	−	2.6 ± 0.4
	200	1	Low		3.1 ± 0.3
	250	0	−	−	≥4
16.2	10	4	High	+	1.3 ± 0.3
	20	4	Medium	+	1.9 ± 0.3
	40	3	Medium	−	2.5 ± 0.4
	60	2	Low	−	2.9 ± 0.3
	80	1	Low	−	3.3 ± 0.5
	90	0	−	−	≥4
20	5	4	High	+	1.2 ± 0.2
	15	3	Medium	+	1.9 ± 0.4
	30	2	Low	−	2.6 ± 0.4
	40	1	Low	−	3.2 ± 0.3
	50	1	Low	−	3.8 ± 0.4
	60	0	−	−	≥4

[a] Standard dose of ca. 1×10^5 oocysts/ml was applied to each of 4 replicate cell monolayers per PUV treatment. Infectivity was determined by both *q*PCR and immunofluorescence (IF) microscopy in HCT-8 cells.
[b] Log reduction in viable *C. pavum* determined by cell culture-*q*PCR assay. As lower limit of detection for standard curve using *Cryptosporidium* DNA is ca. 10 oocysts, the maximum lethality detected is 4 $\log_{10}$ orders. Mean value shown for 4 replicate cell monolayers, ±SD.
[c] −, not detected.

This pattern agrees with the recent findings of Farrell et al. (2009) who investigated the relationship between varying operational parameters and commensurate reductions in numbers of clinically relevant yeast using a similar PUV system. Similar to the PUV-inactivation data reported for the Iowa strain of *C. parvum* in this study, it also took ca. 60 pulses of light to reduce a range of *Candida* species by 4 $\log_{10}$ orders when the PUV system was operated at the highest discharge energy (20 J) at 8 cm distance from the light source. This markedly contrasted for the requirement to use ≤10 pulses under similar operational parameters in order to reduce pre-determined populations of *Escherichia coli* 25922 and *Staphylococcus aureus* 25923 by ca. 7 log10 orders. Lee et al. (2008) also demonstrated that efficacy of PUV for inactivation of *C. parvum* is dependent on positioning of the light source and duration of irradiation, where they used the HCT-8 cell culture and quantitative real-time PCR to show that reductions in oocyst infectivity (6 $\log_{10}$) were maximal when this parasite was irradiated at 20 cm from the pulsed-light source for 60 s, for which the UV dose was 278 mJ/cm^2. Farrell et al. (2009) reported that positioning of the light source at 20 cm distance from the target area exhibited the least amount of inactivation for *Candida* species that appear to exhibit similar PUV tolerances to that of *C. parvum*. However, fluence values reported by Lee et al. (2008) could be considered questionable as these researchers measured UV dose per pulse in stagnant (non-mixed) water samples from 220 to 400 nm in 0.22 nm step using a spectrophotometer as the energy per flash was dissipated within 150 µs, which also appears beyond the measurement capability of radiometric devices. While this UV dose detection strategy has probably been adopted to best determine UV values for rapid ultra-short exposures (as opposed to conventional continuous treatment using collimated beams), it is imperative that accurate measurements and standardization of UV dose for PUV systems is achieved for possible future applications. In order to progress PUV technology further it is important that water-based studies consider key criteria recommended by Bolton and Linden (2003). To reiterate, it is due to this reason that the efficacy of PUV disinfection performances were reported using lamp discharge energies in the present study.

The presence of multiple foci of infection (representative of different life cycle stages of *C. parvum*) was evident in HCT-8 cells that were exposed to large numbers of infectious *C. parvum* or to the untreated control samples containing ca. 10^5 oocysts/ml (Table 1). The designations high, medium and low levels or infectivity in Table 1 relate to the operator interpretations of the degree of infection evident by visual IF microscopic examination of samples. Albeit subjective, the authors feel that it does indicate a measure of infectivity in *C. parvum* post PUV treatments. Similar samples of oocysts that were subjected to heating at 70 °C for 30 min did not infect HCT-8 cells (negative control). Use of the surrogate vital stains revealed overestimation by ca. 1.1 and 1.5$\log_{10}$ between the number of viable oocysts and corresponding number of infectious oocysts where the latter was determined by inoculating similar PUV-treated samples (comprising 10^5 oocysts/ml) in cell culture and in mice, respectively [data not shown].

Rochelle et al. (2002) also observed significant correlation ($r = 0.89$) between infectivity in HCT-8 cells and infectivity in CD-1 mice for the *C. parvum* of the Iowa, TAMU and Moredun isolates at a concentration of 1×10^5 oocysts/ml that had been exposed to UV doses ranging from 0 to 8 mJ/cm^2 using a medium-pressure (MP), continuous (1 kW) UV lamp. The mean level of inactivation obtained at 4 mJ of UV light per cm^2 was ca. 1.6 ± 0.2$\log_{10}$ as measured by HCT-8 cell culture compared to 1.4 ± 0.3 $\log_{10}$ when measured by the CD-1 mouse assay. The average standard deviation for replicate measurements of infectivity in HCT-8 cells and CD-1 mice was 11.9

and 13.3%, respectively, for oocysts exposed to MP-UV light. The latter pattern showed good concordance with average standard deviations for HCT-8 cell culture and mouse data (11.5 and 13.9%, respectively) for infectivity data from similar untreated samples. Indeed, these authors also observed an increase in the amount of infection with an increase in oocyst dose, where the level of infectivity was reported to be 75% and 85% with 50 and 500 oocysts respectively. Mofidi et al. (2001) also used HCT-8 cell cultures and real-time PCR assay to evaluate the efficacy of UV light as a disinfectant against *C. parvum* and demonstrated an average level of inactivation of 94% (1.2 $\log_{10}$) using a polychromatic UV light.

With the exception of this present study and Lee et al. (2008), other published data have utilized low and medium-pressure UV light to inactivate cryptosporidia, where Craik et al. (2001), Keegan et al. (2003), Mofidi et al. (2001) and Rochelle et al. (2005) reported that UV doses of 6, 5.8, 10 and 20 mJ/cm^2, respectively, which provided an average of 2 log reduction in infectivity of *C. parvum*. Variation in PUV-inactivation performances can be attributed to multiple inter-related factors including differences in UV irradiation method and strain of *C. parvum*, the duration of UV exposure at any applied dose appears paramount for reducing or eliminating infectivity. Lee et al. (2008) recently reported that the minimum dose of pulsed UV light required for effective reduction in *C. parvum* infectivity (2 $\log_{10}$) was 15 mJ/cm^2, which was achieved by 5 s of irradiation at 30 cm from the 2 kV light source that operated at 10 pulses/s in each experiment. Therefore, it is quite apparent that effectively reducing or eliminating the threat of low numbers of *C. parvum* in contaminated water at full treatment plant scale level using a possible combined MP-PUV strategy will require more research and development as current data is very limited.

3.2. Use of in vivo mouse-based assay for measuring infectivity of C. parvum post UV treatments

These studies revealed a good agreement between use of the SCID-mouse-infectivity assay and the aforementioned *in vitro* HCT-8 cell culture-*q*PCR assay for determining the degree of infectivity of *C. parvum* post exposure to PUV treatments (Table 2). Indeed, elimination of infectivity in inoculated SCID mice (i.e., as determined by absence of *C. parvum* in the faeces or intestinal villi of mice), also occurred after use of augmented lamp discharge energy and pulsing. Absence of infectivity was also observed after 350, 250, 90 and 60 pulses at 3.2 J, 12.8 J, 16.2 J and 20 J respectively at 8 cm distance from the light source where initial treated dose was ca. 10^5 oocysts/ml (Table 2). Commensurate studies revealed that mice surviving these particular PUV regimes made similar weight gains of ca. 6.2 ± 0.4 g over the 6 week incubation period compared to similar mice that were inoculated with infectious oocysts post UV treatments (ca 4.6 ± 0.3 g) or compared to positive control group mice that received 10^5 infectious oocysts (ca 3.9 ± 0.4 g). It was also observed that mice with lower body weights during these trials excreted more faeces compared to non-infected mice. A UV dose of 32.7 mJ/cm^2 was required to reduce infectivity of *C. parvum* in mouse model by an average of 3 log orders level using the continuous LP system (data not shown). There was also a strong relationship between use of cell culture and the mouse-infectivity bioassay for determining the influence of *C. parvum* population size on PUV disinfection performance at 8 cm distance from light source with lamp discharge energy of 16.2 J (Table 3). However, greater variability between infectivity measurement assays occurred with use of lower oocyst numbers with the animal model appearing to be less sensitive at detecting infective oocysts in these particular samples ($P \leq 0.05$). It was not possible to visually detect survivors using immunofluorescent microscopy alone without the aid of *q*PCR where the dose was ca. 10 viable oocysts. Moreover, significant variable was evident between samples at lower inoculation densities as studies revealed that ca. 50% of HCT-8 cell monolayers were infected by non-PUV treated *C. parvum* when the artificially seeded population was ca. 10 to 40 oocysts/ml. The presence of infective oocysts that survived varying PUV exposure regimes (as reported in Table 2), was detected in the microvilli of treated mice using hematoxlyin and eosin staining (Fig. 2). The presence of humic acid at a concentration above that commonly found in surface water (i.e., 10 ppm) did not affect PUV disinfection performances ($P \leq 0.05$) (Table 3). Previous researchers have also reported that presence of organic matter such as humic acid may reduce the efficacy of UV for inactivating microorganisms due to attenuation of light by the former particles, whereby reducing microbial exposures. A landmark work of King et al. (2008) identified increased dissolved organic content in environmental waters with decreased solar inactivation of *C. parvum* oocysts. However, this present study showed that incorporation of humic acid at a concentration above that commonly found in surface water (i.e., 10 ppm) as stated by Cantwell et al. (2008)) did not significantly affect the inactivation performance of PUV for treating *C. parvum* oocysts suspended in water.

Table 2
Infectivity assessment of *C. parvum* as determined by *in vivo* infectivity in SCID-mouse model post pulsed UV treatments at 8 cm distance from light source.

PUV parameters		No. of SCID mice		Presence of oocysts in treated mice		
Discharge energy (J)	No. of pulses	Dosed	Infected after treatment	Faeces[a]		Intestinal villi[b]
				Shedding	Oocysts/ml	
0	0	4	4	Yes	325 ± 32 A[c]	Yes
3.2	≤250	4	4	Yes	303 ± 24 A	Yes
	300	4	2	Yes	86 ± 11 B	Yes
	350	4	0	No	− D	No
12.8	≤100	4	4	Yes	296 ± 42 A	Yes
	150	4	3	Yes	106 ± 28 B	Yes
	200	4	1	Yes	54 ± 16 C	Yes
	250	4	0	No	− D	No
16.2	50	4	4	Yes	312 ± 18 A	Yes
	60	4	3	Yes	114 ± 30 B	Yes
	90	4	0	No	− D	No
20	25	4	4	Yes	288 ± 34 A	Yes
	50	4	2	Yes	98 ± 33 B	Yes
	60	4	0	No	− D	No

[a] Presence of oocysts in mice faeces as determined by immunofluorescence microscopy of stained faecal pellets using ST103R-Crypto-a-glo™. Dose was standardized at ca. 1×10^5 oocysts/ml for all studies, and studies were performed in triplicate.
[b] Presence of *C. parvum* different life cycle stages in intestinal villi of SCID mice as determined by hematoxylin and eosin staining followed by microscopic examination.
[c] Values with different capitalized letters are significantly different at $P \leq 0.05$. Mean of triplicate counts performed by measuring presence of oocysts in 40 µl of stained faeces. ±, indicates standard deviation, −, oocysts not detected.

Table 3
Relationship between use of PUV (at lamp discharge energy of 16.2 J) and number of pulses required to eliminate the infectivity of different populations of *C. parvum* oocysts as determined by use of *in vitro* HCT-8 cell line assay and *in vivo* SCID-mouse model.

Initial concentration of infectious oocysts (oocysts/ml)[a]	Humic acid conc. (ppm)	Number of pulses required to eliminate infectivity using HCT-8 cell-*q*PCR assay[b]	Number of pulses required to eliminate infectivity using SCID-mouse model
2.3×10^5	0	325 ± 25 A[c]	350 A
2.3×10^5	10	325 ± 25 A	350 ± 25 A
1.8×10^3	0	175 ± 50 B	225 ± 50 B
1.8×10^3	10	200 ± 25 B	275 ± 75 A
2.4×10^2	0	75 ± 25 C	125 ± 50 C
2.4×10^2	10	100 ± 5 C	150 ± 50 B
3.7×10^1	0	50 ± 25[b] D	75 ± 25 C
3.7×10^1	10	50 ± 25[b] D	100 ± 50 C

[a] Mean administered dose (oocysts/ ml) determined by real-time *q*PCR and confirmed using immunofluorescence (IF) microscopy.
[b] Intracellular *C. parvum* stages not detected by visual microscopic assessment of inoculated HCT-8 cell line.
[c] Values with the same uppercase letter do not differ significantly at $P \leq 0.05$ level.

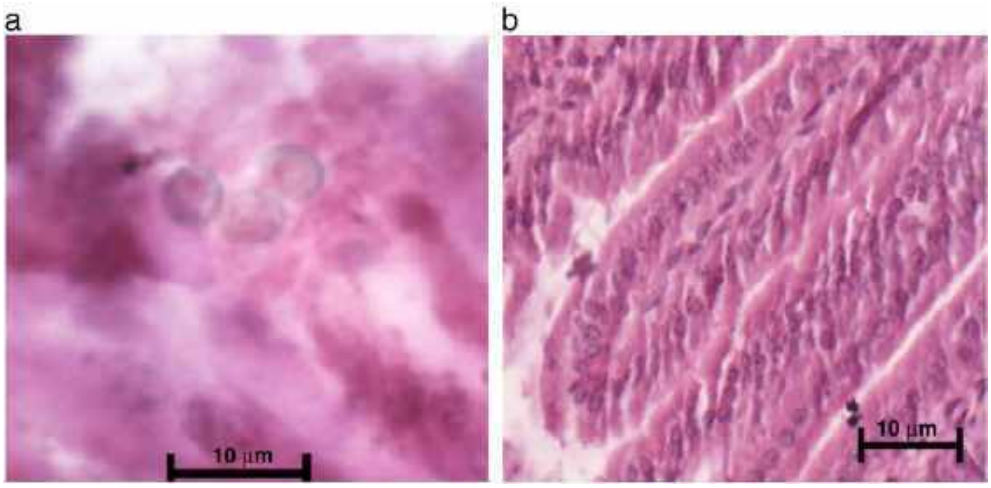

Fig. 2. H and E staining images illustrating presence of *C. parvum* in the intestinal villi of untreated SCID mice (a), and their absence in similar mice subjected to oocysts that had been exposed to a lethal regime of PUV treatment (b).

Findings from this study is also in agreement with the seminal work of Rochelle et al. (2002) who advocated that *C. parvum* disinfection experiments performed with either mice or cell culture infectivity models should be limited to discriminating relatively large differences between treatments and should not try to resolve fine differences in the levels of inactivation between small treatments. In this study we also report on an increased variability between use of cell culture and SCID-mice models for detecting infectivity using deceasing concentrations of oocysts that were initially PUV treated followed by exposure to excystation conditions (acid and bile) before inoculation in cell monolayers or in mice. However, all UV and heating experiments reported in this study relate to exposure of treated oocysts to excystation conditions prior to inoculation in cell line or in mice infectivity models that simulate passage of this Iowa isolate through the human gastrointestinal tract. We have not reported on the efficacy of PUV and monochromatic light to inactivate oocysts that were not exposed to subsequent excystation conditions (i.e., acid and bile exposure) due to the inability of these untreated oocysts to infect the HCT-8 cell monolayers (data not shown). It is possibly due to this inherent variability in untreated oocysts that Lee et al. (2008) exclusively reported on the efficacy of pulsed UV to inactivate oocysts that were all subsequently incubation in acidified HBSS and 4 mM sodium taurocholate before inoculation onto HCT-8 cell monolayers. However, significant lot-to-lot variability of the Iowa isolate was also previously demonstrated by Korich et al. (2000) who reviewed 22 dose response studies with CD-1 mice over a 3 year period, in which the ID_{50}s ranged from 33 to 478 oocysts. Although this study demonstrated that cell culture was equivalent to an animal bioassay for measuring infectivity and inactivation of *C. parvum* when present in samples at ca. 10^5 oocysts/ml, a disadvantage of cell culture is the inability to propagate oocysts *in vitro*. The failure of *C. parvum* to propagate in cell culture is no yet understood but may related to nutritional deficiencies in the culture media, inappropriate redox renditions, or death of the host cells following infection. Therefore, *in vivo* infection in animal bioassays still appears necessary for the production of large numbers of oocysts required for evaluating disinfection performances of established and emerging technologies.

In conclusion, this study demonstrated that there is good agreement between use of *in vitro* cell culture-*q*PCR and the SCID-mouse-infectivity assays for evaluating the disinfection efficacy of pulsed UV, thus reducing the requirement to unnecessarily use animals for these particular research studies. However, further investigations are required to comprehensively demonstrate efficacy of using this novel disinfection UV approach for treating lower concentrations of infectious oocysts representative of different strains and genotypes that may frequently contaminate water supplies. Development of a reliable and repeatable method for measuring fluence values from ultra-short lived pulses of light in water associated with PUV is needed, and the former should take on board critical inter-related factors previously identified by Bolton and Linden (2003) for continuous LP and MP units. A dearth of information also exists on the ability of *C. parvum* to repair post exposure to varying operational conditions associated with PUV treatments combined with possible subsequent survival of sub-lethally inactivated oocysts in the aquatic environment.

Acknowledgements

The authors thank the Irish Environmental Protection Agency (grant no. 2008-PhD-ET-3) for the PhD scholarship of Mary Garvey. We also acknowledge the Department of Health and Children (Ireland) for issuing an animal license [B100/4061] that enabled these studies to be carried out.

References

Amman, R.R., Binder, B.J., Olsen, R.J., Chisholm, S.W., Devereaux, R., Stahl, D.A., 1990. Combination of 16S rRNA-targeted oligonucleotide probes with flow cytometry for analyzing mixed microbial populations. Appl. Environ. Microbiol. 56, 1919–1925.
Bolton, J.R., Linden, K.G., 2003. Standardization of methods for fluence (UV dose) determination in bench-scale UV experiments. J. Environ. Eng. 129, 209–215.
Cantwell, R.E., Hofmann, R., Templeton, M.R., 2008. Interactions between humic acid matter and bacteria when disinfecting water with UV light. J. Appl. Microbiol. 105, 25–35.
Craik, S.A., Weldon, D., Finch, G.R., Bolton, J.R., Belvosevic, M., 2001. Inactivation of *Cryptosporidium parvum* oocysts using medium pressure and low pressure ultraviolet radiation. Water Res. 35, 1387–1398.
Elmnasser, N., Guillou, S., Leroi, F., Orange, N., Bakhrouf, A., Federighi, M., 2007. Pulsed-light system as a novel food decontamination technology: a review. Can. J. Microbiol. 53, 813–821.
Farrell, H., Garvey, M., Rowan, N.J., 2009. Studies on the inactivation of medically important *Candida* species on agar surfaces using pulsed light. FEMS Yeast Res. 9, 956–966.
Gómez-López, V.M., Ragaert, P., Debevere, J., Devlieghere, F., 2007. Pulsed light for food decontamination: a review. Trends Food Sci. Technol. 18, 464–473.
Hunter, P.R., Syed, Q., 2001. Community surveys of self-reported diarrhea can dramatically overestimate the size of outbreaks of waterborne cyptposporidiosis. Water Sci. Technol. 43, 27–30.
Johnson, A.M., Linden, K., Ciociola, K.M., De Leon, R., Widmer, G., Rochelle, P.A., 2005. UV inactivation of *Cryptosporidium hominis* as measured in cell culture. Appl. Environ. Microbiol. 71, 2800–2802.
Keegan, A.R., Fanok, S., Monis, P.T., Saint, P.C., 2003. Cell culture-Taqman PCR assay for evaluation of *Cryptosporidium parvum* disinfection. Appl. Environ. Microbiol. 69, 2505–2511.
King, B.J., Hoefel, D., Daminato, D.P., Fanok, S., Monis, P.T., 2008. Solar UV reduces *Cryptosproidium parvum* oocysts infectivity in environmental waters. J. Appl. Microbiol. 104, 1311–1323.
Korich, D.G., Marshall, M.M., Sterling, C.R., 2000. Lot-to-lot variation of *Cryptosporidium parvum* oocyst viability as assessed by the neonatal mouse infectivity assay.

Proceedings of the American Water Works Association Water Quality Technology Conference, American Water Works Associated, Denver, Colo.
Lee, S.U., Joung, M., Yang, D.J., Park, S.H., Huh, S., Park, W.Y., Yu, J.R., 2008. Pulsed-UV light inactivation of *Cryptosporidium parvum*. Parasitol. Res. 10, 1293–1299.
Mofidi, A.A., Baribeau, H., Rochelle, P.A., De Leon, R., Coffey, B.M., Green, J.F., 2001. Disinfection of *Cryptosporidium parvum* with polychromatic UV light. J. Am. Works Assoc. 93, 95–109.
Nugent, M.J.D., Higginbotham, C.L., 2007. Preparation of a novel freeze thawed poly (vinyl alcohol) composite hydrogel for drug delivery applications. Eur. J. Pharm. Biopharm. 67, 377–386.
Rochelle, P.A., Jutras, E.M., Atwil, E.R., De Leon, R., Stewart, M.H., 1999. Polymorphisms in the β-tubulin gene of *Cryptosporidium parvum*. Appl. Environ. Microbiol. 63, 2029–2037.
Rochelle, P.A., Marshall, M.M., Mead, J.R., Johnson, A.M., Korich, D.G., Rosen, J.S., De Leon, R., 2002. Comparison of *in vitro* cell culture and a mouse assay for measuring infectivity of *Cryptosporidium parvum*. Appl. Environ. Microbiol. 68, 3809–3817.
Rochelle, P.A., Upton, S.J., Montelone, B.A., Woods, K., 2005. The response of *Cryptosporidium parvum* to UV light. Trends Parasitol. 21, 81–87.

Experimental Parasitology 144 (2014) 6–13

Contents lists available at ScienceDirect

Experimental Parasitology

journal homepage: www.elsevier.com/locate/yexpr

Development of a combined *in vitro* cell culture – Quantitative PCR assay for evaluating the disinfection performance of pulsed light for treating the waterborne enteroparasite *Giardia lamblia*

Mary Garvey *, Alessia Stocca, Neil Rowan

Bioscience Research Institute, Athlone Institute of Technology, Dublin Rd, Athlone, Westmeath, Ireland

HIGHLIGHTS

- Pulsed UV light successfully inactivated *Giardia lamblia* cysts as determined by real time PCR.
- *G. lamblia* appears more UV resistant than *Cryptosporidium parvum*.
- The HCT-8 human intestinal cell line acts as a suitable host for *Giardia* infection.
- A reduced level of infectivity was observed with the Caco-2 colon cell line.
- Real Time PCR provided a suitable tool for measuring *Giardia* infectivity *in vitro*.

ARTICLE INFO

Article history:
Received 8 February 2014
Received in revised form 31 May 2014
Accepted 2 June 2014
Available online 11 June 2014

Keywords:
Giardia lamblia
Pulsed UV inactivation
Real time PCR
In vitro
Cell culture

ABSTRACT

Giardia lamblia is a flagellated protozoan parasite that is recognised as a frequent cause of water-borne disease in humans and animals. We report for the first time on the use of a combined *in vitro* HCT-8 cell culture-quantitative PCR assay for evaluating the efficacy of using pulsed UV light for treating *G. lamblia* parasites. Findings showed that current methods that are limited to using vital stains before and after cyst excystation are not appropriate for monitoring or evaluating cyst destruction post PUV-treatments. Use of the human ileocecal HCT-8 cell line was superior to that of the human colon Caco-2 cell line for *in vitro* culture and determining PUV sensitivity of treated cysts. *G. lamblia* cysts were also shown to be more resistant to PUV irradiation compared to treating similar numbers of *Cryptosporidium parvum* oocysts. These observations also show that the use of this HCT-8 cell culture assay may replace use of animal models for determining disinfection performances of PUV for treating both *C. parvum* and *G. lamblia*.

1. Introduction

Giardia lamblia is a flagellated protozoan parasite that is frequently associated with gastrointestinal infection in both developed and developing countries where the main routes of transmission including consumption of contaminated food and water, person-to-person and animal-to-person zoonosis through the faecal-oral route. Waterborne transmission of *Giardia* is the most common cause of outbreaks as *G. lamblia* cysts are abundant in surface and source waters (Shin et al., 2010). Notably, 20 of the 45 European countries have reported the prevalence of *Giardia* in human and water samples with 10 countries reporting its presence in recreational waters. Furthermore, giardiasis has recently been categorised as a "neglected disease" by the World Health Organisation (WHO) (Plutzer et al., 2010). The excretion of extensive numbers of *Giardia* cysts by high numbers of cattle and sheep around water supplies make infected animals an important route of water contamination. Indeed occurrence data from developed and developing countries suggest that *Cryptosporidium* and *Giardia* are commonly found in raw sewage with the latter present in higher numbers more frequently. As with parasites such as *Cryptosporidium parvum* the removal of *Giardia* from water supplies has proven problematic due to its resistance to current water disinfection methods and the low cyst number required for infection to occur.

Indeed it is due to the emergence of such recalcitrant chlorine-resistant pathogens that the need for alternative water disinfection methods has arisen. The use of UV light technology for the treatment of water has proven effective for numerous water borne microorganisms including parasitic protozoan (Craik et al., 2000;

* Corresponding author.
E-mail address: mgarvey@ait.ie (M. Garvey).

http://dx.doi.org/10.1016/j.exppara.2014.06.001
0014-4894/

Garvey et al., 2010). The inactivation of microbial species by UV light involves the alteration of DNA following the absorbance of UV energy by the treated species which in turn inhibits the reproductive abilities of the organism. Standard UV disinfection methods involve the usage of lamps which emit UV in at set wavelength and are termed low press UV. Recent research including that carried out by this research group has focused on the potential of a novel pulsed UV light system as a suitable method of water and waste water disinfection. Pulsed UV operates by storing energy in a capacitor and releasing it as short bursts of energy into the treatment area. Compared to conventional UV light, pulsed light treatment has the advantage of being fast, effective and more efficient at converting electrical energy into photon energy.

Studies on the UV inactivation of organisms such as *Cryptosporidium* and *Giardia* are problematic due to the infective nature of the parasites which require a live host to initiate its reproductive cycle. This coupled with the mode of action of UV light (inducing genetic damage as opposed to cell membrane damage) raises difficulties with accurately determining if *Giardia* has lost its infective abilities following UV exposure.

Research to date on the UV inactivation of *Giardia* has been based on the use of vital dyes, *in vitro* excystation and *in vivo* infection of live rodents with the former consistently proven to overestimate inactivation (Maux et al., 2002) and the latter raising ethical issues as well as the difficulties and time demands associated with animal testing. The use of an *in vitro* cell culture model as an alternative to *in vivo* testing has proven successful for other parasites such as *C. parvum* (Garvey et al., 2010). By providing an *in vitro* environment similar to that of the host intestines, the parasite can be stimulated to infect cells growing in culture and to initiate its life cycle. *Giardia* trophozoites strongly adhere to the epithelial surface of the intestine via a ventral adhesive disc. A number of parasitic surface molecules are engaged in this tight interaction, including giardins (primarily alpha, beta, delta and gamma giardins), as well as a complex network of contractile proteins which play key roles in trophozoite attachment. The extraction and amplification of parasitic DNA via real time PCR may then provide a rapid measurement of infective parasite numbers allowing for the measurement of live or dead parasites. This represents the first study on the use of a combined cell culture - real time PCR *in vitro* assay for the viability assessment of low-pressure and pulsed UV light treated *G. lamblia* cysts using human intestinal derived cell lines. It is envisioned that such an assay may provide an alternative approach to that of *in vivo* testing by allowing for a rapid method of determining parasitic inactivation following UV and other enabling processes for water treatment. Working towards such methods will aid in the treatment and elimination of this pathogenic organism from water supplies by allowing for reproducible studies on the inactivation of *Giardia* cysts for effective water treatment and control.

2. Methods

2.1. Pulsed UV light system

A bench-top pulsed power source (PUV-1, Samtech Ltd., Glasgow) was used to power a low-pressure (60 kPa) xenon-filled flashlamp (Heraeus Noblelight XAP type NL4006 series constructed from a clear UV transparent quartz tube), that produced a high-intensity diverging beam of polychromatic pulsed light, was used in this study as per Garvey et al. (2010, 2012). This delivery system kills microorganisms by using ultra-short duration pulses of an intense broadband emission spectrum that is rich in the UV-C germicidal wavelength. PUV is produced by storing electricity in a capacitor over relatively long times and releasing it as a short duration pulse using sophisticated pulse compression techniques. The pulsed light has a broadband emission spectrum extending from the UV to the infrared region with a rich UV content and its intensity also depends on the level of the voltage applied. The light source has an automatic frequency control function which allows it to operate at 1 pulse per second (pps); this setting was used throughout the study. Light exposure was homogenous as the xenon lamp measuring 9×0.75 cm was longer than the 8.5 cm standard diameter.

2.2. Mammalian cell culture and maintenance of cell lines

Monolayers of the human ileocecal adenocarcinoma cell line HCT-8 (ATCC CCL-244: American Type Culture Collection, Rockville, Md.) were grown with regular sub-culturing in RPMI 1640 growth media with L-glutamine and supplemented antibiotics (penicillin G, 100,000 U/L, streptomycin, 0.5 g/L and amphotericin B, 0.5 g/L), sodium bicarbonate, 2 g/L, and 10% foetal calf serum adjusted to pH7.4. Caco-2 cells (ATCC HTB-37), established from a human colon adenocarcinoma Caco-2 cells were maintained at 37 °C in Dulbecco modified Eagle's medium/Ham's F-12 medium, supplemented with 20% (v/v) foetal bovine serum, 1% 200 mM L-glutamine, 1% (v/v) non-essential amino acids, 0.5% (v/v) penicillin–streptomycin and 0.5% (v/v) amphotericin B (Sigma–Aldrich). Maintenance media was stored at 4 °C and heated to 37 °C prior to use. HCT-8 and Caco-2 cells were cultured and maintained in T75 cm^2 cell culture flasks in a humidified incubator at 37 °C in an atmosphere containing 5% (vol/vol) CO_2 for circa. 24 h until 80 to 90% confluent monolayers had formed. Once confluent, cells were trypsinised to remove the cell monolayer from the flask and seeded into 6 well plates for 24 h at 37 °C at a seeding density of 1×10^6 cells/well for use in real time pcr studies and at a density of 1×10^5 cells/well for chamber slides for infectivity studies using fluorescent stains.

2.3. Viability and infectivity determination of G. lamblia

G. lamblia cysts (derived from experimental infected gerbils) were purchased from Waterborne Inc USA. Cysts were stored in sterile PBS (0.01 M phosphate buffer, containing 0.0027 M KCL and 0.137 MNaCl at a pH of 7.4) with 100 U of penicillin/ml, 100 μg of streptomycin/ml and 100 μg of gentamicin/ml at 4 °C until they were used for UV treatment studies. A combined surrogate dye staining method comprising propidium iodide (PI) 1 mg/ml of 0.1 M sterile PBS, 4′,6′-Diamidino-2-Phenylindole (DAPI) 2 mg/ml in methanol and a fluorescein-labelled mouse-derived monoclonal antibody Giardi-a-Glo™ (having corresponding epitope on cyst cell wall; Waterborne Inc, New Orleans, USA) was used to confirm the viability of cysts. The excystation rate was determined for each batch of cysts by microscopic observation following sequential incubation at 37 °C in acidified hanks balanced salt solution (HBSS) for 1 h as per method of Garvey et al., 2010. All experiments were carried out using cysts with greater than 90% viability, as determined by *in vitro* excystation and the uptake or exclusion of vital dyes. Cysts were counted using a haemocytometer and inverted microscope (Olympus, CKX41) with camera (Olympus, IX2-SLP) attached.

Cell culture infectivity was confirmed by immunofluorescent (IF) staining of treated HCT-8 and Caco-2 cell monolayers following exposure to viable cysts. Cell monolayers were seeded into each of 8 well chambered slides (Lab Tec II, Nunc) at a concentration circa.1×10^5 cells per well. Cysts were stimulated to excyst by re-suspension in acidified HBSS pH 2.7 for 1 h at 37 °C. After one washing step with sterile PBS, cysts were re-suspended in cell culture media containing varying concentrations of proteose and thereafter 350 μl aliquots were then added to each well. Samples were incubated for up to 48 h at 37 °C in 5% (vol/vol) CO_2 atmosphere, to determine optimal conditions for cell infectivity.

At set times each individual well containing a separate monolayer was air dried at room temperature until all moisture had evaporated. After which, 45 μl of Troph-o-Glo™ (Waterborne Inc, UK) which detects different life cycle stages of Giardia *in vitro* was added to each well for 25 min at 37 °C. Slides were rinsed from unbound stain by flooding with 100 μl SureRinse (Waterborne Inc, USA). The inoculated cell monolayers were then counterstained for 1 min with C101 containing Evans blue dye (Waterborne Inc, USA). All slides were examined under fluorescence microscopy (Leitz Diaplan fluorescence microscope) at an excitation wavelength of 460–500 nm and an emission wavelength of 510–560 nm for Troph-o-Glo™ and an excitation wavelength of 550 nm and emissions wavelength of 610 nm for the counterstain C101. All wells containing separate monolayers were examined and noted as positive or negative for sites of parasitic infection.

2.4. UV light treatment of G. lamblia cysts

Petri dishes used in the tests were placed directly below the lamp source for both pulsed and LP UV (low pressure ultraviolet), which ensured full coverage of the plate surface and eliminated possible shading effects. The LP-UV lamp employed in this study is a handheld model (UVGL-55) supplied by UVP Inc, UK. It produces radiations in the wavelength range of 254 nm–365 nm, with maximum emission at the germicidal wavelength, 254 nm. For standard treatments the light source was mounted at 8 cm above the treatment area, as this distance was shown previously to be optimal for inactivation of *C. parvum* (Garvey et al., 2010) for both UV methods. In this study, standard treatments involved suspending predetermined numbers of *G. lamblia* cysts in the range of 1–1,000,000 cysts/ml in sterile phosphate buffered saline (PBS) pH 7 to pulses of UV light. Samples were treated in petri dishes that were then subjected to lamp discharge energies of 16.2 J (900 volts) at 8 cm distance from the light source up to and including a fluence of 22.68×10^{-3} mJ/cm^2 at a rate of 1 pulse per second for PUV studies. The UV dose was adjusted by increasing or decreasing the frequency of the pulsing. In order to ensure that any possible negative effects of such treatment was solely as a result of a UV induced change in the natural environment of the test species, studies were also conducted on heat inactivated (70 °C) samples, which were prepared in the same manner. Measurement of UV fluence rate (μJ/cm^2) at each applied pulse was determined using chemical actinometry as first described by Rahn (2003), with the modifications of Hayes et al. (2012) as the non-continuous emitted spectrum did not facilitate use of a calibrated radiometer. UV dose is reported at mJ/cm^2 for comparative analysis to that of LP-UV. LP-UV inactivation was conducted with a hand help lamp (UVGL-55 handheld UV Lamp) placed 8 cm above the treatment dish, UV dose (mJ/cm^2) was varied by increasing or decreasing the exposure time as required. All studies were conducted in an aseptic environment. Following treatment, treated and untreated controls were viability assessed by fluorescent staining using the method previously described. Parasites were transferred to sterile centrifuge tubes and centrifuged at 10,000 rpm for 15 min to pellet the cysts. The supernatant was removed and the pellet re-suspended in 1 ml of HBSS pH 7.2 for 1 h at 37 °C to initiate cyst excystation. Cell culture infection and real time PCR was then performed in 6 well plates containing a cell monolayer.

2.5. Combined cell culture-quantitative PCR (CC qPCR) assay for enumerating viable G. lamblia

Real-time, Taqman-quantitative PCR (qPCR) was performed using primers (TIB MOLBIOL, Berlin, Germany) specific for the β-giardin region of DNA. Giardins are filamentous proteins with an alpha coiled helix structure and are a component of the attachment mechanism of *G. lamblia* trophozoites to host cells. Real-time PCR reactions are characterised by an increase in fluorescence emission due to probe degradation by DNA polymerase in each elongation step during PCR cycling. The higher the starting copy number of the nucleic acid target, the earlier the fluorescence will reach the predetermined threshold cycle (CT) and the smaller will Ct value will be. The Ct value is the fractional PCR cycle number, at which a significant increase in target signal fluorescence above the baseline is first detected for a sample. Quantification of test samples is performed by determining the Ct value and the use of a standard curve to deduce the starting copy number. Primers coding for β-giardin were used as per method of Bertrand et al., 2009. The Taqman probe with the following sequence: 5′-FAM TCACCCAGACGATGGA CAAGCCCTAMRA-3′ was utilised for this study. Amplification reactions (20 μL) contained 5 μL of sample DNA (0.5 μM of each primer, 0.2 μM of probe) and 15 μL of reaction buffer (Roche Diagnostic, West Sussex, England). Both positive and negative controls were included in RT-PCR to validate the results. DNase–RNase free water was used as negative control throughout.

Cycling parameters were initial denaturation for 10 min at 95 °C followed by 65 cycles of denaturation for 10 s at 95 °C, annealing for 40 s at 40 °C, extension for 1 s at 70 °C and cooling for 30 s at 40 °C on a Nanocycler® device (Roche Diagnostics). Large numbers of cycles were used to ensure detection of low levels of infection. On completion of each RT-PCR run amplification curves were analysed by Nanocycler software (Roche Diagnostics) and a standard curve of oocyst DNA concentration determined.

DNA standards were prepared from fresh cysts ranging in concentration from 10 to 10^7 cysts/ml by dilution in PBS following standard viable count determinations. Aliquots of cysts at different densities were then stimulated to infect the HCT-8 and Caco-2 cell lines that were seeded into 6 well plates at a concentration of circa. 1×10^6 cells/ml at 90% confluency. The latter cell line stimulation occurred by re-suspension and separate incubations for 1 h in acidified HBSS as previously described. 1 ml aliquots of each concentration range of excysted cysts were re-suspended in appropriate cell culture growth media containing varying concentrations of proteose and added to one well of the 6 well plate. Following 48 h incubation at 37 °C in a humidified atmosphere of 5% (vol/vol) CO_2, the cell culture media with non-adherent or internalized *G. lamblia* was removed by aspiration and discarded. Mammalian cells were then washed with sterile PBS and trypsinised using 1 ml of 0.25% (vol/vol) trypsin/EDTA (Sigma) and left for 15 min at 37 °C until complete detachment of the monolayer had occurred. Cells were then centrifuged at 500 rpm for 5 min and re-suspended in 200 μl sterile PBS, thereafter the mammalian cells and *Giardia* cell membranes were lysed using PCR template preparation kit (Roche Diagnostics, West Sussex, England) in order to produce DNA (template) and standard curve following infection in both cell lines. Real time PCR was also conducted on excysted cysts without passage through cell culture to determine the Ct values for serially diluted cysts numbers for comparative analysis. The Ct values for cell culture RT-PCR of each dilution amplified in triplicate were plotted against the logarithm of the starting quantity of cysts. The equation of this standard curve was then used to determine the inactivation of UV treated cysts. The aforementioned cell culture PCR procedure was then repeated to determine infectivity of cysts subjected to varying UV parameters or heating at 70 °C for 30 min (negative control). Log inactivation of oocysts (L) is defined by $L = \log_{10}[Nd/N0]$, where N0 is the initial concentration of cysts and Nd is the concentration of viable infectious oocysts post disinfection treatments as detected by combined cell culture-qPCR assay as per method of Lee et al. (2008).

2.6. Statistical analysis

The log reduction for UV treated cysts was calculated as the $\log_{10}$ of the ratio of the concentration of the non-treated (N_0) and

UV treated (N) samples [$\log_{10}(N_0/N)$]. Student's *t*-tests and ANOVA one-way model (MINITAB software release 16; Mintab Inc., State College, PA) were used to compare the effects of the relationship of independent variables on UV treatments. Student t-tests were used to compare infectivity in both cell lines and parasite types. All experiments were conducted in triplicate in three separate experiments.

3. Results

3.1. Excystation and cell culture infectivity

All cysts were less than 2 weeks old and 100% viable (Fig. 1) before studies were conducted as determined by viability staining using *Giardia* specific IF dyes. Initial excystation methods were conducted as per the methods of Garvey et al., 2010 for the excystation of *Cryptosporidium* and included exposing parasite preparations to HBSS pH2.7 (stomach like environment) followed by resuspension in 1% bovine bile. However it was found that the rate of excystation of *G. lamblia* decreased significantly with an increase in the exposure times to bovine bile as determined by microscopic trophozoite count. Findings showed that maximal cyst excystation occurred in the absence of bile with a 1 h suspension in HBSS pH 2.7 proving sufficient to cause cyst excystation and trophozoite release as determined by trophozoite count via microscopy. Optimal detection of *Giardia* DNA was achieved via RT-PCR without the presence of bile in the excystation step whereas for *C. parvum* it was found that 15 min incubation in 1% bovine bile aided in the excystation of sporozoites as determined by microscopic count and confirmed by RT-PCR amplification of parasitic DNA (Fig. 2). For cell culture infectivity it was found that optimal infectivity of the HCT-8 and Caco-2 cell lines occurred in media which contained 2% proteose for *G. lamblia*. These findings are based on the observation of multiply sites of infection via fluorescent microscopy and the lower Ct readings obtained following PCR amplification of parasitic DNA (Fig. 3). Furthermore, for parasitic cell line infectivity it was found that infection was optimal when cells were exposed to parasites at a ratio of 1:1. The Ct readings for parasitic DNA extracted from cell culture were consistently higher than those extracted from cysts/oocysts without cell culture indicating that a loss of parasite DNA occurred during this step. There was a significant difference ($p < 0.05$) in the amplification values for target DNA from parasites which were stimulated to infect mammalian cells and those which were only stimulated to excyst. Notably, for both cell lines the limit of detection was 10 cysts and oocysts per monolayer for *Giardia* and *Cryptosporidium* respectively (Figs. 3 and 4) with a detection limit of 1 oocyst/cyst without passage through cell culture for both species.

For both parasite species the HCT-8 cell line proved significantly more susceptible to infection than the Caco-2 ($p < 0.05$). This is

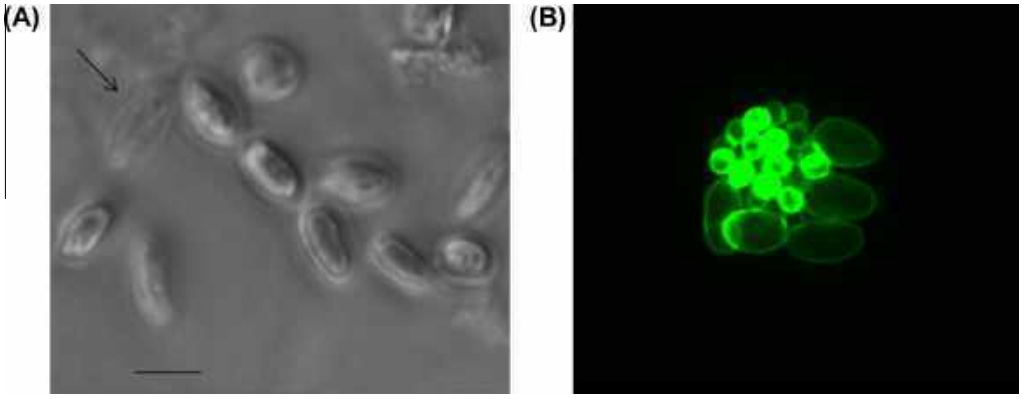

Fig. 1. (A) *Giardia lamia* cysts taken with an inverted microscope, arrow indicates empty cysts structure after excystation (bar is 6 μm). (B) Fluorescent staining of *G. lambia* and *C. parvum* viable parasites using parasite specific dyes.

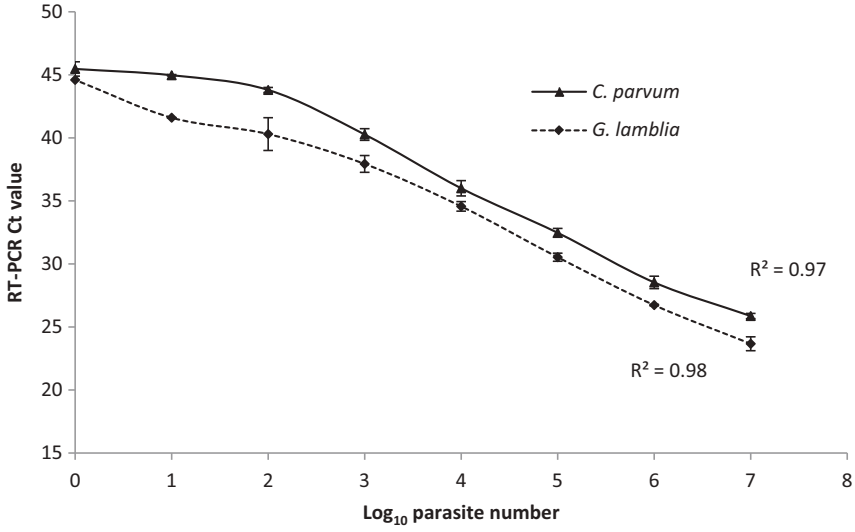

Fig. 2. Standard curve for *Cryptosporidium parvum* and *Giardia lamblia* parasite numbers vs. Ct value as determined by Real Time PCR (±S.D.) using species specific primers. Standard curve obtained without cell culture infectivity.

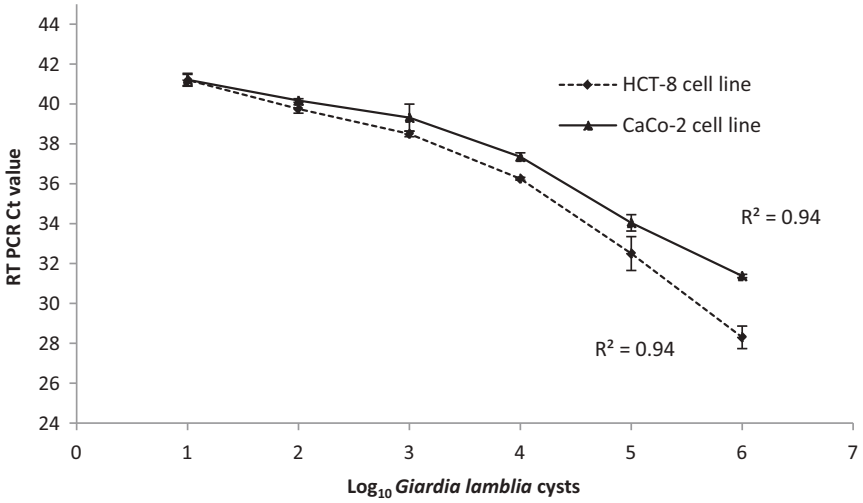

Fig. 3. Standard curve for *Giardia lamblia* infected HCT-8 and Caco-2 cell as detected via real time PCR following 48 h incubation at 37 °C (±S.D.).

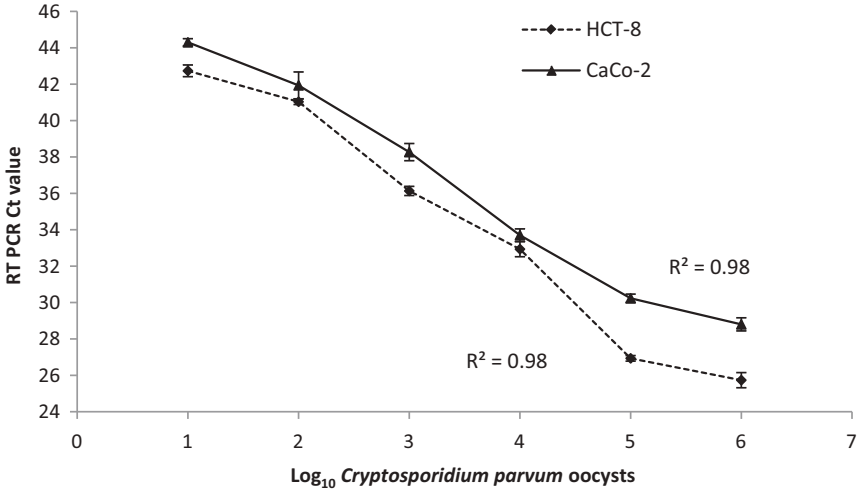

Fig. 4. Standard curve for *Cryptosporidium parvum* infected HCT-8 and CaCo-2 cell as detected via real time PCR following 48 h incubation at 37 °C (±S.D.).

evident from the lower Ct values obtained for PCR amplification following HCT-8 infection, indicating that a larger amount of target DNA was present (Figs. 3 and 4). Fluorescent staining and imaging also indicated that infection of Caco-2 cells was not as prominent with less sites of infection present. Infectivity was graded on a scale of 1 to 4 (Table 1) based on the amount of fluorescent structures present which were not quantifiable due to the high numbers present. Also it was observed that the negative effect of parasitic infection on host cell lines was more noticeable in Caco-2 cells where cell death occurred more rapidly following exposure to parasites, also cells detached from the culture flask with greater ease than the infected HCT-8 cells. Thus suggesting that the Caco-2 host cell monolayer was unable to support infectivity with large numbers of parasites and the resulting loss of cell viability and attachment influenced the rate of infection. This was not observed with HCT-8 cells as they continued to proliferate with monolayer overgrowth occurring in both infected and non-infected cells.

3.2. Real time PCR to determine viability

The use of vital staining techniques on UV treated cysts proved insufficient at determining viability/inactivation following UV treatment (Table 2). Even at maximal UV doses all treated cysts showed levels of dye uptake similar to untreated controls indicating that no inactivation had occurred. These findings correspond to that of Campbell and Wallis, 2002 where vital dye viability assays repeatedly underestimated inactivation. As with Campbell and Wallis, 2002 this confirms that vital dye viability assays should not be used to define inactivation during testing of novel disinfection techniques.

The sensitivity of the real-time RT-PCR assay was examined by performing RT-PCR assays in triplicate with tenfold serial dilution of purified cysts with and without cell culture infection. For β-giardin primer amplification, a linear response ($r^2 = 0.98$) was observed from 1,000,000 to 10 cysts per reaction for both excysted and cell culture PCR assays (Figs. 2 and 3). The detection of target DNA was quicker following excystation with the absence of the cell culture step as evident by the smaller Ct values obtained. However, excystation alone does not give information on the infectivity of the parasite in a host cell environment. Indeed excystation occurred for both treated and untreated *Giardia* at a similar rate suggesting that no UV inactivation had occurred (Table 2). However, with CC-qPCR there was a significant ($p < 0.05$) loss in viability detected with an increase in UV dose indicating a reduction in infective cysts present. This was not achieved with vital dye staining or PCR following excystation alone.

Table 1
Log_{10} reduction and infectivity of treated *Giardia lamblia* via real time PCR and cell culture infectivity IF staining of the HCT-8 cell line following UV treatment (±standard deviation).

Exposure	LP-UV			PUV		
Time seconds	Dose mJ/cm^2	RT-PCR Log_{10} reduction	Cell culture infectivity*	Dose $\times 10^{-3}$ mJ/cm^2	RT-PCR Log_{10} reduction	Cell culture infectivity*
0	0	0	4	0	0	4
10	5.4	1.48 (±0.1)	4	1.08	0.52 (±0.1)	4
20	10.8	1.92 (±0.2)	4	2.15	0.52 (±0.5)	4
30	16.35	2.04 (±0.2)	3	3.24	0.6 (±0.2)	4
60	32.7	1.92 (±0.1)	3	6.48	0.62 (±0.1)	4
90	49	1.84 (±0.1)	3	9.72	1.2 (±0.1)	4
120	65.4	1.84 (±0.3)	4	12.96	1.48 (±0.5)	3
150	81.7	1.88 (±0.2)	4	16.2	2.02 (±0.4)	3
180	98.1	1.74 (±0.1)	4	19.44	2.4 (±0.1)	3
210	113.4	1.74 (±0.2)	4	22.68	2.82 (±0.1)	2

* Infectivity of cells as determined by immune-fluorescent staining of 3 separate HCT-8 monolayers exposed to UV treated and untreated *Giardia lamblia* cysts. Presence of infectivity indicates the presence of viable *Giardia*. Numbers indicate level of infectivity 4 = high, 3 = medium, 2 = low, 1 = very low.

Table 2
Determination of viability of UV treated and untreated *Giardia lamblia* (1×10^5 cysts/ml) via staining with vital dyes DAPI and PI compared to the excystation and cell culture RT-PCR assays.

LP-UV dose mJ/cm^2	Viability			PUV dose μJ/cm^2	Viability		
	DAPI/PI (%)¥	Excystation PCR* Log_{10}	CC-PCR^ Log_{10}		DAPI/PI (%)¥	Excystation PCR* Log_{10}	CC-PCR^ Log_{10}
0	100	4.98 (±0.1)	5 (±0.3)	0	100	5.2 (±0.2)	5 (±0.05)
5.4	100	5.1 (±0.01)	3.52 (±0.05)	1.08	100	5.1 (±0.2)	4.48 (±0.3)
10.8	99	5.1 (±0.1)	3.05 (±0.2)	2.15	100	5.2 (±0.08)	4.48 (±0.1)
16.35	100	5.1 (±0.08)	2.9 (±0.1)	3.24	100	5.2 (±0.1)	4.4 (±0.3)
32.7	100	5.0 (±0.2)	3.08 (±0.5)	6.48	99	5.2 (±0.3)	4.38 (±0.1)
49.0	99	5.0 (±0.1)	3.16 (±0.4)	9.72	100	5.0 (+/-0.2)	3.8 (±0.02)
81.7	100	5.1 (±0.3)	3.12 (±0.2)	16.2	100	5.0 (±0.01)	2.98 (±0.2)
113.4	100	5.1 (±0.1)	3.26 (±0.3)	22.68	98	4.6 (±0.1)	2.18 (±0.01)

¥ Viability measured by vital staining of *Giardia lamblia* pre and post UV exposure, score is the mean of 3 separate replicates of individual experiments. 100 parasite cysts were counted and marked as positive or negative for dye uptake.
* Log_{10} viability as determined PCR amplification of *Giardia lamblia* UV treated and untreated following excystation without passage through a cell line.
^ Log_{10} viability as determined by PCR amplification of *Giardia lamblia* UV treated and untreated following excystation and cell culture infectivity.

3.3. UV inactivation of G. lamblia

The variance in the Ct values following UV exposure allows for the determination of UV inactivation by comparing treated to untreated controls. The equation of the line obtained for the HCT-8 CC qPCR standard curve was used to calculate log_{10} reduction of each UV treated batch. Findings show that both LP-UV and PUV light successfully inactivated the test species. With 5.4 mJ/cm^2 of LP-UV dose a 1.48 log_{10} reduction in viability was achieved for *G. lamblia* as detected via CC-qPCR. With an increase in exposure the rate of inactivation also increased significantly ($p < 0.05$) up to a maximum of 1.88 log_{10}. However, after a UV dose of 65.4 mJ/cm^2 no further increase in *Giardia* inactivation was detected (Table 1). Therefore, a ca. 2 log_{10} inactivation rates was obtained with a UV dose of 113.4 mJ/cm^2 equivalent to a treatment time of 210 s (3.5 min). These findings correspond to that of Craik et al., 2000 and Campbell and Wallis, 2002 where studies show that 99% of *Giardia* inactivation was achieved below 8 mJ/cm^2 and 10 mJ/cm^2 respectively using a medium pressure lamp and *in vivo* infectivity in mice and gerbil modes. At doses exceeding 8 mJ/cm^2 and as high as 130 mJ/cm^2 there was no significant increase in the inactivation of *Giardia* cysts (Craik et al., 2000). The similarities in these findings using a cell culture based assay to that of animal infectivity suggest that the former *in vitro* based approach may indeed show levels of infectivity to that of the *in vivo* test system.

The pulsed UV system resulted in levels of inactivation of *G. lamblia* which were greater than the LP-UV system (Table 1) with significantly less applied UV dose. Indeed a 1.48 log_{10} inactivation was achieved with as little as 12.96×10^{-3} mJ/cm^2 of pulsed UV compared to 5.4 mJ/cm^2 of LP-UV. Noteworthy, the inactivation plateau which was observed with LP-UV did not appear with PUV up to a dose of 22.68×10^{-3} mJ/cm^2 equivalent to a treatment time of 210 s. A ca. 3 log_{10} (99.9%) loss in cyst viability was determined by CC qPCR with a pulsed UV dose of 22.68×10^{-3} mJ/cm^2. Previously published work of Garvey et al., 2010 detailing the inactivation of *C. parvum* reported a 3.3 log_{10} inactivation following a pulsed UV dose of 9.72×10^{-3} mJ/cm^2. This report also showed the correlation between mice infectivity and an *in vitro* HCT-8 CC qPCR assay for the disinfection kinetics of *C. parvum* with pulsed UV light. *G. lamblia* appears more UV resistant than *C. parvum* at doses up to 9.72×10^{-3} mJ/cm^2 with a 1.2 log_{10} and <4 log_{10} inactivation obtained for *Giardia* and *Cryptosporidium* (Garvey et al., 2010) respectively. A similar trend where *C. parvum* showed increased sensitivity to medium pressure UV than *Giardia* was reported by Belosevic et al., 2001.

4. Discussion

According to the European Water Framework Directive, a "good ecological and chemical status of surface water" has to be achieved by 2015. In this context of meeting this important directive, the detection and destruction of emerging recalcitrant pathogens such as chlorine-resistant *Cryptosporidium* and *Giardia* parasites and related issues such as the occurrence of unwanted anthropogenic micropollutants in surface waters via drinking and wastewater treatment plants (WWTPs) has come under the spotlight of scientists as well as politicians (Rowan, 2011; Grummit et al., 2013). Concomitantly, several research projects including the EU project "Poseidon" (Ternes, 2004), the Swiss project "Strategy Micropoll" (Abeeglen et al., 2009) or long-term activities of the NORMAN network (http://www.norman-network.net/) have investigated the efficiency of different innovative technologies in WWTPs such as ozonation or charcoal filters, to specifically lower concentrations

of micropollutants in surface water (Grummit et al., 2013). While the efficiency, practical suitability and respective limitations and strengths were evaluated by several leading scientists in this field of study (Schrank et al., 2009; Stalter et al., 2010), the general consensus reached is that there is concern regarding use of innovative oxidative processes as they create toxic metabolites as well as recognition of the importance of integrating these technologies for destroying emerging recalcitrant microbial pathogens such as parasites and antibiotic resistant microorganisms. We recently reported that pulsed UV light is a superior candidate water treatment technology to that of pulsed-plasma gas-discharge and ozonation as former does not elicit any unwanted geno-, cyto- and ecotoxicological end-points yet effectively and efficiently destroys *C. parvum* oocyts (Hayes et al., 2013). This study also built on our earlier work showing that *in vitro* cell culture can replace use of the gold-standard *in vivo* mice model for assessing efficacy *C. parvum* detection and disinfection post UV irradiation, thus simplifying and standardising processes for parasite destruction (Garvey et al., 2010). However, no prior study had focused on the efficacy of using new innovative disinfection technologies for the destruction of the waterborne *G. lamblia* due in part to the highly complex culture requirement of this flagellated enteroparasite that was limited to using *in vivo* rodent models to interpret infectivity and disinfection efficacy thus limiting developments in this important area. This present study describes the effectiveness of using pulsed light as a novel innovative technology to destroy *G. lamblia* by also reporting for the first time on the use of combined cell culture – qPCR. Application of the findings from this study will also assist the water industry in identifying effective new innovations for disinfection of established and emerging pathogens along with underpinning future risk management, toxicological and ecotoxicological studies.

While there is growing interest in the use of *in vitro* cell culture assays to study the pathogenesis and infectivity of waterborne *Cryptosporidium* parasite infection post disinfection treatments (Hijjawi, 2010; Garvey et al., 2010), there is currently a dearth of critical information on the detection and efficacy of these emerging enabling technologies for removing or destroying *G. lamblia*. The core factor governing choice of appropriate human cell line to address the needs of this study was representativeness of the target area or site of infection, therefore epithelial cells of intestinal origin were selected as they provide a likely matrix for *Giardia* infection. During this study, HCT-8 cells were found to be superior to that of using Caco-2 cells for studying infectivity. Hijjawi (2010) also reported that HCT-8 was superior to that of eleven other human cell lines tested for studying infectivity in *Cryptosporidium* as these particular cells supported all life cycle stages of *Cryptosporidium* growth (Hijjawi, 2010). This present study demonstrated that the mechanism of *Cryptosporidium* cellular infectivity differed to that of *Giardia* where the latter was observed to be not cell membrane invasive but only requiring attachment to epithelial surfaces to initiate and enable infection. An increase or decrease in the amount of host cells available for Giardia significantly affected its infection and subsequent intracellular proliferation, which is mainly attributed to the surface area available for parasite attachment. Loss of viability and detachment which occurred with the Caco-2 cells may have led to the decrease in infectivity that was observed for this cell line following exposure to viable *Giardia* cysts. Exposure of Caco-2 cells to *Giardia* cysts consistently resulted in apoptotic or early phase cell death in this monolayer, which was not observed with similarly challenged HCT-8 cells. Previous studies conducted by Cotton et al. (2011) showed that genes associated with apoptosis are up-regulated in cells exposed to *Giardia* and heightened rates of epithelial apoptosis occurs shortly after exposure to *Giardia* trophozoites, which was observed both *in vitro* and *in vivo*. This marked difference in pathogenesis between these two waterborne parasites may be attributed to *C. parvum* inhibiting apoptosis at the trophozoite stage or promoting apoptosis sporozoite and merozoite stages in HCT-8 cells (Panaro et al., 2007). This may support parasite growth in the early stages after epithelial cell infection, and may explain why greater levels of infectivity were evident for this parasite for each cell line studied. *G. lamblia* predominantly colonises the proximal small intestine and this is the primary site of infection following consumption of the parasite. Therefore, the HCT-8 cell line which is of ileum origin is an ideal candidate for *in vitro* infectivity studies. The Caco-2 cell line has its origin in the colon and this difference in gastrointestinal location may contribute to the ability of the cells to withstand parasitic infection for both the *Giardia* and *Cryptosporidium* species.

Different assays have been used to compare viability and infectivity of *Cryptosporidium* oocysts and *Giardia* cysts. Traditionally neonatal mouse infectivity has been considered the gold standard and most sensitive assay for determining the infectivity of these intestinal parasites. Furthermore, the use of vital dye staining techniques has consistently proven insufficient at determining UV inactivation of these species (Craik et al., 2000). Indeed for many years it was believed that conventional low-pressure generated UV light could not sufficiently inactivate *G. lamblia* based on viability as measured via excystation or vital dye staining (Mofidi et al., 2002). The development of a real time PCR assay for the viability assessment of UV treated parasites allows for a rapid means of assessing disinfection techniques without the need for *in vivo* studies on live hosts. Previously published studies by this and other research groups have shown the correlation between mouse infectivity and *in vitro* cell culture infectivity for *C. parvum* (Garvey et al., 2010; Rochelle et al., 2002). This present bench-scale study demonstrated that PUV effectively destroys *Giardia* and *Cryptosporidium* parasites when suspended in water and therefore offers an exciting opportunity to investigate this approach as a candidate future emerging innovation at water treatment plant level. This has future implications in terms of critical data generation as guiding parameters to include water transmission (presence of suspended or dissolved solids), flow-rates, volume, energy requirements and so forth merit attention as well as the related yet underappreciated area of risk management. Findings of this study will impact positively on water quality and safety and has broad ramifications and/or implications for the water industry moving forward. In order to comprehensively investigate scale up of PUV at water treatment plants one must also consider identifying a surrogate harmless microbial indictor organism of matched or greater resistance to that of *Giardia* or *Cryptosporidium* in order to simulate and conduct important disinfection and monitoring studies. We have recently reported on the use of the harmless bacterial endospore *Bacillus megaterium* which, was shown to be of comparable PUV sensitivity to *C. parvum* suggesting that it may potentially be applied as an alternative surrogate organism to monitor disinfection performances of this complex entero-parasite at drinking and waste water treatment plants (Garvey et al., 2012).

Acknowledgment

This research was funded by the Irish Environmental Protection Agency Strive Programme (2011-W-MS-5).

References

Abeeglen, C., Escher, B., Hollender, J., Koepke, S., Ort, C., Peter, A., Siegrist, H., von Gunten, U., Zimmermann, S., Koch, M., Niederhauser, P., Scharer, M., Braun, C., Galli, R., Junghans, R., Brocker, S., Moser, R., Rensch, D., 2009. Ozonung von gereingtem Abwsser. Schlussbericht Pilotversuch Regensdor. EAWAG 80.

Belosevic, M., Craik, A.S., Stafford, L.J., Newmann, F.N., Kruithof, J., Smith, W.D., 2001. Studies on the resistance/reactivation of *Giardia muris* cysts and

Cryptosporidium parvum oocysts exposed to medium-pressure ultraviolet radiation. FEMS Microbiol. Lett. 204 (1), 197–203.
Bertrand, I., Maux, M.I., Helmi, K., Hoffmann, L., Schwartzbrod, J., Cauchie, M.H., 2009. Quantification of *Giardia* transcripts during in vitro excystation: interest for the estimation of cyst viability. Water Res. 43, 2728–2738.
Campbell, T.A., Wallis, P., 2002. The effect of UV irradiation on human-derived *Giardia lamblia* cysts. Water Res. 36, 963–969.
Cotton, A.J., Beatty, K.J., Buret, G.A., 2011. Host parasite interactions and pathophysiology in *Giardia* infections. Int. J. Parasitol. 41, 925–933.
Craik, A.S., Finch, R.G., Bolton, R.J., Belosevic, M., 2000. Inactivation of *Giardia muris* cysts using medium-pressure ultraviolet radiation in filtered drinking water. Water Res. 34 (18), 4325–4332.
Garvey, M., Clifford, E., O'Reilly, E., Rowan, N., 2012. Efficacy of using harmless *Bacillus* endospores as novel surrogate organisms to indicate the inactivation performance of recalcitrant *Cryptosporidium parvum* oocysts suspended in water using pulsed UV light. J. Parasitol. 99 (3).
Garvey, M., Farrell, H., Cormican, M., Rowan, N., 2010. Investigations of the relationship between use of in vitro cell culture-quantitative PCR and a mouse-based bioassay for evaluating critical factors affecting the disinfection performance of pulsed UV light for treating *Cryptosporidium parvum* oocysts in saline. J. Microbiol. Methods 80 (3), 267–273.
Grummit, T., Kucklehkorn, J., Bahlmann, A., Baumstark-Khan, C., Brack, W., Braunbeck, T., Feles, S., Gartiser, S., Glatt, H., Heinze, R., Hellweg, C.E., Hollert, H., Junek, R., Knauer, M., Kneib-Kissinger, B., Kramer, M., Krauss, M., Kuster, E., Maletz, S., Meinl, W., Noman, A., Prantl, E.M., Redelstein, R., Rettberg, E., Schadenboeck, W., Schmidt, C., Schluze, T., Seiler, T.-B., Spitta, L., Stengel, D., Waldmann, P., Eckhardt, A., 2013. Tox-Box: securing drops of life – an enhanced health-related approach to risk assessment of drinking water in Germany. Eur. Sci. Eur. 25 (27), 1–8.
Hayes, J.C., Garvey, M., Fogarty, A.M., Clifford, E., Rowan, N.J., 2012. Inactivation of recalcitrant protozoan oocysts and bacterial endospores in drinking water using high-intensity pulsed UV light irradiation. Water Sci. Techol: Water Supply 12, 513–522.
Hayes, J., Kirf, D., Garvey, M., Rowan, N., 2013. Cyto-, geno- and ecotoxicological assessment of pulsed-plasma gas-discharge and pulsed UV light treated water containing the waterborne enteroparasite *Cryptosporidium parvum*. J. Microbiol. Methods 94 (3), 325–337.
Hijjawi, N., 2010. *Cryptosporidium*: new developments in cell culture. Exp. Parasitol. 124, 54–60.
Maux, M., Bertrand, I., Gantzer, C., Schwartzbrod, J., 2002. Estimating *Giardia* cyst viability using RT-PCR. Water Sci. Technol. 2 (3), 107–115.
Mofidi, A.A., Meyer, A.E., Wallis, M.P., Chou, I.C., Meyer, P.B., Ramalingam, S., Coffey, M.B., 2002. The effect of UV light on the inactivation of *Giardia lamblia* and *Giardia muris* cysts as determined by animal infectivity assay (P-2951-01). Water Res. 36, 2098–2108.
Panaro, A.M., Cianciulli, A., Mitolo, V., Mitolo, I.C., Acquafredda, A., Brandonisio, O., Cavallo, P., 2007. Caspase-dependent apoptosis of the HCT-8 epithelial cell line induced by the parasite *Giardia intestinalis*. FEMS 51 (2), 302–309.
Plutzer, J., Ongerth, J., Panagiotis, K., 2010. *Giardia* taxonomy, phylogeny and epidemiology: facts and open questions. Int. J. Hyg. Environ. Health 212, 321–333.
Rahn, R.O., 2003. Chemical dosimetry using an iodide/iodate aqueous solution: application to the gamma irradiation of blood. Appl. Radiat. Isot. 58, 79–84.
Rochelle, P.A., Marshall, M.M., Mead, J.R., Johnson, A.M., Korich, D.G., Rosen, J.S., De Leon, R., 2002. Comparison of *in vitro* cell culture and a mouse assay for measuring infectivity of *Cryptosporidium parvum*. Appl. Environ. Microbiol. 68, 3809–3817.
Rowan N.J., 2011. Defining established and emerging microbial risks in the aquatic environment: current knowledge, implications and outlooks. International Journal of Microbiology (published online: <http://www.hindawi.com/journals/ijmb/2011/462832.html>).
Schrank, S.G., Bieling, U., Jose, H.J., Moreira, R.F.P.M., Schroder, H.F., 2009. Generation of endocrine disruptor compounds during ozone treatment of tannery wastewater confirmed by biological effect analysis and substance specific analysis. Water Sci. Technol. 59 (1), 31–38.
Stalter, D., Magdeburg, A., Oehlmann, J., 2010. Comparative toxicity assessment of ozone and activated carbon treated sewage effluents using an in vivo test battery. Water Res. 44 (8), 2610–2620.
Shin, G., Linden, G.K., Faubert, G., 2010. Reactivation of *Giardia lamblia* cysts after exposure to polychromatic UV light. Lett. Appl. Microbiol. 51 (4), 395–399.
Ternes, T. 2004. Assessment of technologies for the removal of pharmaceuticals and personal care products in sewage and drinking water facilities to improve the direct potable water reuse (POSEIDON). Final EU report <http://poseidon.gafg.de/servlet/is/2888/>.

Efficacy of Using Harmless *Bacillus* Endospores to Estimate the Inactivation of *Cryptosporidium parvum* Oocysts in Water

Author(s): Mary Garvey, Eoghan Clifford, Edmond O'Reilly, and Neil J. Rowan
Source: Journal of Parasitology, 99(3):448-452. 2013.
Published By: American Society of Parasitologists
DOI: http://dx.doi.org/10.1645/12-48.1
URL: http://www.bioone.org/doi/full/10.1645/12-48.1

J. Parasitol., 99(3), 2013, pp. 448–452

EFFICACY OF USING HARMLESS *BACILLUS* ENDOSPORES TO ESTIMATE THE INACTIVATION OF *CRYPTOSPORIDIUM PARVUM* OOCYSTS IN WATER

Mary Garvey, Eoghan Clifford*, Edmond O'Reilly*, and Neil J. Rowan

Department of Nursing and Health Science, Athlone Institute of Technology, Westmeath, Ireland. Correspondence should be sent to: *mgarvey@ait.ie*

ABSTRACT: The need to use complex in vitro cell culture, expensive equipment, and highly-trained technicians that are available only to specialist laboratories has significantly limited studies assessing the potential of pulsed UV light (PUV) to inactivate the waterborne parasite *Cryptosporidium parvum* in drinking water. This constitutes the first study to report on the use of different non-pathogenic *Bacillus* endospores as potential surrogate organisms to indicate the PUV inactivation performance of a *C. parvum* oocyst suspended in water. Findings showed that PUV effectively inactivated approximately 5 $\log_{10}$ CFU/ml *Bacillus megaterium* and *Bacillus pumilus* endospores suspended in water at a UV dose of 9.72 $\mu J/cm^2$ that also inactivated statistically similar levels of *C. parvum* oocysts ($P < 0.05$), as determined by combined in vitro HCT-8 cell culture and quantitative PCR. Specifically, this study demonstrated that *B. megaterium* exhibited greater or similar PUV-inactivation kinetic data compared to that of similarly treated *C. parvum* over the UV dose range 6.4 to 12.9 $\mu J/cm^2$. Therefore, the former may be used as an indicator organism for safely investigating the PUV-inactivation performance of this chlorine-resistant, waterborne parasite at the waste-water treatment plant level. Findings presented will impact positively on future water quality studies and on public health.

Protozoan cysts such as *Cryptosporidium* constitute the most commonly identified cause of waterborne diseases in developed countries. *Cryptosporidium* may enter surface waters from urban runoff, agricultural runoff, wastewater discharges, leaking septic systems, and via direct fecal waste from animal and human origin (Sunderland, 2007). In the well-developed countries of America and Western Europe, where drinking water treatment facilities are designed primarily for bacterial removal, the incidence of large-scale waterborne bacterial gastroenteritis is now rare. However, over the recent years there has been increasing concern over the emergence of new forms of enteritis caused by protozoan parasites and enteroviruses. The presence of *Cryptosporidium* oocysts has led to many public health outbreaks in both drinking and recreational waters (Schets et al., 2004). Chlorine-based compounds have, for many years, been widely used as the main disinfectants for drinking water systems. However, the *Cryptosporidium* parasite is resistant to these standard water treatment processes (Méndez-Hermida et al., 2007).

Recently, new approaches such as ozonation and pulsed UV light (PUV) have been developed for the sterilization of drinking water. Studies, including those carried out by this research group, are being conducted on the potential of PUV to inactivate *Cryptosporidium parvum* (Garvey et al., 2010). However, due to the complex nature of the oocysts, the determination of viability post-decontamination has proved challenging and requires sophisticated in vitro cell culture or in vivo mice infection models post-treatments (Garvey et al., 2010). Routine monitoring and detection of (oo)cysts in the aquatic environs have been restricted to specialist laboratories with highly-trained technicians using sophisticated equipment and methodologies (Facile et al., 2000). Current sampling and analytical methods that are available to detect *Cryptosporidium* have proven both insensitive and inaccurate (Nieminski et al., 2000; Schets et al., 2005). The lack of real-time reliable measurements of recalcitrant pathogens in contaminated water inhibits local authorities in reacting to such remedial needs in terms of drinking and waste-water optimization at the treatment plant level. Additionally, oocysts are generally not present in sufficient numbers in water sources to allow direct measurement of *C. parvum* oocysts, which also impacts negatively on the ability to investigate their inactivation performance post-PUV treatments. Consequently, there is a requirement to artificially-spike water at the pilot waste-water treatment plant (WWTP) level with this waterborne pathogen unless a surrogate, less-fastidious microorganism exhibiting similar PUV inactivation kinetic properties to *C. parvum* can be identified. Thus, on-going investigations in our research group have highlighted the need to identify and use an appropriate surrogate microorganism to serve as a harmless indicator model for *C. parvum* oocysts, particularly when investigating scale-up parameters from the laboratory to the pilot WWTP level, thereby avoiding concerns of untreated *C. parvum* being released back into municipal water (Irish EPA grant 2011-W-MS-5).

It has been common practice in the past to use indicator organisms such as coliforms to assess the microbiological quality of treated drinking water. In principle, the surrogate microorganism must share similar or preferably an augmented resistance kinetic profile to that of the target organisms for treatment methods applied, such as PUV. The inactivation kinetics of the non-pathogenic surrogate organism should also be technically easy to measure. Previous studies have assessed the use of aerobic bacterial spores to monitor the efficiency of ozone and concluded that these organisms serve as both reliable and simple indicators to that of both *Giardia* and *Cryptosporidium* under similar treatment conditions (Facile et al., 2000). *Bacillus subtilis* spores and *Clostridium perfringens* spores have been suggested as possible indicators for *Cryptosporidium* due to their observed resistance to disinfectants and to adverse environmental conditions (Verhille et al., 2003). Verhille et al. (2003) also reported that the predominant aerobic spore-forming bacteria present in surface and ground water were members of the genus *Bacillus*, whereas the anaerobic endospores from the genus *Clostridium* were found in lower numbers. Indeed, *Bacillus* and *Clostridium* endospores were routinely isolated in treated water, demonstrating their resistance to commonly-used treatment methods (Verhille et al., 2003). *Clostridium perfringens* is a known pathogen and, therefore, not suitable for water disinfection studies at a treatment plant level. Cryptosporidium are mostly present at low concentrations in raw water; therefore, their monitoring along with the drinking water treatment process

Received 13 August 2012; revised 31 October 2012; accepted 2 November 2012.

* Department of Civil Engineering, National University of Ireland, Galway, Ireland.

DOI: 10.1645/12-48.1

cannot assess large logarithmic removal efficiencies as needed for disinfection–removal studies (Mazoua and Chauveheid, 2005).

Consequently, the aim of this study was to investigate the use and relationship of 2 harmless aerobic endospores-forming *Bacillus* species (namely, *B. pumilus* and *B. megaterium*) as surrogate indicator microorganisms to determine the PUV-inactivation performance of *C. parvum* in artificially-spiked water samples. For comparative PUV-analysis, a pathogenic strain of *Bacillus cereus* was also studied.

MATERIALS AND METHODS

PUV light system

For all studies described, a bench-top pulsed power source (PUV-1, Samtech Ltd., Glasgow, U.K.) was used to power a low pressure (60 kPa) xenon-filled flashlamp (Heraeus Noblelight XAP type NL4006 [Samtech Ltd., Scotland, U.K.] series constructed from a clear UV transparent quartz tube) that produced a high-intensity diverging beam of polychromatic pulsed light, as per Garvey et al. (2010). The pulsed light has a broadband emission spectrum extending from the UV to the infrared region, with a rich UV content, and its intensity also depends on the level of the voltage applied. The light source has an automatic frequency control function that allows it to operate at 1 pulse/sec that was used throughout this study. Light exposure was homogenous, as the xenon lamp measuring 9 cm $\times$ 0.75 cm was longer than the 8.5 cm diameter. Petri dishes used in the tests were placed directly below the lamp, which ensured that full coverage of the plate surface occurred and eliminated possible shading effects. For inactivation studies the light source was mounted at 8 cm above the treatment area, which was set as the minimum threshold distance by the fabricant. In this study, standard treatments involved suspending predetermined numbers of each test species in 20 ml of phosphate-buffered saline (PBS) that were transferred to Petri dishes which were then subjected to lamp discharge energies of 16.2 J at an 8-cm distance from the light source. The UV dose can be adjusted by increasing or decreasing the frequency of the pulsing, the charging voltage, or both.

Preparation and PUV-treatment of vegetative *Bacillus* species

Bacillus megaterium ATCC 14581, *B. pumilus* ATCC 14884, and *B. cereus* ATCC 11778 were sourced from the National Collection of Type Cultures and were selected for this research due to their ability to grow at ambient temperature and for their relatively large size, which facilitates direct microscopic observations. The former 2 strains are non-pathogenic, which allows for their use in the study of water-disinfection techniques. Strains were grown to single colonies on nutrient agar (Oxoid, Hampshire, U.K.) at 30 C and their identity confirmed by determining characteristic morphological, physiological, and biochemical tests as described previously by Rowan et al. (2001). For PUV studies, a single colony of each test strain was separately transferred to 100 ml sterile nutrient broth followed by incubation at 30 C for 24 hr. Samples were then centrifuged at 635.9 *g* for 10 min and the pellet resuspended in 20 ml sterile PBS (0.01 M phosphate buffer, containing 0.0027 M KCL and 0.137 MNaCl, at a pH of 7.4) to give a working stock with approximately 1×10^8 CFU/ml. Neat and PBS-diluted samples were irradiated at 8 cm from the light source at 16.2 J per pulse with 1 pulse delivered per second.

Endospores of *B. cereus*, *B. pumilus*, and *B. megaterium* were cultivated as per the method of Rowan et al. (2001) with modifications. Endospores were prepared by growing test strains in nutrient agar supplemented with 3 mg/L of manganese sulphate for 4 days at 30 C. Spores were then collected by flooding the agar plate with 10 ml sterile PBS (pH 7), mixed gently with a sterile spatula, and then aseptically transferred to sterile, 50-ml polypropylene containers (Sarstedt, Germany). Samples were then heated to 90 C for 25 min to inactivate any residual vegetative cells present and then washed twice by centrifugation at 1,300 *g* for 20 min before resuspending in sterile PBS. The purity of spore suspensions was checked using malachite green spore staining and phase contrast microscopy as described by Rowan et al. (2001). Samples were stored in Microbank™ vials (Pro-Lab Diagnostics, Merseyside, U.K.) at –80 C. PUV studies were performed as described earlier by resuspending endospores at a concentration of approximately 10^8 CFU/ml in 20 ml sterile PBS (determined spectrophotometrically at 580 nm). This allowed for comparative studies to that of *C. parvum* oocysts suspensions in 20-ml volumes. Levels of inactivation were determined by plotting the $\log_{10}$ ratio of survivors against the UV dose ($\mu J/cm^2$) for each experimental organism.

Cryptosporidium parvum oocysts

Cryptosporidium parvum oocysts (Iowa isolate derived from a bovine calf) were purchased from Waterborne Inc., New Orleans, Louisiana. Fresh oocysts (<24 hr after excretion) were stored in sterile PBS with 100 U of penicillin/ml, 100 μg of streptomycin/ml, and 100 μg of gentamicin/ml and stored at 4 C until they were used for UV treatment studies. Oocysts were stored for a maximum of 6 wk and viability was monitored at regular intervals. The excystation rate was determined for each batch of oocysts by microscopic observation following sequential incubation at 37 C in acidified Hanks balanced salt solution for 1 hr and in 0.8% trypsin–0.75% sodium taurocholate for 1 hr, followed by incubation at room temperature for 30 min as described elsewhere (Rochelle et al., 2002). Identification of C. *parvum* oocysts was confirmed by PCR targeting of a 620-base pair (bp) polymorphic region of the β-tubulin gene by previously published procedures (Rochelle et al., 1997, 2002) (data not shown). For negative infection studies, oocysts were inactivated by heating at 70 C for 30 min. All experiments were carried out using oocysts with greater than 80% viability, as determined by in vitro excystation as per Garvey et al. (2010) and Korich et al. (2000).

Combined cell culture-quantitative PCR (CC qPCR) assay for enumerating viable *C. parvum* post treatments

CC *q*PCR was conducted as per described by Garvey et al. (2010) using HCT-8 cell monolayers as host cells for parasitic infectivity followed by real-time PCR. Methods for the growth and maintenance of HCT-8 uninfected and infected cells are therefore not described herein. Real-time, TaqMan®-quantitative PCR (*q*PCR) was performed using primers (TIB MOLBIOL, Berlin, Germany) specific for the 18S region of *Cryptosporidium* following the method of Garvey et al. (2010) and Keegan et al. (2003). The sequence of the TaqMan probe was based on the conserved eukaryotic probe of Amman et al. (1990) with the following sequence: 5′-(6-FAM) ACC AGA CTT GCC CTC C (TAMRA). An aliquot (4 μl) of the LightCycler® TaqMan Master kit (Roche Diagnostics, West Sussex, England) comprising Taq DNA polymerase, reaction buffer, $MgCl_2$, and dNTP was used in each reaction. Cycling parameters were initial denaturation for 10 min at 95 C followed by 50 cycles of denaturation for 10 sec at 95 C, annealing for 40 sec at 40 C, extension for 1 sec at 70 C, and cooling for 30 sec at 40 C on a LightCycler device (Model 1.5, Roche Diagnostics). The large number of cycles was used to ensure detection of low levels of infection. On completion of each *q*PCR run, amplification curves were analyzed by LightCycler software (version 3.5, Roche Diagnostics) and a standard curve of oocyst DNA concentration determined. DNA standards were prepared from fresh oocysts ranging in concentration from 10^1 to 10^7 oocysts/ml by dilution in PBS following standard viable count determinations. Aliquots of oocysts at different densities were then stimulated to infect the HCT-8 cell line that was seeded into 24 well plates (Sarstedt) at a concentration of approximately 1×10^4 cells/ml at 90% confluency as per the method of Garvey et al (2010). One-microliter aliquots of each concentration range of excysted oocysts was re-suspended in RPMI cell culture growth media and added to 1 well of the 24-well plate. Following 48 hr incubation at 37 C in a humidified atmosphere of 5% (vol/vol) CO_2, the cell culture media with non-adherent or internalized *C. parvum* was removed by aspiration and discarded. Mammalian cells were then washed with sterile PBS and trypsinized using 200 μl of 0.25% (vol/vol) trypsin/EDTA (Sigma, Arklow, Ireland) and left for 15 min at 37 C until complete detachment of the monolayer had occurred. Cells were then centrifuged at 70.7 *g* for 10 min and re-suspended in 200 μl sterile PBS; thereafter, the mammalian cells and *C. parvum* sporozoite cell membranes were lysed using a PCR template preparation kit (Roche Diagnostics) in order to produce DNA (template) and a standard curve (Fig. 1). The aforementioned procedure was then repeated to determine infectivity of oocysts subjected to varying UV parameters or to heating at 70 C for 30 min (negative control) as per the method of Garvey et al. (2010). Samples were also re-suspended in PBS containing 10% w/v humic acid (H.A.) in order to investigate the influence of organic matter on microbial inactivation as per Garvey et al. (2010). Log inactivation of oocysts (L) is defined by $L = \log_{10}[Nd/No]$, where No is the initial concentration of oocysts and Nd is the concentration of viable

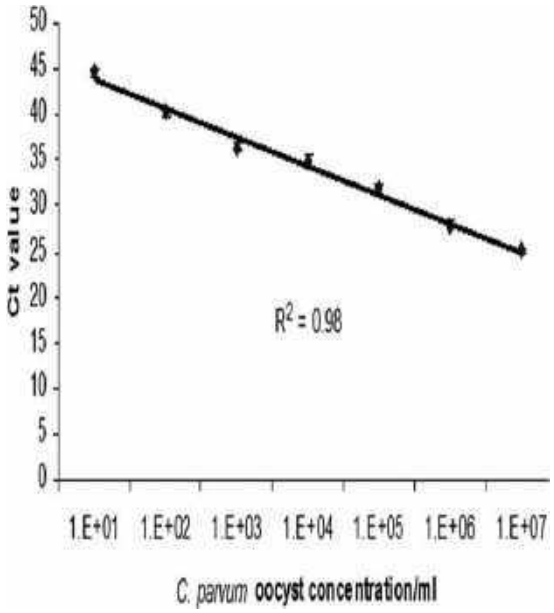

FIGURE 1. Standard curve for *Cryptosporidium parvum* oocyst concentration versus Ct value obtained by real time PCR ultilizing a cell–culture-based assay (±SD).

infectious oocysts post-disinfection treatments as detected by combined CC *q*PCR assay as per the method of Lee et al. (2008).

Statistical analysis

Student's *t*-tests and an ANOVA one-way model (MINITAB software release 16; Mintab Inc., State College, Pennsylvania) were used to compare the effects of the relationship of independent variables on light treatments. Mean results from 3 separate experiments were determined. Linear regression analysis was used to determine the rate of inactivation for each test species under the regime of PUV treatments applied.

RESULTS

PUV inactivation of bacterial endospores and vegetative cells

There was a direct relationship between an increase in UV dose and a corresponding increase in microbial inactivation in all vegetative forms of *Bacillus* strains tested (Table I). A general trend was observed where, at lower UV doses ($\leq$10.8 μJ/cm^2), there was a significant difference in the sensitivity of each vegetative test strain to UV exposure, with *B. cereus* exhibiting more resistance when compared to similarly treated *B. megaterium* and *B. pumilus* ($P < 0.05$) (Table I). However, at higher UV doses, similar rates of inactivation were obtained for all *Bacillus* strains tested. A UV dose of 10.8 μJ/cm^2 was required, producing a 6-log$_{10}$ reduction in CFU/ml for all vegetative strains where the order of sensitivity, from the most resistance to the least, was *B. cereus*, *B. pumilus*, and *B. megaterium* ($P < 0.05$).

A general trend was observed where *Bacillus* endospores proved more UV resistant than did their vegetative state counterparts, whereby an increased UV dose was needed to achieve similar rates of inactivation in similarly PUV-treated vegetative cells (Table II). For example, there was a 0.4, 0.54, and 1-log$_{10}$ reduction in *B. cereus*, *B. megaterium*, and *B. pumilus* at 1.08 μJ/cm^2, respectively, which was approximately 2-log lower compared to similarly PUV-treated vegetative cells. PUV-irradiance at 10.8 μJ/cm^2 produced a 5.1, 5.3, and 6.7-log$_{10}$ reduction in endospore numbers for *B. cereus*, *B. megaterium*, and *B. pumilus* respectively. This general trend also persisted as, with enhanced pulsing, the order of increased resistance to PUV was *B. pumilus*, *B. megaterium*, and *B. cereus* ($P < 0.05$). At higher UV exposures (such as 10.8 μJ/cm^2), a 5.1, 5.3, and 6.7-log$_{10}$ inactivation was obtained for *B. cereus*, *B. megaterium*, and *B. pumilus* spores, respectively. However, at doses exceeding 12.9 μJ/cm^2, there was no significant difference between PUV-inactivation performance for test *B. megaterium* and *B. cereus* endospores. While *B. pumilus* endospores appeared the most UV sensitive for all regimes tested, *B. megaterium* proved the most UV resistant at the uppermost UV doses tested (19.4 μJ/cm^2) (Table II).

Pulsed UV inactivation of *Cryptosporidium parvum* as determined by use of a combined in vitro CC qPCR assay

For relative comparison of samples, a standard curve was generated by inoculating HCT-8 monolayers with different concentrations of *C. parvum* oocysts and by performing linear regression analysis of sample mean CT values plotted against numbers of inoculated oocysts (Fig. 1). A general trend was observed where an increase in UV exposure produced an increase in oocyst inactivation (Table II). A UV dose of 9.72 μJ/cm^2 resulted in approximately 5-log reductions in oocyst viability. At UV doses exceeding 12.96 μJ/cm^2, no parasitic DNA was detected in HCT-8 mammalian cells, indicating that an approximately 6-log$_{10}$ reduction in oocysts had occurred (Table II), thus showing that PUV successfully and repeatedly inactivated *C. parvum* oocysts. At low UV doses ($\leq$4.32 μJ/cm^2), *C. parvum* exhibited greater resistance to similarly-treated *Bacillus* endospores. However, *C. parvum* oocysts exhibited lower or similar resistance to *B. megaterium* endospores over the UV dose range of 6.48 to 12.9 μJ/cm^2 (medium to high PUV-irradiance). The inclusion of 10% w/v H.A. did not affect the PUV-inactivation performance of all test organisms as compared to control samples devoid of H.A. (Fig. 2). *Cryptosporidium parvum* oocysts were significantly more resistant to PUV than were *B. pumilus* at all applied treatment doses.

DISCUSSION

This study reports a general trend where endospores of each *Bacillus* strain tested proved more UV resistant than did their corresponding vegetative form. There was also a significant difference in individual strain sensitivity to UV treatment for both culture forms at lower treatment doses of <10.8 μJ/cm^2. Endospores of *B. pumilus* consistently showed lower levels of resistance to PUV compared to *B. megaterium* and *B. cereus*. In the vegetative state, the order of increasing sensitivity to PUV was as follows: *B. cereus*, *B. pumilus*, and *B. megaterium*. This may be related in part to the larger size of *B. megaterium* cells relative to the other *Bacillus* species tested (Rowan et al., 2001). However, for endospore inactivation studies, the order of increased sensitivity was observed to be *B. megaterium*, *B. cereus*, and *B. pumilus*.

This study also corroborates the findings of Sharifi-Yazdi and Darghahi (2006) who reported that *B. megaterium* endospores proved more resistant to UV irradiation when compared to similarly treated *B. cereus* endospores. These researchers achieved

TABLE I. Log_{10} reduction obtained following PUV treatment of varying strains of *Bacillus* species in their vegetative state (±SD) at a rate of 1 pps and 16.2 J per pulse.

Pulse no. 16.2 J	UV dose ($\mu J/cm^2$)	Log_{10} reduction in microbial test strain		
		Bacillus megaterium	*Bacillus pumilus*	*Bacillus cereus*
0	0	0	0	0
10	1.08	3.38 (±0.3)A	3.39 (±0.4)B	1.77 (±0.3)C
20	2.15	5.18 (±0.5)A	4.69 (±0.2)B	2.81 (±0.2)C
30	3.24	5.31 (±0.3)A	4.66 (±0.5)B	3.06 (±0.5)C
40	4.32	6 (±0.5)A	4.6 (±0.1)B	4.14 (±0.1)C
60	6.48	6.5 (±0.3)A	4.91 (±0.5)B	4.84 (±0.3)C
80	8.64	6.7 (±0.3)A	6.2 (±0.4)B	5.41 (±0.1)C
100	10.8	6.62 (±0.1)A	6.6 (±0.02)A	6.05 (±0.5)A
120	12.96	6.9 (±0.6)A	6.65 (±0.2)A	6.55 (±0.4)A
140	15.12	7.1 (±0.3)A	6.84 (±0.2)A	6.79 (±0.5)A
200	21.6	7.2 (±0.3)A	7.02 (±0.2)A	7.25 (±0.1)A

A, B, C denote a significant difference ($P < 0.05$) in strain sensitivity to UV exposure.

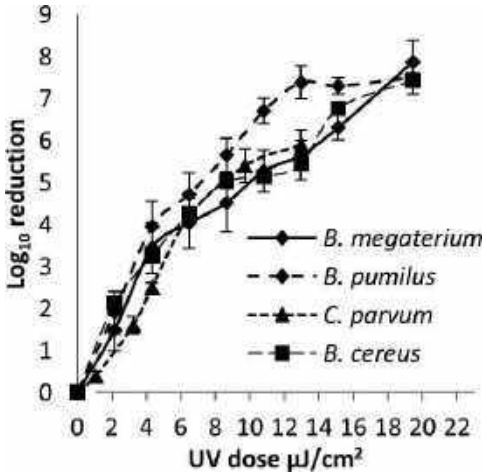

FIGURE 2. Pulsed UV inactivation of *Cryptosporidium parvum* oocysts and *Bacillus* endospores in PBS containing 10% w/v humic acid at lamp discharge energy of 16.2 J using a rate of 1 pulse per second.

a 2-log_{10} CFU/ml reduction of *B. megaterium* with 50 pulses (7.1 $\mu J/cm^2$) and a 5-log_{10} CFU/ml reduction following 25 pulses (3.2 $\mu J/cm^2$) for *B. cereus* at 20 J per pulse. While the mechanisms underpinning destruction of spores differs to that of similarly UV-treated vegetative cells, DNA remains the principal target, with the formation of a lethal adjunct of a thymine dimer in spores as opposed to formation of cyclobutane pyrimidine dimers in vegetative cells. Repair of these photoproducts is an important factor when treating bacterial endospores with UV disinfection techniques. Currently, it is known that endospores possess 3 types of repair mechanisms; recombinational repair (RR), nucleotide excision repair (NER) which is similar to the damage repair system present in vegetative cells, and spore photoproduct lyase (SP lyase) for repair of UV damage to DNA. The importance of these 3 systems varies depending on the damage to be repaired. At present, there is a lack of data on the UV repair potential of PUV-treated endospores. The presence of certain proteins (α/β-type SASP) within the spore structure may also result in the resistance of bacterial spores to many methods of disinfection including heat, chemical, and monochromatic UV (Setlow, 2001). There are high levels of this protein present in the *Bacillus* species including *B. cereus* and *B. megaterium*, and binding of this protein to DNA has been linked to disinfection resistance (Setlow, 2001). The findings of this study also suggest that endospore resistance to disinfection with PUV is not affected by the pathogenicity of the *Bacillus* species studied. Indeed, similar levels of inactivation were obtained for the non-pathogenic and pathogenic strains studied (Table II).

TABLE II. Log_{10} reduction obtained following PUV treatment of varying strains of *Bacillus* species endospores and *Cryptosporidium parvum* (±S.D) at a rate of 1 pps and 16.2 J per pulse.

Pulse no.	UV dose $\mu J/cm^2$	*Bacillus megaterium*	*Bacillus pumilus*	*Bacillus cereus*	*Cryptosporidium parvum*
0	0	0	0	0	0
20	2.159	1.49 (±0.5)A	1.9 (±0.5)B	2.1 (±0.5)C	1.1 (±0.2)D
40	4.32	3.44 (±0.6)A	3.95 (±0.6)B	3.25 (±0.3)A	2.5 (±0.1)D
60	6.48	4.03 (±0.6)A	4.72 (±0.5)B	4.26 (±0.5)A	4.2 (±0.1)A
80	8.64	4.52 (±0.2)A	5.65 (±0.4)B	5.02 (±0.6)C	4.9 (±0.3)C
100	10.8	5.3 (±0.3)A	6.7 (±0.3)B	5.13 (±0.2)A	5.6 (±0.1)A
120	12.96	5.65 (±0.6)A	7.38 (±0.4)B	5.44 (±0.2)A	5.9 (±0.1)A
160	15.12	6.31 (±0.3)A	7.3 (±0.2)B	6.76 (±0.5)A	ND
200	19.44	7.87 (±0.5)A	7.5 (±0.4)A	7.43 (±0.1)A	ND

A, B, C, D denote a significant difference ($P < 0.05$) in strain sensitivity or PUV treatment; ND = no target DNA detected via *q*PCR techniques.

After microbes are entrapped in particles or absorbed to surfaces, they can be shielded from disinfection (Verhille et al., 2003). Therefore, it is reasonable to assume that bacterial endospores would be more resistant in an actual water treatment facility due to their aggregation properties. At present, studies focusing on the UV inactivation of organisms are primarily based on bench-scale inactivation kinetics that are based on laboratory studies using primarily dispersed suspensions of organisms. This highlights the importance of conducting plant-scale studies on problematic pathogenic organisms such as *Cryptosporidium*. However, there are limitations to the extent of PUV studies that can be conducted at a plant level due to the pathogenic nature of *Cryptosporidium* species. This has prevented more in-depth studies that focus on the implementation of the PUV system at an operational plant level.

In conclusion, the findings of this study showed that PUV effectively eliminated high levels of waterborne parasite oocysts and recalcitrant endospores after extended pulsing, suggesting that it is a potential application for use at the WWTP level. These data also suggest that the non-pathogenic *B. megaterium* have similar inactivation rates ($P < 0.05$) to the Iowa strain of *C. parvum* used following exposure to pulsed UV light at 16.2 J. Therefore, *B. megaterium* may allow for future inactivation studies on the optimization of the PUV system at the water–WWTP level by providing a surrogate organism for the PUV inactivation of *C. parvum*. This would allow for full-scale inactivation studies at the plant level using a non-pathogenic organism that is representative of the pathogenic *Cryptosporidium parvum*. Furthermore, it is recommended that studies into the

potential of *Bacillus* endospores to repair genetic damage following PUV treatment be investigated.

ACKNOWLEDGMENTS

The authors wish to thank the Irish Environmental Protection Agency Strive Programme for funding this research (2011-W-MS-5). The authors also wish to acknowledge the assistance of Rosalyn Donnelly.

LITERATURE CITED

Amman, R. R., B. J. Binder, R. J. Olsen, S. W. Chisholm, R. Devereaux, and D. A. Stahl. 1990. Combination of 16S rRNA-targeted oligonucleotide probes with flow cytometry for analyzing mixed microbial populations. Applied Environmental Microbiology **56:** 1919–1925.

Facile, N., B. Barbeau, M. P. Vostm, and B. Koudjonou. 2000. Evaluating bacterial aerobic spores as a surrogate for *Giardia* and *Cryptosporidium* inactivation by ozone. Water Research **34:** 3238–3246.

Garvey, M., H. Farrell, M. Cormican, and N. Rowan. 2010. Investigations of the relationship between use of in vitro cell culture-quantitative PCR and a mouse-based bioassay for evaluating critical factors affecting the disinfection performance of pulsed UV light for treating *Cryptosporidium parvum* oocysts in saline. Journal of Microbiological Methods **80:** 267–273.

Keegan, A. R., S. Fanok, P. T Monis, and C. P. Saint. 2003. Cell culture-TaqMan PCR assay for evaluation of *Cryptosporidium parvum* disinfection. Applied and Environmental Microbiology **69:** 2505–2511.

Korich, D. G., M. Marshall, H. V. Smith, J. O'Grady, Z. Bukhari, C. R. Fricker, J. P. Rosen, and J. L. Clancy. 2000. Inter-laboratory comparison of the CD-1 neonatal mouse logistic dose-response model for *Cryptosporidium parvum* oocysts. Journal of Eukaryotic Microbiology **47:** 294–298.

Lee, S. U., M. Joung, D. J. Yang, S. H. Park, S. Huh, W. Y. Park, and J. R. Yu. 2008. Pulsed-UV light inactivation of *Cryptosporidium parvum*. Parasitology Research **102:** 1293–1299.

Mazoua, S., and E. Chauveheid. 2005. Aerobic spore-forming bacteria for assessing quality of drinking water produced from surface water. Water Research **39:** 5186–5198.

Méndez-Hermida, F., E. Ares-Mazás, K. McGuigan, M. Boyle, C. Sichel, and P. Fernández-Ibáñez. 2007. Disinfection of drinking water contaminated with *Cryptosporidium parvum* oocysts under natural sunlight and using the photocatalyst TiO2. Journal of Photochemistry and Photobiology B: Biology **88:** 105–111.

Nieminski, E. C., W. D. Bellamy, and L. R. Moss. 2000. Using surrogates to improve plant performance. Journal of American Waterworks Association **92:** 67–78.

Rochelle, P. A., D. M. Ferguson, T. J. Handojo, R. De Leon, M. H. Stewart, and R. L. Wolfe. 1997. An assay combining cell culture with reverse transcriptase PCR to detect and determine the infectivity of waterborne *Cryptosporidium parvum*. Applied and Environmental Microbiology **63:** 2029–2037.

———, M. M. Marshall, J. R. Mead, A. M. Johnson, D. G. Korich, J. S. Rosen, and R. De Leon. 2002. Comparison of in vitro cell culture and a mouse assay for measuring infectivity of *Cryptosporidium parvum*. Applied and Environmental Microbiology **68:** 3809–3817.

Rowan, N. J., K. Dean, J. G. Anderson, I. S. Hunter, and T. Chaithong. 2001. Putative virulence factor expression by clinical and food isolates of *Bacillus* species after reconstitution in infant milk formulae. Applied Environmental Microbiology **67:** 3873–3881.

Schets, F. M., G. B. Engels, M. During, and A. M. de Roda Husman. 2005. Detection of infectious *Cryptosporidium* oocysts by cell culture immunofluorescence assay: Applicability to environmental samples. Applied and Environmental Microbiology **71:** 6793–6798.

———, ———, and E. G. Evers. 2004. *Cryptosporidium* and *Giardia* in swimming pools in the Netherlands. Journal of Water and Health **3:** 191–200.

Setlow, P. 2001. Resistance of spores of *Bacillus* species to ultraviolet light. Environmental and Molecular Mutagenesis **38:** 97–104.

Sharifi-Yazdi, M. K., and H. Darghahi. 2006. Inactivation of pathogenic bacteria using pulsed UV-light and its application in water disinfection and quality control. Acta Medica Iranica **44:** 305–308.

Sunderland, D., T. K. Graczyk, L. Tamang, and P. N. Breysse. 2007. Impact of bathers on levels of *Cryptosporidium parvum* oocysts and *Giardia lamblia* cysts in recreational beach waters. Water Research **41:** 3483–3489.

Verhille, S., R. Hofmann, C. Chauret, and R. Andrews. 2003. Indigenous bacterial spores as indicators of *Cryptosporidium* inactivation using chlorine dioxide. Journal of Water and Health **1:** 91–100.

Water and Environment Journal
Promoting Sustainable Solutions
CIWEM

Water and Environment Journal. Print ISSN 1747-6585

Pulsed ultraviolet light inactivation of *Pseudomonas aeruginosa* and *Staphylococcus aureus* biofilms

Mary Garvey, Danny Rabbitt, Alessia Stocca & Neil Rowan

Biomedical Research Institute, Athlone Institute of Technology, Athlone, Ireland

Keywords
biofilms; inactivation; *Pseudomonas aeruginosa*; pulsed UV; *Staphylococcus aureus*

Correspondence
M. Garvey, Athlone Institute of Technology, Dublin road, Athlone, Westmeath, Athlone, Ireland. Email: mgarvey@ait.ie

doi:10.1111/wej.12088

Abstract

Microbial biofilms are complex communities that form when planktonic bacterial species attach to surfaces in many settings where they can provide a source of pathogenicity. The relative ineffectiveness of conventional disinfectants such as free chlorine and monochloramine for the inactivation of some species found in water has led to evaluation of alternative disinfectants for drinking and wastewater treatment. In recent years, novel pulsed power electrotechnologies have been introduced and are being considered as possible alternatives to current methods for inactivating problematic species in water. This study focuses on the ultraviolet (UV) inactivation of bacterial biofilms using a pulsed UV light approach as a potential disinfection method for water treatment operating systems. Biofilms were stimulated to form attached to polyvinyl chloride coupons using a recommended Centre for Disease Control biofilm reactor followed by exposure to a range of UV doses. Findings show that this method is highly effective at inactivating both planktonic and biofilm cells with significant inactivation rates obtained for both test species. Specifically, a 7.2 and 5.9 $\log_{10}$ inactivation was achieved with up to 21.6 $\mu J/cm^2$ UV for *Pseudomonas aeruginosa* and *Staphylococcus aureus*, respectively. Findings from this study highlight the effectiveness of pulsed UV for the inactivation of *Pseudomonas* biofilms among other test species. Research conducted by this group suggests that this pulsed UV system may offer a useful method for the disinfection of drinking and wastewater supplies.

Introduction

Microorganisms are naturally found as either free-floating planktonic cells or within a microbial structure referred to as a biofilm. Biofilms are communities of microorganisms that live attached to surfaces surrounded by a matrix of extracellular polymeric substances (EPSs). This extracellular substance is produced by the organisms and includes proteins, nucleic acids, polysaccharides and amphiphilic polymeric compounds. This matrix is involved in numerous essential processes including attachment to surfaces, cell-to-cell interconnection, quorum sensing, and exchanges between bacterial subpopulations, tolerance and exchange of genetic material (Harmsen *et al*. 2010). Bacterial growth and diversity as well as the development of the biofilm matrix depend on several factors including nutrient availability and hydrodynamic conditions (Schwartz *et al*. 2009). EPS matrices are often negatively charged, gel like and hydrated; thus, the resulting structure can adapt and change its construction under different conditions.

The presence of biofilms on man-made surfaces such as piping, medical equipment and tubing has highlighted their importance in relation to pathogenicity. The formation of biofilms in undesirable places leads to problems in medical and industrial environments as these bacterial communities can resist host cellular immunity (phagocytosis), antimicrobial therapy and biocide treatment (Harmsen *et al*. 2010). Moreover, the presence of biofilms is well documented in the piping associated with water and wastewater treatment plants (Kerr *et al*. 2003) as the drinking water distribution system provides a large surface area for the adhesion of microbial species. Regardless of the fact that nutrient availability is limited, disinfectants are used, and relatively low temperatures are present in water pipes, organisms such as *Pseudomonas aeruginosa* can adhere to the pipe surface and form biofilms. Biofilm formation in drinking water reservoirs and distribution systems can hinder the efficient operation of these systems and can pose a health risk to the users by providing a habitat for pathogenic organisms such as *Cryptosporidium*, *Legionella pneumophila* and *Escherichia*

coli (Coenye & Nelis 2010). The presence of biofilms may increase the bacterial counts in treated water by shielding organisms from standard disinfection methods. Studies by Momba *et al*. (2000) stated that for each planktonic bacterial cell detected, there may be up to 1000 organisms present within a biofilm.

Studies by Momba *et al*. 2000 have shown that the disinfectants used for water treatment are not effective against biofilms. They showed that the presence of residual disinfectant concentrations of 19 ppm hydrogen peroxide, 1 ppm monochloramine and 0.5 ppm free chlorine did not prevent the formation of biofilms on test surfaces (Momba *et al*. 2000). A review by Wingender & Flemming (2011) observed that cells released from biofilms retain the disinfectant resistance obtained while within the EPS matrix and are capable of initiating the formation of new biofilms further down the water system. Biofilm cells were found to be less susceptible to disinfectants than planktonic cells. Therefore, the biofilm serves as a reservoir for the constant contamination of the water flowing through the distribution system. It is also believed that biofilms possess mechanisms that allow associated cells to disperse from the original structure. This is achieved by altering its EPS matrix, allowing sections of the biofilm to separate, relocate and form new biofilm communities downstream. Consequently, the formation and disinfection of biofilms and biofilm-forming organisms such as *Pseudomonas* is an important aspect when assessing the disinfection procedures used in water treatment plant operations.

The disinfection of drinking water may be regarded one of the most important public health measures of this past century as it has radically reduced the occurrence of water borne diseases globally (Momba *et al*. 2000). However, research has shown that the public is still at risk from pathogens such as parasites and viruses that may escape the methods currently in use. Therefore, there is a pressing need for new and alternative disinfection methods. The use of ultraviolet (UV) light for the disinfection of drinking water and wastewater has become more popular because of the microbial inactivation potential of this technology. Recently, a new approach to the delivery of the UV dose termed pulsed UV (PUV) has been investigated (Garvey *et al*. 2012) (Rowan *et al*. 1999). Studies have shown the potential of this PUV technology for the repeated inactivation of numerous microbial species both on sample surfaces and in liquid suspension (Farrell *et al*. 2009). Compared with conventional (continuous) UV light, pulsed light treatment has the advantage of being fast, effective and more efficient at converting electrical energy into photon energy.

P. aeruginosa is part of a large group of free-living bacteria that are abundant in the natural environment. This species is frequently found in natural waters such as lakes and rivers in concentrations of 10 CFU per 100 mL to greater than 1000 CFU per 100 mL and is a well-known cause of the formation of biofilms on pipes and tubing (Coeyne & Nelis 2010). Therefore, it is the organism of choice for this study. This research focuses on determining the efficacy of a PUV system for the inactivation of both planktonic cell and microbial biofilms of *P. aeruginosa* and *Staphylococcus aureus*. *S. aureus* was chosen as a gram-positive biofilm test species to provide comparative data to that of the gram-negative *Pseudomonas*.

Methods

PUV technology

The PUV machine used throughout this study was sourced through Samtech Ltd, Scotland, UK. It operates as a bench-top pulsed power source used to power a low pressure (60 kPa) xenon-filled flashlamp (Heraeus Noblelight XAP type NL4006 series constructed from a clear UV transparent quartz tube) that produces a high-intensity diverging beam of polychromatic pulsed light (Fig. 1). This delivery system kills microorganisms by using ultrashort duration pulses of an intense broadband emission spectrum that is rich in the UV-C germicidal wavelength. PUV is produced by storing electricity in a capacitor over relatively long times and releasing it as a short-duration pulse using sophisticated pulse compression techniques (Rowan *et al*. 1999; Gómez-López *et al*. 2007). The emitted flash has a high peak power and usually consists of wavelengths from 200 to 2600 nm broad spectrum light enriched with shorter germicidal wavelengths (Gómez-López *et al*. 2007) as opposed to low pressure UV that is limited in its wavelength range and therefore cellular targets. The killing effects of pulsed light are caused by the rich and broad-spectrum UV content, the short duration, and the high peak power of the pulse. The system was used as per Garvey *et al*. (2010) and Garvey *et al*. (2012), and is therefore not described in further detail herein.

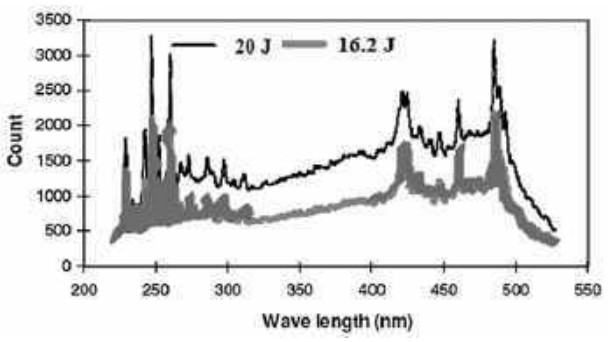

Fig. 1. The spectrum emitted by the pulsed ultraviolet system at a discharge of 20 and 16.2 J per pulse with rich output in the ultraviolet C (UVC) region showing three peaks at 229, 247 and 260 nm.

Centre for Disease Control (CDC) biofilm reactor

The CDC reactor (Biosurface Technologies Corp, Bozeman, MT, USA) is composed of a glass vessel that holds the reactor media. Placed into this vessel is a polyethylene top that holds eight removable polypropylene rods. Each of these rods in turn has three inserts for holding the coupons on which the biofilms form. Therefore, each biofilm reactor has space for 24 coupons equivalent to 24 separate biofilms that makes it an ideal apparatus for inactivation studies. In the centre of the reactor, a magnetic stirrer is present, which provides a continuous flow of nutrients over the colonised surface of the coupons. The CDC reactor is a recognised method for the growth of *P. aeruginosa* biofilms under high shear and continuous flow (Coenye & Nelis 2010), and is the standard method in use by the American Society for Testing and Materials (ASTM).

Preparation of microbial biofilms

P. aeruginosa ATCC 27853 and *S. aureus* ATCC 25923 were sourced, cultured and maintained in nutrient broth. The CDC biofilm reactor (BioSurface Technologies Corp., Bozeman, MT, USA) was used for the formation of microbial biofilms as per the recommended procedure for continuous fluid shear flow biofilm formation (ASTM E2562-12 2012). Specifically, a selected number of polyvinyl chloride (PVC) coupons were inserted into the coupon holes in each reactor rod and firmly secured. To initiate *P. aeruginosa* biofilm formation, 350 mL of 300 mg/L tryptone soya broth (TSB) was added to the reactor ensuring that each coupon was completely submerged. This low concentration of TSB provided a nutrient-depleted environment within the reactor. The reactor was sterilised at 121°C for 15 min. After which, 1 mL of a 12 h microbial culture of *P. aeruginosa* was added to the reactor chamber to ensure that cells were in the log phase of reproduction. Bacterial counts were also conducted to determine the seeding density of the reactor that was ca. 3.4×10^6 CFU/mL. The reactor was incubated at 20°C for 24, 48 and 72 h as required under rotatory conditions (125 rpm). For the formation of *S. aureus* biofilms, 350 mL of TSB supplemented with 0.2% glucose was added to the reactor vessel. Following autoclaving, as previously described, 1 mL of a 12-h culture of known population density of *S. aureus* was added to the reactor media that was then incubated for 48 h at 37°C under rotatory conditions. To allow for comparative analysis, a 48-h biofilm of *P. aeruginosa* that was formed at 37°C was also treated. To allow for the enumeration of CFU per microbial biofilm, all coupons were removed from each reactor rod aseptically and rinsed with sterile phosphate-buffered saline (PBS) to remove any planktonic cells. Biofilms were removed from each coupon by scraping the coupon using a sterile cell scraper into 10 mL of sterile PBS. Serial dilutions were then made, and the standard plate count technique was used to determine the CFU/mL bacterial population in the biofilm as per the recommended procedure (ASTM E2562-12 2012).

PUV inactivation of surface spread and planktonic bacterial suspensions

P. aeruginosa, *S. aureus* and *E. coli* ATCC 25922 cultures were grown and maintained on nutrient agar at 37°C. For PUV studies, a single colony of the test strain was aseptically transferred to 100-mL sterile nutrient broth followed by incubation at 37°C for 12 h at 125 rpm. For surface treatment, 100 μl of an appropriate dilution was spread onto plate count agar. Test plates were then exposed to pulses of UV light at 16.2 J at varying doses at a rate of 1 pulse/s as per Garvey *et al*. (2012). PUV studies were also conducted on samples diluted from the 12 h broth in 20 mL final volumes of sterile PBS at 8 cm from the light source. The applied UV dose (μJ/cm^2) was increased or decreased by adjusting the pulse number.

PUV inactivation of bacterial biofilms

Coupons were aseptically removed from the reactor and transferred to a sterile Petri dish. Samples were exposed to pulses of UV light at 16.2 J at 8 cm from the light source at varying UV doses that were obtained by increasing the pulse number. Once treated, coupons were submerged in 10 mL of sterile PBS and surface-scraped using a sterile cell scraper to remove the treated biofilms and to allow for the determination of inactivated rates. The liquid was then transferred to a sterile 20-mL container and centrifuged at 3000 rpm for 10 min to pellet the cells. The sample was then resuspended and agitated to ensure biofilm dispersion. Serial dilutions were made from the biofilms suspension and 100 μL spread on triplicate agar plates to determine the CFU/mL of treated samples. This process was repeated for coupons at varying UV doses to determine the $\log_{10}$ reduction obtained with increasing UV dose. A cell count was also conducted on the media present in the reactor vessel by spread plate techniques.

Statistical analysis

All the experiments were performed three times with three plate replicates for each experimental data point (allowing for a total of nine replicates for each data point). Mean results from the three separate experiments were determined. The log reduction was calculated as the $\log_{10}$ of the ratio of the concentration (CFU/mL) of the nontreated (N_0) and UV-treated (N) samples [$\log_{10}$ (N_0/N)]. Linear regression analysis was used to determine the rate of inactivation for each test species under the regime of PUV treatments applied.

Student's *t*-tests and ANOVA one-way model (MINITAB software release 16; Mintab, Inc., State College, PA, USA) were used to compare the effects of the relationship between UV treatments and viable/nonviable cells. Student's *t*-tests were used to determine the relationship between the sensitivity of the 24, 48 and 72 h biofilms to UV exposure.

Results and discussion

PUV inactivation of planktonic microbial strains

Substantial rates of inactivation were obtained following the PUV exposure of *P. aeruginosa*, *S. aureus* and *E. coli*, whereby a clear pattern emerged showing an increase in cell death with an increase in UV dose (μJ/cm^2). Findings also show a significant difference ($P < 0.05$) in the sensitivities of each strain tested (Fig. 2) when treated in 20 mL suspensions up to a UV dose of 3.24 μJ/cm^2. At this dose, *P. aeruginosa* proved to be more UV-resistant at a discharge energy of 16.2 J followed by *E. coli* with *S. aureus* proving to be most UV-sensitive. However, exposure to 4.32 μJ/cm^2 resulted in a 5.6 $\log_{10}$ inactivation of both *P. aeruginosa* and *E. coli*, and a marginally increased 7.5 $\log_{10}$ inactivation of *S. aureus*. Results show with doses exceeding 6.48 μJ/cm^2 the level of resistance shown at lower UV doses was obtained again, whereby the order of resistance (from highest to lowest) was as follows: *P. aeruginosa*, *E. coli* and *S. aureus* ($P < 0.05$).

The findings of this study clearly show a significant difference in the rate of inactivation achieved for these test species when exposed to pulses of UV light on agar surfaces to that of microbial suspensions. Gram-negative test species proved to be significantly ($P < 0.05$) more sensitive to UV inactivation when treated on agar surfaces (Fig. 3) as opposed to treatment while in suspension. *E. coli* proved to be most sensitive

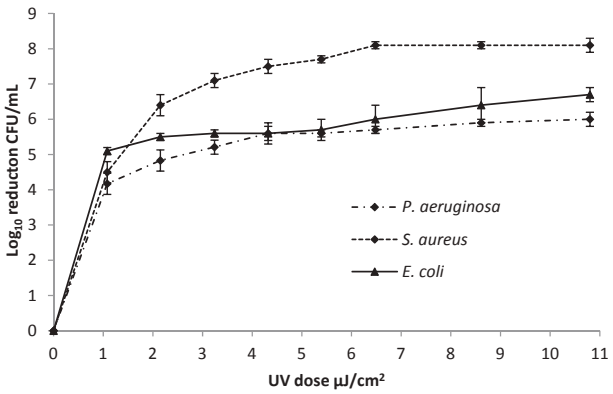

Fig. 2. Pulsed ultraviolet (UV) inactivation given as the $\log_{10}$ reduction in viability of microbial test species suspended in 20 mL volumes at varying UV dose at a discharge energy of 16.2 J per pulse (±standard deviation).

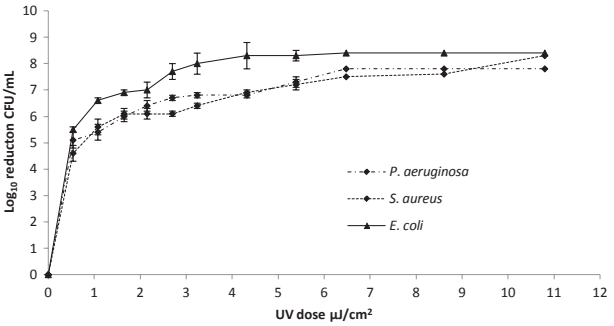

Fig. 3. Pulsed ultraviolet (UV) inactivation given as the $\log_{10}$ reduction in viability of microbial test species spread on agar surfaces at varying UV dose at a discharge energy of 16.2 J per pulse (±standard deviation).

to UV inactivation when treated on agar surfaces with a 6.6 $\log_{10}$ reduction achieved with a dose of 1.08 μJ/cm^2, while a 5.4 and 5.5 $\log_{10}$ inactivation was obtained for *P. aeruginosa* and *S. aureus*, respectively, at this setting. Indeed, *E. coli* proved to be most UV sensitive when exposed on surfaces with *P. aeruginosa* and *S. aureus* consistently showing similar rates of inactivation at all exposures regimes (Fig. 3). With a UV dose of 10.8 μJ/cm^2, a 6.7 $\log_{10}$ inactivation of the gram-negative species, *E. coli* was obtained when treated in suspension compared with an 8.4 $\log_{10}$ inactivation on agar surfaces. This significant difference in inactivation rates was evident for all treatment doses suggesting that *E. coli* is more susceptible to UV inactivation when treated on surfaces. This was also the case for the gram-negative species *P. aeruginosa* where greater inactivation was achieved when the bacteria was treated on agar surfaces. Interestingly for the gram-positive test species *S. aureus*, the inactivation achieved for the surface and suspension studies showed the opposite effect. *S. aureus* appears more UV-sensitive when treated in suspension, whereby a significant difference ($P < 0.05$) in susceptibility was obtained at each dose (Fig. 2). Indeed, a PUV dose of 3.24 μJ/cm^2 provided a 6.4 and 7.1 $\log_{10}$ inactivation of surface spread and microbial suspensions, respectively (Fig. 3). This pattern was evident for all applied doses for this test species. However, with 10.8 μJ/cm^2, maximal inactivation was obtained for both treatment methods with a ca. 8.1 and 8.3 $\log_{10}$ inactivation of *S. aureus* at 16.2 J per UV pulse for microbial suspension and surface-treated samples, respectively.

The results obtained here demonstrate that the xenon flash lamp used in this study is an efficient UV source for the inactivation of the organisms both for agar surface inoculated and liquid suspensions at these set operational parameters. However, the findings have demonstrated that PUV treatment is more effective for the gram-negative species studied on solid agar surfaces with a faster rate of cell death than in liquids. The results also reveal the variations in susceptibility

Table 1 Showing densities of microbial test species at seeding at time 0 h (T0) and following biofilm production at different time points in a Centre for Disease Control biofilm reactor at 20 and 37°C (±standard deviation)

Reactor temperature	20°C			37°C	
Microbial strain	*P. aeruginosa*			*P. aeruginosa*	*S. aureus*
Biofilm age (h)	24	48	72	48	
Initial reactor cell density (T0)	3×10^6 CFU/mL (±0.1)	3×10^6 CFU/mL (±0.1)	9×10^6 CFU/mL (±0.1)	4×10^6 CFU/mL (±0.3)	2×10^6 CFU/mL (±0.1)
Biofilm per coupon cell density	1×10^7 CFU/mL (±0.2)	1×10^8 CFU/mL (±0.1)	1×10^8 CFU/mL (±0.2)	1×10^8 CFU/mL (±0.1)	7×10^6 CFU/mL (±0.2)
Final reactor cell density	1×10^7 CFU/mL (±0.1)	1×10^8 CFU/mL (±0.1)	1×10^7 CFU/mL (±0.1)	6×10^8 CFU/mL (±0.05)	1×10^8 CFU/mL (±0.1)

of these test species to pulses of UV-light. Notably, gram-negative species *E. coli and P. aeruginosa* appears more UV-resistant than the gram-positive *S. aureus* when treated in liquid and more UV-sensitive following surface exposure. Similar studies conducted by Rowan *et al*. (1999) on surface-treated organisms showed a similar order of resistance of these species to UV light.

PUV inactivation of microbial biofilms

The formation of biofilms in the water distribution system raises concerns to the public health, as these biofilms can harbour pathogenic bacteria among other problematic species such as viruses and parasites. Therefore, the inactivation of these resilient microbial communities in water treatment systems is important in order to ensure a safe supply of pathogen-free water for public use. Studies by Paquin *et al*. (1992) showed that the type of piping material and residual chlorine concentrations of up to 0.05 ppm did not affect the formation of biofilms in water distribution systems. Studies by Emitiazi *et al*. (2004) found the formation of *P. aeruginosa* biofilms in distribution systems and in their downstream networks concluded that this source of infection (by these opportunistic pathogens or other species that may be entrapped within the biofilm structure) is of concern in the water treatment setting. Table 1 illustrates the biofilm formation for both strains tested at 20 and 37°C on PVC coupons that are representative of these distribution networks. For *P. aeruginosa*, a seeding density of ca. 1×10^6 CFU/mL resulted in 1×10^7 CFU/mL biofilm following 24-h incubation at 20°C. The cell density increased as the incubation period was extended, resulting in CFU/mL of 1×10^8 following a 48- and 72-h incubation. Notably, there was a change in the viability of the planktonic cells that did not form the biofilm community with a 1 $\log_{10}$ loss in viability following 72-h incubation at 20°C in the reactor broth. This may have occurred due to nutrient depletion of the reactor media. Up to this point, the bacterial count of cells present in the biofilm appeared equal to the planktonic cells present in the reactor (Table 1). It is worth noting that biofilms of similar cell density were formed for both 20 and 37°C incubation temperatures for *Pseudomonas*. Although the gram-positive *S. aureus* formed a relatively densely populated biofilm structure, it did not show a population density comparable with that of *P. aeruginosa*. Following 48-h incubation in suitable media, a ca. 7×10^6 CFU/mL biofilm was formed as opposed to a 1×10^8 CFU/mL structure of *Pseudomonas*. With an initial seeding density of 2×10^6 CFU/mL, there was a 1×10^8 CFU/mL planktonic cell density in the reactor at this 48-h time point for *S. aureus*. *Staphylococcus* biofilms are known to be problematic in the medical setting where they form in lung tissue, and central venous catheters (Gotz 2002). Although by no means extensive, results obtained for these initial studies suggest that for this *Staphylococcus* species at these settings the formation of biofilms was not as typical on this type of material, i.e. PVC as that of *Pseudomonas*.

For PUV inactivation studies, the coupons were exposed to varying UV doses on both sides to ensure complete biofilm exposure. Replicate results indicate that this PUV system was effective at inactivating both test species at 16.2 J per pulse. Indeed, substantial amounts of inactivation were achieved with as little as 2.15 $\mu J/cm^2$ for biofilms of varying ages (Table 2). For this study, it was found that the relatively younger biofilm (24 h) appeared more resistant to UV treatment than the other time frames studied. Table 1 illustrates the inactivation rates for each biofilm, and a clear pattern is evident where biofilms required less exposure with greater inactivation for each 24 h increment. Specifically, a 1.1-, 2.8- and 3.3-$\log_{10}$ inactivation was obtained for 24, 48 and 72 h biofilms of *P. aeruginosa*, respectively, with 6.48 $\mu J/cm^2$ of PUV light at 20°C, and a 2.3- and 2.6-$\log_{10}$ inactivation of *P. aeruginosa* and *S. aureus* at 37°C. This pattern remained consistent for each treatment dose where a significant difference in inactivation rates was obtained for *Pseudomonas* with increasing age where the biofilm cell density increased or remained the same ca. 1×10^7 to 1×10^8 CFU/mL (Table 1). These findings indicate that the initial biofilm structure is more resistant to PUV exposure, and this resistance gradually decreases with age. Indeed, maximal biofilm inactivation (7.2 $\mu J/cm^2$) occurred with a dose of 19.44 $\mu J/cm^2$ for the 72-h biofilm where a 3.8- and 4.7-$\log_{10}$ reduction was achieved for 24 and 48 h, respectively. Findings also demonstrate that the temperature of the biofilm formation did not affect the inactivation kinetics of the *Pseudomonas* test species where

Table 2 Log_{10} reduction of *Pseudomonas aeruginosa* and *Staphylococcus aureus* biofilms of varying ages at 20 and 37°C following exposure to pulsed ultraviolet light at different doses at a discharge energy of 16.2 J per pulse (±standard deviation)

	Temperature 20°C			Temperature 37°C	
	P. aeruginosa			*P. aeruginosa*	*S. aureus*
Uv dose (μJ/cm^2)	24 h	48 h	72 h	48 h	48 h
0	0	0	0	0	0
2.15	0.56 (±0.4)	1.3 (±0.3)	1.7 (±0.2)	1.0 (±0.07)	1.4 (±0.2)
4.32	0.87 (±0.2)	1.9 (±0.1)	1.96 (±0.3)	2.1 (±0.02)	2.6 (±0.1)
6.48	1.1 (±0.3)	2.8 (±0.2)	3.33 (±0.1)	2.3 (±0.07)	2.6 (±0.1)
8.61	2.7 (±0.5)	3.5 (±0.5)	4.06 (±0.06)	2.6 (±0.1)	2.8 (±0.06)
10.8	3.3 (±0.6)	3.7 (±0.2)	4.8 (±0.1)	3.7 (±0.1)	3.6 (±0.01)
12.96	3.4 (±0.4)	3.8 (±0.3)	5.86 (±0.2)	3.9 (±0.1)	3.8 (±0.1)
15.12	3.6 (±0.4)	4.1 (±0.4)	5.86 (±0.2)	4.0 (±0.2)	4.0 (±0.3)
17.28	3.5 (±0.4)	4.1 (±0.3)	6.63 (±0.06)	4.2 (±0.2)	5.4 (±0.2)
19.44	3.8 (±0.3)	4.7 (±0.2)	7.2 (±0.1)	5.25 (±0.2)	5.9 (±0.02)
21.6	3.8 (±0.1)	5.4 (±0.2)	–	5.8 (±0.2)	5.9 (±0.2)
25.92	4.2 (±0.2)	6.2 (±0.1)	–	6.4 (±0.06)	–

similar levels of inactivation were achieved for each UV dose applied (Table 2). Initially, levels of inactivation for 48-h biofilms at 37°C of *P. aeruginosa* and *S. aureus* were obtained where *Pseudomonas* proved to be slightly more resistant up to a UV dose of ≤6.48 μJ/cm^2. However, at doses exceeding this and less than 15.12 μJ/cm^2 (≥6.48 and ≤15.12 μJ/cm^2), there was no significant difference ($P < 0.05$) in sensitivities of these test species.

Wastewater and water treatment plants utilise disinfection approaches and are commonly fitted with medium pressure light sources. Studies by Said *et al*. 2011 on the effects of ultraviolet C on *Pseudomonas* biofilm production showed that biofilm formation was not inhibited after irradiation of *P. aeruginosa* by a recommended dose for water disinfection (40 mJ/cm^2). This result suggests that this dose is insufficient to inhibit the cell-to-cell communication system and therefore biofilm formation (Said *et al*. 2011).

Studies described herein suggest that the PUV light system offers high rates of inactivation at lower energy input to standard UV methods. Implementation of such pulsed systems in conjunction with or as a standalone UV method may be achieved by placing lamps along the piping in sequence to ensure exposure of the treatment area. Operators must guarantee that lamps are pulsed at their uppermost UV dose or fluence settings to disinfect the water at the lamp surface. Plant engineers should also take into account other variable parameters including potential concentration of microbial species present, flow rates, UV transmission and depth of water to be treated to ensure efficient disinfection. All of these factors can influence the disinfection efficiency of the system and need to be assessed. It should be noted that the biocidal light spectrum emitted by pulsed medium pressure and high-voltage xenon light sources are considerably different, and this must be factored into optimised disinfection studies at plant level (Rowan 2011).

Further studies are warranted on the photo reactivation ability of organisms within the biofilm structure following PUV treatment. However, it is worth noting that previously published studies by McDonald & Curry 2001 postulate that the high proton flux from a pulsed light source overwhelms the cellular repair mechanisms of treated organisms. Also, the authors believe that studies are merited to assess the potential of these biofilm structures to harbour other pathogenic organisms such as viruses or parasites within their matrix. Pathogens, even present below the detection limit in water, can accidentally attach to biofilms that then can act as their environmental reservoir and represent a potential source of water contamination. Detachment from biofilms can occur by continuous erosion (Wingender & Flemming 2011). Such studies would allow for a better understanding of the source of these pathogens in drinking water supplies and the ability of this PUV approach to eliminate such problematic species.

Conclusion

This study demonstrated the effectiveness of PUV inactivation of *Pseudomonas* biofilms that were grown by use of the CDC biofilm reactor.

(1) Significant rates of inactivation were obtained for all test organisms following exposure to PUV light in both planktonic and biofilm form.

(2) Significant levels of inactivation were repeatedly obtained for *Pseudomonas* biofilms at with varying UV doses at discharge energy of 16.2 J per pulse at 20 and 37°C.

(3) Findings suggests that this novel technology provides a method for the point of use inactivation of biofilm structures and also as a means of eliminating species that cause the formation of these problematic communities within water treatment networks.

(4) Initial studies conducted on *S. aureus* suggest that it is also sensitive to UV disinfection; however, as this is a more clinically relevant strain, studies are merited on the inactivation of a broader range of *Staphylococcus* species on surfaces more representative of the medical environment.

Acknowledgement

This study was funded by the Irish Environmental Protection Agency Strive Research Programme (2011-W-MS-5).

To submit a comment on this article please go to http://mc.manuscriptcentral.com/wej. For further information please see the Author Guidelines at wileyonlinelibrary.com

References

American Society for Testing and Materials (ASTM) E2562-12 (2012). Standard Test Method for Quantification of *Pseudomonas aeruginosa* Biofilm Grown with High Shear and Continuous Flow Using CDC Biofilm Reactor.

Coenye, T. and Nelis, J.J. (2010) *In Vitro* and *in Vivo* Model Systems to Study Microbial Biofilm Formation. *J. Microbiol. Methods*, **83**, 89–105.

Coeyne, T. and Nelis, J.H. (2010) *In Vitro* and *in Vivo* Model Systems to Study Microbial Biofilm Formation. *J. Microbiol. Methods*, **83**, 89–105.

Emitiazi, F., Schwartz, T., Marten, M.S., Krolla-Sidenstein, P. and Obst, U. (2004) Investigation fo Natural Biofilms Formed during the Production of Drinking Water from Surfacewater Embankment Filtration. *Water Res.*, **38**, 1197–1206.

Farrell, P.H., Garvey, M., Cormican, M., Laffey, G.J. and Rowan, J.N. (2009) Investigation of Critical Inter-Related Factors Affecting the Efficacy of Pulsed Light for Inactivating Clinically Relevant Bacterial Pathogens. *J. Appl. Microbiol.*, **108** (5), 1494–1508.

Garvey, M., Farrell, H., Cormican, M. and Rowan, N. (2010) Investigations of the Relationship between Use of In Vitro Cell Culture-Quantitative PCR and a Mouse-Based Bioassay for Evaluating Critical Factors Affecting the Disinfection Performance of Pulsed UV Light for Treating *Cryptosporidium parvum* Oocysts in Saline. *J. Microbiol. Methods*, **80** (3), 267–273.

Garvey, M., Clifford, E., O'Reilly, E. and Rowan, N. (2012) Efficacy of Using Harmless *Bacillus* Endospores as Novel Surrogate Organisms to Indicate the Inactivation Performance of Recalcitrant *Cryptosporidium parvum* Oocysts Suspended in Water Using Pulsed UV Light. *J. Parasitol.*, **99** (3), 11/2012; doi:10.1645/12-48.1.

Gómez-López, V.M., Ragaert, P., Debevere, J. and Devlieghere, F. (2007) Pulsed Light for Food Decontamination: A Review. *Trends Food Sci. Technol.*, **18**, 464–473.

Gotz, F. (2002) *Staphylococcus* and Biofilms. *Mol. Microbiol.*, **43** (6), 1367–1378.

Harmsen, M., Yang, L, Pamp, J.S. and Tolker-Nielsem, T. (2010) An Update on *Pseudomonas aeruginosa* Biofilm Formation Tolerance, and Dispersal. *FEMS Immunol. Med. Microbiol.*, **59**, 253–268.

Kerr, J.C., Osborn, S.K., Rickard, H.A., Robson, D.G. and Handley, S.P. (2003) Biofilms in Water Distribution Systems. *In* Mara, D. and Horan, N.J. (eds). *The Handbook of Water and Waste Water Microbiology*, pp. 757–777. Elsevier Science Publishing Co. Inc., Atlanta, GA. ISBN 0-12-470100-0.

McDonald, K. and Curry, R. (2001) Comparison of Pulsed and CW Ultraviolet Light Sources to Inactivate Spores on Surfaces. *Pulsed Power Plasma Sci.*, **1**, 604–607.

Momba, M.N.B., Kfir, R., Venter, S.N. and Cloete, T.E. (2000) An Overview of Biofilm Formation in Distribution Systems and its Impact on the Deterioration of Water Quality. *Water SA*, **26** (1), 59–66.

Paquin, J.L., Block, J.C., Haudidier, K., Hartemann, P., Colin, F., Miazga, J. and Levi, Y. (1992) Effet du chlore sur la colonisation bacterienne d'un reseau experimental de distribution d'eau. *Rev. Sci. Eau.*, **5**, 399–414.

Rowan, J.N., MacGregor, J.S., Anderson, J.G., Fouracre, R.A., McIlvaney, L. and Fairish, O. (1999) Pulsed-Light Inactivation of Food-Related Microorganisms. *Appl. Environ. Microbiol.*, **65** (3), 1312–1315.

Rowan, N.J. (2011) Defining Established and Emerging Microbial Risks in the Aquatic Environment: Current Knowledge, Implications and Outlooks. *Int. J. Microbiol.*, Article ID 462832. Published online: http://www.hindawi.com/journals/ijmb/2011/462832.html [accessed 11 April 2014]. [PMID: 209976256].

Said, B.M., Khefacha, S., Maale, L., Daly, I. and Hassen, A. (2011) Effect of Ultraviolet, Electromagnetic Radiation Subtype C (UV-C) Dose on Biofilm Formation by *Pseudomonas aeruginosa*. *Afr. J. Microbiol. Res.*, **5** (25), 4353–4358.

Schwartz, T., Jungfer, C., Heisler, S., Friedrich, F., Faubel, W., and Obst, U. (2009) Combined Use of Molecular Biology Taxonomy, Raman Spectrometry, and ESEM Imaging to Study Natural Biofilms Grown on Filter Materials at Waterworks. *Chemosphere*, **77**, 249–257.

Wingender, J. and Flemming, H. (2011) Biofilms in Drinking Water and their Role as Reservoir for Pathogens. *Int. J. Hyg. Environ. Health*, **214**, 417–423.

International Journal of
Food Science & Technology
International Journal of Food Science and Technology 2012

Original article

Relationship between growth of food-spoilage yeast in high-sugar environments and sensitivity to high-intensity pulsed UV light irradiation

Jennifer C. Hayes,[1] John G. Laffey,[2] Brian McNeil[3] & Neil J. Rowan[1*]

1 Department of Nursing and Health Science, Athlone Institute of Technology, Ireland
2 School of Medicine, Nursing and Health Science, National University of Ireland, Galway, Ireland
3 Strathclyde Institute of Pharmacy and Biomedical Sciences, Strathclyde University, Glasgow, Scotland

(Received 19 November 2011; Accepted in revised form 7 March 2012)

Summary The relationship between prior growth of food-spoilage yeast in high-sugar environments and their subsequent survival postpulsed UV (PUV) irradiation was investigated. Test yeast were separately grown to early stationary phase in YPD broth containing increasing concentrations of glucose (1–50% w/v) and were flashed with ≤40 pulses of broad-spectrum light at lamp discharge energy settings of 3.2, 7.2 and 12.8 J (equivalent to UV doses of 0.53, 1.09 and 3.36 μJ cm^{-2}, respectively) and their inactivation measured. Findings showed that prior growth in high-sugar conditions (≥30% glucose w/v) enhanced the sensitivity of all nine representative strains of *Zygosaccharomyces bailii*, *Z. rouxii* and *Saccharomyces cerevisiae* yeast to PUV irradiation. Significant differences in inactivation amongst different yeast types also occurred depending on amount of UV dose applied, where the order of increasing sensitivity of osmotically stressed yeast to PUV irradiation was shown to be *Z. rouxii*, *Z. bailii* and > *S. cerevisiae*. For example, a 1.2-log order difference in CFU mL^{-1} reduction occurred between *Z. bailii* 11 486 and *S. cerevisiae* 834 when grown in 50% w/v sugar samples and treated with the uppermost test UV dosage of 3.36 μJ cm^{-2}, where these two yeast strains were reduced by 3.8 and 5.0 log orders, respectively, after this PUV treatment regime compared to untreated controls. The higher the UV dose applied the greater the reduction in yeast numbers. For example, a 1.0-, 1.4- and 4.0-log order differences in CFU mL^{-1} numbers occurred for *S. cerevisiae* 834 grown in 15% w/v sugar samples and then treated with PUV dose of 0.53, 1.09 and 3.36 μJ cm^{-2}, respectively. These findings support the development of PUV for the treatment of high-sugar foods that are prone to spoilage by osmotolerant yeast.

Keywords Pulsed light, emerging technologies, osmotolerant stress, yeast, ultraviolet, minimal food processing, high-sugar foods.

Introduction

Other than bacterial pathogens, the control of spoilage yeasts is one of the most important aspects in food preservation particularly as greater amounts of foods are being processed, preserved, stored and transported over long distances before consumption (Fleet, 1992; Pitt & Hocking, 2009; Prakasham *et al.*, 2009). Factors such as low temperature, reduced water activity, addition of preservatives and low pH are all used to inhibit or destroy yeasts and other microorganisms (Martorell *et al.*, 2007). Yeast resistance to such preservation techniques raises problems for the food industry, causing a requirement for either increased preservative levels in low-pH foods and/or the development of an effective alternative decontamination technology to prevent yeast spoilage (Piper *et al.*, 2001; Martorell *et al.*, 2007). Water activity of foods or a_w is also a very important factor affecting yeast growth. While most yeasts will happily grow in 20% w/v glucose, only a limited number of yeasts species are able to grow at low a_w caused by the presence of high concentrations of either sugar (60% w/v) or salt, and these have been referred to as osmotolerant or xerotolerant species (Tilbury, 1980a,b). Previous evidence has shown that fungal growth in high-sugar foods protects yeast cells from extreme temperatures and also cross-protects against the action of preservatives such as sorbic acid and benzoic acid (Gibson, 1973; Corry, 1976; Iwahashi *et al.*, 1995). Taking into account that pasteurisation using heat is the preservation system normally used in candied fruit manufacturing, and widely used in foods and beverages, application of pasteurisation on its

*Correspondent: E-mail: nrowan@ait.ie

doi:10.1111/j.1365-2621.2012.03052.x

own may not be efficient for preservation in very high-sugar foods. These high-sugar food products with sugar concentrations ≥35% are at risk of spoilage from osmotolerant yeast such as *Zygosaccharomyces rouxii* and *Z. bailii* that may aggregate to form more consumer-obvious structures such as flocs, particulates or surface films (Martorell *et al.*, 2007; Pitt & Hocking, 2009; Sperber & Doyle, 2010). On an industrial scale, sugar syrups or syrups of fruit juices are frequently spoiled by osmotolerant yeasts such as *Zygosaccharomyces*, *Candida*, *Pichia* and *Debrayomyces* spp floating undetected as surface films on syrups stored in metal tanks (Sperber & Doyle, 2010). Recent research has demonstrated that use of conventional approaches to decontaminate the aforementioned osmotolerant yeast from high-sugar content foods has proved extremely difficult, particularly as a_w of food decreases the thermotolerance of the spoilage microorganism increases (Coroller *et al.*, 2001; Montiel *et al.*, 2005; Sharma *et al.*, 2005; Gunde-Cimerman *et al.*, 2009).

Martorell *et al.* (2007) showed that all strains of these osmotolerant yeast tested were able to adapt to high levels of sugar and this prior exposure conferred a degree of protection against pasteurisation (enabling survival in what would have otherwise been a lethal treatment) and a high level of resistance to front-line preservatives. Previous researchers have demonstrated that liquid sugar maybe filtered to remove microorganisms and heated but these may impart considerable cost implications to the plant in terms of energy consumption (Sperber & Doyle, 2010). Use of conventional low-pressure UV sources was shown to be of limited effectiveness owing to the requirement to treat at short distances from the contaminated food surfaces, but did not significantly affect the physiochemical quality characteristics of sugar syrups (Giorgi & Gontier, 1980). However, use of an alternative pulsed-power UV approach would offer considerable advantages over low-pressure light sources for this particular application in terms of delivering effective UV doses in a more cost-efficient manner over shorter turnaround periods (Farrell *et al.*, 2010). Furthermore, conventional UV light sources are mercury filled, which raises additional safety concerns if damaged during irradiation of foods. Thus, previous findings suggest that spoilage of high-sugar foods may be better prevented by the combined development of emerging technologies such as pulsed UV light technology along with using biocidal cleaning agents in the factory, rather than treating the food with preservatives where acquired resistance raises problems for the food industry (Piper *et al.*, 2001; Martorell *et al.*, 2007).

Pulsed UV light (PUV) is a nonthermal approach that has received considerable attention as a strategy for decontaminating food, packaging, water and air (Elmnasser *et al.*, 2007; Gómez-López *et al.*, 2007; Oms-Oliu *et al.*, 2010). This approach kills microorganisms by using ultrashort-duration pulses of an intense broad-band emission spectrum that is rich in UV-C germicidal light (200–280 nm band). PUV is produced using techniques that multiply power manifold by storing electricity in a capacitor over relatively long times (fractions of a second) and releasing it in a short time (millionths or thousandths of a second) using sophisticated pulse compression techniques (Rowan *et al.*, 1999). The emitted flash has a high peak power and usually consists of wavelengths from 200 to 1100 nm broad-spectrum light enriched with shorter germicidal wavelengths (Rowan *et al.*, 1999). Thus, significant microbial reductions in ultrashort-treatment times, the limited energy cost of PUV, the lack of residual compounds and its great flexibility are some of the major benefits of this technique for food and water applications (Elmnasser *et al.*, 2007; Lee *et al.*, 2009; Garvey *et al.*, 2010; Oms-Oliu *et al.*, 2010). Recent studies have demonstrated that varying inter-related operational settings will impact significantly on microbial reductions on food surfaces. Farrell *et al.* (2010) observed significant differences in inactivation that largely occurred depending on the level of the applied lamp discharge energy (range 3.2–20 J), the amount of pulsing applied (0–60 pulses) and the distance between the light source and the treatment surface (range 8–20 cm) used. These researchers also observed a difference in sensitivity to PUV irradiation that depended upon the type, age and concentration of cultures treated. Other factors to be considered include whether the targeted microorganism is in a dormant spore-state or is actively growing. Garvey *et al.* (2010) also reported that PUV has limited efficacy in treating highly contaminated samples owing to shading effects of overlapping microorganisms with an upper limit threshold of approximately 10^7 cells mL^{-1} in suspension media.

Based on the aforementioned and given that yeast may encounter various hurdles (stresses) in food processing environments including osmotic stress, it is possible that prior exposure to these inimical stresses may provide cross-protection against normally lethal levels of pulsed UV light. Therefore, the aim of this study was to investigate the relationship (if any) between prior growth in high sugar and subsequent tolerance to normally lethal levels of PUV irradiation in a range of food-spoilage yeasts. The application of high-intensity pulsed UV light may reduce the requirement for use of high levels of a single or multiple preservation steps in the manufacture, packaging and storage of food.

Materials and methods

Pulsed UV light system

A bench-top pulsed-power source (PUV-1, Samtech Ltd., Glasgow, UK) was used to power a low-pressure

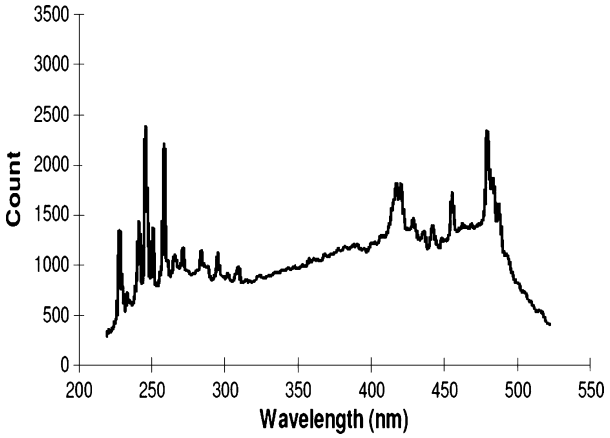

Figure 1 Spectral distribution of postpulsed UV system emitted at 12.8 J per pulse with rich output in the UVC region showing three peaks at 229, 247 and 260 nm.

(60 kPa) xenon-filled flashlamp (Heraeus Noblelight XAP type NL4006 series constructed from a clear UV transparent quartz tube), which produced a high-intensity diverging beam of polychromatic pulsed light, was used in this study as per Wang *et al.* (2005). The pulsed light has a broadband emission spectrum extending from the UV to the infrared region with a rich UV content and its intensity also depends on the level of the voltage applied (Fig. 1). The pulse duration was 80 ns. The fabricant stated that the discharge tube represents a line-source of limited length and consequently the light formed an elliptical, equi-intensity profile over the sample plane eliminating shading effects. This resulted in a approximately 30% variation in luminous intensity between the centre and the edge of the sample. The light source has an automatic frequency-control function that allows it to operate at one pulse per second that was used throughout this study. Light exposure was homogenous as the xenon lamp measuring 9 cm × 0.75 cm was longer than the 8.5-cm-diameter polystyrene Petri dishes used in the tests that were placed directly below the lamp. For standard treatments (unless otherwise noted), the light source was mounted at 8 cm above the treatment area that was designed specifically to accommodate a standard Petri dish and was set as the minimum or lower threshold distance by the fabricant. This was to ensure that full coverage of the sample occurred and to eliminate possible shading effects.

Test organisms, osmotic stress conditions and PUV irradiation regimes

The species of test microorganisms used in these experiments and their origin are summarised in Table 1. All test strains were maintained in Microbank storage vials (Cruinn Diagnostic, Ireland) at −70 °C. Identification of three randomly selected isolates of each yeast strain was confirmed before and after experimental studies by use of the germ-tube assay with occasional use of the VITEK yeast biochemical card and API-32C systems (bioMérieux, France) as per methods described by Hsu *et al.* (2003). To prepare the test samples, yeast test strains were first resuscitated from frozen porous beads taken from Microbank vials stored at −80 °C by overnight enrichment at 25 °C in 100 mL without shaking in yeast extract (1% w/v), peptone (1% w/v) and glucose (1% w/v) broth (YPD) adjusted to pH 5.6 ± 0.2 as per method described previously by Park *et al.* (1997) before streaking to purity on Malt Extract agar (Mea, Oxoid, Basingstoke, UK). An isolated colony was then transferred to separate 100 mL of fresh YPD broth containing 1% w/v, 15% w/v, 30% w/v and 50% w/v glucose adjusted to pH 5.6 ± 0.2 and cultivated without shaking for 2–3 weeks at 25°C to reach early stationary phase as per modified methods described previously (Martorell *et al.*, 2007). This aligned with previous reported studies of Van Zyl *et al.* (1993) and Martorell *et al.* (2007) that advocated use of a 50%

Table 1 Origin and cultivation conditions of test yeast

Test Yeast Name	Code	Origin*	Isolation	BSL†	Growth Temp. (°C)
Zygosaccharomyces bailii	36 947	ATCC	Salad Dressing	1	25
	8766	ATCC	Domestic wine	1	25
	11 486	ATCC	Vinegar	1	25
Zygosaccharomyces rouxii	42 981	ATCC	Miso, Japan	1	25
	46 261	ATCC	Miso, Japan	1	25
	2615	ATCC	Sugar	1	25
Saccharomyces cerevisiae	9763	ATCC	Distillery Yeast	1	25
	26 603	ATCC	Jamaican Cane Juice	1	25
	834	ATCC	Champagne Wine	1	25

*Code for origin of isolates: American Type Culture Collection (ATCC), Rockville, MD, USA. National Collection of Pathogenic Fungi (NCPF), Colindale, London, UK.

†Laboratory Biosafety Level (BSL) designation of test yeast.

w/v to 60% w/v sugar environment to create osmotic stress in test yeast. Growth was measured spectrophotometrically (Model UV 120 02, Shimadzu Corp., Kyoto, Japan) over the 3-week incubation period at 640 nm along with confirming cell numbers using conventional plate count determinations on YPD agar. Ten millilitre samples were serially diluted in 0.1 M phosphate buffered saline (Sigma-Aldrich, Wicklow, Ireland) containing matching percentage of glucose (w/v) to that of original test sample, which were then PUV irradiated at 3.2, 7.2 and 12.8 J over the range 0 (untreated) to ≤40 pulses at 8-cm distance from the light source. Measurement of corresponding fluence (or 'dose') (μJ cm^{-2}) at each applied pulse was determined using chemical actinometry, as the noncontinuous emitted spectrum did not facilitate use of the calibrated UVX digital radiometer (Ultra-Violet Products Inc., Nuffield Road, Cambridge, UK) used in our laboratory. This limitation of digital radiometers and sensors to measure noncontinuous pulsed emission spectra was also reported recently by other researchers in this field of study (Lee *et al*., 2009). Fluence per pulse was measured at 0.0133, 0.027 and 0.084 μJ cm^{-2} at 3.2, 7.2 and 12.8 J lamp discharge energy settings, respectively. The actinometer developed by Rahn (1993) consists of an iodide-iodate solution, the UV photolysis of which results in the formation of triiodide with a quantum yield of 0.73 at 254 nm. The actinometer absorbs UV significantly between 200 and 300 nm, above which absorption decreases sharply. Thus, it is ideally suited for measuring biocidal radiation in the presence of room light (Rahn, 1997; Rahn *et al*., 2003). The fluence is directly proportional to the yield of triiodide, which is determined by measuring the absorbance increase at 352 nm. Care was taken to ensure that 10 ± 0.1 mL of test sample was aseptically transferred by pipette to Petri dishes, thus maintaining standardised depth of volume for all studies.

After treatments, samples were diluted in PBS as described previously and were spread and pour plated onto YPD media and survivors were enumerated after 3-d incubation at 25 °C. The lethality of the PUV process under these varying experimental conditions was determined by enumerating survivors post-treatments (expressed in terms of $\log_{10}$ colony forming units or CFU mL^{-1}). Subtraction of the logarithm of the count after using different combinations of treatment from the logarithm of the count before processing provided a measure of process lethality. The time dependence of log inactivation rate using a fixed lamp discharge energy (J) at 8-cm distance between light source and the treated sample was also measured for all test microorganisms using the model of Kühn *et al*. (2003). These death rate inactivation plots follow a first-order dependence ($\log_{10}(N_t/N_0) = -kt$, where k = rate constant). N_0 is the initial concentration of yeast and N_t is the microbial concentration after pulsing for time t at discharge energy (J). This rate constant k defines the sensitivity of a microorganism to a defined PUV treatment and is unique to each microbial species; the higher the k value the more sensitive the test strain to the treatment process. All experiments were carried out in triplicate using the same culture to avoid sample variability.

Determining repair in PUV-irradiated test yeast

To test the possibility that exposure of treated yeast to sunlight may repair damaged cells through a photoreactivation process, duplicate 10 mL samples from each test yeast were adjusted to approximately 7 $\log_{10}$ CFU mL^{-1} with PBS containing commensurate concentrations of glucose to that of the samples and were exposed to 200 pulses at 3.2 J, 100 pulses at 7.2 J and 32 pulses at 12.8 J to that produced a similar level of UV dose (approximately 2.7 μJ cm^{-2}) at each applied voltage setting. After treatment, the first three plates were immediately wrapped in aluminium foil while the other three similarly treated plates were exposed to direct sunlight by placement on laboratory bench illuminated by sunlight for 4 h. Samples were then plated on YPD media as describe above and were incubated for 72 h at 25 °C before enumeration. Samples were run in triplicate. Heating of the test liquid medium was investigated using a thermocouple and by thermal imaging using IRISYS 4000 Series Imager Software (IRI 4010, Infra-Red Integrated Systems Ltd, Northampton, UK) as per modified method of Nugent & Higginbotham (2007). Plates were positioned 8 cm from light source and were flashed with ≤150 pulses of increasing lamp intensity, namely 3.2, 7.2 and 12.8 J per pulse. There was no discernable rise in temperature observed in treated samples over the UV pulsing regime at and below the fluence levels applied in this study (Fig. 2). Temperature rises were detected in control samples using the higher lamp discharge energy of 20 J, which was therefore not used as a fluence setting in this study.

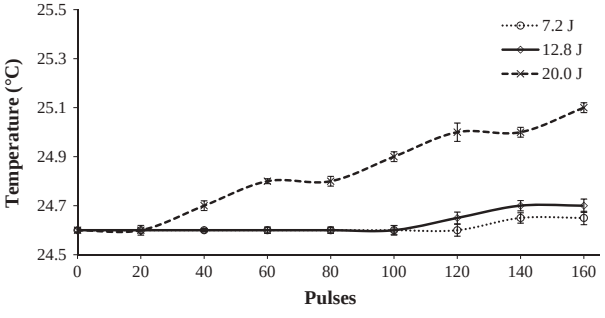

Figure 2 Temperature change in YPD sample containing 50% w/v glucose during exposure to increasing pulses of UV light.

Statistical analysis

A univariate general linear model test along with the Bonferroni method (Minitab software release 13; Minitab Inc., State College, PA, USA) was used to compare the multiple effects of independent variables on pulse-light decontamination efficacy for the various within- and between-subject combination of treatments, where differences between averaged mean values from seven repeated experiments ($n = 7$) were compared and were reported at a significance level of $P < 0.05$. Mean square error was reported at 0.004. Specifically, the univariate general linear model test was performed using one dependent variable that was the average of k values for each combination of independent effects applied, namely yeast type (3), yeast strain (9), sugar level (four concentrations from 0% to 50% w/v glucose) and applied voltage (three levels; 3.2, 7.2 and 12.8 J). Interactions between factors as well as the effects of individual factors were investigated by using the Bonferroni method, which allows many comparison statements to be made (or confidence intervals to be constructed) while still assuring an overall confidence coefficient is maintained. This method applies to an ANOVA situation where linear pairwise combinations or comparisons of treatment level means were investigated.

Results and Discussion

Sensitivity of test yeast to PUV treatments

There were marked variations in sensitivity to treatments amongst species of yeast treated with PUV irradiation (Tables 2, 3 and 4). Greater susceptibility of yeast to PUV treatment occurred with use of increasing discharge energies or UV dose (μJ cm^{-2}) at $P < 0.05$ level, as exhibited by *S. cerevisiae* ATCC 834 (Fig. 3) that had been grown in 15% w/v glucose prior to PUV irradiation. All yeast types and strains also exhibited similar shaped inactivation kinetic plots to Fig. 3 when exposed to increasing lamp discharge

Table 2 Influence of prior exposure to increasing concentrations of glucose on the subsequent resistance of different yeast to pulsed UV light irradiation at 3.2 J (equivalent to a UV dose of 0.5309 μJ cm^{-2})

Yeast Type & Strain		Reduction rate (*k*) values determined at UV dose of 0.5309 μJ cm^{-2} postexposure to increasing concentrations of glucose			
Type	**Strain**	**1% (w/v)**	**15% (w/v)**	**30% (w/v)**	**50% (w/v)**
Zygosaccharomyces bailii	36 947	0.07 ± 0.02	0.07 ± 0.02	0.11 ± 0.01	0.14 ± 0.02
	8766	0.08 ± 0.02	0.07 ± 0.03	0.08 ± 0.02	0.16 ± 0.03
	11 486	0.07 ± 0.02	0.08 ± 0.02	0.08 ± 0.02	0.16 ± 0.02
Zygosaccharomyces rouxii	42 981	0.06 ± 0.01	0.07 ± 0.01	0.10 ± 0.03	0.15 ± 0.01
	46 261	0.07 ± 0.02	0.10 ± 0.02	0.10 ± 0.02	0.16 ± 0.02
	2615	0.08 ± 0.02	0.09 ± 0.02	0.09 ± 0.02	0.13 ± 0.02
Saccharomyces cerevisiae	834	0.10 ± 0.01	0.10 ± 0.02	0.13 ± 0.01	0.19 ± 0.02
	9763	0.08 ± 0.02	0.09 ± 0.02	0.15 ± 0.02	0.20 ± 0.03
	26 603	0.09 ± 0.02	0.09 ± 0.02	0.11 ± 0.01	0.15 ± 0.02

Table 3 Influence of prior exposure to increasing concentrations of glucose on the subsequent resistance of different yeast to pulsed UV light irradiation at 7.2 J (equivalent to a UV dose of 1.093 μJ cm^{-2})

Test Yeast		Reduction rate (*k*) values determined at UV dose of 1.093 μJ cm^{-2} postexposure to increasing concentrations of glucose			
Strain	**Strain**	**1% (w/v)**	**15% (w/v)**	**30% (w/v)**	**50% (w/v)**
Zygosaccharomyces bailii	36 947	0.17 ± 0.03	0.18 ± 0.02	0.23 ± 0.02	0.27 ± 0.02
	8766	0.15 ± 0.03	0.15 ± 0.03	0.18 ± 0.02	0.26 ± 0.02
	11 486	0.15 ± 0.02	0.16 ± 0.02	0.18 ± 0.02	0.25 ± 0.02
Zygosaccharomyces rouxii	42 981	0.08 ± 0.01	0.08 ± 0.02	0.14 ± 0.02	0.18 ± 0.02
	46 261	0.15 ± 0.02	0.14 ± 0.02	0.19 ± 0.02	0.25 ± 0.02
	2615	0.13 ± 0.02	0.13 ± 0.02	0.17 ± 0.02	0.20 ± 0.02
Saccharomyces cerevisiae	834	0.22 ± 0.03	0.23 ± 0.01	0.24 ± 0.01	0.33 ± 0.01
	9763	0.16 ± 0.01	0.17 ± 0.02	0.24 ± 0.02	0.34 ± 0.02
	26 603	0.19 ± 0.03	0.18 ± 0.01	0.25 ± 0.02	0.36 ± 0.02

Table 4 Influence of prior exposure to increasing concentrations of glucose on the subsequent resistance of different yeast to pulsed UV light irradiation at 12.8 J (equivalent to a UV dose of 3.36 μJ cm^{-2})

Test Yeast		Reduction rate (*k*) values determined at a UV dose of 3.36 μJ cm^{-2} postexposure to increasing concentrations of glucose			
Name	**Code**	**1% (w/v)**	**15% (w/v)**	**30% (w/v)**	**50% (w/v)**
Zygosaccharomyces bailii	36 947	0.31 ± 0.03	0.31 ± 0.03	0.34 ± 0.02	0.40 ± 0.02
	8766	0.32 ± 0.04	0.31 ± 0.02	0.37 ± 0.02	0.44 ± 0.02
	11 486	0.25 ± 0.02	0.26 ± 0.01	0.27 ± 0.02	0.35 ± 0.02
Zygosaccharomyces rouxii	42 981	0.24 ± 0.01	0.26 ± 0.01	0.35 ± 0.02	0.48 ± 0.02
	46 261	0.31 ± 0.03	0.32 ± 0.02	0.36 ± 0.02	0.44 ± 0.02
	2615	0.34 ± 0.02	0.36 ± 0.02	0.37 ± 0.02	0.47 ± 0.02
Saccharomyces cerevisiae	834	0.50 ± 0.05	0.51 ± 0.02	0.57 ± 0.02	0.63 ± 0.02
	9763	0.35 ± 0.02	0.34 ± 0.02	0.39 ± 0.01	0.49 ± 0.01
	26 603	0.38 ± 0.04	0.40 ± 0.04	0.50 ± 0.02	0.55 ± 0.02

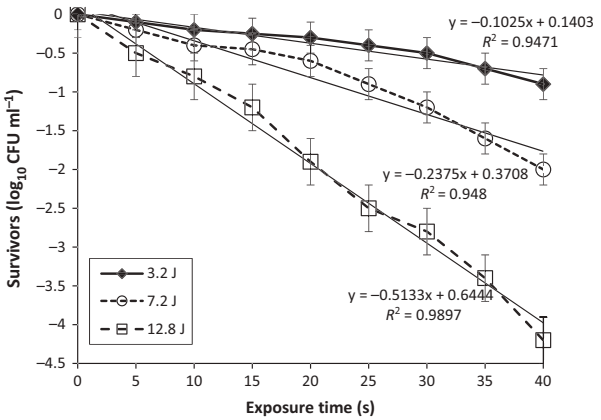

Figure 3 Inactivation kinetic plot of *S. cerevisiae* ATCC 834 grown prior in 15% w/v glucose and pulsed at an 8-cm distances from light source using lamp discharge energies of 3.2 J (♦), 7.2 J (○) and 12.8 J (□). Corresponding rate constant *k* values also illustrated for same treatments. Bars indicate ± SD.

energies for all combinations of sugars studied (data not shown). For ease of interpretation, corresponding death rate constant *k* values are shown in Fig. 1 where the slope (or *k* value shown in bold) of the linearised data plot provides a measure of the log reduction in cell population (log_{10} CFU mL^{-1}) per pulse or second of exposure. The lower the *k* value the greater the resistance of the treated yeast to the applied PUV treatment, and this means of evaluating *in vitro* inactivation performance was used to compare sensitivities of all test yeast under similar studies using increasing lamp discharge energies. Figure 3 illustrates *k* values of 0.10, 0.23 and 0.51 for *S. cerevisiae* ATCC 834 grown prior in 15% w/v glucose after exposure to 3.2, 7.2 and 12.8 J for ≤40 pulses, respectively, (equivalent to UV doses of 0.53, 1.09 and 3.36 μJ cm^{-2}, respectively), which highlights a clear pattern where more rapid reductions in predetermined populations of all test yeast occurred with increased levels of pulsing with use of higher discharge energies. This also correlates to 1.0-, 1.4- and 4.0-log CFU mL^{-1} differences in cell numbers for *S. cerevisiae* ATCC 834 after treatment with forty pulses at 3.2, 7.2 and 12.8 J, respectively, in these 15% w/v sugar samples. For example, it took forty pulses at 3.2 J (equivalent to a UV dose of 0.5309 μJ cm^{-2}) and five pulses at 12.8 J (0.420 μJ cm^{-2}) to obtain the same 1-log reduction in PUV-irradiated yeast numbers (Fig. 3). The levels of susceptibility of test yeast to PUV treatments differed significantly ($P < 0.05$) and are listed in order of decreasing resistance: *Z. rouxii, Z. bailii* > *S. cerevisiae* (Table 2, 3 and 4). A pairwise multiple comparison of means between yeast types using ANOVA showed the *S. cerevisiae* differed significantly in PUV sensitivity to that of similarly treated *Z. rouxii* and *Z. bailii* at $P = 0.024$ and 0.027 levels, respectively. There were no significant differences between *Z. bailii* and *Z. rouxii* for all combinations of strains, sugars and PUV settings tested in this study ($P = 0.953$). ANOVA multiple comparisons between mean values from individual yeast strains from seven replicate experiments revealed that only *S. cerevisiae* 834 differed significantly from *Z. bailii* 11 486 and *Z. rouxii* 42981 at $P = 0.024$ and 0.020, respectively. For example, this represented a 1.2-log order difference in CFU mL^{-1} reductions between these two yeast strains that were grown in 50% w/v sugar samples and then treated with forty pulses at 12.8 J (UV dose of 3.36 μJ cm^{-2}), as *Z. bailii* 11 486 and *S. cerevisiae* 834 were reduced by 3.8 and 5.0 log, respectively, compared to untreated controls. Further molecular-based stress-response studies are needed to ascertain why these particular strains significantly vary in sensitivity to PUV irradiation. That said, differences between *Zygosaccharomyces* spp. and *Saccharomyces cerevisiae* sensitivity to PUV irradiation may be attributed in part to variation in the ability of each species to protect against the plethora of molecular and

cellular insults including PUV-mediated cell membrane leakage, lipid hydroperoxidation, intracellular reactive oxygen species generation, apoptosis and necrosis as observed in PUV-treated *Candida* spp. (Farrell *et al*., 2011). All other combinations of yeast strains examined for sensitivity to PUV at different sugar exposure levels in this study proved not significant at $P < 0.05$ level.

These results presented in Tables 2, 3 and 4 are in agreement with findings from previous studies that demonstrated the efficacy of using PUV at 7 J for inactivating other types of agar-surface irradiated yeast (*Candida lambica, Rhodotorula mucilaginosa*) and fungal spores (*Aspergillus niger*, *A. flavus*, *Botrytis cinerea* and *Fusarium culmorum*) (Oms-Oliu *et al*., 2010). Findings presented in Tables 1, 3 and 4 also corroborate the recent work of Farrell *et al.* (2009) where these researchers reported that PUV effectively inactivates nonstressed clinically relevant yeast cells. Specifically, the latter study showed that levels of susceptibility of test microorganisms to PUV treatments differed significantly ($P < 0.05$) and were listed in the order of decreasing resistance as *Candida krusei* > *C. albicans*, *C. glabrata*, *C. tropicalis*, *C. parapsilosis*, *S. cerevisiae* > *Staphylococcus aureus* > *Escherichia coli*. This present study reports that the food-related yeast *Z. rouxii* ATCC 42981 (Table 2, 3 and 4) exhibited similar levels of PUV tolerance to that of *C. krusei* ATCC 6258, which was reported as the most PUV tolerant of the clinically related *Candida* strains previously studied by Farrell *et al.* (2009). The latter authors also reported that yeast treated at a shorter distance from the treatment surface to the PUV light source were inactivated faster owing to receiving a higher UV dose. In general, it took approximately four times as many pulses to achieve the same level of yeast inactivation at 18 cm as it did for similar studies carried out at 8 cm from the light source. The latter findings were expected as the intensity of the light is inversely proportional to the square of the distance from the light source (Elmnasser *et al*., 2007), as illustrated in Fig. 3. Farrell *et al.* (2009) also reported that the lower the initial starting cell population irradiated, the shorter the time taken to achieve surface sterilisation using PUV. As a distinct tailing or tolerance effect occurred with highly populated yeast samples (approximately 9 $\log_{10}$ CFU cm^{-2}) owing to shading effects, these authors recommended use of ≤ 7 $\log_{10}$ CFU cm^{-2} for PUV inactivation that was a level adopted in this present study. This is in line with the experimental design of present study where a predetermined yeast population of approximately 10^5 $\log_{10}$ cells cm^{-2} was used throughout. All data sets showed no tailing effect within the experimental regime of pulsing in this present study (Fig. 3). Previous researchers also demonstrated the benefit of using greater amounts of pulsing (or higher UV doses) for achieving greater levels of microbial reduction on agar surfaces and in liquid food samples. For example, a 4- to 5-log decrease in yeast numbers was achieved in this present study after forty pulses at 12.8 J (or UV dose of 3.36 μJ cm^{-2}), whereas Farrell *et al.* (2009) demonstrated that a 7-log reduction or greater in yeast numbers can be achieved after ninety pulses using the same lamp discharge energy and distance from the light source (equivalent to a UV dose of 7.56 μJ cm^{-2}). Although the increase in sample temperature of PUV-treated cultures was not found to be discernable in the present study (Fig. 2), localised overheating of the internal cellular constituents cannot be dismissed. For example, Wekhof (2000) proposed that with a fluence exceeding 0.5 J cm^{-2}, the disinfection is achieved through rupture of the bacteria during their momentous overheating caused by absorption of all UV light from a flash lamp. This present study also investigated the efficacy of PUV irradiating early-stationary phase yeast cultures as microorganisms treated in their exponential growth phase were shown previously to be more susceptible to PUV-decontamination treatments compared to older cultures (Farrell *et al*., 2009, 2010). Previous researchers have demonstrated that microorganisms treated when actively growing are more susceptible to range of conventional and novel food processing conditions (Elmnasser *et al*., 2007). This is possibly attributed in part to greater likelihood of inflicting irreversible damage to critical genetic information that governs key metabolic pathways (such as single strand breakages and formation of pyrimidine dimers) along with damaging vital membranes, proteins and other macromolecules, where there is an increased demand for these activities during exponential phase of microbial growth (Farrell *et al*., 2009). Without sufficient repair mechanisms, such damage will result in irreversible events culminating in microbial cell death.

Influence of prior osmotic stress exposure on the sensitivity of test yeast to PUV irradiation

Prior growth of all yeast test strains to a high concentration of glucose (≥30% w/v) significantly enhanced their susceptibility to pulsed UV light irradiation at 3.2 J (Table 2), 7.2 J (Table 3) and 12.8 J (Table 4). Multiple ANOVA analysis of means from pairwise comparisons of the combined effects of sugars and PUV settings revealed that significant differences in sensitivity of yeast to these treatments occurred from 1% w/v to 30% w/v sugar ($P = 0.008$), from 1% w/v to 50% w/v sugar ($P = 0.000$), from 15% w/v to 30% w/v sugar ($P = 0.038$) and from 30% w/v to 50% w/v sugar ($P = 0.006$). No significant difference was evident from comparison of yeast strains treated at all PUV settings when grown prior in either 1% w/v or 15% w/v sugar ($P = 0.119$). Prior exposure of test yeast to 50% (w/v) glucose (uppermost concentration) caused the greatest

reduction in PUV-irradiated samples (Tables 2, 3 and 4). Untreated control yeast samples containing 50% (w/v) glucose were not significantly reduced in cell number (data not shown). The latter finding was expected and is typical of yeast that have sophisticated and efficient osmoregulatory system that maintains cellular water balance that is well understood (Hohmann *et al.*, 2007; Pribylova *et al.*, 2007; Shima & Takagi, 2009). A clear trend emerged where the higher the level of UV dose applied the greater the reduction in yeast samples observed. With the exception of some individual strain differences, the general order of decreasing resistance to PUV irradiation in osmotically stressed yeast samples was *Z. rouxii*, *Z. bailii* > *S. cerevisiae* (Tables 2, 3 and 4). The difference in sensitivity of these PUV-treated *Zygosaccharomyces* spp. compared to that of similarly treated *S. cerevisiae* in high-sugar environments may be attributed to the fact that the former xerophilic yeast have developed a more sophisticated osmoregulatory response system that may provide a degree of cross-protection to that of PUV irradiation (Martorell *et al.*, 2007). While there is a dearth of published papers on the influence of prior food-related stress on subsequent sensitivity to PUV treatments, Hillegas & Demirci (2003) reported that pulsed UV light inactivated 89.4% of *Clostridium sporogenes* bacteria in honey. PurePulse Technology (San Diego, CA, USA) also reported that treating microbial test strains in distilled saline water containing 20% (w/v) glucose effectively enhanced inactivation compared to similar samples that were PUV irradiated in water only (cited in Choi *et al.*, 2010). Marked differences in physiological responses of yeast strains to PUV irradiation and to other conventional stresses are not uncommon (Farrell *et al.*, 2010, 2011) and are likely to be attributed in part to variances in composition and transcription of housekeeping and specific stress-response genes (Rowan, 2011). Findings presented in Tables 2, 3 and 4 also highlight the relationship between prior growth in a stressful food environment (i.e., high-sugar) and subsequent sensitivity of test year to exposure from an additional applied stress (i.e., PUV). This finding markedly contrasts from data presented by other researchers who reported that prior exposure to a homologous sub-lethal stress (such as mild-acid) provides a cross-protective effect to lethal levels of different or heterologous stresses (such as heating, hydrogen peroxide and starvation) (Gibson, 1973; Leistner, 1995; Lou & Yousef, 1997; Rowan, 1999; Hill *et al.*, 2002). While this study reported on the relationship between growth in high-sugar environments and subsequent sensitivity to PUV irradiation under varying operational conditions for directly plated yeast samples only, future studies exploring the use of an additional resuscitation or enrichment step post-PUV treatments are merited. Owing to the fact that PUV appears to kill yeast through a multi-hit cellular process (Farrell *et al.*, 2011), it is highly likely that PUV treatment will produce a mix of sub-lethally injured and killed cells where the former sub-population may not be detected using direct plating techniques unless an appropriate recovery or enrichment stage (Rowan, 2011). These latter resuscitation experiments were not conducted in this study owing to the enormity of additional duplicate samples required for inclusion and analysis.

Influence of PUV on possible microbial photoreactivation repair post-treatments

A clear pattern also emerged where photoreactivation was evident from samples that were treated at the lower discharge energy of 3.2 J with 200 pulses (equivalent to UV dose of 2.66 μJ cm^{-2}), while no significant photoreactivation was observed using similar levels of UV dose after 100 pulses at 7.2 J (UV dose of 2.7 μJ cm^{-2}) and thirty-two pulses at 12.8 J (UV dose of 2.69 μJ cm-^{2}) ($P \leq 0.05$) (Fig. 4). This finding is in agreement with other researchers who reported a difference in the ability of PUV-irradiated yeast and other food-related microorganisms to photorepair and to recover at very low applied voltages (Farrell *et al.*, 2009, 2010). Photoreactivation relates to the ability of PUV-treated microorganisms to enzymatically repair molecular damaged using sunlight. This is a surprising finding as the PUV system was set up to deliver a similar UV dose at each applied voltage setting, and therefore must relate in part to the intensity of the applied voltage used. This latter finding does merit further investigation. Owing to the presence of visible and infrared light (together with UV light) in the pulsed spectrum emitted by the xenon

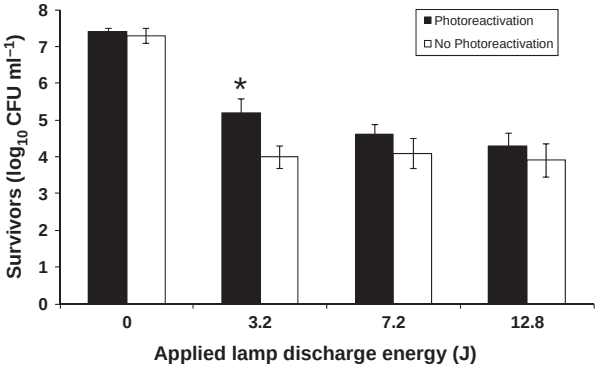

Figure 4 Effect of photoreactivation and repair for *S. cerevisiae* 834 grown in 30% w/v glucose and irradiated at different combinations of applied voltage and pulse number (200 pulses at 3.2 J, 100 pulses at 7.2 J and 32 pulses at 12.8 J) to deliver a similar UV dose of approximately 2.7 μJ cm^{-2}. Bars indicate ± SD. Reductions in populations expressed in log_{10} CFU mL^{-1} with (■) and without provision for conditions inductive to (□) photoreactivation.

lamp, test samples can warm up during flashing. Findings from this study showed that limiting pulse number to ≤40 pulses at lamp discharge energies of 3.2, 7.2 and 12.8 J (equivalent to UV doses of 0.53, 1.09 and 3.36 μJ cm^{-2}) did not have any discernable effect on temperature or heating. A moderate sample temperature increase of 3.2 ± 0.2°C was recorded after 150 pulses at 12.8 J (equivalent to UV dose of 12.6 μJ cm^{-2}) during photoreactivation studies. Therefore, the latter slight increases in sample temperature during treatment did not contribute to the inactivation performances achieved by PUV in this study.

Conclusions

Findings from the present study revealed that prior growth in high-sugar conditions (≥30% w/v glucose) enhances the sensitivity of prominent food-spoilage yeast to high-intensity pulsed UV light irradiation. Specifically, these findings provide evidence to support the further development of PUV combined with traditional preservation approaches for minimal food processing applications, particularly for treatment of high-sugar foods. While the findings from the study demonstrate the effectiveness of using a xenon pulsed light approach for the inactivation of food-spoilage yeast under a limited range of operational settings, future studies investigating the efficacy of treating contaminating yeasts in food environments under a variety of abuse conditions (such as varying surrounding relative humidity, duration of exposure and so forth) are also merited. Further molecular- and cellular-based studies are required to elucidate the underpinning mechanistic or physiological responses governing adaptive tolerance to PUV treatments for xerophilic yeast grown previously in high-sugar environments. Findings from this present study will help to specifically advance the field of nonthermal food processing.

Acknowledgments

The authors thank Technological Sector Research Strand 1 Programme (Ireland) and the Ministry of Agriculture, Fisheries and Food (MAFF) (UK) for funding this research. We also thank Ms Tunku Ahmad for her technical assistance with the statistical analysis element of this study.

References

Choi, M.S., Cheigh, C.I., Jeong, E.A., Shin, J.K. & Chung, M.S. (2010). Nonthermal sterilization of *Listeria monocytogenes* in infant foods by intense pulsed-light treatment. *Journal of Food Engineering*., **97**, 504–509.

Coroller, L., Leguerienel, I. & Mafarat, P. (2001). Effect of water activities of heating and recovery media on apparent heat resistance of Bacillus cereus spores. *Applied and Environmental Microbiology*, **67**, 317–322.

Corry, J.E.L. (1976). The effect of sugars and polyols on the heat resistance and morphology of osmophilic yeasts. *Journal of Applied Microbiology*, **40**, 269–276.

Elmnasser, N., Guillou, S., Leroi, F., Orange, N., Bakhrouf, A. & Federighi, M. (2007). Pulsed-light system as a novel food decontamination technology: a review. *Canadian Journal of Microbiology*, **53**, 813–821.

Farrell, H.P., Garvey, M. & Rowan, N.J. (2009). Studies on the inactivation of medically important *Candida* species on agar surfaces using pulsed light. *FEMS Yeast Research*, **9**, 956–966.

Farrell, H.P., Garvey, M. & Rowan, N.J. (2010). Critical inter-related factors governing the efficacy of pulsed light for the inactivation of clinically relevant bacteria. *Journal of Applied Microbiology*, **108**, 1494–1508.

Farrell, H.P., Hayes, J., Laffey, J.G. & Rowan, N.J. (2011). Studies on the relationship between pulsed UV light and the simultaneous occurrence of molecular and cellular damage in clinically-relevant *Candida albicans*. *Journal of Microbiological Methods*, **84**, 317–326.

Fleet, G. (1992). Spoilage yeasts. *Critical Reviews in Biotechnology*, **12**, 1–44.

Garvey, M., Farrell, H., Cormican, M. & Rowan, N. (2010). Investigations of the relationship between use of in vitro cell culture-quantitative PCR and a mouse-based bioassay for evaluating critical factors affecting the disinfection performance of pulsed UV light for treating Cryptosporidium parvum oocysts in saline. *Journal of Microbiological Methods*, **80**, 267–273.

Gibson, B. (1973). The effect of high sugar concentrations on the heat resistance of vegetative micro-organisms. *Journal of Applied Bacteriology*, **36**, 365–376.

Giorgi, J.C. & Gontier, R. (1980). Preservation of pure sugar syrups by UV irradiation. *International Sugar Journal*, **82**, 86–88.

Gómez-López, V.M., Ragaert, P., Debevere, J. & Devlieghere, F. (2007). Pulsed light for food decontamination: a review. *Trends in Food Science and Technology*, **18**, 464–473.

Gunde-Cimerman, N., Ramos, J. & Plemenitas, A. (2009). Halotolerant and halophilic fungi. *Mycological Research*, **113**, 1231–1241.

Hill, C., Cotter, P.D., Sleator, R.D. & Gahan, C.G.M. (2002). Bacterial stress response in *Listeria monocytogenes*: jumping the hurdles imposed by minimal processing. *International Dairy Journal*, **12**, 273–283.

Hillegas, S.L. & Demirci, A. (2003). Inactivation of *Clostridium sporogenes* in clover honey by pulsed UV-light treatment. *Agricultural Engineering International*, V. Manuscript FP 03 009, 1–7.

Hohmann, S., Krantz, M. & Nordlander, B. (2007). Yeast osmoregulation. *Methods in Enzymology*, **428**, 29–45.

Hsu, M.C., Chen, K.W., Lo, H.J., Chen, Y.C., Liao, M.H., Lin, Y.H. & Li, S.Y. (2003). Species identification of medically important fungi by use of real-time LightCycler PCR. *Journal of Medical Microbiology*, **52**, 1071–1076.

Iwahashi, H., Obuchi., K., Fujii, S. & Komatsu, Y. (1995). The correlative evidence suggesting trehalose stabilizes membrane structure in the yeast *Saccharomyces cerevisiae*. *Cell Molecular Biology*, **41**, 763–769.

Kühn, K.P., Chabreny, I.F., Massholder, K. *et al*. (2003). Disinfection of surfaces by photocatalytic oxidation with titanium dioxide and UVA light. *Chemosphere*, **53**, 71–77.

Lee, S.U., Joung, M., Yang, D.J. *et al*. (2009). Pulsed UV-light inactivation of *Cryptosporidium parvum*. *Parasitology Research*, **10**, 1293–1299.

Leistner, L. (1995). Principles and Applications of Hurdle Technology. In: *New Methods of Food Preservation* (edited by G.W. Gould). Pp. 1–21. Glasgow, UK: Blackie Academic & Professional.

Lou, Y. & Yousef, A.H. (1997). Adaptation of sub-lethal environmental stresses protects against lethal preservation factors. *Applied and Environmental Microbiology*, **63**, 1252–1255.

Martorell, P., Stratford, M., Steels, H., Fernandez-Espinar, M.T. & Querol, A. (2007). Physiological characterization of spoilage strains of *Zygosaccharomyces bailii* and *Zygosaccharomyces rouxii* isolated from high-sugar environments. *International Journal of Food Microbiology*, **114**, 234–242.

Montiel, V., García, R. & Ramos, J. (2005). Mechanisms underlying the halotolerant way of Debaryomyces hansenii Prista C, Loureiro-Dias MC. *FEMS Yeast Research*, **5**, 693–701.

Nugent, M.J.D. & Higginbotham, C.L. (2007). Preparation of a novel freeze thawed poly (vinly alcohol) composite hydrogel for drug delivery applications. *European Journal of Pharmaceutics and Biopharmaceutics*, **67**, 377–386.

Oms-Oliu, G.O., Martin-Belloso, O. & Soliva-Fortuny, R. (2010). Pulsed light treatments for food preservation: a review. *Food Bioprocess Technology*, **3**, 13–23.

Park, J.G., Grant, C.M., Attfield, P.V. & Dawes, I.W. (1997). The freeze-thaw stress response of the yeast *Saccharomyces cerevisiae* is growth phase specific and is controlled by nutritional state via the RAS-cyclic AMP signal transduction pathway. *Applied and Environment Microbiology*, **63**, 3818–3824.

Piper, P., Ortiz Calderon, C., Hatzixanthis, K. & Mollapur, M. (2001). Weak acid adaptation, the stress response that confers yeasts with resistance to organic acid food preservatives. *Microbiology*, **147**, 2635–2642.

Pitt, J.I. & Hocking, A.D. (2009). *Fungi and Food Spoilage*, 3rd edn. New York: Springer Publication Company.

Prakasham, R.S., Sreenivas-Rao, R. & Hubbs, P.J. (2009). Current trends in biotechnological production of xylitol and future aspects. *Current Trends in Biotechnology and Pharmacy*, **3**, 8–36.

Pribylova, L., de Montigny, J. & Sychrova, H. (2007). Osmoresistant yeast *Zygosaccharomyces rouxii*: the two most studied wild-type strains (ATCC 2623 and ATCC 42981) differ in osmotolerance and glycerol metabolism. *Yeast*, **24**, 171–180.

Rahn, R.O. (1993). Use of potassium iodide as a chemical actinometer. *Photochemistry and Photobiology*, **58**, 874–880.

Rahn, R.O. (1997). Potassium Iodide as a chemical actinometer for 254 nm radiation: use of iodate as an electro scavenger. *Photochemistry and Photobiology*, **66**, 450–455.

Rahn, P.O., Bolton, J.R., Goren, E., Shaw, P.S. & Lykke, K.R. (2003). Quantum yield of the iodide-iodate chemical actinometer: dependence on wavelength and concentration. *Photobiology*, **78**, 146–152.

Rowan, N.J. (1999). Evidence that inimical food preservation barriers alters microbial resistance, virulence and cell morphology. *Trends in Food Science and Technology*, **10**, 261–272.

Rowan, N.J. (2011). Defining established and emerging microbial risks in the aquatic environment: current knowledge, implications and outlooks. *International Journal of Microbiology*, **65**, 1–15.

Rowan, N.J., MacGregor, S.J., Anderson, J.G., Fouracre, R.A., McIlvaney, L. & Farish, O. (1999). Pulsed-light inactivation of food-related microorganisms. *Applied and Environmental Microbiology*, **65**, 1312–1315.

Sharma, P., Meena, N., Aggarwal, M. & Mondal, A.K. (2005). *Debaryomyces hansenii*, a highly osmo-tolerant and halo-tolerant yeast, maintains activated Dhog1p in the cytoplasm during its growth under severe osmotic stress. *Current Genetics*, **48**, 162–170.

Shima, J. & Takagi, H. (2009). Stress-tolerance of baker's-yeast (*Saccharomyces cerevisiae*) cells: stress-protective molecules and genes involved in stress tolerance. *Biotechnology and Applied Biochemistry*, **53**, 155–164.

Sperber, W.H. & Doyle, M.P. (eds.) (2010). *Compendium of the Microbiological Spoilage of Foods and Beverages*. Springer: New York, USA.

Tilbury, R.H. (1980a). Xerotolerant yeasts at high sugar concentrations. In: *Microbial Growth and Survival in Extremes of Environment. Society for Applied Bacteriology Technical Series, vol. 15*. (edited by G.W. Gould & J.E.J. Corry). pp. 103–128. London: Academic Press.

Tilbury, R.H. (1980b). Xerotolerant (osmophilic) yeasts. In: *Biology and Activity of Yeasts. Society for Applied Bacteriology, Symposium Series* (edited by F.A. Skinner, S.M. Passmore & R.R. Davenport). Pp. 153–179. London: Academic Press.

Van Zyl, P.J., Kilian, S.G. & Prior, B.A. (1993). Physiological responses of *Zygosaccharomyces rouxii* to osmotic stress. *Applied Microbiology and Biotechnology*, **39**, 235–241.

Wang, T., MacGregor, S.J., Anderson, J.G. & Woolsey, G.A. (2005). Pulsed ultra-violet inactivation spectrum of *Escherichia coli*. *Water Research*, **39**, 2921–2925.

Wekhof, A. (2000). Disinfection with flash lamps. *PDA Journal of Pharmaceutical Science and Technology*, **54**, 264–276.

Use of a Real Time PCR Assay to Assess the Effect of Pulsed Light Inactivation on Bacterial Cell Membranes and Associated Cell Viability

Mary Garvey[1]*, Alessia Stocca[2], Neil Rowan[2]

ABSTRACT: Research into more rapid and effective means of disinfecting water has become necessary due to the recognition that not all pathogenic species are being removed by chemical means. There is an extent of research highlighting the benefits of pulsed light for the disinfection of water. This study aims to determine the ability of a real time polymerase chain reaction assay to evaluate microbial inactivation of pulsed light treated cells. Findings show that pulsed light is a more rapid means of inactivating test species than standard UV lamp systems. A linear relationship between cell number and polymerase chain reaction amplification was obtained. A difference in threshold value (Ct) of approximately 4 ($p \leq 0.05$) was obtained for DNA amplification following the addition of the dye for pulsed ultrviolet (PUV)-treated *Bacillus* cells. Membrane protein leakage proved an effective means of determining membrane damage for both *Bacillus* and *E. coli* test species following PUV treatment. This membrane damage was not evident for cells exposed to low pressure ultraviolet (LPUV). Findings describe suggest that PUV treatment induced a viable but nonculturable state in treated cells. *Water Environ. Res.*, **88,** 168 (2016).

KEYWORDS: pulsed UV, *E. coli, Bacillus*, real time PCR, permeabilization, viable but nonculturable.

doi:10.2175/106143016X14504669767210

Introduction

The use of ultraviolet (UV) light for the inactivation of pathogenic organisms has become common practice for both food and water. The disinfection ability of UV is due to the absorption of UV energy by the genetic material of exposed cells resulting in a photochemical reaction that alters the genetic material (DNA) preventing replication. Standard UV lamps include low pressure (LP) and medium pressure (MP) lamps, which have proven effective for the inactivation of a range of microbial test species. However, it has become increasingly clear that these standard lamps are not as effective for the inactivation of larger protozoa parasite species such as *Cryptosporidium* and *Giardia* (Garvey et al., 2014). Furthermore, microbial species possess DNA repair systems that can repair genetic insult resulting from UV exposure allowing the species to replicate and regain its pathogenic potential. An alternative UV delivery method known as pulsed UV (PUV) light has been recognized as an extremely effective method for the inactivation of fungal, spore, biofilm, and parasite species (Garvey et al., 2014) in a much shorter treatment time. Pulsed UV operates by storing energy in a capacitor and releasing it as short bursts of energy into the treatment area. Compared to standard LPUV lamps, pulsed light treatment has the advantage of being fast, effective, and more efficient at converting electrical energy into photon energy. Furthermore, the use of PUV light is believed to cause irreparable damage to treated species as they have proven unable to reproduce when exposed to an array of repair conditions (Abida et al., 2014). The high potency of pulsed light is believed to stem from damage caused to other essential cellular components such as proteins and cell membranes not achieved with standard UV lamps. Therefore, changes in the physiological state of cells post-PUV treatment should be studied to determine the mechanisms of induced toxicity (Ferrario and Guerrero, 2014).

Furthermore, methods to determine bacterial viability is predominantly reliant on the microbial plate count method, which is often time-consuming. The use of a polymerase chain reaction (PCR) assay may offer a more rapid determination of cell death following disinfection. Polymerase chain reaction assays are based on the amplification of target DNA within a cell providing a direct relationship between the numbers of cells present based on the PCR cycle number. However, the main disadvantage of PCR-based microbial diagnostics is its inability to discriminate between live and dead bacteria following UV treatment. Studies on the use of propidium monoazide (PMA) prior to DNA extraction has been described as a method that allows selective detection of only live cells following chemical disinfection (Kesmen et al., 2011). The dye is nearly completely cell membrane–impermeable and thus can be selectively used to modify exposed DNA from dead cells while leaving DNA from viable cells intact. Once PMA dye enters membrane-damaged cells, it subsequently binds to the DNA of the exposed species, thus preventing subsequent amplification of modified target DNA sequences by PCR. Theoretically, PUV-treated cells exhibiting membrane damage will not be detected via real time PCR (RT-PCR) as opposed to cells with intact membranes, indicating that membrane damage from pulsed light treatment prevented PCR amplification.

Therefore, the aim of this study is to determine PUV-induced membrane damage in treated microbial cells via a PMA RT-PCR assay. This represents the first study to determine the effect of PUV light treatment on bacterial cell membrane structure via

[1*] Department of Life Sciences, Institute of Technology Sligo, Ash Lane, Sligo, Ireland; telephone: +353719305841; e-mail: garvey.mary@itsligo.ie.

[2] Bioscience Research Institute, Athlone Institute of Technology, Dublin Road, Ireland.

PCR and can potentially offer a rapid method to determine disinfection efficacy of pulsed light system for the water or food industry.

Methods

Bacterial Test Species Culture and Maintenance. *Escherichia coli* ATCC 25922 was chosen for this study as it is currently the indicator organism for water contamination. For comparative analysis *Bacillus* strains were also chosen, namely *Bacillus megaterium* ATCC 14581 and *Bacillus cereus* ATCC 11778 to represent both pathogenic and nonpathogenic gram-positive *Bacillus* species. Strains were sourced from the American Type Culture Collection and grown from storage on nutrient agar at 37 °C and identity confirmed via gram stain and standard biochemical tests. To establish a working bacterial culture, a single colony of the test strain was aseptically transferred to 100 mL sterile nutrient broth followed by incubation at 37 °C for 24 hours. Following incubation, test samples were centrifuged at 10 000 rpm for 10 minutes and the pellet resuspended in sterile phosphate buffered saline (0.01 M phosphate buffer, containing 0.0027 M KCl and 0.137M NaCl at a pH of 7.4) (PBS) to give a working stock of ca. 1×10^8 CFU/mL.

UV Light Treatment. Low-pressure UV studies were conducted on 10 mL suspensions using a lab scale UV lamp at 254 nm (UVGL-55 handheld UV lamp) at a distance of 8 cm form the light source. Bacterial suspensions were prepared by placing a 1 in 10 dilution (final volume of 10 mL) from the working solution of ca. 1×10^8 *Bacillus* and *E. coli* respectively in a petri dish followed by exposure to the LPUV lamp (1×10^7 cfu/mL test microbial cell number). The UV dose (mJ/cm^2) was varied by altering the time of exposure as required.

A pulsed lamp system (Samtech Ltd, Glasgow, Scotland, U.K.) was used as described by Garvey et al. (2014) and is, therefore, not described in more detail herein. Pulsed UV studies were conducted on samples diluted from the working stock of ca. 1×10^8 *Bacillus* and *E. coli* in the same manner as LPUV studies of sterile PBS at 8 cm from the light source. Samples were treated at 16.2 J at a rate of 1 pulse per second to determine the relative sensitivity of the test species. Following treatment, 100 µL of serially diluted treated or untreated sample was spread on plate count agar and incubated for 24 hours at 37 °C, after which the colony forming unit (cfu/mL) of survivors was determined. For analysis purposes, the levels of inactivation were determined by plotting the $\log_{10}$ ratio of survivors against UV dose for each experimental organism. Samples were then centrifuged at 10 000 rpm for 10 minutes and the pellet resuspended in 198 µL sterile PBS for PMA binding and PCR analysis. One milliliter of treated and untreated bacterial suspension was also placed on ice to determine protein leakage via the Bradford assay. Additionally, microbial test species were subject to heat treatment at 65 °C for 30 minutes to provide a positive control as heat inactivation is via membrane induced damage.

Propidium Monoazide Cross-Linking. PMA (Biotium Inc., Hayward, California) was dissolved in water to a stock concentration of 10 mM and stored at −20 °C until required. All workings with PMA solution were conducted with minimal light exposure to prevent any potential chemical change in PMA structure, as it is a light-sensitive molecule. Two microliters of PMA dye were added to treated and untreated samples suspended in 198 µL solutions to give a final volume of 100 nM PMA (as recommended by Biotium Inc. for use with the PMA Lite device). Samples were then placed in the Biotium PMA Lite LED photolysis device (Biotium Inc.) and exposed to 475 nm emission for 30 minutes as per manufacturer's instructions. Following exposure, samples were removed from the device and DNA extraction was performed to obtain target DNA prior to PCR amplification.

DNA Extraction. Target DNA extraction was conducted as per kit instructions for *E. coli* and *Bacillus* test species using a Roche DNA extraction kit and HP PCR template preparation kit (Roche Diagnostics, Roche, Ireland). All steps were performed as per manufacturer's instructions with treated and untreated microbial pellets that were suspended in 200 µL of sterile PBS.

Real Time Polymerase Chain Reaction. Real-time polymerase chain reactions are characterized by an increase in fluorescence emission due to probe degradation by DNA polymerase in each elongation step during PCR cycling. The higher the starting copy number of the nucleic acid target, the earlier the fluorescence will reach the predetermined threshold cycle (Ct) and the smaller will the Ct value will be. The Ct value is the fractional PCR cycle number, at which a significant increase in target signal fluorescence above the baseline is first detected for a sample. Quantification of test samples is performed by determining the Ct value and the use of a standard curve to deduce the starting copy number. All primers and probes were sourced from Tib Molbiol, Berlin, Germany. For *E. coli* primers (100 base pairs) coding for the 16s RNA region (16sRNA gene) were used as per Spano et al. (2005); forward primer CAT TGA CGT TAC CCG CAG AA, reverse primer CGC TTT ACG CCC AGT AAT TCC, and a taqman probe sequence: CGT GCC AGC AGC CGC GGT A. For *B. megaterium* and *B. cereus*, the forward primer ACACACGTGCTACAATGGATG and reverse primer AGTTGCAGCCTACAATCCGAA with the taqman probe sequence F-ACAAAGGGCTGCAAGACCGCG—Q coding for the phaC gene was used as per Nayak et al. (2013). Amplification reactions (20 µL) contained 5 µL of sample DNA (0.5 µM of each primer, 0.2 µM of probe) and 15 µL of reaction buffer (Roche Diagnostic, West Sussex, England). Both positive and negative controls were included in RT-PCR to validate the results. DNase and RNase free water was used as negative control throughout. Cycling parameters were initial denaturation for 10 minutes at 95 °C followed by 65 cycles of denaturation for 10 seconds at 95 °C, annealing for 40 seconds at 40 °C, extension for 1 second at 70 °C, and cooling for 30 seconds at 40 °C on a Nanocycler device (Roche Diagnostics). Large numbers of cycles were used to ensure detection of low levels of infection. On completion of each RT-PCR run, amplification curves were analyzed by Nanocycler software (Roche Diagnostics) and a standard curve of DNA concentration versus cell number was determined (Figure 1).

Bicinchoninic Acid (BCA) Protein Assay. The BCA protein assay kit (Fisher Scientific, Ireland) was used as per manufactures instructions. One milliliter of test sample (untreated and treated) was centrifuged for 10 minutes at 8000 *g*, the supernatant was removed to a sterile tube and placed on ice (or stored at −80 °C until required). Bovine serum albumin (BSA) standards were prepared to test concentrations of 500, 250, 125, 50, 25, and 5 ug/mL and run in triplicate on plate with sterile PBS as a blank. Twenty-five microliter aliquots of standards and test samples were transferred to a 96-well plate

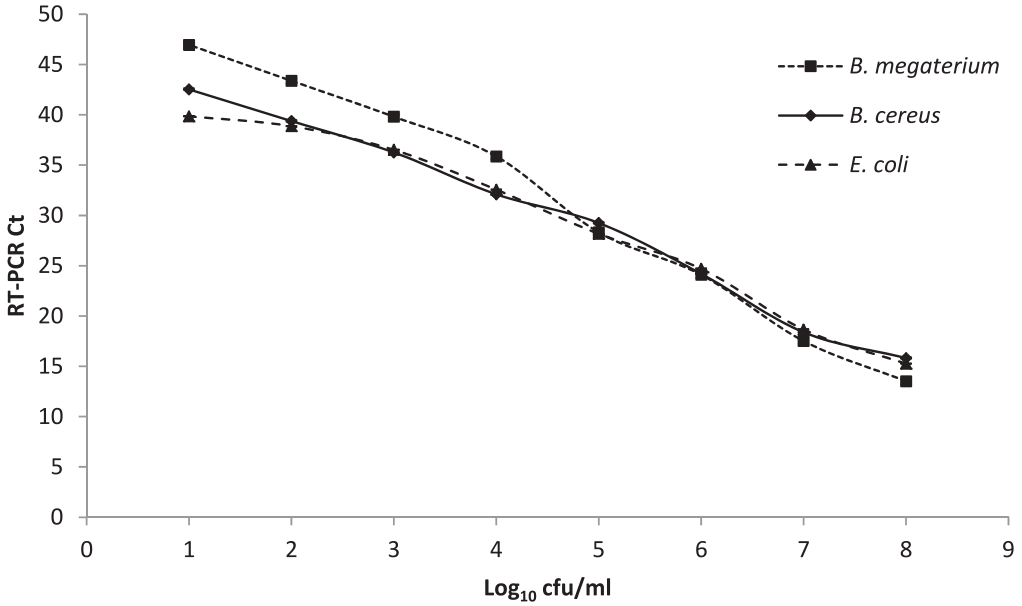

Figure 1—Standard curve as determined by RT-PCR Ct value for *B. megaterium, B. cereus*, and *E. coli* cells (log_{10} cfu/mL) (±S.D) using species specific primers.

in triplicate. A BCA mix was prepared and stored in the dark. Buffer mix (200 μL) was added to each well and incubated at 37 °C for 30 minutes in the dark, after which the absorbance was measured at 562 nm using a multiplate reader (Biotek Synergy HT). Protein concentration in supernatant is calculated using the standard curve equation derived from the protein standards.

Statistics. All the experiments were performed 3 times with three plate replicates for each experimental data point providing a mean result for each experimental batch. The log reduction was calculated as the log_{10} of the ratio of the concentration (cfu/mL) of the nontreated (N_0) and UV-treated (N) samples [log_{10} (N_0/N)]. Linear regression analysis was used to determine the rate of inactivation for each test species under the regime of UV treatments applied at 95% significance level. Student's *t*-tests and ANOVA one-way model (MINITAB software release 16; Mintab Inc., State College, Pennsylvania) were used to compare the relationship between UV treatments and viable/nonviable cells. The slope of the relationship between the protein standard concentrations and absorbance at 562 nm was calculated to determine the protein leakage of treated cells corresponding to UV dose and cell viability.

Results and Discussion

The standard approach determining microbial viability post-disinfection testing has traditionally relied on cultivation-based techniques such as spread plate counts (cfu/mL). In recent years, with the focus on the disinfection of the ever-increasing number of antibiotic resistant microbes, research has sought out speedier assays for disinfection efficacy testing. Polymerase chain reaction methods have gained attention as a rapid and specific method for the quantification of microbial numbers in both food and water samples (Gensberger et al., 2014). However, quantitative PCR (qPCR) does not differentiate between live and dead bacteria; it merely quantifies cell numbers present and is, therefore, not comparable to cultivation techniques. Studies have shown the benefits of DNA intercalating dyes such as EMA and PMA combined with PCR for use in determining viable cell numbers following chemical or heat disinfection. The intercalating dye passes through damaged cell membranes and binds to the DNA, preventing PCR amplification of dead cells. PMA specially binds to double-stranded DNA with high affinity. With photolysis, the photo-reactive azido group on the dye is transformed to an extremely reactive nitrene radical, which then reacts with hydrocarbon moieties at the binding site to form a stable covalent nitrogen–carbon bond, resulting in permanent DNA modification (Taskin et al., 2011). Propidium monoazide is cell membrane–impermeable and can be selectively used to modify exposed DNA only from dead cells while leaving DNA from viable cells intact. At present, there are no studies detailing the use of a PMA PCR assay as a tool to determine pulsed light induced microbial death. Therefore, this study focused on the use of a real-time PCR assay combining PMA dye to determine if PUV treatment causes membrane damage to treated cells. Theoretically, cell membranes damaged by pulsed light should allow for the passage of PMA across the membrane that subsequently binds to the genetic material preventing PCR amplification. *E. coli* is a recognized fecal coliform bacteria used as an indicator for wastewater treatment; additionally *B. megaterium* endospores have been shown to have similar sensitivity to PUV treatment to that of *Cryptosporidium parvum* (Garvey et al., 2012). Therefore, both strains were the focus of this study.

Pulsed Light for Microbial Inactivation. The PUV system used throughout this study proved very effective for the inactivation of all test species when treated in 10 mL suspensions. A 6.2, 7.35, and 8.41 log_{10} inactivation of *B. megaterium, B. cereus*, and *E. coli* was achieved with a PUV dose of 21.6 μJ/cm^2 respectively (Figure 2). Additionally the LP UV system also provided high levels of microbial inactivation with a 6.1, 5.8, and 7.6 log_{10} inactivation of *B. megaterium, B. cereus*, and *E. coli*, respectively, with a UV dose of 392 mJ/cm^2 (Figure 2). For both UV systems *E. coli* proved most UV sensitive to

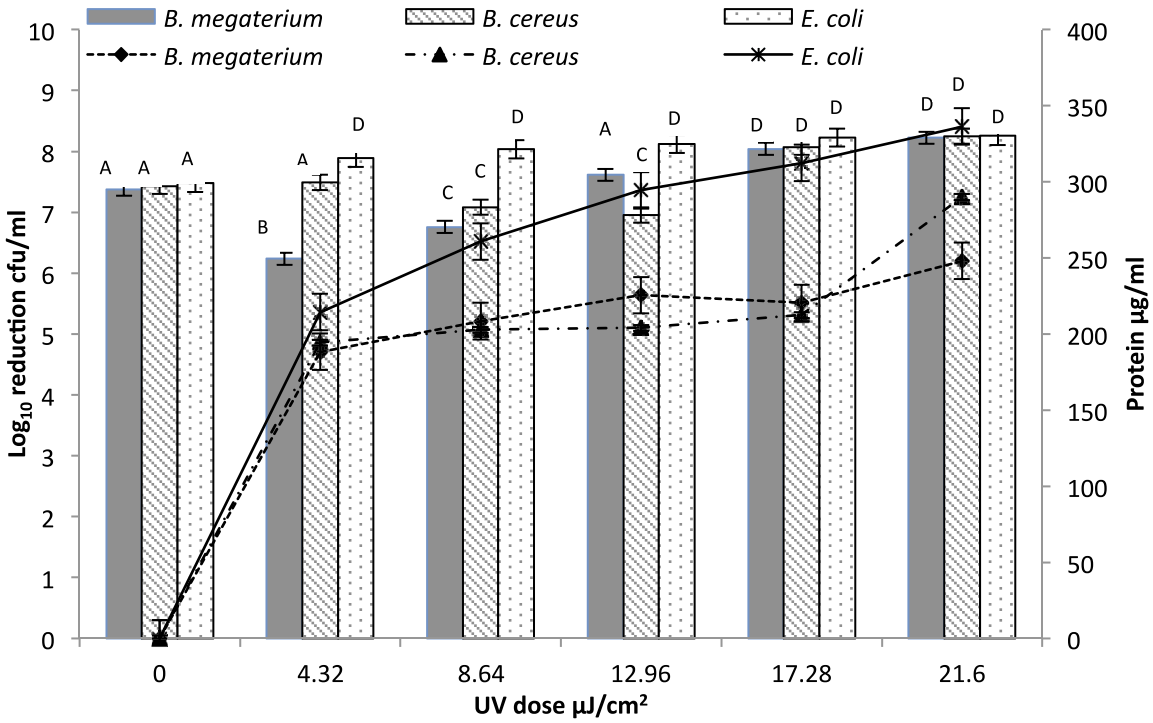

Figure 2—Log_{10} reduction of test strains (line graph) and corresponding membrane protein leakage (column graph) following exposure to PUV light µJ/cm^2. Results are replicate of 3 experiments (±S.D). A, B, C, and D donate significant difference at $p < 0.05$.

treatment followed by *B. cereus*, with *B. megaterium* proving most UV resistant. However, the pulsed light approach provided high levels of inactivation in a much shorter treatment time than the low pressure, 21.6 µJ/cm^2 is equivalent to a treatment time of 1.5 minutes with 392 mJ/cm^2 equivalent to 12 minutes of UV exposure. Gram-positive bacteria were also shown to be more resistant than Gram-negatives to UV inactivation in a study reported by Farrell et al. (2009). The use of UV light for the inactivation of microbial species has proven effective over an array of bacterial strains under varying conditions. Regardless of the delivery approach, light in the UV wavelength range has undeniable antimicrobial properties. However, PUV has not only repeatedly provided higher levels of inactivation of test species in a much-reduced treatment time than its counterparts, it has also demonstrated high levels of inactivation of problematic parasite species such as *Cryptosporidium* and *Giardia* (Garvey et al., 2014). Indeed, this study has shown the significant reduction in time needed to achieve similar levels of inactivation of all test species with PUV compared to LPUV. The increased lethality of PUV compared to standard UV lamps has been accredited to its rich broad-spectrum UV wavelength range, short duration pulses, high peak power, and the ability to control the pulse duration and frequency output of flash lamps (Abida et al., 2014). The broad spectrum of this system with wavelengths ranging from 100 to 1100 nm (Farrell et al., 2011) is believed to play an important role in the irreparable damage caused to treated organisms. However, there is limited information available on the exact microbial insult that occurs. Studies have suggested that damage to cellular membranes plays a key role in microbial inactivation. Krishnamurthy et al. (2008) reported severe cellular damage, cytoplasmic membrane shrinkage, and cellular leakage of *Staphylococcus aureus* as observed via transmission electron microscopy (TEM) and attributed it to the pulsing effect (Krishnamurthy et al., 2008).

Use of Real Time Polymerase Chain Reaction for Viability Assessment. Figure 1 depicts standard curves for viable *E. coli, B. megaterium*, and *B. cereus* obtained via RT-PCR amplification. As shown with a higher cell count (log_{10} cfu/mL), a lower Ct value is obtained indicating that a higher amount of target DNA is present for all test species. A linear response is evident for increasing cell number and corresponding DNA detection (Ct value). Figure 3 depicts protein content for PUV treated cells, while Figure 4a describes the results obtained for log_{10} reduction (cfu/mL) and the resulting Ct value obtained both with and without the addition of the PMA dye and corresponding protein leakage detected (µg/mL) for PUV-treated cells. Similarly, Figure 4b depicts the findings obtained for LPUV-treated test species. For PUV, a clear pattern is evident where an increase in UV dose (µJ/cm^2) resulted in an increase in microbial inactivation. The determination of Ct values with and without the addition of PMA dye did lead to a variation in the PCR results. There was a significant ($p \leq 0.05$) difference in the Ct value for both *Bacillus* strains for treated and untreated cells with the addition of the dye. The untreated control for ca. 1×10^8 *B. megaterium* cells resulted in a Ct value of 13.52 and a value of 13.85 following the addition of the PMA dye. Similarly for *B. cereus*, a Ct value of 15.82 without PMA and 15.49 with PMA was detected for ca. 1×10^8 cfu/mL untreated cells. This Ct value showed good sensitivity for live cells with and without the addition of PMA, with figures corresponding to the untreated standard curve (Figure 1). Following PUV treatment, variations in the Ct values became evident. For the UV dose range of 4.32 to 17.28 µJ/cm^2, there was a Ct value of ca. 15.7 (corresponding to a cfu/mL of 1×10^7 for both *Bacillus* species) for all doses without PMA and

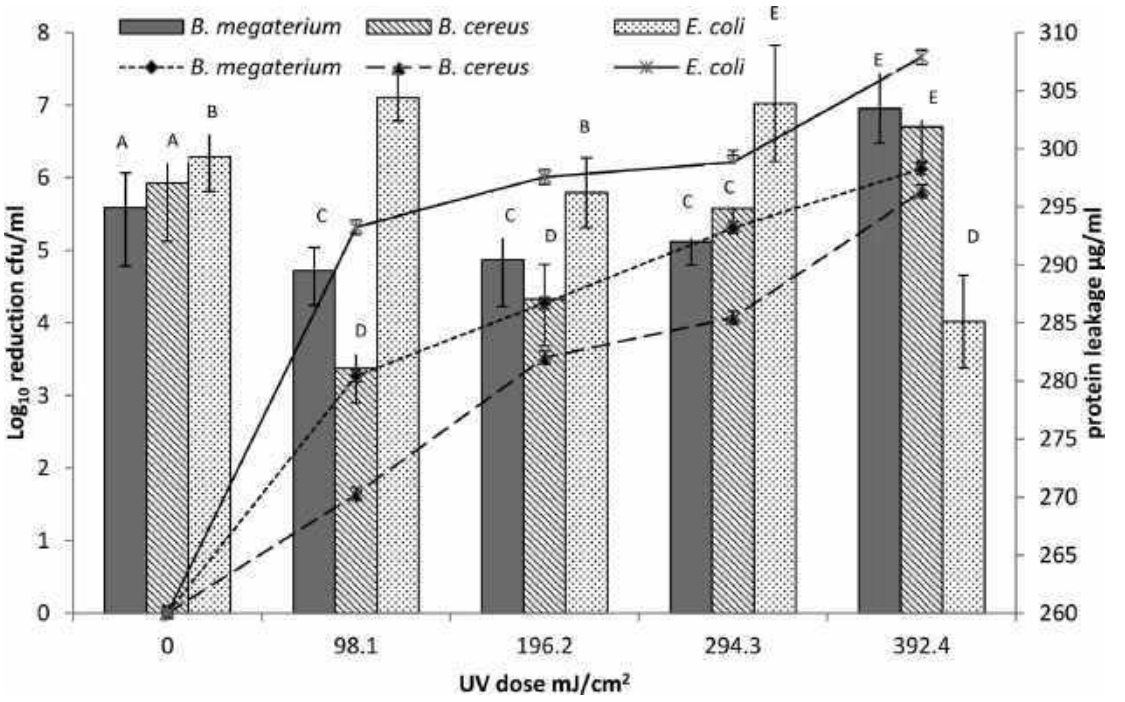

Figure 3—Log_{10} reduction of test strains and corresponding membrane protein leakage following exposure to LPUV light mJ/cm^2. Results are replicate of 3 experiments (±S.D). A, B, C, D, and E donate significant difference at $p < 0.05$.

this increased to approximately 19.5 with the addition of PMA. This corresponds to a Ct value of approximately 4 ($p \leq 0.05$) in the difference following the addition of the dye for PUV-treated cells. In comparison to the standard curve, a Ct value of 19.5 equates to a viable 7 $\log_{10}$ (as determined from Figure 1 equation of the line). Even though there was a difference in values obtained for the PCR for the PUV-treated cells, it was not large enough to correspond to the decrease in viability as determined by the spread plate cell count (cfu/mL). For example, with a PUV dose of 12.96 µJ/cm^2, a 5.6 and 5.1 $\log_{10}$ reduction of *B. megaterium* and *B. cereus* was achieved respectively (Figure 2). The resulting Ct values of 15.7 and 19.4 without and with PMA for *B. megaterium* and 21.1 and 25.89 without and with PMA for *B. cereus* do not correspond to a 5 $\log_{10}$ reduction in viable bacteria. A 5 $\log_{10}$ reduction from an initial population of 1×10^7 viable cells equates to a 2 $\log_{10}$ remaining viable population post-treatment suggesting that a Ct value of ca. 40 should result following the addition of the PMA dye (Figure 1). Similar results

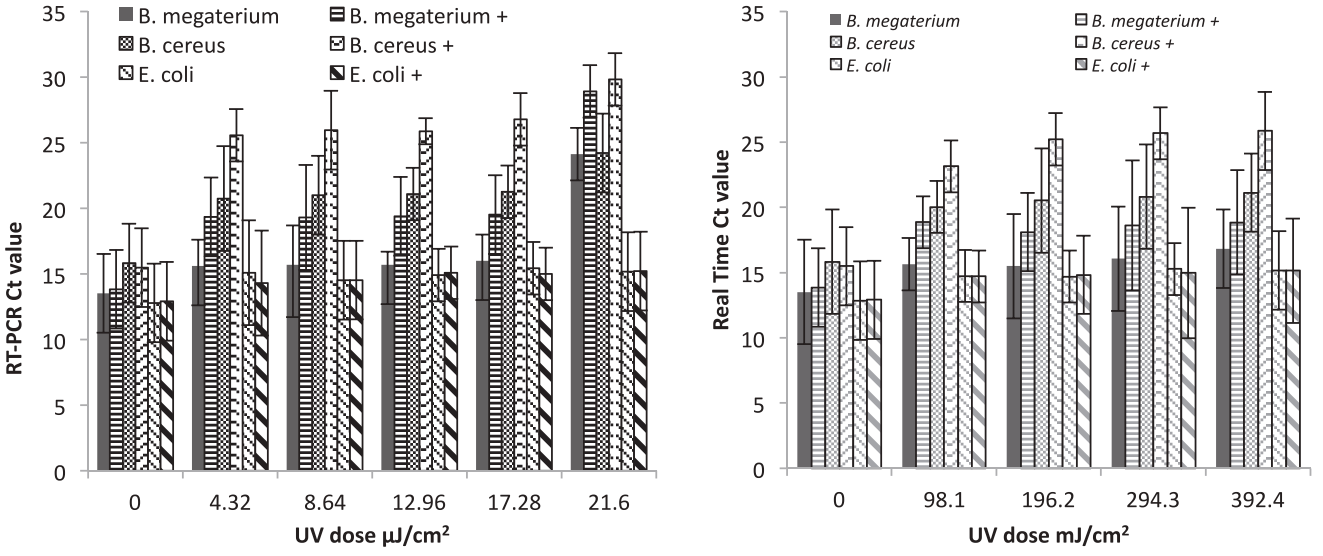

Figure 4—Ct value resulting from RT-PCR analysis of a) PUV-treated and b) LPUV-treated test species with (+) and without the addition of PMA dye as a PCR blocking agent (±S.D).

Table 1—Viability determination of heat inactivated test species (65 °C for 30 minutes) as determined by cfu/mL log_{10} reduction, RT-PCR Ct values and protein leakage (±S.D).

	Viability			
		Ct value		
Test organism	Log_{10} reduction	PMA –	PMA +	Protein (μg/mL)
B. megaterium	0	13.52 (±2.2)[a]	14.85 (±2.1)[a]	294.89 (±2.1)[I]
	7.3 (±0.2)	18.83 (±2.2)[c]	24.22 (±1.2)[d]	392.96 (±1.2)[II]
B. cereus	0	15.82 (±1.1)[b]	15.49 (±1.5)[b]	297.01 (±1.8)[I]
	5.2 (±0.2)	18.62 (±2.2)[c]	24.41(±1.2)[d]	382.27 (±2.2)[III]
E. coli	0	15.82 (±1.1)[b]	15.49 (±1.5)[b]	297.01 (±2.8)[I]
	8.0 (±0.2)	15.65 (±2.2)[a]	15.11 (±2.2)[a]	356.63 (±1.2)[IIII]

[a, b, c, d, I, II, III, IIII] donate significant difference ($p \leq 0.05$).

were seen for the LPUV inactivation of the *Bacillus* test species (Figure 3), although the variation in the Ct values was smaller than that observed with pulsed light. This suggests that the binding of PMA to the DNA of nonviable cells is occurring. Furthermore, for both PUV and LPUV, the Ct values for *E. coli* were very similar with and without the addition of PMA. Indeed there was no significant difference ($p \leq 0.05$) between the values obtained in the absence or presence of PMA dye. This would suggest that the cross-linking of PMA to the DNA either did not occur or did not prevent amplification for *E. coli* even to the extent it did with the *Bacillus* test species. The corresponding viability cell count showed a maximal ca. 8 log_{10} inactivation for both UV methods applied.

Membrane Protein Leakage of Treated Cells. Quantification of protein resulting from membrane leakage pre- and post-UV studies was conducted as a means to verify membrane damage of treated organisms. Additionally, membrane leakage of protein following heat inactivation served as a positive control (Table 1). The equation of the line obtained for protein content versus absorbance was used to calculate the concentration of protein leakage for disinfection studies. There was a significant difference ($p < 0.05$) between the quantity of protein for the untreated control and heat-inactivated bacteria for all test strains. Additionally, this coincided with a significant difference in the Ct value for heat-inactivated *Bacillus* samples with an increase in Ct value following the addition of the PMA dye. As expected, heat inactivation resulted in membrane damage to an extent that allowed for an increase in protein leakage of ca. 100 μg/mL. These findings indicate that the operational conditions of this assay were correct. Furthermore, there was a significant difference in the Ct values (ca. 6 Ct) obtained following PMA binding for *Bacillus*. However, this cross-linking of the PMA with DNA preventing PCR amplification for both *Bacillus* species did not occur to an extent corresponding to the loss in viability as determined via the cultivation method. Similar to the findings of the PUV studies, the difference in Ct value does not correspond to the predicted value for the remaining viable population of cells. Additionally, as observed for the UV studies there was no significant difference in the Ct values with the addition of the PMA dye for *E. coli*. For all PUV-treated samples, there was also a significant difference in protein leakage compared to the untreated control (Table 1). Indeed with a PUV dose of 21.6 μJ/cm^2, the protein content increased to ca. 330 μg/mL for *B. megaterium, B. cereus*, and *E. coli*—an increase of ca. 30 μg/mL protein (Figure 2). This indicates that membrane damage occurred, albeit to a lesser extent than the heat-inactivated cells following PUV treatment for all test strains. Furthermore, the amount of protein leakage following LPUV treatment was not to the same extent as PUV. There was no significant increase in protein leakage for all strains tested with up to and including 12 minutes of LPUV exposure (392.4 mJ/cm^2) (Figure 3). Therefore, studies suggest that PUV light does result in some cellular membrane damage for the Gram-negative and Gram-positive species tested as determined by the quantification of protein leakage. And no such damage was detected for the same species when exposed to LPUV inactivation.

Findings suggest indescrepencies between PCR-detected viability, CFU counts, and protein leakage for UV-treated and heat-inactivated organisms. One possible explanation for this is the presence of viable but nonculturable bacteria. Microbial cells, when under stress conditions such as that caused by extensive UV exposure, can enter a physiological state that prevents normal activities of growth and cell division. In this state, some cells die and some survive, the latter being labelled as viable but nonculturable cells (VBNC), as they cannot be cultured on laboratory media. In this state, metabolic function is reduced to a baseline level, making detecting their presence relatively challenging. Additionally, they may be transported to water and food where they may grow, divide, and, in the case of VBNC, pathogens cause infection (Trevors, 2011). The results of this study show PCR amplification not corresponding to the cell viability as determined by cell count, even though protein leakage occurred suggesting that the PUV system induced membrane damage in the bacteria. Studies by Kramer and Muranyi (2014) showed a significant discrepancy between conventional plate counts and different viability staining parameters for PUV-treated *Listeria* and *E. coli*. The authors concluded that pulsed light treatment does not cause an immediate shutdown of vitality functions even when the number of CFUs already decreased for more than 6 log_{10} sample (Kramer and Muranyi, 2014). Findings showed that oxidative stress with associated damage to the DNA molecule was directly responsible for the loss of cultivability due to pulsed light rather than a direct rupture of cell membranes or inactivation of intracellular enzymes (Kramer and Muranyi, 2014). Additionally, studies by Berney et al. (2006) reported that the cytoplasmic membrane of *E. coli* becomes permeable to dyes as a final outcome of pulsed

light treatment after the cessation of activities such as ATP production, glucose uptake, and the activity of the proton efflux pump (Berney et al., 2006). As a result, a loss in culturability occurred in growth medium before membrane permeability occurred, allowing for the uptake of dyes. In the present study, protein leakage did not occur to the same extent for pulse light–treated cells as did that for heat; therefore, there may have been insufficient membrane damage or permeabilisation caused to allow adequate dye uptake for blocking PCR for the test species. Furthermore, there was significantly less protein leakage for *E. coli* for PUV treatment, suggesting that even less cell permeabilisation occurred for this species. Gram-negative cell structure is different from Gram-positive in its lipid and protein content; this may have affected the ability of the pulsed light to induce membrane damage. Additionally, many studies report on the increased sensitivity of Gram-positive species over Gram-negative when exposed to UV light (Garvey et al., 2012; Rowan et al., 1999).

The findings of this study highlight the importance of using alternative viability indicators, together with culturability, to determine the viability state of treated bacterial cells, particularly when using a method that may induce a viable but nonculturable state in cell populations, because the standard plate count approach may underestimate the actual number of viable cells present.

Conclusions

- Findings described show that PUV provides a much faster inactivation of test species than standard low-pressure lamps.
- Pulsed UV induced membrane damage of all test species as determined via measurement of protein leakage compared to the untreated control. However, the level of protein leakage was not to the same extent as heat-inactivated cells indicating cell permeabilization was reduced.
- This membrane damage was not detected for strains inactivated with an LPUV lamp.
- The RT-PCR assay combining the use of a DNA intercalating dye provided an indication of cell death for the *Bacillus* species to some extent. However, it was not to the same level as the cultivation method using standard plate counts, suggesting a viable but nonculturable state was present.
- There was no significant difference for the RT-PCR results following the addition of the dye for *E. coli*, suggesting that PMA did not prevent the amplification of dead cell DNA.
- Findings may suggest the presence of viable but non-culturable cells within the treated population.

Acknowledgments

All research studies were funded by the Bioscience Research Institute, Athlone Institute of Technology, Athlone, Westmeath, Ireland. The authors would like to acknowledge the assistance of Dr. Niall McGuinness, Institute of Technology, Sligo, Ireland.

Submitted for publication April 14, 2015; revised manuscript submitted July 25, 2015; accepted for publication September 16, 2015.

References

Abida, J.; Rayees, B.; Masoodi, F. A. (2014) Pulsed Light Technology: A Novel Method for Food Preservation. *Int. Food Res. J.*, **21** (3), 839-848.

Berney, M.; Weilenmann, U. H.; Egli, T. (2006) Flow-cytometric Study of Vital Cellular Functions in Escherichia coli During Solar Disinfection (SODIS). *Microbiology*, **152,** 1719-1729. DOI: 10.1099/mic.0.28617-0.

Farrell, P. H.; Garvey, M.; Rowan, N. (2009) *J. Appl. Microbiol*. DOI: 10.1111/j.1365-2672.2009.04545.x.

Farrell H.; Hayes J.; Laffey J.; Rowan, N. (2011) Studies on the Relationship Between Pulsed UV Light Irradiation and the Simultaneous Occurrence of Molecular and Cellular Damage in Clinically-Relevant Candida Albicans. *J. Microbiol. Methods*, **84,** 317-326.

Ferrario, M.; Guerrero, S. (2014) Study of Pulsed Light Induced Damage on Saccharomyces Cerevisiae in Apple Juice by Flow Cytometry and Tramission Electron Microscopy. *Food Bioprocess. Technol.*, **7,** 1001-1011.

Garvey, M.; Clifford, E.; O'Reilly, E.; Rowan, N. (2012) Efficacy of Using Harmless *Bacillus* Endospores as Novel Surrogate Organisms to Indicate the Inactivation Performance of Recalcitrant *Cryptosporidium parvum* Oocysts Suspended in Water Using Pulsed UV Light. *J. Parasit.*, **99** (3).

Garvey, M.; Stocca, A.; Rowan, N. (2014) Development of a Combined in Vitro Cell Culture—Quantitative PCR Assay for Evaluating the Disinfection Performance of Pulsed Light for Treating the Waterborne Enteroparasite Giardia lamblia. DOI: 10.1016/j.exppara.2014.06.001.

Gensberger, T. E.; Polt, M.; Konrad-Keoszler, M.; Kinner, P.; Sessitsch, A; Kosti, T. (2014) Evaluation of Quantitative PCR Combined with PMA Treatment for Molecular Assessment of Microbial Water Quality. *Water Res.*, **67,** 367-376.

Kesmen, Z.; Yetiman, A. E.; Yetim, H. (2011) Determination of Viability of Food-Borne Bacterial Pathogens in Milk by Using PMA/Real-Time PCR Technique. *Curr. Opin. Biotechnol.*, **22,** S100.

Kramer, B.; Muranyi, P. (2014) Effect of Pulsed Light on Structural and Physiological Properties of Listeria innocua and Escherichia coli. *J. Appl. Microbiol.*, **116** (3), 596-611. DOI: 10.1111/jam.12394. Epub 2013 Dec 5.

Krishnamurthy, K.; Tewari C. J.; Irudayaraj, J.; Demirci, A. (2008) Microscopic and Spectroscopic Evaluation of Inactivation of *Staphylococcus aureus* by Pulsed UV Light and Infrared Heating. *Food Bioprocess. Technol.* DOI: 10.1007/s11947-008-0084-8.

Nayak, K. P.; KumarMohanty, A.; Gaonkar, T.; Kumar, A.; Bhosle, N. S.; Garg, S. (2013) Rapid Identification of Polyhydroxyalkanoate Accumulating Members of Bacillales Using Internal Primers for phaC Gene of Bacillus megaterium. *ISRN Bacteriol.*, Article ID 562014, http://dx.doi.org/10.1155/2013/562014 (accessed Sept 21, 2015).

Rowan, J. N.; MacGregor, J. S.; Anderson, J. G.; Fouracre, R. A.; McIlvaney, L.; Fairish, O. (1999) Pulsed-Light Inactivation of Food-Related Microorganisms. *Appl. Environ. Microbiol.*, **65** (3), 1312-1315.

Spano, G.; Beneduce, L.; Terzi, V.; Stanca, M. A.; Massa, S. (2005) Real-time PCR for the Detection of *Escherichia coli* O157:H7 In Dairy and Cattle Wastewater. *Lett. Appl. Microbiol.*, **40,** 164-171. DOI: 10.1111/j.1472-765X.2004.01634.x.

Taskin, B.; Gozen, G. A.; Duran, M. (2011) Selective Quantification of Viable Escherichia coli Bacteria in Biosolids by Quantitative PCR with Propidium Monoazide Modification. *Appl. Environ. Microbiol.*, **77** (13), 4329. DOI: 10.1128/AEM.02895-10.

Trevors, T. J. (2011) Viable but Non-Culturable (VBNC) Bacteria: Gene Expression in Planktonic and Biofilm Cells. *J. Microbiol. Methods*, **86** (2), 266-273.

ELSEVIER

Trends in Food Science & Technology xx (2015) 1–14

TRENDS IN FOOD SCIENCE & TECHNOLOGY

Review

A review of quantitative methods to describe efficacy of pulsed light generated inactivation data that embraces the occurrence of viable but non culturable state microorganisms

Neil J. Rowan[a,1], Vasilis P. Valdramidis[b,2] and Vicente M. Gómez-López[c,*]

[a]Bioscience Research Institute, Athlone Institute of Technology, Dublin Road, Athlone Co., Westmeath, Ireland (e-mail: nrowan@ait.ie)

[b]Department of Food Studies & Environmental Health, Faculty of Health Sciences, University of Malta, Msida, MSD 2080, Malta (e-mail: vasilis.valdramidis@um.edu.mt)

[c]Cátedra Alimentos para la Salud, UCAM Universidad Católica San Antonio de Murcia, Campus de los Jerónimos 135, Guadalupe, 30107, Murcia, Spain (Tel.: +34 968 278 368; e-mail: vmgomez@ucam.edu)

The purpose of this timely review is to critically appraise and to assess the potential significance of best-published microbial inactivation kinetic data generated by pulsed light (PL). The importance of selecting different inactivation models to describe the PL inactivation kinetics is highlighted. Current methods for the detection of viable-but-nonculturable (VBNC) organisms post PL-treatments are outlined along with the limitations of these methods within food microbiology. Greater emphasis should be placed on elucidating appropriate inactivation kinetic model(s) to cater for the occurrence of these VBNC organisms that are underestimated in number using traditional culture-based enumeration methods. Finally, the importance of further molecular and combinational research to tackle the potential threat posed by VBNC organisms with regard to kinetic inactivation modelling and nexus to public health and food safety is presented.

Introduction

Recent developments among consumers regarding the demand for fresh, minimally processed foods with a preferably long shelf life has resulted in emerging research into new non-thermal technologies to ensure appropriate preservation and safety of treated foodstuffs. However, this growing consumer preference for minimally processed foodstuffs is accompanied by public health concerns surrounding efficacy of such approaches to adequately deal with food-borne diseases (Kramer & Muranyi, 2014; Rowan, 2004). The trend towards fresh-cut produce usually cannot be decontaminated by conventional thermal methods, and washing or sanitizing approaches do not provide a sufficient reduction in microbial numbers to afford safety consumers (Sapers, 2001). Therefore, there is a pressing requirement for the development of nonthermal decontamination approaches to meet these demands and to address the requirement for producing safe fresh produce.

Pulsed light (PL) is a non-thermal method for microbial inactivation based in the application of one or several high power ultra-short duration pulses of broad spectrum light between 200 and 1100 nm (Gómez-López, Ragaert,

* Corresponding author.
[1] Tel.: +353 90 647 3081.
[2] Tel.: +356 23401157.

http://dx.doi.org/10.1016/j.tifs.2015.03.006

Debevere, & Devlieghere, 2007). Typical processing times are in the order of few seconds and besides its advantages of rapid and cost-effective treatments, PL does not leave any unwanted residual compounds on foodstuffs. PL is a fast and cost effective process where considerable research has already proved its efficiency for killing various microbial pathogens and spoilage species in or on various matrices (Farrell, Garvey, Cormican, Laffey, & Rowan, 2009; Farrell, Garvey, & Rowan, 2009; Gómez-López, Devlieghere, Bonduelle, & Debevere, 2005; Hayes, Kirf, Garvey, & Rowan, 2013; Hayes, Laffey, McNeil, & Rowan, 2012; Levy, Aubert, Lacour, & Carlin, 2012; Rowan, Kirf, & Tomkins, 2009; Woodling & Moraru, 2007). As many other microbial inactivation technologies, the appropriate characterization of the kinetics of microbial inactivation is fundamental for process optimization.

Data generated for PL inactivation kinetics is represented as function of several parameters, such as fluence, treatment time and number of pulses. As a photochemical process, fluence is the best parameter up to now to characterize PL effects since it provides information on the amount of energy impinging the object, and can allow results intercomparison and scaling up. The latest update of the glossary of terms used in photochemistry of the IUPAC (Braslavsky, 2007) that defines fluence as the radiant energy "incident on a small sphere from all directions divided by the cross-sectional area of that sphere", with SI units in J/m^2, although J/cm^2 is more commonly used in PL. Units such as J/g or J/l refer to dose (absorbed energy) (Braslavsky, 2007), but PL dosimetry usually measures impinging energy and most of the UV light is not absorbed by microorganisms (Bolton & Linden, 2003). The small number of authors using those units should be encouraged to elaborate on the rationale and justification underpinning its use. Nonetheless, the shape of inactivation curves is the same regardless of the use of fluence, time or number of pulses as independent variable or the units using to characterize population changes (CFU/ml or CFU/g) since the dynamics of microbial inactivation depends on the impinging energy.

In order to achieve a safe food, foodborne pathogens must be killed by applying suitable fluence. However, loss of culturability is typically taken as the single criteria for determining cell death where no deeper investigations into associated molecular or physiological contributing factors that underpin PL-mediated killing of treated microbial cells are examined. A performance criteria must be achieved by the treatment, such as the minimum 5-log reduction in pertinent microorganism required by the FDA to cider and juice processors (FDA, 2001). Despite the fact that inactivation curves by PL technology are framed exclusively on culture-based methods, no published study to date has reported on the significance or impact (if any) of variations observed in different inactivation kinetic plots in terms of PL treatment efficacy.

Inactivation mechanism by pulsed light, in brief

Since the kinetics of microbial inactivation is related to the inactivation mechanism, a brief overview of PL inactivation mechanism is provided here. It is generally assumed that the UV component is the most important wavelength region for the bactericidal effects of PL (Gomez-Lopez *et al.*, 2007) as UV illumination causes photochemical modification of microbial genomic material mainly by the photocatalytic formation of cyclobutane thymine dimmers and by causing a variety of mutagenic and cytotoxic DNA lesions (Bohrerova, Shemer, Lantis, Impellitteri, & Linden, 2008). Wang, MacGregor, Anderson, and Woolsey (2005) showed that the maximum inactivation of *Escherichia coli* by PL is obtained at 270 nm, a wavelength that is highly absorbed by DNA. Conversely, studies have also reported on the irreversible disruption of microbial cells by PL implying that destruction is caused by a multi-target process comprising inter-related photochemical, photothermal or photophysical effects (Cheigh, Park, Chung, Shin, & Park, 2012; Farrell, Hayes, Laffey, & Rowan, 2011; Kramer & Muranyi, 2014; Krishnamurthy, Tewari, Irudayaraj, & Demirci, 2010; Takeshita *et al.*, 2003; Wekhof, 2000). Photophysical effects relate to structural damages occasioned by the constant disturbance caused by the high-energy pulses. While photothermal effects relates to the localized heating of microbial cells due to light pulses that can lead to cell explosion (Krishnamurthy *et al.*, 2010). In such instances, exploded microbial cells are incapable of entering the VBNC state.

Models describing the microbial inactivation by pulsed light

Quality and safety kinetics can be described by mathematical models using theoretical analysis and experimental results. Depending on the mechanistic knowledge upon which these models are built, they can be subdivided into deductive or inductive (Hills, 2001), also described as mechanistic or empirical (McDonald & Sun, 1999). Deductive kinetic models are based on the general laws, that is, (bio) chemical/physical, and use them to build realistic mathematical expressions, while inductive models have as a starting point the available data. The exact mechanism of PL induced lethality has not been fully characterized and, most importantly, has not been translated to quantitative measures that could be used for developing equations. For this reasons, most of the published models used to describe inactivation curves by PL treatments have been built on inductive approaches, as they are not based on *a priori* knowledge of the underlying biological mechanisms. Nevertheless, the existing modelling approaches can be further exploited to quantitatively describe the influence of processing conditions on the properties of the studied substrates, e.g., to assess the food safety of a product treated by PL. This review revises the modelling structures published in PL literature so far. These structures are

Please cite this article in press as: Rowan, N. J., et al., A review of quantitative methods to describe efficacy of pulsed light generated inactivation data that embraces the occurrence of viable but non culturable state microorganisms, Trends in Food Science & Technology (2015), http://dx.doi.org/10.1016/j.tifs.2015.03.006

described based on the previous re-parametrisation or normalisation e.g., log transformation of the microbial populations, and transformations advised by the authors of this chapter for permitting easy parameter identification. It is noteworthy that the use of the independent variable changes depending on how the experiments are built and data are collected, in some cases is fluence (in units of J/cm^2) and in others time (in units of second). Hereafter, the models are given in the original version that have been reported in the literature; with appropriate transformation fluence and time could be interchanged. An overview of these mathematical structures and features can be seen in Fig. 1.

The description of each model is given below together with examples of their use to describe PL inactivation kinetics of several microorganisms in different substrates. In order to assess the relation between a certain microorganism-matrix pair and a specific model, one must be aware of the way that such relationship is established because of the variety of analysis approach by the different authors. Some authors report the fitting capacity of a single model, while others test several ones and choose the best fit. Even this approach differs in the use of a variety of statistical indexes. Therefore, for a given dataset, it cannot be excluded that another non-tested model may have had a better fitting capacity. It is important to consider that not all data is considered relevant for performing regression analysis studies. For example, survival data should exhibit at least a reduction of 1 log unit, which is considered to be within the range of the experimental error in plate count data (Mossel, Corry, Struijk, & Baird, 1995). Additionally, for a particular combination of conditions a minimum of 10 data points should be collected and, the majority of them, should be positioned at areas of inflection where the rate of change of the microbial kinetics is maximal (Walker & Jones, 1993).

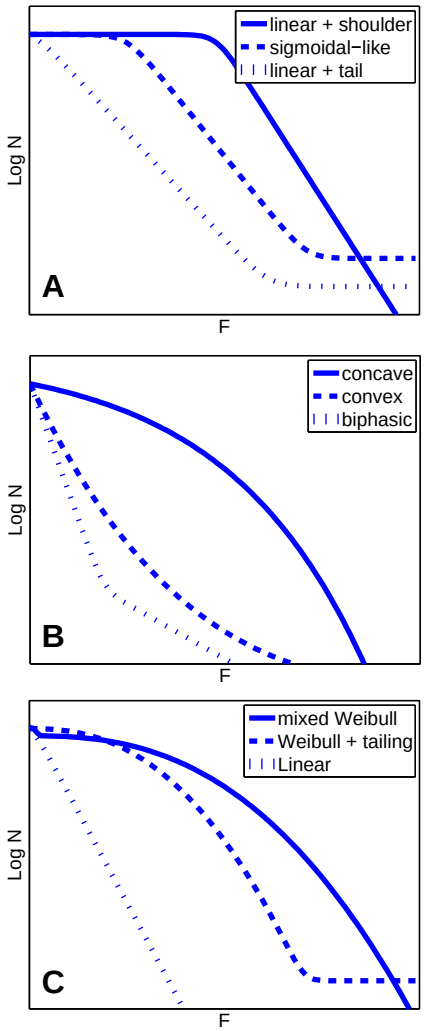

Fig. 1. Commonly observed types of inactivation curves during PL processing expressed as $\log_{10}$ *N* versus *F*. Plot A: sigmoidal-like, linear with a preceding shoulder, log-linear with a tailing. Plot B: biphasic, concave upwards or downwards. Plot C: Linear, Weibull incorporating a tailing effect, two mixed Weibullian distributions.

All current published inactivation curves have been generated in batch systems, in the case of liquids, for example, pouring it in a test cell, which could be a conventional Petri dish. Few cases use an orbital shaker to promote turbulence and generate a homogeneous exposure of the liquid (Miller, Sauer, & Moraru, 2012; Sauer & Moraru, 2009).

Log-linear model

The model of Bigelow (1921) to describe log-linear kinetics has been applied for PL studies, as reported by Izquier & Gomez-Lopez (2011) for decontamination of vegetable surfaces.

$$\log_{10}(N_f) = \log_{10}(N_o) - k_{\max} \cdot \frac{F}{\ln(10)} \quad (1)$$

This version replaces the original use of treatment time as independent variable by F (fluence, J/cm^2). N_f (CFU/g) is the number of survivors, N_0 (CFU/g) is the initial number of microorganisms, and k_{max} is the inactivation rate (cm^2/J).

Table 1 shows the literature where the log-linear model has been used. It is noteworthy that the log-linear pattern has not been identified when foods are the substrate.

Biphasic model

The model of Bigelow (1921) can be extended for describing two subpopulations with different microbial resistances. The biphasic model described originally by Cerf (1977) is a classic example. Ferrario, Alzamora, and Guerrero (2013) used a version that reads as follows:

$$\log_{10}(N_f) = \log_{10}(N_o) + \log_{10}(f \cdot \exp(-k_{\max 1} \cdot t) + (1-f) \cdot \exp(-k_{\max 2} \cdot t)) \quad (2)$$

Where f is the fraction of the initial population corresponding to the subpopulation more sensitive to the treatment, (1-f) is the fraction of the initial population corresponding to the subpopulation more resistant to the treatment and k_{max1}

Please cite this article in press as: Rowan, N. J., et al., A review of quantitative methods to describe efficacy of pulsed light generated inactivation data that embraces the occurrence of viable but non culturable state microorganisms, Trends in Food Science & Technology (2015), http://dx.doi.org/10.1016/j.tifs.2015.03.006

Table 1. Microorganism-matrix combinations following the log-linear model.

Microorganism	Matrix	Reference
E. coli	Water	Otaki *et al.* (2003)
E. coli	Agar	Farrell, Garvey, Cormican, *et al.* (2009)
Listeria monocytogenes	Agar	Bradley, McNeil, Laffey, and Rowan (2012)
Pseudomonas aeruginosa	Buffer	Ben Said and Otaki (2013)
Zygosaccharomyces bailii	Glucose solutions	Hayes *et al.* (2012)
Zygosaccharomyces rouxii	Glucose solutions	Hayes *et al.* (2012)
Saccharomyces cerevisiae	Glucose solutions	Hayes *et al.* (2012)
Coliphage T4	Water	Otaki *et al.* (2003)

and k_{max2} are the specific inactivation rates of the two populations, respectively.

This model has been used by only one research group (Ferrario *et al.*, 2013), which described the kinetics of PL microbial inactivation for *E. coli* in commercial and natural apple juice and commercial orange juice, and *Listeria innocua* and *Saccharomyces cerevisiae* in natural apple juice. It is obvious that the model has only been used to describe the inactivation by PL in fruit juices and by only one research group. These inactivation curves were characterized by a higher sensitive subpopulation ($f > 0.77$).

Sigmoidal model

The microbial responses could be more complicated and follow a more sigmoidal like behaviour, composed by three distinctive phases: a shoulder, a log-linear inactivation phase and a tail. Geeraerd, Herremans, & Van Impe (2000) developed a mathematical structure that can describe this behaviour, and it is presented in the following equation:

$$\log_{10}(N_f) = \log_{10}\left(10^{\log_{10}(N_o)} - 10^{\log_{10}(N_{res})}\right) + \log_{10}\left(\exp(-k_{\max}\cdot t)\cdot\frac{\exp(k_{\max}\cdot S_l)}{1+(\exp(k_{\max}\cdot S_l)-1)\cdot\exp(k_{\max}\cdot t)} + 10^{\log_{10}(N_{res})}\right) \quad (3)$$

This structure (appearing here with the most recent modifications reported by Valdramidis *et al.* (2004)) was considered by Marquenie *et al.* (2003) using t (in seconds) as independent variable. S_l [min] is a parameter that stands for the length of the shoulder. Similarly to the previous models k_{max} is the specific inactivation rate [1/min], and N_{res} is the residual population density [CFU/ml].

This equation can be reduced to the following structure if tailing is not present in the collected data:

$$\log_{10}(N_f) = \log_{10}(N_o) + \log_{10}\left(\exp(-k_{\max}\cdot t)\cdot\frac{\exp(k_{\max}\cdot S_l)}{1+(\exp(k_{\max}\cdot S_l)-1)\cdot\exp(k_{\max}\cdot t)}\right) \quad (4)$$

If tailing is present but not shoulder, the equation takes the following form:

$$\log_{10}(N_f) = \log_{10}\left(10^{\log_{10}(N_o)} - 10^{\log_{10}(N_{res})}\right) + \log_{10}\left(\exp(-k_{\max}\cdot F) + 10^{\log_{10}(N_{res})}\right) \quad (5)$$

The latter structure has been considered by Izquier and Gómez-López (2011) having F as independent variable in the place of t.

The sigmoidal model has been applied for the description of the PL inactivation kinetics on agar of *L. innocua* (Lasagabaster & Martínez, 2014) and *Salmonella* Typhimurium (Luksiene, Gudelis, Buchovec, & Raudeliuniene, 2007), and the fungi *Botrytis cinerea* and *Monilia fructigena* on agar (Marquenie *et al.*, 2003). Nevertheless, this does not imply that all fungi follow this inactivation pattern. For example, Aron-Maftei, Ramos-Villarroel, Nicolau, Martín-Belloso, and Soliva-Fortuny (2014) reported no shoulder in the inactivation of naturally occurring moulds on wheat grain.

Weibull model

The Weibull model is a structure that is commonly used for describing non-linear kinetics. Different notations have been used for describing this model. One of these structures reads as follows:

$$\log_{10}(N_f) = \log_{10}(N_o) - (F/\delta)^p \quad (6)$$

where δ (J/cm^2) is the fluence for the first decimal reduction, and p (dimensionless) is a parameter describing

Please cite this article in press as: Rowan, N. J., et al., A review of quantifying methods to describe efficacy of pulsed light generated inactivation data that embraces the occurrence of viable but non culturable state microorganisms, Trends in Food Science & Technology (2015), http://dx.doi.org/10.1016/j.tifs.2015.03.006

downward or upward concavity of the curve. The same type of equation has been considered from several researchers by using in some cases different notations, for example, a constant multiplied factors (e.g., multiplied by 1/2.303), α instead of δ and p instead of β or sometimes by considering the use of time instead of the fluence as the studied independent variable, e.g., (Bialka, Demirci, & Puri, 2008; Keklik, Demirci, Puri, & Heinemann, 2012; Sauer & Moraru, 2009). The Weibull model is also used (refer to Ferrario *et al*., 2013; Uesugi, Woodling, & Moraru, 2007) in a re-parameterized form (Peleg & Cole, 1998), which reads as follows:

$$log_{10}(N_f) = log_{10}(N_o) - b \cdot t^n \quad (7)$$

In a similar way, the b value in the Weibull distribution function represents the rate of inactivation of the cells, while n indicates the concavity of the survival curve ($n > 1$ refers to downward concavity and $n < 1$ to upward concavity). In all cases reported for microbial inactivation by PL $n < 1$, that means that the inactivation gets slower with the progress of the treatment.

It has to be highlighted that the direct comparison between the different estimated parameters is hampered by the variety of parameterizations and independent variables, which can be overcome by the standardisation of the Weibull model structure used by the different research groups. Previous researchers (refer to Mafart, Couvert, Gaillard, & Leguerinel, 2002) have shown interest on the use of Equation (6) mainly because parameter δ describes the time for the first log reduction and can permit direct comparison between numerous case studies.

The Weibull model is the most frequently used in the literature describing the inactivation of microorganisms by PL (Table 2). It has been applied for the inactivation kinetics of Gram positive and Gram negative bacteria *in vitro* and on food contact surfaces, milk, meat products and fruit and vegetables.

Weibull with tail

Albert and Mafart (2005) extended the Weibull modelling structure for incorporating a tailing effect. When F is the independent variable, the reparameterisation results in the following model:

$$\log_{10}(N_f) = \log_{10}N_o \left[\left(10^{\log_{10}(N_o)} - 10^{\log_{10}(N_{res})}\right) \cdot 10^{\left(-\left(\frac{F}{F_1}\right)^p\right)} + 10^{\log_{10}(N_{res})} \right] \quad (8)$$

Where N_f is the number of CFU after treatment at a fluence F, N_o is the initial number of the tested microorganism (in CFU/mL or CFU/gr depending on how people report their experimental data), N_{res} is the number of surviving cells, F is the fluence applied (J/cm^2), F_1 is the fluence allowing the first $\log_{10}$ reduction and p is a parameter which determines the direction of curve concavity exactly as for equation (7). This equation was studied by Esbelin, Mallea, Ram, and Carlin (2013) to describe the inactivation of *Aspergillus niger* spores, and Cheigh, Hwang, and Chung (2013) for the kinetics of

Table 2. Microorganism-matrix combinations following the Weibull model grouped by its different reparameterizations.

Microorganism	Matrix	Reference
E. coli O157:H7	Strawberry	Bialka *et al.* (2008)
	Cider	Sauer and Moraru (2009)
	Apple juice	
E. coli	Buffer	Hsu and Moraru (2011)
	Skim milk	Miller *et al.* (2012)
	Whole milk	
Listeria monocytogenes	Chicken frankfurters	Keklik *et al.* (2012)
Listeria innocua	Clear liquid	Uesugi *et al.* (2007)
	Buffer	Hsu and Moraru (2011)
	Plastics	Ringus and Moraru (2013)
	Commercial orange juice	Ferrario *et al.* (2013)
	Natural melon juice	
Salmonella Typhimurium	Chicken breast	Keklik *et al.* (2012)
Salmonella Enteritidis	Shell eggs	Keklik *et al.* (2012)
	Natural apple juice	Ferrario *et al.* (2013)
Natural microflora	Lettuce	Izquier and Gómez-López (2011)
	Cabbage	
	Carrots	

Please cite this article in press as: Rowan, N. J., et al., A review of quantitative methods to describe efficacy of pulsed light generated inactivation data that embraces the occurrence of viable but non culturable state microorganisms, Trends in Food Science & Technology (2015), http://dx.doi.org/10.1016/j.tifs.2015.03.006

Listeria monocytogenes inactivation on fillets of salmon, flatfish and shrimp.

Mixed Weibull model

$$\log_{10}N_f = \log_{10}N_o + \log_{10}\left(\frac{1}{1+10^{\alpha}}\right) + \log_{10}\left[10^{\left(-\left(\frac{t}{\delta_1}\right)^{p+\alpha}\right)} + 10^{\left(-\left(\frac{t}{\delta_2}\right)^{p}\right)}\right] \quad (9)$$

Ferrario *et al.* (2013) used the two mixed Weibulian distributions of Coroller, Leguerinel, Mettler, Savy, and Mafart (2006) which could describe the kinetics of subpopulations having different resistance,where t (seconds) is used instead of F, p is a shape parameter, α is the $\log_{10}$ proportion between the sensitive fraction (f) and the resistant one (1 - f), δ_1 and δ_2 are the time for the first decimal reduction of the subpopulation 1 and subpopulation 2, respectively. The authors found that this equation was the best for describing the PL inactivation of *Salmonella* Enteritidis in commercial apple juice and *S. cerevisiae* in that matrix and in natural melon juice.

Interpreting the models

It is not clear why a specific microorganism differs in the pattern of inactivation (applied kinetic model) as function of the substrate. While tailing is more likely to occur in irregular solid opaque substrates than in stirred liquids due to shadow effects, other factors regulating how lethality curves deviate from linearity remain obscure. A clear effect of experimental conditions can be seen in some liquids, where the inactivation curve differs between tests performed under static or turbulent conditions. In the case of *E. coli* inoculated in apple juice, sample shaking causes that tailing occurs at higher inactivation levels in turbulent tests in comparison to static tests leading to a difference higher than 4 log in residual population (Sauer & Moraru, 2009). The turbulence effect is more drastic in milk inoculated with *E. coli*, where tailing appears at about 2 J/cm^2 under static conditions while the inactivation curve is linear even at 14.85 J/cm^2 under turbulence, which is also evidenced by the shape parameter, which is 0.13 for skin milk under static conditions and 0.98 under turbulence (Miller *et al.*, 2012). It is possible that under static conditions only the bacterial cells at the upper levels of the liquid column are reached by light, which gets attenuated when penetrates through the liquid sample. While shaking increase the homogeneity of the exposure of the bacterial population. These results are important from the practical point of view, since PL application to liquids will be likely performed in flow-through systems where turbulence can be promoted.

Subtle differences in data acquisition could lead to different kinetic models, for example, between biphasic and double Weibull, since even though a relatively high number of points could be used to build the inactivation curve, the portions of the curve determining which model yields the best fit could consist of relatively few points. As discussed earlier, the specific models tested in data analysis will not necessarily exclude the appropriateness of the rest. It is known that food matrix affect PL efficacy (Gómez-López *et al.*, 2005) due to competition with bacteria for light absorption, but other extrinsic factors may play a role, such as pH, which can in turn have synergistic or opposite influences in each one of the multi-target lethal inactivation process. Several possible explanations for the occurrence of some features of the PL inactivation curve are given below.

The shoulder phase of PL-generated inactivation kinetic data

While there are different models that include a shoulder, such as the log-linear with shoulder and the biphasic and shoulder (Geeraerd, Valdramidis, & Van Impe, 2005), only the sigmoidal model has been used to describe the PL inactivation kinetics. This fact should not be strange since cases of complete inactivation are very scarce, and the occurrence of tailing is common, and shoulders and tails give place to a sigmoidal pattern. The Weibull model can also fit shoulders although not explicitly (Geeraerd *et al.*, 2005) and could mask their existence, however the kinetic curves analyzed in this revision and described by the Weibull model show a sudden drop of survivor population after the first pulse. Besides the few microorganism-matrix combinations enumerated before, there are other few examples in the literature where shoulders appear evident such as the classical paper of MacGregor *et al.* (1998) on the inactivation of *E. coli*, *E. coli* O157:H7 and *L. monocytogenes*, and those by Farrell, Garvey, Cormican *et al.* (2009) and Farrell, Garvey and Rowan, (2009) on 13 bacteria and the yeast *Candida* respectively, and all of them on agar surfaces.

The biological meaning of the shoulder could be related to the multi-target nature of the microbial inactivation by PL; the damage initially occurring in microbial cells is not enough to make them become unculturable, until a threshold is reached where cells loss the capability to divide. This interpretation is in line with the so-called vitalistic approach (refer also to Geeraerd *et al.*, 2000). This

Please cite this article in press as: Rowan, N. J., et al., A review of quantitative methods to describe efficacy of pulsed light generated inactivation data that embraces the occurrence of viable but non culturable state microorganisms, Trends in Food Science & Technology (2015), http://dx.doi.org/10.1016/j.tifs.2015.03.006

threshold would not be reached until enough photons of adequate energy reach the target points of the microorganisms. The recovery methods can also influence the shoulder of inactivation curves, since there is a possible contributory role of variation in media formulation used for dilution, enumeration and resuscitation of treated cells such as oxygen scavengers. This is relevant as variation in absence or presence of shoulder affects could be attributed to damage of house keeping genes responsible for production of catalase and superoxide dismutase, which affect the ability of sub-populations of PL-treated cells to grow on highly nutritious media. Lewis (2000) described localised metabolic suicide as the ability for stress or damaged cells to tolerate oxygenated environs was decoupled. This, greater consideration must be placed of media design by way of resuscitation to address possible variability seen with shoulder plots.

Besides its biological meaning, it can be considered more important to assess its relevance in PL microbial inactivation. Taking into account the microbial inactivation curves characterized as per fluence basis, (Luksiene *et al.*, 2007) reported a shoulder length of just 0.08 mJ/cm^2, while Lasagabaster and Martínez (2014) reported 0.045–0.073 J/cm^2, which looks relatively irrelevant compared to the value of 12 J/cm^2, which is the maximum allowed by the FDA (1996). Moreover, a possible relationship between the existence of shoulder and the type of bacteria arises from the work of Farrell, Garvey, Cormican *et al.*(2009) where 13 bacteria were tested under similar conditions, the eight Gram positive bacteria exhibited shoulder but the five Gram negative not, with the exception of *Pseudomonas aeruginosa*, which showed a shoulder but only at the lowest lamp discharge, as it has been also reported for several species of *Candida* (Farrell, Garvey & Rowan, 2009).

It is possible that shoulders are missing from several inactivation curves reported in the literature because researchers applied already too high fluences for the first pulse, therefore specific tests using very low fluences could resolve shoulders. However, even though more basic research is needed based on fluence-characterized treatments to elucidate the possible presence of shoulder as a typical feature of PL inactivation curves, those results will be meaningful only from the point of view of fundamental research; from the point of view of practical implementation, very small shoulders could be disregarded for process design. The evidence accumulated so far indicates that shoulders are infrequently observed, and when so, too short to be relevant in practice.

The inactivation phase in PL-mediated inactivation kinetic data

Since all reported inactivation curves have been obtained by using culture methods, the inactivation can be primarily ascribed to the formation of cyclobutane pyrimidine dimmers, which give place to chlonogenic death: the loss of ability of cells to duplicate. Regarding the deviations of linearity, the mechanistic and the vitalistic concepts (developed quite some years ago by Cerf (1977) are the main concepts explaining these phenomena in predictive microbiology. According to the vitalistic concept, on one hand, individual cells are not identical (e.g., due to phenotypic variation between cells (Humpheson, Adams, Anderson, & Cole, 1998)) which can be assigned to a mechanism at the molecular level (Van Boekel, 2002), which may vary between individuals. Consequently, the non-identical behaviour resulting from exposure to stresses, which results to deviations from log linear inactivation kinetics at population level. This variation has been described by some authors in terms of the statistical properties of different underlying distributions (e.g., Weibull) of resistances or sensitivities (Mafart *et al.*, 2002; Peleg & Cole, 1998; Van Boekel, 2002). Possible approaches to validate the vitalistic theory could be to assess the resistance of microorganisms surviving more drastic treatments and compare it with the or assess the resistance of decreasingly smaller fractions of the population in order to determine whether the continuously decreasing death rate curves become progressively exponential as cell counts decrease.

On the other hand, considering the mechanistic theory as it was discussed and reviewed by Geeraerd *et al.* (2000) and Cerf (1977) deviations could be related to the fact that some micro-organisms are inaccessible by the main processing parameter (in the current case light), to acquired microbial resistance during the treatment, or to experimental artefacts, such as, clumping of micro-organisms, the presence of genetically different microbial populations or other experimental protocol issues.

The comparison of results should be performed carefully, especially with data analysed by the Weibull model where diverse reparameterizations have been used. Taken this into account, a limited insight on the effects of different variables on the kinetic parameters can be performed in spite of the relatively high amount of data derived from the Weibull model for PL inactivation. The effect of substrate on PL inactivation kinetics can be observed when *Salmonella enterica* is inactivated upon inoculation on different fruit surfaces. For example, α is 4.16 min on raspberry surface but much lower on strawberry surface (0.05 min), while β is 0.71 and 0.32 for raspberry and strawberry surfaces respectively (Bialka *et al.*, 2008). Another comparison shows also differences in the PL inactivation of *E. coli* in liquid substrates, with α 5.70 for buffer and 1.60 for apple juice (Hsu & Moraru, 2011).

The tail phase in PL-mediated inactivation kinetic data

There are some cases where a residual survival population persists at constant or nearly constant levels no matter how long the treatment is prolonged, which is known as tailing. Tailing seems to be common in the microbial inactivation by PL. From the practical point of view, it implies that once reached the tail, prolonging the treatment will not yield further microbial inactivation but it can deteriorate the

Please cite this article in press as: Rowan, N. J., et al., A review of quantitative methods to describe efficacy of pulsed light generated inactivation data that embraces the occurrence of viable but non culturable state microorganisms, Trends in Food Science & Technology (2015), http://dx.doi.org/10.1016/j.tifs.2015.03.006

food where the microorganism is. Having also in mind this practical implication, the null or nearly null microbial inactivation is not only present in those inactivation models in which the tail is explicitly present (sigmoidal, Weibull plus tail), but also in the inactivation curves where a second inactivation phase can have a very low inactivation rate. Furthermore, it is possible that tailing can emerge in inactivation curves where it has not being identified when higher fluences are applied, since complete inactivation has been rarely reported, Krishnamurthy, Demirci, and Irudayaraj (2007) is an exception.

There are several theories on the possible explanation of tailing, some general and others specific of the PL process. The vitalistic approach supports that the existence of different sub-populations can cause tailing when one sub-population is very resistant to the treatment (Marquenie *et al*., 2003). In the frame of a mechanistic theory, since UV light penetration is poor, any opaque body between the light source and the microorganism can shield it from inactivation, which is known as shadow effect. The shadow effect will then generate a tail in the inactivation curve because part of the microbial population will never be reached by light. In solids, microorganisms can be shielded by surface features such as the achnes of strawberries or the druplets of raspberries (Bialka *et al*., 2008) or by surface irregularities of food contact surfaces (Ringus & Moraru, 2013). In liquids, turbidity and suspended solids area main obstacles for microbial inactivation although appropriate mixing can maximize the exposure to light of all microorganisms present in the liquid mass (Gómez-López, Koutchma, & Linden, 2012). It has also demonstrated that high population densities can produce tailing when microorganisms overlap each other, those at the top get inactivated but simultaneously protect those at the bottom (Cudemos, Izquier, Medina-Martínez, & Gómez-López, 2013; Farrell, Garvey, Cormican *et al*., 2009), the same occurs in liquids when there is cumpling of cells (Uesugi *et al*., 2007). Another approach states that the probability of different targets being reached by photons is reduced when the survivor population is low (McDonald *et al*., 2000).

It is worth mentioning that the tailing could be just an experimental artefact, such asnon-homogeneity in illumination (Unluturk, Atilgan, Handan Baysal, & Tari, 2008). Special care must be taken in non-confounding tailing with reaching the maximum detectable level of inactivation (Lasagabaster & Martínez, 2013). The limit of detection defines the levels in which classical cultural microbiological methods can be performed. Some researchers tried to exclude this artifact by performing additional experiments based on Most Probably Numbers (Sauer & Moraru, 2009) and reporting the same deceleration. It is critical that new microbiological methods are developed to eliminate these experimental artifacts.

Zero or values below statistical significance in an enumeration test based on classical microbiological techniques may consist of artificial below the limit results. These results have been described as censored results that are not quantified but are assumed to be less than a threshold value (Duarte, 2013). Current trends in predictive microbiology are suggesting the use of these data by the applications of imputation, e.g. Lorimer and Kiermeier (2007) or maximum likelihood estimation methods, e.g., (Busschaert, Geeraerd, Uyttendaele, & Van Impe, 2011). These statistical approaches could stand as alternatives to novel microbiological techniques that can contribute to decreasing the levels of detection or enumeration of microbial bacteria.

Relevance of agar plate count culture data

While the foregoing sections have revealed significant differences in kinetic data attributed to PL-treatments, there is also a growing body of evidence to support the viewpoint that food technologies that rely exclusively on such agar plate count or growth-dependent enumeration (kinetic) data may very well be significantly underestimating the proportion of microbial survivors post PL treatments. Recent studies have shown that a still unknown proportion of microorganisms supposedly killed by PL enter what is commonly termed as a viable but not culturable (VBNC) state (Hayes *et al*., 2013; Kramer & Muranyi, 2014; Rowan, 1999, 2004). Consequently, there is a pressing need to establish whether or not existing culture-based kinetic models can be applied to VBNC organisms so that reliable and repeatable determination of their destruction post PL-treatment occurs. According to the early work of Oliver (1993), a bacterium in the VBNC state is defined as "a cell which is metabolically active, which being incapable of undergoing the cellular division required for growth in or on a medium normally supporting grown of that cell". While the relevance and significance of a VBNC microbial state post PL-processes have yet to be fully appreciated, molecular and combinational research suggests that a significant sub-population of non-culturable microorganisms retain pathogenicity that may pose a threat to public health and food safety (Fakruddin, Bin Mannan, & Stewart, 2013; Sardessai, 2005). The acknowledgement of the relevance of this phenomenon in PL treatment also raises questions as to the efficacy of using culture-based data alone for food safety determinations. While only a limited number of studies to date have investigated the impact of PL on microbial viability at the molecular and cellular level (Cheigh *et al*., 2012; Farrell *et al*., 2011; Kramer & Muranyi, 2014; Takeshita *et al*., 2003), they all have revealed alarming discrepancy between conventional plate counts and different viability staining parameters whereby PL-treatment does not cause immediate shutdown of vitality functions even when the number of colony forming units decreased by more than 6 $\log_{10}$ per sample.

Culture dependent vs culture independent methods for assessing pulsed light efficacy

Viable but non-culturable state

The evidence for the existence of VBNC cells has increased since the introduction of this concept by Byrd

and Colwell in the 1980's (Byrd, Xu, & Colwell, 1991), particularly in food and drink that elicits a myriad of inter-related sub-lethal microbial stresses such osmotic stress (Dunaev, Alanya, & Duran, 2008; Rowan, 2011; Sawaya, Kaneko, Fukushi, & Yaguchi, 2008). Microbial pathogens in VBNC state may still retain their capacity to cause infections (Cappelier, Besnard, Roche, Velge, & Federighi, 2007; Rowan, 2011). VBNC state microorganisms cannot be cultured on routine microbiological media, yet maintain their viability and pathogenicity. Unlike semi-starved bacteria, VBNC cells will not resume growth when nutrients and culture-friendly conditions are provided. Fakruddin *et al.* (2013) report that VBNC cells exhibit active metabolism in the form of respiration or fermentation (Besnard, Federighi, & Cappelier, 2000; Rowan *et al.*, 2008; Yaqub, Anderson, MacGregor, & Rowan, 2004), incorporate radioactive substances (Rollins & Colwell, 1986), and have active protein synthesis (Farrell *et al.*, 2011) but cannot be cultured or grown on conventional laboratory media. Albeit currently unknown in terms of its' severity or scope, recent observations reveal that environmentally-stressed pathogenic organisms that exist in the VBNC state may potentially present as yet an undefined risk to consumers. Rowan (2004, 2011) reported previously that VBNC organisms may potentially be more virulent that those grown on artificial laboratory-based culture media due to exposure to adverse environmental stressors that are commonly associated with food processing such as such as high salt or acidity causing enhanced virulence factor expression. Fakruddin *et al.* (2013) reported that VBNC cells pose a distinct threat to public health and food safety dispelling opinion that such pathogens are unable to induce infection/disease despite retaining their virulent properties. Researchers have revealed that when VBNC pathogens pass through an animal host (Baffone *et al.*, 2003), resuscitation and resumption of metabolic activity have led to infections and diseases (Baffone *et al.*, 2003; Sardessai, 2005). The first evidence of pathogenicity of nonculturable cells was demonstrated of fluid accumulation in the rabbit ileal loop assay by VBNC *Vibrio cholera* O1, followed by human volunteer experiments (Amel, Amine, & Amina, 2008). Cappelier *et al.* (2007) also reported that avirulent VBNC cells so *L. monocytogenes* needs to presence of an embryo to be recovered in egg yolk and regain virulence after recovery.

Though historically there has been disputes surrounding the existence of VBNC cells, extensive molecular studies has resolved this debate (Fakruddin *et al.*, 2013; Rowan, 2011). It is now appreciated that VBNC cells represents a distinct survival strategy enabling problematical microorganisms to adapt to adverse environmental conditions (Rowan, 2004). Harsh environmental triggers that have been reported to cause the occurrence of VBNC cells include nutrient starvation, sharp changes in pH or salinity, osmotic stress, oxygen availability, extreme temperatures, exposure to food preservatives and heavy metals, chlorination of wastewater and decontamination processes such as pasteurization of milk (Fakruddin *et al.*, 2013). Recently there has been a growing awareness about the potential for minimal processing technologies such as PL to produce VBNC cells (Kramer & Muranyi, 2014; Rowan, 2011).

Culture dependent vs culture independent methods

Since the landmark work of Rowan *et al.* (1999), most of the published studies to date have used conventional agar-based culture methods for the enumeration of survivors to PL treatments. The purpose of subsequent studies has been to demonstrate efficacy of PL application for microbial destruction at an appropriate technology readiness level (TRL) suitable for market update and deployment. However, measuring of microbial lethality associated with PL treatments has been far from straight forward as inactivation varies depending on operational parameters (such as applied voltage, number of pulses, distance from light source that are collectively captured under the term UV dose or fluence), biological factors (such as type, nature and number of microbial species present, nature of the suspension menstrum, presence of antibiotics or dyes, shading effects), presence of an enrichment/resuscitation phase post treatments to name but a few (Hayes *et al.*, 2013; Rowan, 1999, 2004). Evidence suggests that these harsh environment cues may trigger a switch to the adaptive survival VBNC state in PL treatments (Kramer & Muranyi, 2014; Rowan, 2011). Otaki *et al.* (2003) along with Gómez-López *et al.* (2005) reported the occurrence of photoreactivation after PL treatments. Photoreactivation is the recovery of culturability of PL-treated microorganisms after exposure to visible light. It is limited to small recoveries (<1 log) and to the application of low fluencies. Photoreactivation studies constituted one of the earliest approaches to provide evidence that not all PL-treated microorganisms which are transferred to agar plates retain vital molecular and cellular functions but are incapable of forming colonies.

To complicate the prediction process further, recent evidence clearly shows that PL treatment kills yeast through a multi-hit or mechanistic process that affects cell membrane permeability along with DNA and macromolecule stability and functionality depending on the UV dose applied. Specifically, Farrell *et al.* (2011) reported on the various mechanisms of cellular response in clinical strains of *Candida albicans* to PL treatments. Significant increase in the permeability of the cell membrane as function of the amount of UV pulsing applied was demonstrated by both, propidium iodide uptake and protein leakage (Fig. 2). The latter finding correlated well with increased levels of lipid hydroperoxidation in the cell membrane of PL-treated yeast. PL-treated yeast cells displayed a specific pattern of reactive oxygen species (ROS) production during treatments, where ROS bursts observed during the initial phases of PL treatment was consistent with the occurrence of

Please cite this article in press as: Rowan, N. J., et al., A review of quantitative methods to describe efficacy of pulsed light generated inactivation data that embraces the occurrence of viable but non culturable state microorganisms, Trends in Food Science & Technology (2015), http://dx.doi.org/10.1016/j.tifs.2015.03.006

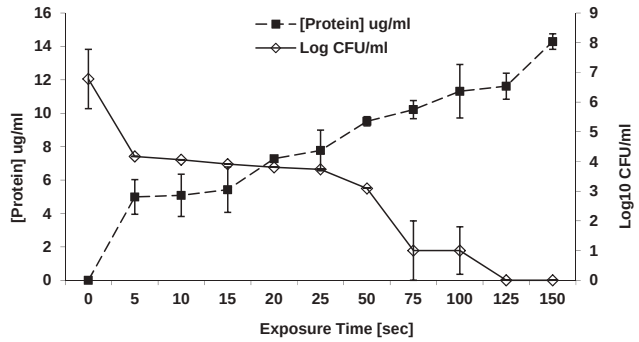

Fig. 2. Reduction in total fungal protein levels (μg/ml) in *C. albicans* D7100 as a consequence of increased pulsing or amount of pulses applied. (Farrell *et al.*, 2011, with permission from Elsevier™, *Journal of Microbiological Methods, 84,* 317–326).

apoptotic cells. Increased amount of PL treatment also resulted in the occurrence of late apoptotic and necrotic cells with commensurate transition from nuclear to cytoplasmic accumulation of ROS and cell membrane leakage. Enhanced nuclear damage was observed in PL-treated cells as determined by the Comet assay. Cellular repair was observed in all yeast during sub-lethal exposure to PL-treatments. These complex structural and physiological studies revealed that microorganisms may survive PL depending on the regime of treatments and in order to comprehensively achieve complete lethality it is important to understand and appreciate all operating conditions including target organism(s) under investigation and to mitigate for VBNC. This will have follow-on implications for effective microbial modelling of survivors post PL treatments and interpreting associated death rate kinetic data.

Ferrario, Guerrero, and Alzamora (2014) studied the inactivation of *S. cerevisiae* using flow cytometry in combination with different fluorescent stains and compared PL-mediated disinfection with conventional plate count enumeration. They found that the loss of culturability was much higher than the correspondent increase in permeabilized cells. Using a similar approach, Kramer and Muranyi (2014) studied the influence of PL treatment on structural and physiological properties of *L. innocua* and *E. coli*. Findings were consistent with the observations of Farrell *et al.* (2011) where a significant discrepancy between conventional plate counts and different viability staining parameters was reported, showing that PL treatment does not cause immediate shutdown of vitality functions even when the number of colony forming units decreased by more than 6 $\log_{10}$ per sample. Kramer and Muranyi (2014) also showed that loss of culturability occurred at considerably lower fluences than shutdown of cellular functions like depolarization of cell membranes, the loss of metabolic, esterase and pump activities or the occurrence of membrane damage. The authors concluded that a considerable proportion of PL-treated bacteria appeared to have entered the VBNC state. While oxidative stress with concomitant damage to DNA molecule were showed to be directly responsible for loss of microbial culturability as opposed to direct rupture of cell membranes or inactivation of intracellular enzymes, it would appear that the microbial lethality occurs due to accumulation of multiple insults inflicted on the treated cells where the rate of onset is influence in part by the amount of fluence applied. This complex cellular response to PL-treatment is reflected in different death rate kinetic data exhibited by microbial food spoilage and pathogens.

Flow cytometric investigations in combination with different fluorescent probes provide valuable insight into the physiological states and are suitable approach to gain further appreciation of the impact of microbial disinfection processes (Kennedy, Cronin, & Wilkinson, 2011; Nocker *et al.*, 2011). Berney, Weilenmann, and Egil (2006) used flow cytometric studies to report statistical different levels of metabolic activity of *L. innocua* and *E. coli* levels detectable after PL treatment despite colony count enumeration data dropping to below the detection limit. However, application of higher energy levels of PL caused a gradual shutdown of cellular functions. Indeed, immediately after applying a fluence of 0.76 J/cm^2, high fractions of both bacterial populations were still able to maintain polarized cell membranes even though colony counts reduced to more than 99.99% in each case. These studies revealed that PL-treated bacteria entering this VBNC state may still show several vital functions, although they are incapable of growth in or on laboratory nutrient media.

Ben Said, Otaki, Shinobu, and Abdennaceur (2010) also reported the occurrence of VBNC bacteria after PL treatments by investigating phage susceptibilities of *Streptococcus typhi*. Infectivity of the host bacteria was still detectable intimating viability although culturability was lost. Kramer & Muranyi (2014) observed that due to highly variable results obtained in different reported studies concerning potential rupture of treated microorganisms by PL, it appears likely that the occurrence of photothermal or photophysical inactivation mechanisms is to some extent likely to be attributed to their size, cellular structure and UV light absorption properties. Besides obvious damages to DNA (Kramer & Muranyi, 2014), microbial inactivation by PL could be linked to alterations of proteins and lipids where researchers reported on the occurrence of lipid peroxides and carbonylated proteins and lipid hydroperoxidation in the cell membrane of treated yeasts (Farrell *et al.*, 2011).

Kramer and Muranyi (2014) reported that measurement of intracellular esterase activity proved to be a weak parameter to investigate cell viability post PL-treatments because high levels of CF-stained bacteria could be detected even when cells were already nonculturable and de-energised. The detection of enzyme activity does therefore not necessarily suggest cell viability. Kramer and Muranyi (2014) also showed that exclusion of the dye PI that is often used as a criterion for live bacteria could not be seen as a suitable marker for viability as high levels of cells with

Please cite this article in press as: Rowan, N. J., et al., A review of quantitative methods to describe efficacy of pulsed light generated inactivation data that embraces the occurrence of viable but non culturable state microorganisms, Trends in Food Science & Technology (2015), http://dx.doi.org/10.1016/j.tifs.2015.03.006

intact membranes were detected after treatment with lethal energy doses. Also, Kramer and Muranyi (2014) reported detection of significant levels of ROS at 0.50 J/cm^2, which corresponds to a fluence where increasing loss of culturability occurred with PL-treatments. This corroborated earlier work of Farrell *et al.* (2011) which demonstrated that augmented levels of ROS were evident in nonculturable cells. The latter authors uniquely reported that the onset of apoptosis is possibly a suitable candidate marker to intimate microbial destruction as this state in PL-treated yeast occurs after lethal doses of PL are delivered.

Recently, PL has also been used for the destruction of the waterborne enteroparasite *Cryptosporidium parvum* that requires either use of complex mammalian *in vitro* cell culture techniques or use of *in vivo* rodent infection models to confirm efficacy of destruction (Garvey, Farrell, Cormican, & Rowan, 2010; Garvey, Hayes, Clifford, Kirf, & Rowan, 2013). An alternative method for assessing viability post PL treatments is the measurement of cellular adenosine triphosphate (ATP), which is the basic unit of energy currency in viable cells. ATP is not present in nonviable cells, as it is degraded after death. ATP has been used as an indicator of viability of microorganisms including *C. parvum* (King, Keegan, Monis, & Saint, 2005). ATP measurement is a likely candidate method for rapidly determining the viability or activity of this parasite pre and post PL disinfection particularly as oocyst excystation requires the generation and use of ATP. Garvey *et al.* (2013) reported on disinfection levels as determined via ATP measurement pre and post UV exposure were also compared with the combined *in vitro* HCT-8 cell culture-qPCR assay which was shown previously to correlate with the gold standard mouse infectivity model (Garvey *et al.*, 2010). Quantitative PCR is growing in popularity as a culture-independent means of assessing microbial lethality post treatments (Garvey *et al.*, 2010, 2013). Their studies showed that PL effectively killed *C. parvum* with a 5.4 $\log_{10}$ loss in oocyst viability after exposure to a UV fluence of 8.5 μJ/cm^2 as determined by the *in vitro* cell culture − *q*PCR assay. The ATP assay was shown to be significantly less effective in measuring loss of oocyst viability in similarly PL-treated samples for all combination of treatment regimes studied. Overestimation of survivors by the ATP assay may suggest that a sub-population of *C. parvum* oocysts may exist in a VBNC state.

How best then to determine the efficacy of PL-treatments to destroy VBNC organisms with the knowledge that traditional culture-based microbial kinetic modelling informs process operational parameters yet are not appropriate for VBNC. Identification of an appropriate model to facilitate enumeration of VBNC post PL treatments using our knowledge acquired from culture-based kinetics would advance the field of food processing and would have far reaching tangential implications for other related domains that are deploying similar PL disinfection approaches including inter alia drinking water. In the very limited number of PL-treatment studies published thus far that reported to occurrence of VBNC, the various vitality markers described plot in a linear fashion and possibly aligned with log-linear kinetic inactivation method (Farrell *et al.*, 2011; Ferrario *et al.*, 2014; Kramer & Muranyi, 2014). One logical approach to connecting VBNC with culture-based kinetic inactivation methods would be to focus of modelling the occurrence of vital markers (such as inter alia onset of apoptosis) and to factor this into operation of PL treatments.

Conclusions

The inactivation kinetic of microbial cells due to PL treatment has been described using different models, frequently non-log-linear. Even though harmonisation between the modelling structures and the right choice of parameters is necessary to compare the effectiveness of the technologies between laboratories worldwide, it appear that the diversity of models is a product of a mechanism of inactivation that is not simple but occurs through a complex multi-targeted molecular and cellular process where the rate of microbial destruction is critically influenced by the level of fluence applied combined with nature of the methods used to enumerate cell survivors. A number of mechanisms have been described associated to photochemical, photophysical and photothermal effects. Therefore, numerous modelling structures have been proposed that can also capture non-linear kinetics.

Increasing evidence recently recognises that significant numbers of microorganisms cannot be cultured successfully with conventional growth dependent techniques such as agar plates, membrane filtration and broth enrichment post PL-treatments. A wide range for nonsporulating Gram positive and negative bacteria can exist in the VBNC state, which is a survival strategy that enables the PL-treated microorganism to employ enhanced resistance to combat adverse conditions that are commonly associated with stresses imposed during food processing. Pathogenicity is maintained by some species during VBNC state inferring that such survivors may still pose a potential threat to consumers is beginning to be considered. The real risk of low numbers of VBNC survivors in minimally processed foods is limited and there is a pressing need to gain a greater appreciation of the true levels of viable organisms in raw materials and the manufacturing environment. However, the full impact of VBNC microorganisms on industrial food processes has not been given consideration due in part to the widespread conventional use of culture dependent growth techniques that are incapable of detecting such organisms. Intensive research is warranted to investigate the most suitable vitality marker(s) for PL-treated cells and to then construct appropriate kinetic curves based on these along with comparing and contrasting kinetic curves produced using traditional culture based techniques under similar experimental conditions to inform process efficacy.

Please cite this article in press as: Rowan, N. J., et al., A review of quantitative methods to describe efficacy of pulsed light generated inactivation data that embraces the occurrence of viable but non culturable state microorganisms, Trends in Food Science & Technology (2015), http://dx.doi.org/10.1016/j.tifs.2015.03.006

A deeper study of PL lethality is therefore needed in order to identify new methods of enumeration and identification with the potential for detecting VBNC organisms post treatments in such foods may bring about a radical reappraisal of processing parameters and detection limits. New research is required to ascertain the ability of VBNC survivors tolerating and replicating within established *in vivo* infection models post PL-treatments. Greater information is also required to elucidate the existence of commonly shared cellular mechanisms (and associated gene expression regulators and gene markers) that govern cellular conversion to this VBNC state. Moreover, there is a dearth of knowledge regarding specific underlying molecular and associated cellular mechanisms governing transition and persistence of food and waterborne microorganisms in this VBNC state, in addition to obviously establishing what specific environmental conditions or triggers cause these changes in culturable state. Further research is, however, also urgently needed to identify a suitable cellular marker to tag microbial cell death and to investigate the relationship (if any) between detection of this 'cell death marker' and corresponding culture dependent plate count data that is currently used in the food industry.

Acknowledgements

This research was partly supported by a Marie Curie FP7-Reintegration-Grant within the 7th European Community Framework Programme under the project Development of novel Disinfection Technologies for Fresh Produce (Di-Tec), while it is also partly funded by the COST ACTION FA1202 BacFoodNet and by the Erasmus + Programme Q-Safe of the European Union, Project No: 2014-1-MT01-KA200-000327. The support of project PMAFI/29/14 sponsored by UCAM is also acknowledged.

References

Albert, I., & Mafart, P. (2005). A modified Weibull model for bacterial inactivation. *International Journal of Food Microbiology, 100*, 197–211.

Amel, B. K., Amine, B., & Amina, B. (2008). Survival of *Vibrio fluvialis* in seawater under starvation conditions. *Microbiological Research, 163*, 323–328.

Aron-Maftei, N., Ramos-Villarroel, A. Y., Nicolau, A. I., Martín-Belloso, O., & Soliva-Fortuny, R. (2014). Pulsed light inactivation of naturally occurring moulds on wheat grain. *Journal of the Science of Food and Agriculture, 94*, 721–726.

Baffone, W., Citterio, E., Vittoria, E., Cassarel, A., Campana, R., Falzona, L., et al. (2003). Retention of virulence in viable but non-culturable halophilic *Vibrio* spp. *International Journal of Food Microbiology, 89*, 31–39.

Ben Said, M., & Otaki, M. (2013). Development of a DNA-dosimeter system for monitoring the effects of pulsed ultraviolet radiation. *Annals in Microbiology, 63*, 1057–1063.

Ben Said, M., Otaki, M., Shinobu, K., & Abdennaceur, H. (2010). Detection of active *Escherichia coli* after irradiation by pulsed UV light using a Qβ phage. *African Journal of Microbiology Research, 4*, 1128–1134.

Berney, M., Weilenmann, H. U., & Egil, T. (2006). Flow-cytometric study of vital cellular functions in *Escherichia coli* during solar disinfection. *Microbiology, 152*, 1719–1729.

Besnard, V., Federighi, M., & Cappelier, J. M. (2000). Evidence of viable but non-culturable state in *Listeria monocytogenes* by direct viable count and CTC-DAPI double staining. *Food Microbiology, 17*, 697–704.

Bialka, K. L., Demirci, A., & Puri, V. M. (2008). Modeling the inactivation of *Escherichia coli* 0157:H7 and *Salmonella enterica* on raspberries and strawberries resulting from exposure to ozone or pulsed UV light. *Journal of Food Engineering, 85*, 444–449.

Bigelow, W. D. (1921). The logarithmic nature of thermal death time curves. *Journal of Infectious Diseases, 29*, 528–536.

Bohrerova, Z., Shemer, H., Lantis, R., Impellitteri, C. A., & Linden, K. G. (2008). Comparative disinfection efficiency of pulsed and continuous-wave UV irradiation technologies. *Water Research, 42*, 2975–2982.

Bolton, J. R., & Linden, K. G. (2003). Standardization of methods for fluence (UV dose) determination in bench-scale UV experiments. *Journal of Environmental Engineering, 129*, 209–215.

Bradley, D., McNeil, B., Laffey, J. G., & Rowan, N. J. (2012). Studies on the pathogenesis and survival of different culture forms of *Listeria monocytogenes* to pulsed UV-light irradiation after exposure to mild-food processing stresses. *Food Microbiology, 30*, 330–339.

Braslavsky, S. E. (2007). Glossary of terms used in photochemistry. *Pure & Applied Chemistry, 79*, 293–465.

Busschaert, P., Geeraerd, A. H., Uyttendaele, M., & Van Impe, J. F. (2011). Hierarchical Bayesian analysis of censored microbiological contamination data for use in risk assessment and mitigation. *Food Microbiology, 18*, 712–719.

Byrd, J. J., Xu, H. S., & Colwell, R. R. (1991). Viable but non-culturable bacteria in drinking water. *Applied and Environmental Microbiology, 57*, 875–878.

Cappelier, J. M., Besnard, V., Roche, S. M., Velge, P., & Federighi, M. (2007). Avirulent viable but non culturable cells of *Listeria monocytogenes* need the presence of an embryo to be recovered in egg yolk and regain virulence after recovery. *Veterinary Research, 38*, 573–583.

Cerf, O. (1977). Tailing of survival curves of bacterial spores. *Journal of Applied Bacteriology, 42*, 1–19.

Cheigh, C. I., Hwang, H. J., & Chung, M. S. (2013). Intense pulsed light (IPL) and UV-C treatments for inactivating *Listeria monocytogenes* on solid medium and seafoods. *Food Research International, 54*, 745–752.

Cheigh, C. I., Park, M. H., Chung, M. S., Shin, J. K., & Park, Y. S. (2012). Comparison of intense pulsed light and ultraviolet (UVC) induced cell damage in *Listeria monocytogenes* and *Escherichia coli* O157:H7. *Food Control, 25*, 654–659.

Coroller, L., Leguerinel, I., Mettler, E., Savy, N., & Mafart, P. (2006). General model, based on two mixed Weibull distributions of bacterial resistance, for describing various shapes of inactivation curves. *Applied and Environmental Microbiology, 72*, 6493–6502.

Cudemos, E., Izquier, A., Medina-Martínez, M. S., & Gómez-López, V. M. (2013). Effects of shading and growth phase on the microbial inactivation by pulsed light. *Czech Journal of Food Sciences, 31*, 189–193.

Duarte, A. (2013). *The interpretation of quantitative microbial data: Meeting the demands of quantitative microbiological risk assessment*. PhD Thesis. Denmark: DTU Food, National Food Institute.

Dunaev, T., Alanya, S., & Duran, M. (2008). Use of RNA-based genotypic approaches for quantification of viable but non-culturable *Salmonella* sp. in biosolids. *Water Science and Technology, 58*, 1823–1828.

Esbelin, J., Mallea, S., Ram, A. F. J., & Carlin, F. (2013). Role of pigmentation in protecting *Aspergillus niger* conidiospores against

pulsed light radiation. *Photochemistry and Photobiology, 89*, 758–761.
Fakruddin, M. D., Bin Mannan, K. S., & Stewart, A. (2013). Viable but nonculturable bacteria: food safety and public health perspective. *ISRN Microbiology, 2013*, (published online Article ID 703813).
Farrell, H. P., Garvey, M., Cormican, M., Laffey, J. G., & Rowan, N. J. (2009). Investigation of critical inter-related factors affecting the efficacy of pulsed light for inactivating clinically relevant bacterial pathogens. *Journal of Applied Microbiology, 108*, 1494–1508.
Farrell, H. P., Garvey, M., & Rowan, N. J. (2009). Studies on the inactivation of medically important *Candida* species on agar surfaces using pulsed light. *FEMS Yeast Research, 9*, 956–966.
Farrell, H., Hayes, J., Laffey, J., & Rowan, N. J. (2011). Studies on the relationship between pulsed UV light irradiation and the simultaneous occurrence of molecular and cellular damage in clinically-relevant *Candida albicans*. *Journal of Microbiological Methods, 84*, 317–326.
FDA. (1996). *Code of federal regulations. 21CFR179.41*.
FDA. (2001). *Code of federal regulations 21CFR120.24*.
Ferrario, M., Alzamora, S. M., & Guerrero, S. (2013). Inactivation kinetics of some microorganisms in apple, melon, orange and strawberry juices by high intensity light pulses. *Journal of Food Engineering, 118*, 302–311.
Ferrario, M., Guerrero, S., & Alzamora, S. M. (2014). Study of pulsed light-induced damage on *Saccharomyces cerevisiae* in apple juice by flow cytometry and transmission electron microscopy. *Food and Bioprocess Technology, 7*, 1001–1011.
Garvey, M., Farrell, H., Cormican, M., & Rowan, N. (2010). Investigations of the relationship between use of *in vitro* cell culture-quantitative PCR and a mouse-based bioassay for evaluating critical factors affecting the disinfection performance of pulsed UV light for treating *Cryptosporidum parvum* oocyts in water. *Journal of Microbiological Methods, 80*, 267–273.
Garvey, M., Hayes, J., Clifford, E., Kirf, D., & Rowan, N. (2013). Efficacy of measuring cellular ATP levels to determine the inactivation of pulsed UV treated *Cryptosporidium parvum* oocysts suspended in water. *Water Science and Technology: Water Supply, 13*, 202–213.
Geeraerd, A. H., Herremans, C. H., & Van Impe, J. F. (2000). Structural model requirements to describe microbial inactivation during a mild heat treatment. *International Journal of Food Microbiology, 59*, 185–209.
Geeraerd, A. H., Valdramidis, V. P., & Van Impe, J. F. (2005). GInaFiT, a freeware tool to assess non-log-linear microbial survivor curves. *International Journal of Food Microbiology, 102*, 95–105.
Gómez-López, V. M., Devlieghere, F., Bonduelle, V., & Debevere, J. (2005). Factors affecting the inactivation of microorganisms by intense light pulses. *Journal of Applied Microbiology, 99*, 460–470.
Gómez-López, V. M., Koutchma, T., & Linden, K. G. (2012). Ultraviolet and pulsed light. In P. J. Cullen, B. Tiwari, & V. Valdramidis (Eds.), *Novel thermal and non-thermal technologies for fluid foods*. Elsevier.
Gómez-López, V. M., Ragaert, P., Debevere, J., & Devlieghere, F. (2007). Pulsed light for food decontamination: a review. *Trends in Food Science and Technology, 18*, 464–473.
Hayes, J. C., Kirf, D., Garvey, M., & Rowan, N. J. (2013). Disinfection and toxicological assessment of pulsed light and pulsed plasma gas discharge treated water containing the waterborne enteroparasite *Cryptosporidium parvum*. *Journal of Microbiological Methods, 94*, 325–337.
Hayes, J. C., Laffey, J. G., McNeil, B., & Rowan, N. J. (2012). Relationship between growth of food-spoilage yeast in high-sugar environments and sensitivity to high-intensity pulsed UV light irradiation. *International Journal of Food Science and Technology, 47*, 1925–1934.
Hills, B. P. (2001). The power and pitfalls of deductive modelling. In L. M. M. Tijskens, M. L. A. T. M. Hertog, & B. M. Nicolaï (Eds.), *Food process modeling* (pp. 3–18). Cambridge, UK: Woodhead Publishing Limited.
Hsu, L., & Moraru, C. I. (2011). A numerical approach for predicting volumetric inactivation of food borne microorganisms in liquid substrates by pulsed light treatment. *Journal of Food Engineering, 105*, 569–576.
Humpheson, L., Adams, M. R., Anderson, W. A., & Cole, M. B. (1998). Biphasic inactivation kinetics in *Salmonella* Enteriditis PT4. *Applied and Environmental Microbiology, 64*, 459–464.
Izquier, A., & Gómez-López, V. M. (2011). Modeling the pulsed light inactivation of microorganisms naturally occurring on vegetable substrates. *Food Microbiology, 28*, 1170–1174.
Keklik, N. M., Demirci, A., Puri, V. M., & Heinemann, P. H. (2012). Modeling the inactivation of *Salmonella* Typhimurium, *Listeria monocytogenes*, and *Salmonella* Enteriditis on poultry products exposed to pulsed UV light. *Journal of Food Protection, 75*, 281–288.
Kennedy, D., Cronin, U. P., & Wilkinson, M. G. (2011). Response of *Escherichia coli, Listeria monocytogenes* and *Staphylococcus aureus* to simulated food processing treatments, determined using fluorescence activated cell sorting and plate counting. *Applied and Environmental Microbiology, 77*, 4657–4668.
King, B. J., Keegan, A. R., Monis, P. T., & Saint, C. P. (2005). Environmental temperature controls *Cryptosporidium* oocyts metabolic rate and associated retention of infectivity. *Applied and Environmental Microbiology, 71*, 3848–3857.
Kramer, B., & Muranyi, P. (2014). Effect of pulsed light on structural and physiological properties of *Listeria innocua* and *Escherichia coli*. *Journal of Applied Microbiology, 116*, 596–611.
Krishnamurthy, K., Demirci, A., & Irudayaraj, J. M. (2007). Inactivation of *Staphylococcus aureus* in milk using flow-through pulsed UV-light treatment system. *Journal of Food Science, 72*, M233–M239.
Krishnamurthy, K., Tewari, J. C., Irudayaraj, J. M., & Demirci, A. (2010). Microscopic and spectroscopic evaluation of inactivation of *Staphylococcus aureus* by pulsed UV light and infrared heating. *Food and Bioprocess Technology, 3*, 93–104.
Lasagabaster, A., & Martínez, I. (2013). Impact of process parameters on *Listeria innocua* inactivation kinetics by pulsed light technology. *Food and Bioprocess Technology, 6*, 1828–1836.
Lasagabaster, A., & Martínez, I. (2014). Survival and growth of *Listeria innocua* treated by pulsed light technology: impact of post-treatment temperature and illumination. *Food Microbiology, 41*, 76–81.
Levy, C., Aubert, X., Lacour, B., & Carlin, F. (2012). Relevant factors affecting microbial surface decontamination by pulsed light. *International Journal of Food Microbiology, 152*, 168–174.
Lewis, K. (2000). Programmed death in bacteria. *Microbiology and Molecular Biology Reviews, 64*, 503–514.
Lorimer, M. F., & Kiermeier, A. (2007). Analysing microbiological data: tobit or not tobit? *International Journal of Food Microbiology, 116*, 313–318.
Luksiene, Z., Gudelis, V., Buchovec, I., & Raudeliuniene, J. (2007). Advanced high-power light device to decontaminate food from pathogens: effects on *Salmonella* Typhimurium viability *in vitro*. *Journal of Applied Microbiology, 103*, 1545–1552.
MacGregor, S. J., Rowan, N. J., McIlvaney, L., Anderson, J. G., Fouracre, J. G., & Farish, O. (1998). Light inactivation of food-related pathogenic bacteria using a pulsed power source. *Letters in Applied Microbiology, 27*, 67–70.
Mafart, P., Couvert, O., Gaillard, S., & Leguerinel, I. (2002). On calculating sterility in thermal preservation methods: application of the Weibull frequency distribution model. *International Journal of Food Microbiology, 72*, 107–113.

Please cite this article in press as: Rowan, N. J., et al., A review of quantitative methods to describe efficacy of pulsed light generated inactivation data that embraces the occurrence of viable but non culturable state microorganisms, Trends in Food Science & Technology (2015), http://dx.doi.org/10.1016/j.tifs.2015.03.006

Marquenie, D., Geeraerd, A. H., Lammertyn, J., Soonthens, C., Van Impe, J. F., Michiels, C. W., et al. (2003). Combinations of pulsed white light and UV-C or mild heat treatment to inactivate conidia of *Botrytis cinerea* and *Monilia fructigena*. *International Journal of Food Microbiology, 85*, 185–196.

McDonald, K. F., Curry, R. D., Clevenger, T. E., Brazos, B. J., Unklesbay, K., Eisenstark, A., et al. (2000). The development of photosensitized pulsed and continuous ultraviolet light decontamination techniques for surfaces and solutions. *IEEE Transactions on Plasma Science, 28*, 89–95.

McDonald, K., & Sun, D. W. (1999). Predictive food microbiology for the meat industry: a review. *International Journal of Food Microbiology, 52*, 1–27.

Miller, B. M., Sauer, A., & Moraru, C. I. (2012). Inactivation of *Escherichia coli* in milk and concentrated milk using pulsed-light treatment. *Journal of Dairy Science, 95*, 5597–5603.

Mossel, D. A. A., Corry, J. E. L., Struijk, C. B., & Baird, R. M. (1995). *Essentials of the microbiology of Foods*. West Sussex: John Wiley and Sons.

Nocker, A., Caspers, M., Esveld-Amanatidou, A., vad der Vossen, J., Schuren, F., Montijn, R., et al. (2011). Multiparameter viability assay for stress profiling applied to the food pathogen *Listeria monocytogenes* F2365. *Applied and Environmental Microbiology, 77*, 6433–6440.

Oliver, J. D. (1993). Formation of viable but nonculturable cells. In S. Kjelleberg (Ed.), *Starvation in bacteria* (pp. 239–272). Springer.

Otaki, M., Okuda, A., Tajima, K., Iwasaki, T., Kinoshita, S., & Ohgaki, S. (2003). Inactivation differences of microorganisms by low pressure UV and pulsed xenon lamps. *Water Science and Technology, 47*, 185–190.

Peleg, M., & Cole, M. B. (1998). Reinterpretation of microbial survival curves. *Critical Reviews in Food Science, 38*, 353–380.

Ringus, D. L., & Moraru, C. I. (2013). Pulsed light inactivation of *Listeria innocua* on food packaging materials of different surface roughness and reflectivity. *Journal of Food Engineering, 114*, 331–337.

Rollins, D. M., & Colwell, R. R. (1986). Viable but non-culturable stage of *Campylobacter jejuni* and its role in survival in the natural aquatic environment. *Applied and Environmental Microbiology, 52*, 531–538.

Rowan, N. J. (1999). Evidence that inimical food preservation barriers alter microbial resistance, virulence and cell morphology. *Trends in Food Science and Technology, 10*, 261–272.

Rowan, N. J. (2004). Viable but non-culturable forms of food and waterborne bacteria: Quo Vadis? *Trends in Food Science & Technology, 15*, 462–467.

Rowan, N. J. (2011). Defining established and emerging microbial risks in the aquatic environment: current knowledge, implications and outlooks. *International Journal of Microbiology*, published online http://www.hindawi.com/journals/ijmicro/2011/462832/.

Rowan, N. J., Espie, S., Harrower, J., Farrell, H., Marsili, L., Anderson, J. G., et al. (2008). Evidence of lethal and sublethal injury in microbial pathogens exposed to pulsed plasma gas discharge treatments. *Letters in Applied Microbiology, 46*, 80–86.

Rowan, N. J., Kirf, D., & Tomkins, P. (2009). Studies on the susceptibility of different culture morphotypes of Listeria monocytogenes to uptake and survival in human polymorphonuclear leukocytes. *FEMS Immunology and Medical Microbiology, 57*, 183–192.

Rowan, N. J., MacGregor, S. J., Anderson, J. G., Fouracre, R. A., McIlvaney, L., & Farish, O. (1999). Pulsed-light inactivation of food-related microorganisms. *Applied and Environmental Microbiology, 65*, 1312–1315.

Sapers, G. M. (2001). Efficacy of washing and sanitizing methods for disinfection of fresh fruit and vegetable products. *Food Technology and Biotechnology, 39*, 3005–3311.

Sardessai, Y. N. (2005). Viable but non-culturable bacteria: their impact on public health. *Current Science, 89*, 1650–1655.

Sauer, A., & Moraru, C. I. (2009). Inactivation of *Escherichia coli* ATCC 25922 and *Escherichia coli* O157:H7 in apple juice and apple cider, using pulsed light treatment. *Journal of Food Protection, 72*, 937–944.

Sawaya, K., Kaneko, N., Fukushi, K., & Yaguchi, J. (2008). Behaviours of physiologically active bacteria in water environment and chlorine disinfection. *Water Science and Technology, 58*, 1343–1348.

Takeshita, K., Shibato, J., Sameshima, T., Fukunaga, S., Isobe, S., Arihara, K., et al. (2003). Damage of yeast cells induced by pulsed light irradiation. *International Journal of Food Microbiology, 85*, 151–158.

Uesugi, A. R., Woodling, S. E., & Moraru, C. I. (2007). Inactivation kinetics and factors of variability in the pulsed light treatment of *Listeria innocua* cells. *Journal of Food Protection, 70*, 2518–2525.

Unluturk, S., Atilgan, M. R., Handan Baysal, A., & Tari, C. (2008). Use of UV-C radiation as a non-thermal process for liquid egg products (LEP). *Journal of Food Engineering, 85*, 561–568.

Valdramidis, V. P., Geeraerd, A. H., Bernaerts, K., Devlieghere, F., Debevere, J., & Van Impe, J. F. (2004). Accurate modelling of non-log-linear survivor curves. *International Dairy Federation Bulletin, 392*, 97–110.

Van Boekel, M. A. J. S. (2002). On the use of Weibull model to describe thermal inactivation of microbial vegetative cells. *International Journal of Food Microbiology, 74*, 139–159.

Walker, S. J., & Jones, J. E. (1993). Protocols for data generation for predictive modelling. *Journal of Industrial Microbiology, 12*, 273–276.

Wang, T., MacGregor, S. J., Anderson, J. G., & Woolsey, G. A. (2005). Pulsed ultra-violet inactivation spectrum of *Escherichia coli*. *Water Research, 39*, 2921–2925.

Wekhof, A. (2000). Disinfection with flash lamps. *PDA Journal of Pharmaceutical Science and Technology, 54*, 264–276.

Woodling, S. E., & Moraru, C. I. (2007). Effect of spectral range in surface inactivation of *Listeria innocua* using broad-spectrum pulsed light. *Journal of Food Protection, 70*, 909–916.

Yaqub, S., Anderson, J. G., MacGregor, S. J., & Rowan, N. J. (2004). Use of fluorescent metabolic stain to assess lethal and sub-lethal injury in food-borne bacteria exposed to pulsed electric fields. *Letters in Applied Microbiology, 39*, 246–251.

Journal of Water Process Engineering 41 (2021) 102070

Contents lists available at ScienceDirect

Journal of Water Process Engineering

journal homepage: www.elsevier.com/locate/jwpe

Bacterial inactivation, photoreactivation and dark repair post flow-through pulsed UV disinfection

Kelly Fitzhenry [a], Eoghan Clifford [a,b,*], Neil Rowan [c], Angeles Val del Rio [a,d]

[a] School of Engineering, NUI Galway, Ireland
[b] Ryan Institute for Environment, Marine and Energy, NUI Galway, Ireland
[c] Bioscience Research Institute, Athlone Institute of Technology, Ireland
[d] School of Engineering, Universidade de Santiago de Compostela, Spain

ARTICLE INFO

Keywords:
Ultraviolet applications
Bacterial disinfection
Wastewater treatment
Cell injury
Pulsed UV
Disease mitigation

ABSTRACT

Pulsed UV (PUV) technology is accepted commercially for disinfection within the food packaging industry, but has yet to be deployed by the water/wastewater sector. This is partly due to a lack of robust, independently validated data for submerged or flow-through treatment applications. This study evaluated the efficacy of PUV for water disinfection under flow-through conditions. Bacterial pathogens of interest in the food and water/wastewater sector, namely *Escherichia coli*, *Staphylococcus aureus* and *Listeria innocua* (surrogate for *L. monocytogenes*) were used to investigate the potential for photoreactivation and/or dark repair post PUV flow-through disinfection. A continuous-flow low-pressure UV was also analysed under similar experimental conditions. Bacterial inactivation via flow-through PUV was dependant on energy output with *E. coli* exhibiting greatest sensitivity to PUV treatment (5.3 log $_{10}$ inactivation after treatment at 1539 mJ/cm ^{2} - output in UV range < 300 nm); *L. innocua* exhibited the highest PUV resistance (3.0 log $_{10}$ inactivation after treatment at 1539 mJ/cm ^{2} – output in UV range < 300 nm) under similar treatment conditions. Greater photoreactivation occurred at lower PUV outputs for both *S. aureus* and *E. coli* after flow-through PUV treatment. Thus exposure of treated bacteria to natural light, immediately post flow-through PUV treatment, should be avoided to minimise photoreactivation. The LPUV demonstrated inactivation of all bacteria below the limit of detection (1 CFU/mL) and inhibited the occurrence of photoreactivation. This study highlights the importance of considering bacterial repair potential and the need for further development of PUV technology for such applications.

1. Introduction

Ultraviolet (UV) disinfection is a well-established technology across a variety of different sectors including aquaculture, ballast water treatment, municipal wastewater treatment, drinking water treatment, agriculture, dairy and the beverage industry [1–3]. UV disinfection is typically seen as being user-friendly, free from toxic/hazardous chemicals, effective against chlorine-resistant microorganisms and exhibiting shorter contact times in comparison to chlorine treatment [4,5]. Low pressure UV (LPUV) and medium pressure UV (MPUV) are currently the de facto UV disinfection systems used for water/wastewater disinfection applications. Typically, UV light is generated within the lamps when a voltage is applied across a mercury gas mixture which results in the discharge of photons. The type of UV light produced is dependent upon the mercury vapour pressure; LPUV lamps produce monochromatic light at 253.7 nm under low vapour pressure while MPUV lamps produce a polychromatic light due to higher vapour pressures [6]. Pulsed UV (PUV) disinfection is a relatively new UV technology which differs to mercury vapour-based LPUV/MPUV light by utilising xenon gas to generate a high energy electron pulse, which typically lasts microseconds. PUV systems generally comprise three parts; the power supply, the pulse configuration system and the flash lamp [7]. An alternating current is stored in a capacitor where energy is discharged to create an intense pulse of light which spans across the polychromatic broad-spectrum of UV, visible and infrared light (200−1000 nm) [8]. The high peak power stored in the capacitor is a trademark of this system, which has been shown in some cases to offer shorter treatment times [9,10]. In addition, the power emitted from pulsed UV lamps is generally at least

* Corresponding author at: School of Engineering, NUI Galway, Ireland.
E-mail addresses: kelly.fitzhenry@nuigalway.ie (K. Fitzhenry), eoghan.clifford@nuigalway.ie (E. Clifford), nrowan@ait.ie (N. Rowan), mangeles.val@usc.es (A. Val del Rio).

https://doi.org/10.1016/j.jwpe.2021.102070
Received 18 November 2020; Received in revised form 19 March 2021; Accepted 5 April 2021

an order of magnitude higher than the power emitted from LPUV lamps; this is reflected in the respective energy outputs of both systems for microbial inactivation [11,12].

The application of PUV light as a microbial disinfection method within the food industry has been approved by the United States Food & Drugs Authority (FDA) under code 21CFR179.41 [7,13]. PUV disinfection is considered a favourable alternative to conventional thermal/-chemical disinfection processes owing to shorter treatment times however currently, it is predominantly applied as a disinfection method for food packaging and to a lesser extent as a decontamination method for food products themselves [14]. The vast majority of the published literature pertaining to PUV studies describe experimentation analysis performed under static conditions i.e. samples are fixed below the lamp. Of those studies which have evaluated the disinfection potential of the system using a continuous 'flow-through' experimental set-up, authors reported log inactivation in terms of flow rates and 'number of passes' through the system; no UV doses were reported. Krishnamurthy et al. [15] investigated the PUV inactivation efficiency of *Staphylococcus aureus* via flow-through milk treatment. Results from this study reported bacterial inactivation rates of between 0.55 and 7.26 $\log_{10}$ CFU/mL which were dependent on the distance of the lamp from the sample, the flow rate and the 'number of passes' i.e. the amount of times the medium was recycled through the system. Complete inactivation of *S. aureus* (7.23$\log_{10}$) was achieved at a lamp distance of 8 cm and a flow rate of 20 mL/min for a 'one-pass' treatment; no UV doses were reported. Uslu et al. [16] evaluated the potential of flow-through PUV for the disinfection of *Escherichia coli* (*E. coli*) and *Bacillus subtilis* (*B. subtilis*) in wastewater. In this case, complete inactivation of *E. coli* (7.23 $\log_{10}$) and *B. subtilis* (7.13 $\log_{10}$) was achieved at a flow rate of 2 L/min for a 'one-pass' treatment in a synthetic wastewater mix. The variation in the sample media used creates difficulty in comparing both studies as UV absorption rates may vary depending on the medium [17]. Further detail on UV dose would also be necessary for comparison, this is an issue which limits wider comparisons within the literature in general. In addition, comparisons were not drawn between PUV flow-through treatment and LPUV disinfection.

While UV treatment is an effective disinfection method which produces no disinfection by-products (typically associated with chemical disinfection), a primary drawback includes that of microbial DNA damage repair post UV disinfection. UV-induced molecular lesions may be repaired or replaced by the microorganism either by (i) using enzymes that require light to repair DNA – i.e. photoreactivation (PHR) or (ii) employing enzymes that replace damaged DNA with undamaged nucleotides; excision or dark repair [18–20]. In the water/wastewater disinfection sector, PHR is of primary concern when incorporating UV systems into disinfection processes as microbial re-growth following exposure to sunlight can influence system effectiveness [21]. Literature investigating the photoreactivation potential of various pathogens in wastewater effluent post LPUV treatment has established the relationship between increasing UV dose and decreasing microbial photoreactivation rates [22–25]. However, in the case of bacterial PHR/dark repair post pulsed UV disinfection, study findings are mixed. Lee et al. [26] reported no PHR or dark repair activity of *E.coli* in distilled water mixed with humic acids after PUV treatment at 9 mJ/cm^2 (dose measured as the portion of UV energy within 200–400 nm range of the broadspectrum lamp), while MacLean et al. [27] confirmed photoreactivation of *S. aureus* after a PUV exposure (320–500 nm wavelength range) of 1500 mJ/cm^2 and also surmised a lower UV output/dose during treatment would most likely result in increased bacterial photoreactivation rates. Kramer et al. [28] investigated the PHR potential of *E. coli* and *L. innocua* after pulsed light exposure on a polysaccharide surface and reported photoreactivation for both test bacteria with relative recovery being PUV energy dependant. In all cases, pulsed UV disinfection analysis took place under static or 'batch' experimental set-up with fixed sample treatment. Indeed, the vast majority of PHR/dark repair studies in water typically involve prior UV disinfection carried out via batch analysis [21,24,29–32]. Limited UV disinfection studies have evaluated the potential of bacterial reactivation after flow-through UV disinfection for liquid treatments and to the best knowledge of the authors, all were performed with conventional UV systems.

In this study the efficiency of UV inactivation for *E. coli*, *S. aureus* and *L. innocua* (pathogens relevant in the food and water/wastewater sectors) was studied using LPUV and PUV systems in single-pass flow-through configuration. This also constitutes the first study to comprehensively compare bacterial photoreactivation and/or dark repair immediately following flow-through pulsed UV treatment. This study would be of general interest to the water/wastewater sector with a particular focus on the implementation of strategies of wastewater reuse.

2. Materials and methods

2.1. LPUV and PUV systems

The PUV system comprised a bench–scale pulsed power source (PUV-01, Samtech Ltd., Glasgow) which was used to power a low pressure (60 kPa) xenon-filled flashlamp (Heraeus Noblelight XAP type NL4006 series constructed from a clear UV transparent quartz tube) and produced a high intensity beam of polychromatic pulsed light (200−1100 nm). The lamp was placed 10.75 cm above a sterilised aluminium flow-through vessel (with a plan surface area of 290 cm^2, sample depth of 5.5 cm and hold-up volume of 750 mL) through which water was pumped with a peristaltic pump at specified flow rates (Fig. 1 (a)). The system was enclosed and a smooth aluminium cover was used on the inside of the lamp cover to reflect UV light onto the sample. The PUV system allowed for the input voltage and the pulse rate to be varied between 400 and 1000 V and for a pulse frequency of between 0.1 and 10 pulses per second (PPS). The energy output of the lamp (total energy and energy in specific wavelength ranges) was calculated by analysing lamp characteristics as supplied and verified by testing (by the manufacturer), the area of the vessel, the pulse frequency and the hydraulic residence time - HRT (Table 1) – see supplementary information for system details (Figure S1 and Table S1). The range of energy outputs chosen for this study were selected based on previous PUV system analysis outlined in Fitzhenry et al. [33] and Fitzhenry [34]. These outputs would approximate low, medium and high energy output capabilities from this lamp. Based on the characteristic curves for the PUV lamp, the expected energy outputs could be calculated to include only the wavelengths below 300 nm (i.e. comprises UV C and some of the UV B spectrum). This was done so provide context for in-situ measurements taken at $<$ 280 nm (described in Section 2.3).

The continuous-flow monochromatic LPUV system deployed in this study (LCD 412 Plus, S.I.T.A., Halpin & Hayward Ltd.) had a fixed power output of 40 W at a UV-C wavelength of 254 nm, an internal empty volume of 2.5 L and chamber dimensions of 95 cm length x6 cm diameter (Fig. 1 (b)). The lamp dimensions were 84.3 cm in length x1.6 cm diameter. The lamp irradiation was 30 mJ/cm^2 (at 1 s residence time). The UV energy output could be altered by varying the influent flow rate thereby altering the HRT and thus the exposure time. The flow rate used in the experiments was the maximum allowable (24.6 L/min) which corresponded to a HRT of 0.47 s. This equates to samples being exposed a UV output of 14 mJ/cm^2 (0.47 s x 30 mJ/cm^2 - this was the lowest exposure energy output achievable and resulted in almost full inactivation for all pathogens) (Table 1).

2.2. Experimental setup

Table 1 summarises the experiments carried out with the LPUV and PUV systems in this study. In the case of the LPUV system, only one energy output was analysed (14 mJ/cm^2). For the flow-through PUV system, four different UV outputs were evaluated ranging from 486 mJ/

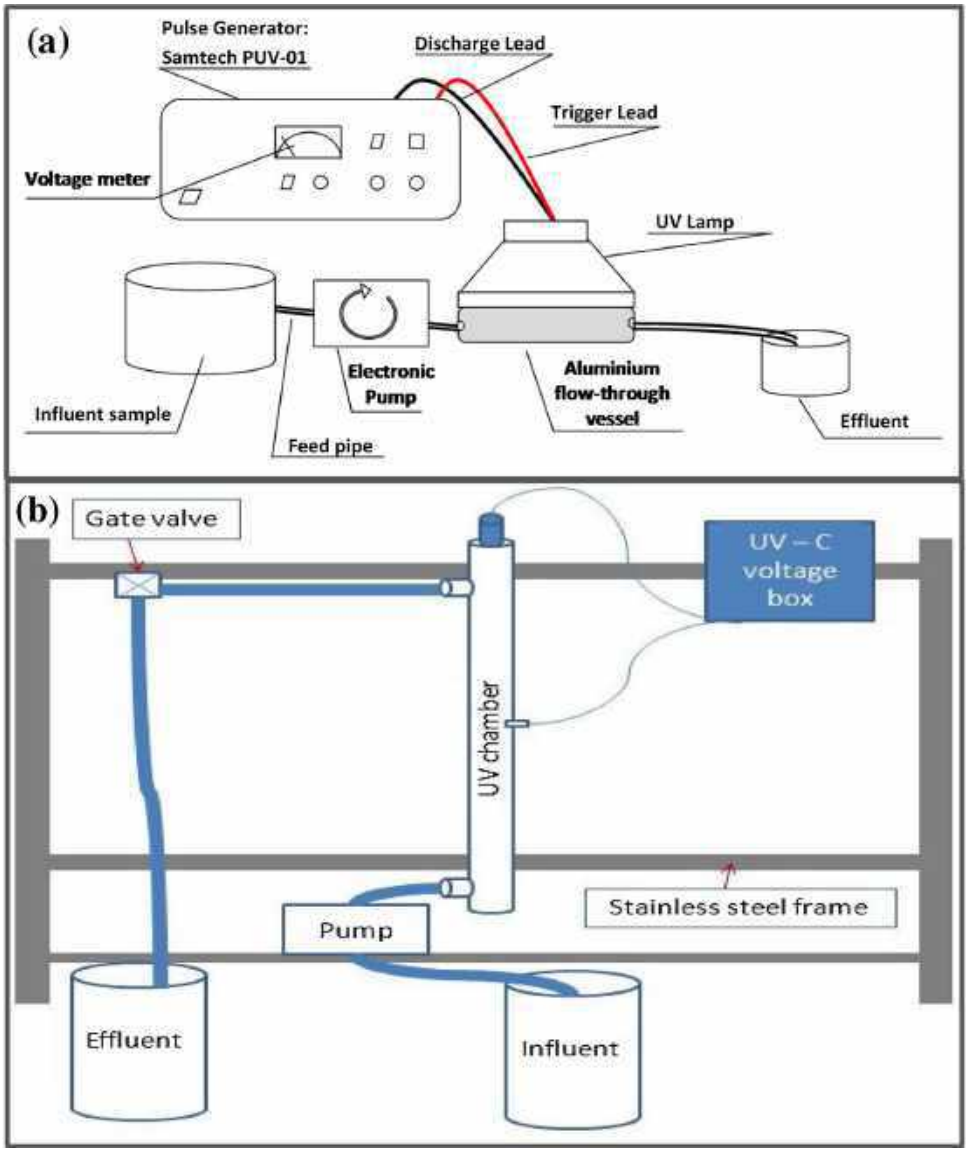

Fig. 1. Schematic of bench-top experimental set-up of (a) PUV system and (b) LPUV system.

cm^2 to 2052 mJ/cm^2.

2.3. UV dose determination of PUV system

The 'UV dose' refers to the UV energy received by the sample (i.e. the UV exposure of the sample). The UV output is energy emitted from the lamp in the UV spectrum. Previous studies have shown the distance of the lamp from the sample to have an impact upon PUV fluence distribution and measurements [35]. Therefore, it was decided to measure the UV dose at the distances used in this study to allow for comparison to the calculated UV output. The UV and UV-C dose received by the sample from the PUV system was analysed using a thermopile power detector (Model: XLP12−3S-H2-IN, Gentec-EO, Quebec, Canada) and Integra software in addition to two longpass colour glass filters; FGL 400 (which filters out wavelengths above 400 nm to give the UV range (200−400 nm)) and FGL 280 (which filters out wavelengths above 280 nm to give the UV-C range (200–280 nm)) (Thorlabs GmbH, Dachau, Germany). The percentage transmission of both filters was as follows; for the 400 nm filter transmission at wavelengths greater than 400 nm was 89 % +/- 4% and for the 280 nm filter transmission for wavelengths greater than 280 nm was 91 % +/- 6% (Thorlabs GmbH, Dachau, Germany). The detector (12 mm aperture) was situated at the bottom of a metal cylinder 5 cm in depth through which the light was directed downwards towards the cylindrical detector surface. The detector was placed on the aluminium vessel, with the sensor being 10.75 cm below the xenon lamp. Pulse energies were measured three times at each voltage and each voltage setting was analysed on three separate occasions (to determine consistency/deviation of detector readings) to give nine broadspectrum energy readings in total after which an average value was obtained. Power was measured in irradiance units (mW/cm^2). The filters were then placed separately directly on top of the detector at the base of the metal tube and the power measurements were taken as previously described. The differences in the power values obtained with and without the filters were used to calculate the power emitted from the lamp within the UV and the UV-C range. The calculated UV output and equivalent measured UV and UV-C dose are listed in Table 2. At a distance of 10.75 cm there is a significant difference between the output of the lamp and the dose measured (as approximated by the inverse square law). Other factors contributing to the relatively low UV (and UV-C) dose relative to the lamp output is the broadspectrum nature of the output and heat generated within the PUV system. This has been previously noted in Fitzhenry et al., (2019) (33). It should be noted that the filters were removed for the disinfection studies and were only used to determine UV dose.

Table 1
Characteristics of the LPUV and PUV flow-through experimental runs performed with the three bacterial strains.

UV system	Voltage (V)	Pulse frequency (PPS)	HRT (s)	Flow rate (L/min)	UV output (mJ/cm^2)	Bacterial strains tested
LPUV	N/A	N/A	0.47	24.60	14.0[1]	*E. coli*, *S. aureus* and *L. innocua*
PUV	800	0.5	120	0.38	486.0[2]	*E. coli*, *S. aureus* and *L. innocua*
	900	1.0	100	0.45	1026.1[2]	*E. coli*, *S. aureus* and *L. innocua*
	900	2.0	75	0.60	1539.2[2]	*E. coli*, *S. aureus* and *L. innocua*
	900	2.0	100	0.45	2052.0[2]	*S. aureus* and *L. innocua*

N/A: Not Applicable.
[1] Output at 254 nm.
[2] Output at < 300 nm.

Table 2
Calculated broadspectrum UV output and equivalent measured UV and UV-C dose for PUV system.

Pulse frequency (PPS)	Residence time (s)	Voltage	Calculated UV Output (from lamp characteristics) $E_{A<300\ nm}$ (mJ/cm^2)	Average measured UV Dose (10.75 cm from lamp)* $E_{A<400\ nm}$ (mJ/cm^2)	Average measured UV-C Dose (10.75 cm from lamp)* $E_{A<280\ nm}$ (mJ/cm^2)
1	60	800	486	42	16
1	100	900	1026	112	18
2	75	900	1539	168	26
2	100	900	2052	269	35

E_A – energy per unit surface area·
* n = 9 for each of these measurements with a standard deviation of less than 2% of the average in each case·

2.4. Bacterial analysis via UV treatment

The bacterial strains used to investigate inactivation, photoreactivation and dark repair post LPUV and PUV disinfection were *Escherichia coli* ATCC 25922, *Staphylococcus aureus* DSM 1104 and *Listeria innocua* DSM 20649. These were chosen as they had been recently identified as pathogens of interest in wastewater streams from dairy processing facilities in Ireland [42]. The strain DSM 20649 was used as a non-pathogenic surrogate for *Listeria monocytogenes* [36]. All three freeze-dried cultures were reconstituted using tryptic soy agar (TSA, Sigma-aldrich, Wicklow, Ireland) and tryptic soy broth (TSB, Fisher Scientific, Dublin, Ireland) at 37 °C for 18−24 hours. Fresh cultures were then inoculated aseptically on to cryobeads (Pro-Lab Microbank, Cruinn Diagnostics, Dublin Ireland) for long-term storage at −80 °C. The fresh cultures were also cultured on TSA slopes as working culture stocks and stored at 4 °C in the fridge. Working stock cultures were discarded every three months and replaced with fresh working cultures to avoid contamination issues.

Prior to the photoreactivation experimentation, the bacteria were exposed to both PUV and LPUV disinfection as a prerequisite to PHR/dark repair analysis. For experimental analysis, one colony of each strain was inoculated into 80 mL of Luria Broth (LB) (Sigma-aldrich, Wicklow, Ireland) for *E. coli* culture and TSB (Fisher Scientific, Dublin, Ireland) for *L. innocua* and *S. aureus*. The broth(s) were cultured on a rotary shaker at 90 rpm for 24 h at 37 °C. For LPUV runs, batches of tap water (20 L) were spiked with 10 mL of broth strains to give a starting bacterial concentration of 6 $\log_{10} \pm 0.5$, while for PUV runs 2.5 L of distillate water was spiked with 1 mL of broth strains to give a starting bacterial concentration of 6 $\log_{10} \pm 0.5$). The distillation system in the laboratory produced a limited volume of water daily and could not meet the volumes required for LPUV analysis thus tap water was used instead. Experimental analysis was carried out to ensure there were no differences in inactivation rates of bacteria (*E. coli* was used as the test strain) via LPUV between both mediums (data not shown). Influent and effluent samples were analysed in duplicate pre and post UV treatment via pour plate technique (1 mL) as per standard methods [43] using Tryptone Bile X-glucuronide (TBX) Agar (VWR, Dublin, Ireland) for *E. coli* and TSA (Sigma-aldrich, Wicklow, Ireland) for *S. aureus* and *L. innocua*. Each UV inactivation experiment was performed at least three times. The limit of detection was 1 CFU/mL, see Section 2.6 for log inactivation calculations.

2.5. Photoreactivation and dark repair analysis

Immediately following UV treatment, effluent samples were placed under light and dark conditions to study potential bacterial PHR/dark repair. For photoreactivation experiments, duplicate sample aliquots (40 mL) were placed into open petri dishes (diameter of 90 mm, surface area of 58 cm^2) at a distance of 9 cm from two compact fluorescent lamps (23 W power, luminous flux (Lm) 1450) which emitted light in the 300–700 nm spectral range (OSRAM model DPRO MITW 23 W/840 E27). Previous studies have reported the photolyase enzyme for bacterial PHR to respond significantly to 'blue light' in the 360–500 nm range [27]. For dark repair experiments, duplicate sample aliquots (20 mL) were aseptically transferred to 60 mL tubes covered with aluminium foil and placed into a sealed box in the dark for the same duration of time as the photoreactivation experiments. Both the light and dark experimental analysis was carried out in the same incubator (Velp Scientifica) at 20 ± 1 °C. Sample volumes of 1 mL were collected aseptically from both the light and dark sample experiments at a series of time intervals ranging from 0 to 120 min post UV treatment. The samples were analysed in duplicate via pour plate technique (1 mL) as per standard methods [43] using TBX agar (VWR, Dublin, Ireland) for *E. coli* and TSA (Sigma-aldrich, Wicklow, Ireland) for *S. aureus*.

2.6. Quantitative analysis

Bacterial inactivation via UV treatment using logarithmic scale and colony forming unit (CFU) /mL was determined using Eq. (1), where N_0 and N are the concentrations (CFU/mL) pre and post disinfection respectively.

$$\text{Inactivation(UV)} = log_{10}(N_0/N) \quad (1)$$

Bacterial photoreactivation and dark repair expressed as a percentage was determined with Eq. (2) adapted from methods used in Maclean et al. [27] and Shafaei et al. [25] where N_t is the concentration at time "t" after the start of the photoreactivation/dark repair experiment (light or dark). Note that at time zero N_t is equal to N.

$$\text{Repair}(\%) = \frac{N_t - N}{N_0 - N} \times 100 \quad (2)$$

3. Results & discussion

3.1. Bacterial inactivation via continuous-flow LPUV and flow-through PUV disinfection

Results for the LPUV system showed almost complete inactivation of all three bacterial strains at the UVC output of 14 mJ/cm^2 (Fig. 2). Log_{10} inactivations of 5.3 ± 0.3, 6.0 ± 0.2 and 5.9 ± 0.1 were observed from starting bacterial populations of 6.0 log_{10} ±0.5 for *S. aureus*, *E. coli* and *L. innocua* respectively at 14 mJ/cm^2. Therefore, given the LPUV system was operating at the shortest HRT (and thus the lowest UV output achievable) – no other HRTs were subsequently investigated. The inactivation of vegetative bacteria in water via LPUV is well established. Previous studies have shown *E. coli* and *S. aureus* to be inactivated by 5–6 log_{10} in water via batch LPUV disinfection at UV doses of < 10 mJ/cm^2 [4,37]. Thus, results in this study are in line with findings in the literature which illustrate vegetative cells are readily inactivated by LPUV disinfection at relatively low UV energies.

Research investigating bacterial inactivation in water/wastewater via flow-through PUV systems is limited. In this study, bacterial inactivation via flow-through PUV disinfection was linearly dependent on energy, with *E. coli* being the most sensitive and *L. innocua* exhibiting the most PUV resistance (Fig. 3).

The maximum inactivation observed for *E. coli* (5.3 ± 0.3 log_{10}) was achieved at a lamp UV output (< 300 nm) of 1539 mJ/cm^2 while a higher UV output (< 300 nm) of 2052 mJ/cm^2 inactivated the Gram-positive bacteria *S. aureus* and *L. innocua* by 5.2 ± 0.6 log_{10} and 4.3 ± 0.3 log_{10} respectively. This finding is consistent with Farrell [38] who reported Gram-positive bacteria (*S. aureus* and *L. monocytogenes*) to be more resistant to PUV light in comparison to Gram-negative bacteria (*E. coli*) in a static experimental set-up. Uslu et al. [17] analysed the inactivation of *E. coli* via flow-through PUV disinfection in synthetic wastewater with the addition of 'multiple pass' analysis whereby the sample was recirculated back under the PUV lamp for a second disinfection step. In the aforementioned study, the UV dose/system output was not described rather the flow rate and broadspectrum energy output (J) per litre treated was given. Results showed complete inactivation of *E. coli* in synthetic wastewater at flow rates of 10 L/min (equivalent to a broadband energy of 39.7 J/L) for a two-pass treatment. A similar study [39] investigated the inactivation of *L. innocua* via flow-through PUV for water treatment. A PUV dose of 4,000 mJ/cm^2 (at a flow rate of 1 L/min) was required for 2 log_{10} *L. innocua* inactivation in water. Krishnamurthy et al. [16] tested the inactivation of *S. aureus* in milk under flow-through PUV experimental conditions and also adopted a multi-pass disinfection method akin to Uslu et al. [17]. Log_{10} reductions were reported as a function of flow-rate, lamp distance and number of sample passes. Complete inactivation of *S. aureus* was obtained at 8 cm sample distance, single pass and 20 mL/min flow rate however no UV dose/energy output

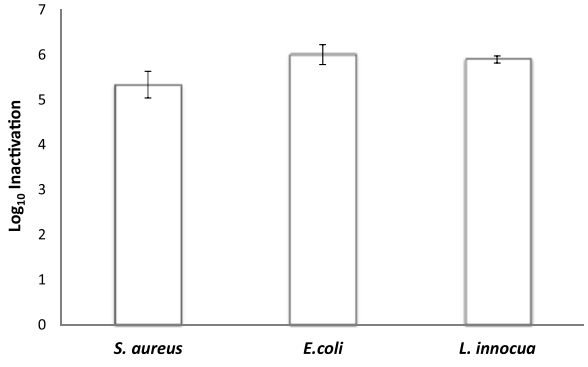

Fig. 2. Log_{10} inactivation of *S. aureus, E. coli* and *L. innocua* via continuous-flow LPUV disinfection at a UV output of 14 mJ/cm^2. Standard error bars shown (n = 3).

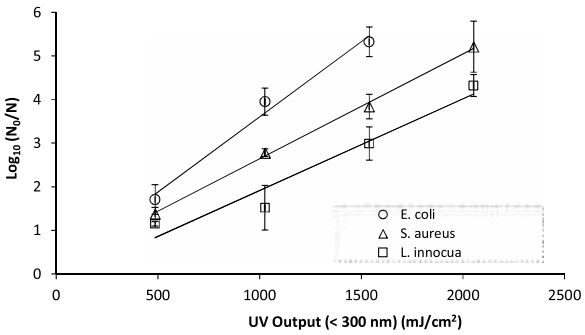

Fig. 3. Bacterial inactivation via flow-through PUV disinfection at various UV outputs. Data points are average values of three independent runs and error bars represent the standard deviation.

was reported. Interestingly, it was also noted that a decrease in PUV energy was a polynomial function of the lamp distance i.e. inactivation rates were higher at 8 cm lamp distance than those achieved at 5 cm lamp distance [16]. Finally, Fitzhenry et al. [33] recently reported a UV output (< 300 nm) of approximately 2,000 mJ/cm^2 was required to inactivate *Bacillus spp*. endospores by approx. 2 log_{10} in water via flow-through PUV disinfection.

These studies show that with flow-through pulsed UV technology (as investigated to date) the use of multi-pass is necessary for the inactivation of S. aureus and E. coli. In the case of L. innocua a single pass may be possible, however, to-date, clear information on the necessary UV dose has not been available. This study presents inactivation rates for various UV outputs for the PUV technology. This data is key as the overall capacity of the lamp in terms of UV energy output will be a key determining factor (alongside the desired pathogen removal rates) as to whether single pass or multi-pass should be deployed.

3.2. Bacterial photoreactivation & dark repair post UV treatment

Experimental results for the potential photoreactivation of the three pathogens following LPUV disinfection at 14 mJ/cm^2 indicated that bacterial concentrations after light and dark repair analysis were negligible (see Supporting Information, Figure S2). Previous research [24] has reported PHR for *E. coli* post LPUV treatment whereby water samples exposed to UV dose of 5 mJ/cm^2 were subsequently placed under sunlight lamps for 4 h before photoreactivation was observed. While photoreactivation of *E. coli* was reported after LPUV treatment at 5 mJ/cm^2, the same study [24] reported a lack of photoreactivation when the bacteria were exposed to a higher UV dose of 15 mJ/cm^2. Sanz et al. [23] reported a similar conclusion when investigating the photorepair potential of total coliforms post LPUV treatment in a wastewater treatment facility. Their results showed a significant decrease of photoreactivation potential at high UV doses indicating the severity of the UV damage at high doses can prohibit DNA lesion repair. Therefore, perhaps in the case of the experimental analysis carried out in this study, the applied LPUV output of 14 mJ/cm^2 may have inhibited the ability of the bacteria to photoreactivate/dark repair. Unfortunately, limitations regarding decreasing the system energy output of the LPUV system did not allow for analysis of bacterial PHR/dark repair post lower LPUV outputs. Nonetheless, considering the high inactivation efficiencies found for the three experimental bacterial strains and the lack of photoreactivation/dark repair at the minimum UV output possible (14 mJ/cm^2), and at a relatively high flow rate (24.6 L/min equating to 0.47 s HRT), the results further highlight the suitability of the LPUV system as an effective technology to inactivate S. aureus, E. coli and L. innocua

The particular strain of *L. innocua* (DSM 20649) selected for this study appeared to be impacted by the photoreactivation experimental conditions. Previous studies have discussed various light sources used in PHR experiments including the spectrum output, the power, the

temperature (which influences sunlight simulation) and the colour of the light. It was noted that the photolyase enzyme for bacterial photoreactivation responds significantly to 'blue light' in the 360–500 nm range and that *L. monocytogenes* and *S. aureus* exhibit maximum photoreactivation potential between 360–380 nm [27], therefore these factors were taken into consideration when deciding the optimum conditions for photoreactivation experiments. Fig. 4a shows the results of the photoreactivation and dark repair experiments for *L. innocua* post flow-through PUV treatments at PUV outputs (< 300 nm) of 486, 1026 and 2052 mJ/cm^2. While minimal dark repair was observed for *L. innocua*, populations of *L. innocua* survivors post PUV irradiation were observed to decrease in numbers during the period of photoreactivation conditions. Upon further investigation, it was confirmed that *L. innocua* was inactivated by the compound fluorescent lamp with no prior UV exposure (Fig. 4b). Thus, it was decided to eliminate it from the photoreactivation analysis. For confirmation purposes, similar analysis was carried out on *E. coli* and *S. aureus* whereby the strains were exposed to the compound light only (without prior exposure to PUV). The results confirmed that the photoreactivation experimental conditions were not impacting upon cell viability as was the case with *L. innocua* (Fig. 4(b)). A previous study reported photoreactivation of the same strain of *L. innocua* as was used in this study [28]. Kramer et al. [28] investigated the photoreactivation of PUV treated *L. innocua* (DSM 20649) and used a 30 W fluorescent lamp with a spectrum output of between 400 and 650 nm for PHR analysis. These results showed photoreactivation rates of between 10^2 and 10^6 CFU/mL after 24 h of lamp exposure on tryptic soy agar at 37 °C depending on the PUV fluence applied.

The reasons for *L. innocua* becoming inactivated under the compound lamp in this study are not entirely clear. Perhaps the slightly lower spectrum output of the lamp and the difference in experimental conditions (illumination on agar and not water as was the case in this study) in the Kramer et al. [28] study were more conducive to *L. innocua* photoreactivation analysis i.e. agar medium designed to enable bacterial growth as opposed to water medium. However, in this study it was considered important to use a lamp with a spectrum below 400 nm due to reasons stated above i.e. photolyase activity and favoured photoreactivation potential at the wavelengths between 360–380 nm. Moreover, *S. aureus* and *E. coli* were not negatively affected by the lamp/photoreactivation conditions. While photoreactivation analysis of *L. innocua* could not be completed in this study, details surrounding the specifics of experimental design and the particular bulbs used for PUV treatments may be noteworthy for future studies.

Photoreactivation was observed for both *E. coli* and *S. aureus* post flow-through PUV treatment at various energy outputs over time (Fig. 5 (a) and 5 (b)). Results for *S. aureus* at the lowest output of 486 mJ/cm^2 showed a sharp increase in PHR between 10 and 60 min after which inactivation were relatively stable. However, this was not constant and the % PHR increased slightly again after this time point. Increases in the

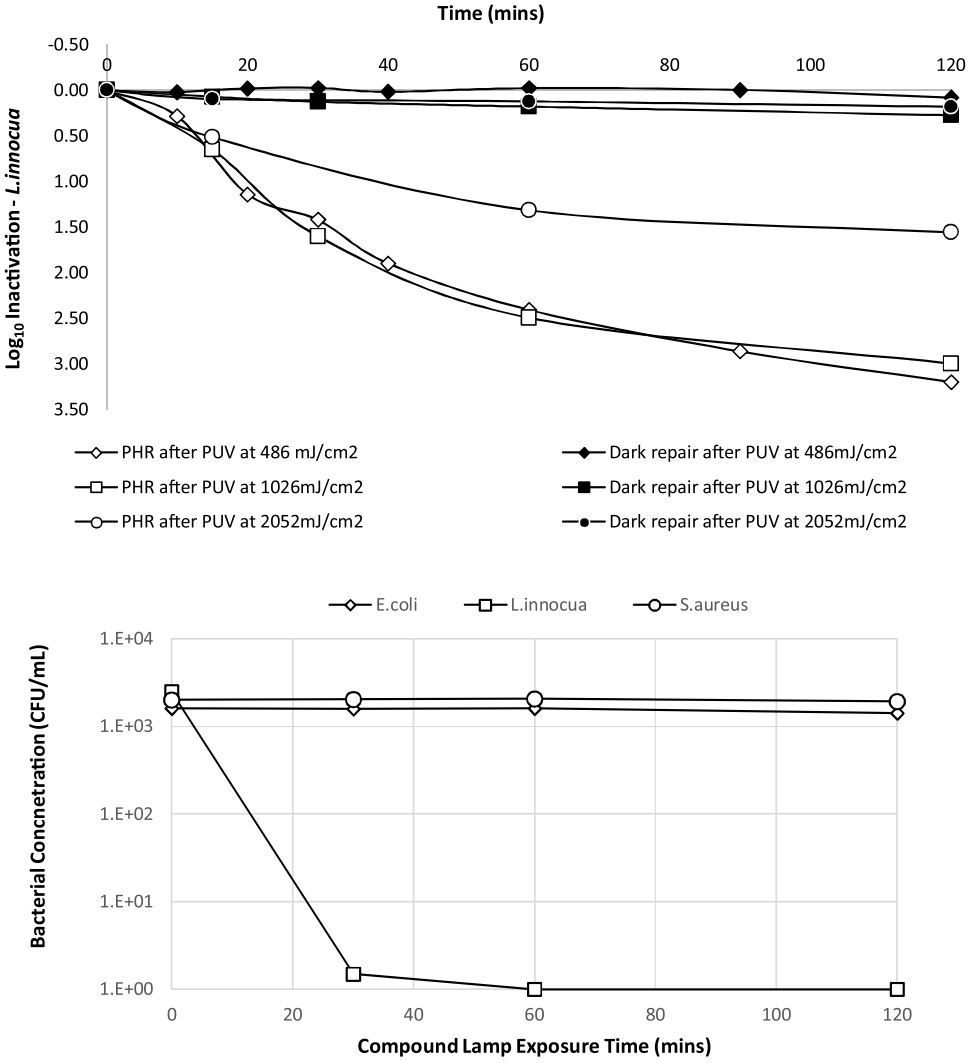

Fig. 4. (a). photoreactivation and dark repair post PUV disinfection at PUV outputs (< 300 nm) of 486, 1026, 2052 mJ/cm^2 and 4(b) inactivation of *L. innocua* under photoreactivation (PHR) lamp only, without any prior PUV treatment.

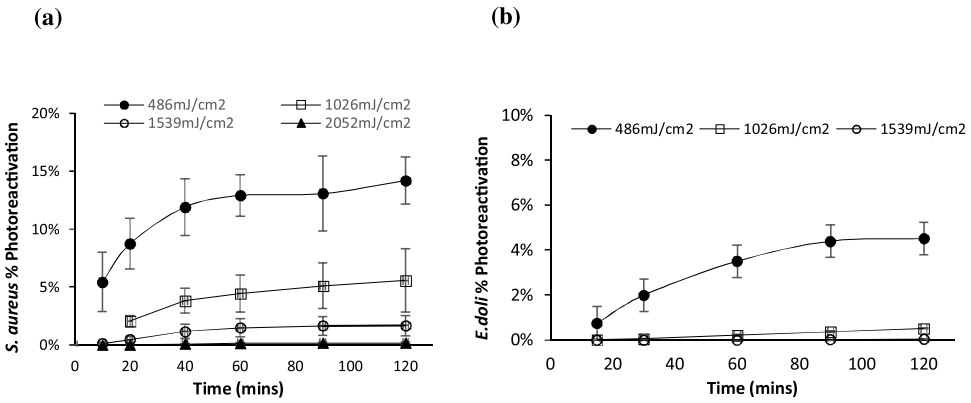

Fig. 5. Percentage photoreactivation over time of (a) *S. aureus* and (b) *E. coli* at various UV outputs (< 300 nm) following flow-through PUV treatment.

percentage photoreactivation of *S. aureus* were less pronounced at higher UV system outputs with negligible PHR occurring at any time point after PUV treatment at 2052 mJ/cm^2 (Fig. 5 (a)). Analysis of *E. coli* photoreactivation over time shows a slightly different trend to that of *S. aureus* post PUV treatment (Fig. 5 (b)). At 486 mJ/cm^2, the PHR of *E. coli* steadily increased between 15 and 90 min before a tailing effect was observed. At 1026 mJ/cm^2 the percentage of photoreactivation *E. coli* was relatively low, while at 1539 mJ/cm^2 it was found to be negligible. Therefore, it was decided to not investigate photoreactivation of *E. coli* at higher UV system outputs. Previous studies [21] have suggested that a time-based comparison for photoreactivation experiments cannot be performed due to variations in lamp intensities i.e. the energy outputs of lamps can vary even where they are the same model. However, in the present research study a time-based comparison between *S. aureus* and *E. coli* was possible as the same experimental set-up and lamp was used for both bacteria and should be noted for future studies of this kind. Photoreactivation has been observed previously [28] for *E. coli* post static PUV treatment on gel mediums with a recovery rate of up to 2 $\log_{10}$ following a PUV dose of 450–1000 mJ/cm^2. Maclean et al. [27] investigated the PHR potential of *S. aureus* and *L. monocytogenes* post PUV treatment under static experimental conditions and observed a photoreactivation response after PUV treatments of 1500 mJ/cm^2 and 3400 mJ/cm^2 (within 320–500 nm range) respectively. The study found approximately 2% of *S. aureus* bacteria photoreactivated after a PUV exposure of 1500 mJ/cm^2 (PHR exposure time not given). Similarly, results in the present study found 1.7 % of the *S. aureus* population photoreactivated after 1500 mJ/cm^2 PUV energy exposure at 90 min. However, in this case, a flow-through experimental set-up was applied. While Maclean et al. [27] did report a low degree of PHR for *S. aureus* at the PUV output energy applied, it was surmised that a less intense UV energy output would likely result in a higher degree of photoreactivation which was the finding in this study. The majority of photoreactivation occurred within the first hour for *S. aureus* and the first 90 min for *E. coli* thus avoiding bacterial exposure to light immediately after flow-through PUV disinfection may be important when attempting to maintain high inactivation rates for both *S. aureus* and *E. coli*. However, it should also be noted that this study did not investigate delayed exposure to light i.e. PHR after some dark incubation, thus caution may need to be exercised in this case also. Nonetheless, as is the case with LPUV disinfection, bacterial photoreactivation is reported to be avoidable when a high UV energy is applied [23,24].

The maximum pathogen photoreactivation and dark repair after 120 min following flow-through PUV treatment is shown in Fig. 6. As indicated in Fig. 5, *S. aureus* exhibited higher PHR rates in comparison to *E. coli*; this trend appeared consistent for dark repair analysis of *S. aureus* at 486 mJ/cm^2 albeit the percentage of reactivated bacteria was low. For example, in the case of *S. aureus*, 0.75 % of the surviving bacterial population (post PUV treatment at 486 mJ/cm^2) repaired under dark

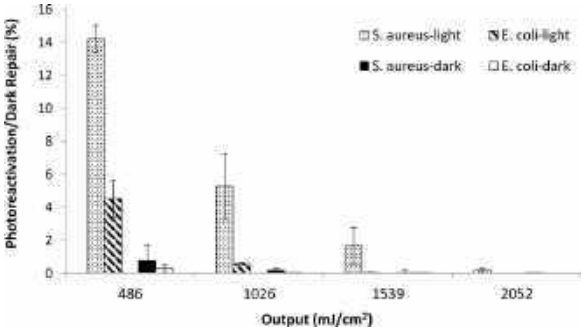

Fig. 6. Photoreactivation (light) and dark repair (dark) after 120 min exposure for *S. aureus* and *E. coli* post flow-through PUV treatment at various UV outputs.

experimental conditions in comparison to 0.29 % of *E.coli* at the same UV output. Aside from slight bacterial reactivation at the lowest PUV output, dark repair for both strains was found to be minimal after PUV flow-through treatments of 1026 mJ/cm^2 and above. Potential reasons for the lack of dark repair exhibited by bacteria in this study may be due the length of dark exposure time applied during the experimental analysis. Jungfer et al. [40] reported the activation of bacterial dark repair mechanisms (*rec*A mRNA protein) to be dependent on experimental incubation time which was found to vary depending on the bacterial strain. For example, a dark incubation time of two hours induced *rec*A in drinking water bacteria *Caulobacter crescentus*. In contrast, *Enterococcus faecium* required an incubation period of six hours before dark repair mechanisms were observed [40]. However, previous studies [23,41] have also reported bacterial dark repair to occur within approximately 100 min of incubation post UV disinfection after which a bacterial decay period was observed. Nebot Sanz et al. [23] confirmed dark repair analysis, carried out in conjunction with photoreactivation analysis, did occur but to a lower degree that in light repair conditions. Moreover, the authors [23] concluded maximum dark repair of bacteria occurred sooner in comparison to maximum bacterial photoreactivation. In this study, stable photoreactivation rates were achieved during the maximum experimental exposure time of 120 min, and for this reason dark repair experimental analysis was also carried out for the same duration. Some of the differences in findings between studies may be attributed to the variation in Gram positive and negative composition in terms of cell membrane(s) and amount of cell wall material present (peptidoglycan) (38).

It is possible that low UV outputs also puts less biocidal stress on the treated bacterial cells with potentially greater ability to repair as less physical, genomic and metabolic damage – lower doses may not cause irreversible damage.

4. Conclusions

This constitutes the first study to demonstrate that bacterial (S. aureus and E. coli) photoreactivation is possible post flow-through PUV disinfection and that the level of bacterial photoreactivation is dependent upon the output energy applied during prior UV disinfection treatment. Furthermore, it was shown that dark repair is less significant when compared to light repair. The results agree with similar studies in the literature involving static and continuous-flow UV disinfection studies whereby the UV dose/output applied during the UV disinfection phase influences the degree to which bacteria can repair. Should flow-through PUV systems be considered for full-scale operation as a disinfection system for water reuse/wastewater treatment, sufficient energy should be applied to avoid bacterial reactivation. The immediate exposure of bacteria to light post flow-through PUV treatment should also be avoided to minimise photoreactivation of both S. aureus and E. coli. The continuous-flow LPUV system used in this study successfully inactivated all three bacteria to a higher degree than the PUV system deployed (with significantly lower energy consumption). The LPUV was also successful in the inhibition of E. coli and S. aureus photoreactivation post LPUV treatment. The study confirmed the suitability of existing LPUV as a technology in achieving adequate inactivation percentages with limited potential for repair in both light and dark conditions. However, further work would be required in the development of PUV systems to enable them be efficiently and cost-effectively deployed in larger scale water/wastewater treatment scenarios. As with all disinfection technology the required doses for adequate removal of targeted pathogens will depend on the nature of the wastewater being treated.

Declaration of Competing Interest

The authors report no declarations of interest.

Acknowledgments

The authors would like to acknowledge the Department of Agriculture, Food and the Marine of Ireland (Ref: 13-F-507) for funding this research. Dr. Val del Rio was supported by the Spanish Government (CTM2014-55397-JIN project co-funded by FEDER) and Xunta de Galicia postdoctoral fellowship.

Appendix A. Supplementary data

Supplementary material related to this article can be found, in the online version, at doi:https://doi.org/10.1016/j.jwpe.2021.102070.

References

[1] H. Chmiel, M. Kaschek, C. Blocher, M. Noronha, V. Mavrov, Concepts for the treatment of spent process water in the food and beverage industries, Desalination 152 (2002) 307–314.
[2] S.T. Summerfelt, M.J. Sharrer, S.M. Tsukuda, M. Gearheart, Process requirements for achieving full-flow disinfection of recirculating water using ozonation and UV irradiation, J. Aquac. Eng. Fish. Res. 40 (1) (2009) 17–27. Available from: http://linkinghub.elsevier.com/retrieve/pii/S0144860908000691.
[3] EPA, BAT Guidance Note on Best Available Techniques for the Dairy Processing Sector, Environmetal Protection Agency, Johnstown Castle Estate, Co. Wexford, Ireland, 2008. ISBN 1840952806.
[4] EPA, Water Treatment Manual: Disinfection, Environmetal Protection Agency, Johnstown Castle, Co. Wexford, Ireland, 2011. ISBN 9781840954210.
[5] WERF, Disinfection of Wastewater Effluent — Comparison of Alternative Technologies, Water Environment Research Foundation, Alexandria, Virginia, USA, 2008. IWAP ISBN: 978-1-84339-799-1/1-84339-799-4.
[6] USEPA, Ultraviolet Disinfection Guidance Manual for the Final Long Term 2 Enhanced Surface Water Treatment Rule, United States Environmental Protection Agency, Washington, USA, 2006. Report EPA 815-R-06-007.
[7] N. Elmnasser, S. Guillou, F. Leroi, N. Orange, A. Bakhrouf, M. Federighi, Pulsed-light system as a novel food decontamination technology: a review, Can. J. Microbiol. 53 (7) (2007) 813–821. Available from: http://www.ncbi.nlm.nih.gov/pubmed/17898836.
[8] T. Wang, S.J. Macgregor, J.G. Anderson, G.a Woolsey, Pulsed ultra-violet inactivation spectrum of Escherichia coli, Water Res. 39 (13) (2005) 2921–2925. Available from: http://www.ncbi.nlm.nih.gov/pubmed/15993922.
[9] Z. Bohrerova, H. Shemer, R. Lantis, Ca Impellitteri, K.G. Linden, Comparative disinfection efficiency of pulsed and continuous-wave UV irradiation technologies, Water Res. 42 (June (12)) (2008) 2975–2982. Available from: http://www.ncbi.nlm.nih.gov/pubmed/18460414.
[10] A.M. Garvey, N. Rowan, Report No. 145 Development of a Pulsed Light Approach As a Novel Solution in Drinking Water Treatment, Environmental Protection Agency, Johnstown Castle, Co. Wexford, Ireland, 2015. ISBN 9781840955828.
[11] A.R. Uesugi, L.C. Hsu, R.W. Worobo, C.I. Moraru, Gene expression analysis for Listeria monocytogenes following exposure to pulsed light and continuous ultraviolet light treatments, LWT - Food Sci Technol 68 (2016) 579–588. Available from: http://www.sciencedirect.com/science/article/pii/S002364381630007X.
[12] J.Y. Yi, N.H. Lee, M.S. Chung, Inactivation of bacteria and murine norovirus in untreated groundwater using a pilot-scale continuous-flow intense pulsed light (IPL) system, LWT - Food Sci Technol 66 (2016) 108–113, https://doi.org/10.1016/j.lwt.2015.10.027. Available from:.
[13] Food and Drug Administration, Irradiation in the Production, Processing and Handling of Food. 21 CFR 179.41, Available from:, 1996 https://www.accessdata.fda.gov/scripts/cdrh/cfdocs/cfcfr/CFRSearch.cfm?CFRPart=179.
[14] V. Heinrich, M. Zunabovic, T. Varzakas, J. Bergmair, W. Kneifel, Pulsed light treatment of different food types with a special focus on meat: a critical review, Crit. Rev. Food Sci. Nutr. 56 (4) (2016) 591–613.
[15] N.J. Rowan, Pulsed light as an emerging technology to cause disruption for food and adjacent industries – quo Vadis? Trends Food Sci. Technol. 15 (9) (2019) 462–467. Available from: https://linkinghub.elsevier.com/retrieve/pii/S0924224418308495.
[16] K. Krishnamurthy, A. Demirci, J.M. Irudayaraj, Inactivation of Staphylococcus aureus in milk using flow-through pulsed UV-light treatment system, J. Food Sci. 72 (7) (2007).
[17] G. Uslu, A. Demirci, J.M. Regan, Disinfection of synthetic and real municipal wastewater effluent by flow-through pulsed UV-light treatment system, J. Water Process Eng. 10 (2016) 89–97. Available from: http://linkinghub.elsevier.com/retrieve/pii/S2214714416300575.
[18] N. Goosen, G.F. Moolenaar, Repair of UV damage in bacteria, DNA Repair (Amst.) 7 (March (3)) (2008) 353–379. Available from: http://www.ncbi.nlm.nih.gov/pubmed/17951115.
[19] R.P. Sinha, D.-P. Häder, UV-induced DNA damage and repair: a review, Photochem. Photobiol. Sci. 1 (4) (2002) 225–236. Available from: http://xlink.rsc.org/?DOI=b201230h.
[20] L.O. Essen, T. Klar, Light-driven DNA repair by photolyases, Cell. Mol. Life Sci. 63 (11) (2006) 1266–1277.
[21] Z. Bohrerova, K.G. Linden, Standardizing photoreactivation: comparison of DNA photorepair rate in Escherichia coli using four different fluorescent lamps, Water Res. 41 (12) (2007) 2832–2838.
[22] Wa M. Hijnen, E.F. Beerendonk, G.J. Medema, Inactivation credit of UV radiation for viruses, bacteria and protozoan (oo)cysts in water: a review, Water Res. 40 (January (1)) (2006) 3–22. Available from: http://www.ncbi.nlm.nih.gov/pubmed/16386286.
[23] E. Nebot Sanz, I. Salcedo Dávila, J.A. Andrade Balao, J.M. Quiroga Alonso, Modelling of reactivation after UV disinfection: effect of UV-C dose on subsequent photoreactivation and dark repair, Water Res. 41 (14) (2007) 3141–3151.
[24] M. Guo, H. Hu, J.R. Bolton, M.G. El-Din, Comparison of low- and medium-pressure ultraviolet lamps: photoreactivation of Escherichia coli and total coliforms in secondary effluents of municipal wastewater treatment plants, Water Res. 43 (3) (2009) 815–821. Available from: http://www.sciencedirect.com/science/article/pii/S0043135408005617.
[25] S. Shafaei, N. Klamerth, Y. Zhang, K. McPhedran, J.R. Bolton, M. Gamal El-Din, Impact of environmental conditions on bacterial photoreactivation in wastewater effluents, Environ. Sci. Process. Impacts 19 (1) (2017) 31–37.
[26] E. Lee, H. Lee, W. Jung, S. Park, D. Yang, K. Lee, Influences of humic acids and photoreactivation on the disinfection of Escherichia coli by a high-power pulsed UV irradiation, Korean J. Chem. Eng. 26 (5) (2009) 1301–1307. Available from: http://link.springer.com/10.1007/s11814-009-0208-5.
[27] M. Maclean, L.E. Murdoch, M.N. Lani, S.J. MacGregor, J.G. Anderson, G. A. Woolsey, Photoinactivation and photoreactivation responses by bacterial pathogens after exposure to pulsed UV-light, Proc 2008 IEEE Int Power Modul High Volt Conf PMHVC (2008) 326–329.
[28] B. Kramer, J. Wunderlich, P. Muranyi, Pulsed light induced damages in *Listeria innocua* and *Escherichia coli*, J. Appl. Microbiol. 119 (4) (2015) 999–1010, https://doi.org/10.1111/jam.12912. Available from:.
[29] J.L. Zimmer, R.M. Slawson, Potential repair of Escherichia coli DNA following exposure to UV radiation from both medium- and low-pressure UV sources used in drinking water treatment potential repair of Escherichia coli DNA following exposure to UV radiation from both medium- and Lo, Appl. Environ. Microbiol. 68 (7) (2002) 3293–3299.
[30] J.L. Zimmer, R.M. Slawson, P.M. Huck, Inactivation and potential repair of Cryptosporidium parvum following low- and medium-pressure ultraviolet irradiation, Water Res. 37 (14) (2003) 3517–3523. Available from: http://www.ncbi.nlm.nih.gov/pubmed/12834745.
[31] J.L. Zimmer-Thomas, R.M. Slawson, P.M. Huck, A comparison of DNA repair and survival of Escherichia coli O157:H7 following exposure to both low- and medium-pressure UV irradiation, J. Water Health 5 (3) (2007) 407, https://doi.org/10.2166/wh.2007.036. Available from:.

[32] M. Guo, J. Huang, H. Hu, W. Liu, J. Yang, UV inactivation and characteristics after photoreactivation of Escherichia coli with plasmid: health safety concern about UV disinfection, Water Res. 46 (13) (2012) 4031–4036. Available from: http://www.ncbi.nlm.nih.gov/pubmed/22683407.

[33] K. Fitzhenry, N. Rowan, A. Val, A. Cremillieux, E. Clifford, Inactivation efficiency of Bacillus endospores via modified flow-through PUV treatment with comparison to conventional LPUV treatment, J Water Process Eng. 27 (November 2018) (2019) 67–76, https://doi.org/10.1016/j.jwpe.2018.11.009. Available from:.

[34] K. Fitzhenry, Evaluation of Modified Flow-through Pulsed UV Technology for Bacterial Inactivation With Comparison to a Standard Continuous-flow Low Pressure UV System, Available from:, National University of Ireland, 2019 https://aran.library.nuigalway.ie/handle/10379/14865.

[35] L. Hsu, C.I. Moraru, Quantifying and mapping the spatial distribution of fluence inside a pulsed light treatment chamber and various liquid substrates, J. Food Eng. 103 (1) (2011) 84–91, https://doi.org/10.1016/j.jfoodeng.2010.10.002. Available from:.

[36] A. Lasagabaster, I. Martínez de Marañón, Comparative study on the inactivation and photoreactivation response of Listeria monocytogenes seafood isolates and a Listeria innocua surrogate after pulsed light treatment, Food Bioprocess Technol. 10 (10) (2017) 1931–1935. Available from: http://link.springer.com/10.1007/s11947-017-1972-6.

[37] A.H. Malayeri, M. Mohseni, B. Cairns, J.R. Bolton, G. Chevrefils, É. Caron, Fluence (UV dose) required to achieve incremental log inactivation of Bacteria, Protozoa, viruses and algae, IUVA News 8 (1) (2016) 38–45. Available from: http://uvsalesinfo.com/Documents/NavLink/UV_Destruction_Chart_uid7102009502412.pdf.

[38] H. Farrell, J. Hayes, J. Laffey, N. Rowan, Studies on the relationship between pulsed UV light irradiation and the simultaneous occurrence of molecular and cellular damage in clinically-relevant Candida albicans, J. Microbiol. Methods 84 (2) (2011) 317–326.

[39] M.L. Artíguez, A. Lasagabaster, I.M.De Marañón, Factors affecting microbial inactivation by Pulsed Light in a continuous flow-through unit for liquid products treatment, Procedia Food Sci. 1 (2011) 786–791, https://doi.org/10.1016/j.profoo.2011.09.119. Available from:.

[40] C. Jungfer, T. Schwartz, U. Obst, UV-induced dark repair mechanisms in bacteria associated with drinking water, Water Res. 41 (1) (2007) 188–196.

[41] I. Salcedo, J.A. Andrade, J.M. Quiroga, E. Nebot, Photoreactivation and dark repair in UV-treated microorganisms: effect of temperature, Appl. Environ. Microbiol. 73 (5) (2007) 1594–1600.

[42] K. Fitzhenry, N. Rowan, W. Finnegan, X. Zhan, E. Clifford, Microbiological characterisation and impact of suspended solids on pathogen removal from wastewaters in dairy processing factories, J. Dairy Res. 85 (3) (2018) 391–395, https://doi.org/10.1017/S0022029918000602.

[43] APHA, Standard methods for the examination of water and wastewater, in: E. W. Rice, R.B. Baird, A.D. Eaton, L.S. Clesceri (Eds.), American Water Works Association (AWWA) and Water Environment Federation (WEF), 22nd edition, American Public Health Association (APHA), Washington, D.C., USA, 2012.

Open Veterinary Journal, (2016), Vol. 6(1): 15-22
ISSN: 2226-4485 (Print)
ISSN: 2218-6050 (Online)
Original Article

Submitted: 20/10/2015 Accepted: 05/01/2016 Published: 27/01/2016

The pulsed light inactivation of veterinary relevant microbial biofilms and the use of a RTPCR assay to detect parasite species within biofilm structures

M. Garvey[1,*], G. Coughlan[2,3], N. Murphy[2] and N. Rowan[3]
[1]*Department of Life Sciences, Institute of Technology Sligo, Sligo, Ireland*
[2]*Department of Parasitology, National University of Ireland Maynooth, Maynooth, Ireland*
[3]*Bioscience Research Institute, Athlone Institute of Technology, Athlone, Ireland*

Abstract
The presence of pathogenic organisms namely parasite species and bacteria in biofilms in veterinary settings, is a public health concern in relation to human and animal exposure. Veterinary clinics represent a significant risk factor for the transfer of pathogens from housed animals to humans, especially in cases of wound infection and the shedding of faecal matter. This study aims to provide a means of detecting veterinary relevant parasite species in bacterial biofilms, and to provide a means of disinfecting these biofilms. A real time PCR assay was utilized to detect parasite DNA in *Bacillus cereus* biofilms on stainless steel and PVC surfaces. Results show that both *Cryptosporidium* and *Giardia* attach to biofilms in large numbers (100-1000 oo/cysts) in as little as 72 hours. Pulsed light successfully inactivated all test species (*Listeria, Salmonella, Bacillus, Escherichia*) in planktonic and biofilm form with an increase in inactivation for every increase in UV dose.
Keywords: Biofilms, *Cryptosporidium*, *Giardia*, PCR, Veterinary.

Introduction

The prevention and control of veterinary related infections is an important aspect of public health and safety due to the occurrence of zoonotic infections. The spread of pathogenic species within veterinary practices can lead to infection of both the housed animals and veterinary staff. Veterinary clinics are a focus for human and animal interaction, often in situations dealing with infected wounds or faecal matter. This is a significant concern for immunocompromised individuals who are animal owners. Animal associated pathogens of concern to immunocompromised persons include *Cryptosporidium, Salmonella, Listeria, Bacillus, Escherichia coli, Campylobacter* and *Giardia* (Grant and Olsen, 1999). Furthermore, many research studies have highlighted the connection between the spread of pathogenic organisms from surfaces to patients (Gebel *et al*., 2013). Consequently, the use of surface disinfectants for the control of pathogens in clinical and veterinary settings has become important due to the increase in antibiotic resistant microbial species and zoonotic infections. However, issues have arisen where some pathogens have shown resistance to commonly used chemical based disinfectants. Such pathogens include the parasites Cryptosporidium and Giardia, bacterial endospores and bacterial biofilm structures (Betancourt and Rose, 2004). Planktonic microbial cells are able to attach to and colonise environmental surfaces by producing an extracellular polymeric substance (EPS), these adherent (sessile) cells are referred to as biofilms. The descriptive terms sessile and planktonic are used to describe surface adherent and free floating bacterial cells respectively. Veterinary important species such as *Listeria, Escherichia, Bacillus* and *Salmonella* are capable of producing these biofilm structures allowing them to gain resistance to standard chemical disinfection methods. Biofilms communities spread largely by breaking of in clumps from the primary structure, these detached biofilm clumps may contain enough bacteria to give an infective dose to housed animals making them a potential health risk. Indeed, biofilms or sessile communities are believed to be the causative agent in diseases such as pneumonia, liver abscesses, enteritis, wound infections and mastitis infections in animals (Clutterbuck *et al*., 2007). Ingestion of a biofilm bacterial clump present in the surrounding environment could play an important role in the transmission of disease. In addition, in hosts with functioning innate and adaptive immune responses, biofilm-based infections are often very persistent and remain unresolved. In fact, surrounding tissues often undergo extensive damage by immune complexes and invading neutrophils when trying to eradicate the infection (Stewart and Costerton, 2001).

The prevention of biofilm formation on surfaces located in areas of animal housing would provide the best control measures for these robust structures; however, there is no agent available that will prevent cell adhesion and biofilm formation. Current methods rely on the use of disinfection agents and regular cleaning of surfaces exposed to possible pathogens. Research has indicated that sessile communities can be

***Corresponding Author:** Dr. Mary Garvey. Department of Life Sciences, Institute of Technology Sligo, Ash Lane, Sligo, Ireland. Tel.: +35371930584 | Email: *garvey.mary@itsligo.ie*

up to 1000 times more resistant to chemotherapeutics such as chlorhexidine than their planktonic counterparts (Garvey *et al*., 2014a). Furthermore, resistant bacteria originated in sessile communities can spread from animal to animal through veterinary staff, veterinary surfaces and equipment or farm equipment such as feeders and water dispensers (Aguilar-Romero *et al*., 2010) resulting in extended infection problems. Biofilm structures are also capable of trapping or incorporating other pathogenic species including enteric noroviruses (Wingender and Flemming, 2011) and parasites such as *Giardia* and *Cryptosporidium* (DiCesare *et al*., 2012). Harbouring of such species shields them from cleaning and disinfection techniques, increasing their already high resistance to such treatments. Studies have shown that aquatic biofilms represent a significant, long-term reservoir for pathogens such as *Cryptosporidium* and *Giardia*, which can be released back into water (Wingender and Flemming, 2011). Thus, explaining the presence of parasites in water networks long after disinfection protocols are completed following an outbreak. Ultraviolet (UV) light is well known for its antimicrobial activity, due to its bacteriostatic properties affecting the DNA of the organism, breaking DNA bonds, causing the formation of DNA adducts thus preventing bacterial cell replication (Ochoa-Velasco *et al*., 2014). Additionally, research focusing on the use of a pulsed light (PL) system for the inactivation of parasite species and bacterial endospores has shown this system to be highly efficient (Garvey *et al*., 2014a). PL technologies differ from standard UV lamps in their mode of delivery, penetration depth and wavelength range (Garvey *et al*., 2014a) making them a more potent disinfection system. Here we report on the use of a PL system for the disinfection of veterinary relevant biofilms on polyvinylchloride (PVC) and stainless steel surfaces. The use of polymerase chain reaction (PCR) methods provides a rapid species specific means of identifying species type and cell numbers present. Indeed, PCR methods have been used extensively to detect and quantify bacterial cells in food products and in biofilms (Pan and Breidt, 2007). Therefore, the present study also utilised a real time PCR assay to determine the extent at which *Bacillus* biofilm structures incorporated parasite species into their matrix, subsequently providing shelter from disinfection techniques.

Materials and Methods

Microbial test species

For this study a range of veterinary relevant biofilm forming microbial species *Listeria monocytogenes* (ATCC 11994), *Bacillus cereus* (ATCC 11778), *Salmonella typhimurium* (ATCC 13311) and *Escherichia coli* (ATCC 11775) were chosen for biofilm formation and PL inactivation studies. All strains were cultured and maintained in nutrient agar and nutrient broth (Cruinn Diagnostics Ltd, Ireland) at 37°C. *Giardia lamblia* cysts and *Cryptosporidium parvum* oocysts were purchased from Waterborne Inc USA. Oocysts and cysts were stored in sterile PBS (0.01 M phosphate buffer, containing 0.0027 M KCL and 0.137 M NaCl at a pH of 7.4) with 100 U of penicillin/ml, 100 µg of streptomycin/ml and 100 µg of gentamicin/ml at 4°C. Prior to use parasite identity was confirmed by a dye staining method comprising of propidium iodide (PI) 1 mg/ml in 0.1 M sterile PBS and 4', 6'-Diamidino-2-Phenylindole (DAPI) 2 mg/ml in methanol and a fluorescein-labelled mouse-derived monoclonal antibody Giardi-a-Glo™ or Crypt-a-Glo™ (Waterborne Inc, New Orleans, USA). Oo/cysts were counted using a haemocytometer and inverted microscope (Olympus, CKX41) with camera (Olympus, IX2-SLP) attached.

Growth of sessile communities using Centers for Disease Control (CDC) biofilm reactor

The CDC biofilm reactor (Biosurface Technologies Corp, Bozeman, Montana, USA) was used for the growth of biofilm structures as per the recommended procedure of the American Society for Testing and Materials (ASTM, 2012). Furthermore, the CDC reactor is a recognised method for the growth of biofilms under high shear and continuous flow (Coenye and Nelis, 2010) and is of sufficient capacity to provide numerous samples of biofilms for disinfection studies. In order to establish a dose response relationship for biofilm inactivation with UV light it is necessary to first obtain biofilm communities which were dense, reproducible and also treatable. For this study both PVC and stainless steel coupons were chosen as biofilm growth surfaces as both materials are commonly used in veterinary settings and are excellent matrixes for biofilm adhesion and proliferation.

For the growth of microbial biofilms methods were followed as per the recommended procedure for continuous fluid shear flow biofilm formation (ASTM E2562-12 2012) and Garvey *et al*., 2014b. The reactor was prepared containing 350 mL of tryptone soy broth (TSB) and 2% glucose as this concentration was previously found to promote biofilm adhesion and proliferation (Senevirantne *et al*., 2013). Once satisfied that the coupons were completely submerged the apparatus was sterilised by autoclaving. 1 mL of a 12 hour microbial culture was added to the reactor chamber to ensure that cells were in the log phase of reproduction. For each test strain the reactor was incubated at 37°C for 72 and 96 hours under rotatory conditions at 125 rpm. To allow for the enumeration of colony forming units (cfu) per microbial biofilm, all coupons were removed aseptically from each reactor rod and rinsed with sterile phosphate-buffered saline (PBS) to remove any planktonic cells. Biofilms were removed from each coupon by scraping the coupon using a sterile cell scraper into 10 mL of sterile PBS. The

standard plate count technique was used to determine the cfu/mL bacterial population in the biofilm as per the recommended procedure (ASTM E2562-12 2012). To allow for the entrapment of parasite test species within the biofilm matrix $1x10^6$ oo/cysts per mL was added to the reactor chamber and incubated for 72 hours. For biofilms containing parasite test species, 1 mL from the 10 mL PBS containing the scrapped biofilm was stained with parasite specific dyes as previously described to confirm identity and numbers present.

Pulsed Ultraviolet* (PUV) *light

The PUV machine used throughout this study was sourced through Samtech Ltd, Strathclyde, Scotland, UK. The bacteriostatic effects of PL are caused by the rich and broad-spectrum UV content, the short duration, and the high peak power of the pulse. The system was used as per Garvey *et al*. (2010) and is therefore not described in further detail herein.

Pulsed light inactivation of planktonic microbial species

E. coli, S. typhimurium, *L. monocytogenes* and *B. cereus* cultures were grown and maintained as previously described. For PUV studies a single colony of the test strain was aseptically transferred to 100 mL of sterile nutrient broth followed by incubation at 37°C for 12 hours at 125 rpm. For surface treatment 100 µL of an appropriate dilution was spread onto agar surfaces. Test plates were then exposed to pulses of UV light at 16.2 J at varying doses (obtained by varying the pulse number) at a rate of 1 pulse per second as per Garvey *et al*. (2014). PUV studies were also conducted on samples diluted from the 12 hour broth in 20 mL final volumes of sterile PBS at 8 cm from the light source, after which 100 µL of treated liquid was transferred to suitable agar and incubated at 37°C for 24 hours.

Pulsed light inactivation of sessile communities

Coupons were aseptically removed from the reactor, rinsed with sterile PBS and transferred to a sterile petri dish. Samples were exposed to pulses of UV light at 16.2J at 8 cm from the light source at varying UV doses which were obtained by increasing the pulse number. Once treated, coupons were submerged in 10 mL of sterile PBS and surface scraped using a sterile cell scraper to remove the treated biofilms and to allow for the determination of inactivated rates. The liquid was then transferred to a sterile 20 mL container and centrifuged at 800 g for 10 minutes to pellet the cells. The sample was then re-suspended and agitated manually to ensure biofilm dispersion. Serial dilutions were made from the biofilms suspension and 100 µL spread on triplicate agar plates to determine the cfu/mL of treated samples. This process was repeated for coupons at varying UV doses (< 8µJ/cm^2) to determine the Log_{10} reduction obtained with increasing UV dose. Plates were incubated for 24 hours at 37°C to allow for the growth of bacterial colonies, which were subsequently gram stained and identify confirmed to ensure no contamination of the rector system had occurred.

Parasite entrapment and DNA extraction from biofilm structures

Biofilms of *B. cereus* were allowed to form while in the presence of $1x10^6$ oo/cysts per mL in the biofilm reactor, to allow for the entrapment of parasite species within the biofilm matrix. This species was chosen due to its enteric pathogenic nature and it greater resistance to PUV inactivation. Following 72 hours incubation, coupons were aseptically removed from the bioreactor to sterile petri dish. Coupons were then aseptically scrapped in to 10 mL volumes of PBS, which was subsequently centrifuged at 800g for 10 minutes to pellet the cells, followed by re-suspension in 200 µl of sterile PCR grade water. Target DNA extraction for *B. cereus, G. lamblia* and *C. parvum* was conducted as per kit instructions for *B. cereus* biofilm suspensions using a Roche DNA extraction kit and HP PCR template preparation kit (Roche Diagnostics, Roche, Ireland). All steps were performed as per manufacturer's instructions with treated and untreated microbial pellets which were suspended in 200 µL of sterile PBS.

Real time PCR

All primers and probes were sourced from Tib Molbiol, Berlin, Germany. For *B. cereus* the forward primer ACACACGTGCTACAATGGATG and reverse primer AGTTGCAGCCTACAATCCGAA with the taqman probe sequence F-ACAAAGGGCTGCAAGACCGCG—Q coding for the phaC gene was used as per Nayak *et al*. (2013). Primers coding for β-giardin of *G. lamblia* were used as per method of Bertrand *et al*. (2009) with the forward primer 5′-AAGCCCGACGACCTCACCCGCAGTGC-3′ and reverse primer 5′-GAGGCCGCCCTGGATCTTCGAGACGAC-3′. The Taqman probe with the following sequence: 5'-FAM TCACCCAGACGATGGA CAAGCCCTAMRA-3 was utilised for this study. For *Cryptosporidium parvum* the 18Si reverse primer 5'- CCTGCTTTAAGCACTTAATTTTC and 18Si forward primer 5'- ATGGACAAGAAATAACAATACAGG as first described by Morgan *et al*. (1997) were utilised as per Garvey *et al*. (2010). The Taqman probe had the following sequence: 5-'-(6-FAM) ACCAGACTTGCCCTCC (TAMRA) as per Keegan *et al*. (2003). Amplification reactions (20 µL) contained 5 µL of sample DNA (0.5 µM of each primer, 0.2 µM of probe) and 15 µL of reaction buffer (Roche Diagnostic, West Sussex, England). Both positive and negative controls were included in RT-PCR to validate the results. DNase–RNase free water was used as negative control throughout. Cycling parameters were initial denaturation for 10 min at 95°C followed by 65 cycles of denaturation for 10 s at 95°C,

annealing for 40 s at 40 °C, extension for 1 s at 70°C and cooling for 30 s at 40°C on a Nanocycler® device (Roche Diagnostics). These cycling parameters were the same for all samples. Additionally, large numbers of cycles were used to ensure detection of low levels of infection. On completion of each RT-PCR run amplification curves were analysed by Nanocycler software (Roche Diagnostics) and a standard curve (Fig. 1) of cell DNA concentration determined. DNA standards were prepared from fresh cells or oo/cysts ranging in concentration from 10 to 10^8 oocysts or cysts/mL by dilution in PBS following standard viable count determinations.

Statistics

All experimental data is an average of 3 experimental replicates with 3 internal replicates. Bacterial inactivation is expressed as $\log_{10}$ reduction of the untreated control. Student's t-tests and ANOVA one-way model (MINITAB software release 16; Mintab Inc., State College, PA) were used to compare the relationship between UV treatments and bacterial inactivation at 95% level of confidence. Student t-tests were used to determine the relationship between the sensitivity of biofilms from different strains to PL treatment.

Results

Sessile communities and parasite detection

All bacterial strains under study formed densely populated sessile communities on both PVC and stainless steel surfaces after 72 hours. Findings also demonstrate (data not shown) that with longer incubation times, exceeding 72 hours (96 hours), there was no increase in cell number of the biofilms as detected by plate counts. Following 72 hours, a ca. 5 and 6.6 $\log_{10}$ biofilm formed for *B. cereus* and *S. typhimurium* respectively, and a 6 $\log_{10}$ for *E. coli* and 6.5 $\log_{10}$ for *L. monocytogenes* on PVC surfaces. A similar level of cell density was detected on stainless steel surfaces, where a ca. 5 $\log_{10}$ to 6.6 $\log_{10}$ biofilm formed for *B. cereus, L. monocytogenes*, *S. typhimurium* and *E. coli*. The determination of cell number for *B. cereus* biofilms via PCR was slightly higher than the standard cell count method. A Ct value of 18.39, corresponding to a cell count of ca. 7 $\log_{10}$ cfu/ml (Fig. 1) for both materials was determined by analysis of the standard curve. An important fact to note is that PCR detects the presence of target DNA, but cannot differentiate between live and dead cells. In contrast, the standard cell count technique reports viable cell numbers only via the enumeration of colonies grown on nutrient agar. The lack of an increase in biofilm cell density after a 72 hours period suggests the presence of a stationary phase or steady state of biofilm growth. PCR analyses showed the presence of total cells (non-viable and viable) at 72 hours, when viable cell counts as determined by the spread plate technique are subtracted from this, a value for non-viable cells can be determined. In this case a biofilm viable cell density of 5 $\log_{10}$ was formed, indicating that approximately 2 $\log_{10}$ of non-viable cells were also present in the biofilm matrix as detected by PCR. The presence of these non-viable cells further confirms that incubation for 72 hours provided an optimal period of time for biofilm formation, after which cell death occurs to some extent. These findings correspond to that of Senevirantne *et al*. (2013), who concluded that 72 hours was also the optimal incubation time for the growth of *Enterococcus faecalis* biofilms. Therefore, the findings of this study suggest that 72 hour duration of incubation is sufficient to reproducibly produce a robust, densely populated biofilm of *B. cereus, E. coli, L. monocytogenes* and *S. typhimurium* using a CDC reactor. Consequently, 72 hour biofilms were used for inactivation studies for all test species.

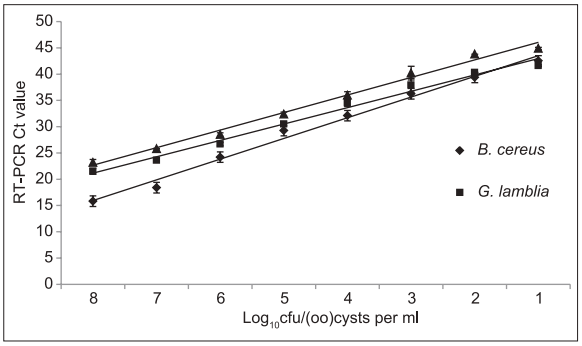

Fig. 1. Linear regression analysis of DNA standard curve as determined by real time PCR analysis for planktonic *Bacillus cereus* ($\log_{10}$ cfu/ml) and the parasite species *Cryptosporidium parvum* ($\log_{10}$ oocysts/ml) and *Giardia lamblia* ($\log_{10}$ cfu/(oo) cysts per ml) (+/-S.D) using species specific primers.

Both parasites species were detected in the *B. cereus* biofilms at a concentration of between 2 and 3 $\log_{10}$ for PVC and stainless steel surfaces by PCR (Fig. 2). Additionally, PCR proved a more efficient reliable method of detecting *Cryptosporidium* and *Giardia* than the use of specific dyes. Fluorescent dye staining of biofilms containing oo/cysts greatly underestimated the number of organisms present. A maximal oo/cyst count of 10 (+/-2) was measured for *C. parvum* and 14 for *G. lamblia* (+/-4) via fluorescent staining. Issues arose in relation to non-specific binding of dyes to biofilm constitutes believed to be EPS components resulting in unreliable counting of parasite numbers.

The impact of PL on microbial species was assessed for surface treated organisms, organisms in suspension and sessile communities. All test strains proved to be susceptible to the pulsed light treatment, albeit with varying levels of sensitivity as shown in (Figs. 3 and 4) *E. coli* showed the greatest level of inactivation on agar surfaces (Fig. 3a) with complete inactivation of an initial concentration of ca. 9 $\log_{10}$ with as little as 5 $\mu J/cm^2$ of pulsed light. The order of decreasing sensitivity for test

strains was *E. coli*, *L. monocytogenes*, *B. cereus* and *S. typhimurium* on surfaces. When treated in suspension this sensitivity changed with *L. monocytogenes* showing the highest resistance to PL treatment and *S. typhimurium* showing the greatest sensitivity to pulsed light (Fig. 3b) for all treatment doses ($p<0.05$). Indeed a maximal 9.6 $\log_{10}$ inactivation of *S. typhimurium* was achieved with 5.39 µJ/cm^2 compared to a 2.73 $\log_{10}$ for *L. monocytogenes*. This same dose resulted in a 3.45 and 5.38 $\log_{10}$ inactivation of *B. cereus* and *E. coli* respectively, highlighting the significant difference in susceptibility to pulsed light. These findings are in conjunction with Cheigh *et al*. (2012) where *E. coli* also proved more sensitive to PL than *L. monocytogenes* when treated in suspension. High levels of biofilm inactivation were also achieved for all test strains present on both surface materials (Fig. 4). For the Gram negative species *E. coli* and *S. typhimurium* a 4.04 and 5.11 $\log_{10}$ reduction in viable cell counts was obtained on PVC surfaces with 5.39 µJ/cm^2 (Fig. 4a). This same dose resulted in a significantly ($p<0.05$) greater level of inactivation of the same species on stainless steel surfaces, with a maximal 4.2 and 6.6 $\log_{10}$ reduction obtained for *E. coli* and *S. typhimurium* respectively (Fig. 4b). Both Gram positive species tested showed increased sensitivity on stainless steel surfaces compared to PVC. A dose of 5.39 µJ/cm^2 resulted in a 3.23 and a 4.34 $\log_{10}$ inactivation on PVC and 5.95 and 4.6 $\log_{10}$ inactivation on stainless steel for *B. cereus* and *L. monocytogenes* respectively. A PL dose of 7.56 µJ/cm^2 resulted in complete inactivation of *L. monocytogenes* and *S. typhimurium* of ca. 6.51 $\log_{10}$ (Fig. 4a) on PVC surfaces.

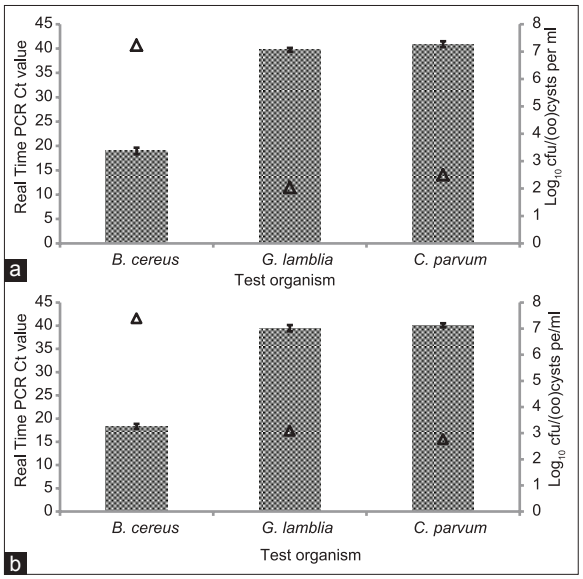

Fig. 2. Real time PCR Ct value (column graph) for microbial test species and corresponding cell count in $\log_{10}$ cfu/(oo)cysts per ml (**Δ**) as determined by using the equation of the line of the standard curves, results show both parasite test species as detected in *B. cereus* biofilms on (a) PVC and (b) stainless steel surfaces (+/- S.D).

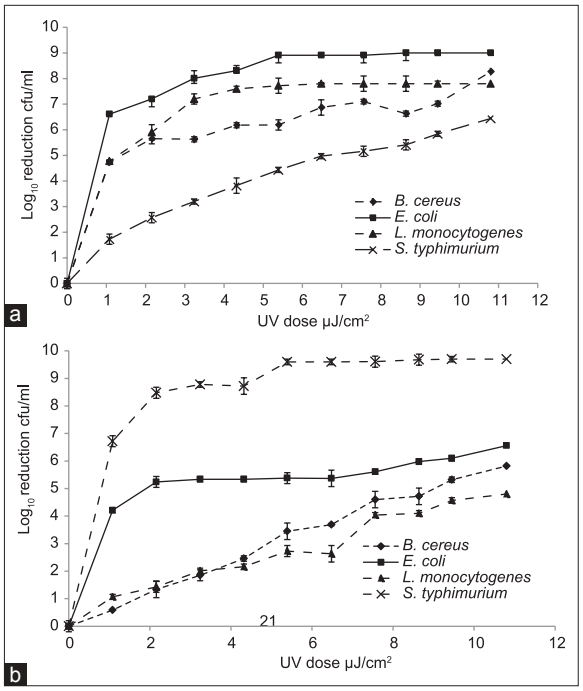

Fig. 3. Pulsed light inactivation of a range of Gram negative and Gram positive test species on (a) agar surfaces and (b) in suspension (+/- S.D).

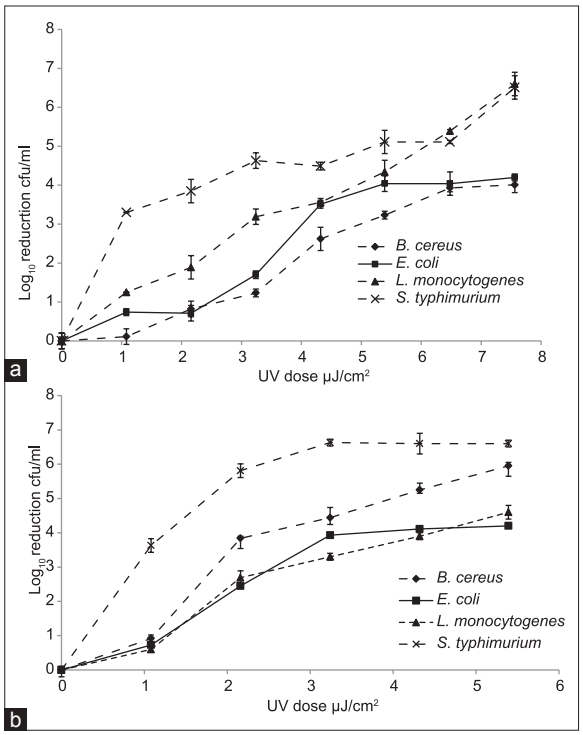

Fig. 4. Pulsed light inactivation of bacterial biofilms of varying test species on (a) PVC surfaces and (b) stainless steel surfaces (+/- S.D).

Discussion

The change from a planktonic free floating cell to that of a biofilm sessile cell induces physiological changes in bacteria, occurring via a series of gene expression alterations including gene repression and induction (Donlan and Costerton, 2002). It is the induction of genes, relating to antibiotic resistance that leads to the increased pathogenicity of sessile bacteria over their planktonic counterparts (O'Leary *et al*., 2015). Consequently, this causes the increased resistance to antibiotics and disinfectants such as chlorine commonly observed with these complex structures (Aguilar-Romero *et al*., 2010). For this reason, it is of the upmost importance to establish alternative ways of eradicating these problematic often pathogenic structures from veterinary surfaces. The pulsed light system used in this study proved successful at disinfecting densely populated biofilms of veterinary relevant microorganisms. Indeed, complete inactivation of a 6.5 $\log_{10}$ biofilm of *L. monocytogenes* and *S. typhimurium* was achieved with 7.56 μJ/cm^2. However, there was a significant difference ($p<0.05$) in the susceptibility of biofilm communities on PVC and stainless steel surfaces. *S. typhimurium* and *B. cereus* proved more sensitive to pulsed light inactivation on stainless steel surfaces compared to PVC. Stainless steel is the predominant material used in veterinary practices as clinical surfaces and animal housing due to their easy to clean nature. Consequently, the higher susceptibility of microbial biofilms on stainless steel surfaces further establishes this materials benefit for use in such environments.

Traditionally, the sensitivity of planktonic cells to disinfection has been used as an indication of biofilm sensitivity and resistance (Buckingham-Meyer *et al*., 2007). However, disinfection studies such as those described herein based on actual biofilm communities is much more representative of the environmental situation. Additionally, high levels of planktonic cell inactivation (4 – 9 $\log_{10}$ cfu/ml) were also achieved following pulsed UV exposure for both surface treated and microbial suspensions. Therefore, pulsed light as a disinfectant has the ability to reduce biofilm formation at the planktonic stage of attachment, which can be assisted by choosing surface materials that are more readily disinfected by this approach such as stainless steel.

The findings of this study confirm that both parasite species studied can quickly attach or become entrapped in bacterial biofilms. This is in keeping with the findings of recently published literate outlining the presence of parasite species in biofilm structures (DiCesare *et al*., 2012; Koh *et al*., 2013). The findings of Koh *et al.* (2013) conclude that biofilm communities accumulate *Cryptosporidium* species over time as determined by qPCR detection. The detection of these pathogens within biofilm structures has important public health implications in relation to animal and human exposure. The infectious dose for *Cryptosporidium* has been established to be less than 20 oocysts (Zambriski *et al*., 2013) with prolonged infection occurring with little success following medical intervention. The robust, chemical disinfection resistant nature of biofilms and these parasites increases the probability that the survival and detachment of biofilm-associated viable parasites may occur at concentrations exceeding that required for infection. This possibility needs to be considered in risk assessments relating to the cleaning of veterinary environments particularly where animals are housed.

Previous studies by this research group reported a ca. 5 $\log_{10}$ inactivation of *Cryptosporidium parvum* (Garvey *et al*., 2013) and ca. 1 $\log_{10}$ inactivation of *Giardia lamblia* (Garvey *et al*., 2014b) with a PL dose of 7.38 μJ/cm^2. Nevertheless, further studies are warranted to determine the exact dose required to inactivate parasites within biofilm matrixes, which will undoubtedly shield parasites to some extent. However, issues are expected to arise in relation to viability determination post treatment and cell culture infectivity. Specifically, issues relating to the sterility of the parasites following extraction from biofilms and subsequent exposure to mammalian cell lines. Nonetheless, PL shows potential for use as a disinfectant for veterinary environments given its highly effective bacteriostatic properties towards bacterial biofilms and parasite species. Regardless of microbial exposure to PL in suspension or on surfaces findings demonstrate that cell inactivation increased significantly ($p<0.05$) with increasing UV dose or treatment time.

In conclusion, the findings reported here contribute to existing literature in many ways:

Firstly, all veterinary relevant strains produced densely populated biofilms structures on both surface materials used.

Secondly, PL repeatedly inactivated the range of test species on surfaces and in suspension. Additionally, it provided high levels of biofilm inactivation on PVC and stainless steel surfaces.

Thirdly, a real time PCR assay proved successful for determining the level of *C. parvum* and *G. lamblia* present in the biofilms of *B. cereus* where fluorescent staining greatly underestimated the numbers present.

Finally, pulsed light doses (7.38 μJ/cm^2) which have been previously shown to inactivate both parasite species (*Cryptosporidium* and *Giardia)*, have also provided complete inactivation of all biofilms tested.

Acknowledgments

All research studies were conducted in the Bioscience Research Institute, Athlone Institute of Technology, Ireland.

Conflict of interest

The authors declare that there is no conflict of interest.

References

Aguilar-Romero, F., Perez-Romero, A.N., Diaz-Aparicio, E. and Hernandez-Castro, R. 2010. Bacterial biofilms: Importance in animal diseases. Current Research, Technology and Education topics in Applied Microbiology and Microbial Biotechnology. A Mendez Vilas Edition, pp: 700-703.

ASTM. 2012. ASTM E2562 - 12: Standard Test Method for Quantification of Pseudomonas aeruginosa Biofilm Grown with High Shear and Continuous Flow Using CDC Biofilm Reactor. In Annual Book of ASTM Standards; ASTM International: West Conshohocken, PA, USA.

Bertrand, I., Maux, M., Helmi, K., Hoffmann, L., Schwartzbrod, J. and Cauchie, H.M. 2009. Quantification of *Giardia* transcripts during *in vitro* excystation: Interest for the estimation of cyst viability. Water Res. 43, 2728-2738.

Betancourt, W.Q. and Rose, J.B. 2004. Drinking water treatment processes for removal of *Cryptosporidium* and *Giardia.* Vet. Parasitol. 126(1-2), 219-234.

Buckingham-Meyer, K., Goeres, D.M. and Hamilton, M.A. 2007. Comparative evaluation of biofilm disinfectant efficacy tests. J. Microbiol. Methods 70, 236-244.

Cheigh, C.I., Park, M.H., Chung, M.S., Shin, J.K. and Park, Y.S. 2012. Comparison of intense pulsed light- and ultraviolet (UVC)-induced cell damage in *Listeria monocytogenes* and *Escherichia coli* O157:H7. Food Control 25(2), 654-659.

Clutterbuck, A.L., Woods, E.J., Knottenbelt, D.C., Clegg, P.D., Cochrane, C.A. and Percival, S.L. 2007. Biofilms and their relevance to veterinary medicine. Vet. Microbiol. 121, 1-17.

Coenye, T. and Nelis J.J. 2010. *In vitro* and *in vivo* model systems to study microbial biofilm formation. J. Microbiol. Methods 83, 89-105.

DiCesare, E.A., Hargreaves, B.R. and Jellison, K.L. 2012. Biofilm roughness determines *Cryptosporidium parvum* retention in environmental biofilms. Appl. Environ. Microbiol. 78(12), 4187-4193.

Donlan, R.M. and Costerton, J.W. 2002. Biofilms: survival Mechanisms of Clinically Relevant Microorganisms. Clin. Microbiol. Rev. 15(2), 167-193.

Garvey, M., Rabbit, D., Stocca, A. and Rowan, N. 2014a. Pulsed Ultraviolet light inactivation of Pseudomonas aeruginosa biofilms. Water Environ. J. 29, 36-42. DOI: 10.1111/wej.12088.

Garvey, M., Stocca, A. and Rowan, N. 2014b. Development of a combined *in vitro* cell culture - quantitative PCR assay for evaluating the disinfection performance of pulsed light for treating the waterborne enteroparasite *Giardia lamblia*. Exp. Parasitol. 144, 6-13.

Garvey, M., Clifford, E., O'Reilly, E. and Rowan, N. 2013. Efficacy of using harmless Bacillus endospores to estimate the inactivation of Cryptosporidium parvum oocysts in water. J. Parasitol. 99(3), 448-452.

Garvey, M., Farrell, H., Cormican, M. and Rowan, N. 2010. Investigations of the relationship between use of *in vitro* cell culture-quantitative PCR and a mouse-based bioassay for evaluating critical factors affecting the disinfection performance of pulsed UV light for treating *Cryptosporidium parvum* oocysts in saline. J. Microbiol. Methods 80(3), 267-273.

Gebel, J., Exner, M., French, G., Chartier, Y., Christiansen, B., Gemein, S., Goroncy-Bermes, P., Harteman, P., Heudorf, U., Kramer, A., Maillard, J.Y., Oltmanns, P., Rotter, M. and Sonntag, G.H. 2013. The role of surface disinfection in infection prevention. GMS Hyg. Infect. Control 8(1): Doc10. doi:10.3205/dgkh000210.

Grant, S. and Olsen, C.W. 1999. Preventing Zoonotic Diseases in Immunocompromised Persons: The Role of Physicians and Veterinarians. Emerg. Infect. Dis. 5(1), 159-163.

Keegan, A.R., Fanok, S., Monis, P.T. and Saint, C.P. 2003. Cell culture-Taqman PCR assay for evaluation of Cryptosporidium parvum disinfection. Appl. Environ. Microbiol. 69, 2505-2511.

Koh, W., Clode, P.L., Monis, P. and Thompson, R.C. 2013. Multiplication of the waterborne pathogen Cryptosporidium parvum in an aquatic biofilm system. Parasit. Vectors. doi: 10.1186/1756-3305-6-270.

Morgan, U.M., Constantine, C.C., Forbes, D.A. and Thompson, R.C. 1997. Differentiation between human and animal isolates of Cryptosporidium parvum using rDNA sequencing and direct PCR analysis. J. Parasitol. 83(5), 825-830.

Nayak, P.K., KumarMohanty, A., Gaonkar, T., Kumar, A., Bhosle, S.N. and Garg, S. 2013. Rapid Identification of Polyhydroxyalkanoate Accumulating Members of Bacillales Using Internal Primers for phaC Gene of Bacillus megaterium. ISRN Bacteriol. 1-12: doi:10.1155/2013/562014.

Ochoa-Velasco, C.E., Cruz-Gonzalez, M. and Guerrero-Beltran, J.A. 2014. Ultraviolet-C light inactivation of Escherichia coli And Salmonella typhimuriumin coconut (Cocos nucifera L.) milk. Innovative Food Sci. Emerg. Technol. 26, 199-204.

O'Leary, D., McCabe, E.M., McCusker, M.P., Martins, M., Fanning, S. and Duffy, G. 2015. Acid environments affect biofilm formation and gene expression in isolates of Salmonella enterica Typhimurium DT104. Int. J. Food Microbiol. 206, 7-16.

Pan, Y. and Breidt, F. 2007. Enumeration of Viable Listeria monocytogenes Cells by Real-Time PCR with Propidium Monoazide and Ethidium

Monoazide in the Presence of Dead Cells. Appl. Environ. Microbiol. 73(24), 8028-8031.

Senevirantne, C.J., Yip, J.W., Chang, J.W., Zhang, C.F. and Samaranayake, L.P. 2013. Effect of culture media and nutrients on biofilm growth kinetics of laboratory and clinical strains of Enterococcus faecalis. Arch. Oral Biol. 58, 1327-1334.

Stewart, P.S. and Costerton, J.W. 2001. Antibiotic resistance of bacteria in biofilms. Lancet 358(9276), 135-138.

Wingender, J. and Flemming, H.C. 2011. Biofilms in drinking water and their role as reservoir for pathogens. Int. J. Hyg. Environ. Health 214(6), 417-423.

Zambriski, J.A., Nydam, D.V., Wilcox, Z.J., Bowman, D.D., Mohammed, H.O. and Littoa, J.L. 2013. *Cryptosporidium parvum*: Determination of ID50 and the dose–response relationship in experimentally challenged dairy calves. Vet. Parasitol. 197, 104-112.

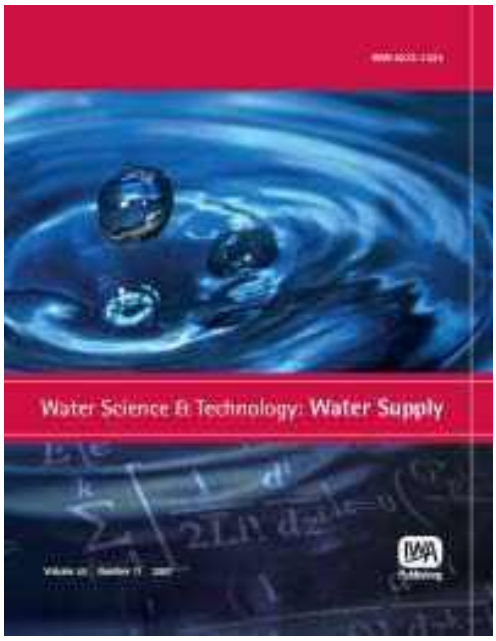

Efficacy of measuring cellular ATP levels to determine the inactivation of pulsed UV treated *Cryptosporidium parvum oocysts* suspended in water

Mary Garvey, Jennifer Hayes, Eoghan Clifford, Dominik Kirf and Neil Rowan

ABSTRACT

This constitutes the first study to report on the use of a novel approach to determine inactivation in PUV-irradiated *Cryptosporidium parvum* oocysts suspended in water based on the measurement of cellular adenosine triphosphate (ATP) concentration. This study also compares the efficiency of a novel ATP assay to that of using the combined *in vitro* HCT-8 cell culture – quantitative polymerase chain reaction (qPCR) method for determining the inactivation in the waterborne pathogen *C. parvum* after exposure to pulsed UV (PUV) treatments. Findings were compared with using the combined cell culture-qPCR approach for determining oocyst viability in similarly treated samples. PUV effectively killed *C. parvum* with a 5.4 $\log_{10}$ loss in oocyst viability after exposure to a UV dose of 8.5 $\mu J/cm^2$ as determined by the *in vitro* cell culture – qPCR assay. The ATP assay was shown to be significantly less effective in measuring loss of oocyst viability in similarly PUV-irradiated samples for all combination of treatment regimes studied. Measurement of cellular ATP is not suitable as an indicator of the disinfection efficiency of PUV-irradiated *C. parvum* oocysts. The levels of ATP present post PUV-irradiated samples suggests that significant cellular activity remained in treated oocysts that are unable to invade human HCT-8 cells. However, further studies are merited to investigate factors that might aid repair post PUV treatments in this water-borne human parasite. Use of this ATP assay offers an interesting insight into loss of infectivity in PUV-treated *C. parvum*. This rapid assay does not appear suitable for investigating or optimizing treatment efficiency under varying operational settings as it detects PUV-treated oocysts at levels significantly higher compared with using the *in vitro* cell culture-qPCR infectivity assay. Overestimation of survivors by the ATP assay may suggest that a sub-population of *C. parvum* oocysts may exist in a viable but non-infectious state or may require a period of resuscitation to facilitate photo-repair (if possible) that may lead to regained ability to infective human hosts.

Key words | ATP assay, combined cell culture-qPCR, *Cryptosporidium*, pulsed UV light, viability

Mary Garvey (corresponding author)
Jennifer Hayes
Dominik Kirf
Neil Rowan
Department of Nursing and Health Science,
Athlone Institute of Technology,
Ireland
E-mail: *mgarvey@ait.ie*

Eoghan Clifford
Department of Civil Engineering,
National University of Ireland,
Galway,
Ireland

INTRODUCTION

Cryptosporidium is a coccidian parasite that is now a well-recognized cause of diarrhoea in immunocompetent and immunocompromised humans (Fayer *et al.* 2007). Also *Cryptosporidium* species have been known to cause serious disease conditions on numerous occasions resulting from the consumption of contaminated drinking water (MacKenzie *et al.* 1994). It has been documented that *Cryptosporidium parvum* represents a threat to public health in the water industry due to the very low infection dose of oocysts and its resistance to standard drinking water treatment methods (Hijjawi 2003; Lee *et al.* 2008). Studies of water sources in the UK and US have found that oocysts

doi: 10.2166/ws.2013.010

commonly occurred in all types of surface water with densities as low as 2.5 oocysts/L (Gray 2005). Also it is known that low levels of *C. parvum* are required for host infectivity (DuPont *et al.* 1995). If the water industry is to make accurate assessments of the risk to public health posed by waterborne *Cryptosporidium* it must be able to determine not just their presence and viability but also whether the oocysts are capable of causing infection. Viability and infectivity assays will also provide the water industry with a tool to measure the efficiency of disinfection protocols (Rochelle *et al.* 1997). Therefore, it is essential to develop such methods that will contribute to the elimination of this parasite from drinking water supplies.

Use of conventional low pressure (LP) UV light has been found to be effective at inactivating a range of problematic organisms including *Cryptosporidium* oocysts but suffers from operational limitations (Rochelle *et al.* 2005). Other novel approaches of UV-irradiation have been developed in recent times such as medium-pressure (MP) and pulsed UV (PUV; Hijnen *et al.* 2006). Optimization of these emerging approaches has been affected by the lack of availability of simple rapid methods to detect and enumerate viability of *C. parvum* post UV treatments, which is currently limited to complex *in vitro* cell culture combined with and real-time quantitative polymerase chain reaction (RT-qPCR) (Keegan *et al.* 2003; Garvey *et al.* 2010). Measurement of oocyst death and associated loss of parasitic infectivity in host tissues is important when investigating the efficiency of traditional and new processes for killing *Cryptosporidium*. Therefore, establishing whether or not treated oocysts in water are viable post-treatments governs decontamination efficiency. Previous studies have reported on the use of range of methods including immunofluorescence microscopy and colorimetric endpoints for detecting *Cryptosporidium* (Fontaine & Guilot 2003) however, these sophisticated non-viability approaches are time-consuming and require use of highly specialist equipment and technique. An animal model using infectivity in mice was developed and considered the gold standard for assessing oocyst viability post decontamination but this approach is also cumbersome and raises significant ethical concerns (Karanis & Aldeyarbi 2011). Therefore, this study explored ways in which to repeatedly and accurately determine oocyst viability following exposure to PUV (Figure 1). One alternative or complimentary candidate method is the measurement of cellular adenosine triphosphate (ATP) levels as all living cells contain ATP, which is the basic unit of energy currency in viable cells. ATP is not present in non-viable cells, as it is degraded after death. ATP has been used as an indicator of viability of microorganisms including *Cryptosporidium* (Holm-Hansen & Booth 1966; Patterson *et al.* 1970; Weddle & Jenkins 1971; King *et al.* 2005). ATP measurement is a likely candidate method for rapidly determining the viability or activity of this parasite pre- and post-disinfection particularly as oocyst excystation requires the generation and use of ATP. Indeed, King *et al.* (2005) reported previously that the quantification of oocyst ATP levels can provide a simple and rapid method to estimate oocyst inactivation post heat treatment. Also, Somiya *et al.* (2000) concluded that the ATP assay is superior to *in vitro* excystation and 4′,6-diamidino-2-phenylindole/propidium iodide (DAPI/PI) permeability assays because of its rapid and simple procedure. Based on the aforementioned, the aim of this study was to assess the potential of an ATP assay to detect the concentration of ATP in treated and untreated *C. parvum* oocysts, in order to determine loss in viability following exposure to PUV irradiation. Use of the ATP measurement may alleviate the strong dependency of complex *in vitro* cell culture and or mice infectivity studies for determining PUV disinfection efficiency. Disinfection levels as determined via ATP measurement pre- and post-UV exposure were also compared with the combined *in vitro* HCT-8 cell culture qPCR assay which was shown previously to correlate with the gold standard mouse infectivity model (Garvey *et al.* 2010).

MATERIALS AND METHODS

Preparation viability staining of *C. parvum* oocysts

C. parvum oocysts (Iowa isolate derived from a bovine calf) were purchased from Waterborne Inc., USA. Oocysts were stored in sterile PBS (0.01 M phosphate buffer, containing 0.0027 M KCL and 0.137 MNaCl at a pH of 7.4) with 100 U of penicillin/ml, 100 μg of streptomycin/ml and 100 μg of gentamicin/ml and stored at 4 °C until they were used for UV treatment studies. Use of a combined surrogate dye staining method comprising PI and a fluorescein-labelled mouse-derived monoclonal antibody A400FLR-1X Crypt-a-Glo™ (having corresponding epitopeon oocyst cell

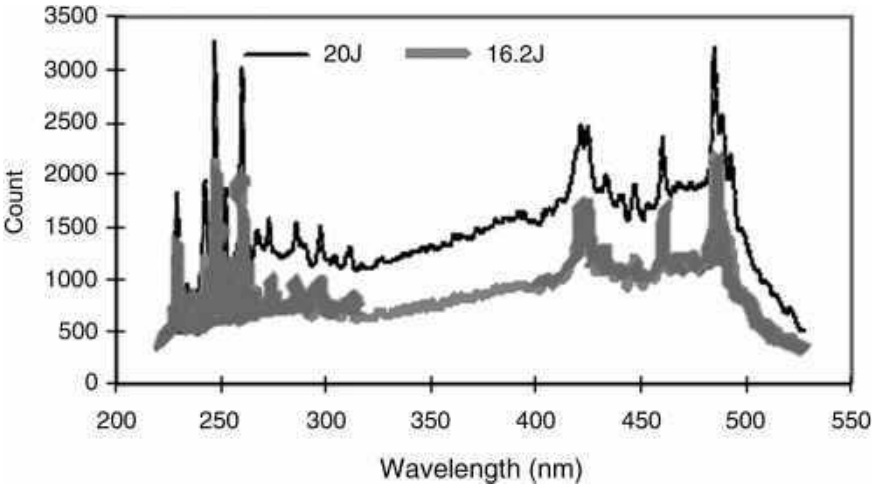

Figure 1 | The spectrum emitted by the PUV system at a discharge of 20 and 16.2 J per pulse with rich output in the UVC region showing three peaks at 229, 247 and 260 nm.

wall; Waterborne Inc., New Orleans, USA) was used to confirm the viability of oocysts. The excystation rate was determined for each batch of oocysts by microscopic observation following sequential incubation at 37 °C in acidified Hanks' balanced salt solution (HBSS) for 1 h and in 0.8% trypsin–0.75% sodium taurocholate for 1 h, followed by incubation at room temperature for 30 min as described elsewhere (Rochelle *et al.* 2002). For negative infection studies, oocysts were inactivated by heating at 70 °C for 30 min. All experiments were carried out using oocysts with greater than 80% viability, as determined by *in vitro* excystation as per Korich *et al.* (2000).

Enumeration and viability of *C. parvum* oocysts

Standard counts were determined for all oocyst stocks. Viable oocysts were enumerated by serial dilution in phosphate buffered saline (PBS) containing the aforementioned antibiotics using both fluorescence microscopy (confocal microscopy, Leica DM 600 CS, Germany), and real-time qPCR post infection in HCT-8 cell line as per method of Garvey *et al.* (2010). Oocyst suspensions at different population sizes were initially centrifuged at 3,000 rpm for 15 min at 4 °C, then re-suspended in acidified HBSS pH 2.7 for 1 h at 37 °C before filtration onto polycarbonate black 0.8 μm pore-size membrane filters (Fischer Scientific) using a filter system (Millipore) at a vacuum pressure of 200 mbar (1 bar = 105 Pa). Ten microlitres of PI (Sigma), prepared by dissolving 1 mg of PI in 1 ml of 0.1 M sterile PBS, and one drop (circa 45 μl) of A400FLR-1X Crypta-Glo™ were then applied to oocysts on the membrane and incubated for 2 h at room temperature in the dark. The membranes were mounted on glass microscope slides with 4 μl mounting medium (glycerol [non-photoreactive], 2 ml; 100 mg of DABCO {1,4-diazabiccyclo[2,2,2] octane} per ml of double distilled water, 2.4 ml; 0.1 ml Tris buffer, 4.8 ml, formalin 0.5 ml; and 5 MNaCl, 0.5 ml) and sealed with coverslips and clear nail varnish. Non-viable oocysts stained bright red due to uptake of PI when viewed at an excitation wavelength of 460–500 nm and an emission spectrum of 510–560 nm. Whereas all viable and non-viable oocysts stained apple-green when stained with A400 FlR-1X at an excitation wavelength of 460–500 nm and an emission wavelength of 510–560 nm. Entire membranes were scanned and all oocysts suspensions were counted by fluorescence microscopy. All counts were determined in triplicate.

Pulsing of *C. parvum* samples with UV rich light

A bench-top pulsed power source (PUV-1, Samtech Ltd, Glasgow) was used to power a LP (60 kPa) xenon-filled flashlamp (Heraeus Noblelight XAP type NL4006 series constructed from a clear UV transparent quartz tube), that produced a high-intensity diverging beam of polychromatic pulsed light, was used in this study as per Garvey *et al.* (2010). The pulsed light has a broadband emission spectrum extending from the UV to the infrared region with a rich UV content and its intensity also depends on the level of the

voltage applied (Figure 1). The light source has an automatic frequency control function that allows it to operate at 1 pulse per second (pps) that was used throughout this study. Light exposure was homogenous as the xenon lamp measuring 9×0.75 cm was longer than the 8.5 cm standard diameter. Petri dishes used in the tests which were placed directly below the lamp, which ensured that full coverage of the agar surface occurred and eliminated possible shading effects. For standard treatments (unless otherwise noted), the light source was mounted at 8 cm above the treatment area, as this distance was shown previously to be optimal for inactivation of *C. parvum* (Garvey *et al.* 2010). In this study, standard treatments involved suspending predetermined numbers of *C. parvum* in 10 ml of PBS that were transferred to Petri dishes that was then subjected to lamp discharge energies of 16.2 J, and 20 J at 8 cm distance from the light source up to and including a fluence of 25.92 and 34 μJ/cm^2 at a rate of 1 per second respectively. Heating of the oocyst suspensions was measured using a thermocouple and by thermal imaging (IRI 4010, InfraRed Integrated Systems Ltd, Northampton, UK) as per modified method of Nugent & Higginbotham (2007). There was no discernable increase in water temperature during each treatment. All studies were run in triplicate.

ATP assay

The ATP Biomass Kit HS (BioThema, Luminescent Assays, Handen, Sweden) was used to detect and quantify ATP in PUV treated and untreated controls following a method of King *et al.* (2005) with modifications. This assay is based on the principle of luminescence utilizing the firefly luciferin-luciferase which is known to be highly specific (Somiya *et al.* 2000). A standard curve of ATP concentration vs. oocysts concentration was prepared by serial dilution of circa. 10^7 oocysts/ml through to 10^1 oocysts/ml in sterile PBS. Final 1 ml volumes of oocyst dilutions were centrifuged at 3,000 rpm for 15 min in a microcentrifuge (Microcentrifuge, MSE Sanyo, Micro Centaur), subsequently the supernatant was removed by careful pipetting and the pellet resuspended in 1 ml of acidified HBSS (pH 2.7). The samples were vortexed for 10 s to disperse the oocyst pellet and a cell count performed using a haemocytometer to ensure that the serial dilutions produced the correct quantity of oocysts per ml. All samples were incubated at 37 °C for 1 h to allow excystation to occur. After incubation, samples were again centrifuged at 3,000 rpm for 15 min, the supernatant was removed and oocysts resuspended in 100 μl of sterile MilliQ water. One hundred microlitres of extractant B/S (ATP Biomass Kit) was added to each sample and vortexed for 10 s, subsequently samples were sonicated (5510 Branson Sonicator) for varying times (30, 60, and 90 s) to determine optimal conditions for ATP extraction (Somiya *et al.* 2000). Following sonication, the ATP assay was conducted as per the manufacturer's instructions with some minor alterations. Specifically, 40 μl of the oocyst extractant solution was removed from the sample container and added to one well of the 96 well plate in triplicate, 160 μl of reconstituted ATP Reagent HS was added to each well containing oocyst samples. The light emission produced by the addition of the ATP reagent to each well containing *C. parvum* ATP was immediately measured using a luminometer (Wallac Victor™, 1420 Multilabel counter). Once the reading was obtained (I_{smp1}) the light emission was again read after 5 s (I_{smp2}) and 10 μl of the 100 nmol/L ATP standard (supplied with kit) was added to each well and the light emission measured ($I_{smp+std}$) after mixing. In triplicate a blank was also run containing only the medium in which the oocysts were suspended, i.e. MilliQ water, the purpose of this was to ensure no external ATP was present in the medium. All ATP studies were conducted in the dark using black 96 well plates as luciferin is rapidly degraded by bright light.

Once the assay was complete the amount of ATP (pmol) per sample was calculated using the equation:

$$\mathrm{ATP}_{\mathrm{sample}} = I_{\mathrm{smp1}} / \left(I_{\mathrm{smp+std}} - I_{\mathrm{smp2}}\right)$$

Pulsed UV inactivation studies were then conducted by treating 1 ml samples containing circa. 10^6 oocysts/ml with a range of pulses at 16.2 and 20 J respectively (corresponding UV doses shown in Tables 1 and 2). After treatment oocyst samples were assayed for ATP content as per the method described above. The amount of ATP (pmol) present after PUV inactivation was used to determine the reduction in oocyst viability post UV exposure by linear regression analysis utilizing the standard curve obtained by measuring ATP (pmol) concentration per oocyst concentration. All studies were conducted in triplicate.

Table 1 | Log_{10} reduction in *C. parvum* viability following exposure to pulses of UV light at varying at UV dose at 16.2 J as detected by a cell culture RT-PCR assay and ATP assay. Results are a mean of 3 replicates (+S.D.)

16.2 J No. of pulses	UV dose μJ/cm²	Log_{10} reduction in viability	
		CC-RT-PCR	ATP assay
0	0	0	0
10	1.08	0.4 ± 0.1	0
30	3.24	1.2 ± 0.1	0
40	4.32	2.5 ± 0.2	0.9 ± 0.1
60	6.48	4.6 ± 0.1	1 ± 0.1
90	9.72	5.4 ± 0.1	1 ± 0.2
120	12.9	–[a]	1.3 ± 0.1
150	16.2	–	1.4 ± 0.1
180	19.44	–	1.6 ± 0.2
210	22.6	–	1.8 ± 0.2
240	25.92	–	3 ± 0.1

[a]No detectable target gene present.

Table 2 | Log_{10} reduction in *C. parvum* viability following exposure to pulses of UV light at varying at UV dose at 20.0 J as detected by a cell culture RT-PCR assay and ATP assay. Results are a mean of 3 replicates (+S.D.)

20 J No. of pulses	UV dose μJ/cm²	Log10 reduction in viability	
		CC-RT-PCR	ATP assay
0	0	0	0
10	1.42	1.2 ± 0.1	0
30	4.26	1.9 ± 0.3	0
40	5.68	3.6 ± 0.3	1
60	8.52	5.6 ± 0.1	1.1 ± 0.2
90	12.78	–[a]	1.3 ± 0.1
120	17.04	–	1.5 ± 0.1
150	21.3	–	2.3 ± 0.2
180	25.5	–	2.5 ± 0.1
210	29.8	–	2.9 ± 0.3
240	34	–	3.8 ± 0.1

[a]No detectable target gene present.

In vitro cell culture infectivity

Cell culture infectivity was confirmed by immunofluorescent staining of treated HCT-8 cell monolayers following exposure to viable oocysts. Monolayers of the human ileocecal adenocarcinoma cell line HCT-8 (ATCC CCL-244: American Type Culture Collection, Rockville, MD) were grown with regular subculturing in RPMI 1640 growth media with L-glutamine and supplemented antibiotics (penicillin G, 100,000 U/L, streptomycin, 0.5 g/L and amphotericin B, 0.5 g/L), sodium bicarbonate, 2 g/L, and 10% foetal calf serum adjusted to pH7.4. HCT-8 cells were grown in T75 cm^{-2} cell culture flasks in a humidified incubator at 37 °C in an atmosphere containing 5% (vol/vol) CO_2 for circa 24 h until 80–90% confluent monolayers had formed. Cell monolayers were then detached with 0.25% (vol/vol) trypsin–EDTA and subsequently seeded into each of eight well chambered slides (Lab Tec II, Nunc) at a concentration circa 1×10^5 cells per well. After UV or heat treatments, the oocysts were stimulated by re-suspension in acidified HBSS (pH 2.7) and then in 1.0% (wt/vol) bile salts (pH 7) for 1 h at 37 °C. After two washing steps with sterile PBS, oocysts were re-suspended in cell culture media and thereafter 350 μl aliquots were then added to each well. Untreated oocysts were also stimulated to infect the cell monolayer as described above and provided a positive control. Duplicate sample of oocysts was heat treated at 70 °C for 30 min and this preparation was used as a negative control as per Rochelle *et al.* (2002). Samples were incubated for up to 48 h at 37 °C in 5% (vol/vol) CO_2 atmosphere, to determine optimal conditions for cell infectivity. At set times each individual well containing a separate monolayer was fixed by flooding with 100% (vol/vol) methanol (Sigma) which was subsequently left to stand for 10 min at room temperature. After removal of methanol, 75 μl of the fluorescein stain Sporo Glo™A600FLR-20X (Waterborne Inc., UK) was added to each well for 45 min (at 37 °C), which detects different life cycle stages of *Cryptosporidium in vitro*. The inoculated HCT-8 cell monolayers were then counterstained for 1 min with C101 containing Evans blue dye (Waterborne Inc., USA). All slides were examined under fluorescence microscopy (Leitz Diaplan fluorescence microscope) at an excitation wavelength of 460–500 nm and an emission wavelength of 510–560 nm for Sporo-Glo™ and an excitation wavelength of 550 nm and emissions wavelength of 610 nm for the counterstain C101. All wells containing separate monolayers was examined and noted as positive or negative for sites of parasitic

infection or foci of infection. Images of *C. parvum* life cycle stages were captured using a camera (Hamamatsu Colour Chilled 3cco camera) mounted on the aforementioned fluorescence microscope. All studies were performed in triplicate.

Combined cell culture-quantitative PCR (CC qPCR) assay for enumerating viable *C. parvum* post treatments

Real-time, TaqMan-quantitative PCR (qPCR) was performed using primers (TIB MOLBIOL, Berlin, Germany) specific for the 18S region of *Cryptosporidium* following the method of Keegan *et al.* (2003) with some slight modifications. Real-time PCR reactions are characterized by an increase in fluorescence emission due to probe degradation by DNA polymerase in each elongation step during PCR cycling. The higher the starting copy number of the nucleic acid target, the earlier the fluorescence will reach the predetermined threshold and the smaller will be Ct. The threshold cycle (CT) is the fractional PCR cycle number at which a significant increase in target signal fluorescence above the baseline is first detected for a sample. Quantification of test samples is performed by determining the Ct value and the use of a standard curve to deduce the starting copy number. The sequence of the TaqMan probe was based on the conserved eukaryotic probe of Amman *et al.* (1990) with the following sequence: 5-′-(6-FAM) ACC AGA CTT GCC CTC C (TAMRA). An aliquot (4 µl) of the Lightcycler TaqMan® Master kit (Roche Diagnostics, West Sussex, UK) comprising *Taq* DNA polymerase, reaction buffer, $MgCl_2$ and dNTP was used in each reaction. Cycling parameters were initial denaturation for 10 min at 95 °C followed by 50 cycles of denaturation for 10 s at 95 °C, annealing for 40 s at 40 °C, extension for 1 s at 70 °C and cooling for 30 s at 40 °C on a LightCycler® device (Model 1.5, Roche Diagnostics, West Sussex, UK). The large number of cycles was used to ensure detection of low levels of infection. On completion of each RT-PCR run amplification curves were analysed by LightCycler® software (version 3.5, Roche) and a standard curve of oocyst DNA concentration determined. When required, PCR amplicons were visualized by UV illumination following electrophoresis in 1% agarose gels containing ethidium bromide. DNA standards were prepared from fresh oocysts ranging in concentration from 10 to 10^7 oocysts/ml by dilution in PBS following standard viable count determinations. Aliquots of oocysts at different densities were then stimulated to infect the HCT-8 cell line that were seeded into 24 well plates at a concentration of circa 1×10^4 cells/ml at 90% confluency. The latter cell line stimulation occurred by resuspension and separate incubations for 1 h in acidified HBSS and in bile salts as described earlier. One millilitre aliquots of each concentration range of excysted oocysts were re-suspended in

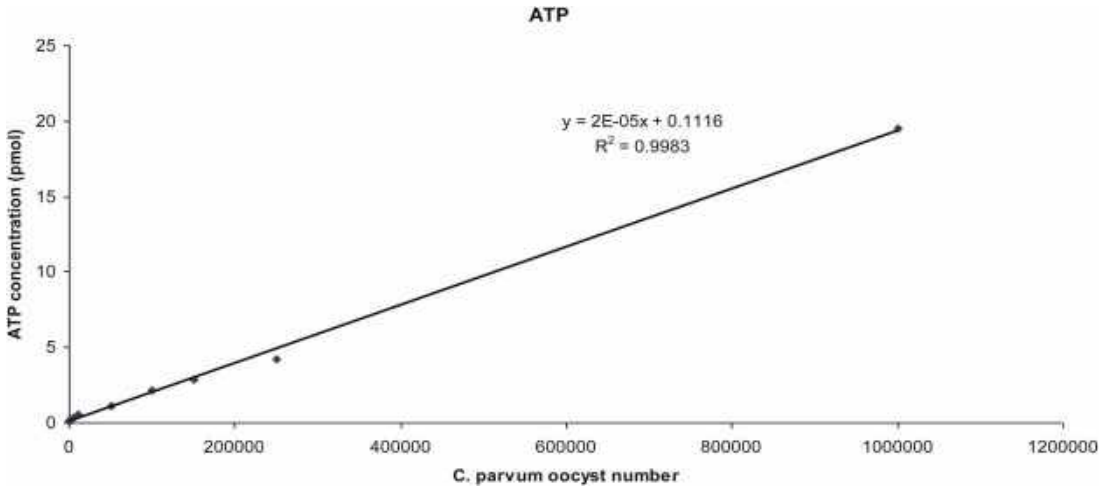

Figure 2 | Standard curve for *C. parvum* oocyst number vs. ATP concentration (pmol).

RPMI cell culture growth media and added to one well of the 24 well plate. Following 48 h incubation at 37 °C in a humidified atmosphere of 5% (vol/vol) CO^2, the cell culture media with non-adherent or internalized *C. parvum* was removed by aspiration and discarded. Mammalian cells were then washed with sterile PBS and trypsinized using 200 µl of 0.25% (vol/vol) trypsin/EDTA (Sigma) and left for 15 min at 37 °C until complete detachment of the monolayer had occurred. Cells were then centrifuged at 1,000 rpm for 10 min and re-suspended in 200 µl sterile PBS, thereafter the mammalian cells and *C. parvum* sporozoite cell membranes were lysed using PCR template preparation kit (Roche Diagnostics, West Sussex, UK) in order to produce DNA (template) and standard curve (Figure 3). The aforementioned procedure was then repeated to determine infectivity of oocysts subjected to varying UV parameters or heating at 70 °C for 30 min (negative control). Log inactivation of oocysts (L) is defined by $L = \log_{10}[N_d/N_0]$, where N_0 is the initial concentration of oocysts and N_d is the concentration of viable infectious oocysts post disinfection treatments as detected by combined cell culture-qPCR assay as per method of Lee *et al.* (2008).

Statistical analysis

Student's *t*-tests and ANOVA one-way model (MINITAB software release 13; Mintab Inc., State College, PA) were used to compare the effects of the relationship of independent variables on light treatments.

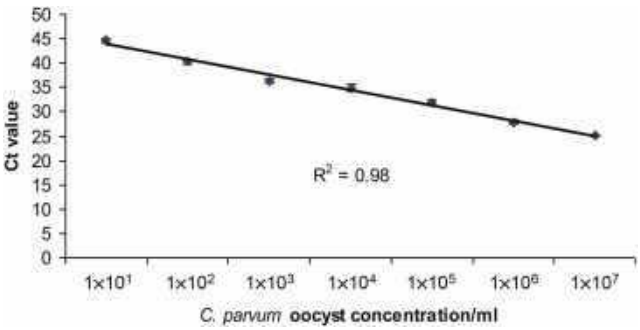

Figure 3 | Standard curve for *C. parvum* oocyst concentration versus Ct value obtained by real-time PCR utilizing a cell culture based assay (+/− S.D.).

RESULTS AND DISCUSSION

Determination of rate of PUV inactivation of *C. parvum* using a combined cell culture real-time PCR *in vitro* assay

A standard curve of *C. parvum* oocyst number and corresponding DNA amplification was generated by using a combined cell culture (CC) – qRT-PCR procedure by inoculating HCT-8 monolayers with different concentrations of *C. parvum* oocysts (Figure 3). Based on the number of oocysts added to each PCR reaction for the DNA standards, relative quantification of infectious oocysts was performed for estimating log inactivation of oocysts during treatment processes. The uninfected HCT-8 cell extract failed to produce a detectable signal in the PCR, indicating no amplification of the host cell DNA with the 18S primers (data not shown). Following UV treatments, the Ct values obtained for PUV-treated oocysts were higher compared with the untreated control suggesting that there was a decrease in the number of viable oocysts present after UV treatment (Table 1). Using the 16.2 J per pulse setting (Table 1), a 1.2 $\log_{10}$ reduction in viability or infectivity was obtained post PUV-irradiation with a UV dose of 3.24 µJ/cm^2 while a maximal 5.4 $\log_{10}$ reduction in oocysts infectivity was achieved using the higher UV dose of 9.72 µJ/cm^2 (Figure 4). At the higher discharge voltage of 1,000 V (or 20 J per pulse) (Table 2), a 1.2 $\log_{10}$ reduction in oocyst infectivity was achieved using a significantly lower UV dose (1.42 µJ/cm^2) and a maximal 5.6 $\log_{10}$ loss in oocyst infectivity occurred after exposure to a UV dose of 8.52 µJ/cm^2. At UV doses 8.52 µJ/cm^2, no *C. parvum* DNA was detected in the host cell monolayer via the combined CC-qPCR compared with untreated controls (Figure 4) suggesting that once complete oocyst inactivation was achieved no cell infectivity occurred resulting in an absence of target DNA for amplification. Mofidi *et al.* (2001) also used HCT-8 cell cultures and real-time PCR assay to evaluate the efficiency of UV light as a disinfectant against *C. parvum* and demonstrated an average level of inactivation of 94% (1.2 $\log_{10}$) using a similar polychromatic UV system that emitted a UV dose of 4 mJ/cm. Therefore, pulsed UV light successfully inactivated *C. parvum* oocysts as determined via the cell

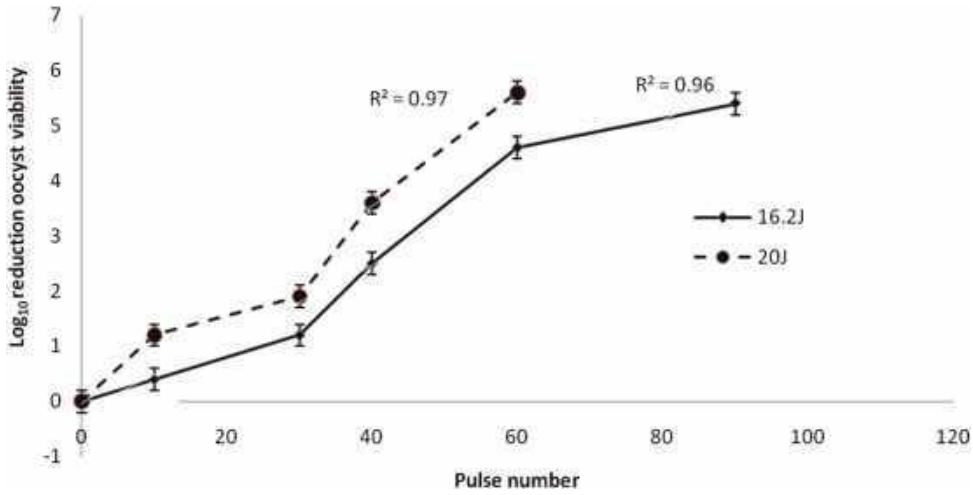

Figure 4 | Reduction in *C. parvum* oocyst viability at 16.2 and 20 J by pulsed UV light at a distance of 8 cm from the light source (+/− SD) as detected by cell culture RT-PCR.

culture qPCR assay, For this PCR assay, the limit of detection was found to be 10 oocysts per monolayer. The log inactivation rate for each type of UV treatment was determined using the equation previously described (Garvey *et al.* 2010). The results demonstrate that the assay was highly reproducible, evident by the linear standard curve obtained for serial dilution of the stock culture (Figure 3). The HCT-8 cell line failed to produce a detectable signal in the PCR, indicating no amplification of host cell DNA with the 18S primers. Also heat inactivated oocysts included as the experimental negative controls were not detected indicating successful removal of oocysts that had not undergone excystation. To date most published data on inactivating *C. parvum* is using LP and MP UV light sources, Craik *et al.* (2001), Keegan *et al.* (2003) and Mofidi *et al.* (2001) reported that a UV doses of 6, 5.8 and 10 mJ/cm^2 respectively provided an average 2 $\log_{10}$ loss of viability of *C. parvum* (Lee *et al.* 2008). The results of this study indicate that with a pulsed UV approach, similar levels of inactivation occur with a greatly reduced applied UV dose, e.g. 1.42 μJ/cm^2 gave a 1.2 $\log_{10}$ loss in viability following a 10 s exposure at 20 J per pulse.

Previous studies conducted comparing *in vitro* cell culture alone or combined cell culture-qPCR to that of measuring infectivity in live severe combined immunodeficiency (SCID) mice found good correlation between PUV inactivation as determined by both these methods (Rochelle *et al.* 2002; Garvey *et al.* 2010). Such studies further support the findings of this research and confirm the disinfection potential of PUV for *C. parvum* and suggest that the optimal method to determine infectivity post treatment is the use of a cell culture based qPCR method. Studies conducted by Fontaine and Guillot (2002) to assess the sensitivity of RT-PCR, for viability of *C. parvum* oocysts also found a similar detection limit to that of this study. Also studies conducted by Keegan *et al.* (2003) observed a detection limit of 10 oocysts per inoculated monolayer using a cell culture qPCR assay, confirming that this assay allows for effective quantification of infection by direct comparison of disinfected and untreated oocysts in cell culture. Therefore, the findings of this study demonstrate that cell culture combined with qPCR allows determination of the inactivation of *C. parvum* oocysts using UV light. These findings are consistent with the findings of Lee *et al.* (2008) and demonstrate that qPCR combined with *in vitro* cell culture is a valuable tool for evaluating disinfection systems for drinking water treatment. While this complex approach is widely accepted as an effective and reliable method for determining inactivation of *C. parvum* oocysts, its usage is restricted to specialist-equipped laboratories operated by highly-trained technicians. Therefore, it is important to assess alternative methods for oocyst inactivation studies.

ATP measurement for viability assessment

Adenosine-5′-triphosphate (ATP) is a multifunctional nucleotide that acts as a coenzyme and an energy source

which is consumed by many enzymes in a multitude of cellular processes. A linear relationship was observed between ATP (pmol) extracted by the method of excystation and sonication and oocyst number over the range of 10,000,000–10 oocysts (Figure 2). These findings correspond to that of Somiya *et al.* (2000) where the ATP sonication procedure used had a linear relationship to that of the DAPI/PI permeability assay for oocyst viability. Tables 1 and 2 show the relationship between UV dose for PUV-treated samples and associated reduction inactivation rates of treated oocysts. As evident from Table 2 and Figure 5, a maximal 3.8 log inactivation rate was achieved using 34 μJ/cm^2 at 20 J (Figure 5) whereas a maximal 3 log reduction in similarly prepared samples was achieved using a UV dose of 25.92 μJ/cm^2 at 16.2 J per pulse (Table 1). The general trend emerged where the ATP assay significantly overestimated survivors compared with using the combined *in vitro* cell culture qPCR infectivity assay. In addition, it took circa seven times more UV dose to register a 3 log reduction in oocyst cell infectivity as detected using the ATP assay compared with using the more sensitive cell culture-qPCR method.

Studies conducted previously by Somiya *et al.* (2000) found that ATP assays also overestimated oocyst viability compared with SCID mouse infectivity models following disinfection with ozone. As with the findings of King *et al.* (2005), the level of sensitivity for the detection of *C. parvum* via measurement of ATP was found to be circa 500 oocysts. The lower level of sensitivity for this test meant that the inactivation data were grossly underestimated. This suggests that the level of ATP degradation within UV treated oocyst does not occur rapidly enough to be used as a viability endpoint post UV treatment. The findings of King *et al.* (2005) suggest that measurement of ATP levels can allow for the assessment of oocyst inactivation following heat treatment of *C. parvum*. These studies reported a decline in oocyst infectivity of HCT-8 cells with a corresponding decline in oocysts ATP levels. King *et al.* (2005) concluded that the quantification of oocyst ATP levels could provide a simple and rapid method for determining oocyst inactivation rates and suggests that ATP is utilized by the parasite following changes in environmental temperature and as a result is not available as an energy source for excystation. However, the mechanisms of heat inactivation are dissimilar to that of UV light where the formation of DNA adducts by the latter prevents parasitic replication. Therefore, the findings of this study suggest that the measurement of ATP may not be a sufficient method to determine oocyst inactivation following PUV-irradiation as determined by comparative cell culture qPCR studies. The inaccuracy of ATP measurement post UV exposure may be related to the rate of degradation of ATP in UV-treated organisms. At present there are limited data available on the cellular activity of UV-treated oocysts, and the fate of such essential cell components as ATP.

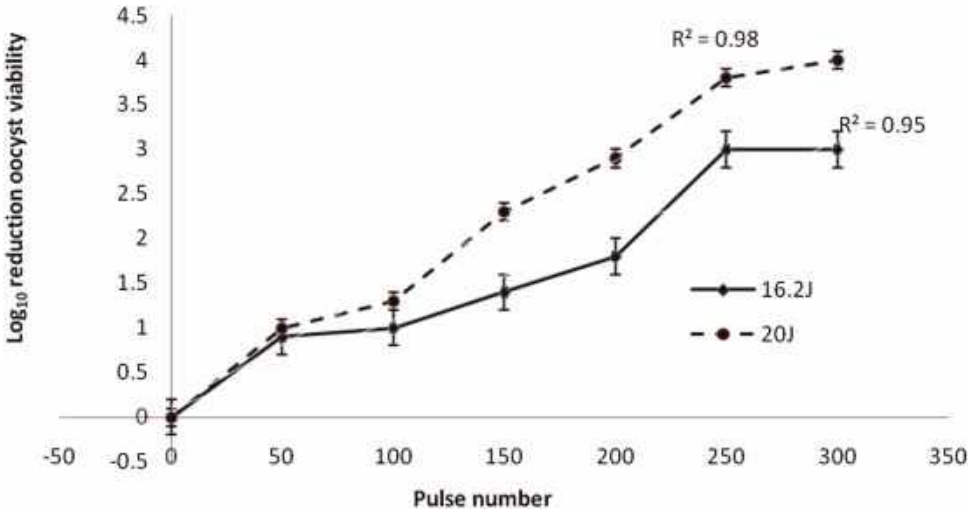

Figure 5 | Reduction in *C. parvum* oocyst viability 16.2 and 20 J by pulsed UV light at a distance of 8 cm from the light source (+/− S.D.) as detected by measurement of ATP.

Due to constant exposure to solar UV, microorganisms have developed mechanisms to repair genetic damage caused by the absorption of photons of UV energy. Conventional UV treatment methods largely affect DNA by means that are reversible under certain conditions, due to exposure to UV light organisms such as *C. parvum* have the ability to conduct DNA repair (Oguma *et al.* 2001). Indeed after treatment with UV light, *C. parvum* will have initiated those repair mechanism. The role of ATP within cells is such that it is essential for all cellular mechanisms. Therefore, the measurement of ATP levels within PUV treated oocysts indicates that damaged oocysts may still remain active but incapable of performing cellular functions such as invading human cells. Studies by Oei & Ziegler (2000) reported that most situations requiring highly efficient DNA repair are accompanied by a dramatic decrease of the cellular ATP concentration. This corresponds with the findings of this study and suggests that the reduction in ATP levels following high doses of UV (Tables 1 and 2) are due to the energy requiring activity within the organism such as photo repair as opposed to actual cell death. Indeed as with the findings of King *et al.* (2005), this may suggest that at higher PUV treatment levels the ATP is no longer available as an energy source for excystation due to the demand for photo-repair. The findings of Waldstein *et al.* (1974) concluded that ATP is required *in vivo* for either the incision step of photo-repair or an enzymatic reaction preceding it in UV treated *E. coli*. Studies conducted by Farrell *et al.* (2011) on the effect of PUV on yeast concluded that pulsed irradiation inactivates *C. albicans* through a multi-hit cellular process that includes inflicting irreversible damage to DNA and destabilizing the functionality and integrity of plasma cell membranes. The decrease in available ATP suggests a secondary method to that of the formation of DNA adducts for the inactivation of *C. parvum* with UV light. Without sufficient energy reserves at the moment of cellular infectivity sporozoites are unable to initiate infection and/or reproduction within a host. To date there is no data on the effect of high doses of pulsed light on the membrane and internal structures of *Cryptosporidium*.

The ability to initiate and conduct repair caused to DNA following UV disinfection is an important aspect to consider when sterilizing drinking water. The comparative qPCR assay used for this study show that at lower PUV doses ($<9.72\ \mu J/cm^2$) no cell infectivity occurred and that *C. parvum* had lost its ability to be infective. The author believes that the depletion of ATP following high UV doses ($34\ \mu J/cm^2$) in this study suggest that research is needed to determine the potential of *Cryptosporidium* to repair any UV-induced genetic damage and to regain infectivity in host cells. These findings have significant implications for PL-technology development, in particular for surface and water decontamination applications.

CONCLUSIONS

- Using an ATP assay, it was possible to measure the intracellular ATP content of viable oocysts where a linear relationship between oocyst number and ATP content was determined. However, the findings of this study demonstrated that the measurement of intracellular ATP is not suitable for the determination of PUV disinfection of *C. parvum* oocysts.
- The level of ATP reduction in PUV-treated oocysts did not correspond to loss of oocyst infectivity as detected by the *in vitro* cell culture q-PCR assay. Specifically, the ATP assay overestimated oocysts numbers post treatments compared with that determined by the cell culture-qPCR approach.
- The measurement of cellular ATP did indicate that cellular activity was present after treatment and suggests that further studies are required to determine the mechanistic effects of oocyst damage inflicted by PUV irradiation. *Cryptosporidium* species possess the ability to repair UV induced DNA damage following treatment with conventional low and MP light sources. Consequently this suggests that studies focusing on the DNA repair mechanisms of *C. parvum* should be conducted following PUV exposure to determine the potential and rate of photo-repair and subsequent possibility of regaining infectivity.
- It has been shown that the cell culture approach has equivalency with the gold standard *in vivo* mice model for measuring loss of oocyst infectivity following UV disinfection.

- This study concludes that ATP measurement is not suitable for assessing oocyst inactivation post PUV-irradiation.

ACKNOWLEDGEMENTS

The authors wish to thank the Irish Environmental Protection Agency Strive Programme for funding this research (2011-W-MS-5).

REFERENCES

Amman, R. R., Binder, B. J., Olsen, R. J., Chisholm, S. W., Devereaux, R. & Stahl, D. A. 1990 Combination of 16S rRNA-targeted oligonucleotide probes with flow cytometry for analyzing mixed microbial populations. *Appl. Environ. Microbiol.* **56**, 1919–1925.

Craik, S. A., Weldon, D., Finch, G. R., Bolton, J. R. & Belosevic, M. 2001 Inactivation of *Cryptosporidium parvum* oocysts using medium- and low-pressure ultraviolet radiation. *Water Research* **35**, 1387–1398.

DuPont, H. L., Chappell, C. L., Sterling, C. R., Okhuysen, P. C., Rose, J. B. & Jakubowski, W. 1995 The infectivity of *Cryptosporidium parvum* in healthy volunteers. *New England Journal of Medicine* **332**, 855–859.

Fayer, R., Santin, M. & Trout, J. M. 2007 Prevalence of Cryptosporidium species and genotypes in mature dairy cattle on farms in eastern United States compared with younger cattle from the same locations. *Veterinary Parasitology* **145**, 260–266.

Farrell, H., Hayes, J., Laffey, J. & Rowan, N. 2011 Studies on the relationship between pulsed UV light irradiation and the simultaneous occurrence of molecular and cellular damage in clinically-relevant *Candida albicans*. *Journal of Microbiological Methods* **84**, 317–326.

Fontaine, M. & Guillot, E. 2002 Development of a TaqMan quantitative PCR assay specific for *Cryptosporidium parvum*. *FEMS Microbiology Letters* **214**, 13–17.

Fontaine, M. & Guillot, E. 2003 An immunomagnetic separation-real-time PCR method for quantification of *Cryptosporidium parvum* in water samples. *Journal of Microbiological Methods* **54**, 29–36.

Garvey, M., Farrell, H., Cormican, M. & Rowan, N. 2010 Investigations of the relationship between use of in vitro cell culture-quantitative PCR and a mouse-based bioassay for evaluating critical factors affecting the disinfection performance of pulsed UV light for treating *Cryptosporidium parvum* oocysts in saline. *Journal of Microbiological Methods* **80**, 267–273.

Gray, N. F. 2005 *Water Technology: An Introduction for Environmental Scientists and Engineers*. Elsevier Butterworth-Heinemann, Oxford.

Hijjawi, N. 2003 *In vitro* cultivation and development of Cryptosporidium in cell culture. In: *Cryptosporidium: From Molecules to Disease* (R. C. A. Thompson, A. Armson & U. M. Morgan-Ryan, eds). Elsevier, Amsterdam.

Hijnen, W. A., Beerendonk, E. F. & Medema, G. J. 2006 Inactivation credit of UV radiation for viruses, bacteria and protozoan (oo)cysts in water: a review. *Water Research* **40**, 3–22.

Holm-Hansen, O. & Booth, C. R. 1966 The measurement of adenosine triphosphate in the ocean and its ecological significance. *Limnology and Oceanography* **11**, 510–519.

Karanis, P. & Aldeyarbi, H. M. 2011 Evolution of *Cryptosporidium in vitro* culture. *International Journal for Parasitology* **41**, 1231–1242.

Keegan, A. R., Fanok, S., Monis, P. T. & Saint, C. P. 2003 Cell culture-Taqman PCR assay for evaluation of *Cryptosporidium parvum* disinfection. *Applied and Environmental Microbiology* **69**, 2505–2511.

King, B. J., Keegan, A. R., Monis, P. T. & Saint, C. P. 2005 Environmental temperature controls *Cryptosporidium* oocyst metabolic rate and associated retention of infectivity. *Applied and Environmental Microbiology* **71**, 3848–3857.

Korich, D. G., Marshall, M. M., Smith, H. V., O'Grady, J., Bukhari, Z., Fricker, C. R., Rosen, J. P. & Clancy, J. L. 2000 Inter-laboratory comparison of the CD-1 neonatal mouse logistic dose-response model for *Cryptosporidium parvum* oocysts. *The Journal of Eukaryotic Microbiology* **47**, 294–298.

Lee, S. U., Joung, M., Yang, D. J., Park, S. H., Huh, S., Park, W. Y. & Yu, J. R. 2008 Pulsed-UV light inactivation of *Cryptosporidium parvum*. *Parasitology Research* **102**, 1293–1299.

MacKenzie, W., Hoxie, N., Proctor, M., Gradus, M., Blair, K. & Peterson, D. 1994 A massive outbreak in Milwaukee of *Cryptosporidium* infection transmitted through the public water supply. *New England Journal of Medicine* **331**, 161–167.

Mofidi, A. A., Baribeau, H., Rochelle, P. A., De Leon, R., Coffey, B. M. & Green, J. F. 2001 *Disinfection of* Cryptosporidium parvum *with polychromatic UV light*. American Water Works Association, Denver, CO.

Nugent, M. J. & Higginbotham, C. L. 2007 Preparation of a novel freeze thawed poly(vinyl alcohol) composite hydrogel for drug delivery applications. *European Journal Pharmaceutics and Biopharmaceutics* **67**, 377–386.

Oei, S. L. & Ziegler, M. 2000 ATP for the DNA ligation step in base excision repair is generated from poly(ADP-ribose). *Journal of Biological Chemistry* **275**, 23234–23239.

Oguma, K., Katayama, H., Mitani, H., Morita, S., Hirata, T. & Ohgaki, S. 2001 Determination of pyrimidine dimers in *Escherichia coli* and *Cryptosporidium parvum* during UV light inactivation, photoreactivation, and dark repair. *Applied and Environmental Microbiology* **67**, 4630–4637.

Patterson, J. W., Brezonik, P. L. & Putnam, H. D. 1970 Measurement and significance of adenosine triphosphate in activated sludge. *Environmental Science and Technology* **4**, 569–575.

Rochelle, P. A., Ferguson, D. M., Handojo, T. J., De Leon, R., Stewart, M. H. & Wolfe, R. L. 1997 An assay combining cell culture with reverse transcriptase PCR to detect and determine the infectivity of waterborne *Cryptosporidium parvum*. *Applied and Environmental Microbiology* **63**, 2029–2037.

Rochelle, P. A., Marshall, M. M., Mead, J. R., Johnson, A. M., Korich, D. G., Rosen, J. S. & De Leon, R. 2002 Comparison of *in vitro* cell culture and a mouse assay for measuring infectivity of *Cryptosporidium parvum*. *Applied and Environmental Microbiology* **68**, 3809–3817.

Rochelle, P. A., Mofidi, A. A., Marshall, M. M., Upton, S. J., Montelone, B., Woods, K. & Di Giovanni, G. 2005 An Investigation of UV Disinfection and Repair in *Cryptosporidium parvum*. American Water Works Association Report 91015F. IWA Publishing, London.

Somiya, I., Fujil, S., Kishimoto, N. & Kim, R. H. 2000 Development of ATP assay as a surrogate indicator of viability of Cryptosporidium parvum oocysts. *Water Science & Technology* **41** (7), 181–188.

Waldstein, E. A., Sharon, R. & Ben-Ishai, R. 1974 Role of ATP in Excision repair of ultraviolet radiation damage in *Escherichia coli*. *Proceedings of the National Academy of Sciences of the United States of America* **71**, 2651–2654.

Weddle, C. L. & Jenkins, D. 1971 The viability and activity of activated sludge. *Water Research* **5**, 621–624.

First received 29 March 2012; accepted in revised form 24 August 2012

Trends in Food Science & Technology 88 (2019) 316–332

Contents lists available at ScienceDirect

Trends in Food Science & Technology

journal homepage: www.elsevier.com/locate/tifs

Review

Pulsed light as an emerging technology to cause disruption for food and adjacent industries – Quo vadis?

Neil J. Rowan

Centre for Disinfection, Sterilisation and Biosecurity, Bioscience Research Institute, Athlone Institute of Technology, Dublin Road, Athlone, Ireland

ARTICLE INFO

Keywords:
Pulsed light
Fresh produce
Post-harvest decontamination
Data harmonisation
Disruptive technology
Life cycle assessment
Pollination
Guidance for reporting studies

ABSTRACT

Background: – Despite verbose amount of publications and having gained approval by Food and Drug Administration (FDA) since 1996 for food-surface disinfection applications, pulsed light (PL) still has not been used on a large scale by industry. Fresh produce remains a leading cause of foodborne illness outbreaks where there is a pressing need for an effective post-harvest decontamination intervention such as PL that can replace or supplement post-harvest washing.

Scope and approach: This review describes current status of PL for non-thermal food-surface treatments. It addresses rationale and efficacy of methods used to assess PL disinfection performance along with addressing interrelated factors that are limiting PL development for these opportunities.

Key findings and conclusions: PL is a promising non-thermal technology for food-surface disinfection. Lack of international harmonisation and consensus on what constitutes priority experimental methods and exposure conditions is hampering commercial development of PL. Previously, many studies have reported on PL-food treatments using a cumulative energy dose or range of UV doses above the FDA recommended 12 J cm^{-2}. Consensus on the choice and relevance of indirect cell and molecular methods to assess injury in PL-treated microorganisms has yet to be reached. This review provides recommendations in reporting experimental data and key parameters governing treatment that enables reporting of sufficient details to extent that other researchers would be able to repeat, compare and evaluate data between studies. Converging developments in adjacent industry sectors that may inform development of PL as a promising future food disruptive technology are described.

1. Introduction

The food sector is the largest manufacturing sector in the EU with €1,098 billion turnover employing 4.24 million people (cited Saguy, Roos, & Cohen, 2018). As our global population continues to grow, so too does the demand for the supply of more safe nutritious food (Michelini, Principato, & Iasevoli, 2018; Richie et al., 2018). This global population growth also brings added challenges including the need to diversify our food supply chain to meet changing diets including growing individualism, diet-related diseases, demand for personalised food products, the rise of 'flexitarianism' (i.e., eating predominantly, but not strictly, vegetarian), an increasing aging population, and greater ethnic or cultural influences. These are projected to bring about a 70% increase in demand for more food over the next 40 years (DBEI, 2018). There has been a commensurate rise in the growth of "Foodomics' to respond to these opportunities (Valdéz, Cifuentes, & León, 2017; Rychilk, Kanawati, & Schmitt-Kopplin, 2017) along with increased digitisation of processes and markets. In addition, future sustaining of our global food supply chain will experience added pressure due to increasing uncertainties associated with impact of global warming on crops, which includes more droughts and flooding. Climate change will also continue to influence choice of innovation with preference for developing less energy-intensive eco-friendly food processes. The aforementioned highlights a trend towards increasing complexity of our food supply chain that requires more international collaboration and harmonisation of management efforts in order to adequately deal with risks to consumers (Quested, Cook, Gorris, & Cole, 2010) including food safety (Richie et al., 2018).

Fresh-cut produce remains the leading cause of foodborne illness outbreaks (Smith DeWall & Bhuiya, 2007; Callejón et al., 2015) surpassing that of meat, dairy and seafood (CDC, 2018). Moreover, fresh food produces are frequently contaminated by a range of potentially hazardous microorganisms including complex chlorine-resistant parasites (Centres for Disease Control and Prevention, 2018; Franssen et al., 2019). Several researchers have previously reported on the open nature of the fresh produce chain where contamination may be introduced at

E-mail address: nrowan@ait.ie.

https://doi.org/10.1016/j.tifs.2019.03.027
Received 30 November 2018; Received in revised form 14 March 2019; Accepted 20 March 2019
Available online 22 March 2019

several points in the production, harvesting and processing, and then passed on to consumers (Murray, Wu, Shi, Xue, & Warriner, 2017; Nuesch-Inderbinen & Stephan, 2016). Best published evidence shows that a critical post-harvest washing step conducted under commercial conditions has limited decontamination efficacy and may potentially lead to unwanted cross-contamination of produce (Gombas et al., 2017; Murray et al., 2017). Although on-farm good agricultural practices (GAP) can reduce contamination in the field and help minimise cross-contamination during post-harvesting handing (Francis et al., 2012), a more effective means to ensure the food safety of fresh produce is to apply post-harvest decontamination interventions that may complement or replace post-harvest washing (Felizani, Lichter, Smilanick, & Ippolito A, 2016; Meireles, Giaouris, & Simoes, 2016; Murray et al., 2017). Worldwide, there is an increasing consumer demand for ready-to-eat fresh-cut fruit and vegetables where this additional commercial processing step presents additional to prevent microbial cross-contamination and to main food safety (Yu, Neal, & Sirat, 2018).

Kramer, Wunderlich, and Muranyi (2017) also suggested several beneficial reasons why PL should be developed as a possible non-thermal technology for surface decontamination of produce including (a) minimally processed foods are typically consumed without additional washing or heating and they mostly display use by dates of several days allowing for growth potentially hazardous microorganisms; (b) the cold chain may not always be properly maintained; (c) plant tissue integrity may be impaired by cutting processes; (d) perishable products such as raw poultry are frequently contaminated with high numbers of pathogenic bacteria such as *Campylobacter* and *Salmonella* species; (e) many minimally processed fresh produce cannot be harshly treated; (f) heating is not applicable for meat, fish or fresh produce, and (g) alternative use of chemical biocides such as chlorine may not be preferred due to potential formation of toxic byproducts like trihalomethanes. Although physical technologies like pulsed electric fields (PEF) and high hydrostatic pressure (HHP) are quite well advanced for commercial scale deployment, these treatments may not be appropriate to meet the surface decontamination and packaging needs of industrially-fabricated ready-to-eat fresh-cut produce. Murray et al. (2017) reported that most approaches to address this food surface decontamination step for ready-to eat fresh-cut produce are typically still at laboratory scale. Increasing research on the use of pulsed light (PL) is a promising but is has yet to reach its' market potential for large scale industrial use despite gaining approval from the Food and Drug Administration (FDA) in 1996 for food surface treatments (Schottroff et al., 2018). PL seeks to achieve a balance between applying effective nonthermal treatment yet maintaining fresh-like food properties as detectable by means of changes in texture, colour, chemical composition or sensory attributes (Kramer et al., 2017; Van Impe, 2018). There are also potential consequences for food safety including evidence of the emergence of viable but not-culturable (VBNC) state microorganisms post PL treatments that may lead to an underestimation of produce microbial quality status (Rowan, Valdramidis, & Gomez-Lopez, 2015; Schottroff et al., 2018; Zhao, Zhong, Wei, Lin, & Ding, 2017).

A related consideration for large scale development of PL technology is the apparent lack of quality of harmonised data surrounding experimental methods and exposure conditions for food treatment technologies that will enable other researchers to repeat, interpret and evaluate data enabling large scale industrial deployment (Schottroff et al., 2018). This appears at odds with the development of similar or different physical treatment technologies in adjacent industries such as the water (TrojanUV, 2016; Fitzhenry, Rowan, Val de Rio, Cremillieux, & Clifford, 2019) or medical technology sectors where there is potential for knowledge transfer. However, there is a trend towards cross-cutting use of innovative technologies such as PL to meet complex food safety challenges including recalcitrant foodborne parasites (Franssen et al., 2019) and other emerging opportunities such as infant milk formulae treatment (McFadden et al., 2017) and even extrusion-based 3-D printing of proteins and fibre-rich materials (Lille, Nurmela, Nordlund, Metsä-Kortelainen, & Sozer, 2018). Therefore, this review will address challenges and opportunities influencing PL development for large scale uptake by the food industry along with providing recommendations for standardising reporting by researchers. Future potential for PL to cause technology disruption is considered.

1.1. Pulsed light as example of emerging technology

Pulsed light (PL) is a nonthermal disinfection technology that has attracted attention over the past 15 years as a promising minimal process to improve the microbial safety or to extend the shelf life of treated foods (Schottroff et al., 2018). PL has been described as a cost-effective, nonthermal technology that does not generate unwanted residuals on treated food surfaces (Hayes, Kirf, Garvey, & Rowan, 2013). PL has also been referred to as high-intensity pulsed UV light (HIPL), pulsed UV light (PUV), high-intensity broad-spectrum UV light (BSPL), intense light pulsed (ILP) and pulsed white light (PWL) (Schottroff et al., 2018). The number of published research on PL technology has substantially increased as attested by 247 citations in Google Scholar in respect of my initial study on use of this innovation for treating foodborne microorganisms (Rowan et al., 1999). PL has been approved by the FDA in the production, processing and handling of foods since 1996 up to cumulative UV dose or fluence of $12\,J\,cm^{-2}$ where emission spectra to be kept between 200 and 1100 nm and pulse duration at $\leq$ 2 ms (Food and Drug Administration, 2015). However, PL has been developed for commercial scale food packaging with little evidence of large scale food treatments. However, emerging applications include ready-to-eat, freshly-cut, fruit and vegetables along with decontamination of meat and fish products and associated packaging (Table 1). The technological principle of pulsed light disinfection is based upon the accumulation of high discharge voltage in a capacitor where the stored energy is delivered in ultra-short pulses through a light source filled with xenon gas. This xenon-light source emits a broad spectrum light flash typically in the range of ca. 200–1100 nm with approximately 25% in the UV range (Kramer et al., 2017). It is considered that PL disinfection efficiency is higher compared with continuous-wave low-pressure UV irradiation (CW-UV) due to its high peak power along with the ability to deliver its stored energy over short durations, typically 1 to 10 pulses per second. The main parameters governing effective PL operational for disinfection are the fluence [J cm^{-2}] over exposure time [s], number of pulsed applied [n], pulsed width [τ], frequency [Hz], and the peak power [W] (Hayes, Laffey, McNeil, & Rowan, 2012a; Hayes, Fogarty, Clifford, & Rowan, 2012b; Hayes, Garvey, Fogarty, Clifford, & Rowan, 2012c; Rowan et al., 2015).

1.2. Development of PL technology for large scale commercial usage in food and other areas

Given that the volume of data published on PL technology for different food surfaces and types is verbose, what are technological gaps or trends in published information that maybe limiting PL development for commercial uptake? A review of existing literature reveals that PL lacks harmonisation and standardisation of data to inform technology acceptance for the food sector for large scale uptake (Table 1). No single PL study to date has holistically addressed reliable and repeatable operation using a broad range of pathogenic and spoilage microorganisms, which demonstrates significant methodological variance where currently there is non-cohesive or consensus for standardised development of PL internationally. These observations also corroborate recent review of Schottroff et al. (2018) who commented that published research outcomes for PL treatments for different foods are incomparable as basic information on parameters is lacking such as details of lamp manufacture, geometry of target matrix and so forth. Table 1 highlights significant variation in PL operational conditions on food quality parameters and targeted microorganisms that generates an enormity of data that is lacking harmonisation and varies in rigor. This particular

Table 1
Variation in parameters measured pre and post PL-treatments of foods and beverages.

Vegetables (n = 15) & Fruit (n = 8)	Food Quality Changes Measured	PL-Operational Settings (n)	PL-mediated Microbial Reduction (CFU)	Meat & Fish Products (n = 13)	Food Quality Changes measured	PL Operational Settings (n =)	PL-mediated Microbial Reduction (CFU)
Greenbell peppers **Iceberg lettuce** **Soybean Sprouts** **Radicchio** **Carrots** **White Cabbage** (Gómez-López, Devlieghere, Bonduelle, & Devevere, 2005)	Increase in respiration rate; sensory deviation during storage (n = 2)	**No fluence reported**. 675 and 2700 pulses at 7 J for 45 and 180s. 7 °C for 9 days under MAP (n = 4)	Aerobic mesophilic count (n = 1)	**Chicken Frankfurters** (Keklik, Demirci, and Puri (2009) Ready-to-eat **Sausages** (Uesugi & Moraru, 2009) **Raw salmon fillets** (Ozer & Demirci, 2006)	Colour; lipid peroxidation (n = 2) Not determined (n = 1) Colour loss; Temperature increase to 100 °C (n = 2)	≤**0.25 cm**$^{-2}$; ≤13 cm (n = 9) **9.4 J cm**$^{-2}$; 48 days; 4 °C or combined Nisin (n = 5) **5.6 J cm**$^{-2}$; ≤60s; ≤ 8 cm (n = 8)	*L. monocytogenes* Scott A (≤1.9 log) (n = 1) *L. innocua* (1.37 log with PL; 4.03 log with Nisin + PL) (n = 1) *E. coli* O157:H7 (≤1.09 log) *L. monocytogenes* Scott A (1.2 log) (n = 2)
Mushrooms (Fresh-cut) (Oms-Oliu, Aguiló-Aguayo, Martín-Belloso, & Soliva-Fortuny, 2010)	Texture, colour, polyphenol oxidase, Vit C, heat damage high fluence (n = 5)	≤**28 J cm**^{2} per pulses up to 60s; up to 13 cm distance; sealed PP-trays, (n = 13)	Native microflora (n = 1)	**Chicken** through plastic films (Haughton et al., 2011)	Discolouration at high treatment intensities	**No fluence reported**. 505 J per pulse; ≤30 s; 3 Hz; (n =	*E. coli* (1.69 log) *Salmonella enteritidis* ATCC 13076 (1.69 log) *Campylobacter jejuni* (1.22 log) (n = 3)
Avocado (Ramos-Villarroel, Martín-Belloso, & Soliva-Fortuny, 2011)	Colour, texture, O_2 and CO_2 increase, reduction ethylene (n = 4)	**0.4 J cm**^{2} per pulse for 15 to 30 pulses, 5 °C dark, 15 days; PP-film/PP-trays (n = 6)	*E. coli* (2.61–2.97 log) *L. innocua* (2.9–3.33 log) (n = 2)	**Beef and Tuna Carpaccio** (Hierro, Ganan, Barroso, & Fernández, 2012)	Sensory attributes and colour parameters (n = 2)	≤**11.9 J cm**$^{-2}$; 4 °C; 28 days (n = 5)	*L. monocytogenes* Scott A ≤0.9 log *E. coli* (≤1.2 log) *S. enterica* serovar Typhimumium (≤1 log) *Vibrio parahaemolyticus* (≤1 log) (n = 4)
Green onions (Xu, Chen, & Wu, 2013)	Not determined	**5 and 14.3** J cm^{2} (dry PL) **56.1 J cm**^{2} (wet PL) *	*E. coli* O157:H7 > 4 log reduction	**Seafood** (shrimp, salmon, catfish) Cheigh et al. (2013)	No impact on colour; Max Temperature rise 5 °C (n = 2)	≤**17.2 J cm**$^{-2}$; ≤9800 pules; ≤1960 s (n = 12)	*L. monocytogenes* KCCM 40307 (≤2.4 log) (n = 1)
Tomatoes (Aguiló-Aguayo, Charles, Renard, Page, & Carlin, 2013)	Softening, increased weight, impact on ascorbic acid, (n = 6),	**2.68 J cm**$^{-2}$; 2.5 k/20 °C; 15 day (n = 2)	Microflora (1 log) *S. cerevisiae* (2.5 log) (n = 2)	**Pork and Salmon** (Nucorescu et al., 2014)	Dose dependent colour change in port and liquid peroxidation in salmon at high fluences (n = 3)	**3, 10 or 30 J cm**$^{-2}$ 3 cm distance from light source, 1 Hz at 4 °C [n = 3]	Aerobic plate count (< 1 log reduction)
Strawberries and **Blueberries** (Huang, Ye, Cao, and Chen (2017)	Not determined (n = 0)	≤**22.5 J cm**$^{-2}$; ≤25s; 16 cm distance (n = 5)	*E. coli* O157:H7 (≤3.8 log) *Salmonella Newport* H1275 (≤4.2log) MNV-1 (≤3.8 log) (n = 3)	**Beef/pork, chicken/ turkey**, and **deer/rabit/ kangaroo** (Tomašević., 2015)	Dose dependent change in sensory and colour change particularly at high fluences (n = 4)	**3.4 cm J cm**$^{-2}$ 6 and 10 cm distance from light source, 1 and 5 pulses, 3 kV (n = 4)	Not determined.
Spinach (Agüero, Jagus, Martín-Belloso, & Soliva-Fortuny, 2016)	Increase respiration, antioxidant capacity, total polyphenolic content, colour (n = 5)	≤**120 kJ cm**$^{-2}$; ≤30 pulses; 8.5 cm distance 4 °C; 10 days (n = 12) PE trays sealed with PP film	*E. coli* (≤2.3 log) *L. innocua* (≤2.6 log) Total plate count (≤2.2 log) (n = 3)	**Apple Juice** (Muñoz et al., 2012)	No impact on pH, nonenzyme browning or total antioxidant activity; colour change (n = 4)	**5.1 J cm**$^{-2}$ but 1.2 J cm^{-2} per pulse under continuous flow rate – distance 1.9 cm; 17 and 13.4 ml min-1; 3 Hz; (n = 4)	*E coli* DSM 1607 (4.9 log reduction)
Mung bean sprouts **Endive Salad** (Kramer et al., 2015a, 2015b)	Colour, respiration due to UV-C content of PL (n = 2)	≤**3 J cm**$^{-2}$, 10 cm, 5 °C, 6 days, (n = 7)	*E. coli* DSM 498 (≤2.34 log) *L. innocua* DSM 20649 (≤1.55 log) Total Viable Count (≤2.46 log) (n = 3)	**Goat Milk** (Kasahara, Carrasco, & Aruilar, 2015)	Aroma changes; no impact upon viscosity, density, pH, moisture, ash (n = 6)	1.3–**10 J cm**$^{-2}$; 0.41 J cm^{-2}per pulse; 20 Hz, 1–8 s; 3 ml sample in quartz cell (n = 4)	*E. coli* DHS (6 log reduction)

(*continued on next page*)

Table 1 (*continued*)

Vegetables (n = 15) & Fruit (n = 8)	Food Quality Changes Measured	PL-Operational Settings (n)	PL-mediated Microbial Reduction (CFU)	Meat & Fish Products (n = 13)	Food Quality Changes measured	PL Operational Settings (n =)	PL-mediated Microbial Reduction (CFU)
Raspberries Strawberries (Bialka & Demirci, 2008)	Weight, colour, sensory attributes (n = 4)	**≤72 J cm^{-2}**; ≤ 60s; ≤ 13 cm distance (n = 13)	*E. coli* O157:H7 (≤3.9 log) *S enterica* (2.8 ≤ log) Several outbreak strains (n = 6)	**Apple, Melon, Orange** and **Strawberry juices** (Ferrario, Alzamora, & Guerrero, 2013)	Temperature increase by up to 16.8 Oc (n = − 4)	**2.4–71.6 J cm^{-2}**; 10 cm distance; 2–60 s; 4.9 ml PL-treated in petri dish (n = 5)	*L. monocytogenes* (≤4.5 log in apple juice; ≤ 1 log orange juice; ≤0.3 log strawberry juice); *E. coli* (≤2 log orange juice);
Raspberries and Strawberries (Huang and Chen, 2015)	No significant discolouration (n = 1)	**≤63.2 J cm^{-2}**; ≤ 60s, water assisted PL alone & combined with 1% H2O2 (n = 12)	*E. coli* O157:H7 *S. entericica* (several outbreak strains) Murine norovirus (≤4.4 log) (n = 3)	**Raw Milk** (Innocente et al., 2014)	Increase by 30 °C (55 °C absolute); up to 94% inactivation of alkaline phosphatase	0.26–**26.25 J cm^{-2}**; 0.5 Hz, 1 cm distance; 3 ml sample (n = 5)	Total microbial count (≤3.2 log unit reduction)

table illustrates broad range of examples from published work on PL treatments to emphasise a trend in metadata where the reader is referred to the comprehensive reviews of Kramer et al. (2017) for a more complete set of findings. Table 1 shows that of the 141 food products tested significant variation is found in log unit reductions that may depend on *inter alia* PL-treated pathogens, level of applied fluence (0.14–580 J cm^{-2}), distance from light source (3 cm–18 cm), food storage temperature (range 3 °C to 28 °C), aerobic or atmospheric packaging, use of combinational treatment technologies such as hydrogen peroxide or preservatives. Review of published research available reveals that many do not include the FDA approved upper threshold fluence value of 12 cm^{-2} in their PL-food treatment studies (Table 1). Moreover, several PL-food treatments studies operated at either a single or range of fluences well above this FDA recommended cumulative energy dosage, yet no rationale for this appears obvious.

A recurring focus was the PL-treatment of artificially-seeded or natural food products in plastic packaging in the format of trays or films that is of commercial interest (Table 1). However, the value of latter data arising of PL-treatment of plastic packing is of limited usefulness given their negative impact on environment and commensurate drive to replace plastics with sustainable alternatives such as with compostable or recyclable material. Some studies report a max temperature rise of 5 °C after 9800 pulses over range 0–17.2 J cm^{-2} with no impact upon seafood colour along with marginal ≤2.4 log unit reductions of *L. monocytogenes* (Cheigh, Hwang, & Chung, 2013). Others describe temperature increases up to 100 °C within 60 s of PL-treatment in raw salmon fillets at 5.6 J cm^{-2} with only modest ca. 1 log CFU reductions in *E. coli* O157:H7 and *L. monocytogenes* Scott A (Ozer & Demirci, 2006), which is surprising given that PL is considered to be a non-thermal process. There appears to be inter-parameter investigation of the contributing role of each factor in terms of statistical significance of disinfection outcome. Evidence-based research from published literature has demonstrated potential for PL to inactivate a range of pathogens on different food types and surfaces along with limited treatments in beverages (Table 1). However, consensus on standardised methods and equipment used that would inform process validation is holding back development of PL technology as there is lack of sufficient data for garnering industrial confidence.

If one delves deeper into published studies many additional factors are described that influence PL treatment of food products (Table 1). Again, there is no one specific study that addresses a broad set of parameters across representative microorganisms of food safety and spoilage interest (Table 2). The focus of previous publications was to apply varying levels of PL treatments to destroy pathogens and to reduce or eliminate spoilage microorganisms under conditions that have minimal impact on nutritional or organoleptic properties for extended shelf life. The overwhelming operational factor governing PL-mediated disinfection is the measured UV dose or fluence (J cm^{-2}) and all future studies should report on findings using this parameter as a measure to move towards international harmonisation. As only 25% of the broad spectrum intense light pulses are in UV range that decreases in efficacy with increased distance from light source to target surface, it is important to standardise and define distances used for food treatments. Currently, distances over the range 3 cm–18 cm from light source to target surface have been reporting in the literature (Table 1). Notwithstanding variances in microbial species and strains reported post PL-treatments, a trend has emerged exhibiting deceasing resistance to PL irradiation roughly in the order fungal spores, bacterial endospores > parasites > viruses > and > vegetative bacteria. Our previous research has demonstrated that pigmentation protects fungal spores against the action of PL as these pigments absorb light optimally in the UV-C region that may be attributed to an evolutionary adaptive trait (Anderson, Rowan, MacGregor, Fouracre, & Farish, 2000). Few studies have focused on complex pathogens such as foodborne parasites or viruses, due to the need for developing alternative and sophisticated in vitro bioassays such as combined RT-qPCR with mammalian cell

Table 2
Variation in the number and types of microorganisms and approach used during PL-treatments of natural and artificially-contaminated fruit and vegetables, meat and fish and beverages.
* Source data, Kramer et al. (2017); -, not tested.

Microorganism or Enumeration Method Applied	Number of food products treated with PL where test microorganism studied*			
	Fruit and Vegetable (n = 80)	Meat and Fish Products (n = 24)	Beverages (n = 37)	Total Food Products (n = 141)
Aerobic Mesophilic Count	19 (23.75%)	1 (4.2%)	2 (5.4%)	22 (15.7%)
E. coli O157:H7	6 (2.5%)	2 (8.3%)	1 (2.7%)	9 (6.4%)
E. coli (non VTEC)	9 (11.25%)	2 (8.3%)	12 (32.4%)	23 (16.4%)
Salmonella enterica	4 (5%)	4 (16.6%)	3 (8.1%)	11 (7.8%)
Microflora	2 (2.5%)	–	1 (2.7%)	3 (2.1%)
Alicyclobacillus acidoterrestris	–	–	1 (2.7%)	1 (0.7%)
Listeria innocua	10 (12.5%)	1 (4.2%)	6 (16.2%)	17 (12.2%)
Listeria monocytogenes	2 (2.5%)	7 (29.1%)	–	9 (6.4%)
Aerobic & Facultative Anaerobic Heterotrophs	–	–	1 (2.7%)	1 (0.7%)
Saccharyomyces cerevisiae	2 (2.5%)	–	4 (10.8%)	6 (4.2%)
Penicillium expansum	–	–	1 (2.7%)	1 (0.7%)
Yeasts and Moulds	10 (12.5%)	–	–	10 (7%)
Bacillus cereus	1 (1.25%)	1 (4.2%)	1 (2.7%)	3 (2.1%)
Pseudomonas aeruginosa	–	–	1 (2.7%)	1 (0.7%)
Total Viable Count	3 (3.75%)	1 (4.2%)	–	4 (2.8%)
Lactobacillus brevis	1 (1.25%)	–	–	1 (0.7%)
Salmonella Newport	4 (5%)	–	–	4 (2.8%)
Murine Norovirus MNV1	2 (2.5%)	–	1 (2.7%)	3 (2.1%)
Total Plate Count	5 (6.25%)	–	–	5 (3.6%)
Salmonella Typhimurium	–	2 (8.3%)	–	2 (1.4%
Campylobacter jejuni	–	1 (4.2%)	–	1 (0.7%)
Vibrio parahaemolyticus	–	1 (4.2%)	–	1 (0.7%)
Clostridium perfringens	–	–	1 (2.7%)	1 (0.7%)
Pseudomonas fluorescence	–	1 (4.2%)	–	1 (0.7%)
Cryptosporidium parvum	–	–	–	1 (0.7%)

culture that also encompasses gold standard mice infectivity studies (Garvey, Farrell, Cormican, & Rowan, 2010). Consequently, several related studies have involved microorganisms such as bacterial endospores as putative surrogates of similar or greater resistance kinetic profiles for the aforementioned parasites that adds to complexity and appropriateness of data (Hayes et al., 2012a, 2012b, 2012c; Garvey et al., 2014a, 2014b). Table 1 further highlights the enormity of data to be considered in terms of ready-to-eat and freshly cut fruit and vegetables (n = 80), meat and fish products (n = 24) and associated PL-impact on quality determinants (n = 37). There appears no standardised approach to investigating or comparing microbial reductions using PL-technology with *E. coli* studied the most as represented by 32 of 141 samples (24.8%), followed by *Listeria innocua* (17/141, 12.2%) as surrogate to the pathogen *Listeria monocytogenes* that was studied in 9 out of 141 food products (6.4%) (Table 2). There is also significant variance in the choice or selection of test organism per food group that makes comparisons between studies on microbial death rate and disinfection efficacy incomparable. This highlights that lack of consensus on an agreed list of test species and strains (such as using a specific ATCC, NCIMB or NCTC reference strain of *E. coli* along with potential inclusion of a recalcitrant endospore as surrogate organism such as a member of the *Bacillus* genus) among international scientific community in order to compare efficacy and understand PL processing. Standardising method for fluence determination is also highly relevant given reported variances from μJ to J cm^{-2}, such as using recent dosimetry method of Gómez-López and Bolton (2016) along with developments in biodosimetry in water industry (TrojanUV, 2016). Moreover, food processors progressing with industrial scale development of PL must also consider 5 log-pathogen reduction performance standard required by the HACCP regulation (Food and Drug Administration, 2003). This 5-log reduction must be targeted to the 'pertinent pathogen', which is the most resistant microorganism of public health concern that may occur in food. For example, the pertinent pathogen may vary with the type of treatment of product such as typically *Salmonella* or *Escherichia coli* O157:H7 for juices. PL as designated control measure can be considered for reduction in the pertinent microorganism by at least 5-log or can be used in combination of control measures that have a cumulative effect of a 5-log reduction and must be accomplished within a single production facility operating under CGMP's. Currently, there appears to be a lack of consideration for the 5-log pathogen reduction performance standard rule in published domain which may relate in part to the inability of PL to achieve a maximum viable count reduction beyond 4 log orders of artificially-inoculated test microorganisms or native microflora on PL-treated food surfaces using xenon light sources and existing equipment configurations (Tables 1 and 2).

There has been an increasing interest in the development of PL technology for surface decontamination of fresh produce given that this as a leading source of foodborne illness (Centres for Disease Control and Prevention, 2018) along with the commensurate worldwide interest in developing an appropriate intervention that would enable effective commercial food-surface decontamination post-harvest handling and packaging (Table 1) including interest in extended shelf-life. It was previously but incorrectly assumed that the post-harvest wash step was sufficient to remove field-acquired contamination with much of the research performed focussed on efficacy of sanitizers (Feliziani et al., 2016; Murray et al., 2018). The impact of PL on the quality attributes of treated fresh produce encompassing fruit and vegetables, meat and fish, and beverages is variable and were typically determined by evaluating changes in texture, colour, chemical composition or sensory attributes (Kramer et al., 2017) (Table 1). Many studies previously reported that increasing fluence intensities negatively influenced several quality parameters in fresh fruit and vegetables including colour of salad (Kramer, Wunderlich, & Muranyi, 2015a, 2015b) or sensory attributes of cut apples (Ignat, Manzocco, Maifreni, Bartolomeoli, & Nicoli, 2014) (Table 1). Kramer et al. (2017) recommended performing specific storage microbial trials under real conditions to include testing quality parameters as significant deterioration is mostly not found immediately post PL exposure, but during storage. PL treatment of plant based fresh produce has also been attributed with formation of health-promoting and nutritive compounds such as carotenoids, lycopene and total phenolic compounds of PL-treated green tomatoes (Pataro et al., 2015) or increased concentrations of phytochemicals in mangoes (Lopes et al., (2016) (Table 1). Kramer et al. (2017) reviewed quality changes in PL-treated meat or fresh fish and noted occurrence of lipid oxidation along with sensory deviations but cannot dismiss the influence of potential overheating from intense PL treatments of the product surface (also presented in Table 1). There have been fewer studies published on the potential impact of PL-treatment on quality attributes of beverages (Table 1). However, mainly changes in colour in PL-treated apple juice or sensory deviations were observed particularly at higher fluence (Kramer et al., 2017). However, pathogen reduction is highly variable due to uneven food surfaces or cavities in surface microstructure that can protect or harbour untreated microorganisms due to shading effects (Murray et al., 2018). For example, pathogen inactivation on cantaloupes and berries is typically restricted to 1 log CFU with fluence of 12 kJ m^{-2} (Adhikari, Syamaladevi, Killinger, & Sablani, 2015) using conventional UV-C light source.

Future sustainability surrounding the development of PL treatment of fresh produce is likely to entail use of different light sources such as LEDs (Kim, Kim, & Kang, 2017) along with using different configuration in treatment chambers design that deliver pulsed light at multiple

Table 3
Factors affecting PL-disinfection performance.

PL- Operational parameters	Microbial and Environmental Parameters	Methods of microbial enumeration, resuscitation and PL-treatment evaluation	Cell and molecular mechanistic factors governing PL-killing
Number of applied light pulses (Elmnasser et al., 2007; Kramer et al., 2017; Bhavya & Umesh-Bebbar, 2017; Van Impe, 2018)	Sequence from high to low-PL resistance. Fungi [Levy, Aubert, Lacour, & Carlin, 2012; Huang et al., 2018]; bacterial spore (Levy et al., 2012); yeasts (Farrell et al., 2011); protozoan parasites (Garvey et al., 2010; Hayes et al., 2012a, 2012b, 2012c); viruses (Huang et al., 2017; Vimont et al., 2015) and vegetative bacteria (Wang, MacGregor, Anderson, & Woolsey, 2005)	Direct viable count (Rowan et al., 2015) Use of selective dyes (Pataro et al., 2011), Antibiotics in lab media (agar and broths) (Farrell, Garvey, Cormican, Laffey, & Rowan, 2010; Rowan et al., 1999) Enrichment and resuscitation (Fitzhenry et al., 2018] Most Probable Number and end-point determinations (McFadden et al., 2017)	Cell Wall Damage using bioassays in *C. albicans* (Farrell et al., 2011) TEM in *L. monocytogenes* Cheigh et al., 2013 and SEM in *S. aureus* Kristnamurthy, Tewari, Irudayaraj, & Demirci, 2010
Applied discharge voltage (Hayes et al., 2012a, 2012b, 2012c; Kramer et al., 2015a, 2015b)	Variation in PL-resistance between microbial genus, species and strains tested (Rowan et al., 2015) along with culture forms (Bradley, Laffey, McNeil, & Rowan, 2012)	Gene expression post PL-treatments using *L. monocytognes* via Whole Genome DNA Microarray Analysis (Uesagi et al., 2016); Expression of *Nox* genes in *Trichophyton rubrum* by 402 nm-PL (Huang et al., 2018)	Cell membrane damage and rupture in *E. coli, S. aureus, B. subtilis, C. albicans* (Farrell et al., 2011; Garvey, Stocca, & Rowan, 2016; Nicorescu et al., 2013; Takeshita et al., 2003; Xu & Wu, 2016).
Distance between target and flash lamp (Rowan et al., 2015, Schottroff et al., 2018)	Population present (homogenous, mixed) (Rowan, 2004)	Flow cytometry to measure cell membrane damage *in L. monocytogenes* [Kramer & Muranyi, 2014]	Lipid peroxidation in *C. albicans* [Farrell et al., 2011]
Spectral range of light flashes – efficacy at 270 nm (Wang et al., 2005); 225–280 nm (Levy et al., 2012); no effect in visible or near infrared (Ramos-Villarroel, Aron-Maftei, Martin-Belloso, & Soliva-Fortuny, 2012)	Environmental parameters such as temperature, osmotic stress (Bradley et al., 2012; Kramer et al., 2017) and illumination conditions bib_Lasagabaster_and_de_Maranon_2014(Lasagabaster and de Maranon (2014)	Confocal and fluorescent microscopy [Nicorescu et al., 2013]	Loss of intracellular constituents including proteins [Farrell et al., 2011; [Cheigh, Park, Chung, Shin, & Park, 2012; Garvey et al., 2016a)
Number of light sources (Rowan et al., 1999)	Presence of organic matter, particle size and turbidity (liquid) negatively impacts upon efficacy (Garvey et al., 2014)	Photoreactivation and repair and length of exposure to daylight or darkness [MacLean et al., 2008; Lasagabaster; de Marañ\u0;n (2014); Fitzhenry et al., 2018)]	UVC- induced DNA damage [Rastogi, Richa, Tyagi, & Sinha, 2010; Farrell et al., 2011] Ramos-Villarroel et al. (2017))
Method of measuring fluence or UV dose (J cm^{-2}) (Hsu et al., 2011; -López and Bolton, 2016)	Older cultured of bacteria less PL-sensitive (Cudemos, Izquier, Medina-Martines, & Gomez-Lopez, 2013; Farrell, Garvey, & Rowan, 2009)	Combined qPCR and cell culture (for complex parasites and viruses) [Garvey et al., 2010; Garvey, Coughlan, Murphy, & Rowan, 2016b]	Indirect damage to cellular components such as proteins or lipids by ROS using fluorescent probes, RT-qPCR, micromorphology and MTT assay (Farrell et al., 2011; Huang et al., 2018; Massier et al., 2013, 2012)
Agar (Aguirre et al., 2015) versus food PL-treatments Kramer et al. (2017)	Gram stain reaction (bacteria) (Rowan et al., 2004)	Modelling of kinetic data such as single, bi and tri-phasic plots [Aguirre et al., 2015; Rowan et al., 2015] Modelling of pulsed light penetration and matrix colour (Aguirre, Herro, Fernandez, & de Fernando, 2014]	Necrosis and apoptosis in *C. albicans* [Farrell et al., 2011]
Statistical power of trials and runs (Rowan et al., 2015)	Planktonic or biofilm (Garvey et al., 2015, ; Montgomery & Banerjee, 2015)	PL-exposed unculturable bacteria expression of proteins in *S. enterica* via synthesis of plasmid-encoded GFP (Kramer et al., 2017)	Loss of esterase activity in *Saccharomyces cerevisiae* (Ferrario et al., 2014)
Liquid treatments including beverages and water (Fitzhenry et al., 2018)	Exposure to prior stress, tempering, sublethal injury (Wutack et al., 2003) generation of VBNC state bacteria (Rowan et al., 2015; Schottroff et al., 2018)	Measurement of ATP [Garvey et al., 2010] Measurement of PL-induced oxidative stress response via proteomic studies (Massier et al., 2012, 2013)	Pigmentation in *P. aeruginosa* [Farrell et al., 2010]. Pigmentation in *A. niger* (Esbelin, Mallea, Ram, & Carlin, 2013). Lipid Peroxidation in *C. albicans* (Farrell et al., 2011)

(*continued on next page*)

Table 3 (*continued*)

PL- Operational parameters	Microbial and Environmental Parameters	Methods of microbial enumeration, resuscitation and PL-treatment evaluation	Cell and molecular mechanistic factors governing PL-killing
Applied frequency of pulses in the range 1–5 Hz (Luksiene, Gedelis, Buchovec, & Raudeliuniene, 2007)	Combination treatments (thermosonication, PEF), PPGD and VBNC phenomenon (Kramer et al., 2015a,b, 2017; Kramer & Muranyi, 2014)	Scanning Electron Microscopy (Huang et al., 2018; Nicorescu et al., 2013) and Transmission Electron Microscopy [Cheigh et al., 2012; Cheigh et al., 2013; Ferrario et al., 2014; Huang et al., 2018]	Possibly over-heating of intracellular fluid (Xu & Wu, 2016)

*Abbreviations – Pulsed Electric Fields (PEF); Pulsed Plasma Gas Discharge (PPGD), Viable but Not Culturable State (VBNC); Green fluorescent Protein (GFP); Real-time quantitative polymerase chain reaction (RT-qPCR); Transmission Electron Microscopy (TEM); Scanning Electron Microscopy (SEM); Reactive Oxygen Species (ROS).

angles to overcome shaded areas (Chen, Loeb, & Kim, 2017). Murray et al. (2018) suggested that additional advantages of using LEDs are the potential to use a range of different wavelengths such as UV-C thereby providing a possible synergistic antimicrobial actions. This approach may be particularly applicable for inactivating complex foodborne parasites where other wavelengths in the pulsed spectrum may also contribute by destroying important cellular macromolecules and structures (Garvey et al., 2010; Rowan et al., 2015). This alternative approach to using Xenon light sources may also help alleviate a tailing' effect that is often observed in PL-mediated microbial dose-response curves due to sub-populations surviving treatment or those harbouring in surface cavities due to protective shading effects, which infers that inactivation is limited to a certain microbial log-reduction threshold irrespective if increased fluence intensity is applied (Rowan et al., 2015). Consideration must also be given to effectiveness of smart packaging for PL food treatments, which was the subject of a recent review by Heinrich et al. (2016) with some informative studies highlighted in Table 1. Effectiveness of existing packaging for food surface decontamination using PL depends upon the type of polymer or combinations thereof employed where use of polypropylene or low-density polyethylene appear suitable as a high proportions of UV-C are transmitted (Kramer et al., 2017). However, data generated from current research using PL should consider that future food packaging is likely to comprise alternative biodegradable materials that are either recyclable or compostable and will replace non-environmental friendly plastics.

Consensus on agreed methods will enable meaningful evaluation between different reported PL-treatments possible and will provide baseline-data suitable for actual and predictive modelling, such as deployment of three-parameter Gaussian model to describe the spatial distribution of total and UV fluence in air and also in liquid substrates (Hsu & Moraru, 2011). Gaining consensus on how to analyse or model metadata generated from emerging technologies such as PL will be informed by advances in data analytics and machine learning (Moral, Hinde, & Demétrio, 2017). Considerable future focus can then be given to comprehensively investigating importance of kinetic inactivation data plots and relevance of single, bi and/or tri-phasic survivor responses during treatments and relevance to food industry (Rowan et al., 2015). Use of freely-available, open-access published data along with exploiting advances in data science and statistics will lead to new approaches for analysing and interpreting large or big-data from new processes that includes identifying key characteristics of observed variables and experimental/sampling designs (Pertea, Kin, Pertea, Leek, & Salzberg, 2016). This will allow for identification of new or extended models and development of new algorithms for global harmonisation of processes. This may inform future digitisation of appropriate metadata for machine interface learning and automation of processes (Keighrey, Flynn, Murray, & Murray, 2017). For example, there are several non-linear inactivation kinetic models that do not consider non-standard random effects that can also be addressed by using mathematics and statistical modelling such as re-parameterising datasets along with use of specific probability distributions. What is also lacking in published domains is goodness-to-fit of the statistical models for fitting data. New models will help researchers better understand the potential significance of the occurrence of shoulder and tailing phases on kinetic plots arising from PL treatments that considers factors that influence efficacy of decontamination performance post-harvest of produce (Moral et al., 2017). The power of harmonised inter-laboratory inter-disciplinary modelling is exemplified by a Dutch research consortium BaSyC that has recently taken on the challenge of building a synthetic biological cell at a project cost of €25 m (Dogertom, 2018). BaySyC consortium recognises that 'A fundamental understanding of life within a cell will bring huge intellectual, scientific and technological rewards', and it is envisaged that gaining a holistic understanding of molecular machinery in cells will inform efficacy of adjacent needs such as control measures.

1.3. What lessons can be gleaned for PL studies conducted at the cell and molecular response level?

In order to advance PL as a food treatment process, there has been a concerted effort to gain an improved understanding of cellular and molecular mechanistic responses in PL-treated foodborne microorganisms, which has also contributed to the enormity of data generated (Table 3). Growth in the number and variety of sophisticated culture and enumeration methods used has been driven in part by observations of significant variances between populations of PL-treated CFU survivors enumerated on conventional laboratory based media and to that of elevated number of test microorganisms exhibiting cellular vitality (Rowan et al., 2015). These differences in microbial survivors become more apparent when applying low or moderate fluence that represents less severe surface processing conditions (Table 3), which has been attributed to the occurrence of viable but non-culturable state (VBNC) in PL treated bacteria. Less stressful operational conditions generally promote photoreactivation effects in several PL-treated microorganisms. The aforementioned has resulted in under-appreciation in the levels of bacterial survivors by as much as 4 log orders in conventional viable count or CFU enumerations (Kramer & Muranyi, 2014). This variance leads to uncertainty in PL-treatment performance that presents significant challenges to the food industry in terms of harmonisation of processes internationally. But what value do complex mechanistic cell and molecular studies offer and is there too much emphasis placed upon these? The ultimate underpinning purpose of their pursuit is to define reliable and repeatable PL-conditions that leads to irreversible destruction of targeted pathogens and reduction of spoilage microorganisms balanced with retention of fresh-like qualities. There lies the conundrum, when is irreversible destruction achieved in PL-treated foods achieved when one considers typical contamination levels? Table 3 highlights current published methods that measures cell and molecular damage in a variety of food-borne and medical-related micro-organisms that are very diverse in design and applicability. There

has been no consensus internationally on what constitutes efficacy for each measurement approach along with use of universal control for validation.

Studies performed thus far to elucidate cellular response of bacteria to PL demonstrates irreparable modifications of treated DNA molecules as a main source for inactivation (Table 3). Kramer & Muranyi, 2014 reported a relationship between onset of PL-induced count reduction in *L. innocua* and occurrence of DNA alterations. However, there is evidence supporting other detrimental damage to macromolecules and cellular structures such as cell membrane or cell wall that are exacerbated with increasing fluence causing irreversible lethal effects (Table 3). However, comparison of details underpinning methods reveals that findings are mostly incomparable due in part to lack of harmonisation of applied fluences reported for various PL systems along with limited information on geometry and configuration of equipment. The rupture of microbial cells after PL treatments is mostly attributed to a combination of photochemical and photophysical effects, resulting in short overheating of microbial cells or the pulsing effect (Kramer et al., 2017). Irreversible rupture of cell member by PL-treatments also brings about loss of vital cellular constituents such as proteins as reported in *C. albicans* (Farrell, Hayes, Laffey, & Rowan, 2011) and *S. cerevisiae* (Ferrario, Guerrero, & Alzamora, 2014). Commensurate indirect cell damage of cellular components such as proteins and lipids also occurs due to formation of reactive oxygen species in PL-treated *E. coli* (Kramer et al., 2015a, 2015b) and *C. albicans* (Farrell et al., 2011). However, a concerted future study employing whole genome sequencing (WGS), bioinformatics and real-time determinations of these cellular responses (such as using flow cytometry combined with magnetic cell sorting) may help elucidate time points associated with occurrence of single and combined cellular effects underpinning sublethal and lethal injury in PL-treated micro-organisms. Selection of markers will be critical to inform automated flow cytometry studies and these panels can eventually be incorporated into MALDI-TOF for international standardisation of processes at cellular level (Fario, Tavanti, Barnini, Ghelardi, & Lupetti, 2018). However, Uesugi, Hsu, Worobo, and Moraru (2016) previously investigated the response of *L. monocytogenes* to PL on the basis of a whole genome DNA microarray analysis, but did not find any distinct differences in gene expression after exposure to PL. While the authors concluded that microbial effects of PL mainly seem to be attributable to UV content, there is increasing evidence to suggest that other cellular damage occurs at higher fluence levels in various PL-treated micro-organisms (Table 3). An understanding of cellular and molecular damage may potentially demarcate occurrence of lethality in PL-treated microorganisms and help unravel significance (if any) of viable but not culturable state (VBNC) in bacteria (Rowan et al., 2015). There has been no data available which shows that VBNC bacteria pose a risk to human health (Kramer et al., 2015a, 2015b).

To date, there has been no published inter-laboratory study that holistically investigated PL treatments in a broad range of foodborne microorganisms that also encompasses a range of cellular responses (Table 3). Farrell et al. (2011) determined occurrence of sequential and combined cell and molecular damage in medically relevant yeast in a single study. The authors reported that increasing fluence levels resulted in PL-mediated lethality through a multi-hit cellular process that did support emphasis on UV-C destruction of genetic material. However, it also demonstrated step wise damage in other PL-treated macromolecules and cellular structures that roughly coincided with the sequence lipid hydroperoxidation of cell membrane, ROS generation, DNA damage, onset of necrosis and apoptosis, rupture of the cell membrane with loss of vital cell constitutes to the environment, and ultimately microbial death. Occurrence of onset of late necrosis and early-phase apoptosis also coincided with total absence of growth in of PL-treated yeast in laboratory media and may possibly constitute a future biomarker for informing real-time indirect lethality in this organism (Table 3).

Future mechanistic cellular information underpinning efficacy of PL-disinfection technology may be informed by whole genome sequencing (WGS) and next-generation sequencing (NGS) that includes high-throughput sequencing of mRNA (RNA-seq) of treated microbial samples post PL-treatments (Mortazavi, Williams, McCue, Schaeffer, & Wold, 2008). Such real-time investigations will benefit from recognising the added value of exploiting shared data from open access and source publishing, open methodology, open data management, open education, open licensing (Angers-Loustau et al., 2018). RNA-seq experiments generates very large, complex data sets that demand fast, accurate and flexible software to reduce the raw data to comprehensive results (Mortazavi et al., 2008). Pertea et al. (2016) describe use of free, open-source software tools, namely HISAT (hierarchical indexing for spiced alignment of transcripts), StringTie and Ballgown for comprehensive analysis of RNA-sequence experiments. This allows scientists to align reads to a genome, assemble transcripts, including novel splice variants, compute the abundance of these transcripts in each sample and compare experiments to identify differently expressed genes and transcripts. Pertea et al. (2016) describes protocol for all steps necessary to process large set of raw sequencing reads and create lists of gene transcripts, expression levels, and differently expressed genes and transcripts that typically takes 45 min of computer time. RNA-seq experiments capture the total mRNA from a collection of treated cells and then sequence that RNA in order to determine which genes were active, or expressed, in those cells. Using high-throughput sequencing machines, a single experiment can capture the expression levels of thousands of genes at once with high efficiency. There experiments generate enormous numbers of raw sequence reads, typically number in the tens of millions, even for a modest sized assay. The number of reads produced from each gene can be used to measure gene abundance that can also easily detect genes and gene variants that are not included in standard annotation, including noncoding RNA genes.

It is envisaged that exploiting whole and next generation sequencing (Ronholm, 2018; Rosen, Friedrich, & Moran-Gilad, 2018) and bioinformatics (Marco-Ramell et al., 2018; Angers-Loustau et al., 2018) may unravel relevance of suite of priority parameters governing PL performance that includes main molecular drivers that are involved in adaptive responses to PL exposure under lethal and sub-lethal conditions. The development of adjacent innovation in automated flow-cytometry (Brascli et al., 2018; Léonard, Bouarab Chibane, Ouled Bouhedda, Degraeve, & Oulahal, 2016) and spectrophotometric analysis (such as high resolution mass spectrometric methods) will also inform PL treatment efficacy under minimal processing conditions. Thus, given advancement in ICT, simple adoption of this bioinformatics protocol can be applied to inform and unravelling complex challenges in microbiology, parasitology and virology from comforts of your own home your personal notepad or computer. For example, cross-cutting research between molecular biologist and ICT are conducted frequently by researchers in our laboratories, which includes ease for remote data analysis by researcher using portable personal computers. Yoon et al. (2017) described how improvements in the quality of WGS for international sharing where bioinformatics tools can then be used to inform processes. These authors introduce an integrated database, called EzBioCloud (www.ezbiocloud.net/), that holds the taxonomic hierarch of bacterial and Archaea, which is presented by quality-controlled 16S rRNA gene and genome sequences. Hino et al. described benefits of 18S rDNA Illumina sequencing for non-culturable species such as parasites where state-of-the-art is predominantly relient upon microscopy and staining technique in fields of ecology, evolutionary biology and epidemiology. Method is easy and quick compared to conventional methods that can be applied to assess biodiversity of parasites in host alimentary tract and allows use of NGS to perform assessment in high-throughput manner. The aforementioned highlights the applicability of new molecular tools for potentially informing PL-technology development for high-throughput processing and validation.

Collectively, the aforementioned studies have produced an enormity of complex 'big data' sets for evaluation and interpretation by food technologies. But, how best to consider relevance, value and impact of

Table 4
PL used for different applications in various domains that potentially demonstrates second order technology disruption.

Application	Description	References
Cosmetic skin treatment	PL used for hair removal, photo rejuvenation (such as treatment of skin pigmentation, sun damage and thread veins) and acne	Barakat, Moftah, El Khayyat, and Abdelhakim (2017)
Optometry and ophthalmology	PL treatment of evaporative dry eye disease due to meibomain gland dysfunction. PL-treatment of keratoconus. PL-treatment of rosacea-associated meibomain gland.	Toyos, McGill, and Briscoe (2015) Seo, Kang, Ha, Chin, and Jung (2018)
Sequelae of breast cancer treatment	Chronic radiodermatitis is common sequelae of breast cancer – PL treated telangiectasia after radiotherapy	Nymann, Hedelund, and Hædersdal (2009)
Treatment of skin cancer	IPL used for photodynamic therapy in treatment of nonmelanoma skin cancer	Piccolo and Kostaki (2018)
Tissue engineering, regenerative medicine, additive manufacturing	Pulsed light for tissue engineered cartilage	Ishihara, Sato, Ishihara, Mochida, & Kikachi, 2007; Ifkovits & Burdick, 2007
Electronics	PL permits a scalable nanotechnology process for treatment of metal nanowire (NW) fusion to increase network activity. PL-sintering of nanoparticles into thin films used in transistors, switches, electronic devices. PL-sintering of CH3NH3Pbl3 solar cells.	Kang, Sowade, & Baumann, 2014; Lavery et al., 2016; Shankar, Salcedo, Berndt, & Choi, 2017; Dexter, Gao, Bansal, Chang, and Malhotra (2018).
Food packaging	PL-treatment of food packaging materials	Heinrich et al. (2016)
Food surfaces and beverages	PL-surface treatment of fresh-cut and whole vegetables, soft fruits, meat and fish	Kramer et al. (2017)
Wastewater treatment	Treatment of wastewater including complex murine noroviruses	Vimont et al. (2015)
Pollination Industry	PL-treatment of pollen to remove complex parasites affecting bumblebees	Naughton, Tiedeken, Garvey, Stout, and Rowan (2017)
Dairy water reprocessing	PL treatment of dairy wastewater for reprocessing	Fitzhenry et al. (2018)
Algal toxins and potentially bloom	PL-treatment and reduction in algal toxin okadiac acid to freshwater crustacean *Daphnia pulex*	Murray et al. (2018)
Freshwater aquaculture	PL-treatment of pond water for reduction of microbial and algal communities	www.morefish.ie (accessed 14/11/2018)

this for commercial uptake of PL? Future-proofing of PL will benefit *inter-alia* from international consensus on key operational parameters that governs effectiveness including (a) full description of equipment and dosimetry underpinning reporting of fluence; (b) agreement on standardise list of test microorganisms for all PL studies to support continuity and inter-study comparisons; (c) agreement on use of appropriate kinetic model to assess efficacy of PL-disinfection performance; and (d) freely-available open access data sources; and (e) specific engagements with industry to produce sufficient quality data to validate process. A more comprehensive suite of recommendations for future reporting of experimental data and exposure conditions for PL treatments is presented in Table 5, which also considers parameters for commercial food treatments. This guidance will enable reporting of sufficient details to extent that other researchers would be able to repeat, compare and evaluate data between studies.

1.4. What lessons can be learned from adjacent medical device sector by way of standardisation and harmonisation of data for commercial deployment of PL technology/

PL and other non-thermal technologies achieve disinfection, which is destruction of pathogens that also leads to reduction in numbers of spoilage microorganisms. These minimal processing approaches apply less severe stresses so as to consider retention of freshly properties with minimal impact on food quality characteristics along with the need for ensuring bioburden reduction for safety considerations (Rowan et al., 2015). Minimal processing technologies are markedly different to commercial sterilisation processes, such as use of gamma, x-ray and electron beam irradiation, and ethylene oxide gas for medical technology (Medtech) industries where it is generally accepted that the latter sterilisation methods are designed to over-process a specific biological indicator (either *Geobacillus stearothermophilus* or *Bacillus atrophaceus*) to ensure log 6 killing that provides sterility assurance to the welfare of the patient (Sella, Vandenberghe, & Soccol, 2015). These biological indicators (BIs) have been included in all terminal sterilisation processes for medical device as the inactivation of such highly-resistant BIs are more resistant to commonly occurring healthcare-associated pathogens and this process follows agreed international sterilisation standards where there is consensus on efficacy (Steris AST, 2018). This concept is in part similar to use of surrogate *Bacillus* endospores (such as *B. megaterium* or *B. subtilis*) described earlier as means of indirectly determining efficacy for PL-treatment of complex parasites where latter is shown or reported to be of lesser resistance to easily cultured endospores (Hayes et al., 2012a, 2012b, 2012c). It is estimated that the Medtech sector demands a market of some $350-400Bn (DBEI, 2108), where sterilised devices have a long history of not contributing to hospital acquired infections. There is also oversight from an International Standards Organisation Technical Committee. It is appreciated that processing technologies including PL for surface decontamination do not need to achieve sterilisation efficacy, and lessons to be gleaned from this adjacent sterilisation domain are of consensus on agreed standards internationally with harmonisation of methods through rigorous validation system (Mendes, Brandão, & Silva, 2007). Recent published evidence suggests that there are emerging opportunities for 3-D printing of heat-sensitive food-derived biologics for adjacent healthcare applicants that will necessitate reduced processing conditions, which may be met by use of pulsed light (Lille et al., 2018).

1.5. Harmonisation and standardisation of data – regulatory and life cycle assessment considerations for PL development

Castro et al. (2018) advocated that there should be governing bodies to regulate and monitor the enforcement of food-processing regulations and to avoid situations where it becomes challenging to interpret relevance of regulations that often only apply to countries belonging to specific organisations. There is also an emerging trend to exploit advances in life cycle analysis (LCA) in order to ascertain impact of traditional and novel food treatment technologies that can extend to highlight future assessment of PL in terms of energy consumption, carbon footprint and environmental impact (Finnegan et al., 2018; Fitzhenry, Rowan, Finnegan, Zhan, & Clifford, 2018; Pardo & Zufia, 2012). This LCA approach can be used to develop and assess more efficient and sustainable food products throughout their whole life cycle including PL surface treatment provision. Future development and exploitation of PL for food surface decontamination should also consider potential impact on the environment including carbon footprint and energy consumption where this information is currently lacking. Additional examples of exploiting LCA to elucidate environmental impact on sustainable technologies include milk powder and butter manufacture (Finnegan, Goggins, Clifford, & Xinmin, 2017), wastewater treatment (McNamara et al., 2016) and aquaculture that includes pulsed light provisions (Tahar et al., 2018; Morefish, 2018). The

Table 5
Recommended information to be reported in studies on microbial inactivation by PL for harmonisation of research and for scalable industry needs.

Microorganism, recovery and enumeration method	Genus, species and strain of microorganism *Provide appropriate culture collection reference number and/or include type strain for test microorganism(s) in studies *Include *Escherichia coli*, *Listeria innocua* and *Bacillus cereus* endospore along with native microflora for food treatments *Confirmation of identify of test microorganisms by biochemical, physiological, morphological, immunological and/or molecular means (provide name of supplier for rapid test kits) *Method of storing cultures (cryoprotectant) and frequency of sub-culturing (using fresh microbial slope every month kept at 4 °C) Initial inoculum ● Description of procedures for microbial cultivation including name of supplier company for media ● Growth medium composition, growth temperature, pH, incubation time, and growth phase (exponential or stationary) ● Growth achieved under static or orbital cultivation (rpm) ● Confirm purity by identifying 3 randomly selected isolates Recovery conditions and enumeration methods ● Composition of media used for recovery to include basal media or physiological saline as diluent ● Time and storage conditions between treatment and microbiological analysis ● Description of procedure for enumerating microorganisms
PL equipment	For commercial: description of power unit used for generating pulses to include equipment name of the supplier company and model For prototype: adequate description of components including treatment chamber, electrical configurations and specifications Auxiliary devices – * Temperature probe * Thermophile power detector and software for total broad-spectrum dose received by sample * Transmissivity sensor to monitor %UV transmittance
PL process parameters	How fluence (J cm^{-2}) over exposure time (t) is calculated/measured ● Recommended use of dosimetry method by Gómez-López and Bolton (2016) Number of pulses applied (n) Applied voltage (V) Frequency of pulsing (Hertz [Hz]) Pulsed width (τ) Peak power (W) Distance of target area from pulsed light source Report absence of heating particularly operating at higher fluence that may contribute to microbial inactivation performance Absorbed 'UV dose' should be lower than calculated power output Specify if UV dose measured relates to full broad-spectrum energy or part thereof such as filtered at 230 nm Description of microbiological indicators or biodosimetry for assessing fluence measurements Consider photoreactivation affects especially when using low PL energy doses and wavelengths between 360 and 380 nm Consider reflectance and roughness of target surfaces that may reduce microbial disinfection during PL Consider influence of improved effectiveness of PL using photosentisers such as titanium dioxide
PL treatment medium properties and conditions	Ensure microbial population density is ≤ 7-log orders to mitigate against influence of protective shading effects Include 5-log pathogen reduction performance standard - however maximum inactivation of ≤3 log for viable counts is typically achieved where complete microbial inactivation is atypical for PL Include description of media composition, pH, aw Composition of menstruum used as diluent for treated samples Sufficient number of treatment trials and replications to provide statistical confidence of findings at 95% level; description of statistic test and version of software package (such as Minitab or SPSS) Description of method used to generate Bacillus endospores (natural aged for 7 days or incorporation of manganese sulphate to expedite conversion of vegetative cells to spores on agar surfaces) Include native microflora along with artificially seeded test microorganisms due to variability in resistance profile to PL Consider occurrence of cavities in plant surface microstructures that may protect microorganisms from incident light due to shading Consider occurrence of residual microorganisms on produce surface that may support outgrowth and affect shelf life
Food raw material	Origins, variety, maturation and storage conditions of raw materials such as plant matrices Plant matrices description to include variety, geographical origin, degree of ripeness, moisture content and storage conditions (temperature, humidity and storage time)
Food quality changes measured post PL treatment	Colour loss or change Lipid peroxidation Total antioxidant activity Sensory attributes such as flavour, aroma and organoleptic properties pH, density, viscosity, moisture, ash and vitamins Enzyme browning or loss of activity such as alkaline phosphatase Choice of single or multilayer films are suitable for PL treatment in package foods (some material permits transmittance of UV-C) Perform specific microbial storage trials under real conditions
For beverage or drink treatments including water	Static or continuous (flow rate) UV transmittance of test material Light source positioned over beverage/water with distance to target (cm) or submerged UV intensity field (light source output and absence of fouling) Composition of inorganic, organic and total suspended solids in beverages and water to include particle size

aforementioned also reflects growing awareness of carbon footprint ranking of food encompassing need for reducing greenhouse gas emissions, preserving the environmental and addressing global warming (Food's Carbon Footprint, 2018). Therefore, future sustainable studies should also consider residual energy after food treatments, including when using and optimising PL for commercial applications.

1.6. Embracing increasing sustaining and disruptive technologies – where does PL potentially reside?

There has been an increasing trend to elucidate innovation that will lead to technology disruption for greater impact, competitiveness and value to businesses (Lauer & D'Agostino, 2013; Yongfu et al., 2017;

Geels, 2018; Li, Porter, & Suominen, 2018; Sousa & Rocha, 2018). This also aligns with the ambitions of many developed countries to sustain growth through innovation for their industries such as Ireland's Food Wise, 2025 Strategy that seeks to achieve 85% increase in food exports to €19 billion, 70% increase in value added to €13 billion, 65% increase in primary production to €10 billion and the creation of 23,000 additional jobs all along the supply chain from producer level to high end value added product development (Food Wise, 2025). Bower and Christensen (1995) initially defined disruptive technologies (DTs), which essentially addressed commercial disruptions in an existing marketplace, where a new product or service (a technology) is introduced into that market. DTs were subsequently redefined by these authors (Christensen, Anthony, & Roth, 2004) and expanded by others (Govindarajan & Kopalle, 2006) to include both high-end and low-end disruptions (Schuelke-Leech, 2018). DT can be referred to as earthquake, game breaking, whirlwind, emergent technologies and are typically those that cause upheaval in the existing market structured and dominant firms by being cheaper, simpler, more convenient and effective than the existing technology (Christensen, 1997; Christensen & Bower, 1996; Schuelke-Leech, 2018).

At the opposite end of the continuum are technologies classified as sustaining technologies (ST) that offer incremental improvements over technologies already in existence. A major distinction between the two forms of technology is that as one moves along the continuum from a sustaining to a disruptive classification. However, few technologies are ever classified as disruptive; as most newly introduced technologies are of sustaining (Garrison, 2009; Schuelke-Leech, 2018). Research demonstrates that disruptive technologies have different key success factors that ST, therefore issues will arise in senior management in terms of variability and uncertainty in their evaluation and adoption of these technologies based on their prior level of familiarity, openness and experience in assessing merits of technologies. Downfall of organisations could be tracked back to poor decision-making with respect towards DT adoption. DTs will have a transformative impact on the way we consider food science and technology and indeed in the future. New innovations and applications arise supporting the delivery and exploitation of new technology-based solutions (Osiyevskyy & Dwwald, 2015). DT are by their nature nascent and only can be revealed as being disruptive in hindsight and therefore provide major problem for technological forecaster or road-mapper as require a degree of insight not required for sustaining technology (albeit still high tech) that follow the established technology product paradigm in a given industry. DT confers regime changes such as new product platform, which is far different from what the market would have experienced with 'only' incremental innovation. Definitions of DT focus on firm-based product technology factors; industry wide-product technology factors and gap between substitutable technological learning curves on cost and performance basis. combination of these. Customers have accepted products and services that have been enable by DT. Schuelke-Leech (2018) described that many of these have been smaller products (may require advances in micro and nanotechnologies), lighter products (advances in material technologies); cheaper products (advances in component technologies and associated manufacturing processes), more flexibility and convenient products (advanced in human factors research, ergonomics, AI), higher unit performance products (advances in chemistry, physics, materials, design, micro and nano-technology manufacturing processes), operationally simple products (may require advances in AI, robotics, and design).

Developing increasing sustaining and disruptive technologies in the agri-food domain are core to underpinning ambitious innovation-driven economies as these create value, problem solve and increase quality of life in dynamically changing global environments. Schuelke-Leech (2018) postulated a conceptual model for understanding the orders of magnitude of disruptive technologies (DT) that are potentially disruptive to business, government and to society. The author looked at these DT at two different levels. The first order disruption is a localised change within a market or industry, which accepts Christensen's conceptualisation or DT, but is not limited by it. An example of first order DT would be use of RT-qPCR for detecting complex parasites and viral pathogens in food produce (Franssen et al., 2018) or use of gas chromatography for detecting low-level chemical contaminants (Tiedeken, Tahar, McHugh, & Rowan, 2017). A first-order DT can come from a start-up, new-entrant to a market, or an existing industry. A second order disruption has much larger and broader influences, affecting many institutions and substantially changing societal norms and institutions (Schuelke-Leech, 2018). Previous definitions of disruptive technologies have focused on disruptions to commercial markets and existing firms, which Schuelke-Leech (2018) stated are on the first order of disruption (Adner, 2002; Christensen, 1997; Danneels, 2004; Dedhayir, Okelainen, & Saju, 2014; King & Baatartogtokh, 2015). Schuelke-Leech (2018) stated that second order disruptions are technological disruptions, where the impacts permeate through society. Understanding and modelling potential disruptions is merited and will require taking a holistic perspective of the socio-technical innovation ecosystems. Future trends in the interpretation of big data from convergence of cross-cutting domains will prove important as to comprehensively evaluate impact of big data from arising from emerging innovations will be challenging. Schuelke-Leech (2018) acknowledged that new innovations that progress to DT designation based upon historical evaluation of individual technologies and how these interacted with other technologies and with other technologies and socio-economic and political factors to produce disruptions. Arguably, many now established innovations would not have been viewed initially as disruptive, such as discoveries in ICT, and it only once the larger societal impacts of a technological disruption is actually known will these be proven. Thus, development of ICT and commensurate modelling of big data will be important for evaluation of DT impact that includes achieving a holistic cross-system understanding of value that embraces convergence of expertise across diversified fields of research and enterprise. Published studies have revealed that there is a trend for development of pulsed light for different applications in food and drink, healthcare, electronics, freshwater aquaculture, pollination and ecosystem services management, and environmental decontamination (such as potential mitigation of algal bloom) that would infer potential for second order technology disruption (Table 4). However, this potential for technology disruption will only be apparent in time with feedback from consumers and other stakeholders post large scale uptake by industry that may also exploit different business models.

1.7. Development of pulsed light for novel applications in pollination industry as an example of possible technology disruption for tackling complex diseases in managed bees

Animal pollinators such as honey bees, bumble bees and solitary bees pollinate our crops and wildflowers, and thus are essential for human wellbeing (Ollerton, Winfree, & Tarrant, 2011). Eighty-seven out of the main 124 crops used directly for human consumption require or benefit from animal pollination: annually, pollinator services contribute €153 billion and €54 million to the global and Irish economies respectively (Gallai, Salles, Settele, & Vaissiere, 2009). However, in Europe, and around the globe, bees face many threats and are often in decline as a result (European Commission Pollinators Initiative, 2018). This is a multi-factorial challenge as bees are predominantly impacted by stresses associated loss of habitat, starvation and diseases (European Commission Pollinators Initiative, 2018) that is a global problem. Parasites and pathogens are not new to wild pollinators as they are naturally exposed to native parasites and pathogens, but strong exposure to non-native species in combination with other pressures like poor nutrition, pesticides and other pollutants can make them more susceptible to this threat. PoshBee (2018) is an example of a pan-European H2020 platform to assess exposure hazard of chemicals, their mixtures, and co-occurrence with pathogens and nutritional stress for

solitary, bumble, and honey bees across two major cropping systems. However, what is underappreciated to the layperson is the complexity presented parasites (including mites), fungi and viruses that affect bees where there is still is no effective intervention or mitigation strategy to address this decline or spread of diseases (Vanbergen and Insect Pollinators Initiative, 2013; Goulson & Hughes, 2015). While such projects will yield important baseline ecological information along with intimating potential add-on complications exacerbated by climate change, these studies have yet to identify a suite of appropriate and affordable solutions to address these problems. The host range, natural geographic range and virulence in different bee hosts are poorly understood for bee parasites that reflects in part the absence of effective mitigation strategies to address this significant problem. It is also of considerable concern that the anthropogenic movement of managed bees for crop pollination purposes has led to the accidental introduction of bee parasites to countries and continents where they do not naturally occur, exposing native bees to parasites which may have little resistance (Goulson & Hughes, 2015). Parasites can move between managed or commercial colonies, and can even spill over into conspecific wild bee populations that is a serious concern. Such disease associations have already occurred between managed ad wild bees, both in the UK (Fürst, McMahon, Osborne, Paxton, & Brown, 2014; Graystock, Goulson, & Hughes, 2014) and Ireland (Murray, Coffey, Kehoe, & Horgan, 2013). Moreover, 73.5% of screened commercial bumble bee colonies imported to Ireland were infected with a least on harmful parasite (Murray et al., 2013). Mitigation measures that reduce parasite loads among managed bees must therefore be developed and implemented in order to protect wild bee populations.

Currently, a critical hazard analysis critical control point (HACCP) approach to identifying key pressure points has revealed potential entry points for new diagnostic, therapeutic and disease mitigation measures for pollinators (Fig. 1). For example, is appreciated that routine parasite screening of commercial, managed and wild bees can help inform extent and scope of challenge for mitigation (Goulson & Hughes, 2015). Co-occurrences of stresses associated with agrochemicals on nutrition and disease in bees can be accurately evaluated, which will include from exploiting advances in whole genome sequencing, bioinformatics and molecular techniques (RT-qPCR) along with flow cytometry (Braschi et al., 2018) will lead to new biomarkers for informing health of bees post exposures. Moreover, although some parasites can be screened using microscopy (Murray et al., 2013), molecular screening via RT-qPCR is the only way to reliably detect all bee parasites at all stages of infection (Goulson & Hughes, 2015). Reliable detection of parasites can only be carried out via destructive screening of bees and it is appreciated that individual steps to alleviate this problem, such as disinfection or sterilize of equipment and honey bee pollen are therefore essential in slowing parasite spread via managed bees (Naughton et al., 2018). Given that there is no current effective cure for any bee parasites (Goulson & Hughes, 2015), the next best option is to employ disinfection technologies to limit disease spread yet it is a sophisticated issue to assess as there is also no in vitro bioassay to pilot studies for mitigation. However, Naughton et al. (2018) conducted pilot studies that showed pulsed light effectively destroys the trypanosome parasite *Crithidia bombi* that affects bumble bees. Use of combined RT-qPCR and cell culture for assessing fluence levels the surrogate enteroparasite *Cryptosporidium parvum* was deployed to inform putative fluence level for the traposome parasite *C. bombi*. Microscopy studies revealed for the first time that PL successfully inactivated *C. bombi* compared to untreated controls, where bumble bees were fed PL-treated samples pre and post-PL treatment. It was also revealed the death in PL-treated *C. bombi* is not always instantaneous due to observations that some samples retained motility, which may be attributed to the possible multi-hit biocidal effect of broad spectrum pulsed light on both parasite DNA and cellular structures. An entry level strategy for PL usage would be non-thermal treatment of pollen that is used for feeding farmed bumble bees (Fig. 1). Recent studies with the use of gamma irradiation for pollen also shows promise in terms of killing complex honey and bumble bee pathogens, namely fungal pathogen *Ascosphaera apis*, the microsporidian *Nosema ceranae* and three honey bee viruses (Deformed wing virus [DWV], Black queen cell virus [BQCV], and Chronic bee paralysis virus [CBPV]) (Simone-Finstrom, Aronstein, Goblirsch, Rinkevich, & de Guzmann, 2018). However, the impact of gamma irradiation on nutritional composition is not yet known. Also PL may also be considered as biocide-free contact surface approach for environmental decontamination. Fig. 1 also highlights other trends in innovation possibly attributed to immunomodulation of bees through fortification of feed and coating of equipment with antimicrobial bioactives that can be subject to non-thermal processes to reduce or eliminate bioburden, such as

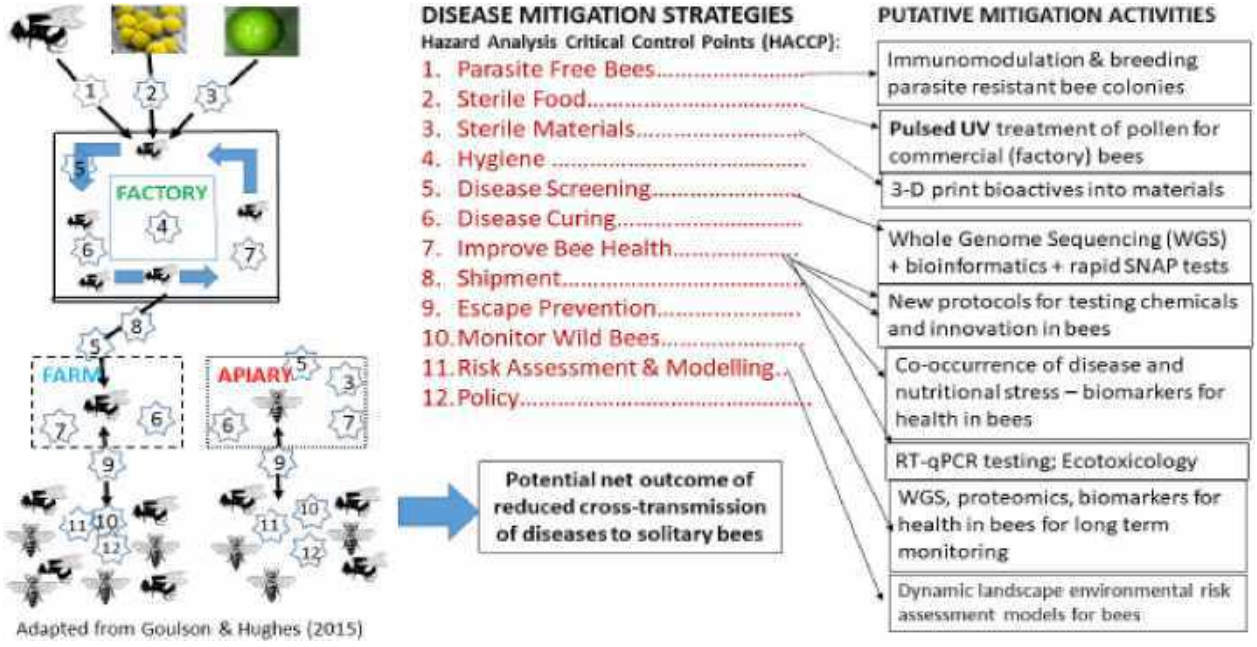

Fig. 1. Putative disease mitigation strategies and activities for promoting bee health and wellbeing that includes use of pulsed UV (PL) for nonthermal pollen treatment and contact surface disinfection.

using PL treatments. Other potential HACCP for mitigation problem may be PL treatment of wax comb that harbours parasites and viruses and is reused from year to year and transferred across beekeeping operations. Few, if any, universal treatments exist for latter control point.

1.8. Potential cross-cutting developments gleaned from the water and waste water industry where PL may lead to technology disruption

There is a commercial niche to consider development of PL as a bolt-on treatment technology for recycled water including dairy rainwater reharvesting applications (Fitzhenry et al., 2018). However, submerged flow-through PL-treatment of water presents challenges due in part to (a) relatively modest UV (25%) efficiency in PL-pulsed spectrum and (b) negative impact on other environmental factors such as presence of inorganic, organic and total suspended solids that influences UV transmittance on PL-performance (Fitzhenry et al., 2019). Conventional low-pressure emits continuously UV with 70% energy efficiency of conversion and has a long history of established success when performing at 40 mJ cm^{-2} that most regulatory bodies specify as required UV dose (TrojanUV, 2016). The potential of PL for water applications can be advanced by knowledge transfer from industry that has a history of testing and developing conventional low-pressure UV systems that includes reactor design, flow rate, UV transmittance of water, UV intensity field within reactor (light source output and fouling) and microbial inactivation for standardised validated processes (TrojanUV, 2016). PL offers additional advantages to the water industry as it produces broad-spectrum biocidal pulse that is effective against chlorine-resistant waterborne enteroparsites *Cryptosporidium parvum* (Garvey et al., 2010) or *Giardia lamblia* (Garvey et al., 2014). Therefore, there is merit in considering standalone or co-deployment of both PL and LPUV for drinking water decontamination (Garvey & Rowan, 2015). There are also other future potential PL applications that includes bespoke bolt-on treatment of contaminated seafood in depuration tanks (Vimont, Fliss, & Jean, 2015). Other contributory factors including extreme weather events (drought and flooding) associated with climate change will also support development of PL as a sustainable technology for water treatments. However, PL process requires validation before water and other industries consider large scale deploying of the technology and there are potential technical issues to be addressed in terms of re-configuring PL for optimised submerged water treatments (Fitzhenry et al., 2019).

Lessons can be gleaned from meeting challenges of detecting, monitoring and mitigating against occurrence of priority and emerging micropollutants or contaminants of concern in receiving waters in terms of embracing innovation, technology validation and commensurate need to balance or negated negative impact on environment, health and wellbeing. This also needs to an enormity of data, notwithstanding additional drivers including need to consider ecotoxicology and uncertainties of climate change. For example, in the Republic of Ireland alone there are ca 1500 waste and drinking water treatment facilities along with several hundred private water supplies that vary in efficacy of innovations for treatments, where use of low pressure UV for end-of-pipe solutions is a preferred treatment option (Tiedeken et al., 2017). What can be gleaned from the water industry for PL –technology development is the trend towards future de-risking and development of risk assessment models to simulate and predict appropriateness of innovation from evidence-based big data analysis given technological and financial constraints. There is a trend for corrective action through exploiting international cooperation of stakeholders including promoting and funding inter-laboratory testing and validation of new approaches based upon review of all data sets that also informs consensus. Such trends can be seen by development of semi-quantitative risk assessment models that considers main factors governing efficacy for mitigating pollutants in water that may also help with understanding and interpretation of enormous data sets generated from PL and other non-thermal technology studies (Tahar, Tiedeken, Cummins, Clifford, & Rowan, 2017). This also helps in simplifying complex issues and for conveying main impactful findings to industry and for policy makers for decision making. Akin to the medical technology domain, the Irish water industry require validation of new innovation before deployment that explains in part why this industry will continue to deploy validated process such as continuous-wave low-pressure UV that has been reliable for the industry. However, PL technology has potential for next-generation UV disinfection technology but requires a platform for independent validation. The latter is attested by growing interest in the use of PL for rainwater harvesting and recirculation in the dairy industry (Fitzhenry et al., 2018) and for aquaculture applications where there is a pressing need for disease mitigation using environmentally-friendly innovation that can be deployed in pond, flow-through and recirculation aquaculture systems (RAS) (cited in Tahar, Kennedy, Fitzgerald, Clifford, & Rowan, 2018a). There is an increasing trend to develop risk assessment models in order to evaluate sustainable technologies for addressing environmental treats for the drinking and wastewater industry where pulsed light can be considered as a candidate control measure post validation (Tahar et al., 2017, 2018b).

2. Conclusions

This review reflects upon some of the key technological developments underpinning PL technology where the food industry is constantly innovating and seeking more rapid, cheaper, efficient and effective outcomes. It specifically focused on the factors influencing the development of PL for the decontamination of fresh produce post-harvest handling. It also provided a set of recommendations for reporting PL studies that will facilitate standardisation and harmonisation of experimental data and exposure conditions that will enable the researcher to repeat and evaluate studies with a commercial orientation. Despite approval from the Food and Drug Administration (FDA) since 1996, there is little evidence that PL technology has not been taken up for large scale commercial treatment of foods. There has been a considerable volume of exciting published information on PL development for food and beverage applications, but there has been a marked lack of collaborative research to yield harmonised data internationally that infers PL technologies currently lead to incomparable findings. Lack of international consensus and harmonisation of data and methods will retard development of PL technology. This infers a pressing need for international networking of academics, industry, regulators and other NGOs, standards bodies such as through EU Cost Action or similar interdisciplinary inter-laboratory platform approach for testing and validating PL internationally. Such collaborative undertakings should exploit freely-available open access sources and the international research community must reach consensus on priority parameters for reliable and repeatable development of PL that recognises FDA recommendations (FDA, 2015). Decisive parameters for describing PL treatment of fresh produce to standardise future research reporting is provided that also considers the importance of including native microflora along with artificially seeded microbial test strains for specific shelf life testing at fluence levels below FDA recommended 12 J cm^{-2}. There is verbose data available on PL treatment conditions from various food produce studies, typically operating at sub-lethal level that eliminates pathogens but retains a population of spoilage microorganisms to reflect co-retention of fresh-like nutritional and organoleptic properties. However, as use of current Xenon-based light sources in current treatment configurations produce a maximum viable count reduction of 3 log orders on food surfaces, there is a pressing need to consider new light sources such as LEDs and different reactor designs to augment effectiveness of fluence to achieve the 5 log reduction standard. Advances in whole genome sequencing, bioinformatics, flow cytometry and spectrometry will help elucidate cell and molecular mechanisms underpinning PL disinfection efficacy that may bring our researcher community closer to understanding dynamic relationship between culturable and VBNC state microorganisms. This may help to inform

effective irreversible PL-decontamination processes for food produce and possible enable extension of shelf life. Agreement upon and advancing microbial inactivation (or kinetic) modelling along with developing possible risk assessment models will also inform efficacy of operational PL parameters and enable comparisons on effectiveness between studies. There is convergence of knowledge and innovation from other adjacent sectors (including medical technologies, wastewater and manufacturing industries) that will facilitate development of PL for food and related disinfection applications. However, there is an increasing trend where such sectors (such as medtech) are also investigating reduction in over-processing conditions associated with terminal sterilisation in order to embrace emerging opportunities for additive manufacturing such as 3-D printing of heat sensitive polymers and treatment of complex medical devices *in situ* in healthcare that responds to growth in personal medicine (Garmulewicz, Holweg, Veldhuis, & Yang, 2018). PL offers exiting opportunities for food and drink including potential for technology disruption in many other areas including freshwater aquaculture, waste reduction and management (rainwater recycling), pollination as putative innovation for tackling disease in bees and treatment of algal bloom. However, such potential will not be realised until agreement has been reached on harmonised methods so as to enable the research to sufficiently compare and validate data. This review also presented an opportunity to consider how PL can be used as a testbed platform for important training, education and evaluation. For example, adjacent advances in artificial intelligence, immersive augmented and virtual reality may transform how workforce training is provided and assessed including development of PL through machine interface learning (Keighrey et al., 2017).

Acknowledgement

I wish to acknowledge funding support from the Department of Agriculture, Food and the Marine, Ireland. Projects DAFM-MOREFISH 14SF872 and DAFM-DAIRYWATER 13F507.

References

Adhikari, A., Syamaladevi, R. M., Killinger, K., & Sablani, S. S. (2015). Ultraviolet-C light inactivation of *Escherichia coli* O157:H7 and *Listeria monocytogenes* on organic fruit surfaces. *International Journal of Food Microbiology, 210*, 138–142.

Adner, R. (2002). When are technologies disruptive? A demand-base view of the emergence of competition. *Strategic Management Journal, 23*(8), 667–688.

Agüero, M. V., Jagus, R. J., Martín-Belloso, O., & Soliva-Fortuny, R. (2016). Surface decontamination of spinach by intense pulsed light treatments: Impact on quality attributes. *Postharvest Biology and Technology, 121*, 118–125.

Aguiló-Aguayo, I., Charles, F., Renard, C. M., Page, D., & Carlin, F. (2013). Pulsed light effects on surface decontamination, physical qualities and nutritional composition of tomato fruit. *Postharvest Biology and Technology, 86*, 29–36.

Aguirre, J. S., de Fernando, G. G., Hierro, E., Hospital, X. F., Ordonez, J. A., & Fernandez, M. (2015). Estimation of the growth kinetic parameters of *Bacillus cereus* spores as affected by pulsed light treatment. *International Journal of Food Microbiology, 202*, 20–26.

Aguirre, J. S., Herro, E., Fernandez, M., & de Fernando, G. D. G. (2014). Modelling the effect of light penetration and matrix colour on the inactivation of *Listeria innocua* by pulsed light. *Innovative Food Science & Emerging Technologies, 26*, 505–510.

Anderson, J. G., Rowan, N. J., MacGregor, S. J., Fouracre, R. A., & Farish, O. (2000). Inactivation of food-borne enteropathogenic bacteria and spoilage fungi using pulsed light. *IEEE Transactions on Plasma Science, 28*(1), 83–88.

Angers-Loustau, A., Petrillo, M., Bengtsson-Palme, J., Berendonk, T., Blais, B., Chan, L.-G., et al. (2018). The challenges of designing a benchmark strategy for bioinformatics pipelines in the identification of antimicrobial resistance determinants using next generation sequencing technologies. *F1000Research, 7*. https://doi.org/10.12688/f1000research.14599.1 Number 459.

Barakat, M. T., Moftah, N. H., El Khayyat, A. M., & Abdelhakim, Z. A. (2017). Significant reduction of inflammation and sebaceous gland size in acne vulgaris lesions after intense pulsed light treatment. *Dermatologic Therapy, 30*(1), e12418.

Bhavya, M. L., & Umesh-Bebbar, H. (2017). Pulsed light of foods for microbial safety. *Food Quality and Safety, 1*(3), 187–201.

Bialka, K. L., & Demirci, A. (2008). Efficacy of pulsed UV-light for the decontamination of Escherichia coli O157:H7 and Salmonella spp. on raspberries and strawberries. *Journal of Food Science, 73*, M201–M207.

Bower, J. L., & Christensen, C. M. (1995). Disruptive technologies: Catching the wave. *Harvard Business Review, 73*(1), 506–520.

Bradley, D., Laffey, J. G., McNeil, B., & Rowan, N. J. (2012). Studies on the cross-relationship between adaptive stress response and efficacy of novel electro-technologies for the inactivation of *Listeria monocytogenes*. *Food Microbiology, 30*, 330–339.

Braschi, G., Patrignani, F., Siroli, L., Lanciotti, R., Schlueter, O., & Froehling, A. (2018). Flow cytometric assessment of the morphological and physiological changes in Listeria monocytogenes and Escherichia coli in response to natural antimicrobial exposure. *Frontiers in Microbiology, 92783*. https://doi.org/10.3389/fmicb.2018.02783.

Callejón, R. M., Rodriguez-Naranjo, M. I., Ubeda, C., Hornedo-Ortega, R., Garcia-Parrilla, M. C., & Troncoso, A. M. (2015). Reported foodborne outbreaks due to fresh produce in the United States and European Union trends and causes. *Foodbourne Pathogens & Disease, 12*, 32–38.

Castro, S. M., Inácio, R. S., Alexandre, E. M. C., Fidalgo, L. G., Periera, S., Quearesma, P., et al. (2018). Environmental footprint of emerging technologies, regulatory and legislative issues. *Innovative technologies for food preservation* (pp. 255–276). Academic Press.

Centers for Disease Control and Prevention (2018). Foodborne Illness and Outbreaks. https://www.cdc.gov/foodsafety/outbreaks/multistate-outbreaks/outbreaks-list.html, Accessed date: 12 January 2019.

Cheigh, C. I., Hwang, H. J., & Chung, M. S. (2013). Intense pulsed light and UV-C treatments for inactivating Listeria monocytogenes on solid media. *Food Research International, 54*, 745–752.

Cheigh, C. I., Park, M. H., Chung, M. S., Shin, J. K., & Park, Y. S. (2012). Comparison of intense pulsed light on ultraviolet (UV-C) inducted cell damage in Listeria monocytogenes and Escherichia coli O157:H7. *Food Control, 25*, 654–659.

Chen, J., Loeb, S., & Kim, J. H. (2017). LED revolution – fundamentals and prospectus for UV disinfection applications. *Environ Sci Water Res Technol, 3*, 188–202.

Christensen, C. (1997). *The innovators dilemma: When new technologies cause great firms to fail.* Boston, MA: Harvard Business School Press.

Christensen, C. M., Anthony, S. D., & Roth, E. A. (2004). *Seeing what's next: Using the theories of innovation to predict industry change.* Cambridge, MA: Harvard Business Press.

Christensen, C. M., & Bower, J. L. (1996). Customer power, strategic investment, and the failure of leading firms. *Strategic Management Journal, 17*(3), 197–218.

Cudemos, E., Izquier, A., Medina-Martines, M. S., & Gomez-Lopez, V. M. (2013). Effects of shading and growth phase on the microbial inactivation of pulsed light. *Czech Journal of Food Sciences, 31*, 189–193.

Danneels, E. (2004). Disruptive technology reconsidered: A critique and research agenda. *Journal of Product Innovation Management, 21*(4), 246–258.

DBEI (2018). https://dbei.gov.ie/en/Publications/Publication-files/Research-Priority-Areas-2018-to-2023.pdf, Accessed date: 27 November 2018.

Dedhayir, O., Okelainen, T. M., & Saju, J. (2014). Disruptive innovations in complex product systems industries: A case study. *Journal of Engineering and Technology Management, 33*(0), 174–192.

Dexter, M., Gao, Z., Bansal, S., Chang, C.-H., & Malhotra, R. (2018). Temperature, crystalline phase and influence of substrate properties of intense pulsed light sintering of copper sulphide nanoparticle thin films. *Scientific Reports, 8*, 2201. https://doi.org/10.1038/s41598-018-206219.

Dogterom, M. (2018). https://www.tudelft.nl/en/2017/tu-delft/dutch-researchers-join-forces-to-build-synthetic-cell/, Accessed date: 27 November 2018.

Elmnasser, N., Guillou, S., Leroi, F., Orange, N., Bakhrouf, A., & Federighi, M. (2007). Pulsed light system as a novel food decontamination technology: A review. *Canadian Journal of Microbiology, 53*, 813–821.

Esbelin, J., Mallea, S., Ram, J., & Carlin, F. (2013). Roe of pigmentation in protecting Aspergillus Niger conidiospores against pulsed light radiation. *Photchem Photobiol, 89*, 758–776.

European Commission Pollinators Initiative (2018). http://ec.europa.eu/environment/nature/conservation/species/pollinators/documents/EU_pollinators_summary_public_consultation.pdf, Accessed date: 27 November 2018.

Fario, W., Tavanti, A., Barnini, S., Ghelardi, E., & Lupetti, A. (2018). Recent advances and ongoing challenges in the diagnosis of microbial infections by MALDI-TOF Mass Spectrometry. *Frontiers in Microbiology, 9*. https://doi.org/10.3389/fmicb.201801097.

Farrell, H. P., Garvey, M., Cormican, M., Laffey, J. G., & Rowan, N. J. (2010). Investigation of critical inter-related factors affecting the efficacy of pulsed light for inactivating clinically relevant bacterial pathogens. *Journal of Applied Microbiology, 198*, 1494–1508.

Farrell, H., Garvey, M., & Rowan, N. (2009). Studies on the inactivation of medically important Candida species on agar surfaces using pulsed light. *FEMS Yeast Res, 9*, 956–966.

Farrell, H. P., Hayes, J., Laffey, J. G., & Rowan, N. J. (2011). Studies on the relationship between pulsed UV light and the simultaneous occurrence of molecular and cellular damage in clinically-relevant *Candida albicans*. *Journal of Microbiological Methods, 84*, 317–326.

Felizani, E., Lichter, A., Smilanick, J., & Ippolito A, L. (2016). Disinfecting agents for controlling fruit and vegetable diseases after harvest. *Postharvet Biology Technol, 122*, 53–69.

Ferrario, M., Alzamora, S. M., & Guerrero, S. (2013). Inactivation kinetics of some microorganisms in apple, melon, orange and strawberry juices by high intensity light pulses. *Journal of Food Engineering, 118*, 302–311.

Ferrario, M., Guerrero, S., & Alzamora, S. M. (2014). Study of pulsed light induced damage on Saccharomyces cerevisiae in apple juice by flow cytometry and transmission electron microscopy. *Food and Bioprocess Technology, 7*, 1001–1011.

Finnegan, W., Clifford, E., Goggins, J., O'Leary, N., Dobson, A., Rowan, N., et al. (2018). Dairywater: Striving for sustainability within the dairy processing industry in the republic of Ireland. *Journal of Dairy Research, 85*(3), 366–374.

Finnegan, W., Goggins, J., Clifford, E., & Xinmin, Z. (2017). Environmental impacts of milk powder and butter manufactured in the Republic of Ireland. *The Science of the Total Environment, 579*, 159–168.
Fitzhenry, K., Rowan, N., Finnegan, W., Zhan, X., & Clifford, E. (2018). Microbial characterisation and impact of suspended solids on pathogen removal from wastewater in dairy processing factories. *Journal of Dairy Research, 85*(3), 391–395.
Fitzhenry, K., Rowan, N., Val de Rio, A., Cremillieux, A., & Clifford, E. (2019). Inactivation efficacy of *Bacillus* endospores via modified flow-through PUV treatment with comparison to conventional LPUV treatment. In: *J. Water. Proc. Eng. 27*, 67–76.
Food Wise. https://www.agriculture.gov.ie/foodwise2025/, Accessed date: 29 November 2018 2025.
Food and Drug Administration (2003). https://www.fda.gov/Food/GuidanceRegulation/GuidanceDocumentsRegulatoryInformation/Juice/ucm072981.htm, Accessed date: 28 December 2018.
Food and Drug Administration (2015). *Code of federal regulations title 21, sec. 179.41*. Pulsed light for treatment of food: 21 CFR179.41.
Foods' Carbon Footprint (2018). http://www.greeneatz.com/foods-carbon-footprint.html, Accessed date: 28 December 2018.
Francis, G. A., Gallone, A., Nychas, G. J., Sofos, J. N., Golellli, G., Amodio, M. L., et al. (2012). Factors affecting quality and safety of fresh-cut produce. *Critical Reviews in Food Science and Nutrition, 52*, 595–610.
Franssen, F., Gerard, C., Cozma-Petrut, A., Vieira-Pinto, M., Režek Jambrak, A., Rowan, N., et al. (2019). Inactivation of parasite transmission stages: Efficacy of treatments on food of animal origin. *Trends in Food Science & Technology, 83*, 114–128.
Fürst, M. A., McMahon, D. P., Osborne, J. L., Paxton, R. J., & Brown, M. J. F. (2014). Disease associations between honeybees and bumblebees as a threat to wild pollinators. *Nature, 506*, 364–366.
Gallai, N., Salles, J.-M., Settele, J., & Vaissiere, B. E. (2009). Economic valuation of the vulnerability of world agriculture confronted with pollinator decline. *Ecological Economics, 68*, 810–821.
Garmulewicz, A., Holweg, M., Veldhuis, H., & Yang, A. (2018). Disruptive technology as an enabler of the circular economy: What potential does 3D printing hold? *California Management Review, 60*(3), 112–132.
Garrison, G. (2009). An assessment of organisational size and sense and response capability on the early adoption of disruptive technology. *Computers in Human Behavior, 25*, 444–449.
Garvey, M., Coughlan, G., Murphy, N., & Rowan, N. (2016b). The pulsed light inactivation of veterinary relevant microbial biofilms and the use of a RTPCR assay to detect parasite species within biofilm structures. *Open Veterinary Journal, 6*(1), 15–22.
Garvey, M., Farrell, H., Cormican, M., & Rowan, N. J. (2010). Investigations of the relationship between use of in vitro cell culture-quantitative PCR and a mouse-based bioassay for evaluating critical factors affecting the disinfection performance of pulsed UV light for treating *Cryptosporidium parvum* oocyts in saline. *Journal of Microbiological Methods, 80*, 267–273.
Garvey, M., Rabbitt, D., Stocca, A., & Rowan, N. (2015). Pulsed ultraviolet light inactivation of Pseudomonas aeruginosa and Staphylococcus aureus biofilms. *Water and Environment Journal, 29*, 36–42.
Garvey, M., & Rowan, N. (2015). A pulsed light system for the disinfection of flow through water in the presence of inorganic contaminants. *Journal of Water and Health, 13*(2), 406–412.
Garvey, M., Stocca, A., & Rowan, N. J. (2014a). Development of a combined *in vitro* cell culture-quantitative PCR assay for evaluating the disinfection performance of pulsed light for treating the waterborne enteroparasite Giardia lamblia. *Experimental Parasitology, 144*(1), 6–13 PMID 24929148.
Garvey, M., Stocca, A., & Rowan, N. (2016). Use of a real-time PCR assay to assess the effect of pulsed light inactivation on bacterial cell membranes and associated cell viability. *Water Environment Research, 88*(2), 168–174.
Garvey, M., Stocca, A., & Rowan, N. (2016a). Use of a real time PCR assay to assess the effect of pulsed light inactivation on bacterial cell membranes and associated cell viability. *Water Environment Research, 88*, 168–174.
Garvey, M., Thokala, N., & Rowan, N. (2014b). A comparative study on the pulsed UV and the low-pressure UV inactivation of a range of microbial species in water. *Water Environment Research, 86*, 2317–2324.
Geels, F. W. (2018). Disruption and low-carbon system transformation; progress and new challenges in socio-technical transitions research and the multi-level perspective. *Energy Research and Social Science, 37*, 224–231.
Gombas, D., Luo, Y., Brennan, J., Shergill, G., Petran, R., Walsh, R., et al. (2017). Guidelines to validate control of cross-contamination during washing of fresh-cut leafy vegetables. *Journal of Food Protection, 80*(2), 312–330.
Gómez-López, V. M., Devlieghere, F., Bonduelle, V., & Devevere, J. (2005). Intense light pulses decontamination of minimally processed vegetables and their shelf life. *International Journal of Food Microbiology, 103*, 79–89.
Gómez-López, V. M., & Bolton, J. R. (2016). An approach to standardize methods for fluence determination in bench-scale light experiments. *Food and Bioprocess Technology, 9*, 1040–1048.
Goulson, G., & Hughes, W. O. H. (2015). Mitigating the anthropogenic spread of bee parasites to protect wild pollinators. *Biological Conservation, 191*, 10–19.
Govindarajan, V., & Kopalle, P. K. (2006). Disruptiveness of innovations: Measurement and an assessment of reliability and validity. *Strategic Management Journal, 27*(2), 189–199.
Graystock, P., Goulson, D., & Hughes, W. O. H. (2014). *The relationship between managed bees and the prevalence of parasites in bumble bees.* PeeJe552.
Hayes, C. J., Fogarty, A., Clifford, E., & Rowan, N. J. (2012b). Inactivation of recalcitrant protozoan oocysts and bacterial endospores in drinking water using high-intensity pulsed UV light irradiation. *Water Science and Technology, 12*(4), 513–522.
Hayes, J. C., Garvey, M., Fogarty, A. M., Clifford, E., & Rowan, N. J. (2012c). Inactivation of recalcitrant protozoan oocyts and bacterial endospores in drinking water using high-intensity pulsed UV light irradiation. *Water Science and Technology, 12*, 513–522.
Hayes, J., Kirf, D., Garvey, M., & Rowan, N. (2013). Disinfection and toxicological assessments of pulsed plasma gas discharge and pulsed UV light treated water containing the waterborne enteroparasite *Cryptosporidium parvum*. *Journal of Microbiological Methods,* (94), 325–337.
Hayes, C. J., Laffey, G. J., McNeil, B., & Rowan, N. J. (2012a). Exposure of yeast to sublethal osmotic stress conditions decreases their ability to survive subsequent high-intensity pulsed UV-light irradiation. *International Journal of Food Science and Technology, 47*(9), 1925–1934.
Heinrich, V., Zunabovic, M., Petschnig, A., Müller, H., Lassenberger, A., Reimhult, E., et al. (2016). Previous homologous and heterologous stress exposure induces tolerance development to pulsed light in Listeria monocytogenes. *Frontiers in Microbiology, 7*, 1–14.
Heinrich, V., Zunabovic, M., Varzakas, T., Bergmair, J., & Kneifel, W. (2016). Pulsed light treatment of different food types with special focus on meat: A critical review. *Critical Reviews in Food Science and Nutrition, 56*(4), 591–613.
Hierro, E., Ganan, M., Barroso, E., & Fernández, M. (2012). Pulsed light treatment for the inactivation of selected pathogens and the shelf-life extension of beef and tuna carpaccio. *International Journal of Food Microbiology, 158*, 42–48.
Hsu, L., & Moraru, C. I. (2011). Quantifying and mapping the spatial distribution of luence inside a pulsed light treatment chamber and various liquid substrates. *Journal of Food Engineering, 103*, 84–91.
Huang, H., Lv, W., Chen, Y., Zheng, X., Hu, Y., Wang, R., et al. (2018). The role of NADPH oxidase in the inhibition of *Trichophyton rubrum* by 420-nm intense pulsed light. *Front. Microbiol. Jan, 9*, 82636. https://doi.org/10.3389/fmicb 2017 02636.
Huang, Y., Ye, M., Cao, X., & Chen, H. (2017). Pulsed light inactivation of murine norovirus, Tulane virus, Escherichia coli O157H7 and Salmonella in suspension and on berry surfaces. *Food Microbiology, 61*, 2491–2498.
Ifkovits, J. L., & Burdick, J. A. (2007). Review. Photopolymerizable and degradable biomaterials for tissue engineering applications. *Tissue Engineering, 13*(10), 2369–2385.
Ignat, A., Manzocco, L., Maifreni, M., Bartolomeoli, I., & Nicoli, M. C. (2014). Surface decontamination of fresh-cut apple by pulsed light: Effects on structure, colour and sensory products. *Postharvest Biology and Technology, 91*, 122–127.
Innocente, N., Segat, A., Manzocco, L., Marino, M., Maifreni, M., Bortolomeoli, I., et al. (2014). Effect of pulsed light on total microbial count and alkaline phosphatase activity in raw milk. *International Dairy Journal, 39*, 108–112.
Ishihara, M., Sato, M., Ishihara, M., Mochida, J., & Kikachi, M. (2007). *Multifunctional evualtion of tissue engineering cartilage using nano-pulsed light for validation of regenerative medicine. Vol. 2006*World Congress of Medical Physics Biomed Eng 33-39-3321.
Kang, H., Sowade, E., & Baumann, R. R. (2014). Direct Intense pulsed light sintering of inkjet-printed copper oxide layers within six milliseconds. *ACS Applied Materials & Interfaces, 6*(3), 1682–1687.
Kasahara, I., Carrasco, V., & Aruilar, L. (2015). Inactivation of Escherichia coli in goat milk using pulsed ultraviolet light. *Journal of Food Engineering, 152*, 43–49.
Keighrey, C., Flynn, R., Murray, S., & Murray, N. (2017). *A QoE evaluation of immersive augmented and virtual reality speech and language assessment applications. 2017 Ninth International Conference on Quality of Multimedia Experience.* https://doi.org/10.1109/QoMEX.2017.7965656.
Keklik, N. M., Demirci, A., & Puri, V. M. (2009). Inactivation of Listeria monocytogenes on unpackaged and vacuum-packaged chicken frankfurters using pulsed UV-light. *Journal of Food Science, 74*, M431–M439.
Kim, D. K., Kim, S. J., & Kang, D. H. (2017). Bactericidal effect of 266-279 nm wavelength UV-C LEDs for inactivation of Gram positive and negative foodborne pathogenic bacteria and yeast. *Food Research International, 97*, 280–287.
King, A. A., & Baatartogtokh, B. (2015). How useful is the theory of disruptive innovation? *MIT Sloan Management Review, 57*(1), 77–90.
Kramer, B., & Muranyi, P. (2014). Effect of pulsed light on structural and physiological properties of *Listeria innocua* and *Escherichia coli*. *Journal of Applied Microbiology, 116*, 596–611.
Kramer, B., Wunderlich, J., & Muranyi, P. (2015a). Pulsed light decontamination of endive salad and mung bean sprouts and impact on colour and respiratory activity. *Journal of Food Protection, 78*, 340–348.
Kramer, B., Wunderlich, J., & Muranyi, P. (2015b). Pulsed light decontamination of endive salad and mung bean sprouts in water. *Food Control, 73*, 367–371.
Kramer, B., Wunderlich, J., & Muranyi, P. (2017). Recent findings in pulsed light disinfection. *Journal of Applied Microbiology, 122*, 830–856.
Kristnamurthy, K., Tewari, J. C., Irudayaraj, T., & Demirci, A. (2010). Microscopic and spectroscopic evaluation of inactivation of Staphylococcus aureus by pulsed UV light and infrared heating. *Food and Bioprocess Technology, 3*, 93.
Lasagabaster, A., & de Maranon, I. M. (2014). Survival and growth of Listeria innocua treated by pulsed light technology: Impact of post-treatment temperature and illumination conditions. *Food Microbiology, 41*, 76–81.
Lauer, M. S., & D'Agostino, R. B. (2013). The randomised registry trial – the next disruptive technology in clinical research. *New England Journal of Medicine, 369*(17), 1579–1581.
Lavery, B. W., Kumari, S., Konermann, H., Draper, G. L., Spurgeon, J., & Druffel, T. (2016). Intense pulsed light sintering of CH3NH3PbI3 solar cells. *ACS Applied Materials and Interfaces, 8*(13), 8419–8426.
Léonard, L., Bouarab Chibane, L., Ouled Bouhedda, B., Degraeve, P., & Oulahal, N. (2016). Recent advances on multi-parameter flow cytometry to characterize antimicrobial treatments. *Frontiers in Microbiology, 7*, 1224. https://doi.org/10.3389/fmicb.2016.01225.

Levy, C., Aubert, X., Lacour, B., & Carlin, F. (2012). Relevant factors affecting microbial surface decontamination by pulsed light. *International Journal of Food Microbiology, 152*, 168–174.
Lille, M., Nurmela, A., Nordlund, E., Metsä-Kortelainen, S., & Sozer, N. (2018). Applicability of protein and fibre-rich food materials in extrusion-based 3D printing. *Journal of Food Engineering, 220*, 20–27.
Li, M., Porter, A. L., & Suominen, A. (2018). Insights into relationships between disruptive technology/innovation and emerging technology: A bibliometric perspective. *Technological Forecasting and Social Change, 129*, 285–296.
Luksiene, Z., Gedelis, V., Buchovec, I., & Raudeliuniene, J. (2007). Advanced high power pulsed light device to decontaminate food from pathogens: Effects on *Salmonella typhimurium* viability in vitro. *J Appl Micrbiol, 103*, 1545–1552.
MacLean, M., Murdoch, L. E., Lani, M. N., MacGregor, S. J., Anderson, J. G., & Woolsey, G. A. (2008). Photoinactivation and photreactivation responses by bacterial pathogens after exposure to pulsed UV light. *2008 proceedings of the IEEE international power modulators and high voltage conference* (pp. 326–329). .
Marco-Ramell, A., Palau-Rodriguez, M., Alay, A., Tulipani, S., Urpi-Sarda, M., Sanchez-Pla, A., et al. (2018). Evaluation and comparison of bioinformatics tools for the enrichment analysis of metablomics data. *BMC Bioinformatics, 19*. https://doi.org/10.1186/s12859-017-2006.0.
Massier, S., Bouffartigues, E., Rince, A., Maillot, O., Feuilloley, M. G. J., Orange, N., et al. (2013). Effects of a pulsed light induced stress on *Enterococcus faecalis*. *Journal of Applied Microbiology, 114*, 186–195.
McFadden, E., Costa-Ramos, A. L., Bradley, D., Vrain, O., McEvoy, B., & Rowan, N. J. (2017). Comparative studies on the novel sterilisation of Irish retailed infant milk formula using electron beam and pulsed light treatments. *International Journal of Science, Environment and Technology, 12*(6), 4375–4377.
McNamara, G., Fitzsimons, L., Horrigan, M., Phelan, T., Delaure, Y., Corcoran, B., et al. (2016). Life cycle assessment of wastewater treatment plants in Ireland. *J. Sustainable Develop Energy Water Environ Systems, 4*(3), 216–233.
Meireles, A., Giaouris, E., & Simoes, M. (2016). Alternative disinfection methods to chlorine for use in the fresh-cut industry. *Food Research International, 82*, 71–85.
Mendes, G. C. C., Brandão, T. R. S., & Silva, C. L. M. (2007). Ethylene oxide sterilisation of medical devices and review. *American Journal of Infection Control, 35*(9), 574–578.
Michelini, L., Principato, L., & Iasevoli, G. (2018). Understanding food sharing models to tackle sustainability challenges. *Ecological Economics, 145*, 205–217.
Montgomery, N. L., & Banerjee, P. (2015). Inactivation of Escherichia coli O157:H7 and Listeria monocytogenes in biofilms by pulsed ultraviolet light. *BMC Research Notes, 8*, 235.
Moral, R. A., Hinde, J., & Demétrio, C. G. B. (2017). Half-normal plots and overdispersed models in R: The hnp package. *Journal of Statistical Software, 81*(10), 1–23.
Morefish (2018). http://www.morefish.ie/, Accessed date: 29 December 2018.
Mortazavi, A., Williams, B. A., McCue, K., Schaeffer, L., & Wold, B. (2008). Mapping and quantifying mammalian transcriptomes by RNA-seq. *Nature Methods, 5*, 621–628.
Murray, T. E., Coffey, M. F., Kehoe, E., & Horgan, F. G. (2013). Pathogen prevalence in commercially reared bumble bees and evidence of spillover in conspecific populations. *Biological Conservation, 159*, 269–276.
Murray, I. M. T., Rowan, N. J., McNamee, S., Campbell, K., & Fogarty, A. (2018). Pulsed light reduces the toxicity of the algal toxin okadaic acid to freshwater crustacean Daphnia pulex. *Environmental Science & Pollution Research, 25*(1) 607-414.
Murray, K., Wu, F., Shi, J., Xue, S. J., & Warriner, K. (2017). Challenges in the microbiological food safety of fresh produce: Limitations of post-harvest washing and the need for alternative interventions. *Food Quality Safety, 1*(4), 289–301.
Muňoz, A., Caminiti, I. M., Palgan, I., Pataro, G., Noci, F., Morgan, D. J., et al. (2012). Effects on Escherichia coli inactivation and quality attributes in apple juice treated by combinations of pulsed light and thermosonication. *Food Research International, 45*, 299–305.
Naughton, J., Tiedeken, E. J., Garvey, M., Stout, J. C., & Rowan, N. J. (2017). Pulsed light inactivation of the bumble bee trypanosome parasite *Crithidia bombi*. *J Apiculture Res, 56*(2), 144–154.
Nicorescu, I., Nguyen, B., Moreau-Ferret, M., Agoulon, A., Chevalier, S., & Orange, N. (2013). Pulsed light inactivation of Bacillus subtilis vegetative cells in suspensions an dspices. *Food Control, 31*, 151–157.
Nuesch-Inderbinen, M., & Stephan, R. (2016). Fresh fruit and vegetables as vehicles of bacterial foodborne disease: A review and analysis of outbreaks registered by proMED-mail associated with fresh produce. *J. Food Safety Food Quality Archiv Fur Lebensmittelhygine, 67*, 32–39.
Nymann, P., Hedelund, L., & Hædersdal, M. (2009). Intense pulsed light vs. long-pulsed laser treatment of telangiectasia after radiotherapy for breast cancer: A randomised split-lesion trial of two different treatments. *British Journal of Dermatology, 160*(6), 1237–1241.
Ollerton, J., Winfree, R., & Tarrant, S. (2011). How many flowering plants are pollinated by animals? *Oikos, 120*, 321–326.
Oms-Oliu, G., Aguiló-Aguayo, I., Martín-Belloso, O., & Soliva-Fortuny, R. (2010). Effects of pulsed light treatments on quality and antioxidant properties of fresh-cut mushrooms (Agaricus bisporus). *Postharvest Biology and Technology, 56*, 216–222.
Osiyevskyy, O., & Dwwald, J. (2015). Explorative versus exploitative business model change: The cognitive antecedents of firm-level responses to disruptive innovation. *Strategic Enterpreneurship Journal*. https://doi.org/10.1002/sej.1192.
Ozer, N. P., & Demirci, A. (2006). Inactivation of Escherichia coli O157:H7 and Listeria monocytogenes inoculated on raw salmon fillets by pulsed UV-light treatment. *International Journal of Food Science and Technology, 41*, 354–360.
Pardo, G., & Zufia, J. (2012). Life cycle assessment of food preservation technologies. *Journal of Cleaner Production, 28*, 198–207.
Pertea, M., Kin, D., Pertea, G. M., Leek, T. J., & Salzberg, S. L. (2016). Transcript-level expression analysis of RNA-seq experiments with HISAT, StringTie and Ballgown. *Nature Protocols, 11*(No. 9), https://doi.org/10.1038/nprot.2016.095 published online 11 August 2016.
Piccolo, D., & Kostaki, D. (2018). Photodynamic therapy activated by intense pulsed light in the treatment of nonmelanoma skin cancer. *Biomedicines, 6*, 18. https://doi.org/10.3390/biomedicines6010018.
PoshBee (2018). *Pan-european assessment, monitoring, and mitigation of stressors on the health of BEEs – H2020 project*. https://cordis.europa.eu/project/rcn/215953_en.html, Accessed date: 23 November 2018.
Quested, T. E., Cook, P. E., Gorris, L. G. M., & Cole, M. B. (2010). Trends in technology, trade and consumption likely to impact on microbial food safety. *International Journal of Food Microbiology, 139*, S29–S42.
Ramos-Villarroel, A., Aron-Maftei, N., Martin-Belloso, O., & Soliva-Fortuny, R. (2012). The role of pulsed light spectral destruction in the inactivation of Escherichia coli and Listeria innocua on fresh-cut mushrooms. *Food Control, 24*, 206–213.
Ramos-Villarroel, A. Y., Martín-Belloso, O., & Soliva-Fortuny, R. (2011). Bacterial inactivation and quality changes in fresh-cut avocado treated with intense light pulses. *European Food Research and Technology, 233*, 395–402.
Rastogi, R. P., Richa, K. A., Tyagi, M. B., & Sinha, R. P. (2010). Pulsed light inactivation of *Listeria innocua* on food packaging materials of different surface roughness and reflectivity. *Journal of Food Engineering, 114*, 331–337.
Richie, S. C., Hacker, J. C., Yearkey, K. L., Shi, Z., Park, S. H., & Rainwater, C. E. (2018). Unraveling food production microbiomes: Concepts and future directions. *Food and feed safety systems and analysis*. Academic Press.
Ronholm, J. (2018). Editorial: Game changer – next generation sequencing and its impact on food microbiology. *Frontiers in Microbiology*. https://doi.org/10.3389/fmicb.2018.00363.
Rosen, J. W. A., Friedrich, A. W., & Moran-Gilad, J. (2018). Practical issues in implementing whole-genome-sequencing in routine diagnostic microbiology. *Clinical Microbiology and Infections, 24*, 355–360.
Rowan, N. J. (2004). Viable but nonculturable forms of food and water-borne bacterial pathogens: Quo vadis? *Trends in Food Science & Technology, 15*, 462–467.
Rowan, N. J., MacGregor, S. J., Anderson, J. G., Fouracre, R. A., McIlvaney, L., & Farish, O. (1999). Pulsed-light inactivation of food-related microorganisms. *Applied and Environmental Microbiology, 65*(3), 1312–1315.
Rowan, N., Valdramidis, V. P., & Gomez-Lopez, V. M. (2015). A review of quantitative methods to describe efficacy of pulsed light inactivation data that embraces the occurrence of viable non-culturable microorganisms. *Trends in Food Science & Technology, 44*(1), 79–92.
Rychilk, M., Kanawati, B., & Schmitt-Kopplin, P. (2017). Foodomics as a promising tool to investigate the mycobolome. *Trends in Analytical Chemistry, 96*, 22–30.
Saguy, I. S., Roos, Y. H., & Cohen, E. (2018). Food engineering and food science and technology: Forward looking journey to future horizons. *Innovative Food Science & Emerging Technologies, 47*, 326–334.
Schottroff, F., Fröhling, A., Zunabovic-Pichler, M., Krottenthaler, A., Schlüter, O., & Jäger, H. (2018). Sublethal injury and viable but non-culturable (VBNC) state in microorganisms during preservation of food and biological materials by non-thermal processes. *Frontiers in Microbiology*. https://doi.org/10.3389/fmicb.2018.02773.
Schuelke-Leech, B. A. (2018). A model for understanding the orders of magnitude of disruptive technologies. *Technological Forecasting and Social Change, 129*, 261–274.
Sella, S. R. B. R., Vandenberghe, L. P. S., & Soccol, C. R. (2015). *Bacillus atrophaeus* main characteristics and biotechnological applications – a review. *Critical Reviews in Biotechnology, 35*(4), 533–545.
Seo, K. Y., Kang, S. M., Ha, D. Y., Chin, H. S., & Jung, J. W. (2018). Long-term effects of intense pulsed light treatment on the ocular surface in patients with rosacea-associated Meibomian gland dysfunction. *Contact Lens and Anterior Eye, 41*(5), 430–435.
Shankar, A., Salcedo, E., Berndt, A., & Choi, A. (2017). *Pulsed light sintering of silver nanoparticles for large deformation for large deformation of printed stretchable electronics*. https://doi.org/10.1007/s42114-017-0012-3.
Simone-Finstrom, M., Aronstein, K., Goblirsch, M., Rinkevich, F., & de Guzmann, L. (2018). Gamma irradiation inactivates honey bee fungal, microsporidian, and viral pathogens and parasites. *Journal of Invertebrate Pathology, 153*, 57–64.
Smith DeWall, C. S., & Bhuiya, F. (2007). Outbreaks by the numbers: Fruits and vegetables 1990-2005. *The Centre for Science in the Public Interest*. Available at: http://www.cspinet.info/foodsafety/Produce%20Outbreaks%2028IAFP%20Poster%2007%29.pdf, Accessed date: 15 September 2018.
Sousa, M. J., & Rocha, A. (2018). Skills for disruptive digital business. *Journal of Business Research*. https://doi.org/10.1016/j.jbusres.2017.12.051.
Steris AST (2018). https://www.steris-ast.com/, Accessed date: 28 November 2018.
Tahar, A., Kennedy, A. M., Fitzgerald, R., Clifford, E., & Rowan, N. (2018a). Longitudinal evaluation of the impact of traditional rainbow trout farming on receiving water quality in Ireland. *PeerJ6*, e5281. https://doi.org/10.7717/peerj.5281.
Tahar, A., Tiedeken, E. J., Cummins, E., Clifford, E., & Rowan, N. J. (2017). Development of a semi-quantitative risk assessment model for evaluating environmental threat posed by the three first EU watch-list pharmaceuticals to urban wastewater treatment plants: An Irish case study. *The Science of the Total Environment, 603*, 627–638.
Tahar, A., Tiedeken, E. J., Cummins, E., Clifford, E., & Rowan, N. J. (2018b). Occurrence and geodatabase mapping of three contaminants of emerging concern in receiving water and at effluent from waste water treatment plants – a first review of the situation in the Republic of Ireland. *The Science of the Total Environment, 616–617*, 187–197.
Takeshita, K., Shibato, J., Sameshima, T., Fukunaga, S., Isobe, S., Arihara, K., et al. (2003). Damage of yeast cells induced by pulsed light irradiation. *International Journal of Food Microbiology, 85*, 151–158.
Tiedeken, E. J., Tahar, A., McHugh, B., & Rowan, N. J. (2017). Monitoring, sources, receptors, and control measures in three Euopean Union Watch list substances of emerging concern in receiving water – a 20 year systematic review. *The Science of the*

Total Environment, 574, 1140–1163.
Tomašević, I. (2015). The effect of intense light pulses on the sensory quality and instrumental color of meat from different animal breeds. *Biotechnology in Animal Husbandry, 31*, 273–281.
Toyos, R., McGill, W., & Briscoe, D. (2015). Intense pulsed light treatment for dry eye disease to Meibomian gland dysfunction – a 3 year restrospective study. *Photomechanical Laser Surgery, 33*(1), 41–46.
TrojanUV (2016). http://www.wstg.ie/wp-content/uploads/2016/10/IW_UV_disinfection_workshop_2016.pdf, Accessed date: 27 November 2018.
Uesugi, A. R., Hsu, L. C., Worobo, R. W., & Moraru, C. I. (2016). Gene expression analysis for *Listeria monocytogenes* following exposure to pulsed light and continuous ultraviolet light treatments. *Lebensmittel-Wissenschaft und -Technologie- Food Science and Technology, 68*, 579–588.
Uesugi, A. R., & Moraru, C. I. (2009). Reduction of Listeria on ready-to-eat sausages after exposure to a combination of pulsed light and nisin. *Journal of Food Protection, 72*, 347–353.
Valdéz, A., Cifuentes, A., & León, C. (2017). Foodomics evaluation of bioactive compounds in foods. *Trends in Analytical Chemistry, 96*, 2–13.
Van Impe, J., Smet, C., Tiwari, B., Greiner, R., Oijha, S., & Stulić, V. (2018). State of the art of nonthermal and thermal processing for inactivation of micro-organisms. *Journal of Applied Microbiology, 125*, 16–35. https://doi.org/10.1111/jam.13751.
Vanbergen, A. J., & Insect Pollinators Initiative (2013). Threats to an ecosystem service: Pressures on pollinators. *Frontiers in Ecology and the Environment, 11*, 251–259.
Vimont, A., Fliss, I., & Jean, J. (2015). Efficacy and Mechanisms of Murine Norovirus inhibition by pulsed light technology. *Applied and Environmental Microbiology, 81*, 2950–2957.
Wang, T., MacGregor, S. J., Anderson, J. G., & Woolsey, G. A. (2005). Pulsed ultra-violet inactivation spectrum of *Escherichia coli. Water Research, 39*, 2921–2925.
Wuytack, E. Y., Phuong, L. D., Aertsen, A., Reyns, K. M. F., Marquenie, D., & De Ketelaere, B. (2003). Comparision of sublethal injury induced by different nonthermal treatments. *Journal of Food Protection, 66*, 31–37.
Xu, W., Chen, H., & Wu, C. (2013). Decontamination of *Escherichia coli* O157:H7 on green onions using pulsed light (PL) and PL-surfactant-sanitizer combinations. *International Journal of Food Microbiology, 166*, 102–108.
Xu, C., & Wu, C. (2016). The impact of pulsed light on decontamination, quality and bacterial attachment of fresh raspberries. *Food Microbiology, 57*, 135–143.
Yongfu, S., Liheng, W., Zongtan, S., Kunsheng, W., Liangyan, H., Jian, C., et al. (2017). *Connotation and selection of disruptive technologies that lead industrial change.* Strategic Study of CARhttps://doi.org/10.153302/J-SSCAE-2017.05.002.
Yu, H., Neal, J. A., & Sirat, S. A. (2018). Consumers food safety risk perceptions and willingness to pay for fresh-cut produce with lower risk of foodborne illness. *Food Control, 86*, 83–89.
Zhao, X., Zhong, J., Wei, C., Lin, C.-W., & Ding, T. (2017). Current perspectives on viable but non-culturable state in foodborne pathogens. *Frontiers in Microbiology, 8*, 580. https://doi.org/10.3389/fmi.2017.00580.

Letters in Applied Microbiology 2000, **31**, 110–114

Pulsed electric field inactivation of diarrhoeagenic *Bacillus cereus* through irreversible electroporation

N.J. Rowan[1], S.J. MacGregor[2], J.G. Anderson[1], R.A. Fouracre[2] and O. Farish[2]

Departments of [1]Bioscience and Biotechnology and [2]Electronic and Electrical Engineering, University of Strathclyde, Glasgow, Scotland, UK

118/2000: received 9 February 2000, revised 14 April 2000 and accepted 20 April 2000

N.J. ROWAN, S.J. MACGREGOR, J.G. ANDERSON, R.A. FOURACRE AND O. FARISH. 2000. The physical effects of high-intensity pulsed electric fields (PEF) on the inactivation of diarrhoeagenic *Bacillus cereus* cells suspended in 0·1% peptone water were examined by transmission electron microscopy (TEM). The levels of PEF-induced microbial cell death were determined by enumeration on tryptone soy yeast extract agar and *Bacillus cereus*-selective agar plates. Following exposure to lethal levels of PEF, TEM investigation revealed irreversible cell membrane rupture at a number of locations, with the apparent leakage of intracellular contents. This study provides a clearer understanding of the mechanism of PEF-induced cellular damage, information that is essential for the further optimization of this emerging food-processing technology.

INTRODUCTION

The increasing incidence of reported food-borne illnesses associated with microbial enteropathogens continues to be an increasing problem (Slutsker *et al.* 1998; Rowan 1999). These events have raised major concerns over food safety problems and their impact on public health. Consequently, the control of microbial contamination of foodstuffs has been given the highest priority in these countries. Also, there is growing consumer preference for minimally processed, fresh food produce, and this has increased interest in non-thermal techniques for food safety and food preservation (Gould 1996; Barbosa-Cánovas 1997).

The potential use of high-intensity, pulsed-power techniques, such as pulsed electric field (PEF) treatment, for food processing applications is currently receiving considerable attention since inactivation of micro-organisms takes place under reduced temperature conditions (Gould 1996; Qin *et al.* 1996; Wouters *et al.* 1999). The advantages of such an electrotechnology include the potential retention of fresh food characteristics and organoleptic qualities such as flavour, aroma and texture (Castro *et al.* 1993). Preliminary studies suggest that such treatment represents a promising non-thermal technique that may supplement or replace conventional pasteurization methods (Castro *et al.* 1993; Qin *et al.* 1995, 1996; Liu *et al.* 1997; Wouters *et al.* 1999). PEF treatment involves the application of pulsed electric fields, with a magnitude usually greater than 20 kV cm^{-1}, for short durations (500 ns to 4 μs), to liquid foods or to appropriate solid foods that can be pumped. A number of recent studies have shown that a range of spoilage and pathogenic micro-organisms are susceptible to PEF, with reductions of $\geq 10^6$ organisms ml^{-1} being reported in both laboratory-based culture media and in certain liquid foodstuffs (Castro *et al.* 1993; Qin *et al.* 1996; Wouters *et al.* 1999).

Although this treatment method has significant potential, the underlying mechanisms of microbial inactivation have still to be fully elucidated (Gould 1996; Schoenbach 1997; Wouters *et al.* 1999). The most commonly suggested theory is that of severe electroporation (i.e. the formation of pores in cell membranes by the action of high voltage electric fields), where local instabilities in the membranes of treated micro-organisms are formed by electromechanical compression and electrical field-induced tension (Wouters *et al.* 1999). PEF inactivation via electroporation is believed to be associated with the migration and accumulation of charge across the cell membrane under the action of an applied electric field. It is generally considered that the critical membrane potential, induced by the electric field, that causes microbial inactivation is about 1 V (Sitzmann 1996). At this level it is thought that the permeability of the membrane increases such that cell death occurs (Schoenbach 1997). The breakdown of biological membranes has been extensively studied with such model systems as liposomes, planar bilayers and phospholipid vesicles (Qin *et al.* 1996). There are a number of theories relating to electroporation,

Correspondence to: N.J. Rowan, Department of Bioscience and Biotechnology, University of Strathclyde, Royal College, 204 George Street, Glasgow G1 1XW, Scotland, UK (e-mail: n.j.rowan@strath.ac.uk).

including dielectric breakdown, transmembrane potential-induced compression of the bilayer or cell membrane, induced changes in the viscoelastic properties of the cell membrane, rearrangement of the fluid mosaic arrangements of the lipids and membranes in the cell membrane; structural defects in the membranes, and colloidal osmotic swelling (Qin *et al.* 1996). The objective of the present study was to assess, by means of transmission electron microscopy, the nature and extent of cellular damage caused by the application of lethal levels of high-intensity pulsed-electric fields, to determine whether PEF treatment results in the formation of irreparable pores in the cell membrane of *Bacillus cereus*.

MATERIALS AND METHODS

Bacterial strains and growth media

The diarrhoeagenic strain of *Bacillus cereus* (NCTC 11145, National Collection of Type Cultures, Colindale, UK) was used in this study. Cells were initially grown in 50-ml tryptone soy broth supplemented with 0·6% (w/v) yeast extract (TSYEB) for 24 h at 30 °C with agitation (125 rev min^{-1}). A 1-ml sample of a 10^{-5} dilution was transferred to fresh 50-ml TSYEB (giving a starting cell population of $\sim 10^3$ cells ml^{-1}), and incubated at 125 rev min^{-1} for 6 h at 30 °C to obtain vegetative cells in the mid-exponential growing phase. Cells were pelleted by centrifugation (3000 *g* for 10 min at 4 °C), washed twice in phosphate-buffered saline (PBS) and resuspended in 0·1% (w/v) peptone water to a cell density of $\sim 10^8$ cells ml^{-1} before transfer to the PEF treatment chamber. The absence of bacterial endospores was confirmed by spore staining of triplicate samples and by heating at 80 °C for 15 min prior to enumeration on TSYEA plates. Stored bacteria were kept at −70 °C in PBS with 20% glycerol (v/v) until used.

Pulsed electric field (PEF) treatment of *Bacillus cereus*

The test cells, suspended in 0·1% peptone water, were subjected to high intensity pulsed electric fields. A 100-kV Glassman high voltage DC generator was used to charge a coaxial cable Blumlein pulse generator through a charging resistance of 10 MΩ. The coaxial cable generator was constructed from 100 m of URM67, 40-kV cable. The high voltage output pulse from the generator was 500 ns in duration, and the generator had an output impedance of 100 Ω, a switching impedance of 50 Ω, and an open circuit gain of 2. The generator was wound inductively on a 30-cm diameter former in order to minimize secondary transmission line losses. The electrical circuit layout is shown schematically in Fig. 1 and the charging circuit was arranged to ensure that the generator charging currents did not flow through the test cells.

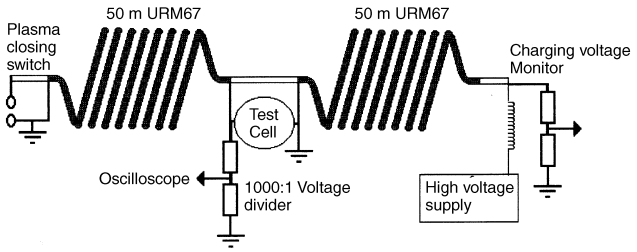

Fig. 1 The electrical circuit layout for PEF treatment

The pulse generator was charged from one end of the cable, and was fired by switching the inner conductor to ground at the opposite end. Although both sides of the test chamber were earthed, the output from the cable generator, which was connected to one side of the test chamber, was transiently decoupled from earth during application of the voltage pulse. The Blumlein generator was fired by a triggered corona stabilized switch. For the present study, the pulse repetition frequency was limited to a maximum value of 5–10 pulses per second in order to ensure that there were no thermal inactivation effects associated with the energy dissipation in the test chamber. The output pulse from the generator was monitored throughout the experiments with a 1000 : 1, Tektronix high voltage probe. The voltage pulse profile used for PEF treatment, measured across the test cell, is shown in Fig. 2.

Test samples of *Bacillus cereus* were subjected to a pulsed electric field at a level of ~ 30 kV cm^{-1} in a uniform-field static test cell. The volume of the test cell was 30 ml and samples of a predetermined cell number were subjected to a range of pulses from 500 to 6000 pulses. A forced air cooling system was used to maintain the test chamber temperature between 25 and 30 °C. A thermocouple was employed throughout the studies in order to verify the temperature of the treated liquid. The levels of microbial inactivation and cell integrity (examined by transmission electron microscopy) were assessed post PEF-treatment. Surviving organisms were enumerated with both the pour and spiral plating techniques on TSYEA and on *Bacillus cereus*-selective agar (BCSA, Oxoid) plates.

Transmission electron microscopy

Bacillus cereus cells treated by PEF were washed twice with PBS and resuspended in sterile-distilled water before application to formvar-coated grids. After the grid was dried, one drop of a solution containing 3% (v/v) tungstopho-

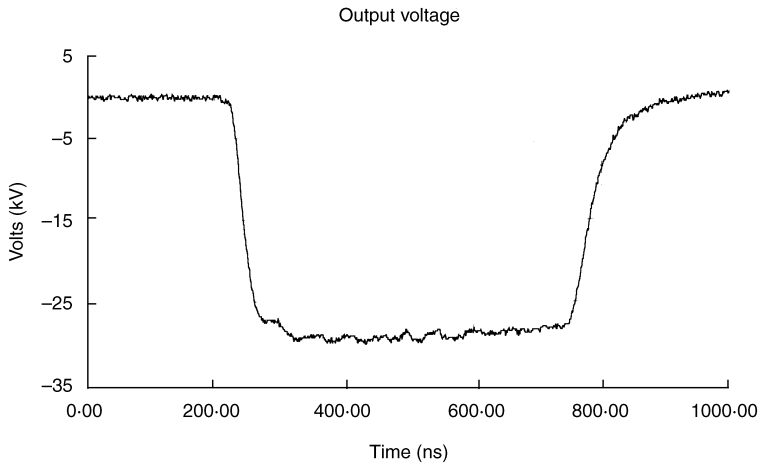

Fig. 2 Measured output pulse waveform applied to the test cell for PEF treatment

sphoric acid and 0·3% (v/v) sucrose (pH 6·8–7·4) was added. The solution was removed after 30–60 s, and the grid was dried and examined on a Zeiss 902 transmission electron microscope.

Statistical analysis

All of the experiments in this study were performed in triplicate and results are reported as averages. Significant differences in the PEF treatment results were calculated at the 95% confidence interval using analysis of variance (one way) with Minitab software Release 11 (Mintab Inc., State College, PA, USA).

RESULTS AND DISCUSSION

The results described in Table 1 show the effect of applying up to 6000 pulses to populations of *B. cereus* with cell survivors enumerated on TSYEA and BCSA plates. A 5·5–6 log order reduction was achieved following the maximum treatment of 6000 pulses. In both sets of cell survivor data, the inactivation was similar and the population reduction increased with the greater the number of pulses applied. The BCSA enumerated data is also observed to be consistently lower than that of the TSYEA data for treatments of 1000 pulses and more. This difference in recovery is possibly due to the added stress of dyes and antibiotics in the selective plating medium (Rowan and Anderson 1998; Rowan 1999).

Transmission electron microscopy (TEM) of untreated (Fig. 3a) and PEF-treated (Fig. 3b) *B. cereus* cells was carried out after 6000 pulses at 30 kV cm^{-1}. TEM results from PEF-treated cells revealed that there was rupture of the cell wall (CW) with irreversible electroporation of the cell membrane with leakage of the intracellular contents or cellular debris (CD) (Fig. 3b). It is significant that PEF-induced pore formation (PF) in the cell envelope was observed at several locations along the length of this rod-shaped bacterium, as well as occurring at the extremities of the rod. In addition to the loss of cytoplasmic and nuclear material by disintegration of the cell envelope (indicated in Fig. 3b as CD). This shrinkage pattern (indicated by → in Fig. 3b) suggests leakage of cytoplasmic and nuclear material from the cell. It is clear that not all PEF-treated bacteria have had their cell wall ruptured, as evident by the presence of an intact *B. cereus* (IBC) cell in this figure, although this should not be interpreted as indicating a viable cell. This observation is in general agreement with

Table 1 Survival data for PEF-treated *Bacillus cereus* cells enumerated on TSYEA and BCSA plates

Number of PEF pulses	Number of cell survivors*		Significance $P < 0·050$
TSYEA†	BCSA†		
0	8·69 (± 0·2)	8·55 (± 0·2)	No
500	7·15 (± 0·2)	6·91 (± 0·3)	No
1000	6·21 (± 0·3)	5·75 (± 0·2)	Yes
3000	5·61 (± 0·3)	4·89 (± 0·3)	Yes
6000	3·25 (± 0·3)	2·44 (± 0·4)	Yes

*Measured as $\log_{10}$ cfu ml^{-1}, where counts were averages of three replicate trials.
†Numbers in parenthesis refer to variation about the mean.

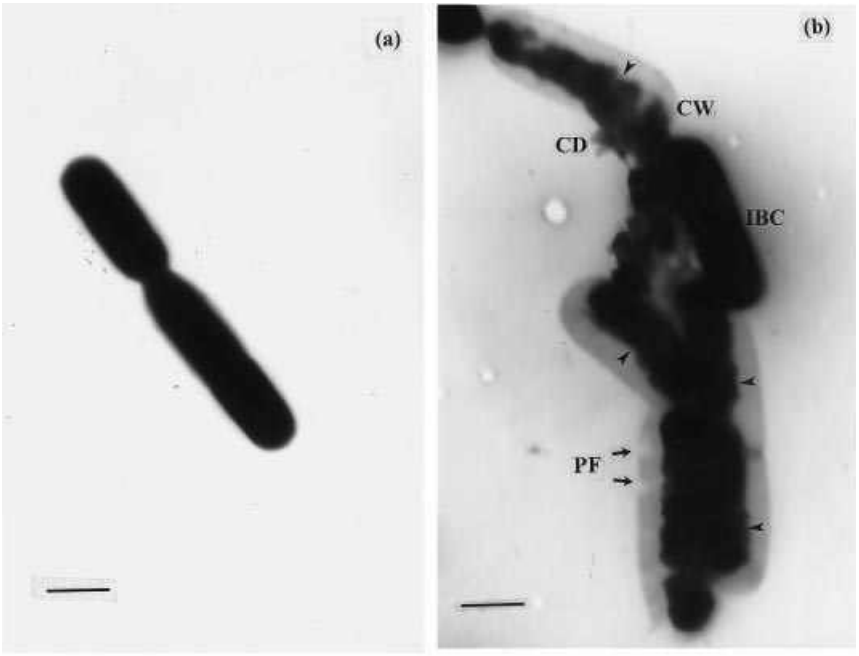

Fig. 3 TEM of untreated (a) and PEF-treated (b) cells of *Bacillus cereus*. Bar, 1·5 μm. CW, cell wall; CD, cellular debris; PF, PEF-induced pore formation; IBC, intact *B. cereus*. Arrowheads (→) indicate shrinkage pattern

the survival data for PEF-treated *B. cereus* shown in Table 1.

The TEM results did reveal some relatively minor shrinkage of the cytoplasmic membrane away from the outer membrane in the treated bacterial cells. There was no visual evidence of any partial or complete disintegration of the cell envelope in these PEF treated organisms. Cells of *Escherichia coli* (ATCC) and *Staphylococcus aureus* (ATCC 6538) suspended in simulated milk ultrafiltrate (SMUF), were observed with scanning (SEM) and transmission (TEM) electron microscopy following electric field treatment at 60 kV cm^{-1}. However, the SEM technique did not indicate any significant differences between PEF-treated and untreated *E. coli* and *Staph. aureus* cells (cited in Barbosa-Cánovas 1997). The TEM results presented here with *B. cereus* are in agreement with the findings of Harrison (1997), who showed that PEF inactivation of the food spoilage yeast *Saccharomyces cerevisiae* (ATCC 16664) occurs by cell envelope rupture and loss of intracellular contents.

In conclusion, studies have been carried out with a simple buffered system that have permitted an assessment to be made on the influence of PEF on the integrity of bacterial cells by TEM. PEF inactivation of diarrhoeagenic *B. cereus* occurs through irreversible electroporation, and causes cell death. The TEM results showed that PEF-induced pore formation occurred randomly in these rod-shaped bacterial cells, resulting in a large-scale leakage of cytoplasmic and nuclear material. This study has provided a clear understanding of the mechanism of PEF-induced lethality in micro-organisms, information that is required in order to allow optimization of this electrotechnology and to help satisfy the regulatory requirements associated with the introduction of such a novel food-processing technology.

ACKNOWLEDGEMENTS

The authors would like to thank D. Cameron, Y. Koutsoubis, A. Dick and D. McLaughlin (University of Strathclyde) for their assistance with this study.

REFERENCES

Barbosa-Cánovas, G.V. (1997) Biological effects and applications of pulsed electric fields for the preservation of foods. In *Nonthermal Preservation of Foods* ed. Barbosa-Cánovas, G.V. pp. 73–112. New York, NY: Marcell Dekker Publishers.

Castro, A.J., Barbosa-Cánovas, G.V. and Swanson, B.G. (1993) Microbial inactivation of foods by pulsed electric fields. *Journal of Food Processing and Preservation* **17**, 47–73.

Gould, G.W. (1996). *New Methods of Food Preservation* ed. Gould, G.W. London: Chapman & Hall Publishers.

Harrison, S.L. (1997) High voltage pulsed electric field induced structural changes and inactivation of *Saccharomyces cerevisiae*. PhD Thesis. Washington State University, USA.

Liu, X., Yousef, A.E. and Chism, G.W. (1997) Inactivation of *Escherichia coli* O157: H7 by the combination of organic acids and pulsed electric fields. *Journal of Food Safety* **16**, 287–299.

Qin, B.-L., Pothakamury, U.R., Vega, H., Barbosa-Cánovas, G.V. and Swanson, B.G. (1996) Nonthermal pasteurisation of liquid foods using high-intensity pulsed electric fields. *Critical Reviews in Food Science and Nutrition* **36**, 603–627.

Qin, B.-L., Pothakamury, U.R., Vega, H., Martín, O., Barbosa-Cánovas, G.V. and Swanson, B.G. (1995) Food pasteurization using high-intensity pulsed electric fields. *Food Technology* **55**, 55–60.

Rowan, N.J. (1999) Evidence that inimical food preservation barriers alters microbial resistance, cell morphology and virulence. *Trends in Food Science and Technology* **10**, 261–270.

Rowan, N.J. and Anderson, J.G. (1998) Effects of above-optimum growth temperature and cell morphology on thermotolerance of *Listeria monocytogenes* cells suspended in bovine milk. *Applied and Environmental Microbiology* **64**, 2065–2071.

Schoenbach, K.H. (1997) The effect of pulsed electric fields on biological cells: experiments and applications. *IEEE Transactions on Plasma Science* **25**, 284–293.

Sitzmann, W. (1996) High voltage pulse techniques for food preservation. In *New Methods of Food Preservation* ed. Gould, G.W. pp. 237–252. London: Chapman & Hall Publishers.

Slutsker, L., Alterkruse, S.F. and Swerdlow, D.L. (1998) Foodborne diseases: emerging pathogens and trends. *Emerging Infectious Diseases* **12**, 199–218.

Wouters, P.C., Dutreux, N., Smelt, J.P.P.M. and Lelieveld, H.L.M. (1999) Effects of pulsed electric fields on inactivation kinetics of *Listeria innocua*. *Applied and Environmental Microbiology* **65**, 5364–5371.

Letters in Applied Microbiology 2004, **39,** 246–251 doi:10.1111/j.1472-765X.2004.01571.x

Use of a fluorescent viability stain to assess lethal and sublethal injury in food-borne bacteria exposed to high-intensity pulsed electric fields

S. Yaqub[1], J.G. Anderson[1], S.J. MacGregor[2] and N.J. Rowan[3]

Departments of [1]Bioscience, and [2]Electronic & Electrical Engineering, University of Strathclyde, Glasgow, UK, and [3]School of Biological Science, Dublin Institute of Technology, Dublin, Ireland

2004/0161: received 13 February 2004, received 19 May 2004 and accepted 20 May 2004

ABSTRACT

S. YAQUB, J.G. ANDERSON, S.J. MACGREGOR AND N.J. ROWAN. 2004.

Aims: To apply scanning electron microscopy, image analysis and a fluorescent viability stain to assess lethal and sublethal in food-borne bacteria exposed to high-intensity pulsed electric fields (PEF).

Methods and Results: A rapid cellular staining method using the fluorescent redox probes 5-cyano-2,3-ditolyl tetrazolium chloride (CTC) and 4′,6-diamidino-2-phylindole was used for enumerating actively respiring cells of *Listeria mononcytogenes*, *Bacillus cereus* and *Escherichia coli*. This respiratory staining (RS) approach provided good agreement with the conventional plate count agar method for enumerating untreated and high-intensity PEF-treated bacteria suspended in 0.1% (w/v) peptone water. However, test organisms subjected to similar levels of lethality by heating at 56°C resulted in *ca* 3-log-unit difference in surviving cell numbers ml^{-1} when enumerated by these different viability indicators. PEF-treated bacteria were markedly altered at the cellular level when examined by scanning electron microscopy.

Conclusions: While PEF-treatment did not produce sublethally injured cells ($P < 0.05$), substantial subpopulations of test bacteria rendered incapable of forming colonies by heating may remain metabolically active.

Significance and Impact of the Study: The fluorescent staining method offers interesting perspectives on assessing established and novel microbial inactivation methods. Use of this approach may also provide a better understanding of the mechanisms involved in microbial inactivation induced by PEF.

Keywords: fluorescent metabolic probes, microbial inactivation, pulsed electric fields, scanning electron microscopy, sublethal injury.

INTRODUCTION

The potential to utilize high intensity, pulsed electric field (PEF) technology for food processing applications is currently receiving considerable attention as this electro-technology may significantly improve the quality of certain liquid food products (Heinz *et al.* 2001; Wouters *et al.* 2001). As an emerging nonthermal food preservation method, PEF pasteurization is of interest to the food industry as this treatment technology has the potential to retain the organoleptic and nutritive properties that are characteristic of fresh food products. PEF treatment involves the application of PEF with a magnitude usually greater than 20 kV cm^{-1}, for very short durations (500 ns to 4 μs), to liquid foods (MacGregor *et al.* 2000; Heinz *et al.* 2001). Numerous research groups have demonstrated the biocidal potential of PEF, having shown that a wide range of food spoilage and pathogenic micro-organisms can be inactivated in test liquids and in various food products (MacGregor *et al.* 2000; Heinz *et al.* 2001; Wouters *et al.* 2001). Whilst the mechanism(s) underlying the inactivation

Correspondence to: N.J. Rowan, School of Biological Science, Dublin Institute of Technology Kevin Street, Dublin 8, Ireland (e-mail: neil.rowan@dit.ie).

of micro-organisms by PEF remains to be fully elucidated, the most commonly suggested theory is that of severe electroporation (i.e. the formation of pores in cell membranes by the action of high voltage electric-fields) (Wouters *et al.* 2001). Despite intensive scientific and developmental interests in PEF-technology, very little research has been directed towards gaining a better understanding of the recovery processes associated with sublethally injured micro-organisms after PEF treatment: previous studies have relied heavily on enumerating microbial survivors using conventional plate count agar techniques.

In this study, image analysis and the novel fluorescent redox probe 5-cyano-2,3-ditolyl tetrazolium chloride (CTC) were used to investigate respiratory activity in *Listeria monocytogenes*, *Bacillus cereus* and *Escherichia coli* cells that were exposed to separate PEF and heat treatments. In particular, enumeration of PEF and heat-injured cells by respiratory staining was compared with similarly treated samples that were enumerated by the conventional plate count agar method. Here, we report that the former epifluorescence approach offers a rapid and quantitative assay for determining the extent of sublethal cellular injury in heat and PEF-treated food-borne bacteria.

MATERIALS AND METHODS

Bacterial strains used

Listeria monocytogenes (NCTC 11994), the diarrhoeagenic strain of *B. cereus* (NCTC 11145), and *E. coli* (NCTC 9001) used in this study were obtained from the National Collection of Type Cultures (Public Health Laboratory Service, Colindale, UK). Cells were initially grown in 50-ml typtone soya broth supplemented with 0·6% yeast extract (TSYEB) for 24 h at 37°C with agitation (125 rev min^{-1}). Following this, a 1-ml sample of the 10^{-5} dilution was transferred to fresh 50-ml TSYEB (giving a starting cell population of *ca* 10^3 cells ml^{-1}), and was incubated at 125 rev min^{-1} for 6 h at 37°C to obtain vegetative cells in the mid-exponential growing phase. Cells were pelleted by centrifugation (3000 *g* for 10 min at 4°C), and were washed three times and resuspended in 0·1% (w/v) peptone water to yield a suspension of 10^7 CFU of test organisms ml^{-1} (determined spectrophotometrically at 540 nm, model UV-120-02 instrument; Shimadzu Corp., Kyoto, Japan) before transfer to the PEF treatment chamber. The absence of bacterial endospores was confirmed by spore-staining of triplicate samples of *B. cereus* and by heating at 80°C for 15 min prior to enumeration on TSYEA plates. Stored bacteria were kept at −70°C in phosphate-buffered saline (PBS) with 20% glycerol (v/v) until used.

PEF treatment of test bacteria

Test bacteria were suspended in 30 ml of 0·1% (w/v) peptone water and were subjected to high voltage, PEF (*ca* 30 kV cm^{-1}) in a circulated, closed-loop system. This comprised a holding reservoir, treatment chamber, interconnections, and peristaltic pump as described previously, with modifications (MacGregor *et al.* 2000). The flow rate of the system was 200 ml min^{-1}, the volume of the system was *ca* 100 ml, and the test or treatment chamber volume was 30 ml. The test chamber consisted of a disk of 10 mm Perspex (SamTech Ltd, Glasgow, UK), with a central hole cut through it to hold the 30 ml volume of sample. Two separate channels were drilled from the outer edge of the Perspex to the central hole, thus allowing for syringe injection and removal of samples. Flat brass plates were fitted on both sides of the central hole, which formed the electrodes of the test chamber. Predetermined cell populations were treated with 7000–8000 pulses at 25°C (in order to achieve *ca* 5 log reduction in CFU of test bacteria ml^{-1} as determined by the conventional plate count method), at a pulse repetition frequency that was limited to 5 pulses per second in order to ensure that there were no thermal inactivation effects associated with the energy dissipation in the test chamber. It should be noted, the PEF system was not optimized for inactivation of test bacteria. The test chamber was immersed in a circulating constant temperature water bath (model HE30; Grant Instruments Ltd, Cambridge, UK) equipped with a thermoregulator capable of maintaining temperature to within ±0·05°C (model TE-8A; Techne Ltd, Cambridge, UK) to maintain the desired treatment temperatures at 25°C. A thermocouple was also employed throughout the studies in order to verify the temperature of the treated liquid. A 100-kV high voltage DC generator (Glassman EH50R02; Glassmann Europe Ltd, Hampshire, UK) was used to charge a co-axial cable Blumlein pulse generator (Type TLG B-01, Samtech Ltd, Glasgow, UK) through a charging resistance of 10 MΩ. The co-axial cable generator was constructed from 100 m of URM67, 40 kV cable (Samtech).

The high voltage output pulse from the generator was 500 ns in duration, and the generator had an output impedance of 100 Ω, a switching impedance of 50 Ω, and an open circuit gain of two. The generator was wound inductively on a 30-cm diameter former in order to minimize secondary transmission line losses. The electrical and charging circuits were arranged to ensure that the generator charging currents did not flow through the test cells. The pulse generator was charged from one end of the cable, and was fired by switching the inner conductor to ground at the opposite end. Although both sides of the test chamber were earthed, the output from the cable generator, which was connected to one side of the test chamber, was

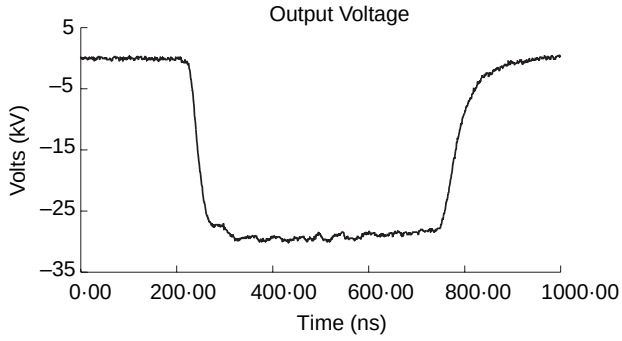

Fig. 1 Measured output pulse waveform applied to the test chamber for PEF treatment

transiently de-coupled from earth during application of the voltage pulse. The Blumlein generator was fired using a triggered corona stabilized switch. The output pulse from the generator was monitored throughout the experiments using a 1000 : 1, Tektronix high voltage probe (Tektronix P6015A; Imex Ltd, Coatbridge, UK). The voltage pulse profile used for PEF treatment, measured across the test cell, is shown in Fig. 1. Recovery of surviving populations (log CFU of test bacteria ml^{-1}), was determined for experimental and control suspensions and dilutions thereof by spread and spiral plating samples (model B; Sprial Systems Inc., Shipley, UK) onto TSYEA agar (Oxoid) plates; these were incubated for 48 h at 37°C before enumeration.

The test bacteria, *L. monocytogenes*, *B. cereus* and *E. coli* were also subjected to heating at 56°C in order to achieve a similar level of inactivation (*ca* 5-log units in CFU ml^{-1}) to that obtained by PEF treatment, according to methods described previously (Rowan and Anderson 1998). Test bacteria were suspended in 1·9 ml of preheated 0·1% (w/v) peptone water to a density of *ca* 10^7 CFU ml^{-1} in 3-ml shrimp cap glass vials (Phase Separations Ltd, Watford, Hertfordshire, UK). The vials were sealed and kept below the level of a circulating constant temperature water bath (model HE30; Grant Instruments Ltd) equipped with a thermoregulator capable of maintaining temperature to within ±0·05°C (model TE-8A; Techne Ltd). The vials were sealed and kept 4 cm below the level in the water bath for the treatment period. Recovery and enumeration of surviving populations of the test bacteria were performed as mentioned above.

Use of image analysis, fluorescent redox probes and conventional plating counting method to enumerate cell numbers after heating and PEF treatment

Image analysis and the fluorescent redox probes CTC and 4′,6-diamidino-2-phylindole (DAPI) were used to investigate cellular activity in the test bacteria according to previously described procedures, with modifications (Rodriguez *et al.* 1992; Gavin *et al.* 2000). One-millilitre cell suspensions were harvested by centrifugation (4°C for 10 min at 3000 *g*) and washed three times with 0·1 M phosphate-buffered saline (PBS). Experimental (i.e. PEF and heat-treated samples) and control preparations, and dilutions thereof, were resuspended in 300 μl of 5 mM CTC (Polysciences, Inc, St Louis, MO, USA) and were incubated for 1 h in the dark at 20°C with agitation (200 rev min^{-1}). CTC is readily reduced to insoluble, highly fluorescent and intracellularly accumulated CTC-formazon, through bacterial respiration. After incubation, experimental and control preparations, and dilutions thereof, were counterstained for 8 min at 20°C with 5 μg of DAPI ml^{-1} (Sigma, St Louis, MO, USA) and were enumerated using methods described previously with modifications (Besnard *et al.* 2000; Gavin *et al.* 2000). Counterstaining with the DNA-binding DAPI allowed concurrent determinations of total (i.e. viable plus nonviable) bacteria and viable (i.e. only cells exhibiting red CTC-formazan fluorescence) bacteria. Epifluorescence observations of CTC-treated preparations were microscopically examined (Nikon Optiphot microscope, Tokyo, Japan) using a blue 420–480-nm excitation filter (combined with a 580-nm dichroic mirror and a 590-nm barrier filter), where eight to 10 fields were counted at a magnification of ×1,000 (expressed in terms of $\log_{10}$ number of corresponding bacteria ml^{-1} of sample). CTC- and DAPI-strained bacteria in the same preparation were also viewed and counted simultaneously with a 365-nm-excitation filter, and emission filter and a 400-nm cutoff filter. Stained cells were distinguished from nonspecific reactions by overlaying the fluorescence and phase-contrast images. The image analysis system comprised a Sony charge-coupled device camera and a Seescan Solitaire image analyser (both Seescan Ltd, Cambridge, UK) with archiving to hard disk. Direct microscopic counts of bacterial suspensions were also carried out by using bright-field microscopy and Thoma counting chamber preparations (Gunasekera *et al.* 2002).

Assessment of PEF-treated bacteria for cellular damage by using scanning electron microscopy

PEF-treated samples were examined visually for cellular damage by using scanning electron microscopy where test bacteria were resuspended for 1 h in 0·1 M phosphate buffer containing 2·5% gluteraldehyde. Fixed cells were subjected to three 5-min washes in 0·1 M phosphate buffer containing 2% (w/v) glucose and were stained for 1 h using 1% osmium tetroxide. Samples were rinsed three times in sterile distilled water and were then treated in the dark for 1 h with 0·5% aqueous uranyl acetate. Samples were then placed on 0·2 μm polycarbonate filters and dehydrated using 10-min

immersions in an increasing series of acetone (30, 50, 70 and 90%, and absolute). Samples were left submerged in dried absolute acetone overnight before transfer to critical point dryer for 1·5 h where the liquid CO_2 was changed every 15 min. Samples were then mounted on carbon double side tape and gold coated using a scanning electron microscopy coating system (Polaran SC515; Quorum Technologies, Newhaven, UK). Samples were viewed using a Philips 500 scanning electron microscope (Eindhoven, the Netherlands).

Statistical analysis

All of the experiments in this study were performed in triplicate, and results are reported as averages. Significant differences in the experimental (heating and PEF treatment) and untreated control results were calculated at the 95% confidence interval using analysis of variance (oneway) with Minitab software Release 11 (Minitab Inc., State College, PA, USA).

RESULTS AND DISCUSSION

Thermal treatment or holding times required to achieve 5 log reductions in cell populations for *L. monocytogenes*, *B. cereus* and *E. coli* at 56°C were 44, 38 and 42 min, respectively. This corresponded to $D_{56°C}$ values (decimal reduction time: the time required to kill a 1-log unit concentration of bacteria) of 8·8, 7·6 and 8·4 min, respectively (data not shown). Good agreement was obtained between the CTC-fluorescence or respiratory staining (RS) method and the conventional plate count agar (PC) method for enumerating untreated cell populations of test bacteria ($P < 0·05$) (Table 1). The PC method demonstrated that heat-treated samples of *L. monocytogenes*, *B. cereus* and *E. coli* were reduced by 5·2, 5·3 and 5·3 log CFU ml^{-1}, respectively: this markedly contrasted with reductions of 2·6, 3·0 and 2·2 log cell numbers of actively respiring bacteria ml^{-1} as determined by the rapid RS ($P < 0·05$) (Table 1). However, no significant difference was observed between conventional PC and rapid RS methods after enumerating PEF-treated *L. monocytogenes*, *B. cereus* and *E. coli* cell populations ($P < 0·05$) (Table 1). Results showed that the 4·2, 5·1, and 3·7 log unit reductions recorded by the PC method for the respective PEF-treated bacteria were similar to that of the respective 3·9, 4·6, and 3·2 log unit reductions determined by the rapid RS approach ($P < 0·05$) (Table 1). While *L. monocytogenes* and *E. coli* appeared equally heat and PEF tolerant, the larger *B. cereus* cells were more susceptible to the lethal action of both PEF treatment. The latter finding is in agreement with other researchers, where larger microbial cells such as yeast are more susceptible to irreversible electroporation (Heinz *et al.* 2001; Wouters *et al.* 2001). Use of image analysis and respiratory staining showed that the PC method did not significantly underestimate the numbers of cell survivors after PEF treatment, which markedly contrasted with the *ca* 3-log unit difference in surviving cell populations that had been heated. The latter results agree with the recent findings of Gunasekera *et al.* (2002), where these researchers used *de novo* expression of a *gfp* reporter gene and membrane integrity based on propidium iodide exclusion as viability indicators to show that a substantial portion of *E. coli* and *Pseudomonas putida* cells in heat-treated milk are metabolically active but are incapable of forming colonies.

Use of fluorescent redox probes for direct visualization of actively respiring bacteria is gaining in popularity amongst research groups investigating the viable but not culturable (VBNC) phenomenon (i.e. stress-injured bacteria which are not capable of the cellular division required for growth in the usual culture media, but, yet remain physically active for several metabolic functions) in food and water-borne bacteria (Besnard *et al.* 2000; Caruso *et al.* 2003). There is increasing evidence for the existence of a VBNC state in microbes, particularly in the stressed environment presented by modern foods with their varied pretreatment and packaging strategies (Rowan 1999). In particular, use has been made of CTC as a metabolic staining technique for reporting the possible existence of VBNC states in *Micrococcus luteus* (Kaprelyants and Kell 1993), *L. monocytogenes* (Besnard *et al.* 2000) and in *E. coli* (Caruso *et al.* 2003): CTC reduction reflects the presence of a functional electron transport (i.e. respiratory) system in the microbial cell

Table 1 Enumeration of *Listeria monocytogenes*, *Bacillus cereus* and *Escherichia coli* cell numbers by respiratory staining (RS) and CFU by conventional plate counting (PC) after heating or PEF treatment

	Log CFU or cell numbers ml^{-1}					
Test bacteria	Untreated (PC)	Untreated (RS)	Heat (PC)	Heat (RS)	PEF (PC)	PEF (RS)
L. monocytogenes	7·3 (±0·2)^{A}	7·5 (±0·3)^{A}	2·1 (±0·3)^{D}	4·9 (±0·3)^{B}	3·1 (±0·5)^{C}	3·6 (±0·4)^{C}
B. cereus	7·1 (±0·2)^{A}	7·0 (±0·1)^{A}	1·9 (±0·4)^{D}	4·8 (±0·4)^{B}	2·0 (±0·5)^{D}	2·4 (±0·3)^{D}
E. coli	6·8 (±0·3)^{A}	7·3 (±0·3)^{A}	1·4 (±0·6)^{D}	3·5 (±0·3)^{C}	1·7 (±0·3)^{D}	2·1 (±0·5)^{D}

Values followed by the same upper case letter in separate columns do not significantly differ at the 95% confidence intervals ($P < 0·05$).

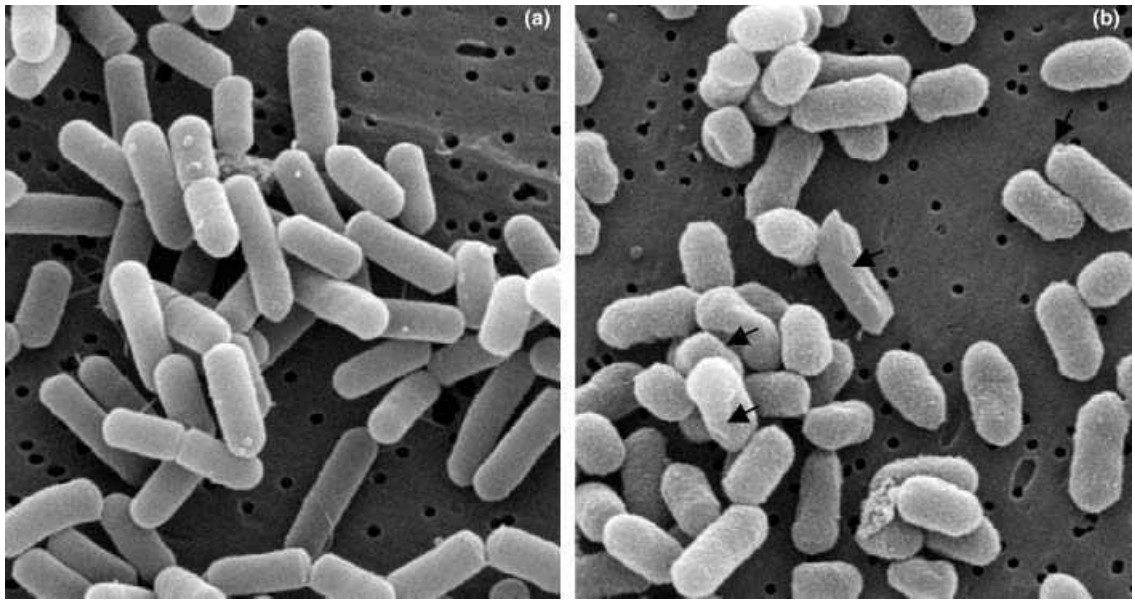

Fig. 2 Scanning electron micrographs of untreated (a) and PEF-treated (b) *Escherichia coli* cells, where arrows indicate points at which significant cellular damage may have occurred. Magnification ×12 000

membrane where insoluble fluorescent CTC-formazan crystals accumulate in metabolically active bacteria in a time-dependent manner. This present study has provided evidence that a significant portion of *L. monocytogenes*, *B. cereus* and *E. coli* cells that are rendered incapable of forming colonies by heat or PEF treatments are metabolically active. These results demonstrate the possible existence of a viable but nonculturable (VBNC) state in vegetative cells of *B. cereus* that has not been reported previously. There is compelling evidence that bacteria in a VBNC state may, in suitable conditions, regain the ability to grow and/or produce toxins that can be pathological to those consuming the food (Booth 1998; Rowan 1999). Results presented previously suggest that this seemingly anomalous situation may result from damage caused by exposure of stress-damaged bacteria to the nutrient-rich conditions in conventional media where this artificial nutritious environment may lead to a decoupling of microbial catabolic and anabolic processes (i.e. some stressed-injured bacterial cells are unable to cope metabolically with nutritious growth media and die through oxidative suicide) (Booth 1998; Rowan 1999). Alternatively, it has been reported that the VBNC state may be a survival mechanism adopted by bacteria when exposed to adverse environmental conditions (Jones *et al.* 1991).

Although there has been considerable research on the design and operation of PEF systems, much less is known about the different types of sublethal damage that PEF exerts on microbial cells (Heinz *et al.* 2001). Whilst the mechanisms underlying the inactivation of micro-organisms by PEF has yet to be fully elucidated, it is generally considered that the formation of irreversible pores in the cell membrane by strong electric fields (i.e. electropermeabilization) contributes significantly to cell death (Rowan *et al.* 2000; Heinz *et al.* 2001). Findings from scanning electron microscopy studies revealed that a significant proportion of PEF-treated bacteria were altered at the cellular level (Fig. 2), where arrows indicate areas of significant cellular damage. While the scanning electron micrographs revealed cellular change as a consequence of exposure to a high intensity electric field (Fig. 2), these images alone do not provide conclusively that irreversible damage occurred. However, when the latter findings are considered in conjunction with the fluorescent CTC-staining data, it is the likely that a single lethal injury (such as electropermeabilization), rather than multiple injuries (associated with thermal inactivation), was responsible for cell death in PEF-treated bacteria. Future use of additional vitality indicator stains such as propidium iodide (Caruso *et al.* 2003), which assesses microbial membrane integrity, may further enhance the accuracy and reliability of metabolic stains in determining the viability status of problematic bacteria in different environments.

In conclusion, results from the present study demonstrate the usefulness of CTC for rapid detection and quantification of actively respiring bacteria that have been subjected to biocidal treatments. The fluorescent staining method offers interesting perspectives on assessing established and novel microbial inactivation methods, particularly when the differentiation between dead and living cells is required for a more precise assessment of treatment or processing efficiency and bacteriological quality. Use of this approach may

also provide a better understanding of the mechanisms involved in microbial inactivation induced by PEF, as well as determining the critical factors influencing inactivation, developing better PEF equipment, and defining the conditions to inactivate micro-organisms in food without over-processing the product.

ACKNOWLEDGEMENTS

We thank Andrew Dick and Douglas Cameron for their excellent technical assistance in conducting these experiments.

REFERENCES

Besnard, V., Federighi, M. and Cappelier, J.M. (2000) Evidence of viable but non-culturable state in *Listeria monocytogenes* by direct viable count and CTC-DAPI double staining. *Food Microbiology* **17**, 697–704.

Booth, I.R. (1998) The bacteria strike back. *The Biochemist* (April), 1–8.

Caruso, G., Mancuso, C.M. and Crisafi, E. (2003) Combined fluorescent antibody assay and viability staining for the assessment of the physiological states of *Escherichia coli* in seawaters. *Journal of Applied Microbiology* **95**, 225–231.

Gavin, J., Button, N.F., Watson-Craik, I.A. and Logan, N.A. (2000) Observation of soft contact lens disinfection with fluorescent metabolic stains. *Applied and Environmental Microbiology* **66**, 874–875.

Gunasekera, T.S., Sørensen, A., Attfield, P., Sørensen, S.J. and Duncan, A.V. (2002) Inducible gene expression by non-culturable bacteria in milk after pasteurisation. *Applied and Environmental Microbiology* **68**, 1988–1993.

Heinz, V., Alvarez, I., Angerbach, A. and Knorr, D. (2001) Preservation of liquid foods by high intensity pulsed electric fields – basic concepts for process design. *Trends in Food Science and Technology* **12**, 103–111.

Jones, M., Sutcliffe, E.M. and Curry, M. (1991) Recovery of viable but non-culturable forms of *Campylobacter jejuni*. *Journal of General Microbiology* **137**, 2477–2482.

Kaprelyants, A. and Kell, D.B. (1993) The use of 5-cyano-2,3-ditolyl tetrazolium chloride and flow cytometry for the visualization of respiratory activity in individual cells of *Micrococcus luteus*. *Journal of Microbiological Methods* **17**, 115–122.

MacGregor, S.J., Farish, O., Fouracre, R., Anderson, J.G. and Rowan, N.J. (2000) Inactivation of pathogenic and spoilage microorganisms in a test liquid using pulsed electric fields. *IEEE Transactions in Plasma Science* **28**, 144–149.

Rodriguez, G.G., Phipps, D., Ishiguro, K. and Ridgway, H.F. (1992) Use of a fluorescent redox probe for direct visualisation of actively respiring bacteria. *Applied and Environmental Microbiology* **58**, 1801–1808.

Rowan, N.J. (1999) Evidence that inimical food-preservation barriers alter microbial resistance, cell morphology and virulence. *Trends in Food Science and Technology* **10**, 261–270.

Rowan, N.J. and Anderson, J.G. (1998) Effects of above-optimum growth temperature and cell morphology on thermotolerance of *Listeria monocytogenes* cells suspended in bovine milk. *Applied and Environmental Microbiology* **64**, 2065–2071.

Rowan, N.J., MacGregor, S.J., Anderson, J.G., Fouracre, R.A. and Farish, O. (2000) Pulsed electric field inactivation of diarrhoeagenic *Bacillus cereus* through irreversible electroporation. *Letters in Applied Microbiology* **31**, 110–114.

Wouters, P.C., Alvarez, I. and Raso, J. (2001) Critical factors determining inactivation kinetics by pulsed electric field food processing. *Trends in Food Science and Technology* **12**, 112–121.

Pulsed Electric Field Inactivation of Spoilage Microorganisms in Alcoholic Beverages

JOSEPH R. BEVERIDGE, KAREN WALL, SCOTT J. MACGREGOR, JOHN G. ANDERSON, AND NEIL J. ROWAN

Invited Paper

In recent years, a number of new applications have emerged where pulsed power is being used in the treatment of waste and effluent, foodstuffs and beverages. One of these emerging applications is pulsed electric field (PEF) inactivation of microorganisms in liquid media. This involves the generation of electric fields of the order of 30 kV/cm across liquids contaminated with microorganisms. This induces a relatively large transmembrane potential that can lead to irreversible electroporation and consequently cell lysis. The nature of the PEF pulse profile is the subject of extensive study, and it has been reported that bipolar square waves provide superior inactivation when compared to monopolar pulses. A previous study, however, has challenged this view, and results will be presented demonstrating that more effective inactivation of bacteria can be achieved using the monopolar pulse. Results will also be given on the effect of monopolar pulse PEF applied to alcoholic beverages containing known spoilage microorganisms. This will highlight an apparent synergistic inactivation effect when microorganisms in alcoholic beverages are exposed to PEF.

Keywords*—*Electronic sterilization, microbial inactivation, pulse profile, pulsed electric field (PEF)

I. INTRODUCTION

The application of pulsed electric field (PEF) treatment as a food technology, although not fully understood, appears to have great potential. PEF treatment inactivates microorganisms in liquid media and is achieved by the generation of electric fields of the order of 30 kV/cm across the liquid. Depending on the type of food or beverage involved, these microorganisms can be pathogens such as *Escherichia coli*, *Salmonella*, and *Listeria monocytogenes* or spoilage microorganisms such as *Zygosaccharomyces bailii*, *Obesumbacterium proteus*, and *Lactobacillus brevis*. The application of PEF induces a relatively large transmembrane potential that can lead to electroporation. The theoretical model widely considered to most accurately describe the process of electroporation is the "transient aqueous pore model." In this model, the edge energy of hydrophilic and hydrophobic pores is considered. Transition from hydrophilic to hydrophobic pores occurs because the latter is an energetically favorable state when the radius of the pore exceeds a critical value. This leads to expansion of the pore and consequently to cell lysis [1].

One of the main advantages of this alternative processing technology is that the organoleptic and nutritional quality of foodstuffs will sustain little or no degradation as a result of treatment [2]. Another potential benefit is increased energy efficiency in food treatment [3]. Finally, PEF may also allow the targeting of specific microorganisms that are resistant to other methods of food treatment.

PEF can be applied using several different waveforms including oscillatory, double exponential, and square wave pulses. Of these, the square wave pulse has been shown in numerous studies to be the most efficient form of PEF delivery [4]. It has also been reported that the bipolar square wave pulse provides superior inactivation when compared to the monopolar pulse [5], [6]. However, other results have shown that this is not the case, with monopolar PEF being at least as effective in bacterial inactivation [7].

The first part of this paper reports on further work that has been undertaken to compare the effectiveness of bipolar and monopolar PEF inactivation. Following the identification of the most effective pulse profile, the paper reports on the potential for the use of PEF in the alcoholic beverage industry. Alcoholic beverages tend to be more resistant to spoilage microorganisms due to their high alcohol content and acidity,

Manuscript received October 16, 2003; revised March 19, 2004. This work was supported by the Engineering and Physical Sciences Research Council.

J. R. Beveridge and S. J. MacGregor are with the Department of Electronic and Electrical Engineering, University of Strathclyde, Glasgow G1 1XW, U.K. (e-mail: joseph.beveridge@strath.ac.uk; s.macgregor@eee.strath.ac.uk).

K. Wall and J. G. Anderson are with the Department of Bioscience and Biotechnology, University of Strathclyde, Glasgow G1 1XW, U.K. (e-mail: karen.wall@eee.strath.ac.uk; j.g.anderson@strath.ac.uk).

N. J. Rowan was with the Department of Bioscience and Biotechnology, University of Strathclyde, Glasgow, G1 1XW, U.K. He is now with the School of Biological Science, Dublin Institute of Technology, Dublin 2, Ireland. (e-mail: neil.rowan@dit.ie).

Digital Object Identifier 10.1109/JPROC.2004.829008

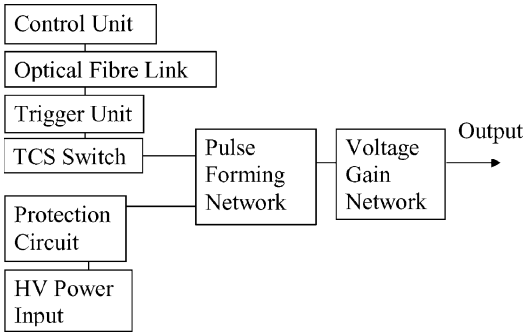

Fig. 1. Diagram of pulse generator system.

but there are still problems associated with spoilage. Current treatment for beer involves thermal pasteurization, but problems do exist at filling and with heat-resistant microorganisms. Wine is currently treated by either heat or the addition of sulphur dioxide, but the former affects taste and many people are sensitive to the latter. One aim of the present study was to explore potential synergistic inactivation effects associated with the application of PEF to the treatment of alcoholic beverages.

II. Experimental Setup

A. Pulse Generator

The pulse generator used in the study is shown schematically in Fig. 1 and consists of a transmission line based pulse-forming network (PFN). This generator has the facility to be configured to produce single or bipolar pulse waveforms of duration of 2 or 3 μs and with a rise time of approximately 200 ns. The bipolar pulse, for a total pulse length of 2 μs, has a negative polarity for 1 μs with a rapid reversal to positive polarity for 1 μs. Samples of the monopolar and bipolar pulses produced by the generator can be seen in Figs. 2 and 3, respectively. The PFN was charged to 29 kV for this series of experiments, and was triggered using a triggered corona-stabilized switch (Samtech Ltd., Glasgow, U.K.) at a repetition rate of 2 or 3 Hz.

B. The Test Chamber System

The test chamber is constructed of aluminum in a parallel plane arrangement with a 1-cm gap spacing and a treatment volume of 5.9 ml. It has a continuous flow design and is fed by a fully controllable peristaltic pump (0–3 ml/s). The test cell system is designed with the following important features.

- Bacteria in the test liquid are exposed to an entirely uniform field within the test chamber. There are, therefore, no dead zones (areas where the field intensity is reduced).
- The test chamber is temperature controlled by pumping cooling water into the electrodes, which have built-in heat sinks, using a flow-rate controllable diaphragm pump.
- The flow regime in the test cell is turbulent to ensure continuous agitation, encouraging temperature uniformity.
- The temperature is monitored at the inlet and outlet of the treatment region.
- Any bubbles occurring in the test fluid are evacuated effectively.
- For a given frequency, variation of the flow rate controls the number of pulses applied to the bacteria.

A schematic diagram of the test chamber setup is shown in Fig. 4.

C. Instrumentation

Voltage monitoring is achieved using a Tektronix P6015A 1000 : 1 high voltage probe connected to a Tektronix TDS 3022 oscilloscope (bandwidth of 300 MHz and peak sample rate of 1.25 GS/s). Fluid temperature is monitored by K-type thermocouples at the inlet and outlet of the treatment chamber. Cooling bath temperature is also monitored throughout.

III. Experimental Procedure

The microorganisms used in the study were *Z. bailii* (MUCL 27 812), a spoilage yeast found in wine, beer, and fruit juices; *L. brevis* (LMG 16 322), a gram-positive, nonmotile rod-shaped bacterium (0.5–1.2 $\times$ 1.0–10.0 μm) which is a recognized beer spoilage microorganism that can also affect wine; and *O. proteus* (LMG 3045), a gram-negative pleomorphic rod (0.8–2.0 $\times$ 1.5–10.0 μm), an important beer spoilage organism that grows alongside pitching yeast and competes for nutrients, resulting in slower fermentation rates. The microorganisms were obtained from Mycotheque de L'Universite Catholique de Louvain (MUCL, Louvain-la-Neuve, Belgium) and Laboratorium voor Microbiologie (LMG, University of Ghent, Ghent, Belgium).

For treatment in beer, wine, and peptone, the microorganisms were grown as follows: *O. proteus* (LMG 3045) was grown to a cell population of 10^8 colony forming units (CFU)/ml in nutrient broth (Oxoid, Basingstoke, U.K.) for 24 h at 30 °C; *Z. bailii* (MUCL 27812) was grown to a population of 10^7 CFU/ml in malt extract broth (Oxoid) for 24 h at 30 °C. *L. brevis* (LMG 16322) was grown to a population of 10^7 CFU/ml in Man, Rogosa, and Sharpe (MRS) broth (Oxoid) for 24 h at 30 °C.

After growth, the cultures were centrifuged for 15 min at 1710 g without refrigeration. The supernatants were discarded and the pellets resuspended in beer, wine, or 1.3% bacteriological peptone.

Prior to testing, the PEF system was cleaned by flushing through 2% hypochloride and then rinsed thoroughly with sterile distilled water. The PEF system was filled with the suspension fluid (without microbes) and primed to the exit of the funnel reservoir. This procedure ensured that all of the contaminated fluid that passed through the chamber had been treated, thereby minimizing cross contamination between treated and untreated media. This also ensured that there was time for the system to reach thermal equilibrium before the bacteria entered the treatment chamber. Sets of exposure times were always run from highest exposure to lowest exposure to make certain that the treated liquid was always progressing from a lower to a higher population, thus ensuring that the microbial count was due to the PEF treatment and not influenced by residual bacteria.

Duplicate samples were taken for each individual data point in a set (three individual data points are produced

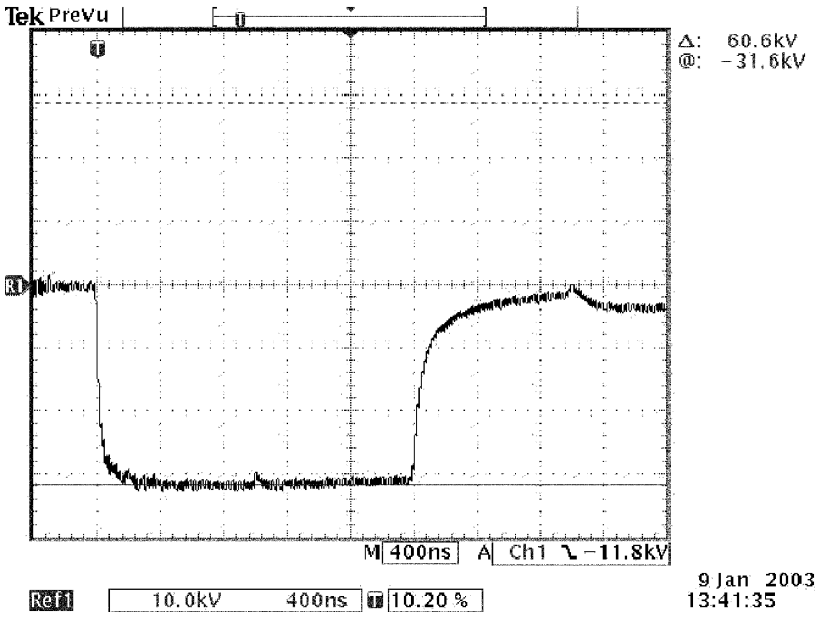

Fig. 2. Two-microsecond monopolar pulse.

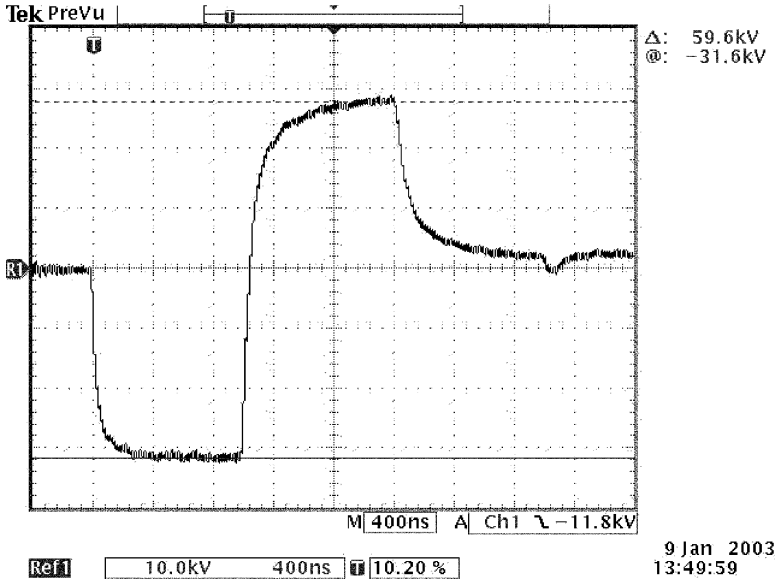

Fig. 3. Two-microsecond bipolar pulse.

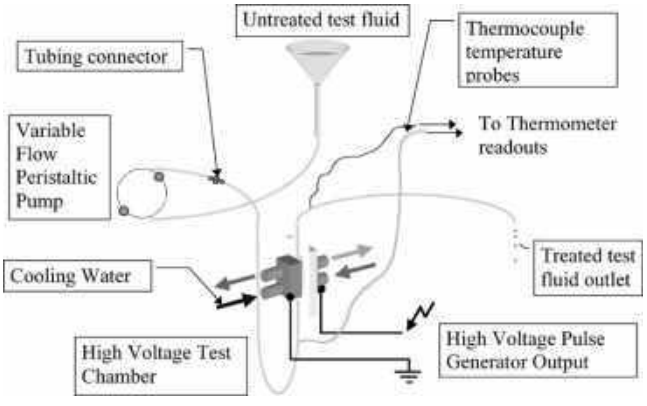

Fig. 4. Schematic diagram of test chamber setup.

for a single data set), and these were plated in triplicate to ascertain the relative levels of inactivation. Treated samples were serially diluted and enumerated by either spiral plating (Model B, Spiral Systems Inc., Cincinnati, OH) or pour plating onto growth media appropriate for the microorganism type and incubated at 30 °C for 48 h. Different dilutions were used depending upon the level of expected population and the method of enumeration. Malt extract agar (MEA) (Oxoid) plates were used for enumeration of *Z. bailii*. MRS agar (Oxoid) plates were used for enumeration of *L. brevis*, and nutrient agar (NA) (Oxoid) plates were used for enumeration of *O. proteus*. The plated colonies were counted and surviving populations expressed as Log_{10} CFU/ml.

An untreated "zero pulse sample" was taken from each microbial suspension at the start of every test and enumerated to determine the starting population. A number of representative tests were undertaken to ensure that microbial cells did not adhere to the internal surfaces of the testing system

Table 1
Treatment Parameters

Organism	Suspension Fluid	Pulse Profile	Frequency Hz	Set of Pulses	Pulse Duration μs	Field Strength kV/cm	Energy per pulse J	Fluid Temp. Range °C
Experiment 1								
Obesumbacterium Proteus	Peptone (1.3%)	Monopolar	2	30,60,130	2	30	16.8	27-37
Obesumbacterium Proteus	Peptone (1.3%)	Bipolar	2	30,60,130	2	30	13.6	27-37
Obesumbacterium Proteus	Peptone (1.3%)	Monopolar	2	30,60,130	3	30	25.2	27-37
Obesumbacterium Proteus	Peptone (1.3%)	Bipolar	2	30,60,130	3	30	23.3	27-37
Experiment 2								
Lactobacillus brevis	Peptone (1.3%)	Monopolar	3	90,200	2	30	16.8	30-42
Lactobacillus brevis	Guiness (Beer)	Monopolar	3	90,200	2	26	16.8	30-42
Lactobacillus brevis	Sauvignon Blanc (wine)	Monopolar	3	90,200	2	25	16.8	30-42
Zygosaccharomyces bailii	Peptone (1.3%)	Monopolar	3	30,60,90	2	30	16.8	30-42
Zygosaccharomyces bailii	Guiness (Beer)	Monopolar	3	30,60,90	2	26	16.8	30-42
Zygosaccharomyces bailii	Sauvignon Blanc (wine)	Monopolar	3	30,60,90	2	26	16.8	30-42

whereby they could affect the accuracy of microorganism recovery. In addition, tests were undertaken to ensure that during the treatment time, the microorganisms did not undergo any significant replication.

A. Treatment Details

The first series of experiments involved a comparison of the effectiveness of bacterial inactivation of *O. proteus* suspended in 1.3% bacteriological peptone using bipolar and monopolar pulses with pulse durations of 2 and 3 μs. The experimental parameters are shown in Table 1.

Because the flow rate is varied to achieve the different pulse numbers, there is a margin of change in the temperature at the chamber outlet; fluid resident in the chamber for a shorter duration is heated less. This is detailed in Table 1 as a temperature range where, for example, outlet fluid temperature was 27 °C for all 30-pulse exposures and 37 °C for all 130-pulse exposures. Therefore, on a given graph, corresponding pulse numbers have corresponding temperatures at outlet; the implication is that any differences between monopolar and bipolar in inactivation are independent of temperature. The fluid temperature at the inlet was measured as 23 °C for all tests in experiments 1 and 2.

The second series of experiments involved a comparison of the effectiveness of PEF inactivation of *L. brevis and Z. bailii* suspended in three menstrua: Bacteriological peptone at 1.3%, which is a suspension fluid with no growth-inhibiting elements and no alcohol; Guinness stout with 4.1% alcohol content; and Sauvignon Blanc at the higher alcohol concentration of 12.5%. Beer and wine are slightly more conductive than the peptone solution used and as indicated in Table 1; lower fields were developed in these suspensions. For this second series of experiments, the 3-μs monopolar pulse was used throughout.

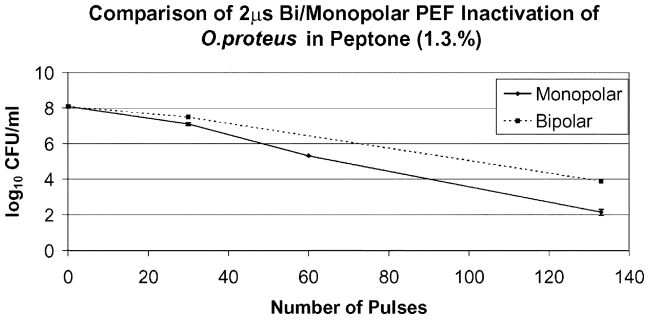

Fig. 5. Two-microsecond pulse bi/monopolar inactivation of *O. proteus*.

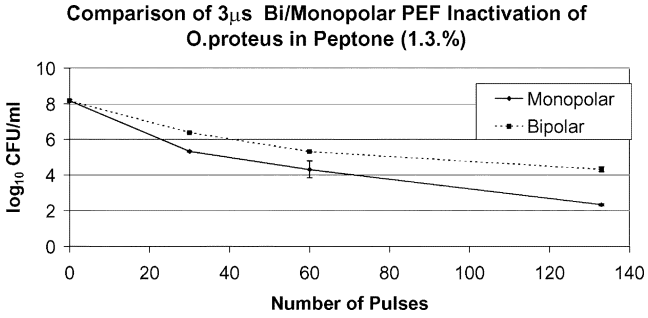

Fig. 6. Three-microsecond pulse bi/monopolar inactivation of *O. proteus*.

IV. Results

The results of the first series of experiments comparing bipolar and monopolar pulses can be seen in Figs. 5 and 6. These show the inactivation of *O. proteus* by bipolar and monopolar pulses using total pulse durations of 2 and 3 μs, respectively. The graphs show the relative inactivation on the basis of the number of pulses applied, and it can be seen that monopolar pulsing causes greater inactivation. For example, with the 2-μs pulse, there was a 6.1 log reduction with

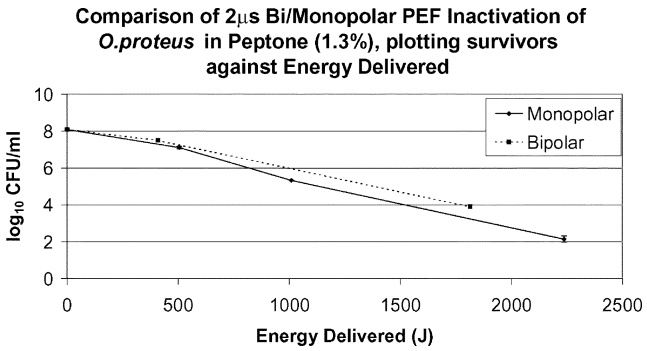

Fig. 7. Two-microsecond pulse bi/monopolar inactivation of *O. proteus* plotting survivors against energy delivered.

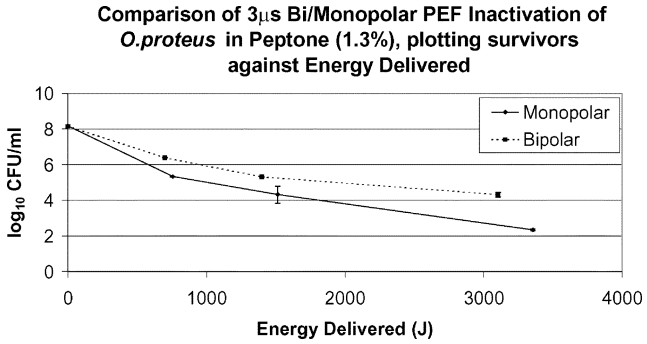

Fig. 8. Three-microsecond pulse bi/monopolar inactivation of *O. proteus* plotting survivors against energy delivered.

monopolar compared to a 4.2 log reduction with bipolar at 130 pulses. Also for the 3-μs pulse, there was a 5.9 log reduction using monopolar compared to a 3.4 log reduction using bipolar.

It can be seen in Table 1 that the energy delivered in the 2-μs bipolar pulse was approximately 80% of that delivered in the 2-μs monopolar pulse, and 90% for 3-μs pulses. This is due to increased losses from the polarity reversal during the bipolar pulse. Figs. 7 and 8 show the inactivation as a function of energy for the two pulse profiles. These graphs, therefore, take into account the difference between a monopolar and a bipolar pulse in terms of the energy delivered and demonstrate that, even when using energy as the criterion for comparison, the use of monopolar pulses results in greater inactivation. PEF-induced inactivation results are normally quoted as a normalized reduction in units of joules/cubic centimeters/log reduction. An analysis of the normalized reduction that takes into account the commutation of the polarity during the bipolar pulse still shows that monopolar is superior to bipolar PEF inactivation. The mean normalized reduction calculated over the three data points of each set is 71 J/cm^3/log reduction for 2-μs monopolar and 95 J/cm^3/log reduction for 2-μs bipolar. Similarly, there is a mean normalized reduction of 70 J/cm^3/log reduction for 3-μs monopolar and 93 J/cm^3/log reduction for 3-μs bipolar.

The results from the second series of experiments are shown in Figs. 9 and 10. These compare the inactivation characteristics of *L. brevis* and *Z. bailii* when suspended in various menstrua and subjected to PEF treatment. It can be seen that *L. brevis* is more resistant to PEF treatment when

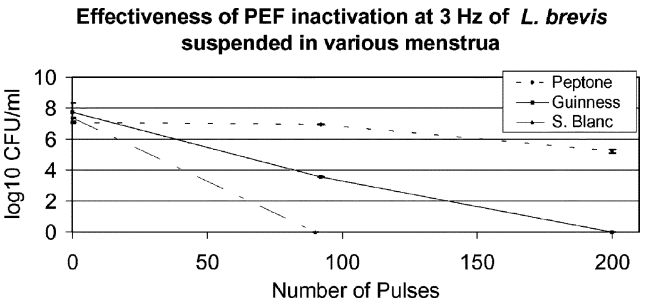

Fig. 9. Inactivation of *L. brevis* in various menstrua using 3-μs monopolar pulses.

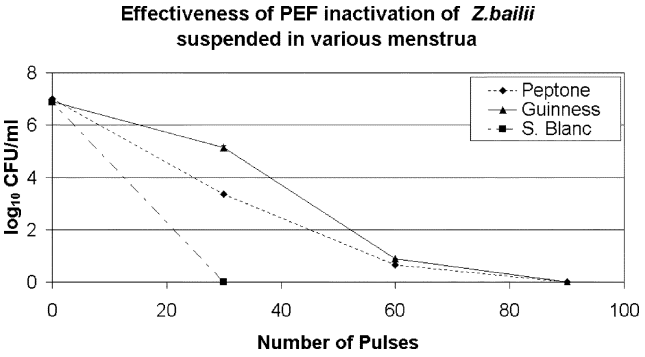

Fig. 10. Inactivation of *Z. bailii* in various menstrua using 3-μs monopolar pulses.

suspended in peptone, yielding only a 1.9 log reduction for 200 pulses. Complete inactivation occurs at 200 pulses in the Guinness and at 90 pulses in the Sauvignon Blanc. Overall, *Z. bailii* was found to be more susceptible than *L. brevis* to the PEF treatment. This microorganism was reduced by about 6 $\log_{10}$ CFU/ml in both peptone and Guinness after 60 pulses, and was completely inactivated in Sauvignon Blanc at 30 pulses.

V. Discussion

In the first series of experiments, the comparison of pulse profiles showed that the monopolar pulse was certainly as effective and apparently superior to the bipolar pulse. The temperature data in Table 1 show the total variation over the experiment. An important point to note is that this temperature is measured at the outlet. Fluid enters the test cell at a temperature of 23 °C, and so the recorded temperature (at the exit) is the maximum achieved. The bacteria are, therefore, exposed to an increasing temperature. The results appear to indicate that the monopolar pulse profile provides more effective delivery of energy in terms of inactivation. Assuming that irreversible electroporation is the mechanism of bacterial inactivation, the difference in inactivation may be due to the longer period available in the monopolar pulse to cause irreversible electroporation. In addition, the second half of the pulse may need to neutralize the charge across the membrane of the previous half pulse, before it can charge the membrane to the opposite polarity and contribute to electroporation. This would further reduce the time available for irreversible electroporation. Although outside the scope of this study, it has been reported by Kotnik *et al.* [8] that with aluminum

electrodes there is reduced electrolytic contamination of the suspension fluid when the bipolar profile is used in preference to the monopolar. The possibility that this might have an effect on microbial inactivation requires further study.

In general, the two spoilage microorganisms studied in the second series of experiments show increased susceptibility to PEF when suspended in the wine and beer. A possible explanation is that the alcoholic beverages could be inducing extra stress on the microbial cell membrane due to the presence of both alcohol and a lower pH. The increased susceptibility to PEF is particularly clear in the case of *L. brevis* where only a 1.9 log reduction was achieved at 200 pulses for peptone but complete inactivation at 200 pulses for Guinness and 60 pulses for wine. The presence or influence of the products of electrolysis is not known, and it is possible that this may have an effect in the synergistic inactivation that the results indicate. As with the first experiment, the exit temperature was maintained within the intended range, so that the points compared on each graph were not affected by temperature.

VI. Summary

In the first series of experiments a comparison of bipolar and monopolar pulses, at both 2- and 3-μs total pulse duration, indicated that the monopolar profile is the more efficient method of delivery of energy as far as inactivation is concerned. These experiments were conducted such that good control of fluid temperature was achieved so that temperature could be discounted as a factor influencing the pulse profile comparison. The second series of experiments in this study investigated the use of PEF for the inactivation of spoilage microorganisms in the alcoholic beverages Guinness and Sauvignon Blanc. Increased susceptibility of both *L. brevis* and *Z. bailii* when suspended in alcoholic beverages and subjected to PEF treatment has been demonstrated.

References

[1] J. C. Weaver and Y. A. Chizmadzhev, "Theory of electroporation: A review," *Bioelectrochem. Bioenerg.*, vol. 41, pp. 135–160, 1996.

[2] D. W. Quass, "Pulsed Electric Processing in the Food Industry: Status Report on PEF," Electric Power Res. Inst., Palo Alto, CA, Rep. No. CR-109 742, 1997.

[3] B. L. Qin, F. J. Chang, G. V. Barbosa Cánovas, and B. G. Swanson, "Nonthermal inactivation of *S. cerevisiae* in apple juice using pulsed electric fields," *Lebensm Wiss Technol.*, vol. 28, no. 6, pp. 564–568, 1995.

[4] Q. H. Zhang, X. Qiu, and S. K. Sharma, *Recent Development in Pulsed Electric Field Processing*. Washington, DC: National Food Processors Assoc., 1997, pp. 31–42.

[5] B. L. Qin, Q. Zhang, G. V. Barbosa-Canovas, and B. G. Swanson, "Inactivation of microorganisms by pulsed electric fields of different voltage waveforms," *IEEE Trans. Dielect. Elect. Insulation*, vol. 1, pp. 1047–1057, Dec. 1994.

[6] S. Y. Ho and G. S. Mittal, "Inactivation of *P. fluorescens* by high voltage electric pulses," *J. Food Sci.*, vol. 60, no. 6, pp. 1337–1340, 1995.

[7] J. R. Beveridge, S. J. MacGregor, L. Marsili, J. G. Anderson, N. J. Rowan, and O. Farish, "Comparison of the effectiveness of biphase and monophase rectangular pulses for the inactivation of micro-organisms using pulsed electric fields," *IEEE Trans. Plasma Sci.*, vol. 30, pp. 1525–1531, Aug. 2002.

[8] T. Kotnik, D. Miklavcic, and L. M. Mir, "Cell membrane electropermeabilization by symmetrical bipolar rectangular pulses – Part II. Reduced electrolytic contamination," *Bioelectrochemistry*, vol. 54, no. 1, pp. 91–95, 2001.

Joseph R. Beveridge was born on January 13, 1978. He received the B.Eng. degree (joint honors) in electrical and mechanical engineering from the University of Strathclyde, Glasgow, U.K., in 2000. He is currently working toward the Ph.D. degree in pathogen inactivation by pulsed electric fields at the University of Strathclyde.

Karen Wall was born on January 4, 1981. She received the B.Sc. degree (joint honors) in biochemistry and microbiology from the University of Strathclyde, Glasgow, U.K., in 2001. She is currently working toward the Ph.D. degree in pathogen inactivation by pulsed electric fields at the University of Strathclyde.

Scott J. MacGregor received the B.Sc. and Ph.D. degrees from the University of Strathclyde, Glasgow, U.K., in 1982 and 1986, respectively.

Since 1986, he has been with the University of Strathclyde. In 1986, he was appointed Pulsed Power Research Fellow. In 1989, he was appointed Lecturer in Pulsed Power Technology. In 1994, he was appointed to the position of Senior Lecturer, with promotion to Reader and Professor of High-Voltage Engineering in 1999 and 2001, respectively. His research interests included high-voltage pulse generation, high-frequency diagnostics, high-power repetitive switching, high-speed switching, and electronic methods for food pasteurization and sterilization.

John G. Anderson was born in Glasgow, U.K., on September 2, 1942. He received the B.Sc. degree in applied microbiology and the Ph.D. degree in fungal physiology from the University of Strathclyde, Glasgow, in 1968 and 1971, respectively.

Since 1971, he has been with the Department of Bioscience, University of Strathclyde, where he is currently a Reader in microbiology as well as Vice-Chairman of the department. He is currently involved in a major interdisciplinary research program on the development of novel electronic pasteurization and sterilization technologies for applications in the food, water, and health care industries. His research interests include various aspects of food, biomedical, and environmental microbiology.

Neil J. Rowan was born in Athlone, Ireland in 1967. He received the B.Sc. degree and the Higher Diploma degree in applied microbiology from the National University of Ireland, Galway, in 1989 and 1990, respectively, and the M.Sc. and Ph.D. degrees in biomedical microbiology from the University of Strathclyde, Glasgow, U.K., in 1992 and 1996, respectively.

He is currently a Lecturer, Department of Bioscience, University of Strathclyde. He has authored or coauthored more than 30 research papers that have appeared in international journals. His current interests are in the physiology and control of food and hospital-borne microbial pathogens, including studies on microbial survival strategies and putative virulence factor expression.

APPLIED AND ENVIRONMENTAL MICROBIOLOGY, June 2001, p. 2833–2836 Vol. 67, No. 6
0099-2240/01/$04.00+0 DOI: 10.1128/AEM.67.6.2833–2836.2001

Inactivation of *Mycobacterium paratuberculosis* by Pulsed Electric Fields

NEIL J. ROWAN,[1]* SCOTT J. MACGREGOR,[2] JOHN G. ANDERSON,[1]
DOUGLAS CAMERON,[1] AND OWEN FARISH[2]

Department of Bioscience and Biotechnology[1] and Department of Electronic and Electrical Engineering,[2] University of Strathclyde, Glasgow, Scotland

Received 21 December 2000/Accepted 19 March 2001

The influence of treatment temperature and pulsed electric fields (PEF) on the viability of *Mycobacterium paratuberculosis* cells suspended in 0.1% (wt/vol) peptone water and in sterilized cow's milk was assessed by direct viable counts and by transmission electron microscopy (TEM). PEF treatment at 50°C (2,500 pulses at 30 kV/cm) reduced the level of viable *M. paratuberculosis* cells by approximately 5.3 and 5.9 $\log_{10}$ CFU/ml in 0.1% peptone water and in cow's milk, respectively, while PEF treatment of *M. paratuberculosis* at lower temperatures resulted in less lethality. Heating alone at 50°C for 25 min or at 72°C for 25 s (extended high-temperature, short-time pasteurization) resulted in reductions of *M. paratuberculosis* of approximately 0.01 and 2.4 $\log_{10}$ CFU/ml, respectively. TEM studies revealed that exposure to PEF treatment resulted in substantial damage at the cellular level to *M. paratuberculosis*.

Mycobacterium paratuberculosis is a chronic enteric pathogen that causes paratuberculosis, commonly known as Johne's disease, in many different species of animals, including primates (3). It has been suggested that the etiological agent in Crohn's disease, a severe inflammatory enteritis in humans that bears extensive clinical, pathological, and systemic similarity to Johne's disease, may be mycobacterial and could be *M. paratuberculosis* (2), but this remains to be proven. Interest in the possible relationship between Crohn's disease and *M. paratuberculosis* has been recently stimulated by the detection of *M. paratuberculosis* DNA in pasteurized cow's milk samples from retail markets in England and Wales (9). Little is known about the levels of *M. paratuberculosis* that may be present in infected milk from cattle suffering from Johne's disease. However, independent research from the United States (14), Northern Ireland (5), and Australia (6) has reported that this pathogen may be capable of surviving commercial high-temperature, short-time (HTST) pasteurization and thus may be present in retail milk supplies. It is presently estimated that between 20 and 40% of U.S. dairy herds are infected with bovine Johne's disease, which may have significant health implications when it is considered that an estimated one-third of U.S. cheese is produced from unpasteurized milk (15).

The potential use of pulsed-power techniques, such as treatment with high-intensity pulsed electric fields (PEF), for food processing is currently receiving considerable attention, since inactivation of problematic microorganisms can take place under reduced-temperature conditions (7, 10). The advantages of such an electrotechnology include the potential retention of fresh-food characteristics and organoleptic qualities such as flavor, aroma, and texture (1). Previous research suggests that the application of PEF (with a magnitude usually greater than 20 kV cm^{-1} for short durations, such as 500 ns to 4 μs) to liquids can inactivate susceptible microorganisms through irreversible electroporation of the cell membrane (7, 10, 12). The present studies were conducted to determine whether the application of PEF at different treatment temperatures (5, 20, and 50°C) effectively kills *M. paratuberculosis* cells in 0.1% (wt/vol) peptone water. *Listeria monocytogenes* cells and *Bacillus cereus* endospores were also treated under similar conditions, as these organisms also occasionally occur in milk and milk products and are of lesser and greater thermal tolerance, respectively, than *M. paratuberculosis* (4, 11). An assessment was made of PEF treatment at 50°C on *M. paratuberculosis* cells in sterilized cow's milk. Susceptibility of *M. paratuberculosis* to the lethal effects of PEF treatment and/or temperature was determined by direct viable counts and by transmission electron microscopy (TEM).

The following two strains of *M. paratuberculosis* were utilized in the PEF studies: strain ATCC 19698 (American Type Culture Collection, Manassas, Va.) and strain Linda (ATCC 43015). Strain 19698 is a laboratory strain of *M. paratuberculosis* originally isolated from ileal tissue of a cow with clinical Johne's disease. Strain Linda (ATCC 43015) was isolated from ileum tissue biopsy from a 15-year-old girl with Crohn's disease. A standard suspension of *M. paratuberculosis* cells was prepared by washing growth from slopes of Middlebrook 7H10 agar medium (containing 10% [vol/vol] Middlebrook OADC [oleic acid, dextrose, and catalase; Becton Dickinson Ltd., Oxford, United Kingdom] and 0.0002% [wt/vol] mycobactin J [Allied Monitor Inc., Fayette, Mo.] per liter) with 0.1% (wt/vol) peptone water. Washed Middlebrook 7H10 agar slopes were centrifuged at 2,500 × *g* for 20 min, and the pellet was resuspended in 0.1% (wt/vol) peptone water to yield a suspension containing approximately 10^6 CFU of *M. paratuberculosis* per ml (determined spectrophotometrically at 540 nm [model UV-120-02 instrument; Shimadzu Corp., Kyoto, Japan]). Similar cell densities of *M. paratuberculosis* were also suspended in commercially pasteurized cow's milk that had been sterilized to

* Corresponding author. Mailing address: Department of Bioscience and Biotechnology, University of Strathclyde, Royal College, 204 George St., Glasgow G1 1XW, Scotland. Phone: 44 (0)141 548 2531. Fax: 44 (0)141 553 4124. E-mail: n.j.rowan@strath.ac.uk.

TABLE 1. Influence of PEF and/or temperature on the inactivation of food-borne bacterial pathogens suspended in 0.1% (wt/vol) peptone water

Bacterial strain	Reduction in viable cell or spore no. (log_{10} CFU/ml) under the following conditions[a]:						
	5°C, 25 min	5°C + PEF[b], 25 min	20°C, 25 min	20°C + PEF, 25 min	50°C, 25 min	50°C + PEF, 25 min	72°C, 25s
M. paratuberculosis ATCC 19698	0 a	1.5 ± 0.2 f	0 a	3.1 ± 0.2 h	0.01 ± 0.01 b	5.1 ± 0.3 j	2.4 ± 0.3 g
M. paratuberculosis Linda (ATCC 43015)	0 a	1.7 ± 0.4 f	0 a	3.3 ± 0.3 h	0.02 ± 0.005 b	5.3 ± 0.5 j	2.8 ± 0.2 g
L. monocytogenes 11994	0 a	1.1 ± 0.1 e	0 a	2.6 ± 0.1 g	0.16 ± 0.05 d	4.1 ± 0.3 i	7.1 ± 0.2[c] k
B. cereus 11145 (endospores)	0 a	0.16 ± 0.02 d	0 a	0.14 ± 0.03 d	0 a	0.17 ± 0.04 d	0.06 ± 0.02 c

[a] Values followed by the same lowercase letter do not differ at the 95% confidence interval ($P < 0.05$). Results are means and standard deviations.
[b] Treatment of suspended bacterial cells with 2,500 pulses at 30 k V/cm.
[c] Reduction of starting population of 7.1 ± 0.2 log_{10} CFU/ml to a nondetectable level when assessed after 15 s at 72°C.

sterility (i.e., three consecutive days of steaming for 30 min). Sterility was confirmed by the absence of microbial growth on plates of tryptone soy agar supplemented with 0.6% (wt/vol) yeast extract that were incubated for 48 h at 37°C prior to cell enumeration. Suspended bacteria were sonicated to disperse clumps prior to PEF or heat treatments, which resulted in more accurate quantification of CFU of bacteria on enumeration media.

M. paratuberculosis cells were suspended in 1.9 ml of 0.1% peptone water or cow's milk and were subjected to high-voltage PEF (~30 kV/cm) in a uniform-field static test chamber. The electrical circuit layout and experimental arrangement for PEF treatment were as described previously (7, 12). The test chamber consisted of a disk of 10 mm Perspex, with a central hole cut through it to hold a 1.9-ml volume of sample. Two separate channels were drilled from the outer edge of the Perspex to the central hole, thus allowing for syringe injection and removal of samples. Flat brass plates were fitted on both sides of the central hole, which formed the electrodes of the test chamber. Predetermined cell populations were treated with 2,500 pulses at 5, 20, and 50°C at a pulse repetition frequency that was limited to 5 pulses per s (5 Hz at 50°C) in order to ensure that there were no thermal inactivation effects associated with the energy dissipation in the test chamber. The test chamber was immersed in a circulating constant-temperature water bath (model HE30; Grant Instruments Ltd., Cambridge, United Kingdom) equipped with a thermoregulator capable of maintaining temperature to within ±0.05°C (model TE-8A; Techne Ltd., Cambridge, United Kingdom) to maintain the desired treatment temperatures at 5, 20, and 50°C. A thermocouple was also employed throughout the studies in order to verify the temperature of the treated liquid. A 100-kV high-voltage DC generator (model EH50R02; Glassmann Europe Ltd., Hampshire, United Kingdom) was used to charge a coaxial-cable Blumlein pulse generator (type TLG B-01; Samtech Ltd., Glasgow, United Kingdom) through a charging resistance of 10 MΩ. The coaxial-cable generator was constructed from 100 m of URM67 40-kV cable (Samtech). The high-voltage output pulse from the generator was 500 ns in duration, and the generator had an output impedance of 100 Ω, a switching impedance of 50 Ω, and an open circuit gain of 2. The generator was wound inductively on a 30-cm-diameter former in order to minimize secondary transmission line losses. The pulse generator was charged from one end of the cable and was fired by switching the inner conductor to ground at the opposite end. Although both sides of the test chamber were grounded, the output from the cable generator, which was connected to one side of the test chamber, was transiently decoupled from ground during application of the voltage pulse. The Blumlein generator was fired using a triggered corona stabilized switch. The output pulse from the generator was monitored throughout the experiments using a 1,000:1 Tektronix P6015A high-voltage probe (Imex Ltd., Coatbridge, United Kingdom). Levels of microbial inactivation and cell integrity (examined with a Zeiss 902 TEM) were assessed after PEF treatment as described previously (12). Recovery of surviving populations (log_{10} CFU of *M. paratuberculosis* per milliliter) was determined for PEF-treated suspensions and dilutions thereof by spread and spiral plating samples (model B; Spiral Systems Inc., Shipley, United Kingdom) onto Middlebrook 7H10 agar plates; these were incubated for 2 months at 37°C before enumeration.

The effect of treatment temperature on the viability of *M. paratuberculosis* cells suspended in 0.1% (wt/vol) peptone water or in tyndallized cow's milk was also determined in the static test chamber. Predetermined cell populations of *M. paratuberculosis* were transferred to the test chamber, which was immersed in a circulating constant-temperature water bath at 5, 20, or 50°C for 20 min as described above; the duration of temperature exposure was similar to that for PEF treatment. Recovery of surviving populations of *M. paratuberculosis* from the test chamber was determined as described earlier. To validate our methods, predetermined populations of *L. monocytogenes* cells (strain 11994; obtained from the National Collection of Type Cultures, Public Health Laboratory Service, Colindale, United Kingdom, and originally isolated from a patient with meningitis) and *B. cereus* endospores (diarrheagenic strain 11145, which was obtained from the National Collection of Type Cultures) were subjected to a regimen of heating and PEF treatment similar to that mentioned above. *L. monocytogenes* was grown in 100 ml of tryptone soy broth supplemented with 0.6% (wt/vol) yeast extract at 37°C for 20 h with shaking (150 rpm). *Listeria* cells were harvested by centrifugation at 3,000 × *g* at 4°C, washed twice, and resuspended in peptone water to a cell density of approximately 10^6 CFU/ml as described above. *B. cereus* endospores were obtained by growth of the bacterium on sporulation medium (nutrient agar supplemented with 0.5 mg of $MnSO_4 \cdot H_2O$ per liter) for 2 weeks at 37°C. The absence of *B. cereus* vegetative cells was confirmed by heating at 85°C for 15 min as described previ-

ously (13). *B. cereus* endospores were washed twice and resuspended in 0.1% (wt/vol) peptone water to a spore density of approximately 10^6 CFU/ml. After heating and PEF treatment, enumeration of surviving populations of *L. monocytogenes* cells and of *B. cereus* endospores was done after 48 h at 37°C on tryptone soy–0.6% (wt/vol) yeast extract agar and on nutrient agar, respectively.

The thermal resistance of *M. paratuberculosis* strains ATCC 19698 and Linda (ATCC 43105), *L. monocytogenes* (strain 11994), and *B. cereus* endospores (strain 11145) was also determined at 72°C for 25 s (HTST pasteurization), according to methods described previously (4, 11). To further validate the present study, *L. monocytogenes* cells were also subjected to 63°C for 30 min. *D* values (decimal reduction time; the time required to kill a 1-log-unit concentration of bacteria) were calculated from the slope of the best-fit line graphically determined by plotting the $\log_{10}$ CFU survivors per milliliter versus time of heat exposure at 63 and 72°C. Test bacteria were suspended in 1.9 ml of preheated 0.1% peptone water to a density of approximately 10^6 CFU/ml in 3-ml crimp cap glass vials (Phase Separations Ltd., Watford, Hertfordshire, United Kingdom). The vials were sealed and kept 4 cm below the level in the water bath for the treatment period. Recovery and enumeration of surviving populations of the test bacteria were done as mentioned above. All of the experiments in this study were performed in triplicate, and results are reported as averages. Significant differences in levels of viable test bacteria recovered after PEF treatment and heating were reported at the 95% confidence interval ($P < 0.05$) using analysis of variance (balanced model) with Minitab software release 11 (Minitab Inc., State College. Pa.).

Results from PEF treatment and heating of *M. paratuberculosis* ATCC 19698 cells suspended in 0.1% peptone water revealed a greater level of cell reduction with increased treatment temperature (Table 1). *M. paratuberculosis* ATCC 19698 cells were reduced by ~5.4 $\log_{10}$ CFU/ml at 50°C after 2,500 pulses at 30 kV/cm. Strain Linda was similarly affected ($P < 0.05$) by PEF treatment at 50°C (Table 1). PEF treatment of *M. paratuberculosis* cells at 5°C resulted in a reduction of ~1.6 $\log_{10}$ CFU/ml, which was the lowest level of cell inactivation achieved using this electrotechnology. The composition and structure of the cell membrane of *M. paratuberculosis* indicate that it may be more rigid at low temperatures, and this may protect the microorganism from membrane rupture by PEF (8). TEM studies of PEF-treated *M. paratuberculosis* cells revealed substantial structural damage at the cellular level (Fig. 1b). Control TEM studies showed that the structural integrity of untreated (Fig. 1a) or heat-treated *M. paratuberculosis* cells remained intact. TEMs of untreated and heat-treated *M. paratuberculosis* cells were similar (data not shown).

Results from comparative studies with other bacteria revealed that *L. monocytogenes* 11194 cells and *B. cereus* 11145 endospores were reduced by 4.07 ± 0.3 and 0.17 ± 0.04 $\log_{10}$ CFU/ml, respectively, after PEF treatment at 50°C (Table 1). This finding suggests that *M. paratuberculosis* cells are more sensitive to the lethal action of PEF than are *L. monocytogenes* cells and *B. cereus* endospores. Thermal studies revealed that *M. paratuberculosis* strains ATCC 19689 and Linda (ATCC 43105) were similarly affected by heating (both strains were reduced by approximately 2.6 $\log_{10}$ CFU/ml at 72°C), which

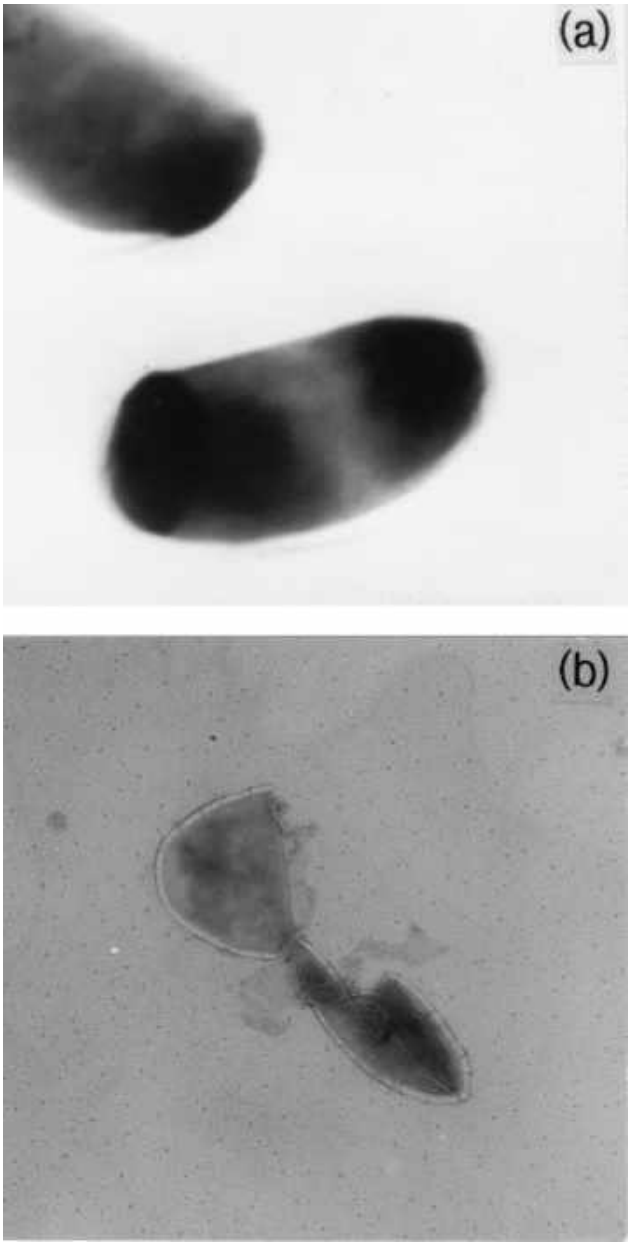

FIG. 1. TEMs of untreated (a) and PEF-treated (b) *M. paratuberculosis* ATCC 19698 cells (magnification, ×25,000).

corroborated the findings of other researchers. Thermal studies showed that *L. monocytogenes* 11994 was effectively killed when examined after 15 s at 72°C (Table 1). The *D* value of *L. monocytogenes* 11994 at 63°C was also determined. The thermal death time curves were linear, and the $D_{63°C}$ of 52.7 s was similar to the $D_{62.7°C}$ of 54 s for *L. monocytogenes* Scott A reported by Donnelly et al. (4). Thus, it can be concluded that the method of thermal death rate or *D* value determination used in the present study is consistent with those used in other studies.

Results from *B. cereus* 11145 endospore heating experiments showed that the dormant spores of this diarrheagenic foodborne enteropathogen were far more heat tolerant than *M.*

paratuberculosis cells; these organisms were reduced by averages of 0.06 ± 0.04 and 2.6 ± 0.3 $\log_{10}$ CFU/ml, respectively. This present study demonstrates that the thermal inactivation of *M. paratuberculosis* cells and *B. cereus* endospores are not similar ($P < 0.001$). Results from PEF treatment of *M. paratuberculosis* ATCC 19698 and Linda (ATCC 43105) cells suspended in tyndallized cow's milk at 50°C revealed reductions of 5.6 ± 0.3 and 5.9 ± 0.4 $\log_{10}$ CFU/ml, respectively (data not shown). PEF treatment of *M. paratuberculosis* cells in cow's milk at 50°C produced a slightly greater level of inactivation than similar treatment in peptone water ($P < 0.05$). This improved PEF-induced killing of *M. paratuberculosis* may be due, in part, to milk having a greater conductivity.

Stimulated by the possible association between Crohn's disease and *M. paratuberculosis*, a number of independent studies from different countries have reported that this thermotolerant bacterium has the potential to survive commercial HTST pasteurization (72°C for 15 s) when suspended in cow's milk (5, 6, 14). Research by Grant et al. (5) showed that *M. paratuberculosis* may survive HTST pasteurization if present in milk at levels of 10^2 to 10^3 CFU/ml prior to heat treatment but will be completely inactivated by HTST pasteurization when low levels (10 CFU/ml) are present. As a consequence of these and other findings, and due to the detection of *M. paratuberculosis* DNA from cow's milk in retail outlets, the United Kingdom dairy industry has responded by extending the pasteurization holding period to 25 s. While the efficacy of this precautionary action has yet to be fully evaluated, it may be worth considering the inclusion of PEF as a complementary treatment to HTST pasteurization. Although the number of pulses applied during the present series of experiments was 2,500, it must be pointed out that no attempt has been made by the investigators to optimize PEF treatment of *M. paratuberculosis* cells. Based on PEF treatment of other organisms (7, 12), it can be expected that if the correct field intensity and PEF pulse frequency content are identified, the number of pulses required could be orders of magnitude lower.

Results from the present study indicate that the application of high-intensity PEF kills *M. paratuberculosis* in a test liquid and in milk and that this treatment is particularly effective when carried out at moderately elevated temperatures. This study has also shown that PEF treatment causes substantial structural damage at the cellular level to *M. paratuberculosis* cells.

We thank Andrew Dick and David Currie for their excellent technical assistance in conducting these experiments.

REFERENCES

1. **Castro, A. J., G. C. Barbosa-Cánovas, and B. G. Swanson.** 1993. Microbial inactivation of foods by pulsed electric fields. J. Food Proc. Preser. **17:**47–73.
2. **Chiodini, R. J.** 1989. Crohn's disease and the mycobacterioses: a review and comparison of two disease entities. Clin. Microbiol. Rev. **2:**90–117.
3. **Cocito, C., P. Gilot, M. Coene, M. De Kesel, P. Poupart, and P. Vannuffel.** 1994. Paratuberculosis. Clin. Microbiol. Rev. **7:**329–345.
4. **Donnelly, C. W., E. H. Briggs, and L. S. Donnelly.** 1987. Comparison of heat resistance of *Listeria monocytogenes* in milk as determined by two methods. J. Food Prot. **50:**14–17.
5. **Grant, I. R., H. J. Ball, and M. T. Rowe.** 1998. Effect of high-temperature, short-time (HTST) pasteurization on milk containing low numbers of *Mycobacterium paratuberculosis*. Lett. Appl. Microbiol. **26:**166–170.
6. **Hope, A. F., P. A. Fulk, and R. J. Condron.** 1996. Pasteurization of *Mycobacterium paratuberculosis* in whole milk, p. 377–382. *In* R. J. Chiodini, M. E. Hines, and M. T. Collins (ed.), Proceedings of the 5th International Colloquium on Paratuberculosis. International Association for Paratuberculosis, Madison, Wis.
7. **MacGregor, S. J., O. Farish, R. A. Fouracre, J. G. Anderson, and N. J. Rowan.** 2000. Inactivation of pathogenic and spoilage microorganisms in a test liquid using pulsed electric fields. IEEE Trans. Plasma Sci. **28:**144–150.
8. **Mamadou, D., and P. Draper.** 1998. The envelope layers of *Mycobacteria* with reference to their pathogenicity. Adv. Microb. Physiol. **39:**131–203.
9. **Millar, D., J. Ford, J. Sanderson, S. Withey, M. Tizard, T. Doran, and J. Hermon-Taylor.** 1996. IS*900* PCR to detect *Mycobacterium paratuberculosis* in retail supplies of whole pasteurized cow's milk in England and Wales. Appl. Environ. Microbiol. **62:**3346–3452.
10. **Qin, B.-L., U. R. Pothakarmury, H. Vega, G. V. Barbosa-Cánovas, and B. G. Swanson.** 1996. Nonthermal pasteurization of liquid foods using high-intensity pulsed electric fields. Crit. Rev. Food Sci. Nutr. **36:**603–627.
11. **Rowan, N. J., and J. G. Anderson.** 1998. Effects of above-optimum growth temperature and cell morphology on thermotolerance of *Listeria monocytogenes* cells suspended in bovine milk. Appl. Environ. Microbiol. **64:**2065–2071.
12. **Rowan, N. J., S. J. MacGregor, J. G. Anderson, R. A. Fouracre, and O. Farish.** 2000. Pulsed electric field inactivation of diarrhoeagenic *Bacillus cereus* through irreversible electroporation. Lett. Appl. Microbiol. **31:**110–114.
13. **Rowan, N. J., and J. G. Anderson.** 1997. Maltodextrin stimulates growth of *Bacillus cereus* and synthesis of diarrheal enterotoxin in infant milk formulas. Appl. Environ. Microbiol. **63:**1182–1184.
14. **Sung, N., and M. T. Collins.** 1998. Thermal tolerance of *Mycobacterium paratuberculosis*. Appl. Environ. Microbiol. **64:**999–105.
15. **U.S. Department of Agriculture.** 1997. Johne's disease on U.S. dairy operations. October report. U.S. Department of Agriculture, Washington, D.C.

Journal of Food Protection, Vol. 70, No. 12, 2007, Pages 2805–2810

Pulsed-Plasma Gas-Discharge Inactivation of Microbial Pathogens in Chilled Poultry Wash Water

N. J. ROWAN,[1]* S. ESPIE,[2] J. HARROWER,[2] J. G. ANDERSON,[2] L. MARSILI,[2] AND S. J. MACGREGOR[2]

[1]*Department of Nursing and Health Science, Athlone Institute of Technology, Dublin Road, Athlone, Ireland; and* [2]*Roberston Laboratories of Electronic Sterilisation Technologies, University of Strathclyde, Glasgow, Scotland*

MS 07-178: Received 30 March 2007/Accepted 7 June 2007

ABSTRACT

A pulsed-plasma gas-discharge (PPGD) system was developed for the novel decontamination of chilled poultry wash water. Treatment of poultry wash water in the plasma generation chamber for up to 24 s at 4°C reduced *Escherichia coli* NCTC 9001, *Campylobacter jejuni* ATCC 33560, *Campylobacter coli* ATCC 33559, *Listeria monocytogenes* NCTC 9863, *Salmonella enterica* serovar Enteritidis ATCC 4931, and *S. enterica serovar* Typhimurium ATCC 14028 populations to nondetectable levels (≤8 log CFU/ml). Although similar PPGD treatments at 4°C also produced significant reductions (≥3 log CFU/ml) in recalcitrant *B. cereus* NCTC 11145 endospore numbers within 30 s, the level of endospore reduction was dependent on the nature of the sparged gas used in the plasma treatments. Scanning electron microscopy revealed that significant damage occurred at the cellular level in PPGD-treated test organisms. This electrotechnology delivers energy in intense ultrashort bursts, generating products such as ozone, UV light, acoustic and shock waves, and pulsed electric fields that have multiple bactericidal properties. This technology offers an exciting complementary or alternative approach for treating raw poultry wash water and for preventing cross-contamination in processing environments.

Salmonella and *Campylobacter* species are leading bacterial causes of human foodborne illness *(14, 23).* The U.S. Department of Agriculture estimates the costs associated with foodborne illness to be approximately $22 billion per year. Outbreaks of enteritis associated with these pathogens have been associated with consumption of contaminated meat, particularly poultry products *(11).* Because of the relatively high frequency of contamination of poultry with these pathogens, raw poultry products are perceived to be responsible for a significant amount of human illness. Enteric pathogens frequently contaminate chicken skin and exposed surfaces during slaughter operation, and an effective process for their reduction or elimination on the surface of poultry is necessary *(23).* Contamination rates of *Campylobacter* spp. on poultry purchased at retail establishments in the United States and the United Kingdom range from 68 to 83% *(7).*

Although various processes have been proposed as alternatives to eliminate or substantially decrease bacterial populations on poultry carcasses *(12),* most of these approaches have not been completely acceptable because of chemical residues, discoloration of chicken carcasses, and/or high cost associated with limited effectiveness. Chlorine rinses generally are used during processing of poultry for pathogen reduction *(23).* However use of chlorine by the food industry is coming under increasing scrutiny by regulators because of toxicity issues and disinfection by-products. Recent surface water rules promulgated by the U.S. Environmental Protection Agency relating to chlorine and chlorine-derived disinfection by-products will undoubtedly stimulate operators to seek technologies that will assure discharge compliance *(9).* The poultry industry also is a large-volume consumer of water, and the potential for reuse or recycling of poultry processing water represents an attractive economic benefit to the industry.

Pulsed electric field technology has been investigated as an important alternative approach to the destruction of microbial pathogens on contaminated surfaces *(18),* in food and drink *(13, 17, 18, 21),* and in potable and waste water *(1, 2, 6)* and the degradation of pollutants *(3).* Electrical discharge treatment of pumpable liquids can be highly effective in terms of microbial reduction and cost. The application of high-voltage pulses to gas-injected test liquids results in the formation of a plasma, which causes the generation of free radicals, free electrons, UV light, acoustic and shock waves, and electric fields at levels of 10 to 40 kV/cm *(1, 2, 4).* The application of high-voltage pulses to gas-sparged test liquids results in partial discharge activity and ionization of the gas, which leads to complete breakdown of the gas in the liquid medium. Through this ionization process, substantial levels of ozone (up to 5,400 ppm) and other physical bactericidal properties are formed in test liquids, which subsequently revert back to water posttreatment *(4).* This technology has been used previously by other researchers for the treatment of potable water artificially contaminated with *Escherichia coli (1).* Although ozone has been successfully used to treat liquids, particularly water, for commercial and industrial applications since the beginning of the last century *(9),* it is very difficult to achieve high ozone transfer rates and high residual dissolved ozone levels in water using conventional

* Author for correspondence. Tel: 00353906471838; Fax: 00353906486135; E-mail: nrowan@ait.ie.

ozone generators because of the properties of ozone and its inherent ability to decompose into its constituent oxygen *(20, 22)*. However, as a highly reactive oxidant, ozone also may lead to the formation of unwanted by-products in the presence of certain organic and mineral compounds *(8)*.

Despite advances made in the development of pulsed power technologies, plasma and plasmochemical processes accompanying electric discharge in water and industrial effluents have received very limited study to date. The aim of this study was to develop an efficient method of decontaminating poultry wash water containing a range of relevant microbial pathogens using a high-voltage pulsed-plasma gas-discharge (PPGD) system. The application of high-voltage pulses to gas-sparged test liquids could result in substantial inactivation of test organisms via several kinds of antimicrobial activity produced during this process.

MATERIALS AND METHODS

Bacterial strains. Single strains of *E. coli* NCTC 9001, *Campylobacter jejuni* ATCC 33560, *Campylobacter coli* ATCC 33559, *Listeria monocytogenes* NCTC 9863, *Salmonella enterica* serovar Enteritidis ATCC 4931, *S. enterica* serovar Typhimurium ATCC 14028, and *Bacillus cereus* NCTC 11145 were used in this study. *E. coli* NCTC 9001 is a nonpathogenic strain and was used in this research for comparative control studies. All test strains were maintained in Microbank storage vials (Cruinn Diagnostic, Dublin, Ireland) at −70°C. Each *Campylobacter* strain was grown to single colonies on modified charcoal-cefoperazone-deoxycholate agar (CCDA) plates (Unipath, Bedford, UK) at 42°C for 48 h in a microaerophilic environment generated by CampyPak gas generators (Unipath) generating 5% O_2, 10% CO_2, and 85% N_2. Strains of *E. coli*, *L. monocytogenes*, and *Salmonella* were grown separately to single colonies on MacConkey agar (MCA; Oxoid, Basingstoke, UK), *Listeria* selective agar (LSA; Oxoid), and xylose lysine desoxycholate agar (XLD; Oxoid), respectively, at 37°C for 48 h aerobically. *B. cereus* was grown at 37°C for 5 days on *B. cereus* selective agar (BCSA, Oxoid) supplemented with 0.5 mg/liter $MnSO_4 \cdot H_2O$, which stimulates endospore formation. Confirmation of *Salmonella* serovars was accomplished with biochemical tests, including triple sugar iron agar slants (Difco, Becton Dickinson, Sparks, Md.) and API 20 E strips (bioMérieux, Inc., Marcy l'Etoile, France), characteristic colony growth on XLD, and subsequent serological reactions with somatic (O) and flagellar (H) antigens (Difco, Becton Dickinson). *E. coli* was confirmed by characteristic colony growth on MCA and use of API 20 E strips. *Campylobacter* strains were confirmed by characteristic colony growth on CCDA and use of an immunolatex assay (Dryspot *Campylobacter* Test, Oxoid). *B. cereus* was confirmed by characteristic colony appearance on BCSA and endospore production under aerobic growth conditions and with API 50CHB and API 20E biochemical strips. *L. monocytogenes* was confirmed by characteristic growth on LSA at 4°C, tumbling motility at 25°C, the Christie-Atkins-Munch-Peterson test reaction, and its API *Listeria* (bioMérieux) profile.

Preparation of inocula. Bacteria were harvested from respective agar plates, washed three times in 0.1 M phosphate-buffered saline (PBS) pH 7.2, and sedimented by centrifugation at 4,000 × *g* for 20 min at 4°C. *Campylobacter* colonies were resuspended in 10 ml of PBS, transferred to a 1.5-liter fermentation vessel containing 500 ml of *Brucella* broth (Difco, Becton Dickinson), and grown in a Bioflow 3000 bioreactor (New Brunswick Scientific, St. Albans, UK) for 24 h at 42°C under the following batch culture settings: agitation at 125 rpm; sparged gas composition of 5% O_2, 10% CO_2, and 85% N_2; and pH 6.8 maintained with 0.1 M NaOH and 0.1 M H_2SO_4. After 24 h of growth (early stationary phase), bacteria were resuspended in 10 ml of sterile distilled water that had been refrigerated overnight at 4°C, and the optical density was adjusted at 540 nm to 2.0 (ca. 10^9 CFU/ml) with a spectrophotometer (model UV-120-02, Shimadzu Corp., Kyoto, Japan). Inocula for the other test bacteria were prepared similarly with the following modifications: cultures were grown at 37°C in Trypticase soy broth supplemented with 3% (wt/vol) yeast extract (Difco, Becton Dickinson) with agitation (250 rpm) using sparged atmospheric air. The presence and degree of endospore formation was confirmed by heat-treating the PBS suspension of *B. cereus* for 15 min at 85°C in a circulating constant temperature waterbath (model HE30, Grant Instruments Ltd., Cambridge, UK) equipped with a thermoregulator capable of maintaining the temperature to within ±0.05°C (model TE-8A, Techne Ltd., Cambridge, UK) and by subsequent enumeration of treated samples on BCSA plates after 48 h at 37°C.

Determination of appropriate sparged gas for subsequent PPGD treatments. Aliquots (10 ml) of OD_{540}-adjusted *B. cereus* endospore suspensions were added to 247 ml of sterile distilled water that had been refrigerated overnight at 4°C before transfer to the coaxial treatment chamber (total volume of 257 ml). The treatment chamber was constructed from 1-in. (2.54-cm)-diameter stainless steel pipe forming the outer grounded electrode, with a 1-mm copper wire forming the coaxial high-voltage electrode. The test chamber was also immersed in a chilled water bath to maintain the temperature at ≤4°C, as monitored with a thermocouple. Once the pulse power system had been activated, the treatment gas was injected into the treatment chamber with a venturi gas injector. Four different treatment gases were investigated separately: nitrogen, carbon dioxide, oxygen, and air. In addition to the four gases used, a control experimental test also was conducted with no gas added to the test liquid, which results in pulsed electric field generation. Plasma discharge activity was achieved in the test liquids using high-voltage pulses that were applied to the coaxial treatment chamber with a pulse-forming line (PFL) circuit, consisting of eight lengths of 12.62-m coaxial cable as described previously with modifications *(5)* (Fig. 1). The PFL was charged with a high-voltage 40-kV DC capacitor charging power supply connected via a resistance-diode protection circuit (RLIM). Using an SF6/air pressurized triggered spark gap switch (Samtech CSS-01, Samtech TG-01(B), the PFL output was connected to the treatment chamber via a further 2-m 50-Ω transmission line. The electrical operating parameters used were a pulse energy of 3.7 J, a PFL charging voltage of 23.5 kV, a pulse rate of 124 pps, and a gas flow rate 10 liters/min. The gas flow rate was controlled with a mass flow controller (model 5851S, Brooks Instruments, Emerson Process Management, Hatfield, Pa.), allowing continual adjustment to compensate for pressure and temperature variances. When the spark gap switch was triggered, a voltage pulse was launched along the transmission line feed cable to the treatment chamber. Upon reaching the treatment chamber, the pulse was applied to suitably contoured electrodes, resulting in ionization of the surrounding gas bubbles in the liquid and leading to ozone formation (depending on gas type used). Samples were taken in triplicate at designated intervals, and after 30 s of treatment time had elapsed, the pulsed power system was shut off and the gas supply was disconnected. The dissolved ozone was measured with a BMT 963AQ ozone-in-water sensor UV photometer (BMT Messtechnik GmbH, Berlin, Germany) as per methods described previously *(4)*. Although the peak ozone level may decay slightly

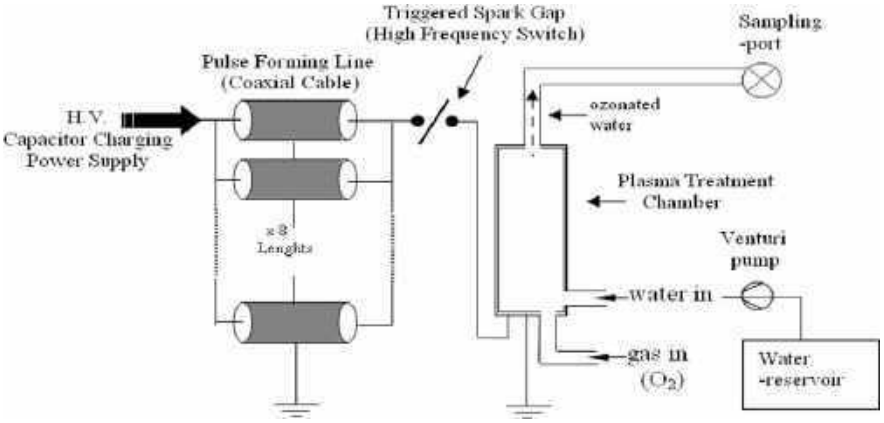

FIGURE 1. *Schematic of pulsed-plasma gas-discharge system for test liquids.*

before measurement, much of the residual ozone remains in solution, allowing the effect of the tested parameters on microbial reduction to be evaluated. Conductivity, pH, and temperature were measured with a WT-50 water test meter (Hanna Instruments, RS Components, Corby, UK), which had the following range and accuracy: temperature, 0 to 60.0°C ± 1°C; pH, 0 to 14.0 ±0.2; conductivity, 0 to 1,999 μS/cm, ±2% full scale.

Chicken wings. Fresh chicken wings were purchased from a local retail store. Representative samples (two chicken wings) selected randomly from the same bag were assayed before inoculation with the bacterial test strains.

PPGD treatments of distilled water and poultry wash water containing test organisms. Three chicken wings (each ca. 8 cm long, 4.5 cm wide, and 45 to 50 g) were submerged in a stomacher bag containing 300 ml of distilled water seeded with a test organism at ca. 10^8 CFU/ml (as confirmed spectrophotometrically). Inoculum for each test strain was prepared as described. The seeded chicken wing suspension was then stomached for 15 s, and a 30-ml sample was added to 270 ml of sterile distilled water that had been refrigerated overnight at 4°C. The mean pH of the poultry wash water containing test bacteria was 6.74 ± 0.18, and the pH of untreated sterile distilled water was 6.03 ± 0.21. A count of total aerobic mesophilic bacteria (enumerates both microbial flora from chicken the seeded test organism) was then performed for duplicate 5-ml samples as described previously *(23)* in addition to enumeration of pretreatment levels of each test organism on appropriate selective agar. A 257-ml sample was then transferred to the plasma chamber for treatment at 4°C. Samples were removed after predetermined exposure times, and bacteria were enumerated. Each test organism was also suspended separately in sterile distilled water only at 4°C to a population of ca. 10^7 CFU/ml and then subjected to plasma treatment and commensurate enumeration. This distilled water experiment was carried out as a control to determine the impact of poultry wash on microbial inactivation. Typical colonies of each test strain were randomly selected from respective selective agar plates after 24 and 48 h at 37°C (42°C for *Campylobacter*) with the highest dilution and were confirmed by use of appropriate physiological and biochemical tests.

Plate count. Treated and control samples were diluted as appropriate in PBS and spiral plated onto appropriate agar using a spiral system (model B, Spiral Systems Inc., Cincinnati, Ohio). Undiluted samples were plated with the pour-plate technique. Populations of surviving bacterial cells and cells in untreated controls were expressed in terms of CFU per milliliter, and corresponding death rate kinetic curves were generated.

Scanning electron microscopy. Test samples were centrifuged (10 min, 10,000 × *g*, 4°C), and the supernatants were discarded. The pellets were washed with PBS twice and fixed with 2.5% gluteraldehyde (Sigma-Aldrich, St. Louis, Mo.). Cells were then filtered onto 0.2-μm-pore-size Isopore GTTP membrane filters (Millipore, Bedford, Mass.). The cells were dehydrated once in 50, 70, 80, and 90% ethanol and twice in 10% ethanol, treated with 100% isoamyl acetate, critical point dried, and then sputter coated with 150-nm gold particles. Preparations were viewed with a model JSM-T200 scanning electron microscope (JEOL, Tokyo, Japan).

Statistical analysis. An analysis of variance balanced model (Minitab. release 14, Minitab Inc., State College, Pa.) was used to compare the effects of PPGD treatments on microbial inactivation. Experiments were replicated three times with duplicate treatments in each replication, and results are reported as means ± standard deviations (SD). Significant differences were reported at the 95% level ($P < 0.05$) and confidence interval.

RESULTS AND DISCUSSION

Effect of sparged-gas composition on pulsed-plasma–induced inactivation of *B. cereus* endospores. The results showed that the presence of oxygen in the sparged gas composition significantly affected the level of reduction of *B. cereus* endospores ($P < 0.05$) achieved in the plasma treatment chamber (Fig. 2). Use of oxygen alone produced the highest level of endospore reduction (3.4 log CFU/ml) after 30 s at 4°C, which may be attributed in part to the

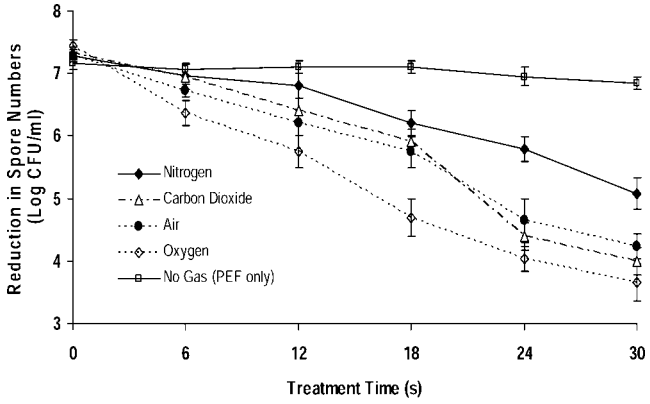

FIGURE 2. *Relationship between sparged-gas composition and the inactivation of* B. cereus *endospores in pulsed-plasma gas-discharge system containing distilled water at 4°C.*

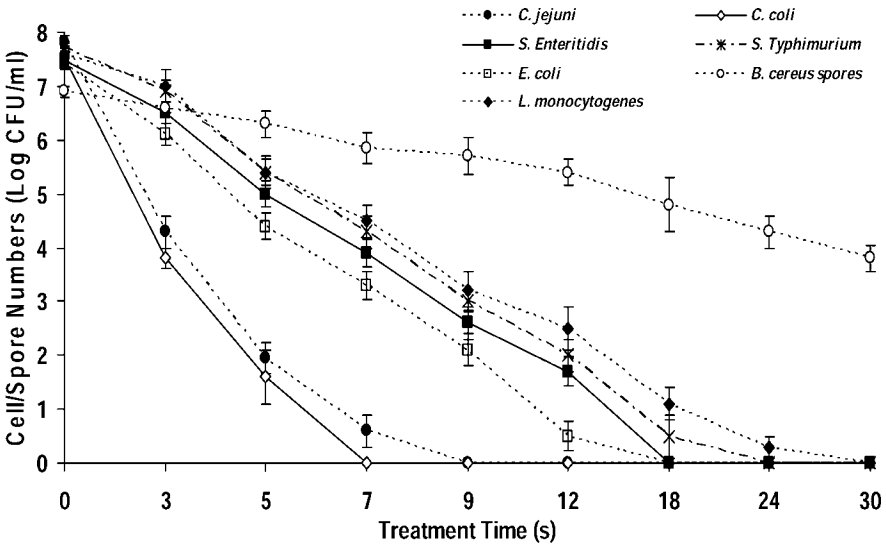

FIGURE 3. *Influence of pulsed-plasma gas-discharge treatment on the inactivation of test bacteria suspended in distilled water at 4°C.*

larger amounts of residual ozone (250 ppm) produced in test liquids sparged with oxygen alone. The significant increase in dissolved ozone from sparged oxygen probably results from the higher number of oxygen molecules present in the treatment gas mix, thus allowing much greater ozone production and hence higher dissolved ozone levels in the test liquid. The higher the number of oxygen molecules present in the treatment chamber, the greater the production and dissolution of ozone. Use of pulsed electric fields alone had no influence on *B. cereus* spore numbers (Fig. 2), a finding that corroborates those of previous studies *(19).*

In addition to the generation of multiple bactericidal properties such as high-intensity UV light, acoustic and shock waves, pulsed electric fields, and free radicals as reported previously *(1, 2, 4)*, production of plasma discharges in sparged water containing *B. cereus* endospores had a notable effect on pH, which was not investigated previously *(1, 2, 4).* The pH of the *B. cereus* spore suspension decreased during plasma treatment at 4°C: the pH measured after 30 s was 3.6, 3.8, 3.9, and 4.4 using sparged N_2, air, O_2, and CO_2, respectively. The pH of untreated sterile distilled water for all gaseous studies was 6.03. The reason why N_2 produced the lowest pH as a result of plasma treatment is not presently known but may be attributed to the availability of oxygen molecules from the breakdown of water during plasma treatment. Under such conditions, N_2-based compounds such as nitrate could be formed during plasma treatment, which would subsequently dissolve into the treated test liquid and produce an acidic solution (e.g., nitric acid) that would promote a rapid reduction in pH. A 3-log reduction in *B. cereus* spores per milliliter also was achieved using sparged CO_2 or air (Fig. 2). Commensurate increases in liquid conductivity occurred during plasma treatment, with 65 μs/cm obtained with CO_2 after 30 s at 4°C. Use of oxygen during plasma treatment resulted in a small but constant increase in conductivity, to 5.8 μs/cm. Water is a very suitable dielectric medium for plasma treatment because of its high permittivity ($\epsilon = 8.01$), which allows for a high-voltage electric field to be generated across the injected gas bubbles of low permittivity ($\epsilon \approx 1$ for most gases) *(4).* Water also have low conductivity (2 and 40 μs/cm for distilled and tap water, respectively), which minimizes energy loss and temperature rise occurring during resistive heating *(1).* Because oxygen alone produced the highest level of endospore reduction in the plasma chamber, this gas was used for the subsequent treatments of other test organisms during this study.

Effect of plasma discharge treatment on the viability of test organisms suspended separately in distilled water and in poultry wash water. Plasma discharge treatment of all vegetative test bacteria suspended separately in sterile distilled water at 4°C resulted in rapid reductions in microbial numbers (by ≤8 log CFU/ml) within 30 s of exposure to nondetectable levels (Fig. 3). The order of increasing sensitivity to pulsed-plasma treatment was *B. cereus* endospores, *L. monocytogenes*, *S. enterica* Typhimurium, *S. enterica* Enteritidis, *E. coli*, *C. jejuni*, and *C. coli.* Reductions in *Campylobacter* numbers (by ≤8 log CFU/ml) were achieved in just 9 s at 4°C, which may be attributable in part to the particular sensitivity of these enteropathogens to highly oxygenated environments *(15).* Suspending untreated (control) test bacteria in sterile distilled water at 4°C for 30 s did not significantly affect population numbers (data not shown). In general, gram-negative test bacteria were more susceptible to the lethal action of PPGD treatment ($P < 0.05$). This reaction may be due to the complexity of the gram-negative bacterial cell envelope, which is targeted by ozone and other oxygenated free radicals *(16).* This hypothesis is supported by scanning electron micrographs (Fig. 4b) of PPGD-treated *Campylobacter*, which reveal significant changes to the outer cell envelope at the cellular level (arrows indicate areas of injury). *L. monocytogenes* was more resistant to the lethal action of PPGD than were other vegetative test bacteria ($P < 0.05$), which corroborates previous findings of the resilience and adaptability of this problematic bacterium to a wide range of applied lethal stresses *(10, 16).* However, the pH of the bacterial suspension in distilled water decreased rapidly from 6.03 (untreated control) to 3.9 during plasma treat-

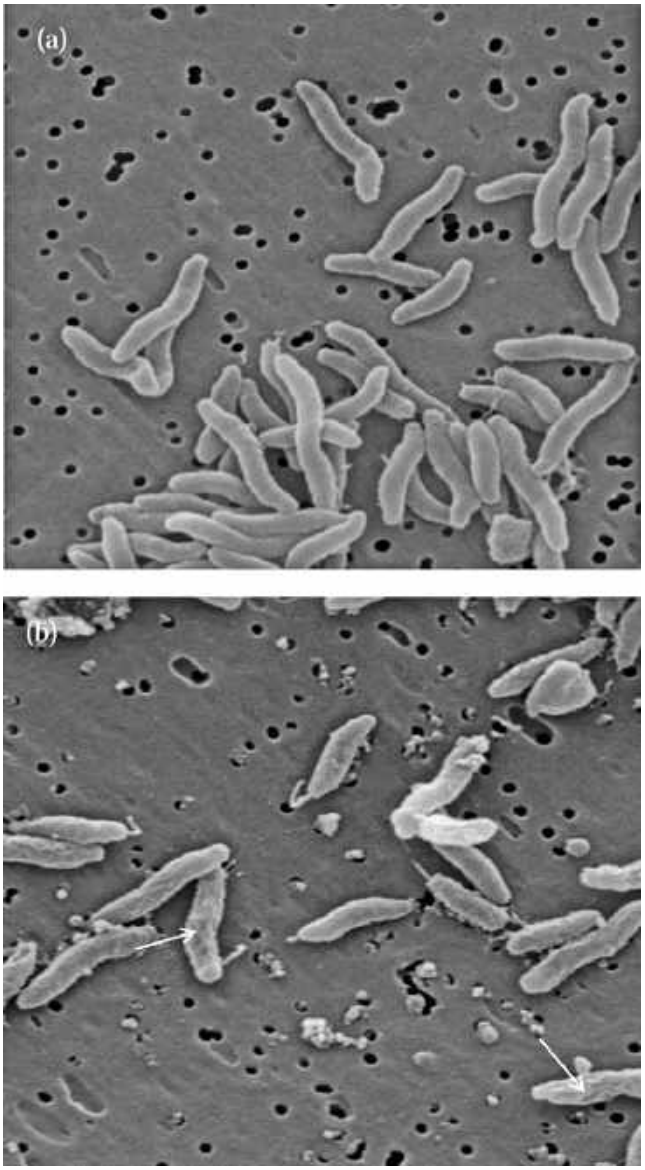

FIGURE 4. *Scanning electron micrographs of PPGD-treated (a) and untreated (b)* C. jejuni *cells (magnification ×12,000; white arrows indicate cellular damage).*

ment, which may have contributed in part to microbial inactivation. *C. jejuni* has been reported to be sensitive to extremes in pH, especially acidic conditions *(23).* Zhao and Doyle *(23)* recently exploited this sensitivity by experimenting with a combination of calcium sulfate and lactic acid (pH 2.1); this treatment was used for the decontamination of *C. jejuni* on artificially contaminated poultry surfaces.

Studies were carried out to investigate the presence of a limited range of toxic by-products in distilled water after treatment with electric discharges as per methods described previously *(1, 4).* The quality of the plasma-treated water met the standards of the European Union (Council directives on the quality of water intended for human consumption 80/778/EEC and the drinking water directive 98/83/EEC), with levels of ammonium (24 μg/liter), Cu (36 μg/liter), Mn (<50 μg/liter), Zn (<20 μg/liter), Pb (<2 μg/liter), Cr (<50 μg/liter), and Fe (<300 μg/liter) within the upper limits for drinking water. The results for Cu and Fe were particularly important because the electrodes in this study were manufactured from stainless steel and copper. These findings corroborate those of Anpilov et al. *(1)*, who found that water samples contained satisfactory levels of ammonium, Fe, Pb, Cr, fluoride, chloride, nitrate, and sulfate after treatment with electric discharges.

However, the present study was not focused on the possibility that application of electric discharges to poultry wash water may generate unwanted by-products such as bromate, which is a recognized carcinogen derived from bromide *(8).* Therefore, future studies should be conducted to investigate the relationship between the application of PPGD and the formation of bromate and other potential carcinogens in treated poultry wash water.

The plasma discharge treatment of all vegetative test bacteria suspended in poultry wash water at 4°C also resulted in rapid reductions in microbial numbers (by ≤8 log CFU/ml) to nondetectable levels within 30 s of exposure (Fig. 5). Although similar inactivation kinetic data were obtained for vegetative test organisms in distilled water (Fig. 3) and in poultry wash water (Fig. 5), in general a more rapid reduction of test bacteria cell numbers was evident

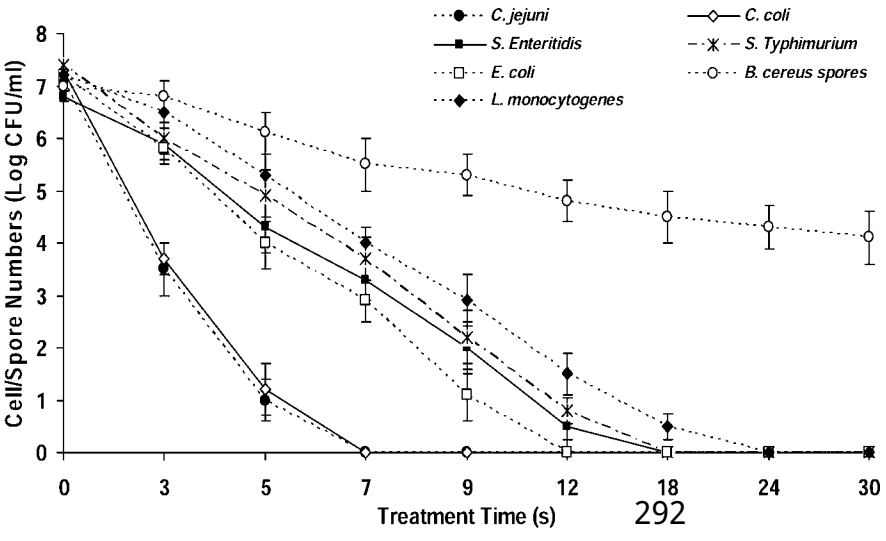

FIGURE 5. *Influence of pulsed-plasma gas-discharge treatment on the inactivation of test bacteria suspended in poultry wash water at 4°C.*

during treatment in the poultry wash water ($P < 0.05$). This finding may be attributed in part to the conversion of oils, fatty acids, and proteins released during poultry washing into associated nitric and carbonic acids during plasma treatment. The multidrug-resistant *S. enterica* Typhimurium strain appeared to be more tolerant to the lethal effects of pulsed-plasma treatment than were the other poultry-related *Campylobacter* and *Salmonella* pathogens tested. The average (±SD) total aerobic mesophilic bacterial count for untreated poultry wash water was 4.3 (±1.1) log CFU/ml, which was reduced to a nondetectable level after 30 s of plasma treatment at 4°C. Similar levels of *B. cereus* endospore reduction (by ca. 3 log CFU/ml) were achieved during plasma treatments in chilled distilled water (Fig. 3) and in poultry wash water (Fig. 5).

Our laboratory-based studies indicate that the use of PPGD was very effective for reducing populations of bacterial enteropathogens in poultry wash water at 4°C within 30s and could act as a critical control point in a hazard analysis critical control point system by preventing cross-contamination of processing environments by killing *Campylobacter* and *Salmonella* in the treated liquids. The potential for poultry wash water to be recycled using this pulsed-plasma approach appears high, particularly because this technology reduces microbial organisms treated to nondetectable levels in a very short time. However, further studies are needed in poultry-processing facilities to validate the efficacy of this plasma treatment under actual use conditions and to confirm that no harmful by-products are produced by this process.

ACKNOWLEDGMENT

We are grateful to David Currie for technical assistance with the electron microscopy.

REFERENCES

1. Anpilov, A. M., E. M. Barkhudarov, N. Christofi, V. A. Kop'ev, I. A. Kossyi, M. I. Taktakishvili, and Y. Zadiraka. 2002. Pulsed high voltage electric discharge disinfection of microbially contaminated liquids. *Lett. Appl. Microbiol.* 35:90–94.
2. Anpilov, A. M., E. M. Barkhudarov, N. Christofi, V. A. Kop'ev, I. A. Kossyi, M. I. Taktakishvili, and Y. V. Zadiraka. 2004. The effectiveness of a multi-spark electric discharge system in the destruction of microorganisms in domestic and industrial wastewaters. *J. Water Health* 4:267–277.
3. Chauchan, S., E. Yankelevich, V. M. Bystritskii, and T. K. Wood. 1999. Degradation of 2,4–5-trichlorophenol and 2,3,5,6-tetrachlorophenol by combining pulse electric discharge with bioremediation. *Appl. Microbiol. Biotechnol.* 52:261–266.
4. Espie, S., L. Marsili, S. J. MacGregor, and J. G. Anderson. 2001. Investigation of dissolved ozone production using plasma discharge in liquid. *Pulsed Power Plasma Sci. Digest Tech. Pap.* 1:616–619.
5. Gupte, A. R., C. L. E. de Rezende, and S. W. Joseph. 2003. Induction and resuscitation of viable but nonculturable *Salmonella enterica* serovar Typhimurium DT104. *Appl. Environ. Microbiol.* 69:6669–6675.
6. Hao, X. L., M. H. Zhou, and L. C. Lei. 2007. Non-thermal plasma-induced photocatalytic degradation of 4-chlorophenol in water. *J. Hazard. Mater.* 141:475–482.
7. Jorgensen, F., R. Bailey, S. Williams, P. Henderson, D. R. A. Wareing, F. J. Bolton, J. A. Frost, L. Ward, and T. J. Humphrey. 2002. Prevalence and numbers of *Salmonella* and *Campylobacter* spp. on raw, whole chicken in relation to sampling methods. *Int. J. Food Microbiol.* 76:151–164.
8. Kim, H. S., H. Yamada, and H. Tsuno. 2006. Control of bromate ion and brominated organic compounds formation during ozone/hydrogen peroxide treatment of secondary effluent. *Water Sci. Technol.* 53:169–174.
9. Kim, J. G., A. E. Yousef, and M. A. Khadre. 2003. Ozone and its current and future application in the food industry. *Adv. Food Nutr. Res.* 45:167–218.
10. Lou, Y., and A. E. Yousef. 1997. Adaptation to sublethal environmental stress protects *Listeria monocytogenes* against lethal preservation factors. *Appl. Environ. Microbiol.* 63:1252–1257.
11. Mead, P. S., L. Slutsker, V. Dietz, L. F. McCaig, J. S. Bresee, C. Shapiro, P. M. Griffin, and R. V. Tauxe. 1999. Food-related illness and death in the United States. *Emerg. Infect. Dis.* 5:607–625.
12. Nauta, M., I. van der Fels-Klerx, and A. Havelaar. 2005. A poultry-processing model for quantitative microbiological risk assessment. *Risk Anal.* 25:85–98.
13. Ordriozola-Serrano, I., S. Bendicho-Porta, and O. Martin-Belloso. 2006. Comparative study on shelf life of whole milk processed by high-intensity pulsed electric field or heat treatment. *J. Dairy Sci.* 89:905–911.
14. Park, H., Y. C. Hung, and R. E. Brackett. 2002. Antimicrobial effect of electrolyzed water for inactivating *Campylobacter jejuni* during poultry washing. *Int. J. Food Microbiol.* 72:77–83.
15. Purdy, D., S. Cawthraw, J. H. Dickinson, D. G. Newell, and S. F. Park. 1999. Generation of a superoxide dismutase (SOD)-deficient mutant of *Campylobacter coli*: evidence for the significance of SOD in *Campylobacter* survival and colonization. *Appl. Environ. Microbiol.* 65:2540–2546.
16. Rowan, N. J. 1999. Evidence that inimical food preservation barriers alters microbial resistance, virulence and cell morphology. *Trends Food Sci. Technol.* 10:261–272.
17. Rowan, N. J., S. J. MacGregor, J. G. Anderson, D. Cameron, and O. Farish. 2001. Inactivation of *Mycobacterium paratuberculosis* by pulsed electric fields. *Appl. Environ. Microbiol.* 65:2833–2836.
18. Rowan, N. J., S. J. MacGregor, J. G. Anderson, R. A. Fouracre, and O. Farish. 1999. Pulsed UV light inactivation of microbial pathogens. *Appl. Environ. Microbiol.* 65:1312–1315.
19. Rowan, N. J., S. J. MacGregor, J. G. Anderson, R. A. Fouracre, and O. Farish. 2000. Pulsed electric field inactivation of diarrhoeagenic *Bacillus cereus* is caused by irreversible electroporation. *Lett. Appl. Microbiol.* 31:110–114.
20. Selma, M. V., D. Beltran, E. Chacon-Vera, and M. I. Gil. 2006. Effect of ozone on the inactivation of *Yersinia enterocolitica* and the reduction of natural flora on potatoes. *J. Food Prot.* 69:2357–2363.
21. Sentandreu, E., L. Carbonell, D. Rodrigo, and J. V. Carbonell. 2006. Pulsed electric fields versus thermal treatment: equivalent processes to obtain equally acceptable citrus juices. *J. Food Prot.* 69:2016–2018.
22. Wade, W. N., A. J. Scouten, K. H. McWatters, R. L. Wick, A. Demirci, W. F. Fett, and L. R. Beuchat. 2003. Efficacy of ozone in killing *Listeria monocytogenes* on alfalfa seeds and sprouts and effects on sensory quality on sprouts. *J. Food Prot.* 66:44–51.
23. Zhao, T., and M. P. Doyle. 2006. Reduction of *Campylobacter jejuni* on chicken wings by chemical treatments. *J. Food Prot.* 69:762–767.

Journal of Microbiological Methods 94 (2013) 325–337

Contents lists available at SciVerse ScienceDirect

Journal of Microbiological Methods

journal homepage: www.elsevier.com/locate/jmicmeth

Disinfection and toxicological assessments of pulsed UV and pulsed-plasma gas-discharge treated-water containing the waterborne protozoan enteroparasite *Cryptosporidium parvum*

Jennifer Hayes, Dominik Kirf, Mary Garvey, Neil Rowan *

Bioscience Research Institute, Athlone Institute of Technology, Dublin Road, Athlone, Ireland

ARTICLE INFO

Article history:
Received 23 April 2013
Received in revised form 11 July 2013
Accepted 12 July 2013
Available online 23 July 2013

Keywords:
Cryptosporidium parvum
Water treatment
Pulsed light
Pulsed-plasma gas-discharge
Cell culture-*q*PCR
Toxicity

ABSTRACT

We report for the first time on the comparative use of pulsed-plasma gas-discharge (PPGD) and pulsed UV light (PUV) for the novel destruction of the waterborne enteroparasite *Cryptosporidium parvum*. It also describes the first cyto-, geno- and ecotoxicological assays undertaken to assess the safety of water decontaminated using PPGD and PUV. During PPGD treatments, the application of high voltage pulses (16 kV, 10 pps) to gas-injected water (N_2 or O_2, flow rate 2.5 L/min) resulted in the formation of a plasma that generated free radicals, ultraviolet light, acoustic shock waves and electric fields that killed ca. 4 log *C. parvum* oocysts in 32 min exposure. Findings showed that PPGD-treated water produced significant cytotoxic properties (as determined by MTT and neutral red assays), genotoxic properties (as determined by comet and Ames assays), and ecotoxic properties (as determined by Microtox™, Thamnotox™ and Daphnotox™ assays) that are representative of different trophic levels in aquatic environment ($p < 0.05$). Depending in part on the type of injected gas used, PPGD-treated water became either alkaline (pH $\leq$ 8.58, using O_2) or acidic (pH $\geq$ 3.21, using N_2) and contained varying levels of reactive free radicals such as ozone (0.8 mg/L) and/or dissociated nitric and nitrous acid that contributed to the observed disinfection and toxicity. Chemical analysis of PPGD-treated water revealed increasing levels of electrode metals that were present at $\leq$30 times the tolerated respective values for EU drinking water. PUV-treated water did not exhibit any toxicity and was shown to be far superior to that of PPGD for killing *C. parvum* oocysts taking only 90 s of pulsing [UV dose of 6.29 μJ/cm^2] to produce a 4-log reduction compared to a similar reduction level achieved after 32 min PPGD treatment as determined by combined in vitro CaCo-2 cell culture-*q*PCR.

1. Introduction

There has been growing international concern about the release of unwanted pharmaceutically-active compounds into the aquatic environment as these are not effectively removed or eliminated at waste water treatment plant level (Sharpe, 2001; EPA, 2005; Fernandez et al., 2007; Rowan, in press). Consumption of water containing endocrine disrupting chemicals (EDC) may cause reproductive disorders in humans (Fernandez et al., 2007). EDCs have been detected worldwide in processed wastewater from domestic treatment plants (WWTPs) at the ng/L level that may cause abnormalities to aquatic organisms (Ternes et al., 1999; Lishman et al., 2006). Previous work conducted by this research group has demonstrated that fish habituating downstream of WWTPs in the Midlands region in Ireland exhibited delayed spermatogenesis compared with fish upstream and intersex (feminization) was discovered in roach (Fogarty and McGee, 2007). Therefore, it is essential that such compounds be efficiently and effectively removed from processed water discharged from WWTPs.

Cryptosporidium parvum is an enteric coccidian parasite that is recognised as a frequent cause of water-borne disease in humans (Hunter and Syed, 2001). The occurrence of the environmentally thick-walled oocyst stage of this parasite has become a world-wide concern due to its resistance to chlorine at concentrations typically applied in drinking water treatment plants (2 to 6 mg/L) (Rowan, 2011). Development of alternative methods of *Cryptosporidium* disinfection for water applications (such as ozone and/or UV) has been hindered in part by the uncertainty surrounding efficacy of using in vitro surrogate viability tests due to their over estimation of oocyst survivors post treatments and lack of critical data on the preferred use of in vitro cell culture and/or in vivo animal-based infectivity assays to determine inter-related factors governing repeatable disinfection of oocysts suspended in water (Garvey et al., 2010).

Development of pulsed UV light has recently received attention as a potential novel strategy for decontaminating water as it offers many

* Corresponding author.
E-mail address: nrowan@ait.ie (N. Rowan).

0167-7012/$ – see front matter © 2013 Elsevier B.V. All rights reserved.
http://dx.doi.org/10.1016/j.mimet.2013.07.012

benefits including rapid microbial reductions and efficiency of energy usage due to high peak-power dissipations (Elmnasser et al., 2007; Rowan et al., 2008a, 2008b; Rowan, in press). Laboratory-based investigations have revealed that critical inter-related factors governing the effective operational use of PUV for disinfecting water include pulse repetition frequency, pulsed duration, applied voltage, distance from the light source, presence of suspended solids, and type and concentration of microbial species present (Garvey et al., 2010; Rowan, 2011; Hayes et al., 2012). Recent studies also reported that PUV inflicts irreversible damage in yeast by a multi-targeted molecular and cellular process (Farrell et al., 2011). There is a dearth of published information on the efficacy of PUV for treating *C. parvum* oocysts in water with particular relevance to lethality of treatment and safety of process.

An alternative or complementary approach to the treatment of drinking and waste water includes the application of high voltage pulses to gas-injected test liquids (or PPGD), which results in the formation of a plasma that causes free radicals such as dissolved ozone and hydrogen peroxide, free electrons, ultraviolet light (UV), acoustic shock waves and electric fields at levels between 10 and 50 kV to be generated in the test liquids (Rowan et al., 2008a, 2008b). Pulsed electric discharge or PPGD has been shown to be effective for the oxidative destruction of structurally-related organic compounds such as dyes, phenol and aniline in aqueous solutions (Willberg et al., 1996; Bubnov et al., 2004; Liu and Xuan Zhen Jian, 2005; Hao et al., 2007; Amin et al., 2007). However, there is also a dearth of information surrounding the ability of PPGD to kill waterborne coccidian parasites.

This constitutes the first study to report on the cyto-, geno- and ecotoxicological quality of PPGD and PUV treated water post inactivating *C. parvum* oocysts.

2. Methods

2.1. Pulsed-plasma gas-discharge system and analytical evaluation of treated test liquids

The pulsed-plasma gas-discharge (PPGD) system (Samtech Ltd, Glasgow, UK) consisted of a prototype HV pulse generator and treatment chamber for low-temperature liquid decontamination which was described previously by Rowan et al. (2008a, 2008b) with modifications. The main components (Fig. 1a) were the high voltage power supply, a set of charging resistors, a trigger generator linked to a corona stabilised switch (CSS) and the pulse generator. This PPGD system produced multiple short-lived biocidal properties in the treatment chamber that includes ozone, acoustic shock waves, UV light and pulsed electric fields as described previously (Rowan et al., 2008a, 2008b). The PPGD test liquid was prepared by combining 95 mL of dH_2O combined with 5 mL of 0.1 M Phosphate Buffered Saline (PBS). The provided high permittivity ($\varepsilon = 80.1$) and low conductivity (1000 μs/cm) supported discharge stability and reduced osmotic stress towards test organisms. The volume of the treatment test liquid was set at 100 mL as this yielded at discharge gap of 5 mm between the electrodes and the surface of the sample for producing a strong and consistent HV discharge. Within the

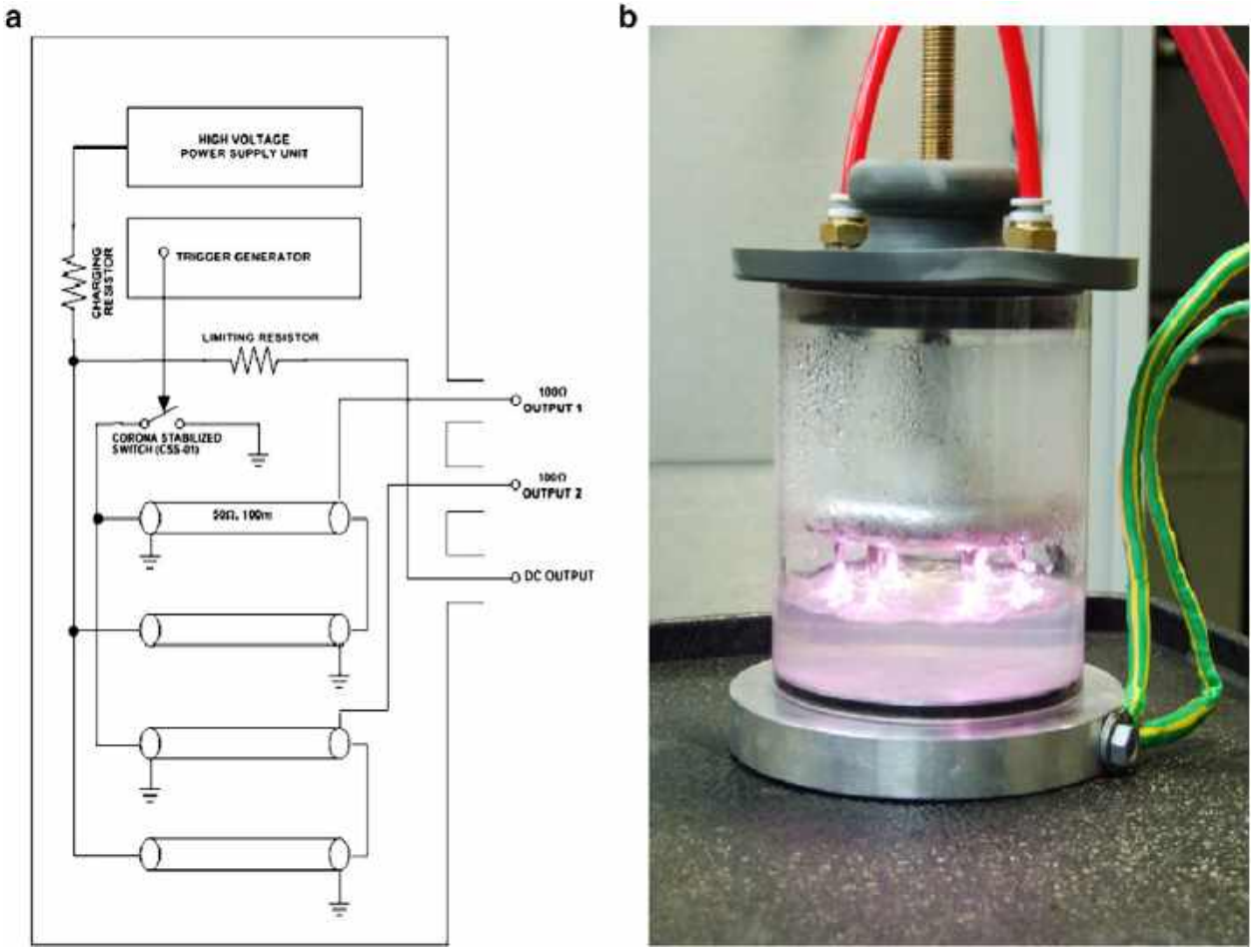

Fig. 1. Schematic of electrical circuitry for pulsed-plasma gas-discharge system (a) and physical appearance of streamer type corona discharge observed during treatment (16 kV, 10 pps, O_2 flow rate at 2.5 L/min).

treatment chamber the PPGD was generated via a multiple needle electrode configuration that was found to produce a positive streamer type corona discharge (Fig. 1b). The electrodes were made of two materials: the upper HV electrode and needle arrangements comprising stainless steel BS316S11 (predominately iron (Fe) with 16–18.5% chromium (Cr), 11–14% nickel, 2–5% molybdenum and a mixture of 2% manganese (Mn), 1% silicon, 0.045% phosphorous, 0.03% sulphur, and 0.03% carbon) with the lower earth electrode comprising aluminium alloy 6082 (predominantly aluminium (Al) with 0.7–1.3% silicon, 0.4–1% Mn, 0.6–1.2% magnesium, a mixture of 0.5% Fe, 0.25% Cr, 0.2% zinc, 0.1% copper and 0.1% titanium).

The possible presence of electrical metal contaminate (namely aluminium, chromium, iron and manganese) released from the treatment fluid during HV operation was determined by an independent laboratory (City Analyst Ltd, Dublin, Ireland). Pure N_2 or O_2 gases (BOC, Ireland) were streamed separately through this electrode gap at a flow rate of 2.5 L/min using a Rate-Master® flowmeter (Dwyer Instruments Inc. UK). The pulsed forming network (PFN) charging voltage and pulse frequency were mainly kept at 16 kV and 10 pps respectively for ≤90 min during this study to avoid internal arcing on the CSS caused by molecular breakdown of sulphur hexafluoride (SF_6) insulation gas that occurred during increased charging voltage and pulse repetitions. The pulse waveform was monitored using a digital oscilloscope (Tektronix TDS 3022). The 100 mL test liquid with and without *C. parvum* was aseptically transferred into the PPGD treatment chamber. Temperature and pH were monitored by using a Eutech® CyberScan pH 510 pH/mV meter with automated temperature control adjustment (Thermo Fischer Scientific, UK). The dissolved ozone (O_3) concentration of gas-discharge treated water was analysed via the dipropyl-p-phenylenediamine (DPD) colorimetric method (Spectroquant® 1.00607, Merck Chemicals, VWR, Ireland), which detects dissolved O_3 within the concentration range 0.01–4.00 mg/L. Ion exchange chromatography (IEC) was used to determine the presence of nitric acid (HNO_3) and nitrous acid (HNO_2) in the gas-discharged water. This chromatographic system was composed of a 761 Compact IC (Metrohm, Ireland) including a conductometric detector and suppressor with peristaltic pump. The utilised mobile phase consisted of a 1 mM sodium bicarbonate ($NaHCO_3$) and 3.5 mM sodium carbonate (Na_2CO_3) in aqueous solution, with ion separation performed in isocratic mode at a 1.2 mL/min flow rate and ambient temperature on a Transgenomic® IC Sep AN2 analytical column. All injections were performed in duplicate with an injection volume of 20 μL and a total run time of 15 min.

2.2. Pulsed ultraviolet light system

The pulsed-UV system used was the PUV-01 (SAMTECH Ltd., Glasgow) and consists of two main components; a treatment chamber and a driver circuit as described previously by Hayes et al. (2012). 20 mL samples were aseptically transferred to a sterile Petri dish and treated in the PUV treatment chamber at a distance of 8 cm from the light source. The number of pulses of light used ranged from 0 (untreated control) to 90 pulses using a lamp discharge energy of 16.2 J that was shown previously to inactivate test *C. parvum* populations by ca. 4 $\log_{10}$ CFU/mL over this treatment regime (Hayes et al., 2012). Measurement of UV fluence rate (μJ/cm^2) was determined using chemical actinometry as described by Hayes et al. (2012) as the non-continuous emitted spectrum did not facilitate use of a calibrated radiometer. Results for both PUV and PPGD were expressed in terms of $\log_{10}$ CFU/mL for reduction in *C. parvum* numbers. Statistical analyses were performed using Minitab Series 15 and reported at 95% confidence intervals, unless otherwise stated.

2.3. Combined cell culture-quantitative PCR (CC qPCR) assay for enumerating viable C. parvum post PPGD and PUV treatments

The combined cell-culture-*q*PCR assay as described recently by Garvey et al. (2010) was used for enumerating viability of *C. parvum* oocysts post treatments. *C. parvum* oocysts (Iowa isolate derived from a bovine calf) were purchased from Waterborne Inc. USA. Fresh oocysts (<24 h after excretion) were stored in sterile PBS with 100 U of penicillin/mL, 100 μg of streptomycin/mL and 100 μg of gentamicin/mL and stored at 4 °C until they were used for treatment studies. The excystation rate was determined for each batch of oocysts by microscopic observation following sequential incubation at 37 °C in acidified Hanks balanced salt solution for 1 h and in 0.8% trypsin—0.75% sodium taurocholate for 1 h, followed by incubation at room temperature for 30 min. Identification of *C. parvum* oocysts was confirmed by PCR targeting of a 620 bp polymorphic region of the β-tubulin gene. For negative infection studies, oocysts were inactivated by heating at 70 °C for 30 min. All experiments were carried using oocysts with greater than 80% viability, as determined by in vitro excystation as per Garvey et al. (2010). Cell culture *q*PCR was conducted as per described by Garvey et al. (2010) using CaCo-2 cell monolayers as host cells for parasitic infectivity followed by real time PCR. Methods for the growth and maintenance of CaCo-2 uninfected and infected cells are therefore not described herein. Real-time, Taqman-quantitative PCR (*q*PCR) was performed using primers (TIB MOLBIOL, Berlin, Germany) specific for the 18S region of *Cryptosporidium* on a LightCycler® device (Model 1.5, Roche Diagnostics, West Sussex, England) following the method of Garvey et al. (2010). Aliquots of oocysts at different densities were then stimulated to infect the CaCo-2 cell line that were seeded into 24 well plates (Sarstedt) at a concentration of ca. 1×10^4 cells/mL at 90% confluency. 1 mL aliquots of each concentration range of excysted oocysts were re-suspended in RPMI cell culture growth media and added to 1 well of the 24 well plate. Following 48 h incubation at 37 °C in a humidified atmosphere of 5% (v/v) CO_2, the cell culture media with non-adherent or internalized *C. parvum* was removed by aspiration and discarded. Mammalian cell was then washed with sterile PBS and trypsinized using 200 μL of 0.25% (v/v) trypsin/EDTA (Sigma) and left for 15 min at 37 °C until complete detachment of the monolayer had occurred. Cells were then centrifuged at 70.7 ×*g* for 10 min and re-suspended in 200 μL sterile PBS, thereafter the mammalian cells and *C. parvum* sporozoite cell membranes were lysed using PCR template preparation kit (Roche Diagnostics, West Sussex, England) in order to produce DNA (template) and standard curve. The aforementioned procedure was then repeated to determine infectivity of oocysts subjected to varying PPGD and PUV parameters or heating at 70 °C for 30 min (negative control) as per method of Garvey et al. (2010). Log inactivation of oocysts (L) is defined by $L = \log_{10}[Nd / No]$, where No is the initial concentration of oocysts and Nd is the concentration of viable infectious oocysts post disinfection treatments as detected by combined cell culture-*q*PCR assay as per method of Garvey et al. (2010).

2.4. Cell culture and treatment of PUV and PPGD test liquids

The hepatoma HepG2 cell line (ATCC, Manassas, USA) and normal keratinocyte, HaCaT cells (Cell Lines Service, Heidelberg, Germany) were grown in Dubeccos Modified Eagle's Medium (DMEM) nutrient mixture Ham's F-12 (1:1) and DMEM respectively. Both media types were supplemented with 10% foetal bovine serum (FBS), 2 mM L-glutamine, 1.25 μg/mL amphotericin B, 25 U/mL penicillin and 25 μg/mL streptomycin and cells were cultured at 37 °C in a 5% CO_2 humidified incubator. Cell culture consumables and media components were sourced from Sarstedt (Drinagh, Ireland) and Sigma-Aldrich (Dublin, Ireland), respectively. 100 mL samples of the test liquid were treated separately with PUV or PPGD in order to produce a ca. 4 $\log_{10}$ reduction in *C. parvum* oocyst numbers as described earlier. For comparative purposes, N_2 and O_2 gases were utilised as discharge gases at a flow rate of 2.5 L/min. 10 mL samples were taken aseptically at the end of each treatment regime (in triplicate) and transferred into a sterile universal that was then centrifuged at 3000 rpm for 10 min. The supernatant was removed and filter sterilized using 0.2 μm filters, before being subjected to toxicity testing. The liquid

was also tested after a 7 day refrigerated storage in order to determine if this incubation period affected toxicity. Untreated samples were used as reference control.

2.5. The MTT cytotoxicity assay

HepG2 and HaCaT cells were seeded in 96-well plates at a density of 1×10^4 and 1.5×10^4 per well (200 μL), respectively. The plates were further incubated for 15 h (HepG2) and 24 h (HaCaT) at 37 °C to facilitate cell attachment. The cells were exposed to undiluted and diluted (cell culture medium) PPGD treated test liquids for varying exposure times at 37 °C. Following removal of test liquid, the cells were rinsed twice with PBS and 100 μL culture medium containing 0.5 mg/mL 3-(4,5-dimethylthiazol-2yl)-2,5-diphenyl-2H-tetrazolium bromide (MTT) (Sigma-Aldrich, Dublin, Ireland) was added to each well and incubated for a further 4 h. After careful removal of MTT medium, 100 μL of dimethyl sulfoxide (DMSO, Sigma-Aldrich, Dublin, Ireland) was added to each well to extract the dye. The plates were agitated for 30 s prior to recording optical densities at 540 nm using a microplate reader (Anthos HTIII, Labtec Instruments GmbH, Wals, Austria).

2.6. The neutral red cytotoxicity assay

Similar to the MTT assay, HepG2 and HaCaT cells were seeded at a density of 1×10^4 and 1.5×10^4 per well (200 μL), respectively and cells were exposed to undiluted and diluted (cell culture medium) PUV and PPGD treated test liquids for varying exposure times at 37 °C. Following removal of extract medium, the cells were rinsed twice with PBS and 100 μL of freshly prepared and filter-sterilized NR solution (100 μg/mL) (Sigma-Aldrich, Dublin, Ireland) was added to each well and incubated for 80 min. After removal of NR solution, the cells were carefully rinsed twice with 200 μL PBS and the dye was extracted by introducing 100 μL of acidified methanol/water solution (1:1) to each well. The plates were then agitated for 30 s prior to recording optical densities at 540 nm using a microplate reader (Anthos HTIII, Labtec Instruments GmbH, Wals, Austria).

2.7. The single cell gel electrophoresis (comet) assay

The Comet assay procedure of Singh et al. (1988) was adopted with minor modifications. 2 mL aliquots of HepG2 and HaCaT cells were seeded at 3×10^4 cells/mL in duplicate wells of a 24-well culture plate and following 24 h incubation culture medium was replaced with 2 mL of PPGD treated test liquids and incubated for further 24 h. In parallel, control cells were treated with 100 μM H_2O_2 for 40 min as positive control. Following treatment, the cells were harvested and cell viability (>80% for all test concentrations) was determined by trypan blue exclusion to avoid false positive responses due to cytotoxicity. Subsequently 200 μL of the cell suspension was diluted with low-melting point agarose and 100 μL cell-aliquots were immediately spread on gel bond strips. The strips were immersed in alkaline lysis solution pH 10 (2.5 M NaCl, 100 mM disodium EDTA, 10 mM Tris–Cl, 1% Triton X-100, 10% DMSO) and incubated at 4 °C for 40 min prior to treatment with 1 mg/mL proteinase K in lysis solution pH 7.4 without Triton X-100 for 2 h at 37 °C. Following alkaline unwinding for 20 min by immersion in electrophoresis buffer (0.1% 8-hydroxyquinoline, 10 mM disodium EDTA, 2% DMSO, 300 mM NaOH, pH 13) the gelbond strips were subject to electrophoresis at 25 V and 300 mA for 12 min. Gel strips were then neutralized with 400 mM Tris–Cl buffer and stained with SYBR Gold for 40 min. Following fixation in methanol, DNA migration was measured via fluorescence microscopy coupled to image analysis software (Comet IV, Perceptive Instruments, UK) and expressed as percentage tail DNA (% tail DNA) and as tail moment. The Comet assay was conducted on duplicate slides with 50 cells scored per slide. Statistical difference between control and treated cells was evaluated with the nonparametric Mann–Whitney test using untransformed Olive tail moment values.

2.8. The Ames mutagenicity assay

The Ames II™ Mutagenicity assay method (Xenometrix) was performed with and without metabolic activation (+/− S9 mix) with slight modifications to a procedure previously described by Flückiger-Isler et al. (2004). The bacterial culture TA98 and TAMix were exposed to the PPGD treated test liquid in the presence and absence of S9 mix. *Salmonella typhimurium* TA98 and TAMix (TA7001-7006) were the chosen tester strains to detect frameshift mutations and base-pair substitutions, respectively. The bacterial cultures were resuscitated in Ames II growth medium containing 50 μg/mL ampicillin. For tests performed in the absence of metabolic activation, 215 μL of Ames II exposure medium was mixed with 25 μL bacterial cultures. For assays performed in the presence of metabolic activation, the volume of the Ames II exposure medium was decreased to accommodate the final S9 mix fraction (Moltox) of 4.5% (v/v). Subsequently, 250 μL of the exposure media (plus tester strains) was pipetted into single wells of a 24-well plate and, following incubation at 37 °C for 90 min with 250 rpm agitation, 2.8 mL of histidine deficient Ames II indicator medium was added to each well. Next, 50 μL of solution from each well was transferred to individual wells of a 348-well plate and following a 48 h incubation period any colour change of the indicator medium from purple to yellow was noted and taken as indicative of revertant bacteria or a positive response. The Ames II™ Mutagenicity test was performed as per manufactures instruction in triplicate.

2.9. Ecotoxicological analysis

A range of commercially-available ecotoxicology assays (MicroBioTests Inc., Gent, Belgium) were used to determine the effect of exposure of various test species to PPGD and PUV-treated water on the various free living organisms representative of taxa in the natural aquatic environment (Table 1). Standard freshwater was prepared as indicated by the supplier. The standard freshwater was used as a hatching medium for the cysts and as dilution medium for the test solutions. Positive control tests were performed using the reference toxicant potassium dichromate ($K_2Cr_2O_7$) or phenol, as recommended by the supplier of the assays. The Thamnotoxkit F™ screening bioassay is a 24 h LC_{50} bioassay performed in multiwell test plates using instar II–III larvae of the fairy shrimp *Thamnocephalus platyurus*. The *T. platyurus* freshwater crustacean toxicity test was performed as per Thamnotoxkit F™ standard operational procedure. The number of dead larvae for each reference toxicant concentration and for each test sample was recorded and the % mortality calculated versus the untreated control. The *Daphtoxkit F™* is a 24 hour acute immobilisation test performed with neonates hatched from dormant eggs/ephippia of *Daphnia magna* in multiwell plates. *Daphnia* spp. are ubiquitous crustaceans in freshwater ecosystems and are key organisms in the aquatic food chain. *Daphtoxkit F™* tests were performed in accordance with recommended test procedures prescribed the supplier. The Microtox™ bioassay is a standardised toxicity system using a luminescent bacterial species, *Vibrio fischeri*, as the toxicity indicator. Microtox determines the acute toxicity of aqueous samples by measuring the changes of light produced naturally in samples exposed to bioluminescent bacterial under standard conditions. The Microtox™ test was carried out as per the suppliers' standard operating procedure (Azur Environmental, 1998). Each test was carried out in triplicate on a Microtox™ 500 analyser (Strategic Diagnostics Incorporation Europe). Phenol was used as a reference chemical and a basic test for phenol was run for every fresh vial of bacteria to ensure the validity of all tests. The acute toxicity data was obtained and analysed using the MicrotoxOmni software (SDI Europe, Hampshire, UK). Five minute and fifteen minute EC_{50} tests were performed. Detection of ecotoxicity for each test is based upon the "median effects level" that is described as either IC_{50}, EC_{50}, or LC_{50} depending upon the test (IC, EC, and LC are abbreviations for inhibition concentration, effect concentration, and lethal

Table 1
Comparison of the $EC_{50}/LC_{50}/IC_{50}$ and $EC_{20}/LC_{20}/IC_{20}$ values obtained from PUV and PPGD-treated water using ecotoxicity and cytotoxicity assays.

Ecotoxicity Tests	PUV	PPGD-treated dH_2O (16 kV/cm, 10 pps, O_2 flow rate at 2.5 L/min)			
	$EC_{20}/LC_{20}/IC_{20}$	$EC_{50}/LC_{50}/IC_{50}$ (% v/v)		$EC_{20}/LC_{20}/IC_{20}$ (% v/v)	
	Immediately post treatment	Immediately post treatment	After 7 days	Immediately post treatment	After 7 days
Thamnotoxkit F™ (fairy shrimp)	100%	12.63% ± 1.016	27.74% ± 0.275	5.10% ± 0.416	15.88% ± 0.176
Daphtoxkit F™ (water flea)	100%	33.73% ± 2.766	55.06% ± 1.684	23.33% ± 1.612	29.63% ± 0.947
Microtox™ (bacteria)	5 min: 100% 15 min: 100%	5 min: 100% 15 min: 100%	5 min: 100% 15 min: 100%	5 min: 29.61% ± 2.097 15 min: 26.75% ± 1.680	5 min: 29.63% ± 3.804 15 min: 31.49% ± 0.507
Cytotoxicity tests					
MTT	100%	25.89% ± 0.652	35.46% ± 2.642	40.54% ± 1.022	56.04% ± 4.175
Neutral red	100%	22.78% ± 0.567	29.71% ± 1.646	35.04% ± 0.883	45.63% ± 2.528

concentration, respectively (British Columbia Ministry of Energy; Tindal, 2007)). The EC_{50} for *D. magna* and *V. fischeri* respectively, LC_{50} for *T. platyurus* and IC_{50} for *Tetrahymena thermophila* were determined for each test as recommended by the microbiotest kit manufacturer. Data for the ecotoxicological analysis of PUV and PPGD treated test liquids are presented as per Slabbert and Venter (1999). 10% effect in the *Daphnia* test and 5% in the protozoan test indicate toxic activity. Effective concentrations of samples (e.g. LC_{50} and EC_{50}) were statistically derived (linear regression) using dose–response curves (% effect versus log concentration). When toxicity was too low to use linear regression, endpoints were presented as LC_{50}: >100% or LC_{50}: 50–100%.

2.10. Statistics

Cytotoxicity assays (MTT, NR) were conducted using six replicates per test sample in three independent experiments, with mean absorbance values expressed as a percentage of untreated control cell values ± standard error of the mean. Homogeneity of variances and normality of data were confirmed with the Levene's test and the Kolmogorov–Smirnov test respectively. Statistical differences compared to control groups were evaluated with one-way ANOVA followed by Dunnett's post-hoc test at 95% confidence level. The Comet assay was conducted on duplicate slides with 50 cells scored per slide. Statistical difference between control and treated cells was evaluated with the nonparametric Mann–Whitney test using untransformed tail moment values. The Ames II™ Mutagenicity test was performed as per manufacturers' instruction in triplicate with statistical differences between treatment groups determined using a one tailed *t*-test. The statistical analysis was performed using Minitab® Version 15. Ecotoxicity analysis was conducted with appropriate number of replicates as recommended by the supplier of the test kits. Differences between treatments and controls were tested by analysis of variance (ANOVA) and Dunnett's test. Median lethal concentrations (LC_{50}) and other lethal concentrations (LC_{20}) were determined by the trimmed Spearman–Karber method, using TOXSTAT software, version 3.4 (Azur, 1995; West Inc. and Gulley, 1994). Statistical analysis for the Microtox ™ test was performed using the Microtox "Chronic Toxicity Testing DOS software", in accordance with guidelines provided by the US Environmental Protection Agency (1994).

3. Results and discussion

3.1. PPGD and PUV-mediated destruction of C. parvum oocysts

Findings showed that the application of PUV and PPGD inactivated ca. 4 log orders of *C. parvum* oocysts after 90 s (equivalent to UV dose of 6.29 μJ/cm^2) (Table 2) and 30 min (16 kV/cm, 10 pps, O_2 flow rate of 2.5 L/min) (Table 3) respectively. Findings demonstrated that *C. parvum* is very recalcitrant requiring the highest test irradiation setting of 120 pulses (UV dose 8.38 μJ/cm^2) to achieve complete disinfection for all test samples. This was equivalent to operating the PUV system at 900 V (or second highest setting) for the duration of pulsing at 8 cm from the light source. This finding will have significant implications for disinfection in a flow-through system such as WWTP as it is likely that the upper threshold level for destruction may be as low as ca. 1 log/mL. Recent studies reported that critical factors to be considered in PUV treatment of microbial species in water include pulsed repetition frequency, applied voltage, distance from the light source, presence of suspended solids and type of microbial species to be treated (Garvey et al., 2010). Recent studies carried out by this research group reported that there is a relationship between pulsed UV light irradiation and the simultaneous occurrence of molecular and cellular damage in treated yeast (Farrell et al., 2011). The latter reported that PUV may be considered as a multi-hit process for inducing lethality in microbial species as these researchers reported cell membrane permeability, lipid hydroperoxidation in the cell membrane, intracellular reactive oxygen species (ROS) generation, the occurrence of late apoptotic and necrotic yeast phenotypes, and significant nuclear damage. Although some level of cellular repair was observed in all test strains during sub-lethal exposure to PUV-treatments (≤20 pulses or UV dose 0.55 μJ/cm^2), this was absent in similar samples exposed to increased amounts of pulsing. While PUV produced superior inactivation performance to similarly treated PPGD samples containing *C. parvum* oocysts under non-flowing or static conditions (Table 2), the specific mechanisms of cellular and molecular destruction in this waterborne enteroparasite remains to be determined.

Previous researchers have revealed that the application of high voltage pulses to gas-injected test liquids (or PPGD) results in the formation of a plasma that causes free radicals such as dissolved ozone and hydrogen peroxide, free electrons, ultraviolet light (UV), acoustic shock waves and electric fields at levels between 10 and 50 kV/cm to be

Table 2
Influence of PUV treatment (16.2 J/pulse) on reduction of *C. parvum* infectivity as determined by use of the combined in vitro $CaCo$-2 cell culture-quantitative PCR assay. PUV treatments were performed at 1 pps.

PUV parameters		CaCo-2 cell culture infectivity assay			
Number of pulses (s)	Fluence (μJ/cm^2)	No. of infected monolayers[a]	IF microscopic detection	Presence of foci of infection	Log_{10} reduction (infectivity)[b]
0	0.000	4	High	+	0
15	1.0484	4	High	+	1.6 ± 0.3
30	2.0969	4	High	+	2.1 ± 0.4
45	3.1454	3	Medium	+	2.4 ± 0.4
60	4.1939	3	Medium	–[c]	2.9± 0.4
75	5.2424	2	Low	–[c]	3.1± 0.3
90	6.2909	1	Low	–[c]	≥4
120	8.3879	0	None	–[c]	≥4

[a] Standard dose of ca. 1×10^5 oocysts/mL was applied to each of the 4 replicate cell monolayers per PUV treatment. Infectivity was determined by both *q*PCR and immunofluorescence (IF) microscopy in CaCo-2 cells.

[b] Log reduction in viable *C. parvum* determined by cell culture-*q*PCR assay. As lower limit of detection for standard curve using *Cryptosporidium* DNA is ca. 10 oocysts, the maximum lethality detected is 4 log_{10} orders. Mean value shown for 4 replicate cell monolayers, ±SD.

[c] Not detected.

Table 3
Influence of PPGD treatment (minutes at 16 kV/cm, 10 pps, O_2 flow rate at 2.5 L/min) on reduction of *C. parvum* infectivity as determined by use of the combined in vitro CaCo-2 cell culture-quantitative PCR assay.

PPGD parameters	CaCo-2 cell culture infectivity assay			
Min [at 16 kV/cm, 10 pps, O_2 flow rate 2.5 L/min]	No. of infected monolayers[a]	IF microscopic detection	Presence of foci of infection	Log_{10} reduction (infectivity)[b]
0	4	High	+	0
8	4	High	+	1.8 ± 0.3
16	3	Medium	+	2.4 ± 0.3
24	2	Medium	–[c]	3.3 ± 0.4
32	1	Low	–[c]	≥4

[a] Standard does of ca. 1×10^5 oocysts/mL was applied to each of the 4 replicate cell monolayers per PPGD treatment. Infectivity was determined both by *q*PCR and immunofluorescence (IF) microscopy in CaCo-2 cells.
[b] Log reduction in viable *C. parvum* determined by cell culture-*q*PCR assay. As lower limit of detection for standard curve using *Cryptosporidium* DNA is ca. 10 oocysts, the maximum lethality detected is 4 log_{10} orders. Mean value shown for 4 replicate monolayers, ± SD.
[c] Not detected.

generated in the test liquids (Rowan et al., 2008a, 2008b). It is likely that the combination of these biocidal properties contributed to the lethal action of PPGD during this study (Table 3). A greater level of *C. parvum* destruction was achieved using prolonged exposure to PPGD (Table 3). Use of O_2 instead of N_2 as the sparged gas produced greater levels of parasite destruction (data not shown). However, findings from this study suggest that the PPGD system used in this study will not be suitable for scale up purposes at WWTP level as this technology took 32 min to produce a 4 log reduction in *C. parvum* oocysts under static conditions. As the UV component of the PPGD treatment process was less intense compared to using a stand-alone PUV approach it is also likely that ultraviolet light played a minor role in the pulsed plasma decontamination process. Pulsed electric discharge or PPGD has been shown to be effective for the oxidative destruction of structurally-related organic compounds such as dyes, phenol and aniline in aqueous solutions (Willberg et al., 1996; Bubnov et al., 2004; Liu and Xuan Zhen Jian, 2005; Hao et al., 2007; Amin et al., 2007), yet there has been no published information on the toxicity or safety of these plasma treated samples. These PPGD and PUV-treated end-point samples were used to conduct extensive cyto-, geno- and ecotoxicity studies described herein.

3.2. Chemical analysis of PUV and PPGD treated water

The concentration of indicator elements in PUV treated water, with and without the presence of inactivated *C. parvum* oocysts, was at acceptable levels for drinking water as dictated by the European Communities (Drinking water) (No. 2) Regulations (2007) (Table 4). However, findings presented in Fig. 2 show that the plasma discharge has a notable effect on the pH of the treated water. When using O_2 as a discharge gas, the pH value increased slightly in an almost linear fashion. The pH increase was dependent on the pulse frequency. The highest pH value of 8.34 was observed after 60 min plasma treatment with 12.5 pps. With the pulse generator adjusted to 10 pps and 7.5 pps the pH increase after a 60 min treatment was found to be 8.06 and 7.87 respectively. The mechanism for this pH change towards alkaline conditions is currently not fully understood yet has been also reported previously by other researchers (Rowan et al., 2008a, 2008b). However, the formation of dissolved hydroxyl ions resulting from the O_2 discharge may have caused the pH increase. In contrast to the O_2 discharge, when using N_2 as discharge gas, a drastic pH drop was observed for all pulse frequencies evaluated. The decrease in pH was also dependent on the pulse frequency. The lowest pH value of 3.21 was observed after a 60 min treatment with 12.5 pps, followed by value of 3.4 and 3.82 for a treatment with 10 pps and 7.5 pps, respectively. The fixation of nitrogen based compounds explains in part the notable decrease in the pH of the PPGD-treated water. The results obtained from the IEC analysis proved that nitrogen compounds were fixed in the treated liquid during N_2 discharge process. The PPGD was potent to activate the gaseous N_2 molecules that were subsequently oxidized to oxygen species originating from the treatment liquid or from residuals at atmospheric O_2 gas within the discharge region. The oxidized nitrogen dissolved in the liquid and caused formation of nitric and nitrous acid which dissociated into detectable NO_3^- and NO_2^-, respectively. Also, research conducted by Bian and Yin (2007) showed that activated nitrogen formed during HV discharge in N_2 gas. Nevertheless, the chemistry behind the production of such compounds during the plasma discharge, and how they dissolve into the aqueous solution, appears to be relatively complex and merits further study.

The efficiency of the PPGD system to produce dissolved ozone in the test water was determined using the DPD colorimetric method (Fig. 3). The results indicate that depending on the type of discharge gas used a substantial difference in ozone production was observed. The higher the applied discharge energy, the greater was the production of ozone during the time duration of the experiment. With varying pulse potency, the concentrations of ozone dissolved in water after a 42 min oxygen discharge treatment were found to be 1.2, 1.0 and 0.6 mg/mL for applied charging voltages of 18, 16 and 14 kV, respectively. PPGD-treated water for cyto-, geno- and ecotox assessments contained 0.8 mg/L ozone (32 min exposure at 16 kV, 10 pps using O_2 at 2.5 L/min) in this study. Small concentrations of ozone (not exceeding 0.14 mg/L at maximum treatment times and discharge conditions) were produced during N_2 mediated discharge which may be explained by oxygen ingress from surrounding ambient air. Also PPGD-treated water contained a possible source for oxygen which can be liberated by the result of the plasma discharge. The latter finding was supported by Takaki et al. (2008) who reported that the efficiency of the ozone production by pulsed plasma depends strongly on the ambient temperature and pressure, the gas used and on the discharge settings itself such as gap-width, applied voltage, the pulse waveforms, electrode surface and electrode material. Ozone is a powerful oxidizing agent that has been used for a variety of applications including purification and disinfection of water (Jyoti and Padnit, 2002). Although ozone itself has good water solubility being 12.5 times more soluble than oxygen, its instability in water makes the determination of the molecule in solution rather complicated (Lin and Nakajima, 2003). However, the DPD colorimetric method employed for

Table 4
Concentration of indicator elements in PUV and PPGD treated test liquids.

Determination	PUV treated[a]	PPGD treatments					
		Untreated control	30 min O_2 treated	90 min O_2 treated	30 min N_2 treated	90 min N_2 treated	PV value[b]
Al (μg/L)	<20	<20	5515	27,150	6546	26,330	200
Fe (μg/L)	<20	<20	98	747	147	500	200
Cr (μg/L)	<5	<5	34	195	44	121	50
Mn (μg/L)	<5	<5	20	90	34	112	50
pH	7.48	7.52	7.69	8.28	4.53	3.09	N/A
Conduct (μs/cm)	987	981	1159	1353	1192	1394	N/A

[a] PUV samples treated with UV dose of 6.29 μJ/cm^2.
[b] PV value is the parametric value taken from European Communities (Drinking water) (No. 2) Regulations (2007) for comparative purposes.

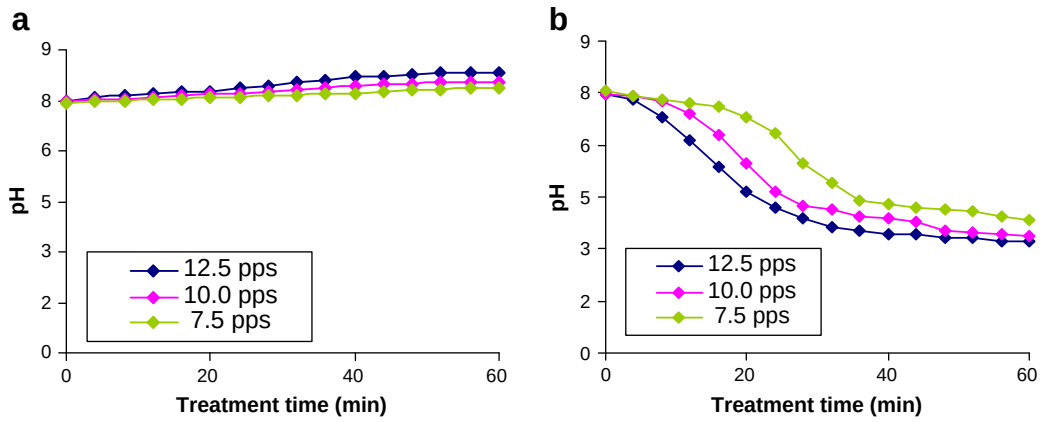

Fig. 2. Effect of PPGD treatment on the pH of treatment fluid using O_2 (a) and N_2 (b) as discharge gas at a flow rate of 2.5 L/min. The pulse generator was charged to 16 kV while varying pulse repetition rates of 7.5, 10 and 12.5 pps were under investigation.

the quantification of dissolved ozone was not suitable to elucidate mechanisms of ozone decay. Preliminary studies undertaken showed that the dissolved ozone levels dropped below detection limit within several hours after the discharge treatment. Ozone, together with its decay products (hydroxyl and superoxide radicals), contributed to *C. parvum* disinfection through oxidation of various essential cellular components including unsaturated fatty acids, amino acids and DNA molecules (Montie et al., 2000) and to toxicity linked to PPGD-treated water.

Electrode degradation is a major problem limiting the performances and lifetime of the electrodes and is caused by erosion events resulting from interactions of electrical discharges with the surface of the electrodes (Shiki et al., 2007). The creation of plasma discharge resulted in a slow but steady shortening of the individual needle electrodes via erosion mechanisms (Fig. 4). The observable damage was believed to result from a mixture of complex electrode erosion events including particle ejection, vaporisation and sputtering as described previously by Lasagni et al., 2004. As most mechanisms leading to electrode erosion are temperature dependent, a way to conserve the electrodes would be to reduce PFN charge and pulse frequency. Also reducing the use of O_2 as discharge gas may diminish oxidative damage. The material degradation resulting from electrode erosion released metals into PPGD-treated water (Table 4). With prolonged PPGD treatments an increasing concentration of electrode contaminants were released into the test liquids in the increasing order Mn, Cr, Fe, and Al. The fact that each electrode-related metal was detected in PPGD-treated water indicated that elements from both the stainless steel HV electrode and the Al earthed electrode were released. The contaminate level increase was dependent on the treatment time suggesting that with every delivered HV pulse material is freed from the electrodes. In comparison with the tolerated metal level in drinking water recommended by the dictated by the European Communities (Drinking water) (No. 2) Regulations (2007), Al concentration was 32 times the recommended value after 30 min operation. All elements were found to exceed the tolerated levels after 90 min treatment where Al exceeded 135 times the maximum tolerated levels. Varying the discharge gas did not seem to cause a major effect on the examined metal levels. Refrigerated storage of PPGD-treated samples for 7 days did not reduce metal contaminant levels in water samples (data not shown). Previous research has reported on the harmful effect of metal ions released from Al or stainless steel electrodes during electrical discharges in aqueous solutions using electroporation equipment for bimolecular cell applications (Friedrich et al., 1998; Lukeš et al., 2006). The use of elkonite or other metals as alternative electrodes may help considerably in reducing toxicity associated with PPGD treatments.

3.3. Ecotoxicological analysis

Ecotoxicology comprises the integration of ecology and toxicology (Baird et al., 1996) and its objectives are to understand and predict effects of chemicals on natural communities under realistic exposure conditions (Chapman, 2002). Ecotoxicity tests measure acute and chronic toxicity and corresponding lethal and sub-lethal effects, detect a wide range of integrated effects of substances released into the freshwater environment, and utilise organisms from different levels of the aquatic food chain as well as cellular and subcellular systems (Slabbert and Venter, 1999). Increasing evidence suggests that it is preferable to carry out ecotoxicological tests on a base-set of taxa utilising target species belonging to different trophic levels as use of a single bioassay will never provide a full picture of the quality of the environment (Chen et al., 2004). Therefore, *V. fischeri* (bacteria), *T. platyurus* (Fairy

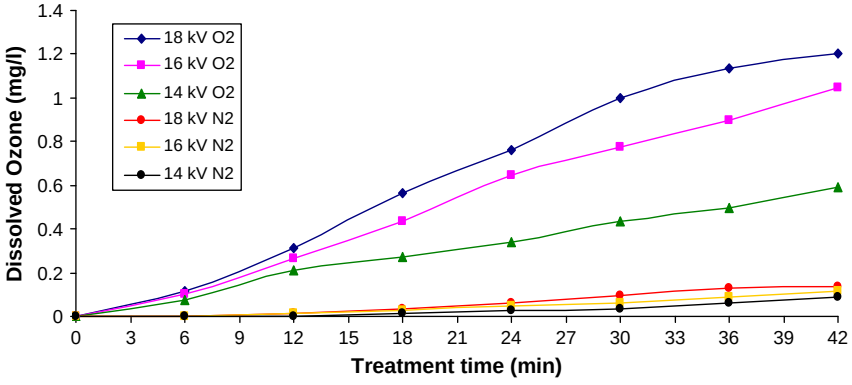

Fig. 3. Dissolved ozone concentration in the test liquid for varying discharge intensities using oxygen and nitrogen gas at a flow rate of 2.5 L/min and a pulse frequency of 10 pps.

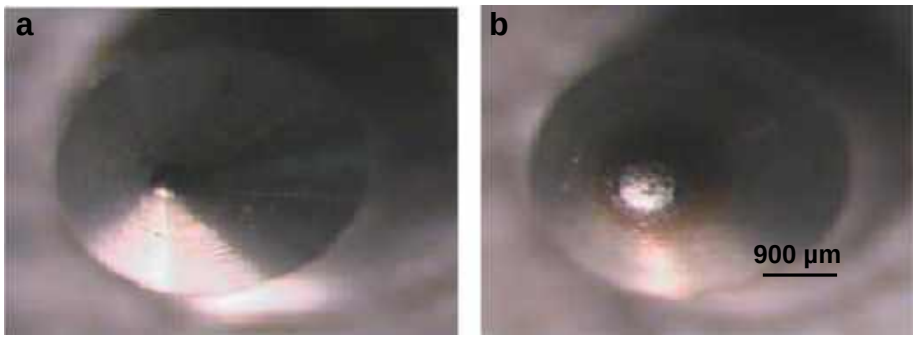

Fig. 4. Unused needle tip of the HV electrode (a). Etched and shortened needle tip after prolonged usage (b).

shrimp) and *D. magna* (water flea) were separately exposed to PPGD and PUV-treated water (Table 1). Testing of pulsed UV treated samples conducted on these battery of test species indicated that no detectable toxicity occurred using these microbiotests (Table 1). This finding again supports the development of PUV as a green-friendly effective technology for decontaminating water containing unwanted *Cryptosporidium* parasites.

In contrast, the PPGD treated samples produced discernible toxic effects (Table 1). The Microtox™ assay was the least sensitive to these toxic effects; an LC_{50} value could not be calculated but the LC_{20} values were determined to be 29.61% (v/v) ± 2.097 (5 min test) and 26.75% (v/v) ± 1.680 (15 min test) immediately post treatment, reducing to 29.63% (v/v) ± 3.804 (5 min test) and 31.49% (v/v) ± 0.507 (15 min test) when tested 7 days post treatment. The Thamnotoxkit F™ assay was the most sensitive to these toxic effects of exposure to PPGD treated water; the LC_{50} value was determined to be 12.63% (v/v) ± 1.016 immediately post treatment, reducing to 27.74% (v/v) ± 0.275 when tested 7 days post treatment. A 12.63% (v/v) concentration of PPGD treated water equates to approximately a 1 in 8 dilution, and that such a high dilution factor would still cause a 50% lethal effect raises serious concerns about the potential safety of PPGD treated water. For all assays/kits the positive control was found to be within the toxic concentration range provided by the kit manufacturers indicating that assay condition were correct for each assay (data not shown). A number of factors are likely to have contributed to the observed PPGD-mediated toxicity that include variations in pH depending on type of streamed gas used, presence of oxygenated free radicals such as ozone and its associated decay products, generation of dissociated nitric and nitrous acid, and high levels of metals released from the electrode. This study also corroborates the findings of Kelly et al. (2004) who reported that the Microtox assay can be effectively used to assess wastewater metal (Cu, Zn, Ni and Cd) toxicity in bench-scale wastewater treatment system. While Velzeboer et al. (2008) used Microtox (bacteria), pulsed-amplitude modulation (algae), Chydotox (crustaceans) and Biolog™ (soil enzymes) to show no appreciable ecotox effects at normal concentrations of up to 100 mg/L for the nanoparticles TiO_2, ZrO_2, Al_2O_3 and CeO_2.

3.4. Cytotoxicological analysis of PUV and PPGD treated samples

The potential of the PUV-treated and PPGD-treated test liquids respectively to induce adverse effects on the human HepG2 and HaCaT cells grown in culture was evaluated using both the MTT and NR endpoints. The MTT endpoint measures mitochondrial function as an indicator of cytotoxicity (Fotakis and Timbrell, 2006), while the NR endpoint assesses the ability of viable cells to incorporate and accumulate the supravital dye NR within lysosomes (Borenfreund and Puerner, 1985). Findings shown in Table 1 indicate that the PUV treated water did not exert any cytotoxic effects on the HepG2 cells. However, following 24 h cell exposure to PPGD-treated test liquid, there was a pronounced effect on the viability of HepG2 cells as determined by measuring MTT (Fig. 5) and NR (Fig. 6) endpoints, respectively. Overall, the trend in toxicity profiles observed via the MTT endpoint was similar to the trend observed in the NR endpoint although the latter assay appeared more sensitive to the cytotoxic effects of the PPGD-treated test liquid. In both assays a dose-dependent decrease in cell viability was observed. Cell exposure to O_2 discharge-treated test liquid (Figs. 5a, 6a) resulted in lower cell viability values compared to cell exposure to test liquids produced using N_2 gas (Figs. 5b, 6b). Using neat samples (i.e. 100% v/v) drawn from the treatment chamber at various time intervals, LC_{50} and LC_{20} values were calculated to reflect the treatment timepoint at which they occur (Table 1). A comparison of the LC_{50} and LC_{20} values of O_2-mediated PPGD treated water for the two cytotoxicity tests in terms of % (v/v) concentration is also presented in Table 1. The LC_{50} value for using the MTT endpoint was determined to be 25.89% (v/v) ± 0.652 immediately post treatment, reducing to 35.46% (v/v) ± 2.642 when tested 7 days post treatment. LC_{20} values using the MTT endpoint were determined to be 40.54% (v/v) ± 1.022 immediately post treatment, reducing to 56.04% (v/v) ± 4.175 when tested 7 days post treatment. The LC_{50} value for using the neutral red endpoint was determined to be 22.78% (v/v) ± 0.567 immediately post treatment, reducing to 29.71% (v/v) ± 1.646 when tested 7 days post treatment. LC_{20} values using the neutral red endpoint were

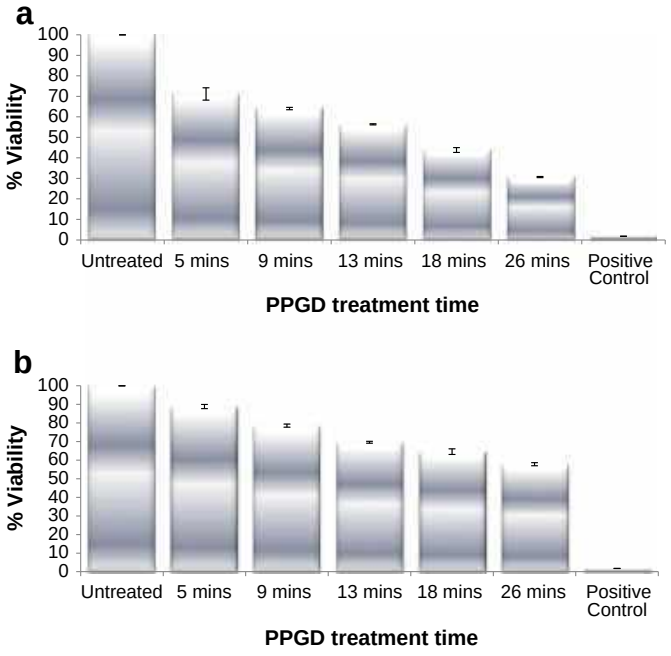

Fig. 5. Findings from MTT assay performed on HepG2 cells exposed to PPGD-treated samples using O_2 (a) and N_2 (b) as sparged gas at flow rate of 2.5 L/min (16 kV/cm, 10 pps).

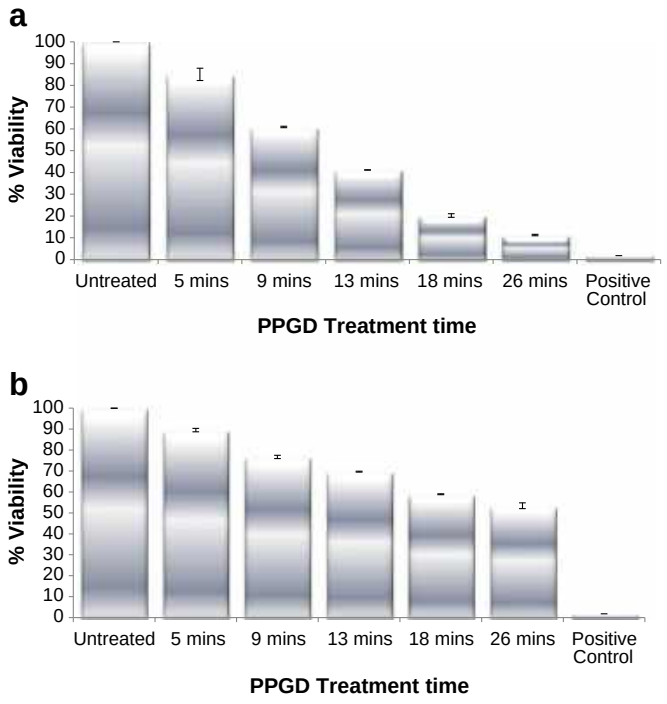

Fig. 6. Findings from neutral red (NR) assay performed on HepG2 cells exposed to PPGD-treated samples using O_2 (a) and N_2 (b) as sparged gas at flow rate of 2.5 L/min (16 kV/cm, 10 pps).

determined to be 35.04% (v/v) ± 0.883 immediately post treatment, reducing to 45.63% (v/v) ± 2.528 when tested 7 days post treatment. Overall, the trend in toxicity profiles observed using HaCaT cells was similar to use of HepG2, where NR assay appeared more sensitive to the cell toxic effects of PPGD-test samples. In both assays a significant ($p < 0.05$ to $p < 0.01$), dose dependent decrease in cell viability was also observed (Figs. 7 and 8). More specifically, as shown in Figs. 7a and 8a, direct exposure to the highest test liquid concentration (40%) prepared with O_2 discharge reduced the cell viability to 21% in the MTT and 4% in the NR assay. In comparison, when incubated for 7 days before exposure, the same concentration resulted in residual cell viability values of 29% and 39% in the MTT and NR assay, respectively. Direct exposure to the highest N_2 treated test liquid concentration (40%) resulted in residual cell viability values of 67% and 61% while exposure after the 7 days of incubation reduced the viability to 77% and 66% for the MTT and NR assay (Figs. 7b and 8b), respectively.

Despite increased interest in the development of non-thermal advanced oxidative processes (such as corona plasma discharges; ozone combined with H_2O_2; low/medium pressure UV combined with H_2O_2 etc.), the authors have been unable to source any published reports on possible toxicological issues associated with use of these new disinfection technologies. Although the observed cell death might be a sum of various effects associated with the plasma treatment, considering the diminished toxicity evident after the 7 day storage period it is likely that reactive chemical species formed during this process played a major role in toxicity. Similar to its deleterious action on microorganisms, ozone and associated free radicals damage mammalian cells mainly by oxidation of fatty acids, DNA, proteins, amines, and thiols (Mehlman and Borek, 1987). Whiteside and Hassan (1988) showed that ozone can lead to the inactivation of intracellular antioxidant enzymes such as catalase and superoxide dismutase thereby enhancing its toxic effects on subcellular structures. Several studies have also reported on the cytotoxic effects of dissolved ozone using mammalian cells in culture (Larini and Bocci, 2005; Zhou et al., 2008) and H_2O_2, was thought to be a major intermediate in the toxicity of ozone (Oosting et al., 1991). However, it was suggested that the effects of ozone depend much on the concentration of antioxidants present in the extracellular fluid (i.e. the cell culture medium) thus making the comparison between other studies difficult (Larini and Bocci, 2005; Zhou et al., 2008). Moreover, with regard to drinking water treatment, other by-products from ozonation may include aldehydes, bromoform, and brominated acetic acids. There is ongoing debate on the relevance of disinfection byproducts compared to the risks of waterborne diseases (Bull et al., 1995). A study by Havelaar et al. (2000) investigated and compared the risk of infection by *C. parvum* and the development of renal cell cancer due to bromate formation from ozonation processes. It was concluded that the benefits of preventing gastroenteritis by proper disinfection outweigh health losses by premature death from renal cell cancer arising from the production of bromate by a factor of >10 (Havelaar et al., 2000).

The presence of dissociated nitric and nitrous acid drastically decreased the pH of the test liquid. It was believed that reactive nitrogen compounds and the resulting acidic conditions played a contributing role in the observed microbial inactivation and toxicity during N_2-mediated PPGD treatment. A study by Bharadwaj et al. (2005) concluded that no significant impact on HepG2 cell viability was observable following 24 h exposure of 1000 mg/L nitrate dissolved in cell culture medium. Nonetheless, two independent studies conducted by Bharadwaj et al. (2005) and Jondeau et al. (2006) provided initial information on the cytotoxic potential of nitrate on human cells in culture (HepG2 cells). Bharadwaj et al. (2005) conducted a NR assay and concluded that no significant impact on HepG2 cell viability was observable following 24 h exposure of 1000 mg/L nitrate dissolved in cell culture medium. Similarly, Jondeau et al. (2006) conducted a range of 20 h exposure tests and showed that a minimum concentration of approximately 2500 mg/L nitrate in cell culture medium was required to cause a 50% reduction in cell viability. In the present study the detected nitrate and nitrite concentrations were found to be 18 and 21 mg/L respectively following PPGD treatment using a charging voltage of 16 kV at 10 pps and a N_2 flow of 2.5 L/min. Of concern is the concentration of nitrite which was detected above the maximum tolerated value (0.5 mg/L) for drinking water within the European Communities (No. 2

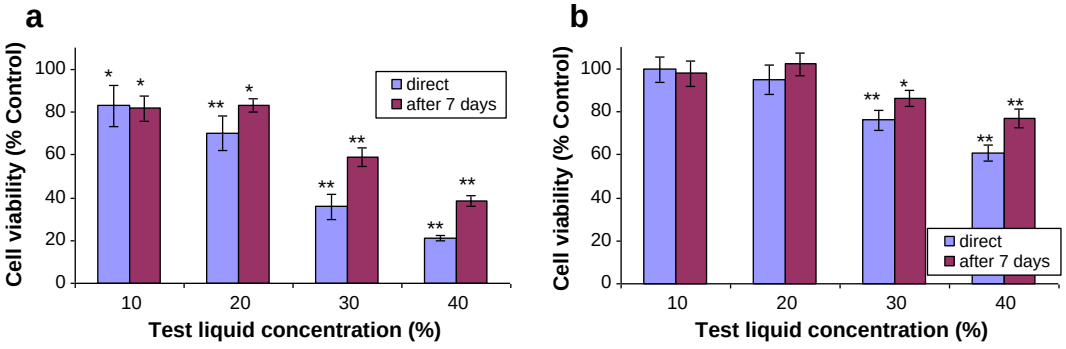

Fig. 7. Effect of O_2 mediated (a) and N_2 mediated (b) PPGD treated liquid on the viability of HaCaT cells following 24 h exposure at 37 °C as assessed using the MTT assay ($n = 18 \pm$ SEM, * denotes a significant difference control * = $p < 0.05$, ** = $p < 0.01$).

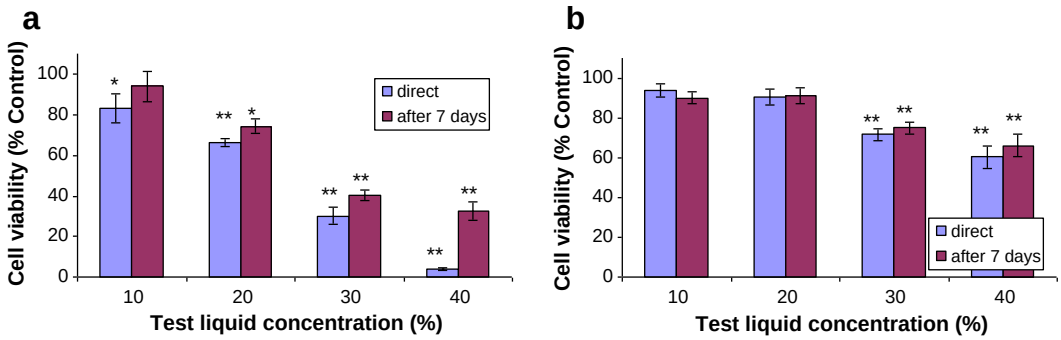

Fig. 8. Effect of O_2 mediated (a) and N_2 mediated (b) PPGD treated liquid on the viability of HaCaT cells following 24 h exposure at 37 °C as assessed using the NR assay (n = 18 ± SEM, * denotes a significant difference control * = $p < 0.05$, ** = $p < 0.01$).

Regulations 2007). Additionally, when dissolved in an aqueous solution the NO_2^- ions are unstable, can decay into smaller reactive nitrogen molecules; but these will, however, eventually be oxidized to form less reactive NO_3^- ions (Cai et al., 2001). Consequently, the decay into less reactive nitrogen compounds may explain the slightly reduced cellular toxicity observed after exposing the cells to N_2 discharge treated liquid which was preincubated for 7 days before exposure. However, it is possible that reactive nitrogen compounds other than nitrate may have contributed to the observed cytotoxicity. Sun et al. (2006) showed that human gastric adenocarcinoma epithelial cell proliferation was inhibited when exposed to 50 mM sodium nitrite. It has also been reported that exposure of cell cultures to sodium nitrite may promote carcinogenesis (Osin'kovskaia et al., 1988). The mutagenicity of sodium nitrite was further demonstrated by Akin and Sumer (1991) using the *Salmonella*/microsome test system. However, similar to sodium nitrite, the toxic action of nitrite in human blood involves nitrite ion oxidizing the ferrous ion in oxyhaemoglobin to ferric ion to produce methaemoglobin (Levin, 2001). The in vitro assessment in this study cannot accurately reflect this haematotoxicity unless human derived blood cells are used to simulate its mechanism in vivo (Lestari et al., 2005).

Another factor that may have affected the cell viability is the presence of metallic electrode degradation products Al, Fe, Cr and Mn within the PPGD treated liquid as mentioned earlier (Table 4). Previous researchers have reported that Al may be a possible etiological factor in neurological disorders such as Alzheimer's disease (Perl and Brody, 1980; Harrington et al., 1994) and dialysis encephalopathy (Stakey, 1987; Deloncle and Guillard, 1990). Hence, several in vitro studies investigated the cytotoxic potential of Al compounds on cells derived from the nervous system (Ohyashiki et al., 2002; Toimela et al., 2004). Previous researchers have also reported on the relationship between metal ions release from electrodes and observed toxicity in mammalian cell lines during electroporation treatments (Loomis-Husselbee et al., 1991; Stapulionis, 1999). Kotnik et al. (2001) investigated the cell toxic effect of Al and Fe ions on DC-3F hamster fibroblast cells and showed that following the 1 h exposure, Fe^{+2} and Fe^{+3} reduced significantly the viability of mammalian cells in culture while Al^{+3} had no effect. It was suggested that biological active ferrous ions could generate free radicals which in turn attack cellular components (Tomov and Tsoneva, 2000). It is likely that a combined action of the aforementioned agents resulted in the observed cytotoxic effects in PPGD-treated water. When exposing cell cultures to vehicles containing a mixture of different substances, toxic responses originating from additive or even synergistic effects cannot be dismissed.

3.4.1. Genotoxicity evaluation of PPGD-treated water

The genotoxic and mutagenic potential of only PPGD-treated water (and dilutions thereof) was investigated using the comet and Ames assay respectively, as PUV-irradiated samples exhibited no discernable cyto- or ecotoxicological properties. Fig. 9 and Table 5 show the results obtained using the comet assay following HaCaT cell exposure to PPGD-treated water. The box plots shown in Fig. 9 indicate that, compared to the untreated control, none of the test sample concentrations from O_2 discharge treated-water caused significantly elevated percentage tail DNA values. Compared to the untreated control, a reduced median and 75 percentile for the percentage DNA distribution were obtained for the highest tested O_2 mediated discharge concentration (20%). The general trend observed in Fig. 9 is further reflected in Table 5 where the whole concentration range of O_2 discharge treated water displayed DNA migration values which did not significantly differ from untreated control values. Table 5 reveals a dose dependent increase in tail moment values. It appears that the level of reactive species was too low to cause a detectable insult on the HaCaT cells DNA. A comet assay study conducted by Diaz-Llera et al. (2002) showed that a dissolved ozone concentration of 42 mg/mL incubated for 1 h was required to induce detectable DNA damage on human leukocytes in culture. However, in the current study, the level of dissolved ozone generated by the PPGD within 30 min of treatment did not exceed a value of 1 mg/mL. Similar

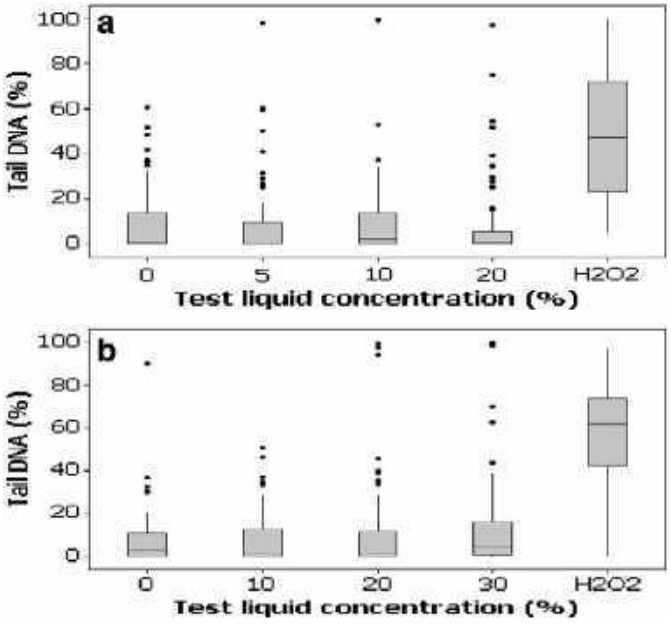

Fig. 9. Box plot presentation of tail DNA (%) obtained following HaCaT cell exposure to increasing concentrations of (a) O_2 and (b) N_2 mediated PPGD treated test liquid (12 h at 37 °C) and 100 μM H_2O_2 (40 min at 4 °C). Each box corresponds to 100 comets measured on two slides and represents 25–75 percentiles, middle line = median, whisker extends to the maximum/minimum data point within 1.5 box heights from the top/bottom of the box. Dots above and below boxes indicate outliers. Asterisk denotes a significant difference from the control ($p < 0.05$).

Table 5
Tail moment and percentage tail DNA obtained in the comet assay after exposure of HaCaT cells to increasing concentrations of PPGD treated test liquid for 12 h and 100 μM of H_2O_2 for 40 min. Results shown are the means (±SEM) of 100 single cells from duplicate slides.

Conc. test liquid (%)	O_2 discharge		N_2 discharge	
	Tail moment (±SEM)	% tail DNA	Tail moment (±SEM)	% tail DNA
0	1.07 (±0.23)	8.49 (±1.35)	1.22 (±0.26)	7.13 (±1.22)
5	1.05 (±0.20)	10.17 (±1.97)	–	–
10	1.35 (±0.33)	9.40 (±1.65)	0.81 (±0.11)	7.81 (±1.12)
20	1.66 (±0.44)	8.51 (±2.03)	1.36 (±0.35)	10.29 (±2.07)
30	–	–	1.98 (±0.47)	11.73 (±1.83)
H_2O_2 100 μM	14.47 (±0.93)*	67.54 (±2.67)*	19.06 (±1.25.)*	55.77 (±2.31)*

* Denotes a significant difference from the untreated control (0%) ($p < 0.05$).

results were obtained following comet assay experiments using N_2 discharge treated liquids (Fig. 9 Table 5). However, Fig. 9 reveals that the highest liquid concentration (30%) caused a slightly elevated percentage tail DNA median and 75 percentile compared to the lower concentrations and the negative control. This effect was also illustrated in Table 5 where again a dose dependent but not significant increase in the mean tail moment values was observable with the highest tail moment value obtained for the 30% test liquid dilution (1.98). The positive control (100 μM H_2O_2) produced the expected response. An extended 40 min exposure at 4 °C resulted in significantly ($p < 0.05$) elevated DNA migration values with mean percentage DNA values approximately 8 times and mean tail moment values 13–20 times higher that the respective values obtained for untreated control cells. An investigation conducted by Spencer et al. (2000) observed significant DNA strand breakage upon exposing 46 mg/L nitrite to human respiratory tract cells in culture at exposure times exceeding 60 min. Nonetheless, within the current study potentially harmful nitrite concentrations above 27 mg/mL could be generated following prolonged PPGD treatment at high energetic discharge conditions. Additionally, it needs to be mentioned that constitutes of culture medium may act as free radical scavengers thus influencing the outcome of the in vitro assays used.

Table 6
Mean values of positive wells (±SEM) obtained from three experiments in the Ames mutagenicity assay following 90 min exposure to increasing concentrations of PPGD treated test liquids and positive controls (±S9). Asterisk denotes a significant difference from the untreated control (0%) ($p < 0.05$).

Conc. test liquid (%)	TA98 (±SEM)		TAMix (±SEM)	
	−S9	+S9	−S9	+S9
O_2 discharge treatment (direct)				
0	1.50 (±0.43)	1.00 (±0.00)	1.80 (±0.88)	1.33 (±0.30)
35	1.67 (±0.33)	1.33 (±0.33)	2.67 (±0.33)	1.33 (±0.88)
45	1.67 (±0.33)	0.67 (±0.33)	3.33 (±0.88)*	1.33 (±0.33)
55	2.00 (±0.58)	1.00 (±0.58)	9.00 (±2.47)*	2.00 (±0.58)
65	2.33 (±0.88)	1.33 (±0.88)	8.33 (±1.45)*	1.67 (±0.66)
Positive control	48.00 (±0.00)*	39.00 (±1.15)*	48.00 (±0.00)*	41.67 (±1.20)*
O_2 discharge treatment (after 7 days)				
0	1.50 (±0.61)	1.33 (±0.33)	1.67 (±0.33)	2.00 (±0.58)
35	1.67 (±0.88)	1.67 (±0.66)	2.00 (±0.00)	1.33 (±0.33)
45	0.67(±0.66)	1.67 (±0.33)	2.33 (±0.33)	0.67 (±0.66)
55	1.00 (±0.58)	1.00 (±0.58)	1.67 (±0.88)	0.67 (±0.33)
65	1.33 (±0.88)	2.33 (±0.66)	2.67 (±0.58)	1.00 (±0.00)
Positive control	47.00 (±0.88)*	36.00 (±3.05)*	48.00 (±0.00)*	34.00 (±2.30)*
N_2 discharge treatment (direct)				
0	2.33 (±0.66)	0.67 (±0.30)	1.67 (±0.88)	1.67 (±0.33)
35	2.67 (±0.88)	0.33 (±0.33)	0.00 (±0.00)	2.00 (±0.58)
45	2.00 (±0.58)	1.67 (±0.88)	1.00 (±0.58)	1.67 (±0.88)
55	1.67 (±0.66)	1.00 (±1.00)	1.67 (±0.66)	1.33 (±0.33)
65	4.00 (±0.58)	1.33 (±0.33)	0.67 (±0.66)	2.00 (±0.00)
Positive control	41.33 (±3.48)*	36.33 (±2.03)*	48.00 (±0.00)*	40.00 (±2.08)*

Table 6 shows the results obtained using the Ames test that were expressed as mean values of positive wells. While the majority of samples tested had no mutagenic activity, significant ($p < 0.05$) mutagenic responses were detected for the O_2 discharged PPGD-treated samples. The positive control chemicals produced the expected mutagenic responses. No increased reversion frequencies were detected following exposure of N_2 discharge treated test liquid to any of the *S. Typhimurium* Ames test strains. In contrast, O_2 discharge treated test liquid caused a positive result in the Ames assay via the induction of missense mutations (TAMix) in the absence of S9. Here, the observed increase in reversion frequency was not very high thus implying weak mutagenicity. It is believed that the mutagenic effect is introduced by the formation of dissolved ozone. These assumptions are strengthen by the negative results obtained for strain exposure to O_2 discharge treated test liquid which had been tested following a 7 day incubation period to allow for ozone decay. The negative results seen with the addition of S9 may be related to a possible detoxifying action of the liver homogenate on reactive oxygen species. Somewhat comparable, an Ames test by Monarca et al. (2000) also demonstrated the mutagenic potential of dissolved ozone at a concentration of 3 mg/L. As the current study is the first of its kind to evaluate the toxicological aspects of PPGD, no directly comparable information was obtainable from existing literature. However, two independent studies by Reyns et al. (2004) and Gusbeth et al., 2009 evaluated the DNA damaging potential of aqueous solutions after antimicrobial PEF treatment. Gusbeth et al. (2009) concluded that PEF treatment used under biocidal conditions did not induced genotoxic or mutagenic byproducts to in PBS buffer solutions and tap water. On the other hand, Reyns et al. (2004) observed a mutagenic effect of PEF treated PBS buffer (TA97 and TA102 strains) and grape juice (TA102 and TA104 strains) via the Ames assay. It was suggested that the genetic insult was caused by reactive oxygen species generated during electrolytic processes.

In terms of the safety evaluation of the PPGD method, a specific hazard could arise from those reactive species, as they may possess the ability to interfere with genetic material. During the last two decades numerous investigations focused on elucidating the DNA damaging mechanisms of several reactive oxygen and nitrogen species (Ohshima, 2003). It was observed that cell exposure to dissolved ozone leads to a dose dependent increase of DNA damage (Ito et al., 2005). Research conducted by Ito et al. (2005) showed that ozone molecules can directly cause DNA base modification. However, it appeared that ozone itself was not fully responsible for the extent of DNA damage observed. It was further suggested that reactions with unsaturated fatty acids and available thiol groups caused the production of reactive intermediaries with H_2O_2 as one of the final products (Diaz-Llera et al., 2002; Ito et al., 2005). This, in turn, traces the DNA damage back to the actions of the OH radical which is generated from H_2O_2 possibly by the redox cycle properties of transition metals (either free or bound to macromolecules such as DNA) (Ohshima, 2003; Ito et al., 2005). Several nitrogen oxides have shown a genotoxic and mutagenic potential in in vitro tests (2003). In contrast to nitrate, in vitro studies revealed a DNA damaging potential of nitrite (Routledge et al., 1994; Spencer et al., 2000; Knaapen et al., 2005). Furthermore, nitrite induced base pair substitutions in the Ames assay (Balimandawa et al., 1994). Also, nitrous acid has the potential to induce point mutations by deamination of DNA bases (Victorin, 1994; Oldreive et al., 1998) and causes DNA strand breaks in mammalian cells (Halliwell, 1999). In this context, metal products released from the electrodes require consideration as they could negatively interfere with the aforementioned reactive species (e.g. redox cycling) or even directly interact with DNA molecules (Moriwaki et al., 2008). Although it has been shown that Al can induce oxidative stress in mammalian cells (Kaneko et al., 2007), information

regarding the genotoxicity and mutagenicity of the element on mammalian cells are scarce and no objective conclusion can be formed.

In conclusion, it was found that PUV-irradiated water samples did not produce any adverse cyto-, geno- or ecotoxicological effects. However, in marked contrast, pulsed-plasma-gas-discharge (PPGD) treated water was shown to produce considerable cyto-, geno- and ecotoxic end-points that varied depending upon the electrical parameters and type of discharged gas used. Significantly diminished toxicity was observed following a 7 day refrigerated storage period, which inferred that the presence of reactive free radicals played a significant role in the observed toxicity observed immediately post treatment. PUV was shown to be a superior technology for the efficient destruction of *C. parvum* as it only required 90 s exposure to produce a 4 log-reduction in oocyst numbers compared to 32-min PPGD treatment to obtain similar lethality. Therefore, as the PPGD described in this study produces considerable toxicological end-points and requires an extensive treatment time and energy input to achieve appropriate levels of microbial inactivation, it is not considered suitable as an effective complementary or alternative approach for water treatment.

Acknowledgments

The authors thank the Irish Environmental Protection Agency (Grant 2011-WS-5) and the Irish Technology Sector Research Strand I programmes for the financial support that enabled this study to be carried out.

References

Akin, A., Sumer, S., 1991. The mutagenic effects of sodium nitrite and monosodium glutamate used as food additives demonstrated by the *Salmonella* microsome test system. Mikrobiyol. Bul. 25, 94–107.
Amin, M.T., Ryu, S., Park, H., 2007. Degradation of phenol and bisphenol-a using discharged water generating system. J. Water Supply Res. Technol. Aqua 56 (3), 203–216.
Azur, E., 1995. Microtox Chronic Toxicity Testing DOS Software, Carlsbad, CA, USA.
AZUR Environmental, 1998. Microtox Acute Toxicity Test, User Manual, 2232 Rutherford Road, Carlsbad, 92008-8883, USA.
Baird, D.J., Maltby, L., Greig-Smith, P.W., Douben, P.E.T., 1996. ECOtoxicology: Ecological Dimensions. Chapman and Hall, London.
Balimandawa, M., de Meester, C., Léonard, A., 1994. The mutagenicity of nitrite in the *Salmonella*/microsome test system. Mutat. Res. 321 (1–2), 7–11.
Bharadwaj, L., Dhami, K., Schneberger, D., Stevens, M., Renaud, C., Ali, A., 2005. Altered gene expression in human hepatoma HepG2 cells exposed to low-level 2,4-dichlorophenoxyacetic acid and potassium nitrate. Toxicol. In Vitro 19, 603–619.
Bian, W., Yin, X., 2007. Nitrogen fixation into HNO_3 and HNO_2 by pulsed high voltage discharge. Plasma Sci. Technol. 9, 288.
Borenfreund, E., Puerner, J.A., 1985. Toxicity determined in vitro by morphological alterations and neutral red absorption. Toxicol. Lett. 24, 119–124.
Bubnov, A.G., Grinevich, V.I., Kuvykin, N.A., 2004. Phenol degradation features in aqueous solutions upon dielectric-barrier discharge treatment, high energy. Chemistry 38 (5).
Bull, R.J., Birnbaum, L.S., Cantor, K.P., Rose, J.B., Butterworth, B.E., Pegram, R., Tuomisto, J., 1995. Water chlorination: essential process or cancer hazard? Fundam. Appl. Toxicol. 28, 155–166.
Cai, Q., Zhang, W., Yang, Z., 2001. Stability of nitrite in wastewater and its determination by ion chromatography. Anal. Sci. 17, 917–920.
Chapman, P.M., 2002. Integrating toxicology and ecology: putting the "eco" into ecotoxicology. Mar. Pollut. Bull. 44, 7–15.
Chen, J., Yu, H., Liu, Y., Jiang, W., Jiang, J., Zhang, J., Hua, Z., 2004. Ecotoxicological evaluation of 4-aminobiphenyl using a test battery. Ecotoxicol. Environ. Saf. 58, 104–109.
Deloncle, R., Guillard, O., 1990. Mechanism of Alzheimer's disease: arguments for a neurotransmitter-aluminum complex implication. Neurochem. Res. 15, 1239–1245.
Diaz-Llera, S., Gonzalez-Hernandez, Y., Prieto-Gonzalezand, E.A., Azoy, A., 2002. A genotoxic effect of ozone in human peripheral blood leukocytes. Mutat. Res. 517, 13–20.
Elmnasser, N., Ritz, M., Leroi, F., Orange, N., Bakhrouf, A., Federighi, M., 2007. Bacterial inactivation using pulsed light. Acta Alimentaria 36, 373–380.
EPA Final Report, 2005. Endocrine Disruptors in the Irish Aquatic Enviornment. Wexford, Ireland.
European Communities (Drinking Water) Regulations (S.I. No. 106 of 2007).
Farrell, H.P., Hayes, J., Laffey, J., Rowan, N.J., 2011. Studies on the relationship between pulsed UV light irradiation and the simultaneous occurrence of molecular and cellular damage in clinically-relevant yeast. J. Microbiol. Methods 84 (2), 317–326.
Fernandez, M.P., Campbell, P.M., Ikonomou, M.G., Devlin, R.H., 2007. Assessment of environmental estrogens and the intersex/sex reversal capacity for Chinook salmon in primary and final municipal wastewater effluents. Environ. Int. 33, 391–396.
Flückiger-Isler, S., Baumeister, M., Braun, K., Gervais, V., Hasler-Nguyen, N., Reimann, R., Van Gompel, J., Wunderlich, H.G., Engelhardt, G., 2004. Assessment of the performance of the Ames IITM assay: a collaborative study with 19 coded compounds. Mutat. Res. 558, 181–197.
Fogarty, A., McGee, C., 2007. Male or female: that is the question? Ir. Sci. 15, 40–44.
Fotakis, G., Timbrell, J.A., 2006. In vitro cytotoxicity assays: comparison of LDH, neutral red, MTT and protein assay in hepatoma cell lines following exposure to cadmium chloride. Toxicol. Lett. 160, 171–177.
Friedrich, U., Stachowicz, N., Simm, A., Fuhr, G., Lucas, K., Zimmermann, U., 1998. High efficiency electrotransfection with aluminium electrodes using microsecond controlled pulses. Bioelectrochem. Bioenergetics 47, 103–111.
Garvey, M., Farrell, H., Cormican, M., Rowan, N., 2010. Investigations of the relationship between use of in vitro cell culture-quantitative PCR and a mouse-based bioassay for evaluating critical factors affecting the disinfection performance of pulsed UV light for treating *Cryptosporidium parvum* oocysts in saline. J. Microbiol. Methods 80, 267–273.
Gusbeth, C., Frey, W., Volkmann, H., Schwartz, T., Bluhm, H., 2009. Pulsed electric field treatment for bacteria reduction and its impact on hospital wastewater. Chemosphere 75, 228–233.
Halliwell, B., 1999. Oxygen and nitrogen are pro-carcinogens. Damage to DNA by reactive oxygen, chlorine and nitrogen species: measurement, mechanism and the effects of nutrition. Mutat. Res. 443, 37–52.
Hao, X.L., Zhou, M.H., Lei, L.C., 2007. Pulsed discharge plasma induced Fenton-like reactions for the enhancement of the degradation of 4-chlorophenol in water. Chemosphere 66, 2185–2192.
Harrington, C.R., Wischik, C.M., McArthur, E.K., Taylor, G.A., Edwardson, J.A., Candy, J.M., 1994. Alzheimer's disease-like changes in tau protein processing: association with aluminium accumulation in brains of renal dialysis patients. Lancet 343, 993–997.
Havelaar, A.H., De Hollander, A.E.M., Teunis, P.F.M., Evers, E.G., Van Kranen, H.J., Versteegh, J.F.M., Van Koten, J.E.M., Slob, W., 2000. Balancing the risk and benefits of drinking water disinfection: disability adjusted life-years on the scale. Environ. Health Perspect. 108, 315–321.
Hayes, J.C., Garvey, M., Fogarty, A.M., Clifford, E., Rowan, N.J., 2012. Inactivation of recalcitrant protozoan oocysts and bacterial endospores in drinking water using high-intensity pulsed UV light irradiation. Water Sci. Technol. Water Supply 12, 513–522.
Hunter, P.R., Syed, Q., 2001. Community surveys of self-reported diarrhoea can dramatically overestimate the size of outbreaks of waterborne cryptosporidiosis. Water Sci. Technol. 43 (12), 27–30.
Ito, K., Inoue, S., Hiraku, Y., Kawanishi, S., 2005. Mechanism of site-specific DNA damage induced by ozone. Mutat. Res. 585, 60–70.
Jondeau, A., Dahbi, L., Bani-Estivals, M.H., Chagnon, M.C., 2006. Evaluation of the sensitivity of three sublethal cytotoxicity assays in human HepG2 cell line using water contaminants. Toxicology 226, 218–228.
Jyoti, K.K., Padnit, A.B., 2002. Ozone and cavitation for water disinfection. Biochem. Eng. J. 18, 9–10.
Kaneko, N., Sugioka, T., Sakurai, H., 2007. Aluminum compounds enhance lipid peroxidation in liposomes: insight into cellular damage caused by oxidative stress. J. Inorg. Biochem. 101, 967–975.
Kelly, C.J., Tumsaroj, N., Lajoie, C.A., 2004. Assessing wastewater metal toxicity with bacterial bioluminescence in a bench-scale wastewater treatment system. Water Res. 38, 423–431.
Knaapen, A.M., Schins, R.P., Borm, P.J., van Schooten, F.J., 2005. Nitrite enhances neutrophil-induced DNA strand breakage in pulmonary epithelial cells by inhibition of myeloperoxidase. Carcinogenesis 26, 1642–1648.
Kotnik, T., Miklavc˘ic, D., Lluis, M., 2001. Cell membrane electropermeabilization by symmetrical bipolar rectangular pulses part II: reduced electrolytic contamination. Bioelectrochemistry 54, 91–95.
Larini, A., Bocci, V., 2005. Effects of ozone on isolated peripheral blood mononuclear cells. Toxicol. In Vitro 19, 55–61.
Lasagni, A., Soldera, F., Mücklich, F., 2004. Quantitative investigation of material erosion caused by high pressure discharges in air and nitrogen. Z. Metallkd. 95, 102.
Lestari, F., Hayes, A.J., Green, A.R., Markovic, B., 2005. In vitro cytotoxicity of selected chemicals commonly produced during fire combustion using human cell lines. Toxicol. In Vitro 19, 653–663.
Levin, B.C., 2001. Smoke and Combustion Products, Patty's Toxicology. John Wiley & Sons, Inc.
Lin, J., Nakajima, T., 2003. An AM1 study of decomposition of aqueous ozone. J. Mol. Struct. (THEOCHEM) 625 (2003), 161–167.
Lishman, L., Smyth, S.A., Sarafin, K., Kleywegt, S., Toito, J., Peart, T., Lee, B., Servos, M., Beland, M., Seto, P., 2006. Occurrence and reductions of pharmaceuticals and personal care products and estrogens by municipal wastewater treatment plants in Ontario, Canada. Sci. Total Environ. 367 (2–3), 544–558.
Liu, Y.J., Xuan Zhen Jian, G., 2005. Phenol degradation by a nonpulsed diaphragm glow discharge in an aqueous solution. Environ. Sci. Technol. 39, 8512–8517 (76).
Loomis-Husselbee, J.W., Cullen, P.J., Irvine, R.F., Dawson, A.P., 1991. Electroporation can cause artifacts due to solubilization of cations from the electrode plates. Biochem. J. 277, 883–885.
Lukeš, P., Člupek, M., Babický, V., Šunka, P., Skalný, J.D., Štefečka, M., Novák, J., Málková, Z., 2006. Erosion of needle electrodes in pulsed corona discharge in water. Czeholovak J. Phys. 56, 916–924.
Mehlman, M.A., Borek, C., 1987. Toxicity and biochemical mechanisms of ozone. Environ. Res. 42, 36–53.
Monarca, S., Feretti, D., Collivignarelli, C., Guzzella, L., Zerbini, I., Bertanza, G., Pedreazzani, R., 2000. The influence of different disinfectants on mutagenicity and toxicity of urban wastewater. Water Res. 34, 4261–4269.
Montie, T.C., Kelly-Wintenberg, K., Roth, J., 2000. An overview of research using the one atmosphere uniform glow discharge plasma (OAUGDP) for sterilization of surfaces and materials. IEEE Trans. Plasma Sci. 28, 41–50.

Moriwaki, H., Osborne, M.R., Phillips, D.H., 2008. Effects of mixing metal ions on oxidative DNA damage mediated by a Fenton-type reduction. Toxicol. In Vitro 22, 36–44.
Ohshima, H., 2003. Genetic and epigenetic damage induced by reactive nitrogen species: implications in carcinogenesis. Toxicol. Lett. 140, 99–104.
Ohyashiki, T., Satoh, E., Okada, M., Takadera, T., Sahara, M., 2002. Nerve growth factor protects against aluminum-mediated cell death. Toxicology 176, 195–207.
Oldreive, C., Zhao, K., Paganga, G., Halliwell, B., Rice-Evans, C., 1998. Inhibition of nitrous acid-dependent tyrosine nitration and DNA base deamination by flavonoids and other phenolic compounds. Chem. Res. Toxicol. 11, 1574–1579.
Osin'kovskaia, N.D., Mittel'man, L.A., Budunova, I.V., 1988. Study in a cell culture of sodium nitrite as a possible promoter of carcinogenesis. Proc. USSR Acad. Sci. 301, 237–240.
Perl, D.P., Brody, A.R., 1980. X-ray spectrometric evidence of aluminum accumulation in neurofibrillary tangle-bearing neurons. Science 208, 297–299.
Reyns, K.F.M.A., Diels, A.M.J., Michiels, C.W., 2004. Generation of bactericidal and mutagenic components by pulsed electric field treatment. Int. J. Food Microbiol. 93, 165–173.
Routledge, M., Mirsky, F.J., Wink, D.A., Keefer, L.K., Dipple, A., 1994. Nitrite-induced mutations in a forward mutation assay concentration and pH. Mutat. Res. Genet. Toxicol. 322, 341–346.
Rowan, N.J., 2013. Defining established and emerging risks in the aquatic environment: current knowledge, implications, and outlooks. Intern. J. Microbiol. (in press) http://dx.doi.org/10.1155/416283. PMID 20976256.
Rowan, N.J., Espie, S., Harrower, J., Farrell, H., Marsili, L., Anderson, J.G., MacGregor, S.J., 2008a. Evidence of lethal and sublethal injury in food-borne bacterial pathogens exposed to high-intensity pulsed-plasma gas discharges. Lett. Appl. Microbiol. 46, 80–86.
Rowan, N.J., Espie, S., Harrower, J., Anderson, J.G., MacGregor, S.J., 2008b. Evidence of lethal and sublethal injury in microbial pathogens exposed to pulsed plasma gas discharge treatments. Lett. Appl. Microbiol. 46, 80–86.
Sharpe, M., 2001. The science of the unclean. J. Environ. Monit. 3 (1), 2N–6N (Feb).
Shiki, H., Motoki, J., Takikawa, H., Sakakibara, T., Nishimura, Y., Hishida, S., Okawa, T., Ootsuka, T., 2007. Electrode erosion in pulsed arc for generating air meso-plasma jet under atmospheric pressure. IEEJ Trans. Fund. Material 127, 567–573.
Singh, N.P., McCoy, M.T., Tice, R.R., Schneider, E.L., 1988. A simple technique for quantitation of low levels of DNA damage in individual cells. Exp. Cell Res. 175 (1), 184–191.
Slabbert, J.L., Venter, E.A., 1999. Biological assays for aquatic toxicity testing. Water Sci. Technol. 39, 367–373.
Spencer, J.P., Whiteman, M., Jenner, A., Halliwell, B., 2000. Nitrite-induced deamination and hypochlorite-induced oxidation of DNA in intact human respiratory tract epithelial cells. Free Radic. Biol. Med. 28, 1039–1050.
Stakey, B.J., 1987. Aluminum in renal disease: current knowledge and future developments. Ann. Clin. Biochem. 24, 337–344.
Stapulionis, R., 1999. Electric pulse-induced precipitation of biological macromolecules in electroporation. Bioelectrochem. Bioenerg. 48, 249–254.
Sun, J., Aoki, K., Wang, W., Guo, A., Misumi, J., 2006. Sodium nitrite-induced cytotoxicity in cultured human gastric epithelial cells. Toxicol. In Vitro 20, 1133–1138.
Takaki, K., Hatanaka, Y., Arimaa, K., Mukaigawaa, S., Fujiwara, T., 2008. Influence of electrode configuration on ozone synthesis and microdischarge property in dielectric barrier discharge reactor. Vacuum 83 (1), 128–132.
Ternes, T.A., Stumpf, M., Mueller, J., Haberer, K., Wilken, R.D., Servos, M., 1999. Behaviour and occurrence of estrogens in municipal sewage treatment plants—I. Investigations in Germany, Canada and Brazil. Sci. Total Environ. 225, 81–90.
Tindal, M., 2007. Updated ecotox database and revised ecological direct contact soil standard for soluble barium. British Columbia Ministry of Energy - Mines and Petroleum Resources.
Toimela, T., Mäenpää, H., Mannerström, M., Tähti, H., 2004. Development of an in vitro blood–brain barrier model-cytotoxicity of mercury and aluminum. Toxicol. Appl. Pharmacol. 195, 73–82.
Tomov, T., Tsoneva, I., 2000. Are the stainless steel electrodes inert? Bioelectrochemistry 51, 207–209.
US Environmental Protection Agency, 1994. Short-term Methods for Estimating the Chronic Toxicity of Effluents and Receiving Water to Freshwater Organisms. EPA 600-4-91-002 3rd ed. (Cincinnati, OH, USA).
Velzeboer, I., Hendriks, J., Ragas, M.J., Van De Meent, D., 2008. Nanomaterials in the environment: aquatic ecotoxicity of some nanomaterials. Environ. Toxicol. Chem. 27, 1942–1947.
Victorin, K., 1994. Review of the genotoxicity of nitrogen oxides. Mutat. Res. Rev. Genet. Toxicol. 317, 43–55.
West, I., Gulley, D.D., 1994. TOXSTAT, Version 3.4. Western Ecosystems Technology, Cheyenne, WY, USA.
Willberg, D.M., Lang, P.S., Höchemer, R.H., Kratel, A., Hoffmann, M.R., 1996. Degradation of 4-chlorophenol, 3,4-dichloroaniline, and 2,4,6-trinitrotoluene in an electrohydraulic discharge reactor. Environ. Sci. Technol. 30 (8), 2526–2534.
Zhou, N., Fu, Z., Sun, T., 2008. Effects of different concentrations of oxygen — ozone on rats' astrocytes in vitro. Neurosci. Lett. 441, 178–182.

Letters in Applied Microbiology ISSN 0266-8254

ORIGINAL ARTICLE

Evidence of lethal and sublethal injury in food-borne bacterial pathogens exposed to high-intensity pulsed-plasma gas discharges

N.J. Rowan[1], S. Espie[2], J. Harrower[2], H. Farrell[1], L. Marsili[2], J.G. Anderson[2] and S.J. MacGregor[2]

1 Department of Nursing and Health Science, Athlone Institute of Technology, Dublin Road, Athlone, Ireland
2 Roberston Laboratories of Electronic Sterilisation Technologies (ROLEST), University of Strathclyde, Glasgow, Scotland

Keywords
fluorescent metabolic probes, HACCP, microbial inactivation, pulsed power electrotechnologies, sublethal injury.

Correspondence
Neil J. Rowan, Department of Nursing and Health Science, Athlone Institute of Technology, Dublin Road, Athlone, Co. Westmeath, Ireland. E-mail: nrowan@ait.ie

2007/1095: received 9 July 2007, revised 9 September 2007 and accepted 10 September 2007

doi:10.1111/j.1472-765X.2007.02268.x

Abstract

Aims: To apply scanning electron microscopy, image analysis and a fluorescent viability stain to assess lethal and sublethal injury in food-borne bacteria exposed to pulsed-plasma gas discharges (PPGD).

Methods and Results: The fluorescent redox probe 5-cyano-2,3-ditolyl tetrazolium chloride (CTC) was used for enumerating actively respiring cells of *Campylobacter jejuni*, *Escherichia coli*, *Listeria monocytogenes*, *Staphylococcus aureus* and *Salmonella* enterica serovar Typhimurium that were suspended in sterile water at 4°C and exposed to separate PPGD and heat treatments. While there was good agreement between use of respiratory staining (RS) and direct-selective agar plate counting (PC) for enumerating untreated bacteria, there were *c.* 1 and 3 log-unit differences in surviving cell numbers per millilitre for test organisms subjected to PPGD and heat treatments respectively, when enumerated by these different viability indicators. PPGD-treated bacteria were markedly altered at the cellular level when examined by scanning electron microscopy.

Conclusions: Use of this RS method revealed that substantial subpopulations of test bacteria rendered incapable of forming colonies by separate PPGD and heat treatments may remain metabolically active.

Significance and Impact of the Study: Use of this RS method offers interesting perspectives on assessing established and novel microbial inactivation methods, and may also provide a better understanding of mechanisms involved in microbial inactivation induced by high-intensity PPGD treatments.

Introduction

Pulsed power technologies have been investigated as major alternative approaches for the destruction of microbial pathogens on contaminated surfaces (Rowan *et al.* 1999), in food and drink (Rowan *et al.* 2001; Sentandreu *et al.* 2006), in domestic and industrial waste water (Aniplov *et al.* 2002, 2004) and for the degradation of pollutants (Hao *et al.* 2007). Albeit limited, some recent studies have reported on the application of high-voltage pulses to gas-injected test liquids that results in microbial inactivation through the formation of a plasma that causes the generation of free radicals, free electrons, ultraviolet light, acoustic and shock waves and electric fields at levels between 10 and 40 kV cm^{-1} (Espie *et al.* 2001; Aniplov *et al.* 2002). The application of high-voltage pulses to gas-sparged test liquids, such as laboratory-based media (Espie *et al.* 2001) and domestic and industrial waster water (Aniplov *et al.* 2002, 2004), results in partial discharge activity and ionization of the gas that leads to complete breakdown of the gas in these liquid media. Previous studies have shown that in addition to the generation of the aforementioned plasmochemical components in test liquids that have recognized antimicrobial properties, substantial levels of ozone also accompany this electrical discharge process when oxygen is used

as the sparged gas (Espie *et al.* 2001). Despite scientific and developmental interests in pulsed-plasma gas discharge (PPGD) technology, very little research has been directed towards gaining a better understanding of the recovery processes associated with sublethally injured micro-organisms after PPGD treatment: previous studies have relied heavily on enumerating microbial survivors using conventional plate count (PC) agar techniques.

In this study, image analysis and fluorescent redox probe 5-cyano-2,3-ditolyl tetrazolium chloride (CTC) were used to investigate respiratory activity in *Listeria monocytogenes*, *Escherichia coli*, *Salmonella enterica se*rovar Typhimurium, *Staphylococcus aureus* and *Campylobacter jejuni* that were exposed to separate PPGD and heat treatments. Here, we report on the use of respiratory staining (RS) for rapidly quantifying the extent of sublethal cellular injury in PPGD and heat-treated food-borne bacteria.

Materials and methods

Bacterial strains used and preparation of inocula

Single strains of *C. jejuni* ATCC 33560, enterotoxigenic *E. coli* NCTC 11601, nonpathogenic *E. coli* K-, *L. monocytogenes* NCTC 9863, *S. enterica* serovar Tpyhimurium ATCC 14028, *Staph. aureus* NCTC 4444 and *B. cereus* NCTC 11145 were used in this study. All test strains were maintained in Microbank storage vials (Cruinn Diagnostic, Ireland) at −70°C. *Campylobacter jejuni* was grown to single colonies on modified charcoal-cefoperazone-deoxycholate agar (CCDA) plates (Unipath, Bedford, UK) at 42°C for 48 h in a microaerophilic environment generated by CampyPak gas generators (Unipath) generating 5% O_2, 10% CO_2 and 85% N_2. Strains of *E. coli*, *L. monocytogenes*, *Staph. aureus* and *Salmonella* spp. were grown separately to single colonies on MacConkey agar (MCA), *Listeria* selective agar (LSA), Baird Parker agar (BPA; Oxoid) and xylose lysine desoxycholate (XLD; Oxoid, Basingstoke, UK) agar, respectively at 37°C for 48 h aerobically. While *B. cereus* was grown at 37°C for 5 days on *B. cereus* selective agar (BCSA; Oxoid) supplemented with 3 mg l^{-1} of $MnSO_4.H_2O$, the latter component stimulates endospore formation.

Bacteria were harvested from respective agar plates, washed thrice in 0·1 mol l^{-1} phosphate-buffered saline (PBS) pH 7·2 and sedimented by centrifugation at 4000 ***g*** for 20 min at 4°C. *Campylobacter jejuni* was resuspended in 10 ml of PBS and transferred to a 1·5-l fermentation vessel containing 500 ml of Brucella broth (Difco Laboratories, Detroit, Michigan, USA), and grown in a Bioflow 3000 bioreactor (New Brunswich Scientific, St Albans, UK) for 24 h at 42°C under the following batch culture settings: agitation 125 rev min^{-1}; sparged gas composition 5% O_2, 10% CO_2 and 85% N_2; and pH was maintained at 6·8 using 0·1 mol l^{-1} NaOH and 0·1 mol l^{-1} H_2SO_4. After 24 h growth (early-stationary phase) bacteria were resuspended in 10 ml of sterile distilled water (dH_2O) at 4°C, and the optical density (OD) was adjusted at 540 nm to 2·0 (*c.* 10^9 CFU ml^{-1}) by spectrophotometric (model UV-120-02 instrument; Shimadzu Corp., Kyoto, Japan) determination. Inocula for the other test bacteria were prepared similarly with the following modifications; growth at 37°C in trypticase soy broth supplemented with 3% (w/v) yeast extract (Difco) with agitation (250 rev min^{-1}) using sparged atmospheric air. The presence and degree of endospore formation was confirmed by heat treating the PBS suspension of *B. cereus* for 15 min at 85°C in a circulating constant temperature waterbath (model HE30; Grant Instruments Ltd, Shepreth, UK) equipped with a thermoregulator capable of maintaining temperature to within ±0·05°C (model TE-8A; Techne Ltd, Cambridge, UK), and by subsequent enumeration of treated samples on BCSA plates after 48 h at 37°C.

PPGD treatment of test bacteria

Ten-millilitre aliquots of OD_{540} adjusted test bacterial suspensions (*c.* $\geq 10^9$ CFU ml^{-1}) were added to 247 ml of sterile dH_2O at 4°C before transfer to the coaxial treatment chamber (total volume 257 ml). Predetermined starting cell populations were prepared similarly for each test bacterium. The treatment chamber was constructed from 2-cm diameter stainless steel pipe forming the outer earthed electrode, with a 1-mm copper wire forming the coaxial high-voltage electrode. The test chamber was also immersed in chilled water bath in order to maintain the temperature at ≤4°C, which was monitored with a thermocouple. Once the pulse power system had been activated, oxygen was injected to the treatment chamber using a venturi gas injector. Plasma discharge activity was achieved in the test liquids using high-voltage pulses that were applied to the coaxial treatment chamber using a pulse-forming line (PFL) circuit, consisting of eight lengths of 12·62 m coaxial cable as described previously, with modifications (Espie *et al.* 2001). The PFL was charged using a high-voltage 40 kV DC capacitor charging power supply, connected via a resistance/diode protection circuit (RLIM). Using an SF6/air-pressurized, triggered spark gap switch [Samtech CSS-01, Samtech TG-01(B)], the PFL output was connected to the treatment chamber via a further 2 m, 50Ω, transmission line. The electrical operating parameters used were pulse energy of 3·7 J, PFL charging voltage of 23·5 kV, pulse rate of 124 pps and gas flow rate of 10 l min^{-1}. The gas flow rate was controlled by use of a Brooks mass flow controller (model 5851S), allowing continual adjustment to compensate for pressure

and temperature variances. When the spark gap switch was triggered, a voltage pulse was launched along the transmission line feed cable to the treatment chamber. Upon reaching the treatment chamber, the pulse was applied to suitably contoured electrodes, resulting in ionization of the surrounding gas bubbles in the liquid leading to ozone formation. Samples were taken in triplicate at designated intervals and after 30 s treatment time had elapsed, the pulsed power system was shut off and the gas supply was disconnected. Measurement of the dissolved ozone level was carried out using a BMT 963AQ ozone-in-water sensor ultraviolet (UV) photometer as per methods described previously (Espie *et al.* 2001). Conductivity, pH and temperature were measured using a Hanna Instruments WT-50 Water Test meter (RS Components, Northants, UK), which had the following ranges and accuracy: temperature, 0 to 60·0°C ± 1°C; pH, –0 to 14·0 ± 0·2; conductivity –0 to 1999 μS cm^{-1}, ±2% full scale. Samples were removed after predetermined exposure times and enumerated as described earlier.

The test bacteria were also subjected to heating at 56°C in order to achieve a similar level of inactivation (*c.* 4 log units in CFU ml^{-1}) to that obtained by PPGD treatment, according to methods described previously, with modifications (Yaqub *et al.* 2004). Test bacteria were suspended in sterile dH_2O to a density of *c.* 10^8 CFU ml^{-1} in 3-ml shrimp cap glass vials (Phase Separations Ltd, Watford, Hertfordshire, UK). The vials were sealed and kept 4 cm below the level of a circulating constant water bath for the treatment period. After separate treatments, heat and PPGD samples were diluted as appropriate in PBS and were spiral-plated onto appropriate agar as described earlier using a spiral system (model B; Spiral Systems Inc., 6740 Clough Cincinnati, USA). Undiluted samples were enumerated using the pour-plate technique. Typical colonies of each test strain were randomly selected from respective selective agar plates after 24 h and 48 h at 37°C (and 42°C for *Campylobacter*) with the highest dilution, and were confirmed by use of appropriate physiological and biochemical tests as described earlier. Survivor cell populations and untreated controls were expressed in terms of colony-forming units per millilitre (CFU ml^{-1}) and the corresponding death rate kinetic curves were generated.

Assessment of PPGD-treated bacteria for cellular damage using scanning electron microscopy

PPGD-treated samples were examined visually for cellular damage by using scanning electron microscopy (SEM). Briefly, test samples were centrifuged (10 min, 10 000 ***g***, 4°C), and the supernatants were discarded. The pellets were washed with PBS twice and fixed with 2·5% gluteraldehyde (Sigma-Aldrich, Gillingham, Dorset, UK). Cells were then filtered onto 0·2-μm-pore-size Isopore GTTP membrane filters (Millipore, Watford, UK). The cells were dehydrated once in 50%, 70%, 80% and 90% ethanol and twice in 10% ethanol, treated with 100% isoamyl acetate, and critical point dried. Finally, cells were sputter-coated with 150-nm gold particles and with the model JSM-T200 SEM (JEOL).

Use of epifluorescence microscopy, image analysis and fluorescence redox probes to enumerate respiring cell numbers after heating and PPGD treatments

Epifluorescence microscopy, image analysis and the fluorescent redox probes CTC and 4′,6-diamidino-2-phenylindole (DAPI) were used to investigate respiratory activity in test strains according to previously described procedures, with modifications (Yaqub *et al.* 2004). One-millilitre cell suspensions were harvested by centrifugation (4°C for 10 min at 3000 ***g***) and washed thrice with PBS. Experimental and control preparations were resuspended in 300 μl of 5 mmol l^{-1} CTC (Polysciences, Inc., St. Louis, MO, USA) and incubated in microaerophilic (for *Campylobacter* only) or aerobic environment for 1·5 h in the dark at 20°C with agitation (200 rev min^{-1}). After incubation, experimental and control preparations, and dilutions thereof, were counterstained for 8 min at 20°C with 5 μg of DAPI (Sigma, St. Louis, MO, USA) per millilitre and the samples were transferred to a Petroff-Hausser counting chamber for enumeration. Counterstaining with the DNA-binding DAPI allowed concurrent determinations of total (i.e. viable plus nonviable) bacteria and viable (i.e. only cells exhibiting red CTC-formazan fluorescence) bacteria. Epifluorescence observations of CTC-treated preparations were viewed using a blue 420–480-nm excitation filter (combined with a 580-nm dichromic mirror and a 590-nm barrier filter) in a Nikon Optiphot microscope. CTC- and DAPI-stained bacteria in the same preparation were viewed simultaneously with a 365-nm excitation filter, and emission filter and a 400-nm cut-off filter. Stained cells were distinguished from nonspecific reactions by overlaying the fluorescence and phase-contrast images. The image analysis system comprised a Sony charge-coupled device camera and a Seescan Solitaire image analyser (Seescan Ltd., Cambridge, UK). Counts were determined from five randomly selected squares on the chamber etched-grid in triplicate experiments and results were expressed as the log number of the corresponding bacteria per millilitre of the sample.

Statistical analysis

Analysis of variance – balanced model (Minitab software Release 14; Minitab Inc., State College, PA, USA) was used to compare the effects of PPGD treatments on

microbial inactivation. Experiments were replicated thrice with duplicate treatments in each replication, and results are reported as means ± standard deviations. Significant differences were reported at the 95% ($P < 0{\cdot}05$) and confidence interval.

Results

Enumeration of heat-treated test bacteria using RS and direct-selective PC

Thermal treatment or holding times required to achieve 4 log reductions in cell populations for *L. monocytogenes* NCTC 11994, nonpathogenic *E. coli* K12, enterotoxigenic *E. coli* NCTC 11601, *C. jejuni*, *Staph. aureus* and *S. enterica* serovar Typhimurium at 56°C were 36·4, 32, 28·8, 31·2, 35·4 and 33·6 min, respectively. This corresponded to $D_{56°C}$ values (decimal reduction time: the time required to kill 1-log unit concentration of bacteria) of 9·1, 8, 7·2, 7·8, 8·8 and 8·4, respectively (data not shown). Good agreement was obtained between the CTC fluorescence or RS method and the conventional direct PC method for enumerating untreated cell populations of test bacteria ($P < 0{\cdot}05$) (Table 1). The PC method demonstrated that heat-treated samples of *C. jejuni*, nonpathogenic *E. coli*, enterotoxigenic *E. coli*, *S. enterica* serovar Typhimurium, *L. monocytogenes* and *Staph. aureus* were reduced by 4·3, 3·7, 3·1, 4·1, 3·9 and 3·6 log CFU ml^{-1}, respectively; this markedly contrasted with reductions of 1·9, 2·7, 1·5, 1·6, 2·7 and 2 log cell numbers of actively respiring bacteria per millilitre as determined by the rapid RS method ($P < 0{\cdot}05$) (Table 1).

Enumeration of PPGD-treated test bacteria using RS and direct-selective PC

PPGD treatments rapidly reduced predetermined populations (≤8 log CFU ml^{-1}) of all vegetative test bacteria suspended separately in sterile dH_2O at 4°C to nondetectable levels within 24 s when enumerated by the PC approach (Fig. 1). Inactivation kinetic data obtained from Fig. 1 was used to determine PPGD exposure times (s) that produced similar levels of lethality (*c.* 4-log units in CFU ml^{-1}) to that obtained by heating: this corresponded to exposure times of 3, 4, 6, 7, 8 and 30 s for *C. jejuni*, nonpathogenic *E.* coli K-12, enterotoxigenic *E. coli*, *S. enterica* serovar Typhimurium, *L. monocytogenes* and *B. cereus* spores, respectively. Findings showed that a similar trend emerged when enumerating PPGD-treated bacteria using the different viability counting methods compared with that of treating similar samples with heating (Table 1). The PC method demonstrated that PPGD-treated samples of *L. monocytogenes*, nonpathogenic *E. coli*, enterotoxigenic *E. coli*, *C. jejuni*, *S. enterica* serovar Typhimurium and *Staph. aureus* were reduced by 3·5, 3·5, 3·2, 3·2, 3·6 and 3·1 log CFU ml^{-1}, respectively, which markedly contrasted with reductions of 2·5, 1·5, 2·0, 2·2, 2·8 and 2·3 log cell numbers of actively respiring bacteria per millilitre as determined by the rapid RS method ($P < 0{\cdot}05$) (Table 1). Mean differences in cell numbers for pooled vegetative test bacteria enumerated by PC and RS methods after heating at 56°C was 3·86 ± 0·49 and 1·98 ± 0·46 log CFU ml^{-1}, respectively. A similar trend emerged for PPGD-treated samples ($P < 0{\cdot}05$), where the mean difference for pooled test bacteria enumerated by PC and RS approaches was 3·5 ± 0·21 and 2·2 ± 0·51 log CFU ml^{-1}, respectively. Whilst heating did not inactivate *B. cereus* spores (data not shown), application of PPGD reduced spore populations by *c.* 3·4 log CFU ml^{-1} after 30 s at 4°C (Fig. 1).

Discussion

In general, it would appear that subpopulations of PPGD- and heat-treated test bacteria (*c.* 1 and 3 log CFU ml^{-1}, respectively) are capable of respiration (which suggests

Table 1 Enumeration of test bacterial cell numbers by respiratory staining (RS) and colony-forming units (CFU) by direct plate counting (PC) after heating and pulsed plasma gas-discharge (PPGD) treatment

	Log CFU or cell members ml^{-1}					
Test bacteria	Untreated (PC)	Untreated (RS)	Heat (PC)	Heat (RS)	PPGD (PC)	PPGD (RS)
Campylobacter jejuni	7·8 (±0·2)^{A}	7·6 (±0·3)^{A}	3·5 (±0·3)^{D}	5·7 (±0·3)^{C}	4·3 (±0·5)^{D}	5·1 (±0·6)^{C}
Escherichia coli K-12	7·6 (±0·3)^{A}	7·3 (±0·2)^{A}	3·9 (±0·7)^{D}	4·6 (±0·3)^{D}	4·1 (±0·3)^{D}	5·8 (±0·4)^{C}
E. coli 11601	7·4 (±0·2)^{A}	7·3 (±0·2)^{A}	4·3 (±0·5)^{D}	5·8 (±0·4)^{C}	4·2 (±0·4)^{D}	5·3 (±0·5)^{C}
Salmonella Typhimurium	7·5 (±0·3)^{A}	7·4 (±0·1)^{A}	3·4 (±0·4)^{D}	5·8 (±0·3)^{C}	4·3 (±0·6)^{D}	5·2 (±0·4)^{C}
Staphylococcus aureus	7·6 (±0·3)^{A}	7·3 (±0·3)^{A}	4·0 (±0·4)^{D}	5·3 (±0·2)^{D}	4·5 (±0·4)^{D}	5·0 (±0·5)^{D}
Listeria monocytogenes	7·7 (±0·3)^{A}	7·5 (±0·3)^{A}	3·8 (±0·6)^{D}	5·3 (±0·3)^{C}	4·1 (±0·5)^{D}	4·7 (±0·4)^{D}
Bacillus cereus (spores)	6·9 (±0·1)^{B}	NA§	6·8 (±0·1)^{B}	NA	4·5 (±0·4)^{D}	NA

Values followed by the same upper case letter in separate columns do not significantly differ at the 95% confidence interval ($P < 0{\cdot}05$).
§Not applicable, as 5-cyano-2,3-ditolyl tetrazolium chloride (CTC)-4′,6-diamidino-2-phenylindole (DAPI) RS does not stain endospores.

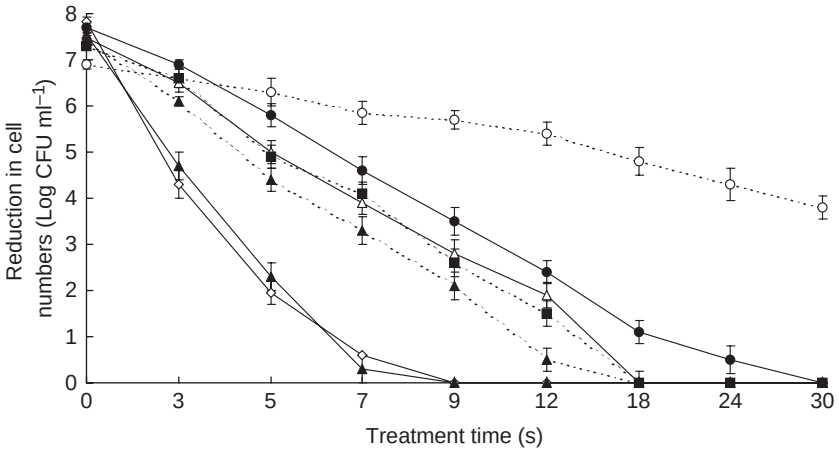

Figure 1 Influence of pulsed plasma gas-discharge treatment on the inactivation of test bacteria suspended in distilled water at 4°C. —◇— *C. Jejuni*; —▲— *E. coli K-12*; —△— *S. typhimurium*; —●— *L. monocytogenes*; ···▲··· *E. coli 11601*; ···○··· *B. cerus* (spores); ···■··· *S. aureus*.

cell viability), but are unable to grow on selective laboratory-based culture media because of sublethal injury. Results from the latter thermal inactivation study agree with the findings of Gunasekera *et al.* (2002), where these researchers used *de novo* expression of a *gfp* reporter gene and membrane integrity based on propidium iodide exclusion as viability indicators to show that a substantial proportion of *E. coli* and *Pseudomonas putida* cells in heat-treated milk are metabolically active but are incapable of forming colonies. These findings are significant as food technologists routinely use agar PC to detect spoilage and pathogenic bacteria (Rowan 2004).

Reductions in *Campylobacter* numbers (≤8 log CFU ml^{-1}) were achieved in just 9 s at 4°C (Fig. 1), which may be attributable in part to the particular sensitivity of this notable enteropathogen to highly oxygenated environments (Purdy *et al.* 1999). In general, both gram-positive and -negative test bacteria appeared similarly susceptible to the effects of plasma treatment, despite there being significant differences in cellular wall structure (Fig. 1). *Listeria monocytogenes* was shown to be more resistant to the lethal action of PPGD compared with other vegetative test bacteria ($P < 0{\cdot}05$), which corroborates previous studies that demonstrated the resilience and adaptability of this problematic bacteria to a wide range of applied lethal stresses (Lou and Yousef 1997). It is interesting to note that the nonpathogenic strain *E. coli* K-12 was more susceptible to the lethal action of PPGD treatment compared with that of the enterotoxigenic *E. coli* NCTC 11601 stain, which is in line with previous studies that investigated the relationship between virulence factor expression and stress tolerance (Rowan 2004).

Use of fluorescent redox probes (such as CTC) for direct visualization of actively respiring bacteria is gaining popularity among research groups investigating the viable but nonculturable (VBNC) phenomenon (i.e. stress-injured bacteria which are not capable of cellular division required for growth in usual culture media, but, yet remain physically active for several metabolic functions) in food- and water-borne bacteria (Chaveerach *et al.* 2003; Gupte *et al.* 2003; Yaqub *et al.* 2004; Cappelier *et al.* 2007). CTC reduction reflects the presence of a functional electron transport (i.e. respiratory) system in the microbial cell membrane where insoluble fluorescent CTC-formazon crystals accumulate in metabolically active bacteria in a time-dependent manner. However, as nonselective agar plates were not used for the recovery of heat- or PPGD-treated test micro-ogranisms, the CTC redox probe used in this present study reports on microbial viability in the context of demonstrating respiration that may not in itself be sufficient to prove growth of living cells post-treatments. This present study has provided evidence that a significant proportion of *C. jejuni*, *L. monocytogenes*, *S. enterica* serovar Typhiumuium and *E. coli* cells that rendered incapable of forming colonies by heat or PPGD treatments are metabolically active. However, previous studies (Yaqub *et al.* 2004) that reported on the use of image analysis and RS showed that the PC method did not significantly underestimate the numbers of cell survivors after pulse electric field (PEF) treatment, which markedly contrasts from the earlier findings where *c.* 2-log unit difference in surviving cell populations was evident after heating or PPGD treatment. While the mechanisms underlying the inactivation of micro-organisms by PPGD have yet to be fully elucidated, it is generally considered that microbial inactivation may be attributed to the combined influence of numerous antimicrobial components formed during this plasma discharge process, such as the generation of ozone and other free radicals, free electrons, ultraviolet light, acoustic and shock waves (Espie *et al.* 2001; Aniplov *et al.* 2004). In this study, the residual ozone level produced during PPGD treatments of test micro-organisms in distilled water after 30 s was

c. 250 ppm. Findings from SEM studies revealed that a significant proportion of PPGD-treated bacteria were altered at the cellular level (data not shown). It should be noted, however, that Aronsson *et al.* (2005) reported that the finally observed irreversible membrane permeabilizaton may not be the initial mechanistic basis for the inactivation of yeast cells. Interestingly García *et al.* (2005) reported on the occurrence of sublethal injury after extended PEF treatments, which depended on the type of the test micro-organism, the treatment medium, pH and the intensity of the treatment investigated. From these and other data it may be inferred that the damage inflicted upon microbial cells such as stresses is multifactorial and that therefore the stress response of the cells will be of a complex nature. Therefore, fundamental insights into the type of damage that inflicts single or multiple injuries in PEF or PPGD-treated micro-organisms merits further experimentation. While a broad spectrum of useful approaches can be pursued to investigate the mode of action, of particular relevance would be the use of genome-wide transcription analysis to assess sublethal conditions in a bacterial model strain such as that described recently by Iwahashi *et al.* (2005).

Albeit limited in scope, previous studies carried out by this (Espie *et al.* 2001) and other research groups (Aniplov *et al.* 2002) demonstrated that quality of plasma-treated water fulfilled the necessary standards of the European Union and was deemed fit for human consumption However, these studies have not focused on the possibility that application of electric discharge to agricultural, municipal or industrial effluents containing organic material may generate unwanted by-products such as bromate which is a recognized carcinogen derived from bromide (Kim *et al.* 2003). The pH of test bacterial suspensions decreased during plasma treatment at 4°C, where the pH values measured after 30 s was 3·9 compared with 6·03 for untreated sterile distilled water. Reasons as to why sparging with oxygen during the electric discharge process resulted in a decrease in pH is not presently known, but may be attributed to the possible formation of weak nitric and carbonic acids from N_2 and CO_2-based compounds present in the microbial milieu during plasma treatment. It is also likely that the rapid reduction in pH to 3·9 may have contributed to microbial inactivation, especially because *C. jejuni* has been reported previously to be sensitive to extremes in pH, especially acidic conditions (Zhao and Doyle 2006).

In conclusion, this is the first study to report on the efficacy of CTC as a rapid approach for quantifying actively respiring food-borne bacteria that were subjected to PPGD treatments. Our studies also indicate that the use of PPGD was very effective not only in rapidly reducing populations of bacterial enteropathogens suspended in sterile distilled water at 4°C, and therefore, could possibly act as a critical control point in a hazard analysis critical control point (HACCP) by preventing cross-contamination of the processing environments.

Acknowledgements

The authors are grateful to David Currie for technical assistance on electron microscopy.

References

Aniplov, A.M., Barkhudarov, E.M., Christofi, N., Kop'ev, V.A., Kossyi, I.A., Taktakishvili, M.I. and Zadiraka, Y. (2002) Pulsed high voltage electric discharge disinfection of microbially contaminated liquids. *Lett Appl Microbiol* **35**, 90–94.

Aniplov, A.M., Barkhudarov, E.M., Christofi, N., Kop'ev, V.A., Kossyi, I.A., Taktakishvili, M.I. and Zadiraka, Y.V. (2004) The effectiveness of a multi-spark electric discharge system in the destruction of microorganisms in domestic and industrical wastewaters. *J Water Health* **4**, 267–277.

Aronsson, K., Rönner, U. and Borch, E. (2005) Inactivation of *Escherichia coli*, *Listeria innocua* and *Saccharomyces cerevisiae* in relation to membrane permeabilization and subsequent leakage of intracellular compounds due to pulsed electric field processing. *Int J Food Microbiol* **99**, 19–32.

Cappelier, J.M., Besnard, V., Roche, S.M., Velge, P.L. and Federighi, M. (2007) Avirulent viable but nonculturable cells of *Listeria monocytogenes* need the presence of an embryo to be recovered in egg yolk and regain virulence after recovery. *Vet Res* **38**, 573–578.

Chaveerach, P., ter Hurrne, A.A., Lipman, L.J. and van Knapen, F. (2003) Survival and resuscitation of ten strains of *Campylobacter jejuni* and *Campylobacter coli* under acid conditions. *Appl Environ Microbiol* **69**, 711–714.

Espie, S., Marsili, L., MacGregor, S.J. and Anderson, J.G. (2001) Investigation of dissolved ozone production using plasma discharge in liquid. *Pulsed Power Plasma Sci – Digest Technical Papers* **1**, 616–619.

García, D., Gómez, N., Maňas, P., Condón, S., Raso, J. and Pagán, R. (2005) Occurrence of sublethal injury after pulsed electric fields depending on the microorganism, the treatment medium pH and the intensity of the treatment investigated. *J Appl Microbiol* **99**, 94–104.

Gunasekera, T.S., Sørensen, A., Attfield, P., Sørensen, S.J. and Duncan, A.V. (2002) Inducible gene expression by nonculturable bacteria in milk after pasteurization. *Appl Environ Microbiol* **68**, 1988–1993.

Gupte, A.R., de Rezende, C.L.E. and Joseph, S.W. (2003) Induction and resuscitation of viable but nonculturable *Salmonella enterica* Serovar Typhimurium DT104. *Appl Environ Microbiol* **69**, 6669–6675.

Hao, X.L., Zhou, M.H. and Lei, L.C. (2007) Non-thermal plasma-induced photocatalytic degradation of 4-chlorophenol in water. *J Haz Mat* **141**, 475–482.

Iwahashi, M., Odani, M., Ishidou, E. and Kitagawa, E. (2005) Adaptation of *Saccharomyces cerevisiae* to high pressure causing growth inhibition. *FEBS Lett* **579**, 2847–2852.

Kim, J.G., Yousef, A.E. and Khadre, M.A. (2003) Ozone and its current and future application in the food industry. *Adv Food Nutr Res* **45**, 167–218.

Lou, Y. and Yousef, A.E. (1997) Adaptation to sublethal environmental stress protects *Listeria monocytogenes* against lethal preservation factors. *Appl Environ Microbiol* **63**, 1252–1257.

Purdy, D., Cawthraw, S., Dickinson, J.H., Newell, D.G. and Park, S.F. (1999) Generation of a superoxide dismutase (SOD)-deficient mutant of *Campylobacter coli*: evidence for the significance of SOD in *Campylobacter* survival and colonization. *Appl Environ Microbiol* **65**, 2540–2546.

Rowan, N.J. (2004) Viable but nonculturable forms of food and water-borne bacterial pathogens: quo vadis? *Trends Food Sci Technol* **15**, 462–467.

Rowan, N.J., MacGregor, S.J., Anderson, J.G., Fouracre, R.A. and Farish, O. (1999) Pulsed UV light inactivation of microbial pathogens. *Appl Environ Microbiol* **65**, 1312–1315.

Rowan, N.J., MacGregor, S.J., Anderson, J.G., Cameron, D. and Farish, O. (2001) Inactivation of *Mycobacterium paratuberculosis* by pulsed electric fields. *Appl Environ Microbiol* **65**, 2833–2836.

Sentandreu, E., Carbonell, L., Rodrigo, D. and Carbonell, J.V. (2006) Pulsed electric fields versus thermal treatment: equivalent processes to obtain equally acceptable citrus juices. *J Food Protect* **69**, 2016–2018.

Yaqub, S., Anderson, J.G., MacGregor, S.J. and Rowan, N.J. (2004) Use of a fluorescent viability stain to assess lethal and sublethal injury in food-borne bacteria exposed to high-intensity pulsed electric fields. *Lett Appl Microbiol* **39**, 246–251.

Zhao, T. and Doyle, M.P. (2006) Reduction of *Campylobacter jejuni* on chicken wings by chemical treatments. *J Food Protect* **69**, 762–767.

Journal of Applied Microbiology

Journal of Applied Microbiology ISSN 1364-5072

REVIEW ARTICLE

Terminal sterilization of medical devices using vaporized hydrogen peroxide: a review of current methods and emerging opportunities

B. McEvoy[1] and N.J. Rowan[2]

1 STERIS Applied Sterilization Technologies, IDA Business and Technology Park, Tullamore, Ireland
2 Bioscience Research Institute, Athlone Institute of Technology, Athlone, Ireland

Keywords
Bacillus, bacterial endospores, medical devices, sterilization, terminal gaseous sterilization, vaporized hydrogen peroxide.

Correspondence
Brian McEvoy, STERIS Applied Sterilization Technologies, IDA Business and Technology Park, Tullamore, Ireland.
E-mail: brian_j_mcevoy@steris.com

2019/0278: received 15 February 2019, revised 3 July 2019 and accepted 25 July 2019

doi:10.1111/jam.14412

Summary

Medical devices are an important and growing aspect of healthcare provision and are increasing in complexity to meet established and emerging patient needs. Terminal sterilization plays a vital role in the provision of safe medical devices. While terminal sterilization technologies for medical devices include multiple radiation options, ethylene oxide remains the predominant nonthermal gaseous option, sterilizing *c.* 50% of all manufactured devices. Vaporized hydrogen peroxide (abbreviated VH2O2 by the International Organization for Standardization) is currently deployed for clinical sterilization applications, where its performance characteristics appear aligned to requirements, constituting a viable alternative low-temperature process for terminal processing of medical devices. However, VH2O2 has operational limitations that create technical challenges for industrial-scale adoption. This timely review provides a succinct overview of VH2O2 in gaseous sterilization and addresses its applicability for terminal sterilization of medical devices. It also describes underappreciated factors such as the occurrence of nonlinear microbial inactivation kinetic plots that may dictate a need to develop a new standard approach to validate VH2O2 for terminal sterilization of medical devices.

Introduction

Medical devices play an important role in the provision of healthcare, where the global market for which is predicted to surpass $400bn by 2020 (International Trade Administration 2016). According to the International Organization for Standardization (ISO 2016b), a medical device may be defined as an 'instrument, apparatus, implement, machine, appliance, implant, reagent for *in vitro* use, software, material or other similar or related article, intended by the manufacturer to be used, alone or in combination, for human beings, for one or more of the specific medical purpose(s)', with such purposes further described in ISO13485:2016 (ISO 2016b). As indicated in the definition, medical devices provide critical care and diagnostic applications through patient contact. An important consideration is safe use, whereby patient infection does not arise as a consequence of such contact. Such hospital-acquired infections (HAIs) are defined by the World Health Organization as infections developing after 48 h of hospitalization that were not present or incubating at the time of admission (Rowan and Anderson, 1998; RAISIN Working Group 2009). HAIs are estimated to affect some 1.7m patients in the United States, with an estimated annual cost to healthcare of $9.8bn (Hensley and Monson 2015). HAIs also impact negatively upon patient health, well-being and quality of life. Infections acquired in hospital may lead to sepsis, a 'life threatening organ dysfunction caused by a dysregulated host response to infection' (Dugani *et al.* 2017; Masterson *et al.* 2019). There are some 750 000 cases of sepsis annually in the United States, with a cost to healthcare of *c.* $20bn (Guirgis *et al.* 2017). While there are many known sources of HAIs (Bauld 2016; Dasenbrock *et al.* 2016), terminally sterilized medical devices are

unlikely to be a point source of infection due to associated rigorous sterilization and validation processes that deliver a sterility assurance level (SAL) far above the minimum requirements to achieve sterilization for patient safety.

Sterility assurance and terminal sterilization processes

Sterility assurance level may be defined as the 'probability of a single viable micro-organism occurring on an item after sterilization' (ISO 2018), and a sterilization process may be defined as a 'series of actions or operations needed to achieve the specified requirements for sterility' (ISO 2018). In order to achieve a required SAL, a sterilization process is applied to medical devices prior to patient use; see Fig. 1. Traditional technologies used in such terminal sterilization processes are described in Table 1 and are Category A sterilization methods according to the US Food and Drug Administration (FDA), as they are well established, they have a long history of use and consensus standards (administered by the ISO) are available. Standards such as ISO14937:2009 help inform manufacturers and users of the key aspects to be evaluated in defining the sterilization process and subsequent qualification and validation. Key considerations such as equipment and process definition, sterilization agent characterization and process validation are described in Table 2.

Medical device sterilization processes

The sterilization marketplace can be subdivided into three broad categories: (i) hospital sterilization, such as point

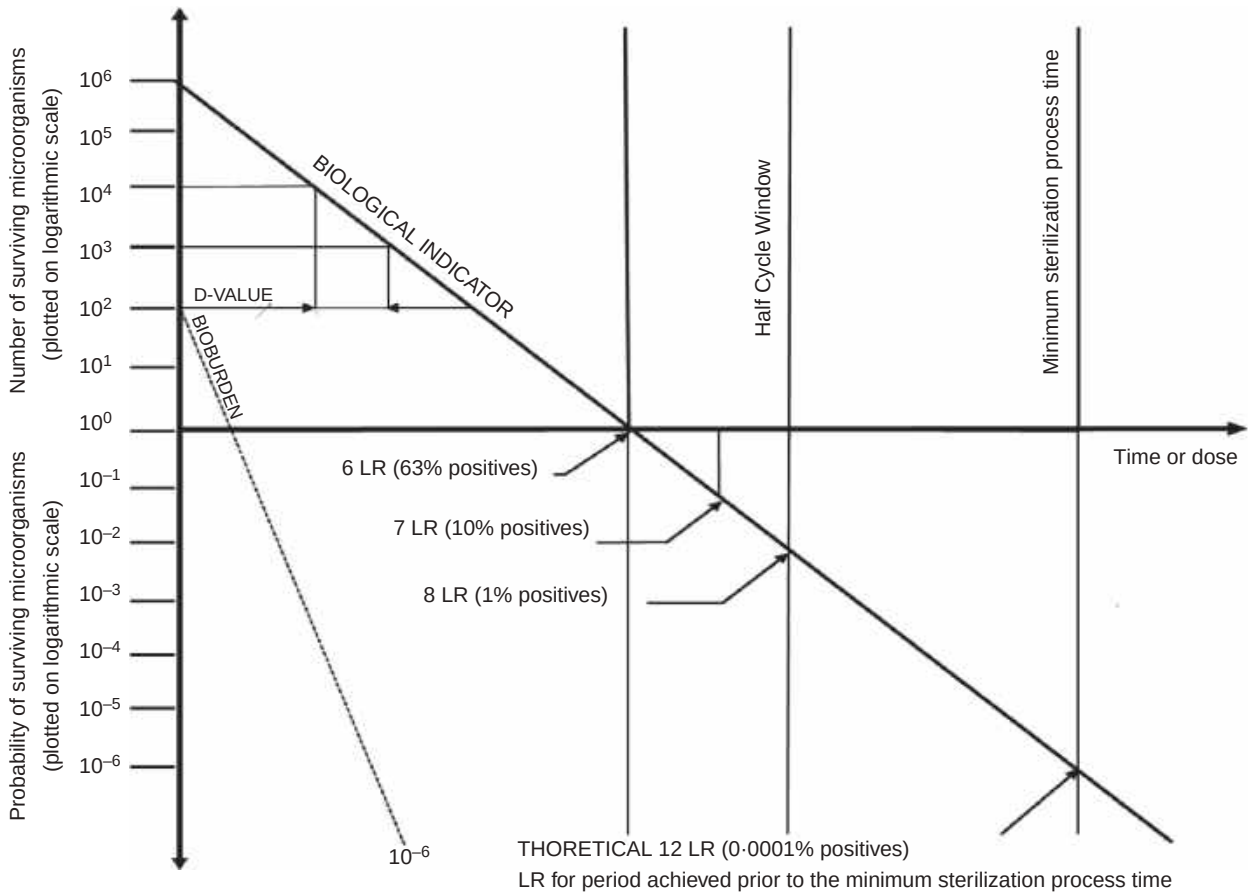

Figure 1 Sterility assurance level and example of the relationship between biological indicator and product bioburden. For illustration purposes, this graphical representation has been obtained from AAMI TIR16:2017. A BI (denoted by full line) has been selected that has a higher population and resistance (*D*-value) than that of the medical device product bioburden (denoted by dashed line). Using an overkill validation method, a sterilization process has been applied at 'half-cycle' parameters with full lethality on the BI. (In EO processing, half-cycle parameter is half of EO exposure time). In order to deliver the required sterility assurance level of $\leq 10^6$, a further 6 log reduction (LR) is applied by doubling the exposure period in the routine process. Note: Microbiological death in EO sterilization follows first-order kinetics and can be approximated by a straight line on a semi-logarithmic plot when the sterilizing conditions (i.e., process temperature, RH, and EO concentration) remain consistent for the duration of the exposure time. (AAMI, 2017)

Table 1 Global contract sterilization market by processing technology (source of Market share data: iia/GIPA (2017); source of other information: STERIS-AST.com (https://www.steris-ast.com/services/technology-comparison/)

	Ethylene Oxide	Gamma	E-beam	X-ray
Market share (%)	50	40·5	4·5	<5
Methodology	Penetration of sterilant gas into packaged product	Irradiation of product using photons from radioisotope	Product sterilized using ionizing energy from electron beam	Products sterilized using high energy X-ray photons
Sterilizaing Agent Penetration	Requires gas-permeable packaging and product design	Good penetration complete even at high densities (>0·4 g per cc)	Efficient penetration at bulk densities between 0·05–0·30 g per cc	Similar to gamma, excellent penetration for all product types
Material Compatibility	Very few material compatibility concerns. Liquids are generally not recommended	Compatible with most materials; plastics need to be evaluated Avoid acetals, PTFE (teflon), unstable polypropylene	Negative effects are frequently less pronounced or eliminated	Similar to gamma, however, negative effects are frequently less pronounced or eliminated
Turnaround time	Days: conventional = 5–10 days. All-in-one processing = 1 day	Hours: time varies based on dose requirements	Minutes: time varies based on dose requirements	Hours: time varies based on dose requirements
Process	Complex process: Variables include exposure time, temperature, humidity and EO concentration. Nonprocess variables impacting lethality include load density, packaging	Simple process: Variables include time in the cell and isotope load	Complex process: Variables include scan height, processing speed, number of passes and product orientation to the beam	Moderately complex process: Variables include processing speed, number of passes and number of pallets on conveyor
Process monitor	Biological indicators and process monitoring	Process parameters confirmed by dosimetry	Process parameters confirmed by dosimetry	Process parameters confirmed by dosimetry
Typical medical devices processed	Wide ranging compatibility: Bulk devices such as surgical procedure packs and trays Drug combination products such as Cardiovascular stents; devices with electronic/ electrical componentry	Some polymer incompatibility but suitable for many medical devices: Orthopaedic polymer and metal implants; Healthcare consumables such as sprays and wipes; labware; complex geometry devices	Wider polymer compatibility and suitable for many medical device types such as: Cardio and neurovascular devices; tissues; biologics	Similar to gamma

of use; (ii) in-house manufacturing sterilization, such as at point of medical device manufacture, often in-line applications; and (iii) contract sterilization, provided by contractors where medical device manufacturers obtain sterilization services along the supply chain after manufacturing. This review focuses on technologies employed in both the contract sterilization and in-house sterilization, specifically the terminal sterilization of medical devices. Terminal sterilization processes are delivered by the medical device manufacturers themselves or by specialist contractors, with a market estimated at over $4bn and growing at a CAGR over 8% a year (Gamma Irradiation Processing Alliance and International Irradiation Association, 2017). As highlighted in Table 1, the selection of terminal sterilization technologies is based on a number of factors, mainly market acceptance, product compatibility and availability. For further insights, see the whitepaper 'A Comparison of Gamma, E-beam, X-ray and Ethylene Oxide Technologies for the Industrial Sterilization of Medical Devices and Healthcare Products' (Gamma Irradiation Processing Alliance and International Irradiation Association 2017).

Use of gamma irradiation and ethylene oxide (EO) constitutes ca. 95% of the terminal sterilization market. In 2008, the US National Research Council determined that there were some 63 panoramic gamma irradiators in the United States, using some 198 million curies of cobalt-60 as a radiation source. It is currently estimated that there are some 400 million curies installed globally for use in gamma radiation facilities (Gamma Irradiation

Processing Alliance and International Irradiation Association 2017). While not all cobalt is dedicated to medical device sterilization, it may be estimated that such a loading of 400 million curies equates to the processing of some 10 million cubic metres of products, with a similar volume in EO processed globally. Although these two sterilization processes are the most widely used, hazards associated with their use require careful organization and control, reflecting the need to address transportation, installation, use and storage of radiation sources. For EO gas, necessary control and environmental abatement measures must be deployed, as it is deemed a carcinogen by the International Agency for Research on Cancer (IARC 2012).

In the field of radiation, much effort is currently underway to further the deployment of alternative accelerator-based technologies to reduce the reliance on isotope processing. Progress has been slow for reasons highlighted by Kroc *et al.* (2017), who offer a comprehensive review of the factors impeding device sterilization using irradiation with accelerator based technology. In gas sterilization technology, while there has been considerable effort by the terminal sterilization industry to control, manage and reduce the required inputs of EO gas, a viable gaseous alternative with similar sterilization efficacy and material compatibility remains elusive.

In the 1990s, a number of authors highlighted the pressing need for an alternative nonhazardous, noncarcinogenic gaseous industrial terminal sterilization (Klapes and Vesley 1990; Rutala and Weber 1996). Rutala and Weber (1998) described the characteristics of an ideal low-temperature industrial sterilization process, which is summarized in Table 3. As much as identifying the need for alternative gaseous sterilization solutions, these authors also proposed alternative methods. Rutala (1996) discussed the use of liquid peracetic acid, hydrogen peroxide (H_2O_2) plasma and a dual gas plasma system sterilization and disinfection in hospitals that potentially fit the criteria for an 'ideal low-temperature sterilization process'. Vaporized hydrogen peroxide (VH2O2) presents a viable alternative to EO that is already widely used in other healthcare applications. VH2O2 has a history of being an effective disinfectant and sterilant: it delivers sterilization in a fast, effective manner without generating carcinogenic or toxic residuals. The IARC has determined that H_2O_2 is not classifiable as to its carcinogenicity to humans (Agency for Toxic Substances and Disease Registry 2019). The advantages of using gaseous H_2O_2 are described by Hultman, Hill and McDonnell (2007): (i) it will have uniform contact with all exposed surfaces, including those with complex topographies; (ii) it may be safely maintained in a chamber environment and (iii) it may be efficiently and quickly removed from a chamber.

Vaporized hydrogen peroxide

History of vaporized hydrogen peroxide in sterilization

The use of H_2O_2 as a biocidal agent originates from the early 1800s following its discovery by French chemist Louis-Jacques Thénard (1777–1857). The work of early pioneers in disinfection, such as Benjamin Ward Richardson (1828–96), helped advance the applications of H_2O_2 (McDonnell 2014). Today, its use as a disinfectant is widespread, with applications including wound antiseptic, general surface disinfectant and dental disinfectant. Hydrogen peroxide is also employed in disinfectant formulations used in contact lens treatment and food postharvesting, and as a packing sterilant in aseptic processing (Linley *et al.* 2012).

The origins of the use of vaporized H_2O_2 in industrial sterilization may be traced back to 1977, when US patent #4 169 123 was granted to Francis Moore and Leon Perkinson for their 'Hydrogen Peroxide Vapor Sterilization Method', which describes a 'cold sterilization process' alternative to EO sterilization and radiation sterilization (Moore and Perkinson 1979). The patent also describes, with examples, the efficacy of the process in delivering a 1×10^{-6} SAL, in line with the FDA recommendation for sterile medical and surgical products.

Subsequently, AMSCO (now part of STERIS) secured rights to use VH2O2 as a sterilant, and further developments of the equipment and process ensued. After the development of the flash vaporizer, AMSCO built the first prototype sterilizer in 1983. Throughout the 1980s, AMSCO worked with researchers, pharmaceutical clients and equipment clients to develop applications for VH2O2. One output of such activities was the release of the 'VHP 1000' Biodecontamination System that was launched to the pharmaceutical customer base in 1991 (AMSCO, 1992). Early work by Rickloff (1989) reported success with sterilization of intravenous sets using a 4·5-h deep vacuum VH2O2 process with *Bacillus subtilis* as an indicator organism (AMSCO, 1992).

From those early years, the application of VH2O2 has evolved into atmospheric and vacuum processes: atmospheric pressure conditions, as is the case for VH2O2 room, isolator, vehicle and building decontamination; or vacuum conditions in low-temperature sterilization applications, such as reusable medical device sterilization (McDonnell, 2014).

Mode of action

Hydrogen peroxide is a clear, water-soluble weak acid that, when concentrated, acts as a strong oxidizing agent. Its properties are described in Table 4 and contrasted

Table 2 Key consideration in process validation (adapted from ISO 2016a)

Consideration	Details
Sterilization equipment	Equipment will be suitable for processing with the sterilizing agent being used (in this case VH2O2) and will do so in a safe and consistent manner. The equipment will contain process control equipment, such as programmable logic controllers and instrumentation, that is capable of both controlling the process to defined parameters and reporting on the data outcomes of the delivered process in such a manner that the user can be confident that the sterilization process was delivered as intended
Sterilization process	A sterilization process is one comprising a 'series of actions or operations needed to achieve the specified requirements for sterility' (ISO 2018). Process parameters with their tolerances are defined in such a manner that they qualify the effectiveness of the sterilization process, and demonstrate the achievement of specification. The process may comprise such things as the sterilizer equipment, measurement devices, biological indicators, chemical indicators and testing, all of which combined are employed to define, control and report upon a sterilization process
Sterilizing agent	ISO14937:2009 requires that the sterilizing agent be described regarding safety, environmental aspects, material effects and microbicidal effectiveness. Regarding the microbicidal effectiveness, a number of key items must be demonstrated: i Demonstration of the lethal action against a range of representative challenge micro-organisms ii Establishment of an 'empirical mathematical relationship defining the microbial inactivation kinetics of identified resistant micro-organisms so that the probability of a micro-organism surviving exposure to a defined treatment can be predicted' per methods defined in Annexes B,C,D of ISO14937:2009) iii Identification of a reference micro-organism that has known high resistance to the sterilizing agent iv Characterization of the process variables that affect the lethal action of the sterilizing agent v Assessment of those factors that can adversely influence the effectiveness of the sterilizing agent based upon physical and/or chemical interactions vi Assessment of those factors that can adversely affect the delivery and/or distribution of the sterilizing agent vii Identification of a means for terminating the activity of the sterilizing agent, if applicable (ISO 2016a)
Process validation	The purpose of validation is to 'demonstrate that the sterilization process established in the process definition can be delivered effectively and reproducibly to the sterilization load (ISO 2016a). The validation process comprises a number of key stages: i installation qualification (IQ), which is performed to demonstrate that equipment is installed in accordance with specified requirements ii operational qualification (OQ), which is performed to demonstrate the capability of the equipment to deliver the specified sterilization process iii performance qualification (PQ), where the process is qualified using product samples and process indicators to demonstrate that the required lethality and subsequent sterility assurance are achieved

with those of EO; note that the boiling point of H_2O_2 is above that of water, and there is currently no evidence of carcinogenicity in humans as attested by assignment of zero classification by IARC. Hydrogen peroxide is an oxidizing agent and, as such, one would expect deleterious effects on biological constituents of micro-organisms: Finnegan *et al.* (2010), in their examination of H_2O_2, peracetic acid and chlorine dioxide, demonstrated that as redox potentials increase in biocides, the level of oxidation of amino acids also increases. While there are direct oxidation effects, there may also be secondary effects such as free-radical generation (McDonnell 2014). The disinfection and sterilization efficacy of H_2O_2 in both aqueous and gas forms from the formation of hydroxyl radicals is well documented (Block 1991; McDonnell 2014). Hydrogen peroxide shows effective antimicrobial activity against a wide range of organisms, including vegetative and bacterial endospores, fungi and viruses (Linley *et al.* 2012; McDonnell 2014); concentrations as low as 25 parts per million have been observed as bacteriostatic, with 3% solution being 'rapidly bactericidal' (Block 1991). However, the mode of inactivation and efficacy differ from gaseous to aqueous form, with gaseous being significantly more effective (Finnegan *et al.* 2010; McDonnell 2014). Finnegan *et al.* (2010) demonstrated how VH2O2 'outperformed' aqueous biocide in the denaturation of bovine serum albumin and postulated that vapour has higher kinetic energies and can more readily penetrate the protein. Furthermore, the work of Fichet *et al.* (2007) observed the formation of monomers (clumping) with the use of liquid biocide for the inactivation of prions and described how such clumping could affect the penetration of liquid sterilant into protein structures, unlike the vapour form.

Some common modes of action are also found between vapour and liquid biocide action. For example, DNA suffers single-strand breaks at phosphodiester bonds (McDonnell 2014). Gaseous H_2O_2 has been shown to

Table 3 Characteristics of an ideal low-temperature industrial sterilization process and VH2O2 sterilization. Criteria for ideal process adapted from Rutala and Weber (1998) into a current context for industrial sterilization process

Characteristic	Definition	VH2O2 sterilization
Efficacious	Being virucidal, bactericidal, tuberculocidal, fungicidal and sporocidal in semi-logarithmic manner, where *D*-values may be determined and hold true for calculation to a defined sterility assurance level	Efficacious disinfection and sterilization process killing microbes (Klapes and Vesley 1990; Cortezzo and Setlow 2005; Meszaros *et al.* 2005), viruses (Heckert *et al.* 1997) and prions (Fichet *et al.* 2004). Sterility assurance may be demonstrated and validated in accordance with ISO14937:2009
Rapid	Achieve sterilization quickly and predictably	'Peroxide processes are significantly faster (than EO) for the overall sterilization times' (McDonnell 2014)
Strong penetrability	Able to penetrate medical device materials and packaging such that surfaces required to be deemed sterile can achieve such a state	'Hydrogen peroxide is less stable and therefore less penetrating than EO' (McDonnell 2007). Number of studies showing penetrability in lumen devices (AMSCO 1992; Alfa *et al.* 1996; Rutala *et al.* 1998; Rutala *et al.* 1999; Penna *et al.* 1999)
Material compatibility	Ideally negligible or at least acceptable changes to the materials such that product functionality characteristics are not negatively impacted	Good compatibility but depends on 'concentration, exposure time and delivery mechanisms' (McDonnell 2014). Information on material compatibility described in AAMI TIR17 (2008) or STERIS Material compatibility factsheet (2002)
Nontoxic and safe	Should be both safe to operate and pose no health risk to those along the manufacturing supply chain or the end user in the hospital environment	See Table 4 for EO *vs* VHP comparison. Biocide readily degrades to water and oxygen (McDonnell 2014)
Process repeatability and monitoring	Sterilization process must be repeatable to ensure validation holds true. Process should also be capable of being monitored routinely to verify compliance to original validation activity	Equipment design, commissioning, validation and operation in compliance with ISO14937:2009, in particular clause 6 (Process and Equipment Characterization) (ISO 2016a)
Compliance	Process must meet requirements of ISO standards (typically ISO14937:2009)	Processes validated in accordance with ISO14937:2009
Cost-effectiveness	Process must be cost-effective with respect to overall manufacturing costs of the product and selling price to end consumers	Equipment and process costs similar to other gaseous modalities such as EO and steam sterilization

denature proteins, whereas in certain test conditions amino acids were not seen to oxidize (McDonnell 2014). In the presence of metals, such as iron, oxidation of amino acids was observed. Less is known about lipids and carbohydrates, but given the known effect of oxidation on lipids, it is expected that there is a similar deleterious oxidation from exposure to H_2O_2. However, additional research is merited to establish proper the oxidative nature and effects of H_2O_2 on the modification and destruction of lipids and proteins that will aid the understanding of the mechanistic mode of lethal action for treated micro-organisms including biological indicators (BI). Previous studies report that aggregated proteins and peptides associated with neurodegenerative disease can generate H_2O_2, apparently through interactions with redox-active metal ions (Tabner *et al.* 2005). Fichet *et al.* (2007) reported use of VH2O2 for prion inactivation. Isotopically coded H_2O_2 has been studied for its contribution to allowing quantitative comparison of cellular prion protein (PrP(C)) and aggregated oligomeric (PrP (β)) forms of prion protein through surface modification approaches (Serpa *et al.* 2014). Duerkop *et al.* (2018) dismissed the role of H_2O_2 in HSA aggregation where the main factors were reported to be cavitation and high shear stress.

Although the focus of this review is the applicability of VH2O2 as a terminal sterilization process, there remains much discussion on the effect of aqueous and vapour phases and the condensation of vapour at material contact and sterilization. For further information on this topic, see Hultman *et al.* (2007), Unger-Bimczok *et al.* (2008), Pottage *et al.* (2010), and Agalloco and Akers (2013).

Vaporized hydrogen peroxide processes

Vapour-based processes may be subdivided into those performed at atmospheric conditions and those in a vacuum environment. One of the key applications of atmospheric VH2O2 is in the area of area or room disinfection: rooms and facilities including isolators and laminar air-flow cabinets, vehicles and aircraft are

disinfected with VH2O2. These applications use an atmospheric-based process (equipment ranges from handheld instruments to industrial-scale units integrated into heating, ventilation and air conditioning systems), where a VH2O2 'fog' is created in the environment being treated. This process has been deployed successfully for the last 30 years as a safer alternative to the use of humidified formaldehyde (McDonnell 2014). A comprehensive description of atmospheric-based processes can be found in McDonnell (2014).

However, it is mostly vacuum-based processes that have been developed and deployed for medical device product applications. As far back as 1988, James Rickloff of the American Sterilizer Company described how successful penetration and sterilization of materials were achieved with deep vacuum processes (AMSCO 1992). Akin to the EO process, a deep vacuum removes air that could impede vapour penetration to surfaces. Deep vacuum also facilitates the removal of ambient humidity, which creates the environment for injecting vaporized H_2O_2 to a maximum level, short of the saturation point after which condensation will occur. The importance of vacuum in drying the load is highlighted by Hultman *et al.* (2007): the 'maximum allowed concentration of peroxide vapour drops from 2·184 to 1·805 mg l^{-1} as moisture content in the carrier gas goes from 0% RH up to 10% RH, ... a 17·4% drop'. A typical vacuum-based process, similar to an EO cycle, comprises three distinct phases of (i) preconditioning, where a vacuum is applied to dry the load being sterilized; (ii) sterilization, where the sterilant vapour is injected to the sterilizer and allowed a period of contact with the product load; and (iii) aeration, where unwanted H_2O_2 is removed through a series of washes using air or steam. Some processes may include additional steps and variances. One is the Sterrad® low-temperature H_2O_2 gas plasma process, where a plasma is created by radiofrequency (RF) power (300W RF power in the case of Sterrad-100S®) and applied after the sterilant dwell phase (Crow and Smith 1995; Lerouge *et al.* 2000). The RF generates an electrical field, which reacts with the chemical sterilant to create a cloud of charged particles. Because the plasma is generated during the postconditioning phase, it is widely thought that its role is associated with the VH2O2 destruction and removal after sterilization (Krebs *et al.* 1998; Lerouge *et al.* 2000; McDonnell 2014).

Table 4 Key properties of EO gas (Linde 2011), and hydrogen peroxide (Seastar 2011); US National Library of Medicine 2018 (https://toxnet.nlm.nih.gov/cgi-bin/sis/search2/r?dbs+hsdb:@term+@DOCNO+547)

	Ethylene oxide gas	Vaporized hydrogen peroxide
Appearance/ Colour	Colourless	Colourless
Odour	Ethereal, poor warning properties at low concentrations	Slightly sharp, irritating
Molecular weight	44 g mol^{-1}	34 g mol^{-1}
Melting point	−112°C	−33°C (35%)
Boiling point	10·4°C	108°C (35%)
Autoignition temperature	440°C	N/A
Flammability range	3% (V)–100% (V)	Does not burn (20–35%)
Vapour pressure 20°C	1·4 bar (20°C)	0·0024 bar (30°C; 35%)
Acute toxicity	May cause irritation to the respiratory tract	Irritating to skin, eyes and respiratory system
LC50 (ppm)	2900 ppm/1 h	2g/m3/4h
Carcinogenic, mutagenic and teratogenic effects	May cause cancer. May cause heritable genetic damage. IARC Group 1 carcinogen	Inadequate evidence in humans for carcinogenicity. Not listed in IARC

Validation of VH2O2 processes

As with all terminal sterilization processes, 100% inspection of processed medical products is not possible. Prior validation of a measurable and repeatable process must, therefore, be performed. VH2O2 processes are qualified in accordance with ISO14937:2009 (ISO 2016a), 'Sterilization of health care products—General requirements for characterization of a sterilizing agent and the development, validation and routine control of a sterilization process for medical devices.' This standard requires the user to characterize the process by selecting an appropriate BI micro-organism of 'known high resistance' that is appropriate in demonstrating the 'microbial effectiveness of the sterilizing agent' (ISO 2016a). This standard is a general validation approach, applicable to many sterilization processes, whereas the more widely adopted traditional modalities of EO and radiation have internationally recognized and dedicated standards, namely ISO11135 (ISO 2014a) and ISO11137 (ISO 2015) respectively.

In the performance of validation activity and routine processing, BIs are employed as measures of microbiocidal efficacy. Previously, there have been investigation and debate on the choice of micro-organism as an appropriate BI. In previous studies, *Bacillus atrophaeus* showed greater resistance to lethal stresses when exposed to aqueous sterilant applications, whereas *Geobacillus stearothermophilus* showed greater tolerances to vapour-based approaches (McDonnell 2007). Considering where vaporized H_2O_2 is currently employed as a sterilization process: in hospital clinical applications regulations such as FDA 510k (FDA 2007) requirements dictate the use of 'the

most resistant organism' and go so far as to recommend *G. stearothermophilus* as appropriate for VH2O2 applications. However, ISO14937:2009 (which is appropriate for medical device terminal sterilization applications), like ISO11137 and ISO11135, requires the consideration of product bioburden, standard resistances and the use of a BI of 'known high resistance'. The selection of a BI as the microbiological challenge in the validation process is significant in that it defines the sterilization process required to meet that challenge. Hence, the appropriateness of the biological indicator challenge merits careful consideration in a validation process.

Opportunities for use of VH2O2 in terminal sterilization applications

When one examines the criteria for an ideal low-temperature gas process (Table 3) and examines the applications of VH2O2 in disinfection, decontamination and sterilization processes, it becomes apparent that VH2O2 offers a possible additional technology to the portfolio of terminal sterilization processes. Its limitations will be discussed later. A key proposition of low-temperature gaseous sterilization over irradiation processes is polymeric material compatibility. Researchers have examined the effect of VH2O2 on materials: various (STERIS 2002); polyurethane catheters, polyethylene tubing, polyvinylchloride (Lerouge *et al.* 2002); PU catheters (Ma *et al.* 2003); poly (D,L-lactic-co-glycolic acid) (Hee *et al.* 2008); steel (Sk *et al.* 2011); titanium dioxide (Junkar *et al.* 2016); and L-polylactic acid/gelatin(PLLA) (Hao *et al.* 2016). Consulting the AAMI TIR17 (2008) or STERIS Material compatibility factsheet (2002) reveals the extensive range of generally used materials employed in medical devices are suited to VH2O2 sterilization.

Where VH2O2 appears to offer many advantages is with the processing of novel materials. Researchers found comparability of VH2O2 with EO: (i) poly(lactic acid) (PLA)—which has been examined for use in sutures, tissue engineering support, orthopaedic applications and drug release—is a polymeric material with a relatively low melting temperature. Savaris *et al.* (2016) observed that sterilization modalities, such as EO, E-beam radiation, H_2O_2 plasma and gamma radiation, induced some variations in material properties, such as crystallinity, colour and contact angle, but were not significant, and therefore such modalities can be used in sterilization of PLA materials. (ii) Nuutinen *et al.* (2002) demonstrated how both EO and VH2O2 plasma offered sterilization options for bioabsorbable fibres that had 'limited effect on the mechanical properties and intrinsic viscosity of the materials tested'. Other researchers found distinct advantages to using VH2O2: Junkar *et al.* (2016), examining titanium nanotubes, found that the structure was preserved with VH2O2 due to lower temperature processing, unlike autoclaving. Hao *et al.* (2016), examining the effect of VH2O2 plasma and EO sterilization on PLLA/gelatin (PLLA/GA) scaffolds, reported that while both technologies were suitable sterilization processes for this material, predominantly due to lower temperature processing, improved cell proliferation was observed on scaffolds sterilized with VH2O2 due to lack of EO residuals and shorter sterilization cycles with VH2O2 processing.

The reduction in processing time, from a minimum 10–15 h in EO to <6 h in a typical VH2O2 process, has the additional benefit of less exposure of medical device materials and packaging to temperature, humidity and vacuum. Bi *et al.* (2013) showed how a VH2O2 process (30°C and six sterilant pulses, each with an exposure time of 5 min—for comparison, a typical EO exposure would be 2–4 h—offered an attractive sterilization technology for treatment of xenograph cancellous bone material ('No obvious changes of architecture or decrease in mechanical strength'), coupled with favourable cytotoxicity observed after treatment with VH2O2.

However, like any terminal sterilization process, while there are many benefits to using VH2O2 (highlighted in Table 3), there are also limitations that must be understood and addressed in process design and validation.

Limitations of VH2O2 in sterilization

Vaporized hydrogen peroxide has been developed and evaluated as an effective sterilization process for healthcare applications over many years (Alfa *et al.* 1996; Rutala and Weber 1998; Schneider 2013; Boiano and Steege 2015), as shown to be an effective agent at sterilizing bacteria (Crow and Smith 1995), prions (Fichet *et al.* 2007) and viruses (Cusinato *et al.* 2016). Klapes and Vesley (1990) reported:

> While aqueous hydrogen peroxide has a long history of use as a sterilant, the concept of vapour phase H2O2 (VPHP) sterilization has been developed within the past decade. VPHP represents a class of nontoxic cold gas sterilant which provides an opportunity to discontinue the use of such toxic or carcinogenic gaseous sterilants as EO and formaldehyde. VPHP technology could have immediate applications for the sterilization of speciality medical products, especially those which would be destroyed by steam sterilization or require lengthy aeration to reduce toxic EO residuals.

In healthcare, VH2O2 technology was successfully deployed into hospital environments with equipment such

as the 'VPro' range from STERIS and STERRAD equipment from Advanced Sterilization Products. Similarly, STERIS provides an extensive range of equipment and product applications for decontamination activities such as VPro hospital sterilizers (STERIS 2019a) and VHP Sterilization and Decontamination equipment (STERIS 2019b). As an example of such deployment, Wallace (2016) reviewed a selected number of 510ks submitted to FDA for sterilization equipment from January 2012 to June 2015, subdividing the sterilization into two categories: high-temperature steam and observed ten 510ks approved for new equipment (mostly for larger chamber sizes), and low-temperature sterilization, which could be subdivided into EO, H_2O_2+ozone and H_2O_2 (predominantly for endoscope processing). In the low-temperature applications, approvals for hydrogen peroxide-based processes outperform EO applications. A survey by Boiano and Steege (2015) of professional practice organizations found that of 373 respondents from healthcare facilities that deployed these gaseous sterilization approaches, 84% used VH2O2, 38% used EO and 22% used both. An extensive search of the literature highlights numerous studies reporting on the efficacy of developing and testing VH2O2 for disinfection and sterilization processes in healthcare settings. But there is a marked gap of published findings on applying VH2O2 terminal sterilization on medical devices, which may be attributed to the limitations described in Table 5. Material compatibility of cellulose-based materials, and ability to penetrate targeted surfaces, are two decisive limitations that have inhibited the advancement of VH2O2 for medical device terminal sterilization. Cellulose is known to degrade VH2O2 so much that it reduces the concentration of H_2O_2 in the vapour phase, rendering the sterilization process ineffective. Reich and Caputo (2005), examining isolator technology, found a 47% reduction in VH2O2 concentration in the presence of cellulose materials (compared to the same experiment in the absence of cellulose). A subsequent outcome of positive BIs dispersed randomly, indicating a resultant 'marginal nonuniform cycle'. Similarly, Corveleyn *et al.* (1997) examined the permeability of water vapour and VH2O2 across a number of packaging materials and observed marked differences in the permeation of VH2O2. Permeation across a Tyvek® package resulted in 87·7% of reference concentration being measured inside the package, compared to 30% with medical paper, most likely due to an 'absorption phenomenon or to the difference in the degradation rate caused by the presence of trace metals acting as catalysts of H_2O_2 breakdown'. With regard to penetration, this is very much linked to the chemistries associated with H_2O_2 in gaseous or liquid form. In the world of room decontamination, there has been much debate as to whether condensation of vapour occurs and the benefits to microbial inactivation.

Agalloco and Akers (2013) in their review of the use of H_2O_2 in room enclosure decontamination and disinfection highlight a number of limitations and associated mis-understandings: Understanding principles such as dew-point and liquid and vapour phases of a two phase system are critical. Hultman *et al.* (2007) provide useful insight into the chemistry associated with this two-phase system. Authors will differ in opinion as to whether condensation is necessary and beneficial to the desired inactivation of micro-organisms: Perspectives on the benefit associated with higher concentrations in the liquid (35% by weight H_2O_2 vapour condenses to approximately 78% by weight liquid at 25°C (Hultman *et al.* 2007)) *vs* the safety and material compatibility issues associated with creation of liquid H_2O_2 on surfaces are discussed.

As identified by Hultman *et al.* (2007), condensation of vapour may result in all surfaces not receiving sterilant

Table 5 Comparison of EO advantages and converse VH2O2 limitation against key sterilization characteristics

Characteristic	EO advantage	VH2O2 limitation	References
Material compatibility	Wide range of material compatibility, from device polymers and metals to packaging materials	Limitation with cellulose-based materials, with degradation of VH2O2	Corveleyn *et al.* (1997); Nuutinen *et al.* (2002); STERIS (2002); Meszaros *et al.* (2005); Reich and Caputo (2005); AAMI (2008); Bi *et al.* (2013); Bertoldi *et al.* (2015); Hao *et al.* (2016); Savaris *et al.* (2016)
Strong penetrability	EO, while a surface sterilant, is stable in gaseous phase sufficiently to reach required inner surfaces such as long lumen lengths, with appropriate cycle parameters of vacuum, temperature, sterilant concentration and time	Maintaining hydrogen peroxide in vapour form, while seeking to contact all required surfaces can be a challenge. Significant efficacy loss upon condensation	Alfa *et al.* (1996); Rutala *et al.* (1998); Penna *et al.* (1999); Rutala *et al.* (1999)
Compliance	In terminal sterilization, the use of EO is provided with extensive ISO guidance in accordance with ISO11135:2014	The application of VH2O2 in a terminal sterilization process demands that ISO14937:2009 be employed	ISO (2014a), ISO (2015), ISO (2016a)

contact: This would be of significant concern with a terminal sterilization application. Therefore, terminal sterilization processes are typically conducted under vacuum with a preconditioning step whereby air and natural humidity is removed and substituted with vapour at a defined temperature and pressure with the goal of maintaining vapour to such an extent that all required surfaces receive contact with the sterilant. Whilst temperature and pressure are important parameters, the calculations performed by Watling *et al.* (2002) demonstrate the importance of reducing the starting relative humidity: The authors found that peak H_2O_2 gas concentration reduces from a value in excess of 1500 ppm to less than 1000 ppm as initial relative humidity increases from 10 to 50%.

Another important consideration is the occurrence of nonlinear microbial inactivation kinetic data plots produced from VH2O2 treatment. This may influence the ability to standardize and validate a process, due to variability in sterilization efficacy.

Microbial inactivation with VH2O2

How VH2O2 affects micro-organisms, prions, protein molecules and other macromolecules is described by Klapes and Vesley (1990), Fichet *et al.* (2007), Finnegan *et al.* (2010) and Linley *et al.* (2012) respectively. The authors compare and contrast inactivation from aqueous H_2O_2 and VH2O2, and the consensus is of enhanced penetrability with VH2O2 and subsequently greater efficacy. Klapes and Vesley (1990), in their work on the use of VH2O2 to sterilize centrifuges, showed that *G. stearothermophilus* is more resistant than *B. subtilis* to VH2O2. Linley *et al.* (2012), in their review of VH2O2 applications, wrote 'The application of VPHP [VH2O2] as a potential sterilant is still clearly in its infancy: definitive knowledge of the mechanism(s) of microcidal action, and the factors which influence it, is lacking'. This re-affirmed Klapes and Vesley's (1990) assertion.

The methods of validation described in the ISO14937:2009 standard include a description of the 'Overkill Approach'. More often such methods are applied in a 'half-cycle approach', where a routine process sterilant dwell period is extrapolated (to 12 spore log reduction) from that used to achieve a 6 log reduction in a 10^6 BI, thus providing a SAL of $\leq 10^{-6}$. However, such an approach relies on achieving linear microbial inactivation kinetic plots, similar to that observed in EO sterilization of BIs of *B. atrophaeus*. A key underpinning assumption is that VH2O2-treated microbial population will show the same resistance to this applied lethal stress, which will be represented by a log linear inactivation kinetic plot (Stone *et al.* 2009). This assumption is frequently made when using homologous populations of *G. stearothermophilus* or *B. atrophaeus* as BIs.

However, as reported by Geeraerd *et al.* (2005) and shown in Fig. 2, microbial inactivation kinetics plots can take different forms. These researchers described nine variations in microbial plots that included both concave- and convex-shaped kinetic inactivation data, with a 'tailing' effect implying the possible occurrence of subpopulations of micro-organisms showing different resistance potentials, or variances under the same exposure conditions that may lead to uneven treatments due to things such as protective effects from microbial aggregation or clumping of cells or spores (Fig. 2).

As described by Stone *et al.* (2009), a commonly held explanation for nonlinear inactivation kinetics lies in the 'vitalistic theory, which holds that the resistance of individual cells in a population is not the same but follows a distribution'. Humpheson *et al.* (1998) further define the vitalistic theory, where in 'a genetically homogeneous population, phenotypic variation exists such that

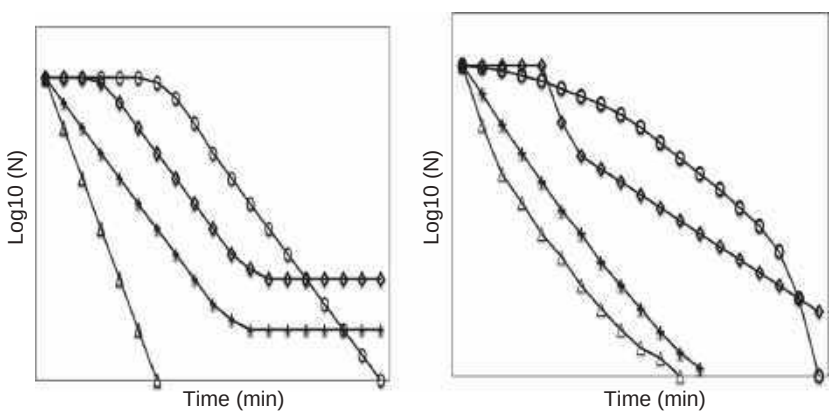

Figure 2 Commonly observed types of inactivation curves. Left plot: linear (r), linear with tailing (X), sigmoidal-like (□), linear with a preceding shoulder (m). Right plot: biphasic (r), concave (X), biphasic with a shoulder (□), and convex (m). (Geeraerd et al., 2005)

resistance to a lethal agent is not uniform'. Hideharu Shintani (Shintani 2014) attributes the biphasic shape of survivor curves to the mechanistic concept of clumping of micro-organisms on a BI, where the low-penetration processes (such as VH2O2) take additional time to reach the inner layers of micro-organisms in the clumps. Similarly, Kramer and Thielmann (2016), using flow cytometry (FCM) techniques, observed the agglomeration of *Listeria innocua* cells upon heat exposure, which then manifested in heat-resistant subpopulations. As described by Humpheson *et al.* (1998) in their review of inactivation of *Salmonella enteritidis*, a minor mutation event during growth is an unlikely source, and tailing may be more likely due to generation of cellular protective proteins (in their case, Heat Shock Proteins, or HSPs) during initial sublethal conditions. These protective proteins, where generated in a subpopulation, cause an increase in resistance. Allan *et al.* (1988) observed that 17 HSPs were generated in response to a heat shock treatment.

A known challenge in the use of VH2O2 is that it does not display linear inactivation kinetics with *G. stearothermophilus* (Agalloco and Akers 2013; Mcleod *et al.* 2017). As highlighted by McLeod *et al.* (2017), the inactivation 'was biphasic in the system used' and likely to be a result of different factors; the authors highlight the challenge of creating a spore monolayer on a small BI surface. Thus, a primary consideration is that the inactivation kinetics must be assessed in the total sterilization system being employed. Krebs *et al.* (1998) attributed the observed tailing to loss of efficiency in the process, with 'binding or consumption' of the sterilant gas.

Where biphasic inactivation is observed in a hydrogen peroxide-based system, it is difficult to negate the importance of VH2O2 in the redox activities and signalling in cells. Dickinson and Chang (2011) describe the extensive and important role fulfilled by H_2O_2 in cellular redox activities, and if one couples that with oxidative stress response (Lee and Helmann 2006; Mols and Abee 2011) and quorum-sensing mechanisms (Huillet *et al.* 2012), there may be many cellular and biochemical activities, yet to be defined, that could explain the biphasic lethality kinetics observed with H_2O_2. As Huillet *et al.* (2012) wrote, 'H_2O_2 stress induces the synthesis of many proteins and enzymes, such as catalase, thioredoxin reductase, ferroxidase and peroxidases, responsible for eliminating H_2O_2 from the cells.' As enzyme activation occurs in the germination and outgrowth phases, further understanding of the sequence of inactivation through the germination and outgrowth lifecycle stages could provide insight.

Another consideration, described by Rowan *et al.* (2015), is the concept of a viable but not culturable state (VBNC) that occurs because of stress in certain micro-organisms: 'evidence suggests that these harsh environment cues (operational parameters of the pulsed light (PL) treatment and biological factors) may trigger a switch to the adaptive survival VBNC state in PL treatments'. The concept of VBNC has been observed in many micro-organism species (Rowan 2004; Rowan *et al.* 2015; Rowan 2019), and one could therefore hypothesize that transitionary phases (rapid inactivation, slower inactivation and VBNC) in a homologous population may occur as a consequence of progressive cellular activity upon contact with a sterilizing agent. Understanding the cellular mechanisms of inactivation, the sequence of the inactivation from spore to outgrowth (and any intermediary states) and the spore defensive responses may also offer insights into why nonlinear inactivation kinetic plots are occasionally observed.

Implications of biphasic lethality with regard to process validation including VH2O2

A combination of factors influencing nonlinear microbial inactivation may also inform predictive microbiology, where decimal time required to achieve one-log reduction in microbial population under fixed lethal sterilizing conditions (or *D*-value), along with extrapolations from half-cycle parameters, are employed to determine SAL (Fig. 1). A problem potentially manifests in the overestimation of achieved SAL using a given challenge micro-organism, where biphasic microbial inactivation kinetic data show two different subpopulation plots. Yet the desired SAL is reached by extrapolation of treatment time in a half-cycle approach, where the *D*-value used is that which includes the less resistant subpopulation. Thus, where such a nonlinear inactivation is known, it needs to be understood and verified in the sterilization system being assessed, before a validation approach is determined. As ISO14937:2009 states, 'For sterilizing agents that do not exhibit linear inactivation kinetics, the nature of the inactivation kinetics should be investigated in order to derive a relationship from which it can be predicted that the specified probability of a microorganism surviving is not exceeded on applying the sterilization process' (ISO 2016a). A potentially important limitation in the above statement is that it appears to identify only the sterilizing agent as the source of the inactivation kinetic plots upon which decisions are made. One could contend that it is the overall sterilization system that contributes to and affects the observed inactivation kinetics. As shown by Humpheson *et al.* (1998), in their heat challenge of *S. enteridis* PT4, biphasic inactivation curves were observed at temperatures of 60°C, but these migrated to linear as temperatures were decreased to 51°C. Previous researchers have also reported on the heterogeneity of endospore germination and occurrence

of super dormant spores from genetically identical populations that can contribute to delayed germination which can also influence microbial inactivation kinetic models (Hong *et al.* 2010; Setlow *et al.* 2012; Zhang and Mathys 2019). Use of combined analytical techniques, such as FCM, phase contrast, fluorescent and transmission electron microscopy, along with use of Raman spectroscopy will help advance this important field of study.

Hence, one must consider the microbial response to the sterilizing agent in the sterilization system. One could expect the response to vary based on various conditions: sterilant concentration, sterilizing conditions (e.g. process temperature, vacuum), micro-organism type, micro-organism population, micro-organism carrier (e.g. BI material or bioburden surface). In their review of the inactivation kinetics of PL on micro-organism populations, Rowan *et al.* (2015) offer insights and review past work examining the vitalistic and mechanistic concepts and theories of microbial inactivation. Given the vitalistic phenotypic expression of subpopulations, and the key factors as cellular activity upon stress conditions, the micro-organism type is a significant factor. If the biphasic

Table 6 Key resistance mechanisms of bacterial spores and interaction with VH2O2

Spore component	Description of resistance mechanisms	Interaction with VH2O2	References
Spore coat resistance	Cross-linking in the coat layer may have some role in chemical and mechanical resistance	Protein structure cross-linked with disulphide bonds shown to house enzymes such as catalase and superoxide dismutase, which play significant roles in oxidative stress. Polycyclic terpenoids (termed sporulenes) as well as various pigments have also been identified in coats and contribute to spore resistance to hydrogen peroxide. Also, a permeability role in providing access to inner membrane	Henriques and Moran (2000); Riesenman and Nicholson (2000); Young and Setlow (2004a); Young and Setlow (2004b); Cortezzo and Setlow (2005); Cybulski *et al.* (2009); Setlow (2011); Leggett *et al.* (2012); Sella *et al.* (2014)
Inner membrane permeability	Acts as barrier in dormancy to small molecules including water, which is crucial to maintaining core conditions.	Cellular location of most significant interaction *Lipid component* Potential role for the phospholipid cardiolipin as a barrier for H_2O_2 access to spore core. As lipids may play a modulation role of important proteins such as germination receptors (GerA, GerB and GerK) as well as SpoVA proteins, any effect on the lipid content may indirectly affect spore germination *Protein–enzyme component* Cortezzo *et al.* (2004) describe how oxidizing agents can damage many proteins and enzymes, attacking both prosthetic groups such as iron–sulphur centres as well as amino acid residues, and such a damage can (i) result in a compromised metabolism during subsequent spore outgrowth, (ii) contribute to the osmotic stress sensitivity of the outgrowing spore and (iii) oxidatively damage proteins A number of authors identify potential damage to key germination proteins such as germinant receptors GerA, GerB and GerK (Young and Setlow 2004b), and GerD (Setlow *et al.* 2013) located in inner membrane As highlighted by McDonnell (2014), 'proteins appear to be an important target in the antimicrobial activity of hydrogen peroxide, both in gas and in liquid form'	Cortezzo *et al.* (2004); Young and Setlow (2004b); Griffiths and Setlow (2009); Setlow *et al.* (2013); Setlow *et al.* (2016)
Spore core	Three key molecules associated with resistance: i Water ii Dipicolinic acid iii Small acid-soluble proteins that saturate and protect DNA	A number of authors have concluded that the cellular target for VH2O2 is 'at or exterior to the spore's inner membrane' SASPs appear to eliminate DNA in the spore core as a site of inactivation with VH2O2 Low water content (27–55%) associated with DPA celated with divalent ions (Ca+) also appears to increase spore resistance to H_2O_2	Popham *et al.* (1995); Setlow (2006); Sella *et al.* (2014); Setlow (2014) Setlow and Setlow (1993); Loshon *et al.* (2001); Genest *et al.* (2002); Melly *et al.* (2002b); Leggett *et al.* (2012)

inactivation is a result of cellular responses, then this could vary by micro-organism type. Therefore, an established industry-standard BI exhibiting the most resistance to lethal sterilization processes may not be the most appropriate challenge micro-organism. Perhaps, greater consideration should be given to using a micro-organism that yields the closest fit to linear inactivation kinetics, while offering an appropriate challenge of 'known high resistance' to the sterilization process.

The purpose of the BI is to offer a higher level of resistance than the product bioburden being killed on a medical device being sterilized and a known challenge to the sterilization process, but also one that can be used in a predictive sense to arrive at the required SAL. While such characterization of the lethality kinetics in a sterilization system can provide clarity and direction on the most appropriate approach to validation and the required SAL, it does not answer the fundamental question of why such a nonlinear inactivation occurs. This is where molecular and cellular investigations on mechanistic activities underpinning sterilization processes, elucidated by microbiologists, can provide critical insights to help engineers design optimal processes as can be informed from adjacent industries (Farrell *et al.* 2011; Hayes *et al.* 2013; Garvey and Rowan 2019).

Interaction of VH2O2 with bacterial endospore cellular constituents

Evidence-based published literature on the effects of H_2O_2 on microbial cellular constituents is summarized in Table 6. However, all the work reviewed and described herein is based on the aqueous form of H_2O_2. Only the work of Fichet *et al.* (2007) examining the effect of VH2O2 gives insight into the vapour form. This lack of investigation into cellular effects from VH2O2 was also highlighted by Linley *et al.* (2012). As Table 6 shows, much of the research has elucidated the spore inner membrane as the likely site of interaction, with the inactivation consequences manifesting during germination (Popham *et al.* 1995; Melly *et al.* 2002a; Cortezzo *et al.* 2004; Cortezzo and Setlow 2005; Setlow *et al.* 2013). Leggett *et al.* (2016) reported that oxidizing agents are commonly used as sporicides and, given specific treatment conditions, can result in spore lysis. However, treatment with H_2O_2 does not necessarily result in spore lysis. Following exposure to this oxidizing agent, spores are left unable to form colonies even after neutralization of the microbiocide. Subsequent lysozyme treatment of such treated spores can often give rise to apparent spore germination, but these germinated spores exhibit little or no metabolic activity and do not outgrow (Setlow *et al.* 2013).

Given their importance as BIs, further work investigating the interaction of VH2O2 with spore components is warranted to understand the location(s) and nature of the sporicidal activity. While the lethality of spores is more often perceived as sporocidal, Leggett *et al.* (2016) have highlighted that manifestation of a cidal effect at outgrowth may be deemed bactericidal or bacteriostatic. Melly *et al.* (2002a), examining the inactivation of *B. subtilis* spores by H_2O_2, have determined that inactivation likely occurs during germination, when high-energy compounds such as ATP are not manufactured in the cell, mostly likely due to lack of core water content necessary for enzyme action. Investigative work by Loshon *et al.* (2001) used assays to try to determine the primary mechanism of spore killing by Sterilox (superoxide water disinfectant). The authors used BacLight stain with propidium iodide to report that inner membrane damage occurs only after endospore germination. Russell (2003) also highlighted that it is important to understand the reactions of different types of micro-organisms to biocidal agents from the point of view of cell structure and physiology, including (i) the mechanisms of action of biocides, (ii) the mechanisms whereby micro-organisms resist biocide action and (iii) the improved usage of biocides in clinical and environmental situations.

Conclusion

The medical device market is one of great importance to healthcare and currently relies on sterilization technologies such as irradiation technologies or gaseous EO. For some time, it has been recognized that there is a need for other gaseous technologies as an alternative to EO. Vaporized hydrogen peroxide sterilization is a widely adopted method in the hospital setting, but it is very much in its infancy in the terminal sterilization of medical devices. VH2O2 has limitations, including cellulosic material compatibility and penetration, which may affect the efficacy of sterilization for established and emerging medical devices that are increasing in complexity. A key consideration in the use of VH2O2 is variance in microbial inactivation kinetics, indicating a need to further understand the mechanism of spore lethality from VH2O2.

While significant investigative work has been conducted into the effect of sterilants at a cellular level (Young and Setlow 2004a, 2004b; Roth *et al.* 2010; Leggett *et al.* 2016; Setlow *et al.* 2016), this work is frequently limited, for instance studying mutants to compare with wild-type micro-organisms to test such things as cellular permeability. Use of such mutants fails to account for the inherent heterogenicity in large micro-organism populations (Cronin and Wilkinson 2008). As Reis *et al.* (2005) write, '*Bacillus* sp. have been found to exhibit a variety of rich

dynamic behaviours including long-term oscillations, multiple steady-states, genetic instability and un-interpretable transients', the consequences of which make process (biotechnology cell culturing) optimization and process prediction 'a difficult task'.

For the past two decades, FCM has been used to investigate micro-organisms. It offers an 'accurate technique to identify spores, vegetative cells and the number of viable and dead cells in the given population' (Majeed *et al.* 2018) and to examine the stages of germination and outgrowth in spore formers (Trunet *et al.* 2017). Traditional techniques such as microbial enumeration and resuscitation approaches offer some insight, but it is expected that newer real-time nonculture-based methods —such as bioinformatics, next-generation sequencing and FCM—may provide greater understanding of cellular responses after VH2O2 processing. The significance and importance of such future work is timely, as the International Organization for Standardization, through the formation of Working Group 16 under Technical Committee 198, seeks to establish a consensus standard for the use of VH2O2 in terminal sterilization processes. Establishing such a standard may move the FDA classification of VH2O2 terminal sterilization from Category B to Category A and subsequently advance the adoption of VH2O2 processes. Investigative work to establish optimal process parameters, including BI selection and associated inactivation kinetics, will provide clear instruction to users on how to correctly validate a VH2O2 process for terminal sterilization applications.

Acknowledgements

The authors acknowledge Athlone Institute of Technology Doctoral Scholarship Programme and funding support from STERIS AST.

Conflict of Interest

There is no conflict of interest.

References

Agalloco, J.P. and Akers, J.E. (2013) Overcoming limitations of vapourised hydrogen peroxide. *Pharma Technol Eur* **37**, 54–65.

Agency for Toxic Substances and Disease Registry (2019). https://www.atsdr.cdc.gov/mmg/mmg.asp?xml:id=304&txml:id=55 (accessed 21 June, 2019).

Alfa, M.J., DeGagne, R.T., Olson, N. and Puchalski, T. (1996) Comparison of ion plasma, VA hydrogen peroxide, and 100% EO sterilizers to the 12/88 ethyle gas sterilizer. *Infect Cont Hosp Epidemiol* **17**, 92–100.

Allan, B., Linseman, M., Macdonald, L.A., Lam, J.S. and Kropinskil, A.M. (1988) Heat shock response of *Pseudomonas aeruginosa*. *J Bacteriol* **170**, 3668–3674.

AMSCO (1992) *VHP Technology: A Collection of Scientific Papers*, 2nd edn. Apex: AMSCO Scientific.

Association for the Advancement of Medical Instrumentation (2008) *AAMI TIR17:2008 Compatibility of Materials Subject to Sterilization*. ISBN 1-57020-321-0. 1110 N. Glebe Road, Suite 220 Arlington, VA 22201-4795: Association for the Advancement of Medical Instrumentation. Approved and published 26 August 2008

Association for the Advancement of Medical Instrumentation (2017) *AAMI TIR16:2017 Microbiological aspects of ethylene oxide sterilization*. ISBN 1-57020-363-6. 1110 N. Glebe Road, Suite 220 Arlington, VA 22201-4795: Association for the Advancement of Medical Instrumentation Approved and published 3 September 2009.

Bauld, T. (2016) A plea for help in reducing hospital-acquired infections. *Biomedical Instrum Technol* **50**, 391.

Bertoldi, S., Farè, S., Haugen, H.J. and Tanzi, M.C. (2015) Exploiting novel sterilization techniques for porous polyurethane scaffolds. *J Mater Sci: Mater Med* **26**, 1–12.

Bi, L., Li, D.-C., Huang, Z.-S. and Yuan, Z. (2013) Effects of sodium hydroxide, sodium hypochlorite, and gaseous hydrogen peroxide on the natural properties of cancellous bone. *Artif Organs* **37**, 629–636.

Block, S.S. (1991). Chapter 9, Peroxygen compounds. In *Disinfection, Sterilization and Preservation*. 4th edn. ed. Block, S.S. pp. 167–181. Philadelphia, PA: Lea & Febiger, ISBN 0-8121-1364-0.

Boiano, J.M. and Steege, A.L. (2015) Ethylene oxide and hydrogen peroxide gas plasma sterilization: precautionary practices in U.S. Hospitals. *Zentralsterilisation (Wiesb)*, **23**, 262–268. HHS Public Access.

Cortezzo, D.E. and Setlow, P. (2005) Analysis of factors that influence the sensitivity of spores of *Bacillus subtilis* to DNA-damaging chemicals. *J Appl Microbiol* **98**, 606–617.

Cortezzo, D.E., Koziol-Dube, K., Setlow, B. and Setlow, P. (2004) Treatment with oxidizing agents damages the inner membrane of spores of *Bacillus subtilis* and sensitizes spores to subsequent stress. *J Appl Microbiol* **97**, 838–852.

Corveleyn, S., Vandenbossche, G.M.R. and Remon, J.P. (1997) Near-Infrared (NIR) monitoring of H2O2 vapor concentration during vapor hydrogen peroxide (VHP) sterilisation. *Pharma Res* **14**, 294–298.

Cronin, U.P. and Wilkinson, M.G. (2008) Monitoring changes in germination and permeability of *Bacillus cereus* endospores following chemical, heat and enzymatic treatments using flow cytometry. *J Rapid Meth Automat Microbiol* **16**, 164–184.

Crow, S. and Smith, J.H. (1995) Gas plasma sterilization: application of space-age technology. *Infect Cont Hosp Epidemiol* **16**, 483–487.

Cusinato, R., Pacenti, M., Martello, T., Fattori, P., Morroni, M. and Palù, G. (2016) Effectiveness of hydrogen peroxide

and electron-beam irradiation treatment for removal and inactivation of viruses in equine-derived xenografts. *J Vir Methods* **232**, 39–46.

Cybulski, R.J., Sanz, P., Alem, F., Stibitz, S., Bull, R.L. and O'Brien, A.D. (2009) Four superoxide dismutases contribute to Bacillus anthracis virulence and provide spores with redundant protection from oxidative stress. *Infect Immun* **77**, 274–285.

Dasenbrock, H.H., Rudy, R.F., Smith, T.R., Guttieres, D., Frerichs, K.U., Gormley, W.B. and Du, R. (2016) Hospital-acquired infections after aneurysmal subarachnoid hemorrhage: a nationwide analysis. *World Neurosurg* **88**, 459–474.

Dickinson, B.C. and Chang, C.J. (2011) Chemistry and biology of reactive oxygen species in signaling or stress responses. *Nat Chem Biol* **7**, 504–511.

Duerkop, M., Berger, E., Duraeur, A. and Jurgbauer, A. (2018) Influence of cavitation and high shear stress on HSA aggreation behaviour. *Eng Life Sci* **18**, 169–178.

Dugani, S., Veillard, J. and Kissoon, N. (2017) Reducing the global burden of sepsis. *Can Med Assoc J* **189**, E2–E3. https://doi.org/10.1503/cmaj.160798

Farrell, H., Hayes, J., Laffey, J.G. and Rowan, N.J. (2011) Studies on the relationship between pulsed UV light irradiation and the simultaneous occurrence of molecular and cellular damage in clinically-relevant *Candida albicans*. *J Microbiol Meth* **84**, 317–326.

Fichet, G., Comoy, E., Duval, C., Antloga, K., Dehen, C., Charbonnier, A. and Deslys, J.P. (2004) Novel methods for disinfection of prion-contaminated medical devices. *Lancet* **364**, 521–526.

Fichet, G., Antloga, K., Comoy, E., Deslys, J.P. and McDonnell, G. (2007) Prion inactivation using a new gaseous hydrogen peroxide sterilisation process. *J Hosp Infect* **67**, 278–286.

Finnegan, M., Linley, E., Denyer, S.P., McDonnell, G., Simons, C. and Maillard, J.Y. (2010) Mode of action of hydrogen peroxide and other oxidizing agents: differences between liquid and gas forms. *J Antimicro Chemother* **65**, 2108–2115.

Food and Drug Adminstration (USA) (2007) *Biological Indicator (BI) Premarket Notification [510(k)] Submissions*. https://www.fda.gov/regulatory-information/search-fda-guidance-documents/biological-indicator-bi-premarket-notification-510k-submissions accessed 10 October 2017.

Gamma Irradiation Processing Alliance, and International Irradiation Association (2017) *A Comparison of Gamma, E-beam, X-ray and Ethylene Oxide Technologies for the Industrial Sterilization of Medical Devices and Healthcare Products, 1–49*. http://iiaglobal.com/wp-content/uploads/2018/01/White-Paper-Comparison-Gamma-Eb-Xray-and-EO-for-Sterilisation.pdf accessed 10 June 2018.

Garvey, M. and Rowan, N.J. (2019) Pulsed UV as a potential surface sanitizer in food production processes to ensure consumer safety. *Curr Opin Food Sci* **26**, 65–70.

Geeraerd, A.H., Valdramidis, V.P. and Van Impe, J.F. (2005) GInaFiT, a freeware tool to assess non-log-linear microbial survivor curves. *Inter J Food Microbiol* **102**, 95–105.

Genest, P.C., Setlow, B., Melly, E. and Setlow, P. (2002) Killing of spores of *Bacillus subtilis* by peroxynitrite appears to be caused by membrane damage. *Microbiology* **148**, 307–314.

Griffiths, K.K. and Setlow, P. (2009) Effects of modification of membrane lipid composition on *Bacillus subtilis* sporulation and spore properties. *Journal of Applied Micro* **106**, 2064–2078.

Guirgis, F.W., Jones, L., Esma, R., Weiss, A., McCurdy, K., Ferreira, J., Gray-Eurom, K. (2017) Managing sepsis: electronic recognition, rapid response teams, and standardized care save lives. *J Crit Care* **40**, 296–302.

Hao, H., Xiaoli, Z., Nian, Q.I.N., Xiaoyan, H.E., Qing, Z. and Qian, H.E. (2016) Effect of ETO and hydrogen peroxide plasma sterilization methods on cell proliferation ability in PLLA/GA scaffolds. *Oxid Comm* **7**, 1–7.

Hayes, J., Kirf, D., Garvey, M. and Rowan, N.J. (2013) Disinfection and toxicological assessment of pulsed UV and pulsed-plasma gas-discharge treated water containing the waterborne enteroparasite *Cryptosporidium pavum*. *J Microbiol Method* **94**, 325–337.

Heckert, R.A., Best, M., Jordan, L.T., Dulac, G.C., Eddington, D.L. and Sterritt, W.G. (1997) Efficacy of vaporized hydrogen peroxide against exotic animal viruses ducted with a variety of viral agents, which included representatives of several virus families. *Orthomyxoviridae* **63**, 3916–3918.

Hee, M., Kim, H., Hwa, C., Ho, S., Koo, J., Jin, S. and Park, J. (2008) Surface and coatings technology effects of low-temperature hydrogen peroxide gas on sterilization and cytocompatibility of porous poly (D, L-lactic-co-glycolic acid) scaffolds. *Surf Coat Technol* **202**, 5762–5767.

Henriques, A.O. and Moran, C.P. (2000) Structure and assembly of the bacterial endospore coat. *Methods* **20**, 95–110.

Hensley, B.J. and Monson, J.R.T. (2015) Hospital-acquired infections. *Surgery* **33**, 528–533.

Hong, L., Zhang, P., Setlow, P. and Li, Y.Q. (2010) Characterization of bacterial spore germination using integrted phase contrast microscopy, Raman spectroscopy, and optical tweezers. *Anal Chem* **82**, 3840–3847.

Huillet, E., Tempelaars, M.H., André-Leroux, G., Wanapaisan, P., Bridoux, L., Makhzami, S., Lereclus, D. (2012) PlcRa, a new quorum-sensing regulator from *Bacillus cereus*, plays a role in oxidative stress responses and cysteine metabolism in stationary phase. *PLoS ONE* **7**, 1–19.

Hultman, C., Hill, A. and McDonnell, G. (2007) The physical chemistry of decontamination with gaseous hydrogen peroxide. *Pharma Eng* **27**, 22–32.

Humpheson, L., Adams, M.R., Anderson, W.A. and Cole, M.B. (1998) Biphasic thermal inactivation kinetics in *Salmonella enteritidis* PT4. *Appl Environ Microbiol* **64**, 459–464.

IARC (2012) Chemical agents and related occupations. IARC Monographs 100F, pp. 379–400. http://monographs.iarc.fr/ENG/Monographs/vol100F/mono100F-28.pdf. Accessed 3 Jan 2018.

International Organization for Standardization (ISO) (2014a) *ISO11135:2014 Sterilization of Health-care Products — Ethylene Oxide — Requirements for the Development, Validation and Routine Control of a Sterilization Process for Medical Devices*. Geneva: ISO.

International Organization for Standardization (ISO) (2015) *ISO 11137–1:2015 Sterilization of Health Care Products — Radiation —Part 1: Requirements for Development, Validation and Routine Control of a Sterilization Process for Medical Devices*. Geneva: ISO.

International Organization for Standardization (ISO) (2016a) *ISO 14937:2009 Sterilization of Health Care Products - General Requirements for Characterization of a Sterilizing Agent and the Development, Validation and Routine Control of a Sterilization Process for Medical Devices*. Geneva: ISO.

International Organization for Standardization (ISO) (2016b) *ISO13485:2016 Medical Devices — Quality Management Systems — Requirements for Regulatory Purposes*. Geneva: ISO.

International Organization for Standardization (ISO) (2018) *ISO11139:2018 Sterilization of Health Care Products — Vocabulary of Terms Used in Sterilization and Related Equipment and Process Standards*. Geneva: ISO.

International Trade Administration (2016) 2016 Top Markets Report Medical Devices: A Market Assessment Tool for U.S. Exporters. https://www.trade.gov/topmarkets/pdf/Medical_Devices_Top_Markets_Report.pdf (accessed 16 Jan 2018)

Junkar, I., Kulkarni, M., Drašler, B., Rugelj, N., Mazare, A., Flašker, A., Iglič, A. (2016) Influence of various sterilization procedures on TiO2 nanotubes used for biomedical devices. *Bioelectrochem* **109**, 79–86.

Klapes, N.A. and Vesley, D. (1990) Vapour-phase hydrogen-peroxide as a surface decontaminant and sterilant. *Appl Environ Microbiol* **56**, 503–506.

Kramer, B. and Thielmann, J. (2016) Monitoring the live to dead transition of bacteria during thermal stress by a multi-method approach. *J Microbiol Meth* **123**, 24–30.

Krebs, M.C., Bécasse, P., Verjat, D. and Darbord, J.C. (1998) Gas-plasma sterilization: relative efficacy of the hydrogen peroxide phase compared with that of the plasma phase. *Inter J Pharma* **160**, 75–81.

Kroc, T.K., Thangaraj, J.C.T., Penning, R.T. and Kephart, R.D. (2017) Accelerator-driven medical sterilization to replace Co-60 sources. Retrieved from http://lss.fnal.gov/archive/2017/pub/fermilab-pub-17-314-di.pdf (accessed 26 Jan 2019).

Lee, J.W. and Helmann, J.D. (2006) The PerR transcription factor senses H_2O_2 by metal-catalysed histidine oxidation. *Nature* **440**, 363–367.

Leggett, M.J., Mcdonnell, G., Denyer, S.P., Setlow, P. and Maillard, J.Y. (2012) Bacterial spore structures and their protective role in biocide resistance. *J Appl Microbiol* **113**, 485–498.

Leggett, M.J., Setlow, P., Sattar, S.A. and Maillard, J.Y. (2016) Assessing the activity of microbicides against bacterial spores: knowledge and pitfalls. *J Appl Microbiol* **120**, 1174–1180.

Lerouge, S., Wertheimer, M.R., Marchand, R., Tabrizian, M. and Yahia, L. (2000) Effect of gas composition on spore mortality and etching during low-pressure plasma sterilization. *J Biomed Mater Res* **51**, 128–135.

Lerouge, S., Tabrizian, M., Wertheimer, M.R., Marchand, R. and Yahia, L. (2002) Safety of plasma-based sterilization: surface modifications of polymeric medical devices induced by Sterrad and Plazlyte processes. *Bio-Med Mater Engin* **12**, 3–13.

Linde (2011) *Safety data sheet – ethylene oxide*. http://hiq.linde-gas.com/en/images/Ethylene%20Oxide%20SDS%20Linde%20EU%20format%20HiQ%20Jan%202011_tcm899-92356.pdf accessed 23 Jan 2019.

Linley, E., Denyer, S.P., McDonnell, G., Simons, C. and Maillard, J.Y. (2012) Use of hydrogen peroxide as a biocide: new consideration of its mechanisms of biocidal action. *J Antimicrob Chemother* **67**, 1589–1596.

Loshon, C.A., Melly, E., Setlow, B. and Setlow, P. (2001) Analysis of the killing of spores of *Bacillus subtilis* by a new disinfectant, Sterilox. *J Appl Microbiol* **91**, 1051–1058.

Ma, N., Petit, A., Huk, O.L., Yahia, L. and Tabrizian, M. (2003) Safety issue of re-sterilization of polyurethane electrophysiology catheters: a cytotoxicity study. *J Biomater Sci, Polymer Edition* **14**, 213–226.

Majeed, M., Majeed, S., Nagabhushanam, K., Punnapuzha, A., Philip, S. and Mundkur, L. (2018) Rapid assessment of viable but non-culturable *Bacillus coagulans* MTCC 5856 in commercial formulations using flow cytometry. *PLoS ONE* **13**, 1–14.

Masterson, C.H., Murphy, E., Major, I., González, H., O'Toole, D., McCarthy, S., Laffey, J.G. and Rowan, N.J. (2019) Purified beta-glucan from the *Lentinus edodes* mushroom attenuates antibiotic resistant *Klebsiella pneumoniae*-induced pulmonary sepsis. *Am Thoracic Soc.* A28. BACTERIAL AND VIRAL LUNG INFECTIONS AND PATHOGENESIS, A1222–A1222.

McDonnell, G. (2007) Chemical sterilization. In *Antisepsis, Disinfection and Sterilization: Types, Action and Resistance* ed. McDonnell, G. pp. 191–216. Washington, DC: ASM Press.

McDonnell, G. (2014) The use of hydrogen peroxide for disinfection and sterilization applications. In *PATAI'S Chemistry of Functional Groups* ed. Rappoport, Z. https://doi.org/10.1002/9780470682531.pat0885

Mcleod, N.P., Clifford, M., Sutton, J.M. and Mcleod, N. (2017) Evaluation of novel process indicators for rapid monitoring of hydrogen peroxide decontamination processes. *PDA J Pharma Sci Technol* **71**, 393–404.

Melly, E., Cowan, A.E. and Setlow, P. (2002a) Studies on the mechanism of killing of *Bacillus subtilis* spores by hydrogen peroxide. *J Appl Microbiol* **93**, 316–325.

Melly, E., Genest, P.C., Gilmore, M.E., Little, S., Popham, D.L., Driks, A. and Setlow, P. (2002b) Analysis of the properties of spores of *Bacillus subtilis* prepared at different temperatures. *J Appl Microbiol* **92**, 1105–1115.

Meszaros, J.E., Antloga, K., Justi, C., Plesnicher, C. and McDonnell, G. (2005) Area fumigation with hydrogen peroxide vapor. *Appl Biosafety* **10**, 91–100.

Mols, M. and Abee, T. (2011) Primary and secondary oxidative stress in *Bacillus*. *Environ Microbiol* **13**, 1387–1394.

Moore, F. and Perkinson, L. (1979) Hydrogen peroxide vapor sterilization method. US Patent 4,169,123. https://patents.google.com/patent/US4169123A/en (accessed 8 Feb 2019).

Nuutinen, J., Clerc, C. and Virta, T. (2002) Effect of gamma, ethylene oxide, electron beam and plasma sterilization on behaviour of SR-PLLA bres in vitro. *J Biomater Sci Polym Ed* **13**, 1325–1336.

Penna, T.C.V., Ferraz, C.A.M. and Cassola, M.A. (1999) The presterilization microbial load on used medical devices and the effectiveness of hydrogen peroxide gas plasma against *Bacillus subtilis* spores. *Infect Cont Hosp Epidemiol* **20**, 1–20.

Popham, D.L., Sengupta, S. and Setlow, P. (1995) Heat, hydrogen peroxide, and UV resistance of *Bacillus subtilis* spores with increased core water content and with or without major DNA-binding proteins. *Appl Environ Microbiol* **61**, 3633–3638.

Pottage, T., Richardson, C., Parks, S., Walker, J.T. and Bennett, A.M. (2010) Evaluation of hydrogen peroxide gaseous disinfection systems to decontaminate viruses. *J Hosp Infect* **74**, 55–61.

RAISIN Working Group (2009) "RAISIN" – a national programme for early warning, investigation and surveillance of healthcare-associated infection in France. *Euro Surveill* **14**:pii=19408. Available: http://www.eurosurveillance.org/ViewArticle.aspx?ArticleId=19408

Reich, R. and Caputo, R.A. (2005) The adverse effects of cellulosic material in isolator barrier technology. *Pharma Technol* **29**, 52–58.

Reis, A., Da Silva, T.L., Kent, C.A., Kosseva, M., Roseiro, J.C. and Hewitt, C.J. (2005) Monitoring population dynamics of the thermophilic *Bacillus licheniformis* CCMI 1034 in batch and continuous cultures using multi-parameter flow cytometry. *J Biotechnol* **115**, 199–210.

Riesenman, P.J. and Nicholson, W.L. (2000) Role of the spore coat layers in *Bacillus subtilis* spore resistance to hydrogen peroxide, artificial UV-C, UV-B, and solar UV radiation. *Appl Environ Microbiol* **66**, 620–626.

Roth, S., Feichtinger, J. and Hertel, C. (2010) Characterization of *Bacillus subtilis* spore inactivation in low-pressure, low-temperature gas plasma sterilization processes. *J Appl Microbiol* **108**, 521–531.

Rowan, N.J. (2004) Viable but non-culturable forms of food and waterborne bacteria: Quo Vadis? *Trend Food Sci Technol* **15**, 462–467.

Rowan, N.J. (2019) Pulsed light as an emerging technology to cause disruption for food and adjacent industries - Quo Vadis? *Trends Food Sci Technol* **88**, 316–332.

Rowan, N.J. and Anderson, J.G. (1998) Growth and enterotoxin production by diarrhogenic *Bacillus cereus* in dietary supplements prepared for hospitalized HIV patients. *J Hosp Infect* **2**, 139–146.

Rowan, N.J., Valdramidis, V.P. and Gómez-López, V.M. (2015) A review of quantitative methods to describe efficacy of pulsed light generated inactivation data that embraces the occurrence of viable but non culturable state microorganisms. *Trends Food Sci Technol* **44**, 79–92.

Russell, A.D. (2003) Similarities and differences in the responses of microorganisms to biocides. *J Antimicrob Chemother* **52**, 750–763.

Rutala, W.A. (1996) Disinfection and sterilization of patient-care items. *Infect Cont Hosp Epidemiol* **17**, 377–384.

Rutala, W.A. and Weber, D.J. (1996) Low-temperature sterilization technologies: Do we need to redefine "sterilization"? *Infect Cont Hosp Epidemiol* **17**, 87–91.

Rutala, W.A. and Weber, D.J. (1998) Clinical effectiveness of low-temperature sterilization technologies. *Infect Cont Hosp Epidemiol* **19**, 798–804.

Rutala, W.A., Gergen, M.F. and Weber, D.J. (1998) Comparative evaluation of the sporicidal activity of new low-temperature sterilization technologies: Ethylene oxide, 2 plasma sterilization systems, and liquid peracetic acid. *Am J Infect Cont* **26**, 393–398.

Rutala, W.A., Gergen, M.F. and Weber, D.J. (1999) Sporicidal activity of a new low-temperature sterilization technology: the Sterrad 50 sterilizer. *Infect Cont Hos Epidemiol* **20**, 514–516.

Savaris, M., dos Santos, V. and Brandalise, R.N. (2016) Influence of different sterilization processes on the properties of commercial poly(lactic acid). *Mater Sci Engin C* **69**, 661–667.

Schneider, P.M. (2013) New technologies and trends in sterilization and disinfection. *Am J Infection Control* **41**, S81–S86.

Seastar (2011) *Material Safety Data Sheet – Hydrogen Peroxide Solution*. http://www.seastarchemicals.com/wpcontent/uploads/2015/03/SSNSSE_10HydrogenPeroxideSDSRev201407.pdf accessed 23 January 2019.

Sella, S.R.B.R., Vandenberghe, L.P.S. and Soccol, C.R. (2014) Life cycle and spore resistance of spore-forming *Bacillus atrophaeus*. *Microbiol Res* **169**, 931–939.

Serpa, J.J., Makepeace, K.A., Borchers, T.H., Wishart, D.S., Pertochencnko, E.U. and Borchers, T.H. (2014) Using isotopically-coded hydrogen peroxide as a surface modification reagent for the structural characterization of prion protein aggregates. *J. Proteomics* **100**, 160–166.

Setlow, P. (2006) Spores of *Bacillus subtilis*: their resistance to and killing by radiation, heat and chemicals. *J Appl Microbiol* **101**, 514–525.

Setlow, P. (2011) Resistance of bacterial spores. In *Bacterial Stress Responses*, 2nd Edition ed. Storz, G. and Hengge, R. pp. 319–332. Washington, DC: ASM Press.

Setlow, P. (2014) Spore resistance properties. Microbiol. *Spectrum* **2**, 1–14. https://doi.org/10.1128/microbiolspec.TBS-0003-2012

Setlow, B. and Setlow, P. (1993) Binding of small, acid-soluble spore proteins to DNA plays a significant role in the resistance of *Bacillus subtilis* spores to hydrogen peroxide. *Appl Environ Microbiol* **59**, 3418–3423.

Setlow, P., Liu, J. and Faeder, J.R. (2012) Heterogenity of bacterial spore populations. In *Bacterial Spores: Current Research and Applications* ed. Abel-Santos, E. pp. 199–214. Norfolk: Caister Academic Press.

Setlow, B., Yu, J., Li, Y.Q. and Setlow, P. (2013) Analysis of the germination kinetics of individual *Bacillus subtilis* spores treated with hydrogen peroxide or sodium hypochlorite. *Lett Appl Microbiol* **57**, 259–265.

Setlow, B., Korza, G., Blatt, K.M.S., Fey, J.P. and Setlow, P. (2016) Mechanism of *Bacillus subtilis* spore inactivation by and resistance to supercritical CO2 plus peracetic Acid. *J Appl Microbiol* **120**, 57–69.

Shintani, H. (2014) Important points to attain reproducible sterility assurance. *Biochem Physiol* **3**, 1–4.

Sk, M.H., Overfelt, R.A., Haney, R.L. and Fergus, J.W. (2011) Hydrogen embrittlement of 4340 steel due to condensation during vaporized hydrogen peroxide treatment. *Mater Sci Engin A* **528**, 3639–3645.

STERIS (2002) Material compatibility with vaporized hydrogen peroxide (VHP®) sterilization: a new option for point-of-manufacture sterilization. Retrieved from www.sterislifesciences.com/~/media/Files/LifeSciences_com/PDF/BiodecontaminationServices/MaterialCompatibilitywithVaporizedHydrogenPeroxide.ashx

STERIS (2019a) *V-PRO® Low-temperature Sterilization Systems*. Retrieved from www.steris.com/healthcare/products/v-pro-sterilizers/

STERIS (2019b) *VHP Sterilization & Biodecontamination*. Retrieved from www.sterislifesciences.com/products/equipment/vhp-sterilization-and-biodecontamination

Stone, G., Chapman, B. and Lovell, D. (2009) Development of a log-quadratic model to describe microbial inactivation, illustrated by thermal inactivation of *Clostridium botulinum*. *Appl Environ Microbiol* **75**, 6998–7005.

Tabner, B.J., El-Agnaf, O.M.A., German, M.J., Fullwood, M.J. and Allsop, D. (2005) Protein aggregation, metals and oxidative stress in neurodegenerative diseases. *Biochem Soc Trans* **33**, 1082–1086.

Trunet, C., Carlin, F. and Coroller, L. (2017) Investigating germination and outgrowth of bacterial spores at several scales. *Trends Food Sci Technol* **64**, 60–68.

Unger-Bimczok, B., Kottke, V., Hertel, C. and Rauschnabel, J. (2008) The influence of humidity, hydrogen peroxide concentration, and condensation on the inactivation of geobacillus stearothermophilus spores with hydrogen peroxide vapor. *J Pharma Innov* **3**, 123–133.

Wallace, C.A. (2016) New developments in disinfection and sterilization. *Am J Infect Con* **44**, e23–e27. https://doi.org/10.1016/j.ajic.2016.02.022.

Watling, D., Ryle, C., Parks, M. and Christopher, M. (2002) Theorethical analysis of the condensation of hydrogen peroxide gas and water vapour as used in surface decontamination. *PDA J Pharma Sci* **56**, 291–299.

Young, S.B. and Setlow, P. (2004a) Mechanisms of *Bacillus subtilis* spore resistance to and killing by aqueous ozone. *J Appl Microbiol* **96**, 1133–1142.

Young, S.B. and Setlow, P. (2004b) Mechanisms of killing of *Bacillus subtilis* spores by Decon and Oxone, two general decontaminants for biological agents. *J Appl Microbiol* **96**, 289–301.

Zhang, Y. and Mathys, A. (2019) Superdomant spores as a hurdle for gentle germination-inactivation based spore control strategies. *Front Microbiol* **9**, 3163. https://doi.org/10.3389/fmicb.2018.0163.

Science of the Total Environment 878 (2023) 162976

Contents lists available at ScienceDirect

Science of the Total Environment

journal homepage: www.elsevier.com/locate/scitotenv

Review

A review of Spaulding's classification system for effective cleaning, disinfection and sterilization of reusable medical devices: Viewed through a modern-day lens that will inform and enable future sustainability

N.J. Rowan [a,b,c,*], T. Kremer [a,d], G. McDonnell [d]

[a] Centre for Sustainable Disinfection and Sterilization, Bioscience Research Institute, Technological University of the Shannon Midlands Midwest, Athlone Campus, Ireland
[b] Department of Nursing and Healthcare, Technological University of the Shannon Midwest Mideast, Athlone Campus, Ireland
[c] SFI-funded CURAM Centre for Medical Device Research, University of Galway, Ireland
[d] Microbiological Quality & Sterility Assurance, Johnson & Johnson, 1000 Route 202, South Raritan, NJ 08869, USA

HIGHLIGHTS

- Cleaning, disinfection and sterilization remain essential for mitigating patient risk from contaminated reusable medical-devices
- Spaulding's classification of 1957 remains applicable, but it needs updating for modern-day challenges and opportunities
- Pressing need for new real-time monitoring and robust cleaning of devices enabled by automation
- Future design thinking of next-generation medical devices should address ease of cleaning, processing efficacy, and sustainability
- Quintuple Helix Hub concept (academia-industry-healthcare-regulators-society) will accelerate innovation and advance device safety

GRAPHICAL ABSTRACT

ARTICLE INFO

Editor: Damià Barceló

Keywords:
Medical devices, sustainability
Spaulding classification, cleaning, processing
Patient risk, endoscopes, reprocessing

ABSTRACT

Despite advances in medicine and innovations in many underpinning fields including disease prevention and control, the Spaulding classification system, originally proposed in 1957, remains widely used for defining the disinfection and sterilization of contaminated re-usable medical devices and surgical instruments. Screening PubMed and Scopus databases using a PRISMA guiding framework generated 272 relevant publications that were used in this review. Findings revealed that there is a need to evolve how medical devices are designed, and processed by cleaning, disinfection (and/or sterilization) to mitigate patient risks, including acquiring an infection. This Spaulding Classification remains in use as it is logical, easily applied and understood by users (microbiologists, epidemiologists, manufacturers, industry) and by regulators. However, substantial changes have occurred over the past 65 years that challenge interpretation and application of this system that includes inter alia emergence of new pathogens (viruses, mycobacteria, protozoa, fungi), a greater understanding of innate and adaptive microbial tolerance to disinfection, toxicity risks, increased number of vulnerable patients and associated patient procedures, and greater complexity in design and use of medical devices. Common cited examples include endoscopes that enable non- or minimal invasive procedures but are highly sophisticated with various types of materials (polymers, electronic components etc), long narrow channels, right angle and

* Corresponding author at: Centre for Sustainable Disinfection and Sterilization, Bioscience Research Institute, Technological University of the Shannon Midlands Midwest, Athlone Campus, Ireland.
E-mail address: nrowan@ait.ie (N.J. Rowan).

http://dx.doi.org/10.1016/j.scitotenv.2023.162976
Received 10 December 2022; Received in revised form 23 February 2023; Accepted 17 March 2023
Available online 22 March 2023

heat-sensitive components and various accessories (e.g., values) that can be contaminated with high levels of microbial bioburden and patient tissues after use. Contaminated flexible duodenoscopes have been a source of several significant infection outbreaks, where at least 9 reported cases were caused by multidrug resistant organisms [MDROs] with no obvious breach in processing detected. Despite this, there is evidence of the lack of attention to cleaning and maintenance of these devices and associated equipment. Over the last few decades there is increasing genomic evidence of innate and adaptive resistance to chemical disinfectant methods along with adaptive tolerance to environmental stresses. To reduce these risks, it has been proposed to elevate classification of higher-risk flexible endoscopes (such as duodenoscopes) from semi-critical [contact with mucous membrane and intact skin] to critical use [contact with sterile tissue and blood] that entails a transition to using low-temperature sterilization modalities instead of routinely using high-level disinfection; thus, increasing the margin of safety for endoscope processing. This timely review addresses important issues surrounding use of the Spaulding classification system to meet modern-day needs. It specifically addresses the need for automated, robust cleaning and drying methods combined with using real-time monitoring of device processing. There is a need to understand entire end-to-end processing of devices instead of adopting silo approaches that in the future will be informed by artificial intelligence and deep-learning/machine learning. For example, combinational solutions that address the formation of complex biofilms that harbour pathogenic and opportunistic microorganisms on the surfaces of processed devices. Emerging trends are addressed including future sustainability for the medical devices sector that can be enabled via a new Quintuple Helix Hub approach that combines academia, industry, healthcare, regulators, and society to unlock real world solutions.

Contents

1. Introduction

Medical devices are of critical importance to patient health, where healthcare is constantly evolving to improve the quality of care provided to patients. Pre COVID-19, there were approximately 54 million outpatient and 46 million inpatient surgical procedures conducted each year in the United States alone (Perry et al., 2012; Pendarkar et al., 2018). International studies have highlighted that addressing the COVID-19 pandemic has resulted in frequent cancellation of surgical service provision and endoscopies due to safety concerns that has placed added enormous pressure on healthcare to meet this backlog and to continue to deliver appropriate care to patients (Ebigbo et al., 2020; Belle et al., 2020). Unexpected patient complications from the use of medical devices further adds to these burdens on healthcare systems worldwide.

The most cited complications are Hospital Acquired Infections (HAIs), which are defined as infections developing after 48 h of a stay at a healthcare facility that was not present or incubating at the time of admission (McDonnell and Hansen, 2020). HAIs are estimated to affect 1.7 million patients in the US annually leading to 99,000 deaths (Bradley and Hensley, 2015; Kathryn Gold, 2013). Medical devices are a common source of HAIs and have accounted for 60 % to 80 % of all bloodstreams, urinary tract, and pneumonia-related HAIs (Kathryn Gold, 2013). Otter et al. (2016) described that transmission routes of pathogens are complicated and have been difficult to assign an assignable cause through investigation.

The medical device industry, encompassing original equipment manufacturers (OEMs) and the connected sterilization industry, is highly regulated to deliver safe and effective products for patient use. For reusable medical devices intended to be processed within a healthcare facility prior to patient use, instructions for use (IFU) and associated labelling provide the important processing requirements to ensure patient safety, including cleaning, disinfection, and/or sterilization that are typically performed by dedicated facility departments (McDonnell and OSMA Anti-Infective Working Group, 2022). Kenters et al. (2018) conducted a worldwide survey on current flexible endoscope reprocessing that identified a large variation in reprocessing practices among healthcare facilities in different countries. Most facilities (82 %) have standard procedure; however, 50 % (n = 165) of reprocessing practitioners identified the need for education and training programme with a competency assessment to prevent reprocessing lapses and to improve patient safety. To mitigate the risk of HAIs, current methods for the safe processing of medical devices still rely upon the guiding classification system of Dr. E. H. Spaulding, originally conceived and published over 50 years ago (Spaulding, 1968). The general applicability of Spaulding's classification system remains logical and practical today. Spaulding's underpinning hypothesis was that healthcare facilities should apply appropriate disinfection and sterilization methods to process medical devices and surgical instruments based on the degree to patient risk of acquiring an infection due to their use. Three categories of risk were proposed, namely critical use [where a device or item enters sterile tissue

and must be sterile], semi-critical use [where a device or item contacts mucous membranes or non-intact skin, and requires at a minimum high-level disinfection], and non-critical [where a device or item comes in contact with intact skin and requires low-to-intermediate level disinfection]. Therefore, this timely review article addresses key pressing technical challenges and embraces emerging opportunities for the sustainable development of medical devices from a reflective lens perspective.

This study drew upon publications across PubMed and Scopus databases using a PRISMA guiding framework. Of the published papers using the key words "Medical Devices" (1,679,481) and "Spaulding Classification" (180) over period 1957 to 2023. Eligibility criteria focused on studies addressing cleaning, processing and sterilization of reusable medical devices and surgical instruments that included microbiology, toxicology, infection transmission, biofilms, antimicrobial resistance and risk assessment. A total of 118 papers were excluded for the reason that reasons that they did not meet eligibility criteria that included bone stress injuries, selective depletion of uropathogenic *E. coli* from the gut, perioperative ultrasonography and echocardiography, theropod furcula, spinal cord injuries; postconcussion and consciousness symptoms and scales, periorbital dirofilariasis, traumatic brain injury, laryngectomy on women, social impact of burns, apraxia, axonal injury, cerebral edema, encephalopathy, peripheral nerve and spinal injuries, parathyroids, avian influenza, Gulf War illness, haemodialysis, schizophrenia, cardiometabolic disease risks, social anxiety, burn recovery, chronic pain, acute phase retinopathy and whole exome sequencing in cerebral palsy for the reasons that these topics did not align with eligibility criteria.

Combining "medical devices + disinfection + risk assessment" generated 301 published results on PubMed and Scopus databases over period 1980 to 2023. Of these, 232 papers were exclude for reasons that they did not align with topic that comprised criteria toilet hygiene, antiseptics and dressings, eyewear contamination, tonometer tips, obstetric infection, acupuncture needles, aseptic technique in microgravity, surgical site infections, chlorhexidine bathing, venous leg ulcers, poultry, personal and protective equipment, COVID-19 management, whole room disinfection, drinking water, corneal staining, waterborne transmission, dental exposure to pesticides, decontamination of beds, swimming pool, dental water lines, military exercise, humidifier disinfectants, oral care, cell sorting in BSL-3 facility, influenza pandemic, diagnostic assays, disposable sterile endosheaths and pulsed UV surface disinfection. Combining the keywords "biofilm", "disinfection" and "medical devices" revealed 203 matching papers on PubMed and Scopus databases over period 1995 to 2023. Also, the incorporation of "antibiotic resistance" generated 80 matching papers in these databases over the period 1972 to 2023 that were screened for eligibility criteria.

2. Spaulding classification for informing appropriateness of disinfection and sterilization of medical devices based upon relationship between use and patient risk

2.1. Current understanding principles and expectations for disinfection and sterilization of devices

This classification system is widely accepted by broad stakeholders including end-users and regulators, such as European Centre for Disease Prevention and Control (ECDC), the U.S. Food and Drug Administration (FDA), and the U.S. Centres of Disease Control and Prevention (CDC), that inform the appropriateness of disinfection and/or sterilization methods to be applied to the reprocessing of reusable medical devices and surgical instruments (McDonnell and Burke, 2011; Klacik, 2019; Rutala, 2019a, 2019b, 2019c; Rutala and Weber, 2016b; Day et al., 2021). Rutala and Weber (2016a) noted that Spaulding's system divides all medical devices into 3 discrete categories based on the severity of perceived risk to patients of acquiring an infection from their use.

1. Critical use items – where a device enters sterile tissue and must be sterile, defined as being free from viable microorganisms (McDonnell and Hansen, 2020). Items contaminated with any microorganism (including bacterial spores), or infectious agent (prion) are referred to as high risk to patients. If they are contaminated and enter sterile tissue or vascular system, they have a high potential for causing disease transmission (Rutala and Weber, 2016b). "Such items should be sterile, such as by using steam sterilization where possible. Examples include surgical instruments. Given that many items contain heat-sensitive materials, other appropriate sterilization modalities should be applied including vaporized hydrogen peroxide (VH2O2), VH2O2 gas plasma, and ethylene oxide gas (EO)" (Rutala and Weber, 2016a). The use of liquid chemical sterilants may also be considered appropriate, such as formulations based on glutaraldehyde (GTA), peracetic acid (PA), hydrogen peroxide (HP), or ortho-phthalaldehyde (OPA). Close attention should be given to the label claims of liquid chemical sterilants as these can vary regionally; they may have the ability to sterilize, depending on their application but may not always be considered practical for routine sterilization.
2. Semi-critical use items– where a device only comes in contact with intact mucus membranes or nonintact skin, it should also be subjected to sterilization, or if this is not feasible due to sensitive material composition or complex design features, then a high-level disinfection (HLD) process must be deployed at a minimum that would be expected to kill all microorganisms except for bacterial endospores (McDonnell and Burke, 2011). Examples of semi-critical items including "respiratory therapy, anaesthesia equipment, some endoscopes, laryngoscope blades and handles, esophageal manometry probes, endocavitary probes, nasopharyngoscopes, prostate biopsy probes, infrared coagulation devices, anorectal manometry catheters, cystoscopies, and diaphragm fitting rings" (Rutala and Weber, 2016b). Depending on regional claim requirements, high level disinfectants should demonstrate broad spectrum antimicrobial activity and typically the ability to eliminate at least 10^6 (or 6-logs) of mycobacterial cells on contaminated surfaces of medical devices. For the vegetative microorganisms and viruses of concern, mycobacteria are typically deemed to exhibit greater resistance to high level disinfectants; thus, mycobacterial cells are recognised as representative (or bio-indicators) for HLD process efficacy. Examples of chemical disinfectants authorized in the USA for HLD use include biocides such as glutaraldehyde, HP, OPA, hypochlorite, and PA with HP (FDA, 2022). It is important to note that the ability to inactivate microorganisms by a disinfectant/sterilant is only part of an overall safe and effective high level disinfection process, as the disinfectant residuals need to be safely removed and the device correctly maintained prior to patient use.
3. Non-critical use items – "where devices contact intact skin (but not mucous membranes), requiring low-level to intermediate-level disinfection. The skin contains intact integumentary layers, and as such, provides a natural barrier to microorganisms. There remains a risk to the skin and as a source of cross-contamination from devices, but this risk is considered low" (Rutala and Weber, 2016a). These risks can be practically reduced by the combination physical removal and disinfection (McDonnell and Burke, 2011). Examples of non-critical use items include blood pressure cuffs, bed surfaces and rails, patient furniture, bedpans, over-bed tables and so forth (Rutala and Weber, 2016b). Such product labelling support disinfection efficacy against a broad spectrum of microbial pathogens that may include methicillin-resistant *Staphylococcus aureus*, vancomycin-resistant enterococci, yeast (*Candida* sp.), mycobacteria, and viruses well within typical label claim for US EPA-registered disinfectants. Physical removal plays an important role in the removal of pathogens with higher levels of natural resistance to disinfectants such as bacterial spores (as highlighted in studies of surface contamination with clostridia; Thomas et al., 2022).

Fig. 1 illustrates the microbial resistance profile to applied disinfection and sterilization modalities. Microorganisms with higher resistance are widely used to challenge and test the effectiveness of disinfection and sterilization methods. Mycobacterial cells, as examples, are used as representative biological indicators (BIs) of microbial resistance for high level disinfection (HDL) such as in the testing of GI endoscopes, bronchoscopes,

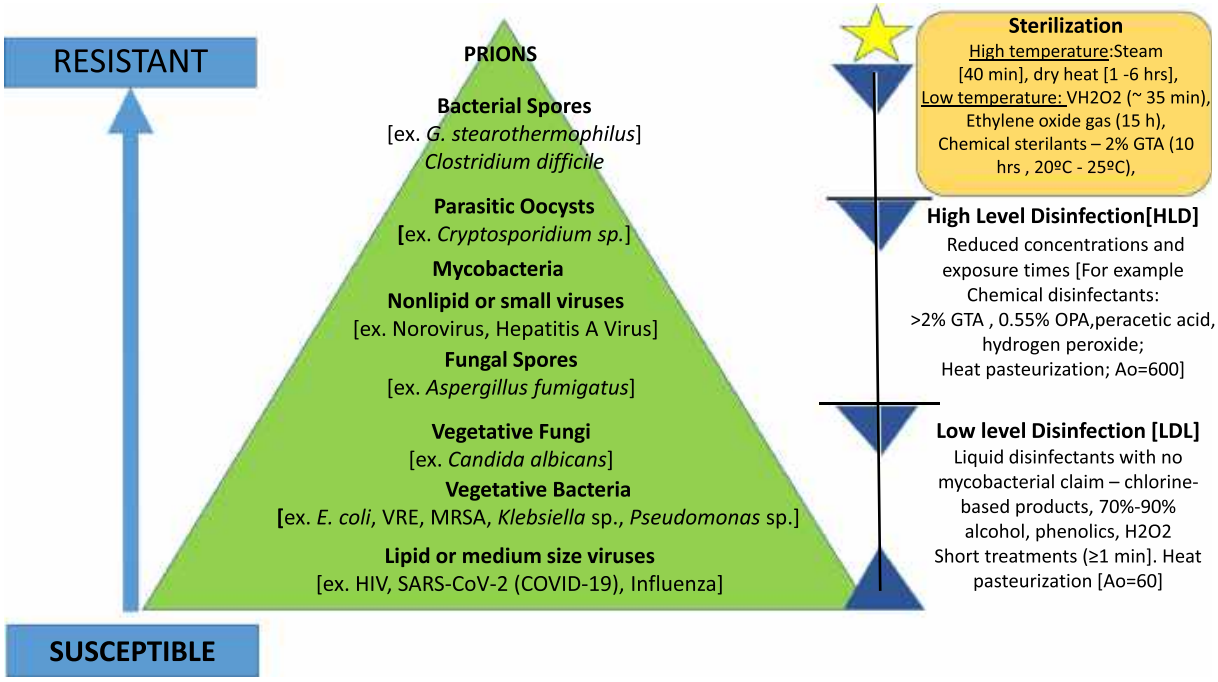

Fig. 1. Pyramid of increasing microbial resistance to disinfectants and sterilants [Noting, this is a guide as the actual levels of resistance depend on the type of disinfection/sterilization process].

and *endo*-cavity probes. Biological indicators are test systems that contain viable microorganisms with a defined resistance to a specific sterilization process (McEvoy and Rowan, 2019; McEvoy et al., 2021; McEvoy et al., 2023). *Bacillus* endospores are used as BIs to confirm sterilization efficacy with heat-tolerant critical (surgical instruments) and heat-sensitive critical and semi-critical patient care items. Although these traditional microbiological tests are useful in establishing the efficacy of such processes and applications, they are limited and there are many benefits in the use of alternative validation approaches such as parametric release or the use of higher classes of chemical indicators (McDonnell and Hansen, 2020). These can provide more robust data insights for the routine control of such processes and lend themselves to automation opportunities. Sterilization addresses the more recalcitrant pathogens that pose serious patient risks transmitted on contaminated devices. Some types of liquid chemical sterilants are frequently used to overcome complex design features associated with heat-sensitive critical and semi-critical devices. At the opposite end, a more wider array of disinfectants can be used at shorter exposure times for chemical liquid disinfection of non-critical patient care items (such as blood pressure cuffs) (Rutala, 2019a, 2019b, 2019c; McDonnell and Hansen, 2020). Some reports have found that certain strains of parasitic oocysts are particularly resistant to chemical disinfectants, but not as much to heat nor UV irradiation (Garvey et al., 2022; McDonnell, 2017). Parasitic oocysts should fall within HLD but may not always be the case; however, they are not routinely required to be tested for any disinfectant claims. It is important to note that the microbial resistance pyramid illustrated in Fig. 1 is only given as a guide as the actual levels of resistance depend on the type of disinfection/sterilization process and the different strains of microorganisms tested. Disinfectant (including HLD) claims are product specific and not just based on certain concentrations and exposure time for the active (e.g., the product formulation and exposure conditions can have a dramatic effect on antimicrobial efficacy).

2.2. Challenges and limitations for modern-day interpretation and application of Spaulding's classification system

Healthcare is constantly scrutinized regarding the effectiveness in the delivery of continuous quality improvements including practices of cleaning, disinfection, and sterilization. HAIs are reported to occur in one out of 25 patients daily on average in the US (CDC, 2014) with over 2 million patients contracting HAIs annually (Vallés and Ferrer, 2009). In the USA alone, the overall incidence of HAIs is estimated to have increased by 36 % in the last two decades (Stone, 2009). In recent times, there have been over 25 outbreaks of multidrug-resistant organisms including carbapenem-resistant Enterobacteriaceae (CRE) in hospitals internationally that have led to significant morbidity and mortality, which have linked to contaminated duodenoscopes. Moreover, contaminated gastrointestinal (GI) endoscopes and bronchoscopes are often considered as semi-critical devices, as they have contact with intact mucous membranes, but have been linked with over 130 outbreaks causing mortalities (Balan et al., 2019). Outbreaks have unfortunately not been limited to flexible endoscopes subjected to HLD but have included critical devices subjected to steam sterilization (Tosh et al., 2011; Dancer et al., 2012).

2.2.1. Failure mode analysis: critical instance case study

There are at least 18 million gastrointestinal endoscopies conduced each year in the United States (Rutala and Weber, 2016b; Rutala, 2019a, 2019b, 2019c). Each of these procedures involves use of surgical instruments or medical devices that contact a patient's sterile tissue or mucous membrane (Rutala and Weber, 2016b). However, there is a major risk of introducing infection to all patients undergoing such procedures if contaminated surgical instruments and medical devices are not appropriately processed (Rutala and Weber, 2016b). For example, a systematic search of the literature conducted during 2018 and 2019 just prior to COVID-19 pandemic, estimated the risk of contracting duodenoscope-associated infections (DAIs) in Dutch practices to be at least 180 times higher than previously published risk estimates due to underreporting of infections caused by multi-drug resistant organisms (MDROs) and sensitive bacteria (Kwakman et al., 2021; Kwakman et al., 2022). The authors advocated greater awareness by healthcare personnel involved in endoscopies, a need for improved endoscope cleaning and new solutions to address technical challenges to prevent occurrence of DAIs.

GI endoscopes can become highly contaminated during use, where the internal long narrow lumen can contain between 7 and 10 $\log_{10}$ enteric microorganisms and the microbial load of colon is ca. 9 to 12 $\log_{10}$/mL

(Rutala, 2019a, 2019b, 2019c; Alfa et al., 1999) The margin of safety associated with processing these endoscopes with semi-critical use designation is negligible and therefore are present higher risk to patients than previously considered. GI endoscopes should be subjected to cleaning and HLD that when conducted correctly can reduce microbial bioburden by ca. 2 to 6 $\log_{10}$ and 4 to 6 $\log_{10}$ respectively; thus, representing a combined maximal microbial reduction of ca. 12 $\log_{10}$ if cleaning is conducted appropriately. As flexible GI endoscopes and bronchoscopes are heat-sensitive devices, they are generally subjected to HLD using chemical disinfectants or by using low-temperature sterilization modalities. But the level of contamination of endoscopes after cleaning and disinfection could be as high as 5 $\log_{10}$/ml when not conducted efficiently. This equates to an estimated 17 $\log_{10}$ reduction of surgical instruments that are cleaned (2–6 $\log_{10}$ microbial reduction), and sterilized (at least a 12 $\log_{10}$ microbial reduction), where surgical device generally present with significantly lower levels of initial microbial contamination given their use (<2 $\log_{10}$; Cloutman-Green et al., 2015; Rutala, 2019a, 2019b, 2019c). In addition, heavily contaminated flexible endoscopes are highly complex and challenge current decontamination methods with complex features such as narrow lumens and valves resulting in approximately 100 processing steps (Ofstead et al., 2017). Overall, this pushes the margin for safety with processing endoscopes to zero. Campbell Westerway and Basseal (2022) noted, as a reusable medical device, the ultrasound transducer (also known as a probe), comes in contact with mucous membranes of vagina, anal cavity and oral cavity, and it can therefore transmit pathogenic viruses, fungi and bacteria by blood, or mucosal, genital or rectal secretions. These authors reported that only a small number of countries worldwide have implemented transducer reprocessing guidelines that adhere to recommended high level disinfection (HLD) for endocavity transducers. This is mainly due to the perception that the infection transmission risk is negligible given that endocavity transducers are covered with a single-use sheath for the procedure, intimating low-level disinfection provides sufficient protection against pathogen transmission. By highlighting the outbreaks arising from tranducer transmission, the authors recommend that HLD should be a global standard of practice. Saliou et al. (2016) reported that the rate of non-compliance of the microbiological tests performed on flexible cystoscopes is relatively high (19.5 %). Thus, there is a need to improve the processing quality of reusable devices (Ball, 2000; Foliente et al., 2001; Rohm-Rodowald and Jakimiak, 2004; Crawford, 2007; Saliou et al., 2016; Snyder et al., 2017; Link, 2018; Sherman et al., 2018; Kenters et al., 2018; Rahman et al., 2019; Pynnonen and Whelan, 2019; Wiktorczyk et al., 2020; Casini et al., 2021).

Outbreaks have been associated with “inadequate cleaning, inappropriate disinfection, and damaged endoscopes, or flaws in the design of endoscopes or automated endoscope reprocessor (AER)” (Rutala, 2019a, 2019b, 2019c). Often these devices have also been linked as causative agents in outbreaks of CRE or other MDROs in which there were no obvious breaches in endoscope reprocessing (Cabronne et al., 2010; Epstein et al., 2014; Smith et al., 2015; Marsh et al., 2015; Kola et al., 2015; Wendorf et al., 2015; Kim et al., 2016; Shenoy et al., 2019). In some instances, transmission was attributed to device design flaws that prohibited appropriate cleaning that enabled persistent contamination. Chemical disinfectants are effective against CRE and MDROs; thus, it likely that failure in HLD processing was attributed to the lack of exposure to sufficient concentration of disinfectants overtime. Rutala (2019a, 2019b, 2019c) intimated that occurrence of surviving MDROs potentially act as indicator or “red-flag” organisms for ineffective reprocessing of complex designed duodenoscopes. This is logical and very plausible given that the occurrence of specific problematic pathogens on processed medical devices, where disinfectants are normally considered to be effective (Wilson and Nayak, 2016). The latter should also be considered in the context of overall surviving cell numbers (or microbial bioburden) on semi-critical devices that presents a high infectious risk to patients. It was noted that 63 % of 249 surveyed endoscopy centres performed double HLD on duodenoscopes and linear echoendoscopes but did not reduce culture positive rates (Rutala, 2019a, 2019b, 2019c). There is also data showing that all the stages in manual endoscope reprocessing are rarely carried out (1.4 % compliance rate) including omission of essential brushing of channels and components (Ofstead et al., 2010). Endoscope decontamination was improved by using AERs, highlighting the benefits of automation and standardization of processes that also addresses shortcomings associated with mundane manual cleaning procedures.

It has been recommended over many years that as duodenoscopes commonly contact mucous membranes and sterile tissue they should be elevated from semi-critical to critical use status that would typically entail use of a low-temperature sterilization modality, replacing the use of HLD. The infection risk to patients is also potentially enhanced by the increased use of endoscopies (such as bronchoscopies) in elderly patients and those with cancers, organ transplantation, severe underlying conditions, host defence abnormalities, or immune-deficient diseases or medications (Rutala, 2019a, 2019b, 2019c). Thus, the margin of safety for processing heavily contaminated flexible endoscopes is too unforgiving to be practical as it demands near perfect compliance with OEM's IFU. Additionally, microbial tolerance to HLD due to the higher risk of the development and protection of microorganisms in biofilms within endoscope channels also presents a challenge for healthcare given that this may lead to decontamination failure of processed endoscopes (da Costa Luciano et al., 2016).

Over the decades since the initial introduction of Spaulding's classification system, there has been commensurate challenges to hurdle including increased device complexity with features that challenge the cleaning process and a better understanding of the intrinsic and acquired mechanisms of biocide tolerance seen in problematic and opportunistic pathogens including development of multidrug-resistance and cross-protection to the applied and dis-similar lethal environmental stresses. These can be further enhanced by the upregulation of microbial virulence in survivors induced by environmental-stress exposures such as drying, the presence of disinfectants (Ladicevic et al., 2022),and biofilm-mediated protection (Alfa and Howie, 2009); emergence of potential disinfectant mediated cross protection against antibiotics (Morrison et al., 2019); fixation of microbial pathogens within protective soils to contaminated surfaces due to specific regimes of cleaning and types of disinfectants (such as aldehydes) that can also potentially anchor more recalcitrant infectious agents (Kremer et al., 2021a, 2021b, 2021c), such as prions; an increasing complex and embattled healthcare environment colonized by antibiotic-resistant bacteria (Rowan and Moral, 2021; Thomas et al., 2022); and greater number of vulnerable patients with diversity of medical needs (McDonnell and Hansen, 2020).

3. Cleaning

The importance of effective cleaning of medical devices prior to disinfection and sterilization is often under-estimated. Reusable device features vary considerably in design complexity (Fig. 2) It is well known that disinfection and sterilization methods will fail if the pre-cleaning stage is not conducted appropriately, but the classification system is more focused on the antimicrobial steps to be deployed based on the device risk. To appropriately apply the Spaulding Classification system based on the patient risk level, a thorough appreciation of the complexity of device cleaning must be considered first (Kremer et al., 2019; Kremer et al., 2022). If a device is not cleaned effectively, not only can the disinfection or sterilization process step be compromised (Alfa, 2019), but residual organic matter from clinical soil may remain in concentrations that may elicit toxicological risks to patients (McDonnell and Burke, 2011; Kremer et al., 2019). Cleaning instructions should be developed and used to ensure the removal of potential residual organic matter or soil (e.g., physical removal of blood, microorganisms, protein, detergents). Moreover, this offers the potential to align with established chemical and physical analysis, along with microbiological, to determine adequate cleaning efficacy. For example, determining microbiological and cellular load reductions including real time use of rapid in vitro approaches beyond current tools that have limited efficacy, such as use of adenosine triphosphate (ATP) biomarkers (Rutala, 2019a, 2019b, 2019c). These ideas require further investigations to ensure adequate correlation.

Fig. 2. Example of the variability in complex design features associated with medical devices: (a) biopsy forceps, and (b) duodenoscope.

Science in this area should adopt a holistic risk-based approach to understand the totality cleaning effectiveness from end-to-end during device lifetime (Fig. 3) where efficiently addressing the constant backlog for medical device processing based on OEM's IFU as a major challenge (Fig. 4).

Cleaning is typically a multi-step process. Treatment at point-of-use is a critical first step to prevent a more challenging cleaning process, device damage or microorganism growth during the wait time prior to cleaning (Association for the Advancement of Medical Instrumentation, 2020a,

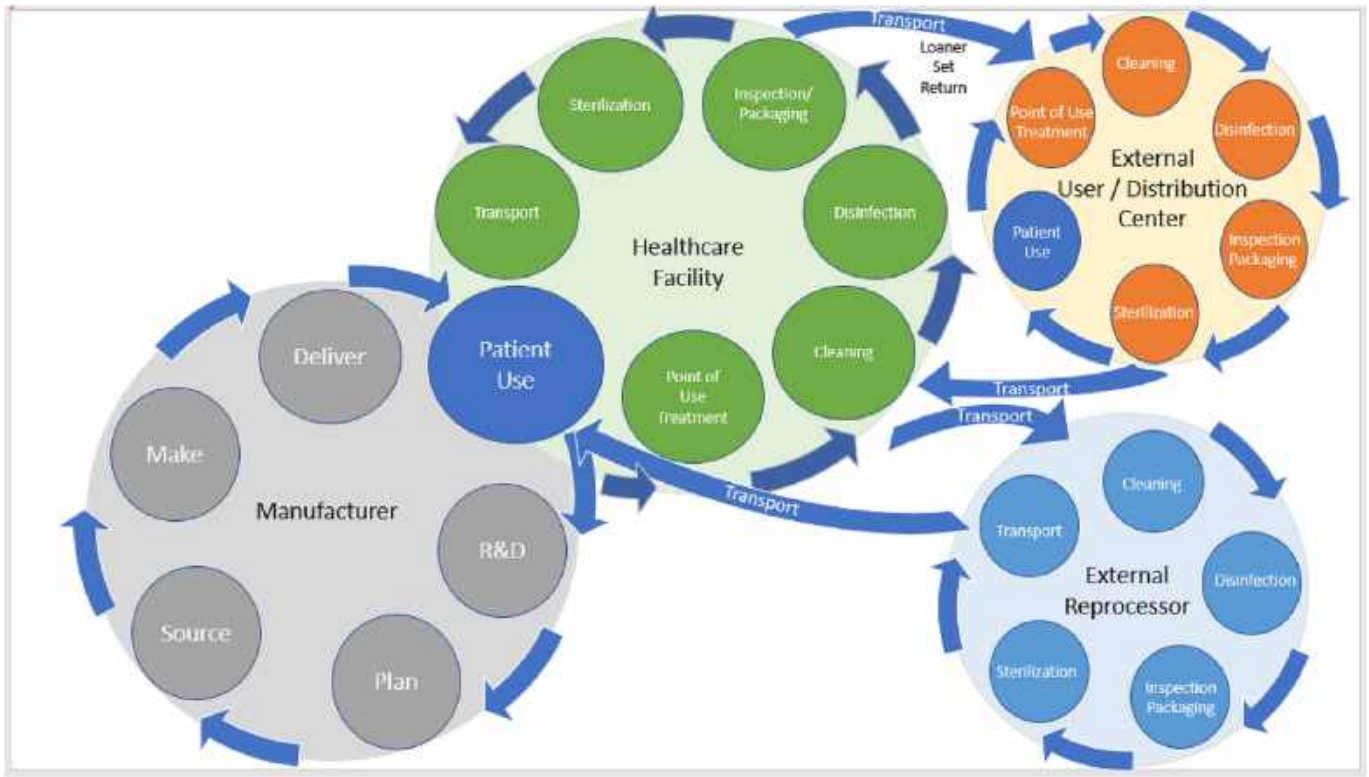

Fig. 3. End-to-end medical device processing cycle.

Fig. 4. Queue for medical device decontamination and inspection in a healthcare Sterile Services Department.

2020b). Most clinical soils, comprising of a multitude of proteins, have shown to be water soluble in a wet and semi-dry condition (Kremer, 2021a, 2021b; Kremer et al., 2022). However, if the soil is allowed to dry, protein is likely to absorb into device material and decrease the soil solubility (Lipscomb, 2007) and reduce the efficacy of cleaning chemistries (Secker, 2015). Transportation and time delays prior to device processing increase the risk of soil drying on the device and increases the challenge.

The validation of associated instructions for use (IFU) is designed to demonstrate that the method of cleaning can consistently remove analytes to a pre-determined level. However, the validation strategy employed, up to recently, was at the discretion of the medical device manufacturer (Kremer et al., 2022). Important industry standards, and commensurate guidance, were developed primarily using the validation experiences of manufacturers, academics, and regulators; however, these new regulatory expectations for device cleanliness may still remain different depending on the geographical location, local requirements, user or regulator experience, availability of cleaning chemistries and equipment, etc. An example of this difference is demonstrated with the acceptance criteria for the cleaning analyte, protein, residuals. In the United States the cleaning specification has been established as 6.4 μg/cm^2 whereas in parts of Europe the value of 50-100 μg/device is the required limit (Kremer et al., 2019). But recent standards and guidance are aligning these requirements (ISO 15883-5).

Cleaning validations have historically been performed under various different guidance and standards that can vary regionally (AAMI TIR30, 2011; ISO 15885-1, 2009b). The guidance provided in these documents was based upon best practices and publications at the time they were published, but often were based on limited independent studies that were performed within the technical competency. Recent updates to these standards (ISO 15883 series, AAMI TIR30, AAMI ST98), have encouraged further investigations to continue to strengthen the scientific foundation for cleaning efficacy. In parallel, there is a need to consider existing and new approaches to help meet the increasing complexity of devices to ensure essential cleaning validation methods generate robust data to substantiate effectiveness. The criticality of the test variables investigated has a relationship to patient safety; thus, if the validation does not appropriately challenge the device, then assurance of patient safety may be compromised. Consider, for example, two very different devices in complexity and the expectation that both have the same consideration for patient risk (Fig. 2). Biopsy forceps have some complex features, such as hinges and mated surfaces, but have one material (e.g., stainless steel) and can be effectively cleaned and terminally sterilized to a very high degree of confidence. The duodenoscope at the other end of the cleaning spectrum has extremely complex features, such as long lumens, electrical parts, restrictive access areas (e.g., encased distal tip) and O-rings that can provide an increase in cleaning challenge (Fig. 2). This highlights the need for a more updated and appropriate classification system that establishes with a relationship between device feature and patient risk from a prior cleaning perspective.

3.1. Biofilms

Biofilm is a common source of infections caused by the ability of microorganisms to adhere to and persist on medical devices (Di Domenico et al., 2022). Microbial cells embedded in the biofilm matrix can be highly tolerant to antimicrobials and, once embedded in a patient may escape or even aggravate the host immune system. The refractory nature of biofilm-related infections (BRIs) still represents a great challenge for clinicians and is a serious health threat worldwide. Despite its importance, the microbiological diagnosis of a BRI is still difficult and not routinely assessed in clinical microbiology. It is estimated that bacterial biofilms may account for 65 and 80 % of microbial and chronic infections with implanted medical devices, respectively (Jamal et al., 2017). A 2012 study suggested that biofilms can serve as a source of infections by periodically releasing planktonic bacterial cells into an environment, even remote to the location of the biofilm (Vickery et al., 2012). The use of disinfectants has already been highlighted as being important to prevent the transmission of infectious pathogens from contaminated surfaces (such as medical equipment) to patients (Rutala, 2019a, 2019b, 2019c). Fig. 5 highlights the role of disinfection in breaking the chain of infection. Thus, despite emphasis on surface disinfection, pathogenic microorganisms have been transmitted to patients through contaminated devices (Quinn et al., n.d.). Within healthcare facilities,

Fig. 5. Role of medical device cleaning, disinfection and sterilization in breaking the chain of infections.

Staphylococcus aureus and *Pseudomonas aeruginosa* are among the most problematic pathogens with *S. aureus* being the second most common pathogen that caused healthcare-associated infections (Dantes et al., 2013). Smith and Hunter (2008) reported that when clinical isolates of MRSA and *P. aeruginosa* were grown as biofilms on discs of materials found in the hospital environment (stainless steel, glass, polyethylene and Teflon) and treated with three commonly used hospital biocides containing benzalkonium chloride (1 % *w/v*), chlorhexidine gluconate (4 % w/v) and triclosan (1 % w/v), these biocides were ineffective for killing these pathogens at label concentration recommended. The diversity of bacteria developing and growing/surviving in biofilms is widely appreciated in the literature (Vickery et al., 2013; Veerachamy et al., 2014; Assefa and Amare, 2022; Dancer, 2022; Alonso et al., 2023). This has even impacted the international definition of biofilms, as a community of microorganisms, rather than the traditional definitions related to Gram negatives and water-systems.

These pathogens have been shown to grow on hard non-porous surfaces and develop an extracellular polymeric matrix that protects the cells from adverse conditions (Su et al., 2022). It has also been shown that the biofilm matrix enhances tolerance to disinfectants by encasing the underlying cells (Abdallah et al., 2015) and by limiting diffusion of disinfectants into the biofilm matrix. The bactericidal efficacy of disinfectants on biofilms is much lower compared to the efficacy of the same disinfectants against planktonic cells (Davison et al., 2010; Fagerlund et al., 2017). The tolerance of biofilms to disinfectants is dependent on the disinfectant active, formulation, temperature, and the type of surface (Abdallah et al., 2015). Moist surfaces have been shown to be more favourable for biofilm growth even though biofilms have also been reported to grow on dry surfaces (Bridier et al., 2011). The behaviour of traditional biofilms, forms under continuously hydrated conditions, differs from a 'dry surface biofilm', defined as the heterogenous accumulation of organisms and other material in a dry matrix, as it less difficult to process (Alfa, 2019). Modeling of dry surface

biofilms demonstrate that some disinfectants are not as effective if a dry surface biofilm is present and can be environmental reservoirs promoting microbial growth and transmission (Alfa, 2019). Disinfectants are primary intervention options against pathogenic microorganisms on surfaces in healthcare facilities and are used as broad-spectrum antimicrobials. Common antimicrobials used for disinfecting surfaces in healthcare facilities include quaternary ammonium compounds, phenolics, and oxidizing agents (e.g., hydrogen peroxide, and chlorine-based products) (McDonnell, 2017; Fagerlund et al., 2017). Claim structure on such disinfectants is well established, but do not generally consider the presence of biofilms (McDonnell and Hansen, 2020). Overall, there are much fewer published studies that investigate the efficacy of disinfectants on bacterial biofilms at label use concentrations and under practical use conditions.

The susceptibility of medical devices by design to recalcitrant biofilm development presents a significant risk to patients from harboured microbial cells that are protected from external stressesand particularly if contaminated surfaces are not appropriately cleaned. The occurrence of biofilms on medical devices can act as protective carrier of planktonic microorganisms leading to infection, which was originally considered by Spaulding in 1957. But our knowledge of the recalcitrance of biofilms is different today. It is well established that failure to eliminate biofilms harbouring microbial cells on contaminated surfaces (such on medical devices) due to appropriate cleaning and disinfection can cause healthcare-associated infections, which can contribute to significant morbidities and mortality (McDonnell and Hansen, 2020). Microbial pathogens in biofilms exist in reduced metabolic or physiological states including dormancy (at their extremes as spores or oocysts), further reducing their sensitivity to chemical disinfection. There is also some evidence of microbial resistance to front line chemical disinfection beyond expected adaptive tolerance that is mediated by expression of specific molecular determinations including by mutation and sharing of genes that promote resistance mechanisms to disinfectants (Table 1). Tolerance to chemical disinfectants by innate and acquired mechanisms has been reported in several problematical microorganisms including *Mycobacterium* species, *Pseudomonas aeruginosa*, *Pseudomonas fluorescens*, *Serratia marcescens*, *Staphylococcus aureus*, *Salmonella* sp., *Escherichia coli*, and *Listeria monocytogenes* (McDonnell, 2017).

Over the past two decades, there has been increased evidence of microbial adaptation to lethal environmental stresses along with subsequent cross-protection against to dis-similar stresses, such as biocides or resistance against antibiotics (McDonnell, 2017). It may be important that the survival of low number of stress-hardened microbial pathogens on devices can present a significant risk to patients. This microbial adaption to applied stress is also evident in adjacent food industry (Rowan, 1999; Yang et al., 2021). Findings suggest that house-keeping functions, such as microbial resistance to environmental stresses and virulence (pathogenesis) are regulated by the same molecular determinants in some pathogens of concern; as an example, *PrfA* expression in L. *monocytogenes* is up-regulated under conditions of environmental stress associated with acid-stress or disinfection conditions (Ladicevic et al., 2022). Microbial pathogens can also change morphologically under conditions of sub-lethal stress that maybe seen as an adaptive response mechanism to the applied stress (Rowan et al., 2000a, 2000b; Rowan et al., 2021). Such mechanisms may be important in the tolerance of mycobacteria to disinfectants, antibiotics, and the immune system (Svetlíkova et al., 2009; Shang et al., 2011). It is also probable that the infection risk to patients is complicated by the occurrence of different types of microbial pathogens that can potentially lead to co-infections in patients, which challenges subsequent disease mitigation and outcomes. Many of these BRIs are likely to be under-reported due to delayed onset in infection development and complexity in effective diagnostics, such as with fungi and mycobacteria (Garvey et al., 2022). This concern is also reflected by the WHO declaring that we are at a crisis point for addressing antifungal drug resistance and as a priority, effective solutions for mitigating against antimicrobial resistant bacteria and fungi are urgently needed (WHO, 2022). Only recently the WHO published the

Table 1
Examples of evidence-based resistance to front line disinfectants and antiseptics used in healthcare applications.

Disinfectant	Microbial resistance to applied disinfection	References
Triclosan	➢ Triclosan resistome – variations in sequencing and structure of FabMG responsible for inefficient binding of triclosan to targets resulting in higher MICs	Kim et al. (2020) Khan et al. (2018).
	➢ A primary target for triclosan is the inhibition of FabI, an enoyl-acyl carrier protein reductase (ENR) involved in bacterial type II fatty acid synthesis essential for survival.	Huang et al. (2016) Ciusa et al. (2012).
	➢ Biochemical and structural basis of triclosan resistance characterized using metagenomics and phylogenetic analysis (*Pseudomonas aeruginosa* that has formed resistance to most conventional antibiotics and forms biofilms)	Gomez et al. (2016)
	➢ Horizontal gene transfer of triclosan resistance in *S. aureus*	
Quaternary Ammonium Compounds (QACs)	➢ Detection of efflux mechanisms such as QacA/B expression *in Enterococcus faecalis*	Bischoff et al. (2012)
	➢ Polyaromatic structural core analogues to activators of QacR, a negative transcriptional regulator of efflux pump QuaA, characterized – thus informing structure-resistance relationships	Forman et al. (2016) Han et al. (2019a, 2019b).
	➢ Detection of QAC resistance gene (*qacEΔ1*), the 1 integron gene (*intI1*), and 12 antibiotic resistance genes informing impact and mechanism of QACs on transmission of antibiotic resistance genes	Tezel and Pavlostathis (2015)
	➢ Novel insight into *qac* and *norA* genotypes in *S. aureus* that relies on plasmid encoded efflux systems for biocide tolerance	Marchi et al. (2015)
	➢ Sub-inhibitory biocide disinfectant concentrations can lead to co-resistance and cross-resistance to antimicrobial agents. Multi-biocide resistance also involves chromosomal gene encoding NorA efflux pump	Pang et al. (2019)
	➢ Use of confocal microscopy to visualize biofilm formation by L. *monocytogenes* and resistance to QACs	Morrison et al. (2019) Minbiole et al. (2016). Pang et al. (2019)
Glutaraldehyde (GTA)	➢ *Mycobacterium massiliense* (recovered post surgical infection) showed high level resistance to 8 % GTA, and likely due to surface modifications reducing biocide penetration/reactivity	De Oliveira Lorena et al. (2010)
	➢ Efflux pumps as potential tolerance mechanisms in *Pseudomonas fluorescens* and *P. aeruginosa* biofilms	Vikram et al. (2015).
	➢ Resistance by unknown mechanisms to GTA found in *P. aeruginosa*, likely due to surface modifications	Kampf et al. (2013)
	➢ Reported *Mycobacterium chelonae* strains from endoscope washer disinfectors with increased resistance to GTA.	Griffiths et al. (1997a, 1997b)
Chlorhexidine (CHX)	➢ *Serratia marcescens* promiscuous INcHI2 mult-resistant plasmid to CHX and other biocides	Allen et al. (2022)
	➢ Genomic Island encoding a homolog of *Pseudomonas MexCD-OprJ* biocide efflux detected in CHX tolerant Serratia	Cieplik et al. (2019)
	➢ *Serratia* isolates possessed a Ser-83 –ile mutation in GyrA conferring fluoroqunolone resistance and increased CHX MICs	
	➢ Mechanisms conferring resistance towards CHX include multidrug efflux pumps and cell membrane changes. For instance, in staphylococci it has been shown that plasmid-borne *qac* genes encode efflux pumps	McDonnell (2017)
Hydrogen peroxide	➢ Adaptive microbial stress tolerance to H2O2, including chemical and enzymatic neutralization	Jacquel et al. (2021)
	➢ Stress induced tolerance to H2O2 in mycobacterial and *Deinococuccus radiodurans*	Li et al. (2014)
	➢ Farnesol induces H2O2 resistance in *Candida albicans* by inhibiting the Ras-cyclic AMP signaling pathway – strains lacking Ras1 or Cyr1 no longer exhibited increased protection against H2O2	Deveau et al. (2010). Wang and Schelborn (1995)

fungal priority pathogens list (WHO FPPL), which is the first global effort to systematically prioritize fungal pathogens, considering their unmet research and development needs and perceived public health importance. The WHO FPPL aims to focus and drive further research and policy interventions to strengthen the global response to fungal infections and antifungal resistance including unlocking appropriate solutions. The list is divided into three categories: critical (*Cryptococcus neoformans*, *Candida auris*, *Aspergillus fumigatus* and *Candida albicans*), high (such as *Candida glabrata*, *Mucorales*, *Fusarium* spp., *Candida tropicalis* and *Candida parapsilosis*) and medium (such as *Coccidioides* spp., *Pichia kudriavzeveii* (*Candida krusei*), and *Cryptococcus gattii*) priority based on a process focused on fungal pathogens that can cause invasive acute and subacute systemic fungal infections for which drug resistance or other treatment and management challenges exist. This list is interesting from a disinfection modality perspective as fungal spores (such as *Aspergillus* sp.) exhibit natural tolerance mechanisms to applied stresses such as UV-irradiation compared with similarly treated non-spore forming fungi (such as *Candida* sp.) (Anderson et al., 2000). This is enhanced resistance is attributed to the expression of a dark pigment in *Aspergillus* spores protecting vital genomic material that has peak absorption at 256 nm, which is natural evolutionary trait to cope with sunlight.

Mitigation strategies for BRIs will depend on the deployment of appropriate regime of verified and validated cleaning procedures before applying high-level disinfection and/or sterilization. Disinfection and sterilization processes can fail if medical device cleaning has not been conducted appropriately, including if they promote fixing of biofilms to surfaces (McDonnell, 2022). Use of life cycle assessment (LCA) tools and 360° degree thinking can help with solutions to this challenge. Innovation can also include sustainable bio-degradable materials or polymers that confer biofilm preventative properties particularly at the early stages of microbial attachment and may even be compatible with cleaning or disinfection (Masterson, 2021). The area of smart materials in medical device design is topical that includes incorporation of functional bioactives and emerging role of 4 D printing (Rtimi et al., 2019; Wang et al., 2022).

3.2. Risk of environmental transmission of cross-contaminated medical devices from a patient perspective

Published findings on the risk to patients from contaminated devices, and cross-transmission leading to outbreak situations, is potentially high (Vonberg et al., 2008; McDonnell and Burke, 2011; Percival et al., 2015). Environmental contamination, including surfaces, has been particularly highlighted over the past decade with increasing investigations with *Clostridium difficile* and extended to include other problematical microbial pathogens (Vonberg et al., 2008; Weber, 2013; Weber et al., 2013; Durovic et al., 2018). For example, Durovic et al. (2018) reported that hospital transmission accounted for 40 % of transmission pathways within the healthcare from review of 24 original articles. Durovic et al. (2018) stated "In healthcare settings, future efforts may need to focus on extending cleaning and disinfection procedures beyond the immediate surroundings of symptomatic carriers". Microbial resilience, survival and the potential for transmission to patients is now well cited in the literature (Seoane-Vazquez et al., 2007; McDonnell et al., 2020). The risks in surgery are often latent, due to the fact that antibiotic prophylaxis is a cornerstone of surgical site infection prevention; but, may often be a crutch to support poor practices in aseptic techniques in surgery (Cohen et al., 2017). This was clearly shown in the last few years with the emergence of outbreaks with carbapenem-resistant Gram negative bacteria, specifically associated with endoscope use (O'Horo et al., 2016; Adrian, 2019). Despite the previous known risk, the levels of overall reported infection outbreaks were considered relatively low; therefore, lapses in best practices evidently occur (McDonnell et al., 2020). However, this trend is now reversed, where changes in these practices are now more supported, particularly in the USA (McDonnell et al., 2020). This risk to patient is not just from an infection point of view, but also potentially toxicity and risk of complications (Seoane-Vazquez et al., 2007). It may also be argued that the overall risk to patients should not be a rationale or excuse to apply best practices in device processing.

4. Addressing microbial challenges – Quo Vadis?

Since the introduction of the Spaulding system, our understanding of microbial challenges to ensuring effective device processing has increased including various types of viruses, mycobacteria, protozoa and fungi (McDonnell and Burke, 2011). The innate resistance mechanisms of microorganisms to disinfection and sterilization methods remains an area of active research, sometimes challenging previous perspectives. In addition, as discussed above, there is evidence of the role of environmental and therapeutic stresses in conferring adaptive microbial tolerance and resistance to established and emerging pathogens (such as CRE and MDROs), that can lead to significant risks, as discussed above (Rutala, 2019a, 2019b, 2019c). There is a gap in information of the types and numbers of surviving pathogens that present a high -infection risk to patients in terms of mortality and morbidity. Healthcare innovation opportunities create a robust evolutionary environment for selecting microbial adaption to front line antimicrobial therapies, including disinfection. An example was reported by West et al. (2018) on inter-strain variability of inhibitory disinfectant concentrations and contact time for clinically relevant MDR strains of *P. aeruginosa* and 4 MRSA strains, with three disinfectant types, when tested at label and reduced contact time. The study underscored the need for a disinfectant validation method that addresses these variances. Chemaly et al. (2014) also reported on the role of the environment in harbouring and transmitting MDR bacteria leading to increased healthcare associated infections (HAIs), higher morbidity and mortality.

New molecular biological-based information, supported by next-generation sequencing highlighted the role of mobile genetic elements in the transfer of disinfectant tolerant genetic mechanisms between similar species and to different bacterial species. This advances our knowledge of the topic beyond earlier insightful reviews (McDonnell and Burke, 2011) where adaption to applied lethal stresses (such as disinfectants) was more so seen as microbial "tolerance" to these deleterious conditions. Such tolerant mechanisms may allow for these microorganisms to survive and persist under normally deleterious conditions. Investigations of outbreaks caused by contaminated duodenoscopes involving CRE and MDROs described persistence was due to lack of contact with microorganisms due to cleaning/device maintenance issues and not a lack of disinfectant effectiveness due to resistance (Rutala, 2019a, 2019b, 2019c). There is also a need to improve detection of genetic variants due to their antibiotic resistance mechanisms that would otherwise have remained undetected. The presence of residual microbial pathogens harboured in biofilm due to inadequate cleaning is of concern as there is reduced efficacy of disinfectants as the latter cannot be delivered at an appropriate concentration. There is justification for changing between the traditional use of aldehydes to oxidative-based disinfectants (such as use of hydrogen peroxide or peracetic acid) due to differences in mechanisms of action and reports of resistance development to aldehydes. A step change to switch to different classes of disinfectants may also promote loss of resistance genes carried on mobile molecular elements. This is similar to the strategic approach for rotational antibiotic use in healthcare or disinfectant rotation in environmental surface applications, as it is recognised that microorganisms will often only express genes only when required, such as in a hostile growth environment (Ciusa et al., 2012; Feng et al., 2021).

New information is required on the molecular and cellular mechanisms potentially involved in adaptive resistance and upregulation of virulence (such as seen in *Listeria monocytogenes*) due to disinfectant exposure where low numbers of microbial stressed survivors present a high infection risk to vulnerable patients. This is particularly relevant as environmental stresses associated with disinfectant use (such as reactive oxygen species [ROS]) are similarly deployed defence tactics used by our front line macrophages to prevent infection (Rowan, 1999; Rowan et al., 2001, 2009; Bradley et al., 2012). Thus, stress-mediated survival post exposure to disinfectants, as used in device processing, may theoretically provide a degree of

cross-protection against our circulating immune cells, which needs to be considered. This highlights the pivotal role of effective automated cleaning and drying, and design-thinking surrounding the creating of the next-generation devices that are less complex with generous built-in margins of safety for to ensure appropriate processing based on IFUs. This should also address simplification and reduction in the workload for healthcare workers in processing departments from a holistic device supply chain perspective, including bespoke training and developing appropriate infection control programs (such as in endoscopy units) (Day et al., 2021). This will also help to ensure the prudent, consistent, and correct use of cleaning, disinfection, and sterilization practices in healthcare facilities, as the literature has many examples of lapses of best practices leading to infection outbreaks. Ongoing and future research should also consider the inclusion of smart polymers and materials that can have antimicrobial or biofilm preventative (or disruptive) properties (Masterson, 2021), as this will reduce risk and may even facilitate compatible disinfection and sterilization processes.

5. Real time monitoring and future automation of processing

There is also a commensurate need to consider real-time monitoring approaches to develop and validate effective processing of devices that encompasses a predictive microbial contamination (or decontamination) function (Kremer et al., 2022). Current methods of assessing cleanliness of devices are typically visual and somewhat primitive, such as the use of various swab tests for analytes such as protein and adenosine triphosphate [ATP], which are unlikely to predict true microbial or soil decontamination (Olfasdottir et al., 2017). Visrodia et al. (2017) reported that ATP correlates poorly with microbiological culture findings, and particularly noted that endoscopes reported as clean by ATP use still had detectable microbial bioburden present (such as up to 1 million bacteria). Other, more sensitive, cleaning validation tools including the extraction and detection of protein, total organic carbon, carbohydrate, haemoglobin, bilirubin, and detecting specific bacterial enzymes.

Advanced studies on cell survival following antimicrobial processes also are of interest. As an example, Farrell et al. (2013) highlighted the potential of addressing a single composite study to address the relationship between use of pulsed UV light irradiation and the simultaneous occurrence of molecular and cellular damage in clinical strains of *Candida albicans*. This is particularly relevant as showed that the occurrence of late apoptotic and necrotic cell phonotypes as detected in real-time using specific markers, coincided with irreversible cell death that can potentially supplement or replace lengthy terminal culture-based methods where there was good agreement between enumeration methods. This constituted the first study to investigate mechanisms of cell destruction caused by pulsed UV using sequential and simultaneous microbial protein leakage assay, lipid hydroperoxidation in cell membrane, specific patterns of reactive oxygen species (ROS) generation, and nuclear damage to treated microbial cells using Comet assay along with detection of specific apoptotic and necrotic stages. Opportunities also exist for this topic in the combined area of photonics and image analysis to assess bioburden on surfaces after device treatment, where such data could also be automated including the provision for artificial intelligence and machine learning for intuitive processing. This reflects increasing smart specialization, such as in additive manufacturing, that embraces the future role of digital transformation including use of robotics that is aligned with the new Industry 5.0 human centric concept (Rowan et al., 2022; Rowan, 2022). For example, Allescher et al. (2022) has recently reported on the potential use of robotics managing the processing of endoscopes. Commensurate development of rapid microbiological methods will also inform real-time determinations of process efficacy for microbial inactivation. However, innovation in this field may be seen as strategically sustaining (or incremental), as opposed to disruptive, to ensure seamless integration of technologies with existing assets from a risk management and corporate operation perspective.

Considerations also need to be given to toxicology given chemical use (e.g., for cleaning and disinfection) and introduction of new biomaterials to support next-generation devices (Kremer et al., 2019). For example, chemical sterilization requires consideration of low non- toxic residues on treated surfaces, in parallel with the benefits of being an antimicrobial process and compatible with a broad range of materials used in medical devices. Some gaseous sterilants, such as VH2O2, have different material compatibility profiles compared with ethylene oxide (EO) (such as packaging materials containing cellulose cannot be practically treated by VH2O2) (McEvoy and Rowan, 2019). Opportunities for new material and biocompatibility research and innovation to advance the medical device industry include material compatibility using alternative sterilization modalities to using EO (such as VH2O2, Nitrogen peroxide, Chlorine dioxide), risk assessment leveraging material compatibility studies between two or more modalities; material compatibility studies of new and novel materials or components (e.g., electronics) in any sterilization modality or modalities; and regulatory case studies related to changing or optimising modalities, or alternative validation approaches. An example of co-application of toxicity testing was reported by Hayes et al. (2013) who developed a range of in vitro toxicity bioassays to assess the efficacy of pulsed plasma gas discharge (oxidative) treatments, where the application of high voltage pulses (16 kV, 10 pps) to gas-injected water (N_2 or O_2, flow rate 2.5 L/min) resulted in the formation of a plasma that generated free radicals, ultraviolet light, acoustic shock waves and electric fields. The antimicrobial effect killed ca. 4 $\log_{10}$ parasitic oocysts in 32 min exposure. Their studies showed the merit of broad toxicity testing including cytotoxic properties (as determined by MTT and neutral red assays), genotoxic properties (as determined by comet and Ames assays), and ecotoxic properties (as determined by Microtox™, Thamnotox™ and Daphnotox™ assays) that supplemented real-time microbial inactivation studies as determined by use of in vitro CaCo-2 tissue culture with qPCR.

6. Use of Quintuple Helix Hubs to advance reprocessing and sterilization of medical device sector

A review of PubMed and Scopus databases over period 2010 to 2023 revealed 78 publications that included the key words “Quadruple Helix”. On review of this list, 70 were not included for the reason that they were not focusing on innovation hubs, for example they included G-quadruplex, telomeric quadruple helix; C-terminal helx, molecular heterogeneity, and metal strings. Exploitation of Quadruple Helix Hub framework has been shown to promote greater engagement with stakeholders and access to specialist equipment for supporting and enabling research and innovation including with a sustainable focus (Malva et al., 2018 Rowan and Casey, 2021; Kulikauskiene, 2021; Zipfel et al. (2022); Cai and Lattu, 2022). Networking of multi-actors to solve challenges presented in the medical device sector can be supported and enabled through a Quintuple-Helix Hub that combines academia, industry, healthcare, regulators and society (Rowan and Casey, 2021). This unifies intellectual and industrial knowledge to holistically address key topics from design to commercialization, where there is a convergence of subject-matter experts with provision for engaging with regulators and society. This concept also ensures that application of digital technologies for transformation of the medtech sector, as applicable, and meets the real-world needs of the industry. This Quintuple Helix can support industry in developing new solutions ranging from compatibility research to new sterilization modalities. This interface between user and regulator can also advance other pressing areas including changes or areas of discussion with international regulatory industries, regulatory innovation approaches with processing (including sterilization) validations or post-market approvals; information and/or promotion of regulatory bodies actively pursuing collaboration to address sterilization capacity issues; use of novel approaches to knowledge management and risk assessment in regulatory submissions; impact of sustainability in the choice and clearance of sterilization modalities; and awareness of benefits of new sustainable sterilization modalities from a societal perspective.

For example, sterilization companies in partnership with universities are developing and deploying state-of-the-art biotechnology tools to unlock real-time microbial inactivation (McEvoy et al., 2021). Immersive (digital)

technologies are also partnering with medtech companies for complex virtual training on specific technical operations. For example, Mersus Technology (Immersive) has partnered with Boston Scientific in Ireland to test and apply an 'Avatar Academy Program' that uses computer gaming to recreate virtual laboratories and cleanrooms; thus, allowing medtech employees to familiarize themselves remotely with a complex work environment and processes. This approach will potentially automate training where one could theoretically run six bespoke training sessions in one day that previously would have taken a month, which can be extrapolated to address the full production chain delivered in a virtual environment (Westmeath Independent, 2020). This Quadruple Helix Hub concept also enables co-creation and design of a life cycle assessment and 360° holistic thinking perspective, thus, unlocking complexity of challenge by converging inputs that is also at the interface between users (OEMS, Healthcare, Sterilization companies, academics) and the regulators. Development and application of living labs concept through this model also addresses knowledge-based innovation systems that includes delivering real-time solutions aligned with Industry 5.0 human centric, such as human interactions with robotics (Archibald et al., 2021; Rowan and Casey, 2021; Kulikauskiene, 2021; Zipfel et al. (2022); Cai and Lattu, 2022). Such an interactive multi-actor model can also address high risk, high gain, deep technical projects that would be relevant to cleaning, disinfection and sterilization including testing and investigating new modalities and new biomaterials for next-generation devices.

There is a need to manage enormous data arising from evaluating cleaning, disinfection and sterilization validations and routine controls, in addition to introducing potentially new design changes to mitigate patient risk, where there are opportunities to manage complex database using artificial intelligence (AI), deep learning/machine learning (ML) and robotics (Gilbert et al., 2021; Aisu et al., 2022; Muehlematter et al., 2021). These sequential or simultaneous steps can be met by applying appropriate statistical analysis and modeling that embraces prediction, simulation, and automation. Such a creative approach to experimental design addresses different control variables, and a decision hierarchy informed by measurements. However, the emergence of AI/ML in medicine also creates system challenges, such as which products should be reviewed by regulators and how can we ensure the safety and effectiveness of AI/ML-based software as a medical device that may change over time as they are applied to new data (Gerke et al., 2020).

7. Sustainability

Supporting "enablers" to sustainability will inform future direction of medical devices. A review of PubMed and Scopus over period 2000 to 2023 revealed 27,804 "Sustainability" publications combined with "reprocessing" and "medical devices" gave 247 publications. Two hundred and fifteen papers were excluded for the reason that they align with specific topic these were focused on life cycle assessment for reprocessed face masks, plastic uses using COVID-9 pandemic, lithium batteries, microbial fuel cells, surgery trays, recycle permeate, photocatalytic treatment of PPE, nuclear waste management, analysis of urine, reusable biosensing element for freshwater toxicity monitoring; toilet flushing, water disinfection; quantum dot fluorescence-based formaldehyde detection; airborne decontamination; contact lens; plastic bedpans; wound care; sustainable energy harvesting techniques; green biocides; detecting organic pollutants; electrochemical membrane bioreactor; hygiene; denture material, germicidal glowsticks; ClO2-generative glovers; haemodialysis; antimicrobial electrospinning, chloroxylenol disinfection by activated sludge; microbial fuel cells; oral candidiasis; central-line associated blood stream infections; spray drying; bioprosthetic heart valves; sustained drug release; electrical potential on chlorine generation; and aerodynamic analysis of SARS-CoV-2 supercritical CO_2 treatment for FFP3s.

Future sustainability for medical device sector can be supported and enabled by the aforementioned Quintuple Helix Hub concept, which is also likely to embrace new digital innovation hubs (for example, where there are 708 new digital innovation hubs in Europe) (Rowan et al., 2022). For example, broad topics of interest that are likely to influence the future sustainability of single-use versus reusable medical devices are presented in Table 2. This highlights the diversity of key topics ranging from resource consumption and emission to global warming impact, which will be met in part through future design thinking, risk modeling and education that also embraces circularity. The recent review of MacNeill et al. (2020) highlighted that the health sector is responsible for 4.6 % of global greenhouse gas emissions of which approximately a quarter originate from the US healthcare system, and appropriately the same proportion of pollutant air emissions. Internationally, a significant proportion of healthcare GHG emissions come from the supply chain; thus, emphasizing this topic of optimal impact for current and future healthcare decarbonization interventions (Watts et al., 2018). The healthcare sector has become increasingly dependent on single-use disposable medical devices, where waste management creates a significant public health burden in terms of environmental pollutants. MacNeill et al. (2020) also noted that such single-use disposable medical devices aptly reflect an inherently unsustainable linear (or "take-make-waste") economy model in which items are produced, used once, and then sent for waste disposable. For example, this linear supply chain model can negatively impact ecology internationally by depleting natural resources along with commensurate excessive production of clinical waste, GHG and other undesirable environmental emissions. An increasing number of life cycle assessment studies comparing single use versus reusable equipment intimate that the former generally result in significantly more petrochemical use and GHG emissions (McGain et al., 2020; Eckelman et al., 2012; Sanchez et al., 2020). A "just-in-time" approach associated with linear supply chain model can reduce storage requirements and product expiration, which reduces healthcare abilities to appropriately manage reusable medical devices. Thus, future consideration should be given to adopting a circular supply chain economy approach in which medical device products are maintained at the highest-value application for as long as possible without sending to disposal. MacNeill et al., 2020 and others (Sherman et al., 2018) have also recently highlighted that reusable medical devices are typically cost-effective over many uses where lifetime costs are significantly lower than that of single-use disposables.

There is an increasing interest in defining and reviewing potential bespoke business models that would be considered potentially appropriate for supporting future sustainability in medical device industry, particularly for the circular economy (Gusso et al., 2020). Healthcare is a resource-intensive and essential ecosystem that generates considerable quantities of diverse waste that varies in non-hazardous to hazardous risk propositions including environmental impact (Minoglou et al., 2017; World Health Organization, 2016). Moultrie et al. (2015) reported that the Medical Device sector significantly contribute to waste generation, particularly when considering single-use plastic and end-of-life devices. Gusso et al. (2020) highlighted the importance of circular strategies for meeting established and emerging sustainable needs of the medical device sector, which are commensurate with the "ecodesign-thinking" concept proposed in this review for medical devices that mitigates waste; yet, satisfies essential functionality and safety requirements from an application and regulatory perspective. Greenhealth Practice (2018) noted that "medical device reprocessing and sterilization of reusable sharps are the main cost-saving initiatives for hospitals in the US". However, it is only recently that a suite of opportunities were suggested in the literature that considers different business model innovations for meeting circularity of single-use and reusable medical devices (Kane et al., 2017; Fargnoli et al., 2018; Gusso et al., 2020). Given the complexity of medical device industry, it remains challenging for healthcare providers to understand and identify a singular appropriate business opportunity that enables and maintains resource cycles. This is complicated by the lack of appropriate published circular case studies that embraces relevant stakeholders (Lewandowski, 2016).

In the medical device industry, the business model structure is a useful conceptual framework to consider real-world circularity applications that must also address risk and safety regulations (Gusso et al., 2020). These authors propose using the main tenets of a business model to consider such strategic opportunities; namely, the value proposition, value creation and

Table 2
Popular topics informing the indicative relevance and future sustainability of single versus reusable medical devices.

Topic(s)	Description of activities	Indicative relevance	Reference
Resource consumption & emissions	➢ Avoiding use of virgin materials and remanufacturing can influence environmental impacts of resource consumption, emissions. ➢ Use of Life Cycle Assessment to inform a pathway to greener processes for medical device and adjacent sectors	Reducing abiotic resource use Contributes new knowledge to the Global Warming impact (GWI) Smart use of LCA tools to inform efficiencies in device design and treatments	Peters (2016) Zhang et al. (2020) Baboudijan (2022)
Circularity assessment environmental Impact assessment LCA assessments	➢ Sustainable studies describe 16 different environmental impact categories highlighting superior use of reprocessed devices over single use in 13 categories (electrophysiology catheter). Also informed by LCA. ➢ Categories include ozone depletion; climate change; photochemical ozone formation; Eutrophication (marine and freshwater), Ionising radiation – human health, land use, non-cancer human effects, resource use, energy carriers, respiratory inorganics [Disease incidences], waste scarcity, Cancer human effects	Healthcare could cut emissions by half for some devices if opting for regulated, reprocessed items. Suite of environmental and technical categories to evaluate relevance of medical devices materials and reusability across technological readiness level from discovery (TRL 1) to commercial deployment (TRL 9).	Schuelke-Leech (2021)
Global warming impact	➢ Comparison between use of medical remanufacturing route and virgin production disposal route (single use) addressing water, sterilization gas, disinfectents, waste treatment, packaging, transport, plastic production/reprocessing, electricity/fuel	New information and approach to pivot device remanufacturing that can inform global warming	Schuelke-Leech, 2021
Economic modeling	➢ Development of appropriate economic modeling for reuse of medical devices and sustainability	Usefulness of using dedicated models to interpret and simulate to inform economics and risk assessment	MacNeill et al. (2020)
Future terminal sterilization of contaminated medical device waste management	➢ Development technologies for decontamination and reuse of contaminated N95s under EUA with provision for future sustainable waste management ➢ Also describes results for a range of modalities and approaches including simple, affordable options suitable for developing countries for PPE reuse under EUA	Future use of a safe and effective technology to reprocess PPE under EUA so as to safety ensure effective waste management	Alt et al. (2022).
Safety Biocompatability	➢ Consider potentially new disinfection and sterilization modalities and future biomaterial composition from a toxicological end-point perspective	Need to consider development of additional biocompatibility tests under ISO standards to inform sustainability.	Hayes et al. (2013)
Recycling challenges	➢ Recycling of complex medical device products needs extensive material flow analysis to make it economically and ecologically reasonable	The more complex a device, the more process steps, energy, and resources are needed for recycling Complex devices may have specific requirements for collection and disposal after use from an infection-prevention perspective and may contain complex materials not suited to municipal waste management & recycling infrastructure (including Green technology)	Gopinath et al., 2020 D'Adamo and Rosa (2016) Eze et al. (2020) Lee et al. (2017)
Profitability, employment opportunities	1. Remanufacturing in medtech sector has high profitability that embraces remanufactured items over virgin products	Potential for increased profitability through remanufacturing over reliance on using virgin products.	D'Adamo and Rosa (2016)
CE concept using R-strategies	➢ Design smarter [Refuse, Rethink, Reduce] ➢ Extend lifetime [Reuse, Repair, Refurbish, Remanufacture, Repurpose] ➢ Circularly end-point activities: Recycle and Recover	R strategies broadly considered relevant for extended and circular use in devices that can be informed by smarter designs.	Potting et al., (2017)
Reuse of PVC	➢ Recycle of Polyvinyl Chloride (PVC) several times (widely used plastic in devices) without loss of critical properties	Opportunities to reuse materials from a resource efficiency perspective	I'Ons (2021)
Design thinking	➢ Design medical devices smarter for circularity that includes appropriateness for reprocessing and sterilization ➢ Design from day one with disassembly and cleaning in mind, including reducing number of device components	Design thinking in medical devices is critical to unlocking efficiencies in usage and automation; thus enabling future sustainability	I'Ons (2021)
Rapid diagnostics Automation	➢ Efficacy for real-time determination of device cleanliness, reprocessing and terminal sterilization potentially reducing disinfectant and sterilant use.	Opportunities to use rapid diagnostics to improve turn-around of reprocessing and potentially amount of sterliant use	McEvoy et al., 2021
Improve energy efficiency	➢ Additive manufacturing can reduce material waste by as much as 90 % compared to conventional manufacturing and can speed up device prototyping and testing	Improving energy efficiency and opting for clean energy source could reduce overall costs	I'Ons (2021)
Logistical and design challenge	➢ Consider device materials in sustainable design	For example, disposable surgical drapes contain polypropylene and polyethylene, each can be recycled, but used together they cannot be recycled	La Plante (2022)
Reduce carbon footprint	➢ Recycled materials can be used without loss of technical properties or need for addition of virgin materials	For example, recycled polyethylene terephthalate (PET) has 79 % lower GHG emissions that virgin PET	La Plante (2022)
Multi-actor collaborations	➢ Work with Medical Device component and OEM manufacturers to advance circular medical device production, and to move away from traditional "take-make-waste" linear systems.	Smart approaches for stakeholders to holistically address issues to inform more efficient means of material use/reuse	La Plante (2022) Rowan and Laffey (2020)
Role of Supply Chain and Transport	➢ Steps are to reduce energy, water and chemical use	For example, reduce transport of waste from used medical devices by recycling in same region to reduce carbon footprint	La Plante (2022)
Microbial inactivation Modeling	➢ Mathematical modeling of inactivation to inform modality efficiencies ➢ Sustainable solutions (e.g, biofilms) for reprocessing	For example, longitudinal modeling to confirm key factors influencing or governing sustainability for device industry and nexus to policy and standards.	Feurhuber et al. (2022) Alfa (2009) Rowan and Moral (2021) Rowan et al. (2015)
Risk Modeling Machine learning Robotics	➢ Use of machine learning to address risks given complexity of database sets spanning processes	Risk characterization for end to end device production	Njage et al. (2019) Zhang et al. (2017) Allescher et al. (2022).

(continued on next page)

Table 2 (*continued*)

Topic(s)	Description of activities	Indicative relevance	Reference
Research translation, Training, Education, Advocacy	➢ Environmental sustainability research in anaesthesia and critical care for circularity ➢ Moving beyond clinical care, energy (renewables vs fossil fuel) and energy efficiency are important influencers in healthcare's ecological footprint.	The critical role of education and training in device manufacture and reuse from an ecological (healthcare) footprint that spans end-to-end cycle.	McGain et al. (2020).

delivery, and value capture. Gusso et al. (2020) also intimated that these business models must also align with 'criticality' according to risk level to the patient with type of contact, which supports and corroborates this review. This criticality analysis dimension considers Spaulding's classification system for devices along with a linked economic orientated endeavour (Kane et al., 2017). This circular framework for medical devices will also facilitate 'green servitization' that considers how device OEMs can also create a supply chain circularity through reprocessing (Benedettini, 2022). Such innovative business models are timely given stakeholder publications focused on defining healthcare guidelines for disinfection and sterilization of instruments in centralized SSD that recognises a pressing need to address single-use medical devices from an environmental footprint and waste management perspective (Ling et al., 2018). Such opportunities also highlight the importance of understanding the pivotal role of OEMs in effective device cleaning and processing. In addition, the challenges of servicing, maintaining and applying reprocessing and sterilization modalities for a plethora of different devices in healthcare facilities are considerable. Moreover, there is a commensurate need to consider training of healthcare staff given increasing complexity of medical equipment and increasing level of sophistication associated with OEM's instructions for use (Ling et al., 2018). Gusso et al. (2020) proposed nine potential circular business models (CBMs) for meeting established and emerging needs of medical devices that considers technical cycles (repair and maintenance, reuse and redistribution, refurbishment and remanufacturing, and recycling), value (high, medium, low), and criticality (critical, semi-critical and non-critical). These CBMs comprise (a) full-care equipment as a service, such as Medigo-Rent, (b) In-house lifecycle, such as STERIS Service contracts, (c) Support for hospital-based reprocessing, such as Medivators-Renatron, (d) mobile solutions, such as Shared Medical Solutions, (e) platform for devices circulation, such as Pioneer Medical Devices, (f) Refurbished system, such as Philips–Smart Path, (g) Full-provision of reprocessed devices, such as Sterimed, a J&J company, (h) End-of-Life Equipment collection, such as Advanced Technology Recycling, and (i) Continued collection of disposable, such as BD ecoFinity Life Cycle Solution (Gusso et al., 2020). Wilson and Nayak (2016) considered pros and cons of reusable medical devices versus single-use items and noted that the former may offer improved clinical performance and are likely to be less expensive; however, reusable devices present a risk of cross-infection, their performance may deteriorate with repeated use, there is environmental costs of decontamination, and healthcare workers are potentially exposed to chemicals and biohazards during decontamination.

However, there is commensurate need to consider the main underpinning tenets of what constitutes increasing sustaining or disruptive business practices in medical device sector in order to comprehensively appreciate and adopt appropriate CBMs for future circularity (Schuelke-Leech, 2018; Rowan, 2019; Schuelke-Leech, 2021). In addition, it is likely that these established and emerging CBMs will be actualized by addressing risk mitigation, corporate governance and digital transformation including Industry 5.0 (Rowan and Galanakis, 2020). Domegan (2021) also noted that in such complex settings, the call to action is large-scale behaviour change. This can be met in part by social marketing that "examines the interface of human and natural systems and their interconnected dynamic forces as a powerful means of influencing behaviours for the accorded transformation and betterment of individuals, communities, society and the planet." In addition, there is a commensurate need to define and include additional sustainable measurement tools beyond LCA for circularity.

8. Summary

Modern medicine and adjacent STEM disciplines are substantially more sophisticated and reflect creativity in meeting complex patient needs in an embattled healthcare environment struggling to also cope with surge in antimicrobial resistance to frontline therapeutic interventions. Our understanding and appreciation of microbial opportunistic pathogens (such as viruses, mycobacteria, protozoa, fungi), and infectious agents (prions), has challenged current definitions and expectations of high, intermediate, and low-level disinfection. The margins of safety appear to be set very tight for cleaning and processing many medical devices with complex features, when performed correctly. Given the increased need to meet a near perfect compliance with manufacturer's IFUs in these cases, combined with over-stretched processing departments that need to implement all processes appropriately, the basis of the Spaulding Classification is challenged. Thus, an understanding of the applicability and limitations of different types of disinfection and sterilization methods is essential to ensure safe, effective and appropriate processing of modern-day devices that will address patient risk of mitigating infection (as per Spaulding's classification).

This paper reviewed challenges and limitations of cleaning, disinfection, and sterilization methods for medical device in the context of modern-day practice using Spaulding's Classification as a guiding framework. Given this challenge in terms of evaluating multiple permutations of data governing processing steps including potentially new features, the need for an updated approach is apparent to accommodate the use of tools including new real-time monitoring and diagnostic interventions to supplement contemporary culture-based methods (such as introduction of robotics, automation, machine learning, and new statistical modeling) for evidence-based decision-making. However, a systems based approach will be required to ensure future AI and deep learning/machine-based trustworthiness occurs for the appropriate regulation of software and its applicability for medical devices. Future proofing the medical device industry will also avail of life cycle assessment (LCA) tools and 360° degree holistic thinking to inform next-generation medical devices that embrace future sustainability. The commensurate role of smart bioactive and biodegradable materials for coating medical devices (including biofilm disruptive properties) combined with sustainable processing methods will contribute towards future solutions. The multi-actor use of a new Quintuple Helix Hubs (combining academia-industry-healthcare-regulators-society) coupled with digital transformation (such as Industry 5.0 – human centric concept) (Rowan et al., 2022) will also contribute to the co-creation of next-generation medical device and management models. Addressing efficacy of new design features from an appropriate end-to-end processing perspective that spans technological, policy and societal readiness levels will meet the pressing needs of medtech sector, and holistically inform future sustainability.

CRediT authorship contribution statement

Neil Rowan (NR), Terra Kremer (TK), Gerard McDonnell (GMcD).

Conceptualization (NR, TK, GMcD), Data Curation (NR, TK, GMcD); Formal Analysis (NR, TK, GMcD); Funding Acquisition (NR, TK); Methodology (NR, TK, GMcD); Writing/Original Draft (NR, TK, GMcD); Writing – Review & Editing (NR, TK, GMcD).

Data availability

Data will be made available on request.

Declaration of competing interest

The authors declare no conflict of interest.

Acknowledgements

The authors acknowledge doctorate support funding from Technological University of the Shannon (TUS) – Johnson and Johnson that was awarded to Terra Kremer. We thank Gillian Keane (Momentum Consultants) for assistance with graphics.

References

Abdallah, M., Khelissa, O., Ibrahim, A., Benoliel, C., Heliot, L., Dhulster, P., Chihib, N.E., 2015. Impact of growth temperature and surface type on the resistance of Pseudomonas aeruginosa and Staphylococcus aureus biofilms to disinfectants. Int. J. Food Microbiol. 214, 38–47.

Adrian, B.J., 2019. Epidemiology of cabapenem-resistant gram-negative infections globally. Curr. Opin. Infect. Dis. 32 (6), 609–616.

Aisu, N., et al., 2022. Regulatory-approved deep learning/machine learning-based medical devices in Japan as of 2020A systematic review. PLoS Digital Health 1 (1), e0000001.

Alfa, M., 2009. Modeling microbial survival in buildup biofilm for complex medical devices. BMC Infect. Dis. 9 (56), 1–14.

Alfa, M.J., 2019. Biofilms on instruments and environmental surfaces: do they interfere with instrument reprocessing and surface disinfection? Review of the literature. Am. J. Infect. Control 47, A39–A45.

Alfa, M., Howie, R., 2009. Modeling microbial survival in buildup biofilm for complex medical devices. BMC Infect. Dis. 9, 56. https://doi.org/10.1186/1471-2334-9-56.

Alfa, M.J., Degagne, P., Olson, N., 1999. Worst-case soiling levels for patient-used flexible endoscopes before and after cleaning. Am. J. Infect. Control 27 (5), 392–401.

Allen, J.L., Doidge, N.P., Bushell, R.N., Browning, G.F., Marenda, M.S., 2022. Healthcare-associated infections caused by chlorhexidine-tolerant Serratia marcescens carrying a promiscuous IncHI2 multi-drug resistance plasmid in a veterinary hospital. PLoS One https://doi.org/10.1371/journal.pone.0264848.

Allescher, H.D., Voigt, F., Mangold, M., Haddadin, S., 2022. Integration of robotic in the reprocessing and transfer of endoscopes. Endosc. Int. Open 10 (8), E1022–E1028. https://doi.org/10.1055/a-1789-0532 PMID: 35979027; PMCID: PMC9377825.

Alonso, V.P.P., et al., 2023. Dry surface biofilm in the food processing industry: an overview on surface characteristics, adhesion and biofilm formation, detection and biofilms, and dry sanitation methods. Compr. Rev. Food Sci. Food Saf. 22 (1), 688–713.

Alt, J., Eveland, R., Fiorello, A., Hass, B., Mezzaros, J., McEvoy, B., Ridenour, C., Shaffer, D., Yirava, W., Ward, L., 2022. Development and validation of technologies suitable for the decontamination and re-use of contaminated N95 filtering facepiece respirators in response to the COVID-19 pandemic. J. Hosp. Infect. 119, 141–148. https://doi.org/10.1016/j.jhin.2021.10.004.

Anderson, J.G., et al., 2000. Inactivation of food-borne enteropathogenic bacteria and spoilage fungi using pulsed-light. IEEE Trans. Plasma Sci. 28 (1), 83–88.

Archibald, M., Wiebe, S., Rieger, K., Linton, J., Woodgate, R., 2021. Protocol for a systematic review of living labs in healthare. BMJ Open 11, e039246. https://doi.org/10.1136/bmjopen-2020-039246.

Assefa, M., Amare, A., 2022. Biofilm-associated multi drug resistance in hospital acquired infections: a review. Infect. Drug. Resist. 31 (15), 5061–5068.

Association for the Advancement of Medical Instrumentation, 2011. AAMI TIR30: 2011 a Compendium of Processes, Materials, Test Methods, and Acceptance Criteria for Cleaning Reusable Medical Devices. Association for the Advancement of Medical Instrumentation, s.l.

Association for the Advancement of Medical Instrumentation, 2020. ANSI/AAMI ST79:2017 & 2020 Amendments A1, A2, A3, A4 (Consolidated Text) Comprehensive Guide to Steam Sterilization and Sterility Assurance in Healthcare Facilities. Association for the Advancement of Medical Instrumentation, s.l.

Association for the Advancement of Medical Instrumentation, 2020. AAMI TIR12:2020 Designing, Testing, and Labeling Reusable Medical Devices for Reprocessing in Health Care Facilities: A Guide for Medical Device Manufacturers. Association for the Advancement of Medical Instrumentation, s.l.

Baboudijan, 2022. Life cycle assessment of resuable and disposable cystoscopies: a path to greener urological procedures. Eur Urol Focus. 20. https://doi.org/10.1016/j.euf.2022.12.006.

Balan, G.G., et al., 2019. Duodenoscope-associated infections beyond the elevator channel: alternative causes for difficult reprocessing. Molecules https://doi.org/10.3390/moloecules24122343.

Ball, K., 2000. Reprocessing anaesthesia instruments and devices. CRNA 11 (1), 20–33.

Belle, A., et al., 2020. Impact of the COVID-19 pandemic on gastrointestional endoscopy activity in France. Endoscopy 52 (12), 1111–1115.

Benedettini, O., 2022. Green servitization in the single-use medical device industry: how device OEMs create supply chain circularity through reprocessing. Sustainability 14. https://doi.org/10.3390/su141912670.

Bischoff, M., et al., 2012. First detection of the antiseptic resistance gene qacA/B in enterococcus faecalis. Microb. Drug Resist. 18 (1). https://doi.org/10.1089/mdr.2011.0092.

Bradley, J., Hensley, J.R.M., 2015. Hospital-aquired infections. Sugery (Oxford) 33 (11), 528–533.

Bradley, D., et al., 2012. Studies on the pathogenesis and survival of different culture forms of listeria monocytogenes to pulsed UV light after exposure to mild-food processing stresses. Food Microbiol. 30 (2), 330–339.

Bridier, A., Briandet, R., Thomas, V., Dubois-Brissonnet, F., 2011. Resistance of bacterial biofilms to disinfectants: a review. Biofouling 27, 1017–1032.

Cabronne, A., Thiolet, J.M., et al., 2010. Control of a multi-hospital outbreak of KPC producing Klebsiella pneumoniae type II in France, sept to october 2009. Euro Surveill. 2010, 15.

Cai, Z., Lattu, A., 2022. Triple helix or quadruple helix: which model of innovation to choose for empirical studies. Minerva 60, 257–280.

Campbell Westerway, S., Basseal, J.M., 2022. Endocavity ultrasound transducers: why high-level disinfection is necessary. Ultrschall Med. 43 (2), 204–208.

Casini, B., et al., 2021. Improving the reprocessing quality of flexible thermolabile endoscopes: how to learn from mistakes. Int. J. Environ. Res. Public Health 18 (5), 2482.

Center for Disease Control, 2014. Healthcare associated infection progress report. CDC. https://www.cdc.gov/hai/surveillance/progress-report/index.html Published 2016. Accessed 5 Nov, 2022.

Chemaly, R.F., et al., 2014. The role of the healthcare environment in the spread of multidrug-resistant organisms: update on current best practices for containment. Ther. Adv. Infect. Dis. 2 (3–4), 79–90.

Cieplik, F., et al., 2019. Resistance toward chlorhexidine in oral bacterial – is there cause for concern. Front. Microbiol. https://doi.org/10.3389/fmicb.2019.00587.

Ciusa, M.L., et al., 2012. A novel resistance mechanism to tricolosan that suggests horizontal gene transfer and demonstrates a potential selective pressure for reducing biocide susceptibility in clinical microorganisms. Int. J. Antimicrob. Agents 40 (3), 210–220.

Cloutman-Green, E., et al., 2015. Biochemical and microbial contamination of surgical devices: a quantitative analsyis. Am. J. Infect. Control 559–661.

Cohen, M.E., et al., 2017. Surgical antibiotic prophylaxis and risk for postoperative antibiotic resistant infections. J. Am. Coll. Surgeons 225 (5), 631–638.

da Costa Luciano, C., et al., 2016. Evaluation of the ability of different detergents and disinfectants to remove and kill organisms in traditional biofilms. Am. J. Infect. Control 44, e243–e249.

Crawford, A., 2007. Decontamination and traceability of flexible endoscopes. J. Perioper Pract. 17 (6), 257–260.

D'Adamo, I., Rosa, P., 2016. Remanufacturing in industry; advices from the field. Int. J. Adv. Manuf. Technol. 86, 2573–2584.

Dancer, S.J., 2022. How do biofilms affect surface cleaning in hospitals. Hygiene 2, 132–135.

Dancer, S.J., Stewart, M., Coulombe, C., Gregori, A., Virdi, M., 2012. Surgical site infections linked to contaminated surgical instruments. J Hosp Infect. 81 (4), 231–238.

Dantes, R., Mu, Y., Belflower, R., Aragon, D., Dumyati, G., Harrison, L.H., Lessa, F.C., Lynfield, R., Nadle, J., Petit, S., Ray, S.M., Schaffner, W., Townes, J., Fridkin, S., 2013. Emerging infections program–active bacterial Core surveillance MRSA surveillance investigators. National burden of invasive methicillin-resistant Staphylococcus aureus infections, United States, 2011. JAMA Intern Med. 173, 1970–1978.

Davison, W.M., Pitts, B., Stewart, P.S., 2010. Spatial and temporal patterns of biocide action against Staphylococcus epidermidis biofilms. Antimicrob. Agents Chemother. 54, 2920–2927.

Day, L.W., et al., 2021. Multi-society guideline on reprocessing flexible GI endoscopes and accessories. Gastrointest. Endosc. 93 (1). https://doi.org/10.1016/j.gie.2020.09.048.

De Oliveira Lorena, N.S., et al., 2010. Mycobacterium massiliense BRA100 strain recovered from postsurgical infections: resistance to high concentrations of glutaraldehyde and alternative solutions for high level disinfection. Acta Cir. Bras. 25 (5), 455–459. https://doi.org/10.1590/S0102-86502010000500013.

Deveau, A., et al., 2010. Farnesol induces hydrogen peroxide resistance in Candida albicans yeast by inhibiting the ras-cyclic AMP signaling pathway. Eukaryot. Cell https://doi.org/10.1128/EC.00321-09.

Di Domenico, E.G., Oliva, A., Guembe, M., 2022. The current knowledge on the pathogenesis of tissue and medical device - related biofilm infections. Microorganisms 10 (7), 1259. https://doi.org/10.3390/microorganisms10071259.

Domegan, C., 2021. Social marketing and behavioural change in a systems setting. Curr. Opin. Environ. Sci. Health 23. https://doi.org/10.1016/j.coesh.2021.100275.

Durovic, A., Widmer, A.F., Tschudin-Sutter, S., 2018. New insights into transmission of Clostridium difficile infection – a narrative review. Clin. Microbiol. Infectin 24 (5), 483–492.

Ebigbo, A., et al., 2020. Impact of the COVID-19 pandemic on gastronintestinal endoscopy in Africa. Endosc. Int. Open. 08 (08), 1097–1101. https://doi.org/10.1055/a-1210-4274.

Eckelman, M., Mosher, M., Gonzalez, A., Sherman, J., 2012. Comparative life cycle assessment of disposable and reusable laryngeal mask airways. Anesth. Analg. 114, 1067–1072.

Epstein, L., Hunter, J.C., et al., 2014. New Delhi metallo-beta-lactamase-producing cabapenem-resistant Escherichia coli associated with exposure to duodenoscopes. JAMA 312, 1447–1455.

Eze, S., Ijomah, W., Wong, T.C., 2020. Remanufacturing: a potential sustainable solution for increasing medical device equipment availability. J. Manuf. 10, 141–159.

Fagerlund, A., Møretrø, T., Heir, E., Briandet, R., Langsrud, S., 2017. Cleaning and disinfection of biofilms composed of listeria monocytogenes and background microbiota from meat processing surfaces. Appl. Environ. Microbiol. https://doi.org/10.1128/AEM.01046-17.

Fargnoli, M., Costantino, F., Di Gravio, G., Tronci, M., 2018. Product service-systems implementation: a customized framework to enhance sustainability and customer satisfaction. J. Clean. Prod. 188, 387–401.

Farrell, H., Hayes, J., Laffey, J., Rowan, N., 2013. Studies on the relationship between pulsed UV light irradiation and the simultaneous occurrence of molecular and cellular damage in clinically-relevant Candida albicans. J. Microbiol. Methods 84 (2), 317–326.

Feng, G., Huang, H., Chen, Y., 2021. Effects of emerging pollutants on the occurrence and transfer of antibiotic resistance genes: a review. J. Hazard. Mater. 420, 126602.

Feurhuber, M., et al., 2022. Mathematically modelling the inactivation of Geobacillus stearothermophlus spores: effects of sterilization environments and temperature profiles. Phys. Med. 13. https://doi.org/10.1016/j.phmed.2021.100046.
Foliente, R.L., et al., 2001. Efficacy of high-level disinfectants for reprocessing GI endoscopes in simulated-use testing. Gastrointest. Endosc. 53 (4), 456–462.
Food and Drug Administration, n.d.Food and Drug Administration (n.d.). FDA-cleared sterilants and high level disinfectants with general claims for processing reusable medical and dental devices. Available from: https://www.fda.gov/medical-devices/reprocessing-reusable-medical-devices-information-manufacturers/fda-cleared-sterilants-and-high-level-disinfectants-general-claims-processing-reusable-medical-and. Accessed November, 2022.
Forman, M.E., et al., 2016. Structure-resistance relationships: interrogating antiseptic resistance in bacteria with multicationic quaternary ammonium dyes. ChemMedChem 11 (), 958–962. https://doi.org/10.1002/cmdc.201600095.
Garvey, M., Meade, E., Rowan, N.J., 2022. Effectiveness of front line and emerging fungal disease prevention and control interventions and opportunities to address appropriate eco-sustainable solutions. Sci. Total Environ. 851 (2). https://doi.org/10.1016/j.scitotenv.2022.158284.
Gerke, S., Babic, B., Evgeniou, T., Cohen, G., 2020. The need for a system view to regulate artificial intelligence/machine learning-based software as medical device. NPJ Digit. Med. 3 (1), 1–4.
Gilbert, S., et al., 2021. Algorithm change protocols in the regulation of adaptive machine learning-based medical devices. J. Med. Internet Res. 23 (10), e30545.
Gomez, A., et al., 2016. Triclosan-induced genes Rv1686c-Rv1687c and Rv3161c are not involved in triclosan resistance in Mycobacterium tuberculosis. Scientific Report 6, 26221. https://doi.org/10.1038/srep26221.
Gopinath, K.P., et al., 2020. A crucial review of the influence of energy, environmental and economic factors on various processes used to handle and recycle plastic wastes: development of a comprehensive index. J. Clean Prod. 274, 123031.
Greenhealth Practice, 2018. Engaged Leadership and the value of sustainable healthcare. https://greenu.miami.edu/_assets/pdf/engaged_leadership_report2018pgh.pdf (accessed 22 Feb, 2023).
Griffiths, P.A., Babb, J.R., Bradley, C.R., Fraise, A.P., 1997. Glutaraldehyde-resistant mycobacterium chelonae from endoscope washer disinfectors. J. Appl. Microbiol. 82, 519–526.
Griffiths, P.A., et al., 1997. Glutaraldehyde-resistant mycobacterium chelonae from endoscope washer disinfectors. J. Appl. Microbiol. 85, 519–526.
Gusso, D., Carvalho, M.M., Balkenende, R., Mascarenhas, J., 2020. Circular business models in the medical device industry: paths towards sustainable healthcare. Resour. Conserv. Recycl. 160. https://doi.org/10.1016/j.resconrec.2020.104904.
Han, Y., et al., 2019. The impact and mechanism of quaternary ammonium compounds on the transmission of antibiotic resistance genes. Environ. Sci. Pollut. Res. 26, 28252–28360.
Han, Y., Zhou, Z.C., Zhu, L., et al., 2019. The impact and mechanism of quaternary ammonium compounds on the transmission of antibiotic resistance genes. Environ. Sci. Pollut. Res. 26, 28352–28360. https://doi.org/10.1007/s11356-019-05673-2.
Hayes, J., Kirf, D., Garvey, M., Rowan, N., 2013. Disinfection and toxicological assessments of pulsed UV and pulsed-plasma gas-discharge treated-water containing the waterborne protozoan enteroparasite Cryptosporidium parvum. J. Microbiol. Methods 94 (3), 325–337. https://doi.org/10.1016/j.mimet.2013.07.012.
Huang, Y.-H., et al., 2016. Functional characterization of triclosan-resistant enoyl-acyl-carrier protein reductase (FabV) in Pseudomonas aeruginosa. Frong. Microbiol. 29. https://doi.org/10.3389/fmicb.2016.01903.
I'Ons, G., 2021. Optimising end-to-end sustainability for single-use devices. Med-Tech Innovation News. https://www.med-technews.com/medtech-insights/medtech-materials-and-assembly-insights/green-goals-optimising-end-to-end-sustainability-for-single-/ (accessed 29 November, 2022).
International Organization for Standardization, 2009. ISO 15883-1 Washer-disinfectors - Part 1: General Requirements, Terms and Definitions and Tests. s.l.: International Organization for Standardization.
Jacquel, B., et al., 2021. A Trade-off Between Stress Resistance and Tolerance Underlies the Adaptive Response to Hydrogen Peroxide. bioRxiv https://doi.org/10.1101/2021.04.23.440814 (accessed 29 November, 2022).
Jamal, M., Ahmad, W., Andleeb, S., Jalil, F., Imran, M., Nawaz, M.A., Hussain, T., Ali, M., Rafiq, M., Kamil, M.A., 2017. Bacteria biofilms and associated infections. J. Chin. Med. Assoc. 81 (1), 7–11.
Kampf, G., Ostermeyer, C., Tschudin-Sutter, S., Widmer, A.F., 2013. Resistance or adaptation? How susceptible is a 'gluteraldehyde-resistant' Psedomonoas aerugionosa isolate in the absence of selection pressure. J. Hosp. Infect. 84, 316–318.
Kane, G.M., Bakker, C.A., Balkenende, A.R., 2017. Towards design strategies for circular medical products. Resour. Conserv. Recycl. 0–1. https://doi.org/10.1016/j.resonrec.2017.07.030.
Kathryn Gold, V.H., 2013. Cleaning assessment of disinfectant cleaning wipes on an external surface of a medical device contaminated with artificial blood or streptococcus pneumonia. Am. J. Infect. Control 41, 901–907.
Kenters, N., et al., 2018. Worldwide practices on flexible endoscope reprocessing. Antimicrobi Resist. Infect. Control 7, 153. https://doi.org/10.1186/s13756-018-0446-6 eCollection 2018.
Khan, R., et al., 2018. Biochemical and structural basis of triclosan resistance in a novel enoyl-acyl carrier protein reductase. Antimicrobial Agents and Chemotherapy. 62, e00648-18. https://doi.org/10.1128/AAC.00648-18.
Kim, S., Russel, D., Mohamadnejad, M., et al., 2016. Risk factors associated with the transmission of carbapenem-resistant enteriobacteriaceae via contaminated duodenoscopes. Gastointest. Edosc. 83, 1121–1129.
Kim, S.-H., et al., 2020. A triclosan-resistance protein from the soil metagenome in a novel enoyl-acyl carrier protein reductase: Structure-guided functional analysis. FEBS J 287, 4710–4728.
Klacik, S.G., 2019. Transitioning from high-level disinfection to sterilization for semi-critical devices. Horizons Summer. 2019 (6).
Kola, A., Piening, B., et al., 2015. An outbreak of carbapenem-resistant OXA-48-producing Klebsiella pneumoniae associated with duodenoscopy. Antimicrob. Resist. Infect. Control 4, 8.
Kremer, T.A., 2021. Material adhesion comparison of test soils for reusable device cleaning efficacy. Zentralsterilization 29 (3), 166–172.
Kremer, T.A., 2021. Thermal disinfection validation: the relationship between A0 and microbial reduction. Biomedical Instrumentation & Technology 29–34.
Kremer, T., et al., 2019. Protein residuals on reusable medical devices and patient saftey impact. Zentral Sterilization 37.
Kremer, T.A., et al., 2021. Material adhesion comparison of test soils for reusable device cleaning efficacy. Zentralsterilization 29 (3), 166–172.
Kremer, T.A., et al., 2021. Assessing detergent residuals for reusable device cleaning validations. Biomed. Instrum. Technol. 165–170.
Kremer, T.A., et al., 2021. Connecting Across Competencies: Leveraging Best Practices for Processing. Industrial Sterilization: Challenging the Status Quo, Driving for Continuous Improvement, pp. 6–11 Volume Spring.
Kremer, T.A., et al., 2022. A standardized method for evaluating test soils used to demonstrate cleaning efficacy. J. Hosp. Infect. 126 (2022), 52–55.
Kulikauskiene, K., 2021. The theoretical quadruple helix model for digital inclusion increase. Sciendo https://doi.org/10.1515/mosr-2021-0002.
Kwakman, J.A., Rauwers, A.W., Klaassen, C.H.W., Bruno, M.J., Vos, M.C., 2021. Investigation of possible transmission of a susceptible microorganism through a contaminated duodenoscope; a case report. Antimicrobial resistance and infection. Control 10 (127). https://doi.org/10.1186/s13756-021-00996-7.
Kwakman, J.A., Erler, N.S., Vos, M.C., Bruno, M.J., 2022. Risk evaluation of duodenoscope-associated infections in the Netherlands calls for a heightened awareness of device-related infections: a systematic review. Endoscopy 54, 148–155.
La Plante, B., 2022. How to design medical devices with sustainability in mind. Med Device Online. https://www.meddeviceonline.com/doc/how-to-design-medical-devices-with-sustainability-in-mind-0001 (accessed 29 Nov, 2022).
Ladicevic, B., de Besten, H.M.W., de Biase, D., 2022. Landscape of stress response and virulence genes among listeria monocytogenes strains. Front. Microbiol. https://doi.org/10.3389/fmicb.2021.738470.
Lee, C.-M., Woo, W.-S., Roh, Y.-H., 2017. Remanufacturing: trends and issues. Int. J. Precis. Manufact. Green Technol. 4, 113–125.
Lewandowski, M., 2016. Designing the business models for circularity economy – towards the conceptual framework. Sustainability https://doi.org/10.3390/su8010043.
Li, X., Tao, J., Han, J., et al., 2014. The gain of hydrogen peroxide resistance benefits growth fitness in mycobacteria under stres. Protein Cell 5, 182–185. https://doi.org/10.1007/s13238-014-0024-5.
Ling, M.L., Ching, P., Widitaputra, A., Stewart, A., Sirijindadirat, N., Thu, L.T.A., 2018. APSIC guidelines for disinfection and sterilization of instruments in health care facilities. Antimicrob. Resist. Infect. Control. 7 (25). https://doi.org/10.1186/s13756-018-0308-2.
Link, T., 2018. Guideline implementation: manual chemical high level disinfection: 1.5 www.Aornjournal.org/content/cme. AORN J. 108 (4), 399–410.
Lipscomb, I.P., 2007. Effect of drying time, ambient temperature and pre-soaks on prion-infected tissue contamination levels on surgical stainless steel: concerns over prolonged transportation of instruments from theatre to central sterile service departments. J. Hosp. Infect. 65, 72–77.
MacNeill, A.J., et al., 2020. Transforming the medical device industry: road map to a circular economy. Health Aff. 39 (12), 2088–2097.
Malva, J.O., et al., 2018. The quadruple helix-based innovation model of reference sites for active and healthy aging in Europe: the Ageing@Coimbra case study. Front. Med. 5, 132. https://doi.org/10.3389/fmed.2018.00132.
Marchi, E., et al., 2015. Novel insight into antimicrobial resistance and sensitivity phenotypes associated with qac and norA genotypes in Staphylococcus aureus. Microbiol. Res. 170, 184–194.
Marsh, J.W., et al., 2015. Genomic epidemiology of an endoscope-associated outbreak of Klebsiella pneumoniae carapenemase (KPC)-producing K. pneumoniae. PLoS One 10, E0144310.
Masterson, K., 2021. Development of a low-temperature extrusion process for production of GRAS bioactive-polymer loaded compounds for targeting antimicrobial-resistant (AMR) bacteria. Sci. Total Environ. 800. https://doi.org/10.1016/j.scitotenv.2021.149545.
McDonnell, G.E., 2017. Antisepsis, Disinfection, and Sterilization: Types, Action, and Resistance. 2nd edition. ASM Press, Washington DC.
McDonnell, G., Burke, P., 2011. Disinfection: is it time to reconsider Spaulding? J. Hosp. Infect. 78, 163–170.
McDonnell, G., Hansen, J., 2020. Block's Disinfection, Sterilization, and Preservation. 6th edition. Wolters Kluwer, Philadelphia.
McDonnell, G., OSMA Anti-Infective Working Group, 2022. Initiating Implant Infection Innovation. Orthopedic Design & Technology. September/October 2022 https://www.odtmag.com/issues/2023-09-01/view_features/initiating-implant-infection-innovation.
McDonnell, G., et al., 2020. Principles of antimicrobial activity. In: Gerald McDonnell, J.H. (Ed.), Block's Disinfection, Sterilization and Preservation, Sixth edition Wolters Kluwer, Philadelphia, pp. 68–119.
McEvoy, B., Rowan, N.J., 2019. Terminal sterilization of medical devices using vaporized hydrogen peroxide: a review of current methods and emerging opportunities. 127 (5), 1403–1420.
McEvoy, B., Lynch, M., Rowan, N.J., 2021. Opportunities for the application of real-time bacterial cell analysis using flow cytometry for the advancement of sterilization microbiology. J. Appl. Microbiol. 130 (6), 1794–1812.
McEvoy, B., Maksimovic, A., Rowan, N.J., 2023. Geobacillus stearothermophilus and Bacillus atrophaeus spores exhibit linear inactivation kinetic performance when treated with an industrial scale vaporized hydrogen peroxide (VH_2O_2) sterilization process. J. Appl. Microbiol. 134 (1), lxac028. https://doi.org/10.1093/jambio/lxac028.

McGain, F., Muret, J., Lawson, C., Sherman, J.D., 2020. Environmental sustainability in anaesthesia and critical care. Br. J. Anaesth. 125 (5), 680–692.
Minbiole, K.P.C., et al., 2016. From antimicrobial activity to mechanism of resistance: the multifaceted role of simple quaternary ammonium compounds in bacterial eradication. Tetrahedron 72, 3559–3566.
Minoglou, M., Gerassimidou, S., Komilis, D., 2017. Healthcare Waste Generation Worldwide and Its Dependence on Socio-economic and Environmental Factors. https://doi.org/10.3390/su9020220.
Morrison, K.R., et al., 2019. More QACs, more questions: recent advances in structure activity relationships and hurdles in understanding resistance mechanism. Tetrahedron Lett. 60. https://doi.org/10.1016/j.tetlet.2019.07.026.
Moultrie, J., Sutcliffe, L., Maier, A., 2015. Exploratory study of the state of environmentally conscious design in the medical device industry. J. Clean. Prod. 108, 363–378.
Muehlematter, U.J., Daniore, P., Vokinger, K.N., 2021. Approval of artificial intelligence and machine-based medical devices in the USA and Europe (2015–20): a comparative analysis. Lancet Digit. Health 3 (3), e195–e203.
Njage, P.M.K., et al., 2019. Improving hazard characterization in microbial risk assessment using next generation sequencing data and machine learning: predicting clinical outcomes in shigatoxigenic Escherichia coli. Int. J. Food Microbiol. 292, 72–82.
O'Horo, J.C., et al., 2016. Carbapenem-resistant enterobacteriaceae and endoscopy: an evolving threat. Am. J. Infect. Control. 44 (9), 1032–1036.
Ofstead, C.I., et al., 2010. Endoscope reprocessing methods: a prospective study on the impact of human factors and automation. Gastroenterol. Nurs. 33, 304–311.
Ofstead, C.L., Quick, M.R., Eiland, J.E., Adams, S.J., 2017. A glimpse at the true cost of reprocessing endoscopes: results of a pilot project. Communique 63–78.
Olfasdottir, L.B., et al., 2017. Adenosine triphosphate quantification correlates poorly with microbial contamination of duodenoscopes. Infect. Control Hosp. Epidemiol. 38, 678–684.
Otter, J.A., et al., 2016. Transmission of SARS and MERS coronaviruses and influenza virus in healthcare settings: the possible role of dry surface contamination. J. Hosp. Infect. 92 (3), 235–250.
Pang, X., et al., 2019. Biofilm formation of listeria monocytogenes and its resistance to quaternary ammonium compounds in a simulated salmon processing environment. Food Control 98, 200–208.
Pendarkar, A.V., et al., 2018. Outpatient spine surgery: defining the outcomes, value and barriers to implementation. Neurosurg. Focus. 44 (5), 1–11. https://doi.org/10.3171/2018.2.FOCUS17790.
Percival, S.L., Suleman, L., Vuotto, C., Donelli, G., 2015. Healthcare-associated infections, medical devices and biofilms, risk, tolerance and control. J. Med. Microbiol. 84 (4). https://doi.org/10.1099/jmm.0.000032.
Perry, A.F., et al., 2012. Burden of gastrointestinal disease in the United States: 2012 update. Gastroenterolology 143, 1179–1187.
Peters, K., 2016. Methodological issues in life cycle assessment for manufactured products: a critical review of existing studies and an illustrative case study. J. Clean. Prod. 126, 21–37.
Potting, J., et al., 2017. Circular Economy: Measuring Innovation in the Product Chain. PBL Publishers: Netherlands Environmental Assessment Agency, The Hauge, The Netherlands.
Pynnonen, M.A., Whelan, J., 2019. Reprocessing flexible endoscopes in the otolaryngology clinic. Otolaryngol. Clin. N. Am. 52 (30), 391–402.
Quinn et al., n.d.Quinn MM, Henneberger PK, National Institute for Occupational Safety and Health (NIOSH), National occupational research agenda (NORA) cleaning and disinfecting in healthcare working group, Braun B, Delclos GL, Fagan K, Huang V, Knaack JL, Kusek L, Lee SJ, Le Moual N, Maher KA, SH MC, Mitchell(n.d.)
Rahman, M.R., Perisetti, A., Coman, R., et al., 2019. Duodenoscope-associated infections: update on an emerging problem. Dig. Dis. Sci. 64 (6), 1409–1418.
Rohm-Rodowald, E., Jakimiak, B., 2004. Assessment of the sterilization of medical devices- an important challenge to health care in Poland. Przegl. Epidemiol. 58 (3), 501–510.
Rowan, N.J., 1999. Evidence that inimical food preservation barriers alter microbial resistance, cell morphology and virulence. Trends Food Sci. Technol. 10 (8), 261–270.
Rowan, N.J., 2019. Pulsed light as an emerging technology to cause disruption for food and adjacent industries – quo vadis? Trends Food Sci. Technol. 88, 316–332. https://doi.org/10.1016/j.tifs.2019.03.027.
Rowan, N.J., 2022. The role of digital technologies in supporting and improving fishery and aquaculture across the supply chain – quo vadis? Aquacult. Fish. https://doi.org/10.1016/j.aaf.2022.06.003.
Rowan, N.J., Casey, O., 2021. Empower eco multiactor HUB: a triple helix 'academia-industry-authority' approach to creating and sharing potentially disruptive tools for addressing novel and emerging new green Deal opportunities under a United Nations sustainable development goals framework. Curr. Opin. Environ. Sci. Health 21. https://doi.org/10.1016/j.coesh.2021.100254.
Rowan, N.J., Galanakis, C.M., 2020. Unlocking challenges and opportunities presented by COVID-19 pandemic for cross-cutting disruption in agri-food and green deal innovations: quo vadis? Sci. Total Environ. 748. https://doi.org/10.1016/j.scitotenv.2020.141362.
Rowan, N.J., Laffey, J.G., 2020. Challenges and solutions for addressing critical shortage of supply chain for personal and protective equipment (PPE) arising from Coronavirus disease (COVID19) pandemic - Case study from the Republic of Ireland. Sci. Total Environ. 127.. https://nam11.safelinks.protection.outlook.com/?url=https%3A%2F%2Fdoi.org%2F10.1016%2Fj.scitotenv.2020.138532&data=05%7C01%7Cp.das%40elsevier.com%7C7b97f5098ab04b9865fd08db2f5e7030%7C9274ee3f94254109a27f9fb15c10675d%7C0%7C0%7C638155854889084994%7CUnknown%7CTWFpbGZsb3d8eyJWIjoiMC4wLjAwMDAiLCJQIjoiV2luMzIiLCJBTiI6Ik1haWwiLCJXVCI6Mn0%3D%7C3000%7C%7C%7C&sdata=reE3sNY%2F9IWsLtU2DUc6y2O%2F1DR1HkUwzp7bx%2BM9sL4%3D&reserved=0.
Rowan, N.J., Moral, R.A., 2021. Disposable face masks and reusable face coverings as non-pharmaceutical interventions (NPIs) to prevent transmission of SARS-CoV-2 variants that cause coronavirus disease (COVID-19): role of new sustainable NPI design innovations and predictive mathematical modeling. Sci. Total Environ. 772. https://doi.org/10.1016/j.scitotenv.2021.145530.
Rowan, N.J., et al., 2000. Virulent rough filaments of listeria monocytogens from clinical and food samples secreting wild type levels of cell-free p60 protein. J. Clin. Microbiol. 38 (7), 2643–2648.
Rowan, N.J., Candlish, A.A., Bubert, A., Anderson, J.G., Kramer, K., McLauchlin, J., 2000 Jull. Virulent rough filaments of listeria monocytogenes from clinical and food samples secreting wild-type levels of cell-free p60 protein. J. Clin. Microbiol. 38 (7), 2643–2648. https://doi.org/10.1128/JCM.38.7.2643-2648.2000.
Rowan, N.J., Anderson, J.G., Candlish, A.A.G., 2001. Cellular morphology of rough forms of listeria monocytogenes isolated from clinical and food samples. Lett. Appl. Microbiol. 31 (40, 319–322.
Rowan, N.J., et al., 2009. Studies on the susceptibility of difference culture morphotypes of listeria monocytogenes to uptake and survival in human polymorphonuclear leukocytes. FEMS Immunol. Med. Microbiol. 57 (2), 183–192.
Rowan, N.J., Valdramidis, V.P., Gomez-Lopez, V.M., 2015. A review of quantitative methods to describe efficacy of pulsed light generated inactivation data that embraces the occurrence of viable but non culturable state microorganisms. Trends Food Sci. Technol. 44 (1), 79–92. https://doi.org/10.1016/j.tifs.2015.03.006.
Rowan, N.J., Meade, E., Garvey, M., 2021. Efficacy of frontline chemical biocides and disinfection approaches for inactivating SARS-CoV-2 variants of concern that cause coronavirus disease with the emergence of opportunities for green eco-solutions. Curr. Opin. Environ. Sci. Health 23. https://doi.org/10.1016/j.coesh.2021.100290.
Rowan, N.J., Murray, N., Qiao, Y., O'Neill, E., Clifford, E., Barcelo, D., Power, D.M., 2022. Digital transformation of peatland eco-innovations ('Paludiculture'): enabling a paradigm shift towards the real-time sustainable production of 'green-friendly' products and services. Sci. Total Environ. 838 (3). https://doi.org/10.1016/j.scitotenv.2022.156328.
Rtimi, S., et al., 2019. Advances in catalytic/photocatalytic bacterial inactivation by nano Ag amd Cu coated surfaces and medical devices. Appl. Catal. B Environ. 240, 291–318.
Rutala, W.A., Weber, D.J., 2016a. Disinfection, sterilization and antisepsis: An overview. Am. J. Infect. Control. 44 (5), 1–6. https://doi.org/10.1016/j.ajic.2015.10.038.
Rutala, W.A., 2019. Reprocessing semicritical items: outbreaks and current issues. Am. J. Infect. Control 47, A79–A89.
Rutala, W.A., Weber, D.J., 2019. Disinfection, sterilization, and antisepsis: an overview. Am. J. Infect. Control 47, A3–A9.
Rutala, W.A., 2019. Best practices for disinfection of noncritical environmental surfaces and equipment in health care facilities: a bundle approach. Am. J. Infect. Prevent. 47, A96–A105.
Rutala, W.A., Weber, D.J., 2016b. Outbreaks of carbapenem-resistant enterobacteriaceae infections associated with duodenoscopes: what can we do to prevent infections? Am. J. Infect. Control 44 (Suppl), 47–51.
Saliou, P., et al., 2016. Microbiological evaluation of cystoscope reprocessing at Brest university hospital from january 2007 through december, 2014. Prog. Urol. 26 (2), 103–107.
Sanchez, S.A., Echelman, M.J., Sherman, J.D., 2020. Environmental and economic comparison of reusable and disposable blood pressure cuffs in multiple clinical settings. Resour. Conserv. Recycl. 155, 104643.
Schuelke-Leech, B.A., 2018. A model for understanding the orders of magnitude of disruptive technologies. Technol. Forecast. Soc. Chang. 129, 261–274.
Schuelke-Leech, B.A., 2021. Disruptive technologies for a green new Deal. Curr. Opin. Environ. Sci. Health 21. https://doi.org/10.1016/j.coesh.2021.100245.
Seoane-Vazquez, E., et al., 2007. Endoscopy-related infections and toxic reactions: an international comparison. Endoscopy 39 (8), 742–778.
Shang, S., Gibbs, Sara, Henao-Tamayo, M., Shanley, C.A., McDonnell, G., Silva Duarte, R., Ordway, D.J., Jackson, M., 2011. Increased virulence of an epidemic strain of Mycobacterium masiliense in mice. PLoS One 6 (9), e24726.
Shenoy, E.S., Pierce, W.M., et al., 2019. Transmission of mobile colistin resistance (mcr-1) by duodenoscope. Clin. Infect. Dis. 68, 1327–1334.
Sherman, J.D., Raibley 4th, L.A., Eckelman, M.J., 2018. Life cycle assessment of costing methods for device procurement: comparing reusable and sing-use disposable laryngoscopes. Anesth. Analg. 127 (2), 434–443.
Smith, K., Hunter, I.S., 2008. Efficacy of common hospital biocides with biofilms of multidrug resistant clinical isolates. J. Med. Microbio. 57 (8), 966–973.
Smith, Z.L., et al., 2015. Transmission of cabapenem-resistant enterbacteriacease during ERCP: time to revisit the current reprocessing guidelines. Gastrointest. Endosc. 81, 1041–1045.
Snyder, G.M., et al., 2017. Randomized comparison of 3 high-level disinfection and sterilization procedures for duodenoscopes. Gastroenterology 153 (4), 1018–1025.
Spaulding, E., 1968. Chemical disinfection of medical and surgical materials. In: Lawrence, C. (Ed.), Block Disinfection, Sterilization, and Preservation. Lea & Febiger, Philadelphia, pp. 517–531.
Stone, P.W., 2009. Economic burden of healthcare-associated infections: an American perspective. Expert Rev Pharmacoecon Outcomes Res 9 (5), 417–422. https://doi.org/10.1586/erp.09.53.
Su, Y., Yrastorza, J.T., Matis, M., Curick, J., Zhao, S., Wang, G., Xie, J., 2022. Biofilms: formation, research models, potential targets, and methods for prevention and treatment. Advanced Science 14. https://doi.org/10.1002/advs.202203291.
Svetlíkova, S., Kovierova, H.Niederweis, Gaillard, J.L., McDonnell, G., Jackson, M., 2009. Role of porins in the susceptibility of Mycobacterium smegmatis and mycobacterium chelonae to aldehyde-based disinfectants and drugs. Antimicrob. Agents Chemother. 53 (9), 4015–4018.
Tezel, U., Pavlostathis, S.G., 2015. Quaternary ammonium compounds disifectants: microbial adaptation, degradation, and ecology. Curr. Opin. Biotechnol. 33, 296–404.
Thomas, R.E., Thomas, B.C., Lorenzetti, D., Conly, J., 2022n. Hospital and long-term care facility environmental service workers' training, skills, activities and effectiveness in cleaning and disinfection: a systematic review. J Hosp Infect. 124, 56–66.

Tosh, P.K., Disbot, M., Duffy, J.M., Boom, M.L., Heseltine, G., Srinivasan, A., Gould, C.V., Berríos-Torres, S.I., 2011c. Outbreak of Pseudomonas aeruginosa surgical site infections after arthroscopic procedures: Texas, 2009. Infect. Control Hosp. Epidemiol. 32 (12), 1179–1186.

Vallés, J., Ferrer, R., 2009. Bloodstream infection in the ICU. Infect. Dis. Clin. N. Am. 23, 557–569.

Veerachamy, S., et al., 2014. Bacterial adherence and biofilm formation on medical implants. Proc. Inst. Mech. Eng. H. 226 (10), 1083–1099.

Vickery, K., Deva, A., Jacombs, A., Allan, J., Valente, P., Gosbell, I.B., 2012. (2012) presence of biofilm containing viable multiresistant organisms despite terminal cleaning on clinical surfaces in an intensive care unit. J. Hosp. Infect. 80 (1), 52–55.

Vickery, K., et al., 2013. A review of bacterial biofilms and their role in device-associated infection. Healthcare Infect. 18, 61–66.

Vikram, A., Bomberger, J.M., Bibby, K.J., 2015. Efflux as a glutaraldehyde resistance mechanism in Pseudomonas fluorescens and Pseudomonas aeruginosa biofilms. Antimicrob. Agents Chemother. 59 (6), 3433–3439.

Visrodia, K., et al., 2017. Duodenoscope reprocessing surveillance with adenosine triphosphate testing and terminal cultures: a clinical pilot study. Gastrointest. Endosc. 86, 180–186.

Vonberg, R.P., Kuijper, E.J., Wilcox, M.H., et al., 2008. Infection control measures to limit the spread of Clostridium difficle. Clin. Microbiol. Infection. 14 (s5), 2–20.

Wang, P., Schelborn, H.E., 1995. Induction of resistance to hydrogen peroxide and radiation in deinococccus radiodurans. Can. J. Microbiol. 41 (2), 170–176. https://doi.org/10.1139/m95-023.

Wang, Y., et al., 2022. Emerging 4D printing strategies for next-generation tissue engineering and medical devices. Adv. Mater. 34 (20), 2109198.

Watts, N., et al., 2018. The lancet countdown on health and climate change from 25 years of inaction to a global transformation for public health. Lancet 391, 581–630.

Weber, W.R., 2013. Assessing the risk of disease transmission to patients when there is a failure to follow recommended disinfection and sterilization guidelines. Am. J. Infect. Control 41, S67–S71.

Weber, D.J., Anderson, D.J., Sexton, D.J., Rutala, W.A., 2013. Role of the environment in the transmission of Clostridium difficile in healthcare facilities. AmericanJ Infect. Control. 41 (5), S105–S110.

Wendorf, K.A., Kay, M., et al., 2015. Endoscopic retrograde cholangiopancreatograph-associated AmpC Escherichia coli outbreak. Infect. Cont. Hosp. Epidemiol 36, 634–642.

West, A.M., Teska, P.J., Lineback, C.B., Olivier, H.F., 2018. Strain, disinfectant, concentration, and contact time quantitatively impact disinfectant efficacy. Antimicrob. Resist. Infect. Control 7, 49. https://doi.org/10.1186/s13756-018-0340-2 (accessed 29 Nov, 2022).

Westmeath Independent, 2020. Second National Award for Mersus. https://www.westmeathindependent.ie/2022/09/23/second-national-award-for-athlone-based-mersus/ (accessed 29th Oct, 2022).

WHO – FPPL, 2022. WHO fungal priority pathogens list to guide research, development and public health action. https://www.who.int/publications/i/item/9789240060241 s.l.: s. n.

Wiktorczyk, N., et al., 2020. Assessment of endoscope cleaning and disinfection efficacy, and the impact of endoscope storage on the microbiological safety level. J. Appl. Microbiol. 128 (5), 1503–1513.

Wilson, A.J., Nayak, S., 2016. Disinfection, sterilization and disposables. Anaesth. Intens. Care Med. 17 (10), 457–479.

World Health Organization, 2016. Decontamination and Reprocessing of Medical Devices for Health-care Facilities. World Health Organization and Pan American Health Organization, Geneva, Switerland.

Yang, H., He, M., Wu, C., 2021. Cross protection of lactic acid bacteria during environmental stresses: stress responses and underlying mechanisms. LWT Food Sci. Technol. 144. https://doi.org/10.1016/j.lwt.2021.111203.

Zhang, J., et al., 2017. Machine learning algorithms define pathogen specific local immune fingerprints in peritoneal dialysis patients with bacterial infections. Kidney Int. 92, 179–191.

Zhang, X., Zhang, M., Zhang, H., Jiang, Z., Liu, C., Cai, W., 2020. A review on energy, environment and economic assessment in remanufacturing based on life cycle assessment method. J. Clean Prod. 255. https://doi.org/10.1016/j.jclepro.2020.120160.

Zipfel, N., et al., 2022. The relationship between the living lab approach and successful implementation of healthcare innovations: an integrative review. BMJ Open 2022 (12), e058630. https://doi.org/10.1136/bmjopen-2021-058630.

Polymer 183 (2019) 121870

Contents lists available at ScienceDirect

Polymer

journal homepage: http://www.elsevier.com/locate/polymer

3D printed polymers are less stable than injection moulded counterparts when exposed to terminal sterilization processes using novel vaporized hydrogen peroxide and electron beam processes

Yuanyuan Chen [a,*], Martin Neff [e], Brian McEvoy [d], Zhi Cao [c], Romina Pezzoli [b], Alan Murphy [c], Noel Gately [b], Michael Hopkins Jnr [b], Neil J. Rowan [f], Declan M. Devine [a]

[a] Materials Research Institute, Athlone Institute of Technology, Ireland
[b] Applied Polymer Technology (APT), Athlone Institute of Technology, Ireland
[c] Centre for Industrial Service & Design (CISD), Athlone Institute of Technology, Ireland
[d] STERIS Applied Sterilization Technologies (AST), Tullamore, Co. Offaly, Ireland
[e] ARBURG Plastic Freeforming (APF), Arburg GmBh & Co KG, Lossburg, Germany
[f] Centre for Disinfection, Sterilization and Biosecurity (CDSB), Athlone Institute of Technology, Ireland

ARTICLE INFO

Keywords:
Sterilization
VHP
E-beam
3D printing
Injection moulded
High density polyethylene
Polyamide 6

ABSTRACT

There is an increasing trend for use of 3D printing processes in healthcare due in part to emergence of customised medical devices and associated low manufacturing cost. However, there is a dearth of knowledge on the efficacy of terminal sterilization processes on such 3D printing processes compared to conventional manufacturing methods, such as injection moulding. Therefore, the goal of this timely work was to compare the mechanical, thermal and chemical effects of vaporized hydrogen peroxide (VHP) and electron beam (E-beam) sterilization processes on the 3D printed and injection moulded high density polyethylene (HDPE) and Polyamide 6 samples. Characterization of materials post sterilization was performed by several analytical methods. Studies found that injection moulded samples exhibited higher tensile strength, higher degree of crystallinity, lower ductility, and higher thermal stability than 3D printed samples due to their tightly packed structures. After VHP and E-beam sterilization processes, oxidation and crosslinking occurred along with yellow colour change. Free hydroxyl radicals and intermolecular carbon bonding were detected by FTIR; the viscosity, storage modulus and loss modulus were increased due to crosslinking; the wettability of all the samples were increased due to the free radicals on the surface. However, the tensile properties of all samples measured were not affected by the VHP or E-beam processes, which was attributed to the low irradiation dosage of E-beam and good resistance to hydrolytic degradation from VHP. Overall, E-beam process resulted in more severe oxidation and crosslinking than VHP process, and sterilized 3D printed samples were less stable compared to injection moulded samples when exposed to terminal sterilization processes, which was evidenced with more new peaks related to oxidation and crosslinking detected by FTIR and the dramatic increase in the degree of crystallinity. These findings highlight the importance of considering choice of industrial terminal sterilization with view to future reduction of processing conditions for emerging additive manufacturing processes, such as in situ 3D printing that is often underappreciated.

1. Introduction

3D printing is a disruptive technology that is revolutionizing the healthcare industry globally. It enables custom-tailored medical devices to be printed to meet personalized needs, expedites surgical procedures, prepares surgeons and physicians with models for some complex cases, reduces the manufacturing cost, and may in time be used to replace human organ transplants in regenerative tissue engineering [1]. Currently, many medical devices are manufactured via 3D printing technology, such as hearing aids, orthopaedic and cranial implants, dental crowns and external prosthetics. As the majority of medical devices require sterilization, the performance of 3D printed devices

* Corresponding author.
E-mail address: yuanyuanchen@ait.ie (Y. Chen).

https://doi.org/10.1016/j.polymer.2019.121870
Received 1 August 2019; Received in revised form 30 September 2019; Accepted 5 October 2019
Available online 7 October 2019
0032-3861/

finished with sterilization compared with traditionally manufactured devices is an important aspect to be considered as the healthcare manufacturing industry seeks to innovate with the 3D printing technology. The findings from this study provided evidence and support for the improvement of the sterilization procedures and standards servicing the fast development of 3D printed medical device industry.

Sterilization is a process by which bacteria or other living microorganisms are either destroyed or completely removed from a treated object [2]. Sterilization methods can be classified into three major groups namely, ionising radiation, gas technologies and heat treatment (steam). Ionising radiation includes gamma radiation, electron beam (E-beam) and X-ray radiation. Gas sterilization technologies comprise plasma, ethylene oxide (EO) and more recently, vaporized hydrogen peroxide (VHP®, a registered trademark of STERIS) [3]. Approximately 50% of medical devices are sterilized by using EO globally [4]. In response to the February 2019 closure of a large device sterilization facility, the FDA announced an innovative challenge to reduce the ethylene oxide emission [5], STERIS Applied Sterilization Technologies have investigated material compatibility with traditional terminal sterilization technologies and VHP appeared to be an alternative sterilization technology to EO. Steam sterilization is typically conducted by use of autoclaves and contrasts from aforementioned processes as relies upon heat for efficacy. This current work focuses on VHP and E-beam sterilization processes.

VHP is a gaseous technology, utilising hydrogen peroxide (H_2O_2) in the form of vapour. H_2O_2 is an extremely powerful oxidant and it generates reactive oxygen species, such as hydroxyl radicals that attack multiple molecular targets, including microbial nucleic acids, enzymes, cell wall proteins and lipids. Typical VHP processes operate at a temperature range of 25–50 °C with an approximate cycle duration of 1.5–4 h, but has limited penetration power [6]. It is suitable for materials that cannot sustain high temperature and moisture from steam sterilization, but it is not suitable for hygroscopic materials that absorb moisture, such as paper, cotton, cellulose, polylactic acid [1,2]. VHP is not classed as a carcinogen and is more environmentally friendly than EO as a sustainable terminal sterilization technology for medical device industry [8].

E-beam radiation is created by the accelerated electrons produced from an electromagnetic filed in an accelerator and the high-energy electrons move through the target material, killing bacteria by breaking the chains of DNA and RNA. However, this process can also lead to significant alternations in the treated materials. The high-energy electrons interact freely with molecules within the target material, ejecting electrons from their orbits and generating free radicals. The free radicals react with the present oxygen, lead to oxidation and degradation [2,3]. The sterilization induced polymer degradation can be cross-linking, chain scission or a combination of both. Polymers with strong bonds such as benzene rings, might regain original configuration following sterilization, while polymers with weak bonds result in chain scission and undergo degradation [2,9].

High density polyethylene (HDPE) in general crosslinks on irradiation, which increases the molecular weight and therefore lower the mobility of molecules and reduce creep. This may raise the tensile strength, increase the hardness and brittleness, but impact strength and shear strength usually decrease or remain relatively unchanged [12]. However, there is a chain scission mechanism as well. It was reported that with 100 kGy radiation dosage, chain scission of HDPE occurred [13].

Polyamides are commonly known as nylon with repeating amide group along the polymer chain. Polyamides are limited to a few cycles of stream or autoclave sterilization because polyamides absorb moisture and hence degrade [14]. Polyamides are reasonably resistant to small doses of irradiation sterilization, typically up to 40–50 kGy, but not for many repeat doses [10,12]. Kubyshkina et al. reported that polyamides are only suitable for a single dose of radiation [15]. Polyamides crosslink and lose crystallinity upon sterilization causing a slow increase in tensile strength but much more rapid drop in impact strength [12].

The effects of sterilization methods on various polymer materials have been studied, but there is a currently a dearth of evidence-based research describing the effects of industrial terminal sterilization processes on 3D printed plastic objects. Shaheen et al. printed tooth replicas, orthognathic splints and surgical cutting guides via PolyJet technology, and sterilized with autoclave (heat/steam sterilization) and VHP. They reported that all 3D printed objects that underwent autoclave and VHP sterilization had indicated shape deformation, and larger differences were observed with autoclave sterilization compared with VHP sterilization [16].

Unlike to conventional medical devices manufacturing techniques, such as machining and injection moulding, 3D printing is an additive method and the material is consequently added in each layer as a thin cross section of a 3D object. This layering process results in various changes in the physical, mechanical, thermal properties of the objects. Several studies have compared the property differences of polymers, including polycarbonate urethane [17], ABS [18], resulted from 3D printing and traditional manufacturing methods.

This current multi-disciplinary study characterises material properties of 3D printed and injection moulded Marlex (HDPE) and 3D printed Grilon (Polyamide 6) samples post terminal VHP and E-beam sterilization. The physical, chemical and thermal properties of the samples were investigated via colorimetry, rheometry, fourier transfer infrared spectroscopy (FTIR), dynamic mechanical thermal analysis (DMTA), differential scanning calorimetry (DSC), thermogravimetric analysis (TGA), and tensile testing. Surface modifications induced by sterilization were studied by scanning electron microscopy (SEM) and goniometry.

2. Materials and methods

2.1. Materials

High density polyethylene (HDPE) (Marlex® HHM 5502BN Polyethylene) was obtained from Chevron Philips Chemical Company LP (Woodlands, US). Polyamide 6 (Grilon F 40 NL) was supplied by EMS-CHEMIE AG (Switzerland). All materials were used as received.

2.2. Injection moulding

ASTM Standard tensile test samples were injection moulded by Arburg™ All-rounder 221K (Arburg, Lossburg, Germany), with the maximal clamping force of 350 kN, a screw diameter of 25 mm, a theoretical stroke volume of 49 cm^3 and a maximum injected part weight of 41 g. Marlex was dried at 70 °C for 8 h prior to injection moulding. The temperature profile for injection moulding increased from 160 °C at the hopper to 200 °C at the nozzle with injection speed of 100 mm/s. The holding pressure used was 600 bar with a holding time of 6.5 s. The cooling time was 10 s with a back pressure of 50 bar. Polyamide 6 Grilon F 40 NL is an extrusion grade polymer and as such inaccurate geometries were obtained from injection moulding. Therefore, the comparison between 3D printed and injection moulded was conducted using Marlex samples only, with the comparative effects of VHP and E-beam on 3D printed parts assessed using both Marlex and Grilon samples.

2.3. 3D printing

3D printed dumbbell-shaped tensile test samples were printed by ARBURG Plastic Freeforming (AKF) (ARBURG GmbH & CO KG, Germany). Marlex samples were printed at 200 °C and Grilon samples were printed at 250 °C. AKF allows molten plastic droplets with a diameter between 0.2 and 0.4 mm to be generated by a stationary nozzle that relies on piezoelectric closure system and deposited on a moving platform to build up 3D objects layer by layer [19].

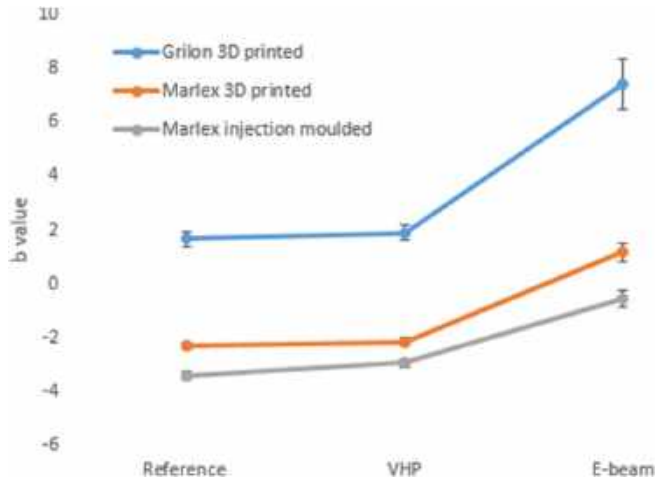

Fig. 1. The b value from colorimetry for Marlex and Grilon samples.

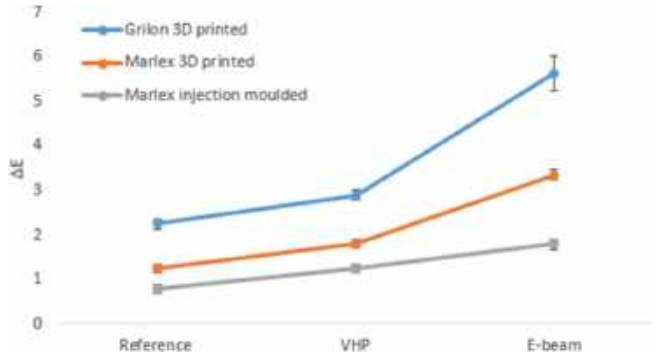

Fig. 2. The ΔE from colorimetry for Marlex and Grilon samples.

2.4. Vaporized hydrogen peroxide (VHP)

The test samples were treated with VHP in a STERIS VHP® LTS-V industrial sterilizer using STERIS VAPROX® hydrogen peroxide (35%) sterilant. The process consisted of a four VHP pulse injection cycle performed in vacuum environment conditions at 30 °C. The process was performed at STERIS Applied Sterilization Technologies, Tullamore, Ireland.

2.5. E-beam

The test specimens were irradiated with E-beam process in STERIS with a Mevex Linac E-beam 10 MeV, 20 kW at a dose of circa 30 kGy in air at ambient temperature. All the specimens were irradiated by E-beam from both sides. The process was performed at STERIS Applied Sterilization Technologies, Tullamore, Ireland.

2.6. Colorimetry

Colour measurements (L*, a*, b* values) of the specimens was determined by using a Lovibond RT Series Reflectance Tintometer (Amesbury, UK) with OnColor software. Prior to measuring the colour of the specimens, the instrument was standardized by placing black and white standard plates and L*, a* and b* colour values were recorded. The L* values correspond to lightness/darkness (0 for black and 100 for white), the a* values correspond to the specimen's colour dimension from red to green (the greater a* value, the redder), the b* values correspond to the specimen's colour dimension from yellow to blue (the greater b* value, the yellower).

2.7. Surface wettability

The surface wettability of all the specimens was assessed using a First 10 Å, FTA32 goniometer (Virginia, US). In this test, the Sessile Drop contact angle technique was utilised with distilled water as the probe liquid and the contact angle value of each specimen was recorded.

2.8. Fourier transfer infrared spectroscopy

Attenuated total reflectance Fourier transform infrared spectroscopy (FTIR) was carried out on a PerkinElmer Spectrum One (Waltham, US) fitted with a universal ATR sampling accessory. All data were recorded at 21 °C in the spectral range of 4000–520 cm^{-1} against air as background, utilising a 4 scan per sample cycle at a resolution of 0.5 cm^{-1} and a fixed universal compression force of 70–80 N. Subsequent analysis was carried out using Spectrum software.

2.9. Differential scanning calorimetry

Differential scanning calorimetry (DSC) was carried out using a DSC 2920 Modulated DSC (TA Instruments, New Castle, US) with a nitrogen flow rate of 20 ml/min to prevent oxidation. Calibration of the instrument was performed using indium as standard. All the samples were dried at 60 °C for 8 h prior to testing. Test specimens weighed between 8 and 12 mg were measured on a Sartorius scales (MC 210 P), capable of being read to five decimal places. Samples were crimped in non-perforated aluminium pans, with an empty crimped aluminium pan used as the reference. The thermal history of Marlex samples was removed by heating samples from 20 °C to 200 °C at the rate of 30 °C/min, and then held isothermally at 200 °C for 10 min. The samples were then cooled down from 200 °C to 0 °C at 30 °C/min. Finally, the thermal properties of the Marlex samples were recorded by heating the samples from 0 °C to 200 °C at the rate of 10 °C/min. Similarly, the Grilon samples were heated initially from 20 °C to 250 °C at the rate of 30 °C/min, then held isothermally at 250 °C for 10 min, followed by cooling down from 250 °C to 0 °C at 30 °C/min. Finally, the Grilon samples were heated again from 0 °C to 250 °C at the rate of 10 °C/min for testing thermal properties. Crystallinity and melting temperature of each sample were analysed. For calculating percentage crystallinity, the melt enthalpy of completely crystalline Marlex was 286.7 J/g and 83 J/g for Grilon.

2.10. Rheometry

An oscillatory rheometer TA Discovery Hybrid Rheometer 2 (New Castle, US) was used for the rheologic analysis of all the samples. The parallel plate rheometer was fitted and calibrated with a geometry of 25 mm diameter steel plate. An amplitude of 1% was applied and previously verified by an amplitude sweep at a frequency of 1.0 Hz. Oscillation frequency sweeps were conducted from 0.1 to 20 rad/s angular frequency at a constant temperature of 260 °C for the Grilon samples and 250 °C for the Marlex samples.

2.11. Dynamic mechanical thermal analysis (DMTA)

The Dynamic mechanical thermal analysis (DMTA) analysis was carried out using PerkinElmer DMA 8000 Analyser (Waltham, US) with Multi-Frequency module – Storage modulus and Strain. The heating profile for Marlex samples was from −150 to 10 °C at 3 °C/min, and the heating profile for Grilon samples was from −10 to 100 °C at 3 °C/min. The storage modulus and loss modulus of all samples were recorded.

2.12. Thermogravimetric analysis

Thermogravimetric analysis (TGA) tests were conducted using PerkinElmer TGA 7 Thermogravimetric Analyzer (Waltham, US), coupled

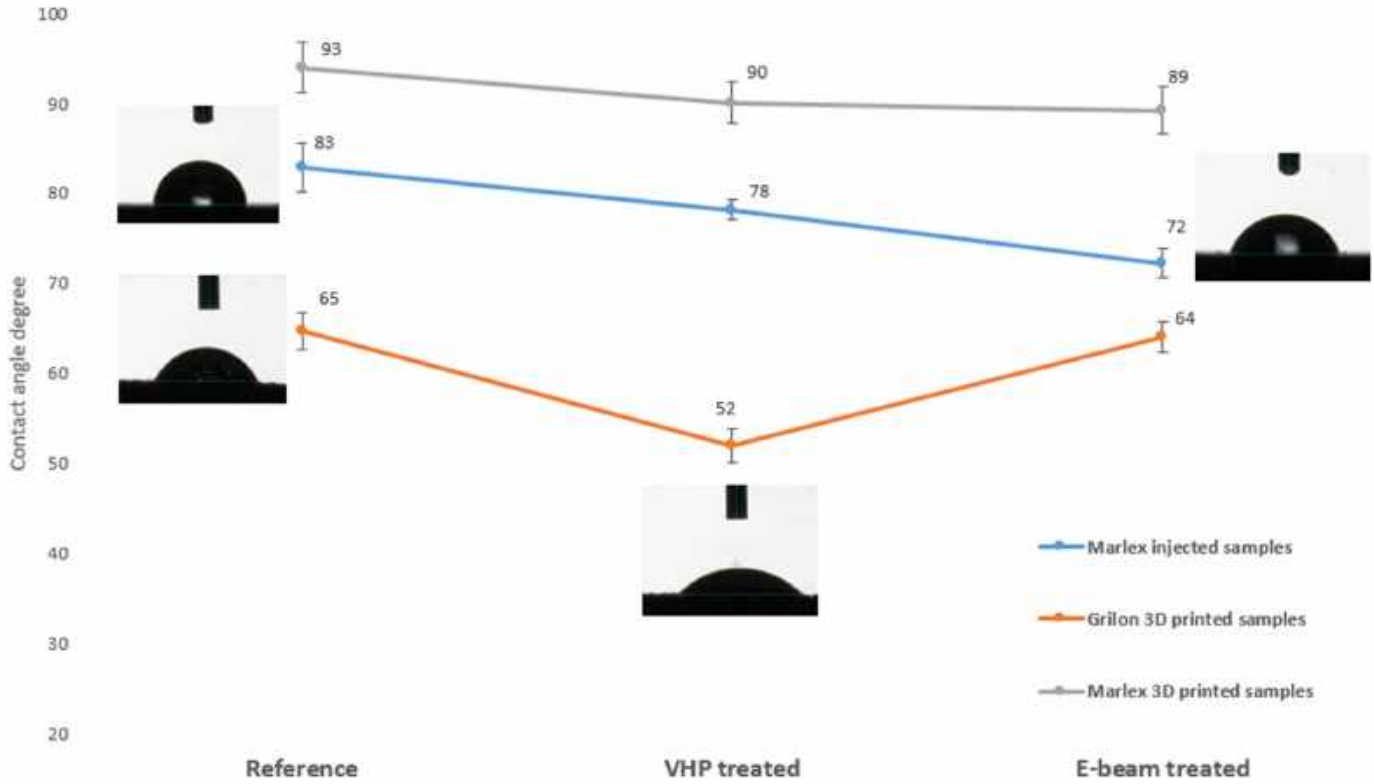

Fig. 3. Contact angle measurements of 3D printed and injection moulded Marlex and Grilon samples upon VHP and E-beam sterilization.

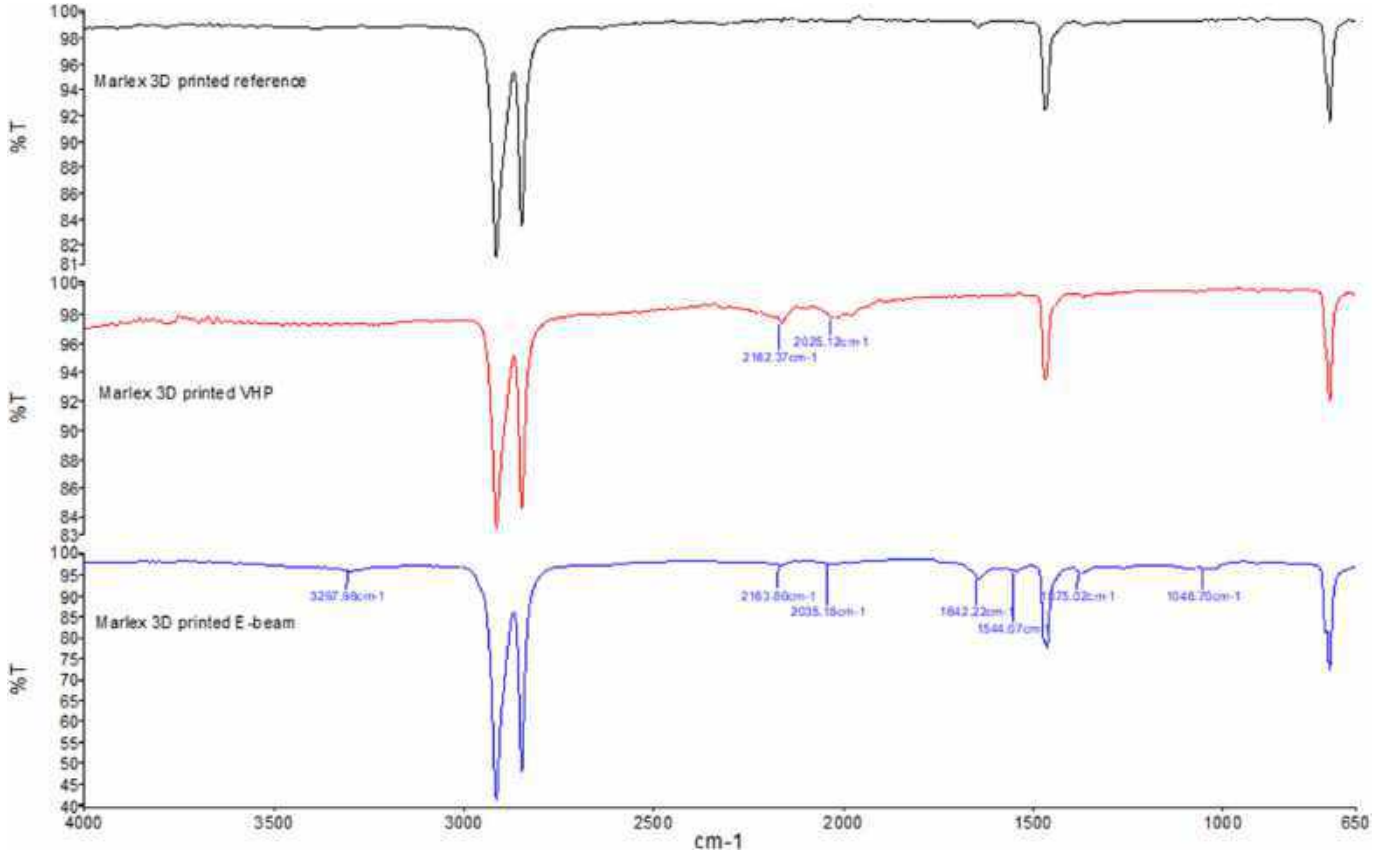

Fig. 4. A: FTIR spectra of Marlex 3D printed samples.

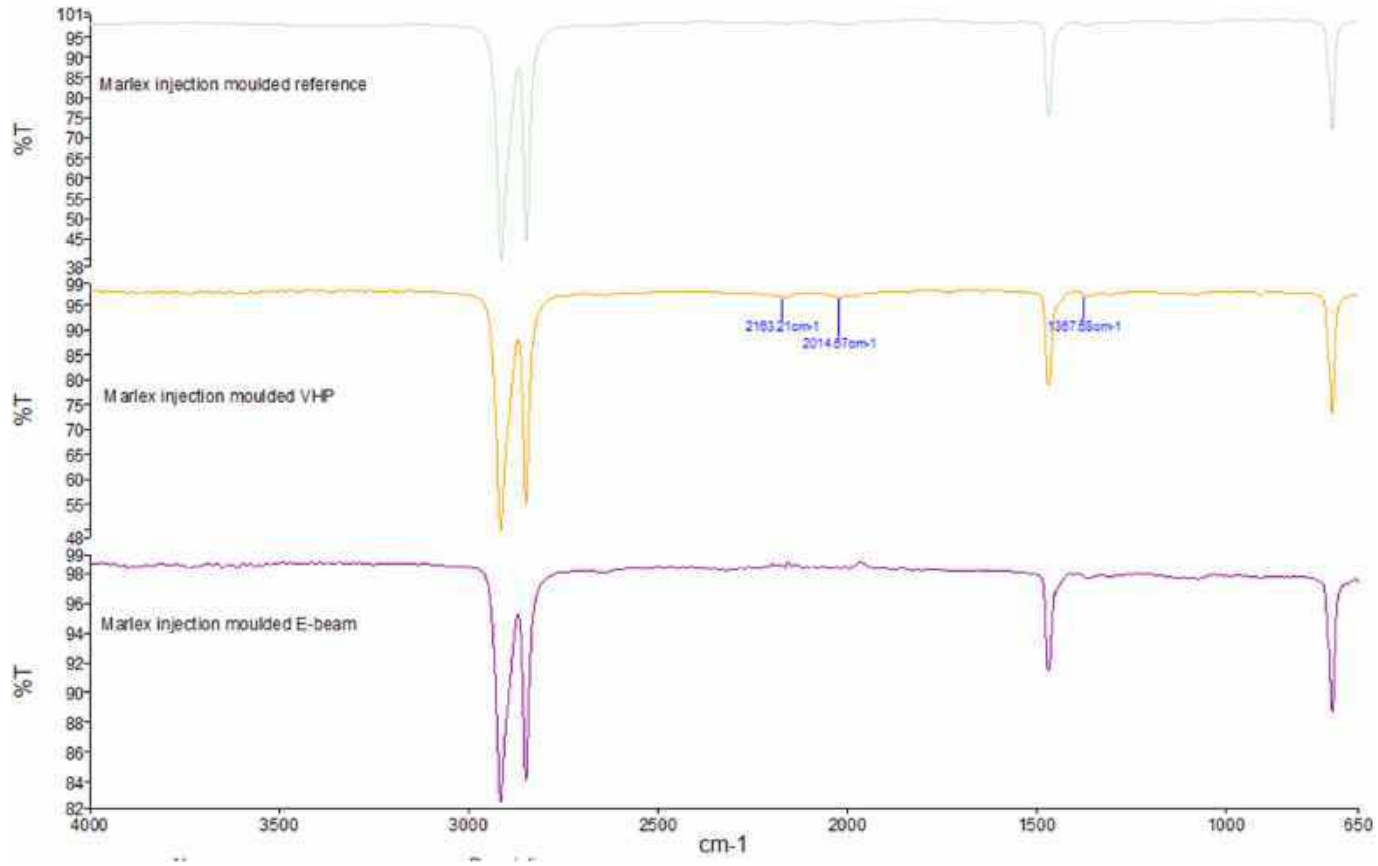

Fig. 5. FTIR spectra of Marlex injection moulded samples.

with a PerkinElmer Thermal Analysis controller TAC7/DX under nitrogen atmosphere. The tests were run from 30 °C to 600 °C, at a heating rate of 10 °C/min. the onset degradation temperature of each sample was recorded.

2.13. Morphology

Scanning electron microscopy (SEM) was performed using a Mira XMU SEM (Tescan™, Czech Republic) in back scattered electron mode for surface analysis. The accelerating voltages utilised were 5 kV and 10 kV. Prior to analysis, test samples were placed on an aluminum stub, and the samples were sputtered with a gold using Baltec SCD 005 for 110 s at 0.1 mbar vacuum before testing.

2.14. Mechanical testing

The mechanical properties of the samples were characterised by tensile tests. Tensile testing was carried out on a Lloyd Lr10k tensometer (Ametek Ltd., West Sussex, UK) using a 2.5 kN load cell on ASTM standard test specimens at a strain rate of 5 mm/min for both 3D printed and injection moulded Marlex samples and 120 mm/min for Grilon samples. Data was recorded using Nexygen™ software. The tensile tests were carried out in adherence to ASTM D 882. Five replicates were analysed per group and prior to testing the thickness of each sample was measured. The percentage strain at maximum load and Young's Modulus of each sample were recorded.

2.15. Statistical analysis

Statistical analysis was performed using one way analysis of variance (ANOVA) with a Tukey Post hoc test to determine differences. Differences were considered significant when $p \leq 0.05$. The software used to perform statistical analysis was SPSS (IBM Version 22) for Windows. All data collected in this study were expressed as mean ± standard deviation. Sample size of 10 was used for colorimetry and contact angle test, while sample size of 5 was used for tensile testing.

3. Results

3.1. Colorimetry

Both VHP and E-beam sterilization processes caused all the specimen turn yellow, and E-beam treated specimen appeared yellower than VHP treated specimen. This was supported by the colorimetric test results, where the b values and ΔE measurements increased dramatically, especially after E-beam treatment, shown in Fig. 1 and Fig. 2 ($p < 0.05$ for all comparison). The b values correspond to the colour of yellow, the greater b value, the yellower.

3.2. Surface wettability

Wettability is the tendency of a material to attract water to its surface, or absorb the water. Contact angle was measured to analyse the wettability of each sample. It can be clearly seen from Fig. 3 that VHP and E-beam sterilization methods decreased the contact angle of 3D printed Marlex samples, injection moulded Marlex samples and 3D printed Grilon samples ($p = 0.021$ for all comparison).

3.3. Fourier transfer infrared spectroscopy

A new peak at 3299 cm^{-1}, which is related to oxidation, appeared in the E-beam treated 3D printed Marlex sample; new peaks at 2022 and 2167 cm^{-1} related to C≡C bonding appeared in both E-beam and VHP treated 3D printed Marlex samples, and new peaks at 1541 and

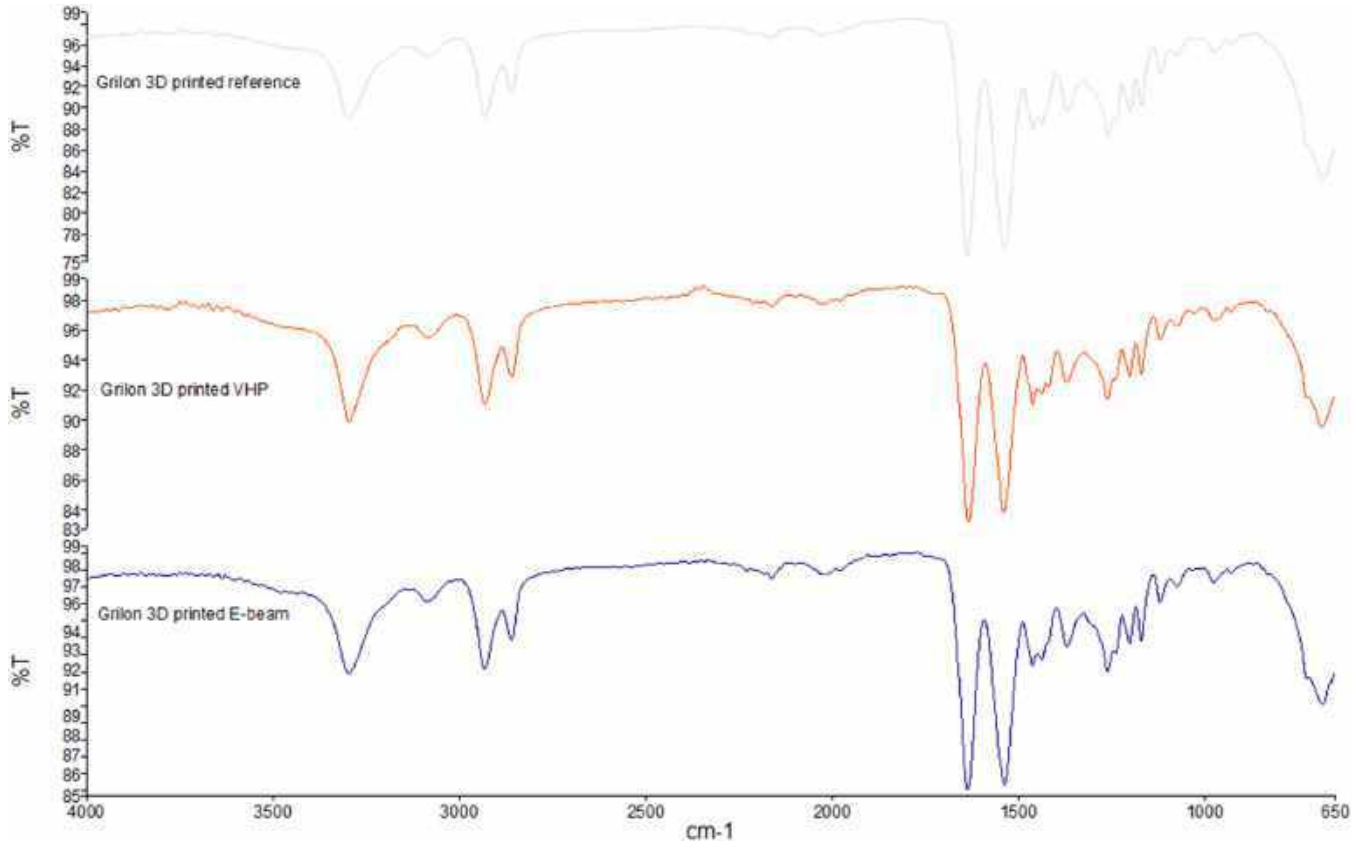

Fig. 6. FTIR spectra of Grilon 3D printed samples.

Table 1
DSC results of 3D printed and injection moulded Marlex and Grilon samples upon VHP and E-beam sterilization.

Samples	Tm	Tc	Xc %
Marlex 3D ref	135	109	64
Marlex 3D VHP	133	111	66
Marlex 3D E-beam	133	110	83
Marlex inject ref	135	111	79
Marlex inject VHP	134	108	83
Marlex inject E-beam	134	105	81
Grilon 3D ref	220	178	72
Grilon 3D VHP	222	178	78
Grilon 3D E-beam	221	176	76

1640 cm^{-1} asociated with C = C strech appeared in E-beam treated 3D printed Marlex samples, shown in Fig. 4. The mentioned new peaks at 3299, 2022 and 2167 cm^{-1} appeared in E-beam treated 3D printed Marlex samples, but not in the E-beam treated injection moulded Marlex samples, shown in Fig. 5. Fig. 6 revealed the chemical bonding in Grilon samples upon VHP and E-beam processes and no great difference can be found.

3.4. Differential scanning calorimetry

DSC was carried out to investigate the thermal characteristics of the test samples. VHP and E-beam processes did not change the T_m of any Marlex samples, but reduced the Tc of injection moulded Marlex samples from 111 °C of reference samples to 108 °C of VHP treated samples and 105 °C of E-beam treated samples, shown in Table 1, Figs. 7 and 8. In addition, it was found that injection moulded Marlex samples had higher degree of crystallinity Xc (%) than 3D printed Marlex samples, and the VHP and E-beam processes increased the Xc of 3D printed Marlex samples from 64% to 66% and 83% respectively, while the VHP and E-beam processes did not cause a dramatic increase in the injection moulded Marlex samples with 79% for pre-sterilization, 83% after VHP treatment and 81% after E-beam process. Fig. 9 illustrated the DSC curves of the 3D printed Grilon samples. Similarly, the T_c and T_m of Grilon samples remained unchanged at 178 and 220 °C respectively, and sterilization processes increased the percentage of crystallinity slightly, with 72% for reference, 78% for VHP treated and 76% for E-beam treated 3D printed Grilon samples.

3.5. Rheometry & dynamic mechanical thermal analysis

The plastic deformation of all the samples were analysed by rheometry and DMTA. The complex viscosity, storage modulus and loss modulus of both 3D printed and injection moulded Marlex and 3D printed Grilon samples increased on both VHP and E-beam sterilization processes. Compared to VHP, E-beam process resulted in higher complex viscosity, storage modulus and loss modulus in all three groups, shown in Figs. 10–12.

3.6. Thermogravimetric analysis

The thermal stability of both 3D printed and injection moulded Marlex and 3D printed Grilon samples was evaluated by TGA. The degradation onset temperature of the injection moulded Marlex samples was 420 °C, which was higher than that of 3D printed Marlex samples (406 °C), shown in Fig. 13. VHP or E-beam processes did not affect the degradation onset temperature of injection moulded Marlex samples, 3D printed Marlex samples and 3D printed Grilon samples (447 °C), shown in Figs. 13 and 14.

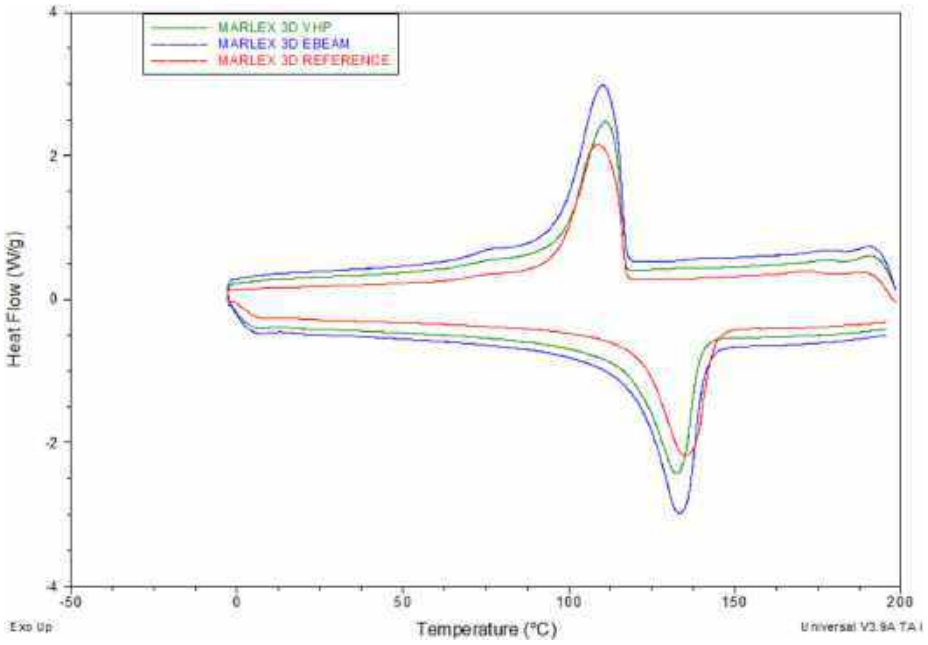

Fig. 7. DSC curves of 3D printed Marlex samples.

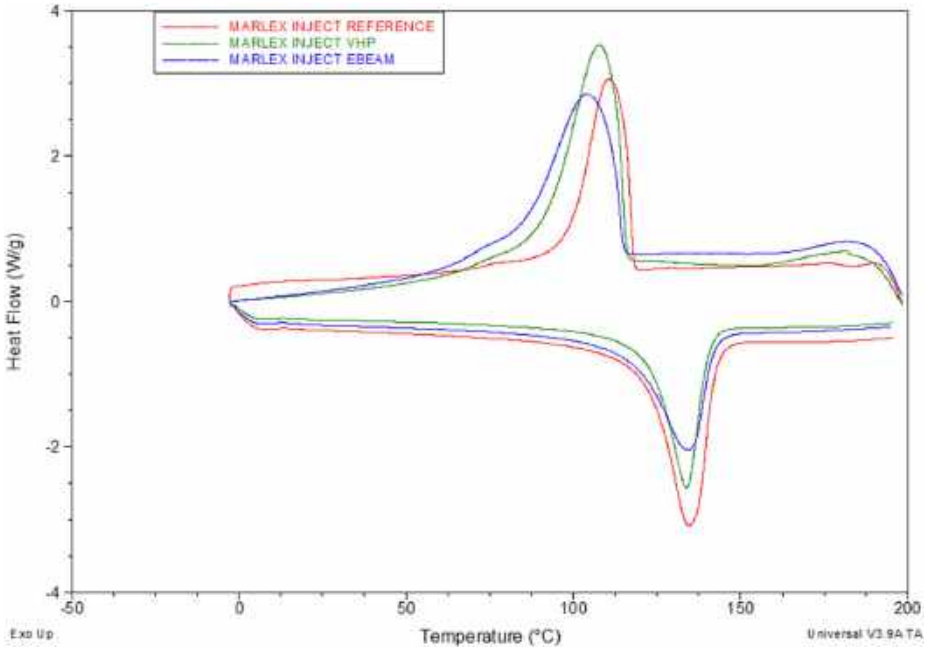

Fig. 8. DSC curves of injection moulded Marlex samples.

3.7. Morphology

No noticeable change (i.e. cracks) was found on the surface of reference, VHP or E-beam treated samples, according to the SEM images, shown in Fig. 15.

3.8. Mechanical testing

Fig. 16 illustrated the tensile test results of 3D printed and injection moulded Marlex samples. It clearly showed that the injection moulded Marlex samples have higher Young's modulus than the 3D printed Marlex samples, but with much lower percentage strain. VHP and E-beam processes did not cause significant change in Young's modulus (E) of 3D printed Marlex (309 ± 73 MPa, $p = 0.996$), injection moulded Marlex (385 ± 35 MPa, $p = 0.998$) or 3D printed Grilon samples (286 ± 96 MPa, $p = 0.699$). Similarly, VHP and E-beam did not cause significant change in their elongations either, with a percentage strain at maximum of 28 ± 1.8, 18.4 ± 1.7 and 375 ± 34 respectively ($p = 1$ for all comparison) (see Fig. 17).

4. Discussion

Oxidation occurred to all the samples after VHP and E-beam sterilization treatments, because all the samples turned yellow post sterilization. The free radicals produced by sterilization reacted with the oxygen diffusing through the material and caused bleaching of the radical based

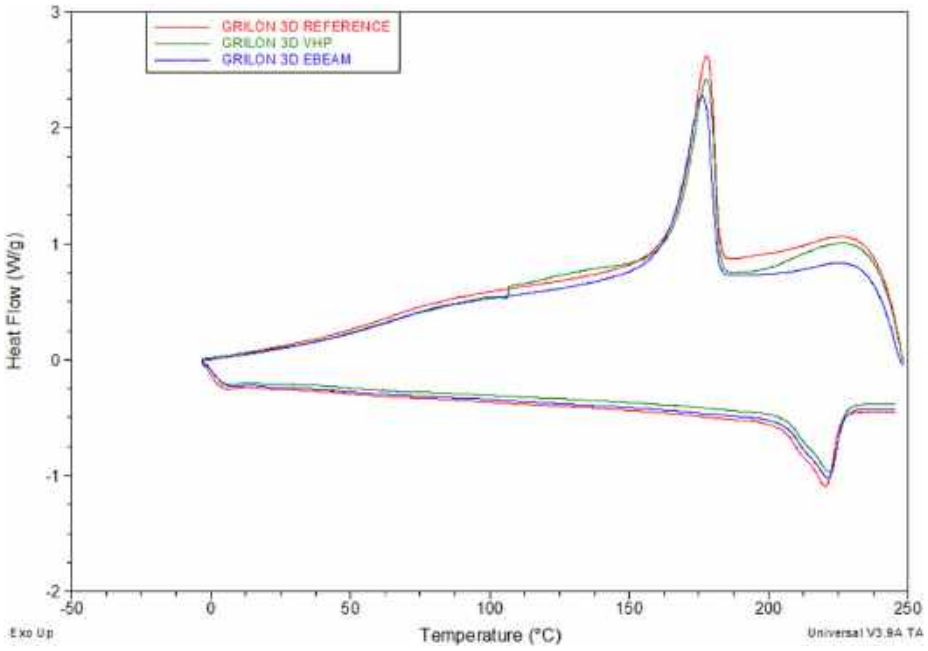

Fig. 9. DSC curves of 3D printed Grilon samples.

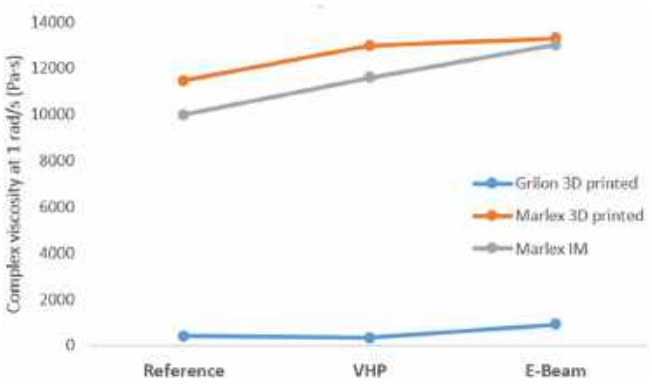

Fig. 10. Complex viscosity of 3D printed and injection moulded Marlex samples and 3D printed Grilon samples.

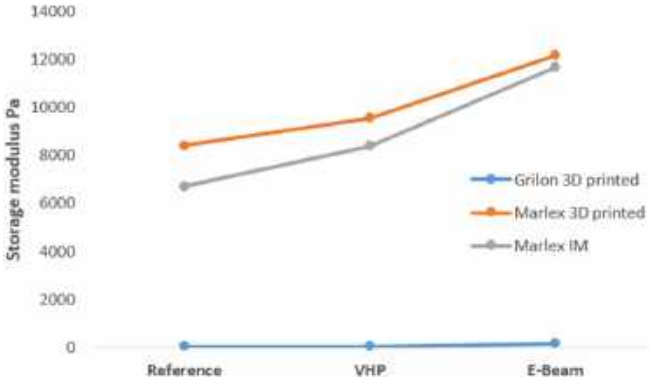

Fig. 11. Storage modulus of 3D printed and injection moulded Marlex samples and 3D printed Grilon samples.

colour centres [20]. These free radicals were also responsible for the increasing hydrophilicity of the material, due to the formation of hydrophilic groups on the material surface by the radicals [11,19]. In some

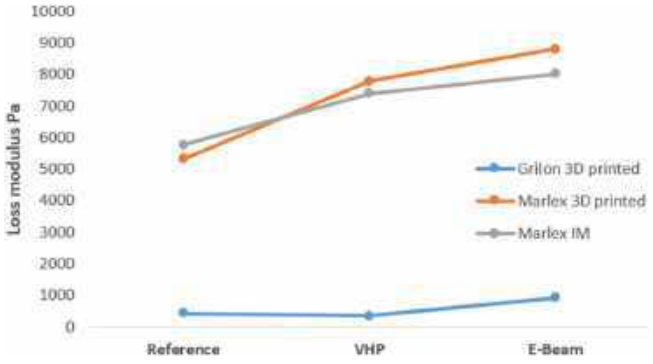

Fig. 12. Loss modulus of 3D printed and injection moulded Marlex samples and 3D printed Grilon samples.

cases, the material became opaque as a consequence of sterilization, but most treated materials changed colour to yellow or brown [9,10]. In this study, E-beam treated samples appeared yellower than VHP treated samples, which may indicate that the E-beam process resulted in more severe oxidation than VHP process.

This can also be proved by FTIR results, where corresponding peaks for oxidation in the range of 3500 and 3100 cm^{-1} [23] were found in E-beam treated Marlex samples, but not in VHP treated Marlex samples. FTIR results also revealed that the sterilization processes resulted in crosslinking. The alkyl and allyl radicals are the predominant free radicals in polyethylene, which are able to bridge two long molecular chains by forming C - C intermolecular bonds or cross-linking that enhance the inter-chain interaction. The cross-linking mechanism of polyethylene involves two main stages. The first stage is the breakdown of the C–H bond on the polyethylene chains to produce hydrogen gas. The second stage is the free radicals react and join together to form cross-linking network [24]. Because some of the peaks related to crosslinking appeared in the E-beam treated 3D printed Marlex samples but not in the E-beam treated injection moulded Marlex samples, it might indicate that the injection moulded samples were more stable than 3D printed samples upon E-beam sterilization process.

The results from DSC also supported that injection moulded samples

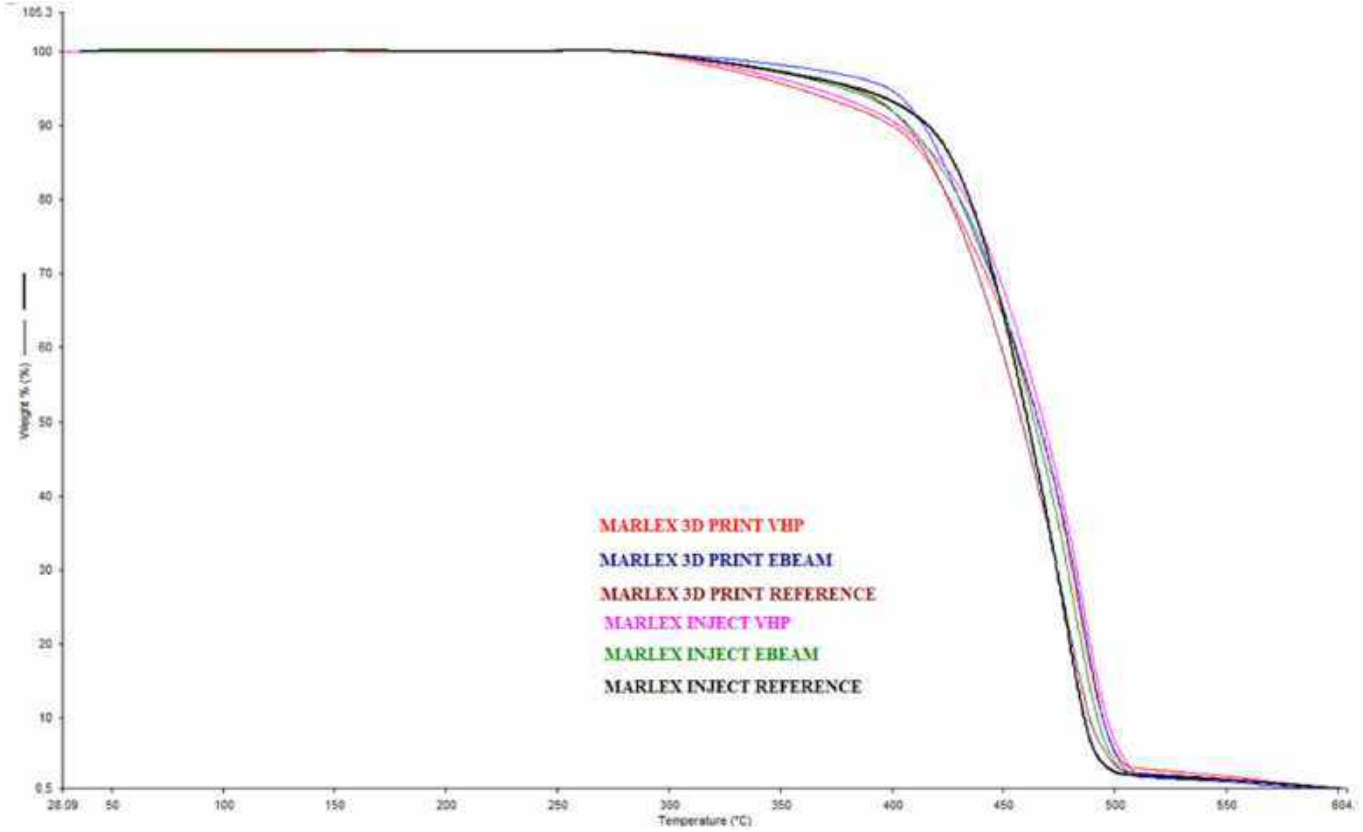

Fig. 13. TGA curves of both 3D printed and injection moulded Marlex samples.

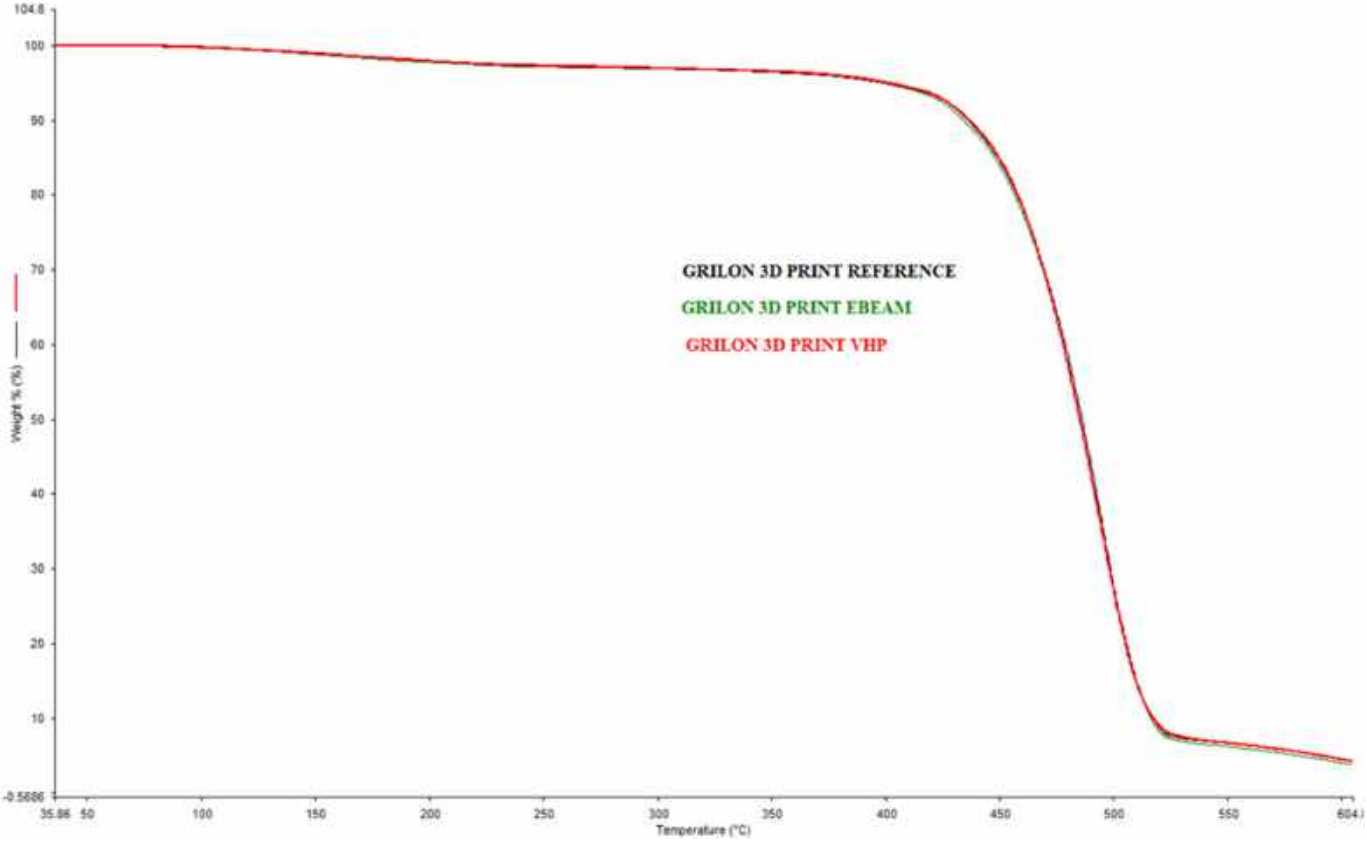

Fig. 14. TGA curve of Grilon samples.

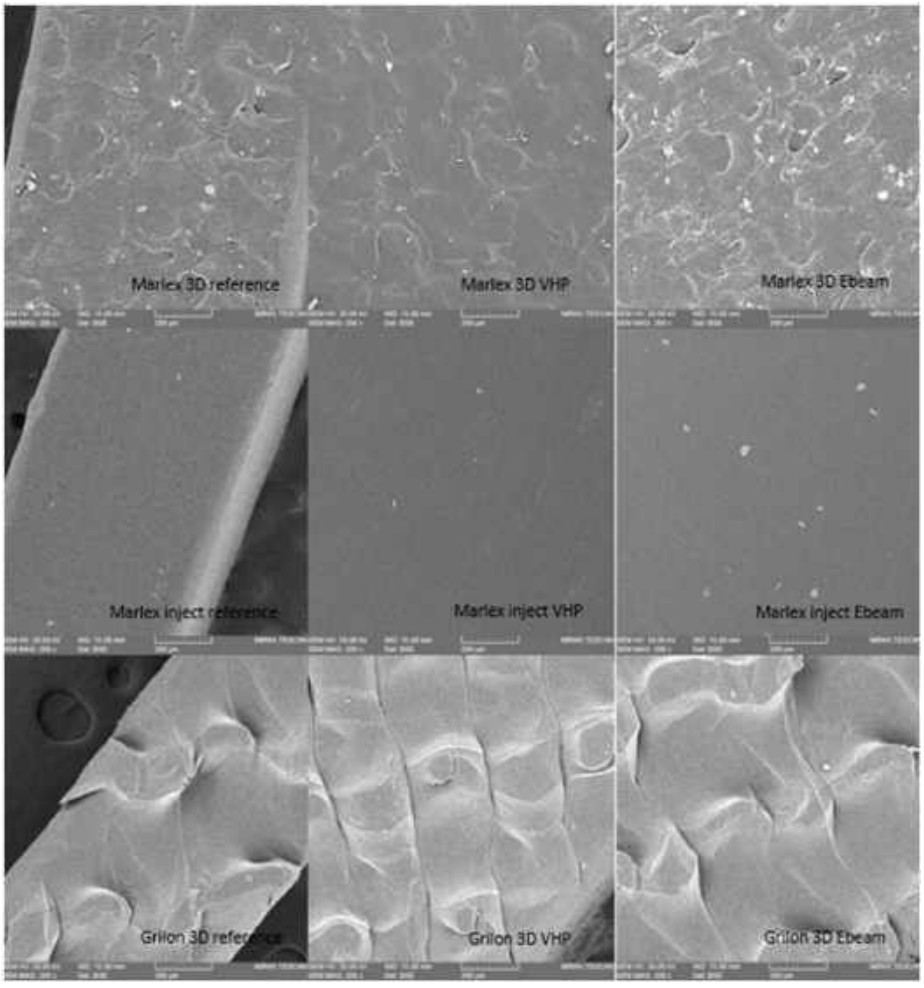

Fig. 15. SEM images of 3D printed and injection moulded Marlex samples and 3D printed Grilon samples.

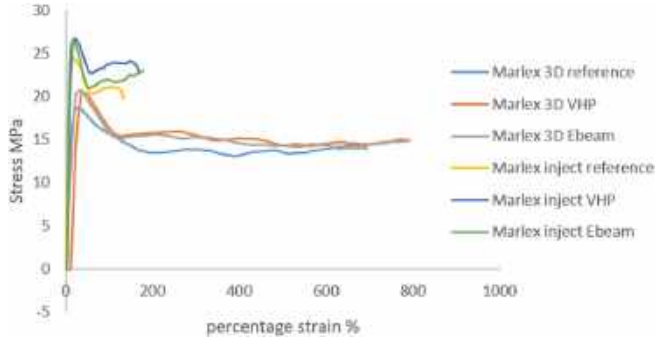

Fig. 16. Tensile test results of Marlex samples.

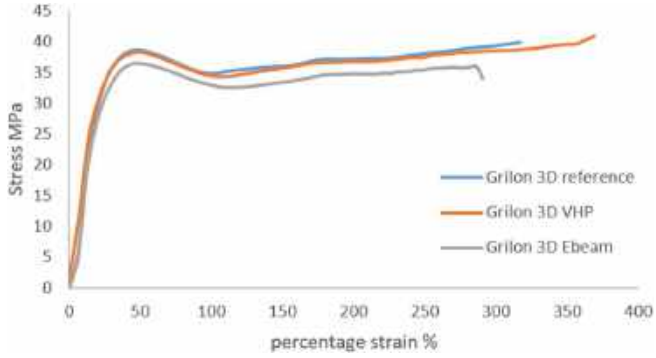

Fig. 17. Tensile test results of Grilon samples.

were more stable than 3D printed samples upon sterilization processes. The E-beam treatment did not influence the percentage of crystallinity of injection moulded samples, but increased that of 3D printed samples dramatically. This can be attributed to the different structures due to the different manufacturing processes. Injection moulded samples have very tight structure due to the high pressure during the manufacturing process, while 3D printed samples are loosely packed with melt droplets. Therefore, there are more voids in 3D printed samples than injection moulded samples, and the voids allow more intermolecular crosslinking occur upon sterilization processes. The heavily cross-linked polymer chains in 3D printed samples hindered the mobility of the chains, resulting in the increase in the percentage of crystallinity [12–15]. Compared to 3D printed Marlex samples, 3D printed Grilon samples did not display a dramatic increase in the percentage of crystallinity. The explanation would be that polyamide 6 tends to be stable upon sterilization methods within the limited cycles of sterilization processes [12, 15].

Crosslinking after sterilization was also detected by rehometry and DMTA, where the viscosity, storage modulus and loss modulus increased after both VHP and E-beam processes. Viscosity refers to the resistance of the molten polymer to flow; the storage modulus and loss modulus are energy stored and energy dissipated in the material, when a deformation

has been imposed. Crosslinking caused extra bonding between polymer chains, resulting in a reduction of molecular chains mobility in the interfacial region, hence causing interfacial stiffness which consequently increased the viscosity and improved the storage modulus of the material [29]. Yakacki et al. also mentioned that crosslinking of the shape memory polymers after gamma irradiation hindered the segmental motion of the polymer chains and resulted in the increase in rubbery modulus of the material [23]. This thermal properties study also revealed that E-beam treatment resulted in higher viscosity, storage modulus and loss modulus than VHP process, which indicated that E-beam process leads to more severe crosslinking effect than VHP treatment.

Despite the oxidation and crosslinking caused by VHP and E-beam treatments, the bulk properties of the samples were not affected, including thermal stability, mechanical properties and surface structure. The explanations are: 1) VHP sterilization process usually cause hydrolytic degradation of the samples, since Marlex and Grilon samples did not absorb moistures during VHP process, the hydrolytic degradation did not occur. It was reported that the molecular weight of polylactic acid (PLA) reduced significantly due to hydrolytic degradation when exposed to VHP treatment, because PLA is hygroscopic [30]; 2) The E-beam dosage of 30 kGy was not high enough to alternate the bulk properties. With a radiation dosage from 100 to 150 kGy, the thermal degradation of HDPE occured [31], small cracks were clearly observed on the surface of HDPE, the tensile strength and elongation at break of HDPE were increased due to crosslinking [13]. A rougher (flaky/scaly) surface of LDPE subsequent to E-beam irradiation at 400 kGy due to oxidative degradation was reported [22]. When the radiation dosage up to 500 kGy, the tensile strength and elongation at break of HDPE reduced significantly due to chain scission [13]. While polyamide 6 was reported not affected with single low radiation dosage, but the hardness, tensile strength, flexural strength and impact resistance of polyamide 6 were improved with the E-beam radiation up to 600 kGy, due to the increased cross-linking caused by radiation [32]. However, high irradiation dosage is not recommonded for sterilization purpose, and in general 25 kGy is a typical dose commonly employed to destroy the microbial load [7].

The tensile test results also revealed that the injection moulded Marlex samples had higher Young's modulus than the 3D printed Marlex samples, but had much lower percentage strain. The weaker mechanical properties of 3D printed objects compared to injection moulded objects can be explained by the layering manufacturing method of the 3D printing technology. The adhesion between layers or polymer strands plays a critical role in the mechanical properties of the 3D printed objects. Shaffer et al. reported that by improving the adhesion between polymer strands the chemical resistance and toughness of the 3D printed objected can be significantly improved [33]. In addition, the injection moulded Marlex samples had higher degree of crystallinity than 3D printed Marlex samples detected by DSC. The polymer chains of the injection moulded Marlex samples were pushed into highly organized structure with high pressure and cooled down quickly to form the shape, which results in high crystallinity, high mechanical strength, but low elongation. While the polymer chains of the 3D printed Marlex samples can move freely and cooled down slowly at room temperature, which results in relatively low crystallinity, low mechanical strength, but high elongation. This structure difference between injection moulded and 3D printed samples determined the different responds to VHP and E-beam processes as discussed above.

5. Conclusion

With the objective to investigate the effects of VHP and E-beam terminal sterilization processes on the 3D printed objects, this research studied the physical, chemical and thermal properties of 3D printed and injection moulded Marlex, and 3D printed Grilon samples upon VHP and E-beam terminal sterilization processes. The main findings were:

1. Oxidation occurred after both VHP and E-beam sterilization. Evidences included the discoloration and increased wettability due to the free radicals on the surface.
2. Crosslinking was caused by both VHP and E-beam sterilization treatment, evidenced with free hydroxyl radicals and intermolecular carbon bonding detected by FTIR; increased viscosity, storage modulus and loss modulus due to crosslinking.
3. E-beam treatment caused more severe oxidation than VHP process. Because the E-beam process resulted in more severe discoloration than VHP process, and the oxidation corresponding peaks detected by FTIR in E-beam treated samples, but not in VHP treated samples.
4. E-beam treatment caused more severe crosslinking than VHP process. Since E-beam process resulted in higher increase in viscosity, storage modulus and loss modulus than VHP treatment studied by rheometry and DMTA.
5. The 3D printed samples were less stable than injection moulded samples upon sterilization processes. Because more crosslinking associated peaks were detected by FTIR in 3D printed samples than in injection moulded samples, and E-beam process caused more dramatic increase in the degree of crystallinity of 3D printed samples than injection moulded samples.
6. Since the 3D printed objects were less stable than traditional manufactured objects, there may be a need to consider a reduction of sterilization parameters, especially for E-beam process, provided sterility assurance achieved.
7. Compared to 3D printed samples, the injection moulded samples exhibited higher tensile strength, higher degree of crystallinity, lower ductility, and higher thermal stability due to the tightly packed structures caused by injection moulding.
8. All the samples displayed a relatively good resistance to single cycle of VHP and E-beam process, evidenced with unaffected tensile properties, thermal stability and surface structure of all the samples.

Declaration of competing interest

The authors declare that there is no conflict of interests regarding the publication of this article, this manuscript has not been published elsewhere and it has not been submitted simultaneously for publication elsewhere. Martin Neff is an employee of ARBURG and Brian McEvoy is an employee of STERIS.

Acknowledgements

This publication has emanated from research conducted with the financial support of Athlone Institute of Technology under the Presidents Seed Fund, Enterprise Ireland funding under the Technology Gateway program, grant number TG-2017-0114 and Science Foundation Ireland (SFI) under Grant Number 16/RC/3918.

References

[1] A. Reichental, How 3D Printing Is Revolutionizing Healthcare as We Know it, TechCrunch, 2018. https://techcrunch.com/2018/04/05/bioprinted-organs-skin-and-drugs-how-3d-printing-is-revolutionizing-healthcare-as-we-know-it/. (Accessed 18 July 2019).
[2] N.P. Tipnis, D.J. Burgess, Sterilization of implantable polymer-based medical devices: a review, Int. J. Pharm. 544 (2018) 455–460, https://doi.org/10.1016/j.ijpharm.2017.12.003.
[3] J. Hayes, D. Kirf, M. Garvey, N. Rowan, Disinfection and toxicological assessments of pulsed UV and pulsed-plasma gas-discharge treated-water containing the waterborne protozoan enteroparasite Cryptosporidium parvum, J. Microbiol. Methods 94 (2013) 325–337, https://doi.org/10.1016/j.mimet.2013.07.012.
[4] Gamma Industry Processing Alliance, International Irradiation Association, White Paper: A Comparison of Gamma, E-Beam, X-Ray and Ethylene Oxide Technologies for the Industrial Sterilization of Medical Devices and Healthcare Products, 2017. www.gipalliance.net. (Accessed 23 July 2019).
[5] U.S. FOOD & DRUG ADMINISTRATION, FDA Innovation Challenge 2: Reduce Ethylene Oxide Emissions, FDA, 2019. https://www.fda.gov/medical-devices/general-hospital-devices-and-supplies/fda-innovation-challenge-2-reduce-ethylene-oxide-emissions. (Accessed 23 September 2019).

[6] N.P. Tipnis, D.J. Burgess, Sterilization of implantable polymer-based medical devices: a review, Int. J. Pharm. 544 (2018) 455–460, https://doi.org/10.1016/j.ijpharm.2017.12.003.
[7] S. Govindaraj, S.M. Muthuraman, Systematic review on sterilization methods of implants and medical devices, Int. J. Chem. Res. 8 (2015) 897–911. https://www.researchgate.net/publication/278242593.
[8] B. McEvoy, N.J. Rowan, Terminal sterilization of medical devices using vaporized hydrogen peroxide: a review of current methods and emerging opportunities, J. Appl. Microbiol. (2019) 14412, https://doi.org/10.1111/jam.14412, jam.
[9] I.V. Puhova, A.V. Kazakov, K.V. Rubtsov, A.V. Medovnik, I. Kurzina, Modification of polymer materials by electron beam treatment, Key Eng. Mater. 670 (2015) 118–125. www.scientific.net/kem.670.118.
[10] M. Sudol, K. Czaja, J. Cybo, P. Duda, Effect of electron-beam irradiation on structure of ultra high molecular weight polyethylene used in medical implants, Polymers 49 (2004) 841–844.
[11] K.J. Hemmerich, Polymer materials selection for radiation-sterilized products, Materials (2000). MDDI Online, https://www.mddionline.com/polymer-materials-selection-radiation-sterilized-products. (Accessed 23 July 2019).
[12] D.W. Plester, Effects of radiation sterilization on plastics, Steriliz. Technol. (1973) 151. https://inis.iaea.org/search/search.aspx?orig_q=RN:5109617.
[13] E.R. Elsharkawy, E.M. Hegazi, A.A.A. El-megeed, Effect of gamma irradiation on the structural and properties of high density polyethylene (HDPE), Int. J. Mater. Chem. Phys. 1 (2015) 384–387.
[14] V.R. Sastri, Engineering thermoplastics: acrylics, polycarbonates, polyurethanes, polyacetals, polyesters, and polyamides, in: Plast. Med. Devices, William Andrew Publishing, 2010, pp. 121–173, https://doi.org/10.1016/B978-0-8155-2027-6.10007-8.
[15] G. Kubyshkina, B. Zupančič, M. Štukelj, D. Grošelj, L. Marion, I. Emri, Sterilization effect on structure, thermal and time-dependent properties of polyamides, J. Biomaterials Nanobiotechnol. 2 (2011) 361–368, https://doi.org/10.1007/978-1-4614-0213-8_3.
[16] E. Shaheen, A. Alhelwani, E. Van De Casteele, C. Politis, R. Jacobs, Evaluation of dimensional changes of 3D printed models after sterilization: a pilot study, Open Dent. J. 12 (2018) 72–79, https://doi.org/10.2174/1874210601812010072.
[17] A.T. Miller, D.L. Safranski, K.E. Smith, D.G. Sycks, R.E. Guldberg, K. Gall, Fatigue of injection molded and 3D printed polycarbonate urethane in solution, Polymer 108 (2017) 121–134, https://doi.org/10.1016/J.POLYMER.2016.11.055.
[18] M. Dawoud, I. Taha, S.J. Ebeid, Mechanical behaviour of ABS: an experimental study using FDM and injection moulding techniques, J. Manuf. Process. 21 (2016) 39–45, https://doi.org/10.1016/J.JMAPRO.2015.11.002.
[19] M. Neff, O. Kessling, Layered functional parts on an industrial scale, Kunstst Int. (2014). www.kunststoffe-international.com. (Accessed 9 May 2019).
[20] R.L. Clough, K.T. Gillen, G.M. Malone, J.S. Wallace, Color formation in irradiated polymers, in: Radiat. Phys. Chem., Pergamon, 1996, pp. 583–594, https://doi.org/10.1016/0969-806X(96)00075-8.
[22] K.A. Murray, J.E. Kennedy, B. Mcevoy, O. Vrain, D. Ryan, R. Cowman, C. L. Higginbothama, Characterisation of the surface and structural properties of gamma ray and electron beam irradiated low density polyethylene, Int. J. Mater. Sci. 3 (2013) 1–8.
[23] C.M. Yakacki, M.B. Lyons, B. Rech, K. Gall, R. Shandas, Cytotoxicity and thermomechanical behavior of biomedical shape-memory polymer networks post-sterilization, Biomed. Mater. 3 (2008) 015010, https://doi.org/10.1088/1748-6041/3/1/015010.
[24] S.-T. Bee, W.-K. Wong, A.R. Rahmat, T.-T. Tee, C.T. Ratnam, J.-X. Lee, L.T. Sin, Effects of electron beam irradiation on the structural properties of polylactic acid/polyethylene blends, Nucl. Instrum. Methods Phys. Res. Sect. B Beam Interact. Mater. Atoms 334 (2014) 18–27, https://doi.org/10.1016/j.nimb.2014.04.024.
[29] N.D. Zaharri, Effect of peroxide cross-linking on viscoelastic behaviour and thermal properties of zeolite filled ethylene vinyl acetate composite, in: Compos. Adv. Manuf. Characterisation, 2016, pp. 177–186, https://doi.org/10.2495/978-1-78466-167-0/018.
[30] D. Bhatnagar, K. Dube, V.B. Damodaran, G. Subramanian, K. Aston, F. Halperin, M. Mao, K. Pricer, N.S. Murthy, J. Kohn, Effects of terminal sterilization on PEG-based bioresorbable polymers used in biomedical applications, Macromol. Mater. Eng. 301 (2016) 1211–1224, https://doi.org/10.1002/mame.201600133.
[31] S.O. Han, D.W. Lee, O.H. Han, Thermal degradation of crosslinked high density polyethylene, Polym. Degrad. Stab. 63 (1999) 237–243, https://doi.org/10.1016/S0141-3910(98)00098-6.
[32] N.K. Pramanik, R.S. Haldar, Y.K. Bhardwaj, S. Sabharwal, U.K. Niyogi, R. K. Khandal, Radiation processing of Nylon 6 by e-beam for improved properties and performance, Radiat. Phys. Chem. 78 (2009) 199–205, https://doi.org/10.1016/j.radphyschem.2008.11.004.
[33] S. Shaffer, K. Yang, J. Vargas, M.A. Di Prima, W. Voit, On reducing anisotropy in 3D printed polymers via ionizing radiation, Polymer 55 (2014) 5969–5979, https://doi.org/10.1016/J.POLYMER.2014.07.054.

International Journal of
Molecular Sciences

MDPI

Review

Pathogenic Drug Resistant Fungi: A Review of Mitigation Strategies

Mary Garvey [1,2] and Neil J. Rowan [3,*]

[1] Department of Life Science, Atlantic Technological University, F91 YW50 Sligo, Ireland
[2] Centre for Precision Engineering, Materials and Manufacturing Research (PEM), Atlantic Technological University, F91 YW50 Sligo, Ireland
[3] Bioscience Research Institute, Technical University Shannon Midlands Midwest, N37 HD68 Athlone, Ireland
* Correspondence: nrowan@ait.ie

Abstract: Fungal pathogens cause significant human morbidity and mortality globally, where there is a propensity to infect vulnerable people such as the immunocompromised ones. There is increasing evidence of resistance to antifungal drugs, which has significant implications for cutaneous, invasive and bloodstream infections. The World Health Organization (WHO) published a priority list of fungal pathogens in October 2022, thus, highlighting that a crisis point has been reached where there is a pressing need to address the solutions. This review provides a timely insight into the challenges and implications on the topic of antifungal drug resistance along with discussing the effectiveness of established disease mitigation modalities and approaches. There is also a need to elucidate the cellular and molecular mechanisms of fungal resistance to inform effective solutions. The established fungal decontamination approaches are effective for medical device processing and sterilization, but the presence of pathogenic fungi in recalcitrant biofilms can lead to challenges, particularly during cleaning. Future design ideas for implantable and reusable medical devices should consider antifungal materials and appropriates for disinfection, and where it is relevant, sterilization. Preventing the growth of mycotoxin-producing fungi on foods through the use of appropriate end-to-end processes is advisable, as mycotoxins are recalcitrant and challenging to eliminate once they have formed.

Keywords: fungi; antifungal drug resistance; decontamination; disease prevention; one health; risk mitigation

Citation: Garvey, M.; Rowan, N.J. Pathogenic Drug Resistant Fungi: A Review of Mitigation Strategies. *Int. J. Mol. Sci.* **2023**, *24*, 1584. https://doi.org/10.3390/ijms24021584

Academic Editor: Rustam I. Aminov

Received: 1 January 2023
Revised: 9 January 2023
Accepted: 11 January 2023
Published: 13 January 2023

1. Introduction

Fungi are eukaryotic microbial species that present in either yeast, mould or dimorphic forms. Yeasts are single celled, and they reproduce by budding, whereas fungi are multicellular with long filaments that are termed hyphae which grow via an apical extension. Fungi are abundant in the natural environment including water, soil and air, and they proliferate easily in warm and humid climates [1]. Indeed, fungi are the primary decomposers present in many ecosystems, releasing degradative enzymes for decomposing actions. Non-pathogenic endophyte fungal species are present in most forms of plant life between the plant cells, where they produce alkaloid toxins which act as insecticides and against other invertebrate animals and vertebrates [2]. Nycorrhizal fungi have a symbiotic relationship with plants, affecting nutrient and water uptake, while other species are plant pathogens, and they are associated with crop destruction, thereby impacting food security [3]. Fungal species are increasingly associated with morbidity and mortality, and they have become a significant public health risk [4]. Annually, fungal pathogens are the cause of approximately 13 million infections and 1.5 million deaths globally [5]. As they are traditionally associated with severe infections of immunocompromised persons, fungal infections are increasingly being associated with immunocompetent persons, with high

mortality rates [1]. Species such as *Cryptococcus*, *Candida*, *Aspergillus*, and *Pneumocystis* are associated with immunocompromised persons, with the dimorphic fungi including *Histoplasma*, *Blastomyces*, *Coccidioides* and *Paracoccidioides*, which affect immunocompetent persons [6].

As the primary or opportunistic pathogens of humans, the resultant disease or mycosis can be superficial, such as infection of skin, hair, nail, mucosal surfaces, and allergic reactions, or invasive fungal infections (IFIs) that affect the internal organs, which are progressive and often fatal [7]. Defects in cell-mediated immunity typically result in a decrease in the activity of CD4+ lymphocytes in HIV patients, and this is the major risk factor for *Pneumocystis* pneumonia [7]. To be classified as an invasive fungal disease (IFD), tissue damage must be observed via a histopathological exam, with the causative agent isolated from clinical samples and cultured [8]. Advances in medical procedures and increasing occurrences of medical surgical procedures and therapeutic treatment protocols have increased the rate of identifying opportunistic infections during intensive treatments [9]. Furthermore, fungal infectious diseases can complicate chronic conditions or co-morbidities in patients with asthma, cirrhosis, diabetes, cystic fibrosis (CF), chronic obstructive pulmonary disease (COPD), cancer, and infectious diseases, including COVID-19 and tuberculosis (TB) [5]. Co-infections with viral pathogens are particularly problematic, and the fungal species *Aspergillus* and *Mucor* are associated with increased mortality in patients presenting with COVID-19 [10]. Fungal meningitis resulting from *Aspergillus fumigatus* has been associated with parenteral injections of corticosteroids, while *Sarocladium kiliense* was detected in fungaemia in oncology patients receiving IV antinausea medication [7]. Blood cancers such as leukemia render the patients at high risk of invasive fungal diseases due to their prolonged and severe neutropenia as a result of anticancer therapeutic treatment [11]. The high prevalence of morbidity and mortality are observed in transplant patients, cancer patients, patients in intensive care units (ICU), and HIV, influenza and COVID-19 patients [12]. The emergence of fungal pathogens is related to climate change, agricultural techniques, occupational hazard, forest erosion, human migration patterns, and soil dispersion, patient immunosuppression, improved disease recognition, and diagnostic tests [13]. Antifungal resistance, antifungal drug tolerance, and biofilm formation directly contribute to rising cases of fungal morbidity and mortality [4]. Antifungal resistance is an absence of a discernable toxic effect on treated fungal species; whereas, antifungal tolerance is the emergence of a partial growth after 24 h that can be seen in susceptibility testing, including at inhibitory drug concentrations [12]. Resistance to one or more of the four antifungal drug classes, polyene, azoles, allylamines and echinocandins, is frequently observed [14]. The chemical structure formulae of related antifungal drugs can be sourced from published reviews [15,16].

In October 2022, the World Health Organisation (WHO) released their fungal priority pathogen list (FPPL), detailing the medium, high, and critically important fungal pathogens [17], highlighting the extent of the public health risk associated with fungal infectious diseases and the antimicrobial resistance (AMR) of major pathogens (Table 1). This timely and important report has three main areas for action including strengthening laboratory capacity and surveillance, sustainable research, development, and innovation, and public health interventions [17]. The rapid diagnosis of fungal diseases is a key factor in the early prevention and control, where tissue cultures and biopsies are the gold standard for diagnosing IFDs [1]. Fungal infections remain frequently underdiagnosed, which results in variable outcomes for patients. This review aims to highlight the clinically important fungal pathogens in line with the WHO FPPL, antifungal resistance, and the importance of preventative and diagnostic procedures to protect public health.

Table 1. WHO priority pathogens, at risk patients, mortality rates, and AMR profile.

Priority	Pathogen	At Risk Patients	Mortality	AMR
Medium	*Scedosporium* spp.	Cystic fibrosis [18] and organ transplant recipients [19]	50% of organ transplant patients [19]	Itraconazole [12]
	Lomentospora prolificans	Cystic fibrosis patients [18], immunocompetent, and immune-suppressed people [13]	46.9% and 87.5% of patients with disseminated disease [13]	MDR, pan resistant [13]
	Coccidioides spp.	COVID-19-infected, pregnant and immunocompromised people [20]	70% of immunocompromised people [20]	Azoles
	Pichia kudriavzeveii (Candida krusei)	Neonates in ICU and immunocompromised people	30% [21]	Innately to fluconazole; Echinocandin resistance often evident [21]
	Cryptococcus gattii	AIDS/HIV patients [7]	10% [22]	Echinocandins [4]
	Talaromyces marneffei	AIDS/HIV patients [23]	13.3% [23]	N/A
	Pneumocystis jirovecii	AIDS/HIV and [5] *Cytomegalovirus* [7] patients	50% of immunocompromised persons [24]	Polyenes-amphotericin B (AMP B) and azoles [4]
	Paracoccidioides spp	AIDS/HIV and immunocompromised [25] patients	from 6.2% to 27% [25]	AMP B, ketoconazole, fluconazole, itraconazole, and sulfamethoxazole [26]
High	*Nakaseomyces glabrata (Candida glabrata)*	Renal failure and ICU patients [27]	54% [27]	Fluconazole, echinocandins [12], and echinocandins [4]
	Histoplasma spp.	AIDS/HIV patients and TB patients [7]	60% of AIDS/HIV patients	Azole
	Eumycetoma-Madurella mycetomatis	Barefoot walking populations of tropical and subtropical countries [28]	Very rare [29]	Prolong treatment needed which can lead to toxicity and surgery [29]
	Mucorales	Immunocompromised, COVID-19-infected [5], and diabetes mellitus patients [7]	80% [4]	Echinocandins [4]
	Fusarium spp.	Immunosuppressed, oncology, and organ transplant patients [30]	37%; disseminated fusariosis cases: 83% [30]	MDR (Garvey et al., 2022), intrinsically to azoles [30]
	Candida tropicalis	Nosocomial patients and oncology patients [31]	64–86% at 10–30 days [31]	Echinocandins [4]
	Candida parapsilosis	Nosocomial patients [32]	26% [32]	Echinocandins [4]
Critical	*Cryptococcus neoformans*	AIDS/HIV patients and TB patients [7]	20%, or 100% if untreated [4]	Fluconazole [12], flucytosine [4]
	Candida auris	Neonates, elderly, chronically ill, and on-therapy patients	70% [4]	Azoles, lower sensitivity to the polyene amphotericin B, MDR [12], echinocandins, and flucytosine [4]
	Aspergillus fumigatus	Cystic fibrosis [18], COVID-19-infected [5], COPD, *Cytomegalovirus*, TB [7], and transplant patients [33]	70% of immunocompromised patients [4]	Triazole resistance [12] and echinocandins [4]
	Candida albicans	TB [7]	30–40% [4])	Echinocandins, flucytosine [4]

2. Clinical Significance of WHO Pathogen List

Like other microbial species, fungi possess impressive genetic plasticity, allowing them to adapt to their environmental niche and rapidly display resistance to chemical insults and AMR [34]. Fungal traits including a short generation time, a broad range of natural habits, and a eukaryotic cell structure makes them extremely virulent, thereby increasing their pathogenicity [12]. Their eukaryotic cell greatly hinders the therapeutic treatments as it predisposes the humans to the toxic side effects of antifungal drugs due to a decrease in the number of selective drug targets [4]. Fungi are associated with cutaneous infections, invasive fungal infections, and nosocomial blood infections or fungemia. Sepsis from fungemia also contributes to high mortality rates, particularly where *Candida* is the causative agent of the disease [35]. Antifungal and biocidal resistance and a lack of biocompatible therapeutic options for IFIs contributes greatly to the disease prevalence, where MDR and pan drug resistance is common amongst many nosocomial species including *Candida albicans*, non-*albicans Candida* strains (NAC), *Cryptococcus, Aspergillus*, and numerous dermatophyte species [4]. As such, emerging IFDs are associated with the difficulty in treating the infections and high rates of mortality globally [7].

2.1. Cutaneous Infection

Cutaneous mycoses are superficial fungal infections of the skin, hair, or nails (onychomycosis), which are the most important causative agents of disease, including dermatophytes species (*Microsporum, Trichophyton,* and *Epidermophyton*), *Malassezia furfur,* and *Candida* (*albicans* and non-*albicans Candida*). The prevalence rate of cutaneous or superficial fungal infections (SFI) is approximately 20–25% globally [36]. Immunocompromised persons are high risk of cutaneous infections, where homeless persons are an often-overlooked high risk group due to malnutrition, lack of healthcare, injury, and co-morbidities [37]. Homeless patients are also high risk for cutaneous fungal infection related complications including cellulitis and osteomyelitis [37]. Importantly, deep cutaneous fungal infections (DCFIs) have high rates of morbidity and mortality, particularly amongst immunocompromised patients, with mortality rates of 4% to 10% in localized infections and ca. 83% to 94% in disseminated cases [38]. Clinically, the diagnosis of cutaneous etiological agents involves both mycological and histological findings [39].

Most of the dermatophyte species are zoonotic, and they are also transmitted via soil and from person to person with associated conditions including tinea capitis, tinea corporis, tinea pedis, tinea unguium, and tinea faciei [40]. Dermatophytes invade the stratum corneum of the epidermis, and they are not typically associated with invasive diseases [41]. The treatment of extensive or invasive dermatophytosis relies on systemic antifungal therapy including griseofulvin, terbinafine, ketoconazole, fluconazole, itraconazole, posaconazole, voriconazole, and ravuconazole antifungals [39]. The dermal commensals *Malassezia* species are the causative agents of pityriasis versicolor (PV), *Malassezia folliculitis*, and seborrheic dermatitis [36]. Topical antifungal creams including zinc pyrithione, ketoconazole, and terbinafine are the primary treatment for PV with oral itraconazole and fluconazole, which is prescribed for persistent cases [42]. *Candida* is associated with oral thrush, vaginal candidiasis, oropharyngeal candidiasis, cutaneous candidiasis, paronychia, and onychomycosis [36]. *Aspergillus* species, namely, *A. fumigatus* or *A. flavus*, with *A. terreus* are associated with cutaneous infections, as they are primary or secondary pathogens [41]. Primary *Aspergillus* disease is related to skin abrasion due to injury, surgery, organ transplant, or burn wounds with secondary diseases associated with an invasive disease of the lungs [41]. Importantly, *Candida* and *Aspergillus fumigatus* are both listed as critically important on the WHO FPPL. Atopic dermatitis (AD) is a prevalent inflammatory skin disease, where chronic conditions can be associated with microbial infection-inducing bacterial and viral species. Studies have observed that the fungal species *Malassezia*, *Candida,* and dermatophyte species can be associated with chronic conditions [43]. Mycetoma is a WHO-recognized neglected tropical disease that is caused by the fungi eumycetoma, and the disease manifests as subcutaneous chronic granulomatous progressively morbid

inflammatory disease affecting the skin, subcutaneous tissue, deep structures, and bones, resulting in the destruction, deformity, loss of function, and it may lead to mortality [29]. The clinical symptoms of skin mycosis can vary across species, and cutaneous infections are often misdiagnosed as skin neoplasms or necrotizing lesions resulting from a lack of a suitable treatment [38].

2.2. Invasive Infection

Aspergillus, Cryptococcus, and *Candida* spp. are the main fungal species associated with invasive fungal infections of the lungs, brain, and bloodstream, respectively [12]. Disseminated infections are typically caused by *Blastomyces*, *Coccidioides*, *Paracoccidioides*, *Histoplasma,* and *Cryptococcus* spp. [44]. The pulmonary system (lungs) are the most common site of IFIs [45]. Triazole-resistant *A. fumigatus* and MDR yeast including *Candida glabrata* and *Candida auris* are of particular concern [46]. IFIs are separated from superficial mycoses due to the involvement of blood and other sterile body tissues or organs, and they are categorized as serious, deep, deep-seated, disseminated, and systemic fungal infections [47]. To cause an IFI in a patient, the fungi must have the ability to grow at or above 37 °C to reach internal tissues, the ability to lyse tissues and absorb their components, and they must be able to evade the host's immune system [7]. Clinically invasive fungal diseases affect many organs and deep tissues, causing endocarditis, meningitis, and respiratory infections, and they are not often detected in blood cultures [46,48]. Furthermore, the insertion of venous catheters and intravascular devices and medical interventions allow for infections with nosocomial IFDs [7]. Cryptococcal meningitis caused by *Cryptococcus neoformans* or *Cryptococcus gattii* is common in HIV patients, where both of the species possess an innate resistance to fluconazole, where a combination therapy with flucytosine is implemented to improve the fungal clearance [12]. Additionally, ca. 7% of systemic *Candida* infections display reduced azole susceptibility [44]. For invasive aspergillosis, voriconazole is typically administered, and amphotericin B (AMPB) and the echinocandins also show anti-aspergillus activity, whereas the *Aspergillus* species possess a resistance to fluconazole [41]. The effective treatment of IFIs is also impacted by the lack of an accurate diagnosis. The diagnosis of IFIs is challenging, as the tests are slow, with limited sensitivity and specificity, and they are typically quite expensive [46]. IFI diagnosis consists of three elements: clinical symptoms (fever, a cough, dyspnea, chest pain, and hemoptysis), which are not always present, imaging results, and the detection of the causative agent [45]. The diagnosis of pulmonary invasive aspergillosis, for example, is achieved via a computed tomography (CT) scan of the chest in a patient with the appropriate risk factors to observe the nodules that are surrounded by a halo, which is a radiological feature [33]. Many A. *fumigatus* isolates are resistant to triazoles and possess pan-azole resistance. *A. niger,* for example, has resistance to oral itraconazole and isovuconazole drugs, with *Aspergillus. terreus* and *Asperguillus nidulans* possessing a resistance to AMPB [49]. The FDA suggests that AMPB is the safest antifungal agent for the treatment of systemic fungal infections, irrespective of its side effects, long half-life, and liver and kidney toxicity [44].

2.3. Bloodstream Infection

The number of bloodstream infections (BSIs) with fungal etiological agents has increased in recent years. *Candida* species are responsible for 90% of the fungal BSIs, and they result in late-onset sepsis etiologies amongst neonates [50]. *Candida* BSIs have a mortality rate of 30–40%, regardless of the therapeutic treatments [51]. Interestingly, studies describe higher mortality rates among countries and regions, where Latin American has a rate of ca. 60% compared to 20% in Spain [52]. Additionally, 80% of *Candida* BSIs occur in immunocompetent patients with nosocomial co-morbidities [7]. Studies have demonstrated the risk factors including diabetes, neoplasm, neutropenia, renal insufficiency, immunosuppression, cardiovascular disease, surgery, and age for fungal BSIs [51]. The incidence rates of BSIs with fungal pathogens are ca. 4.1% and ca. 0.69% in ICU patients in developing and developed countries, respectively [53], and this is directly related to the use of antifungal

drugs, immunosuppression, steroids, placement of central venous catheters, and the low immunity of patients [51]. Echinomycin is recommended for fungal infections, fluconazole, however, is commonly used, particularly in developing countries, and it is associated with high rates of candidemia mortality due to azole resistance [54]. Non-*albicans Candida* species are more and more commonly associated with fungal BSIs, which are causative agents, *Candida parapsilosis* is associated with BSIs or candidemia in younger populations, with *C. glabrata* and *Candidatropicalis* being associated with elderly patient cohorts [51]. *C. tropicalis* is often associated with severe and fatal candidiasis, while *C. parapsilosis* is associated with lower mortality rates [52].

The widespread use of antifungal agents and increasing AMR has encouraged the emergence of non-*albicans Candida* BSIs, and studies have reported the use of echinocandins and azoles in the emergence of *C. parapsilosis* and *C. glabrata*, respectively [50]. Indeed, the multi-antifungal resistant, emerging, biofilm-forming *Candida auris* is listed as critically important by the WHO FPPL, and it is associated with fungal BSIs with high mortality rates [4]. Importantly, the health authorities recognize that *C. auris* is one of the most high-risk nosocomial pathogens due to its high transmissibility, AMR, and biocidal resistance [55]. The occurrence of MDR in fungal species has increased since 2017, particularly in *C. auris* and *C. glabrata*, which demonstrate resistance to the echinocandin drug class and fluconazole, which are the two first-line mono-therapeutic drugs for invasive candidiasis [44]. *Aspergillus* BSIs are not common, and they are typically associated with the dissemination of invasive lung aspergillosis or the infection of critically ill patients [56]. The initiation of a fungal therapy is linked to mortality rates; studies have demonstrated that the effective treatment of fungal BSIs after 12 h of withdrawing blood samples is linked to high mortality rates, while the initiation of therapy within a 12 h period of blood sampling is linked to lower mortality rates [57]. Furthermore, optimal dosing, dosing intervals, and the duration of the treatment are important factors in drug efficacy, reduced patient toxicity, and the prevention of fungal resistance [57].

3. Efficacy of Disinfection Strategies for Addressing Fungal Pathogens

3.1. Reusable Medical Devices and Surgical Instruments

Despite advances in medicine and innovations in many underpinning fields including disease prevention and control, the Spaulding classification system, which was originally proposed in 1957, remains widely used for defining the disinfection and sterilization of contaminated re-usable medical devices and surgical instruments [58]. Medical devices are a common source of hospital acquired infections (HAIs), and they have accounted for between 60% and 80% of all bloodstream-, urinary tract-, and pneumonia-related HAIs [59]. For example, at least 18 million gastrointestinal endoscopies are conducted each year in the United States [60]. Each of these procedures involves use of surgical instruments or medical devices that contact the patient's sterile tissue or mucous membrane [61]. However, there is a marked lack of published information on the relevance of priority WHO fungal pathogens and the contamination of reusable medical devices in terms of transmission post-processing and sterilization. Notably, fungal infections cause over 1.5 million deaths per year, and a quarter million of these deaths are caused by the genus *Candida* [62]. The mortality rate of invasive candidiasis (infections by *Candida*) can be greater than 40% due to there being limited treatment options and increased antifungal resistance [4,62]. To mitigate the risk of HAIs, the current methods for the safe processing of medical devices still rely upon the guiding classification system of Dr E. H. Spaulding, which was originally conceived and published over 50 years ago [61].

Spaulding's underpinning hypothesis was that healthcare facilities should apply appropriate disinfection and sterilization methods to process medical devices and surgical instruments based on the degree of the patients' risk of acquiring an infection due to their use. Spaulding's system divides all of the medical devices into three discrete categories based on the severity of the perceived risk to the patients of acquiring an infection from their use.

Critical use items: Where a device enters the sterile tissue and must be sterile, which is defined as being free from viable microorganisms [58]. Items contaminated with any microorganism (including fungal species) are referred to as high risk to the patients if they are contaminated and enter the sterile tissue or vascular system, and they have a high potential for causing disease transmission [61]. Such items should be sterile, such as by using steam sterilization where it is possible. The examples include surgical instruments. Given that many items contain heat-sensitive materials, other appropriate sterilization modalities should be applied, including vaporized hydrogen peroxide (VH_2O_2), VH_2O_2 gas plasma, and ethylene oxide gas [63]. The use of liquid chemical sterilants may also be considered appropriate, such as formulations based on glutaraldehyde (GTA), peracetic acid (PA), hydrogen peroxide (HP), or ortho-phthalaldehyde (OPA) [61,63].

Semi-critical use items: When a device only comes into contact with the intact mucus membranes or nonintact skin, it should also be subjected to sterilization, or if this is not feasible due to its sensitive material composition or complex design features, then a high-level disinfection (HLD) process must be deployed at a minimum level that would be expected to kill all of the microorganisms, except for the bacterial endospores [63]. The examples of semi-critical items including "respiratory therapy, anaesthesia equipment, some endoscopes, laryngoscope blades and handles, esophageal manometry probes, endocavitary probes, nasopharyngoscopes, prostate biopsy probes, infrared coagulation devices, anorectal manometry catheters, cystoscopies, and diaphragm fitting rings" [61]. Depending on the regional claim requirements, disinfectants should demonstrate a broad spectrum of antimicrobial activity, and typically, the ability to eliminate at least 10^6 (or 6-logs) of the mycobacterial cells on the contaminated surfaces of the medical devices. For the fungi of concern, mycobacteria are typically deemed to exhibit greater resistance to high-quality disinfectants, thus, mycobacterial cells are recognized as being representative (or bio-indicators) of the HLD process efficacy. The examples of chemical disinfectants authorized in the USA for HLD use include biocides such as GTA HP, OPA, hypochlorite, and PA with HP [64].

Non-critical use items: Which includes devices that are in contact with intact skin (but not mucous membranes), requiring low-level-to-intermediate-level disinfection [64]. The skin contains intact integumentary layers, and as such, it provides a natural barrier to the microorganisms. There remains a risk to the skin as a result of cross-contamination from the devices, but this risk is considered to be low. These risks can be practically reduced by the combination of physical removal and disinfection [63]. The examples of non-critical use items include blood pressure cuffs, bed surfaces and rails, patient furniture, and so forth [61].

Figure 1 illustrates the microbial resistance profile to applied disinfection and sterilization modalities. It should be noted that the overall pattern of resistance to applied lethal technologies may vary depending on the modality. Microorganisms with higher resistance are widely used to challenge and test the effectiveness of disinfection and sterilization methods. Mycobacterial cells and *Bacillus* endospores have been used as indicators of HLD and sterilization, respectively [61]. Fungi exhibit greater biocidal resistance to enveloped viruses (such as HIV and SARS-COV-2) and to Gram-positive and -negative vegetative bacterial cells. Fungi present in vegetative- and spore-forming morphologies can be further differentiated based upon these morphologies with increasing exposure to these applied lethal stresses. For example, *Aspergillus* spores are more tolerant to higher doses of UV-irradiation due to the protective peak absorption of pigments at a similar UV-C wavelength to that of DNA (ca. from 250 to 260 nm) [65,66]. However, fungi are considered to be more susceptible to high-level disinfection (HLD) compared to similarly treated non-enveloped viruses (such as norovirus), mycobacterial cells, and parasitic oocysts (*Cryptosporidium* species), or cysts (Giardia species) [67–69].

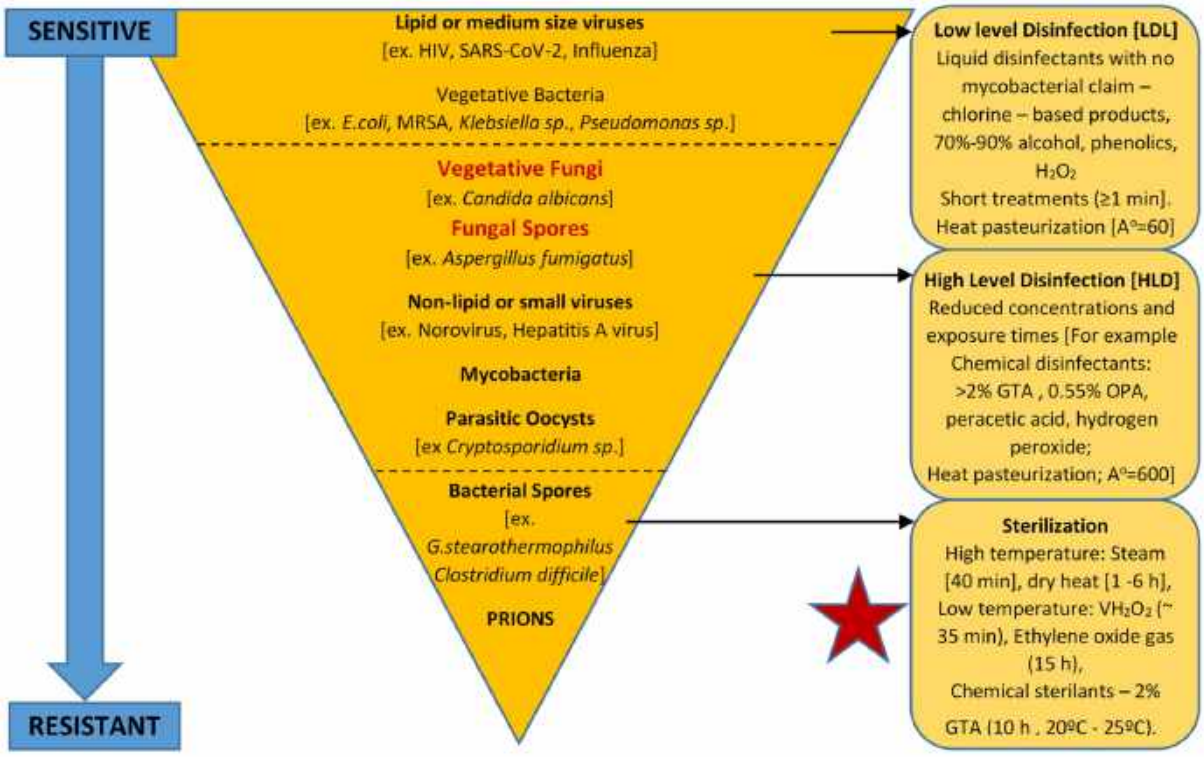

Figure 1. Pyramid of increasing microbial resistance to medical device processing and sterilization stressors.

Over the last few decades, there has been increasing amounts of genomic evidence of innate and adaptive microbial resistance to chemical disinfectant methods along with adaptive tolerance to environmental stresses. For example, this has been particularly evident in bacteria that are exposed to food processing (such as osmotic, acid, heat or UV-stressors) [70] or chemical biocide stresses [71], where the tolerance has been attributed to the expression of specific molecular determinants, ranging from protective stress protein synthesis to antimicrobial efflux pumps. The best published evidence argues that established HLD treatment and sterilization modalities effectively kill the free living fungi [72], however, the presence of fungi in recalcitrant biofilms may harbor these pathogens on the medical devices in the processing conditions used [62,73–75]. This area requires attention in future research. There is also a commensurate need to investigate the efficacy of HLD and sterilization in parallel with new medical design features, material compatibility, and cleaning regimes [76,77].

To reduce these risks of biofilm-mediated infections (including fungal) which are transmitted via contaminated medical devices, it is proposed that we should review the achievable and appropriate instructions of the manufacturers in the cleaning and processing of complex devices, where there can be as many as 100 steps to address by healthcare workers in the Sterile Services Department [61]. This brings the margin of error to near zero, which represents a higher risk to the patients. For example, it has been proposed that we should elevate the classification of high-risk flexible endoscopes (such as duodenoscopes) from semi-critical to critical use, which entails a transition to using low-temperature sterilization modalities instead of routinely using high-level disinfection, thus, increasing the margin of safety for endoscope processing. Gastrointestinal (GI) endoscopes can become highly contaminated during their use, where the internal long narrow lumen can contain between 7 to 10 $\log_{10}$ enteric microorganisms, and the microbial load of colon is ca. 9 to 12 $\log_{10}$/mL [61]. Outbreaks have been associated with medical device transmission where there were no reported links to"inadequate cleaning, inappropriate disinfection, and damaged endoscopes, or flaws in the design of endoscopes or automated endoscope

re-processor" [61]. Often, these devices have also been highlighted as causative agents in outbreaks of multidrug-resistant organisms (MDROs), in which there were no obvious breaches in the endoscope reprocessing procedures [78–85]. However, the role of fungal infections arising from transmission by contaminated reusable medical devices through biofilms needs further research, as where there is a need to co-develop clinical diagnostics may be underappreciated.

3.2. Central Venous and Urinary Catheters

Modern technology has allowed us to use a wider and newer variety of medical devices. The combination of an increasingly aging population and a consistently growing number of inserted devices is likely to escalate the occurrence of infectious complications related to medical devices [86]. The number of indwelling medical devices is increasing, and an increasing proportion of device-related infections are being caused by *Candida* spp. *Candida* spp. produce biofilms on synthetic materials, which facilitates the adhesion of the organisms to the devices and renders them relatively refractory to medical therapy. The management of device-related *Candida* infections can be challenging. The removal of the infected device is generally needed to cure the *Candida* infections caused by the medical devices. However, since the pathogenesis of *Candida* bloodstream infection is complicated, more studies are necessary to determine the role of catheter exchange in patients with both gastrointestinal tract mucositis and indwelling catheters. Kojaic and coworkers [86] noted that *C. albicans* biofilm formation has three developmental phases: the adherence of yeast cells to the device's surface (early phase), the formation of a matrix with dimorphic switching from yeast to hyphal forms (intermediate phase), and the increase in the amount of the matrix material, taking on a three-dimensional architecture (maturation phase). Fully mature *Candida* biofilms have a mixture of morphological forms, and they consist of a dense network of yeasts, hyphae, and pseudohyphae in a matrix of polysaccharides, carbohydrate, protein, and unknown components. The organisms in biofilms behave differently from freely suspended cells with respect to antimicrobial resistance. Both the bacteria and *Candida* cells within biofilms are markedly resistant to antimicrobial agents [86].

C. auris has become a global threat as it can colonize the skin, medical devices, and hospital environments, causing nosocomial outbreaks of blood and urinary tract infections worldwide [62]. *Candida auris* can spread among patients in hospitals, and it is intrinsically resistant to one or more classes of antifungals, which makes it particularly difficult to treat in healthcare settings. Comparative genomics has demonstrated that *C. auris* has expanded families of transporters and lipases, as well as mutations and copy number variants, in genes/enzymes linked to increased resistance and virulence [2]. Understanding the evolution of emerging fungal pathogens such as *C. auris* will be useful for the design of antifungal drugs and therapies for susceptible patients, potentially improving the clinical outcomes.

Piktel et al. [87] reported on the number of antimicrobial agents with the ability to prevent device-associated infections, and these have been proposed as biomaterials coatings. Alternative methods are constantly being developed using established antimicrobial agents. A large number of these applications involve the coating of medical device surfaces with metallic nanoparticles, such as zinc oxide (ZnO NPs)6, silver (Ag NPs)7, copper (Cu NPs), or titanium (TiO_2 NPs), and the mechanism of protective effects of those nanomaterials includes mostly the disruption of the microbial membranes and the prevention of microbial proliferation of the surface of the device or implant. Slamborova et al. [88] combined silver, copper, and titanium dioxide nanoparticles to establish long-term, broad-spectrum antifungal and antibacterial coverage, while maintaining the appropriate mechanical properties of the coating itself. Piktel et al. [87] revealed that a relatively low dose of nanomaterials, i.e., ranging from 0.78 to 0.625 ng mL^{-1}, should be considered as fungicidal and bactericidal, as has been demonstrated for *C. albicans*. Importantly, the minimum biofilm inhibitory concentrations (MBIC) were not significantly higher than the bactericidal ones were; for the majority of strains, the MBIC value was not greater than 0.625 ng mL^{-1}. Owing to their unique physicochemical features and low cytotoxicity, gold nanoparticles (Au NPs)

have been widely used in biological and biotechnological applications as biocidal agents, drug delivery systems, photosensitizer, and molecular diagnostic tools [8]. Piktel et al. [87] assessed the antimicrobial efficiency of non-spherical gold nanoparticles in the shapes of rods (AuR NPs), peanuts (AuP NPs), and stars (AuS NPs), as well as porous spherical-like nanoparticles (AuSph (70C) NPs), which exhibited potent antifungal effects, which contrasts those of previous reports including microgram concentrations (μg mL^{-1}) of gold nanoparticles.

4. Knowledge Gap in Molecular and Cellular Mechanisms Underpinning Disinfection of Fungal Pathogens including AMR Post-Treatment Modalities

Advanced studies on cell survival following antimicrobial processes also are of interest [89]. As an example, Farrell et al. [90] highlighted the potential of addressing a single composite study to address the relationship between the use of pulsed UV light irradiation and the simultaneous occurrence of molecular and cellular damage in clinical strains of *C. albicans*. This is particularly relevant, and it showed that the occurrence of late apoptotic and necrotic cell phonotypes can be detected in real-time using specific representative biomarkers. This coincides with the occurrence of irreversible fungal cell death, which may potentially supplement or replace the lengthy standard culture-based methods where there was good agreement between these indirect biomarker and direct culture-base enumeration approaches. Notably, this constituted the first study to investigate the mechanisms of cell destruction caused by pulsed UV using a sequential and simultaneous microbial protein leakage assay and the lipid hydroperoxidation in the cell membranes, specific patterns of reactive oxygen species generation, and nuclear damage of treated microbial cells using a Comet assay, along with the detection of specific apoptotic and necrotic stages. Design, testing, and validating the real-time markers to demonstrate irreversible fungal death will prove the effectiveness of the disinfection modalities.

5. Need for Improved In Vitro and In Vivo Compatibility Tests for Medical Devices Encompassing Antifungal and Disinfection Efficacy

Researchers have noted that the limitations of in vitro and animal models of chronic device-related infections are important in the context of advancing the med-tech sector, with implications for pressing research and clinical practice [74]. Ramstedt et al. [75] evaluated the efficacy of antimicrobial and antifouling materials for a urinary tract medical device that also enabled the transmission of fungal infections. These authors addressed the challenges of antimicrobial material testing, including surface characterization, biocompatibility, cytotoxicity, in vitro and in vivo tests, microbial strain selection, and hydrodynamic conditions, from the perspective of complying to the complex pathology of device-associated urinary tract infections. Standard assays should be developed that enable us to make comparisons between the inter-laboratory generated results of industries and academia to perform harmonized assessments of the antimicrobial properties of urinary tract devices in a reliable way that includes improving in vitro and in vivo biocompatibility testing. Moreover, the high risk of infection and its associated costs clearly underlines the need to provide patients with devices with the lowest possible risk of infection, and it emphasizes the need for innovative products that reduce the incidence rate of device-associated UTIs. Although standards are available for guiding the development of new devices with respect to biocompatibility (ISO 10993) and material characterization, no such guidance exists for the development of antimicrobial devices [75].

6. Mycotoxins and Appropriate Decontamination Strategies

Mycotoxins are secondary metabolites of mold and fungi; they are generally toxic to living organisms. This term, by general consensus, is used almost exclusively for fungi associated with food products and animal feed, excluding the toxins produced by mushrooms. Mycotoxins are secondary metabolites with no apparent function in the normal metabolism of fungi [91]. They are produced mainly, although not exclusively, when the fungus reaches maturity [91]. They are molecules with structures which vary from simple

heterocyclic rings with molecular weights of up to 50 Da to groups with 6–8 irregularly arranged heterocylic rings with a total molecular weight of >500 Da, and they do not show immunogenicity. Studies have revealed the existence of at least around 400 different mycotoxins [92]. Hundreds of mycotoxins have been identified thus far, with some of them, such as aflatoxins, ochratoxins, trichothecenes, zearalenone, fumonisins, and patulin, being considered agro-economically important [91]. Several factors contribute to the presence of mycotoxins in food, such as climatic conditions, pest infestation, and poor harvest and storage practices. Exposure to mycotoxins, which occurs mostly by ingestion, leads to various diseases, such as mycotoxicoses and mycoses, which may eventually result in death [91,93]. Mycotoxins can enter the human and animal food chains through direct or indirect contamination. The indirect contamination of foodstuffs and animal feed occurs when any ingredient has been previously contaminated with a toxigenic fungus, and even though the fungus has been eliminated during the process, the mycotoxins remain in the final product [92]. Direct contamination, on the other hand, occurs when the product, food, or feed becomes infected with a toxigenic fungus, resulting in the subsequent formation of mycotoxins [94]. Thus, more than a hundred mycotoxins are known, and most of them are produced by some of the species belonging to one of three fungi genera: *Aspergillus*, *Penicillium*, and/or *Fusarium* [95]. According to the available literature the "presence of the following mycotoxins in pollen has been investigated or proved with appropriate analytical methods and analysis: Aflatoxins (AFs), ochratoxins (OTs), fumonisins (FBs), zearalenone (ZEN), deoxynivalenol (DON), and its acetoxy derivative, T-2 toxin (T-2), HT-2 toxin, fusarenon-X, diacetoxyscirpenol, nivalenol, neosolaniol, roridin A, verrucarrin A, α-β-dehydrocurvularin, phomalactone,6-(1-propenyl)-3,4,5,6-tetrahydro-5-hydroxy-4H-pyran-2-one, 5-[1-(1hydroxibut-2-enyl)]-dihydrofuran-2-one and 5-[1-(1-hydroxibut-2-enyl)]-furan-2-one" [96].

The main aflatoxins that are known about are called B1, B2, G1, and G2 based on their fluorescence under ultraviolet light (B = Blue; G = Green) and their mobility during thin-layer chromatography [92]. They are mainly produced by *A. flavus and Aspergillus parasiticus*. It is known that only 50% of the strains of these species produce aflatoxins and that some of the aflatoxigenic isolates produce up to 106 μg/kg of aflatoxins [92]. Due to their capacity to bind with the DNA of cells, aflatoxins affect protein synthesis besides contributing to the occurrence of thymic aplasia (congenital absence of thymus and the parathyroids, with a consequent deficiency in the cell immunity, which is also known as DiGeorge's syndrome) [92]. Aflatoxins have oncogenic and immunosuppressive properties, inducing infections in people who have been contaminated with these substances. Ochratoxin A is a metabolite of *Aspergillus ochraceus*, and it has a chemical structure similar to that of aflatoxins. It is associated with nephropathy in all of the animals that have been studied to date [97]. Besides being recognized as nephrotoxic, ochratoxin A, it also shows hepatoxic, immunosuppressive, teratogenic, and carcinogenic behaviors [92].

Fumonisins are produced by several species of the genus *Fusarium*, especially by *Fusarium verticillioides* (previously classified as *Fusarium moniliforme*), *Fusarium proliferatum and Fusarium nygamai*, besides *Alternaria alternata f.sp. lycopersici* [92]. The presence of fumonisins in corn grains has been associated with cases of oesophageal cancer [98]. Fumonisins are also responsible for leukoencephalomacia in equine species and rabbits [92,99], and hepatotoxic, carcinogenic, and apoptosis (programmed cell death) effects in the livers of rats [100]. Patulin is isolated from *Penicillium griseofluvum*, and albeit inconclusively, it is considered to be toxic to animals and plants [92]. Other mycotoxins of notoriety include ergot alkaloids and trichothecenes, which have been extensively reviewed (such as [91]).

The fungal contamination of different feed/food, including pollen will be more frequent as a result of the occurrence of intensive climatic changes [96]. The quality of pollen can be significantly influenced by the presence of toxigenic fungi. Since it has been proved that the absence of microbial contamination in pollen does not exclude the presence of mycotoxins, mycotoxicological analyses should also be included as a regular control measure, together with microbiological tests. Since aflatoxins and ochratoxins have been proven to be

carcinogenic substances, their presence in pollen is extremely undesirable. Therefore, it is important to monitor the mold and mycotoxin levels in feed/food in order to avoid adverse health effects. The contamination of food and feed by mycotoxins represents a serious health problem for humans and animals, as well as a considerable economic obstacle in African, Asian, and Latin American countries, where the trade balance is based on the exportation of commodities. The recognition of problems caused by mycotoxins in foods destined for human and animal consumption is undoubtedly the first step toward the implementation of programs which enable the adoption of appropriate measures for the prevention and reduction of this problem [92]. The chemical structures of the principal mycotoxins can be found in many published reviews [91,92].

Thus, the consumption of mycotoxins-contaminated feed causes a plethora of harmful responses from acute toxicity to many persistent health disorders with lethal outcomes, such as mycotoxicosis when it is ingested by animals. Therefore, the main task for feed producers is to minimize the concentration of mycotoxins by applying different strategies that are aimed at minimizing the risk of the mycotoxin effects on animal and human health. However, once the mycotoxins enter the production chain, it is hard to eliminate or inactivate them [93]. Notably, mycotoxin-producing fungi are readily destroyed by moderate levels of disinfection. However, given the recalcitrant nature of mycotoxins, emphasis should be placed on ensuring appropriate end-to-end food production and management to prevent the growth of mycotoxin-producing organisms, such as cleaning the grains and removing the kernels that harbor molds. The use of feed additives or supplements that decrease the risk of animal exposure to mycotoxins can be viewed as a means of enhancing animal welfare. These feed supplements are referred to as the substances blended into feed (e.g., mineral clay, microorganism, and yeast cell wall), adsorbing or detoxifying the mycotoxins in the digestive tract of animals (biological detoxification) [93]. In general, mycotoxins are mainly stable compounds under thermal processing conditions used in feed and food [101]. However, the different thermal food and feed treatments that can have different impacts on the mycotoxins include extrusion, cooking, frying, baking, canning, crumbling, pelleting, roasting, flaking, and alkaline cooking. Among the thermal treatments, the utilization of high-temperature processes demonstrates the greatest potential for mycotoxin reduction [93]. Kabak [102] noted that the application of extrusion at a temperature that is higher than 150 °C has a significant impact on the reduction of zearalenone and fumonisins, while the same conditions led to the moderate reduction of aflatoxins and deoxynivalenol. Oxidizing agents such as ozone and hydrogen peroxide have been used to decontaminate mycotoxin-contaminated raw feed and compound feed [103]. The application of microorganisms or enzyme systems to contaminated feeds can detoxify the mycotoxins by metabolism or degradation in their gastrointestinal tract. This process is an irreversible and environmentally friendly method of detoxification, as it does not leave toxic residues or unwanted by-products [93]. However, the levels of particular mycotoxins in feeds have been reduced, but so far, no single technique has been established that is equally efficient against the broad variety of mycotoxins that can co-occur in various commodities [93]. Furthermore, the procedures of detoxication that appear to be efficient in vitro will not necessarily maintain their effectiveness in an in vivo test.

7. Conclusions

Fungal pathogens represent a serious public health risk, where AMR-incorporating biocidal resistance has proliferated the issue. The WHO has announced a fungal priority pathogen list, further highlighting the seriousness of the disease risk of these potentially life-threatening organisms. Antifungal resistance is further augmented by a lack of novel antifungal therapeutic options and associated biocompatibility issues, thereby limiting the medical applications. Without efficient control measures, the critically important WHO listed pathogens such as *C. auris* and *C. neoformans* will continue to result in unacceptably high rates of mortality. Additionally, the emergence of new species such as the non-*ablicans Candida* BSIs will increase, leading to the proliferation of AMR and increasing the death

rates, particularly in immunocompromised persons. As with all of the infectious diseases, prevention is the optimal way to mitigate disease outbreak and transmission. The application of effective disinfection and sterilization regimes, particularly in hospital settings, is vitally important, where a focus on fungal biofilm formation on indwelling medical devices is important. Currently, there is an ongoing drug resistance crisis globally, where fungal AMR is often overlooked in terms of diagnosis and pathogen monitoring. In order to more accurately monitor and respond to the actual number of fungal-mediated infections that is underestimated, there is a need to improve fungal diagnostic and detection methods along with effective communication of same to clinicians. The widespread application of antimicrobial therapeutics without having conducted more investigative studies should not be applied. There is a pressing need to understand the cellular and molecular mechanistic relationship between device reprocessing and the inactivation of biofilm-forming fungi in order to mitigate device-related transmission. Semi-critical devices should be reviewed to reduce the risk to the patient, where there is an unreasonable number of cleaning and processing steps to satisfy the margin of safety in the healthcare setting. Preventing the growth of mycotoxin-producing fungi on foods through the performance of appropriate end-to-end processes is advisable, as mycotoxins are recalcitrant and challenging to eliminate once they have been formed. Adopting the OneHealth approach will support and enable solutions to address this complex societal challenge.

Funding: This review paper was not supported by any funded instrument.

Data Availability Statement: No new data was curated in this review, which was based on a critique of existing best-published information shared in journals and books.

Conflicts of Interest: The authors declare no conflict of interest.

References

1. Huang, J.; Liu, C.; Zheng, X. Clinical features of invasive fungal disease in children with no underlying disease. *Sci. Rep.* **2022**, *12*, 208. [CrossRef] [PubMed]
2. Blackwell, M. The Fungi: 1, 2, 3 . . . 5.1 million species? *Am. J. Bot.* **2011**, *98*, 426–438. [CrossRef] [PubMed]
3. Petrasch, S.; Knapp, S.J.; van Kan, J.; Blanco-Ulate, B. Grey mould of strawberry, a devastating disease caused by the ubiquitous necrotrophic fungal pathogen *Botrytis cinerea*. *Mol. Plant Pathol.* **2019**, *20*, 877–892. [CrossRef] [PubMed]
4. Garvey, M.; Meade, E.; Rowan, N.J. Effectiveness of front line and emerging fungal disease prevention and control interventions and opportunities to address appropriate eco-sustainable solutions. *Sci. Total Environ.* **2022**, *851*, 158284. [CrossRef]
5. Rayens, E.; Norris, K.A. Prevalence and Healthcare Burden of Fungal Infections in the United States, 2018. *Open Forum Infect. Dis.* **2022**, *9*, ofab593. [CrossRef]
6. Alastruey-Izquierdo, A.; Melhem, M.S.C.; Bonfietti, L.X.; Rodriguez-Tudela, J.L. Susceptibility Test for Fungi: Clinical and Laboratorial Correlations in Medical Mycology. *Rev. Inst. Med. Trop. São Paulo* **2015**, *57* (Suppl. 19), 57–64. [CrossRef] [PubMed]
7. Firacative, C. Invasive fungal disease in humans: Are we aware of the real impact? *Mem. Inst. Oswaldo Cruz* **2020**, *115*, e200430. [CrossRef]
8. Donnelly, J.P.; Chen, S.C.; Kauffman, C.A.; Steinbach, W.J.; Baddley, J.W.; Verweij, P.E. Revision and update of the consensus definitions of invasive fungal disease from the European Organization for Research and Treatment of Cancer and the Mycoses Study Group Education and Research Consortium. *Clin. Infect. Dis.* **2019**, *71*, 1367–1376. [CrossRef]
9. Wagner, K.; Springer, B.; Pires, V.P.; Keller, P.M. Molecular detection of fungal pathogens in clinical specimens by 18S rDNA high-throughput screening in comparison to ITS PCR and culture. *Sci. Rep.* **2018**, *8*, 6964. [CrossRef]
10. Meijer, E.F.J.; Dofferhoff, A.S.M.; Hoiting, O.; Buil, J.B.; Meis, J.F. Azole-resistant COVID-19-associated pulmonary *Aspergillosis* in an immunocompetent host: A case report. *J. Fungi* **2020**, *6*, 79. [CrossRef]
11. Abers, M.S.; Ghebremichael, M.S.; Timmons, A.K.; Warren, H.S.; Poznansky, M.C.; Vyas, J.M. A critical reappraisal of prolonged neutropenia as a risk factor for invasive pulmonary aspergillosis. *Open Forum Infect. Dis.* **2016**, *3*, ofw036. [CrossRef]
12. Gow, N.A.R.; Johnson, C.; Berman, J.; Coste, A.T.; Cuomo, C.A.; Perlin, D.S.; Bicanic, T.; Harrison, T.S.; Wiederhold, N.; Bromley, M.; et al. The importance of antimicrobial resistance in medical mycology. *Nat. Commun.* **2022**, *13*, 5352. [CrossRef] [PubMed]
13. Konsoula, A.; Tsioutis, C.; Markaki, I.; Papadakis, M.; Agouridis, A.P.; Spernovasilis, N. *Lomentospora prolificans*: An Emerging Opportunistic Fungal Pathogen. *Microorganisms* **2022**, *10*, 1317. [CrossRef] [PubMed]
14. Fisher, M.C.; Alastruey-Izquierdo, A.; Berman, J.; Bicanic, T.; Bignell, E.M.; Bowyer, P.; Bromley, M.; Brüggemann, R.; Garber, G.; Cornely, O.A. Tackling the emerging threat of antifungal resistance to human health. *Nat. Rev. Microbiol.* **2022**, *20*, 557–571. [CrossRef] [PubMed]

15. Casteli, M.V.; Derita, M.G.; Lopez, S.N. Novel antifungal agents: A patent review (2013–present). *Expert Opin. Ther. Pat.* **2016**, *27*, 415–426. [CrossRef] [PubMed]
16. Van Daele, R.; Spriet, I.; Wauters, J.; Maertens, J.; Mercier, T.; Van Hecke, S.; Bruggemann, R. Antifungal drugs: What brings the future? *Med. Mycol.* **2019**, *57*, S328–S343. [CrossRef] [PubMed]
17. World Health Organization (WHO). WHO Fungal Priority Pathogens List to Guide Research, Development and Public Health Action. 2022. Available online: https://www.who.int/publications/i/item/9789240060241 (accessed on 16 November 2022).
18. de Jong, C.C.M.; Slabbers, L.; Engel, T.G.P.; Yntema, J.B.; van Westreenen, M.; Croughs, P.D.; Roeleveld, N.; Brimicombe, R.; Verweij, P.E.; Meis, J.F.; et al. Clinical relevance of *Scedosporium* spp. and *Exophiala dermatitidis* in patients with cystic fibrosis: A nationwide study. *Med. Mycol.* **2020**, *58*, 859–866. [CrossRef]
19. Sahi, H.; Avery, R.K.; Minai, O.A.; Hall, G.; Mehta, A.C.; Raina, P.; Budev, M. *Scedosporium apiospermum* (*Pseudoallescheria boydii*) Infection in Lung Transplant Recipients. *J. Heart Lung Trans.* **2007**, *26*, 350–356. [CrossRef]
20. Boro, R.; Iyer, P.C.; Walczak, M.A. Current Landscape of Coccidioidomycosis. *J. Fungi* **2022**, *8*, 413. [CrossRef]
21. Douglass, A.P.; Offei, B.; Braun-Galleani, S.; Coughlan, A.Y.; Martos, A.A.R.; Ortiz-Merino, R.A.; Byrne, K.P.; Wolfe, K.H. Population genomics shows no distinction between pathogenic *Candida krusei* and environmental *Pichia kudriavzevii*: One species, four names. *PLoS Pathog.* **2018**, *14*, e1007138. [CrossRef]
22. Hurtado, J.C.; Castillo, P.; Fernandes, F.; Navarro, M.; Lovane, L.; Casas, I.; Quintó, L.; Marco, F.; Jordao, D.; Ismail, M.R.; et al. Mortality due to *Cryptococcus neoformans* and *Cryptococcus gattii* in low-income settings: An autopsy study. *Sci. Rep.* **2019**, *9*, 7493. [CrossRef] [PubMed]
23. Shi, M.; Lin, J.; Wei, W.; Qin, Y.; Meng, S.; Chen, X.; Li, Y.; Chen, R.; Yuan, Z.; Qin, Y.; et al. Machine learning-based in-hospital mortality prediction of HIV/AIDS patients with *Talaromyces marneffei* infection in Guangxi, China. *PLoS Negl. Trop. Dis.* **2022**, *16*, e0010388. [CrossRef] [PubMed]
24. Truong, J.; Ashurst, J.V. Pneumocystis Jirovecii Pneumonia. In *StatPearls [Internet]*; StatPearls Publishing: Treasure Island, FL, USA, 2022.
25. Martinez, R. Epidemiology of Paracoccidioidomycosis. *Rev. Inst. Med. Trop. Sao Paulo* **2015**, *19*, 11–20. [CrossRef] [PubMed]
26. Camacho, E.; Niño-Vega, G.A. *Paracoccidioides* spp.: Virulence Factors and Immune-Evasion Strategies. *Mediat. Inflamm.* **2017**, *2017*, 5313691. [CrossRef] [PubMed]
27. Gupta, A.K.; Foley, K.A. Antifungal Treatment for Pityriasis Versicolor. *J. Fungi* **2015**, *1*, 13–29. [CrossRef]
28. Yadlapati, S.; Chaudhari, S.P. Eumycetoma. [Updated 2022 Aug 8]. In *StatPearls [Internet]*; StatPearls Publishing: Treasure Island, FL, USA, 2022.
29. Elkheir, L.Y.M.; Haroun, R.; Mohamed, M.A.; Fahal, A.H. *Madurella mycetomatis* causing eumycetoma medical treatment: The challenges and prospects. *PLoS Negl. Trop. Dis.* **2020**, *14*, e0008307. [CrossRef]
30. Kim, J.Y.; Kang, C.I.; Lee, J.H.; Lee, W.J.; Huh, K.; Cho, S.Y.; Chung, D.R.; Peck, K.R. Clinical Features and Outcomes of Invasive Fusariosis: A Case Series in a Single Center with Literature Review. *Infect. Chemother.* **2021**, *53*, e4. [CrossRef]
31. Muñoz, P.; Giannella, M.; Fanciulli, C.; Guinea, J.; Valerio, M.; Rojas, L.; Rodríguez-Créixems, M.; Bouza, E. *Candida tropicalis* fungaemia: Incidence, risk factors and mortality in a general hospital. *Clin. Microbiol. Infect.* **2011**, *17*, 1538–1545. [CrossRef]
32. Hirano, R.; Sakamoto, Y.; Kudo, K.; Ohnishi, M. Retrospective analysis of mortality and *Candida* isolates of 75 patients with candidemia: A single hospital experience. *Infect. Drug Res.* **2015**, *8*, 199–205. [CrossRef]
33. Hope, W.; Natarajan, P.; Goodwin, L. Invasive fungal infections. *Clin. Med.* **2013**, *13*, 507–510. [CrossRef]
34. Denning, D.W.; Bromley, M.J. How to bolster the antifungal pipeline. *Science* **2015**, *347*, 1414–1416. [CrossRef]
35. Muderris, T.; Kaya, S.; Ormen, B.; Aksoy Gokmen, A.; Varer Akpinar, C.; Yertsever Gul, S. Mortality and risk factor analysis for *Candida* blood stream infection: A three year retrospective study. *J. Mycol. Méd.* **2020**, *30*, 101008. [CrossRef] [PubMed]
36. Khodadadi, H.; Zomorodian, K.; Nouraei, H.; Zareshahrabadi, Z.; Barzegar, S.; Zare, M.R.; Pakshir, K. Prevalence of superficial-cutaneous fungal infections in Shiraz, Iran: A five-year retrospective study (2015–2019). *J. Clin. Lab. Anal.* **2021**, *35*, e23850. [CrossRef] [PubMed]
37. Rasul, T.F.; Gamret, A.C.; Morgan, O.; Bergholz, D.R.; Eachus, E.; Mathew, M.; Faiz, A.; Elkhadem, A.; Dahl, V.; Motoa, G.; et al. Cutaneous Fungal Infections in Patients Experiencing Homelessness and Treatment in Low-Resource Settings: A Scoping Review. *Cureus* **2022**, *14*, e30840. [CrossRef] [PubMed]
38. Gonzalez Santiago, T.M.; Pritt, B.; Gibson, L.E.; Comfere, N.I. Diagnosis of deep cutaneous fungal infections: Correlation between skin tissue culture and histopathology. *J. Am. Acad. Dermatol.* **2014**, *71*, 293–301. [CrossRef]
39. Rouzaud, C.; Hay, R.; Chosidow, O.; Dupin, N.; Puel, A.; Lortholary, O.; Lanternier, F. Severe Dermatophytosis and Acquired or Innate Immunodeficiency: A Review. *J. Fungi* **2016**, *2*, 4. [CrossRef]
40. Pakshir, K.; Rahimi Ghiasi, M.; Zomorodian, K.; Gharavi, A.R. Isolation and molecular identification of keratinophilic fungi from public parks soil in Shiraz. *Biomed. Res. Int.* **2013**, *2013*, 619576. [CrossRef]
41. Eldridge, M.L.; Chambers, C.J.; Sharon, V.R.; Thompson, G.R. Fungal infections of the skin and nail: New treatment options. *Expert Rev. Anti-Infect. Ther.* **2014**, *12*, 1389–1405. [CrossRef]
42. Gupta, A.; Gupta, A.; Varma, A. *Candida glabrata* candidemia: An emerging threat in critically ill patients. *Indian J. Crit. Care Med.* **2015**, *19*, 151–154. [CrossRef]
43. Thammahong, A.; Kiatsurayanon, C.; Edwards, S.W.; Rerknimitr, P.; Chiewchengchol, D. The clinical significance of fungi in atopic dermatitis. *Int. J. Dermatol.* **2020**, *59*, 926–935. [CrossRef]

44. Hossain, C.M.; Ryan, L.K.; Gera, M.; Choudhuri, S.; Lyle, N.; Ali, K.A.; Diamond, G. Antifungals and Drug Resistance. *Encyclopedia* **2022**, *2*, 1722–1737. [CrossRef]
45. Zhang, H.; Zhu, A. Emerging Invasive Fungal Infections: Clinical Features and Controversies in Diagnosis and Treatment Processes. *Infect. Drug Resist.* **2020**, *13*, 607–615. [CrossRef] [PubMed]
46. Arastehfar, A.; Gabaldón, T.; Garcia-Rubio, R.; Jenks, J.D.; Hoenigl, M.; Salzer, H.J.F.; Ilkit, M.; Lass-Flörl, C.; Perlin, D.S. Drug-Resistant Fungi: An Emerging Challenge Threatening Our Limited Antifungal Armamentarium. *Antibiotics* **2020**, *9*, 877. [CrossRef] [PubMed]
47. Webb, B.J.; Ferraro, J.P.; Rea, S.; Kaufusi, S.; Goodman, B.E.; Spalding, J. Epidemiology and Clinical Features of Invasive Fungal Infection in a US Health Care Network. *Open Forum Infect. Dis.* **2018**, *5*, ofy187. [CrossRef]
48. Jenks, J.D.; Gangneux, J.-P.; Schwartz, I.S.; Alastruey-Izquierdo, A.; Lagrou, K.; Thompson III, G.R.; Lass-Flörl, C.; Hoenigl, M.; European Confederation of Medical Mycology (ECMM) Council Investigators. Diagnosis of Breakthrough Fungal Infections in the Clinical Mycology Laboratory: An ECMM Consensus Statement. *J. Fungi* **2020**, *6*, 216. [CrossRef]
49. Denning, D.W. Antifungal drug resistance: An update. *Eur. J. Hosp. Pharm.* **2022**, *29*, 109–112. [CrossRef]
50. Kotey, F.C.; Dayie, N.T.; Tetteh-Uarcoo, P.B.; Donkor, E.S. *Candida* Bloodstream Infections: Changes in Epidemiology and Increase in Drug Resistance. *Infect. Dis. Res. Treat.* **2021**, *14*, 11786337211026927. [CrossRef]
51. Xiao, G.; Liao, W.; Zhang, Y.; Luo, X.; Zhang, C.; Li, G.; Yang, Y.; Xu, Y. Analysis of fungal bloodstream infection in intensive care units in the Meizhou region of China: Species distribution and resistance and the risk factors for patient mortality. *BMC Infect. Dis.* **2020**, *20*, 599. [CrossRef]
52. Agnelli, C.; Valerio, M.; Bouza, E.; Guinea, J.; Sukiennik, T.; Guimaraes, T.; Queiroz-Telles, F.; Munoz, P.; Colombo, A.L. Prognostic factors of *Candida* spp. bloodstream infection in adults: A nine-year retrospective cohort study across tertiary hospitals in Brazil and Spain. *Lancet Reg. Health—Am.* **2022**, *6*, 100117. [CrossRef]
53. Khan, Z.; Ahmad, S.; Al-Sweih, N.; Joseph, L.; Alfouzan, W.; Asadzadeh, M. Increasing prevalence, molecular characterization and antifungal drug susceptibility of serial *Candida auris* isolates in Kuwait. *PLoS ONE* **2018**, *13* (Suppl. 4), e0195743. [CrossRef]
54. Nucci, M.; Thompson-Moya, L.; Guzman-Blanco, M.; Tiraboschi, I.N.; Cortes, J.A.; Echevarría, J.; Sifuentes, J.; Zurita, J.; Santolaya, M.E.; Matute, T.A.; et al. Recommendations for the management of candidemia in adults in Latin America. *Rev. Iberoam. Micol.* **2013**, *30*, 179–188. [CrossRef] [PubMed]
55. Wurster, S.; Albert, N.D.; Kontoyiannis, D.P. *Candida auris* Bloodstream Infection Induces Upregulation of the PD-1/PD-L1 Immune Checkpoint Pathway in an Immunocompetent Mouse Model. *mSphere* **2022**, *7*, e0081721. [CrossRef] [PubMed]
56. Lin, L.; Zhao, C.H.; Yin, X.Y.; Chen, Y.L.; Zhai, H.Y.; Xu, C.W.; Wang, Y.; Ge, F.J.; Xu, J.M. *Aspergillus niger* bloodstream infection in gastric cancer after common hepatic artery embolization: A case report. *Exp. Ther. Med.* **2017**, *14*, 1427–1432. [CrossRef] [PubMed]
57. Morrell, M.; Fraser, V.J.; Kollef, M.H. Delaying the Empiric Treatment of *Candida* Bloodstream Infection until Positive Blood Culture Results Are Obtained: A Potential Risk Factor for Hospital Mortality. *Antimicrob. Agents Chemother.* **2005**, *49*, 3640–3645. [CrossRef]
58. McDonnell, G.; Hansen, J. *Block's Disinfection, Sterilization, and Preservation*, 6th ed.; Wolters Kluwer: Philadelphia, PA, USA, 2020.
59. Gold, K.M.; Hitchins, V.M. Cleaning Assessment of Disinfectant Cleaning Wipes on an External Surface of a Medical Device Contaminated with Artificial Blood or *Streptococcus pneumonia*. *Am. J. Infect. Control* **2013**, *41*, 901–907. [CrossRef]
60. Rutala, W.A.; Weber, D.J. Outbreaks of carbapenem-resistant Enterobacteriaceae infections associated with duodenoscopes: What can we do to prevent infections? *Am. J. Infect. Control* **2016**, *44* (Suppl. 5), 47–51. [CrossRef]
61. Rutala, W.A.; Weber, D.J. Disinfection, Sterilization, and Antisepsis: An Overview. *Am. J. Infect. Control* **2019**, *47*, A3–A9. [CrossRef]
62. Barrett, T.M.; Tsui, C.K.M. Emerging fungal pathogen: *Candida auris*. *Evol. Med. Public Health* **2021**, *9*, 246–247. [CrossRef]
63. McDonnell, G.; OSMA Anti-Infective Working Group. Initiating Implant Infection Innovation. Orthopedic Design & Technology. September/October 2022. Available online: https://www.odtmag.com/issues/2023-09-01/view_features/initiating-implant-infection-innovation (accessed on 20 December 2022).
64. Food and Drug Administration. FDA-Cleared Sterilants and High Level Disinfectants with General Claims for Processing Reusable Medical and Dental Devices. Available online: https://www.fda.gov/medical-devices/reprocessing-reusable-medical-devices-information-manufacturers/fda-cleared-sterilants-and-high-level-disinfectants-general-claims-processing-reusable-medical-and (accessed on 20 December 2022).
65. Anderson, J.; Rowan, N.; MacGregor, S.; Fouracre, R.; Farish, O. Inactivation of food-borne enteropathogenic bacteria and spoilage fungi using pulsed-light. *IEEE Trans. Plasma Sci.* **2000**, *28*, 83–88. [CrossRef]
66. Rowan, N.J. Evidence that inimical food preservation barriers alter microbial resistance, cell morphology and virulence. *Trends Food Sci. Technol.* **1999**, *10*, 261–270. [CrossRef]
67. Hayes, J.; Kirf, D.; Garvey, M.; Rowan, N. Disinfection and toxicological assessments of pulsed UV and pulsed-plasma gas-discharge treated-water containing the waterborne protozoan enteroparasite *Cryptosporidium parvum*. *J. Microbiol. Methods* **2013**, *94*, 325–337. [CrossRef] [PubMed]
68. Garvey, M.; Farrell, H.; Cormican, M.; Rowan, N. Investigations of the relationship between use of in vitro cell culture-quantitative PCR and a mouse-based bioassay for evaluating critical factors affecting the disinfection performance of pulsed UV light for treating *Cryptosporidium parvum* oocysts in saline. *J. Microbiol. Methods* **2010**, *80*, 267–273. [PubMed]

69. Garvey, M.; Stocca, A.; Rowan, N. Development of a combined in vitro cell culture–quantitative PCR assay for evaluating the disinfection performance of pulsed light for treating the waterborne enteroparasite *Giardia lamblia*. *Exp. Parasitol.* **2014**, *144*, 6–13. [CrossRef] [PubMed]
70. Bradley, D.; McNeill, B.; Laffey, J.G.; Rowan, N.J. Studies on the pathogenesis and survival of different culture forms of Listeria monocytogenes to pulsed UV-light irradiation after exposure to mild-food processing stresses. *Food Microbiol.* **2012**, *32*, 330–339. [CrossRef]
71. Hayes, J.C.; Laffey, J.G.; McNeil, B.; Rowan, N.J. Relationship between growth of food-spoilage yeast in high-sugar environments and sensitivity to high-intensity pulsed UV light irradiation. *Int. J. Food Sci. Technol.* **2012**, *47*, 1925–1934. [CrossRef]
72. Rowan, N.J. Pulsed light as an emerging technology to cause disruption for food and adjacent industries—Quo vadis? *Trends Food Sci. Technol.* **2019**, *88*, 316–332. [CrossRef]
73. Spallone, A.; Schwartz, I.S. Emerging fungal infections. *Infect. Dis. Clin. N. Am.* **2021**, *35*, 261–277. [CrossRef] [PubMed]
74. Stewart, P.S.; Bjarnsholt, T. Risk factors for chronic biofilm-related infection associated with implanted medical devices. *Clin. Microbiol. Infect.* **2020**, *26*, 1034–1038. [CrossRef]
75. Ramstedt, M.; Ribeiro, I.A.C.; Bujdakova, H.; Mergulhão, F.J.M.; Jordao, L.; Thomsen, P.; Alm, M.; Burmølle, M.; Vladkova, T.; Can, F.; et al. Evaluating Efficacy of Antimicrobial and Antifouling Materials for Urinary Tract Medical Devices: Challenges and Recommendations. *Macromol. Biosci.* **2019**, *19*, e1800384. [CrossRef]
76. Kremer, T.A.; Olsen, D.; Summers, C.; Patel, A.; Hoover, H.; Cieslak, M.; Znamensky, D.; McDonnell, G. Assessing detergent residuals for reusable device cleaning validations. *Biomed. Instrum. Technol.* **2021**, *55*, 165–170. [CrossRef]
77. Alfa, M.J. Biofilms on instruments and environmental surfaces: Do they interfere with instrument reprocessing and surface disinfection? Review of the literature. *Am. J. Infect. Control* **2019**, *47*, A39–A45. [CrossRef]
78. Cabronne, A.; Thiolet, J.M.; Fournier, S.; Fortineau, N.; Kassis-Chikhani, N.; Boytchev, I.; Aggoune, M.; Séguier, J.C.; Sénéchal, H.; Tavolacci, M.P.; et al. Control of a multi-hospital outbreak of KPC producing *Klebsiella pneumoniae* type II in France, Sept to October 2009. *Eurosurveillance* **2010**, *15*, 19734.
79. Shenoy, E.S.; Pierce, V.M.; Walters, M.S.; Moulton-Meissner, H.; Lawsin, A.; Lonsway, D.; Shugart, A.; McAllister, G.; Halpin, A.L.; Zambrano-Gonzalez, A.; et al. Transmission of mobile colistin resistance (mcr-1) by duodenoscope. *Clin. Infect. Dis.* **2019**, *68*, 1327–1334. [CrossRef] [PubMed]
80. Smith, Z.L.; Oh, Y.S.; Saeian, K.; Edmiston, C.E., Jr.; Khan, A.H.; Massey, B.T.; Dua, K.S. Transmission of cabapenem-resistant *Enterbacteriacease* during ERCP: Time to revisit the current reprocessing guidelines. *Gastrointest. Endosc.* **2015**, *81*, 1041–1045. [CrossRef]
81. Marsh, J.W.; Krauland, M.G.; Nelson, J.S.; Schlackman, J.L.; Brooks, A.M.; Pasculle, A.W.; Shutt, K.A.; Doi, Y.; Querry, A.M.; Muto, C.A.; et al. Genomic epidemiology of an endoscope-associated outbreak of *Klebsiella pneumoniae* carapenemase (KPC)-producing *K. pneumoniae*. *PLoS ONE* **2015**, *10*, e0144310. [CrossRef] [PubMed]
82. Epstein, L.; Hunter, J.C.; Arwady, M.A.; Tsai, V.; Stein, L.; Gribogiannis, M.; Frias, M.; Guh, A.Y.; Laufer, A.S.; Black, S.; et al. New Delhi metallo-beta-lactamase-producing cabapenem-resistant *Escherichia coli* associated with exposure to duodenoscopes. *JAMA* **2014**, *312*, 1447–1455. [CrossRef]
83. Kola, A.; Piening, B.; Pape, U.-F.; Veltzke-Schlieker, W.; Kaase, M.; Geffers, C.; Wiedenmann, B.; Gastmeier, P. An outbreak of carbapenem-resistant OXA-48-producing *Klebsiella pneumoniae* associated with duodenoscopy. *Antimicrob. Resist. Infect. Control* **2015**, *4*, 8. [CrossRef]
84. Wendorf, K.A.; Kay, M.; Baliga, C.; Weissman, S.J.; Gluck, M.; Verma, P.; D'Angeli, M.; Swoveland, J.; Kang, M.G.; Eckmann, K.; et al. Endoscopic retrograde cholangiopancreatograph-associated AmpC *Escherichia coli* outbreak. *Infect. Control Hosp. Epidemiol.* **2015**, *36*, 634–642. [CrossRef]
85. Kim, S.; Russell, D.; Mohamadnejad, M.; Makker, J.; Sedarat, A.; Watson, R.R.; Yang, S.; Hemarajata, P.; Humphries, R.; Rubin, Z.; et al. Risk factors associated with the transmission of carbapenem-resistant *Enteriobacteriaceae* via contaminated duodenoscopes. *Gastointest. Edosc.* **2016**, *83*, 1121–1129. [CrossRef]
86. Kojic, E.M.; Darouiche, R.O. *Candida* infections of medical devices. *Clin. Microbiol. Rev.* **2004**, *17*, 255–267. [CrossRef]
87. Piktel, E.; Suprewicz, Ł.; Depciuch, J.; Chmielewska, S.; Skłodowski, K.; Daniluk, T.; Król, G.; Kołat-Brodecka, P.; Bijak, P.; Pajor-Świerzy, A.; et al. Varied-shaped gold nanoparticles with nanogram killing efficiency as potential antimicrobial surface coatings for medical devices. *Sci. Rep.* **2021**, *11*, 12546. [CrossRef] [PubMed]
88. Šlamborová, I.; Zajícová, V.; Karpíšková, J.; Exnar, P.; Stibor, I. New type of protective hybrid and nanocomposite hybrid coatings containing silver and copper with an excellent antibacterial effect especially against MRSA. *Mater. Sci. Eng. C Mater. Biol. Appl.* **2013**, *33*, 265–273. [CrossRef] [PubMed]
89. Masterson, K.; Meade, E.; Garvey, M.; Lynch, M.; Major, I.; Rowan, N.J. Development of a low-temperature extrusion process for production of GRAS bioactive-polymer loaded compounds for targeting antimicrobial-resistant (AMR) bacteria. *Sci. Total. Environ.* **2021**, *800*. [CrossRef] [PubMed]
90. Farrell, H.; Hayes, J.; Laffey, J.; Rowan, N. Studies on the relationship between pulsed UV light irradiation and the simultaneous occurrence of molecular and cellular damage in clinically-relevant *Candida albicans*. *J. Microbiol. Methods* **2013**, *84*, 317–326. [CrossRef]
91. Omotayo, O.P.; Omotayo, A.O.; Mwanza, M.; Babalola, O.O. Prevalence of Mycotoxins and Their Consequences on Human Health. *Toxicol. Res.* **2019**, *35*, 1–7. [CrossRef] [PubMed]

92. de Rocha, M.E.B.; da Chagas Oliveira Freire, F.; Maia, F.E.F.; Guedes, M.I.F.; Rondina, D. Mycotoxins and their effects on human and animal health. *Food Control* **2014**, *36*, 159–165. [CrossRef]
93. Čolović, R.; Puvača, N.; Cheli, F.; Avantaggiato, G.; Greco, D.; Đuragić, O.; Kos, J.; Pinotti, L. Decontamination of Mycotoxin-Contaminated Feedstuffs and Compound Feed. *Toxins* **2019**, *11*, 617. [CrossRef]
94. Smith, J.E.; Solomons, G.; Lewis, C.; Anderson, J.G. Anderson Role of mycotoxins in human and animal nutrition and health. *Nat. Toxins* **1995**, *3*, 187–192. [CrossRef]
95. Van Egmond, H.P. Mycotoxins: Risks, regulations and European co-operation. *J. Nat. Sci. Matica Srp. Novi Sad* **2013**, *125*, 7–20.
96. Kostić, A.Ž.; Milinčić, D.D.; Petrović, T.S.; Krnjaja, V.S.; Stanojević, S.P.; Barać, M.B.; Tešić, Ž.L.; Pešić, M.B. Mycotoxins and Mycotoxin Producing Fungi in Pollen: Review. *Toxins* **2019**, *11*, 64. [CrossRef]
97. Reddy, L.; Bhoola, K. Ochratoxins—Food Contaminants: Impact on human health. *Toxins* **2010**, *2*, 771–779. [CrossRef]
98. Pereira, M.M.G.; Carvalho, E.P.; Prado, G.; Rosa, C.A.R.; Veloso, T.; Souza, L.A.F.; Ribeiro, J.M.M. Aflatoxinas em alimentos destinados a bovinos e em amostras de leite da região de Lavras, Minas Gerais—Brasil. *Ciênc. Agrotéc.* **2005**, *29*, 106–111. [CrossRef]
99. Bucci, T.J.; Hansen, D.K.; LaBorde, J.B. Leucoencephalomacia and hemorrhage in the brain of rabbits gavaged with mycotoxin fumonisin B1. *Nat. Toxins* **1996**, *4*, 51–52. [CrossRef] [PubMed]
100. Pozzi, C.R.; Corrêa, B.; Xavier, J.G.; Direito, G.M.; Orsi, R.B.; Matarazzo, S.V. Effects of prolonged oral administration of fumonisin B1 and aflatoxin B1 in rats. *Mycopathologia* **2000**, *151*, 21–27. [CrossRef]
101. Bullerman, L.B.; Bianchini, A. Stability of mycotoxins during food processing. *Int. J. Food Microbiol.* **2007**, *119*, 140–146. [CrossRef] [PubMed]
102. Kabak, B.; Dobson, A.D.W.; Var, I. Strategies to Prevent Mycotoxin Contamination of Food and Animal Feed: A Review. *Crit. Rev. Food Sci. Nutr.* **2006**, *46*, 593–619. [CrossRef] [PubMed]
103. Weltmann, K.-D.; von Woedtke, T. Plasma medicine—Current state of research and medical application. *Plasma Phys. Control. Fusion* **2017**, *59*, 014031. [CrossRef]

Science of the Total Environment 851 (2022) 158284

Contents lists available at ScienceDirect

Science of the Total Environment

journal homepage: www.elsevier.com/locate/scitotenv

Review

Effectiveness of front line and emerging fungal disease prevention and control interventions and opportunities to address appropriate eco-sustainable solutions

Mary Garvey [a,b], Elaine Meade [a,b], Neil J. Rowan [c,d,e,*]

[a] Department of Life Science, Atlantic Technological University, Sligo, Ireland
[b] Centre for Precision Engineering, Materials and Manufacturing Research (PEM), Atlantic Technological University, Sligo, Ireland
[c] Bioscience Research Institute, Technological University of the Shannon Midlands Midwest, Athlone, Ireland
[d] Centre for Decontamination, Sterilization and Biosecurity, Technological University of the Shannon Midlands Midwest, Athlone, Ireland
[e] Empower Eco Sustainability Hub, Technological University of the Shannon Midlands Midwest, Athlone, Ireland

HIGHLIGHTS

- Fungal infections represent an under recognised threat to public health.
- Mycosis represents high incidence of mortality.
- Antifungal resistance is increasing globally.
- New alternative eco-solutions to address pathogenic fungi are needed.

GRAPHICAL ABSTRACT

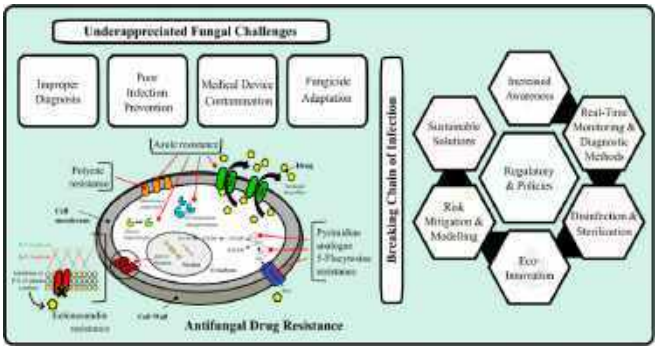

ARTICLE INFO

Editor: Damia Barcelo

Keywords:
Pathogenic fungi
Drug resistance
Environmental toxicity
Disinfection- sterilization
Sustainability

ABSTRACT

Fungal pathogens contribute to significant disease burden globally; however, the fact that fungi are eukaryotes has greatly complicated their role in fungal-mediated infections and alleviation. Antifungal drugs are often toxic to host cells and there is increasing evidence of adaptive resistance in animals and humans. Existing fungal diagnostic and treatment regimens have limitations that has contributed to the alarming high mortality rates and prolonged morbidity seen in immunocompromised cohorts caused by opportunistic invasive infections as evidenced during HIV and COVID-19 pandemics. There is a need to develop real-time monitoring and diagnostic methods for fungal pathogens and to create a greater awareness as to the contribution of fungal pathogens in disease causation. Greater information is required on the appropriate selection and dose of antifungal drugs including factors governing resistance where there is commensurate need to discover more appropriate and effective solutions. Popular azole fungal drugs are widely detected in surface water and sediment due to incomplete removal in wastewater treatment plants where they are resistant to microbial degradation and may cause toxic effects on aquatic organisms such as algae and fish. UV has limited effectiveness in destruction of anti-fungal drugs where there is increased interest in the combination approaches such as novel use of pulsed-plasma gas-discharge technologies for environmental waste management. There is growing interest in developing alternative and complementary green eco-biocides and disinfection innovation. Fungi present challenges for cleaning, disinfection and sterilization of reusable medical devices such as endoscopes where they (example, *Aspergillus* and *Candida* species) can be protected when harboured in build-up biofilm

* Corresponding author at: Bioscience Research Institute, Technological University of the Shannon Midlands Midwest, Athlone, Ireland.
E-mail address: neil.rowan@tus.ie (N.J. Rowan).

http://dx.doi.org/10.1016/j.scitotenv.2022.158284
Received 17 July 2022; Received in revised form 21 August 2022; Accepted 21 August 2022
Available online xxxx

from lethal processing. Information on the efficacy of established disinfection and sterilization technologies to address fungal pathogens including bottleneck areas that present high risk to patients is lacking. There is a need to address risk mitigation and modelling to inform efficacy of appropriate intervention technologies that must consider all contributing factors where there is potential to adopt digital technologies to enable real-time analysis of big data, such as use of artificial intelligence and machine learning. International consensus on standardised protocols for developing and reporting on appropriate alternative eco-solutions must be reached, particularly in order to address fungi with increasing drug resistance where research and innovation can be enabled using a One Health approach.

Contents

1. Introduction

Fungi represent one of the most diverse groups of organisms on the planet with an essential role in ecosystem processes and functioning (Hyde, 2022). The numbers of fungi have always been an intriguing topic; however, 150,000 innocuous, beneficial and harmful fungal species have been described to date enabled by using new DNA sequencing technologies. Despite the fact that problematical fungi infect billions of people annually, there is a significant under appreciation of their aetiological contribution to worldwide diseases (Bongomin et al., 2017). Fungal infections are a significant contributor to sepsis that has increased by 200 % in the United States since 1991 (van der Poll et al., 2017), and is the second most common pathogen to cause cancer related infections (Lortholary et al., 2017). Invasive fungal infections (IFIs) have increased with the widespread use of broad-spectrum antibiotics, immunosuppressive agents, antineoplastic drugs, and in-depth development of organ transplantation, and various invasive diagnostic techniques. *Candida*, *Aspergillus*, *Pneumocystis*, and *Cryptococcus neoformans* are the primary pathogens causing fungal infections, with *Candida* responsible for the largest number of cases, where the infection rates of *Aspergillus*, *Pneumocystis*, and *C. neoformans* have increased.

These IFIs primarily occur in patients with severe underlying diseases, malignant tumours, and other severe diseases compromising immune function and in those undergoing organ transplantation. Fungal infection termed mycosis is increasing globally in immunocompromised and immunocompetent persons, affecting 1 billion people with 1 million deaths yearly (Lass-Flörl et al., 2021). Thus, the immune status of the patient determines the severity of fungal disease, ranging from hypersensitivity, dermal infection, subcutaneous, invasive to disseminated systemic infections (Martinez-Rossi et al., 2018). *Candida* for example, is one of the most common fungal pathogens causing nosocomial bloodstream infections (BSI) or fungemia having a mortality rate of 30–40 % despite an availability of therapeutic options (Galia et al., 2022). Fungal therapeutics consist of 4 classes of antifungal drugs: the polyenes (amphotericin B and nystatin), azoles (fluconazole, itraconazole, voriconazole, posaconazole and isavuconazole), echinocandins (caspofungin, micafungin and anidulafungin) and the pyrimidine analogue 5-flucytosine (Fisher et al., 2022). Bacteraemia and fungemia are the second leading causes of mortality in patients of end stage renal disease receiving dialysis where incidence rates of 4.7 % bacteraemia and fungemia were detected in renal disease patients (Dalgaard et al., 2016).

Fungemia and bacteraemia also lead to severe cases of sepsis in affected patients due to the presence of microbial toxins (Valencia-Shelton and Loeffelholz, 2014).

Similar to bacterial pathogens, fungal pathogens are also displaying alarming rates of antimicrobial resistance (AMR). AMR is the innate or acquired ability of a microbial species (viral, bacterial, fungal, parasitic) to resist antimicrobial therapy, where biocidal resistance is also common amongst AMR pathogens (Meade et al., 2021a, 2021b, 2021c). AMR relates to molecular mechanisms of resistance including efflux pumps, degradative enzymes, target and drug modification, alterations in membrane permeability, biofilm formation and spores (Meade et al., 2021c). Efflux pumps associated with the ATP binding cassette (ABC) transporter superfamily are commonly associated with azole resistance in many fungal species (Nagy et al., 2021). While AMR is a naturally occurring event, the industrial production and mass use of antimicrobials in clinical, veterinary and food production has proliferated the issue beyond measure, making antimicrobials a non-renewable resource. Antifungal and biocidal resistance represents a significant threat to the treatment, transmission, and control of fungal pathogens. Multidrug resistance (MDR) is common in fungal pathogens including *Candida albicans*, non-*albicans Candida* strains (NAC), *Cryptococcus*, *Aspergillus*, and numerous dermatophyte species. Importantly,

Table 1
Outlining antifungal drug therapy options, mode of action and resistance profile of invasive fungal pathogens to be listed as priority pathogens by the WHO.

Drug class (drugs used in clinical practice)	Mode of action	Resistant species	Resistance mechanisms	Additional considerations
Polyenes (AMP B)	Depletes membrane ergosterol (Iyer et al., 2021)	*Pneumocystis jirovecii*	Absence of ergosterol in cell membrane (Helweg-Larsen et al., 2017)	AMP B nephrotoxicity, used in combination with flucytosine, used for treatment of Mucormycosis in humans (Dannaoui, 2017)
Azoles (Triazoles, itraconazole, posaconazole, voriconazole, isavuconazole)	Block ergosterol biosynthesis	*Cryptococcus* spp. (Lee et al., 2020) *Aspergillus* spp. *Candida albicans* and NAC *Pneumocystis jirovecii*	Upregulation of the azole target gene *ERG11*, drug efflux pumps, genetic plasticity (Iyer et al., 2021), exopolysaccharide capsule, formation of large polyploid titan cells (Zafar et al., 2019) Mutations in the *cyp51A* (Romero et al., 2019) *TR34/L98H* mutation, *TR46/Y121F/T289A* mutants (Pinto et al., 2018) *ERG11* point mutations (Wiederhold, 2017), efflux pump Absence of ergosterol in cell (Helweg-Larsen et al., 2017)	Increased expression of membrane transporters and efflux pumps (CaCDR1 and CaCDR2) correlates with azole resistance in many fungal species ATP (adenosine triphosphate)-binding cassette (ABC) family and the major facilitator superfamily (MFS) of efflux pumps also confer biocidal resistance in many microbial species (Meade et al., 2021c) Posaconazole and isavuconazole used to treat Mucormycosis (Dannaoui, 2017)
Echinocandins (anidulafungin, caspofungin, micafungin)	Disrupt cell structural integrity	*Cryptococcus* spp. (Lee et al., 2020) *Aspergillus* spp. *Candida* spp. *Mucorales* spp.	Intrinsic resistance to caspofungin (Meade et al., 2021c) Efflux pumps No in vitro activity (Dannaoui, 2017)	Potent in vitro activity against *Candida* isolates resistant to fluconazole (Wiederhold, 2017) Caspofungin used in combination with clindamycin to treat *Pneumocystis jirovecii* (Li et al., 2016)
Pyrimidine analogue (flucytosine)	Antimetabolite – blocks DNA synthesis	*Cryptococcus* spp. *Candida* spp.	Alterations in capsule biosynthesis in *Cryptococcus* Mutations in *FCY1, FCY2*, and *FUR1* genes (Billmyre et al., 2020)	5-Fluorocytosine is a prodrug converted into toxic 5FU by cytosine deaminase, a fungi specific enzyme (Billmyre et al., 2020)

fungal pathogens are often also extensively drug resistant (XDR), being defined as having resistance to more than one therapeutic agent in three or more antifungal classes (Galia et al., 2022). Importantly, therapeutic failure also relates to antifungal drug properties such as drug pharmacokinetics, pharmacodynamics and drug–drug interactions (Fisher et al., 2022).

The Global Action Plan on AMR and the Global AMR Surveillance System (GLASS) aims to promote standardised AMR surveillance using patient, laboratory, and epidemiology data to analyse the global impact of AMR (World Health, 2019). While bacterial AMR is commonly accepted, GLASS also recognises fungal AMR as a growing major threat where a lack of data increases the risk to public health. Surveillance issues relating to fungal species include poor recovery from blood samples, a lack of accurate identification, lack of susceptibility testing, and a lack of species-specific antifungal breakpoints. Surveillance studies, however, have demonstrated the presence of MDR *C. albicans* and NAC isolates being resistant to more than one therapeutic agent in two antifungal drug classes (Galia et al., 2022). The threat of AMR is recognised at a global scale as having negative impacts on health and wellbeing. The WHO has called for urgent action aligned with the Sustainable Development Goals (SDGs) with AMR listed in the top 10 dangers to public health, along with climate change and global warming (Masterson et al., 2021). The AMR global action plan established by the WHO in 2015 encouraged the United Nations (UN) members to develop and implement national action plans aimed at reducing the emergence and transmission of AMR species (Dutescu, 2021). Undoubtedly, a unified and coordinated action plan is needed to combat the threat of AMR. Additionally, the WHO has called for the establishment of a fungal priority pathogen list (Table 1) to include the following species: *Candida auris*; azole-resistant *Candida* spp., azole-resistant *Aspergillus fumigatus*, *Cryptococcus neoformans*, *Pneumocystis jirovecii*, and Mucorales due to their AMR ability (World Health, 2020). As we move further into a post pandemic era, bacterial and fungal pathogens may be overlooked as medical sectors strive to develop viral vaccine and treatment regimes. Fungal pathogens, and zoonotic cross over species, however, remain an important public health consideration within the One Health approach. A One Health approach is vital to establish the impact of AMR on the Anthropocene (planet, biosphere, atmosphere) and the consequences of the rising consumption rate of antimicrobial agents. Fungal infections of sporotrichosis, histoplasmosis and chromoblastomycosis and MDR dermatophytosis remain important as zoonotic fungal pathogens. Furthermore, the impact of global warming will undoubtedly promote a rise in fungal infectious disease globally negatively impacting public health and food security (Nnadi and Carter, 2021).

2. Growing crisis of antimicrobial resistance (AMR)

AMR is directly responsible for clinical expenses, treatment failures, morbidity, mortality, and economic costs. Reports indicate AMR costs the European Union (EU) healthcare sector approximately €1.5 billion annually with estimates from The World Bank suggesting an annual gross domestic product (GDP) loss of 6.1 trillion dollars by 2050 (Nasereddin, 2021). Reports highlight the mortality of AMR with ca. 5 million deaths involving resistant bacterial species in 2019 with 1.3 million deaths directly related to AMR species (Murray et al., 2022) significantly more than tuberculosis (TB), acquired immune deficiency syndrome (AIDS) and malaria (Iyer et al., 2021). Indeed, predictive modelling studies suggest that 10 million deaths per year will occur due to AMR by 2050, globally (Hillock et al., 2022). The crisis of AMR, therefore, requires a multisectoral approach to mitigation including monitoring, surveillance, novel therapeutic options and optimal prevention and control strategies. While national and global policies have impacted antimicrobial use, studies have shown a startling 65 % increase in antimicrobial use in the period of 2000 to 2015 alone (Dutescu, 2021). Furthermore, developed countries with higher incomes have increased levels of AMR species (Kirby and Herbert, 2013) indicating the effects of neoliberalism on economic policy, the emergence of AMR and the development and production of therapeutics by profit motivated pharmaceutical companies (Dutescu, 2021). Furthermore, the

national political and economic situation impacts on the provision of healthcare and distribution of pharmaceuticals in public and private healthcare settings where the latter may prioritise financial gain over AMR stewardship (Broom et al., 2021). Indeed, in our determination to extend human life, reduce morbidity and obtain optimal healthcare, microbial species are portrayed as loathsome with their commensal and beneficial interactions often overlooked. The extensive use of antimicrobial therapy negatively impacts gastrointestinal (GIT) microbiota, resulting in dysbiosis and associated diseases (autoimmunity, cancer, mental health disorders) leading to morbidity and economic impacts which may be avoided with the absence of prolonged antimicrobial therapy resulting from AMR infections (Meade et al., 2020a). The extensive use of antimicrobial therapy, emergence and re-emergence of resistant microbes has resulted in increasing rates of nosocomial disease where clinician's repertoire of therapeutic options is greatly diminished (Meade et al., 2021a, 2021b, 2021c).

WHO reports indicate nosocomial pathogens including *Escherichia coli* and methicillin resistant *Staphylococcus aureus* frequently display resistance to 3rd generation cephalosporins and fluoroquinolones with the Gram negative *Klebsiella pneumoniae* also displaying resistance to carbapenems (Founou et al., 2017). The ESKAPE pathogens *Enterococcus* spp., *S. aureus*, *K. pneumoniae*, *Acinetobacter baumannii*, *Pseudomonas aeruginosa* and *Enterobacter* spp. represent a significant risk to public health with decreasing treatment options available. Indeed, these species are classed as the most prevalent of the life-threatening pathogens isolated from 72 % of patients in clinical settings (Benkő et al., 2020). Hospital acquired infections (HAIs) or nosocomial infections involving MDR-ESKAPE pathogens are increasing (Zhen et al., 2019) particularly in immune-compromised patients in intensive care units (ICUs) due to non-communicable disease. Emerging and re-emerging pathogens are also unpredictable in their levels of AMR and rates of mortality. *Borrelia burgdorferi* the emerging causative agent of Lyme disease for example displays AMR or antibiotic tolerance (Hodzic, 2015) and is associated with increasing prevalence and chronic morbidity. Advocacy of the continued and proliferating threat of AMR has been somewhat successful, in promoting awareness, driving research, and spurring government and organizations into action, globally. There remains however, a strong focus on antibiotic resistance and bacterial pathogens with fungal species often overlooked in both clinical and in agriculture settings. Even with the evident high mortality rates of fungal infections and ubiquitous nature of mycosis, insufficient funding into the diagnosis and therapy of fungal disease has prevailed for decades (Stone et al., 2021).

2.1. Clinical relevance of fungal AMR – a major underappreciated challenge

Fungal infectious diseases are commonly classified as opportunistic or primary affecting immunocompromised and immunocompetent person respectively, either locally or systemically. Local dermal infections are typically caused by dermatophytes (requiring keratin) and *Malassezia* spp. (requiring fatty acids from host lipids) (White et al., 2014). Systemic fungal infections often involve the opportunistic *Candida*, *Aspergilla*, *Mucorale* and *Fusarium* species. With primary pathogens including *Coccidioides*, *Histoplasma*, *Blastomyces* and *Cryptococcus* causing localised lung infection followed by systemic mycosis in immune competent persons post inhalation of fungal spores. Increasing prevalence of mycosis relates to several factors including increased number of immunocompromised patients, increased longevity, affluence, fungal AMR/MDR, zoonosis and improvement in fungal detection methods (Firacative, 2020). The issue is further proliferated by the increasing number of emerging fungal pathogens including MDR *Candida auris*, *Fusarium* spp. and *Mucorales* (Yousfi et al., 2019). Additionally, rare and emerging moulds including *Lomentospora* spp. and *Scedosporium* species have innate AMR and represent a significant challenge in detection and diagnostics (Hoenigl et al, n.d.). Zoonosis is highly prevalent in fungal species (Table 2) with many species transmitting from food producing and companion animals (Meade et al., 2020b; Meade et al., 2019). The most common species associated with invasive infection, morbidity and mortality include *C. albicans*, *Cryptococcus neoformans*, *Aspergillus fumigatus*, *Pneumocystis jirovecii* and *Mucoromycetes* (Firacative, 2020). Invasive mycosis is a significant challenge in clinical settings due to the vast array of fungal pathogens, limited number of antifungal drug-options, drug biocompatibility and absorption issues in the host.

When the terms funguria or fungal urinary tract infection are used, most physicians are referring to candiduria and urinary tract infections due to *Candida* species (Kauffman, 2014). Other fungi, including yeasts and moulds can involve the kidney during the course of disseminated infection, but rarely cause symptoms referable to the urinary tract. *Candida* species appear to be unique in their ability to both colonize and cause invasive disease in the urinary tract. Candiduria is commonly seen in hospitalized patients and most of the patients are asymptomatic, but it may be due to cystitis, pyelonephritis, prostatitis, epididymo-orchitis or disseminated candidiasis (Odabasi and Mert, 2020). Major risk factors are diabetes mellitus, indwelling urinary catheters, use of broad-spectrum antibiotics, urinary obstruction, and admission to ICUs. *Candida* urinary tract infections can be caused by hematogenous spread following candidemia, or retrograde route via the urethra. *Candida auris*, which was first isolated in 2009, has now become a global health threat with mortality rates of ca. 72 % (Hillock et al., 2022). While *C. albicans* is the leading cause of BSIs, diagnostics increasingly report *C. glabrata* as the cause of invasive fungemia in older patients (Kauffman and Yoshikawa, 2001). Importantly, *C. glabrata* possess innate resistance to fluconazole requiring treatment with echinocandin as drug therapy.

Cryptococcus neoformans and *C. gattii* are the predominant species associated with cryptococcosis where inhalation of the fungal spores leads to pneumonia with dissemination to the central nervous system (CNS) causing meningitis. In immunocompetent persons, the disease is often self-limiting due to the action of innate (neutrophils) and adaptive immunity, like TB; however, persistent infection with chronic systems can occur (Zafar et al., 2019).

Cryptococcus has a 20 % mortality rate in immunocompromised HIV patients (Pasquier et al., 2018) increasing to 100 % if left untreated (Iyer et al., 2021). Furthermore, *Cryptococcus* species are innately resistant to the echinocandins, have acquired resistance to azoles; therefore, treatment is limited to the nephrotoxic amphotericin B (AMPB) (Lee et al., 2020). Efforts to reduce AMP B toxicity and increase efficacy have led to the development of a combination therapy with flucytosine, a liposome bilayer-coated AMPB formulation, and an encochleated oral AMPB a lipid-containing crystal nanoparticle for delivery to the CNS in the treatment of meningitis (Jarvis

Table 2
Zoonotic pathogenic fungal species isolated from food producing and companion animals, where AMR profiles[a] and route of zoonosis are listed.

Isolate		Disease	AMR profile[a]	Route of zoonosis
Fungal species	*Candida albicans*	Canine cutaneous candidiasis	Resistant to FCZ, AMP B and CAS (Meade et al., 2019)	Close contact to the animal, animal bedding and/or excrement
	Candida krusei	Canine candiduria	Resistant to FCZ, AMP B and CAS (Meade et al., 2019)	
	Aspergillus niger	Canine otomycosis	Resistant to FCZ (Meade et al., 2021a, 2021b, 2021c)	
	Malassezia pachydermatis	Canine dermatitis	Resistant to FCZ, AMP B and CAS (Meade et al., 2021a, 2021b, 2021c)	
	Cryptococcus neoformans	Bovine mastitis	Resistant to FCZ, AMP B and CAS (Meade et al., 2020b)	Close contact to the animal, consumption of contaminated milk/dairy

Abbreviations: FCZ - Fluconazole, AMP B - Amphotericin B, CAS - Caspofungin.
[a] AMR profile established via selective agars, and standard disk diffusion and microdilution methods in accordance with EUCAST guidelines.

et al., 2019; Lu et al., 2019). Clinical trials are ongoing where initial studies show promising results (Iyer et al., 2021).

Aspergillus has 4 main manifestations of disease including allergic bronchopulmonary aspergillosis, chronic necrotising pneumonia, aspergilloma (mycetoma) and an invasive aspergillosis (Metodiev, 2012). Invasive aspergillosis commonly resultant from *A. fumigatus* infection has a mortality rate of ca. 70 % in immunocompromised patients (Firacative, 2020) where neutrophil dysfunction and neutropenia are risk factors for disease progression. Importantly, *Aspergillus* pneumonia can result in a chronic necrotizing infection with a mortality rate of 40 % (Latgé and Chamilos, 2019) increasing to 100 % in undiagnosed patients with dissemination to the CNS (Fosses Vuong and Waymack, 2022). Dissemination of aspergillosis resultant in endocarditis, endophthalmitis and abscesses on many organs, soft tissue and bone is also possible (Metodiev, 2012). There is increasing prevalence of azole resistance (fluconazole) in *A. fumigatus* isolates globally (Romero et al., 2019) with this class of drug being the primary treatment option for aspergillosis due to its oral administration, improved biocompatibility, and cost (Wiederhold, 2017). *Pneumocystis jirovecii* is an opportunistic pathogen and the causative agent of Pneumocystis Jirovecii Pneumonia (PJP) a potentially life-threatening pneumonia having a mortality rate of 50 % in immunocompromised persons (Truong and Ashurst, 2022) such as those suffering congenital immunodeficiency, AIDS, or receiving organ transplants (Lee et al., 2015). *P. jirovecii* can be carried asymptomatically by immunocompetent persons who act as reservoirs for transmission. Importantly, ergosterol is absent from the plasma membrane of *P. jirovecii* making many antifungal agents including AMPB and the azoles redundant in the treatment of PJP where anti-protozoan drugs where the mainstay of treatment (Helweg-Larsen et al., 2017).

Currently, standard treatment involves cotrimoxazole which contains sulfamethoxazole (SMX) and trimethoprim (TMP), SMX resistance, however, has become a concern in *P. jirovecii* (Lee et al., 2015). Both these antimicrobial's target the essential enzymes dihydrofolate reductase (DHFR) required for purine synthesis and dihydropteroate synthase. This makes them excellent antimicrobial drug targets, as disruption of thymine synthesis leads to cell death in many microorganisms (Ahmad et al., 1998). Mutations in the *DHFR* gene, however, confer TMP resistance in many microbial species including *P. jirovecii* (Leidner et al., 2021). In non-responsive PCP patients, treatment with a combination of caspofungin and clindamycin may offer some benefit (Li et al., 2016). Additionally, adverse drug reactions are common with cotrimoxazole treatment including fever, nausea, vomiting, neutropenia, thrombocytopenia, and epidermal necrolysis that can be fatal in some cases (Kaplan et al., 2009).

Mucoromycetes are a group of environmental moulds the Mucorales (*Rhizopus*, *Apophysomyces*, *Mucor*, and *Lichtheimia* species) associated with Mucormycosis (previously zygomycosis) a rare, severe, and often fatal fungal infection in humans having an 80 % mortality rate. The incidence of Mucormycosis is increasing however, as the population of immunocompromised patients increases (Skiada et al., 2020). Mucormycosis recently came to light in India in an infection outbreak in thousands of Covid-19 patients (Stone et al., 2021). Prolonged antibiotic and corticosteroid therapy are predisposing factors for Mucormycosis in Covid patients (SeyedAlinaghi et al., 2022) with diabetic patients and patients with hematological malignancies also at risk. A chronic progressive infection caused by *Mucor irregularis* has emerged in immunocompetent persons in China (Skiada et al., 2020). Mucormycosis targets numerous organs including the nasal cavity, paranasal sinuses, orbit fossa, CNS, pulmonary system, GIT, cutaneous, disseminated, and mediastinum (Nagy et al., 2021). The Mucorales have high levels of antifungal resistance with current treatments AMP B, posaconazole and isavuconazole only displaying suboptimal efficacy (Dannaoui, 2017). Drug therapy is therefore often in combination with surgical intervention.

2.2. Food security and fungal AMR

Agriculture is particularly susceptible to fungal infection and destruction leading to loss of production, national economic impacts, and impacts on human health (Gehlot and Singh, 2018). Contamination of the agricultural food chain with fungal species and/or their mycotoxins can result in food wastage, disease outbreak, morbidity, and economic burden. To mitigate the risk of fungal agricultural impacts azole-based fungicides (predominately imidazoles and triazoles) have been in use for decades (Jørgensen and Heick, 2021). Indeed, from a One Health perspective azoles offer effective management of many fungal disease in plants, animals and humans ensuring food security (Verweij et al., 2020). Environmental exposure to the azoles however, used as fungicides in agriculture, has promoted azole resistance in clinical fungal species including *Aspergillus* (Wiederhold, 2017). Such AMR has been observed in *A. fumigatus* which is harmless to plants but causes invasive fungal disease in humans, often fatal in immunocompromised patients (Verweij et al., 2020). Furthermore, disease management is an emerging issue in agriculture as azole resistance occurs in many plant fungal pathogens including *Zymoseptoria tritici*, *Pyrenophora teres* and *Ramularia collocygni* (Rehfus et al., 2019). Indeed, the abundant use of fungicidal agents in agriculture promotes AMR to all classes of antifungal agents including benzimidazoles, anilinopyrimidines, strobilurins, succinate dehydrogenase inhibitors and the sterol demethylation inhibitors (DMIs) (Fisher et al., 2022). While azole use in agriculture varies globally, patterns emerge between the use of azoles and rate of azole resistant strains. Holland for example, where azoles are used abundantly in tulip farming has one of the highest rates of azole resistance strains of *A. fumigatus* (van der Linden et al., 2013). As food security and zero hunger are goals of the UN SDGs there is a need to protect and enhance food production systems in a sustainable way. The introduction of mycopesticides to control insect species as part of sustainable agriculture is one such method. The use of fungal species non-pathogenic to humans may reduce the emergence of AMR species. Mycopesticides used as mycoherbicides (*Collectrichum gloesporioides*, *Phytophthora palmivoraa*), mycoinsecticides (*Beauveria bassiana*) and mycofungicides (*Trichoderma*) certainly offers some benefits towards sustainable agriculture practices (Gehlot and Singh, 2018). The use of entomopathogens has proven beneficial as alternatives to chemical pesticides due to their broad activity, environmental safety, lack of residual on food and safety for human contact. The entomopathogenic fungus *Beauveria bassiana* and bacteria *Bacillus thuringiensis* have displayed a range of possibilities as biopesticides for numerous crop pests (Wang et al., 2021). Entomopathogenic fungi are important regulators of insect populations and biotransformation of ecosystems aiding in biodiversity regulation (Niu et al., 2019). These fungi destroy insect species thereby lowering insect density on crops, preventing crop losses. They are common soil dwellers in natural habitats. Undesirable killings by entomopathogenic fungi are a risk however, where excess usage of these biopesticides may disrupt the biodiversity of soil or harm beneficial insects such as pollinators (Yaman, 2017). Laboratory studies demonstrated that some Beauveria and Metarhizium isolates cause significant mortality to honeybees, but this has not been verified in an environmental setting (Bava et al., 2022). It is essential to fully establish the impact of these fungi on biodiversity and essential species such as pollinators before increasing their widespread application. Additionally, such biopesticides may pose a risk to immunocompromised persons, require approximately 2 weeks to work and have expensive manufacture and storage requirements (Gehlot and Singh, 2018).

2.3. Biocidal AMR considerations

The extensive use of anthropogenic chemicals as biocides represents a great risk to environmental, animal, and human health (Massei et al., 2018). Depending on their application, biocides are categorised as disinfectants, preservatives, pesticides, and other biocidal products such as antifouling agents (Levinskaite, 2012). Such chemical pollution is a significant problem resulting in water and soil pollution, loss of soil fertility, loss of biodiversity, loss of ecosystems and bioaccumulation of fat-soluble chemicals and associated toxicity. Additionally, chemical pollution is believed to have resulted in 9 million premature deaths in 2015 and contribute to the growing trend in neuro-development issues in children including autism, attention deficit disorder, mental retardation, and cerebral palsy

Table 3
Common biocides used for the clinical control of pathogenic species, mode of action and resistance in clinically important species.

Biocide (classification)	Mode of action	Resistance mechanisms	Usage issues relating to AMR	Public health safety issues
Benzalkonium chloride (Quaternary ammonium compound -QAC)	Membrane active agents – membrane destruction (Heinrich et al., 2015) Fungistatic Membrane enzyme alterations Loss of osmo-regulation (Naughton et al., 2017)	Resistance mediated by species specific efflux pumps *Saccharomyces* spp. and fungal spp. *Aspergillus*, *Neurospora* and *Cryptococcus* spp. via efflux pumps (Meade et al., 2021c) Ineffective against planktonic *Candida* spp.	Effective dose must be increased to inactivate pathogens leading to residues in food and noncompliance with MRLs Influenced by bioburden Clinical species and foodborne	Promotes AMR, food pollution exceeding MRL, risk to public health safety
Triclosan (Phenolic compound)	Chlorhexidine is antimicrobial at high concentration, coagulation of cellular contents, nucleic acid and protein precipitation (Lachapelle et al., 2013)	Triclosan induces over expression of MDR efflux pumps (Cameron et al., 2019)	Increased contact time to achieve biocidal action, food pollution with triclosan or toxic triclosan by-products 2, 8-Dichlorodibenzo-p-dioxin and 2, 4-Dichlorophenol (Gómez-López and Bolton, 2016)	Bioaccumulation, foetal toxicity, endocrine toxicity (Chen et al., 2017) CNS toxicity in animals (Franssen et al., 2018) Environmental pollution - detected in aquatic ecosystems Detected in human urine and milk (Cameron et al., 2019)
Chlorhexidine (Biguanide)			No viricidal or sporicidal activity, limited pH range, resistance in *Candida auris* (Meade et al., 2021c)	Dermal irritation, environmental pollution, aquatic toxicity Weak allergen, good skin tolerance
Ethanol	Potent antimicrobial activity at 70–90 % (Sauerbrei, 2020) Decreases the rates of growth and fermentation and cell viability of yeast	Ethanol tolerance present in some species particularly yeast spp.	Exposure time varies ≤ 0.5 and ≥ 5 min. Exposure of up to 5 min - 80 %–90 % ethanol has virucidal/low-level activity - enveloped viruses	
Iodophor PVP-I, (Iodine)	Potent antimicrobial activity at Potent antimicrobial activity at 70-90 % (Sauerbrei, 2020)	A lack of chromosome- or plasmid-mediated resistance.	Dependant on the free iodine concentration. Maximum exposure times are 5 min for bacteria and 60 min for viruses.	Good skin tolerance (Lachapelle et al., 2013)

(Brack et al., 2022). The European Union (EU) implemented the EU Biocidal Products Regulation (BPR) No 528/2012 to regulate the market and use of biocidal products in order to mitigate environmental pollution. Certain unsafe biocides have been withdrawn from use and others are under investigation under this important regulation. Chemical risk assessment is key to establishing the safety profile of biocides where routes of exposure, hazard identification and safety levels are essential factors. The vast range of anthropogenic chemicals and their unpredictable combinations in the environment; however, makes such analysis extremely difficult. The rate of environmental pollution with persistent antimicrobial chemicals such as chlorine and quaternary ammonia compounds (QACs) is extensive, particularly in hotspot locations such as hospital effluent. QACs, which are broad spectrum antimicrobials, are toxic to aquatic species fish, algae and daphnids have been detected in surface and wastewater at 60 ppm (Meade et al., 2021a, 2021b, 2021c). The prevalence of biocidal resistance in AMR species bacterial and fungal (Table 3) is also an alarming trend where resistance to QACs has been shown to promote AMR in species including *E. coli* (Garvey, 2022). Studies report strains of *Pseudomonas aeruginosa*, which were 12 times more tolerant to certain QACs, were also 265 times more resistant to ciprofloxacin due to mutations in the *gyrA* gene (Chen et al., 2021). Indeed, many microbial species display biocidal resistance or tolerance to EPA approved disinfectants evident by increasing minimum inhibitory concentrations (MICs). Exposure to suboptimal or sublethal concentrations allows for the acquisition of AMR in bacterial and fungal species to many of the standard disinfectants including QACs, phenols and chlorine-based solutions (Levinskaite, 2012). The development of alternative green biocides for disinfection purposes may offer some benefits in reducing environmental pollution from disinfection activities (Garvey, 2022).

3. Efficacy of front-line infection preventive interventions

There are several front-line approaches used to inactivate fungal pathogens that vary in efficacy depending on the type of technology used, species of fungi treated, and environmental processing conditions. Emphasis is based on breaking the chain of infection using appropriate technologies and interventions that can be informed by predictive modelling (Rowan et al., 1999) and risk mitigation tools. This is an established HACCP approach that was also successfully used to prevent and control mycotoxins in grains (Matumba et al., 2021) and to addressing important supply chain disruption issues during the COVID-19 pandemic (Rowan and Laffey, 2020; Rowan and Laffey, 2021; Rowan and Moral, 2021). Prevention of fungal infections arising from reuse of medical devices is addressed by appropriate cleaning and reprocessing by the healthcare provider based on following manufacturer's instructions for use (MIFU), which is a highly regulated industry. However, if improperly cleaned and stored, reusable medical devices (such as contaminated endoscopes) can harbour fungal species (such as *Aspergillus* sp., *Candida* sp.) (Marchese et al., 2021) in build-up biofilm that can tolerate reprocessing including use of chemical or gaseous high-level chemical disinfection (Alfa, 2019; Alfa and Singh, 2020; Kwakman et al., 2022). Where appropriate, medical devices are subjected to physical terminal sterilization modalities (such as electron beam, gamma and x-ray irradiation), based on the complexity of design features and heat-sensitive material composition (Chen et al., 2019; McEvoy and Rowan, 2019). The healthcare Sterile Services Department follows MIFUs to understand and apply appropriate cleaning and reprocessing that includes conducting verification testing using artificial soiling procedures (Giles et al., 2018; Alfa, 2019).

Selection of appropriate medical device disinfection or sterilization approaches is informed by the Spaulding Classification system, which is based on the perceived risk to patient acquiring an infection due to use of a contaminated device (Fig. 1). Josephs-Spaulding and Singh, 2021 "Critical (items that contact sterile tissue, such as surgical instruments), semi-critical (items that contact mucous membrane, such as endoscopes), and non-critical (devices that contact only intact skin, such as stethoscopes), items require sterilization, high-level disinfection, and low-level disinfection, respectively" (Rutala, 2019). In terms of the hierarchy

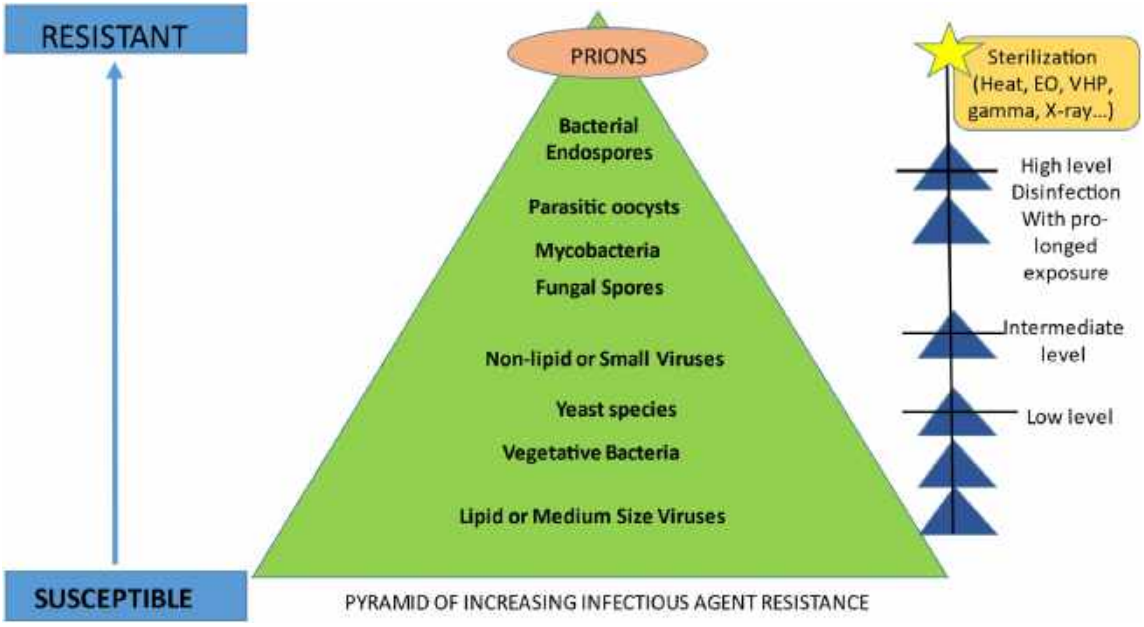

Fig. 1. Pyramid of increasing microbial and infectious agent resistance to disinfection and sterilization.

of susceptibility of different microbial species to the various applied lethal processing technologies, fungal spores are generally considered to be moderately resistant. Yeast cells are of similar resistance to vegetative bacterial cells when exposed to disinfection treatments (Fig. 1). While planktonic occurring yeast are typically killed by low-level disinfection, high-level disinfection or sterilization processes may be required to kill similar yeast species in build-up biofilm on improperly maintained medical devices, such as endoscopes. However, such yeast may survive device reprocessing if improper cleaning precedes high-level disinfection or sterilization. In situ healthcare, and terminal sterilization industry apply the principle of 12 D (Decimal Reduction Time) to ensure all medical devices are sterilized, which is a significantly over-kill approach based upon probability of achieving lethality where biological indicators (such as *Geobacillus stearothermophilus* or *Bacillus atrophaeus*) are treated with high levels of sterilant typically treated for these regulated modalities (Fig. 2). While there is a need to consider the sustainability of sterilant usage, there is also a significant lack of published work on the use of fungi in medical device reprocessing and sterilization.

Indwelling catheters are a high risk of colonization by systemic fungal infections (Kazemzadeh-Narbat et al., 2021). Giles et al. (2018) has

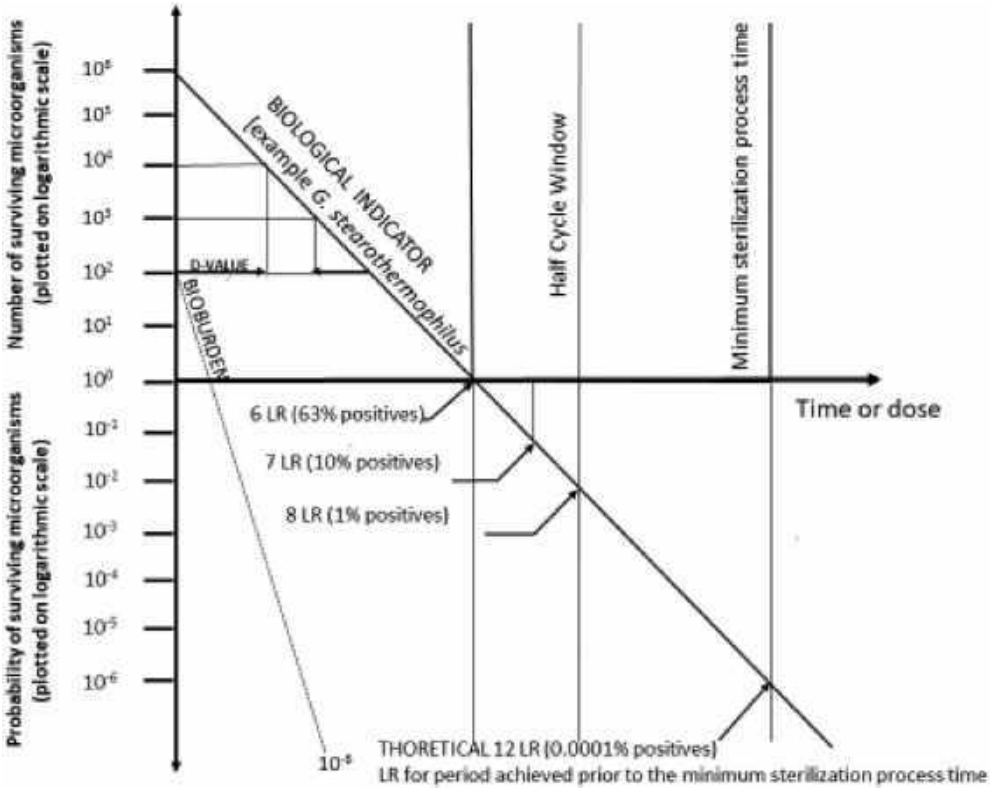

Fig. 2. 12-D microbial inactivation plot for establishing sterility assurance levels in treated devices (adopted from McEvoy and Rowan, 2019).

reported that there is increasing evidence fungal species, particularly *Candida*, can contribute to medical device infections that relate to colonization of devices such as indwelling catheters post insertion in patient. Fungal species can harbour in build-up biofilms that occur in improperly maintained reusable endoscopes where they are protected from high-level disinfection; moreover, these contaminated devices can cause infection particularly in compromised patients (Marchese et al., 2021; Kwakman et al., 2022). High-level disinfection is verified by reducing a pre-determined population of Mycobacterial species by 6 log orders; it does not destroy bacterial endospores Thus, there is a clear need for effective preventative measures, such as thin coatings that can be applied onto medical devices to stop the attachment, proliferation, and formation of device-associated biofilms (Masterson et al., 2021). However, fungi being eukaryotes, the challenge is greater than for bacterial infections because antifungal agents are often toxic towards eukaryotic host cells. While there is extensive literature on antibacterial coatings, a far lesser body of literature exists on surfaces or coatings that prevent attachment and biofilm formation on medical devices by fungal pathogens. Other emerging technologies used in healthcare and adjacent areas to prevent fungal diseases are as follows:

3.1. Light based disinfection technologies

Light based technologies for effectively destroying microbial pathogens including fungal spores have been low-pressure fixed UV (256 nm), broad-spectrum pulsed light (200 to 1100 nm) (Hayes et al., 2012a; Rowan, 2019; Garvey et al., 2010), and more recently, blue light (400 to 500 nm, or fixed at 405 nm) (Trzaska et al., 2017). These are non-thermal technologies that leave no unwanted chemical residuals and have been used for both contact surface and air disinfection (Garvey and Rowan, 2015). Reliable and repeatable destruction of fungal spores depends on duration of exposure, dose, fungal bioburden or population and presence of interfering material or milieu such as organic deposits or biofilm (Farrell et al., 2009; Garvey et al., 2015a). Therefore, prior cleaning of surfaces significantly enhances disinfection performance of light-based technologies, which equally applies for achieving appropriate sterility assurance levels for all modalities (McEvoy and Rowan, 2019). An understanding of inactivation kinetic modelling and performance of UV light sources is critical to achieve appropriate log-reductions in the intended target (Rowan and Moral, 2021; Rowan et al., 2015).

Low pressure, fixed wavelength (256 nm) UV light (LPUV) sources have been used for decades for disinfection of fungal spores on contact surfaces and relies upon the disruptive nature of UV to specifically target and irreversibly damage DNA (Fitzhenry et al., 2019). However, technical drawbacks to using fixed UV light sources include safety to operator due to UV exposure, adaptive molecular and cellular repair mechanisms in treated fungi, and the presence of spore pigmentation that absorbs UV light at the same or similar wavelength to 256 nm protecting the fungus (Anderson et al., 2000). Development of effective adaptive responses by fungi to UV irradiation is well understood given that UV is a constitute wavelength found in sunlight. Fixed-wavelength UV sources is mainly used for inactivation of waterborne pathogens including fungal spores (Wan et al., 2020). There is a gap in knowledge as to whether fungi exhibiting resistance to front-line antifungal drugs are more resistant; however, this is unlikely given LPUV focuses on DNA.

Pulsed UV light (PL) have been reported to effectively destroy a broad range of fungal pathogens, but this has been limited to contact surface disinfection due to safety exposure risk to operators. PL has been approved by the FDA in the production, processing and handling of foods since 1996 up to cumulative UV dose or fluence of 12 J cm^{-2} where emission spectra is to be kept between 200 and 1100 nm and pulse duration at ≤ 2 ms (Food and Drug, 1994). It is used for commercial scale food packaging. The technological principle of pulsed light disinfection is based upon the accumulation of high discharge voltage in a capacitor, where the stored energy is delivered in ultra-short pulses through a light source filled with xenon gas (Hayes et al., 2012b). This xenon-light source emits a broad-spectrum light flash typically in the range of ca. 200–1100 nm, with approximately 25 % in the UV range (Bradley et al., 2012). It is considered that PL disinfection efficiency is higher compared with continuous-wave low-pressure UV irradiation (CW-UV) due to its high peak power along with the ability to deliver its stored energy over short durations, typically 1 to 10 pulses per second (Rowan, 2019). The main parameters governing effective PL operational for disinfection are the fluence [J cm^{-2}] over exposure time [s], number of pulsed applied [n], pulsed width [τ], frequency [Hz], and the peak power [W] (Rowan, 2019; Hayes et al., 2013; Garvey et al., 2015b). Future sustainability surrounding the development of PL treatment is likely to entail use of different light sources such as LEDs (Kim et al., 2017) along with using different configuration in treatment chambers design that deliver pulsed light at multiple angles to overcome shaded areas (Chen et al., 2017). Murray et al. (2018) suggested that additional advantages of using LEDs are the potential to use a range of different wavelengths such as UV-C thereby providing a possible synergistic antimicrobial action (Murray et al., 2018). This approach may be particularly applicable for inactivating complex pathogens, such as fungi or parasites, where other wavelengths in the pulsed spectrum may also contribute by destroying important cellular macromolecules and structures (Garvey et al., 2013).

Farrell et al. (2011) reported on the relationship between pulsed UV light (PL) irradiation and the simultaneous occurrence of molecular and cellular damage in clinical strains of *Candida albicans* (Farrell et al., 2011). Microbial protein leakage and propidium iodide (PI) uptake assays demonstrated significant increases in cell membrane permeability in PL-treated yeast that depended on the amount of UV pulses applied. This finding correlated well with the measurement of increased levels of lipid hydroperoxidation in the cell membrane of PL-treated yeast. PL-treated yeast cells also displayed a specific pattern of intracellular reactive oxygen species (ROS) generation, where ROS were initially localised in the mitochondria after low levels of pulsing (UV dose 0.82 μJ/cm^2) before more wide-spread cytosolic ROS production occurred with enhanced pulsing. Intracellular ROS levels were measured using the specific mitochondrial peroxide stain dihydrorhodamine 123 and the cytosolic oxidation stain dichloroflurescin diacetate. Use of the dihydroethidium stain also revealed increased levels of intracellular superoxide as a consequence of augmented pulsing. The ROS bursts observed during the initial phases of PL treatment was consistent with the occurrence of apoptotic cells as confirmed by detection of specific apoptotic markers, abnormal chromatin condensation and externalisation of cell membrane lipid phosphatidylserine. Increased amount of PL-irradiation (ca. UV does 1.24–1.65 μJ/cm^2) also resulted in the occurrence of late apoptotic and necrotic yeast phenotypes, which coincided with the transition from mitochondrial to cytosolic localisation of ROS and with irreversible cell membrane leakage. Use of the comet assay also revealed significant nuclear damage in similarly treated PL samples. Although some level of cellular repair was observed during sub-lethal exposure to PL-treatments (≤ 20 pulses or UV dose 0.55 μJ/cm^2), this was absent in similar samples exposed to increased amounts of pulsing. Therefore, PL-irradiation inactivates *C. albicans* through a multi-targeted process with no evidence of microbial ability to support cell growth after ≤ 20 pulses. Interesting, the identification of the onset of apoptosis in treated yeast coincided with irreversible cell death, which may be potentially used as a rapid diagnostic test for confirming their destruction, thus alleviating reliance on culture-based enumeration techniques that requires several days to confirm effectiveness (Farrell et al., 2011; Farrell et al., 2009).

Blue light is an emerging technology for destruction of fungal pathogens using spectral wavelengths that are safe for human exposure (Moorhead et al., 2016). Maclean et al. (2009) first reported on the inactivation of bacterial pathogens following exposure to light from a 405 nm light emitting diode, where Gram positive bacteria were more susceptible than similarly treated Gram negative bacteria (Maclean et al., 2009). Trzaska et al. (2017) exposed six-common trauma-associated fungal pathogens (*Rhizopus microsporus*, *Mucor cirinelloides*, *Scedosporium apiosspermum*, *Scedosporium prolificans*, *Fusarium oxysporum*, *Fusarium solari*) along with *Candida albicans* to blue light treatments at 405 nm (Trzaska et al., 2017). While blue light was shown to be highly effective against *Scedosporium*

and *Fusarium* spp., time lapse imaging revealed that *Rhizopus microsporus*, *Mucor circinelloides* and *C. albicans* eventually recovered full growth capacity. The authors noted that once established in the host, IFIs are very difficult to treat and are associated with high levels of morbidity and mortality where they recommended appropriate solutions to decontaminate hospital air, decolonize hospital surfaces to reduce opportunities for wound infection. Blue light appears to be effective against a range of pathogens, including certain fungi, and does not require the need for exogenous photosensitizer that are used in combinational photodynamic therapy (PTD). Zhang and co-workers (2014) demonstrated efficacy of blue light against antibiotic-resistant *Acinetobacter baumannii* in a mouse burn model of infection (Zhang et al., 2014). These authors also demonstrated that bacteria are more susceptible to blue light than keratinocytes, suggesting potential applications in topical treatments. The proposed mechanisms underpinning mechanistic action of blue light is photoexcitation of endogenous porphyrins, generating the production of ROS and cell death; however, this has yet to be elucidated (Moorhead et al., 2016). Moorhead et al. (2016) demonstrated efficacy of blue light for destroying *Trichophyton* and *Aspergillus conidia* by violet-blue light exposure (3380–480 nm) (Moorhead et al., 2016). Blue light technology that underpins High-Intensity Narrow-Spectrum light Environmental Decontamination System (HINS-light EDS) have now been deployed in many hospitals worldwide for the safe disinfection of air (Bache et al., 2012; MacLean et al., 2013). Recently, this technology was proven to completely inactivate the blood borne parasite *Trypanosoma cruzi* (that causes Chagas disease) in stored human platelet concentrates and plasma, which highlights potential for preventing adjacent fungal infections (Jankowska et al., 2020).

3.2. Other established and emerging interventions for preventing fungal infections

Flash heat pasteurization has been successfully used to treat microbial pathogens including fungi for the dairy industry for decades (Garnier et al., 2017), which is particularly relevant for species associated with causing mastitis (Kalińska et al., 2017). However, these authors also reported that prevention and control of the occurrence of fungi is a major concern for industrials and scientists that are looking for efficient eco-solutions. Several traditional methods, also called traditional hurdle technologies, are implemented and combined to prevent and fungal control include good manufacturing and hygiene practices, air filtration, and decontamination systems, while linked control methods encompassing inactivation treatments, and temperature control. While the use of inappropriate and excessive use of antibiotics in dairy cows has contributed to increased resistance of mastitis pathogens (Jamali et al., 2014), the contribution of fungi to disease burden is significantly underestimated and underappreciated as they are frequently overlooked. Other physical emerging technologies considered for reducing fungal pathogens in the environment includes the use of pulsed-plasma gas-discharge (PPGD) treatments, such as for industrial effluents (Rowan et al., 2007), and pulsed electric fields (PEF) (MacGregor et al., 2000; Beveridge et al., 2002). However, Hayes et al. (2013) reported that PPGD treatment can be unsafe for treating industrial effluents as this technology can produce considerable significant cytotoxic properties (as determined by MTT and neutral red assays), genotoxic properties (as determined by comet and Ames assays), and ecotoxic properties (as determined by Microtox™, Thamnotox™ and Daphnotox™ assays), which was attributed to corrosion of the electrodes over time (Hayes et al., 2013). However, Kang et al. (2015) reported on the effective inactivation of fungal spores in water and on seeds by using ozone and arc discharge plasma (Kang et al., 2015). Whereas Dehghani et al. (2007) previously reported on an ultrasound reactor technology to reduce fungi in sewage (Dehghani et al., 2007). The challenges with novel and new emerging technologies are gaining consensus internationally on agreed methodology that will produce harmonized findings that will inform verification for validation of modalities by regulators. This will also impact upon investors for bringing new technologies, including new green-deal innovations to market (Rowan and Galanakis, 2020; Galanakis et al., 2021).

There is commensurate interest the development of antifungal coatings to prevent medical device infections, particularly for *Candida* species (Giles et al., 2018). These authors report that fungal species can form biofilms by themselves or by participating in polymicrobial biofilms with bacteria. Thus, there is a clear need for effective preventative measures, such as thin coatings that can be applied onto medical devices to stop the attachment, proliferation, and formation of device-associated biofilms. However, as fungi are eukaryotes, there is a greater challenge than treating other microbial pathogens as antifungal agents are often toxic towards eukaryotic host cells. These authors noted that while there is extensive literature on antibacterial coatings, a far lesser body of literature exists on surfaces or coatings that prevent attachment and biofilm formation on medical devices by fungal pathogens. A greater appreciation of the molecular understanding of fungal recognition of, and attachment to, suitable surfaces, and of ensuing metabolic changes, is essential for designing rational approaches towards effective antifungal coatings, rather than empirical trial of coatings. With increasing complexity in the design of medical devices comes a commensurate challenge in the effective decontamination and sterilization, including devices for reuse (McEvoy and Rowan, 2019). There is a pressing need to establish appropriate real-time diagnostic technologies that will confirm efficacy of terminal sterilization processes for next-generation medical devices that balances microbial inactivation with maintaining effective material and design functionality of these devices post treatments (McEvoy et al., 2021).

Interest in the development of immunotherapies for addressing complex microbial infections has increased, particularly over the past decade, where invasive infections occur mainly as a result of altered immune status (Armstrong-James et al., 2017; Murphy et al., 2020; Murphy et al., 2021; Casalini et al., 2021). The incidence of IFIs has increased mainly due to the widespread use of immunosuppressive drugs, invasive medical interventions, HIV (Armstrong-James et al., 2017) and COVID-19 (Casalini et al., 2021; Roudbary et al., 2021). Thus, fungal diseases cause life-threatening infections in the context of primary and acquired immunodeficiencies all over the world. Invasive fungal diseases are associated with >50 % mortality that stems mainly from inadequate diagnosis and from clinical shortcomings of existing antifungal drugs (Armstrong-James et al., 2017; Vallabhaneni et al., 2016). However, no clinical vaccine exists for the main genera of fungi causing invasive diseases (*Aspergillus*, *Candida*, *Cryptococcus* and *Pneumocystis*) (Armstrong-James et al., 2017). The close relationship between infection susceptibility and immunocompromised status, combined with poor outcomes and increasing resistance to conventional antifungal chemotherapy, has intensified interest in immunotherapies. The rapid progress in clinical immunotherapy research is creating unprecedented opportunities to exploit existing approaches for treatment of fungal disease—from recombinant cytokines to vaccines, monoclonal antibodies, and engineered T cells (Armstrong-James et al., 2017). However, these authors advocated that the biggest challenge in the next decade will be to test the use of immunotherapy for fungal diseases in carefully designed clinical trials (Armstrong-James et al., 2017). The central role of phagocytic cells in protective innate host response and in the development of adaptive immunity is increasing in focus, where phagocytes are therapeutic targets as their activities can be influenced by soluble immunomodulatory mediators (Wüthrich et al., 2012). The incidence of mycoses is rising because immunomodulatory drugs are increasingly used to treat autoimmune diseases and cancer. New classes of antifungal drugs have only been partly successful in improving the prognosis for patients with fungal infection. Armstrong-James et al. (2017) advocated that adjunctive host-directed therapy is therefore believed to be the only option to further improve patient outcomes (Armstrong-James et al., 2017). Recent advances in the understanding of complex interactions between fungi and host have led to the design and exploration of novel therapeutic strategies in cytokine therapy, vaccines, and cellular immunotherapy, each of which might become viable adjuncts to existing antifungal regimens. However, outcomes of several studies support an association between genetic polymorphisms and increased risk of fungal infections such as patients who have received transplants (Maskarinec et al., 2016), where Armstrong-

James et al. (2017) suggested stratifying patient risk on the basis of immunogenetics (Armstrong-James et al., 2017). In doing so, intensive diagnostic screening alone or combined with prophylactic antifungal therapy can inform targeted immunotherapy to address this issue. Immunotherapy can potentially circumvent increasing prevalence of increased resistance to front line antifungal drugs in infected animals and humans.

3.3. Occurrence, fate and ecological risk of anti-fungal drugs and personal care products

Currently, 400,000 tons of fungicides are applied to food crops globally, which represents 17.5 % of pesticide applications (Gikas et al., 2022). Researchers have reported that popular azole fungicides may reach the receiving environment by direct or indirect discharge of wastewaters; thus, posing significant potential risks to organisms in aquatic ecosystems (Chen and Ying, 2015; Bhagat et al., 2021). Azole fungicides are widely detected in surface water and in sediment of the aquatic environment arising from incomplete destruction or removal in wastewater treatment plants. Assress et al. (2021) reported that azole antifungals may enter the environment through the discharge of domestic, industrial and hospital wastewaters, agricultural runoffs and as leachates in waste-disposal sites. These authors noted that the presence of the azole antifungals poses potential toxicity risks to non-target organisms and plays a critical role in the evolution and/or selection of azole resistant fungal strains in the environment. These fungal drugs were reported to be resistant to microbial degradation but undergo photolysis during exposure to UV irradiation (Chen and Ying, 2015). However, photolysis of azole and effect of its derivatives need to be further studied. Due to variance in physicochemical properties and environmental persistence, these azole drugs could cause toxicity to aquatic organisms such as algae (Nong et al., 2021) and fish (Bhagat et al., 2021). Azole fungicides were recently reported to be potent disrupting chemicals for fish that can significantly affected their reproductive system; moreover, steroid hormone disruption may be novel toxicity in fish (Huang et al., 2022). Toxicities such as inhibition of algal growth, endocrine disruption in fish, CYP450-effected steroidogenesis, modulating sex differentiation in frogs, and reduction of larval body mass and growth rate have been related to azole antifungals (Assress et al., 2021). In addition, the isolation of azole resistant fungi such as *Aspergillus fumigatus* in both the environment and clinic retaining similar mode of molecular drug resistance mechanism has drawn the attention of many researchers (Assress et al., 2021). Therefore, the investigation of the occurrence and distribution of azole antifungals as well as azole resistant environmental isolates of fungi is merited. New solutions are pressing in order to effective remove azole fungicides potentially through alternative treatment technologies such as pulsed plasma gas discharge technologies along with better understanding environmental fate and toxic pathways in aquatic organisms. Multigenerational studies with environmentally relevant concentrations of antifungal drugs such as azole need to be considered (Bhagat et al., 2021). Indeed, based on current knowledge and studies reporting adverse biological effects of antifungal azole on fish, considerable attention is required for better management and effective ecological risk assessment of these emerging contaminants.

3.4. Established and emerging control strategies

Use of antifungal drugs remain the main control intervention for the treatment of disease where this market commands a demand of over $4 billion per year. Based on review of the total market demand, the main antifungal drugs used are azoles that represent over half of this market along with echinocandins and polyenes. However, despite the huge demand for appropriate and effective antifungal drugs, only one anti-fungal drug has been approved for therapeutic use over the past decade (Alanio and Dd, 2020). Approved antimycotics inhibit 1,3-β-d-glucan synthase, lanosterol 14-α-demethylase, protein, and deoxyribonucleic acid biosynthesis, or sequestrate ergosterol (Houšť et al., 2020). These authors reviewed licensed antifungal drugs and summarised their mechanisms of action, pharmacological profiles and susceptibility to specific fungi. The most severe side effects of antifungal drugs are hepatotoxicity, nephrotoxicity, and myelotoxicity. Whereas triazoles exhibit the most significant drug–drug interactions, echinocandins exhibit almost none. The antifungal resistance may be developed across most pathogens and includes drug target overexpression, efflux pump activation, and amino acid substitution (Houšť et al., 2020). These authors advocated that siderophores in the Trojan horse approach, or the application of siderophore biosynthesis enzyme inhibitors represent, the most promising emerging antifungal therapies. Sousa et al. (2020) reported that the high incidence of fungal infections has become a major public health issue (Sousa et al., 2020). These authors noted that despite the availability of drugs on the market to treat these diseases, their efficiency is questionable, and their side effects cannot be neglected. Consequently, it is important to synthetize new and innovative carriers for these antifungal drugs that addresses the emerging fungal infections along with the issue of increased in drug-resistant strains. Sousa et al. (2020) reported that new nano-based drug delivery systems and cellular targets/compounds with antifungal potential are under development (Sousa et al., 2020). However, there are pressing challenges in the translation of these natural compounds into the clinical pipeline.

Fungal urinary tract infections (funguria) are rare in community medicine, but common in hospitals, where 10 to 30 % of urine cultures isolate *Candida* species. Clinical features vary from asymptomatic urinary tract colonization (the most common situation) to cystitis, pyelonephritis, or even severe sepsis with fungemia (Etienne and Caron, 2007). The pathologic nature of funguria is closely relates to host factors, and management depends mainly on the patient's underlying health status. Microbiological diagnosis of funguria is usually based on a fungal concentration of $>10^3/mm^3$ in urine. No cut-off point has been defined for leukocyte concentration in urine. *Candida albicans* is the most commonly isolated species but previous antifungal treatment and previous hospitalization affect both species and susceptibility to antifungal agents. Treatment is recommended only when funguria is symptomatic or in cases of fungal colonization when host factors increase the risk of fungemia. The antifungal agents used for funguria are mainly fluconazole and amphotericin B deoxycholate because other drugs have extremely low concentrations in urine. Primary and secondary preventions are essential. The reduction of risk factors requires removing urinary catheters, limiting antibiotic treatment, and optimizing diabetes mellitus treatment.

The presence of *Candida* species in urine in asymptomatic patients does not warrant antifungal therapy except neutropenic patients, very low-birthweight infants and patients undergoing urologic procedures. Fluconazole is the treatment of choice for symptomatic infections, it achieves high urinary levels. The other azole antifungals and echinocandins do not reach sufficient urine levels. Amphotericin B deoxycholate is the alternative antifungal agent if fluconazole cannot be used because of resistance, allergy or failure.

Fungal pathogens, and zoonotic cross over species, however, remain an important public health consideration within the One Health approach. A One Health approach is vital to address the impact of AMR by way of identifying appropriate alternative solutions and to raise an awareness of the antimicrobial resistance crisis (Masterson et al., 2021). Fungal infections of sporotrichosis, histoplasmosis and chromoblastomycosis and MDR dermatophytosis remain important as zoonotic fungal pathogens. Furthermore, the impact of global warming will undoubtedly promote a rise in fungal infectious disease globally negatively impacting public health and food security.

Emerging opportunities now potentially exist for the development of specific phage therapies to address fungal pathogens (Górski et al., 2019). These authors reported that while the true value of phage therapy (PT) in human bacterial infections still awaits formal confirmation by clinical trials, new data have been accumulating indicating that in the future phage therapy may be applied in the treatment of non-bacterial infections, such as against *Aspergillus* that affect CF patients. Phage therapy will be potentially accelerated by hurdling uncertainty surrounding legal classification of phase therapy from a regulatory approval perspective in the Europe. Species-specific phages can be developed and applied for systemic and for

topical administration. While phages have been developed to treat a variety of significant bacterial infections in animals including poultry, cattle, pigs, sheep, swine, horses and fish (Alomari et al., 2021; Garvey, 2020); the topic remains to be properly advanced as producers are not harmonized where selection of phages is complicated. Xu et al. (2022) have recently reported on the use of phage nanoparticles as a carrier for controlling fungal infections (Xu et al., 2022).

3.5. Detection of fungal species is important in proper diagnosis and treatment

Fungal infections are typically diagnosed late or by chance due to gap of appropriate highly sensitive and specific diagnostic assays (Wen et al., 2020). Moreover, the clinical manifestations of IFIs are frequently non-specific and easily masked by primary underlying diseases (Wen et al., 2020). Early diagnosis is difficult, often resulting in delayed diagnosis, misdiagnosis, and delayed treatment. It is notable that IFIs have a poor prognosis and are associated with high mortality (Ibáñez-Martínez et al., 2017) as attested by ca.1.4 million deaths globally per annum (Sanglard, 2016). Sun et al. (2015) reported that the total mortality rate with invasive fungal species is 13.4 % (Sun et al., 2015), reported that the mortality rates associated with invasive candidiasis (IC) and invasive aspergillosis are 36 % to 63 % and 70 % respectively (Barnes, 2008), which supports the need for improvements in detection methods. Laboratory detection of invasive fungal species mainly involves traditional detection methods including direct microscopy, culture, and histopathology (Clancy and Nguyen, 2013). It is notable that traditional methods have a low positive detection rate along with poor sensitivity that does not enable real time clinical diagnosis (Garey et al., 2006). Serological analysis typically includes use of 1,3-β-D-glucan test (G test), galactomannan test (GM test), and latex agglutination test. While these approaches potentially enable early diagnosis of fungal infections, false-positive results do occur (Taccone et al., 2015) and they are not accurately detecting fungal species. Molecular biology technologies based on PCR have been widely used to detect (Powers-Fletcher and Hanson, 2016). Wen et al. (2020) recently reports on the use of fluorescence PCR melting curve analysis (MCA) as an emerging detection method for identifying fungal species without sequencing (Wen et al., 2020). These authors report that MCA has a high sensitivity, throughput, speed, and accuracy that is cost effective and is applicable for detecting fungal infections. Lengerova and co-workers (2014) noted that this method is based on the principle that different double-stranded DNA molecules have different Tm values, and changes in the shape of the melting curve can be monitored using fluorescent dyes or probes to detect and identify various fungi rapidly and accurately (Lengerova et al., 2014). Researchers have demonstrated efficacy for using combined probe-high resolution melting analysis for detecting *Candida*, *Cryptococcus*, *Aspergillus Mucor*, *Rhizopus*, and endemic diseased-related fungi (Wen et al., 2020; Alonso et al., 2012).

3.6. Mycosis and co-morbidity of COVID-19

Casalini et al. (2021) commensurately reported that IFIs can complicate the clinical course of COVID-19 and are associated with a significant increase in mortality, especially in critically ill patients admitted to an ICU (Casalini et al., 2021). The authors reviewed 4099 cases of IFIs in 58,784 COVID-19 patients involved in 168 studies. COVID-19-associated invasive pulmonary aspergillosis (CAPA) is a diagnostic challenge because its non-specific clinical/imaging features and the fact that the proposed clinically diagnostic algorithms do not really apply to COVID-19 patients. Forty-seven observational studies and 41 case reports have described a total of 478 CAPA cases that were mainly diagnosed based on cultured respiratory specimens and/or biomarkers/molecular biology, usually without histopathological confirmation. Candidemia is a widely described secondary infection in critically ill patients undergoing prolonged hospitalization, and the case reports and observational studies of 401 cases indicate high crude mortality rates of 56.1 % and 74.8 %, respectively. COVID-19 patients are often characterised by the presence of known risk factors for candidemia such as in-dwelling vascular catheters, mechanical ventilation, and broad-spectrum antibiotics. Studies also describe 3185 cases of mucormycosis (including 1549 cases of rhino-orbital mucormycosis (48.6 %)), for which the main risk factor is a history of poorly controlled diabetes mellitus (>76 %). Its diagnosis involves a histopathological examination of tissue biopsies, and its treatment requires anti-fungal therapy combined with aggressive surgical resection/debridement, but crude mortality rates are again high: 50.8 % in case reports and 16 % in observational studies. Roudbary et al. (2021) also patients with severe COVID-19, such as individuals in ICU, are exceptionally susceptible to bacterial and fungal infections (Roudbary et al., 2021). The most prevalent fungal infections are aspergillosis and candidemia. Other fungal species (for instance, *Histoplasma* spp., *Rhizopus* spp., *Mucor* spp., *Cryptococcus* spp.) have recently been increasingly linked to opportunistic fungal diseases in COVID-19 patients. These fungal co-infections are described with rising incidence, severe illness, and death that is associated with host immune response.

Roudbary and co-workers (2021) advocated creating greater awareness of the high risks of the occurrence of fungal co-infections, particularly as to downgrading any arrear in diagnosis and treatment to support the prevention of severe illness and death directly related to these infections (Roudbary et al., 2021). Since the onset of the COVID-19 pandemic, there are still few data on the prevalence of co-infections in patients with COVID-19 pneumonia. Yet, some studies already mention the problem of co-infections and drug resistance, which is the case of *Candida* spp. and COVID-19-associated superinfection mycosis, and its high potential for antifungal resistance (Roudbary et al., 2021; Heard et al., 2020). Indeed, around 21 % of patients who were under treatment with antifungals (voriconazole, isavuconazole, and caspofungin) showed no survival benefit (Rezasoltani et al., 2020). Zhou et al. reported that almost 50 % of mortalities accrued in patients had secondary bacterial and fungal infections (Zhou et al., 2020). This is the reason why antibiotics have been prescribed for hospitalized patients, for example, as a prophylactic measure against secondary infections, regardless of the susceptibility of the microorganism, promoting the emergence of multiple drug-resistant microbial species (Rawson et al., 2021). Roudbary et al. (2021) noted that COVID-19 was highly associated with pulmonary aspergillosis and candidemia (invasive candidiasis), which were increasingly recognised as the main fungal diseases (Roudbary et al., 2021); however, a shift has been occurring towards other fungal infections such as infections related to *Mucor* and *Rhizopus* genera, *Cryptococcus* spp. and other less common species. Generally, these authors noted that COVID-19 patients in ICU seem more susceptible to fungal infections, when compared with patients without ICU admission, due to their immunosuppression status (the same case of HIV patients). Several predisposing factors including diabetes, previous respiratory pathology, nosocomial infection sources and immunosuppressive therapy is associated with co-infections (Roudbary et al., 2021).

4. Additional considerations for developing and labelling eco-friendly biocides and other physical disease mitigation interventions

With such extensive application of fungicides globally to ensure food security and food safety, there must be awareness of the extent of environmental impact of these compounds. Environmental concerns and the need for associated protection have been influencing our approach to exploring new eco-friendly solutions for addressing disease mitigation (Silva et al., 2019; Rowan et al., 2021; Nallal et al., 2022). Both the hydrosphere and biosphere have been experiencing the negative impact of many pollutants, particularly when released to the marine environment (Tiedeken et al., 2017; Silva et al., 2019). Development of new eco-friendly biocides for addressing fungal pathogens need to comply with EU Biocidal Products Regulation (BPR) standards. There is a commensurate need to apply the full battery of ecotoxicology tests on these products that includes appropriate use of in vitro cell culture (Garvey et al., 2015b; Rowan, 2019). Some research has reported on partial use of ecotox batteries for important new innovation and processes (O'Neill et al., 2019), which requires further expansion. Rowan et al. (2021) highlighted key parameters associated with chemical biocides that must be considered for both efficacy and low

environmental impact that included type of biocide, concentration, pH There is growing interest in alternative or complimentary physical treatments for eliminating pathogens in clinical, industrial and municipal effluent; however, care must also be taken to ensure that these modalities do not generate additional toxic residues that may form as part of the biocidal process, such as through electrode erosion when using pulsed plasma gas discharge (Hayes et al., 2013). Nallal et al. (2022) described eco-friendly synthesis of multi-shaped crystalline silver nanoparticles using Hill garlic-Malai Poondu extract along with their potential effective applications against *C. glabrata*, *C. tropicalis*, *C parapsilosis*, *C. krusei* and *C. albincas*. The latter research is representative of increasing activities to the synthesis of metal nanoparticles using greener methodologies. For example, Narayanan and Park (2014) reported on the synthesis of silver nanopartilces using turnip leaf extract and its effectiveness against wood-degrading fungal pathogens. There are increasing opportunities to align development of eco-friendly biocides with sustainability tools such as life cycle assessment, material flow analysis, principle component analysis and so forth in order to provide companies with full risk assessments from a development and business-model perspective, which will inform new Green Deal era (Rowan and Pogue, 2021; Ruiz-Salmon et al., 2021; Laso et al., 2022). There is also a commensurate need to comprehensively consider eco-labelling of these products which are potential vast (Kahhonen and Nordstron, 2008). There is strong potential for combining new eco-friendly innovative biocides with biosurfactants that includes targeting complex biofilms and to prevent biocorrosion (Plaza and Achal, 2020).

5. Other pressing topics associated with ensuring effective prevention and control of fungal infections

Due to the enormity of the challenge at hand, there is a pressing need to develop appropriate digital technologies that will enable end-to-end monitoring of the effectiveness of new prevention and control technologies, and combinations thereof (Rowan et al., 2022). This will enable real-time monitoring of effectiveness that will also inform appropriate design-thinking that will positively transform interdisciplinarity efforts across manufacturers, producers, end-users and regulators for new innovation uptake and regulatory approval. For example, there are opportunities to apply artificial intelligence and to develop robotics in the area of device cleaning and reprocessing that will help remove potential human operator error and will increase the efficiency of reprocessing. Also, the introduction of immersive technologies for upskilling and reskilling workforce that will provide bespoke training to stakeholders including original equipment manufacturers, healthcare staff (such as Sterile Services Department), and external contract service providers (such as terminal sterilization). Candidate digital technologies are likely to emerge for adjacent additive manufacturing, digital twin, agriculture 4.0 and industry 5.0 human centric initiatives that includes digital twin (Rowan, 2020). Digital technologies that will impact positively include internet of things (IoT), cloud-edge computing, artificial intelligence including machine learning, robotics and use of blockchain that will address security of data, risk mitigation and disruptive business model development (Rowan et al., 2022). The generation, modelling and analysis of data governing efficacy of fungal disinfection will improve sustainability, such as by enabling greater reuse of important medical devices along with less use of single-use disposables, which will impart positively on clinical waste management and cost-effectiveness. MacNeill et al. (2020) noted that 'take-make-waste' is inherently unsustainable model of production and consumption as this contributes to global ecological destruction by depleting natural resources and generates excessive solid waste, global greenhouse gases, and other harmful environmental emissions. There is also a pressing need to use machine learning to help apply solutions for real-time decision-making to unlock plethora of complex factors influencing novel non-thermal processing of foods that includes antifungal applications (Gómez-López et al., 2022). Commensurately, there is a need to create a greater awareness in society about the prevalence and significance of fungal diseases including increased resistance to front-line interventions that will improve behaviour change and ultimately, decisions by policy makers (Suanda et al., 2013; Domegan, 2021). Effectively addressing fungal pathogens will contribute significantly to meeting several key Sustainable Development Goals of the United Nations (Rowan and Casey, 2021; O'Neill et al., 2022) including zero hunger, good health and well-being, quality education, industry, innovation and infrastructure, and responsible consumption and production.

6. Concluding remarks

There is increased evidence of adaption and resistance of pathogenic fungi to front-line anti-fungal drugs in animals and humans. IFIs can be particularly problematical in hosts that have a compromised immunity as evidenced by opportunistic IFIs in patients during HIV and COVID-19 pandemics. Greater information is required on appropriate selection and dose of antifungal drugs along with discovering solutions such as immunotherapies. Many front-line biocides are effective for addressing fungal spores; but, there is potential for cross-protection to antifungal drugs. There is a lack of information on efficacy of established disinfection technologies, particularly in the appropriate cleaning of contaminated medical devices that may contain biofilm harbouring infectious fungi. There is intensive research emerging on the development of alternative and complementary innovation that has anti-fungal applications, such as using blue light for air disinfection in healthcare including surgical theatres. Fungal spores present challenges for cleaning and aseptic processing for medical devices; however, the combinational use of terminal sterilization modalities will ensure appropriate sterility assurance levels are achieved. There is a pressing need to develop further appropriate real-time monitoring and diagnostic methods for fungal pathogens and to create a greater awareness as to contribution of fungal pathogens in disease causation, particularly co-infection in immunocompromised patients to improve outcomes. There is also a need to address risk mitigation and modelling to inform efficacy of appropriate intervention technologies that must consider all contributing factors to break the chain of infection including appropriate anti-fungal coatings on indwelling catheters. International consensus must be reached on standardised protocols for developing and reporting on appropriate intervention technologies that embraces emerging anti-fungal resistant strains, such as using a One Health platform.

Funding

The authors thank Interreg Atlantic Area Neptunus Project (EAPA_576/2018) and the Regional University Network - European Universities (RUN_EU) Project for funding supporting relating to this article.

CRediT authorship contribution statement

Conceptualization of this article was by MG and NR. Design, research, and writing of this article was conducted by EM, NR and MG. All authors approve the submission of this article.

Data availability

No data was used for the research described in the article.

Declaration of competing interest

The author declares no conflict of interest.

Acknowledgments

MG and EM would like to acknowledge the PEM centre and ATU Sligo.

References

Ahmad, S.I., Kirk, S.H., Eisenstark, A., 1998. Thymine metabolism and thymineless death in prokaryotes and eukaryotes. Annu. Rev. Microbiol. 52, 591–625.

Alanio, A., Dd, G.F.S.-P.P., 2020. Global Action Fund for Fungal Infections (GAFFI).
Alfa, M.J., 2019. Biofilms on instruments and environmental surfaces: do they interfere with instrument reprocessing and surface disinfection? Review of the literature. Am. J. Infect. Control. https://doi.org/10.1016/j.ajic.2019.02.027.
Alfa, M.J., Singh, H., 2020. Impact of wet storage and other factors on biofilm formation and contamination of patient-ready endoscopes: a narrative review. Gastrointest. Endosc. 91 (2), 236–247. https://doi.org/10.1016/j.gie.2019.08.043.
Alomari, M.M.M., Dec, M., Urban-Chmiel, R., 2021. Bacteriophages as an alternative method for control of zoonotic and foodborne pathogens. Viruses 13 (12), 2348.
Alonso, M., Escribano, P., Guinea, J., Recio, S., Simon, A., Peláez, T., Bouza, E., García de Viedma, D., 2012. Rapid detection and identification of Aspergillus from lower respiratory tract specimens by use of a combined probe-high-resolution melting analysis. J. Clin. Microbiol. 50 (10), 3238–3243.
Anderson, J.G., et al., 2000. Inactivation of food-borne enteropathogenic bacteria and spoilage fungi using pulsed-light. IEEE Trans. Plasma Sci. 28 (1), 83–88. https://doi.org/10.1109/27.842870.
Armstrong-James, D., Brown, G.D., Netea, M.G., Zelante, T., Gresnigt, M.S., van de Veerdonk, F.L., Levitz, S.M., 2017. Immunotherapeutic approaches to treatment of fungal diseases. Lancet Infect. Dis. 17 (12), e393–e402.
Assress, H.A., Selvarajan, R., Nyoni, H., et al., 2021. Antifungal azoles and azole resistance in the environment: current status and future perspectives—a review. Rev. Environ. Sci. Biotechnol. 20, 1011–1041. https://doi.org/10.1007/s11157-021-09594-w.
Bache, S.E., Maclean, M., MacGregor, S.J., Anderson, J.G., Gettinby, G., Coia, J.E., Taggart, I., 2012. Clinical studies of the high-intensity narrow-spectrum light environmental decontamination system (HINS-light EDS), for continuous disinfection in the burn unit inpatient and outpatient settings. Burns 38 (1), 69–76.
Barnes, R.A., 2008. Early diagnosis of fungal infection in immunocompromised patients. J. Antimicrob. Chemother. 61 (Suppl. 1), i3–i6.
Bava, R., Fabio, C., Cristian, P., Vincenzo, M., Carmine, L., Ernesto, P., Domenic, B., Vincenzo, M., 2022. Entomopathogenic fungi for pests and predators control in beekeeping. Vet. Sci. 9 (2), 95. https://doi.org/10.3390/vetsci9020095.
Benkő, R., Gajdács, M., Matuz, M., Bodó, G., Lázár, A., Hajdú, E., Papfalvi, E., Hannauer, P., Erdélyi, P., Pető, Z., 2020. Prevalence and antibiotic resistance of ESKAPE pathogens isolated in the Emergency Department of a Tertiary Care Teaching Hospital in Hungary: a 5-year retrospective survey. Antibiotics (Basel) 9 (9).
Beveridge, J.R., et al., 2002. Comparison of the effectiveness of biphase and monophase rectangular pulses for the inactivation of micro-organisms using pulsed electric fields. IEEE Trans. Plasma Sci. 30 (4), 1525–1531. https://doi.org/10.1109/TPS.2002.804204.
Bhagat, J., Singh, N., Nishimura, N., Shimada, Y., 2021. A comprehensive review on environmental toxicity of azole compounds to fish. Chemosphere 262. https://doi.org/10.1016/j.chemosphere.2020.128335.
Billmyre, R.B., Applen Clancey, S., Li, L.X., Doering, T.L., Heitman, J., 2020. 5-Fluorocytosine resistance is associated with hypermutation and alterations in capsule biosynthesis in Cryptococcus. Nat. Commun. 11 (1), 1–9.
Bongomin, F., Gago, S., Oladele, R.O., Denning, D.W., 2017. Global and multi-national prevalence of fungal diseases—estimate precision. J.Fungi 3 (4), 57.
Brack, W., Barcelo Culleres, D., Boxall, A.B.A., Budzinski, H., Castiglioni, S., Covaci, A., Dulio, V., Escher, B.I., Fantke, P., Kandie, F., Fatta-Kassinos, D., Hernández, F.J., Hilscherová, K., Hollender, J., Hollert, H., Jahnke, A., Kasprzyk-Hordern, B., Khan, S.J., Kortenkamp, A., Kümmerer, K., Lalonde, B., Lamoree, M.H., Levi, Y., Lara Martín, P.A., Montagner, C.C., Mougin, C., Msagati, T., Oehlmann, J., Posthuma, L., Reid, M., Reinhard, M., Richardson, S.D., Rostkowski, P., Schymanski, E., Schneider, F., Slobodnik, J., Shibata, Y., Snyder, S.A., Fabriz Sodré, F., Teodorovic, I., Thomas, K.V., Umbuzeiro, G.A., Viet, P.H., Yew-Hoong, K.G., Zhang, X., Zuccato, E., 2022. One planet: one health. A call to support the initiative on a global science–policy body on chemicals and waste. Environ. Sci. Eur. 34 (1), 21.
Bradley, D., et al., 2012. Studies on the pathogenesis and survival of different culture forms of Listeria monocytogenes to pulsed UV-light irradiation after exposure to mild-food processing stresses. Food Microbiol. 30 (2), 330–339. https://doi.org/10.1016/j.fm.2011.12.024.
Broom, A., Kenny, K., Prainsack, B., Broom, J., 2021. Antimicrobial resistance as a problem of values? Views from three continents. Crit. Public Health 31 (4), 451–463.
Cameron, A., Barbieri, R., Read, R., Church, D., Adator, E.H., Zaheer, R., McAllister, T.A., 2019. Functional screening for triclosan resistance in a wastewater metagenome and isolates of Escherichia coli and Enterococcus spp. from a large Canadian healthcare region. PLoS One 14 (1), e0211144.
Casalini, G., Giacomelli, A., Ridolfo, A., Gervasoni, C., Antinori, S., 2021. Invasive fungal infections complicating COVID-19: a narrative review. J.Fungi 7 (11), 921.
Chen, Z.F., Ying, G.G., 2015. Occurrence, fate and ecological risk of five typical azole fungicides as therapeutic and personal care products in the environment: a review. Environ. Int. 84, 142–153.
Chen, J., Loeb, S., Kim, J.-H., 2017. LED revolution: fundamentals and prospects for UV disinfection applications. Environ. Sci.: Water Res. Technol. 3 (2), 188–202.
Chen, Y., Neff, M., McEvoy, B., Cao, Z., Pezzoli, R., Murphy, A., Gately, N., Hopkins Jnr, M., Rowan, N.J., Devine, D.M., 2019. 3D printed polymers are less stable than injected moulded counterparts when exposed to terminal processes using novel vaporized hydrogen peroxide and electron beam processes. Polymer 183. https://doi.org/10.1016/polymer.2019.121870.
Chen, B., Han, J., Dai, H., Jia, P., 2021. Biocide-tolerance and antibiotic-resistance in community environments and risk of direct transfers to humans: unintended consequences of community-wide surface disinfecting during COVID-19? Environ. Pollut. 283, 117074.
Clancy, C.J., Nguyen, M.H., 2013. Finding the "missing 50%" of invasive candidiasis: how nonculture diagnostics will improve understanding of disease spectrum and transform patient care. Clin. Infect. Dis. 56 (9), 1284–1292.
Fitzhenry, K., et al., 2019. Inactivation efficiency of Bacillus endospores via modified flow-through PUV treatment with comparison to conventional LPUV treatment. J. Water Process Eng. 27, 67–76. https://doi.org/10.1016/j.jwpe.2018.11.009.
Food and Drug, A., 1994. '21 Code of Federal Regulations', Part 21 Current Good Manufacturing Practice for Finished Pharmaceuticals United State.
World Health, O., 2019. Global Antimicrobial Resistance Surveillance System (GLASS): early implementation protocol for inclusion of Candida spp. WHO/WSI/AMR/2019.4).World Health Organization, Geneva Available at https://apps.who.int/iris/handle/10665/326926.
World Health, O., 2020. First Meeting of the WHO Antifungal Expert Group on Identifying Priority Fungal Pathogens: Meeting Report.
Dalgaard, L.S., Nørgaard, M., Povlsen, J.V., Jespersen, B., Jensen-Fangel, S., Ellermann-Eriksen, S., Østergaard, L., Schønheyder, H.C., Søgaard, O.S., 2016. Risk and prognosis of bacteremia and fungemia among peritoneal dialysis patients: a population-based cohort study. Perit. Dial. Int. 36 (6), 647–654.
Dannaoui, E., 2017. Antifungal resistance in mucorales. Int. J. Antimicrob. Agents 50 (5), 617–621.
Dehghani, M.H., Mahvi, A.H., Jahed, G.R., Sheikhi, R., 2007. Investigation and evaluation of ultrasound reactor for reduction of fungi from sewage. J. Zhejiang Univ. Sci. B 8 (7), 493–497.
Domegan, C., 2021. Social marketing and behavioural change in a systems setting. Curr.Opin. Environ.Sci.Health 23, 100275.
Dutescu, I.A., 2021. The antimicrobial resistance crisis: how neoliberalism helps microbes dodge our drugs. Int. J. Health Serv. 51 (4), 521–530.
Etienne, M., Caron, F., 2007. Management of fungal urinary tract infections. Presse Med. 36 (12 Pt 3), 1899–1906.
Farrell, H., Garvey, M., Rowan, N., 2009. Studies on the inactivation of medically important Candida species on agar surfaces using pulsed light. FEMS Yeast Res. 9 (6), 956–966.
Farrell, H., Hayes, J., Laffey, J., Rowan, N., 2011. Studies on the relationship between pulsed UV light irradiation and the simultaneous occurrence of molecular and cellular damage in clinically-relevant Candida albicans. J. Microbiol. Methods 84 (2), 317–326.
Firacative, C., 2020. Invasive fungal disease in humans: are we aware of the real impact? Mem. Inst. Oswaldo Cruz 115.
Fisher, M.C., Alastruey-Izquierdo, A., Berman, J., Bicanic, T., Bignell, E.M., Bowyer, P., Bromley, M., Brüggemann, R., Garber, G., Cornely, O.A., 2022. Tackling the emerging threat of antifungal resistance to human health. Nat. Rev. Microbiol. 1–15.
Fosses Vuong, M., Waymack, J.R., 2022. 'Aspergillosis', StatPearls. StatPearls Publishing Copyright © 2022, StatPearls Publishing LLC, Treasure Island (FL).
Founou, R.C., Founou, L.L., Essack, S.Y., 2017. Clinical and economic impact of antibiotic resistance in developing countries: a systematic review and meta-analysis. PLoS One 12 (12), e0189621.
Franssen, F., Gerard, C., Cozma-Petruţ, A., Vieira-Pinto, M., Jambrak, A.R., Rowan, N., Paulsen, P., Rozycki, M., Tysnes, K., Rodriguez-Lazaro, D., 2018. Inactivation of parasite transmission stages: efficacy of treatments on food of animal origin. Trends Food Sci. Technol. 83 (114–128).
Galanakis, C.M., Rizou, M., Aldawoud, T.M.S., Ucak, I., Rowan, N.J., 2021. Innovations and technology disruptions in the food sector within the COVID-19 pandemic and post-lockdown era. Trends Food Sci. Technol. 110, 193–200.
Galia, L., Pezzani, M.D., Compri, M., Callegari, A., Rajendran, N.B., Carrara, E., Tacconelli, E., Network, C.M.E.-N., 2022. Surveillance of antifungal resistance in candidemia fails to inform antifungal stewardship in European countries. J.Fungi 8 (3), 249.
Garey, K.W., Rege, M., Pai, M.P., Mingo, D.E., Suda, K.J., Turpin, R.S., Bearden, D.T., 2006. Time to initiation of fluconazole therapy impacts mortality in patients with candidemia: a multi-institutional study. Clin. Infect. Dis. 43 (1), 25–31.
Garnier, L., Valence, F., Mounier, J., 2017. Diversity and control of spoilage fungi in dairy products: an update. Microorganisms 5 (3), 42.
Garvey, M., et al., 2015a. Pulsed ultraviolet light inactivation of *Pseudomonas aeruginosa* and *Staphylococcus aureus* biofilms. Water Environ. J. 29 (1), 36–42. https://doi.org/10.1111/wej.12088.
Garvey, M., 2020. Bacteriophages and the one health approach to combat multidrug resistance: is this the way? Antibiotics (Basel) 9 (7).
Garvey, M., 2022. Lameness in dairy cow herds: disease aetiology, prevention and management. Dairy 3 (1).
Garvey, M., Cormican, M., Rowan, N., 2010. Investigations of the relationship between use of in vitro cell culture-quantitative PCR and a mouse-based bioassay for evaluating critical factors affecting the disinfection performance of pulsed UV light for treating Cryptosporidium parvum oocysts in saline. J. Microbiol. Methods 80 (3), 267–273. https://doi.org/10.1016/j.mimet.2010.01.017.
Garvey, M., Hayes, J., Clifford, E., Kirf, D., Rowan, N., 2013. Efficacy of measuring cellular ATP levels to determine the inactivation of pulsed UV treated Cryptosporidium parvum oocysts suspended in water. Water Sci. Technol. Water Supply 13 (2), 202–213.
Garvey, M., Andrade Fernandes, J.P., Rowan, N., 2015b. Pulsed light for the inactivation of fungal biofilms of clinically important pathogenic Candida species. Yeast 32 (7), 533–540.
Garvey, M., Rowan, N., 2015. A pulsed light system for the disinfection of flow through water in the presence of inorganic contaminants. J. Water Health 13 (2), 406–412. https://doi.org/10.2166/wh.2014.176.
Gehlot, P., Singh, J., 2018. Fungi and Their Role in Sustainable Development: Current Perspectives. Springer.
Gikas, G.D., Paraskevas, P., Theodoros, M., Zisis, V., 2022. Particularities of fungicides and factors affecting their fate and removal efficacy: a review. Sustainability 14 (7), 4056. https://doi.org/10.3390/su14074056.
Giles, C., Lamont-Friedrich, S.J., Michl, T.D., Griesser, H.J., Coad, B.R., 2018. The importance of fungal pathogens and antifungal coatings in medical device infections. Biotechnol. Adv. 36 (1), 264–280.
Gómez-López, V.M., Bolton, J.R., 2016. An approach to standardize methods for fluence determination in bench-scale pulsed light experiments. Food Bioprocess Technol. 9 (6), 1040–1048.
Gómez-López, V.M., et al., 2022. Guidelines on reporting treatment conditions for emerging technologies in food processing. Crit. Rev. Food Sci. Nutr. 62 (21), 5925–5949. https://doi.org/10.1080/10408398.2021.1895058.

Górski, A., Bollyky, P.L., Przybylski, M., Borysowski, J., Międzybrodzki, R., Jończyk-Matysiak, E., Weber-Dąbrowska, B., 2019. Perspectives of phage therapy in non-bacterial infections. Front. Microbiol. 9.

Hayes, J.C., Garvey, M., Fogarty, A., Clifford, E., Rowan, N., 2012a. Inactivation of recalcitrant protozoan oocysts and bacterial endospores in drinking water using high-intensity pulsed UV light irradiation. Water Supply 12 (4), 513–522. https://doi.org/10.2166/ws.2012.017.

Hayes, J., Kirf, D., Garvey, M., Rowan, N., 2013. Disinfection and toxicological assessments of pulsed UV and pulsed-plasma gas-discharge treated-water containing the waterborne protozoan enteroparasite Cryptosporidium parvum. J. Microbiol. Methods 94 (3), 325–337.

Hayes, J.C., Laffey, J.G., McNeill, B., Rowan, N.J., 2012b. Relationship between growth of food-spoilage yeast in high-sugar environments and sensitivity to high-intensity pulsed UV light irradiation. Int. J. Food Sci. Technol. 47 (9), 925–934. https://doi.org/10.1111/j.1365-2621.2012.03052.x.

Heard, K.L., Hughes, S., Mughal, N., Moore, L.S.P., 2020. COVID-19 and fungal superinfection. The Lancet. Microbe 1 (3), e107.

Heinrich, V., Zunabovic, M., Bergmair, J., Kneifel, W., Jaeger, H., 2015. Post-packaging application of pulsed light for microbial decontamination of solid foods: a review. Innov.Food Sci. Emerg. Technol. 30, 145–156.

Helweg-Larsen, J., Benfield, T., Kovacs, J., Masur, H., 2017. Drug resistance in Pneumocystis jirovecii. Antimicrobial Drug Resistance. Springer, pp. 1147–1162.

Hillock, N.T., Merlin, T.L., Turnidge, J., Karnon, J., 2022. Modelling the future clinical and economic burden of antimicrobial resistance: the feasibility and value of models to inform policy. Appl. Health Econ. Health Policy 1–8.

Hodzic, E., 2015. Lyme borreliosis: is there a preexisting (natural) variation in antimicrobial susceptibility among Borrelia burgdorferi strains? Bosnian J.Basic Med.Sci. 15 (3), 1–13.

Hoenigl et al., n.d. M. Hoenigl M. Levitz Stuart N. Schuetz Audrey X. Zhang Sean A. Cornely Oliver 'All You Need to Know and More about the Diagnosis and Management of Rare Mold Infections', mBio, 12(1), pp. e02920-20.n.d.

Houšť, J., Spížek, J., Havlíček, V., 2020. Antifungal drugs. Metabolites 10 (3), 106.

Huang, T., Zhao, Y., He, J., Cheng, H., Martyniuk, C., 2022. Endocrine disruption by azole fungicides in fish: a rview of he evidence. Sci. Total Environ. 822. https://doi.org/10.1016/j.scitotenv.2022.153412.

Hyde, K.D., 2022. The numbers of fungi. Fungal Divers. 114, 1. https://doi.org/10.1007/s13225-022-00507-y.

Ibáñez-Martínez, E., Ruiz-Gaitán, A., Pemán-García, J., 2017. Update on the diagnosis of invasive fungal infection. Rev.Esp.Quimioterapia 30.

Iyer, K.R., Revie, N.M., Fu, C., Robbins, N., Cowen, L.E., 2021. Treatment strategies for cryptococcal infection: challenges, advances and future outlook. Nat. Rev. Microbiol. 19 (7), 454–466.

Jamali, H., Radmehr, B., Ismail, S., 2014. Prevalence and antibiotic resistance of Staphylococcus aureus isolated from bovine clinical mastitis. J. Dairy Sci. 97 (4), 2226–2230.

Jankowska, K.I., Nagarkatti, R., Acharyya, N., Dahiya, N., Stewart, C.F., Macpherson, R.W., Wilson, M.P., Anderson, J.G., MacGregor, S.J., Maclean, M., 2020. Complete inactivation of blood borne pathogen Trypanosoma cruzi in stored human platelet concentrates and plasma treated with 405 nm violet-blue light. Front.Med. 7, 617373.

Jarvis, J.N., Leeme, T.B., Molefi, M., Chofle, A.A., Bidwell, G., Tsholo, K., Tlhako, N., Mawoko, N., Patel, R.K.K., Tenforde, M.W., Muthoga, C., Bisson, G.P., Kidola, J., Changalucha, J., Lawrence, D., Jaffar, S., Hope, W., Molloy, S.L.F., Harrison, T.S., 2019. Short-course high-dose liposomal amphotericin B for human immunodeficiency virus–associated cryptococcal meningitis: a phase 2 randomized controlled trial. Clin. Infect. Dis. 68 (3), 393–401.

Jørgensen, L.N., Heick, T.M., 2021. Azole use in agriculture, horticulture, and wood preservation–is it indispensable? Front. Cell. Infect. Microbiol. 806.

Josephs-Spaulding, J., Singh, O.V., 2021. Medical device sterilization and reprocessing in the era of multidrug-resistant (MDR) bacteria: issues and regulatory concepts. Front.Med. Technol. https://doi.org/10.3389/fmedt.2020.587352.

Kahhonen, E., Nordstron, K., 2008. Toward a nontoxic posion: current trends in (European Uniion) biocides regulation. Integr. Environ. Assess. Manag. 4 (4), 471–477.

Kalińska, A., Gołębiewski, M., Wójcik, A., 2017. Mastitis pathogens in dairy cattle - a review. World Sci.News 89, 22–31.

Kang, M.H., Pengkit, A., Choi, K., Jeon, S.S., Choi, H.W., Shin, D.B., Choi, E.H., Uhm, H.S., Park, G., 2015. Differential inactivation of fungal spores in water and on seeds by ozone and arc discharge plasma. PloS one 10 (9), e0139263.

Kaplan, J.E., Benson, C., Holmes, K.K., Brooks, J.T., Pau, A., Masur, H., 2009. Guidelines for prevention and treatment of opportunistic infections in HIV-infected adults and adolescents: recommendations from CDC, the National Institutes of Health, and the HIV Medicine Association of the Infectious Diseases Society of America. MMWR Recomm. Rep. 58 (Rr-4), 1–207 quiz CE1-4.

Kauffman, C.A., 2014. Diagnosis and management of fungal urinary tract infection. Infect. Dis. Clin. 28 (1), 61–74.

Kauffman, C.A., Yoshikawa, T.T., 2001. Fungal infections in older adults. Clin. Infect. Dis. 33 (4), 550–555.

Kazemzadeh-Narbat, M., Cheng, H., Chabok, R., Alvarez, M.M., de la Fuente-Nunez, C., Phillips, K.S., Khademhosseini, A., 2021. Strategies for antimicrobial peptide coatings on medical devices: a review and regulatory science perspective. Crit. Rev. Biotechnol. 41 (1), 94–120.

Kim, D.K., Kim, S.J., Kang, D.H., 2017. Bactericidal effect of 266 to 279nm wavelength UVC-LEDs for inactivation of Gram positive and Gram negative foodborne pathogenic bacteria and yeasts. Food Res. Int. 97, 280–287.

Kirby, A., Herbert, A., 2013. Correlations between income inequality and antimicrobial resistance. PLoS One 8 (8), e73115.

Kwakman, J.A., Erler, N.S., Vos, M.C., Bruno, M.J., 2022. Risk evaluatio of dudenoscope-associated infections in the Netherlands calls for a heightened awareness of device-related infection:a systematic review. Endoscopy 54 (02), 148–2022.

Lachapelle, J.-M., Castel, O., Casado, A.F., Leroy, B., Micali, G., Tennstedt, D., Lambert, J., 2013. Antiseptics in the era of bacterial resistance: a focus on povidone iodine. Clin. Pract. 10 (5), 579.

Laso, J., et al., 2022. Achieving sustainability of the seafood sector in the European Atlantic area by addressing eco-social challenges: the NEPTUNUS project. Sustainability 14 (5). https://doi.org/10.3390/su14053054.

Lass-Flörl, C., Samardzic, E., Knoll, M., 2021. Serology anno 2021—fungal infections: from invasive to chronic. Clin. Microbiol. Infect. 27 (9), 1230–1241.

Latgé, J.P., Chamilos, G., 2019. Aspergillus fumigatus and Aspergillosis in 2019. Clin. Microbiol. Rev. 33 (1).

Lee, S.M., Cho, Y.K., Sung, Y.M., Chung, D.H., Jeong, S.H., Park, J.W., Lee, S.P., 2015. A case of pneumonia caused by Pneumocystis jirovecii resistant to trimethoprim-sulfamethoxazole. Korean J. Parasitol. 53 (3), 321–327.

Lee, Y., Puumala, E., Robbins, N., Cowen, L.E., 2020. Antifungal drug resistance: molecular mechanisms in Candida albicans and beyond. Chem. Rev. 121 (6), 3390–3411.

Leidner, F., Kurt Yilmaz, N., Schiffer, C.A., 2021. Deciphering antifungal drug resistance in Pneumocystis jirovecii DHFR with molecular dynamics and machine learning. J. Chem. Inf. Model. 61 (6), 2537–2541.

Lengerova, M., Racil, Z., Hrncirova, K., Kocmanova, I., Volfova, P., Ricna, D., Bejdak, P., Moulis, M., Pavlovsky, Z., Weinbergerova, B., Toskova, M., Mayer, J., 2014. Rapid detection and identification of mucormycetes in bronchoalveolar lavage samples from immunocompromised patients with pulmonary infiltrates by use of high-resolution melt analysis. J. Clin. Microbiol. 52 (8), 2824–2828.

Levinskaite, L., 2012. Susceptibility of food-contaminating Penicillium genus fungi to some preservatives and disinfectants. Ann. Agric. Environ. Med. 19 (1), 85–89.

Li, H., Huang, H., He, H., 2016. Successful treatment of severe pneumocystis pneumonia in an immunosuppressed patient using caspofungin combined with clindamycin: a case report and literature review. BMC Pulm.Med. 16 (1), 1–6.

Lortholary, O., Renaudat, C., Sitbon, K., Desnos-Ollivier, M., Bretagne, S., Dromer, F., 2017. The risk and clinical outcome of candidemia depending on underlying malignancy. Intensive Care Med. 43 (5), 652–662.

Lu, R., Hollingsworth, C., Qiu, J., Wang, A., Hughes, E., Xin, X., Konrath, K.M., Elsegeiny, W., Park, Y.-D., Atakulu, L., Craft, J.C., Tramont, E.C., Mannino, R., Williamson, P.R., 2019. Efficacy of oral encochleated amphotericin B in a mouse model of cryptococcal meningoencephalitis. mBio 10 (3), e00724-19.

Maclean, M., MacGregor, S.J., Anderson, J.G., Woolsey, G., 2009. Inactivation of bacterial pathogens following exposure to light from a 405-nanometer light-emitting diode array. Appl. Environ. Microbiol. 75 (7), 1932–1937.

MacGregor, S.J., et al., 2000. Inactivation of pathogenic and spoilage microorganisms in a test liquid using pulsed electric fields. IEEE Trans. Plasma Sci. 28 (1), 144–149. https://doi.org/10.1109/27.842887.

MacLean, M., Booth, M.G., Anderson, J.G., MacGregor, S.J., Woolsey, G.A., Coia, J.E., Hamilton, K., Gettinby, G., 2013. Continuous decontamination of an intensive care isolation room during patient occupancy using 405 nm light technology. J. Infect. Prev. 14 (5), 176–181.

MacNeill, A., et al., 2020. Transforming the medical device industry: road map to a circular economy. Health Aff. 39 (9), 2088–2097.

Marchese, V., Di Carlo, D., Fazio, G., Gioe, S.M., Luca, A., Alduino, R., Rizzo, M., Tuzzolino, F., Monaco, F., Conaldi, P.G., Douradinha, B., Di Martino, G., 2021. Microbiological surveillance of endoscopes in a southern Italian transplantation hospital: a retrospective study from 2016 to 2019. Int. J. Environ. Res. Public Health 18 (6). https://doi.org/10.3390/ijerph18063057.

Martinez-Rossi, N.M., Bitencourt, T.A., Peres, N.T.A., Lang, E.A.S., Gomes, E.V., Quaresemin, N.R., Martins, M.P., Lopes, L., Rossi, A., 2018. Dermatophyte resistance to antifungal drugs: mechanisms and prospectus. Front. Microbiol. 9, 1108.

Maskarinec, S.A., Johnson, M.D., Perfect, J.R., 2016. Genetic susceptibility to fungal infections: what is in the genes? Curr.Clin.Microbiol.Rep. 3 (2), 81–91.

Massei, R., Busch, W., Wolschke, H., Schinkel, L., Bitsch, M., Schulze, T., Krauss, M., Brack, W., 2018. Screening of pesticide and biocide patterns as risk drivers in sediments of major European river mouths: ubiquitous or river basin-specific contamination? Environ. Sci. Technol. 52 (4), 2251–2260.

Masterson, K., Meade, E., Garvey, M., Lynch, M., Major, I., Rowan, N.J., 2021. Development of a low-temperature extrusion process for production of GRAS bioactive-polymer loaded compounds for targeting antimicrobial-resistant (AMR) bacteria. Sci. Total Environ. 800, 149545.

Matumba, L., Namaumbo, S., Ngoma, T., Meleke, N., De Boevre, M., Logrieco, A.F., De Saeger, S., 2021. Five keys to prevention and control of mycotoxins in grains: a proposal. Glob. Food Secur. 30, 100562.

McEvoy, B., Rowan, N.J., 2019. Terminal sterilization of medical devices using vaporized hydrogen peroxide: a review of current methods and emerging opportunities. J. Appl. Microbiol. 127 (5), 1403–1420.

McEvoy, B., Lynch, M., Rowan, N.J., 2021. Opportunities for the application of real-time bacterial cell analysis using flow cytometry for the advancement of sterilization microbiology. J. Appl. Microbiol. 130 (6), 1794–1812.

Meade, E., Rawe, S., Slattery, M.A., Garvey, M., 2019. An assessment of alternative therapeutic options for the treatment of prolonged zoonotic fungal infections in companion animals. J. Microbiol. Biotechnol. 4, 000149.

Meade, E., Fowley, C., Savage, M., Slattery, M.A., Garvey, M., 2020a. Antibacterial activity of Roussin's black salt against multidrug resistant zoonotic pathogens isolated from companion animals. Acta Sci.Vet.Sci. 2 (3).

Meade, E., Savage, M., Slattery, M.A., Garvey, M., 2020. Disinfection of mycotic species isolated from cases of bovine mastitis showing antifungal resistance. Cohesive J. Microbiol. Infect. Dis. 3.

Meade, E., Savage, M., Garvey, M., 2021. Effective antimicrobial solutions for eradicating multi-resistant and β-lactamase-producing nosocomial gram-negative pathogens. Antibiotics 10 (11), 1283.

Meade, E., Savage, M., Slattery, M., Garvey, M., 2021. Investigation of alternative therapeutic and biocidal options to combat antifungal-resistant zoonotic fungal pathogens isolated from companion animals. Infect. Dis. Rep. 13 (2), 348–366.

Meade, E., Slattery, M.A., Garvey, M., 2021. Biocidal resistance in clinically relevant microbial species: a major public health risk. Pathogens (Basel, Switzerland) 10 (5), 598.
Metodiev, K., 2012. Immunodeficiency.
Moorhead, S., Maclean, M., MacGregor, S.J., Anderson, J.G., 2016. Comparative sensitivity of trichophyton and aspergillus conidia to inactivation by violet-blue light exposure. Photomed. Laser Surg. 34 (1), 36–41.
Murphy, E.J., Masterson, C., Rezoagli, E., O'Toole, D., Major, I., Stack, G.D., Lynch, M., Laffey, J.G., Rowan, N.J., 2020a. β-glucan extracts from the same edible shiitake mushroom Lentinus edodes produce differential in-vitro immunomodulatory and pulmonary cyto-protective effects—implications for coronavirus disease (COVID-19) immunotherapies. Sci. Total Environ. 732, 139330.
Murphy, E.J., Rezoagli, E., Pogue, R., et al., Simonassi-Paiva, B., 2021. Immunomodulatory activity of beta-glucana polysaccharides isolated from different species of mushroom - a potential treatment for inflammatory lung conditions. Sci. Total Environ. https://doi.org/10.1016/j.scitotenv.2021.152177.
Murray, I.M.T., Rowan, N.J., McNamee, S., Campbell, K., Fogarty, A.M., 2018. Pulsed light reduces the toxicity of the algal toxin okadaic acid to freshwater crustacean Daphnia pulex. Environ. Sci. Pollut. Res. Int. 25 (1), 607–614.
Murray, C.J.L., Ikuta, K.S., Sharara, F., Swetschinski, L., Aguilar, G.R., Gray, A., Han, C., Bisignano, C., Rao, P., Wool, E., 2022. Global burden of bacterial antimicrobial resistance in 2019: a systematic analysis. Lancet 399 (10325), 629–655.
Nagy, G., Kiss, S., Varghese, R., Bauer, K., Szebenyi, C., Kocsubé, S., Homa, M., Bodai, L., Zsindely, N., 2021. Characterization of three pleiotropic drug resistance transporter genes and their participation in the azole resistance of mucor circinelloides. Front. Cell. Infect. Microbiol. 11, 660347.
Nallal, U.V.M., Razia, M., et al., 2022. Eco-friendly synthesis of multishaped crystalline silver nanoparticles using hill garlic extract and their potential application as an antifungal agent. J. Nanomater. 2022. https://doi.org/10.1155/2022/7613210.
Narayanan, K.B., Park, H.H., 2014. Antifungal activity of silver nanoparticles synthesized using turnip leaf extract (Brassica rapa L.) against wood rotting pathogens. Eur. J. Plant Pathol. 140, 185–192. https://doi.org/10.1007/s10658-014-0399-4.
Nasereddin, Y., 2021. Path to a post-antibiotic world. Sustinere 1 (1), 1–17.
Naughton, J., Tiedeken, E.J., Garvey, M., Stout, J.C., Rowan, N.J., 2017. Pulsed light inactivation of the bumble bee trypanosome parasite Crithidia bombi. J. Apic. Res. 56 (2), 144–154.
Niu, X., Xie, W., Zhang, J., Hu, Q., 2019. Biodiversity of entomopathogenic fungi in the soils of South China. Microorganisms 7 (9), 311. https://doi.org/10.3390/microorganisms7090311.
Nnadi, N.E., Carter, D.A., 2021. Climate change and the emergence of fungal pathogens. PLoS Pathog. 17 (4), e1009503. https://doi.org/10.1371/journal.ppat.1009503.
Nong, G.Y., Liu, Y.-A., Qin, U.-T., Mo, L.-Y., Liang, Y.-P., Zeng, H.H., 2021. Toxc mechanism of three azole fungicides and their mixture of green alga Chlorella pyrenoidosa. Chemosphere 262. https://doi.org/10.1016/j.chemosphere.2020.127793.
Odabasi, Z., Mert, A., 2020. Candida urinary tract infections in adults. World J. Urol. 38 (11), 2699–2707.
O'Neill, E.A., Rowan, N.J., Fogarty, A., 2019. Novel use of the alga Pseudokirchneriella subcapitata, as an early-warning indicator to identify climate change ambiguity in aquatic environments using freshwater finfish farming as a case study. Sci. Total Environ. 692, 209–218.
O'Neill, E.A., McKeon-Bennett, Rowan, N.J., 2022. Peatland-based Innovation can potentially support and enable the Sustainable Development Goals of the United Nations: case study from the Republic of Ireland. Case Stud. Chem. Environ. Eng. (accepted for publication).
Pasquier, E., Kunda, J., De Beaudrap, P., Loyse, A., Temfack, E., Molloy, S.F., Harrison, T.S., Lortholary, O., 2018. Long-term mortality and disability in cryptococcal meningitis: a systematic literature review. Clin. Infect. Dis. 66 (7), 1122–1132.
Pinto, E., Monteiro, C., Maia, M., Faria, M.A., Lopes, V., Lameiras, C., Pinheiro, D., 2018. Aspergillus species and antifungals susceptibility in clinical setting in the north of Portugal: cryptic species and emerging azoles resistance in A. fumigatus. Front. Microbiol. 9, 1656.
Plaza, G., Achal, V., 2020. Biosurfactants: eco-friendly and innovative biocides against biocorrosion. Int. J. Mol. Sci. 21 (6), 2152. https://doi.org/10.3390/ijms21062152.
Powers-Fletcher, M.V., Hanson, K.E., 2016. Nonculture diagnostics in fungal disease. Infect. Dis. Clin. N. Am. 30 (1), 37–49.
Rawson, T.M., Wilson, R.C., Holmes, A., 2021. Understanding the role of bacterial and fungal infection in COVID-19. Clin. Microbiol. Infect. 27 (1), 9–11.
Rehfus, A., Matusinsky, P., Strobel, D., Bryson, R., Stammler, G., 2019. Mutations in target genes of succinate dehydrogenase inhibitors and demethylation inhibitors in Ramularia collo-cygni in Europe. J.Plant Dis.Prot. 126 (5), 447–459.
Rezasoltani, S., Yadegar, A., Hatami, B., Asadzadeh Aghdaei, H., Zali, M.R., 2020. Antimicrobial resistance as a hidden menace lurking behind the COVID-19 outbreak: the global impacts of too much hygiene on AMR. Front. Microbiol. 11.
Romero, M., Messina, F., Marin, E., Arechavala, A., Depardo, R., Walker, L., Negroni, R., Santiso, G., 2019. Antifungal resistance in clinical isolates of Aspergillus spp.: when local epidemiology breaks the norm. J.Fungi 5 (2), 41.
Roudbary, M., Kumar, S., Kumar, A., Černáková, L., Nikoomanesh, F., Rodrigues, C.F., 2021. Overview on the prevalence of fungal infections, immune response, and microbiome role in COVID-19 patients. J.Fungi 7 (9), 720.
Rowan, N.J., 2019. Pulsed light as an emerging technology to cause disruption for food and adjacent industries – quo vadis? Trends Food Sci. Technol. 88, 316–332.
Rowan, N.J., 2020. The role of digital technologies in supporting and improving fishery and aquaculture across the supply chain - Quo Vadis? Aquac.Fish. https://doi.org/10.1016/j.aaf.2022.06.003.
Rowan, N.J., Casey, O., 2021. Empower Eco multiactor HUB: a triple helix 'academia-industry-authority' approach to creating and sharing potentially disruptive tools for addressing novel and emerging new Green Deal opportunities under a United Nations Sustainable Development Goals framework. Curr.Opin.Environ.Sci.Health 21, 100254.
Rowan, N.J., Galanakis, C.M., 2020. Unlocking challenges and opportunities presented by COVID-19 pandemic for cross-cutting disruption in agri-food and green deal innovations: Quo Vadis? Sci. Total Environ. 748, 141362.
Rowan, N.J., Laffey, J.G., 2020. Challenges and solutions for addressing critical shortage of supply chain for personal and protective equipment (PPE) arising from coronavirus disease (COVID19) pandemic – case study from the Republic of Ireland. Sci. Total Environ. 725. https://doi.org/10.1016/j.scitotenv.2020.138532.
Rowan, N.J., Laffey, J.G., 2021. Unlocking the surge in demand for personal and protective equipment (PPE) and improvised face coverings arising from coronavirus disease (COVID-19) pandemic – implications for efficacy, re-use and sustainable waste management. Sci. Total Environ. 752. https://doi.org/10.1016/j.scitotenv.2020.142259.
Rowan, N.J., Moral, R.A., 2021. Disposable face masks and reusable face coverings as non-pharmaceutical interventions (NPIs) to prevent transmission of SARS-CoV-2 variants that cause coronavirus disease (COVID-19): role of new sustainable NPI design innovations and predictive mathematical modelling. Sci. Total Environ. 772, 145530.
Rowan, N.J., Johnstone, C.M., McLean, R.C., Anderson, J.G., Clarke, J.A., 1999. Prediction of toxigenic fungal growth in buildings by using a novel modelling system. Appl. Environ. Microbiol. 65 (11), 4814–4821.
Rowan, N.J., Espie, S., Harrower, J., Anderson, J.G., Marsili, L., MacGregor, S.J., 2007. Pulsed-plasma gas-discharge inactivation of microbial pathogens in chilled poultry wash water. J. Food Prot. 70 (12), 2805–2810.
Rowan, N., Pogue, R., 2021. Editorial overview: green new deal era — Current challenges and emerging opportunities for developing sustaining and disruptive innovation. Curr. Opin. Environ. Sci. Health 22. https://doi.org/10.1016/j.coesh.2021.100294.
Rowan, N.J., Valdramidis, V.P., Gómez-López, V.M., 2015. A review of quantitative methods to describe efficacy of pulsed light generated inactivation data that embraces the occurrence of viable but non culturable state microorganisms. Trends Food Sci. Technol. 44 (1), 79–92.
Rowan, N.J., Meade, E., Garvey, M., 2021. Efficacy of frontline chemical biocides and disinfection approahces for inactivating SARS-CoV-2 variants of concern that cause coronavirus disease with the emergence of opportunities for green eco-solutions. Curr.Opin. Environ.Sci.Health 23 10.10.16/j.coesh.2021.100290.
Rowan, N.J., Murray, N., Qiao, Y., O'Neill, E., Clifford, E., Barceló, D., Power, D.M., 2022. Digital transformation of peatland eco-innovations ('Paludiculture'): enabling a paradigm shift towards the real-time sustainable production of 'green-friendly' products and services. Sci. Total Environ. 838, 156328.
Ruiz-Salmon, et al., 2021. Life cycle assessement of fish and seafood products - a review of methodologies and new challenges. Sci. Total Environ. 761. https://doi.org/10.1016/j.scitotenv.2020.144094.
Rutala, W.A., 2019. Disinfection, sterilization, and antisepsis: an overview. Am. J. Infect. Control 47S, A3–A9. https://doi.org/10.1016/j.ajic.2019.01.018 Jun.
Sanglard, D., 2016. Emerging threats in antifungal-resistant fungal pathogens. Front. Med. (Lausanne) 3, 11.
Sauerbrei, A., 2020. Bactericidal and virucidal activity of ethanol and povidone-iodine. Microbiologyopen 9 (9), e1097.
SeyedAlinaghi, S., Karimi, A., Barzegary, A., Pashaei, Z., Afsahi, A.M., Alilou, S., Janfaza, N., Shojaei, A., Afroughi, F., Mohammadi, P., Soleimani, Y., Nazarian, N., Amiri, A., Tantuoyir, M.M., Oliaei, S., Mehraeen, E., Dadras, O., 2022. Mucormycosis infection in patients with COVID-19: a systematic review. Health Sci. Rep. 5 (2), e529.
Silva, E.R., et al., 2019. Eco-friendly non-biocide release coatings for marine biofouling prevention. Sci. Total Environ. https://doi.org/10.1016/j.scitotenv.2018.10.010.
Skiada, A., Pavleas, I., Drogari-Apiranthitou, M., 2020. Epidemiology and diagnosis of mucormycosis: an update. J. Fungi (Basel) 6 (4).
Sousa, F., Ferreira, D., Reis, S., Costa, P., 2020. Current insights on antifungal therapy: novel nanotechnology approaches for drug delivery systems and new drugs from natural sources. Pharmaceuticals 13 (9), 248.
Stone, N., Gupta, N., Schwartz, I., 2021. Mucormycosis: time to address this deadly fungal infection. Lancet Microbe 2 (8), e343–e344.
Suanda, J., Suanda, J., Cawley, D., Domegan, C., Brenner, M., Rowan, N., 2013. A review of the perceived barriers within the health belief model on pap smear screening as a cervical cancer prevention measure. J.Appl.Sci.Res. 3.
Sun, Y., Meng, F., Han, M., Zhang, X., Yu, L., Huang, H., Wu, D., Ren, H., Wang, C., Shen, Z., Ji, Y., Huang, X., 2015. Epidemiology, management, and outcome of invasive fungal disease in patients undergoing hematopoietic stem cell transplantation in China: a multicenter prospective observational study. Biol. Blood Marrow Transplant. 21 (6), 1117–1126.
Taccone, F.S., Van den Abeele, A.M., Bulpa, P., Misset, B., Meersseman, W., Cardoso, T., Paiva, J.A., Blasco-Navalpotro, M., De Laere, E., Dimopoulos, G., Rello, J., Vogelaers, D., Blot, S.I., 2015. Epidemiology of invasive aspergillosis in critically ill patients: clinical presentation, underlying conditions, and outcomes. Crit. Care 19 (1), 7.
Tiedeken, E.J., Tahar, A., McHugh, B., Rowan, N.J., 2017. Monitoring, sources, receptors, and control measures for three European Union watch list substances of emerging concern in receiving waters - a 20 years systematic review. Sci. Total Environ. 574, 1140–1163.
Truong, J., Ashurst, J.V., 2022. 'Pneumocystis Jirovecii Pneumonia', StatPearls. StatPearls Publishing Copyright © 2022, StatPearls Publishing LLC, Treasure Island (FL).
Trzaska, W.J., Wrigley, H.E., Thwaite, J.E., May, R.C., 2017. Species-specific antifungal activity of blue light. PubMedSci. Reports 7 (1), 4605. https://doi.org/10.1038/s41598-017-05000-0 (Accessed 2017/07//).
Valencia-Shelton, F., Loeffelholz, M., 2014. Nonculture techniques for the detection of bacteremia and fungemia. Future Microbiol. 9 (4), 543–559.
Vallabhaneni, S., Mody, R.K., Walker, T., Chiller, T., 2016. The global burden of fungal diseases. Infect. Dis. Clin. 30 (1), 1–11.
van der Linden, J.W.M., Camps, S.M.T., Kampinga, G.A., Arends, J.P.A., Debets-Ossenkopp, Y.J., Haas, P.J.A., Rijnders, B.J.A., Kuijper, E.J., van Tiel, F.H., Varga, J., 2013. Aspergillosis due to voriconazole highly resistant Aspergillus fumigatus and recovery of genetically related resistant isolates from domiciles. Clin. Infect. Dis. 57 (4), 513–520.
van der Poll, T., van de Veerdonk, F.L., Scicluna, B.P., Netea, M.G., 2017. The immunopathology of sepsis and potential therapeutic targets. Nat. Rev. Immunol. 17 (7), 407–420.
Verweij, P.E., Lucas, J.A., Arendrup, M.C., Bowyer, P., Brinkmann, A.J.F., Denning, D.W., Dyer, P.S., Fisher, M.C., Geenen, P.L., Gisi, U., Hermann, D., Hoogendijk, A., Kiers, E., Lagrou, K., Melchers, W.J.G., Rhodes, J., Rietveld, A.G., Schoustra, S.E., Stenzel, K.,

Zwaan, B.J., Fraaije, B.A., 2020. The one health problem of azole resistance in Aspergillus fumigatus: current insights and future research agenda. Fungal Biol.Rev. 34 (4), 202–214.
Wan, Q., Wen, G., Cao, R., Xu, X., Zhao, H., Li, K., Wang, J., Huang, T., 2020. Comparison of UV-LEDs and LPUV on inactivation and subsequent reactivation of waterborne fungal spores. Water Res. 173, 115553.
Wang, H., Peng, H., Cheng, P., Gong, M., 2021. The toxins of Beauveria bassiana and the strategies to improve their virulence to insects. Front. Microbiol. 2375.
Wen, X., Chen, Q., Yin, H., Wu, S., Wang, X., 2020. Rapid identification of clinical common invasive fungi via a multi-channel real-time fluorescent polymerase chain reaction melting curve analysis. Medicine 99 (7).
White, T.C., Findley, K., Dawson, T.L., Scheynius, A., Boekhout, T., Cuomo, C.A., Xu, J., Saunders, C.W., 2014. Fungi on the skin: dermatophytes and Malassezia. Cold Spring Harbor Perspect.Med. 4 (8), a019802.
Wiederhold, N.P., 2017. Antifungal resistance: current trends and future strategies to combat. Infect.Drug Resist. 10, 249.
Wüthrich, M., Deepe Jr., G.S., Klein, B., 2012. Adaptive immunity to fungi. Annu. Rev. Immunol. 30, 115.
Xu, S., Zhang, G., Wang, M., Lin, T., Liu, W., Wang, Y., 2022. Phage nanoparticle as a carrier for controlling fungal infection. Appl. Microbiol. Biotechnol. 1–7.
Yaman, M., 2017. Entomopathogen Biodiversity of Kastamonu Region. Kastamonu University Journal of Forestry Faculty, International Forestry Symposium 2016 Special Issue, pp. 368–372 https://doi.org/10.17475/kastorman.293151.
Yousfi, H., Ranque, S., Rolain, J.-M., Bittar, F., 2019. In vitro polymyxin activity against clinical multidrug-resistant fungi. Antimicrob. Resist. Infect. Control 8 (1), 1–10.
Zafar, H., Altamirano, S., Ballou, E.R., Nielsen, K., 2019. A titanic drug resistance threat in Cryptococcus neoformans. Curr. Opin. Microbiol. 52, 158–164.
Zhang, Y., Zhu, Y., Gupta, A., Huang, Y., Murray, C.K., Vrahas, M.S., Sherwood, M.E., Baer, D.G., Hamblin, M.R., Dai, T., 2014. Antimicrobial blue light therapy for multidrug-resistant Acinetobacter baumannii infection in a mouse burn model: implications for prophylaxis and treatment of combat-related wound infections. J. Infect. Dis. 209 (12), 1963–1971.
Zhen, X., Lundborg, C.S., Sun, X., Hu, X., Dong, H., 2019. Economic burden of antibiotic resistance in ESKAPE organisms: a systematic review. Antimicrob.Resist.Infect.Control 8 (1), 137.
Zhou, F., Yu, T., Du, R., Fan, G., Liu, Y., Liu, Z., Xiang, J., Wang, Y., Song, B., Gu, X., Guan, L., Wei, Y., Li, H., Wu, X., Xu, J., Tu, S., Zhang, Y., Chen, H., Cao, B., 2020. Clinical course and risk factors for mortality of adult inpatients with COVID-19 in Wuhan, China: a retrospective cohort study. Lancet 395 (10229), 1054–1062.

Science of the Total Environment 725 (2020) 138532

Contents lists available at ScienceDirect

Science of the Total Environment

journal homepage: www.elsevier.com/locate/scitotenv

Challenges and solutions for addressing critical shortage of supply chain for personal and protective equipment (PPE) arising from Coronavirus disease (COVID19) pandemic – Case study from the Republic of Ireland

Neil J. Rowan [a,b,*], John G. Laffey [c,d]

[a] Department of Nursing and Healthcare, Athlone Institute of Technology, Ireland
[b] Centre for Disinfection, Sterilization and Biosecurity, Athlone Institute of Technology, Ireland
[c] Lung Biology Group, Regenerative Medicine Institute at CURAM Centre for Medical Devices, National University of Ireland Galway, Galway, Ireland
[d] Anaesthesia and Intensive Care Medicine, University Hospital Galway, Galway, Ireland

HIGHLIGHTS

- There is pressing need to find solutions for reprocessing of PPE for COVID19
- Reprocessing of PPE is challenging as made for one-time-use
- Most sterilization technologies are not suitable for PPE reprocessing
- Use of vaporised hydrogen peroxide and UV irradiation may prove effective for PPE

GRAPHICAL ABSTRACT

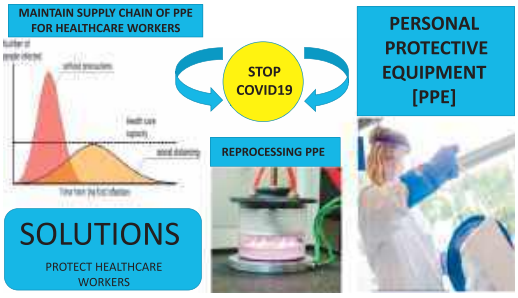

ARTICLE INFO

Article history:
Received 5 April 2020
Accepted 5 April 2020
Available online 6 April 2020

Editor: Damia Barcelo

Keywords:
COVID19
PPE
Sterilization
Healthcare workers
Resource utilization
Sustainability

ABSTRACT

Coronavirus (COVID-19) is highly infectious agent that causes fatal respiratory illnesses, which is of great global public health concern. Currently, there is no effective vaccine for tackling this COVID19 pandemic where disease countermeasures rely upon preventing or slowing person-to-person transmission. Specifically, there is increasing efforts to prevent or reduce transmission to front-line healthcare workers (HCW). However, there is growing international concern regarding the shortage in supply chain of critical one-time-use personal and protective equipment (PPE). PPE are heat sensitive and are not, by their manufacturer's design, intended for reprocessing. Most conventional sterilization technologies used in hospitals, or in terminal medical device sterilization providers, cannot effectively reprocess PPE due to the nature and severity of sterilization modalities. Contingency planning for PPE stock shortage is important. Solutions in the Republic of Ireland include use of smart communication channels to improve supply chain, bespoke production of PPE to meets gaps, along with least preferred option, use of sterilization or high-level disinfection for PPE reprocessing. Reprocessing PPE must consider material composition, functionality post treatment, along with appropriate disinfection. Following original manufacturer of PPE and regulatory guidance is important. Technologies deployed in the US, and for deployment in the Republic of Ireland, are eco-friendly, namely vaporised hydrogen peroxide (VHP), such as for filtering facepiece respirators and UV irradiation and High-level liquid disinfection (Actichlor+) is also been pursed in Ireland. Safeguarding supply chain of PPE will sustain vital healthcare provision and will help reduce mortality.

* Corresponding author at: CDSB, Athlone Institute of Technology, Ireland.
E-mail address: nrowan@ait.ie (N.J. Rowan).

https://doi.org/10.1016/j.scitotenv.2020.138532

1. Introduction

Coronaviruses (CoVs) (order Nidovirales, family Coronaviridae, subfamily Coronavirinae) are enveloped viruses with a positive sense, single-stranded RNA genome (Schoeman and Fielding, 2019). With genome sizes ranging from 26 to 32 kilobases (kb) in length, CoVs have the largest genomes for RNA viruses. Coronavirus is one of the major pathogens that primarily targets the human respiratory system (Rothan and Byrareddy, 2020). Previous outbreaks of coronaviruses (CoVs) include the severe acute respiratory syndrome (SARS)-CoV and the Middle East respiratory syndrome (MERS)-CoV that are a great public health threat (Carty and DiNicolantonio, 2020). A global pandemic status has been recently declared by the World Health Organization (WHO) for COVID19. The first number of cases were identified in Wuhan, a large city of 11 million people in central China in December 2019, which were linked to the Huanan (Southern China) Seafood Wholesale Market (Rothan and Byrareddy, 2020). These were identified by local hospitals using a surveillance mechanism for "pneumonia of unknown etiology", which was established in the wake of the 2003 severe acute respiratory syndrome (SARS) outbreak with the aim of allowing timely identification of novel pathogens such as 2019-nCoV (Li et al., 2020). Globally, the number of confirmed cases as of this writing (3 April 2020) has reached 1,000,249 including 51,515 deaths (https://www.ecdc.europa.eu/en/geographical-distribution-2019-ncov-cases) (Fig. 1). Covid19 is now globally distributed (Fig. 2), suggesting that universal solutions are required to prevent or slowdown its rapid spread until effective control measures are developed and deployed, such as vaccine (Fig. 3). COVID19 is much more lethal than the typical flu, where former has a mortality rate of about 2.92% (Carty and DiNicolantonio, 2020). The annual flu has a mortality rate of just 0.05 to 0.1%, inferring that COVID-19 is around 30 to 60 times more lethal (Carty and DiNicolantonio, 2020). COVID19 causes an inflammatory storm in the lungs and it is this inflammatory storm that leads to acute respiratory distress, organ failure, and death.

Swaminathan et al. (2007) previously considered that while a new influenza pandemic may appear inevitable, critical parameters of transmissibility and attack rate are uncertain. These authors reported that estimates based on extrapolations from the 3 influenza pandemics of the 20th century suggest that healthcare facilities in the United States alone may be required to cope with 314,000–734,000 additional hospitalizations and 18–42 million outpatient visits (Meltzer et al., 1999). During the early containment phase of a pandemic, patients with suspected infection are likely to be referred to hospitals for isolation, diagnosis, and treatment until the transmissibility and virulence of the pandemic strain are known. Although social distancing and school closures may reduce risk in the wider community, healthcare workers (HCWs) are likely to encounter repeated close exposures. Swaminathan et al. (2007) suggested that if hospitals are to continue to function adequately, reliable access to effective personal protective equipment (PPE; gowns, N95 masks, gloves, and eye protection) and antiviral drug therapy will be necessary for an unpredictable period. With awareness of the recent severe acute respiratory syndrome (SARS) outbreak and with growing concern about human deaths from avian influenza (H5N1), governments worldwide have begun to stockpile PPE and antiviral medication.

Key strategies to control the speed and extent of viral spread within healthcare settings have been advocated by national government guidelines and the WHO (Swaminathan et al. (2007). These include rigorous infection control practices, prescriptive instructions for the use of PPE, and dissemination of antiviral medication. These authors reported that information regarding the required quantity and rate of use of these valuable resources in an outbreak situation is lacking, thereby limiting valid assessments of the adequacy of current stockpiles. This was corroborated by a previous simulation study conducted by Mitchell et al. (2012), where a patient with suspected avian or pandemic influenza (API) sought treatment at 9 Australian hospital emergency departments where patient–staff interactions during the first 6 h of hospitalization were observed. Based on World Health Organization definitions and guidelines, the mean number of "close contacts" of the patient was 12.3 (range 6–17; 85% HCWs); mean "exposures" were 19.3 (range 15–26). Overall, 20–25 PPE sets were required per patient, with variable HCW compliance for wearing these items (93% N95 masks, 77% gowns, 83% gloves, and 73% eye protection). These data indicate that many current national stockpiles of PPE and antiviral medication are likely inadequate for a pandemic.

At this time of writing, in the Republic of Ireland, there is a national lockdown imposed by the Irish government where citizens are requested to remain at home to prevent the spread of COVID-19 infection. Where new positive COVID19 cases arise, the role of contact tracing and data analytics are important. Social distancing and cocooning of the elderly and vulnerable groups has been adapted. Only essential services, such as agriculture and fisheries, manufacturing and healthcare, have been granted permission to travel. There is a concerted effort to slow the rate of infection so as align with capacity of healthcare to meet

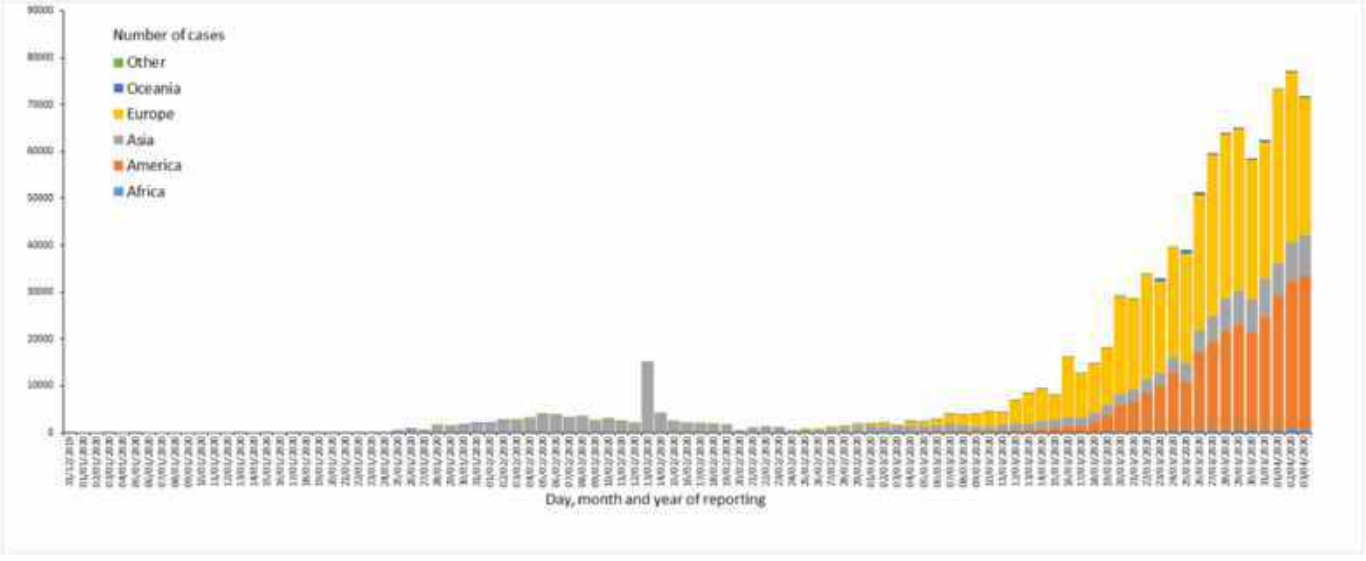

Fig. 1. Distribution of COVID19 worldwide, as of 3 April, 2020.
(Source https://www.ecdc.europa.eu/en/geographical-distribution-2019-ncov-cases)

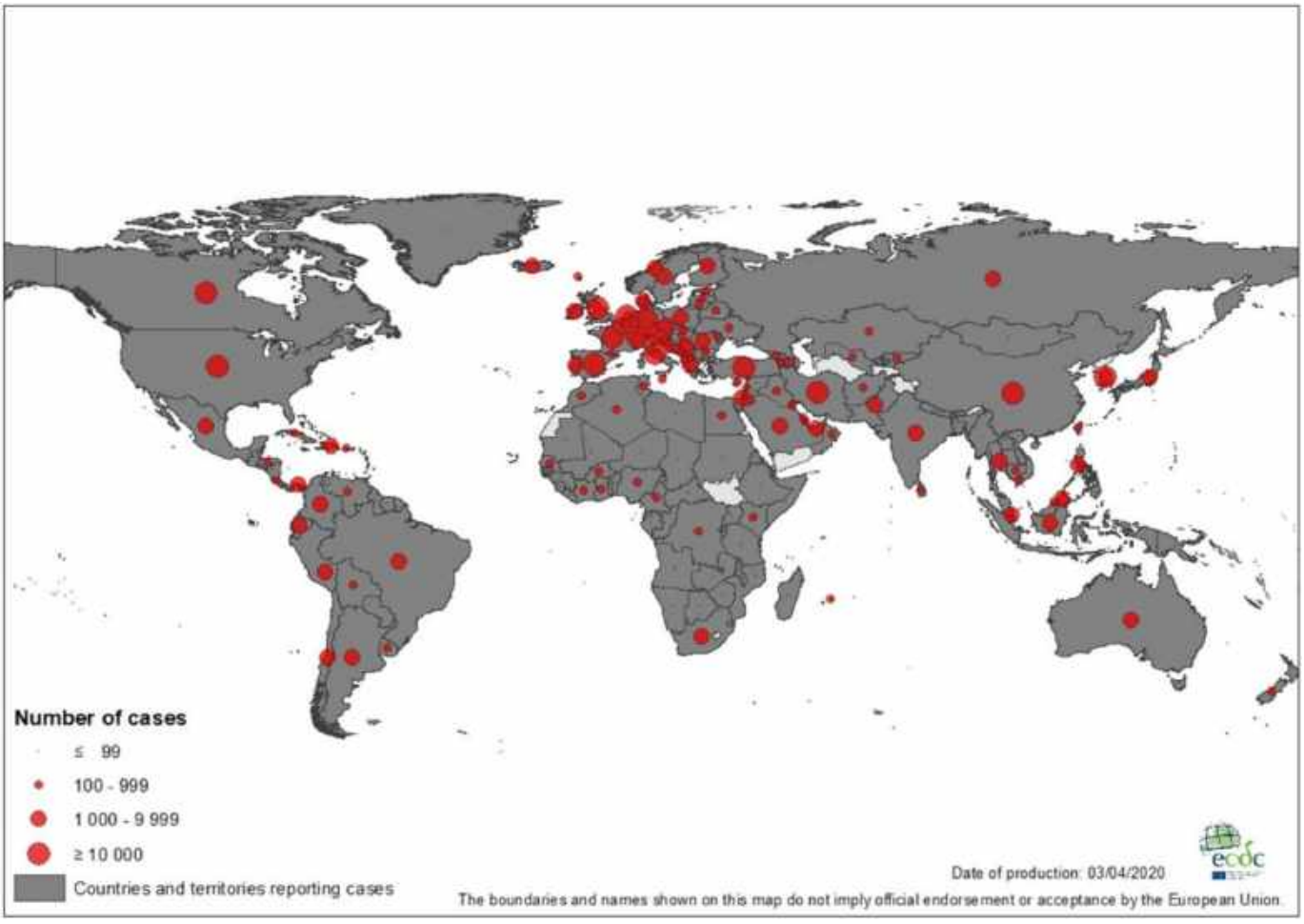

Fig. 2. Geographic distribution of COVID19 worldwide, as of 3rd April, 2020.
(Source, https://www.ecdc.europa.eu/en/geographical-distribution-2019-ncov-cases)

number of cases, thus avoiding a mismatch in early peak in infections (Fig. 3). Given need for react quickly, solutions (where appropriate) are based upon adaptation, blending and re-purposing of existing products, processes, technologies and infrastructures. Solutions and challenges to address shortage of PPE in a regional Irish hospital are described.

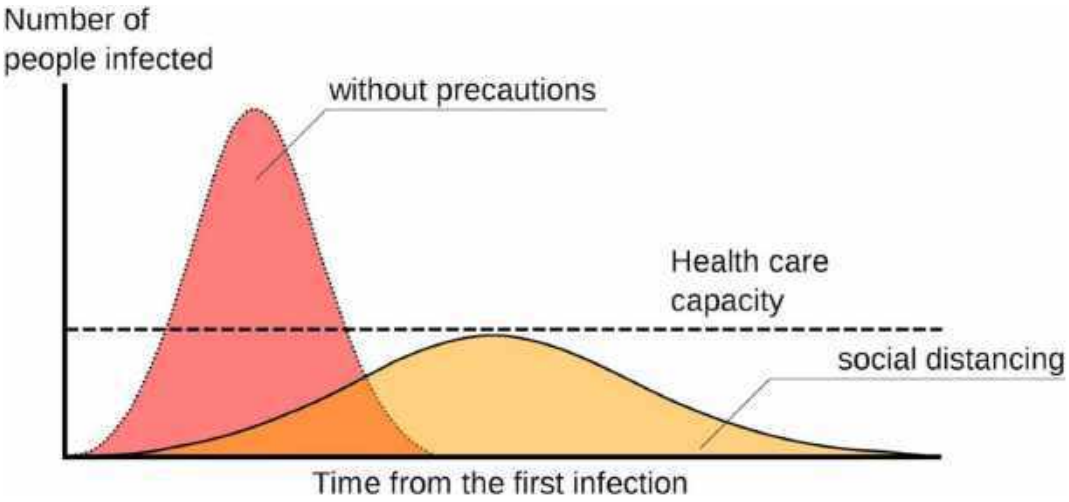

Fig. 3. A sample epidemic curve, with and without social distancing.
(Image credit: Johannes Kalliauer/CC BY-SA 4.0)

Use of smart software and networking with various distribution channels to meet shortfall in PPE and infection prevention and control (IPC) methods.

A new team of experts was formed (designated REA-PPE) to deploy effective solutions in a short time frame, which included those from across academia, healthcare, Enterprise Ireland-funded technology gateways, Science-Foundation-Ireland (SFI)-funded Research Centres (CURAM for Medical Device, COMMAND for software) and industry. REA_PPE team also links with the Crisis Management Team in the regional hospital where solutions is to implemented by manager of the Hospital Sterile Services Department (HSSD). This REA_PPE team comprises experts representative of anaesthesia and intensive care, medical device technology, infection control, hospital disinfection and sterilization, minimal processing; microbiology, toxicology, virology, material science, software engineering, and social marketing Priority initially focused on delineating effective communication channels in order to inform stocks within healthcare from several routes that include use of dedicated webpage [https: //covidmedsupply.org/] established by researchers from NUI Galway and University of Limerick (Ireland) that collects donations of PPE from regional industries and academic institutions. Given volatility in the global supply chain for PPE, Ireland's Health Service Executive (HSE) actively purse PPE orders from China and other sources to meet specific requirements that are quality checked on arrival. Upon arrival, PPE are distributed to primary healthcare, step-back healthcare facilities or nursing homes. HCW aredededicated to one site to avoid risk of cross-infection. Aer Lingus (Ireland's main national airline), made no-stop flights with a team of volunteer rotating pilots to China in order to collect vital PPE stock, where this process was repeated several times in the same week. COVID19 pandemic caused uncertainty to the established norm that is addressed by teamwork, learning, adaptation and adjustment.

Stock usage will also be tracked through a new PPE mobile phone app that uses (1) backend database to save all information on PPE stock and distribution running on a cloud, such as AWS, (2) web-server as a gateway between the mobile app and the database, such as AWS, and (3) two functions for updating the database with latest PPE status along with querying the same database. Provision has been made for use of smart blockchain system to replace the database, if the system becomes too complicated for mobile phone usage, such as data immutability,

2. Bespoke manufacturing of PPE to meet identified shortage in PPE

Where possible, where there was identified shortages in PPE, bespoke production occurred to make these items using medical grade materials, such as Continuous Positive Airway Pressure (CPAP) helmets for use in intensive care. CPAP provides the maximal amount of mean airway pressure without intubation and promotes a more lung-protective ventilation pattern. Various other bespoke manufacturing initiatives have commenced in Ireland linked to international collaborators that included use of crowdfunding by group of researchers and scientists who raised €134,000 in order to develop an easy-to-build and inexpensive ventilator for Covid-19 patients with first prototype now in place (https://www.thejournal.ie/emergency-ventilators-irish-researchers-crowdfund-5061521-Mar2020/). Other Irish researchers in University College Dublin and IT Sligo made easy-to-assemble ventilators using 3D printers and off-the-shelf components that will be validated by Ireland's HSE (https://www.irishtimes.com/business/health-pharma/irish-project-for-easy-to-assemble-covid-19-ventilators-bears-fruit-1.4205999). Facial visors were also made using 3-D printers for use in regional hospitals and nursing homes. At the time of writing, it is uncertain as to what if not all bespoke manufactured PPE in Ireland that will be inspected by HSE before deployment and usage by frontline healthcare workers. The trend by many medical device manufacturers and academic institutions to redeploy expertise and resources to make PPE to address COVID19 crisis is also emerging in other international countries (https://www.cam.ac.uk/business-and-enterprise/help-us-tackle-covid-19).

3. Challenges and solutions for addressing the reprocessing of single-use PPE

At this time of writing, there is a dearth in published literature on efficacy of innovations for reprocessing PPE. This is due to fact that PPE are manufactured for single use. Threfore, there is reliance on information generated by medical device manufacturers and related sterilization industries to help understand how best to address this shortage of PPE and the need for reprocessing in a pandemic. Traditionally, limited knowledge sharing occurs in the medical technology sector due to the need to protect IPR, which is is understandable given nature of commerce and competitiveness. However, there is an increasing trend by leading industries to publish findings that also assists in shaping ISO standards, guidelines and regulations with a focus on future-proofing, greater resource utilization and sustainability (McEvoy and Rowan, 2019; Chen et al., 2019). Original equipment manufacturers (OEMs) of one-time-use PPE have recently provided new information on possible methods for reprocessing these items given the universal need to consider contingency plans arising from shortages during this pandemic (such as 3M Science of Life, 2020).

PPE used in healthcare includes gloves, aprons, long sleeved gowns, goggles, fluid-repellent surgical masks, eye, nose and mouth protection, face visors and respirator masks. Healthcare workers should wear protective clothing when there is a risk of contact with blood, body fluids, secretions and excretions. HCW should select the appropriate PPE based on a risk assessment of the task to be carried out (Table 1). There is particular focus airborne droplets (splatter) liberated through breathing or expelled through sneezing of infected COVID19 patients may travel several meters and remain suspended for ca 30 min and survive on surfaces for potentially several days. Surface, or contact surface, disinfection or sterilization of PPE will suffice, as coronavirus does not penetrate materials. However, greatest challenge to reprocessing on one-time-use PPE relates to ensuring material functionality post effective treatments.

If one considers medical equipment designed for pre-processing, such as endoscope, there is pre-cleaning stage to reduce bioburden in advance of sterilization processes to ensure efficacy. This is relevant as unlike therapeutics (such as vaccines and antibiotics) that rely on a specific mechanistic target for model of action, sterilization modalities are non-specific with reliance upon ensuring that processes run full cycles for achieving sterility assurance level (SAL) of products (McEvoy and Rowan, 2019). For example, the presence of organic matter may affect the oxidative nature of gaseous sterilization processes, such as ethylene oxide (EtO or vaporised hydrogen peroxide (VHP). Pre-cleaning presents an issue in hospitals as there is commensurate need to decontaminate equipment used in this process for COVID19. onsideration was given to use of Actichlor plus as a wash/disinfection phase. To prevent the spread

Table 1
WHO recommendations for HCW barrier precautions, dependent on type of exposure.[a] (Adapted from Swaminathan et al., 2007)

HCW activity	Recommended PPE set
Close contact (<1 m) with potential API-infected patient within or outside of the isolation room or area	Gloves, gown, N95 mask (or equivalent particulate respirator), eye protection
Cleaning	Gloves, either gown of apron
Patient transport within healthcare facilities	Gown, gloves
Specimen transport and processing	Not defined except to use 'safe handling practices', interpreted as use of gloves (minimum) and gown if opening specimen bag

[a] WHO, World Health Organization; HCW, Healthcare worker; PPE, Personal and Protective Equipment, API, Avian or Pandemic Influenza.

of health-care–associated infections, all heat-sensitive endoscopes (e.g., gastrointestinal endoscopes, bronchoscopes, nasopharygoscopes) must be properly cleaned and, at a minimum, subjected to high-level disinfection after each use. High-level disinfection can be expected to destroy all microorganisms, although when high numbers of bacterial spores are present, a few spores might survive (CDC, 2008).

The medical device industry replies upon significant lethality of predetermined populations of a biological indicator (BI) that is typically a recalcitrant bacterial endospore (such as *Geobacillus stearothermophilus* or *Bacillus atrophaeus*). These BIs are carefully selected for this purpose as they are more resistant to that of pathogenic microorganisms including COVID19, which are typically orders of magnitude more sensitive to same applied lethal stress (Fig. 4). These are a highly validated and controlled sterilization processes. However, SAL for these sterilization are endpoint-determination processes that rely upon 12 log reduction in BIs that is excessive duration of treatment for reprocessing single-use PPE (Fig. 5) (McEvoy and Rowan, 2019). There has been no reported cases of patient illness arising from a terminal sterilization of medical devices. Furthermore, sterilization technologies are validated for full treatment regimes. There is an absence of publish knowledge as to the efficacy of operating same sterilization modalities under reduced exposure or cycle conditions, such as for the treatment of PPE. Therefore, use of penetration technologies such as gamma, electron-beam and x-ray will not be appropriate as likely to affect material and functionality of PPE post treatments. Gas-plasma generated hydrogen peroxide vapour will also be unsuitable as the plasma-process affects materials during treatment. STERIS AST have commenced studies on the combined use of real-time flow cytometry with conventional culture-based enumeration methods that will elucidate this gap, which includes frontier microbial inactivation kinetic modelling. Kinetic modelling is important for informing changes in technologies, even for potential disruption potential in emerging innovations, such as in adjacent food industry (Rowan et al., 2015). This pandemic situation will also present emerging minimal treatment opportunities for materials and treatments in medtech and sterilization industries, which will require greater flexibility in approach, such as for in situ 3D printing of medical devices in healthcare. Future reduction in sterilization modality usage would also improve resource utilization and facilitate greater sustainability of the industries. This would also have significant knock-on influence for parametric release of treated products, with quicker turn-around supply time to clients. However, it is essential that future reductions in sterilization processes are informed by best evidence and do not compromise on product safety, which require validation and regulatory approval before usage.

It is appreciated that under pandemic situations, there is a need to do things differently, along with urgency. However, this must be measured, appropriate and best informed by critical information such as that supplied by original manufacturers of single-use devices (such as 3M Announcement, 2020), along with international standards and regulators, such as AAMI and the FDA. There is a gap in knowledge on extensive studies relating to reprocessing by this source too. 3M™ stated that "filtering facepiece respirators (FFRs), such as N95, FFP2, KN95, and similar are commonly used to help provide respiratory protection in a variety of workplaces, including healthcare settings. 3M™ reiterated that a common infection prevention practice employed by healthcare organizations is to utilize FFRs as one-time-use items when worn in the presence of infected patients. In the face of a global pandemic, associated FFR shortage, and based on currently available data, 3M™ does not recommend or support attempts to sanitize, disinfect, or sterilize 3M™ FFRs" (3M announcement, 2020). 3M™ reiterated the importance that such reprocessing methods do not compromise the respirator's filtration performance or the ability of the respirator to seal to the wearer's face as intended. Albeit conducting additional research, 3M did not recommend or support any specific FFR disinfection method at this time (3M Science of Life, 2020). However, 3M™ noted that the U.S. Centers for Disease Control and Prevention (CDC) has published guidance on managing respirators during pandemics including the reuse and extended use of respirators at: https://www.cdc.gov/niosh/topics/hcwcontrols/recommendedguidanceextuse.html

What potential options are available for reprocessing of PPE to address shortage of supply chain arising from this coronavirus disease (COVID19) pandemic?

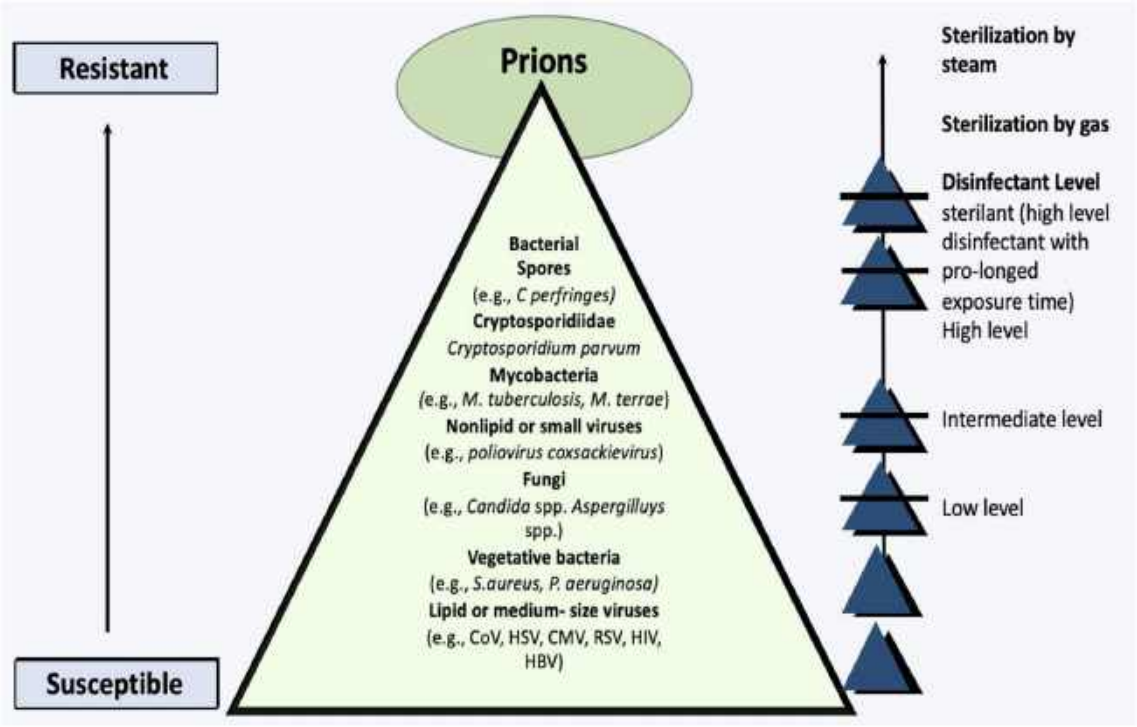

Fig. 4. Pyramid of resistance of increasing resistance to disinfection and sterilization.
(Adapted from Wendt et al., 2015)

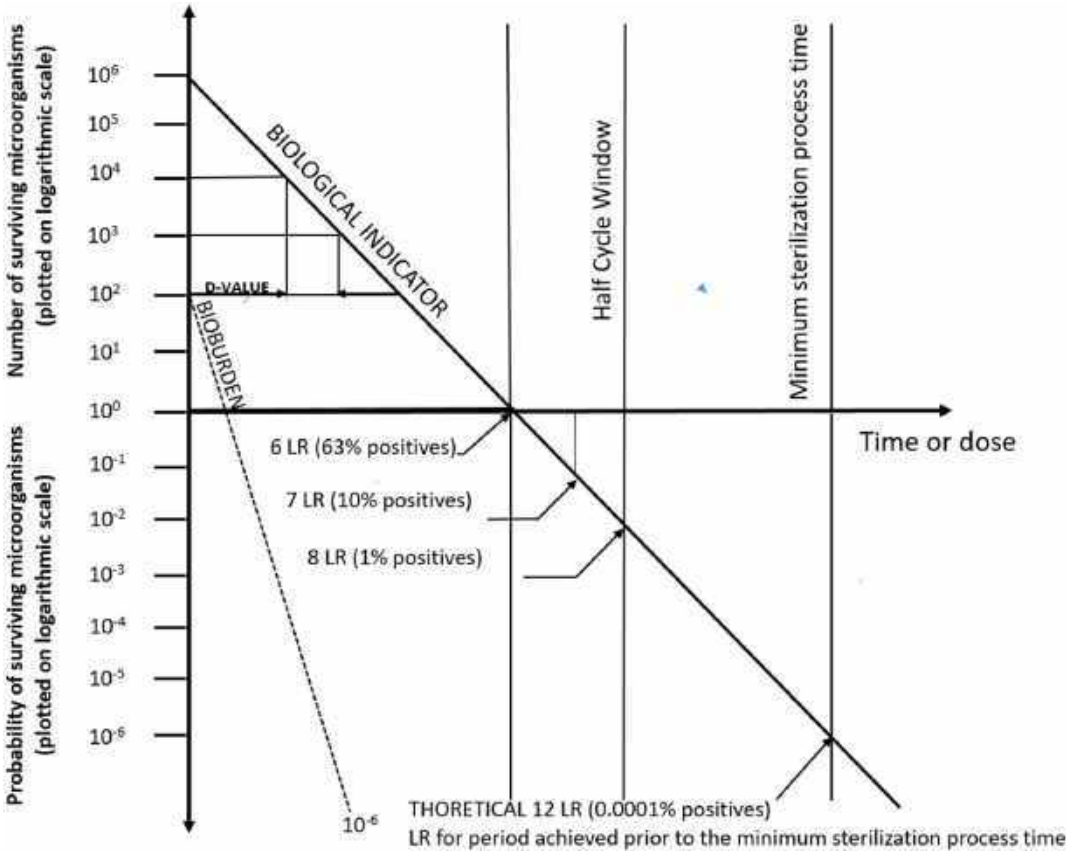

Fig. 5. Sterility assurance level and example of the relationship between biological indicator and product bioburden. For illustration purposes, this graphical representation has been obtained from AAMI TIR16:2017, which was also adapted from McEvoy and Rowan, 2019).

The contingency approach to be adapted by REA_PPE team in Ireland will make provision for the deployment of vaporised hydrogen peroxide, such as for FFRs, on site at or near the hospital. This approach is to align with Columbus-based Battelle process, where it has been reported that up to10,000 N95 masks will be sterilized by VHP in the United States, which has been authorised by the Food and Drug Administration (FDA, 2020a; FDA, 2020b). Final report for the Bioquell hydrogen peroxide vapour decontamination for reuse of N95 respirators is available at FDA (2020a). The FDA (2020b) also released details on enforcement policy for face-masks and respirators during the coronavirus disease (COVID19) public health emergency (revised April 2020) – guidelines for industry and food and drug administration staff. These are important documents to inform reprocessing of PPE. This Battelle approach involves filling a room or enclosed environment (up to 200m^3) with VHP for the treatment of PPE. VHP is an emerging technology for the medical device sterilization industry where its application, opportunities and discussed limitations by McEvoy and Rowan (2019). VHP technology is operative in Ireland now at STERIS AST. However, there is also a pressing need for rapid turn-around for reprocessed PPE on site in the hospitals, such as for critical support in ICU. VHP has potentially additional benefits over use of EtO (which currently sterilizes ca. 50% of medical devices globally) as it is safer and environmentally acceptable from a future sustainability perspective. Use of gamma irradiation and EtO constitutes ca. 95% of the terminal sterilization market (McEvoy and Rowan, 2019). VHP has great promise, but exhibits limitations such as against cellulose-based medical materials whereas EtO has broad material compatability (McEvoy and Rowan, 2019). There is still uncertainty as to ensuring safe distribution of contaminated PPE for external contract VHP sterilization services for treatment that negates reprocessing of PPE at plant level. The RAPPE team have placed an order for BQ50 VHP system, similar to what is been deployed in the US. Strict procurement rules on purchasing of assets over €25 k were relaxed to enable rapid uptake of technologies during this pandemic. Recent studies supports that RNA viruses, including coronavirus, are highly susceptible to hydrogen peroxide exposure where significant lethality is achieved with 0.5% hydrogen peroxide (a fraction to what is used in standard contact lens disinfection) in <1 min on glass. Studies recently reported from China have also revealed that introducing hydrogen peroxide inhalation may improve COVID19 patient outcomes (http://www.adledlight.com/news_show34.html).

REAPPE contingency plan also includes provision for deploying UV-C at 254 nm (Nanoclave cabinet, Ireland) and broad-spectrum pulsed light (Claranor, France) technologies for high-level disinfection of PPE. UV-C technology is a very effective technology for disinfection and used extensively by adjacent food and water industries. Given that coronavirus (COV) and other respiratory viruses are significantly less resistant to that of BIs used in sterilization modalities, the use of high to moderate-level disinfection is conceivable sufficient to meet needs for reprocessing of PPE (Fig. 3). These are also turnkey commercial technologies for ease of operation and integration within hospitals that also considers usage by existing decontamination staff and by the manager of HSSD. Efficacy of UV-irradiation technology is governed by the applied UV dose or fluence (W/m^2) and is affected by shading where it only inactivates what it irradiates – thus, PPE will need to be turned during treatments (Rowan, 2019). Nanoclave chamber has 32 × 30 W and 16 × 25 W Sylvania UVGI lamps that delivers a UV-C dose of 52 W/m^2 for 60s. Nanoclave cabinet was shown to disinfect 3-log viral unit of Adenovirus in 3 min at fixed wavelength of 254 nn that targets vital genetic material, such as RNA (Moore et al., 2012). High intensity, pulsed UV technology (PUV) uses broad spectrum pulsed light that is delivered at ca. 50,000 times the intensity of sunlight at contact surface where treatment time is exceptionally short duration, mere seconds (Farrell et al., 2011; Barrett et al., 2016). Previous researchers have demonstrated efficacy for extensive range of pathogens, but PUV also affected

by shading (Rowan et al., 2015; Rowan, 2019). PUV is currently been used for high-throughput food packaging disinfection commercially (Rowan, 2019). PUV has also been shown to be more effective and environmentally-friendly as a surface disinfection system compared with other minimal processing technologies tested, such as pulsed-plasma gas-discharge that produced short-lived oxidising biocidal water (Hayes et al., 2013; Garvey et al., 2015).

There has been limited studies on use of UV-disinfection technology for PPE treatment. 3M™ recently referred to a previously published study by Bergman et al. (2010) where these authors evaluated a multiple (3-cycle) decontamination processing for filtering facepiece respirators (FFRs) (3M Science of Life, 2020). The UV-germincidal-irradiation (UVGI) method described was operated for 30 min at 254 nm (15-min per side) for 3M™ 1860 and 1870 FFRs where straps on 1870 lost elasticity with a strong burning odour, and the nosefoam compressed on 1860 FFR model. This study did not assess the efficiency of disinfection method to inactivate microorganisms where it would be relevant to report on UV dose over treatment regime. Prolonged and excessive exposure using low-pressure UV light source can produce significant thermal effects along with material damage over repeated use. Bergman et al. (2010) also reported on the use various other unknown FFR makes and models and reported no observable physical change using same (1) UVGI for 15 min at 254 nm using one side of FFR facing lamp with strap removed, (2) ethylene oxide for 1 h in 100% EtO Sterilizer, and (3) VHP treatment for 15 min dewell, 125 min total cycle at 8 g/m^3 concentration. However, it is also unclear as to what specific FFR models were used and functionality post treatments. Fisher and Shaffer (2011) reported on the development of a method to assess model-specific parameters for ultraviolet-C (UV-C, 254 nm) decontamination of filtering facepiece respirators (FFRs). UV-C transmittance was quantified for the distinct composite layers of six N95 FFR models and used to calculate model-specific α-values, the percentage of the surface UV-C irradiance available for the internal filtering medium (IFM). Circular coupons, excised from the FFRs, were exposed to aerosolized particles containing MS2 coliphage and treated with IFM-specific UV-C doses ranging from 38 to 4707 J/m^2. Models exposed to a minimum IFM dose of 1000 J/m^2 demonstrated at least a 3 log reduction in viable MS2. Model-specific exposure times to achieve this IFM dose ranged from 2 to 266 min. Overall, Fisher and Shaffer (2011) found UV-C transmits into and through FFR materials. Log reduction of MS2 was a function of model-specific IFM UV-C doses. The supply of National Institute for Occupational Safety and Health (NIOSH)-certified N95 filtering facepiece respirators (FFRs) may become limited during an influenza pandemic [Institute of Medicine (U.S.) Committee on the Development of Reusable Facemasks for Use During an Influenza (cited in Fisher and Shaffer, 2011). Extending the lifetime of FFRs for multiple uses (e.g. multiple donnings) may help to alleviate the supply demand (Viscusi et al., 2007, 2009a, 2009b). Fisher and Shaffer (2011) also advocated that an option that may permit FFR reuse is the decontamination or removal of the infectious material from the FFR through one or more physical or chemical treatments. For this option to be practical, the decontamination treatment must maintain FFR fit and filtration performance and not leave hazardous residues. Other desired attributes for a decontamination method for FFR reuse would be low cost, high throughput and ease of use (Viscusi et al., 2009b). UVGI technology has been suggested as a viable option for FFR reprocessing application where nine FFR models were evaluated for changes in physical appearance, odour and laboratory performance (filter aerosol penetration and filter airflow resistance) following simulated decontamination using five different methods, including UVGI (Viscusi et al., 2009b). In latter study, UV-C treatment did not affect the filter aerosol penetration, filter airflow resistance or physical appearance of the FFRs. UV-C, as a decontamination method, is affected by several parameters, including the topography of the contaminated surface and the location of the microorganisms within the substrate. The use of UV-C for surfaces is mainly for hard, nonporous substrates (Fisher and Shaffer, 2011). Therefore, at this time of writing, while UVGI and PUV methods appear promising, no validated decontamination methods for FFRs exist.

Lessons can also be gleamed from best-published information and hurdles arising from minimal processing technologies that have been exploited by the food industry for commercial applications (Deng et al., 2019). These technologies rely upon reduced severity of non-thermal treatments that equate to moderate of high-level decontamination (Franssen et al., 2019; Gerard et al., 2019). However, review of best-published approaches suggest that these technologies, in their current configurations, would not be suited for PPE reprocessing. These unsuitable technologies include high hydrostatic pressure, pulsed electric fields, pulsed-plasma gas-discharge, ultrsound and so forth (Deng et al., 2019). Also, the majority of chemical biocides deployed in the food industry as liquid decontaminants for surface- treatments would not be effective for PPE as these cannot be easily used in the hospital setting. However, Kampf et al. (2020) recently reported that coronaviruses persist on inanimate surfaces, such as glass, plastic and metal for up to 9 days, but they are efficiently inactivated on these surfaces with use of 62–72% alcohol, 0.5% hydrogen peroxide, or 0.1% sodium hypochlorite within 1 min exposure. Use of high level disinfection with Actichlor-plus served as both a detergent and biocide for reprocessing Starmed hoods used by COVID19 patients in ICU. Testing of Starmed hoods in heated washer at 90°C caused damage to the PVC component. High level disinfection was applied in advance of lead-time for VHP and UV technologies arriving to HSSD and as use of sodium hypochlorite was suggested as possible approach to cleaning and disinfecting 3M™ powered air purifying respirators following potential exposure to coronaviruses (https://multimedia.3m.com/mws/media/1793956O/cleaning-and-disinfecting-3m-paprs-following-potential-exposure-to-coronaviruses.pdf). There is potential for use of combined HEPA filtration with UV light disinfection for air disinfection in critical areas that will reduce aerobiology or airborne bioburden. However, consideration would need to be given to efficacy of reduction of COVID19 or similar respiratory viruses.

Perceived benefits and future directions for the control of COVID19 with a focus on addressing shortages in supply chain.

The perceived indicative benefits of deploying solutions for reprocessing PPE to address front-line shortage have listed in terms of making potentially significant qualitative and quantitative difference are listed in Table 2. The world, as we know it, will be a changed place post COVID19, where there will be greater focus on mitigation planning for managing pandemics nationally and transnationally with either increased provision and/or less reliance on one-time-use medical devices and PPE. Future provision in hospitals and healthcare will also consider duality of sterilization treatments with reduced processing capability for to deliver if required, high or moderate level of disinfection. There will be increased emphasis on convergence of technologies and knowledge from adjacent disciplines, such as the food industry, to improve our understanding of minimal processing linked to sterilization. This will be framed upon increased demand for evidence-based research and shared publications so to inform validation and new regulations using potentially new smart innovations and services or adapting existing modalities. It is envisaged that there will be a commensurate push to promote more eco-innovations, along with review of exiting sterilization processes, for sustainability of resources and to meet existing needs arising and emerging from this COVID19 pandemic. This pandemic also highlights the value of converging areas of expertise that will inform education and workforce training processes. This pandemic also highlights that despite staggering advancements in innovation, society is still very vulnerable to global treats to our health from what is a microscopic virus. Commensurately, our collective creativity and ingenuity will enables us to countermeasure these challenges.

In summary, providing solutions for the shortages in supply chain for one-time-use PPE is extremely complex. Preference would always be for usage of single-use items as described by the manufacturers as ensuring the safety of our healthcare workers is paramount. Logical

Table 2
Perceived qualitative and quantitative differences to healthcare provision by deploying reprocessing of PPE to address shortages during COVID19 pandemic.

Qualititative	Quantitative
Reduction of infection rates seen in HCW resulting in sustainability of scale and capacity to underpin national strategic plan for addressing the COVID-19 pandemic	Increased availability of PPE and other critical care equipment
Sustainable enhancement of flexible decontamination process linked to (new) education provision in order to hurdle challenges and bottle-neck presented by shortfall in single use PPE for HCW	Reduced impact on environment with less incineration using sustainable eco-sustainable treatment modalities
New transferrable knowledge for replication across healthcare/medtech sectors with global orientation	New technologies and strategies identified as countermeasures to help address and manage COVID-19 – particularly for high risk situations, such as intensive care
Confidence in maintaining health outcomes for frontline HCW and patients	Potential generation of new IP and innovations
Cross-cutting knowledge acquisition from converging areas to address this specific solutions and to inform future policies surrounding preparedness for future pandemics	Increased number of trained experts equipped with new converging knowledge nationally with global orientation
Evolving medical device industry by way of informing need for operating sterilization modalities under reduced processing conditions for this need and for future opportunities	Reduced economic burden in terms of offering alternative options to procurement where there is global pressure on supply chain
Positive disposition towards related mental health issues arising due to uncertainty of existing technologies and provision for front line healthcare staff	Increased number of new policies and guidelines to address pandemic

first step solutions would be to improve communication lines for better stock management of PPE that exploits webpage and mobile phone app development along with dual bespoke production of PPE using medical grade materials where gaps are identified, such as ventilators. However, a pandemic foists untold and unexpected demands on society that includes provision or contingency planning for reprocessing PPE. Under such situations, it is imperative to follow closely advice from original manufacturer of PPE on material composition and design features with view to making reprocessed PPE (where possible), fit for purpose. This also includes adhering to close advice provided by regulators, such as FDA. The majority of existing in house hospital, external terminal sterilization and adjacent minimal processing technologies (as used in food industry) will not be effective for reprocessing PPE. However, review of best evidence suggest that preferred candidate methods for meeting this gap appears to be use of vaporised hydrogen peroxide (VHP) and UV irradiation technologies, which are likely be deployed in the Republic of Ireland.

Funding

Science Foundation Ireland – Rapid COVID19 fund Grant with CURAM edical device Centre.

Authors' contributions

NR and JGL conceptualised the manuscript. NR drafted the manuscript. Both authors read, edited, and approved the final manuscript.

Consent for publication

Not applicable.

Declaration of competing interest

The authors declare that they have no competing or conflict of interests.

Acknowledgements

The authors would like to thank Dr. Emma Murphy for assisting with graphics editing of figures.

References

3M Science of Life, 2020. Disinfection of Filtering Facepiece Respirators, Announcement. https://multimedia.3m.com/mws/media/1816576O/disinfection-of-disposable-respirators-technical-bulletin.pdf, Accessed date: 4 April 2020.
Barrett, M., Fitzhenry, K., O'Flaherty, V., Dore, W., Keaverey, S., Cormican, M., Rowan, N., Clifford, E., 2016. Detection, fate and inactivation of pathogenic norovirus employing settlement and UV treatment in wastewater treatment facilities. Sci. Total Environ. 568, 1026–1036.
Bergman, M.S., Viscusi, D.J., Heimbuch, B.K., Wander, J.D., Sambol, A.Rl, Shaffer, R.E., 2010. Evaluation of multiple (3-cycle) decontamination processing for filtering facepiece respirators. J Engineered Fibers Fabrics 5, 33–41.
Carty, M.F., DiNicolantonio, J.J., 2020. Nutraceuticals have potential for boosting the type 1 interferon response to RNA viruses including influenza and coronavirus. Prog. Cardiovasc. Dis. https://doi.org/10.1016/j.pcad.202.02.007 available online.
Chen, Y., Neff, M., McEvoy, B., Cao, Z., Pezzoli, R., Murphy, A., Gately, N., Hopkins, M., Rowan, N.J., Devine, D.M., 2019. 3D printed polymers are less stable than injected moulded counterparts when exposed to terminal sterilization processing using novel vaporized hydrogen peroxide and electron beam processes. Polymer 183. https://doi.org/10.1016/j.polymer.2019.121870.
Deng, L.-Z., Mujumdar, A.S., Pan, Z., Vidyarthi, S.K., Xu, J., Zielinseka, M., Xiao, H.W., 2019. Emerging chemical and physical disinfection technologies of fruits and vegetables: a comprehensive review. Crit. Rev. Food Sci. Nutr. https://doi.org/10.1080/10408398.2019.1649633.
Farrell, H., Hayes, J., Laffey, J., Rowan, N., 2011. Studies on the relationship between pulsed UV light irradiation and the simultaneous occurrence of molecular and cellular damage in clinically-relevant Candida albicans. J. Microbiol. Methods 84 (2), 317–326.
FDA, 2020a. Final report for the bioquell hydrogen peroxide vapor (HPV) decontamination for reuse of N95 respirators. https://www.fda.gov/media/136386/download, Accessed date: 4 April 2020.
FDA, 2020b. Enforcement Policy for Face Masks and Respirators during the Cornovirus Disease (COVID19) Public Health Emergency (Revised), April, 2020. https://www.fda.gov/regulatory-information/search-fda-guidance-documents/enforcement-policy-face-masks-and-respirators-during-coronavirus-disease-covid-19-public-health, Accessed date: 4 April 2020.
Fisher, E.M., Shaffer, R.E., 2011. A method to determine the available UV-C dose for the decontamination of filtering facepiece respirators. J. Appl. Microbiol. 110 (910), 287–295.
Franssen, F., Gerard, C., Cozma-Petrut, A., Viera-Pinto, M., Jambrak, A.R., Rowan, N.J., Paulsen, P., Rozycki, M., Tsynes, K., Rodriguez-Lazaro, D., Robertson, L., 2019. Inactivation of parasite transmission stages – efficacy of treatments on food of animal origin. Trends Food Sci. Technol. 83, 114–128.
Garvey, M., Hayes, J., Clifford, E., Rowan, N., 2015. Ecotoxicological assessment of pulsed ultraviolet light-treated water containing microbial species and Cryptosporidium parvum using a microbiotest battery. Water Environment Journal 29 (1), 27–35.
Gerard, C., Franssen, F., La Carbona, S., Menterio, S., Cozma-Petrut, A., Utaaker, K.S., Jabmrak, A.R., Rowan, N.J., Rodriguez-Lazaro, D., Nasser, A., Tysnes, K., Robertson, L.J., 2019. Inactivation of parasite transmission stages – efficacy of treatments on foods of non-animal origin. Trends Food Sci. Technol. 91, 12–23.
Hayes, J., Kirf, D., Garvey, M., Rowan, N., 2013. Disinfection and toxicological assessment of pulsed UV and pulsed-plasma gas-discharge treated water containing the waterborne protozoan enteroparasite Cryptosporidium parvum. J. Microbiol. Methods 94 (3), 325–337.
Kampf, G., Todt, D., Pfaemder, S., Steinmann, E., 2020. Persistence of coronavirus on inanimate surfaces and their inactivation with biocidal agents. J. Hosp. Infect. 104 (3), 246–257.
Li, Q., Guan, X., Wu, P., Wang, X., Zhou, L., Tong, Y., Ren, R., Leung, K.S.M., Lau, E.H.Y., Wong, J.Y., Xing, X., Xiang, N., Wu, Y., Li, C., Chen, Q., Li, D., Liu, T., Zhao, J., Liu, M., Tu, W., Chen, C., Jin, L., Yang, R., Wang, Q., Zhou, S., Wang, R., Liu, H., Luo, Y., Liu, Y., Shao, G., Li, H., Tao, Z., Yang, Y., Deng, Z., Liu, B., Wu, J.T., Gao, G.F., Cowling, B.J., Yang, B., Leung, G.M., Feng, M., 2020. Early transmission dynamics in Wuhan, China, of novel coronavirus–infected pneumonia. N. Engl. J. Med. 382, 1199–1207. https://doi.org/10.1056/NEJMoa2001316.
McEvoy, B., Rowan, N.J., 2019. Terminal sterilization of medical devices using vaporized hydrogen peroxide: a review of current methods and emerging opportunities. J. Appl. Microbiol. 127 (5), 1403–1420.
Meltzer, M.I., Cox, N.J., Fukuda, K., 1999. The economic impact of pandemic influenza in the United States: priorities for intervention. Emerg. Infect. Dis. 5, 659–671. https://doi.org/10.3201/eid0505.990507.
Mitchell, R., Ogunreai, T., Astratianakis, S., Bryce, E., Gervais, R., Gravel, D., Johnson, L., Leduc, S., Roth, V., Taylor, G., Vearcombe, M., Weir, C., 2012. Impact of the 2009 influenza A (H1N1) pandemic on Canadian health care workers: a survey on vaccination, illness, absenteeism, and personal protective equipment. Am. J. Infect. Control 40 (7), 611–616.

Moore, G., Ali, S., Cloutman-Green, E.A., Bradley, C.R., Wilkson, M.A., Hatley, J.C., Fraise, A.P., Wilson, A.P., 2012. Use of UVC radiation for disinfecting non-critical patient care items – a laboratory assessment of the Nanoclave Cabinet. BMC Infect. Dis. 3, 12–14.

Rothan, H.A., Byrareddy, S.N., 2020. The epidemiology and pathogenesis of coronavirus disease (COVID-19) outbreak. J. Autoimmun. https://doi.org/10.1016/j.jaut.2020.102433 In press.

Rowan, N.J., 2019. Pulsed light as an emerging technology to cause disruption for food and adjacent industries – quo Vadis? Trends Food Sci. Technol. 88, 316–332.

Rowan, N.J., Valdramidis, V.P., Gomez-Lopez, V.M., 2015. A review of quantitative methods to describe efficacy of pulsed light generated inactivation data that embraces the occurrence of viable but non culturable state microorganisms. Trends Food Sci. Technol. 44 (1), 79–92.

Schoeman, D., Fielding, B.C., 2019. Coronavirus envelope protein – current knowledge. Virol. J. https://doi.org/10.1186/s12985-019-1182-0.

Swaminathan, A., Martin, R., Gamon, S., Aboltins, C., Althan, E., Braitberg, G., Catton, M.G., Cooley, L., Dwyer, D.E., Edmonds, D., Eisin, D.P., Hosking, K., Hughes, A.J., Johnson, P.D., Maclean, A.V., O'Reilly, M., Peter, S.E., Stuart, R.L., Moran, R., Lindsay-Grayson, M., 2007. Personal and protective equipment and antiviral drug use during hospitalization for suspected Avian or Pandemic Influenza. Emerg. Infect. Dis. 13 (10), 1511–1547.

U.S. Centers for Disease Control and Prevention (CDC), 2008. Disinfection of Healthcare Equipment -Guideline for Disinfection and Sterilization in Healthcare Facilities. 2008. https://www.cdc.gov/infectioncontrol/guidelines/disinfection/healthcare-equipment.html, Accessed date: 4 April 2020.

Viscusi, D.J., King, W.P., Shaffer, R.E., 2007. Effect of decontamination on the filtration efficiency of two filtering facepiece respirator models. J Int Soc Respir Prot 24, 93–107.

Viscusi, D.J., Bergman, M.S., Sinkule, E., Shaffer, R.E., 2009a. Evaluation of the filtration performance of 21 N95 filtering face piece respirators after prolonged storage. Am. J. Infect. Control 37, 381–386.

Viscusi, D.J., Bergman, M.S., Eimer, B.C., Shaffer, R.E., 2009b. Evaluation of five decontamination methods for filtering facepiece respirators. Ann. Occup. Hyg. 53, 815–827.

Wendt, C., Frei, R., Widmer, A., 2015. Decontamination, disinfection, and sterilisation. In: Jorgensen, J., Pfaller, M., Carroll, K., Funke, G., Landry, M., Richter, S., Warnock, D. (Eds.), Manual of Clinical Microbiology, Eleventh edition ASM Press, Washington, DC, pp. 183–216. https://doi.org/10.1128/9781555817381.ch13.

Science of the Total Environment 752 (2021) 142259

Contents lists available at ScienceDirect

Science of the Total Environment

journal homepage: www.elsevier.com/locate/scitotenv

Review

Unlocking the surge in demand for personal and protective equipment (PPE) and improvised face coverings arising from coronavirus disease (COVID-19) pandemic – Implications for efficacy, re-use and sustainable waste management

Neil J. Rowan [a,b,c,*], John G. Laffey [d,e]

[a] Department of Nursing and Healthcare, Athlone Institute of Technology, Ireland
[b] Centre for Disinfection, Sterilization and Biosecurity, Athlone Institute of Technology, Ireland
[c] Empower Eco Sustainability Hub, Lough Boora, Co. Offaly, Ireland
[d] Lung Biology Group, Regenerative Medicine Institute at CURAM Centre for Medical Devices, National University of Ireland Galway, Galway, Ireland
[e] Anaesthesia and Intensive Care Medicine, University Hospital Galway, Galway, Ireland

HIGHLIGHTS

- Reprocessing of PPE during COVID-19 for healthcare occurs in many countries under emergency crisis situations
- Social marketing will inform attitudes, barriers and acceptance of PPE reuse by healthcare workers.
- Appropriate decontamination and reuse of face coverings by the public are important disease countermeasures.
- Post-COVID-19, the changes in medical practice will drive high demand for PPE.
- Sustainable PPE, made from bioplastics, will facilitate effective waste management and inform technology disruption.

GRAPHICAL ABSTRACT

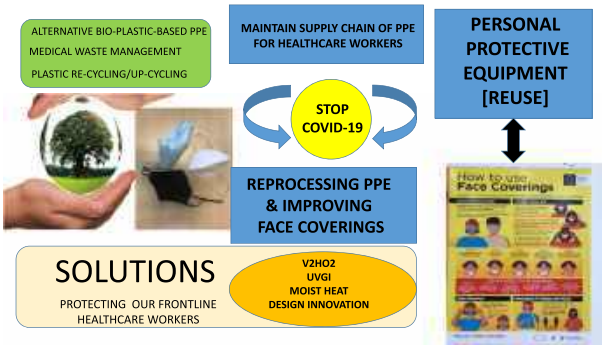

ARTICLE INFO

Article history:
Received 24 July 2020
Received in revised form 4 September 2020
Accepted 5 September 2020
Available online 10 September 2020

Editor: Damia Barcelo

Keywords:
COVID-19
PPE
Face coverings
Reuse
Sustainability
Waste management

ABSTRACT

Currently, there is no effective vaccine for tackling the ongoing COVID-19 pandemic caused by SARS-CoV-2 with the occurrence of repeat waves of infection frequently stretching hospital resources beyond capacity. Disease countermeasures rely upon preventing person-to-person transmission of SARS-CoV2 so as to protect front-line healthcare workers (HCWs). COVID-19 brings enormous challenges in terms of sustaining the supply chain for single-use-plastic personal and protective equipment (PPE). Post-COVID-19, the changes in medical practice will drive high demand for PPE. Important countermeasures for preventing COVID-19 transmission include mitigating potential high risk aerosol transmission in healthcare setting using medical PPE (such as filtering facepiece respirators (FFRs)) and the appropriate use of face coverings by the general public that carries a lower transmission risk. PPE reuse is a potential short term solution during COVID-19 pandemic where there is increased evidence for effective deployment of reprocessing methods such as vaporized hydrogen peroxide (30 to 35% VH2O2) used alone or combined with ozone, ultraviolet light at 254 nm (2000 mJ/cm^2) and moist heat (60 °C at high humidity for 60 min). Barriers to PPE reuse include potentially trust and acceptance by HCWs. Efficacy of face coverings are influenced by the appropriate wearing to cover the nose and mouth, type of material used, number of layers, duration of wearing, and potentially superior use of ties over ear loops. Insertion of a nose clip into cloth coverings may help with maintaining fit. Use of 60 °C for 60 min (such as, use of

* Corresponding author at: CDSB, Athlone Institute of Technology, Ireland.
E-mail address: nrowan@ait.ie (N.J. Rowan).

https://doi.org/10.1016/j.scitotenv.2020.142259

domestic washing machine and spin dryer) has been advocated for face covering decontamination. Risk of virus infiltration in improvised face coverings is potentially increased by duration of wearing due to humidity, liquid diffusion and virus retention. Future sustained use of PPE will be influenced by the availability of recyclable PPE and by innovative biomedical waste management.

Contents

1. Introduction

Since first reported as a cause of serious human pneumonia in Wuhan, Hubei, China in December 2019, the novel coronavirus COVID-19 has spread worldwide with devastating consequences. At the time of writing (29th August 2020), there has been 25.1 million cases of COVID-19 reported (in accordance with the applied case definitions and testing strategies in the affected countries) including 845,343 deaths (European Centre for Disease Control and Prevention, 2020). There is evidence of resurgence of the SARS-CoV-2 globally with the emergence of second waves of infection in many countries (European Centre for Disease Control and Prevention, 2020). Hong Kong is addressing its third wave of COVID-19 infections, where Australia is battling a second wave of infection having previously reduced viral transmission cases close to zero. COVID-19 has also emerged strongly in developing low-resource countries that already have significant healthcare challenges, such as across the African continent that is also challenged with Acquired Immunodeficiency Syndrome (AIDS) and *Mycobacterium tuberculosis* as co-morbidities (African Centre for Disease Control and Prevention, 2020).

Currently, there is still no effective vaccine or anti-viral therapy for COVID-19 with reliance upon the prevention of transmission by way of imposing a lockdown, cocooning, social distancing, and wearing of face masks in order to protect vulnerable groups and to safeguard front-line healthcare professionals (Murphy et al., 2020) Epidemiological studies show that social distancing prevents person-to-person transmission of SARS-CoV-2, which is relevant given that there is growing recognition that asymptomatic carriers may also contribute to this transmission (Li et al., 2020). There is evidence to suggest that COVID-19 is a super-spreader of infectious airborne viral particles where several people can be infected at the same time (Li et al., 2020). Clusters of COVID-19 infection reflect vulnerabilities, such as nursing homes catering for the elderly or meat packing industry (Carswell, 2020), where there are challenges in practicing appropriate safe social distancing. However, recent epidemiology studies for past 14 days from the Health Service Executive in the Republic of Ireland shows that 55% of COVID-19 occurred in people aged below 35 years of age that would not have been considered to be a highly susceptible group earlier, thus highlighting the challenges of reopening countries too quickly. Global studies have revealed that there is insufficient herd immunity to COVID-19 due to low exposure levels typically at ca. 5% of total population (Carswell, 2020). Many countries have introduced innovative approaches to flattening the curve of infection, such as, in the Republic of Ireland where a mobile phone COVID-19 tracker alerts users as to the status of SARS-CoV-2 in the community.

In pandemic situations, such as the ongoing COVID-19 pandemic, hospital resources are frequently stretched beyond capacity (Derraik et al., 2020). There is a pressing need to sustain the supply chain of disposable personal and protective equipment (PPE) in order to prevent the spread of COVID-19 to and from healthcare workers (HCWs) and patients. The availability and effective use of PPE are essential that includes masks, eye protection, gloves, gowns, and, for aerosol generating procedures in particular, N95 and KN95 filtering facepiece respirators (FFRs) or equivalent (Derraik et al., 2020; Rubio-Romero et al., 2020). This interest in PPE reuse, arising from the ongoing COVID-19 pandemic, is also attested by the 52 journal citations that used best-available information provided in our initial opinion article on this topic that was published on 4th April 2020 (Rowan and Laffey, 2020).

Subsequently, there has been a pressing need to provide safe and simple solutions to disinfect and reuse improvised or homemade (non-certified) cloth face coverings in order to prevent person-to-person transmission in the community and workplace. Wearing a face covering reduces the spread of coronavirus in the community as it helps to reduce the spread of respiratory droplets from people infected

with SARS-CoV-2. Use of face coverings helps to stop people who are not aware they have the virus from spreading (HSE, 2020). Face coverings are not recommended for children under the age of 13 unless attending a healthcare setting, as young children may not follow the advice about wearing a face covering correctly such as not touching it. Silva et al. (2020) noted that over 50 countries have mandatory wearing of facemasks or coverings for the general public. Medical face masks are typically worn by healthcare workers and by people in self-isolation who cannot keep a distance of 2 m between themselves and other people in their household (HSE, 2020). For those who find it difficult to wear a cloth face covering, it's appropriate to wear a full face visor or face shield instead. However, use of face shields are not as good as wearing a face covering, but they provide some level of protection (CDC, 2020). The visor should wrap around the sides of your face (ear to ear) and extend to below the chin. Reusable visors should be cleaned after each use and then stored in a clean place until needed. Coordinating the supply chain for PPE in the midst of a pandemic with many closed borders and limited freight compounds the challenge (Derraik et al., 2020). Derraik et al. (2020) also noted that people need to have trust in systems set up to support supply chain for PPE in the workplace. Arising from the unprecedented surge in single-use plastic PPE usage, there also appears to be a need to consider effective waste management and recycling strategies to limit SARS-CoV-2 cross-transmission.

Therefore, given the aforementioned, there is a pressing need to understand the efficacy of disinfection methods and for reuse of medical PPE in high risk healthcare environment where there is a supply chain shortage. Also, to define simple solutions for reuse of non-certified cloth or fabric face coverings used by general public in low risk settings, which the focus of this study. Consequently, we carried out a rapid review to summarize the literature with two inter-related aims – first, to examine the current knowledge about survival of SARS-Cov-2 on surfaces and to provide an update on studies conducted in the Republic of Ireland (Rowan and Laffey), — second, to examine current knowledge on the efficacy and potential barriers for implementing key PPE disinfection methods against SAR-CoV-2; and third, to examine biomedical waste management strategies to meet surge in PPE usage across the globe. Given the very recent discovery of SARS-CoV-2, our study also encompassed appropriate review articles and primary data sources that focused on SARS-CoV-1 as this is sister virus from the same species (Gorbalenya et al., 2020; Derraik et al., 2020).

2. Methods

We carried out a rapid review of the literature to inform the research questions that addressed a search strategy involved Google Scholar, Scopus, Web of Science, and PubMed as per approached described recently by Tiedeken et al. (2017). Searches were restricted to publication from 1 January 2003 (as the first recorded human infection of SARS-1 occurred in November 2002 (as per Derraik et al. (2020)) and 8 August 2020. Titles and/or abstracts were screened by the first author and where appropriate, full text of individual research studies, opinion pieces and reviews were consulted. Key words used were PPE; reuse; reprocessing; disinfection; decontamination; N95; COVID-19; SARS-CoV-1; SARS-CoV-2; UV; hydrogen peroxide vapour (VH2O2); ozone; waste management; recycling. Data extraction and rapid analysis was supplemented by conducting a short observation study where the first author noted the types of facemasks and face coverings worn by the public on entering a large shopping centre in the Republic of Ireland on 14th and 15th August 2020.

3. Knowledge that informed PPE use and potential reuse from a Republic of Ireland perspective

At the time of initial writing (3rd April, 2020) (Rowan and Laffey et al., 2020), the number of confirmed COVID-19 cases had reached 1 million, including 51,515 deaths, which highlights that a 25-fold increase in the prevalence of SARS-Cov-2 has occurred in only 4 months (European Centre for Disease Prevention and Control, 2020). Rowan and Laffey (2020) had predicted an unprecedented high demand for PPE across the globe and therefore, it was prudent to consider PPE reuse as a potential option to meet the critical shortage in the supply chain for frontline HCWs. Rowan and Laffey (2020) intimated that the structure of SARS-Cov-2 is such that is sensitive to harsh environmental stresses. Moreover, the structure of SARS-CoV-2, and related coronaviruses, includes a RNA genome, a protein capsid, and an outer envelope. Viral inactivation is linked to the alteration of one of these structural elements by an environmental stress, such as, heating, ultraviolet light, and biocides (Bentley et al., 2016; Pinon and Vialette, 2018; Gorbalenya et al., 2020). The proteins and lipids of the envelope may be disrupted more easily than the other parts of the virus (Howie et al., 2008; Pinon and Vialette, 2018). Thus, naked viruses are generally more resistant than enveloped viruses (such as SARS-Cov-2 and other coronaviruses) to similar levels of the same or different adverse environmental conditions (Fitzgibbon and Sagripanti, 2008; Pinon and Vialette, 2018). The enveloped structure of SARS-Cov-2 (Meo et al., 2020), and Influenza (cited in Li, 2016), is such that these viruses are more likely to be sensitive to disinfection technologies (Pinon and Vialette, 2018; Rowan and Laffey, 2020). Kampf et al. (2020) had also analysed 22 studies of different human coronaviruses where SARS, MERS, HCoV (but not including COVID-19) were efficiently inactivated by disinfection on variety of contact surface using 62 to 71% ethanol, 0.5% hydrogen peroxide, or 0.1% sodium hypocholorite within 1 min of exposure, but survived on untreated surfaces for up to 9 days. van Doremalen et al. (2020) also conducted tests that showed that SARS-CoV-1 remains on plastic, stainless steel, copper and cardboard for up to 72 h. These and other studies (Zhao et al., 2020) have informed selection of many current disinfection procedures to address SARS-CoV-2 pandemic, including PPE reuse.

Given that disposable, plastic-based, PPE (gowns, eye protection, gloves, face masks, filtering facepiece respirators (FFRs)) are heat sensitive, existing healthcare technologies were considered to be either not available, unsuitable or not configured for reprocessing of PPE in healthcare for emergency use (Rowan and Laffey, 2020). However, potential solutions for effective reprocessing of PPE that considered virus inactivation, material compatibility and device functionality (filtration efficacy, penetration, fit test and so forth) post processing included use of low temperature hydrogen peroxide vapour (VH2O2), ultraviolet germicidal light (UVGI), moist heat, and use of weak bleach for liquid decontamination (Rowan and Laffey, 2020; CDC, 2020). McEvoy and Rowan (2019) had published a comprehensive review on the background and efficacy of VH2O2 for terminal sterilization of medical devices that was used to provide supportive technical information in choice of procedures. This information was supported by prior findings of Bentley et al. (2016) who reported on 4 $\log_{10}$ viral titre reductions for the recalcitrant naked Norovirus in a variety of hospital settings (stainless steel, glass, vinyl flooring, ceramic tile, PVC plastic cornering) using 30% *w*/w hydrogen peroxide vapour. Rowan (2019) had also reviewed potential microbial mechanistic information underpinning UV disinfection that also provided supportive foundation knowledge for the potential use of pulsed light technology for PPE.

Information underpinning these candidate technology solutions included best-published information of efficacy of these approaches to surface disinfection cornoavirus (COVID-19) or related viruses and surrogate biological indicator organisms on different surface materials (Kampf et al., 2020).

The FDA had authorized use of VH2O2 technology, under emergency use authorization (EUA), for the reprocessing of critical N95 face masks in the United States in order to help address COVID-19 transmission. This was informed by Columbus-based Battelle process studies (Battelle, 2016). Given exceptional circumstances, original equipment manufacturers (OEMs) of PPE had also suggested possible appropriate reprocessing strategies, but they also reiterated that their products

had been manufactured with the sole intention of single use. The contingency plan to be adopted in hospitals on the west of Ireland was to procure, install and seek approval from competent authority for the deployment of VH2O2 (Bioquell BQ50 system) for filtering face-piece respirators (FFRs) and surgical gowns, UV technologies (NanoClave low-pressure UVGI system and Claranor Pulsed Light system) for simple PPE such as face shields, and use of mild sodium hypochlorite (4000 ppm) for liquid decontamination of critical Starmed hoods. The VH202, UVGI and mild liquid disinfection strategies have been set up, but there remains a requirement to gain trust and confidence by HCWs for PPE reuse post treatments.

4. Currents status and challenges for the reprocessing of PPE for COVID-19

Coronavirus SARS-CoV-2 transmission has become a significant global challenge where the number of confirmed cases has increased twenty five times in just over 4 months to ca. 25 million cases (Rowan and Laffey, 2020) highlighting the high demand for PPE (European Centre for Prevention and Disease Control, 2020). There has been increasing concerns about the potential exposure to frontline healthcare workers from SARS-CoV-2, and the commensurate need to deploy effective PPE disinfection procedures to ameliorate the threat of cross-transmission and infection (Barceló, 2020; Faridi, 2020). Silva et al. (2020) have reported that over 50 countries across the globe have mandated the use of PPE by the general public to help prevent person-to-person transmission of SARS-CoV2.

Several authors have reported on the viability of SARS-CoV1 and SARS-CoV-2 on various contact surface such as printed paper, printed tissue, cloth, wood, glass, banknotes, plastic, stainless steel, surgical mask layers over different environmental temperatures, relative humidity and durations (Li et al., 2003; Lai et al., 2005; Pagat et al., 2007; Chan et al., 2020; Chin et al., 2020; Fischer et al., 2020; Kasloff et al., 2020; Behzadinasab et al., 2020; Biryukov et al., 2020). In general, lower environmental temperatures support the longer survival of SARS-CoV-2 on materials as reported by Chin et al. (2020) where only a 0.7 $\log_{10}$ reduction was observed for SAR-CoV-2 at 4 °C after 14 days compared with ≥4.5 $\log_{10}$ reduction at 22 °C (room temperature) after 14 days and ≥ 4.5 log reduction at 37 °C after just 2 days. Similarly, Chan et al. (2020) also noted only a 2 $\log_{10}$ reduction of SARS-CoV-1 at 4 °C after 14 days when the virus was inoculated onto glass surfaces. The longer survival of SARS-CoV-2 at colder temperatures may have future implications for viral persistence on contaminated face coverings as we are approaching the winter flu season.

However, public health practices that have been put in place to mitigate the spread of SARS-CoV-2 are likely to have a positive impact on the occurrence of influenza cases given that these viruses share similar modes of transmission to cause illness. Derraik et al. (2020) comprehensively reported on the viability of SARS-CoV-1 and SARS-CoV-2 on different contact surfaces, without and with UV or heat treatments, and noted the importance of virus load and inoculum size on inactivation performance. Lai et al. (2005), who looked specifically at PPE, highlighted the variability in SARS-CoV-1 viability of 2 days on a disposable polypropylene gown and 24 h on a cotton gown for same 6 $\log_{10}$ reduction. Akin to studies reported by Derraik et al. (2020), we also observed that the majority of researchers used medium tissue culture infective dose ($TCID_{50}$) to report inactivation of SARS-CoV-1 and SARS-CoV-2 on various surfaces. Kasloff et al. (2020) simulated typical infectious body fluids of infective patients and showed that to achieve a 5 $\log_{10}$ reduction in SARS-CoV2 at 20 °C (room temperature), it took ca 14 days on nitrile gloves and as much as 21 days on plastic face shields, N100 respirators and polyethylene overalls, with some residual infectivity evident on N95 respirators after 3 weeks. This highlights the importance of safely discarding soiled PPE, which are not fit for reuse.

Surface disinfection studies against SARS-CoV-2, such as use of sodium hypochlorite, hydrogen peroxide or alcohol (Kampf et al., 2020; van Doremalen et al., 2020), have informed the suitability of different technologies for PPE reuse (Table 1). In is notable that Yang et al. (2020) used a chlorine-containing disinfectant spray (2000 mg/L) for treating a variety of contaminated areas in hospitals in Wuhan city, China during SARS-CoV-2 pandemic. All healthcare workers donned significant layers of PPE in the following sequence: white coats, N95 respirator, surgical masks, surgical hat, protective goggles, shoe coverings, isolation gowns, gloves, protective suits, another pair of gloves, protective hoods, and boot coverings where hand disinfection and spraying of 75% ethanol is applied to PPE again on entering the hospital. This highlights the emphasis placed on implementing rigorous infection control strategies to remain safe from SARS-CoV2 and the enormous quantities of PPE used to prevent SARS-CoV-2 transmission.

The U.S. Food and Drug Administration (FDA) led the way in the strategic authorization of PPE and related medical devices processing under Emergency Use Authorization (EUA) where a number of established sterilization companies have been issued authority to meet these critical supply chain needs arising from this COVID-19 pandemic (FDA, 2020). The common reprocessing technology across these sterilization industries is use of hydrogen peroxide in vapour state (VH2O2) for PPE treatment, where Battelle demonstrated it's potential early in pandemic (Rowan and Laffey, 2020). Stryker STERIZONE VP4 Sterilizer, was approved for N95 face mask reprocessing by the FDA under this EUA, which also incorporates the use of ozone combined with VH2O2 for this purpose. As part of this EUA, the FDA reviews the totality of scientific evidence available, including testing data that was submitted within previous applications supporting device clearance for other uses that considers different types of polymer materials, including materials, consistent with those found in compatible N95 respirators. The FDA also reviews performance data such as sporicidal test, residual analysis, bioburden reduction validation demonstrating logarithmic reductions of a non-enveloped virus challenge; testing regarding material compatibility, functionality and filtration performance of compatible N95 respirators after multiple decontamination cycles; and testing regarding VH2O2 residuals after decontamination of compatible N95 respirators. Typically, reprocessed PPE are discarded after ≤10 treatments as per respective factsheet for facilities and personnel furnished to FDA. It is appreciated, that EUA reprocessing of PPE in healthcare settings will reflect supply and demand, if there is sufficient supply of PPE, then the use of reprocessing technologies will not be required. Many countries recommend VH2O2 for N95 respirator decontamination, leaving the decision to health service managers (Kobayashi et al., 2020).

Preparations in the Republic of Ireland for PPE reprocessing are still ongoing with a trajectory towards use of VH2O2 (Bioquell BQ50, UV germicidal irradiation (UVGI, NanoClave) and sodium hypochlorite liquid decontamination by trained healthcare staff within the hospital setting. Challenges observed include unexpected delay in the delivery of reprocessing technologies that took several months, where the low-pressure UVGI system is turn-key innovation for ease and reliability of operation. Standard operating procedures (SOPs) were generated for safe use to meet expected PPE reprocessing needs. It is likely that deployment of the technologies will be met by use of emergency authorization issued by the hospital through infection control and crisis management committee. This would infer that PPE reprocessing technologies, if authorized by this committee, can only be deployed within that specific hospital for fixed purposes under emergency use. Kobayashi et al. (2020) described extended use of N95 respirators, defined as respirator was used, removed, stored and used again at least 1 more time. The maximum duration of extended use of N95 respirators ranged from 4 h (France, New Zealand, and Sweden) to 40 h (Mexico), and the maximum number of cycles of decontamination ranged from 2 (Germany) to 5 (United States).

At the time of writing, there is still no consensus in the Republic of Ireland as to the strategic deployment of these technologies for PPE reuse, such as, for extended community needs where there has been

Table 1
Frequently cited publications for PPE reuse, decontamination, waste management and recycling.[a]

Filtering Facepiece Respirators (FFRs such as N95)			Face Shields or Visors	Cloth or Fabric Face Coverings (Homemade or Commercial)	Surgical and Procedural Masks	PPE (other including Gowns)	Bio-medical waste (including PPE) Management and Recycling
Hydrogen Peroxide Vapor (VH2O2) ± Ozone	UV Germicidal Irradiation (UVGI) UVA, UVB, UVC	Heat-based Procedures					
Boškoski et al. (2020)	Zhao et al. (2020) [N95s]	Liao et al. (2020) [≤85 °C, 30% RH, 10 min]	Flanagan and Ballard (2020) [3D Printed]	Van der Westhuizen et al. (2020)	Sickbert-Bennett et al. (2020]) Filtration efficacy]	Jessop et al. (2020) [PPE reuse]	Horton and Barnes (2020)
Rowan and Laffey (2020)	Mills et al. (2018) [N95s]	de Man et al. (2020) [121 °C]	FDA (2020)	CDC (2020)	Zorko et al. (2020)	Hegde (2020) [choice]	Aeschelmann and Carus (2020)
Rubio-Romero et al. (2020)	Ratnesar-Shumate et al. (2020) UVB	Auerswald et al. (2020)	Perencevich et al. (2020)	Rubio-Romero et al. (2020)	Dangaville et al. (2020) [shortage]	Saini et al. (2020) [overalls]	Barceló (2020)
Saini et al. (2020) [Low Cost]	O'Hearn et al. (2020b)	Price and Chu (2020) dry heat 70 °C/30 min [FFRs	Cook (2020)	WHO (2020)	Elhadi et al. (2020) [low resource countries]	Lockhart et al. (2020) [use In Anaesthesia]	Silva et al. (2020)
Derraik et al. (2020)	Fisher and Shaffer (2011)	Ma et al. (2020)	O'Hearn et al. (2020b)	European Center for Disease Prevention and Control (2020)	Rubio-Romero et al. (2020).	Skrzypczak et al. (2020) 3D printed	Ilyas et al. (2020)
Srinivasan and Peh (2020)	Lowe et al. (2020) [ca 300 mJ/cm^2]	Spanish Society of Preventive Medicine, Public Health and Hygiene (2020)	Saini et al. (2020)		Mueller et al. (2020)	Ahmed et al. (2020)	European Commission (2020)
Schwartz et al. (2020)	Inagaki et al. (2020) [DUV-LEDs]		Toon (2020) [Ozone]	MacIntyre et al. (2015)	Boškoski et al. (2020)	Martín-Rodríguez et al. (2020) [pain]	Ghodrat et al. (2017)
Grossmann et al. (2020) [N95s]	3M™ (2020)			Rengasamy et al., (2010)	Radonovich et al. (2019)	Rowan and Galanakis (2020)	Prata et al. (2020)
FDA (2020c)	Rowan and Laffey (2020)	Rubio-Romero et al. (2020)		Shakya et al. (2017)	Rengasamy et al. (2010)	Suppan et al. (2020) E-learning	Singh et al. (2020)
Steinberg et al. (2020)	Card et al. (2020)	MacKenzie (2020) [Household Use]			MacIntyre et al. (2015)	Toon (2020) [Gowns]	Clark (2020)
Jatta et al. (2020)	Liao et al. (2020)	Batéjat et al. (2020)			FDA (2020)	Park (2020)	Rhee (2020)
CDC (2020) & CDC, 2020)	Steinberg et al. (2020)	Steinberg et al. (2020)			Ou et al. (2020)	Rowan and Laffey (2020) [Surgical Gowns, Starmed Hoods for ICU]	Hutti-Kaul et al. (2020)
Toon (2020) [Ozone]	Ou et al. (2020)	Derraik et al. (2020)					Wang et al. (2020)
Battelle (2016)	Derraik et al. (2020)	Ou et al. (2020)				Barceló (2020)	Liu et al. (2017)
Liao et al. (2020)	Ou et al. (2020)	Kobayashi et al. (2020) [Dry heat]					
Ou et al. (2020)	Ozog et al. (2020)	Daeschler et al. (2020)					
Perkins et al. (2020)	Heilingloh et al. (2020)	Pastorino et al. (2020)					

[a] Powered-air purifying respirators (PARPs); Filtering Facepiece Respirators (FFRs); Relative Humidity (RH).

clusters of infections. However, there has been significant progress made on important guidance documents (NSAI, 2020) that also includes Health Products Regulatory Authority (HPRA) regulatory derogation pathways. The PPE that were observed to be in short supply were surgical gowns and Starmed Hoods for use in ICU, with less pressure on supply of face mask and FFRs. Surgical gowns have similar material consistency to that of surgical wrapping used for reprocessing of endoscopes, but the chamber size of in house plasma-generated VH2O2 is too small to cater for large throughput of PPE for user needs. A limiting factor for bespoke in-house reprocessing of PPE is the ability to test viruses along with biological indicator to confirm efficacy of decontamination along with expertise and capacity to demonstrate functionality (Rowan and Laffey, 2020). There is also a pressing need to explore attitudes, perceptions and possible barriers for use of reprocessed PPE by frontline clinicians and nurses that would entail conducting a social marketing study so as to inform overall acceptance and to overcome behaviour change factors for PPE reuse.

Increased use of face masks by people in communities in Irish society is aligned with similar recommendations in other countries across the globe (Rubio-Romero et al., 2020; Holland et al., 2020; Government of Ireland, 2020). WHO (2020) also advocate that "use of face masks alone are insufficient to provide adequate level of protection, and other measures should also be adopted". WHO (2020) also advises for each country to apply a risk-based approach that considers benefits (such as reduction of potential risk of exposure), along with potential risk (such as self-contamination, false sense of security, impact of PPE shortage) when deciding to use facemasks by general population. The Centre for Disease Control and Prevention (2020) and Health Service Executive (HSE) in the Republic of Ireland (2020) recommends the use of cloth face coverings to help slow down the spread of COVID-19. Face cloths can be decontaminated and reused after putting through a washing machine and dryer where the combination of elevated temperature and use of detergent the virus inactivates SARS-Cov-2 (Zhao et al., 2020).

The WHO (2020b) estimates that approximately 89 million medical masks will be required each month to respond to COVID-19 reflecting general use of these across both community and healthcare. Given that approximately 230,000 new cases of SARS-CoV-2 have been reported daily (European Centre for Disease Prevention and Control, 2020), there has been global interest in gaining an understanding of appropriate procedures for safe PPE reuse (Table 1). It is notable that the term "N95" refers to the US National Institute or Occupational Safety and Health (NOISH) certification (Derraik et al., 2020). N95 filtering facepiece respirators (FFRs) are defined as respirators no resistant to oils, but with a particle filtration efficiency ≥95% when challenged with sodium chloride particles of a median diameter of 0.075 μm at a

flow rate of 85 L/min (Derraik et al., 2020). The equivalent Conformité Européen (CE) certifications are FFP2 and FFP3 respirators that have minimum required particle filtration efficiencies of 94% and 995 respective. Thus, we have referred to this generic group as FFRs.

Disposable PPE are regulated by Regulation (EU) 2016/425 of the European Parliament and repealing Council Directive 89/686/EEC (European Parliament and the Council of the European Union, 2016, which obliges the manufacturer to apply the aforementioned CE marking and to follow the procedure for evaluating and complying with the requirements for that marking. The full suite of European standards and certifications for manufacturer respiratory protective devices are described by Rubio-Romero et al. (2020). However, the European Commission also published specific Commission Recommendations (EU) 2020/43 of March 13, 2020 on conformity assessment and market surveillance procedures with the context of COVID-19 threat to allow for commercialization of PPE or medical devices that comply with non-European standards, even if they do not have CE marking in the event of shortage of supplies, but an adequate level of protection must be guaranteed and the corresponding authority informed (European Commission, 2020). Similarly, the United States government published authorizations to import Non-NIOSH-approved filtering facepiece (FFP) respirators from other countries (Food and Drug Administration, 2020). The situation of widespread shortages of PPE has led civic society making different kinds of improvised facemasks using a variety of materials without any guarantee of certification internationally (Rubio-Romero et al., 2020). In order to help standardize this practice, some standard organization released reference documents such as French Association for Standardization published AFNOR SPEC S-76-001 that addresses mass manufacturer of homemade masks (AFNOR, 2020). Effectiveness of disposable masks varies depending on the type and certification standards, which focuses on the leakage of all particles in the interior at 22%, 8% and 2% for FFP1, FFP2 and FFP3 respectively (Rubio-Romero et al., 2020).

4.1. Translating knowledge from use of medical face masks to informing efficacy of commercial or homemade cloth face coverings

Sickbert-Bennett et al. (2020) recently reported on the aerosol filtration efficiency for FFR alternatives that have been used during the COVID-19 pandemic. Surgical masks with ties were shown to have filtration efficiency (FFE) of 71.5%(±5.5), while procedural masks with ear loops had lower FFE at only 38.1% (±11.4%). The FFE of 3 M's N95 Respirator (Model 1830) was reported to be high at 98.5% (±0.4) (Sickbert-Bennett et al., 2020). Quality improvement studies of 29 fitted face mask alternatives, expired N95 respirator with elastic bands subjected to ethylene oxide or hydrogen peroxide vapour had unchanged fitted filtration efficiency (FFE) of more than 95%, while performance of N95 respirators in wrong size resulted in decreased FFEs between 90 and 95%. As a group, surgical and procedural masks had lower FFEs related to N95 respirators with masks secured with elastic ear loops showing lowest performance. Clinicians and HCWs have voiced concerns about discomfort arising with ear loops from wearing face masks for prolonged period. Thus, there appears merit in use of head ties, instead of ear loops, for securing face masks or face coverings to protect against infectious aerosols harbouring SARS-CoV2.

A short observational study of the types of face masks and face covering used by 1043 shoppers as they entered a large retail centre was conducted in the Irish midlands on 14th and 15th August, 2020. Findings revealed that 461 wore coverings with ear loops, 320 wore procedural masks with elastic ear loops, 140 wore KN95/N95 respirators, 38 wore face shields, 5 wore bandanas, 3 wore scarfs, and 56 shoppers did not wear face coverings. There was no evidence of anyone using surgical masks secured with ties. It was observed that 64 appeared to be wearing face masks or coverings over their mouth only, or below their chin, or were improperly fitting such that these did not cover the nose or mouth. Some shoppers removed their face masks, or raised their face shields to the top of their head, in order to have conversations, which indicated a lack of understanding of their purpose and function. Recnet evidence from Fischer et al. (2020) with FFRs suggests that face masks and face coverings should consider use of adjustable cloth ties, as this design potentially offers better filtration efficacy of the virus compared to using a face coverings that have elasticated ear loops. Creativity in the design of cloth coverings was observed including insertion of a clear panel to facilitate lip reading. Face cloths are likely to be disinfected through use of domestic washing machine for re-use where combination of moist heat above 60 °C and detergent will kill COVID-19 (Zhao et al., 2020; Rubio-Romero et al., 2020). CDC (2020b) report that it is not known if face shields provide any benefit as source control to protect others from the spray of respiratory particles. CDC does not recommend use of face shields for normal everyday activities or as a substitute for cloth face coverings. If face shields are used without a mask, they should wrap around the sides of the wearer's face and extend to below the chin.

5. Reprocessing of PPE during COVID-19 to meet critical shortages in supply chain using different technologies and approaches

Albeit limited, published studies have demonstrated efficacy of various chemical biocides at mild concentrations against several viruses (including SARS, MERS, HCoV) on different inanimate surfaces (Kampf et al., 2020; van Doremalen et al., 2020). This informed PPE re-use studies, such as in the US, where HCWs were provided with 5 FFP respirators to a factor in one usage per day where at the end of the working day, used FFP respirator must be kept in a breathable paper bag and stored by order of usage (Centre for Disease Control and Prevention, 2020). If the workers store and use FFP respirators in order of each day, which would infer that 5 days would have occurred between initial usage of each respirator (Rubio-Romero et al., 2020. The focus of this review is to describe decontamination procedures that are readily scalable for safe PPE reuse based upon best published information.

Procedures that have been reported in the literature for the reuse of PPE in healthcare focus on applying mild treatments that seeks to achieve a balance between exploiting the sensitivity of SARS-CoV-2 with that of ensuring viral bioburden reduction and functionality of PPE post processing. The majority of reported approaches have adopted use of hydrogen peroxide in vapour state (VH2O2) that are authorized by competent authorities (such as FDA), with one company reporting combining VH2O2 with ozone. The authorized use of other processes include moderate heat with steam, low-pressure UV technologies and mild liquid disinfection (CDC, 2020). Physical technologies (such as gamma irradiation) are not been pursued as they affect material functionality of treated PPE (Rowan and Laffey, 2020). The majority of studies have reported on reduction in surrogate microorganisms, but there has been limited publications addressing holistic component aspects such as complex functionality testing such as filtration efficacy of FFRs (Table 1). Several studies have used SARS-CoV-2 as test organism for viability and for reprocessing of PPE with an emphasis on cell culture determinations (Table 1). Others studies have used a range of virial surrogates at different concentrations, such as T1, T7, phi-6 and MS2 bacteriophages, Influenza A H1NI, N5NI, H7N9, MERS-CoV, SARS-CoV, or established bacterial endospore indicators such as *Bacillus atrophaeus* or *G. stearothermophilus* (CDC, 2020; Rowan and Laffey, 2020).

5.1. Reprocessing of PPE using dry and moist heat

Some studies have been reported on the use of different regimes of heating for PPE processing. Heating causes irreversible structural damage in virus proteins that prevents binding to host cells (Derraik et al., 2020); the challenge is for thermal procedures is to eliminate SARS-CoV-2 with damaging PPE. The guiding principle, similar to the concept of pasteurization for use with heat sensitive foods, is that one can achieve a similar one-log reduction in viral load by reducing exposure

time with increasing temperature. For example use 72 °C for 15 s provides similar level of lethality to that of using a holding temperature of 60 °C for 30 min. In general, heat treatment at 60 °C for ≥30 min would lead to ca 4.6 to 7 $\log_{10}$ reduction in SARS-CoV-2 (Table 1). However, doubling exposure duration at 60 °C to 60 min would be prudent given the variability in heat inactivation studies reported for SARS-CoV-1 and SARS-CoV-2 (Derraik et al., 2020). For example, Darnell et al. (2004) reported on residual infectivity after exposure of SARS-CoV-1 to heating at 65 °C for 90 min. Also, there is considerable variability in the manner by which the viruses have been tested by researchers that includes use of artificial solutions, surfaces and materials, with and without soiling, where the lack of harmonized procedures makes it challenging to appreciate significance of findings and relevance to practice, such as PPE (Table 1). Variable factors influencing the efficacy of heat inactivation procedures for SARS-CoV-1 and SARS-CoV-2 include number of viruses present (viral load), presence of organic matter (soiling), temperature, humidity and duration of treatment (Table 1).

Song et al. (2020) reported on the use of heating of face masks in an oven at 56 °C for 30 min combined with hot air from a hair dryer for 30 min to inactivate influenza virus without observing efficacy in filtering capacity. Rubio-Romero et al. (2020) noted that findings from this particular study was used by the International Medical Center of Beijing (2020) and the Spanish Ministry of Labour and Social Economy as basis for indicating that FFRs maintain their filtration efficiency after decontamination at 70 °C for 30 min, although fit and deformation testing is not reported. Price and Chu (2020) and Spanish Society of Preventive Medicine, Public Health and Hygiene (2020) recommend use of dry heat at 70 °C for 30 min in a convection oven to ensure constant and uniform temperature maintenance. However, there is a general lack of information on the effect of dry heat on filtration, fit-test or deformity over several decontamination cycles (N95DECON, 2020a; Rubio-Romero et al., 2020; Derraik et al., 2020).

The CDC (2020) stated that, based on limited research available as of April 2020, moist heat has shown promise as a potential method to decontaminate FFRs. The CDC's National Institute for Occupational Safety and Health (2020) reiterated that before using any decontamination method, it should be evaluated for its ability to retain 1) filtration performance, 2) fit characteristics achieved prior to decontamination, and 3) safety of the FFR for the wearer (e.g. by inactivating SARS-CoV-2). Moist heat, consisting of 60 °C and 80% relative humidity (RH) caused degradation in the filtration and fit performance of tested FFRs (Bergman et al., 2010; Bergman et al., 2011; Viscusi et al., 2011). Heimbuch et al. (2011) disinfected FFRs contaminated with HINI influenza using moist heat of 65 °C and 85% RH that achieved a minimum of 99.99% reduction in the test virus. CDC (2020) noted that one limitation of the most heat method is the uncertainty of disinfection efficacy for various pathogens. This is particularly relevant as there could be more than one respiratory virus or pathogen on contaminated FFRs in healthcare environment and during COVID-19 pandemic.

5.2. Reprocessing of PPE using ozone

Ozone can disrupt lipids and proteins in the cell envelope of viruses exposing vital genetic material, thus causing oxidative inactivation (Rowan, 2019). Zhang et al. (2004) had previously reported on decontamination of FFP respirators using ozone where SARS-CoV1 was inactivated using different concentrations of ozone solution disinfection with efficacy at 27.73 mg/L for 4 min exposure. Toon (2020) also described the efficacy of ozone for decontaminating PPE where the relative humidity needed to be maintained above 50%, Dennis et al. (2020) reported virucidal potential of ozone where they implemented a simple disinfection-box system for treating FFRs. The authors recommended ozone concentrations at 10 to 20 ppm combined with an exposure of at least 10 min. Dennis et al. (2020) note advantages of ozone that include rapid virucidal action that is effective for fibrous material, which included addressing crevices and shading. However, Dennis et al. (2020) also stated that ozone is a lung irritant and can be dangerous to humans, animals, and plants. There is very limited published information on ozone for broader PPE and medical device treatment due possibly to the risk associated with its volatility and lung health implications.

5.3. Reprocessing of PPE using hydrogen peroxide vapour

The majority of authorized approaches advocated by competent bodies deploy hydrogen peroxide vaporization (VH2O2) for emergency reprocessing of PPE where there is critical shortage (Table 1). Jatta et al. (2020) reported on effective filtration efficiency and fit testing of N95 respirators (3 M 8211FF and 9210FF) after 5 and 10 cycles of VH2O2 by V-PRO®maX Low Temperature Sterilization System at higher concentration of 59% VH2O2 to prolong the supply of respirators. Battelle and Duke University had validated hospital protocols for decontaminating respirators using 30 to 35%. VH2O2 (Jatta et al., 2020; Rowan and Laffey, 2020). The background and benefits of using VH2O2 as a reprocessing agent or sterilising modality for medical device application have been comprehensively reviewed by McEvoy and Rowan, 2019. However, VH2O2 compatibility with cellulose-based materials in PPE needs consideration (Zhao et al., 2020).

Grossmann et al. (2020) noted that several VH2O2 sterilization systems are currently approved for use under Emergency Use Authorization (EUA), but these technologies can be difficult to obtain due to the significant demand around the world. Grossmann et al. (2020) described the VH2O2 process (closed and sealed off room using Bioquell Z-2 disinfection cycle) for N95 respirators. These FFRs had been placed in Tyvck pouches where the process includes conditioning, gassing, dwell, and aeration of the VH2O2. Grossmann et al. (2020) demonstrated a reproducible and scalable process for decontaminating N95 respirator within a large academic hospital and healthcare system.

The CDC (2020) reviewed all relevant publications on VHO2H decontamination of FFRs in order to provide evidence of minimal effects to filtration and fit, while demonstrating 99.9999% efficiency in killing bacterial spores. VH2O2 did not reduce the filtration performance of ten N95 FFR models tested while showing a 6-log reduction in *Geobacillus stearothermophilus* spores (Viscusi et al., 2009; Bergman et al., 2010; Battelle et al., 2016; van Doremalen et al., 2020). In a report prepared by Battelle Memorial Institute, the 3 M 1860 FFR was shown to maintain filtration performance for 50 treatment cycles of V2HO2, using the Clarus® R HPV generator form Bioquell (utilizing 30% H2O2). Additionally, FFR fit was shown to be unaffected for up to 20 VH2O2 treatments cycles using NPPTL's Static Advanced Headform (Bergman et al., 2014; Battelle et al., 2016). Strap degradation occurred after 20 treatment cycles. Kenney et al. (2020) contaminated 3 M 1870 FFRs with three bacteriophages, T1, T7, and Phi 6, and decontaminated the FFRs using VHP generated from the Bioquell's BQ-50 system. The V2HO2 treatment was shown to inactivate >99.999% of all phages which was below the limit of detection. Viscusi et al. (2009) found that 9 FFR models (three particulate N95, three surgical N95 FFRs and three P100) exposed to one cycle of VH2O2 treatment using the STERRAD 100S H2O2 Gas Plasma Sterilizer (Advanced Sterilization Products, Irvine, CA) had filter aerosol penetration and filter airflow resistance levels similar to untreated models; however, Bergman et al. (2010) found that three cycles of gas plasma treatment using the STERRAD 100S H2O2 Gas Plasma Sterilizer negatively affected filtration performance. Table 1 lists the most frequently published papers on the decontamination of reuse of PPE using VH2O2.

5.4. Reprocessing of PPE using ethylene oxide (EO)

The CDC (2020) reported that ethylene oxide (EO) is not recommended as a decontamination method for FFRs as it is carcinogenic and teratogenic and may be harmful to the wearer, even at very low concentrations. NIOSH set a low exposure limit due to residual cancer

risk below the quantitative limits of detection, i.e., preferring lowest feasible exposure (CDC, 2020). The CDC reviewed several studies where EO was shown to not harm filtration performance for the 9 tested FFR models. All tests were conducted for one hour at 55 °C with EO gas concentration ranging from 725 to 833 mg/L (Viscusi et al., 2007a; Viscusi et al., 2009; Bergman et al., 2010). Also, six models that were exposed to three cycles of 736 mg/L EtO all passed the filtration performance assessment (Bergman et al., 2010).

5.5. Reprocessing of PPE using ultraviolet light (UV)

Ultraviolet (UV) irradiation causes inactivation of viruses by damaging RNA or DNA via a photo-dimerization process (Darnell et al., 2004). UV decontamination exploits different wavelength bands where UVC (200–280 nm) is superior to UVB (280–300 nm) and UVA (320–400 nm). Optimum irreversible molecular damage occurs around the 254 nm wavelength, hence the reason why this fixed wavelength has been successfully exploited by the water industry for ca. 50 decades (Rowan, 2019). Microbial pigments have evolved for peak absorbance to match 254 nm for to protection, however, viruses (including SARS-CoV-2) do not produce pigments or other defence mechanisms against UV and are not capable of independent lift. Hence, they require a host such as people for replication. Thus, the majority of PPE decontamination studies have focused on exploiting UVC, rather than UVB or UVA (Table 1) Next-generation, pulsed UV light technology exploits an ultra-short, intensive broad light spectrum (ca 200 nm to 1100), and has been previously shown to be superior to conventional low-pressure fixed wavelength UVC methods. However, PUV is an emerging disruptive technology (Rowan, 2019) that is used commercially by the food industry, such as for decontamination of packaging. Only one study, Jinadatha et al. (2015), reported on the disinfection of PPE materials prior to doffing by a pulsed xenon light source that was artificially contaminated with Ebola viral surrogate with reduction in viral load.

There is growing interest in the use of UV technologies for treating COVID-19 with varied findings (Torres et al., 2020; Rubio-Romero et al., 2020; CDC, 2020; Derraik et al., 2020). The CDC (2020) also noted that ultraviolet germicidal irradiation (UVGI) is a promising method for PPE reuse, but stated that not all UV lamps provide the same intensity, thus treatment times would have to be adjusted accordingly (Table 2). Moreover, UVGI is unlikely to inactivate all the viruses and bacteria on an FFR due to shadow effects produced by the multiple layers of the FFR's construction. The CDC (2020) noted that acceptable filtration performance was recorded for eleven FFR models exposed to various UV doses ranging from roughly 0.5–950 J/cm^2 and UVGI was shown to have minimal effect on fit. Heimbuch and Harnish (2019) tested filtration and fit of 15 FFRs and found no adverse effects to FFR performance. An approximate inactivation of 99.9% of bacteriophage MS2, a non-enveloped virus, and H1N1 influenza A/PR/8/34 on FFPs were achieved with approximately UV dose of 1 J/cm^2 (Fisher and Shaffer, 2011; Heimbuch et al., 2011). Heimbuch and Harnish (2019) also tested the performance of 1 J/cm^2 of UVGI against Influenza A (H1N1), Avian influenza A virus (H5N1), Influenza A (H7N9) A/Anhui/1/2013, Influenza A (H7N9) A/Shanghai/1/2013, MERS-CoV, and SARS-CoV and reported virus inactivation from 99.9% to greater than 99.999% (Fisher and Shaffer, 2011). Bodell et al. (2016) also reported on the use of UV technology to destroy HINI influenza viruses where ≥3 log reduction was achieved after 60 to 70 s at irradiance of 17 mW/cm^2. However, these authors reported on significant variably in efficacy depending upon the prototype and operating conditions used. Lindsley et al. (2015) reported treatment of FFP respiratory N95 with low pressure UV light at 950 J/cm^2 produced greater particle penetration (up to 1.25%) and had little effect on flow resistance. However, higher fluence levels (such as 2360 J/cm^2) reduced the strength of filtered layers and the breaking strength of straps. O'Hearn et al. (2020a) conducted systematic review of 13 papers focusing on UV-disinfection of N95 respirators where they recommended a cumulative UV-dose or fluence of 40,000 J/m^2 in future validation studies including filtration, fit and deformation testing.

Card et al. (2020) reported on the potential efficacy of FFP respirator decontamination using UVGI using biosafety cabinets that describes irradiation for 15–20 min per side with a fluence of 100 μW/cm^2. Lowe et al. (2020) reported that use of UVGI effectively inactivates a range of complex human pathogens including coronaviruses with a focus on FFP respirators (N95) disinfection. This online Nebrasca Medicine also reported on fit and functionality efficacy of UVGI-treated N95 were not affected at different levels of fluence (Lowe et al., 2020; N95DECON, 2020a). The Spanish Society of Preventative Medicine recommends decontamination of FFP respirators using UVGI with double lamps at 36 W for 148 s exposure. However, Rowan and Laffey (2020) and Rowan (2019) reported on technical challenges of using UV irradiance for disinfecting complex devices that includes variance in UV fluence and complex shading affects such as presented in filter mesh. The International Medical center of Beijing (2020) does not recommend UV disinfection for FFP respirators as the efficacy of disinfection it produces for COVID-19 is to be determined. The Centres for Disease Control and Prevention (2020) also advocates against use of UV disinfection of filtering facepiece respirators due to "shadowing effects produced by the multiple layers of the filtering respirators construction". Rubio-Romero et al. (2020) noted that the advantages of UV could be that ≥ J/cm^2 of UV-C inactivates viruses similar to SARS-CoV2 on N95s that maintain fit and filtering performance after 10–20 cycles but shadowing may affect disinfection efficacy (N95DECON, 2020b). Straps also become degraded after multiple cycles of UV (Mills et al., 2018).

Zhao et al. (2020) reported on the treatment of N95-rated masks and nonrated surgical masks, where they demonstrated that neither 254 nor 265 nm UV-C irradiation at 1 and 10 J/cm^2 had adverse effects on the masks' ability to remove aerosolized virus-sized particles. The authors noted that additional testing showed no change in polymer structure, morphology, or surface hydrophobicity for multiple layers in the masks and no change in pressure drop or tensile strength of the mask materials. Inagaki et al. (2020) recently reported (via a non-peer reviewed paper), that a deep ultraviolet light-emitting diode (DUV-LED) instrument generating around 250–300 nm wavelength (fluence 3.75 mW/cm^2) showed potential for inactivating (in vitro) a strain of SARS-CoV-2 that had been isolated from a patient who developed COVID-19 in the cruise ship Diamond Princess in Japan in February 2020. This strain was obtained from the Kanagawa Prefectural Institute of Public Health (SARS-CoV-2/Hu/DP/Kng/19–027, LC528233). Proper precautions are required to avoid UVGI exposure to skin or the eyes, as UVGI is harmful. Rowan (2019) described a reliable protocol for harmonizing the UV dose of fluence generated from different technologies in order to enable repeatability. Generally, the consensus for use of UV technologies, is that one needs to apply extended doses of UV light for PPE material decontamination to at least a UV dose of 2000 mJ/cm^2 for efficacy. However, fixed UV lights sources produce significant heat over extended treatments and it is not clear from many of the published studies that focused on UV decontamination of SARS-CoV-1 or SARS-CoV-2 how temperature was monitored and controlled (Table 2). UV technologies are only effective when treating 2D surfaces as they need to irradiate the target; thus, a virus that is trapped in crevices or hidden behind a mesh such as found in the layers of material in FFRs will not be inactivated as it will not have received treatment (CDC, 2020; Rowan, 2019).

5.6. Use of bleach for PPE reuse

Rowan and Laffey (2020) reported on the use of bleach (sodium hypochlorite at ≤4000 ppm), along with a counter water immersion phase to remove residuals, for testing disinfection performance of Starmed Hoods for ICU. While 3 M stated that Viscusi et al. (2009) measured the filtration performance of two FFR models submerged into a range of sodium hypochlorite solutions (0.525% - 5.25% sodium hypochlorite)

Table 2
Recommended information to be reported in studies on microbial/virucidal (SARS-CoV-2) inactivation by UV technologies for harmonization of PPE reuse and for scalability.

Main factors	Recommended information for reporting
Microorganism, recovery and enumeration	Genus, species and strain of microorganism *Provide appropriate culture collection reference number and/or include type strain for test microorganism(s) in studies *Include *Bacillus atrophaeus* and/or *Geobacillus stearothermophilus* endospore along with test organisms *Confirmation of identify of test microorganisms by biochemical, physiological, morphological, immunological and/or molecular means (provide name of supplier for rapid test kits) *Method of storing cultures (cryoprotectant) and frequency of sub-culturing (using fresh microbial slope every month kept at 4 °C where bacterial indicators used) Initial inoculum * Description of procedures for microbial cultivation including name of supplier company for media (to include in vitro analysis) * Growth medium composition, growth temperature, pH, incubation time, and growth phase (exponential or stationary) * Growth achieved under static or orbital cultivation (rpm) * Confirm purity by identifying 3 randomly selected isolates Recovery conditions and enumeration methods for test strains * Composition of media used for recovery to include basal media or physiological saline as diluent * Time and storage conditions between treatment and microbiological analysis * Description of procedure for enumerating viral test strains post treatments, such as use of in vitro tissue culture procedures
UV treatment medium properties and conditions	For commercial: description of power unit used for generating pulses to include equipment name of the supplier company and model For prototype: adequate description of components including treatment chamber, electrical configurations and specifications Auxiliary devices – * Temperature probe * Thermophile power detector and software for total broad-spectrum dose received by sample * Transmissivity sensor to monitor %UV transmittance Ensure microbial population density is ≤5-log orders to mitigate against influence of protective shading effects Include description of media composition, pH, aw Composition of menstruum used as diluent for treated samples Sufficient number of treatment trials and replications to provide statistical confidence of findings at 95% level; description of statistic test and version of software package (such as Minitab or SPSS) Description of method used to generate bacterial endospores (natural aged for 7 days or incorporation of manganese sulphate to expedite conversion of vegetative cells to spores on agar surfaces) Include native microflora along with artificially seeded test microorganisms due to variability in resistance profile to PL Consider occurrence of cavities in plant surface microstructures that may protect microorganisms from incident light due to shading
As part of EUA, the FDA (2020) reviews the totality of scientific evidence for PPE reprocessing including specialist testing	*testing submitted within previous applications supporting device clearance for other uses that considers different types of polymer materials, such as materials consistent with those found in compatible N95 respirators. *performance data such as sporicidal test, residual analysis, bioburden reduction validation demonstrating >3 log reduction of a non-enveloped virus challenge; testing regarding material compatibility, functionality and filtration performance of compatible N95 respirators after multiple decontamination cycles *testing regarding residuals after decontamination of compatible N95 respirators. *Typically, reprocessed PPE are discarded after 10 treatments as per respective factsheet for facilities and personnel furnished to FDA

and noted some degradation in filtration performance, but not below acceptable levels. Viscusi et al. (2009) and Bergman et al. (2010) also examined the performance of multiple FFR models submerged into 6% sodium hypochlorite and found filtration performance not to be affected. However, residual bleach odours and chlorine off-gassing was noticed and Viscusi et al. (2009) concluded that bleach decontamination of FFRs should be further evaluated using lower concentrations of sodium hypochlorite and to consider chemical methods for neutralizing residuals. Based upon published information, use of liquid bleach (sodium hypochlorite) should only be considered for simple PPE configurations, such as visors or starmed hoods, which must have a water rinsing post-process step to ensure residuals are removed in a vented environment so as to remove chlorine vapour. A comparison of different potential approaches for decontaminating PPE is presented in Table 3.

6. Enhanced production of PPE that encompasses improvisation for COVID-19 crisis

There has been a staggering increase in the production of ventilators and supply of single-use PPE to meet unprecedented demands globally (Health Products Regulatory Authority, 2020; Global News Wire, 2020). Cocking (2020) report on the innovative activities of Irish researchers in production of bespoke hoods for ICU and to support decontamination of PPE in healthcare setting. Flanagan and Ballard (2020) also reported that healthcare workers have been improvising and rationing: sometime outside the lines of CDC and FDA guidelines (Ranney et al., 2020). For example, Flanagan and Ballard (2020) have noted that that healthcare workers have worn refuse/bin bags or rain ponchos due to shortage of PPE as healthcare have distributed policies regarding reuse and rationing for frontline staff. In response to FDA not objecting to the distribution of

Table 3
Properties of different decontamination approaches considered for PPE reprocessing and reuse.[a]

	Hydrogen Peroxide Vapour (VH2O2)	Ethylene Oxide (EO)	Ultraviolet Germicidal Light	Moist Heat	Chemical Liquid Disinfectants	Gamma Irradiation
Methodology	Penetration of sterilant gas	Penetration of sterilant gas	Surface irradiation	Penetration by heat (such as 60 °C for 30 min delivers 4 log reduction)	Surface disinfection	Irradiation of product using photons from radioisotope
Efficacy of process	Process efficacy confirmed by biological indicators and/or process monitoring	Process efficacy confirmed by biological indicators and/or process monitoring	Variable, but process efficacy confirmed by biological indicators or monitoring UV dose	Process efficacy confirmed by biological indicators and/or process monitoring	Process efficacy confirmed by international standards on biocide testing	Process parameter confirmed using dosimetry
Penetration (such as use of packaging)	Limited penetration Requires gas permeable packaging and product design	Requires gas permeable packaging and product design	Not suitable for packaged PPE	Suitable for treatment of packaged PPE – but depends upon specific sensitivity of materials	Not applied or suitable for packaged PPE but could be used for surface disinfection	Good penetration complete even at high densities (>0.4 g/cc)
Material Compatibility	Good material compatibility but not with cellulose-based materials as degrades VH2O2	Very few material compatibility concerns	Broad material compatibility – longer exposures affects brittleness of PVC, straps of FFRs	Very broad compatibility	Variable depending upon biocide – but sodium hypochlorite or hydrogen peroxide (≤ 5% compatible with PPE	Compatible with most materials: plastics need to be evaluated. Avoid acetals, PTFE (Teflon), unstable polypropylene
Turnaround Time	All in one day processing	Days: conventional = 9–10 days. All-in-one processing = one day	Relatively short – typically ≤1 h but depends on UV dose	Relatively short, typically ≤1 h	Relatively short (generally ≤30 min)	Hours: time varies based on dose requirement
Process	Complex process that introduces VH2O2 under vacuum, treatment, aeration	Complex process: variables include time, temperature, humidity, and EO concentration	Simple rapid process: delivery of UV dose (J/cm^2) in enclosed chamber	Simple rapid process – duration depends on combination of temp, RH and time	Simple rapid process – but affected by bioburden, pH, temperature	Simple process – variables include time in the cell and isotope load
Mechanisms of destruction	Potent oxidizer of proteins – but mechanism still not fully understood	Alkylation of proteins, enzymes (targeting sulfhydryl groups), DNA, and RNA.	Irreversible RNA damage affecting replication / infection in host	Thermal aggregation of SARS-CoV-2 nucleo-capsid and membrane proteins	Varied depending on biocide - targets cell envelope / capsid protein via coagulation	Physically breaks down viral RNA
Limitation	Not compatible with cellulose-based materials – complex process requiring monitoring and control	Concerns over residuals left on material that are toxic (carcinogenic and teratogenic)	Operator safety due to UV exposure – shading issues with filters of FFRs– need to turn item, but not with PUV	Limited by thermal-sensitivity of materials used in PPE	Certain disinfectants, sanitizers	Adversely affects material
Suitability for PPE Reuse	Yes –	No	Yes – but limited to eye protection	Yes	Yes – limited to Eye Protection; Starmed hood	No

[a] Hydrogen peroxide in vapour (VH2O2); Filtering facepiece respirators (FFRs); ethylene oxide (EO); Relative Humidity (RH). Adapted from McEvoy and Rowan (2019).

improvised face shields as long as they create no 'undue risks' and to support attempts to foster greater availability of PPE for betterment of public health, Flanagan and Ballard (2020) reported on range of innovative activities leading to increased production of face shields including sharing open source face shield designs allowing everyone with a 3D printer to download free design. There has also been an increased surge in the production and wearing of community-made bespoke cloth face masks, where Zhao et al. (2020) advocated decontamination of these through use of domestic washing machines and dryer for their reuse. There is a pressing need for sharing of information globally for harmonization of appropriate best-approaches using open access platforms that will meet need for accelerate rate of usage so as to ensure no undue risks aligned with bringing together multi-actors, particularly competent authorities/regulators. There is a commensurate need for an understanding of the appropriateness and impact of different reprocessing modalities on materials when considering future reprocessing of PPE and medical devices (Rowan and Laffey, 2020).

7. Waste management, resource utilization and environmental impact of existing PPE usage to address COVID-19 with green opportunities for innovative change

There is an unprecedented surge in plastic-based PPE usage, arising a s consequence from the ongoing COVID-19 pandemic, which constitutes a new form of single-use-plastic (SUP) waste that will to plague our oceans posing a threat to our marine ecosystems (Euronews, 2020). Shorelines have been littered with discarded PPE, such as masks and visors, with the gullets of birds stuffed with latex gloves, along with crabs tangled in face masks. Marine conservation organization OceansAsia highlighted the growing number of single-use face masks being discovered during its plastic pollution research in the Soko Islands near Hong Kong (Clark, 2020). To provide context, Republic of Ireland is a small country with a population of ca 4.5 million, yet it's HCWs require 9 million face masks per week at a cost to the exchequer of €1billion a year (Farsaci, 2020). Nzediaegwu and Chang (2020) reported that the number of PPE used daily in Africa is estimated to reach seven hundred million, as several African states with confirmed COVID-19 cases have mandated compulsory facemask use for their citizens. For example, and estimated 171,506,138 facemasks to be used per day in Nigeria with a population of 206 million. These authors noted while developed countries have green and sustainable waste management strategies capable of addressing COVID-19, the risks are much higher in developing countries that have poor waste management.

In developing countries, solid waste are dumped in the open and in poorly managed landfills where waste pickers, without wearing proper PPE, would be exposed to COVID-19 as they scavenge for recyclable materials. Such landfills serve as 'food banks' for livestock and dogs that can

roam about (Word Bank, 2019) that increase chances of exposure to diseases. Rhee (2020) mentioned that PPE used during COVID-19 pandemic is classified as isolation medical waste under South Korea Waste Control Act and is disposed follow principles of sustainability, transparency and safety; this entailed discarding used PPE to containers, thereafter transportation by vehicle for incineration or landfill on the same day as discard. Elhadi et al. (2020) noted that developing countries are struggling to meet PPE needs for their healthcare workers in Libya where they revealed that 56.7% hospitals lacked PPE and 53% of healthcare workers reported that they did not receive proper PPE training. In addition, 70% reported that they were buying the PPE themselves as hospitals did not provide them.

7.1. PPE has added to single-use-plastic global challenges for our environment

Fossil fuel and plastic production are currently integrated where about 80% of manufactured plastic accumulates as waste in landfills and natural environments, presenting an increasing hazard (Karan et al., 2019). Dangaville et al. (2020) need for global engineering and research to exploit innovative polymer degradation and stability fields for PPE to address shortages in supply arising due to COVID-19 pandemic. There is a pressing requirement for access to large scale recycling facilities, effective waste management, and to designate individual usage to match user (Singh et al., 2020). The World Health Organization (2020) projected that supplies of PPE must increase 40% monthly to deal effectively with COVID-19 pandemic. Essential PPE includes an estimated 89 million medical masks, 76 million pairs of medical gloves and 1.6 million pairs of goggles. The increased demand for PPE is expected to be sustained beyond COVID-19 with an estimated compound annual growth of 20% in facial and surgical masks supply from 2020 to 2025 (Singh et al., 2020). It is noteworthy that China produced 240 tons of medical waste daily during peak of pandemic in Wuhan (Singh et al., 2020). Horton and Barnes (2020) reported that microplastics have now been found in the most remote places on earth, far away from human activities. In addition with climate-induced stress, microplastics may lead to enhanced multi-stress impacts, potentially affecting the health and resilience of species and ecosystems. The impact on PPE contamination on the marine environment has yet to be determined where there is significant gaps in knowledge.

Silva et al. (2020) recently reported that single use, plastic-based PPE (such as masks and nitrile gloves) is now adding to anthropogenic pollution threatening environmental sustainability where the COVID-19 precautionary measures are reversing some plastic waste measures. Singh et al. (2020) also note substantial environmental challenges for enormous quantities of used PPE used during COVID-19 pandemic globally. Silva et al. (2020) also noted that the sudden increase in plastic waste and composition (that includes PPE) due to the COVID-19 pandemic undermines the critical need to reinforce plastic reduction policies, to scale up innovation for sustainable and green plastic solutions, along to develop dynamic and responsive waste management systems immediately. This further emphasizes the importance of decoupling plastic production from fossil-fuel resources and to exploit alternative innovation means of meeting pressing need to replace single-use plastic (SUP) that encompasses a holistic community ecosystem approach including Citizen-science. The reader is directed towards the review of Silva et al. (2020) for a comprehensive review on the single-use plastics, plastic waste directives and challenges for the environment arising from COVID-19 including waste management. They noted that without improvements to current system, an estimated 12 billion Mt. of plastic litter will end up in landfills and in the natural environment by 2050, along with green-house gas (GHG) emissions from the entire plastic lifecycle contributing to 15% of the total global carbon budget (Zheng and Suh, 2019). Indiscriminate use and inappropriate disposal or mismanagement SUPs that have low biodegradation have led to accumulation of plastic debris in terrestrial and aquatic ecosystems globally (Singh et al., 2020; Silva et al., 2020). This will affect natural biota, agriculture, fisheries along with threatening human and animal health (Jambeck et al., 2015).

Despite recent progress made in plastic sustainability and waste management, Silva et al. (2020) have noted widespread drawbacks in the use and management of plastics in the fight against COVID-19 pandemic that area associated with government imposed partial and total lockdown of cities/regions/municipalities that has promoted greater use of SUPs, including PPE, by the general public and healthcare workers (Tobías, 2020). There has also been a shift towards mandatory use of PPE by the general public, along with frontline healthcare workers where Silva et al. (2020) noted that over 50 countries are mandated to wear masks in public places. There is also a commensurate need for increased production of PPE globally. World Health Organisation (2020) had expressed concerns about use of masks by general public due to lack of correct handling, and disposal, and the shortage of this material in healthcare materials. Silva et al. (2020) noted that surgical masks should not be worn longer than a few hours (such as 3 h) and should be appropriately discarded to avoid cross-contamination (i.e., in a sealed plastic bag). However, incorrect disposal of PPE is widespread and has been found in several public places and natural environments (Prata et al., 2020; NGO Oceans Asia, 2020). Prata et al. (2020) observed that masks are likely to degraded into smaller microplastic pieces as are made from nonwoven materials (e.g., spunbond and meltdown spunbond) often incorporating polypropylene and polyethylene. These authors also noted that significant enhancement in the usage of PPE and other SUPs is likely to result in an overload increase in waste generation that would disrupt viable options for effective waste management. Many countries have classified all such hospital and household waste potentially contaminated with SARS-CoV2 as infectious that should be incinerated under high temperature (ensuring sterilization), followed by landfilling of residual ash (European Commission, 2020; Silva et al., 2020; Ilyas et al., 2020). Ilyas et al. (2020) reviewed, and reported on the merit, of developing different disinfection technologies for handling COVID-19-generated waste from separate collection to using various physical and chemical steps with view to reducing health and environmental risks.

There is also a significant void in communication channels to general public about appropriate disposal of used face-masks and gloves during COVID-19 that may require user behavioural change, such as exploiting health belief model through social marketing approaches (Suanda et al., 2013; Suanda et al., 2017). However, Silva et al. (2020) noted that not all countries are capable of managing such waste appropriately and are been forced to use direct landfills or open burning as alternative strategies. There is also commensurate concerns about the short, and more longer term, impact of burning considerable amount of plastic that may increase environmental footprint due to release of GHGs and undesirable hazardous compounds (Prata et al., 2020). As some items of PPE are lightweight, there is potential for them to be blown by wind to pollute natural environments including threatening terrestrial and aquatic biota, such as by entanglement. Silva et al. (2020) noted that up 40,000 kg of masks may find their way inappropriately into the natural environment arising from WWF (2020) reporting of inappropriate disposal of only 1% for over 10 million masks introduced to the environment monthly. In order to allay environmental problems arising from COVID-19 due to high demand on SUPs and PPE that produces increased medical waste, Silva et al. (2020) advocated (1) redesigning plastics and decoupling them from fuel-based resources, (2) reduce plastic waste by reducing SUPs and PPE, and (3) optimize plastic waste management. Horton and Barnes (2020) noted that PPE (non-COVID-19 related) have already polluted Antarctica, which are made from synthetic polymer-based fibres, often treated with water repellents such as per/polyfluorinated compounds and flame retardants such as polybrominated diphenyl ethers where their occurrence as contaminations for their toxicity.

7.2. Bio-based plastics as potential alternative sustainable materials for PPE for COVID-19 and future viral pandemics

In the short term, it is important to maintain the PPE supply chain in order to the ensure health and safety of our citizens and our frontline HCWs. However, we now need to look at contingency planning in order to future proof against the potentiale environmental impact of increased single-use plastic (SUP) PPE waste using sustainable solutions. Opportunities will arise to address this challenge through seamlessly connecting research and entrepreneurial ecosystems that will generate a new pipe-line of potentially usable bioplastic products. This could be accelerated through multi-actor innovation hubs linked to healthcare, industry and academia (Rowan and Galanakis, 2020). Silva et al. (2020) noted that the replacement of plastic value chain from fuel-based raw materials and energy has been priorities, which features in many international agreements addressing a green and circular economy. Silva et al. (2020) also noted that bio-based plastics supports are emerging, but at an early stage capturing a market share of ca. 2% due mostly to low-cost of fossil-based plastics, the intense requirement for land use and related financial investment, and undeveloped recycling and/or disposal routes.

Hutti-Kaul et al. (2020) described screening for microbial strains for enhanced hydrolytic and biodegradation abilities for direct conversion of biomass (such as microalgae), extraction of value-added products, and synthesis (polymerisation) process. However, such potentially high-performance bio-based polymers, similar to physical properties of fossil fuel-counterparts (such as low degradability, high durability) (Silva et al., 2020), would need to be characterized and tested for suitability to match design specifications of future PPE including tolerance to thermal processing and potential re-use. OEMs of PPE, academia and regulators should play as strong role in informing the efficacy of bio-based reusable polymers for next-generation products that considers suitability from design, safety and life cycle assessment perspectives. End-of-life strategies need to be consider for waste management and recycling of PPE during COVID-19 used by general public without compromising on safety, where landfill and waste-to-energy should be a last resort option (Silva et al., 2020).

The rapid accumulation of plastic waste is driving international demand for renewable plastics with superior qualities (e.g., full biodegradability to CO_2 without harmful by-products), as part of an expanding circular Bioeconomy (Karan et al., 2019). There has been increasing interest in the identification of alternatives to petroleum-based plastics for various industrial applications where desirable bio-based material properties would include ease of biodegradation and renewability (Emadian et al., 2016; Thakuv et al., 2018).

Bioplastics partly or wholly made from biological materials, and not crude oil, represent an effective way of keeping the huge advantages of conventional plastics but mitigating their disadvantages (Carbon Commentary, 2020). A bioplastic is a plastic that is made partly or wholly from polymers derived from biological sources such as sugar cane, potato starch or the cellulose from trees, straw and cotton (Thakuv et al., 2018). Some bioplastics degrade in the open air, others are made so that they compost in an industrial composting plant, aided by fungi, bacteria and enzymes. Others mimic the robustness and durability of conventional plastics such as polyethylene or PET. Bioplastics can generally be directly substituted for their oil-based equivalent. Bioplastics can generally be made to be chemically identical to the standard industrial plastics (Carbon Commentary, 2020). Bioplastics can be distinguished as two different types in terms of usage (1) items that has the potential to eventually litter such as food where alternative bioplastic could be produced to degrade either in industrial composting units or in the open air or in water, and (2) permanent bioplastics, such as polythene manufactured from sugar cane, can provide a near-perfect substitute for oil-based equivalents in products where durability and robustness is vital. Plastics made from biological materials generally need far smaller amounts of energy to manufacture but are equally recyclable. They use fewer pollutants during the manufacturing process. Per tonne of finished products, the global warming impact of the manufacture of bioplastics is less, and often very substantially less, than conventional plastics (Carbon Commentary, 2020; Emadian et al., 2016). Other emerging sources of bioplastics include seaweed (Thiruchelvi et al. (2020) and microalgae (Rizman et al., 2018). Thiruchelvi et al. (2020) recently reported that seaweed-based bioplastics were found to durable, less brittle and more resistant to microwave radiation. These authors also reviewed the role of seaweed in bioplastic production. Higher plants, microalgae, and cyanobacteria can drive solar-driven processes for the production of feedstocks that can be used to produce a wide variety of biodegradable plastics, as well as bioplastic-based infrastructure that can act as a long-term carbon sink. Karan et al. (2019) noted that well-crafted legislated standards on plastic biodegradability and environmental and animal/human health impacts could fast-track and optimize industry transition. The diversity of bio-based feedstocks opens up the opportunity to produce an expanding range of renewable plastics. However, biodegradable plastics should ideally fully degrade to CO_2 and water without harmful byproducts. Durable bioplastics can act as carbon sinks if well integrated into large-scale long-term infrastructure.

Biorefinery and GMO strategies can support viable business development and the emerging circular Bioeconomy (Karan et al., 2019). Emadian et al. (2016) also reviewed sources of bioplastics for biodegradation in different environment and noted that Actinomyces, bacteria and fungi are key actors responsible for this important activity. Also, the type of bioplastic and environment in which bioplastics are located influences their biodegradation potential. Aeschelmann and Carus (2020) also reviewed bio-based building blocks and biopolymer for capabilities and applications highlighting advances over plastics. However, there is a gap in current information that could be met potentially by conducting comprehensive life cycle assessment (LCA) evaluation of new biopolymers to meet sustainability needs that would include ecotoxicology and ameliorating carbon footprint that follows pathway along biodegradation to CO_2 (Ruiz-Salmón et al., 2020).

There presents an opportunity to exploit the 9 stages of technology readiness developed by NASA (Straub, 2015) to evaluate the sustainability and maturity of emerging innovations for COVID-19 that also addresses environmental friendliness as well as functionality. This strategy is particularly relevant as it address potentially sustainable products from conceptualisation to commercial deployment at higher technology readiness levels: this is particularly relevant given that industry would be familiar with this concept and would allow ease of transitioning for environmental impact. This evaluation of new bioplastics could include life cycle (Ruiz-Salmón et al., 2020) and ecotoxicological (Garvey et al., 2015) assessments of different trophic levels reflecting impact on biodiversity that connects academia with industry partners and policy makers. O'Neill et al. (2020) described development of freshwater aquaculture on cutaway peatlands using organic principles where vast quantities of microalgae, used as natural means of water quality waste remediation, could be used as test system for advancing bioplastic-based PPE innovation and recycling for circular economy developments. Future green innovative research could be extended to new biopolymer-based wrapping and packaging (including for adjacent food industry) to investigate non-thermal treatments that encompass both complex viruses and parasites (Gerard et al., 2019; Franssen et al., 2019). A limiting factor in the production of alternative biomaterials for alternative to single-use PPE relates to thermal stability of materials for fabrication and potential for deformation due to thermal processes. Skrzypczak et al. (2020) recently reported on a new 3D printing approach for meeting such a need where they described an affordable, self-replicating, rapid prototyper that would also make this approach more accessible to home-based 3D printing activities. Chen et al. (2019) also demonstrated potential for exploiting different forms of polymer processing (such as 3D

printing and injection moulding) after novel vapour hydrogen peroxide and electron beam treatments that could be advance next-generation PPE and medical device technologies.

7.3. Medical waste management – a global challenge for PPE

In response to meeting threats of COVID-19, there is substantially increased volumes of medical waste produced that also contains PPE, which presents unprecedented challenges for meeting effective waste management strategies globally with significant potential for overload of systems (Singh et al., 2020; Wang et al., 2020; Silva et al., 2020). Singh et al. (2020) have noted that the unprecedented demand has also impacted other industries reliant upon PPE including manufacturing, construction, oil and gas energy, transportation, firefighting and food production. Singh et al. (2020) also noted that this pandemic has substantially impacted upon how solid-waste management activities are performed as prior to COVID-19 resource recycling and waste management were not regarded as essential services and were placed in lockdown. However, the strategically important disease mitigation role of waste management has been recognised given the need to properly dispose and handle SARS-CoV2 contaminated waste to avoid transmission (Reuters, 2020; Price et al., 2020). The United Nation's Basel Convention on the Trans-boundary Movement of Hazardous Wastes and their Disposal has urged countries to treat waste management amid COVID-19 as urgent and essential public service. These authors noted that PPE includes plastics as major constitutes representing ca 25% by weight, which if not recycled or their disposal may contribute substantially to hazardous environmental pollutants, such as dioxins or toxic metals. Polypropylene is a common constituent of PPEs, such as found in N95 masks, Tyvek protective suits, gloves, and medical face shields. Singh et al. (2020) also noted that the potential for recovery of polymers from mixed healthcare waste including PPE is challenging. This would be further influenced by the low-level of recycling worldwide and lack of government policies. Singh et al. (2020) noted that single-use PPE is not a sustainable practice, however development of safe and sustainable PPE management beyond the healthcare settings under pandemic emergency conditions is nebulous as there are no clear understanding of best practices, monitoring, and enforcement of policy and regulations.

Wang et al., 2020 reviewed efficacy of disinfection technologies and approaches for hospital waste and wastewater that considered use of chlorine and/or incineration for such infectious but negated to mention PPE as particular waste for treatments. These authors observed that hospitals in China are potential sources of environmental pollutants resulting from diagnostic, laboratory and research activities and therefore ensuring effective treatment of waste is important, particularly under the COVID-19 pandemic context. Wang et al. (2020) reviewed different types of technologies for the treatment of hospital wastes and waste water disinfection in China where incineration, chemical and physical disinfection are commonly used for hospital waste disinfection. Typical composition of healthcare waste is approximately 85% general non-infectious, 10% infectious/hazardous, and 5% chemical/radioactive. Factors considered for treating infectious healthcare waste included amount of waste, costs, maintenance of technologies and types of waste. Incineration technologies can be adapted for amount of waste, but if scale of hospital waste is small and investment is limited, then chemical disinfection and high temperature steam disinfection that are easier to maintain are preferred in China. Incineration is widely deployed as is deemed to be safe, simple and effective (Ghodrat et al., 2017) where extreme high temperatures completely kill microorganisms along with converting organic matter into inorganic dust. However, hospitals vary in type of incineration approach depending upon waste preparation and flue gas purification that includes pyrolysis vaporization incinerator where organic components of waste are converted to flammable gases to avoid dust at temperatures above 850 °C that reduces particle emission to air.

Wang et al. (2020) report that these high temperatures is conducive to complete destruction of toxic and hazardous components, thereby reducing production of toxic pollutants such as dioxins due to low temperature combustion (Zhu et al., 2008). In addition, rotary kiln incinerators are deployed that generate temperature as high as 1200 °C or more, where there are advantages that include wide range of applications, good adaptability, handling a different variety of wastes, good gas and solid contact, and uniform reaction, but are not small or medium scale usage with disposal capacity below 8 t/d that investment costs are high and dust content exhaust is higher than pyrolysis incinerator. Plasma incineration technology is novel waste disposal technology that transfers energy through plasma where waste can be rapidly decomposed into small molecules where most of the gases produced are flammable that are sent to secondary combustion chamber and purification, thereafter discharged to atmosphere. Plasma incinerators have higher energy efficiency compared to other incinerators (Messerele et al., 2018).

Wang et al. (2020) described chemical disinfection technologies for treatment of hospital waste that is typically used in combination with mechanical and crushing treatments in China. Generally, crushed hospital waste are mixed with chemical disinfections such as sodium hypochlorite, calcium hypocholorite, chlorine dioxide for fixed contact times during which organic wastes are decomposed and microbial threats inactivated. Chemical disinfection have desirable attributes including low effective concentrations, rapid action, stable performance and broad sterilization efficacy for different types of microorganisms. These chemical disinfectants are generally used as are non-corrosive, safe, easily soluble in water but not easily affected by chemical or physical factors with low toxicity and reported to have no residual hazard post disinfection (Chen and Yang, 2016). Wang et al. (2020) suggest that chemical disinfection technology could be considered when amount of waste is small.

Wang et al. (2020) also reported on use of microwave disinfection as a means of energy saving, low action temperature, slow heat loss, light damage and low environmental pollutions with no residues or toxic wastes after disinfection, but requires strict control by special microwave devices. Wang et al. (2020) stated that microwave technology only used at present for treatment of biohazardous wastes, but the technology is been promoted as effective supplementation technology for incineration to enable diversification of hospital wastes in China. Wang et al. (2020) also reported that microwave technology can achieve logarithmic value for killing complex pathogens such as parasites and viruses at >6 log along with killing of *Bacillus subtilis* endospores at >4 spores. Wang et al. (2020) also reported on high temperature steam disinfection (saturated water vapour with temperatures greater than 100C) to kill microorganisms. In China, a log kill of thermophilic lipobacillus endospores at >5 logs is required. However, this approach has a low volume reduction rate and easily generates toxic volatile organic compounds during disinfection. From perspective of investment and operation costs, as well as economic and social benefit, high temperature incineration is still most popular approach to hospital waste disinfection in China. Thus, there are pressing needs to define effective decontamination strategies for medical waste through appropriate management strategies will also contribute to global collective effort in reducing SARS-COVID-19 transmission along with future safeguarding our environment.

8. Conclusions

There is extraordinary pressure to meet shortages in single-use PPE supply for our frontline clinicians and healthcare workers. PPE treatment is challenging as the constituent material, including single-use plastics (SUPs), are sensitive to harsh decontamination processes. There has been an unprecedented surge in the production of commercial and homemade cloth and fabric face coverings to offset this challenge and to help with preventing person-to-person transmission in

the community setting. Many countries across the globe are extending, decontaminating and reusing PPE where there is critical shortage for frontline healthcare workers (HCWs), but under emergency use only. This unprecedented need will continue given the absence of a vaccine and occurrence of successive waves of SARS-CoV-2 globally; and, the likely high demand for PPE by the medical and nursing profession beyond COVID-19. Table 4 highlights succinctly the main developments surrounding decontamination and reuse of PPE that includes pressure on waste management and recycling. Table 1 also provides a list of key papers that have been published on this topic.

Hydrogen peroxide in vapour (VH2O2), used alone or combined with ozone, has been used for high-throughput decontamination and reuse of complex PPE such as important filtering facepiece respirators (FFRs), such as the popular N95 respirator. VH2O2 has been certified for PPE decontamination under emergency use authorization (EUA) by the FDA in the United States in order to address shortages in supplies arising for ongoing COVID-19 pandemic. Many countries are permitting decontamination and reuse of PPE leaving decision to heath service managers. Ultraviolet (UV) light procedures, particularly using UVC wavelength, have also been reported as potentially appropriate decontamination technology for PPE, but this technology is unlikely to inactivate SARS-CoV-2 if this virus penetrates lower layers of material of FFRs where they would be hidden from the UV. Also, there is significant variability in the reporting of important UV dose (mJ/cm^2) by different researchers using various UV technologies that prevents the harmonization of processes; but, this review provides guidance on standardized reporting. Moist heating at 60 °C to 70 °C combined with high humidity for 60 min is also a promising decontaminating procedure for PPE as it would also enable scalability and high-throughput processing. Use of microwave generated steam would not provide scale for PPE decontamination. Physical irradiation technologies, such as gamma and electron beam, along with ethylene oxide, are not suitable for PPE reprocessing.

Surgical face masks with head ties have been reported to offer superior filtration effectiveness over commonly used procedural face masks that have ear loops. This new information may inform the the effectiveness of commercial and homemade cloth face coverings that may be improved by using ties instead of ear loops that would also help prevent slippage of the face coverings below the nose and mouth. The

Table 4
New developments in PPE decontamination, reuse and waste management.

Trending information on PPE and face coverings reuse, and waste management	Reference
PPE is designed for single-use for medical/nursing staff, but supply chain has been insufficient to meet global needs with many countries adopting reuse practices post deployment of technologies to meet emergency COVID-19 use	Rowan and Laffey (2020); Derraik et al. (2020)
There are limited technologies suitable for PPE reuse that reflects matched efficacy for reprocessing	Rubio-Romero et al. (2020)
Differences in priority usage and decontamination technologies between higher risk medical environment (PPE) and lower risk community settings (face coverings) that have informed selection of technologies and approaches used	Derraik et al. (2020)
Evidence that PPE can be effectively reprocessed using technologies not readily available to public such as VH2O2, O3, low pressure UVC such as UVGI (2000 mJ/cm^2) where variance in determining efficacy of UV dose between UV modalities influencing harmonious acceptance). Generally, is greater disinfection using UVA over UVB and UVA.	Derraik et al. (2020); Rowan, 2019; Rubio-Romero et al. (2020)
High throughput VH2O2 can effectively disinfect, for example,2500 N95 respirators per 12 h shift at 3000–750 ppm hydrogen peroxide	Rubio-Romero et al. (2020) Mackenzie (2020); Perkins et al. (2020)
Recommendation for wearing of face masks and coverings to prevent spread of COVID-19	CDC (2020); Ministry of Health of Spain (2020);
Choice of technologies for reprocessing of PPE healthcare depends on the type and complexity of PPE (functionality, fit test, deformation, filtration efficacy) that are typically single use and thermally-sensitive with increasing challenges in the order face shields, gowns, FFRs (including disposable N95 respirators,)	Derraik et al. (2020); Rubio-Romero et al. (2020)
Evidence of extended use of N95 respirators such as 4 h (France, New Zealand and Sweden) to 40 h (Mexico)	Kobayashi et al. (2020)
Physical irradiation technologies (gamma) and ethylene oxide (EO) are not appropriate for PPE reuse due to non-compatability with material composition or concerns over lingering residual toxic end-points produced during EO	Rowan and Laffey (2020)
Barriers to reuse of PPE by healthcare workers include lack of knowledge to inform acceptance and discomfort over prolonged usage with potential for social marketing studies to inform trust and associated decision making	Rimmer (2020); Mitchell et al. (2012)
Evaluation of fitted filtration efficiency (FFE) showed that surgical masks with ties (71.5 ± 5.5%) and procedural mask with ear loops (38.1 ± 11.4%) exhibit lower FFE post VH2O2 treatment is lower than N95 respirators (98.5 ± 0.4%). This suggests potential benefits of using head ties instead of ear loops for homemade face coverings and would help prevent slippage below nose during wearing.	Sickbert-Bennett et al., 2020
Disinfection performance studies for evaluating PPE reuse over single or several cycles use surrogate viruses or bacterial endospore indicators (bioburden typically at or below 10^6), where most SARS-COV-2 strain(*s*)are studied using in vitro tissue culture infection models. Most researcher won't have access to level 3 containment facilities	Rowan and Laffey (2020); Derraik et al. (2020)
Evaluation of facemask and variety of commonly available non-certified face coverings for filtering expelled droplets during speech, sneezing and coughing revealed that variability from below 0.1% (fitted N95 mask) to 110% (fleece mask). Sequence of decreasing efficacy N95 respiratory, combining cotton-polypropylene-cotton mask; combining layer cotton in pleated style mask; combining 2 layer cotton with pleated style mask; use of single layer cotton masks; knitted masks; double layer bandana; and fleece.	Fischer et al., 2020
Improvised face masks and face coverings should be used as a last solution and for low risk situation as increased duration of wearing may increase risks of virus infiltration due to humidity, liquid diffusion and virus retention	European Centre for Disease Prevention and Control (2020)
Use of common washing machine (ca 60 °C for 30 min) combined with use of spin dryer appear effective for face cloth decontamination and reuse	Zhao et al. (2020); Rubio-Romero et al. (2020); HSE (2020)
SARS-COV2 is sensitive to commonly-used disinfectants on surface. However, lower environmental temperatures promote longer survival on surfaces, which may influence efficacy of mask wearing such as over winter flu season	Derraik et al. (2020)
Face shields are inferior to use of face masks where the latter is particularly relevant for combined use in healthcare settings to prevent infection through the eyes.	Rowan and Laffey (2020)
An increasing trend towards development of smart coatings on materials for inactivation of SARS-CoV-2 and against other future potential pandemic viruses, along with provision for incorporation in PPE, mobile phones and so forth	Behzadinasab et al., 2020.
Over 50 countries are now recommending facemasks by public that presents a new form single-use plastic waste	Silva et al., 2020
Influence of soiling on critical PPE – up to 14 days survival and retention of SARS-CoV-2 on surgical gowns.	Kasloff et al., 2020.
There are opportunities for innovation in new bioplastic-based PPE and waste management as there is likely to be a high demand for PPE post COVID-19	Ilyas et al., 2020
There is an increase trend towards modelling recovery scenarios to investigate the potential impact of lockdown duration that is implemented to protect frontline HCWs against COVID-19 that may include provision for PPE costings against the cost associated with medical staff absenteeism or illness due to inadequate PPE.	Guan et al. (2020); Thomas et al. (2020); Ivanov (2020); Mukerji et al. (2017)
Use of artificial intelligence and deep learning could help identify high-risk patients and suggest appropriate types and use of PPE	Boškoski et al. (2020)

incorporation of a nose bridge and increase number of layers in face cloth design, used by the community, would also improve performance against SARS-CoV-2.

Best published information would also suggest that SARS-CoV-2 will tolerated cold weather, such as 4 °C (refrigeration), better and survival beyond 14 days on materials, which has implications for environmental wearing of masks and face cloths as we enter the winder flu season. Use of a washing machine and spin dryer (60 °C for 60 min) with detergent is likely to decontaminate SARS-CoV-2 on contaminated face cloths where the risk of contamination by this virus is low. Wearing of face coverings by the general public to prevent the person-to-person spread of SARS-CoV-2 is important given increasing evidence that asymptomatic community transmission is contributing to many new cases in countries across the globe. There is a greater need to develop trust and confidence in reuse of PPE by HCWs that can be addressed through engagement in social marketing and knowledge sharing. There is a pressing need to consider new waste management strategies for the huge surge in single-use-plastic PPE that is contaminating our environment. This will create opportunities for using alternative bioplastics that are more environmentally friendly. There are also emerging opportunities to address real-time data analytics through digitization in order to obtain a better holistic understanding of critical shortage of critical supply chain for PPE during this COVID-19 and for future pandemics.

CRediT authorship contribution statement

NR and JGL conceptualised the manuscript. NR drafted the manuscript. Both authors read, edited, and approved the final manuscript.

Funding

The author received no financial support for the research, authorship, and/or publication of this article.

Declaration of competing interest

The authors declared no potential conflicts of interest with respect to the research, authorship, and/or publication of this article.

References

3M Science of Life. Disinfection of filtering facepiece respirators, announcement, 2020. https://multimedia.3m.com/mws/media/1816576O/disinfection-of-disposable-respirators-technical-bulletin.pdf (accessed 4th July, 2020).

Aeschelmann, F., Carus, M., 2020. Bio-based building blocks and polymers in the world: capabilities, production, and applications – status quo and trends towards 2020. Ind. Biotechnol. 11 (3). https://doi.org/10.1089/ind.2018.28999.fae.

AFNOR, 2020. AFNOR SPEC S76-001 Barrier masks. Guide to minimum requirements, test methods, preparation and use for mass manufactured and homemade masks. Association française de Normalisation AFNOR Available on 9th of July 2020 at. https://iv.revistalocal.es/wp-content/uploads/AFNORSpec-S76-001- MascarillasDeProteccion.pdf.

African Centre for Disease Control and Prevention (2020). https://africacdc.org/covid-19/ (accessed 22nd July, 2020).

Ahmed, O., Brockmeier, D., Lee, K., Chapman, W.C., Doyle, M.B., 2020. Organ donation during the Covid-19 pandemic. Am. J. Transplant. https://doi.org/10.1111/ajt.16199.

Auerswald, H., Yann, S., Dui, S., In, S., Dussart, P., Martin, N.J., Karlsson, E.A., Garcia-Rivera, J.A., 2020. Assessment of Inactivation Procedures for SARS-CoV-2. bioRxiv. https://doi.org/10.1101/2020.05.28.120444.

Barceló, D., 2020. An environmental and health perspective for COVID-19outbreak: meteorology and air quality influence, sewage epidemiology indicator, hospitals disinfection, drug therapies and recommendations. Journal of Environmental Chemical Engineering 8. https://doi.org/10.1016/j.jece.2020.104006.

Batéjat, C., Grassin, Q., Manuguerra, J.-C., Leclercq, I., 2020. Heat Inactivation of the Severe Acute Respiratory Syndrome Coronavirus 2. bioRxiv. https://doi.org/10.1101/2020.05.01.067769.

Battelle, 2016. Final report for the bioquell hydrogen peroxide vapor (HPV) decontamination for reuse of N95 respirators. 2016. Available from. https://www.fda.gov/emergency-preparedness-and-response/mcm-regulatory-science/investigating-decontamination-and-reuse-respirators-public-health-emergencies.

Behzadinasab, S., Chin, A., Hosseini, M., Poon, L.L.M., Ducker, W.A.A., 2020. A surface coating that rapidly inactivates SARS-CoV-2. ACS Appl. Mater. Interfaces 12, 34723–34727.

Bentley, K., Dove, B.K., Parks, S.R., Walker, J.T., Bennett, A.M., 2016. Hydrogen peroxide vapour decontamination of surfaces artificially contaminated with Norovirus surrogate feline Calcivurus. J. Hospital Infection 80 (2\), 116–121.

Bergman, M., et al., (2010). Evaluation of multiple (3-cycle) decontamination processing for filtering facepiece respirators. Journal of Engineered Fibers and Fabrics, 2010. 5 (4): p. 33–41.

Bergman, M., et al., 2011. Impact of three cycles of decontamination treatments on filtering facepiece respirator fit. Journal of the International Society for Respiratory Protection 28 (1), 48–59.

Bergman, M.S., et al., 2014. Development of an advanced respirator fit-test headform. J. Occup. Environ. Hyg. 11 (2), 117–125.

Biryukov, J., Boydston, J.A., Dunning, R.A., Yeager, J.J., Wood, S., Reese, A.L., Ferris, A., Miller, D., Weaver, W et al. (2020). Increasing temperature and relative humidity accelerates inactivation of SARS-CoV-2 on surfaces. MSpere, 5, e00441-20. DOI: https://doi.org/10.1128/msphere.00441-20.

Bodell, K., Buckakldian, A.H., Perlmin, S., 2016. Efficacy of an automated multiple whole room ultraviolet C disinfection system against coronavirus MHV and MERS-CoV. Infection Control Hospital Epidemiology 37, 598–599.

Boškoski, I., Gallo, C., Wallace, M. B., Costamagna, G. (2020). COVID-19 pandemic and personal protective equipment shortage: protective efficacy comparing masks and scientific methods for respirator reuse. Gastrointest. Endosc.. https?//doi.org/10.1016/j.gie.2020.04.0048.

Carbon Commentary (2020). Bioplastics – an important component for global sustainability. https://www.carboncommentary.com/blog/2011/09/02/bioplastics-an-important-component-of-global-sustainability (accessed 8th July, 2020).

Card, K.J., Crozier, D., Dhawan, A., Dinh, M., Dolson, E., Farrokhian, N., Gopalakrishnan, V., Ho, E., King, E.S., Krishnan, N., Kuzmin, G., Maltas, J., Pelesko, J., Scarborough, J.A., Scott, J.G., Sedor, G., Weaver, D.T., 2020. UV sterilization of personal protective equipment with idle laboratory biosafety cabinets during the Covid-19 pandemic. MedRxiv https://doi.org/10.1101/2020.03.25.20043489.

Carswell, S. (2020). https://www.irishtimes.com/news/health/coronavirus-ireland-has-no-significant-herd-immunity-study-shows-1.4308216 (accessed 20th July, 2020).

Centers for Disease Control and Prevention (2020). Coronavirus disease – decontamination and reuse https://www.cdc.gov/coronavirus/2019-ncov/hcp/ppe-strategy/decontamination-reuse-respirators.html (accessed 10th July, 2020).

Centres for Disease Control and Prevention (2020). Coronavirus disease (COVID-19): guidance for K-12 school administrators on the use of cloth face coverings in schools. https://www.cdc.gov/coronavirus/2019-ncov/community/schools-childcare/cloth-face-cover.html (Accessed 25th August, 2020).

Chan, K.H., Sridhar, S., Zhang, R.R., Chu, H., Fung, A.Y.F., Chan, G., Chan, J.F.W., To, K.K.W., Hung, I.F.N., Cheng, V.C.C., Yeun, K.Y., 2020. Factors affecting stability and infectivity of SARS-CoV-2. J. Hosp. Infect. 106, 226–231. https://doi.org/10.1016/j.jhin.2020.07.009.

Chen, M., Yang, H., 2016. Current status of medical wastes disinfection and disposal technologies. Chen. J. Disinfect. 33, 171–174.

Chen, Y., Neff, M., McEvoy, B., Cao, Z., Pezzoli, R., Murphy, A., Gately, N., Hopkins, M., Rowan, N.J., Devine, D.M., 2019. 3D printed polymers are less stable than injected moulded counterparts when exposed to terminal sterilization processing using novel vaporized hydrogen peroxide and electron beam processes. Polymer 183. https://doi.org/10.1016/j.polymer.2019.121870.

Chin, A.W.H., Chu, J.T.S., Perera, M.R.A., Hui, K.P.Y., Yen, H.-L., Chan, M.C.W., Peris, M., Poon, L.L.M., 2020. Stability of SARS-Cov-2 in different environmental conditions. Lancet Microbe 1, e10.

Clark, N. (2020). Face masks, gloves and a new breed of plastic pollution. https://www.aljazeera.com/indepth/features/face-masks-gloves-breed-plastic-pollution-200701154052002.html (accessed 8th July, 2020).

Cocking, S. (2020). AIT and NUIG explore PPE decontamination amid global shortage for COVID19. https://irishtechnews.ie/ait-and-nui-galway-ppe-decontamination-covid-19/ (accessed 8th July, 2020).

Cook, M., 2020. Personal protective equipment during the coronavirus disease (COVID) 2019 pandemic – a narrative review. Anaesthesia 75, 920–927.

Daeschler, S.C., Manson, N., Joachim, K., Chin, A.W.H., Chan, K., Chen, P.Z., Tajdaran, K., Minroeini, K., Zhang, J.J., Maynes, J.T., et al., 2020. Effect of moist heat reprocessing on N95 respirators on SARS-CoV-2 inactivation and respirator function. CMAJ https://doi.org/10.1503/cmaj.201203.

Dangaville, T., Spann, K., Celina, M., 2020. Opinion to address the personal and protective equipment shortage in global community during COVID-10 outbreak. Polym. Degrad. Stab. 176. https://doi.org/10.1016/j.polymerdegradstab. 2020.109162.

Darnell, M.E., Subbarao, K., Feinstone, S.M., Taylor, D.R., 2004. Inactivation of the coronavirus that induces severe acute respiratory syndrome, SARS-CoV. Journal of Virology Methods 121, 85–91.

Dennis, B., Cashion, A., Emanuel, S., Hubbard, D., 2020. Ozone Gas: Scientific Justification and Practical Guidelines for Improvised Disinfection using Consumer-Grade Ozone Generators and Plastic Storage Boxes. Journal of Science and Medicine 1 (2). https://doi.org/10.37714/JOSAM.V211.35.

Derraik, J.G.B., Anderson, W.A., Connelly, E.A., Anderson, Y.C., 2020. Rapid Review of SARS-CoV-1 and SARS-CoV-2 Viability, Susceptibility to Treatment, and the Disinfection and Reuse of PPE, Particularly Filtering Facepiece Respirators. Int. J. Environ. Res. Public Health 17, 6117. https://doi.org/10.3390/ijerph17176117.

Elhadi, M., Msherghi, A., Alkeelani, M., Alsuyihili, A., Khaled, A., Buzreg, A., Boughididah, T., Abukhashem, M., Alhashimi, A., Khel, S., Gaffaz, R., Ben Saleim, N., Bahroun, S., Elharb, A., Eisay, M., Alnafati, N., Almiqlash, B., Biala, M., Alghanai, E., Concerns for low-resource countries, with under-prepared intensive care units, facing the COVID-19 pandemic, Infection, Disease & Health, doi:https://doi.org/10.1016/j.idh.2020.05.008.

Emadian, S.M., Onay, T.T., Demirel, B., 2016. Biodegradation and bioplastics in natural environments. Waste Manag. 59, 526–536.

Euronews, 2020. Surge in marine plastic waste as people discard PPE used to ward off COVID-19. https://www.euronews.com/2020/06/25/surge-in-marine-plastic-waste-as-people-discard-ppe-used-to-ward-off-covid-19 (accessed 8th July, 2020).
European Centre for Disease Prevention and Control (2020). COVID-19 situation update worldwide, as of 22nd July 2020. https://www.ecdc.europa.eu/en/geographical-distribution-2019-ncov-cases (Accessed 22nd July, 2020).
European Commission. (2020). Waste management in the context of the coronavirus crisis. https://ec.europa.eu/info/sites/files/waste_management_guidance_dg-env.pdf (Accessed 20th July, 2020).
Faridi, S., 2020. A field indoor air measurement of SARS-CoV-2 in the patient rooms with confirmed Covid-19 in the largest hospital in Iran. Sci. Total Environ. 725 (2020). https://doi.org/10.1016/j.scitotenv.2020.138401.
Farsaci, L. (2020). Coronavirus Ireland: cost of PPE for healthcare workers to hit €1 billion https://www.dublinlive.ie/news/health/coronavirus-ireland-cost-ppe-healthcare-18230287 (accessed 8th July, 2020).
FDA, (2020) Emergency use authorization (EUA) information, and list of all current EUAs https://www.fda.gov/emergency-preparedness-and-response/mcm-legal-regulatory-and-policy-framework/emergency-use-authorization#covidppe (Accessed 8th July, 2020).
FDA, (2020c). Enforcement policy for face masks and respirators during the coronavirus disease (COVID19) public health emergency (revised), April, 2020 https://www.fda.gov/regulatory-information/search-fda-guidance-documents/enforcement-policy-face-masks-and-respirators-during-coronavirus-disease-covid-19-public-health (Accessed 4th April, 2020).
Fischer, E.P., Fischer, M.C., Grass, D., Henrion, I., Warren, S.W., Westman, E., 2020. Low cost measurement of facemask efficiency for following expelled droplets during speed. Sci. Adv. https://doi.org/10.1126/sciadv.abd3083.
Fisher, E.M., Shaffer, R.E., 2011. A method to determine the available UV-C dose for the decontamination of filtering facepiece respirators. J. Appl. Microbiol. 110 (910), 287–295.
Fitzgibbon, J.E., Sagripanti, J.L., 2008. Analysis of the survival of Venezualen equine encephalomyelitis virus and possible viral simulants in liquid suspensions. J. Appl. Microbiol. 105, 1477–1483.
Flanagan, S.T., Ballard, D.H., 2020. 3-D printed face shields – a community response to the COVID-19 global pandemic. Acad. Radiol. 27 (6). https://doi.org/10.1016/j.acra.2020.04.020.
Franssen, F., Gerard, C., Cozma-Petrut, A., Viera-Pinto, M., Jambrak, A.R., Rowan, N.J., Paulsen, P., Rozycki, M., Tsynes, K., Rodriguez-Lazaro, D., Robertson, L., 2019. Inactivation of parasite transmission stages – efficacy of treatments on food of animal origin. Trends Food Sci. Technol. 83, 114–128.
Garvey, M., Hayes, J., Clifford, E., Rowan, N., 2015. Ecotoxicological assessment of pulsed ultraviolet light-treated water containing microbial species and Cryptosporidium parvum using a microbiotest battery. Water and the Environment Journal 29 (1), 27–35.
Gerard, C., Franssen, F., La Carbona, S., Menterio, S., Cozma-Petrut, A., Utaaker, K.S., Jabmrak, A.R., Rowan, N.J., Rodriguez-Lazaro, D., Nasser, A., Tysnes, K., Robertson, L.J., 2019. Inactivation of parasite transmission stages – efficacy of treatments on foods of non-animal origin. Trends Food Sci. Technol. 91, 12–23.
Ghodrat, M., Rashidi, M., Samali, B., 2017. Life cycle assessments of incineration treatment for sharp medical waste. Energy Technology 131–143.
Global News Wire (2020). Medtronic increasing ventilator production to address COVID-19 pandemic.https://www.globenewswire.com/news-release/2020/03/19/2003071/0/en/Medtronic-Increasing-Ventilator-Production-to-Address-COVID-19-Pandemic.html (accessed 8th July, 2020).
Gorbalenya, A.E., Baker, S.C., Baric, R.S., de Groot, R.J., Drosten, C., Guyaeva, A.A., Haagmans, B.L., Lauber, C., Leontovich, A.M., et al., 2020. The species Severa acute respiratory shyndrom-related conronavirus: calssifying 2019-nCoV and naming it SARS-CoV-2. Nat. Microbiol. 5, 536–544.
Government of Ireland, 2020. When to wear cloth face coverings and how to make them. https://www.gov.ie/en/publication/aac74c-guidance-on-safe-use-of-face-coverings/ (Accessed 9th September, 2020).
Grossmann, J., Pierce, A., Mody, J., Gagne, J., 2020. Institution of a novel process for N95 respiratory disinfection with vaporized hydrogen peroxide in the setting of the COVID-19 pandemic at a large academic medical center. J. Am. Coll. Surg. https://doi.org/10.1016/j.jamcollsurg.2020.04.029.
Guan, D., Wang, D., Hallegatte, S., Davis, S.J., Huo, J., Li, S, Bai, Y., Lei, J., Xue, Q,
Health Products Regulatory Authority (2020). Ventilators use in the treatment of COVID-19 – information collated by the HPRA. http://www.hpra.ie/homepage/medical-devices/covid-19-updates/ventilators (accessed 8th July, 2020).
Hegde, S., 2020. Which type of personal protective equipment (PPE) and which method of donning or doffing PPE carries the least risk of infection for healthcare workers? Evidence Based Dentistry 21, 74–76.
Heilingloh, G.S., Aufderhorst, U.W., Schipper, L., Dittmer, U., Witzke, O., et al., 2020. Susceptibility of SARS-CoV-2 to UV Irradiation.
Heimbuch, B.K., et al., 2011. A pandemic influenza preparedness study: use of energetic methods to decontaminate filtering facepiece respirators contaminated with H1N1 aerosols and droplets. Am. J. Infect. Control 39 (1), e1–e9.
Heimbuch, B., Harnish, D., 2019. Research to Mitigate a Shortage of Respiratory Protection Devices During Public Health Emergencies. Applied Research Associates, Panama City, FL, USA, p. 2019.
Holland, M., Zaloga, D.J., Friderici, C.S., 2020. COVID-19 Personal Protective Equipment (PPE) for the emergency physician. Vis. J. Emerg. Med. 19. https://doi.org/10.1016/j.visj.2020.100740.
Horton, A.A., Barnes, D.K.A. (2020). Microplastic pollution in a rapidly changing world: implications for remote and vulnerable marine ecosystems. Sci. Total Environ.. 738. https://https://doi.org/10.1016/j.scitotenv.2020.140349.
Howie, R., Alfa, M.J., Coombs, K., 2008. Survival of enveloped and non-enveloped viruses on surfaces compared with other micro-organisms and impacts of suboptimal disinfection exposure. J. Hospital Infection. 69 (4), 368–376. https://doi.org/10.1159/000484899.
HSE (2020). Face coverings, medical masks and disposable gloves. https://www2.hse.ie/conditions/coronavirus/face-masks-disposable-gloves.html (Accessed 2 Sept, 2020).
Hutti-Kaul, R., Nillson, L.J., Zhang, B., Rehnberg, N., Lundmark, S., 2020. Designing biobased recycling polymers for plastics. Trends Biotechnol. 38, 56–67.
Ilyas, S., Srivastava, R.R., Kim, H., 2020. Disinfection technology and strategies for COVID-19 hospital and bio-medical waste management. Sci. Total Environ. 749. https://doi.org/10.1016/j.scitotenv.2020.141652.
Inagaki, H., Saito, A., Sugiyama, H., Okabayashi, T., Fujimoto, S., 1744-1747. Rapid inactivation of SARS-CoV-2 with deep-UV LED irradiation. Emerging Microbes & Infections 9, 1. https://doi.org/10.1080/22221751.2020.1796529.
International Medical Center of Beijing, 2020. Lets talk about protective function of masks. Accessed on 18th July 2020 at. http://www.imcclinics.com/english/index.php/news/view?id=83.
Ivanov, D., 2020. Predicting the impacts of epidemic outbreaks on global supply chains: a simulation-based analysis of the COVID-19/SARS-CoV2 case. Transp. Res. E https://doi.org/10.1016/j.tre.2020.101922.
Jambeck, J.R., Geyer, R., Wilcox, C., Siegler, T.R., Perryman, M., Andrady, A., Narayan, R., Low, K.L., 2015. Plastic waste inputs from land into the sea. Science 347, 768–771.
Jatta, M., Kiefer, C., Patolia, H., Pan, J., Harb, C., Marr, L.C., Baffoe-Bonnie, A., 2020. N95 reprocessing by low temperature sterilization with 59% vaporized hydrogen peroxide during the 2020 COVID-19 pandemic. AJIC: American Journal of Infection Control https://doi.org/10.1016/j.ajic.2020.06.194.
Jessop, Z.M., Dobbs, T.D., Ali, S.R., Combellack, E., Clancy, R., Ibrahim, N., Jovic, T.H., Kaur, A.J., Nijran, A., O'Neill, T.B., Whitaker, I.S., 2020. Personal protective equipment for surgeons during COVID-19 pandemic: systematic review of availability, usage and rationing. BJS. https://doi.org/10.1002/bjs.11750.
Jinadatha, C., Simmons, S., Dale, C., et al., 2015. Disinfecting personal protective equipment with pulsed xenon ultraviolet as a risk mitigation strategy for health care workers. Am J Infect Control. 43 (4), 412–414. https://doi.org/10.1016/j.ajic.2015.01.013.
Kampf, G., Todt, D., Pfaemder, S., Steinmann, E., 2020. Persistence of coronavirus on inanimate surfaces and their inactivation with biocidal agents. J. Hosp. Infect. 104 (3), 246–257.
Karan, H., Funk, C., Grabert, M., Oey, M., Hankamer, B., 2019. Green bioplastics as part of circular economy. Trends Plant Sci. 24 (3), 237–249.
Kasloff, S.B., Strong, J.E., Funk, D., Cutts, T.A., 2020. Stability of SARS-Cov-2 on critical personal protective equipment. MedRxiv https://doi.org/10.1101/2020.06.11.20128884.
Kenney, P.A., Chan, B.K., Kortright, K., Cinteon, M., Havill, N., Russi, M., Epright, J., Lee, L., Balcezak, T., Martinello, R., 2020. Hydrogen peroxide vapor sterilization of N95 respirators for reuse [e-pub ahead of print]. MedRxiv https://doi.org/10.1001/jamaoto.2020.1423 Accessed 28th July, 2020.
Kobayashi, L.M., Marins, B.M., dos Santos Costa, P.C., 2020. Extended use or reuse of N95 respirators during COVID-19 pandemic: an overview of national regulatory authority recommendations. Infect. Control Hosp. Epidemiol. https://doi.org/10.1017/ice.2020.173.
Lai, M.Y., Cheng, P.K., Lim, W.W., 2005. Survival of severe acute respiratory syndrome coronavirus. Clin. Infect. Dis. 41, e67–e71.
Li, F., 2016. Structure, Function, and Evolution of Coronavirus Spike Proteins. Annual Review of Virology 3 (1), 237–261. https://doi.org/10.1146/annurev-virology-110615-042301.
Li, J., Bao, Z., Liu, S., Zuang, D., Liu, Y., Zhang, W., Jiang, L., 2003. Survival study of SARS virus in vitro. Chin. J. Disinfect 20, 110–112.
Li, Y-K., Peng, S., Li, L-Q., Wang, Q., Ping, W., Zhang, N., Fu, X-N. 2020. Clinical and transmission characteristics of COVID-19 – a retrospective study of 25 cases from a single thoracic surgery department. Current Medical Science, 40 (2), 295-30.
Liao, L., Xiao, W., Zhao, M., Yu, X., Wang, H., Wang, Q., Chu, S., Cui, Y., 2020. Can N95 respirators be reused after disinfection? How many times? ACS Nano 14, 6348–6356.
Lindsley, W.G., Martin, S.B., Thewlis, R.E., Sarkisian, K., Nwoko, J.O., Mead, K.R., Noti, J.D., 2015. Effects of ultraviolet germicidal irradiation (UVGI) on N95 respirator filtration performance and structural integrity. J. Occup. Environ. Hyg. 12, 509–517.
Liu, S., Ren, N., Li, C., Shan, S., Miao, F., Yang, I., Feng, I., Meng, X., Wen, X., Gong, R.E., Xiong, X., Fu, C., Wu, A., 2017. Status of management of medical waste in 125 medical institutions. Chin. J. Noscomial. 27, 4265–4269.
Lockhart, S.L., Duggan, L.V., Wax, R.S., et al., 2020. Personal protective equipment (PPE) for both anesthesiologists and other airway managers: principles and practice during the COVID-19 pandemic. Can J Anesth/J Can Anesth 67, 1005–1015. https://doi.org/10.1007/s12630-020-01673-w.
Lowe, J.J., Paladino, K.D., Farke, J.D., Boulter, K., Cawcutt, K., Emodi, M., Gibbs, S., Hankins, R., Hinkle, L., Micheels, T., Schwedhelm, S., Vasa, A., Wadman, M., Watson, S., Rupp, M.E., 2020. N95 Filtering Facemask Respirator Ultraviolet Germicidal Irradiation (UVGI) Process for Decontamination and Reuse. Nebrasca Medicine. Available on 10th August 2020 at. https://cleanhospital.com/wp-content/uploads/ 2020/03/N-95-decon-process.pdf.
Ma Q-X, Shan H, Zhang C-M. (2020).Decontamination of face masks with steam for mask reuse in fighting the pandemic COVID-19: experimental supports. J. Med. Virol. 2020; 1–4. doi:https://doi.org/10.1002/jmv.25921.
MacIntyre, C.R., Seale, H., Dung, T.C., Hien, N.T., Nga, P.T., Chughtai, A.A., et al., 2015. A cluster randomised trial of cloth masks compared with medical masks in healthcare workers. BMJ Open 5 (4), e006577. https://doi.org/10.1136/bmjopen-2014-006577.
Mackenzie, D., 2020. Reuse of N95 masks. Engineering 6, 593–596.
de Man, P., van Straten, B., van den Dobbelsteen, J., van der Eijk, V., 2020. Sterilization of disposable face masks by means of standardized dry and steam sterilization

processes; an alternative in the fight against mask shortages due to COVID-19. J. Hosp. Infect. 105, 356–357.
Martín-Rodríguez, F., et al., 2020. Blood biomarkers for assessing headaches in healthcare workers after wearing biological personal protective equipment in a COVID-19 field hospital. Research Square https://doi.org/10.21203/rs.3.rs-55229/v1.
McEvoy, B., Rowan, N.J., 2019. Terminal sterilization of medical devices using vaporized hydrogen peroxide: a review of current methods and emerging opportunities. J. Appl. Microbiol. 127 (5), 1403–1420.
Meo, S.A., Alhowikan, A.M., Khlaiwi, T.A.L., Meo, I.M., Halepoto, D.M., Iqbal, M., Usmani, A.M., Hajjar, W., Ahmed, N., 2020. Novel coronavirus 2019-nCoV: prevalence, biological and clinical characteristics comparison with SARS-CoV and MERS-CoV. Eur. Rev. Med. Pharmacol. Sci. https://doi.org/10.26355/eurrev_202002_20379.
Messerele, V.E., Moose, A.L., Ustimenko, A.B., 2018. Processing of biomedical waste in plasma gasifier. Waste Manag. 79, 791–799.
Mills, D., Delbert, A., Harnish, M.S., 2018. Ultraviolet germicidal irradiation of influenza-contaminated N95 filtering facepiece respirators. Am. J. Infect. Control 46 (7), 49–55.
Ministry of Health of Spain, 2020. Action procedure for occupational risk prevention services against exposure to SARS-COV-2. Available on 12th August 2020 at. https://www.mscbs.gob.es/profesionales/saludPublica/ccayes/alertasActual/nCov-China/documentos/PrevencionRRLL_COVID-19.pdf.
Mitchell, R., Ogunreai, T., Astratianakis, S., Bryce, E., Gervais, R., Gravel, D., Johnson, L., Leduc, S., Roth, V., Taylor, G., Vearcombe, M., Weir, C., 2012. Impact of the 2009 influenza A (H1N1) pandemic on Canadian health care workers: a survey on vaccination, illness, absenteeism, and personal protective equipment. Am. J. Infect. Control 40 (7), 611–616.
Mueller, A.V., Eden, M.J., Oakes, J.M., Bellini, C., Fernandez, L.A., 2020. Quantitative Method for Comparative Assessment of Particle Removal Efficiency of Fabric Masks as Alternatives to Standard Surgical Masks for PPE. Matter 3 (3), 950–962. https://doi.org/10.1016/j.matt.2020.07.006.
Mukerji, S., MacIntyre, C.R., Seale, H., et al., 2017. Cost-effectiveness analysis of N95 respirators and medical masks to protect healthcare workers in China from respiratory infections. BMC Infect. Dis. 17, 464.
Murphy, E.J., Masterson, C., Rezoagli, E., O'Toole, D., Major, I., Stack, G.D., Lynch, M., Laffey, J.G., Rowan, N.J., 2020. β-Glucan extracts from the same edible shiitake mushroom Lentinus edodes produce differential in-vitro immunomodulatory and pulmonary cytoprotective effects —implications for coronavirus disease (COVID-19) immunotherapies. Sci. Total Environ. https://doi.org/10.1016/j.scitotenv.2020.139330.
N95DECON, 2020a. Example Processes. Available on 20th April 2020 at. https://www.n95decon.org/example-processes.
N95DECON, 2020b. COVID N95 decon & reuse. UV-C. Available on 10th April 2020 at. https://static1.squarespace.com/static/5e8126f89327941b9453eeef/t/5e85902c0d94fa0516aafa2a/1585811501243/200401_N95DECON_UV_factsheet_v1.2_final.pdf.
NGO Oceans Asia (2020). No shortage of surgical masks at the beach. https://oceansasia.org/beach-mask-coronavirus/ (accessed 20th July, 2020).
NSAI, 2020. Guidance on manufacturing and importing PPE and medical devices - ensuring compliance during the COVID-19 pandemic. https://www.nsai.ie/covid-19-ppe-md/ (Accessed 12th August, 2020).
Nzediaegwu, C., Chang, S.X., 2020. Improper solid waste management increases potential for COVID-19 spread in developing countries. Resour. Conserv. Recycl. https://doi.org/10.1016/j.resconrec.2020.104947.
O'Hearn, K., Gertsman, S., Sampson, M., Webster, R., Tsampalieros, A., Ng, R., et al., 2020a. Decontaminating N95 masks with Ultraviolet Germicidal Irradiation (UVGI) does not impair mask efficacy and safety: A Systematic Review. https://doi.org/10.31219/osf.io/29z6u.
O'Hearn, K., Sampson, M., Webster, R., Tsampalieros, A., Ng, R., Gibson, J., Logos, A.T., Acharya, N., Agarwal, A., Boggs, S., Chamerlain, G., Staykov, E., Sirkora, L., McNally, J.D., 2020b. Decontaminating N95 and SN95 masks with ultraviolet germicidal irradiation does not impair mask efficacy and safety. J. Hosp. Infect. 106, 163–173.
O'Neill, E., Stejskal, V., Clifford, E., Rowan, N.J., 2020. Novel use of peatlands as future locations for the sustainable intensification of freshwater aquaculture production – a case study from the Republic of Ireland. Sci. Total Environ. 706. https://doi.org/10.1016/j.scitotenv.2019.136044.
Ou, Q., Pei, C., Kim, S.C., Abell, E., Pui, D.Y.H., 2020. Evaluation of decontamination methods for commercial and alternative respirator and mask materials – view from filtration aspect. J. Aerosol Sci. https://doi.org/10.1016/j.jaerosci.2020.105609.
Ozog, D., Parker-Miller, S.B., Kohli, I., Lyons, A.B., Narla, S., Torres, A.E., Levesque, M., Lim, H.W., Hamzavi, I.H., 2020. The importance of fit testing in decontamination of N95 respirators: a cautionary note. J. Am. Acad. Dermatol. 83, 672–674.
Pagat, A.-M., Seux-Goepfort, R., Lutsch, C., Lecouturier, V., Saluzzo, J.-F., Kuster, I.C., 2007. Evaluation of SARS-coronavirus decontamination procedures. Appl. Biosafety 12, 100–108.
Park, 2020. Personal protective equipment or healthcare workers during the COVID-19 pandemic. Infection and Chemotherapy 52 (2), 165–182.
Pastorino, B., Touret, F., Gilles, M., de Lamballerie, X., Charrel, R.N., 2020. Heat Inactivation of Different Types of SARS-CoV-2 Samples: What Protocols for Biosafety, Molecular Detection and Serological Diagnostics? Viruses 12. https://doi.org/10.3390/v12070735.
Perencevich, E.N., Diekema, D.J., Edmond, M.B., 2020. Moving personal protective equipment into the community: face shields and containment of COVID-19. JAMA 323 (22), 2252–2253. https://doi.org/10.1001/jama.2020.7477.
Perkins, D.J., Villescas, S., Wu, T.H., Muller, T., Bradfute, S., Hurwitz, I., Cheng, Q., Wilcox, H., Weiss, M., Bartlett, C., Langsjoen, J., Seidenberg, P., 2020. COVID-19 global pandemic planning: decontamination and reuse processes for N95 respirators. Exp. Biol. Med. 245, 933–939.
Pinon, A., Vialette, M., 2018. Survival of viruses in water. Intervirology 61, 214–222.
Prata, J.C., Silva, A.L.P., Walker, T.R., Duarte, A.C., Rocha-Santos, T., 2020. COVID-19 Pandemic Repercussions on the Use and Management of Plastics. Environ. Sci. Technol. 54 (13), 7760–7765. https://doi.org/10.1021/acs.est.0c02178.
Price, A., Chu, L., 2020. Addressing COVID-19 Face Mask Shortages [v1.3]. COVID-19 Evidence Service. Stanford Medicine. Accessed on 18th July 2020 at. https://elautoclave.files.wordpress.com/2020/03/stanford-2020.pdf.
Price, A., Cui, Y., Liao, L., Xiao, W., Yu, X., Wang, H., Zhao, M., Wang, Q., Chu, S., Chu,
Radonovich, L.J., Simberkoff, M.S., Bessesen, M.T., et al., 2019. N95 Respirators vs Medical Masks for Preventing Influenza Among Health Care Personnel: A Randomized Clinical Trial. JAMA 322 (9), 824–833. https://doi.org/10.1001/jama.2019.11645.
Ranney, M.L., Griffeth, V., Jha, A.K., 2020. Critical supply shortage – the need for ventilators and personal and protective equipment during the COVID-19 pandemic. New Englang Journal of Medicine https://doi.org/10.1056/NEJMp2006141.
Ratnesar-Shumate, S., Williams, G., Green, B., Krause, M., Holland, B., Wood, S., Bohannon, J., Boydston, J., Freeburger, D., Hooper, I., 2020. Simulated sunlight rapidly inactivates SARS-CoV-2 on surfaces. Journal of Infectious Disease 222, 214–222.
Rengasamy, S., Eimer, B., Shaffer, R.E., 2010. Simple Respiratory Protection—Evaluation of the Filtration Performance of Cloth Masks and Common Fabric Materials Against 20–1000 nm Size Particles. The Annals of Occupational Hygiene 54 (7), 789–798. https://doi.org/10.1093/annhyg/meq044.
Reuters (2020). Discarded coronavirus masks clutter Hong Kong's beaches and trails. https://www.reuters.com/article/us-healthcoronavirus-hongkong-environme/discarded-coronavirus-masksclutter-hong-kongs-beaches-trails-idUSKBN20Z0PP.2020 (Accessed 20th July, 2020).
Rhee, S.W., 2020. Management of used personal and protective equipment related to COVID-19 in South Korea. Waste Management and Research, 1–5 https://doi.org/10.1177/0734242X20933343.
Rimmer, A., 2020. Covid-19: Experts question guidance to reuse PPE. BMJ 369, m1577. https://doi.org/10.1136/bmj.m1577 (Published 20 April 2020).
Rizman, M., Mujtaba, G., Memon, S.S., Lee, K., Rashid, N., 2018. Exploring the potential of microalgae for new biotechnology applications and beyond: A review. Renewable and Sustainable Energy Reviews 92, 394–404 September 2018.
Rowan, N.J., 2019. Pulsed light as an emerging technology to cause disruption for food and adjacent industries – Quo Vadis? Trends Food Sci. Technol. 88, 316–332.
Rowan, N.J., Galanakis, C.M., 2020. Unlocking challenges and opportunities presented by COVID-19 pandemic for cross-cutting disruption in agri-food and green deal innovations: Quo Vadis? Sci. Total Environ. 748. https://doi.org/10.1016/j.scitotenv.2020.141362.
Rowan, N.J., Laffey, J.G., 2020. Challenges and solutions for addressing critical shortage of supply chain for personal and protective equipment (PPE) arising from Coronavirus disease (COVID19) pandemic – Case study from the Republic of Ireland. Sci. Total Environ. 725. https://doi.org/10.1016/j.scitotenv.2020.138532.
Rubio-Romero, J.C., del Carmen, M., Ferreira, P., Torrecilla, J.A., Santiago, G., Castro, C., 2020. Disposable masks: disinfection and sterilization for reuse, and non-certified manufacturing, in the face of shortages during the COVID-19 pandemic. Sci. Total Environ. https://doi.org/10.1016/j.ssci.2020.104830.
Ruiz-Salmón, I., Margallo, M., Laso, J., Villanueva-Rey, P., Mariño, D., Quinteiro, P., Dias, A.C., Nunes, M.L., Marques, A., Feijoo, G., Moreira, M.T., Loubet, P., Sonnemann, G., Morse, A., Cooney, R., Clifford, E., Rowan, N.J., Méndez-Paz, D., Parga, X., Anglada, C., Martin, J.C., Rubén-Aldaco, A., 2020. Addressing challenges and opportunities of the European seafood sector under a circular economy framework. Current Opinion in Environmental Science & Health 13, 101–106.
Saini, Vikram, Sikri, V., Batra, S.D., Kalra, P., Gautam, K., 2020. Development of a highly effective low-cost vaporized hydrogen peroxide-based method for disinfection of personal protective equipment for their selective reuse during pandemics. Gut Pathogens https://doi.org/10.1186/s13099-020-00367-4.
Schwartz, A., Stiegell, M., Greeson, N., Vogel, A., Thomann, W., Brown, M., Sempowski, G.D., Alderman, A., Condreay, J.P., Burch, J., Wolfe, C., Smith, D., Lewis, S., 2020. Decontamination and reuse of N95 respirators with hydrogen peroxide vapor to address worldwide personal protective equipment shortages during the SARSCoV-2 (COVID-19) pandemic. Applied Biosafety: Journal of ABSA International 25 (2), 67–70.
Shakya, K., Noyes, A., Kallin, R., et al., 2017. Evaluating the efficacy of cloth facemasks in reducing particulate matter exposure. J Expo Sci Environ Epidemiol 27, 352–357. https://doi.org/10.1038/jes.2016.42.
Sickbert-Bennett, E.E., Samet, M., Clapp, P.W., 2020. Filtration efficiency of hospital face mask alternatives available for use during the COVID-19 pandemic. JAMA Intern. Med. https://doi.org/10.1001/jamaintermed.2020.4221.
Silva, A.L.P., Prata, J.C., Walker, T.R., Campos, T.R.W., Duarte, A.C., Soares, A.M.V.M., Barceló, D., Rocha-Santos, T., 2020. Rethinking and Optimising Plastic Waste Management under COVID-19 Pandemic: Policy Solutions Based on Redesign and Reduction of Single-Use Plastics and Personal Protective Equipment. https://doi.org/10.1016/j.scitotenv.2020.140565.
Singh, N., Tang, Y., Ogunseitan, O.A., 2020. Environmentally sustainable management of used personal and protective equipment. Environ. Sci. Technol. 54, 8500–8502.
Skrzypczak, N.G., Tanikella, N.G., Pearce, J.M., 2020. Open source high-temperature reprap for 3-D printing heat-sterilizable PPE and other applications. Basel https://doi.org/10.20944/preprints202005.0479.v1.
Song, W., Pan, B., Kan, H., 2020. Evaluation of heat inactivation of virus contamination on medical masks. J. Microbes Infect 15, 31–33.
Spanish Society of Preventive Medicine, Public Health and Hygiene, 2020. Descontaminación de respiradores de partículas ante desabastecimiento debido a la pandemia COVID-19. Available on 12th August 2020 at. https://www.sempsph.com/ images/REPROCESADO%20FFPS%201.pdf.

Srinivasan, S., Peh, WCG. (2020). N95 filtering facepiece respirators during the COVID-19 pandemic: basics, types, and shortage solutions. Malaysian. Orthopaedic Journal 2020 Vol 14 No 2. doi: doi:https://doi.org/10.5704/MOJ.2007.002.

Steinberg, B.E., Aoyama, K., McVey, M., Levin, D., Siddiqui, A., Munshey, F., Goldenber, N.M., Faraoni, D., Maynes, J. (2020). Efficacy and safety of decontamination for N95 respirator reuse – a systematic literature search and narrative synthesis. Can J. Anaesthesia. https://doi.org.1007/s12630-020-01770-w.

Straub, J., 2015. In search of technology readiness level (TRL) 10. Aerosp. Sci. Technol. 46, 312–320.

Suanda, J., Cawley, D., Domegan, C., Brenner, N., Rowan, N.J., 2013. A review of the perceived barriers within the health belief model on pap smear screening as a cervical cancer prevention measure. Journal of Asian Scientific Research 3, 677–692.

Suanda, J., Cawley, D., Brenner, M., Domegan, C., Rowan, N., 2017. Identification of behavioural change strategies to prevent cervical cancer among Malay women in Malaysia. In: Hastings, Gerard, Domegan, Christine (Eds.), Social Marketing – Rebels with a Cause. Taylor and Francis Group Publishers, pp. 555–567 https://doi.org/10.4324/9781315648590.

Suppan, L., Abbas, M., Stuby, L., Cottet, P., Larribau, R., Golay, E., Iten, A., Harbarth, S., Gartner, B., Suppan, M., 2020. Effect of an E-learning module on personal protective equipment proficiency among prehospital personnel: web-based randomized controlled trial. J. Med. Internet Res. 22 (8), e21265. https://doi.org/10.2196/21265.

Thakuv, S., Chaudhary, J., Sharma, B., Verma, A., Tamulevinus, S., Thakur, V.K., 2018. Sustainability of bioplastics – opportunities and challenges. Current Opinion in Green, Sustainable Chemistry 13, 68–75.

Thiruchelvi, R., Kavitha, K., Shankari, K., 2020. New biotechnological routes for greener bioplastics from seaweed. Research Journal of Pharmacy and Technology 13 (5). https://doi.org/10.5958/0974-360X.2020.00444.8.

Thomas, J.P., Srinivasan, A., Wickranmarachchi, C.S., Dhesi, P.K., Hung, Y.M., Kamath, A., 2020. Evaluating the national personal and protective equipment guidance for NHS healthcare workers during the COVID-19 pandemic. Clinical Medicine 20 (3). https://doi.org/10.7861/clinmed.2020-0143.

Tiedeken, E.J., Tahar, A., McHugh, B., Rowan, N.J. (2017). Monitoring, sources, receptors, and control measures for three European Union watch list substances of emerging concern in receiving waters – a 20 year systematic review. Sci. Total Environ., 574-1140-1163.

Tobías, A., 2020. Evaluation of the lockdown for the SAR-Cov2 epidemic in Italy and Spain after follow up. Sci. Total Environ. 725, 138539. https://doi.org/10.1016/j.scitotenv.2020.138539.

Toon, J., 2020. Ozone disinfection could safely allow reuse of personal protective equipment. Biomedical Safety & Standards 50 (16), 121–123. https://doi.org/10.1097/01.BMSAS.0000696812.81177.fa September 15, 2020.

Torres, A.E., Lyons, A.B., Narla, S., Kohli, I., Parks-Miller, A., Ozog, D., Hamzavi, I.H., Lim, H.W., 2020. Photochemistry and Photobiological Sciences. https://doi.org/10.1039/D0PP00131G.

Van der Westhuizen, H.M., Kotze, K., Tonkin-Crine, S., Gobat, N., Greenhalgh, T. (2020). Face coverings for covid-19: from medical intervention to social practice. BMJ. http://dx.doi.org/10.1136/bmj.m3021.

Viscusi, D.J., King, W.P., Shaffer, R.E., 2007. Effect of decontamination on the filtration efficiency of two filtering facepiece respirator models. J Int Soc Respir Prot 24, 93–107.

van Doremalen, N., Bushmaker, T., Morris, D.H., Holbrook, M.G., Gamble, A., Williamson, B.N., Lloyd-Smith, J.O., 2020. Aerosol and surface stability of SARS-CoV-2 as compared with SARS-CoV-1. N. Engl. J. Med. 382, 1564–1567. https://doi.org/10.1056/NEJMc2004973.

Viscusi, D.J., Bergman, M.S., Sinkule, E., Shaffer, R.E., 2009. Evaluation of the filtration performance of 21 N95 filtering face piece respirators after prolonged storage. Am. J. Infect. Control 37, 381–386.

Viscusi, D.J., et al., 2011. Impact of three biological decontamination methods on filtering facepiece respirator fit, odor, comfort, and donning ease. J. Occup. Environ. Hyg. 8 (7), 426–436 2011.

Wang, J., Shen, J., Ye, D., Yan, X., Zhang, Y., Yang, W., Li, X., Wang, J., Zhang, L. Pan, L. 2020. Disinfection technology of hospital waste and wastewater suggestions for disinfection strategy during Coronavirus Disease-2019 (COVID-19) pandemic in China. Environ. Pollut., 262. https://doi.org./10.1016/j.envpol.2020.114665.

WHO (2020). Transmission of SARS-CoV2: implications for infection control prevention. https://www.who.int/news-room/commentaries/detail/transmission-of-sars-cov-2-implications-for-infection-prevention-precautions (Accessed 25th August, 2020).

WHO, Shortage of personal protective equipment endangering.

World Bank, World Development Indicators. (2019). Solid waste management. Retrieved on July 8th, 2020 from:https://www.worldbank.org/en/topic/urbandevelopment/brief/solid-waste-management.

World Health Organization. (2020). Director General's opening remarks at the media briefing on COVID-19, 11th March, 2020. https://www.who.int/dg/speeches/detail/who-direcot-general-s-opening-remarks-at-the-media-briefing-on-covid-19-11-march-2020 (accessed 20th March, 2020).

WWF (2020). Nello smalltimento di macherine e guanti serve responsabilità. https://www.wwf.int/scoule/?53500%2/FNello-smalltimento-di-macherine-e-guanti-serve-responsabilita World Wide Fund for nature (accessed 20th July, 2020).

Yang, Y., Wang, H., Chen, K., Zhao, J., Deng, S., Wang, Y., 2020. Shelter hospital mode: how to prevent novel corona virus infection 2019(COVID-19) hospital-acquired infection? Infect. Control Hosp. Epidemiol. https://doi.org/10.1017/ice.2020.97.

Zhang, Jia-min, Zheng, Chong-yi, Geng-fu, Xiao, Yuan-quan, Zhou, Gao, Rong, 2004. Examination of the Efficacy of Ozone Solution Disinfectant in Inactivating SARS Virus. Chinese J. Disinfection 2004-01.

Zhao, Z., Zhang, Z., Lanzarini, L., Sinha, S., Rho, H., Herckes, P., Westerhoff, P., 2020. Germicidal ultraviolet light does not damage or impede performance of N95 masks upon multiple uses. Environmental Science and Technology Letters https://doi.org/10.1021/acs.estlett.0c00416.

Zheng, J., Suh, S., 2019. Strategies to reduce the global carbon footprint of plastics. Nat. Clim. Chang. 9, 374–378.

Zhu, Z., Yan, J.H., Jiang, X.G., Lai, Y.E., Cen, K.F., 2008. Study on pyrolysis of typical medical waste materials by using TG-FTIR analysis. J. Hazard. Mater. 153, 670–676.

Zorko, David J., Gertsman, Shira, O'Hearn, Katie, Timmerman, Nicholas, Ambu-Ali, Nasser, Dinh, Tri, Sampson, Margaret, et al., 2020. Decontamination interventions for the reuse of surgical mask personal protective equipment: a systematic review. OSF Preprints https://doi.org/10.31219/osf.io/z7exu April 29.

Science of the Total Environment 772 (2021) 145530

Contents lists available at ScienceDirect

Science of the Total Environment

journal homepage: www.elsevier.com/locate/scitotenv

Review

Disposable face masks and reusable face coverings as non-pharmaceutical interventions (NPIs) to prevent transmission of SARS-CoV-2 variants that cause coronavirus disease (COVID-19): Role of new sustainable NPI design innovations and predictive mathematical modelling

Neil J. Rowan [a,b,c,d,*], Rafael A. Moral [e]

[a] Department of Nursing and Healthcare, Athlone Institute of Technology, Ireland
[b] Centre for Disinfection, Sterilization and Biosecurity, Athlone Institute of Technology, Ireland
[c] Empower Eco Sustainability Hub, Lough Boora, Co. Offaly, Ireland
[d] School of Medicine, National University of Ireland Galway, Ireland
[e] Department of Mathematics and Statistics, Maynooth University, Ireland

HIGHLIGHTS

- Face masks and face coverings are mainstay non-pharmaceutical interventions (NPIs) to help prevent COVID-19.
- Random controlled trials will inform efficacy of relative risk (RR) for single and combined use of NPIs.
- Mathematical modelling will inform efficacy of NPIs to address COVID-19 risk multipliers.
- Surge in new face mask design, functionality and material innovation reflects need for sustainable PPE.
- Other RR factors include emerging winter conditions, religious and cultural events that also challenge NPIs.

GRAPHICAL ABSTRACT

ARTICLE INFO

Article history:
Received 12 October 2020
Received in revised form 25 January 2021
Accepted 26 January 2021
Available online 1 February 2021

Editor: Damia Barcelo

Keywords:
COVID-19
Face masks
Face coverings

ABSTRACT

Best-published evidence supports the combined use of vaccines with non-pharmaceutical interventions (NPIs), to reduce the relative risk of contracting severe acute respiratory syndrome coronavirus 2 (SARS-CoV-2) that causes COVID-19; this will enable a safe transition to achieving herd immunity. Albeit complex, the strategic public health goal is to bundle NPIs to keep the basic reproduction number R_0 below one. However, validation of these NPIs is conducted using random clinical trials, which is challenging in a swiftly moving pandemic given the need for recruiting large participant cohort over a longitudinal analysis period. This review highlights emerging innovations for potentially improving the design, functionality and improved waste management of disposable face masks such as filtering facepiece (FFPs) respirators, medical masks, and reusable face coverings to help prevent COVID-19. It describes use of different mathematical models under varying scenarios to inform efficacy of single and combined use of NPIs as important counter-measures to break the cycle of COVID-19 infection including new SARS-CoV-2 variants. Demand for face masks during COVID-19 pandemic keeps increasing,

* Corresponding author at: Department of Nursing and Healthcare, Athlone Institute of Technology, Ireland.
E-mail address: nrowan@ait.ie (N.J. Rowan).

https://doi.org/10.1016/j.scitotenv.2021.145530

Non-pharmaceutical interventions
Relative risk modelling
Sustainability

especially for FFPs worn by medical workers. Collaborative and well-conducted randomised controlled trials across borders are required to generate robust data to inform common and consistent policies for COVID-19 and future pandemic planning and management; however, current use of systematic reviews of best available evidence can be considered to guide interim policies.

Contents

1. Introduction

At the time of writing (8th December 2020), there has been, 68,225,313, cases of coronavirus disease (COVID-19) reported worldwide, including 1,556,877 deaths (European Centre for Disease Prevention and Control, 2020). COVID-19 pandemic has imposed unprecedented challenges to healthcare systems (Chowdhury et al., 2020), where this respiratory-virus has spread to local communities globally. COVID-19 is primarily a respiratory disease and the spectrum of infection with this virus can range from very mild, non-respiratory symptoms to severe acute respiratory illness, sepsis with organ dysfunction and death (WHO, 2020a). Some people infected have reported no symptoms (WHO, 2020a). There is currently a 7-day average of 204,574 new cases of severe acute respiratory syndrome coronavirus 2 (SARS-CoV-2) in the United States (Johns Hopkins University, 2020), which is the highest affected country for COVID-19. Several of these affected countries are experiencing peak infections rates, such as the United States, Russia and Turkey (Table 1). The occurrence of third waves of COVID-19 infection that affects greater numbers of people is common for many countries globally, which puts added pressure on deploying appropriate disease-prevention counter-measures.

Many countries are appealing for greater compliance with increased and correct wearing of face masks, maintaining social distancing, adopting hand hygiene, use of personal and protective equipment (PPE), along with detection testing and contact tracing that are also referred to as 'non-pharmaceutical interventions' (NPIs) (Rowan and Laffey, 2020a). The combined use of complementary NPIs are deployed to help flatten the curve of COVID-19 infections so as to particularly protect to our frontline healthcare workers (HCWs) and the most vulnerable in society (Rowan and Laffey, 2020a). For example, the WHO (2020a) stated "use of a mask alone is insufficient to provide an adequate level of protection, and other measures should be adopted". The WHO (2020a) advises that each country apply their own risk based-approach when recommending different increasing tiers of NPIs including restrictive lockdowns, which also inflicts significant economic hardship on societies (Rowan and Galanakis, 2020). The emergence of COVID-19-related "behavioural fatigue" or "adherence fatigue" associated with sustained societal compliance with NPIs brings added public health pressures. Michie et al. (2020) described a Google search for "pandemic fatigue" that resulted in approximately 200 million hits, with articles on the first page with titles such as "10 reasons why pandemic fatigue could threaten global health", and "Europe experiencing pandemic fatigue".

Precisely how coronavirus spreads between susceptible individuals remains a matter of debate, but transmission of this respiratory virus may be through contact, droplet, or airborne spread (Asadi et al. 2020). "Direct" modes indicate person-to-person transmission such as via contaminated hands, or indirectly via fomites, which are inanimate or non-living objects or materials (i.e. transfer via a contaminated door handle through touch). If we touch a contaminated surface, we may then potentially transfer the virus onto the face mask if adjusting it, and may then directly inoculate the virus onto mucosal surfaces such as through the touching of the nose or eyes (Wibisono et al., 2020). Droplet and airborne spread occur through the air through sneezing, coughing, singing, talking and exhaling (Chua et al., 2020). It is appreciated that particles larger than 5 μm may fall to the ground within 1 m. However, a "gas cloud" theory has been proposed where aggregated mucosalivary droplets from these different exhalation activities can form a cloud, and potentially be expelled up to 7 to 8 m in combination with environmental factors (Bourouiba, 2020: Dbouk and Drikakis, 2020a, b). Uncertainty surrounding the modes by which these respiratory viruses transmit among humans under varying conditions hinders evaluation of the efficacy of NPIs designed to prevent their spread (Milton et al., 2013; Perencevich et al., 2020).

The first COVID-19 vaccine, manufactured by Pfizer-BioNTech, was administered in the UK today (Diaz, 2020). Priority emphasis has been placed on protecting the most vulnerable to reduce illness and death. While Phase 3 clinical trial data highlights both safety and 95% efficacy for this vaccine, it will take time to observe if it prevents COVID-19 transmission and creates broad herd immunity in communities. Thus, despite this positive news, there will remain a strong reliance on the combined use of NPIs to prevent COVID-19 transmission. The Republic

Table 1
Daily confirmed new cases of COVID-19 (7-day moving average) — outbreak evolution for the current 10 most affected countries (08/12/2020).

Country	Population	7-day mean average (K^{-1}) for COVID-19	Highest 7-day mean average (K^{-1}) for COVID-19	Total number of COVID-19 cases	Total number of COVID-19 deaths	Trend direction of COVID-19 cases in country	Days since first case of COVID-19 reported
United States*	331,002,651	204.574	204.574	14,949,299	283,703	⇑ Up	320
Brazil	212,559,417	39.521	55.891	6,623,911	177,317	⇓ Down	285
India	1,380,004,385	36.001	96,735	9,703,770	140,958	⇓ Down	312
Turkey*	84,339,067	32.736	32.736	860,432	15,103	⇑ Up	271
Russia*	145,934,462	28.701	27.701	2,466,961	43,122	⇑ Up	311
Italy	60,461,826	20.709	37.977	1,742,557	60,606	⇓ Down	311
United Kingdom	67,886,011	17.370	26.870	1,754,911	62,130	⇓ Down	311
Germany	83,783,942	15.971	22.820	1,229,269	20,002	⇓ Down	315
Ukraine	43,732,762	11.928	14.167	843,898	14,208	⇓ Down	279
Iran	83,992,949	11.56	13.961	1,051,374	50,594	⇓ Down	292

Data accessed from Johns Hopkins University on 8th December, 2020 (https://www.coronavirus.jhu.edu/data/new-cases).
* Countries currently experiences peak number of cases of COVID-19.

of Ireland has managed to curtail two waves of COVID-19 through effective implementation of these NPIs, along with enforcing two lockdowns (Government of Ireland, 2020); however, key challenges remain including greater mingling of people due to the opening up of hospitality that coincides with the festive Christmas holiday period. There is sustained pressure on maintaining supply chains of vital personal and protective equipment (PPE) to ensure that frontline healthcare workers, and the most at risk populations are protected (Rowan and Laffey, 2020b; Cook, 2020; Flaxman et al. 2020; Perencevich et al., 2020).

While there is priority emphasis on flattening COVID-19 infections to enable effective roll out of vaccines, there is a commensurate urgency to avoid economic chaos (Guan et al., 2020; Rowan and Laffey, 2020b). Many countries have tried to lift NPIs that has increased the occurrences and likelihood of disease resurgence (Chowdhury et al., 2020). Ensuring continuity in the supply chain for vital personal and protective equipment (PPE) has been a significant challenge that has been met, where possible, by increased production of single-use plastic PPE along with initiatives to safely address their reuse under emergency use authorization (Rowan and Laffey, 2020b). Given the initial gap in knowledge on specific efficacy of existing and emerging counter-measures to combat COVID-19, there has been a commensurate surge of new publications on PPE and other NPIs to meet these public health needs that also has implications for sustainable waste management (Silva et al., 2020). For example, recently research and systematic reviews on these topics approximate 20,000 publications since the first reporting of COVID-19 (such as Silva et al., 2020; Derraik et al., 2020; Rowan and Laffey, 2020a; Rubio-Romero et al., 2020; Chu et al., 2020; Barceló, 2020).

"Face masks are physical barriers to respiratory droplets that may enter the mouth and nose and to the expulsion of mucosalivary droplets from infections individuals" (Chua et al., 2020). The classification of, and technical standards for, different type of disposable masks available according to their intended use, as defined by the European Centre for Disease Prevention and Control (2020), has been comprehensively described by Rubio-Romero et al. (2020). In brief, (a) filtering facepiece (FFP) respirators are classified as PPE and are designed to protect the wearer from exposure to airborne contaminants, such as N95-type respirators; (b) medical face masks (also known as surgical or procedural masks), are classified as a medical device that covers the mouth, nose and chin ensuring a barrier that limits the transition of infective agent between hospital staff and patients; and (c) other face masks (also commonly known as non-medical, home-made cloth or barrier masks) includes various forms of self-made or commercial masks, or face coverings, made of cloth or textiles that are not standardized and not intended for use in healthcare settings (Rubio-Romero et al., 2020) (Fig. 1). The effectiveness of these disposable FFP masks is different depending on type and certification, which is established across 3 levels of protection depending on leakage of all particles into the interior, either through the adjustment of the mask to the face, by the exhalation valve, if any, or penetration through the filter that are 22%, 8% and 2% for FFP1, FFP2 and FFP3 respectively. The effectiveness of two types of medical masks, namely surgical or procedural masks, is defined by bacterial filtration efficiency, differential pressure (Pa/cm^2), splash resistant pressure (kPa) and microbial cleaning. Improvised non-medical face coverings are intended for low-risk cases where the risk of infection can be potentially increased due to humidity, liquid diffusion and virus retention (European Centre for Disease Prevention and Control, 2020b).

Given the aforementioned, the purpose of this review is (1) to highlight key developments surrounding sustainable use of disposable face masks such as PPE, medical masks, and reusable face coverings; (2) to review the role of face masks in the context of other NPIs in breaking the cycle of COVID-19 infection, and; (3) to use relative risk assessment and statistical modelling to inform efficacy of single, and combined NPIs to prevent COVID-19 transmission with particular emphasis on different face mask designs and functionality features. This review does not address non-disposable filtering facepiece (FFP3) respirators.

2. Transmission and survival of SARS-CoV — breaking the chain of infection

2.1. Characteristics of SARS-CoV-2 and survival of contact surfaces

SARS-CoV-2 is a Coronavirus, which is characterised as a positive stranded RNA virus with an envelope containing glycoprotein spikes. Coronaviruses are among the largest RNA viruses comprising a genome of between 26 and 32 kb in size (Jin et al., 2020), and ranges from 60 to 140 nm in size (Chua et al., 2020). Therefore, "face masks and respirators made of materials with larger pore sizes, such as cotton and synthetic material, will not be able to effectively filter these viruses or virus-laden droplets, as compared with those materials with much smaller pore smaller pore sizes". Additionally, face masks and respirators made of, or coated with, water-resistant materials are more effective against large virus-laden respiratory droplets" (Chua et al., 2020). Coronaviruses, such as SARS-CoV-2 comprise complex structural enveloped viruses and it is this complexity that attributes to its sensitivity to popular disinfectants and biocides (Rowan and Laffey, 2020b; Kampf et al., 2020; Van Doremalen et al., 2020). Researchers have reported that the use of conventional disinfectants and biocides inactivate SARS-CoV-2 by disrupting the lipid-containing viral envelope, the capsid, and the genome (Dev Kumar et al., 2020). Indeed, compared to that of naked viruses, enveloped viruses, such as SARS-CoV-2, are generally more sensitive to conventional disinfection strategies and at similar dosages. Thus, in this case, the evolution of greater complexity at the cost of vulnerability can be readily exploited in mitigation approaches (Pinon and Vialette, 2018).

The emergence of SARS-CoV-2 variants in the UK (Volz et al., 2021) and South Africa (WHO, 2020b) may influence viral transmissibility, and possibility pathogenicity. However, it is unlikely that the multiple

Fig. 1. Examples of disposal face masks and reusable cloth face covering: (a) KN95-type filtering face piece mask, (b) medical or procedural mask, and (c) non-medical reusable cloth face covering.

mutations observed in SARS-CoV-2 variants alternating outer surface spike proteins will impact on efficacy of commonly-used disinfection, or penetrating face masks, given that these mutations lead to minor morphological changes to what is still a large enveloped coronavirus from a destructive or preventative perspective. However, an evaluation of variant analysis of SARS-CoV-2 to ensure efficacy of NPIs are merited in order to comprehensively establish same (Koyama et al., 2020). Previous studies have highlighted the importance of the outer lipid membrane in rendering enveloped viruses more susceptible to naked viruses when using disinfectants (Rotter, 2001; Figueroa et al., 2017; Kampf, 2018; Blázquez et al., 2019). WHO (2020b) noted that previous reports of the D614G mutation, and the recent reports of virus variants from the Kingdom of Denmark, the United Kingdom of Great Britain and Northern Ireland, and the Republic of South Africa have raised interest and concern in the impact of viral changes. Moreover, the WHO (2020b) stated "Over a period of several months, the D614G mutation replaced the initial SARS-CoV-2 strain identified in China and by June 2020 became the dominant form of the virus circulating globally. Studies in human respiratory cells and in animal models demonstrated that compared to the initial virus strain, the strain with the D614G substitution has increased infectivity and transmission. The SARS-CoV-2 virus with the D614G substitution does not cause more severe illness or alter the effectiveness of existing laboratory diagnostics, therapeutics, vaccines, or public health preventive measures". Given greater transmissibility of SARS-CoV-2 variants, there is likely to be enhanced pressure on supply chain for personal and protective equipment such as filtering face-piece respiratory (FFR) masks, and stricter adherence to NPIs.

Current evidence shows that disinfectants, such as use of 70% (v/v) alcohol, are effective for hand sanitation and for fomite disinfection (Dev Kumar et al., 2020; Van Doremalen et al., 2020; Kampf et al., 2020). Moreover, several authors are reported on the viability of SARS-CoV-1 and SARS-CoV-2 on different surfaces, such as printed paper, tissue, wood, glass, banknotes, plastic, stainless steel, surgical masks layers under a variety of temperature and relative humidity (RH) conditions (Pagat et al., 2007; Behzadinasab et al., 2020; Chan et al., 2020; Derraik et al., 2020).

In general, SARS-CoV-2 is inactivated on surfaces within 4 days at ambient room temperatures, depending upon the viral load and presence of organic matter or soiling. For example, Chin et al. (2020) used medium tissue culture infective dose ($TCID_{50}$) to report reductions of ≥4.5 $\log_{10}$ for SARS-CoV-2 at room temperature (22 °C, 65% RH) and 37 °C after 14 and 3 days respectively. However, Riddell et al. (2020) measured the survival rates of SARS-CoV-2, suspended in a standard ASTM E2197 matrix, and reported that using initial viral loads broadly equivalent to the highest infectious patients, viable virus was isolated for up to 28 days at 20 °C from common surfaces, such as glass, stainless steel, and both paper and polymer banknotes. This highlights the importance of using hand hygiene and surface disinfection and to avoid touching the outer layer of face masks during the COVID-19 pandemic.

Chin et al. (2020), and other (Chan et al., 2020) highlighted much longer persistence of SARS-CoV-2 on surfaces under colder or refrigeration temperatures (4 °C), where the virus was only reduced by 0.7 to 2 $\log_{10}$ after 14 days. The soiling of face masks and coverings, such as potentially touching the outer surfaces where fingers are coated with natural oils, and possibly with SARS-CoV-2 if contaminated, may contribute to viral persistence. For example, Kasloff et al. (2020) simulated typical infectious body fluids of infective patients and showed that to achieve a 5 $\log_{10}$ reduction of SARS-CoV-2 at room temperature (20 °C), it took 14 days on nitrile gloves, and survival up to 21 days on plastic face shields, N100 filtering facepiece respirators (FFRs) and polyethylene overalls. Some residual SARS-CoV-2 infectivity was evident from the artificially-inoculated FFRs after 3 weeks. Chin et al. (2020), using non-soiling studies, reported that SARS-CoV-2 exhibited residual infectivity on the inner and outer layers of surgical masks after 7 days where there were ≥4.8 $\log_{10}$ and 3 $\log_{10}$ reductions in viral load respectively. Fischer et al. (2020) noted ≥4 $\log_{10}$ reduction ($TCID_{50}$/mL) on SARS-CoV-2 inoculated N95 respirator and stainless steel respirator disks after 24 h and 48 h respectively when held at 21–23 °C, 40% RH. These observations may have implications for longer survival of SARS-CoV-2 when suspended in aerosols or on contact fomite surfaces (such as face coverings), given the transition to the colder winter season in the Northern hemisphere.

2.2. Breaking the chain of infection in the context of non-pharmaceutical interventions (NPIs) to address COVID-19

Adopting key principles of conventional infection control practices has proven effective against COVID-19, namely, breaking the

chains in the infection cycle in at risk settings including use of non-pharmaceutical interventions (NPIs) (Fig. 2). In the context of this infection cycle (Fig. 2), the "infectious agent" is the pathogen, such as SARS-CoV-2, which causes diseases that can be influenced by level of virus or load, transmissibility and virulence of viral variants. The "Reservoir" includes places in the environment where the pathogen resides, such as people, contact surfaces (door handles, and medical equipment (stethoscope, thermometer), where persistence can be influenced by presence of organic matter and environmental factors (temperature, relative humidity). For example, Rowan (2019) reviewed the disruptive potential of pulsed light technology to disinfect contaminated surfaces in healthcare to prevent disease transmission. "Portal of exit" is the way the infectious agent leaves the reservoir, such as through open aerosols, and splatter of body fluids including coughing, sneezing, and saliva (WHO, 2020a). "Mode of transmission" is the means by which the infectious agent can be passed on, such as through direct or indirect contact or by inhalation (WHO, 2020a). There is also the possibility of transmission from people who are infected and the shedding virus, but have not yet developed symptoms; this is called pre-symptomatic transmission (Arons et al., 2020). Lee et al. (2020) quantitatively evaluated SARS-CoV-2 molecular shedding among 303 patients in a community treatment centre in Cheonan, Republic of Korea; of those initially considered asymptomatic, 89 (about 30%) remained healthy throughout the study. Twenty-one others went on to develop symptoms of the virus. The incubation period for COVID-19, which is the time between exposure to the virus and symptom onset, is on average 5–6 days, but can be as long as 14 days (WHO, 2020a). "Portal of entry" is the way the infectious agent can enter a new host, such as, the respiratory tract, mucous membranes or contaminated personal and protective equipment (PPE) (WHO, 2020a). "Susceptible host" can be any person, but the most vulnerable are those who are immune-suppressed or have comorbidities or an aging immune system (elderly) (WHO, 2020a; Murphy et al., 2020). Fig. 2 highlights the important role of NPIs, (such as PPE, face coverings), in breaking multiple inter-connected links in the infection cycle that will prevent COVID-19 transmission.

The main modes of SARS-CoV-2 transmission is through suspension in virus-laden aerosols or droplets that are typically liberated through the nose and mouth of infected spreaders. Airborne spread occurs with pathogens found in exhaled droplets <5 μm in diameter (Chua et al., 2020); where it is generally thought that SARS-CoV-2 can be transmitted in exhaled particles smaller or larger than 5 μm (Leung et al., 2020). A greater risk of SARS-CoV-2 transmission is appreciated through talking, singing, coughing and sneezing where the aerosolised virus can remain airborne due to low sedimentation velocity; thus, highlighting the importance of maintaining a 2 m (6.6 ft) social distancing and the wearing of face masks (WHO, 2020a). The further the distance apart from an infected SARS-CoV-2 spreader, the lower the relative risk of acquiring SARS-CoV-2, such as from airborne aerosols and droplets. Using laser light scattering, Anfinrud et al. (2020) found that there were average emissions of about 1000 droplet particles per second speech, with high emission rates of up to 10,100 droplet particles per second. Stadnytsky et al. (2020) estimated that 1 min of loud speaking generates greater than 1000 droplets containing virus; this was calculated by fitting the time-dependent decrease in particle detected to exponential decay. Chu et al. (2020) conducted a systematic review and meta-analysis of 172 observational studies and found that there is a 12.8% chance of contracting COVID-19 with physical distancing measures of less than 1 m, but this falls to just 2.6% with a distance of 1 m or more. The WHO (2020a) stated that "Droplet transmission

Fig. 2. Breaking the chain of COVID-19 infection: contributions of different NPIs.

occurs when a person is in close contact (within 1 m) with an infected person and exposure to potentially infective respiratory droplets occurs, for example, through coughing, sneezing or very close personal contact resulting in the inoculation of entry portals such as the mouth, nose or conjunctivae (eyes)". This emphasizes the challenges of mitigating transmission of SARS-CoV-2 in the indoor environment as there is a higher risk of viral exposure with the close congregation of potential viral spreaders, and there is limited ability for air treatment or exchange. Thus, improving behavioural change, such as avoiding complacency, when using face masks and face coverings to ensure that both the nose and mouth are kept covered will be beneficial (Rowan and Laffey, 2020b).

SARS-CoV-2 is spread through infectious aerosols (Asadi et al. 2020). Beldomenico (2020) also proposed that superspreaders play an important role in the spread of SARS-CoV-2. The potential variance in individuals to spread SARS-CoV-2 may also explain apparent differences between studies that typically report on low secondary attack rates with homes (11.2% in one Chinese study (Bi et al., 2020) and attack rates in specific clusters of transmission, such as the Skagit County choir where 87% of attendees were affected by one individual (Hamner et al., 2020). Kenyon (2020) highlighted the complexity of quantifying relative risk (RR) for susceptible individuals as there is increasing evidence that a large proportion of SARS-CoV-2 transmissions occur whilst the transmitters have low or no infection (Arons et al., 2020). Thus, it is also increasingly recognised that asymptomatic infected individuals, or symptomless spreaders, may also effectively cross-infect other susceptible people with SARS-CoV-2 (Asadi et al., 2020a,b; Arons et al., 2020), which supports the need for wearing of face masks and improvised face coverings and to follow additional nonpharmaceutical mitigation strategies. However, Perencevich et al. (2020) highlighted that no studies have evaluated the effects or potential benefits of face shields on point source control (i.e., containing a sneeze or cough), when worn by asymptomatic or symptomatic persons. These authors also noted that major recommendations should be evaluated using clinical studies, but it is unlikely that a randomised trial has been conducted to verify efficacy due to restricted time associated with fast moving pandemic conditions; thus, with the introduction of new vaccines, many future randomised control studies that focus on efficacy of NPIs may be retrospective in nature. The type and degree of non-pharmaceutical strategies applied are influenced by the perceived severity of the relative risk; for example, full PPE should be worn in a high-at-risk healthcare setting, such as ICU (Rowan and Laffey, 2020b). Whereas wearing improvised cloth face coverings, hand-sanitation and social distancing are used for lower relative risk community settings. However, the relative contribution of each of these transmission modes remains uncertain, and variance in viral, host, or environmental factor is likely to influence which modality is favoured in different settings (Tellier et al., 2019; Asadi et al., 2020b).

2.3. Aerosol and non-aerosol generating procedures: the role of face mask and face covering including design, features, characteristics and maintenance

Medical masks should be certified according to international and national standards to ensure they offer predictable product performance when used by HCWs, according to the risk and type of procedure in a healthcare setting (WHO, 2020a; Rubio-Romero et al., 2020). "Defined for single use, a medical masks' initial filtration (at least 95% droplet filtration), breathability, and if required, fluid resistance are attributed to the type (e.g. spunbond or meltblown), and layers of manufactured non-woven materials (e.g. polypropylene, polyethylene or cellulose)" (WHO, 2020a). Recent theories suggest that SARS-CoV-2 can also be transmitted by attachment to particles or dust that have been from contaminated surfaces, which have been recently designated as "aerosolized fomites" (Asadi et al., 2020a,b). This, if true, further strengthens the importance of wearing face masks and coverings to prevent infection. The scientific community has been discussing whether the COVID-19 virus, might also spread through aerosols in the absence of aerosol generating procedures (AGPs) (WHO, 2020a). This is an area or active research. It is noteworthy, that the presence of viral RNA is not the same as replication- and infection competent (viable) virus that could be transmissible and capable of sufficient inoculum to initiate invasive infection. High quality research, including randomised trials in multiple settings, are required to address many of the acknowledged research gaps related to AGPs and airborne transmission of the COVID-19 virus (WHO, 2020a). The global spread of COVID-19 has substantially increased the demand for face masks worldwide that has accelerated research and innovation surrounding their efficacy (Rowan and Laffey, 2020a). In general, the term "face mask governs a broad range of protective equipment with a primary function of reducing the transmission of particles or droplets" (Fischer et al., 2020). Fischer et al. (2020) tested 14 commonly available masks, or mask alternatives that included improvised face coverings, using a simple yet cost-effective optical measurement method to evaluate the efficacy of masks to reduce the transmission of respiratory droplets during regular speech. Improvements in preventing droplet transmission was evident using increased layers of cotton-polypropylene and pleats compared to fitted N95, while neck gaiters or bandanas offered very little protection. Fischer et al. (2020) also observed a significant increase in relative droplet count when the N95 respirator was fitted with a value.

The WHO (2020a) have provided comprehensive guidance on use of masks and improvised fabric face coverings in the context of the COVID-19 pandemic. New guidance is provided on non-medical (also referred to as "fabric") mask features and characteristics, including choice of fabric, number and combination of layers, shape, coating and maintenance. "Masks can be used either for protection of healthy persons (worn to protect oneself when in contact with an infected individual) or for source control (worn by an infected individual to prevent onward transmission). However, the use of a mask alone is insufficient to provide an adequate level of protection or source control, and other personal and community level measures should also be adopted to suppress transmission of respiratory viruses. Whether or not masks are used, compliance with hand hygiene, physical distancing and other infection prevention and control (IPC) measures are critical to prevent human-to-human transmission of COVID-19" (WHO, 2020c). While non-medical masks may be made from different combinations of fabrics, layering and are available in diverse shapes; however, few of these combinations of fabrics and materials have been systematically reviewed for filtration and breathability. A non-medical mask standard has been developed by the French Standardization Association (AFNOR, 2020) to define minimum performance in terms of filtration (minimum 70% solid particle filtration or droplet filtration), and breathability (maximum pressure difference of 0.6 mbar/cm^2 or maximum inhalation resistance of 2.4 mbar and maximum exhalation resistance of 3 mbar. It is noted that the lower filtration and breathability standardized requirements and overall expected performances, should be considered for source control (used by infected persons) in community settings, and not for prevention. WHO (2020c) recommended that they can be used ad-hoc for specific activities where social distancing cannot be maintained, and their use should be accompanied to hand hygiene and physical distancing. Dbouk and Drikakis (2020a, b) described a computational fluid dynamic model that takes into account turbulent dispersion forces, droplet phase-change, evaporation, and breaking up in addition to droplet-droplet and droplet-air interactions, mimicking reave events by using data that closely resemble coughing (Table 2). The study showed that criteria employed for assessing face mask performance requires modification to take into account the penetration dynamics and airborne droplet transmission, the fluid dynamics leakage around the filter, and reduction of efficiency during cough cycles. The study proves that use of masks reduce airborne droplet transmission, and will protect the wearer from contaminated droplets; however, many droplets still spread around

Table 2
Published studies on new face mask design, functionality and sustainability factors to help address supply chain shortage and improvements in waste managements presented by ongoing COVID-19 pandemic.

Innovations	Main development(s)	Citing reference(s)
Computational fluid dynamics for face mask filter efficacy	Face mask filters – textile, surgical or respiratory – understanding of droplet dynamics through and around a face mask filters resembling cough many – new criterion for calculating mask efficiency to consider penetration dynamics proposed – masks do not provide complete protection	Dbouk and Drikakis, 2020a, 2020b
Air dispersion distances through patient simulator	Normal cough induces turbulent flow that spreads about 70 cm from the subject – N95 mask prevented air leakage than surgical mask during coughing. But there remains sideway leakage.	Hui et al., 2012
Forward jet of droplets and leakage around mask – droplet transmission	Using the Schlieren optical method, it was shown that wearing a standard surgical mask blocks the forward jet of droplets, but allows leakage around the top, bottom and sides. N95 reduces the droplet leakage around mask edges during coughing – none of the masks entirely prevented penetrating or escaping the mask – i.e., droplet transmission.	Tang et al., 2009
Self-designed triple-layer cotton masks to suppress respiratory droplet levels	Self-designed triple-layer cotton masks worn by respiratory infected person (influenza and COVID-19 participants) were shown to be similar to medical masks for suppressing droplet levels in regular bedroom and a car with air conditioning where cough/sneeze counts were measured	Ho et al. (2020)
Face masks with respiratory valve had lower exchange rate of breathing assistance	Studies to evaluate and characterize the comfort sensation and performance of 12 types of face masks (related to shape, respiratory valve, brand, main materials and protection level) related to breathing assistance for healthcare in fog and haze weather [non-COVID-19] – dynamic changes in airflow rate and breathing resistance were acquired by virtual instrument system- cotton mask had lower rate of breathing assistance than nonwoven fabric masks.	Yao et al., 2019
Mask face detection based on a hybrid AI, deep transfer learning and classic machine learning model	Use of Artificial Intelligence (AI), deep transfer learning and classic machine learning to evaluate mass usage of face masks to potentially inform protection and compliance during COVID-19. Researchers used three data sets: Real-World Masked Face (RMFD) consisting of images of 5000 masked faces and 90,000 unmasked faces; Simulated Masked Face Dataset (SMFD) with 785 for simulated masked faces and 785 for unmasked faces; Labelled Faces in the Wild (LFW) containing 13,000 masked faces of celebrities. Focus was in training for accuracy of face mask detection.	Loey et al., 2021
Use of spray-simulation method (mimicking a sneeze) along with germ-free mice	Development and validation of spray-simulation method (mimicking a sneeze) for determining efficacy of combed-cotton textiles used as two-layer barriers for protecting germ-free mice from bacteria carrying droplets. Authors used aqueous suspension of 12 probiotic-cultured dairy bacteria – authors advocated use of bacteria as they exist in association with respiratory viruses in respiratory fluids – they also used bacteria to quantify number of droplets that escape textile barrier	Rodriguez-Palacios et al., 2020
Surgical and homemade masks, even without fitting, reduces particles emitted via breathing, talking, and coughing	Wearing of surgical masks, or N95 respirators, even without fit-testing, reduces number of emitted expiratory particles from breathing, talking, and coughing from experimental studies. But, efficacy of wearing homemade cloth or paper masks is less clear, and confounded by shedding of masks fibres, with some reductions observed, particularly for larger particles (>0.5 μm). Authors did not measure virus-laden aerosols and droplets, but observations consistent that wearing mask can help with mitigating pandemic-associated with respiratory disease.	Asadi et al., 2020a
Bio-based facemasks – use of electrospinning gluten and carbonization	Suggested sustainable future-use of wheat gluten biopolymer, a by-product of cereal industries, as alternative to using petrochemicals for reusable facemask. Fine mesh nanofilter membrane structure to be achieved via electrospinning and subsequent carbonization at over 700 °C.	Das et al., 2020
Design, velocity and fitness innovation for sustainable face masks including home made	Understanding performance of commercial masks and Advantages of wearing commercial and home-made face coverings during pandemic. Review of masks made from household materials. Limited studies that used randomised control trials for investigating efficacy of cloth masks showing that they are not suitable for HCWs.	Davies et al., 2013; Chughtai et al. (2013); Chua et al., 2020
Cloth masks loose filtration efficacy after frequent washing and drying cycles.	Studies on the effect of washing and drying on cloth mask highlighted a drop in filtration performance that was correlated to pore size and shape of the masks. It was found that the PM10 filtration efficiency dropped by 20% after 4th washing and drying cycle, that was attributed to continuous stretching of the masks, enlarging the pore size, thus impairing mask performance.	Neupane et al., 2019
Engineering multifunctional face masks	Increasing trend for published information that highlights innovation to improve filtering capacity (such as pore size) of mask materials and improving additional functions in terms of design (such as antimicrobial properties, coatings) to enhance user comfort, and convenience (such as introduction of self-cleansing and sensing properties. However, these are laboratory studies.	Chua et al., 2020
Increased super hydrophobicity and transparent qualities of masks materials	Graphene-coated masks shown to exhibit significant superhydrophobic and photothermal performance that can repel incoming aqueous droplets masks exposed up to 80 °C under sunlight illumination can achieve self-sterilisation. Transparent properties included on face masks to improve quality for the hearing impaired such as digital face recognition, human-facing industry.	Son et al., 2020; Zhong et al., 2020; Chua et al., 2020
Differences in FFE for head tie, ear-loop face masks	29 different face masks alternative including expired N95 respirators with intact elastic straps and respirators subjected to ethylene oxide or VH2O22 sterilisation – procedural face masks with elastic ear loops showed lowest fitted filtration efficacy at 38.1%. Thus, highlighting increased risk.	Sickbert-Bennett et al., 2020

and away from the mask cover (Table 2). Therefore, use of a mask does not provide full protection and social distancing remains important during the pandemic.

The WHO (2020c) recognises that many countries have recommended the use of fabric masks/face coverings for the general public, but also recognises that the widespread use of masks by healthy people

in the community is not yet supported by high quality or direct evidence where there are potential benefits and harms to consider. The WHO advises decision-makers to apply risk-based approaches when encouraging the use of for the general public to include, (1) purpose of mask use, (2) risk of exposure to the COVID-19 virus, (3) vulnerability of the mask wearer/population, (4) setting in which the population lives, (5) feasibility, such as availability and cost of masks, and ability of mask wearer to tolerate adverse effects of wearing a mask, and (6) type of mask, such as medical versus-non-medical mask. Examples of where the general public should be encouraged to use medical and non-medical mask in areas with known or suspected community transmission.

2.4. Reprocessing and extended use of PPE and face coverings to meet supply chain shortfall in the context of COVID-19 pandemic

There has been a commensurate interest in reuse of PPE in healthcare, particularly important filtering facepiece respirators (FFRs), such as N95 respirators, to meet supply chain shortages during COVID-19 pandemic (Rowan and Laffey, 2020a; Rubio-Romero et al., 2020). This need for potential extended or reuse of FFRs is likely to be remain beyond COVID-19 given sustained concerns by clinicians and healthcare workers, along with meeting the surge in patients attending health screening (non-COVID-19 related) and requiring medical procedures. Several countries have adopted PPE reuse through reprocessing technologies that address fit testing post treatments along with disinfection and filtration efficacy (Rubio-Romero et al., 2020). A comprehensive review of efficacy and usage of face masks has been conducted by Rubio-Romero et al. (2020). Given the heat sensitivity and complexity of materials used in single-use PPE, only a limited number of reprocessing technologies have been authorized for their emergency reuse by the FDA, such as using hydrogen peroxide in vapor form (30–35% VH2O2) used alone or combined with ozone (FDA, 2020; Rowan and Laffey, 2020a). McEvoy and Rowan (2019) provided an informative and comprehensive review on the use of VH2O2 in the adjacent area of terminal sterilisation of medical devices. Countries are also pursing use of ultra-violet germicidal irradiation technologies (UV dose 2000 μJ/cm^2) (Derraik et al., 2020), but there remains uncertainty surrounding the efficacy of this 2-dimensional irradiation to penetrate complex filtration system associated with FFRs (Rowan and Laffey, 2020b). Use of conventional moist heat at 60 °C (60 min, at high humidity), is also potentially efficacious for safe PPE reprocessing (Derraik et al., 2020; Rowan and Laffey, 2020b).

A limiting factor in harmonized reprocessing of PPE will be the availability of sophisticated technologies, such as VH_2O_2, to meet unprecedented high demand during COVID-19 pandemic (Rowan and Laffey, 2020a; Ilyas et al., 2020). Decisions underpinning PPE reuse are likely to be governed by infection prevention groups in healthcare, in consultation with competent regulatory authority for each country, where critical shortages in supply chain will inform deployment in order to protect frontline healthcare workers (HCWs). However, lack of acceptance by HCWs for the use of reprocessed PPE might be a barrier to general deployment, which can be potentially addressed through education, training and social marketing to highlight efficacy and safety. PPE supply chain shortfalls have been primarily met by enhanced production by original equipment manufacturers (Rowan and Laffey, 2020b). In addition, initiatives and collaborations performed by companies, hospitals, and researchers in utilising 3D printing during the COVID-19 pandemic has contributed to this effort to address supply chain shortfalls in face shields (Tino et al., 2020). Homemade and commercial cloth or fabric face coverings are less complicated, and can be effectively reprocessed by moist heat combined with using a detergent (60 °C for 30 min), such as using a domestic laundry machine combined with spin drying (Rowan and Laffey, 2020a). Face shields are used without a mask, they should wrap around the sides of the wearer's face and extend below the chin. It was recently reported that only those wearing face shields at a Swiss hotel succumbed to COVID-19, where no reported cases occurred for staff and guests who wore face masks in the same hotel. The WHO (2020c), and other authorities, have advised that face shields can offer an added layer of protection, but in addition to a face mask, social distancing, and handwashing, not as a substitute.

2.5. Innovation surrounding face mask design and functionality for future sustainability

Best available evidence supports the effective use of face masks as nonpharmaceutical counter-measures for addressing COVID-19 (Wang et al., 2020a); where there has been advancements on the reprocessing of single-use face masks under Emergency Use Authorisation (Rowan and Laffey, 2020a). However, published evidence shows that masks do no provide 100% protection (Wang et al., 2020b), with significant variance depending on the filtration efficiency and design. There has been a surge in innovation to improve face mask design, comfort, functionality and sustainability, such as improvements in recycling and medical waste management (Table 2). Despite well-conducted studies, there is a pressing need to extensively test and validate these new innovations through regulated multi-actor, collaborating, randomised controlled trials.

Mask efficiency is defined as percentage of a contaminant removed by a mask filter, where mass, weight, number of particles, or volume can quantify this performance (Hutten, 2016) (Table 2). Typically, certification standards (ASTM F1862M-17, 2017; ASTM F201-19, 2019) usually define a surgical mask efficiency as a standard value independent of coughing incidents or cycle. However, Dbouk and Drikakis (2020a, b) noted that these standards neglect fluid flow dynamics effects and droplet leakage through mask openings. Additionally, there is no consideration that mask efficiency can deteriorate considerably over time due to saturation effects; thus, coughing and fluid dynamics need to be considered in calculating fluid efficiency. The main mechanisms of filtering through masks are droplet diffusion, interception and impaction. Also, the frequency of coughs may further challenge efficiency. Continued, or cyclic coughing, increases dynamic flow that can negatively affect efficacy of mask filter performance where a wide range of filter efficiencies have been described (Rengasamy et al., 2010). Previous studies reported that use of surgical masks effectively reduce emission of large droplets and minimize lateral dispersion of droplets (Driessche et al., 2015; Stockwell et al., 2018).

Ho et al. (2020) reported that self-designed triple-layered cotton masks worn by respiratory infected volunteers were similar to participants wearing medical masks (Earloop Procedure Face Mask 1820: 3M, MN, USA) for suppressing respiratory droplet levels in a regular bedroom, and a car with air conditioning. (Table 2). Specifically, 211 adult volunteers with 208 confirmed cases of influenza (influenza A = 188; influenza B = 17) and 6 suspected cases of COVID-19 from Taipei-Keelung metropolitan area were recruited. Four 1-hour repeated measurements of particles with size range 20–1000 nm measured by number concentrations (NC0.002-1), temperature and relative humidity, and cough/sneeze per hour for each volunteer. Authors concluded that cotton masks could potentially substitute for medical masks for respiratory infected person in a microenvironment with air conditioning. Also, healthy individuals may use cotton masks in the community setting as cotton masks are washable and reusable. However, wearing of medical masks is still popular in community settings, globally (Secon, 2020). Previous studies have reported that the oral cavity is the main source of expiratory droplets in the 5 to 100 μm range during speech and cough (Johnson and Morawska, 2009).

Previous studies have shown that towel (100% cotton) and common cloth (70% cotton and 30% polyester) masks showed 40–60% filtration efficiency for polydisperse sodium chloride (NaCl) aerosol particles (75% ± 20 nm count median diameter (CMD) and a geometric standard deviation (GSD) not exceeding 1.86) at 5.5 cm/s face velocity (Rengasamy et al., 2010) (Table 2). Yao et al. (2019) investigated

comfort sensation and performance of face mask related to breathing resistance for healthcare in fog or haze weather (non-COVID-19) (Table 2). The dynamic changes in airflow rate, and the breathing resistance were acquired by a virtual instrument system and a microelectronic system. The researchers used six evaluation indices for defining dynamic performance and comfort sensation of face mask where 12 different types of face masks from four brands with different features were tested, namely shape, respiratory valve, brand, main materials, and protection level. The average breathing frequency was set at 20 times per minute, and the peak flow rate of both exhalation and inhalation was 85 L/min in dynamic measurement. Findings showed that face masks with a respiratory valve had a lower change rate of breathing resistance. Moreover, cotton masks had lower change rate of breathing resistance than the non-woven fabric masks. The cup-type mask had lower change rate of breathing than the folding mask.

A review of best-published information on face masks design and efficacy reveals that face masks prevent, or reduce transmission and contraction of COVID-19, but they should not be considered as a single preventative or counter-disease measure, as they do not guarantee 100% protection. There is considerable surge in published papers on sustainability in face mask design (such as materials, layering), comfort (style), and efficacy of respiratory level of protection, but these studies, for the most part, are based on observational or laboratory studies, and not longitudinal clinical trials (Peebles, 2020). It is envisaged that future robust clinical trials will contribute significantly to this gap in knowledge.

Loey et al. (2021) reported on using artificial intelligence for detecting face mask wearing, which would support studies such as compliance and efficacy in the era of the COVID-19 pandemic (Table 2). Specifically, these authors reported on the development of a hybrid deep transfer learning model with machine learning methods for face mask detection where several thousand images of masked and non-masked individuals were analysed, which were contained in three datasets, namely, Real-World Masked Face Dataset, the Simulated Masked Face Dataset, and the labelled Faces in the Wild. The authors reported on testing and training accuracy for face mask detection at 99.64%, 99.49% and 100% respectively for these datasets.

Rodriguez-Palacios et al. (2020) reported on the use of a functional in vivo test method for assessing facemask/filtration materials using germ free (GF) mice where probiotic bacteria suspended in microdroplets were used, instead of respiratory viruses (Table 2). Use of bacteria, in this instance, was deemed appropriate as bacteria accompany respiratory viruses in respiratory droplets. This study reports on use of an in vivo spray-simulation method (mimicking a sneeze), where combed-cotton textiles used as two-layer barriers covering mice cages prevented the contamination of all GF animals when sprayed with 10–20 bacterial droplet units/cm^2.

Asadi et al. (2020) conducted experimental studies using homemade cotton cloth and paper face masks that showed reductions in number of emitted expiratory particles from breathing, talking, and coughing. However, these observations are not as clear, and confounded by shedding of masks fibres, as compared significant outward particle emission reductions from wearing surgical masks and N95 respirators, even without fit-testing. The authors attest that these observations are consistent with suggestions that mask wearing can help in mitigating pandemic associated respiratory diseases. Also, their results suggest that importance of regular change of disposable masks and washing of homemade masks, and suggest that special care must be taken in removing and changing of masks.

Das et al. (2020) described electrospinning and subsequent carbonization of wheat gluten biopolymer to form nanofiber membranes for bio, or gluten-based facemasks (Table 2). These same gluten materials can be processed into cohesive thin films using plasticiser and hot press. Additionally, lanosol, a naturally-occurring substance, can be added that imparts fire (V−) rating in vertical burn test), and microbial resistance in gluten plastics. Thus, the authors advocate that thin films of flexible gluten with very low amounts of lanosol (<10%) can be bonded together with the carbonised mat and shaped by thermoforming to create the facemasks. Most medical or surgical face masks are made of non-renewable petroleum-based polymers such as polypropylene, polystyrene, polycarbonate, polyethylene, and polyester (Das et al., 2020), which are non-biodegradable and contribute towards environmental pollution. Thus, there is pressing need to rapidly develop facemasks that are fully bio-based and effective along with being low cost, lightweight and comfortable.

For facemasks, filter media is an important component (Table 2). In general, fibrous material are used to create particulate matter (PM) filters, which can be designed according to a particular size of a PM that can be ultrafine (<0.1 μm), fine (0.1–2.5 μm), and course (2.5–10 μm); denoted as $PM_{0.1}$, $PM_{2.5}$ and PM_{10} respectively. Filtration occurs through interception, inertial impaction, diffusion, and inter-molecular/electrostatic/gravitational interactions of the target particles on the surface of the filter medium. However, for virion particles, whose diameter is very small (ca. 20–400 nm), Brownian diffusion is the main filtration mechanism (Mao, 2017). Face masks provide respiratory protection from infected individual by filtration capacity of the media against the aerosol particles. Since the size of coronaviruses are typically in the range 160–200 nm (Pellett et al., 2014), non-woven filter media would be more effective that woven alternatives (Chellamani et al., 2013). Non-woven filters exhibit higher barrier properties compared to cotton and petroleum-based polyesters. Das et al. (2020) noted that these non-woven filter media can be manufactured by the process of electrospinning, which is the most cost-effective and facile methods to create fibrous membranes with a myriad of fibre diameters and porosity. Previous researchers have also used gluten with polyvinyl alcohol (PVA) through electrospinning into nanofibers (Dhandayuthapani et al., 2014; Aziz et al., 2019). Strain et al. (2015) also previously described the use of electrospun recycled polyethylene terephthalate (rPET) to develop fibrous membranes for cigarette smoke filtration. However, for the development of face masks, interdisciplinary research encompassing electrospinning, thermos-chemical conversion, gluten bio-polymer processing, and mask testing would need to addressed (Das et al., 2020). These authors also note the addition of fire retardant and moisture resistance of gluten could be enhanced by adding lanosol, and polyaminoamide epichlorohydrin (PAE), respectively, which are important for face mask using future carbonised gluten fibres.

Gandhi and Rutherford (2020) theorized that face masks could provide some degree of immunity 'variolation', where small doses of the virus potentially penetrate the covering and stimulate the immune response that may help with herd immunity. While this remains to be proven, it is recognised that immune-priming can potentially improve subsequent exposure to larger viral or bacterial loads. This immune-priming concept is also been exploited by researchers as a means of reducing inflammatory responses, such as use of purified β-glucans from medicinal fungi for addressing acute respiratory distress syndrome (ARDS) and sepsis that contributes significantly to severe respiratory systems experienced by critically ill COVID-19 patients (Murphy et al., 2020a; Murphy et al., 2020b; Masterson et al., 2020). Future design innovations may support greater aerosol filtration efficacy for face masks and coverings to help reduce transmission, such as potentially using head ties, instead of ear loops. For example, Sickbert-Bennett et al. (2020) reported that surgical masks with ties had filtration efficiency (FFE) of 71.5% (±5.5), while procedural mask with ear loops had lower FFE at only 38.1% (±1.1) (Table 2). There is a growing interest in evolving face masks and coverings for efficacy and wearer comfort ranging from anti-fogging capacity for those wearing spectacles to evaluating alternative biomaterials to potentially replace plastics in one-time-use PPE. The latter enable improved recycling and waste management (Silva et al., 2020; Wang et al. 2020; Ilyas et al., 2020).

Davies et al. (2013) tested filtration efficacy of house-hold masks made using different materials (including 100% cotton T-shirt, scarf, tea towel, pillowcase, antimicrobial pillowcase, vacuum cleaner bag,

cotton mix, linen and silk) against bacterial (*Bacillus atrophaeus*, 0.95–1.25 μm) and viral (Bacteriophage MS2, 0.023 μm) aerosols (Table 2). All materials were capable of blocking test microorganisms to different extents, and they all worked better in the case of using the larger *B. atrophaeus* endospores. Although surgical mask, as a control sample, exhibited the highest efficacy, cleaner bag, tea towel, and cotton mix also showed filtration efficacy. However, the authors also simultaneously reported on the ease of breathing, which is indicated by pressure drop. The higher the pressure drop, the higher the difficulty for the wearer to breathe. It is observed that despite high filtration efficacy of a vacuum cleaner bag, and tea towel, their high-pressure drop values make them unsuitable for masks. Doubling the layers did not improve filtration efficacy; yet, doubling increased pressure drop, indicating more difficulty for breathing. Wearing a mask can reduce the infection probability yet cannot eliminate the risk of contracting the disease, when used alone as a non-pharmaceutical preventive measures, such as hand hygiene, social distancing, quarantine, and immunization. Chughtai et al. (2013) reviewed cloth masks using randomised clinical trial to evaluate how efficient cloth masks are for protecting HCWs. Findings revealed that respiratory infection was highest in the cloth mask group and that the particle penetration of cloth masks was 97% (versus 44% for medical masks), the authors concluded that cloth masks should not be used for HCWs, especially in highly infectious situations. Neupane et al. (2019) studied the effect of washing and drying of cloth masks on the filtration performance and correlated the performance of the pore size and shape of the masks. These authors concluded that the PM_{10} filtration efficiency dropped by 20% after the 4th washing and drying cycle, which was attributed to the increase in pore size and the lack of microfibers with the pore region. The authors noted that long-term usage of the cloth mask entails continuous stretching of the mask, enlarging the pore size, thus, impairing mask performance. Studies are lacking as to the specific number of times cloth mask can be washed to retain efficacy, but the risk also depends upon the degree of other mitigating non-pharmaceutical counter-measures present. Sickbert-Bennett et al. (2020) evaluated 29 different fitted face mask alternatives showed that surgical and procedural masks had lower fitted filtering performance (FFE) to that of N95 respirators (98.5% FFE), while procedural face masks secured with elastic ear loops showed lowest FFE at 38.1%. Thus, highlighting variance in FFE depending upon head tie and ear loop, which may be considered under risk mitigation for wearer in the context of overall non-pharmaceutical countermeasures and degree of potential exposure to infectious respiratory droplets.

Chua et al. (2020) reviewed innovations in face masks that may improve filtering capacity of mask materials and the addition of functions and properties into the design of masks, including super hydrophobicity (Table 2). These authors expanded upon use of polymer nanofibrous membranes, electret membranes and porous-metal organic framework (MOF)-based filters for masks, compared with existing commercial filters made of thick layers of micron-sized fibres that balance air resistance and filtering performance. Natural-based extracts, such as tea tree oils, extract of olive and *Euscaphis japonica* and *Sophora flavescent* have been sprayed on surfaces of polymeric air filters for antimicrobial properties; however, high loading of antimicrobial herbal extracts may lead to increased pressure drops (Son et al., 2020). Other experimental device-coating studies focus on combinational metal-based nanoparticles for broad spectrum activities, such as incorporation of silver-nanoparticle (AgNP)-impregnated activated carbon cloth (ACC) into a mask resulting in >99.88% virus filtration while having increased air permeability compared to FFP3 mask (US Patent Application US2011011095A1). Currently, many masks, some including a number of types of antimicrobial agents, are commercially available (Chua et al., 2020): however, mask antimicrobial activities have only been studied under strict laboratory conditions. An understanding of day-to-day performance under the actual lived-experience or clinical trial settings is lacking, as are our understanding of potential influence of actors affecting mask reusability including washing, drying or non-thermal processing. Notwithstanding the latter, Chua et al. (2020) recognised that existing models of masks and respirators serve users well in terms of appropriate level of protection against airborne pathogen.

2.6. Mathematical and statistical modelling applied to decision-making with respect to the ongoing COVID-19 pandemic

There is a gap in knowledge on the efficacy of NPIs, in terms of relative risk (RR), in preventing COVID-19 infection. R_0, the reproduction number, has been used as a measure to monitor efficacy of NPIs as it indicates the relative contagiousness of an infectious disease; R_0 denotes the average number of people who will potentially contract a contagious disease from one person with a disease, such as COVID-19 (Perencevich et al., 2020). R_0 specifically applies to a population who previously were free of infection, and were not vaccinated. For example, an R_0 of 7 infers that one infected person may potentially transmit COVID-19 to an average of 7 other susceptible people. Thus, national emergency public health teams carefully track R_0 values daily as a means of assessing how effective the implementation of strategic disease counter-measures have been (example, Government of Ireland, 2020b). This also informs ongoing public health policy decision(s), such as bans on large-in-person gatherings, closure of restaurants and retail stores, and if to implement lockdowns, such as in the Republic of Ireland where citizens have just re-emerged from its second level 5 lockdown period (Government of Ireland, 2020c). Perencevich et al. (2020) also supports that taken as a bundle, the effectiveness of adding face coverings and face shields as a community setting to other NPI containment strategies merits evaluation. The authors noted that his situation is challenging as there is no prior robust template or 'dress rehearsal' to follow, and public health managers and politicians need to make full decisions (100%) on the basis of a diversity of epidemiological data that is probability based; thus, tracking R_0 values provides tangible indicators of efficacy. The implicit goal of NPIs, alone or in combination with other NPIs, should be to interrupt transmission by reducing R_0 to less than 1.

In the context of predicting the variables related to an epidemic (e.g. mortality rate, disease spread, number of infected people, time until herd immunity is reached, etc.), the SIR model of Kermack and McKendrick (1927) and extensions have been used since the 1920s. SIR stands for Susceptible – Infected – Recovered, which are the main compartments individuals may belong to during an epidemic. The general formulation of a SIR model is given by a system of ordinary differential equations (ODEs) describing the instant variation in the populations of each compartment over time (t). The SIR system of ODEs may be written as

$$\frac{dS}{dt} = -\beta \frac{I}{N} S$$

$$\frac{dI}{dt} = \beta \frac{I}{N} - \gamma I$$

$$\frac{dR}{dt} = \gamma I$$

where S, I and R represent the number of susceptible, infected and recovered individuals, N is the total population, i.e. $N = S + I + R$, β is the infection rate and γ is the recovery and/or mortality rate. In practice, the expression $\beta I/N$ is known as the "force of infection", and the system requires the specification of the initial conditions for each compartment, as well as the values for the parameters β and γ, which are estimated from data. Each equation may be seen as the instantaneous rate of change in population size for each compartment. Typically, numerical methods are used to solve the system of ODEs and produce simulated results based on the estimates for β and γ, which are then compared

to the observed data as means of validation. It can then be used to predict future number of cases and deaths, as well as the length of time a particular epidemic is likely to last.

It is often of interest to study the properties of this system and determine conditions for the persistence of the epidemic in the population. By making simple assumptions, it is possible to derive analytical expressions for what is called the "basic reproduction number", better known as R_0. Assuming that the time an infected individual remains in this infected state is exponentially distributed with parameter γ, it is straightforward to show algebraically that the average number of new infections caused by a single infected individual is $R_0 = \beta/\gamma$. When this ratio is greater than 1, the instantaneous change in the number of infected individuals is positive, and therefore an epidemic occurs. Conversely, when it is less than 1, the disease is contained.

More specifically in the context of the COVID-19 pandemic, there have been many attempts to model data from several countries and regions of the world using these epidemiological modelling tools. For example, Katul et al. (2020a, b) used a slightly extended SIR model to calculate an asymptotic global R_0 of 4.5, which shows how important mitigation strategies are for this rapidly growing pandemic. Toda (2020) also used a SIR model and studied the economic impact of the pandemic. He found that under optimal mitigation policies controlling timing and intensity of social distancing, simultaneous infection may be reduced from 28% to 6.2%, thus reducing the risk of overwhelming healthcare systems, but at the same time yielding a longer period of economic burden.

Extensions of the SIR model have also been proposed. For instance, Calafiore et al. (2020) proposed a modified model which added a new compartment "D", for deceased individuals, therefore separating those who recovered from the disease versus those who did not. He et al. (2020a, b), on the other hand, utilised a SEIR system (where "E" is the compartment corresponding to exposed individuals, those who have been infected but are still asymptomatic and uncapable of spreading the virus) and added two extra compartments representing quarantined and hospitalised individuals, as well as split the infected compartment into two, to separate the individuals who became infected during a quarantine phase. They fitted the model to data from the Hubei province in China and found from their parameter estimates that efficiently carried out quarantine measures are helpful to control the spread of the disease. López and Rodó (2020) also included a quarantined compartment in a SEIR-type model, and applied it to data from Spain and Italy. Giordano et al. (2020) proposed a multi-compartment extension called SIDARTHE, which included susceptible, infected, diagnosed, ailing, recognised, threatened, healed and extinct individuals. An important distinction made is between diagnosed versus non-diagnosed individuals, since asymptomatic and/or non-diagnosed people are more likely to spread the disease faster than those who have been diagnosed and are in isolation. Their findings support the combination of NPIs and contact tracing to combat the pandemic.

It is clear that one of the many challenges when modelling the COVID-19 pandemic are the effects of many different confounders acting in concert to result in higher or lower basic reproduction numbers. Of course, it would be ideal to obtain stratified R_0 estimates for different groups, however there is a lack of resolution in most datasets thus not allowing for such approach. We may question how accurate these mechanistic models actually are, and how reliable the long-term projections are. For reasons of parsimony and to avoid parameter estimation problems, only the most important mechanisms and compartments are included in SIR-type models. However, this leaves out potentially important variables that could play an important role. Also, the long-term projections rely upon the current assumptions to remain the same, and it is almost never the case where circumstances do not vary over time. Therefore, the main contribution is not focussed on the reliability of these projections per se, but in understanding what the likely future outcome is so as to avoid it if necessary.

Regarding short-term prediction, different time series models have been proposed to obtain forecasts of number of cases and number of deaths. This can be especially useful to determine possible growth trends in the number of patients requiring healthcare, which in turn can help to avoid the collapse of healthcare systems. Oliveira and Moral (2020) proposed a state-space hierarchical model based on a time-varying autoregressive process and an outlier detection process to forecast the number of daily COVID-19 cases worldwide. Let Y_{it} be the number of reported cases for country i at time t. They assume the distribution of Y_{it}, conditional on the number of reported cases at the previous day $Y_{i,\ t-1}$, to be negative binomial with mean $\mu_{it} = \exp\{\gamma_{it} + \Omega_{it}\}$ and dispersion ψ. The serial autocorrelation is modelled through the parameter $\gamma_{it} = \phi_{it}\gamma_{i,\ t-1} + \eta_{it}$, where η_{it} is a Gaussian white noise process and ϕ_{it} is allowed to vary over time, which introduces novelty to this type of modelling framework. The parameter $\Omega_{it} = \lambda_{it}\omega_{it}$ is an observational-level random effect accounting for extra variability induced by outliers in the time series data, where λ_{it} is a Bernoulli process and assumes value 1 when observation y_{it} is an outlier and 0 otherwise, and ω_{it} is a normal random effect representing the extra variability attributed to outliers. Oliveira and Moral (2020) found that this particular model generates highly accurate and precise forecasts for up to seven days ahead, for most countries of the world. This modelling framework does not incorporate any biological mechanisms and population states, such as the compartment models previously discussed. However, the highly accurate short-term forecasts can be complemented by the long-term projections from SIR-type models to aid decision-making and policy implementation.

Other methods can be used for short-term forecasting. Zeroual et al. (2020) carried out a study comparing six deep learning methods to forecast the daily number of confirmed and recovered cases, using data from Italy, Spain, France, China, the USA and Australia. They found that the variational autoencoder method was superior when compared to simple recurrent neural networks, long and bidirectional short-term memory, and gated recurrent units. These are what we may refer as "black-box" methods. In essence, current data is used to train (or calibrate/estimate) the algorithm, which will be used to produce future forecasts. There is a validation step used to fine tune the algorithm, and this consists of using only part of the data to train the method, and comparing the forecasts with the actual observed data. By providing multiple and extensive validation studies, Oliveira and Moral (2020) highlight their importance for two primary reasons: (1) to ensure the method is fine-tuned to deliver the best possible performance and (2) so that the uncertainty around forecasts is properly described and over-reliance on point estimates is avoided.

An alternative to describe temporal trends and patterns is the use of generalized additive models, a very flexible modelling framework. Let Y_t be the response variable of interest (e.g. number of COVID-19 cases or deaths, viral load, particle concentration etc). We may assume that Y_t follows a particular probability distribution with probability mass function or probability density function $p(\mu_t, \boldsymbol{\theta})$, where μ_t represents the mean response at time t and $\boldsymbol{\theta}$ is a vector of parameters (that may be known or estimated from the data). The mean is modelled as a function of time, such that $g(\mu_t) = f(t;\boldsymbol{\beta})$, where $g(\cdot)$ is a monotonic and differentiable link function, $f(\cdot)$ represents a sum of basis functions, often represented by splines, and $\boldsymbol{\beta}$ a vector of parameters to be estimated (other covariates may also be included if available). The aim is to describe the temporal process with a smooth function, and the degree of smoothness is typically determined via cross-validation or by adding specific penalties to the loss function being optimized (e.g. the log-likelihood or residual sums of squares). For instance, He et al. (2020a, b) fitted a Gaussian generalized additive model to viral load time series data, using cubic splines as the smooth function in the linear predictor, to examine viral shedding temporal trends. They found no significant difference across sex, age groups (over and under 65 years old) or disease severity, however.

Flaxman et al. (2020) implemented a semi-mechanistic hierarchical model to forecast the number of cases and number of deaths for several different countries, and estimated a time-varying basic reproduction number. Here, time series modelling is combined with biological information regarding infectious windows, in what is called a "semi-mechanistic" approach. This results in smooth forecast curves that can accurately depict future trends in the short-term for most countries for up to two weeks ahead. They also included the effects of NPIs in their model and found that lockdowns in particular have had a significant effect driving R_0 below one. In a different approach, Ferguson et al. (2020) adapted individual-based models developed to aid in pandemic influenza planning to COVID-19 and found that R_0 is likely to quickly rebound to being greater than one when NPIs are relaxed.

The hierarchical models discussed above have the inclusion of random effects as a common feature. These are important to accommodate the correlation between observations taken in same experimental or observational units (often referred to as a "grouping factor"), such as patients or geographical regions. The random effects are assumed to be have arisen from a probability distribution with a particular mean and variance (which are often the parameters of interest in the estimation process when assuming Gaussian random effects). This latent distribution is assumed to represent the entire population of interest, of which we have a representative sample in the available data. In the case of meta-analyses, parameter estimates obtained by different studies referring to the description of an effect of interest (e.g. use of face masks, social distancing of at least 1 m, etc.) are combined. Their total variability can be decomposed as between- and within-study variance, with the aid of random effects, and the effects of different characteristics of the studies on the parameter estimates can also be investigated. For instance, Chu et al. (2020) carried out random effects meta-analyses using data from 44 comparative studies worldwide (which included a total of 25,697 patients with COVID-19, SARS or MERS) to assess the effect of different NPIs. They found distancing, use of face masks and eye protection to be favoured in terms of reducing transmission. They highlight, however, the need for robust randomised trials to fill the knowledge gap with respect to effectiveness of different types of NPIs.

It is clear that the combination of different modelling methods is beneficial to understanding the problem as a whole and estimating effects with higher precision (Baker et al., 2018). Therefore, we may look at the short- and long-term projections at the same time using a combination of time series models, deep learning methods and mechanistic compartmental models. There is a problem, however, pertaining to data quality (Vespignani et al., 2020). Precise estimates can only be obtained from good-quality, large datasets. This is especially true when using machine learning black-box methods. These algorithms will reproduce patterns identified in the data, therefore if there is a lack of precision when collecting and/or reporting the data, the algorithms will reproduce the atypical and even non-sensical behaviours found in the data. For instance, Oliveira and Moral (2020) estimate that approximately 12.6% of the daily COVID-19 cases reported worldwide by the European Centre for Disease Control and Prevention (ECDC) represent outliers or points that contribute to extra variability. This reflects poor data collection practices by many countries, and therefore contribute to less accurate future forecasts. Extending the modelling methods discussed above to incorporate different mechanistic processes and NPI effects, therefore, requires good data quality to provide estimates that will be useful when elaborating public policies to prevent the spread of the virus.

Observational public health studies have revealed a number of potentially increasingly problematic factors, or multipliers that merit statistical modelling match with appropriate use of NPIs to break cycle of infections and to reduce R_0, these include inter alia high COVID-19 positivity in community; close proximity and increased numbers of citizens from different households; greater transmissibility of variants; increased pathogenicity of virus across different age groups; presence of co-morbidities; gathering of vulnerable, such as in residential homes; lack or absence of vaccination; reduced testing and contract tracing; non-use of face masks or coverings; absence of hand-hygiene or disinfection; occurrence of superspreaders; COVID-19 public health compliance fatigue; environmental persistence such as prolonged survival at colder temperatures; PPE supply chain shortage; affordability; increasing presence of asymptomatic or pre-symptomatic spreaders (Fig. 2). Statistical modelling that addresses improvements in design and functionality of face coverings and future eco-sustainable, non-plastic, medical or surgical masks will inform efficacy of these counter-measures for a spectrum of increasing risk situations (Table 2). Controlled random studies should also consider extended use, re-use or reprocessing situations along with promoting user behavioural change to any perceived barriers and to improve awareness would also be relevant (Fig. 2). Several other studies have also examined the relationship between COVID-19 and meteorological factors, such as temperature (Ma et al., 2020), humidity (Liu et al., 2020) and air pollution (Zhu et al., 2020). Gupta et al. (2020) also reported on the relationship between weather parameters and COVID-19 spread using daily data of new cases in 50 US states between Jan 1 and April 9, 2020 and found that spread in the US was significant for states with $4 <$ absolute humidity < 6 g/m^3 and number of new cases >10,000.

Chowdhury et al. (2020) investigated dynamic interventions to control the COVID-19 pandemic, where these researchers described a multi-variate prediction model, based on up-to-date transmission and clinical parameters, to simulate outbreak trajectories in 16 countries, from diverse regions and economic categories. In each country, these authors modelled the impacts on intensive care unit (ICU) admissions and death over an 18-month period for the following scenarios: (1) no intervention, (2) consecutive cycles of NPI mitigation measures followed by a relaxation period, and (3) consecutive cycles of suppression measures followed by a relaxation period. Chowdhury et al. (2020) noted that such "schedules" of social distancing might be particularly relevant to low-income countries, where a single, prolonged suppression intervention is unsustainable. These researches advocated that efficient implementation of dynamic suppression interventions can be considered pragmatic options to: (1) prevent critical care overload and deaths, (2) gain time to develop preventive and clinical measures, and (3) reduce economic hardship globally.

At this time of writing, less than 50% of the American population wear face masks and coverings (Cullen, 2020; Donmez, 2020). Use of the Institute of Health Metrics and Evaluation (IHME) model predicts that enforcing non-pharmaceutical interventions, such as face masks and social distancing, can potentially save 122,070 U.S. citizens (Donmez, 2020). Eker (2020) reflected on three popular models from a validity and usefulness perspective in terms of providing a structured framework to understand and interpret the epidemical and social mechanisms behind this COVID-19 pandemic. However, such models cannot be considered as accurate predictions tools, not only because no model is capable of doing this, but also because these models are lacking thorough formal validation. Eker (2020) reported that COVID-19 creates a citation where facts are uncertain, stakes are high, and decisions are very urgent, which is challenging for public health decision makers. Nzediaegwu and Chang (2020) reported that the number of PPE used daily in Africa is also estimated to reach seven hundred million, as several African countries have mandated compulsory face mask usage for their citizens to prevent COVID-19 transmission. Improving compliance with face covering wearing in at-risk settings presents a significant opportunity for reducing infection cases; Silva et al. (2020) noted that wearing of face masks is to be enforced in 50 countries to address COVID-19 transmission. The WHO (2020b) projected supplies of PPE must increase 40% to deal effectively with the COVID-19 pandemic; essential PPE supplies include an estimated 89 million medical masks, 76 million pairs of medical gloves, and 1.6 million pairs of goggles.

2.6.1. Mathematical and statistical modelling applied to studies of the effectiveness of face masks to avoid spreading COVID-19 including enhanced design innovation for mitigating against more transmissible SARS-CoV-2 variants

Regarding the inclusion of facemask use-related parameters within different modelling frameworks, different approaches have been used. Haug et al. (2020) combined statistical modelling and machine learning techniques and estimated that wearing a mask yields a reduction of R_0 between 1.8% and 12%, while social distancing yields an approximate reduction of 20%. However, this does not take into account scenarios of high public adherence and/or high efficiency of facemasks. According to Howard et al. (2021), a combined high mask efficacy and average public adherence, or average mask efficacy and high public adherence, are likely to lead to disease containment. This was confirmed by different studies that included mask efficiency in their mathematical modelling approach. For instance, Stutt et al. (2020) developed a combined modelling approach, involving a branching process based on the negative binomial distribution and a SEIR-type model (discriminating between symptomatic and asymptomatic individuals, as well as two populations: masked and unmasked individuals), and included two parameters in their models, reflecting mask adherence and efficiency. They assume that efficiency in exhalation is greater than 50% on average, but that it is poorer when inhaling. Their assessment indicates that when R_0 is 4, it may only be reduced to below 1 when almost 100% of the population is wearing masks that are more than 50% effective, at all times, even when not displaying symptoms. This is an important distinction, since their findings show that when masks are only used when individuals are symptomatic, even 100% of mask adherence combined with 100% efficiency would not be able to reduce an R_0 of 4 to less than 1. In terms of comparing surgical vs. homemade masks, Eikenberry et al. (2020) developed an extended SEIR-type model, that also included symptomatic/asymptomatic compartments, and masked and unmasked populations. While their results are similar when compared to Stutt et al.'s (2020), they found that the adoption of even very weak masks (20% effectiveness) could be useful when R_0 is relatively small. The assessment of a similar type of extended model developed by Worby and Chang (2020) corroborates this finding, and highlights the importance of optimized distribution, especially when resources are limited. They show that under these circumstances surgical masks should be prioritized for infected and vulnerable individuals. In the absence of current estimates for the efficacy and public adherence to facemasks, these mathematical modelling techniques illustrate possible outcomes of a range of different scenarios, and this proves to be an invaluable tool when developing public policy to contain the spread of the virus.

The combined modelling approach described by Haug et al. (2020) can inform improved efficacy of mask design and functionality, and to compare these innovations with other NPIs based on estimated effectiveness in reducing R_0. For example, disposable surgical mask are commonly produced by using non-woven methods using 20 g^{-2} polyproplyene with spunbound technology, or 25 g m^{-2} non-woven sheet polypropylene using melt-blown technology; the filtration efficiency of surgical masks is influenced by fibre selection, fabrication method, the structure of the web, and the cross-sectional shape of the fibre. Each layer has a different specific function: the middle layer works as a filter; the outermost layer imposes hydrophobicity, and the innermost layer absorbs fluids from the wearer; where all three layers work by restricting transmission of small particles or pathogens from both directions (Chua et al., 2020). Disposable surgical masks consists of folded piles of fabrics that are loose fitting on the user's face, whereas N95 respirator consists of three polypropylene filtering layers and tight-edge fitting. The filter layer is generated from nylon, cotton, polyester and polypropylene where the diameter of fibres affects mechanical filtration characteristics; N95 type respirators operates at approximately 85% efficiency as the pore size of 300 nm is greater than the size of SARS-CoV-2, which is 65 to 140 nm (El-Atab et al., 2020).

For example, electrospun air filters can be modelled as offer better properties; such as the composite air filter membranes generated by electrospinning a mixture of polyvinyl chloride and polyurethane polymer demonstrated good mechanical properties with tensile strength up to 9.9 MPa with excellent air permeability (706.84 nm s^{-1}), a high filtration efficiency (99.5%), and a low pressure drop (144 Pa) (Zhu et al., 2017). Moreover, composite membrane fabricated with Nylon 6 and PAN produced higher filtration efficiency (99.99%), where these approaches might offer improved protection against more transmissible SARS-CoV-2 variants. Wang et al. (2020) applied superhydrophobic electrospun approach using PSU with TiO_2 nanoparticles in multilayers that achieved 99.9997% filtration efficiency with a pressure drop of 45.4 Pa. However, these general electrospinning fabrication methods still use non-environmentally friendly polymers. Eco-friendly materials can be substituted with natural polymers such as polysaccharides, glutens, proteinaceous materials, biosynthetic polymer materials, and chemical synthesis of polymers (Wibisono et al., 2020). Lv et al. (2019) produced an eco-friendly electrospun membrane using polyvinyl alcohol (PVA), konjac glucomannan (KGM), and ZnO nanoparticles that increased filtration efficiency to 99.9% and increased pressure drop by 130 Pa (300 nm particles). The additions for anti-viral functional materials to layers (Table 2) can also be evaluated for improved protection. Haug et al. (2020) modelling approach can also inform development of cloth masks including number of layers, layer density, and facial fitness, and yet at the same time still considering breathability, washability and reusability. Advancement of non-medical cloth masks by combining fabric materials, such as cotton-silk, cotton-chiffon, and cotton-flannel, can potentially increase filtration efficiency to 80% (<300 nm particles (Feng et al., 2020). Currently, the most efficient face coverings are 100% cotton masks, which is based on filtration efficiency and pressure drop (Wibisono et al., 2020).

2.7. Random controlled trials and risk mitigation

Wang et al. (2020b) was one of the earliest retrospective cohort studies (28 February to 27 March 2020 in Beijing, China) of 335 people in 124 to investigate community mask wearing, hand washing, and social distancing on COVID-19 risk reduction within families. This study confirmed that the highest risk of transmission prior to symptom onset, and provided first evidence of the effectiveness of mask use, disinfection and social distancing in preventing COVID-19. The overall secondary attack rate was 23.0% (77/335). Face masks were 79% effective and disinfection was 77% effective in preventing transmission, while calculated R0 showed that close frequent contact increased the risk of transmission 18.26 times. Household crowding was also significant; results demonstrated the involvement of pre-systematic infectiousness of COVID-19 patients (Wang et al., 2020b).

Chu et al. (2020) conducted a systematic review and meta-analysis to investigate the optimum distance for avoiding person-to-person SARS-CoV-2, SARS-CoV, and MERS-CoV transmission, and to assess the use of face masks and eye protection to prevent transmission of these viruses. These authors used meta-analysis of associations of by pooling risk ratios, or adjusted odds ratios, depending on the availability from 172 observational studies across 16 countries and six continents (n = 25,697 participants), using DerSimonian and Laird random-effects models. Chu et al. (2020) also used the Newcastle-Ottawa scale to rate risk of bias for comparative non-random studies. Risk of transmission of these viruses was lower with physical distancing of 1 m or more, compared with a distance of less than 1 m; protection was increased as distance was lengthened; face mask use could result in a large reduction in risk of infection, with stronger associations with N9 or similar respirators compared with disposable surgical masks or similar (e.g., reusable 12–16 layer cotton masks; and eye protection was associated with less infection. The primary limitation of this Chu et al. (2020) study was that all studies were non-randomised, not always adjusted, and may suffer from recall and measurement bias (e.g., direct contact

in some studies may not be measuring near distance). However, the authors found that unadjusted, adjusted, frequentist, and Bayesian meta-analyses all supported the main findings, and this approach supported the recording of large or very large effects.

Bungaard et al. (2020) recently reported on randomised controlled trial involving Danish participants to assess whether recommending surgical masks use outside the home reduces wearers' risk of SARS-COV-2 infection in a setting where masks were uncommon and not among recommended public health measures. A total of 3030 participants were randomly assigned to the recommendation of wear masks, and 2994 were assigned to the control group; 4862 completed the study. Infection with SARS-CoV-2 occurred in 42 participants recommended to wear masks (1.8%) and 53 control participants (2.1%). Participants were adults spending more than 3 h per day outside the home without occupational mask use. Participants were encouraged to follow social distancing measures for COVID-19, but it is not possible to prove that this as achieved. The primary measurement outcome was detection of SARS-CoV-2 in the mask wearer at 1 month by antibody testing, polymerase chain reaction (PCR), or hospital diagnosis. The secondary outcome was PCR- positivity for other respiratory viruses. The authors concluded that the recommendation to wear surgical masks to supplement other public health measures did not reduce the SARS-CoV-2 rate among wearers by more than 50% in a community with modest infection rates, some degree of social distancing, and uncommon general mask use. Loeb (2020) also described a randomised controlled trial that is ongoing in Canada in which 576 nurses will be randomised to either medical masks, or N95 respirators, when providing care to patients with COVID-19, which is due for completion on April 1, 2021. Inclusion criteria are nurses who work >37 h per week in medical, emergency, paediatric units; while exclusion criteria are nurses with one or more comorbidities, and nurses who cannot pass an N95 respirator fit test. Ultimately, researchers have concluded that globally collaborative and well conducted studies, including randomised trials, of different personal protective strategies are needed regardless of challenges, but the current use of systematic appraisals of best available evidence could be considered to inform interim guidance (Chu et al., 2020).

The WHO (2020b) noted that "all viruses, including SARS-CoV-2, change over time, most without a direct benefit to the virus in terms of increasing its infectiousness or transmissibility, and sometimes limiting propagation. The potential for virus mutation increases with the frequency of human and animal infections. Reducing transmission of SARS-CoV-2 by using established disease control methods as well as avoiding introductions to animal populations, are critical aspects to the global strategy to reduce the occurrence of mutations that have negative public health implications. Preliminary data suggest that the growth rate and effective reproductive number is elevated in areas of the United Kingdom with community circulation of the novel variant VOC-202012/01. In South Africa, genomic data highlighted that the 501Y.V2 variant rapidly displaced other lineages circulating, and preliminary studies suggest the variant is associated with a higher viral load, which may suggest potential for increased transmissibility; however, this, as well as other factors that influence transmissibility, are subject of further investigation". The WHO has reported that epidemiologic investigations are underway to understand the increase in cases in these communities and the potential role of increased transmissibility of these variants as well as the robustness of implementation of control measures. "While initial assessment suggests that 202012/01 and 501Y.V2 do not cause changes in clinical presentation or severity, if they result in a higher case incidence, this would lead to an increase in COVID-19 hospitalizations and deaths" (WHO, 2020b). More intensive public health measures may be required to control transmission of these variants. Further investigations are required to understand the impact of specific mutations on viral properties and the effectiveness of diagnostics, therapeutics, vaccines along with disinfection and NPI modalities.

Use of risk assessment (RA) to evaluate complex environmental threats is increasing in popularity. For example, Tahar et al. (2017) reported on the development of a semi-quantitative risk assessment model for evaluating the environmental threat posed by three EU watch list pharmaceutical compounds to aquatic ecosystems. This RA model adopts the Irish EPA's Source-Pathway-Receptor concept to define relevant parameters for calculating practical low, medium or high risk scores for each agglomeration of wastewater treatment plant (WWTPs), which includes complex catchment, treatments, operational and management factors. This provides a working example where RA modelling may potentially strategically be used to unlock complex scenarios for policy decisions, such as to identify WWTPs that post a particular risk as regards releasing disproportionally high levels of pharmaceutical chemicals, and to help identify priority locations for introducing or upgrading control counter-measures (Tiedeken et al., 2017; Tahar et al., 2018; Rowan, 2019).

3. Non-pharmaceutical interventions and use of vaccines to deliver safe herd immunity in context of COVID-19 pandemic

Herd immunity is a key concept for epidemic control and is achieved when one infected person in a population generates less than one secondary case on average (Fontanet and Cauchemez, 2020). These authors described a mathematical model for forecast predications on the current COVID-19 pandemic as to how and when immunity can be achieved, and at what cost. This is also risk based, wearing face masks reduce the number of individuals who would also be more likely to get infected and to transmit because they have more contact, such as super spreaders, would be likely to be infected first. Thus, face coverings protect the population of susceptible individuals, who would typically get rapidly depleted, thus slowing the pace of transmission. Population immunity is typically estimated through cross-sectional surveys of representative samples using serological test that measure humoral immunity (Fontanet and Cauchemez, 2020). Surveys performed in countries affected during the COVID-19 epidemic, such as Italy and Spain, suggest a nationwide prevalence of antibodies ranges from 1 to 10%, with up to 15% in heavily affected urban areas Byambasuren et al. (2020). Another unknown, is whether pre-existing immunity to common cold coronaviruses may provide some level of cross-protection. However, Fontanet and Cauchemez (2020) noted that given that we do not know how long naturally acquired immunity to SARS-CoV-2 lasts. Immunity to seasonal coronaviruses is usually relatively short lived, particularly among those who had mild forms of the disease, and it may take several rounds of reinfection before robust immunity is attained.

Wearing face coverings and masks, and adopting other non-pharmaceutical interventions, are important to safeguard citizens prior to, and supplementary to, the use of effective vaccines until herd immunity is achieved. The introduction of the Pzifer-BioNTech vaccine today is a positive news with an efficacy of 95%. It is envisaged that random controlled studies focusing on the added benefits of combined use of NPIs to help manage transition to point where 'herd immunity' is achieved would be informative. Commensurately, face masks, and combined use of other NPIs is likely to remain essential for countries in the Northern hemisphere that are entering the autumn/winter seasons due to greater viral circulation, along with addressing greater transmissibility of SARS-CoV-2 variants as emerging in the UK due to spike protein mutation in variant 614G (Volz et al., 2021). Volz et al. (2021) did not find any indication that patients infected with the spike 614G variant have higher COVID-19 mortality or clinical severity, but 614G is associated with higher viral load and younger age of patients.

4. Conclusion and recommendations

As the first COVID-19 vaccine is distributed across the UK and other countries, the use of combined non-pharmaceutical interventions (NPIs) will remain important for preventing COVID-19 transmission globally. Wearing of face masks and improvised cloth or face coverings

reduce the relative risk of COVID-19, but systematic reviews and limited randomised control studies show that they do not provide 100% protection to susceptible individuals when used alone. There remains pressure on supply chains for medical face masks, and N95 respirators, where many COVID-19 affected countries are increasing greatly in new cases. Use of single-use plastic face masks are polluting the environment that has stimulated a surge in new sustainable innovations, which includes recycling and improved waste management (Ilyas et al., 2020). Globally, deployment of the type and degree of different NPIs, from a measured tiered response approach, will be informed by relative risk evaluations and monitoring of reproduction number (R_0), for example, as used by the Republic of Ireland (Government of Ireland, 2020). Mathematical models require verbose data to inform efficacy of NPIs, and potential higher relative risk 'multiplier factor' situations.

Recommendations arising from this study include:

Randomised controlled trials are merited to comprehensively evaluate, and validate, the single and combined use of NPIs, along with vaccines, in order to safety reach herd immunity.

Many countries significantly affected by COVID-19 will still need to consider reprocessing of PPE under EUA, where there are critical shortages.

There is pressing need to conduct global collaborative studies to appreciate, and validate new design, functionality and sustainability innovations for face masks that may be informed by life cycle assessment (LCA) and mathematical modelling.

Robust empirical data is required to inform predictive modelling and commensurate efficacy of appropriate combinational use of NPIs, including disinfection approaches, which also addresses emergence of new SARS-CoV-2 variants that appear to be replacing less transmissible variants globally. The emergence of new sustainable design innovations in face masks and coverings need to considered in the context of increasing relative risk scenarios where there is increased pressure on PPE supply chain. Greater transmissibility, and possibility pathogenesis, associated with emerging SARS-CoV-2 variants will necessitate enhanced deployment and monitoring of NPIs.

Improve behavioural change in order to avoid complacency when using face coverings in community settings with emphasis on covering both the nose and mouth, along with maintaining social distance at 2 m, to combat greater threat posed by more transmissible airborne SARS-CoV-2 variants; this can be supplemented with health literacy and education.

There should also be greater use of mathematical modelling, including relative risk assessment, to inform other factors that may potentially affect efficacy of NPIs, such as greater persistence of SARS-CoV-2 variants on surfaces due to colder winter weather, or forecasting for increased person-to-person gatherings due to celebrating religious or culture events.

There are significant opportunities to converge cross-cutting academia with innovators that will be supported and accelerated by an 'invest and enable' approach to driving new innovation.

Adjacent social science research is merited at a community level to inform behavioural change that includes emergence of 'COVID-19 fatigue', and barriers to new potential innovation (e.g., reprocessing of PPE in the Republic of Ireland for reuse did not occur due mainly to lack of confidence and understanding of new reprocessing technologies by nursing staff). There is increasing evidence that shows growing emotional stress in various cohorts in the context of COVID-19 pandemic (Shanahan et al., 2020); thus, studies such as to discern the influence (if any) of extended, or re-use of PPE to frontline HCWs, including comfort levels, are merited. However, Wang et al. (2020c) compared levels of psychological impact of the pandemic and levels of anxiety and depression between 1210 Chinese 1056 Polish participants who were encouraged and discouraged to wear masks respectively during initial stage of COVID-19. It was observed that use of face masks may safeguard better physical and mental health.

The emergence of strategic climate action and sustainable funding initiatives, such as the EC's Green Deal funding, will provide opportunities to develop clusters of complimentary expertise to deliver solutions: however, it is also envisaged that the efficacy of many of these new innovations may be validated through retrospective random controlled trials, possibly post COVID-19.

Reprocessing technologies for treating single-use PPE in healthcare under emergency conditions are currently limited to using VH_2O_2, and potentially UVGI, and moist heat. These reprocessing modalities should also be considered for treating new sustainable PPE from initial design stage as materials used may not be compatible with the treatment technologies.

Improvised face coverings appear to contribute to preventing COVID-19 transmission, but potentially carry a higher relative risk compared to that of wearing face masks due to lower filtration efficacy. Further testing of new face covering design innovations, such as multiple layers of materials containing anti-viral bioactive, along with breathability, are required to be met through random controlled trials. There is pressing need to improve and share data in real-time transnationally, such as through use of blockchain, machine learning, IoT, and AI that will harmonize and inform adoption of common and consistent policies. Connecting outputs by combined use of mathematical models and development of IT systems with improve global preparedness and responses to future pandemics. This will also support and enable key challenges and relative risks, such as relationship between emergence of more transmissible SARS-CoV-2 variants and the type of countermeasures to be deployed that includes NPIs in conjunction with vaccination.

Consent for publication

Not applicable.

Declaration of competing interest

The authors declare that they have no competing or conflict of interests.

Acknowledgment

The authors acknowledge the assistance of Chloe Rowan and Gillian Keane in the preparation of graphics used in this review paper.

References

AFNOR, 2020. SPEC S76-001. Masque barrière, Guide d'exigence minimales, de méthode d'essais, de confection et d'usage. https://masques-barrieres.afnor.org/home/telechargement.

Anfinrud, P., Stadnystskyi, V., Bax, B.E., Bax, A., 2020. Visualizing speech-generated oral fluid droplets with laser light scattering. N. Engl. J. Med. 382 (21), 2061–2063.

Arons, M.M., Hatfield, K.M., Reddy, S.C., Kimball, A., James, A., Jacobs, J.R., et al., 2020. Presymptomatic SARS-CoV-2 infections and transmissions in a skilled nursing facility. N. Engl. J. Med. 382, 2081–2090. https://doi.org/10.1056/NEJMoa2008457.

Asadi, S., ben Hnia, N.G., Barre, R.S., Wexler, A.S., Ristenpart, W.D., Bouvier, N.H., 2020a. Influenza A virus is transmissible via aerosolized fomites. Nat. Commun. https://doi.org/10.1038/s41467-020-17888-w.

Asadi, S., Cappak, C.D., Barreda, S., Wexler, A., Bouvier, N.M., Ristenpart, W.D., 2020b. Efficacy of masks and face coverings in controlling outward aerosol particle emission from expiratory activities. Sci. Rep. Nat. Res. https://doi.org/10.1038/s414598-020-72798-7.

ASTM F1862M-17 (2017), Standard Test Method for Resistance of Medical Face Masks to Penetration by Synthetic Blood (Horizontal Projection of Fixed Volume at a Known Velocity), ASTM International, West Conshohocken, PA, 2017.

ASTM F201-19 (2019), Standard Test Method for Evaluating the Bacterial Filtration Efficiency (BFE) of Medical Face Mask Materials, Using a Biological Aerosol of *Staphylococcus aureus*, ASTM International, West Conshohocken, PA. 2019.

Aziz, S., Hosseinzadeh, L., Arkan, E., Azandaryani, A.H., 2019. Preparation of electrospun nanofibers based on wheat gluten containing azathioprine for biomedical application. Int. J. Polym. Mater. Polym. Biomater. 68, 639–646.

Baker, R.E., Peña, J.M., Jayamohan, J., Jérusalem, A., 2018. Mechanistic models versus machine learning, a fight worth fighting for the biological community? Biol. Lett. 14, 20170660.

Barceló, D., 2020. An environmental and health perspective for COVID-19 outbreak: meteorology and air quality influence, sewage epidemiology indicator, hospitals disinfection, drug therapies and recommendations. J. Environ. Chem. Eng. 8. https://doi.org/10.1016/j.jece.2020.104006.

Behzadinasab, S., Chin, A., Hosseini, M., Poon, L.L.M., Ducker, W.A.A., 2020. A surface coating that rapidly inactivates SARS-CoV-2. ACS Appl. Mater. Interfaces 12, 34723–34727.

Beldomenico, P.M., 2020. Do superspreaders generate new superspreaders? A hypothesis to explain the progation pattern of COVID. Int. J. Infect. Dis. https://doi.org/10.1016/j.ijid.2020.05.025.

Bi, Q., Wu, Y., Mei, S., Ye, C., Zou, X., Zhang, Z., et al., 2020. Epidemiology and transmission of COVID-19 in 391 cases and 1286 of their close contacts in Shenzhen, China: a retrospective cohort study. Lancet Infect Dis. 20, 911–919. https://doi.org/10.1016/S1473-3099(20)30287-5.

Blázquez, E., Rodríguez, C., Ródenas, J., Navarro, N., Riquelme, C., Rosell, R., Campbell, J., Crenshaw, J., Segales, U.J., Pujols, J., Polo, J., 2019. Evaluation of the effectiveness of the SurePure Turbulator ultraviolet-C irradiation equipment on inactivation of different enveloped and nonenveloped viruses inoculated in commercially collected liquid animal plasma. PLoS One 14 (2), e0212332. https://doi.org/10.1371/journal.pone.0212332.

Bourouiba, L., 2020. Turbulent gas clouds and respiratory pathogen emissions: potential implications for reducing transmission of COVID-19. JAMA 323 (18), 1837–1838.

Bundgaard, H., Bundgaard, J.S., Raaschou-Pedersen, D.E.T., von Buchwald, C., Todsen, T., Norsk, J.B., Pries-Heje, M.M., Vissing, C.R., Ringgard, A., Anderson, P., Goecke, N.B., Trebbien, R., Skovgaard, K., Benfield, T., Ullum, H., Torp-Pedersen, C., Iversen, K., 2020. Effectiveness of adding a mask recommendation to other public health measures to prevent SARS-CoV-2 infection in Danish mask wearers — a randomized controlled trial. Ann. Intern. Med. https://doi.org/10.72326/M20-6817.

Byambasuren, O., et al., 2020. Estimating the seroprevalence of SARS-CoV-2 infections: systematic review. Preprint at. medRxiv https://doi.org/10.1101/2020.07.13.20153163.

Calafiore, G.C., Novara, C., Possieri, C., 2020. A time-varying SIRD model for the COVID-19 contagion in Italy. Annu. Rev. Control. 50, 361–372.

Chan, K.H., Sridhar, S., Zhang, R.R., Chu, H., Fung, A.Y., Chan, G., Chan, J.F., To, K.K., Hung, I.F., Cheng, V.C., Yuen, K.Y., 2020. Factors affecting stability and infectivity of SARS-CoV-2. J. Hosp. Infect. https://doi.org/10.1016/j.jhin.2020.07.009.

Chellamani, K.P., Veerasubramanian, D., Balaji, R.S.V., 2013. Surgical face masks: manufacturing methods and classification. J. Acad. Indust. Res. 2, 320–324.

Chin, A.W.H., Chu, J.T.S., Perera, M.R.A., Hui, K.P.Y., Yen, H.-L., Chan, M.C.W., Peris, M., Poon, L.L.M., 2020. Stability of SARS-Cov-2 in different environmental conditions. Lancet Microbe 1, e10.

Chowdhury, R., Heng, K., Shawon, M.S.R., Goh, G., Okonofua, D., Ochoa-Rosales, C., Gonzales-Jaramillo, V., Bhuiya, A., Reidpath, D., Prathapan, S., Shahzad, S., Athaus, C.L., Gonzalez-Jaramillo, N., Franco, O.H., 2020. Dynamic interventions to control COVID-19 pandemic: a multivariate prediction modelling study comparing 16 worldwide countries. Eur. J. Epidemiol. 35, 389–399.

Chu, D.K., Akl, E.A., Duda, S., Solo, K., Yaacoub, S., Schunemann, H.J., 2020. Physical distancing, face masks, and eye protection to prevent person-to-person transmission of SARS-CoV-2 and COVID-19: a systematic review and meta-analysis. Lancet 395, 1973–1987.

Chua, M.H., Cheng, W., Goh, S.S., Kong, J., Li, B., Lim, J.Y.C., Mao, L., Wang, S., Xue, K., Yang, L., Ye, E., Zhang, K., Cheong, W.C.D., Tan, B.H., Li, Z., Tan, B.H., Loh, Z.J., 2020. Face masks in the new COVID-19 normal: materials, testing and perspectives. AAAS Res. https://doi.org/10.34133/2020/7286735.

Chughtai, A.A., Seale, H., MacIntyre, C.R., 2013. Use of cloth masks in the practice of infection control — evidence and policy gaps. Int. J. Infect. Control 9 (3).

Cook, T.M., 2020. Personal protective equipment during coronavirus disease (COVID) 2019 pandemic - a narrative review. Anaesthesia 75 (7), 920–927.

Cullen, P., 2020. Ireland may see 1,200 more Covid-19 deaths by 2021 if face mask use doesn't improve — US experts. https://www.irishtimes.com/news/health/ireland-may-see-1-200-more-covid-19-deaths-by-2021-if-face-mask-use-doesn-t-improve-us-experts-1.4347042.

Das, O., Neiziany, R.E., Capezza, A.J., Hedenqvist, M.S., Forsth, M., Xu, Q., Jiang, L., Ji, D., Ramakrishna, S., 2020. The need for fully bio-based facemasks to counter-coronavirus outbreaks: a perspective. Sci. Total Environ., 736 https://doi.org/10.1016/j.scitotenv.2020.139611.

Davies, A., Thompson, K.A., Giri, K., Kafotas, G., Walker, J., Bennett, A., 2013. Testing the efficacy of homemade masks; would they protect in an influenza pandemic? Dis. Med. Publ. Health Prep. 7 (4), 413–418.

Dbouk, T., Drikakis, D., 2020a. On repiratory droplets and face masks. Phys. Fluids 32. https://doi.org/10.1063/5.0015044.

Dbouk, T., Drikakis, D., 2020b. On coughing and airborne droplet transmission in humans. Phys. Fluids 32 (5), 053310.

Derraik, Y.G.B., Anderson, W.A., Connelly, E.A., Anderson, Y.C., 2020. Rapid review of SARS-CoV-1 and SARS-CoV-2 viability, susceptibility to treatment, and the disinfection and reuse of PPE, particularly filtering facepiece respirators. Int. J. Environ. Res. Public Health 17, 6117. https://doi.org/10.3390/ijerph17176117.

Dev Kumar, G., Mishra, A., Dunn, L., Townsend, I., Oguadinma, C., Bright, K.R., Gerba, C.P., 2020. Biocides and novel antimicrobial agents for the mitigation of coronaviruses. Front. Microbiol. 11, 1351. https://doi.org/10.3389/fmicb.2020.01351.

Dhandayuthapani, B., Mallampati, R., Sriramulu, D., Dsouza, R.F., Valiyaveettil, S., 2014. PVA/gluten hybrid nanofibres for removal of nanoparticles from water. ACS Sustain. Chem. Eng. 2, 1014–1021.

Diaz, D., 2020. U.K. begings nationwide coronavirus immunization, latest in nation's history. https://www.npr.org/sections/coronavirus-live-updates/2020/12/08/944125280/u-k-begins-nationwide-coronavirus-immunization-largest-in-nations-history?t=1607636443459.

Donmez, B.B., 2020. US: model predicts 400,000 COVID-19 deaths by January. https://www.aa.com.tr/en/americas/us-model-predicts-400-000-covid-19-deaths-by-january/1963459.

Driessche, K.V., Hens, N., Tilley, P., Quon, B.S., Chilvers, M.A., deGroot, R., Cotton, M.F., Marais, B.J., Speert, D.P., Zlosnik, J.E.A., 2015. Surgical masks reduce air-borne spread of Pseudomonas aeruginosa in colonized patients with cystic fibrosis. Am. J. Respir. Crit. Care Med. 192, 897–899.

Eikenberry, S.E., Mancuso, M., Iboi, E., Phan, T., Eikenberry, K., Kuang, Y., Kostelich, E., Gumel, A.B., 2020. To mask or not to mask: modeling the potential for face mask use by the general public to curtail the COVID-19 pandemic. Infect. Dis. Modell. 5, 293–308.

Eker, S., 2020. Validity and usefulness of COVID-19 models. Human. Soc. Sci. Commun. https://doi.org/10.1057/s41599-020-00535-4.

El-Atab, N., Qaiser, N., Badghaish, H., Shaikh, S.F., Hussain, M.M., 2020. Flexible nonporous template for the design and development of reusable anti-COVID-19 hydrophobic face masks. ACS Nano 14, 7659–7665.

European Centre for Disease Prevention and Control, 2020. New COVID-19 situation dashboard. https://www.ecdc.europa.eu/en/covid-19-pandemic (accessed 11th October, 2020).

European Centre for Disease Prevention and Control, 2020b. Cloth face masks and masks sterilisation as options in case of shortage of surgical masks and respirators. Available on 8th September 2020 at. https://www.ecde.europa.eu/en/publications-data/cloth-masks-sterilisation-options-shortage-surgical-masks-respirators.

FDA, 2020. Emergency use authorization (EUA) information, and list of all current EUAs. https://www.fda.gov/emergency-preparedness-and-response/mcm-legal-regulatory-and-policy-framework/emergency-use-authorization#covidppe (Accessed 8th October, 2020).

Feng, S., Shen, C., Xia, N., Song, W., Fan, M., Cowling, B., 2020. Rational use of face masks in the COVID-19 pandemic. Lancet Respir. Med. 8, 434–436.

Ferguson, N., Laydon, D., Nedjati-Gilani, G., Imai, N., Ainslie, K., Baguelin, M., Bhatia, S., Boonyasiri, A., Cucunubá, Z., Cuomo-Dannenburg, G., Dighe, A., Dorigatti, I., Fu, H., Gaythorpe, K., Green, W., Hamlet, A., Hinsley, W., Okell, L.C., van Elsland, S., Thompson, H., Wang, H., Wang, Y., Walker, P.G.T., Walters, C., Winskill, P., Whittaker, C., Donnelly, C.A., Riley, S., Ghani, A.C., 2020. Report 9: impact of non-pharmaceutical interventions (NPIs) to reduce COVID-19 mortality and healthcare demand. Imp. Coll. Lond. 10, 77482.

Figueroa, A., Hauck, R., Saldias-Rodriguez, J., Gallardo, R.A., 2017. Combination of quaternary ammonium and glutaraldehyde as a disinfectant against enveloped and non-enveloped viruses. J. Appl. Poul. Res. 26, 491–497.

Fischer, E.P., Fischer, M.C., Grass, D., Henrion, I., Warren, S.W., Westman, E., 2020. Low cost measurement of facemask efficiency for following expelled droplets during speed. Sci. Adv. https://doi.org/10.1126/sciadv.abd3083.

Flaxman, S., et al., 2020. Estimating the effects of non-pharmaceutical interventions of COVID-19 in Europe. Nature 584, 257–261.

Fontanet, A., Cauchemez, S., 2020. COVID-19 herd immunity: where are we? Nat. Rev. Immunol. https://doi.org/10.1038/s41577-020-00451-5 (October, 2020).

Gandhi, M., Rutherford, G.W., 2020. Facial masking for Covid-19 — potential for "variolation" as we await a vaccine. N. Engl. J. Med. https://doi.org/10.1056/NEJMp2026913.

Giordano, G., Blanchini, F., Bruno, R., Colaneri, P., Di Filippo, A., Di Matteo, A., Colaneri, M., 2020. Modelling the COVID-19 epidemic and implementation of population-wide interventions in Italy. Nat. Med. 26, 855–860.

Government of Ireland, 2020. Latest charts and maps on COVID-19 in Ireland. https://www.gov.ie/en/service/0039bc-view-the-covid-19-coronavirus-dashboard-showing-the-latest-stats-and/ (Accessed 8th December, 2020).

Government of Ireland, 2020b. Ireland placed on level 5 of the plan for living with COVID-19. https://www.gov.ie/en/press-release/66269-ireland-placed-on-level-5-of-the-plan-for-living-with-covid/ (Accessed 8th December, 2020).

Government of Ireland, 2020c. Resilience and Recovery 2020–2021 — Plan for Living With COVID-19 file:///C:/Users/Neil/Downloads/87128_0d3f8c17-2c95-40c3-9311-e3fbb2c0fae5.pdf (Accessed 8th December, 2020).

Guan, D., Wang, D., Hallegatte, S., Davis, S.J., Huo, S., Li, L., Bai, Y., Lei, T., Xue, Q., Coffiman, D., Cheng, D., Chen, P., Liang, X., Xu, B., Lu, X., Wang, S., Hubacek, K., Cong, P., 2020. Global supply-chain effects of COVID-19 control measures. Nat. Hum. Behav. https://doi.org/10.1038/s41562-020-0896-8.

Gupta, S., Raghuwanshi, G.S., Chanda, A., 2020. Effect of weather on COVID-19 spread in the US: a prediction model for India in 2020. Sci. Total Environ. 728. https://doi.org/10.1016/j.scitotenv.2020.138860.

Hamner, L., Dubbel, P., Capron, I., Ross, A., Jordan, A., Lee, J., et al., 2020. High SARS-CoV-2 attach rate following exposure at a choir practice – Skagit County, Washington, March 2020. MMWR Morb. Mortal. Wkly Rep. 89, 606–610.

Haug, N., Geyrhofer, L., Londei, A., Dervic, E., Desvars-Larrive, A., Loreto, V., Pinior, B., Thurner, S., Klimek, P., 2020. Ranking the effectiveness of worldwide COVID-19 government interventions. Nat. Hum. Behav. 4 (12), 1303–1312.

He, S., Peng, Y., Sun, K., 2020b. SEIR modeling of the COVID-19 and its dynamics. Nonlin. Dynam. 101, 1667–1680.

He, X., Lau, E.H., Wu, P., Deng, X., Wang, J., Hao, X., Lau, Y.C., Wong, J.Y., Guan, Y., Tan, X., Mo, X., Chen, Y., Liao, B., Chen, W., Hu, F., Zhang, Q., Zhong, M., Wu, Y., Zhao, L., Zhang, F., Cowling, B.J., Li, F., Leung, G.M., 2020a. Temporal dynamics in viral shedding and transmissibility of COVID-19. Nat. Med. 26 (5), 672–675.

Ho, K.-F., Lin, L.-Y., Weng, S.-P., Weng, S.-P., Chuang, K.J., 2020. Medical mask versus cotton masks for preventing respiratory droplet transmission in micro-environments. Sci. Total Environ. https://doi.org/10.1016/j.scitotenv.2020.139510.

Hui, D.S., Chow, B.K., Chu, L., Ng, S.S., Lee, N., Gin, T., Chan, M.T.V., 2012. Exhaled air dispersion during coughing with and wearing surgical or N95 mask. PLoS One 7, 050845.

Hutten, I.M., 2016. Chapter 6 — Testing of nonwoven filter media. In: Hutten, I.M. (Ed.), Handbook of Nonwoven Filter Media, 2nd ed. Butterworth-Heineman Publishers, pp. 343–408.
Ilyas, S., Srivastava, R.R., Kim, H., 2020. Disinfection technology and strategies for COVID-19 hospital and bio-medical waste management. Sci. Total Environ. 749. https://doi.org/10.1016/j.scitotenv.2020.141652.
Jin, Z., Du, X., Xu, Y., Deng, Y., Liu, M., Zhao, Y., et al., 2020. Structure-based drug design, virtual screening and high-throughput screening rapidly identify antiviral leads targeting COVID-19. bioRziv https://doi.org/10.1101/2020.02.26.964882.
Johns Hopkins University, 2020. New cases of COVID-19 in word countries (7 day moving average). https://coronavirus.jhu.edu/data/new-cases. (Accessed 12 August 2020).
Johnson, G.R., Morawska, L., 2009. The mechanism of breath aerosol formation. J. Aerosol. Med. 22, 229–237.
Kampf, G., 2018. Efficacy of ethanol against viruses in hand disinfection. J. Hosp. Infect. 98 (4), 331–338.
Kampf, G., Todt, D., Pfaemder, S., Steinmann, E., 2020. Persistence of coronavirus on inanimate surfaces and their inactivation with biocidal agents. J. Hosp. Infect. 104 (3), 246–257.
Kasloff, S.B., Strong, J.E., Funk, D., Cutts, T.A., 2020. Stability of SARS-Cov-2 on critical personal protective equipment. MedRxiv https://doi.org/10.1101/2020.06.11.20128884.
Katul, G.G., Mrad, A., Bonetti, S., Monoli, G., Parolari, J., 2020a. Global convergence of COVID-19 basic reproduction number and estimation from early-time SIR dynamics. PLoS One 15 (9), e0239800. https://doi.org/10.1371/journal.pone.0239800.
Katul, G.G., Mrad, A., Bonetti, S., Monoli, G., Parolari, J., 2020b. Global convergence of COVID-19 basic reproduction number and estimation from early-time SIR dynamics. PLoS One 15 (9), e0239800. https://doi.org/10.1371/journal.pone.0239800.
Kenyon, C., 2020. The prominence of asymptomatic superspreaders in transmission mean universal face masking should be part of COVID-19 de-escalation strategies. Int. J. Infect. Dis. https://doi.org/10.1016/j.ijid.2020.05.102.
Kermack, W.O., McKendrick, A.G., 1927. A contribution to the mathematical theory of epidemics. Proc. R. Soc. Lond. Ser. A 115, 700–721.
Koyama, T., Platt, D., Parida, L., 2020. Variant analysis of SARS-CoV-2 genomes. Bull. World Health Org. 98 (7), 495–504 July 1. https://www.ncbi.nlm.nih.gov/pmc/articles/PMC7375210/pdf/BLT.20.253591.pdf.
Lee, S., Kim, T., Lee, E., Lee, C., Kim, H., Rhee, H., Park, Y.P., Son, H.-J., Yu, S., Park, J.W., Choo, E.J., Park, S., Loeb, M., Kim, T.H., 2020. Clinical course and molecular viral shredding among asymptomatic and symptomatic patients with SARS-CoV-2 infection in a community treatment Centre in the Republic of Korea. JAMA Intern. Med. 180 (1), 1447–1452.
Leung, N.H.L., Chu, D.K.W., Shiu, E.Y.C., et al., 2020. Respiratory virus shedding in exhaled breath and efficacy of face masks. Nat. Med. 26 (5), 676–680.
Liu, J., Zhou, J., Yao, J., Zhang, Z., Li, L., Zu, X., Wang, B., Fu, S., Niu, T., Wan, U.J., Shi, Y., Ren, Z., Niu, J., Zhu, W., Li, S., Luo, B., Zhang, K., 2020. Impact of meteorological factors on the COVID-19 transmission: a multi-city study in China. Sci. Total Environ. 726, 138513.
Loeb, M., 2020. Medical masks versus N95 respirators to prevent 2019 Novel Coronavirus Disease (COVID-19) in healthcare workers: a randomized trial. https://ichgcp.net/clinical-trials-registry/NCT04296643.
Loey, M., Monogaran, G., Taha, M.H.N., Khalifa, N.E.M., 2021. A hybrid deep transfer learning model with machine learning methods for face mask detection in the era of the COVID-19 pandemic. Measurement. 167. https://doi.org/10.1016/j.measurement.2020.108288.
López, L., Rodó, X., 2020. A modified SEIR model to predict the COVID-19 outbreak in Spain and Italy: simulating control scenarios and multi-scale epidemics. Results in Physics 25. https://doi.org/10.1016/j.rinp.2020.103746.
Lv, D., Wang, R., Tang, G., Mou, Z., Lei, J., Han, J., Smedt, S., Xiong, R., Huang, C., 2019. Eco-friendly electrospun membranes loaded with visible-light response nano-particles for multi-functional usages; high-efficient air filtration, dye scavenger, and bactericide. ACS Appl. Mater. Interfaces 11, 12880–12889.
Ma, Y., Zhao, Y., Liu, J., He, X., Wang, B., Fu, S., Yan, J., Niu, J., Zhou, J., Luo, B., 2020. Effects of temperature variation and humidity on the death of COVID-19 in Wuhan, China. Sci. Total Environ. 724, 138226.
Mao, N., 2017. Nonwoven fabric filters. In: Brown, P.J., Cox, C.L. (Eds.), Fibrous Filter Media. Woodhead Publishing, pp. 133–171.
Masterson, C.M., Murphy, E., Gonzalez, H., Major, I., McCarthy, S.D., O'Toole, D., Laffey, J.G., Rowan, N.J., 2020. Purified β-glucans from the Shiitake mushroom ameliorates antibiotic-resistant *Klebsiella pneumoniae*-induced pulmonary sepsis. Lett. Appl. Microbiol. https://doi.org/10.1111/lam.13358.
McEvoy, B., Rowan, N.J., 2019. Terminal sterilization of medical devices using vaporized hydrogen peroxide: a review of current methods and emerging opportunities. J. Appl. Microbiol. 127 (5), 1403–1420.
Michie, S., West, R., Harvey, N., 2020. The concept of "fatigue" in tackling covid-19. BMJ https://doi.org/10.1136/bmj.m4171.
Milton, D.K., Fabian, M.P., Cowling, B.J., Grantham, M.L., McDevitt, J.J., 2013. Influenza virus aerosols in human exhaled breath: particle size, culturability, and effect of surgical masks. PLoS Pathog. 9, e1003205.
Murphy, E., Masterson, C., Rezoagli, E., Major, I., Stack, G., O'Toole, D., Laffey, J.G., Rowan, N.J., 2020a. β-Glucan Extracts From the Same Edible Shiitake Mushroom *Lentinus edodes* Produce Differential In-vitro Immunomodulatory and Pulmonary Cytoprotective Effects — Implications for Coronavirus Disease (COVID-19) Immunotherapies. https://doi.org/10.1016/j.scitotenv.2020.139330.
Murphy, E., Rezoagli, E., Major, I., Laffey, J.G., Rowan, N.J., 2020b. β-Glucan metabolic and immunomodulatory properties and potential for clinical application. J. Fungi. 6, 356. https://doi.org/10.3390/jof6040356.
Neupane, B.B., Mainali, S., Sharma, A., Giri, B., 2019. Optical microscopic study of surface morphology and filtering performance of face masks. PeerJ 7, e7142.
Nzediaegwu, C., Chang, S.X., 2020. Improper solid waste management increases potential for COVID-19 spread in developing countries. Resour. Conserv. Recycl. https://doi.org/10.1016/j.resconrec.2020.104947.
Oliveira, T.P., Moral, R.A., 2020. Global short term forecasting of Covid-19 cases. arXiv: 2006.00111.
Pagat, A.-M., Seux-Goepfort, R., Lutsch, C., Lecouturier, V., Saluzzo, J.-F., Kuster, I.C., 2007. Evaluation of SARS-coronavirus decontamination procedures. Appl. Biosafety 12, 100–108.
Peebles, L., 2020. What the data say about wearing face masks. Nature 586, 186–189.
Pellett, P.E., Mitra, S., Holland, T.C., 2014. Chapter 2 — Basics of virology. In: Tselis, A.C., Booss, J. (Eds.), Handbook of Clinical Neurology. 123. Elsevier, pp. 45–66.
Perencevich, E.N., Diekema, D.J., Edmond, M.B., 2020. Moving personal protective equipment into the community — face shields and containment of COVID-19. JAMA 323 (2). https://doi.org/10.1001/jama.2020.7477.
Pinon, A., Vialette, M., 2018. Survival of viruses in water. Intervirology 61, 214–222.
Rengasamy, S., Eimer, B., Shaffer, R.E., 2010. Simple respiratory protection — evaluation of the filtration performance of cloth masks and common fabric materials against 20–1000 nm size particles. Ann. Occup. Hyg. 54, 789–798.
Riddell, S., Goldie, S., Hill, A., Eagle, D., Drew, T.W., 2020. The effect of temperature on persistence of SARS-CoV-2 on common surfaces. Virol. J. 17. https://doi.org/10.1186/s12985-020-01418-7.
Rodriguez-Palacios, A., Conger, M., Cominelli, F., 2020. Germ-free mice under two-layer textiles are fully protected from bacterial in sprayed microdroplets: a functional in vivo test method of facemask/filtration materials. Front. Med. 7, 504. https://doi.org/10.3389/fmed.2020.00504.
Rotter, M.L., 2001. Arguments of alcoholic hand disinfection. J. Hosp. Infect. 48, S4–S8.
Rowan, N.J., 2019. Pulsed light as an emerging technology to cause disruption for food and adjacent industries — quo vadis? Trends Food Sci. Technol. 88, 316–332.
Rowan, N.J., Galanakis, C.M., 2020. Unlocking challenges and opportunities presented by COVID-19 pandemic for cross-cutting disruption in agri-food and green deal innovations: quo vadis? Sci. Total Environ. 748, 141362. https://doi.org/10.1016/j.scitotenv.2020. 141362.
Rowan, N.J., Laffey, J.G., 2020a. Challenges and solutions for addressing critical shortage of supply chain for personal and protective equipment (PPE) arising from coronavirus disease (COVID19) pandemic — case study from the Republic of Ireland. Sci. Total Environ. 725 (2020). https://doi.org/10.1016/j.scitotenv.2020.138532.
Rowan, N.J., Laffey, J.G., 2020b. Unlocking the surge in demand for personal and protective equipment (PPE) and improvised face coverings arising from coronavirus disease (COVID-19) pandemic — implications for efficacy, re-use and sustainable waste management. Sci. Total Environ. 752 (2020). https://doi.org/10.1016/j.scitotenv.2020.142259.
Rubio-Romero, J.C., del Carmen, M., Ferreira, P., Torrecilla, J.A., Santiago, G., Castro, C., 2020. Disposable masks: disinfection and sterilization for reuse, and non-certified manufacturing, in the face of shortages during the COVID-19 pandemic. Sci. Total Environ. https://doi.org/10.1016/j.ssci.2020.104830.
Secon, H., 2020. People are racing to buy face masks amid the coronavirus outbreak, but they probably won't protect you from illness. Bus. Insid Available from. https://ww.businessinsider.com/wuhan-coronavirus-face-masks-not-entirely-effective-2020-1.
Shanahan, L., Steinhoff, A., Bechtiger, L., Murray, A.L., Nivette, A., Hepp, U., Ribeaud, D., Eisner, M., 2020. Emotional distress in young adults during COVID-19 pandemic: evidence of risk and resilience from a longitudinal cohort study. Psychol. Med., 1–10 https://doi.org/10.1017/S003329172000241X.
Sickbert-Bennett, E.E., Samet, M., Clapp, P.W., 2020. Filtration efficiency of hospital face mask alternatives available for use during the COVID-19 pandemic. JAMA Intern. Med. https://doi.org/10.1001/jamaintermed.2020.4221.
Silva, A.L.P., Prata, J.C., Walker, T.R., Campos, T.R.W., Duarte, A.C., Soares, A.M.V.M., Barceló, D., Rocha-Santos, T., 2020. Rethinking and Optimising Plastic Waste Management Under COVID-19 Pandemic: Policy Solutions Based on Redesign and Reduction of Single-use Plastics and Personal Protective Equipment. https://doi.org/10.1016/j.scitotenv.2020.140565.
Son, B.C., Park, C.H., Kim, C.S., 2020. Fabrication of antimicrobial nanofiber air filter using activated carbon and cinnamon essential oil. J. Nanosci. Nanotechnol. 20 (7), 4376–4380.
Stadnytsky, V., Bax, B.E., Bax, A., Anfinrud, A., 2020. The airborne lifetime of small speech droplets and their potential importance in SARS-CoV-2 transmission. Proc. Natl. Acad. Sci. 117 (22), 11875–11877.
Stockwell, R.E., Knibbs, M.E., He, C., Sherrard, L.J., Ballard, E.I., Kidd, T.J., Johnson, G.R., Knibbs, L.D., Morawska, L., Bell, S.C., 2018. Face masks reduce the release of Pseudomonas aeruginosa cough aerosols when worn for clinically relevant periods. Am. J. Respir. Crit. Care Med. 198, 1339–1342.
Strain, I.N., Wu, Q., Pourrahimi, A.M., Hedenqvist, M.S., Olsson, R.T., Andersson, R.I., 2015. Electrospinning of recycled PET to generate tough mesomorphic fibre membranes for smoke filbration. J. Mater. Chem. A3, 1632–1640.
Stutt, R.O., Retkute, R., Bradley, M., Gilligan, C.A., Colvin, J., 2020. A modelling framework to assess the likely effectiveness of facemasks in combination with 'lock-down'in managing the COVID-19 pandemic. Proc. Royal Soc. A 476 (2238), 20200376.
Tahar, A., Tiedeken, E.J., Clifford, E., Cummins, E., Rowan, N., 2017. Development of a semi-quantitative risk assessment model for evaluating environmental threat posed by the three first EU watch-list pharmaceuticals to urban wastewater treatment plants: an Irish case study. Sci. Total Environ. 603–604, 627–638.
Tahar, A., Tiedeken, E.J., Rowan, N.J., 2018. Occurrence and geodatabase mapping of three contaminants of emerging concern in receiving water and at effluent from waste water treatment plants — a first overview of the situation in the Republic of Ireland. Sci. Total Environ. 616–617, 187–197.

Tang, J.W., Liebner, T.J., Craven, B.A., Settles, G.S., 2009. A Schlieren optical study of the human cough with and without wearing mask for aerosol infection control. J. R. Soc. Interface 6, 727–736.

Tellier, R., Li, Y., Cowling, B.J., Tang, J., 2019. Recognition of aerosol transmission of infectious agents: a commentary. BMJ Infect. Dis. 19, 101.

Tiedeken, E.J., Tahar, A., McHugh, B., Rowan, N.J., 2017. Monitoring, sources, receptors, and control measures for the three European Union watch list substances of emerging concern in receiving waters — a 20 year systematic review. Sci. Total Environ. 574, 1140–1163.

Tino, R., Moore, R., Antoline, S., Ravi, P., Wake, N., Ionita, C.N., Morris, J.M., Decker, S.J., Sheikh, A., Rybicki, F.J., Chepelev, L.L., 2020. COVID-19 and the role of 3D printing in medicine. 3D Print Med. https://doi.org/10.1186/s41205-020-00064-7.

Toda, A.A., 2020. Susceptible-infected-recovered (SIR) dynamics of COVID-19 and economic impact. arXiv:2003.11221.

Van Doremalen, N., Bushmaker, T., Morris, D., Holbrook, M., Gamble, A., Williamson, B. et al. 2020. Aerosol and surface stability of HCoV-19 (SARS-CoV-2) compared to SARS-CoV-1. N. Engl. J. Med. 382, 1564–1267. doi:https://doi.org/10.1056/NEJMc2004973.

Vespignani, A., Tian, H., Dye, C., Lloyd-Smith, J.O., Eggo, R.M., Shrestha, M., Scarpino, S.V., Gutierrez, B., Kraemer, M.U., Wu, J., Leung, K., Leung, G.M., 2020. Modelling COVID-19. Nat. Rev. Phys. 2, 279–281.

Volz, E., Hill, V., McCrone, J.T., Price, A., Jorgensen, D., O'Toole, A., Southgate, J., Johnson, R., Jackshon, B., Nascimento, F.F., Rey, S.M., Nicholls, S.M., Colquhoun, R.M., Filipe, A., Shepherd, J., Pascall, D.J., Shah, R., Jesudason, N., Li, K., Jarrett, R., Pacchiarini, N., Bull, N., Geidelbergy, L., Siveroni, I., 2021. Evaluating the effects of SARS-CoV-2 spike mutation D614G on transmissibility and pathogenicity. Cell 184 (1), 64–75.

Wang, C., Chudzicka-Czupala, A., Grabowski, D., Pan, R., Adamus, K., Wan, X., Hetnal, M., Tan, Y., Olszewska-Guisso, A., Xu, L., McIntyre, R.S., Quek, J., Ho, R., Ho, C., 2020c. The association between physical and mental health and face mask use during the COVID-19 pandemic: a comparison of two countries with different views and practices. Front. Psychiat. 11, 569981. https://doi.org/10.3389/fpsyt.2020.569981.

Wang, J., Shen, J., Ye, D., Yan, X., Zhang, Y., Yang, W., Li, X., Wang, J., Zhang, L., Pan, L., 2020b. Disinfection technology of hospital waste and wastewater suggestions for disinfection strategy during Coronavirus Disease-2019 (COVID-19) pandemic in China. Environ. Pollut. 262. https://doi.org/10.1016/j.envpol.2020.114665.

Wang, Y., Tian, H., Zhang, L., Zhang, M., Guo, D., Wu, W., Zhang, X., Kan, G.L., Jia, L., Hoo, D., Liu, B., Wang, X., Sun, Y., Wang, Q., Yang, P., MacIntyre, R., 2020a. Reduction of secondary transmission of SARS-CoV-2 in households by face mask use, disinfection and social distancing: a cohort study in Beijing, China. BMJ Glob. Health 5, e002794. https://doi.org/10.1136/bmjgh-2020-002794.

Wibisono, Y., Fadila, C.R., Saiful, S., Bilad, M.R., 2020. Facile approaches of polymeric face masks reuse and reinforcements for micro-aerosol droplets and virus filtration: a review. Polymers 12, 2516. https://doi.org/10.3390/polym12112516.

Worby, C.J., Chang, H.H., 2020. Face mask use in the general population and optimal resource allocation during the COVID-19 pandemic. Nat. Commun. 11 (1), 1–9.

World Health Organization, 2020a. Advice on the use of masks in the context of COVID-19 pandemic. Interim guidance 4 July, 2020. https://apps.who.int/iris/rest/bitstreams/1279750/retrieve accessed 10th October, 2020.

World Health Organization, 2020b. SARS-CoV-2 variants — emergencies preparedness response. https://www.who.int/csr/don/31-december-2020-sars-cov2-variants/en/ (accessed 31 December, 2020).

World Health Organization, 2020c. Transmission of SARS-CoV2: implications for infection control prevention. https://www.who.int/news-room/commentaries/detail/transmission-of-sars-cov-2-implications-for-infection-prevention-precautions accessed 25th August, 2020.

Yao, B.G., Wan, Y.-X., Ye, X.-Y., Zhang, F., Peng, Y.-L., 2019. Impact of structural features on dynamic breathing resistance of healthcare face mask. Sci. Total Environ. 689, 743–753.

Zeroual, A., Harrou, F., Dairi, A., Sun, Y., 2020. Deep learning methods for forecasting COVID-19 time-series data: a comparative study. Chaos, Solitons Fractals 140, 110121.

Zhong, H., Zhu, Z., Lin, J., 2020. Reusable and recyclable graphene masks with outstanding superhydrophobic and photothermal performances. ACS Nano 14 (5), 6213–6221.

Zhu, M., Han, J., Hang, F., Shao, W., Xiong, R., et al., 2017. Electrospun nanofibers membranes for effective air filtration. Macromol. Mater. Eng. 302, 1600353.

Zhu, Y., Zie, J., Huang, F., Cao, L., 2020. Association between short-term exposure to air pollution and COVID-19 infection: evidence from China. Sci. Total Environ. 727, 138704.

Section Three – Scaling Disinfection and Sterilisation Technologies

The **third section** of this describes 'large scale disinfection, sterilisation and demonstration technologies. Studies describe development and evaluation of Vaporised Hydrogen Peroxide as new sterilisation modality for terminal treatment of medical devices. Commensurate studies revealed, for the first time, that VHP produces log-linear inactivation kinetic plots after 6 decimal (D) log-reductions inferring that sterility assurance can be appropriately assumed for extrapolation to 12 D sterility. These studies have provided foundational data for regulatory approval of VHP as 'Class A' sterilization technology and linkage on the use of 'families' of similar treatment devices as master files for parametric release. Studies revealed that the dose from VHP, gamma and electron irradiation can be similarly applied for achieving reduction of *Bacillus* bioindicators for device sterilization (*Geobacillus stearothermophilus* and *Bacillus atrophaeus* spores). Studies were reported on the use of electron beam and VHP for use in combination with 3 D printing or injection moulding for parts for medical devices that informs appropriate ad-hoc use in healthcare setting for flexible disease prevention and control of devices. The VHP technology is now deployed commercially by STERIS AST for medical device and pharma product treatments globally. Studies also report on development of a new cleaning classification system for reprocessed medical devices based on complexity and gaining access to device features given that many of the current manufacturers IFUs are too complicated for healthcare facility to meet these processing expectations that can lead to unwanted infections (such as contaminated endoscopes that can harbour pathogens in device features/biofilms). I described implications for modern medical microbiology for use of sterilization modalities in clinical practice given that it still relies on 1957 classification system of Earl Spaulding. Such understanding of critical knowledge on technologies elucidates and develops appropriate technologies for adjacent societal challenging applications. Studies in this section also describe the first effective use of PUV for treating heat sensitive pollen contaminated with complex parasites affecting bees along with commensurate reporting on positive effects on the bee's gut microbiome and immunological status post consumption of PUV-treated pollen by these pollinators. This is relevant given the lack of solutions for pollination and ecosystem service management globally. Studies are also described on rapid methods and decontamination technologies for treatment of complex bacterial and viral pathogens in shellfish at depuration. This section also used subject-matter understanding and knowledge to describe appropriate innovations and methods to safely reprocess PPE arising from critical supply chain shortage during COVID-19 pandemic that helped guide and support

US FDA's recommendation for use of these vital technologies under Emergency Use Authorization. An understanding of fungal physiology also informed studies describing elucidation, development and application on the first use of computational model to predict occurrence of toxigenic mould growth in buildings that was used as European Reference model. The latter reflected my time at Strathclyde University and collaborations with Prof Joe Clarke. Studies report on digital tools and educational technologies to advance the development of medical devices including meeting shortcomings including bespoke training and sustainability. The role of digital health in addressing self-management of diseases in respiratory patients is described.

Science of the Total Environment 899 (2023) 165614

Contents lists available at ScienceDirect

Science of the Total Environment

journal homepage: www.elsevier.com/locate/scitotenv

Studies on the novel effects of electron beam treated pollen on colony reproductive output in commercially-reared bumblebees (*Bombus terrestris*) for mass pollination applications

J. Eakins [a,b], M. Lynch [a], J.C. Carolan [b], N.J. Rowan [a,*]

[a] Centre for Disinfection and Sterilization, Faculty of Science and Health, Technological Institute of the Shannon, Midlands Campus, Ireland
[b] Department of Biology, Maynooth University, Maynooth, Co. Kildare, Ireland

ARTICLE INFO

Editor: Damià Barceló

Keywords:
Pollination
Commercial bumblebees
Pollen
electron-beam
Colony reproductive outputs
Food security

ABSTRACT

Commercially-reared bumblebees provide an important pollinator service that helps support food production and security. The deployment of an appropriate non-thermal disinfection technology for the bulk treatment of pollen collected from honeybees for the feeding of commercial bumblebees is important in order to mitigate against complex diseases and unwanted pathogen spillover to native bees. High level disinfection of pollen was achieved using an electron (e)-beam dose of 100 kGy that corresponded to 78 % loss of cellular viability of bee pathogens before feeding to bumblebees as measured by the novel in vitro use of flow cytometry (FCM). Novel findings showed that e-beam treated-pollen that was fed to bumblebees produced fewer females, gynes and exhibited an absence of males when compared to control bumblebee colonies that were fed untreated commercial pollen. A similar trend emerged in bumblebee colony reproductive outputs when using membrane filtered washed pollen. Proteomic analysis of bumblebees from individual colonies fed with treated-pollen revealed a differential abundance of proteins associated with stress, immunity and metabolism when compared to the untreated pollen control group. Microbiome analysis of the bumblebee gut content revealed differences in microbiota between treated and untreated pollen in bumblebee colony studies. This novel study evaluated the impact of industrial e-beam treated-pollen on complex bee disease mitigation where physically treated-pollen fed to bumblebees was shown to substantially affect colony reproductive outputs.

1. Introduction

Pollination is a vital resource provided by many insects including bees with 87.5 % of angiosperm species benefiting from insect pollination (Theodorou et al., 2020). Animal pollination is required for up to 40 % of global crop production (Krams et al., 2022), and bee pollinators, such as managed honeybee (*Apis mellifera*) and various bumblebees (*Bombus* species) and solitary bees, play a critical role. The western honeybee alone is estimated to be worth $15–$20 billion to the US economy, where it pollinates >90 % of almond, blueberry and apple crops. The honeybee is extremely important on a global scale for crop production; however, there is evidence of regional declines in both Europe and the USA (Murphy and Stout, 2019). Consequently, the commercial production of bumblebees has increased substantially (Hidalgo et al., 2020). Several bumblebee species have also been adapted to commercial pollination with over 2 million commercial bumblebee colonies used on an annual basis to pollinate over 20 crop types worldwide (Trillo et al., 2021). Bumblebees are efficient pollinators and have the ability to forage at low temperatures and in adverse weather conditions. In addition, some species of bumblebee have the ability to buzz pollinate that is necessary for pollination and to increase the yield of many fruit crops such as tomatoes, and peppers (De Luca and Vallejo-Marin, 2013). Due to their size, *Bombus terrestris* has the ability to carry more pollen on their body surfaces relative to honeybees (Knapp et al., 2019) (Stern et al., 2021). Previous Irish surveys reported that commercial bumblebees pollinate strawberries (60 %), apples (25 %) and tomatoes (20 %) (Biodiversity and Series, 2009).

However, bees are one of many pollinators that are under treat in the world today (Peso et al., 2018). The decline in honey bees was first reported in 2006 that was referred to as colony collapse disorder (CCD) (VanEngelsdorp et al., 2017; Tong et al., 2018). Since then, losses have been observed in bee colonies in several countries (Staveley et al.,

* Corresponding author.
E-mail address: neil.rowan@tus.ie (N.J. Rowan).

https://doi.org/10.1016/j.scitotenv.2023.165614
Received 12 June 2023; Received in revised form 12 July 2023; Accepted 16 July 2023
Available online 19 July 2023

2014), and have raised conservation concerns (Murray et al., 2012). Several factors, such as pesticides, parasites, viruses, climate change, habitat loss and a lack of quality nutrition have been linked with poor colony survivorship (Runckel et al., 2011; Tong et al., 2018; Reeves et al., 2018; Peso et al., 2018). The decline of bee pollinators is an alarming development given their critical role in food security and economic prosperity. Hidalgo et al. (2020) noted that a "concern related to the commercial rearing of bumblebees is the possibility of microbial contamination of food used in the rearing, including pollen obtained from domesticated honeybees". These commercial bumblebees have a high parasite prevalence (41 % of individuals infected) of trypanosomatids, microsporidians, and neogregarines, posing a potential risk to wild pollinators (Trillo et al., 2021).

A key factor influencing bee decline is their susceptibility to diseases caused by parasites and viruses (Walderdorff et al., 2018). Bumblebees tend to be predominantly infected by the parasite *Crithidia bombi* while *Nosema ceranae* and *Varroa* mites tend to infect honeybees. There is evidence to suggest that these pathogens can cross bee species to cause infection (Graystock et al., 2015). *Nosema ceranae* is a significant fungal parasite that shortens the life span of the bee by causing energetic stress (Youngsteadt et al., 2015). This fungal bee pathogen also suppresses bee immunity, disrupts foraging behaviour, and negatively impacts on the synthesis of vital molecules and cellular signalling. *Nosema* infections have been traditionally treated therapeutically such as using fumagillin; however, this has since been banned by the European Union due to its toxicity. It is appreciated that there is currently no technology or intervention that has been proven to effectively disinfect the broad array of complex bee pathogens, such as those contamination wax combs or pollen (Burnham, 2019; Simone-Fintrom et al., 2018). This is due to multiple factors including the lack of interdisciplinary research to inform testing and development of appropriate industrial-scale disinfection technologies commensurate with using bee infectivity colony studies (Goblirsch et al., 2021); the lack of a relevant in vitro bioassay for real-time determination of complex pathogen destruction that will inform appropriate treatment dosage (Simone-Fintrom et al., 2018); the variability in pathogen resistance to applied treatment technologies (Hidalgo et al., 2020); lack of simultaneous or sequential cellular and molecular information on the response of complex bee pathogens to sublethal and lethal treatment doses appropriate for killing pathogens in bee host (that maybe significantly lower dose when required for artificial in vitro disinfection studies (Naughton et al., 2017; Simone-Fintrom et al., 2018); and the lack of consensus on appropriate standard methods to reporting disinfection efficacy that includes future use of potential indicator reference strain(s) representative of different bee pathogen types informing comparative and repeatable studies enabling the relevant testing and development of appropriate breakthrough treatment technologies.

Pollen is an important natural source of protein and lipids for honeybees, where the amount of pollen collected is related to the number of larval and adult bees present in the hive (Ghosh et al., 2020). Commercial pollen is sourced from honey bees and this is then used to feed bumblebees (Pereira et al., 2019a). In natural environments, pollen is exposed to a broad range of microorganisms including pathogens to the extent that pollen collected by honeybees harbour complex microbial bee pathogens that maybe transmitted to the bee colony (Graystock et al., 2013; Graystock et al., 2015). More than 200 tonnes of honeybee-collected pollen is used annually (Velthuis and van Doorn, 2006). Commercial pollen has been found to contain a variety of bee pathogens that are economic importance in that they contaminate bumblebee colonies produced by mass rearing for export to other countries. These bee pathogens include inter alia *N. ceranae*, and *Crithidia mellificae*, *Apicystis bombi* and viruses *Deformed wing virus* (DWV), *Israeli acute paralysis virus* (IAPV), Chronic bee paralysis virus and *Sacbrood virus* (SBV) (Pereira et al., 2019b).

Determining an appropriate and effective method for the non-thermal treatment of natural pollen gathered by honeybees for the mass rearing of commercial bumblebees is a complex challenge (Hidalgo et al., 2020; Goblirsch et al., 2021). There are limited number of industrial-scale technologies that can potentially treated large quantities (tonnes) of pollen, such as on pallets, without affecting its nutritional constituents for this important pollination application (Goblisrsch et al., 2021). However, limited studies thus far have pursed use of irradiation technologies (Hidalgo et al., 2020) that have been applied and regulated for food applications that includes important knowledge transfer from the adjacent medical device sector (McEvoy et al., 2023). Hidalgo et al. (2020) have reported that gamma irradiation at a dose of 7 kGy effectively killed the majority of aerobic bacteria and the spores of fungi that contaminated commercial pollen when treating small sample quantities; however, aerobic endospore forming bacteria survived treatment at 9 kGy, particularly *Bacillus pumilus*. Meeus et al. (2014) reported that gamma irradiation of pollen is capable of reducing the pathogenicity of honey bee virus IAPV, and two commercial bumblebee produces (Biobest, Waesterloo, Belgium; Koppert B. V, Verkel en Rodenrijs, The Netherlands), have started to use this method for pollen sterilization in Europe. Other researchers have also noted that gamma irradiation reduces viral incidences in bumblebee mass rearing, along with reducing the level of other bee pathogens, such as *C. bombi*, *A. bombi*, *N. bombi*, *Nosema apis*, *N. ceranae*, deformed wing virus (DWV), Kashmir bee virus (KPV), black queen cell virus (BQCV), sacbrood virus (SQB), Ascosphaera fungi, and American foulbrood and European foulbrood bacterial (Graystock et al., 2016). However, Simone-Fintrom et al. (2018) reported that the recalcitrant Chronic bee paralysis virus and the Black queen cell virus can withstand 25 kGy gamma irradiation delivered over 9 h 45 min (standard dose used for sanitation purpose; ISO#13409 2002); however, this dosage was reported to effectively inactivate the fungus *Ascosphaera apis*, the microsporidian gut parasite *Nosema ceranae*, and Deformed wing virus.

Yook et al. (1998) previously reported that gamma treatment of pollen at 7.5 kGy dose did not significantly affect the nutritional composition of pollen; thus, intimating that this irradiation method offers potential as a sterilization process for mass rearing of commercial bumblebees. McFadden et al. (2016) reported that electron-beam treatments of heat sensitive infant milk formulae at 10 kGy did not substantially affect nutritional composition. However, there is a marked gap in appropriate experimental studies that focus on bee colony stability, and potential hereditary effects, post consumption of treated pollen by commercial bumblebees.

McEvoy and Rowan (2019) compared the effectiveness of irradiation technologies for large scale medical device applications that would be potentially similar in high through-put treatment of honey-bee gathered pollen destined for mass rearing of commercial bumblebees. E-beam uses high energy electrons emitted via an accelerator or ^{60}Co isotope as its radiation source (McEvoy and Rowan, 2019). It has advantages over gamma-treatments that include short exposure periods (usually minutes), fast cycle times, flexible batch size, good radiation dose distribution, simple validation process, no quarantine period and enables real-time monitoring (McEvoy and Rowan, 2019). E-beam is a non-thermal sterilization method for high-throughput treatment of medical devices and pharmaceutical drugs (McEvoy et al., 2023). E-beam efficiently penetrates bulk densities between 0.05 and 0.3 g per cc (McEvoy and Rowan, 2019). Electron-beam treatment of pollen for rearing commercial bumblebees was investigated in this study due also to the proximity of a large-scale industrial terminal sterilization process that also facilitated fast transportation of samples for analysis and usage in nearby specialist laboratories. In addition, McEvoy et al. (2023b) recently reported that X-ray, gamma and e-beam are comparable in terms of their microbicidal efficacy at equivalent respective dosages for medical device applications where these authors used recalcitrant bacterial endospore bioindicators (*Bacillus* species) that may potentially use in the future as an umbrella in vitro approach representative of the different complex bee pathogens that require an in vivo host (bee) for culture. The determination of bee disease inactivation by treatment

technologies and approaches is challenging given that there is reliance on using bees as host where there is limited information of appropriate in vitro assays. Determining the infectivity of complex pathogens, such as parasites, is generally very difficult as there is a lack of an appropriate in vitro infection models (Gerard et al., 2019; Franssen et al., 2019). Naughton et al. (2017) used a novel combined qPCR and cell culture assay for *Cryptosporidium parvum* oocysts (a waterborne enteroparasite), where survivor plots were used to scope appropriate pulsed UV dose for inactivating the bumblebee trypanosome parasite *Crithidia bombi* prior to using bumblebee infectivity studies. Pulsed UV is not deemed suitable as a technology for bulk pollen treatment due to lack of depth of UV penetration (Rowan, 2019). We report here, an assessment of the effectiveness of industrial electron beam technology for the decontamination of commercial pollen destined for bulk use in feeding commercial bumblebees. The subsequent impact of electron beam-treated and membrane-filtered washed pollen on commercial bumblebee colony reproductive outputs that includes influencing changes in bee types, fatbody proteome and bee gut microbiome composition, is reported. The insect fatbody plays a key role in protection against oxidative stress, accumulation of toxic compounds, nutrient and energy storage and mobilization, which is necessary for biosynthesis of molecules (Strachecka et al., 2021). This makes the fatbody an ideal tissue for the detection of molecular fluctuations associated with dietary changes.

2. Materials and methods

2.1. Industrial electron-beam sterilization

Pollen was obtained from a commercial supplier treated in an industrial electron beam site (STERIS AST, Tullamore Industrial Park, Ireland), and transported to the lab for analysis and use. E-beam treatments of 1 kg pollen samples were conducted at 1.5 kGy, 5 kGy, 10 kGy, 25 kGy, 50 kGy, 75 kGy and 100 kGy. This study was repeated in triplicate. The effectiveness of reducing microbial burden in these e-beam treatment regimes was determined using flow cytometry where propidium iodide (PI) was used to confirm loss of cellular viability as per McEvoy et al. (2021). Noting, there were limited opportunities to investigate treatment doses due to restricted access as it coincided with COVID-19 pandemic where there was increased need for treating medical devices at this industrial e-beam terminal sterilization site.

2.2. Membrane filtration of pollen

Untreated pollen was placed on a 5 μm cut-off filter (Whatman) and washed with sterile water. The water mixes with the pollen, and passes through the membrane filter, while the pollen is retained. It was hypothesised that this process could reduce pathogen load, as small microorganisms can readily pass through the 5 μm pores of the filter.

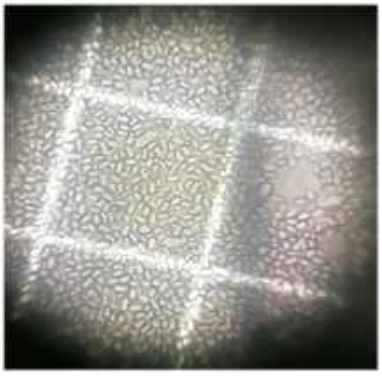

Fig. 1. Microscopic visualization of microbial load suspended in sterile water that was extracted from commercial pollen using membrane filtration.

Microbial contamination present in the filtered water was confirmed using a haemocytometer, where 1×10^6 microbes/mL were counted (Fig. 1). The washed pollen product was blotted dry using Whatman filter paper.

All pollen treatment types were stored in separate containers at 4 °C for the duration of the experiment. All challenged bumblebee colonies were fed on pollen used from the same batch, and fil pollen was made up every three days, using sterile water and 5 μm filter paper.

2.3. Bumblebee colonies

Research grade colonies of *Bombus terrestris audax* were sourced from Agralan with 40–50 bees per colony. These bumblebees had ad libitum access to feeding tubes filled with 40 % (w/v) sucrose. All bumblebee colonies were kept at 24 ± 2 °C and 58 ± 5 % relative humidity in the dark. For the first week, colonies were fed daily with 4 g of pollen, and 8 g of pollen thereafter. Twelve bumblebee colonies were used that were divided them into 3 groups, #1 to 4 were fed untreated pollen (control); Bumblebee colonies #5 to 8 were fed the same commercial pollen that had been treated with a 100 kGy dose of e-beam radiation. Bumblebee colonies #9 to 12 were fed washed pollen. Observations were made on each colony every second day, for a total of 28 days. Colonies were monitored for weight (once a week) and reproductive output (every second day) through visual observations and counting. Reproductive output was determined through counting of eggs, larvae and pupae.

2.4. Tagging callows and dissection for microbiome analysis

Newly emerged bees (callows) can be distinguished from adult bees due to their grey phenotype compared to the adult yellow and black phenotype. Callows were anesthetised under CO_2, tagged and reintroduced into the colony. Tagged callows were removed from the colony after 2 weeks, snap frozen in liquid nitrogen and stored at −80 °C until required.

2.5. DNA extractions for microbiome analysis

Bees were removed from −80 °C storage, pinned to a wax bed through the thorax and stinger prior to thawing. The abdomen was extended slightly and cut along the dorsal and ventral plane to reveal the abdominal contents. The digestive tract was located, transferred toa sterile 1.5 mL tube containing 200 μl of the ATL buffer from the DNeasy Blood and Tissue Kit (Qiagen) and homogenised using a motorised pestle. 100 μl of lysozyme was added and the sample was incubated at 36 °C for 40 min. The remainder of the DNA extraction procedure followed the manufacturer's instructions. Extracted DNA was stored at −20 °C before submission to Novogene Europe (UK) Ltd. for and ITS and 16S amplicon sequencing to determine the bacterial and fungal species present. Five replicate samples per treatment were sequenced. Sequencing data are available from NCBI BioProject PRJNAXXXXXXX. DNA quality control studies exhibited range values between 1.9 and 2.1 for untreated (control), e-beam and filtered-treated samples for Abs 260 and Abs 280 ratios (Supplementary Table 1).

2.6. Proteomic sample preparation

For fatbody collections, bees were prepared and pinned as they were for the digestive tracts. Fat body cells were collected from the inside the dorsal and ventral cuticles using sterilized pins and tweezers and transferred to individual 1.5 ml tubes containing 300 μl of lysis buffer comprising 6 M urea, 2 M thiourea and 1 tablet of Complete™, Mini Protease Inhibitor Cocktail (Roche Diagnostics). Samples were snap frozen in liquid nitrogen and stored at −20 °C. When all dissections were complete the samples were thawed on ice, homogenised for 30 s each using a motorised pestle, and centrifuged at 10000 rpm for 5 min to pellet any remaining cellular debris. Supernatants were aliquoted into

sterile 1.5 mL tubes and stored at −80 °C.

Protein quantification was conducted using a Qubit® fluorometer version 2.0 following manufacturer guidelines. 100 μg of protein was removed from each sample and processed with a 2-D clean up kit (GE HealthCare) to remove biological impurities. The resulting pellet was resuspended in 50 μl resuspension buffer (6 M urea, 0.1 M Tris HCl, pH 8.0), of which 20 μl was used for protein digestion. 115 μl of 50 mM ammonium bicarbonate was added to each sample. Proteins were reduced and alkylated by adding 0.5 M dithiothreitol (DTT) at 56 °C for 20 min followed by 0.5 M iodoacetamide (IAA) and incubated at RT for 15 min in the dark. 1 μl of 1 % (w/v) Protease Max (Promega) and 1 μl sequence grade trypsin (Promega) were added to each sample and incubated at 37 °C for 16 h. Subsequently, 1 μl of 100 % trifluoroacetic acid (TFA) was added to each sample to terminate digestion and the samples were incubated at room temperature for 5 min and centrifuged at 10,800 rpm for 10 min. The resulting supernatants were purified using Pierce C18 spin columns (Thermo Scientific) following manufacturer guidelines and the eluted purified peptides were dried using a vacuum concentrator (Thermo Scientific Savant DNA 120) and stored at 4 °C. Peptides were resuspended in a volume of loading buffer (2 % (v/v) acetonitrile and 0.05 % (v/v) TFA) to yield a concentration of 0.5 μg/μl, sonicated for 2 min and centrifuged at 13,400 rpm for 5 min.

2.7. Mass spectrometry analysis

1 μg of peptide mix for each sample was eluted onto the Q Exactive (Thermofisher Scientific, USA) high resolution accurate mass spectrometer connected to a Dionex Ultimate 3000 (RSLCnano) chromatography system. An increasing acetonitrile gradient was used to separate peptides on a Biobasic C18 Picofrit™ column (200 mm length, 75 mm ID), using a 120-minute reverse phase gradient at a flow rate of 250 nL/min. All data were acquired with the mass spectrometer operating in automatic data dependent switching mode. A high-resolution MS scan (300–2000 Da) was carried out to select the 15 most intense ions prior to MS/MS. MaxQuant version 1.6.17.0 (www.maxquant.org) was used for protein identification and LFQ normalisation of all MS/MS data. The Andromeda search algorithm in MaxQuant was used to correlate all MS/MS data against protein reference sequences obtained from the National Centre for Biotechnology to correlate the data against the protein reference sequences derived from the *B. terrestris* genome (Saad et al., 2015) obtained from the National Centre for Biotechnology Information (NCBI) repository (17,508 entries, downloaded September 2021). The mass spectrometry proteomics data have been deposited to the ProteomeXchange Consortium via the PRIDE partner repository with the dataset identifier PXDXXXXXX).

2.8. Proteomic data analysis

Perseus version 1.6.1.1 was used for data visualization and statistical analysis. Normalised LFQ intensity values were used as a measure of protein abundance. The data was filtered for the removal of contaminants and peptides identified by site. LFQ intensity values were $\log_2$ transformed and samples were allocated to groups corresponding to treatment. Proteins absent from any samples in at least one group were not used for further analysis. A data imputation step was conducted to replace missing values with values that simulate signals of low abundant proteins chosen randomly from a distribution specified by a downshift of 2.1 times the mean standard deviation (SD) of all measured values and a width of 0.1 times this SD. Normalised intensity values were used for principal component analysis. A two-sample *t*-test was performed using a cut-off value of $p \leq 0.05$ to identify statistically significant differentially abundant (SSDA) proteins. Volcano plots were produced by plotting –Log *p*-values on the y-axis and Log_2 fold-change values on the x-axis to visualize differences in protein abundance between treatment groups. Hierarchical clustering of SSDA proteins was performed using z-score normalised intensity values to produce a heat map of protein abundance.

2.9. Functional annotation

The Search Tool for the Retrieval of Interacting Genes/proteins (STRING) version 11 (Szklarczyk et al., 2019) (www.string-db.org) was used to map protein-protein interaction networks. Protein sequences were inputted into the STRING database and protein-protein interactions were analysed using the homologous *Apis mellifera* match for each identified *B. terrestris* protein. STRING clusters were inspected for the protein sets of higher or lower abundance in fatbodies from bees fed *E*-beam-treated or washed pollen with respect to the control pollen. The gene ontology categories enriched with each set (Fisher's Exact test; $p < 0.05$) were obtained for molecular function, biological process, cellular compartment, KEGG term and others where appropriate to determine the pathways and processes affected by the different pollen treatments.

3. Results

3.1. Preliminary screening and assessment of treatments for pollen sterilization

E-beam technology was tested for its suitability to decontaminate bulk honeybee gathered pollen for the purpose of feeding commercial bumblebees. E-beam treatment was carried out on pre-determined microbial and parasitic bee pathogens extracted from bulk pollen at Steris Advanced Sterilization Technologies (AST), Tullamore, Ireland. E-beam treatments were not effective at lower treatment doses (≤25 kGy), where there was increased level of inactivation achieved using 50 kGy, 75 kGy and 100 kGy doses that were equivalent to 36.6 %, 51.2 % and 77.9 % loss of cellular activity respectively using flow cytometry (Fig. 2). E-beam samples left in storage at room temperature revealed no mold growth after 8 months compared to untreated pollen where fungal growth was observed after one-month storage (Fig. 3). Due to this study coinciding with the COVID-19 pandemic, it was not possible to access the industrial e-beam facility for additional optimisation. Accordingly, a dose of 100 kGy for e-beam treatment of pollen was selected that would provide a fixed dosage for maximal destruction of pathogens in the pollen based on initial findings.

3.2. Colony reproductive output

Bumblebee colonies were observed every second day for changes in brood development with the changes in eggs clumps, larvae and pupae numbers noted and recorded. A reduction in the number of larvae and pupae being produced in both treated colonies (e-beam treated and washed pollen) compared to untreated colonies was observed after four weeks (Fig. 4). A change in egg, larvae, and pupae colour was also observed. Eggs from colonies fed with treated pollen failed to develop into larvae. Colonies fed untreated pollen continued to produce eggs, larvae and pupae.

Colonies fed on e-beam treated and washed pollen produced significantly more eggs compared to those fed on control pollen (Fig. 4A) ($P \leq 0.05$). However, control colonies produced significantly more larvae than e-beam-treated and washed pollen-fed colonies ($P \leq 0.001$, $P \leq 0.05$) (Fig. 4B). Control colonies also produced significantly more pupae ($P \leq 0.001$) (Fig. 4C).

3.3. Colony numbers and sex typing

Colonies were examined post-experiment and sex typed bees that had died during the course of the experiment were included in the overall count, but were not typed due to the poor condition of their bodies. These were seen mainly in the control colonies (Fig. 5). Colonies fed on treated pollen produced fewer males, while control groups produced males in all 4 colonies. Female bees that were deemed to be larger

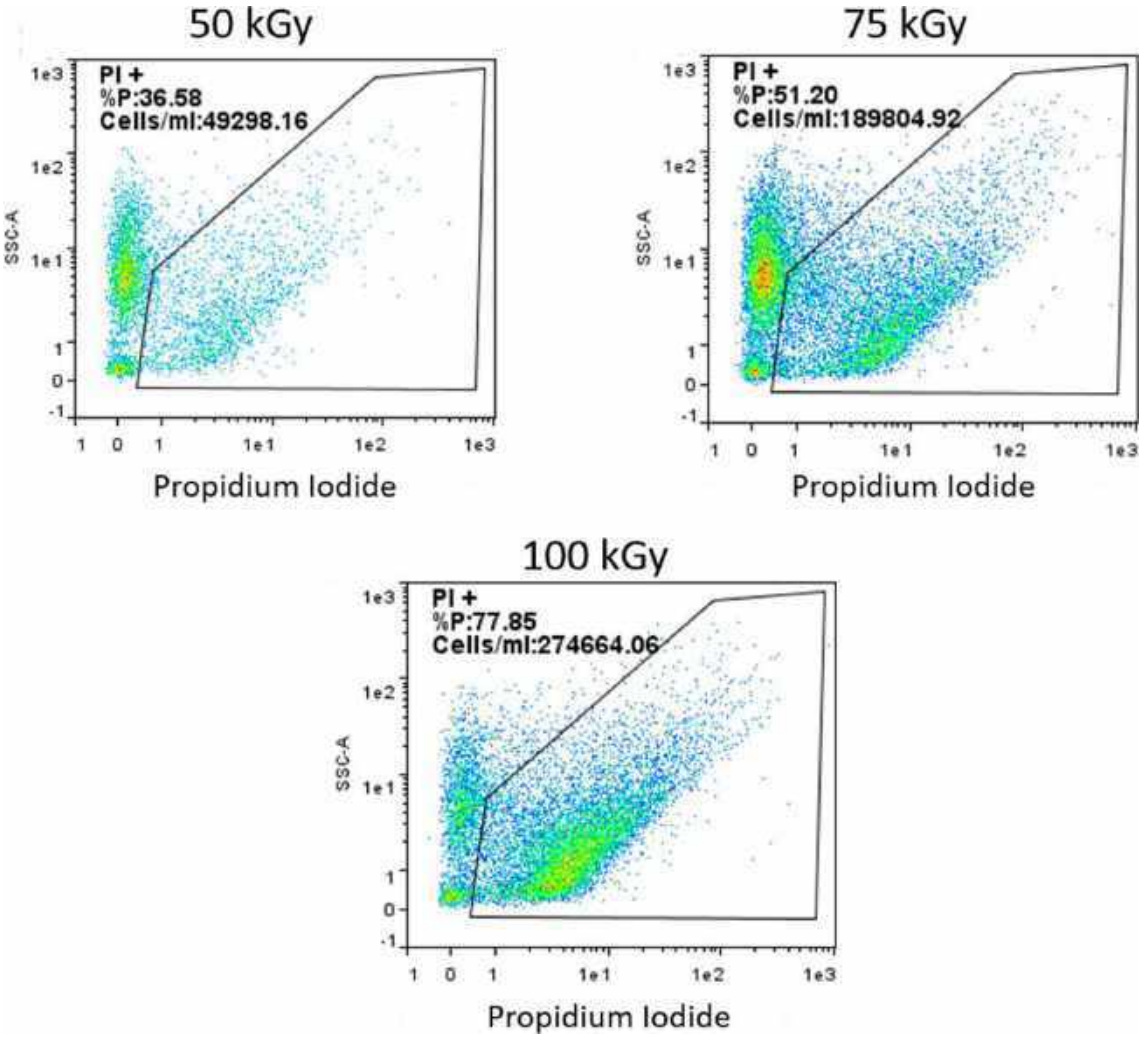

Fig. 2. E-beam treatments were administered to microbial samples derived from industrial pollen at intensities of 50, 75 and 100 kGy. Samples were prepared for flow cytometry analysis by staining with viability dye Propidium Iodide (PI). Dot plots show percentages and total cell numbers positive for PI fluorescence, representative of cell damage/death.

Fig. 3. Pollen treated with E-beam radiation and control untreated pollen was stored in sealed containers for 9 months post-treatment. Pollen treated with E-beam exhibited no fungal growth 9 months post treatment. Untreated pollen exhibited a small amount of fungal growth 1-month post treatment and major growth 9 months post treatment.

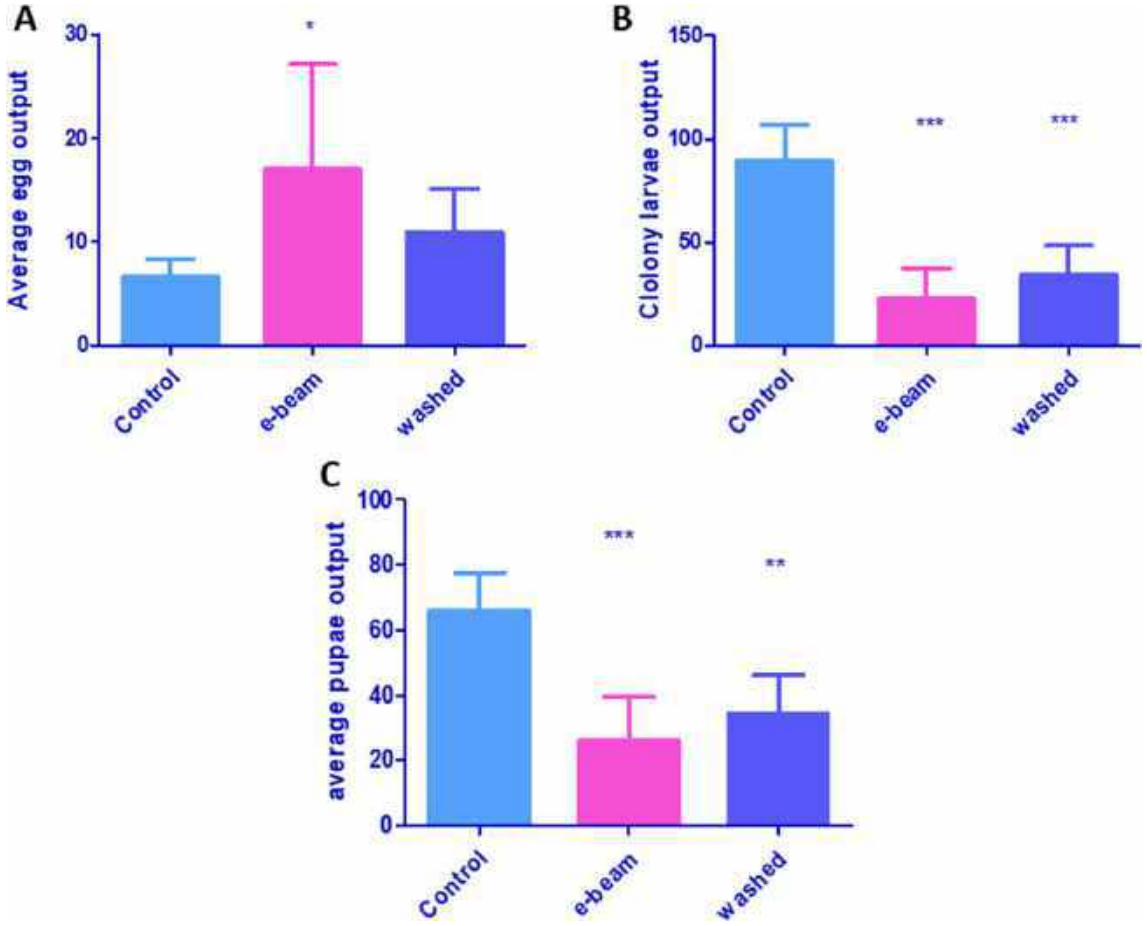

Fig. 4. Colony reproductive output was measured after 28 days of feeding on untreated, e-beam treated, and washed pollen. Both e-beam and washed colonies produced significantly more eggs ($P \leq 0.05$) than the control colony (A). The control colony produced significantly more larvae compared to the e-beam treated pollen fed colony ($P \leq 0.001$), and washed pollen fed colony ($p \leq 0.05$) (B), as well as significantly more pupae ($P \leq 0.001$) (C). Colonies were analysed using a one-way ANOVA repeated measure test.

than average were denoted as Gyne/Queen. Each colony had 1 queen and any other bee of similar size within that colony was labelled as a gyne. In the control group three of the four colonies produced gynes. In the treated colonies, only the colony fed washed pollen produced a single gyne, which was found in colony 11. In total, control groups produced 781 females, 856 males and 39 queens/gynes, compared to e-beam producing 379 females, 11 males and 4 queens/gynes and washed pollen fed colonies producing 661 females, 2 males and 5 queens/gynes (Fig. 5B).

3.4. E-beam pollen vs control pollen proteomic analysis

A total of 177 statistically significant differentially abundant (SSDA) proteins were identified in fatbodies from e-beam treated pollen fed and control bees (relative fold change (RFC) range: +21.7 to −169.2). There were 103 proteins with increased abundance and 74 with decreased abundance. The top 15 proteins that were upregulated were associated with toxicity, immunity, translation and sex hormone production (Table 1). The top 15 proteins that were downregulated in colonies fed on e-beam treated pollen were associated with bee venom, chitin degradation, exoskeleton, peptidoglycan recognition, cellular respiration and heat shock. Cytochrome b5 was detected in high abundance in the e-beam treated pollen fed colonies. Cytochrome enzymes are generally associated with detoxification.

Proteins that were in lower abundance in the e-beam treated pollen fed group included melittin (RFC-168.9), Chitinase 2 (RFC-10.5) and proteins involved in defence and immunity such as the serine proteinase Chymotrypsin (RFC-4.3) and Peptidoglycan recognition protein (RFC-4.6). It is suggestive of an upregulation of detoxification proteins within the e-beam treated pollen fed group coupled with a downregulation of proteins involved in immunity.

3.5. Washed pollen vs control pollen analysis

A total of 523 (SSDA) proteins were identified in fatbodies from washed and control pollen fed bees (RFC range: +47.5 to −394.3). There were 337 proteins with increased abundance and 185 with decreased. The top 15 proteins that were upregulated were associated with toxicity, immunity, translation and sex hormone production, with clusters in proteasomal upregulation and amino acid biosynthesis being identified (Table 2, Fig. 6). The top 15 proteins that were downregulated in colonies fed on e-beam treated pollen were associated with bee venom, chitin degradation, exoskeleton, peptidoglycan recognition, cellular respiration and heat shock.

The most prominent microbiota identifed in individual bumblebee colonies were *gilliamella*, *snodgrassella*, *lactobacillus*, chloroplast and mitochondria. *Gilliamella* was more abundant in e-beam treated pollen fed colonies (0.3992) compared to washed pollen fed colonies (0.3665) and control colonies (0.2568). *Snodgrassella* was more abundant in control colonies (0.3505) compred to e-beam (0.1714) and washed (0.2710). *Lactobacillus* was more abundant in e-beam treated colonies (0.2670) compared to washed (0.2313) and control colonies (0.1245), (Fig. 7A). The mean abundant differences between species from various genera of microbiota found in the digestive tracts of bees fed on either

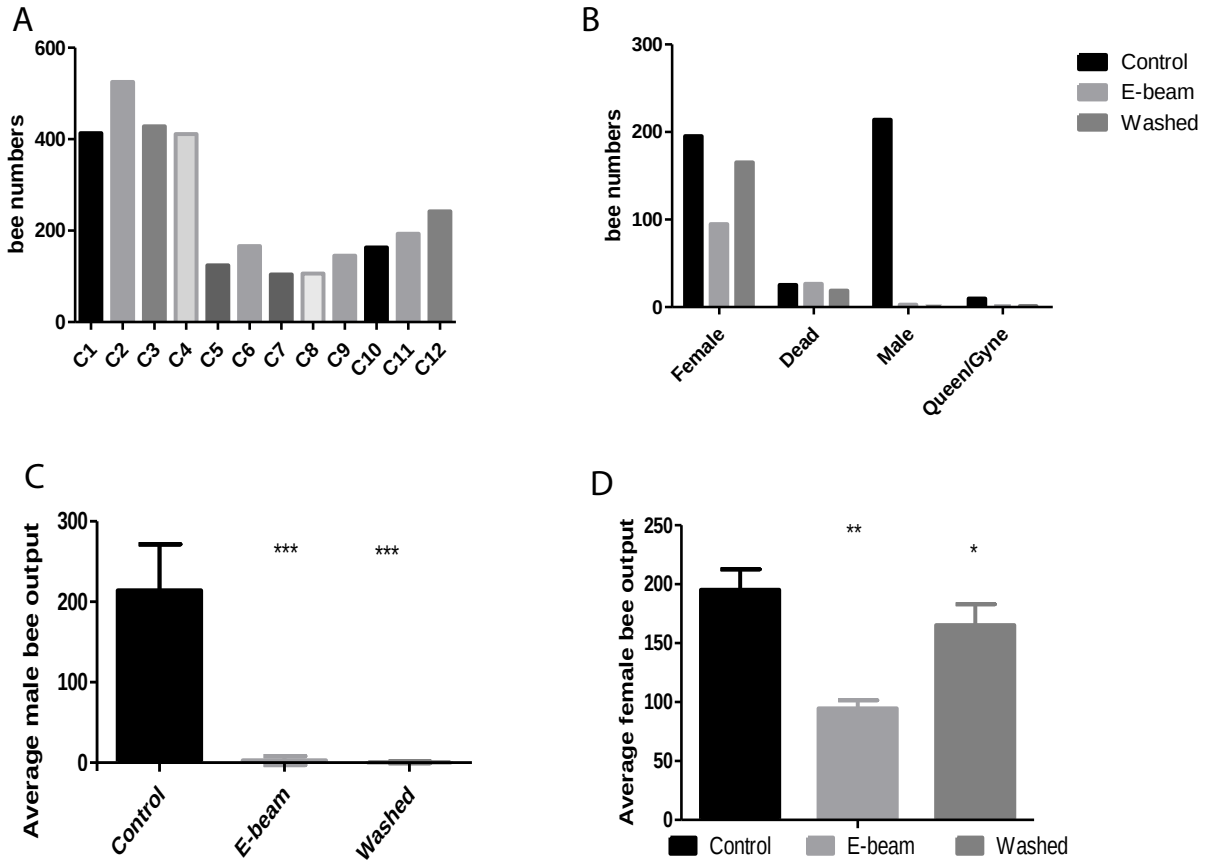

Fig. 5. Bee output from colonies fed on untreated, e-beam treated, or washed pollen. The differences observed for individual colonies total bee counts (A) and the categories they were divided into via treatment (B). Treated colonies as a whole failed to produce male bees (C), whereas control colonies produced more males compared to females. Fewer females were also produced in e-beam and washed colonies (D). Data was analysed using one-way ANOVA, Turkey's method.

untreated, e-beam treated pollen or washed pollen were recorded with confidence intervals between the groups of a upper limit of 95 % (Fig. 8).

The abundance and diversity of fungi present varied per colony and per pollen source. *Zygosaccharomyces* averaged in control colonies (0.2482), e-beam (0.0041) and washed (0.2759), *Rhizopus* ranged in the control (0.0004), e-beam (0) and washed (0.1085), *Wickerhamomyces* ranged in the control (0.0172), e-beam (0.0049) and washed (0.1339), *Kazachstania* ranged in the control (0), e-beam (0.0129) and washed (0), *Candida* ranged in the control (0.0002), e-beam (0.0096) and washed (0.0010). *Bettsia* was not present in the control (0) or washed (0), while small amounts were detected in e-beam (0.0037). *Neoascochyta* was also found in e-beam (0.0074) with a smaller amount found in the control (0.00003) and none detected in washed (0). A total of 10 genus were identified In bees fed on control pollen 8 of the 10 were present, 9 of the 10 in bees fed on e-beam treated pollen and 7 of the 10 in the bees fed on washed pollen. Bees fed on e-beam treated pollen also had the greatest number of unidentified fungi (Fig. 7B).

4. Discussion

4.1. Decontamination efficacy

This study investigated e-beam sterilization as a novel non-thermal technology for the purpose of sterilizing pollen for commercial bumblebee rearing application. Samples treated with 100 kGy exhibited no microbial growth 2 months post treatment when compared to untreated controls, based on light microscopy observations. The microbial burden treated at 100 kGy exhibited a residual vitality at ca. 22 % of treated population as measured by flow cytometry that intimates high level disinfection; however, it is likely that this high dosage possibly killed bee pathogens such as complex parasites through a multi-hit biocidal process. There were no survival of bee parasites when treated bumblebees were monitored over a 30 day period. Naughton et al. (2017) observed lingering viability in the bumblebee trypanosome parasite *Crithidia bombi* when treated with high intensity pulsed UV (PUV). Simone-Fintrom et al. (2018) noted that it is critical to determine appropriate physicochemical and operational parameters that inform an effective dose for gamma irradiation of honey bee fungal agent causing chalkbrood disease, the microsporodium gut parasite Nosema spp. and several viruses in the bee host where studies were conducted at 25 kGy for disinfecting wax combs with reported survival of Black queen cell virus (BQCV) and Chronic bee paralysis virus (CBPV).

There is currently a reliance on use of surrogate in vitro methods to estimate inactivation of broad range of pathogens without properly considering the ability of treated pathogens to elicit an infection process in the bee host. For example, Farrell et al. (2011) reported that lethal action of pulsed light is attributed to a multi-hit biocidal process in treated *Candida albicans* where increased fluence or UV dose enhanced the severity of simultaneous or sequential sub-lethal stresses (namely membrane-lipid peroxidation, membrane permeabilization, reactive oxygen species accumulation, DNA damage, necrosis and apoptosis) to a point of irreversible lethality, and death. This study reported on the novel use of flow cytometry for determining total microbial bioburden lethality; for example, an e-beam treatment dose of 100 kGy achieved 78 % lethality based on DNA and membrane stability staining. However, it is possible that a much lower treatment dose may have been effective at killing various types of bumblebee pathogens present in the contaminated pollen if challenged in bumblebees. Interestingly, the

Table 1
The top 15 SSDA proteins in bees from e-beam treated and control pollen fed colonies. Positive relative fold change (RFC) values indicate proteins with higher abundances in fatbodies from bees fed with the e-beam treated pollen whereas negative RFCs indicate proteins with reduced abundances in bees fed with the e-beam treated pollen in comparison to those fed the non-treated control pollen.

Accession number	Protein name	Relative fold change
XP_003397300.2	Uncharacterized protein	21.1
XP_012176245.1	Cytochrome b5	6.9
XP_012163499.1	Vitellogenin	6.4
XP_020721756.1	Uncharacterized protein	6.1
XP_003396646.1	Uncharacterized protein	5.0
XP_003393261.1	Mitochondrial coenzyme A transporter SLC25A42	4.3
XP_003395337.1	1-acyl-sn-glycerol-3-phosphate acyltransferase gamma	4.3
XP_003393699.1	Cytochrome P450 9e2	4.3
XP_003399652.1	PRA1 family protein 3	3.7
XP_003398970.1	long chain fatty acid transport protein 1	3.7
XP_012164498.1	ADP-ribosylation factor 2	3.5
XP_012164498.1	Chaoptin	3.2
XP_020723232.1	60S ribosomal protein L39	3.2
XP_003402576.2	Serine protease inhibitor 3/4 partial	3.2
XP_003401025.1	Ornithine amninotransferase	3.0
XP_020718386.1	Melittin	−168.9
XP_003395447.1	Epididymal sercretory protein E1	−17.1
XP_003400637.1	Probable chitinase 2	−10.5
XP_003395094.1	Uncharacterized protein	−9.8
XP_012165909.1	Uncharacterized protein	−9.2
XP_020718419.1	Glycine rich cell wall structural protein 1	−9.2
XP_003397852.1	Nicotinamidase	−9.2
XP_020718442.1	Transmembrane protease serine 9	−8.6
XP_012169980.1	Protein lethal(2) essential for life	−7.0
XP_12172148.1	Uncharacterized protein	−5.3
XP_003400160.1	Peptidoglycan recognition protein	−4.6
XP_003394953.1	Cuticle protein 16.5	−4.6
XP_012169306.1	Uncharacterized protein	−4.6
XP_020718419.1	Glycine rich cell wall structural protein 1	−4.6
XP_003402742.1	Chymotrypsin	−4.3

Table 2
The top 15 SSDA proteins in bees from washed and control pollen fed colonies. Positive relative fold change (RFC) values indicate proteins with higher abundances in fatbodies from bees fed with the washed pollen whereas negative RFCs indicate proteins with reduced abundances in bees fed with the washed pollen in comparison to those fed the non-treated control pollen.

Accession number	Protein name	Relative fold change
XP_003395548.1	Insulin gf binding protein acid labile subunit	48.5
XP_020721715.1	Putative fatty acyl CoA reductase CG8306	17.1
XP_012164498.1	Chaoptin	16
XP_012163499.1	Vitellogenin	13.9
XP_020718283.1	Membrane metallo-endopeptidase 1	12.1
XP_003402924.1	UDP = Gluctonosyltransferase 2B15	11.3
XP_003399880.1	Putative fatty acyl CoA reductase	11.3
XP_012175289.2	Retinol dehydrogenase 14	9.8
XP_003396646.1	Uncharacterized protein	9.1
XP_003402892.1	Glucosylceramidase	8.5
XP_003395752.1	Ribosomal protein S29	8
XP_003397300.2	Uncharacterized protein	7.4
XP_020723232.1	Ribosomal protein	7.4
XP_003398436.1	Pancreatic lipase relasted protein 4	6.9
XP_003395762.1	Omega conotoxin protein 3	6.9
XP_020718386.1	Melittin	−388.0
XP_020718442.1	Transmembrane protease serine 9	−27.8
XP_003400637.1	Probable chitinase 2	−27.8
xp_012170989.1	Phospholipase A2	−18.3
XP_003402742.1	Chymotrypsin 1	−14.9
XP_003400160.1	Peptidolycan recognition protein	−13.9
XP_003393535.1	Chymotrypsin 1	−12.9
XP_003398056.1	DNA-directed RNA polymearse II subunit RPB1	−10.5
XP_003394953.1	Cuticle protein 16.5	−9.8
XP_003394058.1	Probable salivary secreted peptide	−9.8
XP_003401050.2	Serine protease 53	−9.8
XP_003395094.1	Uncharacterized protein	−8
XP_003402225.2	Maltase A1	−8
XP_003399666.1	Collagen alpha (IV) chain	−7.4
XP_012165896.1	Uncharacterized protein	−7.4

detection of a bioactive to represent occurrence of an irreversible death phase in treated pathogens (such as apoptosis) may also indirectly inform future process efficacy that may negate the need for using complex surrogate in vitro assays. A dose of 100 kGy was selected in this study as it produced the greatest level of microbial lethality and there was limited opportunities to test less severe dosages due to the COVID-19 pandemic where the industrial e-beam facility was prioritised for medical device sterilization. Albeit limited, studies using gamma irradiation of pollen (Hildago et al., 2020), or wax combs (Simone-Fintrom et al., 2018), using ca 10 kGy (a standard dose employed by commercial bumblebee producers) maybe of a sufficient intensity for achieving the desired high level disinfection or sterilization of treated pathogens in the bee host itself; however, it is likely that higher treatment doses are potentially required given the resistance profile of recalcitrant viruses as exhibited by BQCV and CPBV in related honey bee inactivation studies (Simone-Fintrom et al., 2018). Hildago et al., (2018) reported the survival of *Bacillus pumilus* endospores in wax comb studies at 9 kGy; thus, inferring the potential use of this particular bacterial species as a bio-indicator of sterilization efficacy for bee disease migitation where these particular spore-forming bacteria are used to confirm sterility assurance levels for the adjacent medical device sector (McEvoy et al., 2023; Rowan et al., 2023).

It is recognised that the doses of e-beam ranging from 7 kGy to 44 kGy have been applied for treating foods (Lee et al., 2017); however, the higher dose of 100 kGy was also selected in this study to assure sterilization (or high-level disinfection) so as to avoid any unnecessary use of test bumblebees. Use of flow cytometry was used to indirectly measure or gauge disinfection of complex parasites as there is no specific in vitro infection model for studying bee parasites. Interestingly, use of flow cytometry has also been used as a rapid in vitro enumeration method for medical device sterilization (McEvoy et al., 2021). Naughton et al. (2017) also used a surrogate approach for determining efficacy of destroying *C. bombi* parasites where these researchers used a waterborne protozoan parasite as the challenge bioindicator where survivors were determined using in vitro combined cell culture-qPCR infectivity assay. Recent studies have reported on the development of honey bee and bumblebee cell lines that may inform future in vitro infectivity studies that would inform scoping in vitro studies to limit use of actual bumblebees (Goblirsch and Adamczyk, 2023).

Bumblebee colonies fed on either e-beam treated or washed pollen, produced significantly fewer females, gynes and males compared to bees fed on non-treated pollen. They also produced significantly fewer larvae and pupae, despite producing more eggs. This is likely due to the eggs failing to develop into larvae, meaning a constant egg count was observed in treated colonies. The failure to produce adult bees in these colonies presents the risk of having fewer workers and nurses to tend to the brood, and a lack of gynes means there is less chance of new colonies being founded. The lack of males will also heavily impact on reproduction as the primary role of males in a bumblebee colony is to mate with the queen (Amin et al., 2010). There was a significant difference in thorax width and intertegular distance between colonies fed on treated and control pollen. As sucrose was readily available across all colonies, the differences noted in size and reproductive output could be due to nutritional alterations in the pollen, with key components either being washed out or denatured. It is possible that the microbial community that inhabits commercial pollen plays a key role in nutrition, which is required for reproductive output too. Changes in the proteome were observed, likely due to microbial and nutritional alterations in the polled due to treatment. Several pathways involved in stress and metabolism, growth and development and immunity were altered in bees fed on

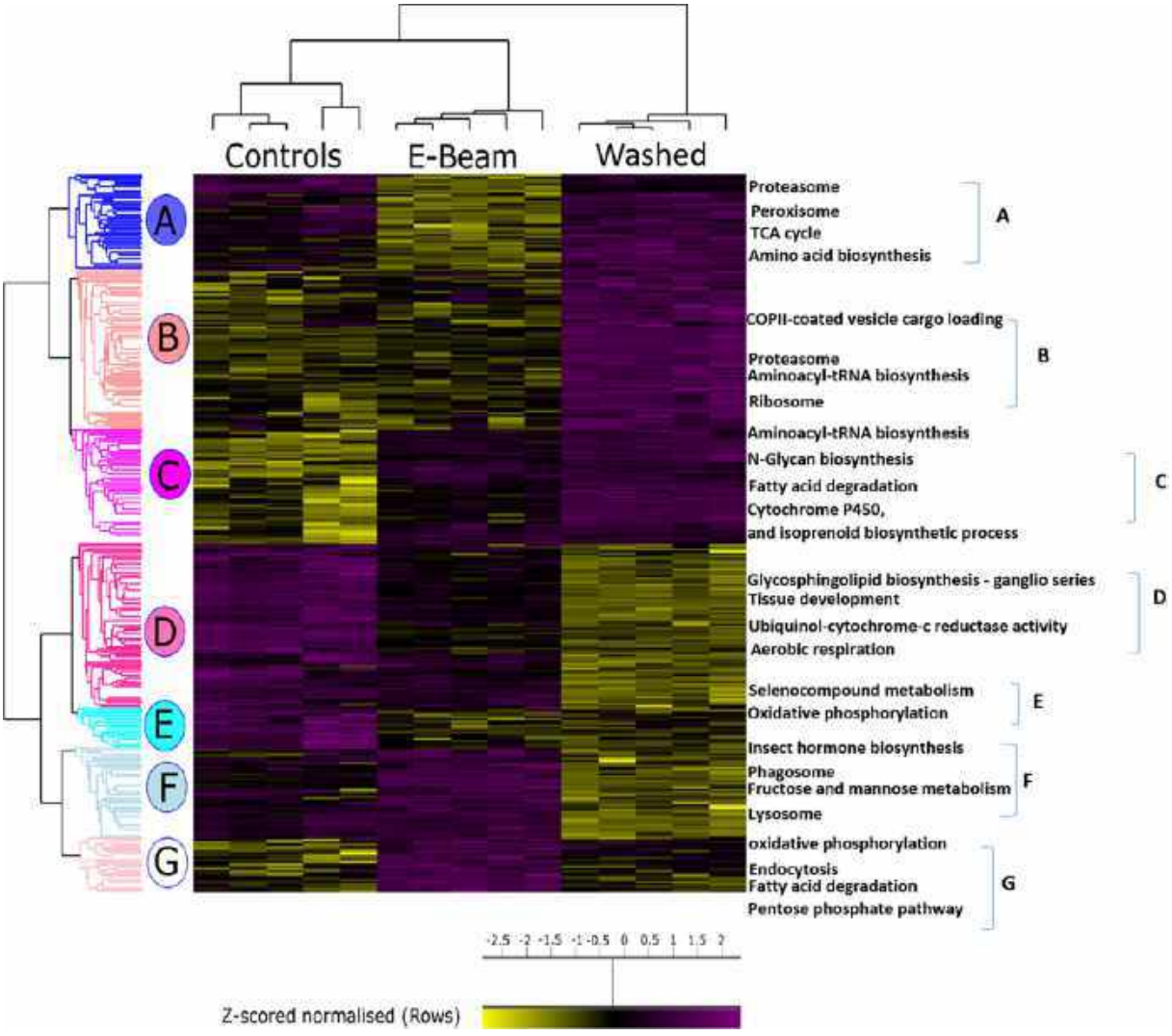

Fig. 6. Heat map of treated clusters from fat body analysis showing proteins divided into clusters sorted by abundance. Clusters in black/dark purple are normalised, with yellow denoting proteins and pathways of low abundance and bright purple denoting proteins and pathways of high abundance. Pathways involved in immunity, stress and metabolism were upregulated or downregulated depending on pollen type fed to the commercial bumble bee colonies.

treated pollen compared to those fed on control pollen.

4.2. Increased abundance in E-beam treated pollen fed colonies

4.2.1. Metabolism

Colonies fed on e-beam treated pollen exhibited upregulation in oxidative phosphorylation, endocytosis, fatty acid degradation and the pentose phosphate pathway. The pentose phosphate pathway is a key pathway in the formation of molecules for nucleic acid and amino acid biosynthesis while the non-oxidative pathway can supply glycolysis with the necessary metabolites required for normal function. Fructose and mannose metabolism was upregulated in the colonies fed on e-beam treated pollen, perhaps due to an excess of both sugars in the diet, or a dependency on both sugars in the diet in order to maintain energy levels for normal function. Mannose and fructose metabolism was downregulated in the washed group and normalised in the control, suggesting e-beam treated pollen is altered and affecting the metabolism of the colonies. An upregulation of cytochrome *b*5 in e-beam treated pollen fed colonies could be a direct result of fatty acid degradation. If bees in these colonies were facing a nutrient deficit, then it is possible that fatty acids are being broken down to generate ATP, and a remodelling of degraded fatty acids is occurring to maintain lipid metabolism. Mitochondrial coenzyme A transporter SLC25A42 was upregulated. This mitochondrial inner membrane protein transports both cytosolic dephosphoCoA (dPCoA) and coenzyme A (CoA), with CoA playing a role in fatty acid and cholesterol biosynthesis, fatty acid oxidation and amino acid metabolism (Philip et al., 2012). This suggests that there is a breakdown and restructuring of various fatty acids in order to maintain homeostasis.

4.2.2. Stress-related protein upregulation

Vitellogenin (Vg), which is vital for egg maturation and embryonic development (Wu et al., 2021), was upregulated in e-beam treated pollen fed colonies. It not only plays a role in egg maturation, but also in protecting against oxidative stress, and can act as a pathogen recognition receptor (PRR) in *Apis mellifera* (Wu et al., 2021). It is possible that Vg upregulation was in response to stress conditions, as an upregulation in phagosome, lysosome and oxidative phosphorylation was observed in the heat maps. This could be a result of poor nutrition and Vg could be acting as sensor for sugar.

Other proteins upregulated included members of the cytochrome *p*450 family cytochrome p4509e2, which metabolise toxins and promote tolerance. In *Apis mellifera*, these enzymes play a role in detoxification of pesticides (Mao et al., 2011). A change in the molecular makeup of the pollen due to e-beam treatment may be inducing toxic effects on the

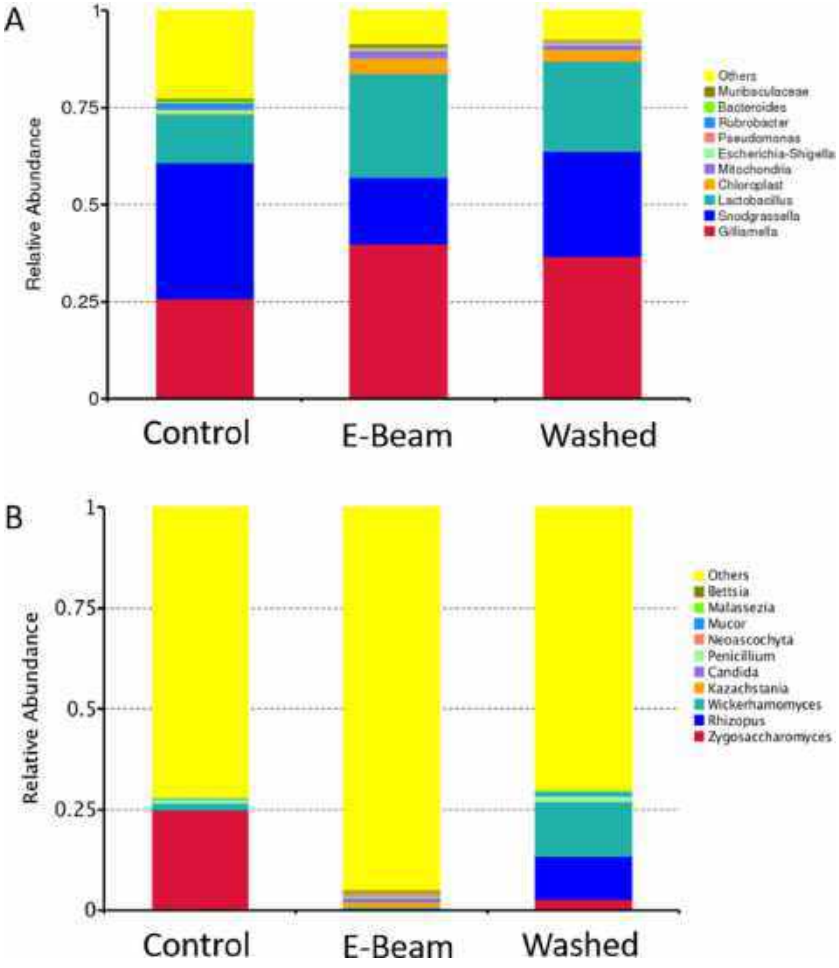

Fig. 7. The relative abundance of the microbiome (A) and mycobiome (B) from the gut of bees fed on either control, e-beam treated or washed pollen. Genus distribution varied depending on the type of pollen the colonies were fed. The three core bacteria *Gilliamella*, *Snodgrassella* and *Lactobacillus* made up the majority of the microbiota present, with differences being observed in the numbers present depending on the type of pollen the bees were fed. Bees fed on e-beam treated pollen had the greatest diversity of fungi in their mycobiome.

colonies. Indeed, e-beam treated pollen visually differed from non-treated commercial pollen, it had a waxy glow, resembling plasticine and took on a darker colour.

4.3. Increased abundance in washed pollen fed colonies

4.3.1. Unsaturated fats and fatty acids biosynthesis

Biosynthesis of fatty acids and unsaturated fats were upregulated in bumblebees fed on washed pollen, they had a less diverse gut microbiome, and a greater abundance of *Firmicutes* and *Bacteroidota* compared to control colonies. High *Firmicutes* and *Bacteroidota* levels are an indicator of a high fat diet (HFD). An increase in saturated fatty acids (SFA) in the diet decreases microbiota diversity (Wang et al., 2021). When considered together, this suggests that bees fed on washed pollen are potentially living on a HFD/SFA diet. The upregulation in the biosynthesis of unsaturated fats is possibly a direct result of nutrition defects within the pollen. Upregulation of fatty acid biosynthesis along with fatty acid degradation may suggest that the pollen diet is driving a change in metabolism and a reliance on fat stores in order to maintain homeostasis.

4.3.2. Metabolism

Proteins associated with the TCA cycle, amino acid biosynthesis, the peroxisome and proteasome were upregulated in washed pollen fed colonies. Pollen has been shown to affect amino acid levels, with non-essential amino acid production being increased in pollen fed honeybees (Gage et al., 2020). While additional research is required to determine amino acid profiles, altered pollen may not provide enough nutrition for sufficient the same level of amino acids as good quality pollen. Previous studies have shown altered amino acid profiles in the brains of bees deprived of pollen.

4.3.3. Growth and development

Insulin like growth factor (IGF) plays a role in growth development, reproduction, stress resistance and lifespan, and was upregulated in colonies fed on washed pollen. This could be why larger bees were observed in these colonies compared to control colonies. IGF works to promote body and tissue growth during development, in response to the nutritional status (Naoki Okamoto, 2018). Glucosylceramidase breaks down glucosylceramide (GlcCer) to glucose and ceramide, and play roles in cell adhesion, recognition, growth, development and inflammation (Reza et al., 2021). Deficiencies in glucosylceramidase can impair memory, and movement via accumulation of glucosylceramide (Reza et al., 2021). Glycosphingolipid biosynthesis was downregulated in colonies fed on washed pollen and upregulated in control colonies, suggesting further negative impacts on colonies fed washed pollen.

4.4. Decreased abundance in E-beam treated pollen fed colonies

4.4.1. Immunity

Proteins associated with inflammatory responses and immunity were down regulated in e-beam treated pollen fed colonies. Chymotrypsins are a family of proteins that have developed in response to defence mechanisms of plants against insects that feed on them (Kim et al., 2022). It is possible that mechanisms produced by pollen such as proteinase inhibitors and defensive enzymes (Kim et al., 2022) have been deactivated by e-beam sterilization process. Peptidoglycan recognition proteins were downregulated, potentially because the nutrient quality is

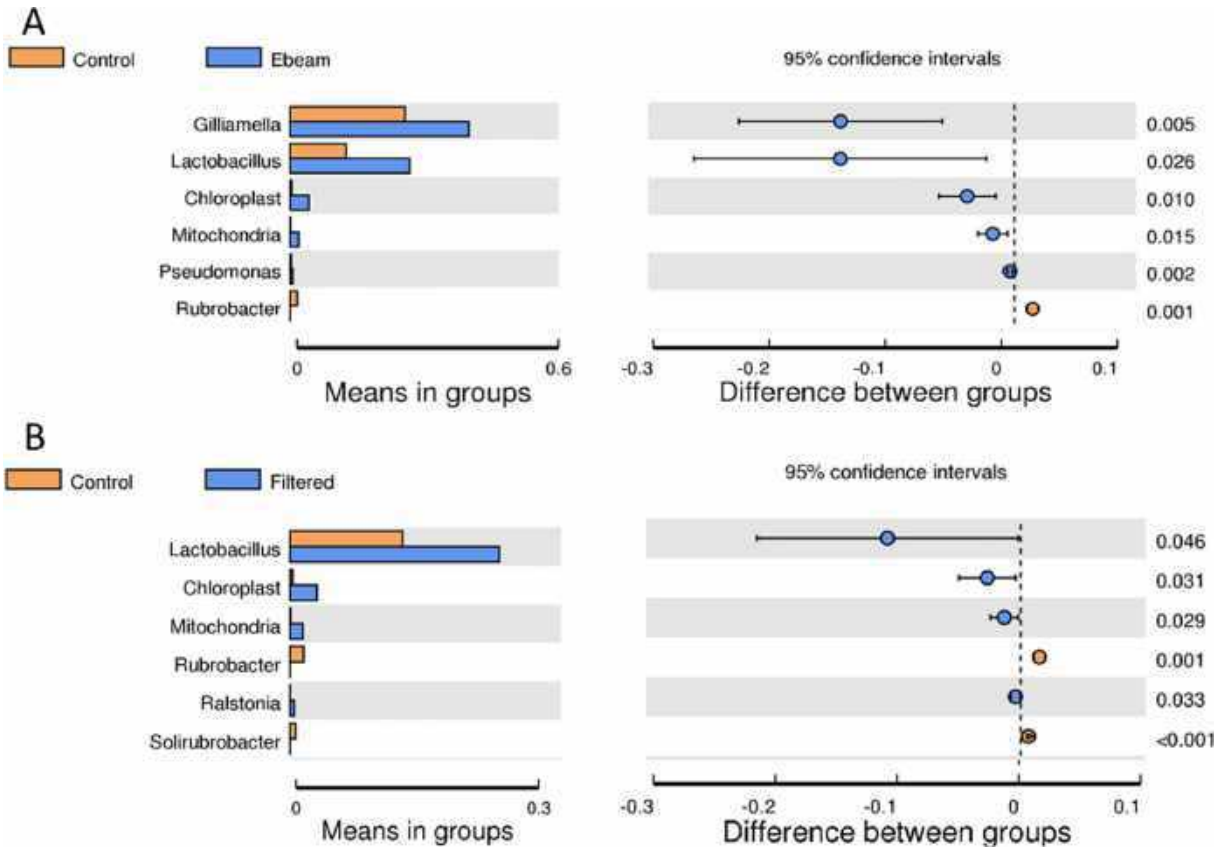

Fig. 8. The mean abundance of microbiota species from the digestive tracts of bees fed on e-beam treated pollen compared to control pollen (A) and fed on washed pollen (B). The confidence interval of between group variation demonstrates the lower and upper confidence limits of the 95 % confidence interval, with the centre representing the difference of the mean value.

poor, and the necessary precursors for maintaining homeostasis are not available. Fatty acid degradation was upregulated, suggesting that starvation is playing a role in protein regulation and the immune pathways are being downregulated in favour of maintaining pathways for fatty acid degradation for ATP generation.

4.5. Decreased abundance in washed pollen fed colonies

4.5.1. Immunity studies

The fatbody proteomic profile is similar to what was observed in the bees fed on e-beam treated pollen, with a downregulation of proteins that play a role in innate immunity. These included serine proteases, chymotrypsin, peptidoglycan recognition, phospholipase and chitinase. There is upregulation of proteins involved with ATP generation and lipid degradation suggests that bees also generate energy through alternative pathways under stressful conditions.

4.6. Microbiomes studies

Bacteria belonging to the Genus *Gilliamella*, *Snodgrassella* and *Lactobacillus* were all present in each treatment group, but varied in relative abundance. In each group, several fungi were identified with the greatest diversity of fungal species evident in bees that were fed on e-beam treated-pollen. Bumblebee colonies fed with untreated control pollen exhibited the greatest abundance of *Snodgrassella* in their digestive tracts, whereas bees fed on treated pollen had a greater abundance of *Gilliamella*. This organism has been previously reported to degrade polysaccharides and can trigger host immune responses (Zhang et al., 2022). There was no clear dominant fungal genus present in the e-beam treated group; whereas *Rhizopus* and *Wickerhamomyces* were found at elevated levels in the washed group compared to the e-beam and untreated control group. Adding sterile water to the pollen during the filtration step increases the water activity value, and would have supported greater growth of fungal and other microbial organisms retained on the pollen.

The food spoiling yeast *Zygosaccharomyces* was the dominant fungal species present in bees fed with untreated pollen. *Zygosaccharomyces* has been detected in bee bread and offers a possible transmission route to newly emerging bees; it has the ability to grow in pollen due to its high osmotolerance (Detry et al., 2020). These fungal pathogens appear to have been fully inactivated in e-beam treated pollen. However, the presence of colonizing microorganisms (such as yeast and bacteria) in the gut microbiome of bees is beneficial as this aids digestion such as fermentation of complex sugars (Tauber et al., 2019).

5. Conclusion

Identifying an appropriate and effective non-thermal decontamination technology for pollination industry remains a complex but critical challenge. This constitutes the first study to provide an initial insight into the impact of decontaminating honeybee pollen, and subsequent effects on colony reproductive outputs in commercial-reared bumblebees. A range of reproductive and colony level changes were observed in bumblebees fed e-beam treated pollen. This coincided with changes in the bumblebee proteome and microbiome, which appear to impact negatively on bee health. A similarity between test bumblebees fed e-beam treated and washed pollen was observed where no males were produced. A failure to produce males is most possibly evident of stunt in colony stage development. Fewer females were also recorded within treated colonies and this failure to produce offspring would most likely affect colony productivity with less workers to attend the brood and then less foragers to gather food from the developing brood. Also, the failure

to produce gyne (virgin queens) would most likely mean that new colonies would not be established. While this might not necessarily be a negative factor for commercial colony establishment or production, as they are only required for a single growing season; however, it does post the question that if these effects are being observed at the colony and individual organism level, then what is potentially happening at the molecular level. It also poses the question as to whether or not a change in the chemical or nutritional makeup of the pollen was a driver for changes at the colony level, or perhaps the removal of other microorganisms that be beneficial to bee nutrition. Currently, there is a strategic need to identify appropriate decontamination technology for appropriately treating bulk pollen so as to mitigate potential transfer of complex parasites and viruses to native pollinators (bees). It appears that a high-intensity e-beam sterilization dosage (100 kGy) is not appropriate for treating pollen that was informed by using an artificial in vitro flow cytometry enumeration approach; thus inferring that additional research is required focused on studying lower doses of industrial scale e-beam or gamma irradiation.

5.1. Future related studies should address

Conduct extensive comparative testing and development of industrial-scale gamma irradiation and electron-beam treatment of pollen over a range of (appropriate) dosages that targets and measures the inactivation performance of different types of problematical bumblebee pathogens. There is also a possible future role for the use of X-ray technology for bulk pollen treatment as demonstrated by McEvoy et al., 2023b in the adjacent medical device area.

Commensurate physicochemical characterization and visualization of pollen post treatments to confirm no structural or nutritional changes in treated pollen for rearing commercial bumblebees, such as combined novel use of scanning electron microscopy and image analysis. Studies revealed that physically treating pollen affects colony outputs; thus to co-monitoring of pollen structure over treatment regimes is important.

Identification of an appropriate non-thermal technology and treatment dosage that will support and enable bee disease mitigation without affecting colony reproductive outputs, possibly the use of combinational industrial treatments such as X-ray or vaporized hydrogen peroxide (such as McEvoy et al., 2021).

Co-creation and development of an appropriate in vitro diagnostic method for studying pathology and physiology of complex bee pathogens post treatments, such as possibly the future use of cell lines derived from bumblebees similar to approaches adopted from honey bee (such as Goblirsch and Adamczyk, 2023).

Investigate simultaneous and sequential occurrence of lethal stresses in treated bee pathogens to inform appropriate dosage for killing similar problematical pathogens in the bee host.

Investigate the potential relationship between producing super clean or sterilized pollen on subsequent bee immunity that may affect critical housekeeping activities such as foraging in bumblebee colonies fed these artificially-treated resources.

Investigate the potential relationship between floral types and bee parasite and virus contamination of gathered pollen with implications for effective disease mitigation for the pollinator industry.

Establish stakeholder consensus on the use and adoption of appropriate decontamination technologies for the pollinator industry, such as for treating bulk pollen, hive equipment and wax combs.

Investigate the development of digital (twin) tools for end-to-end sterility assurance of pollen and commercially reared bumblebees including monitoring for decision-making.

Investigate the sustainable development of appropriate sterilization technologies for pollination and ecosystem service management including applying life cycle assessment and other key performance indicator tools (such as intimated in adjacent areas by Rowan and Pogue, 2021; Garvey et al., 2022; McEvoy et al., 2023; McEvoy et al., 2023b; Rowan, 2023).

CRediT authorship contribution statement

Jack Eakins (JE), Mark Lynch (ML), James Carolan (JC), Neil J Rowan (NR).

Conceptualization (NR, JC); Research methods (JE, ML, JC, NR); Data generation (JE), Data analysis (JE, ML, JC, NR); research funding (NR), research supervision (NR, JC, ML), draft research paper writing, review (JE, ML, JC, NR).

Declaration of competing interest

The authors declare no competing conflict of interests.

Data availability

Data will be made available on request.

Acknowledgements

The authors acknowledge co-funding support from EPA (Project Number 2018-NC-PhD-8) and the Technological University of the Shannon (TUS) Presidential Doctoral Scholarship initiative. Use of Q-Exactive Quantitative Mass Spectrometer was funded under the SFI Research Infrastructure Call 2012; Grant Number: 12/RI/2346(3).

Appendix A. Supplementary data

Supplementary data to this article can be found online at https://doi.org/10.1016/j.scitotenv.2023.165614.

References

Amin, M.R., Than, K.K., Kwon, Y.J., 2010. Mating status of bumblebees, Bombus terrestris (Hymenoptera: Apidae) with notes on ambient temperature, age and virginity. Appl. Entomol. Zool. 45 (3), 363–367. https://doi.org/10.1303/aez.2010.363.

Biodiversity, N., & Series, D. (2009). Guidelines for users of imported bumblebee colonies What is the All-Ireland Pollinator Plan? 21.

Burnham, A.J., 2019. Scientific advances in controlling Nosema ceranae (microsporidia) infections in honey bees (Apis mellifera). Frontiers in Veterinary Science. https://doi.org/10.3389/fvets.2019.00079.

De Luca, P., Vallejo-Marin, M., 2013. What's the 'buzz' about? The ecology and evolutionary significance of buzz-pollination. Curr. Opin. Plant Biol. 16 (4), 429–435.

Detry, R., Simon-Delso, N., Bruneau, E., Daniel, H.M., 2020. Specialisation of yeast genera in different phases of bee bread maturation. Microorganisms 8 (11), 1–14. https://doi.org/10.3390/microorganisms8111789.

Farrell, H., Hayes, J., Laffey, J., Rowan, N., 2011. Studies on the relationship between pulsed UV light irradiation and the simultaneous occurrence of molecular and cellular damage in clinically-relevant Candida albicans. J. Microbiol. Methods 84 (2), 317–326.

Franssen, F., Gerard, C., Cozma-Petrut, A., Vieira-Pinto, M., et al., 2019. Inactivation of parasite transmission stages: efficacy of treatments on food of animal origin. Trends inf Food Science and Technology 83, 114–128.

Gage, S.L., Calle, S., Jacobson, N., Carroll, M., DeGrandi-Hoffman, G., 2020. Pollen alters amino acid levels in the honey bee brain and this relationship changes with age and parasitic stress. Front. Neurosci. 14 (March), 1–14. https://doi.org/10.3389/fnins.2020.00231.

Garvey, M., Meade, E., Rowan, N.J., 2022. Effectiveness of front line and emerging fungal disease prevention and control interventions and opportunities to address appropriate eco-sustainable solutions. Sci. Total Environ. 851 (2) https://doi.org/10.1016/j.scitotenv.2022.158284.

Gerard, C., Franssen, F., La Carbona, S., Monteiro, S., et al., 2019. Inactivation of parasite transmission stages: efficacy of treatments on food of non-animal origin. Trends Food Sci. Technol. 19, 12–23.

Ghosh, S., Jeon, H., Jung, C., 2020. Foraging behaviour and preference of pollen sources by honey bee (Apis mellifera) relative to protein contents. J. Ecol. Environ. 44 (4). https://doi.org/10.1186/s41610-020-0149-9.

Goblirsch, M., Adamczyk, J.J., 2023. Using the Honey Bee (*Apis mellifera* L.) Cell Line AmE-711 to Evaluate Insecticide Toxicity. Environ. Toxicol. Chem. 42 (1), 88–99. https://doi.org/10.1002/etc.5500.

Goblirsch, M., Eakins, J., Rowan, N.J., 2021. Disease-mitigating innovations for the pollination service industry: Challenges and opportunities. Curr. Opin. Environ. Sci. Health 22. https://doi.org/10.1016/j.coesh.2021.100265.

Graystock, P., Blane, E.J., McFrederick, D.S., Goulson, D., Hughes, W.O.H., 2016. Do managed bees drive parasite spread and emergence in wild bees? Int. J. Parasitol. Parasites Wildl. 5 (1), 64–75. https://doi.org/10.1016/j.ijppaw.2015.10.001.

Graystock, P., Goulson, D., Hughes, W.O.H., 2015. Parasites in bloom: flowers aid dispersal and transmission of pollinator parasites within and between bee species. Proc. R. Soc. B Biol. Sci. 282 (1813) https://doi.org/10.1098/rspb.2015.1371.

Graystock, P., Yates, K., Evison, S., E.F., Darvill, B., Goulson, D., Hughes, O.H. (2013). The Trojan hives: pollinator pathogens, imported and distributed in bumblebee colonies. J. Appl. Ecol., 50 (5), 1207–1215.

Hidalgo, E.Q., Hernandez-Flores, J.L., Andrade Moreno, V.D., et al., 2020. Gamma irradiation effects on the microbial content in commercial bee pollen used for bumblebee mass rearing. Radiat. Phys. Chem. 168 https://doi.org/10.1016/j.radphyschem.2019.108511.

Kim, E.Y., Jung, J.K., Hyeon Kim, I., Kim, Y., 2022. Chymotrypsin is a molecular target of insect resistance of three corn varieties against the Asian corn borer, Ostrinia furnacalis. PLoS One 17 (4 April), 1–21. https://doi.org/10.1371/journal.pone.0266751.

Knapp, J.L., Becher, M.A., Rankin, C.C., Twiston-Davies, G., Osborne, J.L., 2019. Bombus terrestris in a mass-flowering pollinator-dependent crop: a mutualistic relationship? Ecology and Evolution 9 (1), 609–618. https://doi.org/10.1002/ece3.4784.

Krams, R., Gudra, D., Popovs, S., Willow, J., Krama, T., Munkevics, M., Megnis, K., Jõers, P., Fridmanis, D., Garduño, J.C., Krams, I.A., 2022. Dominance of fructose-associated Fructobacillus in the gut microbiome of bumblebees (Bombus terrestris) inhabiting natural forest meadows. Insects 13 (1). https://doi.org/10.3390/insects13010098.

Lee, E.-J., Ameer, K., Kim, G.-R., Chung, M.-S., Kwon, J.-H., 2017. Effects of approved dose of e-beam irradiation on microbiological and physicochemical qualities of dried laver products and detection of their irradiation status. Food Sci. Biotechnol. 27, 233–240.

Mao, W., Schuler, M.A., Berenbaum, M.R., 2011. CYP9Q-mediated detoxification of acaricides in the honey bee (Apis mellifera). Proc. Natl. Acad. Sci. U. S. A. 108 (31), 12657–12662. https://doi.org/10.1073/pnas.1109535108.

McEvoy, B., Rowan, N.J., 2019. Terminal sterilization of medical devices using vaporized hydrogen peroxide: a review of current methods and emerging opportunities. J. Appl. Microbiol. 127, 1403–1420.

McEvoy, B., Lynch, M., Rowan, N.J., 2021. Opportunities for the application of real-time bacterial cell analysis using flow cytometry for the advancement of sterilization microbiology. J. Appl. Microbiol. 130 (6), 1794–1812.

McEvoy, B., Maksimovic, A., Rowan, N.J., 2023. *Geobacillus stearothermophilus* and *Bacillus atrophaeus* spores exhibit linear inactivation kinetic performance when treated with an industrial scale vaporized hydrogen peroxide (VH2O2) sterilization process. J. Appl. Microbiol. 134 (1), 1–11. https://doi.org/10.1093/jambio/lxac028.

McEvoy, B., Maksimovic, A., Howell, D., Reppert, P., Ryan, D., Rowan, N., Michel, H., 2023b. Studies on the comparative effectiveness of X-rays, gamma rays and electron beam to inactivate microorganisms at different dose rates in industrial sterilization of medical devices. Radiat. Phys. Chem. 208 https://doi.org/10.1016/j.radpnhschem.2023.100915.

McFadden, E., Costa Ramos, A.-L., Bradley, D., Vrain, O., McEvoy, B., Rowan, N.J., 2016. Comparative studies on the novel sterilization of Irish retailed infant milk formulae using electron beam and pulsed UV treatments. International Journal of Science, Environment and Technology 5 (6), 4375–4377.

Murphy, A. J. T., & Stout, J. C. (2019). Report No. 275 Assessing Market and Non-market Values of Pollination Services in Ireland: Pollival Literature Review (Issue 275). http://www.epa.ie/pubs/reports/research/biodiversity/Research_Report_291.pdf.

Meeus, I., Mosallanejad, H., Niu, J., de Graaf, D.C., Wackers, F., Smagghe, G., 2014. Gamma irradiation of pollen and eradication of Israeli acute paralysis virus. J. Invertebr. Pathol. 121, 74–77.

Murray, T.E., Fitzpatrick, Ú., Byrne, A., Fealy, R., Brown, M.J.F., Paxton, R.J., 2012. Local-scale factors structure wild bee communities in protected areas. J. Appl. Ecol. 49 (5), 998–1008. https://doi.org/10.1111/j.1365-2664.2012.02175.x.

Naoki Okamoto, N.Y., 2018. 乳鼠心肌提取 HHS public access. Physiol. Behav. 176 (1), 139–148. https://doi.org/10.1016/j.cois.2015.08.001.Nutrition-dependent.

Naughton, J., Tiedeken, E.J., Garvey, M., Stout, J.C., Rowan, N.J., 2017. Pulsed light inactivation of the bumblebee trypansome parasite Crithidia bombi. Journal of Apiculture Research 56 (2), 144–154.

Pereira, K. de S., Meeus, I., Smagghe, G., 2019a. Honey bee-collected pollen is a potential source of Ascosphaera apis infection in managed bumble bees. Sci. Rep. 9 (1), 1–9. https://doi.org/10.1038/s41598-019-40804-2.

Pereira, K. de S., Meeus, I., Smagghe, G., 2019b. Honey bee-collected pollen is a potential source of Ascosphaera apis infection in managed bumble bees. Sci. Rep. https://doi.org/10.1038/s41598-019-40804-2.

Peso, M., Grassl, J., Holt, S., Hahne, D., Cremen, N., Baer, B., 2018. Synergistic effects of pathogen and pesticide exposure on honey bee (Apis mellifera) survival and immunity. J. Invertebr. Pathol. 159 (October), 78–86. https://doi.org/10.1016/j.jip.2018.10.005.

Philip, L.P., Keith, H.J.C., Colleen, L.M., Yuezhou, Y., Donald, T., 2012. Partial pyridoxine responsiveness in PNPO deficiency. JIMD Reports 4, 113–116. https://doi.org/10.1007/8904.

Reeves, A.M., O'Neal, S.T., Fell, R.D., Brewster, C.C., Anderson, T.D., 2018. In-hive Acaricides alter biochemical and morphological indicators of honey bee nutrition, immunity, and development. Journal of Insect Science (Online). https://doi.org/10.1093/jisesa/iey086.

Reza, S., Ugorski, M., Suchański, J., 2021. Glucosylceramide and galactosylceramide, small glycosphingolipids with significant impact on health and disease. Glycobiology 31 (11), 1416–1434. https://doi.org/10.1093/glycob/cwab046.

Rowan, N.J., 2019. Pulsed light as an emerging technology to cause disruption for food and adjacent industries - Quo Vadis? Trends Food Sci. Technol. 88, 316–332. https://doi.org/10.1016/j.tifs.2019.03.027.

Rowan, N.J., 2023. The role of digital technologies in supporting and improving fishery and aquaculture across the supply chain – Quo Vadis? The role of digital technologies in supporting and improving fishery and aquaculture across the supply chain - Quo Vadis? Aquac. Fish. 8 (4), 365–374. https://doi.org/10.1016/j.aaf.2022.06.003.

Rowan, N.J., Kremer, T., McDonnell, G., 2023. A review of Spaulding's classification system for effective cleaning, disinfection and sterilization of reusable medical devices: viewed through a modern-day lens that will inform and enable future sustainability. Sci. Total Environ. 878 https://doi.org/10.1016/j.scitotenv.2023.162976.

Rowan, N.J., Pogue, R., 2021. Editorial overview: Green new deal era — Current challenges and emerging opportunities for developing sustaining and disruptive innovation. Curr. Opin. Environ. Sci. Health 22. https://doi.org/10.1016/j.coesh.2021.100294.

Runckel, C., Flenniken, M.L., Engel, J.C., Ruby, J.G., Ganem, D., Andino, R., DeRisi, J.L., 2011. Temporal analysis of the honey bee microbiome reveals four novel viruses and seasonal prevalence of known viruses, Nosema, and Crithidia. PLoS One. https://doi.org/10.1371/journal.pone.0020656.

Saad, B.M., Barribeua, S.M., et al., 2015. The genomes of two key bumblebee species with primitive eusocial organization. Genome Biol. 16 (76) https://doi.org/10.1186/s13059-015-0623-3.

Simone-Fintrom, M., Aronstein, K., Goblirsch, M., Rinkevich, F., de Guzman, L., 2018. Gamma irradiation inactivates honey bee fungal, microsporidian, and viral pathogens and parasites. J. Invertebr. Pathol. 153, 57–64.

Staveley, J. P., Law, S. A., Fairbrother, A., Menzie, C. A., Staveley, J. P., Law, S. A., Fairbrother, A., Menzie, C. A., Staveley, C. J. P., Law, S. A., Fairbrother, A., Menzie, C. A., Staveley, J. P., Law, S. A., Fairbrother, A., & Menzie, C. A. (2014). A Causal Analysis of Observed Declines in Managed Honey Bees (*Apis mellifera*) A Causal Analysis of Observed Declines in Managed. 7039. doi:https://doi.org/10.1080/10807039.2013.831263.

Stern, R. A., Rozen, A., Eshed, R., Zviran, T., Sisai, I., Sherman, A., Irihimovitch, V., & Sapir, G. (2021). (Persea americana) Pollination.

Strachecka, A., Olszewski, K., Kuszewska, K., Chobotow, J., Wójcik, Ł., Paleolog, J., Woyciechowski, M., 2021. Segmentation of the subcuticular fat body in Apis mellifera females with different reproductive potentials. Sci. Rep. https://doi.org/10.1038/s41598-021-93357-8.

Szhlarczyk, D., Gable, A.L., et al., 2019. STRING v11: protein-protein association networks with increased coverage, supporting functional discovery in genome-wide experimental datasets. Nucleic Acids Res. 47 (D1), D607–D613. https://doi.org/10.1093/nar/gky1131.

Tauber, J.P., Nguyen, V., Lopez, D., Evans, J.D., 2019. Effects of a resident yeast from the honeybee gut on immunity, microbiota, and Nosema disease. Insects 10 (9). https://doi.org/10.3390/insects10090296.

Theodorou, P., Radzevičiūtė, R., Lentendu, G., Kahnt, B., Husemann, M., Bleidorn, C., Settele, J., Schweiger, O., Grosse, I., Wubet, T., Murray, T.E., Paxton, R.J., 2020. Urban areas as hotspots for bees and pollination but not a panacea for all insects. Nat. Commun. 11 (1), 1–13. https://doi.org/10.1038/s41467-020-14496-6.

Tong, Z., Duan, J., Wu, Y., Liu, Q., He, Q., Shi, Y., Yu, L., Cao, H., 2018. A survey of multiple pesticide residues in pollen and beebread collected in China. Sci. Total Environ. 640–641, 1578–1586. https://doi.org/10.1016/j.scitotenv.2018.04.424.

Trillo, A., Bartomeus, I., Ortiz-Sanchez, F.J., Belmonte, J., Vila, M., 2021. No detectable impact of parasite-infected commercial bumblebees on wild bees in areas adjacent to greenhouses despite diet overlap. Agric. Ecosyst. Environ. 320. https://doi.org/10.1016/j.agee.2021.107604.

VanEngelsdorp, D., Traynor, K.S., Andree, M., Lichtenberg, E.M., Chen, Y., Saegerman, C., Cox-Foster, D.L., 2017. Colony Collapse Disorder (CCD) and bee age impact honey bee pathophysiology. PLoS One. https://doi.org/10.1371/journal.pone.0179535.

Velthuis, H.H.W., van Doorn, A., 2006. A centuray of advances in bumblebee domestication and the economic and environmental aspects of its commercialization for pollination. Apidologie 37 (4), 421–451. https://doi.org/10.1051/apido:2006019.

Walderdorff, L., Laval-Gilly, P., Bonnefoy, A., Falla-Angel, J., 2018. Imidacloprid intensifies its impact on honeybee and bumblebee cellular immune response when challenged with LPS (lippopolysacharide) of Escherichia coli. J. Insect Physiol. 108 https://doi.org/10.1016/j.jinsphys.2018.05.002.

Wang, X., Zhong, Z., Chen, X., Hong, Z., Lin, W., Mu, X., Hu, X., Zheng, H., 2021. High-fat diets with differential fatty acids induce obesity and perturb gut microbiota in honey bee. Int. J. Mol. Sci. 22 (2), 1–15. https://doi.org/10.3390/ijms22020834.

Wu, Z., Yang, L., He, Q., Zhou, S., 2021. Regulatory mechanisms of vitellogenesis in insects. Frontiers in Cell and Developmental Biology 8 (January), 1–11. https://doi.org/10.3389/fcell.2020.593613.

Yook, H.-S., Lim, S.I.L., Byun, M.-W., 1998. Changes in microbiological and physicochemical properties of bee plllen by application of gamma irradiation and ozone treatment. J. Food Prot. 61 (2), 217–220.

Youngsteadt, E., Appler, R.H., López-Uribe, M.M., Tarpy, D.R., Frank, S.D., 2015. Urbanization increases pathogen pressure on feral and managed honey bees. PLoS One. https://doi.org/10.1371/journal.pone.0142031.

Zhang, Z., Guo, Y., Yang, F., Li, J., 2022. Pan-genome analysis reveals functional divergences in gut-restricted Gilliamella and Snodgrassella. Bioengineering 9 (10). https://doi.org/10.3390/bioengineering9100544.

Journal of Apicultural Research

ISSN: 0021-8839 (Print) 2078-6913 (Online) Journal homepage: http://www.tandfonline.com/loi/tjar20

Pulsed light inactivation of the bumble bee trypanosome parasite Crithidia bombi

John Naughton, Erin J Tiedeken, Mary Garvey, Jane C Stout & Neil J Rowan

To cite this article: John Naughton, Erin J Tiedeken, Mary Garvey, Jane C Stout & Neil J Rowan (2017) Pulsed light inactivation of the bumble bee trypanosome parasite Crithidia bombi, Journal of Apicultural Research, 56:2, 144-154, DOI: 10.1080/00218839.2017.1289668

To link to this article: http://dx.doi.org/10.1080/00218839.2017.1289668

Journal of Apicultural Research, 2017
Vol. 56, No. 2, 144–154, http://dx.doi.org/10.1080/00218839.2017.1289668

ORIGINAL RESEARCH ARTICLE

Pulsed light inactivation of the bumble bee trypanosome parasite *Crithidia bombi*

John Naughton[a], Erin J Tiedeken[a,b], Mary Garvey[c], Jane C Stout[d] and Neil J Rowan[a]*

[a]*Bioscience Research Institute, Athlone Institute of Technology, Athlone, Ireland;* [b]*National Biodiversity Data Centre, Waterford, Ireland;* [c]*Department of Life Sciences, Institute of Technology Sligo, Waterford, Ireland;* [d]*Discipline of Botany, School of Natural Sciences, Trinity College Dublin, Dublin, Ireland*

(*Received 27 September 2016; accepted 16 December 2016*)

The anthropogenic movement of managed bees has led to the introduction and global spread of parasites with significant adverse effects on the health of both managed and wild species. This constitutes the first study to report on the use of high-intensity pulsed light (PL) for the inactivation of the trypanosome parasite *Crithidia bombi*, a pest of wild and managed bees. Through initial PL range-finding studies we identified a putative effective UV dose of 12.96 μJ/cm^2 for *C. bombi* treatment. This was a result of tests on waterborne protozoan *Cryptosporidium parvum*, and was determined using *in vitro* combined cell culture-qPCR infectivity assays. This irradiance produced ca. ≥4 $\log_{10}$ oocyst reductions of *C. parvum*. To confirm this dose as appropriate for treatment of *C. bombi*, we used the buff tailed bumble bee (*Bombus terrestris*) as an animal infectivity model. *C. bombi* was collected from the feces of wild *B. terrestris* queens and used to inoculate 30 commercially supplied workers (*B. terrestris audux*) in order to obtain a colony-specific *C. bombi* inoculum. This was used for subsequent tests on 60 randomly-selected unparasitised workers, which were divided evenly and fed either PL-treated or untreated (control) *C. bombi* inoculant. Of the 28 surviving workers fed with pooled *C. bombi* untreated inoculum, 25 exhibited infection as confirmed by detection of the parasite in fecal samples after 9 days, where the remaining two did not excrete feces. Twenty-eight of 30 (93%) workers fed PL-treated *C. bombi* at 12.96 μJ/cm^2 under similar test conditions were uninfected after the same time period (the remaining two workers did not produce feces for testing). Thus we demonstrate for the first time, that PL is potentially a reliable and efficient technology for the non-thermal inactivation of *C. bombi* for the pollination industry. Although *in vivo* treatment of whole bees with PL is not possible, the use of this technology on equipment used in commercial bumble bee breeding facilities could potentially reduce infection rates, therefore contributing to making the industry more sustainable and less of a risk to wild pollinators.

Inactivación del parásito tripanosomátido de abejorros, *Crithidia bombi*, mediante luz pulsada

El movimiento antropogénico de las abejas manejadas ha llevado a la introducción y expansión global de parásitos con efectos adversos significativos sobre la salud de las abejas tanto manejadas como silvestres. Éste constituye el primer estudio que informa sobre el uso de luz pulsada de alta intensidad (LP) para la inactivación del parásito tripanosomátido *Crithidia bombi*, una plaga de abejas silvestres y manejadas. A través de la búsqueda inicial del rango de LP, encontramos un efecto putativo de tratamiento de *C. bombi* con una dosis UV de 12.96 J/cm^2. Éste fue el resultado de pruebas con el protozoo trasladado en barcos, *Cryptosporidium parvum*, que combinaron el cultivo de células *in vitro* con los ensayos de infectividad por qPCR. Esta irradiación produjo aproximadamente una reducción de ≥4 $\log_{10}$ en los oocistos de *C. parvum*. Para confirmar que la dosis era apropiada en el tratamiento de *C. bombi*, usamos el abejorro *Bombus terrestris* como animal modelo de infección. Se colectó *C. bombi* de las heces de reinas de *B. terrestris* silvestres y se usó para inocular 30 obreras de nidos comerciales *(B. terrestris audax)* para obtener un inóculo *C. bombi* específico de colonia. Este inóculo se usó en las pruebas consiguientes en 60 obreras sin parásitos elegidas aleatoriamente, que se dividieron equitativamente y se alimentaron con inóculos tratados con LP o sin tratar (control). De las 28 obreras supervivientes alimentadas con el inóculo de *C. bombi* sin tratar, se confirmó la infección en 25 mediante la detección de parásitos en muestras fecales a los 9 días, mientras que los dos restantes no excretaron heces. Veintiocho de 30 (93%) obreras alimentadas con *C. bombi* tratada con LP a 12.96 J/cm^2 bajo condiciones similares no estaban infectadas después del mismo período de tiempo (las dos obreras restantes no produjeron heces para comprobarlo). Así, demostramos por primera vez que la LP es una tecnología potencialmente segura y eficiente para la inactivación no-térmica de *C. bombi* en la industria polinizadora. Aunque el tratamiento *in vivo* de las abejas enteras con LP no es posible, el uso de esta tecnología en el equipamiento usado para criar abejorros comerciales podría potencialmente reducir las tasas de infección, y contribuir de esta manera a hacer la industria más sostenible y reducir el riesgo para los abejorros silvestres.

Keywords: bumble bee; *Bombus terrestris audux*; *Crithidia bombi* parasite; pulsed light; disinfection; pollination industry

Introduction

Pollination is a critical ecosystem process for the maintenance of biodiversity and is economically important for the production of crops used for human consumption (Gallai, Salles, Settele, & Vaissière, 2009; Klein et al., 2007; Ollerton, Winfree, & Tarrant, 2011). Wild bees are often the most effective crop pollinators (Garibaldi et al., 2013), but honey bees have been introduced and

*Corresponding author. Email: nrowan@ait.ie

are managed worldwide for commercial crop pollination (Goulson & Hughes, 2015). In the 1980s, commercial rearing and importation of bumble bee colonies for pollination of certain crops began and now commercial bumble bee colonies are imported by over 50 countries (Murray, Coffey, Kehoe, & Horgan, 2013; Velthuis & van Doorn, 2006). However, recent colony losses of honey bees and declines in many wild bee species have sparked widespread concern for food security worldwide (Brown et al., 2016; Vanbergen & Insect Pollinators Initiative, 2013). A critical contributing factor to bee declines is an increase in the spread of a broad range of parasites, including mites, protozoans, bacteria, fungi and viruses (Daszak, Cunninghan, & Hyatt, 2000; Goulson & Hughes, 2015). Furthermore the host range, natural geographic range and virulence in different bee hosts are poorly understood for many bee parasites (Otterstatter & Thomson, 2008), making it difficult to develop effective mitigation strategies (Goulson & Hughes, 2015).

The main bee species that are moved by man are the western honey bee, *Apis mellifera*, and two species of bumble bee, the European *Bombus terrestris* and the North American *Bombus impatiens*. The mass-breeding of commercial or managed bees allows for rapid spread of pests as well as the development of pathogens and parasites that are resistant to current treatment methods (Meeus, Brown, De Graaf, & Smagghe, 2011). This problem hinders the productivity of the industry and must be controlled in order to increase its sustainability. Managed bees are kept in high densities often at suboptimal conditions, ideal environments for parasite infection (Meeus et al., 2011). Parasites can move between managed colonies, and can also spill over into conspecific wild bee populations. This has already occurred, for example, in Canada (Colla, Otterstatter, Gegear, & Thomson, 2006), the UK (Fürst, McMahon, Osborne, Paxton, & Brown, 2014; Graystock, Goulson, & Hughes, 2014) and Ireland (Murray et al., 2013).

The anthropogenic movement of managed bees for crop pollination purposes has also led to the accidental introduction of non-native bee parasites to places where they do not naturally occur, exposing native bees to parasites to which they may have little resistance (Goulson & Hughes, 2015). For example, In North America, the accidental importation of a non-native strain of the parasite *N. bombi* via commercial bees has been implicated in the dramatic decline of five bumble bee species (Thorp, 2005; Thorp & Shepherd, 2005; Winter et al., 2006); declines occurred soon after the global commercial trade of bumble bees began (Cameron et al., 2011). Additionally, the arrival of the European *B. terrestris* into South America appears to have contributed to the rapid local extinction of the native *Bombus dahibomii* (Schmid-Hempel et al., 2014), possibly as a result of pathogen spillover (Goulson & Hughes, 2015). While the identity of these pathogen(s) remains uncertain, Schmid-Hempel et al. (2014) reported high prevalence of the trypanosome *Crithidia bombi* in the invading *B. terrestris* populations. Mitigation measures that reduce parasite loads among managed bees must therefore be developed and implemented in order to reduce risk to wild bee populations. Currently there are few if any effective and reliable intervention strategies to cope with bumble bee parasites in particular (Goulson & Hughes, 2015).

Pulsed light (PL) technology has received considerable attention as a promising next-generation approach for decontaminating food, packaging and air (Garvey, Farrell, Cormican, & Rowan, 2010; Rowan, Valdramidis, & Gomez-Lopez, 2016). This approach kills microorganisms using ultrashort duration pulses of an intense broadband emission spectrum that is rich in UV-C germicidal light (200–280 nm). PL is produced using techniques that multiply power manifold by storing electrical energy in a capacitor over relatively long times (fraction of a second) and releasing it in a short time (millionths or thousands of a second) using sophisticated pulse compression techniques (Rowan et al., 2016). The emitted light flash has a high peak power and usually consists of wavelengths of 200–1100 broad spectrum light enriched with shorter biocidal wavelengths (Hayes, Kirf, Garvey, & Rowan, 2013). A strong advantage of using pulsed xenon lamps over continuous low to medium pressure conventional UV lamps is that the former has a peak power dissipation, which allows for more microbial inactivation (Garvey, Stocca, & Rowan, 2014). Despite significant interest in the development of PL as an alternative or complementary means of disinfection, most published studies to date have focused on bacteria or fungi that grow on conventional agar plates, yet there is a dearth in PL-sanitation data for food and waterborne parasites that require more complex culture techniques.

In this study, we tested pulsed light for the destruction of *C. bombi*, a Trypansome parasite that infects wild and commercial bumble bees via the fecal-oral transmission route. *C. bombi* is a prevalent gut parasite of *B. terrestris* (Shykoff & Schmid-Hempel, 1991a), widespread throughout Europe and North and South America. Transmission is carried out between colonies via flowers (Durrer & Schmid-Hempel, 1994), and within colonies by contact with infected fecal material, and occurs by ingestion of cells that are shed in the feces of infected bees. Infection by *C. bombi* has a number of subtle, context-dependent pathogenic effects, including reduced ovary growth and slower colony growth at the start of the season (Brown, Schmid-Hempel, & Schmid-Hempel, 2003; Shykoff & Schmid-Hempel, 1991b). According to Brown, Loosli, and Schmid-Hempel (2000), *C. bombi* dramatically increases host mortality when bumble bees are under starvation (stress) conditions. Studies also show that colony-level impacts of *C. bombi* infection include significantly reduced colony size and male production as well as a reduction of overall fitness by up to 40% (Brown, Schmid-Hempel, et al., 2003). These colony-level impacts may be a result of the negative impact *C. bombi* infection can have on foraging

behavior of host bumble bees (Gegear, Otterstaffter, & Thompson, 2005, 2006). For example, Gegear et al. (2006) found that natural and experimental infections with *C. bombi* impaired the ability of bumble bee host foragers to learn color rewarding flowers and thus make effective and economic foraging decisions. Thus even though *C. bombi* is seemingly a benign gut parasite, this highly contagious protozoan has the potential to negatively impact bee health at a colony and even population level.

As there is currently no combined *in vitro* cell culture-qPCR infectivity assay for parasites in the pollinator industry, initial range finding PL-sanitation studies were required to determine an indicative UV dose. Thus the specific aims of this study were:

(1) Determine the indicative UV dose for treatment of *C. bombi* using the protozoan parasite *Cryptosporidium parvum* as a surrogate indicator organism.
(2) Using the bumble bee *B. terrestris*, to test the effectiveness of PL for *in vitro* treatment of *C. bombi*, and to develop a method that avoids unnecessary use of bumble bees.

Materials and methods

Pulsed light

A portable pulsed power source (PUV-1, Samtech Ltd., Glasgow) was used to power a low-pressure (60 kPa) xenon-filled flashlamp (Heraeus Noblelight XAP type NL4006 series constructed from a clear UV transparent quartz tube) that produced a high-intensity diverging beam of polychromatic pulsed light (as per Garvey et al., 2010). This delivery system kills microorganisms by using ultra-short duration pulses of an intense broadband emission that is rich in the UV-C germicidal wavelength. Pulsed light (PL) is produced by storing electricity in a capacitor over relatively long times and releasing it as a short duration pulse using sophisticated pulse compression techniques. The PL has a broadband emission spectrum extending from the UV to the infrared with a rich UV content, and its intensity also depends on the level of voltage applied. The light source has an automatic frequency control function which allows it to operate at 1 pulse per second (pps); this setting was used throughout the study. Light exposure was homogenous as the xenon lamp measuring 9.75 cm was longer that the 8.5 cm standard diameter Petri dish used to treat the solutions.

Mammalian cell culture and maintenance of cell lines for growth of the protozoan parasite C. parvum

The recalcitrant protozoan parasite *C. parvum* was used as a potential surrogate organism to simulate disinfection of the bumble bee parasite *C. bombi*, as there is currently no *in vitro* diagnostic infectivity assay for the latter. Similar to *C. bombi*, *C. parvum* is an obligate intercellular parasite that requires a human or animal host to support growth (Garvey et al., 2010). Monolayers of the human ileocecal adenocarcinoma cell line HCT-8 (ATCC CCL-224: American Type Culture Collection, Rockville, MD) were grown with regular sub-culturing in RPMI 1640 growth media with L-glutamine and supplemented antibiotics (penicillin G, 100,000 U/l, streptomycin, 0.5 g/l and amphotericin B, 0.5 g/l), sodium bicarbonate, 2 g/l and 10% fetal calf serum adjusted to pH 7.4. Caco-2 cells (ATCC HTB-37), established from a human colon adenocarcinoma Caco-2 cells, were maintained at 37 °C in Dulbecco modified Eagle's medium/Ham's F-12 medium, supplemented with 20% (v/v) fetal bovine serum, 1% 200 mM L-glutamine, 1% (v/v) non-essential amino acids, 0.5% (v/v) penicillin-streptomycin and 0.5% (v/v) amphotericin B (Sigma-Aldrich). Maintenance media was stored at 4 °C and heated at 37 °C prior to use. HCT-8 and Caco-2 cells were cultured and maintained in T75 cm^2 cell culture flasks in a humidified incubator at 37% in an atmosphere containing 5% (v/v) CO_2 for ca. 24 h until 80 to 90% confluent monolayers had formed. Once confluent, cells were trypsinised to remove the cell monolayer from the flask and seeded into 6 wells for 24 h at 37 °C at a seeding density of 1×10^6 cells/well for use in real-time PCR studies and at a density of 1×10^5 cells/well for chamber slides for infectivity studies using fluorescent stains.

Viability and infectivity determination of C. parvum *oocysts post PL treatments*

C. parvum oocysts (Iowa isolate derived from a bovine calf) were purchased from Waterborne Inc., USA. Ooysts were stored in sterilized PBS (0.01 M phosphate buffer, containing 0.027 M KCL and 0.137 M NaCl at a pH of 7.4) with 100 U of penicillin/ml, 100 μg of streptomycin/ml and 100 μg of gentamicin/ml, and stored at 4 °C until they were used for UV treatment studies. A combined surrogate dye staining method comprising propidium iodide (IP) and a fluorescent-labelled mouse derived monoclonal antibody A400FLR-1-X Crypt-a-GloTM (having corresponding epitope on oocyst cell wall; Waterborne Inc., New Orleans, USA) was used to confirm viability of oocysts. The excystation rate was determined for each batch of oocysts by microscopic observation following sequential incubation at 37 °C in acidified Hanks balanced salt solution (HBSS) for 1 h as per method of Garvey et al. (2010). All experiments were carried out using oocysts with greater than 90% viability, as determined by *in vitro* excystation and the uptake of or exclusion of vital dye. Oocysts were counted using a haemocytometer and inverted microscope (Olympus, CKX41) with camera (Olympus, 1X2-SLP) attached.

In this study, standard treatments involved suspending pre-determined numbers of *C. parvum oocysts* in

10 ml of PBS that were transferred to Petri dishes that was then subjected to UV doses at 8 cm distance from the light source with discharge energy of 16.2 J at a rate of 1 pulse per second for PL studies. In order to ensure that any possible negative effects of such treatment was solely as a result of UV induced change in the natural environment of the test species, studies were also conducted on heat inactivated (70 °C) samples, which were prepared in the same manner as per Rochelle et al. (2002). Measurement of UV dose rate ($\mu J/cm^2$) was determined using chemical actinometry as first described by Rahn (2003), with the modifications of Hayes, Garvey, Fogarty, Clifford, and Rowan (2012) as the non-continuous emitted spectrum did not facilitate use of a calibrated radiometer. Following treatment, treated and untreated controls were viability assessed by fluorescent staining using the method described earlier. Treated and untreated oocysts were stimulated by re-suspension in acidified HBSS and then in 1.0% (wt/v) bile salts (Sigma, pH 7) for 1 h at 37 °C. After two washing steps and sterile PBS, oocysts were re-suspended in cell culture media and thereafter 350 µl aliquots were then separately added to each HCT-8 and Caco-2 well. Samples were incubated for 48 h at 37 °C in 5% (v/v) CO_2 atmosphere, which included addition of fresh RPMI media after 24 h. Each individual well containing separate monolayer was fixed by flooding with 100% (v/v) methanol (Sigma) and left to stand for 10 min at room temperature. After removal of methanol, 75 µl of the fluorescein stain Sporo-GloTM A600FLR-20X (Waterborne Inc., UK) was also added to each well for 45 min (at 37 °C), which detects different life cycle stages of *C. parvum in vitro*. The inoculate cell monolayers were then counterstained for 1 min with C101 containing Evans blue dye (Waterborne Inc., USA). All slides were examined under fluorescence microscopy (Leitz Diaplan fluorescence microscope) at an excitation wavelength of 460–500 nm and an emission wavelength of 510–560 nm for Spore-GloTM and an excitation wavelength of 610 nm for the counterstain C101. All wells containing separate monolayers were examined and noted as positive or negative for sites of parasitic infection or foci of infection. All studies were performed in triplicate.

Combined cell culture – quantitative PCR assay for enumerating viable C. parvum *post treatments*

Real-time, Taqman-quantitative PCR (qPCR) was performed using primers (TIB MOLBIOL, Berlin, Germany) specific for the 18S region of *C. parvum* following method of Keegan, Fanok, and Monis (2003) with some modification. The Taqman probe, based on the conserved eukaryotic probe of Amman et al. (1990) with the following sequence: - 5′-(6-FAM) ACC AGA CTT GCC CTC C (TAMRA), was used in this study. Real-time PCR reactions are characterized by an increase in fluorescence emission due to probe degradation by DNA polymerase in each elongation step during PCR cycling as described in Garvey et al. (2010). The higher the starting copy number of the nucleic acid target, the earlier the fluorescence will reach the predetermined threshold cycle (Ct) and the smaller the Ct value will be. The Ct value is the fractional PCR cycle number, at which a significant increase in target signal fluorescence above the baseline is first detected for a sample. Quantification of the test sample is performed by determining the Ct value and the use of a standard curve to deduce the starting copy number. Amplification reactions (20 µl) contained 5 µl of sample DNA (0.5 µM of each primer, 0.2 µM of probe) and 15 µl of reaction buffer (Roche Diagnostic, West Sussex, England). Both positive and negative controls were included in RT-PCR to validate the results. DNase-RNase free water was used as a negative control throughout. Cycling parameters were initial denaturation for 10 min at 95 °C followed by 50 cycles of denaturation for 10 s at 95 °C, annealing for 40 s at 40 °C, extension for 1 s at 70 °C and cooling for 30 s at 40 °C on a Nanocycler device (Roche Diagnostics). Large numbers of cycles were used to ensure detection of low levels of infection. On completion of each RT-PCR run amplification curves were analyzed by Nanocycler software (Roche Diagnostics) and a standard curve of *C. parvum* oocyst DNA concentration prepared. DNA standards were prepared from fresh oocysts ranging in concentration from 10^1 to 10^7 oocysts/ml by dilution in PBS following standard viable count determinations. Aliquots of oocysts at different densities were then stimulated to infect Caco-2 and HCT-8 cell lines that were seeded into 24 well plates (Sarstedt) at a concentration of ca. 1×10^4 cells/ml at 90% confluency. The latter cell line stimulation occurred by re-suspension and separate incubations for 1 h in acidified HBSS and bile salts as described earlier. One milliliter aliquots of each concentration range of excysted oocysts were re-suspended in RPMI cell culture growth media and added to on well of a 24 well plate. Following a 24 h incubation at 37 °C, in a humidified atmosphere of 5% (v/v) CO_2, the cell culture media with non-adherent or internalized *C. parvum* was removed by aspiration and discarded. Mammalian cells were then washed with sterile PBS and trypsinised using 200 µl of 0.25% (v/v) trypsin/EDTA (Sigma) and left for 15 min at 37 °C until complete detachment of the monolayer had occurred. Cells were then centrifuged at 1000 rpm for 10 min and re-suspended in 200 µl sterile PBS, thereafter the mammalian cells and *C. parvum* sporozoite cell membranes were lysed using PCR template preparation kit (Roche Diagnostics; West Sussex, UK) in order to produce DNA (template) and standard curve following infection in both cell lines. The Ct values of cell culture RT-PCR of each dilution amplified in triplicate were plotted against logarithm of the starting quantity of oocysts. The equation of this standard curve was then used to determine the inactivation of UV treated oocysts. The aforementioned cell culture PCR

procedure was then repeated to determine infectivity of oocysts subjected to varying UV doses or heating at 70 °C for 30 min (negative control). Log inactivation of oocysts (L) is defined by $L = \log_{10} [N_d/N_0)$, where N_0 is the initial concentration of oocysts and N_d is the concentration of viable infectious oocysts post disinfection treatments as detected by combined cell culture-qPCR assay as per method of Lee et al. (2008).

Bumble bees and parasite infectivity assay

We investigated how consumption of untreated and PL-treated inoculant containing a common bumble bee parasite, *C. bombi*, impacted parasite loads of the buff tailed bumble bee *B. terrestris*. *B terrestris* was used as a model system as (a) this species is an important native pollinator in Ireland and other EU countries, and (b) it is reared as a commercial pollinator and distributed throughout Europe, and thus has the potential to become infected with and spread pathogens/parasites to wild bees. Bumble bee colonies were obtained from a commercial supplier (Unichem, Ireland), who source the native subspecies *B. terrestris audax* from Koppert Biological Control (The Netherlands). Upon arrival, the colony was screened for parasites by examining fecal samples using established microscopy methods (as in Tiedeken et al., 2016) from 10 workers. No ethical approval or licenses are required at the state or institutional level for insect bioassays, but researchers complied with good research practices.

Stocks of the parasite *C. bombi* were obtained from wild-caught, infected queen bumble bees. Sixty-six wild *B. terrestris* queens were caught while foraging between 3 March and 14 April 2016 in Merrion Square and the National Botanic Gardens (Glasnevin) in Dublin, Ireland. Captured queens were transported in individual 650 ml plastic containers (160 × 110 × 45 mm) under chilled conditions to Trinity College Dublin for parasite screening as per Tiedeken et al. (2016). Queens were screened for *C. bombi* infection by examining a fecal sample under a phase-contrast microscope (400× magnification). Infected queens were kept in individual plastic containers at 25–30 °C and 24 h darkness and fed ad libitum commercial pollen and 50% diluted Apiinvert sugar water. Aseptic conditions were maintained when handling bees and all equipment.

To obtain *C. bombi* inoculum, fecal samples from infected queens were obtained and used to infect stock workers from the commercial colony as per Tiedeken et al. (2016). Fecal samples from 11 infected native queens were mixed and diluted with 50% Apiinvert to a concentration of 2500 *Crithidia* cells/µl (determined using a Neubaumer Improved Haemocytometer, VWR, Ireland) (Logan, Ruiz-Gonzalez, and Brown, 2005; Schmid-Hempel & Schmid-Hempel, 1993). Thirty stock workers from the *B. terrestris* colony were removed, starved for 2 h and fed with 10 µl of standard inoculum. Stock workers were kept in a wooden box (10 cm × 7 × 6 cm) for 10 days and fed *ad libitum* pollen and 50% Apiinvert until they reached peak infection (Otterstatter & Thomson, 2008). Thereafter, fecal samples were pooled from the stock workers for subsequent PL treatment and control studies. Fecal samples were kept for no longer than 48 h under refrigerated conditions to ensure the parasite remained viable.

PL treatment of the parasite C. bombi *for bumble bee (B. terrestris) infectivity assay*

Sixty uninfected workers from the commercial colony were randomly divided into two groups of 30, kept individually in plastic containers, and starved for up to 6 h, as described above. Pooled fecal material from *C. bombi* infected stock workers was diluted in 3 ml of sugar water and two samples of equal volume were transferred to 8.5 cm Petri dishes. One of these dishes was subjected to pulsed light treatment at a UV dose (µJ/cm^2) found in this study to be optimal for recalcitrant parasite disinfection using *C. parvum* (see above). The control sample was kept under the same conditions but was not exposed to PL treatment. Thirty worker bees each were individually fed 10 µl of treated or untreated sugar water containing 2.5×10^4 *C. bombi* cells, and then returned to individual containers. Each bee was screened 9 days post exposure (peak infection) for *C. bombi* by collecting a fecal sample and determining parasite load using haemocytomer counts. Mortality was recorded in both PL-treated and control samples.

Statistical analysis

The log reduction for UV treated *Cryptosporidium* oocysts was calculated as $\log_{10}$ of the ratio of the concentration of the non-treated (N_0) and PL-treated (N) samples ($\log_{10}$ (N_0/N). Student's *t*-tests and ANOVA one-way model (MINITAB software release 16; Mintab Inc., State College, PA) were used to compare the effects of the relationship of independent variables on PL treatment. Student *t*-tests were used to compare infectivity in both cell lines. All range finding PL-experiments using surrogate *C. parvum* oocysts were conducted in triplicate in three separate experiments.

Results

Pulsed light range-finding disinfection studies using recalcitrant waterborne parasite C. parvum *as surrogate indicator of efficacy for* C. bombi

Findings revealed that the HCT-8 cell line proved significantly more susceptible to infection than the Caco-2 ($p < 0.05$). This is evident from the lower Ct values obtained from PCR amplification following HCT-8 infection, indicating a larger amount of target DNA was present (Figure 1). The limit of detection for both cell lines was 10 oocysts per monolayer for both cell lines. Fluorescent staining and imaging demonstrated that

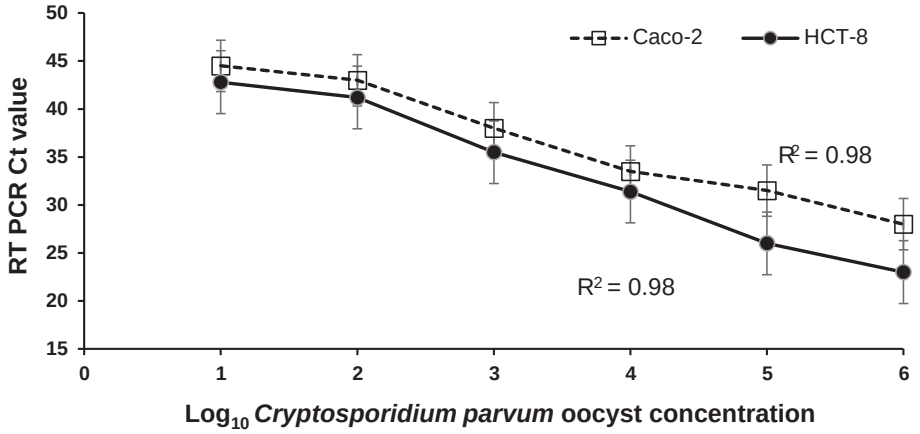

Figure 1. Standard curve for *C. parvum* infected Caco-2 and HCT-8 cells as detected via real time PCR following 46 incubation at 37 °CC (±SD).

Table 1. Log_{10} reduction and infectivity of treated *C. parvum* via real time PCR and cell culture infectivity IF staining of separate Caco-2 and HCT-8 cell lines following PUV treatments (±standard deviation).

	Cell culture infectivity assay							
	No. of infected monolayers[a]		IF microscopic detection		Presence of foci of infection		RT-PCR Log_{10} reduction[b]	
PUV dose (μJ/cm^2)	Caco-2	HCT-8	Caco-2	HTC-8	Caco-2	HTC-8	Caco-2	HCT-8
0.00	4	4	High	High	+	+	0	0
1.08	4	4	High	High	+	+	1.1 ± 0.2	1.2 ± 0.3
2.15	4	4	High	Medium	+	+	1.6 ± 0.4	1.8 ± 0.3
4.32	3	3	Medium	Medium	+	+	2.3 ± 0.4	2.5 ± 0.4
6.48	2	2	Medium	Low	—[c]	—[c]	2.8 ± 0.3	3.0 ± 0.4
8.64	1	1	Low	Low	—[c]	—[c]	3.4 ± 0.4	3.5 ± 0.3
9.72	1	0	Low	—[c]	—[c]	—[c]	≥4	≥4
12.96	0	0	—[c]	—[c]	—[c]	—[c]	≥4	≥4

[a]Standard dose of ca. 1×10^5 oocysts/ml was applied to each of the 4 replicate cell monolayers per PUV treatment. Infectivity was determined by both qPCR and immunofluorescence (IF) microscopy of Caco-2 and HCT-8 cells.
[b]Log reduction in viable *C. parvum* determined by cell culture-qPCR assay. As lower limit of detection for standard curve using *Cryptosporidium* DNA is ca. 10 oocyts, the maximum lethality detected is 4 log_{10} orders. Mean value shown for 4 replicate cell monolayers, ±SD.
[c]Not detected.

infection in Caco-2 cells was less pronounced as there were less sites of infection present. Also, cell death attributed to negative effective of parasitic infection on Caco-2 occurred more rapidly with following exposure to *C. parvum*. Caco-2 host cell monolayers were unable to support infectivity with large numbers of parasites (>5 log_{10} oocysts per monolayer), which resulted in loss of viability. This was not observed with HCT-8 cells that continued to proliferate with monolayer outgrowth occurring in both infected and non-infected cells. It was found that destruction of recalcitrant *C. parvum* oocysts at lower infective dose of 5 log_{10} oocysts per monolayer by pulsed light requires an augmented UV dose of 12.96 μJ/cm^2, which was the highest level of irradiance used in this study (Table 1). Absence of foci of infection in both cell lines occurred post exposure to UV dose of 6.84 μJ/cm^2, which produced a ca. 2.8 log_{10} reduction in oocysts infectivity. There was good agreement between use of Caco-2 or HCT-8 mammalian cells for the quantification of PL-treated *C. parvum* oocyst infectivity using this *in vitro* combined cell culture-qPCR assay where the infective dose used was 5 log_{10} oocysts per monolayer (Table 1). Based upon these findings, the uppermost UV dose of 12.96 μJ/cm^2 was used for pulsed-light treatment of the bumble bee parasite *C. bombi* in this study.

*Use of the bumble bee (***B. terrestris audax***) animal infectivity assay to demonstrate efficacy of* C. bombi *inactivation by pulsed light treatment*

Findings from this present study showed that 11 of 66 (16.7%) of wild queen bumble bees (*B. terrestris*) captured in Dublin, Ireland were infected with the parasite *C. bombi*. Of these 66 captured queens, 27 (1 infected (2.56%)) and 39 (10 infected (25.66% infected) were captured in Merrion Square and in the Botanic Gardens respectively, where locations are separated by 4.6 km.

Table 2. Infectivity status of *B. terrestris* at day 9 after consumption of PL-treated or untreated *C. bombi* parasite (ca. 25,000 cells in 10 µl sugar water) on day 1.

Infectivity of bumble bee (*B. terrestris*)					
Untreated Control with *Crithidia bombi*			PL-treated *Crithidia bombi*		
Worker No.	*C. bombi* detected in feces (cells/µl)	*B. terrestris* infectivity status	Worker No.	*C. bombi* detected in feces (cells/µl)	*B. terrestris* infectivity status
1	14,500	+[d]	31	ND[c]	–[e]
2	25,000	+[d]	32	ND[c]	–[e]
3	15,000	+[d]	33	ND[c]	–[e]
4	2000	+[d]	34	ND[c]	–[e]
5	45,000	+[d]	35	ND[c]	–[e]
6	–[a]	Not known	36	ND[c]	–[e]
7	2500	+[d]	37	ND[c]	–[e]
8	–[a]	Not Known	38	ND[c]	–[e]
9	16,500	+[d]	39	ND[c]	–[e]
10	14,500	+[d]	40	ND[c]	–[e]
11	–[b]	Deceased	41	–[a]	Not known
12	–[b]	Deceased	42	ND[c]	–[e]
13	12,000	+[d]	43	ND[c]	–[e]
14	1500	+[d]	44	ND[c]	–[e]
15	11,000	+[d]	45	ND[c]	–[e]
16	17,500	+[d]	46	ND[c]	–[e]
17	10,000	+[d]	47	ND[c]	–[e]
18	6500	+[d]	48	ND[c]	–[e]
19	37,500	+	49	ND[c]	–[e]
20	–[b]	Deceased	50	–[a]	Not known
21	21,000	+[d]	51	ND[c]	–[e]
22	12,500	+[d]	52	ND[c]	–[e]
23	9500	+[d]	53	ND[c]	–[e]
24	3500	+[d]	54	ND[c]	–[e]
25	500	+[d]	55	ND[c]	–[e]
26	1000	+[d]	56	ND[c]	–[e]
27	12,500	+[d]	57	ND[c]	–[e]
28	26,000	+[d]	58	ND[c]	–[e]
29	15,000	+[d]	59	ND[c]	–[e]
30	18,500	+[d]	60	ND[c]	–[e]

[a]Unable to obtain fecal sample from worker to establish presence or absence of infection.
[b]Worker died during infection monitoring period.
[c]ND, no detection of *C. bombi* by light microscopy (×400) observation of fecal samples.
[d]+, visual confirmation of infectivity of *B. terrestris* by light microscopy (×400) by detection of *C. bombi* in feces.
[e]–, visual confirmation of non-infectivity of *B. terrestris* by light microscopy (×400) by absence of *C. bombi* in feces.

Uninfected queens were released back to the wild after two replicate parasite screens. Findings showed that the commercial colony of *B. terrestris* used for this study was not infected with *C. bombi* when it was initially imported. Of the 30 workers fed PL-treated *C. bombi* using UV dose of 12.96 µJ/cm^2, none were shown to be infected after 13 days post infection, as determined by the absence of this parasite in faces via microscopy methods (Table 2). It was not possible to obtain fecal samples from 2 of the 30 workers in this treatment group. A few *C. bombi* examined immediately post PL-treatment by phase contrast microscopy was shown to be still motile prior to ingestion by *B. terrestris* workers at commencement of bee survival assay. PL-treated *C. bombi* were observed to be altered in appearance at the cellular level (Figure 2). In marked contrast, of the 30 control workers fed untreated *C. bombi* under the same conditions, 25 workers excreted the parasite in feces where the remaining 5 either died (2) or did not excrete samples (3) during monitoring period (Table 2).

Discussion

For the first time this study reports on the effective use of high-intensity pulsed light (PL) to deactivate the bumble bee parasite *C. bombi*. We demonstrate through an animal infectivity model that PL-treatment of feces containing *C. bombi* cells irreversibly kills the parasite at a UV dose of 12.98 µJ/cm^2. Given that there are currently few if any effective and reliable cures for treating any bumble bee parasites (Goulson & Hughes, 2015), the development and deployment of disinfection technologies such as PL in order to limit the spread of disease via infected feces is of great importance.

Our experiment demonstrates proof-of-concept for the use of PL technology in the pollinator industry, however to determine the best application for this disinfection technology the transmission of the target parasite must be well understood. Research to date indicates that the fecal-oral route is the exclusive transmission pathway for *C. bombi* in bumble bees; thus,

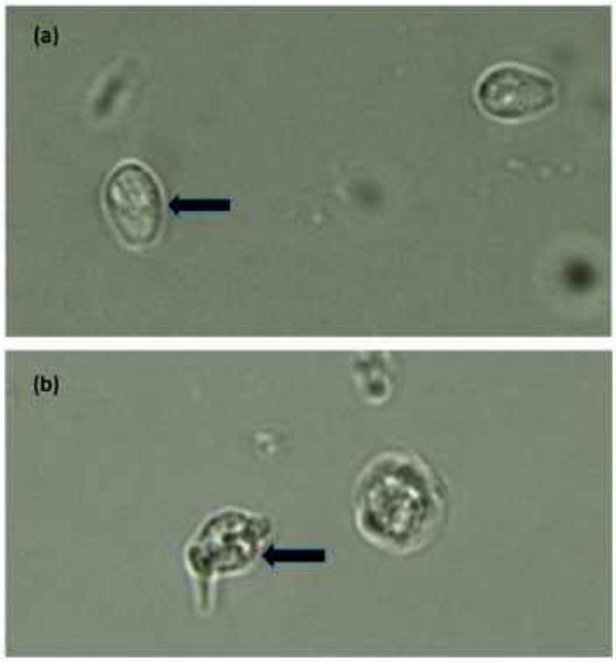

Figure 2. Untreated (a) and PL- treated *C. bombi* at 12.96 μJ/cm^2 (b). *C. bombi*, occurring in choanomastigote life cycle phase, are highlighted with arrow (1000× magnification).

bees contract this parasite by ingesting cells that are shed in the feces of infected bees (Brown, Moret, & Schmid-Hempel, 2003; Brown, Schmid-Hempel, et al., 2003; Gegear et al., 2006). The spread of *C. bombi* infection within bumble bee colonies occurs when uninfected workers are exposed to infected nest materials (Schmid-Hempel, 2001) or via direct contact with infected workers (Otterstatter & Thomson, 2007). Transmission between colonies is believed to occur almost exclusively at flowers via contaminated nectar (Durrer & Schmid-Hempel, 1994). While *in vivo* treatment of bees with PL would likely be fatal to the hosts, the technology could alternatively be used to disinfect equipment in commercial bumble bee breeding facilities. Some parasite spores have been shown to contaminate and spread via equipment and clothing of honey bee breeders (Aronstein & Murray, 2010). The application of PL to reusable equipment in commercial bumble bee breeding facilities could thus decrease infection rates and transmission of *C. bombi*. Ultimately this would reduce the risk of disease spread to wild pollinator populations via importation of commercial bumble bee colonies.

Another application of PL technology is in regards to the use of contaminated honey bee pollen by commercial bumble bee breeding facilities. Honey bee pollen is commonly used as the protein source used to rear commercial bumble bees, however it is likely to be contaminated with a wide variety of parasites, including both those that infect honey bees and other bees (Goulson & Hughes, 2015; Singh et al., 2010). Some commercial producers of bumble bees now freeze or routinely treat honey bee pollen with gamma radiation before feeding it to their bumble bees in an attempt to reduce parasite levels (Meeus, de Miranda, de Graaf, Wäckers, & Smagghe, 2014; reviewed in Goulson & Hughes, 2015). However, there is a shortage of information on the nutritional status of gamma irradiated pollen along with variability in sanitation efficacy for parasite reduction (Meeus et al., 2014). In addition, gamma or electron-beam sterilization commonly require off-site sterilization treatment, thus are not appropriate for *in situ* usage (McFadden et al., 2016). PL is a non-thermal processing technology, hence investigations into potential uses for minimizing the levels of viable parasites in pollen, without harming the nutritional value of the pollen, should be carried out.

Mediation technologies that can reduce the *C. bombi* bioburden to lower the intensity of infections have the potential to influence important ecological behavioral processes and decision-making in bumble bees. For example, Gegear et al. (2005) reported that low intensities of *C. bombi* infections (1–1000 cells) had no effect on the ability of bumble bees (*B. impatiens*) to learn floral handing methods; however, high intensities of infection (>1000 cells) significantly reduced both motor-learning rate and maximum handling proficiency. Thus the commercial bumble bee industry should prioritize decreasing *C. bombi* infection intensity in its colonies to reduce the risk to wild pollinators and increase the quality of the colonies it provides to growers. Based on Gegear et al.'s (2005) infectivity categorization, *C. bombi* was present at both low and high intensities in feces samples prior to destruction using PL-technology in our study. Reduction or elimination of parasites is important as it could also influence a variety of other important host behaviors including foraging, mate choice and predator avoidance (Baracchi, Brown, & Chittka, 2015).

In our study, observation of PL-treated *C. bombi* samples by phase contrast microscopy revealed that many parasites were still motile. It is therefore plausible that subsequent loss of infectivity in workers consuming PL-treated *C. bombi* is attributed to a combination of lethal effects incurred by this complex parasite. Previous evidence supporting this theory of a PL-mediated, multi-hit, lethal cellular process is provided by Farrell and co-workers (Farrell, Hayes, Laffey, & Rowan, 2011) where pre-determined populations of the yeast *Candida albicans* treated with low UV doses were capable of recovery, yet application of higher UV doses caused irreversible cell and molecular damage. Farrell et al. (2011) showed that this lethality was attributed to the nature of the broad spectrum light pulse (200–1100 nm), which was delivered at high UV dose killed PL-treated yeast through a combination of irreversible cell membrane damage or permeabilisation (with loss of vital cellular constituents), lipid peroxidation, toxic free radical generation, necrosis, apoptosis and DNA damage. It is envisaged that application of PL irradiation delivered at high intensities will also cause similar irreversible cell and molecular damage in other established and emerging

pathogens that infect pollinators, as PL technology was recently reported to destroy viruses (Barrett et al., 2016), fungi (Rowan et al., 2016), bacteria (Hayes et al., 2013) and other recalcitrant food and waterborne protozoan parasites (Garvey et al., 2014; Wainwright et al., 2007). PL technology also offers considerable advantages over other conventional UV irradiation approaches in terms of biocidal efficacy. Low and medium pressure UV approaches inactivate pathogens by attacking DNA; however, many microorganisms have evolved sophisticated protective cellular mechanisms to fixed wavelength exposures, thus enabling unwanted repair of UV treated pathogens (Garvey, Thokala, & Rowan, 2014; Rowan et al., 2016).

A technological challenge for the pollinator industry is to develop appropriate disinfection biocides and technologies for obligate bee parasitoids and parasites that are not easily cultured under laboratory conditions. The focus of this study, the bumble bee protozoan-parasite *C. bombi*, presents a challenge akin to other recalcitrant foodborne parasites; it is difficult to establish a reliable *in vitro* assay for its propagation that will help inform disease mitigation technologies. Thus, in this study, we exploited knowledge *of in vitro* infectivity in the waterborne protozoan-parasite *C. parvum* to inform an indicative UV dose for subsequently killing *C. bombi*. The diagnostic approaches used to ascertain infectivity for food and waterborne parasite under *ex vivo* conditions, such as combined cell culture-qPCR used in this study for *C. parvum*, are more advanced at this point in time. Use of *C. parvum*, as an initial *in vitro* screening surrogate approach for informing disinfection efficacy of *C. bombi*, also avoided unnecessary use of bumble bee colonies for considerable PL range-finding killing studies. Gaining and understanding of disinfection kinetics (Rowan et al., 2016) and relative standing of bumble bee parasites with other established foodborne microbial organisms would greatly assist hazard analysis critical control point modelling, risk assessment and management, and would inform new disinfection innovations for the commercial pollination industry that would impact positively on conservation.

Concluding remarks: PL is an effective mitigation technology for the inactivation of the bumble bee parasite *C. bombi*. Use of the waterborne protozon parasite *C. parvum* provided an effective surrogate for informing PL-inactivation of fastidious *C. bombi*. PL potentially offers an innovative option for the destruction of established and emerging parasites for the pollination industry. Moreover, given that infection by *C. bombi* has a number of pathogenic effects on bumble bees at the individual and colony level, the development of a disinfection technology that can be used in commercial bumble bee breeding facilities is urgently required. Further investigations of effective mitigation measures for pollinator parasites are necessary in order to protect both managed and wild pollinators and ultimately the vital service they provide.

Disclosure statement

No potential conflict of interest was reported by the authors.

Funding

This study was funded by an Athlone Institute of Technology Postgraduate Scholarship initiative [project number 11/2014 AIT].

ORCID

Neil J Rowan http://orcid.org/0000-0003-1228-3733

References

Amman, R.R., Binder, B.J., Olsen, R.J., Chisholm, S.W., Devereaux, R., & Stahl, D.A. (1990). Combination of 16s rRNA-targeted oligonucleotide probes with flow cytometry for analysing mixed microbial populations. *Applied and Environmental Microbiology, 56*, 1919–1925.

Aronstein, K.A., & Murray, K.D. (2010). Chalkbrood disease in honey bees. *Journal of Invertebrate Pathology, 103*, S20–S29.

Baracchi, D., Brown, M.J.F., & Chittka, L. (2015). Behavioral evidence for self-medication in bumble bees? *F1000Research, 4*, 73. doi:10.12688/f1000research.6262.1

Barrett, M., Fitzhenry, K., O'Flaherty, V., Dore, W., Keavaney, S., Cormican, M., … Clifford, E. (2016). Detection, fate and inactivation of pathogenic norovirus employing settlement and UV treatment in waste water treatment facilities. *Science of the Total Environment, 568*, 1026–1036. doi:10.1016/j.scitotenv.2016 06.067

Brown, M.J.F., Dicks, L.V., Paxton, R.J., Baldock, K.C.R., Barron, A.B., Chauzat, M.-P., … Stout, J.C. (2016). A horizon scan of future threats and opportunities for pollinators and pollination. *PeerJ, 4*, e2249.

Brown, M.J.F., Loosli, R., & Schmid-Hempel, P. (2000). Condition-dependent expression of virulence in a trypanosome infecting bumble bees. *Oikos* 91, 421–427.

Brown, M.J.F., Moret, Y., & Schmid-Hempel, P. (2003). Activation of host constitutive immune defence by an intestinal trypanosome parasite of bumble bees. *Parasitology, 126*, 253–260.

Brown, M.J.F., Schmid-Hempel, R., & Schmid-Hempel, P. (2003). Strong context-dependent virulence in a host-parasite system: Reconciling genetic evidence with theory. *Journal of Animal Ecology, 72*, 994–1002.

Cameron, S.A., Lozier, J.D., Strange, J.P., Koch, J.B., Cordes, N., Solter, L.F., & Griswold, T.L. (2011). Patterns of widespread decline in North American bumble bees. *Proceedings of the National Academy of Sciences, 108*, 662–667.

Colla, S.R., Otterstatter, M.C., Gegear, R.J., & Thomson, J.D. (2006). Plight of the bumble bee: Pathogen spillover from commercial to wild populations. *Biological Conservation, 129*, 461–467.

Daszak, P., Cunninghan, A.A., & Hyatt, A.D. (2000). Wildlife ecology—Emerging infectious diseases of wildlife—Threats to biodiversity and human health. *Science, 287*, 443–449.

Durrer, S., & Schmid-Hempel, P. (1994). Shares use of flowers leads to horizontal pathogen transmission. *Proceedings of the Royal Society B: Biological Sciences, 258*, 299–302.

Farrell, H.P., Hayes, J., Laffey, J.G., & Rowan, N.J. (2011). Studies on the relationship between pulsed UV light and the simultaneous occurrence of molecular and cellular damage in clinically-relevant *Candida albicans*. *Journal of Microbiological Methods, 84*, 317–326.

Fürst, M.A., McMahon, D.P., Osborne, J.L., Paxton, R.J., & Brown, M.J.F. (2014). Disease associations between honey

bees and bumble bees as a threat to wild pollinators. *Nature, 506*, 364–366.
Gallai, N., Salles, J.-M., Settele, J., & Vaissière, B.E. (2009). Economic valuation of the vulnerability of world agriculture confronted with pollinator decline. *Ecological Economics, 68*, 810–821.
Garibaldi, L.A., Steffan-Dewenter, I., Winfree, R., Aizen, M.A., Bommarco, R., Cunningham, S.A., … Klein, A.M. (2013). Wild pollinators enhance fruit set of crops regardless of honey bee abundance. *Science, 339*, 1608–1611.
Garvey, M., Farrell, H., Cormican, M., & Rowan, N.J. (2010). Investigations of the relationship between use of *in vitro* cell culture-quantitative PCR and a mouse-based bioassay for evaluating critical factors affecting the disinfection performance of pulsed UV light for treating *Cryptosporidium parvum* oocyts in saline. *Journal of Microbiological Methods, 80*, 267–273.
Garvey, M., Stocca, A., & Rowan, N.J. (2014). Development of a combined *in vitro* cell culture-quantitative PCR assay for evaluating the disinfection performance of pulsed light for treating the waterborne enteroparasite *Giardia lamblia*. *Experimental Parasitology, 144*, 6–13. doi:10/1016/j.exppara.2014.06.001
Garvey, M., Thokala, N., & Rowan, N.J. (2014). A comparative study on pulsed UV and low pressure UV inactivation of waterborne microorganisms. *Water Environment Research, 86*, 2317–2324.
Gegear, R.J., Otterstaffter, M.C., & Thompson, J.D. (2005). Does parasitic infection impair the ability of bumble bees to learn flower-handling techniques. *Animal Behavior, 70*, 2009–2215.
Gegear, R.J., Otterstatter, M.C., & Thomson, J.D. (2006). Bumble bee foragers infected by a gut parasite have an impaired ability to utilize floral information. *Proceedings of the Royal Society B: Biological Sciences, 273*, 1073–1078.
Goulson, D., & Hughes, W.O.H. (2015). Mitigating the anthropogenic spread of bee parasites to protect wild pollinators. *Biological Conservation, 191*, 10–19.
Graystock, P., Goulson, D., & Hughes, W.O.H. (2014). The relationship between managed bees and the prevalence of parasites in bumble bees. *PeerJ*, e552.
Hayes, J., Kirf, D., Garvey, M., & Rowan, N. (2013). Disinfection and toxicological assessments of pulsed plasma gas discharge and pulsed UV light treated water containing the waterborne enteroparasite *Cryptosporidium parvum*. *Journal of Microbiological Methods, 94*, 325–337.
Hayes, J. C., Garvey, M., Fogarty, A.M., Clifford, E., & Rowan, N.J. (2012). Inactivation of recalcitrant protozoan oocysts and bacterial endospores in drinking water using high-intensity pulsed UV light irradiation. *Water Science and Technology: Water Supply, 12*, 513–522.
Keegan, A.R., Fanok, S., & Monis, P.T. (2003). Cell culture-Taqman PCR assay for evaluation of Cryptosporidium parvum disinfection. *Applied and Environmental Microbiology, 69*, 2505–2511.
Klein, A.-M., Vaissiere, B.E., Cane, J.H., Steffan-Dewenter, I., Cunningham, S.A., Kremen, C., & Tscharntke, T. (2007). Importance of pollinators in changing landscapes for world crops. *Proceedings of the Royal Society B: Biological Sciences, 274*, 303–313.
Lee, S.U., Joung, M., Yang, D.J., Park, S.H., Huh, S., Park, W.Y., & Yu, J.R. (2008). Pulsed-UV light inactivation of *Cryptosporidium parvum*. *Parasitology Research, 102*, 1293–1299.
Logan, A., Ruiz-Gonzalez, M.X., & Brown, M.J. (2005). The impact of host starvation on parasite development and population dynamics in an intestinal trypanosome parasite of bumble bees. *Parasitology, 130*, 637–647.
McFadden, E., Costa-Ramos, A.L., Bradley, D., Vrain, O., McEvoy, B., & Rowan, N.J. (2016). Comparative studies on the novel sterilization of Irish retailed infant milk formula using electron beam and pulsed light treatments. *International Journal of Science, Environment and Technology, 12*, 4375–4377.
Meeus, I., Brown, M.J., De Graaf, D.C., & Smagghe, G.U.Y. (2011). Effects of invasive parasites on bumble bee declines. *Conservation Biology, 25*, 662–671.
Meeus, I., de Miranda, J.R., de Graaf, D.C., Wäckers, F., & Smagghe, G. (2014). Effect of oral infection with Kaskmir bee virus and Israeli acute paralysis virus on bumble bee (*Bombus terrestris*) reproductive success. *Journal of Invertebrate Pathology, 121*, 64–69.
Murray, T.E., Coffey, M.F., Kehoe, E., & Horgan, F.G. (2013). Pathogen prevalence in commercially reared bumble bees and evidence of spillover in conspecific populations. *Biological Conservation, 159*, 269–276.
Ollerton, J., Winfree, R., & Tarrant, S. (2011). How many flowering plants are pollinated by animals? *Oikos, 120*, 321–326.
Otterstatter, M.C., & Thomson, J.D. (2007). Contact networks and transmission of an intestinal pathogen in bumble bee (*Bombus impatiens*) colonies. *Oecologia, 154*, 411–421.
Otterstatter, M.C., & Thomson, J.D. (2008). Does pathogen spillover from commercially reared bumble bees threaten wild pollinators? *PLoS ONE, 3*, e2771.
Rahn, R.O. (2003). Chemical dosimetry using an iodide/iodate aqueous solution: Application to the gamma irradiation of blood. *Applied Radiation and Isotopes, 58*, 79–84.
Rochelle, P.A., Marshall, M.M., Mead, J.R., Johnson, A.M., Korich, D.G., Rosen, J.S., & De Leon, R. (2002). Comparison of *in vitro* cell culture and a mouse assay for measuring infectivity in *Cryptosporidium parvum*. *Applied and Environmental Microbiology, 68*, 3809–3817.
Rowan, N., Valdramidis, V.P., & Gomez-Lopez, V.M. (2016). A review of quantitative methods to describe efficacy of pulsed light inactivation data that embraces the occurrence of viable non culturable microorganisms. *Trends in Food Science and Technology, 44*, 79–92.
Schmid-Hempel, P. (2001). On the evolutionary ecology of host-parasite interactions: Addressing the question with regard to bumble bees and their parasites. *Naturwissenschaften, 88*, 147–158.
Schmid-Hempel, P., & Schmid-Hempel, R. (1993). Transmission of a pathogen in Bombus terrestris, with a note on division of labour in social insects. *Behavioral Ecology and Sociobiology, 33*, 319–327.
Schmid-Hempel, R., Eckhardt, M., Goulson, D., Heinzmann, D., Lange, C., Plischuk, S., … Schmid-Hempel, P. (2014). The invasion of southern South America by imported bumble bees and associated parasites. *Journal of Animal Ecology, 83*, 823–837.
Shkoff, J.A., & Schmid-Hempel, P. (1991a). Parasites and the advantage of genetic variability within social insect colonies. *Proceedings of the Royal Society of London Series B Biology Sciences, 243*, 55–58.
Shykoff, J.A., & Schmid-Hempel, P. (1991b). Genetic relateness and euscociality: parasite-mediated selection on the genetic composition of groups. *Behavioral Ecology and Sociobiology, 28*, 371–376.
Singh, R., Levitt, A.L., Rajotte, E.G., Holmes, E.C., Ostiguy, N., vanEngelsdorp, D., … Cox-Foster, D.L. (2010). RNA viruses in hymenopteran pollinators: Evidence of inter-taxa virus transmission via pollen and potential impact of non-Apis hymenopteran species. *PLoS ONE, 5*, doi:10.1371/journal.pone.0014357
Thorp, R.W. (2005). Species profile*: Bombus franklini*. In M.D. Shepherd, D.M. Vaghan, & S.H. Black (Eds.), *Red list of pollinator insects of North America* (pp. 1–8). Portland, OR: The Xerces Society for Invertebrate Conservation.

Thorp, R.W., & Shepherd, M.D. (2005). Profile: Subgenus *Bombus*. In M.D. Shepherd, D.M. Vaughan, & S.H. Black (Eds.), *Red list of pollinator insects of North America* (pp. 9–17). Portland, OR: The Xerces Society for Invertebrate Conservation.

Tiedeken, E.J., Egan, P.A., Stevenson, P.C., Wright, G.A., Brown, M.J., Power, E.F., … Stout, J.C. (2016). Nectar chemistry modulates the impact of an invasive plant on native pollinators. *Functional Ecology, 30*, 885–893.

Vanbergen, A.J., & Insect Pollinators Initiative. (2013). Threats to an ecosystem service: Pressures on pollinators. *Frontiers in Ecology and the Environment, 11*, 251–259.

Velthuis, H.H.W., & van Doorn, A. (2006). A century of advances in bumble bee domestication and the economic and environmental aspects of its commercialization for pollination. *Apidologie, 37*, 421–451.

Wainwright, K.E., Lagunas-Solar, M., Miller, M.A., Barr, B.C., Gardner, I.A., … Conrad, P.A. (2007). Physical inactivation of *Toxoplama gondii* cysts in water. *Applied and Environmental Microbiology, 76*, 5140–5147.

Winter, K., Adams, L., Thorp, R.W., Inouye, D., Day, L., Ascher, J., & Buchmann, S. (2006). *Importation of non-native Bumble bees into North America: Potential consequences of using* Bombus terrestris *and other non-native bumble bees for greenhouse crop pollination in Canada, Mexico and the United States*. A white paper of the north American Pollinator Protection Campaign (NAPPC).

Available online at www.sciencedirect.com

ScienceDirect

Current Opinion in
Environmental Science & Health

Disease-mitigating innovations for the pollination service industry: Challenges and opportunities

Mike Goblirsch[1], John Eakins[2] and Neil J. Rowan[2,a]

Abstract

Commercially reared bumblebees are often deployed for fruit, vegetable, and seed crop pollination. Commercial bumblebee pollination contributes significantly to economic and nutritional security; thus, maintaining healthy stocks should be a priority for bumblebee producers. Honey bee–collected pollen is used as a nutritional source for bumblebee rearing, but potential contamination of pollen with pathogens requires mitigation to limit spread of infectious diseases. Gamma irradiation is the primary means of sterilizing pollen, but limitations, including off-site access to cobalt-60, warrant exploration into alternatives. Sterilization technologies used in the food safety and medical device sectors, such as pulsed UV and electron beam, offer options with the potential to deliver safe, effective, and less restrictive mitigation. Adopting these alternatives could ultimately support healthy bumblebee stocks and reduce pathogen transmission to other bees.

Addresses

[1]USDA-ARS Thad Cochran Southern Horticulture Laboratory, 810 Hwy 26 W, Poplarville, MS, 39470, USA
[2]Bioscience Research Institute, Athlone Institute of Technology, Dublin Road, Athlone, Co. Westmeath, Ireland

Corresponding author: Goblirsch, Mike (michael.goblirsch@usda.gov)
[a] Given his role as Guest Editor Neil J. Rowan had no involvement in the peer-review of this article and has no access to information regarding its peer-review. Full responsibility for the editorial process for this article was delegated to Robert Pogue.

Current Opinion in Environmental Science & Health 2021, **22:**100265

This review comes from a themed issue on **Environmental Toxicology 2021:Disruptive Green Deal Innovations**

Edited by **Neil J. Rowan** and **Robert Pogue**

For a complete overview see the Article Collection

https://doi.org/10.1016/j.coesh.2021.100265

Keywords

Decontamination, Sterilization, Emerging infectious diseases, Insect viruses, Pathogenic microbes.

Introduction

Contamination of pollen with pathogens: a source of opportunity

Bumblebees reared commercially, mainly *Bombus impatiens* and *Bombus terrestris*, are essential contributors to global food production. Visitation of greenhouse, high tunnel, and field crops such as tomatoes, peppers, cucurbits, and soft fruits by bumblebees results in highly efficient pollination. This pollination efficiency is partly explained by the ability of bumblebees to buzz pollinate or produce thoracic vibrations that trigger the release of pollen held tightly within the anthers of these flowering plants [1]. Moreover, bumblebee colonies can be produced year-round in commercial facilities, and containment of individual colonies in small, transportable units simplifies deployment to meet growers' demand. There are more than one million bumblebee colonies reared globally every year, and pollination by commercially produced bumblebees increases crop yield and quality, promoting economic and nutritional security [2–4].

Initiating bumblebee colonies artificially requires that queens be confined to small nesting boxes provisioned with food (Figure 1). Diet quality and quantity are essential for queen nesting success and subsequent colony growth [5–8]. Unlike managed honey bees (e.g. *Apis mellifera*), artificial diets are not available to successfully rear bumblebee colonies [3]. Queens cannot forage freely during rearing confinement; therefore, their diet is provided to them and consists of sugar solution, which serves as a source of carbohydrates, and pollen harvested from honey bee colonies, which provides proteins, lipids, and micronutrients (Figure 2).

One concern of feeding commercially reared bumblebees honey bee–collected pollen is pathogens in pollen. Honey bee–collected pollen can be contaminated with viruses (e.g. black queen cell virus and deformed wing virus), bacteria (e.g. *Paenibacillus larvae*, the causative agent of American foulbrood), fungi (e.g. *Ascosphaera apis*, the causative agent of chalkbrood disease), Microsporidia (e.g. *Nosema* spp.), and protozoa (e.g. *Crithidia* spp.) [9–12]. Pathogens found in honey bee–collected pollen can infect bumblebees, which may pose a risk of transmission among managed and wild bee populations [9,10,13–18]. Although our understanding of the impact of pathogens on bee health is best characterized in managed bees [19,20], much remains unknown about their effects on several thousand species of wild bees [13,21–24]. As pathogens are a leading contributor to declining populations of both managed and wild bees [25–27], there is a precedent for mitigating infection

Figure 1

An early stage in the development of a bumblebee colony reared artificially. A queen incubates the brood raised atop a mass of honey bee–collected pollen. Two of the first workers have emerged to the adult stage and will assist the queen in caring for the brood. Photo Credit: Elaine Evans.

Figure 2

Collected pollen dislodged from the corbicula of honey bee foragers that have returned to their colony. A pollen-trapping device placed on the colony restricts the passage of returning pollen foragers into their nest, causing the pollen to become dislodged from their corbiculae. Significant quantities of pollen 'pellets' are harvested using this mechanism. Trapped pollen is the primary source of nutrition for rearing bumblebees. Photo Credit: University of Minnesota Bee Laboratory.

and transmission in honey bee–collected pollen provisioned to commercial bumblebee colonies.

Challenges and potentially disruptive pollen sterilization technologies

Reducing the incidence and spread of pathogens among bumblebee colonies reared commercially is a priority for producers. Goulson and Hughes [3] illustrate critical control points in the flow of pathogens among managed bees where abatement is possible and that could reduce transmission to other bees. Honey bee–collected pollen is a point for control in this scheme [3]. The most common approach to sterilizing pollen is exposure to gamma irradiation [28]. Although effective, there are drawbacks to this technology (see the following section). Limitations of gamma treatment prompt exploration of alternative technologies, especially those used in the medical device and food production sectors (Table 1), for their efficacy in inactivating bee pathogens. Before technologies are adopted to treat honey bee–collected pollen, studies should establish effective doses and determine whether there are adverse effects on nutritional quality and associated dietary microbiota [29–32].

Biological surrogates and complementary techniques to optimize sterilization processes for honey bee–collected pollen

Researchers have historically approached sterilization efficacy through biological surrogates, such as *Bacillus* spp. endospores [33–35] or oocysts of waterborne protozoa [36,37]. Biological surrogates are innocuous microbes exhibiting greater resistance to applied inactivation stresses and provide a safe substitute over intended target pathogens for validating sterilization processes [38]. For example, a biological surrogate is exposed to conditions of a sterilization process, and the inability of the surrogate to grow in culture after treatment confirms the process is effective. Biological surrogates used in the food safety and healthcare sectors could serve as calibrators for adapting sterilization processes against complex pathogens that affect bees [39,40]. Biological surrogates would help resolve factors mediating inactivation of target pathogens, such as highly infectious *P. larvae* spores. These factors are multifaceted and include operational (e.g. applied dosage, system configuration, nonthermal modality), environmental (e.g. temperature, pH, water activity), and biological considerations (e.g. amount of organic matter, diversity and abundance of parasites present, inclusion of recalcitrant life stages) [41,42]. The addition of highly sensitive and specific molecular techniques, such as quantitative polymerase chain reaction (qPCR), and cell culture could complement the use of surrogates and permit reliable post-treatment quantification of the pathogen load and reduction in viability and infectivity [38,41]. The appropriateness of complementary *in vitro* systems will depend on the cell line selected. In the case of bees, demonstrating inhibition of infectivity and growth of treated pathogens using cell lines established from bee tissues could be highly useful [43]. Moreover, modeling inactivation kinetics of treated-bee pathogens by flow cytometry would help evaluate sterilization modalities as it will provide real-

Table 1

Properties of different decontamination approaches considered for treating honey bee–collected pollen.[a]

Process considerations	Hydrogen peroxide vapor (VH_2O_2)	Ethylene oxide (EO)	Pulsed UV light	Moist heat	Electron beam	Gamma irradiation
Methodology	Penetration of sterilant gas	Penetration of sterilant gas	Surface irradiation	Penetration by uniform heating	Ionizing energy from electron beam	Irradiation using photons from radioisotopes
Efficacy of process	Efficacy confirmed by biological indicators and/or process monitoring	Efficacy confirmed by biological indicators and/or process monitoring	Variable, but efficacy confirmed by biological indicators or dosimetry	Efficacy confirmed by biological indicators and/or process monitoring	Efficacy confirmed by biological indicators	Process parameters confirmed using dosimetry
Penetration	Limited penetration; gas-permeable packaging/ product design required	Gas-permeable packaging and product design required	Limited penetration	Suitable for treatment of packaged products but depends on material sensitivity	Efficient penetration at bulk densities between 0.05 and 0.03 g/cc	Penetration at high densities (>0.4 g/cc)
Material compatibility	Good material compatibility except cellulose-based materials	Broad material compatibility	Broad material compatibility	Broad material compatibility, but heat can affect nutrients in pollen	Negative effects are less pronounced or eliminated based on packaging.	Broad material compatibility except plastics such as acetals, PTFE, polypropylene
Turnaround time	One-day processing	Conventional treatment requires 9–10 days.	Relatively short, typically $\leq$1 h depending on the dose	Relatively short, typically $\leq$1 h	Very short, several minutes depending on the dose	Relatively short, several hours depending on the dose
Process	Complex process that introduces VH_2O_2 under vacuum or aerosol	Complex process; variables include time, temperature, humidity, and [EO].	Simple, rapid process; delivery of UV (J/cm^2) in an enclosed chamber	Simple, rapid process; duration depends on time, temperature, and RH.	Complex process; variables include scan height, processing speed, number of passes, beam-product alignment	Simple process; variables include time and isotope load.
Putative mechanisms of pathogen inactivation	Potent oxidizer of proteins, but mechanism is not fully understood.	Proteins, enzymes, and nucleic acid alkylation (targets sulfhydryl groups)	Irreversible damage to RNA affecting replication and infection	Thermal aggregation of viral nucleocapsid and membrane proteins	Extensive degradation of RNA and DNA — but yet to elucidate mechanisms properly	Extensive degradation of RNA and DNA molecules
Limitation	Complex process requiring monitoring and control, not for *in situ* application	Toxic residuals (carcinogenic and teratogenic), not recommended for *in situ*	Operator safety due to UV exposure, shading issues, can be used *in situ*	Limited by thermal sensitivity of materials (e.g. pollen)	Not often used *in situ* but more as an external contract service	Adversely affects material, not recommended for *in situ*

PTFE, polytetrafluoroethylene; RH, Relative humidity.

[a] Modified from the study by McEvoy and Rowan [31*].

time cellular and molecular mechanistic information underpinning the killing process [35,44].

Gamma irradiation

Although various sterilization technologies are applied toward mitigating pathogens found in honey bee–collected pollen and equipment, gamma irradiation using cobalt-60 is the current standard [28]. Gamma irradiation causes irreparable breaks in nucleic acids and has been reported to inactivate several bee pathogens, including some but not all bee viruses [45–48]. Gamma treatment has been evaluated as safe for food production for more than 30 years (US Food and Drug Administration; URL: https://fda.gov/food/buy-store-serve-safe-food/food-irradiation-what-you-need-know), and direct exposure of bees or nest materials does not affect bee survivorship [28,49]. Gamma treatment improves food safety and extends the shelf life by reducing or eliminating microorganisms. Furthermore, treatment does not make foods radioactive, compromise nutritional quality, or noticeably change taste, texture, or appearance (US Food and Drug Administration; URL: https://fda.gov/food/buy-store-serve-safe-food/food-irradiation-what-you-need-know). Gamma irradiation facilities can accommodate large batch sizes, and treatment is compatible with high-density materials, with excellent penetration into nonuniform packaging [33]. However, treatment must be conducted at regulated facilities, requires relatively long processing periods (hours), and potentially degrades products through the release of heat. Owing to the shortage of cobalt-60 supply, medical devices are given priority for gamma treatment, making it prudent to investigate alternative approaches for pollen sterilization.

Hydrogen peroxide in vapor form

Vaporized hydrogen peroxide (VHP) is an environmentally gaseous process used for sanitation of hospitals and health-care facilities [51,49]. The mode of action stems from the generation of free hydroxyl radicals that cause oxidation of DNA, proteins, and lipids [52]. It is effective against adenovirus and avian flu virus [53] and sporicidal when distributed evenly into areas where manual cleaning is impractical [54]. There are two types of VHP sterilization: exposure to 30–35% vapor produced by heating hydrogen peroxide (H_2O_2) or evaporation of H_2O_2 droplets from a 5–7% aerosol. These treatments have long been explored for use in factories for packaging and machinery sterilization [55] and decontamination of meat processing facilities, with varying, but potential, efficacy, against *Listeria monocytogenes* [51]. VHP is most efficacious on inanimate objects but would likely be unsuitable for pollen treatment as exposure to condensate or heat (55–60 °C) would cause structural damage to pollen [55] and nutrient degradation (Eakins and Rowan, personal communication, December 9, 2020).

Moist heat

Moist heat uses either plant, process, or pure steam [56] and is used in the pharmaceutical industry for vaccine and medical device sterilization and in the food industry for pasteurization. Most vegetative microorganisms are inactivated between 55 and 65 °C using moist heat, with more resistant microbes and spores requiring temperatures ≥70 °C and 100 °C, respectively, to achieve inactivation [56]. Owing to pollen's organic nature and denaturation of matrix proteins at >60 °C [57], moist heat could be an obstacle, but further investigation is warranted. As mentioned previously, pollen will form a dough-like mass after exposure to condensate, which may provide opportunistic microbes a substrate for growth that leads to nutrient degradation and spoilage. Studies should determine if bees are attracted to pollen treated with moist heat.

Ethylene oxide gas

Ethylene oxide (EO) is a gaseous process traditionally used for sterilization of spices and now predominately for medical devices [58,59]. EO effectively diffuses through solid matter without causing damage to heat- or moisture-sensitive materials [58,60]. EO is an explosive, highly flammable gas and is highly toxic, carcinogenic, and mutagenic. It is an alkylating agent that interacts with biomolecules, such as nucleic acids and proteins. The addition of alkyl groups to these structures prevents regular cellular activity and inhibits microbial reproduction [61]. The compatibility of EO with moisture-sensitive products is of potential interest for pollen treatment. However, the generation of toxic byproducts, such as ethylene glycol, when EO interacts with water, would require further safety considerations [58,61]. Other potential drawbacks of EO include cost and cycle length [58]. Despite the compatibility with a broad range of materials, this modality will likely be reduced or replaced because of ongoing environmental and sustainability considerations.

Pulsed UV light

Pulsed UV (PUV) technology dissipates stored energy in ultrashort bursts of broad-spectrum light. Currently, PUV is used for high-throughput sterilization of packaging for the food industry [38]. PUV inactivates various complex pathogens [39,40], including those associated with bees [62]. Brief PUV exposure reduces the viability of surrogate oocysts of the trypanosome *Cryptosporidium parvum* [37] and the trypanosome *Crithidia bombi*, a common bumblebee parasite [62]. PUV is considered nontoxic and environmentally friendly based on an increased understanding of the relationship between the UV dose and inactivation of cellular mechanisms [38,41,63]. PUV can be delivered from a fixed source *in situ* or in an adjustable configuration via a handheld device to achieve maximum exposure; however, penetration depth is limited by nontarget materials obstructing the flow of UV radiation

[38]. These drawbacks could restrict usage to surface disinfection, but PUV has several advantages compared with gamma irradiation, including *in situ* application and relatively short processing time. Further studies are required to determine the potential of PUV for pollen sterilization.

Electron beam

High-energy electrons emitted from an accelerator (E-beam) are an alternative to gamma irradiation [33]. E-beam operates through standard electricity, negating the need for radioactive isotopes [33], and is a continuous process technology for sterilizing medical devices and pharmaceuticals [64]. E-beam reduces bacterial pathogens on fresh foods, including *Bacillus cereus* endospores using doses of 3.65 kGy (broccoli) and 4.8 kGy (red radish) [65]. It also reduces porcine epidemic diarrhea virus in contaminated feed [66] and causes minimal changes to powdered infant formula [67]. E-beam lacks the penetrative power of gamma sterilization, and as an *in situ* process, there is potential for recontamination of treated products during redistribution [65]. Despite these drawbacks, E-beam has several advantages compared with gamma irradiation and includes short exposure periods (minutes), fast cycle time, flexible batch size, even distribution of dose, simple validation, no quarantine, and real-time monitoring. Rapid processing of low-density materials and greater operational flexibility can make E-beam a cost-effective approach for pollen treatment.

Conclusions

Development and application of effective, nonthermal sterilization of contaminated pollen would be a potentially powerful tool to help sustain the health of commercial bumblebee stocks and reduce pathogen transmission to other managed and wild bees. Currently, there is a lack of efficacy data for emerging sterilization technologies, and research that addresses the complex morphology and culture requirements of bee pathogens is needed. This review highlights the potential benefits of alternatives to gamma irradiation for pollen treatment, but additional studies should address appropriate dosage, treatment configurations, and mechanistic information underpinning cellular and molecular damage to pathogenic microorganisms and viruses. There remains a reliance on using live bees to confirm treatment effect; however, advances in *in vitro* diagnostics may enable surrogate approaches as a screening tool. Novel processes will be informed by applying technology, policy, and society readiness level framework that considers the intended environment and sustainability of innovation. Ultimately, the deployment of sustainable decontamination technologies to treat honey bee–collected pollen used to rear bumblebees would contribute a vital countermeasure to reduce pollinator decline.

Author contributions

MG, JE, and NJR conceived and proposed the topics of the manuscript. MG, JE, and NJR wrote the article. MG and NJR provided funding and resources.

Equal employment opportunity (eeo)/non-discrimination statement

The U.S. Department of Agriculture prohibits discrimination in all its programs and activities on the basis of race, color, national origin, age, disability, and where applicable, sex, marital status, familial status, parental status, religion, sexual orientation, genetic information, political beliefs, reprisal, or because all or part of an individual's income is derived from any public assistance program. (Not all prohibited bases apply to all programs.) Persons with disabilities who require alternative means for communication of program information (Braille, large print, audiotape, etc.) should contact USDA's TARGET Center at (202) 720-2600 (voice and TDD). To file a complaint of discrimination, write to USDA, Director, Office of Civil Rights, 1400 Independence Avenue, S.W., Washington, D.C. 20250-9410, or call (800) 795-3272 (voice) or (202) 720-6382 (TDD). USDA is an equal opportunity provider and employer.

Declaration of competing interest

The authors declare that they have no known competing financial interests or personal relationships that could have appeared to influence the work reported in this paper.

Acknowledgements

The authors appreciate the input of Dr. Chris Werle, Dr. Elaine Evans, and Dr. Marla Spivak and two anonymous reviewers for reading and offering suggestions that helped improve this manuscript. NJR and JE acknowledge funding support from the Environmental Protection Agency (2018-NC-PhD-8 project), Ireland.

References

Papers of particular interest, published within the period of review, have been highlighted as:

* of special interest
** of outstanding interest

1. Vallejo-Marín M: **Buzz pollination: studying bee vibrations on flowers**. *New Phytol* 2019, **224**:1068–1074, https://doi.org/10.1111/nph.15666.

2. Velthuis HHW, van Doorn A: **A century of advances in bumblebee domestication and the economic and environmental aspects of its commercialization for pollination**. *Apidologie* 2006, **37**:421–451, https://doi.org/10.1051/apido:2006019.

3. ** Goulson D, Hughes WHO: **Mitigating the anthropogenic spread of bee parasites to protect wild pollinators**. *Biol Conserv* 2015, **191**:10–19, https://doi.org/10.1016/j.biocon.2015.06.023.
Illustrates critical control points in the flow of pathogens from managed

honey bee and commercially-reared bumblebee colonies with the potential for spillover to wild bee populations. Offers suggestions for mitigating pathogens at these control points to improve stocks of managed bees and reduce transmission to wild bees.

4. Strange JP: ***Bombus huntii, Bombus impatiens*, and *Bombus vosnesenskii* (Hymenoptera: Apidae) pollinate greenhouse-grown tomatoes in Western North America**. *J Econ Entoml* 2015, **108**:873–879, https://doi.org/10.1093/jee/tov078.

5. Kämper W, Werner PK, Hilpert A, Westphal C, Blüthgen N, Eltz T, Leonhardt SD: **How landscape, pollen intake and pollen quality affect colony growth in *Bombus terrestris***. *Landsc Ecol* 2016, **31**:2245–2258, https://doi.org/10.1007/s10980-016-0395-5.

6. Moerman R, Vanderplanck M, Fournier D, Jacquemart A-L, Michez D: **Pollen nutrients better explain bumblebee colony development than pollen diversity**. *Insect Conserv Divers* 2017, **10**:171–179, https://doi.org/10.1111/icad.12213.

7. Vaudo AD, Farrell LM, Patch HM, Grozinger CM, Tooker JF: **Consistent pollen nutritional intake drives bumble bee (*Bombus impatiens*) colony growth and reproduction across different habitats**. *Ecol Evol* 2018, **8**:5765–5776, https://doi.org/10.1002/ece3.4115.

8. Watrous KM, Duennes MA, Woodard SH: **Pollen diet composition impacts early nesting success in queen bumble bees *Bombus impatiens* Cresson (Hymenoptera: apidae)**. *Environ Entomol* 2019, **48**:711–717, https://doi.org/10.1093/ee/nvz043.

9. ** Singh R, Levitt AL, Rajotte EG, Holmes EC, Ostiguy N, Vanengelsdorp D, Lipkin WI, Depamphilis CW, Toth AL, Cox-Foster DL: **RNA viruses in hymenopteran pollinators: evidence of inter-taxa virus transmission via pollen and potential impact on non-*Apis* hymenopteran species**. *PloS One* 2010, **5**:e14357, https://doi.org/10.1371/journal.pone.0014357.
A study on the distribution of honey bee viruses in honey bees, honey bee-collected pollen, and several species of non-*Apis* hymenopterans. Viruses detected in pollen was shown to be infective when given to virus-free honey bee colonies.

10. Andrade VDM, Flores JLH, López MAR, Hernández AC, Gómez SR, Medina RPC, Calvillo RPM, Martínez AGE, Pérez JC, Hernández IA, Hidalgo EÁ, Osuna CÁ, Jones GH, Guillén JC: **Evaluation of the presence of *Paenibacillus larvae* in commercial bee pollen using PCR amplification of the gene for tRNA(Cys)**. *Braz J Microbiol* 2019, **50**:471–480, https://doi.org/10.1007/s42770-019-00039-9.

11. Pereira KS, Meeus I, Smagghe G: **Honey bee-collected pollen is a potential source of *Ascosphaera apis* infection in managed bumble bees**. *Sci Rep* 2019, **9**:4241, https://doi.org/10.1038/s41598-019-40804-2.

12. Syromyatniko MY, Savinkova OV, Panevina AV, Solodskikh SA, Lopatin AV, Popov VN: **Using bumblebee microcolonies and molecular approaches reveals no correlation between pollen quality and pathogen presence**. *J Econ Entomol* 2019, **112**:49–59, https://doi.org/10.1093/jee/toy345.

13. Graystock P, Yates K, Darvill B, Goulson D, Hughes WHO: **Emerging dangers: deadly effects of an emergent parasite in a new pollinator host**. *J Invertebr Pathol* 2013, **114**:114–119, https://doi.org/10.1016/j.jip.2013.06.005.

142. * Fürst MA, McMahon DP, Osborne JL, Paxton RJ, Brown MJ: **Disease associations between honeybees and bumblebees as a threat to wild pollinators**. *Nature* 2014, **506**:364–366, https://doi.org/10.1038/nature12977.
Pathogens of managed honey bees are widespread and suggests spillover to wild bumblebees. Levels of the honey bee virus Deformed wing virus and the microsporidian *Nosema ceranae* were positively correlated between managed honey bees and wild bumblebees with implications of spillover of emerging infectious disease for populations of wild bees.

15. Graystock P, Goulson D, Hughes WO: **The relationship between managed bees and the prevalence of parasites in bumblebees**. *Peer J* 2014, **2**, https://doi.org/10.7717/peej.522. e522.

16. Alger SA, Burnham PA, Boncristiani HF, Brody AK: **RNA virus spillover from managed honeybees (*Apis mellifera*) to wild bumblebees (*Bombus* spp.)**. *PloS One* 2019:14, https://doi.org/10.1371/journal.pone.0217822. e0217822.

17. Graystock P, Ng WH, Parks K, Tripodi AD, Muñiz PA, Fersch AA, Myers CR, McFrederick QS, McArt SH: **Dominant bee species and floral abundance drive parasite temporal dynamics in plant-pollinator communities**. *Nat Ecol Evol* 2020, **4**:1358–1367, https://doi.org/10.1038/s41559-020-1247-x.

18. Tehel A, Streicher T, Tragust S, Paxton RJ: **Experimental infection of bumblebees with honeybee-associated viruses: no direct fitness costs but potential future threats to novel wild bee hosts**. *R Soc Open Sci* 2020, **7**:200480, https://doi.org/10.1098/rsos.200480.

19. Genersch E: **Honey bee pathology: current threats to honey bees and beekeeping**. *Appl Microbiol Biotechnol* 2010, **87**:87–97, https://doi.org/10.1007/s00253-010-2573-8.

20. Gisder S, Genersch E: **Viruses of commercialized insect pollinators**. *J Invertebr Pathol* 2017, **147**:51–59, https://doi.org/10.1016/j.jip.2016.07.010.

21. Ravoet J, De Smet L, Meeus I, Smagghe G, Wenseleers T, de Graaf DC: **Widespread occurrence of honey bee pathogens in solitary bees**. *J Invertebr Pathol* 2014, **122**:55–58, https://doi.org/10.1016/j.jip.2014.08.007.

22. Brettell LE, Riegler M, O'Brien C, Cook JM: **Occurrence of honey bee-associated Pathogens in *Varroa*-free pollinator communities**. *J Invertebr Pathol* 2020a, **171**:107344, https://doi.org/10.1016/j.jip.2020.107344.

23. Brettell LE, Schroeder DC, Martin SJ: **RNAseq of Deformed wing virus and other honey bee-associated viruses in eight insect taxa with or without *Varroa* infestation**. *Viruses* 2020b, **12**:1229, https://doi.org/10.3390/v12111229.

24. Ngor L, Palmer-Young EC: **Burciaga Nevarez R, Russell KA, Leger L, Giacomini SJ, Pinilla Gallego MS, Irwin RE, McFrederick QS: Cross-infectivity of honey and bumblebee-associated parasites across three bee families**. *Parasitology* 2020, **147**:1290–1304, https://doi.org/10.1017/S0031182020001018.

25. * Goulson D, Nicholls E, Botías C, Rotheray EL: **Bee declines driven by combined stress from parasites, pesticides, and lack of flowers**. *Science* 2015, **347**:1255957, https://doi.org/10.1126/science.1255957.
A review of factors that contribute to decline and failing health of bee pollinators. Stressors do not act alone but form complex interactions. The effect of chronic exposure to several stressors simultaneously in bee pollinators is a societal challenge that should promote discoveries that help preserve pollinator, and ultimately ecosystem, health.

26. Steinhauer N, Kulhanek K, Antúnez K, Human H, Chantawannakul P, Chauzat M-P, van Engelsdorp D: **Drivers of colony losses**. *Curr Opin Insect Sci* 2018, **26**:142–148, https://doi.org/10.1016/j.cois.2018.02.004.

27. Botías C, Jones JC, Pamminger T, Bartomeus I, Hughes WOH, Goulson D: **Multiple stressors interact to impair the performance of bumblebee *Bombus terrestris* colonies**. *J Anim Ecol* 2020, **90**:415–431, https://doi.org/10.1111/1365-2656.13375.

28. Graystock P, Jones JC, Pamminger T, Parkinson JF, Norman V, Blane EJ, Rothstein L, Wäckers F, Goulson D, Hughes WO: **Hygienic food to reduce pathogen risk to bumblebees**. *J Invertebr Pathol* 2016, **136**:68–73, https://doi.org/10.1016/j.jip.2016.03.007.

29. Hamdi C, Balloi A, Essanaa J, Crotti E, Gonella E, Raddadi N, Ricci I, Boudabous A, Borin S, Manino A, Bandi C, Alma A, Daffonchio D, Cherif A: **Gut microbiome dysbiosis and honeybee health**. *J Appl Entomol* 2011, **135**:524–533, https://doi.org/10.1111/j.14390418.2010.01609.x.

30. McFrederick QS, Mueller UG, James RR: **Interactions between fungi and bacteria influence microbial community structure**

in the *Megachile rotundata* larval gut. *Proc R Soc B* 2014, **281**: 20132653, https://doi.org/10.1098/rspb.2013.2653.

31. Steffan SA, Dharampal PS, Diaz-Garcia LA, Currie CR, Zalapa JE, Hittinger CT: **Empirical, metagenomic, and computational techniques illuminate the mechanisms by which fungicides compromise bee health**. *JoVE* 2017, https://doi.org/10.3791/54631. e54631.

32. Dharampal PS, Carlson C, Currie CR, Steffan SA: **Pollen-borne microbes shape bee fitness**. *Proc Biol Sci* 2019, **286**:20182894, https://doi.org/10.1098/rspb.2018.2894.

33. * McEvoy B, Rowan N: **Thermal sterilization of medical devices using vaporized hydrogen peroxide: a review of current methods and emerging opportunities**. *J Appl Microbiol* 2019, **127**:1403–1420, https://doi.org/10.1111/jam.14412.
Comparative evaluation of the effectiveness of using vaporized hydrogen peroxide to that of using other sterilization technologies for treating heat-sensitive medical devices. This provides state-of-the-art knowledge on operational parameters and limitations for each technology for medical device applications where there are translational implications for food and pollination industry for commercial deployment.

34. Mendes-Oliveira GM, Jensen JL, Keener KM, Campanella OH: **Modelling the inactivation of *Bacillus* spores during cold plasma sterilization**. *Innovat Food Sci Emerg Technol* 2019, **52**: 334–342, https://doi.org/10.1016/j.ifset.2018.12.011.

35. * McEvoy B, Lynch M, Rowan NJ: **Opportunities for the application of real-time bacterial cell analysis using flow cytometry for the advancement of sterilization microbiology**. *J Appl Microbiol* 2020, https://doi.org/10.1111/jam.14876.
Comprehensive analysis, supplemented with research data from the group, on the use of flow cytometry as a real-time diagnostic for enumerating complex microorganisms, including parasites and viruses, post treatment to sterilization technologies operated under reduced conditions. This provides critical insight into real-time monitoring of treated pathogens where there has traditionally been a delay in enumeration due to limitations in conventional culture techniques.

36. Garvey M, Farrell H, Cormican M, Rowan N: **Investigations of the relationship between use of *in vitro* cell culture-quantitative PCR and a mouse-based bioassay for evaluating critical factors affecting the disinfection performance of pulsed UV light for treating *Cryptosporidum parvum* oocysts in saline**. *J Microbiol Methods* 2010, **80**:267–273, https://doi.org/10.1016/j.mimet.2010.01.017.

37. Hayes J, Kirf D, Garvey M, Rowan N: **Disinfection and toxicological assessments of pulsed UV and pulsed-plasma gas-discharge treated-water containing the waterborne protozoan parasites *Cryptosporidium parvum***. *J Microbiol Methods* 2013, **94**:325–337, https://doi.org/10.1016/j.mimet.2013.07.012.

38. * Rowan NJ: **Pulsed light as an emerging technology to cause disruption for food and adjacent industries – Quo Vadis?** *Trends Food Sci Technol* 2019, **88**, https://doi.org/10.1016/j.tifs.2019.03.027. 316-32.
A critical review of main developments in pulsed light technology as a novel non-thermal sterilization technology including areas for improving innovation for application in the field, such as the pollination industry. Key operational parameters for using pulsed light are described for addressing complex pathogens highlighting the potential of this innovation for *in situ*, handheld applications.

39. Franssen F, Gerard, Cozma-Petrut A, Vieria-Pinto M, Jambrak AR, Rowan N, Paulsen P, Rozycki M, Tysnes K, Rodriquez-lazaro D, Robertson L: **Inactivation of parasite transmission stages: efficacy of treatments on food of animal origin**. *Trends Food Sci Technol* 2019, **83**:114–128, https://doi.org/10.1016/j.tifs.2019.06.015.

40. Gerard C, Franssen F, Carbona SL, Monteiro S, Cozma-Petrut A, Utaaker KS, Jambrak AR, Rowan N, Rodriguez-Lazaaro D, Nasser A, Tysnes K, Robertson LJ: **Inactivation of parasite transmission stages: efficacy of treatments on foods of non-animal origin**. *Trends Food Sci Technol* 2019, **91**:12–23, https://doi.org/10.1016/j.tifs.2019.06.015.

41. ** Farrell H, Hayes J, Laffey J, Rowan N: **Studies on the relationship between pulsed UV light irradiation and the simultaneous occurrence of molecular and cellular damage in clinically-relevant *Candida albicans***. *J Microbiol Methods* 2011, **88**:317–326, https://doi.org/10.1016/j.mimet.2010.12.02.
First study to comprehensively report on the use of pulsed light over different treatment regimes (e.g., UV doses) for causing irreversible damage in microorganisms. It highlights the broad-spectrum nature of pulsed light for killing targeted pathogens that includes simultaneous molecular and cellular damage. A key finding was the detection of onset of apoptosis as a point of irreversible damage in treated pathogens and the full description of novel *in vitro* bioassays.

42. Bahrami A, Baboli ZM, Schimmel K, Jafari SM, Williams S: **Efficiency of novel processing technologies for the control of *Listeria monocytogenes* in food products**. *Trends Food Sci Technol* 2020, **96**:61–78, https://doi.org/10.1016/j.tifs.2019.12.009.

43. * Guo Y, Goodman CL, Stanley DW, Bonning BC: **Cell lines for honey bee virus research**. *Viruses* 2020, **12**:236, https://doi.org/10.3390/v12020236.
Cell culture systems established from managed and wild bee tissues are lacking for the pollinator research community. Development and use of continuous cell lines established from honey bees and other bees could be used to further our understanding of host-pathogens interactions and promote exploration of mitigation strategies.

44. Rowan NJ, Valdramidis VP, Gómez-López VM: **A review of quantitative methods to describe efficacy of pulsed light generated inactivation data that embraces the occurrence of viable but non culturable state microorganisms**. *Trends Food Sci Technol* 2015, **44**:79–92, https://doi.org/10.1016/j.tifs.2015.03.006.

45. de Guzman ZM, Cervancia CR, Dimasuay KGB, Tolentino MM, Abrera GB, Cobar MLC, Fajardo Jr AC, Sabino NG, Manila-Fajardo AC, Feliciano CP: **Radiation inactivation of *Paenibacillus larvae* and sterilization of American foul brood (AFB) infected hives using Co-60 gamma rays**. *Appl Radiat Isot* 2011, **69**:1374–1379, https://doi.org/10.1016/j.apradiso.2011.05.032.

46. Meeus I, Mosallanejad H, Niu J, de Graaf DC, Wäckers F, Smagghe G: **Gamma irradiation of pollen and eradication of Israeli acute paralysis virus**. *J Invertebr Pathol* 2014, **121**: 74–77, https://doi.org/10.1016/j.jip.2014.06.012.

47. Simone-Finstrom M, Aronstein K, Goblirsch M, Rinkevich F, de Guzman L: **Gamma irradiation inactivates honey bee fungal, microsporidian, and viral pathogens and parasites**. *J Invertebr Pathol* 2018, **153**:57–64, https://doi.org/10.1016/j.jip.2018.02.011.

48. de Guzman LI, Simone-Finstrom M, Frake AM, Tokarz P: **Comb irradiation has limited, interactive effects on colony performance or pathogens in bees, *Varroa destructor* and wax based on two honey bee stocks**. *Insects* 2019, **10**:15, https://doi.org/10.3390/insects10010015.

49. Gagnaire B, Bonnet M, Tchamitchian S, Cavalié I, Della-Vedova C, Dubourg N, Adam-Guillermin C, Brunet JL, Belzunces LP: **Physiological effects of gamma irradiation in the honeybee, *Apis mellifera***. *Ecotoxicol Environ Saf* 2019, **174**: 153–163, https://doi.org/10.1016/j.ecoenv.2019.02.031.

50. Doll M, Morgan DJ, Anderson D, Bearman G: **Touchless technologies for decontamination in the hospital: a review of hydrogen peroxide and UV devices**. *Curr Infect Dis Rep* 2015, **17**:498, https://doi.org/10.1007/s11908-015-0498-1.

51. Møretrø T, Fanebust H, Fagerlund A, Langsrud S: **Whole room disinfection with hydrogen peroxide mist to control *Listeria monocytogenes* in food industry related environments**. *Int J Food Microbiol* 2019, **292**:118–125, https://doi.org/10.1016/j.ijfoodmicro.2018.12.015.

52. Linley E, Denyer SP, McDonnell G, Simons C, Maillard JY: **Use of hydrogen peroxide as a biocide: new consideration of its mechanisms of biocidal action**. *J Antimicrob Chemother* 2012, **67**:1589–1596, https://doi.org/10.1093/jac/dks129.

53. Goyal SM, Chander Y, Yezli S, Otter JA: **Evaluating the virucidal efficacy of hydrogen peroxide vapour**. *J Hosp Infect* 2014, **86**:255–259, https://doi.org/10.1016/j.jhin.2014.02.003.

54. Fu TY, Gent P, Kumar V: **Reply to Destrez: efficacy, efficiency and safety aspects of hydrogen peroxide vapour and aerosolized hydrogen peroxide room disinfection systems**.

J Hosp Infect 2012, **82**:300, https://doi.org/10.1016/j.jhin.2012.07.021.

55. Scaramuzza N, Cigarini M, Mutti P, Berni E: **Sanitization of packaging and machineries in the food industry: effect of hydrogen peroxide on ascospores and conidia of filamentous fungi**. *Int J Food Microbiol* 2020, **316**:108421, https://doi.org/10.1016/j.ijfoodmicro.2019.108421.

56. Shintani H: **Validation study and routine control monitoring of moist heat sterilization procedures**. *Biocontrol Sci* 2012, **17**: 57–67, https://doi.org/10.4265/bio.17.57.

57. Proffen BL, Perrone GS, Fleming BC, Sieker JT, Kramer J, Hawes ML, Murray MM: **Effect of low-temperature ethylene oxide and electron beam sterilization on the *in vitro* and *in vivo* function of reconstituted extracellular matrix-derived scaffolds**. *J Biomater Appl* 2015, **30**:435–449, https://doi.org/10.1177/0885328215590967.

58. Shintani H: **Ethylene oxide gas sterilization of medical devices**. *Biocontrol Sci* 2017, **22**:1–16, https://doi.org/10.4265/bio.22.1.

59. Horakova J, Mikes P, Saman A, Jencova V, Klapstova A, Svarcova T, Ackermann M, Novotny V, Suchy T, Lukas D: **The effect of ethylene oxide sterilization on electrospun vascular grafts made from biodegradable polyesters**. *Mater Sci Eng C Mater Biol Appl* 2018, **92**:132–142, https://doi.org/10.1016/j.msec.2018.06.041.

60. Dai Z, Tian Y, Sethi B, Cao X: **Sterilization techniques for biodegradable scaffolds in tissue engineering applications**. *J Tissue Eng* 2016, **7**:1–13, https://doi.org/10.1177/2041731416648810.

61. Mendes GCC, Brandao TRS, Silva CM: **Ethylene oxide sterilization of medical devices: a review**. *Am J Infect Contr* 2007, **35**: 574–581, https://doi.org/10.1016/j.ajic.2006.10.014.

62. Naughton J, Tiedeken EJ, Garvey M, Stout JC, Rowan NJ: ** **Pulsed light inactivation of the bumble bee trypanosome parasite *Crithidia bombi***. *J Apicult Res* 2017, **56**:144–154, https://doi.org/10.1080/00218839.2017.1289668.
First study to report on the effective use of pulsed light for the irreversible killing of the trypanosome *Crithidia bombi*, which is a complex parasite affecting bumblebees. Quantitative(q)-PCR for assessing appropriate pulsed UV dose against dormant waterborne *Cryptosporidium parvum* oöcysts was used to intimate a relevant pulsed UV dose for treating *Crithidia bombi*. This constitutes the first use of a surrogate parasite affecting the water industry to inform innovation in the pollination industry.

63. Garvey M, Rowan N: **A pulsed light system for the disinfection of flow through water in the presence of inorganic contaminants**. *J Water Health* 2015, **13**:406–412, https://doi.org/10.2166/wh.2014.176.

64. Marín-Huachaca N, Delincée H, Mancini-Filho J, Villavicencio ALCH: **Use of the DNA comet assay to detect beef meat treated by ionizing radiation**. *Meat Sci* 2005, **71**:446–450, https://doi.org/10.1016/j.meatsci.2005.04.019.

65. Silindir M, Özer AY: **Sterilization methods and the comparison of E-beam sterilization with gamma radiation sterilization**. *Fabad J Pharm Sci* 2009, **34**:43–53.

66. Trudeau MP, Verma H, Sampedro F, Urriola PE, Shurson GC, McKelvey J, Pillai SD, Goyal SM: **Comparison of thermal and non-thermal processing of swine feed and the use of selected feed additives on inactivation of Porcine epidemic diarrhea virus (PEDV)**. *PloS One* 2016, **11**, https://doi.org/10.1371/journal.pone.0158128. e0158128.

67. McFadden E, Costa-Ramos A-L, Bradley D, Vrain O, McEvoy B, Rowan NJ: **Comparative studies on the novel sterilisation of Irish retailed infant milk formula using electron beam and pulsed light treatments**. *Int J Sci Environ Technol* 2016, **12**: 4375–4377. research.thea.ie/handle/20.500.12065/3297.

Journal of Applied Microbiology, 0, 2022, lxac028

doi: 10.1093/jambio/lxac028
Advance Access Publication Date: 0 2022
Original Article

ORIGINAL ARTICLE

Geobacillus stearothermophilus and *Bacillus atrophaeus* spores exhibit linear inactivation kinetic performance when treated with an industrial scale vaporized hydrogen peroxide (VH_2O_2) sterilization process

Brian McEvoy[1,2], Ana Maksimovic[1,*] and Neil J Rowan[2]

[1]STERIS Applied Sterilization Technologies, IDA Business and Technology Park, Tullamore, Ireland and [2]Bioscience Research Institute, Technological University of the Shannon Midlands Midwest, Athlone Campus, Ireland

*Corresponding author. STERIS Applied Sterilization Technologies, IDA Business and Technology Park, Tullamore, Ireland. R35×865. Tel/Fax: +353852755825; E-mail: ana_maksimovic@steris.com

Keywords: Vaporized hydrogen peroxide sterilization; *Geobacillus*; bacterial endospores; terminal gaseous sterilization; medical devices; inactivation kinetics

Introduction

Many medical devices are supplied as sterile for safe patient care (McEvoy and Rowan 2019). The global sterilization services market is projected to reach USD 5.5 billion by 2026, growing at a compound annual growth rate (CAGR) of 6.0%, primarily driven by increasing surgical procedures, the prevalence of hospital-acquired infections and increased outsourcing of sterilization services (Anon 2021, McEvoy *et al*. 2021). A sterilization process may be defined as a "series of actions or operations needed to achieve the specified requirements for sterility" (ISO 2018). Sterility is not an absolute; therefore, it must be predicted and expressed in terms of the probability of achieving the inactivation of microbial and other infectious agents post-sterilization treatment (McEvoy and Rowan 2019). Moreover, the underpinning sterility assurance level (SAL) is defined as the 'probability of a single viable microorganism occurring on an item after sterilization' (ISO 2018). A sterilization process is validated whereby a pre-determined SAL is demonstrated through a series of process evaluations (McEvoy and Rowan 2019). In accordance with ISO14937:2009, microbicidal effectiveness must be established such that it is plausible to predict the probability of a defined resistant microorganism surviving exposure to a defined treatment.

In radiation processing, validation is performed through verification of the appropriateness of a delivered dose of sterilant to inactivate the microorganisms occurring on medical devices, where it is assumed that the commensurate microbial inactivation kinetics have been demonstrated as first order (Tallentire *et al*. 2010, Tallentire and Miller 2015, Hansen *et al*. 2020). Such first-order microbial inactivation has been demonstrated through the dose-related killing of *Bacillus pumilus* as a representative challenge microorganism. The best evidence indicates that nucleic acids are the main target of biocidal action for some sterilization modalities, such as radiation and ethylene oxide where first-order relationships can occur (Mosley 2003). Biological indicators (BIs) are employed to demonstrate microbicidal efficacy in gaseous and vapour sterilization processes such as ethylene oxide, steam, and vaporized hydrogen peroxide (VH_2O_2) processes. BIs are enclosed in process challenge devices (PCDs) during the validation of industrial sterilization modalities to provide sufficient resistance to the applied process (Shintani 2017).

With VH_2O_2 processing, a BI-containing *Geobacillus stearothermophilus* is selected and validated, due to its higher endospore

Received: 28 July 2022; **Revised:** 5 September 2022

resistance (D-value) compared to the bioburden that contaminates medical devices, which is carried out in accordance with ISO14937:2009 and ISO22441:2022. A D-value is defined as the exposure time to achieve a one-log reduction in the treated microbial population using a fixed dose of sterilant (McEvoy *et al*. 2021). Using what is typically an 'overkill' validation method in terms of the applied sterilant dose, a sterilization process is performed at 'half-cycle' parameters where full lethality of the treated BI is achieved that encompasses a minimum of 6-log reduction. Sterilant exposure is then doubled to achieve a theoretical 12 log reduction, where the additional 6-log reduction is extrapolated where it is assumed that inactivation follows first-order linear kinetics. Such a 12D process can be approximated based on an understanding of inactivation kinetics on a semi-logarithmic plot when the sterilizing conditions (i.e. process temperature, RH, and VH_2O_2 concentration) remain consistent for the duration of the exposure time (McEvoy and Rowan 2019). While, international sterilization standards such as ISO14937 require the establishment of the 'mathematical relationship defining the microbial inactivation', first-order log-linear microbial inactivation kinetics are often assumed to achieve predictability, allowing for the extrapolation to the desired SAL. Given the criticality of extrapolation to a desired SAL, the threshold for linearity, as determined by the coefficient of determination (R^2) of the survivor curve, should not be less than 0.8 (ISO 2019).

However, it has been previously demonstrated that first-order linear inactivation-type kinetic data may not be readily achieved, such as when microorganisms are exposed to relatively mild inactivation conditions that can stress-harden these microorganisms to subsequent lethal applied doses of the same or different processing stress, which can yield a low number of survivors (Rowan 1999, Rowan *et al*. 2007, Bradley *et al*. 2012, Garvey *et al*. 2015, Fitzhenry *et al*. 2019, Rowan 2019). Under such non-linear conditions that can be experienced using non-thermal food processing technologies, inactivation kinetic data curves can exhibit pronounced initial shoulders, extended tails, or sigmoid curves that are challenging to fit the primary data (Rowan *et al*. 2015). Non-linear inactivation has been previously reported for VH_2O_2 treatments, where the phenomenon of biphasic inactivation was described, which was being attributed to a number of potential sources including micro-condensation (Unger-Bimczok *et al*. 2008, Dufresne and Richards 2016), and the physiological factors associated with the treated BIs (Agalloco and Akers, 2013; Shintani 2014). However, the cellular and molecular mechanisms underpinning the VH_2O_2-mediated destruction of bacterial endospores remain to be fully understood (Linley *et al*. 2012, McEvoy and Rowan 2019).

Previous researchers have reported the use of chemical biocides that produced non-linear inactivation curves (Rowan *et al*. 2021) that were attributed to different theoretical models, namely, the 'vitalistic theory' that describes the phenotypic variation of microorganisms (Cerf 1977, Humpheson *et al*. 1998, Stone *et al*. 2009) and the 'mechanistic theory' that describes influencing factors that were associated with the applied sterilization process. The latter theory encompasses concepts such as superdormancy, biocide quenching, microorganism clumping, and biocidal action itself as possible contributing sources underpinning non-linear sterilization processing (Johnston *et al*. 2000, Lambert and Johnston 2000, Dhar and McKinney 2007, Shintani 2014).

Previous researchers have also reported on the use of predictive microbiology to address non-linear inactivation kinetic plots by applying various mathematical models that reflect the shape of different curves such as Weibull, Hom, and Gompertz (Lambert and Johnston 2000, Geeraerd *et al*. 2005, Coroller *et al*. 2006, Stone *et al*. 2009, Bevilacqua *et al*. 2015). Effective modeling of microbial inactivation arising from physical, chemical, or gaseous treatment modalities typically requires the plot to encompass a 6-log reduction in microbial count (or survival ratio) versus time data (Buzrul 2017). This is important as a dose-response curve is necessary to address the potential occurrence of microbial variance and possible resistance to the applied stress that may exhibit different inactivation shapes, which can be interpreted through a mathematical best-fit (Garre *et al*. 2020, Feurhuber *et al*. 2022). Additionally, numerous log reductions of treated BIs are required to effectively interpret and fit the inactivation plots (Rowan *et al*. 2015, Rowan 2019), which also supports international standardization of processes.

Thus, this constitutes the first detailed study to report on the inactivation kinetics of *G. stearothermophilus* spores that were subjected to VH_2O_2 treatment in an industrial sterilization process. Inactivation kinetic data for *Bacillus atrophaeus* were also determined using similar VH_2O_2 treatments to establish if first-order kinetics produced are specific to the treated microorganism. The impact of sterilant residues was elucidated to establish that the observed VH_2O_2-mediated inactivation was solely attributed to the sterilization process. In addition, scanning electron microscopy was employed to determine if a uniform monolayer of dispersed BI spores occurred during VH_2O_2 treatments where this occurrence provides additional insights into the potential impact of this sterilization process on treated endospore morphology.

Materials and methods

PCD preparation

PCDs were prepared by placing a BI of *G. stearothermophilus* (ATCC 12980) steel coupon (STERIS, Mentor, USA, Lot: AH-126) along with a Sterafirm VH2O2 chemical indicator (STERIS, Mentor, OH, USA,) into a 10 ml Luer lock syringe (Becton Dickinson, Franklin Lakes, NJ, USA) with a 15 cm flexible PVC lumen (3.5 mm internal diameter) attached. A PCD with a 15 cm lumen was determined to be an appropriate challenge following initial trials with lumens of various lengths (unpublished data). The syringe was sealed [150°C [+/−2°C], 40 psi [+/−5 psi] for 1 s] within a vented foil pouch (Nelipak, Ireland) (Fig. 1). Similarly, PCDs containing a BI of *B. atrophaeus* (ATCC 9372) steel coupon (MesaLabs, Bozeman, USA, Lot AG-022) were prepared by placing into a 10 ml luer lock syringe with varying lengths of flexible PVC lumen for PCD evaluation.

Inactivation of *Geobacillus stearothermophilus* PCDs with VH_2O_2

PCDs were fixed to the VH_2O_2 loading cart using Sellotape; thereafter, the cart was loaded to the industrial LTS-V VH_2O_2 sterilizer (STERIS, Mentor, USA) that had a chamber volume of 2025 l. VH_2O_2 processing was performed in the chamber supplied with 35% Vaprox sterilant (STERIS, Mentor, OH, USA). A standardized VH_2O_2 process consisting of the parameters of 35°C, minimum vacuum 4 millibars, and 5-pulse aeration was developed (Fig. 2). Sterilant concentration varied by injection of a fixed number of pulses (from one to a maximum of five pulses), each with approximately 5 mg l^{-1} VH_2O_2. Following processing, PCD samples were removed, and BI coupons were enumerated and

Figure 1 PCD comprising of a chemical and biological indicator placed into a 10 ml syringe with 15 cm lumen length (left), which is then sealed inside a SteriVent pouch with a Tyvek window (right).

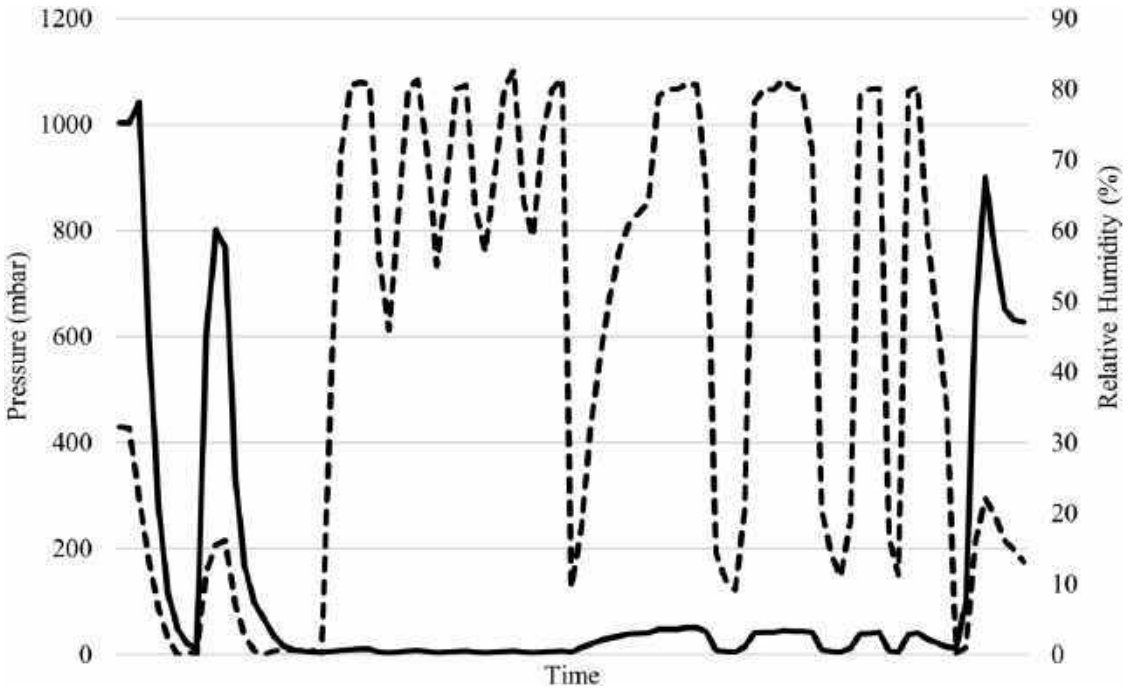

Figure 2 Schematic of the pressure and relative humidity (RH) profile of a 5-pulse VH_2O_2 process. Parameters: chamber pressure (—); chamber RH (—).

imaged by Scanning Electron Microscopy, while chemical indicators were visually examined for colour change. VH_2O_2 inactivation cycles were performed for both microorganism types and in triplicate for each survivor curve data point. To generate sufficient data points to meet a first survivor curve, 10 replicates (BIs) were used in each of the 1–5 pulse cycles. The number of replicates was reduced to 7 in the second and third VH_2O_2 processing runs.

Inactivation of *Bacillus atrophaeus* PCDs with VH_2O_2

PCDs of varying lumen lengths (15, 20, 25 cm) were trialled using varying combinations of sterilant pulses and survivor growth was enumerated to compare with kinetic inactivation data achieved using *G. stearothermophilus* PCDs. Thus, following the selection of an appropriate PCD, a survivor curve was generated by exposure to varying pulses of VH_2O_2 (1–5 pulses), in triplicate. A total of seven replicates (BIs) were used for each survivor curve data point. Representative samples during VH2O2 treatments were also recovered for imaging by SEM.

Enumeration of biological indicators

Geobacillus stearothermophilus enumeration

G. stearothermophilus BIs were aseptically removed from packaging and transferred into individual sterile glass test tubes containing 10 ml sterile purified water, which were then sonicated (Transsonic T890, Germany) for 25 min at 35 kHz. After sonication, 1:10 serial dilutions were prepared in sterile purified water. Selected dilutions were pour plated in duplicate in Tryptic soy agar (TSA; Biokar, France) cooled to approximately 45°C. Solidified plates were incubated inverted at 55–60° C for 48 h (48 h was determined in pre-study trials to be an appropriate incubation period for the BIs being tested following fractional treatment with VH_2O_2), after which plates were counted. For each treatment point, catalase was used to establish if any residual VH_2O_2 was absorbed onto the carrier to consider if this had any detrimental effect on spore viability, where studies were conducted in triplicate. Tubes of sterile dH_2O were replaced with Phosphate Buffer Saline (pH 7.1–7.5, Sigma Lifescience Ireland) containing 0.2 mg bovine liver catalase (2000–5000 units/mg protein; Sigma Aldrich, Germany) as similarly described by the method of Malik *et al.* 2013.

Bacillus atrophaeus enumeration

B. atrophaeus BI coupons (MesaLabs, Apex discs GRS-090) were aseptically removed from packaging and transferred into individual sterile glass test tubes containing 5 ml sterile Tween-80 (0.1%) and four 6 mm sterile glass beads. Tubes were sonicated for a minimum of 3 min at 35 kHz followed by vortexing for a minimum of 5 min. Then 5 ml of sterile purified water was added and tubes were vortexed for an additional 30 s. Thereafter, 1:10 serial dilutions were prepared in sterile purified water and selected dilutions were pour plated in duplicate in TSA (Biokar, France) cooled to approximately 40°C. Solidified plates were incubated at 30–35°C for 48 h, after which plates were counted.

Microbial inactivation kinetic data determination and statistical analysis and statistics

Microbial survivor curves were generated by plotting the logarithm of the survivor fraction ($\log_{10} N/N_o$) against the number of pulses of VH_2O_2 (or VH_2O_2 concentration); where N_o represents untreated spores and N represents the surviving fraction of VH_2O_2-treated spores. By using the ideal gas law ($pV = nRT$), VH_2O_2 concentration was calculated for each pulse. Survivor curves were generated separately for both BIs using triplicate VH_2O_2 processing runs. Microbial survivor curves were also generated for the treated *G. stearothermophilus*, where catalase was used to determine the impact of sterilant residue on spore inactivation. Regression analyses were performed and the average D-values were calculated from the slope of VH_2O_2-generated survivor plots (ISO 11138–7:2019) for each treated BI. Statistical analysis was conducted to determine the impact of VH_2O_2 residues on spore viability via Minitab software using *t*-testing at the 95% confidence level (alpha of 0.05).

Scanning electron microscopy

Non-destructive SEM EDX (Energy Dispersive X-ray) analysis was performed using a TESCAN SEM (Brno, Czech Rep.) with an EDX detector for elemental profiling set at 20 keV. Stainless steel BI specimens were mounted onto aluminium sample stubs coated with a surface adhesive to hold them in place. Images were obtained at 10 000× and 40 000× and examined for structural modification following treatment with VH_2O_2.

Results

Inactivation of *Geobacillus stearothermophilus* spores using VH_2O_2 treatments

Findings reveal that the spore populations of *G. stearothermophilus* were gradually decreased following treatments with 1–5 pulses of VH_2O_2, as shown in Fig. 3. The microbial inactivation plot follows a first-order linear kinetic shape where the R^2 coefficient was measured at 0.91. Moreover, the number of recovered BIs (n) has also declined with an increased number of applied VH_2O_2 pulses (Table 1). For example, all *G. stearothermophilus* BIs were recovered (96.83%) after 1-pulse cycle, while only 15.24% of BIs were recovered after a 5-pulse cycle.

The rapid inactivation of BI spores corresponds to the increasing sterilant concentration from zero to 1 pulse (Fig. 3). Subsequent examination of the pulse duration revealed that not all pulses were of equal duration or sterilant concentration. This is attributed to how the sterilizer controls the process: as part of the preconditioning step prior to sterilant injection, relative humidity (RH) is reduced to a level of 0.0%–0.1% RH. In the first pulse, the sterilant is injected from this starting RH and a vacuum set-point of 4 millibar (mb) to a control endpoint of 80% RH. However, for all other pulses thereafter, vacuums are pulled to a set-point of 4 mb, but RH does not reduce to zero as there are no additional preconditioning steps. With each vacuum, RH reduces to a typical value of 46%–56% RH. Consequently, with an injection set-point of 80%, the injection on pulses after pulse 1 is less (delta injection of only 34%–24% RH), with less sterilant and less overall exposure time. Thus, when accounting for this variance in sterilant concentration by pulse, inactivation plotted against sterilant concentration revealed an improved linearity value of R^2=0.98 (Fig. 4). The appearance of chemical indicators is shown in Fig. 5, demonstrating VH_2O_2 penetration of the 15 cm lumen PCD after two pulses.

Effect of residual VH_2O_2 on the survivor curve

During the preparation of the initial VH_2O_2-mediated survivor curve for *G. stearothermophilus*, a second set of samples was enumerated with the incorporation of catalase as a sterilant

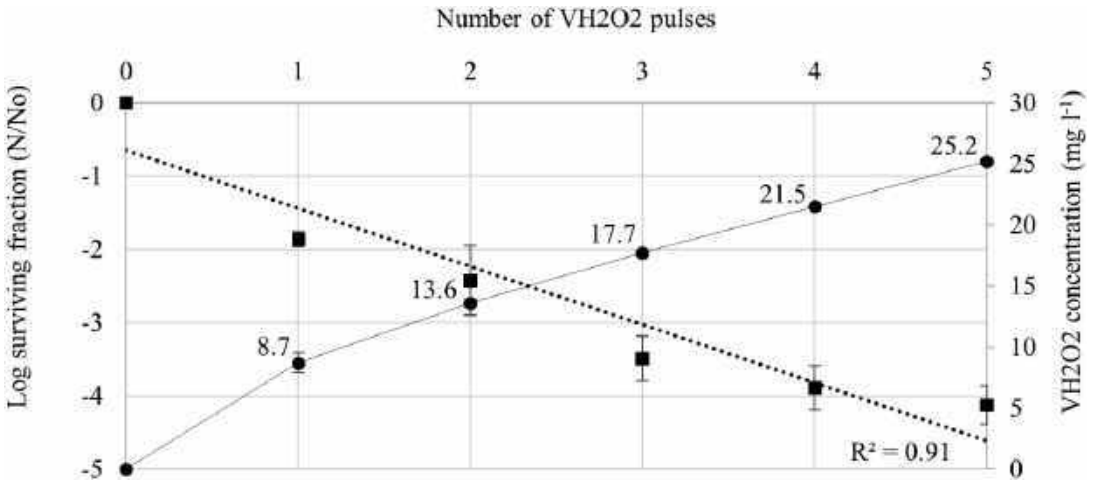

Figure 3 Survivor curve of *G. stearothermophilus* following treatment with pulses of VH_2O_2. *G. stearothermophilus* log surviving fraction in a 15 cm PCD (■) with vertical error bars showing standard deviation of N/N_o; calculated VH_2O_2 concentration (mg l^{-1}; •; values also shown) with error bars showing standard deviation of sterilant concentration; linear fit for *G. stearothermophilus* 15 cm PCD (•••).

Table 1 Percent recovery of *G. stearothermophilus* and *B. atrophaeus* BI spores following treatment with 1–5 pulses of VH_2O_2 sterilant.

Biological indicator	Number of pulses ± SD	Average exposure time (min)	Recovered biological indicators from triplicate runs (%)			
			Run 1	Run 2	Run3	Average
G. stearothermophilus	1	8.59 ± 0.49	100.00	100.00	90.48	96.83
	2	14.86 ± 0.66	90.00	100.00	82.38	90.79
	3	20.64 ± 0.36	70.00	100.00	90.00	86.67
	4	27.00 ± 0.50	30.00	71.43	38.57	46.67
	5	32.63 ± 0.70	20.00	14.29	11.43	15.24
B. atrophaeus	1	9.35 ± 1.01	100.00	100.00	57.14	85.71
	2	15.07 ± 1.22	100.00	100.00	100.00	100.00
	3	23.78 ± 1.29	42.86	42.86	42.86	42.86
	4	30.01 ± 2.18	42.86	57.14	71.43	57.14
	5	35.88 ± 2.53	85.71	28.57	14.29	42.86

Note: Pulses also expressed as average exposure time from triplicate runs.

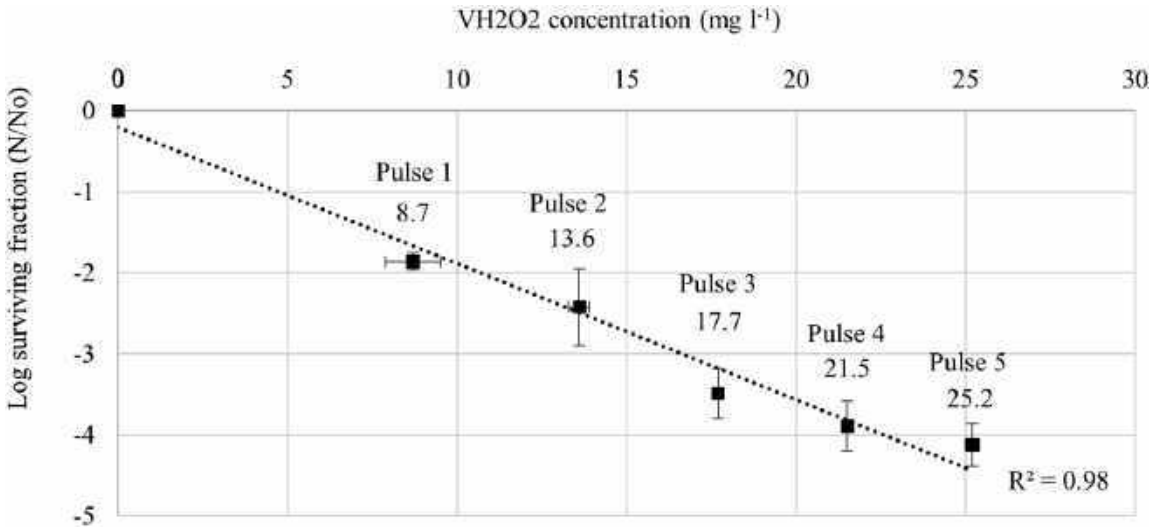

Figure 4 Survivor curve of *G. stearothermophilus* following treatment with incremental doses of VH_2O_2 sterilant. *G. stearothermophilus* log surviving fraction in a 15 cm PCD (■); linear fit for *G. stearothermophilus* 15 cm PCD (•••). Vertical error bars show standard deviation of N/N_o; horizontal error bars show standard deviation of sterilant concentration. Data labels show sterilant concentration (mg l^{-1}) and corresponding pulse number.

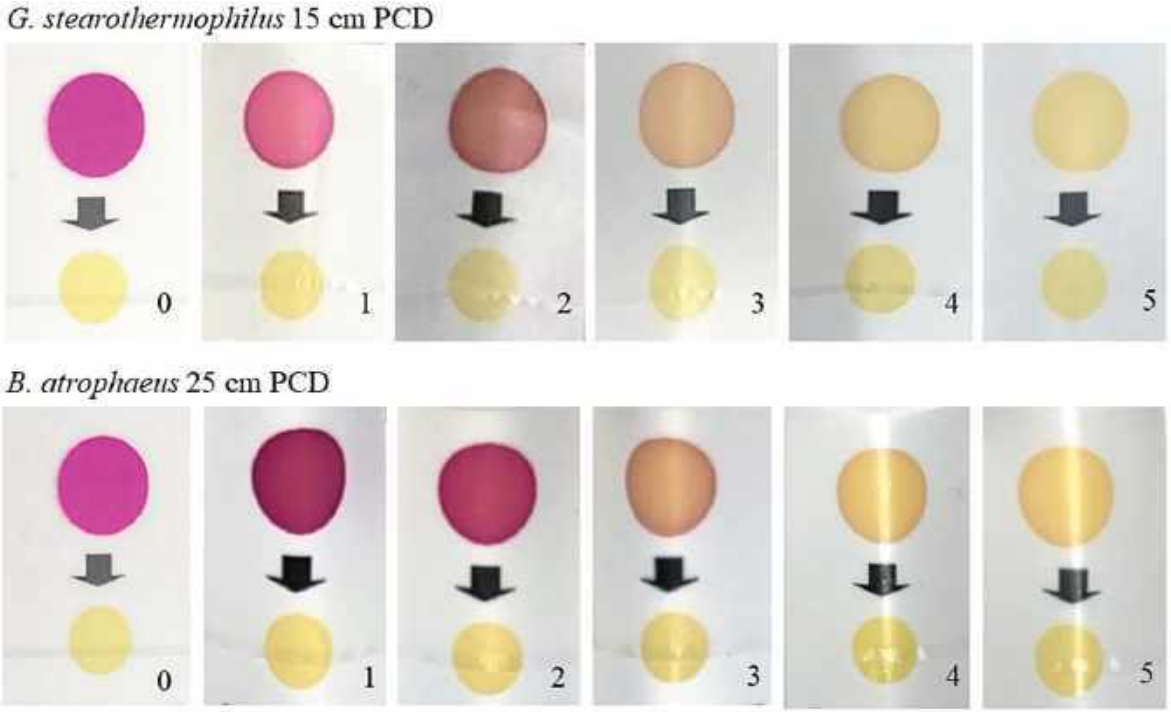

Figure 5 The appearance of untreated chemical indicator (0) and chemical indicators treated in 1, 2, 3, 4 and 5 pulse cycle. The labels 0–5 stand for the number of pulses used in the cycle. Chemical indicators used with *G. stearothermophilus* (top) were placed in the 15 cm PCD, while chemical indicators used with *B. atrophaeus* were placed in a 25 cm PCD (bottom).

quencher. Samples treated with catalase revealed that there was no statistical difference in these treatments ($P > .05$). It was noted that even if hydrogen peroxide had absorbed onto the BI carrier, this did not affect the VH_2O_2-treated spore viability.

Inactivation of *Bacillus atrophaeus* with VH_2O_2

Following the establishment of a microbial survivor plot using G. *stearothermophilus*, a range of PCDs containing *B. atrophaeus* were evaluated to find one appropriate for generating an appropriate measurable inactivation data plot over the required range of 1–5 pulses of VH_2O_2. The tested PCD types were as follows: syringe with 15, 20, 25, and 30 cm lumen length. First, all trialled PCDs were subjected to a 1-pulse cycle to establish the initial reduction in population and compared with the results obtained for *G. stearothermophilus* after 1-pulse cycle (Fig. 6). PCD with a lumen length of 30 cm was excluded from further analysis as it was deemed to be too technically challenging, whereas *B. atrophaeus* BIs in the shorter lumen length PCDs were enumerated following a 3-pulse cycle for lumen lengths of 15 and 20 cm, and a 4-pulse cycle for PCDs of 25 cm to determine their capacity to survive extensive VH_2O_2 treatment where these were compared with *G. stearothermophilus* data sets. As shown in Fig. 6, a PCD comprising of 25 cm lumen was found to closely match the established inactivation plot of G. *stearothermophilus*. Other lumen lengths were found to be either too challenging that required many pulses to achieve an inactivation plot over the 6-log regime or were deemed to be not sufficiently challenging as reflected in achieving inactivation after too few pulses to generate a clear microbial kinetic plot.

A survivor inactivation plot was generated using the PCD of 25 cm lumen with *B. atrophaeus*, (Fig. 7), where surviving BI fractions were plotted using the delivered sterilant concentration per pulse over the range of 1 to 5 pulses that were shown to exhibit $\log_{10}$ linear inactivation shape (R^2 coefficient, 0.93). The colour change of chemical indicators retrieved from this same VH_2O_2 process is shown in Fig. 5.

D-value calculations of *Geobacillus stearothermophilus* 15 cm PCD and *Bacillus atrophaeus* 25 cm PCD

D-values were calculated from the inverse of the slope of the survivor curve and summarized in Table 2.

SEM of *Geobacillus stearothermophilus* and *Bacillus atrophaeus* treated with VH_2O_2

SEM images of untreated, VH_2O_2 treated, and fully inactivated *G. stearothermophilus* and *B. atrophaeus* spores are shown in Fig. 8.

Upon visual observation of SEM images of the untreated and VH_2O_2-treated BIs, a well-distributed monolayer of spores was evident with no apparent change to the level of clumping or aggregation with regard to the inactivation process (the number of H_2O_2 pulses applied) (Fig. 9). Similar observations were made from SEM images of *B. atrophaeus* BIs treated with fractional and sterilization doses of vaporized hydrogen peroxide (VHP) and ethylene oxide gas (unpublished data).

Discussion

Following the establishment of an appropriate PCD and VH_2O_2 process, experimental studies were found to be very repeatable and were appropriate for producing a survivor plot of kinetic inactivation range using one to five pulses of VH_2O_2. As shown in Fig. 3, a first-order log-linear inactivation was observed for

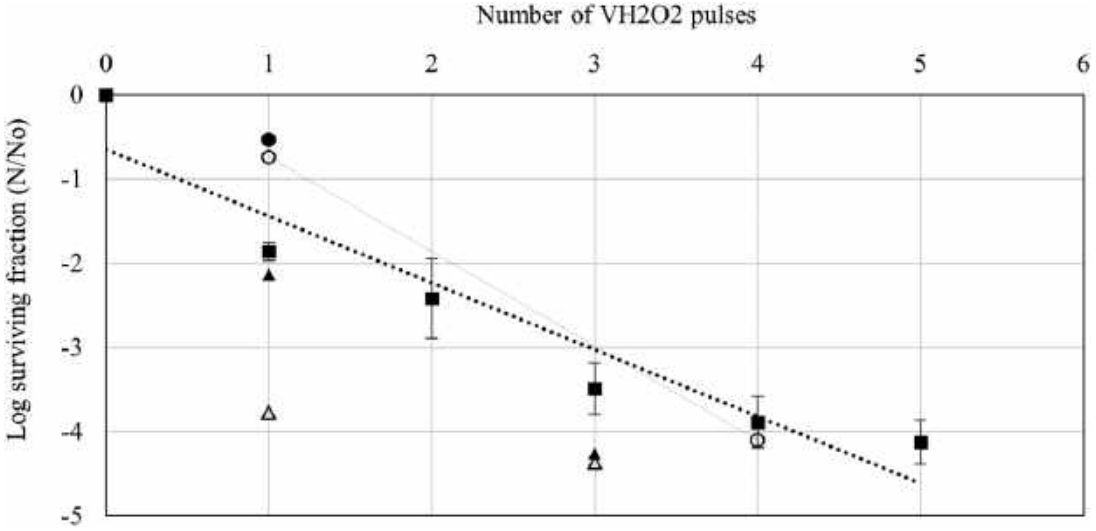

Figure 6 Survivor inactivation plots of PCDs containing *B. atrophaeus* that were compared with similarly treated *G. stearothermophilus* spore populations. A range of PCDs containing pre-determined numbers of *B. atrophaeus* spores with different degrees of resistance (15, 20, 25, and 30 cm lumen) were trialled to establish a PCD with a level of resistance comparable to *G. stearothermophilus*. As shown on the figure: *G. stearothermophilus*, 15 cm PCD (■); *B. atrophaeus*, 15 cm PCD (△); *B. atrophaeus*, 20 cm PCD (▲); *B. atrophaeus*, 25 cm PCD (■); *B. atrophaeus*, 30 cm PCD (●); linear fit *G. stearothermophilus*, 15 cm PCD (●●●); linear fit *B. atrophaeus*, 25 cm PCD (—).

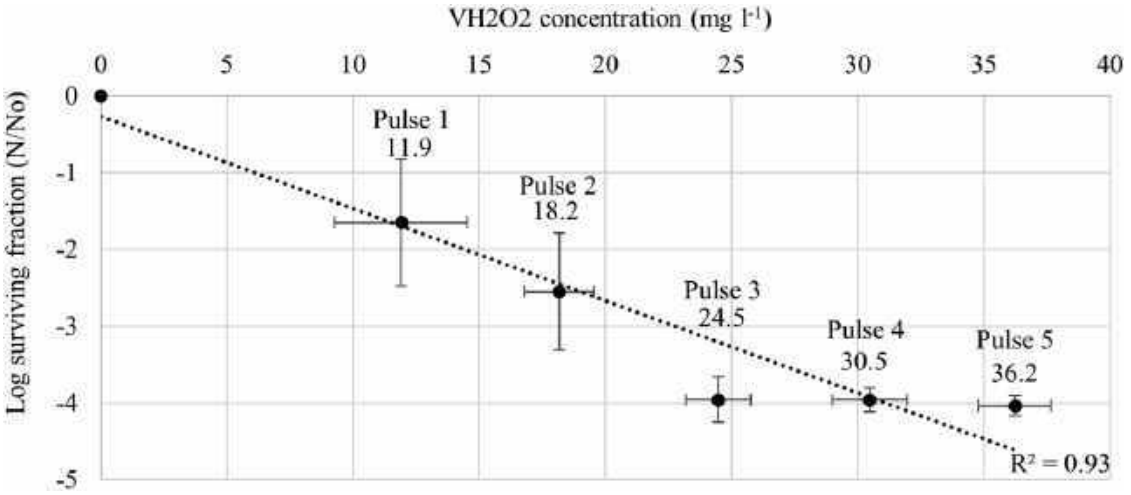

Figure 7 Survivor inactivation plot of *B. atrophaeus* following treatment with VH_2O_2 with increasing sterilant concentration. *B. atrophaeus* log surviving fraction in a 25 cm PCD (●); linear fit for *B. atrophaeus* in a 25 cm PCD (●●●). Vertical error bars show standard deviation of N/N_o; horizontal error bars show standard deviation contact time ($n = 3$). Data labels show sterilant concentration.

Table 2 Comparison of D-values and sterilization processing requirements, pulses of VH_2O_2 required for processing of PCDs containing *G. stearothermophilus* and *B. atrophaeus*.

Sterilization processing requirements	*G. stearothermophilus*	*B. atrophaeus*
BI D-value (min) (Manufacturer claim)	1.4	0.3
PCD	15 cm lumen	25 cm lumen
D-value (min)	7.75	8.72
12 SLR (Routine process time required for sterilization) (min)	93	104.64
Average pulse time from survivor curve (min)	7.24	7.90
VH_2O_2 Sterilization Process (Pulses of sterilant)*	13	14

*VH_2O_2 pulses are calculated based on 12 SLR time/average pulse time. Fractions of pulses are positively rounded to full integers.

the BI, *G. stearothermophilus* contained in a PCD comprising of a 10 ml syringe with a 15 cm lumen attached that was contained in a vented pouch. In compliance with ISO11138-7:2019, an R^2 coefficient of determination greater than 0.8 was achieved. Further examination of the duration and concentration of sterilant delivered in each VH_2O_2 pulse revealed that not all pulses were equal in these properties; therefore, the survivor inactivation

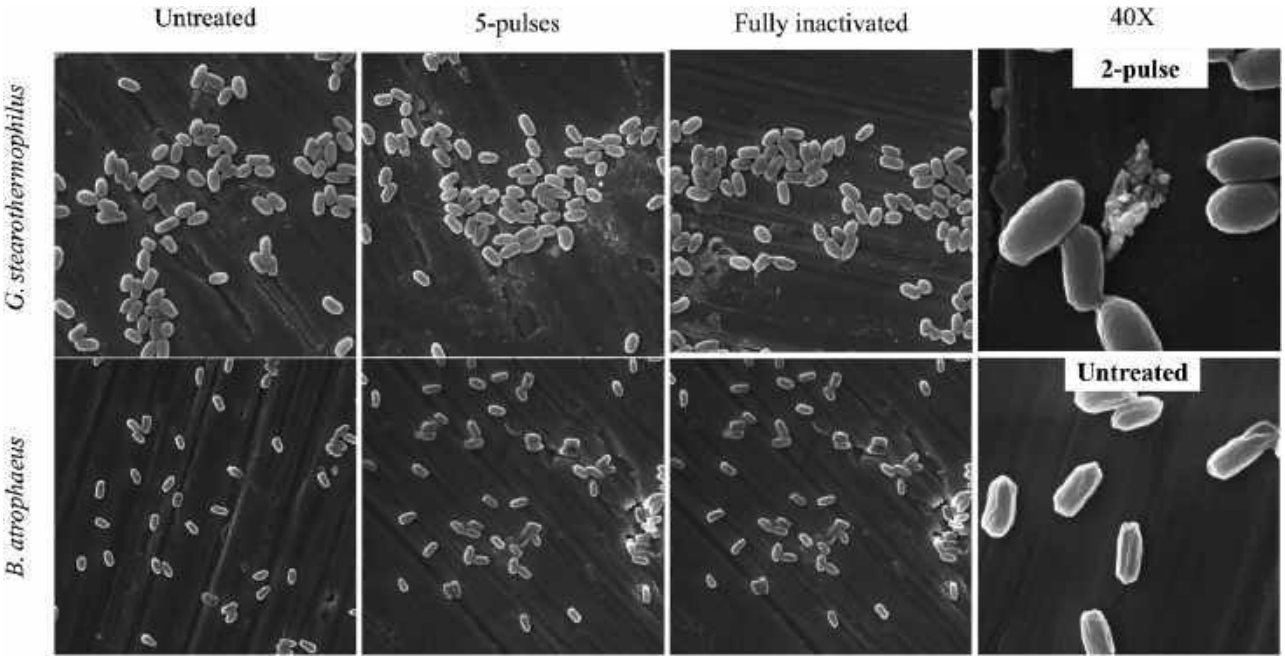

Figure 8 SEM images (10k×) of untreated *B. atrophaeus* and *G. stearothermophilus*, treated with five pulses and fully inactivated with VH_2O_2. Higher magnification (40k×) also shown of selected samples.

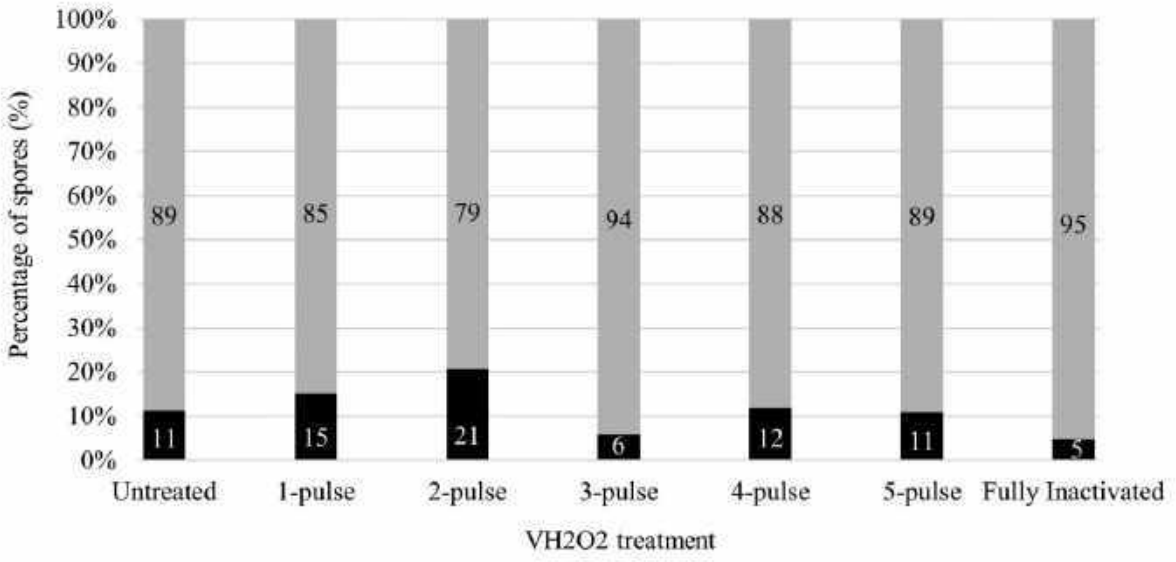

Figure 9 Count of *G. stearothermophilus* single spores (■) and grouped spores (≥ 2; ■) from SEM images (10 000×). Data are provided for untreated spores, fully inactivated spores, and spores treated in VH_2O_2 cycles ranging from one to five pulses.

data were re-plotted to log survivor versus sterilant concentration that resulted in an improvement in R^2 of 0.98 (Fig. 4). This demonstrates the importance of establishing the most appropriate measure of 'sterilant dose' when assessing inactivation. In this work, pulses are not equal due to how the process is controlled by the sterilizer with the inactivation of the spores being a consequence of sterilant concentration and exposure time, which is potentially under-appreciated in the field of sterilization microbiology (McEvoy and Rowan 2019). The novel finding of the degree of linearity of the inactivation applies to industrial-scale sterilization with VH_2O_2 and demonstrates the appropriateness of the use of validation methods such as half-cycle overkill as described in ISO14937:2009. The D-value for VH_2O_2 sterilant exposure time of 7.75 min (SD = 0.40) was calculated to deliver 12 spore log reductions (or 12D), which is equivalent to a SAL of 10^{-6} in 93.00 min. With an average exposure time per pulse of 7.24 min, this equates to a routine sterilization process of 12.85 pulses. Similarly, D-value may be calculated in terms of sterilant concentration (M = 5.84 mg l^{-1}; SD = 0.22), and with an average concentration per pulse of 5.78 mg l^{-1}, determined to require a process of 12.12 pulses. Thus, to provide a SAL of 10^{-6} to the described PCD a routine process of 13 pulses must be programmed on the sterilizer. Furthermore, the demonstration of linearity also confirms that fractional methods

of D-value determination such as Holcomb–Spearman–Karber Procedure, Limited Holcomb–Spearman–Karber Procedure, and Stumbo–Murphy–Cochran Procedure may be applied (ISO 2019).

A range of PCDs was evaluated for *B. atrophaeus* by interpreting the linked survivor kinetic data generated from VH_2O_2-treated *G. stearothermophilus* in this study (Fig. 6). Given the lower D-value of the *B. atrophaeus* BI (D-value = 0.3 minutes) versus *G. stearothermophilus* BI (D-value = 1.4 min), a more challenging PCD was selected for survivor kinetic data plot generation: following treatment with one and four pulses of VH_2O_2, a 25 cm lumen PCD containing *B. atrophaeus* was found to yield a similar inactivation as the 15 cm PCD containing *G. stearothermophilus*. A survivor curve was constructed yielding an R^2 value of 0.93, in compliance of the requirements of ISO11138-7:2019.

The type of sterilization process and associated experimental conditions are significant factors that inform the reliable and repeatable linear destruction of BIs over a period of approximately 45 min in industrial-scale sterilization using PCDs. This contrasts with previously reported studies where biphasic microbial inactivation kinetic plots were observed over much shorter durations of treatments such as within less than 5 min (Dufresne and Richards 2016). It is plausible that if the zero to one pulse range of this study was more closely examined in a BI evaluation resistometer (BIER) in the absence of a PCD, non-linear inactivation may potentially be observed: this is due to the inactivation kinetics being significantly shortened when the resistance of the PCD is removed and D-values more aligned to the BI manufacturer stated values, e.g., 1.4 min for *G. stearothermophilus* BI used in this study. In contrast, this present study has been performed in an industrial sterilizer with PCDs that are typically used to increase the microbiological challenge in the validation of such a sterilization process in accordance with the relevant ISO14937 standard.

As described by Shintani *et al.* (2010) and Shintani (2014), experimental artefact of spore clumping has been described as a potential source of non-linear inactivation kinetics, whereby the aggregation of spores result in reduced penetration of the sterilant vapour. Furthermore, the work of Johnston *et al.* (2000) demonstrated the significance of microbial load and the possibility for biocide quenching by the inoculum: as quenching occurs, the amount of available biocide for further inactivation of the population reduces at a microbial cellular level, thus resulting in the appearance of a more resistant sub-population of treated BIs. This was also evident for pulsed-plasma gas-discharge treated microbial samples that contained short-lived oxygenated free radicals (Rowan *et al.* 2007; Hayes *et al.* 2013). SEM may be effectively used as an investigative tool to provide visual data on the effect of sterilization processes on spore shape and surface topography; e.g. this was demonstrated for *Mycobacterium paratuberculosis* cells by pulsed electric field treatments (Rowan *et al.* 2001) and for *Campylobacter jejuni* cells treated with pulsed-plasma gas-discharge exposures (Rowan *et al.* 2008). In this work, the analysis of SEM images revealed (i) an evenly distributed monolayer of spores in treated and untreated BIs and (ii) no significant change to the distribution of spores on the BI carrier material either before or after treatment (Figs. 8 and 9). This is consistent with the findings of others who examined treatment with VHP and ethylene oxide (EO) sterilant and noticed no noticeable morphology differences or clumping of cells (Reich and Akkus 2013). Furthermore, the inclusion of catalase in the test method confirmed the absence of any observed sterilant residual effect on spore enumeration.

The appropriateness of *B. atrophaeus* as a potential BI system for use in VH_2O_2 is demonstrated in the survivor plot with rapid inactivation from one to three pulses of *B. atrophaeus* (Fig. 7). While the cycles in which *B. atrophaeus* were treated had somewhat higher VH_2O_2 concentration (Fig. 7) in the chamber, it is important to note that VH_2O_2 concentration in the chamber does not necessarily correspond to the VH_2O_2 concentration within the PCD. This was evident in the colour change in the chemical indicators: unlike *G. stearothermophilus*, no colour change was observed in the *B. atrophaeus* PCDs after two pulses (Fig. 5). This would indicate that the longer 25 cm lumen was effective in impeding the ingress of vapour. However, once vapour penetrated the PCD lumen, inactivation of the *B. atrophaeus* BI was rapid due to its lower intrinsic resistance, with a D-value of only 0.3 min as compared to *G. stearothermophilus* of 1.4 min (Table 2). This may also explain why spore inactivation is observed with 1- and 2- pulses of VH_2O_2 treatment even though limited penetration with sterilant. Thus, while the overall resistance of a PCD is a combination of the BI resistance and the PCD materials, the contribution of each constituent component may require some consideration when assessing both D-value and linearity.

Calculation of D-value for the *B. atrophaeus* PCD yielded a conservative figure of 8.72 min or 14 pulses for a routine sterilization process yielding SAL of 10^{-6}. If only pulses 1–3 were considered in the calculation of the slope of the line, then D-value would adjust to 6.07 min and 10 pulses. Thus, this demonstrates that experimental limitations conservatively add to the final process being delivered such that in this case it is likely that approximately four additional logs of kill are being delivered to the process, resulting in a SAL of 10^{-10}.

Furthermore, as shown by this research, the use of a 'most resistant organism', in this case *G. stearothermophilus*, does not seem to be the most important factor as it is the overall resistance of the PCD relative to the medical device being sterilized, which is of most importance when quantifying D-values and extrapolating to a required SAL. In this research, by modifying the lumen length of the PCD, similar D-values were obtained using two different biological indicator species. Hence, it may be argued that the criteria for an appropriate BI for use in industrial sterilization are one of (i) known high resistance within a PCD, (ii) known inactivation kinetics and linearity of the PCD, and (iii) one that may be qualified as equivalent or greater resistance relative to the natural microbiological challenge of the medical device itself. The generation of critical data points for VH_2O_2 sterilization will also inform the future automation of this process including the uses of digital technologies such as artificial intelligence enabled by machine learning (Rowan *et al.* 2022).

In conclusion, this constitutes the first study to examine the inactivation of two types of BI spores contained in PCDs and processed with an industrial VH_2O_2 sterilizer. Findings supported the occurrence of linear BI inactivation plots post-VH202 treatments, which is important given that validation methods underpinning terminal medical device sterilization rely upon this linear microbial death-rate assumption. Thus, this study provides additional rigour and confidence that an appropriate sterility level can be achieved using biological indicators using standard validation methods as described in the recently published ISO22441 standard for sterilization with VH_2O_2. Hence, this work furthers the advancement of VH_2O_2 for the terminal sterilization of medical devices that is critical for patient care.

Acknowledgements

The authors would like to acknowledge the team at STERIS who assisted with VH_2O_2 sterilization processing. For the support with SEM analysis, the authors would like to thank Dr.

Emer O'Neill and Dr. Alan Murphy of TUS. The authors acknowledge the Technological University of the Shannon Midlands Midwest Doctoral Scholarship Programme and funding support from STERIS AST.

References

Agalloco JP, Akers JE. Overcoming limitations of vaporized hydrogen peroxide: hydrogen peroxide is highly potent and highly problematic. *Pharm Technol* 2013;**9**:46–56.

Anon. Sterilization services market by method (ETO, gamma, steam, X-ray), type (contract sterilization, validation services), mode of delivery (off-site, on-site), end user (Hospitals and clinics, pharmaceuticals) - Global Forecasts (2022 - 2026). *Markets and Markets* 2021. https://www.marketsandmarkets.com/Market-Reports/sterilization-service-market-183597324.html?gclid=EAIaIQobChMI_6ifsb2H-AIVgQCLCh1jCw2OEAAYASAAEgK6DPD_BwE (30 May 2022, date last accessed).

Bevilacqua A, Speranza B, Sinigaglia M *et al.* A focus on the death kinetics in predictive microbiology: benefits and limits of the most important models and some tools dealing with their application in foods. *Foods* 2015;**4**:565–80.

Bradley D, McNeill B, Laffey JG *et al.* Studies on the pathogenesis and survival of different culture forms of listeria monocytogenes to pulsed UV-light irradiation after exposure to mild-food processing stresses. *Food Microbiol* 2012;**30**:330–9.

Buzrul S. Evaluation of different dose-response models for high hydrostatic pressure inactivation of microorganisms. *Foods* 2017;**79**:1–15.

Cerf O. Tailing of survival curves of bacterial spores. *J Appl Bacteriol* 1977;**42**:1–19.

Coroller L, Leguerinel I, Mettler E *et al.* General model, based on two mixed weibull distributions of bacterial resistance, for describing various shapes of inactivation curves. *Appl Environ Microbiol* 2006;**72**:6493–502.

Dhar N, McKinney JD. Microbial phenotypic heterogeneity and antibiotic tolerance. *Curr Opin Microbiol* 2007;**10**:30–38.

Dufresne S, Richards T. The first duel-sterilant low-temperature sterilization system. *Can J Infect Control* 2016;**3**:169–74.

Feurhuber M, Neuschwander R, Taupitz T *et al.* Mathematically modelling the inactivation kinetics of *Geobacillus stearothermophilus* spores: effects of sterilization environments and temperature profiles. *Phys Med* 2022;**13**:p.100046.

Fitzhenry K, Rowan N, de Rio AV *et al.* Inactivation efficacy of Bacillus endospores via modified flow-through PUV treatment with comparison to conventional LPUV treatment. *J Water Process Eng* 2019;**27**:67–76.

Garre A, Zwietering MH, den Besten HMW. Multilevel modelling as a tool to include variability and uncertainty in quantitative microbiology and risk assessment. Thermal inactivation of listeria monocytogenes as proof of concept. *Food Res Int* 2020;**137**:1–13.

Garvey M, Rabbity D, Stocca A *et al.* Pulsed light inactivation of *Pseudomonas aeruginosa* and *Staphylococcus aureus*. *Water Environment J* 2015;**29**:36–42.

Geeraerd AH, Valdramidis VP, van Impe JF. GInaFiT, a freeware tool to assess non-log-linear microbial survivor curves. *Int J Food Microbiol* 2005;**102**:95–105.

Hansen JM, Fidopiastis N, Bryans T *et al.* Radiation sterilization: dose is dose. *Biomed Instrum Technol* 2020;**54**:45–52.

Hayes J, Kirf D, Garvey M, Rowan NJ. Disinfection and toxicological assessments of pulsed UV and pulsed-plasma gas-discharge treated-water containing the waterborne protozoan enteroparasite *Cryptosporidium parvum*. *J Microbiol Methods* 2013;**94**:325–37.

Humpheson L, Adams MR, Anderson WA *et al.* Biphasic thermal inactivation kinetics in *Salmonella enteritidis* PT4. *Appl Environ Microbiol* 1998;**64**:459–64.

International Organization for Standardization (ISO). ISO22441:2022. *Sterilization of health care products—low temperature vaporized hydrogen peroxide—requirements for the development, validation and routine control of a sterilization process for medical devices*. Geneva: ISO, 2022.

International Organization for Standardization (ISO). ISO11138-7:2019. *Sterilization of health care products—biological indicators—Part 7: Guidance for the selection, use and interpretation of results*. Geneva: ISO, 2019.

International Organization for Standardization (ISO). ISO11139:2018. *Sterilization of health care products—vocabulary of terms used in sterilization and related equipment and process standards*. Geneva: ISO, 2018.

International Organization for Standardization (ISO). ISO14937:2009. *Sterilization of health care products—general requirements for characterization of a sterilizing agent and the development, validation and routine control of a sterilization process for medical devices*. Geneva: ISO, 2009.

Johnston MD, Simons EA, Lambert RJW. One explanation for the variability of the bacterial suspension test. *J Appl Microbiol* 2000;**88**:237–42.

Lambert RJW, Johnston MD. Disinfection kinetics: a new hypothesis and model for the tailing of log-survivor/time curves. *J Appl Microbiol* 2000;**88**:907–13.

Linley E, Denyer SP, McDonnell G *et al.* Use of hydrogen peroxide as a biocide: new consideration of its mechanisms of biocidal action. *J Antimicrob Chemother* 2012;**67**:1589–96.

McEvoy B, Lynch M, Rowan NJ. Opportunities for the application of real-time bacterial cell analysis using flow cytometry for the advancement of sterilization microbiology. *J Appl Microbiol* 2021;**130**:1794–812.

Malik DJ, Shaw CM, Rielly CD *et al.* The inactivation of *Bacillus subtilis* spores at low concentrations of hydrogen peroxide vapour. *J Food Eng* 2013;**114**:391–6.

McEvoy B, Rowan NJ. Terminal sterilization of medical devices using vaporized hydrogen peroxide: a review of current methods and emerging opportunities. *J Appl Microbiol* 2019;**127**:1403–20.

Mosley GA. Microbial lethality: when it is log-linear and when it is not. *Biomed Instrum Technol* 2003;**37**:451–3.

Reich MS, Akkus O. Sporicidal efficacy of genipin: a potential theoretical alternative for biomaterial and tissue graft sterilization. *Cell Tissue Bank* 2013;**14**:381–93.

Rowan NJ, Espiec S, Harrower J *et al.* Evidence of lethal and sublethal injury in food-bonre bacterial pathogens exposed to high-intensity pulsed-plasma gas-discharges. *Lett Appl Mirobiol* 2008;**46**:80–86.

Rowan NJ, Valdramidis VP, Gomez-Lopez VM. A review of quantitative methods to describe efficacy of pulsed light generated inactivation data that embraces the occurrence of viable but non culturable state microorganisms. *Trends Food Sci Technol* 2015;**44**:79–92.

Rowan NJ. Pulsed light as an emerging technology to cause disruption for food and adjacent industries—quo vadis? *Trends Food Sci Technol* 2019;**88**:316–32.

Rowan NJ, MacGregor SJ, Anderson JG *et al*. Inactivaion of *Mycobacterium paratuberculosis* by pulsed electric fields. *Appl Environ Microbiol* 2001;**67**:2833–6.

Rowan NJ, Espie S, Harrower J *et al*. Pulsed plasma gas discharge inactivation of microbial pathogens in chilled poultry wash water. *J Food Prot* 2007;**70**:2805–10.

Rowan NJ. Evidence that inimical food-preservation barriers alter microbial resistance, cell morphology and virulence. *Trends Food Sci Technol* 1999;**10**:261–70.

Rowan NJ, Meade E, Garvey M. Efficacy of frontline chemical biocides and disinfection approaches for inactivating SARS-CoV-2 variants of concern that cause coronovirus disease with the emergence of opportunities for green eco-solutions. *Curr Opin Environ Sci Health* 2021;**23**:1–13.

Rowan NJ, Murray N, Qiao Y *et al*. Digital transformation of peatland eco-innovations ('Paludiculture'): enabling a paradigm shift towards the real-time sustainable production of 'green-friendly' products and services. *Sci Total Environ* 2022;**3**:1–20.

Shintani H, Sakudo A, Burke P *et al*. Gas plasma sterilization of microorganisms and mechanisms of action. *Exp Ther Med* 2010;**1**:731–8.

Shintani H. Important points to attain reproducible sterility assurance. *Biochem Physiol* 2014;**03**:135.

Shintani H. Ethylene oxide gas sterilization of medical devices. *Biocontrol Sci* 2017;**22**:1–16.

Stone G, Chapman B, Lovell D. Development of a log-quadratic model to describe microbial inactivation, illustrated by thermal inactivation of *Clostridium botulinum*. *Appl Environ Microbiol* 2009;**75**:6998–7005.

Tallentire A, Miller A. Microbicidal effectiveness of X-rays used for sterilization purposes. *Radiat Phys Chem* 2015;**107**:28–130.

Tallentire A, Miller A, Helt-Hansen J. a comparison of the microbicidal effectiveness of gamma rays and high and low energy electron radiations. *Radiat Phys Chem* 2010;**79**:701–4.

Unger-Bimczok B, Kottke V, Hertel C, Rauschnabel **3**, 123-133. The influence of humidity, hydrogen peroxide concentration, and condensation on the inactivation of *Geobacillus stearothermophilus* spores with hydrogen peroxide vapor. *J Pharm Innov* 2008;**3**:123–33.

Radiation Physics and Chemistry 208 (2023) 110915

Contents lists available at ScienceDirect

Radiation Physics and Chemistry

journal homepage: www.elsevier.com/locate/radphyschem

Studies on the comparative effectiveness of X-rays, gamma rays and electron beams to inactivate microorganisms at different dose rates in industrial sterilization of medical devices

Brian McEvoy [a], Ana Maksimovic [a,*], Daniel Howell [b], Pierre Reppert [c], Damien Ryan [a], Neil Rowan [d], Hervé Michel [c]

[a] STERIS, IDA Business & Technology Park, Tullamore, R35 X865, Ireland
[b] STERIS, Roydsdale Way, Euroway Trading Estate, Bradford, W. Yorkshire, BD4 6SE, UK
[c] STERIS, Hogenweidstrasse 6, 4658, Däniken, Switzerland
[d] Bioscience Research Institute, Technological University of the Shannon Midlands Midwest, Athlone Campus, Ireland

ARTICLE INFO

Handling Editor: Piotr Ulanski

Keywords:
Ionizing radiation
Industrial sterilization
Medical device
Dose rate
Microbicidal effectiveness
Technology transfer

ABSTRACT

The radiation resistance of *Bacillus pumilus* spores to gamma rays, X-rays, and electron beam (e-beam) was investigated using industrial irradiators operating at various dose rates. The dose rates were as follows: gamma 1 and 10 kGy/h; X-ray 10 and 200 kGy/h; e-beam 2000 kGy/h. The regression analysis showed that survivor curves were $\log_{10}$ linear for all three sources within the investigated absorbed dose range of 1–6 kGy, irrespective of the dose rate applied. All irradiation technologies were equally efficient to inactivate the spores, which is reflected in their comparable D-values ($p > 0.05$), and dose rate had no impact on the microbicidal efficacy. These results suggest that wherever a specified minimum dose is delivered, the sterilization dose can be transferred between irradiation technologies in industrial sterilization of medical devices without any impact on product sterility. These findings from a novel single study encompassing all available industrial radiation technologies for the purpose of medical devices sterilization, advance our understanding of microbial destruction as related to exposure to important sterilization modalities, which will help inform future applicability of these technologies for emerging industry opportunities.

1. Introduction

Sterilization by radiation is employed as the means of achieving required sterility assurance for some 50% of single use medical devices, with gamma irradiation being the most widely used technology (GIPA-Gamma Industry Processing Alliance, 2017). However, in the past number of years certain challenges regarding Cobalt-60, the raw material for gamma processing, have been identified (Dethier, 2016; BPSA, 2021). Such challenges have culminated in the advancement of accelerator based technologies, such as X-ray and electron beam (e-beam) (McEvoy et al., 2020). In particular, X-ray has been established as a sustainable supplement to gamma due to many similarities between the two photon-based technologies (McEvoy et al., 2020). Many potential changes are considered when migrating to X-ray, including the effect on materials, any potential induced radioactivity, the effect of dose rate, temperature impacts, and processing time. Considerable focus has been placed on material effects (Murray et al., 2012, 2014; Fifield et al., 2021) and induced radioactivity in materials processed with energy above 5 MeV (Michel et al., 2021). Currently, the Association for the Advancement of Medical Instrumentation (AAMI) is generating a Technical Information Report (TIR104) to provide guidance to users when considering a change of radiation technology (Montgomery et al., 2021). That entails performing a risk assessment to identify and quantify the potential impact on the functionality and performance of the medical devices following the terminal sterilization process (Montgomery et al., 2021). Among other factors to be considered when products are moved to X-ray, it is imperative to ensure that the sterility assurance level (SAL) is achieved. Dose rate is a key differential parameter between gamma, electron beam and X-ray, and its effect on sterilization efficacy should be considered (Kroc et al., 2017). Dose rate is defined as the quantity of radiation absorbed per unit of time, and while it can take hours to sterilize products with gamma, the treatment can be completed within

* Corresponding author.
E-mail address: Ana_Maksimovic@steris.com (A. Maksimovic).

https://doi.org/10.1016/j.radphyschem.2023.110915
Received 16 April 2022; Received in revised form 6 March 2023; Accepted 11 March 2023
Available online 17 March 2023

minutes with an X-ray (Dethier, 2016) and seconds with an e-beam. Furthermore, a recent paper by the Irradiation Panel on gamma and electron irradiation (2020) has re-emphasised the need to consider the effect of higher dose rates. With regard to medical device sterilization, researchers have found that microbicidal efficacy is primarily a dose dependant activity. In their work, Tallentire et al. (2010) and Tallentire and Miller (2015) found that microbiological responses for water hydrated *B. pumilus* spores were the same for all types of industrial irradiators, while Hansen et al. (2020) demonstrated microbicidal equivalence of gamma and e-beam when microorganisms were irradiated in a dry state. However, such studies investigating the microbicidal efficacy of irradiation technologies under conditions typical for industrial sterilization of medical devices are scarce, and more research is needed to evaluate the possibility of transfer of minimum doses required for inactivation between irradiators of the same and/or different irradiation sources. Therefore, in this study, the microbicidal efficacy of all relevant industrial irradiators (gamma, X-ray, and e-beam), operating at different dose rates, have been directly compared in terms of decimal reduction time (D-value) utilizing a single biological indicator reference microorganism. A D-value can be defined as the time or dose required under given conditions to achieve inactivation of 90% (or 1 log) of a population of the test microorganisms (ISO 11139:2018) and is commonly used in sterilization microbiology to express the sterilization efficacy of the process. As a reference microorganism, *Bacillus pumilus* spores were selected due to its high radiation resistance and irradiated in a dry state, as being representative for industrial sterilization processes. Moreover, other sterilization parameters such as temperature and energy level were also assessed regarding their impact on microbial inactivation. The findings from this novel study herein are expected to further substantiate our understanding of the sterilization efficacy of industrial irradiators.

2. Experimental

2.1. Pre-trial to determine the stability of irradiated spores

Prior to executing the experiment, a pre-trial was carried out to determine the stability of irradiated spores, i.e., to establish a time frame within which irradiated spores need to be microbiologically analysed. Spores (biological indicator Lot P102, Crosstex, USA) had a certified population of 2.2×10^6 and a D-value of 1.6 kGy. The manufacturer's spore population claim was verified, and samples were prepared and irradiated with e-beam at a nominal dose of 3.5 kGy. Irradiated samples were immediately (within 30 min) incubated at 2–8 °C and microbiologically analysed at designated time intervals: 0, 24, 48, 72 and 96 h. Grown colonies were enumerated and colony forming units (CFU) calculated. Viable counts (CFU) recovered at different time points were statistically compared to determine the population stability over time. Spore population claim verification, sample preparation, irradiation and microbiological analysis were carried out as described in the current paper.

2.2. Sample preparation

Commercial *Bacillus pumilus* (ATCC 27142) biological indicator (BI) paper strips were used in this study. Spores were supplied by Crosstex (USA, Lot P104) as a certified population containing 2.6×10^6 viable spores (colony forming units (CFU)) per paper strip with a D-value of 1.7 kGy based on the manufacturers test method. The spore population claim was verified following the manufacturer's instructions prior to running the experiment. In brief, the procedure was carried out as described for *B. pumilus* recovery with the addition of a heat shock treatment where biological indicators were first incubated at 65–70 °C for 15 min and then rapidly cooled to below 4 °C. *B. pumilus* samples for X-ray and gamma irradiation were prepared as described by Tallentire et al. (2010) and Tallentire and Miller (2015) with modifications. Briefly, individual *B. pumilus* spore strips were carefully secured in the middle of a Petri dish, without breaking the sterile barrier. Absorbed dose was measured with Alanine dosimeters (Harwell Dosimeters, UK), placed in a Petri dish next to each spore strip (Fig. 1). Samples were prepared differently for e-beam irradiation: two WINdose dosimeters (GEX, USA) were secured to a spore strip (each from one side) and then taped to the middle of a paper envelope (Fig. 1). Two new spore strips were then taped, one on the left and the other on the right side of the dosimeter. Duplicate spore strips were used for microbiological analysis, while the strip placed between two dosimeters was only used for reference dose measurement.

2.3. Irradiation of Bacillus pumilus spores

Dose mapping experiments were conducted for all technologies to determine the maximal and minimal dose zones, reproducibility, and dose rate of the process. Different configurations were designed and trialled to establish a set-up capable of precise dose delivery (data not shown). Once the configuration was established, spore strips were irradiated in duplicates, either placed in Petri dishes (X-ray and gamma) or as duplicate BI's placed in a paper envelope (e-beam). Petri dishes have been processed in static mode with a fix irradiation field dose rate for the X-ray or gamma at 1 kGy dose increments. Each set of duplicates received a nominal dose of 1, 2, 3, 4, 5 or 6 kGy. After exposure to the nominal dose for a particular set of duplicates was achieved, *B. pumilus* spore strips were retrieved for microbiological analysis, while Alanine dosimeters were retrieved for measurement of the absorbed dose. To evaluate the impact of dose rate on inactivation efficacy, samples were treated at different fixed dose rates: 1 or 10 kGy/h with gamma, and 10 or 200 kGy/h with X-ray. The X-ray dose rate is directly proportional to the electron beam current, and it was modified by changing this current. E-beam treatment was performed at 2000 kGy/h, and samples received a nominal dose (1, 2, 3, 4, 5 or 6 kGy) with a single conveyance through the electron field. All irradiated *B. pumilus* spore strips were kept at 2–8 °C and microbiologically analysed within 72 h of treatment. Spore samples were transported in temperature controlled boxes (2–8 C°; Peli Biothermal, UK).

2.4. X-ray, gamma, and e-beam irradiation systems

STERIS AST Radiation Technology Center (RTC) in Däniken (Switzerland), Tullamore (Ireland) and in Bradford (UK) were utilized for X-ray, e-beam, and gamma treatment, respectively. With X-ray, *B. pumilus* spore strips were treated with photons achieving a maximal energy of 7 MeV (560 kW) using a Rhodotron TT1000 (IBA, Belgium) electron accelerator. Radiation source for gamma was Cobalt-60, with an activity of approximately ~330 kCi. E-beam treatment was performed using a 10 MeV (5 kW) electron accelerator (Mevex, Canada) with a horizontal beam delivery. All treatments were carried out at ambient atmosphere and temperature. Temperature indicators (GEX, USA) with a detection range of 27.5 °C–65 °C were used to measure the maximal temperature achieved during treatment.

2.5. Evaluation of the absorbed dose

For gamma and X-ray, Alanine dosimeters (detection range 0.1–100 kGy) were analysed using an electron spin resonance spectroscopy dosimetry system (Aerial/Bruker MS5000). For e-beam, GEX B3 WINdose radiochromic thin film dosimeters were measured using a dosimetry system based on a visible spectrophotometer (Thermo Fisher Genesys 20). Dosimetry systems were calibrated for condition of use against the National Physics Laboratory (NPL, UK). Dosimetry system uncertainty has been assessed at 4% ($k = 2$) for Alanine and at 6% ($k = 2$) for GEX dosimetry.

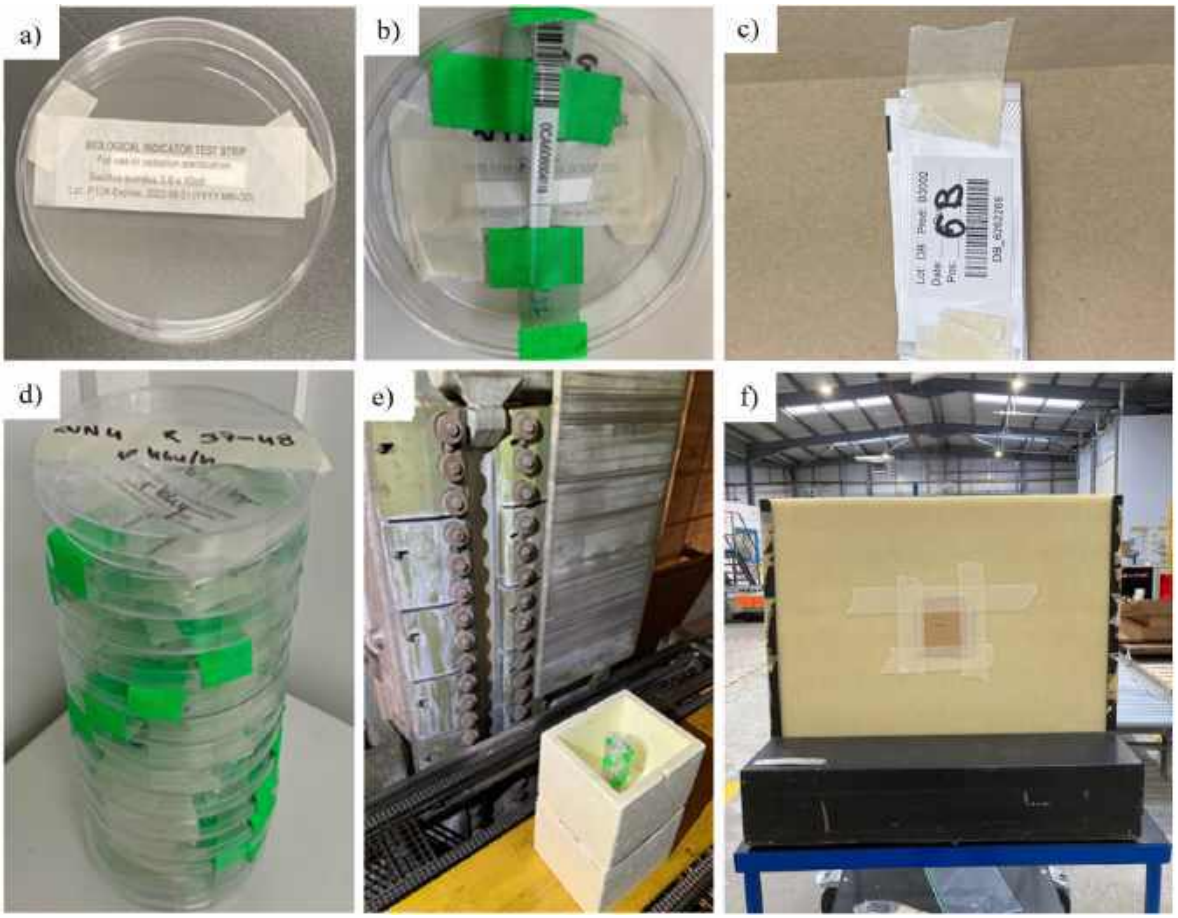

Fig. 1. Experimental set-up. Sample preparation (configuration) was identical for X-ray and gamma: biological indicators were placed in a Petri dish (a) together with dosimeters (b), and stacked Petri dishes were irradiated (d). Placement at X-ray in static mode in front of the beam is shown in panel e. For e-beam irradiation, one biological indicator was placed in between two dosimeters and taped in the middle of a paper envelope (c), while two individual biological indicators used for microbiological analysis were then taped, one on the left and the other on the right side of the dosimeter (not shown in the figure). Sample placement on the carrier (paper envelope fixed to the middle of the carrier) for e-beam treatment is shown in panel f.

2.6. Bacillus pumilus recovery, plotting a survivor curve and D-value calculation

Untreated *B. pumilus* (N_o) and surviving fraction of treated spores (N) were recovered from spore strips and cultured in Tryptic soy agar (TSA, Biokar, France). First, the spore strips were transferred into a sterile test tube containing 5 mL of sterile dH_2O and 10 sterile 6-mm glass beads. The tube was vortexed until the strip was pulped, and another 5 mL of water was added. Then the tube was vortexed again until a homogeneous suspension was achieved. Serial 1:10 dilutions were aseptically prepared using sterile water and 1 mL of the appropriate dilution was inoculated in TSA agar, in duplicates. Plates were incubated at 30–35 °C, enumerated after 48h of incubation, and colony forming units (CFU) were calculated to quantify the viable bacteria. The survivor curve was generated by plotting the logarithm of the survivor fraction ($\log_{10} N/N_o$) against the absorbed dose. Regression analyses were performed, and average D-values calculated from the slope of the obtained curve (ISO 11138-7:2019), for each technology and dose rate combination.

2.7. Statistical analysis

Student's T-test was used to determine the statistical significance between the population recovered immediately after irradiation (0 h) and after incubation at 2–8 °C (24, 48, 75 and 96 h). Analysis of variance (one-way ANOVA) was used to determine the statistical significance between the obtained D-values. Tests were performed at confidence level (or intervals) alpha of 0.05, using Minitab Statistical Software.

3. Results

3.1. Stability of irradiated spores

The stability of irradiated spores was tested over a time period of 96 h. Spore samples were irradiated with e-beam, at an average absorbed dose of 3.4 ± 0.08 kGy. No statistical difference was found when population recovered immediately after irradiation (CFU at 0 h) was compared with population obtained after designated incubation period at 2–8 °C (CFU at 0, 24, 48, 72 and 96 h). The population was approximately at 4.4 log CFU up to 96 h of incubation, when it increased to 4.6

Table 1
A viable population (CFU) of spores recovered immediately after irradiation (0 h) and after 24, 48, 72 and 96 h of treatment. Spores were incubated at 2–8 °C.

Runs	Log CFU at investigated time points				
	0 h	24h	48h	72 h	96 h
Run 1	4.48 ± 0.05	4.39 ± 0.17	4.48 ± 0.15	4.41 ± 0.07	4.43 ± 0.01
Run 2	4.42 ± 0.20	4.44 ± 0.03	4.37 ± 0.01	4.53 ± 0.20	4.65 ± 0.14
Run 3	4.42 ± 0.18	4.37 ± 0.01	4.41 ± 0.11	4.43 ± 0.08	4.74 ± 0.06
Average	4.44	4.40	4.42	4.46	4.61

log CFU (Table 1). Although the increase in CFU was not statistically significant, for the purpose of this study a time point of 72 h was selected as the last stable point. Therefore, further microbiological analysis was carried out within 72 h of irradiation.

3.2. Absorbed doses

Considering that accurate dose delivery is crucial for obtaining reliable results in inactivation experiments, the absorbed dose of each sample was monitored in the study. The absorbed doses during treatment at each nominal dose are shown in Table 2.

3.3. Temperature

During treatment with gamma and e-beam, the temperature was below the detection limit for GEX temperature indicators (27.50 °C). During X-ray processing at 10 kGy/h, the temperature was observed to increase from an average starting temperature of 32 ± 2 °C to 36 ± 2 °C at the end of irradiation. Similarly, at a dose rate of 200 kGy/h, the temperature increased from 29 ± 1 °C to 34 ± 3 °C.

3.4. B. pumilus survivor curves and resistance to irradiation with regards to irradiation technology and dose rate

The regression analysis indicated that all survivor curves were $\log_{10}$ linear (ISO 11138-7:2019) within the investigated dose range, irrespective of the dose rate applied, with all $R^2 \geq 0.95$. The curves with corresponding R^2 values are shown in Fig. 2. Based on the slope of the obtained curves, the D-values were calculated and compared (Fig. 3). No statistical difference ($p > 0.05$) was found between irradiation sources, irrespective of the dose rate applied.

4. Discussion

To ensure that the microbiological growth response is a valid representation of the sterilization efficacy of the process, there should be adequate control over the biological indicator recovery system (Caputo et al., 1980). Namely, there should be a control over the length of time elapsed between exposure to a sterilant and growth testing, and the temperature at which microorganisms are incubated before the microbiological analysis, as these factors are known to impact the recovery of treated microorganisms (Caputo et al., 1980). In this study, the recovery of irradiated spores (CFU) was comparable for all tested time points. A slight increase in CFU was observed at 96 h post treatment, and although this change was not statistically significant, the previous time point (72 h) was selected as a timeframe for carrying out microbiological analysis. Therefore, all spore samples in this study were incubated at 2–8 °C immediately after irradiation (within 30 min of treatment), transported at temperature-controlled conditions and microbiologically analysed within 72 h of irradiation.

Table 2
Absorbed doses of samples during irradiation with gamma-rays, X-rays, and electron beam radiation at different dose rates. Data are shown as means of three independent runs ±1 standard deviation.

Radiation technology	Dose rate (kGy/h)	Absorbed dose during treatment at each nominal dose (kGy)					
		1	2	3	4	5	6
Gamma	1	1.00 ± 0.02	2.00 ± 0.03	2.95 ± 0.06	3.91 ± 0.08	4.86 ± 0.11	5.86 ± 0.11
	10	1.02 ± 0.02	2.07 ± 0.03	3.06 ± 0.08	4.03 ± 0.05	5.09 ± 0.06	6.15 ± 0.10
X-ray	10	1.01 ± 0.01	2.00 ± 0.01	2.97 ± 0.04	3.99 ± 0.06	5.04 ± 0.06	6.10 ± 0.12
	200	0.98 ± 0.04	2.09 ± 0.20	2.87 ± 0.08	3.92 ± 0.04	4.97 ± 0.15	6.34 ± 0.22
E-beam	2000	0.92 ± 0.10	2.05 ± 0.10	3.02 ± 0.08	4.12 ± 0.13	5.10 ± 0.10	6.0 ± 0.00

The resistance ofB. pumilus was examined under the following experimental conditions: gamma 1 kGy/h; gamma 10 kGy/h; X-ray 10 kGy/h; X-ray 200 kGy/h and e-beam 2000 kGy/h. The configuration used in the experiment supported accurate and uniform dose delivery, which is evidenced by the absorbed dose results (Table 2), but also in the clear clustering of data points when recovered microorganisms were plotted against the absorbed dose (Fig. 2, panel f). The regression analysis indicated that all inactivation curves were $\log_{10}$ linear ($R^2 \geq 0.95$) within the investigated dose range of 1–6 kGy. A $\log_{10}$ linear correlation between bacterial inactivation and the treatment dose of ionizing radiation was previously reported by others (Tallentire et al., 2010; Zhang et al., 2020). A non-linear (biphasic) inactivation curve for *B. pumilus* has been reported by Tallentire and Miller (2015); however, the inactivation still followed the first-order kinetics up to about 6 kGy, whereas for doses above 6 kGy, inactivation occurred at an increased rate. Findings from this study support first order model, where a plot of the logarithm of surviving fraction against time yields a straight line, and the inactivation rates are expressed in terms of decimal reduction time, or D-value, which is the reciprocal of the specific inactivation rate at a particular dose of the agent. However, there are many exceptions to the simple first-order type kinetics, especially when microorganisms are exposed to relatively mild inactivation that frequently yield a low number of log reductions (Rowan, 2019) that can produce non-log linear inactivation curves; moreover, these inactivation curves may exhibit pronounced initial shoulders, extended tails, or sigmoid curves that are challenging to fit to the primary data (Rowan et al., 2015). Effective modelling of microbial inactivation arising from physical, chemical or gaseous treatment modalities typically requires the plot to encompass a 6 log microbial count (or survival ratio) versus time data (Buzrul, 2017) for several reasons. Firstly, such a dose-response curve is necessary to address the potential occurrence of microbial variance and resistance to the applied stress that may take different inactivation shapes interpreted through a mathematical best-fit (Garre et al., 2020). A large number of log-reductions are required to effectively interpret and fit inactivation plots (Rowan, 2019), and 6 log reduction has also been shown to support and enable the irreversible destruction of treated microorganisms by way of demonstrating simultaneous occurrence of cellular and molecular damage through 'lethal hits' (Farrell et al., 2011; Hayes et al., 2013; Gérard et al., 2019; Franssen et al., 2019; Fitzhenry et al., 2021). As evident from these findings, when microorganisms are exposed to irradiation, the concentration of surviving *B. pumilus* spores decreases exponentially with dose. This infers the inactivation process reflects a first-order reaction where lethal events occur at random over time with a defined population of spores, which are similarly susceptible to the agent (Klotz et al., 2007). As reported in this study, the first order kinetics are aligned with the physical nature of the process. Thus, when a uniform suspension of microorganisms is irradiated, quanta of radiant energy interact with spores in a random stochastic, which from first principles, implies that lethal 'hits' are distributed in a Poissonian manner (Klotz et al., 2007). These findings suggest that spores in a pre-determined population are equally susceptible to death resulting from a single hit in a dried treatment state. In contrast to radiation, moist heat may differ where treated microorganisms do not all receive the same dose of energy per unit time, as the kinetic energy of water molecules are distributed according to the Mazwell-Botzmann distribution (Klotz et al., 2007).

No significant statistical difference was detected between the obtained D-values, indicating that all radiation technologies (gamma, X-ray, and e-beam) were equally effective at inactivating the challenge microorganism, regardless of the dose rate applied. D-values were

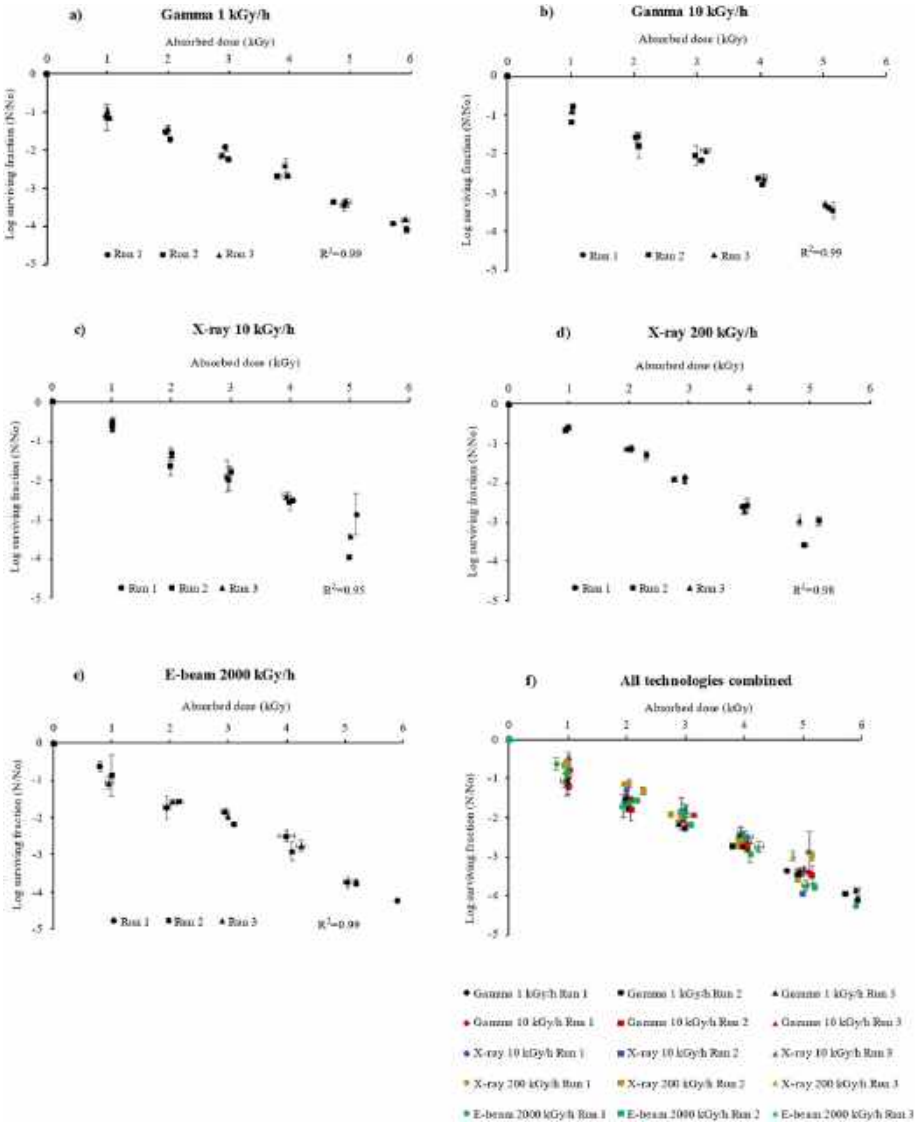

Fig. 2. Inactivation of *B. pumilus* spores treated with (a) Gamma 1 kGy/h, (b) Gamma 10 kGy/h, (c) X-ray 10 kGy/h, (d) X-ray 200 kGy/h and (e) e-beam 2000 kGy/h. Data points for all investigated technologies are plotted together in panel f. Error bars represent the standard deviations for absorbed dose (horizontal) and counts of microorganisms (log CFU; vertical). R^2 values are calculated as means of three independent runs (panels a–e).

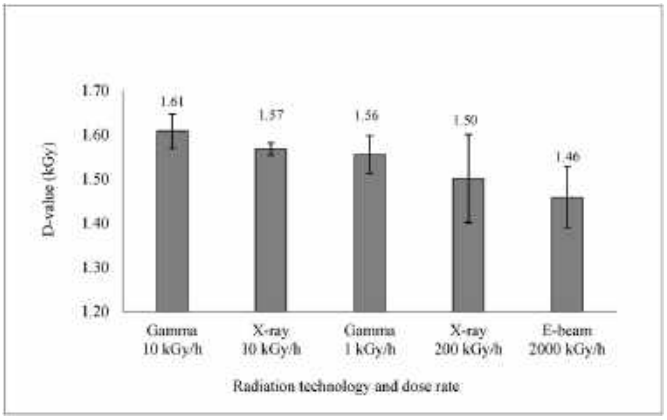

Fig. 3. D-values of *B. pumilus* treated with gamma, X-ray, and e-beam at different dose rates. Data are shown as means ± standard deviation.

within a range of 1.46–1.61 kGy. The finding that dose rate had no impact on microbial inactivation supports the possibility of dose transfer between technologies. Other researchers have obtained similar results for B. pumilus *treated with industrial irradiators (gamma and* 10 MeV *e-beam)*; for example, Tallentire et al. (2010) reported a D-value of 1.5 for both technologies, while Hansen et al. (2020) also found the two technologies to be comparable and reported D-values within a range of 1.2–1.5 kGy. On the other hand, some authors have reported results showing variance when investigating the dose-rate effect and microbicidal efficacy of radiation technologies (Jung et al., 2015; Song et al., 2016; Kyung et al., 2019; Begum et al., 2020). However, such results are often difficult to compare as studies have been carried out under differing test conditions (not always applicable to industrial sterilization settings) and product types.

Although dose rate is a critical parameter, other factors, including temperature and energy level, may also differ between the technologies. The bactericidal effects of ionizing radiation may be enhanced at elevated temperatures (usually above 45 °C), however, this synergistic effect is characteristic for vegetative cells, while spores are impacted to a much lesser extent, as pointed out by Emborg (1974) and Silva Aquino (2012). To evaluate the potential impact of such parameters on the

radiation resistance of *B. pumilus*, spores were treated with gamma and X-ray operating at the same dose rate, and temperature was monitored during treatment. However, it is not possible to determine the exact temperature difference between the two technologies due to the limitations of the measuring system. A higher temperature was detected in the X-ray bunker, where spores were exposed to at least ~5 °C higher temperature than gamma at the beginning and at least ~9 °C higher temperature at the end of the treatment. More importantly, the maximum temperature detected in this study was 36 °C which is unlikely to influence the rate of inactivation of the spores. Regarding the differences in the energy level of the two radiation sources, gamma emits two wavelengths of high energy rays (1.17 and 1.33 MeV), while 5–10 MeV X-ray emits a spectrum of photon energies with a peak occurring at approximately 0.3 MeV, as highlighted by Meissner et al. (2000) and McEvoy et al. (2020). Considering that comparable D-values ($p > 0.05$) were obtained for both technologies operating at 10 kGy/h, the results suggest that when the potential impact of the dose rate was excluded, the variability in temperature and energy levels used in this research had no impact on microbicidal effectiveness of the source.

As previously pointed out by Tallentire et al. (2010), in industrial sterilization of medical devices the microorganisms are commonly irradiated in a "dry" state, although "dryness" is not precisely defined, and it is often a function of the ambient relative humidity. The goal of this study was to evaluate biological indicator spores in a 'dry' physiological state, as being representative of a significant microbiological challenge in industrial sterilization processing. Hence, based on the experimental conditions, results reported in this study suggest that the sterilization dose can be transferred between modes of irradiation in industrial sterilization of medical devices, without causing any impact on the sterility assurance level (SAL), as long as the specified dose is delivered. This finding is particularly relevant to the ecosystem of industry, but also regulators and academia, who seek evidence-based findings to further enable and advance a transition from gamma to X-ray.

5. Conclusions

All investigated technologies (gamma, X-ray, and e-beam) showed log-linear inactivation kinetics ($R^2 \geq 0.95$) and were equally efficient to inactivate *B. pumilus*, which is indicated in comparable D-values ($p > 0.05$), regardless of the dose rate applied.

Considering that dose rate had no impact on sterilization efficacy, the data suggests that an easier transition can be obtained within different ionizing radiation technologies without extensive work related to the sterilization effects as a function of the dose rate. That is, the results reported herein suggest that transfer of minimum doses required for inactivation is possible between irradiators of the same and/or different irradiation source without impacting the sterility assurance level (SAL), in accordance with ISO11137-2:2013.

Funding

This research did not receive any specific grant from funding agencies in the public, commercial, or not-for-profit sectors.

Authors contribution statement

Brian McEvoy participated in designing the experiment, interpreting the results and took the lead in writing the manuscript. Ana Maksimovic carried out microbiological analysis and participated in interpreting the results and writing the manuscript. Daniel Howell, Pierre Reppert, Damien Ryan, and Hervé Michel carried out irradiation experiments. Neil Rowan assisted in writing and reviewing the manuscript and supported the research through all stages. All authors provided critical feedback and helped shape the research, analysis, and manuscript.

Declaration of competing interest

The authors declare that they have no known competing financial interests or personal relationships that could have appeared to influence the work reported in this paper.

Data availability

Data will be made available on request.

Acknowledgments

We gratefully acknowledge the support of STERIS personnel at gamma Radiation Technology Centre (RTC) Bradford, X-ray RTC Däniken and e-beam RTC Tullamore sites for their help with dosimetry and sample treatment. We are thankful to personnel working in STERIS laboratories (Thorne and Tullamore) for their help with microbiological analysis and logistical support.

References

Begum, T., Follett, P.A., Hossain, F., Christopher, L., Salmieri, S., Lacroix, M., 2020. Microbicidal effectiveness of irradiation from Gamma and X-ray sources at different dose rates against the foodborne illness pathogens *Escherichia coli, Salmonella Typhimurium* and *Listeria monocytogenes* in rice. LWT (Lebensm.-Wiss. & Technol.) 132, 1–6. https://doi.org/10.1016/j.lwt.2020.109841.

BPSA, 2021. X-Ray Sterilization of Single-Use Bioprocess Equipment. Part I-Industry Need, Requirements and Risk Evaluation. BPSA; Bio-Process System Alliance.

Buzrul, S., 2017. Evaluation of different dose-response models for high hydrostatic pressure inactivation of microorganisms. Foods 6 (9), 79. https://doi.org/10.3390/foods6090079.

Caputo, R.A., Rohn, K.J., Mascoli, C.C., 1980. Recovery of biological indicator organisms after sublethal sterilization treatment. PDA J. Pharm. Sci. Technol. 34, 304–307.

Dethier, P., 2016. Industrial Gamma and X-Ray: Same but Different. IBA whitepaper.

Emborg, C., 1974. Inactivation of dried bacteria and bacterial spores by means of gamma irradiation at high temperatures. Appl. Microbiol. 5, 830–833. https://doi.org/10.1128/am.27.5.830-833.1974.

Farrell, H., Hayes, J., Laffey, J., Rowan, N., 2011. Studies on the relationship between pulsed UV light irradiation and the simultaneous occurrence of molecular and cellular damage in clinically-relevant Candida albicans. J. Microbiol. Methods 84 (2), 317–326. https://doi.org/10.1016/j.mimet.2010.12.021.

Fifield, L.S., Pharr, M., Staack, M., Pillai, S.D., Nichols, L., McCoy, J., Faucette, T., Bisel, T.T., Huang, M., Hasan, M.K., Perkins, L., Cooley, S.K., Murphy, M.K., 2021. Direct comparison of gamma, electron beam and X-ray irradiation effects on single-use blood collection devices with plastic components. Radiat. Phys. Chem. 180, 1–26. https://doi.org/10.1016/j.radphyschem.2020.109282.

Fitzhenry, K., Clifford, E., Rowan, N., Va del Rio, A., 2021. Bacterial inactivation, photoreactivation and dark repair post flow-through pulsed UV disinfection. Bacterial inactivation, photoreactivation and dark repair post flow-through pulsed UV disinfection. J. Water Process Eng. 41 https://doi.org/10.1016/j.jwpe.2021.102070.

Franssen, F., Gerard, C., Cozma-Petrut, Vieira-Pinto, V., Rezek Jambrak, A., Rowan, N., Paulsen, P., Rozycki, M., Tysnes, K., Rodriguez-Lasaro, Robertson, L., 2019. Inactivation of parasite transmission stages: efficacy of treatmen. Trends Food Sci. Technol. 83, 114–128. https://doi.org/10.1016/j.tifs.2018.11.009ts on food of animal origin.

Garre, A., Zwietering, M.H., den Besten, H.M.W., 2020. Multilevel modelling as a tool to include variability and uncertainty in quantitative microbiology and risk assessment. Thermal inactivation of Listeria monocytogenes as proof of concept. Food Res. Int. 137, 1–13. https://doi.org/10.1016/j.foodres.2020.109374.

Gérard, C., Franssen, F., La Carbona, S., Monteiro, S., Cozma-Petrut, A., Utaaker, J., Rezek Jambrak, A., Rowan, N., Rodriguez-Lazaro, D., Nasser, A., Tysnes, K., Robertson, L.J., 2019. Inactivation of parasite transmission stages: efficacy of treatments on foods of non-animal origin. Trends Food Sci. Technol. 91, 12–23. https://doi.org/10.1016/j.tifs.2019.06.015.

GIPA-Gamma Industry Processing Alliance, 2017. A Comparison of Gamma, E-Beam, X-Ray and Ethylene Oxide Technologies for the Industrial Sterilization of Medical Devices and Healthcare Products. Whitepaper.

Hansen, J.M., Fidopiastis, N., Bryans, T., Luebke, M., Rymer, T., 2020. Radiation sterilization: dose is dose. Biomed. Instrum. Technol. 45–52 https://doi.org/10.2345/0899-8205-54.s3.45.

Hayes, J., Kirf, D., Garvey, M., Rowan, N., 2013. Disinfection and toxicological assessment of pulsed UV and pulsed-plasma gas-discharge treated-water containing the waterborne protozoan enterparasite Cryptosporidium parvum. J. Microbiol. Methods 94 (3), 325–337. https://doi.org/10.1016/j.mimet.2013.07.012.

International Organization for Standardization (ISO), 2013. ISO11137-2:2013. Sterilization of Health Care Products-Radiation-Part 2: Establishing the Sterilization Dose. ISO, Geneva.

International Organization for Standardization (ISO), 2018. ISO11139:2018. Sterilization of Health Care Products — Vocabulary of Terms Used in Sterilization and Related Equipment and Process Standards. ISO, Geneva.

International Organization for Standardization (ISO), 2019. ISO11138-7:2019. Sterilization of Health Care Products-Biological Indicators-Part 7: Guidance for the Selection, Use and Interpretation of Results. ISO, Geneva.

Jung, K., Song, M.M., Kim, M.J., Moon, B.G., Go, S.M., Kim, J.J., Lee, Y.J., Park, J.H., 2015. Effect of X-ray, gamma ray, and electron beam irradiation on the hygienic and physicochemical qualities of red pepper powder. LWT (Lebensm.-Wiss. & Technol.) 63, 846–851. https://doi.org/10.1016/j.lwt.2015.04.030.

Klotz, B., Pyle, D.L., Mackey, B.M., 2007. New mathematical modelling approaching for predicting microbial inactivation by high hydrostatic pressure. Appl. Environ. Microbiol. 73 (8), 2468–2478.

Kroc, T.K., Thangaraj, J.C.T., Penning, R.T., Kephart, R.D., 2017. Accelerator-driven Medical Sterilization to Replace Co-60 Sources. Fermilab-Fermi National Accelerator Laboratory.

Kyung, H.K., Ramakrishnan, S.R., Kwon, J.H., 2019. Dose rates of electron beam and gamma ray irradiation affect microbial decontamination and quality changes in dried red pepper (*Capsicum annuum* L.) powder. J. Sci. Food Agric. 2, 632–638. https://doi.org/10.1002/jsfa.9225.

McEvoy, B., Michel, H., Howell, D., Roxby, P., 2020. X-Ray: an effective photon. Biomed. Instrum. Technol. 54, 23–30. https://doi.org/10.2345/0899-8205-54.s3.23.

Meissner, J., Abs, M., Cleland, M.R., Herer, A.S., Jongen, Y., Kuntz, F., Strasser, A., 2000. X-ray treatment at 5 MeV and above. Radiat. Phys. Chem. 57, 647–651. https://doi.org/10.1016/S0969-806X(99)00431-4.

Michel, H., Kroc, T., McEvoy, B.J., Patil, D., Reppert, P., Smith, M.A., 2021. Potential induced radioactivity in materials processed with X-ray energy above 5 MeV. Biomed. Instrum. Technol. 55, 17–26. https://doi.org/10.2345/0899-8205-55.s3.17.

Montgomery, A., Bolle-Reddat, R., Formica, S., Lundahl, B., McDonnell, G., 2021. Regulatory approach for transitioning from gamma ray to X-ray radiation sterilization. Biomed. Instrum. Technol. 55, 58–66. https://doi.org/10.2345/0899-8205-55.s3.58.

Murray, K.A., Kennedy, J.E., McEvoy, B., Olivier, V., Ryan, D., Higginbotham, C.L., 2012. The effects of high energy electron beam irradiation on the thermal and structural properties of low density polyethylene. Radiat. Phys. Chem. 8, 962–966. https://doi.org/10.1016/j.radphyschem.2011.09.011.

Murray, K.A., Kennedy, J.E., McEvoy, B., Vrain, O., Ryan, D., Cowman, R., Higginbotham, C.L., 2014. The influence of electron beam irradiation on the mechanical and thermal properties of Poly (ether-block-amide) blends. Radiat. Phys. Chem. 1993, 26–30. https://doi.org/10.1016/jradphyschem201304009.

Panel on gamma and electron irradiation (The irradiation panel), 2020. Change of Irradiation Modalities in Radiation Sterilization of Medical Devices– Normative Requirements and Aspects in EN ISO 11137-1.

Rowan, N.J., 2019. Pulsed light as an emerging technology to cause disruption for food and adjacent-industries – quo Vadis? Trends Food Sci. Technol. 88, 316–332. https://doi.org/10.1016/j.tifs.2019.03.027.

Rowan, N.J., Valdramidis, V.P., Gomez-Lopez, V.M., 2015. A review of quantitative methods to describe efficacy of pulsed light generated inactivation data that embraces the occurrence of viable but non culturable state microorganisms. Trends Food Sci. Technol. 44 (1), 79–92. https://doi.org/10.1016/j.tifs.2015.03.006.

Silva Aquino, K. A. da, 2012. Sterilization by gamma irradiation. In: Gamma Radiation. InTech. https://doi.org/10.5772/34901.

Song, B.S., Lee, Y., Moon, B.G., Go, S.M., Park, J.H., Kim, J.K., Jung, K., Kim, D.H., Ryu, S., 2016. Comparison of bactericidal efficiency of 7.5 MeV X-rays, gamma-rays, and 10 MeV e-beams. Radiat. Phys. Chem. 106–108. https://doi.org/10.1016/jradphyschem201603022.

Tallentire, A., Miller, A., 2015. Microbicidal effectiveness of X-rays used for sterilization purposes. Radiat. Phys. Chem. 107, 128–130. https://doi.org/10.1016/j.radphyschem.2014.09.012.

Tallentire, A., Miller, A., Helt-Hansen, J., 2010. A comparison of the microbicidal effectiveness of gamma rays and high and low energy electron radiations. Radiat. Phys. Chem. 79, 701–704. https://doi.org/10.1016/j.radphyschem.2010.01.010.

Zhang, Y., Huber, N., Moeller, R., Stulke, J., Dubovcova, B., Akepsimaidis, G., Meneses, N., Drissner, D., Mathys, A., 2020. Role of DNA repair in *Bacillus subtilis* spore resistance to high energy and low energy electron beam treatments. Food Microbiol. 87, 1–7. https://doi.org/10.1016/j.fm.2019.103353.

Journal of Applied Microbiology

Journal of Applied Microbiology ISSN 1364-5072

REVIEW ARTICLE

Opportunities for the application of real-time bacterial cell analysis using flow cytometry for the advancement of sterilization microbiology

B. McEvoy[1], M. Lynch[2] and N.J. Rowan[2]

1 STERIS Applied Sterilization Technologies, IDA Business and Technology Park, Tullamore, Ireland
2 Centre for Disinfection, Sterilization and Biosecurity, Athlone Institute of Technology, Athlone, Ireland

Keywords
bacterial endospores, flow cytometry, medical devices, real-time monitoring, sterilization, terminal gaseous sterilization, vaporized hydrogen peroxide, VH2O2, VHP.

Correspondence
Brian McEvoy, STERIS Applied Sterilization Technologies, IDA Business and Technology Park, Tullamore, Ireland.
E-mail: brian_j_mcevoy@steris.com

2020/1089: received 28 May 2020, revised 10 September 2020 and accepted 21 September 2020

doi:10.1111/jam.14876

Abstract

Medical devices provide critical care and diagnostic applications through patient contact. Sterility assurance level (SAL) may be defined as the probability of a single viable micro-organism occurring on an item after a sterilization process. Sterilization microbiology often relies upon using an overkill validation method where a 12-log reduction in recalcitrant bacterial endospore population occurs during the process that exploits conventional laboratory-based culture media for enumeration. This timely review explores key assumptions underpinning use of conventional culture-based methods in sterilization microbiology. Consideration is given to how such methods may limit the ability to fully appreciate the inactivation kinetics of a sterilization process such as vaporized hydrogen peroxide (VH2O2) sterilization, and consequently design efficient sterilization processes. Specific use of the real-time flow cytometry (FCM) is described by way of elucidating the practical relevance of these limitation factors with implications and opportunities for the sterilization industry discussed. Application of FCM to address these culture-based limitation factors will inform real-time kinetic inactivation modelling and unlock potential to embrace emerging opportunities for pharma, medical device and sterilization industries including potentially disruptive applications that may involve reduced usage of sterilant.

Introduction

Background to sterilization microbiology and the industry

The sterilization marketplace can be subdivided into hospital sterilization (such as point of use), in-house manufacturing sterilization (such as at point of medical device manufacture, often inline applications) and contract sterilization, provided by contractors where medical device manufacturers obtain sterilization services along the supply chain after manufacturing (McEvoy and Rowan 2019). Central to sterilization microbiology is the treatment of medical devices where associated global market is estimated to exceed $400bn (International Trade Administration 2016). An important consideration is the safe use of sterile medical devices that provide critical care and diagnostic applications, whereby patient infection does not arise as a consequence of such patient contact. Addressing hospital-acquired infections (HAIs) and sepsis is a global challenge with an estimated annual cost to healthcare in the United States at $9.8bn (Hensley and Monson 2015) and $20bn (Guirgis *et al.* 2017), respectively. HAIs and sepsis are estimated to affect 1.7 m and 700 000 cases in the United States, respectively. While factors associated with the occurrence of these serious infections are varied, terminal sterilization modalities are unlikely to be point-of-infection due to comprehensive sterilization and validation processes (cited McEvoy and Rowan 2019).

Sterilization microbiology underpinning these processes delivers sterile assurance far above minimum requirements to achieve sterilization for patient safety. To achieve a required sterility assurance level (SAL), a

sterilization process is applied to medical devices prior to patient use. Sterilization validation typically relies upon using an overkill validation method, as shown in Fig. 1, where the process demonstrates a 12-log reduction in recalcitrant bacterial endospore population enumerated on artificial laboratory-based media, where it is assumed that the shape of the inactivation kinetic plot is a straight line and semi-logarithmic when the sterilizing conditions remain consistent for the duration of the exposure time (AAMI 2017). Thus, conventional microbiology assumes the process is predicable based upon probability of linear inactivation kinetic death rate plot. Terminal sterilization processes such as Gamma irradiation, Electron-beam irradiation, X-ray irradiation, gaseous ethylene oxide (EO) and hydrogen peroxide in vapour state are discussed by McEvoy and Rowan (2019).

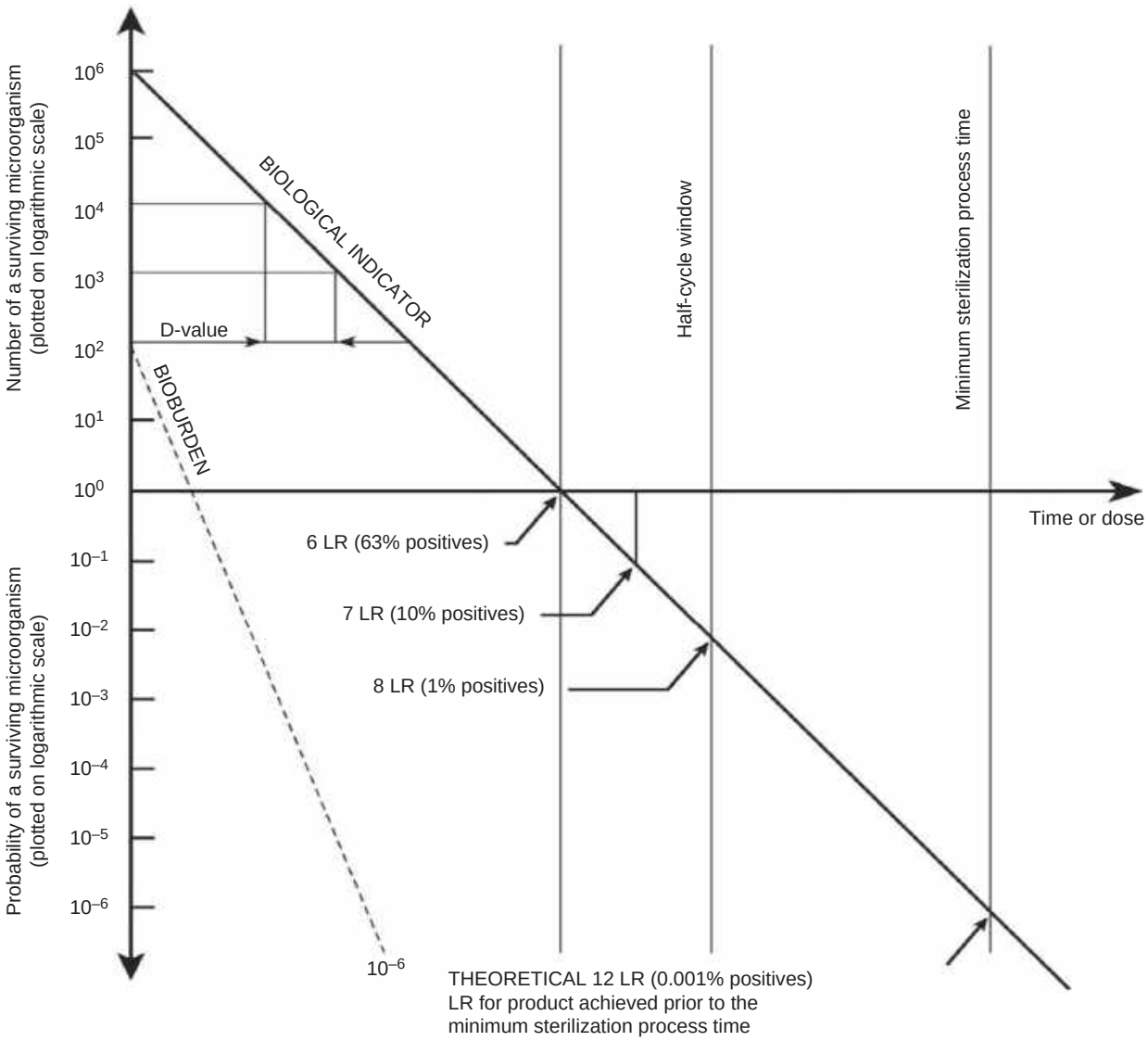

Figure 1 Sterility assurance level and example of the relationship between biological indicator and product bioburden. For illustration purposes, this graphical representation has been obtained from AAMI TIR16:2017. A BI (denoted by full line) has been selected that has a higher population and resistance (*D*-value) than that of the medical device product bioburden (denoted by dashed line). Using an overkill validation method, a sterilization process has been applied at 'half-cycle' parameters with full lethality on the BI. (In EO processing, half-cycle parameter is half of EO exposure time). To deliver the required sterility assurance level of $\leq 10^{-6}$, a further 6 log reduction is applied by doubling the exposure period in the routine process. Microbiological death generally follows first-order kinetics and can be approximated by a straight line on a semi-logarithmic plot when the sterilizing conditions (i.e. process temperature, relative humidity and EO concentration) remain consistent for the duration of the exposure time (AAMI 2017).

SAL is defined as the 'probability of a single viable micro-organism occurring on an item after sterilization' (International Organization for Standardization [ISO] 2018a), and a sterilization process defined as a 'series of actions or operations needed to achieve the specified requirements for sterility' (ISO 2018b). Traditional technologies used in terminal sterilization include EO sterilization and radiation processing using Gamma, Electron beam or X-ray irradiation and are described as Category A sterilization processes by US Food and Drug Administration (FDA), as they are well established, they have a long history of use, and consensus standards (administered by the ISO) are available. Standards such as ISO11135:2014 help (ISO 2014) inform manufacturers and users of the key aspects to be evaluated in defining the sterilization process and subsequent qualification and validation. Underpinning the validation of a sterilization process, in accordance with an ISO standard, is the microbiology assessment of the challenge presented by the medical device and the microbicidal effect of that process on the measured challenge and or where a biological indicator (BI) is chosen to represent such a challenge.

Limitations of current techniques in sterilization microbiology

Uniformity of microbial distribution, bioburden and predictability

Many of the sterilization standards are underpinned by the associated microbiological testing standards such as ISO11737-1 and ISO11737-2, which govern the testing of bioburden and sterility, respectively (ISO 2018a, 2019). Bioburden testing refers to the quantification of natural microflora residing on a medical device product. During a sterilization, a validation process is applied and qualified. As part of the qualification exercise, 'Tests of Sterility' may be applied as part of the demonstration of the process inactivation. Upon completion of such tests, it may be possible to plot an inactivation curve such as that demonstrated in Fig. 1 (McEvoy and Rowan 2019). However, conventional sterilization processes such as EO often require use of a BI population of reasonable uniformity that are reliably predictable in an end-point analysis such as a fractional sterilization process performed during validation.

Microbial diversity, heterogenicity and environmental-stress adaptation

Micro-organisms range in size, form, complexity and diversity including variety of physicochemical and environmental growth requirements for those capable of sustaining independent life, all with individual phenotypic identities. Some micro-organisms are highly complex, such as viruses and parasites, which do not grow on standard laboratory-based media. These fastidious micro-organisms require mammalian cell culture or an appropriate host to propagate, where molecular biology tools are typically used as indirect means of enumerating their number (Garvey *et al.* 2013, 2015). Micro-organisms can respond to changes in the environment where prior exposure to sub-lethal amount of stress has been shown to temper or harden the same micro-organisms against subsequent lethal levels of the same of different stresses (Rowan 1999, 2019). Micro-organisms can communicate to each other via quorum sensing (Wu *et al.* 2015) that further illustrates the importance of each single cell in any population. The heterogenicity of bacterial cells in an evenly distributed homologous culture may be viewed as a consequence of gene expression and cell-to-cell interactions, such as quorum sensing. Consequently, the need for analysis at a single cell level is often required for greater insight that includes both mechanistic and cellular responses to applied or lethal stresses (Farrell *et al.* 2011; Wu *et al.* 2015). As highlighted by Geier *et al.* (2008), 'social interactions among bacteria are more specific than interactions with the environment', through signalling compounds called auto-inducers. In addition, research by García-Contreras *et al.* (2015) highlights the role for quorum sensing in protecting cells from a wide range of environmental stresses. The phenotypic outcomes of such responses to stress environments, further add to the complexity of micro-organism populations, particular those in stressed state as would be expected during sterilization inactivation. The importance of phenotypic heterogenicity can manifest in the inactivation kinetics of a population to an environmental stress such as a disinfectant or sterilization process: Stone *et al.* (2009) offered an explanation for nonlinear inactivation kinetics due to the 'vitalistic theory, which holds that the resistance of individual cells in a population is not the same but follows a distribution'. Humpheson *et al.* (1998) further define the vitalistic theory, where in 'a genetically homogeneous population, phenotypic variation exists such that resistance to a lethal agent is not uniform'. Furthermore, when one considers superdormant spores as a microbial defence mechanism, the importance of heterogenicity in phenotypic composition with varying germinant receptors is apparent (Dembek *et al.* 2013; Ghosh and Setlow 2009; Zhang *et al.* 2012). Hence, such phenotypic variation in a population should be considered in sterilization microbiology. Most sterilization methods rely on 'overkill', or in other words a conservative over-processing with sterilant to provide the greatest level of assurance. However, as a consequence of that over-processing is the over

application of a hazardous sterilant like EO gas or a material affecting radiation such as gamma. If in the future, workers may seek to deliver reduced and targeted processes, and therefore the need to fully appreciate the behaviours of the microbiological target becomes even more pressing. As researchers strive for greater levels of understanding of inactivation kinetics to deliver more measured and potentially reduced processes, understanding of the aforementioned microbial mechanisms and behaviours in sterilization microbiology must be considered.

Binary growth of micro-organism and culture conditions post-treatment

Cell culture techniques in sterilization microbiology provide binary information, namely 'growth' and 'no-growth'. Microbial viability is determined by counting live cells based upon their ability to grow on artificial-laboratory-based media such as agars or broths under aerobic cultivation over a typical 48-h incubation at optimal temperature, where failure of similarly treated populations of micro-organisms to grow are presumed dead (Hayouni *et al.* 2008; Rowan *et al.* 2015; Léonard *et al.* 2016). Furthermore, culture-based techniques assume that one colony forming unit has emanated from a single cell, which may not be the case as a colony can arise from one or more cells. This limitation has been highlighted by many authors such as Ou *et al.* (2017); Laflamme *et al.* (2005); Mtimet *et al.* (2017); Reis *et al.* (2005) and therefore has the potential to underestimate the microbiological population being examined. Furthermore, as identified by both Ou *et al.* (2017) and Laflamme *et al.* (2005), culturability is inherently dependent on culture conditions. The binary nature of traditional culture techniques in sterilization microbiology provides little information regarding the heterogenicity of a population, phenotypic states as a micro-organism transitions from live to dead, or environmental conditions such as presence or absence of oxygen (Rowan 1999; Rowan *et al.* 2015).

Ability to recover and understand intermediate microbial states post-treatment

The ability to recover or resuscitate micro-organisms following a sterilization treatment is a key consideration, in that it may influence the ability to quantify and/or verify the efficacy of sterilization treatment (McEvoy and Rowan 2019). The risks associated with non-recovery of viable micro-organisms may be minimized with the use of reference micro-organisms, such as BIs, as recovery may be well characterized and prescribed with culture conditions. Investigations into BI grow-out times by Gillis *et al.* (2010) highlight some of the considerations with recovery of damaged micro-organisms. The authors identify that out-growth of a non-sterile BI is a function of (i) initiation of spore germination, (ii) conversion to the cell form and (iii) cellular metabolism and cell division and multiplication (Gillis *et al.* 2010). Therefore, if one considers a traditional sterility test where a BI is immersed in test media and the goal is to be able to recover a single viable micro-organism, then these multiple events must occur, successfully. The authors postulate that delayed outgrowth of BIs is likely to be a consequence of the delayed germination time of a damaged spore. If this is a correct assumption, then the significance of the test media and its ability to provide required conditions for the germination apparatus to operate effectively, should not be underestimated. If, however, natural bioburden population is being examined, an understanding of the identity of the micro-organisms is necessary to ensure culture conditions for recovery are appropriate. If one considers the proposal of Keller and Zengler (2004); 'As we now understand, >98% of the micro-organisms in our environment cannot be kept in culture, culture-independent technologies are required that can characterize (micro-organisms) precisely' (Müller and Nebe-Von-Caron 2010). These and other authors (Taimur Khan *et al.* 2010; Rowan 2011; Wilkinson 2018) highlighted that some micro-organisms may fail to grow in culture media simply due to fact that they may be missing a special requirement such as a growth factor or a symbiotic support.

Micro-organisms may exist in a viable but not culturable (VBNC) state, which has been observed as a consequence of applying a lethal or sub-lethal stress, such as that experienced during a decontamination or process technology (Rowan *et al.* 2015). The authors postulated that 'evidence suggests that these harsh environment cues (operational parameters of the pulsed light treatment and biological factors) may trigger a switch to the adaptive survival VBNC state in PL (pulsed light) treatments'. The concept of VBNC has been observed in many micro-organism species (Rowan 2004; Oliver 2005; Rowan *et al.* 2015) and one could therefore hypothesize that transitionary phases (rapid inactivation, slower inactivation and VBNC) in a homologous population may occur as a consequence of progressive cellular activity upon contact with a sterilizing agent. Stress conditions result in other subpopulations and phenotypes such as VBNC which have lost their ability to grow on culture media, but continue to demonstrate metabolic activity (Léonard *et al.* 2016). Therefore, aside from the significance of not being capable of recovering a viable fraction of the treated population, this limitation also hinders the understanding of inactivation kinetics and the true mechanisms of the lethal agent in the life cycle of the micro-organism and cellular responses to stress.

Bacterial 'Viability' versus 'Vitality'

Bacterial viability may be defined as the ability to grow whereby key properties of structural, genetic, metabolic function to facilitate growth (Wilkinson 2018). Traditional culture techniques are able to detect such viability, for a given set of culture conditions. As already stated, many micro-organisms cannot be recovered or maintained in culture due to fastidious nutrient and condition needs. Hence, as stated by Wilkinson (2018), we arrive at a new term of 'Vitality'. The work of Kramer and Thielmann (2016) investigated the cellular activity associated with vitality in food relevant bacteria being treated with mild heat: Using non-culture techniques such as flow cytometry (FCM), the researchers were able to monitor cellular functions and structures such as membrane potential or respiratory activity. Hence, measurement of such cellular vitality indicators at a single cell level can elucidate detailed information regarding microbial inactivation.

Ability to examine mixed cultures

Traditional cell culture techniques seek to segregate and purify culture through the use of selective media and creation of distinct colonies for counting purposes. This unfortunately eliminates possibilities to understand the micro-organism type to micro-organism type interactions, including quorum sensing that may be happening *in situ*. The ability to understand such interactions has been shown to be particularly relevant in bioprocessing such as that described by Rodriguez and Thornton (2008).

Speed of analysis: lack of real-time monitoring and assessment

Traditional culture techniques are a 'time-consuming multiday process', that 'does not provide timely information that is required in applications such as industrial manufacturing, research and medical diagnoses' (Ou *et al.* 2017). This time lag between point of sampling and obtaining any results or information regarding the micro-organism population often renders the information as retrospective. However, the more significant issue is that the information gained from the recovery of a cell or population of cells on a culture plate is not representative of the state of the micro-organism at the point of sampling, as the micro-organisms more often have been recovered and artificially grown on nutrient-enriched media. In industrial bioprocesses, having real-time data allow decision-making during the real-time operation of the bioprocess (Díaz *et al.* 2010). Thus, as a consequence of such limitations, the need for more advanced real-time tools and methods that provide detailed phenotypic insights is merited. One such method with growing application is flow cytometry.

Flow Cytometry

History of Flow Cytometry

If one considers the optics developed by Leeuwenhoek in 1600s, and combine with the experimental apparatus of John Tyndall in the 1800s, the early design of flow cytometry can be imagined (Müller and Nebe-Von-Caron 2010). In the late 1940s, flow cytometers were generated to identify bacterial aerosols in warfare. Through the 1970s, the technology was further developed to a point of being able to detect large viruses. Since the 1980s, flow cytometry has been deployed to many applications with extensive publication of its use (Müller and Nebe-Von-Caron 2010). The review paper by Picot *et al.* (2012) offers a very detailed chronological history of the development of FCM.

As described by Picot *et al.* (2012) and Kalina *et al.* (2020), while many early applications focussed on mammalian cells, flow cytometry has extended to many clinical applications (Brown and Wittwer 2000; Suo *et al.* 2020). Furthermore, there is an increasing evidence that flow cytometry has been extensively used to advance routine microbiology laboratory analysis (Mejuto *et al.* 2017) real-time in vivo clinical determinations (Brown and Wittwer 2000; Kalina *et al.* 2020; Suo *et al.* 2020), and in field environmental monitoring (Safford and Bischel 2019). For example, Kalina *et al.* (2020) have reported on the effective use of FCM in primary immunodeficiencies, immunophenotyping, diagnostics and functional studies. Mejuto *et al.* (2017) have reported on the use of FCM as an effective alternative approach for urine culture in routine clinical microbiology laboratory. Álvarez-Barrientos *et al.* (2000) describe the application of FCM for parasite and virus detection in clinical specimens. Similarly, Glier and Holada (2012) describe how anti-prion monoclonal antibodies conjugates may enable FCM screening of clinical blood samples for prion disease. Safford and Bischel (2019) reviewed the potential of FCM to radically inform applications in waste treatment and reuse. Léonard *et al.* (2016) have reviewed the potential opportunities presented by FCM in the examination of the effect of antimicrobials on sub-populations of micro-organisms.

Principles of Flow Cytometry

Flow cytometry is best described as automated microscopy where thousands of cells can be analysed in a second. FCM quantitatively measures the optical characteristics of cells as they pass in single file in front of a focused light

beam (Veal *et al.* 2000). By measuring fluorescence, either natural or induced by use of fluorescent markers, cells may be differentiated based on size, shape or phenotypic characteristics. The flow cytometer consists of three main components, namely Fluidics, Optics and Electronics for measurement (Goure 2013).

The key aspect of flow cytometry is the measurement of scattered light following impact of the beam from a light source with the individual cells being analysed. Light that is scattered at acute angles, called 'forward scatter' gives an indication of the particle size, whereas light scattered at wider angles, called 'side scatter is proportional to the particles roughness and complexity' (Ambriz-Aviña *et al.* 2014). Even though measurement of light scatter can yield very useful information about bacterial cells, it is unfortunately non-specific to bacterial species. Therefore, fluorescent dyes must be employed in combination to achieve further specificity in the analysis. Cell viability, protein identity and enzymatic activity have been measured in such a manner (Ambriz-Aviña *et al.* 2014).

Another useful advancement of flow cytometry is 'Fluorescence Activated Cell Sorting (FACS)' whereby cells are differentiated and sorted by means of detection of a fluorescent marker using flow cytometry. For the past two decades, flow cytometry (FCM) has been used to investigate micro-organisms and offers an 'accurate technique to identify spores, vegetative cells and the number of viable and dead cells in the given population' (Majeed *et al.* 2018). FCM is a sensitive technique operating in real time that can examine individual cells at rates of 100–1000 cells per second.

Light Scatter

Cell characterization using flow cytometry is achieved by means of measuring light scatter or fluorescence signals (Díaz *et al.* 2010). Examining cells with light scatter yields useful information regarding cell morphology and size: Forward scatter is normally assumed to be proportional to cell size, whereas 'side scatter light has been shown to be affected by intracellular structure and inclusion body formation' (Díaz *et al.* 2010).

Light scatter alone can yield important information about micro-organisms and can be an early differentiator of phenotypic populations. Reis and co-workers observed bimodal side scatter with vegetative cells of *Bacillus licheniformis* (Reis *et al.* 2005). Similarly, Hewitt *et al.* (1999) and Schenk *et al.* (2011) observed a bimodal distribution of side scatter light with *Escherichia coli*, which is characteristic of rod-shaped micro-organisms explained by Hewitt *et al.* (1999), as most likely due to 'an elongated cell's orientation as it travels through the laser beam can vary in range from the major to the minor axis'. Comas-Riu and Vives-Rego (2002) observed bimodal light distribution of forward scatter light from *Paenibacillus polymyxa* spores, and upon further investigation with a staining protocol using propidium iodide (PI) and Syto 13, observed two distinct phenotypic populations, one permeable to PI (and weakly permeable to Syto13) and the other sub-population impermeable to both dyes. Hence, light scatter in this case (unlike that in Reis and Hewitt studies) served as an early indication of phenotypic variation, which was then confirmed by further exploratory work.

FCM analysis of light scatter may also detect autofluorescence of micro-organisms. As highlighted by Magge *et al.* (2009), autofluorescence may occur in some species as a consequence of spore coat components such as dityrosine which cross-links through oxidation activities involving peroxidase and oxidase. Hence, in the design of a FCM experiment, it may be necessary to consider the addition of a negative control for autofluorescence as adopted by Zhang *et al.* (2020) in the execution of their research.

Use of Fluorescent probes

However, when looking at microbial cells, given their size, light scatter profiles alone may yield insufficient information. Hence, the use of fluorescent probes has proved to be a useful methodology when combined with flow cytometry. Fluorescent probes work from the principle that the wavelength of emission will be longer than that of excitation and the difference between the two, described as the Stokes shift, determines the effectiveness of the probe (Davey and Kell 1996; Adan *et al.* 2017).

Various fluorescent probes may be used to determine the physiological state of the organism and help differentiate a population by viability state. Probes such as those examples described in Table 1, may be used based on cell interaction characteristics to identify a population or may even be used to count micro-organisms. Probes used in flow cytometry studies may be divided into two broad groups: (i) nucleic-acid-binding dyes and (ii) metabolic/cellular/protein-binding dyes (Mathur *et al.* 2016).

Trevors (2003) describes the advantages and limitations of the use of fluorescent probes in bacterial research. Combinations of dyes may be used to generate 'multiparametric data' from individual cells in a heterogeneous population (Wilkinson 2018). The key properties favourable in a fluorescent probe include (i) biologically inert, (ii) a high extinction coefficient and a high quantum yield so that small concentrations of the stain can be detected within the cell, (iii) a narrow emission spectrum to avoid overlapping, (iv) photostability, (v) low toxicity and (vi) solubility in water (Díaz *et al.* 2010).

Table 1 Selection of Fluorescent stains commonly used with flow cytometry

Probe	Property	Cell fraction identified	References
Carboxyfluorescein diacetate (cFDA)	Intracellular esterase activity	Viable cell fraction	Majeed *et al*. (2018); Cronin and Wilkinson (2008); Wilkinson (2018)
DiBAC4	Anionic structure which enters cell and binds to intracellular proteins	Membrane potential	Buysschaert *et al*. (2016)
Dihydroethidium (HE)	Oxidation of HE results in formation of ethidium which, in turn, binds with DNA yielding fluorescence	Reactive oxygen species	Buysschaert *et al*. (2016)
Ethidium Bromide (EB)	Positively charged monovalent compound used to evaluate efflux pump system. Enters intact cells but is pumped out. However, where membrane and efflux pump is damaged, intracellular DNA is stained	Efflux pump and membrane activity	Léonard *et al*. (2016)
Fluorescein	Binds to proteins	Protein	Cronin and Wilkinson (2008)
Hoechst 33342	Binds to DNA	DNA	Cronin and Wilkinso (2008)
Propidium Iodide (PI)	PI is a commonly used dye for detection of dead or damaged cells as evidenced by permeabilization of the inner membrane. PI contains two positive charges normally excluded from the cells due to divalence. Therefore, PI can only enter permeabilized inner membranes	Dead or damaged cells	Leonard *et al*. (2016); Majeed *et al*. (2018)
Rhodamine 123	Cationic dye that only accumulates in cells with active membrane potential and reciprocally can be pumped back out of cells	Membrane potential	Buysschaert *et al*. (2016)
Sybr Green	DNA	Total cell counting	Buysschaert *et al*. (2016)
SYTO BC SYTO 9	Nucleic Acid stain (both DNA and RNA)	Total cells—intact and damaged cells	Majeed *et al*. (2018); Trevors (2003); Wilkinson (2018)
SYTO BC + polystyrene microspheres	Nucleic acid stain (both DNA and RNA)	Total cell counting	Majeed *et al*. (2018)

Fluorescent dyes used in flow cytometry

Membrane integrity and permeabilization

Membrane integrity is often employed as a definitive measure of cell viability. Thus, as a consequence, dyes typically fall into two categories, namely cell permeant and cell impermeant, depending on their ability to penetrate an intact cell membrane (Buysschaert *et al*. 2016). Membrane integrity indicates that cells continue to display metabolic activity by maintaining potential without guaranteeing cell replication (which is required for cell culturing techniques). Cells with damaged or compromised membranes are unable to maintain the electrochemical gradient across the membrane and are therefore considered as dead (Díaz *et al*. 2010). Dyes employed typically work on the principle of exclusion from a viable cell membrane and permeabilization through a damaged membrane. Propidium iodide is a commonly used dye for detection of dead cells as evidenced by permeabilization of the inner membrane. PI contains two positive charges and is 'normally excluded from the cells due to divalence'. Therefore, PI can only enter permeabilized inner membranes (Léonard*et al*. 2016). Viability may be determined through combination with dyes such as PI (membrane impermeant) where fluorescence indicates non-viability (Buysschaert *et al*. 2016).

Membrane permeant dyes may be used to combine with cellular nucleic acids: Sybr green binds to DNA while Syto9 binds to both DNA and RNA to fluoresce green (Buysschaert *et al*. 2016; Wilkinson 2018). Such dyes yield total counts as nucleic acids may be present in dead and damaged cells. Furthermore, the asymmetric cyanine-based dyes such as Syto are non-fluorescent until such time as they bind with nucleic acid, whereas DAPI or Sybr-based dyes enhance their fluorescence upon binding to nucleic acids (Díaz *et al*. 2010). This may be a consideration when trying to differentiate very small bacterial cells from background noise.

Cell structure and differences between gram-positive and gram-negative bacteria is an important consideration when design staining strategies (Berney *et al.* 2007; Buysschaert *et al.* 2016; Léonard *et al.* 2016). Gram-negative cells present greater challenge to staining, often requiring a time-dependant protocol due to presence of the outer membrane. Buysschaert *et al.* (2016) found that uptake of Syto dyes was immediate in gram-positive micro-organisms, whereas approximately 15-min incubation was required with Gram-negative bacteria. Even allowing sufficient time for dye uptake in gram negative may be insufficient to see homogeneous staining and therefore protocols may require addition of EDTA to chelate the LPS layer of Gram-negative bacteria (Berney *et al.* 2007; Buysschaert *et al.* 2016). As described by Buysschaert *et al.* (2016), work is required to determine the appropriate EDTA and dye concentration, and in their research they found that EDTA improved uptake in Gram-negative bacteria at lower dye concentrations. However, Davey and Kell (1996) highlight the impact of the EDTA sample preparation in terms of cell viability, change to side scatter profiling, cell-sorting and re-growth which should be considered.

Membrane potential/Energization

Membrane potential is often used to determine cell viability where viable cells maintain ion potential across the cell membrane, necessary in ATP synthesis and essential molecule transport (Buysschaert *et al.* 2016). Given the link between membrane potential and cell respiration and ATP synthesis, this may be considered a more appropriate measure of viability given the criticality of respiration (Hammes *et al.* 2011). When the difference between the ions inside and outside the cell decreases to zero, it serves as an indication that the membrane is structurally damaged (Díaz *et al.* 2010). Cationic dyes such as $DiOC_n$ are able to cross the cell membrane of viable cells and accumulate inside polarized cells. However, as advised by Magge *et al.* (2009), care should be taken with dyes such as $DiOC_6$, as non-specific binding to the spore coat was observed during their studies, further emphasizing the importance of understanding a selected dye and its site of action.

Metabolic Activity

As part of metabolic activity, cells operate a suite of esterases and dehydrogenases whose activity may be detected and measured with dyes and flow cytometry. Like nucleic acids stains, enzymes may still be active after cell death (Buysschaert *et al.* 2016). Therefore, staining protocols should be carefully designed and more often involve multi-stain approach. Carboxfluorescein diacetate (cFDA) is cleaved by esterases to release the fluorescent fluorescein. cFDA is a viability stain that is effectively retained in the cell, but staining protocols should consider pH conditions as it may affect fluorescence emission intensity with pH 9 being most intense (Buysschaert *et al.* 2016). Another enzymatic activity of interest is that of superoxide dismutase in responding to reactive oxygen species (ROS) during oxidative stress. An increase in ROS may be detected using dihydroethidium (HE), where the oxidation of HE results in the cleavage of ethidium which fluoresces with the intercalation with DNA (Buysschaert *et al.* 2016).

Multi-staining strategies

Single staining strategies may overestimate populations or suggest incomplete determinations of phenotypic fractions whereby intermediate states are elucidated (Díaz *et al.* 2010; Léonard *et al.* 2016). Through the use of multiple fluorescent probes, different functional properties or morphological states may be assessed simultaneously and used to form a more complete understanding of the micro-organism (Buysschaert *et al.* 2016). An often used staining kit is Live/Dead® BacLight™ kit which uses a combination of SYTO9 and PI to distinguish intact live cells from permeabilized dead cells. Thus, multiple fluorochromes are often used in combination to label cellular components or properties and subsequently assist in differentiation. As shown by the work of Quirós *et al.* (2007) the dual staining of *Lactobacillus hilgardii* and *Saccharomyces cerevisiae* using CV6 and PI shows the value in elucidating cell fractions such as damaged and VBNC cells, not observed in cell culture plates. The authors were able to gain a fuller understanding of the culture kinetics in the bioprocess being examined.

As highlighted by Wilkinson (2018), micro-organism types may uptake stains differently and this should be considered in any protocol. The author highlighted some reliability challenges with PI. Hence, multi-stain strategies should be considered whereby fractions may be triangulated and validated. For example, a strategy might be to perform total stain with Syto, a non-viable stain with PI and a viable stain with cFDA. Majeed *et al.* (2018) utilized such a strategy whereby they were able to validate their staining strategy by comparing cFDA fraction to the Syto-PI fraction (each representing viable cell numbers).

In our own work, we have used multiple dyes to examine fractions of *Geobacillus stearothermophilus*. In this work, biological indicators of *G. stearothermophilus* were treated with vapourized hydrogen peroxide sterilization and examined with flow cytometry to elucidate fractions recovered in Tryptone Soya media broth. As shown in Fig. 2, the benefit of having a multi-stain strategy is apparent: Syto BC plots as expected show total count of cells due to the nucleic acid staining, while PI shows dead

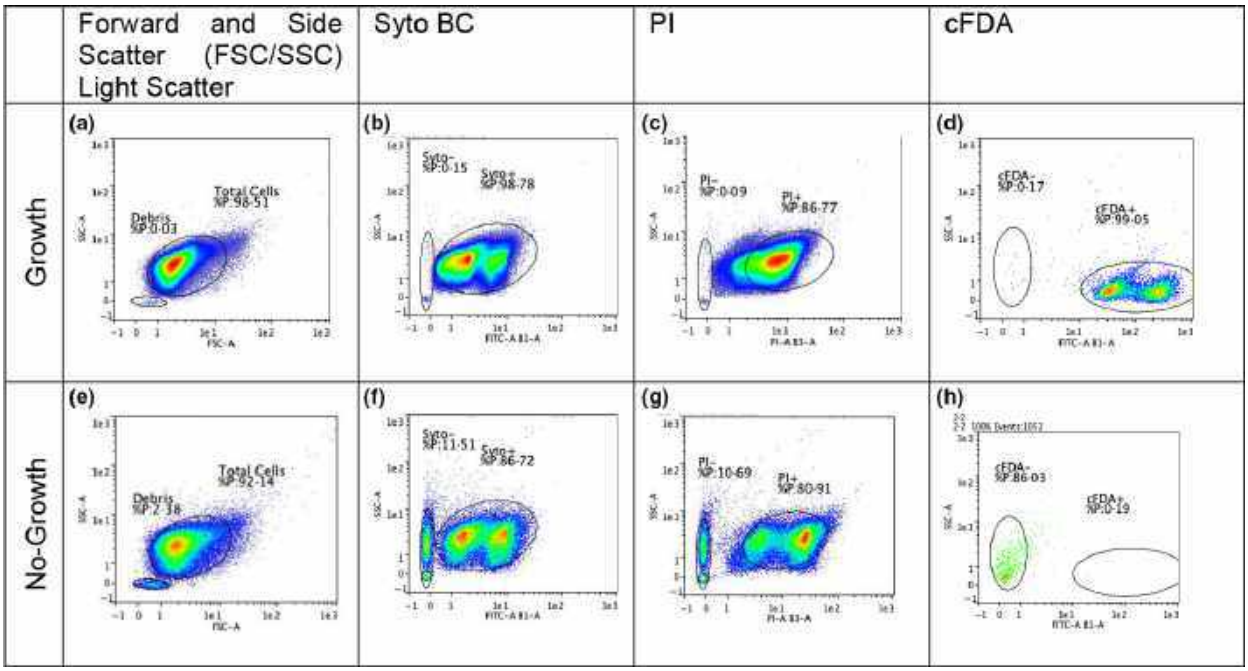

Figure 2 Flow cytometry of *Geobacillus stearothermophilus* biological indicators treated with vapourized hydrogen peroxide and incubated in TSB. Plots (a–d) are of from TSB tubes where growth was observed after 24 h. Plots (e–h) are from TSB tubes where no growth was observed after 48 h. [Colour figure can be viewed at wileyonlinelibrary.com]

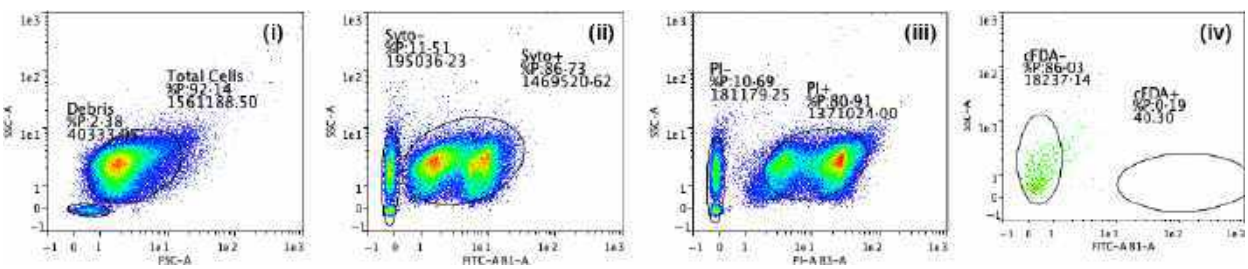

Figure 3 Flow cytometry of plates E–H (Fig. 2) unstained (i) and stained with Syto BC (ii); PI (iii); CFDA (iv) and including values for cells per ml. (i)–(iii) performed as same experimental test with Syto BC and PI applied as a dual stain. CFDA applied as separate experiment with differing dilution: When CFDA events are corrected to same dilution as Syto/PI experiment, a $CFDA^-$ cell count of $1{\cdot}47 \times 10^6$ is obtained. [Colour figure can be viewed at wileyonlinelibrary.com]

and damaged cells due to the penetration of the dye through the inner membrane of the cell. In panel G of Fig. 2, PI stained positive as expected for a tube that yielded no viable growth and this was verified by the cFDA—population elucidated in panel H. However, in the TSB tube where growth was observed, PI-positive cells (Fig 2c) were also observed which was also somewhat expected to indicate damaged cells. Again, cFDA acted to confirm that albeit the cells were damaged, they were capable of metabolic activity.

As much as one can observe the ability of FCM and fluorescent probes to elucidate various fractions as shown in Fig. 2, the accuracy at which it elucidates such fractions is also a considerable benefit of using flow cytometry. Again, in our own research studies, a test tube of TSB containing a biological indicator of *G. stearothermophilus* was examined by flow cytometry with stains of CFDA, Syto BC and PI. The results of the examination of this tube are shown in Fig. 3.

When CFDA experiment is corrected for dilution, a similar population is observed for Syto BC^+, PI^+ and $CFDA^-$. This therefore indicates a population of total cells (Syto BC^+) of approximately $1{\cdot}5 \times 10^6$ cells of *G. stearothermophilus* that have damaged inner cell

membranes (PI^+) to such an extent that the cells are not viable ($CFDA^-$).

In defining a protocol for multiple staining, careful consideration should be given to (i) the individual staining protocols for each dye, (ii) the possibility for overspill of fluorescence and the need for compensation, (iii) the interference of one dye with another, for example, electron quenching, (iv) dye stability and (v) the potential for cellular metabolic activity to affect the staining protocol (Buysschaert *et al*. 2016; Kirchhoff and Cypionka 2017).

For example, Kirchhoff and Cypionka (2017) observed viable cells of *Dinoroseobacter shibae* and *Bacillus subtilis* being stained with PI and attributed this to a 'boosted membrane potential', that is, an amplified ion-motive force leading to permeability of the PI cation. In the case of *B. subtilis*, this phenomenon was observed when cells were in early growth phase (similar to our TSB culture stained after 24 h; Kirchhoff and Cypionka 2017). Again, this further highlights (i) the careful selection of appropriate stains, (ii) the definition of an appropriate protocol and (iii) the benefit of using multiple stains. In the case of our work, the use of CFDA acts as the ultimate arbitrator of viability, and subsequently, confirmation of the other fractions obtained.

Key advantages with Flow Cytometry

Key advantages may be summarized as (adapted from Wilkinson 2018) rapid test time and data generation (min); high numbers of test cells (in excess of 10 000); single cell analysis; real-time analysis; minimal sample volumes; significant data generation; detailed Data analysis tools; and multi-parameter analysis.

With regard to the examination of bacteria, the key advantage is appropriately summarized by Díaz *et al.* (2010), as 'the assessment of structural and/or functional cell properties such as metabolic activity, membrane potential and integrity or macro-molecules biosynthesis leads to a deeper characterization of cell populations'.

Challenges with FCM in sterilization microbiology

With regard to the examination of bacteria with flow cytometry, there are a number of challenges that must be considered and strategized for, particularly, bacterial size, staining protocols and creating a partial picture.

Bacterial Size

Bacteria are some three times smaller than mammalian cells in mass and therefore contain less cellular constituents, such as nucleic acids, where fluorescent probes are often targeted. As a consequence of this, the areas of light scatter of interest are often either close to the instrumentation noise or the cellular debris detected as events by the flow cytometer (Tracy *et al.* 2008; Ambriz-Aviña *et al.* 2014).

Staining Protocols

The importance and moreover the significance and impact of the staining protocol on the final result are highlighted by many researchers. For example, Nescerecka *et al.* (2016) identified that the use of solvents such as DMSO may affect the permeability of the cell and subsequently affect results. Other researchers have reported bleaching of probes over time, for example, Stiefel *et al.* (2015) observed loss of SYTO9 in *Staphylococcus aureus* and *Pseudomonas aeruginosa* cells over time of 10–130 min with a loss of 4–8% every 5 min. In some studies, cellular and metabolic interference was observed. As described already, ion motive force can potentially result in misleading results with PI. Similarly, Stiefel *et al.* (2015) describe how Gram-negative micro-organisms with two cell membranes may limit the permeabilization of SYTO9. Also, the same workers observed variances in uptake of SYTO9 in live and dead cell populations. Background fluorescence may also impact results. Again, related to the size of the bacterial cell, the impact of background fluorescence must be known and accounted for. For example, PI yields high fluorescence in the unbound form (Stiefel *et al.* 2015). Regarding the probes themselves, emission spectra wavelengths may overlap and therefore compensation must be applied to yield accurate determinations. Additionally, spores themselves have proved to be challenging to analyse. Bacterial endospores have many protective strategies deployed during dormancy including spore coat, dormant metabolic activity, nucleic acid protected with small acid soluble proteins. All of these mechanisms make it somewhat difficult to stain with FCM probes, consequently with mixed results being observed in the literature (Comas-Riu and Vives-Rego 2002; Cronin and Wilkinson 2007; Mathys *et al.* 2007; Majeed *et al.* 2018; Trunet *et al.* 2019; Young and Setlow 2004b). Some researchers were unable to stain endospores while others had some success with specific probes, staining protocols and use of germinants. As expected, an understanding of the action and target of the probes is imperative: Laflamme *et al.* (2004) found that while Syto9 penetrates free endospores, DiBAC did not work, not because the molecule could not pass the spore coat but because the mechanism it is testing namely efflux pump is dormant in a dormant endospore.

Creating a partial picture

In the research field of Food sterilization and preservation, flow cytometry has been used as an investigative

tool quite extensively (Borch-Pedersen *et al.* 2017; Lv *et al.* 2019; Zhang *et al.* 2020). The very recent work of Zhang *et al.* (2020) demonstrates how FCM can be employed to elucidate various phenotypic fractions observed during an inactivation treatment. FCM can also show the sequence of events from intact spores to germinated spores (high fluorescence with Syto) to an intermediate (moderate fluorescence) 'unknown state' to finally an inactivated state (PI positive). However, it can equally be observed that a limitation resides with FCM, where one fraction is often labelled 'unknown'—it is known from a stain fluorescence perspective but not fully resolved from a phenotypic or vitality state. Some authors determine this to be the VBNC fraction accounting for differences with cell counts from conventional plate count techniques. Zhang *et al.* (2020) examined the cultivability of each fraction to further inform, and arrived at the conclusion that this fraction is likely to be 'germinated with partial sublethal damage'. Our work to date, as shown in Figs 2 and 3, demonstrates elucidation of various fractions with Syto and PI stain and viability assessment using CFDA. However, like many others have identified, FCM is one of the necessary tools that may be used to inform but other investigative tools and approaches are needed to form the rich picture about bacterial state in a sterilization or decontamination process. Comas-Riu and Vives-Rego (2002) observed how FCM could differentiate culture fractions such as vegetative cells and spores, all of varying degrees of viability in a way that microscopic or electric particle analysis were not able to do. The authors, using cell sorting and examination under SEM, were able to clearly identify the various fractions in the culture of *P. polymyxa* being examined, hence demonstrating the complementarity of using multiple techniques. Table 2 describes some of the other tools and techniques that may be employed to help form such a rich picture.

As shown in Table 2, additional information can be obtained using complementary techniques such as quantitative PCR and image analysis techniques that have been successfully used in adjacent fields of environmental and food microbiology. Techniques such as RAMAN spectroscopy, Maldi time-of-flight (tof) Mass Spectrometry along with use of scanning and transmission electron microscopy can provide important cellular and mechanistic information on spore composition and destruction post-treatments (De Gelder *et al.* 2007; Lasch *et al.* 2008; Hutchison *et al.* 2014). Raman bands of calcium dipicolinate and amino acids such as phenylalanine and tyrosine are more intense in the spectra of sporulating bacteria compared with those of bacteria from earlier phases of growth and therefore can be used to detect sporulation of cells by a characteristic band at 1018 cm(−1) from calcium dipicolinate. The increase in amino acids could possibly be explained by the formation of small acid-soluble proteins that saturate the endospore DNA (De Gelder *et al.* 2007). These rapid approaches can also be used to detect intermediate morphological and physiological states and therefore complement FCM in providing a more complete picture.

Opportunities for real-time FCM in sterilization microbiology

As much as researchers should understand and address limitations, the benefits of flow cytometry in the examination of micro-organisms cannot be overlooked. As stated by Wilkinson (2018), 'FCM data may reflect differing properties such as the extent of cell membrane integrity, functionality of membrane potential, presence of intracellular enzyme activity and DNA base composition'.

As highlighted by Majeed *et al.* (2018) 'intermediate states between viable and dead bacteria like injured and stressed cells are difficult to detect by the plating method and are often termed as viable but nonculturable' (VBNC). Hence, we arrive at another classification based on the term 'vitality' or the degree to which a cell can perform various aspects of metabolic, physiological and genetic functionality and the extent of structural and morphological integrity (Kramer and Thielman 2016).

While significant investigative work has been conducted by a number of researchers regarding the effect of sterilants at a cellular level (Roth *et al.* 2010; Leggett *et al.* 2016; Setlow *et al.* 2016; Young and Setlow 2004a, 2004b), often this work is limited to the use of mutants to compare to wild-type micro-organisms to test such things as cellular permeability for instance. As identified by Cronin and Wilkinson (2008), the use of such mutants still fails to account for the inherent heterogenicity in large micro-organism populations. Some traditional polymerase chain reaction (PCR)-based methods may be limited in differentiating genetic material from viable and non-viable cells (Wilkinson 2018). As highlighted by Wang *et al.* (2017), quantitative-PCR (q-PCR) will not differentiate between viable and non-viable cells, whereas PCR in combination with a nucleic-acid-binding dye such as ethidium monoazide bromide offers potential for differentiation. EMA-q-PCR works on the same principle of membrane permeabilization where EMA intercalates into the DNA of permeabilized membranes preventing amplification by nucleic acids (Pisz *et al.* 2007). Therefore, while EMA-q-PCR offers potential assessment of viability, detection of injured (and viable cells) may be limited, similar to the use of PI in FCM. Hence, FCM using a combination of dyes not just those based on membrane permeabilization as an indicator of viability

Table 2 Potential use of real-time flow cytometry as a tool to address assumptions and limitations underpinning use of conventional culture-based media in sterilization microbiology. Complementary methods to FCM are also described

	Enumeration method for determining survivor populations		
Assumption or limitation	Gold standard culture-based method (Agar, Broth)	Flow cytometry	Other complementary methods
Binary growth of biological indicator	Conventional plate counts assume colonies occur from a single cell every time (Rowan 2019). Broth cultures, for end-point determinations, also assume culture are drawn from single cells. No information may be obtained from non-cultured states	While plate counts can only detect viable cells, FCM counts all cells as events, whether dead or alive. FCM staining strategy (e.g. PI and CFDA) stain will elucidate whether cells are alive, dead, or in an intermediate state, giving exact numbers for each sub population. Ability to elucidate non-culturable states	RAMAN spectroscopy (De Gelder *et al*. 2007)
Characterization of viable endospores and other complex micro-organisms	Endospores are dormant so assumptions is these forms would have all germinated and grown in broth or media—but little understanding of potential sub-lethal damage when an inactivation process is applied (McEvoy and Rowan 2019)	FCM can readily detect unstained viable spores. Spores that are damaged may be stained with PI and germinated spores with other viability stains such as CFDA	RAMAN spectroscopy (De Gelder *et al*. 2007) RNA transcription (Dembek *et al*. 2013) SEM (Rowan *et al*. 2008; Hutchison *et al*. 2014) TEM (Rowan *et al*. 2001; Hutchison *et al*. 2014) Maldi-Tof MS (Lasch *et al*. 2008)
Detection of intermediate morphological and physiological states	Standard culture-based approaches do not enumerate intermediate or viable non-culturable states (Bradley *et al*. 2012; Rowan *et al*. 2015)	PI stain can differentiate a gradient of live-damaged-dead cells depending on degree of PI uptake. Various stains can inform about the physiological state, for example, CFDA regarding metabolic activity	Redox stains (Yaqub *et al*. 2004) ATPase and PCR (Garvey *et al*. 2016) TEM (Sahin *et al*. 2012; Reineke *et al*. 2013) SEM (Reineke *et al*. 2013; Georget *et al*. 2014)
Environmental conditions and microbial stress-adaptation	Prior exposure to sub-lethal stresses may harden microbes to lethal levels of the same stress (Rowan 1999; Rowan *et al*. 2015); ; . Growth in oxygen-rich environment may cause metabolic suicide for some aerobic organisms where vital catalase and superoxide dismutase genes damaged, yet are capable of growth under reduced oxygen conditions (Rowan 1999)	FCM with targeted staining protocols will help elucidate environment and stress responses: PI stain, which stains damaged/dead cells, will give an indication of the ability of the organism to adapt to stress. CFDA may be employed to indicate vitality by demonstrating metabolic activity	Gene-chip microarray for microbial genotypes and species in communities, bioinformatics (Aspedon *et al*. 2006) Microfluidic technologies for microbial community monitoring (Dhar and Lee 2018). qPCR for gene expression under stress conditions (Rowan 2019)
Homogeneity versus Heterogeneity	Natural bioburden may be a mixed culture of different cell types and species. In sterilization microbiology, it is assumed that homogeneity of Biological Indicators (BIs) as a reference micro-organism, compensates for this (McEvoy and Rowan 2019)	Microbes of different size/population will separate out on dot plots making it possible to examine heterogenicity in microbial populations, including those from natural bioburden	Multiplex PCR assays (Diercks *et al*. 2009), MinION for microbial whole genome sequencing (Tyler *et al*. 2018) Immunoassays (Bartholomew *et al*. 2017) Maldi-TOF (Kryazhevskikh *et al* (2015); Li *et al* (2019)
Speed of enumeration post-sterilization treatment	Treated samples require up to 24- or 48-hr incubation before enumeration of survivors (McEvoy and Rowan 2019)	FCM gives total, and population, cell counts in real time, as the sample is analysed	PCR is more time-consuming, but can give complimentary data (Garvey *et al*. 2010)

(Continued)

Table 2 (Continued)

Assumption or limitation	Enumeration method for determining survivor populations		
	Gold standard culture-based method (Agar, Broth)	Flow cytometry	Other complementary methods
Uniformity of cell distribution	CFU counts on agar or broth cultures assume uniformity of cell distribution (Farrell *et al*. 2011; McEvoy and Rowan, 2019)	FCM will give indication of how uniform (size/granularity) cells with FSC indicating size and SSC the granularity of the cells. SSC-Height v SSC-Area to gate out duplets and aggregates (Zhang *et al*. 2020)	Microscopy, SEM, qPCR and combined cell culture (Garvey *et al*. 2013) Image analysis (Rowan *et al*. 2000; Wan-Mohtar *et al*. 2016)
Viability versus vitality	Treated micro-organisms may retain vital functions, but are not capable of growing on artificial laboratory media, thus underestimating population of potential survivors (Rowan 1999; Rowan *et al*. 2015)	Fluorescent probes may be used to target specific cell functions that only operate in alive cells. For example: EB is used to verify a functioning efflux pump (Léonard *et al*. 2016)	Quantitative PCR for specific genes related to vitality (Garvey *et al*. 2010, 2016)

and therefore offers complementary technological insights to addressing complex environmental microbiology challenges.

In their analysis of the effectiveness of disinfectants on nosocomial bacterial species, Massicotte *et al*. (2017) compared traditional culture techniques and FCM, and came to the conclusion that the ability of FCM to detect intermediary states between live and dead cells is a very important aspect given the hypothesis that some organisms such as *Enterococcus faecalis*, in a sub-lethal state had the potential to provide a 'biocharge of bacteria' for future nosocomial infection or food poisoning.

In our investigative work looking at the inactivation of biological indicators of *G. stearothermophilus* using vapourized hydrogen peroxide, the usefulness of FCM as an informative tool cannot be overstated. As shown in Fig. 2e–h, from a test tube of TSB showing no growth and therefore, no useful information from such a traditional technique, FCM has provided a rich picture of information regarding cell numbers, viability and damage. As described by McEvoy and Rowan (2019), investigation of the cellular location of lethality of VH2O2 is an important aspect of understanding sterilization kinetics and one which traditional cell culture techniques simply cannot inform. FCM is already providing valuable insights through the use of various fluorescent probes. However, it is equally recognized that the usefulness of FCM is further accelerated when used in combination with other investigative techniques.

Furthermore, sterilization microbiology often relies on the use of reference micro-organisms in the form of Biological indicators. BIs are often chosen as their resistance to a given sterilization or decontamination method is known and the method for micro-organism recovery is well described (McEvoy and Rowan 2019). However, as sterilization methods are designed to be more efficient and more tailored to the microbiology challenge of the healthcare product being processed, the reliance on BIs for process validation becomes less. As a consequence, the natural microbiology flora is used to define the minimum processing requirement. Use of traditional microbiology techniques that relies upon an understanding of different microbial species present may necessitate providing an enormity of different culture conditions for enumerating and resuscitating the variety of micro-organisms present that have either complex growth requirements or fail to grown in laboratory-based culture media (Tyler *et al*. 2018; Rowan 2019). There is evidence that some lethal or sub-lethally treated-bacteria may be adversely affected by environmental culture conditions (Rowan 2004; Rowan *et al*. 2015).

FCM can be used to discern microbial homogeneity through real-time dot plots of different cell populations. FCM combined with other techniques (Table 2) can effectively monitor, profile and investigate changes in microbial ecosystems. When assessing inactivation from a sterilization or decontamination process, FCM can rapidly assess survivors and those bacteria that may enter a viable but non-culturable state, thus yielding important information during the examination of the inactivation kinetics during process design.

Conclusion

Sterilization validation relies on the demonstration of a measured inactivation of micro-organisms, whether micro-organisms from the natural microflora of the device being sterilized or that of a reference BI (McEvoy

Box 1: Steps to be considered in the design of an FCM experiment.

a Understand the interaction of the probe and the micro-organism being studied and recognizing the growth stage of the micro-organism
b Include sufficient negative and positive control to subtract any background fluorescence, including autofluorescence from the micro-organism itself (Zhang *et al*. 2020).
c Have a multiple staining and counterstaining strategy to triangulate results.
d Assess the requirement for signal compensation (Alvarez *et al*. 2010; Adan *et al*. 2017).
e Design the protocol optimizing conditions, for example, temperature, probe concentration and appropriateness of materials, for example, TRIS buffers as opposed to DMSO (Nescerecka *et al*. 2016).
f Use other methods such as light microscopy, electron microscopy, Raman microscopy, PCR, etc. (to further inform the results obtained from FCM (see Table 2).

and Rowan 2019). To deliver more precise and efficient sterilization processes, a deeper understanding of the inactivation must be understood. On account of the heterogenicity and fastidiousness of micro-organisms, current traditional culture-based methods are limited: They offer a binary assessment of growth or no growth, not taking into account intermediate states that may exist during an inactivation process. As described by Reis *et al.* (2005), '*Bacillus* spp. have been found to exhibit a variety of rich dynamic behaviour including long-term oscillations, multiple steady-states, genetic instability and un-interpretable transients' and the consequences of which make process (Biotechnology cell culturing) optimization and process prediction 'a difficult task'. In addition, culture-based methods are time-consuming and often require a prior knowledge of the microflora species to design experimental recovery methods that are capable of recovering viable cells, in particular those that may be only sub-lethally impacted by the inactivation process (Rowan 2004; Rowan *et al.* 2015).

FCM can inform limitations associated with conventional sterilization microbiology. The use of FCM with appropriate fluorescent probes such as PI offers the opportunity to examine the heterogenous sub-populations including population transitions from viable to dead cells upon treatment with a sterilization process such as VH2O2. The use of FCM multi-parameter analysis using multiple fluorescent probes and alternative methods helps provide a rich picture of the 'vitality' states in heterogenous populations, and such a picture can potentially help inform the inactivation kinetics observed with VH2O2 treatment. However, FCM is not without its own limitations. Such limitations may be addressed by the researcher taking the appropriate steps in protocol design (see Box 1) and/or adding complementary investigative techniques and tools such as those described in Table 2.

Adjacent techniques described in Table 2 include Raman spectroscopy and new omics technologies, such as metagenomics and transcriptomics, which will advance efficacy and application of FCM analysis. Raman spectroscopy may complement FCM analysis of membrane permeability by providing insights into chemical composition (CaDPA) changes within the cell through measurement of Raman shifts (De Gelder *et al.* 2007; Piktel *et al.* 2017). Similarly, developments in omics (transcriptomics, proteomics and metabolomics) of micro-organisms may provide complementary mechanistic cellular information regarding stress resistance and genetic modifications in biomarkers during an inactivation treatment (den Besten *et al.* 2018). Zhang *et al.* (2010) describe how multi-omic strategies may help decipher complex microbial metabolism. Rowan (2019) described the benefits of omics technologies in advancing pulsed light as a potential disruptive decontamination technology for agri-food, water and healthcare applications, where use of FCM would provide valuable real-time determinations. For example, automated FCM analysis would offer considerable complementary determinations when used with metagenomics profiling and next-generation sequencing (Breitwieser *et al.* 2018). As described by Hammes and Egli (2010), 'cultivation-independent viability analysis on the single cell level is one of the finest uses of FCM', *and with* careful experimental design, coupled with complementary techniques such as Raman spectroscopy or omics, FCM may be employed to further inform sterilization microbiology and ultimately aid the improvement of decontamination and sterilization processes.

Acknowledgements

The authors acknowledge Athlone Institute of Technology Doctoral Scholarship Programme and funding support from STERIS for same.

Conflict of Interest

There is no conflict of interest.

References

Adan, A., Alizada, G., Kiraz, Y., Baran, Y. and Nalbant, A. (2017) Flow cytometry: basic principles and applications. *Crit. Rev. Biotechol* **37**, 163–176.

Alvarez, D.F., Helm, K., DeGregori, J., Roederer, M. and Majka, S. (2010) Publishing flow cytometry data. *Am J Physiol – Lung Cell Mol Physiol* **298**, 127–130.

Álvarez-Barrientos, A., Arroyo, J., Cantón, R., Nombela, C. and Sánchez-Pérez, M. (2000) Applications of flow cytometry to clinical microbiology. *Clin Microbiol Rev.* **13**, 167–195.

Ambriz-Aviña, V., Contreras-Garduño, J.A. and Pedraza-Reyes, M. (2014) Applications of flow cytometry to characterize bacterial physiological responses. *BioMed Res Int* **2014**, 1–14.

Aspedon, A., Palmer, K. and Whiteley, M. (2006) Microarray analysis of the osmotic stress response in *Pseudomonas aeruginosa*. *J. Bacteriol* **188**, 2721–2725.

AAMI(2017) AAMI TIR16:2017 Microbiological aspects of ethylene oxide sterilization. ISBN 1-57020-363-6. Association for the Advancement of Medical Instrumentation. Approved and published 3 september 2009.

Bartholomew, R.A., Ozanich, R.M., Arce, J.S., Engelmann, H.E., Heredia-Langner, A., Hofstad, B.A., Hutchison, J.R., Jarman, K. *et al.* (2017) Evaluation of immunoassays and general biological indicator tests for field screening of *Bacillus anthracis* and Ricin. *Heal Secur* **15**, 81–96.

Berney, M., Hammes, F., Bosshard, F., Weilenmann, H.U. and Egli, T. (2007) Assessment and interpretation of bacterial viability by using the LIVE/DEAD BacLight kit in combination with flow cytometry. *Appl Environ Microbiol* **73**, 3283–3290.

den Besten H.M.W., Amézquita A., Bover-Cid S., Dagnas S, Ellouze M., Guillou S., Nychas G., O'Mahony C. *et al.* (2018) Next generation of microbiological risk assessment: Potential of omics data for exposure assessment. *International Journal of Food Microbiology*, **287**, 18–27. http://dx.doi.org/10.1016/j.ijfoodmicro.2017.10.006.

Borch-Pedersen, K., Mellegård, H., Reineke, K., Boysen, P., Sevenich, R., Lindbäck, T. and Aspholm, M. (2017) Effects of high pressure on *Bacillus licheniformis* spore germination and inactivation. *Appl Environ Microbiol* **83**, 1–13.

Bradley, D., McNeil, B., Laffey, J.G. and Rowan, N.J. (2012) Studies on the pathogenesis and survival of different culture forms of *Listeria monocytogenes* to pulsed UV-light irradiation after exposure to mild-food processing stresses. *Food Microbiol* **30**, 330–339.

Breitwieser, F.P., Lu, J. and Salzberg, S.L. (2018) A review of methods and databases for metagenomic classification and assembly. *Brief Bioinform* **20**, 1125–1139.

Brown, M. and Wittwer, C. (2000) Flow cytometry: principles and clinical applications in hematology'. *Clin Chem* **46**, 1221–1229.

Buysschaert, B., Byloos, B., Leys, N., Van Houdt, R. and Boon, N. (2016) Reevaluating multicolor flow cytometry to assess microbial viability. *Appl Microbiol Biotechnol* **100**, 9037–9051.

Comas-Riu, J. and Vives-Rego, J. (2002) Cytometric monitoring of growth, sporogenesis and spore cell sorting in *Paenibacillus polymyxa* (formerly *Bacillus polymyxa*). *J Appl Microbiol* **92**, 475–481.

Cronin, U.P. and Wilkinson, M.G. (2007) The use of flow cytometry to study the germination of *Bacillus cereus* endospores. *Cytom Part A* **71**, 143–153.

Cronin, U.P. and Wilkinson, M.G. (2008) Monitoring changes in germination and permeability of *Bacillus cereus* endospores following chamical, heat and enzymatic treatments using flow cytometry. *J Rapid Methods Autom Microbiol* **16**, 164–184.

Davey, H.M. and Kell, D.B. (1996) Flow cytometry and cell sorting of heterogeneous microbial populations: the importance of single-cell analyses. *Microbiol Rev* **60**, 641–696.

De Gelder, J., Scheldeman, P., Leus, K., Heyndrickx, M., Vandenabeele, P., Moens, L. and De Vos, P. (2007) Raman spectroscopic study of bacterial endospores. *Anal Bioanal Chem* **389**, 2143–2151.

Dembek, M., Stabler, R.A., Witney, A.A., Wren, B.W. and Fairweather, N.F. (2013) Transcriptional analysis of temporal gene expression in germinating *Clostridium difficile* 630 endospores. *PLoS One* **8**, e64011

Dhar, B.C. and Lee, N.Y. (2018) Lab-on-a-chip technology for environmental monitoring of microorganisms. *Biochip J* **12**, 173–183.

Díaz, M., Herrero, M., García, L.A. and Quirós, C. (2010) Application of flow cytometry to industrial microbial bioprocesses. *Biochem Eng J* **48**, 385–407.

Diercks, A., Kostner, H. and Ozinsky, A. (2009) Resolving cell population heterogeneity: real-time PCR for simultaneous multiplexed gene detection in multiple single-cell samples. *PLoS One* **4**, e6326.

Farrell, H., Hayes, J., Laffey, J. and Rowan, N. (2011) Studies on the relationship between pulsed UV light irradiation and the simultaneous occurrence of molecular and cellular damage in clinically-relevant *Candida albicans*. *J Microbiol Methods* **84**, 317–326.

García-Contreras, R., Nuñez-López, L., Jasso-Chávez, R., Kwan, B.W., Belmont, J.A., Rangel-Vega, A., Maeda, T. and Wood, T.K. (2015) Quorum sensing enhancement of the stress response promotes resistance to quorum quenching and prevents social cheating. *ISME J* **9**, 115–125.

Garvey, M., Farrell, H., Cormican, M. and Rowan, N. (2010) Investigations of the relationship between use of in vitro cell culture-quantitative PCR and a mouse-based bioassay for evaluating critical factors affecting the disinfection performance of pulsed UV light for treating *Cryptosporidium parvum* oocysts in saline. *J Microbiol Methods* **80**, 267–273.

Garvey, M., Hayes, J., Clifford, E., Kirf, D. and Rowan, N. (2013) Efficacy of measuring cellular ATP levels to determine the inactivation of pulsed UV treated *Cryptosporidium parvum* oocysts suspended in water. *Water Sci. Technol. Water Supply* **13**, 202–213.

Garvey, M., Rabbitt, D., Stocca, A. and Rowan, N. (2015) Pulsed ultraviolet light inactivation of *Pseudomonas aeruginosa* and *Staphylococcus aureus* biofilms. *Water Environ J* **29**, 36–42.

Garvey, M., Coughlan, G., Murphy, N. and Rowan, N. (2016) The pulsed light inactivation of veterinary relevant microbial biofilms and the use of a RTPCR assay to detect parasite species within biofilm structures. *Open Vet J* **6**, 15–22.

Geier, H., Mostowy, S., Cangelosi, G.A., Behr, M.A. and Ford, T.E. (2008) Autoinducer-2 triggers the oxidative stress response in *Mycobacterium avium*, leading to biofilm formation. *Appl Environ Microbiol* **74**, 1798–1804.

Georget, E., Kapoor, S., Winter, R., Reineke, K., Song, Y., Callanan, M., Ananta, E., Heinz, V. *et al.* (2014) In situ investigation of *Geobacillus stearothermophilus* spore germination and inactivation mechanisms under moderate high pressure. *Food Microbiol* **41**, 8–18.

Ghosh, S. and Setlow, P. (2009) Isolation and characterization of superdormant spores of *Bacillus* species. *J. Bacteriol* **191**, 1787–1797.

Gillis, J.R., Mosley, G.A., Kowalski, J.B., Krushefski, G., Nirgenau, P.T. and Mccauley, K.J. (2010) Understanding biological indicator grow-out times. *Pharm Tech Europe* **34**, 1–8.

Glier, H. and Holada, K. (2012) Blood storage affects the detection of cellular prion protein on peripheral blood leukocytes and circulating dendritic cells in part by promoting platelet satellitism. *J Immunol Methods* **380**, 65–72.

Goure, J.P. (ed.) (2013) Optics in Instruments: Applications in Biology and Medicine. New York: John Wiley and Sons Inc. ProQuest Ebook Central. Accessed 26 May 2020.

Guirgis, F.W., Jones, L., Esma, R., Weiss, A., McCurdy, K., Ferreira, J., Cannon, C., McLauchlin, L. *et al.* (2017) Managing sepsis: Electronic recognition, rapid response teams, and standardized care save lives. *J Crit Care* **40**, 296–302.

Hammes, F., Berney, M. and Egli, T. (2011) Cultivation-independent assessment of bacterial viability. In *High Resolution Microbial Single Cell Analytics* ed. Müller, S. and Bley, T., pp. 123–150. Berlin, Heidelberg: Springer, Berlin Heidelberg.

Hammes, F. and Egli, T. (2010) Cytometric methods for measuring bacteria in water: advantages, pitfalls and applications. *Anal Bioanal Chem* **397**, 1083–1095.

Hayouni, E.A., Bouix, M., Abedrabba, M., Leveau, J.Y. and Hamdi, M. (2008) Mechanism of action of *Melaleuca armillaris* (Sol. Ex Gaertu) Sm. essential oil on six LAB strains as assessed by multiparametric flow cytometry and automated microtiter-based assay. *Food Chem* **111**, 707–718.

Hensley, B.J. and Monson, J.R.T. (2015) Hospital-acquired infections. *Surgery* **33**, 528–533.

Hewitt, C.J., Nebe-Von Caron, G., Nienow, A.W. and McFarlane, C.M. (1999) The use of multi-parameter flow cytometry to compare the physiological response of *Escherichia coli* W3110 to glucose limitation during batch, fed-batch and continuous culture cultivations. *J. Biotechnol* **75**, 251–264.

Humpheson, L., Adams, M.R., Anderson, W.A. and Cole, M.B. (1998) Biphasic thermal inactivation kinetics in *Salmonella enteritidis* PT4. *Appl Environ Microbiol* **64**, 459–464.

Hutchison, E.A., Miller, D.A. and Angert, E.R. (2014) Sporulation in bacteria: beyond the standard model. *Microbiol. Spectr*, **2**, 1–15.

International Organization for Standardization (ISO) (2014) *ISO11135:2014 Sterilization of Health-Care Products—Ethylene Oxide—Requirements for the Development, Validation and Routine Control of a Sterilization Process for Medical Devices*. Geneva: ISO.

International Organization for Standardization (2018a) *ISO11737-1:2018 Sterilization of Health Care Products—Microbiological Methods—Part 1: Determination of a Population of Microorganisms on Products*. Geneva: ISO.

International Organization for Standardization (2018b) *ISO11139:2018 Sterilization of Health Care Products—Vocabulary of terms used in sterilization and related equipment and process standards*. Geneva: ISO.

International Organization for Standardization (2019) *ISO11737-2:2019 Sterilization of health care products—Microbiological methods— art 2: Tests of sterility performed in the definition, validation and maintenance of a sterilization process*. Geneva: ISO.

International Trade Administration (2016) Top markets report medical devices: a market assessment tool for U.S. exporters. https://www.trade.gov/topmarkets/pdf/Medical_Devices_Top_Markets_Report.pdf (accessed 16 Jan 2018).

Kalina, T., Abraham, R.S., Rizzi, M. and van der Burg, M. (2020) Editorial: application of cytometry in primary immunodeficiencies. *Front Immun* **11**, 1–4.

Keller, M. and Zengler, K. (2004) Tapping into microbial diversity. *Nat Rev Microbiol* **2**, 141–150.

Kirchhoff, C. and Cypionka, H. (2017) Propidium ion enters viable cells with high membrane potential during live-dead staining. *J. Microbiol Methods* **142**, 79–82.

Kramer, B. and Thielmann, J. (2016) Monitoring the live to dead transition of bacteria during thermal stress by a multi-method approach. *J Microbiol Methods* **123**, 24–30.

Kryazhevskikh, N.A., Loiko, N.G., Demkina, E.V., Mulyukin, A.L., Lebedev, A.T., Gaponov, A.M., and El'-Registan, G. I.(2015) Applicability of MALDI mass spectrometry for diagnostics of phase variants in bacterial populations. *Microbiology* **84**, 328–346.

Laflamme, C., Lavigne, S., Ho, J. and Duchaine, C. (2004) Assessment of bacterial endospore viability with fluorescent dyes. *J Appl Microbiol* **96**, 684–692.

Laflamme, C., Ho, J., Veillette, M., De Latrémoille, M.C., Verreault, D., Mériaux, A. and Duchaine, C. (2005) Flow cytometry analysis of germinating *Bacillus* spores, using membrane potential dye. *Arch Microbiol* **183**, 107–112.

Lasch, P., Nattermann, H., Erhard, M., Stämmler, M., Grunow, R., Bannert, N., Appel, B. and Naumann, D. (2008) MALDI-TOF mass spectrometry compatible inactivation method for highly pathogenic microbial cells and spores. *Anal Chem* **80**, 2026–2034.

Leggett, M.J., Setlow, P., Sattar, S.A. and Maillard, J.Y. (2016) Assessing the activity of microbicides against bacterial spores: Knowledge and pitfalls. *J Appl Microbiol* **120**, 1174–1180.

Léonard, L., Chibane, L.B., Bouhedda, B.O., Degraeve, P. and Oulahal, N. (2016) Recent advances on multi-parameter flow cytometry to characterize antimicrobial treatments. *Front Microbiol* **7**, 1–16.

Li, Y., Shan, M., Zhu, Z., Mao, X., Yan, M., Chen, Y., Gu, B. (2019) Application of MALDI-TOF MS to rapid identification of anaerobic bacteria. *BMC Infect Dis* **19**, 1–11.

Lv, R., Wang, D., Zou, M., Wang, W., Ma, X., Chen, W., Liu, D. (2019) Analysis of *Bacillus cereus* cell viability, sublethal injury, and death induced by mild thermal treatment. *J. Food Saf* **39**, 1–8.

Magge, A., Setlow, B., Cowan, A.E. and Setlow, P. (2009) Analysis of dye binding by and membrane potential in spores of *Bacillus* species. *J Appl Microbiol* **106**, 814–824.

Majeed, M., Majeed, S., Nagabhushanam, K., Punnapuzha, A., Philip, S. and Mundkur, L. (2018) Rapid assessment of viable but non-culturable *Bacillus coagulans* MTCC 5856 in commercial formulations using Flow cytometry. *PLoS One* **13**, 1–14.

Massicotte, R., Mafu, A.A., Ahmad, D., Deshaies, F., Pichette, G. and Belhumeur, P. (2017) Comparison between flow cytometry and traditional culture methods for efficacy assessment of six disinfectant agents against nosocomial bacterial species. *Front Microbiol* **8**, 1–14.

Mathur, H., Rea, C.M., Fallico, V., Cotter, P.D., Hill, C. and Ross, R.P.(2016) Flow cytometry as a tool to study the effects of bacteriocins on prokaryotic and eukaryotic Cells. *J Mol Biomark Diagn* **S8**, 1–8.

Mathys, A., Chapman, B., Bull, M., Heinz, V. and Knorr, D. (2007) Flow cytometric assessment of *Bacillus* spore response to high pressure and heat. *Innov Food Sci Emerg Technol* **8**, 519–527.

Mejuto, P., Luengo, M. and Díaz-Gigante, J. (2017) Automated flow cytometry: an alternative to urine culture in a routine clinical microbiology laboratory? *Int. J Microbiol* **2017**, 1–8.

McEvoy, B. and Rowan, N.J. (2019) Terminal sterilization of medical devices using vaporized hydrogen peroxide: a review of current methods and emerging opportunities. *J Appl Microbiol* **127**, 1403–1420.

Mtimet, N., Trunet, C., Mathot, A.G., Venaille, L., Leguérinel, I., Coroller, L. and Couvert, O. (2017) Walking dead: permeabilization of heat-treated *Geobacillus stearothermophilus* ATCC 12980 spores under growth-preventing conditions. *Food Microbiol* **64**, 126–134.

Müller, S. and Nebe-Von-Caron, G. (2010) Functional single-cell analyses: flow cytometry and cell sorting of microbial populations and communities. *FEMS Microbiol Rev* **34**, 554–587.

Nescerecka, A., Hammes, F. and Juhna, T. (2016) A pipeline for developing and testing staining protocols for flow cytometry, demonstrated with SYBR Green I and propidium iodide viability staining. *J Microbiol Methods* **131**, 172–180.

Oliver, J.D. (2005) The viable but nonculturable state in bacteria. *J Microbiol* **43**, 93–100.

Ou, F., McGoverin, C., Swift, S. and Vanholsbeeck, F. (2017) Absolute bacterial cell enumeration using flow cytometry. *J Appl Microbiol* **123**, 464–477.

Picot, J., Guerin, C.L., Le Van Kim, C. and Boulanger, C.M. (2012) Flow cytometry: Retrospective, fundamentals and recent instrumentation. *Cytotechnology* **64**, 109–130.

Piktel, E., Pogoda, K., Roman, M., Niemirowicz, K., Tokajuk, G., Wróblewska, M., Szynaka, B., Kwiatek, W.M. *et al.*(2017) Sporicidal activity of ceragenin CSA-13 against *Bacillus subtilis*. *Sci Rep* **7**, 1–12.

Pisz, J.M., Lawrence, J.R., Schafer, A.N. and Siciliano, S.D. (2007) Differentiation of genes extracted from non-viable versus viable micro-organisms in environmental samples using ethidium monoazide bromide. *J Microbiol Methods* **71**, 312–318.

Quirós, C., Herrero, M., García, L.A. and Díaz, M. (2007) Application of flow cytometry to segregated kinetic modeling based on the physiological states of microorganisms. *Appl Environ Microbiol* **73**, 3993–4000.

Reineke, K., Ellinger, N., Berger, D., Baier, D., Mathys, A., Setlow, P. and Knorr, D. (2013) Structural analysis of high pressure treated *Bacillus subtilis* spores. *Innov Food Sci Emerg Technol* **17**, 43–53.

Reis, A., Da Silva, T.L., Kent, C.A., Kosseva, M., Roseiro, J.C. and Hewitt, C.J. (2005) Monitoring population dynamics of the thermophilic *Bacillus licheniformis* CCMI 1034 in

batch and continuous cultures using multi-parameter flow cytometry. *J Biotechnol* **115**, 199–210.

Rodriguez, S.B. and Thornton, R.J. (2008) Use of flow cytometry with fluorescent antibodies in real-time monitoring of simultaneously inoculated alcoholic-malolactic fermentation of Chardonnay. *Lett Appl Microbiol* **46**, 38–42.

Roth, S., Feichtinger, J. and Hertel, C. (2010) Characterization of *Bacillus subtilis* spore inactivation in low-pressure, low-temperature gas plasma sterilization processes. *J Appl Microbiol* **108**, 521–531.

Rowan, N.J. (1999) Evidence that inimical food-preservation barriers alter microbial resistance, cell morphology and virulence. *Trends Food Sci Technol* **10**, 261–270.

Rowan, N.J., Candlish, A.A.G., Bubert, A., Anderson, J.G., Kramer, K. and Mclauchlin, J. (2000) Virulent rough filaments of *Listeria monocytogenes* from clinical and food samples secreting wild-type levels of cell-free p60 protein. *J Clin Microbiol* **38**, 2643–2648.

Rowan, N.J., MacGregor, S.J., Anderson, J.G., Cameron, D. and Farish, O. (2001) Inactivation of *Mycobacterium paratuberculosis* by Pulsed Electric Fields. *Appl Environ Microbiol* **67**, 2833–2836.

Rowan, N.J. (2004) Viable but non-culturable forms of food and waterborne bacteria: Quo Vadis? *Trends Food Sci Technol* **15**, 462–467.

Rowan, N.J., Espie, S., Harrower, J., Farrell, H., Marsili, L., Anderson, J.G. and MacGregor, S.J. (2008) Evidence of lethal and sublethal injury in food-borne bacterial pathogens exposed to high-intensity pulsed-plasma gas discharges. *Lett Appl Microbiol* **46**, 80–86.

Rowan, N.J. (2011) Defining established and emerging microbial risks in the aquatic environment: current knowledge, implications, and outlooks. *Int J Microbiol* **2011**, 1–15.

Rowan, N.J., Valdramidis, V.P. and Gómez-López, V.M. (2015) A review of quantitative methods to describe efficacy of pulsed light generated inactivation data that embraces the occurrence of viable but non culturable state microorganisms. *Trends Food Sci Technol* **44**, 79–92.

Rowan, N.J. (2019) Pulsed light as an emerging technology to cause disruption for food and adjacent industries – Quo vadis? *Trends Food Sci Technol* **88**, 316–322.

Safford, H.R. and Bischel, H.N. (2019) Flow cytometry applications in water treatment, distribution, and reuse: A review. *Water Res* **151**, 110–133.

Sahin, O., Yong, E.H., Driks, A. and Mahadevan, L. (2012) Physical basis for the adaptive flexibility of *Bacillus* spore coats. *J R Soc Interface* **9**, 3156–3160.

Suo, Y., Gu, Z. and Wei, X. (2020) Advances of in vivo flow cytometry on cancer studies. *Cytom Part A* **97**, 15–23.

Schenk, M., Raffellini, S., Guerrero, S., Blanco, G.A. and Alzamora, S.M. (2011) Inactivation of *Escherichia coli*, *Listeria innocua* and *Saccharomyces cerevisiae* by UV-C light: study of cell injury by flow cytometry. *LWT – Food Sci Technol* **44**, 191–198.

Setlow, B., Korza, G., Blatt, K.M.S., Fey, J.P. and Setlow, P. (2016) Mechanism of *Bacillus subtilis* spore inactivation by and resistance to supercritical CO_2 plus peracetic acid. *J Appl Microbiol* **120**, 57–69.

Stiefel, P., Schmidt-Emrich, S., Maniura-Weber, K. and Ren, Q. (2015) Critical aspects of using bacterial cell viability assays with the fluorophores SYTO9 and propidium iodide. *BMC Microbiol* **15**, 36.

Stone, G., Chapman, B. and Lovell, D. (2009) Development of a log-quadratic model to describe microbial inactivation, illustrated by thermal inactivation of *Clostridium botulinum*. *Appl Environ Microbiol* **75**, 6998–7005.

Taimur Khan, M.M., Pyle, B.H. and Camper, A.K. (2010) Specific and rapid enumeration of viable but nonculturable and viable-culturable Gram-negative bacteria by using flow cytometry. *Appl Environ Microbiol* **76**, 5088–5096.

Tracy, B.P., Gaida, S.M. and Papoutsakis, E.T. (2008) Development and application of flow-cytometric techniques for analyzing and sorting endospore-forming clostridia. *Appl Environ Microbiol* **74**, 7497–7506.

Trevors, J.T. (2003) Fluorescent probes for bacterial cytoplasmic membrane research. *J Biochem Biophysical Meth* **57**, 87–103.

Trunet, C., Ngo, H. and Coroller, L. (2019) Quantifying permeabilization and activity recovery of *Bacillus* spores in adverse conditions for growth. *Food Microbiol* **81**, 115–120.

Tyler, A.D., Mataseje, L., Urfano, C.J., Schmidt, L., Antonation, K.S., Mulvey, M.R. and Corbett, C.R. (2018) Evaluation of Oxford Nanopore's MinION sequencing device for microbial whole genome sequencing applications. *Sci Rep*, **8**, 1–12.

Veal, D.A., Deere, D., Ferrari, B., Piper, J. and Attfield, P.V. (2000) Fluorescence staining and flow cytometry for monitoring microbial cells. *J. Immunol Methods* **243**, 191–210.

Wang, H., Bédard, E., Prévost, M., Camper, A.K., Hill, V.R. and Pruden, A. (2017) Methodological approaches for monitoring opportunistic pathogens in premise plumbing: a review. *Water Res* **117**, 68–86.

Wan-Mohtar, W.A.A.Q.I., Ab Kadir, S. and Saari, N. (2016) The morphology of *Ganoderma lucidum* mycelium in a repeated-batch fermentation for exopolysaccharide production. *Biotechnol Reports* **11**, 2–11.

Wilkinson, M.G. (2018) Flow cytometry as a potential method of measuring bacterial viability in probiotic products: a review. *Trends Food Sci. Technol* **78**, 1–10.

Wu, L., Wang, S., Song, Y., Wang, X. and Yan, X. (2015) Applications and challenges for single-bacteria analysis by flow cytometry. *Sci China Chem* **59**, 30–39.

Yaqub, S., Anderson, J.G., MacGregor, S.J. and Rowan, N.J. (2004) Use of a fluorescent viability stain to assess lethal and sublethal injury in food-borne bacteria exposed to high-intensity pulsed electric fields. *Lett Appl. Microbiol* **39**, 246–251.

Young, S.B. and Setlow, P. (2004a) Mechanisms of *Bacillus subtilis* spore resistance to and killing by aqueous ozone. *J Appl Microbiol* **96**, 1133–1142.

Young, S.B. and Setlow, P. (2004b) Mechanisms of killing of *Bacillus subtilis* spores by Decon and Oxone, two general decontaminants for biological agents. *J Appl Microbiol* **96**, 289–301.

Zhang, P., Kong, L., Wang, G., Scotland, M., Ghosh, S., Setlow, B., Setlow, P. and Li, Y.Q. (2012) Analysis of the slow germination of multiple individual superdormant *Bacillus subtilis* spores using multifocus Raman microspectroscopy and differential interference contrast microscopy. *J Appl Microbiol* **112**, 526–536.

Zhang, W., Li, F. and Nie, L. (2010) Integrating multiple "omics" analysis for microbial biology: Application and methodologies. *Microbiology* **156**, 287–301.

Zhang, Y., Delbrück, A.I., Off, C.L., Benke, S. and Mathys, A. (2020) Flow cytometry combined with single cell sorting to study heterogeneous germination of bacillus spores under high pressure. *Front Microbiol* **10**, 1–13.

International Journal of Science, Environment and Technology, Vol. 5, No 6, 2016, 4375 – 4377

ISSN 2278-3687 (O)
2277-663X (P)

COMPARATIVE STUDIES ON THE NOVEL STERILISATION OF IRISH RETAILED INFANT MILK FORMULA USING ELECTRON BEAM AND PULSED LIGHT TREATMENTS

Emily McFadden[1], Ana-Luisa Costa Ramos[2], Derek Bradley[3], Olivier Vrain[4], Brian McEvoy[5] and Neil J. Rowan[6*]

[1,3]Postgraduate Student, [6]Professor,
Bioscience Research Institute, Athlone Institute of Technology, Ireland
[2]Postgraduate Student, Faculdade de Ciẽncias e Techologieas, Universidade do Algarve, Faro, Portugal
[4]Technical Operations Manager, STERIS Advanced Sterilisation Technologies, Tullamore, Co. Offaly, Ireland
[5]Senior Director Globla Technologies, STERIS Advanced Sterilisation Technologies, Tullamore, Ireland
E-mail: nrowan@ait.ie (**Corresponding Author*)

Abstract: This constitutes the first study to compare use of electron beam (EB) irradiation and pulsed light (PL) for novel sterilisation of infant mik formula retailed in Ireland. The microbiological quality of 60 powdered infant milk formula (PIMF), representative of two leading brands available in Ireland, were analyzed immediately after reconstitution and were shown to exhibit a total aerobic mesophilic count of $<10^4$ CFU/g (mean 3.3×10^2 CFU/g) and a *Bacillus cereus* count of $<10^3$ CFU/g powder (mean 2.2×10^2 CFU/g). Only 7 of 60 PIMF samples of Irish PIMF were free of *Bacillus* sp; while the pathogenic bacteria *Cronobacter sakazakii* and *Listeria monocytogenes* were not detected in any samples. Application of EB irradiation at 10 kGy sterilised the aforementioned PIMF. Pulsed light was not suitable for PIMF sterilisation due to turbidity, but did successfully kill *C. sakazakii, L. monocytogenes* and test *Bacillus* species when suspended and treated in saline solution. D_{10} values [dosage required to elicit a one $\log_{10}$ reduction in microbial numbers], for EB varied over the range 1.4 to 2.5 kGy for *Bacillus* species treated. Nutritional studies of EB-treated of PIMF samples at upper 10 kGy revealed no discernible difference in appearance, moisture, protein, ash, vitamin C, total fat and total carbohydrate content compared with untreated controls. The results indicate that EB treatment of Irish retailed infant milk formula at 10 kGy destroyed *Bacillus* endospores in these products without affecting nutritional status or appearance.

Keywords: infant milk formula, electron beam, pulsed light, nutritional status, sterilisation.

I. INTRODUCTION

The global baby and infant food market is projected to grow substantially [1]. In 2015, China imported over 175,000 tonnes of infant formula, this demand is driven by a high level of consumer confidence in product produced outside China. Nielsen Company estimated global

*Received Nov 15, 2016 * Published Dec 2, 2016 * www.ijset.net*

baby food and formule sales reached 35 billion U.S. dollars in 2015. This market surge is linked with socioeconomic development in these countries commensurate with growing number of working women and policy changes such as the one child policy in China. Ireland currently produces approximately 10% of products for the global infant formula market. However, reconstituted powdered infant formula (PIMF) are considered to be a food class of high risk due to the susceptibility of the infant population to enteric bacterial pathogens such as *Cronobacter sakazakii* and *Clostridium botulinum*, severe response to toxins and increased mortality [2, 3]. Since the first reported *Cronobacter* infection outbreak in 1958, PIMF has been identified as a source of these outbreaks resulting in many recalls of products worldwide. China recently ceased milk powder importants from New Zealand and Australia over concerns with PIMF contamination; Chinese public have grown increasingly distrusful of domestically-produced food since 2008, when ca. 300,000 people were poisoned resulting in 6 infant deaths from consumption of baby formula and milk containing melamine and poisonings from important products [4]. Despite the elevated temperatures employed in the manufacture of PIMF, there have been a number of food related illnesses where PIF has been implicated as the vehicle of infection [5 – 10].

Generally, PIMF are known to be predomintly contaminated with aerobic spore-formers of the genus *Bacillus* [11 – 13], and thus, are not sterile. The application of non-thermal food processing technologies may potentially enable elimination of bacterial endospores in PIMF rendering them sterile. Electron-beam irradiation (EBI) is a novel food decontamination technology that uses low-dose ionizing radiation in the treatment of crops or foods, to eliminate contamination [14]. Pulsed light (PL) has also been applied for water and disinfection of food surfaces owing to its' ability to delivery high-intensity, broad-spectrum biocidal lighr [15]. Irradation has been approved by the United States Food and Drug Administration (USFDA), United Nations Food and Agriculture Organisation (FAO) and World Health Organisation for food decontamination [14]. However, from a perspective of food safety, it must be proven that these food decontamination technologies not only eliminate microorganisms but also exert no adverse effects on the nutrition or residual radiation in the food, before it is applied in food processing industry. The aim of this study was to assess the efficacy of EBI and PL as novel non-thermal methods for sterilising infant milk formula produced in Ireland.

II. METHODOLOGY

Microbiological quality of reconstituted PIMF samples

The survey was composed of 60 powdered infant milk formula (PIMF), representative of two leading brands available in the Republic of Ireland, were prepared as per methods described previously [13], with slight modifications. Briefly, 25 g of PIMF was reconstituted in 225 ml sterile distilled water at a water temperature 45ºC by shaking 25 times through an excursion of 30 cm. Following a 30 min cooling period triplicate aliquots of 1 ml was removed for total aerobic mesophilic counts (TAMCs) and for other bacteriological enumerations as outlined below The reconstituted PIF were then incubated at either 25ºC and 35ºC for periods up to and including 24 h. Total aerobic mesophilic bacteria in PIF were enumerated and identified at 0, 8, 14 and 24 h sample time intervals by pour and spread plating, decimal diluted samples in buffered peptone water (BPW) and plating on Tryptone Soya Agar supplemented with 0.6% Yeast Extract (TSYEA; Cruinn Diagnostics, Ireland) followed by aerobic incubation of plates at 37ºC for 48 h. This procedure was repeated in duplicate for three separate samples analyzed from the same PIF. *Bacillus* spp present in these PIMF samples were identified as per methods described previously [11]. The identity of each Bacillus isolate was confirmed using the API 50 CHB and API 20 E galleries (bioMérieux Ltd.). PIMF were also examined for the presence of *Cronobacter sakazakii* using conventional isolation method as according to Haughton et al. [13]. Staphyococcal isolates were identified based on Gram reaction, ability to produce catalase and oxidase and coagulase activity, with subsequent use of API Staph (BioMerieux) to confirm identity. Efficacy of bacterial detection was evaluated in PIMF using positive control strains comprising *C. sakazakii* (NCTC 8155), *L. monocytogenes* NCTC 11994, *Salmonella Enteritidis* NCTC 3046, *Escherichia coli* ATCC 29522, *Staphylococcus aureus* ATCC 29523 and *Bacillus cereus* NCTC 11145. PIMF samples were coded based on microbiogical quality for subsequent electron beam irradiation and pulsed light treatments.

Electron-beam irradiation (EBI)

A Mevex high energy electron beam irradiator (combined 10/12 MeV unit, 30 kW) was used to irradiate 25 g samples of IMF at doses of 1.5, 5, 10 and 25 kGy. A range of representative test microorganisms were also artificially-seeded in 25 ml reconstituted IMF (and phosphate buffered saline) samples where starting populations was ca. 10^7 vegetative cells or endospores per millilitre in order to determine the D_{10} values for each test test organism post EB

treatment (average dose to reduce microbial numbers by 1 $\log_{10}$ order expressed in kGy). All samples were irradiated at room temperature in the presence of air at STERIS Advanced Sterilisation Technology plant (Tullamore, Ireland).

Pulsed light (PL) treatments

Powdered and reconstituted IMF samples (25 g/ml) were treated using pulsed light (PL) at UV doses of 4.32, 10.8, 12.98 µJ/cm^2 as described in Garvey et al. [16], with modifications. A pulsed power source (PUV-1, Samtech Ltd., Glasgow) was used to power a low-pressure (60kPa) xenon-filled flashlamp (Heraeus Noblelight XAP type NL4006 series constructed from a clear UV transparent quartz tube) that produced a high-intensity diverging beam of polychromatic pulsed light. This delivery system produced ultra-short duration pulses of an intense broadband emission that is rich in the UV-C germicidal wavelength. PL is produced by storing electricity in a capacitor over relatively long times and releasing it as a short duration pulse using sophisticated pulse compression techniques. The light source has an automatic frequency control function which allows it to operate at 1 pulse per second (pps); this setting was used throughout the study.

Nutritional and cytotoxicity status of irradiated PIMF samples

Powdered IMF samples subjected to EBI were independently analysied for nutritional content changes at ALS Food and Pharmaceutical testing laboratory (Chatteris, Cambridgeshire, England); these tests comprised moisture, energy, protein, ash, vitamin C (as ascorbic acid), total fat and total carbohydrate content. Changes in physical appearance and texture was also examined. Untreated and EBI-treated samples were encoded post treatment and transported to this independent, accredited food testing facility under refrigeration conditions. Cytotoxicity tests of EBI-treated IMF was determined using MTT (3-(4, 5 dimethylthiazol-2-yl)-2,5-diphenyl-tetrazolium bromide) assay following exposure to human HepG2 liver cells as described previously [17]. IMF was reconstituted at 13% w/v (as recommended by manufacturer), 1.0% w/v and 0.1% w/v and exposed to HepG2 cells; release the purple formazan product was measured spectrophotometrically at 490nm after addition of 100ul decolouriser (DMSO).

Statistical analysis

The Fisher's exact test was used to compare the bacteriological quality (where total aerobic counts for 60 PIMF were pooled and compared as a unit under these conditions), differences in treatment technologies (PB, PL) were examined using two-way analysis of variance

(ANOVA, Minitab version 13.1, Minitab Ltd, State College, Pennyylvania, USA). All significant differences were reported at the 95% level of confidence ($p<0.05$).

III. RESULTS

All 60 PIMF examined immediately after reconstitution were of satisfactory bacteriological quality as per new guidelines recommended by Codex Alimentarius Commission code of hygienic practice for powdered formulae for infants and young children [18]. All PIMF had a total aerobic mesophilic counts less than the 1 x 10^4 bacteria per gram (Table 1). While the latter Codex does not recommend an action limit for *B. cereus*, all PIMF were shown to have a count less than 10^3 CFU/g power for this pathogen that is below the safety limit of 10^4 CFU/g recommended by the Association of Dietetic Food Industries of the European Community (IDAEC). The PIMF examined, which were representative of two leading brands currently available in the Republic of Ireland were of similar bacteriological quality ($p<0.05$). The largest concentration of organisms present in any PIMF product was 4.9x10^3 CFU/g (consisting solely of *B. subtilis*), while the mean total aerobic plate count for all 60 infant foods analyzed was 3.5x10^2 CFU/g (Table 1). *Bacillus cereus* was present in 38 of 60 PIMF examined (mean *B. cereus* 2.2x10^2 CFU/g), where the largest number of *B. cereus* recovered from any formulation was 4.7 x10^2 CFU/g (Table 1). The microbial flora of PIMF before reconstitution consisted mainly of aerobic spore-formers of the genus *Bacillus*.

Bacillus species exhibited varying D_{10} values (average dose in kGy that caused a reduction in microbial numbers by 1 $\log_{10}$ order) to EB irradiation over the range 0.5 to 2.8 kGy where endospores were shown to be more resistant compared to vegetative cell forms ($p<0.05$) (Table 2). Initial EBI range finding studies was conducted at 25 kGy that was too high a dose for D_{10} determinations. Treatment of *Bacillus* endospores in reconstituted IMF provided protection compared with similar EB irradiated samples in PBS ($p<0.05$). *Cronobacter sakazakii* and *Listeria monocytogenes* exhibited similar EBI sensititiy to that of vegetative cells of *Bacillus* species tested. There was no significant difference between retailed IMF1 and IMF2 products in terms of efficacy of EBI treatments ($p<0.05$). EB irradiation at 10 kGy sterilised retailed powdered IMF of *Bacillus* endospores present.

Retailed PIMF treated with EB at 10 kGy were not altered in moisture (2.8 g versus 2.8 g treated), ash (2.2 g versus 2.3 g treated), energy (497 kcal versus 497 treated), vitamin C (71.5 mg versus 69.4 mg treated), total fats (23.4 g versus 23.5 treated), total carbohydrates (62.1 versus 61.8 treated) or physical compared with untreated controls. There was no discernible

cytotoxicity difference in untreated and EB irradiated infant formula at 10 kGy when challenged with human HepG2 liver cells post treatments (Fig. 1).

Pulsed light (PL) produced ca. 6 $\log_{10}$ CFU/ml reduction in *Bacillus* endospores when treated in phosphate buffered saline at varying UV doses over range 4.32 to 12.98 µJ/cm^2, but was significantly less effective at destroying these endospores when PL-treated in reconstituted IMF at same UV dose (p<0.05) (Table 3]. Similar to EBI, *Bacillus* in endospore state were more tolerant of UV irradiance compared to vegative cells. The inability of PL to reduce bacterial load in reconstituted IMF is attributed to poor transmissivenss and penetration ability of this system, which is turbid (Fig. 2).

IV. DISCUSSION

The pathogenic bacterium *Cronobacter sakazakii* was not isolated from 60 reconstituted PIMF in this study, findings agree with the work of O'Brien and coworkers [19] where these researchers did not detect *C. sakazakii* in 468 samples representative of 31 different milk and soya-based infant formula products commercially available in European countries. Maximum allowed levels for *B. cereus* in dried infant feeds have also been set in several countries, ranging from an acceptable threshold of 10^3 CFU of *B. cereus* per gramme (e.g., Finland) to 10^4 in Sweden [12]. Veda and co-workers also showed that the most frequently isolated organisms from dried baby formulae in Japan were *B. licheniformis* and *B. subtilis*, while other *Bacillus* recovered included *B. cereus, B. pumilus, B. megaterium, B. circulans* and *B. coagulans* [cited in 11]. Thus, isolation of aerobic endospores is commonplace for IMF products globally.

Pulsed light is a promising next generation approach for contact surface and water decontamination [15], but is not applicable as sterilisation technology for powdered foods due to lack of ability to penetrate this product. However, irradiation of retailed powdered IMF at dose of 10 kGy can effectively destroy *Bacillus* endospores. There is a significant gap in scientific research on the application of irradiation to powdered foods [14]. Hong et al. [20] reported on the use of EB for inactivation of *C. sakazakii*, *B. cereus* and *Salmonella typhimurium* in powdered weaning food where D_{10} values were 4.83, 1.22 and 0.98 kGy, respectfully. This reported D_{10} value is *C. sakazakii* is approximately 9 times greater to that reported for a different strain of this foodborne pathogen in this study, which highlights the importance of investigating a broad range of species to EBI in powdered infant formula. Sarrias and coworkers [21] revealed that EB can effectively be deployed for rice sterilisation

at 7.5 kGy as it destroys *Bacillus* and *Clostrida* endospores and fungi. Helfinstine et al. [22] previously demonstrated that EB irradiation can effectively destroy *Bacillus atrophaeus* endospores in envelopes under a biodefence study, where D_{10} value of 1.53 kGy was determined for this species that is similar to D_{10} values reported in this study for *Bacillus* species. Other researchers compared the tolerance of multiple bacterial strains to EBI and found variability in tolerances depending on species type such as *Listeria monocytogens* (D10 = 1.09 kGy), *Listeria innocua* (D_{10} – 0.38 kGy), *Salmonella enterica* Poona (D_{10} = 0.38 kGy), *E. coli* O157:H7 (D_{10} = 0.36) and *Salmonella* LT2 (D_{10} = 0.12 kGy) [23]. Lung et al. [14] reported that EBI does not significantly affect nutritional or appearance properties of various treated foods. However, D_{10} value determinations for EB treatments of foods should also consider other varying factors including food composition, water activity, storage temperature and presence of oxygen [24]. While there is gap in current knowledge as to how EB destroys *Bacillus* endospores at molecular level, studies focusing on vegative cell inactivation by Shehata et al. [25] revealed DNA is the principal target govering loss of viability post EB irradiation. Electron beam irradiation has many advantages such as relatively short processing time, in-line process, highly effective, involves few variables, low heat, short release time, low equipment cost and controlled dose [14]. Future studies in this area should consider broadening microbial targets to encompass anaerobic *Clostridia* endospores that may occasionally contaminate powdered infant formula; use of human duodenal Caco2 cells instead of HepG2 cells for cytotoxicity studies; and expand nutritional compostion studies pre and post EBI.

ACKNOWLEDGMENTS

The authors would like to acknowledge funding support from Athlone Institute of Technology’s Postgraduate Scholarhip Initiaive (15AIT2014

REFERENCES

[1] Kent, G. 2015. Global infant formula: monitoring and regulating the impacts to protect human health. International breastfeeding Journal, 10:6 (open access).

[2] Townsend, S, Barron, J.C, Loc-Carrillo, C., Forsythe, S. 2007. The presence of endotoxin in powdered infant milk formulae and the influence of endotoxin and *Enterobacteri sakazakii* on bacterial translocation in the infant rat. Food Microbiology. *24*, 67-74.

[3] Norberg, S., Staunton, C., Hill, C., Fitzgerald, G.F., Cotter, P.D. 2012. *Cronobacter* species in powdered infant formula. J. Food Protect. 3, 438-620.

[4] Wu, Y-N., Zhao, Y-F., Li, J-G., 2009. A survey on occurrence of melanine and its analogues in tainted infant formula in China. Biomedical and Environmental Sciences, 22(2), 95-99.

[5] Rowe, B. 1987. Salmonella ealing infections associated with consumption of infant dried milk. Lancet October, 900-903.

[6] Louie, K.K. 1993. *Salmonella* serotype tennesse in powdered milk products and infant formula-Canada and the United States, JAMA. 270:4:432.

[7] Gerike, B., Thurn, V. 1994. Identification of infant food as a vehicle in a nosocomial outbreak of *Citrobacter freundii*: epidemiological subtyping by allozyme whole cell protein and antibiotic resistance. Journal of Applied Bacteriology. 76,553-558.

[8] Van Archer, J., De Smet, F., Muyldermans, G.,Gougatef, A., Naessens, A.,, Lauwers, S. 2001. Outbreak of necrotizing enterocolitis associated with *Enterobacter sakazakii* in powdered milk formula. Journal of Clinical Microbiol. 39, 293-297.

[9] Himelright, I., Harris, E., Lorch, V., Anderson, M. 2002. *Enterobacter sakazakii* infections associated with the use of powdered infant formulae – Tenessee, 2001. J. Am Med Assoc. 287, 2204-2205.

[10] Caubilla-Barron, J., Hurrell, E., Townsend, S., Cheetham, P., Loc-Carrillo, C., Fayet, O., Frere, M.F., Forsythe, S.K. 2007. Genotypic and phenotypic analysis of *Enterobacter sakazakii* strains from an outbreak resulting in fatalities in a neonatial intensive care unit in France. Journal of Clinical Microbiology. 45, 3979-3985.

[11] Rowan, N. J., Anderson, J. G., Anderton, A. 1997. Bacteriological quality of infant milk formulae examined under a variety of preparation and storage conditions. Journal of Food Protection. 60, 1089-1094.

[12] Shaheen R., Andersson, M.A., Apetroaie, C., Schulz, A., Ehling-Schulz, M., Ollilainen, V.M., Salkinoja-Aalonen, M.S. 2006. Potential of selected inant food formulas for production of *Bacillus cereus* emetic toxin, cereulide. International Journal of Food Microbiology. 107, 287-294.

[13] Haughton, P., Garvey, M., Rowan, N.J. 2010. Emergence of Bacillus Cereus as a Dominant Organism in Irish Retailed Powdered Infant Formulae (Pif) When Reconstituted and Stored under Abuse Conditions, Journal of Food Safety, 30(4), 814--831.

[14] Lung, H-M., Cheng, Y-C., Chang, Y-H., Huang, H-W., Yang, B.G., Wang, C.Y. (2015). Microbial decontamination of food by electron beam irradiation. Frends in Food Science and Technology, 44, 66-78.

[15] Rowan, N., Valdramidis, V.P., Gomez-Lopez, V.M. 2015. A review of quantitative methods to describe efficacy of pulsed light generated inactivation data that embraces the occurrence of viable but non culturalbe state microorganisms. Trends Food Science and Technology, 44 (1), 79-92.

[16] Garvey, M., Fernandes, A., Rowan, N.J. 2015. Pulsed light for the inactivation of fungal biofilms of clinically important pathogenic Candida species. Yeast 32 (7), 533-40.

[17] Kirf, N., Higginbotham, C.L., Rowan, N., Devery, S. 2015. Cyto and gentoxicological assessment and functional characterization of N-vinyl-2-pyrrolidone-acrylic acid based copolymeric hydgrogels with potential for future use in wound healing applications. Biomedical Materials, 5 (open access)

[18] CODEX ALIMENTARIUS COMMISSION (2009). Code of hygiene practice for powdered formulae for infants and young children (CAC/RCP 66 – 2008).

[19] O'Brien, S., Healy, B., Negredo, C, Anderson, W., Fanning, S, Iversen, C. 2009. Prevalence of *Cronobacter* species (*Enterobacter sakazakii*) in follow-on infant formulae and infant drinks. Letters in Applied Microbiology 48, 538-541.

[20] Hong, Y.H., Park, J.Y., Park, J.H., Chung, M.S., Kwon, K.S., Chung, K., Won, M.., Song, K.B. 2008. Inactivation of *Enterobacter sakazakii*, *Bacillus cereus*, and Salmonella typhimurium in powdered weaning food by electron-beam irradiation, Radiation Physics and Chemistry, 77 (9), 1097-1100.

[21] Sarrias, J., Valero, M., Salmeron, M.C. (2003). Elimination of *Bacillus cereus* contamination in raw rice by electron beam irradiation. Food Microbiology, 20 (3) 327-332.

[22] Helfinstine, S. L., Vargas-Aburto, C., Uribe, R. M. and Woolverton, C. J. (2005) 'Inactivation of Bacillus endospores in envelopes by electron beam irradiation. Applied Envirnmental Microbiology, 71(11), 7029-7032

[23] Rodriguez, O., Castell-Perez, M.E., Ekpanyaskun, N., Moreira, R.G.., Castillo, A. 2006. Surrogates for validation of electron beam irradation of foods. International Journal of Food Microbiology, 110, 117-122.

[24] Yim, D.G., Yo, C., Kim, H.J., Chen, J.S., Kim, H.C., Nam, K.C. (2015). Combined effect of irradiation and aging condition on physiochemical and microbial quality on Hanwoo eye of round. Korean Journal of Food Science, 35(3), 406-412.

[25] Shehata, M.K., Gomaa, F.A.M., Helal, Z.H. (2011). Effects of gamma and electron beam irradiation on viability and DNA elimination of S. aureus. Archives of Clinical Microbiology (2), 6.3, doi 10.3823/244.

Table 1: Variation in aerobic plate counts for named bacterial species in 60 Powdered IMF (30 IMF1 & 30 IMF2) enumerated immediately after reconstitution at a water temperature of 45ºC

Bacterial spp.	**Number of PIF where named bacterial spp had total aerobic count (log_{10} CFU/g) in the below ranges**								**Total Aerobic Count (log_{10} CFU/g) Mean[a]**	
	< 2		**2**		**2 - 3**		**3 - 4**			
	IMF1	**IMF2**	**IMF1**	**IMF2**	**IMF1**	**IMF2**	**IMF1**	**IMF2**	**IMF1**	**IMF2**
B. licheniformis	8	5	11	7	11	6	3	1	2.1±1.1	2.2±1.4
B. subtilis	6	7	6	7	5	5	0	1	2.2±0.6	2.4±0.5
B. pumilus	1	1	3	3	2	2	0	1	2.0±1.0	2.4±0.5
B. cereus	7	7	7	8	6	5	1	1	2.4±0.4	2.5±0.3
B. mycoides	2	1	2	1	1	2	0	0	2.0±0.7	1.9±0.5
B. megaterium	4	2	3	3	2	2	0	0	2.4±0.7	2.3±0.4
B. sphaericus	1	3	3	4	1	1	0	0	1.9±0.3	2.0±0.6
B. circulans	2	0	2	0	1	0	0	0	2.0±0.4	2.0±0.4
Staphylococcus spp.	3	2	2	1	3	3	0	0	1.8±0.5	1.8±0.3
Listeria spp.	ND	ND	ND	ND	ND	ND	ND	ND	ND	ND
Cronobacter spp.	ND	ND	ND	ND	ND	ND	ND	ND	ND	ND

[a] Mean ± SD refer to variation in total aerobic counts (log_{10} CFU/g) among PIMF in each brand prepared at water temperature of 45ºC (n=30). No significant difference in microbial numbers was observed between brands of PIMF. ND, not detected.

Table 2: D_{10} value determinations for EB irradiated (kGy) test bacteria in vegetative and endospore state suspended in reconstituted infant milk formula (RIMF) or phosphate buffered saline (PBS)

Test Bacterium	Morphological State	D_{10} value (kGy)*		
		PBS	IMF1	IMF2
C. sakazakii NCTC 8115	Vegetative cell	0.488±0.04	0.492±0.07	0.531±0.06
L. monocytogenes NCTC 11994	Vegetative cell	0.554±0.04	0.705±0.04	0.562±0.05
B. cereus NCTC 11145	Vegetative cell	0.771±0.03	0.632±0.04	0.618±0.05
B. cereus NCTC 11145	Endospore	1.588±0.04	1.674±0.11	1.666±0.14
B. cereus NR3	Vegetative cell	0.513±0.04	0.816±0.08	0.926±0.12
B. cereus NR3	Endospore	1.658±0.05	1.236±0.24	1.257±0.17
B. cereus EMF2	Vegetative cell	0.504±0.06	0.554±0.08	0.611±0.07
B. cereus EMF2	Endospore	1.018±0.08	1.294±0.06	1.898±0.31
B. cereus NCTC 11143	Vegetative cell	0.501±0.03	0.536±0.07	0.528±0.06
B. cereus NCTC 11143	Endospore	1.506±0.10	2.155±0.28	2.08±0.24
B. cereus NB40	Vegetative cell	0.678±0.11	0.690±0.09	0.674±0.13
B. cereus NB40	Endospore	1.526±0.04	1.722±0.19	2.51±0.05
B. cereus NB51	Vegetative cell	0.561±0.05	0.554±0.08	0.601±0.12
B. cereus NB51	Endospore	1.466±0.06	1.309±0.16	2.281±0.15
B. coagulans NB11	Vegetative cell	0.466±0.05	0.528±0.08	0.518±0.05
B. coagulans NB11	Endospore	1.521±0.04	1.239±0.14	1.428±0.06
B. licheniformis NCTC 10341	Vegetative cell	0.540±0.11	0.590±0.06	0.612±0.08
B. licheniformis NCTC 10341	Endospore	1.408±0.10	1.622±0.24	1.630±0.13
B. subtilis NCTC 3610	Vegetative cell	0.582±0.06	0.602±0.04	0.598±0.06
B. subtilis NCTC 3610	Endospore	1.455±0.03	1.612±0.11	1.550±0.8

*The D_{10} value indicates the average dose (kGy) it takes to reduce the bacterial load by 1-Log

Table 3: Log_{10} reduction in microbial numbers (CFU/ml) of test bacteria treated in phosphate buffered saline (PBS) at different UV doses ($\mu J/cm^2$) produced by pulsed light

Test Bacterium	**Morphological State (Vegetative cell or Endospore)**	**Log_{10} reduction (CFU/ml) of test bacteria at varying UV doses ($\mu J/cm^2$)**		
		4.32 $\mu J/cm^2$	**10.8 $\mu J/cm^2$**	**12.96 $\mu J/cm^2$**
C. sakazakii NCTC 8115*	Vegetative cell	5.6±0.3	7.2±0.6	7.4±0.3
L. monocytogenes NCTC 11994*	Vegetative cell	5.3±0.6	6.9±0.5	7.3±0.3
B. cereus NCTC 11145	Vegetative cell	4.2±0.2	6.0±0.5	6.5±0.4
B. cereus NCTC 11145	Endospore	2.5±0.5	5.6±0.4	5.9±0.3
B. cereus NR3	Vegetative cell	5.4 ±0.4	6.4 ±0.3	6.9±0.2
B. cereus NR3	Endospore	3.4 ±0.1	5.3±0.5	5.6±0.5
B. cereus EMF2	Vegetative cell	5.1±0.3	6.2±0.4	6.7±0.4
B. cereus EMF2	Endospore	2.3±0.5	5.0±0.4	5.3±0.3
B. cereus NCTC 11143	Vegetative cell	5.0±0.5	5.8±0.3	6.7±0.2
B. cereus NCTC 11143	Endospore	3.2±0.4	5.1±0.6	5.5±0.2
B. cereus NB40	Vegetative cell	4.9±0.1	5.5±0.5	6.4±0.4
B. cereus NB40	Endospore	2.2±0.3	5.1±0.3	5.5±0.2
B. cereus NB51	Vegetative cell	5.3±0.2	6.2±0.2	7.0±0.1
B. cereus NB51	Endospore	3.2±0.5	5.4±0.5	5.8±0.3
B. coagulans NB11	Vegetative cell	4.3±0.4	6.0±0.4	6.4±0.4
B. coagulans NB11	Endospore	2.4±0.4	5.4±0.5	5.7±0.3
B. licheniformis NCTC 10341	Vegetative cell	4.6±0.5	6.6±0.4	6.9±0.2
B. licheniformis NCTC 10341	Endospore	3.9±0.1	5.7±0.3	6.1±0.5
B. subtilis NCTC 3610	Vegetative cell	4.3±0.5	6.1±0.6	6.7±0.2
B. subtilis NCTC 3610	Endospore	3.3±0.3	5.3±0.5	5.6±0.3
*Non-endospore forming pathogenic bacteria				

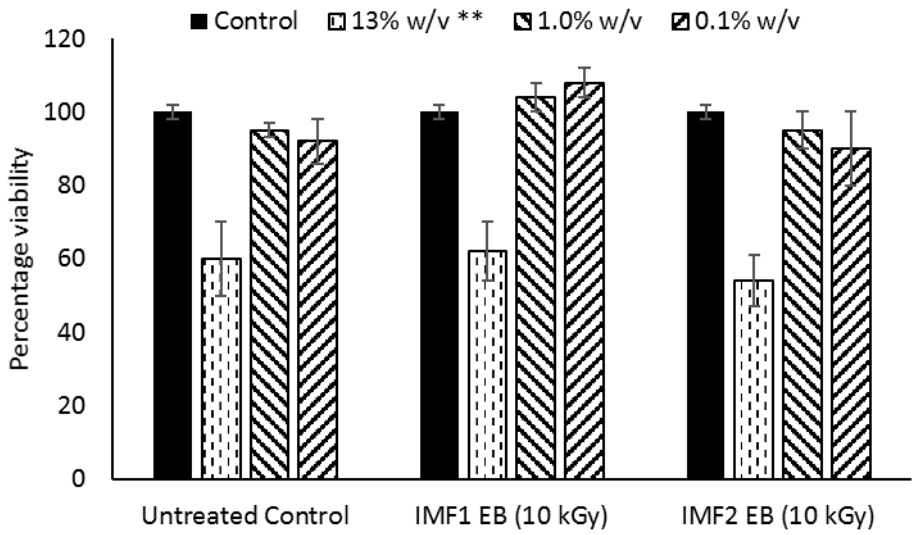

Figure 1 Percentage viability of human HepG2 liver cells exposed to varying dilutions of IMF1 and IMF2 pre and post EB irradiation at 10 kGy. **intimates recommended preparation mix for reconstituting powdered IMF products

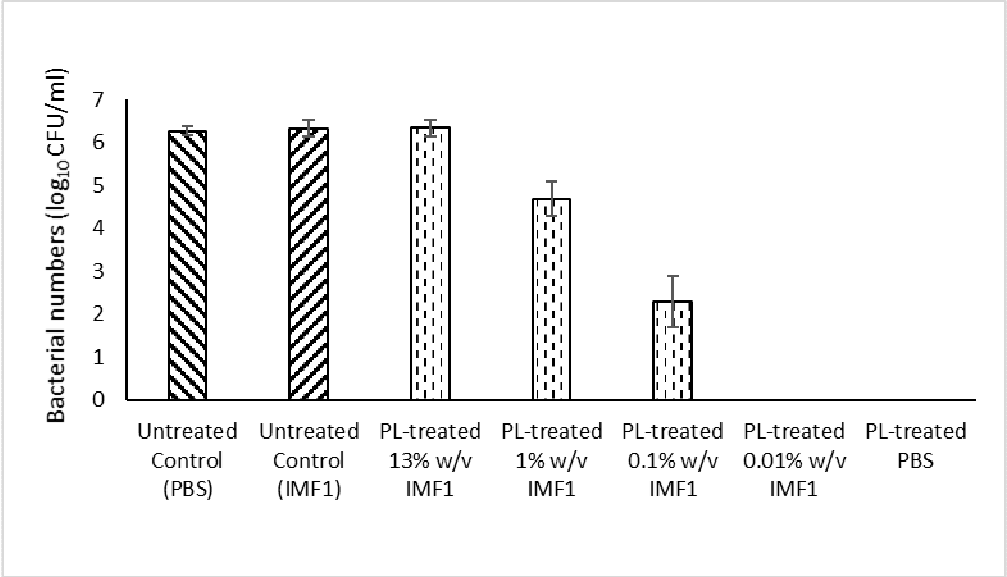

Figure 2 Log_{10} order reduction, expressed in CFU/ml of *Bacillus cereus* (NB3), for serially diluted infan t formula and PBS treated with a pulsed light UV dose of 12.98 µJ/cm^2.

Journal of Hospital Infection 145 (2024) 88—98

Available online at www.sciencedirect.com

Journal of Hospital Infection

journal homepage: www.elsevier.com/locate/jhin

Review

A proposed cleaning classification system for reusable medical devices to complement the Spaulding classification

T. Kremer [a,d,*], **N.J. Rowan** [a,b,c], **G. McDonnell** [d]

[a] *Centre for Sustainable Disinfection and Sterilization, Bioscience Research Institute, Technological University of the Shannon Midlands Midwest, Athlone, Ireland*
[b] *Department of Nursing and Healthcare, Technological University of the Shannon Midwest Mideast, Athlone, Ireland*
[c] *SFI-funded CURAM Centre for Medical Device Research, University of Galway, Galway, Ireland*
[d] *Microbiological Quality and Sterility Assurance, Johnson & Johnson, Raritan, NJ, USA*

ARTICLE INFO

Article history:
Received 21 June 2023
Accepted 22 November 2023
Available online 14 December 2023

Keywords:
Spaulding
Cleaning
Reusable medical device
Hospital-acquired infections
Disinfection
Sterilization
Patient risk

SUMMARY

A central tenet in infection prevention is application of the Spaulding classification system for the safe use of medical devices. Initially defined in the 1950s, this system defines devices and surfaces as being critical, semi-critical or non-critical depending on how they will be used on a patient. Different levels of antimicrobial treatment, defined as various levels of disinfection or sterilization, are deemed appropriate to reduce patient risk of infection. However, a focus on microbial inactivation is insufficient to address this concern, which has been particularly highlighted in routine healthcare facility practices, emphasizing the underappreciated importance of cleaning and achieving acceptable levels of cleanliness. A deeper understanding of microbiology has evolved since the 1950s, which has led to re-evaluation of the Spaulding classification along with a commensurate emphasis on achieving appropriate cleaning. Albeit underappreciated, cleaning has always been important as the presence of residual materials on surfaces can interfere with the efficacy of the antimicrobial process to inactivate micro-organisms, as well as other risks to patients including device damage, malfunction and biocompatibility concerns. Unfortunately, this continues to be relevant, as attested by reports in the literature on the occurrence of device-related infections and outbreaks due to failures in processing expectations. This reflects, in part, increasing sophistication in device features and reuse, along with commensurate manufacturer's instructions for use. Consequently, this constitutes the first description and recommendation of a new cleaning classification system to complement use of the traditional Spaulding definitions to help address these modern-day technical and patient risk challenges. This quantitative risk-based classification system highlights the challenge of efficient cleaning based on the complexity of device features present, as an isolated variable impacting cleaning. This cleaning classification can be used in combination with the Spaulding classification to improve communication of cleaning risk of a reusable medical device between manufacturers and healthcare facilities, and improve established cleaning practices. This new cleaning classification system

* Corresponding author. Address: Microbiological Quality and Sterility Assurance, Johnson & Johnson, 1000 Route 202 S Building 930, East Raritan, NJ 08869, USA.
E-mail address: tkremer@its.jnj.com (T. Kremer).

https://doi.org/10.1016/j.jhin.2023.11.018

will also inform future creation, design thinking and commensurate innovations for the sustainable safe reuse of important medical devices.

Introduction

The safe use of any medical device always requires collaboration between the manufacturer and the healthcare user. For sterile, single-use medical devices, the product is provided ready for use; however, safety can only be assured when the device is handled correctly during storage and use at the healthcare facility. The requirement for this collaboration becomes even greater with medical devices intended to be processed prior to use or reuse by the healthcare facility. For reusable medical devices, greater responsibility for the mitigation of infection risk lies with the healthcare facility. This transfer of responsibility is communicated through manufacturer's instructions for use (IFU). As described in international standards, the medical device manufacturer must provide detailed processing instructions to ensure that, when followed correctly, the risk of patient infection or other complications is minimized [1–3]. The processing IFU are intended to standardize the quality of the medical device as appropriate to patient use. Product, including microbiological, quality is a qualitative concept that encompasses all activities which provide confidence that a medical device is safe for its intended use, and is more than just a consideration of the presence or absence of micro-organisms potentially remaining on a product. It includes residual chemicals or particulates which may remain on a device following use and processing that may also elicit an immune response in a patient [4].

Earle H. Spaulding defined a classification system to address the microbiological quality of medical devices processed within a healthcare facility in the 1950s [5]. This system needs to evolve in order to respond appropriately to the increasing complexity of reusable medical devices (e.g. endoscopes) since the late 1960s [5]. The Spaulding classification system for medical devices is based on the risk of transmission of infections [1]. This risk is based on the level of contact the device has with the patient. Devices are classified as critical, semi-critical or non-critical [6].

Critical devices include those that contact 'sterile' tissues (including blood and internal body spaces) during their use. Examples include surgical devices. It is recommended that these devices should be adequately cleaned, inspected and sterilized prior to patient use [1,5,7,8]. Semi-critical devices may only contact mucous membranes or non-intact skin. Examples include flexible colonoscopes, gastroscopes and respiratory equipment. It is also recommended that these devices should be adequately cleaned and sterilized prior to use. However, in many cases, they may be subjected to terminal high-level disinfection (HLD) instead of sterilization [1,5,7,8]. The purpose of HLD is to remove pathogens safely, but this may or may not include all dormant micro-organisms such as bacterial spores. Non-critical devices or instruments may contact intact skin but do not penetrate it. Examples include blood pressure cuffs, stethoscopes and skin electrodes (non-critical patient care devices). They also include a variety of equipment and environmental surfaces that may not contact the patient directly, but can become contaminated during use or over time in clinical practice (non-critical environmental surfaces). Recommended processing steps can include cleaning alone or cleaning with disinfection, where the level of disinfection can vary depending on the risk to patient or staff safety, as well as country-specific requirements [1,5,7,8].

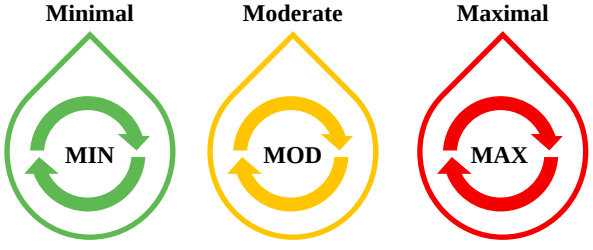

Figure 1. Examples of potential cleaning classification symbols.

The Spaulding classification focuses on the resistance of, and risks with, known micro-organisms (specifically pathogens) in parallel with the criticality of the device in clinical use. Although more information about microbial resistance profiles to inactivation is known today, this classification system, which focuses on use of disinfection and sterilization practices, is just as applicable today as it was when it was developed over 50 years ago [5]. However, criticism on the foundational resistance profiles of micro-organisms to inactivation has shown variability depending on the type of antimicrobial process being employed (especially with chemical disinfectants) [5]. It has been reported previously that exposure to implicit stresses can enable treated micro-organisms to adapt otherwise-lethal biocidal processes, particularly when embedded in complex biofilms [9]. Another topic of debate is the persistence of micro-organisms on environmental surfaces [10]. Despite being 'non-critical' surfaces, the transmission of micro-organisms from these surfaces to patients and staff has highlighted the importance of surface disinfection, particularly with bacterial spores (e.g. *Clostridioides difficile*), meticillin-resistant *Staphylococcus aureus* and, increasing problematic, Gram-negative bacteria (e.g. *Pseudomonas aeruginosa*). In these situations, it is not necessary or practical to ensure that these surfaces are treated with sporicidal disinfectants/sterilants, but does emphasize the importance of physical removal (cleaning). Overall, these examples remind us to remain vigilant in our understanding of microbiology and the potential for unwanted microbial adaptation to frontline therapeutics and disinfection practices. It is rare that reports of failure of the Spaulding classification system have led to patient infections, when applied correctly. Unfortunately, it is more common that reports of device-associated infections and other patient complications with reusable devices/surfaces have arisen due to incorrect processing practices [7]. A review of the literature highlights common examples, such as inadequate device design

or maintenance, poor water quality used at important stages of processing, use of inappropriate processing methods or antimicrobial technologies, and poor environmental controls during storage and handling of devices. Moreover, the most frequent reports appear to be related to failure of adequate cleaning, where a keyword search was completed using 'processing' and 'reusable medical device'. Of the 56 results, 18 were relevant (Table I). It should be noted that an important, yet underappreciated, consideration underpinning the earliest use of Spaulding's classification was that medical devices are clean prior to disinfection or sterilization. This assumption does not take into consideration the increasing number of different medical devices with highly complex device features that are not easy to clean, which reflects the dynamic and evolving needs of modern-day medicine.

Cleaning, defined as the removal of soil to the extent necessary for further processing or for intended use [11], is essential, and it has been demonstrated repeatedly in the literature that cleaning failures are a root cause of failing decontamination of reusable medical devices [5,12]. Many articles over the last 50 years have highlighted the need for more attention on the cleaning process related to medical devices with complex features, with increasing focus on the relationship between cleaning difficulty and hospital-acquired infections (HAIs) [13].

How clean is safe?

At the time the Spaulding classification was widely adopted, the detailed measurement techniques or endpoints for determining cleanliness had yet to be established. Visual cleanliness was the expectation, and the Spaulding classification system was established with the foundational assumption that all devices would be visibly clean prior to the microbial reduction step of disinfection or sterilization. It was assumed that vigorous cleaning would always be performed, and, in many cases, devices (and their associated features) could be inspected quickly during or following the cleaning process. If the device was visibly clean, it was assumed that the residual soil level was sufficiently low to ensure that the antimicrobial process would be effective, even in the presence of some residual soil. In regulatory approval requirements worldwide [39,40], the effectiveness of disinfection or sterilization products/methods was required to demonstrate activity in the presence of residual soil. Microbial reduction studies (i.e. disinfection and sterilization) are typically investigated under laboratory conditions with little (e.g. micro-organism titre with 5% bovine serum) or no soil remaining on the device. The resistance profile of the most resistant micro-organism to the process may change in the presence of soil, depending on soil components, as demonstrated by spore survival studies [32].

Another example centres on the development of complex biofilms in or on device surfaces harbouring problematic micro-organisms, a concept that was not considered initially by Spaulding. Roberts *et al.* described traditional conditions required for biofilms to develop, including the presence of colonizing micro-organisms, surface to be colonized, sufficient nutrients and water, temperature conditions for growth, and time required for development [33]. Micro-organisms harboured in biofilms exhibit reduced metabolism or switch to a dormant state (if endospore formers), and can be protected from the otherwise-lethal action of biocides at typical labelled doses (e.g. chemicals, ultraviolet light) [29]. It is now known that dry biofilms are also a concern with reusable device processing [34]. If biofilms are allowed to develop within a device, the cleaning challenge is increased, as well as limitations to the access of antimicrobial processes for disinfection and even sterilization [33,35,36]. For example, Otter *et al.* [37] reviewed the contribution made by interfering substances in supporting microbial survival (e.g. surface-attached cells and biofilms) on hospital contact surfaces and reducing biocidal efficacy. The authors advocated that new approaches to hospital cleaning and disinfection are required, including the potential use of appropriate novel materials to reduce microbial attachment to surfaces. There is also a commensurate need to elucidate the complex nature and physiology of microbes on dry hospital surfaces, which takes into consideration the prevalence and composition of biofilms and cleaning/disinfection.

There has also been interest in defining the scientific endpoints for cleaning in the last 30 years. Part of this was due to the characterization of proteinaceous infectious particles (prions), and particular emphasis on risks of protein contamination on reusable medical devices in the wake of the bovine spongiform encephalopathy crisis in the UK and other countries [19]. However, in parallel, there continued to be reports of outbreaks and potential patient risks with surgical devices that may not have been cleaned effectively, and the risks of transmission of blood-borne pathogens. It is known from experience that many such episodes occurred but were not published, so the published literature may have underestimated the true extent of the risk to patients. To address the risk of devices not being cleaned effectively, efforts have since been completed at international level to establish cleaning performance requirements during the processing of reusable medical devices and medical device manufacturers/healthcare facilities to establish and monitor the effectiveness of the cleaning instructions. For washer-disinfectors (WDs), the International Standards Organization (ISO) 15883 series was first published in 2006 by an international group of experts [38]. The intention of this standard series was to require WD manufacturers and users to have shared responsibility for the effectiveness of cleaning (and disinfection) of the equipment. However, even at the time of publication, there was no consensus agreement on the definition of 'clean', the acceptable endpoints for a cleaning process, and validation methods to demonstrate cleanliness under laboratory or clinical conditions. The standards at this stage deferred to country-specific guidance that varied widely.

Following initial publication, a concerted effort was made by these committees to gain an internationally harmonized consensus on cleaning requirements. This culminated successfully in the recently published updated versions of ISO 15883-1 and ISO 15883-5. While ISO 15883-1 provides general requirements for all WDs, ISO 15883-5 focuses solely on the cleaning requirements. This includes a two-phase evaluation for cleaning efficacy with performance criteria commensurate to patient safety. The two phases include simulative (type testing) and clinical or typical use conditions (performance qualification). A major consideration in simulative testing is the choice and method of application of test soils to WD loads, chamber walls and load carriers [39]. The test soil is expected to be proteinaceous (unless otherwise justified for the intended use of the equipment), justified based on its relevance to

Table I
Examples of reports of healthcare-associated infections due to lapses in medical device decontamination

Source	Micro-organism(s)/ contaminate involved	Outbreak or infection summary	Patient impact	Device issue
Srinivasan *et al.*, 2003 [14]	*P. aeruginosa*	Outbreak of *P. aeruginosa* associated with lapses in processing best practices including a contaminated, loose biopsy port cap in bronchoscopes. Bronchoscopes were cleaned by trained personnel in accordance with national guidelines and the manufacturer's recommendations (Olympus America). Bronchoscopic and reprocessing procedures were observed during random, unannounced visits. No significant breaches in technique were observed.	A total of 414 patients underwent 665 bronchoscopic procedures during the outbreak. The rate of recovery of *P. aeruginosa* from bronchoalveolar lavage specimens obtained using endoscopy suite bronchoscopes increased from a mean of 10.4% at baseline to 31.0% during the outbreak. There were 48 infections among 39 of the 414 patients (9.4%) in the 2 weeks after bronchoscopy. Based on the authors' definition, exposure to a potentially contaminated bronchoscope may have had a role in the death of three patients, all of whom were critically ill at the time of bronchoscopy.	The contamination appeared to be related to a loose biopsy port cap on the bronchoscopes, which may have sheltered organisms and thus rendered disinfection procedures ineffective.
Muscarella, 2008 [15]	*P. aeruginosa*	Literature review following laryngoscopy and suggestion for increased standardization for manufacturer's processing instructions.	Authors focused on a single case study where 15 infants were infected, with two fatalities [16]. Literature review recommended the use of sterile disposable sheaths to mitigate contamination risk.	Rigid laryngoscopes within the USA are classified as Class 1 devices and are exempt from the Food and Drug Administration oversight. Decontamination instructions, therefore, vary widely from manufacturer to manufacturer. The handle and blade of laryngoscopes have been reported with residual soil.
Cabronne *et al.*, 2010 [17]	*K. pneumoniae*	KPC-producing *K. pneumoniae* type 2 multi-hospital outbreak due to what was suspected to be an ineffectively processed duodenoscope.	Within 6 weeks, 12 patients were identified as having an HAI with the same molecular typing.	The duodenoscope was the only device used commonly among the infected patients. Although culturing of the duodenoscope did not recover the micro-organism, it was suspected that this was due to reprocessing after the contamination, and ineffective cleaning of the channels was the primary cause of the outbreak. The duodenoscope was sent back to the manufacturer for repair, so no additional analysis was completed.
Williams *et al.*, 2010 [18]	*Enterococcus spp.* *S. aureus* *Klebsiella* spp. *Acinetobacter* spp.	Evidence demonstrating HAI risk from lack of decontamination of laryngoscope handles.	Patient-ready laryngoscopes were cultured using a swabbing technique to demonstrate that 86% of the handles were contaminated with one or more species of bacteria.	The design feature of the handle was evaluated, resulting in a higher occurrence of bacteria residing on the knurled surface compared with the smooth surface. When in the closed position, the patient-contacting blade folds against the handle. This study

(*continued on next page*)

Table I (*continued*)

Source	Micro-organism(s)/ contaminate involved	Outbreak or infection summary	Patient impact	Device issue
				confirms that laryngoscope handles can be a vector for transmission of infection.
Kovaleva *et al.*, 2013 [19]	Most commonly: *Salmonella* spp. *P. aeruginosa* Mycobacteria	Literature review of the challenges with flexible endoscopy. This meta-analysis is a comprehensive review of 379 sources evaluating the infection risk from flexible endoscopes.	It is estimated that 6% of patients will experience an HAI due to improper infection control procedures.	Endoscopes have a complex design with internal lumens and multiple channels that are easy to damage and difficult to clean.
Lowman and Venter, 2013 [20]	*Enterobacter* spp. *A. baumannii*	Ineffective decontamination of laryngoscope blades is a source of microbial contamination and patient risk.	A contamination rate of 57.3% in a South African healthcare facility was reported from a total of 110 laryngoscope blades swabbed for micro-organism recovery.	Guidelines within the region specify that laryngoscope blades should be cleaned and disinfected as a semi-critical device. Blades were soaked and scrubbed prior to rinsing and high-level disinfection. The rate of contaminated samples indicates that either the decontamination procedure for the blades is ineffective, or there is contamination from the unprocessed handle or from handling during assembly.
Negri de Sousa *et al.*, 2013 [21]	Non-specific literature review	Literature review of cross-infection risk from laryngoscope blades and handles. 20 studies were evaluated.	Non-specific literature review.	As summarized in this literature review, the laryngoscope is comprised of many pieces that have features of varying complexity, including rows and furrows, that may hinder the decontamination process.
Magill *et al.*, 2014 [22]	*C. difficile*	Additional study by authors to look at multiple facilities (183 hospitals) for the detection of HAIs. Of the 11,282 patients, 4% were identified with an HAI.	Surveys conducted in 183 hospitals found that, out of 11,282 patients, 452 experienced an HAI (4.0%). Device-associated infections accounted for 25.6%.	Device-specific information was not provided in this analysis, but the authors recommend that devices should be reviewed as a vector for infection transmission.
Kola *et al.*, 2015 [23]	*K. pneumoniae*	Investigation of a German outbreak with the root cause being a contaminated duodenoscope.	7 of 13 cases of *K. pneumoniae* in two French hospitals were associated with a contaminated duodenoscope. Extraction of the scope channels was conducted by flushing 100 mL of sterile water through the channel and collecting it for microbial cultures.	Duodenoscopes must be thoroughly dried and reprocessed after a long period of storage. Special handling is required to reduce the contamination risk for duodenoscopes.
Marsh *et al.*, 2015 [24]	*K. pneumoniae*	HAI outbreak investigation with root cause being endoscopes.	Pulsed-field gel electrophoresis and multi-locus sequencing were used to evaluate 43 *K. pneumoniae* patient isolates. Two clusters were recovered from endoscopes.	Authors state that this evidence supports the growing body of literature that endoscopes are a risk for bacterial transmission.
Ofstead *et al.*, 2015 [25]	Protein Total organic carbon Adenosine triphosphate	Monitoring of 60 colonoscopes and gastroscopes in a clinical setting with demonstration of microbial contamination despite compendial processing protocols.	Individual channels were swabbed and extracted using the flush—brush—flush method with 20 mL of water and a 6-mm brush. Samples were collected after each cleaning step (i.e. bedside, manual,	Contamination was reduced with each stage of the reprocessing step. However, patient-ready devices, disinfected and stored, contained microbial contamination. Cleaning of endoscope channels is time-

			disinfected and stored). Of the 60 samples collected, 92% of the scopes cleaned at the bedside, 46% of scopes manually cleaned, 64% of scopes that underwent high-level disinfection and 9% of stored scopes contained micro-organisms.	consuming and can be overlooked in practice. The distal end of duodenoscopes provides a particular challenge for cleaning due to the elevator guidewire. Colonoscopes and gastroscopes have multiple channels, ports and valves that increase the risk of ineffective cleaning.
Davis, 2017 [26]	Non-specific literature review	Compilation of data reporting the rate of bioburden per patient claim records. There is an increasing trend of bioburden prevalence.	Meta-analysis of reported events related to surgical instruments. An increase in incident reporting is evident.	Authors hypothesize that the medical device design, which includes compound hinges, gaps, channels and lumens, can result in bioburden accumulation and subsequent development of biofilm.
Rauwers *et al.*, 2018 [27]	*E. cloacae* *E. coli* *K. pneumoniae*	Dutch study where duodenoscopes within the clinical setting were cultured and demonstrated high levels of bioburden post processing.	73 Dutch ERCP centres submitted duodenoscopes for microbial screening. Samples were collected by flushing the channels with sterile physiological saline. 15% of the duodenoscopes from 39% of the facilities had microbial contamination in a patient-ready state.	Results indicated that a specific design feature on the TJF-Q180V did not allow for adequate cleaning and disinfection. In addition to the design features being a risk factor, the age of the device is also a contributing factor. The brush, forceps elevator and protection cap had the highest occurrence of microbial contamination.
Rahman *et al.*, 2019 [28]	*P. aeruginosa*	Literature review of duodenoscope-associated HAIs due to difficult-to-remove biofilm.	16 publications were included in this literature review from 2000 to 2018 focusing on ERCP-associated outbreaks.	The elevator channel is a key feature that predisposes the duodenoscope to contamination.
Shenoy *et al.*, 2019 [29]	*K. pneumoniae*	HAI investigation with transmission associated with a duodenoscope.	Case study where the transmission of mcr-1-positive *K. pneumoniae* for two patients was caused by a contaminated duodenoscope as the epidemiological link. *K. pneumoniae* was recovered from the biopsy channel and distal tip.	The distal cap defect likely allowed material to penetrate a sealed area that was not accessible for cleaning. Authors advocate increased awareness of duodenoscope design with an emphasis of single-use components.
Ofstead *et al.*, 2020 [30]	Non-specific literature review	Literature review of duodenoscope-related HAIs and discussion around risk mitigation.	Literature review consisting of evidence suggesting the rate of infection is 1 in 1765 or as many as 10% of ERCP procedures.	Reprocessing failures may occur as a result of the complex design that includes elevator mechanisms in the distal end and open wires/channels that are exposed to patient soil. Suction-biopsy channels are also a source of residual contamination.
Okamoto *et al.*, 2022 [31]	*S. aureus* *S. lugdunensis* B-haemolytic streptococcus, *Enterococcus* spp.	US study investigating the contamination rate of duodenoscopes after processing.	859 new-model duodenoscopes (TJF-Q180V) and 850 older model duodenoscopes (TJF-160F/VF) were extracted for microbial contamination using the flush—brush—flush method with sterile water. The detected contamination rate for these patient-ready duodenoscopes was 5.3%.	The authors witnessed reprocessing errors in 27.7% of the procedural reviews, and recommend increased awareness of the processing instructions with ongoing staff training programmes.

P. aeruginosa, Pseudomonas aeruginosa; K. pneumoniae, Klebsiella pneumoniae; S. aureus, Staphylococcus aureus; A. baumannii, Acinetobacter baumannii; C. difficile, Clostridioides difficile; E. cloacae, Enterobacter cloacae; E. coli, Escherichia coli; S. lugdunensis, Staphylococcus lugdunensis; HAI, hospital-acquired infection; ERCP, endoscopic retrograde cholangiopancreatography.

the intended use [40] as protein is the major contaminant detected on reusable devices following clinical use [41]. In addition, the test soil must meet new performance criteria [40,42]. The test method was developed by an interlaboratory collaboration, and based on investigations using coagulating blood as a widely used test soil and protein concentration as the analyte criteria.

The testing conditions in which the WD is challenged are intended to simulate worst-case conditions for the devices expected to be cleaned in the WD. As performance testing is carried out in both a laboratory setting and a clinical setting, the choice of challenge test soil is a critical element of the evaluation. Using the soil validation test method in Annex B of ISO 15883–5:2021 and the soil analyte concentration from the literature [41,43], a comparison of soil performance allows for standardization when assessing both phases of the cleaning efficacy test. In addition to the choice of test soil, the device is expected to be soiled as it would be in normal use. For example, the medical device should be soiled in a manner that is representative of clinical use with actuation, exposure to extreme temperatures (e.g. to simulate cauterization), simulated use of accessory chemicals (e.g. lubricants or other chemicals used during surgery), and drying prior to cleaning. The effectiveness of the method to remove the analyte from the device (i.e. extraction) [44] and the analyte detection method must also be evaluated [45]. WDs can be designed for the cleaning of single or multiple devices with various device features (e.g. lumens or internal moving parts) that can be a challenge to cleaning effectiveness; therefore, representative worst-case loads should be defined for testing purposes. This programme for standardization demonstrates confidence across the supply chain that the WD equipment will perform as expected under worst-case conditions.

In addition to the traditional requirement for visual cleanliness, the ISO 15883 series now defines acceptance criteria for specific analytes when measuring cleaning efficacy. Quantitative, analytical test methods are justified for use based on a risk assessment, with protein detection being highlighted as a recommended analyte. The acceptance criteria for analytes have been defined as both alert and action levels (Table II). Detection levels of analytes below alert levels over multiple test cycles are considered 'clean', but those falling between alert and action levels are to be further investigated as they are considered to be at high risk of failure over time. This was designed to minimize the risk of soil accumulation or periodic, insufficient cleaning during normal use of the WD. These levels have been defined, but the standard does note that country-specific requirements may also need to be considered, such as levels of total protein per device [46] or device side [47].

Table II
Analyte acceptance criteria for cleaning efficacy

Analyte	Alert level	Action level
Protein	$\geq$3 μg/cm^2	$\geq$6.4 μg/cm^2
Total organic carbon	$\geq$6 μg/cm^2	$\geq$12 μg/cm^2
Carbohydrate	$\geq$0.9 μg/cm^2	$\geq$1.8 μg/cm^2
Haemoglobin	$\geq$1 μg/cm^2	$\geq$2.2 μg/cm^2
ATP	$\geq$10 femtomoles ATP/cm^2	$\geq$22 femtomoles ATP/cm^2
Endotoxin	$\geq$2.2 EU/device	$\geq$20 EU/device

Processing residuals are also assessed to evaluate patient impact [48] or an impact on further processing.

The ISO 15883-5 acceptance criteria have also been harmonized in the requirements established recently in the USA for the validation of cleanliness requirement for reusable medical devices [49]. ANSI/AAMI ST98:2022 and the US Food and Drug Administration guidelines detail the conditions in which the processing steps for cleaning must be challenged to mitigate the risk of residuals past the point of visual cleanliness for reusable medical devices [8,49].

The established industry acceptance criteria are supported by the literature, where the primary analyte (i.e. protein) has been evaluated for patient safety [50], and the other analytes have been established as clinically relevant and measurable [51]. The two levels of acceptance criteria provide a level of safety within the test system that accounts for variability in the analyte detection method as well as test system variables that can impact detectability (e.g. sample extraction [44]). A risk assessment allows the appropriate level to be identified to ensure patient safety. For example, if during the cleaning validation medical device manufactures must be below the action level with the most challenging cleaning conditions included in the experimental design, it may be appropriate during verification testing at a healthcare facility to obtain results below the alert level for an extra margin of safety.

Evaluation of risk

ISO 14971 describes the evaluation of risk as being a process of comparing an estimated risk against a risk criteria to determine the acceptability of that risk [52]. The hazardous situations at the healthcare facility leading to the inadequate processing of a reusable medical device can include human factors (e.g. inadequate training) leading to the inability to execute the required cleaning process [13], the time before or during the decontamination process that can lead to increased cleaning challenge [53], available processing equipment, and effective process monitoring practices. The estimated risk for inadequate decontamination is expressed in terms of patient risk for potential infection/biofilm formation, other adverse immune responses (e.g. tissue damage or toxicity reactions from process residuals), or surgical complications/cancellations/delays or device damage. Medical device manufacturers, when developing the IFU, should assess the acceptability of the risk of inadequate cleaning, and mitigate any significant risk by either including device designs with features that are compatible for cleaning, or providing robust instructions that are validated to be reproducible.

It is reasonable to expect that processing instructions will be followed faithfully at the healthcare facility, defined by AAMI ST79 as any 'specialized facility where professionals deliver services utilizing medical devices' [54], using validated equipment that accommodates many decontamination processes. However, this has many challenges, including a wide range of staff training, in-depth knowledge of each device/set of instructions, and the fact that processing instructions can vary significantly between manufacturers. The reality is that sterile or device processing personnel are juggling many products, and handle products the best they can, in established processes that have been put in place for the efficient throughput of their facility [55]. This challenge is compounded when an increasing number of devices with unique processing

instructions are purchased, even though they have many similarities in device complexity. The pressures on equipment and sterile processing departments to meet healthcare needs cannot be underestimated. In these cases, it seems logical to increase throughput and consistency such that groups of devices can be processed together using the same steps and obtain the same endpoints despite the IFU provided [56]. There is currently no global industry guidance for how to adopt devices into such processes using a family grouping strategy. ISO 17664-1 outlines what instructions must be included in the device IFU based upon risk to provide sufficient instructions for device processing [1]. As such, it is left to the discretion of the device manufacturer to identify the level of detail provided. For example, complex devices may have pages of cleaning instructions, whereas simple devices have a single paragraph. It remains the expectation that each IFU will be followed exactly [54], but this is not practical considering the number of devices processed each day.

Standardization efforts to develop decontamination process flows based on device risk have been an initiative of various standard committees over the last 10 years, and some have been deployed based on the geographical region. For example, the US guidance for device manufacturers, AAMI TIR 12 Annex D and E, recommends processing instructions depending on the device category and based on difficulty of cleaning [57]. In Germany, the responsibility shifts to the healthcare facility, with the requirement of a process qualification to validate the cleaning process. The qualification is an assessment of cleaning performance for the processing steps, and will typically use a worst-case device or surrogate device as the process challenge device. There is often a stronger emphasis placed on complete automated processes for cleaning, and the associated requirements for qualification of cleaning processes are described in ISO 15883-1 [39]. However, it is still at the discretion of the healthcare facility to group devices and adopt them into the appropriate processing procedures.

Device manufacturers have a similar barrier in validating each device within a product portfolio that may be comprised of thousands of devices. An efficient approach to this is the identification and use of representative product families, and validation of the worst-case designs with demonstrated commonality in device materials, design features, intended use and clinical soil exposure. Processing instructions must be the same for each device in such product families [1,8,57].

Cleaning classification

When the Spaulding classification was introduced, it provided a necessary framework for manufacturers, regulators and healthcare personnel to consistently deliver an appropriate microbiological reduction for devices. However, when using the Spaulding classification alone, the entirety of the microbiological quality of the reusable medical device is not considered, as the risk to ensure cleaning is not considered in detail. The introduction of a complementary cleaning classification system would allow for effective communication between medical device manufacturers and healthcare facilities on the proper risk mitigation for associated cleaning processes.

For each device design and associated cleaning process, there is a probability of soil retention. This relationship can be quantified to assess risk. This relationship has been well described in the literature [58], and evaluated by standards organizations with the intent to inform medical device manufacturers on the cleaning steps that may need to be included in the cleaning IFU based on the device features. Michels *et al.* described an example based on current validations for reusable medical devices, regarding how they can be grouped based on feature, but did not assess the probability of the risk of soil accumulation based on the feature [59]. AAMI TIR12:2020 Annex D logically describes three device categories based on cleaning processes designated by device complexity. Category 1 devices are simple devices that can be processed using manual or automated cleaning methods. Category 2 devices have features that require human intervention, such as brushing, to remove soil which is difficult to clean. Category 3 devices require sonication to aid in the removal of soil that is not accessible or is difficult to remove using brushing and flushing [57]. The categorization of these groups was completed by evaluating the cleaning IFU for marketed devices, and applying them to the complexity of device features of the medical device. The assumption of this evaluation is that the IFU contains all necessary steps for cleaning the applicable device, but no guidance is given regarding how to assess the device for each category.

A cleaning risk-based approach is proposed that considers the probability of risk for residual soil to remain on or in the various design features of a device following cleaning. For effective cleaning to occur, the cleaning chemistry (cleaning agent and water) must have access to the soil with enough exposure (e.g. spray, soak) or force (e.g. brush, flush, sonication) to solubilize and remove the residual soil for surface removal. The device feature is, therefore, the key variable of a reusable medical device that can influence this relationship. Three categories have been established to describe this risk, and are described in Table III.

The cleaning classification uses device features as the key elements for risk analysis for the device cleaning process. As described previously, the device feature approach provides a more conservative estimate of residual analytes on a reusable medical device, and allows for identification of the most probable location for soil accumulation, and thereby risk to the cleaning process. This approach allows the medical device manufacturer to assess the risk during the development and

Table III
Cleaning classification

Risk category	Description
Maximal	Complex device features with a high probability of soil accumulation with a medical device
Moderate	Accessible device features that require specific intervention (e.g. brushing or flow through lumens, mated surfaces requiring disassembly or opening/closing to ensure access)
Minimal	Low-risk reusable medical devices where all features are exposed without specific intervention for cleaning

validation of the device processing IFU, and to bring the attention of the healthcare personnel to these high-risk areas (e.g. focus on inspection protocol) [60]. Consider a device where the geometry seems simple but, when evaluating the features for the cleaning challenge, the device contains a lumen [the most difficult-to-clean feature [61] with a junction point (i.e. bend)]. If evaluating the entire device during the cleaning validation, the surface area of the whole device may dilute the residual protein concentration from the lumen, and under-report patient risk [59].

For example, if a medical device is used to flush a solution into a patient, the lumened portion of the device is the highest risk feature, as the fluid pathway of the lumen will deposit fluid into the patient whereas the rest of the device is only communicating externally. Although other features within the device may be difficult to clean, if the surface of the lumen has direct contact with the fluid being flushed through it, remaining soil in the lumen is of the highest risk to the patient. Once fluid flows through the lumen, any residual soil solubilized in the fluid pathway and inserted into the patient becomes a major concern. When using the typical recommended method to determine cleaning efficacy, it is typical for the entire surface area of the device (or, in some cases, each side of a device) to be used to calculate the residual concentration compared with the surface area [49]. This method may under-report the concentration of residual soil in the most difficult-to-clean portion of the device, diluting the analyte to below the limit of detection for the test method. However, when using the device feature approach, the most difficult-to-clean area of the medical device is scrutinized for cleanability, and reported against the established acceptance criteria. The device feature approach is therefore the most appropriate and conservative method for a risk assessment.

This cleaning classification is a quantitative risk-based categorization approach utilizing the probability of soil accumulation for the challenging device feature. It can provide guidance to manufacturers to improve the design for cleanability, and how to label the medical device within the IFU to communicate the cleaning risk effectively to healthcare personnel. Examples of associated symbols with a description of the device feature that resulted in the categorization are suggested for inclusion within the IFU (Figure 1). Communication of this information to the healthcare facility can inform the device risk for cleaning, and alert when special considerations for equipment or training are required to ensure effective and consistent processing. Using the medical device example from above, the cleaning classification might be set as 'maximal', leading the manufacturer to require enhanced visual inspection steps (e.g. use of borescope) to assess it for cleanliness and mitigate risk.

Decontamination risk mitigation

Ineffective device processing is a major risk for HAIs and other patient complications. Complex features of devices can make visual inspection and monitoring for cleanliness difficult, thereby increasing the risk of soil accumulation and biofilm development. Medical device manufacturers can use this cleaning classification in conjunction with the Spaulding definitions to assess the risk for the entire decontamination process for reusable medical devices. This can improve cleaning and disinfection/sterilization validation methods, improve device design, and ensure that risks are clearly communicated and mitigated at healthcare facilities. The Spaulding classification provides an easy mechanism to connect manufacturers and healthcare facilities regarding how devices must be validated and processed. By complementing this with a classification to assess the cleaning risk in more detail, the appropriate processing methods can be defined and optimized, thereby further decreasing the risk to patient safety. This combined approach can help safeguard against and tackle the emergence of increasingly recalcitrant microbial pathogens, including drug-resistant fungi [62,63].

Conflict of interest statement
None declared.

Funding sources
None.

References

[1] International Organization for Standardization. ISO 17664-1. Processing of health care products — information to be provided by the medical device manufacturer for the processing of medical devices. Geneva: ISO; 2021.
[2] International Organization for Standardization. ISO 17664-2. Processing of health care products — information to be provided by the medical device manufacturer for the processing of medical devices. Part 2: Non-critical medical devices. Geneva: ISO; 2021.
[3] World Health Organization. Decontamination and reprocessing of medical devices for health-care facilities. Geneva: WHO; 2016.
[4] McDonnell G, Hansen J. Principles of antimicrobial activity. In: McDonnell G, Hansen J, editors. Block's disinfection, sterilization and preservation. 6th ed. Philadelphia: Wolters Kluwer; 2020. p. 68—119.
[5] Spaulding E. Chemical disinfection and antisepsis in the hospital. J Hosp Res 1957;9:5—31.
[6] Rowan N, Kremer T, McDonnell G. A review of Spaulding's classification system for effective cleaning, disinfection, sterilization or reusable medical devices: viewed through a modern-day lens that will inform and enable future sustainability. Sci Total Environ 2023;878:162976.
[7] Spaulding E. Chemical disinfection of medical and surgical materials. In: Lawrence C, editor. Block disinfection, sterilization, and preservation. Philadelphia: Lea & Febiger; 1968. p. 517—31.
[8] Food and Drug Administration. Reprocessing medical devices in health care settings: validation methods and labeling guidance for industry and Food and Drug Administration staff. White Oak, MD: FDA; 2015.
[9] McEvoy B, Rowan N. Terminal sterilization of medical devices using vaporized hydrogen peroxide: a review of current methods and emerging opportunities. J Appl Microbiol 2019;127:1403—20.
[10] Donskey C. Does improving surface cleaning and disinfection reduce health care-associated infections? Am J Infect Control 2013;41:S12—9.
[11] McDonnell G, Baseman H, Cordie-Bancroft L. Words matter: a commentary on a glossary of definitions for microbiological quality. Biomed Instrum Technol 2021;55:143—64.
[12] McDonnell G, Burke P. Disinfection: is it time to reconsider Spaulding? J Hosp Infect 2011;78:163—70.
[13] Kremer T, Murray N, Buckley J, Rowan N. Blending immersive and educational technologies to unlock appropriate training for effective cleaning and processing of reusable medical devices that safeguards patient health — quo vadis? Sci Total Environ 2023;900:165673.

[14] Srinivasan A, Wolfenden L, Song X, Mackie K, Hartsell T, Jones H, et al. An outbreak of *Pseudomonas aeruginosa* infections associated with flexible bronchoscopes. N Engl J Med 2003;348:221—7.
[15] Muscarella L. Reassessment of the risk of healthcare-acquired infection during rigid laryngoscopy. J Hosp Infect 2008;68:101—7.
[16] Chang A. Hospital policy eyed in L.A. outbreak. Associated Press; 21 December 2006.
[17] Cabronne A, Thiolet JM, Fournier S, Fortineau N, Kassis-Chikhani N, Boytchev I, et al. Control of a multi-hospital outbreak of KPC producing *Klebsiella pneumoniae* type II in France, Sep to Oct 2009. Euro Surveill 2010;15:19734.
[18] Williams D, Dignley J, Jones C, Berry N. Contamination of laryngoscope handles. J Hosp Infect 2010;74:123—8.
[19] Kovaleva J, Peters F, van der Mei H, Degener J. Transmission of infection by flexible gastrointestinal endoscopy and brochoscopy. Clin Microbiol Rev 2013;26:231—54.
[20] Lowman W, Venter LSJ. Bacterial contamination of re-usable laryngoscope blades during course or daily anaesthetic practice. S Afr Med J 2013;103:386—9.
[21] Negri de Sousa A, Levy C, Freitas M. Laryngoscope blades and handles as sources of cross-infection: an integrative review. J Hosp Infect 2013;83:269—75.
[22] Magill S, Edwards J, Stat M, Bamberg W, Beldavs Z, Dumyati G, et al. Multistate point-prevalence survey of health care-associated infections. N Engl J Med 2014;370:1198—208.
[23] Kola A, Piening B, Pape U, Veltzke-Schlieker W, Kaase M, Geffers C, et al. An outbreak of carbapenem-resistant OXA-48-producing *Klebsiella pneumoniae* associated to duodenoscopy. Antimicrob Resist Infect Control 2015;4:8.
[24] Marsh J, Krauland M, Nelson J, Schlackman J, Brooks A, Pasculle A, et al. Genomic epidemiology of an endoscope-associated outbreak of *Klebsiella pneumoniae* carbapenemase (KPC)-producing *K. pneumoniae*. PLoS One 2015;10:e0144310.
[25] Ofstead C, Wetzler H, Doyle E, Rocco C, Visrodia K, Baron T, et al. Persistent contamination on colonoscopes and gastroscopes detected by biologic cultures and rapid indicators despite reprocessing performed in accordance with guidelines. Am J Infect Control 2015;43:794—801.
[26] Davis J. Retained bioburden on surgical instruments after reprocessing: are we just scraping the surface? Pennsylvania Patient Safety Advisory 2017;14:71—5.
[27] Rauwers A, Voor In 't Holt A, Buijs J, de Groot W, Hansen B, Bruno M, et al. High prevalence rate of digestive tract bacteria in duodenoscopes: a nationwide study. Gut 2018;67:1637—45.
[28] Rahman M, Perisetti A, Coman R, Bansal P, Chhabra R, Goyal H. Duodenoscope-associated infections: update on an emerging problem. Dig Dis Sci 2019;61:1409—18.
[29] Shenoy ES, Pierce WM, Walters MS, Moulton-Meissner H, Lawsin A, Lonsway D, et al. Transmission of mobile colistin resistance (mcr-1) by duodenoscope. Clin Infect Dis 2019;68:1327—34.
[30] Ofstead C, Buro B, Hopkins K, Eiland J, Wetzler H, Lichtenstein D. Duodenoscope-associated infection prevention: a call for evidence-based decision making. Endosc Int Open 2020;8:E1769—81.
[31] Okamoto N, Sczaniecka A, Hirano M, Benedict M, Baba S, Horino Y, et al. A prospective, multicenter, clinical study of duodenoscope contamination after reprocessing. Infect Control Hosp Epidemiol 2022;43:1901—9.
[32] Nicholson W, Munakata N, Gorneck G, Melosh HSP. Resistance of bacillus endospores to extreme terrestrial and extraterrestrial environments. Microbiol Mol Biol Rev 2000;64:548—72.
[33] Roberts C. The role of biofilms in reprocessing medical devices. Am J Infect Control 2013;41:S77—80.
[34] Alonso V, Goncalves M, de Brito F, Barboza G, Rocha L, Silva N. Dry surface biofilms in the food processing industry: an overview on surface characteristics, adhesion and biofilm formation, detection of biofilms, and dry sanitization methods. Compr Rev Food Sci Food Saf 2023;22:688—713.
[35] Alfa M. Biofilms on instruments and environmental surfaces: do they interfere with instrument reprocessing and surface disinfection? Review of the literature. Am J Infect Control 2019;47:A39—45.
[36] Vickery K, Hu H, Jacombs A, Bradshaw D, Anand D. A review of bacterial biofilms and their role in device-associated infection. Healthcare Infect 2013;18:61—6.
[37] Otter J, Cickery J, Walker J, deLancy Pulcini E, Stoodley P, Goldenberg S, et al. Surface-attached cells, biofilms and biocide susceptibility: implications for hospital cleaning and disinfection. J Hosp Infect 2015;89:16—27.
[38] International Organization for Standardization. ISO 15883-1. Washer-disinfectors — Part 1. General requirements, terms and definitions and tests. Geneva: ISO; 2006.
[39] International Organization for Standardization. ISO/DIS 15883-1. Washer-disinfectors — Part 1. General requirements, terms and definitions and tests. Geneva: ISO; 2021.
[40] International Organization for Standardization. ISO 15883-5. Washer-disinfectors — Part 5. Performance requirements and test method criteria for demonstrating cleaning efficacy. Geneva: ISO; 2021.
[41] Cloutman-Green E, Canales M, Zhou Q, Ciric L, Hartley J, McDonnell G. Biochemical and microbial contamination of surgical devices: a quantitative analsyis. Am J Infect Control 2015;43:559—661.
[42] Kremer T, Bancroft R, Patel Z, Owen M, McDonnell G. A standardized method for evaluating test soils used to demonstrate cleaning efficacy. J Hosp Infect 2022;126:52—5.
[43] Kremer T, Tortora A, Yeung Y, McDonnell G. Material adhesion comparison of test soils for reusable device cleaning efficacy. Zentral Steril 2021;29:166—72.
[44] Kremer T, Kulkarni K, Ratanski C, Floyd L, Anderson C. Connecting across competencies: leveraging best practices for processing. Biomed Instrum Technol 2021;55(Suppl. 3):6—11.
[45] Kremer T, Kimble A, Ratanski C. Improving protein assay methods to more accurately assess medical device cleanliness. Biomed Instrum Technol 2023;57:122—8.
[46] German Society for Hospital Hygiene (DGKH), German Society for Sterile Supply (DGSV), Working Group Instrument Preparation (AKI). Hygiene requirements for the reprocessing of medical devices. Federal Institute for Drugs and Medical Devices: Bonn, Germany; 2012.
[47] Department of Health. Health Technical Memorandum 01-01. Management and decontamination of surgical instruments (medical devices) used in acute care. London: DoH; 2016.
[48] Kremer T, Olsen D, Summers C, Patel A, Hoover J, Cieslak M, et al. Assessing detergent residuals for reusable device cleaning validations. Biomed Instrum Technol 2021;55:165—70.
[49] Association for the Advancement of Medical Instrumentation. ANSI/AAMI ST98 Cleaning validation of health care products — requirements for development and validation of a cleaning process for medical devices. Arlington, VA: AAMI; 2022.
[50] Kremer T, Patel A, Summers C, Quin M, Lemons K, McDonnell G. Protein residuals on reusable medical devices and patient safety impact. Zentral Steril 2019;27:178—83.
[51] Lappalainen S, Gomatam S, Hitchens V. Residual total protein and total organic carbon levels on reprocessed gastrointestinal (GI) biopsy forceps. J Biomed Mater Res B Appl Biomater 2009;89:172—6.
[52] International Organization for Standardization. Medical devices — application of risk management to medical devices. Geneva: ISO; 2019. p. 14971.
[53] Kremer T, Carfaro C, Klacik S. Effects of time, temperature, and humidity on soil drying on medical devices. Biomed Instrum Technol 2023;57:58—66.
[54] Association for the Advancement of Medical Instrumentation. ANSI/AAMI ST79:2017 & 2020 Amendments A1, A2, A3, A4 (Consolidated

Text). Comprehensive guide to steam sterilization and sterility assurance in healthcare facilities. Arlington, VA: AAMI; 2020.
[55] Bancroft R, Spencer W. Practical issues with instructions for use (IFU) for reusable medical devices. Zentral Steril 2022;30:97—101.
[56] Alfred M, Catchpole K, Huffer E, Fredendall L, Taaffe K. Work systems analysis of sterile processing: decontamination. BMJ Qual Saf 2020;29:320—8.
[57] Association for the Advancement of Medical Instrumentation. AAMI TIR12:2020. Designing, testing, and labeling reusable medical devices for reprocessing in health care facilities: a guide for medical device manufacturers. Arlington, VA: AAMI; 2020.
[58] Southworth P. Infections and exposures: reported incidents associated with unsuccessful decontamination of reusable surgical instruments. J Hosp Infect 2014;88:127—31.
[59] Michels W, Roth K, Eibl R. Assessment of cleaning efficacy based on the protein—surface relationship. Central Service 2013;3:212—5.
[60] Kremer T, Felgar F, Rowan N, McDonnell G. Validation of the device feature approach for reusable medical device cleaning evaluations. Biomed Instrum Technol 2023;57:143—52.
[61] Alfa M, Degagne P, Olson N. Worst-case soiling levels for patient-used flexible endoscopes before and after cleaning. Am J Infect Control 1999;27:392—400.
[62] Garvey M, Meade E, Rowan N. Effectiveness of front line and emerging fungal disease prevention and control interventions and opportunities to address appropriate eco-sustainable solutions. Sci Total Environ 2022;851:158284.
[63] Garvey M, Rowan N. Pathogenic drug resistant fungi: a review of mitigation strategies. Int J Mol Sci 2023;24:1584.

Validation of the Device Feature Approach for Reusable Medical Device Cleaning Evaluations

Terra A. Kremer, Jeff Felgar, Neil Rowen, and Gerald McDonnell

Abstract

The identification of worst-case device (or device set) features has been a well-established validation approach in many areas (e.g., terminal sterilization) for determining process effectiveness and requirements, including for reusable medical devices. A device feature approach for cleaning validations has many advantages, representing a more conservative approach compared with the alternative compendial method of testing the entirety of the device. By focusing on the device feature(s), the most challenging validation variables can be isolated to and studied at the most difficult-to-clean feature(s). The device feature approach can be used to develop a design feature database that can be used to design and validate device cleanliness. It can also be used to commensurately develop a quantitative cleaning classification system that will augment and innovate the effectiveness of the Spaulding classification for microbial risk reduction. The current study investigated this validation approach to verify the efficacy of device cleaning procedures and mitigate patient risk. This feature categorization approach will help to close the existing patient safety gap at the important interface between device manufacturers and healthcare facilities for the effective and reliable processing of reusable medical devices. A total of 56,000 flushes of the device features were conducted, highlighting the rigor associated with the validation. Generating information from design features as a critical control point for cleaning and microbiological quality will inform future digital transformation of the medical device industry and healthcare delivery, including automation.

This study sought to validate a device feature approach to be used in cleaning validations for reusable medical devices.

Reusable medical devices are required to be cleaned, disinfected, and/or sterilized between patient exposure and can include those used directly on a patient during surgery or items that have minimal patient contact (e.g., blood pressure cuffs) or contact surfaces indirectly (e.g., monitor or piece of equipment).[1] Medical devices that are not properly cleaned have demonstrated an increased challenge for disinfection/sterilization and can lead to transmission of infectious disease.[2]

To comply with international standards, manufacturers of medical devices for which processing is required prior to patient use must provide validated processing instructions to the customer. These instructions for use (IFUs) are used to process medical devices in a healthcare facility so they are safe and functional for subsequent patient use.[3] Manufacturers validate cleaning IFUs by developing a test system that challenges each step of the cleaning process with worst-case conditions. The process steps for the cleaning IFUs, which must be defined, may include initial treatment at point of use (pretreatment), preparation before cleaning (e.g., disassembly), manual and/or automated cleaning, rinsing, drying, and visual inspection.[1]

During the cleaning validation, the following test conditions are selected to mitigate human factors that may affect the efficacy of the cleaning process within a healthcare setting[3]:

- Device conditioning (i.e., simulated use): Repetition of processing prior to validation to place the device in a used state and account for soil accumulation.[3]
- Soil formulation: The formulation of the of the test soil (i.e., substitute for a contaminate found on a device after clinical use[3]) should be representative of the clinical soil expected during use and validated.[4,5]
- Soil volume: The soil volume must be sufficient to adequately challenge the cleaning of the device as it would be used in a clinical setting and be representative of the clinically relevant analyte concentrations.[3]

***Terra A. Kremer**, BS, is the director of microbiological quality in Microbiological Quality & Sterility Assurance at Johnson & Johnson in Raritan, NJ, and a PhD candidate at the Technological University of the Shannon in Athlone, Ireland. Email: tkremer@its.jnj.com*
Corresponding author

***Jeff Felgar**, BS, MS, is a staff scientist in Microbiological Quality & Sterility Assurance at Johnson & Johnson in Warsaw, IN. Email: jfelgar@its.jnj.com*

***Neil Rowan**, PhD, is the director of the Bioscience Research Institute at the Technological University of the Shannon located in Athlone, Ireland. Email: neil.rowan@tus.ie*

***Gerald McDonnell**, BsC, PhD, is a senior director of microbiological quality and sterility assurance at Johnson & Johnson in Raritan, NJ. Email: gmcdonne@its.jnj.com*

- Soiling location: The most challenging areas of the device to clean, including areas of test soil and fluid ingress accumulation.[6] Identifying these areas is of critical importance.
- Soil application: The method of applying the test soil should be representative of the most challenging (worst-case) clinical use.[7]
- Device articulation: Physical manipulations (e.g., actuations, flexures) of the device during soiling, thereby allowing for soil migration.[3]
- Soil conditioning/drying: Conditions during use (e.g., heating) that can make the test soil more difficult to remove should be mimicked, and the length of time and environmental conditions related to the drying of test soil on the device should represent the most appropriate challenge.[8]

In addition to the preparation of the test samples, the cleaning parameters should also be selected to simulate the most challenging cleaning conditions. If the cleaning IFUs provide a range of processing parameters, the validation should be completed at practical worst-case parameters.[3] Examples include:

- Detergent preparation: If the IFU states to dilute the detergent to obtain a concentration range, then the weakest detergent concentration should be used.
- Flushing: If the device is to be flushed for a specific time or until visibly clean, then the indicator of visual cleanliness should be specified in the validation, including use of a timing element.
- Soaking: If a device is intended to be submersed for a specified time range (e.g., soak for 5–10 min), then the time selected should be the most rigorous (e.g., 5-min soak selected for validation).
- Volume: If volume of fluid is specified (e.g., flush lumen with 60 mL prepared detergent), then a volume slightly below the volume specified should be used in the validation (e.g., 59 mL detergent used in the validation procedure).
- Temperature: If a temperature is specified, the condition representing the most rigorous challenge would be selected (e.g., devices specified to be cleaned in a cleaning chemistry at a specific temperature [45°C ± 5°C]), then the most extreme condition should be selected (e.g., 40°C, as it is below the optimal temperature for enzyme performance).

By stacking the most challenging cleaning validation parameters, a more robust validation of the cleaning process can be developed and inform more reliable IFUs.

Device Feature Validation Approach

ANSI/AAMI/ISO 17664-1:2022 describes methods to classify devices for validation by using a risk-based approach (e.g., the Spaulding classification) or challenging the process based on the device design.[1] AAMI TIR12:2020 provides design considerations that may pose additional challenges during the cleaning process.[9] Michels et al.[6] expanded on the latter method by grouping devices into the following six groups: (1) instruments without joints (cavities/lumens), (2) instruments with joints, (3) sliding-shaft instruments, (4) tubular instruments, (5) microsurgical instruments, and (6) complex instruments. This categorization was developed by analyzing the residual protein levels obtained from cleaning validations.

The concept of specifically targeting variables related to the most challenging portion of the medical device has been used for many years in validating sterilization parameters.[10] The process challenge location is defined as a "site chosen within a load as the position at which the least microbiological inactivation is expected to be delivered," and a process challenge device is defined as an "item providing a defined resistance to a cleaning, disinfection, or sterilization process and is used to assess performance of the process."[11] The cleaning method for a reusable medical device can be validated using the actual medical device or surrogate devices that are well-designed comparators.[1,3]

As demonstrated by Michels et al.,[6] underreporting of the residual soil level on devices can occur if the validation method is not focused on the most difficult-to-clean area of the device, which also represents the greatest risk to the patient. By using the entirety of the device to evaluate cleanliness, the surface area of easy-to-clean areas may dilute the most challenging-to-clean features

or process challenge location,[6] thus underestimating appropriateness.

The design feature validation approach focuses exclusively on the device feature(s) that poses a known challenge to cleaning, without including the surface area from other exposed parts of the actual device that are not considered a challenge for cleaning. This approach also minimizes the volume of extraction fluid required, thereby optimizing the limit of quantification. The results of the feature testing then can be directly applied during the evaluation of actual devices to validate by equivalency. If the features of the candidate device are equal to or less challenging than the validated features, the candidate device can be considered validated, hence delivering a well-designed comparator.

Residual analyte concentrations on soiled devices with multiple features are expected to be equal to or less than concentrations for individual challenging features. This hypothesis is due to the increased surface area from the multiple features and the area of other, nonchallenging surfaces. Theoretically, the device feature approach can be used to isolate the most difficult-to-clean feature while considering patient risk to evaluate the entirety of the device. Although this approach has been widely accepted in similar processes for reusable medical devices, literature is lacking on mathematical approaches for cleaning validations.

Material and Methods

To investigate the device feature approach, a dead-end (i.e., blind) lumen was selected as the most challenging-to-clean feature (as demonstrated in the literature[12,13]). The test coupon design is shown in Figure 1. To be removed from the feature, a dead-end lumen requires a backflow of the eluent flush after it reaches the dead end. This requires competing pressure gradients in the lumen and can limit sheer force of the liquid over the surface, resulting in ineffective soil removal.[14] The longer the lumen and the smaller the diameter, the more challenging this feature becomes to clean. As the diameter narrows, the competing flow of the liquid increases. The length of the lumen will require more force for the liquid to reach the dead end with enough flow velocity for the liquid to exit the lumen.

The null hypothesis of this experiment was that the protein-per-surface-area relationship for a single feature would be statistically similar to that of a device with multiple features. To challenge this hypothesis, two types of coupons were used:

1. Single feature: 300 series stainless steel block (6 mm × 6 mm × 50 mm) with a 2-mm diameter hole drilled in the top center (Figure 1).
2. Multiple features: 300 series stainless steel block (30 mm × 30 mm × 50 mm) with 25 holes (2 mm each) drilled in the top (Figure 2).

To challenge the flow velocity of the lumen, each coupon type had three challenge lumen lengths (depth) of 20 mm, 30 mm, and 40 mm, for a total of six coupon types to be tested.

As specified in ANSI/AAMI ST98:2022,[3] the surface area of the device was used to normalize the analyte concentration by applying a constant to evaluate the cleaning efficacy of the device against the established

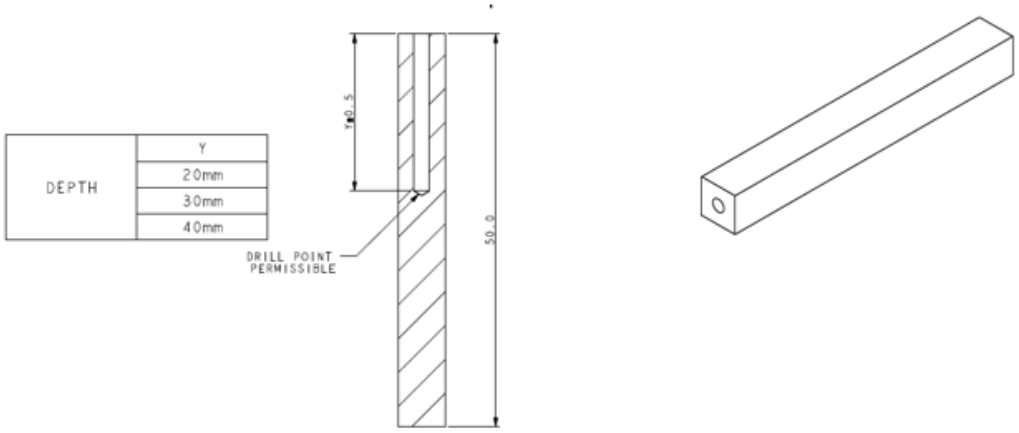

Figure 1. Single-feature test coupon with a dead-end lumen.

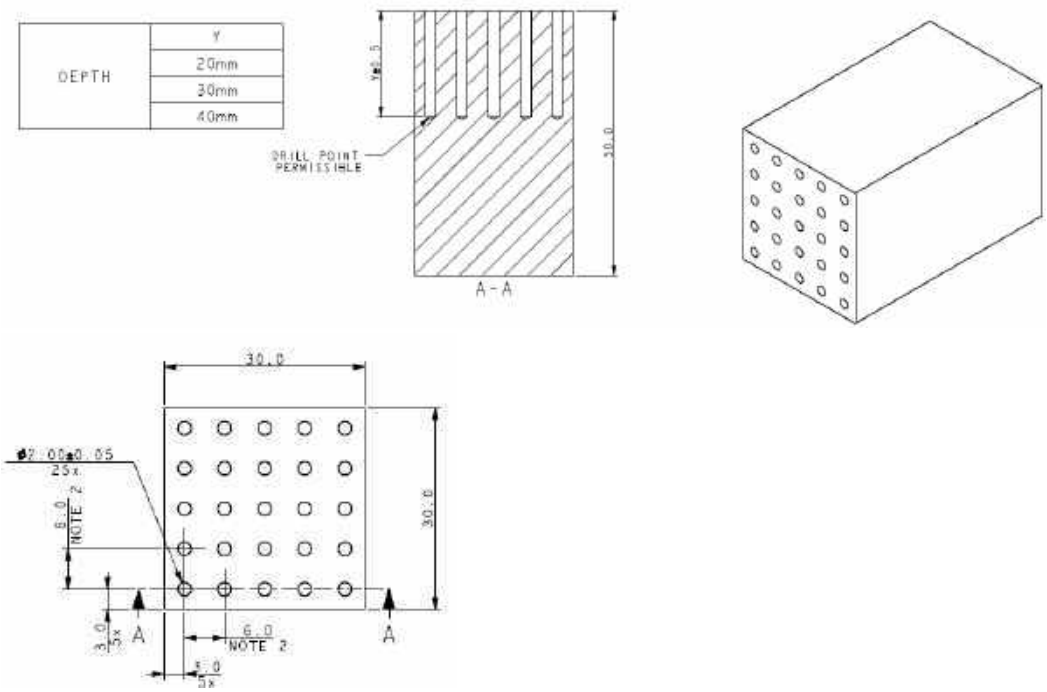

Figure 2. Multiple-feature test coupon with individual dead-end lumens.

acceptance criteria (reported in µg/cm²). The single-feature-only surface area was calculated using the feature alone. For the multiple-feature coupons, the 25 features were added for a total feature surface area. The surface area for the whole device was calculated using the surface area for the entire exterior stainless-steel block and that for the feature (Table 1).

In preparation for soiling, the devices were rinsed under running critical water[15] for 1 minute while brushing the lumen with a 2.2 mm × 12 inch lumen brush (Key Surgical, Eden Prairie, MN). Devices then were immersed in a 10 mL/L concentration of alkaline cleaning agent (NeoDisher; Dr. Weigert, Hamburg, Germany), and each lumen was flushed with the cleaning agent solution using a 16.5-G needle and 3-mL syringe. Following a 60-minute soak, the lumens were again flushed with 10 mL of the detergent solution and sonicated for 15 minutes at 45 kHz in a fresh batch of the alkaline cleaning agent. Then, they were rinsed under running critical water[15] and each lumen was flushed two times. The lumens were dried using medical-grade compressed air and inspected for cleanliness using a borescope.

Modified coagulated blood soil has been previously described[5] and was identified as the most difficult-to-remove soil due to the complexity of water-soluble and -insoluble protein complexes, resulting from fibrin in

	Surface Area (cm²)	
Coupon Type	**Single Feature Only**	**Whole Device**
Single feature: 20 mm	1.257	13.977
Single feature: 30 mm	1.885	14.605
Single feature: 40 mm	2.513	15.233
Multiple features: 20 mm	31.416	109.416
Multiple features: 30 mm	47.124	125.124
Multiple features: 40 mm	62.832	140.832

Table 1. Surface area by coupon type.

the coagulated blood.[4] The soil was prepared by mixing 100 mL fresh egg yolk (Eggland's Best, Malvern, PA) with 100 mL sheep blood (Rockland, Royersford, PA; with 0.1 mL heparin), and 2 g dehydrated hog mucin (Sigma-Aldrich, St. Louis, MO) in a blender. The soil was stored at 4°C to 8°C and brought to room temperature prior to coagulation. The soil was poured into a bowl and mixed well with 0.05 mL of 100% powdered protamine sulphate (Thermo Scientific, Waltham, MA) for each 5 mL of blood. The soil was applied immediately and typically would coagulate in 10 to 15 minutes. The test soil was applied within 10 minutes of preparation (i.e., before coagulation) with a pipette. When depositing the test soil, the pipette tip was inserted as far as it would go into the lumen. The coupon was gently tapped on the counter to promote the migration of the test soil to the dead end of the lumen. The devices then were dried under the most challenging conditions (72 hours at 22°C/50% relative humidity).[8]

The amount of test soil used in a cleaning efficacy should be an appropriate challenge but also must be representative of soil levels following clinical use. That is, the challenge protein concentration should be equivalent to clinical protein concentration levels and quantifiable via a validated protein residual test method. For surgical devices, protein analyte levels of approximately 244 µg/cm^2 are representative of clinical use.[16] The approximate protein concentration of modified coagulated blood soil was 108,747 µg/mL, as measured using the micro-BCA protein assay (Thermo Scientific). The minimum soil volume for the device was calculated using the following equation, resulting in the volumes shown in Table 2.

$$\text{Soil volume per lumen (mL)} = \frac{\text{Protein analyte level}\left(\frac{\mu g}{cm^2}\right) \times \text{Lumen surface area (cm}^2\text{)}}{\text{Soil protein concentration}\left(\frac{\mu g}{mL}\right)}$$

The cleaning procedure began with a prerinse, where each lumen was flushed with 10 mL water and bushed five times using a 2.2 mm × 12 inch lumen brush with a twisting motion. The devices then were immersed in a 4-mL/L concentration-neutral pH cleaning agent solution (Valsure Neutral; STERIS, St. Louis, MO) at less than 40°C for 5 minutes. While immersed, a 2.2 mm × 12 inch lumen brush was used to clean all traces of test soil from the lumen and exterior surface using a twisting motion five times for a minimum of 1 minute. To rinse, the devices were immersed in critical water (<40°C) for a minimum of 1 minute. An ultrasonic bath was prepared with the neutral pH cleaning agent at a concentration of 4 mL/L. The lumens were flushed with the cleaning agent solution using a 50-mL syringe before being sonicated for 5 minutes at 40 kHz. The devices then were immersed in critical water (<40°C) for a minimum of 1 minute while the lumens were flushed with 50 mL water. The lumens in the devices were dried by flushing the lumen with air using a 16.5-G needle until no droplets exited the lumen, and the outside of the device was dried using a lint-free cloth.

To account for the water-soluble and -insoluble protein present in the test soil postdrying, an additive extraction was validated. This was performed by first extracting with high-purity water (<50 ppb total organic carbon), followed by a second extraction of 2% alkaline sodium dodecyl sulfate (SDS) at a pH 10. The alkaline SDS solution is an aggressive extraction eluent and was validated to remove the residual protein remaining on the device.[17] The first and second extraction then were added together to deliver the total residual protein concentration. The validated extraction efficiencies are shown in Table 3 using a sample size of 30 coupons.

The extraction volume used within a cleaning efficacy is a critical test variable.

Lumen Depth	Surface Area for Feature Only (cm^2)	Minimum Soil Volume (µL)	Applied Soil Volume (µL)
20 mm	1.257	2.82	3.00
30 mm	1.885	4.23	5.00
40 mm	2.513	5.64	6.00

Table 2. Minimum soil volume, rounded to the nearest microliter.

Device	Sample Size (No. Coupons)	Protein Residual Concentration (µg/cm²) Mean ± SD	95% CI for mean (µ)
Single feature: 20 mm	30	27.350 ± 10.71	23.35–31.35
Single feature: 30 mm	*30*	23.710 ± 4.493	22.03–25.39
Single feature: 40 mm	*30*	24.870 ± 9.990	21.14–28.60
Multiple features: 20 mm	30	25.829 ± 7.750	22.93–28.72
Multiple features: 30 mm	30	23.837 ± 4.815	22.04–25.64
Multiple features: 40 mm	30	19.022 ± 17.44	12.51–25.54

Table 3. Protein residual results. Abbreviation used: CI, confidence interval; SD, standard deviation.

Too little eluent can result in incomplete removal of the residual protein, whereas too much will dilute the analyte, causing detectability issues.[18] To account for this situation, the limit of quantification established for the protein residual method (2.5 µg/mL) was divided into the analyte method acceptance criteria (6.4 µg/cm²) to establish the maximum extraction ratio.[3] The ratio then was multiplied by the surface area to calculate the maximum extraction volume for each lumen.

$$\text{Device maximum extraction volume (mL)} = \frac{\text{Device surface area (cm}^2\text{)} \times \text{Method acceptance criteria } \left(\frac{\mu g}{cm^2}\right)}{\text{Method LOQ } \left(\frac{\mu g}{mL}\right)}$$

The resulting extraction volumes for the devices are shown in Table 3.

Cleaned devices were extracted using the validated method of flushing three times; thus, the extraction volume was divided by three to deliver the flush volume per lumen per flush (Table 3). The device was inserted into the Whirl-pak extraction bag (Nasco, Madison, WI) with the lumen to the side of the bag. Using a 16.5-G needle and 3-mL syringe, the lumen(s) were flushed. The device was oriented so that the lumen opening was completely covered by the extraction fluid, then the bag was closed and sonicated for 15 minutes at 40 kHz. Following sonication, the devices were placed so that the lumen was oriented to the bag opening and an additional flush was completed. The bag was again sealed and sonicated for an additional 15 minutes at 40 kHz. After the second sonication, the device was again flushed with extraction fluid. The extraction fluid was measured for protein residuals using the standard addition micro-BCA protein assay[18] using a SpectraMax Plus 384 UV-VIS Spectrophotometer and the Pierce BCA Protein Assay Kit (Thermo Scientific). Testing was completed with a sample size of 30 coupons, and the results were calculated with Minitab 19 using a one-sample *t* test and a one-way analysis of variance.

Results

A negative sample control, negative device control, positive sample control, and positive device control were evaluated within the test system to verify whether the lumen was appropriately challenged and the test system would yield accurate results.[3] The results for the controls for both water and SDS extraction eluents demonstrated that each validation test system was in a state of control and that the devices were appropriately challenged.

The calculation method using the device feature approach was compared with the compendial method, which uses the surface area of the entire device (Figure 3). The results for the total lumen concentration with standard deviation and 95% confidence interval for the mean (µ) are reported in Table 4.

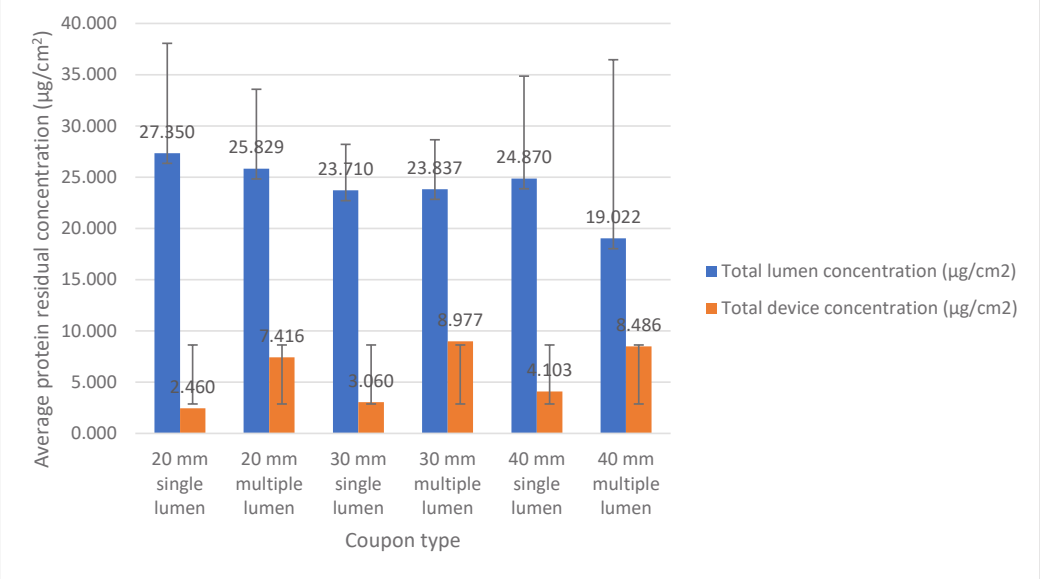

Figure 3. Protein residual concentration: design feature approach versus compendial method.

The data from both coupon types at 20, 30, and 40 mm was normally distributed, as demonstrated by the probability density of results. Comparing the cleaning efficacy of the devices with a 20-, 30-, and 40-mm single lumen with the results from the devices with 25 lumens (20, 30, and 40 mm) showed that the associated surface areas were statistically similar ($P = 0.534$ for the 20-mm devices, $P = 0.925$ for the 30-mm devices, and $P = 0.079$ for the 40 mm devices). All means, except for 40-mm devices with multiple features, were statistically similar ($P = 0.368$).

Discussion

When comparing the residual protein concentrations between the device feature approach and the compendial method, it is evident that the concentration of protein is diluted when using the surface area of the entire device. Using the device feature approach, only the surface area from the difficult-to-clean feature was used to calculate the extraction volume and soil application amount in the test system. The surface area then was used to calculate the residual protein level (per cm²). The compendial method used the entirety of the

Device	Surface Area for Feature Only (cm²)	Maximum Extraction Volume (mL)	Used Extraction Volume per Lumen (mL)	Flush Volume per Lumen per Flush (mL)	Total Extraction Volume (mL)	Extraction Efficiency (%) Mean ± SD
Single feature: 20 mm	1.257	2.56	2.4	0.8	2.4	93.418 ± 4.942
Single feature: 30 mm	1.885	4.83	4.5	1.5	4.5	87.837 ± 5.178
Single feature: 40 mm	2.513	6.28	6.0	2.0	6.0	88.214 ± 4.133
Multiple features: 20 mm	31.416	64.00	2.4	0.8	60	98.039 ± 0.973
Multiple features: 30 mm	47.124	120.75	4.5	1.5	112.5	96.477 ± 2.671
Multiple features: 40 mm	62.832	157.00	6.0	2.0	150.0	93.282 ± 3.713

Table 4. Maximum extraction volume per coupon and validated extraction efficiency.

device, including easy-to-clean features and surfaces of the device. As such, the entire surface area of the device was included in the calculations. This dilution of the analyte in the case of the entire device can provide misleading passing results when the most challenging device feature continues to harbor residual soil in a concentration above the acceptable level at that location.

To our knowledge, this constitutes the first published study demonstrating that the device feature approach is a more conservative method with less risk for determining analyte residuals than the compendial whole-device approach. These data also demonstrated that if a device has multiple features, the challenge to the most difficult-to-clean feature (or combination of features) can be representative of the cleaning performance of the entire device with multiple features. The device feature approach therefore is a conservative approach to validating a reusable medical device.[3] This approach also provides a new insight into the practicalities of addressing a complex device feature for cleaning validation. It is envisaged that the effectiveness of such an approach will be further corroborated, such as by using advanced surface imaging or specific measurement of analytes or bioindicator(s).

Next Steps

As demonstrated by comparing the results for the whole device with those for the device feature approach (Figure 3 and Table 4), the device feature approach—as a method to assess cleaning efficacy of isolated device features—can allow new devices to be assessed and validated by equivalency. For example, a device that contains multiple lumens without any other challenging features can be validated by equivalency using the results from one lumen feature validation—if the lumen feature is more challenging than the lumens found on the actual device. As the number of lumens increase, so does the surface area, keeping the amount of analyte (e.g., protein per cm^2) the same. Further, the amount of analyte (per cm^2) likely will decrease given the addition of any smooth surface area that is not a challenge for cleaning.

Using the device feature approach will also allow for the creation of a design feature database to be used in new device assessments and as guidance to device designers for determining which new designs will need testing or unique cleaning steps before the final assessment. Such a database would facilitate designing a device for cleanability and cleaning validations. As new, more challenging features are used in device designs, they can be further validated and represent a new master challenge feature. Devices consisting of a combination of features, and creating a more challenging scenario compared each individual feature, will be treated as a compound feature and have their own validation. Similarly, complex design features that consist of many individual components and, as a result, are difficult to assess can be isolated and validated as an individual feature.

A design feature database such as the one noted here could also be used to assess previously validated devices to establish a new cleaning classification with associated patient risk.[19] By providing information regarding the device feature cleaning efficacy, location within the device, and patient exposure, this database would provide a quantitative method to establish device cleaning requirements and/or acceptable analyte residual concentrations.

The design of device categories for cleaning validations will help in reducing the risks associated with cleaning steps in device processing and allow for minimization of the cleaning process. As medical devices become increasingly complex, it is necessary to develop a body of evidence and rigorous data to give designers, device users, and regulators the scientific support needed to ensure consistency in device processing. The current Spaulding classification system is not optimal in considering the complexity of device design and risks of inadequate cleaning; therefore, a subsequent classification may be established to ensure patient safety.[19]

Operationally, the practical impact of the device feature approach is to assess the proposed risk to patients. Using this approach, device features can be assessed as part of risk management, thus allowing developers to design medical device for

cleanability in a manner that mitigates risk during processing at healthcare facilities.

The risk assessment performed by device manufacturers must include an analysis of human factors that can lead to the inability to properly clean medical devices. Devices that are too complex may require additional mitigation steps, such as intensive training or special equipment, to fully mitigate cleaning risk when complex features are present. In addition, understanding the risk of the most challenging device feature will facilitate communication with healthcare facilities as part of the shared responsibility of ensuring the appropriate microbiological quality of reusable medical devices during execution of manufacturers' IFUs.

Conclusion

The device feature approach is a conservative method for validating the cleaning requirements of reusable medical devices and validates the use of reliable surrogate(s) for a whole device. This method can improve the reliability of device processing by helping to facilitate a design feature database for validation, IFU development, and a newly established quantitative cleaning classification system.

Acknowledgments

To the following Johnson & Johnson–affiliated individuals, who consulted on and performed the 56,000 flushes completed within this experimental design: Allan Kimble, Lorraine Floyd, Marcin Cieslak, Chris Carfaro, Spenser Chen, Chris Ratanski, Holyfield Agyekum, Stephen Kinyanjui, Gracie Ahrens, Cindy Rodriguez, Emily Garcia, Saachi Shibad, Margaret McCauley, Oliver Kremer, Elliott Kremer, and Zonia Rueda.

References

1. ANSI/AAMI/ISO 17664-1:2022. *Processing of health care products—Information to be provided by the medical device manufacturer for the processing of medical devices—Part 1: Critical and semi-critical medical devices*. Arlington, VA: Association for the Advancement of Medical Instrumentation.
2. AAMI TIR30:2011/(R)2016. *A compendium of processes, materials, test methods, and acceptance criteria for cleaning reusable medical devices*. Arlington, VA: Association for the Advancement of Medical Instrumentation.
3. ANSI/AAMI ST98:2022. *Cleaning validation of health care products—Requirements for development and validation of a cleaning process for medical devices*. Arlington, VA: Association for the Advancement of Medical Instrumentation.
4. Kremer T, Tortora A, Yeung Y, McDonnell G. Material adhesion comparison of test soils for reusable device cleaning efficacy. *Zentralsterilization*. 2021;29(3)166–72.
5. Kremer T, Bancroft R, Patel Z, et al. A standardized method for evaluating test soils used to demonstrate cleaning efficacy. *J Hosp Infect*. 2022;126:52–5.
6. Michels W, Roth K, Eibl R. Assessment of cleaning efficacy based on the protein-surface relationship. *Central Service*. 2013;21(3):212–5.
7. Kremer TA, Ratanski C. Test soil application and material affinity for reusable device cleaning validations. *Biomed Instrum Technol*. In press.
8. Kremer TA, Carfaro C, Klacik S. Effects of time, temperature, and humidity on soil drying on medical devices. *Biomed Instrum Technol*. 2023;57(2):58–66.
9. AAMI TIR12:2020. *Designing, testing, and labeling medical devices intended for processing by health care facilities: A guide for device manufacturers*. Arlington, VA: Association for the Advancement of Medical Instrumentation.
10. ANSI/AAMI/ISO 17665-1:2006/(R)2013. *Sterilization of health care products—Moist heat—Part 1: Requirements for the development, validation and routine control of a sterilization process for medical devices*. Arlington, VA: Association for the Advancement of Medical Instrumentation.
11. ISO 11139:2018. *Sterilization of health care products—Vocabulary of terms used in sterilization and related equipment and process standards*. Geneva, Switzerland: International Organization for Standardization.
12. Ofstead CL, Wetzler HP, Doyle EM, et al. Persistent contamination on colonoscopes and gastroscopes detected by biologic cultures and rapid indicators despite reprocessing performed in accordance with guidelines. *Am J Infect Control*. 2015;43(8):794–801.
13. Lopes LK, Costa DM, Tipple AV, et al. Complex design of surgical instruments as barrier for

cleaning effectiveness, favouring biofilm formation. *J Hosp Infect*. 2019;103(1):e53–60.

14. Hariharan P, Paruchuri SS, Topoleski LD, et al. A test method to assess the contribution of fluid shear stress to the cleaning of reusable device surfaces. *J Biomed Mater Res B Appl Biomater*. 2019;107(4):1132–40.

15. AAMI TIR34:2014/(R)2021. *Water for the reprocessing of medical devices*. Arlington, VA: Association for the Advancement of Medical Instrumentation.

16. Cloutman-Green E, Canales M, Zhou Q, et al. Biochemical and microbial contamination of surgical devices: A quantitative analsyis. *Am J Infect Control*. 2015;43(6):659–61.

17. Hoover J, Drosnock MA, Carfaro C, Kremer TA. Cleaning challenges: can extended soil dry times be reversed? *Biomed Instrum Technol*. 2023;57(2):44–51.

18. Kimble A, Ratanski C, Kremer TA. Chemical changes over time associated with protein drying. *Biomed Instrum Technol*. 2023;57(2):52–7.

19. Rowan NJ, Kremer T, McDonnell G. A review of Spaulding's classification system for effective cleaning, disinfection and sterilization of reusable medical devices: Viewed through a modern-day lens that will inform and enable future sustainability. *Sci Total Environ*. 202320;878:162976.

APPLIED AND ENVIRONMENTAL MICROBIOLOGY, Nov. 1999, p. 4814–4821 Vol. 65, No. 11
0099-2240/99/$04.00+0

Prediction of Toxigenic Fungal Growth in Buildings by Using a Novel Modelling System

NEIL J. ROWAN,[1]* CAMERON M. JOHNSTONE,[2] R. CRAIG MCLEAN,[2] JOHN G. ANDERSON,[1] AND JOE A. CLARKE[2]

Department of Bioscience and Biotechnology[1] and Department of Mechanical Engineering,[2] University of Strathclyde, Glasgow, Scotland

Received 26 February 1999/Accepted 27 August 1999

There is growing concern about the adverse effects of fungal bioaerosols on the occupants of damp dwellings. Based on an extensive analysis of previously published data and on experiments carried out within this study, critical limits for the growth of the indoor fungi *Eurotium herbariorum*, *Aspergillus versicolor*, and *Stachybotrys chartarum* were mathematically described in terms of growth limit curves (isopleths) which define the minimum combination of temperature (T) and relative humidity (RH) at which growth will occur. Each growth limit curve was generated from a series of data points on a T-RH plot and mathematically fitted by using a third-order polynomial equation of the form $RH = a_3T^3 + a_2T^2 + a_1T + a_0$. This fungal growth prediction model was incorporated within the ESP-*r* (Environmental Systems Performance [*r* stands for "research"]) computer-based program for transient simulation of the energy and environmental performance of buildings. For any specified location, the ESP-*r* system is able to predict the time series evolution of local surface temperature and relative humidity, taking explicit account of constructional moisture flow, moisture generation sources, and air movement. This allows the predicted local conditions to be superimposed directly onto fungal growth curves. The concentration of plotted points relative to the curves allows an assessment of the risk of fungal growth. The system's predictive capability was tested via laboratory experiments and by comparison with monitored data from a fungus-contaminated house.

In developed countries, people spend a substantial proportion of time indoors, and it is now generally accepted that indoor air quality can have a significant impact on human health (8, 13–15, 18, 22, 27, 41, 50, 52, 53). The indoor environment can contain numerous potentially harmful substances, such as dust mite and cat allergens, formaldehyde, ozone, and volatile organic vapors (1, 28, 38, 42). In the present context, attention is drawn primarily to the presence, growth, and prediction of the xerophilic fungus *Eurotium herbariorum* and the mycotoxigenic fungi *Aspergillus versicolor* and *Stachybotrys chartarum* (15, 20, 22, 27, 34).

There is currently a substantial body of evidence to support the view that fungi in buildings can have severe and wide-ranging effects on the general health of occupants (7, 14, 15, 20, 22, 43, 53). Respiratory, allergenic, and other symptoms, including nausea and vomiting, have been diagnosed (14, 15, 18, 22, 43). Several major investigations have concluded that there is a significant correlation between the incidence of high levels of airborne fungal spores containing mycotoxins, particularly from *A. versicolor* or *S. chartarum*, and ill health (13–15, 18, 20, 22, 27, 29). For example, in some damp and moldy buildings, airborne concentrations of viable *S. chartarum* spores containing stachybotryotoxins can reach levels of up to 18,000 CFU/m^3 (23). Recent research has focused on the health status of workers in water-damaged office environments after exposure to fungal bioaerosols (13, 28, 42), especially *A. versicolor* or *S. chartarum* and their toxigenic metabolites (22, 27). It was concluded that prolonged and intense exposure to these toxigenic fungi is associated with reported disorders of the respiratory and central nervous systems and of the mucous membranes and the cellular and humoral immune system, suggesting a possible immune competency dysfunction (22, 27).

Clearly, the prevention of fungal development and mycotoxin production within buildings is a priority. While the use of biocidal compounds may be appropriate to prevent the problem from occurring in new buildings and to alleviate existing problems, it is generally agreed that the preferred strategy is the elimination of conditions which can lead to fungal growth (1, 46). A key element in such a strategy would be a model which could predict the likelihood and extent of toxigenic fungal growth for any given set of conditions (24). Such a model could be used to critically evaluate a building at the design stage for inherent problems, allowing appropriate changes to be made early in the project. It could also be applied to existing problematic buildings to determine the most effective remedial action.

Through the International Energy Agency's Annex 24 program, advanced computer models which can be used to simulate the moisture behavior of structures have been developed (25). However, the main focus of that research has been on the passage of moisture through walls and the prediction of moisture content and condensation within them (25). Until recently, little consideration was given to the prediction of fungal growth within an integrated building simulation model, probably because of the perceived difficulties involved in combining the biological and physical parameters which contribute to the conditions suitable for fungal development.

The present interdisciplinary study was undertaken to develop a prototype fungal prediction program for the built environment. First, growth limit curves for the fungi *E. herbariorum*, *A. versicolor*, and *S. chartarum* were mathematically described within a fungal growth prediction (FGP) database. Second, the FGP database was incorporated into the ESP-*r* environmental modelling system to produce a model that can

* Corresponding author. Mailing address: Department of Bioscience and Biotechnology, University of Strathclyde, Royal College Building, 204 George St., Glasgow G1 1XW, Scotland. Phone: 44 (0) 141 548 2531. Fax: 44 (0) 141 553 4124. E-mail: n.j.rowan@strath.ac.uk.

identify local environmental conditions under which fungal development may occur. Third, the efficacy of the system's predictive capability was tested by laboratory-based experiments and by comparison of real and simulated data from a building exhibiting visible fungal growth.

MATERIALS AND METHODS

The ESP-*r* system. ESP-*r* is an advanced transient energy and environmental simulation computer package (11, 26, 56) which is used extensively in building performance appraisal. Since its inception, the system has been the subject of a comprehensive development and validation process. This has included long-term involvement in the research portfolio of the European Community, which resulted in the selection of ESP-*r* as the European reference model for two major building and environmental research programs (10, 11, 26, 51, 56). The ESP-*r* system is comprised of the following elements: the "project manager," an interface that allows the user to define the problem being investigated, within the context of the computer language required for processing, and the displaying of results once the problem has been solved; the "simulator," a numerical solver which mathematically solves the problem under investigation; and a number of supporting programs and databases containing information required by the numerical solver (e.g., thermophysical properties of building materials, glazing systems, climate).

ESP-*r* is capable of analyzing the heat, power, and air flow in a building and the operation of the associated environmental control systems (e.g., air-conditioning, heating). Typically, the building being investigated is configured within the system in terms of geometry, construction, layout, and usage. Flow paths, which represent air and moisture transfers in the building and the distribution of environmental systems and electrical power, are defined. This configuration is then analyzed under specified climate and control conditions (e.g., thermostat and time-clock settings), and the results are fed to the project manager for user interpretation. This analysis technique is equally applicable to both existing buildings and new designs, and it allows the efficacy of measures aimed at improving the energy and environmental performance of a building to be specifically quantified.

In the present context, a building can be modelled within ESP-*r* at any specified level of resolution. An enhanced resolution can be used at locations of particular concern (e.g., where there are local moisture sources or where insulation levels are low). Taking explicit account of moisture movement through walls, internal moisture generation, and air movement, ESP-*r* can predict changes in local surface temperature and relative humidity at a specified location(s) for any climatic condition. ESP-*r* is widely available at no cost to researchers, and further information and access can be gained through ESRU@strath.ac.uk.

ESP-*r* model of the test house. Comparative environmental monitoring and mycological studies were conducted for a selected fungus-contaminated surface in a late-1940's prefabricated three-bedroom, semidetached dwelling located on a housing estate in Edinburgh, Scotland. Information relating the house's design, form, and fabric (e.g., hygrothermal properties); occupancy behavior (e.g., moisture production); building environmental systems (e.g., heating, ventilation); and outdoor climate were incorporated and simulated in ESP-*r*. The house was of steel frame construction, which is prone to condensation. The windows were steel framed, with high resultant air infiltration rates, and insulation levels were generally poor. The lower floor consisted of a hall, kitchen, bathroom, storeroom, and living room, while the upper floor consisted of three bedrooms and a hall. The house was heated by a 3-kW electric heater in the living room and a 1-kW electric heater in the upstairs hallway. During the study, two people resided in the test house.

Environmental monitoring of the test house. The selected test location was a fungus-contaminated surface at the junction of a north-facing wall and ceiling in one of the bedrooms. The local environmental conditions were monitored for surface temperature and relative humidity at 1.5-h intervals over a 7-day period in March by using a dedicated thermocouple (±0.5°C) and relative humidity sensor (±0.5%) attached to a recording device (data logger, model XT 102; ACR Systems Inc., Shepshed, United Kingdom). Simultaneous monitoring of external climatic conditions also took place, by using an on-site weather station consisting of global horizontal and diffuse solar irradiance measurement (Kipp and Zonen [St. Albans, United Kingdom] type CM11 pyranometers and shadow band), wet and dry bulb temperature measurement (Vector Instruments [Rhyl, United Kingdom] type H301 aspirated psychrometer), and wind velocity and direction measurement (Vector Instruments type A100R switching anemometer and type W200P potentiometer windvane). These instruments were connected to a data logger (model DL2; Delta-T Devices Ltd., Cambridge, United Kingdom).

Mycological examination of the test house. During the same 7-day monitoring period in March, the types of fungi on the test surface and their minimum relative humidity (RH) growth requirements were determined by using dichloran rose bengal chloramphenicol agar (DRBCA) and 2% malt extract agar (MEA) contact plates (Oxoid Products). The equilibrated relative humidity (ERH) (which is equivalent to the more commonly used biological term water activity [a_w]) was adjusted for the agar to 98.7, 94.5, 93, 90.5, 88.5, 84.5, 81, 78.5, 76.1, 74.5, 71.2, and 67.8% by the addition of glycerol. The final ERH was confirmed with an a_w-Wert Messer Chamber (Lufft). During the monitoring study, the DRBCA and MEA plates were pressed against areas of confluent fungal growth at the test location. The contact plates were positioned on metal rack supports over 50 ml of appropriate saturated salt solutions, as described by Grant et al. (19), in crystallizing chambers (100 mm in diameter by 60 mm in depth) which controlled the ERH in the culture media at the aforementioned levels. In preparing and maintaining the humidity chambers, the stipulations made by Wexler and Hasegawa (54) and Winston and Bates (55) regarding the control and accuracy of ERH were carefully observed. A check was made on the ERH level attained in each chamber by using a model DP680 hygrometer (Protimeter Ltd., Marlow, United Kingdom) and Solomat (Bishops Stortford, United Kingdom) model MPM2000 and was found to agree within a 1% margin. The contact plates were subsequently incubated in the above-mentioned atmospheric controlled chambers at 20°C for 25 days. The plates were examined periodically for the presence of fungal growth, and the emerging yeasts and molds were identified by conventional mycological techniques (44).

Lowest relative humidity value supporting growth of building-isolated fungi on woodchip wallpaper. This study was designed to compare the minimum RH requirements for the growth of fungi isolated from the test surface on nutritionally rich laboratory-based culture media with the minimum water requirements when grown on the nutritionally inferior building material woodchip wallpaper. The test molds were grown and sporulated on MEA slants after 10 days at 25°C, while the yeast cultures were grown on MEA for 3 days at 25°C. Strips of woodchip wallpaper (40 by 40 mm) were placed in minimal salt solutions, as described in Grant et al. (19), after autoclaving at 109°C for 10 min and drying overnight. The squares of woodchip wallpaper were positioned in atmospheric chambers that were controlled at the above-mentioned series of ERH values. After equilibration for 10 days, duplicate squares were separately centrally inoculated with the test fungi by using a sterile needle. The chambers were incubated and examined for growth over 110 days at 20°C. The identities of the emerging fungi were confirmed as described earlier.

Statistical analysis. Analysis of variance, balance model (Minitab software release 11; Minitab Inc., State College, Pa.), was used to compare the minimum relative humidity requirements for the test fungi growing on MEA, DRBCA, and woodchip wallpaper. The studies were performed in duplicate with duplicate samples examined at each trial. Analysis of variance, two-way model, was used to compare minimum moisture requirements reported by previous researchers with limiting RH values obtained for the same fungi during this study. A paired *t* test was used to compare simulated and real RH and temperature data from the test house. All significant differences were reported at the 95% ($P < 0.05$) confidence interval.

RESULTS

Development of the fungal growth prediction program. An analysis of previously published data (1–6, 9, 12, 16, 17, 19, 21, 23, 24, 30–32, 34, 36–40, 48, 49) and experiments conducted in this study were used to derive growth limit curves (isopleths), which define the minimum combination of local-surface relative humidity and temperature for which growth of the toxigenic fungi *A. versicolor* and *S. chartarum* and the xerophilic atoxigenic fungus *E. herbariorum* will occur (Fig. 1). Each growth limit curve was generated from a series of data points on a temperature-versus-relative-humidity (T-RH) plot and was mathematically fitted by using a third-order polynomial equation of the form $RH = a_3T^3 + a_2T^2 + a_1T + a_0$. Curve fitting for the isopleths was undertaken by using the curve-fitting package within Microsoft Excel 97. The above-mentioned third-order polynomial gave both the closest match (for all the data analyzed) and required profile for the control data points used ($R^2 = 0.96$).

Mycological verification of fungal growth limits incorporated within ESP-*r*. The types of fungi isolated from the test house and the lowest RH levels at which each fungus grew at 20°C on MEA, DRBCA, and woodchip wallpaper after 25 and 110 days of incubation are given in Table 1. There was no significant difference ($P < 0.05$) between the lowest RH values supporting growth of the test fungi on MEA and DRBCA (Table 1). Due to the absence of *S. chartarum* in the test house, the minimum RH limit for the growth of *S. chartarum* IMI 032542 (obtained from the International Mycological Institute, CABI International, Egham, Surrey, United Kingdom) was examined with MEA, DRBCA, and woodchip wallpaper under the ERH-controlled atmospheres described earlier. The re-

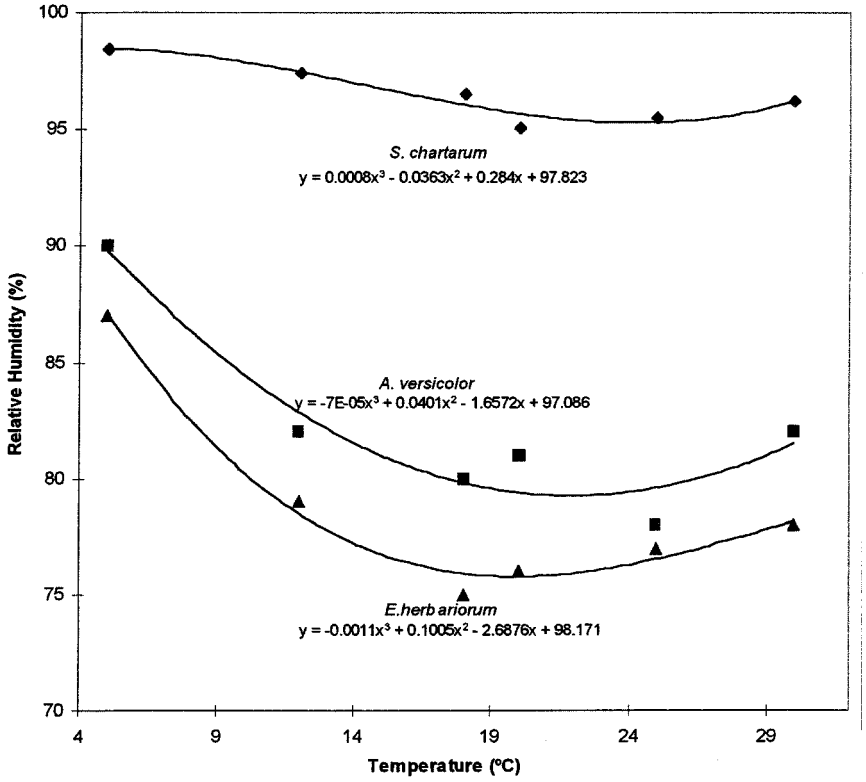

FIG. 1. Third-order fit of relative humidity and temperature which limit growth of *E. herbariorum*, *A. versicolor*, and *S. chartarum* on building materials (data points obtained from this study and from previously published research).

sults of this study are consistent with the isopleths shown in Fig. 1, where the minimum RH levels supporting growth of *E. herbariorum*, *A. versicolor*, and *S. chartarum* are fully consistent with the predictions of the model, as is the lack of any fungal growth at 74.5% and below (Table 1).

Ten different mold species and two yeasts (*Hansenula anomala* and *Rhodotorula glutinis*) were isolated from the test surface (Table 1). Significant variation ($P < 0.05$) in the abilities of the test fungi to grow at different humidity levels was apparent (Table 1). This ranged from growth at ≤81% RH for the molds *A. versicolor*, *E. herbariorum*, *Penicillium brevicompactum*, and *Penicillium spinulosum* to failure for some molds (*Mucor plumbeus*, *Phoma herbarum*, and *S. chartarum*) and the aforementioned yeasts to sustain growth at less than 93% RH. Despite prolonged incubation of inoculated woodchip wallpaper (110 days) at 20°C, the fungi *Cladosporium cladosporiodies*,

TABLE 1. Minimum relative humidity requirements for growth of different building-isolated fungi on MEA and DRBCA after 25 days and on woodchip wallpaper after 110 days of incubation at 20°C

Fungus isolated from test house	Minimum RH (%) supporting growth on[a]			Significant difference ($P < 0.05$)[b]
	MEA	DRBCA	Woodchip wallpaper	
Cladosporium cladosporioides	84.5	85.5 ± 2	89 ± 1	Yes
Cladosporium herbarum	85.5 ± 2	85.5 ± 2	88.5	Yes
Alternaria alternata	88.5	88.5	89.5 ± 1.2	No
Aureobasidium pullulans	88.5	89 ± 1	88.5	No
Penicillium brevicompactum	81.8 ± 1.8	82.7 ± 2	85.5 ± 2	Yes
Penicillium spinulosum	81	81	84.5	Yes
Aspergillus versicolor	81	81	82.2 ± 1.2	No
Eurotium herbariorum	76.1	76.7 ± 1.2	77.3 ± 1.2	No
Phoma herbarum	93	93.8 ± 0.8	93.8 ± 0.8	No
Mucor plumbeus	93.8 ± 0.8	93.8 ± 0.8	94.1 ± 0.8	No
Hansenula anomala	92.4 ± 1.3	93	94.5	Yes
Rhodotorula glutinis	91.7 ± 1.7	92.5 ± 1	93	No
Stachybotrys chartarum IMI 032542[c]	94.5	94.5	96.5 ± 2.3	Yes

[a] Values are averages of four replicate samples representing two trials.

[b] Difference between lowest humidity value supporting growth of fungus on woodchip wallpaper and those supporting growth on MEA and DRBCA. No significant difference between minimum RH values obtained from MEA and DRBCA at the 95% confidence interval was found ($P < 0.05$).

[c] Fungal culture obtained from the International Mycological Institute, CABI International, Egham, Surrey, United Kingdom.

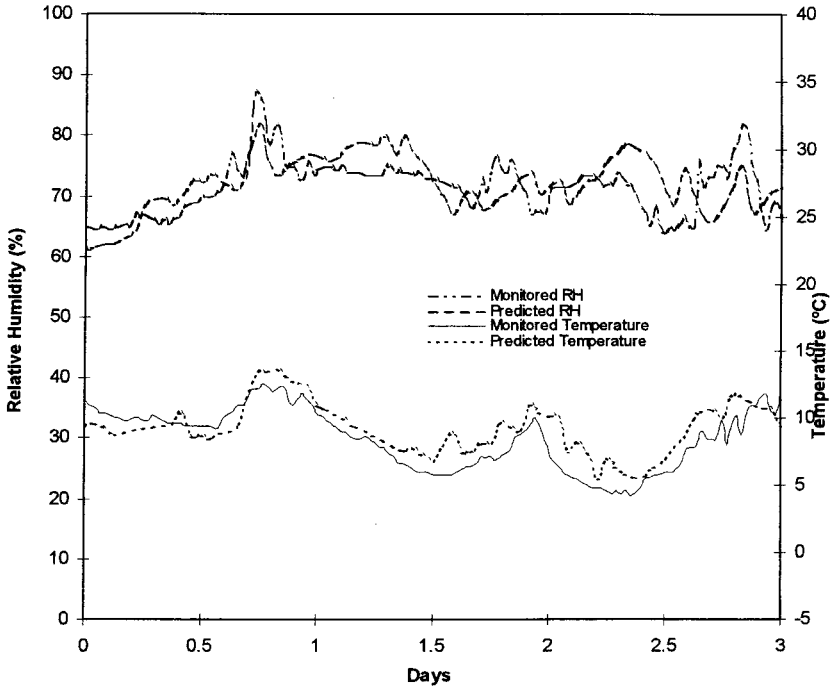

FIG. 2. Monitored and predicted relative humidity and temperature data at surface of concern in test house (period in March).

Cladosporium herbarum, *P. brevicompactum*, *P. spinulosum*, *H. anomala*, and *S. chartarum* grew at lower RH values on the nutritionally rich MEA and DRBCA over the shorter 25-day period (Table 1).

Comparison of simulated and real relative humidity and temperature data from the test house. A simulation of the mold-contaminated test house was run against the externally monitored climatic data for the 7-day period in March. The predicted-versus-real temperature and relative humidities at the test location for part of this period are shown in Fig. 2. It is evident from Fig. 2 that the simulated and real data are in relatively close agreement ($P < 0.05$). On this basis, simulated data from ESP-*r* could be taken as providing a good representation of the temperature and relative humidity occurring at the test location over any stipulated period of time.

Testing the predictions of the fungal program. In order to compare the predictions of the ESP-*r* fungal program against the types of fungal species isolated from the test location, the monitored (i.e., real) surface relative humidity and temperature data for the 7-day period in March are shown superimposed on the growth limit curves in Fig. 3. While the model successfully predicted fungal growth at the test location, on the basis of the range of plotted RH data in Fig. 3, only fungi with a growth limit of below 83% RH would have been predicted to occur. This upper RH measurement of 83% does not account for the isolation of hydrophilic molds such as *Cladosporium*, *Alternaria*, *Aureobasidium*, *Phoma*, and *Mucor* or the yeasts *Hansenula* and *Rhodotorula*, which were shown to have minimum moisture requirements of 89, 89.5, 88.5, 93.8, 94.1, 94.5, and 93% RH, respectively, on woodchip wallpaper (Table 1). In order to explain the occurrence of these molds, a simulation employing 1-h intervals and climatic data for a 3-day period in January was performed. The simulated conditions of surface relative humidity and temperature at the test location are shown superimposed on the growth limit curves in Fig. 4. On the basis of this plot (where surface relative humidity values reach as high as ~96%), a user would have correctly predicted the likely presence of the aforementioned hydrophilic fungi (Table 1), in addition to predicting the growth of *E. herbariorum* and *A. versicolor* and the absence of *S. chartarum*. The user would therefore have predicted an extensive development of different types of fungi spanning a wide range of T-RH growth categories, which is in agreement with the outcome of the mycological tests.

DISCUSSION

The most commonly occurring fungi which contaminate damp buildings in North America and Europe are those that form true cell walls of the group Eumycota (43, 46). While fungi from all subdivisions of Eumycota are often present in damp dwellings, the majority of these fungi belong to the class Hyphomycetes of the subdivision Deuteromycotina, such as *Penicillium*, *Aspergillus*, *Cladosporium*, and *Stachybotrys* (1, 43, 46). Fungal growth in buildings has been shown previously to be essentially a surface phenomenon (1). Fungal spores germinate and form active mycelia on hygroscopic building materials or interior finishes when certain critical growth parameters are satisfied (1, 46). On internal wall surfaces, the principal controlling factors governing fungal growth are relative humidity (which governs the free water availability) and temperature (1, 19, 24).

This study has addressed the prediction of local environmental conditions that encourage fungal growth on internal surfaces. Critical limits for the growth of the indoor fungi *E. herbariorum*, *A. versicolor*, and *S. chartarum* were mathematically described in terms of growth limit curves, or isopleths, that define the minimum combination of temperature and relative humidity for which growth will occur. Each growth limit curve was generated from a series of data points on a T-RH plot and was mathematically fitted by using a third-order polynomial equation of the form $RH = a_3T^3 + a_2T^2 + a_1T + a_0$

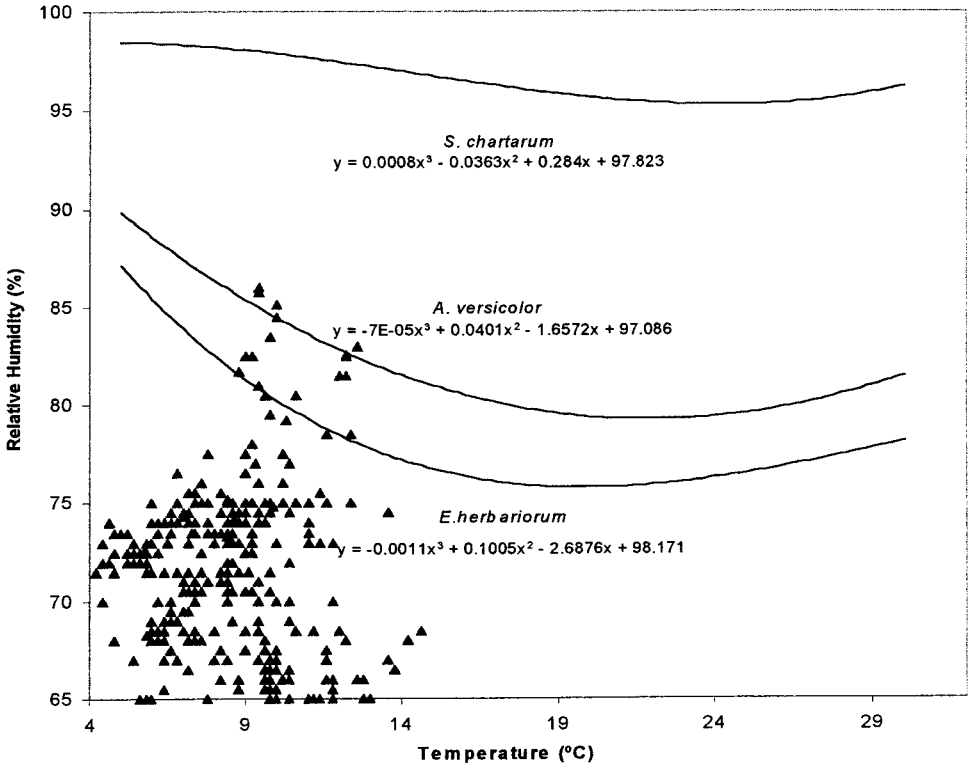

FIG. 3. Monitored environmental data for test house superimposed on growth limit curves in ESP-*r*. Each point represents a recorded temperature/relative humidity value collected at 1.5-h intervals at the test location over a 7-day period in March.

(Fig. 1). The data points were derived from previously published research data (1–6, 9, 12, 16, 17, 19, 21, 23, 24, 30–32, 34, 36–40, 48, 49) and from experiments carried out in this study (Table 1). It is evident from Fig. 1 that the three fungi differ in their minimum RH and T requirements to sustain growth on building materials. For example, *E. herbariorum* requires a minimum of 76.1% RH to sustain growth at 20°C, whereas *A. versicolor* and *S. chartarum* require a minimum of 81 and 96.5% RH, respectively, to grow at the same temperature. Local surface T-RH values occurring below the growth limit curve for each fungus prevent the organism from either initiating or sustaining growth. Both Adan (1) and Grant et al. (19) have postulated that fungal growth will be prevented if RH and surface temperature conditions within buildings are maintained such that internal wall surfaces remain below 80% RH. The limit of 80% RH for the prevention of fungal growth in buildings (1, 19) is 5% greater than the prediction limit for fungal growth set by the ESP-*r* model. Our recommendation of 75% RH for limiting fungal growth in buildings is based on our findings shown in Table 1.

In relation to the minimum moisture requirements for food spoilage and building-related fungi, many researchers have previously reported that the mold *E. herbariorum* can grow at very low RH values (1, 43, 44, 46). Therefore, relative humidity values occurring consistently below the isopleth for this highly xerophilic fungus will result in the indoor surface remaining free of all fungal growth. The concept of using RH-versus-T isopleth curves for predicting germination, growth, and asexual sporulation of toxigenic and nontoxigenic fungi on nutrient media and in foodstuffs has been exploited by a number of previous workers (2, 5, 6, 36). Ayerst (6) showed that growth of a wide variety of food spoilage fungi was governed by controlling the limiting combinations of a_w (ERH) and temperature, and each fungus had an optimal value for both of these parameters at which the growth rate was maximized. Adan (1) found that the maximum tolerance to low moisture conditions was exhibited on materials of a high nutritional content under optimum temperature. In the context of this study and to our knowledge, this is the first time this concept has been employed to predict fungal growth in buildings.

Minimum a_w values (converted to ERH) obtained by previous researchers for the growth of fungi on nutrient media at temperatures of 20 to 25°C are compared with the findings of this study in Table 2. These minimum relative humidity values limiting growth of the test fungi were shown to be in good agreement ($P < 0.05$) with minimum moisture requirements reported for the same fungi by other researchers (Table 2). Many of these workers showed that these fungi also differed in moisture requirements for each stage in their growth cycle, where differences of ~2% RH between spore germination, hyphal growth, and sporulation were recorded (1, 2, 24, 45). However, the findings of this study do not agree with the work of Nikulin et al. (34), who examined growth of *S. chartarum* and its toxin production on some building materials and in animal fodder under different RH conditions. Nikulin et al. (34) reported that *S. chartarum* was capable of growth (and in some instances, toxin production) on wallpaper, pine panel, and paper at 78% RH, while all previous studies reported that this fungus required a minimum RH of 91% or above to sustain growth (6, 9, 19, 23, 36). It is also recognized that *S. chartarum* is not a xerophilic organism (19, 24, 44), which, according to the definition of Pitt and Christian, is "a fungus capable of growth under at least one set of environmental conditions at 85% RH or less" (40).

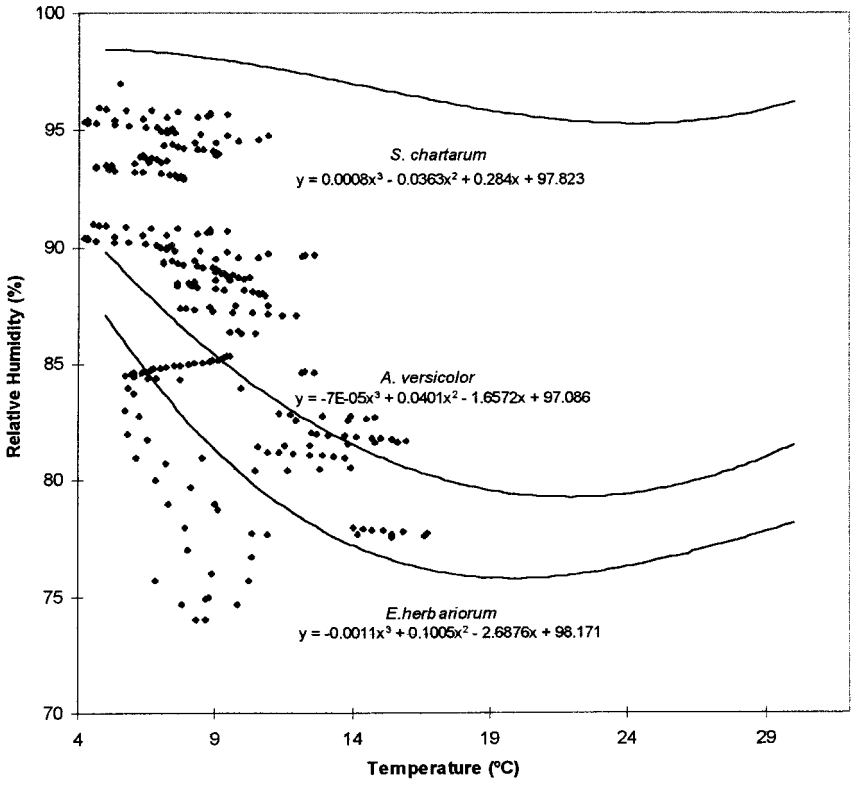

FIG. 4. Predicted environmental data for test house superimposed on growth limit curves by ESP-*r*. Each point represents a temperature/relative humidity value predicted by ESP-*r* at 1-h intervals at the test location with actual climatic data for a 3-day period in January.

On the basis of the methodology described by Nikulin et al. (34), it is possible that the moisture limit for growth of *S. chartarum* was greater than the reported 78% RH. The authors inoculated the building materials with a 1-ml volume of spores suspended in a highly nutritious aqueous wash which had been equilibrated for only 3 days to reach 78% RH (the final and subsequent RH values not being monitored in the chambers). This procedure goes against the usual convention of using a dried-spore suspension to avoid altering the moisture content of the samples. It would further appear that the samples were incubated at 20 to 23°C, which may have permitted this fungus to grow before the saturated salt solution reduced the atmosphere to less than 90% RH. Therefore, it is possible that the actual RH may have been significantly higher than the reported 78%. Nikulin et al. (34) showed that *S. chartarum* was capable of growth and of producing stachybotryotoxins on wallpaper, gypsum board, hay, and straw.

The fungal prediction model used in the present study and containing the growth limit curves, which is incorporated within ESP-*r*, operates by using information from two sources. First, as previously described, ESP-*r* can predict, from an appropriate representation of the building, changes in local sur-

TABLE 2. Minimum a_w values (converted to ERH) obtained in this and previous studies for growth of test fungi over the temperature range 20 to 25°C

Fungus	Minimum RH (%) supporting growth			Significant difference ($P < 0.05$)
	Previous studies			
	Value(s) (reference[s])	Avg ± SD	Values found in this study[a]	
Aspergillus versicolor	78 (9, 19, 30), 79 (23), 80 (4), 83 (36)	79.3 ± 2	81	No
Alternaria alternata	85 (24, 37), 88 (30)	86 ± 1.7	88.5	No
Cladosporium cladosporioides	88 (30), 84 (19, 23)	85.3 ± 2.3	84.5	No
Cladosporium herbarum	84 (19), 88 (36), 90 (30)	87.3 ± 3	85.5	No
Mucor plumbeus	93 (9, 24)	93	93.8 ± 0.8	No
Penicillium brevicompactum	79 (23), 81 (9), 82 (24), 83 (19)	81.3 ± 1.7	81.8 ± 0.8	No
Penicillium spinulosum	79 (19), 80 (9)	79.5 ± 0.7	81	No
Phoma herbarum	92 (16), 93 (19, 23)	92.6 ± 0.6	93	No
Stachybotrys chartarum	94 (6, 9, 36), 93 (19, 23)	93.6 ± 0.5	94.5	Yes
Aureobasidium pullulans	89 (23), 88 (44)	88.5 ± 0.7	88.5	No

[a] Values shown are for growth on MEA over a 25-day period at 20°C.

face temperature and relative humidity at any specified location for any set of climatic data. Second, the mathematical functions defining the isopleths (Fig. 1) are contained within the FGP database. This allows the predicted local conditions to be superimposed directly on the growth limit curves, as illustrated in Fig. 4. The concentration of plotted points relative to the isopleths allows an assessment of the risk and extent of possible fungal growth.

Environmental monitoring study of the fungus-contaminated test house (Fig. 2) showed that the comparison between simulated and real surface temperature and relative humidity data over a 7-day period in March was relatively good ($P < 0.05$). It should be noted, however, that due to the lack of some information, this simulation could not be regarded as constituting a strict test of the model, which has been subjected to strictly controlled validation exercises (56). For example, due to the age of the building, some of the structural properties were not readily ascertainable and values for similar representative materials had to be substituted (24). Other uncertainties arose because it was not possible to obtain definite information on the influence of the occupants on the internal environment, e.g., additional heat and moisture from washing and cooking, etc. With this information, a more accurate prediction would have been possible.

Conclusions. Overall, the present study has verified the feasibility of a computer-based approach to the prediction of toxigenic fungal growth in problematic buildings and has demonstrated the usefulness of the prototype ESP-*r* program. However, the continued development of the prototype into a comprehensive prediction model will require an upgrading of the current FGP database. First, there is very limited information currently available on the effects of fluctuations in temperature and relative humidity on fungal growth, sporulation, and mycotoxin production in buildings. Second, a large number of fungi, hitherto regarded as harmless and which commonly occur indoors, have recently been implicated as the cause of human ill health; e.g., some *Fusarium*, *Acremonium*, and *Penicillium* spp. have been shown to be agents of hyalohyphomycosis (53). It is envisaged that additional isopleths for the prediction of these emerging filamentous fungal pathogens will be incorporated within the FGP database. Such information will enhance ESP-*r*'s fungal prediction capability, thus allowing the program to make a more accurate assessment of the risk or probability of toxigenic fungal growth in existing and new buildings.

ACKNOWLEDGMENTS

We express gratitude to Scottish Homes, which funded this research.

Thanks go also to Kerr McGregor and Alex Taylor of Napier University, Edinburgh, Scotland, for assistance in obtaining the monitored environmental data for the test house.

REFERENCES

1. **Adan, O. C. G.** 1994. Fungal disfigurement of interior finishes. Ph.D. thesis. University of Eindhoven, Eindhoven, The Netherlands.
2. **Andrews, S., and J. I. Pitt.** 1987. Further studies on the water relations of xerophilic fungi, including some halophiles. J. Gen. Microbiol. **133:**233–238.
3. **Armolik, N., and J. G. Dickson.** 1965. Minimum humidity requirements for germination of conidia of fungi associated with storage of grain. Phytopathology **46:**462–465.
4. **Avari, G. P., and D. Allsopp.** 1983. The combined effect of pH, solutes, and water activity (Aw) on the growth of some xerophilic *Aspergillus* species, p. 548–555. *In* T. A. Oxley and S. Barry (ed.), Biodeterioration 5, John Wiley, Chichester, United Kingdom.
5. **Ayerst, G.** 1966. Influence of physical factors on determination of molds. Soc. Chem. Ind. Monogr. **23:**14–20.
6. **Ayerst, G.** 1969. The effects of moisture and temperature on growth and spore germination in some fungi. J. Stored Prod. Res. **5:**127–141.
7. **Burr, M. I., J. Mullins, T. G. Merrett, and N. C. H. Scott.** 1988. Indoor molds and asthma. J. R. Soc. Health **3:**99–101.
8. **Canadian Public Health Association.** 1987. Significance of fungi in indoor air: report of a working group. Can. J. Public Health **78:**S1–S14.
9. **Christian, J. H. B.** 1980. Reduced water activity, p. 79–90. *In* Microbial ecology of foods 1. Factors affecting life and death of microorganisms. Academic Press, London, United Kingdom.
10. **Clarke, J. A., and J. L. M. Hensen.** 1991. An approach to the simulation of coupled heat and mass flow in buildings. Int. J. Indoor Air Quality Climate **3:**283–296.
11. **Clarke, J. A.** 1985. Energy simulation in building design. Adam Higher Publishers, Bristol, United Kingdom.
12. **Coppock, J. B. M., and E. D. Cookson.** 1951. The effect of humidity on mold growth on constructional materials. J. Sci. Food Agric. **2:**534–537.
13. **Croft, W. A., B. B. Jarvis, and C. S. Yatawars.** 1986. Airborne outbreak of trichothecene toxicosis. Atmos. Environ. **20:**549–552.
14. **Dales, R. E., R. Burnett, and H. Zwanenburg.** 1991. Adverse health effects among adults exposed to house dampness and molds. Am. Rev. Respir. Dis. **143:**505–509.
15. **Dales, R. E., H. Zwanenburg, R. Burnett, and C. A. Franklin.** 1991. Respiratory health effects of home dampness and molds among Canadian children. Am. J. Epidemiol. **134:**196–203.
16. **Eveleigh, D. E.** 1961. The growth requirements of *Phoma violacea*, with reference to its disfigurement of painted surfaces. Ann. Appl. Biol. **49:**412–423.
17. **Ezeonu, I. M., J. A. Nobel, R. B. Simmons, D. L. Price, S. A. Crow, Jr., and D. G. Ahearn.** 1994. Effect of relative humidity on fungal colonization of fiberglass insulation. Appl. Environ. Microbiol. **60:**2149–2151.
18. **Flannigan, B., E. M. McCabe, and F. McGarry.** 1991. Allergenic and toxigenic microorganisms in houses. J. Appl. Bacteriol. Symp. Suppl. **20:**615S–735S.
19. **Grant, C., C. A. Hunter, B. Flannigan, and A. F. Bravery.** 1989. The moisture requirements of molds isolated from domestic dwellings. Int. Biodeterior. **25:**259–284.
20. **Hendry, K. M., and E. C. Cole.** 1993. A review of mycotoxins in indoor air. J. Toxicol. Environ. Health **38:**183–198.
21. **Hocking, A. O., and J. I. Pitt.** 1979. Water relations of some *Penicillium* species at 25°C. Trans. Br. Mycol. Soc. **73:**141–145.
22. **Hodgson, M. J., P. Morey, M. Y. Leung, L. Morrow, D. Miller, B. B. Jarvis, H. Robbins, J. F. Halsey, and E. Storey.** 1998. Building-associated pulmonary disease from exposure to *Stachybotrys chartarum* and *Aspergillus versicolor*. J. Occup. Environ. Med. **40:**241–249.
23. **Hunter, C. A., C. Grant, B. Flannigan, and A. F. Bravery.** 1988. Moulds in buildings, the air spora of domestic dwellings. Int. Biodeterior. **24:**81–101.
24. **International Energy Agency.** 1991. Condensation and energy. *In* H. Hens (ed.), International Energy Agency: Annex 14 Programme. Laboratorium Bouwfysica Publishers, Leuven, Belgium.
25. **International Energy Agency.** 1996. Heat, air, and moisture transfer through new and retrofitted insulated envelope parts. *In* H. Hens (ed.), International Energy Agency: Annex 24 Programme. Laboratorium Bouwfysica Publishers, Leuven, Belgium.
26. **Jensen, S. O.** 1993. The PASSYS Project. Subgroup model validation and development. Final report, parts I and II, 1986–1992. Commission of the European Communities DGXII.
27. **Johanning, E., R. Biagini, D. Hull, P. Morey, B. Jarvis, and P. Landsbergis.** 1996. Health and immunology study following exposure to toxigenic fungi (*Stachybotrys chartarum*) in a water-damaged office environment. Int. Arch. Occup. Environ. Health **68:**207–218.
28. **Lacey, J., and J. Dutkiewicz.** 1994. Bioaerosols and occupational lung-disease. J. Aerosol Sci. **25:**1371–1404.
29. **Lewis, C. W., J. E. Smith, J. G. Anderson, and Y. M. Murad.** 1994. The presence of mycotoxin-associated fungal spores isolated from the indoor air of the damp domestic environment and cytotoxic to human cell lines. Indoor Environ. **3:**323–330.
30. **Magan, N., and J. Lacey.** 1984. Effect of temperature and *p*H on water relations of field and storage fungi. Trans. Br. Mycol. Soc. **82:**71–81.
31. **Mislivec, P. B., and J. Tuite.** 1970. Temperature and relative humidity requirements of species of *Penicillium* isolated from yellow dent corn. Mycologia **62:**75–88.
32. **Mislivec, P. B., C. T. Dieter, and V. R. Bruce.** 1970. Effect of temperature and relative humidity on spore germination of mycotoxic species of *Aspergillus* and *Penicillium*. Mycologia **67:**1187–1189.
33. **Nakhi, A. E.** 1995. Adaptive construction modelling within whole building dynamic simulation. Ph.D. thesis. University of Strathclyde, Glasgow, Scotland.
34. **Nikulin, M., A.-L. Pasanen, S. Berg, and E.-L. Hintikka.** 1994. *Stachybotrys atra* growth and toxin production in some building materials and fodder under different relative humidities. Appl. Environ. Microbiol. **60:**3421–3424.
35. **Northolt, M. D.** 1979. The effect of water activity and temperature on the production of some mycotoxins. Ph.D. thesis. University of Wageningen, Wageningen, The Netherlands.
36. **Northolt, M., and L. B. Bullerman.** 1982. Prevention of mold growth and

toxin production through control of environmental conditions. J. Food Prot. **45:**519–526.
37. **Panasenko, V. T.** 1967. Ecology of microfungi. Bot. Rev. **33:**189–215.
38. **Pasanen, P., A. Korpi, P. Kalliokoski, and A. L. Pasanen.** 1997. Growth and volatile metabolite production of *Aspergillus versicolor* in house dust. Environ. Int. **23:**425–432.
39. **Pitt, J. I.** 1975. Xerophilic fungi and spoilage of foods of plant origin, p. 273–307. *In* R. B. Duckworth (ed.), Water relations of foods. Academic Press, London, United Kingdom.
40. **Pitt, J. I., and J. H. B. Christian.** 1968. Water relations of xerophilic fungi isolated from prunes. Appl. Microbiol. **16:**1853–1858.
41. **Platt, S. D., C. J. Martin, S. M. Hunt, and C. W. Lewis.** 1989. Damp housing, mold growth and symptomatic health state. BMJ **298:**1673–1678.
42. **Rautiala, S., T. Reponen, A. Hyvarinen, A. Nevalainen, T. Husman, A. Vehvilainen, and P. Kalliokoski.** 1996. Exposure to airborne microbes during the repair of moldy buildings. Am. Ind. Hyg. Assoc. J. **57:**279–284.
43. **Samson, R. A.** 1985. Occurrence of molds in modern living and working environments. Eur. J. Epidemiol. **1:**54–61.
44. **Samson, R. A., and E. S. van Reenen-Hoekstra.** 1989. Introduction to foodborne fungi. Centraalbureau voor Schimmelcultures, Baarn, The Netherlands.
45. **Scott, W. J.** 1957. Water relations of food spoilage microorganisms. Adv. Food Res. **7:**83–127.
46. **Singh, J.** 1995. The built environment and the developing fungi, p. 1–21. *In* J. Singh (ed.), Building mycology. Spon Publishers, London, United Kingdom.
47. **Smith, J. E., G. L. Solomons, C. W. Lewis, and J. G. Anderson.** 1994. Mycotoxins in human nutrition and health. European Commission DGXII, Science Research and Development.
48. **Smith, S. L., and S. T. Hill.** 1982. Influence of temperature and water activity on germination and growth of *Aspergillus restrictus* and *A. versicolor*. Trans. Br. Mycol. Soc. **79:**558–559.
49. **Snow, D.** 1949. The germination of mould spores under controlled humidities. Ann. Appl. Biol. **36:**1–13.
50. **Sorenson, W. G.** 1990. Mycotoxins as potential occupational hazards. Dev. Ind. Microbiol. **31:**205–211.
51. **Strachan, P.** 1993. ESP-*r* validation using the PASSYS test cells. Building Environ. **28:**153–165.
52. **Sudakin, D. L.** 1998. Toxigenic fungi in a water-damaged building: an intervention study. Am. J. Ind. Med. **34:**183–190.
53. **Warnock, D. W., and C. K. Campbell.** 1996. Centenary review: medical mycology. Mycol. Res. **100:**1153–1162.
54. **Wexler, A., and S. Hasegawa.** 1954. Relative humidity—temperature relationships of some saturated salt solutions in the temperature range 0 to 50°C. J. Res. Natl. Bur. Stand. **53:**19–26.
55. **Winston, P. W., and D. H. Bates.** 1960. Standard solutions for the control of humidity in biological research. Ecology **41:**232–237.
56. **Wouters, P., L. Vandaele, and B. Geerincks.** 1996. The contribution of PASSYS to future building performance evaluation. Procedures of Building Environmental Performance, York, United Kingdom.

Science of the Total Environment 926 (2024) 171672

Contents lists available at ScienceDirect

Science of the Total Environment

journal homepage: www.elsevier.com/locate/scitotenv

Review

Digital technologies to unlock safe and sustainable opportunities for medical device and healthcare sectors with a focus on the combined use of digital twin and extended reality applications: A review

Neil J. Rowan *

Centre for Sustainable Disinfection and Sterilization, Technological University of the Shannon, Midlands Campus, Ireland
CURAM SFI Research Centre for Medical Devices, University of Galway, Ireland

HIGHLIGHTS

- Reusable medical devices have increased complexity for patient risk.
- Improvements in device deign and effective training enabled by digital tools.
- Digital twin and extended reality can help unlock end-to-end cycle opportunities.
- Integrated multi-actor HUB approach to sustainable development of medical devices.

GRAPHICAL ABSTRACT

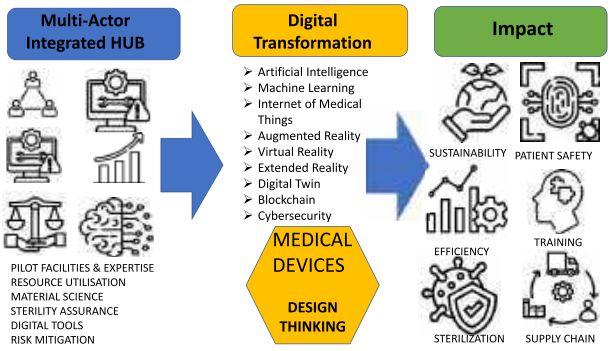

ARTICLE INFO

Editor: Damià Barceló

Keywords:
Medical devices
Digital transformation
Design thinking
Sterilization
Sustainability
Circularity

ABSTRACT

Medical devices have increased in complexity where there is a pressing need to consider design thinking and specialist training for manufacturers, healthcare and sterilization providers, and regulators. Appropriately addressing this consideration will positively inform end-to-end supply chain and logistics, production, processing, sterilization, safety, regulation, education, sustainability and circularity. There are significant opportunities to innovate and to develop appropriate digital tools to help unlock efficiencies in these important areas. This constitutes the first paper to create an awareness of and to define different digital technologies for informing and enabling medical device production from a holistic end-to-end life cycle perspective. It describes the added-value of using digital innovations to meet emerging opportunities for many disposable and reusable medical devices. It addresses the value of accessing and using integrated multi-actor HUBs that combine academia, industry, healthcare, regulators and society to help meet these opportunities. Such as cost-effective access to specialist pilot facilities and expertise that converges digital innovation, material science, biocompatibility, sterility assurance, business model and sustainability. It highlights the marked gap in academic R&D activities (PRISMA review of best publications conducted between January 2010 and January 2024) and the actual list of U.S. FDA's approved and marketed artificial intelligence/machine learning (AI/ML), and augmented reality/virtual reality (AR/VR) enabled-medical devices for different healthcare applications. Bespoke examples of benefits underlying

* Corresponding author at: Centre for Sustainable Disinfection and Sterilization, Technological University of the Shannon, Midlands Campus, Ireland
E-mail address: neil.rowan@tus.ie.

https://doi.org/10.1016/j.scitotenv.2024.171672
Received 14 February 2024; Received in revised form 9 March 2024; Accepted 10 March 2024
Available online 12 March 2024

future use of digital tools includes potential implementation of machine learning for supporting and enabling parametric release of sterilized products through efficient monitoring of critical process data (complying with ISO 11135:2014) that would benefit stakeholders. This paper also focuses on the transformative potential of combining digital twin with extended reality innovations to inform efficiencies in medical device design thinking, supply chain and training to inform patient safety, circularity and sustainability.

1. Design thinking for improve patient safety

The medical device industry constitutes a multi-billion sector globally that has increased in sophistication to meet the evolving and diverse needs of modern healthcare (Garvey, 2024). Meeting such healthcare needs has underpinned end-to-end supply chains along with the manufacture of new complex reusable and single-use medical devices (Rowan et al., 2023a). However, healthcare acquired infections (HAIs) linked to contaminated use of some medical devices (particularly reusable items) continues to contribute towards patient morbidity and mortality (Garvey, 2024). While single use medical devices can cause HAIs due to cross-contamination issues in healthcare (such as urinary tract infections), there is a greater probability of patient infection arising from using reusable medical equipment such as endoscopes and duodenoscopes (Garvey, 2024). Disposable medical devices undergo effective sterility assurance; however, these can subsequently cause post-operative and other medical-device related infection due to contamination in healthcare environment. For example, surgical site infections (SSIs) due to intra-operative contamination from single use devices have been ascribed to airborne microbial contamination of surgeon's hands and instruments (Chauveaux, 2015). SSIs are surgery-related infections occurring within 30 days of the surgical intervention, or within one year after the introduction of a medical implant (Chua et al., 2022). While terminal modalities effectively sterilize single-use medical devices; prevention from device-related-infections in patients due to subsequent environmental and user-mediated contamination is challenging where those with comorbidities are particularly vulnerable (Chua et al., 2022). Healthcare contaminated devices include central venous access devices, cardiac-implantable electronic devices, Ommaya reservoirs, external ventricular drains, breast implant plus tissue expanders, ureteral and esophageal stents, biliary stents and so forth (Viola et al., 2023).

General recommendations for the prevention of device-related infections include hand washing, infection control and prevention programs, MRSA screening and decolonization, perioperative antisepsis protocols, and perioperative antibacterial prophylaxis (Viola et al., 2023). For example, central venous devices that are used in at least 4 million patients in the U.S. are left in place for several months are essential for patients living with cancer. However, incorporating specific device-related antimicrobial interventions and procedures by infection control team to address such complex infections in patients is challenging (Patal et al., 2023; Whitaker et al., 2023). The introduction of U. S. Food and Drug Administration (FDA) approved antimicrobial-impregnated catheters (AICs) has added protective layer against life-threatening catheter-related bloodstream infections. Use of antimicrobial envelope (such as TYRX, Medtronic) that locally releases a high concentration of minocycline and rifampin has helped patients at high risk of developing cardiac-implantable electronic-device related infections (Blomstrom-Lundqvist et al., 2022). The ability to visualize, model, design simulate, develop, sterilize, test, verify and validate such medical devices from an end-to-end process perspective will remain essential and would substantially benefit from an integrated multi-actor effort that connects clinicians, healthcare professionals, sterilization providers, manufacturers, SMEs/entrepreneurs, patients and regulators. Given this complexity, the application of appropriate digital innovation would help address key needs (many in real-time) including improving efficiencies, resource utilization, safety and security (Table 1).

In 1957, Earle Spaulding introduced a new infection prevention classification based on the need to establish safe guidelines for the use of medical devices (Rowan et al., 2023a). This system describes types of device and instruments as non-critical, semi-critical and critical to reflect how these items will be used on patients (Table 2). This classification system has been adopted by industry into appropriate standards for decades that informs manufacturers' instructions for use (MIFUs) in dialogue with healthcare providers and regulators. However, MIFUs for complex medical devices typically have a substantial number of complicated steps that may not align with healthcare capabilities to efficiently clean and process, such as for duodenoscopes (Rowan et al., 2023a; Kremer et al., 2023a). This is attested by the documented occurrences of device-related infections where there were no documented failures reported in reprocessing by the healthcare provider (Garvey, 2024). Recent research has emphasized the role of effective and appropriate device cleaning with complex design features. Such 'difficult-to-reach' features may be potentially contaminated with recalcitrant biofilms harbouring microbial pathogens (Kremer et al., 2023a). Kremer et al. (2022) noted that cleaning and associated validation requirements are essential for the safe use of reusable devices. However, test methods and associated endpoint for cleaning validations have varied worldwide. Kremer et al. (2022) reiterated the importance of ensuring end-users to keep an awareness of appropriate international standards that have updated the requirements to include cleaning endpoints, and for the use of test soils for demonstrating cleaning efficacy of washer-disinfectors. Medical devices will continue to evolve to support clinicians for better patient outcomes (Kremer et al., 2023d). Moreover, given the complexity and number of MIFUs steps for some medical devices, it is becoming increasing challenging to ensure that we can appropriately mitigate risk to patients of contracting a device-related infection in the healthcare environment (Rowan et al., 2023a).

Different antimicrobial measures are applied to mitigate patient risk of infection arising from use of medical devices that are met by high-level disinfection or sterilization modalities (Fig. 1) (Rowan et al., 2023a; McLaren, 2020). The role of a sterility assurance subject-matter-expert with a full appreciation of the end-to-end device process including supply chain and material science will remain critical (McLaren et al., 2021). However, there is increasing evidence of unwanted infections attributed to the reuse of processed medical devices due to failures in processing and sterilizing expectations. Therefore, despite recent advancements in the development of new international standards by stakeholders, there remains significant technical and logistical challenges to address effective cleaning and processing of complex reusable device devices for safe patient use (Kremer et al., 2023a). Recently, there has been a focus on the suitability for cleaning, reprocessing and sterilization for reusable devices at the initial design thinking stage; however, there is a need to consider this in the context of use and reuse in the end-to-end supply chain and sterility assurance, such as developing, testing and validating alternative sterilization modalities (McLaren, 2020; McLaren et al., 2021; Kremer et al., 2023d). There are many complicated and interrelated factors influencing the safe and effective processing of medical devices that increases the chances of operational and processing errors (McLaren et al., 2021). There are also considerable opportunities to develop sustainable 'green' medical devices that considers use of new biomaterials based on appropriate selection of medical device sterilization modality to ensure effective design for satisfying customer needs, supplier selection, management (scheduling, production, distribution, after sale-customer care) (Rowan et al., 2023a; Kremer et al., 2023c). This also considers a greater spot light on increasing healthcare resuse options given the surge and

Table 1
Digital technologies — definitions and applications in medical device and healthcare sectors.

Digital technology definitions*	Examples of benefits and applications
Information and communications technology (ICT) encompasses the capture, storage, retrieval, processing, display, representation, presentation, organization, management, security, transfer, and interchange of data and information.	■ Mobile health (mHealth) – smart devices, apps, and wearables, health information technology, telehealth, personalized medicine; biosensors, ECG monitors; blood pressure monitors and so forth ■ smart hospital management (bed occupancy, device usage, equipment status, operational data.
Internet of medical things (IoMT) – network of smart, interconnected devices and services capable of sensing or listening to requests and perform actions using actuators. IoMT enables network sensors to remote connect, track and manage products and systems.	■ Remote patient monitoring (heart rate, temperature glucose) ■ Robotic surgery ■ Connected inhalers ■ Smart connected contact lens ■ Hand hygiene monitoring
Cloud computing – use of tools and applications (such as data storage, servers, databases, software) based on a network of severs through the internet. It enables user to rent computer resources on demand to store files and applications in a virtualised servers and access all data via the internet.	■ Accelerates clinical analyses and care processes (e.g., electronic health records) ■ Automates data processing & scalability. ■ Increases patient data accessibility ■ Reduces network equipment/staff costs ■ Reduces risks of data loss ■ Integrates physical, digital and data platforms for patient experience ■ Cloud computing for clinical R&D (Azure platform for patient analytics – HoloLens 2 projects holographic images for wearer) ■ Amazon Web Services to create cloud solutions
Artificial Intelligence (AI) defines machines achieving human-like cognitive functions (ex. learning, reasoning, interacting) that comprises different forms of cognition and meaning understanding (such as speech recognition) and human interaction (signal sensing, smart control, simulators) rooted in algorithms and software.	■ Data management ■ Remote surgery and patient monitoring ■ Early detection of patient health issues ■ Diagnostic and procedural assisting ■ Clinical trials ■ Improve device manufacturing efficiency ■ Reduce risk through Machine Learning ■ Advancing wearable technology and medical device — can monitor vital signs and collect patient data in real time ■ Non-destructive sampling (device materials) during design/production
Machine learning (ML) – a subset of AI, use and development of computer systems that learn and adapt without following explicit instructions, by using algorithms and statistical models to analyse and draw inferences from patterns in data. Noting, 10 guiding Good machine learning practices (GMLP) have been identified by U.S. FDA, Health Canada, and UK's Medicines and Healthcare Regulatory Agency (MHRA) for A/ML-driven medical devices. These GMLPs will identify specific areas where International Medical Device Regulators Forum (IMDRF), International Organization for Standardization (ISO) and other collaborative bodies will advance medical device development.	■ 171 AI and ML enabled medical devices marketed in the US added to FDA list and insights (FDA 2023). ■ The devices in this list have met the FDA's applicable premarket requirements, including a focused review of the devices' overall safety and effectiveness, which includes an evaluation of appropriate study diversity based on the device's intended use and technological characteristics. ■ Through the end of July 2023, 79 % of AI/ML-enabled devices authorized (FDA) in 2023 are in Radiology (85), 9 % in Cardiovascular (10), 5 % in Neurology (5), 4 % in Gastroenterology/Urology (4), 2 % in Anesthesiology (2), and 1 % each in Ear, Nose and Throat (1), and Ophthalmic (1)
Big data – continuous increase in data & technologies that needs to be collected, stored, managed and analysed. Complex and multidimensional that impacts processes, technologies. Characterized by Volume (amount of data sets), Velocity (speed of data processing), Variety (types/sources of data), Veracity (quality of data analysed).	■ Better patient care, improved research, smarter treatment plans, reduced costs for patients and health providers ■ Healthcare source of Electronic heath records (EHRs) ■ Apply predictive analytics to create machine learning (ML) models such as likelihood of patient infection ■ Real-time alerts to medical staff by continuously monitoring patient conditions ■ Transforming supply chain logistics ■ Enhancing security of sensitive data (ex insurance claims, design innovation of device)
Blockchain is a shared digital, immutable ledger that facilitates the process of recording transitions and tracking assets in a business network using cryptographic algorithms). Blockchain protocols aggregate, validate, and relay transactions within the blockchain network. The blockchain system records the transactions in sequence. A transaction may contain a value transfer or a smart contract invocation.	■ Traceability ■ Training ■ New business models
Augmented reality – is a real-world augmented experience with overlaying or mixing simulated digital imagery with the real world as seen through a camera or display, such as a smartphone or head-mounted or heads-up display (HUD). Digital imagery may be able to interact with real surroundings (often controlled by users). This is sometimes referred to as mixed or merged reality.	■ Training ■ Visualization of design features/process ■ Overlying medical images onto a patient during an operation to help guide surgery
Virtual Reality – the computer-generated simulation of a 3D image or environment that can be interacted with in a seemingly real or physical way by a person using special electronic equipment, such as helmet with screen inside or gloves fitted with sensors.	■ Bespoke training in safe setting ■ Used to treat post-traumatic stress disorder in army veterans ■ VR rehabilitation therapy – simulates real-life situations to improve physical functions for patients (e.g., physical disability caused by a stroke)
Extended Reality (XR)	■ 3D visual training, spatial audio combining AR, VR and mixed reality (or parts thereof) for monitoring and training (see Tables 3 and 4). ■ Make procedures less invasive (AR/VR) ■ Accelerate diagnosis ■ Allow for self-directed care ■ Possible risks (cybersickness, head and neck strain, cybersecurity risks, privacy risk, distraction in operating room). ■ Future design thinking, visualization, use
Robotics – a branch of technology that deals with the design, construction, operation and application of robots. In multi-robot or swarm robot systems, the robot collaborate to complete predefined tasks.	■ Robot-assisted surgery (precision) such as da Vinci system ■ Robot-assisted radiotherapy (reposition patient without need have anyone in room), reduces procedure time ■ Laboratory automation (reduces human error, expedites processes, removes repetitive tasks, improves staff satisfaction, reduces overall costs, improves safety.

(*continued on next page*)

Table 1 (*continued*)

Digital technology definitions*	Examples of benefits and applications
Cobot, or collaborative robot, is a robot intended for direct human robot interaction with a shared space, or where humans and robots are in proximity.	■ Prosthetics – robotic appendages (grabbing, walking) ■ Rehabilitation and exoskeletons for helping patients recover from surgery, or deal with disability. Can sense electric pulse allowing rebuilding of muscles. ■ Social support – care robots meeting emotional needs of patients (elderly, isolated) ■ Hospital robots – nursing robots can address mundane and repetitive tasks ■ AI training and coaching – see VR. ■ Microbots – help recovery time at cellular level during surgery (Sorimuthu, 2023). ■ Cost savings from staff overtime, extended hospital stays, physical therapy, home care, travel etc. ■ Cleaning and disinfection robots in healthcare facilities (UV-C) ■ Improving cost efficiency, quality, and safety in high production processes ■ Cobots contribute to development and delivery of innovative/reliable devices ■ Addressing labor shortages by optimize limited human resources ■ Cost effective, rapid development such as plug-and-play style to automation ■ Offer flexibility to adjust capacity, throughput avoiding over investment or underutlizaiton of resources ■ Scalability, lower maintenance costs. ■ Flexibility and quick redeployment ■ Efficient use of floorspace/infrastructure ■ High precision (ex assembly applications)
Digital twin – a digital win is a virtual model designed to accurately reflect a physical object.	■ Software for data traceability ■ Real time monitoring ■ Design think and visualization ■ Preventative maintenance ■ Design validation and planning ■ Optimizing operational needs (Table 3)
Edge Cloud/Intelligence – Edge computing is developed as complement to cloud computing, encompassing storage and compute assets located at the edge and interconnected by a scalable, application-aware network that can sense and adapt to changing needs, securely & in real time. The "edge" of network is element of network infrastructure furthest from core.	■ Real-time secure remote monitoring (medical devices or received urgent alert) ■ Patient data/device processed by on site edge compute resources ■ Analysis of patient data (ex. wearables) ■ Detect early signs of illness or disease ■ Smartwatches, fitness trackers ■ Reduce data latency ■ Maintain high availability (via Cloud service) ■ IoT sensors, smart cameras, uCPE equipment, servers and processors
Cybersecurity or information technology (IT) security – is the practice of protecting critical systems and sensitive information from digital attack. It is how individuals and organisations reduce the risk of a cyber attack where cyber security code function protects the devices (smartphones, laptops, tables).	■ Essential component of healthcare and medical devices so as to guarantee systems are secure and shielded from cyber threats. ■ Maintaining precision and dependability of medical equipment and systems ■ Keeping patients secure, protecting financial information, private medical data, confidential patient information.
Cyber-physical systems refer to systems where software and hardware components are seamlessly integrated towards performing well-defined tasks.	Helps safeguard healthcare from malware and ransomware assaults resulting in patient care disruptions, system failure, data breaches

* Adopted in part from Rowan et al. (2023b).

reliance on single-use disposable items (Greene et al., 2022). Consequently, this timely paper provides both an awareness of and describes the use of digital innovation to effectively advance existing medical devices and to unlock opportunities with new design thinking with a lens on sustainability. It also focuses on the potential innovate use of digital tools to help inform and advance reusable and disposable medical devices for existing and future needs including sustainability.

2. Use of an integrated Quintuple helix HUB approach to address appropriate digital solutions

Integration of key actors from different specialist backgrounds, such as manufacturers, academics, industry (including sterilization providers), policy-makers (regulators), healthcare (including Sterile Services Department, clinicians), SMEs/entrepreneurs and patients can help inform opportunities and solutions across the entire production and logistical supply-chain for medical devices from conception to market product launch including supporting regulatory approval (Table 3). The benefits of adopting an integrated multi-disciplinary approach for addressing knowledge and innovation gaps (example, quadruple helix) has been well articulated in the published domain that includes improving efficiencies and cost saving on "testing the tech" before investing by accessing specialist equipment (example, RAMAN Spectroscopy, Flow cytometry, 3D printing, injection moulders, automated washers and pilot sterilization modalities, extended reality suite and so forth) and subject-matter-experts (such as immersive or extend reality technologists, advanced imaging or polymer scientists) (such as highlighted by Rowan and Casey, 2021). The core indicative activities highlighted in Table 3 would be overseen by an experienced HUB manager with appropriate knowledge of underpinning sterility assurance embedded in the academic hosting framework for enabling and accelerating appropriate networking, partnerships with industry, manufacturers, entrepreneurs, regulators and so forth (McLaren et al., 2021). The CURAM SFI Medical Device Research Centre in Ireland represents a typical example of such an effective multi-actor HUB that includes considerable experience in addressing appropriate intellectual property protection and management from data generated for various users. This would also facilitate the testing of new materials with existing or alternative sterilization modalities for optimizing time and costs in alignment with FDA guidance titled "submission and review of sterility information in premarket notification 510(k) – submission for devices labelled as sterile (U.S. FDA, 2024)". For example, the sterilization modalities established in Category A are ethylene oxide (EO), vaporized hydrogen peroxide (VH_2O_2), dry and moist heat, and radiation), established Category B include ozone, hydrogen peroxide, ozone, and flexible bag systems, and novel sterilization modalities include vaporized peracetic acid, microwave radiation, sound waves, low pressure and pulsed UV light (McLaren, 2020). There is also considerable opportunities for introducing non-destructive sampling for medical device development that includes important sterility assurance provision (Table 3) — this includes use of specialist imaging and spectroscopy equipment that can be linked to machine learning models.

The integrated multi-actor approach avoids the traditional 'silo' approach that focused on use of specific aspect(s) of the device process

Table 2
Examples of applications of the Spaulding Classification system for medical devices encompassing type of decontamination or sterilization modality to mitigate patient risk of acquiring an infection.

Risk category	Description	Type of decontamination or sterilization modality required to address risk
Critical use items	• Where a device enters sterile tissue and must be sterile, defined as being free from viable microorganisms (McDonnell and Hansen, 2020) • Items contaminated with any microorganism (including bacterial spores), or infectious agent (prion) are referred to as high risk to patients. If they are contaminated and enter sterile tissue or vascular system, they have a high potential for causing disease transmission (Rutala and Weber, 2019). Such items should be sterile, such as by using steam sterilization where possible. Examples include surgical instruments • Close attention should be given to the label claims of liquid chemical sterilants as these can vary regionally; they may have the ability to sterilize, depending on their application but may not always be considered practical for routine sterilization.	• Given that many items contain heat-sensitive materials, other appropriate sterilization modalities should be applied including vaporized hydrogen peroxide (VH_2O_2), VH_2O_2 gas plasma, and ethylene oxide gas (EO). • The use of liquid chemical sterilants may also be considered appropriate, such as formulations based on glutaraldehyde (GTA), peracetic acid (PA), hydrogen peroxide (HP), or ortho-phthalaldehyde (OPA).
Semi-critical use items*	• Where a device only comes in contact with intact mucus membranes or nonintact skin, it should also be subjected to sterilization, or if this is not feasible due to sensitive material composition or complex design features, then a high-level disinfection (HLD) process must be deployed at a minimum that would be expected to kill all microorganisms except for bacterial endospores (McDonnell and Burke, 2011). • Examples of semi-critical items including "respiratory therapy, anaesthesia equipment, some endoscopes, laryngoscope blades and handles, esophageal manometry probes, endocavitary probes, nasopharyngoscopes, prostate biopsy probes, infrared coagulation devices, anorectal manometry catheters, cystoscopies, and diaphragm fitting rings" (Rutala and Weber, 2019).	• Depending on regional claim requirements, high level disinfectants should demonstrate broad spectrum antimicrobial activity and typically the ability to eliminate at least 10^6 (or 6-logs) of mycobacterial cells on contaminated surfaces of medical devices. • For the vegetative microorganisms and viruses of concern, mycobacteria are typically deemed to exhibit greater resistance to high level disinfectants; thus, mycobacterial cells are recognised as representative (or bio-indicators) for HLD process efficacy. • Examples of chemical disinfectants authorized in the USA for HLD use include biocides such as glutaraldehyde, HP, OPA, hypochlorite, and PA with HP (Rowan et al., 2023a).**
Non-critical use items	• Where devices contact intact skin (but not mucous membranes), requiring low-level to intermediate-level disinfection. The skin contains intact integumentary layers, and as such, provides a natural barrier to microorganisms. There remains a risk to the skin and as a source of cross-contamination from devices, but this risk is considered low (Rowan et al., 2023a) • These risks can be practically reduced by the combination physical removal and disinfection (McDonnell and Burke, 2011). Examples of non-critical use items include blood pressure cuffs, bed surfaces and rails, patient furniture, bedpans, over-bed tables and so forth (Rutala and Weber, 2019). • Such product labelling support disinfection efficacy against a broad spectrum of microbial pathogens that may include methicillin-resistant *Staphylococcus aureus*, vancomycin-resistant enterococci, yeast (Candida sp.), mycobacteria, and viruses well within typical label claim for US EPA-registered disinfectants.	• Physical removal plays an important role in the removal of pathogens with higher levels of natural resistance to disinfectants such as bacterial spores (as highlighted in studies of surface contamination with clostridia; Thomas et al., 2022).

Modifed in part from information furnished in Rowan et al. (2023a).
** It is important to note that the ability to inactivate microorganisms by a disinfectant/sterilant is only part of an overall safe and effective high level disinfection process, as the disinfectant residuals need to be safely removed and the device correctly maintained prior to patient use.

(McLaren et al., 2021); thus, creating new opportunities to holistically (360°) consider "design thinking" across all key activities over the entire end-to-end lifecycle for complex devices. This approach allows opportunities for introducing transformative beyond-state-of-the-art innovation from adjacent industries, such as digital twin (Table 4)). Yet also ensures that appropriate international standards for development, manufacturing and validation are applied and interpreted correctly. Table 4 also describes key activities and benefits for manufacturers' instructions for use (MIFUs) that will close the innovation gap for meeting client/patient needs. The inclusion of clean room and pilot facilities for cleaning, disinfection and sterilization of new medical devices that connects stakeholders would be beneficial, such as design thinking and sterility assurance informing selection of sterilization modality to meet the safe intended use for patients including functionality, material composition (AAMI TIR17:2017), biocompatibility (ISO 10993), and sustainability (McLaren et al., 2021). An example of appropriate medical device modality selection to meet complexity of medical device design and patient needs is represented in the adapted viewpoint paper of McLaren (2020) (Fig. 1). Such a holistic approach would save on costly manufacturing revisions to medical devices and unlock situations where new-biomaterials in design features can be tested from a development, testing, validation perspective (510k) in dialogue with regulators. Application of approaches that improve efficiencies and data sharing including collaborative partnerships across manufacturing, healthcare, sterility assurance and so forth will impact positively on intended product functionality, shortened timeliness for regulatory approval, efficiencies in resources and risks (McLaren et al., 2021).

This interdisciplinary hub approach is also highly relevant for manufacturers, small companies, entrepreneurs, doctorate research candidates across different disciplines who want to test new ideas using appropriate equipment, methods following appropriate international standards. This would also entail keeping pace with international standards updates. This would also help de-risk for financially viable innovations and investments. It would mitigate against potential unforeseen reputational damage due to possible misinterpretation of appropriate methods for new devices medical devices by inventors as it would have appropriate sterility assurance embedded from commencement of the project for addressing key activities. For example, Smith et al., 2023 (representative of medical device industry), recently expressed concern about the reporting findings from a published study (Deasy et al., 2022), as the test methods and claims in the report were inconsistent with international standards for cleaning and disinfection of reusable devices in washer-disinfectors (WDs) (BS EN ISO 15883-1:2006, 2006; BS EN ISO 15883-2:2009, 2006; BS EN ISO 15883-5:2021, 2022). Deasy et al. (2022) had stated that there are no specific standards for dental head-pieces (DHPs); however, Smith et al. (2023) noted that DHPs, as medical devices, are given as examples of the type of devices in the WD standard series BS EN ISO 15883-2:2009, 2006), and specifically as powdered devices. Smith et al. (2023) also stated that "cleaning and disinfection requirements in these standards therefore apply. For example, cleaning validation using defined test soils and disinfection efficacy requirements described in the standards (BS EN ISO 17664-1:, 2021) are applicable to these reusable medical devices".

3. Digital transformation of the medical device and health care sectors

There is increased interest in the application and development of digital technologies to improve efficiencies and to unlock sustainable opportunities in the medical device and connected sectors (Tables 1 and 4). Definitions of the different types of digital innovation for enabling development of medical devices are articulated in Table 1 in addition to highlighting benefits and applications. Adapting and integrating these digital technologies will help transform supply chain logistics, improve medical device design and production, improve workflows and efficiencies, reduce uncertainties, save costs, reduce resources and errors, improve education and training, reduce waste, improve user satisfaction, improve security, and mitigate for enhanced patient safety. The real-time application of these digital technologies will also enhance knowledge and innovation exchange such as through Open Access shared publishing platforms (Kremer et al., 2023c) that will help stakeholders appreciate the utility of generated data for manufacturing, verification and validation applications, including informing important standards in consultation with regulators. For example, robotics and automation are transforming surgery and radiography through precision and by alleviating fatigue (Table 5). It addresses mundane yet important tasks such as cleaning that can be further aided by applying machine learning. Internet of medical things (IoMT) addresses many key patient needs including digital health (wearables) (Table 1).

The U.S. FDA has acknowledged the role of digital technologies in enabling development of the medical devices sector, for example, 171 artificial intelligence (AI) and machine learning (AI/ML)-enabled medical devices were recently added their list marked in the US hat recognises their ability to create new and important insights from the vast amount of data generated during the delivery of healthcare provision (FDA, 2023a). A central tenet of the FDA's public health mission is to ensure that these potentially transformative devices are "safe and effective which includes an evaluation of the appropriate study diversity based on the device's intended use and technological characteristics. Over the past decade, the FDA has reviewed and authorized an increasing number of devices (marketed via 510(k) clearance, granted De Novo request, or premarket approval) with AI/ML across many different fields of medicine". They FDA noted that no device has been authorized that uses generative AI or artificial general intelligence (AGI) or powered by large language models. Currently the number of AI/ML enabled devices authorized through the end of July 2023 appear in the decreasing sequence radiology (n = 85, 79 %), cardiovascular (n = 10, 9 %), neurology (n = 5, 5 %), gastroenterology/urology (n = 4, 4 %), anaesthesiology (n = 2 %), ear, nose and throat (n = 1, 1 %), ophthalmic (n = 1, 1 %). In general, ML are increasing in complexity including deep learning models that included more hybrid approaches combining different algorithms to achieve safe and effective devices results (e.g., combining use one model to address classification and another model to generate features".

It is important to discern when AI should be applied to safely address a specific societal challenge, particularly in a highly-regulated world of medical devices and healthcare comprising multiple actors. Retursdottir (2024) noted that AI/ML technologies "need to be able to integrate seamlessly into a clinical setting, be easy to use for patients, and have safety critical algorithms that are transparent and explainable to regulator." Moreover, this author noted (1) do AI/ML technologies solve a real problem that is appreciated by stakeholder; (2) do they align with Principle of "Design Thinking" to address feasibility, viability and desirability, and (3) does it use different reputable and reliable state-of-the-art technical research approaches to confirm that AI/ML is the right solution for a problem as opposed to a non-specific technique without purpose. Activities to improve confidence and reliability in AI/ML including avoiding use of bad quality datasets (invalid, missing, non-inclusive or too small) that will affect the reliable performance of ML-model, for example with the development of next generation medical devices such sensitive data can be challenging to obtain for stakeholders (see Table 4 for desirable attributes for enabled devices including training and evaluating machine learning models). For example, in addition to being needed by stakeholders to accurately solve a recognised healthcare problem, AI and ML models need to be explainable as end-users and regulators will need to understand the foundational basis as to how such AI-based medical devices are making specific decisions. Ten guiding principles have been identified by the FDA and MHRA for

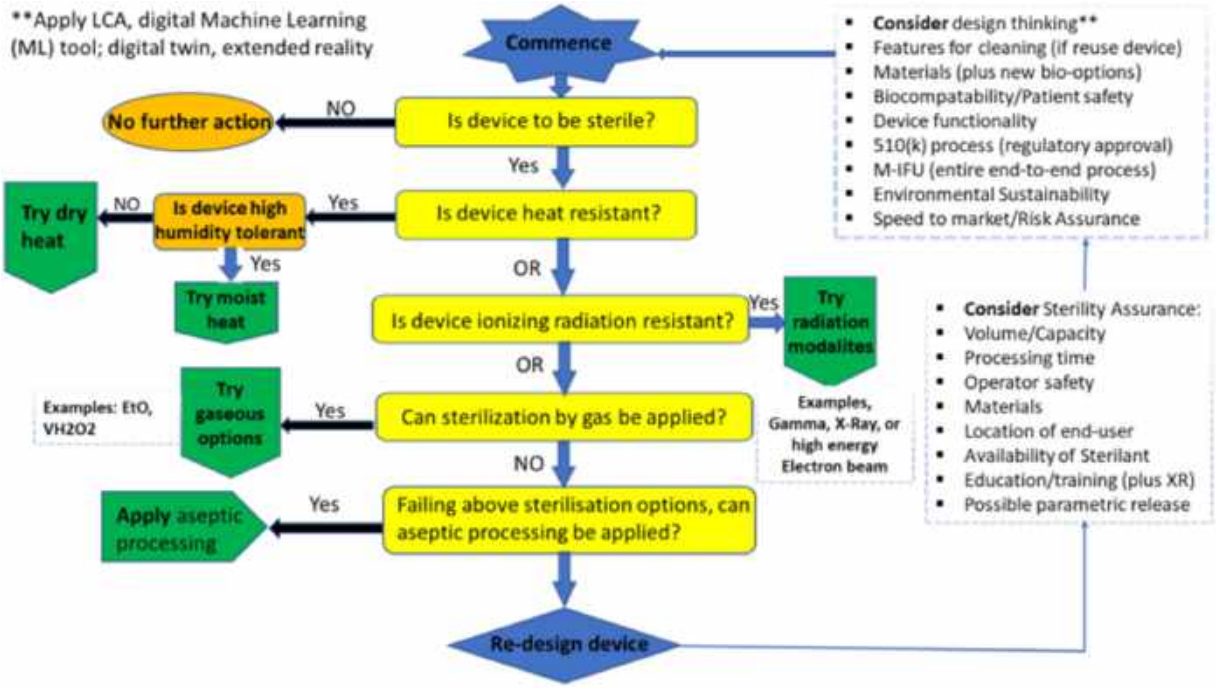

Fig. 1. Flow path of sterilization modality options depending on factors underpinning medical devices design and intended use informed by digital tools. (Adapted from McLaren, 2020).

Table 3
Meeting oppotunities through integrated access and use of multi-actor hub including industry, academics, healthcare, manufacturers, policy (regulators), entrepreneurs, society.

Activity	Description	Benefits
Multi-actor approach	■ Integrated academic, industry, manufacturers, policy (regulators), healthcare, society approach	■ Multi-actor (specialist) inputs
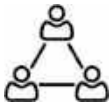	■ Appoint expert HUB manager	■ End-to-end full cycle (aligned with needs of MIFUs, healthcare)
	■ Step change physical infrastructure & support systems	■ Supporting existing and future Healthcare/industrial sterilization
	■ Modelling, simulations, prediction, verification, validation	■ Networking/conferencing
	■ Education & holistic training programs (End-to-End Cycle)	■ Holistic problem solving
	■ Mentorship opportunities	■ Leverage access to specialist equipment/staffing (cost savings)
	■ Ideation & design thinking to align with TRL, manufacturer needs etc. Appropriate methods/Standards	■ Clustering of resources
		■ De-risking/risk-assessment
		■ Suits small to large operations
Technical	■ Digital transformation	■ Update existing/new medical device design (parts/process)
	■ DT and XR specialist equipment & expert staffing	■ Specialist training (physical to virtual) safe-efficient.
	■ Modelling, simulation, automation	■ Automation, efficiencies, uncouple uncertainties, de-risk
	■ Machine Learning for real time data analysis, prediction and performance	
	Pilot disinfection/sterilization modalities:	■ Pilot testing of new products, (bio-) materials combination with new modalities
	■ Chemical biocides	■ Alternative sterilization products for manufacturers
	■ Steam/dry heat	■ End-to-end design thinking including functionality, biocompatibility
	■ Low temp technology options: such as	
	■ Electron beam	■ Limiting re-testing of devices,
	■ Vaporized hydrogen peroxide (VH_2O_2)	■ Reduction in cost
	■ Testing alternative sterilization modalities (including informing implementation, validation, regulatory requirements)	■ Opportunities for new "Green" (sustainability) testing, verification, validation for products, services
	■ A nexus to commercial large-scale treatments (Gamma, X-ray, EtO etc)	
	3D printing healthcare applications including devices and APIs	■ Medical applications, modelling, simulations, testing, verification
	Advanced (bio-) materials characterization for devices and packaging (pre and post processing/sterilization)	■ Developing methods, products, informing standards (ISO working groups), SWOT, risk mitigation, sustainability (reduced waste)
	Dosimetry (mapping) and software/ future parametric release	Appropriate disinfection, sterilization – group as "family" products for dose
	Automation (washer disinfectors (WD)	Improved efficiencies, reliabilities
	Challenge testing (PCDs) including bioburden using appropriate BIs	Training and innovation on core supporting applied sciences
	Design thinking (devices)	■ Efficiency, reduced risk to patients and environment
		■ Material reuse/eco-efficient process
	Biocompatability (ISO 10993)	In vitro/in vivo (regulatory) including scope for new 3D printing (implants)
	Skills, training and development	End-to-end processing; complex procedures
Regulatory	Advice on existing and updated ISO Standards	■ Appropriate methodology
	Understanding new regulations and rules (example sustainable use of EtO)	■ Reputational integrity
		■ Risk Management
		■ Avoids misinterpretation
		Verification, validation
Business & dissemination	■ Test the tech/test before invest	■ Financial viable product/value proposition (cost structures)
	■ Business model canvas and SWOT	■ Inform certainties on cost and timelines
	■ Integrated ecosystem building	■ Providing key resources
	■ Intellectual property management	■ Providing key activities
	■ Access to finance/investments	■ Networking key partnerships
	■ Appropriate dissemination and communication channels including infographics	■ De-risking and optimized value stream
		■ Market research and needs analysis
	■ Grant and specialist writing supports.	
Sustainability	■ Energy and carbon footprint (LCA)	■ Eco-friendly parts, products, services, processes
	■ Technical, political, societal LCAs	■ Effective waste management
	■ Safe and Sustainable by Design (SSbD) framework approach	■ Educational and training
	■ Waste management (recycling/reuse)	■ Corporate Social Responsibility
	■ Staffing (training)	■ Green product "sustainability testing" to validation
	■ Informing polices, standards	■ Lean six sigma for medical waste
Ethics	■ Artificial Intelligence (AI) trustworthiness	■ Increases productivity
	■ Safeguarding against reputational damage from using incorrect methods, or their misinterpretation	■ Attracts outstanding employees
		■ Employee loyalty
	■ Supporting Regulatory affairs	■ Better reputation
	■ Gender and cultural Inclusiveness	■ Integrity and responsibility
		■ Provides competitive advantage
		■ Attracts more investors
Social Sciences	■ Social marketing	■ Engage with and learn your audience
	■ Social enterprises	■ Promote innovation/customer service
	■ Society engagement and acceptance	■ Understand competition
	■ Outreach activities	■ Build appropriate partnerships
	■ Citizen Science	■ Acquire talent
		■ Impact sales
		■ Keep up with industry trends

(*continued on next page*)

Table 3 (*continued*)

Activity	Description	Benefits
Educational technologies 	■ Specialist healthcare/sterilization training ■ Supports diversity of short courses (micro-credentials) to postgraduate qualification (ex sterility assurance) ■ Wide choice of learner tools ■ Adaptive learning/new skills/new knowledge ■ Prepares learners for future ■ Enhance engagement/satisfaction	■ Training and educational opportunities for experienced staff and newcomers ■ University design by learning (UDL) ■ Enhanced Productivity ■ Boost and improve collaboration ■ Stay current with new technologies ■ Blended with XR/DT innovation
Infection control 	■ Addressing pressing healthcare challenges from holistic multi-actor approach (such as potential microbial MDR and biofilm issues with processed devices ■ Improved device cleaning, processing and sterilization ■ Infection control team kept current ■ Updates on policies and guidelines ■ Offers new suite of preventative solutions to complex microbial challenges where many front-line antibiotics are at crisis point	■ Allows solutions (pivoting) to address key healthcare needs and for unforeseen (ex. Pandemics) ■ Improve healthcare efficiencies ■ Reduces mobidity, mortality ■ Reduces patient risks ■ Improves healthcare savings/spend ■ Reduces patient anxiety and stress ■ Prevents occurrence/spread of HAIs

DT (digital twin); Extended Reality (XR), BIs (Biological Indicators), CIs (Chemical Indicators); Life Cycle Assessment (LCA); EtO (ethylene oxide); AI (Artificial Intelligence); ML (Machine Learning); Manufacturers instructions for use (MIFUs); TRL (technology Readiness level).; Multi-drug resistance (MDR); healthcare acquired infections (HAIs); APIs (Active Pharmaceutical Ingredients).

Table 4
Digital twin and extend reality innovation attributes and benefits for medical device development and testing.

Digital twin (DT)	Extended reality (XR)
Virtual copy of physical entity interconnected via exchange of data in real time	Delivery of 360° visuals, spatial audio – allowing learner active participation using virtual or augment reality scenarios/simulations
■ Real-time monitoring ■ Design + validation of new/existing entity ■ Enables end to end planning for devices ■ Optimizing for solutions in real time ○ DT can foresee defects and faults in advance ○ Accessibility – can be controlled ○ monitored + remotely accessed using DT ○ not restricted by geographical location ○ not limited by remote access ○ Informs preventative maintenance ○ Safer – than physical counterpart if working with hazardous situation thus reduces risk	■ Monitors and reports on frequency of training in real time ■ Training -duration ■ Completion ■ Learner tasks performed ■ Questions answered ■ Deep level of virtual and augmented learning ■ Monitor engagement and cognative levels using wearable sensor technologies ■ Eye gaze ■ Head movements ■ Physiological measurement indicators (Heart rate)
■ Decision making of complex multifactorial scenarios in real time ■ Realistic/holistic measurement of unforeseen and unpredicted scenarios ■ Waste reduction – DT simulates and tests products in virtual environ reducing waste, development costs, time to market	■ Decision-making – level of competencies achieved and potential need for retraining ■ Supporting risk management (ISO 14971:2019) ■ 3D simulation of real experience
■ Optimizing operations – in depth analysis of physical twin ■ Increased multi-user engagements ■ Fusing information and technical innovation ■ Integrated multiscale, multidiscipline, multi-physical simulation of entity (product)/process ■ Bidirectional transfer/sharing of qualitative and quantitative data between physical and DT	■ Strong effects on human perception and behaviour ■ Influences performance, satisfaction, motivation, concentration ■ Informs and advances robotic training ■ Improves training-based outcomes and education including micro-credentials to doctorate provision ■ Reduced anxiety in learning process where there is a complex setting
■ Tracks status of physical twin through life cycle ■ Prediction and optimization of part, product, and process ■ Better understanding by synchronizing data in real time across software applications, database, hard copies	■ Improved design, verification, validation and manufacture of medical devices ■ VR provides low cost, high fidelity training with improved accuracy and task completion ■ VR used to assess, model and implement safety risk assessments/mitigation
■ Reduction in errors, uncertainties, inconsistencies, expenses in product/process ■ Avoids component failures and predicts different stages in life cycle (complex parts, multiple materials).	■ Mimics stress clinical setting for training for enhanced patient safety, reduced errors ■ High fidelity visual/sensory feedback
■ Holistic training – more efficient, safer, illustrative linked to education	■ Address limitation of cognitive overload in trainees due to continuous changes in attention
■ Removes 'silos' in process ■ Expediting prototyping, product re-design ■ Close knowledge gap between experienced staff and newcomers (across departments)	■ AR headset remotely train clinicians ■ Develop manufacturers IFUs ■ Improvements in evaluation/assessment in simulated training

good machine learning practices (GMLP) that underlie development of AI/ML based medical devices (Gampa, 2023). Retursdottir (2024) reported that of the 343 medical devices with AI/ML capabilities on the FDA list, 95 % were marked between 2015 and 2021 with majority addressing diagnostic medical imaging needs. FDA approved AI/ML enabled devices involved "locked" algorithms, intimating that given the same input, the model will always give the same output. However, the future of AI/ML innovation must also embrace evolving these models to meet increasing needs of patients and healthcare professionals. Retursdottir (2024) stated that there are "no harmonized standards that regulate use of ML in medical applications and devices where companies are not required to classify their technology as AI/ML based".

Artificial intelligence and ML will be used to help understand risk assessment and mitigation in device manufacture from an end-to-end perspective. Combined use of digital twin (DT) and extended reality (XR) innovations can help understand and meet the need to safely use

and embrace rapid AI and ML-driven devices in terms of aligning with patients' needs and stringent regulatory requirements (Gampa, 2023). Combining use of immersive and educational technologies will also help maintain a critical focus on devices' quality, security, and safety aspects from end to end device production and supply chain perspective. Gampa (2023) noted that failure to meet these requirements will lead to device recalls and hefty fines from regulatory agencies. Thus, physical to virtual enabling innovations that includes simulating real-world devices using replicated avatars can help device manufacturers incorporate AI/ML into innovations will ultimately comply with market entry by adhering to relevant government laws, regulations, and GMLP.

The accelerated interest in AI/ML as rising and promising medical devices will require marked shift in regulatory approach in addition to consideration of risks and potential consequences of inaccurate models (Retursdottir, 2024), particularly addressing continuously learning AI algorithms for healthcare. AI technology has developed leaps and bounds since first coined at the Dartmouth Summer project in 1956, where it can now interpret medical images 10,000 times faster than the average radiologist and can improve patient diagnostics and care by augmenting digital pathologies (Retursdottir, 2024). However, despite enormous potential, AI technology has a considerable journey remaining to grapple with human health and all its complexities. Moreover, Gampa (2023) reported that "the complexity of regulatory requirements for AI/ML-integrated medical devices has skyrocketed and has, in turn, posed significant challenges for manufacturers in terms of data security, patient safety, and device quality, hindering their access to global markets". The U.S. FDA, Health Canada (HC), and the U.K.'s Medicines and Healthcare Regulatory Agency (MHRA) have united to identify 10 guiding principles with a converging aim of developing good machine learning practices (GMLP) addressing the unique nature of AI/ML-driven devices. This coming together of key regulatory actors adopts or tailors for good practices from other adjacent sectors, or it creates new practices specific for the medical technology or healthcare sectors that also identifies areas where International Medical Device Regulatory Forum (IMDRF), International Organization for Standardization (ISO), and other collaborative bodies can advance GMLP for medical devices development (see Table 5). Clark et al. (2023) conducted a systematic review of 119 public 510(k) application summaries and corresponding marketing materials, where devices with significant software components similar to devices flagged in FDA's published AI and ML-enabled devices where 12.6 %, 6.7 % and 80.6 % were considered discrepant, contentious and consistent respectively between marketing and FDA 510(k) clearance summaries (Table 6). The authors noted that the aim of the study was not to intimate designers or developers were creating or marketing unsafe or untrustworthy devices, but to highlight the need for more harmonized guidelines addressing marketing of such AI/ML devices. The role of end-user perception and understanding of such digital health innovation would also be beneficial (Byrne et al., 2023).

While this is a fascinating topic in the context of all potential digital tools, this paper will mainly focus on the role of combining digital twin with immersive technologies to visualize and unlock the complexities of medical device design including transforming training for healthcare staff for improved patient safety. The application of digital twin and immersive technologies can also help manufacturers introduce more

Table 5
Examples of relevant digital tools informing medical device research, innovation and applications appearing in PubMed database (2010 to 2024).

Combination	Description and relevance	References
VR + AR + MR	Applications in spinal surgery	Sakai et al. (2020)
	Objective performance measurement and subjective evaluation in manual assembly tasks	Daling and Schlittmeier (2024)
XR + MD	Head-mounted devices for medical education	Barteit et al. (2021)
	Medical device safety training using quick XR based technology	Saurio et al. (2019)
	Develop software management app for medical devices that supports XR including neurosurgery	Sugimoto and Sueyoshi (2023)
	Accurate mixed reality surgical guidance	Brown et al. (2023)
	3D printed devices for patient specific applications	Moreta-Martinez et al. (2018)
	Immersive and educational training for healthcare applications including rehabilitation	Bryant et al. (2024)
DT + MD	Regulatory oversight and ethical concerns surrounding software as medical devices and DT technology interface and interpretation	Lal et al. (2022)
	Design of digital twin – human-machine interface server with intelligent finger gesture recognition	Mo et al. (2023)
	Parameter personalization for implantable cardiac defribillation	Lai et al. (2022)
	Visualization of use of DTs to inform medical device development from in silico clinical trial perspective	Bordukova et al. (2024)
	Computational modelling for active implantable medical devices	Nguyen et al. (2023)
	Visualize, develop and validate kinematically accurate upper-limb exoskeleton including Stroke rehabilitation	Grimm et al. (2021)
	Automated creation of individual computations and applications in CT organ dosimetry	Fu et al. (2021)
	Modelling and visual design for miniaturizing medical implants including materials	Kazarinov et al. (2022)
VR + MD + AR	AR in vascular and endocascular surgery informed by device	Eves et al. (2022)
	Applying AR technologies to medical images and models	Sutherland et al. (2019)
	Design and evaluation of AR to medical devices	Escalada-Hernandez et al. (2019)
SUS + MD + XR	Educational tools combined with immersive technologies for specialist medical device training on cleaning and processing	Murray et al. (2019)
		Kremer et al. (2023a)
		Kremer et al. (2023b)
DT + XR	Metaverse wearables for immersive digital healthcare applications	Kim et al. (2023)
	Intelligent radiotherapy applications including dosimetry	Chen et al. (2022)
		Chaudhuri et al. (2023)
	Work-based occupational learning from errors in safe environment	Goppold et al. (2022)
AI + MD	FDA-cleared AI and ML-based medical devices and their 510(k) predicate network	Muehlematter et al. (2023)
	AI and Internet of Medical Things assisted biomedical systems in intelligent healthcare to make devices intelligent and efficient for performing tasks	Manickam et al. (2022)
	Are clinical studies on AI-based medical devices comprehensive enough supporting full health technology assessment	Farah et al. (2023)
	AI software to for advancing medical devices – focus on laparscopic cholecystectomy surgical phase recognition	Shinozuka et al. (2022)
	FDA-approved AI and ML enabled devices an update on status	Joshi et al. (2024)
	Marketing of US FDA cleared AI and ML-enabled software as medical devices – 119 devices reviewed highlighting a degree of variance between marketing and FDA 510(k) summary details	Clark et al. (2023a)

Noting that extent and scope of publications in PubMed particularly address research, development and applications, but this underestimates the level (amount) of actual commercial innovation as reflected by FDA List of approved and marketed AG/VR enabled medical devices (FDA, 2023a; FDA, 2023b).

sustainable materials both in terms of reusable and single-use devices.

4. Selection and application of potential digital solutions for medical devices

A PRISMA approach was adopted to review papers published in PubMed database over the period January 2010 to Jan 2024 using key words medical device (MD, 786,727), sustainability (SUS, 402,083), artificial intelligence (AI, 187,208), digital twin (DT, 1649), augmented reality (AR, 5266), virtual reality (VR, 19,032), mixed reality (MR, 6884), extended reality (XR, 1726), sterilization (STER, 114,448), DT + XR (10), DT + MD (135), XR + MD (124); SUS + MD (19,571), AI + MD (12,267), SUS + MD + STER (221), and VR + MD + STER (11). Publications dismissed due to lack of alignment with specific theme described home monitoring (asthma), visualization museum specimens, precision public health, self-balancing low limb exoskeleton, tooth preparation, hormone delivery, sterile bag use, sterile wash flow, digital brain technology, cardiac electrophysiology, stroke and tele-rehabilitation, finite element modelling, haemodialysis, modelling of healthcare buildings, predictive oncology, infrastructure disaster prevention/reconstruction, historical document reconstruction, bioreactor contamination, organ-on-a-chip devices, bioink exopolysaccharides, gynaecological sterilization technologies, membrane reactors and waste water, laser to clean healthcare furnishings, pain and anxiety during vasectomy, 3D surgical instrument supply chain tracking, toilet flushing, plasma approaches for wound healing, visualising hydraulic systems, sustained activities and therapies for COVID-19.

4.1. Digital twin use in medical devices and healthcare

Digital twin (DT) is seen as the virtual copy or model of any physical entity (digital twin) where both are interconnected through the exchange of data (Singh et al., 2021a). From a medical device evolution perspective, it enables design, planning, predictive maintenance, training, decision-making, risk analysis, in depth data analysis, safety, reliability, multi-actor accessibility, waste reduction and cost efficiency by the bidirectional sharing of quantitative and qualitative data between the physical counterpart (medical device) and its digital twin (Table 4). It provides a safe remote virtual environment to develop and track status of new medical device from design, materials, processing through its full life time. Thus, enabling the visualization, production and testing of parts, product or process for intended purpose that limits or avoids component or process failures that includes provision for preventive maintenance and improved performance. Digital twin (DT) was born out of the Industry 4.0 era from the aerospace industry where its' global market size is projected to reach USD 16.44 billion in 2024 (Businesswire, 2024).

Table 4 highlights key performance benefits and opportunities from applying DT to meet needs in the medical device sector. It is envisaged that these will inform future key performance indicators for the industry that will help regulators understand its applicability for shaping future medical devices that will potentially lead to updating existing and generating new ISO standards with stakeholders. However, appropriate device communication and data collection/sharing standards that define its quality requires standardization for uniformity to make it accessible to regulators to approve process without compromising security (Wagner et al., 2019). Additionally, future challenges for developing DT to unlock opportunities for medical device applications relates to confidentiality, privacy, transparency and ownership of unique data that will be influenced by company policies (Singh et al., 2018). Table 4 provides examples as to how DT has specifically informed the development of medical devices. Singh et al. (2021b) have highlighted the real versus virtual costs of device prototyping that clearly intimates positivity developers and investors. DT sought-after characteristics include high fidelity (a near-identical copy of its physical counterpart), dynamic (changes with respect to time and needs), self-evolving with its counter physical twin over life span, uniquely identifiable based on its physical twin and vice versa over the full life cycle, multiscale, multidisciplinary and multiphysical and hierarchical. The latter relates to the integrated nature of parts or sub-models of the DT that make up the final product or process. Despite its apparent benefits, DT is still an emerging innovation that requires buy-in from stakeholders to meet its potential. DT is initially an expense investment as the end-to-end process requires significant investment in ultra-high-fidelity computer models to create DT that is specialist labour intensive and time consuming.

4.2. Extended reality use in medical device and healthcare sector

Extended reality (XR) innovation is an overarching term that combines virtual reality (VR), augmented reality (VR) and mixed reality (MR) that have the potential to transform medical device and healthcare sectors (for example, Tables 4 and 5 provide definitions and examples of applications). The FDA has noted that these approaches deliver new types of treatments, and diagnostics that can change how and where care is delivered. These holistic 360° virtually visual innovations have the ability to "deliver standard and radically new types of technical content in highly immersive and realistic ways, remotely, and specifically tailored" to meet pressing healthcare and clinical needs for different end-users (industry, policy-makers, physicians, patients, caregivers and so forth). Table 4 provides a summary of key benefits and activities for existing and future applications in medical device and healthcare sectors that contrast markedly from DT innovation. However, when considered together, DT and XR innovations can provide powerful training tools for complex medical device design processes delivered in a safe and reliable virtual environment. Kremer et al. (2023c) highlighted the benefits of applying immersive and education technologies to unlock opportunities particularly in training and smart of next generation reusable medical devices through the lens of entire end-to-end process. However, the use and interpretation of XR is highly subject matter (expert) driven where effective blending of these real-world augmented and virtual-world experiences would likely to be met by specific digital companies engaging with medtech industry and healthcare end-users. This can be also be enabled by collaborating through multi-actor innovation HUBs that will reduce costs along with providing a considerable number of other benefits (Table 3). For example, learner experiences can be monitored by evaluating physiological parameters (eye gaze, heart rate, etc.) that will inform efficacy of training undertaken, and potentially the need for retraining, or additional training delivered in a safe remote environment.

Real-world examples highlighted by the FDA for XR applications that are already being used to treat patients include AR system that overlays medical images onto a patient during an operation to help guide surgery, VR rehabilitation therapy simulating real-life situations to improve physical functions for patients who have experienced disability associated with stroke or other medical conditions (FDA, 2023b) (Table 4). Moreover, the FDA noted the increasing number of treatment domains used to treat and help patients including pediatric diagnostics and treatments, pain management, mental health, neurological disorders, surgery planning, intraoperative procedures, ophthalmic diagnostics, telemedicine, virtual care, post-operative and other rehabilitation therapies. Table 4 highlights experienced and potential benefits of XR applications. Different examples of XR innovations both reviewed and approved by the FDA for marketing of devices through 510(k) clearance, granted De Novo request, or Premarket approval across different fields of medicine and healthcare is found at FDA, 2023b, where it expects this trend to continue.

4.3. Digital tools to help inform device design for improved cleaning, processing and patient risk

Application of machine learning will help the real-time evaluation of complex device features for effective cleaning of complex reusable

Table 6
Ten good guiding machine learning practices (GMLP) for AI/ML based devices in context of design/training (as framed by FDA, HC, MHRA).

GMLP no.	Description	Relevance to AI/ML based device design and training
1	Leverage multidisciplinary expertise throughout the product life cycle	■ Important to have sterility assurance along with in depth knowledge and understanding of AI/ML for device development for design, clinical workflow, benefits, potential risk for patients ■ DT/XR training will also help stakeholders understand knowledge gap including regulatory requirements that can inform safe and effective clinical meaningful needs over full life cycle. ■ This ensures compliance with QMS, consensus standards, applicable regulatory requirements
2	Implement good software and engineering practices for AI/ML-based medical devices	■ Data security, integrity, and privacy over product life cycle of AI/ML enabled devices and for AI/ML software including good software engineering practices, data quality assurance, data management, robust cybersecurity practices that should address methodological risk management and design processes including ensuring data authenticity and integrity.
3	Represent the intended patient population through clinical study participants and data sets	■ In clinical study, training, and test data sets, manufacturers mush appropriately represent relevant characteristics of intended patient population, use, and measurement inputs in a sample of adequate size including managing bias, assess usability, and identify circumstances where model may underperform (list of potential biases are highlighted in Gampa, 2023)
4	Maintain training data sets as independent from test data sets	■ Selecting and maintaining training and test data such that they are independent of one another (role of digital training, educational technologies (Kremer et al., 2023c). ■ Consider all potential sources of dependence, data acquisition, site factors – test data for ML model accuracy. ■ Manufacturers should validate that test and training data meet specified criteria encompassing descriptive statistics and addressing label leakage (use of DT/XR to visualize full process to help understanding independence of data sets and for maintaining related training).
5	Use the best available methods for selected reference data sets	■ Use of DT/XT training to represent well-characterized and clinically relevant data for medical device and use that can help inform and develop specific use of AI/ML software including evaluation and testing that will promote model robustness and for intended use.
6	Tailor the model design to the available data and ensure that it reflects the device's intended use	■ Potential use of digital tools to visualize and inform mitigation of known risks, such as overfitting, performance degradation, and security risks that helps model design to suit available data. ■ The real time holistic perspective offered by digital tools can be tailored to reflect greater or thorough understanding of clinical benefits and risks related to the device where model can derive clinically meaningful performance goals and testing. ■ Potential use of integrated multi-mode XR connectivity of end-users can help inform global and local performance of the device, uncertainty or variability in device's impacts and outputs, intended patient populations, and clinical use conditions.
7	Focus on the performance of the human–AI team	■ Potential greater involvement of model in "human in the loop" that embraces human factors and human interpretability of models' outputs. ■ XR innovation also helps mitigate against just the performance of ML model in isolation. ■ Other digital visualization technologies can help manufacturers identify risk related to usability of the device and evaluate safety-relevant use scenarios.
8	Use testing to demonstrate the device's performance during clinically relevant conditions	■ DT and XR innovations can help potentially help inform accuracy of AI model selection that includes evaluation metrics, optimizing parameters and testing where such performance activities play central rol in obtaining adequate and compliant data required to gain regulatory approvals.
9	Provide users with clear, essential information	■ DT and XR can help establish and provide clear and contextually relevant information will help users (healthcare providers and patients ○ Products intended use and indications of use ○ Performance of model for appropriate subgroups ○ Characteristics of data used to train and test the model ○ Acceptable inputs ○ Known limitations ○ User interface interpretation ○ Clinical workflow integration of the model ■ In addition to enabling device modifications and for updating from real-world performance monitoring that adds to deep learning models that also provides feedback loop for developer to improve and address concerns.
10	Monitor deployed models for performance and manage re-training risks	■ Deploying of monitored AI/ML models can help with accuracy of safety and performance based on real world use that can also inform models used by human-AI team for periodic and continually training purposes such as post-market surveillance plan, incident response plan, configuration controls, over-fitting, unintended use, or data set drift (degradation). ■ Combined use of DT/XR innovation can help visualize and test design changes for managers based on regulatory requirements before implementing them.

Adoption based on responding to details of Gampa (2023) reflecting GMLP content based on FDA, HC and MHRA expert inputs.

devices from end-to-end process that represents a more conservative approach compared with the alternative compendial method for testing the entirety of the device (Kremer et al., 2023a). Rowan et al. (2023a) reported that the Spaulding's classification approach is sub-optimal for informing appropriate patient risks using some complex devicees as it fails to appreciate the role of device features in effective cleaning that can affect overall sterility assurance and patient safety (Table 2). Kremer et al. (2023a) evaluated a total of 56,000 flushes of the device features (n23) highlighting both the rigor and the enormity of big data generated from studies encompassing several analysed factors where machine learning would help with simultaneous data modelling, simulations and evaluations for informing validation. The complexity of device features is a central issue to consider for designers and manufacturers in their instructions for use (MIFU). Thus, this features categorization approach will help address the existing patient gap at this important interface between device manufacturers and healthcare facilities for effective cleaning, and reliable processing of reusable medical device devices. Digital technologies can be used to evaluate critical data for addressing key cleaning steps in processes including device conditioning, soil formulation, soil volume, soiling location, soil application, device articulation, and soil conditioning/drying. Manufacturers cleaning IFUs also provide a range of processing parameters for validation including detergent preparation, flushing, soaking, volume, temperature for validation. Future application of robots and automation will help with

addressing precision and mundane tasks associated with device cleaning.

Use of Internet of medical things (IoMT) will also potentially transform supply chain logistics where reusable devices are queued and staked in healthcare prior to cleaning, and processing that will help mitigate against device drying. Kremer et al. (2023d) proposed the grouping of device features in families representing different designated bands reflecting accessibility to soiling on a device surface and effectiveness of cleaning regime to mitigate risks. Again, this would be informed by an automated learning processing for precision (such as ML). Michels et al. (2013) also categorized cleaning processes based on groups of complex features based on analysing residual protein levels, namely instruments with joints, instruments without joints (lumens and cavities), sliding-shaft instruments, tubular instruments, microsurgical instruments, and complex instruments. Use of digital tools to facilitate data generation and sharing on this important topic will help inform ANSI/AAMI/ISO 17664-1:2022, AAMI RIT12:2020 and other future ISO standards on device cleaning that focuses on resuable device features and risk mitigation. There is increased interest in determining the efficacy of manual and automated cleaning of complex device features including addressing recalcitrant biofilm removal (de Melo Costa et al., 2022b). de Melo Costa et al. (2022b) advocated that for sterilizing service units, with no access to automated cleaning equipment, it is important to brush the inner hinge during manual cleaning.

5. Digital practices in medical device sterilization

5.1. Applications in sterility assurance

Sterilization is defined as conducting a validated safe monitored process to render a product free of viable microorganisms, which is a critical function underpinning device safety and for considering new innovations such as material science, biocompatibility, functionality and potential parametric release (McEvoy et al., 2023a; Rowan et al., 2023a). Achieving desired sterility assurance level (SAL) is the probability of a single viable microorganism occurring on an item post sterilization (Rowan et al., 2023a; Garvey, 2024). Moreover, SAL is seen as the probability of one viable microorganism surviving on the challenge device surface in a microbial population of million treated bacteria (6 D reduction). Determination of appropriate sterilant dose reflects decontamination efficacy or bioburden (organic material and artificially-inoculated recalcitrant biological indicators or BIs) in test devices where correction factors are applied. However, SAL is conventionally determined post microbial growth responses using lengthy incubation of treated biological indicator (BI, such as *B. atrophaeus*, or *G. stearothermophilus*) from sampled challenge devices in tandem with monitoring dosimetry readings (Rowan et al., 2023a). Chemical and physical indicators are also used to confirm the appropriate sterilant is applied within tolerances over treatment time for validation of processes. Developing new device innovation is challenging given the complexities of meeting scalability for volume of device throughput (industrial providers or healthcare end-users) using appropriate sterilization modalities that could be informed by using pilot facilities with stakeholders, such as for new design innovations according to appropriate ISO standards. Recent important studies have shown that vaporized hydrogen peroxide (VHP, also represented by VH_2O_2) sterilization modality exhibits log -linear inactivation kinetic data supporting the standing statistical probability that the applied gaseous sterilant kills treated biological indicators in a uniform manner (McEvoy et al., 2023b). McEvoy et al. (2023c) have also recently reported that the dose produced by X-ray, electron beam and gamma-irradiation can be interchangeably considered for to treating medical devices for appropriate microbial reduction. This supports the important concept of sustainable sterilization where selection of the type of modality can be made to meet the design features, material composition and functionality, which must also satisfy regulatory approval (Karimi Estahbanati, 2023).

5.2. Future potent in parametric release of sterilized products

McEvoy et al. (2023a) noted that this approach can be potentially adopted to accelerate product (or parametric) release that relies on use of process data, and to potentially reduce sterilant dose based on linked bioburden studies. Parametric release (according to ISO 11139: 2018) reflects appropriate records demonstrating a product is sterile based on sterilization processes delivered within specified tolerances. Adoption of parametric release by the sterilization industry has been thus far slow where integrated use of digital innovation could contribute to expediting this process, such as through modelling, simulations, and machine learning for real-time analysis of data. For example, potential real-time use of digital innovation with parametric release based on analysis of monitored and calculated data offers advantages including (1) eliminates the time, risks, and costs associated with BI, sterility testing and dosimetry analysis, (2) reduces the amount of unreleased inventory, and (3) allows for continuous demonstration of process control (McEvoy et al., 2023a). It is still a current requirement in ISO 11135:2014 to directly monitor EO concentration. McEvoy et al. (2023a) recently highlighted how data provided during sterilization of devices (described through examples for ethylene oxide (EO), VH_2O_2 (or VHP) and radiation may be better used to inform parametric release implementation. The authors noted that “EO and VHP demonstrated the ability to the sterilization equipment to deliver validated parameters repeatedly after load presented was validated”. This study also highlighted benefits of this approach that considers variability that has not been addressed in performance qualification (PQ). A key tenet underpinning device validation and potential use of the ‘calculated’ parametric release approach is the generation of sufficient appropriate data that demonstrates repeatability of the validated process; moreover, the more quality data generated the better digital tools such as machine learning algorithms and models can precisely inform this complex process. McEvoy et al. (2023a) also noted that radiation processes are also on a trajectory for implementing parametric release, however use of current photon delivery is not appropriate for measuring all critical parameters for this purpose. McEvoy et al. (2021) also separately reported on the potential use of real time enumeration technologies such as using flow cytometry for assessing efficacy of VHP on treated BIs where such initiatives have the future potential to inform automation.

This integrated approach will also serve to reduce ethylene oxide dose for a more sustainable process where EO produces toxicological end-points that requires abatement before product release (Garvey, 2024). For example, EO is broadly applicable for the sterilization of medical devices having a variety of complex materials, whereas use of VH_2O_2 is sensitive to cellulose (McEvoy and Rowan, 2019). The use of new cleaning classification system (Kremer et al., 2023d) with sustainable sterilization modalities will inform future applications in reusable medical devices in healthcare. It will also inform automation and in situ decontamination of 3D printed devices, such as for surgery or for organ printing to offset current need for use of animals in biocompatibility testing of implantable devices (Table 3). However, heathcare budget needs to reflect upon the need to pivot for enhanced reuse and in situ decontamination and innovation. International standards, such as TIR17 addressing materials will require frequent updating, such as for the alternative use of more sustainable biomaterials combined with using appropriate sterilization modalities in order to unlock our next-generation of green medical devices and circularity. A critical understanding of material science is important for applying appropriate sterilization modality underpinning a validated process for medical device products (Murray et al., 2013; Murray et al., 2014; Murray et al., 2018). The application of advanced imaging and spectroscopy may also inform non-destructive sampling (NDS) of materials in the use of medical devices including opportunities for machine learning to rapidly evaluate and inform efficiencies and applications (Manley, 2014; Yan

et al., 2022).

5.3. Digital modelling of data for simulations and to inform innovations

Development and application of appropriate digital tools that permits the simultaneous modelling, simulation and monitoring of holistic data can inform the appropriateness of new medical device design and functionality, including addressing key areas to enable sustainability (Table 3). The role of design thinking and specialist training will help unlock challenges in medical device design, processing, supply chain and for patient safety (Rowan et al., 2023a; Kremer et al., 2023d). Addressing such opportunities, including the potential for automation, can be met by precisely and safely replicating physical data for the intended new medical device design in a virtual environment (digital twin), such as for 3D printable devices, which also dually includes provision for undertaking immersive virtual training (or re-training) to achieve desirable learner competency (Murray et al., 2019; Kremer et al., 2023d).

Recent advances in our understanding of molecular and cellular mechanistic responses of *Bacillus atrophaeus* spores to H_2O_2 revealed that the formation of reactive oxygen species from this sterilant is the rate limiting factor in oxidative spore death. Bertz et al. (2024) used non-destructive optical sensing with trapping Raman spectroscopy in real-time to show that H_2O_2 mediated spore death to occur in two phases: (a) initial fast release of dipicolinic acid (DPA), a major spore bioindicator indicating irreversible rupture of spore's core, and (b) the oxidation of remaining spore material leading to fragmentation of the spore's coat. These finding was corroborated using optical microscopy. Hydrogen peroxide is effective in gas and liquid phases, with low temperature vaporized hydrogen peroxide (VH_2O_2) recently been approved for terminal sterilization of medical devices as Cat A process that offers more sustainable environmental benefits compared to the long-standing use of ethylene oxide gas. The future use of machine learning models to potentially monitor simultaneous damage caused by VH_2O_2 for treated bioindicators spores will also inform trajectory towards parametric release of treated devices. Such studies would require validation using appropriate challenge devices, bioburden testing and so forth; however, future deployment of Raman spectroscopy does provide exciting opportunities given that use of existing laboratory-based microbial culture responses for bioburden testing/validation require lengthy incubation periods to determine VH_2O_2-mediated spore death. Additionally, sensor-based approaches that monitor spore viability/damage by H_2O_2 in the gas or liquid phase (such as piezoelectric and impedimetric sensors, potentometric chemosensors) "all suffer from the fact that they have response times of a least several to tens of minutes (which precludes real-time validation of spore degradation) or are incompatible with in situ experiments, such as gaseous conditions (Bertz et al., 2024)". The non-destructive trapped Raman spectroscopy approach hurdles this technical limitation. Additionally, H_2O_2 is a strong oxidising agent that decomposes into reactive species such as hydroxyl/hydroperoxyl radicals that non-selectively oxidizes spore material. However, microbial catalase and superoxide dismutase that counteract these oxygenated free radicals may be damaged where use of standard nutritious agar and aerobic incubation may promote microbial autolytic suicide at sub-lethal treatment doses — thus, the real-time use of Raman spectroscopy with ML modelling combined with conventional biorburden/SAL culture-based testing will potentially reliably confirm irreversible spore lethality over the entire end-to-end sterilization process in addition to informing parametric release for families of different devices geometries/design shown to be reliably killed over particular treatments sterilant doses for appropriate SALs. Thus highlighting the role of advancing imaging, spectroscopy and machine learning in advancing conventional sterilization microbiology for treated medical devices including testing for new design thinking and introducing new biomaterials (such as packaging). Desirable to progress towards sustainable sterilization practices including selection of materials and dosage particularly to address new innovation in material science and polymers – beyond steam and dry heat sterilization modalities there is suite low temperature physical and gaseous options for designers and end-users to embrace (Fig. 1).

There is a growing interest in the potential use of spectroscopy and digital imagery as non-destructive testing (NDT) approaches for reliable inspection of small-scale material defects (such as targeting dimensions below 100 μm), which is crucial for structural safety of critical components in high-value applications (Ines Silva et al., 2023). These NDT can also be considered in end-to-end design thinking for next generation devices that encompasses sterilization modality. Robust and reliable NDT can reduce safety concerns and preventative maintenance costs for equipment over whole lifecycle (Wang et al., 2020). Early defects are often possible to repair, contributing for the circular economy and sustainability by allowing extended life and reuse of components. Ines Silva et al. (2023) noted that "distinguishable high detection accuracy and resolution is provided by computed tomography paired with computer laminography, scanning thermal microscopy paired with Raman spectroscopy, and NDT techniques paired with machine learning and advanced post-processing signal algorithms". Yan et al. (2022) highlighted opportunities for use of machine learning (explainable AI and Gaussian mixture models) in microplastic identification using Attenuated Total Reflection Fourier Transform Infrared Spectroscopy (ATR-FTIR) enabling real-time monitoring using spectral data augmentation approaches. Other promising NDTs are near-infrared (NIR) spectroscopy (Manley, 2014), time-of-flight diffraction, thermoreflectance thermal imaging, advanced eddy currents probes, micro magnetic bridge probe used in magnetic flux leakage, driven-bacterial cells, Quantum dots and hydrogen-as-a-probe. Wang et al. (2020) reported that the role of intelligence and automated inspection systems with high accuracy and efficient data processing capabilities will help shape future innovations. Interestingly, Cebi et al. (2023) described combined use of FTIR, NIR and Raman spectroscopy for rapid non-destructive metabolomic fingerprinting in adjacent field of food screening.

6. Digital tools to inform sustainability in medical device — quo vadis?

Digital innovation will help advance established and transform future medical devices from end-to-end design thinking to supply chain logistics including addressing enhanced patient safety, effectiveness and sustainability subject to satisfying regulatory review and approval requirements. The application of AI and ML will add significant value to future LCA studies informing important quantitative assessments for sustainability across the medical device sector. Romeiko et al. (2024) reviewed forty published studies from across adjacent fields that reported on quantitative assessments using combinations of LCA and ML including addressing life cycle inventories, computing characterization factors, estimating life cycle impacts, and supporting life cycle interpretation. The authors noted the value of continuous collection of big data to improve reliable ML modelling, prediction accuracy, pattern discovery and computational efficiency and pattern discovery; such as, potential future ML use of data generated by Kremer et al. (2023d) on use of 56,000 flushes from different device features to determine effective new cleaning classification for reusable families of medical devices with nexus to informing and improving patient risk. Future sustainability research using combined ML and LCAs should clearly report on selection criteria for ML models to match device intended use and to also report on ML model uncertainty analysis (Romeiko et al., 2024). These authors also noted that the increasing "complexity of environmental challenges demands adoption of interdisciplinary collaborative research to achieve deep integration of ML into LCA to support sustainability development" as exemplified by use of quintuple helix hub approach for stakeholders. Friedericy et al. (2022) reported on the reduced environmental impact of sterilization packaging for surgical instruments in the operating room where comparative LCA of rigid

sterilization containers were far more environmentally friendly than disposable polypropylene packaging (blue wrap) in terms of carbon footprint and eco-costs.

The healthcare sector has become increasing reliant on using disposables where meeting supply chain frequently dominates budget spend with significant consequences for medicine's carbon footprint and our fragile environment (Greene et al., 2022). Modern medicine enterprises are distinctively wasteful where enhanced use for many disposable items have been born out of convenience and efficiency with minimal evidence to support the superiority of some disposable supplies over thoroughly sterilized reusable ones (Greene et al., 2022). This is particularly relevant for general non-critical use items. These authors noted that "discarded material that are disposable rather than reusable comprise 85% of medical waste. Moreover, enormous volumes of plastic packaging, single use-tools, and diagnostic devices produce greenhouse gases when incinerated or while decomposing in landfills and oceans". Pickler et al. (2019) reported that the healthcare sector is a major environmental polluter where it represents ca. 5.5 % of the total national carbon footprint of countries. It is estimated that blue wrapping for sterilization of surgical equipment results in staggering environmental pollution with 115 million kg of plastic waste on an annual basis in the U.S. (Kagoma et al., 2012).

The application of suite of digital technologies intimated in Tables 4 and 5 will potentially help improve the implementation of European Medical Device Regulation (MDR) where Deirdre Clune MEP raised concerns about lack of progress in approval of new devices. In addition, efforts to a establish a more robust and transparent European MDR framework needs to unlock more timely pathways for accessing new medical devices prioritizing safety, health and innovation that will also impede sustainability. "The current European MDR lacks predictability and efficiency, and fails to keep pace with the required innovation to develop medical device innovation resulting in increased cost affecting SMEs that alarming implications for patients due to lack of availability of medical devices" (Deirdre Clune, MEP, 2024). There are over 700 digital innovation hubs in Europe that presents future opportunity for consolidation, convergence and pivoting to address sustainable needs for supporting and enabling innovation across the medical device and healthcare sectors (Rowan et al., 2023b).

Combining use of DT and XR innovation from a holistic end-to-end design thinking and training perspective offers significant potential for saving on resources, energy and time including opportunities for introducing appropriate new sustainable biomaterials. Pilot device testing, development and validation would typically require appropriate use of sterilization modality, where access to a subject-matter sterility assurance expert, such as hub manager and/or terminal sterilization industry expert, would help designers and manufactures address an effective process (McLaren et al., 2021). This would also de-risk for decision making and investments; for example, device cleaning and sterilization are appropriately built into the new design thinking from creation (TRL1) to market deployment (TRL9) avoiding situations where the material composition of new devices are non-sterilisable, or non-functional or appropriate for intended use or where more sustainable or alterative modalities (such as aseptic approaches) may be applied for production and packaging of devices including supply chain logistics (Fig. 1). Researchers have also highlighted the potential of implementing educational and immersive technologies to inform bespoke training for end-to-end medical device production including addressing key bottleneck areas such as cleaning for improved patient safety and sustainability (Murray et al., 2019; Kremer et al., 2023d).

Ibn-Mohammed et al. (2023) reported despite the fact that functional materials and devices (FM&Ds) have critically important roles in different devices and products improving patient safety and quality of life, these also place a significant environmental burden on our fragile natural ecosystems prompting enhanced use of LCA from a more quantified value chain perspective. These authors highlighted that bottom-up LCA framework models for informing medical device sustainability are frequently limited in scope that are typically static or retrospective. As volume of FM&Ds that are manufactured increase this is likely to present situations that proxy values will be used to fill data gaps; thus limiting their appropriateness in terms of relevance, accuracy and quality of results. These shortcomings across all phases in the environmental sustainability LCA model can be addressed by using computationally guided parameterized models enabled by AI/ML. "Smart materials constitute non-living stimuli-responsive material systems endowed with sensing, actuation, logic, and control functions to respond adaptively to environment to which they are exposed, in a manner that is usually repetitive and beneficial" (Strock, 1996). The role of AI/ML in each phase of bottom up LCA can be applied for determining the environmental burden of devices covers inventory analysis, characterization, normalization, impact assessment and interpretation.

Efficient real-time deployment of digital technologies will also help company compliance with future EU Corporate Sustainability Reporting Directive from a business model perspective such as use of blockchain. In addition to addressing sustainable R&D activities for medical devices, collaborative use of an interdisciplinary integrated HUB approach will also facilitate an awareness of key ISO standards (and updates), and strategic policies/directives for stakeholders including manufacturers and end-users. Lean six sigma (LSS) strategy for boosting efficiencies in medical waste stream that can also help cut costs through measured performance and analysis of root causes that will inform sustainable improvements and establish appropriate controls (McDermott et al., 2022). McGrane et al. (2022) adopted LLS framework to address potential barriers and bottlenecks for regulatory environment for informing effective project management, continuous improvement, and engineering changes in medical device manufacturing industry. Skalli et al. (2023) described positive environmental, social and economic impacts of interlinking LSS, the circular bioeconomy with Industry 4.0 technologies on sustainable organizational performance within manufacturing firms.

McGain and McAlister (2023) noted that several published LCA studies (McGain et al., 2017; Donahue et al., 2020; Rizan and Bhutta, 2022) revealed that disposable items have a greater impact from raw material extraction and manufacturing compared to reusable medical devices. The authors also highlighted that in terms of carbon footprint and material sustainability, reusable medical devices offer 300 times more desirable outcomes for our environment. Brenner et al. (2023) highlighted the challenges of identifying and achieving broad stakeholder recognition of key performance indicators (KPIs) including end-user acceptance of digital health technologies as attested by only five of 2192 reviewed publications either mentioning or considering harmonized KPIs. The critical role of end-user (patients, clinicians) experience and acceptance of digital health technology will also inform applications and future sustainability practices (Byrne et al., 2023). Alt et al. (2022) also highlighted the potential safe use of VH_2O_2 for decontaminating single-use medical devices contaminated with SARS-CoV2 from a sustainable waste management perspective.

7. Summary

The potential for digital technologies to enable and to advance expectations and opportunities in real-time for medical devices and healthcare sectors is enormous, which will potentially transform safety, precision and efficiencies across the entire end-to-end process. Reusable medical devices will benefit from new design innovations for improved patient safety and sustainability that will be informed by digital transformation of processes and approaches with stakeholders, such as blending new Kremer cleaning classification with Spaulding's sterilization system for next generation devices. Moreover, the combined role of using digital twin and extended reality innovation will advance training, diagnostics and interventions in real-time that will be enabled through access to and use of integrated multi-actor HUB facilities for testing new technologies with subject matter experts, such as sterility assurance. A

PRISMA review of best-published journal papers revealed a marked disparity and underappreciation as to the extent of new digital health technologies when compared to current lists shared by the FDA that reviewed and approved these innovations for marketing at 510(k) clearance, granted De Novo requests, or Premarket approval. Bespoke examples of benefits underlying future use of digital tools includes potential use of machine learning for supporting and enabling real-time parametric release of complex sterilization monitored and calculated data with correct processes that would benefit manufacturers, sterilization providers and patients. This paper also highlights an awareness and knowledge gap for stakeholders (particularly academics) on the actual range and variety of different digital innovations used in real-world situations in terms of validated, marketed and applied digital technologies for patient use in medicine and healthcare. Similarly, there appears to be a lack of appreciation by academic/researcher communities as to the central importance of using appropriate and up-to-date ISO standards that presents potential scenarios where appropriate methods may not be correctly applied or that methods may be misinterpreted, particularly from a 'silo' academic R&D perspective. This further emphasises the importance of adopting a multi-actor approach encompassing beneficiaries and end-users such as industry, healthcare, policy-makers, academics and society for effectively addressing solutions across the medical device and healthcare sectors. Such a holistic integrated HUB proposition will also facilitate engagements by experts in informing future sustainability needs such as performing appropriate LCAs using different materials, sterilization modalities and so forth for effective waste mitigation and reuse/recycling. The knowledge shared by leading actors such as terminal sterilization industry is extremely valuable and will continue to drive new developments The future is very promising for digital health technologies as attested by the public health mission of the FDA recognizing that "these innovations are playing an increasingly significant central role in many facets of our health and daily lives – ensuring that these innovative devices are safe and effective, and that they can reach the full potential to help people".

CRediT authorship contribution statement

Neil J. Rowan: Writing – review & editing, Writing – original draft, Visualization, Resources, Methodology, Formal analysis, Conceptualization.

Declaration of competing interest

The author declares no conflict of interest.

Data availability

Data will be made available on request.

Acknowledgement

The author acknowledges Irelands' CÚRAM SFI Medical Devices Research Centre.

References

Alt, J., Eveland, R., Fiorello, A., Haas, B., Meszaros, J., McEvoy, B., Ridenour, C., Shaffer, D., Yirava, W., Ward, L., 2022. Development and validation of technologies suitable for the decontamination and re-use of contaminated N95 filtering facepiece respirators in response to the COVID-19 pandemic. J. Hosp. Infect. 119, 141–148.a.

Barteit, S., Lanfermaan, L., et al., 2021. Augmented reality, mixed and virtual reality based head mounted devices for medical education: systematic review. JMIR Serious Games 9 (3), e29080. https://doi.org/10.2196/29080.

Bertz, M., Molinnus, D., Schoning, M.J., Homma, T., 2024. Real-time monitoring of H_2O_2 sterilisation of individual *Bacillus atrophaeus* spores by optical sensing with trapping Raman spectroscopy. Chemosensors 11, 445. https://doi.org/10.3390/chemosensors11090445.

Blomstrom-Lundqvist, C., Traykov, V., Erba, P.A., et al., 2022. European Heart Rhythm Association (EHRA) international consensus document onn how to prevent, diagnose, and treat cardiac implantable electronic device infections-endorsed by the Heart Rhytum Society, the Latin American Heart Rhythm Society, International Society for Cardiovascular Infectious Disease and the European Society for Clinical Microbiology and Infections Disease in collaboration with the European Association of Cardio-thoracic Surgery. Eurospace 22 (4), 515–549.

Bordukova, M., Makarov, N., et al., 2024. Generative artificial intelligence empowers digital twins in drug discovery and clinical trials. Expert Opin. Drug Discov. 19 (1), 33–42. https://doi.org/10.1080/17460441.2023.2273839.

Brenner, M., Weir, A., et al., 2023. Development of the key performance indicators for digital health interventions: a scoping review. Digit. Health. https://doi.org/10.1177/20552076231152160.

Brown, E.J., Fujimoto, K., Blumenkopf, B., Kim, A.S., Kontson, K.L., Benz, H.L., 2023. Usability assessments for augmented reality head-mounted displays in open surgery and interventional procedures: a systematic review. Multimodal Technol. Interact. 7, 49. https://doi.org/10.3390/mti7050049.

Bryant, L., Sedlarevic, N., Stubbs, P., Bailey, B., Nguyen, V., et al., 2024. Collaborative co-design and evaluation of an immersive virtual reality application prototype for communication rehabilitation (DISCOVR prototype). Disabil. Rehabil. Assist. Technol. 19, 90–99. https://doi.org/10.1080/17483107.2022.2063423.

BS EN ISO 15883-1:2006, 2006. Washer-Disinfectors Part 1: General Requirements, Terms and Definitions and Tests 2006. British Standards Institute, London.

BS EN ISO 15883-2:2009, 2006. Washer-disinfectors Part 2: Requirements and Tests for Washer-disinfectors Employing Thermal Disinfection for Surgical Instruments, Anaesthetic Equipment, Bowls, Dishes, Receivers, Utensils, Glassware, Etc. British Standards Institute, London.

BS EN ISO 15883-5: 2021, 2022. Washer-disinfectors Part 5: Performance Requirements and Test Method Criteria for Demonstrating Cleaning Efficacy. British Standards Institute, London (Incorporating corrigendum January).

BS EN ISO 17664-1, 2021. Processing of Health Care Products — Information to be Provided by the Medical Device Manufacturer for the Processing of Medical Devices. Part 1: Critical and Semi-critical Medical Devices.

Businesswire, 2024. Global digital twin market size is projected to reach USD 16.44 billion by 2024, growing at a CAGR of almost 38%. https://www.businesswire.com/news/home/20201105005766/en/Global-Digital-Twin-Market-Size-is-Projected-to-Reach-USD-16.44-billion-by-2024-Growing-at-a-CAGR-of-Almost-38#:~:text=Global%20Digital%20Twin%20Market%20Size%20is%20Projected%20to,November%2006%2C%202020%2012%3A45%20AM%20Eastern%20Standard%20Time (accessed 18 Jan, 2024).

Byrne, T., Murray, N., McDonnell-Naughton, M., Rowan, N.J., 2023. Perceived factors informing the pre-acceptability of digital health innovation by aging respiratory patients: a case study from the Republic of Ireland. Front. Public Health 11. https://doi.org/10.3389/fpubh.2023.1203937.

Cebi, N., Bekiroglu, H., Erarslan, A., 2023. Nondestructive metabolomic fingerprinting: FTIR, NIR and Raman specroscopy in food screening. Moleculares 28 (23). https://doi.org/10.3390/molecules28237933.

Chaudhuri, A., Pash, G., Hormuth, D.A., et al., 2023. Predictive digital twin for optimizing patient-specific radiotherapy regimens under uncertainty in high grade gliomas. Front. Artif. Intell. 6, 122612 https://doi.org/10.3389/2Ffrai.2023.1222612.

Chauveaux, D., 2015. Preventing surgical-site infections: measures other than antibiotics. Orthop. Traumatol. Surg. Res. 101 1, S77–S83.

Chen, G., Cui, J., et al., 2022. Rapid progress in intelligent radiotherapy and future implementation. Cancer Investig. 40, 425–436. https://doi.org/10.1080/07357907.2022.2044842.

Chua, R.A.H.W., Lim, S.K., Chee, C.F., Chin, S.P., Kiew, L.V., Sim, K.S., Tay, S.T., 2022. Surgical site infection and development of antimicrobial sutures: a review. Eur. Rev. Med. Pharmacol. Sci. 26, 828–845.

Clark, P., Kim, J., Aphinyanaphongs, Y., 2023a. Marketing and US Food and Drug Administration clearance of artificial intelligence and machine learning enabled software in and as medical devices: a systematic review. JAMA Netw. Open 6 (7), e2321792. https://doi.org/10.1001/jamanetworkopen.2023.21792. Jul 3.

Daling, L.M., Schlittmeier, S.J., 2024. Effects of augmented reality, virtual reality, and mixed reality-based training on objective performance measures and subjective evaluations in manual assembly tasks: a scoping review. Hum. Factors 66 (2), 589–626.

Deasy, E.C., Scott, T.A., Swan, J.S., O'Donnell, J.M., Coleman, D.C., 2022. Effective cleaning and decontamination of the internal air and water channels, heads and head-gears of multiple contra-angle dental headpieces using an enzyme detergent and automated washer-disinfection in a dental hospital setting. J. Hosp. Infect. 128, 80–88.

Donahue, L.M., Hilton, S., et al., 2020. A comparative carbon footprint analysis of disposable and reusable varinal specula. Am. J. Obstet. Gynecol. 223, 225.e1–225.e7.

Escalada-Hernandez, P., Ruiz, N.S., Martin-Rodrigues, L., 2019. Design and evaluation of a prototype of augmented reality applied to medical devices. Int. J. Med. Inform. 128, 87–92.

Eves, J., Sudarsanam, A., Shalhoub, J., Amiras, D., 2022. Augmented reality in vascular and endovascular surgery: scoping review. JMIR Serious Games 10 (3), e34501. https://doi.org/10.2196/34501.

Farah, L., Davaze-Schneider, J., Martin, T., Nguyen, P., Borget, I., Martelli, N., 2023. Are current clinical studies on artificial intelligence-based medical devices comprehensive enough to support a full health technology assessment? A systematic review. Artif. Intell. Med. 140, 102547 https://doi.org/10.1016/j.artmed.2023.102547.

FDA, 2023a. Artificial intelligence and machine learning (AI/ML) enabled medical devices. U.S. Food and Drug Administration. https://www.fda.gov/medical-device

s/software-medical-device-samd/artificial-intelligence-and-machine-learning-aiml-enabled-medical-devices (accessed 14th Feb, 2024).
FDA, 2023b. Augmented reality and virtual reality in medical devices. United States Food and Drug Administration. https://www.fda.gov/medical-devices/digital-health-center-excellence/augmented-reality-and-virtual-reality-medical-devices#:~:text=Examples%20of%20probable%20benefits%3A,Fulfill%20unmet%20medical%20needs (accessed 29th January, 2024).
Friedericy, H., van Egmond, C.W., Vogtlander, J.G., van der Eijk, A.C., Jansen, F.W., 2022. Reducing the environmental impact of sterilization packaging for surgical instruments in the operating room: a comparative life cycle assessment of disposable versus reusable systems. Sustainability 14, 430. https://doi.org/10.3390/su14010430.
Fu, W., et al., 2021. iPhantom: a framework for automated creation of individualized computational phantoms and its application to CT organ dosimetry. IEEE J. Biomed. Health Inform. 25 (8), 3061–3072. Aug. 2021. https://doi.org/10.1109/JBHI.2021.3063080.
Gampa, S. (2023). The 10 guiding principles of th GMLP identified by the FDA, HC and MHRA. Med Device Online. https://www.meddeviceonline.com/doc/the-guiding-principles-of-gmlp-identified-by-the-fda-hc-and-mhra-0001 (accessed 10th Feb, 2023).
Garvey, M., 2024. Medical device-associated healthcare infections: sterilization and the potential of novel biological approaches to ensure patient safety. Int. J. Mol. Sci. 25 (1), 201. https://doi.org/10.3390/ijms25010201.
Goppold, M., Herrman, J.-P., Tackenberg, S., 2022. An error-based augmented reality learning system for work-based occupational safety and health education. Work 72 (4), 1563–1575. https://doi.org/10.3233/WOR-211243.
Greene, J., Skolnik, C.L., Merritt, M.W., 2022. The art of medicine – how medicine becomes trash – disposability in health care. Lancet 400, 1298–1299.
Grimm, F., Kraugmann, J., Naros, G., Gharabaghi, A., 2021. Clinical validation of kinematic assessments of post-strok upper limb movements with a multi-joint arm exoskeleton. J. Neuroeng. Rehabil. 18 (92) https://doi.org/10.1186/s12984-021-00875-7.
Ibn-Mohammed, T., Mustapha, K.B., Abdulkareem, K., et al., 2023. Toward artificial intelligence and machine learning-enabled frameworks for improved predictions of lifecycle environmental impacts of functional materials and devices. MRS Commun. 13, 795–811. https://doi.org/10.1557/s43579-023-00480-w.
Ines Silva, M., Malitckii, E., Santos, T.G., Vilaca, P., 2023. Review of conventional and advanced non-destructive testing techniques for detection and characterization of small scale defects. Prog. Mater. Sci. 138 https://doi.org/10.1016/j.pmatsci.2023.101155.
Joshi, G., Jain, A., Araveeti, S.R., Adhikari, S., Garg, H., Bhandari, M., 2024. FDA-approved artificial intelligence and machine learning (AI/ML)-enabled medical devices: an updated landscape. Electronics 13, 498. https://doi.org/10.3390/electronics13030498.
Kagoma, Y., Stall, N., et al., 2012. People, planet and profits: the case for greening operating rooms. CMAJ 184, 1905–1911.
Karimi Estahbanati, M.R., 2023. Advances in vaporized hydrogen peroxide reusable medical device sterilization cycle development: technology review and patent trends. Microoorganisms 11, 2566. https://doi.org/10.3390/microorganisms11102566.
Kazarinov, N., Stotskiy, A., et al., 2022. Finite element modeling for virtual design to miniaturize medical implants manufactured of nanostructured titanium with enhanced mechanical performance. Materials (Basel) 15 (21), 7417. https://doi.org/10.3390/ma15217417.
Kim, K., Yang, H., Lee, J., Lee, W.G., 2023. Metaverse wearables for immersive digital healthcare: a review. Adv. Sci. 10 (31) https://doi.org/10.1002/advs.202303234.
Kremer, T., Felgar, J., Rowan, N., McDonnell, G., 2023a. Validation of the device features approach for reusable medical devices cleaning evaluations. Biomed. Instrum. Technol. 57 (4), 143–152.
Kremer, T., Rowan, N.J., McDonnell, G., 2023c. A proposed cleaning classification for reusable medical devices to complement the Spaulding Classification. J. Hosp. Infect. https://doi.org/10.1016/j.jhin.2023.11.018.
Kremer, T., Murray, N., Buckley, J., Rowan, N.J., 2023b. Use of real-time immersive digital training and educational technologies to improve patient safety during the processing of reusable medical devices: quo vadis? Sci. Total Environ. 900 https://doi.org/10.1016/j.scitotenv.2023.165673.
Kremer, T.A., Bancroft, R., Patel, Z., Owen, M., McDonnell, G., 2022. A standard method for evaluating test soils used to demonstrate cleaning efficacy. J. Hosp. Infect. 126, 52–55.
Kremer, T.A., Carfaro, C., Klacik, S., 2023d. Effects of time, temperature and humidity on soil drying on medical devices. Biomed. Instrum. Technol. https://doi.org/10.2345/0899-8205-57.2.58.
Lai, M., Yang, H., Gu, J., et al., 2022. Digital-twin-based online parameter personalization for implantable cardiac defibrillators. In: 2022 44th Annual International Conference of the IEEE Engineering in Medicine & Biology Society (EMBC), Glasgow, Scotland, United Kingdom, pp. 3007–3010. https://doi.org/10.1109/EMBC48229.2022.9871142.
Lal, A., Dang, J., et al., 2022. Regulatory oversight and ethical concerns surrounding software as medical device (SaMD) and digital twin technology in healthcare. Ann. Transl. Med. 10 (18) https://doi.org/10.21037/2Fatm-22-4203.
Manickam, P., Mariappan, S.A., Murugesan, S.M., Hansda, S., Kaushik, A., Shinde, R., Thipperudraswamy, S.P., 2022. Artificial Intelligence (AI) and internet of medical things (IoMT) assisted biomedical systems for intelligent healthcare. Biosensors (Basel) 12 (8), 562. https://doi.org/10.3390/bios12080562. Jul 25.
Manley, M., 2014. Near-infrared spectroscopy and hyperspectral imaging: non-destructive analysis of biological materials. R. Soc. Chem. 43, 8200–8214.
McDermott, O., Antony, J., et al., 2022. Lean six sigma in healthcare: a systematic literature review on motivations and benefits. Processes 10 (10), 1910. https://doi.org/10.3390/pr10101910.
McDonnell, G., Burke, P., 2011. Disinfection: is it time to reconsider Spaulding? J. Hosp. Infect. 78, 163–170.
McEvoy, B., Rowan, N.J., 2019. Terminal sterilizaition of medical devices using vaporized hydrogen peroxide: a review of current methods and emerging opportunities. J. Appl. Microbiol. 127 (5), 1403–1420.
McEvoy, B., Lynch, M., Rowan, N.J., 2021. Opportunities for the application of real-time bacterial cell analysis using flow cytometry for the advancement of sterilization microbiology. J. Appl. Microbiol. 130 (6), 1794–1812.
McEvoy, B., Maksioovic, A., Howell, D., Michel, H., 2023a. Principles of parametric release: emphasis on data collection and interpretation. Biomed. Instrum. Technol. 57 (4), 163–170. https://doi.org/10.2345/0899-8205-57.4.163.
McEvoy, B., Maksimovic, A., Rowan, N.J., 2023b. *Geobacillus stearothermophilus* and *Bacillus atrophaeus* spores exhibit linear inactivation kinetic performance when treated with an industrial scale vaporized hydrogen peroxide (VH_2O_2) sterilization process. J. Appl. Microbiol. 134 (1) https://doi.org/10.1093/jambio/lxac028.
McEvoy, B., Maksimovic, A., Howell, D., Reppert, P., Ryan, D., Rowan, N., Michel, H., 2023c. Studies on the comparative effectiveness of X-rays, gamma rays and electron beams to inactivate microorganisms at different dose rates in industrial sterilization of medical devices. Radiat. Phys. Chem. 208 https://doi.org/10.1016/j.radphyschem.2023.110915.
McGain, F., McAlister, S., 2023. Reusable versus single-use ICU equipment: what's the environmental footprint? Intensive Care Med. 49, 1523–1525.
McGain, F., Story, D., Lim, T., McAlister, S., 2017. Financial and environmental costs of reusable and single-use anaesthetic equipment. Br. J. Anaesth. 118, 862–869.
McGrane, V., McDermott, O., Trubetskaya, A., Rosa, A., Sony, M., 2022. The effect of medical device regulations on deploying a Lean Six Sigma project. Processes 10, 2303. https://doi.org/10.3390/pr10112303.
McLaren, J., 2020. Medical device sterilization modality selection decision process. Biomed. Instrum. Technol. 54 (s1), 6–14. https://doi.org/10.2345/0899-8205-54.s3.6.
McLaren, J., Hansen, J.M., Le, V., 2021. Sterilization modality selection: role of sterilization assurance subject matter expert. Biomed. Instrum. Technol. https://doi.org/10.2345/0899-8205-55.s3.67.
de Melo Costa, D., Castillo, R., Vichery, K., Ferreira Velga Tipple, A., de Oliveira Lopes, L. K., Hu, H., 2022b. Hinged surgical instruments: efficacy of double manual cleaning versus automated cleaning on biofilm removal. J. Hosp. Infect. 124, 67–71.
Michels, W., Roth, K., Eibl, R., 2013. Assessment of cleaning efficacy based on the protein-surface relationship. Cent. Serv. 21 (3), 212–215.
Mo, D.-H., Tien, C.-L., et al., 2023. Design of digital twin human-machine interface sensor with intelligent finger gesture recognition. Sensors 23 (7), 3509. https://doi.org/10.3390/s23073509.
Moreta-Martinez, R., García-Mato, D., García-Sevilla, M., Pérez-Mañanes, R., Calvo-Haro, J., Pascau, J., 2018. Augmented reality in computer-assisted interventions based on patient-specific 3D printed reference. Healthc. Technol. Lett. 5 (5), 162–166. https://doi.org/10.1049/htl.2018.5072. PMID: 30464847; PMCID: PMC6222179.
Muehlematter, U.J., Bluethgen, C., Vokinger, K.N., 2023. FDA-cleared artificial intelligence and machine learning-based medical devices and their 510(k) predicate networks. Lancet Digit Health. 5 (9), e618–e626. https://doi.org/10.1016/S2589-7500(23)00126-7. Sep.
Murray, K.A., Kennedy, J.E., McEvoy, B., Vrain, O., Ryan, D., Cowaman, R., Higginbotham, C.L., 2013. Effects of gamma ray and electron beam irradiation on the mechanical, thermal, structural and physicochemical properties of poly (ether-block-amide) thermoplastic elastomers. J. Mech. Behav. Biomed. Mater. 17, 252–268.
Murray, K.A., Kennedy, J.E., McEvoy, B., Vrain, O., Ryan, D., Cowaman, R., Higginbotham, C.L., 2014. Influence of gamma and electron beam sterilization on the stability of a premixed injectable calcium phosphate cement for trauma indications. Mater. Sci. Eng. C 39, 380–394.
Murray, K.A., Collins, M.N., O'Sullivan, R.P., Ren, G., Devine, D.M., Murphy, A., et al., 2018. Influence of gamma and electron beam sterilization on the stability of a premixed injectable calcium phosphate cement for trauma indications. J. Mech. Behav. Biomed. Mater. 77, 116–124.
Murray, N., Buckley, J., Seery, N., Rowan, N.J., 2019. Blending immersive and educational technologies to inform sustainability and diversification of workforce training through machine interface using sterilization as model — quo vadis?. In: 10th Kilmer Conference, Dublin, Ireland https://research.thea.ie/handle/20.500.12065/3280.
Nguyen, M.H., Onken, A., Wulff, A., Foremny, K., Torgau, P., Schütte, H., Hild, S., Doll, T., 2023. Computational modeling of diffusion-based delamination for active implantable medical devices. Bioengineering (Basel) 10 (5), 625. https://doi.org/10.3390/bioengineering10050625.
Patal, P.K., Advani, S.D., Kofman, A.D., Lo, E., et al., 2023. Strategies to prevent catheter-associated urinary tract infections in acute-care hospitals: 2022 update. Infect. Control Hosp. Epidemiol. 44, 1209–1231.
Pickler, P.P., Jaccard, J.S., Weisz, U., Weisz, H., 2019. International comparison of health care carbon footprints. Environ. Res. Lett. 14, 064004.
Retursdottir, T., 2024. Developing machine learning and AI for medical devices. https://www.team-consulting.com/insights/developing-ai-and-machine-learnging-for-diagnostic-devices/.
Rizan, C., Bhutta, M.F., 2022. Environmental impact and life cycle financial cost of hybrid (resuable/single-use) instruments versus single-use equivalents in laparoscopic cholecystectomy. Surg. Endosc. 36, 4067–4078.

Romeiko, X.X., Zhang, X., Pang, Y., Gao, F., Xu, M., Lin, S., Babbitt, C., 2024. A review of machine learning applications in life cycle assessment studies. Sci. Total Environ. https://doi.org/10.1016/j.scitotenv.2023.168969.

Rowan, N.J., Casey, O., 2021. Empower Eco multiactor HUB: a triple helix 'academia-industry-authority' approach to creating and sharing potentially disruptive tools for addressing novel and emerging new Green Deal opportunities under a United Nations Sustainable Development Goals framework. Curr. Opin. Environ. Sci. Health 21. https://doi.org/10.1016/j.coesh.2021.100254.

Rowan, N.J., Kremer, T., McDonnell, G., 2023a. A review of Spaulding's classification system for effective cleaning, disinfection and sterilization of reusable medical devices: viewed through a modern-day lens that will inform and enable future sustainability. Sci. Total Environ. 878 https://doi.org/10.1016/j.scitotenv.2023.162976.

Rowan, N.J., Murray, N., Qiao, Y., O'Neill, E., Clifford, E., Barcelo, D., Power, D.M., 2023b. Digital transformation of peatlands eco-innovations ("Paludiculture"): enabling a paradigm shift towards the real-time sustainable production of 'green-friendly' products and services. Sci. Total Environ. 838 (3) https://doi.org/10.1016/j.scitotenv.2022.156328.

Rutala, W.A., Weber, D.J., 2019. Disinfection, sterilization, and antisepsis: an overview. Am. J. Infect. Control 47, A3–A9.

Sakai, D., Joyce, K., Wananabe, M., et al., 2020. Augmented, virtual and mixed reality in spinal surgery: a real-world experience. J. Orthop. Surg. https://doi.org/10.1177/2309499020952698.

Saurio, R., Jutila, M., et al., 2019. Medical Device Safety Training by using quick response codes and extended reality-based technologies. In: Healthcare Transformation with Informatics and Artificial Intelligence published in International Conference on Informatics, Management and Technology in Healthcare, pp. 323–326. ISBN 978-64368-401-7.

Shinozuka, K., Turuda, S., Fujinaga, A., Nakanuma, H., Kawamura, M., Matsunobu, Y., Tanaka, Y., Kamiyama, T., Ebe, K., Endo, Y., Etoh, T., Inomata, M., Tokuyasu, T., 2022. Artificial intelligence software available for medical devices: surgical phase recognition in laparoscopic cholecystectomy. Surg. Endosc. 36 (10), 7444–7452. https://doi.org/10.1007/s00464-022-09160-7. Oct.

Singh, M., Fuenmayer, E., Hinchy, E.P., Qiao, Y., Murray, N., Devine, D., 2021a. Digital twin: origin to future. Appl. Syst. Innov. https://doi.org/10.3390/asi4020036.

Singh, M., Fuenmayer, E., Hinchy, E.P., Qiao, Y., Murray, N., Devine, D., 2021b. Digital twin: origin to future. Appl. Syst. Innov. 4, 36. https://doi.org/10.3390/asi4020036.

Singh, S., Shehab, E., Higgins, N., et al., 2018. Challenges of digital twin in high value manufacturing, 0148-7191. In: SAE Technical Paper. SAE International, Warendale, PA, USA.

Skalli, D., Charkaoui, A., Anass, C., Garza-Reyes, J.A., 2023. Analysing the integrated effect of circular economy, Lean Six Sigma and Industry 4.0 on sustainable manufacturing performance from a practice-based view perspective. Bus. Strateg. Environ. https://doi.org/10.1002/bse.3546.

Smith, A., Bancroft, R., Ingle, D., Kirk, B., McDonnell, G., Smith, S., 2023. Misinterpretation of medical device cleaning standards. J. Hosp. Infect. https://doi.org/10.1016/j.hin.2023.02.009.

Sorimuthu, A.P.K., 2023. How robotic applications are changing medical devices. Medical device and diagnostic industry. https://www.mddionline.com/robotics/how-robotic-applications-are-changing-medical-devices.

Strock, H.B., 1996. Emerging smart materials systems. Am. Ceram. Soc. Bull. 75 (4).

Sugimoto, M., Sueyoshi, T., 2023. Development of holoeyes holographic image guided surgery and telemedicine system: clinical benefits of extended reality (virtual reality, augmented reality, mixed reality), the metaverse, and artificial intelligence in surgery, with a systematic review. Med. Res. Arch. 11 (7) https://doi.org/10.18103/mra.v11i7.1.4045 [online].

Sutherland, J., Belec, J., Sheikh, A., et al., 2019. Applying modern virtual and augmented reality technologies to medical images and models. J. Digit. Imaging 32, 38–53. https://doi.org/10.1007/s10278-018-0122-7.

Thomas, R.E., Thomas, B.C., Lorenzetti, D., Conly, J., 2022. Hospital and long-term care facility environmental service workers' training, skills, activities and effectiveness in cleaning and disinfection: a systematic review. J. Hosp. Infect. 124, 56–66.

U.S. FDA, 2024. Submission and Review of Sterility Information in Premarket Notification (510(k)) Submissions for Devices Labeled as Sterile - Guidance for Industry and Food and Drug Administration Staff. Document Issued on January 8, 2024.

Viola, G.M., Szvalb, A.D., et al., 2023. Prevention of device-related infections in patients with cancer: current practice and future horizons. CA Cancer J. Clin. 73 (2), 147–163. https://doi.org/10.3322/caac.21756.

Wagner, R., Schleich, B., et al., 2019. Challenges and potentials of digital twins and industry 4.0 in product design and production for high performance products. Procedia CIRP 84, 88–93.

Wang, B., Zhong, S., Mi, J., et al., 2020. Non-destructive testing and evaluation of composite materials/structures: a state-of-the-art review. Adv. Mech. Eng. 12 (4) https://doi.org/10.1177/1687814020913761.

Whitaker, A., Colgrove, G., Scheutzow, M., Ramic, M., Monaco, K., Hill, J., 2023. Decreasing Catheter-Associated Urinary Tract Infection (CAUTI) at a community academic medical centre using a multidisciplinary team employing a multi-pronged approach during COVID-19 pandemic. Am. J. Infect. Control 51, 319–323.

Yan, X., Cao, Z., Murphy, A., Qiao, Y., 2022. An ensemble machine learning method for microplastics identification with FTIR spectrum. J. Environ. Chem. Eng. 10 (4) https://doi.org/10.1016/j.jece.2022.108130.

Trends in Food Science & Technology 83 (2019) 114–128

Contents lists available at ScienceDirect

Trends in Food Science & Technology

journal homepage: www.elsevier.com/locate/tifs

Review

Inactivation of parasite transmission stages: Efficacy of treatments on food of animal origin

Frits Franssen[a,*], Cédric Gerard[b], Anamaria Cozma-Petruţ[c], Madalena Vieira-Pinto[d], Anet Režek Jambrak[e], Neil Rowan[f], Peter Paulsen[g], Miroslaw Rozycki[h], Kristoffer Tysnes[i], David Rodriguez-Lazaro[j], Lucy Robertson[i]

[a] Centre for Zoonotic Diseases and Environmental Microbiology, National Institute for Public Health and the Environment, Antonie van Leeuwenhoeklaan 9, 3721, MA, Bilthoven, the Netherlands
[b] Food Safety Microbiology, Nestlé Research, Vers-chez-les-Blanc, 1000, Lausanne 26, Switzerland
[c] Department of Bromatology, Hygiene, Nutrition, "Iuliu Haţieganu" University of Medicine and Pharmacy, 6 Pasteur Street, 400349, Cluj-Napoca, Romania
[d] Department of Veterinary Science, University of Trás-os-Montes e Alto Douro (UTAD), 5001-801, Vila Real, Portugal AND Animal and Veterinary Research Center, UTAD, Portugal
[e] Faculty of Food Technology and Biotechnology, University of Zagreb, Pierotti Street 6, Zagreb, Croatia
[f] Centre for Disinfection, Sterilisation and Biosecurity, Athlone Institute of Technology, Dublin Road, Athlone, Co. Westmeath, Ireland
[g] Institute for Meat Hygiene, University of Veterinary Medicine Vienna, Veterinärplatz 1, 1210, Vienna, Austria
[h] National Veterinary Research Institute in Pulawy (PIWet), Poland
[i] Parasitology, Department of Food Safety and Infection Biology, Faculty of Veterinary Medicine, Norwegian University of Life Sciences, Adamstuen Campus, PO Box 369 Sentrum, 0102, Oslo, Norway
[j] Microbiology Division, Department of Biotechnology and Food Science, Faculty of Science, University of Burgos, Burgos, Spain

ARTICLE INFO

Keywords:
Foodborne
Parasite
Inactivation
Control measure
Meat
Fish

ABSTRACT

Background: One third of parasitic outbreaks with known source in the US are attributable to food of animal origin (FoAO). Among 24 foodborne parasites ranked by FAO/WHO, 14 are associated with FoAO. Management of these biological hazards is essential for food safety.

Scope and approach: Control measures to inactivate the 12 most relevant parasites in FoAO are evaluated, including cooking, freezing, curing, and traditionally applied food-processing techniques, as well as high-pressure treatment and irradiation.

Key findings and conclusions: How inactivation is determined may affect results, however efficacy of freezing and heating depends on parasite species and developmental stage, as well as temperature and time conditions. Cooking at core temperature 60–75 °C for 15–30 min inactivates parasites in most matrices. Freezing at −21 °C for 1–7 days generally inactivates parasites in FoAO, but cannot be relied upon in home situations. Parasitic stages are sensitive to 2–5% NaCl, often augmented by lowering pH. Gamma irradiation at > 0.1–0.5 kGy is effective for fish parasites, except *Anisakis* (10 kGy); > 0.4–6.5 kGy control meatborne parasites. More research is needed to investigate and improve irradiation technologies using sustainable energy sources. Literature data are diverse and insufficient to model survival as response to treatment. Research on foodborne parasites should be improved to standardize experimental approaches for evaluation of inactivation techniques and methods to monitor inactivation.

1. Introduction and the growing awareness of foodborne parasites

In 2010, parasitic infections were estimated to cause 91.1 million cases of human disease and 51,909 deaths globally per year; excluding enteric protozoa, 48% of cases were foodborne, of which ascariasis and toxoplasmosis were the most common parasitic diseases (Torgerson, 2015). However, there were considerable regional differences and low-income countries suffered the highest disease burden.

* Corresponding author. Centre for Zoonotic Diseases and Environmental Microbiology, National Institute for Public Health and the Environment, Antonie van Leeuwenhoeklaan 9, 3721, MA, Bilthoven, the Netherlands.
E-mail addresses: frits.franssen@rivm.nl (F. Franssen), Cedric.Gerard@rdls.nestle.com (C. Gerard), anamaria.cozma@umfcluj.ro (A. Cozma-Petruţ), mmvpinto@utad.pt (M. Vieira-Pinto), arezek@pbf.hr (A.R. Jambrak), nrowan@ait.ie (N. Rowan), peter.paulsen@vetmeduni.ac.at (P. Paulsen), mrozycki@piwet.pulawy.pl (M. Rozycki), kristoffer.tysnes@nmbu.no (K. Tysnes), drlazaro@ubu.es (D. Rodriguez-Lazaro), lucy.robertson@nmbu.no (L. Robertson).

https://doi.org/10.1016/j.tifs.2018.11.009
Received 8 March 2018; Received in revised form 1 November 2018; Accepted 4 November 2018
Available online 09 November 2018

Among foodborne disease events reported in the EU between 2007 and 2011, foods of animal origin (FoAO) were associated with 90% of outbreaks, 74% of cases, 65% of hospitalizations, and 54% of deaths (Da Silva Felicio et al., 2015). Appraisal of foodborne illness data from USA between 1998 and 2008, indicated that FoAO were associated with approximately 48% of cases, 52% of hospitalizations, and 49% of deaths (Painter et al., 2013). However, these data cover the spectrum of infectious agents, and the USA data also include foodborne illnesses associated with chemicals.

The food vehicle is unknown for most foodborne parasitic diseases in the USA, but where identified, FoAO account for around one third (Painter et al., 2013). Some foodborne parasites may have a considerable health-related impact, but do not often cause outbreaks (e.g. *Toxoplasma*). As data were derived from outbreaks, human health impacts from foodborne parasites are probably underestimated.

Among 24 (potentially) foodborne parasites listed for risk-ranking by FAO/WHO in 2012 (FAO/WHO, 2014), transmission of 14 of them (58%) can be associated with FoAO. These include parasites associated with both marine and freshwater finfish (Anisakidae, Diphyllobothriidae, Heterophyidae, and Opistorchiidae), parasites associated with freshwater crustacea (*Paragonimus* spp.), parasites associated with pork (*Trichinella spiralis*, other *Trichinella* species, *Toxoplasma gondii*, *Taenia solium*, and *Sarcocystis suihominis*), parasites associated with beef (*Taenia saginata, Toxoplasma gondii*, and *Sarcocystis bovihominis*), parasites associated with meat from small ruminants (*Toxoplasma gondii*), parasites associated with meat from game animals (*Trichinella* spp. and *T. gondii*), and parasites associated with frog and snake meat (*Spirometra* spp.). In addition, some parasites have been associated with contamination of molluscs that can accumulate excreted transmission stages (e.g. *Giardia duodenalis*), and have also been associated with milk (*Cryptosporidium parvum* and *T. gondii*).

Although certain types of fresh produce are more frequently associated with raw consumption or minimal processing than FoAO, intentional or unintentional under-cooking of FoAO is well recognized. In particular, consumption of raw fish has become a global culinary trend, with the rise in popularity of sushi, sashimi, and ceviche, and since fish that is commonly eaten raw may contain infective parasites, e.g. *Anisakis simplex* (Mo et al., 2014), this may result in increased exposure of consumers to fishborne parasites (Robertson, 2018). Although consumption of raw meat occurs in several culinary cultures (e.g. steak tartare from France, *carpaccio* from Italy, *mett* in Germany, *koi soi* in Thailand, *kitfo* from Ethiopia etc.), more common is consumption of rare meat (cooked briefly to a temperature below 60 °C). This may be insufficient to inactivate transmission stages of pathogens, including some parasites. In addition, meat may be inadvertently undercooked.

Given that some cooking techniques or other preparation of FoAO (e.g. fermentation, drying, freezing, etc.) may be insufficient to inactivate parasite transmission stages, knowledge on the effects of these different procedures at inactivating different parasite transmission stages is of interest, and of particular relevance, given the globalization of the food chain (Dorny, 2009).

The present study intends to provide a comprehensive overview of the 12 most relevant parasites in FoAO that have been ranked globally and regionally for Europe (FAO/WHO, 2014; Bouwknegt et al., 2018). Although it is clear that the highest burden from foodborne parasitic infections is in lower income countries, our focus is directed towards foodborne parasites of greatest relevance in European countries, as an output from a Eurocentric COST Action (see acknowledgements). Nevertheless, treatments that are effective in Europe, will also be effective elsewhere, so the assessment of treatments is of global relevance.

Many of the more recent review papers and recommendations by food safety organisations (e.g. EFSA, FDA, ANSES and others) are based on the same, sometimes old, original papers, with more recent studies lacking for many parasites.

Testing for parasitic infections at meat inspection to prevent zoonotic parasites entering the food chain is mandatory for *Trichinella* in Europe, according to Regulation EU 2015/1375 (European-Commission, 2015). Testing for some other parasites may be relevant, but may not be routinely implemented, and some parasites are tested for, but with limited sensitivity (e.g., tapeworm cysts). In this review we provide an overview of inactivation techniques with the potential to prevent transmission of parasitic infections due to consumption of FoAO. This review does not take into account parasite-derived health hazards other than infection, such as allergic reactions provoked by Anisakidae sp. Or toxins associated with *Sarcocystis* species.

2. Reference inclusion criteria

A non-systematic literature review was used to gather scientific publications, reports, and official documents relevant for this article. Original papers were included that quantified effects of methods for parasite inactivation over a wide range of topics; different parasites, different matrices, different inactivation methods, and different ways of assessing inactivation.

With such a breadth of cover, ensuring reference quality is difficult. Should only references answering to our highest quality requirements be included (i.e., recent papers providing detailed quantification of parasite inactivation determined by bioassay), some parasites, matrices, and different methods (e.g. heat inactivation of Heterophyidae, freeze inactivation of *Opisthorchis* spp., all inactivation methods for Anisakidae), would have no reference material and therefore would not be included at all. On the other hand, references that have been founding papers in their field (e.g., Kotula et al. (1983) and Kotula et al. (1990) for *Trichinella* control), provide time/temperature combinations for complete inactivation of *Trichinella* in pork, but lack quantitative details regarding parasite inactivation. Such information could be used to model inactivation as part of a QMRA, to reflect consumer behaviour. In the example of *Trichinella*, not all consumers will cook their meat to safe time/temperature combinations, which will result in partial inactivation of muscle larvae. Moreover, legal requirements exist for some parasites, and official authorities conduct tests, like for *Trichinella*; whereas for others, it is the sole responsibility of the food business operators to establish a risk-based limit and to adjust their control measures accordingly.

3. Current state of knowledge

The reader is referred to Annex 7 of the FAO/WHO multi-criteria based ranking for risk management of foodborne parasites (FAO/WHO, 2014), for a comprehensive overview of parasite biology, geographical distribution, disease in humans, relevance for trade and impact on economically vulnerable populations, concerning the parasites of FoAO included in the current review.

4. Key aspects of preventive measures

Many different parasites may be transmitted by FoAO, with a wide range of different transmission stages. Developing universally applicable measures to prevent infection with these parasites is therefore challenging. The key steps in preventive measures in primary production of FoAO are environmental hygiene, hygienic production, personnel hygiene, facility cleaning and maintenance, and monitoring/surveillance (FAO/WHO, 2016).

Several important parasites transmitted by meat form infectious tissue stages in animals, for which a main intervention is to prevent food production animals from being infected. This has been particularly effective in animals that can be kept confined, e.g. pigs and poultry, whereas for grazing animals, such as sheep, it may be difficult or impossible to avoid exposure. *Trichinella* is now generally absent in meat from pigs kept indoors in many European countries (Pozio, 2014). Recent trends in consumer preferences, favouring organic production

and improved animal welfare, have led to changes in pig farming, with an increase in pigs raised outdoors (Park, Min, & Oh, 2017). This may result in greater *Trichinella* exposure of these pigs, and thereby increased human *Trichinella* infection. As sheep are mainly kept outdoors, and restricting the access of cats (definitive host of *T. gondii*) to sheep farms can be impossible, *T. gondii* is a continuous challenge in sheep production and for food safety.

Tissue parasites are also potentially problematic in the aquaculture industry, including farmed and wild-caught fish. Anisakidae are mainly a hazard in wild-caught fish. It has been argued that *Anisakis* infection is not a problem in farmed fish production, as these fish have minimal access to the parasite's intermediate hosts (crustaceans and smaller fish). Nevertheless, 0.7% *Anisakis pegreffii* infestation was reported recently in farmed sea bass from the Mediterranean Sea (Cammilleri, 2018) and *Anisakis simplex* has been found in farmed salmon (Mo, 2015). Although closed breeding facilities may reduce exposure of farmed fish to parasite infective stages such as *Anisakis* spp., it has not yet been implemented at a large scale, but may become a future industry standard.

5. Evaluation of inactivation

Unlike bacteria and viruses, the infective unit for parasites may be one individual (e.g. amoeba), one egg or one larval stage (helminths), or four to eight individuals (mature oocysts of coccidians). For parasites that form tissue cysts, one infective unit (the tissue cyst) may contain a few to 1000 individuals per tissue cyst (e.g. *Toxoplasma*). Because of this variation in units of infection, using the standard log reduction measure for inactivation, as commonly applied for bacteria and viruses, is not a uniform measure for inactivation of individual parasites. However, log reduction may still be used mentioning the unit of infection (e.g. tissue cyst, cyst, oocyst, egg). Parasites on or in foods do not grow or replicate during storage, unlike bacterial contaminations that may increase to very high numbers. As a result, a two or three log reduction that may be considered marginal for bacteria, may be highly relevant for parasitic contamination.

Transmission stages of most foodborne parasites require an animal host and are not suitable for laboratory cultivation. The gold standard to evaluate parasite (stage) inactivation is method-induced elimination of infectivity in bioassays. In recent decades, use of experimental animals has become controversial, and in more recent studies, infection experiments have been replaced by surrogate indicators. Such indicators may be loss of a parasite's ability to proceed in development (e.g. oocyst sporulation), evaluation of motility or morphological integrity as determined by microscopy, or molecular methods to evaluate genetic activity (Rousseau et al., 2018), which should be validated in relation to the gold standard.

6. Conventional processing

6.1. Heat treatment

Heat treatment remains one of the most reliable methods to control parasites in FoAO (Gajadhar, 2015). Table 1 provides an overview of reported data on the efficacy of different heat treatments to inactivate parasites in a variety of food matrices of animal origin.

For *Anisakis*, heating at ≥ 60 °C core temperature of fishery products for at least 1 min is sufficient to kill the larvae (Bier, 1976; EFSA, 2010); consequently, fish fillets 3 cm thick should be heated for 10 min to reach and maintain 60 °C in the core (Wootten, 2001).

Metacercariae of trematodes seem more tolerant to heat, since for *Heterophyes* in fish, temperatures as high as 100 °C for more than 15 min are required to kill the metacercariae (Hamed & Elias, 1970), whereas isolated metacercariae of *Opisthorchis viverrini* are inactivated at 70 °C for 30 min or at 80 °C for 5 min (Waikagul, J., 1974, cited in: Abdussalam, Käferstein, & Mott, 1995). Metacercariae of *Ascocotyle* were inactivated by heating at ≥60 °C for 15 min (Novo Borges, Corrêa Lopes, & Portes Santos, 2018).

Several studies (Table 1) have highlighted the efficacy of microwave heating in killing some parasites in FoAO, like *Anisakis* in Arrowtooth flounder (Adams, Miller, Wekell, & Dong, 1999; Vidacek et al., 2011). However, heating in standard domestic microwave ovens (2450 MHz, 700 W) may not penetrate all areas of the food, resulting in hot and cold spots, and thus some parasites may evade inactivation (Vidacek et al., 2011). *Toxoplasma* cysts in mutton steaks processed in a microwave oven at 65 °C remained infective (Lunden & Uggla, 1992) and microwave exposures for 1–3 s (43.2–62.5 °C) partially, but not significantly, reduced infectivity of *Cryptosporidum parvum* oocysts in oysters for neonatal mice, but treatment above 43.2 °C caused unacceptable changes in oyster meat texture and colour (Collins, Flick, Smith, Fayer, Rubendall, et al., 2005).

Larvae isolated from pork chops cooked at 71–82 °C core temperature in the microwave oven (2.9–3.1 min) did not prevent *T. spiralis* infection of rats (Kotula, Murrell, Acosta-Stein, Lamb, & Douglass, 1983b). Inactivation temperatures for *T. spiralis* may vary from 60 °C for roasted pork (Carlin, Mott, Cash, & Zimmermann, 1969; Kotula, Murrell, Acosta-Stein, Lamb, & Douglass, 1983a) to 66 °C for pork chops prepared in a conventional oven, convection oven, and flat grill, and 77 °C for char broiler or deep fat fryer (Kotula et al., 1983b).

Several studies highlight that heating duration is as important as temperature, and should be chosen such that desired temperatures are reached, maintained, and evenly distributed throughout the meat (Kotula et al., 1983a). Heat inactivation of *T. spiralis* in pork was tested at a range for both time (2 min–6 h) and temperature (49–63 °C) on 2 mm thick pieces of experimentally infected pork (Kotula et al., 1983a). In that study, the intrinsic freeze sensitivity for *T. spiralis* in pork was defined by linear regression as $\mathrm{Log}(t) = 17.3 - 0.302T$, where t represents time (hours) and T temperature (°C). By this equation, it is possible to define time/temperature combinations to which pork should be exposed for complete *T. spiralis* inactivation (Table 1). Notably, these time - temperature combinations refer to the conditions in the core of the meat piece. More recently, Franssen et al. (2018, under review) developed a heat-inactivation model based on experimental data including bioassay in mice. According to this model, consumer cooking of portions of pork for a total time of 15 min would expose *Trichinella* muscle larvae to 60 °C during 10 min, inactivating 99% (*T. britovi*) or 96% (*T. spiralis*) of *Trichinella* larvae.

Based on the work of Kotula et al. (1983a), *Taenia* cysticerci can be inactivated by cooking whole cuts of beef and pork to at least 62.8 °C core temperature and subsequent rest for at least 3 min (FDA, 2012). Nevertheless, both higher and lower temperature values can also be found in the literature (Table 1).

The US Department of Agriculture recommends that whole cuts of pork, lamb, veal, or beef are cooked to an internal temperature of 62.8 °C, with a 3-min rest to inactivate *T. gondii* in meat (Jones & Dubey, 2012), based on the work of Kotula et al. (1983a). Dubey, Kotula, Sharar, Andrews, and Lindsay (1990) exposed 20 g samples of *Toxoplasma gondii* infected and spiked pork, compressed to 2 mm in thickness, to temperatures ranging from 49 to 67 °C for 0.01–96 min. Parasite inactivation was evaluated by bioassay in mice. *T. gondii* tissue cyst inactivation was characterised in that study as $\mathrm{Log}(t) = 7.918–0.146T$. Following this equation, time/temperature combinations to which *T. gondii* in pork should be exposed for complete parasite inactivation were provided, e.g. > 61 °C for 3.6 min (Dubey et al., 1990). However, in their experiments, *T. gondii* tissue cysts survived 64 °C for 3 min once and therefore, Jones and Dubey (2012) advised that whole cuts of pork, lamb, veal, or beef, should be cooked to an internal temperature of at least 65.6 °C, with a 3-min rest.

C. parvum oocysts in either water or milk lose infectivity when held at 71.7 °C for 5 s or more, indicating that conditions used in commercial pasteurization (71.5-72 °C for 15 s) are sufficient to inactivate *C. parvum* oocysts in milk (Harp, Fayer, Pesch, & Jackson, 1996); milkborne

Table 1
Effects of conventional processing on parasites in FoAO. Control measure: Heat treatment.

Transmission stage	Condition	Method	Effect	Log reduction	Matrix	Ref
Anisakis						
Larvae	≥60 °C; 1 min 60 °C; 10 min, fillet 3 cm thick 70 °C; 7 min, fillet 3 cm thick	n.s.[a]	Kills Anisakis	n.s.	Fish	Wootten, 2001
	60 °C; 700-W microwave heating	Larvae viability (with ultraviolet light)	Kills 69% Anisakis larvae, initial log population: 1.81 Kills 89% Anisakis larvae; initial log population: 1.91	0.51 0.96	Fish: Arrowtooth flounder fillets	Adams et al. (1999)
	77 °C; 700-W microwave heating	Fluorescence under UV light; Microscopic motility examination under mechanical or glacial acetic acid stimulation	Kills 100% Anisakis larvae in food	1.78	Fish: whole fillets of Arrowtooth flounder	
	70 °C; 3 min (microwave heating at maximum 1000 W)	Motility, emission of fluorescence under UV light, scanning electron microscopy	Kills Anisakis (L3)	1.08	Fish: infected hake muscle sandwiches	Vidacek et al. (2011)
Heterophyidae						
Metacercariae	50 °C; > 180 min 100 °C; > 10 min	Microscopic detection Metacercariae movement	Kills metacercariae	n.s.	Flesh of mullet	Hamed and Elias (1970)
	≥60 °C; 15 min	Metacercariae movement				Novo Borges et al. (2018)
Sarcocystis spp.						
Sarcocysts	40–60 °C; 20–25 min (heart muscle)	Bioassay (dogs)	Sarcocystis levinei sarcocysts still infective	n.s.	Buffalo heart	Srivastava et al. (1986)
	65 °C; 20–25 min (heart muscle)	Bioassay (dogs)	S. levinei sarcocysts non-infective			
	60 °C; 20min (thigh muscles).	Bioassay (dogs)	Sarcocystis miescheriana sarcocysts non-infective		Pork	Saleque, Juyal, and Bhatia (1990)
Taenia spp.						
Cysticerci	Cooking to 60 °C	n.s.	Controls T.solium and T.saginata in meat	n.s.	Pork and beef	Murrell and Crompton (2009)
	> 65 °C Cooking roast pork (cochinita pibil) or pork and beans (frijol con puerco)	In vitro evaluation of metacestode movement and scolex evagination	Damages T. solium metacestodes in both cases		Pork	Rodriguez-Canul et al. (2002)
Trichinella spp						
Muscle larvae	≥60 °C (internal temperature, oven cooked)	Larvae viability (after digestion) and bioassay	Inactivates *T. spiralis* larvae in meat	n.s.	Pork loin	Carlin et al. (1969)
	49 °C; 6 h 52 °C; 47 min 55 °C; 6 min 60 °C; 2 min	Bioassay (rats)	Destruction of *T. spiralis* infectivity		Pork	Kotula et al. (1983a)
	70 °C (core temperature	n.s.	Inactivates Trichinella in pork, game and horse meat		Pork, game meat, horse	Blackburn and McClure (2009)
	71.1 °C (core temperature)		Inactivates Trichinella in pork and any wild game that may be infected with trichinae		Pork, game meat	Doyle (2003)
	71–82 °C; 3 min internal temperature)	Bioassay (rats)	Did not inactivate *T. spiralis* larvae in pork chops		Pork	Kotula et al. (1983b)
Cryptosporidium						
Oocysts	43.2 °C; 1sec 54 °C; 2 s (microwave heating)	Bioassay (neonatal mice)	Not effective in reducing the infectivity of C. parvum	0.00	Shucked oysters	Collins et al. (2005)
	62.9 °C for 3 s; microwave heating		Partially reduces oocysts viability; initial log population: 4.58, log reduction: 0.15	0.15		
	71.7 °C; 5 s 71.7 °C; 10 s 71.7 °C; 15 s (conditions of commercial pasteurization)		Inactivates oocysts heat treated in milk	5	Milk	Harp et al. (1996)

(*continued on next page*)

Table 1 (*continued*)

Transmission stage	Condition	Method	Effect	Log reduction	Matrix	Ref
Sarcocystis spp.						
Sarcocysts	65–75 °C; 20–25 min	Bioassay (dogs)	Sarcocystis levinei sarcocysts become non-infective to pups	n.s.	Buffalo heart	Srivastava, Saha, and Sinha (1986)
	70 °C; 15 min 100 °C; 5 min		Sarcocystis miescheriana sarcocysts become non-infective to pups		Pork (minute pieces)	Saleque et al. (1990)
Toxoplasma gondii						
Tissue cysts	65 °C; Microwave oven	Bioassay (mouse)	Not always effective, partial inactivation of cysts	n.s.	Naturally infected sheep	Lunden and Uggla (1992)
	52 °C; 9.5 min (internal temperature) thickness of 2 mm	Bioassay (mice)	Does not eliminate infectivity to mice	n.s.	Pork from infected pigs mixed with infected mouse brains and homogenized	Dubey et al. (1990)
	58 °C; 9.5 min (internal temperature) thickness of 2 mm		Eliminates infectivity to mice			
	> 61 °C; 3.6 min (internal temperature) thickness of 2 mm		Eliminates infectivity to mice			
	64 °C; 3 min (internal temperature - thickness of 2 mm)		Partial inactivation of Tissue cysts			

[a] n.s.: not stated.

cryptosporidiosis outbreaks have been exclusively associated with unpasteurized milk.

6.2. Freezing

Table 2 gives an overview of freezing to inactivate parasites in FoAO.

Anisakis spp. in fish have been inactivated in a blast freezer at −35 °C for ≥15 h or at −20 °C for at least 24 h (Deardorff & Throm, 1988; McClelland, 2002). *Anisakis* spp. inactivation was evaluated by observing larval movement after physical stimulation. Some larvae seen to be moving after freeze-treatment at −35 °C for 1 h were considered moribund. Subsequent sub-zero storage after freezing is recommended for complete inactivation of anisakidae larvae (Deardorff & Throm, 1988).

Trematode metacercariae appear to be more resistant to freezing temperatures, although not many studies have been performed to date. *Clonorchis sinensis* in fish and fishery products are considered to be inactivated at −10 to −20 °C for 5–20 days (EFSA, 2010). However, *C. sinensis* metacercariae in fish that had been frozen at −12 °C for 10–18 days or at −20 °C for 5–7 days remained viable and infective in bioassays using rats and rabbits. Only 20 days of freezing at −12 °C or 3 days of freezing at −20 °C followed by thawing and another freeze treatment for 4 days at −20 °C eliminated infectivity in rabbit and rat bioassays (Fan, 1998). Freeze-treatment of mullet fillets for 30 h at −10 or −20 °C is not effective at inactivating *Heterophyes* metacercariae (Table 2). At temperatures below −20 °C for 2–32 h, the viability of *Opisthorchis* spp. in fish has been markedly, but not completely, reduced (Table 2). Although anecdotal evidence, an outbreak of opisthorchiasis in Italy was due to consumption of infected fish that had been frozen in a household freezer at −10 °C for 3 days (Armignacco, Caterini, Marucci, Ferri, et al., 2008).

In contrast, larval stages of cestodes appear more sensitive to freeze treatment, although primary literature is scarce; one paper describes inactivation of isolated *Diphyllobothrium* spp. plerocercoids (Table 2). *Taenia solium* cysticerci in pork are inactivated by freezing at −24 to −5 °C for 1–4 days, whereas inactivation of *Taenia saginata* cysticerci in beef requires freezing at −5 to −25 °C for 10–15 days (Table 2).

Freeze inactivation of *T. spiralis* in pork was tested at a wide range for both time (1 s–182 days) and sub-zero temperatures (−1 to −193 °C) on 2 mm thick pieces of experimentally infected pork (Kotula et al., 1990). In that study, the intrinsic freeze sensitivity for *T. spiralis* in pork was defined by linear regression as $\mathrm{Log}(t) = 5.98 + 0.40T$, where t represents time (hours) and T temperature (°C). Using this equation, time/temperature combinations have been defined to which *T. spiralis* in pork should be exposed for complete parasite inactivation (Table 2). Note that the time needed to reach the desired temperature in pork must be determined for each situation and should be added to the calculated inactivation time. Based on the work of Kotula et al. (1990), the International Commission on Trichinellosis (ICT) recommends freezing at −21 °C for 7 days for complete inactivation of *T. spiralis* in pork. However, freeze inactivation of *Trichinella* in bulk packages may need lower temperatures or longer exposure times (e.g. −29 °C for 6 days to −15 °C for 30 days) to ensure safety, depending on meat thickness and stacking height in industrial freezers (ICT, 2006). These recommendations have been included in EU recommendation 2015/1375 (European-Commission, 2015), laying down specific rules on official controls for *Trichinella* in meat regarding freeze treatment, and its previous version (EU Recommendation 2075/2005).

Inactivation studies on *Trichinella* spp. in other matrices than pork are less elaborated and limited in number. *T. spiralis* and *T. britovi* in experimentally infected wild boars, 24 weeks post infection, were inactivated by freezing at −21 °C for 1 week as determined by mouse bioassay (Lacour et al., 2013). Freezing to inactivate *Trichinella* species other than *T. spiralis* in pork, game, and horse meat, cannot be relied upon. Frozen wild boar meat from a naturally *T. britovi*-infected animal

Table 2
Effects of conventional processing on food borne parasites. Control measure: Freezing.

Transmission stage	Condition	Method	Effect	Log reduction	Matrix	Ref
Anisakis						
Larvae	−35 °C; 15 h; followed by −18 °C; 24 h	Movement after stimulation with dissection needle	Kills Anisakis larvae, 6/3545 survived after 1 h of freezing; after 24 h no larvae survived	2.77	Fish: Sockeye salmon and canary rockfish	Deardorff and Throm (1988)
Clonorchis sinensis						
Metacercariae	−12 °C; 18 days	Bioassay (rats)	Metacercariae only marginally inactivated	0.00	Fish	Fan (1998)
	−12 °C; 10 days	Bioassay (rats)	Metacercariae survival	0.00		
	−20 °C, 7 days	Bioassay (rats)	100% of rats infected by metacercariae	0.00	Fish	
	−12 °C, 20 days	Bioassay (rabbits)	Eliminates infectivity for rabbits; 160 metacercariae inoculated, no flukes recovered	2.20		
	−20 °C for 3 days, thawing, and refreezing for 4 days	Bioassay (rats)	Eliminates infectivity for rats; 400 metacercariae inoculated, no flukes recovered	2.60		
Diphyllobothrium spp.						
Plerocercoid larvae	−10 °C; 5 min	Bioassay (golden hamster)	Inactivates plerocercoids	n.s.	Fish fillets (isolated plerocercoids)	Salminen (1970)
Heterophyidae						
Metacercariae	−10 °C or −20 °C; 30 h	Motility	Inefficient, metacercariae can survive	0.00	flesh of mullet	Hamed and Elias (1970)
Opistorchis spp.						
Metacercariae	−28 °C; 20 h −35 °C; 8 h −40 °C; 2 h	n.s.	Viability markedly reduced, but not completely inhibited	n.s.	Fish	Fattakhov (1989)
Sarcocystis fusiformis						
Sarcocysts	−20 °C; 3 days	Bioassay (cats)	Complete loss of infectivity	n.s.	Beef	Gestrich and Heydorn (1974)
Sarcocystis spp.						
Sarcocysts	−2 °C; 24 h	Bioassay (dogs)	Meat containing sarcocysts still infective	0.00	Buffalo heart	Srivastava et al. (1986)
	−4 °C; 48 h		Inactivates S. levinei sarcocysts	n.s.		
	−4 °C; 2 days		Inactivates S. miescheriana sarcocysts	3.1	Pork	Saleque et al. (1990)
	−20 °C; 1 day			3.1		
Taenia saginata						
Cysticerci	−5 °C; 360 h −10 °C; 216 h ≤ −15 °C; 144 h	In vitro viability assay	Inactivates T.saginata cysticerci	n.s.	Beef carcasses	Hilwig, Cramer, and Forsyth (1978)
Taenia solium	0 °C or above		Does not affect parasite survival in culture	0.00		
Tissue cysts		In vitro culture assay			Pork	Sotelo et al. (1986))
	−15 °C; 3 days		Inactivates cysts	2.24		
	−24 °C; 1 day			2.25		
	−5 °C; 4 days			2.50		
Trichinella spp.						
Muscle larvae	−21 °C; 7 days	Bioassay (mice)	Inactivates T. britovi muscle larvae	1.50	Wild boar meat	Lacour et al. (2013)
	−20 °C; up to 20 months	Bioassay (guinea pigs)	Does not inactivate T. nativa muscle larvae	n.s.	Walrus meat	Leclair et al. (2004)
	−20 °C; 4 months	Bioassay (pigs)	Does not inactivate T. nativa muscle larvae	n.s.	Bear meat	Hill, Gamble, Zarlenga, Coss, and Finnigan (2005)
	−10 °C; 4 days, excluding cooling down time −15 °C; 57 min, excluding cooling down time −20 °C; 1 min, excluding cooling down time	Bioassay (mice)	Inactivates *T. spiralis* muscle larvae	n.s.	Pork	Kotula et al. (2010)
	−21 °C; 7 days	Bioassay (mice)	Inactivates *T. spiralis* muscle larvae	2.19[a]	Wild boar meat	Lacour et al. (2013)

(*continued on next page*)

Table 2 (*continued*)

Transmission stage	Condition	Method	Effect	Log reduction	Matrix	Ref
Toxoplasma gondii						
Tissue cysts	−12 °C; 3 days	Bioassay (cats)	Inactivates tissue cysts	n.s.	Meat: Experimentally infected pigs	Dubey et al. (1988)
	−7 °C to −12 °C; 4 days	Bioassays (cats and/or mice)			Pork	Kuticic and Wikerhauser (1996)
	−20 °C for 54 h and thawed overnight at 4 °C	Bioassay (mice)			Mutton	Lunden and Uggla (1992)
	−8 °C; 3 days −7 °C; 17 days,	Bioassay (mice)			Pork	Kotula, Sharar, Andrews, Shen, and Lindsay (1991)
Cryptosporidium parvum						
Oocysts	Ice cream mixing, freezing and hardening at −20 °C for 24 h	Exclusion of fluorochrome propidium iodide	Inactivation of oocysts	3.90	Dairy products: ice cream matrix	Deng and Cliver (1999)
Cyclospora cayetanensis						
Oocysts	−15 °C; 24 h	Oocyst sporulation	No inactivation of oocyst sporulation	0.00	Dairy substrates	Ortega and Sanchez (2010)
	−15 °C; 2 days		Inactivates oocysts	2.00	Dairy products: diluted milk substrate Dairy products: milk matrix Dairy products: whipped cream matrix	Sathyanarayanan and Ortega (2006)

[a] Note that log reduction has been calculated from infectivity index data (number of *Trichinella* larvae recovered/number inoculated), as no parasite counts were available (Lacour et al., 2013).

Table 3
Effects of enzymatic and chemical preservation on the infectivity of parasite stages in meat and fish products. Control measure: Marination, Pickling, Smoking, Fermentation and Salting.

Transmission stage	Condition	Evaluation method	Effect	Log reduction	Matrix	Ref
Anisakis						
Larvae	Marination in 2.6% acetic acid and 5–6% salt for 12 weeks Marination in 2.6% acetic acid and 8–9% salt for 6 weeks	n.s.	Inactivates Anisakis larvae	n.s.	Fish (herring)	Doyle (2003)
	6% acetic acid (v/v) (vinegar); 12% salt for 13 days, 4 °C 10% acetic acid; 12% NaCl for 5 days 20% acetic acid; 12% NaCl for 3 days 30% acetic acid; 12% NaCl for 3 days 40% acetic acid; 12% NaCl for 2 days	Movement; determination of stress protein levels; bioassay (rat)	Inactivates Anisakis larvae	1.78	Fish: anchovies	Sanchez-Monsalvez et al. (2005)
	Storage in brine with 6.3% salt and 3.7% acetic acid in the aqueous phase of the fish for 28 days	Motility	Inactivates Anisakis larvae	n.s.	Fish: herring	Karl, .Roepstorff, Huss, and Bloemsma (1994)
	5% NaCl; > 17 weeks 6–7% NaCl; 10–12weeks	Motility	Inactivates Anisakis larvae	n.s.	Fish: Herring	Karl et al. (1994)
	6% acetic acid, 10% NaCl for 24 h followed by the addition of sunflower seed oil and refrigeration at 4 °C for 13 days	Motility	Inactivates Anisakis larvae	n.s.	Fish: Sardines	Arcangeli (1996)
	Pickled herring; 28 days	Motility in 1% acetic acid and staining	Inactivates Anisakis larvae	≥2.60	Fish, anchovies	Karl and Leinemann (1989)
	21% NaCl; 15 days	Motility and scanning electron microscopy	Inactivates Anisakis pegreffi larvae	n.s.	Fish, anchovies	Anastasio et al. (2016)
	13% NaCl brine; 5 °C; 24 h plus dry salt maturation at 5° for 15 days	Motility	Inactivates Anisakis larvae	n.s.	Fish, cod	Smaldone et al. (2017)
Clonorchis sinensis metacercariae Opistorchis viverrini	3 g NaCl/10 g fish flesh; 8 days	Bioassay (rat)	Inactivation of metacercariae	n.s.	Freshwater fish	Fan (1998)

(*continued on next page*)

Table 3 (*continued*)

Transmission stage	Condition	Evaluation method	Effect	Log reduction	Matrix	Ref
metacercariae	13.6% NaCl, 48 h	Bioassay (hamster)	Reduced infectivity of metacercariae	n.s.	Fermented fish	Kruatrachue et al. (1982)
	20% NaCl, 5 h	Bioassay	metacercariae non-infectious	n.s.	Fermented fish	Tesana, Kaewkes, and Phinlaor (1986)
	7.5% NaCl, glutinous rice; keeping fish 3 days refrigerated plus 4 days fermentation time at room temperature	Bioassay (hamster)	metacercariae non-infectious	n.s.	Fermented fish (plasom)	Onsurathum et al. (2016)
Taenia solium metacestodes	7–10.5% NaCl at 30 °C	microscopy	Inactivation overnight	n.s.	pork	Ockerman and Basu (2017)
Trichinella spp.						
Larvae	2.8% nitrite-curing salt (99.5% NaCl, 0.5% $NaNO_2$); initial larva count 1090/g	Examination of digested larvae and bioassay (mice)	Larvae lose motility between days 7–10; no larvae recovered from mice fed with salami ripened for 10 or more days (a_W ca. 0.942; pH 5.4)	n.s.	Raw pork sausage	Lötzsch and Rödel (1974)
	2.8% nitrite-curing salt; initial larva count 530/g		Larvae lose motility between days 4–7; no larvae recovered from mice fed with cervelat ripened for 10 or more days (a_W ca. 0.932; pH 5.4)			
	2.8% nitrite-curing salt; initial larva count 200/g		Kills *T. spiralis* larvae in 55–75 mm diameter salami ripened for 6 days (a_W ca. 0.931/0.944; pH 5.7/5.4			
	2.8% nitrite-curing salt; initial larva count 200/g		Kills *T. spiralis* larvae in 55–75 mm diameter cervelat ripened for 7–9 days (a_W ca. 0.948; pH 5.4/5.2)			
	2.8% nitrite-curing salt; initial larva count 800/g		Kills *T. spiralis* larvae in 75 mm diameter Mailänder Salami ripened for 11 days (a_W ca. 0.939; pH 5.1)			
	≥1.3% NaCl; pH 4.6; initial larva count 181 - 447/g		Kills *T. spiralis* larvae in 8 days (a_w 0.935–0.961)		Cured pork sausage	Hill et al. (2017)
	≥1.3% but < 1.8% NaCl; 4.6 < pH ≤ 5.2; initial larva count 386–390/g		Kills *T. spiralis* larvae in 11 days (a_w 0.965)			
	≥1.8% but < 2.8% NaCl; 4.6 < pH ≤ 5.2; initial larva count 181–447/g		Kills *T. spiralis* larvae in 9 days (a_w 0.943–0.961)			
	≥2.8% NaCl; 4.6 < pH ≤ 5.2; initial larva count 322 -323		Kills *T. spiralis* larvae in 8 days (a_w 0.935–0.945)			
	storage at 10 °C; initial larva count 400–700/g		Kills *T. spiralis* larvae in dry-cured ham in 21 (aW 0,948; pH 5.5) to 57 (a_W 0.922; pH 5.6) days, according to ham type		Dry ham	Lötzsch and Leistner (1979)
	6% NaCl cure, then storage at 10 °C; total 75 days; 8.5 kg initial ham weight; initial larva count 390–440/g		Infective in rat bioassay		Dry ham	Lin et al., 1990a; Lin et al., 1990b
	6% NaCl cure, then storage at 10 °C; total 90 days; 8.5 kg initial ham weight; initial larva count 390–440/g		Kills *T. spiralis* larvae			
	6% NaCl cure, then storage at 10 °C; total 90 days; 11.1 kg initial ham weight; initial larva count 380–525/g				Dry ham	
	6% NaCl cure, then storage at 23.9 °C; total 5 days; 11.1 kg initial ham weight; initial larva count 380–525/g					
	4.4% NaCl cure, storage at 23.9 °C; total 23 days; 11.1 kg initial ham weight; initial larva count 600/g				Bag-cured ham	
Toxoplasma gondii						
Tissue cysts	2% NaCl	Bioassay (mice)	Viable at day 8	n.s.	Muscle from mice in tissue culture medium	Lötzsch and Rödel (1974)
	2.5% and 3% NaCl		Inactivation within one day			
	2.5% nitrite-curing salt		Inactivation within 4 days			
	2% NaCl or 1.4% sodium- or potassium lactate in the loin; 7 days	Bioassay (cats)	Inactivation of tissue cysts		Pork loin	Hill et al., 204
	3–5% NaCl; 64 h	Bioassay (mice)	Inactivation of tissue cysts		Mutton meat	Lunden and Uggla (1992)
	4.2–6.2% NaCl; 12, 14 and 16 months		Inactivation of tissue cysts		Parma ham	Genchi et al. (2017)

(3 larvae per gram), kept at −35 °C for one week, caused clinical trichinellosis in six people (Gari-Toussaint et al., 2005). Moreover, *Trichinella nativa,* associated with human trichinellosis after consumption of walrus meat or bear meat, was found to be infective by bioassay after naturally infected walrus or bear meat was stored frozen at −20 °C for up to 20 months. In contrast, *T. nativa* muscle larvae in experimentally infected pig meat were inactivated by freezing for 106 h at −17.7 °C (0 °F), as determined by mouse bioassay (Table 2).

Toxoplasma gondii in pork, mutton, and other meat is completely inactivated by freezing at between −7 and −13 °C for 2–4 days (Table 2). After freezing at −2 °C for 24 h, *Sarcocystis levinei* tissue cysts in buffalo meat remained infective to dogs, but freezing of beef, buffalo, and pork at −4 to −20 °C for 2–4 days renders *Sarcocystis* spp. tissue cysts inactive (Table 2).

Parasites such as *C. parvum* and *Cyclospora cayetanensis* may play a role as foodborne pathogens through faecal contamination of milk and other dairy products. Oocysts of these protozoan parasite species have been spiked into dairy products to evaluate their freeze inactivation, mimicking ice cream production. Freezing at −15 °C for 2 days inactivated oocysts of both *C. parvum* and *Cyclospora cayetanensis* in milk matrices (Table 2).

More work is needed to evaluate techniques such as rapid chilling to very low temperatures, which is commonly used in food processing industries.

6.3. Enzymatic and chemical preservation

Parasites in FoAO do not grow during storage, but they are able to survive for days to weeks under cold storage conditions (> 0 °C) in meat or fish flesh (Hamed & Elias, 1970; Fan, Ma, Kuo, & Chung, 1998; Neumayerová et al., 2014). This means that production of ready-to-eat-foods from animal origin at the production plant must ensure parasite absence or inactivation. Some traditionally applied food-processing techniques, such as marination, fermentation, smoking etc., have parasite-inactivating potential, often as a result of a combination of several mechanisms, occasionally acting synergistically. Table 3 gives an overview of the effects of enzymatic and chemical inactivation of foodborne parasites in meat and fish products. Both drying and addition of salt reduce the amount of available water and increase osmotic pressure, which is detrimental for all living cells. Marination can be defined as treatment of meat or fish with brines containing salt, organic acids, and, occasionally, essential oils. Fermentation is an enzyme-driven breakdown of the main constituents of flesh, most notably degradation of carbohydrates to lactic acid. The resultant acidification and oxygen consumption have major immediate effects (Ockerman & Basu, 2017).

Marination of fish is a traditional processing method with some effect on nematode larvae. As regards composition of brine, ranges in NaCl and acetic acid of 5–20%, and 2.6–40%, respectively, have been studied (Table 3). With increasing salt concentrations, time to inactivation decreases (AESAN, 2007; CEVPM, 2005; Karl, 1998; Karl, Roepstorff, Huss, & Bloemsma, 1994), but is still in the range of more than one week. In herring, an NaCl content of 20% in the fish tissue water phase resulted in a 1 log reduction in *Anisakis* larvae motility within 14 days, and a > 2 log reduction in 28 days (Karl & Leinemann, 1989). In contrast, when the fish tissue water phase contained 15% NaCl, the reduction was less than 1 log after 21 days. In cod, a combination of brine salting (13% NaCl) at 5 °C for 24 h, in combination with dry-salting for another 14 days, inactivated *Anisakis* larvae (Smaldone, Marrone, Palma, Sarnelli, & Anastasio, 2017).

Even for dry-salted herring, 20 days of storage is recommended in order to ensure inactivation of *Anisakis* larvae (CEVPM, 2005). For dry-salted anchovies, 15 days of storage inactivated *Anisakis pegreffii* at a salt concentration of 21% in the anchovies fillets (Anastasio et al., 2016). Also Marination in vinegar (6% acetic acid) for 4–24 h is considered insufficient to inactivate larvae (AESAN, 2007), and recommended procedures comprise marinating for 31 days in brine with 2.5% NaCl and 6% acetic acid or 6% NaCl and 12% acetic acid for 13 days.

Essential oils have proven antibacterial properties, and there is evidence that such substances can inactivate parasites. Giarratana, Muscolino, Beninati, Giuffrida, and Panebianco (2014) were able to inactivate third stage larvae of *Anisakis* in 5 and 10% solutions of essential oils of *Thyme vulgaris* (containing mostly thymol, linalool and pinens) in sunflower seed oil with 14 and 7 h, respectively (Giarratana et al., 2014). Anisakis L3 larvae were inactivated after 2 h in 1% and 5% solutions of essential oils of *Tagetes minuta* (containing mostly β-ocimene, limonine and (Z)-tagetone) in saline solution, and after 4 h in 0.1–5% essential oil in an industrial marinating solution (water and vinegar 1:1, with 3% NaCl and 1% citric acid), but not in sunflower oil (Giarratana et al., 2017). Inactivation was assessed by motility and electron-microscopic observation of structural damages of the cutis in both studies. Even when this anti-*Anisakis* effect might be delayed in a fish flesh matrix, there should be ample time during the time periods of food distribution and display in the shelves before it reaches the consumer.

Inactivation of *Clonorchis sinensis* metacercariae in heavily-salted freshwater fish (3 g NaCl/10 g fish) at 6 °C took at least 8 days (Fan, 1998). Inactivation of *Opisthorchis* metacercariae in fish flesh salted with 13.6% NaCl was observed after 24 h (Kruatrachue, Chitramvong, Upatham, Vichasri, & Viyanant, 1982), whereas 20% NaCl for 5 h was less effective (Tesana, 1986). In fermented fish, inactivation was influenced by the duration of both cold storage of the fish and the fermentation time (Onsurathum et al., 2016). As could be expected, among the traditional salted fish products in Thailand, those salted and stored for 2–3 months (Sithithaworn & Haswell-Elkins, 2003) have the least risk to contain viable metacercariae.

Due to the highly variable conditions for above described methods to inactivate parasites in fish, EU Regulation (EC) 853/2004 and its amendment (EC) 1276/2011 demand that fishery products intended for raw consumption, cold smoking preparation (< 60 °C), or processing by marinating and/or salting, must be frozen at −20 °C in all parts of the product for at least 24 h or at −35 °C for at least 15 h to inactivate other parasites than trematodes (European-Commission, 2004, 2011). As shown in section 6.2 and Table 2, trematodes require exposure to freezing during longer time periods for complete inactivation.

For *Trichinella*, most studies refer to *T. spiralis*, although other species might occur in meat. Zimmermann (1971) studied salt content, drying time and temperature and concluded that 28 days curing with 40 g NaCl/kg, plus re-salting at day 14, followed by 7 days drying at 37 °C or above would render *Trichinella* larvae non-infectious (bioassay in mice). The procedure was not safe when drying was performed at room temperature. Lin et al. (1990b) studied *Trichinella* survival in dry- (hind legs of 8.5–11.1 kg initial weight) and bag-cured (11.1 kg initial weight) hams. Pork contained 300–525 larvae/g. The dry curing process included covering the ham with a cure mix (40 g NaCl/kg ham and additional 20 g NaCl/kg at day 10) for 28–39 days (according to ham weight) at 2.2 °C, followed by rinsing and an equalisation period to allow even distribution of salt in the muscle, whereas for bag curing, hams with 11.1 kg weight were salted with 44 g NaCl/kg and then stored in wrapped condition (Lin et al., 1990a). Dry hams were stored at 10–32.2 °C for up to 90–11 days; storage at 10 °C was only effective after 90 days, whereas this was considerably shorter when hams were stored at 23.9 °C (Table 3).

European dry ham production generally relies on low aging temperatures. In a German study, pork with 400–700 larvae/g was cured by injection or immersion and stored at 10 °C (Lötzsch & Leistner, 1979); depending on the type of ham, no infectivity was demonstrated in mouse bioassay at day 10 of storage (a_W 0,904; pH 5.6) or day 29 (a_W 0.921; pH 5.6). The time to loss of infectivity of *T. spiralis* in fermented sausages made with 2.8% nitrite curing salt and 0.5% sugar, ranged from 6 to 14 days with NaCl content from 3.2 to 3.8% in the finished

products (Table 3). Since inactivation was observed at a_W of 0.93–0.95 for fermented sausages and 0.90–0.92 for dried hams, it was suggested that a_W of 0.90 and 0.87 could be used as threshold levels for fermented sausage and dried hams, respectively (Lötzsch & Leistner, 1979).

The United States Department of Agriculture (USDA) requires that cured pork products are produced with pork that tested negative for *Trichinella* muscle larvae at meat inspection, or have been produced according to validated procedures (Hill et al., 2017). To determine *Trichinella* muscle larva inactivation in cured ready-to-eat dry type sausage, Hill et al. (2017) performed a validation study monitoring five parameters during curing: salt/brine concentration, a_w, pH, temperature and time, using experimentally *Trichinella* infected pork for the production of batter. In their experiments, pH ranged 4.6–5.2 and salt varied between 1.3% and 2.8%. Loss of infectivity of *T. spiralis* in fermented sausages was determined by mouse bioassay after 0–11 days. From these experiments, key conditions could be defined for the production of cured dry sausages that simultaneously inactivated *T. spirals* muscle larvae. These included NaCl concentrations > 1.3% and fermentation to pH ≤ 5.2 for complete *T. spiralis* inactivation after 7–10 days post-stuffing (Hill et al., 2017, Table 3). However, there are also raw sausages with no fermentation or only short-term fermentation, such as “Teewurst” or “Mettwurst” types. For Teewurst sausages (2.8% nitrite-curing-salt) containing 950 larvae/g, 21 days of ripening were required for loss of infectivity (bioassay in mice), corresponding to a_W of around 0.949 and pH of 5.3 (Lötzsch & Rödel, 1974), whereas in the same product with 200 larvae/g, 14 days of ripening (a_w ca. 0.944; pH 5.3) were sufficient. Nöckler and Kolb (2000) studied larval survival in sausage batter starter culture manufactured with lower content of nitrite-curing-salt (2%). The number of viable larvae decreased markedly between the 4th and 7th day after manufacture. Loss of motility of digested larvae and of infectivity in mice were observed from the 9th day onwards. Although these studies indicate that Teewurst sausages with respect to *Trichinella* would be a safe product after 9–14 days of storage, such products are usually placed on the market and consumed before this period. In sum, a_W of 0.92 is reported as the limit for survival of *Trichinella* larvae (species not specified), which corresponds to dry, rather than semi-dry to fresh, fermented sausages (Ockerman & Basu, 2017). Control of this parasite for fermented meats can also be achieved by the use of industrially deep-frozen meat for production or from pig production systems of adequate biosecurity level to ensure a lack of *Trichinella* in the pork.

Rodriguez-Canul et al. (2002) reported inactivation of *Taenia solium* cysts in pork salted with 70–105 g/kg and left overnight at ca. 30 °C. The authors observed structural changes in the cyst and inability of the scolex to evaginate. They attributed this inactivation to changes in osmotic pressure rather than to the pH decline from about 6.0 to 5.3. For cysts of *T. saginata* in beef, a water activity of 0.98 is regarded as the limit for survival (Ockerman & Basu, 2017).

Protozoan parasite stages in meat and fish flesh are sensitive to salt concentration. *Toxoplasma* tissue cysts in muscle of mice were inactivated within 1 day at 2.5% NaCl (Pott et al., 2013). Nitrite-curing salt (99.5% NaCl with 0.5% $NaNO_2$) proved more effective than NaCl alone. In contrast, *Toxoplasma* tissue cysts have a high pH tolerance: at lower pH (pH 5 and 6 compared to pH 7), infectivity was not reduced with exposure for 24–26 days at 4 °C. This finding was regarded as relevant, not only for fresh meats, but also for fermented meats where the pH can be around 5.0. In cured-dried and cured-cooked meats, the pH is typically at 6 or above, but the infectivity of tissue cysts in loin has been demonstrated to decrease rapidly with exposure to 2% NaCl. *Toxoplasma* tissue cysts in pork loin that was injected with brine to give 2% NaCl or 1.4% sodium- or potassium lactate (injection volume 10% of loin weight) followed by storage for 7 days at 4 °C, were not infectious when the pork was fed to cats (Hill, Sreekumar, Gamble, & Dubey, 2004). Moreover, it was shown that inactivation of cysts (assessed via bioassay) in pork loins held at 4 °C with addition of 2% sodium chloride or 1.4% potassium or sodium lactate occurs within the first 8 h after treatment (Hill et al., 2006). In contrast, infectivity of positive controls (infected, but injected with 0.85% NaCl only) was demonstrated at least partially, even after 45 days of storage. Sodium triphosphate and sodium diacetate, both common compounds in meat enhancers, had no effect. A study on processing of mutton (Lunden & Uggla, 1992) indicated that in meat cured for 64 h at 4 °C with 30–50 g sodium chloride and 25–40 g sucrose for 200–360 g of meat, cysts lost infectivity. Also, warm-smoking at above 50 °C for 24–48 h inactivated *Toxoplasma* tissue cysts in brine-injected mutton (as assessed via bioassay in mice). The survival and infectivity of *Toxoplasma* tissue cysts in ham from experimentally infected pigs after the standard curing process required for Parma ham (storage for 12, 14 and 16 months and typical average NaCl contents from 4.2 to 6.2%) was recently assessed (Genchi et al., 2017). Bioassay in mice and *in vitro* culture followed by PCR were used to determine infectivity and viability. None of the mice became infected and the *in vitro* culture/PCR did not provide evidence that the *Toxoplasma* were viable after the curing process (Genchi et al., 2017). Thus, a_w below 0.95 and/or pH below 5.3 are recognized as being detrimental to survival of *Toxoplasma* tissue cysts (Ockerman & Basu, 2017).

7. High pressure and irradiation

With the survival of some parasites under the conditions of traditional inactivation methods for FoAO, such as freezing and curing, there is interest in alternative approaches. However, data are relatively limited, and there is a clear need for further testing.

7.1. High pressure processing (HPP)

High pressure processing (HPP) is a non-thermal processing technique that uses a liquid compression medium and constant pressure to treat vacuum-packaged food products. Typically, a pressure range from 200 to 600 MPa is used. Time, temperature, decompression time and liquid temperature vary, depending on product and food composition. During HPP, pressure is transmitted uniformly and instantly with little variation in temperature, independent of food shape or size (Rendueles et al., 2011). In general, temperature increases approximately 3 °C per 100 MPa pressure increase, depending on food composition.

Table 4 provides an overview of the efficacy of HPP on parasites in fish, meat, and oysters, although only a limited number of parasites has been investigated. *Anisakis* larvae in fish filets were killed at a pressure of 200–300 MPa for 5–10 min at a temperature between 0 and 15 °C using motility as an indicator of larval death. *Cryptosporidium parvum* oocysts have been HPP treated at pressures of 305–550 MPa for ≥ 180 s, which significantly reduced infectivity to mouse pups in a bioassay, but could not totally prevent infection.

Significant inactivation of *T. spiralis* larvae isolated from infected pork using hydrodynamic pressure (Hydrodyne process, method for tenderising meat or fish using explosion induced shock waves in water) has been reported, although the pressure generated (55–60 MPa) did not eliminate the infectivity to mice as determined by bioassay. *Toxoplasma gondii* tissue cysts in ground pork were successfully inactivated using 300–400 MPa for 30 s, whereas 100 and 200 MPa were ineffective (Table 4).

7.2. Electron beam irradiation

Electron beam (E-Beam) is a process used for microbial inactivation that utilizes high-energy electrons, accelerated to close to light speed. The resulting high energies (up to 12 million electron volts) are capable of uniformly penetrating food materials. Foodstuffs are typically placed on pallets for large throughput and the dose received is controlled by manipulating the beam current and the beam scanning length, along with the under-beam conveyor speed (McFadden et al., 2017; Murray et al., 2015).

Collins et al. (2005) examined the efficacy of E-Beam irradiation on the viability of the Beltsville strain *C. parvum* oocysts as artificial contaminants of Eastern Oysters (*Crassostrea virginica*), by feeding E-beam treated oyster tissues to neonatal mice. A dose of 2 kGy completely eliminated *C. parvum* infectivity and did not adversely affect the visual appearance of the oysters (Table 5).

7.3. Gamma irradiation

The inactivation effect of gamma irradiation is quite diverse, as reflected in the huge variation of the observed minimum effective dose (MED) and directly related to the type of parasite, the parasite stage, and food product assayed (Table 5).

The radio resistance of *A. simplex* is high; doses as high as 2–10 kGy, on isolated *Anisakis* larvae in physiological salt produced a reduction in penetration ability and infectivity in rats (up to 70% worm recovery rate), but a dose of 2 kGy was not fully effective to prevent infection in rabbits (up to 25% recovery rate; Chai, Hong, & Lee, 1991). When salted fish products were assayed, similar results were observed; doses as high as 6 kGy were not effective for larvae in salted herring, with substantial numbers surviving the treatment (Table 5).

The radio resistance of trematodes varies depending on parasite species and whether the treatment is applied to meat or another matrix. Metacercariae of *Clonorchis sinensis* were three-fold less susceptible to gamma irradiation when encysted in the flesh of fish than when they were isolated from the fish; i.e. the MED for metacercariae in fish was 0.15 kGy, but 0.02 KGy when metacercariae had been isolated from the fish (Table 5). A similar situation was observed for *Paragonimus westermani;* the MED for metacercariae in crab was 25 times higher than that for metacercariae isolated from the crustacean (2.5 kGy vs 0.1 kGy). Thus, the higher dose is required for practical application. However, identical MED (0.1 kGy) were required for inactivating *Opisthorchis viverrini* metacercariae in fish or after isolation from fish (Table 5).

The MED needed to inactivate *Trichinella* in heavily contaminated pork carcasses is 0.3 kGy (Table 5). The US FDA approved irradiation for the control of *T. spiralis* in pork under Regulation 21 CFR 179 in 1985, allowing treatments of 0.3 kGy as minimum and 1 kGy as maximum.

The MED for *Taenia saginata* cysticerci in beef varied significantly, ranging from 3.7 to 6.5 kGy. Doses of 0.2–0.6 KGy on *Taenia solium* cysticerci produce an irreversible effect on the development of the adult worms, affecting the viability of the cells in the neck region (Table 5).

Studies of inactivation of *T. gondii* by gamma irradiation in meat demonstrated that intermediate irradiation doses (0.1–1 kGy) significantly reduce the infectivity of bradyzoites and tissue cysts in pork products. However, differences in radio resistance between *T. gondii* strains have been observed, with MEDs ranging from 0.4 to 0.7 kGy (Table 5).

8. Future perspectives

Bioassay is regarded the gold standard for evaluation of treatment efficacy of parasites in food. However, 65% of the people questioned in a 2016 UK survey accepted the use of experimental animals for medical research, but, at the same time, 35% of respondents think that experimental animal use should be banned on animal welfare grounds and 75% agreed that more needs to be done to search for alternatives to experimental animal use (Clemens & Leaman, 2016). Alternative methods to evaluate parasite inactivation include morphological examination of structure integrity, evaluation of movement after mechanical stimulation, or *in vitro* essays to evaluate parasite development into the next life stage. However, sensitivity and specificity of alternative indicators remain to be determined in most cases and more research is needed to evaluate such indicators in comparison with the gold standard. Future efforts to modify and advance treatment methods may benefit from next-generation sequencing (NGS) and bioinformatics regarding (absence of) gene expression, although finding anti-parasitic targets using NGS would be more relevant. Free availability and open access data that come with NGS will improve standardization and harmonization of research efforts.

Although low doses of irradiation were long ago found to be

Table 4
Effects of high pressure and irradiation on foodborne parasites. Control measure: High Pressure Processing.

Transmission stage	Condition	Evaluation method	Effect	Log reduction	Matrix	Ref
Anisakis						
Larvae	140 MPa; 1 h 150 MPa; 30 min 200 MPa; 10 min 170 MPa; 3 x 2 min 180 MPa; 2 x 2 min 190 MPa; 15 min	Motility tests, methylene blue fluorescence	Inactivates Anisakis larvae	Low numbers used; log reductions cannot be calculated	Fish: Nile perch fillet	Molina-Garcia and Sanz (2002)
	100 MPa; 5 min 200 MPa; 5 min 300 MPa; 5 min	Motility test	8% larval inactivation 97% larval inactivation 100% larval inactivation	Low numbers used; log reductions cannot be calculated	Fish: Mackerel filet	Brutti et al. (2010)
Cryptosporidium						
Oocysts	400 MPa; 3 min 370 MPa; 3 min 480 MPa; 3 min 305 MPa; 3 min 550 MPa; ≥3 min	Bioassay (mice)	Reduction of infected mice by 40% 57% 57% 48% ≥65%	Low numbers used; log reductions cannot be calculated	Shellfish: Oysters	Collins et al. (2005)
Trichinella spp.						
Larvae	55–60 MPa	Bioassay (mice)	Does not inactivate *Trichinella spiralis*	n.s.	Pork	Gamble, Solomon, and Long (1998)
Toxoplasma gondii						
Tissue cysts	300 MPa; 30 s 400 MPa; 30 s	Bioassay	Inactivates tissue cysts	n.s.	Meat: Ground pork	Lindsay, Collins, Holliman, Flick, and Dubey (2006)

Table 5
Effects of high pressure and irradiation on foodborne parasites. Control measure: E-beam and gamma irradiation.

Transmission stage	Condition	Evaluation method	Effect	Log reduction	Matrix	Ref
E-BEAM IRRADIATION						
Cryptosporidium parvum						
Oocysts	From 1 to 1.5 kGy	Bioassay (neonatal mice)	No significant reduction in oocyst viability	0.10 (1 KGy) to 0.25 (1.5 KGy)	In shell Oysters	Collins et al. (2005)
	From 1 kGy to 2 KGy		Infectivity reduction from 47 to 57% (1 KGy) to 100% (2 kGy)	0.32 (1 KGy) to 1.78 (2 KGy)	Oysters (in shell and shucked)	
GAMMA IRRADIATION						
Anisakis simplex						
Larvae	3–6 kGy	Visual inspection	6 kGy: reduction on the number of larvae but still substantial numbers of nematodes survived	n.s.	Fish: salted herring	Van Mameren and Houwing (1968)
Clonorchis sinensis						
Metacercariae	0.01–0.20 kGy (^{137}Cs; ^{60}Co)	Bioassay (albino rats, guinea pigs)	MED was 0.15 kGy; complete control of the infectivity. The LD_{50} was established at 0.05 kGy	n.s.	Fish	Chai et al., 1991; Lee, Park, Sohn, Hong, & Chai, 1989
Opisthorchis viverrini						
Metacercariae	0.05–0.1 kGy (^{60}Co)	Bioassay (hamsters, rabbits, cats)	MED: 0.1 kGy	n.s.	Fish	Sornami, Impand, and Bundisting (1993)
Paragonimus westermani						
Metacercariae	0.05–0.1 kGy (60Co)	Bioassay (albino mice)	MED: 2.5 kGy		Crab (Potamon spp.)	Song, Duan, et al. (1993)
Trichinella spp.						
Larvae	0.1–0.8 kGy (^{60}Co, ^{137}CS)	Bioassay (rats)	MED: 0.5 kGy 0.15–0.3 kGy block production of larval progeny 0.3–0.6 kGy inactivates Trichinella larvae	n.s.	Pork	Brake et al., 1985; Kasprzak et al., 1993; Murrell & Dubey, 1991
Taenia spp.						
Cysticerci	1–6 kGy (^{137}Co)	Bioassay (gerbils)	MED: 3.7 KGy; total inactivation of Taenia saginata	n.s.	Meat	Alabay, Emre, Çerçi, Ersen, and Mutluer (1993)
	0.2–0.6 kGy (^{60}Co)	Bioassay (Human volunteers)	MED: 0.5 kGy		Cooked meat previously frozen	Geerts, De Borchgrave, Brandt, and Kumar (1993)
	0.2–1.40 kGy	Bioassay (golden hamsters)	MED: 0.60 kGy Taenia solium		Pork meat	Verster, Du Plessis, and Van Den Heever (1976)
	0.5–11 kGy (^{60}Co)	Bioassay (golden hamsters)	MED: 6.5 kGy Taenia solium 0.5–0.7 kGy does not kill cysticerci but inhibits infection		Pork meat	De Aluja, Nunez, and Villalobos (1993)
Toxoplasma gondii						
Tissue cysts	0.1–1 kGy (^{60}Co)	Bioassay (NIH mice)	MED: 0.55 kGy Elimination of infection	n.s.	Pork products	Song et al., 1993; Murrell & Dubey, 1993
	0.1–0.5 kGy (^{137}Cs, ^{60}Co)	Bioassay (cat)	MED: 0.5 kGy At 0.25 kGy: elimination of infection in cats, at 0.4 kGy 10,000-fold reduction of infectivity in mice and cat; 0.5 kGy no detectable infective Toxoplasma in mice		Pork	Dubey, Brake, Murrell, and Fayer (1986)
	0.4–0.7 kGy (^{60}Co)	Bioassay (cats, mice)	Complete inactivation depending on T. gondii isolate			Wikerhauser, Kuticic, Razem, Orsanic, and Besvir (1993)
	0.1–1 kGy (^{60}Co)	Bioassay (NIH mice)	MED: 0.55 kGy Elimination of infection	n.s.	Pork products	Song et al., 1993; Murrell & Dubey, 1993

effective at inactivating at least seven genera of parasites, this methodology has barely been considered for use in controlling foodborne parasites in FoAO. This is partly due to considerable controversy concerning the safety of irradiated food. Fierce opposition against the use of irradiation from consumer groups in Europe is often based on old information and plays on consumer fear (Roberts, 2014). Although irradiation is increasingly used for treatment of various foods globally, its use in the European Union is limited and even decreasing; strict legislation only permits irradiation treatment of dried herbs and frog legs (Feliciano, 2018).

E-beam is a potential methodology that circumvents the need of radioactive isotopes, but E-beam electrons have a limited penetration depth of, at most, 5 cm, considerably below that of X-rays (penetration depth 60–400 cm, depending on the energy used) (Collins, Flick, Smith, Fayer, Rubendall, et al., 2005). However, this limited penetration has been proven appropriate for some foods (e.g. oysters). E-beam irradiation doses ≥2.0 kGy may be used in commercial processes, but irradiation at 2 kGy changes meat tenderization, colour, and flavour (Yim et al., 2015). In industrialized regions especially, such as the US and Europe, a trend towards more critical consumer attitudes regarding sustainability of food products and production methods is ongoing, with increasing demands for freshness and “naturalness” of foods, thereby excluding additives and human intervention (e.g. irradiation, but also freezing) (Román, Sánchez-Siles, & Siegrist, 2017). This calls for better communication and more research to investigate and improve irradiation technologies. Using sustainable energy sources may improve public acceptance of irradiation treatment of foods. Indeed, evaluation of electrical equipment to generate E-beam and X-ray irradiation to replace Cobalt-60 use for irradiation of foods is ongoing (Feliciano, 2018).

High pressure processing (300 MPa for 0.5–5 min) may be used to inactivate Anisakidae larvae in fish and *Toxoplasma* tissue cysts in (minced) meat, but *Cryptosporidium* oocysts in oysters appear to be highly resistant to HPP. Also here, more research is needed to evaluate applicability of HPP to inactivate parasites in FoAO.

Research on foodborne parasites should be improved towards standardization of experimental approaches to evaluate inactivation methods, but also towards standardization of methods to monitor inactivation. Literature data are diverse and are currently generally insufficient for modelling survival as a response to treatment. Although inactivation effects vary considerably between parasites and methods, modelling may help to determine minimal effective treatment parameters to ensure food safety for FoAO.

9. Conclusions

Based on our extensive literature review, information on the effects of different inactivation techniques on 12 most relevant parasites in FoAO has been assimilated. The efficacy of time-temperature combinations for freezing and heating procedures is influenced by parasite species and developmental stage, but, in general, heating to 60–75 °C for 15–30 min or freezing at −21 °C for 1–7 days inactivates parasites in meat or fish, as determined using bioassays. USDA recommends heating meat at a core temperature of 62.8–73.9 °C or freezing at −18 °C to inactivate parasites in meat or fish, but freezing cannot be relied upon for total inactivation in home situations. Industrial pasteurization of fluids (15 sec 71.7 °C) or fish and crabs (175–65 min 85–92.2 °C) is effective for control of parasites in milk and in fish.

Meat- and fishborne parasitic stages are generally sensitive to NaCl contents of 2–5%, associated with higher osmotic stress and often augmented by lowering pH (fermentation or organic acids). Literature on high pressure treatment and E-beam to inactivate parasites in animal origin matrices is scant. The minimal effective dose for gamma radiation ranges > 0.1–0.5 kGy for fish parasites except *Anisakis* (10 kGy) and > 0.4–6.5 kGy for meatborne parasites. Literature data are currently insufficient for modelling survival as response to treatment.

This assimilation of data clearly shows that research on foodborne parasites should be improved, and efforts should be directed towards sustainable novel inactivation methods for parasites in FoAO and standardization of experimental approaches for the evaluation of inactivation methods.

Declaration of interests

The authors declare that they have no conflict of interests.

Acknowledgements

This work was performed in collaboration within the framework of the European Network for Foodborne Parasites in Europe (EURO-FBP), COST Action FA 1408.

References

Abdussalam, M., Käferstein, F. K., & Mott, K. E. (1995). Food safety measures for the control of foodborne trematode infections. *Food Control, 6*(2), 71–79. https://doi.org/10.1016/0956-7135(95)98910-S.

Adams, A. M., Miller, K. S., Wekell, M. M., & Dong, F. M. (1999). Survival of *Anisakis simplex* in microwave-processed arrowtooth flounder (*Atheresthes stomias*). *Journal of Food Protection, 62*(4), 403–409.

AESAN (2007). Sobre medidas para reducir el riesgo asociado a la presencia de Anisakis. *Informe del Comité Científico de la Agencia Española de Seguridad Alimentaria y Nutrición (AESAN)*.

Alabay, B. M., Emre, Z., Çerçi, H., Ersen, S., & Mutluer, B. (1993). Inhibition of viability and infectivity of *Cysticercus bovis* by irradiation of meat. In: *Proc. Final research coordination meeting on use of irradiation to control infectivity of food-borne parasites, Mexico city* (pp. 15–22). Vienna: (IAEA).

Anastasio, A., Smaldone, G., Cacace, D., Marrone, R., Lo Voi, A., Santoro, M., et al. (2016). Inactivation of Anisakis pegreffii larvae in anchovies (Engraulis encrasicolus) by salting and quality assessment of finished product. *Food Control, 64*, 115–119.

Arcangeli, G., Galuppi, A., Bicchieri, M., Gamberini, R., & Presicce, M. (1996). Prove sperimentali sulla vitalità di larve del genere *Anisakis* in semiconserve ittiche. *Industria Conserve, 71*, 502–507.

Armignacco, O., Caterini, L., Marucci, G., Ferri, F., Bernardini, G., Raponi, G. N., et al. (2008). Human illnesses caused by Opisthorchis felineus flukes, Italy. *Emerging Infectious Diseases, 14*(12), 1902–1905. https://dx.doi.org/10.3201/eid1412.080782.

Bier, J. W. (1976). Experimental anisakiasis: Cultivation and temperature tolerance determinations. *Journal of Milk and Food Technology, 39*, 132–137.

Blackburn, C., & McClure, P. J. (2009). Foodborne pathogens: Hazards, risk analysis and control. *Foodborne pathogens: Hazards, risk analysis and control*(2nd ed.). Elsevier.

Bouwknegt, M., Devleesschauwer, B., Graham, H., Robertson, L. J., van der Giessen, J. W. B., & the Euro-FBP workshop participants (2018). Prioritization of food-borne parasites in Europe, 2016. *Euro Surveillance, 23*(9).

Brake, R. J., Murrell, K. D., Ray, E. E., Thomas, J. D., Muggenburg, B. A., & Sivinski, J. S. (1985). Destruction of *Trichinella spiralis* by low dose irradiation of infected pork. *Journal of Food Safety, 7*, 127–143.

Brutti, A., Rovere, P., Cavallero, S., D'Amelio, S., Danesi, P., & Arcangeli, C. (2010). Inactivation of Anisakis simplex larvae in raw fish using high hydrostatic pressure treatments. *Food Control, 21*, 331–333.

Cammilleri, G., Costa, A., Graci, S., Buscemi, M. D., Collura, R., Vella, A., et al. (2018). Presence of *Anisakis pegreffi* in farmed sea bass (*Dicentrarchus labrax* L.) commercialized in southern Italy: A first report. *Veterinary Parasitology, 259*, 13–16.

Carlin, A., Mott, C., Cash, D., & Zimmermann, W. (1969). Destruction of *Trichinella* larvae in cooked pork roasts. *Journal of Food Science, 34*, 210–212.

CEVPM (2005). *Etude des conditions de destruction des larves d'Anisakis simplex dans le hareng salé au sel sec destiné à la fabrication de harengs saurs traditionnels.* Centre d'Expérimentation et de valorisation des Produits de la Mer.

Chai, J., Hong, S., & Lee, S. (1991). Effects of gamma irradiation on the survival and development of Clonorchis sinensis metacercariae. *Final FAO/IAEA research Co-ordination meeting on use of irradiation to control infectivity of food-borne parasites* (pp. 33–41). Vienna: IAEA.

Clemens, M., & Leaman, J. (2016). *Public attitudes to animal research in 2016.* Department for Business, Energy & Industrial Strategy and Ipsos MORI Social Research Institutehttps://www.ipsos.com/sites/default/files/publication/1970-01/sri-public-attitudes-to-animal-research-2016.pdf.

Collins, M. V., Flick, G. J., Smith, S. A., Fayer, R., Croonenberghs, R., O'Keefe, S., et al. (2005a). The effect of high-pressure processing on infectivity of *Cryptosporidium parvum* oocysts recovered from experimentally exposed Eastern oysters (*Crassostrea virginica*). *The Journal of Eukaryotic Microbiology, 52*(6), 500–504. https://doi.org/10.1111/j.1550-7408.2005.00059.x.

Collins, M. V., Flick, G. J., Smith, S. A., Fayer, R., Rubendall, E., & Lindsay, D. S. (2005b). The effects of E-beam irradiation and microwave energy on Eastern Oysters (*Crassostrea virginica*) experimentally infected with *Cryptosporidium parvum*. *The Journal of Eukaryotic Microbiology, 52*(6), 484–488. https://doi.org/10.1111/j.1550-7408.2005.00056.x.

Da Silva Felicio, M. T., Hald, T., Liebana, E., Allende, A., Hugas, M., Nguyen-The, C., et al.

(2015). Risk ranking of pathogens in ready-to-eat unprocessed foods of non-animal origin (FoNAO) in the EU: Initial evaluation using outbreak data (2007-2011). *International Journal of Food Microbiology, 195*, 9–19. https://doi.org/10.1016/j.ijfoodmicro.2014.11.005.

De Aluja, A. S., Nunez, F., & Villalobos, A. N. M. (1993). Use of gamma irradiation to prevent infectivity of metacestodes of *Taenia solium* in pork. In: *Proc. Final research co-ordination meeting on use of irradiation to control infectivity of food-borne parasites, Mexico city 24–28 June 1991* (pp. 23–32). Vienna: IAEA.

Deardorff, T. L., & Throm, R. (1988). Commercial blast-freezing of third-stage *Anisakis simplex* larvae encapsulated in salmon and rockfish. *The Journal of Parasitology, 74*(4), 600–603.

Deng, M. Q., & Cliver, D. O. (1999). *Cryptosporidium parvum* studies with dairy products. *International Journal of Food Microbiology, 46*(2), 113–121. https://doi.org/10.1016/S0168-1605(98)00187-1.

Dorny, P., Praet, N., Deckers, N., & Gabriel, S. (2009). Emerging food-borne parasites. *Veterinary Parasitology, 163*, 196–206.

Doyle, M. E. (2003). *Foodborne parasites - a review of the scientific literature.* Madison: FRI Briefings - Food research institute - University of Wisconsin.

Dubey, J. (1988). Long-term persistence of *Toxoplasma gondii* in tissues of pigs inoculated with *T. gondii* oocysts and effect of freezing on viability of tissue cysts in pork. *American Journal of Veterinary Research, 49*(6), 910–913.

Dubey, J. P., Brake, R. J., Murrell, K. D., & Fayer, R. (1986). Effect of irradiation on the viability of *Toxoplasma gondii* cysts in tissues of mice and pigs. *American Journal of Veterinary Research, 47*(3), 518–522.

Dubey, J. P., Kotula, A. W., Sharar, A., Andrews, C. D., & Lindsay, D. S. (1990). Effect of high temperature on infectivity of *Toxoplasma gondii* tissue cysts in pork. *The Journal of Parasitology, 76*(2), 201–204.

EFSA (2010). Opinion of the scientific panel on biological hazards on"Risk assessment of parasites in fishery products. *EFSA Journal, 8*(4), 1543.

European-Commission (2004). Regulation (EC) No 853/2004 of the European parliament and of the Council of 29 April 2004 laying down specific hygiene rules for on the hygiene of foodstuffs. *Official Journal of the European Union, 139*, 55–205.

European-Commission (2011). COMMISSION REGULATION (EU) No 1276/2011 of 8 December 2011 amending Annex III to Regulation (EC) No 853/2004 of the European Parliament and of the Council as regards the treatment to kill viable parasites in fishery products for human consumption. *Official Journal of the European Union, 327*, 39–41.

European-Commission (2015). Commission Regulation (EC) No 2015/1375 of 10 august 2015 laying down specific rules for *Trichinella* in meat. *Official Journal of the European Union, 212*, 7–34.

Fan, P. C. (1998). Viability of metacercariae of *Clonorchis sinensis* in frozen or salted freshwater fish. *International Journal for Parasitology, 28*(4), 603–605. https://doi.org/10.1016/S0020-7519(97)00215-4.

Fan, P. C., Ma, Y. X., Kuo, C. H., & Chung, W. C. (1998). Survival of *Taenia solium* cysticerci in carcasses of pigs kept at 4 C. *The Journal of Parasitology, 84*(1), 174–175.

FAO/WHO (2014). *Multicriteria-based ranking for risk management of food-borne parasites. [Food and agriculture organization of the united nations/world health organization] - microbiological risk assessment series, N° 23 rome*.

FAO/WHO (2016). Guidelines on the application of general principles of food hygiene to the control of foodborne parasites. *Codex Alimentarius* CAC/GL 88-2016.

Fattakhov, R. G. (1989). Low-temperature regimens for the decontamination of fish of the larvae of *Opisthorchis*. *Med Parazitol (Mosk)*, (5), 63–64.

FDA, U. (2012). *Handbook of foodborne pathogenic microorganisms and natural toxins* (2nd ed.). Bad Bug Book (online).

Feliciano, C. P. (2018). High-dose irradiated food: Current progress, applications and prospects. *Radiation Physics and Chemistry, 144*, 34–36.

Franssen, F., Deng, H., Swart, A., Bonacic Marinovic, A., Liu, X., Liu, M., et al. (2018). Inactivation of Trichinella muscle larvae at different time-temperature heating profiles. *Food Microbiology* (submitted for publication).

Gajadhar, A. A. E. (2015). *Foodborne parasites in the food supply web: Occurrence and control.* Woodhead Publishing.

Gamble, H. R., Solomon, M. B., & Long, J. B. (1998). Effects of hydrodynamic pressure on the viability of *Trichinella spiralis* in pork. *Journal of Food Protection, 61*(5), 637–639.

Gari-Toussaint, M., Tieulie, N., Baldin, J., Dupouy-Camet, J., Delaunay, P., Fuzibet, J. G., et al. (2005). Human trichinellosis due to *Trichinella britovi* in southern France after consumption of frozen wild boar meat. *Euro Surveillance, 10*(6), 117–118 550 [pii].

Geerts, S., De Borchgrave, J., Brandt, J., & Kumar, V. (1993). Susceptibility of *Taenia saginata* metacestodes to gamma irradiation and shelf-life extension of the treated meat. In: *Proc. Final research co-ordination meeting on use of irradiation to control infectivity of food-borne parasites, Mexico city 24–28 June 1991* (pp. 49–54). Vienna: (IAEA).

Genchi, M., Vismarra, A., Mangia, C., Faccini, S., Vicari, N., Rigamonti, S., et al. (2017). Lack of viable parasites in cured 'Parma Ham' (PDO), following experimental *Toxoplasma gondii* infection of pigs. *Food Microbiology, 66*, 157–164. https://doi.org/10.1016/j.fm.2017.04.007.

Gestrich, R., & Heydorn, A. O. (1974). Studies on the survival time of *Sarcocystis* in the meat of slaughter animals. *Berliner und Münchener Tierärztliche Wochenschrift, 87*(24), 475–476.

Giarratana, F., Muscolino, D., Beninati, C., Giuffrida, A., & Panebianco, A. (2014). Activity of *Thymus vulgaris* essential oil against Anisakis larvae. *Experimental Parasitology, 142*, 7–10.

Giarratana, F., Muscolino, D., Ziino, G., Giuffrida, A., Marotta, S. M., Lo Presti, V., et al. (2017). Activity of *Tagetes minuta* Linnaeus (Asteraceae) essential oil against L3 *Anisakis* larvae type 1. *Asian Pacific Journal of Tropical Medicine, 10*(5), 461–465.

Hamed, M. G. E., & Elias, A. N. (1970). Effect of food-processing methods upon survival of the trematode *Heterophyes* sp. in flesh of mullet caught from brackish Egyptian waters. *Journal of Food Science, 35*(4), 386–388.

Harp, J. A., Fayer, R., Pesch, B. A., & Jackson, G. J. (1996). Effect of pasteurization on infectivity of *Cryptosporidium parvum* oocysts in water and milk. *Applied and Environmental Microbiology, 62*(8), 2866–2868.

Hill, D. E., Benedetto, S. M., Coss, C., McCrary, J. L., Fournet, V. M., & Dubey, J. P. (2006). Effects of time and temperature on the viability of *Toxoplasma gondii* tissue cysts in enhanced pork loin. *Journal of Food Protection, 69*(8), 1961–1965.

Hill, D. E., Gamble, H. R., Zarlenga, D. S., Coss, C., & Finnigan, J. (2005). *Trichinella nativa* in a black bear from Plymouth, New Hampshire. *Veterinary Parasitology, 132*, 143–146.

Hill, D. E., Luchansky, J., Porto-Fett, A., Gamble, H. R., Fournet, V. M., Dawkins-Cooper, D. S., et al. (2016). Curing conditions to inactivate *Trichinella spiralis* muscle larvae in ready-to-eat pork sausage. *Food and Waterborne Parasitology*. https://doi.org/10.1016/j.fawpar.2017.06.001.

Hill, D. E., Sreekumar, C., Gamble, H. R., & Dubey, J. P. (2004). Effect of commonly used enhancement solutions on the viability of *Toxoplasma gondii* tissue cysts in pork loin. *Journal of Food Protection, 67*(10), 2230–2233.

Hilwig, R. W., Cramer, J. D., & Forsyth, K. S. (1978). Freezing times and temperatures required to kill cysticerci of *Taenia saginata* in beef. *Veterinary Parasitology, 4*(3), 215–219. https://doi.org/10.1016/0304-4017(78)90048-1.

ICT (2006). *Recommendations on methods for the control of Trichinella in domestic and wild animals intended for human consumption.* ICT (International Commission on Trichinellosis).

Jones, J. L., & Dubey, J. P. (2012). Foodborne toxoplasmosis. *Clinical Infectious Diseases, 55*(6), 845–851. https://doi.org/10.1093/cid/cis508.

Karl, H., Roepstorff, A., Huss, H. H., & Bloemsma, B. (1994). Survival of *Anisakis* larvae in marinated herring fillets. *International Journal of Food Science and Technology, 29*(6), 661–670. https://doi.org/10.1111/j.1365-2621.1994.tb02107.x.

Karl, H., & Leinemann, M. (1989). Survival of nematode larvae at the production of salted herring [In German]. *Archiv für Lebensmittelhygiene, 20*, 104–120.

Karl, H., & Leinemann, M. (1998). Survival of nematode larvae in the production of salted herring (Überlebensfähigkeit von Nematodenlarven bei der Herstellung von gesalzenen Heringserzeugnissen) [In German]. *Archiv für Lebensmittelhygiene, 20*, 104–120.

Kasprzak, W., Pozio, E., Rauhut, W., Nowosad, P., Gustowska, L., & Golinska, Z. (1993). Effect of low dose irradiation on *Trichinella* isolates. In: *Proc. Final research co-ordination meeting on use of irradiation to control infectivity of food-borne parasites, Mexico city 24–28 June 1991* (pp. 55–72). Vienna: (IAEA).

Kotula, A. W., Murrell, K. D., Acosta-Stein, L., Lamb, L., & Douglass, L. (1983a). *Trichinella spiralis*: Effect of high temperature on infectivity in pork. *Experimental Parasitology, 56*(1), 15–19.

Kotula, A. W., Murrell, K. D., Acosta-Stein, L., Lamb, L., & Douglass, L. (1983b). Destruction of *Trichinella spiralis* during cooking. *Journal of Food Science, 48*, 765–768.

Kotula, A. W., Sharar, A. K., Andrews, C. D., Shen, S. K., & Lindsay, D. S. (1991). Effect of freezing on infectivity of *Toxoplasma gondii* tissue cysts in pork. *Journal of Food Protection, 54*(9), 687–690. https://doi.org/10.4315/0362-028X-54.9.687.

Kotula, A. W., Sharar, A. K., Paroczay, E., Gamble, H. R., Murrell, K. D., & Douglass, L. (1990). Infectivity of Trichinella spiralis from frozen pork. *Journal of Food Protection, 53*(7), 571–573.

Kruatrachue, M., Chitramvong, Y. P., Upatham, E. S., Vichasri, S., & Viyanant, V. (1982). Effects of physico-chemical factors on the infection of hamsters by metacercariae of *Opisthorchis viverrini*. *Southeast Asian Journal of Tropical Medicine and Public Health, 13*(4), 614–617.

Kuticic, V., & Wikerhauser, T. (1996). Studies of the effect of various treatments on the viability of *Toxoplasma gondii* tissue cysts and oocysts. *Current Topics in Microbiology and Immunology, 219*, 261–265.

Lacour, S. A., Heckmann, A., Mace, P., Grasset-Chevillot, A., Zanella, G., Vallee, I., et al. (2013). Freeze-tolerance of *Trichinella* muscle larvae in experimentally infected wild boars. *Veterinary Parasitology, 194*(2–4), 175–178. https://doi.org/10.1016/j.vetpar.2013.01.049.

Lecleir, D., Forbes, L. B., Suppa, S., Proulx, J. F., & Gajadhar, A. A. (2004). A preliminairy investigation of the infectivity of *Trichinella* larvae in traditional preparations of walrus meat. *Parasitology Research, 93*, 507–509. https://doi.org/10.1007/s00436-004-1179-4.

Lee, S. H., Park, Y. H., Sohn, W. M., Hong, S. T., & Chai, J. Y. (1989). The effects of gamma irradiation on the survival and development of *Clonorchis sinensis* metacercariae. *Kisaengch'ung Hak Chapchi, 27*(3), 187–195.

Lindsay, D. S., Collins, M. V., Holliman, D., Flick, G. J., & Dubey, J. P. (2006). Effects of high-pressure processing on *Toxoplasma gondii* tissue cysts in ground pork. *The Journal of Parasitology, 92*(1), 195–196. https://doi.org/10.1645/GE-631R.1.

Lin, K. W., Keeton, J. T., Craig, T. M., Gates, C. E., Gamble, H. R., Custer, C. S., et al. (1990a). Physicochemical composition of dry-cured ham processed under minimal aging time-temperature conditions. *Journal of Food Science, 55*(2), 285–288.

Lin, K. W., Keeton, J. T., Craig, T. M., Huey, R. H., Longnecker, M. T., Gamble, H. R., et al. (1990b). Bioassay analysis of dry-cured ham processed to affect *Trichinella spiralis*. *Journal of Food Science, 55*(2), 289–292.

Lötzsch, R., & Leistner, L. (1979). Survival of *Trichinella spiralis* in raw sausages and raw ham depends on water activity (Aw Value) [Überleben von *Trichinella spiralis* in Rohwurst und Rohschinken in Abhängigkeit von der Wasseraktivität (aW Wert)]. *Fleischwirtschaft, 69*, 231–233.

Lötzsch, R., & Rödel, W. (1974). Evaluation of *Trichinella spiralis* survival in raw sausages in relation to water activity [Untersuchungen über die Lebensfähigkeit von *Trichinella spiralis* in Rohwürsten in Abhängigkeit von der Wasseraktivität]. *Fleischwirtschaft, 64*, 1203–1208.

Lunden, A., & Uggla, A. (1992). Infectivity of *Toxoplasma gondii* in mutton following

curing, smoking, freezing or microwave cooking. *International Journal of Food Microbiology, 15*(3–4), 357–363.
McClelland, G. (2002). The trouble with sealworms (*Pseudoterranova decipiens* species complex, nematoda): A review. *Parasitology, 124*(Suppl), S183–S203.
McFadden, E., Costa-Ramos, A. L., Bradley, D., Vrain, O., McEvoy, B., & Rowan, N. J. (2017). CoMParative studies on the novel sterilisation of Irish retailed infant milk formula using electron beam and pulsed light treatments. *International Journal of Science, Environment and Technology, 12*(6), 4375–4377.
Mo, T. A., Gahr, A., Hansen, H., Hoel, E., Oaland, Ø., & Poppe, T. T. (2014). Presence of Anisakis simplex (rudolphi, 1809 det. Krabbe, 1878) and hysterothylacium aduncum (rudolphi, 1802) (nematoda; anisakidae) in runts of farmed atlantic salmon, Salmo salar *L. Journal of Fish Diseases, 37*(2), 135–140.
Molina-Garcia, A. D., & Sanz, P. D. (2002). *Anisakis simplex* larva killed by high-hydrostatic-pressure processing. *Journal of Food Protection, 65*(2), 383–388.
Murray, K. A., Kennedy, J. E., Barron, V., McEvoy, B., Vrain, O., Ryan, D., et al. (2015). Effects of electron beam irradiation on the property behaviour of poly(ether-block-amide) blended with various stabilisers. *Radiation Physics and Chemistry, 110*, 24–37. https://doi.org/10.1016/j.radphyschem.2015.01.009.
Murrell, D., & Crompton, D. (2009). Foodborne helminth infections. In C. Blackburn, & P. J. McClure (Eds.). *Foodborne pathogens: Hazards, risk analysis and control*(2nd ed.). Elsevier.
Murrell, D., & Dubey, J. P. (1993). Epidemiology and control of trichinellosis and toxoplasmosis. In: *Proc. Final research co-ordination meeting on use of irradiation to control infectivity of food-borne parasites, Mexico city 24–28 June 1991* (pp. 73–79). *Vienna:* (IAEA).
Neumayerová, H., Jurankova, J., Salakova, A., Gallas, L., Kovarcik, K., & Koudela, B. (2014). Survival of experimentally induced *Toxoplasma gondii* tissue cysts in vacuum packed goat meat and dry fermented goat meat sausages. *Food Microbiology, 39*, 47–52. https://doi.org/10.1016/j.fm.2013.11.001.
Nöckler, K., & Kolb, H. (2000). Survival of *Trichinella spiralis* in raw sausage production. *Fleischwirtschaft, 80*, 102–105.
Novo Borges, J., Corrêa Lopes, K., & Portes Santos, C. (2018). Viability of *Ascocotyle* (*Phagicola*) *longa* (Trematoda: Heterophyidae) metacercariae from mullets (*Mugil liza*) from Rio de Janeiro, Brazil after exposure to freezing and heating in the temperature range from 35 °C to 180 °C. *Food Control, 89*, 117–122.
Ockerman, H., & Basu, L. (2017). Technology of fermented meat products. In N. Zdolec (Ed.). *Fermented meat products: Health aspects* (pp. 15–48). Boca Raton – London, New York: CRC Press.
Onsurathum, S., Pinlaor, P., Haonon, O., Chaidee, A., Charoensuk, L., Intuyod, K., et al. (2016). Effects of fermentation time and low temperature during the production process of Thai pickled fish (pla-som) on the viability and infectivity of *Opisthorchis viverrini* metacercariae. *International Journal of Food Microbiology, 218*, 1–5. https://doi.org/10.1016/j.ijfoodmicro.2015.11.001.
Ortega, Y. R., & Sanchez, R. (2010). Update on *Cyclospora cayetanensis*, a food-borne and waterborne parasite. *Clinical Microbiology Reviews, 23*(1), 218–234. https://doi.org/10.1128/CMR.00026-09.
Painter, J. A., Hoekstra, R. M., Ayers, T., Tauxe, R. V., Braden, C. R., Angulo, F. J., et al. (2013). Attribution of foodborne illnesses, hospitalizations, and deaths to food commodities by using outbreak data, United States, 1998-2008. *Emerging Infectious Diseases, 19*(3), 407–415. https://doi.org/10.3201/eid1903.111866.
Park, H., Min, B., & Oh, S. (2017). Research trends in outdoor pig production - a review. *Asian-australasian Journal of Animal Sciences, 30*(9), 1207–1214. https://doi.org/10.5713/ajas.17.0330 Epub 2017 Jul 17.
Pott, S., Koethe, M., Bangoura, B., Zoller, B., Daugschies, A., Straubinger, R. K., et al. (2013). Effects of pH, sodium chloride, and curing salt on the infectivity of *Toxoplasma gondii* tissue cysts. *Journal of Food Protection, 76*(6), 1056–1061. https://doi.org/10.4315/0362-028X.JFP-12-519.
Pozio, E. (2014). Searching for *Trichinella*: Not all pigs are created equal. *Trends in Parasitology, 30*(1), 4–11. https://doi.org/10.1016/j.pt.2013.11.001.
Rendueles, E., Omer, M., Alvseike, O., Alonso-Calleja, C., Capita, R., & Prieto, M. (2011). Microbiological food safety assessment of high hydrostatic pressure processing: A review. *Food Science and Technology, 44*, 1251–1260. https://doi.org/10.1016/j.lwt.2010.11.001.
Roberts, P. B. (2014). Food irradiation is safe: Half a century of studies. *Radiation Physics and Chemistry, 105*, 78–82.
Robertson, L. J. (2018). Parasites in food: From a neglected position to an emerging issue. *Advances in Food & Nutrition Research, 86*, 1043–4526. https://doi.org/10.1016/bs.afnr.2018.04.003.
Rodriguez-Canul, R., Argaez-Rodriguez, F., Pacheco De La Gala, D., Villegas-Perez, S., Fraser, A., Craig, P. S., et al. (2002). *Taenia solium* metacestode viability in infected pork after preparation with salt pickling or cooking methods common in Yucatán, México. *Journal of Food Protection, 65*(4), 666–669.
Román, S., Sánchez-Siles, L. M., & Siegrist, M. (2017). The importance of food naturalness for consumers: Results of a systematic review. *Trends in Food Science & Technology, 67*, 44–57.
Rousseau, A., La Carbona, S., Dumètre, A., Robertson, L. J., Gargala, G., Escotte-Binet, S., et al. (2018). Assessing viability and infectivity of foodborne and waterborne stages (cysts/oocysts) of giardia duodenalis, Cryptosporidium spp., and Toxoplasma gondii: A review of methods. *Parasite, 25*https://doi.org/10.1051/parasite/2018009.
Saleque, A., Juyal, P. D., & Bhatia, B. B. (1990). Effect of temperature on the infectivity of *Sarcocystis miescheriana* cysts in pork. *Veterinary Parasitology, 36*(3–4), 343–346.
Salminen, K. (1970). The infestiveness of heat and cold exposed *Diphyllobothrium latum* plerocercoids on golden hamster. *Acta Veterinaria Scandinavica, 11*(2), 247–253.
Sanchez-Monsalvez, I., de Armas-Serra, C., Martinez, J., Dorado, M., Sanchez, A., & Rodriguez-Caabeiro, F. (2005). A new procedure for marinating fresh anchovies and ensuring the rapid destruction of *Anisakis larvae. Journal of Food Protection, 68*(5), 1066–1072.
Sathyanarayanan, L., & Ortega, Y. (2006). Effects of temperature and different food matrices on *Cyclospora cayetanensis* oocyst sporulation. *The Journal of Parasitology, 92*(2), 218–222. https://doi.org/10.1645/GE-630R.1.
Sithithaworn, P., & Haswell-Elkins, M. (2003). Epidemiology of *Opistorchis viverrini. Acta Tropica, 88*, 187–194.
Smaldone, S., Marrone, R., Palma, G., Sarnelli, P., & Anastasio, A. (2017). Preliminary study on the inactivation of anisakid larvae in baccalà prepared according to traditional methods. *Italian Journal of Food Safety, 6*(6964), 195–198.
Song, C., Duan, Y., Shou, G., & Zhu, H. (1993a). Studies on the use of 60Co irradiation on the infectivity of *Paragonymus westermani* metacercariae. In: *Proc. Final research co-ordination meeting on use of irradiation to control infectivity of food-borne parasites, Mexico city 24–28 June 1991* (pp. 99–104). Vienna: IAEA.
Song, C., Yuan, X., Shen, L., Gan, X., & Ding, J. (1993b). The effect of cobalt-60 irradiation on the infectivity of *Toxoplasma gondii. International Journal for Parasitology, 23*(1), 89–93.
Sornami, S., Impand, P., & Bundisting, C. (1993). Irradiation of fish to control the infectivity of the liver fluke *Opisthorchis viverrini.* In: *Proc. Final research co- ordination meeting on use of irradiation to control infectivity of food-borne parasites, Mexico city* (pp. 115–128). Vienna: IAEA.
Sotelo, J., Rosas, N., & Palencia, G. (1986). Freezing of infested pork muscle kills cysticerci. *Journal of the American Medical Association, 256*(7), 893–894.
Srivastava, P. S., Saha, A. K., & Sinha, S. R. (1986). Effects of heating and freezing on the viability of sarcocysts of *Sarcocystis levinei* from cardiac tissues of buffaloes. *Veterinary Parasitology, 19*(3–4), 329–332.
Tesana, S., Kaewkes, S., & Phinlaor, S. (1986). Infectivity and survivorship of *Opisthorchis viverrini* metacercariae in fermented fish. *Journal of Parasitology of the Tropical Medical Association Thailand, 9*, 21–30.
Torgerson, P. R., Devleesschauwer, B., Praet, N., Speybroeck, N., Willingham, A. M., Kasuga, F., et al. (2015). World health organization estimates of the global and regional disease burden of 11 foodborne parasitic diseases, 2010: A data synthesis. *PLoS Medicine.* https://doi.org/10.1371/journal.pmed.1001920.
Van Mameren, J., & Houwing, H. (1968). Effect of irradiation on *Anisakis larvae* in salted herring. *Elimination of harmful organisms from food and feed by irradiation (international atomic energy agency (IAEA)* (pp. 73–80). Vienna: IAEA.
Verster, A., Du Plessis, T. A., & Van Den Heever, L. W. (1976). The effect of gamma radiation on the cysticerci of *Taenia solium. Onderstepoort Journal of Veterinary Research, 43*(1), 23–26.
Vidacek, S., De Las Heras, C., Solas, M. T., Garcia, M. L., Mendizabal, A., & Tejada, M. (2011). Viability and antigenicity of *Anisakis simplex* after conventional and microwave heating at fixed temperatures. *Journal of Food Protection, 74*(12), 2119–2126. https://doi.org/10.4315/0362-028X.JFP-11-108.
Wikerhauser, T., Kuticic, V., Razem, D., Orsanic, L., & Besvir, J. (1993). Irradiation to control infectivity of *Toxoplasma gondii* in murine brains and edible porcine tissues. In: *Proc. Final research co- ordination meeting on use of irradiation to control infectivity of food-borne parasites, Mexico city* (pp. 133–136). Vienna: IAEA.
Wootten, R.,C. D. (2001). *Round worms in fish. FAO - (torry advisory note No. 80 : Round Worms in fish, ministry of agriculture, fisheries and food).*
Yim, D. G., Jo, C., Kim, H. J., Cha, J. S., Kim, H. C., & Nam, K. C. (2015). Combined effect of irradiation and ageing condition on physicochemical and microbial quality of Hanwoo eye of round. *Korean Journal for Food Science of Animal Resources, 35*(3), 406–412. https://doi.org/10.5851/kosfa.2015.35.3.406.
Zimmermann, W. J. (1971). Salt cure and drying-time and temperature effects on viability of *Trichinella spiralis* in dry-cured hams. *Journal of Food Science, 36*, 58–62.

Trends in Food Science & Technology 91 (2019) 12–23

Contents lists available at ScienceDirect

Trends in Food Science & Technology

journal homepage: www.elsevier.com/locate/tifs

Review

Inactivation of parasite transmission stages: Efficacy of treatments on foods of non-animal origin

Cédric Gérard[a,*], Frits Franssen[b], Stephanie La Carbona[c], Silivia Monteiro[d], Anamaria Cozma-Petruţ[e], Kjersti S. Utaaker[f], Anet Režek Jambrak[g], Neil Rowan[h], David Rodríguez-Lazaro[i], Abidelfatah Nasser[j], Kristoffer Tysnes[f], Lucy J. Robertson[f]

[a] Food Safety Microbiology, Nestlé Research, Vers-chez-les-Blanc, 1000 Lausanne 26, Switzerland
[b] Centre for Zoonotic Diseases and Environmental Microbiology, National Institute for Public Health and the Environment, Antonie van Leeuwenhoeklaan 9, 3721 MA, Bilthoven, the Netherlands
[c] ACTALIA Food Safety Department, 310 rue Popielujko, 50000, Saint-Lô, France
[d] Instituto Superior Tecnico, Laboratorio Analises, Universidade Lisboa, Lisbon, Portugal
[e] Department of Bromatology, Hygiene, Nutrition, "Iuliu Haţieganu" University of Medicine and Pharmacy, 6 Pasteur Street, 400349, Cluj-Napoca, Romania
[f] Department of Food Safety and Infection Biology, Faculty of Veterinary Medicine, Norwegian University of Life Sciences, Adamstuen Campus, PO Box 369 Sentrum, 0102, Oslo, Norway
[g] Faculty of Food Technology and Biotechnology, University of Zagreb, Pierotti Street 6, Zagreb, Croatia
[h] Bioscience Research Institute, Athlone Institute of Technology, Dublin Road, Athlone, Co. Westmeath, Ireland
[i] Microbiology Division, Department of Biotechnology and Food Science, Faculty of Science, University of Burgos, Burgos, Spain
[j] Institute of Natural Sciences, Beit Berl College of Education, Beitberl, Israel

ARTICLE INFO

Keywords:
Foodborne
Parasite
Inactivation
Control measure
Fresh produce

ABSTRACT

Background: Among 24 foodborne parasites ranked by FAO/WHO, 15 are associated with food of non-animal origin (FoNAO). Control of these hazards is essential for food safety.

Scope and approach: Control measures to inactivate parasites in FoNAO are reviewed. Preventing contamination is key to ensuring the safety of fresh produce. However, additional control measures can further reduce the likelihood of occurrence of infectious parasites in FoNAO.

Key Findings and Conclusions: The efficacy of treatments depends on parasite species, developmental stage, matrix, and application conditions. Conventional pasteurization (72 °C; 15 s) inactivates parasites in most matrices, although some parasites are more heat resistant, and this may be an inappropriate method for many FoNAO that are intended for eating fresh and raw. Freezing at −20 °C for 2 days inactivates most, but not all, parasites, and some are highly resistant to freezing. Parasites generally survive chemical disinfection, making its application at effective doses often unsuitable at an industrial scale. Ozone and chlorine dioxide are the most promising in terms of efficacy and dosage, nevertheless challenges remain in their application especially for the most fragile produce. High-pressure processing is an efficient technology, providing good inactivation of parasites. Further research should focus on standardizing experimental approaches for evaluation of inactivation techniques and development of methods to measure parasite inactivation in food matrices.

1. Introduction and the growing awareness of food of non-animal origin as a vehicle for parasite infection

Foodborne diseases encompass a wide range of acute and chronic syndromes that differ greatly in their prevalence, duration, and severity. WHO estimates that 31 bacterial, viral, parasitic and chemical global hazards caused a total of 600 million foodborne illnesses in 2010, of which 15% were due to parasites (WHO, 2015). Although fish and meat are often associated with biological hazards, foods of non-animal origin (FoNAO), such as fresh produce, are particularly associated with foodborne parasites (FBP) (Van Pelt et al., 2018). One third of domestically acquired parasitic foodborne illnesses in the US have

* Corresponding author.
E-mail addresses: cedric.gerard@rdls.nestle.com (C. Gérard), frits.franssen@rivm.nl (F. Franssen), s.lacarbona@actalia.eu (S. La Carbona), silvia.monteiro@tecnico.ulisboa.pt (S. Monteiro), anamaria.cozma@umfcluj.ro (A. Cozma-Petruţ), kjersti.utaaker@nina.no (K.S. Utaaker), arezek@pbf.hr (A. Režek Jambrak), nrowan@AIT.IE (N. Rowan), drlazaro@ubu.es (D. Rodríguez-Lazaro), abid@beitberl.ac.il (A. Nasser), kristoffer.tysnes@nmbu.no (K. Tysnes), lucy.robertson@nmbu.no (L.J. Robertson).

https://doi.org/10.1016/j.tifs.2019.06.015
Received 28 January 2019; Received in revised form 26 June 2019; Accepted 26 June 2019
Available online 28 June 2019

been attributed to FoNAO (Painter et al., 2013); by extrapolation from the WHO estimates, this corresponds to around 30 million illnesses globally during 2010. Among the 24 FBP listed for risk-ranking by FAO/WHO in 2014 (FAO/WHO, 2014, p. 302) or the 25 FBP ranked by Bouwknegt et al. for Europe in 2016 (Bouwknegt et al., 2018), transmission of 15 of them, particularly those for which the transmission stage is shed in the feces of the definitive host, can be associated with FoNAO. Contamination of FoNAO may occur along the farm-to-fork continuum, either directly from infected handlers with poor hygiene (e.g., *Cryptosporidium* and *Cyclospora* oocysts, *Giardia* cysts, and *Ascaris* and *Taenia* eggs) or from feces of infected animals (e.g., *Cryptosporidium* and *Toxoplasma* oocysts, *Echinococcus* and *Toxocara* eggs), or indirectly via contaminated irrigation water, or use of sewage as fertiliser. Most FBPs have a low infective dose and robust transmission stages. Thus, implementing measures that prevent contamination with parasites during primary food production, by following Good Agricultural Practices, is generally preferable to relying upon removal/inactivation of parasite transmission stages in subsequent stages of the food chain (EFSA, 2018).

As various different types of fresh produce, particularly salad vegetables and fruits such as berries, are often consumed with minimal preparation, any measures implemented along the farm to fork continuum to prevent, remove, or inactivate parasites may provide a measure of protection of consumer health and should be considered in the frame of Hazard Analysis and Critical Control Points (HACCP) studies. With greater demand and current food trends advising consumers to increase their intake of fresh produce, in combination with global sourcing and improved transport chains, the possibility of fruit and vegetables contaminated with parasite transmission stages being distributed more widely may be increasing. The probability of introduction of new strains or species into non-endemic areas is also likely to rise. Control procedures in the fresh-produce chain mostly concern spoilage and pathogenic bacteria. However, whether those procedures affect the survival of parasite transmission stages has seldom been addressed. Furthermore, distinction between whether parasites on fresh produce have become non-viable (as assessed by a viability study) or non-infectious (as assessed using an infection model) is also of relevance, and seldom addressed. In this companion paper to an already published article addressing foods of animal origin (FoAO; Franssen et al., 2018), we provide an in depth review of treatments for inactivation of parasite transmission stages in FoNAO, emphasizing where data are insufficient and drawing attention to relevant new technologies.

2. Reference inclusion criteria

As with the FoAO companion paper (Franssen et al., 2018), a non-systematic literature review was used to gather relevant information from scientific publications, reports, and official documents. Articles were included that attempted to quantify parasite inactivation effects of different treatments for FoNAO. However, given the breadth of cover, addressing different parasites, different matrices, different inactivation methods, and different ways of assessing inactivation, it was difficult to ensure the quality of all the references. Including only those references that corresponded to our highest quality requirements (i.e., recent papers with detailed quantification of parasite inactivation using bioassay), some parasites, matrices, and different methods would have had no reference material and would thus have been excluded. Information from relevant articles was aggregated into a database that is presented in Tables 1–4.

3. Current state of knowledge

As with the article on FoAO (Franssen et al., 2018), we do not describe parasite biology, geographical distribution, disease in humans, relevance for trade, and impact on economically vulnerable populations in this article. The relevant information on these aspects for parasites that may be transmitted via FoNAO is available in Annex 7 of the FAO/WHO multi-criteria based ranking for risk management of foodborne parasites (FAO/WHO, 2014, p. 302).

4. Avoiding contamination and key aspects of removal

Clearly, and from the HACCP perspective, prevention of contamination is essential in reducing transmission of parasites with FoNAO. Measures that may reduce contamination are ensuring that personnel in contact with FoNAO are not themselves infected, ensuring that appropriate hygiene facilities are available for farm workers, keeping animals out of food facilities, including at the farm level, using non-contaminated water within the food chain, from irrigation to washing prior to packing etc.

Should contamination occur, a proportion of parasites transmission stages may be removed from FoNAO by washing procedures without the requirement for an inactivation procedure. Generally, washing procedures in the fresh produce industry are intended to remove dirt, pesticide residues, and microorganisms responsible for quality loss (Gil, Selma, Lopez-Galvez, & Allende, 2009). Additionally, washing is used to pre-cool cut produce and remove cell exudates that may support microbial growth. Such procedures include spraying or deluging in water, and sometimes mechanical treatment of surfaces by brushes or spray washers, followed by rinsing; sanitizer treatments may also be involved. The water used for these purposes must also be clean (potable standard), so that it does not become a vehicle for contamination. Washwater quality, especially if recycled and not treated prior to reuse, is a concern of the fresh produce industry (Parish et al., 2003). Methods for sanitizing washwater are not the focus of this document and not considered further.

Although hardy items of fresh produce can be brush-washed, a process in which oscillating brushes are used to scrub surfaces for physical removal of soil and microorganisms (Parish et al., 2003), this is not suitable for fresh produce such as lettuce and soft fruit. Addition of particles to washwater to increase abrasion is impractical, as additional wastewater treatment and particle recovery would be needed. However, introducing air into liquid provides additional cleaning forces and modern aeration ‘jacuzzi’ washers reduce bacterial loads on vegetables by between 1 and 2 logs (Gil et al., 2009). Since bacteria are smaller than parasite transmission stages, it can be speculated that shear forces should be larger, and thus the parasites would be easier to remove, and use of this technology should be explored regarding parasites. However, the transmission stages of many parasites, are “sticky”, and thus may be more difficult to remove than bacteria. It should also be noted that various characteristics of the surfaces of the fresh produce (cracks, crevices, hydrophobic tendency, texture etc.) may affect the ability of the washing procedure to remove adherent parasites.

Despite removal of bacteria from fresh produce by washing being given considerable attention, investigations on removal of parasites from fresh produce surfaces by washing procedures are largely lacking. Among helminths, the adhesive properties of *e.g. Taenia* eggs (OIE, 2018), *Echinococcus* eggs (Eckert & Deplazes, 2004), and *Ascaris* eggs (Jimenez, 2007) are well recognized. However, one older study found some washing approaches were successful at removing *Fasciola* metacercaria from leafy greens (el-Sayad, Allam, & Osman, 1997).

Studies on removal of protozoa from the fresh produce surfaces are also sparse, but removal of *Cryptosporidium* oocysts from the surface of apples has been explored (Macarisin, Santin, Bauchan, & Fayer, 2010). None of the washing methods tested removed all oocysts from apple peel, with the most efficient removal achieved either by rigorous manual washing in water with a detergent or agitation in an orbital shaker with tris-sodium dodecyl sulfate buffer. Scanning electron microscopy revealed that some oocysts were in deep natural crevices in the apple exocarp, and some oocysts were closely associated with an amorphous substance with which they appeared to be attached to the

Table 1
Effects of chemical inactivation methodologies on foodborne parasites. Control measures: chlorine dioxide, hydrogen peroxide.

Transmission stage	Condition	Method for determining inactivation/viability	Effect	Log reduction	Matrix	Ref
CHLORINE DIOXIDE						
Cryptosporidium						
oocysts	CT = 82 mg min/L. Spot inoculation; vegetables placed in a chamber in presence of gas	Cell culture assay	2.60 Log reduction (Log MPN/g) of oocysts infectivity	2.60	basil	Ortega et al. (2008)
			3.31 Log reduction (Log MPN/g) of oocysts infectivity	3.31	lettuce	
HYDROGEN PEROXIDE						
Cryptosporidium						
oocysts	0.03% H_2O_2; for 1 h; acids added to juices in granular form on a weight/volume basis	Excystation	0.33 log reduction in oocysts excystation	0.33	apple cider	Kniel et al. (2003)
			0.44 log reduction in oocysts excystation	0.44	orange juice	
			0.48 log reduction in oocysts excystation	0.48	purple grape juice	
			0.47 log reduction in oocysts excystation	0.47	white grape juice	
		Cell culture	3.5 log reduction of oocysts infectivity	3.50	apple cider	
			4.4 log reduction of oocysts infectivity	4.40	orange juice	
			4.1 log reduction of oocysts infectivity	4.10	purple grape juice	
			4.0 log reduction of oocysts infectivity	4.00	white grape juice	
	0.025% H_2O_2; for ≥ 6 h; acids added to juices in granular form on a weight/volume basis	Excystation	0.55 log reduction in oocysts excystation	0.55	purple grape juice	
			0.46 log reduction in oocysts excystation	0.46	apple cider	
		Cell culture	> 5.9 log reduction of oocysts infectivity	> 5.90	orange juice purple grape juice white grape juice	
			3 log reduction of oocysts infectivity	3.00	apple cider	
	0.03% H_2O_2; for ≥ 2 h; acids added to juices in granular form on a weight/volume basis	Excystation	0.60 log reduction in oocysts excystation	0.60	purple grape juice	
			0.56 log reduction in oocysts excystation	0.56	apple cider	
			0.53 log reduction in oocysts excystation	0.53	orange juice	
			0.54 log reduction in oocysts excystation	0.54	white grape juice	
		Cell culture	≥5.9 log reduction of oocysts infectivity	5.90	orange juice purple grape juice white grape juice apple cider	

Table 2
Effects of thermal inactivation methodologies on foodborne parasites. Control measure: heat treatment.

Transmission stage	Condition	Method for determining inactivation/viability	Effect	Log reduction	Matrix	Ref
Cryptosporidium						
oocysts	70 °C; 5 s;	semiquantitative in vitro infectivity assay: bovine kidney cells infected with heat-treated oocysts, followed by examination by indirect fluorescent antibody staining	3 log reduction of oocysts infectivity	3.00	apple cider	Deng and Cliver (2001)
	71.7 °C; 5 s;		4.8 log reduction of oocysts infectivity	4.80		
	≥70 °C and above; ≥ 10 s		> 4.9 log reduction of oocysts infectivity	4.90		
	Microwave heating; 2450 MHz; 850 W; 5 min	propidium iodide (PI) staining	93.23% oocysts PI positive in average (6 replicates)	1.19	green pepper	Duhain et al. (2012)
	200 ppm; 40 s washing + microwave heating; 2450 MHz; 850 W; 5 min		98.10% oocysts PI positive in average (6 replicates)	1.72		
	Blanching; 96 °C; 3 min		93.53% oocysts PI positive in average (6 replicates)	1.17		
Cyclospora cayetanensis						
oocysts	Water bath, minimum internal berry temperature of 80 °C maintained for 1 h; (*Eimeria acervulina* used as a surrogate)	bioassay: heat-treated oocysts fed to chicks, followed by evaluation of duodenal lesions or oocysts in cecal contents or in fecal contents	Absence of *E. acervulina* oocysts in feces of chicks, at 6 days postinoculation. Initial concentration between 400 and 650 oocysts.	n.s.	raspberries	Lee & Lee (2001)
	70 °C; 15 min	percentage of sporulation as an indicator of viability	0% sporulation; counts made on counting cell on 100–150 organisms - at least 2 log inactivation	2.00	basil	Sathyanarayanan & Ortega (2006)
	100 °C; 15 min					
Echinococcus						
eggs	25 °C; in air of 27% relative humidity; 48 h	bioassay: voles orally infected with eggs	eliminates infectivity for voles, 3 voles inoculated with eggs, none infected	n.s.	in vitro	Veit et al. (1995)
	43 °C; suspended in water; 4 h		eliminates infectivity for voles, 7 voles inoculated with eggs, none infected			
	43 °C; in air of 15% relative humidity; 2 h		eliminates infectivity for voles, 8 voles inoculated with eggs, none infected			
	45 °C; in air of 85–95% relative humidity; 3 h		eliminates infectivity for voles, 3 voles inoculated with eggs, none infected			
	65 °C; suspended in water; 180 min	sodium hypochlorite resistance test to assess in vitro egg viability at inoculation, then evaluation of infectivity of oncospheres by subcutaneous inoculation in mice	eggs lose infectivity			Federer et al. (2015)
	70 °C; suspended in water; 30 min					
	75 °C; suspended in water; 15 min					
	80 °C; suspended in water; 7.5 min					

n.s.: not stated.

Table 3
Effects of thermal inactivation methodologies on foodborne parasites. Control measure: freezing.

Transmission stage	Condition	Method for determining inactivation/viability	Effect	Log reduction	Matrix	Ref
Cryptosporidium						
	Exposure to 200 ppm chlorine; 40 s washing + Blast freezing; −20 °C; 4 min	propidium iodide staining	did not affect significantly the viability of the oocysts	~0.00	green pepper	Duhain et al. (2012)
	Blast freezing; −20 °C; 4 min, then thawing in 4 °C water for 3 min		0.10 log reduction of oocysts viability	0.10		
Cyclospora cayetanensis						
oocysts	−18 °C; (*Eimeria acervulina* used as a surrogate of *Cyclospora*)	bioassay: heat-treated oocysts fed to chicks, followed by evaluation of duodenal lesions or oocysts in cecal contents or in fecal contents	Absence of *E. acervulina* oocysts in feces of chicks, at 6 days postinoculation. Initial concentration between 400 and 650 oocysts.	n.s.	raspberries	Lee & Lee (2001)
	−70 °C; 1 h	percentage of sporulation as an indicator of viability	0% sporulation; counts made on counting cell on 100–150 organisms - at least 2 log inactivation	2.00	basil	Sathyanarayanan & Ortega (2006)
	−20 °C; 2 days		< 1% can sporulate; counts made on counting cell on 100–150 organisms - at least 2 log inactivation			
Echinococcus						
eggs	−196 °C; 20 h	bioassay: voles orally infected with eggs	eliminates infectivity for voles, 10 voles inoculated with eggs, none infected	n.s.	in vitro	Veit et al. (1995)
	−83 °C; 48 h		eliminates infectivity for voles, 30 voles inoculated with eggs, none infected	n.s.		
Tripanosoma cruzi						
trypomastigotes	−20 °C; 26 h	bioassay: trypomastigotes administered intraperitoneally, orally, or by gavage to immunodeficient mice/parasitemia quantified by Brener method	do not affect trypomastigotes infectivity for mice	0.00	açai pulp	Barbosa et al. (2012)

n.s.: not stated.

Table 4
Effects of non-thermal inactivation methodologies on foodborne parasites. Control measure: drying, high pressure processing, gamma irradiation.

Transmission stage	Condition	Method for determining inactivation/viability	Effect	Log reduction	Matrix	Ref
DRYING						
Giardia						
cysts	Room temperature; 24 h	Vital dyes	Almost 50% die-off	0.30	lettuce	Utaaker et al. (2017)
HIGH PRESSURE PROCESSING						
Cryptosporidium						
oocysts	550 MPa; 30 s	cell cuture infectivity assay	gives 99.959% inactivation, reduction of oocysts infectivity	3.40	apple juice	Slifko et al. (2000)
	550 MPa; ≥ 60 s		gives > 99.992% inactivation, reduction of oocysts infectivity	> 4.10		
	550 MPa; 30 s		gives 99.993% inactivation, reduction of oocysts infectivity	> 4.10	orange juice	
	550 MPa; ≥ 60 s		gives > 99.994% inactivation, reduction of oocysts infectivity	> 4.20		
Cyclospora cayetanensis						
oocysts	550 MPa; 2 min; 40 °C (*Eimeria acervulina* used as a surrogate of *Cyclospora*)	in vivo infection	eliminates oocysts infectivity for birds; no oocysts in feces, initial load 6 log	n.s.	raspberries basil	Kniel et al. (2007)
Toxoplasma						
oocysts	340 MPa or above; 60 s	Mice bio-assay	eliminate infectivity for mice	n.s.	raspberries	Lindsay et al. (2008)
GAMMA IRRADIATION						
Cyclospora cayetanensis						
oocysts	1 kGy and above; (*Eimeria acervulina* used as a surrogate of *Cyclospora*)	Chicks bioassay	No duodenal lesions detected in natural host, no infectivity of *Eimeria acervulina* oocysts for chicks. Initial concentration between 400 and 650 oocysts.	n.s.	raspberries	Lee & Lee (2001)
Toxoplasma						
oocysts	0.5 kGy	Mice bioassay	kills oocysts on raspberries	n.s.	raspberries	Dubey et al. (1998)
	≥0.2 kGy	Cell culture plaque assay	reductions of ≥4 log PFU/g	4	Blueberries	Lacombe et al. (2017)

n.s.: not stated.

apple surface. Another study demonstrated strong adherence of *Cryptosporidium* oocysts to spinach leaves, and also internalization of oocysts through the stomata, such that washing was ineffective for removal (Macarisin, Bauchan, & Fayer, 2010). In addition (Armon, Gold, Brodsky, & Oron, 2002), reports that *Cryptosporidium* oocysts are difficult to remove from the outer surfaces (skins) of courgettes (zucchini), possibly due to the hairs (trichomes) on the surfaces. Both apples and spinach are of relevance to *Cryptosporidium* transmission due to outbreaks of cryptosporidiosis associated with apple cider and with spinach leaves in salad.

Although no studies have directly investigated removal of *Cyclospora* oocysts from fresh produce by washing, an experiment in which *Eimeria acervulina,* a coccidian parasite of chickens, was used as a surrogate for *Cyclospora* on raspberries demonstrated that washing was generally inadequate (Lee & Lee, 2001). *Cyclospora* oocysts have been visualized attached to the surface of vegetables after washing and it has been reported that *Cyclospora* oocysts are "stickier" than *Cryptosporidium* oocysts, although the adhesins responsible for enhanced attachment have not been identified (Ortega & Sanchez, 2010). Experiments investigating removal of *Toxoplasma* oocysts from fresh produce by washing showed they adhere to berries, with greater attachment to raspberries than blueberries, presumably due to surface differences between the two berry types (Kniel et al., 2002).

5. Chemical inactivation methodologies

Although washing fresh produce with tap water can remove part of the indigenous microbiota, chemical disinfectants are usually added in the fresh produce industry to improve efficacy and to limit re-contamination of produce, the use of which depends on national regulations. Although washing with disinfectant decreases the concentration of microbial hazards, these strategies are insufficient to ensure microbiological safety of fresh produce, because the efficacy of the treatment will depend on several factors, including: i) the microbial target and initial load; parasite transmission stages are often more resistant than bacteria or fungi; ii) the conditions of application (type of disinfectant, concentration of disinfectant and contact time (CT value), pH, temperature); iii) the food matrix itself, which may protect the microorganism and/or modify the action of the chemicals. Thus, efficacy data obtained for pathogens in simple matrices (buffers, water) cannot be extrapolated to food matrices. Nevertheless, most studies concerning parasites only assess the efficacy of chemicals in simple matrices. Although the studies are informative, often the results cannot be directly transferred and applied to fresh produce.

5.1. Chemical oxidizers

5.1.1. Chlorine

Chlorine is the most widely used disinfectant in the fresh produce industry to sanitize food-processing environments and washwaters. Treatment efficiency depends on the concentration of free chlorine (i.e., hypochlorous acid, HClO) which varies with pH, temperature, exposure time, and the presence of organic matter. Although various studies have investigated the effect of chlorine on parasites (particularly *Cryptosporidium* and *Giardia*) in aqueous solutions, and generally found that very high CT are required to inactivate them, very few studies have investigated the effects on fresh produce. Only one study investigated the efficacy of chlorine at inactivating *Cryptosporidium parvum* oocysts inoculated onto green peppers, and an insignificant reduction in viability was reported with a CT of 67 mg min/L (100 mg/mL of free chlorine for 40 s), as determined by propidium iodide staining (Duhain, Minnaar, & Buys, 2012). In the minimally processed vegetable industries, chlorine is commonly used at concentrations of 50–200 ppm for 1–2 min, pH < 8.0 (CT from 50 to 400 mg min/L) and low temperatures (5–8 °C) (Goodburn & Wallace, 2013). Based on the experimental data available, these conditions would probably not result in inactivation of parasites in FoNAO.

5.1.2. Chlorine dioxide

Chlorine dioxide (ClO_2) is a gas used for its powerful oxidizing properties. Table 1 presents results investigating the efficacy of chlorine dioxide to inactivate parasites on surfaces of vegetables or in various types of juice.

Ortega et al. (2008) found that basil and lettuce exposed to relatively low concentrations of gaseous chlorine dioxide for 20 min (CT of 82 mg min/L) led to 2.6–3.31 log reduction in infectivity of *Cryptosporidium* oocysts. Although high concentrations seem to be effective at controlling bacterial pathogens on apples, tomatoes, and onions without compromising their sensory quality, its use seems limited with other vegetables and berries because of the sensory impacts on the fresh produce. Although the infectious *Cryptosporidium* load was significantly reduced, *Cyclospora* sporulation was not affected. Thus, it was concluded that chlorine dioxide was not suitable as a sanitizer against parasitic contamination in the fresh produce industry (Ortega, Mann, Torres, & Cama, 2008).

5.1.3. Electrolyzed water

Electrolyzed water is a technique based on electrolysis of water containing sodium chloride to form hypochlorous acid and sodium hydroxide. The bactericidal effects have been tested on fresh produce by (Huang, Hung, Hsu, Huang, & Hwang, 2008), who found that disinfection efficacy may be reduced in the presence of organic matter due to formation of monochloramines. However, its efficiency at inactivating parasites on fresh produce is unknown.

5.1.4. Hydrogen peroxide and peroxyacetic acid

Hydrogen peroxide (H_2O_2) is a strong oxidizer, commonly used for disinfection purposes. Addition of hydrogen peroxide to fruit juices at concentrations as low as 0.025%–0.03% has been reported to result in a 25%–99.9% reduction of *C. parvum* infectivity, depending on duration of treatment, ranging from 1 to over 6 h. Exposure of *Cryptosporidium* oocysts to 0.03% H_2O_2 for 1 h resulted in 0.33–0.48 log inactivation in various fruit juices as measured by excystation, whereas a reduction of 3.5–4.4 log was measured by cell-culture infectivity (Kniel et al., 2003). Although exposure to hydrogen peroxide may inactivate *Cryptosporidium* oocysts, the exposure time and concentrations necessary seem unsuitable for treating FoNAO.

Peroxyacetic acid or peracetic acid ($C_2H_4O_3$) is a mixture of acetic acid (CH_3COOH) and hydrogen peroxide (H_2O_2) in aqueous solution that is used as a disinfectant in the food industry. However, its probable efficiency at inactivating parasite transmission stages on fresh produce seem low as (Briancesco, Veschetti, Ottaviani, & Bonadonna, 2005) found that peracetic acid (CT of 120 mg min/L) had only a marginal effect on reducing the viability of *Cryptosporidium* oocysts and *Giardia* cysts in effluent water.

5.1.5. Ozone

Ozone (O_3) is an inert gas with a high oxidant power and a short half-life (30 min at 15 °C, pH 7.0). The growing interest in ozone, rather than chlorine, for drinking water treatment is due to: i) its disinfection potential, enabling shorter contact times and lower concentrations; ii) its inactivation efficacy against a wide range of microbes; iii) the formation of relatively few toxic byproducts; iv) the possibility to treat large volumes of water. However, whether this can be extrapolated to FoNAO is less clear. Compared with chlorine, the disinfection rate of ozone is less affected by pH and temperature variations. However, ozone reacts rapidly with most organic and many inorganic compounds, decreasing persistence. Application of a high concentration for a short contact time is usually considered preferable. Although it has been used for reducing bacterial contamination of fresh produce for a considerable period, and is considered to be a safe option for use (Glowacz & Rees, 2016), to date, the efficacy of ozone at inactivating

parasites has been studied only in simple matrices such as water, and has not, to our knowledge been tested for its efficacy on parasites contaminating fresh produce.

5.2. Organic acids alone or in combination

Organic acids, such as acetic, malic, tartaric, or citric acids, have been tested as natural sanitizers (Uyttendaele, Neyts, Vanderswalmen, Notebaert, & Debevere, 2004). They are thought to inactivate cells by decreasing the pH, damaging membrane functions and key enzymes.

Acetic acid or vinegar is a natural, inexpensive readily available product with known sanitizing properties. However, little information exists on its efficacy at inactivating FBP, with only a few reports published. Zanini and Graeff-Teixeira (2001) investigated the larvicidal effect of wine vinegar on *Angiostrongylus costaricensis*, by incubating *A. costaricensis* L3 larvae at 20 °C for 1 h in red wine vinegar, with 1.5% (v/v) aqueous bleach solution and saturated cooking salt solution as controls and using mouse infectivity to evaluate inactivation. Incubation in vinegar resulted in a 1.25 log reduction in infectivity (Zanini & Graeff-Teixeira, 2001).

The efficacy of undiluted vinegar (4% v/v acetic acid) and diluted vinegar solutions at inactivating *G. duodenalis* cysts has been investigated (Costa, Thomaz-Soccol, Paulino, & Alcantara de Castro, 2009) Undiluted vinegar resulted in complete inactivation of the cysts following incubation for 60 min at 21 °C corresponding to 5.7 log reduction as measured by excystation. Thus, although very few studies have investigated the use of acetic acid/vinegar for inactivating FBP transmission stages on FoNAO, results available indicate that the efficacy depends on the organism, temperature, time, and concentration.

Citric acid, a major component of orange juice, has antimicrobial activity and has long been used in different food applications (Davidson, Sofos, & Branen, 2005). However, investigations on its ability to inactivate FBP are scarce and focus only on *Cryptosporidium*. The potential mechanisms and interactions between citric acid and *Cryptosporidium* oocysts have been discussed; an acidified environment may damage oocyst walls thereby reducing infectivity (Kato, Jenkins, Ghiorse, & Bowman, 2001; Kniel et al., 2003) (Friedman, Patten, Rose, & Barney, 1997). Although incubation in orange juice for 24 h at 4 °C failed to inactivate *C. parvum* oocysts completely, the methods used for determining viability gave conflicting results, with in vitro excystation indicating higher viability than dye staining. Kniel et al. (2003) tested the disinfection potential of organic acids, including citric acid, at inactivating *C. parvum* oocysts in juice. Citric acid was added to orange juice in concentrations ranging from 1 to 5% (w/v) at 4 °C and infectivity was measured in cell culture using human ileocecal adenocarcinoma cells. Infectivity decreased with increasing acid concentration, but complete inactivation was not achieved, even at the highest concentration. The addition of 5% citric acid resulted in a 23% decrease in *C. parvum* infectivity (Kniel et al., 2003). Dawson, Samuel, Scrannage, and Atherton (2004) investigated citric acid from 0.017 M at pH 7.0 to 0.089 M at pH 2.6 for inactivation of *C. parvum* oocysts. Viable sporozoites were detected after 14 days of contact time indicating a lack of efficacy at inactivating oocysts. Reductions in viability ranged from 17% at pH 7.0 (22 °C) to 52% at pH 2.6 (22 °C) or pH 7.0 (4 °C) (Dawson et al., 2004).

Levulinic acid is an inexpensive acid produced from renewable feedstocks (Bozell & Moens, 2000; Fang & Hanna, 2002) with known antimicrobial properties (Zhao, Zhao, & Doyle, 2009). It has been classified by the U.S. Food and Drug Administration as generally recognized as safe for direct addition to food as a flavoring substance or adjuvant (FDA, 2017). Ortega et al. (2011) evaluated the effects of levulinic acid alone or in combination with sodium dodecyl sulfate on the viability of *C. parvum* oocysts, using different contact periods from 30 min to 2 h and two concentrations (3% levulinic acid with 2% SDS and 2% levulinic acid with 1% SDS). Using cell culture to assess infectivity, the combination of 3% levulinic acid and 2% SDS decreased oocyst viability by 0.41 log after 1 h of treatment (Ortega, Torres, & Tatum, 2011). These results suggest that levulinic acid and SDS are unlikely to be effective at inactivating *Cyptosporidium* oocysts on FoNAO, and other parasites that are more robust than *Cryptosporidium* are also likely to survive levulinic acid treatment.

Malic acid is an organic acid produced by all organisms and is partly responsible for the taste of fruits. Although known to inhibit fungi and bacteria, presumably due to pH alterations, studies on its effects on FBP are scarce. Kniel et al. (2003) investigated the effect of different concentrations (1, 3 and 5% w/v) of malic acid on *C. parvum* oocysts in apple cider, with oocyst viability evaluated by cell culture using HCT-8 cells. Infectivity reduction ranged between 0.11 log for 1% to 0.81 log for 5% (Kniel et al., 2003). Therefore, although malic acid is effective against bacteria and fungi, its effect on the viability of parasite transmission stages is probably insufficient in treating FoNAO against FBP.

As for the other organic acids, information on the effects of tartaric acid against FBP is scarce, with only one publication to date (Kniel et al., 2003). Tartaric acid is an organic compound occurring naturally in many plants and added to foods as an antioxidant. Again, antimicrobial properties of tartaric acid are associated with lowering of the pH (Davidson et al., 2005). The effect of tartaric acid on *C. parvum* oocyst viability was investigated by increasing the concentration of tartaric acid in purple and white grape juice (Kniel et al., 2003). Complete abrogation of infectivity was not achieved. In purple grape juice, 5% tartaric acid increased inactivation of *C. parvum* from around 57% to about 77%, whereas for white grape juice, addition of 5% tartaric acid increased inactivation of *C. parvum* viability from around 30% to about 55%. These data indicate that tartaric acid is probably unsuitable for treating FoNAO against FBP.

6. Thermal inactivation methodologies

6.1. Heat treatment

Adequate heat treatment can destroy parasites that contaminate FoNAO (Gajadhar, 2015). Table 2 presents available data on thermal treatments that have been reported for parasites on fresh produce. For all the high temperatures listed, it should be noted that these may be of minimal relevance for fresh produce such as salad vegetables and soft fruit that are intended for raw consumption.

Commercial pasteurization (71.7 °C, 15 s) has been demonstrated to be effective in inactivating *Cryptosporidium* oocysts in apple cider (Deng & Cliver, 2001), whereas blanching at 96 °C for 3 min has been shown to inactivate 93% of *Cryptosporidium* oocysts inoculated onto green peppers (Duhain et al., 2012).

Cyclospora cayetanensis oocysts appear to be susceptible only to higher temperatures. Heating *Cyclospora* oocysts on basil at 50 °C for 1 h did not prevent sporulation, but temperatures of 70 °C or 100 °C for 15 min, were effective in preventing sporulation (Sathyanarayanan & Ortega, 2006). For raspberries contaminated with *Eimeria acervulina* oocysts as *Cyclospora* surrogate, inactivation was achieved by heating to a minimal internal temperature of 80 °C maintained for 1 h (Lee & Lee, 2001).

Heat may not always be that effective at inactivating *Echinococcus multilocularis* eggs on FoNAO; although the eggs appear to lose infectivity at temperatures even as low as 43 °C, low humidity conditions may also be required (Veit et al., 1995). This aspect is important, particularly as *Echinococcus* eggs on fresh produce may be in contact with water droplets. Indeed, *E. multilocularis* eggs suspended in water have relatively high heat tolerance, showing infectivity after exposure to 65 °C for up to 120 min (Federer, Armua-Fernandez, Hoby, Wenker, & Deplazes, 2015). However, eggs were demonstrated to lose infectivity following heat exposure at 65 °C for 180 min or at 70, 75 and 80 °C for 30, 15 or 7.5 min (Federer et al., 2015). EFSA recommend heating of food for at least 3 h at 65 °C to ensure that potential contaminant *Echinococcus* eggs are inactivated (EFSA, 2018).

Microwave heating also has shown promise in the decontamination of some parasites on FoNAO, being effective in inactivating 93% of *Cryptosporidium* oocysts inoculated onto green peppers and microwaved in a domestic microwave oven (2450 MHz; 850 W) for 5 min. Pretreatment with chlorine increased the efficacy of inactivation to 98% (Duhain et al., 2012). These results suggest that industrial microwave blanching, as well as home microwave heating of fresh produce, could represent efficient treatments in parasite decontamination, should sufficient time and temperature variables be applied.

Few data are available on the effect of heat treatment on trematodes transmitted via FoNAO, such as *Fasciola hepatica* or *Fasciolopsis buski*. However, there are recommendations to boil water plants for 1–2 min prior to consumption to kill metacercaria of *F. buski* (Weng, Zhuang, Jiang, Lin, & Lin, 1989), or to cook aquatic plants thoroughly before eating, to control foodborne trematodes (Keiser & Utzinger, 2009).

6.2. Freezing

Freezing is another thermal methodology that can be efficient in controlling some parasites on FoNAO, although, as with heating, this treatment may not always be appropriate for FoNAO due to altered sensory properties (Gajadhar, 2015). Table 3 presents data on the control of parasites on fresh produce at varying combinations of time and low temperatures. *Cyclospora* oocysts on basil were able to sporulate following storage at - 20 °C for up to 2 days, but were inactivated by exposure to −70 °C for 1 h (Sathyanarayanan & Ortega, 2006).

Oocysts of *C. parvum* and *T. gondii*, and *T. cruzi* trypomastigotes have also been shown to tolerate temperatures as low as - 20 °C. For example, infectivity of *T. cruzi* trypomastigotes in açaí pulp was unaffected by exposure to −20 °C for 26 h (Barbosa et al., 2012), and Duhain et al. (2012) reported that blast freezing at - 20 °C for 4 min was not sufficient to kill *C. parvum* oocysts inoculated onto surfaces of green peppers (Duhain et al., 2012).

Regarding helminths, *Echinococcus multilocularis* eggs have been found to tolerate - 18 °C for 240 days, but lost infectivity following exposure to - 83 °C for 48 h (Veit et al., 1995).

As domestic freezers have average operating temperatures of between - 13 °C and - 18 °C (Evans, Foster, & Brown, 2014), household freezers should not to be expected to inactivate all parasites in FoNAO. Indeed, EFSA recommend deep freezing at −80 °C for a minimum of 24 h in order to inactivate potentially contaminant *Echinococcus* eggs (EFSA, 2018); something that cannot be achieved in a domestic freezer. However, for industrial freezing, the paucity of information indicates that further studies are required.

7. Non-thermal inactivation methodologies

Table 4 presents results investigating the efficacy of various non-thermal technologies.

7.1. Drying

Among protozoan FBP, it has been shown that air-drying of *Giardia* cysts on lettuce results in viability abrogation within less than 24 h with almost 50% die-off of *Giardia* cysts recorded within the first 24 h; however, as the lettuce also became unpalatable under these conditions, it is not an appropriate methodology for this, and various other types of fresh produce (Utaaker, Skjerve, & Robertson, 2017). The effects of drying on other FBP on fresh produce are lacking, and it would be of particular interest to investigate how the viability of the more robust parasites (cestode and nematode eggs) are affected by the drying conditions used for producing “dried” fresh produce (e.g., dried fruit occurring in cereals, “trail mix”, herbs etc.). There have been various outbreaks of foodborne disease associated with dried fruits and vegetables, and although none of those reported are parasitoses, that various bacteria can survive drying processes indicates that this is also relevant for parasite transmission stages (Bourdoux, Li, Rajkovic, Devlieghere, & Uyttendaele, 2016).

7.2. High-pressure processing (HPP)

In high-pressure processing (HPP), also known as pascalization, bridgmanization, or application of high hydrostatic pressure (HHP), foods are subjected to pressures from 100 to 800 MPa. The processing temperature during treatment can be from below 0 °C to above 100 °C, with exposure times ranging from a few seconds to 20 min and longer, depending on process conditions. Nutritive values and sensory properties of food often remain unaffected by HPP.

The studies on the effectiveness of HPP in inactivating FBP have often used surrogate organisms, particularly for helminths, and often have not investigated the process on a relevant FoNAO matrix, although initial data have suggested that this technology could be of use for inactivating nematode eggs contaminating FoNAO (Rosypal, Bowman, Holliman, Flick, & Lindsay, 2007).

With regards to protozoa, Slifko et al. (2000) evaluated the effects of HHP at 550 MPa for 0, 30, 45, 60, 90, and 120 s on *C. parvum* oocysts suspended in apple and orange juice. HHP inactivated *C. parvum* oocysts by at least 3.4 log after 30 s of treatment, and after at least 60 s of treatment more than 4.2 log inactivation was observed as assessed by cell culture (Slifko, Raghubeer, & Rose, 2000).

For *Toxoplasma gondii* oocysts, Lindsay et al. (2008) inoculated raspberries with 5×10^4 oocysts of the *T. gondii* VEG strain exposed to 500, 400, 340, 300, 270, 250, 200, 100 MPa for 60 s and showed 340 MPa resulted in the oocysts becoming non-infectious for mice (Lindsay et al., 2008).

For *Cyclospora,* the only investigations on HPP have used *Eimeria acervulina* oocysts as a surrogate. Sporulated *E. acervulina* oocysts inoculated onto basil and raspberries at high (10^6 oocysts) and low (10^4 oocysts) levels and treated with 550 MPa at 40 °C for 2 min resulted in apparent abolition of infectivity to chickens (Kniel, Shearer, Cascarino, Wilkins, & Jenkins, 2007).

7.3. X-ray irradiation

X-rays are produced by reflecting a high-energy stream of electrons off a target substance (usually one of the heavy metals) into foods. The adverse effects on nutritional or organoleptic (sensory) properties associated with thermal processes are likely to be reduced as x-rays do not produce heat.

Although some studies on inactivation of FBP by x-ray treatment have been performed, none have been conducted on parasites contaminating FoNAO with the intention of investigating the suitability of this process for food treatment.

7.4. Gamma irradiation

Gamma rays used for food treatments are emitted from radioactive forms of the radionuclide elements, usually cobalt-60 or, very rarely, caesium-137. A few studies have investigated the effects of gamma irradiation on survival of FBP as contaminants of fresh produce, including *Toxoplasma* oocysts on raspberries irradiated with doses of ≥0.4 kGy (cesium-137) failed to cause infections in mice (Dubey, Thayer, Speer, & Shen, 1998), despite antibodies being produced in some mice. Lacombe et al. (2017) showed that irradiation at ≥ 0.2 kGy (caesium-137) led to at least 4 log PFU/g inactivation of *Toxoplasma* oocysts on blueberries as evaluated by cell culture plaque assay (Lacombe et al., 2017). For *Cyclospora* oocysts, the only data rely on experiments using *Eimeria* oocysts as surrogates, inoculated onto raspberries and these indicate that irradiation at 1 kGy or higher is needed to ensure complete abrogation of infectivity (Lee & Lee, 2001).

7.5. Ultraviolet irradiation

The effect of ultraviolet irradiation (UV) on the viability and infectivity of FBP is diverse and related to parasite species, stage, and the matrix assayed. Reductions in infectivity have been observed for protozoa that may be transmitted by FoNAO, but inactivation varies depending on the species tested and the matrix; the sensitivity of *Cryptosporidium* and *Giardia* to UV light has resulted in this becoming a standard treatment for drinking water. However, extrapolation to parasites as contaminants of food is less clear, particularly due to shading effects. However, experiments with raspberries spiked with *Cryptosporidium* oocysts and exposed to a pulsed UV light of total fluence 4J/cm^2, have reported a 2 log reduction or 3 log reduction in infectivity, with initial levels of 10^3 or 10^4 oocysts respectively (Le Goff et al., 2015). Raspberries have also been spiked with 2×10^4 oocysts *Eimeria acervulina* oocysts, as a surrogate organism for *Cyclospora*, and treated with UV at doses up to 261 mw/cm^2; in this experiment, infectivity was reduced at the higher UV doses, as demonstrated by lower oocyst excretion in infected chickens and a lower lesion score at autopsy; however when the inoculum was 2×10^6 oocysts, oocyst excretion was not affected (Kniel et al., 2007). In experiments with a similar set up, but 2×10^6 oocysts inoculated onto basil leaves, similar results were obtained as for raspberries, but when the inoculum size was lower (2×10^4 oocysts), a UV dose of 160 mw/cm^2 was used, the effect was greater on the oocysts on the basil than on the raspberries (Kniel et al., 2007). As discussed by the authors, this may well be due to the shadowing effect and that basil provides a planar surface for irradiation, where as raspberries are irregular and oocysts in crevices between drupules may avoid the UV irradiation.

Helminths seem to be less sensitive to UV exposure than protozoa, although data from food matrices is lacking. *Ascaris* eggs are among the most UV-resistant pathogens, although exposure to 400 mJ/cm^2 can reduce embryonation of *Ascaris suum* by at least 2.23 logs (Brownell & Nelson, 2006).

7.6. Ultrasound

Ultrasound is used in many applications in the food industry. Depending on the frequency used, ultrasound may be used to stimulate cellular activity, for extraction and emulsification, and for cellular destruction and cleaning, amongs others (Mason, Paniwnyk, & Lorimer, 1996). Ultrasound parasite inactivation tests on fresh produce are lacking, but experiments conducted on aqueous matrices have suggested that ultrasound may affect the viability of *Cryptosporidium* oocysts. Continuous sonication of real and filtered municipal water treatment plants effluents with 20 kHz power for 10 min was able to achieve around 1 log reduction of viability of *C. parvum* oocysts (Abeledo-Lameiro, Ares-Mazás, & Goméz-Couso, 2018).

7.7. Supercritical fluid-state gases

Supercritical fluids exist when the temperature and pressure are such that distinct liquid and gas phases do not exist; the temperature (and thus molecular kinetic energy) is sufficiently high that condensation will not occur, but the pressure is sufficiently high that the substance does not remain in pure gaseous state. Although supercritical fluid-state gases have properties suitable for various applications, the mechanisms behind their known antimicrobial effects are poorly understood. Supercritical carbon dioxide (SC CO_2) treatment has been recognized as a promising non-thermal treatment technology for the food industry, particularly for extraction process, but also inactivating a large variety of microorganisms, particularly in combination with ultrasound (Koubaa, Mhemdi, & Fages, 2018). More recently, an alternative supercritical fluid, supercritical nitrous oxide (SC N_2O), has been shown to have a similar microbicidal effect as that of SC CO_2, but without affecting pH change. Although we are lacking information on use of this technology on parasites in food matrices, the efficacy of supercritical CO_2 and N_20 at inactivating *Ascaris suum* eggs has been investigated, and a strong ovicidal effect was observed after 1 min exposure, with both gases achieving 2.4 log inactivation evaluated by embryonation (Mun, Lee, & Yoon, 2012).

8. Future trends and novel technologies in inactivation of parasites on food

Better understanding of the extent of contamination of FoNAO and survival of transmission stages on these matrices, along with methods for inactivation of potentially contaminated produce and assessment of the efficacy of such methods, are important for safeguarding public health. However, the application of Good Agricultural practices and HACCP approaches are essential for minimizing contamination of FoNAO.

Due to the lack of efficacy of chlorine-based traditional processes for disinfection of FBP in the fresh produce industries, coupled with the need to find alternatives to chlorine for health concerns, other directions have been explored (De Corato, 2019). Temperature (heat, freezing) and desiccation may be appropriate for some FoNAO, but not appropriate for produce such as leafy salad vegetables or fresh berries. Although technologies such as irradiation technologies (X-ray, gamma, UV), high pressure processing, and ultrasound may be effective, these are also associated with some difficulties, related to their efficacy on food matrices, their applicability within an industrial food setting, and their effects on the organoleptic and sensory properties of the FoNAO. Although X-ray is reliable and efficient at processing large volumes of produce, there is considerable consumer mistrust and its use is relatively expensive. Use of electron beam as alternative irradiation source to gamma has not yet been investigated for inactivation of FBP on FoNAO but some characteristics of this technology indicate that it may provide more rapid effects. Various novel technologies have been investigated for other pathogens, such as bacteria, that may be transmitted via FoNAO but have yet to be investigated for parasites. Such technologies include non-thermal/cold plasma and plasma activated water. For both of these, reactive oxygen species (ROS) are usually considered as the major inactivating agent in combination with a high positive oxidation reduction potential and low pH resulting in oxidative stress in microbial cells, and thus damage to DNA, proteins, and lipids (Ma et al., 2015). Another technology that may be of relevance is pulsed electric field (PEF) technology; whereas PEF has been considered as an important, non-thermal food processing technology for decades, particularly for beverage production (Aneja, Dhiman, Aggarwal, & Aneja, 2014); advances in this methodology, such as nanosecond PEF (nsPEF) and microchip PEF (MCPEF) are considered to be effective membrane disruptors. These may have better potential for eliminating microbial contaminants, either alone or in combination with other technologies, without affecting sensory qualities (Zhu et al., 2019).

Although, data on the use of these novel methods against other foodborne pathogens is being steadily accrued, for FBP the data tend to be scattered, inconsistent, or, more often, entirely absent. One important aspect is that suitable methods for determining survival and infectivity of relevant FBP will need to be developed, such that we have a good basis for evaluating the effects of such exciting technologies on this important pathogen group in FoNAO (Rousseau et al., 2018). Without appropriate viability/infectivity assessment methods, it is very difficult to determine the efficacy of novel methods; for most parasites, infectivity remains the gold standard – but this has associated ethical issues, and is not possible for parasites such as *Cyclospora*, for which no animal model is available. In parallel, investigations on the use of appropriate surrogates, may help to circumvent the difficulty in obtaining some parasites and would help in assessing the efficacy of processes at industrial scale for relevant parasitic targets (Busta et al., 2003).

9. Conclusions

Based on our extensive literature review, information on the effects of different inactivation techniques on relevant parasites on FoNAO has been assimilated. Given that contamination of FoNAO with transmission stages of FBP occurs relatively frequently, that they survive well under storage, and are difficult to remove by washing procedures, it is important to consider the efficacy of potential inactivation methods that may be used on FoNAO without affecting their intrinsic qualities.

Chemical oxidizers have some effects on survival of FBP, but the concentrations and contact times required to ensure inactivation are not appropriate for FoNAO. Organic acids and other chemicals are ineffective at inactivating FBP on FoNAO. Data from water studies suggest that ozone may be suitable for inactivation of several foodborne parasites, and could be promising for use in fresh produce industries. The application conditions (around 5 °C) and the requirement to maintain the aqueous ozone concentration among various levels of organic matter are critical parameters in the context of minimally processed fresh produce industries. Citric acid studies have investigated the effects of various parameters, but none demonstrated total elimination of *C. parvum* oocyst viability, indicating that treatment of FoNAO with citric acid would be unlikely to reduce the risk of infection should the food be contaminated with viable oocysts.

Among physical treatments, heat particularly, and for some parasites, freezing and desiccation may be effective, but are not appropriate for FoNAO that are to be eaten raw, such as lettuce or berries. And some important FBP, such as *Echinococcus* eggs, are resistant to elevated or decreased temperatures. Although technologies such as irradiation technologies (X-ray, gamma, UV), high pressure processing, and ultrasound may be effective, the data are sparse and mostly derived from water matrices rather than actual FoNAO, and the range of FBP tested are limited. Furthermore, these technologies are associated with some difficulties, associated with applicability within an industrial food setting, cost and effect on the organoleptic and sensory properties of the FoNAO, but also consumer perception limitating the applicability of irradiation technologies.

This assimilation of data indicates that research on the inactivation of FBP transmitted by FoNAO should be expanded, with efforts directed towards developing reliable and useful methods for assessing effects of methods, such that investigations of current and novel inactivation methods used for other pathogens on their effects on parasites in FoNAO enables the production of useful, comparable data of relevance for industrial applications.

Declaration of interests

The authors declare that they have no conflict of interests.

Acknowledgements

This article is based upon work from COST Action FA1408 - A European Network for Foodborne Parasites in Europe (Euro-FBP), supported by COST (European Cooperation in Science and Technology; www.cost.eu).

References

Abeledo-Lameiro, M. J., Ares-Mazás, E., & Goméz-Couso, H. (2018). Use of ultrasound irradiation to inactivate *Cryptosporidium parvum* oocysts in effluents from municipal wastewater treatment plants. *Ultrasonics Sonochemistry, 48*, 118–126. https://doi.org/10.1016/j.ultsonch.2018.05.013.

Aneja, K. R., Dhiman, R., Aggarwal, N. K., & Aneja, A. (2014). Emerging preservation techniques for controlling spoilage and pathogenic microorganisms in fruit juices. *International Journal of Microbiology*. https://doi.org/10.1155/2014/758942 2014.

Armon, R., Gold, D., Brodsky, M., & Oron, G. (2002). Surface and subsurface irrigation with effluents of different qualities and presence of *Cryptosporidium* oocysts in soil and on crops. *Water Science and Technology, 46*(3), 115–122. https://doi.org/10.2166/wst.2002.0067.

Barbosa, R. L., Dias, V. L., Pereira, K. S., Schmidt, F. L., Franco, R. M. B., Guaraldo, A. M. A., et al. (2012). Survival *in vitro* and virulence of *Trypanosoma cruzi* in açaí pulp in experimental acute chagas disease. *Journal of Food Protection, 75*(3), 601–606. https://doi.org/10.4315/0362-028X.JFP-11-233.

Bourdoux, S., Li, D., Rajkovic, A., Devlieghere, F., & Uyttendaele, M. (2016). Performance of drying technologies to ensure microbial safety of dried fruits and vegetables. *Comprehensive Reviews in Food Science and Food Safety, 15*(6), 1056–1066. https://doi.org/10.1111/1541-4337.12224.

Bouwknegt, M., Devleesschauwer, B., Graham, H., Robertson, L. J., & van der Giessen, J. W. The Euro-Fbp Workshop. (2018). Prioritisation of food-borne parasites in Europe, 2016. *Euro Surveillance, 23*(9), https://doi.org/10.2807/1560-7917.ES.2018.23.9.17-00161.

Bozell, J. J., & Moens, L. (2000). Production of levulinic acid and use as a platform chemical for derived products. *Resources, Conservation and Recycling, 28*(3–4), 227–239. https://doi.org/10.1016/S0921-3449(99)00047-6.

Briancesco, R., Veschetti, E., Ottaviani, M., & Bonadonna, L. (2005). Peracetic acid and sodium hypochlorite effectiveness in reducing resistant stages of microorganisms. *Central European Journal of Public Health, 13*(3), 159–162.

Brownell, S. A., & Nelson, K. L. (2006). Inactivation of single-celled *Ascaris suum* eggs by low-pressure UV radiation. *Applied and Environmental Microbiology, 72*(3), 2178–2184. https://doi.org/10.1128/AEM.72.3.2178-2184.2006.

Busta, F. F., Suslow, T. V., Parish, M. E., Beuchat, L. R., Farber, J. N., Garrett, E. H., et al. (2003). The use of indicators and surrogate microorganisms for the evaluation of pathogens in fresh and fresh-cut produce. *Comprehensive Reviews in Food Science and Food Safety, 2*(s1), 179–185. https://doi.org/10.1111/j.1541-4337.2003.tb00035.x.

Costa, A. O., Thomaz-Soccol, V., Paulino, R. C., & Alcantara de Castro, E. (2009). Effect of vinegar on the viability of *Giardia duodenalis* cysts. *International Journal of Food Microbiology, 128*(3), 510–512. https://doi.org/10.1016/j.ijfoodmicro.2008.10.001.

Davidson, P. M., Sofos, J. N., & Branen, A. L. (2005). *Antimicrobials in foods* (3rd ed.). Boca Raton: CRC Taylor and Francis.

Dawson, D. J., Samuel, C. M., Scrannage, V., & Atherton, C. J. (2004). Survival of *Cryptosporidium* species in environments relevant to foods and beverages. *Journal of Applied Microbiology, 96*(6), 1222–1229. https://doi.org/10.1111/j.1365-2672.2004.02281.x.

De Corato, U. (2019). Improving the shelf-life and quality of fresh and minimally-processed fruits and vegetables for a modern food industry: A comprehensive critical review from the traditional technologies into the most promising advancements. *Critical Reviews in Food Science and Nutrition,* 1–36. https://doi.org/10.1080/10408398.2018.1553025.

Deng, M. Q., & Cliver, D. O. (2001). Inactivation of *Cryptosporidium parvum* oocysts in cider by flash pasteurization. *Journal of Food Protection, 64*(4), 523–527. https://doi.org/10.4315/0362-028X-64.4.523.

Dubey, J. P., Thayer, D. W., Speer, C. A., & Shen, S. K. (1998). Effect of gamma irradiation on unsporulated and sporulated *Toxoplasma gondii* oocysts. *International Journal for Parasitology, 28*(3), 369–375. https://doi.org/10.1016/S0020-7519(97)83432-7.

Duhain, G. L. M. C., Minnaar, A., & Buys, E. M. (2012). Effect of chlorine, blanching, freezing, and microwave heating on *Cryptosporidium parvum* viability inoculated on green peppers. *Journal of Food Protection, 75*(5), 936–941. https://doi.org/10.4315/0362-028X.JFP-11-367.

el-Sayad, M. H., Allam, A. F., & Osman, M. M. (1997). Prevention of human fascioliasis: A study on the role of acids detergents and potassium permenganate in clearing salads from metacercariae. *Journal of the Egyptian Society of Parasitology, 27*(1), 163–169.

Eckert, J., & Deplazes, P. (2004). Biological, epidemiological, and clinical aspects of echinococcosis, a zoonosis of increasing concern. *Clinical Microbioly Reviews, 17*(1), 107–135. https://doi.org/10.1128/CMR.17.1.107-135.2004.

EFSA BIOHAZ Panel (EFSA Panel on Biological Hazards)Koutsoumanis, K., Allende, A., Alvarez-Ordnez, A., Bolton, D., Bover-Cid, S., Chemaly, M., et al. . (2018). Scientific Opinion on the public health risks associated with food-borne parasites. *EFSA Journal, 16*(12), 5495. https://doi.org/10.2903/j.efsa.2018.5495 113.

Evans, J. A., Foster, A. M., & Brown, T. (2014, June). Temperature control in domestic refrigerators and freezers. Refrigeration Science and Technology Proceedings. *3rd IIR international conference on sustainability and the cold chain, London, UK* (pp. 142–149). .

Fang, Q., & Hanna, M. A. (2002). Experimental studies for levulinic acid production from whole kernel grain sorghum. *Bioresource Technology, 81*(3), 187–192. https://doi.org/10.1016/S0960-8524(01)00144-4.

FAO/WHO [Food and Agriculture Organization of the United Nations/World Health Organization] (2014). *Multicriteria-based ranking for risk management of food-borne parasites. Microbiological Risk Assessment Series, No 23. Rome*.

FDA (2017). *Electronic code of federal regulation.* https://www.ecfr.gov/cgi-bin/text-idx?SID=47c9f6a3f4e8dcb8f0f4fae3b15eee09&mc=true&node=se21.3.172_1515&rgn=div8, Accessed date: 13 May 2019.

Federer, K., Armua-Fernandez, M. T., Hoby, S., Wenker, C., & Deplazes, P. (2015). In vivo viability of *Echinococcus multilocularis* eggs in a rodent model after different thermotreatments. *Experimental Parasitology, 154*, 14–19. https://doi.org/10.1016/j.exppara.2015.03.016.

Franssen, F., Gerard, C., Cozma-Petruț, A., Vieira-Pinto, M., Režek, J.,A., Rowan, N., ... Robertson, L. (2018). Inactivation of parasite transmission stages: Efficacy of treatments on food of animal origin. *Trends in Food Science & Technology, 83*, 114–128. https://doi.org/10.1016/j.tifs.2018.11.009.

Friedman, D. E., Patten, K. A., Rose, J. B., & Barney, M. C. (1997). The potential for *Cryptosporidium parvum* oocysts survival in beverages associated with contaminated tap water. *Journal of Food Safety, 17*(2), 125–132. https://doi.org/10.1111/j.1745-4565.1997.tb00181.x.

Gajadhar, A. A. E. (2015). *Foodborne parasites in the food supply web: Occurrence and control* (1st ed.). Cambridge: Elsevier Woodhead Publishing.

Gil, M. I., Selma, M. V., Lopez-Galvez, F., & Allende, A. (2009). Fresh-cut product sanitation and wash water disinfection: Problems and solutions. *International Journal of Food Microbiology, 134*(1–2), 37–45. https://doi.org/10.1016/j.ijfoodmicro.2009.05.021.

Glowacz, M., & Rees, D. (2016). The practicality of using ozone with fruit and vegetables. *Journal of the Science of Food and Agriculture, 96*(14), 4637–4643. https://doi.org/10.1002/jsfa.7763.

Goodburn, C., & Wallace, C. A. (2013). The microbiological efficacy of decontamination methodologies for fresh produce: A review. *Food Control, 32*(2), 418–427. https://doi.org/10.1016/j.foodcont.2012.12.012.

Huang, H. R., Hung, Y. C., Hsu, S. H., Huang, Y. W., & Hwang, D. F. (2008). Application of electrolyzed water in the food industry. *Food Control, 19*, 329–345. https://doi.org/10.1016/j.foodcont.2007.08.012.

Jimenez, B. (2007). Helminth ova removal from wastewater for agriculture and aquaculture reuse. *Water Science and Technology, 55*(1–2), 485–493. https://doi.org/10.2166/wst.2007.046.

Kato, S., Jenkins, M. B., Ghiorse, W. C., & Bowman, D. D. (2001). Chemical and physical factors affecting the excystation of *Cryptosporidium parvum* oocysts. *The Journal of Parasitology, 87*(3), 575–581. https://doi.org/10.1645/0022-3395(2001)087[0575:CAPFAT]2.0.CO;2.

Keiser, J., & Utzinger, J. (2009). Food-borne trematodiases. *Clinical Microbiology Reviews, 22*(3), 466–483. https://doi.org/10.1128/CMR.00012-09.

Kniel, K. E., Lindsay, D. S., Sumner, S. S., Hackney, C. R., Pierson, M. D., & Dubey, J. P. (2002). Examination of attachment and survival of *Toxoplasma gondii* oocysts on raspberries and blueberries. *The Journal of Parasitology, 88*(4), 790–793. https://doi.org/10.1645/0022-3395(2002)088[0790:EOAASO]2.0.CO;2.

Kniel, K. E., Shearer, A. E. H., Cascarino, J. L., Wilkins, G. C., & Jenkins, M. C. (2007). High hydrostatic pressure and UV light treatment of produce contaminated with *Eimeria acervulina* as a *Cyclospora cayetanensis* surrogate. *Journal of Food Protection, 70*(12), 2837–2842. https://doi.org/10.4315/0362-028X-70.12.2837.

Kniel, K. E., Sumner, S. S., Lindsay, D. S., Hackney, C. R., Pierson, M. D., Zajac, A. M., et al. (2003). Effect of organic acids and hydrogen peroxide on *Cryptosporidium parvum* viability in fruit juices. *Journal of Food Protection, 66*(9), 1650–1657. https://doi.org/10.4315/0362-028X-66.9.1650.

Koubaa, M., Mhemdi, H., & Fages, J. (2018). Recovery of valuable components and inactivating microorganisms in the agro-food industry with ultrasound-assisted supercritical fluid technology. *The Journal of Supercritical Fluids, 134*, 71–79. https://doi.org/10.1016/j.supflu.2017.12.012.

Lacombe, A., Breard, A., Hwang, C. A., Hill, D., Fan, X., Huang, L., et al. (2017). Inactivation of Toxoplasma gondii on blueberries using low dose irradiation without affecting quality. *Food Control, 73*, 981–985. https://doi.org/10.1016/j.foodcont.2016.10.011.

Le Goff, L., Hubert, B., Favennec, L., Villena, I., Ballet, J. J., Agoulon, A., et al. (2015). Pilot-scale pulsed UV light irradiation of experimentally infected raspberries suppresses *Cryptosporidium parvum* infectivity in immunocompetent suckling mice. *Journal of Food Protection, 78*(12), 2247–2252. https://doi.org/10.4315/0362-028X.JFP-15-062.

Lee, M. B., & Lee, E. H. (2001). Coccidial contamination of raspberries: Mock contamination with *Eimeria acervulina* as a model for decontamination treatment studies. *Journal of Food Protection, 64*(11), 1854–1857. https://doi.org/10.4315/0362-028X-64.11.1854.

Lindsay, D. S., Holliman, D., Flick, G. J., Goodwin, D. G., Mitchell, S. M., & Dubey, J. P. (2008). Effects of high pressure processing on *Toxoplasma gondii* oocysts on raspberries. *The Journal of Parasitology, 94*(3), 757–758. https://doi.org/10.1645/GE-1471R.1.

Macarisin, D., Bauchan, G., & Fayer, R. (2010). *Spinacia oleracea* L. Leaf stomata harboring *Cryptosporidium parvum* oocysts: A potential threat to food safety. *Applied and Environmental Microbiology, 76*(2), 555–559. https://doi.org/10.1128/AEM.02118-09.

Macarisin, D., Santin, M., Bauchan, G., & Fayer, R. (2010). Infectivity of *Cryptosporidium parvum* oocysts after storage of experimentally contaminated apples. *Journal of Food Protection, 73*(10), 1824–1829. https://doi.org/10.4315/0362-028X-73.10.1824.

Mason, T. J., Paniwnyk, L., & Lorimer, J. P. (1996). The uses of ultrasound in food technology. *Ultrasonics Sonochemistry, 3*(3), S253–S260. https://doi.org/10.1016/S1350-4177(96)00034-X.

Ma, R., Wang, G., Tian, Y., Wang, K., Zhang, J., & Fang, J. (2015). Non-thermal plasma-activated water inactivation of food-borne pathogen on fresh produce. *Journal of Hazardous Materials, 300*, 643–651. https://doi.org/10.1016/j.jhazmat.2015.07.061.

Mun, S., Lee, Y. W., & Yoon, J. (2012). Ovicidal activities of supercritical CO_2 and N_2O on *Ascaris suum* eggs. *Journal of Industrial and Engineering Chemistry, 18*(1), 504–508. https://doi.org/10.1016/j.jiec.2011.11.032.

OIE. (2018). *Manual of diagnostic tests and vaccines for terrestrial animals 2018*. http://www.oie.int/standard-setting/terrestrial-manual/access-online/, Accessed date: 13 May 2019.

Ortega, Y. R., Mann, A., Torres, M. P., & Cama, V. (2008). Efficacy of gaseous chlorine dioxide as a sanitizer against *Cryptosporidium parvum, Cyclospora cayetanensis*, and *Encephalitozoon intestinalis* on produce. *Journal of Food Protection, 71*(12), 2410–2414. https://doi.org/10.4315/0362-028X-71.12.2410.

Ortega, Y. R., & Sanchez, R. (2010). Update on *Cyclospora cayetanensis*, a food-borne and waterborne parasite. *Clinical Microbiology Reviews, 23*(1), 218–234. https://doi.org/10.1128/CMR.00026-09.

Ortega, Y. R., Torres, M. P., & Tatum, J. M. (2011). Efficacy of levulinic acid-sodium dodecyl sulfate against *Encephalitozoon intestinalis, Escherichia coli* O157:H7, and *Cryptosporidium parvum*. *Journal of Food Protection, 74*(1), 140–144. https://doi.org/10.4315/0362-028X.JFP-10-104.

Painter, J. A., Hoekstra, R. M., Ayers, T., Tauxe, R. V., Braden, C. R., Angulo, F. J., et al. (2013). Attribution of foodborne illnesses, hospitalizations, and deaths to food commodities by using outbreak data, United States, 1998-2008. *Emerging Infectious Diseases, 19*(3), 407–415. https://doi.org/10.3201/eid1903.111866.

Parish, M. E., Beuchat, L. R., Suslow, T. V., Harris, L. J., Garret, E. H., Farber, J. N., et al. (2003). Methods to reduce/eliminate pathogens from fresh and fresh-cut produce. *Comprehensive Reviews in Food Science and Food Safety, 2*(s1), 161–173. https://doi.org/10.1111/j.1541-4337.2003.tb00033.x.

Rosypal, A. C., Bowman, D. D., Holliman, D., Flick, G. J., & Lindsay, D. S. (2007). Effects of high hydrostatic pressure on embryonation of *Ascaris suum* eggs. *Veterinary Parasitology, 145*(1–2), 86–89. https://doi.org/10.1016/j.vetpar.2006.11.001.

Rousseau, A., La Carbona, S., Dumètre, A., Robertson, L. J., Gargala, G., Escotte-Binet, S., et al. (2018). Assessing viability and infectivity of foodborne and waterborne stages (cysts/oocysts) of *Giardia duodenalis, Cryptosporidium* spp., and *Toxoplasma gondii*: A review of methods. *Parasite, 25*. https://doi.org/10.1051/parasite/2018009.

Sathyanarayanan, L., & Ortega, Y. (2006). Effects of temperature and different food matrices on *Cyclospora cayetanensis* oocyst sporulation. *The Journal of Parasitology, 92*(2), 218–222. https://doi.org/10.1645/GE-630R.1.

Slifko, T. R., Raghubeer, E., & Rose, J. B. (2000). Effect of high hydrostatic pressure on *Cryptosporidium parvum* infectivity. *Journal of Food Protection, 63*(9), 1262–1267. https://doi.org/10.4315/0362-028X-63.9.1262.

Utaaker, K. S., Skjerve, E., & Robertson, L. J. (2017). Keeping it cool: Survival of *Giardia* cysts and *Cryptosporidium* oocysts on lettuce leaves. *International Journal of Food Microbiology, 255*, 51–57. https://doi.org/10.1016/j.ijfoodmicro.2017.05.009.

Uyttendaele, M., Neyts, K., Vanderswalmen, H., Notebaert, E., & Debevere, J. (2004). Control of *Aeromonas* on minimally processed vegetables by decontamination with lactic acid, chlorinated water, or thyme essential oil solution. *International Journal of Food Microbiology, 90*(3), 263–271. https://doi.org/10.1016/S0168-1605(03)00309-X.

Van Pelt, A. E., Quiñones, B., Lofgren, H. L., Bartz, F. E., Newman, K. L., & Leon, J. S. (2018). Low prevalence of human pathogens on fresh produce on farms and in packing facilities: A systematic review. *Frontiers in Public Health, 23*, 6–40. https://doi.org/10.3389/fpubh.2018.00040.

Veit, P., Bilger, B., Schad, V., Schäfer, J., Frank, W., & Lucius, R. (1995). Influence of environmental factors on the infectivity of *Echinococcus multilocularis* eggs. *Parasitology, 110*(1), 79–86. https://doi.org/10.1017/S0031182000081075.

Weng, Y. L., Zhuang, Z. L., Jiang, H. P., Lin, G. R., & Lin, J. J. (1989). Studies on ecology of *Fasciolopsis buski* and control strategy of fasciolopsiasis. *Zhongguo Ji Sheng Chong Xue Yu Ji Sheng Chong Bing Za Zhi, 7*(2), 108–111.

WHO (2015). *WHO estimates of the global burden of foodborne diseases - foodborne disease burden epidemiology reference group 2007 - 2015*. http://apps.who.int/iris/bitstream/handle/10665/199350/9789241565165_eng.pdf?sequence=1/, Accessed date: 13 May 2019.

Zanini, G. M., & Graeff-Teixeira, C. (2001). Inactivation of infective larvae of *Angiostrongylus costaricensis* with short time incubations in 1.5% bleach solution, vinegar or saturated cooking salt solution. *Acta Tropica, 78*(1), 17–21. https://doi.org/10.1016/S0001-706X(00)00165-0.

Zhao, T., Zhao, P., & Doyle, M. P. (2009). Inactivation of *Salmonella* and *Escherichia coli* O157:H7 on lettuce and poultry skin by combinations of levulinic acid and sodium dodecyl sulfate. *Journal of Food Protection, 72*(5), 928–936. https://doi.org/10.4315/0362-028X-72.5.928.

Zhu, N., Zhu, Y., Yu, N., Wei, Y., Zhang, J., Hou, Y., et al. (2019). Evaluation of microbial, physicochemical parameters and flavor of blueberry juice after microchip-pulsed electric field. *Food Chemistry, 274*, 146–155. https://doi.org/10.1016/j.foodchem.2018.08.092.

Science of the Total Environment 900 (2023) 165673

Contents lists available at ScienceDirect

Science of the Total Environment

journal homepage: www.elsevier.com/locate/scitotenv

Discussion

Use of real-time immersive digital training and educational technologies to improve patient safety during the processing of reusable medical devices: Quo Vadis?

T. Kremer [a,c,*], N. Murray [b], J. Buckley [b], N.J. Rowan [c,d]

[a] Microbiological Quality & Sterility Assurance, Johnson & Johnson, 1000 Route 202 South Raritan, NJ 08869, USA
[b] Faculty of Engineering and Informatics, Technological University of the Shannon, Midlands West, Athlone Campus, Ireland
[c] Centre for Sustainable Disinfection and Sterilization, Bioscience Research Institute, Technological University of the Shannon, Midlands Midwest, Athlone Campus, Ireland
[d] Department of Nursing and Healthcare, Technological University of the Shannon, Midlands Midwest, Athlone Campus, Ireland

ARTICLE INFO

Editor: Damia Barcelo

Keywords
Medical device
Educational immersive technologies
Robotic instrumentation
Patient safety
Decontamination

ABSTRACT

Hospital acquired infections stemming from contaminated reusable medical devices are of increasing concern. This issue is exaggerated with the introduction of complex medical devices like endoscopes and robotic instrumentation. Although medical device manufacturers validate their cleaning instructions for use, evidence in the literature demonstrates that effective device processing is not being performed consistently within sterile processing departments in clinical settings. The result is increased risks to patient safety. As a solution to this problem, focused one-on-one training increases compliance to the medical device manufacturer's processing instruction. However, often this is not a practical solution for the volume of healthcare staff responsible for device processing activities. This constitutes the first paper to address the blended use of educational and digital technologies to address these challenges and as a result inform safety and sustainability for the medical device sector. Cognitive learning theory is an evidence-based framework for learning. It supports the use of immersive educational experiences using emerging extended reality technologies (e.g., virtual or augmented reality) to increase learning comprehension. The delivery of educational content via these technologies provides an innovative option for repeatable leaning and training outcomes. The motivation is to decrease patient risk of contaminated reusable medical devices. The proposed approach while primary motivated by safety can also enhance sustainability and efficiency enabled by artificial intelligence and robotic instrumentation.

1. Introduction

Medical devices are of critical importance to patient health where healthcare is continually evolving to enhance the quality of care for patients (Kremer et al., 2019; Rowan et al., 2023). However, despite advances in innovation and service provision, healthcare is constantly scrutinized so as to improve and evolve products for diverse patient needs. In particular, the effectiveness of quality improvements where inappropriately cleaned, processed and sterilized medical devices have been frequently cited as the source of transmitting significant microbial infections leading to morbidity and mortalities (McDonnell and Hansen, 2020). Hospital acquired infections (HAIs) are defined as infections that develop 48 h after a stay at a healthcare facility that was not present or incubating at the time of admission. HAIs are estimated to affect 1.7 million patients in the US annually leading to 99,000 deaths (Hensley and Monson, 2015). Contaminated medical devices are a common source of HAIs and have accounted for 60 to 80 % of all bloodstreams, urinary tract, and pneumonia-related HAIs (Gold and Hitchins, 2013). Although these statistics are related to the US as an example, similar studies can be found globally (e.g., France (Cabronne et al., 2010)). To reduce this risk, reusable medical devices are decontaminated (i.e., cleaned, disinfected and/or sterilized) before being used on the next patient.

1.1. Reusable medical device decontamination

Before reusable medical devices (e.g., surgical instruments) can be effectively disinfected or sterilized they must be thoroughly cleaned

* Corresponding author at: Microbiological Quality & Sterility Assurance, Johnson & Johnson, 1000 Route 202 South Raritan, NJ 08869, USA.
E-mail address: tkremer@its.jnj.com (T. Kremer).

https://doi.org/10.1016/j.scitotenv.2023.165673
Received 3 March 2023; Received in revised form 17 July 2023; Accepted 18 July 2023
Available online 20 July 2023

(Association for the Advancement of Medical Instrumentation, 2020) (World Health Organization, 2016). Cleaning is defined in the medical device industry as the "removal or contaminants to the extent necessary for further processing or intended use" while clean is defined as "visually free of soil and below specified levels of analytes" (International Organization for Standardization, 2018). These specified levels have been set by industry consensus in ANSI/AAMI ST98 (Association for the Advancement of Medical Instrumentation, 2022) and ISO 15883-5 (International Organization for Standardization, 2021). Device manufacture's hold the responsibility to validate these cleaning instructions for use and demonstrate they can be reliably achieved within a healthcare setting with consideration of human factors (Association for the Advancement of Medical Instrumentation, 2014).

Regardless of the validation requirements, HAI outbreaks have still been associated with inadequate cleaning and inappropriate disinfection of particularly challenging to clean devices, i.e., endoscopes (Rutala and Weber, 2019; Rowan et al., 2023). Often these devices have also been linked as causative agents in outbreaks of multi-drug resistant microorganisms (MDROs) in which there was no apparent breach reported in endoscope reprocessing (Cabronne et al., 2010; Marsh et al., 2015; Shenoy et al., 2019). This occurrence also coincides with the continued rise in antimicrobial resistance (AMR) in problematical bacteria and fungi that has reached crisis point globally (Masterson et al., 2021; Garvey et al., 2022; Garvey and Rowan, 2023). Notably, there can be as many as 100 complex cleaning and reprocessing steps for decontaminating medical devices (as per Original Manufacturers' Instructions for Use [IFU]) where the margin for patient safety post processing and sterilization is near zero (Rutala and Weber, 2019). The presence of recalcitrant biofilm that harbours pathogenic microorganisms adds to this reprocessing challenge (McDonnell and Hansen, 2020). In Oct 2022, the World Health Organization (2016) highlighted a new priority list of key fungal pathogens (such as *Candida* sp.) that can also be present and harboured in recalcitrant biofilms exacerbating safety and technical challenges for medical device cleaning and processing in healthcare.

1.2. Complex medical devices

As device features, geometric features of a medical device, continue to gain in complexity, the cleaning process also becomes more difficult for health care facilities to perform. Device manufacturers must reach a delicate balance in their instructions for use (IFU) between being too vague and risking improper cleaning or too detailed and being too restrictive and risk noncompliance (Bancroft and Spenser, 2022). As described by White et al. (2021), an ideal situation would be for medical device manufactures to improve the design of devices for ease of effective processing; but it is often evident from the literature that the efficacy of device processing is typically only evaluated at the end of the device design process where the design features are fixed. This also has implications for material selection in medical device design to ensure appropriateness for effective functionality, cleaning, processing and sterilization (McEvoy and Rowan, 2019; McEvoy et al., 2021) (Table 2).

An example of the evolution of complex device features is the flexible gastroscope, introduced by Dr. Rudolph Schindler in 1932 (Olympus, 2022). The application of a camera with flexible lumens allows for visualisation during clinical procedures that dramatically changed the standard of care over the last 90 years using many types of flexible endoscopes. These devices were designed for functionality during the clinical procedure, may not always considered fully the required processing steps necessary to ready them for subsequent patient use with repeated and constant use. As such, over the last 20 years there has been a plethora of research documenting the challenges with the cleaning process and the increased risk of HAIs as a result (Fig. 3).

A literature search using the terms "endoscope" and "cleaning" currently results in 1906 results with 384 of these articles being relevant to cleaning/disinfection or the prevention of HAIs through appropriate processing practices. Narrowing the scope to include the word "duodenoscope" in the search results in 88 results with all of them relevant. The topic of how to appropriately process endoscopes to prevent HAIs has been a subject of much debate since the early 2000s in the medical device community. Prior to 2015 there was not a standard practice for how device manufacturers were expected to validate the cleaning process. The inconsistencies in experimental designs led to conflicting information from the manufactures to what was observed within the clinical setting (Alfa, 2016). Throughout the globe, studies investigating unsuccessful decontamination began to populate the literature in addition to linking studies to the occurrence of patient HAIs (Rutala and Weber, 2019; Rowan et al., 2023). It is noteworthy that failure to effectively clean medical devices can contribute to the build-up of recalcitrant biofilms harbouring unwanted microbial pathogens that can challenge the sterility assurance process leading to HAIs and potentially sepsis (Vickery et al., 2013; Roberts, 2013; Dancer, 2014; Protano et al., 2019; Rowan et al., 2023). In 2015 the US Food and Drug Administration published a guidance applicable to endoscope medical device manufacturers. This standardization of the validation process for cleaning IFU allowed the health care facilities to focus their attention on the implementation of the validated processing instructions within the sterile processing departments as the root cause for the associated HAIs. Publications on the appropriate processing requirements for endoscopes has continues to steadily increase over the last 45 years (Fig. 1).

There is increasing interest and focus on the potential use of digital technologies to improve the effectiveness and sustainability of medical devices including environmental waste management and circularity (Rowan et al., 2023). This discussion paper addresses the novel role of combining immersive and educational technologies to improve and evolve cleaning of medical devices. More specifically, through enhanced and active training, the target is to improve efficacy and sustainability. For example, immersive virtual reality training has been reported to inform design, verification, validation and manufacturing of medical devices with safety to the fore (Keefe et al., 2010). Immersive training informed educational programs and motivated workers (Matthew and Pillai, 2020; Pears and Konstantinidis, 2022; Ovunc et al., 2021; Ndhaief et al., 2022; Tang et al., 2022) and provide insight into environmental impact (Afolabi et al., 2022). Digital innovations and the rapid evolution of devices and tools requires to include critical thinking about sustainability (Barats et al., 2020) that includes novel opportunities to introduce of 3D printed polymers, digital twin (Chen et al., 2019) and sustainable sterilization modalities (McEvoy et al., 2023). Thus, there is a growing interest in leveraging digital tools to communicate simple, engaging and sustainability messages to large populations and to different appropriate stakeholders (such as Rowan, 2023; Rowan et al., 2023). Moreover, appropriate omni-channel messaging is relevant for embracing environmental issues, sustainable development and climate change (George et al., 2021) that includes considering real-time opportunities for improving safety of medical devices such as through design thinking and automation (O'Neill et al., 2022; Schuelke-Leech, 2021; Rowan et al., 2023). Life cycle assessment (LCA) contributes to the environmental assessment of higher order effects of ICT applications that includes behavioural change effects (Pohl et al., 2019), which includes modelling the environmental effects of services and products throughout their life cycle. Researchers have noted the importance of applying digital solutions to facilitate development of new digital tools beyond LCA (Cooney et al., 2023; Rowan et al., 2022, 2023) where there is provision for harmonized training and problem solving such as the use of extended reality applications (Table 3).

1.3. Risk mitigation

Effective decontamination continues to be an important industry discussion as the literature continues to explore a root cause analysis for the HAIs. At the World Federation Hospital Sterilization Sciences Congress held in Barcelona, Spain in November 2022, Annette Rittich of Olympus discussed a collaboration with French authorities to

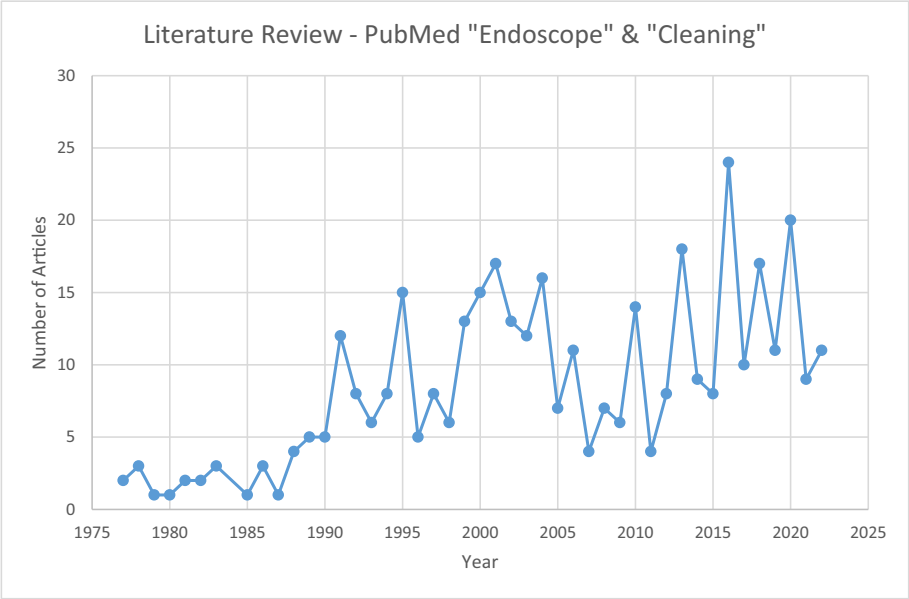

Fig. 1. PubMed literature review – key words, "Endoscope + Cleaning".

investigate 2017 HAIs associated with endoscopy. The key findings of their investigation showed that cleaning steps were not being performed correctly or were missing from the process due to a lack of training or awareness. Mitigation showed that with direct training from the medical device company on performing processing, effective decontamination could be achieved (World Federation for Hospital Sterilization Sciences, 2022). Singh et al. (2022) noted challenges faced by the medical device industry presented by the COVID-19 pandemic and the importance of safety (Table 4).

The occurrence of HAIs has direct medical cost impact on hospital finances and many researchers perform analysis to understand the economic benefits of the investment of an infection control program. In a 2009 summary report based on 2002 HAI data, the consumer price index (CPI) for inpatient hospital service ranged from $35.7 billion to $45 billion, while the benefits of prevention ranged from $25.0 billion to $31.5 billion (Scott, 2009).

Immersive and educational technologies will support and enable the application of appropriate risk management for medical devices in terms of training on important techniques and design features. These technologies can help ensure safety of the device throughout the product lifecycle by identifying device design problems from a risk-based cleaning and processing decisions perspective prior to distribution. This underpins risk analysis, which is a regulatory requirement where FDA requires risk analysis information (Rowan et al., 2023). This risk management specifically relates to ISO 14971:2019 Standard and rigor associated with this guiding document that essentially reduces the probability of device failure and patient risk (harm) due to the occurrence and severity of this hazard or hazardous situation. Using blended immersive and educational approaches, this will also help towards visualisation holistic situation in virtual real-time that will inform and help reduce the possibility of failure of the device by way of design, use and re-use including reducing margins of error with end-to-end use of the device. This approach will also allow specialist end-users, such as nurses, surgeons, contribute to design and training from an integrated real-time solutions perspective that will help reduce risk for patients. These digital and cognitively informed approaches will also help provide specialist situational training on devices as it relates to understand the potential source of harm (hazard) and the sequence of events that may lead to or prevent this hazardous situation to reduce probability of occurrence. Immersive technologies will provide real-time interactive experiences simulating actual device cleaning and processing that will contribute to risk-based decisions such as identifying design outputs for proper functioning of the device that may be difficult to clean, or by defining the type and extent of control to be exercised over product and for end-users (FDA). The complementarity of digital and educational technologies will also help understand and implement an appropriate quality system including subject-matter training addressing necessary process control and simplification of steps to ensure major equipment and processes are validated appropriately. These can seamlessly help contribute to informing necessary approvals for in-process acceptance based on feedback from virtual training experience. These tools can also potentially provide training including efficacy of new product designs, labelling and instructions for use for appropriate risk controls to reduce and mitigate unacceptable risks. These technologies can also help regulators (FDA) for risk make risk-based decisions surrounding core management activities including device and recall classifications and can also provide an insight the role of AI in terms of usage and appreciation for trustworthiness (Rowan et al., 2023). These risks management activities can also be extended to help with critical inspectional decisions from a training and devices features perspective, particularly with complex devices that may be more prone to supporting biofilm build-up due to challenges associated with cleaning that may bring margin of error to zero for meeting all steps defined by manufacturers' IFUs. Immersive and educational tools also can support greater understanding, visualisation and training on risk management techniques such as Fault Tree Analysis (FTA) to hazard identification, Failure Mode and Effective Analysis (FMEA) to identify and help evaluate individual fault modes in hazardous situations, and FDA Benefit-Risk Analysis that is used to assess medical device risk(s) once all measures to reduce risk (s) have been applied. For example, given the complexity of the de-risking situation, these virtual and cognitive approaches can also help inform determinations in pre-market approval applications (PMA) and De Novo classifications along with supporting appropriate training that may contribute to determining substantial equivalence in premarket notifications (510(k)). These technologies can help unlock efficiencies, such as through enhanced collaborations with multi- and inter-disciplinary stakeholders that will streamline compliance including risk-based requirements under ISO 13485: 2016.

The growing application of artificial intelligence (AI) in healthcare including the virtually-created paradigm has brought technological breakthroughs to traditional training, diagnosis and treatments. However, it is accompanied by risks and challenges. Where medical data are

Table 1
Scopus database search of keywords blending use of immersive and educational technologies with medical devices up to 2023.

Year	Frequency of keyword cited in published abstracts and full length papers[a]					
	"Medical devices"	"Immersive technology"	"Virtual reality"	"Infection control"	"Educational technologies"	"Training"
2023	10,252	1337	19,939	16,031	11,635	100,155
2022	25,306	2964	32,880	42,432	30,540	264,875
2021	23,857	2123	26,789	43,116	26,666	226,265
2020	20,666	1300	21,765	35,726	22,952	199,371
	Combinations of keywords cited in published abstracts and full length papers					
	√	√	√	√	√	√
2023	0					
2022	0					
2021	0					
2020	0					
	√[+Ed Technol]		√[All four marked]		√	√[+MedDev + Ed]
2023	23		2			10
2022	70		3			18
2021	68		3			21
2020	56		7			29
	√		√			[+√]
2023	90					3
2022	183					14
2021	131					16
2020	88					6
	√		√	√		
2023	1					
2022	2					
2021	1					
2020	0					

[a] Search conducted 25/5/2023; √ indicates key word used in combination; + indicates a combination used with other marked keywords for that search.

unstructured, lack uniformity and standardization annotation there is potential for such data to directly affect the quality of medical AI algorithm models. These authors noted that opacity of algorithms affects patients' trust in medical AI where algorithmic errors or security vulnerabilities can pose significant risks and harm to patients. There is a commensurate need to "make medical AI trustworthy, at the ethical level. At the important regulatory level, strengthening data quality management, improving algorithm transparency and traceability to reduce algorithm bias, and reviewing the whole process of the AI industry to control risk" is appropriate. Use of the virtual environment created by immersive technologies may potentially provide a case study environment for multiple stakeholders to discuss and assess AI risks and social impacts through international cooperation and communication for service end-users. Effective use of education and enabling technologies will help stakeholders understand and compensate for perceived risks associated with AI trustworthiness (Table 2).

2. Educational and digital technologies - training and innovation in device design, cleaning and processing

Training and competence development remains mostly grounded in traditional methods of training against a backdrop of highly innovative processes and technology advancements. Likewise, the provision of specialist training in the healthcare workforce merits innovative approaches using technology as a tool in competence development. A systematic review of publications in Scopus databases using combinations of the keywords 'immersive', 'medical devices', 'virtual reality', 'infection control', 'educational technologies' and 'training' using a PRISMA framework (Rowan et al., 2023) revealed a surge in increased published outputs (Table 1). These activities and applications have been applied to help with end-user understanding, testing, risk management, competencies, and satisfaction with conducting complex procedures, such as simulated device use in surgery and infection control that includes improved patient safety (Table 2).

For example, in the context of specialist training and educational programs, Extended Reality technologies such as Virtual reality (VR) are emerging as potential platforms to deliver learning content in a more ecologically valid manner. This is based on their delivery of 360° visuals, spatial audio, and allowing the learner to move beyond the passive mode towards an active participant in their learning experience (Braga Rodrigues et al., 2020). These technologies in conjunction with various wearable sensor technologies support the capture of various user physiological measures in addition to task performance and user interaction to facilitate a true "human-in-the-loop" system that supports adaptive, personalized while maintaining context-based learning (Egan et al., 2016; Salgado, 2018). The capture system identifies, at the individual level, key abilities of the learner (by moving beyond binary pass/fail reporting towards understanding a specific individual learning needs). This then informs how the presentation system challenges the learner; thus, optimizing the learner experience. It identifies opportunities for improved training including future provision for operator retraining (Tables 1 and 2).

To ensure efficacy, it is paramount that any training agenda adopts a suitable evidence based theoretical framework to guide educational design, implementation, and evaluation. Having already been used or advocated for across several industries such as the food (Galanakis et al., 2021), manufacturing (Carvalho et al., 2020), and automotive industries (Atici-Ulusu et al., 2021), Cognitive Load Theory (CLT) (Sweller, 1988) provides a suitable framework for this general purpose.

2.1. Cognitive Load Theory (CLT)

CLT is based on the view of learning being a change in long-term memory, i.e., that a goal of education or training is for important and relevant knowledge to become stored [learned] in a learner or trainees' long-term memory and therefore be retrievable when necessary. The purpose of CLT is to underpin the efficiency of this process through ensuring an appropriate instructional design of educational materials and approaches.

CLT is premised on the limitations of peoples' working memory and thus their restrictions to contend with excessive amounts of information or excessive complexity in information to be learned. It is regarded as one of the most evidence-informed educational theories for teaching and learning and underpins several explicit pedagogical practices (Weinstein et al., 2018). It is considered specifically pertinent to medical education (Young et al., 2014; Young and Sewell, 2015), notably in terms of

Table 2
Examples of immersive and educational technologies informing training and behavioural change for complex medical device applications including patient safety and risk management.

Description of activities and applications	Reference(s)
Use of VR as optimal solution in neuroscience, psychology, medicine and sports rehabilitation with ecological validation, smart interface with other medical devices; 3D simulation of real-life experience; strong effects on human perception and behaviour	Fusco and Gaetano (2022)
VR relevant as learning and practicing tool for improving infection control procedures including influencing performance, motivation, concentration	Omori et al. (2023)
Systematic review of 287 approaches (VR, AR, EX) published from 2011 to 2022 in field of Industry 4.0 intimated emergence of benefits including high performance on human tasks with focus on XR applications - opportunities for improving algorithms, ergonomic features, built-in cameras/sensors	Cardenas-Robledo et al. (2022)
VR induced post-stroke patients will illusion of painting masterpieces for motor rehabilitation in upper limbs	Losa et al. (2020)
Immersive VR treatment on balance and pasture by inducing stroke patients illusion of motivation and rehabilitation	Yeung et al. (2021)
Robotic training to inform and to improve rehabilitation	Slater and Sanchez-Vives (2016)
VR, AR, mixed reality and extended reality (XR) mechanization in healthcare sector demonstrated students using these immersive technologies improved training-based learning outcomes and education; motivated students; created positive interactions; reduced anxiety in learning process complex setting (medical professionals), improved engagement and satisfaction	Khan and Lippert (2022)
Deployment of HoloSens2 MR deadest device to support delivery of remote care in COVID-19 hospital environment – highlighted role of MR in minimizing exposure to nosocomial infection, optimizing use of PPE, and enhanced aspects of care. Addressed content-specific security, infection control, user experience and workflow integration for clinical end-users.	Martin et al. (2020)
Immersive VR informed design, verification, validation and manufacture of medical devices including new high risk, high-payoff design. Aligned with goals of FDA where simulation played role in engineering, manufacturing and science. 3D interface and visualisation to inform training.	Keefe et al. (2010)
126 articles reviewed showing that Immersive Technologies (VR, AR, MR, XR) used mainly to inform education and training in surgery and anatomy-related subjects for doctors, medical students and interns	Tang et al., 2022
Use of VR for medical students to improve learning motivation, competencies and transferrable skills such as for complex operation theatre	Matthew and Pillai (2020)
VR **visualisation** of complex CFD simulated blood flow in cerebral aneurysms treated with flow diverted stents	Baheri Islami et al. (2021)
Immersive technologies informed training and competencies in First Responders and Physiotherapists	Wilkerson et al. (2008) Pappa and Papodopoulos (2019)
VR provided low cost, high-fidelity surgical training skills, improved procedure time task completion, accuracy, satisfaction and low discomfort.	Mao et al. (2021)
Training with cognitive load improves performance under similar conditions in a real surgical task, improved pre-, post and retention tests	Sankaranarayanan et al. (2020)
Immersive technologies and AI allowed autonomous support for trainees to accelerate their skills tailored to learners with minimal time and expense	Pears and Konstantinidis (2022)
VR training proven to be low cost option for microbiologist in teaching	Damasceno et al. (2023)
Immersive technologies improved perioperative anxiety, acute and chronic pain management	Alqudimat et al. (2021)
VR supported rapid upskilling of Healthcare professionals during COVID-19 pandemic	Young and Aquilina (2021)
VR relevant as learning and practicing tool for improving infection control procedures including performance, motivation, concentration	Omori et al. (2023)
Virtual reality infection control (IC) simulation used in donning and doffing of PPE during COVID-19 for respiratory care in paediatric patients – informed knowledge, IC performance and self-efficacy for nursing students	Yu and Yang (2022)
Immersive technologies used to assess, model and implement safety risk mitigation (adjacent construction industry)	Afolabi et al. (2022)
Immersive simulation exercises improved student skills and patient safety; created safe and supportive environment replacing real life	Mitchell and Assadi (2021)
Use of immersive technologies in robotic surgery and training to improve patient safety	A. Chen et al. (2021)
Immersive technology used in surgery training (mimics actual stressful clinical setting) to enhance patient safety and reduce errors; high-fidelity visual/sensory feedback – thus providing all 3 levels of human behaviour	Dargar et al. (2015)
Training using VR to prevent HAIs focusing on hand hygiene – providing visual feedback about complex microbial-transmission and intervention	Clack et al. (2021)
Development of VR simulation on program for high-risk neonatal infection control education – VR combines digital learning with simulation to provide situated learning in 3D interactive experience, informs clinical skills in deliberate and repetitive manner, promotes problem solving for nurses	Yu and Mann (2020)
Reduction in visual changes while learning in XR environments – research describes addresses XR limitation of cognitive overload in trainees due to continuous changes in attention.	Bautista et al. (2023)
Engineering design and evaluation of the process evaluation method of auto repair professional training in VR environ – this traditional vocational training limitations saving time and resources.	Xiang et al. (2022).
Immersive (IM) technologies improves safety training by increasing motivation, engagement and skills development – albeit only 10 of 44 studies published on comparing IM training to traditional learning (PRISMA)	Garcia Fracaro et al. (2022)
Addresses improvements in evaluation and assessment for simulated training and development and performances from this experience	Akdere et al. (2022)
VR simulation of high tibial osteotomy for medical training with outstanding result through interaction between surgical tools/sites verified by surgeons.	Han et al. (2022)
A scoping review addressing current state of XR is in Otolaryngology head and neck (OHNS) surgery training that defined as fully-immersive (VR) using head-mounted displays, non-immersive and semi-immersive VR, AR, or MR. Current educational applications of XR in OHNS are limited to VR, do not fully immerse participants with need for shared definition of VR technology.	Zagury-Orly et al. (2023)
Used AR to reduce risk of contamination from airborne disease agents on surfaces with novel application of 3D sensing technology in real time	Yu et al. (2021)
Used task models to understand the interaction of numeracy skills and technical competence with medical device design where interactive systems are safety critical (syringe drivers and infusion pumps for IV medication). Helped prevent errors through ensuring system behaviours are consistent with user requirements – highlights major role in training medical personnel	Bowen and Coben (2021)
Digital factory – VR environments for industrial training and maintenance – highlighting benefit this platform as intuitive and immersive human-computer interface for complex training using low-cost applicability	Shamsuzzoha et al. (2021)
Use of AR headset to successfully remotely train clinicians on medical devices using anatomic models – two way training with the proctor and student using their own platforms – AR eliminates need to travel and may mitigate risks of infectious exposures, reduce training cost and increase proctor availability, allowing training from own institute or clinic.	Stone et al. (2022).
Use of digital technologies and 3D simulation to train medical staff on new technologies and tools (practice of lumbar puncture, childbirth)	Ndhaief et al. (2022)
VR training for assembly of hybrid medical devices with positive experience.	Ho et al. (2018)
Use of Immersive technologies to develop medical educational materials.	Ovunc et al. (2021)
VR as psychological intervention for mental health disturbances during COVID-19 pandemic alleviating face-to-face challenges – conceptual.	Hatta et al. (2022)
Use of handheld educational technologies (digital) in medical schools.	Relan et al. (2004)
IR trauma simulation using MR for next level of medical skills training.	Uhl et al. (2023)
VR, AR and MR applications in surgery increased operative accuracy and improved safety by decreasing procedure-related complications "innovations in computer-assisted surgery (CAS)".	Verhey et al. (2020)

Abbreviations: virtual reality (VR), augmented reality (AR), mixed reality (MR), extended reality (XR), hospital acquired infections (HAIs), infection control (IC).

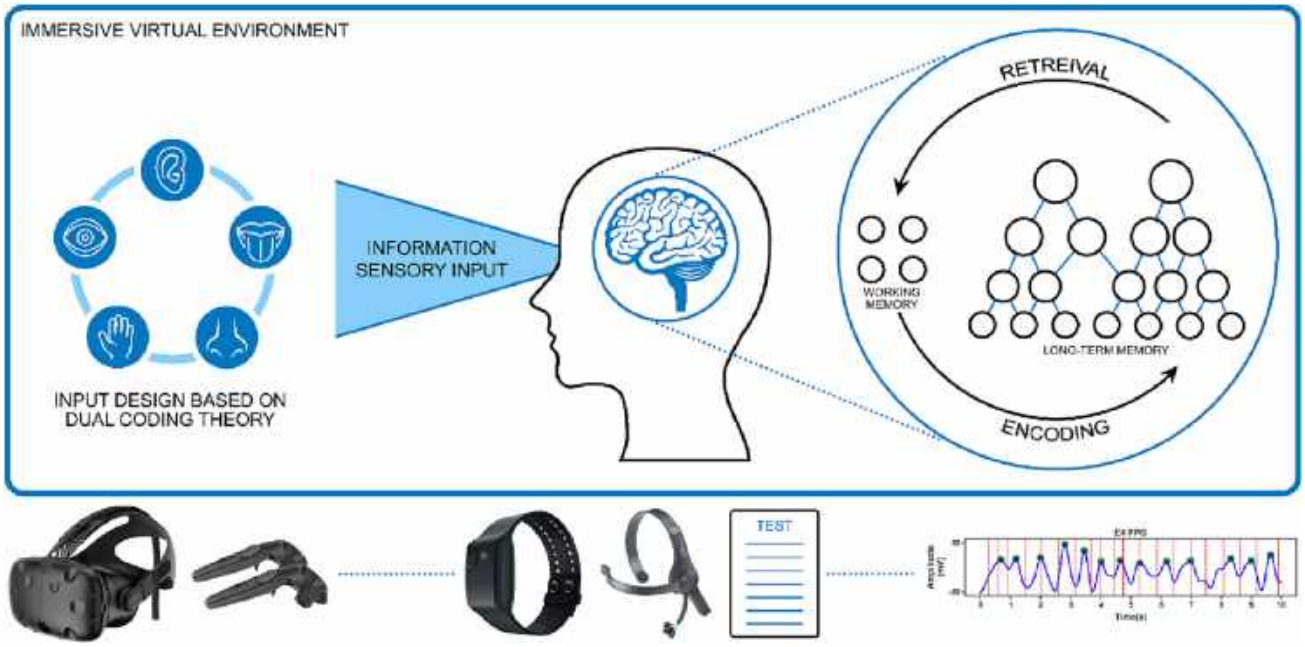

Fig. 2. Virtual reality training.

curriculum design (Leppink and Duvivier, 2016), clinical training (Mancinetti et al., 2019), and simulation design (Fraser et al., 2015). It has also been foundational to research within the medical device industry where Fenik et al. (2013) used CLT to guide a randomized control trial in which novice clinicians use of pre-packaged all-inclusive central line catheter kits was compared with their use of kits containing only the catheter components and with all other components separately packaged and provided in a materials cart.

Specialist training through IM for the medtech industry has developed using the assumption of CLT that humans have working-memory limitations and the learning science assumptions that human information processing system has two channels, visual/pictorial and verbal/auditory (dual-channel assumption). Therefore, humans need to actively engage in cognitive processing to learn and not just be passive recipients of knowledge (active processing assumptions). These assumptions were evolved into the Cognitive Theory of Multimedia Learning (Mayer, 2014). The utility of this theory lies in its capacity to be translated into evidence-informed techniques for education and training where immersive technologies specifically are being used. Mayer and Moreno's (2003) seminal work provides 9 explicit techniques with associated effect sizes which can be immediately adopted within the design of IM-based training. Examples of these include segmenting – allowing time between bite-sized segments of multimedia information for cognitive processing, synchronizing – presentation narration simultaneously to animation to reduce the trainee's need to mentally hold representations in their memory, and off-loading – moving some essential information from the visual to auditory channel or vice-versa to avoid overloading a singular channel and permit more efficient cognitive processing.

2.2. Advantages of CLT

Immersive technologies utilize physiological and psychological measurements to provide insight into learning and performance data and CLT is directly associated with the cognitive capacity of trainees. This combined underpinning framework allows for a seamless integration of an educational paradigm within Medtech training. It is envisaged that such immersive approaches to training and development could deliver significant benefit to healthcare industry in highly technical areas such as aseptic manufacturing, cleanroom control, sterilization processing and laboratory testing. The key aim of various assistive technology (AT) systems is to augment an individual's functioning while supporting an enhanced quality of life (QoL). In recent times, we have seen the emergence of Virtual Reality (VR) based assistive technology systems made possible by the availability of commercially available Head Mounted Displays (HMDs) (Salgado, 2018). The use of VR for AT aims to support levels of interaction and immersion not previously possibly with more traditional AT solutions. Crucial to the success of these technologies is understanding, from the user perspective, the influencing factors that affect the user Quality of Experience (QoE). In addition to the typical QoE metrics, other factors to consider are human behaviour like mental and emotional state, posture, and gestures. In terms of trying to objectively quantify such factors, there are wide ranges of wearable sensors that can monitor physiological signals and provide reliable data. Salgado has previously demonstrated, captured and presented the users EEG, heart Rate, EDA, and head motion during the use of AT VR application from a learning perspective (Salgado, 2018). The prototype is composed of the sensor and presentation systems: for acquisition of biological signals constituted by wearable sensors and the virtual wheelchair simulator that interfaces to a typical LCD display. Hynes et al. (2020) describes an evaluation of lower facial micro expressions as an implicit QoE metric for an augmented reality (AR) procedure assistance application, such as for device cleaning. Augmented reality (AR) has been identified as a key technology to enhance worker utility in the context of increasing automation of repeatable procedures. The development of AR will also be commensurately important for enabling human-robotic interaction for high-level remote robotic operation (HRI) (Xue et al., 2020), which is a critical component for delivering reliable and cost effective HRI system in adjacent smart factories of the future. Vijayakumar et al. (2022) have also recently proposed complementary AI-derived QoE prediction-based on measuring and assessing human physiological signals for immersive multimedia experiences. Specifically, the authors describe use of advanced machine learning techniques to predict QoE from physiological signals using a multimodal digital model. Vijayakumar et al. (2020) also describe commensurate wearable technology research that focuses on using peripheral physiological signals for emotion recognition that has real-time applications in healthcare. Adapting to the learner needs in a context aware manner by employing various AI and machine learning techniques to process the aforementioned human responses to predict the user state will facilitate the next generation of human in the loop

Table 3
Potential benefits and limitations of educational immersive technologies.

Potential benefit	Example (Ref)
Increased training motivation	Virtual reality has been shown to increase medical student motivation in learning activities (Sattar et al., 2019) with motivation being significantly linked to transfer to learning and competency (Vansteenkiste et al., 2009).
Overcoming of language barriers	Mobile AR applications have been developed to permit live language translation, permitting instructional and training materials to be made more generally accessible. Applications extend from written and verbal language (Fragoso et al., 2011) to sign language (Soogund and Joseph, 2019).
Cost and time savings to industry with potential safety implications	Immersive technologies can enable off-site training reducing the need for production line downs, the development of physical training equipment which can be less mobile, travel expenses, and where relevant the need to place novices in high risk situations for realistic training exercises (Kizil and Joy, 2001).
Responsivity to individual training needs	Use adaptive difficulty scaling of virtual reality task in proof-of-concept stage (Knobel et al., 2021) illustrates potential for immersive training tasks to respond live to individual trainee needs.
Just-in-time information provision	AR applications can provide relevant information in real time of working procedures for device usage (Nakai and Suzuki, 2016; Rochlen et al., 2017) and/or instructional steps for produce assembly (Radkowski et al., 2015) to operators or trainees.

Potential limitations	Example (Ref)
Sub-optimal presence/ immersion	Quality and level of user-experienced immersion is associated with feelings of presence in immersive technologies (Cummings and Bailenson, 2016). Higher levels of immersion is linked to improved task performance and error reduction in procedural training tasks (Sowndararajan et al., 2008) however excessive feelings of presence can lead to users being distracted hindering learning and subsequent performance (Parong and Mayer, 2021)
Potential high costs	Cost of immersive technology includes a wide range of factors to be considered on case-by-case basis which can vary based on industry/company size, sector, training needs, and dedicated budgets. These include technology investment costs, training and operator costs, re-use potential of the technology over time, and number of trainees availing of the technology (Garcia Fracaro et al., 2022).
Trainee safety	The use of head-mounted displays has been shown to present side effects of nausea in immersive simulations which can need to be resolved prior to clinical or industry implementation (Nunnerley et al., 2017)
Cybersecurity risks	Predominantly highlighted through the use of the Metaverse (includes immersive technologies, artificial intelligence, and blockchain) is the potential cybersecurity threat via internet communications (Jaipong et al., 2023; Pooyandeh et al., 2022).

intelligent reality experiences. Nowadays, potential opportunities exist to employ the use of digitized "feedback" modalities to help a user to "understand" improved techniques. A critical requirement emerges to consider the quality of feedback from the user perspective i.e., how they process, understand, and react to the feedback.

For example, medical device companies in partnership with universities are developing and deploying state-of-the-art biotechnology tools to unlock real-time microbial inactivation (McEvoy et al., 2021). Immersive (digital) technology providers are also partnering with medtech companies for complex virtual training on specific technical operations. For example, Mersus Technology has partnered with Boston Scientific in Ireland to test and apply an 'Avatar Academy Program' that uses computer gaming to recreate virtual laboratories and cleanrooms; thus, allowing medtech employees to familiarize themselves remotely with a complex work environment and processes. This approach will potentially automate training where one can could theoretically run six bespoke training sessions in one day that previously would have taken a month, which can be extrapolated to address the full production chain delivered in a virtual environment (Westmeath Independent, 2022). Thus, there is a significant opportunity to combine immersive and educational technologies for informing and shaping the future of device cleaning and reprocessing (Murray et al., 2019), which will help to safeguard patient health and will support e-innovation with future potential for technology disruption.

This combined educational and immersive technology approach to medical device cleaning and processing training is rooted in digitalization, which is commonly recognized as "Digital Twin" (DT) and is gaining in popularity across industries (Singh et al., 2022). The term 'Digital Twin' (DT) has gained popularity recently in academic as well as industrial circles, even though it was conceptualized decades ago. In 2002, Michael Grieves, who introduced the concept of DT, defined it as "*A set of virtual information constructs that fully describes a potential or actual physical manufactured product from the micro atomic level to the macro geometrical level. At its optimum, any information that could be obtained from inspecting a physically manufactured product can be obtained from its Digital Twin*" (Grieves and Vickers, 2017). Singh et al. (2022) defined DT as comprising three components: (a) physical twin – a real world entity (living/non-living) such as part, produce, machine, process (such as device cleaning), organization or human; (b) digital twin – the digital representation of the physical twin with the capability to mimic/mirror its physical counterpart in real-time; (c) linking mechanism – the bidirectional flow of data between the two with operates automatically in real-time. DT offers benefits in reducing operational costs and time, increasing productivity of existing system, informs decision making into opportunities for automation, improves maintenance schedules and activities, provides, and enables remote access including bespoke training, makes for a safer working/operational environment (including potential for medical product/reprocessing, and promotes sustainability (such as resource utilization) (Singh et al., 2022). As reported by Grand View Research (2021), the global market of DT was estimated at USD 5.04 billion in 2020 and is expected to reach USD 86.09 billion by 2028, with a compound annual growth rate of 42.7 % from 2021 to 2028. Combined use of digital technologies to inform design and processing has the potential to cause business and technology disruption by optimizing the learner's experience leading to significance increase in the device processing instruction retention. For example, Rowan (2019) noted the potential of developing novel processes for food and health applications where the author defined differences between sustaining and disruptive innovation). Fig. 2 depicts the methodology behind immersive learning with example technologies. Table 3 provides the benefits and limitations of immersive and educational technologies for this purpose, which compliments the extensive range of potential applications that was highlighted in Table 1.

2.3. Application of immersive technologies in healthcare

During the 2019 Kilmer Conference, a concept of how augmented reality could be applied to improve the training for the processing steps associated with reusable medical devices was presented. The authors described how the user experiences the real-world environment with an overlay of information that provides instruction (Patel and Flynn, 2019). This enhancement of instruction would allow for the substitution of device manufacturer's representative providing direct training and provide a greater opportunity for enhanced training (Fig. 3).

The complexity of reusable medical devices continues to advance with the introduction of robotic surgeries. The instruments used with the robotic are particularly difficult to clean as they often cannot be fully dismantled and require specific instructions for decontamination (White

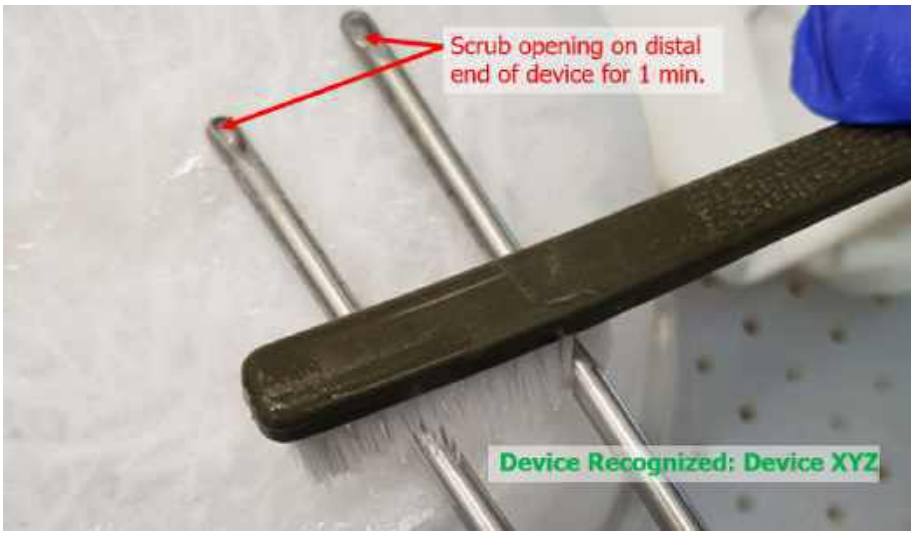

Fig. 3. Viewing example of proposed device processing augmented reality.

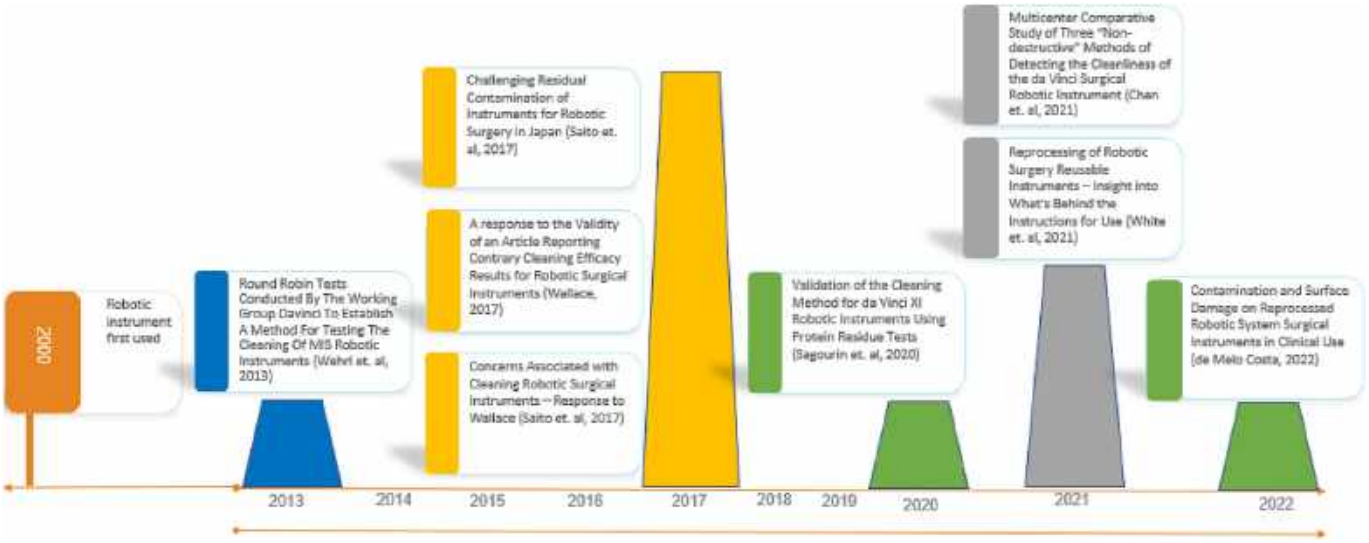

Fig. 4. Robotic instruments cleaning publication timeline (Wehrl et al., 2014; Wallace, 2017; Saito, 2017a,b; Chen et al., 2021b; de Melo Costa, 2022; Sagourin et al., 2021; White et al., 2021).

et al., 2021), so although there may be a benefit to the patient for the surgical procedure, the risk of an HAI originating from a contaminated robotic instrument is higher than with less complex, manual devices.

With endoscopes the literature demonstrates that without proper training for the sterile processing personnel there is an increased risk of the endoscopes not being fully decontaminated leading to HAIs. Robotic instruments are on a similar path of discovery. Like endoscopes, publications and conference proceedings are beginning to highlight the presence of residual soil after the decontamination process and the inability of health care facilities to properly clean these devices.

Performing literature search, like that for endoscopes, using the terms "robotic instrument" and "cleaning" results in 118 articles with 5 being relevant to cleaning. Although currently smaller in number, the articles are controversial with investigations from the clinical setting claiming the instruments cannot be cleaned, whereas the instrument manufacturer defends the cleaning process defined within the IFU. Robotic surgery is a fast-growing area of innovation and therefore, the problems associated with the decontamination of the instruments may grow exponentially over time (Fig. 4). Like other complex devices (i.e., endoscopes) effective training on performing the cleaning instructions will mitigate the risk of HAIs associated with this type of reusable medical device.

The medical industry has learned a lot over the years about the need for effective training from the introduction of endoscopes. To be appropriately trained the evidence shows that training must be personalized and interactive. The traditional way of training through seminar instruction is not sufficient for individuals to demonstrate competency, and the training issue is becoming increasingly more important with the introduction of robotic instruments.

CLT demonstrates that using immersive educational experiences like virtual or augmented reality will increase the competency of the trainees and are an innovative training process that can complement technological advancements. Individual leading supports active and engaged training that allows for the trainee to demonstrate competency without risk to patient safety. Compared to the cost of manufacturers providing individualized training, educational technologies have a lower cost and are more consistent with knowledge transfer (Table 1). Application of this educational technology to the processing instructions for complex medical devices, such as endoscopes or robotic instrumentation, is an ideal way to reduce patient safety risk.

Table 4
Indicative key performance indicators (KPIs) to assess impact of educational and immersive technologies on medical device.

Indicative key performance indicator (KPIs)	Relevant related reference(s)
Reduction in waste, resources and increased cost efficiency in healthcare – such as through eco-design	MacNeill et al. (2020) Gusso et al. (2020) Ling et al. (2018) Benedettini (2022)
Informing reduction in number of complicated steps for effective reprocessing of devices	Rowan et al. (2023)
Reduction in the margin of error for safety on device reprocessing through robust training combined with design thinking	Rowan et al. (2023)
Reduction in the number of hospital-acquired infections (HAIs) associated with use of reusable medical devices	Rowan et al. (2023)
Increased satisfaction, competence and standardization in the delivery of effective procedures through virtual/educational platform	Mao et al. (2021) Khan and Lippert (2022)
Increased productivity and product quality, optimized cost and time. Combining immersive technologies with *Lean tools* such as for improving layout and flow, supply chain enhancement, reduction of waste, improving quality, expedite operations, standardization and '6S' practices, continuous improvement, increased competitiveness, work-in-progress reduction.	Trubetskaya et al. (2022).
Increased number of inter-disciplinary publications that harness use of IM and Educational technologies to support measurable KPI (outcomes) for device cleaning and processing – including use of Quadruple Helix framework	Rowan and Casey (2021)
Efficiency in patient scheduling and reduction in waiting times for medical device intervention (including related reduction in patient anxiety).	Wu et al. (2014)
Reduction in Development cost and time (including human resources, material and machine expenditures).	Peel and Eggbeer (2016)
End-user satisfaction (such as surgeon)	Garnica-Bohorquez et al. (2019).
Medical device maintenance performance (life cycle) monitoring including types of maintenance strategies (scheduled, corrective), dependability criteria, failure rate category, maintenance costs, and risks.	Iadanza et al. (2019)
Number of short advanced programmes (SAPs), micro-credentials and mobility of staff for subject-specific training on immersive and educational technologies informing infection control procedures and outcomes	Perla et al. (2023) Rowan et al. (2022)
Number of sustaining or potentially disruptive innovations (including high risk/high gain, deep tech) envisioned through virtual end-to-end processing and training and connectivity between immersive and living (complex) labs	Schuelke-Leech (2018) Schuelke-Leech (2021)
Increased number of businesses from diverse disciplines developing coherent, appropriate and relevant partnerships for medical device innovation	Auer and Jarmai (2018)
Number of engagements with regulatory authorities including ISO standards informed by embracing education and immersive technologies including risk mitigation and MI/AI trustworthiness	Guerra-Bretana and Florez-Rendon (2019)
Use of IM + Educational technologies used in combination with other measurement tools (such as LCA) for informing appropriate sustainable solutions (HACCP) in medical device innovation with a training focus	Hemberg et al. (2023)
Increased awareness and appreciation of use of IM and Educational technology for an E-health considering including patient perspective and behavioural change including provision of learner/end-user interactive tools	Brenner et al. (2023)
Increased number of educational modules delivered across university curriculum that recognizes digital technologies for device devices including sterility assurance	Lambert et al. (2021)
Reduction in occurrence in device-associated sepsis as a consequence of effective bespoke immersive training	Rivers et al. (2015)
Simplification and potential standardization of many complex steps under manufacturers' IFUs that reduces risk of error in healthcare in cleaning and processing	Rutala and Weber, 2019 Rowan et al. (2023)
Number of dedicated interdisciplinary workshops and networking activities on use of IM and Educational technologies to address a harmonized approach to achieving consensus on appropriate KPIs for stakeholders including training and device features	Brenner et al. (2023)
Use of IM + Educational Technologies to inform increased number of trained technologists, engineers, clinicians, interns and nurses to simplify complex procedures from medical device cleaning/processing, to surgery/anaesthesia.	Tang et al. (2022)

Abbreviations: IM (Immersive technologies); HACCP (Hazard Analysis Critical Control Point); HAIs (Hospital-acquired infections); AI (Artificial Intelligence); LCA (Life Cycle Assessment); IFUs (Instructions for Use).

Brenner et al. (2023) recently conducted a systematic review of 2165 publications in this emerging domain of digital health, yet found only 5 papers that address or suggest tangible key performance indicators (KPIs) (Table 2). However, the medical device industry is very much an established rigorous domain that is highly regulated including risk management through ISO 14971: 2019 and more recently, ISO 14971: 2020. Table 4 provides a list of established and potentially new KPIs for the medical device industry that can be informed by use of novel immersive and educational technologies. Use of digital tools and automation will be informed by use of appropriate biosensors (Anand et al., 2022).

3. Summary

Effective cleaning and reprocessing of medical devices is essential to mitigate the risk to patient safety. Despite technological advancements, contaminated medical devices can transmit pathogenic microorganisms and have caused outbreak infections despite the fact that no defect in the medical device was detected, nor were there deviations from cleaning and processing steps. Device cleaning and processing comprises many complicated steps in healthcare where the margin to patient safety is often near zero, such as for gastroendoscopes subjected to cleaning and disinfection. There is a pressing need to improve training and innovation including design that can be met through future combined use of educational and training technologies that will also inform automation. This holistic approach to education and innovation has the potential to impact positively on future sustainability for the medical device sector along with commensurately benefiting patient safety. Development of health using these "E-Technologies" and digital twin innovations constitutes a healthcare domain of special interest as society begins to engage in more meaningful manners with "Metaverse" technologies, a concept initially conceived by Neal Stephenson in 1992.

CRediT authorship contribution statement

T. Kremer: Conceptualization, Writing – original draft. **N. Murray:** Writing – review & editing. **J. Buckley:** Writing – review & editing. **N.J. Rowan:** Writing – original draft.

Declaration of competing interest

The authors declare that they have no known competing financial interests or personal relationships that could have appeared to influence the work reported in this paper.

Data availability

Data will be made available on request.

Acknowledgements

The authors acknowledge doctorate support funding from Technological University of the Shannon (TUS) – Johnson and Johnson that was awarded to Terra Kremer. We thank Gillian Keane (Momentum Consultants) for assistance with graphics.

References

Afolabi, A.O., Nnaji, C., Okoro, C., 2022. Immersive technology implementation in the construction industry: modeling paths of risk. Buildings 12, 363. https://doi.org/10.3390/buildings12030363.

Akdere, M., Jiang, Y., Lobo, F.D., 2022. Evaluation and assessment of virtual reality-based simulated training: exploring the human–technology frontier. Eur. J. Train. Dev. 46 (5–6), 434–449.

Alfa, M., 2016. Current issues result in a paradigm shift in reprocessing medical and surgical instruments. Am. J. Infect. Control 44, e41–e45.

Alqudimat, M., Mesaroli, G., Lalloo, C., et al., 2021. State of the art: immersive technologies for perioperative anxiety, acute, and chronic pain management in pediatric patients. Curr. Anesthesiol. Rep. 11, 265–274. https://doi.org/10.1007/s40140-021-00472-3.

Anand, U., Chandel, A.K.S., Oleksak, P., et al., 2022. Recent advances in the potential applications of luminescence-based, SPR-based, and carbon-based biosensors. Appl. Microbiol. Biotechnol. 106, 2827–2853. https://doi.org/10.1007/s00253-022-11901-6.

Association for the Advancement of Medical Instrumentation, 2014. AAMI TIR55 Human Factors Engineering for Processing Medical Devices. AAMI, s.l.

Association for the Advancement of Medical Instrumentation, 2020. ANSI/AAMI ST79: 2017 & 2020 Amendments A1, A2, A3, A4 (Consolidated Text) Comprehensive Guide to Steam Sterilization and Sterility Assurance in Healthcare Facilities. Association for the Advancement of Medical Instrumentation, s.l.

Association for the Advancement of Medical Instrumentation, 2022. AAMI ST98 Cleaning Validation of Health Care Products - Requirements for Development and Validation of a Cleaning Process for Medical Devices. Association for the Advancement of Medical Instrumentation, Arlington, VA.

Atici-Ulusu, H., Ikiz, Y.D., Taskapilioglu, O., Gunduz, T., 2021. Effects of augmented reality glasses on the cognitive load of assembly operators in the automotive industry. Int. J. Comput. Integr. Manuf. 34 (5), 487–499.

Auer, A., Jarmai, K., 2018. Implementing responsible research and innovation practices in SMEs: insights into drivers and barriers from the Austrian medical device sector. Sustainability 10 (1), 17. https://doi.org/10.3390/su10010017.

Baheri Islami, S., Wesolowski, M., Revell, W., Chen, X., 2021. Virtual reality visualization of CFD simulated blood flow in cerebral aneurysms treated with flow diverter stents. Appl. Sci. 11, 8082. https://doi.org/10.3390/app11178082.

Bancroft, R., Spenser, W., 2022. Practical issues with instructions for use (IFU) for reusable medical devices. Zentral Sterilization 30 (2), 97–101.

Barats, C., Schafer, V., Fickers, A., 2020. Fading away – the challenge of sustainability in digital studies. Digit. Humanit. Quart. 14 (3).

Bautista, L., Maredei, M., Pedraza, G., 2023. Strategies to reduce visual attention changes while learning and training in extended reality environments. Int. J. Interact. Design Manuf. 17 (1), 17–43.

Benedettini, O., 2022. Green servitization in the single-use medical device industry: how device OEMs create supply chain circularity through reprocessing. Sustainability 14. https://doi.org/10.3390/su141912670.

Bowen, J., Coben, D., 2021. Using task models to understand the intersection of numeracy skills and technical competence with medical device design. Interact. Comput. 33 (1), 40–54.

Braga Rodrigues, T., Catháin, C.Ó., O'Connor, N.E., Murray, N., 2020. A Quality of Experience assessment of haptic and augmented reality feedback modalities in a gait analysis system. PLoS One 23 (Mar).

Brenner, M., Weir, A., McCann, M., Doyle, C., Hughes, M., Meon, A., Ingvar, M., Nauwelaerts, K., Turk, E., McCabe, C., 2023. Development of the key performance indicators for digital health interventions: a scoping review. Digital Health 9, 1–8.

Cabronne, A., et al., 2010. Control of a multi-hospital outbreak of KPC producing *Klebiella pneumoniae* type II in France, Sep to Oct 2009. Euro Surveill. 15.

Cardenas-Robledo, L., Uribe, H.O., Reta, C., Cantoral-Ceballos, A.J., 2022. Extended reality applications in industry 4.0 – a systematic literature review. Telematics Inform. 73 https://doi.org/10.1016/j.tele.2022.101863.

Carvalho, A.V., Chouchene, A., Lima, T.M., Charrua-Santos, F., 2020. Cognitive manufacturing in industry 4.0 toward cognitive load reduction: a conceptual framework. Appl. Syst. Innov. 3 (4).

Chen, Y., Neff, M., McEvoy, B., Cao, Z., et al., 2019. 3D printed polymers are less stable than injection moulded counterparts when exposed to terminal sterilization processes using novel vaporized hydrogen peroxide and electron beam processes. Polymer 183 (21). https://doi.org/10.1016/j.polymer.2019.121870.

Chen, A., et al., 2021a. Multicenter comparative study of three "non-destructive" methods of detecting the cleanliness of the da Vinci surgical robotic instrument. Glan. Surg. 10 (12), 3305–3313.

Chen, I.H.A., Ghazi, A., Sridhar, A., et al., 2021b. Evolving robotic surgery training and improving patient safety, with the integration of novel technologies. World J. Urol. 39, 2883–2893. https://doi.org/10.1007/s00345-020-03467-7.

Clack, L., Hirt, C., Kunz, A., Sax, H., 2021. Experiential training of hand hygiene using virtual reality. In: Brooks, A.L., Brahman, S., Kapralos, B., Nakajima, A., Tyerman, J., Jain, L.C. (Eds.), Recent Advances in Technologies for Inclusive Well-Being. Intelligent Systems Reference Library, vol. 196. Springer, Cham. https://doi.org/10.1007/978-3-030-59608-8_.

Cooney, R., de Sousa, D.P., Fernandez-Rios, A., et al., 2023. A circular economy framework for seafood waste valorization to meet challenges and opportunities for intensive production and sustainability. J. Clean. Prod. 393 https://doi.org/10.1016/j.jclepro.2023.136283.

Cummings, J.J., Bailenson, J.N., 2016. How immersive is enough? A meta-analysis of the effect of immersive technology on user presence. Media Psychol. 19 (2), 272–309. https://doi.org/10.1080/15213269.2015.1015740.

Damasceno, E.F., Fernandes, L., Silva, A.P.d., Días, J.B., Feb. 2023. A systematic mapping study on low-cost immersive virtual reality for microbiology. In: IEEE Revista Iberoamericana de Tecnologias del Aprendizaje, 18, no. 1, pp. 62–69. https://doi.org/10.1109/RITA.2023.3250551.

Dancer, S.J., 2014. Controlling hospital-acquired infection: focus on the role of the environent and new technologies for decontamination. Clin. Microbiol. Rev. 27 (4), 665–690.

Dargar, S., Kennedy, R., Lai, W., et al., 2015. Towards immersive virtual reality (iVR): a route to surgical expertise. J. Comput. Surg. 2, 2. https://doi.org/10.1186/s40244-015-0015-8.

de Melo Costa, D., et al., 2022. Contamination and Surface Damage on Reprocessed Robotic System Surgical Instruments in Clinical Use. Barcelona, Spain (s.n.).

Egan, D., et al., 2016. An evaluation of Heart Rate and ElectroDermal Activity as an objective QoE evaluation method for immersive virtual reality environments. In: Eighth International Conference on Quality of Multimedial Exprience (QoMEX).

Fenik, Y.C.N., et al., 2013. Prepackaged central line kits reduce procedural mistakes during central line insertion: a randomized controlled prospective trial. BMC Med. Educ. 13 (1), 60.

Fragoso, V., Gauglitz, S., Zamora, S., Kleban, J., Turk, M., 2011. TranslatAR: a mobile augmented reality translator. In: 2011 IEEE Workshop on Applications of Computer Vision (WACV), pp. 497–502. https://doi.org/10.1109/WACV.2011.5711545.

Fraser, K.L., Ayres, P., Sweller, J., 2015. Cognitive load theory for the design of medical simulations. Simul. Healthc. 10 (5), 295–307.

Fusco, A., Gaetano, T., 2022. Challenges and perspectives for clinical applications of immersive and non-immersive virtual reality. J. Clin. Med. 11 (15), 4540. https://doi.org/10.3390/jcm11154540.

Galanakis, C., et al., 2021. Innovations and technology disruptions in the food sector within the COVID-19 pandemic and post-lockdown era. Trends Food Sci. Technol. 110, 193–200.

Garcia Fracaro, S., Jarka, G., Fristel, B., 2022. Immersive technologies for the training of operators in the process industry: a systematic literature review. Comput. Chem. Eng. 160 https://doi.org/10.1016/j.compchemeng.2022.107691.

Garnica-Bohorquez, I., Lopez-Gualdron, C.I., Martinez-Gomez, J.M., 2019. Key performance indicators at manufacturing workflow in specific medical devices: a systematic literature review. In: 5th International Conference on Modern Approaches to Science, Technology and Engineering, 29–31 August, Berlin, Germany, pp. 35–48.

Garvey, M., Rowan, N.J., 2023. Pathogenic drug resistant fungi: a review of mitigation strategies. Int. J. Mol. Sci. 24 (2), 1584. https://doi.org/10.3390/ijms24021584.

Garvey, M., Meade, E., Rowan, N.J., 2022. Effectiveness of front-line and emerging fungal disease prevention and control interventions and opportunities to address appropriate eco-sustainable solutions. Sci. Total Environ. 851 https://doi.org/10.1016/j.scitotenv.2022.158284.

George, G., Merrill, R.K., Schillebeechx, S.J.D., 2021. Digital sustainability and entrepreneurship: how digital innovations are helping tackle climate change and sustainable development. Entrepreneur. Theory Pract. 45 (5), 999–1027.

Gold, K., Hitchins, V., 2013. Cleaning assessment of disinfectant cleaning wipes on an external surface of a medical device contaminated with artificial blood or *Streptococcus pneumonia*. Am. J. Infect. Control 41, 901–907.

Grand View Research, 2021. Digital Twin Market Size Worth $86.09 Billion by 2028 | CAGR: 42.7%: Grand View Research, Inc. https://www.prnewswire.com/news-releases/digital-twin-market-size-worth-86-09-billion-by-2028–cagr-42-7-grand-view-research-inc-301293274.html. (Accessed 20 July 2023).

Grieves, M., Vickers, J., 2017. Digital twin: mitigating unpredictable, undesirable emergent behavior in complex systems. In: Kahlen, J., Flumerfelt, S., Alves, A. (Eds.), Transdiscipl. Perspect. Complex Syst. Springer, Cham. https://doi.org/10.1007/978-3-319-38756-7_4.

Guerra-Bretana, R.M., Florez-Rendon, A.L., 2019. Impact of regulations on innovation in the field of medical devices. Res. Biomed. Eng. 34 (4) https://doi.org/10.1590/2446-4740.180054.

Gusso, D., Carvalho, M.M., Balkenende, R., Mascarenhas, J., 2020. Circular business models in the medical device industry: paths towards sustainable healthcare. Resour. Conserv. Recycl. 160 https://doi.org/10.1016/j.resconrec.2020.104904.

Han, S.W., Sung, S.-K., Shin, B.-S., 2022. Virtual reality simulation of high tibial osteotomy for medical training. Mob. Inf. Syst. 2022 https://doi.org/10.1155/2022/3055898.

Hatta, M.H., Sidi, H., Sharip, S., Das, S., Saini, S.M., 2022 Feb 18. The role of virtual reality as a psychological intervention for mental health disturbances during the COVID-19 pandemic: a narrative review. Int. J. Environ. Res. Public Health 19 (4), 2390. https://doi.org/10.3390/ijerph19042390.

Hemberg, L., Wessberg, N., Leire, C., Bentzer, P., 2023. Environmental impact of single-use and reusable items in central venous catheter insertion kits: a life cycle assessment. Intensive Care Med. https://doi.org/10.1007/s00134-023-07078-9.

Hensley, B., Monson, J., 2015. Hospital-aquired infections. Sugery (Oxford) 33 (11), 528–533.

Ho, N., Wong, P.-M., Chua, M., Chui, C.-K., 2018. Virtual reality training for assembly of hybrid medical devices. Multimed. Tools Appl. 77 (23), 30651–30682. https://doi.org/10.1007/s11042-018-6216-x.
Hynes, E., Flynn, R., Lee, B., Murray, N., 2020. A QoE Evaluation of an Augmented Reality Procedure Assistance Application. In: Twelfth International Conference on Quality of Multimedia Experience (QoMEX), Athlone, Ireland, 2020, pp. 1–4. https://doi.org/10.1109/QoMEX48832.2020.9123097.
Iadanza, E., Gonnelli, V., Satta, F., Gherardelli, M., 2019. Evidence-based medical equipment management: a convenient implementation. Med. Biol. Eng. Comput. 57, 2215–2230.
International Organization for Standardization, 2018. ISO 11139 Sterilization of Heath Care Products - Vocabulary. International Organization for Standardization, s.l.
International Organization for Standardization, 2021. ISO 15883-5 Washer-Disinfectors - Part 5: Peformance Requirements and Test Method Criteria for Demonstrating Cleaning Efficacy (s.l.: s.n.).
Jaipong, P., Siripipattanakul, S., Sriboonruang, P., Sitthipon, T., 2023. A review of metaverse and cybersecurity in the digital era. Int. J. Comput. Sci. Res. 7 (1), 1125–1132.
Keefe, D.F., Sotiropoulos, F., et al., 2010. A process for design, verification, validation, and manufacture of medical devices using immersive VR environments. J. Medical Devices 4 (4), 045002. https://doi.org/10.1115/1.4002561.
Khan, M.N.R., Lippert, K.J. (2022). Immersive technologies in healthcare education. in Intelligent Systems and Machine Learning for Industry – Advancements, Challenges and Practices. Ist edition, CRC Press, Anisha, P.P. et al. (ISBN 9781003286745).
Kizil, M.S., Joy, J., 2001. What Can Virtual Reality Do for Safety? University of Queensland, pp. 1–12. http://citeseerx.ist.psu.edu/viewdoc/download?doi=10.1.1.466.8522&rep=rep1&type=pdf.
Knobel, S.E.J., Kaufmann, B.C., Gerber, S.M., Urwyler, P., Cazzoli, D., Müri, R.M., Nef, T., Nyffeler, T., 2021. Development of a search task using immersive virtual reality: proof-of-concept study. JMIR Serious Games 9 (3), e29182. https://doi.org/10.2196/29182.
Kremer, T., Patel, A., Summers, C., Quin, M., Lemons, K., McDonnell, G., 2019. Protein residuals on reusable medical devices and patient safety impact. Zentral Sterilization 37.
Lambert, B.J., Hansen, J.M., Bryans, T.D., Lam, S., 2021. Sterility assurance across sectors - new paradigms and tools. Front. Med. Technol. 3 https://doi.org/10.3389/fmedt.2021.622710.
Leppink, J., Duvivier, R., 2016. Twelve tips for medical curriculum design from a cognitive load theory perspective. Med. Teacher 38 (7), 669–674.
Ling, M.L., Ching, P., Widitaputra, A., Stewart, A., Sirijindadirat, N., Thu, L.T.A., 2018. APSIC guidelines for disinfection and sterilization of instruments in health care facilities. Antimicrob. Resistance Infect. Control. 7 (25) https://doi.org/10.1186/s13756-018-0308-2.
Losa, M., Aydin, M., Candelise, C., et al., 2020. The Michelangelo effect: art improves the performance in a virtual reality task developed for upper limb neurorehabilitation. Front. Psychol. https://doi.org/10.3389/fpsyg.2020.611956.
MacNeill, A.J., et al., 2020. Transforming the medical device industry: road map to a circular economy. Health Aff. 39 (12), 2088–2097.
Mancinetti, M., Guttormsen, S., Berendonk, C., 2019. Cognitive load in internal medicine: what every clinical teacher should know about cognitive load theory. Eur. J. Internal Med. 60, 4–8.
Mao, R.Q., Lan, L., Kay, J., Lohre, R., Ayeni, O.R., Goel, D.P., de Sa, D., 2021. Immersive virtual reality for surgical training: a systematic review. J. Surg. Res. 268, 40–58. https://doi.org/10.1016/j.jss.2021.06.045.
Marsh, J., et al., 2015. Genomic epidemiology of an endoscope-associated outbreak of *Klebsiella pneumoniae* carapenemase (KPC) - producing *K. pneumoniae*. PLoS One 10 (E0144310).
Martin, G., Koizia, L., Kooner, A., et al., 2020 Aug 14. Use of the HoloLens2 mixed reality headset for protecting health care workers during the COVID-19 pandemic: prospective, observational evaluation. J. Med. Internet Res. 22 (8), e21486 https://doi.org/10.2196/21486.
Masterson, K., Meade, E., Garvey, M., Lynch, M., Major, I., Rowan, N.J., 2021. Development of a low-temperature extrusion process for production of GRAS bioactive-polymer loaded compounds for targeting antimicrobial-resistant (AMR) bacteria. Sci. Total Environ. 800 https://doi.org/10.1016/j.scitotenv.2021.149545.
Matthew, P.S., Pillai, A.S., 2020. Role of immersive (XR) technology in improving healthcare competencies: a review. In: Virtual and Augmented Reality in Education, Art and Museums. https://doi.org/10.4018/978-1-7998-1796-3.ch002.
Mayer, R., 2014. Cognitive theory of multimedia learning. In: The Cambridge Handbook of Multimedia Learning, pp. 43–71.
Mayer, R., Moreno, R., 2003. Nine ways to reduce cognitive load in multimedia learning. Educ. Psychol. 38 (1), 43–52.
McDonnell, G., Hansen, J., 2020. Principles of antimicrobial activity. In: Gerald McDonnell, J.H. (Ed.), Block's Disinfection, Sterilization and Preservation, Sixth edition. Wolters Kluwer, Philadelphia, pp. 68–119.
McEvoy, B., Rowan, N.J., 2019. Terminal sterilization of medical devices using vaporized hydrogen peroxide: a review of current methods and emerging opportunities. J. Appl. Microbiol. 127 (5), 1403–1420.
McEvoy, B., Lynch, M., Rowan, N., 2021. Opportunities for the application of real-time bacterial cell analysis using flow cytometry for the advancement of sterilization microbiology. J. Appl. Microbiol. 130 (6), 1794–1812.
McEvoy, B., Maksimovic, A., Howell, D., Reppert, P., Ryan, D., Rowan, N., Michel, H., 2023. Studies on the comparative effectiveness of X-rays, gamma rays and electron beams to inactivate microorganisms at different dose rates in industrial sterilization of medical devices. Radiat. Phys. Chem. 208 https://doi.org/10.1016/j.radphyschem.2023.110915.
Mitchell, A., Assadi, G., 2021. Using simulation exercises to improve student sills and patient safety. Br. J. Nurs. 30 (20) https://doi.org/10.12968/bjon.2021.30.20.1198.
Murray, N., Buckley, J., Seery, N., Rowan, N., 2019. Blending Immersive and Educational Technologies to Inform Sustainability and Diversification of Workforce Training Through Machine Interface Learning Using Sterilization Technologies as Model - Quo Vadis?. City West, Dublin (s.n.).
Nakai, A., Suzuki, K., 2016. Instructional information system using AR technology for chemical plants. Chem. Eng. Trans. 53, 199–204. https://doi.org/10.3303/CET1653034.
Ndhaief, N., Rezg, N., Dsiri, C., Pitekelabou, E.H., 2022. Towards the digitialization of the healthcare learning process using 3D experience. In: 2022 International Conference on Microelectronics, ICM 2022, 4th December, pp. 152–155.
Nunnerley, J., Gupta, S., Snell, D., King, M., 2017. Training wheelchair navigation in immersive virtual environments for patients with spinal cord injury – end-user input to design an effective system. Disabil. Rehab. Assist. Technol. 12 (4), 417–423. https://doi.org/10.1080/17483107.2016.1176259.
Olympus, 2022. Olympus - history of Olympus products - endoscopes [Online] Available at: https://www.olympus-global.com/technology/museum/endo/?page=technology_museum.
Omori, K., Shigemoto, N., Kitagawa, H., et al., 2023. Virtual reality as a learning tool for improving infection control procedures. Am. J. Infect. Control 51 (2), 129–134. https://doi.org/10.1016/j.ajic.2022.05.023.
O'Neill, E.A., McKeon-Bennett, M., Rowan, N.J., 2022. Peatland-Based Innovation Can Potentially Support and Enable the Sustainable Development Goals of the United Nations: Case Study From the Republic of Ireland, p. 6. https://doi.org/10.1016/j.cscee.2022.100251.
Ovunc, S.S., Yolcu, M.B., Emre, S., Elicevik, M., Celayir, S., Ovunc, S.S., Yolcu, M.B., Emre, S., Elicevik, M., Celayir, S., 2021. Using immersive technologies to develop medical education materials. Cureus 13 (1). https://doi.org/10.7759/cureus.12647.
Pappa, D., Papodopoulos, H., 2019. A use case of the application of advanced gaming and immersion technologies for professional training: the GAMEPHARM training environment for physiotherapists. EJEL 17 (3). https://doi.org/10.34190/JEL.17.2.08.
Parong, J., Mayer, R.E., 2021. Learning about history in immersive virtual reality: does immersion facilitate learning? Educ. Technol. Res. Dev. 69 (3), 1433–1451. https://doi.org/10.1007/s11423-021-09999-y.
Patel, R., Flynn, S., 2019. A new approach to reusable medical device reprocessing instructions for use. In: City West Ireland, Kilmer Conference.
Pears, M., Konstantinidis, S., 2022. The future of immersive technology in global surgery education. Indian J. Surg. 84 (Suppl. 1), 281–285. https://doi.org/10.1007/s12262-021-02998-6.
Peel, S., Eggbeer, D., 2016. Additively manufactured maxillofacial implants and guides - achieving routine use. Rapid Prototyp. J. 22 (1), 189–199.
Perla, L., Vinci, V., Scarinci, A., 2023. Innovating university teaching with micro-credentials - an ongoing research experimentation. Res. Educ. Media 15 (1), 72–79.
Pohl, J., Hilty, L.M., Finkbeiner, M., 2019. Howe LCA contributes to the environmental assessment of higher order effects of ICT applications: a review of different approaches. J. Clean. Prod. 219, 698–712.
Pooyandeh, M., Han, K.-J., Sohn, I., 2022. Cybersecurity in the AI-based metaverse: a survey. Appl. Sci. 12 (24), 24 https://doi.org/10.3390/app122412993.
Protano, C., Cammalleri, V., Romano Spica, V., Valeriani, F., Vitali, M., 2019. Hospital environment as a reservoir for cross transmission: cleaning and disifection procedures. Ann. Ig. 31 (5), 436–448.
Radkowski, R., Herrema, J., Oliver, J., 2015. Augmented reality-based manual assembly support with visual features for different degrees of difficulty. Int.l J. Hum.–Comput. Interac. 31 (5), 337–349. https://doi.org/10.1080/10447318.2014.994194.
Relan, A., Parker, N., Wali, S., Guiton, G., Fung, C.C., 2004. Supporting handheld technologies in a medical school curriculum: lessons from three years of design, development and implementation. In: The 2nd IEEE International Workshop on Wireless and Mobile Technologies in Education, 2004. Proceedings, pp. 51–58. https://doi.org/10.1109/WMTE.2004.1281333.
Rivers, E.P., McIntyre, L., Morro, D.C., Rivers, K.K., 2015. Early and innovative interventions for severe sepsis and septic shock: taking advantage of a window of opportunity. CMAJ 173 (9), 1054–1065.
Roberts, C.G., 2013. The role of biofilms in reprocessing medical devices. Am. J. Infect. Control 41 (5 Supp), S77–S80.
Rochlen, L.R., Levine, R., Tait, A.R., 2017. First-person point-of-view–augmented reality for central line insertion training: a usability and feasibility study. Simul. Healthc. 12 (1), 57. https://doi.org/10.1097/SIH.0000000000000185.
Rowan, N.J., 2019. Pulsed light as an emerging technology to cause disruption for food and adjacent industries – Quo vadis? Trends Food Sci. Technol. 88, 316–332.
Rowan, N.J., 2023. The role of digital technologies in supporting and improving fishery and aquaculture across the supply chain – quo Vadis? Aquac. Fish. 8 (4), 365–374.
Rowan, N.J., Casey, O., 2021. Empower Eco multiactor HUB: a triple helix 'academia-industry-authority' approach to creating and sharing potentially disruptive tools for addressing novel and emerging new Green Deal opportunities under a United Nations Sustainable Development Goals framework. Curr. Opin. Environ. Sci. Health 21. https://doi.org/10.1016/j.coesh.2021.100254.
Rowan, N.J., Murray, N., Qiao, Y., O'Neill, E., Clifford, E., Barcelo, D., Power, D.M., 2022. Digital transformation of peatland eco-innovations ('Paludiculture'): enabling a paradigm shift towards the real-time sustainable production of 'green-friendly' products and services. Sci. Total Environ. 838 (3) https://doi.org/10.1016/j.scitotenv.2022.156328.
Rowan, N.J., Kremer, T., McDonnell, G., 2023. A review of Spaulding's classification system for effective cleaning, disinfection and sterilization of reusable medical devices: viewed through a modern-day lens that will inform and enable future

sustainability. Sci. Total Environ. 878 https://doi.org/10.1016/j.scitotenv.2023.162976.
Rutala, W., Weber, D., 2019. Reprocessing semicritical items: outbreaks and current issues. Am. J. Infect. Control 47, A79–A89.
Sagourin, P., Viallet, A., Batista, R., Talon, D., 2021. Validation of the cleaning method for Da Vinci XI robotic instruments using protein residue tests. Zentral Sterilization 29 (1), 48–53.
Saito, Y., et al., 2017a. Challenging residual contamination of instruments for robotic surgery in Japan. Infect. Control Hosp. Epidemiol. 38 (2), 143–146.
Saito, Y., et al., 2017b. Concerns associated with cleaning robotic surgical instruments-response to Wallace. Infect. Control Hosp. Epidemiol. 38 (8), 1014–1015.
Salgado, D.P., 2018. A QoE assessment method based on EDA, heart rate and EEG of a virtual reality assistive technology system. s.l., s.n., pp. 517–520.
Sankaranarayanan, G., Odlozil, C.A., Wells, K.O., et al., 2020. Training with cognitive load improves performance under similar conditions in a real surgical task. Am. J. Surg. 3, 620–629. https://doi.org/10.1016/j.amjsurg.2020.02.002.
Sattar, M.U., Palaniappan, S., Lokman, A., Hassan, A., Shah, N., Riaz, Z., 2019. Effects of virtual reality training on medical students' learning motivation and competency. Pak. J. Med. Sci. 35 (3), 852–857. https://doi.org/10.12669/pjms.35.3.44.
Schuelke-Leech, B.A., 2018. A model for understanding the orders of magnitude of disruptive technologies. Technol. Forecast. Soc. Chang. 129, 261–274.
Schuelke-Leech, B.A., 2021. Disruptive technologies for a Green Gew Deal. Curr. Opin. Environ. Sci. Health 21. https://doi.org/10.1016/j.coesh.2021.100245.
Scott, D., 2009. The Direct Medical Costs of Healthcare-Associated Infections in U.S. Hospitals and the Benefits of Prevention. Division of Healthcare Quality Promotion National Center for Preparedness, Detection, and Control of Infectious Diseases Coordinating Center for Infectious Diseases Center for Disease Control and Prevention, s.l.
Shamsuzzoha, A., Toshev, R., Vu Tuan, V., Kankaanpaa, T., Helo, P., 2021. Digital factory–virtual reality environments for industrial training and maintenance. Interact. Learn. Environ. 29 (8), 1339–1362.
Shenoy, E.S., et al., 2019. Transmission of mobile colistin resistance (mcr-1) by duodenoscope. Clin. Infect. Dis. 68, 1327–1334.
Singh, M., Srivastava, R., Fuenmayor, E., Kuts, V., et al., 2022. Applications of digital twin across industries: a review. Appl. Sci. 12 (11), 5727. https://doi.org/10.3390/app12115727.
Slater, M., Sanchez-Vives, M.V., 2016. Enhancing our lives with immersive virtual reality. Front. Robot. AI 3, 74.
Soogund, N.-U.-N., Joseph, M.H., 2019. SignAR: a sign language translator application with augmented reality using text and image recognition. In: 2019 IEEE International Conference on Intelligent Techniques in Control, Optimization and Signal Processing (INCOS), pp. 1–5. https://doi.org/10.1109/INCOS45849.2019.8951322.
Sowndararajan, A., Wang, R., Bowman, D.A., 2008. Quantifying the benefits of immersion for procedural training. In: Proceedings of the 2008 Workshop on Immersive Projection Technologies/Emerging Display Technologies, pp. 1–4. https://doi.org/10.1145/1394669.1394672.
Stone, N.N., Wilson, M., Griffith, S.H., et al., 2022. Remote surgical education using synthetic models combined with an augmented reality headset. Surg. Open Sci. 10, 27–33.
Sweller, J., 1988. Cognitive load during problem solving: effects on learning. Cogn. Sci. 12 (2), 257–285.
Tang, Y.M., Chau, K.Y., Kwok, A.P.K., Zhu, T., Ma, X., 2022. A systematic review of immersive technology applications for medical practice and education—trends, application areas, recipients, teaching contents, evaluation methods, and performance. Educ. Res. Rev. 35, 100429 https://doi.org/10.1016/j.edurev.2021.100429.
Trubetskaya, A., Manto, D., McDermott, O., 2022. A review of lean adoption in the Irish MedTech industry. Processes 10. https://doi.org/10.3390/pr10020391.
Uhl, J.C., Schrom-Feiertag, H., Regal, G., Gallhuber, K., Tscheligi, M., 2023. Tangible immersive trauma simulation: is mixed reality the next level of medical skills training?. In: Proceedings of the 2023 CHI Conference on Human Factors in Computing Systems, pp. 1–17. https://doi.org/10.1145/3544548.3581292.
Vansteenkiste, M., Sierens, E., Soenens, B., Luyckx, K., Lens, W., 2009. Motivational profiles from a self-determination perspective: the quality of motivation matters. J. Educ. Psychol. 101, 671–688. https://doi.org/10.1037/a0015083.
Verhey, J.T., Haglin, J.M., Verhey, E.M., Hartigan, D.E., 2020. Virtual, augment, and mixed reality applications in orthopaedic surgery. Int. J. Med. Robot. 16 (2), e2067 https://doi.org/10.1002/rcs.2067.
Vickery, K., Hu, H., Simone Jacombs, A., Bradshaw, D.A., Deva, A.K., 2013. A review of bacterial biofilms and their role in device-associated infection. Healthc. Infect. 18 (2), 61–66.
Vijayakumar, S., Flynn, R., Murray, N., 2020. A Comparative Study of Machine Learning Techniques for Emotion Recognition from Peripheral Physiological Signals. In: 31st Irish Signals and Systems Conference (ISSC), Letterkenny, Ireland, 2020, pp. 1–6. https://doi.org/10.1109/ISSC49989.2020.9180193.
Vijayakumar, S., Corcoran, P., Flynn, R., Murray, N., 2022. AI-derived quality of experience prediction based on physiological signals for immersive multimedia experiences: research proposal. In: Proceedings of the 13th ACM Multimedia Systems Conference, pp. 403–407.
Wallace, B., 2017. A response to the validity of an article reporting contrary cleaning efficacy results for robotic surgical instruments. Infect. Control Hosp. Epidemiol. 38 (5), 625–626.
Wehrl, M., et al., 2014. Round robin tests conducted by the working group DaVinci to establish a method for cleaning of MIS robotic instruments. Central Service 3, 173–179.
Weinstein, Y., Madan, C.R., Sumeracki, M.A., 2018. Teaching the science of learning. Cogn. Res. Princ. Implic. 3 (1), 2. https://doi.org/10.1186/s41235-017-0087-y (Epub 2018 Jan 24. PMID: 29399621; PMCID: PMC5780548).
Westmeath Independent, 2022. Second award for Mersus [Online] available at: https://www.westmeathindependent.ie/2022/09/23/second-national-award-for-athlone-based-mersus/ (accessed 29 October 2022).
White, S., Jubeli, E., Slack, M., 2021. Reprocessing of robotic surgery resuable instruments - insight into what's behind the instructions for use. Zentral Sterilization 29 (5), 288–293.
Wilkerson, W., Avstreih, D., et al., 2008. Using immersive simulation for training first resonders of mass casualty incident. Acad. Emerg. Med. 1152–1159 https://doi.org/10.1111/j.1553-2712.2008.00223.x.
World Federation for Hospital Sterilization Sciences, 2022. World congress 2022 - Barcelona, Spain [Online] Available at: https://wfhss.com/world-congress-2022-barcelona-spain/.
World Health Organization, 2016. Decontamination and Reprocessing of Medical Devices for Health-Care Facilities. World Health Organization and Pan American Health Organization, Geneva, Switerland.
Wu, Y., Dong, M., Zheng, Z., 2014. Patient scheduling with periodic deteriorating maintenance on single medical device. Comput. Oper. Res. 49, 107–116.
Xiang, Q., Feyue, Q., et al., 2022. Engineering design and evaluation of the process evaluation method of auto repair professional training in virtual reality environment. Appl. Sci. 12 (13) https://doi.org/10.3390/app122312200.
Xue, C., Qiao, Y., Murray, N., 2020. Enabling Human-Robot-Interaction for Remote Robotic Operation via Augmented Reality. In: IEEE 21st International Symposium on "A World of Wireless, Mobile and Multimedia Networks" (WoWMoM), Cork, Ireland, 2020, pp. 194–196. https://doi.org/10.1109/WoWMoM49955.2020.00046.
Yeung, A.W.K., Tosevska, A., Klager, E., Eibensteiner, F., Laxar, D., Stoyanov, J., Glisic, M., Zeiner, S., Kulnik, S.T., Crutzen, R., et al., 2021. Virtual and augmented reality applications in medicine: analysis of the scientific literature. J. Med. Internet Res. 23, e25499.
Young, A., Aquilina, A., 2021. Use of virtual reality to support rapid upskilling of healthcare professionals during COVID-19 pandemic. Management for Professionals. In: Jung, Timothy, Dalton, Jeremy (Eds.), XR Case Studies, edition 1. Springer, pp. 137–145.
Young, J., Sewell, J., 2015. Applying cognitive load theory to medical education: construct and measurement challenges. Perspect. Med. Educ. 3 (1), 107–109.
Young, J.Q., Van Merrienboer, J., Durning, S., Ten Cate, O., 2014. Cognitive Load Theory: Implications for medical education. In: Implications for Medical Education: AMEE Guide No. 86 Medical Teacher, 36(5), pp. 371–384.
Yu, M., Mann, J.S., 2020. Development of virtual reality simulation program for high-risk neonatal infection control education. Clin. Simul. Nurs. 50, 19–26. https://doi.org/10.1016/j.ecns.2020.10.006.
Yu, M., Yang, M.R., 2022. Effectiveness and utility of virtual reality infection control simulation for children with COVID-19: quasi-experimental study. JMIR Serious Games 10 (2), e36707. https://doi.org/10.2196/36707.
Yu, Kevin, Ostler, Daniel, Fuchtmann, Jonas, Zapaishchykova, Anna, Berlet, Maximilian, Navab, Nassir, Feussner, Hubertus, Wilhelm, Dirk, 2021. Clean-AR: using augmented reality for reducing the risk of contamination from airborne disease agents on surfaces. Curr. Direct. Biomed. Eng. 7 (1), 6–10. https://doi.org/10.1515/cdbme-2021-1002.
Zagury-Orly, I., Soninski, M.A., Nguyen, L.H.P., et al., 2023. What is the current state of extended reality use in otolaryngology training? A scoping review. Laryngoscope 133 (2), 227–234.

frontiers | Frontiers in Public Health

TYPE Original Research
PUBLISHED 24 October 2023
DOI 10.3389/fpubh.2023.1203937

OPEN ACCESS

EDITED BY
Colin K. Drummond,
Case Western Reserve University, United States

REVIEWED BY
Arkers Kwan Ching Wong,
Hong Kong Polytechnic University,
Hong Kong SAR, China
Vegard Engen,
Bournemouth University, United Kingdom

*CORRESPONDENCE
Tara Byrne
✉ tara.byrne2@hse.ie

RECEIVED 11 April 2023
ACCEPTED 22 September 2023
PUBLISHED 24 October 2023

CITATION
Byrne T, Murray N, McDonnell-Naughton M and Rowan NJ (2023) Perceived factors informing the pre-acceptability of digital health innovation by aging respiratory patients: a case study from the Republic of Ireland.
Front. Public Health 11:1203937.
doi: 10.3389/fpubh.2023.1203937

Perceived factors informing the pre-acceptability of digital health innovation by aging respiratory patients: a case study from the Republic of Ireland

Tara Byrne[1,2,3]*, Niall Murray[3], Mary McDonnell-Naughton[2] and Neil J. Rowan[2]

[1]Saolta University Healthcare Group, HSE, Galway, Ireland, [2]Department of Nursing and Healthcare, Technological University of the Shannon (TUS), Athlone, Ireland, [3]Faculty of Engineering and Informatics, Technological University of the Shannon, (TUS), Athlone, Ireland

It is appreciated that digital health is increasing in interest as an important area for efficiently standardizing and developing health services in Ireland, and worldwide. However, digital health is still considered to be in its infancy and there is a need to understand important factors that will support the development and uniform uptake of these technologies, which embrace their utility and ensure data trustworthiness. This constituted the first study to identify themes believed to be relevant by respiratory care and digital health experts in the Republic of Ireland to help inform future decision-making among respiratory patients that may potentially facilitate engagement with and appropriate use of digital health innovation (DHI). The study explored and identified expert participant perceptions, beliefs, barriers, and cues to action that would inform content and future deployment of living labs in respiratory care for remote patient monitoring of people with respiratory diseases using DHI. The objective of this case study was to generate and evaluate appropriate data sets to inform the selection and future deployment of an ICT-enabling technology that will empower patients to manage their respiratory systems in real-time in a safe effective manner through remote consultation with health service providers. The co-creation of effective DHI for respiratory care will be informed by multi-actor stakeholder participation, such as through a Quintuple Helix Hub framework combining university-industry-government-healthcare-society engagements. Studies, such as this, will help bridge the interface between top-down digital health policies and bottom-up end-user engagements to ensure safe and effective use of health technology. In addition, it will address the need to reach a consensus on appropriate key performance indicators (KPIs) for effective uptake, implementation, standardization, and regulation of DHI.

KEYWORDS

digital health, respiratory health, education, living labs, quintuple Helix hub, aging

1. Introduction

The impact of chronic disease on healthcare systems internationally is well documented (1–3). Effective and resource-efficient long-term management of multimorbidity is one of the greatest health-related challenges facing patients, health professionals, and society more broadly (3). Respiratory disease represents a diverse range of acute and chronic diseases that are a major cause of morbidity and mortality (4). This situation has been exacerbated by the COVID-19 pandemic (5). Respiratory diseases are responsible for a large proportion of the overall health burden of illness, both in Ireland and globally (6). It is estimated that respiratory disease causes one in five deaths nationally which is 38.2% higher than the EU-28% average. In 2018, a report titled "Respiratory Health of the Nation" found that respiratory disease accounted for 14.3% ($n = 92,391$) of inpatient hospitalizations and 15.8% ($n = 578,319$) of bed days. Comparable figures for cardiovascular disease were 8.2 and 11.3%, and for non-respiratory cancers 4.7 and 8.0% (7).

The delivery of healthcare services has witnessed an accelerated evolution in recent years. Healthcare professionals have had to exercise creativity to meet the changing needs of service users (8). For example, there is a commensurate interest in implementing strategies to support remote patient monitoring and telemedicine to help service users at home and to provide follow-up consultations. Digital health is defined by the WHO as a field of knowledge and practice associated with the development and use of digital technologies to improve health (9) There is evidence to suggest that these programs can improve the quality of care and compliance, reduce the financial burden and ultimately improve patients quality of life (10). Remote healthcare is an evolving concept that is seeing clinicians move toward remote monitoring for service users outside of the hospital setting. Malasinghe et al. (11) propose that there are many advantages to this type of healthcare. These include real-time detection of illnesses, prevention of worsening of illness/ untimely deaths, and reduced hospital admission. Noah et al. (12) reported that remote patient monitoring has many positive outcomes; however, caution must be taken by clinicians using remote patient monitoring and further research is required.

According to the report titled "Health in the 21st Century; Putting Data to Work for Stronger Health Systems" recently published by OECD (13), intelligent use of data and digital technology improves the safety and quality of care provided in healthcare. It also helps address unmet health needs and makes accessing services easier. It supports informed health system stewardship and the development of policies. Effective data collection also assists researchers to develop safer and better treatments, and enables more robust disease prevention and public health, resulting in healthier and more productive populations. The Irish government has faced challenges as to how this country will appropriately address its overwhelmed health service as attested by extensive and lengthy patient waiting lists for elective surgery and consultations. Moreover, there is also a growing concern surrounding future predictions of extreme burden due to the prolonged lifespan of the aging population. The concept of "living labs" in health care has been proposed as a framework to connect governmental, public-sector organizations, industry, higher education institutions, community-based organizations, and clinicians. The aim is to create an environment of creativity that encourages a collaborative approach in the developmental process of a product, service, or system.

Globally, the adoption of digital technologies varies significantly (8). There is evidence to suggest that the adoption of wearable technologies has significantly lagged in comparison to other established technologies such as smartphones and tablets. Cheung et al. (14) noted that when it comes to healthcare, researchers have inadequate knowledge of the adoption intentions of service users. A high proportion of the research conducted has a primary focus on the technical development of the device; therefore, there is an inadequate understanding of the diffusion process. This contrasts with the marketing research conducted for smart technologies, which is primarily focused on consumer adoption, resulting in a much quicker diffusion process. Brenner et al. (8) highlighted the significant gap in evidenced-based published literature across 10 databases on the development of key performance indicators for the development of digital health interventions where only five references were eligible. Key performance indicators play a central role in the evaluation, measurement, and improvement of healthcare quality and service performance. This also intimates a gap in knowledge concerning the service users adoption of technology within healthcare. Lycett et al. (15) suggest the use of psychological theory can enhance the effectiveness of digital interventions and ultimately result in more successful outcomes such as increased consumer adoption. The systematic review concluded with a future recommendation for researchers to further evaluate how the application of theory in the development of digital interventions impacts their overall effectiveness. It is suggested that the use of a psychological framework to gain insight and understanding into consumer adoption will lead to positive engagement with digital health technologies. More recently, future recommendations by Nadal et al. (16) identified that the gap in the current body of knowledge was in the pre-acceptance of technologies. A main thrust of research has focused on understanding people's perspectives before and after using digital health innovations (DIH) where the initial emphasis has been placed on establishing appropriate multi-actor partnerships with relevant stakeholders including end-users, developing models for evaluation and monitoring, informed by best-published evidence, and the generation of key performance indicators (KPI's) for measuring the effectiveness and appropriateness of DHI that is currently lacking (8). However, if the main goal is to access the effectiveness of DHI, it cannot be assumed that the service user will engage with the technology long term, or indeed at all. Dundon et al. (17) noted that digital tools for diagnosis and management of respiratory conditions are an important area for research and development; however, the long-term success in this domain will depend on identifying real needs and integrating the often-divergent interests of the various partners in healthcare systems worldwide. Thus, the overarching aim of this novel study is to gain an understanding of the pre-acceptability of respiratory patients to digital health technologies in the Republic of Ireland by interviewing key subject matter experts encompassing respiratory care and digital health.

2. Methodology

2.1. Research approach including philosophical underpinning

A reflective thematic analysis framework (18) that addresses flexibility within data analysis while maintaining the integrity of the

method was used in this study. This method for health research is supported by the literature and deemed "*an interpretive method firmly situated within a qualitative paradigm that would also have broad applicability within a range of qualitative health research designs*" (19). This study used a phenomenological approach to explore the participants' intentions, perceived thinking, and reactions toward digital health. Subsequently, experiences were captured without any prejudice and participants were provided ample space and time to share their experiences. In line with a phenomenological approach, the phase of the study provides a detailed description of participants' experiences from analysis through to contextualized findings (20).

2.2. Participants

Purposive sampling was used in the study to select the participants which has allowed the researcher to choose appropriate members with selected levels of expertise. Samples were not chosen randomly as not every member of the particular specialty is eligible to partake in this study. Pursuing random sampling also needs significantly more time and information, beyond the capacity of this project which led the researcher to use purposive sampling. Saturation is reached at a point where similar themes were provided as answers to the questions posed (21). However, in this particular study, not all questions that had reached saturation were void, as some were retained to expand themes and help with the discovery of new information. Saturation points were discovered as the transcription process occurred simultaneously during the interview process.

2.3. Inclusion and exclusion criteria

Participants in this study were Irish women and men. Each participant was invited to partake in the study, as they will have been identified to subject matter experts who possess particular qualities or skills relevant to the digital health technology field and /or Respiratory disease. Subject matter experts participating in this study encompassed a respiratory physician, psychologist, digital health expert, technological expert, respiratory nurse specialist, health innovation representative, and a government representative.

2.4. Ethics statement

In qualitative research, ethics is one essential part that must be considered. Ethical approval is important for all types of research to result in a benefit and to minimize the risk of harm, by protecting participants' information by informing the participants of everything about the study and their roles as participants, and minimizing the misuse of the information given. It is equivalent to a moral contract when it comes to dealing with humans (22). Ethical applications were first sent to the Technological University of the Shannon Research Ethics Committee, and thereafter the clinical sites. The completed submissions were made on 12th Dec 2021 and were approved *via* email on January 15^{th,} 2022. The researcher carried out data collection (interviews) from March 2022 to May 2022. Ethical approval number C.A.2734.

2.5. Data collection

Semi-structured interviews were carried out with the participants. The qualitative phase was a crucial level in which the researcher gained a better understanding of behaviors and knowledge among the targeted population (23). Data collection was conducted in English, as it is the first language spoken in Ireland. Before the interviews commenced, participants were first informed through the information sheet that all the information gained from the interviews would be kept completely confidential. Besides informing participants about the study, the information sheet is a comprehensive reference for the participants to refer to; if anything ever happened to them after the interview session. It is also mentioned in that particular document about confidentiality and how the information will be stored and kept confidential using coding to respect anonymity. Participants were also informed of their rights to withdraw from the study at any stage (Protocol included in Supplementary material).

2.6. Study setting

The reasons for choosing a small number of participants for this study are as follows. Firstly, it is valuable to understand peoples experiences within their area of expertise in this topic. This helped the researcher gain valuable insight into diverse areas within the area of digital health technology and indeed technology specific to the area of respiratory diseases. It took at least one to 2 days to explore and draw a conclusion after each conversation before starting a new interview. Also, the time schedule for interviews depended on what free time the participant had, and not all who were invited could or were willing to participate in the interview. Secondly, because the locations were separated geographically, the researcher's time to interview participants was limited, therefore the option of a virtual interview was offered. Thirdly, there were a small number of participants who had the most valuable experiences and were to deliver the expectations of the researcher purposefully. Interviews were carried out until data saturation was reached. Lastly, it is relevant that the number of interviewed participants met the research objectives and fulfilled the research aim. Data collected and analyzed at this qualitative phase 1 were aimed at developing an instrument for a future quantitative phase II. The data collection was performed primarily through Zoom narrative interviews, using open-ended questions. In the interview sessions, questions were asked according to the interview protocols. Participants responses also generated further questions about the study topic. Each interview was recorded, guided by an interview protocol and guide, and also by the recommendation of the regional ethics committees.

2.7. Bracketing

In, bracketing is essential for understanding the phenomenology method. In Braun and Clarke's phenomenological research method, the application of bracketing is a process to prove the validity and to demonstrate the phenomenological approach through the research process, not only during the data collection but also during data analysis. In this particular study, bracketing began to take place as soon as the interview started. Bracketing is important for the researcher to avoid pre-judgment and assumptions.

2.8. Reflection

After utilizing bracketing, the researcher used reflection to help improve her understanding of the outcome and the meaning of the findings of this study (20). This activity involves thorough and deep thought of any factor that might contribute toward respondents' reactions about the studied topic (24). Reflection is an important activity, especially for social science research, where the relationship with scientific needs was established in exploring thoughts through culture (25). The environment and experiences are real and natural; thus, it is categorized as valuable and rich. It also involves recalling and extracting participants' details such as: who said that, how, when, where, and why. Through this research, the researcher came to learn and appreciate the art of reflection and practiced this process through the analysis of the project findings for phase 1.

2.9. Data analysis

Data was analyzed in agreement with Braun and Clarke's data analysis framework. The researcher explored the data analysis tools available and decided to adapt Braun and Clarke's framework. Braun and Clark's framework is one of the most popular frameworks and is used widely by qualitative researchers to gain reliable results. In this study, the adaption of Braun and Clarke's phenomenological analysis method is appreciated and translated into the following steps: the interviews were conducted and the researcher practiced bracketing during the particular time to ensure original experiences and thoughts were produced by the participants. The raw data from the audio were then transcribed. Subsequently, the researcher decided to use computer-aided qualitative data analysis to help with coding and theming. Through coding, themes emerged accordingly and supported the aim of this study. Emerging themes were either similar or different from one participant to another. Transcripts were uploaded into NVivo to allow the process. NVivo also helped the researcher to see the statements made by the participants being placed under certain themes. Coding data using NVivo saves the researcher time and also helps to organize complex data. From there, themes were extracted, sub-themes were reorganized and data was organized under the identified gaps. These statements were then gathered under matrices. Finally, themes were organized again and this stage eliminated the redundancy of themes, also, all codes evolved were clustered in a bigger theme. The steps have considered the application of NVivo computer-aided data analysis software to aid the analysis process, especially in theming the transcribed data.

3. Findings

3.1. Surrounding key themes emerging from semi-structured interviews with subject matter-experts in respiratory care and digital health on beliefs and barriers to uptake of digital health technologies by patients

3.1.1. Utility and patient understanding

Participants commented on the ability of patients to appreciate and use digital technologies for personal management of their respiratory symptoms, for example, Participant 1 believed" *I think there's a little bit of work to be done first before they are given the device around getting them to understand that they can affect change or they can make something at least improve something even if they have a chronic illness that they have control over exacerbation of symptoms.*"

3.1.2. Digital literacy

Digital literacy was noted as a key consideration to the acceptability of technology. Digital health literacy has been identified within the literature as being a factor that influences the adoption of digital health technology but it also is a significant barrier. Slevin et al. (26) explore this theory within their study, where findings suggest that individuals with previous experience with technology, perceived these skills enhanced their digital literacy abilities, therefore empowering them to engage with digital health technology. In the same study, digital literacy was reported to be a significant adoption barrier to digital health technology.

Participant 6 in this study stated "*The ability of the person to use the device is an important consideration. "I have just seen a 47-year-old lady who does not know how to send an email when I tried to give her contact details of how best to contact somebody in an emergency or if they have a question.*"

3.1.3. Data privacy and trustworthiness

Participants noted that despite concerns, the use of technology can have a relatively positive impact on people's lives as noted by Participant *5 "Technology has changed our lives, you know technology is a good idea for the most part.*"

Korpershoek et al. (27) suggest that individuals do not feel that digital health technology can be trusted. Data privacy is commonly discussed and an area that internationally raises concern. The Data Protection Acts 1988–2018 are designed to protect people's privacy. The legislation confers rights on individuals concerning the privacy of their data as well as responsibilities on those persons holding and processing such data. It is assumed that individuals may have strong opinions on their health data and how it may be used; however, to note this is only an assumption and confirmation would be beneficial. Interestingly multiple subject matter experts in this study did not feel that service users would have significant data privacy concerns.

Participant *4* believed that *"I'm not sure about privacy, I do not think that's as big an issue as it may be, for some people, but not for everyone, I think it's getting across and understanding what it is in the first instance, and how your data is being used, and when it is your health data for the people who are the controllers and are the ones who are making these decisions for their clinical team, they need this information.*"

Participant 5 stated *"I do not know if the service users in the patient cohort have huge data concerns. I do not feel like you know patients come in and say God that looks amazing but I'm worried that the Russians are looking you know I mean I just do not.*"

Participant 6 stated "*No, I would not have said that in fact, I would consider the consultation, a lot more privacy on digital technology, because there's a lot of security and protection there for patients with the GDPR concerns some may have, so no I think there's much more privacy sitting in a room on their own.*"

3.1.4. Equality

Equal and fair access to the necessary amenities to engage in digital health technology is ambiguous. This is a common theme among other studies. Multiple authors such as Mathar et al. (28) and

Disler et al. (29) explore the concept that individuals claim that they have no access to technology due to their location and age, but also that they would have little to no confidence in their ability to use any device. It is somewhat unclear what individuals define as "access to." On one hand, individuals are insinuating that they do not own a piece of technology such as a computer to access some of the available online resources, however, the lack of internet access was also highlighted. None of the studies in the literature made specific reference to the access to internet and the reasons why this was an issue. It is very unclear if the participants in the studies which vary across multiple international countries such as the United Kingdom, Australia, Denmark Norway to name a few, were from an urban or rural geographical location. One study however conducted by Sönnerfors et al. (30) in Sweden, does however mention that data were collected in rural and urban areas however no differentiation was made in the discussion of the results. This study was unique also, as it reported that access to the internet and access to technology was a significant facilitator to the adoption of technology. The author highlights to the reader that in Sweden, approximately only 4% of the population are seldom or non-users of the internet. It is also worth noting that the Swedish government has a national vision of e-health for 2025, in which the government pledges to assist and support the population, to have increased access to the internet and digital devices. This would suggest that the successful adoption of digital health technology would require commitment and support from local government to invest in both rural and urban infrastructure and internet access. It would be safe to assume that rural Ireland would lack similar resources and most definitely requires investment.

Similarly in this study, participants believed that not every individual in Ireland has equal and fair access to digital technologies.

Participant 4″ *"The IT infrastructure might be challenging particularly in rural parts of the country."*

Participant 6 stated "*high-speed broadband so even though you are kind of maybe saying okay mine maybe that brilliant for the older population, it might be that brilliant for the younger population, because they cannot afford to engage in it."*

Participant 7 *"Absolutely not and that goes back to you know I'm in a Council House and I am not getting the wifi because they are going to make me commit to 12 months, but the Council said, I have to move out of here in 3 months so I'm not going to sign up there."*

3.1.5. Education

Education, or more specifically IT education, is mentioned within the literature as both a facilitator and barrier to the adoption of digital health technology. Slevin et al. (26) report from an Irish study that participants perceived that IT education should be personalized for everyone. Personalized early IT education would result in a higher uptake of engagement with digital health technology, as it would instill competence and confidence in individuals when presented with digital health technology.

Participant 6 stated, "*I mean, even in my career like I'm self-learning every single bit of it that I've ever done."* Education regarding the use of technology and the intention that it is in place to support and is not intended to replace the HCP is warranted to negate any ill feeling toward technology.

Participant 1 comments *"I think, as soon as they are put on something that is remote so away from a person and they are feeling like their issues are being trivialized in some way. They need to see that it does not have to be an all or nothing, it can be supported by a person and use of technology."*

Participant 4 believed that "*a lack of protocol on the clinical side and a lack of understanding or awareness of what was happening on the service user side."*

A summary of the themes emerging from the interviews with subject-matter expert participants in this project, on reaching data saturation, is shown in Figure 1.

The data analyzed from these semi-structured interviews highlighted many key themes among the subject matter experts on the role and potential effectiveness of DHI for remote patient use. There was a strong concern that people's awareness of digital technologies and their perceived usefulness could be poor. There was also concern that poor awareness could hinder the acceptance of technology as people were somewhat blinkered to the advantages. The literature suggests that the increased knowledge and awareness of disease resulted in better self-management, better reported quality of life, and improved continuity of care from healthcare professionals (31). However, not all studies acknowledged this as a facilitator of the adoption to digital health technology. A qualitative study conducted in the United Kingdom by Sanders et al. (32) reflects the perception that engagement with digital health technology poses a threat to an individual's identity, autonomy, and ability to self-care. It was believed that the use of digital health technology would result in a lifestyle that put too much focus on ill health and would encourage a high degree of dependency on the technology. Individuals were also keen to distance themselves from technology to avoid negative stereotypes of ill health and aging. The increased access to health data and focus in symptom awareness was seen as an aggravating factor for anxiety for some individuals (32) whereas counter-argument was made by Slevin et al. (33) who insinuates that engagement with digital health technology was seen to reduce an individual's experience of anxiety. It can be concluded that an individual's perception of usefulness is a significant element that should be considered as a facilitator, but, also a barrier to the adoption of digital health technology. The follow on quantitative phase of this study will encompass translating information from these semi-structured interviews into a questionnaire for respiratory patient participation attending both rural and urban health service clinics. The questionnaire will be developed using data from this study and will apply the Health Information Technology Acceptance Model. This framework is an amalgamation of TAM and HBM (34).

3.2. The role of living labs in supporting and enabling development and use of digital health interventions in respiratory care

Living labs are a relatively new concept within healthcare despite their existence since the early 2000s. There is no commonly accepted definition of living labs, however frequently used adjectives include, open innovation, user-centric, co-creation, test innovation, and real-life context (35). The idea of living labs facilitates the collaboration of knowledge sharing and research design which delivers a user-centered open innovation system. Broadly speaking the key concept of living labs is the idea that a safe space is created to facilitate knowledge exchange, co-ideation, and testing between diverse stakeholder groups

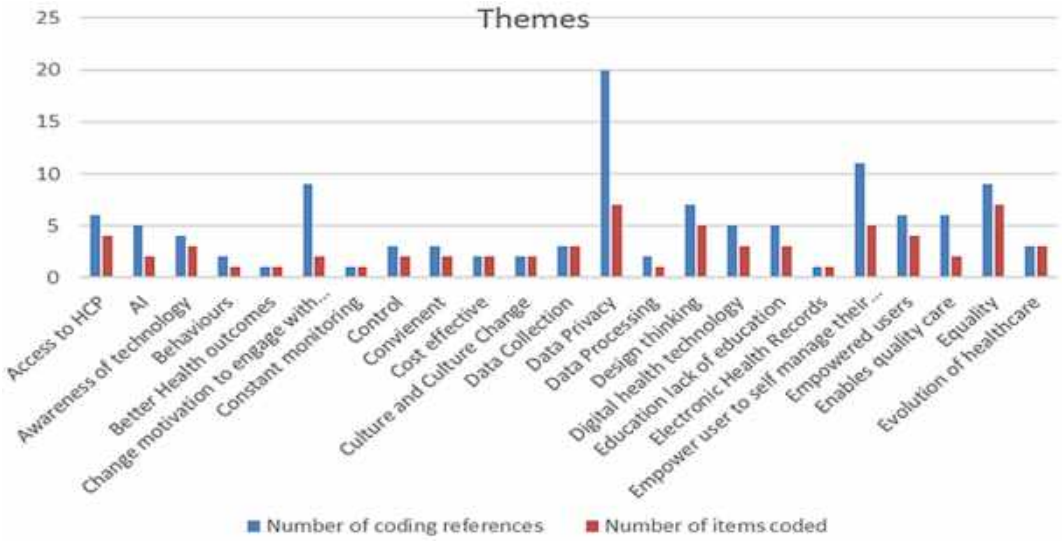

FIGURE 1
Themes emerging from semi-structured interviews with subject-matter expert participants in this study.

in real-life settings (36) The underpinning goal of living labs is to establish and accelerate networking and collaborations of key stakeholders resulting in greater and faster societal impact inclusive of service providers and service users. In Ireland, there are currently nine different living labs focusing on different aspects of digital health. While the type of disease supported varies, the main aim of the living labs is to facilitate the use of technology for remote monitoring, data collection, telehealth, and assistant apps for the older population. Respiratory living labs facilitate actively transferring the research into action. The development of a living laboratory for respiratory care management and intervention in Ireland will be informed by data generated from this study. Key candidate digital technologies to be used and developed in this digital respiratory health library include the Internet of Things (IoT) which includes personalized mobile phone apps; artificial intelligence and machine learning (algorithms) for real-time analysis and intuitive use of big data to promote ease of use and for patient risk mitigation; Edge end-to-end monitoring of data and the use of block chain to develop both business models and to address data trustworthiness; and immersive technologies to help patients and service providers understand new e-technologies. The living lab established for this respiratory patient project or DHI provides access to specialist training environments and subject-matter experts (including immersive technologies), for healthcare and industry through a university interface that also responds to community needs informed by regional policies (Figure 2).

Moreover, the increasing availability and sophistication of mobile health technology continue to garner research interest (37). Liao et al. (37) noted that mobile technology has become a ubiquitous part of everyday life and is challenging the way we offer clinical and health services internationally. However, meeting the challenges posed by unprecedented access to data and the commensurate influx of wearable device data requires a multidisciplinary team of researchers, clinicians, software developers, information technologists, and statisticians. Adoption of digital health technologies in Ireland will also be accelerated by the use of open access and by knowledge transfer from adjacent domains that are more advanced in living laboratories including additive manufacturing and smart agri-food systems (38, 39). The studies of Flott et al. (40) also corroborate the necessity for using this Quintuple Helix Hub encompassing living laboratories as a flexible patient-centered framework for evaluating the digital maturity of health services. Digital maturity is the extent to which digital technologies are used as enablers to deliver a high-quality health service. Flott et al. (40) noted that measurement systems that do exist are limited to evaluating digital programs within one service or care setting, intimating that digital maturity evaluation is not accounting for the needs of patients across their care pathways.

The use of big data and artificial intelligence is under study to stratify the delivery of healthcare. In Ireland, programs have been funded through Horizon (2020), an example being the CLARIFY project which aims to identify risk factors that impact cancer patients´ quality of life after oncological treatment by using Big Data and AI. Data from more than 15,000 survivors of breast, lung, and lymphoma cancer will be reviewed. The objective is to help to stratify cancer survivors by risk to personalize their follow-up by better assessment of their needs.

3.3. Quintuple Helix hub framework for support and enabling living labs in respiratory health

The Quintuple Helix Hub framework combines academia-industry-government-healthcare and society thus providing an integrated multi-actor environment enabling digital transformation of living laboratories, such as for bespoke respiratory care and management. There is a pressing need to embrace national digital transformation strategies, particularly for healthcare; however, there is a gap at the interface between top-down strategic policies and bottom-up healthcare and end-users. This framework operates as a one-stop-shop to cross-cut different disciplines that include specialist infrastructure and equipment sharing, subject-matter expertise, demonstrator facilities, human capital building, training and mobility,

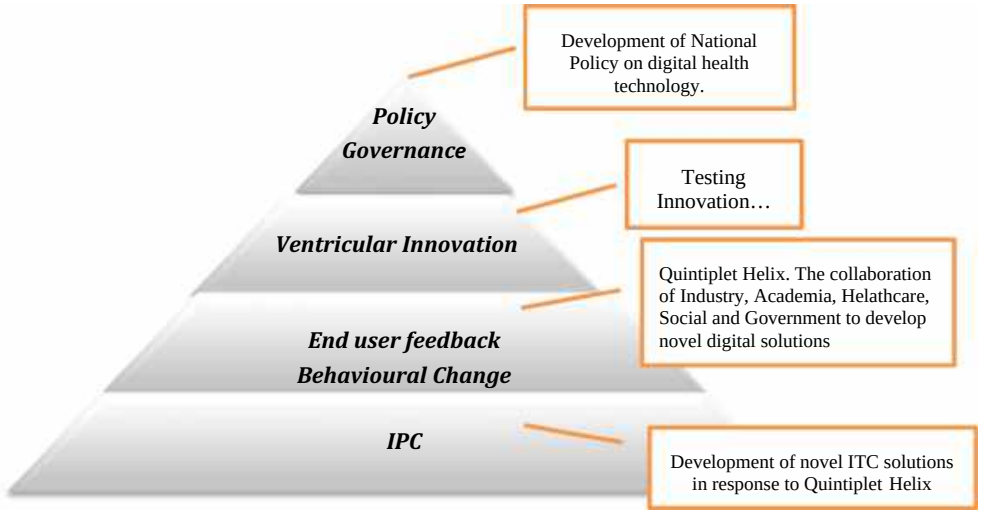

FIGURE 2
Addressing the interface between top-down digital health policies and service end-user needs, such as through a Quintuple Helix Hub Framework.

test-the tech, funding and investing (41, 42). The Quintuple Helix has its' foundations in previous N-Tuple helices (namely Triple and Quadruple) that are explanatory and active models for facilitating and analyzing knowledge-based economies (43). This author reported that "the Triple Helix model of university-industry-government relations measures the extent to which innovation has become systematic instead of assuming the existence of national (or regional) systems of innovations on a priority ground." This model also addresses the system of innovation patterns that embraces integrating (such as functions of wealth creation, knowledge production, and normative control taking place at organizational interfaces) and differentiating factors (such as exchanges on the market, scholarly communication in knowledge production, and political discourse) (43). One can determine whether innovation systems are technology-specific or sector-based by review of indicators, such as co-authorship data arising from the Science Citation Index. Leysdesdorff and Sun (44), previously showed that in Japan, "university scholars have increasingly co-authored with foreign colleagues, thus favoring internationalization above relevance when considering the triple helix model of university-industry-government." It is appreciated that defining selection environments for delineating performing indicators for deploying effective digital health technology beyond the Triple helix of university-industry-government as it will require substantive specification and operational in terms of potentially relevant data that may require the development of additional relevant indicators. However, to effectively deploy appropriate digital technologies, consideration must be given to the additional subject domains of healthcare and society for both subject-matter appreciation, appropriateness, and socio-economic value for tax-payers; thus, inferring development of a Quintuple Helix framework for digital health in Ireland.

This present project addresses key themes for remote patient uptake of digital health innovations including informing future key performance indicators for living labs for respiratory care under a digital health living-lab framework. This challenge is not insignificant, for example, Rowan et al. (39) have noted that there are 706 digital innovation hubs in Europe under varying degrees of maturity. Yet, Brenner et al. (8) highlighted that of the 2,192 publications reviewed and analyzed (PRISMA) between May 2021 and August 2021, only five papers have addressed approaches to inform key performance indicators for the applicability of digital health innovations. Further reading of these five mainly European publications reveals that they mainly focused on developing multi-stakeholder frameworks exploiting literature reviews and expertise meetings to classify indicators (45) and completing interviews with individual stakeholders followed by an interdisciplinary brainstorming session (46). Vedluga (47), applied the Activity Pyramid, Kane's Model Affinity Diagrams, and Critical quality requirements tree to identify stakeholders, their needs and to determine KPIs for Lithuania's national eHealth information system. Carrion (48), and Bradway (49), did not include methods to identify KPIs, but described DHI assessment based on principles of technical readiness and maturity, risks, benefits, and resources needed. Thus, there remains a knowledge gap in assessing both the benefits and barriers to supporting and enabling remote respiratory patient monitoring using digital technologies in a Quintuple Helix framework that also addresses appropriate KPIs for reporting on their effective implementation and management, which also embraces feedback to government on policies at the interface with end-users. This present study reports on the first qualitative phase through interviews with subject-matter experts to guide remote aging respiratory patient usage and their empowerment.

Living labs will also be supported and accelerated by digital twin (DT) activities that refer to the "virtual copy or model of any physical entity (physical twin) both of which are interconnected *via* the exchange of data in real-time. Applications of DT include real-time monitoring, designing/planning, optimization, maintenance, remote access, and so forth" (50). Operating an effective living laboratory that exploits digital technologies including digital twin applications for healthcare can increase productivity and efficiency. This Quintuple Helix Hub framework may potentially also operationally meet clinical programs and electronic medical records for the effective commensurate implementation of appropriate technologies into clinical workflow and allow feedback to measure the impact including key performance indicators on clinical outcomes (37). This hub

framework can also address the nexus to personalized home healthcare options for smart service delivery and patient-centered monitoring (51), such as respiratory care management. Alexandru and Ianculescu (51), noted that as the number of older adult patients increases with a broad spectrum of needs and specificities, the number of available or caretakers diminishes; thus, the healthcare and social system needs to evolve to meet these trends including informing appropriate and efficient decision making such as financial and human resources.

In the context of specialist training and educational programs delivered in living labs supporting eHealth, Extended Reality technologies such as Virtual reality (VR) are emerging as potential platforms to deliver learning content in a more ecologically valid manner. This is based on their delivery of 360° visuals, spatial audio, and allowing the learner to move beyond the passive mode toward an active participant in their learning experience (52). These technologies in conjunction with various wearable sensor technologies support the capture of various user physiological measures in addition to task performance and user interaction to facilitate a true "human-in-the-loop" system that supports adaptive, personalized while maintaining context-based learning (53, 54). The capture system identifies, at the individual level, key abilities of the learner (by moving beyond binary pass/fail reporting toward understanding a specific individual learning needs). This then informs how the presentation system challenges the learner; thus, optimizing the learner experience. It identifies opportunities for improved training including future provision for operator retraining. The Quadruple Helix Hub framework also supports and enables the integrated knowledge translation (IKT) approach that proposes researcher/knowledge user collaboration as a key step in achieving population impact and a way for society to direct science. IKT shifts from a paradigm where the researcher is an expert to one where researchers and knowledge users are both experts bringing complementary knowledge and skills to the team (55).

3.4. Role of DHI as an enabler to informing sustainability for respiratory health

Sustainability is referred to as a societal goal to enable co-existence. More often than not, it is a term more commonly used when referring to global warming and detrimental environmental changes that need radical change. The Irish healthcare system is a constant topic for Government debate which already is at a crisis point. Indeed, with the projected rise in the aging population, the future of Healthcare appears to be grim. The growth of the aging population in the Republic of Ireland has accelerated in comparison to other EU countries. In 2019 the estimated population of individuals greater than 65 in the Republic of Ireland was 696,300 people, which represents approx. 14% of the total population. This is estimated to reach 1.6 million by 2051 (56). This level of growth is likely to increase the already lengthy waiting lists, delay elective surgeries, overburden our emergency departments, and results in poor quality care provision. The current data from January 2023 shows that 505,545 adults and 84,125 children are currently waiting time for Outpatient appointments in Ireland (57). The number of patients waiting for a Respiratory Consultant appointment is estimated to be 19,200. To put this into context, currently, One in eight of the Irish population is waiting for medical intervention. This is 12.5% of the Irish population. Healthcare is at the core of the success of sustainability in many other areas as it is the main beneficiary and contributor to development. It is suggested that ultimately health is determined by a range of environmental, social, and economic influences, and the health of people, places, and the planet are interdependent (58). However, for healthcare to contemplate sustainability, changes need to be radial and imminent.

The introduction and inclusion of technology in the form of digital solutions into how healthcare is delivered is an exciting and welcome innovation currently being explored internationally. Digital solution goals have such diversity, therefore requiring the inclusion of stakeholders who have a particular interest in digital solutions interests (59). Collaboration is the key to success, such as through the Quadruple Helix Hub framework.

3.5. Summary

This study aimed to explore the perspectives of subject matter experts and their view of the factors that influence the pre-acceptability of digital health technology in the aging respiratory patient. The common themes identified in the literature were digital literacy, perceived usefulness, education, and access to and reliability of technology. Each theme uniquely impacts an individual's compliance with digital health technology. Participants discussed the difficulties that they experienced in gaining access to technology and also the lack of availability to the Internet. Most studies in best-published literature did not explore this theme in detail; therefore, it is unclear the reasons for this difficulty. Is it age? Is it geographical? Each of the subject matter experts raised awareness that the availability of appropriate infrastructure was a concern and that not all service users would have access to the internet or technological devices. Lack of digital literacy skills, IT education, and/or access to technology were also identified as concerns that may lead to poor engagement by service users. This topic is somewhat under-researched, and there are very limited Irish studies available for review. Data privacy was also a common theme among the participants in this study, but not a concerning one. It was suggested that service users may be very forthcoming about sharing their health data for the purposes of obtaining support and guidance from healthcare professionals and ultimately disease control. Healthcare is significantly evolving into the world of digital health technology; however, it is very unlikely that service users are evolving as rapidly to evoke change; understanding is needed of the perspectives of the service users to encourage engagement with digital health technology. It is imperative to ensure not only the success of digital health technology but also the sustainability of the Irish healthcare system so that the service users are identified as key stakeholders. Investment in digital health technology is futile if it is not accepted by the end user. Given the increasing emergence of digital innovation hubs across Ireland and Europe ($n = 206$), applying an effective Quintuple Helix Hub framework that encompasses living lab activities will help define datasets and domains for improved utility and data trustworthiness.

This constituted the first study to identify themes believed to be relevant by respiratory care and digital health experts in Ireland to help inform future decision-making among a cohort of respiratory patients in the Irish midlands and Western region that may potentially facilitate engagement with an appropriate use of digital health technology. The study explored and identified expert participant perceptions, beliefs, barriers, and cues to action that would inform content and future deployment of living labs in respiratory care and related strategies for remote patient monitoring of people with respiratory diseases. The

ultimate goal of this case study was to generate and evaluate appropriate data sets to inform the selection and future deployment of an ICT-enabling technology that will empower patients to manage their respiratory systems in real-time in a safe effective manner through remote consultation with health service providers. Findings will advance Digital Health Strategies in Ireland and Europe and will have a global orientation. This study focused on respiratory patients only as it is the area of expertise of the researcher in nursing. The researcher is working full-time as an Advanced Nurse Practitioner and is undertaking this study independently. Leave has not been permitted to expand this study; therefore, this novel study focuses on the group of participants that are accessible.

Data availability statement

The raw data supporting the conclusions of this article will be made available by the authors, without undue reservation.

Ethics statement

The studies involving humans were approved by Technical University of the Shannon Saolta Hospital Group ethics committee. The studies were conducted in accordance with the local legislation and institutional requirements. The participants provided their written informed consent to participate in this study.

Author contributions

TB, NR, NM, and MM-N contributed to the ideation, methods development, and review of first draft, proof editing and final review. NR and TB generated first draft of paper. TB obtained funding via PhD project. NR, NM, and MM-N supervised PhD for data generation and paper synthesis. All authors contributed to the article and approved the submitted version.

Acknowledgments

TB acknowledges funding support from Technical University of the Shannon and Ireland's Health Service Executive (HSE) for this Doctorate study.

Conflict of interest

The authors declare that the research was conducted in the absence of any commercial or financial relationships that could be construed as a potential conflict of interest.

Publisher's note

Supplementary material

The Supplementary material for this article can be found online at: https://www.frontiersin.org/articles/10.3389/fpubh.2023.1203937/full#supplementary-material

References

1. Bauer UE, Briss PA, Goodmand RA, Bowman BA. Prevention of chronic disease on the 21st century: elimination of the leading preventable causes of premature death and disability in the USA. *Lancet*. (2014) 384:45-52/. doi: 10.1016/S0140-6736(14)60648-6

2. Durrani H. Healthcare and healthcare systems: inspiring progress and future prospects. *Mhealth*. (2016) 2:3. doi: 10.3978/j.issn.2306-9740.2016.01.03

3. McPhail SM. Multimorbidity in chronic disease: impact on health care resources and costs. *Risk Manage Healthc Policy*. (2016) 9:143–56. doi: 10.2147/RMHP.S97248

4. Bellani G, Laffey JG, Pham T, Fan E, Brochard L, Esteban A, et al. Epidemiology, patterns of care, and morbidity for patients with acute respiratory distress syndrome in intensive care units in 50 countries. *JAMA*. (2016) 315:788–800. doi: 10.1001/jama.2016.0291

5. Verma R. eHealth literacy among older adults living with cancer and their caregivers: A scoping review. *J. Geriatr. Oncol*. (2022) 13:555–562. doi: 10.1016/j.jgo.2021.11.008

6. Gibson GJ, Loddenkemper R, Lundbäck B, Sibille Y. Respiratory health and disease in Europe: the new European lung white book. *Eur Respir J*. (2013) 42:559–63. doi: 10.1183/09031936.00105513

7. Respiratory health and disease in Europe: the new European Lung White Book | European Respiratory Society (2018). Available at: https://erj.ersjournals.com/content/42/3/559 (Accessed January 13, 2023).

8. Brenner M, Weir A, McCann M, Doyle C, Hughes M, Moen A, et al. Development of the key performance indicators for digital health interventions: a scoping review. *Digit Health*. (2023) 9:205520762311521–8. doi: 10.1177/20552076231152160

9. WHO. (2022), *Monitoring the implementation. Of digital health*. An overview of selected national and international methodologies Monitoring the implementation of digital health: an overview of selected national and international methodologies (who.int).

10. Ferrua M, Minvielle E, Fourcade A, Lalloué B, Sicotte C, Di Palma M, et al. How to design a remote patient monitoring system? A French case study. *BMC Health Serv Res*. (2020) 20:434. doi: 10.1186/s12913-020-05293-4

11. Malasinghe LP, Ramzan N, Dahal K. Remote patient monitoring: a comprehensive study. *J. Ambient. Intell. Humaniz. Comput*. (2019) 10:57–76. doi: 10.1007/s12652-017-0598-x

12. Noah B. Impact of remote patient monitoring on clinical outcomes: an updated meta-analysis of randomized controlled trials. *NPJ Digital Medicine*. (2018) 1:20172. doi: 10.1038/s41746-017-0002-4

13. OECD (2019) Health in the 21st Century: Putting Data to Work for Stronger Health Systems. OECD (OECD Health Policy Studies). doi: 10.1787/e3b23f8e-en

14. Cheung ML. 'Examining Consumers' Adoption of Wearable Healthcare Technology: The Role of Health Attributes. *Int. J. Environ. Res. Public Health INT J ENV RES PUB HE*. (2019) 16:2257. doi: 10.3390/ijerph16132257

15. Lycett HJ. Theory-Based Digital Interventions to Improve Asthma Self-Management Outcomes: Systematic Review. *J. Med. Internet Res*. (2018) 20:e9666. doi: 10.2196/jmir.9666

16. Nadal C, Sas C, Doherty G. Technology acceptability, acceptance and adoption - definitions and measurement (2019).

17. Dundon A, Cipollla D, Mithell J, Lyapustina S. Reflections on digital health tools for respiratory applications. *J Aerosol Med Pulm Drug Deliv*. (2020) 33:127–32. doi: 10.1089/jamp.2020.1597

18. Braun V, Clarke V. Using thematic analysis in psychology. *Qual Res Psychol*. (2006) 3:77–101. doi: 10.1191/1478088706qp063oa

19. Campbell K, Orr E, Durepos P, Nguyen L, Li L, Whitmore C, et al. Reflexive thematic analysis for applied qualitative Health Research. *Qual Rep*. 26:2011–28. doi: 10.46743/2160-3715/2021.5010

20. Dowling M. From Husserl to van Manen. A review of different phenomenological approaches. *Int. J. Nurs. Stud.* (2007) 44:131–142. doi: 10.1016/j.ijnurstu.2005.11.026

21. Mason M. Sample Size and Saturation in PhD Studies Using Qualitative Interviews. *Forum Qualitative Sozialforschung/Forum: Qualitative Social Research*. (2010) 11. doi: 10.17169/fqs-11.3.1428

22. Gregory I. *Ethics in Research*. A&C Black, London (2003).

23. Creswell JW. *How Interpretive Qualitative Research Extends Mixed Methods Research* (2006).

24. Bulman C, Schutz S. *Reflective Practices in Nursing*. Chichester, West Sussex, UK: Published John Wiley & Sons Ltd (2012).

25. Watson C, Gatti SN, Cox M, Harrison M, Hennes J. "Reflective supervision and its impact on early childhood intervention," in *Early Childhood and Special Education*. Bingley: Emerald Group Publishing Limited. (2014) 18:1–26. doi: 10.1108/S0270-402120140000018001

26. Slevin P, Kessie T, Cullen J, Butler MW, Donnelly SC, Caulfield B. Exploring the potential benefits of digital health technology for the management of COPD: a qualitative study of patient perceptions. *ERJ Open Res*. (2019) 5:239. doi: 10.1183/23120541.00239-2018

27. Korpershoek YJG, Vervoort SCJM, Trappenburg JCA, Schuurmans MJ. Perceptions of patients with chronic obstructive pulmonary disease and their health care providers towards using mHealth for self-management of exacerbations: a qualitative study. *BMC Health Serv Res*. (2018) 18:757. doi: 10.1186/s12913-018-3545-4

28. Mathar H, Fastholm P, Sandholm N. A qualitative study of televideo consultations for COPD patients. *Br. Med. J.* (2015) 24. doi: 10.12968/bjon.2015.24.4.205

29. Disler RT, Inglis SC, Newton P, Currow DC, Macdonald PS, Glanville AR, et al. Older patients' perspectives of online health approaches in chronic obstructive pulmonary disease. *Telemed J E Health*. (2019) 25:840–6. doi: 10.1089/tmj.2018.0098

30. Sönnerfors P, Skavberg Roaldsen K, Ståhle A, Wadell K, Halvarsson A. Access to, use, knowledge, and preferences for information technology and technical equipment among people with chronic obstructive pulmonary disease (COPD) in Sweden. A cross-sectional survey study. *BMC Med Inform Decis Mak*. (2021) 21:185. doi: 10.1186/s12911-021-01544-4

31. Gale N, Sultan H. Telehealth as 'peace of mind': embodiment, emotions and the home as the primary health space for people with chronic obstructive pulmonary disorder. *Health Place*. (2013) 21:140–7. doi: 10.1016/j.healthplace.2013.01.006

32. Sanders C, Rogers A, Bowen R, Bower P, Hirani S, Cartwright M, et al. Exploring barriers to participation and adoption of telehealth and telecare within the whole system demonstrator trial: a qualitative study. *BMC Health Serv Res*. (2012) 12:220. doi: 10.1186/1472-6963-12-220

33. Slevin P, Kessie T, Cullen J, Butler MW, Donnelly SC, Caulfield B. A qualitative study of chronic obstructive pulmonary disease patient perceptions of the barriers and facilitators to adopting digital health technology. *Digit Health*. (2019) 5:71729. doi: 10.1177/2055207619871729

34. Kim J. *Living labs for health: an integrative literature review* (2012) 9.

35. Zipfel N, Horreh B, Hulshof CTJ, De Boer AGEM, Van der Burg-Vermeulen SJ. The relationship between the living lab approach and successful implementation of healthcare innovations: an integrative review. *BMJ Open*. (2022) 12:e058630. doi: 10.1136/bmjopen-2021-058630

36. Archibald MM, Wittmeier K, Gale M, Ricci F, Russell K, Woodgate RL. Living labs for patient engagement and knowledge exchange: an exploratory sequential mixed methods study to develop a living lab in paediatric rehabilitation. *BMJ Open*. (2021) 11:e041530. doi: 10.1136/bmjopen-2020-041530

37. Liao Y, Thompson C, Peterson S, Mandrola J, Shaalan M. The future of wearable technologies and remote monitoring in healthcare. *Am Soc Clin Oncol Educ Book*. (2019) 39:115–21. doi: 10.1200/EDBK_238919

38. Rowan NJ. The role of digital technologies in supporting and improving fishery and aquaculture across the supply chain–quo Vadis? *Aquac Fisheries*. (2022) 8:365–74. doi: 10.1016/j.aaf.2022.06.003

39. Rowan NJ, Murray N, Qiao Y, O'Neill E, Clifford E, Barcelo D, et al. Digital transformation of peatland eco-innovations ('Paludiculture'): enabling a paradigm shift towards the real-time sustainable production of 'green-friendly' products and services. *Sci Total Environ*. (2022) 838:156328. doi: 10.1016/j.scitotenv.2022.156328

40. Flott K, Callahan R, Darzi A, Mayer E. A patient-centered framework for evaluating digital maturing of health services: a systematic review. *J Med Internet Res*. (2016) 18:e57. doi: 10.2196//jmir.5047

41. Rowan NJ, Casey O. Empower eco multifactor HUB: a triple helix 'academia-industry-authority' approach to creating and sharing potentially disruptive tools for addressing novel and emerging new green Deal opportunities under a United Nations sustainable development goals framework. *Curr Opin Environ Sci Health*. (2021) 21:100254. doi: 10.1016/j.coesh.2021.100254

42. O'Neill E, McKeon-Bennett M, Rowan NJ. Peatland-based innovation can potentially support and enable the sustainable development goals of the United Nations: Case study from the Republic of Ireland. *Case Studies in Chemical and Environmental Engineering*. (2022) 6. doi: 10.1016/j.cscee.2022.100251

43. Leydesdorff L. The triple Helix, quadruple Helix,….And an N-tuple of helices: explanatory models for analyzing the knowledge-based economy. *J Knowl Econ*. (2012) 3:25–35. doi: 10.1007/s13132-011-0049-4

44. Leydesdorff L, Sun Y. National and international dimensions of the Teiple Helix in Janpan: university-industry-government versus international co-authorship relations. *J Am Soc Inf Sci Technol*. (2009) 60:778–88. doi: 10.1002/asi.20997

45. Hyppönen H, Ammenwerth E, Keizer N. Exploring a methodology for eHealth indicator development. *Stud Health Technol Inform*. (2012) 180:338–42.

46. Farinango CD, Benavides J, Cerón J, López DM, Álvarez RE. Human-centereddesign of a personal health record system for metabolic syn-drome management based on the ISO 9241-210:2010 standard. *J Multidiscip Health*. (2018) 11:21–37. doi: 10.2147/JMDH.S150976

47. Vedluga T, Mikulskiene B. Stakeholder driven indicatorsfor eHealth performance management. *Eval Program Plann*. (2017) 63:82–92. doi: 10.1016/j.evalprogplan.2017.03.001

48. Carrion C, Bradway M, Vallespin B, Puigdomènech E. mHealthAssessment: conceptualization of a global framework. *Int J Integr Care*. (2016) 16:S9. doi: 10.5334/ijic.2556

49. Bradway M, Carrion C, Vallespin B, Saadatfard O, Puigdomènech E, Espallargues M, et al. Mhealth assessment:conceptualization of a global framework. *JMIR Mhealth Uhealth*. (2017) 5:e60. doi: 10.2196/mhealth.7291

50. Singh M, Faurnmayer E, Hinchy HP, Qiao Y, Murray N, Devine D. Digital twin: origin to future. *Appl Syst Innov*. (2021) 4:36. doi: 10.3390/asi4020036

51. Alexandru A, Lianculescu M. Personalized home healthcare options for smart service delivery and patient-centered monitoring. *J E Health Manage*. (2019) 2019:1–11. doi: 10.5171/2019.630156

52. Braga Rodrigues T, Catháin Ó, O'Connor NE, Murray N. A quality of experience assessment of haptic and augmented reality feedback modalities in a gait analysis system. *PLoS One*. (2020) 15:e0230570. doi: 10.1371/journal.pone.0230570

53. Egan D, Brennan S, Barrett J, Qiao Y, Timmerer C, Murray N (2016). *An evaluation of heart rate and ElectroDermal activity as an objective QoE evaluation method for immersive virtual reality environments. Eighth international conference on quality of multimedial Exprience (QoMEX)*. 2016 Eighth International Conference on Quality of Multimedia Experience (QoMEX).

54. Salgado DP. *A QoE assessment method based on EDA, heart rate and EEG of a virtual reality assistive technology system. MMSys 18 proceedings of the 9th ACM multimedia systems conference, June, pp. 517–520*. (2018).

55. Graham ID, Kothari A, McCutcheon CIntegrated Knowledge Translation Research Network Project Leads. Moving knowledge into action for more effective practice, programmes and policy: protocol for a research programme on integrated knowledge translation. *Implement Sci*. (2018) 13:22. doi: 10.1186/s13012-017-0700-y

56. Sheehan A, O'Sullivan R. (2020) Ageing and Public Health – an overview of key statistics in Ireland and Northern Ireland. Dublin: Institute of Public Health.

57. National Treatment Purchase Fund (2023). Outpatient/Waiting List – Hospitals. On behalf of the Integrated Knowledge Translation Research Network Project Leads, Graham, I.D. Available at: https://www.ntpf.ie/home/outpatient_group.htm (Accessed September 28, 2023).

58. Health Service Executive – National Service Plan 2023 (2023). Available at: https://www.hse.ie/eng/services/publications/serviceplans/national-service-plan-2023.pdf (Accessed September 28, 2023).

59. Kulikauskienė K. The theoretical quadruple Helix model for digital inclusion increase. *Manag Organ Syst Res*. (2021) 85:13–32. doi: 10.1515/mosr-2021-0002